



Match-mismatch dynamics and the relationship between ocean-entry timing and relative ocean recoveries of Central Valley fall run Chinook salmon

William H. Satterthwaite^{1,2,*}, Stephanie M. Carlson³, Shanae D. Allen-Moran¹,
Simone Vincenzi², Steven J. Bograd⁴, Brian K. Wells¹

¹Fisheries Ecology Division, Southwest Fisheries Science Center, National Marine Fisheries Service, NOAA, 110 Shaffer Rd, Santa Cruz, CA 95060, USA

²Center for Stock Assessment Research, Applied Math and Statistics, University of California, Santa Cruz, CA 95064, USA

³Department of Environmental Science, Policy, and Management, University of California Berkeley, 130 Mulford Hall #3114, Berkeley, CA 94720, USA

⁴Environmental Research Division, Southwest Fisheries Science Center, NOAA, Pacific Grove, CA 93950, USA

ABSTRACT: The match-mismatch hypothesis suggests there is an optimal window for organisms to undergo key life cycle events. Here, we test the importance of match-mismatch dynamics in the timing of salmon arrival to the ocean, relative to ecosystem phenology, for the ocean survival rates of hatchery-origin fall run Chinook salmon originating from California's Central Valley. Specifically, we considered tag recovery data for releases of coded-wire tagged fish released into the San Francisco Estuary during the years 1978 to 2010. We determined a time lag for each release relative to the local spring transition date (initiation of net upwelling). Additionally, we obtained information on fish condition and size at release, the number of fish released corresponding to distinct tag codes, and yearly stock-specific harvest rate estimates. We used generalized linear models, generalized additive models, and cross-validation to identify the best-supported models for the effects of release timing and other covariates on age-3 ocean fishery recovery rates, a proxy of ocean survival rates. Release time is a useful predictor of within-year variation in survival rates, above and beyond the effects of size at release, presence of disease, and the use of net pens, and the lag relative to spring transition was a slightly better predictor than year-day. The optimal release timing appeared to occur around the end of May, and the optimal time lag appeared to be approximately 70 to 115 d after the spring transition date. However, timing is only one of many factors that affected within- and among-year variation in survival.

KEY WORDS: Timing · Mismatch · Recruitment · Phenology · Salmon · Survival · Fishery · GAM

Resale or republication not permitted without written consent of the publisher

INTRODUCTION

It has been long recognized that the environment plays a significant role in the variability of fish production. Specifically, when exposed to a poor environment at a critical time, the mortality rate of a population will be great, and ultimately, recruitment will be low (Hjort 1914, Cushing 1990). While these may

be tenets in the fishery literature, most fisheries management is still based on information gleaned only from the population dynamics of the fish (Beverton & Holt 1957) without an explicit consideration of environmental drivers. In the last few decades, however, environmental data series have been widely available to explore the impact of the environment on stock dynamics (Quinn & Deriso 1999, Deriso et al.

*Corresponding author: will.satterthwaite@noaa.gov

2008) and have been at times incorporated into management (Jacobson & MacCall 1995, Logerwell et al. 2003). One recurring challenge in incorporating environmental variables into fisheries management models is that correlations between environmental drivers and fishery dynamics have a tendency to break down over time (Myers 1998). Focusing on explicit mechanistic hypotheses for the relationship between environment and fishery dynamics may increase the ability of environmental covariates to improve our understanding of fish population dynamics and management based upon these dynamics.

Here, we examine the relationship between the phenology of upwelling and the survival of juvenile salmon. The timing of ocean entry is a key life history trait that can profoundly influence the early marine survival of anadromous salmon (Bilton et al. 1982, 1984, Whitman 1987, Quinn 2005, Scheuerell et al. 2009). For example, Scheuerell et al. (2009) reported that Columbia River Chinook salmon and steelhead migrating to the ocean early in the season (early to mid-May) experienced 4- to 50-fold higher survival than individuals migrating late in the season (mid-June). They also noted, however, that the timing of peak survival varied among years and hypothesized that the cause was interannual variation in nearshore conditions—especially variation in physical conditions and trophic dynamics. The natural spread in the timing of ocean entry ensures some degree of match between salmon arrival to the ocean and the timing of favorable ocean conditions but also some degree of mismatch (i.e. match-mismatch hypothesis *sensu* Cushing 1990). Indeed, this natural variation in the timing of ocean entry among and within stocks can be thought of as a bet-hedging strategy that spreads risk of mortality among individuals arriving at different times and thus minimizes the possibility of a complete mismatch between salmon arrival to the ocean and the availability of their prey.

Anthropogenic activities that influence the ocean arrival timing of salmon might then have large consequences for the survival of salmon populations. Such influences might include altered migration timing due to slowed passage around dams (e.g. Raymond 1979, 1988), altered river flows and temperatures from water management (Zabel & Williams 2002, Williams 2008, Petrosky & Schaller 2010), or changes to hatchery release strategies (Rechisky et al. 2012). Another management activity that directly affects salmon ocean arrival timing is barging (e.g. on the Columbia River; Budy et al. 2002) or trucking of the fish from the hatchery for direct release into the estuary (e.g. the California

Central Valley; California Hatchery Scientific Review Group 2012).

Chinook salmon originating from the California Central Valley have shown great variability in abundance in recent years, and mismatch dynamics have been invoked as among the potential explanations for this pattern (Lindley et al. 2009, Woodson et al. 2013). For example, juvenile salmon entering the ocean in 2000 and 2001 produced 2 of the greatest recruitment events on record, while only 5 yr later, early survival was so low that the stock collapsed to record low numbers, leading to an unprecedented emergency closure of commercial and recreational salmon fishing off the coasts of California and southern Oregon (Lindley et al. 2009). The proximate cause identified for this collapse, and likely a major contributor to variation over the longer term, is upwelling dynamics, including strength, duration, and timing (Barth et al. 2007, Lindley et al. 2009, Woodson et al. 2013). Previous work in this system has revealed that upwelling intensity relates to variability in a number of salmon vital rates, including growth (Wells et al. 2007, 2008) and recruitment (Logerwell et al. 2003, Wells et al. 2012, Burke et al. 2013). Here, we focus on the role of variability in the match between the timing of upwelling initiation and the time that emigrating juveniles enter the ocean. Upwelling strength and timing are indirectly and directly related to forage and predator dynamics in central coastal California (Croll et al. 2005, Wells et al. 2008, 2012, Thompson et al. 2012, Woodson et al. 2013). Increased nutrients associated with the initiation of the upwelling season positively correlate to zooplankton prey abundance in the Monterey Bay months later (Croll et al. 2005). Wells et al. (2008) and Thompson et al. (2012) demonstrate that, in addition to the indirect positive effect of providing nutrients for primary production, upwelling has a positive and direct effect on zooplankton and forage fish abundance in central California. The direct relationship is partly a result of physical forcing and advective properties associated with the interaction of wind strength and geographic features, such as Point Reyes, which provide an upwelling shadow in which a forage community can develop and be retained (Graham & Largier 1997, Wing et al. 1998, Santora et al. 2012, in press). Juvenile salmon diet composition, condition, and abundance respond positively to the increased prey associated with upwelling (Thompson et al. 2012, Wells et al. 2012), and when prey is delayed or absent from the region, significant increases in mortality of juvenile salmon have been documented (Lindley et al. 2009, Woodson et al. 2013).

A better understanding of how ocean entry timing affects marine survival is important for informed management of salmon stocks and in particular for managing anthropogenic activities that determine ocean entry timing and its influence on fish survival. Our goal is to examine linkages between hatchery release timing, environmental variability including upwelling linked to food web dynamics, and performance of the Central Valley Chinook salmon stock complex.

To quantify match-mismatch dynamics in this system, we compare the distribution of release dates to the spring transition date. We hypothesize that the phenology of upwelling in this system influences salmon survival by determining the availability of salmon prey in the coastal ocean (Croll et al. 2005). We test this hypothesis by examining success of hatchery-released salmon from the Central Valley with respect to release timing. Furthermore, considering the 30 yr period, we ask if there is an optimal time lag between the timing of release and the spring transition date that maximizes the early marine survival of juvenile salmon. While numerous other factors undoubtedly affect salmon survival, and different factors will moderate the effects of timing on survival differentially across years, our primary question is whether the effect of timing is strong and consistent enough that a clear signal emerges, on average, even in the presence of numerous confounding factors. Given the demonstrated importance of upwelling in this system, we further ask whether the initiation of upwelling, as measured by the spring transition date, captures enough information about important ecosystem drivers and phenology that models measuring time relative to the spring transition date can better explain variability in the data than models based on calendar date alone.

MATERIALS AND METHODS

To examine how marine survival and recruitment to the fishery are affected by release timing and lags relative to ocean phenology as characterized by the timing of initiation of upwelling, we considered ocean recovery rates of individual release groups, identified by unique coded-wire tags (CWT; Johnson 1990, Lapi et al. 1990, Nandor et al. 2010). CWT are small pieces of wire injected into the snouts of juvenile salmon, and each tag is etched with a unique batch-code that identifies all individuals released in a given group (hereafter 'release group'). The Regio-

nal Mark Identification System (RMIS, www.rmpc.org) is an online repository for CWT release and recovery data for the Pacific coast. Associated with each CWT in the RMIS database are descriptors such as the release date(s), total number of marked fish that were released, average weight of fish at release, developmental stage of fish at release, source hatchery, location of release, and a comments field that includes various notes including, for example, whether fish in a release group showed signs of disease or poor condition.

Release groups identified by coded-wire tags

We analyzed CWT groups released directly into San Francisco Bay for which the approximate time of ocean entry is known and results are not influenced by variability in survival during downstream migration. We queried the RMIS for all releases of CWT Central Valley fall run Chinook salmon released into the San Francisco Estuary through 2010. Note that all of these fish were of hatchery origin.

Ocean recovery rates

We also queried RMIS for all recoveries of CWT fish in the ocean recreational or troll fisheries reported by California Department of Fish and Game (CDFG; now the California Department of Fish and Wildlife [CDFW]) or the Oregon Department of Fish and Wildlife (ODFW) and calculated ocean recoveries $O_{i,a}$ as the sum of the 'estimated number' (i.e. expanded for subsampling of the harvest) reported for each recovery of an age a fish from the release group i in the ocean fishery, repeated over all age-year combinations subject to the fishery. To recover the tags, adults are sampled from commercial and sport fisheries. A known fraction, typically ~20%, of the harvest is examined for the presence of CWT. This allows calculation of a sample expansion factor that estimates how many CWT fish from a particular release group were likely in the total sampling stratum for each CWT read. Thus, for every CWT from a particular release group recovered in a particular sampling stratum with sample rate f , it is assumed that $1/f$ fish were caught. We then use the sum of these $1/f$ values across strata to estimate total recoveries. Ages are calculated as the difference between recovery year and brood year, where brood year is the year of spawning and fish are typically released the next calendar year.

Covariates and confounding issues

Our direct interest is in the relationship between release timing and survival as indicated by ocean recovery rates. We characterized years on the basis of spring transition (Schwing et al. 2006, Bograd et al. 2009) at 39°N, 125°W. Spring transition is defined as the day in each calendar year that the cumulative coastal upwelling index (for that year, integrated daily values starting January 1) first starts increasing from its minimum value, and this transition day is highly variable across years (Fig. 1). We hypothesized that 'time lag', the difference between the year-day (i.e. day of year) of release and the spring transition date, would provide a better predictor of relative survival than year-day alone.

We excluded individual release groups whose release dates spanned >30 d since no single release date could be assigned to such groups (amounting to only ~6% of all records). For the remaining groups, we determined the total number of marked fish in each release group N_i released on year-day t of year y . When a release group was released over multiple days, we characterized the group based on the midpoint of the release dates.

Our analyses also allowed for expected effects of numerous covariates, such as the use of acclimation (net) pens prior to release, and notes of disease or poor condition associated with individual release groups. Many studies (Ward et al. 1989, McGurk 1996) have found an effect of size at emigration on survival (but see Tomaro et al. 2012), so we included weight as a covariate as well. We removed data for release groups with no weight information (~2% of records).

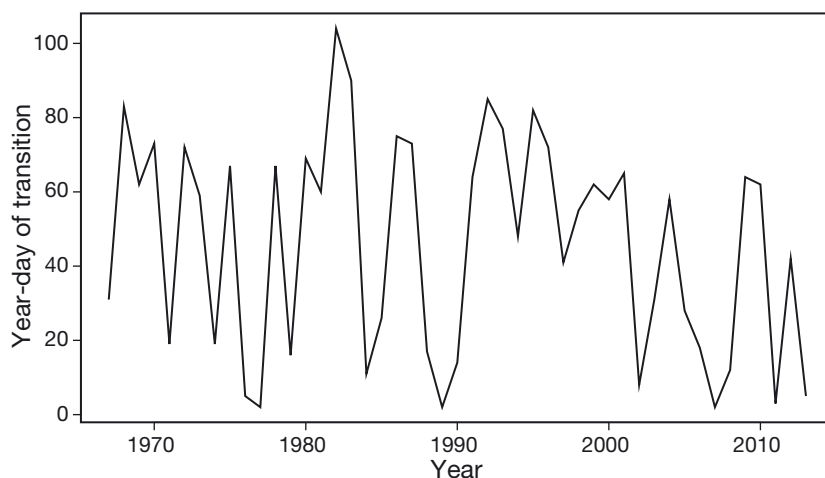


Fig. 1. Annual variation in spring transition date measured at 39°N, 125°W (see 'Materials and methods: Covariates and confounding issues' for methodological details); 'year-day' = day of year

Because release times varied among hatcheries, and some hatcheries had a very restricted range of release dates, we restricted our analysis to Feather River Hatchery releases, which released fish over a protracted period (see Supplement 1 at www.int-res.com/articles/suppl/m511p237_supp.pdf for further details). To reduce the collinearity between weight and release timing, we restricted our analysis to fish released as 'fingerlings' or 'advanced fingerlings' which make up the majority of releases (~90%), rather than the much larger smolts or much smaller fry. We considered only age 3 ocean recoveries because prior to being caught at age 3, the predominant source of mortality is from natural causes, and recoveries of age 2 and age 4 fish are comparatively rare (Supplement 1; age 3 recoveries typically an order of magnitude higher than age 2 and age 4, with negligible recoveries of other ages). We excluded releases from years 2006 and 2007 due to closures of the fishery in 2008 and 2009, precluding recovery of age 3 fish. Data filtering is described more fully in Supplement 1.

We also integrated into our analysis an approximation of Sacramento River fall run Chinook (SRFC) adult harvest rate based on the Sacramento Index (see 'Modeling recoveries' below) (O'Farrell et al. 2013). SRFC harvest rates were applied to recovery years of age 3 fish. Yearly estimates of SRFC harvest rates do not exist prior to 1983, limiting data to fish released after 1980.

Finally, one observation was excluded in which the year-day of release was far greater than other release groups. In total, we used information from 164 Feather River Hatchery release groups that were released in years 1981 to 2010 (Table 1).

Modeling recoveries

The expected number of age a ocean recoveries of release group i ($O_{i,a}$) is a product of the probability of surviving until being caught in ocean fisheries ($s_{i,a}$), the conditional probability of a live fish being caught at age a after being released in year y ($c_{y,a}$, accounting for fishery effects in year $(y-1) + a$), and the number released (N_i). We assume the conditional probability of being caught at age 3 is proportional to the SRFC harvest rate ($c_{y,3} = \phi h_y$), where ϕ is a constant of

Table 1. Annual number of release-groups released directly into San Francisco Bay by each California Central Valley fall Chinook hatchery (CM: Coleman; MC: Merced; MK: Mokelumne; NB: Nimbus; TC: Tehema-Colusa; FE: Feather). Releases spanning >30 d were excluded, as were releases without information on release weight or those that reached age 3 in years before the Sacramento River fall run Chinook (SRFC) harvest rates were estimated. Only fingerling (finger.) and advanced fingerling (adv. finger.) releases from Feather River Hatchery were included in the models presented in this study (see Supplement 1 at www.int-res.com/articles/suppl/m511p237_supp.pdf)

Re- lease year	CM	MC	MK	NB	TC	FE All	FE (finger. and adv. finger. only)
1981	2	0	1	0	0	6	5
1982	3	0	1	0	0	6	5
1983	0	1	1	3	0	7	5
1984	0	1	0	3	0	3	3
1985	0	1	3	2	0	9	9
1986	0	0	2	2	2	4	4
1987	0	0	0	2	0	2	2
1988	1	0	0	3	0	2	2
1989	1	0	2	4	0	2	2
1990	1	0	0	4	0	0	0
1991	1	0	0	0	0	0	0
1992	1	0	0	0	0	0	0
1993	0	0	0	0	0	2	2
1994	0	0	0	0	0	9	9
1995	0	0	0	0	0	10	10
1996	0	0	2	0	0	9	9
1997	0	0	1	0	0	6	6
1998	0	0	2	0	0	2	2
1999	0	0	1	0	0	11	11
2000	0	0	2	0	0	6	5
2001	0	0	2	6	0	10	9
2002	0	0	0	3	0	7	7
2003	0	0	0	0	0	10	10
2004	0	0	0	0	0	5	5
2005	0	0	0	0	0	11	11
2006	0	0	0	0	0	22	22
2007	0	0	1	4	0	17	17
2008	1	0	5	3	0	13	13
2009	2	0	0	4	0	8	7
2010	2	0	0	2	0	12	12

proportionality, and the yearly SRFC harvest rate (h_y) is the estimated number of age 3 to age 5 SRFC caught as a proportion of an index of yearly abundance (O'Farrell et al. 2013). If we further assume the fates of fish are independent, ocean recoveries of age 3 fish from N_i number of tagged releases are binomially distributed:

$$O_{i,3} \sim \text{Bin}(N_i, s_{i,3}\phi h_y) \quad (1)$$

Since the unconditional probability of being caught ($s\phi h$) is small, the number of recoveries can be well approximated by a Poisson distribution (Raff 1956). However, due to the non-independent fates of individual fish, the presence of measurement error, and

the complex forces and interactions acting on ocean survival, there is likely to be much unexplained variation. For these reasons, we allow the variance (σ^2) of the Poisson to be greater than the mean (μ) (Ver Hoef & Boveng 2007). The variance of the related overdispersed Poisson distribution is calculated as follows:

$$\sigma^2 = \theta\mu \quad (2)$$

such that θ is an estimated overdispersion parameter ($\theta > 1$).

Age 3 ocean recoveries (count data) are then modeled as an overdispersed (quasi) Poisson regression with mean μ . We chose to use a quasi-Poisson distribution to allow for overdispersion rather than a negative binomial distribution due to its better computational performance and the lack of specific motivation for using a negative binomial. Our data do not allow separate estimation of ϕ and s ; thus, we assume constant ϕ and interpret their product (which is itself modeled as a function of various covariates) as a measure of relative survival. Thus, the expected number of fish recovered (μ) from an initial release of N fish is $s\phi hN$, yielding the following relation:

$$\log(\mu) = \log(Nh) + \log(\phi s) \quad (3)$$

In the null model, no covariates other than year affect survival, resulting in the following relation:

$$\log(\mu) = \log(Nh) + \gamma_y \quad (4)$$

where γ_y is the combined effect of release year y to recovery year $y + 2$, and $\log(Nh)$ is treated as a model offset. Year effects (γ_y) are modeled as random effects and include unaccounted effects of natural mortality prior to being caught, exploitation and maturation of age 2 fish, ignored interacting effects between release timing and year, and temporal deviations in the proportional difference (otherwise assumed constant at ϕ) between conditional recovery probabilities and the SRFC harvest rate.

Additional models are based on the null model and include a linear effect of release weight ($\beta_1 W$), an additive effect of net pens (β_n), and/or an effect of disease/poor condition (β_d). Also, 2 other suites of

models include either an effect of year-day of release or an effect of time lag relative to spring transition date. Without the effects of weight, disease, or net pens, the mean of a model that includes the effect of time lag (i.e. year-day of release $[t]$ – year-day of spring transition $[\tau]$) is generalized as follows:

$$\log(\mu) = \log(Nh) + f(t - \tau, \nu) + \gamma_y$$

$f()$ is a smooth function of a generalized additive model (GAM; Wood 2011) allowing for nonlinear effects of release timing on survival with a maximum of ν degrees of freedom, where ν ranges from 1 to 5 or is unspecified (i.e. unconstrained), and the maximum possible number of knots is $\nu + 1$. This results in a total of 104 models, 8 with no release timing effects, 48 with potentially nonlinear effects of year-day of release, and 48 with similar effects of time lag.

One assumption of these models is that different release groups from the same year are equally vulnerable to fisheries (and thus that release timing does not have major effects on ocean distribution or size-at-age, affecting the proportion of fish reaching legal size). Similar ocean distributions might be expected for similar run types originating from the same or adjacent watersheds, based on the results of Weitkamp & Neely (2002) and Satterthwaite et al. (2014). Previous work (Hankin 1990) has suggested that later releases may be smaller than earlier releases in subsequent years (since later releases have spent less time growing in the more favorable ocean environment) but also found that later releases more often exhibit delayed maturation. Another assumption is an equal effect of release timing across years. For interpretability, we did not consider an interaction between release time and year (aside from that implied by changing the measure of release time to the lag from the spring transition date, which varies by year), but in Fig. 2, we present the relationship between release time and recovery rates standardized by SRFC harvest rates for individual years without a formal analysis.

Models were fit using the *mgcv* package (Wood 2011) in R 2.15.1 (R Development Core Team 2012).

We used Monte Carlo cross-validation rather than Akaike's information criterion due to concerns about non-independence of different release groups and a tendency for Akaike's criterion to favor overparameterized models (Shao 1993). The Monte Carlo cross-validation method involves randomly splitting the data into k subsets and calculating the prediction error for each subset. This is repeated over a number of iterations. We performed 1500 Monte Carlo cross validation iterations, each time randomly selecting

41 subsets (k) with 4 data points per subset. Then, for each subset, we quantified the error when predicting a single subset (4 data points) from a model fitted to the remaining 40 subsets. The median number of releases per brood year is 6; thus, $k = 41$ mostly ensures that if data from a particular release year are included in the validation subset, they are also included in the training data. Model errors for a validation subset were not calculated if release years in the validation subset were not included in the training data. Our model selection criterion is the minimum root weighted mean squared prediction error (RWMSE). Since release groups varied in size and thus in the certainty with which recovery proportions could be estimated, we weighted each datum on the basis of the number of total fish present in the corresponding initial release. We also consider a cross validation metric similar to R^2 , denoted R_{CV}^2 (equivalent to OCV^* in Rupp et al. 2012). Diagnostic plots for the best-supported model are presented in Supplement 2 at www.int-res.com/articles/suppl/m511p237_supp.pdf.

RESULTS

Combining data from a wide range of release years (1981 to 2010) for Feather River Hatchery releases, the relationship between release timing and age 3 ocean recovery rates standardized by SRFC harvest rates appeared to vary across years (Fig. 2). This illustrates that, given current practices and covariation among factors, there is no consistent optimal release time that applies for all years, with 'optimal' defined as yielding the greatest availability to the fishery.

The best-supported model when applied to releases from Feather River Hatchery included the effects of net pen, disease, and release time as measured by time lag rather than year-day. This model had a mean RWMSE of 0.0037 and a mean R_{CV}^2 of 0.60 (Table 2). A similar model with release year-day in place of time lag was less supported ($\overline{RWMSE} = 0.0047$ and $\overline{R_{CV}^2} = 0.45$), but including either measure of release timing was better than including none at all ($\overline{RWMSE} = 0.0051$ and $\overline{R_{CV}^2} = 0.41$).

The earliest releases appeared to survive poorly (Fig. 3a,b), and releases approximately 90 d after the spring transition appeared to do better than even later releases (Fig. 3a). Very late releases may have also fared well (Fig. 3a,b), but there were few data points driving this part of the curve and most points were from early release years. Releases of heavier

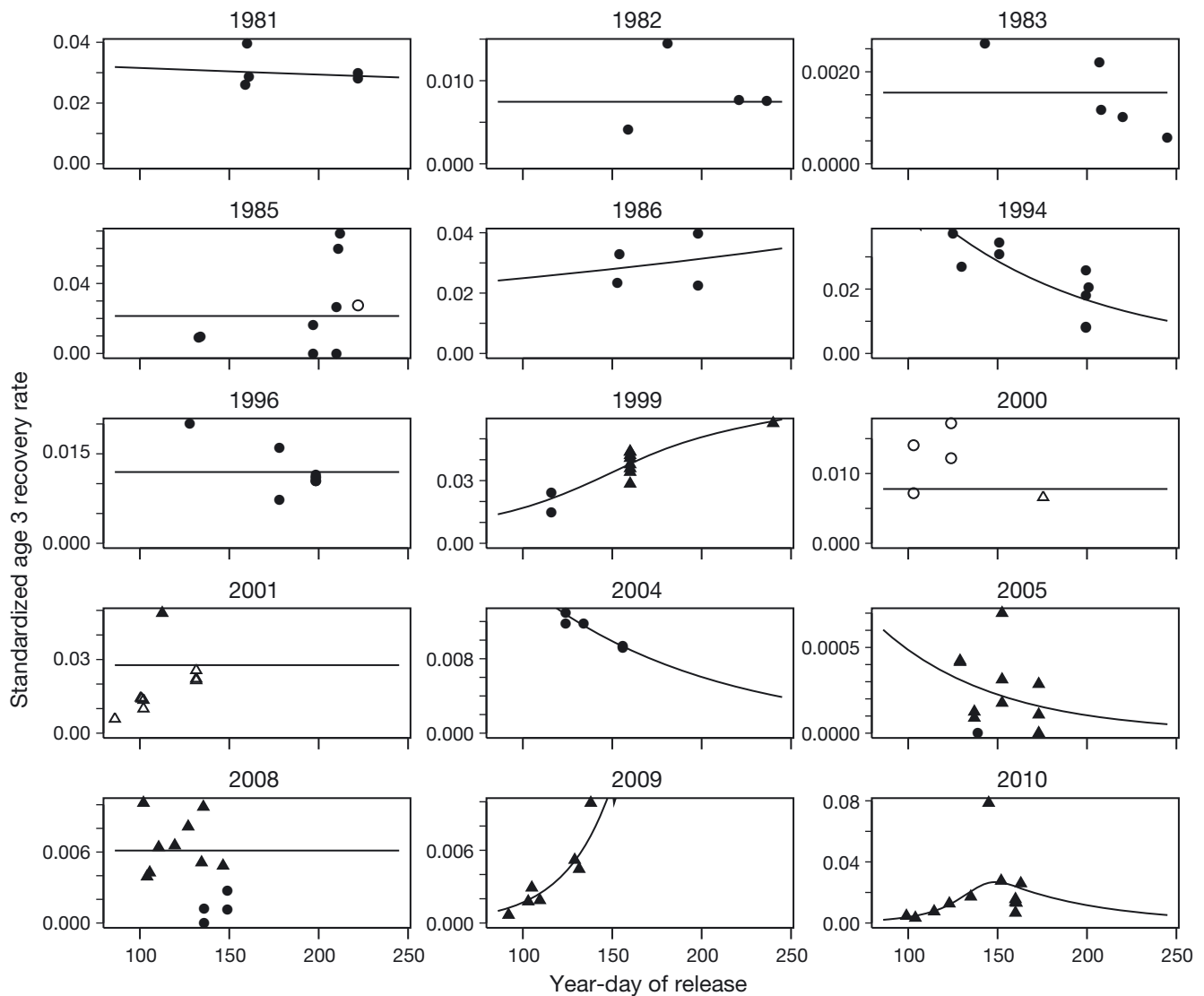


Fig. 2. Age 3 ocean recovery rates standardized by SRFC harvest rates as a function of release date (year-day) for Feather River Hatchery releases. Releases spanning >30 d were excluded, as were release groups with missing weight information and those released as smolts or fry. Open symbols denote mention of disease or poor condition, and triangles denote releases that were acclimated in net-pens. Filled circles are fish that were not diseased and not acclimated in pens. Fitted lines are intercept-only or GAM models chosen based on leave-one-out cross validation and minimum root weighted mean squared error (RWMSE). Note that y-axis scales vary among panels

fish had higher survival rates (Fig. 3c), and fish with disease were less likely to survive (Fig. 3d). Fish acclimated in net pens may have had poorer survival but not significantly so (Fig. 3e). Even after accounting for these effects, there was substantial variation in estimated year effects on recovery (Fig. 4).

DISCUSSION

The overall goal of this study was to investigate the importance of ocean arrival timing on salmon sur-

vival to test the hypothesis that timing relative to ecosystem phenology would influence salmon ocean survival. We found support for the importance of arrival timing relative to spring transition to driving intra-annual variation in salmon survival (i.e. our 'Time lag' model received the strongest support; Table 2), but we also found an effect of calendar date irrespective of ocean phenology (i.e. our 'Year-Day' model received more support than a model without any time effect; Table 2).

The use of model comparison techniques and GAMs allowing for nonlinear relationships provided

Table 2. Results of model comparison analyzing Feather River Hatchery releases for release years 1981 to 2010. Top models with the lowest mean prediction errors (ranked by \overline{RWMSE}) and their associated mean cross validation R^2 values ($\overline{R^2}_{cv}$) are shown. (*) indicates a particular term was included in the model; (-) indicates it was excluded. v: maximum degrees of freedom, with ∞ denoting unconstrained degrees of freedom

Year	Weight	Time, v	Net pen	Disease	\overline{RWMSE}	$\overline{R^2}_{cv}$
*	*	Lag, 4	*	*	0.00367	60.1
*	*	Lag, 5	*	*	0.00370	59.7
*	*	Lag, ∞	*	*	0.00370	60.1
*	*	Lag, 4	-	*	0.00371	59.8
*	-	Lag, 4	*	*	0.00372	59.0
*	-	Lag, 5	*	*	0.00373	59.0
*	-	Lag, ∞	*	*	0.00373	59.4
*	*	Year-day, 3	-	*	0.00471	44.8
*	*	Year-day, 3	*	*	0.00475	44.6
*	-	-	-	*	0.00505	41.3

strong support for a relationship between ocean entry timing and survival, inferred by recovery rates in ocean fisheries standardized by SRFC harvest rates. At the same time, we note very strong year effects (i.e. controlling for modeled effects of release time and other covariates such as fish size) on survival rates irrespective of timing. For example, the central 90% of year effects corresponded to predicted age 3 survival rates that varied 19-fold according to the best-supported model applied to the full dataset (Fig. 4a). Note that this period excluded 2 years of very low recovery rates corresponding to the recent salmon collapse and fishery closure

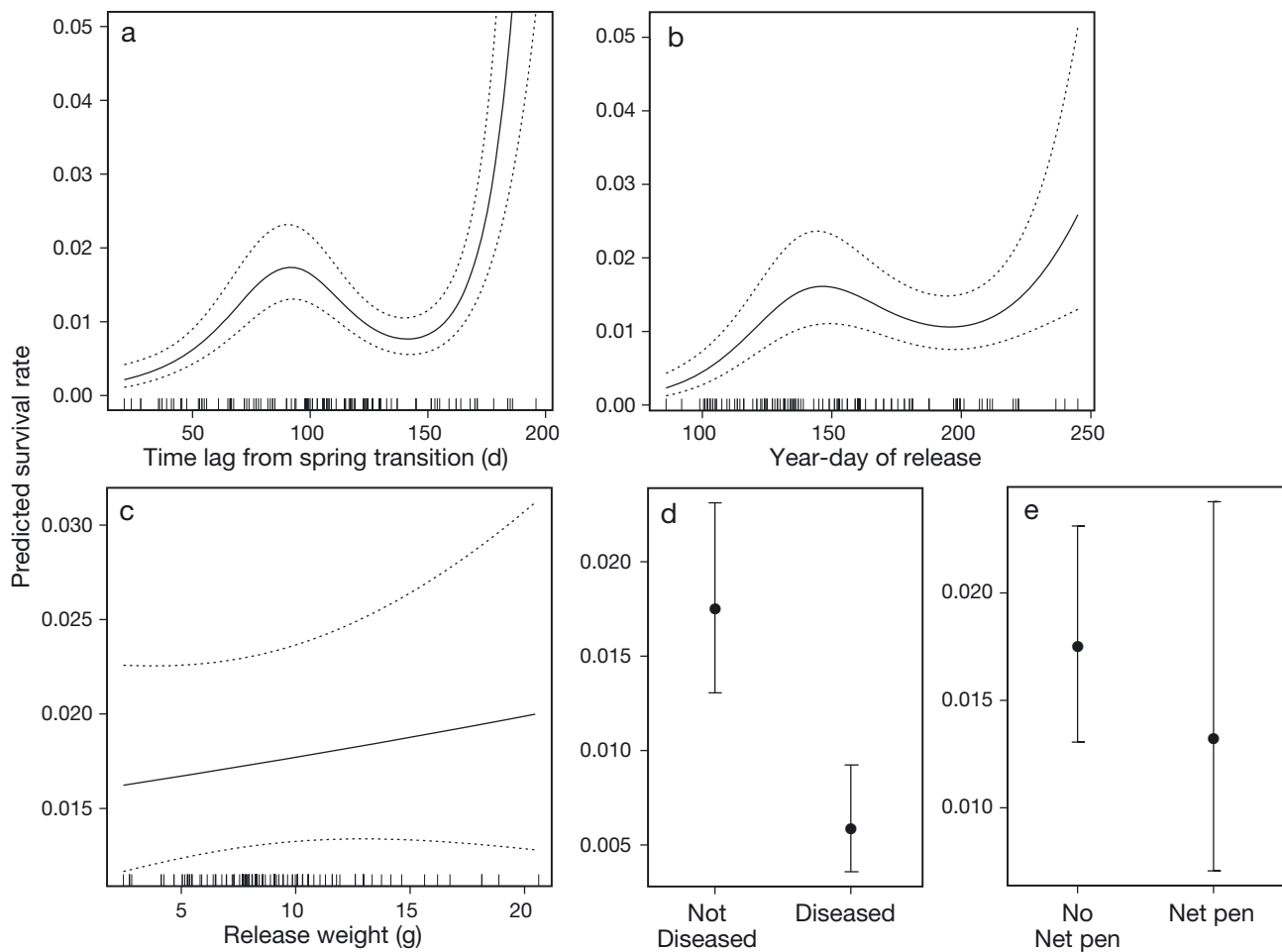


Fig. 3. Model predicted survival rate (harvest-adjusted recovery rates with approximate 95% predictive intervals) illustrating the fitted effects of timing measured as (a) time lag from spring transition, (b) timing measured as year-day, (c) release weight, (d) the presence of disease, and (e) the use of net pens. Predictions are for the year with median fitted year effect (1996), and at the optimal time lag of 92 days (all but a and b), median release weight (all but c), without disease (all but d), or without net pen (all but e). The rug-plots represent values of the independent variable with associated data

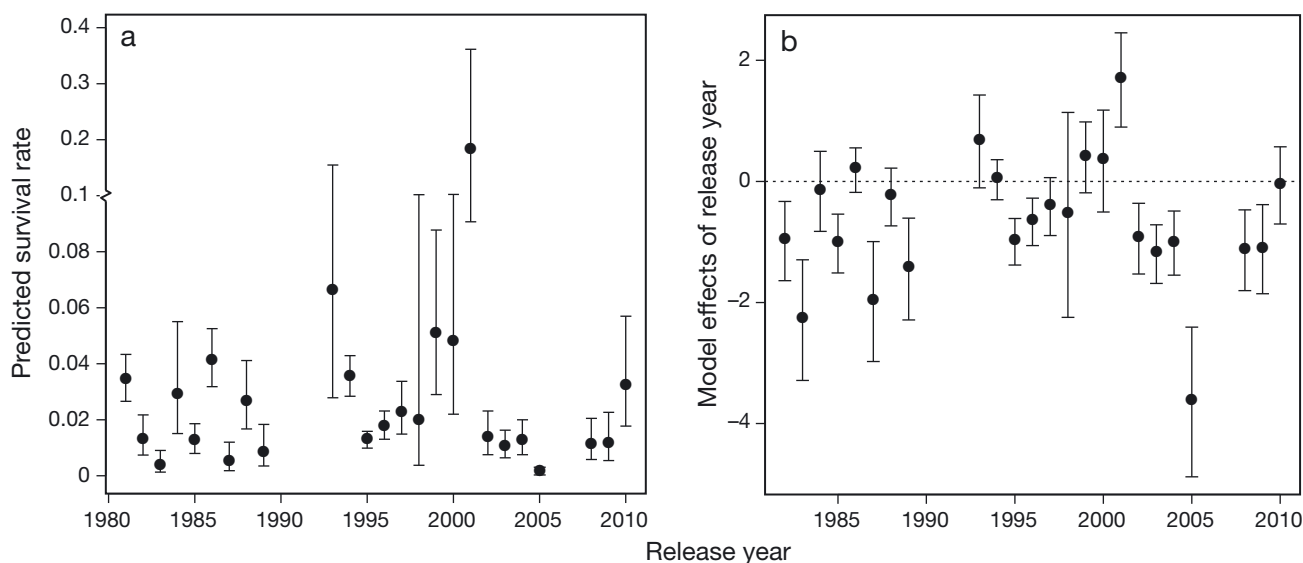


Fig. 4. Fitted year effects in the best-supported model, presented as (a) predicted harvest-adjusted recovery rates (with approximate 95 % prediction intervals) given release of non-diseased, non-net pen, median-weight fish at the optimal time lag from the spring transition date (92 d). Also presented are (b) model year effects (with approximate 95 % prediction intervals) on the log scale

(Lindley et al. 2009), so overall variation in year effects may be even greater.

The degree of variation in year effects is not surprising given the numerous ecological factors acting at longer time scales that may affect early ocean survival—for example, important effects of upwelling intensity, mixing, mesoscale activity, and advection are apparent in this system (Santora et al. 2011, 2012, in press, Ralston et al. 2013), as are preconditioning effects carried over from the previous year (Schroeder et al. 2009, 2013). For instance, the most extreme year effect is associated with release year 2005 and is highly negative (Fig. 4b); while the timing of spring transition was earlier than average in 2005, upwelling that followed was particularly weak (Lindley et al. 2009). This year was also characterized by anomalous poleward transport during the winter 2005 and low krill survival in spring (Dorman et al. 2011). Apparent year effects on age 3 recovery may also reflect temporal variation in age 2 maturation, natural mortality, and/or exploitation, but we do not attempt to model age 2 dynamics due to limited data, as described in Supplement 1.

While our results provide strong support for the existence of a nonlinear relationship between release timing and survival rates within years, there is some ambiguity regarding the explanatory power of timing per se (i.e. year-day) versus timing relative to characteristics of ecosystem phenology (here, using the spring transition date as a metric of phenology).

In addition, effects of release time on survival rates are not fully consistent across years (see Fig. 2; variation among years was also reported by Scheuerell et al. 2009). Indeed, previous studies have reported effects of smolt size or early growth rates on marine survival in some years but not others (in particular, size or growth rate may only be strong predictors in stressful years: Holtby et al. 1990, Tomaro et al. 2012, Woodson et al. 2013), so it is not surprising that relationships between release timing and survival may vary across years as well. Thus, variable timing of ocean entry may amount to little more than making the most of a bad situation in some years.

Further, the apparent effects of timing and release weight are complicated by the collinearity between release time and fish size, although with $r = 0.50$, the observed correlation in the analyzed dataset is below the threshold often invoked as problematic (Dormann et al. 2013). In this case, our results suggested poor survival of either very early releases or releases of small fish, which tend to occur together. Teasing apart the relative influence of timing versus size is challenging because these traits are often correlated. However, in a series of experimental releases designed to test the relative importance of timing versus size, Bilton et al. (1984) and Morley (1988) reported stronger effects of timing than size on survival of coho salmon and Whitman (1987) found similar results for Chinook salmon.

Even using cross validation methods, the very large apparent sample sizes made possible by multiple CWT release groups can easily lead to overfitting if the assumption of statistical independence is violated, making it difficult to unambiguously identify the most important predictors of survival or rigorously quantify their effects. An additional concern is the leverage of extreme values when our dataset contains only a few late releases from early years. Finally, the unbalanced design is a concern, both in terms of potentially conflating year effects with covariates unequally distributed among years and differential influence on overall model results of years with different sample sizes and temporal spread of releases. Unfortunately, uncertainty and sensitivity to model specification and choice of dataset is an unavoidable consequence of using ocean recovery rates to infer survival, a problem affecting this and other studies with important management implications. We are attempting to address a complicated problem with data collected by a fishery, not a planned sampling scheme executed in the context of a designed experiment. Thus, we did not attempt to fit even more complicated models including year-by-timing interactions or additional environmental covariates.

Nevertheless, despite the presence of numerous confounding factors we did not attempt to model directly, we found evidence for a relationship between ocean entry or hatchery release timing and survival rates that was strong enough for a clear signal to emerge for the average effect. In addition, there appeared to be an optimal time after accounting for other effects such as body size, with some suggestion that this optimal timing within a given year could be predicted relative to the spring transition date. A similar analysis by Ryding & Skalski (1999) also supported optimal conditions for early marine survival of coho salmon related to the date of spring transition. Even though the predicted effects of small changes in release timing are generally small, given very large total releases (average 32 million yr^{-1} from 2000 to 2010 across all 5 hatcheries; E. Huber & S. Carlson unpubl.), a small change in survival may still translate into a large number of returning adult fish. Of course, regardless of release timing, we expect reduced survival overall in years of generally poor ocean conditions (e.g. Barth et al. 2007, Lindley et al. 2009).

Translating these results into advice on hatchery practices may prove difficult for several reasons. For example, the effects of timing described here were generally small aside from poor survival of the earli-

est releases and the apparent but uncertain increase in survival of the very late releases (Fig. 3a,b). Specifically, survival rates increase 2.3-fold when time lag decreases from the local minimum of 149 d to the local maximum of 92 d, compared to a 19-fold difference in survival due to year effects. Beyond a weak effect of timing, the 'peaks' corresponding to optima were generally broad. Moreover, spring transition date is variable from year to year (Fig. 1) and may not be known far enough in advance to alter hatchery conditions such that fish will be prepared for release at a target time. Further, we found significant effects of fish size, which is difficult if not impossible to manipulate independently of release time (i.e. releasing fish at a later date often involves releasing them at a larger size).

In addition, our results suggest that the relationship between relative survival and release timing does not always show a consistent within-year pattern (Fig. 2), and this variability combined with a lack of prior knowledge of spring transition timing might argue for staggered release times. Such staggering might be accomplished through direct staggering of release timings by hatchery managers or by increased on-site releases, as has been advocated recently for other reasons (California Hatchery Scientific Review Group 2012). Indeed, different release strategies among hatcheries could contribute relevant variation to the portfolio effect in this system, akin to stock or run-specific variation typical of less-impacted systems (Hilborn et al. 2003). On-site releases would also tend to staggered ocean entry timing as fish made their individual paths down the river, although on-site releases do face added mortality risks in rivers. Williams (2006, his Fig. 5-28) notes that Chinook believed to be fall or spring run are recovered in San Francisco Bay all year, but recoveries peak in April or May and are very low before February or after July (consistent with the full distribution of Feather River Hatchery release dates analyzed but wider than a typical single year; Fig. S1 in the Supplement). In addition, fish migrating downstream may be able to adjust their transit time in response to environmental cues, possibly allowing fish to arrive during more favorable conditions.

Acknowledgements. This work was supported by funding from California Sea Grant (R/FISH-217) and the California Sea Grant Ocean Protection Council. We thank A. Grover, D. Hankin, M. Mohr, M. O'Farrell, and I. Schroeder for helpful discussions and assistance with accessing data and O. Shelton and A. Winhip for helpful comments on earlier drafts of the manuscript.

LITERATURE CITED

- Barth JA, Menge BA, Lubchenco J, Chan F and others (2007) Delayed upwelling alters nearshore coastal ocean ecosystems in the northern California Current. *Proc Natl Acad Sci USA* 104:3719–3724
- Beverton RJH, Holt SJ (1957) On the dynamics of exploited fish populations. *Fishery Investigations Ser II Vol XIX*. Ministry of Agriculture, Fisheries and Food, London
- Bilton HT, Alderdice DF, Schnute JT (1982) Influence of time at release of juvenile coho salmon (*Oncorhynchus kisutch*) on returns at maturity. *J Fish Res Board Can* 39: 426–447
- Bilton HT, Morley RB, Coburn AS, van Tyne J (1984) The influence of time and size at release of juvenile coho salmon (*Oncorhynchus kisutch*) on returns at maturity; results from releases from Quinsan River Hatchery, B.C., in 1980. *Fisheries and Oceans Canada, Nanaimo, BC*
- Bograd SJ, Schroeder I, Sarkar N, Qiu X, Sydeman WJ, Schwing FB (2009) Phenology of coastal upwelling in the California Current. *Geophys Res Lett* 36:L01602, doi:10.1029/2008GL035933
- Budy P, Thiede G, Bouwes N, Petrosky CE, Schaller H (2002) Evidence linking delayed mortality of Snake River salmon to their earlier hydrosystem experience. *N Am J Fish Manag* 22:35–51
- Burke BJ, Peterson WT, Beckman BR, Morgan C, Daly EA, Litz M (2013) Multivariate models of adult Pacific salmon returns. *PLoS ONE* 8:e54134
- California Hatchery Scientific Review Group (2012) California Hatchery Review Report. Prepared for the US Fish and Wildlife Service and Pacific States Marine Fisheries Commission, CA
- Croll DA, Marinovic B, Benson S, Chavez FP, Black N, Ter-nullo R, Tershy BR (2005) From wind to whales: trophic links in a coastal upwelling system. *Mar Ecol Prog Ser* 289:117–130
- Cushing DH (1990) Plankton production and year-class strength in fish populations: an update of the match/mismatch hypothesis. *Adv Mar Biol* 26:249–293
- Deriso RB, Maunder MN, Pearson WH (2008) Incorporating covariates into fisheries stock assessment models with application to Pacific herring. *Ecol Appl* 18:1270–1286
- Dorman JG, Powell TM, Sydeman WJ, Bograd SJ (2011) Advection and starvation cause krill (*Euphausia pacifica*) decreases in 2005 Northern California coastal populations: implications from a model study. *Geophys Res Lett* 38:L04605, doi:10.1029/2010GL046245
- Dormann CF, Elith J, Bacher S, Buchmann C and others (2013) Collinearity: a review of methods to deal with it and a simulation study evaluating their performance. *Ecography* 36:27–46
- Graham WW, Largier JL (1997) Upwelling shadows as near-shore retention sites: the example of northern Monterey Bay. *Cont Shelf Res* 17:509–532
- Hankin DG (1990) Effects of month of release of hatchery-reared Chinook salmon on size at age, maturation schedule, and fishery contribution. *Info Rep Number 90-4*. Oregon Department of Fish and Wildlife, Portland, OR
- Hilborn R, Quinn TP, Schindler DE, Rogers DE (2003) Bio-complexity and fisheries sustainability. *Proc Natl Acad Sci USA* 100:6564–6568
- Hjort J (1914) Fluctuations in the great fisheries of northern Europe, viewed in the light of biological research. *Rapp P-V Reun Cons Int Explor Mer* 20:1–228
- Holtby LB, Andersen BC, Kadowaki RK (1990) Importance of smolt size and early ocean growth to interannual variability in marine survival of coho salmon (*Oncorhynchus kisutch*). *Can J Fish Aquat Sci* 47:2181–2194
- Jacobson LD, MacCall AD (1995) Stock-recruitment models for Pacific sardine (*Sardinops sagax*). *Can J Fish Aquat Sci* 52:566–577
- Johnson JK (1990) Regional overview of coded wire tagging of anadromous salmon and steelhead in northwest America. *Am Fish Soc Symp* 7:782–816
- Lapi L, Hamer M, Johnson B (1990) Data organization and coding for a coastwide mark-recovery data system. *Am Fish Soc Symp* 7:720–724
- Lindley ST, Grimes CB, Mohr MS, Peterson W and others (2009) What caused the Sacramento River fall Chinook stock collapse? NOAA Tech Memo NOAA-TM-NMFS-SWFSC-447
- Logerwell EA, Mantua N, Lawson PW, Francis RC, Agostini VN (2003) Tracking environmental processes in the coastal zone for understanding and predicting Oregon coho (*Oncorhynchus kisutch*) marine survival. *Fish Oceanogr* 12:554–568
- McGurk MD (1996) Allometry of marine mortality of Pacific salmon. *Fish Bull* 94:77–88
- Morley RB (1988) The influence of time and size at release of juvenile coho salmon (*Oncorhynchus kisutch*) on returns at maturity: results of studies on three brood years at Quinsam Hatchery, B.C. *Can Tech Rep Fish Aquat Sci* 1620
- Myers RA (1998) When do environment–recruitment correlations work? *Rev Fish Biol Fish* 8:285–305
- Nandor GF, Longwill JR, Webb DL (2010) Overview of the coded wire tag program in the greater Pacific region of North America. In: Wolf KS, O’Neal JS (eds) PNAMP Special Publication: tagging, telemetry and marking measures for monitoring fish populations—A compendium of new and recent science for use in informing technique and decision modalities. Pacific Northwest Aquatic Monitoring Partnership, Duvall, WA, p 5–46
- O’Farrell MR, Mohr MS, Palmer-Zwahlen ML, Grover AM (2013) The Sacramento Index (SI). NOAA Tech Memo NOAA-TM-NMFS-SWFSC-512
- Petrosky CE, Schaller HA (2010) Influence of river conditions during seaward migration and ocean conditions on survival rates of Snake River Chinook salmon and steelhead. *Ecol Freshw Fish* 19:520–536
- Quinn TP (2005) The behavior and ecology of Pacific salmon and trout. American Fisheries Society and University of Washington, Seattle, WA
- Quinn TJ, Deriso RB (1999) Quantitative fish dynamics. Oxford University Press, New York, NY
- R Development Core Team (2012) R: a language and environment for statistical computing. R Foundation for Statistical Computing, Vienna
- Raff MS (1956) On approximating the point binomial. *J Am Stat Assoc* 51:293–303
- Ralston S, Field JC, Sakuma K (2013) Interannual variation in pelagic juvenile rockfish abundance—going with the flow. *Fish Oceanogr* 22:288–308
- Raymond HL (1979) Effects of dams and impoundments on migrations of juvenile chinook salmon and steelhead from the Snake River, 1966 to 1975. *Trans Am Fish Soc* 108:505–529
- Raymond HL (1988) Effects of hydroelectric development and fisheries enhancement on spring and summer chi-

- nook salmon and steelhead in the Columbia River Basin. *N Am J Fish Manag* 8:1–24
- Rechisky EL, Welch DW, Porter AD, Jacobs-Scott MC, Winchell PM, McKern JL (2012) Estuarine and early-marine survival of transported and in-river migrant Snake River spring Chinook salmon smolts. *Sci Rep* 2:448
- Rupp DE, Wainwright TC, Lawson PW, Peterson WT (2012) Marine environment-based forecasting of coho salmon (*Oncorhynchus kisutch*) adult recruitment. *Fish Oceanogr* 21:1–19
- Ryding KE, Skalski JR (1999) Multivariate regression relationships between ocean conditions and early marine survival of coho salmon (*Oncorhynchus kisutch*). *Can J Fish Aquat Sci* 56:2374–2384
- Santora JA, Sydeman WJ, Schroeder ID, Wells BK, Field JC (2011) Mesoscale structure and oceanographic determinants of krill hotspots in the California Current: implications for trophic transfer and conservation. *Prog Oceanogr* 91:397–409
- Santora JA, Field JC, Schroeder ID, Sakuma KM, Wells BK, Sydeman WJ (2012) Spatial ecology of krill, micronekton and top predators in the central California Current: implications for defining ecologically important areas. *Prog Oceanogr* 106:154–174
- Santora JA, Schroeder ID, Field JC, Wells BK, Sydeman WJ (in press) Spatio-temporal dynamics of ocean conditions and forage taxa reveals regional structuring of seabird-prey relationships. *Ecol Appl*, doi:10.1890/13-1605.1
- Satterthwaite WH, Mohr MS, O'Farrell MR, Anderson EC and others (2014) Use of genetic stock identification data for comparison of the ocean spatial distribution, size-at-age, and fishery exposure of an untagged stock and its indicator: Klamath River versus California Coastal Chinook salmon. *Trans Am Fish Soc* 143:117–133
- Scheuerell MD, Zabel RW, Sandford BP (2009) Relating juvenile migration timing and survival to adulthood in two species of threatened Pacific salmon (*Oncorhynchus* spp.). *J Appl Ecol* 46:983–990
- Schroeder ID, Sydeman WJ, Sarkar N, Thompson SA, Bograd SJ, Schwing FB (2009) Winter pre-conditioning of seabird phenology in the California Current. *Mar Ecol Prog Ser* 393:211–223
- Schroeder ID, Black BA, Sydeman WJ, Bograd SJ, Hazen EL, Santora JA, Wells BK (2013) The North Pacific High and wintertime pre-conditioning of California Current productivity. *Geophys Res Lett* 40:541–546
- Schwing FB, Bond NA, Bograd SJ, Mitchell T, Alexander MA, Mantua N (2006) Delayed coastal upwelling along the US West Coast in 2005: a historical perspective. *Geophys Res Lett* 33:L22SO1, doi:10.1029/2006GL026911
- Shao J (1993) Linear model selection by cross-validation. *J Am Stat Assoc* 88:486–494
- Thompson SS, Sydeman WJ, Santora JA, Black BA and others (2012) Linking predators to seasonality of upwelling: using food web indicators and path analysis to infer trophic connections. *Prog Oceanogr* 101:106–120
- Tomaro LM, Teel DJ, Peterson WT, Miller JA (2012) When is bigger better? Early marine residence of middle and upper Columbia River spring Chinook salmon. *Mar Ecol Prog Ser* 452:237–252
- Ver Hoef JM, Boveng P (2007) Quasi-Poisson vs. negative binomial regression: How should we model overdispersed count data? *Ecology* 88:2766–2772
- Ward BR, Slaney PA, Facchin AR, Land RW (1989) Size-biased survival in steelhead trout (*Oncorhynchus mykiss*): back-calculated lengths from adults' scales compared to migrating smolts at the Keogh River, British Columbia. *Can J Fish Aquat Sci* 46:1853–1858
- Weitkamp L, Neely K (2002) Coho salmon (*Oncorhynchus kisutch*) ocean migration patterns: insight from marine coded-wire tag recoveries. *Can J Fish Aquat Sci* 59:1100–1115
- Wells BK, Grimes CB, Waldvogel JB (2007) Quantifying the effects of wind, upwelling, curl, sea surface temperature and sea level height on growth and maturation of a California Chinook salmon (*Oncorhynchus tshawytscha*) population. *Fish Oceanogr* 16:363–382
- Wells BK, Field JC, Thayer JA, Grimes CB and others (2008) Untangling the relationships among climate, prey and top predators in an ocean ecosystem. *Mar Ecol Prog Ser* 364:15–29
- Wells BK, Santora JA, Field JC, MacFarlane RB, Marinovic BB, Sydeman WJ (2012) Population dynamics of Chinook salmon *Oncorhynchus tshawytscha* relative to prey availability in the central California coastal region. *Mar Ecol Prog Ser* 457:125–137
- Whitman RP (1987) An analysis of smoltification indices in fall chinook salmon (*Oncorhynchus tshawytscha*). MS thesis, University of Washington, Seattle, WA
- Williams JG (2006) Central Valley salmon: a perspective on Chinook and steelhead in the Central Valley of California. *San Francisco Estuar Watershed Sci* 4:1–398
- Williams JG (2008) Mitigating the effects of high-head dams on the Columbia River, USA: experience from the trenches. *Hydrobiologia* 609:241–251
- Wing SR, Botsford LW, Ralston SV, Largier JL (1998) Mero-planktonic distribution and circulation in a coastal retention zone of the northern California upwelling system. *Limnol Oceanogr* 43:1710–1721
- Wood SN (2011) Fast stable restricted maximum likelihood and marginal likelihood estimation of semiparametric generalized linear models. *J R Stat Soc B* 73:3–36
- Woodson L, Wells BK, Johnson RC, Weber P, MacFarlane RB, Whitman G (2013) Size, growth, and origin-dependent mortality of juvenile Chinook salmon *Oncorhynchus tshawytscha* during early ocean residence. *Mar Ecol Prog Ser* 487:163–175
- Zabel RW, Williams JG (2002) Selective mortality in Chinook salmon: What is the role of human disturbance? *Ecol Appl* 12:173–183

Editorial responsibility: Konstantinos Stergiou,
Thessaloniki, Greece

Submitted: January 13, 2014; Accepted: July 1, 2014
Proofs received from author(s): September 15, 2014

The following supplements accompany the article

Match-mismatch dynamics and the relationship between ocean-entry timing and relative ocean recoveries of Central Valley fall run Chinook salmon

William H. Satterthwaite^{1,2,*}, Stephanie M. Carlson³, Shanae D. Allen-Moran¹, Simone Vincenzi², Steven J. Bograd⁴, Brian K. Wells¹

¹Fisheries Ecology Division, Southwest Fisheries Science Center, National Marine Fisheries Service, NOAA, 110 Shaffer Rd, Santa Cruz, CA 95060, USA

²Center for Stock Assessment Research, Applied Math and Statistics, University of California, Santa Cruz, CA 95064, USA

³Department of Environmental Science, Policy, and Management, University of California Berkeley, 130 Mulford Hall #3114, Berkeley, CA 94720, USA

⁴Environmental Research Division, Southwest Fisheries Science Center, NOAA, Pacific Grove, CA 93950, USA

*Corresponding author: will.satterthwaite@noaa.gov

Marine Ecology Progress Series 511:237–248 (2014)

Supplement 1. Data Filtering

In addition to the 5 extant Central Valley hatcheries producing fall run Chinook (Coleman National Fish Hatchery, Feather River Hatchery, Nimbus Hatchery, Mokelumne River Fish Installation, and the Merced River Fish Facility) and the discontinued Tehama-Colusa Spawning Channel, the RMIS identifies 2 additional ‘hatcheries’: the Tiburon Minor Port and Tiburon Net pens, which release only Feather River Hatchery-sourced fish. We recategorized these fish as Feather River Hatchery.

We compared the distribution of release times across hatcheries to identify the potential confounding of source hatchery and release timing. There were clear differences among hatcheries in their release times (Fig. S1; ANOVA $F_{3,284}=13.4$, $p < 0.01$). Among the 2 hatcheries with substantial variability in release times, nearly all of the variation for the Mokelumne River Hatchery was across years rather than within years (Fig. S2), while the Feather River Hatchery had substantial within-year variability, although releases tended to occur earlier and with less temporal spread in later years (Fig. S2). We therefore focused our analysis on Feather River Hatchery releases, since such releases provide the majority of the available data (Table 1 in the main article) and cover the widest range of release times (Fig. S1).

In general, later releases tend to be of larger fish. To reduce the collinearity between weight and release timing, we restricted our analysis to fish released as ‘fingerlings’ or ‘advanced fingerlings’, which make up the majority of releases (~90%), rather than the much larger smolts or much smaller fry. Excluding fish released as smolts or fry substantially reduces the extent of collinearity between release weight and release timing of release groups (from $r = 0.73$ for year-day and release weight, $r = 0.63$ for time lag and release weight to $r = 0.52$ for year-day and release weight, $r = 0.40$ for time lag and release weight).

Historically, estimates of age 2 recoveries are, on average, ~0.1% (SD = 0.14) of tagged releases, whereas recoveries of age 3 fish are ~0.9% (SD = 0.93). Age 4 recovery rates are similar to those for age 2 (mean \pm SD = $0.1 \pm 0.13\%$). Estimating such low recovery rates of age 2 and age 4 fish could result in relatively high sampling errors. Thus, we restricted our analysis to age 3 recoveries. However, age 3 availability is affected by (generally low) harvest or early maturation of age 2 fish, potentially confounding the effects on survival. Another concern is the amount of time that different release groups spend in the ocean (i.e. greater cumulative daily mortality can accrue for earlier releases), but for recoveries at age 3 or later, the differences in cumulative time spent in the ocean are relatively small. An additional reason for restricting our analysis to age 3 ocean recoveries is that age 2 harvest data are more uncertain due to generally low recoveries and uncertainty in how much age 2 harvest actually occurred in a sampling stratum from which no age 2 tags were recovered, but only a fraction of the harvest was examined for tags. In addition, age 3 fish are nearly always of legal size to retain in the fishery but age 2 fish often are not, so attempting to model age 2 harvest would introduce major confounding due to annual variability in fish

size, variation from year to year in minimum size limit regulations, and variability in the relative magnitude of recreational versus commercial fisheries which have substantially different minimum size limits and thus very different relative impacts on age 2 versus older fish.

It should be noted that O'Farrell et al. (2013) define fish as reaching age 3 in September 2 yr after the brood year; thus, the harvest metric h was calculated including a small number of fish harvested toward the end of the calendar year in which we would still refer to them as age 2 using the aging convention in this paper. Similarly, we would consider a fish harvested in October 3 yr after the brood year to be age 3, but in the O'Farrell et al. (2013) calculation, such fish would be considered age 4. However, since the majority of the fishery occurs in spring and summer, the vast majority of harvest would be considered age 3 under either designation, and the calculations and assumptions underlying the calculation of h in O'Farrell et al. (2013) do not distinguish age 3 from age 4 and older fish.

Fig. S1. Box-and-whisker plot of release dates of different release groups (not of individual fish) by hatchery. Thick lines denote median release date, boxes the central 50%, whiskers the furthest data points within 1.5 times the interquartile range, and open circles any outliers beyond this

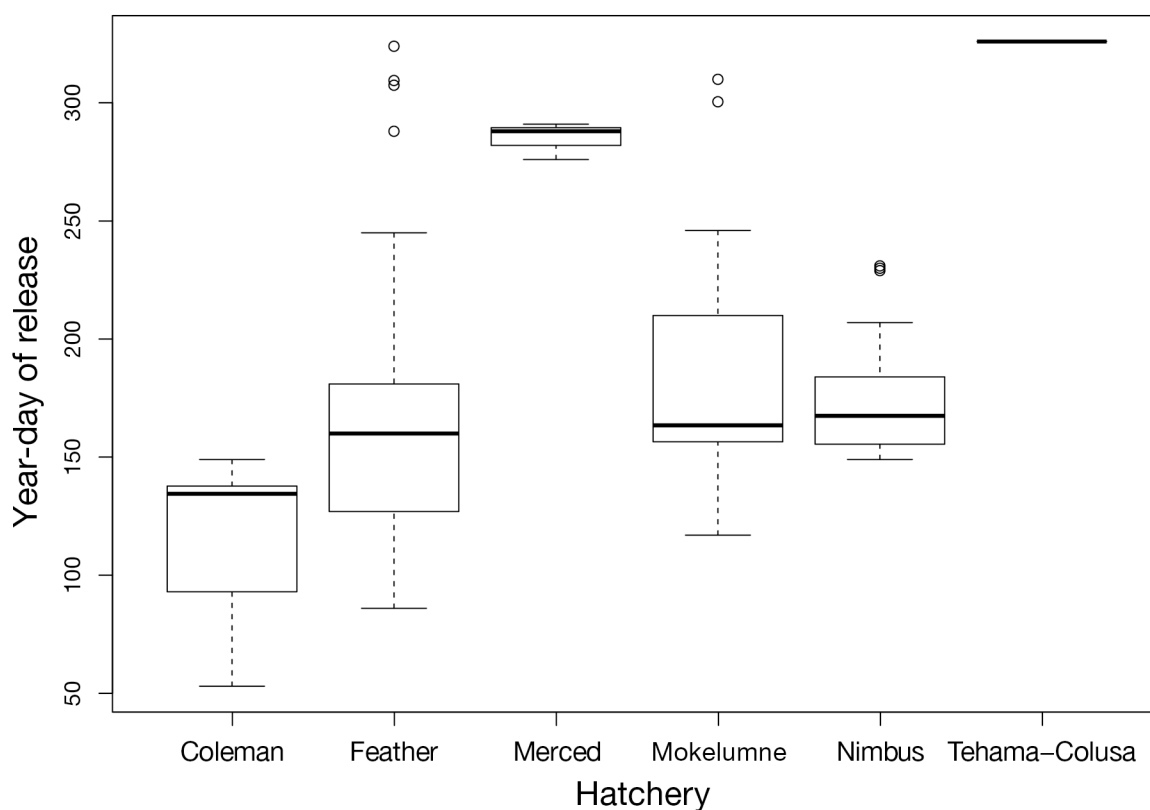
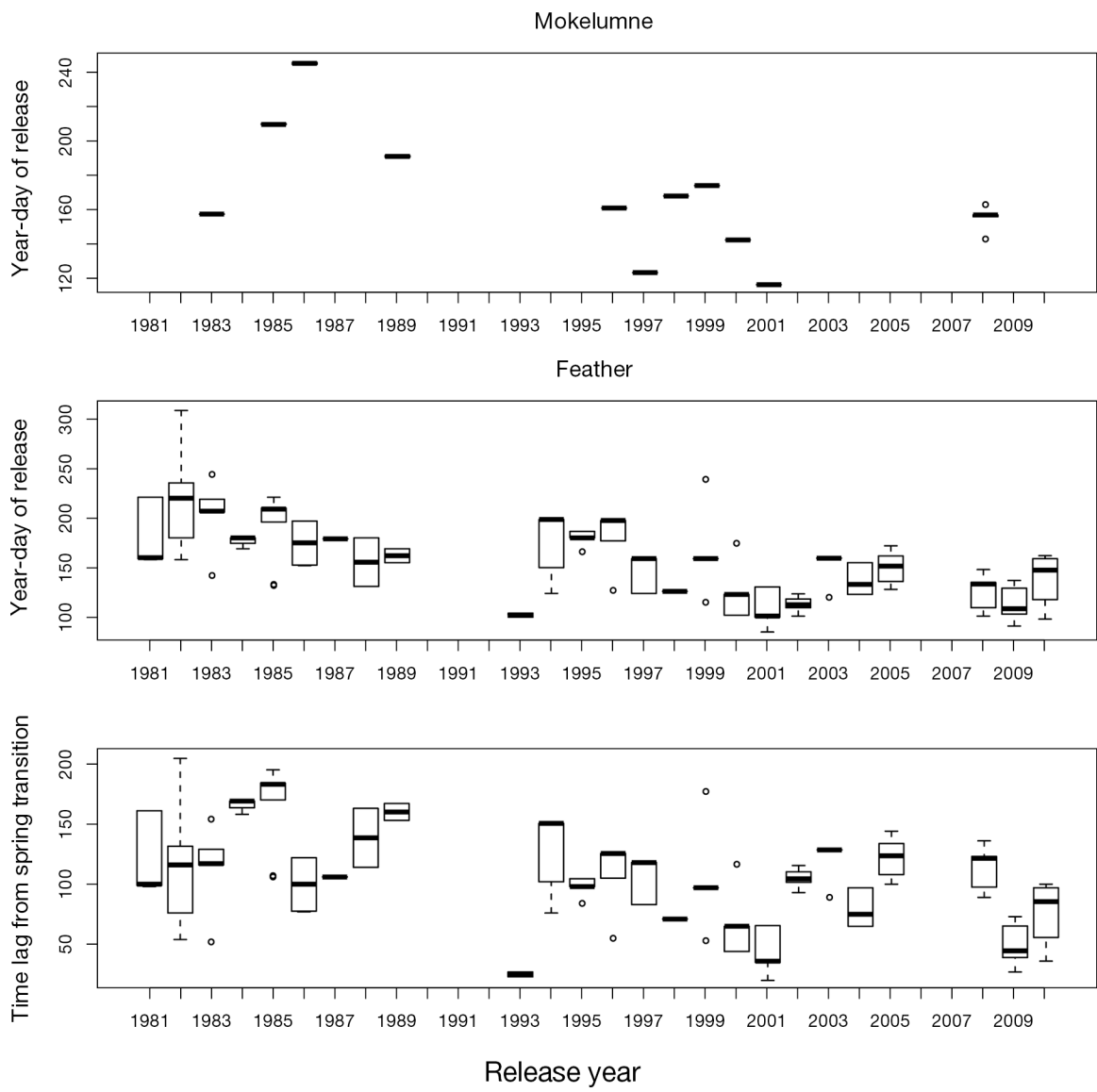
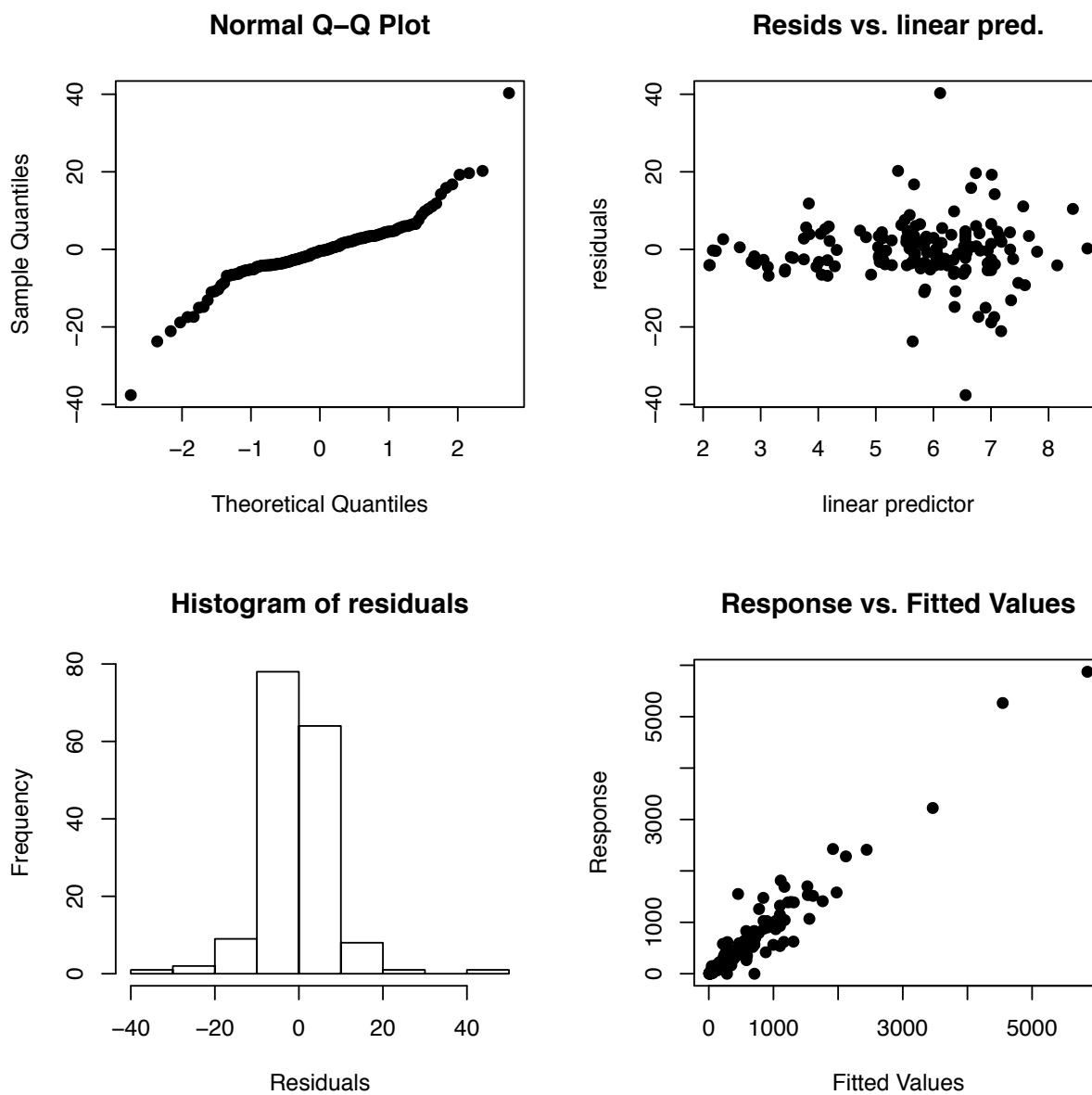


Fig. S2. Box-and-whisker plot of release dates of different release groups (not of individual fish) by year for Mokelumne and Feather hatcheries (the hatcheries with the largest range in reported release dates) and time lag from spring transition for Feather River Hatchery only. Releases spanning >30 d were excluded, as were release groups with missing weight information and those released as smolts or fry (see 'Materials and Methods'). Thick lines denote median release date, boxes the central 50%, lines the furthest data points within 1.5 times the interquartile range, and open circles any outliers beyond this. In most years, the Mokelumne River hatchery released all its fish in a single day



Supplement 2. Diagnostic Plots

Fig. S3. Diagnostic plots for the best-supported model for releases from Feather River Hatchery that included a nonlinear effect of time lag from spring transition day, a linear effect of weight, and fixed effects of net pen and disease. Releases spanning >30 d were excluded, as were release groups with missing weight information and those released as smolts or fry



See discussions, stats, and author profiles for this publication at:
<http://www.researchgate.net/publication/225450174>

Population Status of North American Green Sturgeon, *Acipenser medirostris*

ARTICLE *in* ENVIRONMENTAL BIOLOGY OF FISHES · JULY 2007

Impact Factor: 1.57 · DOI: 10.1007/s10641-006-9062-z

CITATIONS

31

READS

70

6 AUTHORS, INCLUDING:



Peter B. Adams

National Oceanic and Atmospheric Ad...

38 PUBLICATIONS 480 CITATIONS

SEE PROFILE



Churchill B. Grimes

National Oceanic and Atmospheric Ad...

74 PUBLICATIONS 1,968 CITATIONS

SEE PROFILE



Joseph E. Hightower

North Carolina State University

104 PUBLICATIONS 1,096 CITATIONS

SEE PROFILE



Steve Lindley

National Oceanic and Atmospheric Ad...

81 PUBLICATIONS 2,750 CITATIONS

SEE PROFILE

Population status of North American green sturgeon, *Acipenser medirostris*

Peter B. Adams · Churchill Grimes ·
Joseph E. Hightower · Steven T. Lindley ·
Mary L. Moser · Michael J. Parsley

Received: 18 July 2005 / Accepted: 6 April 2006 / Published online: 8 July 2006
© Springer Science+Business Media B.V. 2006

Abstract North American green sturgeon, *Acipenser medirostris*, was petitioned for listing under the Endangered Species Act (ESA). The two questions that need to be answered when considering an ESA listing are; (1) Is the entity a species under the ESA and if so (2) is the “species” in danger of extinction or likely to become an endangered species in the foreseeable future throughout all or a significant portion of its range? Green sturgeon genetic analyses showed strong differentiation between northern and southern populations, and therefore, the species was divided into Northern and Southern Distinct Population Segments (DPSs). The Northern DPS includes populations in the Rogue, Klamath-Trinity, and Eel rivers, while the Southern DPS only includes a

single population in the Sacramento River. The principal risk factors for green sturgeon include loss of spawning habitat, harvest, and entrainment. The Northern DPS is not considered to be in danger of extinction or likely to become an endangered species in the foreseeable future. The loss of spawning habitat is not large enough to threaten this DPS, although the Eel River has been severely impacted by sedimentation due to poor land use practices and floods. The two main spawning populations in the Rogue and Klamath-Trinity rivers occupy separate basins reducing the potential for loss of the DPS through catastrophic events. Harvest has been substantially reduced and green sturgeon in this DPS do not face substantial entrainment loss. However there are significant concerns due to lack of information, flow and temperature issues, and habitat degradation. The Southern DPS is considered likely to become an endangered species in the foreseeable future. Green sturgeon in this DPS are concentrated into one spawning area outside of their natural habitat in the Sacramento River, making them vulnerable to catastrophic extinction. Green sturgeon spawning areas have been lost from the area above Shasta Dam on the Sacramento River and Oroville Dam on the Feather River. Entrainment of individuals into water diversion projects is an additional source of risk, and the large decline in numbers of green sturgeon entrained since 1986 causes additional concern.

P. B. Adams (✉) · C. Grimes · S. T. Lindley
NMFS, Southwest Fisheries Science Center, Santa
Cruz, California, USA
e-mail: Pete.Adams@noaa.gov

J. E. Hightower
USGS, North Carolina Cooperative Fish and Wildlife
Research Unit, Raleigh, North Carolina, USA

M. L. Moser
NMFS, Northwest Fisheries Science Center, Seattle,
Washington, USA

M. J. Parsley
USGS, Western Fisheries Research Center, Columbia
River Research Laboratory, Cook, Washington, USA

Keywords Green sturgeon · Population status · Endangered Species Act · Distinct population segment

Introduction

The North American green sturgeon, *Acipenser medirostris*, have been petitioned for listing under the Endangered Species Act (ESA) and this is a review of the scientific considerations that the National Marine Fisheries Service uses to consider listing. Sturgeons in general have a life history that is susceptible to overharvesting and degradation of freshwater habitat and a number of species have some kind of protection or conservation status (Secor et al. 2002). In the United States, there are five ESA listed sturgeon: short-nose sturgeon, *A. brevirostrum*, Endangered (USFWS 1967); Pallid sturgeon, *Scaphirhynchus albus*, Endangered (USFWS 1990); Gulf sturgeon, *A. oxyrinchus desotoi*, Threatened (USFWS and NOAA 1991); white sturgeon, Kootenai River Population, *A. transmontanus*, Endangered (USFWS 1994); and Alabama sturgeon, *S. suttkusi*, Endangered (USFWS 2000). Green sturgeon has a status designation of Special Concern in Canada (Houston 1988) because of its population characteristics that make it particularly sensitive to human activities or natural catastrophic events. Sakhalin sturgeon, *A. mikadoi*, a species that was at one time synonymized with green sturgeon, is extirpated throughout Japan, Korea, and China. In Russia, Sakhalin sturgeon now only occurs in the Tumnin River where there is a hatchery supporting it.

There are two key questions that must be addressed in determining whether a listing under the ESA is warranted: (1) Is the entity in question a “species” as defined by the ESA, and (2) if so, is the “species” in danger of extinction or likely to become an endangered species in the foreseeable future throughout all or a significant portion of its range? For the purpose of the ESA, a species is defined as “any subspecies of fish or wildlife or plants, or any distinct population segment (DPS) of any species of vertebrate fish or wildlife which interbreeds when mature.” The ESA allows listing of “distinct population segments” of

vertebrates as well as named species and subspecies. Two elements are necessary for a decision to identify separate DPSs (USFWS and NOAA 1996): discreteness and significance of the population segment to the species. A DPS may be considered discrete if it is markedly separate from other populations of the same taxon as a consequence of physical, physiological, ecological, or behavioral factors or if it is delimited by international governmental boundaries. If a population segment is considered discrete, its biological and ecological significance will be considered on the basis of considerations including, but not limited to its persistence, evidence that loss of the DPS would result in a significant gap in spatial structure, evidence of the DPS representing the only surviving natural occurrence of a taxon, or evidence that the DPS differs markedly in its genetic characteristics.

The ESA defines the term “endangered species” as “any species which is in danger of extinction throughout all or a significant portion of its range.” The term “threatened species” is defined as “any species which is likely to become an endangered species within the foreseeable future throughout all or a significant portion of its range.” In evaluating the level of risk faced by a species or DPS, important considerations include (1) absolute numbers and their spatial and temporal distribution; (2) current abundance in relation to historical abundance and carrying capacity of the habitat; (3) any spatial and temporal trends in abundance; (4) natural and human-influenced factors that cause variability in survival and abundance; (5) possible threats to genetic integrity (e.g., artificial rearing); and (6) recent events (e.g., a drought or a change in management) that have predictable short-term consequences for abundance of the species. Additional risk factors, such as disease prevalence or changes in life history traits, may also be considered in evaluating risk to populations. The determination of whether a species as “in danger of extinction” or “likely to become an endangered species within the foreseeable future” should be made on the basis of “the best scientific and commercial information” available regarding its current status. The use of “best scientific and commercial information” is a standard makes the risk assessment process

fundamentally different than typical scientific investigation. This standard requires the gathering of all information possible, including some that would not meet traditional scientific guidelines, and requires making recommendations based on imperfect and incomplete information.

Green sturgeon life history

Green sturgeon is the most widely distributed member of the sturgeon family Acipenseridae. Like all sturgeons, they are anadromous, but are also the most marine oriented of the sturgeons. The only known green sturgeon spawning locations are in Oregon and California rivers where they experience anthropogenic impacts similar to other anadromous fishes (Moyle 2002). Adults migrate into their spawning rivers, peaking in May–June, and then hold in deep pools or “holes” in the mainstem of large turbulent rivers to stage for spawning (Erickson et al. 2002). Eggs are likely broadcast spawned over large cobble substrate where they settle into the spaces between the cobbles. Fecundity is lower than other sturgeons, but the egg size is larger (Deng 2000). The large egg size provides more yolk stores for the nourishment of embryos, presumably resulting in more viable larvae. The adhesiveness of green sturgeon eggs is lower than that of white sturgeon and the eggs may not attach to the substrate after fertilization like white sturgeon, but become trapped in crevices and gravel during embryo development. The juveniles spend from 1–4 years in freshwater, before migrating to the ocean. Once in the ocean, green sturgeon range in coastal waters from Mexico to the Bering Sea (Moyle 2002). Tagging has shown that they make long migrations in the ocean, generally to the north¹ and analyses of Oregon trawl catch found them almost exclusively inside the 110-m contour (Erickson and Hightower in press). Recent hydro-acoustic tagging information has shown that green sturgeon congregate near the Brooks

Peninsula, and immediately north of Vancouver Island.² Green sturgeon congregate in coastal bays and estuaries in late summer and early fall, with particularly large concentrations in the Columbia River Estuary, Willapa Bay, and Grays Harbor.³ The reasons for these concentrations are unclear. Green sturgeon have delayed sexual maturity, somewhere between 13 and 20 years, and they apparently only spawn every 2–5 years (Moyle 2002).

What is the “species” unit for ESA listing?

Review of “species” data

Green sturgeon that occur within United States and Canadian waters are now known to be a geographically isolated and genetically distinct species. The species was first described as *Acipenser medirostris* by Ayres (1854) from San Francisco Bay. The North American form was considered conspecific with a previously described Asian species Sakhalin sturgeon, *A. mikadoi*, and the two forms were synonymized (Berg 1948). More recent molecular data on three mitochondrial genes show large differences between the North American and Asian forms (Birstein and DeSalle 1998), and these two forms are now considered separate species. Morphometric data shows differences between the two forms with the snout of the Asian form being longer (North et al. 2002). Other morphometric and meristic data between the two forms are similar. Both Green and Sakhalin sturgeon occur in coastal waters and in estuaries. The only currently documented Sakhalin sturgeon spawning population occurs in the Tumnin River, Russia, which also has a hatchery for this species.

Sturgeons are known to have strong homing capabilities and this leads to high spawning site fidelity (Bemis and Kynard 1997). It is common to

¹ Adams, P.B., C.B. Grimes, J.E. Hightower, S.T. Lindley, and M.L. Moser. 2002. Status Review for the North American green sturgeon. Final Report to Southwest Region, NOAA Fisheries. Long Beach, CA. 50 p.

² S. Lindley and M. Moser. 11/22/2004. NOAA Fisheries, Santa Cruz, CA.

³ Moyle P., P. J. Foley, and R. M. Yoshiyama. 1992. Status of green sturgeon, *Acipenser medirostris*, in California. Final Report submitted to National Marine Fisheries Service. 11 p. University of California Davis.

have a large numbers of genetically separated races or morphs within a species (Wirgin et al. 1997). The trend of sturgeon homing to individual rivers is so strong that river by river analysis is common in sturgeon ESA recovery plans. This general pattern in sturgeon population genetics led to consideration that green sturgeon might have multiple DPSs.

The actual historical and current geographical extent of green sturgeon spawning is difficult to assess because green sturgeon make non-spawning movements into coastal lagoons and bays in the late summer to fall, and because their original spawning distribution may have been reduced due to harvest and other anthropogenic effects. Green sturgeon commonly occur in coastal waters from San Francisco Bay to Canada,¹ but actual spawning has only been documented (by the presence of juveniles) in the Rogue (Erickson et al. 2002), Klamath (Scheiff et al. 2001), Trinity (Scheiff et al. 2001), Sacramento,⁴ and Eel⁵ rivers. The historical status of the Umpqua, Feather, and San Joaquin rivers as green sturgeon spawning areas remains unknown.

In late summer and early fall, green sturgeon commonly occur in estuaries where there has been no known spawning. The exact reason for this behavior is not known, but it greatly complicates identification of natal rivers and designation of DPSs. Green sturgeon have occurred in many estuaries where there are no records of their occurrence further up the river system. Therefore, we used the presence of juveniles to confirm green sturgeon spawning in a given river system.

Historic green sturgeon spawning distribution may never be known due to sturgeon's vulnerability to overharvest and other anthropogenic impacts (Boreman 1997, also see extinction risk section). Smaller less productive populations may

have extirpated by harvest and habitat degradation long before there was any scientific recognition of their existence.

Green sturgeon population genetic analyses have recently become available (Israel et al. 2004, also⁶), but these analyses are limited by small sample size and mixed samples of different spawning populations in different years. Genetic samples were analyzed from the Klamath River, from San Pablo Bay, juveniles from the Sacramento River, from the Rogue River, from the Columbia River estuary, and from the Umpqua River estuary. Nine microsatellite loci were amplified for analysis of allele frequencies; six of these loci were tetrasomic and therefore do not permit standard genetic analysis. The genetic analyses of existing samples are problematic in those samples from estuaries since these fish may be a mixture of different spawning stocks. Ideally, coast-wide genetic studies should be conducted on juveniles collected in their natal rivers.

The results of the genetic analyses showed strong separation between a northern and southern group of spawning fish (Israel et al. 2004, this volume). The northern group contains spawning populations in the Klamath and Rogue rivers that have similar genetic composition. Non-spawning green sturgeon sampled in Umpqua Bay are also grouped with the northern group because of similar genetic composition. The southern group, which contains the Sacramento River juveniles samples and fish from San Pablo Bay, has a distinctly different genetic composition from the northern group.

The genetic data showed a complex relationship between Columbia River green sturgeon samples and samples from San Pablo Bay and the Sacramento River. There was no significant genotypic differentiation detected between San Pablo Bay and Columbia River collections. However, the San Pablo Bay samples were not identical to the Sacramento River samples from juveniles. There are a number of possible explanations for these results. One is that Columbia River fish generally come from the Sacramento River. Another is that both Columbia River and

⁴ California Department of Fish and Game (CDFG). 2002. California Department of Fish and Game Comments to NMFS Regarding Green Sturgeon Listing. Sacramento, CA, 129 pp.

⁵ Puckett, L. K. 1976. Observations on the downstream migrations of anadromous fishes within the Eel River system. California Department of Fish and Game. Memorandum Report. 35 p. California Department of Fish and Game, Eureka, CA.

⁶ J. Israel and B. May. 2005. Univ. of California, Dept. of Animal Science, Davis, CA.

San Pablo Bay are a mixture of other spawning populations. Finally, it is possible that by chance, the small number of Columbia River samples come largely from fish that were spawned in the Sacramento River.

Conclusions and discussion on the “species” question

North American green sturgeon are clearly a species under the ESA. The North American species, *A. medirostris*, is a separate species from the western Pacific Tumnin River population, *A. mikadoi*, due to the lower chromosome number (Birstein et al. 1993) and morphological differences (North et al. 2002).

Current evidence justifies the separation of green sturgeon into Northern and Southern DPSs. Sturgeons generally show fidelity to their spawning sites so they have a general pattern of multiple DPSs (Bemis and Kynard 1997). The Northern DPS includes populations from the Rogue, Klamath-Trinity, and Eel rivers, and the Southern DPS currently includes only the Sacramento River population (Fig. 1). The Eel River, for which there is no genetic information, is assigned to the Northern DPS on an “isolation by distance” argument since the mouth of the Eel River is much closer to the Northern DPS. The ESA “discreteness” test that populations are markedly separated from each other is clearly met by the genetic data discussed earlier. The ESA “significance” test is also clearly met by genetic evidence, distribution, and adaptation to different habitats. The Northern and Southern DPSs represent the northern and southern extent of the green sturgeon’s range. The loss of either of these DPSs would result in a significant shrinkage of the species distribution and would be considered the loss of a portion of the species’ range. The two DPSs are also significantly separate because spawning occurs in very different habitats. The Northern DPS spawning occurs in the more coastal Klamath Mountain Province, a cooler, wetter area that supports a number of uniquely adapted salmonids (Busby et al. 1996). The Southern DPS spawning occurs in the dry, hot California Central Valley that has experienced large anthropogenic change (Lindley et al. 2006).

The loss of ability to spawn in either of these different habitats would be a major loss of adaptation. There may be green sturgeon spawning locations and population structure that are not apparent now and which may cause this assessment of DPS structure to change in the future.

What is the level of “extinction risk”?

Review of “extinction risk” data

Loss of spawning habitat

The amount of lost green sturgeon spawning habitat is unclear. Although there have been claims that as many as twice the number of green sturgeon spawning populations have been extirpated as currently remain,⁷ these claims are impossible to evaluate because it is unknown how many spawning populations there were and if spawning populations are actually extirpated. In the Northern DPS, there is no evidence of green sturgeon spawning north of the Umpqua River, Oregon. Spawning does appear to occur in the Umpqua River, but probably is rare. There are two confirmed records of green sturgeon captured above tidal influence in the Umpqua River,⁸ approximately 150 km up river. However, Oregon Department of Fish and Wildlife sampled the Umpqua River in 2002, 2003, and 2004 using gill nets, beach seines, snorkeling, and underwater video and did not collect any green sturgeon above tidal influence. Green sturgeon in the South Fork of the Trinity River were reportedly extirpated by the 1964 flood (Moyle 2002), but juvenile green sturgeon are captured at Willow Creek on the Trinity River (Scheiff et al. 2001). These fish could be coming from either the South Fork or the Trinity River. Green sturgeon still appear to occasionally occupy the Eel River.

⁷ Environmental Protection Information Center (EPIC), Center for Biological Diversity, and Waterkeepers Northern California. 2001. Petition to list the North American green sturgeon (*Acipenser medirostris*) as an endangered or threatened species under the ESA. National Marine Fisheries Service. Long Beach, CA. 63 pp.

⁸ T. Rien. 11/16/2004. ODFW, Clackamas, OR.

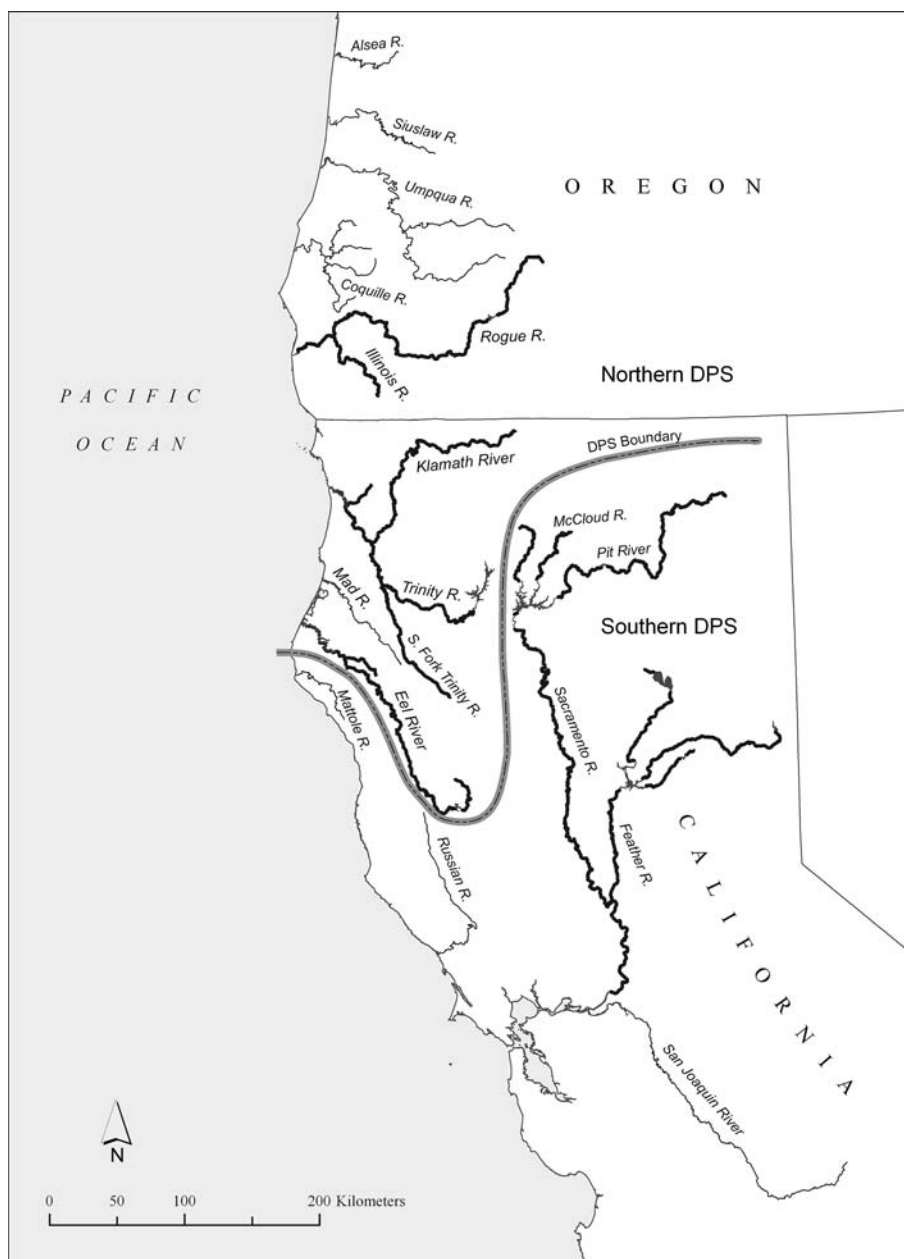


Fig. 1 Green Sturgeon DPSs. The Northern DPS includes populations from the Rogue, Klamath-Trinity, and Eel rivers. The Southern DPS includes a single population in the Sacramento River

Adult green sturgeon were sighted on the mainstem Eel River near Fort Seward (rkm 101) during snorkel surveys in 1995 and 1996.⁹ Two juvenile green sturgeon (282 mm and 510 mm FL)

were captured in the Eel River Estuary in 1994 by trawl.¹⁰ This is in addition to the previously reported capture of 26 juvenile green sturgeon near Fort Seward in 1967 and 1968.⁵

⁹ S. Downie 10/8/2004. CDFG, Fortuna, CA.

¹⁰ S. Cannata. 11/5/2004. CDFG, Fortuna, CA.

In the Southern DPS, recent habitat evaluations conducted in the upper Sacramento River for salmonid recovery planning suggests that significant potential green sturgeon spawning habitat was made inaccessible or altered by dams (historical habitat characteristics, temperature, and geology summarized in Lindley et al. (2004, 2006). This spawning habitat may have extended up into the three major branches of the Sacramento River; the Little Sacramento River, the Pitt River system, and the McCloud River. Green and white sturgeon adults have been observed periodically in small numbers in the Feather River¹¹ There are no records of larval or juvenile sturgeon of either species, even prior to the 1960's when Oroville Dam was built.¹² There are reports that green sturgeon may reproduce in the Feather River during high flow years, but these are not specific and are unconfirmed.⁴ California Department of Fish and Game regards the Feather River to be “the most likely loss of spawning habitat [of green sturgeon in the Central Valley]”.⁴ They suggests that Oroville Dam blocks access to potential spawning habitat and that Thermalito Afterbay warm water releases may increase temperatures to levels that are undesirable for green sturgeon spawning and incubation. No green sturgeon has ever been documented in the San Joaquin River or its tributaries.^{4, 11} Small numbers of adult sturgeon occur in the San Joaquin River, but all those identified to date have been white sturgeon. Two juvenile white sturgeon caught at Woodbridge on the Mokelumne River (rkm 63) in 2003 are the first confirmation of sturgeon reproduction in the San Joaquin River system.¹¹ The San Joaquin River and its tributaries have been heavily modified in ways that reduce suitability for sturgeon since the 1940's, so the lack of contemporary information cannot be

considered evidence of historical green sturgeon absence.

Harvest

Green sturgeon harvest is now almost entirely bycatch in three fisheries: white sturgeon commercial and sport fisheries, Klamath Tribal salmon gill-net fisheries, and coastal groundfish trawl fisheries (Table 1). Historically, the larger take was bycatch from white sturgeon commercial and sport fisheries. Large commercial fisheries developed in the late 1800's for previously unexploited white sturgeon, and these fisheries collapsed because fishing mortality far exceeded sustainability (Galbreath 1985). The excessive white sturgeon fishing mortality likely caused an accompanying decline in green sturgeon, but the degree of green sturgeon decline is unknown. Green sturgeon do have longer ocean residence than white sturgeon and therefore may be less available to fisheries. A smaller part of the harvest occurs directly on spawning fish as bycatch to the Klamath River Yurok and Hoopa tribal gill-net salmon fishery. The tribal salmonid fishery is used for subsistence.

The total average annual harvest of green sturgeon declined substantially from 6494 fish in 1985–1989 to 1072 fish in 2000–2003 (Table 1) and has continued to decline to 512 in 2003. Historically, harvest came predominately from the Columbia River (51%), coastal trawl fisheries (28%), the Oregon fishery (8%), and the California Tribal fishery (8%). Much of the harvest reduction in recent years is due to increasingly restrictive Columbia River fishing regulations. Coastal trawl fisheries have declined to low levels since 1999 (Rein 2002). In 2003, Klamath and Columbia River Tribal fisheries accounted for 65% of the total catch.

The California Klamath Tribal fishery has historically accounted for approximately 8% of green sturgeon harvest (Table 1). This fishery is especially important because the Klamath fishery operates directly on what is thought to be the largest green sturgeon spawning population. Harvest averaged 279 fish annually with no apparent trend from 1985 to 2003. There was one extremely high catch in 1981 of 810 fish. Green

¹¹ Beamesderfer, R.C.P., Simpson, G. Kopp, J. Inman, A. Fuller, and D. Demko. 2004. Historical and current information on green sturgeon occurrence in the Sacramento and San Joaquin rivers and tributaries. S.P. Cramer & Associates, Inc. Gresham, OR. 46 p.

¹² A. Seesholtz. 2005. California Department of Water Resources. Sacramento, CA.

Table 1 Harvest of green sturgeon (numbers) from California, Oregon, and Washington from 1985 to 2003

Year	California		Oregon ¹³		Washington ¹⁴								Total			
	Klamath ¹⁵		Sport	Trawl	Columbia River ¹⁶		Willapa Bay		Greys Harbor							
	SF Bay ¹	Yurok			Hoop	Sport	Comm.	Comm.	Sport	Treaty ¹⁷	Comm.	Sport	Treaty ¹⁸	Trawl	Other ¹⁸	
1985	Few	351	10	726	533	1600	1289			227	5	348	67	5156		
1986	Few	421	30	153	190	407	6000	925	1	626	3	142	167	9065		
1987	Few	171	20	170	124	228	4900	877		770	8	52	349	7669		
1988	Few	212	20	258	120	141	3300	1598	4	609	4	1	34	6514		
1989	Few	268	30	202	210	84	1700	461	4	870	12	2	133	4067		
1990	Few	242	20	157	143	86	2200	953	2	734	4	9	66	4736		
1991	Few	312	11	366	242	22	3190	957	0	1527	0	3	99	6788		
1992	Few	212	3	197	94	73	2160	1002	0	737	0	3	66	4551		
1993	Few	417	36	293	250	15	2220	290	32	542	112	3	37	4267		
1994	Few	293	6	160	154	132	240	268	13	6	17	25	22	5	1	1342
1995	Few	131	6	78	29	21	390	78	8	374	96	7	3	65	1286	
1996	Few	119	8	210	182	63	610	129	24	137	70	132	1	7	1692	
1997	Few	306	16	158	400	41	1614	16	4	316	105	198	6	19	3199	
1998	Few	335	10	103	77	73	894	65	12	2	25	28	55	0	1692	
1999	Few	204	28	73	21	93	967	9	5	0	29	58	4	1491		
2000	Few	162	31	15	12	32	1224	224	5	0	38	50	3	1796		
2001	Few	268	10	NA	17	50	342	106	9	0	27	32	1	862		
2002	Few	273	5	NA	14	51	163	0	48	7	0	131	4	696		
2003	Few	287	16	NA	17	52	46	43	NA	2	NA	46	5	514		

See footnotes for data sources

sturgeon catch is incidental to the chinook gill-net fishery by the Yurok and Hoopa Tribes on the lower portions of the Klamath and Trinity rivers. The green sturgeon catch is monitored but there is no direct regulation of the fishery for green sturgeon. In 2004, the tribal fisheries adopted additional conservation measures that will change the character of the catch time series.

California sport catch of green sturgeon, primarily in San Pablo Bay, is not monitored, but is thought to be only a few fish each year.⁴ Until very recently, there has been no differentiation between green and white sturgeon in the regulations and the current slot limits are 117 cm to 183 cm (46 to 72 in.). In 2006, California announced an emergency closure of recreational fishing for green sturgeon.

Harvest data provide limited information about population status. Average length of Columbia River commercially caught green sturgeon has been increasing since 1990 (Rien et al. 2001), and the largest average sizes have been in recent years. In the California Klamath Tribal fishery, the percentage of green sturgeon over 175 cm TL remained unchanged from 1984 to 2001. Larger fish are increasing in proportion to the total catch in recent years.

¹³ Farr et al. (2002), T. Rien., ODFW, 11/16/2004. Clackamas, OR.

¹⁴ Washington Department of Fish and Wildlife (WDFW). 2002. Letter to Ms. Donna Darm. 5 pp. (plus enclosures, 28 p.). WDFW. 2002. Letter to Dr. Peter Adams. 5 pp.

¹⁵ USFWS (1994) Klamath River fisheries investigation program, Annual Report—1992. Acraata, CA. 63 pp; Hillemeier, D. 2004. Yurok Tribe green sturgeon unpublished catch data. Yurok Tribe. Orcutt, CA.; Kautsky, G. 2004. Hoopa Tribe green sturgeon unpublished catch data. Hoopa, CA. 2 pp.

¹⁶ D. Ha 2002. Personel Communitation. VIMS. Gloucester Point, VI.

¹⁷ Frank, B. Jr. 2002. Northwest Indian Fisheries Commission unpublished green sturgeon catch data, 2 pp.

¹⁸ Rien, T. 2002. Lower Columbia River green sturgeon catch rates from commercial landings tickets. Memorandum. Oregon Dept. of Fish and Wildlife. 14 p.

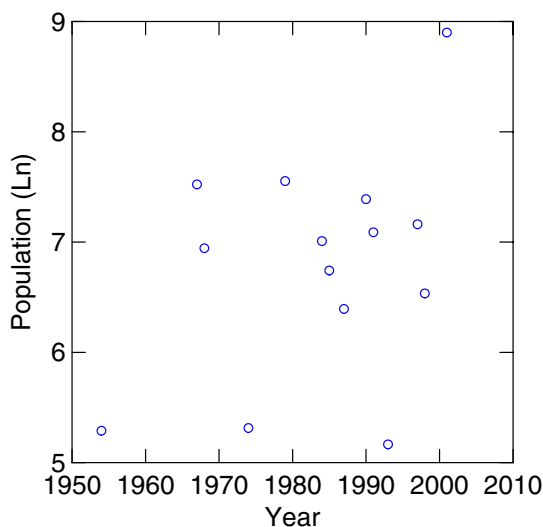


Fig. 2 CDFG San Pablo Bay green sturgeon (<102 cm) population estimates (\log_e transformed) from mark and recapture white sturgeon estimates (see text) conducted intermittently from 1954 to 2001

Population abundance

Musick et al. (2000) state that green sturgeon suffered “an 88% decline in most of their range.” The statement¹⁶ comes from the fact that “the abundance of all west coast sturgeons, including green, suffered approximately an 88% decline in California, inferred from commercial catch rates (Cech 1992).” However, the only statistics in the Cech (1992) article are the reduction of all commercial sturgeon landed (white and green, but primarily white) from 1.63 million pounds in 1887 to 0.2 million pounds in 1901 an 88% reduction. If these statistics are the basis of the 88% population decline reported in Musick et al. (2000), then these claims are hard to relate to current green sturgeon status.

The only estimates of green sturgeon population size are made incidentally to white sturgeon monitoring in San Pablo Bay.⁴ These estimates are calculated from a multiple-census or Peterson mark-recapture estimate of legal-size white sturgeon taken by trammel nets. The tagging experiments have been conducted irregularly since 1954, but since 1990, tagging has been conducted for 2 years consecutively and then the next 2 years are skipped. Over this period, a total of 536 green sturgeon were captured and

233 were tagged. The green sturgeon estimate was obtained by multiplying the ratio of legal-size green sturgeon to legal-size white sturgeon caught in the tagging program by the legal-size white sturgeon population estimate. There is no long-term trend in legal-size green sturgeon abundance, ($r^2 = 0.146$, slope = 0.029, $P = 0.177$, Fig. 2) even though the highest value occurred in 2001, based on linear regression¹⁹ These estimates have a number of potential biases; the most important being the assumption of equal vulnerability of both species to the gear. Green sturgeon concentrate in estuaries only during summer and fall whereas white sturgeon may remain in estuaries year around and therefore, the temporal and spatial vulnerabilities of the two species can be very different.

Two additional green sturgeon harvest population time series were analyzed because of their length, their relative lack of bias, and their geographical importance. These were the Klamath Yurok Tribal fishery catch and catch-per-unit-effort (CPUE) series and Columbia River commercial landings. Both of these population time series came from fisheries targeting other species. The raw catch time series suffers from changing regulations and effort levels. Also, green sturgeon are not an abundant species, and therefore the numbers captured are small and variable with a large number of zero observations. Simple linear regressions were calculated for each time series providing a slope with a standard error and confidence intervals.

The Klamath Yurok Tribal fishery catch and CPUE are the most consistent green sturgeon data sets. Catch and CPUE data are available from 1984 to 2003 and it is the time series least impacted by changes in regulations.²⁰ Analyses were performed on \log_e -transformed catch and CPUE from April and May. This time period was considered to be the most representative of the green sturgeon presence in the river. The regression analyses¹⁹ for the \log_e -transformed catch

¹⁹ Undated analysis from S. Heppel and L. Hoffman. 2002. Green Sturgeon Status Assessment. Final Report for the Southwest Fisheries Science Center, Santa Cruz, CA. 41 p.

²⁰ D. Hillemeier. 2004. Yuork Tribe green sturgeon unpublished catch data. Yurok Tribe. Orcut, CA.

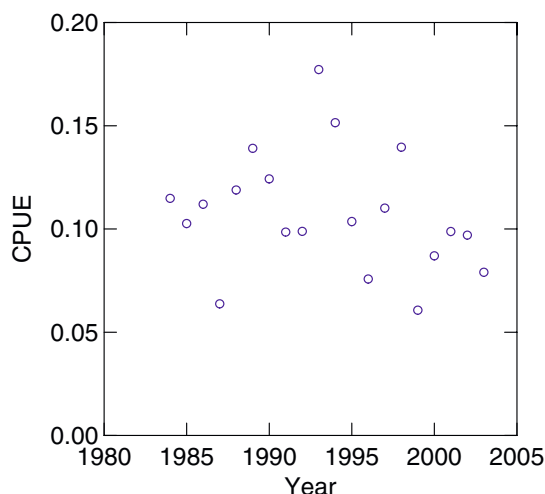


Fig. 3 Yurok Tribal green sturgeon April and May CPUE (numbers/gill net set) for 1984 to 2003 regressed against year

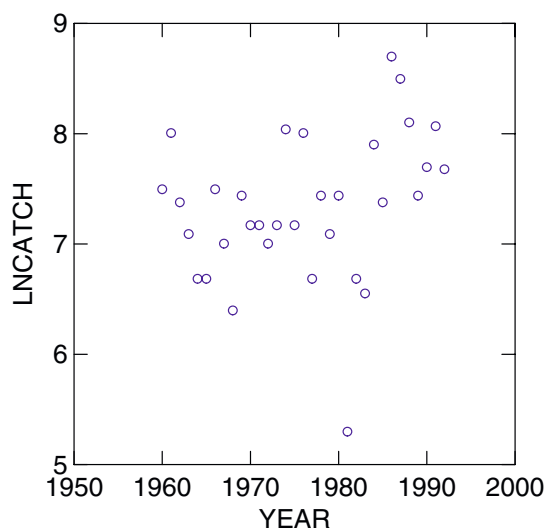


Fig. 4 Columbia River green sturgeon catch (\log_e transformed) in numbers (see text) regressed against year. The time period ends in 1992 due to regulatory changes in the fishery

($r^2 = 0.494$, slope = 0.053, $P = 0.012$) and CPUE ($r^2 = 0.055$, slope = -0.0008 , $P = 0.320$, Fig. 3) both had slopes that were not significantly different from 0. \log_e transformed catch and CPUE were not well correlated with each other ($r^2 = 0.166$). Length–frequency data over this time period showed no trends.¹

The Columbia River commercial landings are the longest green sturgeon time-series available

and represent the largest source of removals from the population (Fig. 4). Landings were recorded in pounds in early years, but catch in numbers were estimated by Oregon Department of Fish and Wildlife (Rien et al. 2001). Fishery regulations drastically changed in 1993, so the regression was only conducted until 1992. Catch in numbers is not only affected by effort and size regulations, but also by the amount and timing of green sturgeon occurrence in the estuary during the summer. The regression analysis¹⁹ of \log_e -transformed catch in numbers on years was not significant ($r^2 = 0.082$, slope = 0.020, $P = 0.108$, Fig. 4). There was a significant positive trend ($r^2 = 0.083$, slope = 0.022, $P < 0.0001$) when the commercial landings were adjusted for total sturgeon effort based on trip tickets¹⁸ Length–frequency distribution of catch from 1985 to 2001 showed no trend (Rien et al. 2001).

Entrainment

Substantial numbers of green sturgeon were killed in pumping operations at state and federal water export facilities in the Sacramento-San Joaquin River Delta (Table 2). Green sturgeons taken in both water export facilities are juvenile fish in the 28 cm to 38 cm FL size range.¹ These numbers are higher in the period prior to 1986 than from 1986 to the present (CDFG 2002). For the state facility (1968–2001), the average number of green sturgeon taken per year prior to 1986 was 732; while the average number was 47 from 1986 on. For the federal facility (1980–2001), the average number prior to 1986 was 889; while the average number was 32 from 1986 on. Trends at each facility were similar with or without adjustment for volume of water pumped (per 1 000 acre-feet). Further examination of the salvage estimates founded that the actual number of actual green sturgeon observed were three-and-one-half times higher in the pre-1986 period.²¹ However, a General Linear Model (GLM) analysis of the green sturgeon estimates compared to observed fish in the pre-1986 period showed that one observed fish was

²¹ P. Adams, unpublished analysis. 2006. NMFS, Santa Cruz, CA.

Table 2 Green sturgeon numbers and numbers per 1000 acre-feet of water exported from the State and Federal water export facilities at the Sacramento-San Joaquin River Delta Annual estimates are expansions of brief sampling periods⁴

Year	State facility		Federal Facility	
	Numbers	Numbers per 1000 acre-feet	Numbers	Numbers per 1000 acre-feet
1968	12	0.0162		
1969	0	0		
1970	13	0.0254		
1971	168	0.2281		
1972	122	0.0798		
1973	140	0.1112		
1974	7313	3.9805		
1975	2885	1.2033		
1976	240	0.1787		
1977	14	0.0168		
1978	768	0.3482		
1979	423	0.1665		
1980	47	0.0217		
1981	411	0.1825	274	0.1278
1982	523	0.2005	570	0.2553
1983	1	0.0008	1475	0.653
1984	94	0.043	750	0.2881
1985	3	0.0011	1374	0.4917
1986	0	0	49	0.0189
1987	37	0.0168	91	0.0328
1988	50	0.0188	0	0
1989	0	0	0	0
1990	124	0.0514	0	0
1991	45	0.0265	0	0
1992	50	0.0332	114	0.0963
1993	27	0.0084	12	0.0045
1994	5	0.003	12	0.0068
1995	101	0.0478	60	0.0211
1996	40	0.0123	36	0.0139
1997	19	0.0075	60	0.0239
1998	136	0.0806	24	0.0115
1999	36	0.0133	24	0.0095
2000	30	0.008	0	0
2001	54	0.0233	24	0.0106

converted to 48 estimated fish (coefficient = 47.9, $F = 303$ with 16 df, $P = 0.001$). The same analysis for the period from 1986 on showed that one observed fish was converted into 9.7 estimated fish (coefficient = 9.7, $F = 12.4$ with df = 14, $P = 0.003$). So while the numbers of green sturgeon still were higher in the pre 1986 period, it appears that the expansion procedure exaggerated that difference. These entrainment estimates suffer from problems of species identification (green sturgeon were not identified until 1981 at the federal facility), and the estimates are expanded catches from brief sampling periods.⁴ Additional entrainment must also occur from a large number of smaller, unmonitored water diversions on the Sacramento River.

Conclusions and discussion on the “extinction risk” question

Species wide threats

Ocean and estuarine green sturgeon harvest is considered a species wide threat since its impact could not be apportioned to one particular DPS (except for the Klamath tribal in-river catches). Even catches in San Pablo Bay could be fish that originated in the Northern DPS. Harvest impact could be very different if there were disproportionately high harvest of only one DPS. Current total harvest has been reduced to 6% of its 1986 value of 9065 fish. The recent reductions are due in large part to newly imposed fishing regulations

in Oregon and Washington. Commercial fisheries targeting sturgeon have not been allowed in the Columbia River or Willapa Bay since 2001. Klamath tribal catch has remained relatively constant during the entire time series, but recently instituted conservation measures will decrease that catch in the future. The very recent closure of the California recreational fishery will reduce catch even further. The decrease in catch due to changes in regulations and conservation measures represents a reduction in risk to green sturgeon.

No estimates of fishing mortality or exploitation rates exist for green sturgeon, although an annual survival rate of about 85% has been suggested by examining preliminary age data for the Klamath River.²² Secor et al. (2002) note that sturgeon populations can be harvested on a sustainable basis, but only if sufficient spawner escapement is maintained. They noted that sturgeon populations typically can not tolerate more than 5% fishing mortality during spawning runs. Similar rates of annual survival (S) have been assumed in population models for adult Gulf sturgeon in the Suwannee River, Florida ($S = 0.84$, maximum age 25; Pine et al. 2001) and age-1 + shortnose sturgeon ($S = 0.865$, max age 37; Gross et al. 2002). Higher survival rates were assumed in models for Hudson River Atlantic sturgeon ($S = 0.93$, max age 60; Gross et al. 2002) and lower Columbia River white sturgeon ($S = 0.91$, max age 100; Gross et al. 2002). Fishing mortality rates for green sturgeon are affected by slot limit regulations that restrict harvest of adults. In terms of population impacts, however, it is worth noting that sturgeon populations can be substantially affected by harvest of subadults, because of the long interval prior to maturity (Gross et al. 2002; Secor et al. 2002).

One way to judge the impact of fishing is to examine age structure and consider how many opportunities an adult sturgeon would have to spawn. This is particularly critical for sturgeon species, given that strong year classes occur infrequently and adults may only spawn every 3–

5 years. Based on preliminary age data,²⁰ female green sturgeon in 1999–2000 Klamath River catches ranged in age from 17 to 33 although most were 25–31. Using a female maturity of age 20 and their 5 year spawning periodicity, most female green sturgeon would only spawn twice. In comparison, a restoration goal for Atlantic sturgeon (NMFS 1998) is to have at least 20 adult age classes in the spawning stock prior to any consideration of lifting the current harvest moratorium.

The northern green sturgeon DPS

The Northern DPS has two known well-established spawning populations, one in the Rogue River and one in the Klamath-Trinity River system. This spreads the risk over more than one spawning area. In addition, the two systems are not geographically close and thus do not share the same risks of catastrophic events. Spawning appears to occur infrequently in the Umpqua and Eel rivers. The principal threats to green sturgeon in this DPS are flow and temperature factors, habitat degradation, and harvest (Table 3).

The extent of green sturgeon spawning in the Rogue River has only been recently documented (Erickson et al. 2002). The river is less manipulated and habitat seems to be of better quality than in other green sturgeon spawning rivers. Blockages to migration do not seem to be limiting and habitat seems to be roughly what it was historically. Other anadromous fishes are generally doing well in the Rogue River (Weitkamp et al. 1995; Busby et al. 1996; Myers et al. 1998).

The Klamath River is considered to have the largest green sturgeon spawning population. The Yurok catch data were judged to be the most representative available population measure, since the data were based on spawning fish rather than on fish involved in their summer concentration behavior. Neither catch nor CPUE had a negative slope, but trends for both were also not statistically significant. The length data did not indicate that large fish were decreasing within the population, but sample sizes were very small. Spawning still occurs upstream to the historical limit of its habitat range (Ishi Pishi Falls). Out-

²² R. Beamsederfer and M. Webb. 2002. Green sturgeon status review information. S. P. Cramer and Associates, Inc. Gresham, OR. 46 p.

Table 3 Historical and current spawning status of green sturgeon within the Northern DPS, including specific threats to river systems (but excluding ocean and estuarine harvest, which is considered as a coastwide threat)

River system	Historical spawning status	Present spawning status	Threats/changes
Fraser River	No evidence	No evidence ²³	Availability of appropriate habitat and degradation or alterations to the habitat (Houston 1988). Local harvest
Chehalis River	No evidence	No evidence ²⁴	Local harvest
Umpqua River	Known spawning	Known spawning ²⁵	Local harvest
Rogue River	Known spawning	Known spawning ²⁶	Common to Savage Rapids ²³ and known to occur to Lost Creek Dam ²⁷ Flow management and hydro effects ²⁸ Local Harvest
Klamath River	Known spawning	Known spawning ²⁹	Increased temperatures ³⁰ Reduced oxygen concentrations ³¹ Flow regime change ³² In-river harvest ¹ Reduced flows ³⁴
- Trinity River	Known spawning	Known spawning ³³	See Klamath River Threats
-SF Trinity	Suspected spawning ³⁵	Suspected spawning ³⁶	1955 and 1964 floods ³ See Klamath River Threats
Eel River	Known spawning ⁵	Suspected spawning ⁹	1955 and 1964 floods ³⁷ Flow management and water transfers ³⁸ Sediment and TMDL ³⁹

migrant juvenile green sturgeon are captured each year in screw traps at Big Bar (Scheiff et al. 2001). There are concerns about the temperature and flow regime in the Klamath River, a major

issue for salmonids that have been highlighted by recent fish kills (NRC 2004).

The Trinity River has far less data than the Klamath. The Hoopa Tribe has a small in-river

²³ Fraser River green sturgeon are from U.S. spawning populations, but do occur as far north as the Skeena River (D. Lane. 2004. Malaspina University, Nanaimo, British Columbia).

²⁴ Washington Department of Fish and Wildlife. 2004. Letter to Mr. James Lecky from R. Fuller, 4 pp.

²⁵ T. Rien. 2004. Oregon Department of Fish and Wildlife. Clackamas, OR. Two juvenile green sturgeon (approximately 10 cm long) were regurgitated from two small-mouth bass caught at rkm 134 on the Umpqua River, in June 2000.

²⁶ Erickson et al. (2002).

²⁷ R. Reisenbichler. 2004. U. S. Geological Service. Seattle, WA.

²⁸ Oregon Department of Fish and Wildlife. 2002. NMFS Status Review for North American Green Sturgeon. ODFW Memorandum, 5 pp.

²⁹ Spawning to Ishi Pishi Falls (Moyle 2002). Juveniles taken annually at Big Bend (Scheiff et al. 2001).

³⁰ Increased summer temperatures due to lower flows (NRC 2004).

³¹ Oxygen concentration decreased due to flow and degradable organic material below Irongate Dam (NRC 2004).

³² Shift in peak flows from April to March (NRC 2004).

³³ Spawning to Greys Falls (Moyle 1992). Juveniles taken in most years at Willow Creek (Scheiff et al. 2001).

³⁴ Trinity River flows reduced 88% (NRC 2004).

³⁵ 1978 CDFG Letter (referenced in USFWS 1981, Klamath River fisheries investigation program, Annual Report—1980 Arcata, CA, 105 pp, but not located).

³⁶ Willow Creek trap located down stream of S.F. Trinity confluence (Scheiff et al. 2001)

³⁷ Historic reductions to chinook populations from which they never recovered (Moyle 2002).

³⁸ Summer flows are lower and decrease earlier than historical flows (National Marine Fisheries Service. 2002. Biological opinion for the proposed license amendment of the Potter Valley project. Southwest Region. Long Beach, CA. 135 pp).

³⁹ Loss of habitat due to sedimentation from land use practices and large scale floods (NMFS 2002).

Table 4 Historical and current spawning status of green sturgeon within the Southern DPS, including specific threats to river systems (but excluding ocean and estuarine harvest, which is considered as a coastwide threat)

River system	Historical spawning status	Present spawning status	Threats/changes
Sacramento River	Known spawning	Known spawning ¹	Impassible barriers (Keswick and Shasta dams) ²¹ Adult migration barriers ⁴⁰ Insufficient flow ²¹ Increased temperatures ⁴¹ Juvenile entrainment ¹ Exotic species (e.g., striped bass) ⁴ Poaching ¹ Pesticides and heavy metals ²¹ Local Harvest
Feather River	Suspected spawning ⁴	No evidence ¹¹	Impassible barriers (Oroville Dam) ⁴² See Sacramento River Threats
San Joaquin River	No evidence ^{1,43}	No evidence ¹¹	Impassible Barriers (Friant Dam) ⁴⁴ Extreme low flow ⁴⁵ See Sacramento River Threats

fishery that takes less than 30 adult green sturgeon each year (Table 1). Juvenile out-migrant green sturgeon are captured in most years in small numbers at Willow Creek (Scheiff et al. 2001). There are similar concerns about the temperature and flow regime here as there are in the Klamath (NRC 2004).

The Eel River is the southern most known spawning area in the Northern DPS. Moyle

(2002) suggested that green sturgeon were lost from the Eel River following the 1964 flood. This event along with the 1955 flood and poor land use practices brought large amounts of sediment into the Eel River, and this high sediment level is present today. Some portion of the deep holes that green sturgeon use for holding must have been filled in by these events, but the extent is unknown. Green sturgeon do not appear to be extirpated from the Eel River since there were sightings of adults in both 1995 and 1996 and juveniles in the estuary in 1994. The adult surveys were only conducted in those years and the estuary surveys were only conducted in one other year. Nevertheless, green sturgeon are almost certainly severely reduced in the Eel River from historical levels.

Green sturgeon in the Northern DPS are not considered in danger of extinction now nor are they likely to become endangered in the foreseeable future throughout all of their range, although the lack of data introduces a great deal of uncertainty into this decision. The risk of catastrophic events is spread over a larger geographically area in this DPS, because there are two known spawning populations in the Rogue and Klamath-Trinity rivers. Population trends are not

⁴⁰ Other barrier that are not impassible, RBBB and ACID. Also, sturgeon attracted to stranding areas such as Yolo Bypass. J. McLain. 2004. NOAA Fisheries, Sacramento, CA.

⁴¹ High water temperatures previous to winter-run chinook flow management (J. McLain. 2004. NOAA Fisheries, Sacramento, CA.

⁴² No evidence of spawning but continued presence of green sturgeon in the Feather and Yuba rivers suggest that they are trying to migrate into presumed spawning areas now blocked by Oroville Dam.

⁴³ Adult presence documented in Delta.¹ Evidence of white sturgeon spawning in San Joaquin.¹¹ Accounts of unspecified sturgeon sport catch in San Joaquin River as far as the Merced River (Kohlhorst 1976).

⁴⁴ San Joaquin River and tributaries block by dams (Yoshiyama et al. 2001).

⁴⁵ Vernalis flows as low as 17% of minimum targets. J. McLain. 2004. NOAA Fisheries, Sacramento, CA.

negative and harvest has been reduced. Green sturgeon populations in this DPS face serious potential threats (Table 3) that are particularly worrisome given the lack of data to adequately monitor population status. We recommend that appropriate monitoring of these populations be implemented so that a serious decline in population status could be detected in a timely manner.

The southern green sturgeon DPS

Green sturgeon face a larger number and severity of threats in the Southern DPS (Table 4). The principal threat to this DPS comes from the reduction of green sturgeon spawning to a single area in the Sacramento River. The Sacramento River has impassible barriers blocking green sturgeon access to what were almost certainly historical spawning grounds upstream from Shasta and Keswick dams constructed in the 1940's and 50's.⁴⁶ The same is also true for Feather River and Oroville Dam,⁴⁷ completed in 1968.⁴⁸ In addition, there are also other migration barriers such as Red Bluff Diversion Dam (RBDD) and Anderson-Cottonwood Irrigation District Dam that do not complete block migrations or only block fish seasonally. The Sacramento River now has both reduced and controlled flow.²¹ A strong correlation has been found between mean daily temperature and white sturgeon year-class strength.²¹ Similar relationships may exist for green sturgeon. High temperatures may be less of a problem that it once was due to the installation of the Shasta Dam temperature control device in 1997, although Shasta Dam has a limited storage capacity and cold-water reserves could be depleted in long droughts. Temperatures at RBDD have not been

higher than 16 °C since 1995. This is near green sturgeon egg and larvae optimal temperatures of 15–19 °C (Mayfield and Cech 2004). However, green sturgeon reproduction before 1995 probably was adversely affected by temperature. This may have caused population reductions that could still affect the overall population size and age-structure even now. The average number of juvenile green sturgeon entrained at both the state and federal facility prior to 1986 were higher than they were from 1986 on. There are no apparent reasons for the large reduction in numbers entrained. Exotic species are an ongoing problem in the Sacramento-San Joaquin River and Delta systems (Cohen and Carlton 1998). Probably, the largest problems with exotic species regard the replacement of native food items. The exotic bivalve *Potamocorbula amurensis*, introduced in 1988, has become the most common food of white sturgeon and was found in the only green sturgeon examined.⁴ Moreover, the overbite clam is known to bioaccumulate selenium, a toxic metal (Linville et al. 2002). Green sturgeon may also experience predation by introduced species including striped bass. Sturgeon have high vulnerability to fisheries and the trophy status of large white sturgeon makes them the target of poachers.⁴ Green sturgeon are caught incidentally in these white sturgeon fisheries and may also be taken in illegal fisheries. Pollution within the Sacramento River increased substantially in the mid-1970s when application of rice pesticides increased.²¹ Estimated toxic concentrations for the Sacramento River during 1970–1988 may have deleteriously affected striped bass larvae (Bailey 1994). White sturgeon may also accumulate PCB and selenium,⁴⁹ substances know to be impair embryonic development.

The Sacramento River supports the only known green sturgeon spawning population in this DPS. There has almost certainly been a substantial loss of spawning habitat behind Keswick and Shasta dams.²¹ The historical habitat data has been

⁴⁶ U.S. Fish and Wildlife Service. 1994. Recovery Plan for Sacramento-San Joaquin Native Fishes. Portland, OR. 142 p.

⁴⁷ U.S. Fish and Wildlife Service. 1995. Working Paper on Restoration Needs: Habitat Restoration Actions to Double Natural Production of Anadromous Fish in the Central Valley of California. Vol. 3. Prepared for the U. S. Fish and Wildlife Service under the direction of the Anadromous Fish Restoration Program Core Group. Stockton, CA. 544 p.

⁴⁸ California Data Exchange Center. <http://cdec.water.ca.gov/>. California Department of Water Resources, Division of Flood Management. Sacramento, CA.

⁴⁹ J. White, P. Hoffmann, K Urquhart, D. Hammond, and S. Baumgartner. 1989. Selenium verification study, 1987–1988. A report to the California State Water Resources Control Board from the California Department of Fish and Game, April 1989. 60 p.

summarized in Lindley et al. (2004). Green sturgeon occur up to the impassible barrier at Keswick Dam. It is unlikely that green sturgeon historically reproduced in their current spawning area based on the historical temperature regime that occurred before the construction of Shasta and Keswick dams. At the present, water temperatures in the current spawning area are lower due to cool-water releases from Shasta Dam. Green sturgeon almost certainly spawned further up the mainstem that they do now. It possible that the additional habitat behind Shasta Dam in the Little Sacramento, Pitt, and McCloud systems would have supported separate populations or at least, a single larger population that was less vulnerable to catastrophes than the current one.

Green sturgeon almost certainly no longer spawn in the Feather River. Access to a substantial amount of habitat in the Feather River was lost with the construction of Oroville Dam. California Department of Fish and Game concluded that the Feather River spawning habitat was most likely lost due to habitat blockage by Oroville Dam and from thermal barriers created by the Thermaltio Afterbay facility.⁴ U.S. Fish and Wildlife Service stated¹⁷ that “Evidence also suggests that sturgeon reproduction occurs in both the Feather and Bear rivers.” in reference to white sturgeon prior to dam construction. Again, it must be assumed that a similar conclusion could be made for green sturgeon in the face of the paucity of data. Sturgeon (including some documented green sturgeon) still regularly occur in the Bear and Yuba rivers^{4,11} and therefore must migrate through the Feather River. Threats to green sturgeon are similar to those faced in the Sacramento River.

There is not sufficient information to establish whether the San Joaquin River system ever had supported a viable green sturgeon population. There is no evidence of green sturgeon occurrence or spawning in the San Joaquin River.^{1,4,11} White sturgeon do occur in the San Joaquin River system, particularly in wet years⁴ and the first record of white sturgeon spawning in the San Joaquin system was made in 2003.¹¹ Moyle (2002) suggests that green sturgeon reproduction may have taken place in the San Joaquin River because adult green sturgeon were captured at Santa Clara Shoal and Brannan Island

Recreational Area in the Delta. If green sturgeon occurred in the San Joaquin system, the potential threats would be similar in nature to those faced in the Sacramento River, but would probably be more extreme.

The green sturgeon Southern DPS population trend information was less definitive than in the Northern DPS, and less convincing. The San Pablo Bay population estimates had a slightly positive trend, which was not statistically significant, even though the 2001 estimate was the highest on record. The usefulness of these estimates was reduced because they are based on the green sturgeon’s summer concentrations, a situation which is not understood. In addition, unequal vulnerabilities to sampling gear of these two species make these estimates less reliable.

Green sturgeon in the Southern DPS are likely to become an endangered species in the foreseeable future. The Southern DPS is at substantial risk, primarily because green sturgeon are confined to a single spawning area in the Sacramento River. Potential threats faced by green sturgeon are substantially greater in the Southern DPS than in the Northern one. Threats in this DPS include vulnerability due to concentration of spawning, smaller population size, lack of population data, potentially growth-limiting and lethal temperatures, harvest concerns, loss of spawning habitat, entrainment by water projects and influence of toxic material and exotic species. Catastrophic events have occurred in this DPS, such as the large-scale Cantara herbicide spill which killed all fish in a 10-mile stretch of river upstream from Shasta Dam, and the 1977–1978 drought that caused year-class failure of winter-run chinook salmon. Population sizes are unknown in this DPS, but are clearly much smaller than in the northern one and therefore this DPS is much more susceptible to catastrophic events. As is the case for the Northern DPS, the Southern DPS is in need of adequate population monitoring.

References

- Ayres WO (1854) Descriptions of three new species of sturgeon San Francisco. Proc California Acad Nat Sci 1:14–15 (1854–1857)

- Bailey HC, Alexander C, DiGiorgio C, Miller M, Doroshov SI, Hinton DE (1994) The effect of agricultural discharge on striped bass (*Morone saxatilis*) in California's Sacramento-San Joaquin drainage. *Ecotoxicology* 3:123–142
- Bemis WE, Kynard B (1997) Sturgeon rivers: an introduction to acipenseriform biogeography and life history. *Environ Biol Fish* 48:167–183
- Berg LS (1948) Freshwater fishes of the U.S.S.R. and adjacent countries, vol I, 4th edn. Academy of Sciences of the U.S.S.R. Zoological Institute. Published for the National Science Foundation, Washington, D.C. by the Israel Program for Scientific Translations, Jerusalem 1962
- Birstein VJ, Poletaeov AI, Goncharov BF (1993) DNA content in Eurasian sturgeon species determined by flow cytometry. *Cytometry* 14:377–383
- Birstein VJ, DeSalle R (1998) Molecular phylogeny of Acipenserinae. *Mol Phylogenetics Evol* 9:141–155
- Boreman J (1997) Sensitivity of North American sturgeons and paddlefish to fishing mortality. *Environ Biol Fishes* 46:399–405
- Busby PJ, Wainwright TC, Bryant GJ, Lierheimer LJ, Waples RS, Waknitz FW, Lagomarsino IV (1996) Status review of West Coast Steelhead from Washington, Idaho, Oregon, and California. NOAA-NWFSC Tech. Memo. 27, 261 pp
- Cech JJ Jr (1992) White sturgeon. In: Leet WS, Dewees CM, Haugen CW (eds) California's living marine resources and their utilization. California Sea Grant, Sea Grant Extension Publication UCSGEP-92-12, pp 70–72
- Cohen AN, Carlton JT (1998) Accelerating invasion rate in a highly invaded estuary. *Science* 279:555–558
- Deng X (2000) Artificial reproduction and early life stages of the green sturgeon (*Acipenser medirostris*). Unpublished. Master of Science thesis. University of California. Davis, CA. 61 pp
- Erickson DL, North JA, Hightower JE, Weber J, Lauck L (2002) Movement and habitat use of green sturgeon *Acipenser medirostris* in the Rogue River, Oregon, USA. *J Appl Ichthyol* 18:565–569
- Erickson DL, Hightower JE (in press) Oceanic distribution and behavior of green sturgeon (*Acipenser medirostris*). In: Munro J, Hatin D, McKown K, Hightower J, Sulak KJ, Kahnle AW, Caron F (eds) Symposium on anadromous sturgeons. American Fisheries Society, Symposium. Bethesda, Maryland
- Farr RA, Hughes ML, Rien TA (2002) Green sturgeon population characteristics in Oregon. Annual Progress Report. Sport Fish Restoration Project F-178-R. 27 pp
- Galbreath JL (1985). Status, life history, and management of Columbia River white sturgeon, *Acipenser transmontanus*. In: Binkowski FP, Doroshov SI (eds). North American sturgeons. Dr. W. Junk Publishers, Dordrecht, pp 119–125
- Gross MR, Repka J, Robertson CT, Secor DH, Van Winkle W (2002) Sturgeon conservation: insights from elasticity analysis. *Am Fish Soc Symp* 28:13–30
- Houston JJ (1988) Status of green sturgeon, *Acipenser medirostris*, in Canada. *Can Field-Nat* 102:286–290
- Israel JA, Blumberg M, Cordes J, May B (2004) Geographic patterns of genetic differentiation among western U.S. collections of North American green sturgeon (*Acipenser medirostris*). *North Am J Fish Manage* 24:922–931
- Lindley ST, Schick R, May BP, Anderson JJ, Greene S, Hanson C, Low A, McEwan D, MacFarlane RB, Swanson C, Williams JG (2004) Population structure of threatened and endangered chinook salmon ESUs in California's Central Valley basin. NOAA TM NMFS SWFSC 360. 56 pp
- Lindley ST, Schick RS, Agrawal A, Goslin M, Pearson T, Mora E, Anderson JJ, May BP, Greene S, Hanson C, Low A, McEwan D, MacFarlane RB, Swanson C, Williams JG (2006) Historical population structure of Central Valley steelhead and its alteration by dams. *San Francisco Estuary Watershed Science* 4(1)
- Linville RG, Luoma SN, Cutter L, Cutter GA (2002) Increased selenium threat as a result of invasion of the exotic bivalve *Potamocorbula amurensis* into the San Francisco Bay-Delta. *Aqua Toxicol* 57:51–64
- Mayfield RB, Cech JJ Jr (2004) Temperature effects on green sturgeon bioenergetics. *Trans Am Fish Soc* 133:961–970
- Moyle PB (2002) Inland fishes of California. University of California Press, Berkeley, CA. 502 pp
- Musick JA, Harbin MM, Berkeley SA, Burgess GH, Eklund AM, Findley L, Gilmore RG, Golden JT, Ha DS, Huntsman GR, McGovern JC, Parker SJ, Poss SG, Sala E, Schmidt TW, Sedberry GR, Weeks H, Wright SG (2000) Marine, estuarine, and diadromous fish stocks at risk of extinction in North America (exclusive of Pacific salmonids). *Fisheries* 25:6–30
- Myers JM, Kope RG, Bryant GJ, Teel D, Lierheimer LJ, Wainwright TC, Grant WS, Waknitz FW, Neely K, Lindley ST, Waples RS (1998) Status review of chinook salmon from Washington, Idaho, Oregon, and California. NOAA-NWFSC Tech. Memo. 35. 443 pp
- National Marine Fisheries Service (NMFS) (1998) Status review of Atlantic sturgeon (*Acipenser oxyrinchus oxyrinchus*). National Marine Fisheries Service, Gloucester, MA, 126 pp
- National Research Council (NRC) (2004) Endangered and threatened fishes in the Klamath River Basin: causes of decline and strategies for recovery. Committee on Endangered and Threatened Fishes in the Klamath River Basin. National Academies Press, Washington, D.C., 424 pp
- North JA, Farr RA, Vescei P (2002) A comparison of meristic and morphometric characters of green sturgeon *Acipenser*. *J Appl Ichthyol* 18:234–239
- Pine WE III, Allen MS, Dreitz VJ (2001) Population viability of the Gulf of Mexico sturgeon: inferences from capture-recapture and age-structured models. *Trans Am Fish Soc* 130:1164–1174
- Rien TA, Burner LC, Farr RA, Howell MD, North JA (2001) Green sturgeon population characteristics in Oregon. Annual Progress Report. Sportfish Restoration Project F-178-R, 41 pp
- Scheiff AJ, Lang JS, Pinnix WD (2001) Juvenile salmonid monitoring on the mainstem Klamath River at Big

- Bar and mainstem Trinity River at Willow Creek 1997–2000. USFWS, AFWO, Arcata, CA 95521, 114 pp
- Secor DH, Anders PJ, Van Winkle W, Dixon DA (2002) Can we study sturgeons to extinction? What we do and don't know about the conservation of North American sturgeons. *Am Fish Soc Symp* 28:3–10
- United States Fish and Wildlife Service (USFWS) (1967) Endangered and Threatened Wildlife and Plants; Endangered Status for the Shortnose Sturgeon. *Federal Register* 32:4001
- United States Fish and Wildlife Service (USFWS) (1990) Endangered and threatened wildlife and plants; determination of endangered status for the Pallid Sturgeon. *Federal Register* 55(173):36641–36647
- United States Fish, Wildlife Service (USFWS) (1994) Endangered and threatened wildlife and plants; determination of endangered status for the Kootenai River Population of the White Sturgeon. *Federal Register* 59(171):45989–46022
- United States Fish and Wildlife Service (USFWS) (2000) Endangered and threatened wildlife and plants; final rule to list the Alabama sturgeon as endangered. *Federal Register* 65(88):26437–26461
- United States Fish and Wildlife Service (USFWS) and National Oceanic and Atmospheric Administration (NOAA) (1991) Endangered and threatened wildlife and plants; threatened status for the Gulf Sturgeon. *Federal Register* 56(189):49653–49658
- United States Fish and Wildlife Service (USFWS) (1996) Policy regarding the recognition of distinct Vertebrate Population Segments Under The endangered species Act. *Federal Register* 61(26):4721–4725
- Weitkamp LA, Wainwright TC, Bryant GJ, Milner GB, Teel DJ, Kope RG, Waples RS (1995) Status review of Coho Salmon from Washington, Oregon, and California. NOAA-NWFSC Tech Memo-24, 258 pp
- Wirgin II, Stabile JE, Waldman JR (1997) Molecular analysis in the conservation of sturgeons and paddlefish. *Environ Biol Fish* 48:385–398
- Yoshiyama RM, Gerstung ER, Fisher FW, Moyle PB (2001) Historical and present distribution of chinook salmon in the Central Valley Drainage of California. *CDFG, Fish Bull* 179(1):71–176

Recommended Streamflow Schedules To Meet the AFRP Doubling Goal in the San Joaquin River Basin

27 September 2005

Introduction

The goal of the Anadromous Fish Restoration Program (AFRP) is to make all reasonable efforts to at least double natural production of anadromous fish in California's Central Valley streams on a long-term, sustainable basis. However, production of fall-run Chinook salmon (Chinook Prod) between 1992 and 2004 has declined by 28% in the Stanislaus River, 46% in the Tuolumne River, and increased by only 4% in the Merced River, which is a hatchery supported stream, compared to the 1967-1991 baseline period. Evidence is provided here that the declines in salmon production primarily resulted from a reduction in the frequency and magnitude of spring flooding in the San Joaquin River Basin during the 1992-2004 period compared to the baseline period. Additional evidence is provided that the most likely means of increasing adult production would be to increase flows during February and March to substantially increase the survival of juveniles in the lower half of the tributaries and the San Joaquin River and thereby increase the production of smolts, and then to increase flows between April and mid-June to increase smolt survival. It is also likely that production can be further increased by (1) providing fall pulse flows that help minimize the number of adult salmon that stray to the Sacramento Basin when Delta export rates are high and minimize delays of adults in the Delta that may impair gamete viability; (2) gradually ramping down spring flows during June to facilitate riparian vegetation recruitment and thereby increase the input of allochthonous organic matter and food into the aquatic habitat; and (3) increasing summer flows to increase the survival of juvenile Central Valley steelhead and Chinook yearlings.

The population models described below suggest that the physical habitat in the Stanislaus, Tuolumne, and Merced rivers can support the progeny of no more than 2,000 spawners. If true, restoring the spawning, rearing, and/or floodplain habitats should substantially increase salmonid production in all three tributaries. However, it is likely that habitat restoration by itself will not increase juvenile production, unless flows are increased to increase the amount of rearing habitat, the frequency of floodplain inundation, and thereby increase juvenile survival.

There is also a slight possibility that increasing flows during spawning in early November to increase the amount of habitat with suitable water temperatures would reduce redd superimposition and thereby increase juvenile production; however, screw trap data from the Stanislaus River, which are presented below, do not support this hypothesis.

Ten analyses that were used to justify and determine the flow schedules needed to help achieve the AFRP doubling goal are summarized below:

1. Relationships between salmon recruitment and flow in the Stanislaus and Tuolumne rivers;
2. Relationships between juvenile survival and flow in the Stanislaus River;
3. Salmon production models for the San Joaquin River Basin;
4. Spring flows required to double fall-run Chinook salmon populations;
5. Fall pulse flows required for adult passage through the Delta;
6. Fall flows required for spawning and incubation habitat;
7. Ramping down spring flows to promote riparian vegetation;
8. Summer flows required to increase habitat for yearling steelhead and salmon;
9. The effect of Delta Exports rate reductions on Chinook salmon production; and
10. Comparison of Flow Schedules for a 53% increase in production and doubling.

1. Relationships Between Salmon Recruitment And Flow In The Stanislaus And Tuolumne Rivers

Fall-run Chinook salmon production in the San Joaquin River Basin is well correlated with flow, particularly in the San Joaquin River at Vernalis, during the spring when the juveniles are migrating from the tributaries (Mesick 2005). Mesick's analysis converts production, which consists of several different cohorts of fish that all return to spawn in the tributaries during the same year, into recruitment, which consists of same-aged adults that all migrated through the Basin as juveniles during the same year. This conversion requires age data to segregate escapement into cohorts, which was not collected on the Merced River until 1988; therefore, these analyses that compare the baseline and post-baseline periods could only be done for the Tuolumne and Stanislaus rivers.

Comparing the regressions of average flow in the San Joaquin River at Vernalis for the March through May period and salmon recruitment suggests that the slope of the regressions has declined by about 10% for the Stanislaus River (Figure 1) and 20% for the Tuolumne River (Figure 2); however, statistical tests cannot be conducted to determine the significance of the declines because the tests can only be conducted if the variances of the two regressions are not significantly different (Snedecor and Cochran 1989) and *F*-tests indicate that the variances of the baseline and 1992-2002 regressions were significantly different ($p \leq 0.01$). Therefore, most if not all of the declines in production observed in the Stanislaus and Tuolumne rivers since 1992 are a result of a lower frequency of wet years during the 1992-2004 period compared to the baseline period. For example, the average March through May flows at Vernalis during the slightly wet years (San Joaquin River Index of 4.0 to 5.0 million acre feet) ranged between 5,000 and 10,000 cfs during the 1992-2004 period and between 15,000 and 20,000 cfs during the baseline period (Figure 3). The lower flood magnitudes observed after 1992 are primarily due to differences in climate because the large San Joaquin reservoirs that capture all or most of flood flows were all completed prior to 1992: New Melones was completed in 1980, New Don Pedro was completed in 1971, and New Exchequer was completed in 1966.

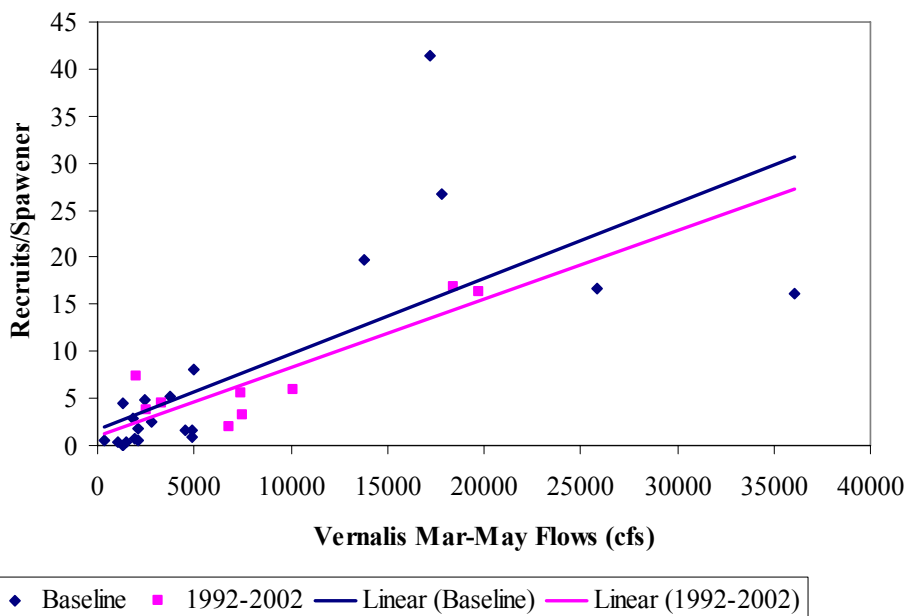


Figure 1. The relationship between the number of fall-run Chinook salmon recruits/spawner to the lower Stanislaus River and the average flow in the San Joaquin River at Vernalis between 1 March and 31 May during the 1967-1991 baseline period and the 1992-2002 AFRP period. The lines labeled as “linear” show the linear regression models for each period. The adjusted R-Squared for the linear regression model is 0.50 for the 1967 to 2002 dataset.

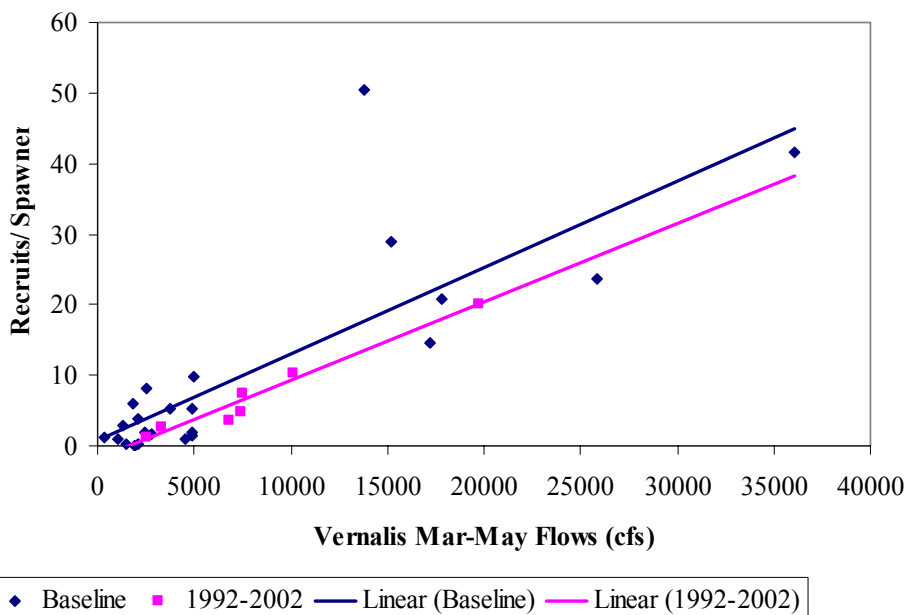


Figure 2. The relationship between the number of fall-run Chinook salmon recruits/spawner to the lower Tuolumne River and the average flow in the San Joaquin River at Vernalis between 1 March and 31 May during the 1967-1991 baseline period and the 1992-2002 AFRP period. The lines labeled as “linear” show the linear regression models for each period. The adjusted R-Squared for the linear regression model is 0.59 for the 1967 to 2002 dataset.

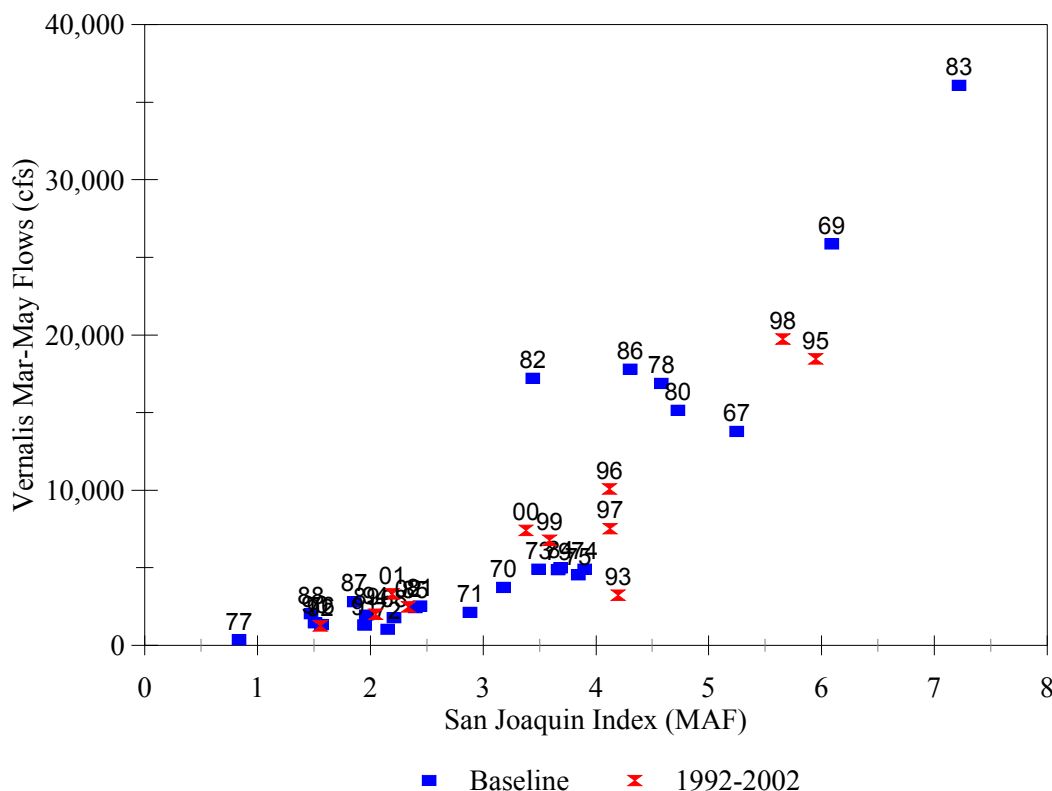


Figure 3. The relationship between the mean March through May flow in the San Joaquin River at Vernalis and the San Joaquin Index in millions of acre-feet (MAF) for the baseline and 1992-2002 periods.

2. Relationships between juvenile survival and flow in the Stanislaus River

The survival of fry and parr migrating and rearing in the Stanislaus River between Oakdale and Caswell State Park is highly dependent on flow between March and early June and presumably the same is true for the Tuolumne and Merced rivers. Many more fry, parr, and smolts were captured in the Stanislaus River at the Caswell traps when the flow at Ripon in February and March ranged between 1,000 and 5,000 cfs during above normal and wet years (1998-2000) than when it was typically less than 600 cfs during dry and normal years (2001-2004; Appendix 1). The fact that more juveniles passed the downstream Caswell trap (RM 5) than the upstream Oakdale trap (RM 40) in April and May during the above normal and wet years strongly suggests that high February and March flows may be needed for fry and parr to rear in the lower river. It is also likely that the extended periods of high flows in April, May and early June during the above normal and wet years were responsible for the high survival rates of migrating smolts. Supporting evidence is provided by the strong correlations between adult recruitment and Vernalis flows in March, April, May, and June (Mesick 2005). The relatively weak correlations between recruitment and Vernalis flows in February suggest that February

flows may be as important as those between March and mid June. It is assumed that high flows in February through mid June would also be important for juvenile salmonids in the Tuolumne and Merced rivers as well.

3. Salmon production models for the San Joaquin River Basin

Regression equations were computed for the number of Chinook salmon recruits per spawner in each of the San Joaquin River tributaries (Mesick 2005) and the average flow at Vernalis during April and May for the purpose of estimating the amount of flow required to double populations. It was assumed that the magnitude of flow during April and May was more directly related to juvenile salmon survival because this is the period when most of the smolt-sized fish are migrating¹ and water temperatures are in the range that may affect smolt survival². Vernalis flows were used in the model instead of tributary reservoir releases for two reasons. First, juvenile survival in the Stanislaus River is much more highly correlated with flow at Vernalis (adjusted-R² = 0.53) than with flow at Goodwin Dam in the Stanislaus River (adjusted-R² = 0.16), which suggests that Delta flows are more important than tributary flows (Mesick 2005). Second, there were insufficient flow data at Snelling to estimate reservoir releases in the Merced River during the entire AFRP baseline period, which precludes model development based on tributary flows.

Stanislaus River model: $\text{Recruits/Spawner} = 0.0008611 * \text{April-May Vernalis Flows} + 1.17688$. The adjusted-R² was 0.53 with a probability level of 0.0000 for the model developed with the estimates for 1983 to 2002. Recruitment was computed by multiplying the model's predicted number of recruits/spawner by the number of spawners. It was assumed that recruitment increased linearly until 2,000 spawners, after which and there was no further change in recruitment as the number of spawners exceeded 2,000 fish. This assumption reflects the relationship between stock and the total estimated number of juveniles passing the Oakdale Screw trap between 1996 and 2004 (Mesick 2005). Figure 4 compares the recruitment estimates based on escapement surveys (Mesick 2005) with the model results.

Tuolumne River model: $\text{Recruits/Spawner} = 0.00140 * \text{April-May Vernalis Flows} + 0.18957$. The adjusted-R² was 0.65 with a probability level of 0.0000 for the model developed with the estimates for 1980 to 2002. Recruitment was computed by multiplying the estimated number of recruits/spawner by the estimated number of spawners. It was assumed that recruitment increased linearly until 2,000 spawners, after which there was no further change in recruitment as the number of spawners exceeded 2,000 fish. This assumption was made because the model's adjusted-R² declined to 0.44 and then to 0.32 as the spawner-recruit inflection point was increased to 3,000 and 4,000 spawners respectively. Figure 5 compares the recruitment estimates based on escapement surveys (Mesick 2005) with the model results.

¹ CDFG Mossdale Trawl Data presented to the State Water Resources Control Board in Spring 2005.

² Vernalis Adaptive Management Plan technical reports produced by the San Joaquin River Group Authority.

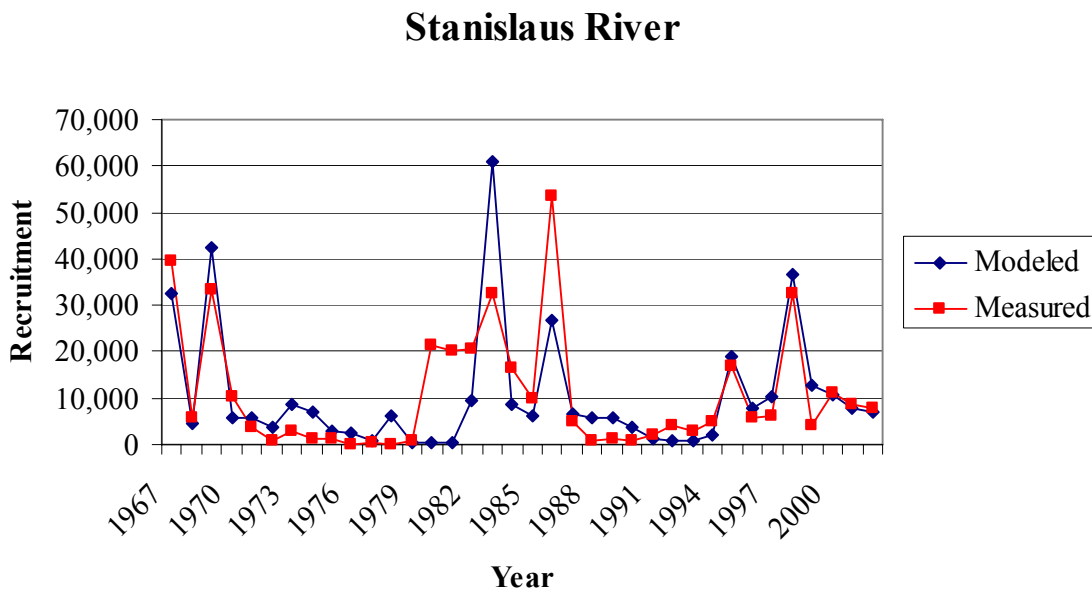


Figure 4. Adult Chinook salmon recruitment to the Stanislaus River from 1967 to 2002 based on escapement surveys (Measured) and regression model predictions (Modeled).

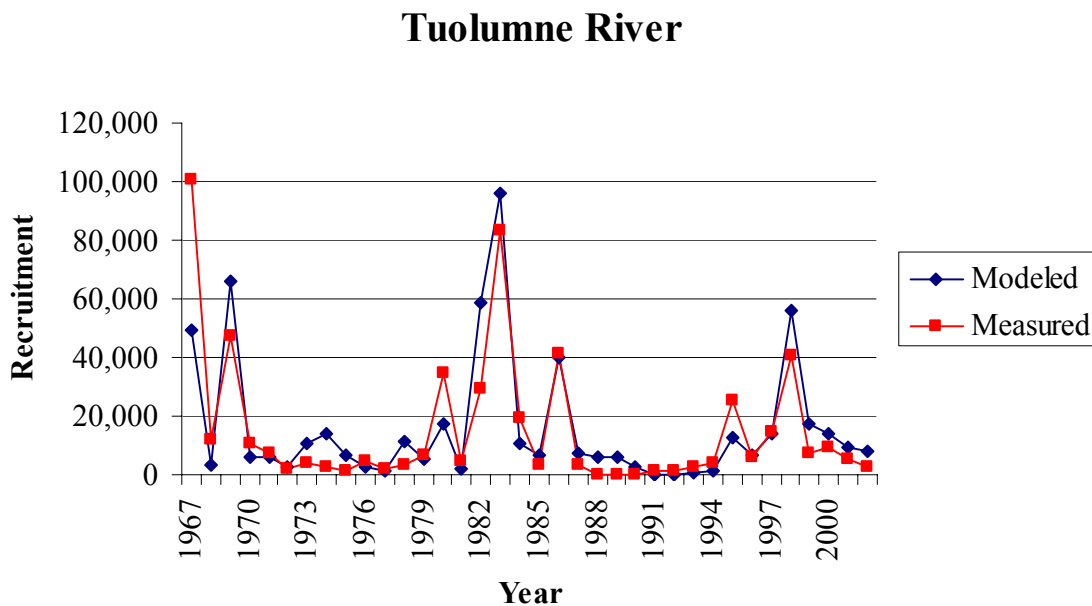


Figure 5. Adult Chinook salmon recruitment to the Tuolumne River from 1967 to 2002 based on escapement surveys (Measured) and regression model predictions (Modeled).

Merced River model: $\text{Recruits/Spawner} = 0.000554 * \text{April-May Vernalis Flows} + 0.07938$. The adjusted- R^2 was 0.61 with a probability level of 0.0000 for the model developed with the estimates for 1980 to 2002. The recruitment estimates between 1980

and 1986 were based on Age 2 estimates from the Tuolumne River whereas the later estimates were based on length-frequency derived Age 2 estimates from the Merced River (Mesick 2005). Recruitment was computed by multiplying the estimated number of recruits/spawner by the estimated number of spawners. It was assumed that each fish collected in the Merced River Fish Hatchery, up to the approximate hatchery's capacity of 1,000 spawners, contributed twice the in-river production compared to naturally spawning adults. It was also assumed that recruitment increased linearly until 2,000 in-river spawners, after which there was no further change in recruitment after the number of spawners exceeded 2,000 fish. This assumption was made because the physical condition of the spawning and rearing habitat in the Merced River is more degraded than those habitats in the Stanislaus and Tuolumne rivers³. In addition, the number of recruits produced per spawner in the Merced River is substantially lower than in the Tuolumne and Stanislaus rivers, and so it is highly unlikely that the habitat in the Merced River can support the progeny of more than 2,000 spawners. Figure 6 compares the recruitment estimates based on escapement surveys (Mesick 2005) with the model results.

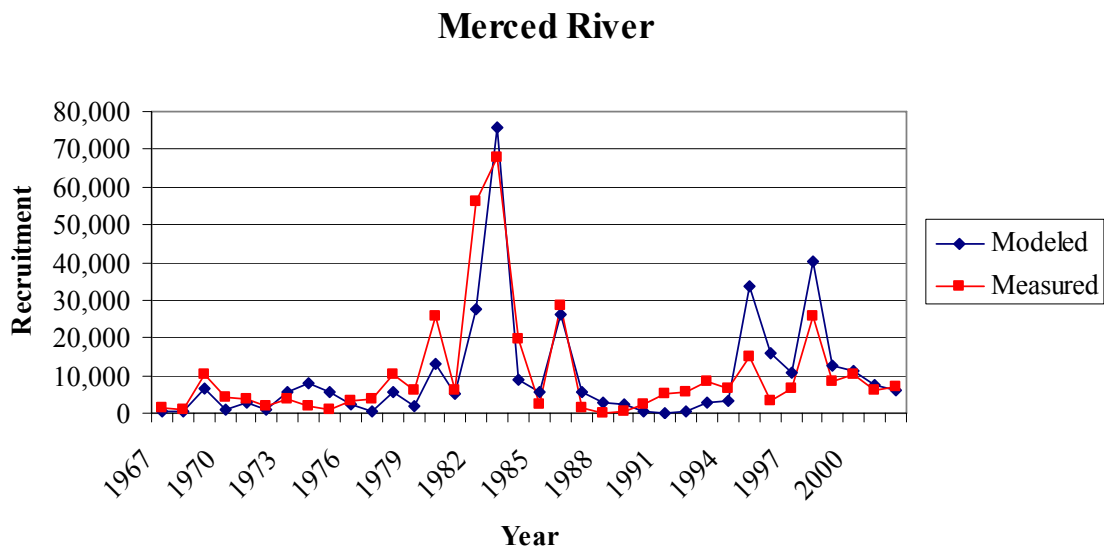


Figure 6. Adult Chinook salmon recruitment to the Merced River from 1967 to 2002 based on escapement surveys (Measured) and regression model predictions (Modeled).

4. Spring flows required to double fall-run Chinook salmon populations

To use the above recruitment models to estimate the amount of flow at Vernalis that would be needed to double salmon production in the San Joaquin Basin, it is necessary to maintain the historical conditions that formed the basis of the model. This means that each of the three San Joaquin River tributaries must maintain the similar contributions to Vernalis flows as well as maintain a similar hydrograph. Based on the estimated annual unimpaired flows, the Stanislaus River contributes 28%, the Tuolumne River contributes

³ The physical condition of the Merced, Tuolumne, and Stanislaus rivers was visually assessed by Carl Mesick, USFWS, during boat surveys in 2005, 2004, and 2002 respectively.

49%, and the Merced River contributes 23% of Vernalis flows historically. To convert the modeled flows into monthly averages for March, April, and May in a functional flow schedule, a constant percentage of the average unimpaired historical flow (1901 to 2004) was used for each month. For example, the Merced River Model indicates that an average flow of 3,480 cfs would be needed for the months of April and May during wet years to double production. The flow schedule was determined by multiplying the average unimpaired flow during wet years by 76.86%, which computes to a March flow of 2,279 cfs, an April flow of 2,559 cfs, and a May flow of 4,402 cfs. Suitable February flows were assumed to be either half of March flows or a minimum of 350-500 cfs, which was slightly lower than the recommended March flow.

Two sets of recommended flows were developed. The first set of flows simply extended the Vernalis flow standards in the State Water Resources Control Board's 1995 Water Quality Control Plan from April 15 to May 15 to April 1 to May 30, and then proportioned the flow during each month between March and May to match the natural hydrograph. Based on all three recruitment models, the total modeled population for the San Joaquin River Basin would increase by 53% from 36,494 fish during the AFRP baseline period to 55,945 fish, if the flows in Table 1 were implemented. The increase in recruitment varies between the three tributaries: 59% for the Stanislaus River, 42% for the Tuolumne River, and 57% for the Merced River, because the populations respond differently in terms of the effects of flow on juvenile survival and increases in spawner abundance. Historically, spawner abundance limited recruitment more frequently on the Stanislaus and Merced rivers than in the Tuolumne River and so an increase in flow would improve both spawner abundance as well as smolt survival in the Stanislaus and Merced rivers to a greater degree than for the Tuolumne River, and thereby, produce the largest increases in recruitment in the Stanislaus and Merced rivers. The rate that recruitment increases with flow would be expected to decline after spawner abundance consistently reaches the habitat's capacity of 2,000 fish.

The second set of flows would be expected to double the total predicted San Joaquin Basin recruitment from 36,494 fish during the AFRP baseline period to 72,916 fish. The increase in recruitment varies considerably between the three tributaries: 114% for the Stanislaus River, 86% for the Tuolumne River, and 112% for the Merced River. The following table indicates the average flow for February, March, April, and May in the Stanislaus, Tuolumne, and Merced rivers that would be expected to double salmon production for the basin.

Table 1. The average flow (cfs) for February, March, April, and May for the Stanislaus, Tuolumne, and Merced rivers that would be expected to achieve a 53% increase in total predicted Chinook salmon production for the basin.

	<u>WET</u>	<u>ABOVE NORMAL</u>	<u>BELOW NORMAL</u>	<u>DRY</u>	<u>CRITICAL</u>
Stanislaus					
February	674	500	500	500	450
March	1,348	814	571	545	462
April	1,641	1,364	1,109	1,065	814
May	2,541	1,902	1,520	1,146	845
Tuolumne					
February	1,060	638	500	500	500
March	2,119	1,276	883	922	874
April	2,532	1,881	1,792	1,586	1,420
May	4,284	3,605	2,646	2,395	1,702
Merced					
February	600	500	450	350	300
March	1,200	613	480	383	329
April	1,347	1,022	832	808	654
May	2,317	1,687	1,339	1,038	783
Total					
February	2,333	1,638	1,450	1,350	1,250
March	4,667	2,703	1,933	1,850	1,665
April	5,520	4,266	3,733	3,459	2,888
May	9,142	7,194	5,505	4,579	3,331

Table 2. The average flow (cfs) for February, March, April, and May in the Stanislaus, Tuolumne, and Merced rivers that would be expected to double the total predicted Chinook salmon production for the basin.

	<u>WET</u>	<u>ABOVE NORMAL</u>	<u>BELOW NORMAL</u>	<u>DRY</u>	<u>CRITICAL</u>
Stanislaus					
February	1,280	787	514	500	500
March	2,560	1,573	1,028	927	785
April	3,117	2,636	1,998	1,811	1,385
May	4,827	3,676	2,738	1,950	1,438
Tuolumne					
February	2,013	1,212	794	784	744
March	4,027	2,424	1,589	1,568	1,487
April	4,811	3,574	3,225	2,696	2,415
May	8,139	6,850	4,763	4,072	2,895
Merced					
February	1,140	582	500	500	500
March	2,279	1,165	864	651	559
April	2,559	1,941	1,498	1,375	1,112
May	4,402	3,205	2,410	1,766	1,332
Total					
February	4,433	2,581	1,809	1,784	1,744
March	8,866	5,162	3,481	3,146	2,832
April	10,487	8,151	6,721	5,883	4,912
May	17,369	13,732	9,912	7,787	5,665

5. Fall pulse flows required for adult passage through the Delta

Poor water quality in the deep-water ship channel near Stockton and excessive exports at the State Water Project and Central Valley Project at Tracy in October can either delay the upstream migration of adults or cause them to stray to the Sacramento River basin.

Delayed Adult Migration

Hallock and others (1970) showed that radio-tagged adult Chinook salmon delayed their migration at Stockton whenever dissolved oxygen (DO) concentrations were less than 5 mg/l and/or water temperatures exceeded about 65 °F in October. DO concentrations near Stockton in October were greater than 5 mg/l from 1983, when DWR began

monitoring, to 1990, but were lower than 5 mg/l for most of October in 1991 and 1992. The Head of the Old River Barrier was installed in fall 1992 to maximize flows in the deep water ship channel, but it did not correct the problem until late October (Figure 7). In 1993, DO levels were low until about 10 October and it is likely that pulse flows that raised Vernalis flows to about 4,000 cfs on 7 October were responsible for increasing DO levels at Stockton (Figure 7). Similarly in 1994, DO levels were low until 15 October when pulse flows raised Vernalis flows to about 2,000 cfs (Figure 7). In 1995, DO levels were at least 6 mg/l in October when Vernalis flows ranged about 3,000 cfs to 6,000 cfs through mid October. DO levels were low or greatly fluctuated in 1996 until 13 October when pulse flow releases increased Vernalis flows from 2,000 to about 3,000 cfs (Figure 7).

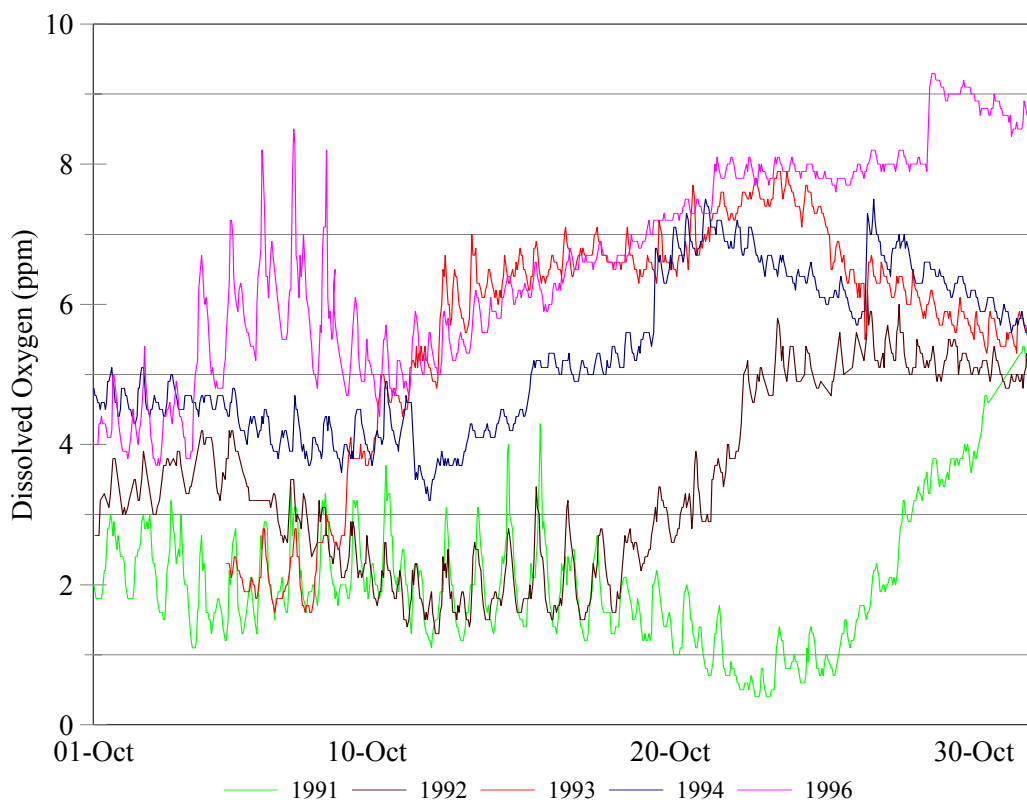


Figure 7. Hourly dissolved oxygen measurements at the Department of Water Resources' Burns Cut Off Road monitoring station during October in 1991 through 1994 and in 1996.

There are concerns that delaying the migration of adult salmon in the deep-water ship channel near Stockton may reduce gamete viability if the fish are exposed to high temperatures for prolonged periods. Egg survival at the Merced River Hatchery increased from a mean of 46% from 1990 to 1992 during the peak of the drought to a mean of 77% from 1993 to 1999 after fall pulse flows were made⁴. A more in-depth

⁴ Merced River Hatchery Production Reports by CDFG

analysis should be conducted to determine whether the mid-October pulse flows help maintain gamete viability in Chinook salmon migrating in the Delta.

Adult Straying

Delta export rates at the State Water Project and Central Valley Project were increased to near maximum (about 9,600 cfs) in fall 1996 and in subsequent years to “make-up” for reduced pumping rates during the spring outmigration period to improve salmon smolt survival (Mesick 2001). The adult fall-run salmon are migrating upstream through the Delta primarily in October typically when San Joaquin River flows at Vernalis are low (Mesick 2001). It is likely that when exports are high relative to San Joaquin River flows, little if any San Joaquin River water reaches the San Francisco Bay where it may be needed to help guide the salmon back to their natal stream. An analysis by Mesick (2001) of the recovered adult salmon with coded-wire-tags (CWT) that had been reared at the Merced River Fish Facility and released in one of the San Joaquin tributaries suggests straying occurred when more than 400% of Vernalis flows were exported at the CVP and SWP Delta pumping facilities. The analysis indicates that during mid October from 1987 through 1989 when export rates exceeded 400% of Vernalis flows, straying rates ranged between 11% and 17% (Figure 8). In contrast, straying rates were estimated to be less than 3% when Delta export rates were less than about 300% of San Joaquin River flow at Vernalis during mid-October. Between 1993 and 2002, pulse flow releases from the San Joaquin tributaries and/or reductions in Delta exports for 10 days in mid-October have kept Delta export rates to less than 300% of the San Joaquin River flow at Vernalis (Figure 8).

To maintain high levels of gamete viability in migrating salmon and minimize straying during periods of high exports (i.e., export no more than 300% of Vernalis flows), it is recommended that a 1,000-cfs pulse flow should be released for 10 days in mid-October from each of the three San Joaquin River tributaries.

6. Fall flows required for spawning and incubation habitat

Adult Chinook salmon typically crowd into the uppermost six miles of habitat in the Tuolumne and Merced rivers, and to a lesser extent the Stanislaus River, in early November. Crowding of spawning is thought to be detrimental because the rate of redd superimposition, where females either destroy or bury the eggs in pre-existing redds, would be abnormally high and thereby reduce the production of juvenile fish. Crowding may be a result of inadequate fall spawning flows that result in excessively warm temperatures in the downstream areas. Although the percentage of spawners that use the downstream areas increases as water temperatures decline with declining air temperatures, there is no evidence that increased fall flows reduces spawner crowding or improves juvenile production (Figure 9).

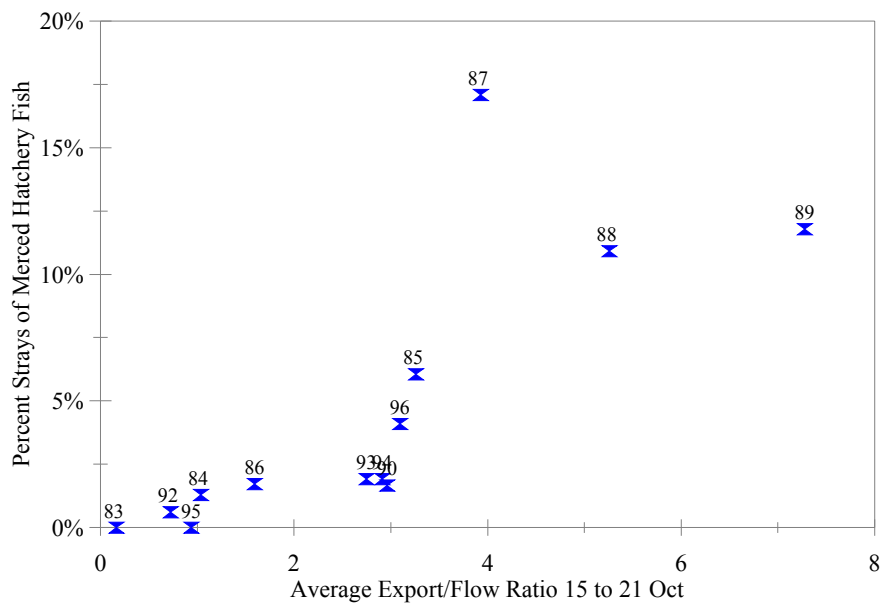


Figure 8. Estimated percent of adult CWT Chinook salmon that were reared at the Merced River Hatchery, released in the San Joaquin basin as juvenile salmon, and subsequently strayed to the Sacramento River and eastside tributary basins to spawn relative to the average ratio of the export rate at the CVP and SWP pumping facilities in the Delta to the flow rate in the San Joaquin River at Vernalis between 15 and 21 October from 1983 to 1996.

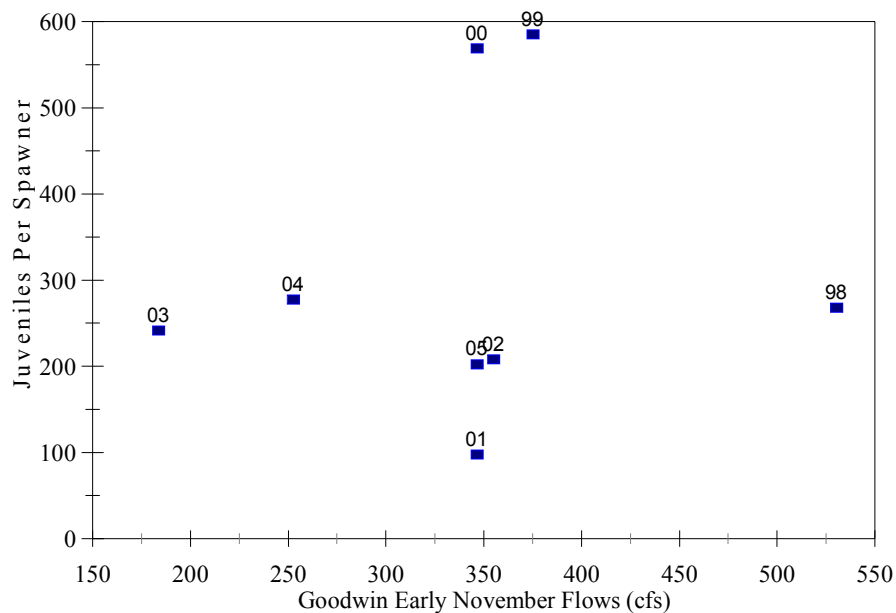


Figure 9. Relationship between the estimated number of juvenile salmon passing Oakdale per spawner and the Goodwin Dam flow release in early November in the Stanislaus River from 1998 to 2004.

It is recommended that studies should be conducted to determine the relationship between the magnitude of fall spawning flows and juvenile production in the Tuolumne and Merced rivers where spawner crowding is high. In the meantime, it is recommended that fall flows should be based on the optimum amount of physical habitat as determined by the PHABSIM model: 300 cfs for the Stanislaus River, 175-300 cfs for the Tuolumne River, and 200-250 cfs for the Merced River. These flows should be implemented from late October following the pulse flows until the end of January when flows begin to increase for juvenile rearing.

7. Ramping down spring flows to promote riparian vegetation

A likely benefit of spring flooding is the flushing of food and organic matter that produces food from the floodplains into the rivers where it can benefit juvenile salmonids. A healthy riparian forest is an integral component of the food chain.

A key factor for successful riparian recruitment is ensuring that the general rate of stage decline during the recession limb of flood control releases is gradual enough to support riparian seedling establishment. Another important issue is the timing of the recession limb. Recruitment flows should be targeted from mid-April to late-May to improve cottonwood recruitment and mid-May to late June to benefit black willow.

Research on a variety of cottonwood and willow species suggests that 1 to 1.5 inches/day is the maximum rate of water table decline for seedling survival (McBride et al. 1989; Segelquist et al. 1993; Mahoney and Rood 1992, 1998; Amlin and Rood 2002). However, a recent manipulation experiment of Fremont cottonwood, black willow, and narrow leaf willow seedlings found that water table declines of one inch or more resulted in 80% mortality within 60 days, even when the water table was maintained near the soil surface for several weeks before drawdown (Stillwater Sciences, unpublished data). Therefore more conservative rates may be appropriate. Flow recession rates of 100 to 300 cfs/day in the San Joaquin Basin are thought to prevent seedling desiccation under the assumed 1 inch/day maximum root growth rate.

A secondary benefit of a gradual ramp down of flows during June would be to increase juvenile salmon survival. Juvenile salmon migrate from the tributaries through early June and it is likely that they require 10 to 14 days to complete their migration through the Delta.

To promote the riparian vegetation recruitment and enhance the survival of juvenile salmon through the Delta, it is recommended that flows should be gradually ramped down at a constant rate between May 31 and June 30.

8. Summer flows required to increase habitat for yearling steelhead and salmon

Naturally produced juvenile steelhead typically rear in fresh water for two years before smolting and it is likely that successful rearing must occur in the tributaries because of

the unsuitable conditions that occur in the Delta during the summer. The physical habitat is most suitable for rearing steelhead in the 12-mile reach below the lowermost dams in the Stanislaus, Tuolumne, and Merced rivers. Although it would be preferable to provide water that is cooler than 65°F throughout the entire 12-mile reach during all water year types, doing so would require an unreasonable volume of water and could possibly exhaust the cold water pool in the primary reservoirs. A more reasonable alternative would be to maintain suitable water temperatures in at least a 5-mile reach, which presumably would be sufficient to sustain a population.

It is recommended that a block of water should be allocated in each of the tributaries to manage flows on a daily basis so that water temperatures do not exceed 65°F in the uppermost 5-mile reach between July 1 and mid October when the pulse flows begin. Flow management should be based on the new water temperature model for the Stanislaus River and on empirical flow-water temperature data for the Tuolumne (Figure 10) and Merced rivers until new models can be developed. It is anticipated that summer flows will range between 150 and 325 cfs depending on air temperatures and the desired length of river with suitable water temperatures.

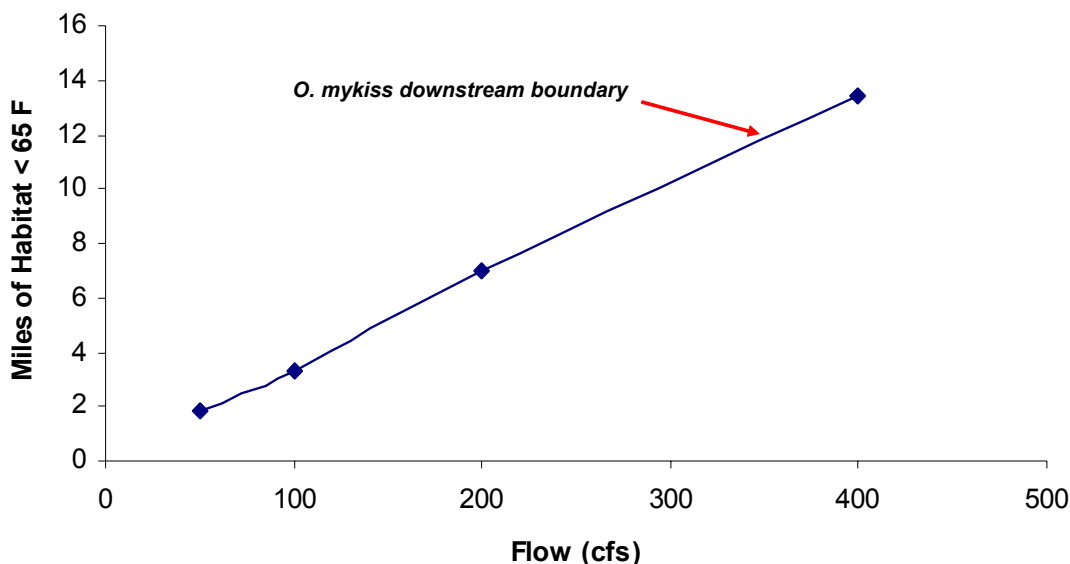


Figure 10. Relationship between the flow from La Grange Dam and the amount of habitat with water temperatures less than 65°F in the Tuolumne River based on a simple water temperature model (EA Engineering, Science, and Technology 1991).

9. The effect of Delta Exports rate reductions on Chinook salmon production

Export rates at the State's Harvey O. Banks pumping facilities (SWP) and the Federal pumping facilities at Tracy (CVP) have been substantially reduced during the VAMP period (typically April 15 to May 15) since 1996 to improve the survival of outmigrating smolts. However, the numbers of recruits-per-spawners in the Stanislaus and Tuolumne rivers are similar since the export reductions began in 1996 compared to the years when

exports were high prior to 1996 (Figures 11 and 12). This suggests that reducing exports below 400% of Vernalis flows for 31 days has had no detectable affect on adult recruitment. If true, experimental water transfers that increase flows in the San Joaquin Basin tributaries as prescribed above could be captured at the SWP and CVP pumping facilities without affecting the expected increase in salmonid recruitment.

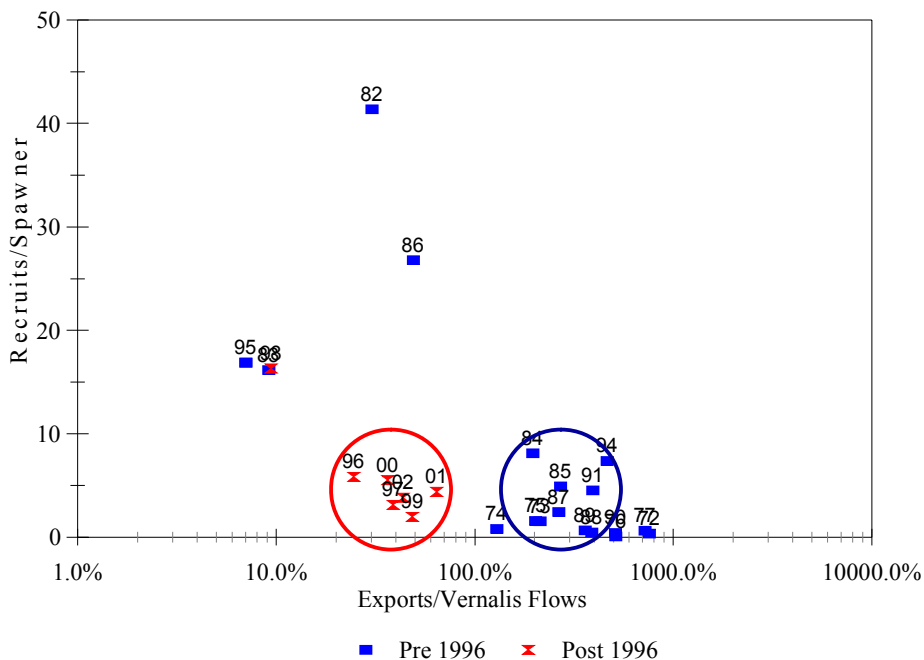


Figure 11. The relationship between the number of fall-run Chinook salmon recruits/spawner to the lower Stanislaus River and the average ratio of combined CVP and SWP exports to the flow in the San Joaquin River at Vernalis between 15 April and 15 May from 1972 to 2002. Exports were reduced during this period since 1996 (Blue Symbols) to improve the survival of outmigrating smolts.

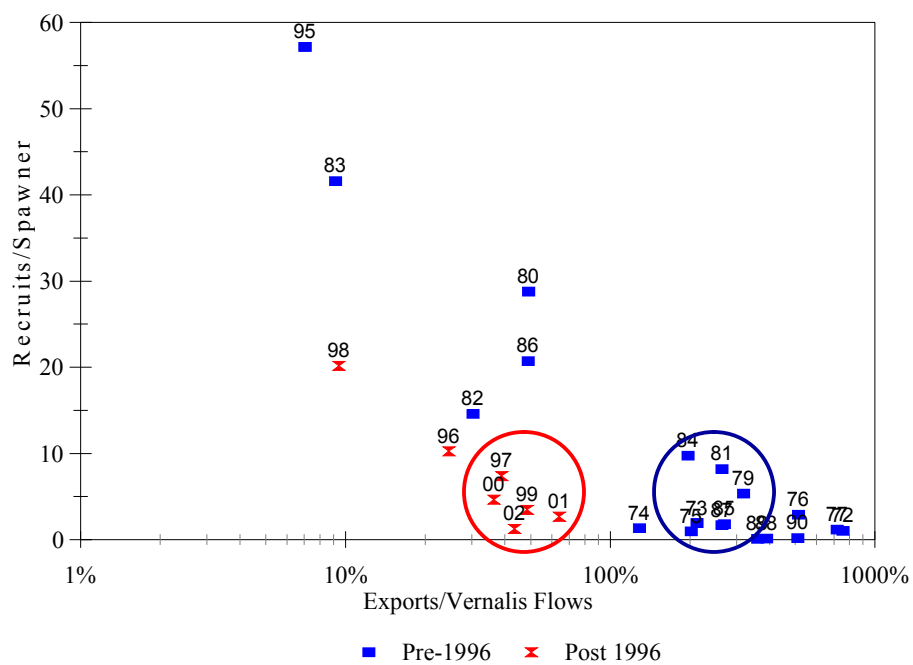
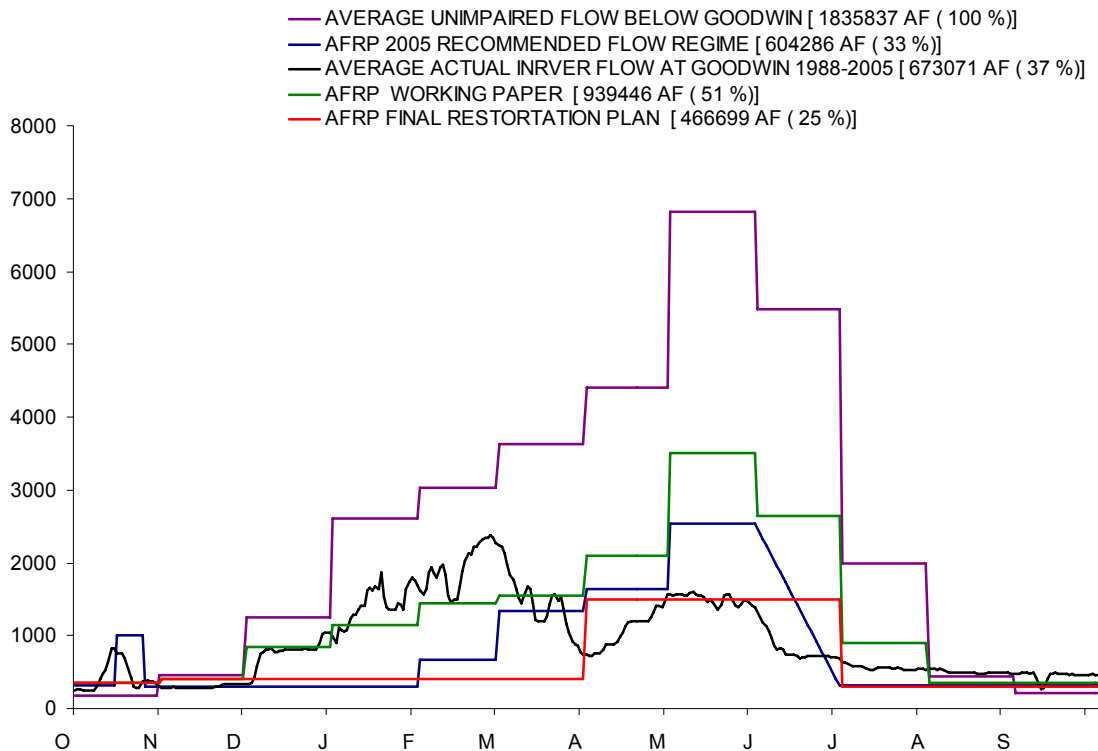


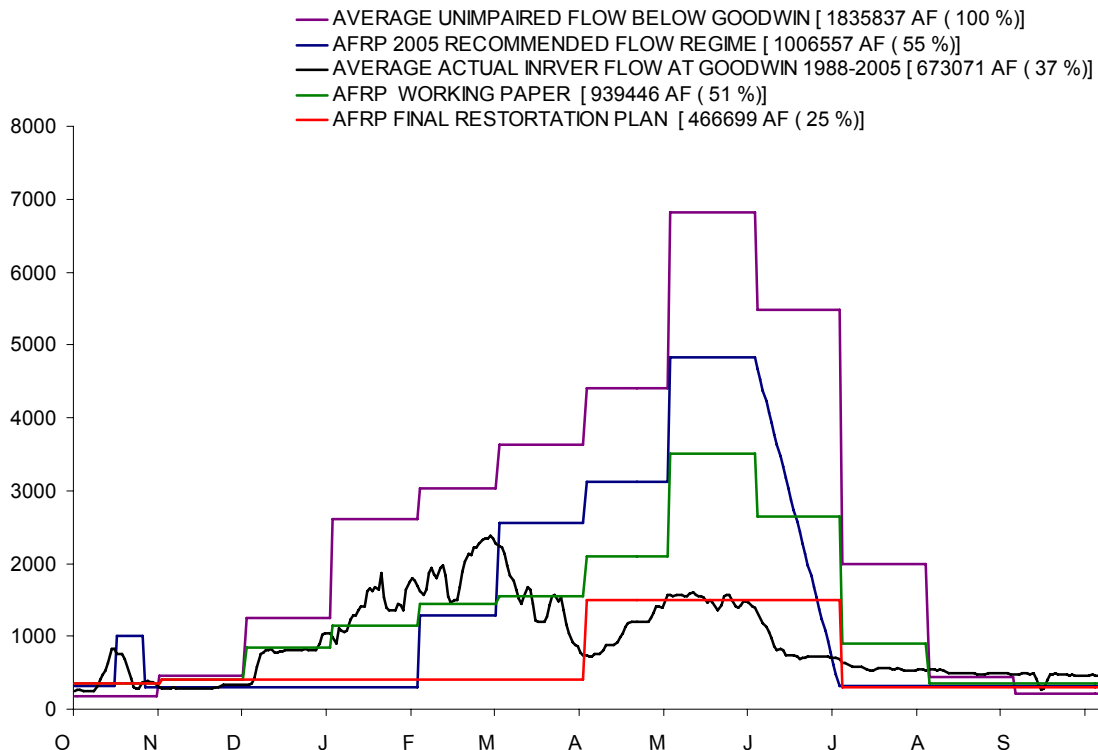
Figure 12. The relationship between the number of fall-run Chinook salmon recruits/spawner to the lower Tuolumne River and the average ratio of combined CVP and SWP exports to the flow in the San Joaquin River at Vernalis between 15 April and 15 May from 1972 to 2002. Exports were reduced during this period since 1996 (Blue Symbols) to improve the survival of outmigrating smolts.

10. Comparison of Flow Schedules: Stanislaus River

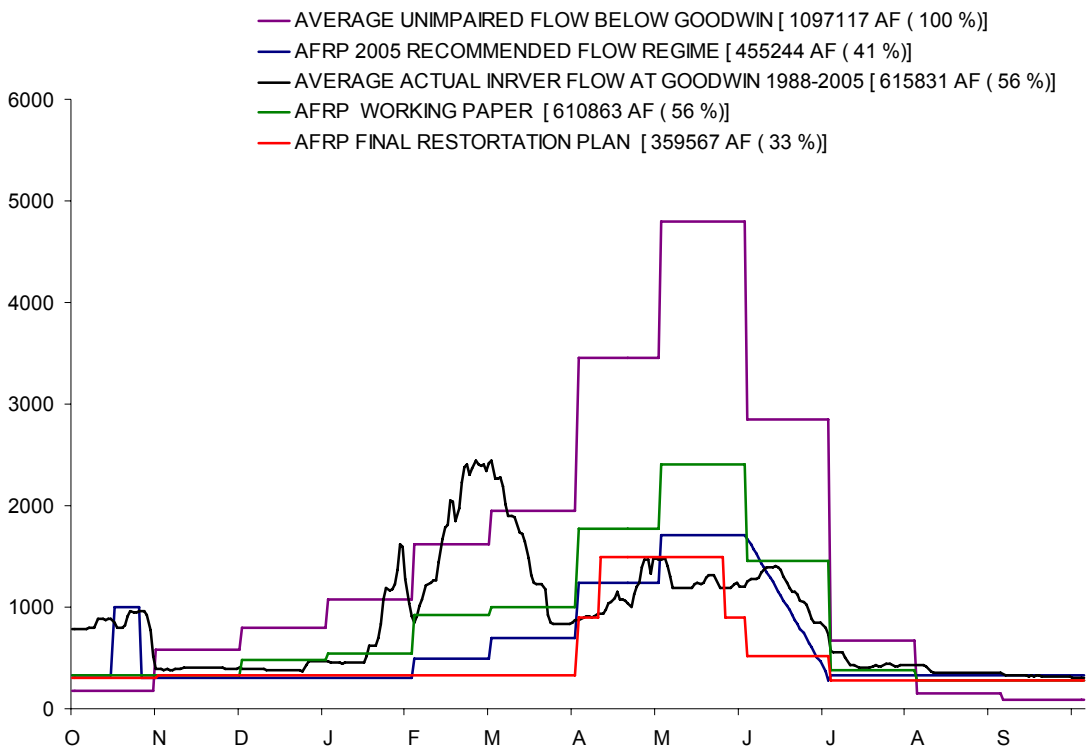
Wet Year – 69% Increase



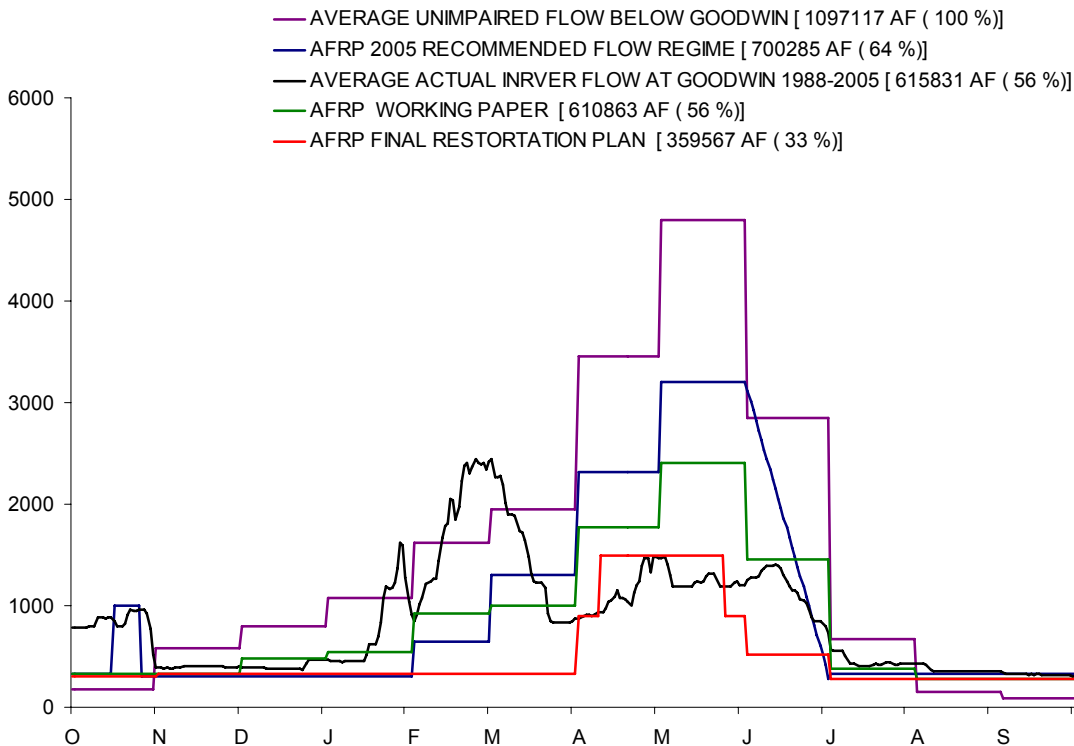
Wet Year – Doubling (114%)



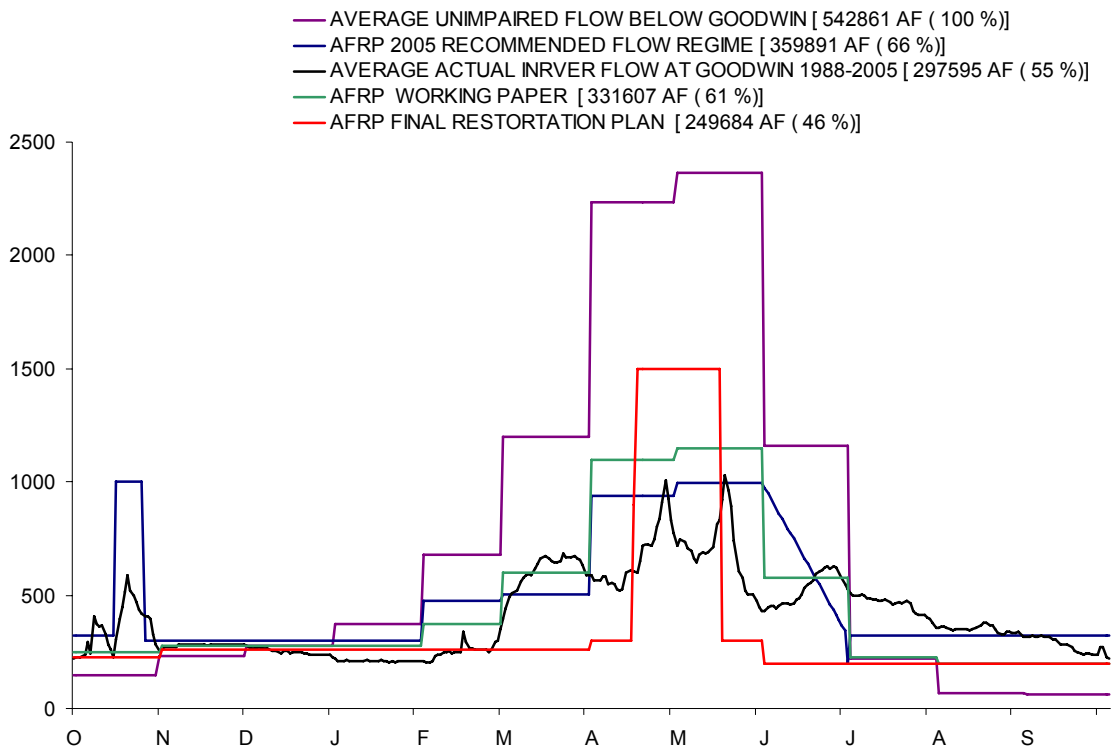
Stanislaus River: Normal Year – 69% Increase



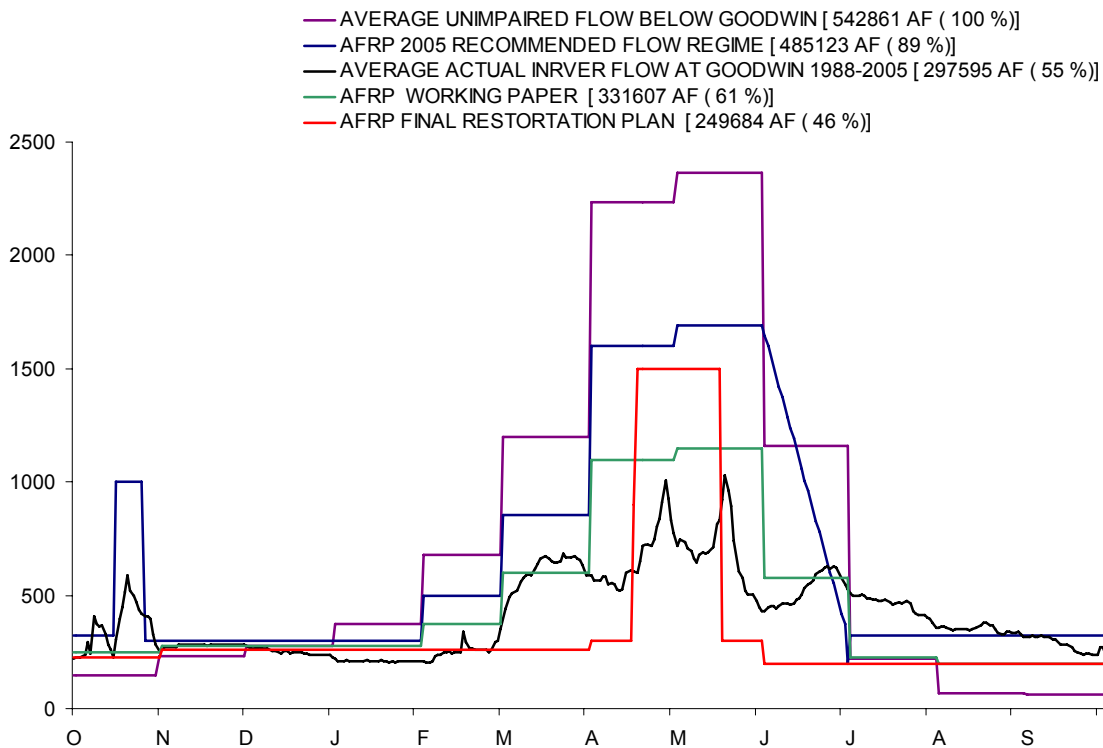
Normal Year – Doubling (114%)



Stanislaus River: Dry Year – 69% Increase

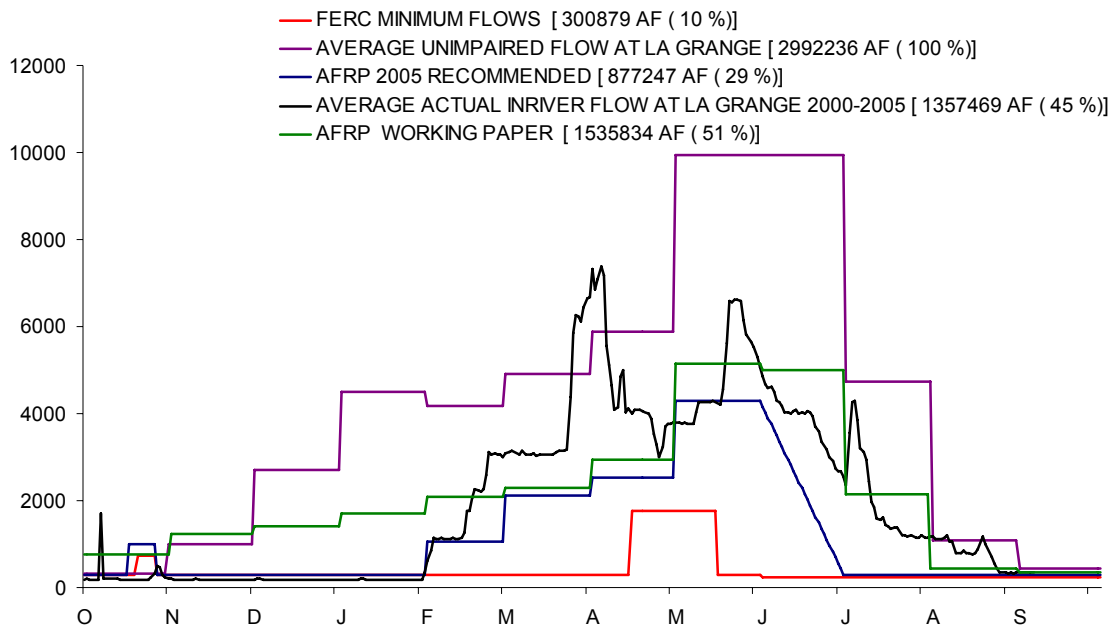


Dry Year – Doubling (114%)

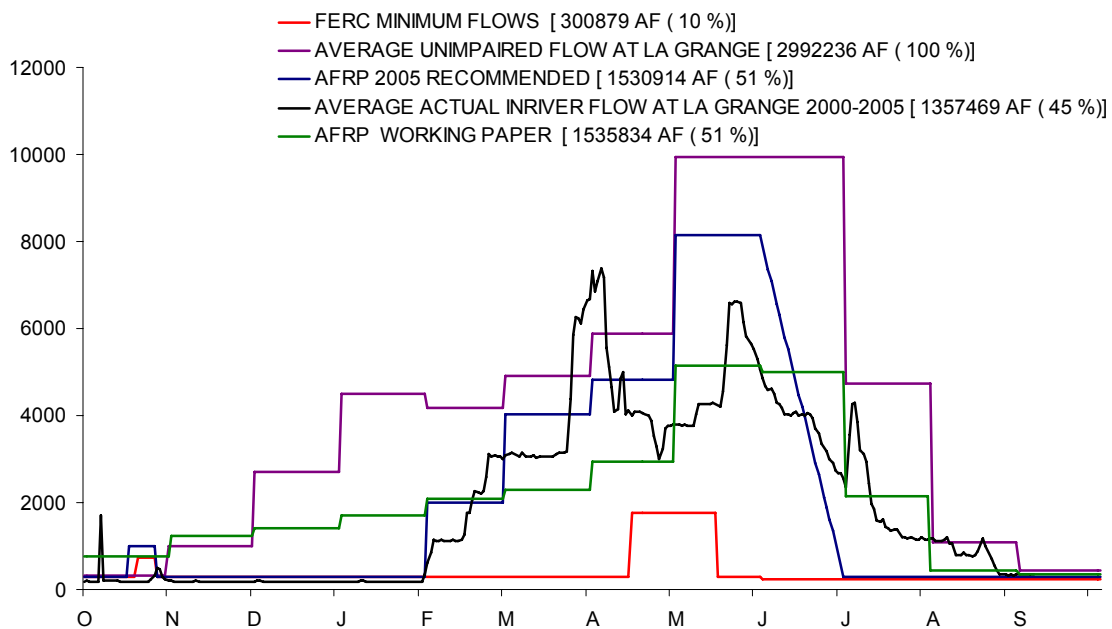


11. Comparison of Flow Schedules: Tuolumne River

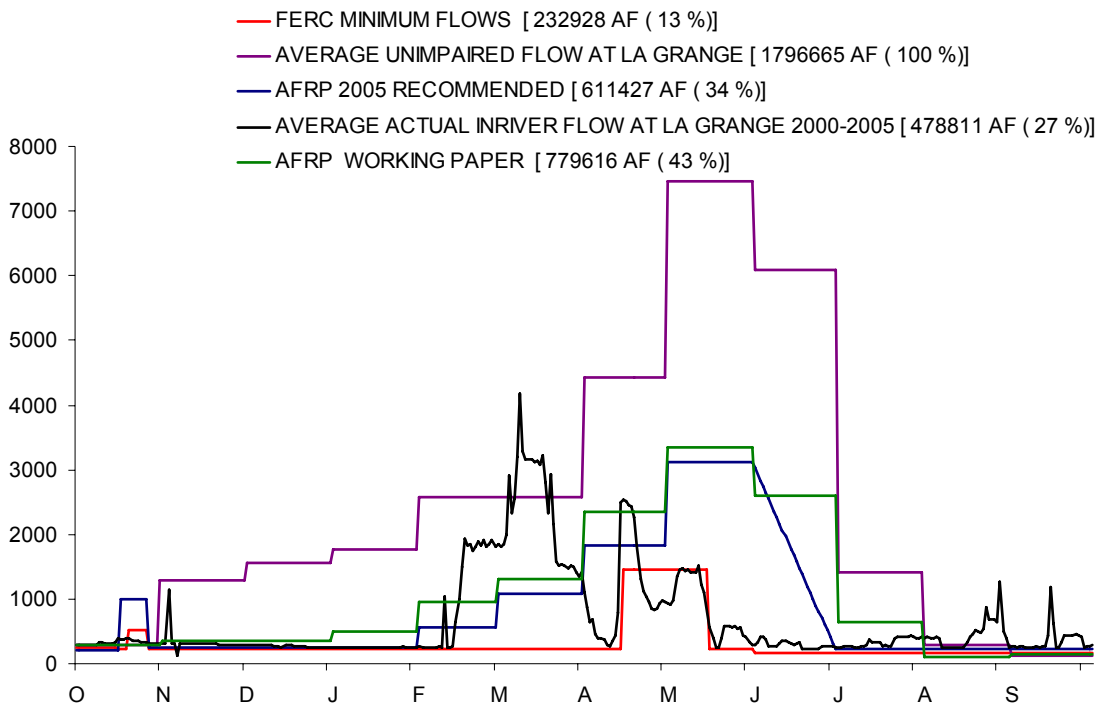
Wet Year – 42% Increase



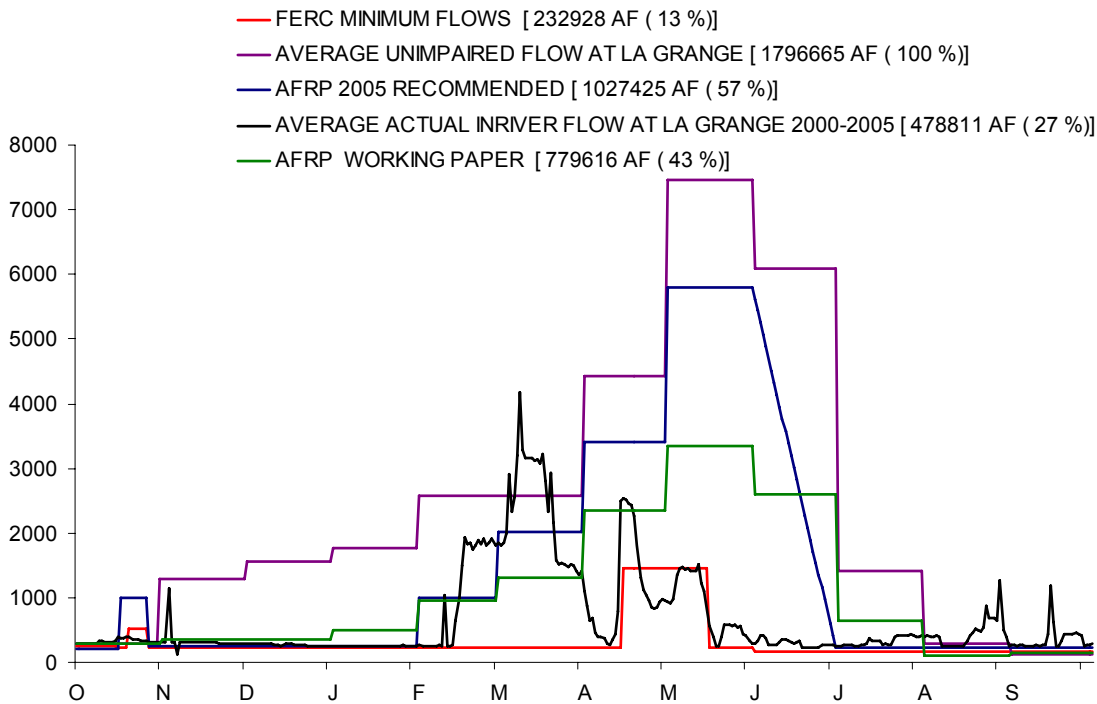
Wet Year – Doubling (86%)



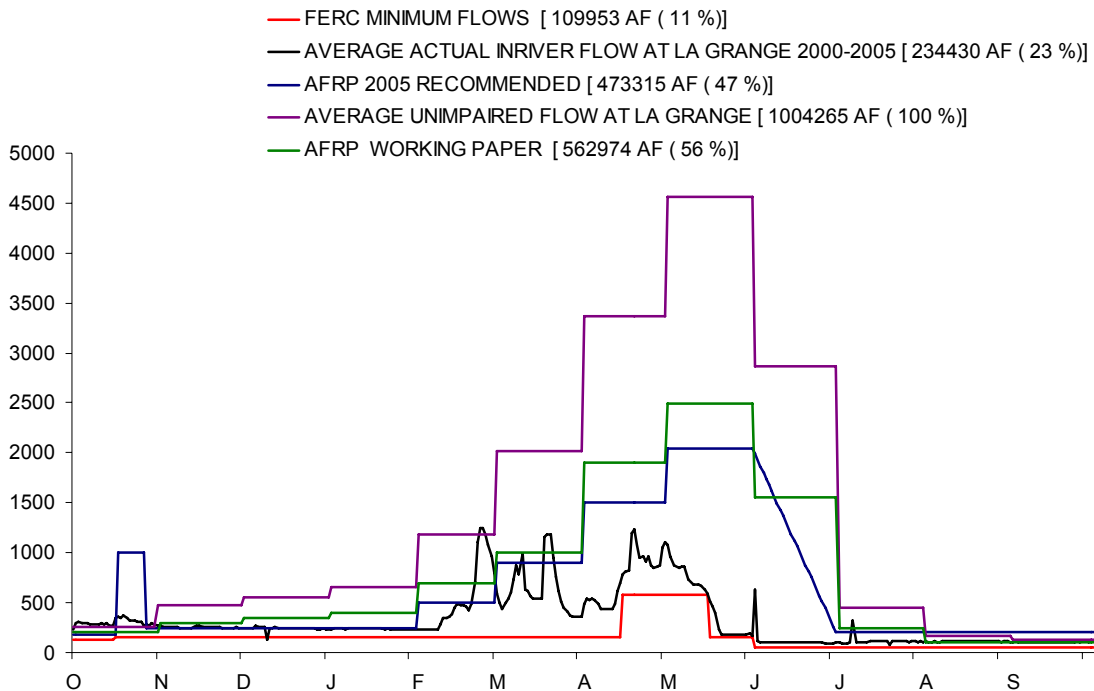
Tuolumne River: Normal Year – 42% Increase



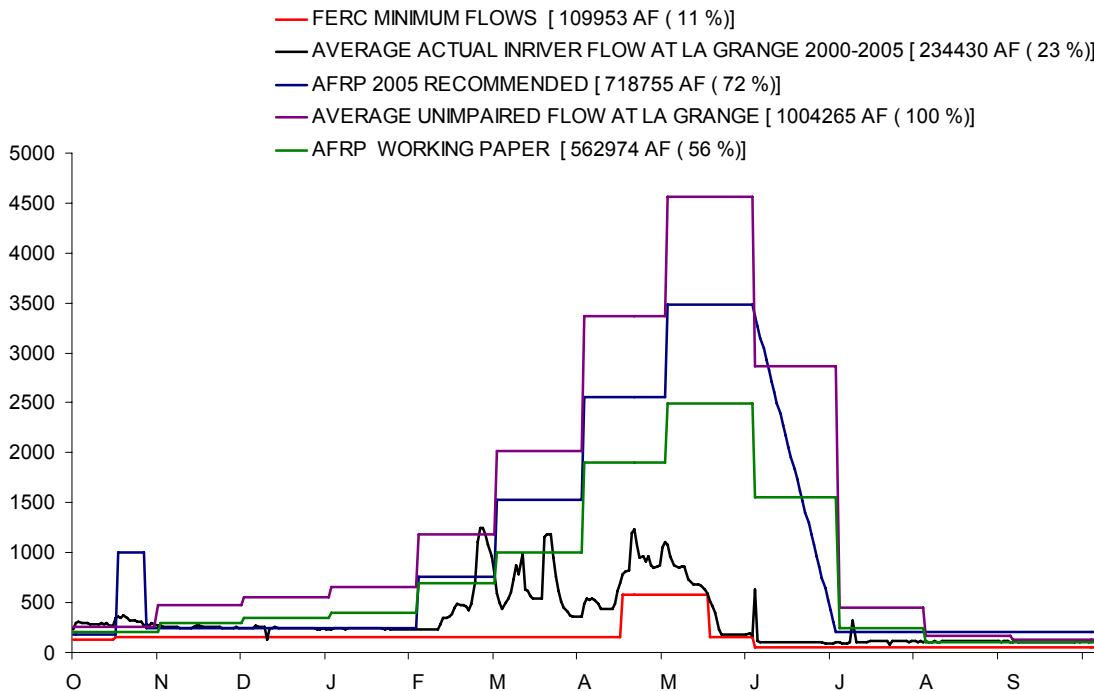
Normal Year – Doubling (86%)



Tuolumne River: Dry Year – 42% Increase

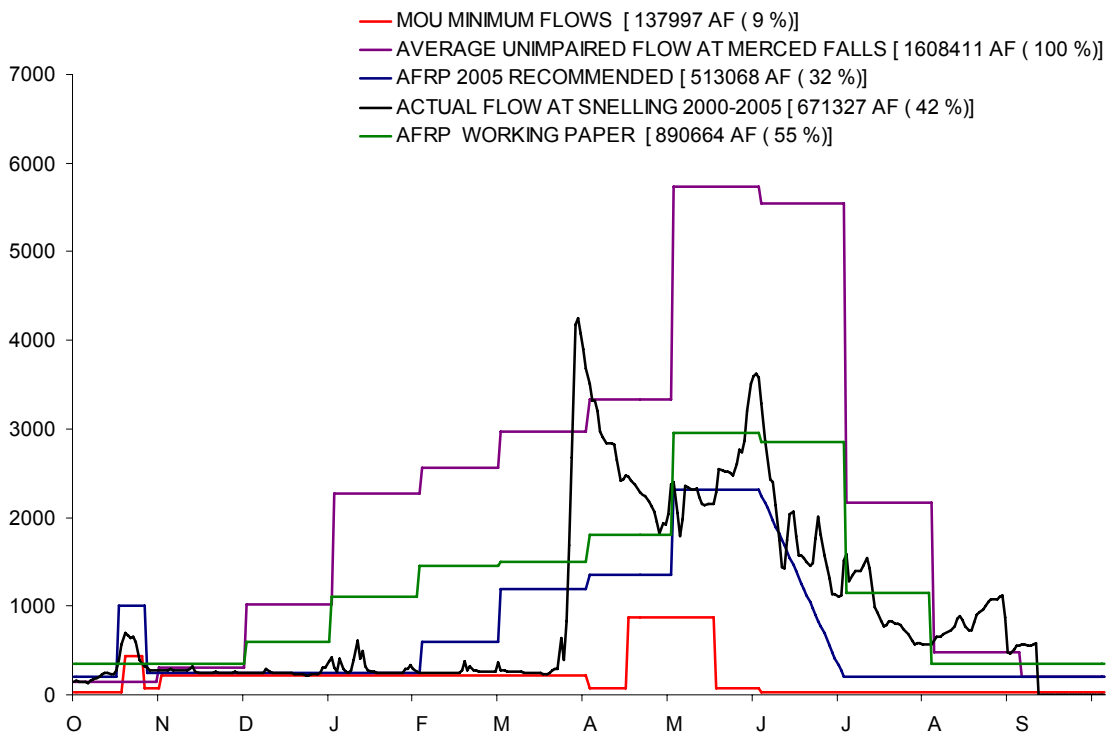


Dry Year – Doubling (86%)

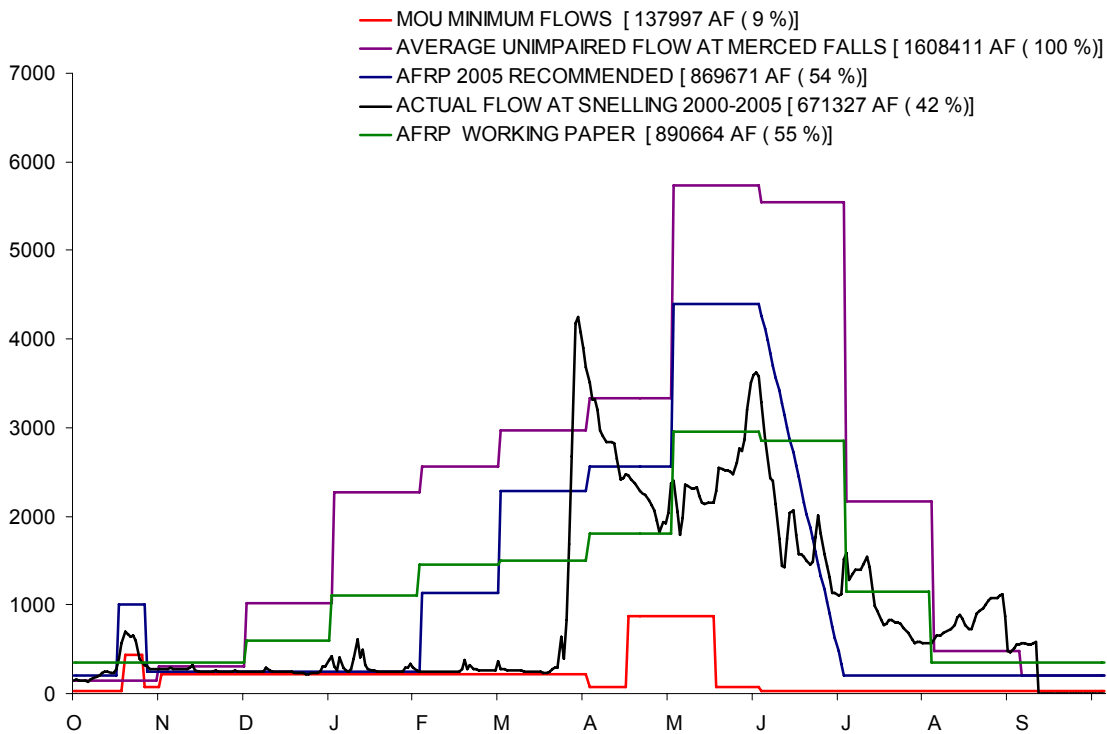


12. Comparison of Flow Schedules: Merced River

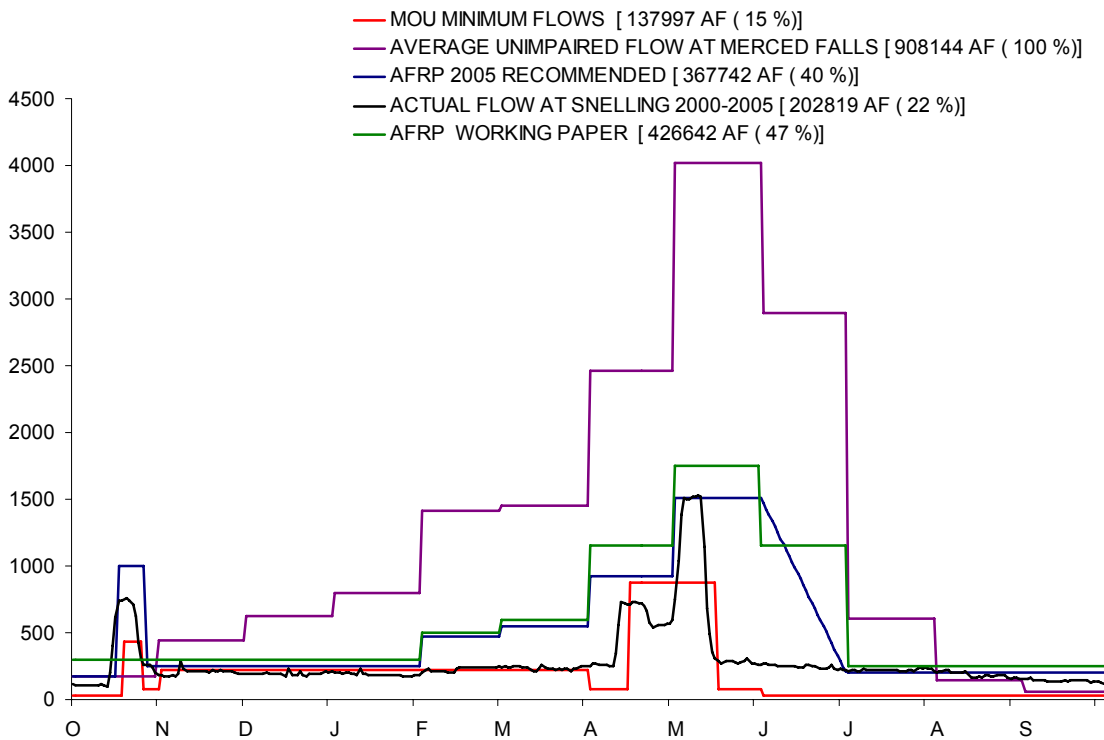
Wet Year – 85% Increase



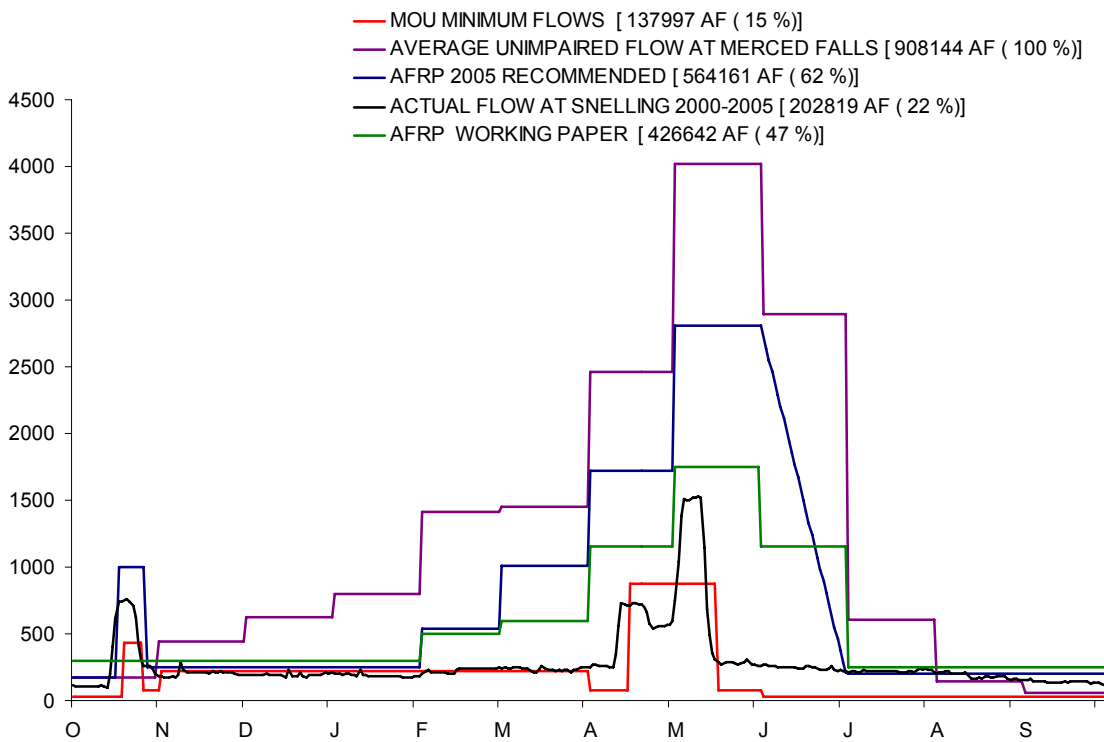
Wet Year – Doubling (134%)



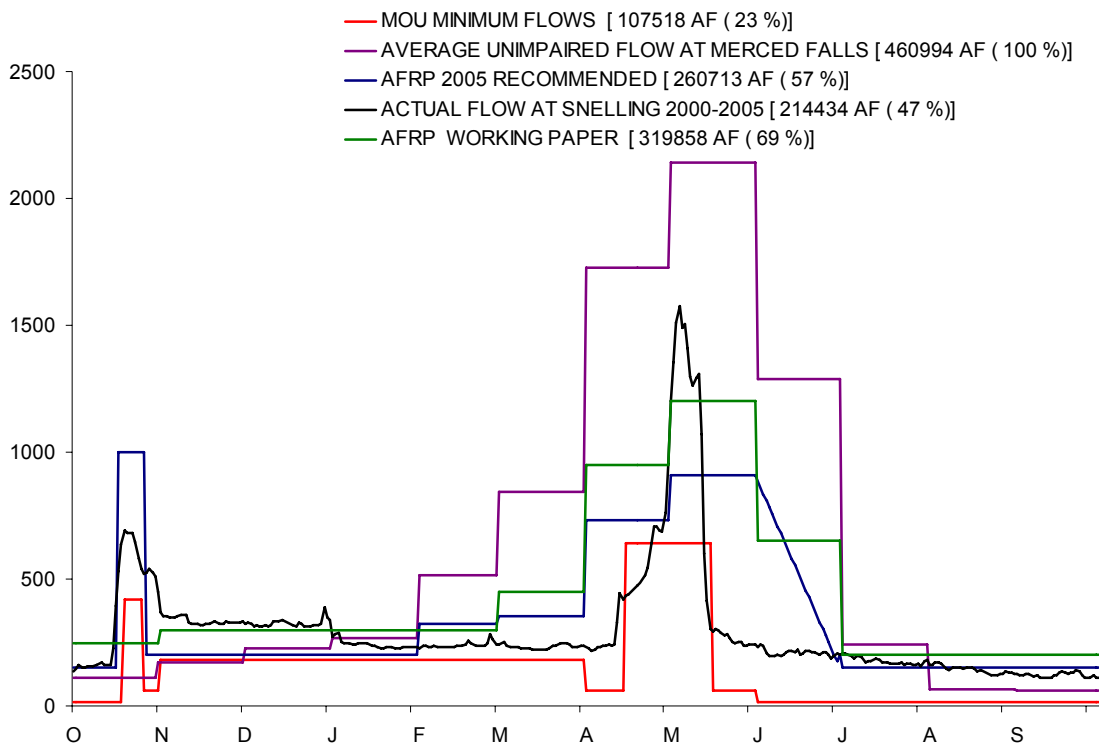
Merced River: Normal Year – 85% Increase



Normal Year – Doubling (134%)



Merced River: Dry Year – 85% Increase



Dry Year – Doubling (134%)

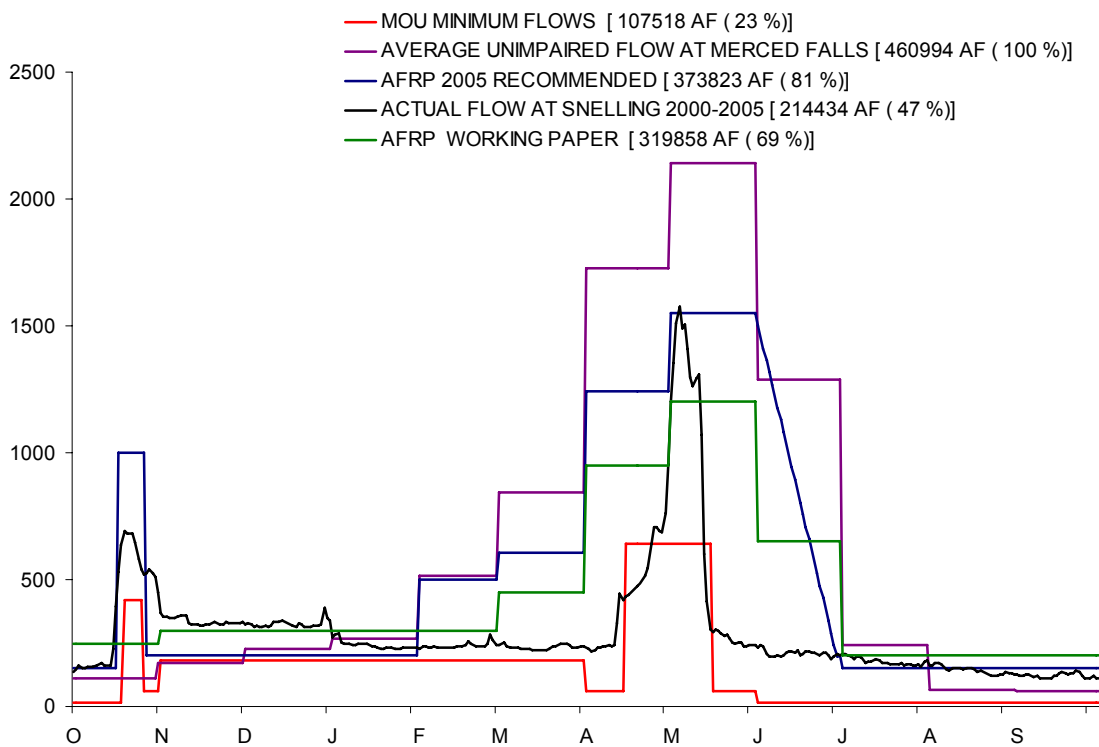


Table 3. The total annual volume of water (acre-feet) and percentage of unimpaired flows required to increase Chinook production by an average of 53% and 100% in the Stanislaus, Tuolumne, and Merced rivers.

	WET	ABOVE NORMAL	BELOW NORMAL	DRY	CRITICAL
53% Increase					
Stanislaus	604,286 33%	487,578 38%	422,911 48%	384,882 60%	334,899 73%
Tuolumne	877,247 29%	673,275 32%	549,579 37%	510,996 44%	435,634 50%
Merced	513,068 32%	394,518 38%	340,966 47%	279,861 52%	241,566 61%
Doubling					
Stanislaus	1,006,557 55%	785,985 62%	614,584 70%	525,231 82%	445,016 97%
Tuolumne	1,530,914 51%	1,169,192 55%	885,659 59%	783,854 68%	653,656 76%
Merced	869,671 54%	624,749 59%	503,572 69%	404,055 75%	343,591 86%

Appendix 1

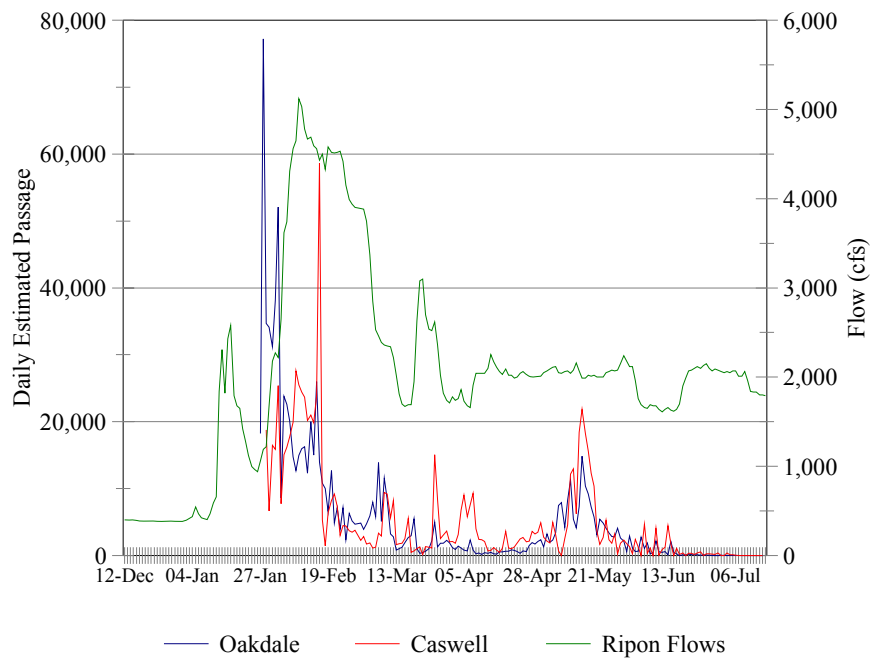


Figure 1. The relationship between the estimated daily passage at the Oakdale and Caswell Park screw traps and the mean daily flow at Ripon in the Stanislaus River between 12/12/97 and 7/15/98, a wet year. Overall juvenile survival between the Oakdale and Caswell traps was 95% in 1998.

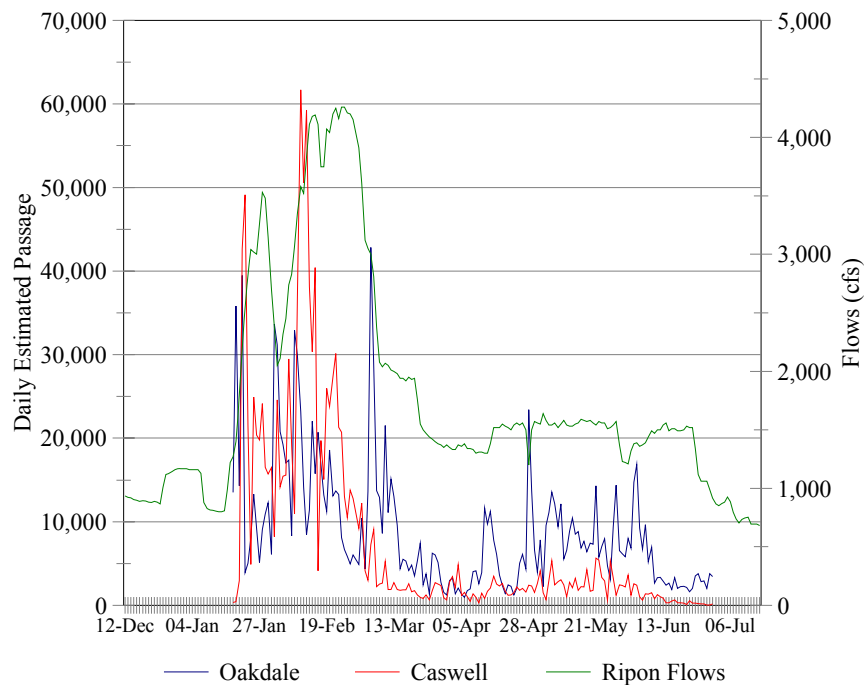


Figure 2. The relationship between the estimated daily passage at the Oakdale and Caswell Park screw traps and the mean daily flow at Ripon in the Stanislaus River between 12/12/98 and 7/15/99, an above normal year. Overall juvenile survival between the Oakdale and Caswell traps was 83% in 1999.

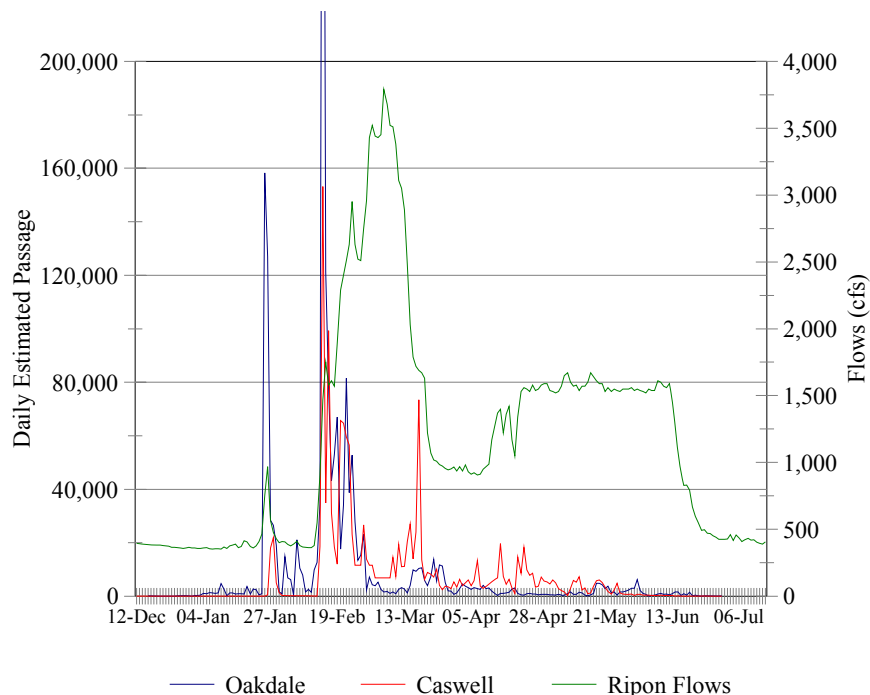


Figure 3. The relationship between the estimated daily passage at the Oakdale and Caswell Park screw traps and the mean daily flow at Ripon in the Stanislaus River between 12/12/99 and 7/15/00, an above normal year. Overall juvenile survival between the Oakdale and Caswell traps was 74% in 2000.

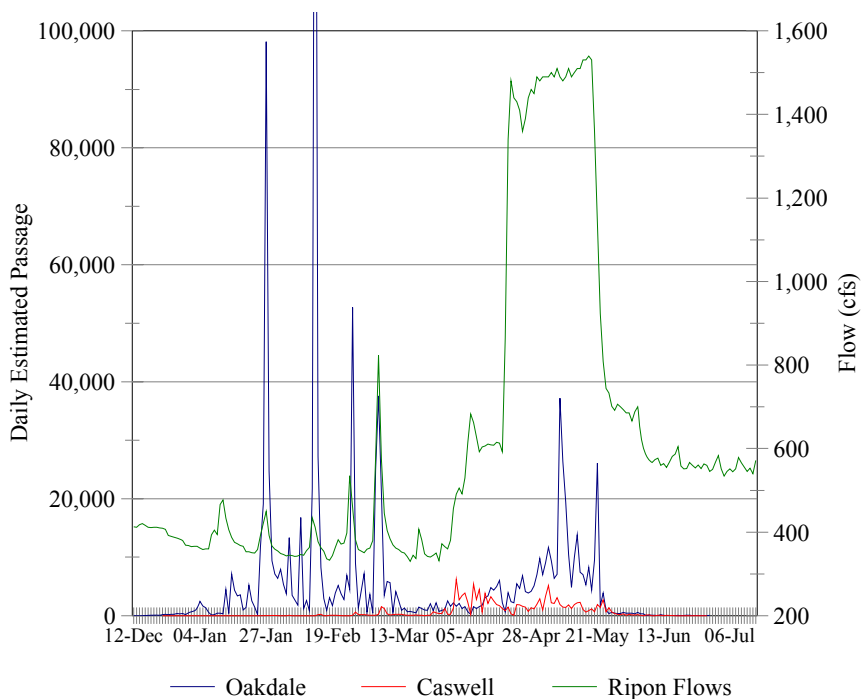


Figure 4. The relationship between the estimated daily passage at the Oakdale and Caswell Park screw traps and the mean daily flow at Ripon in the Stanislaus River between 12/12/00 and 7/15/01, a dry year. Overall juvenile survival between the Oakdale and Caswell traps was 11% in 2001.

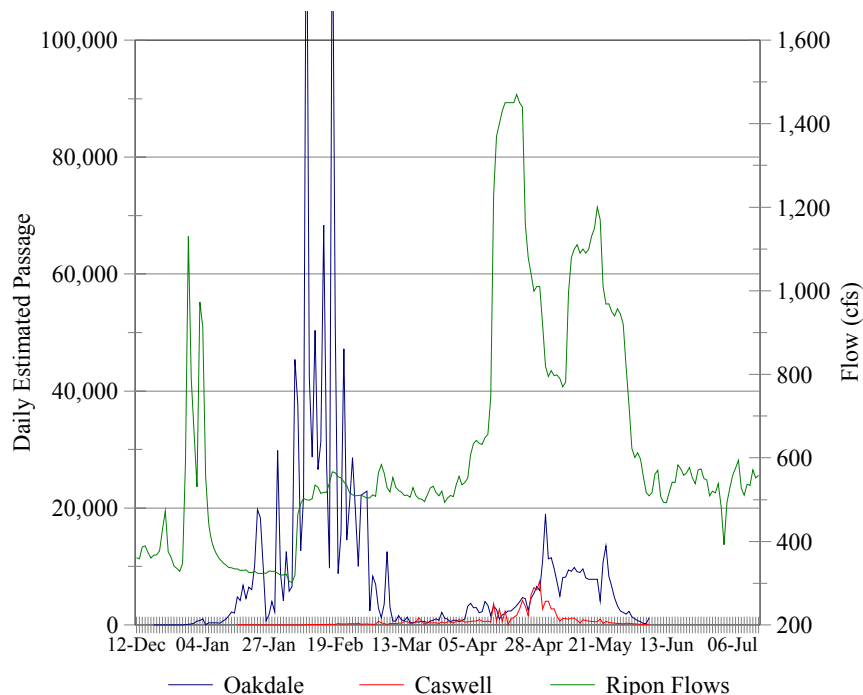


Figure 5. The relationship between the estimated daily passage at the Oakdale and Caswell Park screw traps and the mean daily flow at Ripon in the Stanislaus River between 12/12/01 and 7/15/02, a dry year. Overall juvenile survival between the Oakdale and Caswell traps was 7% in 2002.

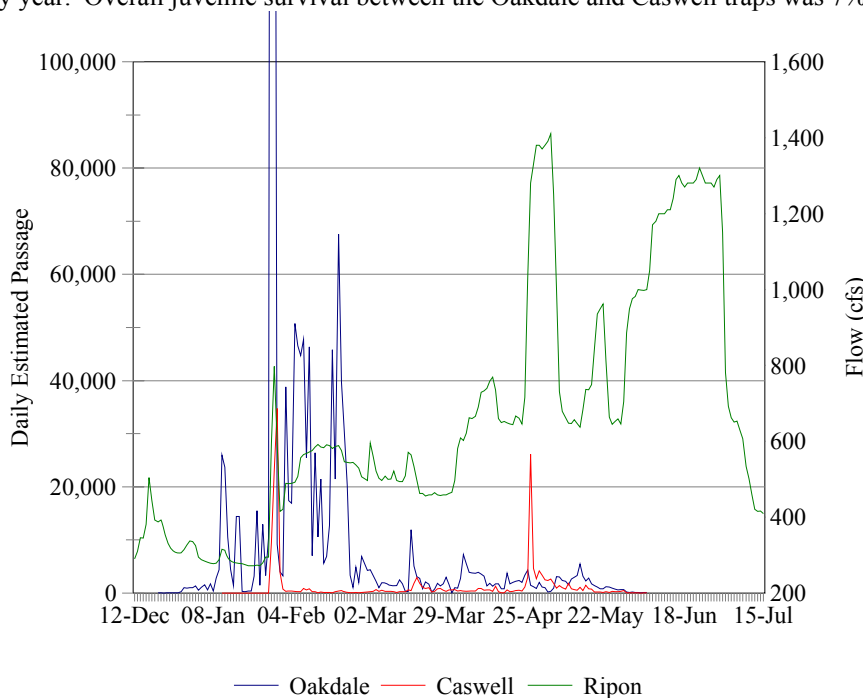


Figure 6. The relationship between the estimated daily passage at the Oakdale and Caswell Park screw traps and the mean daily flow at Ripon in the Stanislaus River between 12/12/02 and 7/15/03, a below normal year. Overall juvenile survival between the Oakdale and Caswell traps was 11% in 2003.

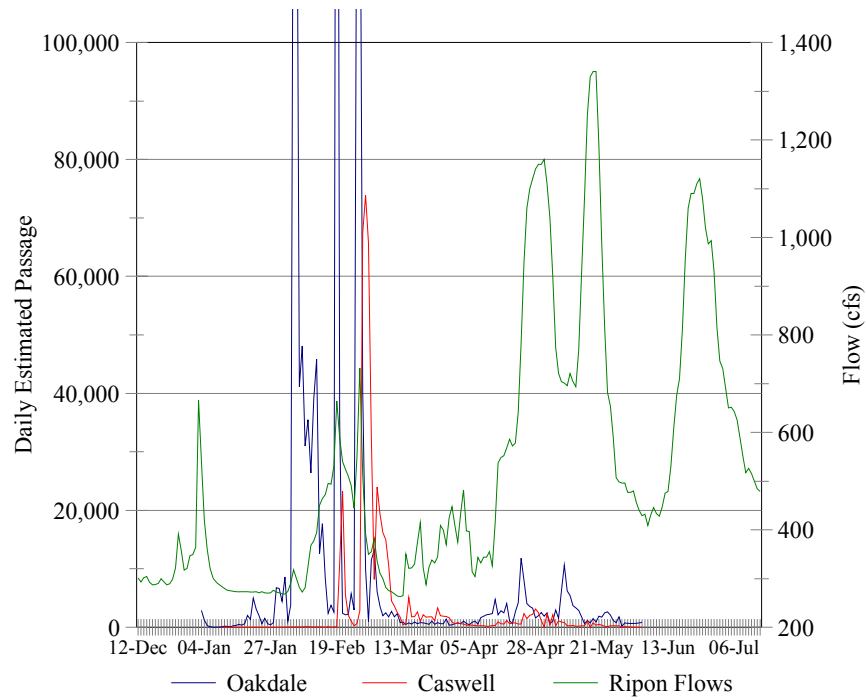


Figure 7. The relationship between the estimated daily passage at the Oakdale and Caswell Park screw traps and the mean daily flow at Ripon in the Stanislaus River between 12/12/03 and 7/15/04, a dry year. Overall juvenile survival between the Oakdale and Caswell traps was 30% in 2004.

Phytoplankton growth rates in a light-limited environment, San Francisco Bay

Andrea E. Alpine, James E. Cloern

US Geological Survey MS496, 345 Middlefield Road, Menlo Park, California 94025, USA

ABSTRACT: San Francisco Bay has a high degree of spatial variability in physical properties (e.g. suspended sediment concentrations, water depths, vertical mixing rates) that affect biological processes. We used this setting to test the hypothesis that light availability is the primary control of phytoplankton growth in this turbid nutrient-rich estuary. In situ incubations (24 h), designed to simulate vertical mixing over the water column at 2 rates, were done at 4 sites. The photic depth to mixed depth ratio ($Z_p:Z_m$) at the 4 sites ranged from 0.12 to 1.1. Phytoplankton growth rates were estimated by ^{14}C assimilation and by changes in cell number. Growth rates were highest (approximately 2 divisions d^{-1}) where the photic depth was large relative to the mixed depth, and small or negative where $Z_p:Z_m$ was small. Growth rate increased with total daily light exposure and fit a hyperbolic function that predicts maximum specific growth rate of about 2 divisions d^{-1} and a compensation irradiance of about $1.4 \text{ Einst. m}^{-2} \text{ d}^{-1}$.

INTRODUCTION

Phytoplankton cells reside in a turbulent medium partitioned into an upper photic zone that sustains photosynthesis, and a lower aphotic zone that does not. In estuaries, vertical mixing rates between these 2 zones can be rapid (< 1 generation time) because of tidal stirring and because the mixing depth is generally shallow. Moreover, the photic depth is characteristically shallow in estuaries because of the high seston concentrations that typify these systems (e.g. Cloern 1987). Hence the mean light exposure of phytoplankton cells, and their rates of photosynthesis and growth in estuaries, should be related to the ratio of photic depth Z_p to mixing Z_m (defined as either the water column depth, or the surface layer depth in a stratified estuary).

Grobbelar (1985) has measured phytoplankton production in turbid waters and used the ratio $Z_p:Z_m$ as a simple index to quantify the degree of light limitation. Harris and his colleagues have examined in detail the importance of the $Z_p:Z_m$ ratio in lakes for influencing variability of phytoplankton production and photosynthetic parameters (Harris et al. 1980), and variability of species composition both temporally (Harris & Piccinin 1980) and spatially (Haffner et al. 1980). Phytoplankton growth rates have only rarely been measured

in estuaries (Malone 1977, Furnas 1982, Harding et al. 1986) where cycling rates between the photic and aphotic zones can be much faster than in lakes or the open ocean.

This study was motivated by the need for quantitative measures of phytoplankton population growth rate in an estuarine environment, and was designed around the presumption that growth rates can be related empirically to light exposure. We conducted the study in San Francisco Bay (California, USA), which has large horizontal gradients in light availability ($Z_p:Z_m$) typical of many coastal plain estuaries, and nutrient concentrations that often exceed those presumed to limit phytoplankton growth (Cloern et al. 1985). We tested the hypothesis that light availability is the primary control of phytoplankton growth, and that previous estimates of growth rate based on the ratio of productivity to biomass (Cloern et al. 1985) are realistic. Specifically, we wanted to verify that growth rate varies spatially along horizontal gradients of light availability indexed as $Z_p:Z_m$, such that phytoplankton turnover rate is rapid in shallow clear areas (high $Z_p:Z_m$) and slow in deep turbid areas (low $Z_p:Z_m$). We used an in situ incubation technique which simulated vertical mixing, and measured both changes in cell number and carbon production as independent estimates of growth rate across a range of $Z_p:Z_m$ ratios.

METHODS

Experimental design. San Francisco Bay has a central deep (10 to 30 m) channel flanked by a broad expanse of subtidal shoals (< 3 m depth). It also has a wide range of SPM (suspended particulate matter) concentrations reflected in contours of the light extinction coefficient k (e.g. Fig. 1). To examine growth rates over a range of light environments (i.e. $Z_p:Z_m$ ratios), 4 experimental sites (Fig. 1) were chosen: 2 channel sites (depth 10 m), one each in the extremely turbid North Bay and the less turbid South Bay; and 2 shoal sites (depth 2 m), one from each bay. Four $Z_p:Z_m$ ratios were used in these experiments (Fig. 2), based upon measured mean k at each site during 1980 (Cloern et al. 1985). Although the deep channel of San Francisco Bay can be density stratified, particularly during the winter-spring period of high river discharge, the upper estuary and South Bay are well mixed or only weakly stratified during the dry summer-autumn (Walters et al. 1985). Our experiments were designed to simulate conditions

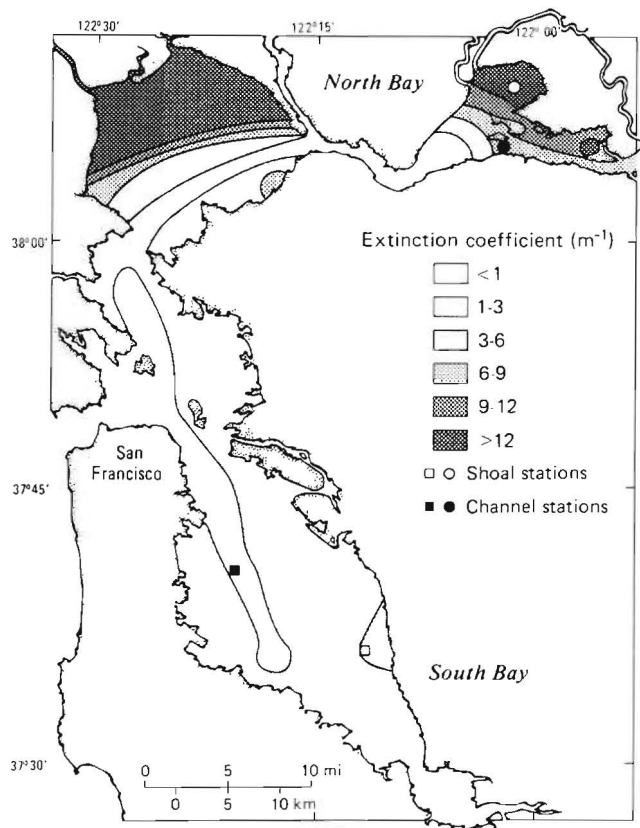


Fig. 1. Contours of the light extinction coefficient measured in San Francisco Bay during August 1980, representative of the summer-fall season. Turbidity measurements were made at 94 sites throughout the estuary with a nephelometer. These measurements were calibrated against extinction coefficients obtained with a LiCor 192S quantum sensor. Also shown are the 4 sampling sites for the experiments described here.

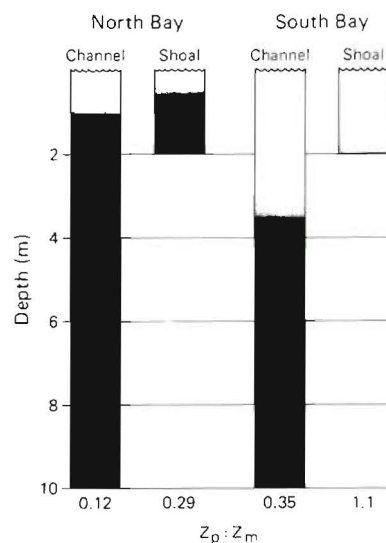


Fig. 2. Photic depth to mixed depth ratio ($Z_p:Z_m$) at the 4 experimental sites.

of a well-mixed estuary (i.e. $Z_m =$ water depth). These experiments were done in September to represent the summer-autumn period when growth rates are presumably maximal in San Francisco Bay (Cloern et al. 1985), and when freshwater inflow and stratification are minimal.

Growth rates were measured by incubating samples in situ and simulating high frequency variations in light exposure that phytoplankton cells mixed throughout a turbulent water column might experience. Our incubation technique was not designed to measure changes in photoadaptive parameters as a function of mixing speed (e.g. Lewis et al. 1984), but rather was a technique to simulate transport of phytoplankton between the photic and aphotic zones so that dark processes (respiration) would be included in the growth estimates. This approach differed from previous studies (e.g. Jewson & Wood 1975, Marra 1978, Gallegos & Platt 1982) which simulated mixing within the photic zone only. Preliminary numerical experiments from computer models indicated that results of such measurements can be sensitive to vertical mixing rates (i.e. nature of light exposure during incubations), so we chose 2 mixing rates that correspond to the range in vertical eddy diffusivities over the neap-spring tidal cycle. These vertical speeds were calculated as depth Z_m divided by the estimated time scale for vertical mixing in a homogenous water column (Walters et al. 1985). Because the eddy diffusivity scales with tidal current speed, and hence water depth (Walters et al. 1985), a different range of mixing speeds was specified for the channel (1.0 and 5.0 $m h^{-1}$) and shoal sites (0.5 and 1.5 $m h^{-1}$). Although these estimates of vertical mixing rate are crude approximations, they are within

the range calculated by Denman & Gargett (1983) for turbulent mixing in the upper ocean. It should be noted, however, that these mixing speeds are considerably slower than other researchers have used to simulate organized motions such as those of Langmuir circulation cells (e.g. Marra 1978, Yoder & Bishop 1985).

The incubation experiments were designed to simulate high frequency variations in light exposure due to vertical motions as well as diurnal changes in surface irradiance, for mean summer-autumn conditions in San Francisco Bay. To do this, we incubated water samples in situ and moved the incubation bottles vertically during the course of the experiment according to a prescribed schedule using the following equation (Parsons et al. 1977):

$$I_t = I_{\max}[\sin^3\{(\pi/D)t\}]e^{-kz} \quad (1)$$

where I_t = prescribed irradiance at time t (h); I_{\max} = surface irradiance at solar noon (= 2000 $\mu\text{Einst. m}^{-2} \text{ s}^{-1}$); D = photoperiod (= 13 h); and k = mean extinction coefficient specific to each site. In calculating these schedules of light exposure, the depth variable z (m) was changed every 15 min based on an initial starting position in the water column and an incremental displacement using the prescribed vertical mixing rate. These schedules defined circular trajectories of movement in the water column and included no random component of vertical motion. It is important to note that these experiments were designed to measure *potential* maximum growth rates, not mean in situ rates. This was done by using that mixing schedule which maximized daily light exposure (typically this meant that incubation bottles were near the surface at solar noon).

Previous estimates of growth rates in San Francisco Bay have been based on carbon production normalized to biomass (Cloern et al. 1985). Other researchers have shown that carbon production and cell division may not be tightly coupled (Pruder & Bolton 1980, Cosper 1982, Reynolds et al. 1985), so we measured both change in cell number and carbon productivity as independent estimates of growth rate.

Experimental procedure. From each site, surface water samples were collected with buckets and screened through 60 μm mesh to remove macrozooplankton. Polycarbonate bottles of 4 l capacity were filled and incubated in situ for 24 h beginning at dawn. Vertical mixing was simulated by manually moving the bottles every 15 min according to the schedule prescribed for each experiment, using irradiance measurements with LiCor quantum sensors (192S) attached to each incubation rack. Instantaneous irradiance was recorded every 15 min and integrated over the day to obtain total irradiance I .

Carbon production was determined using the ^{14}C

acid bubbling technique (Schindler et al. 1972). Following incubation, aliquots (3 ml) from each bottle were placed in scintillation vials. Unincorporated ^{14}C was stripped from the sample and the residual activity measured with a scintillation counter. Duplicate chlorophyll samples were taken at each site, also pre-screened with 60 μm mesh. Chlorophyll *a*, corrected for pheopigments, was determined spectrophotometrically (Lorenzen 1967, Riemann 1978).

Samples for phytoplankton identification and enumeration were preserved with Lugol's solution. Aliquots (150 ml) were collected from each initial sample, each incubated bottle, and a 'dark' bottle (incubated at in situ temperatures and kept in total darkness). At least 300 algal cells were enumerated both at 1000 \times and 80 \times using an inverted microscope. The historical estimate of precision (i.e. average coefficient of variation for triplicate counts) is 8% (Wong & Cloern 1982).

Growth rates (divisions d^{-1}) based on cell division (μ_1) and based on carbon production (μ_2) were calculated as follows:

$$\mu_1 = \log_2[N_t/N_d] \quad (2)$$

where N_t = mean cell density after in situ incubation; and N_d = mean cell density after dark incubation (to correct for cell divisions unrelated to light exposure);

$$\mu_2 = \log_2[(C_i + (C_p - C_d))/C_i] \quad (3)$$

where C_p = production (mg C m^{-3}) during in situ incubation; C_d = carbon assimilation in the dark; and C_i = initial phytoplankton biomass as carbon (mg m^{-3}). Phytoplankton biomass was calculated as the product of the initial chlorophyll *a* concentration and an estimated mean carbon to chlorophyll *a* ratio of 50 (Wienke & Cloern 1987).

RESULTS

The initial conditions for each experiment are shown in Table 1. Salinity was about 3 in the North Bay and 30 in the South Bay; water temperature was 22°C in both

Table 1. Initial experimental conditions

	North Bay		South Bay	
	Channel	Shoal	Channel	Shoal
Salinity	3.5	2.4	30.3	31.1
Temperature (°C)	22.2	—	22.0	—
Chlorophyll <i>a</i> ($\mu\text{g l}^{-1}$)	13.9	18.4	2.3	1.9
DIN ^a ($\mu\text{g-at l}^{-1}$)	5.46	0.43	21.56	1.56
PO ₄ ($\mu\text{g-at l}^{-1}$)	1.90	1.67	11.70	9.30
SiO ₃ ($\mu\text{g-at l}^{-1}$)	130	130	111	105

^a DIN (dissolved inorganic nitrogen) = $\text{NH}_4^+ + \text{NO}_3^- + \text{NO}_2^-$

embayments. Chlorophyll *a* concentrations ranged from $1.9 \mu\text{g l}^{-1}$ at the South Bay shoal site to $18.4 \mu\text{g l}^{-1}$ at the North Bay shoal site. Concentrations of dissolved inorganic nutrients (N, P, Si) at the channel locations exceeded those presumed to limit phytoplankton growth. However dissolved inorganic nitrogen concentration was low ($< 0.5 \mu\text{g-at l}^{-1}$) at the North Bay shoal site (Table 1). As observed historically, diatoms and small cryptophytes were the dominant phytoplankton throughout the estuary.

Fig. 3 details the light exposure of each incubation

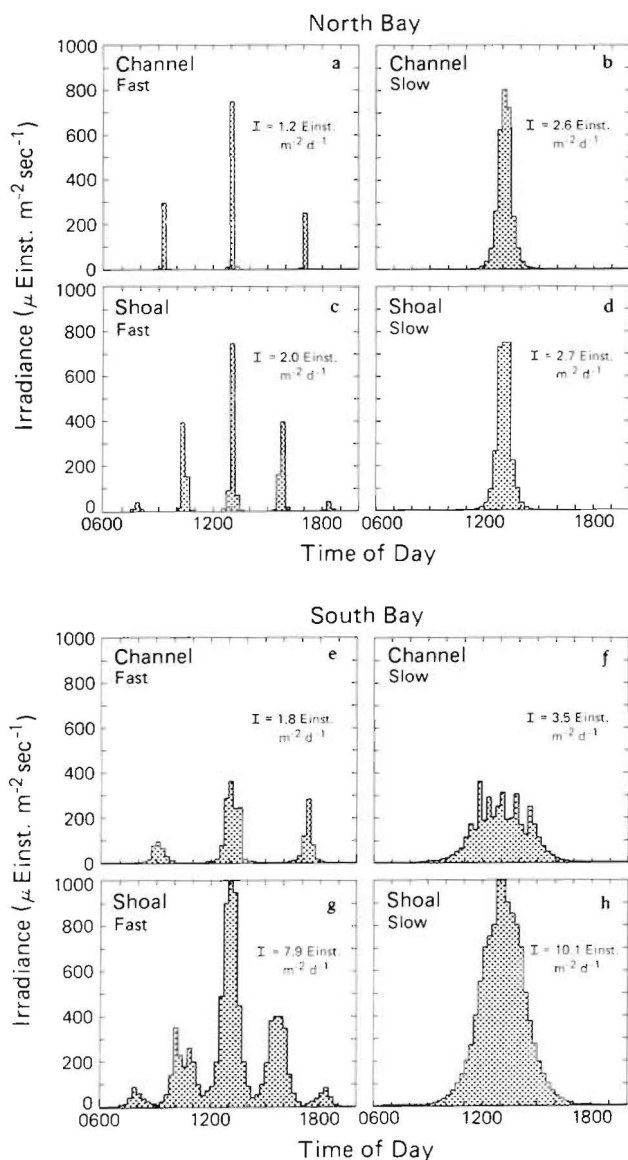


Fig. 3. Light exposure of each incubation bottle during the course of vertical mixing experiments (Irradiance = I_t). Left panels (a, c, e, g) represent high frequency (fast vertical mixing rate) light exposure; right panels (b, d, f, h) represent the light exposure from vertical mixing at the slowest rates. Also shown is total daily irradiance (I) for each incubation bottle

bottle during the course of the 24 h experiments. Both the amount of light received and the timing of the exposure varied with Z_m (i.e. between channel and shoal sites), with Z_p (i.e. between embayments), and with mixing rate. In general, light exposure with the slow mixing rates was characterized by one broad peak centered around solar noon, reflecting the diurnal cycle (e.g. Figs. 3d, h). At the other extreme, rapid vertical mixing generated more variable light exposures such that the incubation bottles were moved between the photic and aphotic zone repeatedly over the photoperiod (e.g. Fig. 3c, g). Total irradiance ranged from 1.2 to $10.1 \text{ Einst. m}^{-2} \text{ d}^{-1}$, which encompasses the range in average water column light intensities found in this estuary (Cloern et al. 1985).

Table 2. Phytoplankton growth rates based on cell division (μ_1) and biomass-normalized carbon production (μ_2) using 2 mixing rates at 4 sites within San Francisco Bay. I : total irradiance (PAR) for each mixing rate. Fast mixing rate (F) = 5 m h^{-1} (channel) or 1.5 m h^{-1} (shoal). Slow mixing rate (S) = 1 m h^{-1} (channel) or 0.5 m h^{-1} (shoal)

	North Bay				South Bay			
	Channel		Shoal		Channel		Shoal	
	F	S	F	S	F	S	F	S
μ_1 (div. d^{-1})	-0.1	0.5	0.4	0.2	0.8	1.2	1.9	1.8
μ_2 (div. d^{-1})	0.2	0.3	0.2	0.3	0.6	1.1	1.7	1.3
I (Einst. $\text{m}^{-2} \text{ d}^{-1}$)	1.2	2.6	2.0	2.7	1.8	3.5	7.9	10.1

Phytoplankton growth rates differed among the 4 locations, ranging from -0.10 to 1.9 divisions d^{-1} based on cell counts and 0.17 to 1.7 divisions d^{-1} based on carbon production (Table 2). The spatial variation in growth rates tracked the variation in the $Z_p:Z_m$ ratio. The fastest growth rates were found in the shoals of the South Bay where $Z_p:Z_m > 1$, and the slowest growth rates were measured in the channel of the North Bay where $Z_p:Z_m = 0.12$. Because the mixing schedules optimized light exposure to each incubation bottle, these measured growth rates represent upper limits rather than mean growth rates for the given mixing rates and $Z_p:Z_m$ ratios.

In these experiments we used 2 methods to measure phytoplankton growth: one based on cell division and one based on biomass-normalized carbon assimilation. These 2 methods yielded growth rates of similar magnitude (Fig. 4), and the 2 measures were highly correlated ($r^2 = 0.93$). The regression slope (Eq. 4) indicates that cell division was faster ($1.3\times$) than the calculated turnover rate of phytoplankton carbon measured by ^{14}C uptake:

$$\mu_2 = 0.04 + 0.76\mu_1 \quad (4)$$

Asynchrony between cell division and photosynthesis has been demonstrated in the laboratory with culture

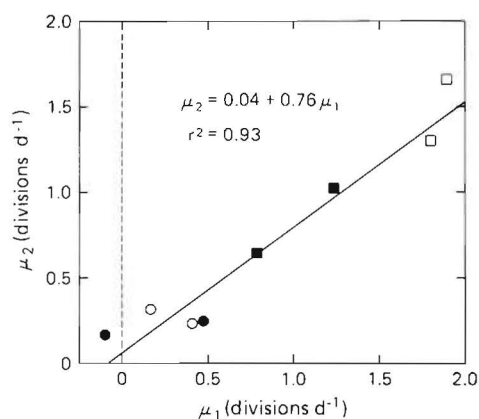


Fig. 4. Regression of μ_2 (growth rate based on carbon production normalized to biomass) against μ_1 (growth rate based on changes in cell numbers). Symbols represent the stations as in Fig. 1

experiments (e.g. Pruder & Bolton 1980, Langdon 1987). However generalities about cell division occurring more rapidly than carbon production, from field studies such as this, should be made with caution. Estimates of μ_2 (from productivity) are based on an assumed ratio of phytoplankton carbon:chlorophyll *a*, which was specified here as 50. However the 2 methods would yield identical mean growth rates (regression slope of 1) given a carbon:chlorophyll *a* ratio of 38, which is within the range expected for natural phytoplankton populations (e.g. Malone 1977, Cullen 1982, Welschmeyer & Lorenzen 1984).

DISCUSSION

Because the 2 methods for measuring phytoplankton growth rate agreed well, we conclude that the traditional approach of estimating μ_1 from productivity:biomass is reasonable. Results of these experiments further demonstrate that estuarine phytoplankton populations have the potential to increase biomass very quickly (i.e. 2 divisions d^{-1}) where the photic depth is large relative to the mixed depth. Conversely, we found small or negative growth rates in the turbid channel of the North Bay where $Z_p:Z_m$ is small. These results support our hypotheses that phytoplankton growth rates can be highly variable spatially, rapid in clear shallow waters (e.g. South Bay shoals) and extremely slow in turbid deep waters (e.g. North Bay channel).

Among others, Cole & Cloern (1987) have shown that phytoplankton productivity is controlled largely by light availability in a wide range of estuarine environments. An objective of this study was to test the hypothesis that variations in phytoplankton growth rate are similarly controlled largely by variations in

light availability. Our results demonstrate a quantitative relationship between growth rate and light exposure. Over a range of light exposure frequencies (Fig. 3), measured growth rates increased with total daily light exposure and fit a hyperbolic function (Fig. 5) that predicts a maximum specific growth rate of about 2 divisions d^{-1} as daily irradiance *I* approaches 10 $Einst. m^{-2} d^{-1}$. A similar hyperbolic relation between growth and irradiance has been observed by Langdon (1987), who measured both particulate organic carbon increase and cell division rate in cultures. Our results also follow the pattern demonstrated by many others (e.g. Bannister 1974, Platt & Jassby 1976, Malone & Neale 1981, Peterson et al. 1987) for the relation between photosynthesis and irradiance. This function also predicts zero growth rate when $I < 1.4$ $Einst. m^{-2} d^{-1}$. Hobson & Guest (1983) have reported daily compensation irradiance (I_{comp}) values between 0.08 and 1.9 $Einst. m^{-2} d^{-1}$ for neritic phytoplankton. Our results are also within the range (0.06 to 1.76 $Einst. m^{-2} d^{-1}$) that Langdon (1987) found in a laboratory study of 3 phytoplankton species: a diatom, a chrysophyte and a dinoflagellate.

Given the protocol of experiments described here, we conclude that an apparent minimum irradiance of about 1.4 $Einst. m^{-2} d^{-1}$ is required to sustain phytoplankton population growth in San Francisco Bay. By knowing this minimum irradiance value (i.e. $I_{comp} = 1.4$ $Einst. m^{-2} d^{-1}$) and substituting it for *I* in Eq. (5), which gives the mean irradiance in a totally absorbing water column, we can estimate the critical $Z_p:Z_m$ ratio needed to sustain growth:

$$I = (I_0 \times Z_p:Z_m) / 4.61 \quad (5)$$

For an average summer day (surface irradiance $I_0 = 40$ $Einst. m^{-2} d^{-1}$) we calculate that the critical $Z_p:Z_m = 0.16$, which is consistent with the critical $Z_p:Z_m$ ratio for photosynthesis (Cloern 1987). This implies that when

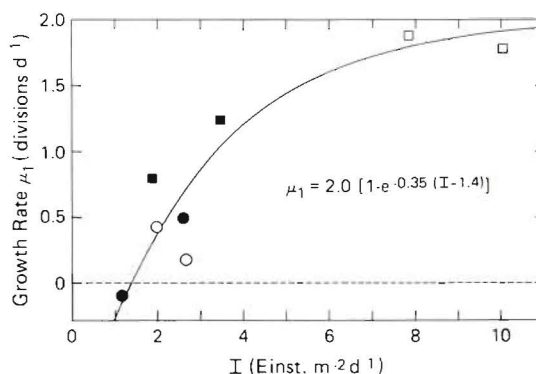


Fig. 5. Phytoplankton growth rate as a function of irradiance during simulated vertical mixing. Measurements were made at 4 sites (see Fig. 1) during September 1984 using 2 vertical mixing rates per site

the photic depth is less than approximately 16 % of the mixed depth, phytoplankton growth cannot be sustained.

Our results demonstrate that phytoplankton population dynamics can be strongly influenced by the ratio $Z_p:Z_m$ in estuaries, as in lakes (e.g. Harris et al. 1980, Horn & Paul 1984, Grobbelaar 1985). We can measure Z_p accurately but do not yet have an equivalent capability to quantify the mixed depth Z_m , particularly when density gradients are present in the water column. Even if Z_m is well defined, it remains difficult to use physical properties (e.g. vertical density or velocity gradients) to infer trajectories of movement, and therefore mean light exposure, of phytoplankton populations. Experimental results such as those presented here emphasize the need for collaborations between phytoplankton ecologists and physical scientists to better characterize the vertical motions of phytoplankton, and thus enhance the utility of empirical functions (e.g. Fig. 5) to estimate phytoplankton growth rates in nature.

Acknowledgements. We gratefully acknowledge Ray Wong, Brian Cole and the crew of the RV 'Polaris' who assisted in this study. We thank J. Thompson and T. Hollibaugh for manuscript reviews.

LITERATURE CITED

- Bannister, T. T. (1974). A general theory of steady state phytoplankton growth in a nutrient saturated mixed layer. *Limnol. Oceanogr.* 19: 13-30
- Cloern, J. E., Cole, B. E., Wong, R. L. J., Alpine, A. A. (1985). Temporal dynamics of estuarine phytoplankton: a case study of San Francisco Bay. *Hydrobiol.* 129: 153-176
- Cloern, J. E. (1987). Turbidity as a control on phytoplankton biomass and productivity in estuaries. *Cont. Shelf Res.* 7: 1367-1381
- Cole, B. E., Cloern, J. E. (1987). An empirical model for estimating phytoplankton productivity in estuaries. *Mar. Ecol. Prog. Ser.* 36: 299-305
- Cosper, E. (1982). Influences of light intensity on diel variations in rates of growth, respiration and organic release of a marine diatom: comparison of diurnally constant and fluctuating light. *J. Plankton Res.* 4: 705-724
- Cullen, J. J. (1982). The deep chlorophyll maximum: comparing vertical profiles of chlorophyll *a*. *Can. J. Fish. aquat. Sci.* 39: 791-803
- Denman, K. L., Gargett, A. E. (1983). Time and space scales of vertical mixing and advection of phytoplankton in the upper ocean. *Limnol. Oceanogr.* 28: 801-815
- Furnas, M. J. (1982). Growth rates of summer nanoplankton (< 10 μ m) populations in lower Narragansett Bay, Rhode Island, USA. *Mar. Biol.* 70: 105-115
- Gallegos, C. L., Platt, T. (1982). Phytoplankton production and water motion in surface mixed layers. *Deep Sea Res.* 29: 65-76
- Grobbelaar, J. U. (1985). Phytoplankton productivity in turbid waters. *J. Plankton Res.* 7: 653-663
- Haffner, G. D., Harris, G. P., Jarai, M. K. (1980). Physical variability and phytoplankton communities. III. Vertical structure in phytoplankton populations. *Arch. Hydrobiol.* 89: 363-381
- Harding, L. W., Meeson, B. W., Fisher, T. R. (1986). Phytoplankton production in two east coast estuaries: photosynthesis-light functions and patterns of carbon assimilation in Chesapeake and Delaware Bays. *Estuar. coast. Shelf Sci.* 23: 773-806
- Harris, G. P., Haffner, G. D., Piccinin, B. B. (1980). Physical variability and phytoplankton communities. II. Primary productivity by phytoplankton in a physically variable environment. *Arch. Hydrobiol.* 88: 393-425
- Harris, G. P., Piccinin, B. B. (1980). Physical variability and phytoplankton communities. IV. Temporal changes in the phytoplankton community of a physically variable lake. *Arch. Hydrobiol.* 89: 447-473
- Hobson, L. A., Guest, K. P. (1983). Values of net compensation irradiation and their dependence on photosynthetic efficiency and respiration in marine unicellular algae. *Mar. Biol.* 74: 1-7
- Horn, H., Paul, L. (1984). Interactions between light situation, depth of mixing and phytoplankton growth during the spring period of full circulation. *Int. Revue ges. Hydrobiol.* 69: 507-519
- Jewson, D. H., Wood, R. B. (1975). Some effects on integral photosynthesis of artificial circulation of phytoplankton through light gradients. *Verh. int. Verein. Limnol.* 19: 1037-1044
- Langdon, C. (1987). On the causes of interspecific differences in the growth-irradiance relationship for phytoplankton. Part I. A comparative study of the growth-irradiance relationship of three marine phytoplankton species: *Skeletonema costatum*, *Olisthodiscus luteus* and *Gonyaulax tamarensis*. *J. Plankton Res.* 9: 459-482
- Lewis, M. R., Horne, E. P. W., Cullen, J. J., Oakey, N. S., Platt, T. (1984). Turbulent motions may control phytoplankton photosynthesis in the upper ocean. *Nature, Lond.* 311: 49-50
- Lorenzen, C. J. (1967). Determination of chlorophyll and phaeo-pigments: spectrophotometric equations. *Limnol. Oceanogr.* 12: 343-346
- Malone, T. C. (1977). Environmental regulation of phytoplankton productivity in the Lower Hudson Estuary. *Estuar. coast. Mar. Sci.* 5: 151-171
- Malone, T. C., Neale, P. J. (1981). Parameters of light-dependent photosynthesis for phytoplankton size fractions in temperate estuarine and coastal environments. *Mar. Biol.* 61: 289-297
- Marra, J. (1978). Phytoplankton photosynthetic response to vertical movement in a mixed layer. *Mar. Biol.* 46: 203-208
- Parsons, T. R., Takahashi, M., Hargrave, B. (1977). *Biological oceanographic processes*, 2nd edn. Pergamon Press, Oxford
- Peterson, D. H., Perry, M. J., Bencala, K. E., Talbot, M. C. (1987). Phytoplankton productivity in relation to light intensity: a simple equation. *Estuar. coast. Shelf Sci.* 24: 813-832
- Platt, T., Jassby, A. D. (1976). The relationship between photosynthesis and light for natural assemblages of coastal marine phytoplankton. *J. Phycol.* 12: 421-430
- Pruder, G. D., Bolton, E. T. (1980). Difference between cell division and carbon fixation rates associated with light intensity and oxygen concentration: implications in the cultivation of an estuarine diatom. *Mar. Biol.* 59: 1-6
- Reynolds, C. S., Harris, G. P., Gouldney, D. N. (1985). Comparison of carbon-specific growth rates and rates of cellular increase of phytoplankton in large limnetic enclosures. *J. Plankton Res.* 7: 791-820

- Riemann, B. (1978). Carotenoid interference in the spectrophotometric determination of chlorophyll degradation products from natural populations of phytoplankton. *Limnol. Oceanogr.* 23: 1059–1066
- Schindler, D. W., Schmidt, R. V., Reid, R. A. (1972). Acidification and bubbling as an alternative to filtration in determining phytoplankton production by the ^{14}C method. *J. Fish. Res. Bd Can.* 29: 1627–1631
- Walters, R. A., Cheng, R. T., Conomos, T. J. (1985). Time scales of circulation and mixing processes of San Francisco Bay waters. *Hydrobiologia* 129: 13–36
- Welschmeyer, N. A., Lorenzen, C. J. (1984). Carbon-14 labeling of phytoplankton carbon and chlorophyll *a* carbon: determination of specific growth rates. *Limnol. Oceanogr.* 29: 135–145
- Wienke, S. M., Cloern, J. E. (1987). The phytoplankton component of seston in San Francisco Bay. *Neth. J. Sea Res.* 21: 25–33
- Wong, R. L. J., Cloern, J. E. (1982). Plankton studies in San Francisco Bay. IV. Phytoplankton abundance and species composition. January 1980–February 1981 U.S. Geol. Survey Open-File Report 82–443: 1–152
- Yoder, J. A., Bishop, S. S. (1985). Effects of mixing-induced irradiance fluctuations on photosynthesis of natural assemblages of coastal phytoplankton. *Mar. Biol.* 90: 87–93

This article was submitted to the editor; it was accepted for printing on March 4, 1988

SAN FRANCISCO BAY CONSERVATION AND DEVELOPMENT COMMISSION

455 Golden Gate Avenue • Suite 10600 • San Francisco, California 94102 • (415) 352-3600 • Fax: (415) 352-3606 • www.bcdc.ca.gov

May 23, 2014

TO: Commissioners and Alternates

FROM: Lawrence J. Goldzband, Executive Director (415/352-3653 lgoldzband@bcdc.ca.gov)
Joe LaClair, Chief Planning Officer (415/352-3656 joel@bcdc.ca.gov)

**SUBJECT: Staff Recommendation on Comments on the Bay Delta Conservation Plan
Environmental Documents**
(For Commission consideration on June 5, 2014)

Staff Recommendation

Staff recommends that the Commission direct staff to submit the following comments on the Bay Delta Conservation Plan (BDCP) Environmental Impact Report/Statement (EIR/S) with any revisions from the Commission.

The Commission received a briefing from Paul Helliker from the Department of Water Resources (DWR) on the BDCP at its February 20, 2014 meeting, and held a panel discussion on the BDCP at its May 1, 2014 meeting. At these briefings, Commissioners raised several questions about how the proposed project may directly affect the San Francisco Bay and Suisun Marsh. The BDCP is undergoing state and federal environmental review. Commission laws and policies call for adequate fresh water inflows from the Delta to Suisun Marsh and the Bay to maintain proper salinity levels and water circulation patterns, to flush pollutants, and to maintain related ecosystem functions. Based on Commissioner comments and questions, and staff review of the environmental documents prepared for the BDCP, staff prepared the following proposed comments on these environmental documents. Attached to this report is a memo from Paul Helliker providing some additional information on the BDCP issues raised at the Commission's briefings.

Staff Report

Bay-Delta Conservation Plan Project Description. The Bay-Delta Conservation Plan (BDCP) is being prepared to meet the requirements of the federal and state Endangered Species Acts. It is the first attempt in the nation to prepare a habitat conservation plan that includes aquatic habitats. The plan lays out a framework for conserving certain species, both listed and non-listed, and authorizes take of listed species under certain circumstances. Regulated entities (DWR and the US Bureau of Reclamation, state and federal water contractors, other users of Delta water) and resource agencies (California Natural Resources Agency, state and federal fishery agencies) and non-governmental organizations developed the plan.



BDCP's long-term goal is to preserve, restore and enhance aquatic, riparian and associated terrestrial natural communities and ecosystems that support a wide range of species of concern. It intends to provide a stable regulatory environment for water projects, standardize mitigation and compensation requirements, and provide a less costly and more efficient approach to conservation than project-by-project and species-by-species reviews.

The BDCP Environmental Impact Report/Statement (EIR/S) evaluates sixteen project alternatives, including fifteen that vary over different project components. These variations include: four different water conveyance configurations; different intake locations and alignment options; four different diversion capacities ranging from 3,000 to 15,000 cubic feet per second (cfs); eight various operational scenarios based upon guiding water supply parameters, diversion flows, operational demands, and water quality requirements; and, three different habitat restoration plans ranging from 113,000 to 163,000 acres. The alternatives have varying implications for biological resources, hydrology, and interactions with the human environment. Alternative 4, the proposed project of the BDCP, includes using a pipeline/tunnel system to convey water from the Sacramento River over forty miles south, under the Delta, to the California Aqueduct system, which supplies much of the state's water. The comment period on the BDCP draft EIR/S ends June 13, 2014.

Project Impacts. Potential effects of the BDCP on water bodies downstream of the Delta were analyzed and the EIR/S states that the project may affect the following downstream resources:

- Flow;
- Sediment inputs;
- Food;
- Temperature; and
- Dissolved oxygen.

The analysis in the EIR/S concludes that there would be no significant adverse effects on San Francisco Bay. Therefore, areas downstream of the Delta (e.g., San Pablo Bay, San Francisco Bay south to the Golden Gate Bridge and Bay Bridge) were considered, but were not included as a part of the BDCP's analysis.

Staff Comments

Staff would like to commend the authors for this ground-breaking plan. As the first ever aquatic Habitat Conservation Plan/Natural Communities Conservation Plan (HCP/NCCP), in one of the most ecologically, legally and culturally complex areas in the world, the BDCP represents an incredible first effort at crafting a solution to many of the complex Delta issues. We believe there are some pieces missing, and our comments address those. As a responsible agency under CEQA, BCDC should comment on the EIR/S. The Commission will need to issue permits or consistency determinations for the conservation measure projects located in the Suisun Marsh or San Francisco Bay. Based on Commissioner comments and questions, the Commission's laws and policies, and staff review of the EIR/S prepared for the BDCP, staff prepared the following proposed comments on these environmental documents. The relevant, applicable policies are quoted in the following section.

San Francisco Bay and Suisun Marsh Effects. The EIR/S states that there would be no significant effects on San Francisco Bay. Commissioners, staff, other state agencies and members of the public raised concerns about possible project impacts west of the Delta in the Suisun Marsh and downstream in the San Francisco Bay. Some of these effects would be significant. Potential significant impacts could include effects on salinity, sediment supply, and the consequences (intended and unintended) of various restoration programs, and further impacts

on Bay habitats and species. The Delta Stewardship Council's (DSC) Independent Science Board (ISB) concluded that more research and analysis is needed on areas west of the Delta in order to get a more complete picture of the cumulative effects of the BDCP. The ISB noted that "the hydrodynamic modeling needs to capture the entire domain of effects. The current Effects Analysis does not consider the influence of shifting timing of withdrawals on San Francisco Bay circulation patterns and ecology. This is a significant omission with ecologically important implications."

The ISB also noted that the BDCP evaluates "three geographic regions: upstream of the Delta, the legal Delta, and the State Water Project (SWP) and Central Valley Project (CVP) service areas. Areas downstream of the Delta (i.e., San Francisco Bay) were not included even though the National Research Council (NRC) scientific review specifically stated that this area should be included. Adequate justification for lack of consideration of impacts to San Francisco Bay was not provided ... in the document, although there are potential impacts. For example, the expected reduction in sediment supply has the potential impacts of: (1) tidal marshes in the Bay could be less resilient to sea level rise and; (2) increased water clarity in the Bay could render it more responsive to nutrient inputs." The EIR/S should better assess the potential effects on the Marsh and the Bay, and identify potential impacts on salinity, sediment delivery and Bay species as potentially significant, and evaluate strategies to avoid or mitigate these effects.

Water Quality and Salinity. Biological opinions from the National Marine Fisheries Service and the US Fish and Wildlife Service determined that habitat degradation in the Marsh for multiple sensitive species is due, in part, to reduced freshwater inflows from the Delta. Current Delta fresh water outflows seem inadequate to support or recover endangered species. Studies project that the salinity in San Francisco Bay could increase by 0.30-0.45 practical salinity unit (psu) per decade due to the compounding effects of decreasing freshwater inflow and rising sea level (projected by Cloern et al. 2011 to rise approximately 4 inches per decade). Climate change will affect future Bay salinity and the restoration and conservation measures proposed in the EIR/S. Higher salinity in the Suisun Marsh due to high diversion years would affect managed wetlands, and the Bay's native species, such as the Dungeness Crab, that use the lower salinity of the Bay as a nursery. However, these species are not included in the BDCP's analysis. Also, waterfowl that rely on the lower salinity/freshwater of the Marsh as breeding habitat may be at risk, as higher salinity levels have been shown to be dangerous to ducklings.

The EIR/S states that the BDCP would be implemented using a "decision tree process, a focused form of adaptive management that will be used to determine at the start of new operations, the fall and spring outflow criteria that are required to achieve the conservation objectives of the BDCP for delta smelt and longfin smelt and to promote the water supply objectives of the BDCP. Other BDCP-covered fish species, including salmonids and sturgeon, may also be affected by outflow. Their outflow needs will also be investigated as part of the decision tree process." The EIR/S should clarify how the proposed pipelines will be managed in the long term (e.g., 50 years), if there are recurring droughts that require changes in future flow regimes. The BDCP should evaluate flow scenarios that provide greater freshwater flows to the Bay beyond the requirements of D1641¹ to recover declining fish populations. Decreased reliance on Delta freshwater diversions may become necessary for the protection of sensitive and threatened species. Scenario F (Alternative 8: pipeline/tunnel alignment, dual conveyance, intakes at 2, 3 & 5, with 9,000 cfs diversion) would increase Delta outflow up to 1.5 million acre-feet annually. A project alternative that provides for greater Delta outflows is likely necessary to meet the policy objectives in the *San Francisco Bay Plan* (Bay Plan) and the *Suisun Marsh*

¹ D1641 refers to a State Water Board water rights Decision of 2005 that set water quality (salinity) standards for various monitoring stations in the Bay and Delta and amends certain water rights by assigning responsibilities to the persons or entities holding those rights to help meet the salinity objectives.

Protection Plan (Marsh Plan). Also, the EIR/S should evaluate potential impacts on non-listed Marsh and Bay species that rely on salinity levels characteristic of the Bay and the Marsh as required by current X2 standards.

Conservation Measures. Most Conservation Measures are discussed at a programmatic level, rather than at a project level in the EIR/S. The ISB noted that, "the difference in level of detail [of restoration project analyses] presented effectively treats the co-equal goals unequally. We are concerned that the merely programmatic analysis of habitat restoration provides too little basis for decision-making by the Delta Stewardship Council and other parties. Furthermore, the benefits of habitat restoration are assumed when a beneficial cumulative impact is concluded under NEPA or a less than significant cumulative impact is concluded under CEQA. Achieving beneficial conservation measures requires understanding limiting factors, ecosystem processes, sequencing, adaptive management responses, thresholds for certain actions, and interactions and other consequences of these actions...to describe how major uncertainties will be resolved." Also, the Effects Analysis recognizes that suspended sediment has been declining in the Sacramento River, but no analysis of the potential for corresponding increased algal blooms is addressed.

Specific locations for habitat improvements are not discussed in the restoration opportunity areas, including those in the Suisun Marsh. The EIR/S would benefit from further analysis of restoration patterns in the Marsh to determine how they affect salinity patterns in the Marsh and Delta. This may help focus the restoration efforts to specific regions of the Marsh to limit salinity intrusion. There is little discussion in the EIR/S of the effects of climate change on conservation measures. Some Conservation Measures that involve habitat restoration or enhancement should be addressed at a project level of detail in the EIR/S so that they can be implemented early in the project cycle, in timeframes consistent with Conservation Measure 1. Also, additional conservation measures may be needed to address project effects on the Marsh and the Bay, particularly those related to sediment management.

Sediment. The BCDP EIR discusses a potential reduction in suspended sediment transport to the Suisun Marsh and San Francisco Bay of approximately eight to ten percent. The EIR/S does not characterize this change as a significant impact. The ISB report to the Delta Stewardship Council raises this as a significant issue. USGS researchers have observed a steep reduction in Bay suspended sediment concentrations and characterize San Pablo Bay as erosional. With projected sea level rise, further reduction in Bay sediment inputs should be considered significant, given Bay wetland restoration targets, current subsided diked-baylands, and the overall Bay-Delta sediment budget. Given sediment settling in the new northern forebay, the relocation of flows from channels into underground pipes, new pumping regimes and proposed restorations together and separately will alter sediment transport, delivery, and rate of deposition downstream. Reduced suspended sediment in the Bay will exacerbate nutrient loading problems caused from the sewage treatment plants discharging into the Bay.

Construction of restoration projects, which are highly desirable in the Delta upstream of the Bay, will likely create sediment sinks, thus further reducing sediment flows to the Marsh and San Francisco Bay. The cumulative impacts analysis should consider this, using science-based thresholds of significance.

Cumulative Effects. There are several related projects that, cumulatively, could exacerbate effects of BDCP and adversely affect the Bay and the Marsh that are not addressed in the EIR/S. These projects include, but are not limited to, dredging the Baldwin Ship Channel (between San Pablo Bay and the Port of Stockton) that may include constructing a sill in the Carquinez Strait; proposals to construct seasonal drought barriers or gates in the Delta; and several proposed water storage projects on existing dams and reservoirs. The issue of storage should be addressed within BDCP, particularly planned projects. The EIR/S should address cumulative impacts of all relevant related projects.

Next steps. The authors of the EIR/S will review the comments from the many agencies, organizations and members of the public providing input and will determine whether to recirculate a draft or prepare a final environmental document, in either case, that responds to the comments provided. If a draft EIR/S is circulated, then another round of comments will follow, before a final document is prepared, or a final document will be prepared and issued later this year or early next year.

BCDC's Relevant Policies and Related Agreements

Bay Plan Findings and Policies. The Commission's Bay Plan recognizes the tremendous ecological value of the Bay-Delta estuary and the importance of fresh water inflows from the Delta to the survival of fish and wildlife in the Bay and Suisun Marsh.

Bay Plan findings on Tidal Marshes and Tidal Flats state, in part, that "San Francisco Bay is a substantial part of the largest estuary along the Pacific shore of North and South America and is a natural resource of incalculable value" and that "the sheltered waters of estuaries support unique communities of plants and animals specially adapted for life in the region where rivers meet the coast."

Bay Plan findings and policies recognize the importance of fresh water inflows to the ecosystem of the Bay. Bay Plan findings on Fish, Other Aquatic Organisms and Wildlife state, in part, that "conserving fish, other aquatic organisms and wildlife depends, among other things, upon availability of ...proper fresh water inflows, temperature, salt content, water quality, and velocity of the water." Fresh Water Inflow Finding A states that "[f]resh water flowing into the Bay, most of which is from the Delta, dilutes the salt water of the ocean flowing into the Bay through the Golden Gate....This delicate relationship between fresh and salt water helps to determine the ability of the Bay to support a variety of aquatic life and wildlife in and around the Bay."

Bay Plan findings and policies also recognize the impact of pollutants passing through the Delta into the Bay. Bay Plan findings on Water Quality state, in part, that "water from approximately 40 percent of California drains into San Francisco Bay carrying with it pollutants from point and nonpoint sources" and that "harmful effects of pollutants reaching the Bay can be reduced by maximizing the Bay's capacity to assimilate, disperse, and flush pollutants by maintaining and increasing...the volume and circulation of water flowing in and out with the tides and in fresh water inflow."

The Bay Plan's Fresh Water Inflow policies require limits on water diversions, preservation of the Suisun Marsh, and cooperation with the State Water Board to ensure adequate fresh water inflow. Policy 1 states that "[d]iversions of fresh water should not reduce the inflow into the Bay to the point of damaging the oxygen content of the Bay, the flushing of the Bay, or the ability of the Bay to support existing wildlife." Policy 2 states that "[h]igh priority should be given to the preservation of Suisun Marsh through adequate protective measures, including maintenance of fresh water inflows." Finally, Policy 3 states, in part, that the "Bay Commission should cooperate with the State Board and others to ensure that adequate fresh water inflows to protect the Bay are made available."

Suisun Marsh Preservation Act. The Nejedly-Bagley-Z'berg Suisun Marsh Preservation Act of 1974 directed BCDC and the California Department of Fish and Game (CDFG) to develop the Suisun Marsh Protection Plan, which was codified into law as the Suisun Marsh Preservation Act of 1977. The Act recognizes the important role of the Suisun Marsh in providing wintering habitat for waterfowl using the Pacific Flyway and critical habitat for other wildlife, including rare and endangered species.

The Suisun Marsh, where salt and fresh water meet and mix, contains approximately 85,000 acres of tidal marsh, managed wetlands, and waterways in southern Solano County. It is an important part of the Bay-Delta ecosystem and requires adequate fresh water inflows to maintain its fish and wildlife habitat.

Section 29003 of the Act finds that continued wildlife use of Suisun Marsh requires, among other things, “[p]rovision for future supplemental water supplies and related facilities to assure that adequate water quality will be achieved within the wetland areas.”

Section 29010 finds that “[w]ater quality in the marsh is dependent on the salinity of the water in sloughs of the marsh, which depends in turn on the amount of fresh water flowing in from the Delta.”

Suisun Marsh Protection Plan. The Plan recognizes that Suisun Marsh contains “the unique diversity of fish and wildlife habitats characteristic of a brackish marsh.” The Plan emphasizes the need to maintain adequate fresh water inflows to preserve this unique habitat.

Water Supply and Quality Finding 2 of the Plan states, in part, that “[t]he most important source of fresh water inflow to the Suisun Marsh is the outflow from the Sacramento-San Joaquin River Delta.”

Finding 9 states, in part, that “[t]he State Water Resources Control Board in its Delta Decision, and the Environmental Protection Agency and the Regional Water Quality Control Board in the Water Quality Control Plan for the San Francisco Bay Basin, have set water and soil salinity standards for the Marsh.”

Finding 10 states, in part, that “[a]ssuring that sufficient quantities of fresh water will be available to the Marsh to meet the standards and marsh management requirements is as important as determining appropriate water quality standards for the Marsh.”

Water Supply and Quality Policy 1 states, in part, “there should be no increase in diversions by State or Federal Governments that would cause violations of existing Delta Decision or Basin Plan standards.”

Policy 2 states, “Adequate supplies of fresh water are essential to the maintenance of water quality in the Suisun Marsh. Therefore, the State should have the authority to require the Bureau of Reclamation to comply with State and Federal water quality standards for the Delta and the Marsh. This should be accomplished through Federal legislation if necessary.”

Policy 4 states, in part, that “[w]ater quality standards in the Marsh should be met by maintaining adequate inflows from the Delta.”

Suisun Marsh Preservation Agreement. In 1987, DWR, CDFG, the Bureau, and the Suisun Resource Conservation District signed the Suisun Marsh Preservation Agreement to mitigate impacts on Marsh salinity from the CVP, SWP, and other upstream diversions. The objectives of the agreement are:

- To assure that the Bureau and DWR maintain a water supply of adequate quantity and quality for managed wetlands within the Marsh. This is to mitigate adverse effects on these wetlands from operation of the CVP and SWP as well as a portion of the adverse effects of other upstream diversions;
- To improve Marsh wildlife habitat on these managed wetlands;
- To define the obligations of the Bureau and DWR necessary to assure the water supply, distribution, management facilities, and actions necessary to accomplish these objectives; and
- To recognize that water users in the Marsh (i.e., existing landowners) divert water for wildlife habitat management within the Marsh.

In 2005, the Revised Suisun Marsh Preservation Agreement was signed to make its water salinity requirements consistent with water quality standards adopted in 1999 (see “Bay-Delta Beneficial Uses” in Bay-Delta Management section below) and to replace proposed large scale water management facilities with landowner water and management activities to meet the Agreement objectives in the western Marsh.

X2 Water Quality Standards. X2 refers to the salinity level of 2 parts per thousand, which corresponds to the mixing zone of fresh and salt water. Maintaining X2 within Suisun Bay between February and June is considered beneficial for the reproductive success and survival of the early life stages of many estuarine species, including Delta smelt. The CCMP recommended the adoption of these standards, which became an element of the 1994 Bay-Delta Accord.

The US Fish and Wildlife Service listed the Delta Smelt as threatened under the federal Endangered Species Act in 1993, and designated portions of the Delta as critical habitat for the smelt in 1994. The US Environmental Protection Agency and FWS established the X2 water quality standards in 1995. The standards require X2 to be maintained at particular locations within the Delta between February and June depending on the amount of precipitation.

To: BCDC Commissioner and Alternates

From: Paul Helliker, Deputy Director, California Department of Water Resources

Subject: Summary Responses to Issues Raised at the May 1, 2014 Meeting and BDCP Panel Discussion

Relationship to the Suisun Marsh Plan

- The BDCP would restore up to 11,500 acres in Suisun Marsh to tidal wetlands over 50 years; the Suisun Marsh Plan (SMP) calls for 5,000-7,000 acres over 30 years.
- The BDCP would preserve and enhance 8,100 acres of managed wetlands.
- The BDCP can help implement the SMP restoration component.
- SMP and BDCP modeling show that location of restoration is one of the most important factors in managing salinity in the Marsh.

Sediment

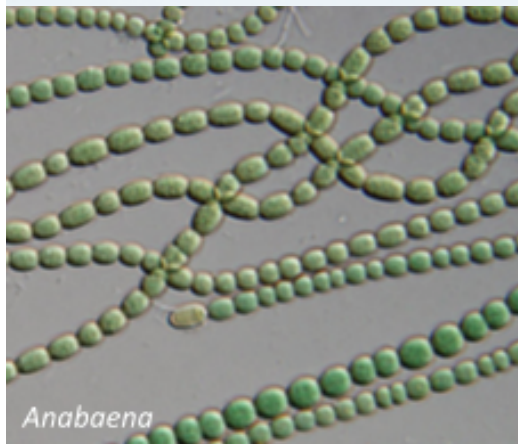
- The BDCP North Delta Intake would reduce the sediment load into the Plan Area (Delta) by around 8-10%. However, that material could be reintroduced into the Plan Area for restoration or other beneficial uses. The actual net reduction in sediment is likely to be less than 8-10%.
- Specific hydrodynamics and restoration locations and designs will dictate how suspended sediments move, including if areas will be sediment sinks or sources.
- Recent work by McKee et al. (2013) using updated methods to improve sediment load estimates beyond previous efforts suggests that, despite their small watershed area (5% of total area) and fluvial flow (7% of total flow), the smaller urbanized and tectonically active tributaries to San Francisco Bay are the major contributors (61% of total) of sediment load into San Francisco Bay compared to upstream sources that are affected by SWP and CVP operations (remaining 39% of sediment load). For San Pablo Bay, which is farther upstream, the proportional contribution of sediment load from upstream was estimated by Schoelhamer et al. (2008) to be approximately 50%.

Inflows

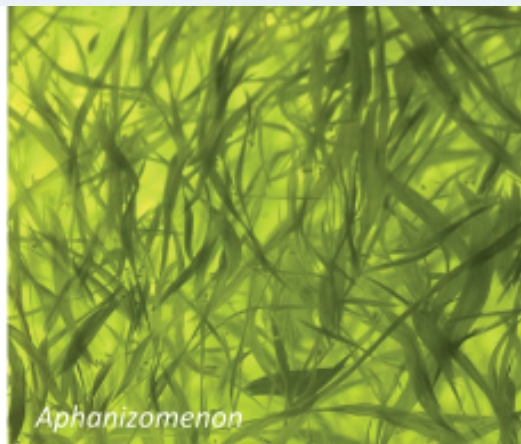
- According to the *Delta Atlas* (DWR 1995), average historical tidal flow through the Golden Gate Bridge is 2,300,000 cubic feet per second (cfs) and average historical tidal flow at Chipps Island is 170,000 cfs. According to BDCP CALSIM modeling, the greatest mean monthly reduction in Delta outflow due to BDCP (compared to a baseline that includes the Fall X2 standard [EBC2]) would be 5,613 cfs during September under the low outflow scenario (LOS), which would not include the Fall X2 standard. This equates to 0.2% and 3% of average tidal flow at the Golden Gate Bridge and Chipps Island, respectively.
- Under all outflow scenarios, the BDCP would comply with D-1641. Under the high outflow scenario, spring and fall outflows would be greater than D-1641.

Factors Affecting Growth of Cyanobacteria

With Special Emphasis on the Sacramento-San Joaquin Delta



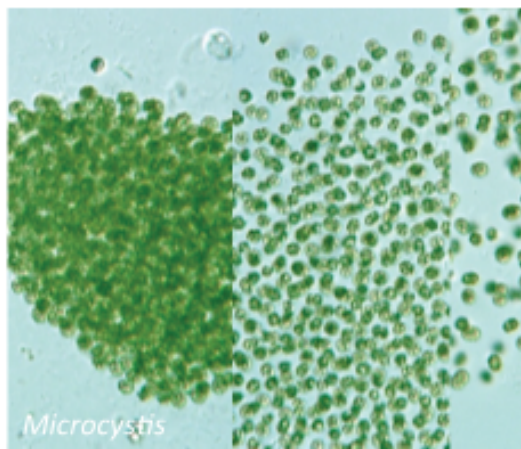
Anabaena



Aphanizomenon



Microcystis



Microcystis

Mine Berg
Martha Sutula

Southern California Coastal Water Research Project

SCCWRP Technical Report 869

Factors Affecting the Growth of Cyanobacteria with Special Emphasis on the Sacramento-San Joaquin Delta

**Prepared for:
The Central Valley Regional Water Quality Control Board
and
The California Environmental Protection Agency
State Water Resources Control Board
(Agreement Number 12-135-250)**

Mine Berg
Applied Marine Sciences

Martha Sutula
Southern California Coastal Water Research Project

August 2015
Technical Report 869

ACKNOWLEDGEMENTS

The authors of this document wish to thank the members of the Cyanobacteria Technical Advisory Group for their excellent review and discussion of this topic. This report was produced under California State Water Board contract to the Southern California Coastal Water Research Project (Agreement Number 12-135-250).

This report should be cited as:

Berg M and Sutula M. 2015. Factors affecting the growth of cyanobacteria with special emphasis on the Sacramento-San Joaquin Delta. Southern California Coastal Water Research Project Technical Report 869 August 2015.

EXECUTIVE SUMMARY

A world-wide increase in the incidence of toxin-producing, harmful cyanobacterial blooms (cyanoHABs) over the last two decades has prompted a great deal of research into the triggers of their excessive growth. Massive surface blooms are known to decrease light penetration through the water, cause depletion of dissolved oxygen following bacterial mineralization of blooms, and cause mortality of aquatic life following ingestion of prey with high concentrations of toxins. Additionally, humans coming in contact with the water may develop digestive and skin diseases, and it may affect the drinking water supply.

The Central Valley Regional Water Quality Control Board (Water Board) is developing a science plan to scope the science needed to support decisions on policies governing nutrient management in the Delta. Blooms of cyanoHABs are one of three areas, identified by the Water Board, that represent pathways of potential impairment that could be linked to nutrients. The Water Board commissioned a literature review of the factors that may be contributing to the presence of cyanoHABs in the Delta. The literature review had three major objectives:

- 1) Provide a basic review of biological and ecological factors that influence the prevalence of cyanobacteria and the production of cyanotoxins;
- 2) Summarize observations of cyanobacterial blooms and associated toxins in the Delta;
- 3) Synthesize literature to provide an understanding of what ecological factors, including nutrients, may be at play in promoting cyanobacterial blooms in the Delta.

This review had four major findings:

#1. Five principal drivers emerged as important determinant of cyanobacterial blooms in a review of the global literature on factors influencing cyanobacteria blooms and toxin production. These include: 1) Water temperature, 2) Water column irradiance and water clarity, 3) Stratified water column coupled with long residence times, 4) Availability of N and P in non-limiting amounts; scientific consensus is lacking on the importance of N: P ratios as a driver for cyanoHABs, and 5) Salinity regime.

#2. Existing information is insufficient to fully characterize the threat of CyanoHABs to Delta ecosystem services because cyanoHABs are not routinely monitored. Based on existing data, the current risk to Delta aquatic health is of concern and merits a more thorough investigation. This observation is based total microcystin levels found in Delta fish tissues that are within the range of sublethal effects to fish as recently reviewed by the California Office of Environmental Health Hazards (OEHHA 2009), and dissolved toxin concentrations that occasionally exceed both the OEHHA action level and the World Health Organization (WHO) guideline of 1000 ng L⁻¹ in certain “hotspots” of the Delta.

#3. Comprehensive understanding of the role of nutrients vis-à-vis other environmental factors in influencing cyanoHAB presence in the Delta is severely hampered by the lack of a routine monitoring program. Drawing on available information on the five factors influencing cyanoHABs, we can conclude the following:

- Temperature and irradiance appear to exert key roles in the regulation of the onset of blooms. Cyanobacteria require temperatures above 20°C for growth rates to be competitive with eukaryotic phytoplankton taxa, and above 25°C for growth rates to be competitive with diatoms. In addition, they require relatively high irradiances to grow at maximal growth rates.
- It appears that N and P are available in non-limiting amounts in the Delta; moreover, concentrations, or ratios, do not change sufficiently from year-to-year in order to explain year-to-year variation *Microcystis* biomass or occurrence. Therefore the initiation of *Microcystis* or other cyanoHAB blooms are probably not associated with changes in nutrient concentrations or their ratios in the Delta. However, as with all phytoplankton blooms, once initiated, cyanoHABs cannot persist without an ample supply of nutrients.
- Salinity is controlling the oceanward extent of cyanobacteria blooms in the Delta, but salinity gradients do not explain the spatial distribution of cyanoHABs in the Delta. Notably, salinity regime is not a barrier to toxin transport, as cyanotoxins have been detected in SF Bay.
- Turbidity, low temperatures, and higher flows during most of the year are likely restricting cyanobacteria blooms to the July-August time period.

#4. Climate change and anthropogenic activity associated with land use changes have the potential to alter cyanoHAB prevalence in the future. Climate change will likely result in warmer temperatures and increased drought, the latter of which could result in reduced flows, increased residence time and water column stability leading to higher light availability in the Delta. Both temperature and reduced flows would presumably result in a greater prevalence of cyanoHABs. It's noteworthy that phytoplankton biomass and primary productivity are depressed relative to available nutrients in the Delta, so it's unclear what the effect of modifying nutrient loads will have on frequency and intensity of cyanoHAB occurrence in the future.

Given these findings, two major science recommendations are proposed:

R1: Implement Routine Monitoring of CyanoHABs. DWR is currently conducting a monitoring program which routinely samples many of the variables of interest known to influence cyanoHABs. Comprehensive cyanoHAB monitoring should be added as a component to this program. To begin, a work plan should be developed which specifically scopes the needed changes in the program to comprehensively monitor cyanoHABs. This report details specific components that should be considered in this workplan. The workplan should also consider monitoring needed to develop and calibrate an ecosystem model to further investigate controls

on primary productivity and phytoplankton assemblage (see R2 below). The workplan should be peer-reviewed by subject matter experts. After an initial period of 3-5 years, the monitoring data should be used to comprehensively report on the status and trends of cyanoHABs and the factors that favor bloom occurrence in the Delta.

R2: Develop an Ecosystem Model of Phytoplankton Primary Productivity and HABs Occurrence to further Inform Future Risk and Hypotheses on Factors Controlling

CyanoHABs. Because nutrients are not currently limiting cyanobacterial blooms, it is critical that an improved understanding is gained of the factors that are controlling phytoplankton primary productivity in the Delta, since increased phytoplankton growth could lead to increased risk of cyanoHAB blooms. To inform management action moving into the future, an ecosystem model of phytoplankton primary productivity and HABs occurrence should be developed. This model should have the capability to provide information on primary productivity and biomass as well as planktonic food quality and transfer of carbon to higher trophic levels. To step into model development, three actions should be taken: 1) examine existing models already available to determine suitability for this task, 2) utilize existing data to explore, to the extent possible, the relationships between chlorophyll a, phytoplankton composition, climate variables *et al.* factors. This analyses should inform hypotheses that can be tested through model development as well as potential future scenarios, and 3) a work plan should be developed that lays out the modeling strategy, model data requirements, and implementation strategy.

TABLE OF CONTENTS

Acknowledgements	i
Executive Summary	iii
List of Tables	vii
List of Figures	viii
1. Introduction, Purpose and Organization of the Review	1
1.1 <i>Background and Context</i>	1
1.2 <i>Goal and Organization of Cyanobacterial Literature Review</i>	3
2. Basic Biology and Ecology of Cyanobacteria	4
2.1 <i>Overview</i>	4
2.2 <i>General Characteristics</i>	5
2.2.1 <i>Classification, Distribution and Akinete Production</i>	5
2.2.2 <i>Light Harvesting, Photosynthesis and Carbon Fixation</i>	7
2.2.3 <i>Buoyancy Regulation</i>	8
2.2.4 <i>Nitrogen Metabolism</i>	9
2.2.5 <i>Cellular Nitrogen:Phosphorus (N:P) Requirement</i>	13
2.2.6 <i>Toxin Production</i>	15
3. Factors Influencing Cyanobacterial Blooms and Toxin Production	21
3.1 <i>Salinity</i>	21
3.2 <i>Nutrient Concentrations and Ratios</i>	22
3.2.1 <i>Influence of N and P Loadings and Concentrations in Stimulating Cyanobacterial Growth</i>	22
3.2.2 <i>Influence of Changes in N:P Ratios on Stimulation or Limitation of Cyanobacterial Growth</i>	23
3.2.3 <i>Influence of Type of N on Growth of Cyanobacteria</i>	26
3.3 <i>Irradiance and Water Clarity</i>	27
3.4 <i>Factors Impacting Toxin Production and Degradation</i>	29
3.4.1 <i>Toxin Production</i>	29
3.4.2 <i>Toxin Degradation</i>	30
3.5 <i>Temperature</i>	31
3.6 <i>Stratification and Residence Time</i>	32
3.6.1 <i>Stratification</i>	32
3.6.2 <i>Residence Time</i>	33
3.7 <i>Other Factors</i>	33

4. Prevalence of CyanoHABs and Potential for Effects on Ecosystem Services in the Delta.....	34
4.1 Ecosystem Services	34
4.2 Prevalence and Trends of CyanoHABs in the Delta.....	35
4.2.1 Spatial Distribution of Microcystis throughout the Delta	35
4.2.2 Interannual variability in Microcystis biomass in the Delta.....	37
4.2.3 Microcystin toxin concentrations in the Delta and San Francisco Bay.....	39
4.2.4 Potential for CyanoHAB Risk to Delta Beneficial Uses.....	41
4.2.5 Summary of Potential for Adverse Effects on Delta Beneficial Uses	42
5.0 Synthesis of Factors Influencing CyanoHABs presence and Toxin Production in the Delta.....	43
5.1 Present and Future Factors associated with cyanoHAB prevalence in the Delta	43
5.1.1 Flow and mixing.....	43
5.1.2 Temperature.....	44
5.1.3 Water Clarity.....	46
5.1.4 Nutrient Concentrations	46
5.2 Summary.....	47
6.0 Recommendations	50
R1: Implement Routine Monitoring of CyanoHABs	50
R2: Develop an Ecosystem Model of Phytoplankton Primary Productivity and HAB Occurrences to further Inform Future Risk and Hypotheses on Factors Controlling CyanoHABs.....	51
7.0 Literature Cited.....	52
Appendix A	75
Appendix B	80
Appendix C	97

LIST OF TABLES

Table 2.1. Cyanobacterial groupings based on morphological traits. Adapted from Rippka <i>et al.</i> 1979.....	5
Table 2.2. Toxins produced by cyanobacteria. Based on data from Cox <i>et al.</i> 2005, Sivonen and Borner 2008, Cheung <i>et al.</i> 2013.	16
Table 2.3. Common cyanobacterial toxins. ND: Not determined.....	18
Table 4.1. Action levels developed by OEHHA (2009) for human health exposure to cyanotoxins compared with the WHO guidance level for microcystins and the EPA 10-day average exposure threshold.....	42
Table 5.1. Summary of general physiological drivers of cyanobacterial growth, how they are manifested in population growth and competition with diatoms, and how they compare with environmental drivers observed to be operating in the Delta.....	49

LIST OF FIGURES

Figure 1.1. The Sacramento-San Joaquin Delta Region.....	2
Figure 2.1. Akinetes of a) <i>Anabaena cylindrica</i> culture grown in medium without nitrogen; A=akinetete; H=heterocyst; V=vegetative cell (picture from Tomatini <i>et al.</i> 2006), b) <i>Anabaena lemmermanni</i> , and c) <i>Cylindrospermopsis raciborskii</i> in lake sediments under light microscopy and hybridized with probe under fluorescence microscopy; scale bar is 10µm (pictures from Ramm <i>et al.</i> 2012).....	7
Figure 2.2. Cellular N:P ratios (mole:mole) in different phytoplankton taxa. Dashed red line indicates the average phytoplankton cellular N:P ratio of 16, also called the Redfield ratio. Data from Hillebrand <i>et al.</i> 2013.	14
Figure 3.1. Conceptual model of factors affecting cyanobacteria blooms including warmer water, drought and decreased flow, decreased mixing, increased residence time, and increased N and P inputs from agricultural, industrial and urban sources. From Paerl <i>et al.</i> 2011.	21
Figure 3.2. Conceptual diagram of interaction of nutrient inputs, cycling processes, and limitation of primary production along the freshwater to marine continuum. From Pearl <i>et al.</i> 2014b.	23
Figure 3.3. Difference in growth rates of <i>Cylindrospermopsis raciborskii</i> when growth on NO ₃ ⁻ (red bars) versus NH ₄ ⁺ (blue bars) for eight different strains. Data from Saker and Neilan 2001 and Stucken <i>et al.</i> 2014.	27
Figure 3.4. Photosynthesis as a function of irradiance in three cyanoHAB species. Data from Wu <i>et al.</i> 2009.	28
Figure 3.5. Concentration of dissolved microcystin-LR equivalents in bioassays as a function of time after addition of purified microcystin (top panel) or lysed bloom material (bottom 3 panels) to lake water containing natural microbial assemblages. Shaded area corresponds with time period of degradation of 95% of original microcystin concentration. Data from Christoffersen <i>et al.</i> 2002.	31
Figure 3.6. Changes in growth rate with temperature for diatoms (red ± 0.35 d ⁻¹ , T _{opt} = 20 ± 1.8 °C), Chlorophytes (green ± 0.21 d ⁻¹ , T _{opt} = 29 ± 3.8), Cyanobacteria (cyan ± 0.13 d ⁻¹ , T _{opt} =29 ± 4.5) and dinoflagellates (orange ± 0.1 d ⁻¹ , T _{opt} = 21 ± 2.8). Data from Kudo <i>et al.</i> 2000, Butterwick <i>et al.</i> 2005, Yamamoto and Nakahara 2005, Boyd <i>et al.</i> 2013, Lurling <i>et al.</i> 2013.	32
Figure 4.1. The Sacramento-San Joaquin Delta Region. Red bubbles mark locations with greatest Microcystis-associated surface Chl a concentrations (largest bubble=0.55 µg Chl a L ⁻¹). Data from Lehman <i>et al.</i> 2005.	36
Figure 4.2. Interannual changes in surface Chl a due to abundance of Microcystis colonies. Means and standard deviations of 9 different stations in the San Joaquin River (Antioch (D12), Jersey Point (D16), Frank's Tract (D19), Potato Point (D26), Prisoners Point (D29), San Joaquin River at Turner Cut, Sand Mound Slough, Mildred Island, and Old River at Rancho del Rio (D28). Data from Lehman <i>et al.</i> 2005, 2013.	37

Figure 4.3. Comparison of environmental variables and Chl a in Clear Lake (Cyan) and the Delta (orange) using in-patch grab samples during the summer months of 2011. (A) Temperature, (B) Secchi disk depth, (C) Chl a. Data from Mioni <i>et al.</i> 2012.	38
Figure 4.4. Percent toxin-producing strains in <i>Microcystis</i> assemblage at stations AT, Antioch (D12); BI, Brannan Island (D23); MI, Mildred Island; and OR, Old River at Rancho del Rio (D28). Data from Baxa <i>et al.</i> 2010.....	39
Figure 4.5. Microcystin toxin concentrations determined with grab samples (blue/cyan) and with SPATT resin (red/orange) at three stations in Clear Lake, during and after a <i>Microcystis</i> bloom, and at one station (D12, Antioch) in the Delta. Data from Mioni <i>et al.</i> 2012.	40
Figure 5.1. Variation in flow at Brandt Bridge in the Delta (years 2009 and 2012) illustrating the low- and reverse-flow window in July-August (shaded grey). Data and plot from Spier <i>et al.</i> 2013.....	44
Figure 5.2. Deviation from the annual mean of maximum water temperatures at Stockton in the Central Delta. Grey shaded area indicates period from 1999 onwards with increased positive temperature deviations. Data from Brooks <i>et al.</i> 2011.....	45

1. INTRODUCTION, PURPOSE AND ORGANIZATION OF THE REVIEW

1.1 Background and Context

The Sacramento–San Joaquin River Delta, is an inland river delta and estuary approximately 1300 square miles in size, found in Northern California. Formed at the western edge of the Central Valley by the confluence of the Sacramento and San Joaquin Rivers, the Delta is a key component of the State’s water resource infrastructure and a region that is rapidly urbanizing, yet serves as critical habitat for fish, birds and wildlife. Water from the 45,000 square mile Delta watershed fuels both local and statewide economies, including important agricultural commodities. The Delta is widely recognized as in “crisis” because of human effects on the environment and competing demands for the Delta’s resources. The consequences of these competing demands include point and non-point discharges, habitat fragmentation and loss, modified flow regimes, introduction of non-native species, all of which combine to threaten ecosystem health, including the continued decline of threatened and endangered species

In 2009 the California legislature passed the Delta Reform Act creating the Delta Stewardship Council. The mission of the Council is to implement the coequal goals of the Reform Act and provide a more reliable water supply for California while protecting, restoring, and enhancing the Delta ecosystem. The Council wrote and adopted a Delta Plan in 2013 to implement these goals. Chapter 6 of the Delta Plan deals with water quality and contains recommendations to implement the coequal goals of the Delta Reform Act. Recommendation # 8 states, in part, “...the State Water Resources Control Board and the San Francisco Bay and Central Valley Regional Water Quality Control Boards (Water Board) should prepare and begin implementation of a study plan for the development of objectives for nutrients in the Delta ... by January 1, 2014. Studies needed for development of Delta... nutrient objectives should be completed by January 1, 2016. The Water Boards should adopt and begin implementation of nutrient objectives, either narrative or numeric, where appropriate, in the Delta by January 1, 2018. Potential nutrient related problems identified in the Delta Plan for evaluation are:

- 1) Decreases in algal abundance and shifts in algal species composition,
- 2) Increases in the abundance and distribution of macrophytes, including water hyacinth and Brazilian waterweed,
- 3) Increases in the magnitude and frequency of cyanobacterial blooms

To provide better scientific grounding for the study plan, the Water Board commissioned two literature reviews centered on these three potential areas of impairment. This document provides a synthesis of literature on cyanobacterial blooms in the Delta. Technical Advisory Group and Stakeholder comments on the review are provided in Appendices B and C, respectively.

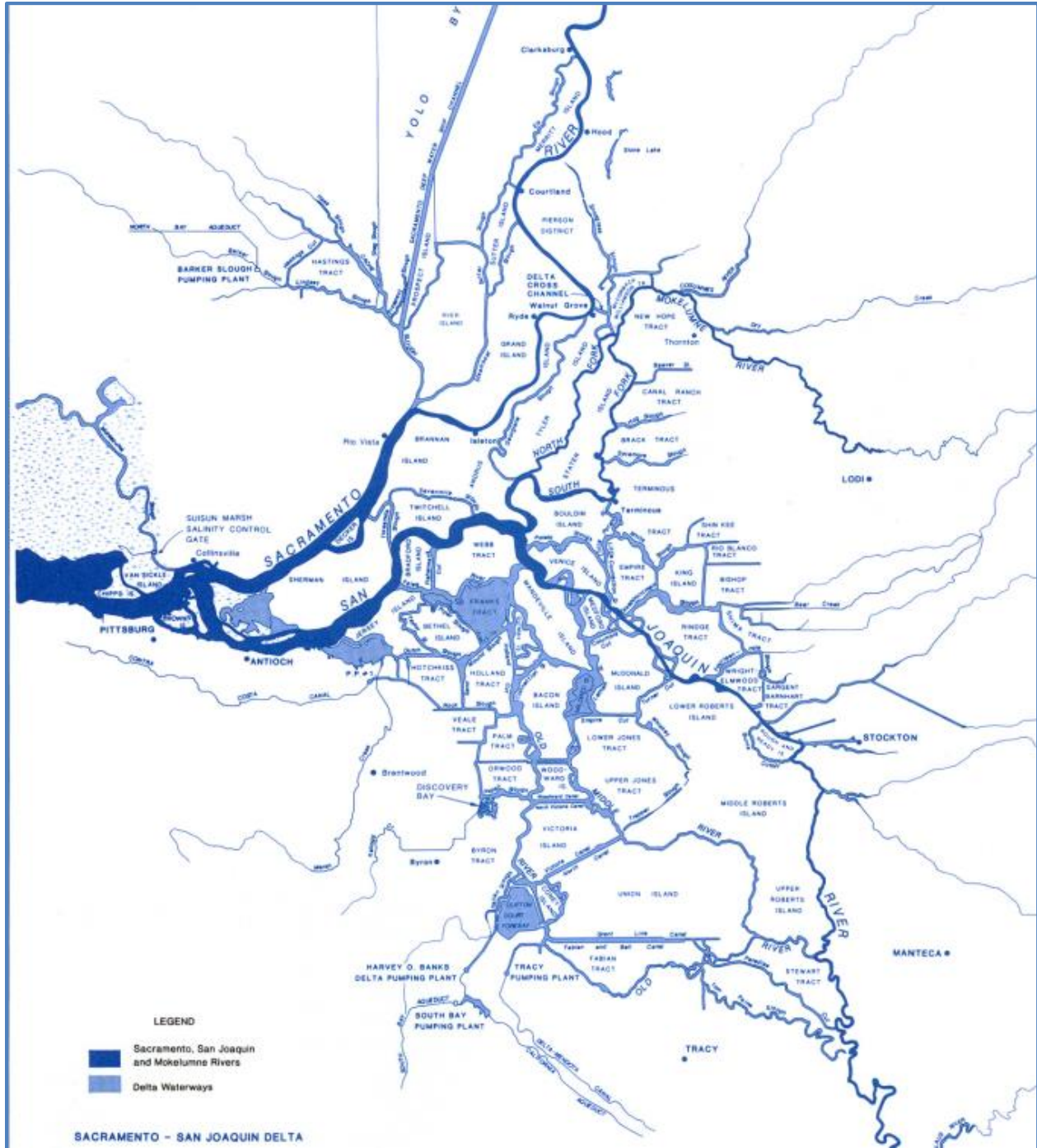


Figure 1.1. The Sacramento-San Joaquin Delta Region.

1.2 Goal and Organization of Cyanobacterial Literature Review

The goal of the cyanobacterial literature review is to synthesize available information to provide insight into cyanobacterial blooms in the Delta. The review had three major objectives:

- 1) Provide a basic review of biological and ecological factors that influence the prevalence of cyanobacteria and production of cyanotoxins;
- 2) Summarize observations of cyanobacteria blooms and associated toxins in the Delta;
- 3) Synthesize literature to provide an understanding of what ecological factors, including nutrients, may be at play in promoting cyanobacteria blooms in the Delta.

This review, and the recommended next steps, will contribute to a science plan to determine whether or how to proceed with the development of nutrient objectives for the Delta. The document is organized as follows:

Section 1: Introduction, Purpose and Organization of the Review

Section 2: Basic Biology and Ecology of Cyanobacteria

Section 3: Factors Influencing Cyanobacterial Blooms and Toxin Production

Section 4: Prevalence of CyanoHABs and Potential for Effects on Ecosystem Services in the Delta

Section 5: Synthesis of Factors Influencing CyanoHABs Presence and Toxin Production in the Delta

Section 6: Recommendations

Section 7: Literature Cited

2. BASIC BIOLOGY AND ECOLOGY OF CYANOBACTERIA

2.1 Overview

Cyanobacteria are a versatile group of bacteria that were the ancient colonizers of Earth and the photosynthetic ancestors of chloroplasts in eukaryotes such as plants and algae. As pioneers of photosynthesis, cyanobacteria were responsible for oxygenating Earth's atmosphere 2.5 billion years ago. In addition to being photosynthetic, cyanobacteria can differentiate into specialized cell types called heterocysts and fix nitrogen (N), exhibit gliding mobility, and tolerate a wide range of temperatures as evidenced by their ability to thrive in hot springs and ice-covered Antarctic lakes. Cyanobacteria also produce an array of bioactive compounds, some of which possess anti-microbial, anti-cancer and UV protectant properties. However, a subset of these bioactive compounds is highly toxic to humans and wildlife.

Blooms of cyanobacteria that produce these toxins, collectively known as harmful cyanobacterial algal blooms (cyanoHABs), has garnered a great deal of attention due to their increased occurrence in recent decades (Chorus and Bartram 1999, Carmichael 2008, Paerl and Huisman 2008, Hudnell 2010). The geographical distribution of these blooms has also increased with blooms appearing in areas previously unaffected (Lehman *et al.* 2005, Lopez *et al.* 2008). CyanoHABs can have major negative impacts on aquatic ecosystems. Toxins produced by cyanobacteria can lead to mortality in aquatic animals, waterfowl and domestic animals (Havens 2008, Miller *et al.* 2010). Moreover, toxins in drinking water supplies can pose a variety of adverse health effects and therefore require expensive treatment options such as filtration, disinfection, and adsorption with activated carbon (Cheung *et al.* 2013). In addition to the threat of toxins, oxygen depletion due to organic matter decomposition following the die-off of blooms can result in massive fish kills. CyanoHABs can also lead to revenue losses and impact local economies by reducing business in affected water bodies during the peak of tourism season. Considerable costs are associated with mitigation of blooms and lake restoration (Dodds *et al.* 2009).

The San Francisco Bay Delta is an area where cyanoHABs were previously undetected but have become commonplace since early 2000 (Lehman *et al.* 2005). In addition to providing a home for several species of pelagic fish and other wildlife, the Delta serves as a critical source of drinking water, and freshwater for irrigation of farms, to communities locally as well as farther south including the Los Angeles Metropolitan Water District. In concert with the occurrence of cyanoHABs, concentrations of the toxins they produce have been detected in the water and in higher trophic levels including zooplankton and fish (Lehman *et al.* 2010). The purpose of the following sections summarizes the basic biology of cyanobacteria beginning with classification, light harvesting, carbon metabolism, buoyancy regulation, nitrogen metabolism, cellular N:P ratios and toxin production, in order to build fundamental concepts that are later utilized in the review.

2.2 General Characteristics

2.2.1 Classification, Distribution and Akinete Production

Classification

Traditionally, morphological traits have been used to subdivide the cyanobacteria into five subgroups (Rippka *et al.* 1979). The major division is between cyanobacteria that are single celled and/or colonial and those that grow filaments (Table 2.1). Each category contains a mixture of marine and freshwater species. In the former category are the Group I Croococcales including the freshwater *Microcystis* and *Synechocystis*, and the marine *Synechococcus* and *Prochlorococcus*. Group II Pleurocapsales include *Pleurocapsa* and *Xenococcus* (Table 2.1). The filamentous algae, Groups III, IV, and V, are further subdivided into the Oscillatoriales that produce only vegetative cells, including the freshwater planktonic *Planktothrix* species, the benthic *Oscillatoria* and *Lyngbya* species, as well as the marine *Trichodesmium* sp. (Table 2.1). Group IV, the Nostocales, contain filamentous algae that differentiate into heterocysts and fix N₂. This group includes *Aphanizomenon*, *Anabaena*, *Nostoc* and *Cylindrospermopsis* (Table 2.1). Additionally, the Nostocales is known for differentiation into resting cells called akinetes during unfavorable conditions. Group V, the Stigonematales include species with filaments that grow in complex branching patterns.

Table 2.1. Cyanobacterial groupings based on morphological traits. Adapted from Rippka *et al.* 1979.

Croococcales Unicellular, reproduce by binary fission		GROUP 1	<i>Gloeotheca</i> (N) <i>Microcystis</i> <i>Prochlorococcus</i> <i>Prochloron</i>	<i>Synechococcus</i> <i>Synechocystis</i>
Pleurocapsales Unicellular, reproduce by multiple fission		GROUP 2	<i>Pleurocapsa</i> <i>Staniera</i> (N) <i>Xenococcus</i> (N)	
Filamentous chain (trichome) forming; reproduce by random trichome breakage, hormogonia, germination of akinetes	Trichome composed of vegetative cells	Oscillatoriales 1 plane division GROUP 3	<i>Lyngbya</i> (N) <i>Oscillatoria</i> (N) <i>Phormidium</i> <i>Prochlorothrix</i> <i>Trichodesmium</i> (N)	
	In the absence of fixed N, trichome contains heterocysts; some produce akinetes	Nostocales 1 plane division GROUP 4	<i>Aphanizomenon</i> <i>Anabaena</i> <i>Cylindrospermum</i> <i>Nodularia</i> <i>Nostoc</i>	
		Stigonematales Division in more than 1 plane GROUP 5	<i>Chlorogleopsis</i> <i>Fisherella</i>	

It was originally thought that N₂ fixation primarily existed in the Nostocales which had the ability to differentiate into heterocyst cells. More recent investigations tracking the *nifD* and *nifH* gene diversity has uncovered that N₂ fixation occurs in a range of unicellular, non-filamentous cyanobacteria dispersed throughout the five original groups first proposed by Rippka *et al.* (1979). These species are indicated by an (N) after their name in Table 2.1. Depending on which functionality of the cyanobacteria is emphasized, recent gene-based groupings of cyanobacteria have created as many as ten different sub-categories (Turner *et al.* 1999, Tomatini *et al.* 2006). However, there appears to exist no general consensus over the best manner in which to categorize the cyanobacteria based on functionality and marker genes. Most cyanobacteria are planktonic and are dispersed throughout the five groups. The benthic cyanobacteria are found mainly in the Oscillatoriales subgroup. The toxic cyanoHAB-forming cyanobacteria are mostly freshwater planktonic species dispersed throughout groups I, III and IV and include the N₂ fixing genera *Anabaena*, *Aphanizomenon*, *Cylindrospermopsis*, and *Nodularia*; the benthic N₂ fixing genera *Lyngbya* and some *Oscillatoria*; and the non-N₂ fixing genera *Microcystis* and *Planktothrix* (Paerl and Paul 2012).

Akinete formation

Akinetes are the resting cells produced by the Nostocales in order to survive adverse environmental conditions such as cold and desiccation (Tomatini *et al.* 2006). Akinete cells maintain low levels of metabolic activity (Thiel and Wolk 1983, Sukenik *et al.* 2007), are dispersed in sediments (Baker 1999, Kim *et al.* 2005, Rucker *et al.* 2009), and are distinguishable from vegetative cells by their larger size (Figure 2.1). They germinate in response to improved environmental conditions such as light and temperature (Baker and Bellifemine 2000, Karlsson-Elfgren *et al.* 2004, Yoshimasa and Nakahara 2005, Kaplan-Levy *et al.* 2010) and provide an inoculum of Nostocales vegetative cells to the water column from the sediments where the akinete “seed bank” may remain viable for decades (Stockner and Lund 1970, Livingstone and Jaworski 1980). Therefore, eradication of Nostocales from a system once it has become “infected” is very difficult.

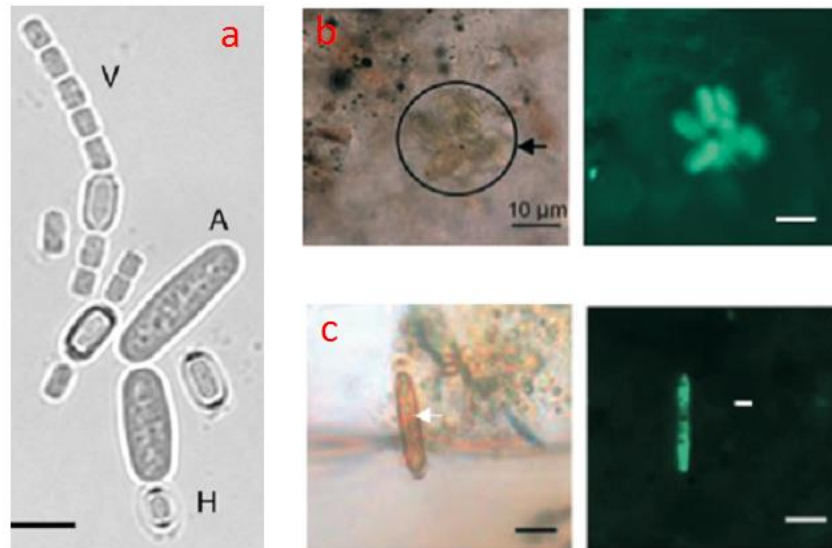


Figure 2.1. Akinetes of a) *Anabaena cylindrica* culture grown in medium without nitrogen; A=akinete; H=heterocyst; V=vegetative cell (picture from Tomatini *et al.* 2006), b) *Anabaena lemmermanni*, and c) *Cylandrospermopsis raciborskii* in lake sediments under light microscopy and hybridized with probe under fluorescence microscopy; scale bar is 10µm (pictures from Ramm *et al.* 2012).

2.2.2 Light Harvesting, Photosynthesis and Carbon Fixation

Cyanobacteria are distinct from all other algae in that most of them possess two light harvesting systems (as opposed to one). Maintaining two light harvesting system is costly in terms of protein and N requirements and manifests strongly in their cell biology. For example, the extra protein requirement means that cyanobacteria have a high tissue nitrogen:phosphorus (N:P) ratio and a high N requirement for growth (discussed below). Despite this, light harvesting is necessary in photosynthetic organisms to 1) collect light energy from the sun and 2) convert it to chemical energy in the form of electrons and ATP that can be used to power carbon fixation.

Light harvesting pigments and photosynthesis

Light harvesting is performed by chlorophyll *a* (Chl *a*) pigment molecules that are associated with two photosystems (PSI and PSII) that comprise the centers of the photosynthetic process which starts with the liberation of an electron from the splitting of water and ends with the production of ATP. Sitting in each of the photosystems is a specialized Chl *a* molecule that initiates the flow of electrons through the electron transport chain that eventually powers ATP synthesis. The other Chl *a* molecules, 40 and 90, together with 12 and 22 carotenoid pigment molecules, in PSI and PSII respectively, funnel light energy to the reaction core (DeRuyter and Fromme 2008). This complex of Chl *a* and carotenoid pigment molecules, coordinated by a large number of proteins, is very similar in its structure to the light-harvesting complex (LHC)

embedded into the thylakoid membranes of vascular plants and eukaryotic phytoplankton (Fromme *et al.* 2001, 2002).

What makes the cyanobacteria unique is that they have a second light harvesting antenna complex peripheral to the thylakoid membrane that is water soluble (e.g. not membrane bound). This pigment complex, comprised of pigmented proteins arranged in rods fanning out from a core attached to the thylakoid membrane, called the phycobilisome (PBS), is what gives cyanobacteria their name (Grossman *et al.* 1993, Grossman 2003). Similar to the carotenoid pigments mentioned above, the PBS chromophores absorb light inbetween the Chl *a* absorption peaks of 440nm and 670nm (Grossman *et al.* 1993). Interestingly, the PBS proteins are not exclusive to cyanobacteria; they also occur in photosynthetic eukaryotes.

Up to 50% of cyanobacterial cellular protein content is bound in the PBS complex taking a large proportion of the cell's resources, particularly its nitrogen (N) allocation. Therefore, under stress condition such as N starvation, the entire PBS can be degraded within a few hours and the N can become reused within the cell (Sauer *et al.* 1999). When conditions improve, the PBS will be re-synthesized and re-assembled (Collier and Grossman 1994, Grossman *et al.* 2001).

Carbon fixation

The ATP produced and the electrons liberated during photosynthesis are used to power the fixation of carbon into sugars in the Calvin Cycle. They are also used to reduce oxidized sources of N to ammonia during N assimilation (discussed below). The primary and rate-limiting enzyme in carbon fixation is Rubisco which catalyzes the first step in the Calvin Cycle. To deal with the rate-limiting nature of Rubisco, cyanobacteria have evolved specialized structures called carboxysomes. In addition to housing Rubisco, the carboxysomes contain a number of other enzymes that help concentrate CO₂ in its vicinity to speed its reaction rate (Kaplan and Reinhold 1999). Cyanobacteria fix carbon to provide the skeletons needed to assimilate N into amino acids and build protein and cellular biomass; fixed carbon can also be used to accumulate carbohydrate storage products (carbohydrate ballasting) in order to make the cell heavier during buoyancy regulation.

2.2.3 Buoyancy Regulation

One distinct advantage of many cyanobacterial genera such as *Microcystis*, *Planktothrix*, *Anabaena* and *Aphenizomenon* is their ability to regulate their buoyancy by a combination of producing gas vesicles and carbohydrate storage products (Oliver 1994, Beard *et al.* 1999, Brookes *et al.* 1999). The former renders them positively buoyant whereas the latter does the opposite (Walsby 1994, 2005). The carbohydrate storage products are derived from C-fixation and the amount produced varies depending on the species and on irradiance (Howard *et al.* 1996, Visser *et al.* 1997, Wallace and Hamilton 1999). At an irradiance that is specific to each species and strain, the amount of carbohydrate storage product will perfectly balance the upward lift

created by the gas vesicles and the cyanobacteria will become neutrally buoyant (Walsby *et al.* 2004). In addition to producing and storing the carbohydrates, cyanobacteria also consume the storage products to produce energy.

By regulating the amount of carbohydrate storage products consumed, cyanobacteria control their vertical position in the water column (Thomas and Walsby 1985, Konopka *et al.* 1987, Wallace and Hamilton 1999). Models demonstrate that filamentous cyanobacteria can sink or float at speeds up to 0.3 m per day in order to position them at a depth where irradiance is such that it maximizes their growth potential (Walsby 2005). These speeds are only achievable for filaments of a certain size and weight; picocyanobacteria and small filaments do not have enough momentum to respond by vertical repositioning to changes in irradiance (Walsby 2005). Of course, carbohydrate production, therefore buoyancy regulation, is affected by nutrient availability; nitrogen starved cells have excess carbohydrate stores and tend to lose buoyancy more easily than nutrient sufficient cells (Klemer *et al.* 1982, Brookes *et al.* 1999, Brookes and Ganf 2001).

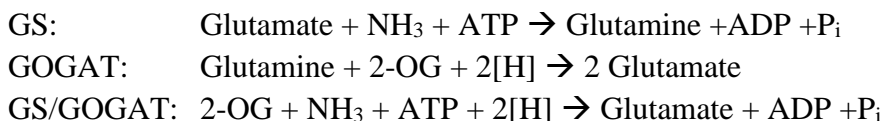
2.2.4 Nitrogen Metabolism

Cyanobacteria use a wide variety of N sources for growth including ammonium (NH_4^+), nitrate (NO_3^-), nitrite (NO_2^-), urea, amino acids, cyanate, and several species are also capable of dinitrogen gas (N_2) fixation to satisfy their cellular N demand. Below we discuss the pathways of N transport, metabolism and assimilation, and their regulation.

Ammonium transport and assimilation of N into amino acids

Being a charged molecule, NH_4^+ cannot diffuse freely into the cell and has to be transported via active transport. Transport of NH_4^+ into cyanobacteria (as well as in eukaryotic algae) occurs via the Amt family of transporters. These transporters are either expressed constitutively or differentially depending on external N concentrations. At environmental concentrations, most of the NH_4^+ is transported into the cell via the high-affinity transporter Amt1 encoded by the gene *amt1* (Muro-Pastor *et al.* 2005).

Before it can be assimilated, all N sources, whether N_2 , NO_3^- or organic N containing molecules, first have to be converted to NH_4^+ . The NH_4^+ is then assimilated into amino nitrogen through the GS/GOGAT pathway. The primary NH_4^+ assimilating enzymes in cyanobacteria (as well as in vascular plants and eukaryotic algae) are glutamine synthetase (GS) and glutamate synthase (also called glutamine-2-oxoglutarate-amido transferase, GOGAT) acting in concert to aminate 2-oxoglutarate (2-OG). Photosystem I (PSI)-reduced ferredoxin (Fd_{red}) is typically used as a reductant in this reaction:



An alternate route of NH_4^+ assimilation involves the enzyme glutamate dehydrogenase (GDH) but it's postulated that this occurs only during select conditions such as stationary growth:



In all photosynthetic cells the link between the carbon (C) and N cycles in the cell occurs at the GS/GOGAT reactions because the two key ingredients in N assimilation is 1) 2-OG derived from carbon fixation, and 2) Fd_{red} derived from PSI. GOGAT (and also GDH) will not proceed without their presence, which avoids wasteful consumption of glutamine, and ensures that even in the presence of excess N, assimilation will not proceed unless an adequate supply of C skeletons is available (Flores and Herrero 2005, Muro-Pastor *et al.* 2005).

Nitrate transport and reduction to NH_4^+

As NO_3^- is also a charged molecule it's transported into the cell via active transport. Cyanobacteria use two different transport systems. Most freshwater species, including *Anabaena*, *Synechocystis* and *Gloebacter*, use the high affinity ATP-binding cassette (ABC) transporter NrtABCD (Flores *et al.* 2005). Most marine species (*Synechococcus* and others) take up NO_3^- and NO_2^- via the major facilitator superfamily transporter NrtP, also a high-affinity transporter (Flores *et al.* 2005). Some species also have a NO_2^- -specific transporter NIT (Maeda *et al.* 1998). Nitrate uptake is tightly regulated by the external concentration of NH_4^+ ; when NH_4^+ becomes available, cells cease NO_3^- uptake and switch to use NH_4^+ which is preferred. This process is regulated at the level of NO_3^- uptake (Flores and Herrero 1994). In addition, CO_2 -fixation (regulated by irradiance) is required to maintain active NO_3^- uptake, a regulatory link that ensures that the product of NO_3^- reduction (ammonium) can be incorporated into carbon skeletons (Luque and Forchhammer 2008).

Reduction of NO_3^- to NH_4^+ is a two-step process catalyzed by the enzymes nitrate reductase (NR) and nitrite reductase (NiR). The power for the reduction reaction, in the form of 2 electrons for NR and 6 electrons for NiR, is provided by Fd_{red} via PSI providing a strong link between the light reactions and NO_3^- use by the cell (Flores *et al.* 2005).

In cyanobacteria, the genes encoding NR, narB, and Nir, nirA, and the NO_3^- transporter NrtP, are typically clustered in the same operon. An operon is a unit that tells the cells to transcribe a sequence of genes simultaneously. In cyanobacteria, the transcription of operons associated with N metabolism is tightly regulated by the transcription factor NtcA (discussed below).

The only cyanobacteria discovered to date that is not able to use NO_3^- is *Prochlorococcus* which lives in the open ocean. While it was initially thought that some species could assimilate NO_2^- , sequencing of their genomes demonstrates that they all lack the *nirA* genes and therefore cannot reduce NO_2^- (Garcia-Fernandez *et al.* 2004).

Urea transport and metabolism

Many, but not all, cyanobacteria can use urea as a source of N for growth. Because urea is not a charged molecule it diffuses freely into the cell; however, environmental concentrations are not such that diffusion can supply the needed concentration of urea for the urease enzyme (based on its K_m). Both in freshwater and marine cyanobacteria, an ABC-type active transport system specific for urea has been identified (Valladares *et al.* 2002). The subunits of this transporter are encoded by the five genes *urtA-E*. In *Anabaena*, the urea transporter genes are in the same NtcA-activated promoter and subject to metabolic repression by NH_4^+ (Valladares *et al.* 2002). Urea is metabolized to two molecules of NH_3 and CO_2 by the enzyme urease, also called urea amidohydrolase (Mobeley *et al.* 1995). The urease enzyme is well-conserved throughout the bacteria and eukaryotic organisms and consists of two small and one large subunit encoded by at least seven genes, three which encode the structural subunits (*ureA*, *ureB*, *ureC*) and the other four (*ureD*, *ureE*, *ureF*, *ureG*) encoding accessory polypeptides required for the assembly of the nickel metallocenter (Collier *et al.* 1999, Palinska *et al.* 2000).

Amino acid transport

All cyanobacteria tested to date have at least one transport system for amino acids. These transporters appear to have broad specificity (i.e. they can transport more than one type of amino acid) and different species have different combinations of transporters (Herrero and Flores 1990, Montesinos *et al.* 1997). For example, freshwater *Synechocystis* sp. has four different amino acid transporters, including the ABC transporter Nat for glutamine and histidine, the ABC transporter Bgt for basic amino acids, and two glutamate-specific transporters GHS and Gtr (Quintero *et al.* 2001). Once in the cell, cyanobacteria possess a variety of deaminase enzymes that can deaminate the amino acids to NH_3 which then enters the GS/GOGAT pathway.

Cyanate transport and metabolism

Cyanobacteria, including freshwater and marine species, can use cyanate (a toxin) as a N source for growth since they have the genes encoding a transporter (*cynA*, *cynB*, *cynC*) and the gene encoding the cyanase enzyme (*cynS*) which hydrolyzes cyanate to NH_3 and CO_2 (Kamennaya and Post 2011). In freshwater cyanobacteria, these genes are repressible by NH_4^+ suggesting that they are under NtcA regulation.

Nitrogen fixation

Arguably the most expensive (energetically speaking) source of N for cyanobacteria is molecular dinitrogen gas (N_2). Nitrogen fixation, the process of reducing N_2 to NH_3 , is catalyzed by the nitrogenase enzyme. The nitrogenase has two subunits. The first is the dinitrogenase subunit which catalyzes the reduction of N_2 to NH_4^+ , composed of the NifD and NifK polypeptides encoded by the *nifD* and *nifK* genes. The dinitrogenase contains an iron-molybdate active site and two iron-sulfur clusters. The second is the dinitrogenase reductase subunit (NifH polypeptide

encoded by the *nifH* gene) which contains a central iron-sulfur cluster whose function it is to donate electrons derived from ferredoxin to dinitrogenase. Reduction of N₂ to NH₃ requires 8 electrons and 15 molecules of ATP in the following reaction:



It was recently discovered that under conditions of molybdate limitation, some *Anabaena* species express an alternative nitrogenase containing a vanadium-iron cofactor instead of the molybdate-iron cofactor (Thiel 1993, Boison *et al.* 2006). Both these variants require iron cofactors to function and N₂ fixation cannot proceed under iron-limiting conditions.

The nitrogenase enzyme is very sensitive to oxygen (O₂), and O₂ is evolved as a byproduct of the water-splitting reactions at photosystem II (PSII), requiring the nitrogenase enzyme to be kept separate from PSII. Accordingly, freshwater cyanobacteria have evolved heterocysts (Wolk *et al.* 1994). These are specialized cells where PSII is inactivated, the PBS antenna proteins are degraded, and energy to power the cell is derived from cyclic electron flow around PSI. Rates of respiration in these cells are also high to scavenge any O₂. The ATP and reductant needed for N₂ reduction is generated by carbohydrate metabolism inside the heterocyst. The carbohydrate is synthesized in the non-heterocyst, vegetative cells flanking the heterocyst and transported inside. In turn, NH₃ produced inside the heterocyst is exported to the vegetative cells in the form of amino acids (Wolk *et al.* 1994). However, many species of cyanobacteria that fix N₂ do not form heterocysts; these species either separate N₂ fixation from photosynthesis in time (e.g. by fixing N₂ at night such as *Lyngbya aestuarii* and *Crocospaera watsonii*) or in different regions of filaments as is hypothesized to be the case for *Trichodesmium* sp. (Frederiksson and Bergman 1997).

Because nitrogen fixation is such an energy expensive process, from the formation of the heterocysts to the reduction of N₂, it is tightly regulated by NtcA and is only induced under N starvation and in the absence of any other fixed N source (Herrero *et al.* 2004).

Regulation of nitrogen metabolism

As evident from the preceding sections, the transcription factor NtcA (encoded by the gene *ntcA*) regulates most of the cyanobacterial genes associated with nitrogen uptake and assimilation, and is therefore considered the master regulator of N metabolism (Herrero *et al.* 2004). NtcA binds to and activates the operons for heterocyst differentiation, N₂ fixation, NO₃⁻ uptake and reduction, urea uptake and hydrolysis, and glutamine synthetase to mention a few. In other words, none of the genes related to N metabolism are transcribed and their enzymes synthesized unless NtcA binds to their promoter in the genome (Luque *et al.* 1994, Wei *et al.* 1994, Forchammer 2004, Luque and Forchammer 2008). The exception to this rule are some NH₄⁺ transport proteins which are not under NtcA control and are transcribed constitutively, i.e.

always “on” (Herrero *et al.* 2001). NtcA also controls signaling proteins that fine-tune cellular activities in response to fluctuating C/N conditions (Herrero *et al.* 2001).

NtcA is under negative control by NH_4^+ , meaning that when NH_4^+ is detectable by the cell, *ntcA* gene transcription is repressed (Herrero *et al.* 2001, Lindell and Post 2001). There is an inverse relationship between NH_4^+ concentration and *ntcA* expression in all cyanobacteria tested to date, with basal levels of *ntcA* expression observed in the presence of high external NH_4^+ concentrations and maximal levels of *ntcA* expression observed under N starvation (Frias *et al.* 1994, Lindell *et al.* 1998, Lee *et al.* 1999, Sauer *et al.* 1999, Lindell and Post, 2001). Ammonium regulates expression of *ntcA* via 2-OG which is synthesized in the Calvin cycle and consumed in the GS/GOGAT cycle. Thus 2-OG is at the crossroads between C and N metabolism and is ideally suited to “sense” NH_4^+ concentrations (Vazquez-Bermudez *et al.* 2002, Tanigawa *et al.* 2002, Forchhammer 2004).

The repression of *ntcA* expression by NH_4^+ places NH_4^+ at the top of the hierarchy of N substrates utilized and assimilated by cyanobacteria. The order in which N substrates other than NH_4^+ is assimilated differs depending on species. For example, in N_2 fixing cyanobacteria, NH_4^+ represses both N_2 fixation and NO_3^- assimilation. Nitrate, in turn, represses N_2 fixation. Therefore N_2 fixation is at the bottom of the hierarchy in some cyanobacteria (Ramasubramanian *et al.* 1994). But in others such as marine *Trichodesmium* sp., NO_3^- does not repress N_2 fixation genes and the process of N_2 fixation is on a more even footing with NO_3^- assimilation (Post *et al.* 2012).

2.2.5 Cellular Nitrogen:Phosphorus (N:P) Requirement

In 1958 Redfield published his discovery that phytoplankton particulate matter was composed of N and P in a molar ratio of 16, similar to the ratio of dissolved N:P in the water (Redfield 1958). Redfield suggested that the ratio of dissolved N:P in the ocean was driven by the remineralization of phytoplankton particulate matter, a theory which has since taken hold (Falkowski 2000, Geider and LaRoche 2002). Given that the average N:P ratio was discovered to be 16 in phytoplankton, it was deduced that under nutrient limiting conditions phytoplankton would become limited by N at dissolved N:P less than 16 and limited by P at dissolved N:P ratios greater than 16.

Shortly after Redfield’s discovery of the universality of the N:P ratio of 16, investigators turned to phytoplankton cultures to examine how closely phytoplankton cellular N:P ratios varied around 16. Parsons *et al.* (1961) published the first investigation demonstrating variability in cellular N:P ratios depending on the phytoplankton species. Subsequent investigations noted that diatoms and dinoflagellates tended to have cellular N:P ratios below 16 whereas chlorophytes and cyanobacteria typically had ratios above 25 (Geider and LaRoche 2002; Ho *et al.* 2003; Quigg *et al.* 2003; Klausmeier *et al.* 2004; Hillebrand *et al.* 2013; Figure 2.2). This difference

among the taxa stems from slight variations in macromolecular composition of the phytoplankton, principally in their ratio of protein, the largest store of N in the cell, to nucleic acids, the largest store of P in the cell (Terry *et al.* 1985, Falkowski 2000, Elser *et al.* 2000, Geider and LaRoche 2002). As mentioned above in section 2.2.2, cyanobacteria have two light-harvesting complexes requiring a greater association of proteins with the light-harvesting pigments compared with eukaryotic cells which only have one light harvesting complex (Raven 1984, Geider and LaRoche 2002). The “excess” protein associated with the peripheral phycobilisomes substantially increase the cellular N:P ratios of cyanobacteria. Once it was realized that there were significant departures in the cellular N:P ratio depending on taxa, it also became clear that the ratio of N:P uptake differed with respect to taxa and that this was a major basis of resource-based competition among taxa (Rhee 1978). That phytoplankton take up N:P in proportion to their tissue composition was subsequently confirmed in culture experiments (Droop 1974, Elrifi and Turpin 1985, Tett *et al.* 1985, Quigg *et al.* 2003, Leonardos and Geider 2004). In other words, phytoplankton do not take up nutrients according to the ratio that occurs in water, but rather the ratio dictated by the macromolecular composition of their tissues.

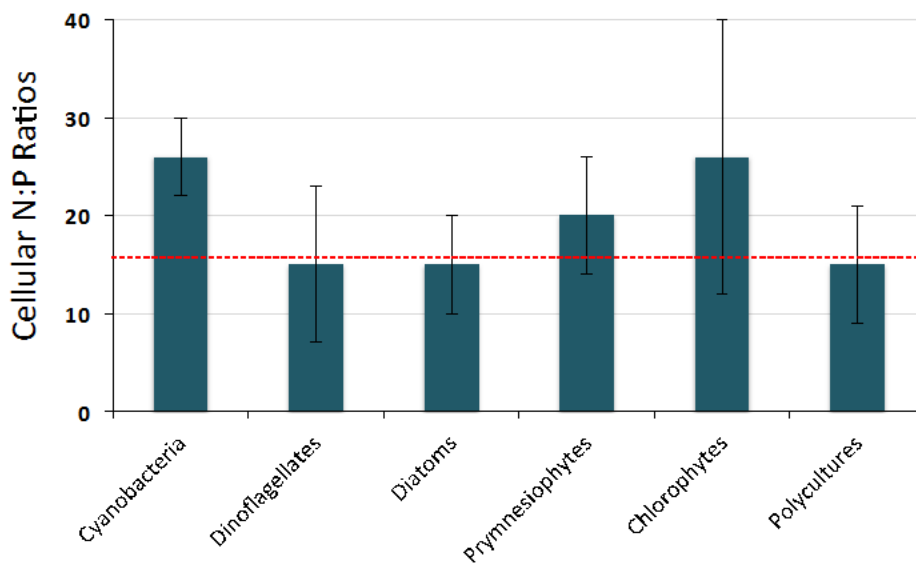


Figure 2.2. Cellular N:P ratios (mole:mole) in different phytoplankton taxa. Dashed red line indicates the average phytoplankton cellular N:P ratio of 16, also called the Redfield ratio. Data from Hillebrand *et al.* 2013.

Tissue N:P composition is not a fixed trait and phytoplankton are able to adjust it, within certain limits, in order to keep growing when environmental conditions change for the suboptimal. When limited for a nutrient, uptake of the non-limiting nutrient can proceed for a while skewing cellular ratios. But, severe limitation by one nutrient will eventually prevent the uptake of the other, non-limiting nutrient, even when the other is present in excess. This quirk of nature

constrains the extent to which cellular ratios vary (Droop 1974, Tett *et al.* 1985, Leonardos and Geider 2004, Hillebrand *et al.* 2013). For example, a summary of nearly 50 phytoplankton studies demonstrates that the N:P ratio of P-limited phytoplankton converge around 28 and the N:P ratio of N-limited phytoplankton converges around 16 (Hillebrand *et al.* 2013).

Irradiance may also change the cellular N:P ratio through its influence on the cellular protein content (LaRoche and Geider 2002). Pigments (Chl *a* and light harvesting antenna pigments) are bound in pigment-protein complexes rich in N that increase as irradiance decreases, and decrease under high light as cells reduce the size of the light harvesting complex to avoid photodamage (Wynne and Rhee 1986, Falkowski and LaRoche 1991, Nielsen 1992, Leonardos and Geider 2004). The irradiance-dependent change in N:P ratios is even more pronounced among cyanobacteria due to the greater association of protein with the phycobilisome than in the eukaryotic light harvesting complex (Raven 1984, Geider and LaRoche 2002).

In contrast with limiting nutrient concentrations or changes in irradiance, changes in the medium N:P ratio when nutrient concentrations are in excess of demand was found not to affect cellular N:P ratios in phytoplankton in early experiments (i.e. Tilman *et al.* 1982, Tett *et al.* 1985, Reynolds 1999, Roelke *et al.* 2003, Sunda and Hardison 2007) and has not been pursued by the scientific community.

2.2.6 Toxin Production

Cyanobacteria produce a large variety of toxins with a number of different actions in animals and humans leading to significant health risks and drinking water issues globally (c.f. Chorus and Bartram 1999, Chamichael 2008, Cheung *et al.* 2013). The toxin-producing cyanobacteria, and the suite of different toxins that each species produces, is discussed below.

Toxin-producing taxa

The cyanobacterial toxins were named according to the species that they were originally discovered in and isolated from. For example, microcystin was discovered in *Microcystis aeruginosa* and anatoxin was originally isolated from *Anabaena*. However, most cyanobacteria produce several different types of toxins, with the exception of nodularin which is only produced by *Nodularia spumigena*.

The toxin most widely produced by different cyanobacterial taxa is the recently discovered neurotoxin Beta-N-methylamino-L-alanine (BMAA, Cox *et al.* 2005). This is followed by the microcystins which are produced by nine different taxa (Table 2.2). Chief among the microcystin producing taxa are *Microcystis* (the toxin was originally isolated from *Microcystis aeruginosa*), followed by *Planktothrix* and *Anabaena*. Another widely distributed toxin is anatoxin-a, which is produced by eight different cyanobacterial taxa, principally *Anabaena*, the genus from which the toxin was originally isolated.

Table 2.2. Toxins produced by cyanobacteria. Based on data from Cox *et al.* 2005, Sivonen and Borner 2008, Cheung *et al.* 2013.

	Microcystin	Nodularin	Cylindro-spermopsin	Anatoxin-a	Anatoxina(S)	Saxitoxin	Dermatotoxin	BMAA
<i>Microcystis</i>	X							X
<i>Planktothrix</i>	X			X		X		X
<i>Anabaena</i>	X		X	X	X	X		X
<i>Nostoc</i>	X							X
<i>Anabaenopsis</i>	X							
<i>Radiocystis</i>	X							X
<i>Synechococcus</i>	X							X
<i>Phormidium</i>	X			X				X
<i>Oscillatoria limosa</i>	X			X				
<i>Oscillatoria</i>				X			X	
<i>Nodularia</i>		X						X
<i>Cylindro-spermopsis</i>			X			X		X
<i>Aphanizomenon</i>			X	X		X		X
<i>Raphidiopsis</i>			X	X				X
<i>Cylindro-spermum</i>				X				X
<i>Lyngbya</i>						X	X	X
<i>Shizothrix</i>							X	
<i>Umezakia natans</i>			X					

Anabaena species, including *flos-aquae/ lemmermannii/ circinalis*, may be the most toxically versatile of all the cyanobacteria as they can produce all the toxins, including BMAA, microcystins, cylindrospermopsin, anatoxin-a, anatoxin-a(S) and saxitoxins, save nodularin (Table 2.2). Nodularin is only produced by *Nodularia spumigena*. Another versatile toxin producer is *Aphanizomenon flos-aquae* which produces BMAA, cylindrospermopsin, anatoxin-a and saxitoxins (Table 2.2). *Planktothrix* also produces four different toxins including BMAA, microcystins, anatoxin-a and saxitoxins. The cyanobacteria *Cylindrospermopsis raciborskii* from whence cylindrospermopsin was originally isolated also produces saxitoxins (Table 2.2). Benthic cyanobacteria are also versatile when it comes to toxin production. For example, *Oscillatoria limosa* can produce microcystins as well as anatoxin-a while *Lyngbya wollei* can produce saxitoxins and dermatotoxins (Table 2.2).

Toxin types and their biosynthetic pathways

The toxins produced by cyanobacteria can be divided into three main groups: hepatotoxins that damage the liver of the organisms ingesting them, neurotoxins that cause respiratory arrest, and dermatotoxins that cause rashes and inflammations. Each is discussed separately below.

Hepatotoxins. The most well-known hepatotoxins are microcystins and nodularin which are serine/threonine protein phosphatase inhibitors (Table 2.3). A large variety of different microcystins (close to 80) have been identified, with the most toxic being microcystin-LR. These cyclic heptapeptides contain seven amino acids, including a unique beta amino acid ADDA (MacKintosh *et al.* 1990, Yoshizawa *et al.* 1990). In contrast with microcystins, only a few varieties of nodularin have been identified (Yoshizawa *et al.* 1990). The toxicity of cyanobacterial toxins is typically measured by injecting them into mice and calculating the lethal dosage to half the population (LD₅₀; Table 2.3).

Biosynthesis of the microcystin and nodularin peptides occurs by non-ribosomal peptide synthases (NRPS) and polyketide synthases (PKS) found mainly in bacteria (Welker and von Dohren 2006). Both of these enzyme classes are needed for both the microcystin and nodularin biosynthesis pathways which have been sequenced from a number of cyanobacterial species including *Microcystis*, *Planktothrix* and *Anabaena* (Borner and Dittman 2005). For example, the *mcyA*, *mcyB* and *mcyC* genes encode the NRPS that synthesize the pentapeptide portion of microcystins. The *mcyD*, *mcyE*, *mcyF* genes encode the PKS which synthesize the ADDA amino acid unique to microcystins. Finally, the *mcyF*, *mcyG*, *mcyH*, *mcyI*, *mcyJ* genes encode the proteins that tailor and transport specific microcystins (Table 2.3). Similarly, the *nda* gene cluster specific to nodularin encode the NRPS and PKS synthases as well as the tailoring and transport proteins (Table 2.3). Although not verified through functional investigations, the cylindrospermopsin gene cluster, encoding the genes *cyrA*, *cyrB*, *cyrC*, has recently been characterized in *Aphanizomenon flos-aquae* (Stuken and Jakobsen 2010).

Table 2.3. Common cyanobacterial toxins. ND: Not determined.

Toxin	Chemical Class	Action	Effect	LD ₅₀	Reference	Gene Name	Gene Reference
Micro-cystins	Cyclic heptapeptides; 80 variants; microcystin-LR is most toxic	Serine/threonine protein phosphatase (1 and 2A) inhibitors	Hepatotoxin; damages liver	50 µg kg ⁻¹	MacKintosh <i>et al.</i> 1990, Yoshizawa <i>et al.</i> 1990	<i>mcyA-I</i>	Tillett <i>et al.</i> 2000, Christiansen <i>et al.</i> 2003
Nodularin	Cyclic pentapeptide; only a few variants identified	Serine/threonine protein phosphatase 1 and 2A inhibitor	Hepatotoxin; damages liver	50 µg kg ⁻¹	Yoshizawa <i>et al.</i> 1990	<i>ndaA-I</i>	Moffitt and Neilan 2004
Cylindrospermopsin	Cyclic guanidine alkaloid	Protein synthesis inhibitor	Hepatotoxin/Cytotoxin; affects liver as well as kidney, spleen, thymus and heart	200 µg kg ⁻¹ at 6 days 2000 µg kg ⁻¹ at 24 hrs	Runnegar <i>et al.</i> 1994, Terao <i>et al.</i> 1994, Ohtani <i>et al.</i> 1992	<i>cyrA-C</i>	Stuken and Jakobsen 2010
Anatoxin-a	Alkaloid	Competitive inhibitor of acetyl choline	Neurotoxins: causes death by respiratory arrest	200-250 µg kg ⁻¹	Devlin <i>et al.</i> 1977, Carmichael <i>et al.</i> 1990, Skulberg <i>et al.</i> 1992	<i>ana</i>	Mejean <i>et al.</i> 2010
Anatoxin-a(S)	Phosphate ester of cyclic N-hydroxyguanine	Anticholinesterase	Neurotoxins: causes death by respiratory arrest	20 µg kg ⁻¹	Carmichael <i>et al.</i> 1990	<i>ana</i>	Mejean <i>et al.</i> 2010
Saxitoxins	Carbamate alkaloids; the most potent are saxitoxins and neosaxitoxins	Sodium channels blocker	Neurotoxin	10 µg kg ⁻¹	Sivonen and Jones 1999	<i>stxA-Z</i>	Kellmann <i>et al.</i> 2008
BMAA	Non-protein amino acid		Neurotoxin: linked with neuro-degenerative diseases (e.g. Parkinson's Dementia Complex)	ND	Cox <i>et al.</i> 2005	ND	
Dermato-toxins	Aplysiatoxins	Protein kinase C activators	Dermatotoxin: tumor promoters; dermatitis and oral/gastrointestinal inflammations	ND	Mynderse <i>et al.</i> 1977, Fujiki <i>et al.</i> 1990	ND	

Neurotoxins. By far the most potent toxins are the neurotoxin saxitoxin that causes paralytic shellfish poisoning (PSP) syndrome and respiratory arrest in humans and animals. This neurotoxin is produced both by cyanobacteria and dinoflagellates and is an alkaloid that acts as a sodium channel blocker. Another alkaloid neurotoxin, anatoxin-a, competitively inhibits acetyl choline, and a variant, anatoxin-a(S), acts as an anti-cholinesterase (Devlin *et al.* 1977, Mynderse *et al.* 1977, Carmichael *et al.* 1990, Sivonen and Jones 1999). The LD₅₀ of these toxins vary from 200-250 µg kg⁻¹ in the case of anatoxin-a, 20 µg kg⁻¹ in the case of anatoxin-a(S), to 10µg kg⁻¹ in the case of saxitoxins (Table 3). The gene clusters encoding the saxitoxin biosynthesis and anatoxin biosynthesis pathways were very recently elucidated via functional homology and each contains 20 or more genes (Kellmann *et al.* 2008, Mejean *et al.* 2010). The recently discovered neurotoxin BMAA, a non-protein amino acid that is potentially linked to neurodegenerative diseases such as Parkinson Dementia Complex (PDC), is produced in almost all cyanobacteria tested to date (Cox *et al.* 2005).

Dermatotoxins. Benthic cyanobacteria, including *Lyngbya*, *Oscillatoria* and *Schizothrix*, produce a number of different toxins including aplysiatoxins, debromoaplysiatoxins and lyngbyatoxin-a. These toxins are protein kinase C activators that cause dermatitis and oral and gastrointestinal inflammations, and can also promote tumor formation (Mynderse *et al.* 1977, Cardellina *et al.* 1979, Fujiki *et al.* 1990). The pathways and genes involved with the production of the dermatotoxins have yet to be elucidated.

Potential functions of toxin production

Interestingly, researchers have not been able to determine the purpose of toxin production in cyanobacteria, or under what conditions toxins are most likely to be produced (Sivonen and Borner 2008). Moreover, under environmental conditions cyanobacteria that produce toxins co-exist with cyanobacteria of the same genus that do not produce toxins; it's unclear whether the possession of, or lack of, the toxins confers an ecological advantage (Sivonen and Borner 2008, Baxa *et al.* 2010).

Despite these complications, several explanations for the potential function of toxin production exist. Originally it was thought that cyanotoxins acted as allelochemicals and that their secretion into the surrounding water would suppress the growth of competitors (Keating 1977, Keating 1978, Flores and Wolk 1986, Klein *et al.* 1995). But, when the distribution of toxins, such as microcystins, was compared between cells and the surrounding medium using immunodetection combined with electron microscopy, most of the toxin was found to be cell-bound (Rapala *et al.* 1997, Wiedner *et al.* 2003, Tonk *et al.* 2005, Gerbersdorf 2006). Because, live (i.e. non-lysed) cyanobacteria do not secrete the toxins they produce it is doubtful that they act as allelopathic chemicals. Consistent with this notion, most investigations that demonstrate allelopathic effects do so at concentrations of extracted toxins far above what is ecologically relevant, leading

investigators to conclude that the ability of cyanobacterial toxins to work as allelopathic chemicals appears unlikely (Babica *et al.* 2006, Berry *et al.* 2008, Holland and Kinnear 2013).

One explanation that is gaining ground is that the primary role of toxins is probably not to be toxic (Llewellyn 2006). Rather, investigators are hypothesizing that toxins may be produced to protect the cells from abiotic stresses. For example, microcystins are produced during all phases of growth but the greatest accumulation typically occurs under conditions that support optimal growth, including growing under optimal light levels (Sivonen and Jones 1999, Wiedner *et al.* 2003). Several lines of evidence point towards increases in irradiance as being a trigger for microcystin production. These include accumulation of intracellular microcystin-LR with increased irradiance, the association of intracellular microcystins with the thylakoid membranes, and increased microcystin gene expression with increased irradiance (Kaebernick *et al.* 2000, Tonk *et al.* 2005, Borner and Dittman 2005, Gerbersdorf 2006). As such, it makes sense that microcystins are produced across a number of cyanobacterial taxa, such as *Microcystis*, *Anabaena*, and *Planktothrix*, that grow well in high-light environments (Paerl and Paul 2012).

Microcystins may also be implicated in preventing iron-stress by acting as siderophores to scavenge iron (Utkilen and Gjolme 1995, Lyck *et al.* 1996), an idea supported by the discovery that the iron-regulator factor Fur binds to the genes that produce microcystins in cyanobacteria (Martin-Luna *et al.* 2006). As such, microcystin production may provide an advantage to cyanobacteria in early stages of iron-limiting conditions (Alexova *et al.* 2011, Holland and Kinnear 2013) vis-à-vis eukaryotic competitors (Molot *et al.* 2014).

Another potential role for cyanotoxins is to act as a grazing deterrent (Burns 1987, Gilbert 1996). However, recent research using *Microcystis aeruginosa*, has demonstrated that it's not the toxic microcystins that deters *Daphnia* from grazing *M. aeruginosa* but other substances it produces. In other words, the substances causing toxicity and deterrence are not identical and the non-toxic substances may be much important in terms of grazing deterrence (Rohrlack *et al.* 1999, 2003).

While the toxic substances are by far the most well-known, there are hundreds of other, secondary metabolites similar in structure to the toxins that are produced by cyanobacteria. Just as the toxins, these cyclic or linear peptides may not be needed for growth but may serve protective functions. For example, the grazing deterrents discussed above belong to a class of depsipeptides called microviridins (originally isolated from *Microcystis viridis*) and has since their isolation been found in a range of cyanobacteria (Rohrlack *et al.* 2003). These secondary metabolites may also have important pharmacological applications. An alkaloid produced by *Nostoc*, called nostocarboline, is a cholinesterase inhibitor which has an effect comparable to galanthamine, a drug approved for Alzheimer's disease (Becher *et al.* 2005). Also isolated from *Nostoc* is a compound called cyanovirin-N which has antiviral activity and is under development as an antiviral agent against HIV (Boyd *et al.* 1997, Bolmstedt *et al.* 2001).

3. FACTORS INFLUENCING CYANOBACTERIAL BLOOMS AND TOXIN PRODUCTION

The world-wide increase in the incidence of cyanoHABs such as the N₂ fixing genera *Anabaena*, *Aphanizomenon*, *Cylindrospermopsis*, and *Nodularia*; the benthic N₂ fixing genera *Lyngbya* and some *Oscillatoria*; and the non-N₂ fixing genera *Microcystis* and *Planktothrix* has prompted a great deal of research into the conditions that favor the growth of these species (Chorus and Bartram 1999; Carmichael 2008; Paerl and Huisman 2008; Hudnell 2008, 2010; O'Neill *et al.* 2012; Paerl and Paul 2012). These conditions typically include favorable salinity, ample supply of nutrients, calm water and stratified conditions, plenty of irradiance and warm water temperatures (Figure 3.1). In contrast, the most successful strategies to mitigate blooms of cyanoHABs include reducing the supply of nutrients, increasing the flow of water to promote mixing and destratify the water column (Figure 3.1). In the following sections, we will focus on the conditions that are favorable for the growth of the cyanoHAB genera.

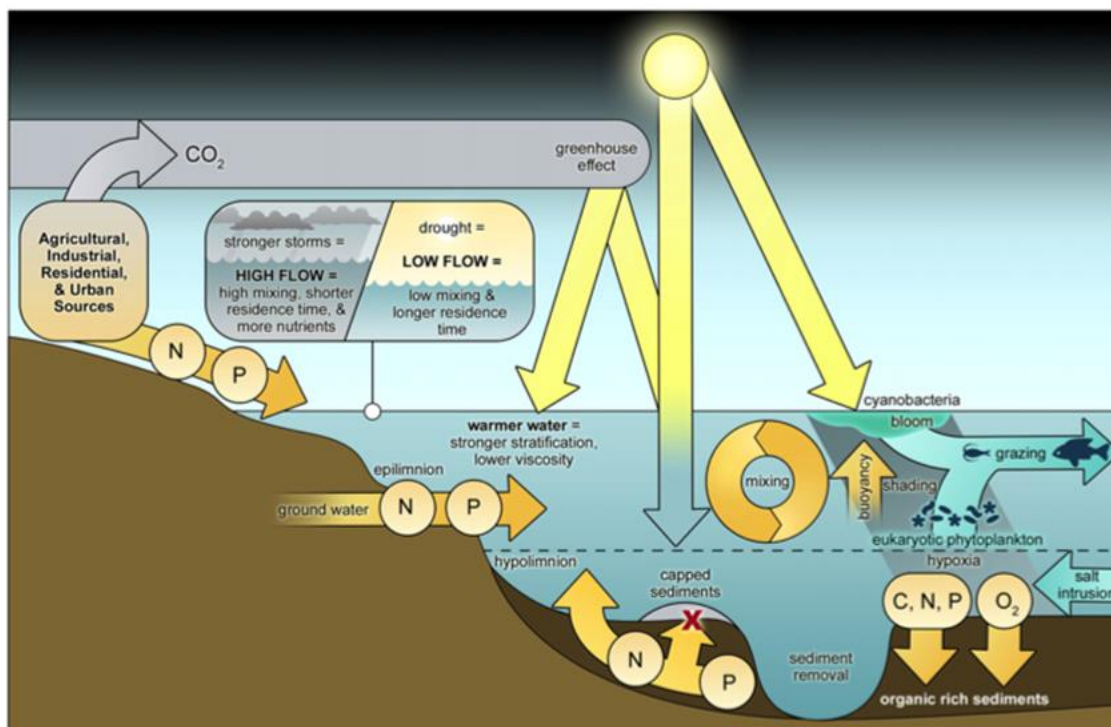


Figure 3.1. Conceptual model of factors affecting cyanobacteria blooms including warmer water, drought and decreased flow, decreased mixing, increased residence time, and increased N and P inputs from agricultural, industrial and urban sources. From Paerl *et al.* 2011.

3.1 Salinity

Most harmful algal bloom-forming and toxin-producing cyanobacteria (cyanoHABs) are freshwater species. In contrast, marine cyanobacteria such as *Prochlorococcus*, *Synechococcus* sp. and *Trichodesmium* sp. are not toxic and do not form cyanoHABs. However, laboratory investigations of freshwater cyanoHAB species demonstrate that these have quite wide salinity

tolerance ranges. For example, the least tolerant, *Cylindrospermopsis* only thrives up to 2.5 ppt salinity, but the most tolerant, *Anabaenopsis* and *Nodularia* spp., thrive at salinities from 5-20 ppt (Moisander *et al.* 2002). *Microcystis aeruginosa* tolerates up to 10 ppt salinity without a change in its growth rate compared to that on freshwater (Tonk *et al.* 2007). What these studies suggest is that given optimal growth conditions, these species could also bloom in brackish-water regions. Indeed, recent decades have witnessed a spread in the geographical extent of these species into the mesohaline (5-15 ppt) reaches of coastal systems (Paerl and Paul 2012). For example, blooms of *Microcystis aeruginosa* have occurred in the Baltic Sea (Maestrini *et al.* 1999) and the San Francisco Estuary (Lehman *et al.* 2013) suggesting 1) that factors other than salinity are regulating their geographical distribution and that 2) those factors are currently changing to allow cyanoHAB growth to occur in regions where they previously did not exist. In summary, salinity may not be the strongest “barrier” in terms of restricting the occurrence and geographical distribution of toxic cyanoHABs.

3.2 Nutrient Concentrations and Ratios

As with other photosynthetic phytoplankton, given optimal temperatures and irradiance, cyanobacterial biomass accumulation is directly proportional to the amount of nutrients (N and P) available in the water column. Therefore, strategies to reduce the accumulation of cyanoHAB biomass and severity of their blooms frequently focus on reductions of nutrient concentrations (Paerl 2008).

3.2.1 Influence of N and P Loadings and Concentrations in Stimulating Cyanobacterial Growth

Cyanobacterial growth in freshwater systems (rivers and lakes), which tend to become limited by P sooner than by N, is frequently linked with excessive P loading (Likens 1972, Schindler 1977, Edmondson and Lehman 1981, Elmgren and Larsson 2001, Paerl 2008, Schindler *et al.* 2008). In contrast with freshwater systems, estuarine and marine systems tend to be more sensitive to N loading (Figure 3.2), and eutrophication due to cyanobacterial growth is frequently linked with excessive N loading (Ryther and Dunstan 1971, Nixon 1986, Suikkanen *et al.* 2007, Paerl 2008, Conley *et al.* 2009, Ahn *et al.* 2011).

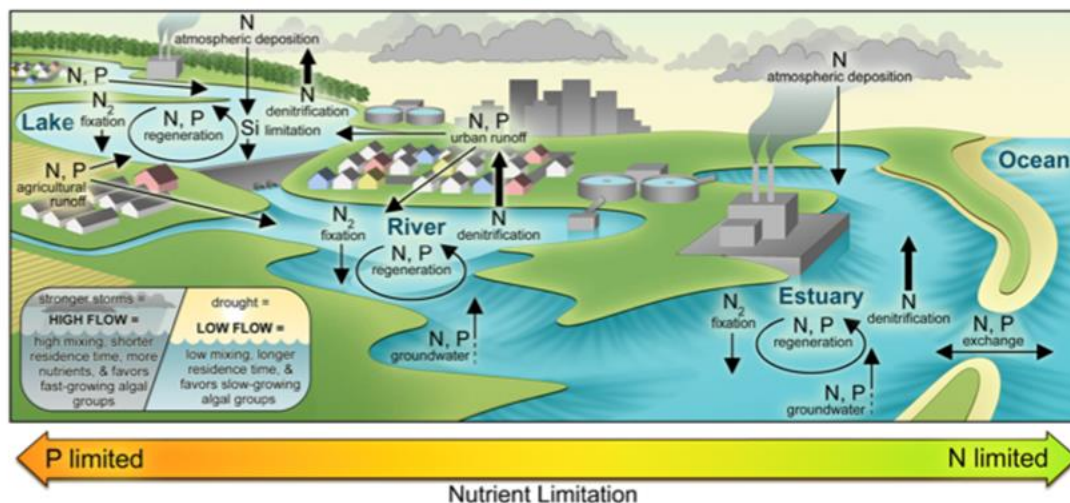


Figure 3.2. Conceptual diagram of interaction of nutrient inputs, cycling processes, and limitation of primary production along the freshwater to marine continuum. From Pearl *et al.* 2014b.

However, both non-point and point source nutrient contributions, such as agriculture and wastewater effluent, tend to increase N and P concentrations simultaneously (Paerl and Paul 2012, Paerl *et al.* 2014b). For example, human population growth-induced intensification of wastewater discharge and agriculture has led to hypereutrophication of China's third largest lake, Taihu (Qin *et al.* 2007). Increased nutrient loads, combined with low water column depth and increased water temperatures, has led to an explosive growth of cyanobacteria and a change in total phytoplankton community composition from being mainly diatom-dominated to being dominated by *Microcystis aeruginosa* (Qin *et al.* 2010, Paerl *et al.* 2014a). Bioassay experiments during summer months when cyanobacterial biomass is at its maximum, and nutrient concentrations at a minimum, demonstrate that N and P exert equal control over biomass accumulation in this system (Paerl *et al.* 2014a).

In general, dominance of both N₂-fixing and non-N₂ fixing cyanobacteria such as *Aphenizomenon flos aquae*, *Nodularia spumigena*, *Microcystis aeruginosa* and *Cylindrospermopsis raciborskii*, have increased world-wide in concert with increased loads of both N and P (Chapman and Schelske 1997, Jacoby *et al.* 2000, Gobler *et al.* 2007, Burford *et al.* 2006, Burford and O'Donahue 2006, Hong *et al.* 2006, Suikkanen *et al.* 2007, O'Neill *et al.* 2012).

3.2.2 Influence of Changes in N:P Ratios on Stimulation or Limitation of Cyanobacterial Growth

At low and intermediate nutrient loadings, reduction in only N or P may be sufficient to control blooms of cyanobacteria. But with elevated loadings of both N and P, reduction of only one type of nutrient can lead to an imbalance in the N:P ratio of the water column potentially leading to a

worsening of the cyanoHAB problem, or even lead to a eukaryotic HAB problem (Smith 1983; Paerl 2008; Pearl *et al.* 2011, 2014b).

Low nutrient concentrations

Pioneering studies by Smith (1983, 1990) predicted that phytoplankton community composition would be dominated by cyanobacteria when N:P ratios were < 15 , and by eukaryotic phytoplankton when N:P ratios > 20 . This was because many nuisance freshwater cyanobacteria that fix N_2 were hypothesized to thrive at very low ambient concentrations of fixed N, therefore at N:P < 15 . In comparison, growth rates of eukaryotic phytoplankton that could not fix N_2 were predicted to slow down at N-limiting concentrations, resulting in eukaryotic species becoming outcompeted at N:P < 15 . At N:P > 20 , growth rates of eukaryotic phytoplankton would not be limited by N and therefore they could dominate phytoplankton community composition (Smith 1983, 1990). These predictions suggested that one could control growth of cyanobacteria by increasing the dissolved N:P ratio above 20. Consequently, many investigators who study lakes with low to intermediate nutrient loadings advocate for reductions in “P only” as a way to control cyanobacterial growth (Schindler 1977, Schindler *et al.* 2008). However, increasing the dissolved N:P ratio > 15 becomes less important as a way to control cyanobacterial growth at high concentrations of nutrients, for a number of reasons, including: 1) nutrient concentrations are high relative to biomass and non-limiting; 2) the prevalence of N_2 fixation in N_2 -fixing cyanobacteria is not as great as initially hypothesized; 3) the cellular N:P ratio of cyanobacteria, and their N requirement, is high; 4) analysis of lake data by several investigators have demonstrated that absolute concentrations of N and P are more important in supporting blooms of N_2 fixing cyanobacteria rather than specific ratios of dissolved N:P.

High and non-limiting nutrient concentrations

In order for changes in nutrient ratios to affect phytoplankton growth, nutrient concentrations must be so low (relative to the phytoplankton biomass) that either P or N will eventually limit their growth rates. In the last decades, both N and P loadings have increased to the point that they exceed the assimilative capacity of the resident phytoplankton in many systems (Chapman and Schelske 1997, Jacoby *et al.* 2000, Burford *et al.* 2006, Burford and O’Donahue 2006, Hong *et al.* 2006, Gobler *et al.* 2007, Suikkanen *et al.* 2007, Paerl 2008, Paerl *et al.* 2011, Dolman *et al.* 2012, O’Neill *et al.* 2012, Paerl and Paul 2012, Paerl *et al.* 2014a). Therefore, changes in the N:P ratio have little effect on the growth of any of the phytoplankton taxa present in the water column (Paerl 2008, Davidson *et al.* 2012, but see also Glibert *et al.* 2011 with respect to diatoms).

Prevalence of N_2 fixation

An assumption that must be met in order that N_2 fixing cyanobacteria dominate the community at low N:P ratios (and N limiting conditions) is that they mostly use N_2 gas rather than fixed N for growth. However, investigations demonstrate that the proportion of the N demand of N_2

fixers that is met by N₂-fixation is typically less than 25% (Levine and Lewis 1987, Findlay *et al.* 1994, Laamanen and Kuosa 2005). For example, in Baltic Sea phytoplankton communities dominated by the N₂ fixers *Aphanizomenon flos aquae* and *Nodularia spumigena*, less than 20% of N utilization is due to N₂ fixation under N-limiting conditions (Sorensen and Sahlsten 1987; Berg *et al.* 2001, 2003; Laamanen and Kuosa 2005). As mentioned in section 2.2.4, N₂ fixation is repressed in the presence of NH₄⁺; culture studies of the N₂ fixing cyanobacterium *Cylindrospermopsis raciborskii* demonstrate that N₂ fixation is shut down in the presence of NH₄⁺ and that it's competitive for fixed N (Sprosser *et al.* 2003, Moisander *et al.* 2008). Based on a wide range of investigations, the assumption that most of the N demand of cyanobacteria is met by N₂ fixation does not hold.

Cellular N:P composition

As discussed above (Section 2.2.5), the cellular N:P requirement of cyanobacteria is greater than any other eukaryotic group due to the large protein demand of the peripheral light harvesting antennae. At N-limiting conditions, cyanobacteria would need to provide most, if not all, of their N demand by N₂ fixation in order to meet their high tissue N demand. This would lead to a sharp divide in the distribution of genera that fix N₂ from those that do not; the latter group would be much better suited to dominate high N:P ratio (>25) than low N:P ratio environments. On the flip side, many genera of eukaryotic phytoplankton, such as diatoms and dinoflagellates, have relatively high tissue P requirements and have cellular N:P ratios <16 (Geider and LaRoche 2002, Quigg *et al.* 2003, Hillebrand *et al.* 2013) rendering them better suited for environments with N:P <16 (Arrigo *et al.* 1999, Mills and Arrigo 2010). Based on their cellular N:P ratios, cyanobacteria are better suited to dominate high N:P ratio systems (>25) and some eukaryotes low N:P ratio systems (<16) which is opposite of the conclusions reached by Smith (1983).

Confounding factors

Because the height of a phytoplankton bloom, including blooms of N₂ fixers, frequently coincides with a depletion in N and N:P <15, it is often assumed that the major control on the cyanobacteria is the nutrient ratio, rather than the other way around. Additionally, there may be time lags between nutrient uptake and increased biomass such that a correlation between the two variables at a given point in time may not imply causality. Blooms of N₂ fixers also coincide with a warm, stratified water column coupled with adequate or high irradiance. Because all these parameters (warm water, high irradiance, stratification, depletion of N, overall increase in Chl *a*) occur in concert, it's difficult to separate out the impact of nutrients from other co-occurring environmental variables in order to quantify the most important effect on increases in cyanobacterial biomass. Investigations that separate out the effect of changes in absolute concentrations from ratios, find that changes in absolute concentrations of nutrients, or changes in total Chl *a* biomass, are more strongly related to changes in cyanobacterial biomass than changes in the ratio of N:P (Trimbee and Prepas 1987, Downing *et al.* 2001, Dolman *et al.* 2012).

Meta analyses of Lake Studies

Consistent with the problems of assigning shifts in phytoplankton community composition to changes in N:P ratios described above, Trimbee and Prepas (1987) and Downing *et al.* (2001) demonstrated that changes in cyanobacterial biomass was more strongly associated with changes in the absolute concentrations of N and P than with changes in the dissolved N:P ratio in 99 different freshwater systems. In a study of 102 lakes in Germany, Dolman *et al.* (2012) found that the more enriched in both N and P the lakes were, the greater was their total cyanobacterial biomass. The cyanobacterial taxa that responded most to nutrient enrichment included *Planktothrix agardhii*, *Microcystis* and *Anabaenopsis*. Moreover, differences between cyanobacterial taxa were not consistent with the hypothesis that N fixing taxa were favored in low N:P conditions as the greatest biomass of *Aphaenizomenon* and *Cylindrospermopsis raciborskii* were found lakes with the greatest N:P ratios (Dolman *et al.* 2012).

3.2.3 Influence of Type of N on Growth of Cyanobacteria

As previously mentioned, NtcA is central in cyanobacterial N regulation and is under negative control by NH_4^+ (Section 2.2.4). Other than NH_4^+ -transporters, transcription of all N related enzymes requires binding of the NtcA transcription factor in order to be transcribed. Therefore, uptake and metabolism of sources other than NH_4^+ does not take place unless NH_4^+ is at limiting concentrations (Lindell and Post 2001, Lindell *et al.* 2005). In contrast, NH_4^+ transporters are constitutively expressed, or always “on”, regardless of external concentration of NH_4^+ (Berg *et al.* 2011). In addition, the *amt1* NH_4^+ transporter gene is one of the most highly expressed in cyanobacterial genomes. In the marine cyanobacteria *Synechococcus* and *Prochlorococcus*, *amt1* is expressed on par with, or at a greater level, respectively, than the gene encoding the C-fixation enzyme Rubisco (Berg *et al.* 2011). Considering the countless other critical processes happening within cells, it is noteworthy that the protein responsible for NH_4^+ uptake is one of the most abundant proteins in cyanobacteria.

Given that NH_4^+ exerts such a strong control over the use of other N sources in cyanobacteria, is the preference for NH_4^+ reflected in different rates of growth on different N sources? There is no clear answer to this question. From a theoretical perspective it should not be the case because the magnitude of reductant and ATP needed for carbon fixation dwarfs the energetic costs of N assimilation, even assimilation of “expensive” sources such as NO_3^- or N_2 gas (Turpin 1991). The type of N should not affect the rate of growth other than under conditions of very low irradiance where assimilation of NO_3^- may compete with carbon fixation for reductant and ATP, thereby lowering the growth rate (Turpin 1991). Culture investigations appear to bear this out as faster rates of growth are typically not observed when cyanobacteria are grown on NH_4^+ versus NO_3^- (i.e. Berman and Chava 1999, Hawkins *et al.* 2001, Post *et al.* 2012, Saker and Neilan 2001, Solomon *et al.* 2010). Differences in growth rates when growing on NO_3^- versus on NH_4^+ are frequently detected for individual strains (i.e. Saker and Neilan 2001), but there is no pattern that can be generalized with respect to cyanobacteria as a whole. Even within the same species,

some strains may be growing faster on NH_4^+ and some on NO_3^- , but the difference with N source in most cases is smaller than the difference in growth rate among different strains (Figure 3.3). Therefore, observations of fast growth of cyanobacteria using NH_4^+ in the field are most likely due to 1) factors that promote fast growth of cyanobacteria generally (i.e. high temperature and high irradiance) combined with 2) high enough availability of NH_4^+ such that NtcA is repressed and only NH_4^+ is taken up and utilized by the cell.

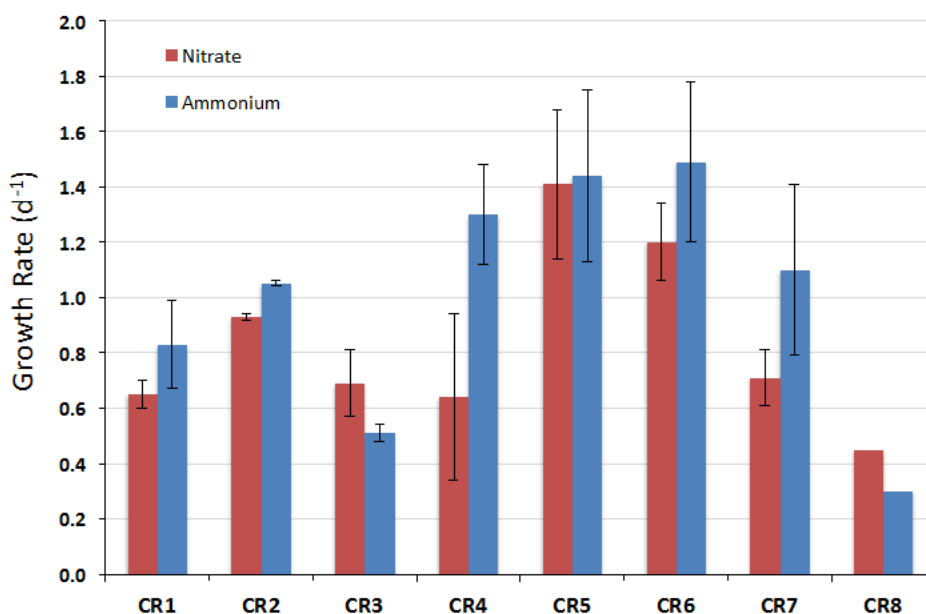


Figure 3.3. Difference in growth rates of *Cylindrospermopsis raciborskii* when growth on NO_3^- (red bars) versus NH_4^+ (blue bars) for eight different strains. Data from Saker and Neilan 2001 and Stucken *et al.* 2014.

3.3 Irradiance and Water Clarity

Cyanobacteria have a distinct advantage with respect to other photosynthetic organisms in the amount of carotenoid pigments per cell volume (Section 2.2.2). These pigments serve a photoprotective function by dissipating excess light energy when required allowing cyanobacteria to be exposed to high irradiances without experiencing photoinhibition (Paerl *et al.* 1983, 1985). Recent investigations also demonstrate that the toxic peptides produced by cyanoHAB species accumulate in the thylakoid membranes potentially serving a role in photoprotection of the cells (Kaebernick *et al.* 2000, Borner and Dittman 2005, Gerbersdorf 2006). Interestingly, many cyanoHAB species are not strong competitors for light in a well-mixed environment due to their poor light absorption efficiency (Huisman *et al.* 1999, Reynolds 2006). Among the cyanoHAB species tested to date, *Microcystis* appears to possess the least efficient rate of photosynthesis for a given light intensity (Figure 3.4). The upshot of these traits

is that cyanobacteria grow ineffectively at low and mixed light, but very effectively when exposed to high light, particularly the toxic peptide-producing varieties (Huisman *et al.* 2004, Reynolds 2006, Carey *et al.* 2012).

Aided by their positive buoyancy, cyanobacteria such as *Microcystis*, can grow very close to the surface by tolerating irradiance levels that are inhibitory to other members of the phytoplankton community. As a result, these cyanobacteria can increase their cell densities past the point where they would ordinarily become light-limited by self-shading. Growing close to the surface can also help cyanobacteria avoid light limitation if there is a high concentration of suspended sediment matter in the water. In contrast, phytoplankton that are not positively buoyant can become shaded by the cyanobacteria growing at the surface (Carey *et al.* 2012).

In contrast with *Microcystis* and *Aphanizomenon*, other cyanoHAB species such as *Cylindrospermopsis raciborskii* and *Planktothrix* sp. are good competitors at low light. Cultures of *C. Raciborskii* can grow at optimal rates at very low irradiances (Briand *et al.* 2004, Dyble *et al.* 2006, Wu *et al.* 2009) and it grows well in deep water columns where it's exposed to fluctuating light levels as it mixes from the surface to the bottom (McGregor and Fabbro 2000, Burford and Donohue 2006, O'Brien *et al.* 2009). Not only is the rate of photosynthesis in *C. raciborskii* efficient at low irradiances, it's also efficient at high irradiances, making this a very versatile cyanoHAB species (Figure 3.4).

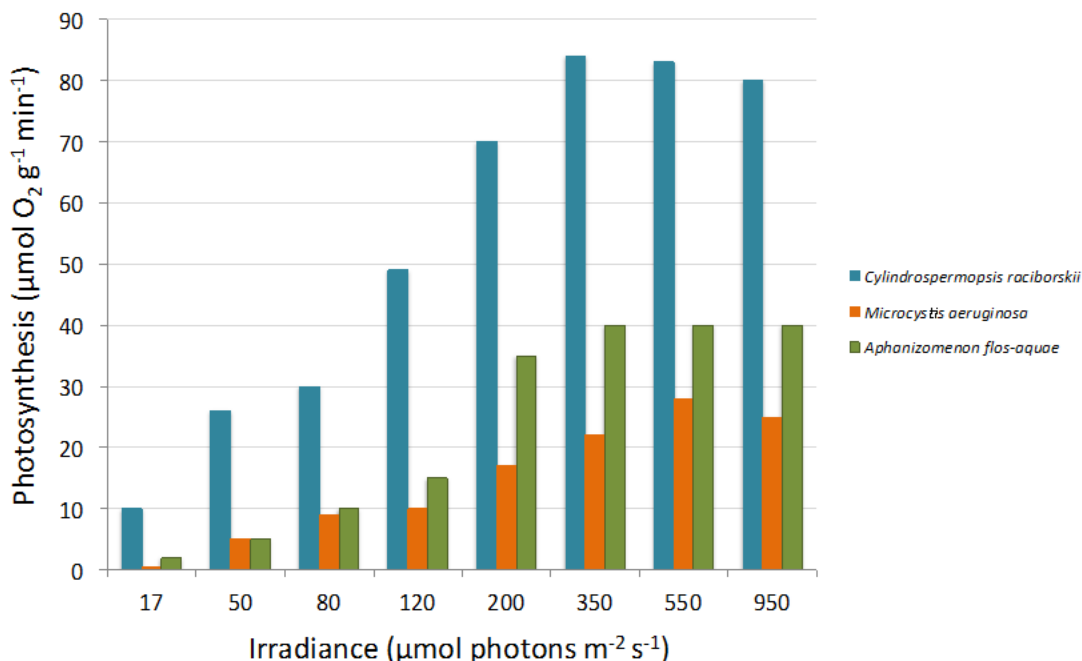


Figure 3.4. Photosynthesis as a function of irradiance in three cyanoHAB species. Data from Wu *et al.* 2009.

3.4 Factors Impacting Toxin Production and Degradation

While a large number of different toxins are produced by cyanoHAB species, the literature is heavily tilted towards investigations of factors impacting the production and degradation of microcystins. Therefore the information presented here is focused on microcystin-LR.

3.4.1 Toxin Production

Just as there is substantial discussion surrounding the purpose of toxin production in cyanobacteria, the conditions under which toxin production is enhanced is also vigorously debated. Previous studies have concluded that the greatest intracellular toxin concentrations are detected under favorable growth conditions, including high irradiance as discussed above, with maximal toxin production occurring at maximal rates of cell division and in late log phase (Watanabe and Oishi 1985, Orr and Jones 1998, Sivonen and Jones 1999, Van Der Westhuizen and Eloff 1985).

Investigations specifically focused on changes in nutrient concentrations and ratios, demonstrate that microcystin content reaches a maximum under maximum growth rates, regardless of medium N:P ratio, but that the microcystin content of the cells correlates with total cellular N and protein content (Lee *et al.* 2000, Vezie *et al.* 2002, Downing *et al.* 2005). These results make sense as the toxins, being peptides, require ample N in order to be synthesized. Consistent with this, total toxin production per cell decreases at N-limiting concentrations (Tonk *et al.* 2008).

Not only does toxin concentration per cell vary in strains that produce toxins (i.e. are toxigenic), but natural populations are typically comprised of a mix of toxigenic and non-toxigenic strains of the same species. It is also of interest to know whether the proportion of toxigenic:non-toxigenic strains within a population changes with nutrient concentrations or ratios. Laboratory culture investigations comparing growth of toxigenic and non-toxigenic strains of *Microcystis* demonstrated that toxigenic strains of *Microcystis* grew faster than non-toxigenic strains at N concentrations of 6000 $\mu\text{moles L}^{-1}$ and at N:P ratios $\gg 200$ (Vezie *et al.* 2002). The reason for this is not clear, but could include microcystin conferring protection from NO_3^- toxicity in the toxin-producing strains at such unnaturally high concentrations of NO_3^- .

While results obtained with unnaturally high nutrient concentrations and ratios do not easily translate to natural systems, a nutrient enrichment bioassay investigation has demonstrated that toxigenic strains within a *Microcystis* population were promoted to a greater degree with N (and P) additions than non-toxigenic strains (Davis *et al.* 2010). However, the pattern of selective stimulation of toxigenic strains with increased nutrient concentrations is not evident in natural communities which typically exhibit a high degree of variability across small spatial scales in the proportion of toxigenic:non-toxigenic strains within a population. This variability appears not to be related to nutrient concentrations or ratios which do not exhibit the same spatial variability (Vezie *et al.* 1998, Baxa *et al.* 2010, Mbedi *et al.* 2005, Dolman *et al.* 2012).

3.4.2 Toxin Degradation

Together with labile dissolved organic carbon, toxins are rapidly degraded by the natural microbial community following sedimentation (and subsequent release of cellular material) of a cyanobacterial bloom (Jones *et al.* 1994, Rapala *et al.* 2005). In addition to non-specific degradation by the whole community, specific degradation of toxin peptides occurs due to bacteria belonging to the *Sphingomonadaceae* family (Bourne *et al.* 1996, 2001), and other more recently discovered families (Rapala *et al.* 2005, Yang *et al.* 2014). Bacteria that degrade microcystins may also degrade nodularin (Rapala *et al.* 2005). The predominance of these specialized bacteria in the microbial community may determine the length of time it takes (i.e. lag period) before bacterial degradation of toxins takes place. For example, Rapala *et al.* (1994) found the lag time decreased in waters with previous cyanobacterial blooms, compared with no previous cyanobacterial blooms, presumably due to a greater proportion of toxin-degradating bacteria in the former environment. Once degradation of toxin commences, it proceeds rapidly and toxin concentrations typically decrease in an exponential fashion (Figure 3.5), with a loss rate of 0.5 to 1 d⁻¹, corresponding to a half-life of only one day (Christoffersen *et al.* 2002, Jones and Orr 1994). While 95% of the toxins may be degraded within the first 3 days, a more recalcitrant fraction may remain for 20 days or more (Jones and Orr 1994). Other sinks for microcystin-LR include UV degradation (Tsuji *et al.* 1995), and adsorption onto clay particles (Morris *et al.* 2000). In the absence of bacteria, clay particles and UV light, microcystins are very stable in the environment and degrade slowly. At temperatures below 40°C the half-life of microcystin toxin increases to 10 weeks; this conservative estimate is used by the Office of Environmental Health Hazard Assessment to determine the risk of the toxin to wildlife (OEHHA 2009). Because there probably exists a great deal of variation in the relative importance of biological, chemical and physical processes in the degradation of microcystins depending on location, accounts in the literature regarding the half-life and recalcitrance of cyanoHAB toxins tend to be conflicting (i.e. Jones and Orr 1994, Gible and Kudela 2014). Added to this uncertainty is the difference in toxin concentrations obtained using different methods of measurements (See Section 4.2.3 below).

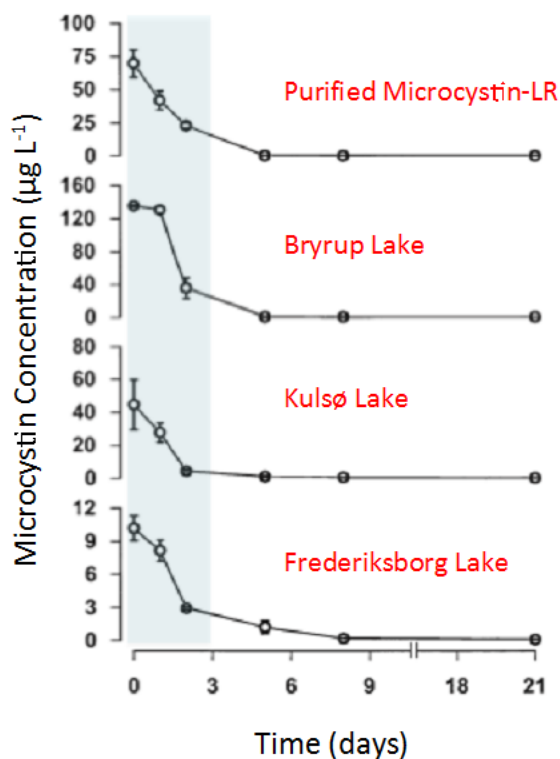


Figure 3.5. Concentration of dissolved microcystin-LR equivalents in bioassays as a function of time after addition of purified microcystin (top panel) or lysed bloom material (bottom 3 panels) to lake water containing natural microbial assemblages. Shaded area corresponds with time period of degradation of 95% of original microcystin concentration. Data from Christoffersen *et al.* 2002.

3.5 Temperature

Perhaps one of the most important factors in controlling the growth rate of cyanobacteria is temperature (Robarts and Zohary 1987, Butterwick *et al.* 2005, Reynolds 2006, Paerl and Huisman 2008). Cyanobacteria isolated from temperate latitudes (i.e. excluding polar regions) typically have temperature growth optima between 25 and 35°C (Reynolds 2006, Lurling *et al.* 2013). For example, in a survey of eight cyanobacteria the growth optima of two *Microcystis aeruginosa* strains were 30-32.5°C and that of *Aphanizomenon gracile* was 32.5°C. Lower growth temperature optima were observed in *Cylindrospermopsis raciborskii* and *Planktothrix agardhii*, both at 27.5°C while *Anabaena* sp had an optimum of 25°C (Lurling *et al.* 2013). The optima of these freshwater HAB-forming cyanobacteria are greater than for marine cyanobacteria which typically have growth temperature optima ranging from 20-27.5°C (Breitbarth *et al.* 2007, Boyd *et al.* 2013).

Compared with other phytoplankton taxa, cyanobacteria typically demonstrate lower growth rates at colder temperatures and higher growth rates at higher temperatures. For example, diatoms typically have a 6-fold higher growth rate at 15°C, 3-fold higher growth rate at 20°C and

a similar growth rate at 25°C, compared with cyanobacteria (Figure 3.6). Growth rates of dinoflagellates typically peak at 25°C. Above 25°C both chlorophytes and cyanobacteria have faster growth rates than diatoms and dinoflagellates (Figure 3.6). The difference in the optimum growth temperatures of the various phytoplankton taxa is hypothesized to become increasingly important in determining phytoplankton community composition as global temperatures continue to increase above 20°C (Lehman *et al.* 2005, Paerl and Huisman 2008). For example, the acceleration of growth rate with a 10°C increase in temperature (Q_{10}) commonly varies from 1-4 for cyanobacteria and 1-3 for chlorophytes (Reynolds 2006). However, it varies from 4-9 for *M. aeruginosa*, the highest recorded for any phytoplankton (prokaryotic or eukaryotic) species (Reynolds 2006). These data suggest that in a mixed phytoplankton assemblage, all else being equal, cyanobacteria will be able to grow faster and outcompete other phytoplankton taxa as the temperature increases. With continued climate change and global warming, there's an increased risk that cyanoHABs will become increasingly competitive vis-à-vis diatoms which often dominate community composition in temperate regions.

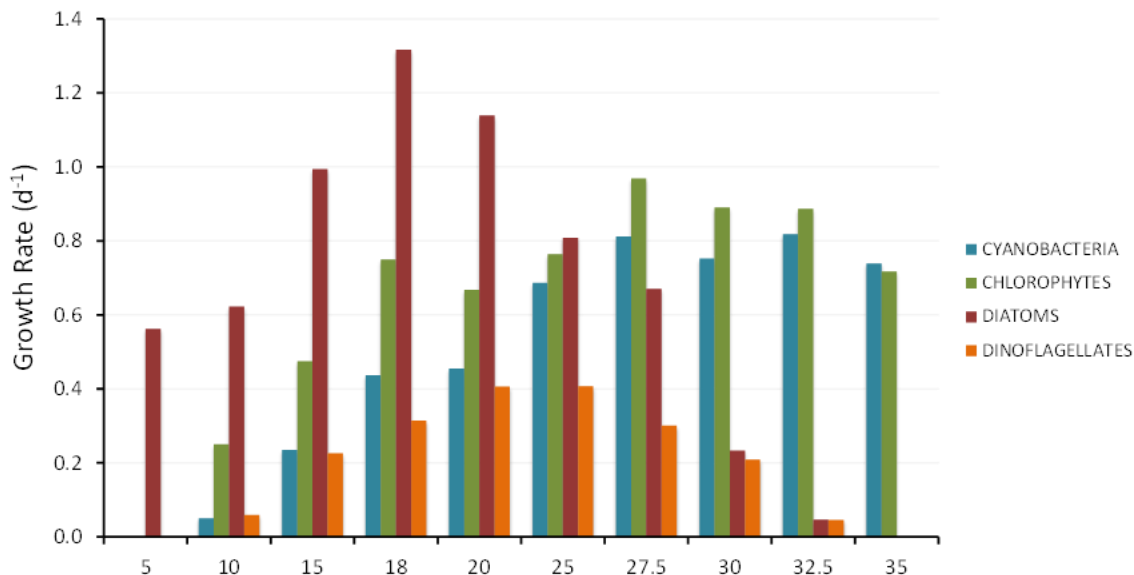


Figure 3.6. Changes in growth rate with temperature for diatoms (red ± 0.35 d⁻¹, $T_{opt}= 20 \pm 1.8$ °C), Chlorophytes (green ± 0.21 d⁻¹, $T_{opt}= 29 \pm 3.8$), Cyanobacteria (cyan ± 0.13 d⁻¹, $T_{opt}=29 \pm 4.5$) and dinoflagellates (orange ± 0.1 d⁻¹, $T_{opt}= 21 \pm 2.8$). Data from Kudo *et al.* 2000, Butterwick *et al.* 2005, Yamamoto and Nakahara 2005, Boyd *et al.* 2013, Lurling *et al.* 2013.

3.6 Stratification and Residence Time

3.6.1 Stratification

CyanoHAB blooms tend to occur during times of calm, stratified water columns (Huber *et al.* 2012). The degree of stratification and water column stability increases with increased temperature, therefore stratification and temperature are closely linked (Paerl and Huisman

2008). The reasons that stratified conditions promote blooms of cyanobacteria are at least three-fold. First, growth rates will increase as a result of the increase in the temperature in the top layer of the water column. Second, cyanobacteria will remain in the top layer of the water column where irradiance is greater, and not become mixed down to the bottom and into lower light, allowing them to maintain higher growth rates. Third, stratification may be a sign of increased residence times (reduced flushing rates), which minimizes loss of cyanobacterial biomass from the system and allows cyanobacteria to use all the nutrients available in the water column (Jeppesen *et al.* 2007). In other words, it's likely that stratification does not directly promote cyanobacterial blooms, but rather it promotes blooms indirectly through increased temperatures, irradiance and reduced loss rates (Elliott 2010).

3.6.2 Residence Time

Because residence time is determined by the flushing rate, the direct effect of increased residence time is to decrease the loss rate of cyanobacteria (Romo *et al.* 2013). Indirect effects of residence time are the same as those for stratification; this is because residence time and stratification typically covary such that stratification is maximal when residence time is minimal, and vice versa. Studies that report on the effect of residence time suggest that cyanobacterial abundance, cell size and toxin concentration are positively related to increased residence time (Elliott 2010, Romo *et al.* 2013).

3.7 Other Factors

Additional to the above-mentioned factors, a number of others may influence cyanobacterial blooms including grazing by higher trophic levels and exposure to toxic compounds such as herbicides and pesticides. Grazing in the Delta region is dominated by *Corbicula fluminea* (Jassby 2008). It is not known to what extent *C. fluminea* impacts cyanoHAB species versus the rest of the phytoplankton community in the Delta. The same is true for grazing by zooplankton. Another factor that may differentially impact cyanoHAB species versus the rest of the phytoplankton community is resistance to herbicides and pesticides. Investigations demonstrate substantial variability in sensitivity to herbicides of cyanobacteria compared with other phytoplankton such as green algae and diatoms (Peterson *et al.* 1997, Lurling and Roessink 2006)

4. PREVALENCE OF CYANOHABS AND POTENTIAL FOR EFFECTS ON ECOSYSTEM SERVICES IN THE DELTA

The Sacramento-San Joaquin Delta (hereafter Delta) is formed at the intersection of two of California's largest rivers, the Sacramento and the San Joaquin Rivers, and contains 700 miles of sloughs and waterways that drain 47% of the runoff in the State of California (Figure 1.1). The land surrounding the waterways is composed of 57 leveed island tracts, many of which provide wildlife habitat. In the Delta, freshwater from the rivers mix with saltwater from the San Francisco Bay; together the Bay and the Delta form the West Coast's largest estuary.

4.1 Ecosystem Services

The Delta region has many ecosystem services including agriculture, drinking water supplies, and wildlife habitat, all of which translate directly to the beneficial uses designated in the Water Board Basin Plan (Appendix A). The population surrounding the Delta region, numbering 500,000 people, is principally engaged in agriculture and produce crops that bring in revenues exceeding \$500 million annually. While there is some local demand on the water from the Delta, most of the water is distributed via the State Water Project and Federal Central Valley Projects to the Central Valley to irrigate farmland and to provide drinking water to Southern California (<http://www.water.ca.gov/swp/delta.cfm>). According to the California Department of Water Resources, about two thirds of Californians and millions of acres of irrigated farmland rely on the Delta for their water. Besides acting as a source of drinking water, the Delta is a popular recreation spot and many people use it for sport fishing.

In addition to the human demand, the Delta supplies critical habitat to a large wildlife ecosystem and intersects migration paths for several fish species, including salmon, traveling between the Pacific Ocean and the Sacramento River and beyond. This habitat is in a fragile state with close to 20 of its endemic species listed as endangered. A recent and unexpected decline in four pelagic fish species including the endangered Delta Smelt and the Longfin Smelt, as well as juvenile-Striped Bass and Threadfin Shad, has caused concern among resource managers and renewed calls for conservation of the fragile Delta ecosystem (Sommer *et al.* 2007).

Set against this backdrop of competing resource use by human populations and wildlife, a new threat to Delta ecosystem services and designated beneficial uses is emerging in the form of toxic cyanoHABs. The impact of toxic cyanobacteria on the aquatic ecosystem differs widely depending on whether their density is low or high. At low concentrations, they are not dense enough to affect light penetration or dissolved O₂ concentration; therefore, they do not affect the growth of other members of the aquatic community. However, even at low concentrations toxins released (upon death and cell lysis, or by grazing) can accumulate in tissues of higher trophic levels (Lehman *et al.* 2010). At high densities, cyanoHABs increase the turbidity of the water column to the point where light penetration is severely restricted suppressing the growth of other

phytoplankton, macrophytes, and benthic microalgae (Jeppesen *et al.* 2007, Paerl and Paul 2012). CyanoHABs also can cause night-time dissolved oxygen depletion via bacterial decomposition and respiration of dense blooms which results in fish kills and loss of benthic fauna (Paerl 2004, Paerl and Fulton 2006). At dense concentrations, mortality to aquatic animals such as sea otters, birds and seals may result from liver failure following ingestion of prey with high concentrations of toxin, or coming into physical contact with the toxin (Jessup *et al.* 2009, Miller *et al.* 2010). Humans coming in contact with the water may develop digestive and skin diseases (Section 2.2.6) and it may affect the drinking water supplies (Cheung *et al.* 2013). In the following sections, cyanoHAB abundance and toxin levels in the Delta vis-à-vis published guidance on alert levels are summarized in order to place the threat of cyanoHABs in the Delta into context.

4.2 Prevalence and Trends of CyanoHABs in the Delta

Since 1999 blooms of the toxin producing cyanobacteria *Microcystis aeruginosa* in the Delta have been observed by the Department of Water Resources (DWR), and have been reported in the scientific literature. In the beginning, only blooms of *Microcystis* were observed; these were documented visually appearing as little flakes of lettuce in the water (Lehman and Waller 2003). Later investigations (post 2005) employing microscopic enumeration and molecular characterizations have documented blooms comprised of a mix of *Aphanizomenon* sp. and *Microcystis*, with *Anabaena* sp. also present in much smaller densities (Lehman *et al.* 2010, Mioni *et al.* 2012).

While environmental indicators such as salinity, turbidity, temperature, total phytoplankton biomass (as Chl *a*), and phytoplankton species composition are monitored on a monthly basis by DWR, surface concentrations of cyanobacteria and cyanotoxins, which require special sampling, are not routinely monitored. As such, the information on the chronology of cyanoHAB occurrences presented here is taken from a handful of publications and reports, and varies somewhat in geographical extent according to where the authors sampled. Because *Aphanizomenon* and *Anabaena* densities have only been documented for two time points, the following sections will focus on *Microcystis* biomass and microcystin toxin concentrations. Additionally, these sections will focus on aquatic health rather than human health whose risks may be better evaluated from sampling of surface scums.

4.2.1 Spatial Distribution of *Microcystis* throughout the Delta

The Central Delta, between Antioch and Mildred Island, is typically the region with the highest surface *Microcystis* and *Aphanizomenon* concentrations. In 2003, the stations with the greatest recorded abundance of Chl *a* due to *Microcystis* (as determined by horizontal surface tows with a 75- μ m mesh plankton net) were Jersey Point (D16), Mokelumne River Mouth and Navigation Marker 13 in the San Joaquin River, followed by San Mound Slough, Mildred Island, (D29) and Rancho del Rio (D28) in Old River (Figure 4.1). In following years, greatest abundance of

Microcystis has repeatedly occurred in the same areas in the San Joaquin and Old Rivers (Lehman *et al.* 2008, Mioni *et al.* 2012, Lehman *et al.* 2013). In 2012, abundant *Microcystis* colonies were also observed in the South-East Delta region in the Turning Basin of the Stockton Shipping Channel (Spier *et al.* 2013). Moving west from Antioch into Suisun Bay, *Microcystis* abundance decreases substantially to almost non-detectable by Chipps Island (Lehman *et al.* 2005, 2008, 2010). The same holds true when moving north where abundances detected at Antioch decline to almost zero by Collinsville at the entrance of the Sacramento River (Figure 4.1).

Whether or not the spatial distribution of *Microcystis* and other cyanoHAB species is affected favorably or unfavorably by concentrations of herbicides entering the Delta as run-off, or from the Sacramento and San Joaquin Rivers is not known. Recent reports suggest that a broad swath of herbicides and fungicides associated with agriculture is present at concentrations high enough to affect aquatic life (Orlando *et al.* 2014). As such, the impact of herbicides common to the Delta in selectively promoting certain phytoplankton species, including possibly cyanoHAB species, may deserve greater attention.

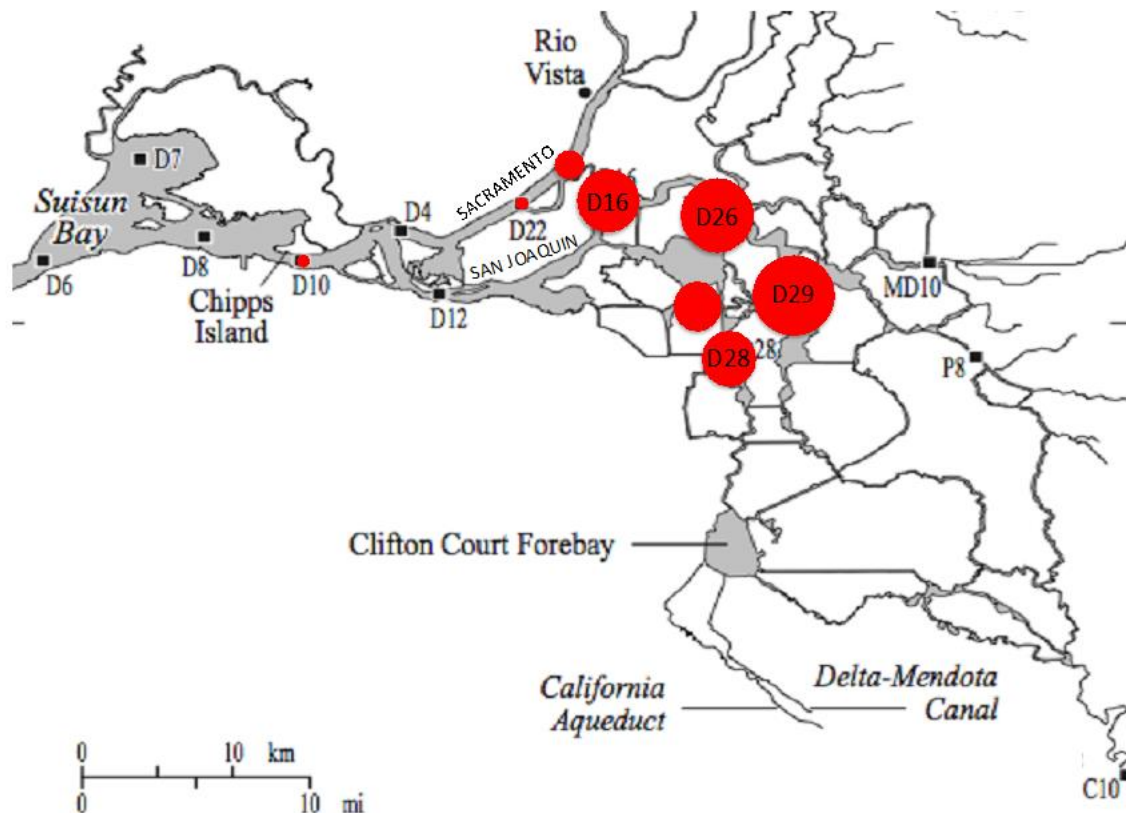


Figure 4.1. The Sacramento-San Joaquin Delta Region. Red bubbles mark locations with greatest *Microcystis*-associated surface Chl a concentrations (largest bubble= $0.55 \mu\text{g Chl a L}^{-1}$). Data from Lehman *et al.* 2005.

4.2.2 Interannual variability in *Microcystis* biomass in the Delta

Since 2003, *Microcystis* cell abundance in depth-integrated surface waters has varied from $4\text{--}40 \times 10^3$ cells mL^{-1} in the Delta (Lehman *et al.* 2008). The biomass (as surface Chl *a*) has also varied approximately 10-fold (Figure 4.2). Not only is *Microcystis* biomass patchy between years, its distribution in the years that it blooms is also variable. Even within a station, the distribution of *Microcystis* colonies is patchy, as evidenced by the low concentration of surface Chl *a*, sampled with horizontal net-tows normalized to total towed volume, which to date has not been above $0.6 \mu\text{g Chl } a \text{ L}^{-1}$ (Figure 4.2). In the years following 2005, *Microcystis* was also present in the phytoplankton community together with *Aphanizomenon flos-aqua*, and to a lesser extent *Anabaena* sp. (Lehman *et al.* 2008, Mioni *et al.* 2012).

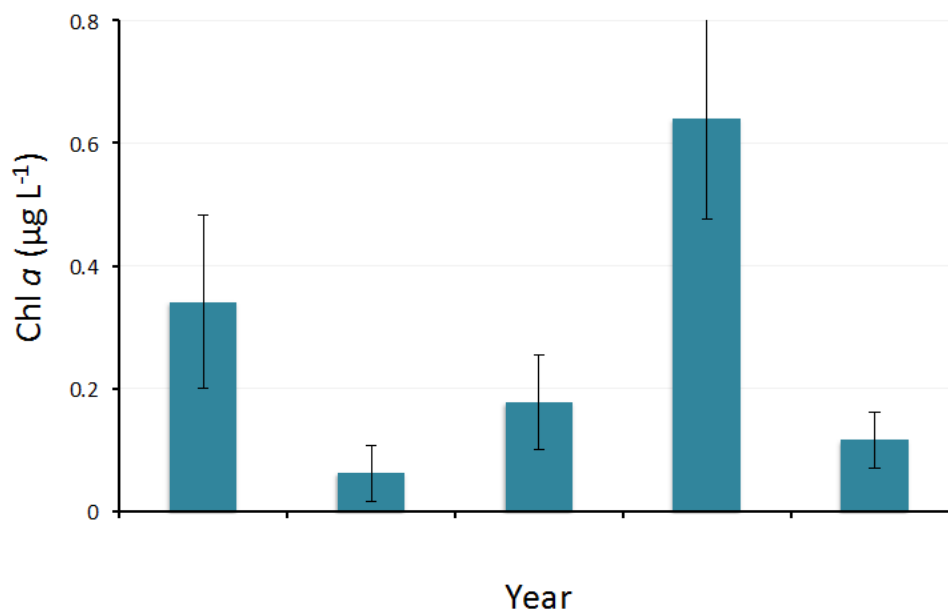


Figure 4.2. Interannual changes in surface Chl *a* due to abundance of *Microcystis* colonies. Means and standard deviations of 9 different stations in the San Joaquin River (Antioch (D12), Jersey Point (D16), Frank's Tract (D19), Potato Point (D26), Prisoners Point (D29), San Joaquin River at Turner Cut, Sand Mound Slough, Mildred Island, and Old River at Rancho del Rio (D28). Data from Lehman *et al.* 2005, 2013.

In addition to a high degree of horizontal variability, *Microcystis* cell densities and biomass also varies vertically in the water column, decreasing from the surface to almost zero at 1 m depth. The density of *Microcystis* in surface waters at the Central Delta Stations does not affect phytoplankton community composition in a measurable way. For example, at four stations where *Microcystis* dominated abundance of phytoplankton at the surface, the communities at 1m depth was a variable mix of different species of phytoplankton that was equally variable at stations containing no *Microcystis* in the surface. Rather than decreasing, the biomass of other

phytoplankton taxa increased in tandem with increasing *Microcystis* biomass (Lehman *et al.* 2010).

Compared with lakes widely recognized for severe CyanoHAB problems, *Microcystis* (and other cyanoHAB species) biomass appears low. For example, in Clear Lake spring and early summer Chl *a* concentrations average $11.5 \pm 8 \mu\text{g Chl } a \text{ L}^{-1}$ but increase to $352 \pm 295 \mu\text{g Chl } a \text{ L}^{-1}$ in the summer once *Microcystis* starts to bloom (Figure 4.4). Here, *Microcystis*-associated Chl *a* concentration is a factor of 100 to 1000 greater than it is in the Delta (Figure 4.4). One important caveat with respect to determining surface Chl *a* concentrations is that it depends on the method used to collect the surface Chl *a*. The difference between using a surface net tow (akin to what is used in Lehman *et al.* 2013) and a grab sample from the middle of a patch (akin to Mioni *et al.* 2012) can be close to be 100-fold, i.e. $0.2 \mu\text{g Chl } a \text{ L}^{-1}$ versus $20 \mu\text{g Chl } a \text{ L}^{-1}$, respectively. This is because the former is an integrated measure and the latter is not, suggesting that the “coverage” of *Microcystis* colonies in surface waters of the Central Delta is around 1%. This is in sharp contrast with Clear Lake where surface Chl *a* is uniformly high (above $150 \mu\text{g Chl } a \text{ L}^{-1}$) at all stations during a bloom (Richerson 1994, Mioni *et al.* 2012).

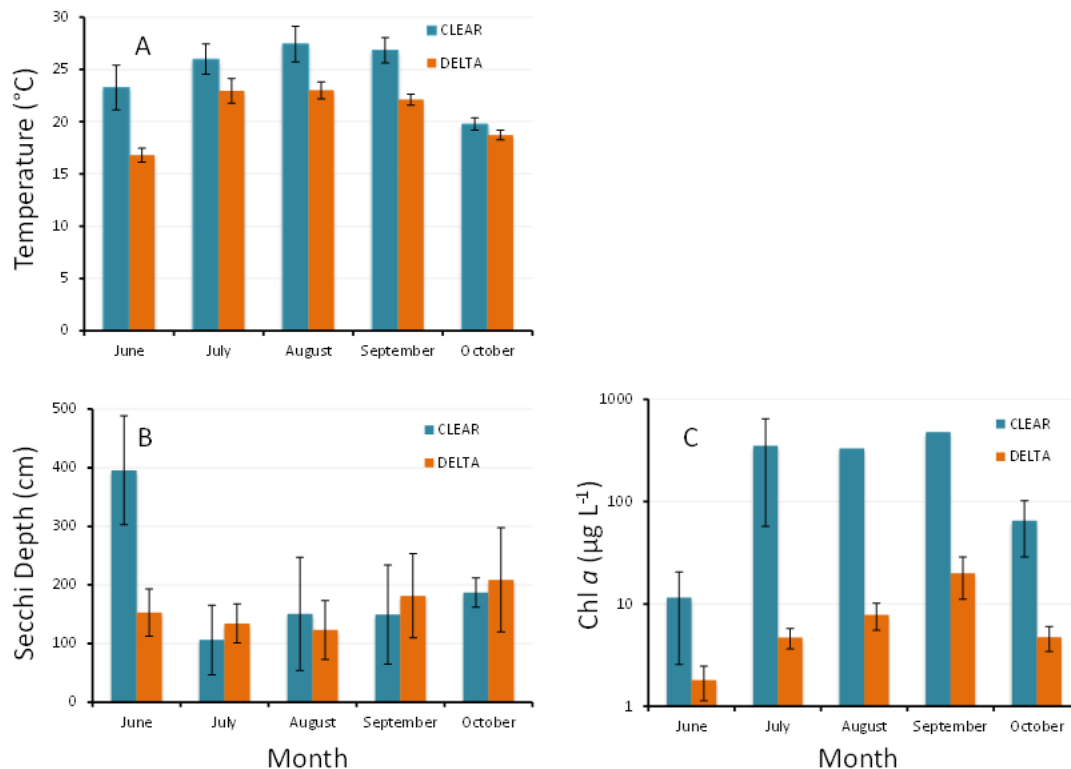


Figure 4.3. Comparison of environmental variables and Chl *a* in Clear Lake (Cyan) and the Delta (orange) using in-patch grab samples during the summer months of 2011. (A) Temperature, (B) Secchi disk depth, (C) Chl *a*. Data from Mioni *et al.* 2012.

4.2.3 Microcystin toxin concentrations in the Delta and San Francisco Bay

Given the number of different toxins produced by each cyanoHAB species, and the number of different genera present in Central California, one would expect a number of different toxins to be present in the water column. However, toxins other than microcystin are not frequently encountered (Kudela pers. com, Gibble and Kudela 2014). Based on the data available for the Delta, this section describes total microcystin concentrations and how they relate to *Microcystis* cell abundance.

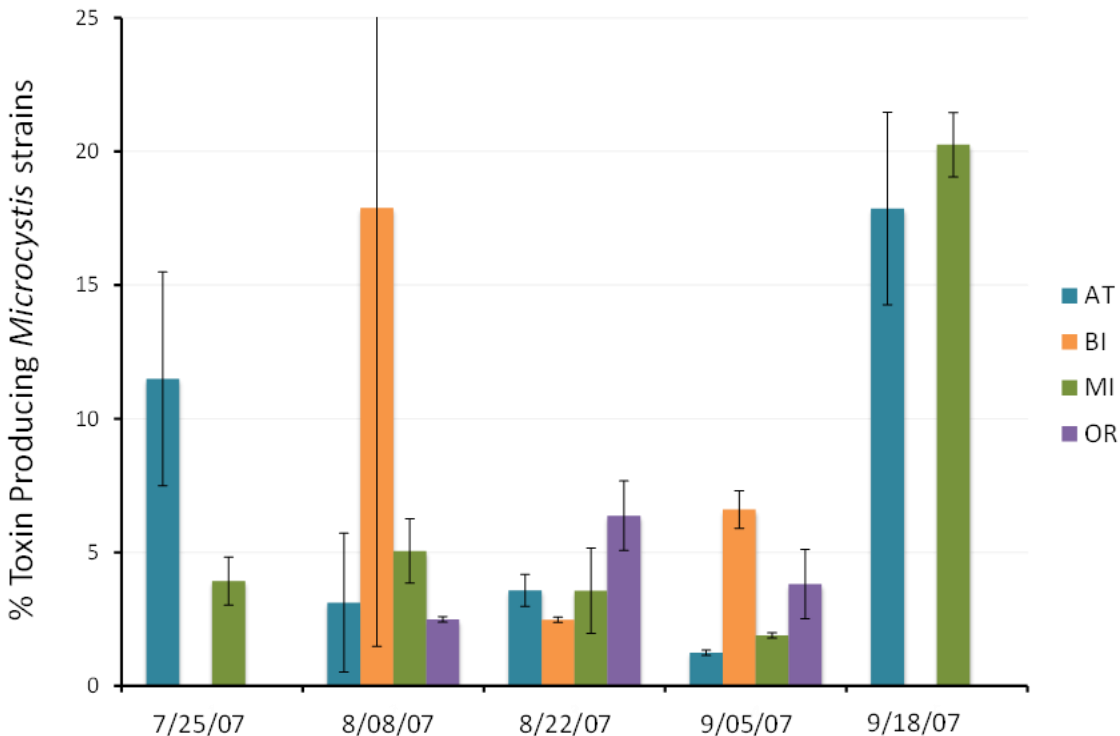


Figure 4.4. Percent toxin-producing strains in *Microcystis* assemblage at stations AT, Antioch (D12); BI, Brannan Island (D23); MI, Mildred Island; and OR, Old River at Rancho del Rio (D28). Data from Baxa *et al.* 2010.

Microcystis produces approximately 100-400 ng microcystin per μg Chl *a* in toxin producing strains (Sivonen and Jones 1999). Just as with other regions where *Microcystis* occurs, the strains that occur in the Delta are a mix of toxigenic and non-toxigenic strains (Baxa *et al.* 2010). Toxigenic strains generally comprise 2-20% of the total number of *Microcystis* strains present. This variation in the proportion of toxigenic strains is observed everywhere (i.e. at every station) and at all times (Figure 4.4). No single station stands out as consistently producing a greater proportion of toxigenic strains compared with other stations (Figure 4.4). Accordingly, total microcystin concentrations reflect total *Microcystis* cell abundance, typically varying from 10-50 ng L^{-1} (Lehman *et al.* 2008). However, in 2012 concentrations approaching 2000 ng L^{-1} were detected in the Stockton shipping channel during a *Microcystis* event (Spier *et al.* 2013).

In the Sacramento River, intermediate concentrations of total microcystins have been detected at a station close to Rio Vista (Brannon Island) where *Microcystis* cell abundance is low to non-detectable (Lehman *et al.* 2008, 2010). This station is connected via a channel to the San Joaquin River and the Frank's Tract area. Physical mixing of water directly from the San Joaquin River with brackish water at this station situated at the entrance to the Sacramento River may bring toxins but establishment of *Microcystis* populations may be prevented by the conditions in the Sacramento River including colder water, greater flow rates, mixing down to the bottom, and lower water clarity (Lehman *et al.* 2008).

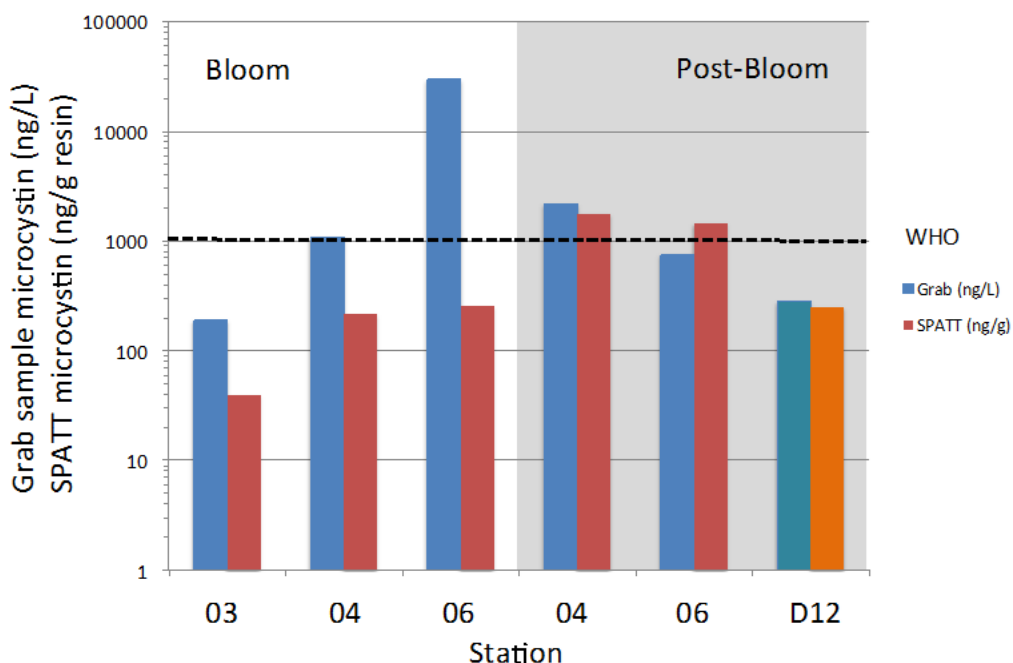


Figure 4.5. Microcystin toxin concentrations determined with grab samples (blue/cyan) and with SPATT resin (red/orange) at three stations in Clear Lake, during and after a *Microcystis* bloom, and at one station (D12, Antioch) in the Delta. Data from Mioni *et al.* 2012.

Microcystin toxin has also been detected at low concentrations throughout the Delta and the San Francisco Estuary using the novel Solid Phase Adsorption Toxin Tracking (SPATT) technique which integrates exposure of dissolved toxins over longer time spans (Kudela 2011). While valuable to indicate a potential for exposure to cyanotoxins, the comparison of SPATT to existing guidelines for human and aquatic health is problematic because SPATT detected concentrations are not directly comparable to traditional, instantaneous grab samples. For example, in Clear Lake microcystin detected with SPATT (ng/g resin) was 5-115 times lower than grab samples (ng/L) taken the last day of the SPATT deployment during the height of a *Microcystis* bloom (Figure 4.5). Post bloom, microcystin detected with SPATT was either comparable to, or double, levels measured in grab samples (Figure 4.5). While microcystin was

detectable both with SPATT and with grab samples in Clear Lake, microcystin was detectable with SPATT in the Delta, at similar levels as in Clear Lake, but not with grab samples. In the former system *Microcystis* was very abundant and in the latter it was not. The above example illustrates that given longer equilibration times, SPATT becomes more sensitive than grab samples at lower concentrations of toxins. Although difficult to “translate” directly into effects on aquatic life (i.e. Echols *et al.* 2000), SPATT detection may be a very useful system for identifying regions at risk for harm to aquatic life from toxin exposure (Gibble and Kudela 2014).

4.2.4 Potential for CyanoHAB Risk to Delta Beneficial Uses

Characterization of the risk of cyanoHABs to Delta beneficial uses is generally poor. While no guidelines for toxicity of cyanotoxins to aquatic life have been established for California, total microcystin levels found in the Delta are within the range of potential impacts to aquatic health, as recently reviewed by the California Office of Environmental Health Hazards (OEHHA 2009). For example, microcystins are acutely toxic to fish at concentrations as low as a fraction of a microgram per liter (OEHHA 2009). Chronic exposures can also be problematic; embryos and larval fish appear to be very sensitive to chronic exposures to microcystins, resulting in oxidative stress, reduced growth, developmental defects, and lethality; exposures as low as 0.25 µg/L resulted in oxidative stress to zebrafish embryos (OEHHA 2009).

Consumption of prey items with body burdens of cyanotoxins can also be a potential pathway of impact. Lehman *et al.* (2010) traced increasing concentrations of microcystins from the water (25-50 ng L⁻¹) to zooplankton (0.4-1.5 µg g dry wt⁻¹) to striped bass muscle tissue (1-3.5 µg g dry wt⁻¹) at Central Delta Stations. These values are within the range of sublethal microcystin doses to fish (2.5 µg g dry wt⁻¹; OEHHA 2009). The striped bass caught at stations where *Microcystis* cells comprised 100% of the surface Chl *a* had tumor lesions in their liver tissue, consistent with the sublethal effects caused by microcystin-LR toxin (OEHHA 2009, Lehman *et al.* 2010). This is consistent with fish feeding studies which demonstrate that microcystin-LR spiked diets result in lesions of the liver (Deng *et al.* 2010; Acuna *et al.* 2012a,b).

Zooplankton are also acutely sensitive to *Microcystis aeruginosa* cells; diets consisting of 50% toxigenic and non-toxigenic *Microcystis* strains result in 100% mortality in the copepods *Eurytemora affinis* and *Pseudodiaptomus forbesi* (Ger *et al.* 2010). Interestingly, when fed diets containing only 10-25% *Microcystis* cells, both copepods demonstrate significantly greater survival on the toxigenic strain than the non-toxigenic strain, suggesting that bioactive compounds other than the microcystin toxin exert a greater adverse impact on the zooplankton (Ger *et al.* 2010). This is consistent with a number of the studies of the effect of cyanoHABs on zooplankton mentioned in Section 2.2.6.

Determination of risk to human health in the Delta is problematic because cyanoHABs monitoring has been focused on aquatic health (depth-integrated sampling) rather than human

health (via surface-scum sampling). With this caveat, toxin concentrations of 10-50 ng L⁻¹ (Lehman *et al.* 2008) are 16-80 times lower than the Office of Environmental Health Hazard Assessment (OEHHA) Action Level for human health (Table 4.1), but the 2012 concentrations approaching 2000 ng L⁻¹ in the Stockton shipping channel (Spier *et al.* 2013) exceed both the OEHHA Action level and the WHO guideline of 1000 ng L⁻¹ (Table 4.1).

Table 4.1. Action levels developed by OEHHA (2009) for human health exposure to cyanotoxins compared with the WHO guidance level for microcystins and the EPA 10-day average exposure threshold.

Toxin	OEHHA Recreational Use (µg/L water)	OEHHA Consumption Level (ng/g fish)	WHO recreational Use (µg/L water)	EPA 10-day average (µg/L)
Microcystins	0.8	10	1.0	0.3
Cylindrospermopsin	4	70		
Anatoxin-a	90	5000		

4.2.5 Summary of Potential for Adverse Effects on Delta Beneficial Uses

A thorough characterization of the risks for adverse effects on Delta beneficial uses is hindered by the fact that cyanoHAB prevalence and toxin concentrations are currently not routinely monitored in the Delta; moreover, sampling has been focused on aquatic health and does not include sampling for human health risks. Determination of risk to human health is not possible at this time because surface scums are not currently being monitored. The current risk to Delta aquatic health is of concern and merits a more thorough investigation. This observation is based on total microcystin levels found in Delta fish tissues that are within the range of sublethal effects to fish as recently reviewed by the California Office of Environmental Health Hazards (OEHHA 2009). In addition, dissolved toxin concentrations (10- 50 ng L⁻¹) that are generally 16-80 times below the OEHHA action level, occasionally exceed both the OEHHA action level and the WHO guideline of 1000 ng L⁻¹ in certain “hotspots” of the Delta. Whether or not these hotspots are expanding is currently not known and merits further investigation and monitoring.

5.0 SYNTHESIS OF FACTORS INFLUENCING CYANOHABS PRESENCE AND TOXIN PRODUCTION IN THE DELTA

The charge of the cyanobacterial workgroup, as outlined in the Delta Nutrient Management Charter, is to “assess whether observed increases in the magnitude and frequency of cyanobacterial blooms in the Delta is the result of long-term changes in nutrient concentrations and whether management of nutrient loads can remedy the problems associated with cyanobacteria.” The best way to characterize the relationship between the extent and frequency of bloom occurrence and nutrient concentrations is by regression analysis. Ideally, this type of analysis ought to be performed in multiple locations for longer time scales. Given that temperature, irradiance and water column clarity are such powerful triggers of blooms, stepwise multiple regression analysis to test the influence of several environmental indicators simultaneously on cyanoHAB cell densities would be even more useful in order to ascertain key triggers of the blooms in the Delta region.

While environmental indicators such as salinity, turbidity, temperature, total phytoplankton biomass (as Chl *a*), and phytoplankton species composition are monitored on a monthly basis by DWR, surface concentrations of phytoplankton, which requires special sampling, are not routinely monitored in this program. Therefore, the statistical analyses needed to answer the charge of the cyanobacterial working group cannot be performed at this time. Instead, this section focuses on summarizing factors known to favor cyanobacterial prevalence (from Section 2) and synthesizing available literature on the extent to which those factors may also be at play in the Delta.

5.1 Present and Future Factors associated with cyanoHAB prevalence in the Delta

5.1.1 Flow and mixing

Environmental and population drivers that promote growth of cyanoHABs in freshwater bodies around the world also play key roles in regulating growth of cyanoHABs in the Delta (Table 5.1). Chief among these is low flow. For example, Lehman *et al.* (2013) noted that increased abundance of *Microcystis* is associated with up to a 50% reduction in flow of water in the San Joaquin River. In 2004, *Microcystis* only appeared in the Central Delta when stream flow was 1-35 m³ s⁻¹ (Lehman *et al.* 2008). In addition to direct effects of decreased flow such as increased stratification of the water column, changes in flow and mixing also impart indirect effects that may influence cyanobacterial growth. These include changes in turbulence, sediment resuspension (therefore turbidity), chemical constituents, and water temperature to mention a few. Changes in these parameters typically cannot be separated from that of flow to determine their relative importance. For example, in the Delta, reduction in flow is accompanied by a 50% reduction in turbidity and volatile suspended solids. Decreased flow also leads to increased water temperatures. Conditions of decreased flow occur more predictably in dry years (Lehman *et al.*

2013). Within the summer season, reduced flows typically occur in the July-August time frame (Figure 5.1) and set the stage for the two factors necessary for bloom initiation, including increased water column temperature and water column clarity (decreased turbidity). While decreased flow may increase the abundance of *Microcystis*, increasing rates of flow decrease its abundance because of the negative effects of water column mixing, such as light limitation, on its growth. Artificial mixing is even used as a strategy to mitigate blooms of harmful cyanobacteria in lakes and reservoirs (Reynolds *et al.* 1983, Burford and O'Donohue 2006). In the Delta, natural mixing rates may be sufficient to restrict the abundance of *Microcystis* to 10-15% of the total phytoplankton community.

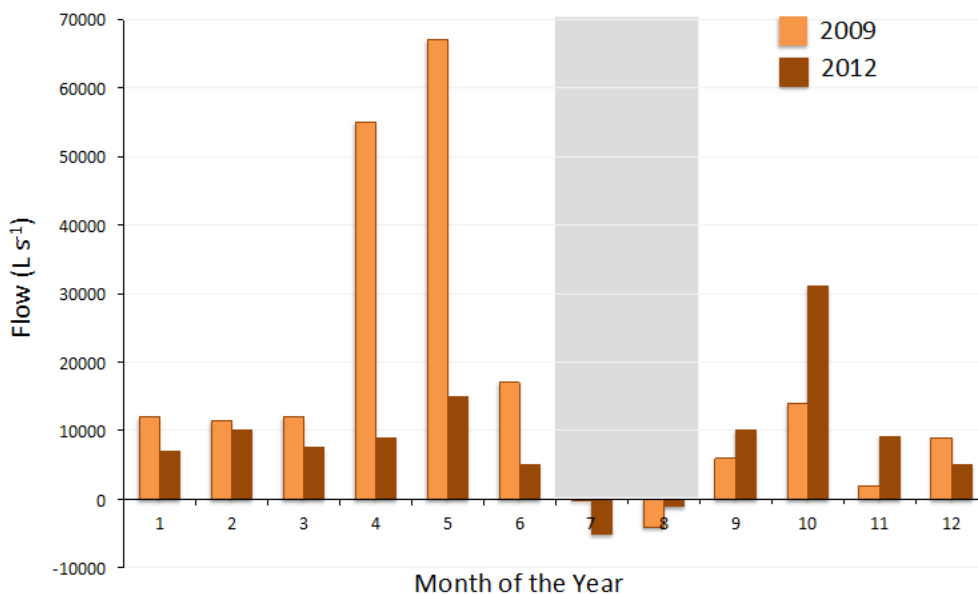


Figure 5.1. Variation in flow at Brandt Bridge in the Delta (years 2009 and 2012) illustrating the low- and reverse-flow window in July-August (shaded grey). Data and plot from Spier *et al.* 2013.

5.1.2 Temperature

Aside from the rate of water flow, water temperatures have increased globally over the last few decades as a result of global warming (Gille 2002, Hansen *et al.* 2005). In the Central Delta, a change from mainly negative deviations in the water temperature from the long-term mean to positive deviations occurred in 1999 (Figure 5.2). This local change in the water temperature may be part of the larger-scale global patterns and/or the Pacific Decadal Oscillation weather pattern which also changed sign in the same year (Cloern *et al.* 2007).

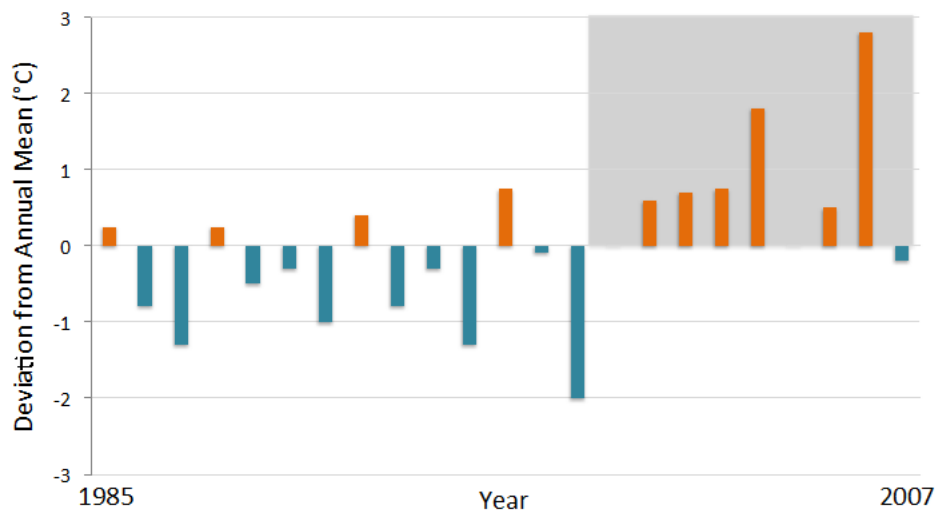


Figure 5.2. Deviation from the annual mean of maximum water temperatures at Stockton in the Central Delta. Grey shaded area indicates period from 1999 onwards with increased positive temperature deviations. Data from Brooks *et al.* 2011.

The interesting question with respect to changes in water temperatures is whether they are great enough to affect competition between cyanobacteria and other members of the phytoplankton community in the Central Delta. Presently, 40-75% of the phytoplankton community in the Delta is comprised of diatoms, followed by chlorophytes (15-30%), cyanobacteria (15-40%), cryptophytes (5-10%) and flagellates (0-10%), including dinoflagellates (Lehman 2007). In order for cyanoHAB species to grow faster than diatoms and displace diatoms as the dominant member of the phytoplankton community, they would have to be able to accelerate their growth rates up to 2-3 fold. Alternatively, a scenario where the growth rate of diatoms would decrease and cyanobacteria would increase is necessary. Examining variation in growth rates with changes in environmental data, temperature appears the most likely candidate for bringing about such a change. Data from Figure 3.6 indicates that a doubling in cyanobacterial growth rates occurs with an increase in temperature from 20-27°C, whereas diatom growth rates decrease over the same temperature range. Therefore, a rise in temperature is a scenario under which cyanobacteria are able to outcompete diatoms.

This scenario is consistent with differences in temperature between a system, such as Clear Lake, where cyanoHABs dominate community composition, and the Delta. Comparing the 2011 environmental variables from Clear Lake and the Central Delta, two pre-bloom (June) differences become immediately clear. One is that the water temperature in Clear Lake is 7°C degrees warmer than the Delta (Figure 4.3). The other is that the Secchi disk depth is 2.6-fold greater in Clear Lake compared with the Delta (Figure 4.3). This difference in water clarity disappears in July when the *Microcystis* bloom takes off in Clear Lake, increasing Chl *a* 35-fold and decreasing the water clarity (Figure 4.3). Lehman *et al.* (2013) also predicted that the two

factors that potentially would make the greatest impact on accelerating the growth of *Microcystis*, and increase the frequency and duration of blooms in the Delta, would be increased water temperatures and increased water column clarity. The earlier in the growth season that these increases would occur the greater the window of opportunity for growth would become (see also Peeters *et al.* 2007).

5.1.3 Water Clarity

The Central Delta is highly turbid due to large amounts of sediments transported into the upper estuary via the Sacramento River as well as due to sediment resuspension. However, as more and more of the sediment load is being caught behind dams, sediment transport is on the decline and the upper estuary is becoming less turbid (Schoellhamer *et al.* 2012). Since 1975, turbidity at Stations D26 and D28 has declined by on average 2 and 4% per year, respectively (Jassby 2008). These average declines are accentuated by declines in turbidity of up to 50% during the low flow months (Lehman *et al.* 2013). If these present declines in turbidity in the Central Delta continue into the future, they may substantially promote growth of cyanoHAB species.

5.1.4 Nutrient Concentrations

If water temperatures did not increase above the summer-time average of 18-20°C, could there be a 2-fold acceleration in cyanobacterial growth rates with changes in N source, or with N:P ratio, at non-limiting nutrient concentrations that would enable them to outcompete diatoms and become dominant? To answer this question, we can 1) look to growth results from culture investigations and 2) investigate how nutrient ratios differ between a system that is overwhelmed by *Microcystis* (such as Clear Lake) compared with the Delta.

- 1) Culture investigations demonstrate that there is no significant, or consistent, change in growth rates with change in N source, or N:P ratios, at nutrient concentrations in excess of demand (Tilman *et al.* 1982, Tett *et al.* 1985, Reynolds 1999, Saker and Neilan 2001, Roelke *et al.* 2003, Sunda and Hardison 2007).
- 2) Comparing the ratios of dissolved N:P between the Delta and Clear Lake, 3.6 ± 0.6 and 2.9 ± 0.8 , respectively, it's clear that these are essentially the same (Mioni *et al.* 2012). Nutrient ratios also do not vary from pre-bloom to bloom in the Delta, indicating that nutrients are in excess of phytoplankton demand for the entire summer season (Lehman *et al.* 2008, Mioni *et al.* 2012). Moreover, nutrient concentrations, or ratios, do not change sufficiently from year-to-year in order to explain year-to-year variation *Microcystis* biomass or occurrence. For example, since 1994 there has been no change in concentrations or ratios of nutrients in the Central Delta (Appendix A).

Therefore, the initiation of *Microcystis* blooms around 1999 in the Delta was probably not associated with changes in nutrient concentrations or their ratios. However, as with all

phytoplankton blooms, once initiated, cyanoHABs cannot persist without an ample supply of nutrients. It is important to keep in mind that while nutrient reduction may not limit the onset or frequency of bloom occurrence, it will limit bloom duration, intensity and possibly also geographical extent. If, in the future, nutrient concentrations were to decrease to the point where they start to limit phytoplankton biomass, then the magnitude of the nutrient pool, as well as seasonal changes in the magnitude, would impact cyanoHAB concentration, distribution and bloom duration.

Interestingly, the long-term record for station D26 demonstrates that a decline in Chl *a* and corresponding increases in nitrogen concentrations (NH_4^+ and NO_3^-) and N:P ratios occurred in the period from 1985-1994 (Appendix A). Jassby (2008) reported similar changes in Chl *a* (decrease) and nitrogen (increase) at Central Delta Stations D16 and D28 between the years 1985 and 1994. Van Nieuwenhuysse (2007) hypothesized that the changes in N:P ratios and Chl *a* were driven by a decrease in phosphorus loadings to the Sacramento River that occurred in 1994; however the step change in P loading that year does not explain the gradual decrease in Chl *a* that started prior to 1994 (Appendix A).

Gradual decreases in Chl *a* concentrations may have been brought about by relative changes in flow and benthic grazing, leading to a new and lower Chl *a* equilibrium by the mid-1990's (Lucas and Thompson 2012). According to Lucas and Thompson (2012) the areas of the Delta where benthic grazing typically overwhelms phytoplankton growth rates are the same as those where *Microcystis* tends to bloom (Figure 4.1; Lehman *et al.* 2005). Because *Microcystis* floats at the very surface, it may avoid being grazed by clams in contrast with other phytoplankton that are distributed throughout the water column. It's important to bear in mind that large-scale (temporal and spatial) variation in environmental factors such as flow and grazing by clams may have a more profound impact on phytoplankton standing stocks, and competition among different phytoplankton taxa, compared with many of the autecological adaptations discussed in this review.

5.2 Summary

In the review of the global literature on factors influencing cyanobacterial blooms and toxin production, five principal drivers emerged as important determinants:

- 1) Water temperatures above 19°C
- 2) High irradiance and water clarity
- 3) Availability of N and P in non-limiting amounts; scientific consensus is lacking on the importance of N:P ratios and nutrient forms (e.g. ammonium) as a driver for cyanoHABs
- 4) Long residence times and stratified water column
- 5) Low salinity (<10 ppt) waters

Comprehensive understanding of the role of nutrients vis-à-vis other environmental factors in influencing cyanoHAB presence in the Delta is severely hampered by the lack of a routine monitoring program. The DWR monitoring program currently measures many of the environmental factors of interest, except cyanobacterial abundance and toxin concentration, which require a different approach than that used in standard phytoplankton monitoring. Drawing on the five factors influencing cyanoHABs, we can conclude the following:

- Because of the large effects of temperature and irradiance on accelerating, and decelerating, the growth rates of cyanoHABs, these two factors appear to exert key roles in the regulation of the onset of blooms. Cyanobacteria require temperatures above 20°C for growth rates to be competitive with eukaryotic phytoplankton taxa, and above 25°C for growth rates to be competitive with diatoms (Table 5.1). In addition, they require relatively high irradiance to grow at maximal growth rates. This is in contrast with diatoms that are able to keep near-maximal growth rates at irradiances limiting to cyanoHABs in the Delta, e.g., 50 $\mu\text{mol phot m}^{-2} \text{ s}^{-1}$ (Table 5.1).
- It appears that N and P are available in non-limiting amounts in the Delta; moreover concentrations, or ratios, do not change sufficiently from year-to-year to explain year-to-year variation in *Microcystis* biomass or occurrence. Therefore, the initiation of *Microcystis* blooms and other cyanoHABs are probably not associated with changes in nutrient concentrations or their ratios in the Delta. However, as with all phytoplankton blooms, once initiated, cyanoHABs cannot persist without an ample supply of nutrients. As long as temperatures, flow rates and irradiance remain favorable for growth, the size of the nutrient pool will determine the magnitude and extent of cyanoHAB blooms.
- Salinity is controlling the oceanward extent of cyanobacterial blooms in the Delta, but salinity gradients do not explain the spatial distribution of cyanoHABs in the Delta (Table 5.1). Notably, salinity regime is not a barrier to toxin transport, as cyanotoxins have been detected in San Francisco Bay.
- Higher flows, turbidity and lower temperatures during most of the year are likely restricting cyanobacterial blooms to the July-August time period.

Climate change and anthropogenic activity associated with land use changes have the potential to alter cyanoHAB prevalence in the future. Climate change will likely result in warmer temperatures and increased drought, the latter of which could result in reduced flows, increased residence time and water column stability leading to higher light availability in the Delta. Both higher temperatures and reduced flows would presumably result in a greater prevalence of cyanoHABs. It's noteworthy that phytoplankton biomass and primary productivity are depressed relative to available nutrients in the Delta, so it's unclear what the effect of modifying nutrient loads will have on frequency and intensity of cyanoHAB occurrence in the future.

Table 5.1. Summary of general physiological drivers of cyanobacterial growth, how they are manifested in population growth and competition with diatoms, and how they compare with environmental drivers observed to be operating in the Delta.

Physiological Driver	Population Driver	Observations in the Delta
Growth significantly slower below 20°C, and greater above 25°C, compared with eukaryotic phytoplankton taxa	Requires temperatures above 25°C for growth rates to be competitive with diatoms	Not observed at temperatures <19°C
Cyanobacteria have greater cellular N:P ratios than diatoms due to two light harvesting systems and peptide toxin production	At non-limiting nutrient concentrations, changes in ratios of nitrogen substrates or N:P does not affect competition among species or taxa	Nutrient concentrations, nitrogen speciation, and dissolved N:P ratios have not changed in the Delta over the last 25 years
Production of bioactive peptide compounds (toxic and non-toxic) results in high N demand of cells	Toxin production per cell is greatest at maximal growth rates; linked with external N concentrations and decrease at N limiting conditions; cyanoHABs do not secrete toxin	Inorganic N and P concentrations are at non-limiting concentrations for growth and toxin production; Variation in toxin produced per cell or in number of toxigenic vs non-toxigenic strains is not related to any specific environmental condition
Inefficient photosynthesis, low alpha; efficient at dissipating excess light energy via high concentration of carotenoid pigments in photosystems (<i>Microcystis</i>, <i>Anabaena</i> and <i>Aphanizomenon</i>)	CyanoHABs (<i>Microcystis</i> , <i>Anabaena</i> and <i>Aphanizomenon</i>) require high irradiance to grow; diatoms able to keep near-maximal growth rates at irradiances limiting to cyanoHABs (e.g. 50 $\mu\text{mol phot m}^{-2} \text{s}^{-1}$)	High rate of water flow and mixing most of the growing season restricting blooms to low-flow periods (July-August), when turbidity is < 50 NTU, flow is <30 $\text{m}^3 \text{s}^{-1}$ and irradiance > 50 $\mu\text{mol phot m}^{-2} \text{s}^{-1}$ (Central Delta 2004-2008)
Growth optimal at salinities <10 ppt for most cyanoHAB species	CyanoHABs generally restricted to freshwater habitats and estuaries with salinities <10 ppt (Baltic Sea, San Francisco Delta, North Carolina)	Does not proliferate outside the Delta in the Sacramento River (freshwater) or Suisun Bay (mesohaline) suggesting that the primary agent restricting its spread is not salinity

6.0 RECOMMENDATIONS

The goal of this review is to synthesize available information to provide insight into cyanobacterial bloom occurrence in the Delta. The review has three major objectives:

- 1) Provide a basic review of biological and ecological factors that influence the prevalence of cyanobacteria and the production of cyanotoxins;
- 2) Summarize observations of cyanobacterial blooms and associated toxins in the Delta;
- 3) Synthesize literature to provide an understanding of what ecological factors, including nutrients, may be at play in promoting cyanobacterial blooms in the Delta.

This review found that the lack of a routine monitoring of cyanoHAB occurrence in the Delta greatly hindered our ability to summarize, with confidence, the status and trends of cyanoHABs in the Delta (Objective 2), and to what extent nutrients versus other factors were controlling their occurrence (Objective 3). Given this finding, our recommendations are focused on two principal actions:

- 1) Strengthening routine monitoring; and
- 2) Development and use of an ecosystem model, coupled with routine monitoring and special studies, to 1) understand controls on primary productivity and phytoplankton assemblage in the Delta and 2) test hypotheses regarding factors promoting or curtailing growth of cyanobacteria.

R1: Implement Routine Monitoring of CyanoHABs

DWR is currently conducting a monitoring program that routinely samples many of the variables of interest known to influence cyanoHABs. Comprehensive cyanoHAB monitoring should be added as a component to this program to fully evaluate risk to human and aquatic health as well as better understand linkages to factors that may be promoting or maintaining blooms.

To begin, a work plan should be developed which specifically scopes the needed changes in the program to comprehensively monitor cyanoHABs. Monitoring should include enumeration of major cyanobacterial species (e.g. *Microcystis*, *Aphanizomenon* and *Anabaena*). Sampling of toxins should include water column concentrations as well as mussel tissue concentrations or other important taxa that represent sentinels for bioaccumulation in the food web. Analyses of toxin concentrations should be expanded to include the six major cyanotoxins of concern identified in the OEHHA guidance in year 1 then adjusted based on the most commonly encountered toxins thereafter. In addition, selective sampling for analysis of concentrations of herbicides and fungicides commonly encountered in the Delta should be considered. The workplan should also consider monitoring needed to develop and calibrate an ecosystem model to further investigate controls on primary productivity and phytoplankton assemblage (see R2 below).

After an initial period of 3-5 years, the monitoring data should be used to comprehensively report on the status and trends of cyanoHABs and the factors that favor bloom occurrence in the Delta.

R2: Develop an Ecosystem Model of Phytoplankton Primary Productivity and HAB Occurrences to further Inform Future Risk and Hypotheses on Factors Controlling CyanoHABs

The Delta is at an advantage with respect to management of cyanoHABs in that naturally occurring high rates of flow and turbulence act to keep cyanobacteria in check. Despite this, future increases in temperature and residence time associated with climate change, increasing the degree and duration of stratification events, may substantially degrade the effectiveness of the Delta's breaking mechanism and increase the risk of cyanoHAB occurrences. Because nutrients are not currently limiting cyanobacterial blooms, it is critical that an improved understanding is gained of the factors that are controlling phytoplankton primary productivity in the Delta, since a relaxation of those factors followed by increased growth of phytoplankton could lead to increased risk of cyanoHABs.

To inform management actions moving into the future, an ecosystem model of phytoplankton primary productivity and HAB occurrences should be developed. This model should have the capability to provide information on primary productivity and biomass as well as planktonic food quality and transfer of carbon to higher trophic levels. Moreover, such a model could be used to assess the relative importance of environmental factors such as benthic grazing, flow, water column stability, temperature, to mention a few, at various times and locations in the Delta, on cyanobacterial growth. To step into model development, four steps should be taken: 1) examine existing models already available to determine suitability for this task, 2) utilize existing data from the Central Delta to explore, to the extent possible, the relationships between Chl *a*, phytoplankton composition, climate variables and other factors at stations where cyanoHABs are known to occur (e.g. D26, D28 and turning basin in the Stockton Shipping Channel). 3) Develop hypotheses regarding the environmental conditions in those areas that promote cyanoHABs. In addition, develop hypotheses regarding conditions needed to curtail cyanoHABs; including the effect of reducing nutrient loads on the entire phytoplankton community (including cyanobacteria) and on the transfer of carbon to higher trophic levels. These hypotheses can subsequently be tested through model development as well as potential future scenarios, and 4) a work plan should be developed that lays out the modeling strategy, model data requirements, and implementation strategy.

7.0 LITERATURE CITED

- Acuna, S., D. Baxa and S. Teh. 2012a. Sublethal dietary effects of microcystin producing *Microcystis* on threadfin shad, *Dorosoma petenense*. *Toxicon* 60:1191-1202.
- Acuna, S., D.F. Deng, P. Lehman and S. Teh. 2012b. Sublethal dietary effects of *Microcystis* on Sacramento splittail, *Pogonichthys macrolepidotus*. *Aquatic Toxicology* 110-111:1-8.
- Ahn, C.Y., H.M. Oh and Y.S. Park. 2011. Evaluation of environmental factors on cyanobacterial bloom in eutrophic reservoir using artificial neural networks. *Journal of Phycology* 47:495-504.
- Alexova, R., M. Fujii, D. Birch, J. Cheng, T.D. Waite, B.C. Ferrari and B.A. Neilan. 2011. Iron uptake and toxin synthesis in the bloom-forming *Microcystis aeruginosa* under iron limitation. *Environmental Microbiology* 13:1064-1077.
- Arrigo, K.R., D.H. Robinson, D.L. Worthen, R.B. Dunbar, G.R. DiTullio, M. VanWoert and M.P. Lizotte. 1999. Phytoplankton community structure and the drawdown of nutrients and CO₂ in the Southern Ocean. *Science* 283:265-367.
- Babica, P., L. Blaha and B. Marsalek. 2006. Exploring the natural role of microcystin – a review of effects on photoautotrophic organisms. *Journal of Phycology* 42:9-20.
- Baker, P.D. 1999. Role of akinetes in the development of cyanobacterial populations in the lower Murray River, Australia. *Marine & Freshwater Research* 50:265-279.
- Baker, P.D. and D. Belliferrine. 2000. Environmental influences on akinete germination of *Anabaena circinalis* and implications for management of cyanobacterial blooms. *Hydrobiologia* 427:65-73.
- Baxa, D., T. Kurobe, K.A. Ger, P.W. Lehman and S.J. Teh. 2010. Estimating the abundance of toxic *Microcystis* in the San Francisco Estuary using quantitative real-time PCR. *Harmful Algae* 9:342-349.
- Beard, S.J., B.A. Handley, P.K. Hayes and A.E. Walsby. 1999. The diversity of gas vesicle genes in *Planktothrix rubescens* from Lake Zurich. *Microbiology* 145:2757-2768.
- Becher, P.G., J. Beuchat, K. Gademann and F. Juttner. 2005. Nostocarboline: isolation and synthesis of a new cholinesterase inhibitor from *Nostoc* 78-12A. *Journal of Natural Products* 68:1793-1795.
- Berg, G.M., P.M. Glibert, N.O.G. Jorgensen, M. Balode and I. Purina. 2001. Variability in inorganic and organic nitrogen uptake associated with riverine nutrient input in the Gulf of Riga, Baltic Sea. *Estuaries* 24:204-214.
- Berg, G.M., M. Balode, I. Purina, S. Bekere, C. Bechemin and S.Y. Maestrini. 2003. Plankton community composition in relation to availability and uptake of oxidized and reduced nitrogen. *Aquatic Microbial Ecology* 30:263-274.

Berg, G.M., J. Shrager, G. van Dijken, M.M. Mills, K.R. Arrigo and A.R. Grossman. 2011. Responses of *psbA*, *hli*, and *ptox* genes to changes in irradiance in marine *Synechococcus* and *Prochlorococcus*. *Aquatic Microbial Ecology* 65:1-14.

Berman, T. and S. Chava. 1999. Algal growth on organic compounds as nitrogen sources. *Journal of Plankton Research* 21:1423-1437.

Berry, J.P., M. Gantar, M.H. Perez, G. Berry and F.G. Noriega. 2008. Cyanobacterial toxins as allelochemicals with potential applications as algicides, herbicides and insecticides. *Marine Drugs* 6:117-146.

Boison, G., C. Steingen, L.J. Stal and H. Bothe. 2006. The rice field cyanobacteria *Anabaena azotica* and *Anabaena* sp. CH1 express vanadium-dependent nitrogenase. *Archives of Microbiology* 186:367-376.

Bolmstedt, A.J., B.R. O'Keefe, R.S. Shenoy, J.B. Memahon and M.R. Boyd. 2001. Cyanoviridin-N defines a new class of antiviral agent targeting N-linked, high-mannose glycans in an oligosaccharide-specific manner. *Molecular Pharmacology* 59:949-954.

Borner, T. and E. Dittmann. 2005. Molecular biology of cyanobacterial toxins. pp. 25-40 in: J. Huisman, H.C.P. Matthijs and P.M. Visser (eds.), *Harmful Cyanobacteria*. Springer. New York, NY.

Boyd, M.R., K.R. Gustafson, J.B. McMahon, R.H. Shoemaker, B.R. O'Keefe, T. Mori, R.J. Gulakowski, L. Wu, M.I. Rivera, C.M. Laurencot, M.J. Currens, J.H. Cardellina, R.W. Buckheit, Jr., P.L. Nara, L.K. Pannell, R.C. Sowder and L.E. Hendersong . 1997. Discovery of cyanovirin-N, a novel human immunodeficiency virus-inactivating protein that binds viral surface envelope glycoprotein gp 120: potential applications to microbicide development. *Antimicrobial Agents Chemotherapy* 42:1521-1530.

Boyd, P.W., T.A. Ryneerson, E.A. Armstrong, F. Fu, K. Hayashi, Z. Hu, D.A. Hutchins, R.M. Kudela, E. Litchman, M.R. Mulholland, U. Passow, R.F. Strzepak, K.A. Whittaker, E. Yu and M.K. Thomas. 2013. Marine phytoplankton temperature versus growth responses from polar to tropical waters – outcome of a scientific community-wide study. *PLoS ONE* 8(5): e63091 doi:10.1371/journal.pone.0063091.

Bourne, D.G., G.J. Jones, R.L. Blakely, A. Jones, A.P. Negri and P. Riddles. 1996. Enzymatic pathway for the bacterial degradation of the cyanobacterial cyclic peptide toxin microcystin LR. *Applied Environmental Microbiology* 62:4086-4094.

Bourne, D.G., P. Riddles, G.J. Jones, W. Smith, R.L. Blakely. 2001. Characterisation of a gene cluster involved in bacterial degradation of the cyanobacterial toxin microcystin LR. *Environmental Toxicology* 16:523-524.

- Breitbarth, E., A. Oschlies and J. LaRoche. 2007. Physiological constraints on the global distribution of *Trichodesmium* – effect of temperature on diazotrophy. *Biogeosciences* 4:53-61.
- Briand, J.F., C. Lebourlanger, J.F. Humbert, C. Bernard and P. Dufour. 2004. *Cylindrospermopsis raciborskii* (cyanobacteria) invasion at mid-latitudes: selection, wide physiological tolerance, or global warming. *Journal of Phycology* 40:231-238.
- Brookes, J.D. and G.G. Ganf. 2001. Variations in the buoyancy response of *Microcystis aeruginosa* to nitrogen, phosphorus and light. *Journal of Plankton Research* 23:1399-1411.
- Brookes, J.D., G.G. Ganf, D. Green and J. Whittington. 1999. The influence of light and nutrients on buoyancy, filament aggregation and flotation of *Anabaena circinalis*. *Journal of Plankton Research* 21:327-341.
- Brooks, M.L., E. Fleishman, L.R. Brown, P.W. Lehman, I. Werner, N. Scholz, C. Mitchelmore, J.R. Lovvorn, M.L. Johnson, D. Schlenk, S. van Drunick, J.I. Drever, D.M. Stoms, A.E. Parker and R. Dugdale. 2011. Life histories, salinity zones, and sublethal contributions of contaminants to pelagic fish declines illustrated with a case study of San Francisco Estuary, California, USA. *Estuaries and Coasts* DOI 10.1007/s12237-011-9459-6.
- Burford, M.A., K.L. McNeale and F.J. McKenzie-Smith FJ 2006. The role of nitrogen in promoting *Cylindrospermopsis raciborskii* in a subtropical water reservoir. *Freshwater Biology* 51:2143-2153.
- Burford, M.A. and M.J. O'Donohue. 2006. A comparison of phytoplankton community assemblages in artificial and naturally mixed subtropical water reservoirs. *Freshwater Biology* 51:973-982.
- Burns, W.C. 1987. Insights into zooplankton-cyanobacteria interactions derived from enclosure studies. *New Zealand Journal of Marine and Freshwater Research* 21:477-482.
- Butterwick, C., S.I. Heaney and J.F. Talling. 2005. Diversity in the influence of temperature on the growth rates of freshwater algae, and its ecological relevance. *Freshwater Biology* 50:291-300.
- Cardellina, J.H., F.J. Marner and R.E. Moore. 1979. Seaweed dermatitis, structure of lyngbyatoxin-A. *Science* 204:193-195.
- Carey, C.C., B.W. Ibelings, E.P. Hoffmann, D.P. Hamilton and J.D. Brookes. 2012. Eco-physiological adaptations that favour freshwater cyanobacteria in a changing climate. *Water Research* 46:1394-1407.
- Carmichael, W.W. 2008. A world overview one-hundred-twenty seven years of research on toxic cyanobacteria – Where do we go from here? *in*: H.K.Hudnell (ed.), *Cyanobacterial Harmful Algal Blooms: State of the Science and Research Needs*. *Advances in Experimental Medicine & Biology*, 619. Springer. New York, NY.

- Carmichael, W.W., N.A. Mahmood and E.G. Hyde. 1990. Natural toxins from cyanobacteria (blue-green algae). pp. 87-106 *in*: S. Hall and G. Strichartz (eds.), *Marine Toxins, Origin, Structure and Molecular Pharmacology*, vol. 418. American Chemical Society USA. Boston, MA.
- Chapman, A.D. and C.L. Schelske. 1997. Recent appearance of *Cylindrospermopsis* (Cyanobacteria) in five hypereutrophic Florida lakes. *Journal of Phycology* 33:191-195.
- Cheung, M.Y., S. Liang and J. Lee. 2013. Toxin-producing cyanobacteria in freshwater: a review of the problems, impact on drinking water safety, and efforts for protecting public health. *Journal of Microbiology* 51:1-10.
- Chorus, I. and J. Bartram. 1999. *Toxic Cyanobacteria in Waters: a Guide to Public Health. Significance, Monitoring and Management*, London: The World Health Organization E and FN Spon.
- Christiansen, G., J. Fastner, M. Erhard, T. Borner and E. Dittmann. 2003. Microcystin biosynthesis in *Planktothrix*: genes, evolution, and manipulation. *Journal of Bacteriology* 185:564-572.
- Christoffersen, K., S. Lyck and A. Winding. 2002. Microbial activity and bacterial community structure during degradation of microcystins. *Aquatic Microbial Ecology* 27:125-136.
- Cloern, J.E., A.D. Jassby, J.K. Thompson and K.A. Hieb. 2007. A cold phase of the East Pacific triggers new phytoplankton blooms in San Francisco Bay. *Proceedings of the National Academy of Sciences USA* 104:18561-18565.
- Collier, J.L. and A.R. Grossman. 1994. A small polypeptide triggers complete degradation of light-harvesting phycobiliproteins in nutrient-deprived cyanobacteria. *The EMBO Journal* 13:1039-1047.
- Collier, J.L., B. Brahmsha and B. Palenik. 1999. The marine cyanobacterium *Synechococcus* sp. WH7805 requires urease (urea amidohydrolase, EC 3.5.1.5) to utilize urea as a nitrogen source: molecular-genetic and biochemical analysis of the enzyme. *Microbiology* 145:447-459.
- Conley, D.J., H.W. Paerl and R.W. Howarth, D.F. Boesch S.P. Seitzinger, K.E. Havens, C. Lancelot and G.E. Likens 2009. Controlling eutrophication: nitrogen phosphorus. *Science* 323:1014-1015.
- Cox, P.A., S.A. Banack, S.J. Murch, *et al.* 2005. Diverse taxa of cyanobacteria produce b-N-methylamino-L-alanine, a neurotoxic amino acid. *Proceedings of the National Academy of Sciences USA* 102:5074-5078.
- Davidson, K., R.J. Gowen, P. Tett, E. Bresnan, P.J. Harrison, A. McKinney, S. Milligan, D.K. Mills, J. Silke and A.M. Crooks. 2012. Harmful algal blooms: how strong is the evidence that

nutrient ratios and forms influence their occurrence? *Estuarine, Coastal and Shelf Science* 115:339-413.

Davis, T.W., M.J. Harke, M.A. Marcoval, J. Goleski, C. Orano-Dawson, D.L. Berry and C.J. Gobler. 2010. Effects of nitrogenous compounds and phosphorus on the growth of toxic and non-toxic strains of *Microcystis* during bloom events. *Aquatic Microbial Ecology* 61:149-162.

Deng, D.F., K. Zheng, F.C. Teh, P.W. Lehman and S.J. Teh. 2010. Toxic threshold of dietary microcystin (-LR) for quart medaka. *Toxicol* 55:787-794.

DeRuyter, Y.S. and P. Fromme. 2008. Molecular structure of the photosynthetic apparatus. pp. 217-269 in: A. Herrero and E. Flores (eds.), *The Cyanobacteria Molecular Biology, Genomics and Evolution*. Caister Academic Press. Norfolk, UK.

Devlin, J.P., O.E. Edwards, P.R. Gorham, M.R. Hunter, R.K. Pike and B. Stavrlic. 1977. Anatoxin-a, a toxic alkaloid from *Anabaena flos-aquae* NCR-44h. *Canadian Journal of Chemistry* 55:1367-1371.

Dodds WK, Bouska WW, Eitzmann JI et al. (2009) Eutrophication of U.S. freshwaters: Analysis of potential economic damages. *Environ Sci Technol* 43:12-19

Dolman, A.M., J. Rucker, F.R. Pick, J. Fastner, T. Rohrlack, U. Mischke and C. Wiedner. 2012. Cyanobacteria and cyanotoxins: the influence of nitrogen versus phosphorus. *PLoS ONE* 7(6):e38757. doi:10.1371/journal.one.0038757.

Downing, T.G., C.S. Sember, M.M. Gehringer and W. Leukes. 2005. Medium N:P ratios and specific growth rate comodule microcystin and protein content in *Microcystis aeruginosa* PCC7806 and *M. aeruginosa* UV027. *Microbial Ecology* 49:468-473.

Downing, J.A., S.B. Watson and E. McCauley. 2001. Predicting cyanobacteria dominance in lakes. *Canadian Journal of Fisheries and Aquatic Sciences* 58:1905-1908.

Droop, M.R. 1974. The nutrient status of algal cells in continuous culture. *Journal of the Marine Biological Association of the United Kingdom* 55:541-555.

Dyble, J., P.A. Tester and R.W. Litaker. 2006. Effects of light intensity on cylindrospermopsin production in the cyanobacterial HAB species *Cylindrospermopsis raciborskii*. *African Journal of Marine Science* 28:309-312.

Echols, K.R., R.W. Gale, T.R. Schwartz, J.N. Huckins, L.L. Williams, J.C. Meadows, D. Morse, J.D. Petty, C.E. Orazio and D.E. Tillitt. 2000. Comparing Polychlorinated Biphenyl Concentrations and patterns in the Saginaw River using sediment, caged fish, and semipermeable membrane devices. *Environmental Science & Technology* 34:4095-4102.

Edmondson, W.R. and J.T. Lehman. 1981. The effect of changes in the nutrient income on the condition of Lake Washington. *Limnology and Oceanography* 26:1-29.

Elliott, J.A. 2010. The seasonal sensitivity of cyanobacteria and other phytoplankton to changes in flushing rate and water temperature. *Global Change Biology* 16:864-876.

Elmgren, R. and U. Larsson. 2001. Nitrogen and the Baltic Sea: managing nitrogen in relation to phosphorus. *The Scientific World* (1S2):371-377.

Elrifi, I.R. and D.H. Turpin. 1985. Steady-state luxury consumption and the concept of optimum nutrient ratios: a study with phosphate and nitrate limited *Selenastrum minutum* Chlorophyta). *Journal of Phycology* 21:592-602.

Elser JJ, Sterner RW, Gorokhova E et al. (2000) Biological stoichiometry from genes to ecosystems. *Ecological Letters* 3:540-550

Falkowski, P.G. 2000. Rationalizing elemental ratios in unicellular algae. *Journal of Phycology* 36:3-6.

Falkowski P.G. and J. LaRoche. 1991. Acclimation to spectral irradiance in algae. *Journal of Phycology* 27:8-14.

Findlay, D.L., R.E. Hecky, L.L. Hendzel, M.P. Stainton and G.W. Regehr. 1994. Relationships between N₂-fixation and heterocyst abundance and its relevance to the nitrogen budget of Lake 227. *Canadian Journal of Fisheries and Aquatic Sciences* S1:2254-2266.

Flores, E. and A. Herrero. 1994. Assimilatory nitrogen metabolism and its regulation. pp. 488-517 in: D.A. Bryant (ed.), *The Molecular Biology of Cyanobacteria*. Kluwe Academic Publishers. New York, NY.

Flores, E. and A. Herrero. 2005. Nitrogen assimilation and nitrogen control in cyanobacteria. *Biochemical Society Transactions* 33:164-167.

Flores, E. and C.P. Work. 1986. Production, by filamentous, nitrogen-fixing cyanobacteria, of a bacteriocin and of other antibiotics that kill related strains. *Archives of Microbiology* 145:215-219.

Flores, E., J.E. Frias, L.M. Rubio and A. Herrero. 2005. Photosynthetic nitrate assimilation in cyanobacteria. *Photosynthesis Research* 83:117-133.

Forchhammer, K. 2004. Global carbon/nitrogen control by PII signal transduction in cyanobacteria: from signals to targets. *FEMS Microbiology Reviews* 28:319-333.

Frederiksson, C. and B. Bergman. 1997. Ultrastructural characterization of cells specialized for nitrogen fixation in a non-heterocystous cyanobacterium, *Trichodesmium* spp. *Protoplasma* 197:76-85.

- Frias, J.E., E. Flores and A. Herrero. 1994. Requirement of the regulatory protein NtcA for the expression of nitrogen assimilation and heterocyst development genes in the cyanobacterium *Anabaena* sp. PC 7120 *Molecular Microbiology* 14:823-832.
- Fromme, P., P. Jordan and N. Krauss. 2001. Structure of photosystem I. *Biochimica et Biophysica Acta* 1507 5-31.
- Fromme, P., J. Kern, B. Loll, J. Biersiadka, W. Saenger, H.T. Witt, N. Krauss and A. Zouni. 2002. Functional implications on the mechanism of the function of photosystem II including water oxidation based on the structure of Photosystem II. *Philosophical Transactions of the Royal Society of London. Series B-Biological Sciences* 357:1337-1344.
- Fujiki, H., M. Suganuma, H. Suguri *et al.* 1990. New tumor promoters from marine natural products. pp. 232-240 *in*: S. Hall and G. Strichartz (eds.), *Marine Toxins, Origin, Structure and Molecular Pharmacology*, vol. 418. American Chemical Society USA. Boston, MA.
- Garcia-Fernandez, J.M., N. Tandeau De Marsac and J. Diez. 2004. Streamlined regulation and gene loss as adaptive mechanisms in *Prochlorococcus* for optimized nitrogen utilization in oligotrophic environments. *Microbiology and Molecular Biology Reviews* 68:630-638.
- Geider, R. and J. La Roche. 2002. Redfield revisited: variability of C:N:P in marine microalgae and its biochemical basis. *European Journal of Phycology* 37:1-17.
- Gerbersdorf, S.U. 2006. An advanced technique for immuno-labelling of microcystins in cryosectioned cells of *Microcystis aeruginosa* PCC 7806 (cyanobacteria): Implementations of an experiment with varying light scenarios and culture densities. *Toxicon* 47:218-228.
- Ger, K.A., S.J. Teh, D.V. Baxa, S. Lesmeister and C.R. Goldman. 2010. The effect of dietary *Microcystis aeruginosa* and microcystin on the copepods of the upper San Francisco Estuary. *Freshwater Biology* doi:10.1111/j.1365-2427.2009.02367.x.
- Gibble, C.M. and R.M. Kudela. 2014. Detection of persistent microcystin toxins at the land-sea interface in Monterey Bay, California. *Harmful Algae* 39:146-153.
- Gilbert, J.J. 1996. Effect of temperature on the response of planktonic rotifers to a toxic cyanobacterium. *Ecology* 77:1174-1180.
- Glibert, P.M., D. Fullerton, J.M. Burkholder, J.C. Cornwell and T.M. Kana. 2011. Ecological stoichiometry, biogeochemical cycling, invasive species, and aquatic food webs: San Francisco Estuary and comparative systems. *Reviews in Fisheries Science* 19:358-417.
- Gille, S.T. 2002. Warming of the Southern ocean since the 1950s. *Science* 295:1275-1277.
- Gobler, C.J., Davis, T.W., Coyne, K.J., and G.L. Boyer. 2007. The interactive influences of nutrient loading and zooplankton grazing on the growth and toxicity of cyanobacteria blooms in a eutrophic lake. *Harmful Algae* 6, 119–133.

- Grossman, A.R. 2003. A molecular understanding of complementary chromatic adaptation. *Photosynthesis Research* 76:207-215.
- Grossman, A.R., M.R. Schaefer, G.G. Chiang and J.L. Collier. 1993. The phycobilisome, a light-harvesting complex responsive to environmental conditions. *Microbiology Reviews* 57:725-749.
- Grossman, A.R., D. Bhaya and Q. He. 2001. Tracking the light environment by cyanobacteria and the dynamic nature of light harvesting. *Journal of Biological Chemistry* 276:11449-11452.
- Hansen, J., L. Nazaernko, R. Ruedy, M. Sato, J. Willis, A. Del Genio, D. Koch, A. Lacis, K. Lo, S. Menon, T. Novakav, J. Perlwitz, G. Russell, G.A. Schmidt and N. Tausnev. 2005. Earth's energy imbalance: confirmation and implications. *Science* 308:1431-1435.
- Havens, K.E. 2008. Cyanobacteria blooms: effects on aquatic ecosystems. Cyanobacterial Harmful Algal Blooms: State of the Science and Research Needs, EPA, Adv. Exp. Med. Biol. 619, Springer Press, NY Chapter 33:733-747.
- Hawkins, P.R., E. Putt, I. Falconer and A. Humpage. 2001. Phenotypical variation in a toxic strain of the phytoplankter *Cylindrospermopsis raciborskii* (Nostocales, Cyanophyceae) during batch culture. *Environmental Toxicology* 16:460-467.
- Herrero, A. and E. Flores. 1990. Transport of basic amino acids by the dinitrogen-fixing cyanobacterium *Anabaena* PCC 7120. *Journal of Biological Chemistry* 265:3931-3935.
- Herrero, A., A.M. Muro-Pastor and E. Flores. 2001. Nitrogen control in cyanobacteria. *Journal of Bacteriology* 183:411-425.
- Herrero, A., A.M. Muro-Pastor, A. Valladares and E. Flores. 2004. Cellular differentiation and the NtcA transcription factor in filamentous cyanobacteria. *FEMS Microbiology Reviews* 28:469-487.
- Hillebrand H, Steinert G, Boersma M, Malzahn A, Meunier CL, Plum C, Ptacnik R 2013. Goldman revisited: faster-growing phytoplankton has lower N:P and lower stoichiometric flexibility. *Limnology and Oceanography* 58:2076-2088.
- Ho, T.Y., A. Quigg, Z.V. Finkel, A.J. Milligan, K. Wyman, P.G. Falkowski and M.M. Morel. 2003. The elemental composition of some marine phytoplankton. *Journal of Phycology* 39:1145-1159
- Holland, A. and S. Kinnear. 2013. Interpreting the possible ecological role(s) of cyanotoxins: compounds for competitive advantage and/or physiological aide? *Marine Drugs* 11:2239-2258.
- Hong, Y.A., R.R. Jonker, A. Inman, B. Biddanda, R. Rediske and G. Fahnenstiel. 2006. Occurrence of the toxin-producing cyanobacterium *Cylindrospermopsis raciborskii* in Mona and Muskegon Lakes, Michigan. *Journal of Great Lakes Research* 32:645-652.

- Howard A, Irish AE, Reynolds CS. 1996. A new simulation of cyanobacterial underwater movement (SCUM'96). *Journal of Plankton Research* 18: 1373–1385.
- Huber, V., C. Wagner, D. Gerten and R. Adrian. 2012. To bloom or not to bloom: contrasting responses of cyanobacteria to recent heat waves explained by critical thresholds of abiotic drivers. *Oecologia* 169:245-256.
- Hudnell, H.K. (ed.). 2008. Cyanobacterial Harmful Algal Blooms: State of the Science and Research Needs. *Advances in Experimental Medicine & Biology*, 619. Springer. New York, NY.
- Hudnell, H.K. 2010. The state of U.S. freshwater harmful algal blooms assessments, policy and legislation. *Toxicon* 55:1024-1034.
- Huisman, J., R.R. Jonker, C. Zonneveld and F.J. Weissing. 1999. Competition for light between phytoplankton species: experimental tests of mechanistic theory. *Ecology* 80:211-222.
- Huisman, J., J. Sharples, J.M. Stroom, P.M. Visser, W.E.A. Kardinaal, J.M.H. Verspagen and B. Sommeijer. 2004. Changes in turbulent mixing shift competition for light between phytoplankton species. *Ecology* 85:2960-2970.
- Jacoby, J.M., Collier, D.C., Welch, E.B., Hardy, F.J., and M. Crayton,. 2000. Environmental factors associated with a toxic bloom of *Microcystis aeruginosa*. *Can. J. Fish. Aquat. Sci.* 57, 231–240.
- Jassby, A. 2008. Phytoplankton in the upper San Francisco Estuary: Recent biomass trends, their causes and their trophic significance. *San Francisco Estuary and Watershed Science* 6(1) <https://escholarship.org/uc/item/71h077r1>.
- Jeppesen, E., B. Kronvang, M. Meerhoff, M. Sondergaard, K.M. Hansen, H.E. Andersen, T.L. Lauridsen, L. Liboriussen, M. Beklioglu, A. Ozen and J.E. Olesen. 2007. Climate change effects on runoff, catchment phosphorus loading and lake ecological state, and potential adaptations. *Journal of Environmental Quality* 38:1930-1941.
- Jessup D.A., Miller M.A., Ryan J.P. et al. 2009. Mass stranding of marine birds caused by a surfactant-producing Red Tide. *PLoS One* 4(2): e4550. doi:10.1371/journal.pone.0004550
- Jones, G.J., D.G. Bourne, R.L. Blakely and H. Coelle. 1994. Degradation of the cyanobacterial hepatotoxin microcystin by aquatic bacteria. *Natural Toxins* 2:228-235.
- Jones, G.J. and P.T. Orr. 1994. Release and degradation of microcystin following algicide treatment of a *Microcystis aeruginosa* bloom in a recreational lake, as determined by HPLC and protein phosphatase inhibition assay. *Water Research* 28:871-876.
- Kaebnick, M., B.A. Neilan, T. Borner and E. Dittmann. 2000. Light and the transcriptional response of the microcystin gene cluster. *Applied Environmental Microbiology* 66:3387-3392.

- Kamennaya N.A. and A.F. Post. 2011. Characterization of cyanate metabolism in marine *Synechococcus* and *Prochlorococcus* spp. *Applied and Environmental Microbiology* 77:291-301
- Kaplan, A. and L. Reinhold. 1999. The CO₂ concentrating mechanisms in photosynthetic microorganisms. *Annual Review of Plant Physiology and Plant Molecular Biology* 50:539-570.
- Kaplan-Levy, R.N., O. Hadas, M.L. Summers, J. Rucker and A. Sukenik. 2010. Akinetes: Dormant cells of cyanobacteria. pp. 5-28 *in*: E. Lubzens, J. Cerda and M. Clark (eds.), *Dormancy and Resistance in Harsh Environments*. Topics in Current Genetics. Vol. 21. Springer-Verlag. Heidelberg, GE.
- Karlsson-Elfgren, I., K. Rengefors and S. Gustafsson. 2004. Factors regulating recruitment from the sediment to the water column in the bloom-forming cyanobacterium *Gloeotrichia echinulata*. *Freshwater Biology* 49:265-273.
- Keating, K.I. 1977. Allelopathic influence on blue-green bloom sequence in a eutrophic lake. *Science* 196:885-887.
- Keating, K.I. 1978. Blue-green algal inhibition of diatom growth: transition from mesotrophic to eutrophic community structure. *Science* 199:971-973.
- Kellmann, R., T.K. Mihali, Y.J. Jeon, R. Pickford, F. Pomati and B.A. Neilan. 2008. Biosynthetic intermediate analysis and functional homology reveal a saxitoxin gene cluster in cyanobacteria. *Applied Environmental Microbiology* 74:4044-4053.
- Kim, B.H., W.S. Lee, Y.O. Kim, H.O. Lee and M.S. Han. 2005. Relationship between akinete germination and vegetative population of *Anabaena flos-aquae* (Nostocales, Cyanobacteria) in Seokchon reservoir (Seoul, Korea). *Archiv fur Hydrobiologie* 163:49-64.
- Klausmeier, C.A., E. Litchman, T. Daufresne and S.A. Levin. 2004. Optimal nitrogen-to-phosphorus stoichiometry of phytoplankton. *Nature* 429:171-174.
- Klein, D., D. Daloz, J.C. Braekman, L. Hoffmann and V. Demoulin. 1995. New hapaindoles from the cyanophyte *Hapalasiophon laingii*. *Journal of Natural Products* 58:1781-1785.
- Klemer, A.R., J. Feuillade and M. Feuillade. 1982. Cyanobacterial blooms: carbon and nitrogen limitation have opposite effects on the buoyancy of *Oscillatoria*. *Science* 215:1629-1631.
- Konopka, A., J. Kromkamp and L.R. Mur. 1987. Regulation of gas vesicle content and buoyancy in light- or phosphate-limited cultures of *Aphanizomenon flos-aquae* (Cyanophyta). *FEMS Microbial Ecology* 45:135-142.
- Kudela, R.M. 2011. Characterization and deployment of Solid Phase Adsorption Toxin Tracking (SPATT) resin for monitoring of microcystins in fresh and saltwater. *Harmful Algae* 11:117-125.

- Kudo, I., M. Miyamoto, Y. Noiri and Y. Maita. 2000. Combined effects of temperature and iron on the growth and physiology of the marine diatom *Phaeodactylum tricornutum* (Bacillariophyceae). *Journal of Phycology* 36:1096-1102.
- Laamanen M, Kuosa H 2005. Annual variability of biomass and heterocysts of the N₂-fixing cyanobacterium *Aphanizomenon flos-aquae* in the Baltic Sea with reference to *Anabaena* spp. and *Nodularia spumigena*. *Boreal Environment Research* 10:19-30.
- Lee, S.J., M.H. Jang, H.S. Kim, B.D. Yoon and H.M. Oh. 2000. Variation of microcystin content of *Microcystis aeruginosa* relative to medium N:P ratio and growth stage. *Journal of Applied Microbiology* 89:323-329.
- Lee, H.M., M.F. Vazquez-Bermudez and N. Tandeau de Marsac. 1999. The global nitrogen regulator NtcA regulates transcription of the signal transducer PII (GlnB) and influences its phosphorylation level in response to nitrogen and carbon supplies in the cyanobacterium *Synechococcus* sp. strain PCC 7942. *Journal of Bacteriology* 181:2697-2702.
- Lehman, P. W. 2007. The influence of phytoplankton community composition on primary productivity along the riverine to freshwater tidal continuum in the San Joaquin River, California. *Estuaries and Coasts* 30: 82-93.
- Lehman, P.W. and S. Waller. 2003. Microcystis blooms in the Delta. *IEP Newsletter* 16:18-19.
- Lehman, P.W., G. Boyer, C. Hall, S. Waller and K. Gehrts. 2005. Distribution and toxicity of a new colonial *Microcystis aeruginosa* bloom in the San Francisco Bay Estuary, California. *Hydrobiologia* 541:87-99.
- Lehman, P.W., G. Boyer, M. Satchwell and S. Waller. 2008. The influence of environmental conditions on the seasonal variation of *Microcystis* cell density and microcystins concentration in San Francisco Estuary. *Hydrobiologia* 600:187-204.
- Lehman, P.W., S.J. Teh, G.L. Boyer, M.L. Nobriga, E. Bass and C. Hogle. 2010. Initial impacts of *Microcystis aeruginosa* blooms on the aquatic food web in the San Francisco Estuary. *Hydrobiologia* 637:229-248.
- Lehman, P.W., K. Marr, G.L. Boyer, S. Acuna and S.J. Teh. 2013. Long-term trends and causal factors associated with *Microcystis* abundance and toxicity in San Francisco Estuary and implications for climate change impacts. *Hydrobiologia* 718:141-158.
- Leonardos, N. and R.J. Geider. 2004. Responses of elemental and biochemical composition of *Chaetoceros muelleri* to growth under varying light and nitrate:phosphate supply ratios and their influence on critical N:P. *Limnology and Oceanography* 49:2105-2114.
- Levine, S.N. and W.M. Lewis. 1987. A numerical model of nitrogen fixation and its application to Lake Valencia, Venezuela. *Freshwater Biology* 17:265-274.

- Lewellyn, L.E. 2006. Saxitoxin, a toxic marine natural product that targets a multitude of receptors. *Natural Products Report* 23:200-220.
- Likens, G.E., 1972. Eutrophication and aquatic ecosystems. In: Nutrients and Eutrophication: The Limiting-Nutrient Controversy, *Limnology and Oceanography Special Symposium*, vol. 1. pp. 3–13.
- Lindell, D. and A.F. Post. 2001. Ecological aspects of *ntcA* gene expression and its use as an indicator of the nitrogen status of marine *Synechococcus* spp. *Applied Environmental Microbiology* 67:3340-3349.
- Lindell, D., E. Padan and A.F. Post. 1998. Regulation of *ntcA* expression and nitrite uptake in the marine *Synechococcus* sp. Strain WH7803. *Journal of Bacteriology* 180:1878-1886.
- Lindell, D., S. Penno, M. Al-Qutob, E. David, T. Rivlin, B. Lazar and A.F. Post. 2005. Expression of the N-stress response gene *ntcA* reveals N-sufficient *Synechococcus* populations in the oligotrophic northern Red Sea. *Limnology and Oceanography* 50:1932-1944.
- Livingstone, D. and G.H.M. Jaworski. 1980. The viability of akinetes of blue-green algae recovered from the sediments of Rostherne Mere. *European Journal of Phycology* 15:357-364.
- Lopez, C.B., Jewett, E.B., Dortch, Q., Walton, B.T., Hudnell, H.K. 2008. Scientific Assessment of Freshwater Harmful Algal Blooms. Interagency Working Group on Harmful Algal Blooms, Hypoxia, and Human Health of the Joint Subcommittee on Ocean Science and Technology. Washington, DC.
- Lucas, L.V. and J.K. Thompson. 2012. Changing restoration rules: exotic bivalves interact with residence time and depth to control phytoplankton productivity. *Ecosphere* 3(12):117.
- Luque, I. and K. Forchhammer. 2008. Nitrogen assimilation and C/N sensing. pp 334-382 in: A. Herrero and E. Flores (eds.), *The Cyanobacteria Molecular Biology, Genomics and Evolution*. Caister Academic Press. Norfolk, UK.
- Luque, I., E. Flores and A. Herrero. 1994. Molecular mechanisms for the operation of nitrogen control in cyanobacteria. *The EMBO Journal* 13:2862-2869.
- Lurling, M., F. Eshetu, E.J. Faassen, S. Kosten and V.M. Huszar. 2013. Comparison of cyanobacterial and green algal growth rates at different temperatures. *Freshwater Biology* 58:552-559.
- Lurling, M. and I. Roessink. 2006. On the way to cyanobacterial blooms: Impact of the herbicide metribuzin on the competition between a green alga (*Scenedesmus*) and a cyanobacterium (*Microcystis*). *Chemosphere* 65:618-626.
- Lyck, S., N. Gjørlme and H. Utkilen. 1996. Iron starvation increases toxicity of *Microcystis aeruginosa* CYA 228/1 (Chroococcales, Cyanophyceae). *Phycologia* 35:120-124.

- MacKintosh, C., K.A. Beattie, S. Klumpp, P. Cohen and G.A. Codd. 1990. Cyanobacterial microcystin-LR is a potent and specific inhibitor of protein phosphatase 1 and 2A from both mammals and higher plants. *FEBS Letters* 264:187-192.
- Maeda, S.I., M. Okamura, M. Kobayashi and T. Omata. 1998. Nitrite-specific active transport system of the cyanobacterium *Synechococcus* sp. Strain PCC 7942. *Journal of Bacteriology* 180:6761-6763.
- Martin-Luna, B., E. Sevilla, J.A. Hernandez, M.T. Bes, M.F. Fillat and M.L. Peleato. 2006. Fur from *Microcystis aeruginosa* binds in vitro promoter regions of the microcystin biosynthesis gene cluster. *Phytochemistry* 67:876-881.
- Mbedi, S., M. Welker, J. Fastner and C. Wiedner. 2005. Variability of the microcystin synthetase gene cluster in the genus *Planktothrix* (Oscillatoriales, Cyanobacteria). *FEMS Microbiology Letters* 245:299-306.
- McGregor GB, Fabbro LK 2000. Dominance of *Cylindrospermopsis raciborskii* (Nostocales, Cyanoptokaryota) in Queensland tropical and subtropical reservoirs: implications for monitoring and management. *Lakes and Reservoirs: Research and Management* 5:195-205.
- Mejean, A., R. Mazmouz, S. Mann, A. Calteau, C. Medigue and O. Ploux. 2010. The genome sequence of the cyanobacterium *Oscillatoria* sp. PCC 6506 reveals several gene clusters responsible for the biosynthesis of toxins and secondary metabolites. *Journal of Bacteriology* 192:5264-5265.
- Miller, M.M., R.M. Kudela, A. Mekebri, D. Crane, S.C. Oates, M.T. Tinker, M. Staedler, W.A. Miller, S. Toy-Choutka, C. Dominik, D. Hardin, G. Langlois, M. Murray, K. Ward and D.A. Jessup. 2010. Evidence for a novel marine harmful algal bloom: cyanotoxin (microcystin) transfer from land to sea otters. *PLoS ONE* 5(9):e12576. Doi:10.1371/journal.pone.0012576.
- Mills, M.M. and K.R. Arrigo. 2010. Magnitude of oceanic nitrogen fixation influenced by the nutrient uptake ratio of phytoplankton. *Nature Geoscience* DOI: 10.1038/NGEO856.
- Mioni, C., R. Kudela and D. Baxa. 2012. Harmful cyanobacteria blooms and their toxins in Clear Lake and the Sacramento-San Joaquin Delta (California). Surface Water Ambient Monitoring Program Report 10-058-150.
- Mobeley, H.I., M.D. Island and R.P. Hausinger. 1995. Molecular biology of microbial ureases. *Microbiological Reviews* 59:451-480.
- Moffitt, M.C. and B.A. Neilan. 2004. Characterization of the nodularin synthetase gene cluster and proposed theory of the evolution of cyanobacterial hepatotoxins. *Applied Environmental Microbiology* 70:6353-6362.

- Moisander, P.H., E. McClinton and H.W. Paerl. 2002. Salinity effects on growth, photosynthetic parameters, and nitrogenase activity in estuarine planktonic cyanobacteria. *Microbial Ecology* 43:432-442.
- Moisander, P.H., H.W. Paerl and J.P. Zehr. 2008. Effects of inorganic nitrogen on taxa-specific cyanobacterial growth and *nifH* expression in a subtropical estuary. *Limnology and Oceanography* 53:2519-2522.
- Molot L.A., Watson S.B., Creed I.F. et al. 2014. A novel model for cyanobacteria bloom formation: the critical role of anoxia and ferrous iron. *Freshwater Biology* 59:1323-1340
- Morris, R.J., D.E. Williams, H.A. Luu, C.F.B. Holmes, R.J. Andersen and S.E. Calvert. 2000. The adsorption of microcystin-LR by natural clay particles. *Toxicon* 38:303-308.
- Montesinos, M.L., A. Herrero and E. Flores. 1997. Amino acid transport in taxonomically diverse cyanobacteria and identification of two genes encoding elements of a neutral amino acid permease putatively involved in recapture of leaked hydrophobic amino acids. *Journal of Bacteriology* 179:853-862.
- Muro-Pastor, M.I., J.C. Reyes and F.J. Florencio. 2005. Ammonium assimilation in cyanobacteria. *Photosynthesis Research* 83:135-150
- Mynderse, J.S., R.E. Moore, M. Kashiwagi and T.R. Norton. 1977. Antileukemia activity in the Oscillatoriaceae, isolation of debromoaplysiatoxin from *Lyngbya*. *Science* 196:538-540.
- Nielsen, M.V. 1992. Irradiance and daylength effects on growth and chemical composition of *Gyrodinium aureolum* Hulbert in culture. *Journal of Plankton Research* 14:811-820.
- Nixon, S.W. 1986. Nutrient dynamics and the productivity of marine coastal waters. pp. 97-115 in R. Halwagy, D. Clayton and M. Behbehani (eds). *Marine Environment and Pollution*. The Alden Press. Oxford, UK.
- O'Brien, K.R., M.A. Burford and J.D. Brookes. 2009. Effects of light history on primary productivity in a *Cylindrospermopsis raciborskii*-dominated reservoir. *Freshwater Biology* 54:272-282.
- OEHHA 2009. Microcystins: A brief overview of their toxicity and effects, with special reference to fish, wildlife, and livestock. Integrated Risk Assessment Branch. Office of Environmental Health Hazard Assessment. Ecotoxicology Program. California Environmental Protection Agency. January 2009.
- Ohtani, I., R.E. Moore and M.T.C. Runnegar. 1992. Cylindrospermopsin, a potent hepatotoxin from the blue-green alga *Cylindrospermopsis raciborskii*. *Journal of the American Chemical Society* 114:7941-7942.

- Oliver, R.L. 1994. Floating and sinking in gas-vacuolate cyanobacteria. *Journal of Phycology* 30:161-173.
- O'Neill, J., T.W. Davis, M.A. Burford and C.J. Gobler CJ 2012. The rise of harmful cyanobacteria blooms: the potential roles of eutrophication and climate change. *Harmful Algae* 14:313-334.
- Orlando, J.L., M. McWayne, C. Sanders and M. Hladik. 2014. Dissolved pesticide concentrations entering the Sacramento–San Joaquin Delta from the Sacramento and San Joaquin Rivers, California, 2012–13: U.S. Geological Survey Data Series 876, 28 p., <http://dx.doi.org/10.3133/ds876>.
- Orr, P.T. and G.J. Jones. 1998. Relationship between microcystin production and cell division rates in nitrogen-limited *Microcystis aeruginosa* cultures. *Limnology and Oceanography* 43:1604-1614.
- Paerl HW 2004. Estuarine eutrophication, hypoxia and anoxia dynamics: causes, consequences and controls. In: Rupp GL, White MD (eds) Proceedings of the 7th International symposium on fish physiology, toxicology and water quality. EPA Office of Research and Development, Athens, Georgia, USA EPA/600/R-04/049.
- Paerl, H.W. 2008. Nutrient and other environmental controls of harmful cyanobacterial blooms along the freshwater-marine continuum. *Advances in Experimental Medicine and Biology* 619:216-241.
- Paerl, H.W., P.T. Bland, N.D. Bowles and M.E. Haibach. 1985. Adaptation to high-intensity, low wavelength light among surface blooms of the cyanobacterium *Microcystis aeruginosa*. *Applied Environmental Microbiology* 49:1046-1052.
- Paerl, H.W. and R.S. Fulton III. 2006. Ecology of harmful cyanobacteria. pp. 95-107 in: E. Graneli and J. Turner (eds.), *Ecology of Harmful Marine Algae*. Springer-Verlag, Berlin.
- Paerl, H.W., N.S. Hall and E. Calandrino. 2011. Controlling harmful cyanobacterial blooms in a world experiencing anthropogenic and climatic-induced change. *Science of the Total Environment* 40:1739-1745.
- Paerl, H.W., N.S. Hall, B.L. Peierls, and K.L. Rossignol. 2014b. Evolving paradigms and challenges in estuarine and coastal eutrophication dynamics in a culturally and climatically stressed world. *Estuaries and Coasts* 37:243-258.
- Paerl, H.W. and J. Huisman. 2008. Blooms like it hot. *Science* 320:57-58.
- Paerl, H.W. and V.J. Paul. 2012. Climate change: links to global expansion of harmful cyanobacteria. *Water Research* 46:1349-1363.

Paerl, H.W., J. Tucker and P.T. Bland. 1983. Carotenoid enhancement and its role in maintaining blue-green algal (*Microcystis aeruginosa*) surface blooms. *Limnology and Oceanography* 28:847-857.

Paerl, H.W., H. Xu, N.S. Hall, G. Zhu, B. Qin, Y. Wu, K.L. Rossignol, L. Dong, M.J. McCarthy and A.R. Joyner. 2014a. Controlling cyanobacterial blooms in hypertrophic Lake Taihu, China: will nitrogen reductions cause replacement of non-N₂ fixing by N₂ fixing taxa? *PLoS ONE* 9(11):e113123 doi:10.1371/journal.one.0113123.

Palinska, K.A., T. Jahns, R. Rippka and N. Tandeau De Marsac. 2000. *Prochlorococcus marinus* strain PCC 9511, a picoplanktonic cyanobacterium, synthesizes the smallest urease. *Microbiology* 146:3099-3107.

Parsons, T.R., K. Stephens and J.D.H. Strickland. 1961. On the chemical composition of eleven species of marine phytoplankters. *Journal of the Fisheries Research Board of Canada* 18:1001-1016.

Peeters, F., D. Straile, A. Lorke and D.M. Livingstone. 2007. Earlier onset of the spring phytoplankton bloom in lakes of the temperate zone in a warmer climate. *Global Change Biology* 13:1898-1909.

Peterson, H.G., C. Boutin, K.E. Freemark and P.A. Martin. 1997. Toxicity of hexazinone and diquat to green algae, diatoms, cyanobacteria and duckweed. *Aquatic Toxicology* 39:111-134.

Post, A.F., B. Rihman and Q. Wang. 2012. Decoupling of ammonium regulation and ntcA transcription in the diazotrophic marine cyanobacterium *Trichodesmium* sp. IMS101. *The ISME Journal* 6:629-637.

Qin, B.Q., P.Z. Xu, Q.L. Wu, L.C. Luo and Y.L. Zhang. 2007. Environmental issues of Lake Taihu, China. *Hydrobiologia* 581:3-14.

Qin, B., G. Zhu, G. Gao, Y. Zhang, W. Li, H.W. Paerl and W.W. Carmichael WW 2010. A drinking water crisis in Lake Taihu China: linkage to climatic variability and Lake management. *Environmental Management* 45:105-112.

Quigg, A., Z.V. Finkel, A.J. Irwin Y. Rosenthal, T.-Y. Ho, J.R. Reinfelder, O. Schofield, F.M.M. Morel and P.G. Falkowski . 2003. The evolutionary inheritance of elemental stoichiometry in marine phytoplankton. *Nature* 425:291-294.

Quintero, M.J., M.L. Montesinos, A. Herrero and E. Flores. 2001. Identification of genes encoding amino acid permeases by inactivation of selected ORFs from the *Synechocystis* genomic sequence. *Genome Research* 11:2034-2040.

Ramasubramanian, T.S., T.F. Wei and J.W. Golden. 1994. Two *Anabaena* sp. strain PCC 7120 DNA-binding factors interact with vegetative cell- and heterocyst-specific genes. *Journal of Bacteriology* 176:1214-1223.

Ramm, J., A. Lupu, O. Hadas, A. Ballot, J. Rucker, C. Wiedner and A. Sukenik. 2012. A CARD-FISH protocol for the identification and enumeration of cyanobacterial akinetes in lake sediments. *FEMS Microbiology Ecology* 82:23-36.

Rapala J., Lahti K., Sivonen K., and S.I. Niemelä. 1994. Biodegradability and absorption on lake sediments of cyanobacterial hepatotoxins and anatoxin-a. *Letters in Applied Microbiology* 19: 423 – 426

Rapala J., Berg K.A., Lyra C. et al. 2005. *Paucibacter toxinivorans* gen. nov., sp. nov., a bacterium that degrades cyclic cyanobacterial hepatotoxins microcystins and nodularin. *International Journal of Systematic and Evolutionary Microbiology* 55:1563-1568.

Rapala, J., K. Sivonen, C. Lyra and S.I. Niemela. 1997. Variation of microcystins, cyanobacterial hepatotoxins, in *Anabaena* spp. as a function of growth stimuli. *Applied Environmental Microbiology* 63:2206-2012.

Raven, J.A. 1984. A cost-benefit analysis of photon absorption by photosynthetic cells. *New Phytologist* 98:593-625.

Redfield, A.C. 1958. The biological control of chemical factors in the environment. *Am Sci* 46:205-221.

Reynolds, C.S. 1999. Non-determinism to probability, or N:P in the community ecology of phytoplankton. *Archiv fur Hydrobiologie* 146:23-35.

Reynolds, C.S. 2006. *Ecology of Phytoplankton*. Cambridge University Press. Cambridge, UK.

Reynolds, C.S., S.W. Wiseman, B.M. Godfrey and C. Butterwick. 1983. Some effects of artificial mixing on the dynamics of phytoplankton populations in large limnetic enclosures. *Journal of Plankton Research* 5:203-232.

Rhee, G.Y. 1978. Effects of N:P atomic ratios and nitrate limitation on algal growth, cell composition, and nitrate uptake. *Limnology and Oceanography* 23:10-25.

Richerson, P.J., Suchanek, T.H. and Why, S.J. 1994. *The causes and control of algal blooms in Clear Lake*. Final report, July 28, 1994. Clean Lake Diagnostic/Feasibility Study for Clear Lake, California. pp.182.

Rippka R., Deruelles J., Waterbury J. B., Herdman M. and R. Y. Stanier. 1979. Generic assignments, strain histories and properties of pure cultures of cyanobacteria. *Journal of General Microbiology* 111:1-61

Robarts, R.D. and T. Zohary. 1987. Temperature effects on photosynthetic capacity, respiration and growth rates of phytoplankton of bloom-forming cyanobacteria. *New Zealand Journal of Marine and Freshwater Research* 21:391-401.

- Roelke, D.L., S. Augustine and Y. Buyukates. 2003. Fundamental predictability in multispecies competition: The influence of large disturbance. *The American Naturalist* 162:615-623.
- Rohrlack, T., K. Christoffersen, P.E. Hansen, W. Zhang, O. Csarnecki, M. Henning, J. Fastner, M. Erhard, B.A. Neilan and M. Kaebernick. 2003. Isolation, characterization, and quantitative analysis of microviridin J, a new *Microcystis* metabolite toxic to *Daphnia*. *Journal of Chemical Ecology* 29:1757-1770.
- Rohrlack, T., E. Dittmann, M. Henning, T. Borner and J.G. Kohl. 1999. Role of microcystins in poisoning and food ingestion inhibition of *Daphnia galeata* caused by the cyanobacterium *Microcystis aeruginosa*. *Applied Environmental Microbiology* 65:737-739.
- Romo, A., J. Soria, F. Fernandez, Y. Ouahid and A. Baron-Sola. 2013. Water residence time and the dynamics of toxic cyanobacteria. *Freshwater Biology* 58:513-522.
- Rucker, J., E.I. Tingwey, C. Wiedner, C.M. Anu and B. Nixdorf. 2009. Impact of the inoculum size on the population of Nostocales cyanobacteria in a temperate lake. *Journal of Plankton Research* 31:1151-1159.
- Runnegar, M.T., S.M. Kong, Y.Z. Zhong, J.E. Ge and S.C. Lu. 1994. The role of glutathione in the toxicity of a novel cyanobacterial alkaloid cylindrospermopsin in cultured rat hepatocytes. *Biochemical and Biophysical Research Communications* 201:235-241.
- Ryther, J.H. and W.M. Dunstan. 1971. Nitrogen, phosphorus and eutrophication in the coastal marine environment. *Science* 171:1008-1112.
- Saker, M.L. and B.A. Neilan. 2001. Varied diazotrophies, morphologies, and toxicities of genetically similar isolates of *Cylindrospermopsis raciborskii* (Nostocales, Cyanophyceae) from northern Australia. *Applied Microbiology* 67:1839-1845.
- Sauer, J., M. Gori and K. Forchhammer. 1999. Nitrogen starvation in *Synechococcus* PCC 7942: involvement of glutamine synthetase and NtcA in phycobiliprotein degradation and survival. *Archives of Microbiology* 172:247-255.
- Schindler, D.W. 1977. Evolution of phosphorus limitation in lakes. *Science* 195:260-262.
- Schindler, D.W., R.W. Hecky, D.L. Findlay *et al.* 2008. Eutrophication of lakes cannot be controlled by reducing nitrogen input: results of a 37 year whole ecosystem experiment. *Proceedings of the National Academy of Sciences USA* 105:11254-11258.
- Schoellhamer, D.H., S.A. Wright and J. Drexler. 2012. A conceptual model of sedimentation in the Sacramento-San Joaquin Delta. *San Francisco Estuary and Watershed Science* 10(3): <https://escholarship.org/uc/item/2652z8sq>.

Sivonen, K. and T. Borner. 2008. Bioactive compounds produced by cyanobacteria. pp. 159-197 *in*: A. Herrero and E. Flores (eds.), *The Cyanobacteria Molecular Biology, Genomics and Evolution*. Caister Academic Press. Norfolk, UK.

Sivonen K. and G.J. Jones. 1999. Cyanobacterial toxins. pp. 41-111 *in*: I. Chorus and J. Bertram (eds.), *Toxic Cyanobacteria in Water: Guide to Public Health Consequences, Monitoring and Management*. The World Health Organization E & FN Spon. London, UK.

Skulberg, O.M., W.W. Carmichael, R.A. Anderson, S. Matsunaga, R.E. Moore and R. Skulberg. 1992. Investigations of a neurotoxic Oscillatorian strain (cyanophyceae) and its toxin. Isolation and characterization of homo-anatoxin-a. *Environmental Toxicology and Chemistry* 11:321-329.

Smith, V.H. 1983. Low nitrogen to phosphorus ratios favor dominance by blue-green algae in lake phytoplankton. *Science* 221:669-671.

Smith, V.H. 1990. Nitrogen, phosphorus, and nitrogen fixation in lacustrine and estuarine ecosystems. *Limnology and Oceanography* 35:1852-1859.

Solomon, C.M., J.L. Collier, G.M. Berg and P.M. Glibert. 2010. Role of urea in microbial metabolism in aquatic systems: a biochemical and molecular review. *Aquatic Microbial Ecology* 59:67-88.

Sommer, T., C. Armor, R. Baxter, R. Breuer, L. Brown, M. Chotkowski, S. Culberson, F. Feyrer, M. Gingras, B. Herbold, W. Kimmerer, A. Mueller-Solger, M. Nobriga and K. Souza. 2007. The collapse of pelagic fishes in the upper San Francisco Estuary. *Fisheries* 32:270-277.

Sorensson, F. and E. Sahlsten. 1987. Nitrogen dynamics of a cyanobacterial bloom in the Baltic Sea: new versus regenerated production. *Mar Ecol Prog Ser* 37:277-284.

Spier, C., W. Stringfellow, J. Hanlon, M. Estiandan, T. Koski and J. Kaaria. 2013. Unprecedented bloom of toxin-producing cyanobacteria in the Southern Bay-Delta Estuary and its potential negative impact on the aquatic food web. University of the Pacific Ecological Engineering Research Program Report 4.5.1.

Sprosser, P., H.M. Shafit, M. Presing, A.W. Kovacs and S. Herodek. 2003. Nitrogen uptake and fixation in the cyanobacterium *Cylindrospermopsis raciborskii* under different nitrogen conditions. *Hydrobiologica* 506-509:169-174.

Stockner, J.G. and J.W.G. Lund. 1970. Live algae in postglacial lake deposits. *Limnology and Oceanography* 15:41-58.

Stucken K., John U., Cembella A., Soto-Liebe K. and M. Vasquez. 2014. Impact of nitrogen sources on gene expression and toxin production in the diazotroph *Cylindrospermopsis raciborskii* CS-505 and non-diazotroph *Raphidiopsis brookii* D9. *Toxins* 6:1896-1915.

- Stuken, A. and K.S. Jakobsen. 2010. The cylindrospermopsin gene cluster of *Aphanizomenon* sp. strain 10E5: Organization and recombination. *Microbiology* 156:2438-2451.
- Suikkanen, S., M. Laamanen and M. Huttunen. 2007. Long-term changes in summer phytoplankton communities of the open northern Baltic Sea. *Estuarine, Coastal and Shelf Science* 71:580-592.
- Sukenik, A., J. Beardall and O. Hadas. 2007. Photosynthetic characterization of developing and mature akinetes of *Aphanizomenon ovalisporum* (Cyanoprokaryota). *Journal of Phycology* 43:780-788.
- Sunda, W.G. and D.R. Hardison. 2007. Ammonium uptake and growth limitation in marine phytoplankton. *Limnology and Oceanography* 52:2496-2506.
- Tanigawa, R., M. Shirokane, S.S. Maeda, T. Omata, K. Tanaka and H. Takahashi. 2002. Transcriptional activation of NtcA-dependent promoters of *Synechococcus* sp. PCC 7942 by 2-oxoglutarate in vitro. *Proceedings of the National Academy of Sciences USA* 99:4251-4255.
- Terao, K., S. Ohmori, K. Igarashi, I. Ohtani, M.F. Watanabe, K.I. Harada, E. Ito and M. Watanabe. 1994. Electron microscopic studies on experimental poisoning in mice induced by cylindrospermopsin isolated from the blue-green alga *Umezakia natans*. *Toxicon* 32:833-843
- Terry KL, Laws EA, Burns DJ (1985) Growth rate variation in the N:P requirement ratio of phytoplankton. *Journal of Phycology* 21:323-329
- Tett, P., S.I. Heaney and M.R. Droop. 1985. The Redfield ratio and phytoplankton growth rate. *Journal of the Marine Biological Association of the United Kingdom* 65:487-504.
- Thiel, T. 1993. Characterization of genes for an alternative nitrogenase in the cyanobacterium *Anabaena variabilis*. *Journal of Bacteriology* 175:6276-6286.
- Thiel, T. and C.P. Wolk. 1983. Metabolic activities of isolated akinetes of the cyanobacterium *Nostoc spongiaforme*. *Journal of Bacteriology* 156:369-374.
- Thomas RH, Walsby AE. 1985. Buoyancy regulation in a strain of *Microcystis*. *Journal of General Microbiology* 131: 799–809.
- Tillett, D., E. Dittmann, M. Erhard, H. von Dohren, T. Borner and B.A. Neilan. 2000. Structural organization of microcystin biosynthesis in *Microcystis aeruginosa* PCC 7806: an integrated peptide-polyketide synthase system. *Chemical Biology* 7:753-764.
- Tilman, D., S.S. Kilham and P. Kilham. 1982. Phytoplankton community ecology: the role of limiting nutrients. *Annual Review of Ecology, Evolution, and Systematics* 13:349-372.
- Tomatini, A., A.H. Knoll, C.M. Cavanaugh and T. Ohno. 2006. The evolutionary diversification of cyanobacteria: Molecular-phylogenetic and paleontological perspectives. *Proceedings of the National Academy of Sciences USA* 103:5442-5447.

- Tonk, L., K. Bosch, P.M. Visser and J. Huisman. 2007. Salt tolerance of the harmful cyanobacterium *Microcystis aeruginosa*. *Aquatic Microbial Ecology* 46:117-123.
- Tonk, L., D.B. van de Waal, P. Slot, J. Huisman, H.C. Matthijs and P.M. Visser. 2008. Amino acid availability determines the ratio of microcystin variants in the cyanobacterium *Planktothrix agardhii*. *FEMS Microbiology Ecology* 65:383-390.
- Tonk, L., P.M. Visser, G. Christiansen, E. Dittmann, E.O.F.M. Snelder, C. Wiedner, L.R. Mur and J. Huisman. 2005. The microcystin composition of the cyanobacterium *Planktothrix agardhii* changes toward a more toxic variant with increasing light intensity. *Applied Environmental Microbiology* 71:5177-5181.
- Trimbee, A.M. and E.E. Prepas. 1987. Evaluation of total phosphorus as a predictor of the relative biomass of blue-green algae with emphasis on Alberta lakes. *Canadian Journal of Fisheries and Aquatic Sciences* 44:1337-1342.
- Turner S., Pryer K.M., Miao V.P. and J.D. Palmer. 1999. Investigating deep phylogenetic relationships among cyanobacteria and plastids by small subunit rRNA sequence analysis. *Journal of Eukaryotic Microbiology* 46:327-338.
- Turpin, D.H. 1991. Effects of inorganic N availability on algal photosynthesis and carbon metabolism. *Journal of Phycology* 27:14-20.
- Tsuji, K., T. Watanuki, F. Kondo, M.F. Watanabe, S. Suzuki, H. Nakazawa, M. Suzuki, H. Uchida, and K.-I. Harada. 1995. Stability of microcystins from cyanobacteria II. Effect of UV light on decomposition and isomerization. *Toxicon* 33:1619-1631.
- Utkilen, H. and N. Gjørlme. 1995. Iron-stimulated toxin production in *Microcystis aeruginosa*. *Applied Environmental Microbiology* 61:797-800
- Valladares, A., M.L. Montesinos, A. Herrero and E. Flores. 2002. An ABC-type, high-affinity urea permease identified in cyanobacteria. *Molecular Microbiology* 43:703-715.
- Van Der Westhuizen, A.J. and J.N. Eloff. 1985. Effect of temperature and light on the toxicity and growth of the blue-green alga *Microcystis aeruginosa* (UV006). *Planta* 163:55-59.
- Van Nieuwenhuysse, E.E. 2007. Response of summer chlorophyll concentration to reduced total phosphorus concentration in the Rhine River (Netherlands) and the Sacramento-San Joaquin Delta (California, USA). *Canadian Journal of Fisheries and Aquatic Sciences* 64:1529-1542.
- Vazquez-Bermudez, M.F., A. Herrero and E. Flores. 2002. 2-Oxoglutarate increases the binding affinity of the NtcA (nitrogen control) transcription factor for the *Synechococcus* glnA promoter. *FEBS Letters* 512:71-74.

- Vezie, C., L. Briant, K. Sivonen G. Bertru, J.-C. Lefeuvre and M. Salkinoja-Salonen. 1998. Variation of microcystin content of cyanobacterial blooms and isolated strains in Lake Grand-Lieu (France). *Microbial Ecology* 35:126-135.
- Vezie, C., J. Rapala, J. Vaitomaa, J. Seitsonen and K. Sivonen. 2002. Effect of nitrogen and phosphorus on growth of toxic and nontoxic *Microcystis* strains and on intracellular microcystin concentrations. *Microbial Ecology* 43:443-454.
- Visser, P.M., J. Passarge and L.R. Mur. 1997. Modelling vertical migration of the cyanobacterium *Microcystis*. *Hydrobiologia* 349-99-109.
- Walsby, A.E. 1994. Gas vesicles. *Microbiological Reviews* 58:94-144.
- Walsby, A.E. 2005. Stratification by cyanobacteria in lakes: a dynamics buoyancy model indicates size limitations met by *Planktothrix rubescens* filaments. *New Phytologist* 168:365-376.
- Walsby, A.E., G. Ng, C. Dunn and P.A. Davis. 2004. Comparison of the depth where *Planktothrix rubescens* stratifies and the depth where the daily insolation supports its neutral buoyancy. *New Phytologist* 162:133-145.
- Wallace, B.B. and D.P. Hamilton. 1999. The effect of variation in irradiance on buoyancy regulation in *Microcystis aeruginosa*. *Limnology and Oceanography* 44:273-281.
- Watanabe, M.F. and S. Oishi. 1985. Effects of environmental factors on toxicity of a cyanobacterium (*Microcystis aeruginosa*) under culture conditions. *Applied Environmental Microbiology* 49:1342-1344.
- Wei, T.F., T.S. Ramasubramanian and J.W. Golden. 1994. *Anabaena* sp. strain PCC 7120 ntcA gene required for growth on nitrate and heterocyst development. *Journal of Bacteriology* 176:4473-4482..
- Welker, M. and H. von Dohren. 2006. Cyanobacterial peptides – Nature’s own combinatorial biosynthesis. *FEMS Microbiology Reviews* 30:530-563.
- Wiedner, C., P.M. Visser, J. Fastner, J.S. Metcalf, G.A. Codd and L.R. Mur. 2003. Effects of light on the microcystin content of *Microcystis* strain PCC 7806. *Applied Environmental Microbiology* 69:1475-1481.
- Wolk, C.P., A. Ernst and J. Elhai. 1994. Heterocyst metabolism and development. pp. 769-823 in: D.A. Bryant (ed.), *The Molecular Biology of Cyanobacteria*. Kluwe Academic Publishers. New York, NY.
- Wu, Z., J. Shi and R. Li. 2009. Comparative studies on photosynthesis and phosphate metabolism of *Cylindrospermopsis raciborskii* with *Microcystis aeruginosa* and *Aphanizomenon flos-aquae* 2009. *Harmful Algae* 8:910-915

Wynne, D. and G.Y. Rhee. 1986. Effects of light intensity and quality on the relative N and P requirement (the optimum N:P ratio) of marine planktonic algae. *Journal of Plankton Research* 8:91-103

Yamamoto Y. and H. Nakahara. 2005. The formation and degradation of cyanobacterium *Aphanizomenon flos-aquae* blooms: the importance of pH, water temperature, and day length. *Limnology* 6:1-6.

Yang, F., Y. Zhou, L. Yin, G. Zhu, G. Liang and Y. Pu. 2014. Microcystin-degrading activity of an indigenous bacterial strain *Stenotrophomonas acidaminiphila* MC-LTH2 isolated from Lake Taihu. *PLoS ONE* 9(1): e86216. doi:10.1371/journal.pone.0086216

Yoshimasa, Y. and H. Nakahara. 2005. The formation and degradation of cyanobacterium *Aphanizomenon flos-aquae* blooms: the importance of pH, water temperature, and day length. *Limnology* 6:1-6.

Yoshizawa, S., R. Matsushima, M.F. Watanabe, K. Harda, A. Ichihara, W.W. Carmichael and H. Fujiki. 1990. Inhibition of protein phosphatases by microcystin and nodularin associated with hepatotoxicity. *Journal of Cancer Research and Clinical Oncology* 116:609-614.

APPENDIX A

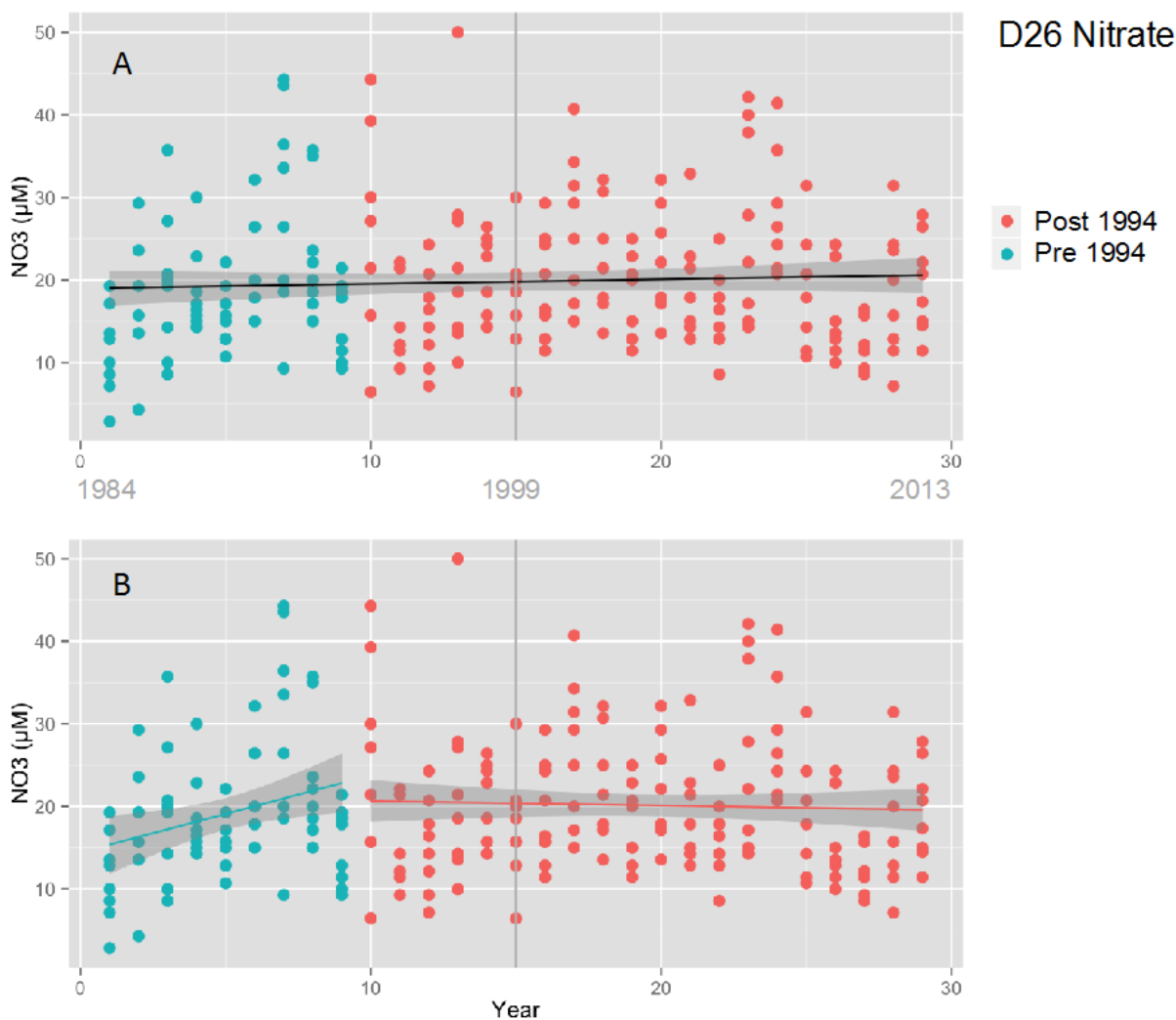


Figure A-1. Changes in the concentration of nitrate (NO_3^-) over time (1985-2013) at station D26 in the Delta. Green filled circles denote period before 1994 and red filled circles denote the period after 1994. Vertical grey line denotes the year 1999 when *Microcystis* started occurring. A) Regression of NO_3^- versus time for the period 1985-2013 (black line) with 95% confidence interval in grey. B) Regression of NO_3^- versus time for the period 1985-1994 (green line) and the period 1994-2013 (red line). Slopes significantly different from zero in bold in regression table:

Nitrate	1985-2013	1985-1994	1994-2013
Slope	0.09066	1.374	-0.02962
Probability	0.226	0.00149	0.832
multi- R^2	0.00424	0.09127	0.0001988

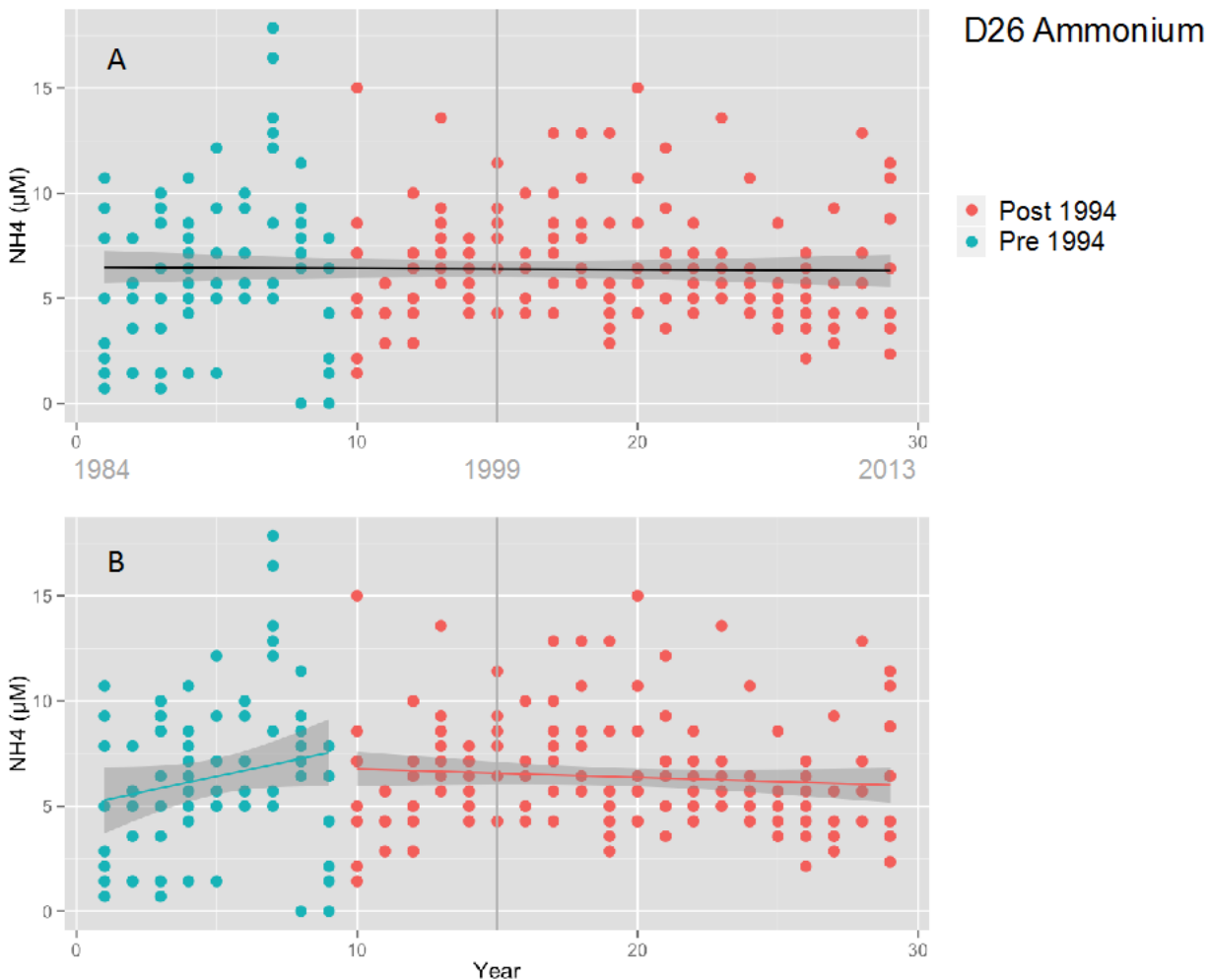


Figure A-2. Changes in the concentration of ammonium (NH_4^+) over time (1985-2013) at station D26 in the Delta. Green filled circles denote period before 1994 and red filled circles denote the period after 1994. Vertical grey line denotes the year 1999 when *Microcystis* started occurring. A) Regression of NH_4^+ versus time for the period 1985-2013 (black line) with 95% confidence interval in grey. B) Regression of NH_4^+ versus time for the period 1985-1994 (green line) and the period 1994-2013 (red line). Slopes significantly different from zero in bold in regression table:

Ammonium	1985-2013	1985-1994	1994-2013
Slope	-0.038	0.3801	-0.03525
Probability	0.108	0.023	0.358
multi- R^2	0.007448	0.04779	0.00374

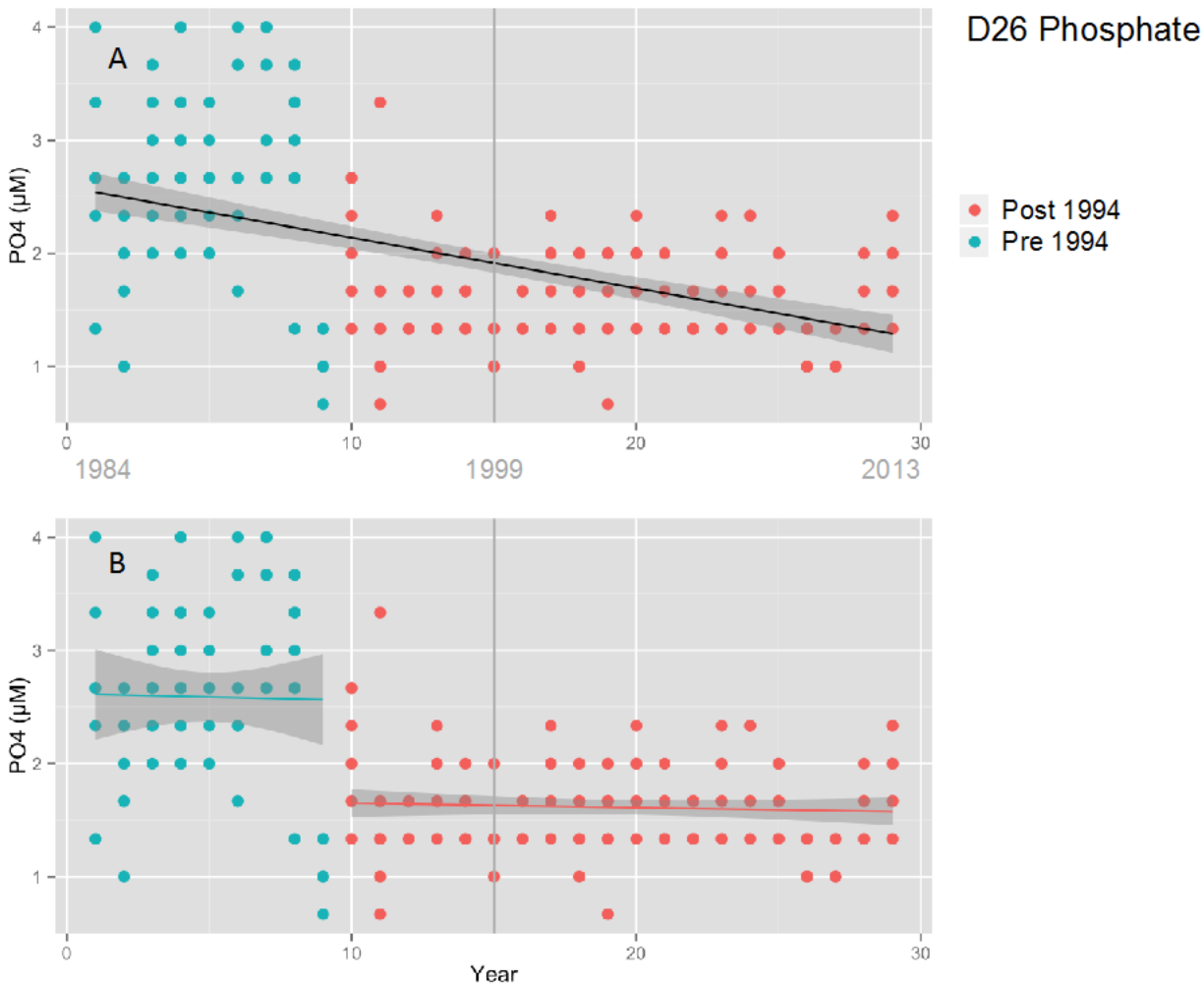


Figure A-3. Changes in the concentration of phosphate (PO_4^{3-}) over time (1985-2013) at station D26 in the Delta. Green filled circles denote period before 1994 and red filled circles denote the period after 1994. Vertical grey line denotes the year 1999 when *Microcystis* started occurring. A) Regression of PO_4^{3-} versus time for the period 1985-2013 (black line) with 95% confidence interval in grey. B) Regression of PO_4^{3-} versus time for the period 1985-1994 (green line) and the period 1994-2013 (red line). Slopes significantly different from zero in bold in regression table:

Phosphate	1985-2013	1985-1994	1994-2013
Slope	-0.048906	0.03673	-0.008772
Probability	2.00E-16	0.263	0.157
multi- R^2	0.2594	0.01183	0.008855

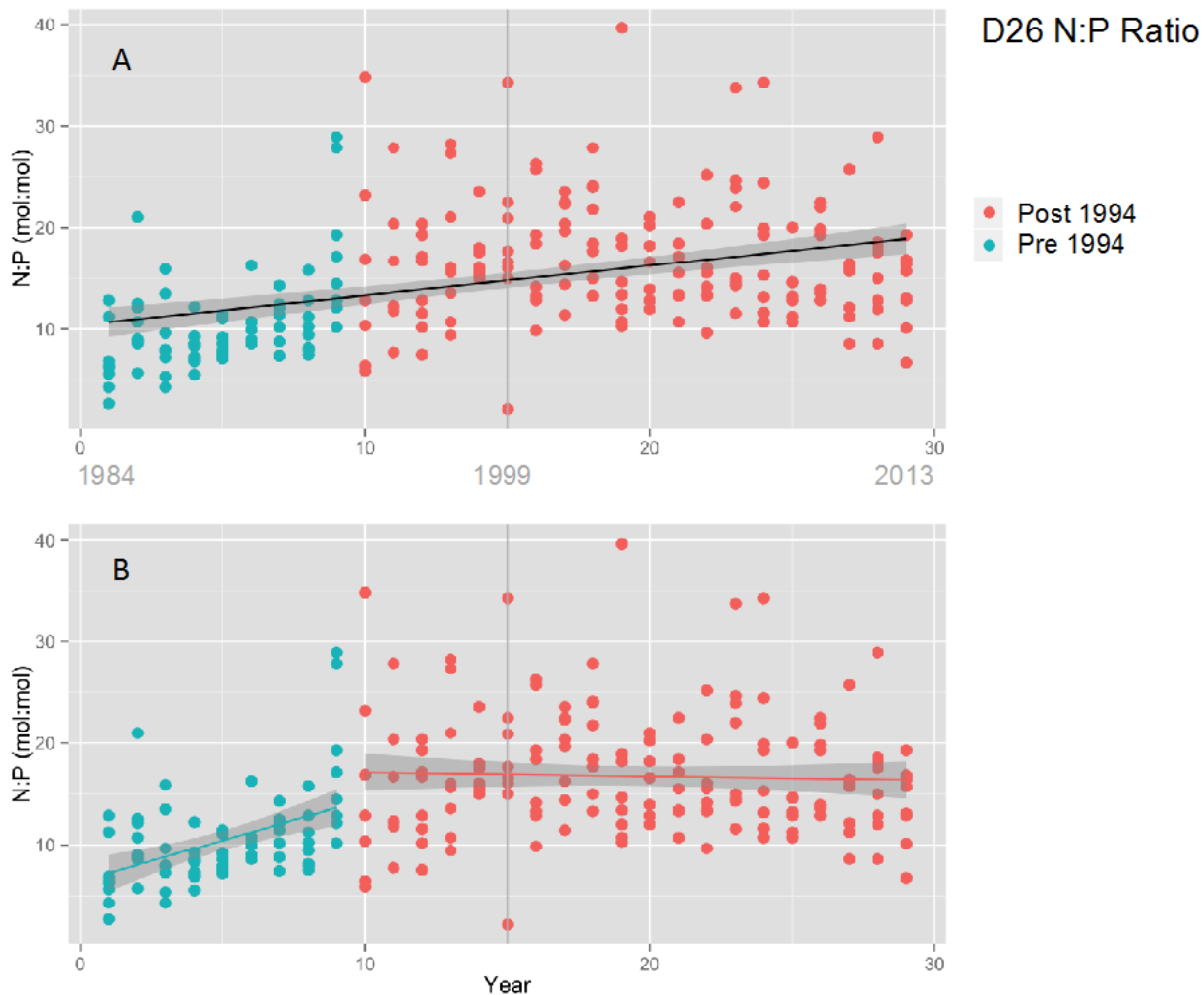


Figure A-4. Changes in the N:P ratio (mol:mol) over time (1985-2013) at station D26 in the Delta. Green filled circles denote period before 1994 and red filled circles denote the period after 1994. Vertical grey line denotes the year 1999 when Microcystis started occurring. A) Regression of N:P ratio versus time for the period 1985-2013 (black line) with 95% confidence interval in grey. B) Regression of N:P ratio versus time for the period 1985-1994 (green line) and the period 1994-2013 (red line). Slopes significantly different from zero in bold in regression table:

N:P Ratio	1985-2013	1985-1994	1994-2013
Slope	0.3726	0.6236	0.02932
Probability	3.79E-16	0.000572	0.736
multi- R ²	0.1747	0.1064	0.0005047

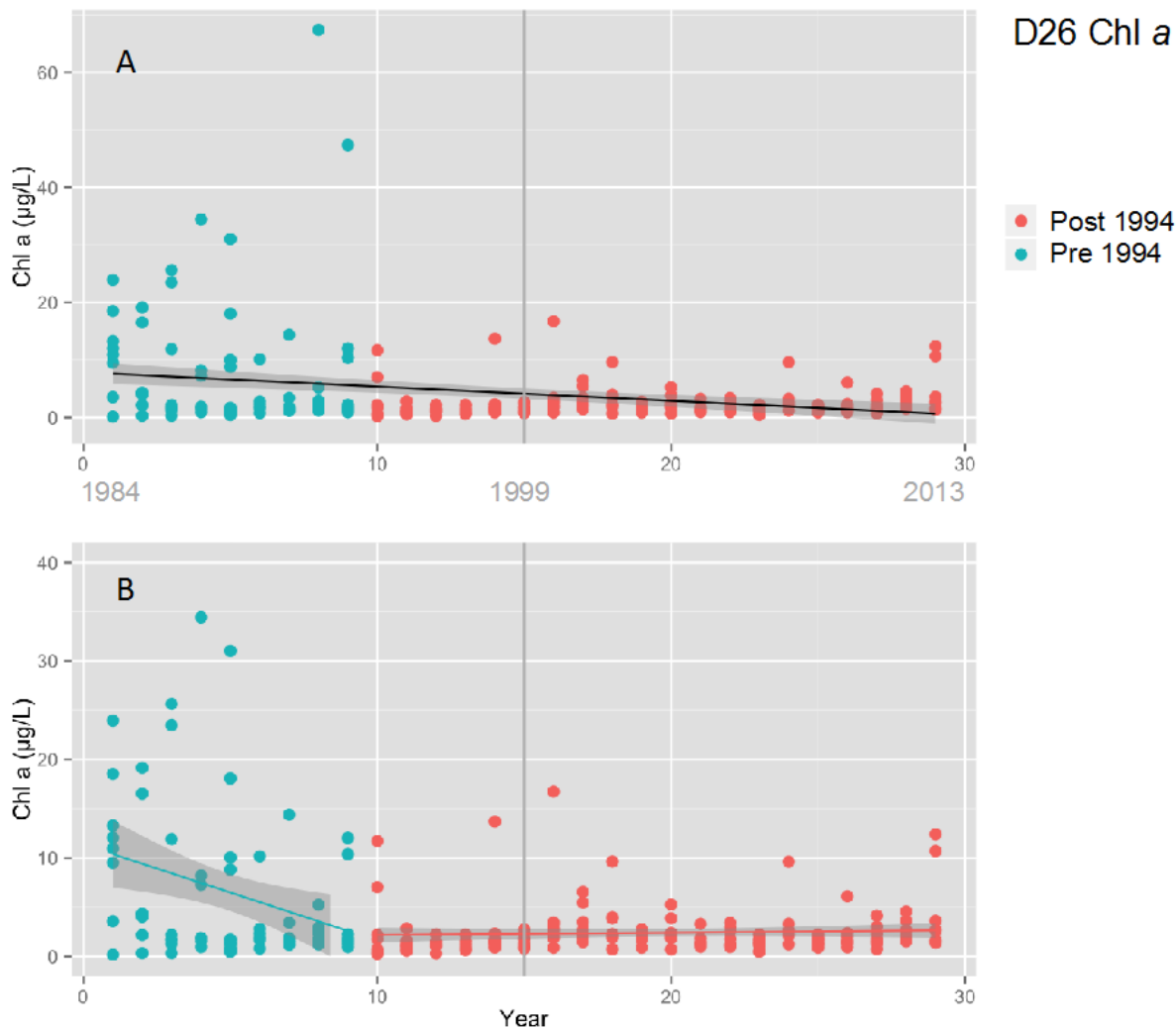


Figure A-5. Changes in the concentration of Chlorophyll a (Chl a) over time (1985-2013) at station D26 in the Delta. Green filled circles denote period before 1994 and red filled circles denote the period after 1994. Vertical grey line denotes the year 1999 when Microcystis started occurring. A) Regression of Chl a versus time for the period 1985-2013 (black line) with 95% confidence interval in grey. B) Regression of Chl a versus time for the period 1985-1994 (green line) with two of the high values from 1994 removed, and the period 1994-2013 (red line). Slopes significantly different from zero in bold in regression table:

Chl a	1985-2013	1985-1994	1994-2013
Slope	-0.1676	-0.7386	0.03936
Probability	2.87E-05	0.00759	0.1148
multi- R ²	0.05143	0.07266	0.01116

APPENDIX B

Comments from the Scientific Working Group and responses from the authors.

Author	Page	Comment	Response
Anonymous	iii	Under Finding #3, second bullet, regarding ratios of N and P in Delta: I'm reading this to mean ratios of total N and total P (including various forms of each). I don't know that enough research has been done to determine if the ratios of the different forms can be an important driver.	Ratios of N:P are important drivers when one nutrient is in limiting supply and slows the growth rate down. Ratios of different forms of the same nutrient are important if a certain form produces a lower growth rate than the other; research on this topic is discussed under section 3.2.3 p24.
Foe	11	Under section 2.2.5, first paragraph, last sentence: Add something like this to last sentence on page 11, "it was deduced that <i>under nutrient limiting conditions</i> phytoplankton would become ..."	Done
Foe	19	On pages 19, 22, and 38 you note that nutrient concentrations are one factor constraining the accumulation of cyanoHAB biomass. Can you estimate either from information from the delta or other waterbodies what range of N and P concentrations would be needed to limit cyanoHAB biomass and toxin levels below a low or moderate probability of human and wildlife health effects? Presumably there are a number of complicating factors including the fact that cyanoHABs co occur with blooms of other algal species which would also pull down nutrient levels. I understand that your estimate is likely to be fairly gross. Would it be possible to refine the range through a series of laboratory and/or field experiments? Could this be considered an information gap? Maybe discuss this somewhere around page 37?	I tried to do this in the original version where based on measurements of microcystin toxin that was harmful to aquatic life (0.8 µg/L) I calculated the amount of Microcystis-associated surface Chl a needed to produce that amount (7 µg/L). Because the science group did not like this estimation I've removed it from the paper. However, using 7 µg/L surface Chl a as a rough estimate, you would need greater or equal to 7 moles N/L to sustain such a level; this is not discussed in the current version
Foe	29	Second paragraph: You might note that Ger <i>et al.</i> , 2010 found that both toxin producing and non-toxin producing strains of Microcystis reduced the survival of both <i>Eurytemora affinis</i> and <i>Pseudodiaptomus forbesi</i> in 10 day lab bioassays. This suggests that the presence of other microcystis metabolites also contribute to overall toxicity.	A new section (4.2.4) on p39 entitled "Potential for CyanoHAB Risk to Delta Beneficial Uses" has been where the Ger (2010) paper and additional papers mentioned by Peggy Lehman are discussed
Foe	32	Under section 4.2.3, second paragraph: Brannan Island is located inside the legal boundary of the delta.	This sentence has been changed to read "Sacramento River" instead
Foe	35	Under section 4.2.4 under potential adverse effects on Delta beneficial uses: What can be concluded about the potential toxicity of cyanoHABs to aquatic organisms including zooplankton and larval fish in the Delta? Presumably there is the possibility of both direct and indirect effects. See Ger et al 2010 for an example of direct toxicity and Acuna et al (2012) and Deng et al (2010) for examples of bioaccumulation related effects. Peggy gave citations for all these papers. If uncertainty exists about the extent of	These effects and papers are discussed in a new section (4.2.4) on p39 entitled "Potential for CyanoHAB Risk to Delta Beneficial Uses". I think uncertainty exists regarding 1) whether the organisms reflect concentrations that are in the water column or 2) they bioaccumulate the toxin 3) what affects the zooplankton - toxic or non-toxic cells

		potential toxicity, then should this be listed as an information gap? What information is most important to collect first?	
Foe	38	Figure 5.2 shows nutrient trends at station D26 in the delta between 1994 and 2014. The conclusion is that nutrients concentrations are not changing. Longer term nutrient analysis suggest otherwise. Nutrient concentrations, N speciation, and dissolved N:P ratios have changed in the delta over the last 40 years. More DIN, more NH4, less SRP and an increase in the N:P ratio (Jassby 2008; Glibert, 2010 ³ ; Van Nieuwenhuyse, 2007 ⁴) ³ Reviews in Fishery Science, 18:211-232 ⁴ Canadian journal of fisheries and aquatic science 64:1529-1542	I reanalyzed the nutrient data going back to 1985. My new interpretation is in section 5.1.4 on p43. I included the Van Nieuwenhuyse and Jassby citations. Appendix A provides plots of NO3, NH4, PO4, N:P, and Chl a from station D26. I demonstrate that one can draw different conclusions from these data depending on whether they are broken into separate time periods or analyzed as one long time course.
Foe	39	Around page 39. You note that cyanoHAB growth rates are a positive function of water clarity. The Delta has become clearer. The delivery of suspended sediment from the Sacramento River to the Delta has decreased by about half during the period between 1957 and 2001 (Wright and Schoellhamer (2004) ¹ and this has resulted in a statistically significant -2 to -6 percent decrease per year in SPM between 1975 and 2005 (Jassby, 2008) ² . Of course, it is uncertain whether the trend will continue. Might this increase in clarity also increase the frequency and magnitude of cyano blooms in Delta and make other factors like nutrients more important? ¹ San Francisco Estuary and Watershed Science, 2004 volume 2, issue 2 ² San Francisco Estuary and Watershed Science, 2006 volume 6, issue 1	This is true and I've added a new section (5.1.3) entitled Water Clarity (p 43) where this additional information is discussed.
Joab	ii	Second paragraph, second sentence. Add "the" between "by" and "Water Board".	Done
Joab	ii	Under Finding #2, item 1), change "e.g." to e.g.,"	Removed
Joab	1	Under section 1.1, first sentence. Add "in" between "found" and "Northern California".	Done
Joab	1	Last paragraph, first sentence regarding the commissioning of literature reviews: Actually we only commissioned two white papers (to date) on cyano	Changed to "two"

		and macrophytes. We are working on commissioning the third.	
Joab	4	Under section 2.1, first paragraph, fourth sentence. In sentence, "Cyanobacteria also produce and array..." Change "and" to "an".	Done
Joab	5	In Table 2.1, under the Nostocales (Group 4), is <i>Cylindrospermum</i> the correct name?	It is the correct name; however, I could just as easily have mentioned <i>Cylindrospermopsis</i> which is a more recognizable species.
Joab	6	Second paragraph, second sentence. You identify Group 5 as having toxic cyanoHAB-forming cyanobacteria: Don't you mean Group 4 based on the species identified in Table 2.1? Also, which group is <i>Planktothrix</i> in? I did not see them identified in the table - can they be added?	I did mean Group 4; it's been changed. I've also indicated in the text which subgroup <i>Planktothrix</i> belongs to
Joab	8	Under Ammonium transport section, third paragraph. Change "alterate" to "alternate".	Done
Joab	8	Under Nitrate transport and reduction section, last sentence regarding nitrate uptake: What concentrations of ammonia are relevant? Are these concentrations in the cells or the water column?	External; sentence changed to reflect this
Joab	9	First paragraph, first sentence: Carbon fixation seems to be very important in the nutrient uptake process. What controls carbon fixation? Is there some way to reduce their carbon fixation?	Irradiance controls CO ₂ fixation; this has been mentioned
Joab	9	Fourth paragraph, last sentence. Remove "have" between "their genomes" and "demonstrates".	Done
Joab	10	Under Nitrogen fixation, second paragraph, last sentence relating to n ₂ fixation under iron-limiting conditions: What is the iron-limiting condition? Do we know?	Where iron is not enough to support cell division
Joab	10	Under nitrogen fixation, last paragraph, seventh sentence. Correct the spelling of "heterocyst".	Done
Joab	11	First paragraph: What are the conditions for N starvation?	When N concentration is not enough to support cell division of available biomass
Joab	19	In Figure 3.1, step 6 states to add grazers: Are their cyanobacteria grazing fish and zooplankton?	This figure was very busy and included many processes not discussed in the White Paper; I've substituted a new and simpler figure
Joab	38	Under section 5.2, first paragraph, first sentence: This citation is now 8 years old. Is there any recent information to suggest if these percentages have changed significantly?	Not that I'm aware
Joab	39	First paragraph: Correct the spelling of "cyanoHABs" to "cyanoHABs". Do global search in document to check spelling of cyanoHAB.	Done
Joab	39	Second full paragraph: In sentence, "In Clear Lake, Both N and P..." delete capital B and make lowercase.	Sentence changed

Joab	41	In Table 5.1, Observations in the Delta "temperatures above 25° C rarely occur." - Temperatures in the San Joaquin River near Stockton have over the past 3 years (2012-2014) reached over 25°C from June through October, most likely due to this persistent drought and overall increase in temperature.	Sentence has been removed
Kudela	31	Figure 4.2. I think this is an issue with Peggy's original figure, because I remember seeing it before, but the chlorophyll units don't make much sense. 0.1 ng/L is barely detectable under the best of circumstances.	Y-axis corrected to µg/L
Kudela	N/A	The toxin table is very thorough, but it might be worth pointing out that, based on available information, Central California seems to be dominated by microcystins. We have all of those genera present but we don't very often see saxitoxins or anatoxin-a. Admittedly we don't look that often either, but we have tested some samples from Clear Lake, SF Bay, and Pinto Lake. We very rarely get low levels of STX, and one low hit for anatoxin-a in Clear Lake. We did see low levels of anatoxin-a in Lake Chabot also, and if you go further north, anatoxin-a becomes dominant in the Eel River basin. This supports Mine's decision to focus on microcystins in the report, but the implication of that section is that we could see a wide variety of toxins, and we usually don't.	This has been pointed out in the first paragraph of section 4.2.3
Kudela	N/A	Temperature. While I completely agree with Mine's summary, bear in mind that we do see toxin at low temperatures (this is documented in Kudela 2012 and Gibble and Kudela 2014). We were not tracking species, but it seems likely that it's related to a shift in composition to more cold-tolerant species such as Planktothrix. We tend to get two peaks of toxicity—one at lower biomass and cooler temperatures, and the second (larger) when Microcystis is dominant.	I was not aware of the Gibble Kudela paper; would like to add appropriate discussion
Kudela	N/A	Marine toxins. I'm not sure I completely believe it but there is a recent article (which I can't find right now—looking for it) that documents presence of microcystins in marine waters, from marine cyanobacteria.	Noted

Kudela	N/A	I'd be very supportive of developing an ecosystem model, but for CHABs in particular you probably need a fairly complex model that can parameterize both end-members (riverine and marine). A good hydrodynamic model would be a great place to start. I'm not sure how easy or difficult it would be to add a biological model on top of that, or whether you'd need two models, etc. It's probably my own bias but I would start with assembling all the available data and run statistical analyses on that (Peggy's done quite a bit of this already) to see what variables emerge as most important. Cecile Mioni has been attempting that with the Bay/Delta data and it's been interesting, in that there are no clear physical drivers related to cell abundance or toxicity. She looked at all the usual ones, temperature, salinity, nutrients, etc. suggesting that either there's not enough data (a real possibility) or that it's not a simple relationship. That of course leads back to the need for more monitoring and modeling.	Noted
Mussen	iii	Under Finding #4, third sentence regarding increased nutrient loading: With continued regulatory controls on nutrient loads into the system, we should not necessarily expect nutrient loading to increase substantially in the future.	This has been removed
Mussen	1	Under section 1.1, in fourth sentence "The Delta is widely recognized as in "crisis" because of competing demands..." Add "human effects on the environment and" between "because of" and "competing".	Done
Mussen	4	Last paragraph, second sentence. Add "in local communities" between "irrigation of farms" and "as well as". Plus, remove the words "drinking water to" after the words "as well as".	Sentence has been revised
Mussen	7	Under Carbon Fixation, fifth sentence. Add "near" between "concentrate CO2" and "its vicinity".	Sentence has been revised
Mussen	28	Under section 4.1 Ecosystem Services, second paragraph, third sentence: Change "Striped Bass" to "juvenile-Striped Bass".	Done
Mussen	29	First paragraph, fourth sentence: "At high densities...(Paerl 2004, Paerl and Fulton 2006)" is a repeat from text in the paragraph above on page 28.	Noted; the repeat text has been removed
Mussen	29	First paragraph, sixth sentence "At dense concentrations..." - If low nutrient concentrations can be used to limit the magnitude of future cyanoHAB blooms, the effects of lower nutrient concentrations must also be considered for all other plant and algae species growing in the system (this is especially important for the period followin onset of a future cyanoHAB blooms where nutrients in the area would be fully depleted).	Noted; this point has been brought up in the recommendations section (6.0) in conjunction with hypotheses development

Mussen	38	Under section 5.2, second paragraph, first sentence referring to growth of cyanoHABs versus diatoms: Without nutrient limitation, growth rates may not determine which phytoplankton species is dominant in the system. Other factors such as light availability, buoyancy, temperature, salinity and grazing pressure may determine the dominant species.	This sentence, presently in section (5.1.4) has been revised to clarify point
Mussen	40	Under second bullet, third sentence concerning blooms not persisting without ample supply of nutrients: Once a bloom consumes the available nutrients, would nutrient remineralization be able to sustain some lower concentration of cyanoHABs presence throughout the remainder of the growth season? Could cyanoHABs persist at harmful levels in this manner?	I think typically not; harmful levels require a certain level of biomass to be sustained
Mussen	40	Under second bullet, third sentence: Add "flow rates," between "temperatures," and "and irradiance".	Done
Mussen	40	Under second bullet, third sentence: Remove "s" from word "remains".	Done
Mussen	40	Last paragraph, fourth sentence starting with "Increase nutrient loading...": Please see my comment above on increased nutrient loading.	This has been removed
Mussen	42	Under R1, second paragraph discussing enumeration of cell counts: What about the inclusion of "and average biomass?"	Controversy regarding how it is to be measured; could be discussed under recommendations
Mussen	43	Under R2, first paragraph, second sentence: Replace "higher chlorophyll a" with "increased phytoplankton growth in the Delta".	Done
Mussen	43	Last paragraph, first sentence concerning informing management actions: It is also important to model expected nutrient levels with levels of reduced loading. The time required for a reduction and the amount of nutrient regeneration in a system can be highly variable.	Section expanded in order to note this point
Mussen	43	Last paragraph, first sentence. Add "s" to "action" making it "actions".	Done
Mussen	43	Last paragraph, second sentence regarding modeling primary productivity and biomass: CyanoHAB growth rates under ideal conditions (which may be used as the basis for a model design) can be quite different from their growth rates at near-limiting nutrient conditions. Do we know what low nutrient concentrations (thresholds) would be necessary to prevent the overgrowth of different cyanoHABs? How would other plants and algae in the system be affected by low nutrient concentrations? With limited nutrients, can we predict which phytoplankton species would be dominant in the system, and how the dominant species may change with climatic factors such as temperature, flow, and turbidity, or with differing grazing rates?	Section expanded in order to note this point

Orr	iii	Under #3, first bullet - During the last meeting lower temperatures (18°C) were discussed. Are there references for the blooms at lower temperatures in the delta?	None that I'm aware of
Orr	28	For the last sentence on page 28 under section 4.1. Ecosystem Services, "CyanoHABs also can cause night-time dissolved oxygen depletion via bacterial decomposition and respiration of dense blooms which results in fish kills and loss of benthic fauna (Paerl 2004, Paerl and Fulton 2006) - Does this occur in the Delta or is flow mixing sufficient to prevent the issue?	This is an example of an adverse effect noted in other systems
Orr	29	In the second paragraph, the sentences starting with "At low concentrations...(Lehman <i>et al.</i> 2010)" are already in the preceding paragraph. Consider removing.	This has been removed
Orr	29	Regarding the third sentence at the top of the page, "However, even at low concentrations, toxins released (upon death and cell lysis, or by grazing) can bioaccumulate in higher trophic levels (Lehman <i>et al.</i> 2010) - There is some disagreement on this topic in the literature. Based on the Lehman paper alone it seems unclear whether the toxins bioaccumulate or simply occur in tissue at concentrations that are not greater than the surrounding environment. In other systems it depends on the particular toxin and species in question. I recommend removing the "even at low concentrations" to make a more conservative statement. Another option would be to state they have been observed in higher trophic levels in the delta and leave the bioaccumulation to be addressed in recommendations or further research.	This sentence has been modified
Orr	32	Under section 4.2.3, last sentence in first paragraph "Using the relationship 115 ng microcystin μg surface Chl a^{-1} (Figure 4.4), <i>Microcystis</i> -associated surface Chl a concentration of 7 $\mu\text{g L}^{-1}$ (sampled using a horizontal net tow) would produce enough microcystin (800 ng L^{-1}) to reach the OEHHA Action Level, and constitute an action level for the Delta." I am concerned with the concept of using Chl a to determine actions levels. While Chl a and microcystin levels are related the correlation is not linear and does not take other cyanotoxins into account. Whether or not chl a correlates with other toxins would be an interesting question.	This can be discussed further; to be on the safe side I removed Figure 4.4 and the calculation of a surface Chl a level that could potentially constitute an action level

Orr	36	Under section 5.1, last half of paragraph relating to flow and turbidity - Is there data to suggest that increased turbidity reduces risk of HABs in the delta that is independent of flow rate or temperature? HABs are common in other water bodies with high turbidity. The observation the HABs are controlled by turbidity may be an artifact of higher flows and lower temps. In low flows and turbid water could buoyancy regulating species stay near the surface to receive the necessary light intensity?	Yes, I do think that the effect of turbidity cannot be separated from the effect of flows in the Delta; whether turbidity alone has the same effect is not clear. I have revised this statement to reflect that the two covary
Orr	42	Under R1, second paragraph discussing monitoring - Consider not listing species. If the plan is long term the species of concern may change or expand.	Adaptive management strategies should take care of that; the species are listed as an example
Orr	42	Under R1, last sentence in first paragraph, correct the misspelling of "calibrate".	Done
Orr	N/A	The introductory sections have a broad perspective regarding toxigenic algal species. However, the discussion of factors influencing cyanobacterial blooms appears to focus on microcystins as a model for all blooms. I think the discussion of other species should be increased.	The literature is heavily tilted towards microcystins therefore the white paper as well. However, Kudela noted in his comments that cyanobacterial toxins other than microcystins are almost not detected in the Delta; a statement to this effect has been added in the first paragraph of section 4.2.3
Orr	N/A	I am concerned about how turbidity is discussed. If data is available I recommend discussing it separately from flow and temperature. If turbidity related data is not available avoid general assumptions regarding its influence on blooms.	I have repeated previously published statements regarding turbidity and Microcystis in the Delta; the assumptions in the published work are stated. A new section (5.1.3) on water clarity in the Delta has been added.
Orr	N/A	It was unclear to me what the end goal of the monitoring program is. If a clearer question(s) can be developed I encourage adding a more specific monitoring plan.	To be discussed at the next meeting
Orr	N/A	I heard some monitoring questions from the group and am interested in how common these questions are among the group. I suspect there will be some disagreement about the hypothesized answers but the questions seemed shared. (See 4 questions below)	Noted
Orr	N/A	1. When and where do we reach the required surface temperatures for a bloom? (microcystis exclusively?) a. What is the appropriate depth to measure temperature?	Noted
Orr	N/A	2. Do nutrient limited conditions occur during blooms in the delta? Presumed not to. a. Does this occur in some areas but not others? b. Are we close enough for this to occur in near future? c. Is this question species or nitrogen source dependent in a non-limited system?	Noted
Orr	N/A	3. Spatially where are both temperature and nutrients high and do we need more spatial resolution?	Noted

Orr	N/A	4. Is chlorophyll a the right parameter to be measuring? a. Does it correlate with microcystin concentrations?	Noted
Taberski	iii	Delete "already exists" under the section R1, first sentence.	Done
Taberski	1	Add "of" under section 1.1, 4th sentence "...Delta is widely recognized as in "crisis" because of competing demands..."	Done
Taberski	1	Delete "d" in word "declined" under section 1.1, last sentence "...including the continued declined of ..."	Done
Taberski	22	The paragraph under sub-section "Confounding factors:" is not clear, particularly the last sentence is confusing.	This sentence has been revised
Taberski	29	In the 5th sentence at the top of the page, insert a space in the word "watercolumn".	Done
Taberski	32	In table 4.1, I think you should also include the OEHHA thresholds.	Table below has OEHHA thresholds
Taberski	39	Under the last paragraph for section 5.2, the last sentence "...nutrients are unlikely to play a role in the onset or frequency of bloom occurrence in the Delta." - I agree. Nutrient concentrations would play a role, though, in the magnitude (concentration) and duration of a bloom. If nutrients were lower, they would be depleted more quickly and the bloom would crash. This was stated in the Summary bullet #2. That clarification should be added to this paragraph.	This has been added
Taberski	40	Under the second bullet, in the third sentence, correct the misspelling of "initiated".	Done
Taberski	40	In the last paragraph, in the second sentence, put a space in the word "watercolumn".	Done
Taberski	40	In the last paragraph, in the third sentence, change the sentence to read as "Both <i>higher</i> temperatures and reduced ..."	Changed
Taberski	42	Under R1, first sentence, delete the wording "already exists".	Done
Taberski	N/A	A section should be added on risk to aquatic life.	Done
Taberski	N/A	Historical data should be analyzed based on driving factors to evaluate risk (areas with high temperatures/low turbidity/long residence time)	Example analysis of nutrient concentrations at station D26 performed; included in Appendix A
Taberski	N/A	Recommended monitoring should be based on specific management questions related to status and trends, hotspots, risks to humans, animals and aquatic life, and directing management actions.	Noted
Taberski	N/A	Monitoring information should be collected on processes and projections needed for modeling cyanoHABs and directing management actions. The SF Bay RMP's management questions could be used as a model for developig management questions for cyanoHABs. The RMP's management questions are:	Noted

Taberski	N/A	<p>1. Are chemical concentrations in the Estuary at levels of potential concern and are associated impacts likely?</p> <p>a. Which chemicals have the potential to impact humans and aquatic life and should be monitored?</p> <p>b. What potential for impacts on human and aquatic life exists due to contaminants in the Estuary ecosystem?</p> <p>c. What are appropriate guidelines for protection of beneficial uses?</p> <p>d. What contaminants are responsible for observed toxic responses?</p>	Noted
Taberski	N/A	<p>2. What are the concentrations and masses of contaminants in the Estuary and its segments?</p> <p>a. Do spatial patterns and long-term trends indicate particular regions of concern?</p>	Noted
Taberski	N/A	<p>3. What are the sources, pathways, loadings, and processes leading to contaminant-related impacts in the Estuary?</p> <p>a. Which sources, pathways, and processes contribute most to impacts?</p> <p>b. What are the best opportunities for management intervention for the most important contaminant sources, pathways, and processes?</p> <p>c. What are the effects of management actions on loads from the most important sources, pathways, and processes?</p>	Noted
Taberski	N/A	<p>4. Have the concentrations, masses, and associated impacts of contaminants in the Estuary increased or decreased?</p> <p>A. What are the effects of management actions on the concentrations and mass of contaminants in the Estuary?</p> <p>B. What are the effects of management actions on the potential for adverse impacts of humans and aquatic life due to Bay contamination?</p>	Noted
Taberski	N/A	<p>5. What are the projected concentrations, masses, and associated impacts of contaminants in the Estuary?</p> <p>A. What patterns of exposure are forecast for major segments of the Estuary under various management scenarios?</p> <p>B. Which contaminants are predicted to increase and potentially cause impacts in the Estuary?</p>	Noted
Thompson	ii	You only have four, not five, major findings identified in the Executive Summary section	Corrected
Thompson	iii	Under Finding #3, first bullet, second sentence relating to temperature for growth: Should we specify the time frame over which the temperature is measured? e.g., instantaneous, daily average, daily max or min. This will matter more when we get to modeling phytoplankton dynamics.	Save for the modeling

Thompson	19	Under section 3, first sentence: Correct spelling of word "prompted" by adding a "p" between "m" and "t".	Done
Thompson	20	Under section 3.1, in sentence "Indeed, recent decades has witnessed..." Replace word "has" with "have".	Done
Thompson	20	Under section 3.2.1, first paragraph, reference Edmondson and Lehman 1981 was not included in the reference section.	Done
Thompson	21	Under Cellular N:P composition section: Reference Mills <i>et al.</i> was not included in the reference section and date missing in citation.	Corrected; citation added
Thompson	22	Under Confounding Factors, third sentence: Should we introduce the concept that there may be time lags between nutrient uptake and increased biomass, such that a correlation between two variables at a given point in time may not imply causality?	Good idea; sentence added under confounding factors on page 23 of revised manuscript.
Thompson	22	Under Confounding Factors, third sentence discussing parameters: Is there a diagram from a paper or textbook that we could borrow and reference, that shows the patterns of these variables over time before, during and after a bloom? (e.g., temperature, nutrient concentration, nutrient uptake rate, phytoplankton biomass). Something to show phytoplankton biomass peaking as nutrients draw down.	I found one diagram that showed a dinoflagellate peaking as nutrients were drawn down but nothing for cyanobacteria; after looking for the same pattern for cyanobacteria for half day I gave up
Thompson	27	Last paragraph under section 3.6 on stratification and residence time: Suggest adding a brief discussion of the potential role of ferrous iron. See Molot <i>et al.</i> 2014. A novel model for cyanobacteria bloom formation: the critical role of anoxia and ferrous iron. <i>Freshwater Biology</i> 59:1323-1340. The article mainly deals with lakes but there is a section on page 1330 that mentions shallow, nearshore regions of lakes, including harbors, inshore areas of Lake Erie, and embayments of Georgian Bay (Lake Huron). [Text from Introduction shown on next line.]	The potential role of toxins acting as siderophores and aiding cyanobacteria with iron uptake providing an advantage in competition with eukaryotes is discussed in a new expanded paragraph on p. 19 and the Molot <i>et al.</i> citation has been added to this section.

		<p>Here's some text from the Introduction:</p> <p>"We cannot predict with any certainty when a cyanobacteria bloom will begin once temperatures are warm enough to support growth or the duration of a bloom except through empirical observations from previous years. Nor do we know why the problem is worsening in some mesotrophic systems."</p> <p>"Clearly, the predictive state of cyanobacteria science is unsatisfactory. This dissatisfaction may have contributed to the recent debate challenging the supremacy of the P paradigm in eutrophication management. Wurtsbaugh, Lewis, Paerl, and their colleagues argue that N plays a major role alongside P in promoting cyanobacteria blooms and that both N and P should be controlled (refs). This argument has been vigorously challenged in return by Schindler and his colleagues who claim that controlling N to control cyanobacteria will not work because N-fixation by cyanobacteria will compensate to a large extent for induced N shortages (refs). The outcome of this on-going debate can be expected to influence the direction of billions of dollars in public expenditures to remedy nutrient loading."</p> <p>"Our purpose here is to present a novel model that does not supplant the important roles of P and N as major macronutrients, but instead weaves additional ideas into older ones to create a novel and more comprehensive conceptual framework with much more explanatory power that spans the range of conditions where cyanobacteria blooms have been observed."</p>	
Thompson	27		Noted
Thompson	28	Under section 4.1 Ecosystem Services, second paragraph, Reference Sommer <i>et al.</i> 1997 not included in reference section.	Citation added
Thompson	30	Figure 4.1 - Can we get a higher resolution version of this map? It was blurry in the original Word version, prior to becoming a Google doc.	Will investigate
Thompson	36	Under section 5.0, first paragraph, last sentence: Should we specify that the variables may need to be time-lagged in order for the correlations to be apparent?	I actually prefer to be vague in case entirely different statistics are needed
Thompson	38	Under section 5.2, first paragraph, second sentence referring to Microcystis and Aphanizomenon becoming more common: Is the reference for this statement the Lehman 2007 paper? I think it would be worth referencing it again at the end of this sentence, or adding an additional reference as necessary.	This is based on Lehman's 2008 paper and the Mioni <i>et al.</i> 2012 report; these citations have been added
Thompson	38	Under section 5.2, second paragraph, second and fourth sentence referring to Figure 2: I think this is now [Figure] 3.3. Check Figure number.	Corrected: now figure 3.6

Thompson	39	Second full paragraph, reference to Figure 4.5: This information is not shown in this figure. Check your Figure number.	Correct, the reference to this figure has been deleted
Thompson	39	Second full paragraph, last sentence related to culture investigations: It would strengthen the point to reference (re-reference) some key papers here.	Done
Thompson	41	In Table 5.1, Observations in the Delta "when turbidity is <50 NTU, flow is <30 m ³ s ⁻¹ and irradiance >50 μmol phot m ⁻² s ⁻¹ ": Please briefly state where in the Delta this was measured, and over what spatial and temporal scale.	Done
Ward	N/A	<p>Comment 1: Of the five questions the Work Group is tasked with answering, the first is to determine whether the principal physical and biological factors promoting cyanobacteria blooms and toxin production in the Delta have been identified. My reading of the current work in this area leads me to conclude that these factors have not yet been adequately characterized. More importantly, the critical task of accurately gauging the relative weight of various factors that are known to influence/control the formation of toxigenic (or other) blooms still seems beyond our capability at present, whether in the Delta or in other waterbodies for which some relevant data is available. These deficiencies are particularly problematic for the development of a model that has practical utility.</p> <p>The field work and laboratory studies on Delta water quality and Delta species involved with the Pelagic Organism Decline that were cited in the draft white paper and/or distributed to the Work Group are largely "Microcystis-centric" and "microcystin-centric". There is, in my view, a very large risk in attributing (1) all significant microcystin production to Microcystis in the Delta, and; (2) focusing on microcystin(s) to the exclusion of the effects of other possible toxigenic genera and other cyanotoxins. Dr. Berg's draft white paper duly notes the existence of many other toxigenic genera and other cyanotoxins, but it seems the Delta-specific research on these possibilities may not yet be available for review.</p>	Noted; Please see new comment under section 4.2.3 on toxin data available from Central California demonstrating that very few detections of toxins other than microcystins have been made in the Delta

Ward	N/A	<p>Comment 1 continued: This is not a trivial point: for example, various Aphanizomenon strains can produce saxitoxin, microcystin(s), cylindrospermopsin, BMAA, and anatoxin-a (Paerl & Otten, 2013), and Lehman <i>et al.</i> have noted the presence of this genus in the estuary, bay and/or Delta. Though it is quite possible that I have overlooked Delta-specific studies on Aphanizomenon strains which examined the possibility that one or more of these toxins is present, if it is true that these studies have not been conducted yet, it would be ill-advised to presume that microcystin(s) are some sort of "model" toxin that can be regarded as a generic equivalent of all of the others in a subsequent modeling exercise, especially given their chemical and toxicological heterogeneity. Similarly, the diazotrophic cyanobacteria such as Aphanizomenon may respond rather differently to "nutrient limitation" (of nitrogen) than the non-diazotrophic genera such as Microcystis. If both genera produce microcystins, then microcystin production per se may continue in a water body as nitrogen becomes more limiting for Microcystis.</p> <p>Comparisons of diazotrophic cyanobacteria with non-nitrogen fixing cyanobacteria to nitrogen-limited conditions tend to show the following pattern: diazotrophs (e.g., Aphanizomenon) tend to produce toxins such as microcystin under nitrogen-limited conditions, whereas non-nitrogen fixers such as Microcystis and Planktothrix increase toxin production under non-limiting conditions.</p>	Not necessarily; please see Dolman 2012 citation for patterns of abundance of various species and toxin production in over 100 lakes in Germany under different N:P scenarios described in "Meta analyses of Lake Studies" on page 24.
Ward	N/A	<p>Comment 1 continued (references): Holland, A., Kinnear, S. Interpreting the possible ecological role(s) of cyanotoxins: compounds for competitive advantage and/or physiological aide? <i>Marine Drugs</i> 2013, 11(7), 2239-2258 http://www.mdpi.com/1660-3397/11/7/2239 Paerl, H. Otten, T. Harmful Cyanobacterial Blooms: Causes, Consequences, and Controls. <i>Microbial Ecology</i> 2013 May;65(4):995-1010 http://www.unc.edu/ims/paerllab/research/cyanohabs/me2013.pdf Leao, P. <i>et al.</i> The chemical ecology of cyanobacteria. <i>Natural Products Reports</i>, 2012 Mar;29(3):372-91 http://www.ncbi.nlm.nih.gov/pmc/articles/PMC4161925/pdf/nihms-599340.pdf</p>	
Ward	N/A	<p>Comment 2: Given my time limitations for reviewing more recent work on how/whether nutrient management can reduce the magnitude and frequency of cyanobacteria blooms and toxin formation, I was unable to conduct the review I had originally anticipated on this question.</p>	Noted

Ward	N/A	<p>Comment 3: I believe the draft white paper correctly examines and compares the relative significance of various factors in controlling the growth and development of toxigenic blooms based on the limited data now available on this subject that is “Delta-specific”. However, as stated in answer to Question 1 (above), I also believe the factors considered, while appropriate, are nevertheless an incomplete list. At our meeting I mentioned the apparent role of competition for iron as a factor in bloom formation and dominance in freshwater ecosystems, and provided a citation for this. Other factors which should be considered include the differences in sensitivity to herbicides between cyanobacteria and other phytoplankton that are being reported in studies conducted elsewhere, and the role of allelopathy in bloom formation, dominance, and senescence. Allelopathy is also discussed in references provided in answer to Question 1. For pesticides – in this case, I focused on herbicides – please refer to references provided below.</p>	<p>Allelopathy was discussed in the original version of the White paper under "Potential Functions of toxin production" on page 18. Two new references have been added to the previous references on allelopathy in this section.</p>
Ward	N/A	<p>Comment 3 continued (references): The USGS maintains an online geo-referenced database which charts the most commonly-used pesticides in CA as they have continued to change in recent years that is current through 2012: http://water.usgs.gov/nawqa/pnsp/usage/maps/compound_listing.php Lurling, M., Roessink, I. On the way to cyanobacterial blooms: Impact of the herbicide metribuzin on the competition between a green alga (<i>Scenedesmus</i>) and a cyanobacterium (<i>Microcystis</i>). <i>Chemosphere</i>, 2006, 65:4, 618-626. Peterson, H. <i>et al.</i> Toxicity of hexazinone and diquat to green algae, diatoms, cyanobacteria and duckweed. <i>Aquatic Toxicology</i>, 1997, 39(2), 111-134. Arunakumara, K. <i>et al.</i> Metabolism and degradation of glyphosate in aquatic cyanobacteria: a review <i>African Journal of Microbiology Research</i>, 2013 Vol. 7(32), pp. 4084-4090. http://www.academicjournals.org/article/article1380269900_Arunakumara%20et%20al.pdf</p>	<p>The potentially important influence of herbicides and fungicides on the prevalence of cyanobacteria vis-à-vis other phytoplankton is discussed in a new Section 3.7 on p. 31 and again under Section 4.2.1 p 33. Because concentrations of herbicides in the Delta have been demonstrated to be quite high, a recommendation has been added that selective sampling for herbicides and pesticides be instituted in the Delta.</p>
Ward		<p>Comment 4: In answer to this question, please see the additional references supplied in answer to Questions (1) and (3).</p>	<p>A citation by Holland and Kinnear (2013) has been added on the benefits of toxin production under iron limiting conditions as mentioned in previous comments.</p>

<p>Ward</p>	<p>N/A</p>	<p>Comment 5: Overall, I agree with the draft recommendation put forward regarding monitoring of CyanoHABs (Recommendation 1), but would place more emphasis on monitoring for more immediate threats to public health e.g., intakes for drinking water treatment plants either within the bloom-prone areas of the Delta. The waterboard’s drinking water program staff has informed me that some public water supply systems are struggling to successfully contend with this issue elsewhere in California, and this may also be a recurrent problem for smaller communities in the Delta. With perennially limited resources, public health protection should be given the highest priority, followed closely by protection of beneficial uses such as threatened/endangered species already impacted by the Pelagic Organism Decline, and a (seasonal?) surveillance program for areas of the Bay/Delta which experience periods of frequent and prolonged recreational uses water-contact uses, fishing, etc.</p> <p>With respect to Recommendation 2, I am unclear as to what the model being described is intended to accomplish: will it, if properly deployed, facilitate successful toxigenic bloom “forecasting”? Will use of whatever model results from this development process be of assistance, say, to managers of local public water supplies whose intakes are situated in the Delta? Having worked on this issue for ten years, I am concerned that our scarce resources are not being directed at immediate (& often seasonally recurrent) cyanotoxin hazards, and that local public health officials and water system managers have too few resources to respond effectively, and in a timely manner, when these episodes occur.</p>	<p>Noted</p>
-------------	------------	--	--------------

<p>Ward</p>	<p>N/A</p>	<p>Comment 5 continued: As an example, last year the public water supply system for 400,000 people in the greater Toledo area were shut down, causing a public emergency and immediate potable water shortage for the entire population, when a microcystin-producing <i>Microcystis</i> bloom swamped the treatment plant's capacity to remove it in the "finished" drinking water. The National Guard was called-up to help deliver potable to this large urban population, and the problem did not abate for several days. Prior to this episode, NOAA had been doing quite a bit of modeling, bloom-forecasting, and other scientific investigations on these recurrent toxigenic blooms on western portion of Lake Erie where Toledo area residents obtain their public water supplies. The NOAA investigations remain on-going, and no doubt have provided much useful information on the role of various environmental factors in bloom formation: their "mission", however, is not to protect specific public water supplies from catastrophic events such as this episode. http://www.washingtonpost.com/news/post-nation/wp/2014/08/04/toledos-water-ban-and-the-sensitivity-of-our-drinking-systems/</p>	<p>Noted</p>
-------------	------------	---	--------------

APPENDIX C

Comments from the Stakeholder and Technical Advisory Group (STAG) members and responses from the authors.

Author	Page	Comment	Response
Lee	N/A	Overall Comment: The findings expressed in the draft white papers are consistent with our many years of experience investigating nutrient-related water quality, our findings in investigating Delta nutrient impacts and control of excessive aquatic plants, as well as with the findings expressed in presentations made at the CWEMF Delta Nutrient Modeling Workshop discussed below.	Noted
Lee	N/A	There remains little ability to quantitatively and comparatively describe the role of nutrients (N and P) in controlling the excess fertilization of the Delta waters.	Noted
Lee	N/A	There is considerable misinformation in the professional arena on the relative roles of N and P concentrations and loads, and the ratios of N to P in affecting water quality in the Delta; some of the information presented on nutrient/water quality issues is biased toward preconceived positions.	Noted
Lee	N/A	Based on the results of the US and international OECD eutrophication study and our follow on studies of more than 600 waterbodies worldwide (lakes, reservoirs, estuarine systems) the planktonic chlorophyll levels in the Central Delta are well-below those that would be expected based on the phosphorus loads to the Delta.	Noted
Lee	N/A	There is a lack of understanding of the quantitative relationship between nutrient loads and fish production in the Delta.	Noted
Lee	N/A	The Delta Stewardship Council's timetable for developing Delta nutrient water quality objectives by January 1, 2016, and to adopt and begin implementation of nutrient objectives, either narrative or numeric as appropriate, in the Delta by January 1, 2018 is unrealistically short.	Noted
Lee	N/A	There is need for substantial well-funded, focused, and intelligently guided research on Delta nutrient water quality issues over at least a 10-yr period in order to develop the information needed to generate a technically sound and cost-effective nutrient management strategy for the Delta.	Noted
Lee	N/A	As discussed in our writings, some of which are noted below, it will be especially difficult to develop technically valid and cost-effective nutrient control programs for excessive growths of macrophytes in the Delta.	Noted

Mioni	3	#2: pH may also be important (I see some correlations and I think Raphe mentioned a report). I believe some cyanobacteria can be more competitive when pH increases due to CO ₂ concentrating mechanism. I think Alex Parker did some research on the Delta pH... Also, the residence time may be affected by the pumping station located near the EMP Old River D28 station (a station with typically high Microcystis abundance).	Noted
Mioni	13	last paragraph: Please talk to Anke Mueller-Solger. I believe Microcystis was there before 2000 but was simply not monitored as closely or did not cause such bloom.	Noted
Mioni	16	Carbon fixation: I would include a few reference to the cyanobacteria carbon concentrating mechanism.	Noted
Mioni	16	Table 2.3: Microcystin LD50 varies depending on the variant	Noted
Mioni	20	typo "preceding"	Noted
Mioni	21	N:P ratio: I would cite Hans Paerl as well. I believe he has shown (in Lake Taihu?) that the N:P ratios were not so fixed for cyanobacteria.	Noted
Mioni	29	Salinity: I think Pia Moissander did phylogenetic studies in the SFBD and has shown that there were two types of Microcystis, one of those was associated with higher salinity.	Noted
Mioni	31	I agree that absolute concentrations of nutrients is more relevant than N:P ratios with regards to cyanobacteria. I believe Hans Paerl also demonstrated this (Nature paper? I can't recall the exact source).	Noted
Mioni	37	last paragraph: typo "water column"	Noted
Mioni	39	Old River stn (D28) usually has the highest abundance based on my monitoring. Antioch also has a high abundance of Microcystis. Pia Moisaner's paper show that there may be two different strains (different requirements?) between antioch and other stations. It varies between years at other stations (see attached examples but please do not use as this is for the paper I am writing...)	Noted

Mioni	40	<p>It really depends on the year. Aphanizomenon was very sporadic before 2011 and I focused on enumerating Microcystis which was the dominant cyanoHAB. But in 2011, Aphanizomenon was pretty significant. The tricky part here is that the Aphanizomenon cells are much larger than Microcystis so even if Aphanizomenon doesn't reach the cell density of Microcystis, it doesn't mean they are not dominating the bloom (e.g. 2011, it would clog my filters pretty quickly at some stations)... In 2012, Microcystis abundance was higher than in 2011 but Apha was still pretty abundant. I think that the "bloom" classification based on cell density should be revised to take into account the biovolume... Cell counts can be misleading.</p>	Noted
Mioni	44	<p>There is definitely variations explained by the method but there are also variations due to heterogeneity, patchiness and temporal variation. In Clear lake, while on station (within maybe 30min or less), we could see the scum moving very quickly with the wind. Also, the two net samples mostly applies to colonial forms of Microcystis although it occurs also as single cells and microcolonies. Another bias is the cell count. Prior to do my cell counts, I was homogenizing the samples by dislocating the colonies physically (based on prior research and comparison). I suspect that not dislocating the colonies prior to do the cell count may result in bias as the person enumerating the cells may not be able to count accurately as colonies can be more 3D than 2D (I hope it makes sense)... Although there is a bias in all methods, I do not think I ever collected samples in the same time than Peggy and at the same location. Thus, the comparison is a little puzzling to me. We never did intercomparison of the cell enumeration from the same samples. It would be more relevant to compare methods for the toxicology work since we did intercomparison of methods for the same samples.</p>	Noted
Mioni	48	<p>"colonial Microcystis have been more common", see my comments regarding the bias of tow net sampling versus grad raw water samples...</p>	Noted

Mioni	4 & 35	#3 and page 35, temperature: Lenny Grimaldo generated a logistic model based on my CALFED data (see attached) which shows that Microcystis bloom probability raises to 50% when surface water temperature reaches 25C. Also, I suspect there is a minimum temperature that would need to be sustained for several days if not week for a bloom to initiate.	Noted
Mioni	42-43	I think the SWAMP report could be cited, especially for the SPATT results.	Noted
Mioni	Fig 4.5	Figure 4.5: the axis are not labelled and I have trouble understanding this figure.	Noted
Mioni	48	I could not find the figure 2 mentioned here...	Noted

Factors Controlling Submersed and Floating Macrophytes in the Sacramento-San Joaquin Delta

Prepared for:

The Central Valley Regional Water Quality Control Board

And

The California Environmental Protection Agency

State Water Resources Control Board

(Agreement Number 12-135-250)

Katharyn Boyer

Romberg Tiburon Center for Environmental Studies

San Francisco State University

Martha Sutula

Southern California Coastal

Water Research Project

Revised Draft Technical Report XXX

July 2015

Acknowledgements

The authors of this document wish to thank the members of the Submersed and Floating Macrophyte Science Working Group and Stakeholder and Technical Advisory Group for review and input. This report was produced under California State Water Board contract to the Southern California Coastal Water Research Project (Agreement Number 12-135-250).

DRAFT

This report should be cited as:

Boyer K and Sutula M. 2015. Factors Controlling Submersed and Floating Macrophytes in the Sacramento-San Joaquin Delta. Southern California Coastal Water Research Project Technical Report No. XXX. XXXX 2015.

Executive Summary

The Central Valley Regional Water Quality Control Board (Water Board) is developing a plan to generate the science needed to support decisions on policies governing nutrient management in the Delta. Non-native, invasive floating and submersed aquatic vegetation (SAV) are one of three areas, identified by Water Board, that represent pathways of potential ecosystem impairment that could be linked to nutrients. The Water Board commissioned a literature review of the factors that may be controlling the prevalence of floating and SAV. This literature review addresses three major questions:

- 1) How do submersed and floating aquatic vegetation support or adversely effect ecosystem services and related beneficial uses?
- 2) What is known about the spatial and temporal trends in submersed and floating aquatic vegetation in the Delta?
- 3) What is the relative importance of nutrients versus other factors in promoting observed trends in submersed and floating aquatic vegetation in the Delta?

This review had seven major findings:

#1. Native submersed and floating vegetation are beneficial components of the Delta; however, non-native species have been found to adversely affect Delta ecosystem services and associated beneficial uses at the high densities at which they typically occur. Adverse effects include: 1) changes to water chemistry including diurnal swings in pH and dissolved oxygen, 2) changes to physical properties of water including flow and turbidity 3) outcompetition of native SAV, phytoplankton, and other benthic primary producers, 3) changes to the food web, 4) impedece of navigation and obstruction of industrial intake pipes and 5) poor aesthetics.

#2. Two invasive species, *Egeria densa* (Brazilian waterweed, a submersed species) and *Eichhornia crassipes* (water hyacinth, a floating species) are widely recognized as problematic in the Delta, and appear to be increasing in abundance despite control efforts. *E. densa* coverage was estimated at ~2000 hectares in 2007 and 2900 hectares in 2014. *E. crassipes* covered ~200 hectares between 2004-2008 and 800 hectares in 2014.

#3. Additional invaders may also have reached high enough abundance to be considered problematic, especially *Ludwigia* spp. (water primrose). *Ludwigia* spp. (unknown proportion of *L. peploides* and *L. hexapetala*, and possibly *L. grandiflora*) are now equal in floating coverage to water hyacinth (800 hectares each estimated in 2014), whereas the native pennywort was much more common than *Ludwigia* during the period of 2004-2008. *Ludwigia* spp. are not part of a control program in the Delta at this time.

#4. Data on spatial and temporal trends in invasive aquatic plants have been collected only sporadically in space and time and without adequate detail. Remote sensing may be adequate to estimate of coverage of floating vegetation, but submersed vegetation requires a much greater, field-

based effort to distinguish species. Both types of vegetation require estimates of biomass or preferably primary production if we are to understand patterns in abundance and rates of turnover.

#5. Existing scientific literature has documented a number of environmental and management-related factors that have control over the growth of invasive aquatic plants worldwide. These include: 1) light, 2) temperature, 3) salinity, 4) dissolved inorganic carbon (for SAV), 5) nutrients, 6) flow and residence time, 7) interaction with other species, and 8) control efforts.

#6. Studies have documented the importance of a subset of these factors in the Delta, but insufficient evidence exists to determine the relative importance of nutrients versus other factors in promoting the expansion of these species. Drawing on available information, we can conclude the following:

- Conditions in the Delta, including seasonal low flow, low turbidity, warm temperatures, and a freshwater (low salinity) regime, appear to favor the establishment and growth of invasive macrophytes.
- Aquatic plants require macronutrients (nitrogen, N and phosphorus, P) for growth. N and P are available in relatively high concentrations in the Delta ($\sim 0.5 \text{ mg l}^{-1}$ dissolved inorganic N, DIN, and 0.05 mg l^{-1} DIP), and available nutrients may not limit growth. However, it is difficult to discern the relative influence of nutrients versus other factors, making uncertain the effect that nutrient management could have on growth and persistence of these invasive aquatic plants. Recent rapid expansion of invasive macrophyte acreage, despite evidence that concentrations of NH_4^+ , NO_3^- , PO_4^+ , and ratios of N:P within Delta waters have been steady over the last decade, suggest other factors besides nutrients are contributing to the extensive plant growth at the scale of the whole Delta.

#7. Climate change and anthropogenic activity associated with land use changes have the potential to further increase the prevalence of invasive macrophytes. Climate change will likely result in warmer temperatures, reduced frequency of frost, and increased drought, the latter of which could result in reduced flows, increased residence time and water column stability in the Delta. These factors would provide a favorable environment for increased prevalence of *E. densa* and *E. crassipes*, and perhaps other invaders. However, increased salinity intrusion into the west Delta would favor native species of aquatic vegetation, in particular the pondweed *Stuckenia pectinata*.

Given these findings, three major science recommendations are proposed:

R1: Implement routine monitoring of invasive floating and submersed aquatic vegetation. Routine monitoring of floating and submersed aquatic vegetation should be undertaken to assess trends over time and to support ecosystem modeling of the Delta. Grant-funded efforts have been sporadic and there is no plan for on-going rigorous evaluation of patterns and trends. Monitoring should be comprised of a combination of remotely sensed areal coverage and field-based transects to estimate biomass or, ideally, net primary production (through repeated measures of biomass over time to determine rates of turnover), as well as species composition. Estimates of biomass/production and areal cover should be conducted in combination with measures of the major factors that control growth of

these primary producers, including water column and sediment nutrients. Early actions should include the development of a workplan to lay out the key indicators and cost estimates required for monitoring.

R2: Develop a biogeochemical model of the Delta, focused on nutrient and organic carbon fate and transport. Understanding of factors controlling floating and SAV is critically hampered by the lack of information on nutrient and carbon budgets for the Delta and its subregions. In particular, it is important to quantify the storage in the compartments of the ecosystem (i.e. water, sediment, plant biomass, etc.) and fluxes or exchanges between compartments at varying seasonal and spatial scales and with a variety of water flow and residence time scenarios. This information will provide an understanding of whether management of nutrients is likely to aid in control of floating and SAV. To step into model development, three actions should be taken: 1) examine existing models already available to determine suitability for this task, 2) develop a work plan that lays out the modeling strategy, model data requirements, and implementation strategy, and 3) conduct special studies and other monitoring needed to support model development. This includes special studies that quantify N, P, and organic carbon associated with ecosystem compartments as well as uptake, release and flux rates that characterize different reaches of the Delta. Lab and field experiments that test whether macrophyte growth is limited by nutrients in Delta waters could help inform management and predict problem areas. These analyses and experiments should inform hypotheses that can be tested through model development as well as potential future scenarios. The monitoring and modeling teams should collaborate closely to collect high priority data to inform the models.

Comment [KB1]: Point of discussion: John Madsen said “the authors are assuming that nutrients are limiting plant growth without knowing this. It is doubtful that an ecosystem model will indicate if nutrients are limiting either water hy or egeria. It is far more common to see luxury consumption of nutrients by submersed and floating aquatic plants than nutrient limitation”.

R3. Review current and potential future control strategies for invasive aquatic macrophytes in the Delta, including mechanical, chemical, biological control, and integrated control methods, as well as barriers that reduce movement of vegetation into sensitive areas or those with heavy human use. Depending on the outcome of R2, nutrient management may be ineffective in controlling invasive floating and SAV. While monitoring, modeling and special studies are under way, determine the degree to which control strategies are supporting beneficial uses and nutrient management objectives going forward. This work should begin by evaluating current and planned control strategies to determine effectiveness at both reducing live biomass and minimizing recycling of nutrients from dead material into additional growth in areas with high residence time. A current USDA-ARS program on integrated control methods for both *E. densa* and *E. crassipes* could help to inform the proposed review.

Table of Contents

Acknowledgements.....	i
Executive Summary.....	ii
List of Tables.....	vii
List of Figures.....	vii
1. Introduction, Purpose and Organization of the Review	1
1.1 Background and Context	1
1.2 Goal and Organization of Macrophyte Literature Review.....	3
2. General Ecology and Trends in the Distribution of Submersed and Floating Aquatic Vegetation in the Delta	4
2.1 Classification of Aquatic Vegetation and Scope of Review.....	4
2.2 Overview of Species Found in the Delta.....	4
2.3 Habitat Types in Which They are Characteristically Found	10
2.4 Spatial and Temporal Trends in their Distribution and Abundance	13
3. Role of Submersed and Floating Aquatic Vegetation in Supporting Delta Ecosystem Services	17
3.1 Conceptual View of Positive and Negative Effects of Submersed and Floating Aquatic Vegetation on Ecosystem Services.....	17
3.1.1 Changes to Water Chemistry	18
3.1.2 Changes to physical properties of water	20
3.1.3 Effects on algae and native macrophytes	21
3.1.4 Trophic support.....	22
3.1.5 Navigation and industry.....	23
3.1.6 Aesthetics.....	24
4. Factors Contributing to the Prevalence of Submersed and Floating Aquatic Vegetation in the Delta	24
4.1 Conceptual Models of Growth, Propagation and Environmental Characteristics that Enhance or Limit Growth	24
4.1.1 Light.....	27
4.1.2 Temperature	28
4.1.3 Salinity.....	29
4.1.4 Dissolved inorganic carbon	31

4.1.5 Nutrients 31

4.1.6 Flow, residence time, substrate stability, and slope 37

4.1.7 Interactions with other submersed or floating species 38

4.1.8 Chemical, mechanical, and biological control..... 41

4.2 *Relative Importance of Nutrient Subsidies Versus Other Factors in Promoting Observed Trends* . 42

5. Recommendations43

6. Literature Cited45

6.1 *Peer-reviewed literature and grey literature (reports)*..... 45

6.2 *Local and regional press reports*..... 55

DRAFT

List of Tables

Table 2.1. Submersed and floating vegetation in the Sacramento-San Joaquin Delta. N = Native, I = Introduced. * Indicates the most abundant introduced and native species, on which this review is focused.	5
--	---

List of Figures

Figure 1.1 The Sacramento-San Joaquin Delta Region.....	2
Figure 2.1. Rake detections and other data on abundance of submersed species at sampling points within the central Delta (left). Excerpted from Santos et al. 2011	6
Figure 2.2. Relative abundance of submersed plant species in the west Delta and Suisun Bay (see map inset to interpret site abbreviations from west to east) in 2012 as estimated with a rake sampling method (Kenow et al. 2007). Species abbreviations as in Fig. 2.1, with the addition of <i>Stuckenia foliosus</i> (STFO), the green alga <i>Cladophora</i> (CL), and <i>Ruppia</i> sp. (RU). (Figure from Boyer et al. 2013)	7
Figure 2.3. Species central to this review. Top: Two abundant non-native aquatic species, <i>Egeria densa</i> (left, photo Katharyn Boyer) and <i>Eichhornia crassipes</i> (right, photo Bob Case). Bottom: Two abundant native species, <i>Ceratophyllum demersum</i> (left, photo Ron Vanderhoff) and <i>Stuckenia</i> sp. (right, photo Katharyn Boyer).....	Error! Bookmark not defined.
Figure 2.4. Submersed vegetation (primarily <i>E. densa</i>) coverage of up to 560 hectares within Franks Tract in the central Delta, 2003-2007 (figure from Santos et al. 2009).....	11
Figure 2.5. Spatial distribution of <i>Stuckenia</i> sp. from Ryer Island in Suisun Bay to Sherman Lake in the west Delta, as determined from digitizing and ground truthing aerial imagery (Google Earth), 2012. Coverage is estimated to be ~ 500 hectares in this region. Image unpublished, based on data in Boyer et al. 2015.	12
Figure 2.6. Decadal changes in coverage of <i>Stuckenia</i> sp. within Suisun Bay, as mapped using digitized and ground-truthed Google Earth images. From Boyer et al. 2015	15
Figure 2.7. Decadal changes in coverage of <i>Stuckenia</i> sp. within the western portion of the Delta, as mapped using digitized and ground-truthed Google Earth images. From Boyer et al. 2015.....	16
Figure 3.1. Conceptual model of the effects of Delta macrophyte canopy structure on provision of fish habitat. Arrows show direction and primary effect caused by interaction of each “ecological type” of aquatic plant on fish (red, dashed = negative effect, green, solid = positive effect. From Anderson 2008	18
Figure 3.2. Conceptual model hypothesizing loss of function in invasive <i>Egeria densa</i> versus native <i>Stuckenia</i> sp. beds	Error! Bookmark not defined.
Figure 3.3. Green filamentous algal mats attached to <i>Egeria densa</i> in Sherman Lake, May 2012. Photo, Katharyn Boyer	22
Figure 4.1 Aquatic plant resource requirements for establishment, growth and dispersal, as described in a draft conceptual model by Anderson (2008)	25
Figure 4.2. Sub models describing important drivers of establishment, growth, and dispersal in submersed (A) and floating (B) aquatic vegetation. From draft conceptual model by Anderson (2008)	26
Figure 4.3. Response of <i>Egeria densa</i> to a range of temperature conditions applied at increasingly high salinity conditions at the end of 6 weeks in aquaria. From Borgnis and Boyer, in revision.....	28
Figure 4.4. Salinity effects on growth characteristics and nitrogen and phosphorus content and ratio of <i>Egeria densa</i> and <i>Stuckenia</i> sp. (gross morphological characteristics most closely matched <i>S. filiformis</i>) at the end of mesocosm experiment that ran June-August 2012. ND = no data; <i>E. densa</i> tissue nutrients could not be	

measured at the higher salinities due to insufficient tissue availability. From Borgnis and Boyer, in revision
 30

Figure 4.5. Effects of salinity on growth characteristics of *Egeria densa* (EDGE) and *Stuckenia* sp. (presumed to be *S. filiformis* based on gross morphological characteristics, STFI), grown separately and together, at the end of a mesocosm experiment running June-August 2012. From Borgnis and Boyer, in 38

Figure 4.6. Left: Effect sizes reflecting change in coverage with 25% increases or decreases in water hyacinth (*Eichhornia crassipes*) from remote sensing data (dark region of background indicates a strong effect). Changes are shown for water (blue), submersed vegetation (red, predicted to be primarily *Egeria densa*), emergent and senescent plants (green), native pennywort *Hydrocotyle umbellata* (yellow), and introduced water primrose (*Ludwigia* spp.). Right: Conceptual model of successional pathways of *E. crassipes* growth and expansion, with effects on other floating and submersed plants. From Khanna et al. 2012..... 40

DRAFT

1. Introduction, Purpose and Organization of the Review

1.1 Background and Context

The Sacramento–San Joaquin River Delta (hereto referred to as “the Delta”), is an inland river delta and estuary approximately 1300 square miles in size, found in Northern California (Fig. 1.1). Formed at the western edge of the Central Valley by the confluence of the Sacramento and San Joaquin Rivers, the Delta is a key component of the State’s water resource infrastructure and a region that is rapidly urbanizing, yet serves as critical habitat for fish, birds and wildlife. Water from the 45,000 square miles of Delta watershed fuels both local and statewide economies, including important agricultural commodities. The Delta is widely recognized as being in a state of “crisis” because of competing demands for the Delta’s resources (Delta Plan 2013). The consequences of these competing demands include point and non-point discharges, habitat fragmentation and loss, modified flow regimes, introduction of non-native species, all of which combine to threaten ecosystem health, including the continued decline of native fish (Delta Plan 2013).

In 2009 the California legislature passed the Delta Reform Act creating the Delta Stewardship Council. The mission of the Council is to implement the coequal goals of the Reform Act and provide a more reliable water supply for California while protecting, restoring, and enhancing the Delta ecosystem. The Council wrote and adopted a Delta Plan in 2013 to implement these goals. Chapter 6 of the Delta Plan deals with water quality and contains recommendations to implement the coequal goals of the Delta Reform Act. Among these include a recommendation to consider development of nutrient objectives for the Delta.

Potential nutrient related problems identified in the Delta Plan for evaluation are:

1. Decreases in phytoplankton abundance and shifts in algal species composition,
2. Increases in the abundance and distribution of macrophytes, including water hyacinth and Brazilian waterweed, and
3. Increases in the magnitude and frequency of cyanobacterial blooms

To provide better scientific grounding for the study plan, the Water Board commissioned two literature reviews centered on the latter two potential areas of impairment. This document provides a synthesis of literature on submersed and floating macrophytes in the Delta.

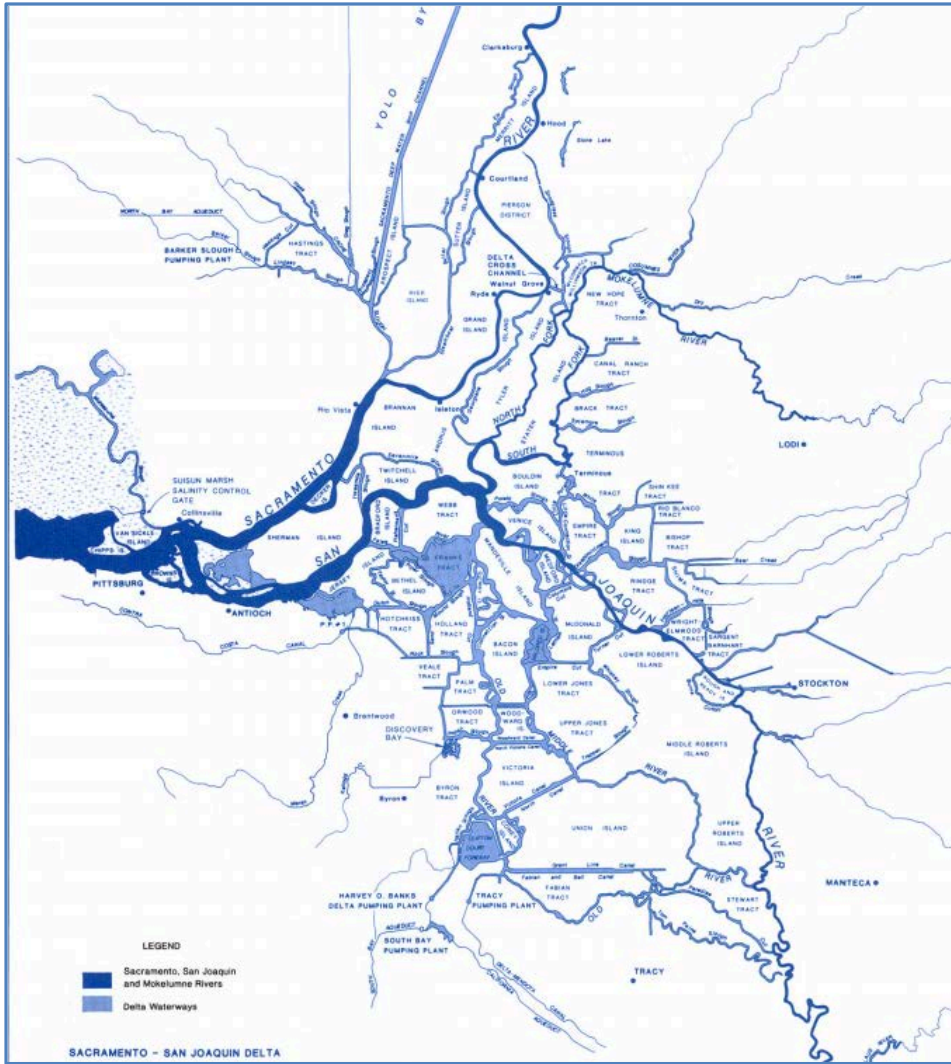


Figure 1.1 | The Sacramento-San Joaquin Delta Region

Comment [KB2]: Consider replacing figure – Shruti said hard to read (and I agree). What was ultimately used in the cyano review?

1.2 Goal and Organization of Macrophyte Literature Review

This review aims to assess whether there is evidence that the perceived increase in the abundance and distribution of submersed or floating aquatic macrophytes in the Delta is the result of long term changes in nutrient or organic matter loading relative to other factors and to ascertain whether management of nutrient loads might be used to remedy the problems associated with these macrophytes. This review will be evaluated and utilized by a Science Working Group to develop recommendations for a research plan to resolve outstanding questions regarding the need for nutrient management to reduce the impacts of invasive aquatic macrophyte species; a Stakeholder and Technical Advisory Group (STAG) will review and contribute to the research plan.

This review addresses the following key questions:

- 1) How do submersed and floating aquatic vegetation support or adversely effect ecosystem services and related beneficial uses?
- 2) What is known about the spatial and temporal trends in submersed and floating aquatic vegetation in the Delta?
- 3) What is the relative importance of nutrients versus other factors in promoting observed trends in submersed and floating aquatic vegetation in the Delta?
- 4) What are the key data gaps and recommended future studies?

The document is organized as follows:

Section 1: Introduction, Purpose and Organization of the Review

Section 2: General Ecology and Trends in the Distribution of Submersed and Floating Aquatic Vegetation in the Delta

Section 3: Role of Submersed and Floating Aquatic Vegetation in Supporting Ecosystem Services

Section 4: Factors Contributing to the Prevalence of Submersed and Floating Aquatic Vegetation in the Delta

Section 5: Recommendations

Section 6: Literature Cited

2. General Ecology and Trends in the Distribution of Submersed and Floating Aquatic Vegetation in the Delta

2.1 Classification of Aquatic Vegetation and Scope of Review

This review pertains to the fully aquatic vegetation in the Delta, including those submersed and rooted plant species in the sediments and those floating on the surface. It does not include emergent species such as sedges, rushes, and broad-leafed forbs that are rooted along the Delta's shores but do not extend across the water surface beyond where they are rooted. The focus is on the most common species and especially the prolific invaders for which management measures leading to a reduction in abundance and distribution, if feasible, would be deemed acceptable and desirable to resource agencies, scientists, and the general public. We consider only the vascular plants; macro- and microalgae are outside of the scope of this review, although they are mentioned in terms of macrophyte effects on them.

2.2 Overview of Species Found in the Delta

There are at least nineteen species of submersed or floating aquatic plants in the Delta (Table 2.1) as identified in the peer-reviewed and grey literature (Anderson 1990, 2011; Jassby and Cloern 2000; Ustin et al. 2007, 2008; Santos et al. 2011; Khanna et al. 2012, Khanna, pers. comm. 2015; Boyer et al. 2012, 2013; Cohen et al. 2014). About half of those species are rooted and submersed beneath the water surface except at low tides. Roughly half of the species are introductions from other regions.

No studies have estimated abundance of all these species Delta-wide, but patterns in relative abundance have been evaluated within particular regions. Two studies focused on submersed species (Santos et al. 2011; Boyer et al. 2013) used a rake method in which the number of tines occupied by each species is used to determine relative abundance (Kenow et al. 2007). *Egeria densa* was by far the most abundant submersed species found in the central Delta study, with detections at 70-90% of sampling points (Santos et al. 2011; Fig. 2.1). Similarly, *E. densa* was detected up to 100% of the time within the submersed vegetation beds sampled at four west Delta locations (Boyer et al. 2013; Fig. 2.2). Recent remote sensing data indicate that submersed vegetation covers ~2900 hectares of the Delta, with *E. densa* dominant among the species (Khanna and Ustin 2014, unpublished data; CA State Parks Division of Boating and Waterways [DBW]). Other submersed, non-native species are typically much less abundant (Fig. 2.1, 2.2), but both *Potamogeton crispus* and *Myriophyllum spicatum* are species of potential concern (see Santos et al. 2011). Distinguishing among submersed species in mixed stands is problematic, leading to concerns about accuracy of coverage estimates, as further discussed below.

Ceratophyllum demersum (coontail) was the most frequently encountered submersed native species within both the central and west Delta studies described above, and was more common than all the introduced species other than *E. densa* (Fig. 2.1, Santos et al. 2011; Fig. 2.2, Boyer et al. 2013). In the same central Delta region that harbored 383 hectares of *E. densa* in fall 2007, *C. demersum* covered 284 hectares (Santos et al. 2011; Fig. 2.1). In 2014, *C. demersum* was found in 45% of all sampled points for

submersed aquatic vegetation with an average cover of 30% (Khanna and Ustin, unpublished data). We know of no Delta-wide estimates of acreage for this species.

Table 2.1. Submersed and floating vegetation in the Sacramento-San Joaquin Delta. N = Native, I = Introduced. * Indicates the most abundant introduced and native species, on which this review is focused.

Species	Common name	Submersed/ Floating	N/I
<i>Cabomba caroliniana</i>	Carolina fanwort	Submersed	I
<i>Egeria densa</i> *	Brazilian waterweed	Submersed ¹	I
<i>Eichhornia crassipes</i> *	Water hyacinth	Floating	I
<i>Limnobiium laevigatum</i>	South American sponge plant	Floating	I
<i>Ludwigia hexapetala</i> *	Uruguay water primrose	Floating	I
<i>Ludwigia peploides</i> *	Water primrose	Floating	I ²
<i>Myriophyllum aquaticum</i>	Parrot's feather	Floating	I
<i>Myriophyllum spicatum</i>	Eurasian watermilfoil	Submersed	I
<i>Potamogeton crispus</i>	Crisped or curly-leaf pondweed	Submersed	I
<i>Azolla</i> sp.	Water fern	Floating	N
<i>Ceratophyllum demersum</i> *	Coontail	Submersed ³	N
<i>Elodea canadensis</i>	Common waterweed	Submersed	N
<i>Hydrocotyle umbellata</i> *	Pennywort	Floating	N
<i>Lemna</i> sp.	Duckweed	Floating	N
<i>Ludwigia palustris</i>	Water purslane	Floating	N
<i>Potamogeton foliosus</i>	Leafy pondweed	Submersed	N
<i>Potamogeton nodosus</i>	Long-leaf or American pondweed	Submersed ⁴	N
<i>Ruppia maritima</i>	Widgeongrass	Submersed	N
<i>Stuckenia pectinata</i> *	Sago pondweed	Submersed	N

1 *E. densa* is typically rooted but fragments can form floating mats.

2 There is confusion over the identification of native and non-native species of water primrose; this species has been designated as introduced in this review as it has by other authors (e.g., Khanna et al. 2012).

3 *C. demersum* is the one submersed species that is not rooted in the sediment; it is found loose in the water column.

4 *P. nodosus* is rooted in the sediment but its leaves float at the surface of the water.

In addition, the native submersed pondweed *Stuckenia pectinata* was relatively common in the Delta sites (Fig. 2.1, Santos et al. 2011) and is typically the only aquatic plant species found within the open Suisun Bay (Fig. 2.2; Boyer et al. 2012, 2013). Although this species has been referred to as *S. filiformis* based on gross morphology, or *Stuckenia* spp. because of difficulty in identification, recent genetic analyses indicate *S. pectinata* is the correct species identification for a morphologically broad range of samples throughout Suisun Bay and the Delta (Patten and Boyer, unpublished; see below). Because *S. pectinata* occurs in monotypic stands in the open Suisun Bay and the plants are clearly visible from the surface of the water during summer low tides, Google Earth images show the beds well; these were digitized and systematically ground-truthed by boat and were found to very accurately represent the

acreage present (Boyer et al. 2012). Approximately 200 hectares occur within Suisun Bay as determined through this digitizing and ground-truthing activity during 2011-2014 (Boyer et al. 2012, 2015). Such methodology could be effective in open water, high flow regions of the Delta as well, as *S. pectinata* occurs there at 100% relative abundance (Khanna, pers. comm., based on 2014 remote sensing and ground truthing). Estimating acreage remotely becomes much more difficult in semi-enclosed flooded islands and other embayments within the Delta where many more species are present; however, a rough estimate is that another 350 hectares of *S. pectinata* occur within the Delta region (Boyer et al. 2015). *S. pectinata* occurring in island interior sloughs and in Suisun Marsh is not included in these estimates.

Comment [KB3]: Ask Shruti if she can give an estimate

In terms of floating species, *Eichhornia crassipes* (water hyacinth) has become notorious for its role in clogging channels, marinas, and water supply pipes within the Delta (see Literature Cited, Local and Regional Press Reports, for many recent articles centered around the Stockton area). Worldwide, it is ranked as one of the worst invaders (OTA 1993). As of 2014 it covers ~800 hectares, based on remote sensing and ground truthing of point locations (Khanna and Ustin, unpublished). Its prevalence and nuisance effects in areas of high human activity have led to high interest in understanding factors that control it.

Number of detections, relative frequency (in percent) from point samples, area (ha) and percent cover of the submersed aquatic plant species detected in the Sacramento-San Joaquin River Delta (waterways area is 639.89 ha)

Scientific name	Code	Status	Fall 2007			Summer 2008		
			Detections (%)	Area (ha)	% cover	Detections (%)	Area (ha)	% cover
<i>Egeria densa</i>	EGDE	Non-native	339 (89)	382.49	59.77	300 (69)	99.64	15.6
<i>Cabomba caroliniana</i>	CACA	Non-native	1 (0.3)	NA	NA	36 (8)	1.41	0.2
<i>Myriophyllum spicatum</i>	MYSP	Non-native	32 (8)	68.03	10.6	78 (18)	20.4	3.2
<i>Potamogeton crispus</i>	POCR	Non-native	52 (14)	50.8	7.9	53 (12)	10.03	1.6
Total			424	382.9	59.8	467	174.08	27.2
<i>Ceratophyllum demersum</i>	CEDE	Native	107 (28)	283.77	44.3	180 (41)	59.14	9.2
<i>Potamogeton nodosus</i>	PONO	Native	1 (0.3)	NA	NA	10 (2)	6.04	0.9
<i>Elodea canadensis</i>	ELCA	Native	19 (5)	34.28	5.36	10 (2)	18.29	2.9
<i>Stuckenia</i> spp.	STSPP	Native	24 (6)	73.02	11.4	32 (7)	69.84	10.9
Total			151	294.29	45.9	232	157.04	24.5
Total submersed species			575	388.35	60.7	699	239.6	37.4

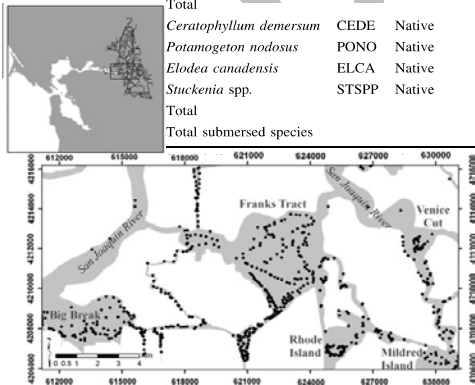


Figure 2.1. Rake detections and other data on abundance of submersed species at sampling points within the central Delta (left). Excerpted from Santos et al. 2011

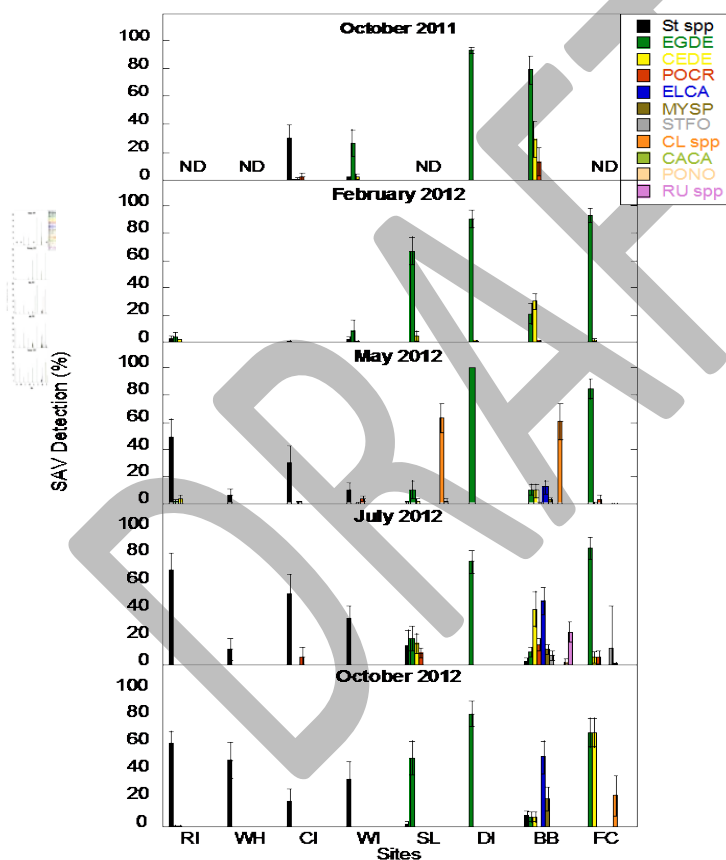
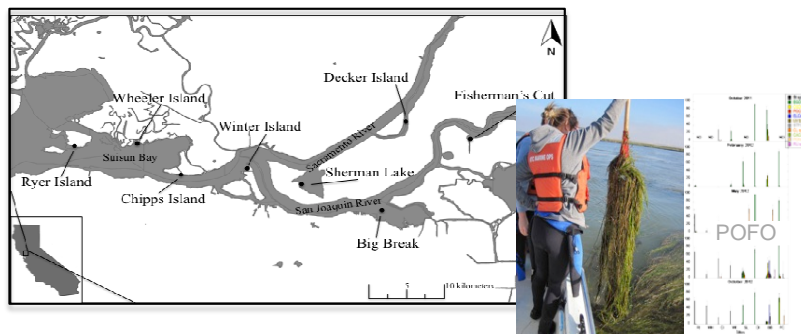


Figure 2.2. Relative abundance of submersed plant species in the west Delta and Suisun Bay (see map inset to interpret site abbreviations from west to east) in 2012 as estimated with a rake sampling method (Kenow et al. 2007). Species abbreviations as in Fig. 2.1, with the addition of the native Potamogeton foliosus (POFO), the green alga Cladophora spp. (CL), and Ruppia spp. (RU). (Figure from Boyer et al. 2013)

Recently, another floating invader, *Ludwigia* spp. (water primrose), has become very common in the Delta as well. As of 2014, it covered about the same acreage as *E. crassipes* (800 hectares; Khanna and Ustin, unpublished data). Rooted at the shoreline, this combination of *L. hexapetala*, *L. peploides*, and perhaps *L. grandiflora* (Khanna and Ustin, unpublished data), has now become a subject of concern, although there is not yet a program to control the plants.

The floating native species, *Hydrocotyle umbellata* (pennywort), was common during recent years and nearly as abundant as *E. crassipes*. Currently, it is much less abundant than both *E. crassipes* and *Ludwigia* spp. (Khanna and Ustin, unpublished data).

These six species, the submersed *Egeria densa*, *Ceratophyllum demersum* and *Stuckenia pectinata* and the floating *Eichhornia crassipes*, *Ludwigia* spp. and *Hydrocotyle umbellata*, will be the primary subjects of this review (Fig. 2.3), with a special focus on the invaders. A botanical description of each of these species is given below (from the Jepson Manual and Flora of North America, plus unpublished genetic work on *Stuckenia pectinata* from San Francisco State graduate student Melissa Patten).

Egeria densa (Brazilian waterweed) is native to warm temperate South America in southeastern Brazil, Argentina, and Uruguay. It grows with trailing stems up to 5 m long, producing roots at intervals along the stem. Although it is typically rooted in the sediment, it can also form mats of detached fragments. The leaves are produced in whorls of four to eight, 1–4 cm long and 2–5 mm broad, with an acute apex. It is dioecious, with staminate and pistillate (sometimes referred to as “male” or female”, respectively) flowers on separate plants; however, all plants outside the native range, including California, are believed to be “male”, with reproduction accomplished only through fragmentation. The flowers are 12–20 mm diameter, with three broad, rounded, white petals, 8–10 mm long.

Ceratophyllum demersum (coontail) is a submersed, native perennial that grows in still or very slow-moving water. The stems reach lengths of 1–3 m, with numerous side shoots making a single specimen appear as a large, bushy mass. The leaves are produced in whorls of six to twelve, each leaf 8–40 mm long, simple, or forked into two to eight thread-like segments edged with spiny teeth; they are stiff and brittle. The flowers are small, 2 mm long, with eight or more greenish-brown petals; they are produced in the leaf axils. The fruit is a small nut 4–5 mm long, usually with three spines, two basal and one apical, 1–12 mm long. *C. demersum* is not rooted; it can be found free-floating beneath the water surface, often among other plant species.

Stuckenia pectinata (sago pondweed) is a monocot, perennial rhizomatous herb native to California, with long stems (2–4 m in summer) and a submersed canopy of thin leaves near the water surface. *S. pectinata* was historically an important food for Canvasback ducks in ponds within Suisun Marsh (Jepson 1905) but was not recorded in the open waters of the San Francisco Estuary until very recently (Boyer et al. 2012, 2015). Morphology of these plants is quite variable, and a form outwardly resembling *Stuckenia filiformis* is common, with little to no secondary branching, leaves frequently > 1.5 mm and often 2–3 mm or more wide (with extremes to 3.7 mm), olive in color and blunt-tipped (fruits are seldom found but should be 2–3 mm in size with style and stigma reduced to a broad flattened disk at the top of fruit).



Figure 2.3. Species central to this review. Left, submersed species: *Egeria densa* (top; photo Katharyn Boyer), *Ceratophyllum demersum* (middle, photo Ron Vanderhoff), and *Stuckenia pectinata* (bottom; photo Katharyn Boyer). Right, floating species: *Eichhornia crassipes* (top; photo Bob Case), *Ludwigia* spp. (center), *Hydrocotyle umbellata* (bottom)

In contrast, a form more closely resembling keys for *Stuckenia pectinata* is also present, and has a forking “zig-zag” (wide branch angle) pattern of branching, multiple orders of very leafy branches, with leaves 1 mm wide or less and seldom exceeding 1.5 mm, brighter green in color with more acutely-pointed leaf tips (fruits are seldom found but should be 2.5-5 mm with pronounced beaks resulting from

persistent styles). Many specimens observed to date do not precisely match keys for either species, and the few fruits available have been intermediate between the two species (large but not beaked) (Boyer et al. 2015); however, recent genetic data (using the CO1 region of the mitochondrial DNA) indicate that samples representing a wide range of morphologies are all *Stuckenia pectinata* (Patten and Boyer, unpublished data). Additional analyses underway using microsatellite data will help to reveal whether there are fine-scale genetic differences across the region within this species that could lead to different observed morphologies, while common garden experiments are examining the degree of phenotypic plasticity that results from variation in flow velocities (Patten and Boyer, unpublished data).

Eichhornia crassipes (water hyacinth) is a free-floating perennial aquatic plant native to tropical and sub-tropical South America. With broad, thick, glossy, ovate leaves, water hyacinth may rise above the surface of the water as much as 1 meter in height. The leaves are 10–20 cm across, and float above the water surface on long, spongy and bulbous stalks. The feathery, freely hanging roots are purple-black. An erect stalk supports a single spike of 8-15 conspicuously attractive flowers, mostly lavender to pink in color with six petals. When not in bloom, water hyacinth may be mistaken for the smaller South American sponge plant (*Limnobium laevigatum*), recently discovered in the Delta (Anderson 2011). One of the fastest growing plants known (a mat of 10 plants can produce 650,000 in one growing season; Penfound and Earle 1948), water hyacinth reproduces primarily by way of runners or stolons, which eventually form daughter plants. Although each plant can produce thousands of seeds each year, these have a low germination rate outside their native range and seedlings grow slowly, taking a full growing season to produce flowers. The stembase can lie under water during winter and initiate rapid growth in the new growing season (Madsen, pers. comm.).

***Ludwigia* spp.** (water primrose) is well known as a noxious weed that invades and clogs waterways. It is perennial herb that grows in moist to flooded areas. The stem can creep over 2 meters long, sometimes branching. It spreads to form mats on the mud, or floats ascending in the water. The leaves are several centimeters long and are borne in alternately arranged clusters along the stem. The flower has 5 to 6 lance-shaped sepals beneath a corolla of 5 or 6 bright yellow petals up to 2.4 centimeters long. The fruit is a hard, cylindrical capsule. In the Delta, *Ludwigia peploides* and *L. hexapetala* are the primary species, but *L. grandiflora* may also be present (Khanna, pers. comm.).

Hydrocotyle umbellata (pennywort) is a perennial herb that is native to California and is also found elsewhere in North America and beyond. It can also be found growing as an introduced species and sometimes a noxious weed on other continents. It can be found creeping or floating with round leaves generally 1–5 cm wide. Its inflorescences are open umbels with up to 60 individual flowers on them.

2.3 Habitat Types in Which They are Characteristically Found

Egeria densa is found throughout the Delta in areas of moderate and low flow, along the margins of larger sloughs and in more protected areas such as smaller sloughs and breached islands (e.g., Sherman Lake, Franks Tract: Fig. 2.4). It can be found as far west as the confluence of the Sacramento and San Joaquin Rivers around Winter Island (Boyer et al. 2013). It grows densely throughout the water column

in waters up to 7 m deep (Parsons and Cuthbertson 1992), but grows nearer to the surface in turbid waters (Bossard et al. 2000; Khanna, pers. comm.). Typically, it is rooted in the substratum throughout its distribution but it can also be found as a free-floating mat (Bossard et al. 2000).

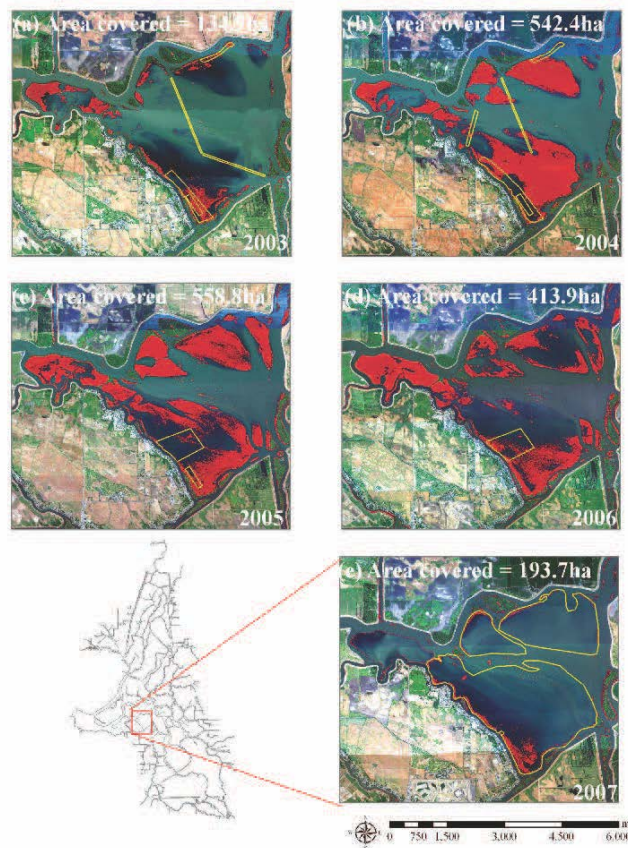


Figure 2.4. Submersed vegetation (primarily *E. densa*) coverage of up to 560 hectares within Franks Tract in the central Delta, 2003-2007 (figure from Santos et al. 2009)

Ceratophyllum demersum has been documented as abundant in the west and central Delta in areas of low flow (Santos et al. 2011; Boyer et al. 2013). This species was found with roughly half the frequency of *Egeria densa* within the central Delta region in one study (Santos et al. 2011). It is free-floating and may benefit from water column stability through co-occurrence with other submerged vegetation; in one survey, it more often occurred along with other species such as *E. densa* than on its own (Santos et al. 2011).

Stuckenia pectinata is less commonly found in the Delta than the other species described above, but still more common than all other native species besides *Ceratophyllum demersum*. It was found at about 25% of the frequency of *C. demersum* in a survey of the central Delta (Santos et al. 2011). With high

salinity tolerance (maintaining its biomass even at a salinity of 15; Borgnis and Boyer, in revision), it forms large beds in the west Delta (e.g., Sherman Lake) and along shoals and island shores throughout much of the open Suisun Bay, as well as in sloughs interior to islands and the Suisun Marsh (Fig. 2.5; Boyer et al. 2015).

Eichhornia crassipes is found throughout the Delta in calm waters, but can be dislodged by boating

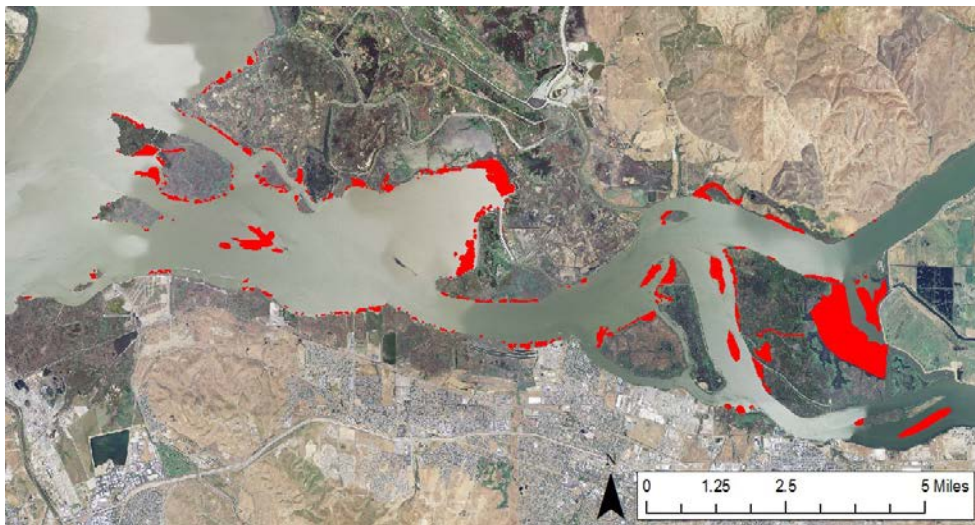


Figure 2.5. Spatial distribution of *Stuckenia* sp. from Ryer Island in Suisun Bay to Sherman Lake in the west Delta, as determined from digitizing and ground truthing aerial imagery (Google Earth), 2012. Coverage is estimated to be ~500 hectares in this region. Image unpublished, based on data in Boyer et al. 2015.

activity, high tides, or wind, and can be seen rafting through open waters with its stout leaves acting as sails (Boyer, pers. obs.). It has been extremely abundant near the city of Stockton in the last several years (see Literature Cited, Local and Regional Press Reports, for many news articles). It has also been very abundant near the Tracy Fish Collection Facility and River's End Marina on Old River (see Literature Cited). It is typically found along channel edges with more stable flow conditions, thus minimizing wash out, or in narrow channels or low flow basins (e.g., marinas, breached island interiors, inside of tule islands) where there is protection from higher velocity flows. Water depth alone is not a limitation, as it does not root in the sediment.

Ludwigia spp. is also found throughout the Delta in calm waters and can be found interspersed with *E. crassipes* and *Hydrocotyle umbellata*. It is typically found in shallow water where it is rooted in the sediment and has creeping stems that reach across the water surface. It often grows in matted stands, with thick white spongy roots at floating nodes. It frequently climbs over other plants.

Hydrocotyle umbellata is found in similar habitats to *Ludwigia* spp., attached to the sediments in shallow water and creeping across the water.

2.4 Spatial and Temporal Trends in their Distribution and Abundance

A regular, comprehensive mapping program for aquatic vegetation does not exist for the Delta region. Several grant-funded efforts to conduct remote sensing have provided valuable information, and have led to improvements in mapping techniques. In particular, recent work to incorporate hyperspectral imagery has aided in the distinction of some of the native submersed species (*Ceratophyllum demersum* and *Potamogeton nodosus*) from non-native ones (*Egeria densa*, *Myriophyllum spicatum*, *Potamogeton crispus*). However, distinction among the non-native species was not well achieved, especially in the western region of the Delta where green algae obscured the spectral signal of *Egeria densa* and *Myriophyllum spicatum* was confused with *E. densa* (Santos et al. 2012). Further, although the native *Stuckenia* sp. (presumed to be *S. pectinata* based on recent genetic work; Patten and Boyer unpublished) had a distinct spectral signature in greenhouse tanks, patches were too small to be detected by remote sensing in the area of the Delta studied (Santos et al. 2012). Mixed species stands are also problematic for remotely determining species presence and extent as described above. Hence, on the ground monitoring of relative abundance, biomass, and preferably, primary production (through multiple biomass estimates over time to estimate turnover) is necessary to complement the remote sensing work.

Below, we summarize what is known of the spatial and temporal extent of each of the six species emphasized in this review, primarily resulting from individual grant-funded efforts that provided a window into the distribution over, at most, a few years at a time.

Egeria densa is thought to have been introduced to the Delta in 1946 (Light et al. 2005) through aquarium dumping and has spread throughout the region (Anderson 1990; Foschi et al. 2004; Santos et al. 2009). It was discussed without signs of alarm in a CA Department of Water Resources report that described water quality conditions over a 30-year period (DWR 1993); however, by 1996, Grimaldo and Hymanson (1999) described thick stands harboring many non-native centrarchid fish. It may have replaced native submersed aquatic plants in much of this area (Lund et al. 2007). In terms of interannual trends, there has been a major expansion in acreage over the last several years. In 2007, submersed vegetation dominated by *E. densa* covered ~2000 hectares (~8%) of Delta waters (Santos et al. 2009) and this number increased to ~2900 hectares (~11%) according to remote sensing and ground-truthing in 2014 (Khanna and Ustin, unpublished data). Application of herbicide (by the California Department of Boating and Waterways, now the CA Department of Parks and Recreation Division of Boating and Waterways, DBW) in areas such as Franks Tract has the potential to reduce acreages locally, especially if conducted in spring (Santos et al. 2009; see Fig. 2.4, acreage was reduced by >50% after fluridone application in April 2007, as opposed to after July 1 in the other years). However, a very small proportion of the Delta is included in the management program, with the most area treated in any year covering only 4-5% of the Delta waterways (DBW 2005). During periods of drought, this species shifts further east into the Delta (Boyer, pers. obs.), as its survivorship is very low at salinities of 5 and above (Borgnis and Boyer, in revision; see Chapter 4). In terms of seasonal trends, one study documented a greater acreage and percent cover in the central Delta in fall (October 2007) than in the summer (June 2008) (Santos et al. 2011, see Fig. 2.1). Though its biomass declines in winter, it maintains aboveground shoots (Pennington and Systma 2009; Santos et al. 2011; Boyer et al. 2013, see Fig. 2.2).

Ceratophyllum demersum was documented to change in abundance seasonally, with greater acreage and percent cover in October 2007 (284 ha, 44% cover of the waterways sampled) than in June 2008 (59 hectares, 9%) within the same central Delta region (Fig. 2.1, Santos et al. 2011). A similar pattern was found at Fisherman's Cut, with rake detections at 70% in October 2012, but little to no presence in February, May, and July 2012 (Fig. 2.2, Boyer et al. 2013). However, its frequency of occurrence at Big Break varied considerably seasonally, with 40, 10, 30, and 5% detection over the four sampling periods in 2012, respectively. In the same study there were no detection at Decker Island, and less than 10% detection at Sherman Lake in any season (Fig. 2.2, Boyer et al. 2013). We found no records of *C. demersum* variation in abundance in the Delta over longer periods of time.

Stuckenia pectinata appears to have increased in acreage over the last several decades (Fig. 2.6, from Boyer et al. 2015). Comparing digitized imagery over time for Suisun Bay, and in doing so assuming that historical stands were essentially monotypic as they are at present, there was little change in acreage between 1993 and 2002. However, there was about a 30% increase in acreage (43 hectares) in the Suisun Bay region between 2002 and 2012, with many new, mostly small beds occurring along nearly every stretch of shoreline and large increases in acreage in the cove on the southwest side of Ryer Island and along the south sides of Simmons and Chipps Islands. In the west Delta, a similar increase in acreage (37 hectares) appears to have occurred over the decade ending in 2012, a 13% increase since 2002; however, this increase is less certain due to the many species present within Sherman Lake that make accurate estimates much more difficult. Still, there appeared to have been large gains in *S. pectinata* acreage in Sherman Lake, offshore and to the west of Sherman Island, and to the west of Winter and Browns Islands (Fig. 2.7). In a 2014 remote sensing survey followed by groundtruthing of point locations, *S. pectinata* was found in 26% of sampled points in the Delta (Khanna and Ustin, unpublished data). In that survey it was found to have an average relative cover of 50%, but 100% in open water areas of the Delta, perhaps suggesting a distinct environmental niche (Khanna and Ustin, unpublished data; Khanna, pers. comm.). It is not clear why *Stuckenia pectinata* acreage would be expanding over the last 20 years, although increased water clarity and thus greater light availability may be partially responsible (Wright and Schoellhamer 2004; Schoellhamer 2011; Hestir et al. 2013; see Chapter 4).

Eichhornia crassipes was introduced to the Sacramento River in 1904 by horticulturalists (Finlayson 1983; Cohen and Carlton 1998; Toft et al. 2003) or perhaps through garden escape (Light et al. 2005). It was estimated to cover 160-300 hectares of the Delta (~1% of the water area) during the period of 2004-2008 (Santos et al. 2009); however, this species has expanded in coverage, with ~800 hectares in 2014, or about 3% of the water area (Khanna and Ustin, unpublished data). This increase in cover may be partly attributable to a delay in chemical treatment over two years (2011 and 2012) owing to permitting issues (Llaban, pers. comm.); however, in general, these control methods seem to have little impact on year-to-year coverage of water hyacinth (Khanna pers. comm., unpublished data). There also seem to have been favorable conditions during the years of rapid increase in cover, including but not limited to a low occurrence of frost in winter (Khanna, pers. comm.). Positions of colonies can shift within a season and from year to year due to drifting and movement on the tides and with wind or other disturbance (Santos et al. 2009).

Comment [KB4]: Ask Shruti if she'd like us to cite the SOTER side bar that has these trends. I have cited the 2014 changes as unpublished data throughout at this point

Ludwigia spp. has expanded greatly in coverage between remote sensing surveys conducted in 2008 and 2014 (Khanna and Ustin, unpublished data). It had low coverage during the period of 2004 to 2008, but is now equal in coverage to *E. crassipes*, with ~800 hectares present in 2014 (Khanna and Ustin, unpublished data).

Hydrocotyle umbellata has declined in coverage between the remote sensing surveys conducted in 2008 and 2014 (Khanna and Ustin, unpublished data). Between 2004 and 2008, *H. umbellata* was comparable in coverage to *E. crassipes*. Considering the large increases in *Ludwigia* spp. seen in 2014, it is possible that *Ludwigia* has a competitive advantage over *H. umbellata* under current conditions.

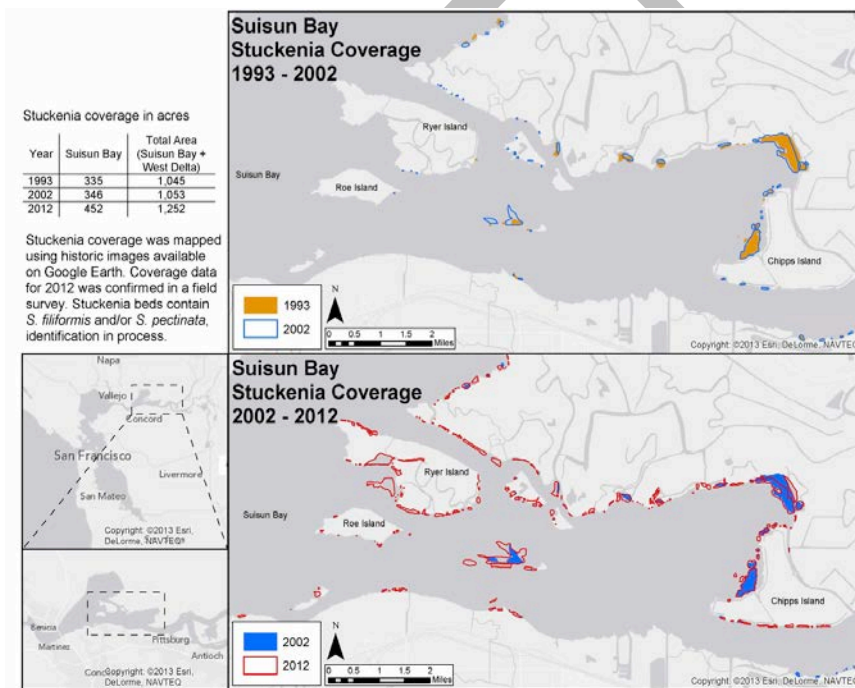


Figure 2.6. Decadal changes in coverage of *Stuckenia* sp. within Suisun Bay, as mapped using digitized and ground-truthed Google Earth images. From Boyer et al. 2015

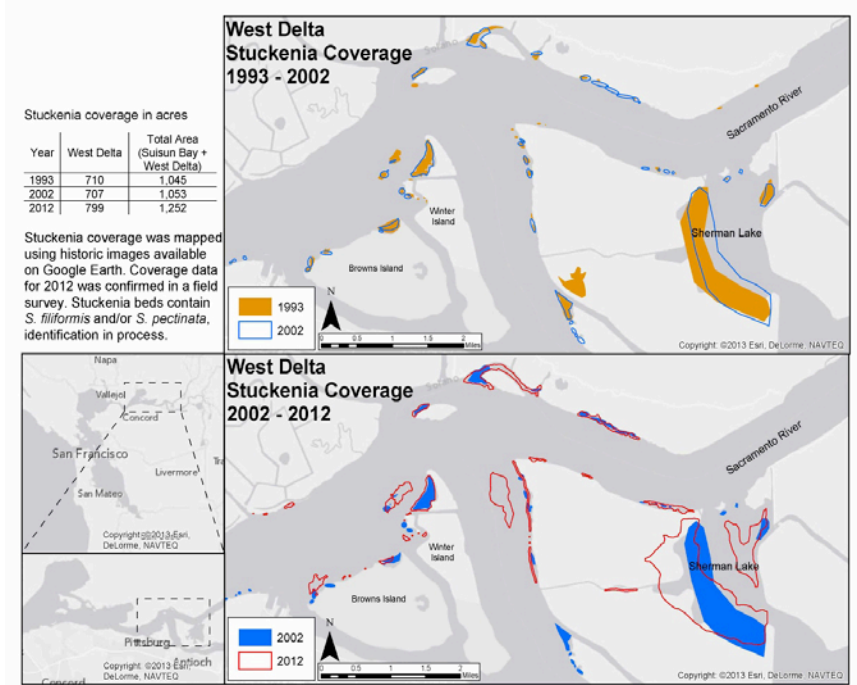


Figure 2.7. Decadal changes in coverage of *Stuckenia* sp. within the western portion of the Delta, as mapped using digitized and ground-truthed Google Earth images. From Boyer et al. 2015

3. Role of Submersed and Floating Aquatic Vegetation in Supporting Delta Ecosystem Services

Submersed and floating aquatic vegetation are natural components of estuaries, providing benefits in the form of carbon storage, uptake of nutrients, oxygenation of waters, trophic support through direct consumption by grazers or contributions to the detrital food web, provision of surfaces for algal and invertebrate attachment (also providing trophic support), and predation refuge for small fish. Negative effects tend to emerge in the case of non-native species that have invaded large areas and that have characteristics unlike those of the native species (especially when the invaders are at high densities), thus leading to undesirable changes in a number of factors, including nutrient dynamics and food web support. Here we review both the positive and negative effects of submersed and floating vegetation, based on the published literature from other regions as well as local studies where available.

3.1 Conceptual View of Positive and Negative Effects of Submersed and Floating Aquatic Vegetation on Ecosystem Services.

Anderson (2008) proposed a draft conceptual model of the effects of submersed, floating, and emergent vegetation on water quality and fish habitat in the Delta (Fig. 3.1). In general, low to moderate densities or open growth forms of any species may have beneficial functions, including provision of habitat and food web support, but the dense stands typical of the worst invaders tend to produce negative effects. For example, dense canopies of the floating *Eichhornia crassipes* may shade phytoplankton and exclude submersed native plants such as *Stuckenia*. Dense stands of submersed plants (primarily *Egeria densa*) can draw down oxygen at night, increase water temperatures by increasing water residence time, increase pH to the benefit of plants that can utilize bicarbonate as a carbon source (e.g., *E. densa*, see Section 4.1.4), and harbor large non-native fish in the shadows of the canopy, which could possibly lead to predation on smaller adult and juvenile native fish. In contrast, the open water beneath naturally sparse canopies of native submersed species such as *Stuckenia pectinata* may provide a more stable dissolved oxygen setting, accessible invertebrate food resources, and a paucity of large predator hiding places – in all, it has the potential to provide more suitable habitat for native fish species than dense *E. densa* beds (Fig. 3.1). As expected in a conceptual modeling exercise, there is not necessarily data to support all of the effects and feedbacks (e.g., there is no detailed dataset for the composition or abundance of fish species that utilize *Stuckenia* beds); in these cases, the model can be used to identify hypotheses that should be tested with further data collection and experimentation.

Below, we detail a number of adverse effects that may result from introduced macrophyte species when they become dense and widespread in invaded regions. Potential adverse effects include changes to water quality, a decline in phytoplankton and native plants, a change in the physical structure of the habitat, alterations of trophic interactions, impediments to navigation and industry, and visual impacts.

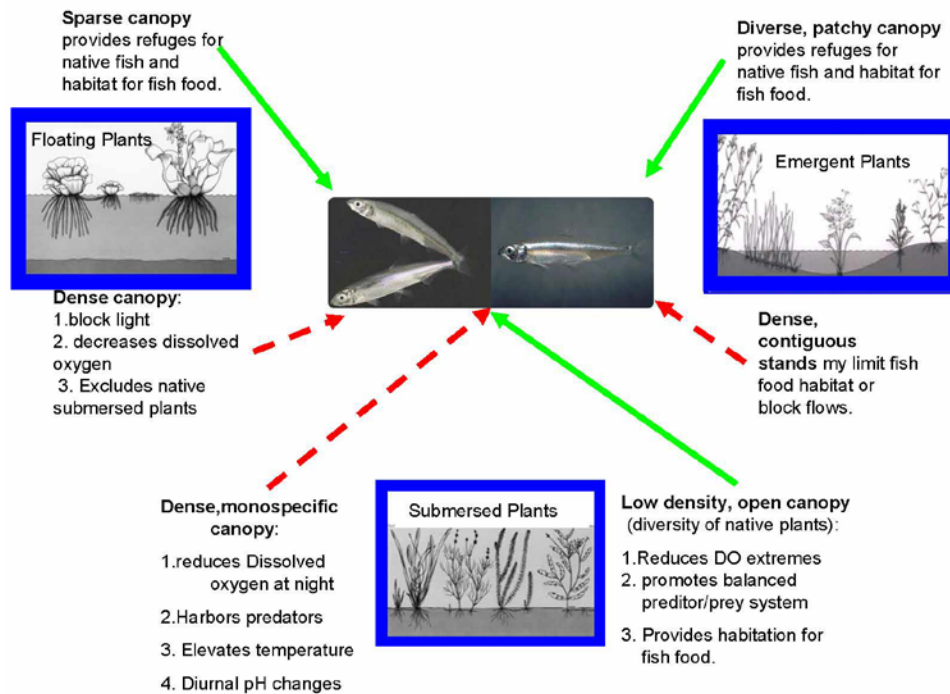


Figure 3.1. Conceptual model of the effects of Delta macrophyte canopy structure on provision of fish habitat. Arrows show direction and primary effect caused by interaction of each "ecological type" of aquatic plant on fish (red, dashed = negative effect, green, solid = positive effect. From Anderson 2008

3.1.1 Changes to Water Chemistry

Dissolved oxygen

Submersed species such as *E. densa* have the potential to greatly draw down dissolved oxygen levels within thick mats (e.g., Getsinger 1982). Dissolved oxygen in plant beds declines at night due to a lack of photosynthetic oxygen production to counter oxygen needs for respiration, and these diurnal swings can be especially pronounced in high density submersed macrophyte beds (Fig. 3.1). Interestingly, *E. densa* was promoted as a way to oxygenate waters for fish during its early introduction period (Cook and Urmikönig 1984).

Dense mats of *E. crassipes* can lead to large reductions in dissolved oxygen through drawdown at night as well as prevention of gas exchange at the water's surface (Madsen 1997; Hunt and Christiansen 2000; Perna and Burrows 2005) and through shading photosynthetic species in the water including phytoplankton and submersed vascular plants (Malik 2007). In the Delta, drawdown of dissolved oxygen has been documented in areas of rapid *E. crassipes* growth, even in places with significant tidal

exchange (Dow Wetland, directly off the mainstem of the San Joaquin River, with 1-2 m tidal variation; Greenfield et al. 2007). Further, decomposition of *E. crassipes* following mechanical treatment can lead to high biological oxygen demand and drawdown of oxygen in areas with low flow, creating unfavorable conditions for fish and invertebrates and even fish kills (dissolved oxygen concentration $<2.3 \text{ mg l}^{-1}$; US EPA 1986). For example, Greenfield et al. (2007) found dead bluegill sunfish and carp during weeks of anoxic waters after an experimental *E. crassipes* shredding operation at the low-flow Lambert Slough. With this in mind, the CA Parks Division of Boating and Waterways must monitor dissolved oxygen levels during weed control, maintaining a minimum of $5\text{-}7 \text{ mg l}^{-1}$, as mandated by the Central Valley Water Quality Control Board (Moran, pers. comm.).

Comment [KB5]: Is there a citation for this?

Notably, decreased oxygen in the sediments can increase mobility of phosphorus, contributing to nutrient loading (Scheffer and Van Ness 2007). In support of this concept, Cornwell found high phosphorus release in soils of submersed macrophyte beds in the Delta; if conditions conducive to phosphorus release develop over time in these beds, they could promote a positive feedback in which phosphorus is supplied to the plants, especially through porewater uptake (Cornwell et al. 2014; J. Cornwell, pers. comm.).

pH

High abundance of submersed macrophytes can lead to increased pH as CO_2 is drawn down during photosynthesis, leading to diurnal swings in pH and to bicarbonate (HCO_3^-) becoming the primary form of dissolved inorganic carbon (DIC) available (Sand-Jensen 1989; Santamaria 2002). This can work to the advantage of species that can use bicarbonate efficiently as their carbon source (e.g., *Egeria*, Cavalli et al. 2012). We are not aware of data on pH within submersed macrophyte beds in the Delta to date, but expect both the changes in pH and these effects on the form of available DIC would be greatest in thick *E. densa* beds and in places with limited water flow.

Nutrients

Both *Egeria densa* and *Eichhornia crassipes* are known for their abilities to take up nutrients and store them for later use (e.g., Gopal 1987; Reddy et al. 1987). *E. crassipes* has been used in a number of regions as a tool to remove nutrients from the water column, both in pilot and demonstration scale projects and in full scale wastewater treatment (reviewed by Malik 2007). Despite this propensity for nutrient uptake, Delta-wide effects of these species on water column nutrient removal could be relatively low considering only about 3% of Delta waters contain *E. crassipes* and 11% contain *E. densa* as of 2014 (Khanna and Ustin, unpublished data). To understand the contribution of these species to nutrient cycling, including in comparison to other producer groups (e.g., ~9500 hectares or 37% of Delta waters contained emergent plant species in 2014; Khanna and Ustin, unpublished), data on productivity rates, sequestration of nutrients within perennial tissues, and recycling within tissues and from the water column and sediments would be needed. One Florida study comparing nutrient removal effects over a range of macrophyte species found *E. crassipes* to rank much higher than many others (including *Hydrocotyle umbellata* and *Egeria densa*) in N removal during summer (Reddy and DeBusk 1985). P removal was also higher in *E. crassipes* than in all other species in summer. Interestingly, in winter, *H.*

umbellata was higher in both N and P removal rates than all the other species (Reddy and de Busk 1985).

In areas of densely growing macrophytes, intraspecific competition can lead to continuous shedding of dead tissues that decompose in place and may serve as a source of remineralized nutrients to the existing plant bed as well as other producers (Carignan and Neiff 1992; Rommens et al. 2003). Seasonal senescence of *Eichhornia crassipes* is generally slow and occurs during fall and winter (Carignan and Neiff 1992; Pinto-Coelho and Greco 1999; Battle and Mihuc 2000; Spencer 2005). *Egeria densa* sheds tissues in winter even though it does not fully senesce within the Delta region (Fig. 2.2, Boyer et al. 2013; Santos et al. 2011). In both cases, natural senescence is likely to result in a slow release of dissolved organic compounds from plants in the water column that may be utilized by the macrophytes or other producers locally, or transported away with water flow. Accumulation of dead organic matter within sediments of the beds appears limited in open water areas; sediment flux measures by Cornwell et al. (2014) in Sherman Lake, Big Break, and Franks Tract (all sites with substantial *E. densa* populations) did not suggest high rates of sediment respiration or nitrogen release, although rates tended to be higher than in non-vegetated areas measured in Suisun Bay. However, rapid deposition of dead macrophyte tissue in low flow areas may be a significant source of nutrients fueling macrophyte growth. For example, control methods that leave large quantities of shredded water hyacinth material in place can lead to increased water column nutrients, especially total P (up to 5-fold increases) and organic P (up to 2-fold increases) and to a lesser extent, total N (3-fold increase at one site) (Greenfield et al. 2007). This elevated nutrient effect was found to be short-lived (<4 days) where there was tidal exchange but water column nutrients were elevated at least several weeks after treatment in a quiescent site (Greenfield et al. 2007) where a related study documented significant quantities of the shredded debris even after six months (Spencer et al. 2006). These studies highlight that water residence time and flow rates at any one location will critically affect the degree to which macrophyte biomass accumulates and releases nutrients within the beds, whether as a result of control efforts or other abrupt changes in conditions (e.g., extended periods of frost for *E. crassipes*, or increased salinity for *E. crassipes* or *E. densa*; see Chapter 4) that cause rapid plant mortality.

3.1.2 Changes to physical properties of water

Flow

In general, dense submersed vegetation has the potential to slow the velocity of water, thereby initiating a positive feedback loop in which the favorable lower flows permit greater growth and spread (e.g., *E. densa*, Roberts et al. 1999). The density of the vegetation throughout the water column influences the degree to which water flow is affected (>40% reduction in dense *E. densa* beds; Wilcock et al. 1999) and varies with both plant morphology and density. Submersed plants may also facilitate the establishment and spread of floating plants through reduction in flow, permitting floating plants to better remain in place and spread locally (see Khanna et al. 2012, and Chapter 4). Dense floating macrophytes also can reduce flow under already moderately low flow conditions (Penfound and Earle 1948).

Light

Dense floating and submersed vegetation greatly reduce light penetration through the water column, shading other plants beneath. However, *E. densa* is also capable of reducing suspended sediment, creating clearer water in the vicinity of the plants (Tanner et al. 1993; Hestir et al. 2013). Grimaldo and Hymanson (1999) found secchi depth increased to 2 m in patches of *E. densa* in Franks Tract (central Delta), up from 0.5-1 m outside of patches.

Temperature

E. crassipes infestations lead to increased water surface temperatures through reduction in water flow (Penfield and Earle 1948). *E. densa*, too, causes increased water temperatures during the day, which helps to reduce heat loss at night (Grimaldo and Hymanson 1999).

3.1.3 Effects on algae and native macrophytes

A number of changes to the local environment by nuisance aquatic macrophytes could impact other species of primary producers, including native vascular plants and algae. First, shading of the water column by dense stands of floating or submersed macrophytes can reduce the light available to native submersed species, which tend to have more sparse growth forms and less potential to shade other species themselves (see Anderson 2008 conceptual model, Fig. 3.1). Shading of phytoplankton and benthic microalgae could also result from dense canopies or mats of aquatic macrophytes such as *Egeria densa* or *Eichhornia crassipes*. *E. densa* can reduce suspended sediment concentrations through baffling of particles out of suspension (Hestir et al. 2013); however, shading from thick mats could minimize any potential positive effects of sediment removal to other submersed primary producers. Second, thick mats of *E. densa* reduce water flow, and although floating vegetation is less likely to reduce water motion, a dense coverage over the water can reduce the generation of wind waves across the water surface. Third, reductions in dissolved oxygen within *E. densa* mats or beneath *E. crassipes* could also limit other producers among or below these plants. Fourth, a number of submersed and floating macrophytes, including *Eichhornia crassipes*, have been noted to have allelopathic effects on algae and microbes (Shanab et al. 2010). Removal of *E. crassipes* may lead to increases in *E. densa* abundance (Khanna et al. 2012), most likely due to increased light, but perhaps due to a combination of factors described above. Chapter 4 further describes the interactions between species that may influence abundance of introduced and native macrophyte species.

Submersed vegetation and the roots of floating vegetation provide surfaces for the growth of epiphytic algae and attachment points for filamentous algae where there is sufficient light (Fig. 3.2). These in turn affect the habitat and food availability to invertebrates and fish, and can influence nutrient cycling; e.g., filamentous algae attached to *Potamogeton crispus* was found to increase phosphorus retention of an experimental pondweed assemblage (Engelhardt and Richie 2002). These algae can also be considered



Figure 3.2. Green filamentous algal mats attached to *Egeria densa* in Sherman Lake, May 2012. Photo, Katharyn Boyer

nuisance species if they become overly abundant. Observations of thick green algal mats attached to *E. densa* have been made in a number of locations within the Delta (Santos et al. 2012; Boyer unpublished, Fig. 3.2; Llaban and DBW staff, pers. comm.).

3.1.4 Trophic support

Macrophyte invasion can lead to changes in structural complexity of the habitat, altering composition and abundance of invertebrates, which can have effects on higher trophic levels (e.g., Toft et al. 2003; Schultz and Dibble 2012). Direction and magnitude of change are difficult to predict in terms of desirable food for fish; however, thick stands of *Egeria densa* are thought to make access to invertebrate food resources difficult for fish, while locally clear water and dark, shadowy hiding places appear to increase predation risk compared to other habitats (Grimaldo and Hymanson 1999; Brown 2003; Nobriga and Feyrer 2007). The degree to which these modifications to food and predator conditions impact native fish in particular is unclear, nor have there been comparable studies in native SAV beds (e.g., *Stuckenia pectinata*) to support the assertion that the typically more open native plant canopies and greater turbidity (expected to be less reduced through baffling of sediment particles out of the water column) create more favorable habitat for native fish (Fig. 3.1). There is evidence that thick stands of *Egeria densa* impede the movement of small (including juvenile) fish, including natives such as salmonids, splittail, and Delta smelt (Brown 2003). It is possible that *E. densa* could be managed to maintain lower densities, and that this would permit increased access to food resources and reduce predation risk as the more open native plant canopies are hypothesized to do (Fig. 3.1).

Eichhornia crassipes may also modify the food resources available to higher trophic levels. Floating macrophyte invasion of open water can increase the surface area available for epiphytic invertebrate colonization (Brendonck et al. 2003). However, when native floating macrophytes are replaced, there can be a large change in species composition of the invertebrate assemblage. For example, in the Delta, large differences in the epiphytic invertebrate assemblage were found on *E. crassipes* versus the native floating species, pennywort (*Hydrocotyle umbellata*) (Toft et al. 2003). Microcrustacean zooplankton can be more abundant with no vegetation than with *E. crassipes* present (Brendonck et al. 2003). A study in Uruguay found calanoid and cyclopoid copepods to be less abundant at sites with *E. crassipes* than with *Stuckenia pectinata* or no vegetation (Meerhoff et al. 2003). Still, the literature on *E. crassipes* effects on zooplankton are inconsistent, perhaps because there are many factors that might interact to affect zooplankton, including the effects of density of *E. crassipes* on predator abundance (Villamagna and Murphy 2010).

In terms of food web support for fish, consumption of *E. crassipes* appears to be minimal, as it is a nutritionally poor diet choice for herbivorous fish (Cox 2003). For carnivorous fish, the presence of *E. crassipes* may change the invertebrate foods available relative to those on the native *Hydrocotyle umbellata* (Toft et al. 2003). Although both assemblages are dominated by amphipods, large drawdowns in dissolved oxygen (see Section 3.1.1) make *E. crassipes* a less favorable location for feeding due to physiological constraints on the fish (Simenstad et al. 1999). In fact, dissolved oxygen under dense or decomposing mats of *E. crassipes* can be dangerously low for fish (lower than 4.8 mg l^{-1} ; reviewed by Villamagna and Murphy 2010). The abundance of *E. crassipes* is linked to the value of the habitat it creates for fish; at some (undefined, and probably site-specific) lower level of abundance, adequate light for phytoplankton production to support zooplankton, surfaces for algae and invertebrate attachment, and dissolved oxygen all support fish presence and diets, while at higher abundance these features are diminished or even threatening to fish (McVea and Boyd 1975; Brown and Maceina 2002).

Similarly, for birds, presence of *Egeria densa* or *Eichhornia crassipes* may benefit certain birds through provision of invertebrate or fish prey attracted to the physical structure; however, access to these prey becomes diminished when canopies become excessively dense (Brendonck et al. 2003), and declines in dissolved oxygen (see Chapter 3) that affect prey would also limit value to birds. Neither of these species is known to be a valuable food source for birds themselves although American coots are known to eat *E. crassipes* (Villamagna 2009). In contrast, *Stuckenia pectinata*, a native species subject to replacement by these two invaders, is a very nutritious food source that was heavily used by canvasback ducks historically (Jepson 1905).

3.1.5 Navigation and industry

Submersed and floating vegetation both have the capacity to clog navigation channels, marinas, intake pipes for potable water supply, industry, and agriculture. Highly productive aquatic plant beds can have devastating effects on local economies and quality of life for recreational users of waterways. Thick mats of *Egeria densa* hinder a wide variety of recreational and commercial activities, including boating, fishing, swimming and water pumping for potable supply and irrigation (Bossard et al. 2000). *Eichhornia crassipes* can grow so densely on the water's surface that it impedes navigation by recreational

motorboats and ships, becomes entrained in water pumps, and chokes irrigation channels (Bossard et al. 2000; Toft et al. 2003). In turn, boating and shipping activities can facilitate spread of these invaders; *E. crassipes* can become dislodged from colonies and drift to other locations, and *E. densa* can be chopped into fragments that can become propagules for establishment elsewhere through water movement.

3.1.6 Aesthetics

Some invasive macrophytes are very attractive, but lose their aesthetic appeal when there is a loss of commercial, industrial, municipal, and recreational use. *Eichhornia crassipes*, in particular, has very showy and attractive purple flowers, a likely reason for its original introduction in many areas of the world.

4. Factors Contributing to the Prevalence of Submersed and Floating Aquatic Vegetation in the Delta

4.1 Conceptual Models of Growth, Propagation and Environmental Characteristics that Enhance or Limit Growth

There are a number of factors known to influence aquatic vegetation in low salinity and fresh regions of an estuary. Anderson (2008) developed a draft conceptual model to describe the ways in which submersed, floating, and emergent species are likely to respond to and modify conditions within the Delta. This effort included a general model for establishment, growth, and dispersal, reprinted here as Fig. 4.1. To briefly review this model, both submersed and floating macrophytes are influenced by light levels, with submersed plants adapted to lower light conditions. Carbon dioxide limits photosynthesis especially for submersed plants in thick stands where drawdown and high pH reduce availability, but many submersed species are capable of substituting bicarbonate as a source of inorganic carbon. Water quality conditions, including nutrient levels, are known to strongly influence growth of these species. Sediment characteristics, including nutrients and grain size distribution affect growth and anchoring of submersed vegetation. Local flow conditions help to maintain floating plants in place and help submersed species to accumulate large quantities of biomass.

Anderson (2008) described “sub models” for submersed and floating species which further detailed important determinants of establishment, growth, and dispersal for each vegetation type. These are reprinted here as Fig. 4.2A and B. Below we review these sub models in detail and the literature supporting each of them.

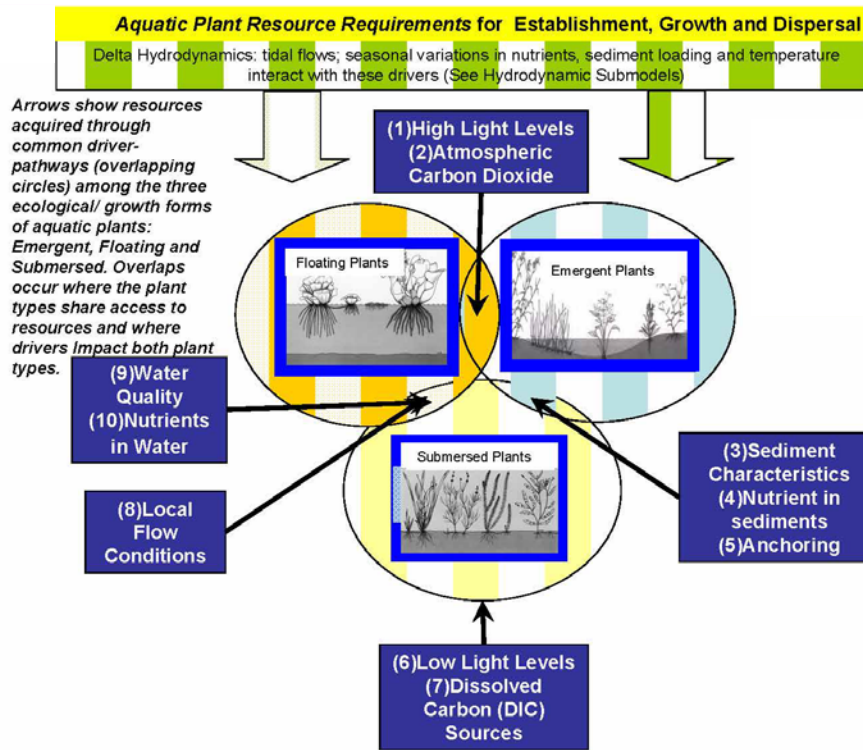


Figure 4.1 Aquatic plant resource requirements for establishment, growth and dispersal, as described in a draft conceptual model by Anderson (2008)

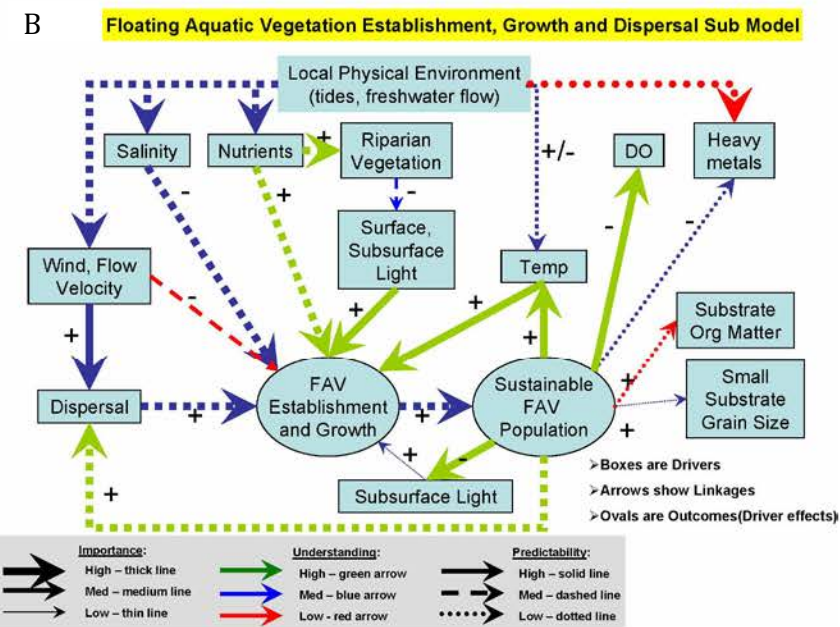
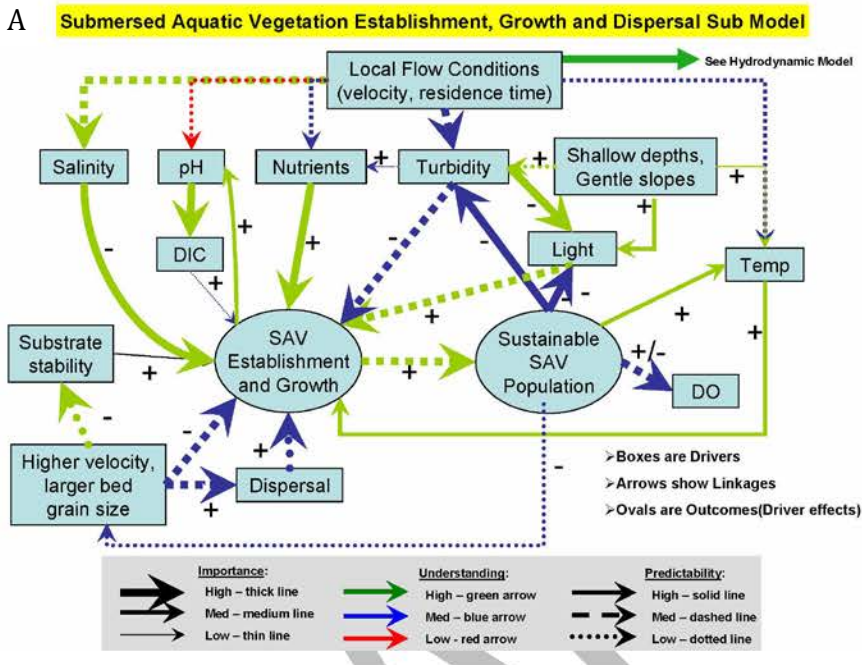


Figure 4.2. Sub models describing important drivers of establishment, growth, and dispersal in submersed (A) and floating (B) aquatic vegetation. From draft conceptual model by Anderson (2008)

4.1.1 Light

Light is essential to photosynthesis in all plants and is generally adequate for floating species such as *Eichhornia crassipes*, although periods of reduced light due to extended cloud cover (during El Niño years) have been implicated in a major decline in this species' vigor and cover in Lake Victoria in Africa (Williams et al. 2005, 2007). Floating species can benefit by shading submerged plants (see Section 4.1.7 below), which frees other resources such as nutrients and favors development of sustainable floating macrophyte populations (Fig. 4.2B).

Submersed species must cope with lower light conditions than floating species due to attenuation of photosynthetically-active radiation (wavelengths of 400-700 nm, PAR) through water. PAR is further attenuated by particles in the water, including sediments and phytoplankton. Light availability is very important to establishment of submersed species at the sediment surface (Fig. 4.2A), whether from seeds, turions, or vegetative fragments, depending on the species. After establishment, dense plant growth can lead to self-shading of tissues lower in the water column. However, *E. densa* reduces turbidity of the water, leading to greater light penetration (Fig. 4.2A; Hestir et al. 2013), which is likely to represent a positive feedback toward greater growth even at depth. *Stuckenia pectinata* has its canopy of leaves within the upper portion of the water column, which provides access to higher light levels near the surface, and its relatively sparse leaf growth minimizes self-shading. This sparse leaf growth does not appear to reduce the turbidity of the water based on measures of PAR inside and outside of *S. pectinata* beds (Boyer unpublished data). However, species-specific effects on light conditions are not well known for this or other species in the Delta.

Studies also support that light is likely to be quite limiting to lower portions of plant tissue in dense *Egeria densa* beds. In one local experiment testing light effects, *E. densa* had 4-fold lower biomass under conditions comparable to those measured in beds in the Delta at 1 m depth ($215.5 \mu\text{M quanta m}^{-2}\text{s}^{-1}$) compared to light levels 2x greater (Borgnis and Boyer, unpublished data). Although Durand (2014) found an ambiguous relationship between turbidity and *E. densa* growth, he found a low probability of establishment at depths below 5 m. In a New Zealand mesocosm study, reduced light (25% reduced from 50% incident level) was found to be a more important factor controlling *E. densa* than was temperature (tested at 20, 26, and 30°C) (Riis et al. 2012). Interestingly, a Brazilian study found the highest rates of elongation for apical shoots of *E. densa* occurred under reduced light conditions ($<30 \mu\text{M quanta m}^{-2}\text{s}^{-1}$), suggesting a mechanism by which *E. densa* may extend its canopy upward through the water column (Rodrigues and Thomaz 2010).

Waters in the Delta have become clearer over at least the last fifty years. The delivery of suspended sediment from the Sacramento River to the Delta has decreased by about half during the period between 1957 and 2001 (Wright and Schoellhamer 2004) and this has resulted in a statistically significant (2 to 6 percent) decrease per year in suspended particulate matter between 1975 and 2005 (Jassby 2008). It is unclear whether this increase in water clarity has increased the biomass and distribution of submerged macrophytes already, or how it will influence other important factors in plant growth, including nutrients.

4.1.2 Temperature

Warm temperatures are expected to favor the establishment and growth of both floating and submersed species and to produce localized warming of waters through reduction in water flow, which in turn should benefit plant growth (Fig. 4.2A-B). However, high water temperatures within the range found currently in the Delta might limit growth of some species, and temperatures are expected to increase with climate warming (Knowles and Cayan 2002; Wagner et al. 2011). A 2012 experiment testing water temperature effects on growth of *E. densa* apical shoot sections in aquaria showed substantial increases over time in aboveground biomass, total shoot length, and mean root length at a water temperature of 22°C (the average measured in the west Delta in summer) in fresh water, with similar effects at 26°C, although much less of a biomass response (Fig. 4.3, Borgnis and Boyer in revision). In contrast, there were great reductions in all these measures at 30°C (Fig. 4.3), which is within the current range of maximum temperatures measured for the west Delta (Borgnis and Boyer, in revision). Further, testing these temperatures at a salinity of 5, which can be found in the west Delta in drought years (e.g., 2012-2014), led to a reduction in root length at all temperatures. At a salinity of 10, the negative effects of high temperature (30°C) were amplified and led to greatly reduced aboveground biomass (Fig. 4.3). As for cold temperatures, we are not aware of any local data; in other regions, night-time freezing, especially in shallow water was found to be highly stressful to *E. densa* (Leslie 1982).

We know of no local experiments testing temperature effects on *Eichhornia crassipes*, *Ceratophyllum demersum*, or *Stuckenia pectinata*. In other regions, *Eichhornia crassipes* has been shown to benefit from warming above ambient conditions within limits. In China, *E. crassipes* rates of relative growth and clonal propagation increased by 15% with an increase in water temperature from 24 to 26-27°C in mesocosms (You et al. 2014). However, at

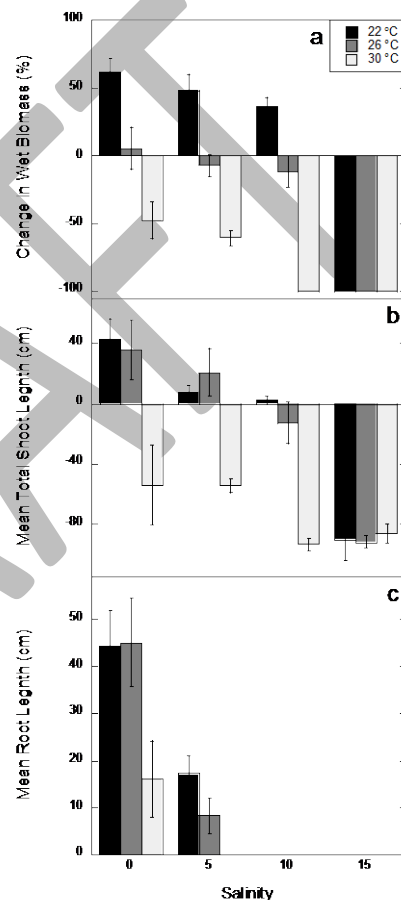


Figure 4.3. Response of *Egeria densa* to a range of temperature conditions applied at increasingly high salinity conditions at the end of 6 weeks in aquaria. From Borgnis and Boyer, in revision

temperatures above 33-34 C, *E. crassipes* loses nutrients from the roots and experiences negative growth (Moran, pers. comm.). *E. crassipes* is also limited by cold temperatures in the range of 10°C (Gopal 1987; Wilson et al. 2005). Frost can cause mortality of leaves and whole plants (Bock 1969; Ueki and Oki 1979; Spencer 2005), although stem bases can survive and serve as propagules for growth in the next year (Spencer 2005). Large rafts of *E. crassipes* have been observed floating seaward from the Delta during periods of freezing night-time conditions, suggesting deterioration of the ability to remain in cohesive mats under these conditions (Foe, pers. comm.). Further, a three-week period of night-time frost in 2007 appeared to have contributed to a significant decline in *E. crassipes* in the next year (Khanna, pers. comm.).

4.1.3 Salinity

In general, species in much of the Delta experience fresh water maintained with little seasonal variation through water management practices to support potable, industrial, commercial, and agricultural uses (Moyle et al. 2010). This is in contrast to the historic condition of seasonal and interannual salinity variation prior to water management practices. In the past several years of drought, late-summer water salinities of 5 or more have reached east to the Sherman Lake region of the Delta. Salinity could further increase in the Delta through several mechanisms stemming from climate change and water management. Sea-level rise and shifts in magnitude and timing of snowmelt events are projected to increase salinity levels by 1-3 in this region by 2090 (Knowles and Cayan 2002). In addition, extended periods of drought could lead to increased salt penetration not counteracted by reservoir releases during the summer months. There is also potential for levee failures through erosion or earthquakes, leading to a higher volume of saline tidal waters reaching up-estuary. Finally, management actions that inadvertently or deliberately reduce fresh water releases during the dry season could increase salinity in this region. Summer and fall salinity has already increased in the last 25 years due to reduction in fresh water releases from water control structures (Knowles and Cayan 2002; Contra Costa Water District 2010). C&H Sugar Refining Company (Crockett, CA) has long tracked salinity in order to access fresh water for its refining process; its data show annual salinity intrusion now occurs much earlier in the year in Suisun Bay (beginning of March) compared to the early 1900s (beginning of July) (Department of Water Resources 2010).

As mentioned, *Egeria densa* is strongly limited by salinity. As in the six-week temperature-controlled aquaria experiment described above, a three-month experiment conducted in large tanks in a greenhouse in 2012 showed *E. densa* negative responses to a salinity of 5, with a 5-fold decrease in biomass relative to the freshwater treatment over the three months (Fig. 4.4, Borgnis and Boyer, in revision). At salinities of 10 and 15, mortality and decomposition occurred within three weeks. This was in contrast to 5-fold increases in shoot biomass in freshwater over the three months, and nearly 10-fold increases in the number of shoots and in root biomass (Fig. 4.4). Tissue nitrogen (N) concentration stayed constant at salinities of 0 and 5; however, tissue phosphorus (P) increased at a salinity of 5 (and thus N:P also), suggesting that P taken up could not be utilized and thus accumulated in the tissues, perhaps another indication of stress at this higher salinity.

Of all aquatic macrophyte species found within the Delta, *Stuckenia pectinata* is expected to have the greatest tolerance for salinity. This assumption is due in part to its nearly monotypic distribution in waters that can reach salinities of 15 within Suisun Bay. Further, in six weeks in greenhouse mesocosms, *S. pectinata* biomass accumulated greatly (~4x initial) at salinities of 0 and 5, doubled at 10, and was unchanged at 15 (Fig. 4.4; Borgnis and Boyer, in revision). Increases in both N and P concentrations in tissues at higher salinities (Fig. 4.4) suggests an inability to utilize all available nutrients, and perhaps the accumulation of N as “compatible solutes” to balance water potential as is common in saline wetland plants.

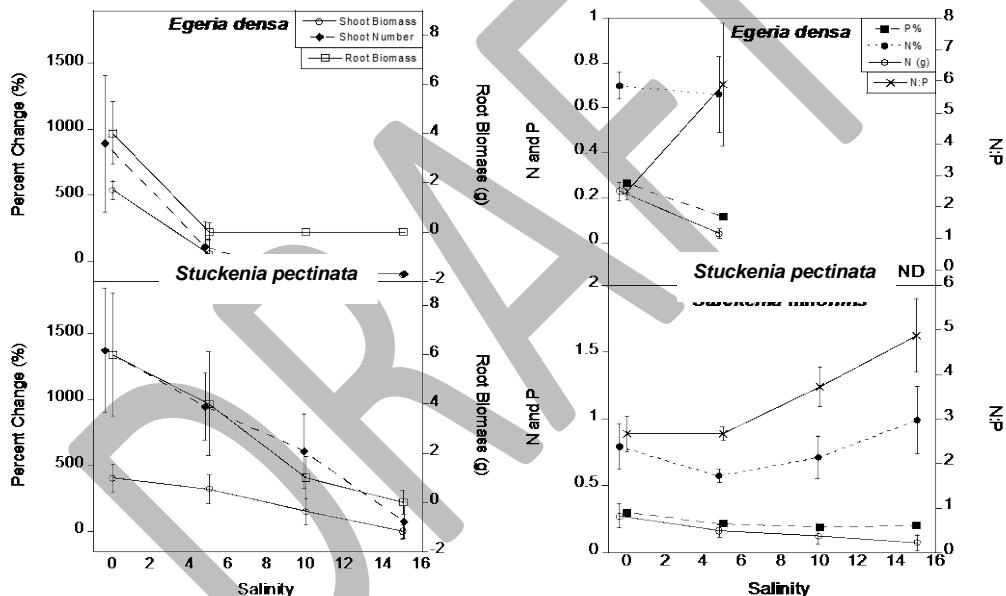


Figure 4.4. Salinity effects on growth characteristics and nitrogen and phosphorus content and ratio of *Egeria densa* and *Stuckenia pectinata* at the end of mesocosm experiment that ran June-August 2012. ND = no data; *E. densa* tissue nutrients could not be measured at the higher salinities due to insufficient tissue availability. From Borgnis and Boyer, in revision

We are not aware of any local studies of salinity tolerance on *Ceratophyllum demersum* or *Eichhornia crassipes*. Studies in other regions have found that *E. crassipes* undergoes stress at salinities as low as 2.5 (Haller et al. 1974) and that salinities above 6-8 are lethal (Muramoto et al. 1991; Olivares and Colonnello 2000).

4.1.4 Dissolved inorganic carbon

Floating vegetation should be able to access adequate carbon dioxide to fuel photosynthesis; however, availability of dissolved inorganic carbon (DIC) can be an important limiting factor to submersed species. The forms of carbon dissolved in the water are determined by pH (Barko and Smart 1981; Sand-Jensen 1989). Although CO₂ is the form of DIC preferred by all autotrophic organisms (Raven 1970), drawdown of CO₂ leads to increased pH. This is because CO₂ in solution is in equilibrium with carbonic acid (H₂CO₃), which becomes more common, leading to removal of protons from the water (thus a higher pH). This, in turn, has an effect on the relative concentrations of the other DIC forms in the water and bicarbonate (HCO₃⁻) becomes the primary form of DIC available (Sand-Jensen 1989; Santamaria 2002). Species that can utilize bicarbonate efficiently should have an advantage in the waters of the Delta. Both *Egeria densa* and *Ceratophyllum demersum* are able to efficiently utilize bicarbonate as a DIC source (Cavalli et al. 2012), which may partly explain their success within the Delta, with the heightened pH in dense beds leading to further advantage over time through positive feedback (Fig. 4.2A). We are not aware of pH measures within macrophyte beds in the Delta, but heightened pH and diurnal swings in both pH and CO₂ would be expected to be greatest within dense beds of *E. densa* and in settings with limited water flow.

4.1.5 Nutrients

The primary nutrients that limit plant growth are nitrogen (N) and phosphorus (P). Limitation is typically determined by adding one or more nutrients to ascertain if the potential rate of net primary production has been achieved (Howarth 1988); in other words, if the plant grows with added nutrients, then it has greater potential for production than what its ambient nutrient environment allows. At temperate latitudes, phosphorus is generally considered the primary limiting element to system primary production in freshwater, and nitrogen is considered the primary limiting element in marine systems, although there is variation in this pattern (Smith 1984). N may be less limiting in freshwater due to a greater importance of N fixation there (Howarth et al. 1995, 1999; Paerl et al. 1995), and a greater efficiency of sediments in sequestering P than in marine systems (Caraco et al. 1990); however, both N and P have been shown to be important in estuaries (McComb et al. 1981; D'Elia et al. 1986) under different conditions and seasonally (Conley 2000).

The San Francisco Estuary is an example of a system replete in both N and P, and yet depauperate in phytoplankton production (Cloern 2001). The annual loading rates of both N and P are higher in San Francisco Estuary than in the Chesapeake, and yet large phytoplankton blooms and mortality common in Chesapeake, followed by large drawdowns in dissolved oxygen concentration, do not typically occur in the San Francisco Estuary (Cloern et al. 2001). Thus, San Francisco Estuary is not considered to be a eutrophic system in terms of algal production; phytoplankton may be limited by high levels of turbidity, abundant consumers including introduced clams (Jassby and Cloern 2000), and possibly by the ratios of species of N available (i.e., ammonium versus nitrate, Wilkerson et al. 2006).

Although adequate nutrient supply is necessary to fuel growth of macrophytes in the Delta, the degree to which nutrients trigger or exacerbate extensive growth of the invasive *Egeria densa* and *Eichhornia crassipes* (and now *Ludwigia* spp. as well) within Delta waters is unclear. Acreage of all these invasive

Comment [KB6]: John Durand said "limited at times in N Delta off Sac plume" – need clarification or reference

macrophytes has expanded in recent years, and especially during the time between two mapping events in 2008 and 2014 (Khanna and Ustin, unpublished data). Although there has been an increase in NH_4^+ and a decrease in the N:P ratio over a 30 year period through 2006, especially in the upper Sacramento River, this trend was not evident in the last decade of that time period (Glibert 2010; Fig. 4.5). A closer look at the last decade (through 2013) shows no trends in any form of inorganic nutrients or N:P ratios in the central Delta region (Berg and Sutula 2015, Figure A-1 through A-4). Thus, it does not seem that overall increasing acreages of invasive macrophytes can be related to changes in ambient dissolved inorganic nutrient concentration, form, or ratios during the same time period.

DRAFT

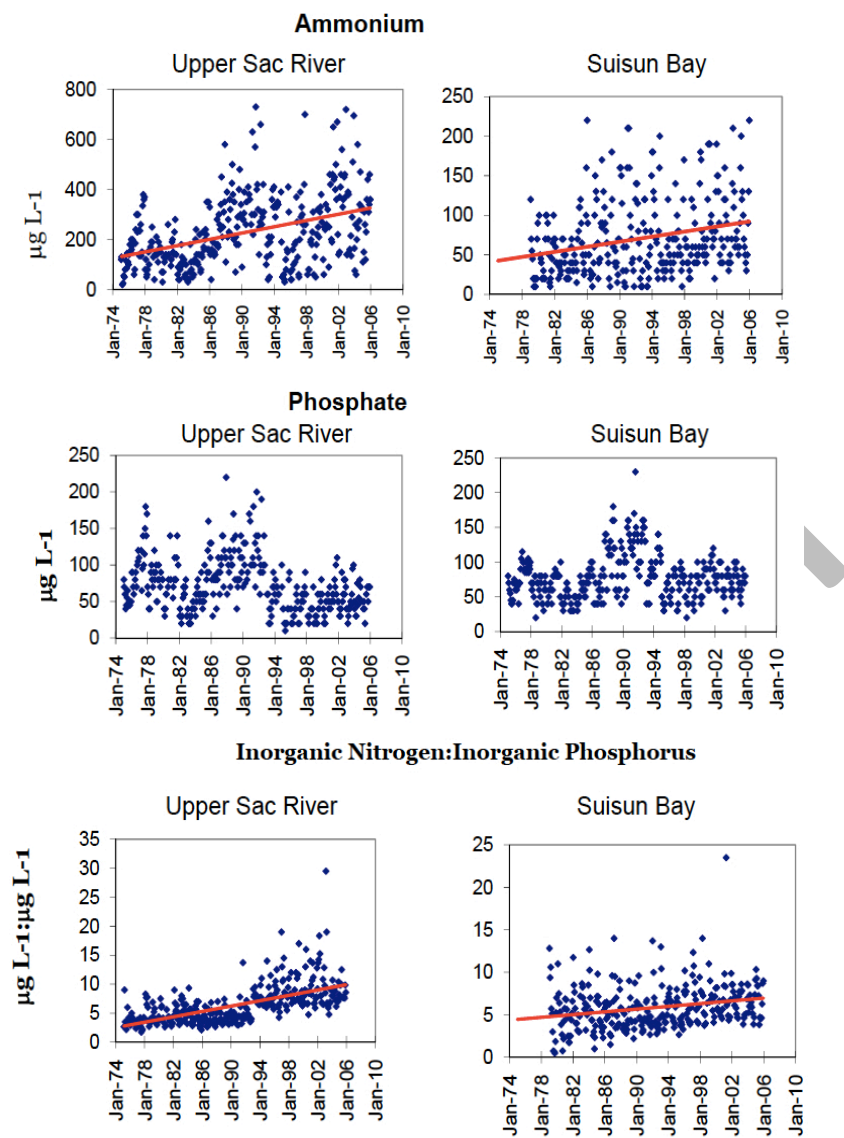


Figure 4.5. Patterns in ammonium, phosphate, and ratios of inorganic N to P over time at two locations, upper Sacramento River and Suisun Bay. From Glibert 2010.

Water nutrient concentrations vary across the geographical extent of these species, with at least a 3-fold difference in all three of the primary inorganic nutrient forms, ammonium (NH_4^+), nitrate (NO_3^-) and phosphate (PO_4^+) from the upper Sacramento River to Chipps Island (Foe et al. 2010; Figs. 4.6, 4.7).

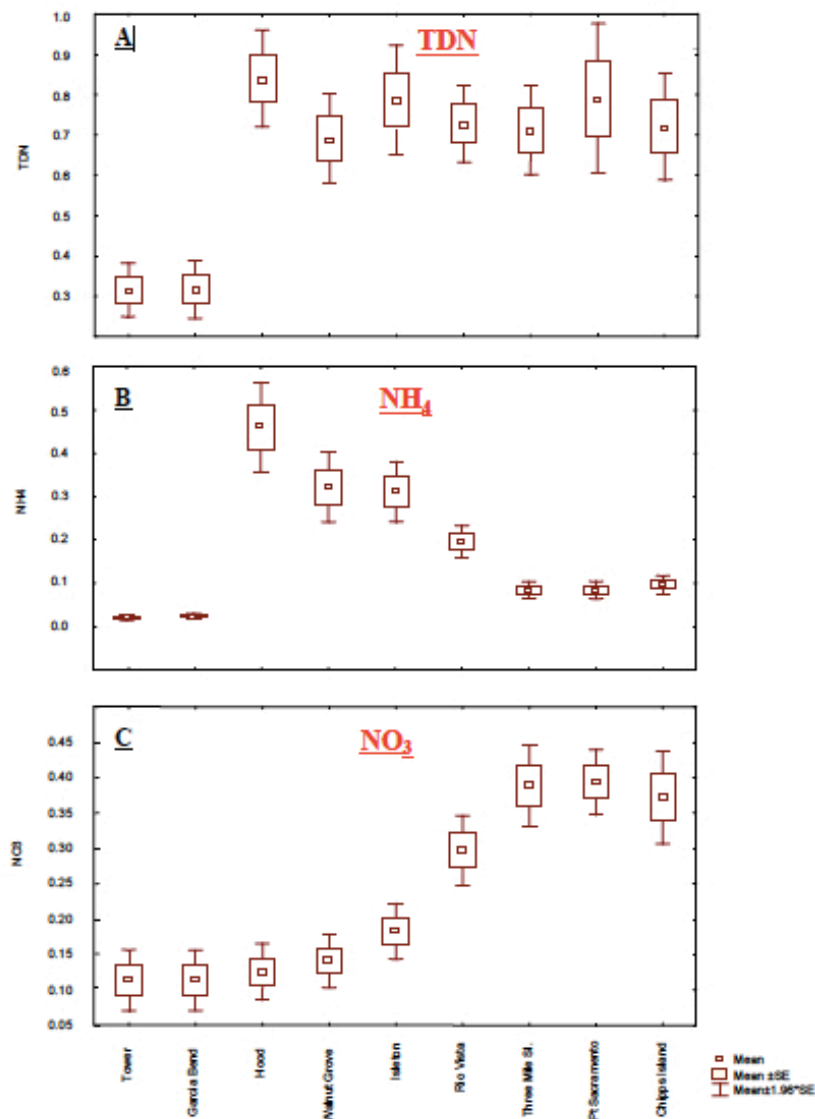


Figure 4.6. Mean annual total dissolved nitrogen (TDN), NH_4 and NO_3 concentrations in the Delta between Tower Bridge (north Sacramento River) and Chipps Island (Suisun Bay) between March 2009 and February 2010. Tower and Garcia Bend sites are above the discharge of the Sacramento River Water Treatment Plant. From Foe et al. 2010.

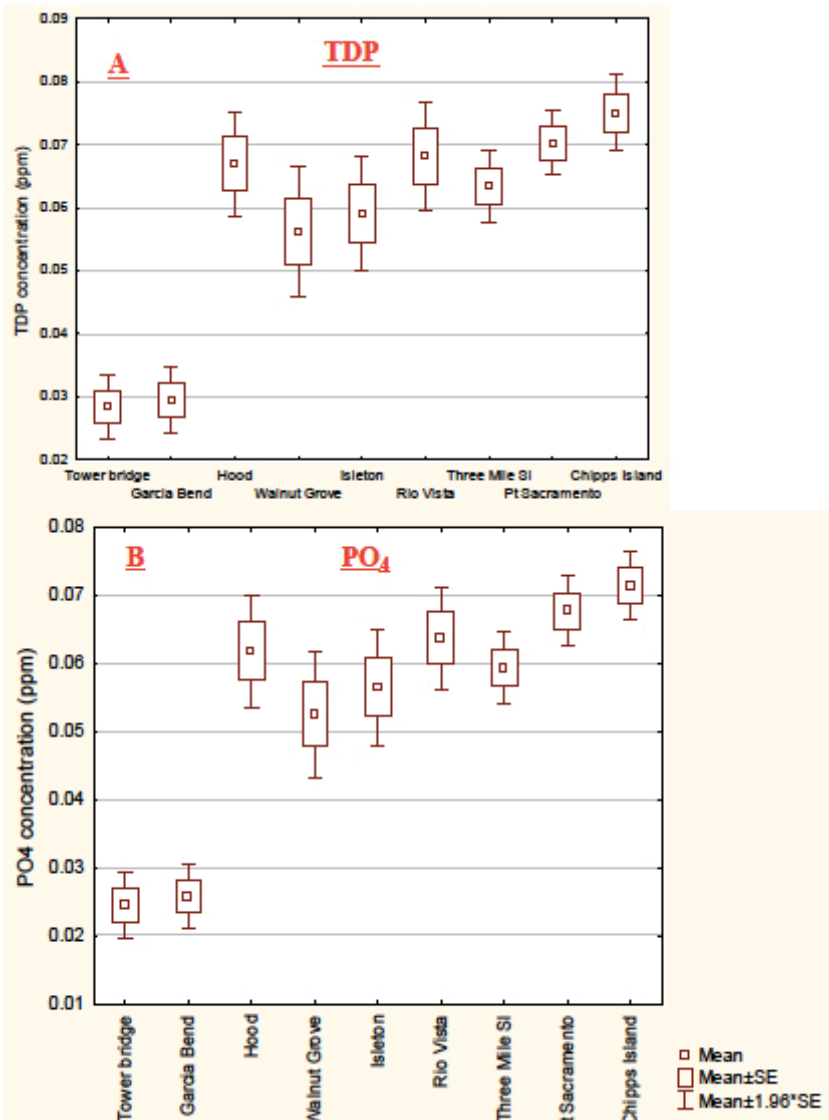


Figure 4.7. Mean annual total dissolved phosphorus (TDP) and PO₄ across sites as in Fig. 4.5. From Foe et al. 2010.

It is possible that acreages of these species could be examined in relation to nutrient supply to determine if there is a correlation between changes in abundance and nutrient patterns at specific locations, but it would be difficult to tease apart other co-occurring patterns in environmental conditions that may vary with nutrients.

Egeria densa is able to take up nutrients through its leaves and roots, thus accessing water column nutrients from both the water column and the sediment. Studies differ on whether it preferentially takes up nutrients from its roots (Barko and Smart 1980) or shoots (Feijoo et al. 2002). *Eichhornia crassipes* accesses nutrients through its roots hanging at the surface of the water column (Klumpp et al. 2002; Rommens et al. 2003). Although many experiments have tested the effects of nutrients on phytoplankton growth under different scenarios of light, temperature and other variables in the Delta (e.g., Wilkerson et al. 2006), we know of no comparable local experiments conducted on aquatic macrophytes.

Researchers in other regions have evaluated nutrient limitation of *E. densa* through experiments in which nutrients were added to test the plant's response. In *E. densa*'s native range in highly enriched Pampean streams in Argentina, biomass and nutrient content were positively correlated with nutrient concentrations (phosphate and ammonium) in the water and in sediments (as total N) (Feijoo et al. 1996). An experiment by that same group found ambient levels of phosphate (0.3 mg l^{-1}) led to significantly greater biomass than phosphate at half of ambient concentrations (Feijoo et al. 2002). In a separate experiment, they found that ammonium was absorbed more readily than nitrate (added at ambient concentrations of 6 mg DIN l^{-1} , separately), leading to higher concentrations of tissue N with ammonium; however, this did not translate to differences in biomass (Feijoo et al. 2002). A comparison across the two experiments found phosphate was more readily absorbed by *E. densa* than nitrogen in either form, and that water column uptake was greater than from sediments (Feijoo et al. 2002). A study in Florida also found *E. densa* to prefer ammonium over nitrate when both were present in the water in equal amounts at concentrations considered to be non-limiting (10.5 mg l^{-1} of each DIN source, plus phosphate at 3 mg l^{-1} , as found in sewage effluent, Reddy et al. 1987). In a separate experiment, these authors varied concentration of ammonium and phosphate (range of $1\text{-}4 \text{ mg N}$ and $0.2\text{ to }0.8 \text{ mg P l}^{-1}$, respectively); although they did not report biomass data, they noted that biomass was *greater* at low nutrient concentrations than at high. N and P removal rates were estimated to be $186\text{-}408 \text{ mg N m}^{-2} \text{ day}^{-1}$ and $122\text{-}228 \text{ mg P m}^{-2} \text{ day}^{-1}$ from the water column (Reddy et al. 1987). *E. densa* uptake of both nutrients was similar in summer and winter experiments. A Florida mesocosm experiment repeated in two different seasons (April-June and October-December) found no effects of fertilizer (N:P:K of 15-9-12 in slow release fertilizer) added to the sediment in a range of concentrations from 0 to 4 kg/g sediment) on *E. densa* biomass (Mony et al. 2007).

Taken together, these studies of *E. densa* suggest that nutrient uptake from water may be preferred over uptake from sediment, that ammonium may be preferred over nitrate, and that phosphate may be more readily absorbed than either form of N. The tests of water column nutrient effects in all the above studies were conducted at very high concentrations, which may explain the limited growth responses. Although concentrations vary among sites in the Delta, typical DIN levels are 0.5 mg l^{-1} and DIP levels are 0.06 mg l^{-1} (annual means of ~monthly sampling in 2009-2010; Figs. 4.6, 4.7; Foe et al. 2010), with an

annual average as high as 1.43 mg l⁻¹ DIN and 0.18 mg l⁻¹ DIP at one site (Foe 2010). However, the studies described in the previous paragraph evaluated *E. densa*'s responses under higher ambient nutrient conditions and thus they tell us little about water column nutrient thresholds for macrophyte biomass expansion in the Delta. In addition, little is understood about the role that dissolved organic nutrients may play in supporting macrophyte growth. Moreover, we suspect rooted species like *E. densa* with the capability of accessing nutrients from both the water column and the sediments would be very difficult to manage by only reducing water column nutrient supply, especially in quiescent areas where dead biomass can accumulate and possibly provide an extended period of remineralizable nutrients. Further, the positive feedback of declines in dissolved oxygen making sediment-bound P more available (see Chapter 3) suggests that this important nutrient will continue to be sourced from the sediments (Cornwell et al. 2014), especially in places where decomposing macrophyte tissues accumulate.

Eichhornia crassipes, with access to nutrients only from the water column, is perhaps a simpler case. A number of studies have shown *E. crassipes* to readily absorb added N (Carignan and Neiff 1994; Heard and Winterton 2000; Reddy et al. 1989, 1990; Moran 2006) and to sometimes be limited by P (Srivastava et al. 1994; but see Moran 2006, who did not find an association between DIP and P uptake). In a mesocosm study on *E. crassipes* in China, nutrient additions to lake water comparable in nutrients to the Delta (0.6 mg l⁻¹ total N and 0.05 mg l⁻¹ total P), raising N to 5 mg l⁻¹ (using NH₄NO₃) and P to 0.5 mg l⁻¹, led to 30% increases in both relative growth rate and clonal propagation rate (You et al. 2014). Notably, the same elevated N level combined with a much higher P enrichment (1.0 mg l⁻¹) led to 150% increases in these measures relative to ambient conditions simulated. In that same study, warming by 2-3 degrees had a much smaller positive effect on growth rate (15%) and some effects of elevated temperature (increased shoot:root and foliar N) were found only when nutrient levels were also elevated (You et al. 2014). A study that explored water N concentration in relation to *E. crassipes* growth rates (Aoyama et al. 1986; see review and modeling by Wilson et al. 2005) suggests that *E. crassipes* growth rates in the Delta could be reduced with lower DIN concentrations than are typically found there (0.5 mg l⁻¹, Foe et al. 2010). This work also estimated that N becomes limiting for *E. crassipes* growth at an N:P ratio in water of <7 (Wilson et al. 2005); assuming 0.5 and 0.06 mg l⁻¹ DIN and DIP in Delta waters on average (Foe et al. 2010), respectively, an N:P ratio of about 8 suggests that N supply is not currently limiting. Although water column nutrients are the only source available to *E. crassipes*, sediment fluxes can supply both N and P (the latter enhanced by low oxygen conditions) to the water column. Hence, while management of water column nutrient supply might seem to be a straightforward solution that could reduce *E. crassipes* abundance, perhaps more easily than for *E. densa*, biogeochemical coupling with the sediments must also be considered.

4.1.6 Flow, residence time, substrate stability, and slope

Flow velocity and residence time of water within a given area are expected to influence both floating and submersed species. Propagules need to be able to stay in place to initiate bed establishment, which succeeds to a greater degree in more protected areas. Two studies found flow rates above 0.3 or 0.49 ms⁻¹ limiting to establishment of *Egeria densa* (Durand 2014 and Hestir 2010, respectively). Substrate stability is necessary for submersed plant establishment and persistence, and larger grain size (sand) can

lead to less stable bed conditions, especially under higher flow regimes. Development of an aquatic plant bed slows flow in the immediate vicinity, a positive feedback loop that further supports bed development. Although the draft conceptual model of Anderson (2008) indicates the importance of substrate stability, it does not indicate the importance of this positive feedback (Fig. 4.2A). Densely growing submersed macrophytes like *Egeria densa* can reduce flow by 40% (Wilcock et al. 1999; Champion and Tanner 2000), favoring their continued presence and spread within the area. However, higher flow is important to dispersal of propagules of all aquatic macrophytes to new areas (Fig. 4.2A) and water movement is essential for growth by bringing nutrients and dissolved carbon to the leaves by mass transport.

Depth and slope of shores can also limit submersed species (Fig. 4.2A). *Egeria densa* can grow to depths of 6 m (Carrillo et al. 2006) and 40% slope, but this seems to be the extreme (in tropical, high elevation lakes). *Eichhornia crassipes* vegetative propagation is not limited by water depth, but propagules accumulate along shores due to greater protection from washing out. Although sexual reproduction contributes little to population growth in the Delta, germination and seedling growth require shallow water over gentle sloping shorelines to maximize light availability (Barrett 1980).

4.1.7 Interactions with other submersed or floating species

A factor not summarized in the draft conceptual models of Anderson (2008) is interaction among species of aquatic macrophytes. Several recent studies suggest these could be quite important in determining the abundance of some species or guilds of species. For example, experimental work in mesocosms suggests that *Egeria densa* has strong negative effects on *Stuckenia* sp. growth under fresh water conditions. When grown together with *Egeria densa* in fresh water, *Stuckenia* sp. produced 75% less biomass than in monoculture, and significantly more nodal roots, suggesting increased nutrient foraging (Fig. 4.5, Borgnis and Boyer in revision). At a salinity of 5, a decline in *E. densa* performance (see above) coincided with a doubling of *Stuckenia* sp. shoot

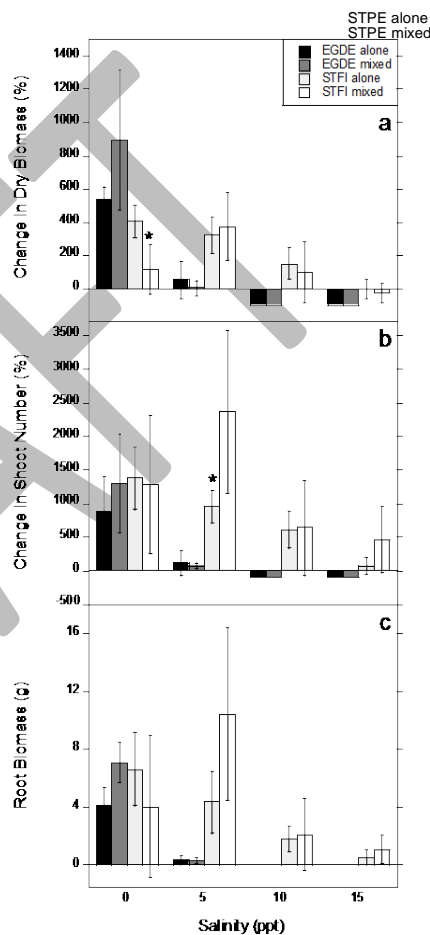


Figure 4.5. Effects of salinity on growth characteristics of *Egeria densa* (EGDE) and *Stuckenia pectinata* (STPE), grown separately and together, at the end of a mesocosm experiment running June-August 2012. From Borgnis and Boyer, in revision

density. These results suggest that *S. pectinata* might be more abundant in the fresh waters of the Delta in places where *E. densa* currently dominates.

There may be other possibilities of important interactions within the submersed plant community. As previously mentioned, *Egeria densa* maintains substantial biomass during the winter, perhaps increasing its competitive ability among species that undergo winter senescence, such as *Stuckeina pectinata*. However *E. densa* may facilitate other species in some cases. In one study, *Ceratophyllum demersum* was found to occur more frequently with other species, especially *Egeria densa*, than it occurred on its own (Santos et al. 2011), suggesting it may derive some benefit from other species.

In addition, remote sensing data tracking changes in the coverage of the floating species *Eichhornia crassipes* indicated a large loss of submersed species with an increase of 25% in *E. crassipes* and conversely a large increase in submersed species with 25% decrease (Fig. 4.6, Khanna et al. 2012). The possibility that one of these invaders will replace the other and vice versa with management is an important issue to consider. In contrast, there were no consistent effects on other floating species: the native *Hydrocotyle umbellata* or the introduced *Ludwigia* spp. (Fig. 4.6). A conceptual model was developed to show the hypothesized relationships between *E. crassipes* and submersed vegetation with succession and treatment (Fig 4.6). An interesting new trend of reduced *H. umbellata* accompanied by large increases in *Ludwigia* spp. suggests that there may be feedbacks between these two species as well (Khanna and Ustin, unpublished data).

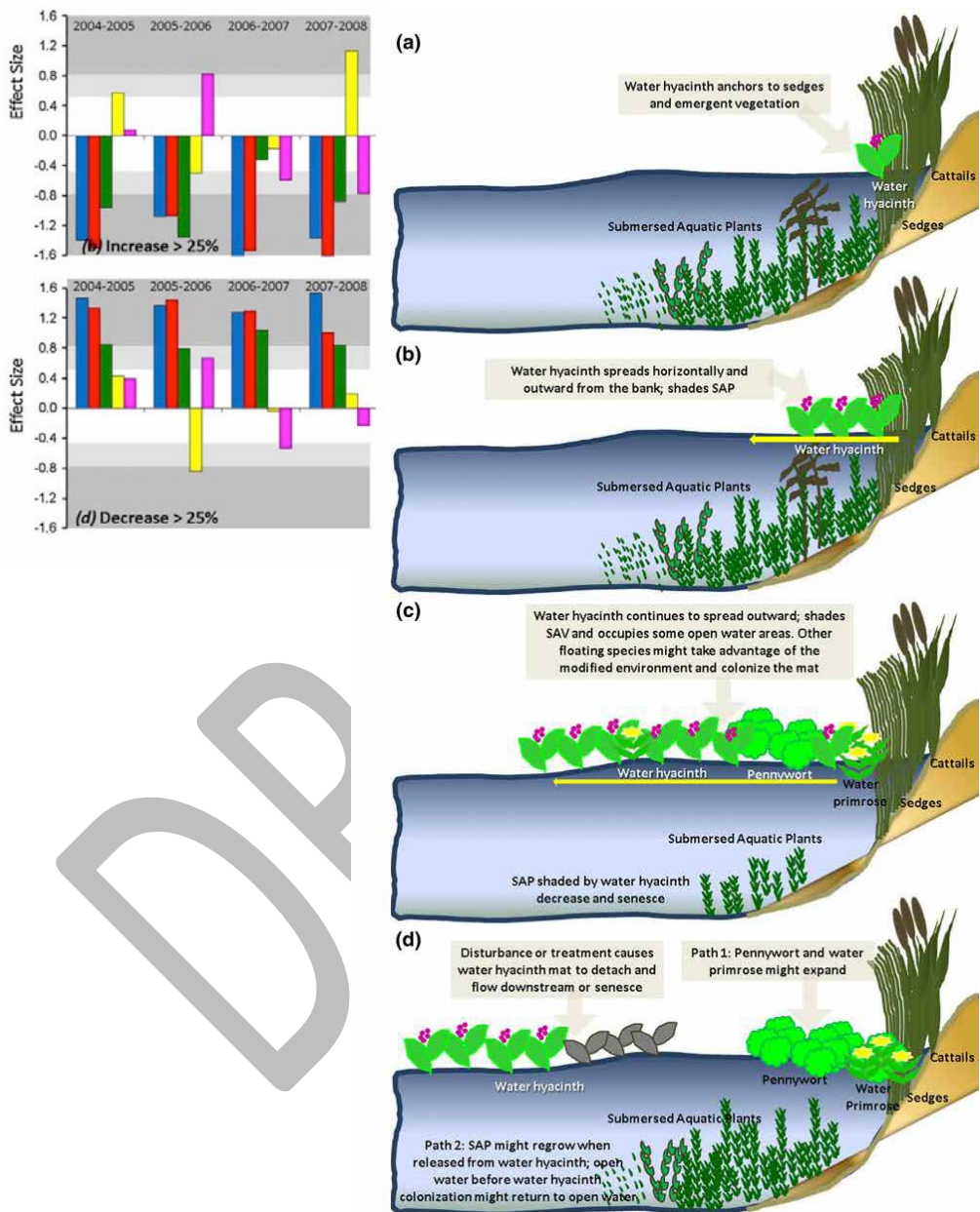


Figure 4.6. Left: Effect sizes reflecting change in coverage with 25% increases or decreases in water hyacinth (*Eichhornia crassipes*) from remote sensing data (dark region of background indicates a strong effect). Changes are shown for water (blue), submersed vegetation (red, predicted to be primarily *Egeria densa*), emergent and senescent plants (green), native pennywort *Hydrocotyle umbellata* (yellow), and introduced water primrose (*Ludwigia* spp., pink). Right: Conceptual model of successional pathways of *E. crassipes* growth and expansion, with effects on other floating and submersed plants. From Khanna et al. 2012

4.1.8 Chemical, mechanical, and biological control

Herbicide application has been the most common means of attempted control for both *Egeria densa* and *Eichhornia crassipes* to date (Anderson 1990, DBW 2005). Legal challenges to herbicide control have led to new permitting and monitoring requirements (Siemering et al. 2005), and a re-evaluation of alternative control methods (Greenfield et al. 2007).

Mechanical removal of *Egeria densa* has been attempted in the Delta, but tends to produce fragments that then can become propagules for further spread locally and in distant locations through water movement (Anderson 2003). Such harvesting also has the potential to remove or damage non-target organisms. Mechanically gathering and harvesting *Eichhornia crassipes* can be effective in limited areas, but it is expensive to remove the heavy masses of plants with very high water content (Gopal 1987). Shredding of this species using shredder boats and leaving the plant material in place may be one option, although the resulting biomass and source of remineralizable nutrients as well as dissolved oxygen implications are both concerns in areas with limited flow (Greenfield et al. 2007; see above). Further, such shredding can leave viable propagules that can survive and regrow (Spencer et al. 2006). Benthic barriers have been used to limit small infestations of *E. densa* around high use areas such as docks, boat launches and swimming areas in other regions but have not been used in the Delta to our knowledge.

There is an extensive literature on the use of biological agents as controls for *Eichhornia crassipes*. There are two commonly used weevil species from the plant's native range in use for biological control, in the genus *Neochetina* (Sosa et al. 2012). Typically, mechanical or chemical treatment is used first, making initial conditions more manageable for biological control (Adekoya et al. 1993). In the Delta, several species intended for biological control of *E. crassipes* were introduced in the early 1980s; of these, the weevil *Neochetina bruchi* has become established but does not appear to have much impact (Stewart et al. 1988). Although this weevil is likely to have its nutritional needs met through adequate plant nutrient levels in the Delta (Spencer and Ksander 2004), its immature stages have poor survivorship during winter conditions (Akers and Pitcairn 2006). The US Department of Agriculture (USDA-ARS) and the California Department of Food and Agriculture (CDFA) are investigating other potential biological control agents, and are beginning to release a planthopper, *Megamelus scutellaris* for *E. crassipes* control (P. Moran, USDA-ARS Exotic and Invasive Weeds Research Unit, Albany, CA, pers. comm.). This planthopper is considered to be sufficiently host-specific in Florida, where it is now widely established, and impact evaluations there are ongoing (Tipping et al. 2014a; Moran, pers. comm.).

To date, besides the above biological control attempts in the Delta on *E. crassipes*, no other introductions have been made for control of other invasive macrophytes. Biological control studies are underway for *E. densa* under lab conditions; an ephydrid fly larva is one species being evaluated (D. Dubose, USDA-ARS, pers. comm.).

Although biological control methods may be desirable to avoid the concerns of non-target species effects of chemical application, the resulting biomass can still be an issue to contend with. *Neochetina* spp. weevils reduce buoyancy of *Eichhornia crassipes*, making it sink to the bottom and decompose (Wilson et al. 2007). As with chemical control or natural causes of plant death (e.g., freezing

Comment [KB7]: Cite – Llaban suggested Biology and Control of Aquatic Plants. A Best Management Practices Handbook

temperatures), if there is mortality and accumulation of dead material, decomposition can lead to a drawdown of oxygen and a release of nutrients, mainly in quiescent areas where the material is not washed out (Greenfield et al. 2007). Further, biological control has been shown to reduce the size of *E. crassipes* plants over several generations, which could reduce the biomass of live plants that can lead to low oxygen conditions beneath the floating mats (Tipping et al. 2014b).

4.2 Relative Importance of Nutrient Subsidies Versus Other Factors in Promoting Observed Trends

Our review indicates that there are a number of important factors that affect the biomass and distribution of nuisance aquatic species. There are a few factors that can lead to large losses of biomass in a short period of time, including increased salinity for *E. densa* and *E. crassipes* and freezing temperatures for the latter. Two papers reported on state shifts resulting from dramatic losses of these two species. As described above, *E. crassipes* suffered a major decline largely attributed to reduced light due to extended cloud cover (during El Niño years) in Lake Victoria in Africa (Williams et al. 2005, 2007). *E. densa* disappeared from a wetland in its native range in southern Chile, probably due to desiccation exacerbated by low rainfall and cold temperatures (Marin et al. 2009). It is possible that there are management actions that could be used in some areas of the Delta to control these species to some degree. For example, water levels could be controlled in some locations, in order to attempt to desiccate *E. densa*, and salinity could be permitted to intrude for brief periods of time if that were politically acceptable (Moyle et al. 2010), which could shift west Delta *E. densa* stands to the native *Stuckenia pectinata*. Species interactions are also worth considering in manipulations; e.g., are there management actions that could shift composition toward native or desirable species? However, there is also the possibility of a “zero sum game” if managing *E. crassipes* leads to further invasion by *E. densa* and vice versa, or other undesirable species are benefitted through a management action.

Nutrients are certainly important to the growth of all plant species and our review suggests that the nutrient levels currently found in the Delta are probably not limiting these plants. Studies of nutrient addition to *Eichhornia crassipes* show clear signs of a direct relationship of water column nutrients to accumulation of biomass as well as clonal propagation, and it may be possible to reduce growth rates through nutrient reductions. However, studies of *Egeria densa* biomass at realistic nutrient levels for the Delta are very limited, and thus do not provide convincing evidence that a reduction in water column nutrients will result in a reduction in *E. densa* production. Further, for both these species, we have very limited understanding of the relative importance of new nutrient supply versus the cycling of nutrients within beds, including the release of P from sediments within macrophyte beds (Cornwell et al. 2014). Finally, have very limited information on the relative importance of nutrients versus other factors in controlling growth and biomass expansion of any of the nuisance invaders within the Delta. The fact that DIN, DIP, and N:P have remained quite steady over the last decade, while there have been great expansions in areal extent of *E. densa*, *E. crassipes* and *Ludwigia* spp. during the latter part of this period, suggest that nutrient management alone will not be sufficient to control any of these species.

5. Recommendations

The goal of this review is to synthesize available information to provide insight into major factors controlling the expansion of invasive floating and submerged aquatic vegetation in the Delta. The review addressed three major questions:

1. How does submersed and floating aquatic vegetation support or adversely affect ecosystem services and related beneficial uses?
2. What is known about the spatial and temporal trends in submersed and floating aquatic vegetation in the Delta?
3. What is the relative importance of nutrients versus other factors in promoting observed trends in submersed and floating aquatic vegetation in the Delta?

This review found that the lack of routine monitoring of aquatic macrophytes greatly hindered our ability to summarize, with confidence, the status and trends of floating and SAV in the Delta (Question 2), and to what extent nutrients versus other factors were controlling their occurrence (Question 3).

Given this finding, our recommendations are focused on three principal actions:

1. Implement routine monitoring of macrophytes as well as the major factors that control them.
2. Develop and use a biogeochemical model, coupled with routine monitoring and special studies, to understand the spatial and seasonal nutrient and organic carbon budgets vis a vis major sources of nutrients fueling floating and SAV growth.
3. Conduct a literature review and a pilot research program in floating and SAV control programs.

R1: Implement Routine Monitoring of Invasive Floating and Submersed Aquatic Vegetation. Routine monitoring of floating and submersed aquatic vegetation should be undertaken to assess trends over time and to support ecosystem modeling of the Delta. Grant-funded efforts have been sporadic and there is no plan for on-going rigorous evaluation of patterns and trends. Monitoring should be comprised of a combination of remotely sensed areal coverage and field-based transects to estimate biomass or, ideally, net primary production (through repeated measures of biomass over time to determine rates of turnover). Despite recent advances in remote sensing to include image spectrometry (i.e., hyperspectral remote sensing), problems with misclassification among non-native SAV as well as poor detection of species that occur in smaller patches (e.g., *Stuckenia* sp.) suggest that transect and quadrat monitoring is also needed to follow trends in species composition in space and time. Estimates of biomass/production and areal cover should be conducted in combination with measures of the major factors that control growth of these primary producers, including water column and sediment nutrients and other standard water quality measures (e.g., temperature, salinity, pH, dissolved oxygen), as well as flow rates. Early actions should include the development of a workplan to lay out the key indicators and cost estimates required for monitoring.

R2: Develop a Biogeochemical Model of the Delta, focused on Nutrient and Organic Carbon Fate and Transport. Understanding of factors controlling floating and SAV is critically hampered by the lack of information on nutrient and carbon budgets for the Delta and its subregions. In particular, it is important to quantify the storage in the compartments of the ecosystem (i.e. water, sediment, plant biomass, etc.) and fluxes or exchanges between compartments at varying seasonal and spatial scales and with a variety of water flow and residence time scenarios. Early actions should include the development of a workplan to lay out the key indicators and cost estimates required for monitoring. This information will provide an understanding of whether management of nutrients is likely to aid in control of floating and SAV. To step into model development, three actions should be taken: 1) examine existing models already available to determine suitability for this task, 2) develop a work plan that lays out the modeling strategy, model data requirements, and implementation strategy, and 3) conduct special studies and other monitoring needed to support model development. This includes special studies that quantify N, P, and organic carbon associated with ecosystem compartments as well as uptake, release and flux rates that characterize different reaches of the Delta. Lab and field experiments that test whether macrophyte growth is limited by nutrients in Delta waters could help inform management and predict problem areas. These analyses and experiments should inform hypotheses that can be tested through model development as well as potential future scenarios. The monitoring and modeling teams should collaborate closely to collect high priority data to inform the models.

R3. Review current and potential future control strategies for invasive aquatic macrophytes in the Delta, including mechanical, chemical, biological control, and integrated control methods, as well as barriers that reduce movement of vegetation into sensitive areas or those with heavy human use. Depending on the outcome of R2, nutrient management may be ineffective in controlling invasive floating and SAV. While monitoring, modeling and special studies are under way, determine the degree to which control strategies are supporting beneficial uses and nutrient management objectives going forward. This work should begin by evaluating current and planned control strategies to determine effectiveness at both reducing live biomass and minimizing recycling of nutrients from dead material into additional growth in areas with high residence time. A current USDA-ARS program on integrated control methods for both *E. densa* and *E. crassipes* could help to inform the proposed review.

6. Literature Cited

6.1 Peer-reviewed literature and grey literature (reports)

Akers, R. P., and M. J. Pitcairn. 2006. Biological control of water hyacinth in the Sacramento-San Joaquin Delta year 3 - final report. California Department of Food and Agriculture, Sacramento, California, USA.

Anderson, L. W. J. 1990. Aquatic weed problems and management in the Western United States and Canada. Pages 371–391 in A. H. Pieterse and K. J. Murphy, eds. *Aquatic Weeds: The Ecology and Management of Nuisance Aquatic Vegetation*. New York: Oxford University Press.

Anderson, L. W. J. 2008. Draft conceptual model for DRERIP.

Anderson, L. 2011. Spongeplant: A new aquatic weed threat in the Delta. Cal-IPC News, Spring 2011.

Aoyama, I., H. Nishizaki, and M. Yagi. 1986. Uptake of nitrogen and phosphate, and water purification capacity by water hyacinth (*Eichhornia crassipes* (Mart.) Solms). Vol. 19. *Berichte des Ohara Instituts für landwirtschaftliche Biologie*, Okayama Universität, pp. 77–89.

Barrett, S.C.H. 1980. Sexual reproduction in *Eichhornia crassipes*. II. Seed production in natural populations. *Journal of Applied Ecology* 17:113-124.

Bini, L. M. and S. M. Thomaz. 2005. Prediction of *Egeria najas* and *Egeria densa* occurrence in a large subtropical reservoir (Itaipu Reservoir, Brazil-Paraguay). *Aquatic Botany* 83:227-238.

Borgnis, E. and K. E. Boyer. Salinity tolerance and competition drive distributions of native and invasive submerged aquatic vegetation in the upper San Francisco Estuary. In revision at *Estuaries and Coasts*.

Bossard, C. C., J. M. Randall and M. C. Hoshovsky. 2000. *Invasive plants of California's wildlands*. University of California Press, Berkeley.

Boyd, C. E. 1970. Vascular aquatic plants for mineral nutrient removal from polluted waters. *Economic Botany* 23(1):95-103.

Boyd, C. E. 1976. Accumulation of dry matter, nitrogen and phosphorus by cultivated water hyacinths. *Economic Botany* 30(1):51-56.

Boyer, K. E., J. Lewis, W. Thornton and R. Schneider. 2012. San Francisco Bay Expanded Inventory of Submerged Aquatic Vegetation (Part 1). Final Report for NOAA National Marine Fisheries, Southwest Region Habitat Conservation Division.

Boyer, K. E., E. Borgnis, J. Miller, J. Moderan, and M. Patten. 2013. Habitat Values of Native SAV (*Stuckenia* spp.) in the Low Salinity Zone of San Francisco Estuary. Final Report prepared for the Delta Science Program.

Boyer, K.E., J. Miller, M. Patten, J. Craft, J. Lewis, and W. Thornton. 2015. San Francisco Bay Expanded Inventory of Submerged Aquatic Vegetation, Part 2: Trends in Distribution and Phenotypic

Plasticity. Final Report for NOAA/National Marine Fisheries Service, Southwest Region, Habitat Conservation Division.

Brown, L. R. 2003. Will tidal wetland restoration enhance populations of native fishes? *San Francisco Estuary and Watershed Science* 1(1):1-42.

Brown, L. R. and D. Michniuk. 2007. Littoral fish assemblages of the alien-dominated Sacramento– San Joaquin Delta, California, 1980–1983 and 2001–2003. *Estuaries and Coasts* 30:186-200.

Carignan, R. and J. J. Neiff. 1992. Nutrient dynamics in the floodplain ponds of the Parana River (Argentina) dominated by the water hyacinth *Eichhornia crassipes*. *Biogeochemistry* 17:85-121.

Carr, G. M., H. C. Duthie, and W. D. Taylor. 1997. Models of aquatic plant productivity: a review of the factors that influence growth. *Aquatic Botany* 59:195-215.

Carrillo, Y., A. Guarin, and G. Guillot. 2006. Biomass distribution, growth and decay of *Egeria densa* in a tropical high-mountain reservoir (NEUSA, Colombia). *Aquatic Botany* 85:7-15.

Casabianca, M.-L. and T. Laugier. 1995. *Eichhornia crassipes* production on petroliferous wastewaters: Effects of salinity. *Bioresource Technology* 54:39-43.

Cavalli, G., T. Riis, and A. Baattrup-Pedersen. 2012. Bicarbonate use in three aquatic plants. *Aquatic Botany* 98:57-60.

Center, T. D. and F. A. Dray Jr. 2010. Bottom-up control of water hyacinth weevil populations: Do the plants regulate the insects? *Journal of Applied Ecology* 47:329-337.

Choudhury, M. I., X. Yang, and L.-A. Hansson. 2014. Stream flow velocity alters submerged macrophyte morphology and cascading interactions among associated invertebrate and periphyton assemblages. *Aquatic Botany* 120:333-337.

Clary Jr., R. F. and H. A. George. 1983. Ten years of testing for waterfowl food plants in California. *Cal-Neva Wildlife Transactions* 1983:91-96.

Coetzee, J. A., M. Byrne, and M. P. Hill. 2007. Impact of nutrients and herbivory by *Ecritotarsus catarinensis* on the biological control of water hyacinth, *Eichhornia crassipes*. *Aquatic Botany* 86:179-186.

Cohen, A. N. and J. T. Carlton. 1998. Accelerating invasion rate in a highly invaded estuary. *Science* 279: 555–558

Cohen, R. A., F. P. Wilkerson, A. E. Parker, and E. J. Carpenter. 2014. Ecosystem-scale rates of primary production within wetland habitats of the northern San Francisco Estuary. *Wetlands* 34:759-774.

Cook, C. D. K. and K. Urmi-Kořnig. 1984) A revision of the genus *Egeria* (Hydrocharitaceae). *Aquatic Botany* 19:73–96.

- Cornwell, J. C., P. M. Glibert, and M. S. Owens. 2014. Nutrient fluxes from sediments in the San Francisco Bay Delta. *Estuaries and Coasts* 37:1120-1133.
- Cornwell, D. A., J. Zoltek Jr., C. D. Patrinely, T. deS. Furman, and J. I. Kim. 1977. Nutrient removal by water hyacinths. *Journal of the Water Pollution Control Federation* 49(1):57-65.
- [DBW] California Department of Boating and Waterways. 2005. *Egeria densa* Control Program. Sacramento, CA. 70 p.
- DeBusk, T. A. and F. E. Dierberg. 1989. Effects of nutrient availability on water hyacinth standing crop and detritus deposition. *Hydrobiologia* 174:151-159.
- Desougi, L. A. 1984. Mineral nutrient demands of the water hyacinth (*Eichhornia crassipes* (Mart.) Solms) in the White Nile. *Hydrobiologia* 110:99-108.
- Durand, J. R. 2014. Restoration and reconciliation of novel ecosystems: Open water habitat in the Sacramento-San Joaquin Delta. Ph.D. dissertation, University of California, Davis.
- [DWR] Department of Water Resources. 1970-2000 Water quality conditions in the Sacramento-San Joaquin Delta. Sacramento, CA.
- Engelhardt, K. A. M. and M. E. Ritchie. 2002. The effect of aquatic plant species richness on wetland ecosystem processes. *Ecology* 83:2911-2924.
- Enright, C. and S. D. Culbertson. 2010. Salinity trends, variability, and control in the northern reach of the San Francisco Estuary. *San Francisco Estuary and Watershed Science* 7(2):1-28.
- Feijóo, C., M. E. García, F. Momo, and J. Toja. 2002. Nutrient absorption by the submerged macrophyte *Egeria densa* Planch.: Effect of ammonium and phosphorus availability in the water column on growth and nutrient uptake. *Limnetica* 21(1-2):03-104.
- Ferreiro, N., C. Feijoo, A. Giorgi, and L. Leggieri. 2011. Effects of macrophyte heterogeneity and food availability on structural parameters of the macroinvertebrate community in a Pampean stream. *Hydrobiologia* 664:199-211.
- Finlayson B. J. 1983. Water hyacinth: threat to the Delta? *Outdoor California* 44:10-14.
- Foe, C., A. Ballard, and S. Fong. 2010. Nutrient concentrations and biological effects in the Sacramento-San Joaquin Delta. Central Valley Regional Water Quality Control Board.
- Foschi, P. G., G. Fields, G., and H. Liu. 2004. Detecting a spectrally variable subject in color infrared imagery using data-mining and knowledge-engine methods. *PRRS04-018*.
- Frost-Christensen, H. and K. Sand-Jensen. 1995. Comparative kinetics of photosynthesis in floating and submerged *Potamogeton* leaves. *Aquatic Botany* 51:121-134.

- Gantes, H. P. and A. S. Caro. 2001. Environmental heterogeneity and spatial distribution of macrophytes in plain streams. *Aquatic Botany* 70:225-236.
- Getsinger, K. D. 1982. The life cycle and physiology of the submersed angiosperm *Egeria densa* Planch. in Lake Marion, South Carolina. PhD. Dissertation. Clemson University, 104 pp.
- Glibert, P. M. 2010. Long-term changes in nutrient loading and stoichiometry and their relationships with changes in the food web and dominant pelagic fish species in the San Francisco Estuary, California. *Reviews in Fisheries Science* 18:211-232.
- Gopal B. 1987. Water hyacinth. Elsevier, Amsterdam.
- Grace, J. B. and R. G. Wetzel. 1978. The production biology of Eurasian Watermilfoil (*Myriophyllum spicatum* L.): A review. *Journal of Aquatic Plant Management* 16:1-11.
- Greenfield, B. K., G. S. Siemering, J. C. Andrews, M. Rajan, S. P. Andrews Jr., and D. F. Spencer. 2007. Mechanical shredding of water hyacinth (*Eichhornia crassipes*): Effects on water quality in the Sacramento-San Joaquin River Delta, California. *Estuaries and Coasts* 30:627-640.
- Grimaldo, L. and Z. Hymanson. What is the Impact of the Introduced Brazilian Waterweed *Egeria densa* to the Delta Ecosystem? Interagency Ecological Program Newsletter.
- Grimaldo, L. F., A. R. Stewart, and W. Kimmerer. 2009. Dietary segregation of pelagic and littoral fish assemblages in a highly modified tidal freshwater estuary. *Marine Coastal Fisheries: Dynamics, Management & Ecosystems Sciences* 1:000-000.
- Gruber, R. K. and W. M. Kemp. 2010. Feedback effects in a coastal canopy-forming submersed plant bed. *Limnology and Oceanography* 55(6):2285-2298.
- Gunnarsson, C. C. and C. M. Peterson. 2007. Water hyacinths as a resource in agriculture and energy production: A literature review. *Waste Management* 27:117-129.
- Haller, W. T. and D. L. Sutton. 1973. Effect of pH and high phosphorous concentrations on growth of waterhyacinth. *Hyacinth Control Journal* 11:59-61.
- Heard, T. A. and S. L. Winterton. 2000. Interactions between nutrient status and weevil herbivory in the biological control of water hyacinth. *Journal of Applied Ecology* 37:117-127.
- Henninger, T. O., P. W. Froneman, N. B. Richoux, and A. N. Hodgson. 2009. The role of macrophytes as a refuge and food source for the estuarine isopod *Exosphaeroma hylcoetes* (Barnard, 1940). *Estuarine, Coastal and Shelf Science* 82:285-293.
- Hestir, E. L. 2010. Trends in estuarine water quality and submerged aquatic vegetation invasion Dissertation, University of California, Davis. 146 p.

- Hestir, E. L., S. Khanna, M. E. Andrew, M. J. Santos, J. H. Viers, J. A. Greenberg, S. S. Rajapakse, and S. L. Ustin. 2008. Identification of invasive vegetation using hyperspectral remote sensing in the California Delta ecosystem. *Remote Sensing of Environment* 112:4034–4047.
- Hestir, E. L., D. H. Schoellhamer, T. Morgan-King, and S. L. Ustin. 2013. A step decrease in sediment concentration in a highly modified tidal river delta following the 1983 El Niño floods. *Marine Geology* 345:304-313.
- Hill, J. M. 2014. Investigations of growth metrics and $\delta^{15}\text{N}$ values of water hyacinth (*Eichhornia crassipes*, (Mart.) Solms-Laub) in relation to biological control. *Aquatic Botany* 114:12-20.
- Hofstra, D. E., J. Clayton, J. D. Green, and M. Auger. 1998. Competitive performance of *Hydrilla verticillata* in New Zealand. *Aquatic Botany* 63:305-324.
- Hussner, A., H. P. Hoelken, and P. Jahns. 2010. Low light acclimated submerged freshwater plants show a pronounced sensitivity to increasing irradiances. *Aquatic Botany* 93:17-24.
- Hussner, A., D. Hofstra, P. Jahns, and J. Clayton. 2014. Response capacity to CO₂ depletion rather than temperature and light effects explain the growth success of three alien Hydrocharitaceae compared with native *Myriophyllum triphyllum* in New Zealand. *Aquatic Botany* 120:205-211.
- Jassby 2006. *San Francisco Estuary and Watershed Science* (6)1.
- Jassby, A. D. and J. E. Cloern. 2000. Organic matter sources and rehabilitation of the Sacramento-San Joaquin Delta (California, USA). *Aquatic Conservation* 10:323-352.
- Jassby A. D., J. E. Cloern, and B. E. Cole. 2002. Annual primary production: patterns and mechanisms of change in a nutrient rich tidal ecosystem. *Limnology and Oceanography* 47:698–712.
- Jepson, W. L. 1905. Where ducks dine. *Sunset Magazine*.
- Julien, M. H., M. P. Hill, T. D. Center, and D. Jianqing, eds. 2001. Biological and integrated control of water hyacinth, *Eichhornia crassipes*. Proceedings of the Second Meeting of the Global Working Group for the Biological and Integrated Control of Water Hyacinth, Beijing, China.
- Kato-Noguchi, H., M. Moriyasu, O. Ohno, and K. Suenaga. 2014. Growth limiting effects on various terrestrial plant species by an allelopathic substance, loliolide, from water hyacinth. *Aquatic Botany* 117:56-61.
- Kennedy, T. L., L. A. Horth, and D. E. Carr. 2009. The effects of nitrate loading on the invasive macrophyte *Hydrilla verticillata* and two common, native macrophytes in Florida. *Aquatic Botany* 91:253-256.
- Kenow, K. P., J. E. Lyon, R. K. Hines, and A. Elfessi. 2007. Estimating biomass of submersed vegetation using a simple rake sampling technique. *Hydrobiologia* 575:447-454.

- Khanna, S., M. J. Santos, E. L. Hestir, and S. L. Ustin 2012. Plant community dynamics relative to the changing distribution of a highly invasive species, *Eichhornia crassipes*: a remote sensing perspective. *Biological Invasions*.
- Kim, Y. and W.-J. Kim. 2000. Roles of water hyacinths and their roots for reducing algal concentration in the effluent from waste stabilization ponds. *Water Research* 34(13):3285-3294.
- Lund, J., E. Hanak, W. Fleenor, R. Howitt, J. Mount, and P. Moyle. 2007. Envisioning futures for the Sacramento-San Joaquin Delta. Public Policy Institute of California, San Francisco, California.
- Madsen, J. D. 1997. Methods for management of nonindigenous aquatic plants. Pp. 145–171. In J. O. Luken and J. W. Thieret (eds.), *Assessment and Management of Plant Invasions*. Springer, New York.
- Malik, A. 2007. Environmental challenge vis a vis opportunity: The case of water hyacinth. *Environment International* 33:122-138.
- Marín, V. H., A. Tironi, L. E. Delgado, M. Contreras, F. Novoa, M. Torres-Gómez, R. Garreaud, I. Vila, and I. Serey. 2009. On the sudden disappearance of *Egeria densa* from a Ramsar wetland site of Southern Chile: A climatic event trigger model. *Ecological Modelling*
- Marlina, D., M. P. Hill, B. S. Ripley, A. J. Strauss, and M. J. Byrne. 2013. The effect of herbivory by the mite *Orthogalumna terebrantis* on the growth and photosynthetic performance of water hyacinth (*Eichhornia crassipes*). *Aquatic Botany* 104:60-69.
- Martin, G. D. and J.A. Coetzee. 2014. Competition between two aquatic macrophytes, *Lagarosiphon major* (Ridley) Moss (Hydrocharitaceae) and *Myriophyllum spicatum* Linnaeus (Haloragaceae) as influenced by substrate sediment and nutrients. *Aquatic Botany* 114:1–11.
- Matheson, F. E., M. D. de Winton, J. S. Clayton, T. M. Edwards, and T. J. Mathieson. 2005. Responses of vascular (*Egeria densa*) and non-vascular (*Chara globularis*) submerged plants and oospores to contrasting sediment types. *Aquatic Botany* 83:141-153.
- Meerhoff, M., Mazzeo N., Moss B. et al. 2003. The structuring role of free-floating versus submerged plants in a subtropical shallow lake. *Aquatic Ecology* 37:377–391.
- Mony, C., T.J. Koschnick, W.T. Haller, and S. Muller. 2007. Competition between two invasive Hydrocharitaceae (*Hydrilla verticillata* (L.f.) (Royle) and *Egeria densa* (Planch)) as influenced by sediment fertility and season. *Aquatic Botany* 86:236–242.
- Moran, P.J. 2006. Water nutrients, plant nutrients, and indicators of biological control on waterhyacinth at Texas field sites. *Journal of Aquatic Plant Management* 44: 109-114.
- Nobriga, M. L. 2009. Bioenergetic modeling evidence for a context-dependent role of food limitation in California's Sacramento-San Joaquin Delta. *California Fish and Game* 95(3):111-121.

- Nobriga, M. L., F. Feyrer, R. D. Baxter, and M. Chotkowski. 2005. Fish community ecology in an altered river delta: spatial patterns in species composition, life history strategies, and biomass. *Estuaries* 28(5):776-785.
- Ogg Jr., A. G., V. F. Bruns, and A. D. Kelley. 1969. Response of sago pondweed to periodic removal of topgrowth. *Weed Science* 17(2):139-141.
- [OTA] Office of Technology Assessment. 1993. Harmful Non-Indigenous Species in the United States. Washington, DC: U.S. Congress.
- Penfound W. T. and T. T. Earle. 1948. The biology of water hyacinth. *Ecological Monographs* 18:447-472.
- Pennington, T. G. and M. D. Sytsma. 2009. Seasonal changes in carbohydrate and nitrogen concentrations in Oregon and California populations of Brazilian *Egeria* (*Egeria densa*). *Invasive Plant Science and Management* 2:120-129.
- Petrucio, M. M. and F. A. Esteves. 2000. Uptake rates of nitrogen and phosphorous in the water by *Eichhornia crassipes* and *Salvinia auriculata*. *Revista Brasileira de Biologia* 60(2):229-236.
- Pierini, S. A. and S. M. Thomaz. 2004. Effects of inorganic carbon source on photosynthetic rates of *Egeria najas* Planchon and *Egeria densa* Planchon (Hydrocharitaceae). *Aquatic Botany* 78:135-146.
- Reddy, K. R. 1983. Fate of nitrogen and phosphorus in a waste-water retention reservoir containing aquatic macrophytes. *Journal of Environmental Quality* 12:137-141.
- Reddy, K. R. and W. F. DeBusk. 1984. Growth characteristics of aquatic macrophytes cultured in nutrient-enriched water: I. water hyacinth, water lettuce, and pennywort. *Economic Botany* 38(2):229-239.
- Reddy, K. R. and W. F. DeBusk. 1985. Nutrient removal potential of selected aquatic macrophytes. *Journal of Environmental Quality* 14(4):459-462.
- Reddy, K. R. and J. C. Tucker. 1983. Productivity and nutrient uptake of water hyacinth, *Eichhornia crassipes* I. effect of nitrogen source. *Economic Botany* 37(2):237-247.
- Reddy, K. R., J. C. Tucker, and W. F. DeBusk. 1987. The role of *Egeria* in removing nitrogen and phosphorous from nutrient enriched waters. *Journal of Aquatic Plant Management* 25:14-19.
- Reddy, K. R., M. Agami and J. C. Tucker. 1989. Influence of nitrogen supply rates on growth and nutrient storage by waterhyacinth (*Eichhornia crassipes*) plants. *Aquatic Botany* 36:33-43.
- Reddy, K. R., M. Agami and J. C. Tucker. 1990. Influence of phosphorous on growth and nutrient storage by water hyacinth (*Eichhornia crassipes* Mart. Solms.) plants. *Aquatic Botany* 37:355-265.
- Rierner, D. N. and S. J. Toth. 1969. A survey of the chemical composition of *Potamogeton* and *Myriophyllum* in New Jersey. *Weed Science* 17(2):219-223.

- Riis, T., B. Olesen, J. S. Clayton, C. Lambertini, H. Brixa, and B. K. Sorrell. 2012. Growth and morphology in relation to temperature and light availability during the establishment of three invasive aquatic plant species. *Aquatic Botany* 102:56-64.
- Ripley, B. S., E. Muller, M. Behenna, G. M. Whittington-Jones, and M. P. Hill. 2006. Biomass and photosynthetic productivity of water hyacinth (*Eichhornia crassipes*) as affected by nutrient supply and mirid (*Eccritotarus catarinensis*) biocontrol. *Biological Control* 39:392-400.
- Rodrigues, R. B. and S. M. Thomaz. 2010. Photosynthetic and growth responses of *Egeria densa* to photosynthetic active radiation. *Aquatic Botany* 92:281-284.
- Rogers, H. H. and D. E. Davis. 1972. Nutrient removal by waterhyacinth. *Weed Science* 20(5):423-428.
- Santos M. J., Khanna S., E. L. Hestir, M. E. Andrew, S. S. Rajapakse, J. A. Greenberg, L. W. J. Anderson, and S. L. Ustin. 2009. Use of hyperspectral remote sensing to evaluate efficacy of aquatic plant management in the Sacramento-San Joaquin River Delta, California. *Invasive Plant Science and Management* 2:216–229.
- Santos, M. J., L. W. Anderson, and S. L. Ustin. 2011. Effects of invasive species on plant communities: an example using submersed aquatic plants at the regional scale. *Biological Invasions* 13:443-457.
- Scheffer, M., E. Jeppesen. 2007. Regime shifts in shallow lakes. *Ecosystems* 10:1–35.
- Schultz, R. and E. Dibble. 2012. Effects of invasive macrophytes on freshwater fish and macroinvertebrate communities: the role of invasive plant traits. *Hydrobiologia* 684:1-14.
- Schoellhamer, D. H. 2011. Sudden clearing of estuarine waters upon crossing the threshold from transport to supply regulation of sediment transport as an erodible sediment pool is depleted: San Francisco Bay, 1999. *Estuaries and Coasts* 34:885–899.
- Shanab, S. M. M., E. A. Shalaby, D. A. Lightfoot, and H. A. El-Shemy. 2010. Allelopathic effects of water hyacinth [*Eichhornia crassipes*]. *PLoS ONE* 5(10): e13200.doi:10.1371/journal.pone.0013200
- Smart, R. M. and J. W. Barko. 1990. Effects of water chemistry on aquatic plants: Interactive effects of inorganic carbon and nitrogen on biomass production and plant nutrition. Department of the Army, Technical Report A-90-4.
- Smith, S. D. P. 2014. The roles of nitrogen and phosphorus in regulating the dominance of floating and submerged aquatic plants in a field mesocosm experiment. *Aquatic Botany* 112:1-9.
- Sosiak, A. 2002. Long-term response of periphyton and macrophytes to reduced municipal nutrient loading to the Bow River (Alberta, Canada). *Canadian Journal of Fisheries and Aquatic Science* 59:987-1001.

- Sousa, W. T. Z., S. M. Thomaz, and K. J. Murphy. 2010. Response of native *Egeria najas* Planch. and invasive *Hydrilla verticillata* (L.f.) Royle to altered hydroecological regime in a subtropical river. *Aquatic Botany* 92:40-48.
- Spencer, D. F., G. G. Ksander. 2005. Seasonal growth of waterhyacinth in the Sacramento/San Joaquin Delta, California. *Journal of Aquatic Plant Management* 43:91–94.
- Spencer, D. F., G. G. Ksander, M. J. Donovan, P. S. Liow, W. K. Chan, B. K. Greenfield, S. B. Shonkoff, and S. P. Andrews. 2006. Evaluation of waterhyacinth survival and growth in the Sacramento Delta, California, following cutting. *Journal of Aquatic Plant Management* 44:50-60.
- Steinhardt, T. and U. Selig. 2011. Influence of salinity and sediment resuspension on macrophyte germination in coastal lakes. *Journal of Limnology* 70:11-20.
- Stewart, R. M., A. F. Cofrancesco, and L.G. Bezark. 1988. Biological control of waterhyacinth in the California Delta. U.S. Army Corps of Engineers Waterways Experiment Station, Technical Report A-88-7. U.S Army Corps of Engineers, Washington, D.C.
- Summers, J. E., R. G. Ratcliffe, and M. B. Jackson. 2000. Anoxia tolerance in the aquatic monocot *Potamogeton pectinatus*: Absence of oxygen stimulated elongation in association with an unusually large Pasteur effect. *Journal of Experimental Botany* 51(349):1413-1422.
- Tipping, P. W., A. Sosa, E. N. Pokorny, J. Foley, D. C. Schmitz, J. S. Lane, L. Rodgers, L. McCloud, P. Livingston, M. S. Cole, and G. Nichols. 2014a. Release and establishment of *Megamelus scutellaris* (Hemiptera: Delphacidae) on waterhyacinth in Florida. *Florida Entomologist* 97:804-806.
- Tipping, P. W., M. R. Martin, E. N. Pokorny, K. R. Nimmo, D. L. Fitzgerald, F. A. Dray, Jr., and T. D. Center. 2014b. Current levels of suppression of waterhyacinth in Florida, USA. *Biological Control* 71:65-69.
- Thomaz, S. M., P. A. Chambers, S. A. Pierini, and G. Pereira. 2007. Effects of phosphorus and nitrogen amendments on the growth of *Egeria najas*. *Aquatic Botany* 86:191-196.
- Thouvenot, L., C. Puech, L. Martinez, J. Haury, and G. Thiébaud. 2012. Strategies of the invasive macrophyte *Ludwigia grandiflora* in its introduced range: Competition, facilitation or coexistence with native and exotic species? *Aquatic Botany* 107:8-16.
- Toft, J. D., C. A. Simenstad, J. R. Cordell, and L. F. Grimaldo. 2003. The effects of introduced water hyacinth on habitat structure, invertebrate assemblages, and fish diets. *Estuaries* 26:746–758.
- Ustin, S. L., J. A. Greenberg, E. L. Hestir, S. Khanna, M. J. Santos, M. E. Andrew, M. Whiting, S. Rajapakse, and M. Lay. 2007. Mapping invasive plant species in the Sacramento-San Joaquin Delta using hyperspectral imagery. California Department of Boating and Waterways, Sacramento, CA.
- Ustin, S.L., J. A. Greenberg, M. J. Santos, S. Khanna, E. L. Hestir, P. J. Haverkamp, and S. Kefauver. 2008. Mapping invasive plant species in the Sacramento-San Joaquin Delta using hyperspectral imagery. California Department of Boating and Waterways, Sacramento, CA.

- Van, T. K., G. S. Wheeler, and T. D. Center. 1997. Competition between *Hydrilla verticillata* and *Vallisneria americana* as influenced by soil fertility. *Aquatic Botany* 62:225-233.
- Vanderstukken, M., N. Mazzeo, W. van Colen, S. A. J. Declerck, and K. Muylaert. 2011. Biological control of phytoplankton by the subtropical submerged macrophytes *Egeria densa* and *Potamogeton illinoensis*: a mesocosm study. *Freshwater Biology* 56:1837-1849.
- Villamagna, A. M., and B. R. Murphy. 2010. Ecological and socio-economic impacts of invasive water hyacinth (*Eichhornia crassipes*): a review. *Freshwater Biology* 55:282-298.
- Wagner, R. W., M. Stacey, L. R. Brown, and M. Dettinger. 2011. Statistical models of temperature in the Sacramento-San Joaquin Delta under climate-change scenarios and ecological implications. *Estuaries and Coasts* 34:544-556.
- Weragoda, S.K., N. Tanaka, K. B. S. N. Jinadasa, and Y. Sasaki. 2008. Impacts of plant (*Egeria densa*) density and nutrient composition on nitrogen transformation mechanisms in laboratory microcosms. *Journal of Freshwater Ecology* 24:393-401.
- Wilkerson, F. P., R. C. Dugdale, V. E. Hogue, and A. Marchi. 2006. Phytoplankton blooms and nitrogen productivity in San Francisco Bay. *Estuaries and Coasts* 29:401-416.
- Williams, A. E., H. C. Duthie, and R. E. Hecky. 2005. Water hyacinth in Lake Victoria: Why did it vanish so quickly and will it return? *Aquatic Botany* 81:300-314.
- Williams, A. E., H. C. Duthie, and R. E. Hecky. 2007. Water hyacinth decline across Lake Victoria—Was it caused by climatic perturbation or biological control? A reply. *Aquatic Botany* 87:94-96.
- Wilson, J. R. U., O. Ajuonu, T. D. Center, M. P. Hill, M. H. Julien, F. F. Katagira, P. Neuenschwander, S. W. Njoka, J. Ogwang, R. H. Reeder, and T. Van. 2007. The decline of water hyacinth on Lake Victoria was due to biological control by *Neochetina* spp. *Aquatic Botany* 87:90-93.
- Wilson, J. R., N. Holst, and M. Rees. 2005. Determinants and patterns of population growth in water hyacinth. *Aquatic Botany* 81:51-67.
- Wright and Schoellhamer. 2004. San Francisco Estuary and Watershed Science (2)2.
- Wu, Z., P. Deng, X. Wu, S. Luo, and Y. Gao. 2007. Allelopathic effects of the submerged macrophyte *Potamogeton malaianus* on *Scenedesmus obliquus*. *Hydrobiologia* 592:465-474.
- Xie, Y., M. Wen, D. Yu, and Y. Li. 2004. Growth and resource allocation of water hyacinth as affected by gradually increasing nutrient concentrations. *Aquatic Botany* 79:257-266.
- Xie, Y. and D. Yu. 2003. The significance of lateral roots in phosphorus (P) acquisition of water hyacinth (*Eichhornia crassipes*). *Aquatic Botany* 75:311-321.

Yarrow, M., V. H. Marin, M. Finlayson, A. Tironi, L. E. Delgado, and F. Fischer. 2009. The ecology of *Egeria densa* Planchon (Liliopsida: Alismatales): A wetland ecosystem engineer? *Revista Chilena de Historia Natural* 82: 299-313.

You, W., D. Yu, D. Xie, L. Yu, W. Xiong, and C. Han. 2014. Responses of the invasive aquatic plant water hyacinth to altered nutrient levels under experimental warming in China. *Aquatic Botany* 119:51-56.

Zhang, M., T. Cao, L. Ni, P. Xie, G. Zhu, A. Zhong, J. Xu, and H. Fu. 2011. Light-dependent phosphate uptake of a submersed macrophyte *Myriophyllum spicatum* L. *Aquatic Botany* 94:151-157.

6.2 Local and regional press reports

Anderson, L. and P. Akers. 2011. Spongeplant: A new aquatic weed threat in Delta. *Cal-IPC News* 19(1):45.

Breitler, A. 2012, December 22. Entangled: Owner of marina says water hyacinth, bureaucracy choking life out of business. *The Record*. Retrieved from http://www.recordnet.com/article/20121222/A_NEWS/212220315

Breitler, A. 2014, October 22. Bill Wells: Hyacinth a 'disaster,' possible national security threat. *The Record*. Retrieved from <http://www.recordnet.com/>

Breitler, A. 2014, October 24. Legislators: Help us with hyacinth. *The Record*. Retrieved from <http://www.recordnet.com/>

Breitler, A. 2014, October 28. Another hyacinth plan hatches. *The Record*. Retrieved from <http://www.recordnet.com/>

Breitler, A. 2014, November 8. Stockton mayor floats an idea: Bring in manatees. *The Record*. Retrieved from <http://www.recordnet.com/>

Breitler, A. 2014, November 14. Feds, state may join the hyacinth fray. *The Record*. Retrieved from <http://www.recordnet.com/>

Breitler, A. 2014, December 15. Delta: As hyacinth clears out, focus turns to next year. *The Record*. Retrieved from <http://www.recordnet.com/>

Burgarino, P. 2013, December 6. State begins using mechanical harvesters to control water hyacinth in Delta trouble spots. *Contra Costa Times*. Retrieved from http://www.contracostatimes.com/contracosta-times/ci_24673609/state-begins-using-mechanical-harvesters-control-water-hyacinth

Daly, T. 2014, October 27. State claims it's doing everything possible to eradicate water hyacinth. *ABC News10*. Retrieved from <http://www.news10.net/>

Ibarra, R. 2014, November 17.

Task force to control hyacinth in the delta. *Capital Public Radio*. Retrieved from <http://www.caprado.org/>

Martinez, L. 2014, November 3. Removing hyacinth clogging Port of Stockton a slow process as dry year has plant thriving. *CBS Sacramento*. Retrieved from <http://sacramento.cbslocal.com/>.

Ruhstaller, L. 2014, November 22. Guest view: Solution to weedy problem? *The Record*. Retrieved from <http://www.recordnet.com/>

Theuri, M. 2013. Water hyacinth – Can its aggressive invasion be controlled? UNEP Global Environmental Alert Service (GEAS).

(No author). 2014. Our viewpoint: Green water = problem, *The Record*. Retrieved from http://www.recordnet.com/article/20141015/OPINION/141019724/101034/A_OPINION.

DRAFT

7.0 Appendices

7.1 Comment Matrix and Responses to Science Working Group

Author	Page	Comment	Response
Conrad	ii	Executive Summary, first paragraph, second sentence - What type of impairment? Ecosystem?	added word "ecosystem"
Conrad	ii	Executive Summary, first paragraph, last sentence - Only three (major) questions follow (not four).	fixed
Conrad	ii	Executive Summary, Finding#2: Lack of a routine monitoring program hampers our ability to discern recent spatial and temporal trends. - This seems like a recommendation rather than a finding. The finding is that Egeria and water hyacinth dominate the macrophyte community in the Delta and may be expanding. The lack of adequate monitoring is addressed in your recommendations below so I suggest removing this sentence here.	changed the findings section to incorporate this
Conrad	iii	Executive Summary, Finding#5: first sentence - Sea level rise should also be mentioned here, perhaps?	did not mention; much less important to species that can grow in range of depths than other factors
Conrad	1	Under Chapter 1, Section 1.1, fourth sentence: The Delta is widely recognized as in "crisis"... - Incomplete sentence.	fixed
Conrad	3	Under Chapter 1, Section 1.2, Second paragraph - Re-start numbering (of key questions) at #1.	fixed
Conrad	4	Under section 2.1, the first two sentences were highlighted by the commenter but no comment provided.	not sure why highlighted by reviewer either
Conrad	11	Figure 2.5 caption - The caption says that the Google Earth imagery was "digitized and ground truthed." How was the ground-truthing conducted? It seems hard to believe that a species-level determination of submersed vegetation can be done from visual review of Google Earth imagery, especially given that analysis of hyperspectral imagery was not always reliable for species determination of SAV. The reference for this is Boyer et al. 2015, which is not provided in the Google Drive of references. Is it possible to see this information.	additional explanation added. Species level is pretty easy to determine within Suisun Bay, as ground-truthing (visiting all areas) by boat, and performing rake sampling in a subset of these areas confirmed that <i>Stuckenia pectinata</i> is nearly mono-typic there. In the Delta where there are many more species, this methodology does not work well as described by Ustin research group. Yes, all references will be added to the Google Drive.
Conrad	12	4th paragraph, reference to Breiter 2014 - This citation is not provided in the Literature Cited.	fixed

Conrad	13	Second paragraph on <i>Stuckenia sp.</i> , first sentence - See comment above on Fig. 2.5. Was <i>Stuckenia</i> coverage in 1993 and 2002 also ground-truthed?	No, it was not. Additional explanation added that we assumed that <i>Stuckenia</i> was the only species present then as in 2011-2012 time period. The distinct growth form of <i>Stuckenia</i> can be seen in the previous images
Conrad	15	Section 3.1, first paragraph, highlighted sentences from "In contrast, dense canopies... to "...leading to predation on smaller adult and juvenile native fish" - Some of the following paragraph (e.g., highlighted passage) reads as if these conceptual ideas have been well established. Not the case for all of these assertions. Suggest revising the language to be less absolute.	Revised to clearly state where conceptual ideas have not been backed up by data.
Conrad	16	Under section 3.1.1, first paragraph, fourth sentence " <i>E. densa</i> sheds some biomass in winter but does not fully senesce (Fig. 2.2) - Santos et al. 2011 may be another reference to use for this assertion.	Added this reference
Conrad	17	Section 3.1.3 - Consider re-naming this "Effects on hydrodynamic and sediment processes" or some version of this. "Habitat" can mean a lot of things- from substrate to food web to water quality. I expected this section to address vegetation effects on water quality given that it addressed suspended sediment. Also, it seems more intuitive to discuss effects of vegetation on the physical habitat (like water velocity) and water quality before discussing food web effects. Right now the organization discusses food web ("trophic support") in the middle of these physical aspects.	Revised the names and order of the sections in this chapter.
Conrad	17	Under section 3.1.3, third sentence, "Submerged plants may also ..." - I think Shruti Khanna's 2012 paper present a conceptual model that expresses this idea	yes, cited and this is discussed in detail in chapter 4
Conrad	18	Under section 3.1.3, last paragraph on floating vegetation - This is a very short section on habitat alteration by floating vegetation. Check Shruti Khanna's paper for more detail that could be fleshed out here...	additional detail added.
Conrad	18	Under section 3.1.4, first paragraph, first sentence - A useful reference that could be included in this synthesis is: Schultz, R., and E. Dibble. 2012. Effects of invasive macrophytes on freshwater fish and macroinvertebrate communities: the role of invasive plant traits. <i>Hydrobiologia</i> 684:1-14.	thanks, added the reference.
Conrad	19	Under section 3.1.4, Second paragraph under <i>Eichhornia crassipes</i> , 2nd sentence - Awkward sentence, should be revised. Shift invertebrate	sentence revised

		foods available relative to what?	
Conrad	19	Under section 3.1.4 third paragraph under <i>Eichhornia crassipes</i> - This section seems fairly brief, given the amount of published work on the subject. To help readers process the host of effects that aquatic veg can have on water quality, it may be useful to deal with each water quality parameter one by one, and highlight the important results (e.g. subsections for DO, pH, nutrients. And what about temperature? It seems that should be discussed as well if there is literature suggesting the AV may have effects. Examples help too...	Each effect now discussed one by one.
Conrad	19	Under section 3.1.5. Changes in Water Quality, 1st paragraph, first sentence - These effects should be described in more detail here, with citations. I expected the rest of this paragraph to delve into effects on DO, but instead the next sentence shifts gears into nutrients.	More detail and citations added.
Conrad	19	Under section 3.1.5. Changes in Water Quality, 1st paragraph, 2nd sentence - Interesting...is there a citation for this?	yes, added citations
Conrad	20	Under section 3.1.5 2nd paragraph, 1st sentence - Does SAV contribute DO or limit it? There are diurnal swings in DO in dense <i>Egeria</i> beds.	expanded this section and discussed diurnal swings
Conrad	20	Under section 3.1.5, 2nd paragraph, 1st sentence (Meerhoff et al. 2003) - This reference is not listed in the Literature Cited section.	fixed
Conrad	24	Under section 4.1.1 Light, 2nd paragraph, last two sentences - Seems like it's worth noting here that rigorous study of species-specific effects on local water quality conditions (such as turbidity) have not been done- perhaps this is an area worthy of more study?	yes, added this
Conrad	24	Under section 4.1.1. Light, third paragraph, second sentence - The difference between treatments in the study described is unclear in this sentence. 2x greater...depth...light?	clarified in the text
Conrad	24	Under section 4.1.1 Light, third paragraph, last sentence - Again, the conditions tested in this experiment are not completely clear in this sentence. Why not state what the light exposure treatments were?	light exposure treatments now given

Conrad	24	Under section 4.1.2 Temperature, reference for Knowles and Cayan 2002 - This reference is missing in the literature cited section. Also, a more recent reference that projects Delta water (rather than air) temperatures is: 1. Wagner RW, Stacey M, Brown LR, Dettinger M (2011) Statistical models of temperature in the Sacramento-San Joaquin Delta under climate-change scenarios and ecological implications. <i>Estuaries and Coasts</i> 34: 544-556.	added this citation
Conrad	25	Under section 4.1.3 Salinity, first paragraph, first sentence - This first paragraph provides helpful background on how this aspect of water quality responds to current management practices and how it has been changing over time. It also puts the Delta plant life in context. I think this would be nice to do for light (i.e., turbidity) and for temperature as well. There are several papers that discuss a trend of water clearing in the Delta. You already do this to some extent with temperature, but it could be expanded a little (see above comment for an updated reference).	did some expanding of these sections
Conrad	25	Under section 4.1.3 Salinity, first paragraph, sentence related to summer and fall salinity in last 25 years due to management of fresh water - Reduction?	yes, reduction
Conrad	26	Under section 4.1.3 Salinity, second paragraph, reference to Figure 4.4 - I find the axes below of % change a bit confusing. What is the reference condition? What does 1000% change at 0ppt mean?	change from initial conditions over 3 month experiment. Tried to make this more clear in the text.
Conrad	27	Under section 4.1.3 Salinity, first paragraph, second sentence - Similar to (Engle's) above comment: I understand this text, but I don't see this message reflected in Fig. 4.4. It looks like a declining trend in <i>Stuckenia</i> biomass with increasing salinity.	there was no change in biomass at a salinity of 15 over the course of the experiment. There was a great increase in biomass at all lower salinities. Yes, there is a declining biomass with increasing salinity.
Conrad	27	Under section 4.1.3 Salinity, second paragraph - Given that there is little detail above on the distribution of these species, I'm not sure what this surmising is based on.	added citations for tolerances
Conrad	27	Under section 4.1.4, first paragraph, second sentence - And what are primary factors determining pH in the Delta?	did not address this -- out of my scope
Conrad	28	Under section 4.1.5, third paragraph, second sentence - Add a ")" after the words "0 to 4 kg/g sediment"	added

Conrad	29	Under section 4.1.6 Flow, first paragraph, second sentence - Erin Hestir's dissertation includes an analysis of maximum water velocity thresholds for SAV establishment in the Delta (I have a copy if you would like to review): 1. Hestir EL (2010) Trends in estuarine water quality and submerged aquatic vegetation invasion [Dissertation]. Davis: University of California, Davis. 146 p.	edited and added citation
Conrad	31	Under section 4.1.8, second paragraph regarding reference to Santos et al. 2011 - An important result from this paper that I don't see highlighted here is that Egeria sustains its biomass in the fall/winter, giving it a head-start in growth in the following spring compared to other species.	yes, had this elsewhere but added it here
Conrad	35	Under section 5. Recommendations, R2 - More detail of the vision here? See major comment in the accompanying Word File (my general comment #4)	Tried to give more detail for this recommendation. Note that I did not receive a Word file with general comments from Louise
Cornwell	N/A	General Comments: Overall, this is a good analysis of control of invasive/native macrophytes in the Bay/Delta. As a biogeochemist, my comments are focused on nutrient-related regulation of plant success and the effects of invasive plants on Bay/Delta nutrient cycling and balances. My lab's recent publication in sediment biogeochemistry may be of some help, I didn't emphasize macrophyte effects because we also saw large effects of benthic microalgae in areas with submersed vegetation.	Cited Cornwell paper mentioned here and discussed in multiple places in revised paper
Cornwell	N/A	Specific Comment 1. The biogeochemical feedback of increased plant biomass on water quality, especially low dissolved oxygen and higher nutrient remineralization/release is of concern. Often, as in the Hydrilla invasion of the Potomac River, the results can be beneficial for nutrient balances. I think the concern of poor sediment quality, i.e. high rates of respiration/nutrient release/poor habitat for benthos, is perhaps less of a worry. Our sediment flux work (Cornwell et al. 2014) in several locations with (albeit sparse) submersed aquatic vegetation (Sherman Lake, Big Break, Franks Tract) did not suggest extremely high rates of sediment respiration or nitrogen release, although rates tended to be higher than in non-vegetated Suisun Bay environments. The macrotidal nature of much of this estuary might lead to export of decaying macrophyte biomass "downstream", with only a very modest effect on nutrient balances in the plant bed. However, these concerns are easily tested.	Cited this paper and indicated that a sediment pool of decomposing macrophytes probably only contributes to nutrient balances in quiescent areas

Cornwell	N/A	Specific Comment 2. Evaluating the role of nutrients in the spread of invasive macrophytes is a massive challenge. In the Chesapeake, the loss of water clarity from phytoplankton and the proliferation of epiphytes lead to a collapse of grasses; understanding the enhancement of macrophytes by nutrients is more difficult. The hypothesis that enhanced P release from increasing metabolic rates for <i>E. densa</i> is interesting, and in fact we observed high P releases in March 2012 in areas with macrophytes. If plant beds develop conditions conducive to P release over time, with the buildup of organic matter, there may be a strong supply of P, especially from pore water uptake. Thus, there could be a positive feedback.	Agreed, a massive challenge. Cited Cornwell work showing sediment P release in areas with macrophytes
Cornwell	N/A	Specific Comment 3. The absence for routine monitoring of plant biomass, spatial extent, species composition, and relatively standard water quality measures (oxygen, salinity, pH, chlorophyll a, nutrients) in plant beds is the greatest source of uncertainty in the report and an absolute necessity to move forward with modeling and control strategies. This is perhaps the key investment that needs to be made; without this, the extent of the problems will be poorly understood. Any potential investments in more research, modeling, or management suggestions need this basic information.	Yes, beefed up recommendation that a routine monitoring program for the macrophytes should include standard water quality measures
Cornwell	N/A	Specific Comment 4. The suggestion of developing a biogeochemical model of the Delta has been made in this report and from our work, it appears to be a key needed advance. There exist many different models for estuarine ecosystems, and I would suggest that off the shelf models might work well for large scale nutrient cycling and balances. Modeling macrophyte communities remains a huge challenge in estuarine science. The biogeochemical effects of given plant species and biomass are becoming better understood, but models also need to the temporal and spatial patterns of macrophyte abundance.	Yes, emphasized need for information on temporal and spatial patterns in macrophyte abundance needed for modeling efforts
Cornwell	N/A	Overall Comment and Reference: Overall, this is a useful assessment of the state of knowledge regarding Delta macrophytes, with a number of modest caveats from committee members that were expressed at our meeting. The report includes all plausible environmental controls on biomass, as well as biogeochemical feedbacks. Cornwell, J. C., P. M. Glibert, and M. S. Owens. 2014. Nutrient Fluxes from Sediments in the San Francisco Bay Delta. <i>Estuaries and Coasts</i>	Included citation and discussed its findings in several places

		37:1120-1133.	
Durand	iii	Under Recommendation #4, first bullet on conditions in Delta favoring growth: low turbidity?	added
Durand	iii	Under R1: We need routine nutrient monitoring on a finer scale than we have, too.	yes, added to recommendation
Durand	iv	Under R3: Item 2 in last sentence: Suggestions for control strategies: chemical, mechanical, gated restoration planning, etc.	all now included
Durand	1	Under 1.1: first paragraph, last sentence - Typo on declined [change "declined" to "decline"], wording for "threatened and endangered" to native? desirable?	typo fixed. yes, native used instead
Durand	1	Under 1.1, second paragraph - need an end quote on sentence "...the State Water Resources...".	fixed
Durand	1	Under Potential nutrient related problems, item 1. Decreases in algal abundance - Do you mean phytoplankton?	yes, clarified
Durand	1	Under Potential nutrient related problems, item 3. Increases in the magnitude and frequency of cyanobacterial blooms - Do you mean Microcystis?	wording in the Delta Plan is "cyanobacterial blooms" -- probably means Microcystis
Durand	5	Last paragraph, last sentence - I am certain that it has greatly expanded during the drought.	acreage updated using Shruti's 2014 data
Durand	10	Under section 2.3 third sentence on egeria densa related to growth response under red light - ... or conditions with sufficient turbidity to shade out blue light.	revised to say it grows nearer to the surface in turbid water
Durand	12	3rd paragraph on page starting with "egeria densa is thought to have been introduced to the Delta in 1946". - But worth noting that DWR reports from 1993 (Department of Water Resources. 1970-2000. Water Quality Conditions in the Sacramento-San Joaquin Delta. Sacramento, CA.) mention Egeria without alarm; however by 1996 Grimaldo and Hymanson (1999) noted thick stands with lots of alien centrarchids. My point being that some shift in the late century began accelerating the spread of this plant.	Added this
Durand	13	2nd paragraph on Stuckenia sp., first sentence - Louise' (Conrad) comments notwithstanding, this is an interesting way to compare...can you do something like this with Egeria...and how reliable are your estimates?	Can be done with monotypic stands of Stuckenia in Suisun but not in places where Egeria is mixed with other species
Durand	15	Under Chapter 3, first paragraph, second sentence on negative effects - ...usually facilitated by very high densities of alien SAV	yes, clarified

Durand	15	Section 3.1, first paragraph, sentence "In contrast, the open water beneath sparse canopies of native <i>Stuckenia</i> sp. may provide ..." - I am not sure how well these statements are supported by the literature as well. For example, I am not sure if we have any idea that native fish are particularly associated with <i>Stuckenia</i> . Adverse effects of alien SAV on fishes are more consistent with the literature...but even some of that may have been overstated. For example, while high densities of predators may lurk in SAV patches, there is no evidence to suggest that this is responsible for populations effects of vulnerable native fishes like smelt or salmon.	okay, point taken. Tempered this whole section
Durand	16	Under section 3.1.1, first paragraph, fourth sentence " <i>E. densa</i> sheds some biomass in winter but does not fully senesce (Fig. 2.2) - Freezing can make a huge impact. Years (like the last) without a freeze had limited die back. I think Shruti has some documentation or a ref for this.	<i>E. crassipes</i> is greatly affected by freezing. Is this comment referring to <i>E. crassipes</i> or <i>E. densa</i> ?
Durand	18	Under section 3.1.4, first paragraph, second sentence on cascading effects - not sure what you mean by this: trophic cascades are typically top down	took "cascading" out
Durand	18	Under section 3.1.4, first paragraph, fourth sentence on thickly growing stems - But it's reasonable to think about this as a management question, because, as we have said, at intermediate densities it probably provides more food access with limited risk. Also, at reasonable densities, it can provide prey refuge, I suspect. the question I have is: how often does it occur at "reasonable densities" and if so, can we find that as an intermediate ideal?	added a sentence on this
Durand	18	Under section 3.1.4, first paragraph, last sentence with effects on the food web - predation effects	added
Durand	19	Under section 3.1.4 under <i>Eichhornia crassipes</i> first paragraph, 3rd sentence - I wonder how much this matters to predators? Matt Young at UCD has a lot of insight into this. [Matt's email] mjyoung@ucdavis.edu	have not contacted Matt Young at this point. Toft paper discusses this somewhat and I added more detail from it.
Durand	20	Under section 3.1.5, 2nd paragraph, 1st sentence - [In reference to Conrad's comments on DO] ...especially at night.	yes, added
Durand	24	Under section 4.1.1 Light - For what it's worth, my model using Santos' data showed an ambiguous relationship with turbidity, a low probability of establishment at depths below 5 m and a rapidly decreasing probability of establishment with increasing flows.	added this information and cited Durand thesis

Durand	25	<p>Under section 4.1.3 Salinity, first paragraph, second sentence -[In reference to Shruti Khanna's comment] Not sure what you mean Shruti, but the Delta was not necessarily fresher before the 1970's. It had more intra and inter-annual variability than we see now. One of the famous early pieces of evidence for this is the Martinez C&H Sugar plant records which document how far up the Delta they needed to go for freshwater. After project implementation, the Vernalis agreement established a salinity standard, legally prohibiting the intrusion of salinity past a certain point. Clearly, Egeria responds well to the more stable salinity regime.</p> <p>We have recommended salinity variability as a way of controlling a number of alien species. Generally, this has been shot down because of legal implications, in Delta consumptive use and the cost of water.</p>	added more about lowered variability in salinity
Durand	27	Under section 4.1.5, second paragraph, first sentence - But limited at times, in the north Delta, that is, off of the Sac plume.	Not sure what this is referring to; need a reference or more information from JD
Durand	29	Under section 4.1.6 Flow, first paragraph, second sentence - [In reference to Conrad's comments on Hestir's dissertation reference] Hestir found a dramatic decrease at .49 ms ⁻¹ , I found a decrease at around .3 ms ⁻¹ .	added both values to text
Durand	31	Under section 4.1.8, first paragraph, first sentence - [his comments on the words "is interactions"] case	fixed

Durand	34	<p>Under section 5. Recommendations - Are there really no concrete recommendations that we can bring, at least in the form of hypotheses, about management of the two main invasives? The "more research is needed" is understandable, but not really adequate, given the time and money currently invested in research and management of this beast.</p> <p>I believe we can say a number of things about SAV/FAV distributions, even if we have to qualify the recommendations with a certain amount of uncertainty, or state explicitly that some recommendations remain disputed or controversial.</p> <p>For example, restorations with limited flow and shallow water 1 and 5 meters are going to get a lot of Egeria. Small embayments or eddies on the lee side of channels are going to be heavily impacted by E. crassipes.</p> <p>Regions that can utilize flow pulses of water will be able to "reset". Managed wetlands are able to "reset" by draining.</p> <p>Chemical management is not very effective except for short periods, and is quite spotty in terms of its impact.</p> <p>Mechanical harvesting is slow and the effect is only good for short periods (how long?), but the effect is targeted where it is most needed. The waste can be re-used as fertilizer to subsidize the harvest.</p> <p>Etc, etc. I am sure that at this point, we can describe these and other hypo-recommendations either as targeted research questions or for interim management recommendations....</p>	<p>Information about distributions given. If more information is available that this reviewer wants included, please provide additional comment and citations. Have not given these detailed recommendations but considering whether to do so</p>
Durand	34	<p>Under section 5. Recommendations, first listed item #3 - This may not be your charge, but a fourth question worth considering is how aq. veg will affect restoration and how restoration sites can be managed or designed in anticipation of this.</p>	<p>consider this to be outside scope of this review</p>
Durand	34	<p>Under section 5. Recommendations, second paragraph, second listed item #1 - I said this before, but routine monitoring should include continuous water quality monitoring, flow conditions, and nutrient compositions across the estuary. The SFE is really behind in these basic observational elements.</p>	<p>yes, added this to recommendation</p>

Durand	35	Under section 5. Recommendations, R2 - Also a widely available hydrodynamic model, which will be necessary to understand stand development and dispersal	yes, I think this is covered now
Engle	iii	Under R1: Second sentence on monitoring: We have to be able to quantify the net primary production (changes in biomass over small time periods using tagged whole rosettes or internodes) , expected growth increments based on (standing biomass at "Time A")x(measured NPP), and then compare the expected growth increment to standing biomass at next time point (Time B). This provides NPP and turnover rate. Without those you cant know what the carbon or nutrient flux into and out of the plant biomass is. In other words, standing biomass can be absolutely static even while huge quantities of carbon and nutrients are being fixed in tissue and rapidly turning over.	Agreed, added that ideally primary production would be measured to estimate turnover
Engle	3	Under section 1.2, originally item 6) of the following key questions: What is the relative importance of nutrients and organic matter accumulation ... - Not sure that "organic matter accumulation" is meant to be described here as "a factor promoting trends" in the vegetation. At our meeting, it was being discussed as a potential result of vegetation but not the cause of it.	revised accordingly
Engle	5	Last paragraph, first sentence in references (see Literature Cited...) - Rephrase to "Literature Cited, Local and regional press reports"	rephrased
Engle	15	Section 3.1, first paragraph - Floating macrophyte beds also provide a substrate near the water surface for a diverse and large biomass of attached microalgae that can exceed the biomass of phytoplankton in adjacent open water (on a per m2 basis). We may not fully understand how the epiphytic community contributes to production at higher trophic levels. Certainly in my own experience there can be thousands of microcrustaceans and other invertebrates (especially insect larvae) per dry gram of root tissue in floating macrophyte beds. If you would like some references from analogous systems in the Amazon, let me know.	added more on the habitat value of roots and community that develops on it.

Engle	15	Section 3.1, first paragraph, last sentence discussing excessive organic matter accumulation - As we discussed during the meeting, I am not sure if there is accumulation of organic matter in the Delta channels where this stuff grows. I'm sure there is a "rain" of detritus, however - what is the evidence that there is organic sediment build up? It is just as likely that the turnover of biomass yields primarily DOC that is exported downstream. This is the predominant fate of macrophyte-fixed carbon in the Amazon system.	revised to say that it could be a factor where high residence time and minimal export
Engle	16	Under section 3.1.1, first sentence on sediments over time - See my comments above. Are we really getting organic matter build up in Delta sediments? If we are going to emphasize a sediment feedback hypothesis as leading to impairment I would like to see some citations from the Delta confirming that there is organic matter accumulation in the sediments, or this should be couched as hypothesis and a data gap. Also, in a lotic system, nutrients released from sediment into the water column aren't preferentially used by macrophytes...they are available to any primary producer in the downstream environs. In general I find myself wishing for more discussion of fate and transport processes related to elemental stocks in macrophytes since the Delta is a "fluid" system (no pun intended).	greatly reduced this section and discussed likelihood that organic matter fuels nutrient recycling only low flow areas if there is a mechanism of biomass accumulation
Engle	16	Under section 3.1.1, first paragraph, last sentence on page "As aquatic vegetation expands in coverage, this large contribution of organic matter from both natural senescence and management of these abundant plants represents eutrophication. - I really am uncomfortable with this assertion unless we can demonstrate that the macrophyte bed carbon metabolized in adjacent water is causing the Delta waterways to be net heterotrophic.	removed this and reduced whole section it was in
Engle	17	Under section 3.1.2., 1st paragraph, 1st sentence - See my earlier comment regarding macrophyte beds providing a platform for attached microalgae that are maintained near the surface and get plenty of light. In fact, there may be more primary production in attached microalgae being held near the surface than there is in the turbid, mixed water column in adjacent waters.	added this
Engle	19	Section 3.1.5 Changes in Water Quality - Since this paper will be used in a nutrient standard setting purpose, it is important that this section be robust and supported by citations.	increased detail and added citations

Engle	19	Under section 3.1.5 Changes in Water Quality, 1st paragraph, 3rd sentence - The Greenfield citation is about effects of mechanical shredding. Natural senescence is not likely to have the same water quality effects. There ought to be sufficient literature to support a hypothesis about large beds naturally "sinking" - if not, we should leave this out. In my experience, aquatic macrophytes usually lose most of their labile elemental mass while still in the water column as they senesce - which means lots of transport downstream through dissolved organic compounds. You dont usually find hearty masses of decaying stems and other tissues sitting around on the bottom unless there has been a physical disturbance. If massive sinking occur in the Delta in undisturbed beds - it should be backed up with a citation.	point taken. This section heavily edited
Engle	21	Under section 4.1, first paragraph, last sentence - Back in the days when BDCP was generating its conservation measures, they relied heavily on a threshold velocity for Egeria establishment of 0.49 meter per second (m/s) to model the effects of their future operations scenarios on Egeria distribution. This threshold was cited to come from: Hestir, E. L., D. H. Schoellhamer, J. A. Greenberg, T. Morgan-King, and S. L. Ustin. 2010. Interactions between Submerged Vegetation, Turbidity, and Water Movement in a Tidal River Delta. Water Resources Research, (in review) I dont find that this paper ultimately appeared in the literature, but the threshold received lots of publicity in the arena of BDCP-management scenarios and I would like to know if the macrophyte-mavens in the Delta support acknowledgement of this threshold in the white paper. I see further down that this threshold is brought up by other reviewers and came from Hestir's thesis.	incorporated Hestir and Durand findings of thresholds for Egeria establishment. I couldn't find the Hestir paper mentioned so have cited her dissertation
Engle	24	Under section 4.1.2 Temperature - If you take Louise's suggestion about adding water management aspects to the other "factors", you might want to look at the BDCP modeling outcomes for temperature under operations scenarios. They modeled the operations effects on Microcystis (not saying I agree or disagree with their conclusions) by calculating how many days temperature would exceed certain thresholds in the Delta in the future. Cant remember if they published temperature scenarios that include climate change.	Have not reviewed these modeling outcomes at this time

Engle	27	Under section 4.1.3 Salinity, first paragraph, second sentence -Should you let people know you are using PSU, if you are?	Oceanographers I work with insist that salinity has no units and thus psu is not appropriate
Engle	27	Under section 4.1.4, second paragraph - Are there any direct diel measurements of pH inside macrophyte beds in the Delta? If not, this should be acknowledged. I'm skeptical of dissolved-gas mediated changes in water chemistry in lotic settings, although in flooded islands and back sloughs less skeptical.	I have not found direct diel measurements of pH inside macrophyte beds locally. I added a caveat that changes would be greatest in dense beds in quiet waters
Engle	29	Under section 4.1.5, first paragraph on section related to organic loading of sediments - My usual saw...this is highly speculative unless there is evidence that there is continual organic loading of sediments going on in this system (as opposed to rapid export), with subsequent higher release rates of DIN and DIP from sediments where macrophytes are growing.	revised this section to indicate that most organic matter losses are likely to be mostly in dissolved form
Engle	29	Under section 4.1.5, second paragraph on <i>Eichhornia crassipes</i> - I dont have time by today to look into Eichhornia dosing experiments, but its seems that there should be more than 1 citation out there regarding Eichhornia dosing experiments. I suspect Shruti may have provided some resources. Given the "charge" to guide the Central Valley Board regarding whether nutrients are driving macrophytes - this nutrient section should be beefed up with a more thorough literature review - and the experimental conditions placed in context of DIN and DIP concentrations from monitoring stations in the Delta to see if any of them are environmentally relevant.	yes, added more citations
Engle	30	Under section 4.1.7 third paragraph, first sentence - Is there a review paper or two to cite, or even the proceedings of some symposia or another?	added citations
Engle	31	Under section 4.1.8, third paragraph, first sentence - It seemed from our meeting that there is concern that the "niche" occupied by Eichhornia would be occupied by SAV if Eichhornia was effectively managed. This "zero sum game" aspect of the Delta macrophyte issue should be discussed more fully in this white paper, in my view.	yes, this shift in composition was already described but it is more explicitly discussed now

Engle	33	Under section 4.2 - There seem to be only a few examples where a hyacinth or SAV-dominated system experienced a state-change to plankton-dominated. In the cases I am aware of, climatic perturbations seem to be a driver, not nutrient management. One case is the state change to low hyacinth in Lake Victoria in the late 1990s. The explanations for this state change have been debated in the literature (bio-control, meteorologic event like an El Nino?). In addition, there was a regime shift from Egeria dominance to turbid open water in the Rio Cruces wetland in Chile that may have been prompted by a climatic event (Marin et al. - citation was among those posted for the group). I think the white paper should have at least a brief section acknowledging cases where some kind of perturbation actually DID result in disappearance of FAV or SAV - it could be instructive for management debate here.	agreed, added that state shifts have been noted for both species
Engle	33	Under section 4.2, third sentence on accumulation of biomass as well as clonal propagation - But at environmentally relevant concentrations for the Delta?	revised as described in previous sections
Engle	34	Under section 5. Recommendations, R1 - Please see my comment about NNP and turnover measurements in the executive summary	revised as suggested
Engle	39	Reference for Marina, V.H. et al. 2009 - spelling is Marin; This paper is not referenced in the paper, but should be regarding regime shifts having to do with climatic perturbations. I wonder if there are other references here that are not cited in the text?	fixed. Citations updated.
Foe	24	You note that light availability is important for successful colonization of Egeria densa, and maximizing its tissue growth and biomass. The Delta has become clearer. The delivery of suspended sediment from the Sacramento River to the Delta has decreased by about half during the period between 1957 and 2001 (Wright and Schoellhamer (2004) ¹ and this has resulted in a statistically significant 2 to 6 percent decrease per year in SPM between 1975 and 2005 (Jassby, 2008) ² . Of course, it is uncertain whether the trend will continue. Might this increase in clarity also increase the biomass and distribution of submerged macrophytes like E. densa? Could this increase in clarity make other factors like nutrients more important? 1 San Francisco Estuary and Watershed Science, 2004 volume 2, issue 2 2 San Francisco Estuary and Watershed Science, 2006 volume 6, issue 1	discussed under sections on light

Foe	24-25	I have observed large rafts of Eichornia crassipes being tidally moved seaward out of the Delta to San Francisco bay in late fall with the first cold snaps. I assumed that colonies lost their cohesive stability under freezing night time conditions. This seems like a potentially significant biomass loss mechanism. Is this true? Is there any mention of this in the literature?	added a description of effects of cold temps, including this observation
Foe	28	Second paragraph - You say, "High nutrient availability is often cited...." Can you give a reference to support this assertion?	took statement out because hearsay
Foe	29	Redfield ratios are often used in phytoplankton studies to determine which nutrient will become limiting as the nutrient pool is exhausted. Typical phytoplankton N:P Redfield ratios are 7.5:1 (wt:wt) although the number may change somewhat based upon algal growth stage and species. DIN to DIP ratios for Suisun Bay are around 6:1 (Glibert et al 2010). Ratios for the delta are more variable but range between 5 and 10 (Foe et al., 2010). You can get more data from Alex Parker and Dick Dugdale at the Romberg Tiburon Center. N:P ratios are 2 to 3 for Stuckenia sp and E densa in figure 4.4. If so, it seems that macrophytes may have a higher P requirement than phytoplankton and may be more likely to become P limited in the Delta if consuming mostly waterborne nutrients. Can you comment?	added N:P of water thought to be limiting for E crassipes, but otherwise this is still a gap
Foe	29	It would be nice to include a summary table of the key factors controlling macrophytes in the Delta. Left column would be a list of primary macrophyte species and across the top the primary drivers. These might be light, temperature, salinity, DIC, and nutrients. In the cells give the ranges that restrict plant establishment and growth.	I have not done this and most of these numbers could only be very rough with little local data on how the factors work specifically in the Delta.
Foe	34	I think the recommendations are fine but are too general. I suspect that both the monitoring and modelling should be accompanied by special studies to help interpret and inform the results. Maybe under monitoring you could list specific high priority questions in bullet form. For example: Do N and P concentrations limit E. crassipes growth and biomass anywhere in the Delta now? To determine this conduct amendment experiments in the laboratory and/or in field mesocosms to determine growth as a function of nutrient concentrations and compare these with levels found in and around macrophyte beds in the Delta now. What is the limiting nutrient? Are these conclusions robust under different light and temperature regimes typical of	expanded the recommendations to be more detailed, but not as detailed as suggested here

		the delta?	
Foe	N/A	<p>I think the nutrient discussion would be improved by including a paragraph or two on ambient nutrient concentrations and trends over time in the Delta. Annual average DIP and DIN concentrations at key locations in the Delta range between 0.02-0.09 mg/l and 0.13-1.10 mg/l (Foe et al., 2010)¹. Typical DIN and DIP concentrations are 0.5 and 0.05 mg/l, respectively, but talk with dick dugdale from the Romberg Tiburon Center for more information. All the amendment experiments cited in the review paper are at higher concentrations than occur in the delta and this may affect the interpretation of the results. The results obtained by You et al. for E. crassipes are particularly interesting and suggest the possibility of nutrient limitation in the delta now. You et al. increased N and P concentrations above 0.6 and 0.05 mg/l and observed a 30% increase in growth and clonal propagation. If these findings are confirmed by additional experiments, then nutrient management might be an option for reduce the severity of the water hyacinth problem. Please comment.</p> <p>¹ http://www.waterboards.ca.gov/centralvalley/water_issues/delta_water_quality/ambient_ammonia_concentrations/foe_nutrient_conc_bio_effects.pdf</p>	<p>added several figures on nutrient concentrations in the Delta including ones from Glibert and from Foe. Would like to add a figure like what is in the cyano report if I can get those data. Added more on nutrient limitation and that E. crassipes is unlikely to be limited under current conditions.</p>
Foe	N/A	<p>About trends, nutrient concentrations, N speciation, and dissolved N:P ratios have changed in the delta over the last 40 years. More DIN, more NH₄, less SRP and an increase in the N:P ratio (Jassby 2008; Glibert, 2010²; Van Nieuwenhuysse, 2007³). Could these changes in concentrations be partially responsible for the emerging macrophyte problem?</p> <p>² Reviews in fishery Science, 18:211-232 ³ Canadian journal of fisheries and aquatic science 64:1529-1542</p>	<p>Although there has been an increase in NH₄⁺ and a decrease in the N:P ratio over a 30 year period through 2006, especially in the upper Sacramento River, this trend was not evident in the last decade of that time period (Glibert 2010; Fig. 4.5). A closer look at the last decade (through 2013) shows no trends in any form of inorganic nutrients or N:P ratios in the central Delta region -- this comes from the more recent data shown in the Cyano white paper, which I am trying to get.</p>
Foe	N/A	<p>The modelers are going to need specific data to be collected to help inform model development. This paper should note and recommend that there be collaboration between the monitoring and modeling team to collect high priority information to inform the models.</p>	<p>yes noted this</p>

Joab	1	Under 1.1 - In sentence "...critical habitat or fish.." Change "or" to "for".	fixed
Joab	1	Under section 1.1, last paragraph - The Water Board only commissioned two not three literature reviews.	fixed
Joab	3	Under section 1.2, listing for Section 3: Insert "to" between "Contributing" and "the" and capitalize the words "submersed", "floating", "aquatic", and "vegetation" to be consistent in formatting.	fixed
Joab	4	Under section 2.2, first sentence - Only 17 species are identified in Table 2.1, not eighteen. Please correct text or Table 2.1.	19 now with addition of 2 by Shruti
Joab	17	Under section 3.1.1., last sentence - "identified" spelled incorrectly.	
Joab	All	Global Comment: I found numerous references cited in document that were not included in the Chapter 6 Literature Cited. Please compare all references in text and Chapter 6.	fixed
Khanna	iv	Under R3: Item 2 in last sentence: adding information to Durand's comments on control strategies: also biological	added
Khanna	1	Under 1.1 - In sentence, "...45,000 square mile" change "mile" to "miles."	fixed
Khanna	1	Under 1.1, second paragraph - the sentence "Studies needed for development of Delta..." seems incomplete - difficult to understand.	need to pull up the language used in this document to fill this in and make more clear
Khanna	2	Figure 1.1 - Maybe pick a different figure? I can't read any of the text in this figure.	can the water board suggest another figure that would be more clear?
Khanna	4	Heading of section 2.1 - "Classification" is misspelled.	fixed
Khanna	4	Under section 2.2, second paragraph reference to Hestir et al. 2010 - As I remember, this figure actually comes from some other paper that Erin might have cited in her paper. I know she did not herself harvest biomass and determine the % coming from Egeria. Moreover, this original paper is even older. I think the timeline is important. I think when you mention cover, biomass ratios, any information pertaining specifically to the Delta, it is better to mention which year this study comes from. Because the Delta is so dynamic and what was true 10 years ago, might no longer be true. Same goes for the Santos et al. 2009 study.	revised this. Tried to always indicate year that data came from.
Khanna	4	Under section 2.2, last paragraph, first sentence on Coontail being the most frequently encountered native species - In 2014, (coontail) found in 45% of all sampled SAV points. Average cover where sampled - 30%.	added
Khanna	4	Under section 2.2, last paragraph, last sentence - What is the citation for these numbers (284 hectares)?	Santos et al. 2011. cited it again.

Khanna	5	Table 2.1 - There are two more species we have documented which I don't see mentioned here - one is water purslane (which is similar to water primrose and floating - genus Ludwigia), the other is parrotfeather (genus myriophyllum), which is actually a floating species.	added to table
Khanna	5	General comment on figures - for new figures, see total area of floating in the excel sheet I forwarded and divide by half to get appx. water hyacinth area. Other half is water primrose.	included these new estimates from the excel sheet from Shruti throughout
Khanna	10	Under section 2.3, last sentence on egeria densa on range of depths in turbid and clear water - but maybe to a shallower depth in turbid water.	added
Khanna	11	Under section on Stuckenia sp. - 2014 survey: Sago or fineleaf found in 26% of sampled points. Avergae cover where samples: 50%. Especially in the open bay. It is found as 100% cover so it looks like it's niche is at least partially unique from all other submerged species.	added
Khanna	11	Figure 2.5 caption - I agree with Louise's comment. We have not been able to differentiate between SAV species even with hyperspectral data. I'd like to see this reference.	see my clarifications on this, and response to Louise's comment
Khanna	12	Thirrd paragraph, fourth sentence " <i>Egeria</i> coverage expanded during the years between 2003 and 2007" - I haven't read Maria's paper recently but according to the numbers I have (see the xls file), <i>Egeria</i> was abundant until 2006 then decreased quite a bit in 2007 and even more in 2008.	revised to reflect numbers in Shruti's spreadsheet
Khanna	12	Fourth paragraph, second sentence on <i>Eichhornia crassipes</i> , reference to Santos et al 2009 study - Maria's study was hazy about the efficacy of water hyacinth control. My study found that control had no impact on year-to-year cover of water hyacinth. The decline of cover in 2007 was mainly due to a 3 week period of continuous frost nights in Jan 2007. There are several studies that back up the claim that water hyacinth is vulnerable to frost.	added reference to Khanna study on lack of year-to-year change from control efforts. Added references on frost.
Khanna	12	Fourth paragraph, second sentence on <i>Eichhornia crassipes</i> with mention on estimates of acreage - Take estimates from the SOTER report or the xls file. I have a comment on this earlier.	done
Khanna	15	Section 3.1, first paragraph, highlighted sentences from "In contrast, dense canopies..." to "...leading to predation on smaller adult and juvenile native fish" - [Following Louise Conrad's statement] Moreover, doesn't each of these statements require a citation?	greatly revised this section to address concerns of Louise and John D

Khanna	16	Under section 3.1.1, first paragraph, 4th sentence " <i>E. densa</i> sheds some biomass in winter but does not fully senesce (Fig. 2.2) - [In reference to John Durand's comment that Shruti may have references.] Yes, check the annotated bibliographies. There are examples from Florida and Louisiana.	added references
Khanna	17	Under section 3.1.3, fourth sentence "Dense submersed vegetation is ..." - There are a couple of new Hestir et al. papers on the relationship between SAV and turbidity e.g. Hestir, E. L., D. H. Schoellhamer, T. Morgan-King, and S. L. Ustin. 2013. A step decrease in sediment concentration in a highly modified tidal river delta following the 1983 El Niño floods. <i>Marine Geology</i> 345:304-313.	added reference
Khanna	19	Under section 3.1.5 Changes in Water Quality, first paragraph, second sentence - [In reference to Conrad's comments on citations for this section] Yes, many. Kathy, check out the bibliography. If not there, then the Gopal book should have a ton. I think he has a chapter on the use of water hyacinth as a secondary water pollutants purifier.	added references
Khanna	20	Under section 3.1.5, second paragraph, first sentence - [In reference to Conrad's comments on DO] I also seem to remember that <i>Egeria</i> mats can depress oxygen levels.	yes, added
Khanna	20	Under section 3.1.5, second paragraph, third sentence on decomposition of <i>E. crassipes</i> following senescence - Even in a healthy mat, the growth rate of hyacinth is so obscene that there is material constantly dripping from the root system and a thick mat can cause part of its own mat to senesce due to intra-species competition.	agreed, added
Khanna	24	Under section 4.1.1 Light, second paragraph, last two sentences - [In reference to Conrad's comments on these statements] I agree. I think the <i>Stuckenia</i> comment can still stand but maybe instead of <i>Egeria</i> , you can say SAV mats? Especially since <i>Elodea</i> , a native that has increased in the Delta over the past six years, also forms dense canopies identical to <i>Egeria</i> . Also Hestir et al. paper cited in a previous comment.	yes, changed to SAV mats. Added Hestir citation
Khanna	24	Under section 4.1.2 Temperature - For water hyacinth, lower air temperatures can be pretty limiting and this is insufficiently discussed here. I have some references on the subject in the bibliography.	added info and refs on cold temps/frost

Khanna	25	Under section 4.1.3 Salinity, first paragraph, second sentence -This is a matter of debate. The historic delta used to be a lot more of freshwater and the X2 line was much farther away. Only in times of drought would part of the Delta become brackish. And the reason was that the water had a much longer route to take through meandering narrow channels and did not meet with the bay waters as readily. By dredging the Sacramento river and getting most of the water out quickly into the bay, we have reduced the residence time of the water in the Delta thereby ironically increasing the salt intrusion. The thing different in the part was the strong seasonal variability in the salinity - especially more salinity during low-flow. Now the delta is fresh all year long. This is the crucial change. References?? I have a bibliography on the Delta too, I think. I'll send it to you directly.	Durand had conflicting view. Added info about salinity variability being decreased.
Khanna	27	Under section 4.1.3 Salinity, second paragraph - there are many salinity studies for eichhornia and they are all mentioned in my annotated bibliography. Please take a look.	added more citations
Khanna	27	Under 4.1.3 Salinity, second paragraph - [In reference to Conrad's comment on this section] probably field data?	yes, field data but weak so added citations from other regions
Khanna	28	Under section 4.1.5, second paragraph - There are many studies of Eichhornia with nutrients but in a slightly different set of literature - paper on water purification plants. I'm not sure if I have much in my bibliography but if you research use of water hyacinth in water purification, you'll get some good references.	added more citations
Llaban	ii	Under Major Finding #1, first sentence - Native floating aquatic vegetation (i.e. pennywort) can also be a beneficial component (invertebrate habitat and trophic support). Toft et al 2003 found higher insect densities in pennywort vs. hyacinth and that invertebrates associated with pennywort occurred more often in diets of adjacent fish.	yes, added native floating to sentence indicating it is typically beneficial. Toft reference cited in another section to help capture the comment
Llaban	iv	Under R3 - Mechanical removal/harvesting of water hyacinth is already being implemented by DBW in the Delta as a part of an integrated pest management program (Water Hyacinth Control Program).	added this
Llaban	1	Under 1.1, first paragraph, last sentence on Delta Plan - Please include a full reference under literature cited.	need to add
Llaban	3	Under section 1.2 regarding key questions 4-7 - Should these questions be numbered starting from 1?	fixed

Llaban	11	Under Eichhornia crassipes paragraph, first sentence on windy periods- High tides can also cause water hyacinth to dislodge from shores or tule islands and move with the tidal flux. Disturbance from boating activity can also cause water hyacinth to detach and float around. (DBW staff observations)	added
Llaban	11	Under Eichhornia crassipes, paragraph, second sentence regarding abundance - Also has been historically abundant near USBR's Tracy Fish Collection Facility and River's End Marina (Old River) due to hydrodynamics and waterway characteristics. Related news articles at http://www.recordnet.com/article/20121222/A_N_EWS/212220315 http://www.contracostatimes.com/contracosta-times/ci_24673609/state-begins-using-mechanical-harvesters-control-water-hyacinth	added these locations
Llaban	11	Under Eichhornia crassipes paragraph, third sentence regarding channel edges - Also can be found around tule islands in the middle of a channel.	added
Llaban	12	Under Egeria densa paragraph concerning active management spraying - Suggest avoiding the word "spraying" and rephrase to "herbicide application" or "herbicide treatment". Egeria densa treatments are done with application of granular (pellet) formulations of herbicide, rather than spraying of liquid herbicide. In the rest of the paragraph change "spraying/sprayed" to "treatment".	done
Llaban	12	Under Eichhornia crassipes paragraph, second to last sentence regarding "spraying over several years" - Please change the word "several" to "two". 2011 and 2012 were years where there were delays in permitting between DBW and federal agencies.	done
Llaban	15	Under section 3.1, first paragraph, third sentence regarding shading of phytoplankton - Can also decrease dissolved oxygen in water (as depicted in Figure 3.1).	added discussion of DO effects
Llaban	18	Under section 3.1.3, first paragraph, last sentence on west Delta - Also observed by DBW staff in east Delta.	added pers. comm.
Llaban	20	Under section 3.16, third sentence referencing "boating" - In return, boating activity can facilitate spread of egeria densa by production of plant fragments from propeller disturbance.	added
Llaban	24	Under section 4.1.1, third paragraph, last sentence on E. densa expanding more rapidly - Under what conditions? Low light?	yes, fixed

Llaban	27	<p>Under second paragraph, first sentence regarding local studies - Found a report from a UC Berkeley student on salinity effects on water hyacinth.</p> <p>http://nature.berkeley.edu/classes/es196/projects/2004final/Cheng.pdf</p> <p>This is not a peer-reviewed article and appears to be a class project, so I'm unsure if it can be used as a reference.</p>	have not reviewed this report yet to determine appropriateness
Llaban	30	<p>Under section 4.1.7, first paragraph, last sentence - This section should include a description of benthic barriers as an alternative control measure (cultural control) to control small infestations of <i>Egeria densa</i> in or around high-use areas such as docks, boat launches and swimming areas.</p> <p>I'm not aware of use of benthic barriers in the Delta, but it has been used in Emerald Bay to control Eurasian watermilfoil.</p>	added. Still need to search for info from other locations like Emerald Bay.
Llaban	30	<p>Under section 4.1.7, second paragraph, first sentence on mechanical removal - In general, there are concern about impacts to non-target plant species and by catch of non target organisms, that should be addressed in this section. A useful reference: <i>Biology and Control of Aquatic Plants. A Best Management Practices Handbook.</i></p>	added. Have not been able to get this book.
Llaban	30	<p>Under section 4.1.7, second paragraph, last sentence on concerns - Another concern is potential survival and regrowth of cut water hyacinth.</p> <p>Reference: Spencer et al 2006. Evaluation of Waterhyacinth Survival and Growth in the Sacramento Delta, California, Following Cutting. <i>Journal of Aquatic Plant Management</i> 44:50-60.</p>	added to text and cited
Llaban	30	<p>Under section 4.1.7, third paragraph, fifth sentence regarding no biological control methods - USACE released <i>Neochetina bruchi</i> in the Delta in the early 1980s. USDA-ARS also has done some releases of <i>Neochetina</i>.</p>	updated this whole section on biological control
Llaban	32	<p>Figure 4.6 - Left figure is cutoff. Please resize to present the complete 2007-2008 data.</p>	fixed

Llaban	33	<p>Under section 4.1.9, first paragraph, last sentence - Vegetative growth is not limited by depth and bank slope. However, water hyacinth seed germination and seedling establishment can be limited by depth and requires shallow water. Although vegetative reproduction is likely the primary means of reproduction, factors affecting sexual reproduction should be considered.</p> <p>Barret 1980 conducted a study of seed production germination in the Delta near Stockton, Ca. S.C.H. Barrett. 1980. Sexual Reproduction in Eichhornia Crassipes. II. Seed Production in Natural Populations. Journal of Applied Ecology. 17:113-124.</p>	Added and cited.
Llaban	34	Under section 5 Recommendations - Section title is inconsistent with title on pg. 3 - "Section 5: Key Data Gaps and Research Recommendations". Please revise either title for consistency.	fixed
Llaban	36	Under section 6 Literature Cited - Many references within the body of the paper are missing from the literature cited section. Please revise the literature cited to ensure consistency with referenced literature.	done
Madsen	5	Recommendation 1. Aerial remote sensing, whether by satellite or aircraft, provide useful data on water hyacinth distributions, but perform extremely poorly on egeria or any other submersed plant communities. Species discrimination with remote sensing is still insufficient to categorize species composition without significant ground truthing. The recommendation does not indicate how biomass estimates would be derived from transects, nor does what technique is planned for transect.	clarified throughout document. Added more detail on biomass estimates
Madsen	5	Recommendation 2. The authors are assuming that nutrients are limiting plant growth without knowing if this, in fact, is the case. It is doubtful that an ecosystem model will indicate if nutrients are limiting either water hyacinth or egeria. It is far more common to see luxury consumption of nutrients by submersed and floating aquatic plants than nutrient limitation.	Need help from SWG to decide how to address

Madsen	6	Recommendation 3. Why do the authors want to reinvent the wheel on management of invasive species? Why select a management technique that is already known to kill fish – namely, harvesting? USDA ARS has already been doing this research for decades, as has the US Army Engineer Research and Development Center. This recommendation is made, yet no citations of existing best management practices manuals are included in this report. The Journal of Aquatic Plant Management has 2,000 articles on the biology and management of aquatic macrophytes, and has ONE citation in the report. The San Francisco Estuary Institute had a multi-year project to investigate harvesting to replace herbicides for management in the early part of the last decade, and concluded that harvesting was not a replacement for herbicides.	changed this recommendation to suggest a review of existing and planned methods of control with an eye to effectiveness in meeting nutrient objectives and increasing beneficial uses
Madsen	17	Rake methods. Rake methods to “estimate biomass” are poor substitutes for actually measuring biomass.	true, but this is the method that has been done
Madsen	19	Coontail does not “attach to other plants.” It might wrap around other plants. It lies on the surface of the sediment.	fixed
Madsen	22-23	<i>Egeria densa</i> . I realize that, in trying to be understood by non-scientists, many people use the term “male” and “female” plant or flower, but the plant or flower itself is not male or female. The plant or flower is correctly referred to as either “staminate” or “pistillate,” not male or female.	yes, corrected
Madsen	23	Water hyacinth. While water hyacinth does produce a large number of seeds, outside of their native range they have very low germination rates, and the seedlings take exceedingly long to grow. A seedling may not be capable of producing a flower until the end of the year. For overwintering, the importance of the stembase cannot be overstated. The stembase can lie underwater during the cold season, and initiate growth rapidly in the new growing season.	added both these points
Madsen	23	Coontail does not attach to other plants. It is neither epiphytic nor saprophytic.	fixed
Madsen	26	Line 5. <i>M. spicatum</i> is misspelled as <i>spicatam</i> . Repeatedly.	fixed (2 locations)
Madsen	26	Line 23. Submersed herbicide application is inaccurately described as “spraying,” when in fact liquid herbicides for submersed plants are injected beneath the water’s surface using trailing weighted hoses. Since most of the fluridone in the past decade has been applied as a granular formulation, “spraying” is even more inaccurate.	fixed

Madsen	27	Stuckenia distribution. Unless remote sensing is ground truthed, it is not a reliable method for estimating the distribution of submersed plants. More than half of the population will be out of detection, and the amount remaining undetected will vary based on water clarity and other issues.	Stuckenia is well predicted within Suisun Bay where it is nearly monotypic; in Delta this is only true in open water areas according to Shruti
Madsen	N/A	Global Comment. By the way, most of the figures did not download from Google Documents.	True, hopefully he was able to look at original version sent out
Madsen	N/A	Global Comment. About half of the Literature Cited citations are incomplete, making it impossible for me to look up these citations.	fixed
Moran	i	Acknowledgments: Does the author mean this Macrophyte Science Working Group? Or is there a separate Submersed and Floating Macrophyte Technical Advisory Group?	There is a Science Working Group and also a Stakeholder and Technical Advisory Group. This was clarified.
Moran	ii	Executive Summary: Text indicates four major questions, but only three are listed.	fixed
Moran	ii	Executive Summary: Major Finding #2, aquatic weed coverage values are too low -CDBW-CA Parks estimates <i>Egeria densa</i> coverage at 10,000-15,000 acres or 4,050-6,075 ha. -Water hyacinth coverage in the Delta is much more than 200 ha. In 2014, for example, the Division of Boating and Waterways-CA Parks treated 2,617 acres or 1,060 ha. In 2015, they plan to treat close to 3,400 acres or 1,377 ha. DBW estimates at least 5,000 acres or 2,025 ha in the Delta. See comments from Ustin lab for more precise estimates of coverage. Provide information on increase in coverage from mid-2000s to now. [See reference below.]	Updated with Shruti's numbers in excel sheet
Moran	ii	Ustin Ian, UC Davis, estimates 2000 ha, 1/2 Water hyacinth, 1/2 Ludwigia -This study should consider other important aquatic invasive macrophytes for which there is currently no control program, especially Ludwigia spp., which is likely as widespread or more widespread than water hyacinth and equally damaging (and the two weeds co-occur and appear to benefit from each other's presence)	Ludwigia now addressed. Pointed out as a finding that there are additional problematic invasive species that have not received much attention.
Moran	iii	Recommendation R1: (Comment for discussion) Remote sensing data for water hyacinth are being collected by NASA as part of the USDA-ARS Areawide Project for improved control of aquatic weeds in the Delta. R1: Check spelling of "areal" (correct is "arial")	areal was intended -- it means across an area
Moran	iii-iv	Recommendation R2: This should be communicated to the Modeling Work Group. The Macrophyte work Group could identify data requirements.	yes, added this in recommendation

Moran	iv	Recommendation R3: The USDA-ARS Areawide Delta Aquatic Weed Management Project is conducting pilot studies on integrated control.	added that current and planned control methods should be evaluated relative to nutrient objectives
Moran	3	Under Introduction Section 1.2 Goal and Organization of Macrophyte Literature Review - Key Questions: Why are they numbered 4,5,6, and 7?	some kind of auto-formatting--fixed
Moran	5	Information on coverage of water hyacinth, see above and information from Ustin lab on correct coverage estimates.	used estimates provided by Shruti
Moran	10	Under Chapter 2 General Ecology and Trends, Section 2.3 Habitat Types in which they are typically found - <i>Egeria densa</i> some of the information here is redundant with page 8.	fixed
Moran	12	Under Chapter 2 General Ecology and Trends, Section 2.4 Spatial and Temporal Trends in Distribution and Abundance - DBW-CA Parks is treating up to 4-5% of Delta area for <i>Egeria densa</i> .	added this percentage
Moran	13-14	Under Chapter 2 General Ecology and Trends, Section 2.4 Spatial and Temporal Trends in Distribution and Abundance - Are there specific causes of the <i>Stuckenia</i> expansion over the past 20+ years? Describe here or in Section 4.	added text that it could be increased water clarity but that we don't know
Moran	16	Under Chapter 3 Role of Submersed and Floating Aquatic Vegetation in Supporting Delta Ecosystem Services 3.1.1 Organic matter subsidy/accumulation - For more information on seasonal growth and senescence of water hyacinth, see also Spencer, D. 2005. Seasonal growth of water hyacinth in the Sacramento/San Joaquin Delta, California. <i>J. Aquat Plant Manage.</i> 43:91-94.	Added this citation
Moran	17	Under Chapter 3 Role of Submersed and Floating Aquatic Vegetation in Supporting Delta Ecosystem Services 3.1.3 Habitat alteration - Can <i>Egeria densa</i> alter habitat in ways that helps it outcompete <i>Stuckenia</i> and other submersed natives? Refer reader to Section 4.1.8	referred to chapter 4 here
Moran	17	Under Chapter 3 Role of Submersed and Floating Aquatic Vegetation in Supporting Delta Ecosystem Services 3.1.3 Habitat alteration - Water hyacinth and <i>Ludwigia</i> often grow together, although one dominates. Could mention here and refer to Section 4.1.8.	about half each in 2014 -- already mentioned
Moran	18	Under Chapter 3 Role of Submersed and Floating Aquatic Vegetation in Supporting Delta Ecosystem Services 3.1.4 Trophic support - Redundant information in the paragraph about <i>Egeria densa</i> providing hiding habitat for predatory non-native fish.	fixed

Moran	19	<p>Under Chapter 3 Role of Submersed and Floating Aquatic Vegetation in Supporting Delta Ecosystem Services</p> <p>3.1.5 Changes in water quality - Consider more references here and in the more detailed nutrient section later on to support statement of use of water hyacinth to remove nutrients from sewage or other nutrient-rich water.</p> <p>Reddy, K. R., M. Agami and J. C. Tucker. 1989. Influence of nitrogen supply rates on growth and nutrient storage by waterhyacinth (<i>Eichhornia crassipes</i>) plants. <i>Aquat. Bot.</i> 36:33-43.</p> <p>Reddy, K. R., M. Agami and J. C. Tucker. 1990. Influence of phosphorous on growth and nutrient storage by water hyacinth (<i>Eichhornia crassipes</i> Mart. Solms.) plants. <i>Aquat. Bot.</i> 37:355-265.</p> <p>Moran, P. J. 2006. Water nutrients, plant nutrients, and indicators of biological control on waterhyacinth at Texas field sites. <i>J. Aquat. Plant Mgmt.</i> 44:109-115. 2006. (This paper, based on Texas field sites, supports earlier work by other authors in tanks showing a positive association between dissolved inorganic N in water and % N content in water hyacinth leaves, although in this study no associations were found between soluble water P and plant % P, in contrast to a number of other studies. This study did not examine plant growth; however no associations were found between water N or P and plant size)</p>	added citations here and in Chapter 4
Moran	20	<p>Under Chapter 3 Role of Submersed and Floating Aquatic Vegetation in Supporting Delta Ecosystem Services</p> <p>3.1.5 Changes in water quality - The DBW-CA Parks aquatic weed control programs include DO monitoring requirements and follows thresholds established by the CVRWQCB or other agencies for minimum DO levels under which treatments may be conducted (5-7 ppm)</p>	added this information
Moran	25	<p>Under Chapter 4 Factors Contributing to the Prevalence of Submersed and Floating Aquatic Vegetation in the Delta</p> <p>4.1.2 Temperature - Not local, but studies have been done to show that above about 33-34 C, water hyacinth loses nutrients from the roots and experiences negative growth.</p>	added pers. comm., need citation

Moran	27	<p>Under Chapter 4 Factors Contributing to the Prevalence of Submersed and Floating Aquatic Vegetation in the Delta</p> <p>4.1.2 Temperature - One past review indicates that water hyacinth cannot tolerate salinity above 2 ppt. This may not be accurate in the Delta.</p> <p>Wilson, J. R., Rees, M., Holst, N., Thomas, M. B., Hill, G. 2001. Waterhyacinth population dynamics. pp. 99-103 in Julien MH, Hill M. P., Center T. D., Jianqing, D. (eds.), Biological and Integrated Control of Water Hyacinth, Eichhornia crassipes. Proceedings of the Second Meeting of the Global Working Group for the Biological and Integrated Control of Water Hyacinth, Beijing, China, 9-12 October, 2000. ACIAR, Canberra, Australia.</p>	couldn't get this review
Moran	28	<p>Under Chapter 4 Factors Contributing to the Prevalence of Submersed and Floating Aquatic Vegetation in the Delta</p> <p>4.1.5 Nutrients - Can you provide information on average and range of N and P values in the Delta, and compare to averages for other key estuaries such as Chesapeake? What do you mean by "high" nutrient levels?</p>	added info on average and range of N and P values in the Delta. Added reference to impairment indices. Did not compare to other estuaries such as Chesapeake because absolute values of nutrient concentrations not useful unless there is info on water clarity, phytoplankton blooms, filter feeding ,etc.... which is beyond what we want to get into here
Moran	29	<p>Under Chapter 4 Factors Contributing to the Prevalence of Submersed and Floating Aquatic Vegetation in the Delta</p> <p>4.1.5 Nutrients - The conclusion that E. densa management cannot likely be improved much using nutrient management is important and should be restated at the end.</p>	done

Moran	30	<p>Under Chapter 4 Factors Contributing to the Prevalence of Submersed and Floating Aquatic Vegetation in the Delta</p> <p>4.1.7 Chemical, mechanical, and biological control - Major errors in fact regarding biological control</p> <p>-The U.S. Army Corps of Engineers and CDFA released three agents for water hyacinth in the early 1980s in the Delta:</p> <p>Stewart, R. M., A.F. Cofrancesco, and L.G. Bezark. 1988. Biological control of waterhyacinth in the California Delta. U.S. Army Corps of Engineers Waterways Experiment Station, Technical Report A-88-7. U.S Army Corps of Engineers, Washington, D.C.-CDFA conducted surveys in the early 2000s and found that only one agent, the weevil <i>Neochetina bruchi</i>, is established in the Delta. It is widespread but is not having sufficient impact. A key reason appears to be the inability of immature stages to survive winter conditions in the Delta.</p> <p>Akers, R. P., and M. J. Pitcairn. 2006. Biological control of water hyacinth in the Sacramento-San Joaquin Delta year 3 - final report. California Department of Food and Agriculture, Sacramento, California, USA.</p>	added this info and citations
Moran	30	<p>Section 4.1.7 Chemical, mechanical and biological control - Major errors in fact regarding biological control</p> <p><u>Continued comment from above:</u></p> <p>-Plant nutrient levels in water hyacinth in the Delta are likely sufficient for <i>Neochetina</i> weevil development:</p> <p>Spencer, D. F., and G. S. Ksander. 2004. Do tissue carbon and nitrogen limit population growth of weevils introduced to control waterhyacinth at a site in Sacramento-San Joaquin Delta, California? <i>Journal of Aquatic Plant Management</i> 42:45-48.</p> <p>CDFA and the USDA-ARS are beginning to release a planthopper, <i>Megamelus scutellaris</i>, for biocontrol of water hyacinth. This insect was discovered and characterized as being sufficiently host-specific to water hyacinth by the USDA-ARS in Florida, where it is now widely established, with impact evaluations ongoing.</p> <p>Tipping, P. W., A. Sosa, E. N. Pokorny, J. Foley, D. C. Schmitz, J. S. Lane, L. Rodgers, L. McCloud, P. Livingston, M. S. Cole, and G. Nichols. 2014b. Release and establishment of</p>	added this info and citation

		Megamelus scutellaris (Hemiptera: Delphacidae) on waterhyacinth in Florida. Florida Entomologist 97:804-806.	
Moran	30	<p>Section 4.1.7 Chemical, mechanical and biological control - Major errors in fact regarding biological control</p> <p>Continued comment from above: (and Patrick Moran, USDA-ARS Exotic and Invasive Weeds Research Unit, Albany, CA, pers. comm.)</p> <p>-No biocontrol agents have been released for any of the other non-native weeds listed. -Biocontrol using non-native natural enemies is not be an option for control of native aquatic plants that may sometimes be invasive/cause problems, such as coontail and pennywort. Biocontrol using native natural enemies that are reared and released in large numbers (such as a native fungus or a plant-feeding insect) may be an option.</p>	added this info
Moran	30	Gopal 1987 book cited here is not listed in Literature Cited.	fixed
Moran	30	<p>The conclusion that biocontrol poses a unique risk to DO is flawed. Biocontrol of water hyacinth reduces the size of plants over several generations of growth: Tipping, P. W., M. R. Martin, E. N. Pokorny, K. R. Nimmo, D. L. Fitzgerald, F. A. Dray, Jr., and T. D. Center. 2014a. Current levels of suppression of waterhyacinth in Florida, USA. Biological Control 71:65-69. Biocontrol does not cause rapid sinkage that would be associated with DO declines. Also, biomass accumulation in sediments in areas of water hyacinth invasion will occur in either the presence or absence of biocontrol, in areas of low flow; biocontrol will reduce the problems caused by living plants. In any event, biocontrol would not pose any greater DO hazard than herbicidal control, and in fact would pose less of a hazard.</p>	revised text and added citation.
Moran	32	<p>Under Chapter 4 Factors Contributing to the Prevalence of Submersed and Floating Aquatic Vegetation in the Delta</p> <p>4.1.8 Interactions with submersed or other floating species - Fig 4.6 (Left, Bar charts). I assume that Ludwigia is the pink bars after yellow, but this is missing in legend. The figure is partially cut off on the right.</p>	figure placement fixed. Color coding is identified in the caption

Moran	34-35	Under R1, include monitoring of water and plant nutrient content and analysis of their relationships. Also water flow. Possibly also rates of growth.	added
Moran	34-35	R3 is already underway through the USDA-ARS Areawide Project focused on water hyacinth and Egeria densa.	mentioned this
Moran		General Comment on the evaluation factor - All of the major water quality problems caused by the proliferation of water hyacinth and Brazilian waterweed in the Delta have been identified. "Yes"	good
Moran		General Comment on the evaluation factor - All physical and biological factors that influence the abundance and distribution of these invasive aquatic weeds have been identified. "YES, but little quantitative information is provided on the environmental tolerances of the aquatic weeds in terms of salinity, water flow, turbidity, may be other factors such as temperatures. Information could be provided on what is known for the Delta (lots of gaps), and what is known from other areas."	these topics more extensively reviewed now
Moran		General Comment on the evaluation factor - Evidence is presented that ambient nutrient concentrations influence or do not influence the growth, distribution and abundance of aquatic weeds. More quantitative information is needed on typical nutrient levels in the Delta, and nutrient requirements/concentration ranges in the aquatic weeds, and effects on plant growth (not well-studied in the Delta, so would be mostly from other regions).	quite a bit added on this
Moran		General Comment on the evaluation factor - The White Paper findings are fully supported by the literature and there is no additional unreferenced information that either supports or refutes the findings. Additional references have been suggested.	Added many more citations
Moran		General Comment on the evaluation factor - The prioritized list of nutrient recommendations include all questions that need to be resolved before it can be concluded that nutrient management will reduce the severity of the invasive aquatic weed problem in the Delta. NO, the monitoring plan under R1 needs to include water nutrient, plant nutrient, and plant growth information. Also, studies are needed on nutrient changes resulting from control-killed plants being left in place vs removed.	Included

Moran		Additional Questions from the STAG: Is nutrient management necessary for management of macrophytes UNCERTAIN a. Yes or No? b. If so, what level?	okay
Moran		Additional Questions from the STAG: Is nutrient management alone sufficient to control macrophytes? UNLIKELY	okay
Moran		Additional Questions from the STAG: What combinations of management actions (nutrient and non-nutrient) are likely to achieve equal levels of benefit with regard to macrophyte management? What are the likelihoods, costs, and potential unintended consequences of these different strategies?	no comment made
Moran		Additional Questions from the STAG: How do stands of macrophytes affect nutrient dynamics in surrounding waters? Include under R2	done
Moran		Additional Questions from the STAG: How do stands of macrophytes affect higher-level organisms, including POD species? Some studies underway as part of USDA-ARS Areawide Project. Invertebrates in water hyacinth roots before/after chemical herbicide control.	did not discuss at this point

7.2 Comment Matrix and Responses to Stakeholder and Technical Advisory Group

Author	Comment	Response
Bedore	Specific Comment 1. The White Paper provides a general description of the types of impairments that can be associated with macrophyte over-abundance, but there should be greater detail provided on the actual nature of macrophyte-related impairments in the Delta itself. The impairments should be linked to the Beneficial Uses of the Delta as they are described in the Water Quality Control Plan for the Sacramento and San Joaquin River Basins (2011), and the frequency, magnitude, and geographic extent of macrophyte-related impairments should be described for each Beneficial Use. It should also be determined, to the best degree possible, the level of macrophyte management that is necessary to fully achieve these Beneficial Uses.	Did my best to increase the detail in this. Have not linked them to the Beneficial Uses of the Delta document mentioned. I do not have the information on frequency, magnitude and geographic extent of macrophyte related impairments. I don't think we can determine at this time the level of management needed to achieve beneficial uses.
Bedore	Specific Comment 2. A detailed life history for each macrophyte of interest is also recommended to provide context for describing why various physical and biological factors influence their abundance and distribution. Details particular to the life cycles of macrophytes in the Delta would be most helpful.	Life history info has been added, but probably not to the degree desired here. I need to be careful to not exceed my charge or scope.

Bedore	Specific Comment 3. A more thorough review of all known and relevant efforts related to macrophyte management in estuaries should be provided. From this review it could then be determined under what conditions nutrient management or management of other factors (physical removal, herbicide treatments, hydrological controls, etc.) are likely to be successful, and whether control of those factors is possible and/or likely to be effective for the Delta given its unique hydrology and water quality. This information should then be used to rank the probable efficacy of possible macrophyte management options for the Delta.	Added detailed information about management in the Delta. Added a recommendation to review the current and planned control methods with respect to nutrient objectives.
Bedore	Specific Comment 4. Recommendations to expend resources on nutrient/macrophyte-related research should consider the overall probability that nutrient management, relative to other management options, is likely to provide an effective means for addressing the known macrophyte impairments in the Delta.	added more discussion of the fact that there have been massive increases in problematic species during a period when increased nutrients or changes in ratios has not been observed. Suggests that nutrient management may have limited effects compared to other factors controlling the macrophytes.
Lee	Overall Comment: The findings expressed in the draft white papers are consistent with our many years of experience investigating nutrient-related water quality, our findings in investigating Delta nutrient impacts and control of excessive aquatic plants, as well as with the findings expressed in presentations made at the CWEMF Delta Nutrient Modeling Workshop discussed below.	good to hear
Lee	Basically, the water quality/beneficial use of the Delta is seriously degraded by excessive growths of aquatic plants that are caused by excessive nutrient loads to, and within, the Delta.	We have not been able to make the link that excessive nutrient loads are the leading reason for excessive macrophyte growth, although we have not ruled out that they contribute
Lee	There remains little ability to quantitatively and comparatively describe the role of nutrients (N and P) in controlling the excess fertilization of the Delta waters.	that's right
Lee	There is considerable misinformation in the professional arena on the relative roles of N and P concentrations and loads, and the ratios of N to P in affecting water quality in the Delta; some of the information presented on nutrient/water quality issues is biased toward preconceived positions.	do not know what biases are being referred to
Lee	Based on the results of the US and international OECD eutrophication study and our follow on studies of more than 600 waterbodies worldwide (lakes, reservoirs, estuarine systems) the planktonic chlorophyll levels in the Central Delta are well-below those that would be expected based on the phosphorus loads to the Delta.	yes, this is mentioned in the review

Lee	There is a lack of understanding of the quantitative relationship between nutrient loads and fish production in the Delta.	probably true, not sure what the specific comment is here
Lee	The Delta Stewardship Council's timetable for developing Delta nutrient water quality objectives by January 1, 2016, and to adopt and begin implementation of nutrient objectives, either narrative or numeric as appropriate, in the Delta by January 1, 2018 is unrealistically short.	A comment for Chris to address
Lee	There is need for substantial well-funded, focused, and intelligently guided research on Delta nutrient water quality issues over at least a 10-yr period in order to develop the information needed to generate a technically sound and cost-effective nutrient management strategy for the Delta.	A comment for Chris to address
Lee	As discussed in our writing, some of which are noted below, it will be especially difficult to develop technically valid and cost-effective nutrient control programs for excessive growths of macrophytes in the Delta.	okay

DRAFT

2012 South Delta Chinook Salmon Survival Study

Rebecca Buchanan, University of Washington;
Pat Brandes, Mike Marshall, J. Scott Foott, Jack Ingram and David LaPlante,
U.S. Fish and Wildlife Service;
Josh Israel, U.S. Bureau of Reclamation;
Compiled and edited by Pat Brandes, U.S. Fish and Wildlife Service

Introduction

The Vernalis Adaptive Management Plan (VAMP) as part of the San Joaquin River Agreement has been measuring juvenile salmon survival through the Delta since 2000 (SJRG 2013). Prior to 2000, similar south Delta coded-wire-tag (CWT) studies were funded by the Interagency Ecological Program and others (Brandes and McLain 2001). Since 2008, survival of juvenile Chinook Salmon through, or in, the Delta has been measured using acoustic tags. The main objective of the VAMP was to better understand the relationship between Chinook Salmon smolt survival through the Delta and San Joaquin River flows and combined CVP and SWP exports in the presence of the physical head of Old River barrier (HORB). The San Joaquin River Agreement and the VAMP study ended in 2011.

In 2012, the main objective of the Chinook Salmon survival study was to estimate survival through the Delta during the San Joaquin River Flow Modification Project (USBR 2012), during which the Merced River flows were augmented between April 15 and May 15, and compare it to survival, without the flow augmentation (after May 15), in the presence of the HORB. As part of the National Marine Fisheries Service and California Department of Water Resources Joint Stipulation Regarding South Delta Operations during April and May of 2012

(http://www.westcoast.fisheries.noaa.gov/central_valley/water_operations/ocapstip.html; accessed 8/27/15), the physical HORB was installed in 2012. The barrier had eight culverts in 2012, compared to between two and six culverts as in past years. Funding for this study was provided by the restoration fund of the Central Valley Project Improvement Act, the California Department of Water Resources (CDWR) and the U.S. Bureau of Reclamation (USBR).

These salmon studies also estimated route selection at some channel junctions in the south Delta along the main stem San Joaquin River and provided information on how route selection into some reaches influences overall survival through the Delta to Chipps Island. Recent advances in acoustic technology have allowed investigators to evaluate the influence of route selection and reach-specific survival of salmon to overall survival through the Sacramento-San Joaquin Delta (Perry et al. 2010). In this study, the hypothesis focused on the impact of changes in hydrology with the HORB, as the primary factor relative to juvenile salmon survival however we are aware that many other factors also influence survival through the Delta.

Goals and Objectives

The goal of this study was to determine if there were differences in survival resulting from changes in hydrology (i.e. increased flow) with the HORB installed.

Objectives:

1. Determine survival of emigrating salmon smolts from Mossdale to Chipps Island during two time periods (prior to May 15 and after May 15) in the presence of the HORB to determine if there was a benefit from the flow augmentation from the Merced River in the spring of 2012.
2. Assess whether the higher flows resulted in a reduction in travel time; a potential mechanism for why survival may be higher with higher flows.
3. Identify route selection at HOR and Turner Cut under the two periods with varied flows to determine its effect on survival to Chipps Island in 2012.
4. Assess the influence of flow on survival between Mossdale and Jersey Point with the HOR barrier installed in 2012 and compare it to past years to further evaluate if the increased flow from the Merced River flow augmentation likely resulted in higher smolt survival through the Delta.

Background

Survival during the smolt life-stage was assumed to be the link associated with two statistically significant relationships between San Joaquin basin escapement and 1) San Joaquin River flow at Vernalis and 2) the ratio of San Joaquin River flow to Central Valley Project and State Water Project exports, 2 ½ years earlier (Figures 5-20 and 5-21 in SJRGA 2007). It is these relationships between flow and flow/exports and escapement that are the basis for the hypothesis that increasing flow and decreasing exports during the smolt outmigration would increase adult escapement and production in the San Joaquin basin.

The early, pre-VAMP studies compared survival of CWT Feather River Hatchery (FRH) smolts released into upper Old River to those released on the main stem San Joaquin River at Dos Reis. Dos Reis is located on the San Joaquin River downstream of the head of Old River. These studies were conducted between 1985 and 1990 and suggested that survival was higher for salmon smolts released on the main stem San Joaquin River at Dos Reis than for fish released into Old River (Brandes and McLain 2001). The results of these studies were the basis for recommending a rock barrier at the head of Old River (HORB) to prevent juvenile salmon from migrating down Old River where survival appeared to be less.

CWT releases made at Dos Reis were also used to assess the survival of salmon smolts on the San Joaquin River downstream of Old River. Although it is assumed that fish released at Dos Reis migrated downstream via the main stem San Joaquin River, there is the potential for fish released at Dos Reis to have moved upstream into Old River on flood tides, especially during periods of low San Joaquin River flows and high exports or into the interior Delta via Turner or Columbia Cuts or other downstream connections to the interior Delta. Data from 1989 to 1999 indicated that as San Joaquin River flows increased downstream of Old River, survival increased from Dos Reis to Jersey Point (Figure 5-14 in SJRGA 2007). These data provided the basis for the hypothesis that increased flow in the San Joaquin

River would increase salmon smolt survival. However, with the addition of more recent data (2005 and 2006) from recoveries in the trawls (as there were no or limited recovery data from the ocean fishery due to fishery closures in 2008 and 2009), the strength of this relationship appeared to lessen (Figure 5-13 in SJRGA 2007).

With the HORB in place, the majority of the fish migrating downstream would stay on the main stem San Joaquin River at the junction between the San Joaquin River and the head of Old River. With the HORB, a statistically significant relationship between CWT survival in the reach between Mossdale or Durham Ferry and Jersey Point and San Joaquin River flow at Vernalis has been observed ($r^2 = 0.73$, $p < 0.01$; Figure 5-11 in SJRGA 2007), further supporting our hypothesis that increased flow in the San Joaquin River would increase juvenile salmon survival in the Delta.

In 2010, as part of the VAMP peer review, a statistical model was used to model survival through the Delta as a function of flow and exports, based on the CWT releases in the south Delta (Appendix 1). The results of this modeling also suggested survival was generally higher on the San Joaquin River than in Old River and flow tended to improve survival in the San Joaquin River route, but there was a lot of environmental noise (low signal to noise ratio). This modeling also supported our hypothesis that a HORB would improve survival, because it would reduce the number of smolts migrating through Old River.

Conceptual Model

Our hypothesis in 2012 was that survival would increase with increased flow from the Merced River flow augmentation in the presence of the HORB. Flows were an average of 3,543 cfs during the flow augmentation period and 2,327 cfs afterwards. A potential mechanism for increased survival with increased flow is that increased flow results in shorter travel times (i.e. increased migration rates) through the riverine parts of the Delta, and thus reduces the period of exposure to mortality factors such as high water temperature, predation and toxics (Figure 1). Increased flow is also expected to reduce the effect of the mortality factors by 1) decreasing water temperatures to less stressful levels for juvenile salmon, 2) decreasing the impacts of predation due to lower metabolic rates of predators at lower water temperatures and 3) reducing toxicity concentrations through dilution (Figure 1). Survival through the entire Delta (i.e. to Chipps Island) was expected to increase with the higher flows in 2012 as a consequence of higher survival through the riverine portion of the Delta because of these hypothesized relationships.

The higher flows provided by the Merced flow augmentation in 2012 may also have resulted in the tidal prism moving further downstream, because most of the increased flow would have stayed in the San Joaquin River at the head of Old River (HOR) junction with the HORB, in contrast to when there is no HORB and a large majority of the flow moves into Old River at that junction. The shift in the tidal prism's position serves to increase the portion of the Delta that is riverine and the portion of the migration pathway that potentially responds to decreases in travel time in response to increased flow (Figure 1). It is unclear how far the tidal prism would be moved downstream from the increase in flow of approximately 1200 cubic feet per second (cfs) from the Merced flow augmentation in 2012. Additionally, the shifted position of the tidal prism further downstream, which is dependent on the magnitude of the increased flow, could also potentially reduce the proportion of flow and tagged fish

that enter Turner Cut (Figure 1). In summary, survival through the entire Delta was expected to increase as the riverine component of the Delta increased and the proportion of water and fish that were diverted into Turner Cut was reduced from a positional shift of the tidal prism downstream from higher flows.

Once fish enter the interior Delta or into the strongly tidally influenced San Joaquin River, residence times are hypothesized to increase and survival is hypothesized to decrease compared to the river reaches. The increased residence times are anticipated to increase the exposure time of juvenile salmonids to predation or other mortality factors. The incremental increase in flow from the Merced River flow augmentation was not anticipated to decrease water temperatures or dilute toxics in the tidally dominant areas of the Delta as much as the riverine reaches because inflow is a much lower proportion of overall flow in these tidally dominated regions. Lastly, the change to the flow patterns at the HOR from the installation and operation of the HORB was expected to result in fewer tagged fish being salvaged or entrained at the CVP and SWP in 2012 because a low proportion of the San Joaquin flow (~ 5%) and tagged fish enter Old River when the HORB is in place.

Study Design and Methods

This study was conducted in conjunction with a separate, but coordinated study assessing the HORB in 2012 (CDWR, 2015). As part of this HORB assessment, other groups of juvenile salmon were tagged with Hydroacoustic Technology Incorporated (HTI) tags prior to, during, and after the salmon tagging as part of this study (with VEMCO V5 tags). While the methods and results of the HTI study will not be discussed in this report, we have listed when the HTI fish were released with our study fish (Table 1).

Sample Size Analyses

A unique sample size analyses was not conducted for the 2012 study, instead we used information derived from the 2011 VAMP sample size analyses to guide release numbers for the 2012 study (SJRG 2013). For a single release at Durham Ferry it was determined that a sample size of 475 fish would allow estimation of parameters for low route specific survival (0.05), with high detection probability (90-97%) at Chipps Island. To estimate a relative effect of 100%, between two routes (San Joaquin and Old River), 790 fish would need to be tagged with low survival and 410 for medium survival (SJRG 2013). To estimate a relative effect between the two routes of 50%, 3,510 would need to be released in years with low survival and 1,800 would need to be released in years with medium survival (SJRG 2013). We did not have the resources to purchase enough tags to provide the power to estimate the relative effects between routes at either of these levels for the two groups released in 2012.

Study Fish

Study fish were obtained from the Merced River Hatchery (MRH) and transported to the Tracy Fish Collection Facility (TFCF) of the CVP on April 20 and May 7 for tagging. Fish were kept in chilled, ozonized, Delta water (14-15 ° C) until 3-4 days before tagging to minimize the progression of

proliferative kidney disease (PKD). Low water temperatures inhibit the development of PKD (Ferguson 1981): PKD is progressive at temperatures greater than 15° C (Ferguson 1981). Thus 3-4 days before tagging, tanks holding the fish were slowly switched to ambient Delta water so that they could acclimate to Delta water temperatures prior to tagging and transport to the release site. Fish were sorted such that they were greater than 13 grams (~105 mm forklength [FL]) prior to tagging. Tagged study fish averaged 18.0 grams (SD = 3.7), and 112.8 mm FL (SD = 7.2). Fish were taken off feed 24 hours prior to moving them from MRH to the TFCF and 24 hours prior to surgery.

Tags

Juvenile salmon were tagged with VEMCO V5 180 kHz transmitters that weighed 0.66 grams (g) in air on average (SD = 0.012). Tags were 12.7 millimeters (mm) long, 4.3 mm in height, and 5.6 mm wide (<http://vemco.com/products/v4-v5-180khz/>; accessed 6/15/15). The percentage of tag weight to body weight averaged 3.8% (SD = 0.7%) for the 960 fish tagged, well below the recommended 5%. Only 3% (34 of the 960 fish) had a tag weight to body weight ratio slightly greater than 5%, with all less than 5.4%.

Tags were custom programmed with two separate codes; a traditional Pulse Position Modulation (PPM) style coding along with a new hybrid PPM/High Residence (HR) coding. The HR component of the coding allows for detection at high residence receivers. High residence receivers were placed where tag signal collisions (i.e. many tags emitting signals at the same time to the same receiver) were anticipated (CVP, CCF). The transmission of the PPM identification code was followed by a 25-35 second delay, followed by the PPM/HR code, followed by a 25-35 second delay, and then back to the PPM code, etc. The PPM code consisted of 8 pings approximately every 1.2 to 1.5 seconds. The PPM/HR code consisted of 1 PPM code and 8 HR codes (all the same for each individual fish) with 8 pings approximately every 1.2-1.5 seconds.

Tags were soaked in saline water for at least 24 hours prior to tag activation. Tags were activated using a VEMCO tag activator approximately 24 hours prior to tag implantation. For the first week of releases, time of activation was estimated to the nearest hour, whereas tag activation was identified to the nearest minute for the second group of releases.



Photo credit: Jake Osborne

Tagging training

Training those who conducted the tagging occurred between April 9 and April 13 at the TFCF using Chinook Salmon from MRH. Three hundred fish were used for training, and were brought to the TFCF on April 4. The training was conducted by staff from the U.S. Geological Survey (USGS)'s Columbia River Research Laboratory (CRRL). During training, the CRRL refined standard operating procedures, (SOP), and trained personnel to surgically implant acoustic tags (Liedtke 2012). Returning taggers received a refresher course on training during which they were required to tag a minimum of 35 fish. New taggers received a more thorough training on surgical techniques and were required to tag a minimum of 75 fish during training. Training included sessions on knot tying, tagging bananas, tagging dead fish and finally tagging live fish, holding them overnight and necropsying them to evaluate techniques and provide feed-back. Lastly, a mock tagging session was held on April 13 to practice logistic procedures and to identify potential problems and discuss solutions.

Tagging

In 2012, two groups of 480 Chinook Salmon were tagged with VEMCO V5 tags over two weekly periods: May 1-5 and May 16-20. Each group of salmon was tagged in 3 days, over a 6 day period; Chinook Salmon were tagged every other day, to facilitate survival comparisons between Chinook Salmon and steelhead (the comparison between salmon and steelhead will not be discussed in this report). Two sessions of tagging were conducted for salmon: one in the morning and one in the afternoon. Morning and afternoon tagging sessions were further divided into shifts with each shift incorporating groups of salmon tagged with either VEMCO or HTI tags. The salmon tagged as part of this study were tagged on May 1, May 3, May 5 and May 16, May 18 and May 20 (Table 1). Tagging was conducted at the TFCF as was done since 2009. Four surgeons were used to tag the fish and each surgeon had an assistant. Three additional individuals (runners) helped to move fish into and out of the tagging operation.

Tags were inserted into the fish body cavity after the fish had been anesthetized with between 6.0 and 6.5 milliliters (ml) of tricaine methanesulfonate (MS-222) buffered with sodium bicarbonate,

until they lost equilibrium. Fish were weighed (to the nearest 0.1 g) and measured to the nearest mm (FL). Surgeries took between 1 minute 20 seconds and 6 minutes 57 seconds, but most were within 2 to 3 minutes. Tagging was done using standard operating procedures (SOP) developed by the CRRL and refined during the training week. The SOP (Appendix 2) directed all aspects of the tagging operation and was based on Adams et al. (1998) and Martinelli et al (1998) and modified as needed.



Photo credits: Pat Brandes



Photo credit: Pat Brandes



Photo credit: Jake Osborne



Photo credit: Pat Brandes



Photo credit: Jake Osborne

Transmitter Validation

After the surgical implantation of tags, one or two fish were placed into 19 liter (L) (5 gal) perforated buckets with high dissolved oxygen concentrations (110-130%) and allowed to recover from anesthesia for 10 minutes. During this time, tag codes were verified using a 180 khz hydrophone connected to a VR100. Tags that would not verify using the VR100 were replaced with a new tag in a new fish. After validation, a pair of buckets containing either one or two fish was combined to create a bucket of 3 fish. The bucket was then moved into a holding flume of circulating water to await loading to the transport truck once the tagging session was completed.



Photo credits: Pat Brandes

Transport to Release Site

After tagging, the 19L perforated buckets, which usually contained three tagged Chinook Salmon each, were held in a flume at the TFCF until they were loaded into transport tanks at the end of each tagging session (morning or afternoon). Immediately prior to loading, all fish were visually inspected for mortality or signs of poor recovery from tagging (e.g. erratic swimming behavior). Fish that died or were not recovering from surgery were replaced with a new tagged fish.

In order to minimize the stress associated with moving fish and for tracking smaller groups of individually tagged fish, two specially designed transport tanks were used to move Chinook Salmon from the TFCF, where the tagging occurred, to the release site at Durham Ferry. The transport tanks for Chinook Salmon were designed to securely hold a series of 19 L perforated buckets filled with fish. Tanks had an internal frame that held 21 or 30 buckets in individual compartments to minimize contact between containers and to prevent tipping. Buckets were covered in the transport tanks with stretched cargo nets to assure buckets did not tip over and lids did not come off. Both transport tanks were mounted on the bed of a 26 foot flatbed truck that was equipped with an oxygen tank and hosing to deliver oxygen to each of the tanks during transport. Two trips to the release site were made each tagging day, with the morning and afternoon sessions of tagged fish being transported separately (Table 1).



Photo credits: Jake Osborne



Photo credits: Jake Osborne



Photo credit: Pat Brandes

After loading buckets into the transport tank, de-chlorinated ice was usually added to the transport tanks to either 1) reduce water temperatures during transport such that they would be closer to the river temperature at the release site, or 2) to prevent water temperatures from increasing during transport. Water temperature and dissolved oxygen (DO) in the transport tanks were recorded after loading buckets and ice (if added) into transport tanks; before leaving the TFCF and at the release site after transport, prior to unloading buckets. The temperature and DO were also measured in the river at the holding/release site.

Transfer to Holding Containers

Once at the release site, the perforated buckets, which typically contained three Chinook Salmon each, were removed from the transport tanks and moved to the river. For all releases, perforated buckets were placed into “sleeves” in a pick-up truck and driven a short distance to the river’s edge. A “sleeve” is a similar-sized, non-perforated bucket that allows more water to stay in the perforated bucket than would be the case without placing it in a “sleeve”. Perforated buckets in sleeves were unloaded from the pick-up truck and carried to the river. Perforated buckets were then separated from the sleeves at the shoreline and submerged in-river to be transported to the holding containers which were anchored one to two meters from shore. Water temperature and dissolved oxygen levels were measured in the river prior to placing the salmon into the holding containers in the river.

Once at the river’s edge, the tagged Chinook Salmon were transferred from the perforated buckets to the holding containers; 120 L (32 gal) perforated plastic garbage cans held in the river. These holding containers were perforated with hole sizes of 0.64 cm in diameter. Five buckets containing fish were emptied into each perforated garbage can. Only four of the five buckets emptied into the garbage cans contained VEMCO tagged fish while the fifth bucket of each group held 3 to 4 HTI fish. Each bucket and garbage can was labeled to track the specific tag codes and assure fish were transferred to the correct holding can for later release at the correct time. Tagged salmon were held in the perforated garbage cans for approximately 24 hours prior to release. Steelhead for the 6 Year Study were held at the same location and released either the day before or the day after the releases of Chinook Salmon; steelhead were released May 1-2, May 3-4, and May 5-6, and May 18-19, May 20-21, and May 22-23.



Photo credit: Pat Brandes

Fish Releases

The Chinook Salmon, held in perforated garbage cans, were transported downstream by boat to the release location which was in the middle of the channel downstream of the holding location. The fish were released downstream of the holding site to potentially reduce initial predation of tagged fish immediately after release, under the assumption that predators may congregate near the holding location. Releases were made every 4 hours after the 24 hour holding period, at approximately 1500, 1900, 2300 hours (the day after tagging), and 0300, 0700, and 1100 hours (2 days after tagging)(Table 1). Fish releases were made at these four-hour increments through-out the 24-hour period to spread the fish out and to better represent naturally spawned fish that may migrate downstream through-out the 24 hour period. The Chinook Salmon releases were made on May 2-3, May 4-5, May 6-7 and May 17-18, May 19-20, May 21-22 (Table 1).

Immediately prior to release, each holding container was checked for any dead or impaired fish. At the release time, the lid was removed and the holding container was rotated to look for mortalities. The container was then inverted to allow the fish to be released into the river. After the holding container was inverted, the time was recorded. As the holding containers were flipped back over, they were inspected to make sure that none of the released fish swam back into the container. Some exceptions to this procedure occurred as one group was released from shore due to high winds and waves, and three groups were released from shore due to a dead battery in the boat (Table 1).

Once the release was completed, the information on any dead fish was recorded and the tags removed. The tags were bagged and labeled and returned to the tagging location or office for tag code identification.



Photo credit: Pat Brandes

Dummy-tagged fish

In order to evaluate the effects of tagging and transport on the survival of the tagged fish, several groups of Chinook Salmon were implanted with inactive (“dummy”) transmitters. Dummy tags in 2012 were systematically interspersed into the tagging order for each release group. For each day of tagging and transport, 15 fish were implanted with dummy transmitters and included in the tagging process (Table 1). Procedures for tagging these fish, transporting them to the release site, and holding them at the release site were the same as for fish with active transmitters. Dummy-tagged fish were evaluated for condition and mortality after being held at the release site for approximately 48 hours. After being held, dummy tagged fish were assessed qualitatively for percent scale loss, body color, fin hemorrhaging, eye quality, and gill coloration (Table 2). In addition, two additional groups of 15 dummy-tagged fish (tagged on the same day) were held for approximately 48 hours and assessed for pathogens and other diseases (discussed below).

Fish Health Assessment

As a part of the 2012 South Delta Chinook Salmon Survival Study, the U.S. Fish and Wildlife Service’s CA-NV Fish Health Center (CNFHC) conducted a general pathogen screening and smolt physiological assessment on dummy-tagged fish held at the release site for 48 hours. The health and physiological condition of the study fish can help explain their performance and survival during the studies. Pathogen screenings during past VAMP studies using MRH Chinook Salmon have regularly found infection with the myxozoan parasite *Tetracapsuloides bryosalmonae*, the causative agent of Proliferative Kidney Disease (PKD). This parasite has been shown to cause mortality in Chinook Salmon with increased mortality and faster disease progression in fish at higher water temperatures (Ferguson 1981; Foott et al. 2007). The objectives of this element of the project were to evaluate the juvenile Chinook Salmon used for the studies for specific fish pathogens including *Tetracapsuloides bryosalmonae* and assess smolt development from gill $\text{Na}^+ - \text{K}^+$ -ATPase activity to determine potential differences in health between groups. For a complete description of methods see Appendix 4.

Tag life tests

Two tag life tests were conducted in conjunction with this study. The first tag-life study began on May 16, with 43 tags. The second tag-life study began on May 24, with 40 tags. Tags were activated and then put into mesh bags and held in holding tanks at the TFCF containing ambient Delta water. A VEMCO VR2W was installed in each tank for recording detections of each individual tag. Files of detections were reviewed to identify the tag failure of each individual tag used in the tag life study. These results were then compared to observed tag travel times of the tags used in the study to estimate their tag life and make any necessary corrections to fish survival estimates.

Tag retention test

On May 25, 2012, each of the 4 surgeons tagged 9 to 10 fish with dummy tags to assess tag retention and longer-term mortality of tagged fish. Thirteen of these fish were held in each of 3 separate tanks for 30 days to determine if there was any longer-term mortality of the tagged fish and whether any tags were expelled. Fish were held in tanks at the TFCF for the duration of the 30 days.

Receiver deployment, retrieval, and receiver database

The 2012 Chinook Salmon Survival Study, in conjunction with the 6-Year Steelhead Study used receivers at 26 locations in the lower San Joaquin River and South Delta to Chipps Island (i.e. Mallard Slough) for detecting juvenile salmon and steelhead as they migrated through the Delta (Figure 2). These receivers were placed at key locations throughout the south Delta and similar to those used in VAMP in 2010 and 2011 (Figure 2). Although locations of receivers are similar, the VAMP study used an HTI receiver array, whereas the 2012 study used a VEMCO receiver array. The USBR funded the USGS to deploy, maintain and remove all of the receivers in the array, including receivers at both Jersey Point and Chipps Island in 2012. The detections of tagged salmon on these receivers allowed survival of juvenile salmon to be estimated from Durham Ferry to Chipps Island.

Data processing and survival model

This study used the tag detection data recorded on the receiver array to populate a release-recapture model similar to that used in the 2010 and 2011 VAMP studies (SJGRA 2011, 2013). The release-recapture model used the pattern of detections among all tags to estimate the probabilities of route selection, survival, and transition in various reaches and detection probability at receivers. Parameter estimates were then combined to calculate estimates of reach-specific survival, route-specific survival, and total survival through the Delta to Chipps Island. The release-recapture model (described in more detail below) is a multi-state model based on the models of Cormack (1964), Jolly (1965), and Seber (1965), in combination with the route-specific survival model of Skalski et al. (2002). Tags that appeared to be in predators were identified, and the model was fit first to the complete data set that included all detections, including those from predators, and then to the reduced data set that omitted detections that appeared to come from predators. This allowed comparison of estimates of survival and route selection probabilities with and without tags that appeared to come from predators in order to assess the potential bias associated with predator detections; this approach was similar to that used in the 2010 and 2011 VAMP studies (SJGRA 2011, 2013). More details on all statistical methods follow.

Statistical Methods

Data Processing for Survival Analysis

The University of Washington (UW) received the database of tagging and release data from the US Fish and Wildlife Service (USFWS). The tagging database included the date and time of tagging surgery for each tagged Chinook Salmon released in 2012, as well as the name of the surgeon (i.e., tagger), and the date and time of release of the tagged fish to the river. Fish size (length and weight), tag size, and any notes about fish condition were included, as well as the survival status of the fish at the time of release. Tag serial number and three unique tagging codes were provided for each tag, representing codes for various types of signal coding. Tagging data were summarized according to release group and tagger, and were cross-checked with Pat Brandes (USFWS) for quality control.

Acoustic tag detection data collected at individual monitoring sites (Table 3) were transferred to the USGS in Sacramento, California. A multiple-step process was used to identify and verify detections of fish in the data files, and produce summaries of detection data suitable for converting to tag detection histories. Detections were classified as valid if two or more pings were recorded within a 30 minute time frame on the hydrophones comprising a detection site from any of the three tag codes associated with the tag. The UW received the primary database of autoprocessed detection data from the USGS. These data included the date, time, location, and tag codes and serial number of each valid detection of the acoustic Chinook Salmon tags on the fixed site receivers. The tag serial number was linked to the acoustic tag ID, and was used to identify tag activation time, tag release time, and release group from the tagging database.

The autoprocessed database was cleaned to remove obviously invalid detections. The UW identified potentially invalid detections based on unreasonable travel times or unlikely transitions between detections, and queried the USGS processor about any discrepancies. All corrections were noted and made to the database. All subsequent analysis was based on this cleaned database.

The information for each tag in the database included the date and time of the beginning and end of each detection event when a tag was detected. Unique detection events were distinguished by detection on a separate hydrophone or by a time delay of 30 minutes between repeated hits on the same receiver. Separate events were also distinguished by unique tag encoding schemes (e.g., PPM vs. hybrid PPM/HR). The cleaned detection event data were converted to detections denoting the beginning and end of receiver “visits,” with consecutive visits to a receiver separated either by a gap of 12 hours or more between detections on the receiver, or by detection on a different receiver. Detections from receivers in dual or redundant arrays were pooled for this purpose, as were detections using different tag coding schemes.

Distinguishing between Detections of Salmon and Predators

The possibility of predatory fish eating tagged study fish and then moving past one or more fixed site receivers complicated analysis of the detection data. The Chinook Salmon survival model depended on the assumption that all detections of the acoustic tags represented live juvenile Chinook Salmon, rather than a mix of live salmon and predators that temporarily had a salmon tag in their gut. Without removing the detections that came from predators, the survival model would produce potentially biased

survival estimates of actively migrating juvenile Chinook Salmon through the Delta. The size and type (positive or negative) of the bias would depend on the amount of predation by predatory fish and the spatial distribution of the predatory fish after eating the tagged salmon. In order to minimize bias, the detection data were filtered for predator detections, and detections assumed to come from predators were identified.

The predator filter used for analysis of the 2012 data was based on the predator filter designed and used in the analysis of the 2011 data (SJRG 2013). That predator filter in turn was based on predator analyses presented by Vogel (2010, 2011), as well as conversations with fisheries biologists familiar with the San Joaquin River and Delta regions and the predator decision processes used in previous years (SJRG 2010, 2011). The filter was applied to all detections of all tags. Two data sets were then constructed: the full data set including all detections, including those classified as coming from predators (i.e., “predator-type”), and the reduced data set, restricted to those detections classified as coming from live Chinook Salmon smolts (i.e., “smolt-type”). The survival model was fit to both data sets separately. The results from the analysis of the reduced “smolt-type” data set are presented as the final results of the 2012 Chinook Salmon tagging study. Results from analysis of the full data set including “predator-type” detections were used to indicate the degree of uncertainty in survival estimates arising from the predator decision process.

The predator filter was based on assumed behavioral differences between salmon smolts and predators such as striped bass and white catfish. All detections were considered when implementing the filter, including detections from acoustic receivers that were not otherwise used in the survival model. As part of the decision process, environmental data including river flow, river stage, and water velocity were examined from several points throughout the Delta (Table 4), as available. Hydrologic data were downloaded from the California Data Exchange Center website (<http://cdec.water.ca.gov/selectQuery.html>) and the California Water Data Library (www.water.ca.gov/waterdatalibrary/) on 27 September 2013. Environmental data were reviewed for quality, and obvious errors were omitted.

For each tag detection, several steps were performed to determine if it should be classified as predator or salmon. Initially, all detections were assumed to be of live smolts. A tag was classified as a predator upon the first exhibition of predator-type behavior, with the acknowledged uncertainty that the salmon smolt may actually have been eaten sometime before the first obvious predator-type detection. Once a detection was classified as coming from a predator, all subsequent detections of that tag were likewise classified as predator detections. The assignment of predator status to a detection was made conservatively, with doubtful detections classified as coming from live salmon. In general, the decision process was based on the assumptions that (1) salmon smolts were unlikely to move against the flow, and (2) salmon smolts were actively migrating and thus wanted to move downriver, although they may have temporarily moved upstream with reverse flow.

A tag could be given a predator classification at a detection site on either arrival or departure from the site. A tag classified as being in a predator because of long travel time or movement against the flow was typically given a predator classification upon arrival at the detection site. On the other hand, a tag classified as being in a predator because of long residence time was given a predator classification upon departure from the detection site. Because the survival analysis estimated survival

within reaches between sites, rather than survival during detection at a site, the predator classifications on departure from a site did not result in removal of the detection at that site from the reduced data set. However, all subsequent detections were removed from the reduced data set.

The predator filter used various criteria on several spatial and temporal scales, as described in detail in previous reports (e.g., SJRGA 2013). Criteria fit under various categories, described in more detail in SJRGA (2013): fish speed, residence time, upstream transitions, other unexpected transitions, travel time since release, and movements against flow. The criteria used in the 2011 study were updated to reflect river conditions and observed tag detection patterns in 2012 (Table 5a and 5b). Differences between the 2011 filter and the filter used for the 2012 study (in addition to those identified in Table 5a and 5b) were:

1. Minimum migration rates on upstream-directed transitions were set to 0.1-0.2 km/hr for most upstream transitions. Upstream transitions in Old River from the Highway 4 area to the CVP trashracks and in the Sacramento or San Joaquin River from Threemile Slough to Chipps Island were limited to migration rates no less than 0.5 km/hr.
2. Maximum regional residence times allowed for smolts were set at 60 hours for the San Joaquin River upstream of the head of Old River, and 360 hours in all other regions. In most cases, the maximum regional residence time allowed for smolts making a downstream-directed transition was set at 3 – 5 times the maximum allowable near-field residence time.
3. A maximum of 3 upstream forays and 15 upstream river kilometers was imposed.
4. Maximum allowable travel time since release at Durham Ferry was set at 15 days (360 hours).

The predator scoring and classification method used for the 2011 study was used again for the 2012 study, resulting in tags being classified as in either a predator or a smolt upon arrival at and departure from a given receiver site and visit; for more details, see SJRGA (2013). All detections of a tag subsequent to its first predator designation were classified as coming from a predator, as well.

The criteria used in the predator filter were spatially explicit, with different limits defined for different receivers and transitions (Table 5a and 5b). General components of the approach to various regions are described below. Only regions with observed detections are described; regions that follow the general guidelines described in SJRGA (2013) are not highlighted here.

DFU, DFD = Durham Ferry Upstream (A0) and Durham Ferry Downstream (A2): ignore flow and velocity measures, allow long travel time to accommodate initial disorientation after release, and allow few if any repeat visits.

SJL = San Joaquin River near Lathrop (A5): upstream transitions from Stockton sites are not allowed.

ORE = Old River East (B1): repeat visits are not allowed.

SJG = San Joaquin River at Garwood Bridge (A6): transitions from upstream require arrival on flood tide

SJNB = San Joaquin River at Navy Bridge Drive (A7): allow longer residence time if arrive at slack tide; repeated visits require arriving with opposite flow and velocity conditions to departure conditions.

MAC, MFE/MFW = MacDonald Island (A8), Medford Island (A9): repeated visits require arriving with opposite flow and velocity conditions to departure conditions.

TCE/TCW = Turner Cut (F1): should not move against flow; repeated visits require arriving with opposite flow and velocity conditions to departure conditions.

ORS = Old River South (B2): repeated visits require arriving with opposite flow and velocity conditions to departure conditions.

CVP = Central Valley Project (E1): allow multiple visits; transitions from downstream Old River should not have departed Old River site against flow; no repeat visits or arrivals from downstream if not pumping.

JPE/JPW, FRE/FRW = Jersey Point (G1), False River (H1): no flow/velocity restrictions; allowed for transition from Threemile Slough (TMS/TMN)

Constructing Detection Histories

For each tag, the detection data summarized on the “visit” scale was converted to a detection history (i.e., capture history) that indicated the chronological sequence of detections on the fixed site receivers throughout the study area. In cases in which a tag was observed passing a particular receiver or river junction multiple times, the detection history represented the final route of the tagged fish past the receiver or river junction. Detections from the receivers comprising certain dual arrays were pooled, thereby converting the dual arrays to redundant arrays: the San Joaquin River near Mossdale Bridge (MOS, site A4), Lathrop (SJL, A5), and Garwood Bridge (SJG, A6); and Old River East near the head of Old River (ORE, B1). For some release groups, the receivers comprising the dual array just downstream of the initial release site (DFD, A2) were also pooled in order to achieve a better model fit; in other cases, very low detection probabilities at this site required omitting this site from analysis. Likewise, in some cases the dual arrays at either MacDonald Island (MAC, A8) or Old River South (B2) were pooled in order to improve model fit.

Survival Model

A two-part multi-state statistical release-recapture model was developed to estimate salmon smolt survival and migration route parameters throughout the study area. The full two-part model incorporates all receivers, with the exception of the San Joaquin River receiver just upstream of the head of Old River (HOR = B0), the northern-most receivers in Old and Middle rivers (OLD = B4 and MRE = C3) and the Threemile Slough receivers (TMS/TMN = T1) (Table 3, Figure 2). Because many acoustic receivers in the interior delta had no or few detections, a reduced model was developed by simplifying

the full model and limiting it to receivers with sufficient detections for analysis. The full model is described in detail first, and then the reduced model is presented.

Full Model

The full release-recapture model is a slightly simplified version of the model used to analyze 2011 steelhead data (Buchanan 2013), and similar to the model developed by Perry et al. (2010) and the model developed for the 2009 – 2011 VAMP studies (SJRG 2010, 2011, 2013). Figure 2 shows the layout of the receivers using both descriptive labels for site names and the code names used in the survival model (Table 3). The survival model represents movement and perceived survival throughout the study area to the primary exit point at Chipps Island (i.e., Mallard Island) (Figure 3, Figure 4). Individual receivers comprising dual arrays were identified separately, using “a” and “b” to represent the upstream and downstream receivers, respectively. Not all sites were used in the survival model, although all were used in the predator filter.

Fish moving through the Delta toward Chipps Island may have used any of several routes. The two primary routes modeled were the San Joaquin River route (Route A) and the Old River route (Route B). Route A followed the San Joaquin River past the distributary point with Old River near the town of Lathrop and past the city of Stockton. Downstream of Stockton, fish in the San Joaquin River route (Route A) may have remained in the San Joaquin River past its confluence with the Sacramento River and on to Chipps Island. Alternatively, fish in Route A may have exited the San Joaquin River for the interior Delta at any of several places downstream of Stockton, including Turner Cut, Columbia Cut (just upstream of Medford Island), and the confluence of the San Joaquin River with either Old River or Middle River, at Mandeville Island. Of these four exit points from the San Joaquin River between Stockton and Jersey Point, only Turner Cut was monitored and assigned a route name (F, a subroute of route A). Fish that entered the interior Delta from any of these exit points may have either moved north through the interior Delta and reached Chipps Island by returning to the San Joaquin River and passing Jersey Point and the junction with False River, or they may have moved south through the interior Delta to the state or federal water export facilities, where they may have been salvaged and trucked to release points on the San Joaquin or Sacramento rivers just upstream of Chipps Island. All of these possibilities were included in both subroute F and route A.

For fish that entered Old River at its distributary point on the San Joaquin River just upstream of Lathrop (route B), there were several pathways available to Chipps Island. These fish may have migrated to Chipps Island either by moving northward in either the Old or Middle rivers through the interior Delta, or they may have moved to the state or federal water export facilities to be salvaged and trucked. The Middle River route (subroute C) was monitored and contained within Route B. Passage through the State Water Project via Clifton Court Forebay was monitored at the entrance to the forebay and assigned a route (subroute D). Likewise, passage through the federal Central Valley Project was monitored at the entrance trashracks and in the facility holding tank and assigned a route (subroute E). Subroutes D and E were both contained in subroutes C (Middle River) and F (Turner Cut), as well as in primary routes A (San Joaquin River) and B (Old River). All routes and subroutes included multiple unmonitored pathways for passing through the Delta to Chipps Island.

Several exit points from the San Joaquin River were monitored and given route names for convenience, although they did not determine unique routes to Chipps Island. The first exit point encountered was False River, located off the San Joaquin River just upstream of Jersey Point. Fish entering False River from the San Joaquin River entered the interior Delta at that point, and would not be expected to reach Chipps Island without subsequent detection in another route. Thus, False River was considered an exit point of the study area, rather than a waypoint on the route to Chipps Island. It was given a route name (H) for convenience. Likewise, Jersey Point and Chipps Island were not included in unique routes. Jersey Point was included in many of the previously named routes (in particular, routes A and B, and subroutes C and F), whereas Chipps Island (the final exit point) was included in all previously named routes and subroutes except route H. Thus, Jersey Point and Chipps Island were given their own route name (G). Three additional sets of receivers located in Old River (Route B) and Middle River (Subroute C) north of Highway 4 and in Threemile Slough (Route T) were not used in the survival model. The routes, subroutes, and study area exit points are summarized as follows:

- A = San Joaquin River: survival
- B = Old River: survival
- C = Middle River: survival
- D = State Water Project: survival
- E = Central Valley Project: survival
- F = Turner Cut: survival
- G = Jersey Point, Chipps Island: survival, exit point
- H = False River: exit point
- T = Threemile Slough: not used in survival model

The release-recapture model used parameters that denote the probability of detection (P_{hi}), route entrainment (ψ_{hi}), Chinook Salmon survival (S_{hi}), and transition probabilities equivalent to the joint probability of movement and survival ($\phi_{kj,hi}$) (Figure 3, Figure 4, Table A5-1). Unique detection probabilities were estimated for the individual receivers in a dual array: P_{hia} represented the detection probability of the upstream array at station i in route h , and P_{hib} represented the detection probability of the downstream array.

The model parameters are:

P_{hi} = detection probability: probability of detection at telemetry station i within route h , conditional on surviving to station i , where $i = ia, ib$ for the upstream, downstream receivers in a dual array, respectively.

S_{hi} = perceived survival probability: joint probability of migration and survival from telemetry station i to station $i+1$ within route h , conditional on surviving to station i .

ψ_{hl} = route entrainment probability: probability of a fish entering route h at junction l ($l=1, 2$), conditional on fish surviving to junction l .

$\phi_{kj,hi}$ = transition probability: joint probability of route entrainment, and survival; the probability of migrating, surviving, and moving from station j in route k to station i in route h , conditional on survival to station j in route k .

A variation on the parameter naming convention was used for parameters representing the transition probability to the junction of False River with the San Joaquin River, just upstream of Jersey Point (Figure 2). This river junction marks the distinction between routes G and H, so transition probabilities to this junction are named $\phi_{kj,GH}$ for the joint probability of surviving and moving from station j in route k to the False River junction. Fish may arrive at the junction either from the San Joaquin River or from the interior Delta. The complex tidal forces present in this region prevent distinguishing between smolts using False River as an exit from the San Joaquin and smolts using False River as an entrance to the San Joaquin from Frank's Tract. Regardless of which approach the fish used to reach this junction, the $\phi_{kj,GH}$ parameter (e.g. $\phi_{A9,GH}$) is the transition probability from station j in route k to the junction of False River with the San Joaquin River via any route; ψ_{G1} is the probability of moving downstream toward Jersey Point from the junction; and $\psi_{H1} = 1 - \psi_{G1}$ is the probability of exiting (or re-exiting) the San Joaquin River to False River from the junction (Figure 3).

Because of the complexity of routing in the vicinity of MacDonald Island (referred to as "Channel Markers" in reports from previous years, e.g., SJRGA 2013) on the San Joaquin River, Turner Cut, and Medford Island, and the possibility of reaching the interior Delta via either route A or route B, the full survival model that represented all routes was decomposed into two submodels for analysis. Submodel I modeled the overall migration from release at Durham Ferry to arrival at Chipps Island without modeling the specific routing from the lower San Joaquin River (i.e., from the Turner Cut Junction) through the interior Delta to Chipps Island, although it included detailed subroutes in route B for fish that entered Old River at its upstream junction with the San Joaquin River (Figure 3). In Submodel I, transitions from MacDonald Island (A8) and Turner Cut (F1) to Chipps Island were interpreted as survival probabilities ($S_{A8,G2}$ and $S_{F1,G2}$) because they represented all possible pathways from these sites to Chipps Island. Submodel II, on the other hand, focused entirely on Route A, and used a virtual release of tagged fish detected at the San Joaquin River receiver array near Lathrop, (SJL) to model the detailed routing from the lower San Joaquin River near MacDonald Island and Turner Cut through or around the interior Delta to Jersey Point and Chipps Island (Figure 4). Submodel II included the Medford Island detection site (A9), which was omitted from Submodel I because of complex routing in that region.

Reduced Model

Detection data of tagged Chinook Salmon in the interior Delta in 2012 were very sparse. There were very few detections at the downstream Old and Middle river sites (OR4 [model code B3] and MR4

[C2]) and Central Valley Project (model codes E1 and E2) receivers, and no detections in Middle River at its head (C1) or radial gates (D1 and D2) receivers. There were also no detections at False River (H1) used in the survival analysis because all False River detections were followed by detections either at Jersey Point (G1) or Chipps Island (G2). With so few detections in the Old River route and the interior Delta portions of the San Joaquin River route, it was not possible to fit the full release-recapture model to the 2012 Chinook Salmon data set. Instead, it was necessary to omit all detection sites in the Old River route other than the first two sites in that route: ORE (B1) and ORS (B2). The simplified submodel I (Figure 5) includes the overall probability of surviving from the Old River receivers near the head of Middle River (ORS) to Chipps Island, $S_{B2,G2}$. This parameter includes all ways of getting from ORS (site B2) to Chipps Island (site G2), and is interpreted as the sum of products of the $\phi_{k_i,hi}$ parameters from the full Submodel I:

$$S_{B2,G2} = \phi_{B2,D1}\phi_{D1,D2}\phi_{D2,G2} + \phi_{B2,E1}\phi_{E1,E2}\phi_{E2,G2} + (\phi_{B2,B3}\phi_{B3,GH} + \phi_{B2,C2}\phi_{C2,GH})\psi_{G1}\phi_{G1,G2}.$$

The reduced Submodel I does not decompose $S_{B2,G2}$ into its route-specific components because of sparse data.

The reduced Submodel II focuses on transitions in and from the lower portions of the San Joaquin River, and omits transitions from this region to the interior Delta or water export facilities (Figure 6). While the full Submodel II included transitions from MacDonal Island, Medford Island, and Turner Cut to the interior Delta and water export facilities, insufficient observations of tags making these transitions made it necessary to omit these pathways from the reduced model. Thus, the reduced Submodel II models transitions only to the Jersey Point/False River junction from the MacDonal Island/Medford Island/Turner Cut region. In fact, because no tags were observed exiting the system at False River, it was not possible to separate the probability of getting to the Jersey Point/False River junction ($\phi_{hi,GH}$) from the probability of turning toward Jersey Point (ψ_{G1}); instead, only the product was estimable: $\phi_{hi,G1} = \phi_{hi,GH}\psi_{G1}$, for transitions from site i in route h . Thus, the reduced Submodel II used parameters $\phi_{A8,G1}$, $\phi_{A9,G1}$, and $\phi_{F1,G1}$, which jointly include all routes from the lower San Joaquin River receivers to Jersey Point, including those past the interior Delta receivers in northern Old and Middle rivers (B3 and C2). Likewise, without detections at the head of Middle River receiver (MRH, code C1), it was not possible to separately estimate the probability of surviving from the head of Old River to the head of Middle River (S_{B1}) from the probability of remaining in Old River at the head of Middle River (ψ_{B2}). Only the product was estimate: $\phi_{B1,B2} = S_{B1}\psi_{B2}$. Finally, there were insufficient detections at the receivers upstream of the Durham Ferry release site (DFU, code A0), so the A0 site was removed from the simplified submodel I (Figure 5).

The two simplified submodels I and II were fit concurrently using unique detection and transitions probabilities at shared receivers: SJG (A6), SJNB (A7), MAC (A8), TCE/TCW (F1), and MAE/MAW (G2). Parameters at these sites were estimated separately for the two submodels to avoid “double-counting” tags used in both submodels.

In addition to the model parameters, derived performance metrics measuring migration route probabilities and survival were estimated as functions of the model parameters. Both route entrainment and route-specific survival were estimated for the two primary routes determined by routing at the head of Old River (routes A and B). Route entrainment and route-specific survival were also estimated for the major subroutes of route A; subroutes were not distinguishable for route B. These subroutes were identified by a two-letter code, where the first letter indicates routing used at the head of Old River (i.e., A), and the second letter indicates routing used at the Turner Cut junction: A or F. Thus, the route entrainment probabilities for the route A subroutes were:

$\psi_{AA} = \psi_{A1}\psi_{A2}$: probability of remaining in the San Joaquin River past both the head of Old River and the Turner Cut Junction, and

$\psi_{AF} = \psi_{A1}\psi_{F2}$: probability of remaining in the San Joaquin River past the head of Old River, and exiting to the interior Delta at Turner Cut, where $\psi_{F2} = 1 - \psi_{A2}$.

Route entrainment probabilities were estimated on the large routing scale, as well, focusing on routing only at the head of Old River. The route entrainment parameters were defined as:

$\psi_A = \psi_{A1}$: probability of remaining in the San Joaquin River at the head of Old River

$\psi_B = \psi_{B1}$: probability of entering Old River at the head of Old River.

The probability of surviving from the entrance of the Delta near Mossdale Bridge (site A4, MOS) through an entire migration pathway to Chipps Island was estimated as the product of survival probabilities that trace that pathway:

$S_{AA} = S_{A4}S_{A5}S_{A6}S_{A7}S_{A8,G2}$: Delta survival for fish that remained in the San Joaquin River past the head of Old River and Turner Cut,

$S_{AF} = S_{A4}S_{A5}S_{A6}S_{A7}S_{F1,G2}$: Delta survival for fish that entered Turner Cut from the San Joaquin River, and

$S_B = S_{A4}\phi_{B1,B2}S_{B2,G2}$: Delta survival for fish that entered Old River at its head.

The overall probability of surviving through the Delta in the San Joaquin River route was defined using the subroute-specific survival probabilities and the probabilities of taking each subroute:

$S_A = \psi_{A2}S_{AA} + \psi_{F2}S_{AF}$: Delta survival (from Mossdale to Chipps Island) for fish that remained in the San Joaquin River at the head of Old River.

The parameters $S_{A8,G2}$ and $S_{F1,G2}$ used in S_{AA} and S_{AF} represent the probability of getting to Chipps Island (i.e., Mallard Island, site MAE/MAW) from A8 and F1, respectively. Both parameters represent multiple pathways around or through the Delta to Chipps Island (Figure 2). Fish that were detected at the A8 receivers (MacDonald Island) may have remained in the San Joaquin River all the way to Chipps Island, or they may have entered the interior Delta downstream of Turner Cut. Fish that entered the interior Delta either at Turner Cut or farther downstream may have migrated through the interior Delta to Chipps Island via Frank's Tract or Fisherman's Cut, False River, and Jersey Point; returned to the San Joaquin River via its downstream confluence with either Old or Middle River at Mandeville Island; or gone through salvage and trucking from the water export facilities. All such routes are represented in the $S_{A8,G2}$ and $S_{F1,G2}$ parameters, which were estimated directly using Submodel I.

The route-specific survival probability for the Old River route, S_B , includes a transition probability, $\phi_{B1,B2}$, as a factor. As indicated above, $\phi_{B1,B2}$ is the product of a survival probability and a route entrainment probability: $\phi_{B1,B2} = S_{B1}\psi_{B2}$. No tags were detected on the Middle River receivers near the head of Middle River (site C1). However, if some tags actually had entered Middle River at its head without detection, then $\psi_{B2} < 1$ and $\phi_{B1,B2} < S_{B1}$, resulting in S_B being a minimum estimate of true Delta survival in the Old River route.

Using the estimated migration route probabilities and route-specific survival for these two primary routes (A and B), survival of the population from A4 (Mosssdale) to Chipps Island was estimated as:

$$S_{Total} = \psi_A S_A + \psi_B S_B.$$

Survival was also estimated from Mosssdale to Jersey Point, although this was estimable only for fish in the San Joaquin River route. Survival through this region ("Mid-Delta" or MD) was defined as follows:

$S_{A(MD)} = \psi_{A2} S_{AA(MD)} + \psi_{F2} S_{AF(MD)}$: Mid-Delta survival for fish that remained in the San Joaquin River past the head of Old River,

where

$$S_{AA(MD)} = S_{A4} S_{A5} S_{A6} S_{A7} (\phi_{A8,G1} + \phi_{A8,A9} \phi_{A9,G1}), \text{ and}$$

$$S_{AF(MD)} = S_{A4} S_{A5} S_{A6} S_{A7} \phi_{F1,G1}.$$

Survival was also estimated through the southern portions of the Delta ("Southern Delta" or SD), although once again this was estimable only for fish in the San Joaquin River route:

$$S_{A(SD)} = S_{A4} S_{A5} S_{A6} S_{A7}.$$

The probability of reaching Mossdale from the release point at Durham Ferry, ϕ_{A1A4} , was defined as the product of the intervening reach survival probabilities:

$$\phi_{A1,A4} = \phi_{A1,A2} S_{A2} S_{A3}.$$

This measure reflects a combination of mortality and possible residualization upstream of Old River, although the Chinook Salmon in this study were assumed to be migrating (i.e., no residualization). In cases where the first detection site A2 (DFD) had to be removed from analysis, the alternative model parameter $\phi_{A1,A3} = \phi_{A1,A2} S_{A2}$ was used:

$$\phi_{A1,A4} = \phi_{A1,A3} S_{A3}.$$

Individual detection histories (i.e., capture histories) were constructed for each tag as described above. Each detection history consisted of one or more fields representing initial release (field 1) and the sites where the tag was detected, in chronological order. Detection on both receivers in a dual array was denoted by the code “ab”, detection on only the upstream receiver was denoted “a0”, and detection on only the downstream receiver was denoted “b0”. For example, the detection history DF A2a0 A5 A7 A8ab A9b0 G1a0 G2ab represented a tag that was released at Durham Ferry and detected at the first (but not the second) receiver just downstream of the release site (A2a0), at one or both of the receivers near Lathrop (A5), at the single receiver in the San Joaquin River near the Navy Drive Bridge (A7), both receivers at MacDonald Island (A8ab), the downstream receiver at Medford Island (A9b0), the upstream receiver at Jersey Point (G1a0), and both receivers at Chipps Island (G2ab). A tag with this detection history can be assumed to have passed by certain receivers without detection: A2b, A3, A4, A6, A9a, and G1b. In Submodel I, the detections at A9 and G1 were not modeled, yielding Submodel I parameterization:

$$\phi_{A1,A2} P_{A2a} (1 - P_{A2b}) S_{A2} (1 - P_{A3}) S_{A3} (1 - P_{A4}) S_{A4} \psi_{A1} P_{A5} S_{A5} (1 - P_{A6}) S_{A6} P_{A7} S_{A7} \psi_{A2} P_{A8a} P_{A8b} S_{A8,G2} P_{G2a} P_{G2b}.$$

In Submodel II, this detection history was parameterized starting at the virtual release at site A5 and included detections at A8, A9, and G1:

$$S_{A5} (1 - P_{A6}) S_{A6} P_{A7} S_{A7} \psi_{A2} P_{A8a} P_{A8b} \phi_{A8,A9} (1 - P_{A9a}) P_{A9b} \phi_{A9,G1} P_{G1a} (1 - P_{G1b}) \phi_{G1,G2} P_{G2a} P_{G2b}.$$

Another example is the detection history DF A2ab A4 A5 A6 A7 G2b0. A fish with this detection history was released at Durham Ferry, migrated downstream in the San Joaquin River past the head of Old River with detections at the receivers just downstream of the release site (A2ab), as well as at the Mossdale Bridge (A4), Lathrop (A5), Garwood Bridge (A6), and Navy Drive Bridge (A7) before being detected on the second Chipps Island receiver (G2b0). This fish passed the Turner Cut junction but we have no information on which route it took there, so both routes must be parameterized in both submodels. This fish presumably passed Jersey Point without being detected on either receiver there.

This detection history is modeled partially in Submodel I and partially in Submodel II. In Submodel I, the probability of this detection history is

$$\phi_{A1,A2} P_{A2a} P_{A2b} S_{A2} (1 - P_{A3}) S_{A3} P_{A4} S_{A4} \psi_{A1} P_{A5} S_{A5} P_{A6} S_{A6} P_{A7} S_{A7} \theta P_{G2a} P_{G2b},$$

where $\theta = \psi_{A2} (1 - P_{A8}) S_{A8,G2} + \psi_{F2} (1 - P_{F1}) S_{F1,G2}$, $1 - P_{A8} = (1 - P_{A8a})(1 - P_{A8b})$, and $1 - P_{F1} = (1 - P_{F1a})(1 - P_{F1b})$.

In Submodel II, this detection history is parameterized

$$S_{A5} P_{A6} S_{A6} P_{A7} S_{A7} \left[\psi_{A2} (1 - P_{A8}) (\phi_{A8,G1} + \phi_{A8,A9} \phi_{A9,G1}) + \psi_{F2} (1 - P_{F1}) \phi_{F1,G1} \right] (1 - P_{G1}) \phi_{G1,G2} (1 - P_{G2a}) P_{G2b},$$

where $1 - P_{G1} = (1 - P_{G1a})(1 - P_{G1b})$.

A final example is the detection history DF A3 A4 B1 B2a0. A fish with this detection history was released at Durham Ferry, passed the first receivers without detection, passed the receivers at Banta Carbona (A3) and Mossdale Bridge (A4) with detection, entered Old River through the barrier and was detected on at least one receiver at the first Old River site (B1) and on the upstream receiver at the Old River South site (B2a0). The fish was not detected again after passing the Old River South site. It may have died between that site and Chipps Island (the next site modeled), or it may have reached Chipps Island but evaded detection there. Both possibilities must be included in the model parameterization. This detection history is parameterized only in Submodel I:

$$\phi_{A1,A2} (1 - P_{A2}) S_{A2} P_{A3} S_{A3} P_{A4} S_{A4} (1 - \psi_{A1}) P_{B1} \phi_{B1,B2} P_{B2a} (1 - P_{B2b}) \left[1 - S_{B2,G2} P_{G2} \right],$$

where $1 - P_{A2} = (1 - P_{A2a})(1 - P_{A2b})$ and $P_{G2} = 1 - (1 - P_{G2a})(1 - P_{G2b})$.

Under the assumptions of common survival, route entrainment, and detection probabilities and independent detections among the tagged fish in each release group, the likelihood function for the survival model for each release group is a multinomial likelihood with individual cells denoting each possible capture history.

Parameter Estimation

The multinomial likelihood model described above was fit numerically to the observed set of detection histories according to the principle of maximum likelihood using Program USER software, developed at the UW (Lady et al. 2009). Point estimates and standard errors were computed for each parameter. Standard errors of derived performance measures were estimated using the delta method (Seber 2002: 7-9). Sparse data prevented some parameters from being freely estimated for some release groups. Transition, survival, and detection probabilities were fixed to 1.0 or 0.0 in the USER model as appropriate, based on the observed detections. The model was fit separately for each release.

For each release, the complete data set that included possible detections from predatory fish was analyzed separately from the reduced data set restricted to detections classified as Chinook Salmon smolt detections. Population-level estimates of parameters and performance measures, representing both release groups, were estimated by fitting the model to the pooled detection data from both release groups. For each model fit, goodness-of-fit was assessed visually using Anscombe residuals (McCullagh and Nelder 1989). The sensitivity of parameter and performance metric estimates to inclusion of detection histories with large absolute values of Anscombe residuals was examined for each release group individually.

For each release group and for the pooled data set, the effect of primary route (San Joaquin River or Old River) on estimates of survival to Chipps Island was tested with a two-sided Z-test on the log scale:

$$Z = \frac{\ln(\hat{S}_A) - \ln(\hat{S}_B)}{\sqrt{\hat{V}}},$$

where

$$V = \frac{\text{Var}(\hat{S}_A)}{\hat{S}_A} + \frac{\text{Var}(\hat{S}_B)}{\hat{S}_B} - \frac{2\text{Cov}(\hat{S}_A, \hat{S}_B)}{\hat{S}_A \hat{S}_B}.$$

The parameter V was estimated using Program USER. Also tested was whether tagged Chinook Salmon smolts showed a preference for the San Joaquin River route using a one-sided Z-test with the test statistic:

$$Z = \frac{\hat{\psi}_A - 0.5}{SE(\hat{\psi}_A)}.$$

Statistical significance was tested at the 5% level ($\alpha=0.05$).

Analysis of Tag Failure

The first of two tag-life studies began on May 16 with 43 tags; the last tag failure was recorded on July 6. The second tag-life study began on May 24 with 40 tags, and the last tag failure was recorded on July 12. Observed tag survival was modeled using the 4-parameter vitality curve (Li and Anderson 2009). Stratifying by tag-life study (mid-May or late May) versus pooling across studies was assessed using the Akaike Information Criterion (AIC; Burnham and Anderson 2002).

The fitted tag survival model was used to adjust estimated fish survival and transition probabilities for premature tag failure using methods adapted from Townsend et al. (2006). In Townsend et al. (2006), the probability of tag survival through a reach is estimated based on the average observed travel time of tagged fish through that reach. For this study, travel time and the probability of tag survival to Chipps Island were estimated separately for the different routes (e.g., San Joaquin route

vs. Old River route). Standard errors of the tag-adjusted fish survival and transition probabilities were estimated using the inverse Hessian matrix of the fitted joint fish-tag survival model. The additional uncertainty introduced by variability in tag survival parameters was not estimated, with the result that standard errors may have been slightly low. In previous studies, however, variability in tag-survival parameters has been observed to contribute little to the uncertainty in the fish survival estimates when compared with other, modeled sources of variability (Townsend et al. 2006); thus, the resulting bias in the standard errors was expected to be small.

Analysis of Tagger Effects

Tagger effects were analyzed in several ways. The simplest method used contingency tests of independence on the number of tag detections at key detection sites throughout the study area. Specifically, a lack of independence (i.e., heterogeneity) between the detections distribution and tagger was tested using a chi-squared test ($\alpha=0.05$; Sokal and Rohlf 1995). Detections from downstream sites were pooled for this test in order to achieve adequate cell counts, and the chi-squared test was performed via Monte Carlo simulations to accommodate remaining low cell counts.

Lack of independence may be caused by differences in survival, route entrainment, or detection probabilities. A second method visually compared estimates of cumulative survival throughout the study area among taggers. Sparse detection data in the Old River route for individual taggers prevented estimating reach survival within the Old River route by tagger, so only the overall survival to Chipps Island was estimated for route B for this analysis. A third method used Analysis of Variance to test for a tagger effect on individual reach survival estimates, and an F-test to test for a tagger effect on cumulative survival throughout each major route (routes A and B). Tagger effects on estimates of individual parameters were also assessed using an F-test. Finally, the nonparametric Kruskal-Wallis rank sum test (Sokal and Rohlf 1995, ch. 13) was used to test for whether one or more taggers performed consistently poorer than others, based on individual reach survival or transition probabilities through key reaches. In the event that survival was different for a particular tagger, the model was refit to the pooled release groups without tags from the tagger in question, and the difference in survival estimates due to the tagger was tested using a two-sided Z-test on the lognormal scale. The reduced data set (without predator-type detections), pooled over release groups, was used for these analyses.

Testing Effect of Release Group on Parameter Estimates

The effect of release group on the values of the model survival and transition probability parameters was examined by testing for a statistically significant decrease in parameter estimates for the second release group. For each model survival and transition probability parameter θ , where $\theta = \phi_{kj,hi}$ or $\theta = S_{hi}$, the difference in parameter values between the first and second release groups was defined as

$$\Delta_{\theta} = \theta_1 - \theta_2 ,$$

for model parameter θ_R for release group R ($R = 1, 2$). The difference was estimated by $\hat{\Delta}_\theta = \theta_1 - \theta_2$. The null hypothesis of no difference was tested against the alternative of a positive difference (i.e., higher parameter value for the first release group):

$$H_{0\theta} : \Delta_\theta = 0$$

vs

$$H_{A\theta} : \Delta_\theta > 0.$$

A family-wise significance level of $\alpha=0.10$ was selected, and the Bonferroni multiple comparison correction was used, resulting in a test-wise significance level of 0.0071 for 14 tests (Sokal and Rohlf 1995).

Analysis of Travel Time

Travel time was measured from release at Durham Ferry to each detection site. Travel time was also measured through each reach for tags detected at the beginning and end of the reach, and summarized across all tags with observations. Travel time between two sites was defined as the time delay between the last detection at the first site and the first detection at the second site. In cases where the tagged fish was observed to make multiple visits to a site, the final visit was used for travel time calculations. When possible, travel times were measured separately for different routes through the study area. The harmonic mean was used to summarize travel times.

To evaluate our hypotheses that reduced travel times increased survival, we compared average travel time and survival for the different reaches to see if they were different ($p < 0.05$) for the two release groups. Given that the lengths of the reaches were different we also standardized the length of each reach and survival in the reach by the distance of each reach (in km) prior to comparing average travel time per km to survival per km ($S^{(1/\text{km})}$) across reaches.

Route Entrainment Analysis

A physical barrier was installed at the head of Old River in 2012. The barrier was designed to keep fish from entering Old River, but included culverts that allowed limited fish passage. Only 11 of the 959 (1%) tags released in juvenile Chinook Salmon in 2012 were detected entering the Old River route in 2012, while 449 (47% of 959) were detected in the San Joaquin River route. Because of the barrier and the low number of tags detected in the Old River route, no effort was made to relate route entrainment at the head of Old River to hydrologic conditions in 2012. A route entrainment analysis was performed for the Turner Cut junction instead.

The effects of variability in hydrologic conditions on route entrainment at the junction of Turner Cut with the San Joaquin River were explored using statistical generalized linear models (GLMs) with a binomial error structure and logit link (McCullagh and Nelder 1989). The acoustic tags used in this analysis were restricted to those detected at either of the acoustic receiver dual arrays located just downstream of the Turner Cut junction: site MAC (model code A8) or site TCE/TCW (code F1). Tags

were further restricted to those whose final pass of the Turner Cut junction came from either upstream sites or from the opposite leg of the junction; tags whose final pass of the junction came either from downstream sites (e.g., MFE/MFW) or from a previous visit to the same receivers (e.g., multiple visits to the MAC receivers) were excluded from this analysis. Tags were restricted in this way in order to limit the delay between initial arrival at the junction, when hydrologic covariates were measured, and the tagged fish's final route selection at the junction. No Chinook Salmon tags were observed moving from one junction leg to the other, so in fact only tags that came from upstream were used in this analysis. Predator-type detections were also excluded. Detections from a total of 89 tags were used in this analysis: 79 from release group 1, and 10 from release group 2.

Hydrologic conditions were represented in several ways, primarily total river flow (discharge), water velocity, and river stage. These measures were available at 15-minute intervals from the TRN gaging station in Turner Cut, maintained by the USGS (Table 4). The Turner Cut acoustic receivers (TCE and TCW) were located 0.15 – 0.30 km past the TRN station in Turner Cut. No gaging station was available in the San Joaquin River close to the MAC receivers. The closest stations were PRI (13 km downstream from the junction), and SJG (18 km upstream from the junction) (Table 4). These stations were considered too far distant from the MAC receivers to provide measures of flow, velocity, and river stage sufficiently accurate for describing localized conditions at the Turner Cut junction for the route entrainment analysis. Thus, while measures of hydrologic conditions were available in Turner Cut, measures of flow proportion into Turner Cut were not available.

Additionally, there was no measure of river conditions available just upstream of the junction that might inform about the environment as the fish approached the junction. Instead, gaging data from the SJG gaging station (18 km upstream of the junction) were used as a surrogate for conditions upstream of the junction. Because of the distance between the SJG station and the Turner Cut junction, and the fact that the San Joaquin River becomes considerably wider between the SJG station and the junction, conditions at SJG were used only as an index of average conditions during the time when the fish was in this reach. In particular, no measure of tidal stage or flow direction was used at SJG. Instead, the analysis used the average magnitude (measured as the root mean square, RMS) of flow and velocity at SJG during the tag transition from the time of tag departure from the SJG acoustic receiver (model code A6) to the time of estimated arrival at the Turner Cut junction.

Conditions at the TRN gaging station were measured at the estimated time of arrival at the Turner Cut junction. The location (named TCJ for Turner Cut Junction) used to indicate arrival at the junction was located in the San Joaquin River 1.23 km from the TCE receiver and 2.89 km upstream of the MACU receiver. Time of arrival at TCJ (t_i) was estimated for tag i by a linear interpolation from the observed travel time from the SJNB or SJG acoustic receivers upstream to detection on either the MAC or TCE/TCW receivers just downstream of the junction. Linear interpolation is based on the first-order assumption of constant movement during the transition from the previous site. In a tidal area, it is likely that movement was not actually constant during the transition, but in the absence of more precise spatiotemporal tag detection data, the linear interpolation may nevertheless provide the best estimate of arrival time.

The TRN gaging station typically recorded flow, velocity, and river stage measurements every 15 minutes. Linear interpolation was used to estimate the flow, velocity, and river stage conditions at the estimated time of tag arrival at TCJ:

$$x_i = w_i x_{t_{1(i)}} + (1 - w_i) x_{t_{2(i)}}$$

where $x_{t_{1(i)}}$ and $x_{t_{2(i)}}$ are the two observations of metric x ($x = Q$ [flow], V [velocity], or C [stage]) at the TRN gaging station nearest in time to the time t_i of tag i arrival such that $t_{1(i)} \leq t_i \leq t_{2(i)}$. The weights w_i were defined as

$$w_i = \frac{t_{2(i)} - t_i}{t_{2(i)} - t_{1(i)}},$$

and resulted in weighting x_i toward the closest flow, velocity, or stage observation.

In cases with a short time delay between consecutive flow and velocity observations (i.e., $t_{2(i)} - t_{1(i)} \leq 60$ minutes), the change in conditions between the two time points was used to represent the tidal stage (Perry 2010):

$$\Delta x_i = x_{t_{2(i)}} - x_{t_{1(i)}}$$

for $x = Q, V$, or C , and tag i .

Negative flow measured at the TRN gaging station was interpreted as river flow being directed into the interior Delta, away from the San Joaquin River (Cavallo et al. 2013). Flow reversal (i.e., negative flow at TRN) was represented by the indicator variable U (Perry 2010):

$$U_i = \begin{cases} 1, & \text{for } Q_i < 0 \\ 0, & \text{for } Q_i \geq 0 \end{cases}$$

Prevailing flow and velocity conditions in the reach from the SJG acoustic receiver to arrival at the Turner Cut junction were represented by the root mean square (RMS) of the time series of observed conditions measured at the SJG gaging station during the estimated duration of the transition:

$$x_{RMS(i)} = \sqrt{\frac{1}{n_i} \sum_{j=T_{1(i)}}^{T_{2(i)}} x_j^2}$$

where x_j = observed covariate x at time j at the SJG gaging station ($x = Q$ or V), $T_{1(i)}$ = closest observation time of covariate x to the final detection of tag i on the SJG acoustic receivers, and $T_{2(i)} =$

closest observation time of covariate x to the estimated time of arrival of tag i at TCJ. If the time delay between either $T_{1(i)}$ and final detection of tag i on the SJG acoustic receivers, or $T_{2(i)}$ and estimated time of arrival of tag i at TCJ, was greater than 1 hour, then no measure of covariate x from the SJG gaging station was used for tag i .

Daily export rate for day of arrival of tag i at TCJ was measured at the Central Valley Project (E_{iCVP}) and State Water Project (E_{iSWP}) (data downloaded from DayFlow on November 5, 2013). Fork length at tagging L_i and release group RG_i were also considered. Finally, arrival time (day vs. night) at the Turner Cut Junction site (TCJ) was measured based on whether the tagged Chinook Salmon first arrived at TCJ between sunrise and sunset (day_i).

All continuous covariates were standardized, i.e.,

$$\tilde{x}_{ij} = \frac{x_{ij} - \bar{x}_j}{s(x_j)}$$

for the observation x of covariate j from tag i . The indicator variables U , RG , and day were not standardized.

The form of the generalized linear model was

$$\ln\left(\frac{\psi_{iA}}{\psi_{iF}}\right) = \beta_0 + \beta_1(\tilde{x}_{i1}) + \beta_2(\tilde{x}_{i2}) + \dots + \beta_p(\tilde{x}_{ip})$$

where $\tilde{x}_{i1}, \tilde{x}_{i2}, \dots, \tilde{x}_{ip}$ are the observed values of standardized covariates for tag i (covariates 1, 2, ..., p , see below), ψ_{iA} is the predicted probability that the fish with tag i selected route A (San Joaquin River route), and $\psi_{iF} = 1 - \psi_{iA}$ (F = Turner Cut route). Route choice for tag i was determined based on detection of tag i at either site A8 (route A) or site F1 (route F). Estimated detection probabilities for the two release groups were 0.97 – 1.00 for site A8 and 1.00 for site F1 (Appendix 5, Table 5A-2), so no groups were omitted because of low detection probability.

Single-variate regression was performed first, and covariates were ranked by P-values from the appropriate F-test (if the model was overdispersed) or χ^2 test (McCullagh and Nelder 1989). Covariates found to be significant alone ($\alpha=0.05$) were then analyzed together in a series of multivariate regression models. Because of high correlation between flow and velocity measured from the same site, and to a lesser extent, correlation between flow or velocity and river stage, the covariates flow, velocity, and river stage were analyzed in separate models. The exception was that the flow index in the reach from SJG to TCJ (Q_{SJG}) was included in the river stage model. Exports at CVP and SWP had low correlation over the time period in question, so CVP and SWP exports were considered in the same models. The general forms of the three multivariate models were:

$$\text{Flow model: } Q_{TRN} + Q_{SJG} + \Delta Q_{TRN} + U + day + E_{CVP} + E_{SWP} + L + RG$$

$$\text{Velocity model: } V_{TRN} + V_{SJG} + \Delta V_{TRN} + U + day + E_{CVP} + E_{SWP} + L + RG$$

$$\text{Stage model: } C_{TRN} + Q_{SJG} + \Delta C_{TRN} + U + day + E_{CVP} + E_{SWP} + L + RG.$$

In general, only terms that were significant in the single-variate models were included as candidates in the flow, velocity, and stage models. However, the flow, velocity, and stage metrics from the TRN gaging station were included as candidates in their respective models, regardless of their significance in the single-variate models. Backwards selection with F-tests was used to find the most parsimonious model in each category (flow, velocity, and stage) that explained the most variation in the data (McCullagh and Nelder 1989). Main effects and two-way interaction effects were considered. The model that resulted from the backwards selection process in each category (flow, velocity, or stage) was compared using an F-test to the full model from that category to ensure that all significant main effects were included. AIC was used to select among the flow, velocity, and stage models. Model fit was assessed by grouping data into discrete classes according to the independent covariate, and comparing predicted and observed frequencies of route entrainment into the San Joaquin using the Pearson chi-squared test (Sokal and Rohlf 1995).

Comparison of survival between Mossdale and Jersey Point in 2012 compared to past years.

A multiple regression was run on the combined data set of survival estimates from Mossdale to Jersey Point with the HORB using CWT's in 1994, 1997, 2000-2004 (SJRGA 2013) and using acoustic tags for the two releases in 2012 to determine if tag type (acoustic tag or coded wire tag) was a significant factor in addition to flow for predicting survival. We also compared the results observed in 2012 to those predicted from the CWT relationship with flow at the same flow levels as those experienced by tagged fish in the two 2012 releases. The data were also plotted and the two regression lines were compared; CWT data only and the CWT data combined with the 2012 acoustic tag data.

Results

Transport to Release Site

No mortalities were observed after transport to the release site. Water temperatures ranged from 16.8°C to 20.3° C after loading, prior to transport. Water temperatures ranged from 16.5°C to 20.5°C after transport and before unloading at the release site. Water temperature in the river at the release site ranged from 17.5°C to 20.7°C, with the average during the first week being lower (18.3°C) than for the second week (19.7°C) (Table 6). By adding ice, water temperatures did not change substantially during transport (Table 6 and Appendix 3) and water temperatures in the transport tanks when arriving at the release site were usually within a degree C of the water temperature in the river (Table 6). During transport water temperatures did not rise or lower more than 0.5°C, and transport

tank temperatures were similar between tanks within about 0.5 °C (Appendix 3). Dissolved oxygen levels ranged between 8.73 and 11.89 mg/l for all measurements in the transport tanks or in the river (Table 6).

Fish Releases

No mortalities occurred after holding and prior to release in the 2012 Chinook Salmon study (Table 6).

Dummy Tagged fish

None of the 60 dummy-tagged Chinook Salmon were found dead when evaluated after being held for 48 hours (Table 7). Three fish from the May 20 group had abnormal gill coloration. All remaining fish were found swimming vigorously, had normal gill coloration, normal eye quality, normal body coloration and no fin hemorrhaging. Mean scale loss for all fish assessed ranged from 2.3 to 5.5%. Eight of the 60 examined fish were found to have stitched organs. Mean FL of the four groups of dummy tagged fish ranged from 108.2 to 112.0 mm. These data indicate that the fish used for the Chinook Salmon study in 2012 appeared to be in generally good condition (Table 7).

Fish Health

Pathogen testing conducted on dummy-tag cohorts of acoustic tagged MRH juvenile Chinook Salmon used in studies corresponding to May 7 and May 23 releases showed no virus or *Renibacterium salmoninarum* infection detected in the fish. The May 23 group had 37% prevalence of both suture abnormalities and *Aeromonas – Pseudomonas* sp. infection however there was little correlation between the two findings. As in the past, *Tetracapsuloides bryosalmonae* infection was highly prevalent ($\geq 97\%$) and the associated Proliferative Kidney Disease became more pronounced in the May 23 sample. No mortality occurred to these fish prior to assessment after they had been held for 48 hours for either sample date. Gill Na-K-ATPase data was not reported due to a problem with a key assay reagent. The combination of kidney impairment and poor suture condition of the May 23 salmon indicates that health of the two release groups was not equivalent. See Appendix 4 for more detail on the results of the fish health evaluations.

Tag retention test

Of the 39 dummy tagged fish held for 30 days, 3 died within the first 5 days after tagging. No other mortality was observed during the 30 day period. This suggests that the tagging process alone may have caused some (less than 10%) of the mortality observed during the study. None expelled their tag.

Detections of Acoustic-Tagged Fish

There were 960 acoustic tags released in juvenile Chinook Salmon at Durham Ferry in 2012, but one was removed from the analyses due to the tag “looking odd” resulting in data from only 959 being analyzed. Of these, 713 (74%) were detected on one or more receivers either upstream or downstream of the release site (Table 8), including any predator detections. A total of 707 tags (74%) were detected at least once downstream of the release site, and 482 (50%) were detected in the study area from

Mossdale to Chipps Island (Table 8). Although more tags from the second release group were detected between the release site and the upstream boundary of the study area (Mossdale), considerably more tags from the first release group were detected in the study area than from the second release group (301 vs. 181) (Table 8).

The large majority of the tags detected in the study area were detected in the San Joaquin River route (449 of 482), while only 11 tags were detected in the Old River route (Table 8). Additionally, some tags were detected in the study area near Mossdale Bridge but not downstream of the head of Old River. In general, tag detection counts in the San Joaquin River route decreased as distance from the release point increased. Of the 449 tags observed in the San Joaquin River route, 449 were detected on the receivers near Lathrop; 310 were detected on one or both of the receivers near Stockton (SJG or SJNB); 111 were detected on the receivers in the San Joaquin River near MacDonald Island or in Turner Cut; and 47 were detected at Medford Island (Table 9).

Some of the 449 tags detected in the San Joaquin River downstream of the head of Old River were not assigned to that route for survival analysis because they were subsequently observed upstream of Old River and had no later downstream detections (Table 8). Overall, 446 of the 449 tags observed in the San Joaquin River downstream of Old River were assigned to that route for survival analysis. Of these, 13 tags were observed exiting the San Joaquin River at Turner Cut, three were observed at the Old or Middle River receivers near of Empire Cut, one was observed at the Old and Middle River receivers near Highway 4, one was observed at the CVP trashrack, and none were observed at the radial gates at the entrance to the Clifton Court Forebay (Table 9). A total of 28 San Joaquin River route tags were detected at the Jersey Point/False River receivers, including seven detections on the False River receivers (Table 9). However, all of the tags detected at False River were later detected either at Jersey Point or at Chipps Island, and so no San Joaquin River route tags were used in the survival model at False River (Table 10). A total of 14 San Joaquin River route tags were eventually detected at Chipps Island, including predator-type detections (Table 9).

Only 11 tags were detected in the Old River route, and all but one, were assigned to that route for survival analysis (Table 8). Nine (9) tags were detected both at the Old River East receivers near the head of Old River (ORE) and the Old River receivers near the head of Middle River (ORS). Four tags were detected at the CVP trashracks, and none at the radial gates at the entrance to the Clifton Court Forebay (Table 9). One tag from the Old River route was detected at both the Old River sites near Highway 4 and near Empire Cut; it was last detected at Empire Cut. No tags from the Old River route were detected at any of the Middle River sites (Table 9). One of the 11 tags in the Old River route was observed at Chipps Island, and it passed through the holding tank at the Central Valley Project (Tables 9 and 10).

In addition to the Old and Middle receivers located near Empire Cut, the Threemile Slough receivers recorded detections of tags but were purposely omitted from the full survival model. Six tags were detected on the Threemile Slough receivers: four came directly from the San Joaquin River receivers at Medford Island and MacDonald Island, and two were last detected at Jersey Point before being detected at Threemile Slough (Table 9). Those that had come from Medford Island and MacDonald Island continued on to either Jersey Point or Chipps Island, while those that came upriver to Threemile Slough from Jersey Point had no subsequent detections.

The predator filter used to distinguish between detections of juvenile Chinook Salmon and detections of predatory fish that had eaten tagged smolts classified 130 of the 959 tags released (14%) as being detected in a predator at some point during the study (Table 11). Of the 482 tags detected in the study area (i.e., at Mossdale or points downstream), 95 tags (20% of 482) were classified as being in a predator, and the majority (94 of 95) were first classified as being in a predator within the study area. The remaining tag was classified as a predator at Banta Carbona (upstream of the study area) but was later detected in the San Joaquin River at the Lathrop receiver (SJL). Approximately 7% (36 of 535) of the tags detected upstream of Mossdale were classified as being in a predator in that region (Table 11). Two of the tags that were first classified as predators in the study area were subsequently detected upstream of Mossdale. Two of the nine tags detected at upstream Old River sites (ORE and ORS) were classified as in a predator (Table 11).

Within the study area, the detection sites with the largest number of first-time predator-type detections were Lathrop (14 of 449, 3%), Garwood Bridge (18 of 310, 6%), Navy Drive Bridge (23 of 241, 10%), and MacDonald Island (18 of 100, 18%) (Tables 9 and 11). The majority of predator classifications at these four sites were assigned on tag departure from the detection site in question because of long residence times and movements against the flow. Because those detections that are assigned the predator classification only on departure are not removed from analysis in the survival model, only a few detections were actually removed from these sites.

When the predator-type detections were removed, slightly fewer detections were available for the survival analysis (Tables 12-14). With the predator-type detections removed, 697 of the 959 (73%) tags released were detected downstream of the release site, and 480 (50% of those released) were detected in the study area from Mossdale to Chipps Island (Table 12). A similar percentage of the tags from each release group were detected anywhere as a smolt (73% and 72% for the two release groups). Considerably more tags from the first release group were detected in the study area than from the second release group (63% vs. 37%) (Table 12).

Removing predator-type detections did not appreciably change the spatial patterns in the detection counts. The large majority of the tags detected in the study area were detected in the San Joaquin River route (444 of 480, 93%) and assigned to that route for the survival analysis. Only 11 tags were observed in the Old River route (Table 12). Another 25 tags were detected at the Mossdale receivers, but not downstream of the head of Old River (Table 12). Most of the changes to detection counts introduced by removing predator-type detections occurred at receivers in the San Joaquin River, both upstream and downstream of the head of Old River (Tables 9 and 13). There was no change in tag counts at Jersey Point, False River, and Chipps Island. There were very few detections at receivers throughout the western and northern regions of the interior Delta (Table 13), and somewhat fewer once detections were formatted for survival analysis (Table 14). Whether predator-type detections were included or not, detections from those sites had to be omitted from the survival model (Tables 10 and 14) (See *Statistical Methods: Survival Model – Reduced Model*).

Tag-Survival Model and Tag-Life Adjustments

The Akaike Information Criterion (AIC) indicated that pooling data from both tag-life studies (AIC = 18.1) was preferable to stratifying by study month (AIC = 33.4). Thus, a single tag survival model was

fitted and used to adjust fish survival estimates for premature tag failure. The estimated mean time to failure from the pooled data was 41.7 days ($SE = 7.5$ days) (Figure 7).

The complete set of detection data, including predator-type detections, contained some detections that occurred after the tags began dying (Figures 8 and 9). The sites with the latest detections were Banta Carbona and the San Joaquin River receivers near the Lathrop, Garwood Bridge, Navy Bridge and MacDonald Island. Some of these late-arriving detections may have come from predators. Tag-life corrections were made to survival estimates to account for the premature tag failure observed in the tag-life studies. All estimates of reach survival for the acoustic tags were greater than 0.99 (out of a possible range of 0 – 1). Thus, there was very little effect of either premature tag failure or corrections for tag failure on the estimates of salmon reach survival in 2012.

Tagger Effects

Fish in the release groups were evenly distributed across tagger (Table 15). For each tagger, the number tagged was distributed evenly across the two release groups. A chi-squared test found no evidence of lack of independence of tagger across the release groups ($\chi^2 = 0.0279$, $df=3$, $P=0.9988$). The distribution of tags detected at various key detection sites or regions of the study area was well-distributed across taggers, showing no evidence of a tagger effect on survival, route entrainment, or detection probabilities at these sites ($\chi^2 = 16.8759$, simulated P-value = 0.5372; Table 16).

Estimates of cumulative survival throughout the San Joaquin River route to Chipps Island showed generally small, non-significant effects of tagger through the system (Figure 10). Tagger C had consistently higher point estimates of cumulative survival through the receiver at Navy Drive Bridge, after which cumulative survival from this tagger were no greater than from the other taggers. Despite the higher point estimates of survival observed for Tagger C, the differences were not statistically significant (ANOVA, $P = 0.1944$). Furthermore, rank tests found no evidence of consistent differences in reach survival across fish from different taggers either upstream of the head of Old River ($P=0.9217$) or in the San Joaquin River route ($P=0.9704$). Fish tagged by Tagger B had significantly lower survival estimates through the San Joaquin River reach from the Navy Bridge to the Turner Cut junction (i.e., MacDonald Island and Turner Cut) (F-test: $P = 0.0078$); however, fish from Tagger B showed no difference in survival estimates in other reaches or to Chipps Island overall compared to the other taggers (Figure 10).

In particular, there was no difference in overall survival to Chipps Island among taggers through the San Joaquin River route ($P=0.4655$). Only one fish was observed to arrive at Chipps Island via the Old River route, so no tagger effects could be explored for that route. The survival model was fit to the data pooled from all taggers without Tagger B, and estimates of four key performance measures were compared to results found with Tagger B: S_{Total} , S_A , S_B , and $\phi_{A1,A4}$. Statistical Z-tests on the log-scale found no significant difference between estimates of these parameters with and without data from fish tagged by Tagger B ($P \geq 0.5835$).

Survival and Route Entrainment Probabilities

As described above, detections from the receivers at the entrances to the water export facilities and in the holding tank at the Central Valley Project were removed from the survival model because of sparse data, as were detections from the Old and Middle River receivers near Highway 4. In some cases, there were too few detections at the dual array just downstream of Durham Ferry (DFD, site A2) to include this site in the model. In these cases, the model used the composite parameter

$\phi_{A1,A3} = \phi_{A1,A2} S_{A2}$ in place of $\phi_{A1,A2}$ and S_{A2} . Also, in several cases analysis of model residuals showed that incorporating the full dual receiver array at some detection sites reduced the quality of the model fit to the data. In such cases when it was possible to simplify the data structure and still attain useful and valid parameter estimates, detections from the dual array in question were pooled to create a redundant array for better model fit. This occurred at the downstream Durham Ferry site (A2), MacDonald Island (A8), Old River South (near the head of Middle River, B2), and Jersey Point (G1).

No tags from the second release group (released in mid-May) were detected at Chipps Island in 2012, yielding a total Delta survival estimate of 0 ($SE = 0$) for that group whether or not predator-type detections were included. The first release group (released in early May) had positive survival ($S_{total} = 0.05$; $SE = 0.01$), yielding a population estimate for all fish in the tagging study of 0.03 ($SE = 0.01$) (Table 17). Using only those detections classified as coming from juvenile Chinook Salmon and excluding the predator-type detections, the estimated probability of remaining in the San Joaquin River at the junction with Old River ($\psi_A = \psi_{A1}$) was 0.98 ($SE = 0.01$) for both release groups (Table 17), and both release groups demonstrated a significant preference for the San Joaquin River route ($P < 0.0001$ for each group). The estimated survival from Mossdale to Chipps Island via the San Joaquin River route (S_A) was 0.05 ($SE = 0.01$) for the first release group, and 0 ($SE = 0$) for the second group; the overall population estimate was 0.03 ($SE = 0.01$) (Table 17). Very few fish took the Old River route (11 overall). Although the point estimate of survival to Chipps Island via this route ($S_B = 0.16$) was relatively high compared to the estimated survival via the San Joaquin River route ($S_A = 0.05$), the small number of fish observed taking the Old River route resulted in very high uncertainty in the Old River route survival estimate ($SE = 0.15$ for S_B); thus no significant difference in route-specific survival was detected for the first release group ($P = 0.1977$). The estimated route-specific survival to Chipps Island via the Old River route was 0 for the second release group, yielding a population estimate of $S_B = 0.11$ ($SE = 0.10$); again, there was no significant difference in population survival estimates between the two routes ($P = 0.1999$) (Table 17).

Survival in the Old River route used the parameter $\phi_{B1,B2}$ in place of S_{B1} because there were no detections at site C1 (MRH) (see *Statistical Methods*). The transition parameter $\phi_{B1,B2} = S_{B1} \psi_{B2}$, so if $\psi_{B2} < 1$, then S_B is underestimated using this formulation. For the first release group, $\phi_{B1,B2} = 1$ ($SE =$

0), so both $S_{B1} = 1$ and $\psi_{B2} = 1$, and S_B is not underestimated (Table A5-2). For the second release group, $\phi_{B1,B2} = 0.67$ ($SE = 0.27$), implying that either $S_{B1} < 1$ or $\psi_{B2} < 1$, or both (Table A5-2). However, there was only a single tag detected at site B1 (ORE) that was not later detected as a smolt at site B2 (ORS), and this tag was actually detected at B2 with a predator classification at that site. Thus, there is no evidence that $\psi_{B2} < 1$ for either release group, and so it is reasonable to interpret estimates of S_B as unbiased rather than as minima. Furthermore, the lack of detections of tags from the second release group at Chipps Island would yield $S_B = 0$ for that release group in any event. Thus, there is no reason to assume that survival to Chipps Island via the Old River route is underestimated.

Survival was estimated to Jersey Point for fish that used the San Joaquin River route. This survival measure ($S_{A(MD)}$) was estimated at 0.09 ($SE = 0.02$) for the first release group, 0.01 ($SE = 0.01$) for the second release group, and 0.06 ($SE = 0.01$) overall (Table 17). No estimates were available for the Old River route. Survival ($S_{A(SD)}$) to the receivers just downstream of the Turner Cut junction on the San Joaquin River (i.e., MacDonald Island and Turner Cut receivers) was estimated at 0.33 ($SE = 0.03$) for the first release group, 0.07 ($SE = 0.02$) for the second release group, and 0.23 ($SE = 0.02$) overall (Table 17). Thus it is apparent that survival was low both to the Turner Cut junction and from that junction to Jersey Point, especially for fish from the second release group.

Survival was lower for the second release group than for the first group throughout the San Joaquin River. Estimated survival from the release site to Mossdale ($\phi_{A1,A4}$) was considerably lower ($p < 0.0001$) for the second release group (0.37 for the second group vs. 0.63 for the first group), as was survival through the Southern Delta (0.07 vs. 0.33; $p < 0.0001$), Middle Delta to Jersey Point (0.01 vs. 0.09; $p < 0.0001$), and the entire Delta to Chipps Island (0 vs. 0.05; $p < 0.0001$) (Table 17). Estimated survival was also lower through the modeled portions of the Old River route, i.e., from the head of Old River to the head of Middle River for the second release group. For the first release group, estimated survival through this reach was 1.0; for the second release group, it was 0.67 ($SE = 0.27$); however, the difference was not statistically significant ($p = 0.1106$) (Table A5-2). Although the estimate for this reach for the second release group had high uncertainty, the point estimate fits the pattern observed in the San Joaquin River of lower survival for the second release group relative to the first release group.

Including predator-type detections in the analysis produced very similar results on all spatial scales, including survival to Chipps Island, Jersey Point, and the Turner Cut junction (Table 18). The largest difference was in estimates of San Joaquin River survival through the Southern Delta to the Turner Cut junction ($S_{A(SD)}$), which increased by 0.01 for both release groups and overall (overall estimate = 0.24, $SE = 0.02$) (Table 18). Including predator detections did not alter the comparisons between release groups; estimated survival was lower for the second release group throughout the various San Joaquin River regions (Table 18; $P < 0.0001$).

Parameter estimates were significantly (family-wise $\alpha=0.10$) higher for the first release group compared to the second release group for parameters S_{A2} , S_{A3} , S_{A4} , S_{A5} , S_{A7} , $\phi_{A8,G1}$, and $\phi_{G1,G2}$ (Table 19).

Travel Time

Average travel time through the system from release at Durham Ferry to Chipps Island was 5.75 days based on 11 detections ($SE = 0.41$ days) (Table 20a). Travel time to Chipps Island ranged from 4.1 days to 10.4 days, all from the first release group. The large majority of tags that reached Chipps Island came via the San Joaquin River route; the single tag that arrived at Chipps Island via the Old River route had a total travel time of 4.12 days, which was faster than any of the 14 tags that arrived via the San Joaquin River route. All tags observed at Jersey Point arrived via the San Joaquin River route in 3 – 9 days, with an average of approximately 6 days (Table 20a).

Travel time from release to the Mossdale Bridge receivers ranged from 0.3 to 3.9 days, and averaged 0.53 days (harmonic mean; $SE = 0.01$ days) (Table 20a). Fish with the longer travel times to Mossdale tended to come from the second release group, although both release groups included fish that arrived in under 8 hours. Travel time from release to the Turner Cut junction receivers (i.e., to Turner Cut or MacDonald Island) ranged from 1.5 days to 8.2 days, and averaged between 2 and 4 days (Table 20a). Fish with the longer travel times to Mossdale tended to come from the second release group, although both release groups included fish that arrived in under 8 hours. Travel time from release to the Turner Cut junction receivers (i.e., to Turner Cut or MacDonald Island) ranged from 1.5 days to 8.2 days, and averaged between 2 and 4 days (Table 20a).

Only 2 tags were detected at the Old River receivers near Highway 4 (OR4). One of these tags came via the Old River route and arrived 4.3 days after release, while the other tag arrived via Turner Cut from the San Joaquin River route 5.1 days after release. For the few tags that were detected at the entrance to the Central Valley Project, tags that came via the Old River route tended to have shorter travel times than tags that arrived via the San Joaquin River route (Table 20a). Sample sizes were too small to draw definitive conclusions, but these observations may have been expected because of the longer route to the interior and western receivers via the San Joaquin River route.

Including predator-type detections had only a small effect on average travel times through the system (Table 20b). Travel times to the San Joaquin River receivers at MacDonald Island and Turner Cut were generally slightly longer when predator-type detections were included. This was because travel times were measured to the beginning of the tag's final visit to each site, and many tags classified as being in predators at those sites were observed making multiple visits to those sites. The longer travel times observed for the data set that includes the predator-type detections reflect the assumption used in the predator filter that predators are more likely than smolts to exhibit long travel times.

Average travel time through reaches for tags classified as being in smolts ranged from 0.01 days (approximately 20 minutes) for the single tag observed moving from the Central Valley Project trashracks to the holding tank, to over 2 days for tags moving from MacDonald Island to Jersey Point, and over 3 days for tags moving from MacDonald Island and Medford Island to Chipps Island (Table 21a). While there were several tags that moved from MacDonald Island to Jersey Point in under 2 days, there

were also several tags that took over 5 days to make the journey. Similar travel times were observed from the Medford Island receivers to the Jersey Point receivers, although the average travel time was somewhat lower from Medford Island (approximately 1.54 days over both release groups) (Table 21a). The reach from MacDonald Island to Jersey Point was one of the longer reaches in the study area (approximately 26 rkm), so it not surprising that it had some of the longer observed travel times. However, the reach from Jersey Point to Chipps Island was also approximately 26 rkm in length, and travel time through this reached tended to be shorter, ranging from 16 hours to 2.1 days and averaging 1.21 days ($SE = 0.14$ days) (Table 21a). The region between Jersey Point and Chipps Island is strongly affected by tides, which may delay migrating fish, but it is nevertheless channelized. The region between MacDonald Island and Jersey Point, on the other hand, includes Frank's Tract, and it is possible that migrating Chinook Salmon smolts are delayed there for a considerable time. In general, there were too few detections in the interior Delta to make comparisons of travel time through reaches in that region with travel time through reaches contained within the San Joaquin River route. Including predator-type detections did not greatly affect the pattern of observed travel times through the various reaches (Table 21b).

There was a significant negative relationship ($p < 0.05$) between travel time per km and survival per km in river reaches upstream of the Lathrop/Old River junction for the second release group, suggesting as travel time per km increased, survival per km decreased (Figure 11, Table 22). Survival also decreased as travel time increased in reaches between Durham Ferry and Lathrop/Old River junction for the first release group, but the regression line was not significant at the $p < 0.05$ level. Survival was higher for the first release group, than for the second release group in these three reaches of the river (Figure 11, Table 19). Also there appeared to be a slight increase in travel time (slower migration rate) between Mossdale and Lathrop/Old River junction and between Banta Carbona and Mossdale for the second release group relative to the first release group (Figure 11, Table 22).

In contrast, there did not appear to be a relationship between travel time per km and survival per km for reaches between the Lathrop/Old River junction and Jersey Point (tidal reaches) for either of the release groups in 2012 (Figure 12). While survival through the reach (or joint probability of moving to and surviving to the downstream location) was significantly higher (Table 19) for the first release group for three of these reaches in the San Joaquin River downstream of Lathrop (Lathrop to Garwood Bridge, S_{A5} ; Navy Drive Bridge to MacDonald Island or Turner Cut, S_{A7} ; and the reach between MacDonald Island to Jersey Point, $\phi_{A8,G1}$ [not shown on Figure 12]), others were not significantly higher (e.g. Garwood Bridge to Navy Bridge Drive [S_{A6}], MacDonald Island to Medford Island [$\phi_{A8,A9}$], and Medford Island to Jersey Point [$\phi_{A9,G1}$]) (Table 19). Travel times in these reaches were similar for the two release groups (Figure 12).

Route Entrainment Analysis

River flow (discharge) at the TRN gaging station in Turner Cut ranged from -4,402 cfs to 3,361 cfs (average = -1070 cfs) during the estimated arrival time of the tagged Chinook Salmon at the Turner Cut junction location (TCJ) in 2012. Water velocity in Turner Cut was highly correlated with river flow ($r = 0.999$), and velocity values ranged from -0.8 ft/s to 0.6 ft/s (average = -0.1 ft/s). The flow in Turner

Cut was negative (i.e., directed to the interior Delta) upon arrival at TCJ of approximately 61% (54 of 89) tags in this analysis. River stage measured in Turner Cut was moderately correlated with both river flow and velocity ($r=-0.70$), and ranged from 6.7 ft to 10.9 ft (average = 9.1 ft). Changes in river stage in the 15-minute observation period containing the arrival of the tagged Chinook Salmon to the TCJ ranged from -0.2 ft to 0.2 ft (average = 0 ft). Changes in river stage were not correlated with stage ($r=-0.13$). The index of river flow in the reach from Stockton to Turner Cut was uncorrelated with flow and velocity in Turner Cut upon arrival at TCJ ($r= 0.01$), and only moderately correlated with river stage at Turner Cut ($r= -0.29$). The flow index in the Stockton-Turner Cut reach ranged from 2,324 cfs to 3,400 cfs (average = 2,785 cfs).

The daily export rate at CVP ranged from 821 cfs to 1,016 cfs (average = 960 cfs); exports at CVP were generally low in both early and late May, and was greatest in mid-May. The daily export rate at the State Water Project (SWP) ranged from 507 cfs to 3,698 cfs (average = 1,908 cfs). SWP exports were more variable than CVP exports but also peaked in the third week of May. Exports from CVP and SWP were uncorrelated ($r= -0.01$). Neither CVP nor SWP exports was correlated with either flow ($r=0.09$ for CVP, $r=-0.03$ for SWP) or river stage ($r=0.00$ for CVP, $r=-0.14$ for SWP) in Turner Cut. The majority of tags (66 of 89, 74%) arrived at the Turner Cut junction during daylight hours.

The single-variate analyses found no significant effects ($\alpha=0.05$) of any of the covariates considered ($P>0.40$ for all covariates; Table 23). This negative result may reflect the true lack of a relationship between environmental variables and route selection at Turner Cut, or it may be an artifact of the low degrees of freedom available and the resulting low statistical power; because only 11 fish were observed entering Turner Cut (out of 89), there were only 11 degrees of freedom total. A study with a larger sample size and more fish observed using Turner Cut may provide evidence of a relationship between one or more of the covariates and route selection at this junction in future.

Comparison of Delta Survival to Past Years

In a multiple regression, tag type (acoustic or CWT) did not come out as an important variable affecting survival, whereas flow did (Table 24). Using the relationship developed from the CWT data (Figure 13), we calculated what survival from Mossdale to Jersey Point was expected to be at the two flow levels in 2012: predicted survival was 0.12 at flows of 3543 cfs and 0 at flows of 2327cfs, very close to what we observed (0.09, $SE = 0.02$, at the higher flow and 0.01, $SE = 0.01$, at the lower flow). The relationships between flow at Vernalis and survival from Mossdale to Jersey Point with the HORB, developed from the historical CWT data and from all of the data (historic CWT data and acoustic tag data added from 2012), were similar (Figure 13). The slopes of the two linear regression lines were the same (0.0001), and the intercepts were similar (-0.2345 for the CWT data only and -0.2295 for the combined data (Figure 13)) . Both relationships were statistically significant ($p < 0.01$).

Discussion

The similarity between parameter estimates with and without predator-type detections raises questions about the predator filter. One possible explanation for the similar estimates is that the

majority of the mortality was not directly caused by the predatory fish used to build the predator filter, or that many of the predatory fish feeding on the tagged salmon merely evaded detection. Chinook Salmon smolts may have been eaten by sedentary predators, birds, or mammals (e.g., otters), or by predatory fish that moved about the Delta but evaded the acoustic receivers. Alternatively, Chinook Salmon smolts may have died due to disease or habitat quality. In either case, the tags of the deceased salmon smolts may have settled on the river bottom away from the acoustic receivers; in these cases, the predator filter would correctly identify existing detections of these tags as in smolts rather than predators, and the survival model estimates would be unbiased.

Another possibility is that the filter missed detections of predators, and thus the resulting filtered data set (which supposedly has no detections from predators) is only artificially similar to the unfiltered data set (which includes detections from predators). If this is the case, then survival estimates for the (presumed) smolt-only data set would be biased because they would be based partially on predator detections. The type of bias depends on where the predator filter failed. For example, none of the tags detected at Chipps Island were classified as being in predators by the existing filter. A filter that recategorizes some of those detections as predator detections may yield survival estimates to Chipps Island that are lower than that estimated in this study (0.03). This would happen as long as the revised filter agreed with the original filter in upstream regions. On the other hand, if the predator filter was inefficient (i.e., wrong) upriver of Mossdale such that detections passed by the filter as smolts were actually detections of predators, then it is possible that true survival to Chipps Island was actually higher than estimated (0.03); this may happen if there were fewer actual smolts starting at Mossdale than appeared from the original filter. Of the 959 tags released at Durham Ferry, only 480 (50%) were detected at Mossdale, and 478 of them were classified as in smolts upon arrival at Mossdale (Tables 9 and 13). Only 15 of these tags were detected at Chipps Island. Adjusting the predator filter cannot add more detections at Chipps Island, but it may remove detections at Mossdale. A revised filter that used more stringent criteria upstream of Mossdale was constructed and implemented on the detection data. The revisions to the filter were:

- no upstream-directed transitions allowed upstream of Mossdale
- no repeat visits to sites upstream of Mossdale
- maximum residence time of 2 hours at any site upstream of Mossdale
- maximum regional residence time of 15 hours upstream of Mossdale
- minimum migration rate of 0.2 km/hr for all transitions upstream of Mossdale

This stricter filter resulted in 477 of the 480 detections at Mossdale being classified as in smolts, compared to 478 classified as in smolts using the original predator filter. The Delta survival estimate from the stricter predator filter was 0.03 for the population (i.e., both release groups pooled), unchanged from the estimate using the original filter. Thus, it is unlikely that errors in the predator filter resulted in the similar results with and without the predator-type detections.

Our first objective of the 2012 study was to determine survival of emigrating salmon smolts from Mossdale to Chipps Island during two time periods (prior to May 15 and after May 15) in the presence of the HORB to determine if there was a benefit from the flow augmentation from the Merced

River in 2012. Average river flow measured at the Vernalis gaging station when fish from the first release group were traveling through the Delta to Chipps Island (from release through approximately 10 days after the end of release period) was 3,543 cfs, while for the period of comparable length for the second release group was 2,327 cfs (Figure 14). Survival was higher ($p < 0.0001$) through the Delta (S_{Total}) for the first release group (0.05) relative to the second release group (0.00) (Table 17). Thus these findings appear to support our hypothesis that the increased flow from the Merced River flow augmentation increased survival through the Delta.

Our second objective was to assess whether the higher flows from the Merced River flow augmentation resulted in a reduction in travel time and higher survival, specifically in the riverine reaches of the Delta, and resulted in higher through-Delta survival. Shorter travel times would reduce the time tagged fish were exposed to mortality factors such as predation, high water temperatures, and toxics. Travel times in reaches of the Delta between Durham Ferry and a series of downstream locations (Mosssdale, Lathrop, Garwood Bridge, Navy Drive Bridge, and MacDonald Island) were all significantly less (i.e. faster migration) for the first release group than the second release group (Table 20a; $p < 0.05$). The travel times in these reaches appeared to be strongly influenced by the travel time for the reach between Lathrop (SJL) and Garwood Bridge (SJG). Travel time between SJL and SJG was significantly less ($p < 0.05$) for the first release group (0.60; $SE = 0.02$) which experienced the higher flows, than for the second release group (0.86; $SE = 0.05$) which experienced the lower flows (Table 21a). Survival through this reach was also higher for the first release group (0.81; $SE = 0.02$) relative to the second release group (0.48; $SE = 0.04$) ($p < 0.0001$) (S_{A5} ; Table A5-2). Thus, the data in this specific, partly riverine, reach of the Delta are consistent with our hypothesis that an increase in flow would reduce travel time and be associated with higher survival.

To further evaluate the possible relationship between travel time and survival in the remaining reaches, travel time and survival were standardized to a per-km basis. With this standardization, we found that as travel time per km increased, survival decreased for both release groups in the three riverine reaches between Durham Ferry and the Lathrop/Old River junction (Figure 11). Travel time per km was greater for the second group relative to the first group for two of the three reaches; (Banta Carbona to Mosssdale and Mosssdale to Lathrop/Old River, but not Durham Ferry to Banta Carbona) whereas survival was always lower for the second release group (lower flows) relative to the first group (higher flows) for these three reaches (Figure 11, Table 22). Thus the difference in travel time per km for the first group relative to the second did not always support our hypotheses that the higher survival per km resulted from a decrease in travel time per km from the higher flows in these riverine reaches.

Travel time per km was somewhat less and survival greater for the first release group relative to the second release group in two reaches: 1) between Lathrop and Garwood Bridge (discussed above) and 2) between Garwood Bridge and Navy Bridge Drive (Figure 12, Table 22); the shorter travel time from the increased flow may partially explain the higher point estimate of survival for release 1 compared to release 2 between Garwood Bridge and Navy Bridge, although the increase in survival is not statistically significant at the 5% level (Table 19); however, it is not possible to determine causation from this study.

Once fish enter the interior Delta or into the strongly tidally influenced San Joaquin River, travel times were expected to increase and survival was expected to decrease. While we did generally see longer travel times per km in the tidal reaches (reaches downstream of Navy Bridge Drive), it was not always greater (Table 22; e.g. travel time per km was shorter from MacDonald Island to Medford Island than it was from Lathrop to Garwood Bridge). Travel time per km was also less for the second release group than for the first, even though survival was generally higher for the first group relative to the second in all reaches downstream of Navy Bridge Drive, except between MacDonald Island and Medford Island, when survival per km was higher for the second group (Table 22). Since the increased flow probably was not enough to change velocities significantly in the downstream tidal reaches, the increased survival of the first group relative to the second in most of these tidal reaches suggests there are other mechanisms either associated with flow or other factors that resulted in the increases in survival in these tidal reaches of the Delta.

Once fish move into the interior Delta, they are exposed to flows moving toward the export facilities, which may increase their travel time and reduce their survival to Jersey Point or Chipps Island. While many of the tagged fish may have been diverted from the San Joaquin River into the interior Delta downstream of Turner Cut, we were only able to identify those entering the interior Delta through Turner Cut. We had hypothesized that tagged fish moving into the interior Delta (e.g. Turner Cut) would have increased travel times over those not being diverted into Turner Cut. Since none of the tagged fish that entered Turner Cut survived to Chipps Island for either the first or second release group, we could not compare travel times between release groups or for the Turner Cut route relative to the other routes. One fish that entered Turner Cut from the first release group was observed in the CVP holding tank, but did not survive to reach Chipps Island. We were also not able to assess the impact on survival of tagged fish being routed to the SWP and CVP as detections from the receivers at the entrances to the water export facilities and in the holding tank at the Central Valley Project were removed from the survival model because of sparse data due to the presence of the HORB.

The results of comparing travel time to survival suggests that the increased flow during the first release did not always result in decreased travel times, although it did coincide with an increase in survival in more of the riverine reaches. It was the higher survival in the majority of the reaches (both riverine and tidal) during the first release that resulted in a higher overall survival through the Delta for the first release group relative to the second release group.

However, there are other possible hypotheses for the lower survival in the second release group compared to the first release group, including differences in fish condition, tagging and release procedures, and other environmental conditions. The same tagging and release procedures were used for both release groups, including the same taggers, presumably with the same skill set, so that does not appear to be responsible for the differences in survival we observed. Fish from the second release group were slightly larger on average than fish from the first release group (mean FL = 109.9 mm and 115.7 mm for the first and second release groups, respectively), so it was reasonable to expect higher survival for the second release group rather than lower survival, but we did not observe this. Although the two release groups were released only two weeks apart, they experienced different environmental conditions other than flow. During the same two time periods, combined exports at CVP and SWP varied from 1,513 cfs to 5,054 (mean = 3,200 cfs), with similar means in the two periods. However,

exports tended to be high toward the end of the first period, when relatively few fish from the first release were still migrating, and also high near the beginning of the second period, when the majority of fish from the second release group were migrating (Figure 15).

It is also possible that the difference in flow conditions may have resulted in the different survival rates via a mechanism other than travel time, such as temperature, increased predation or toxicity. We had hypothesized that the higher inflow from the Merced flow augmentation would potentially reduce the effects of these mortality factors by reducing temperature stress, diluting toxics or reducing predator metabolic demands from the lower water temperatures. Water temperature measured at the San Joaquin River gage near Lathrop was almost 2 degrees higher on average for the second release group (67.5 °F [19.7°C]) than for the first group (65.6 °F [18.7°C]), which may have negatively affected the survival of the second release group, and been a consequence of the lower flows experienced by the second release group (Figure 16). We were unable to assess the hypothesis that increased metabolic demands from predators due to the warmer water temperatures was the cause for the increased mortality for the second release group relative to the first release group.

To assess the hypothesis that the increased flow from the Merced River flow augmentation may have diluted toxicity in the Delta, we observed that survival was significantly higher for the first group relative to the second group in the reach between SJL and SJG (Table 19). This reach from SJL to the SJG is one of the longer reaches of the Delta at 18 km (Table 22), and it includes a variety of habitats. It is not entirely riverine, but includes the transition to tidal habitat, depending on inflow. The reach is more riverine at higher inflows, and more tidal at lower inflows. The Stockton Wastewater treatment plant releases its effluent in the lower part of this reach which may have an effect on survival, especially during periods of low flow. During periods of low flow the movement of the tidal prism upstream may result in concentration of the effluent in this reach and dilution from flow would be less. There is also the possibility that increased temperatures exacerbate the toxicity effects of the effluent on juvenile salmon survival. Further evaluation of water quality in this reach may be warranted, building on studies conducted near there in 2008 (SJRG 2009) after a significant die-off of acoustic tags near this location in 2007 – a low flow year (SJRG 2008).

In addition, it is possible that the higher incidence of PKD infection for the second release group reduced their survival to Chipps Island relative to the first release group. Infection does not necessarily lead to death but would reduce fitness from anemia, kidney dysfunction, and immune suppression even if the fish survived the disease (Angelidis et al 1987, Hedrick and Aronstien 1987 as cited in Nichols et al 2012). The increase in water temperature may have contributed to the higher incidence of PKD infection for the second release group relative to the first as PKD is a progressive disease at water temperatures greater than 15°C (Okamura and Wood 2002 as cited in SJRG 2013).

Unfortunately, PKD infection is not just a problem for the experimental fish we used in 2012, but was noted as a problem in monitoring on the Merced River. Smolts caught in the Hopeton rotary screw trap on the Merced River (presumably wild stock) also had high levels of PKD infection in 2012 (Nichols et al. 2012). This is also not new, as 90-100% of naturally produced fish in a 2001 survey of Merced outmigrant salmonid health were observed to be infected with PKD (Nichols and Foott 2002 as cited in Nichols et al. 2012). Even some of salmon transferred from MRH to the lab at the Fish Health Center soon after ponding in February of 2012, developed light infections of PKD (Nichols et al 2012).

However, the worst infections identified in the 2012 study were later in the season, with gross clinical signs of PKD (anemia and swollen kidney) observed for naturally produced fish on May 9 (2 out of 24), and high numbers of parasites observed for both naturally produced (May 9 and May 15) and hatchery fish (May 15) (Nichols et al. 2012).

PKD is caused by infection by the endoparasitic myxozoan, *Tetracapsuloides bryosalmonae*. Reducing byrzoan habitat directly upstream of the hatchery and in the Merced River could be a viable disease management strategy (Foott et al. 2007). Increasing flows, if they result in decreasing water temperatures, would serve to reduce the severity of PKD for both experimental and wild fish emigrating from the San Joaquin basin. Higher water temperatures in the river and at the hatchery may have increased the severity of the PKD infection for the second group of tagged fish in 2012, relative to the first group; this may account for some of the increased mortality observed in the second group. Higher water temperatures are affected by both flow and air temperature upstream of the Delta. Cold water releases from the upstream reservoir on the Merced River may have reduced the water temperatures for the first release group over what they would have been without the water release.

Our third objective of the 2012 study was to identify route selection at HOR and at Turner Cut under the two different periods with varying flows and exports. Since the physical HORB was in place in 2012, route selection into the San Joaquin River was high for both groups (0.98; $SE = 0.02$) and did not vary between release groups (Table 17) or when predator type detections were included (Table 18). Route selection at Turner Cut was 0.11 ($SE = 0.03$) for the first release group, and 0.16 ($SE = 0.11$) for the second release group (Table 17) when predator-type detections were removed and similar when predator-type detections were included (0.12; $SE = 0.03$ for the first release group and 0.14; $SE = 0.04$ for the second release group) (Table 18). Differences in the proportion diverted into Turner Cut at the TCJ between release groups were not statistically different: with 11 to 16% of the tagged fish diverted into Turner Cut, none of which survived to Chipps Island ($S_{F1,G2}$; Tables A5-2 and A5-3). Zero probability of survival to Chipps Island for the tagged fish that entered Turner Cut negatively affected total through-Delta survival for both release groups. A study with a larger sample size and more fish observed using Turner Cut may provide evidence of a relationship between one or more covariates (e.g. flow, and tides) and route selection at this junction in future.

It is possible that the lower flows, higher water temperatures, higher toxicity, higher incident of disease (PKD) and possibly higher export rates during the time of peak migration may have combined to negatively affect salmon survival from the second release. Diversion into Turner Cut decreased survival of both groups. With only two release groups and observational data, however, it is not possible to conclude more. Combining these results with those from additional years may shed light on possible causes of mortality in the Delta. The Interagency Ecological Program has funded a multi-year analysis of the data from 2010, 2011, 2012 and 2013 and results will be forthcoming.

Based on the results of this study in 2012, naturally spawned or hatchery juvenile salmonids from the San Joaquin tributaries likely experienced variable survival within the migration period through the Delta, with greater survival during the Merced River flow augmentation period and lower survival during the later remainder period of migration. Higher flows appeared to benefit survival through

multiple intertwined mechanisms including shorter travel times, lower water temperatures, and reduced disease impacts.

The comparison of estimates of survival from Mossdale to Jersey Point for the two release groups in 2012, to estimates generated using CWT's with the HORB, suggests that survival observed in 2012 was within that expected based on the past CWT relationship, and that differences in flow between the two releases in 2012 likely increased survival over what it would have been without the flow pulse. However, without direct manipulation and further replication, cause and effect cannot be determined. While this comparison supports our hypothesis that the increased flow from the flow augmentation in the Merced River during the first release group increased survival, it also shows that survival for both groups in 2012 was relatively low, compared to that measured in other years with the HORB (Figure 13). These data suggest a higher flows of approximately 6,000 cfs with the HORB, are needed to achieve survival through the Delta of approximately 0.40. Additional studies, especially during higher flow periods, with the HORB in place, are needed to confirm these results.

List of References

- Adams, N.S., D.W. Rondorf, S.D. Evans, and J.E. Kelly (1998). Effects of surgically and gastrically implanted radio tags on growth and feeding behavior of juvenile Chinook Salmon: Transactions of the American Fisheries Society, v.127, p. 128-136.
- Brandes, P.L. and J.S. McLain (2001). Juvenile Chinook Salmon abundance, distribution, and survival in the Sacramento-San Joaquin Estuary. Contributions to the Biology of the Central Valley Salmonids, Fish Bulletin 179: Volume 2.
- Buchanan, R. (2013). OCAP 2011 Steelhead Tagging Study: Statistical Methods and Results. Prepared for Bureau of Reclamation, Bay Delta Office, Sacramento CA. August 9, 2013. 110 p.
- Burnham, K. P., and D. R. Anderson (2002). Model selection and multimodel inference: A practical information-theoretic approach. 2nd edition. Springer. New York, NY. 488 pp.
- California Department of Water Resources (2015). Final: An Evaluation of Juvenile Salmonid Routing and Barrier Effectiveness, Predation, and Predatory Fishes at the Head of Old River, 2009-2012. Prepared by AECOM, ICF International and Turnpenny Horsfield Associates.
http://baydeltaoffice.water.ca.gov/sdb/tbp/web_pg/tempbar/horbereport.cfm
- Cavallo, B., P. Gaskill, and J. Melgo (2013). Investigating the influence of tides, inflows, and exports on sub-daily flow in the Sacramento-San Joaquin Delta. Cramer Fish Sciences Report. 64 pp. Available online at: http://www.fishsciences.net/reports/2013/Cavallo_et_al_Delta_Flow_Report.pdf.
- Cormack, R.M. (1964) Estimates of survival from the sighting of marked animals. Biometrika 51, 429-438.
- Ferguson, HW. (1981). The effects of water temperature on the development of Proliferative Kidney Disease in rainbow trout, *Salmo gairdneri* Richardson. Journal of Fish Disease 4: 175-177
- Foott JS, R Stone and K Nichols (2007). Proliferative Kidney Disease (*Tetracapsuloides bryosalmonae*) in Merced River Hatchery juvenile Chinook Salmon: mortality and performance impairment in 2005 smolts. California Fish and Game 93: 57-76.
- Jolly, G.M. (1965) Explicit estimates from capture-recapture data with both death and immigration - Stochastic model. Biometrika 52: 225-247.
- Lady, J. M., and J. R. Skalski (2009). USER 4: User-Specified Estimation Routine. School of Aquatic and Fishery Sciences. University of Washington. Available from
<http://www.cbr.washington.edu/paramest/user/>.
- Li, T., and J. J. Anderson (2009). The Vitality model: A Way to understand population survival and demographic heterogeneity. Theoretical Population Biology 76: 118-131.

Liedtke, T. (2012). 2012 South Delta Study Tagger Training and QA/QC Summary. Prepared by Theresa Liedtke, U.S. Geological Survey, Western Fisheries Research Center, Columbia River Research Laboratory 5501A Cook-Underwood Road, Cook, WA 98605, for J. Israel, USBR Bay-Delta Office, 801 I Street, Suite 140, Sacramento, CA 95814. 97pgs.

Martinelli, T.L., H.C. Hansel, and R.S. Shively (1998). Growth and physiological responses to surgical and gastric radio tag implantation techniques in subyearling Chinook Salmon: *Hydrobiologia*, v. 371/372, p. 79-87.

McCullagh, P., and J. Nelder (1989). Generalized linear models. 2nd edition. Chapman and Hall, London.

Nichols, K., A. Bolick and J.Scott Foott (2012). FY2012 Technical Report: Merced River juvenile Chinook Salmon health and physiology assessment, March-May 2012. December 2012. US Fish and Wildlife Service, California-Nevada Fish Health Center, 24411 Coleman Hatchery Road, Anderson CA 96007.

Perry, R. W. (2010). Survival and Migration Dynamics of Juvenile Chinook Salmon (*Oncorhynchus tshawytscha*) in the Sacramento-San Joaquin River Delta. University of Washington, Ph.D. dissertation. 2010. 223 p.

Perry, R. W., J. R. Skalski, P. L. Brandes, P. T. Sandstrom, A. P. Klimley, A. Ammann, and B. MacFarlane (2010). Estimating survival and migration route probabilities of juvenile Chinook Salmon in the Sacramento-San Joaquin River Delta. *North American Journal of Fisheries Management* 30: 142-156.

San Joaquin River Group Authority (2007). 2006 Annual Technical Report: On Implementation and Monitoring of the San Joaquin River Agreement and the Vernalis Adaptive Management Plan (VAMP). Prepared for the California Water Resources Control Board. Available at www.sjrg.org.

San Joaquin River Group Authority (2008). 2007 Annual Technical Report: On Implementation and Monitoring of the San Joaquin River Agreement and the Vernalis Adaptive Management Plan (VAMP). Prepared for the California Water Resources Control Board. Available at www.sjrg.org.

San Joaquin River Group Authority (2010). 2009 Annual Technical Report: On Implementation and Monitoring of the San Joaquin River Agreement and the Vernalis Adaptive Management Plan (VAMP). Prepared for the California Water Resources Control Board. Available at www.sjrg.org.

San Joaquin River Group Authority (2011). 2010 Annual Technical Report: On Implementation and Monitoring of the San Joaquin River Agreement and the Vernalis Adaptive Management Plan (VAMP). Prepared for the California Water Resources Control Board. Available at www.sjrg.org.

San Joaquin River Group Authority (2013). 2011 Annual Technical Report: On Implementation and Monitoring of the San Joaquin River Agreement and the Vernalis Adaptive Management Plan (VAMP). Prepared for the California Water Resources Control Board. Available at www.sjrg.org.

Seber, G. A. F. (2002). The estimation of animal abundance. Second edition. Blackburn Press, Caldwell, New Jersey.

Seber, G.A. F. (1965) A note on the multiple recapture census. *Biometrika* 52, 249-259.

Skalski, J. R., R. Townsend, J. Lady, A. E. Giorgi, J. R. Stevenson, and R. D. McDonald (2002). Estimating route-specific passage and survival probabilities at a hydroelectric project from smolt radiotelemetry studies. *Canadian Journal of Fisheries and Aquatic Sciences* 59: 1385 - 1393

Sokal, R. R., and Rohlf, F. J. (1995). *Biometry*, 3rd ed. W.H. Freeman and Co., New York, NY, USA.

Townsend, R. L., J. R. Skalski, P. Dillingham, and T. W. Steig (2006). Correcting Bias in Survival Estimation Resulting from Tag Failure in Acoustic and Radiotelemetry Studies. *Journal of Agricultural, Biological, and Environmental Statistics* 11: 183-196.

US Bureau of Reclamation (2012). San Joaquin River Flow Modification Study. Finding of No Significant Impact. Division of Planning, Mid Pacific Region, Sacramento CA. 3 p.

Vogel, D. A. (2010). Evaluation of acoustic-tagged juvenile Chinook Salmon movements in the Sacramento-San Joaquin delta during the 2009 Vernalis Adaptive Management Program. Technical Report for San Joaquin River Group Authority. 72 p. Available <http://www.sjrg.org/technicalreport/> (accessed 13 December 2011).

Vogel, D. A. (2011). Evaluation of acoustic-tagged juvenile Chinook Salmon and predatory fish movements in the Sacramento-San Joaquin Delta during the 2010 Vernalis Adaptive Management Program. Technical report for San Joaquin River Group Authority. Available <http://www.sjrg.org/technicalreport/> (accessed 13 December 2011).

Acknowledgements:

Funding for the project came from the restoration funds of the Central Valley Project Improvement Act, the U.S. Bureau of Reclamation, and the Department of Water Resources. Several individuals from a variety of agencies made this project possible. Those agencies and individuals who participated in the tagging and release components of the project were; USFWS: Amber Aguilera, Denise Barnard, Crystal Castle, Dustin Dinh, David Dominguez, Kyle Fronte, Garrett Giannetta, Jack Ingram, Carlie Jackson, Joseph Kirsch, David LaPlante, Jerrica Lewis, Mike Marshall, Louanne McMartin, Greg Nelson, Jacob Osborne, Lori Smith, Brent Trim, and Rob Wilson; California Department of Water Resources: Roxanne Kesler, Bryce Kozak, and Matt Silva; AECOM: Curtis Yip; and USBR: Raymond Bark and Josh Israel. USGS provided training for the surgeons (Theresa [Marty] Liedtke) and was responsible for the deployment, maintenance and retrieval of the receiver array (Jon Burau, Chris Vallee, Jim George and Norbert VandenBranden). Mike Simpson, retired from USGS, processed the data prior to giving it to Rebecca Buchanan of University of Washington for analyses.

Figures

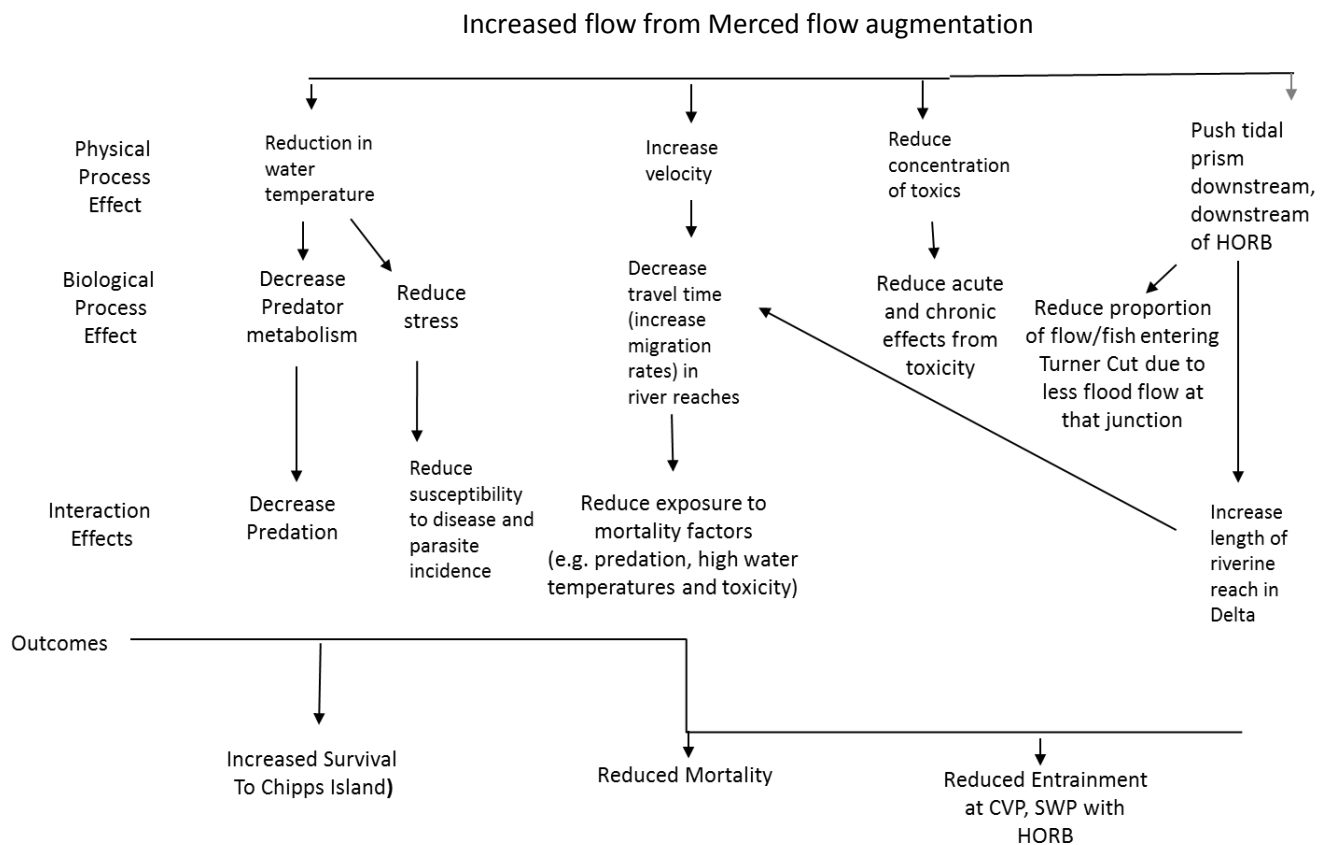


Figure 1: Conceptual model of mechanisms for increased survival from increasing Vernalis Flow with the head of Old River barrier in place.

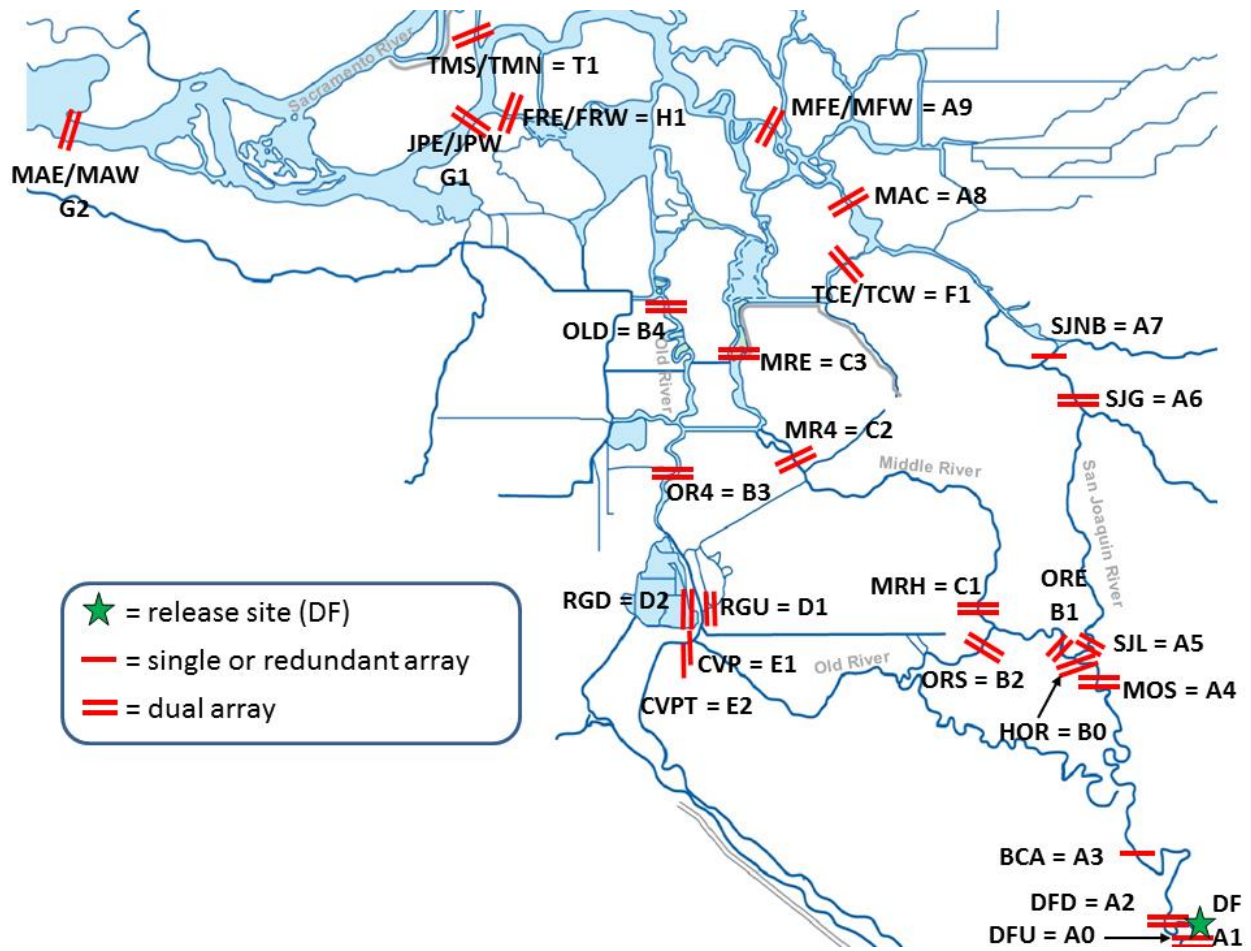


Figure 2. Locations of acoustic receivers and release site used in the 2012 Chinook Salmon study, with site code names (3- or 4-letter code) and model code (letter and number string). Site A1 is the release site at Durham Ferry. Sites B0, B4, C3, and T1 were excluded from the survival model.

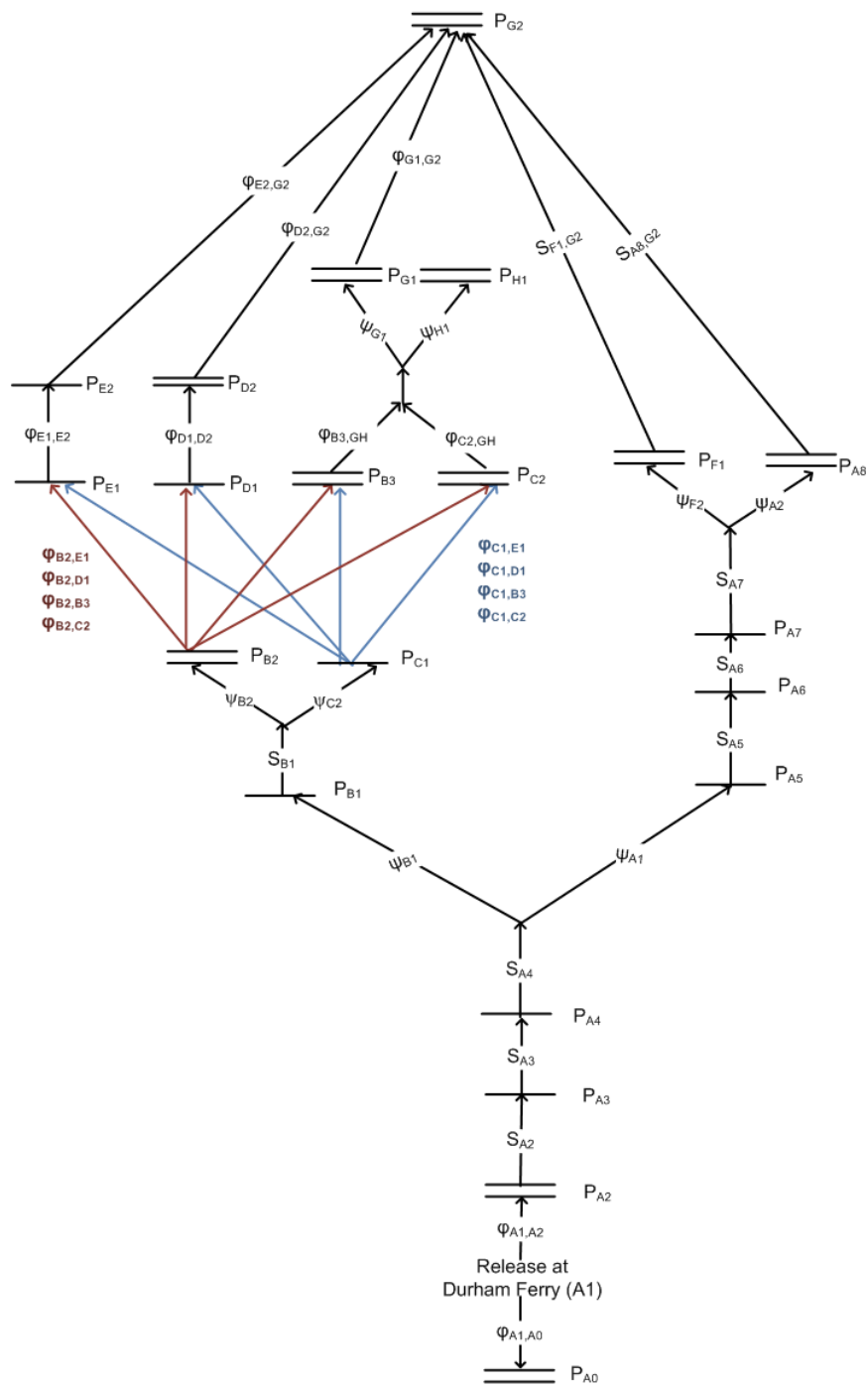


Figure 3. Schematic of 2012 mark-recapture Submodel I. Single lines denote single-array or redundant double-line telemetry stations, and double lines denote dual-array telemetry stations. Names of telemetry stations correspond to site labels in Figure 2. Migration pathways to sites B3 (OR4), C2 (MR4), D1 (RGU), and E1 (CVP) are color-coded by departure site.

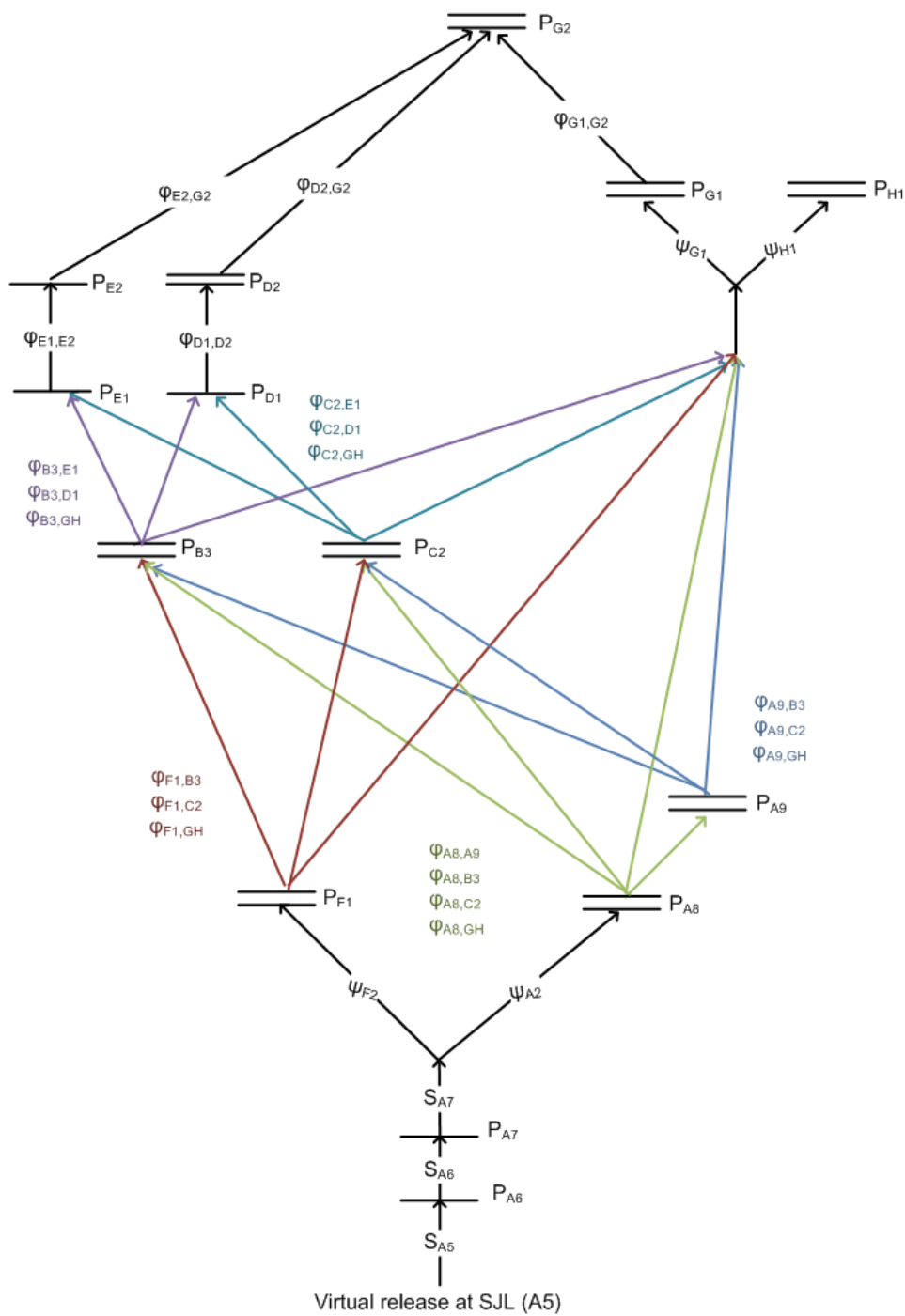


Figure 4. Schematic of 2012 mark-recapture Submodel II with estimable parameters. Single lines denote single-array or redundant double-line telemetry stations, and double lines denote dual-array telemetry stations. Names of telemetry stations correspond to site labels in Figure 2. Migration pathways to sites B3 (OR4), C2 (MR4), D1 (RGU), and E1 (CVP) are color-coded by departure site.

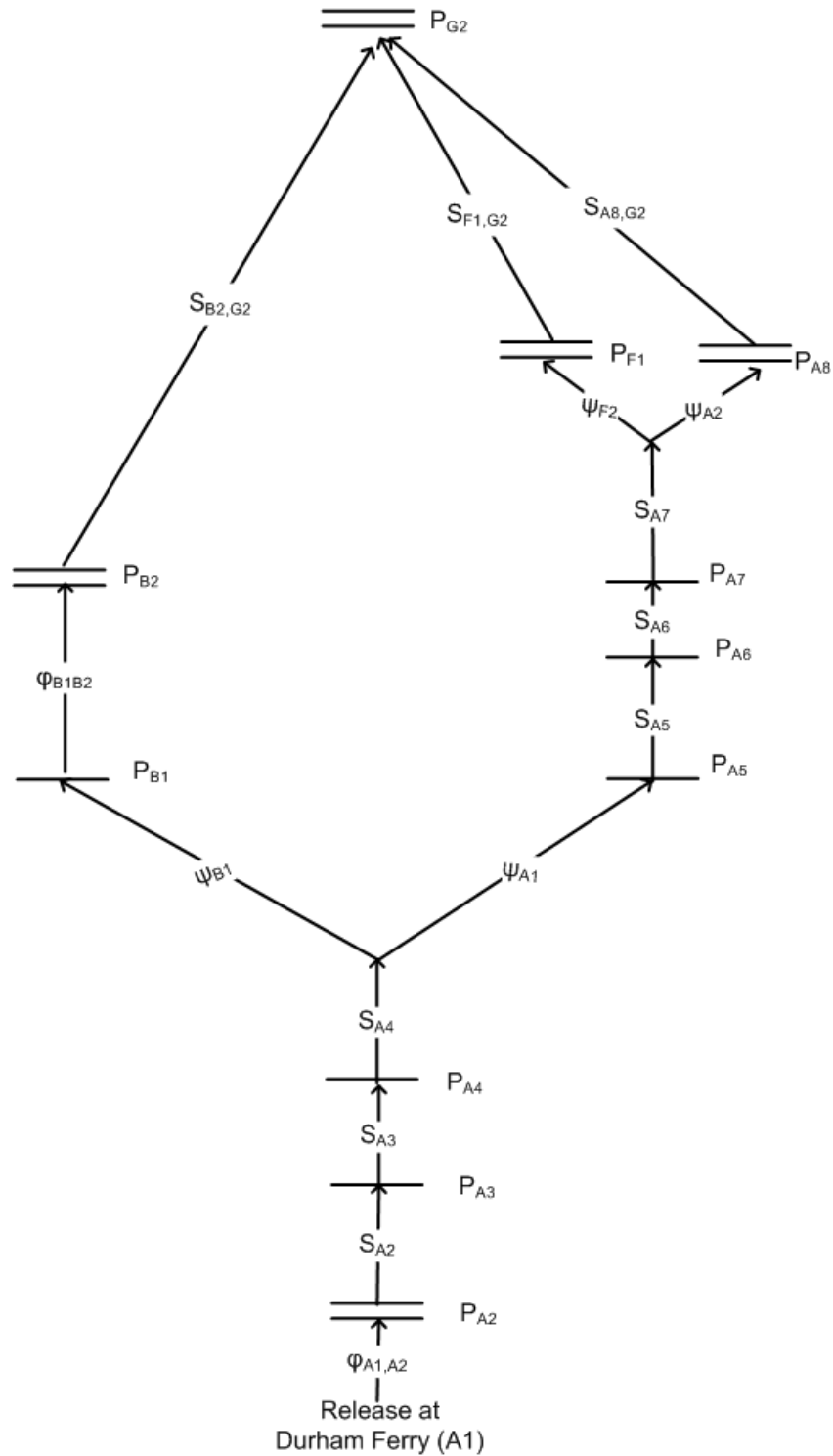


Figure 5. Schematic of reduced 2012 mark-recapture Submodel I with estimable parameters. Single lines denote single-array or redundant double-line telemetry stations, and double lines denote dual-array telemetry stations. Names of telemetry stations correspond to site labels in Figure 2.

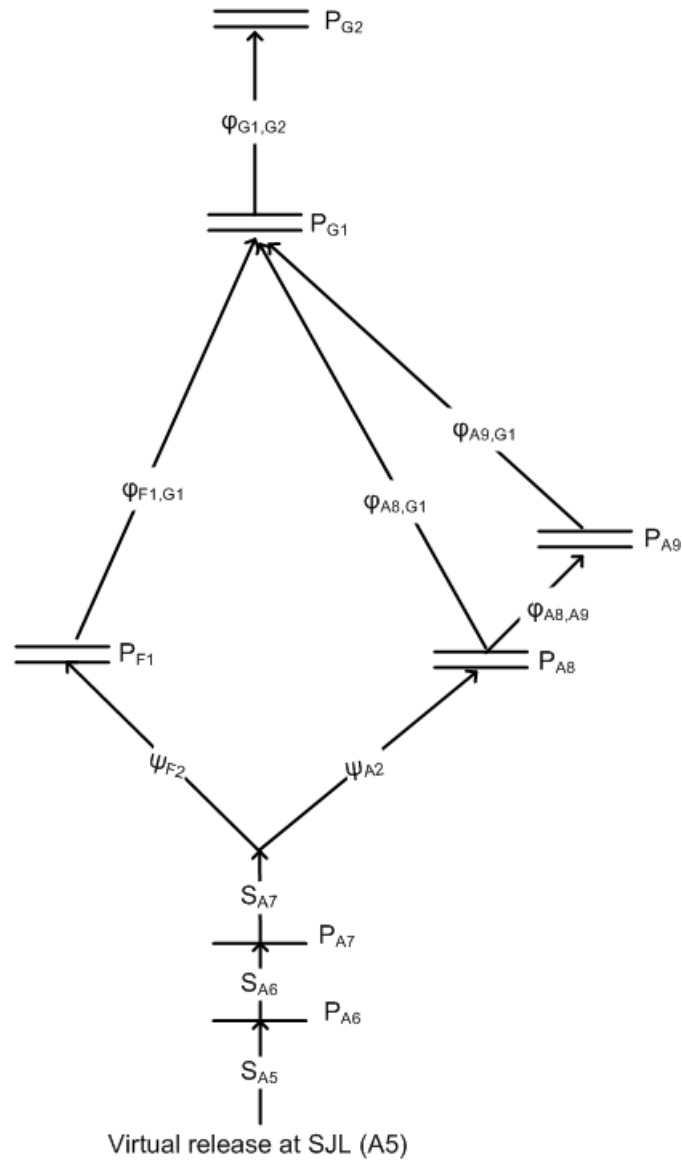


Figure 6. Schematic of reduced 2012 mark-recapture Submodel II with estimable parameters. Single lines denote single-array or redundant double-line telemetry stations, and double lines denote dual-array telemetry stations. Names of telemetry stations correspond to site labels in Figure 2.

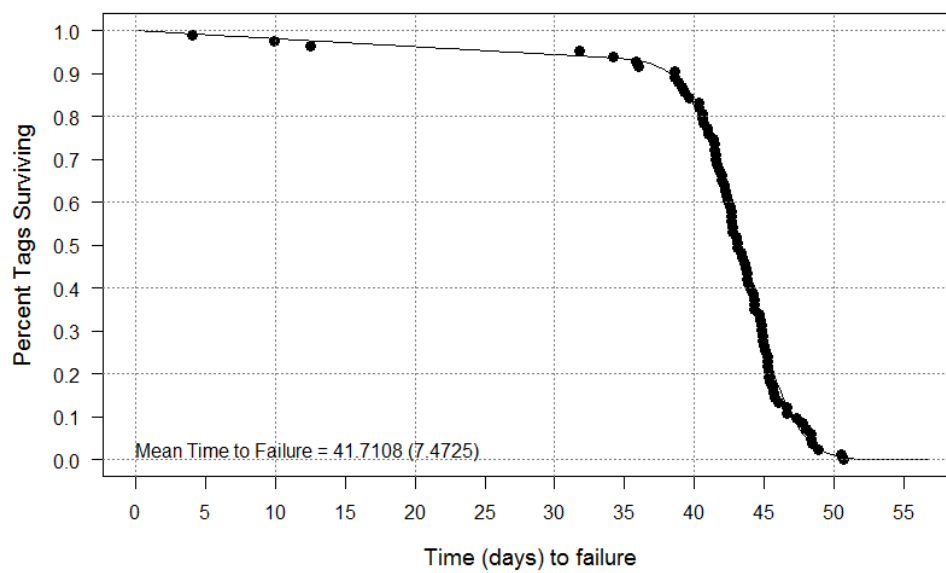


Figure 7. Observed tag failure times from the 2012 tag-life studies, pooled over the two studies, and fitted four-parameter vitality curve.

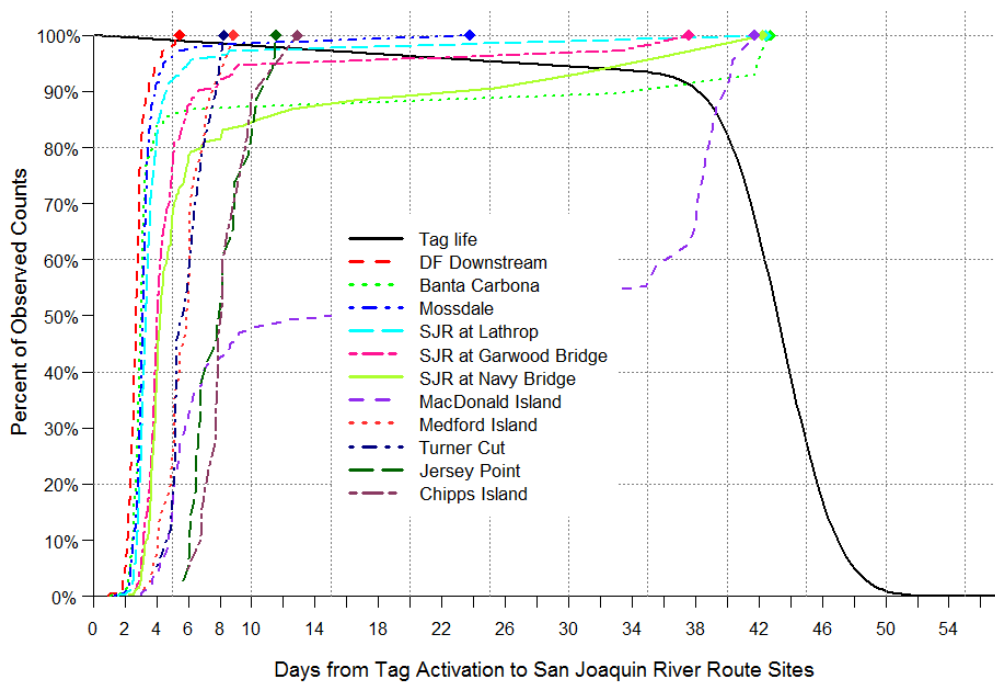


Figure 8. Four-parameter vitality survival curve for tag life, and the cumulative arrival timing of acoustic-tagged juvenile Chinook Salmon at receivers in the San Joaquin River route to Chipps Island in 2012, including detections that may have come from predators.

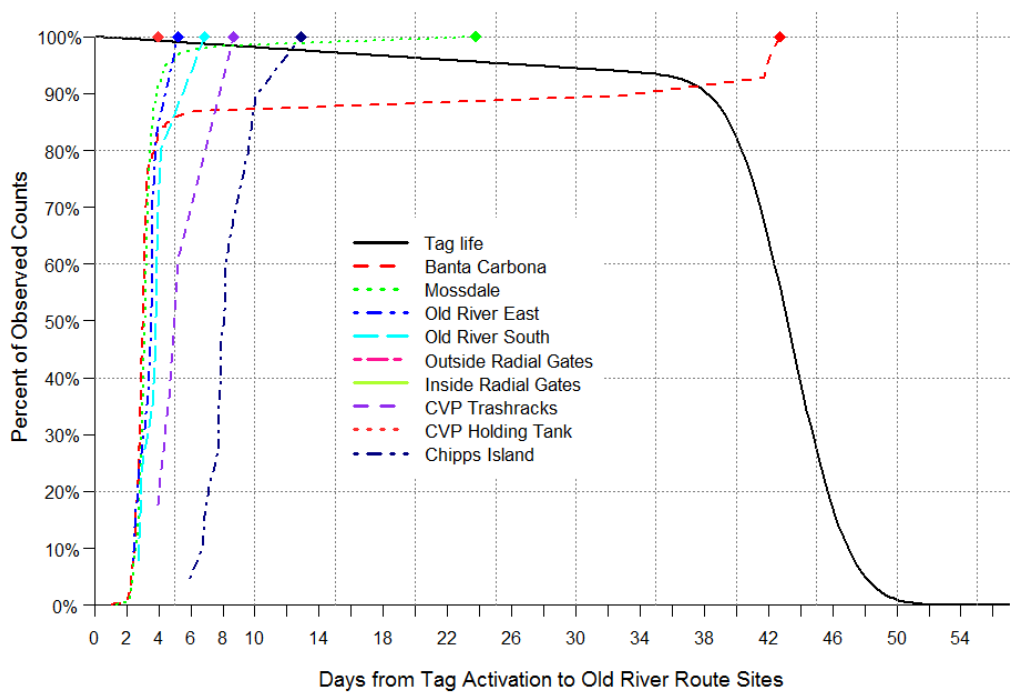


Figure 9. Four-parameter vitality survival curve for tag life, and the cumulative arrival timing of acoustic-tagged juvenile Chinook Salmon at receivers in the Old River route to Chipps Island in 2012, including detections that may have come from predators.

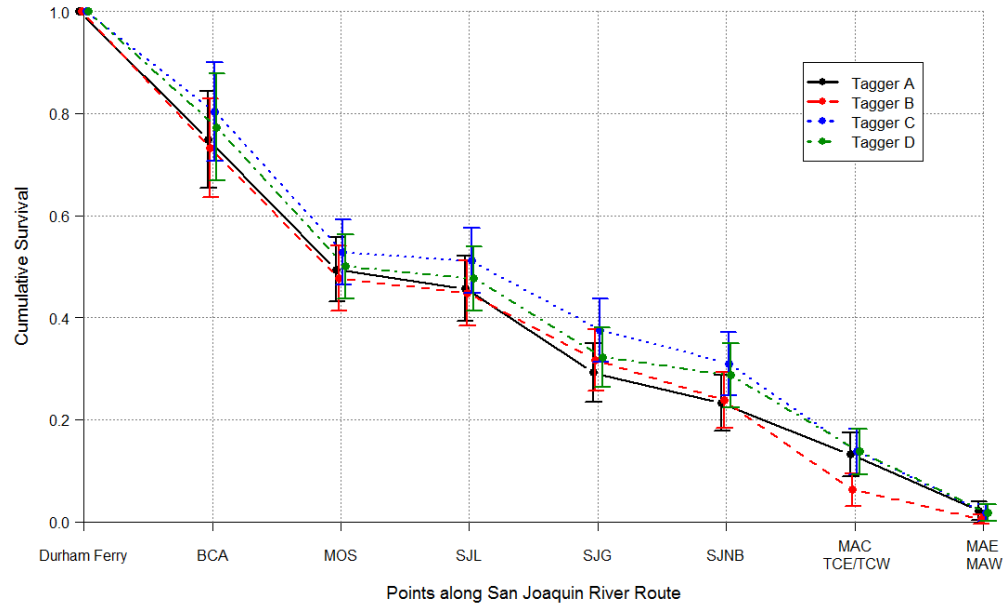


Figure 10. Cumulative survival from release at Durham Ferry to various points along the San Joaquin River route to Chipps Island, by tagger. Error bars are 95% confidence intervals.

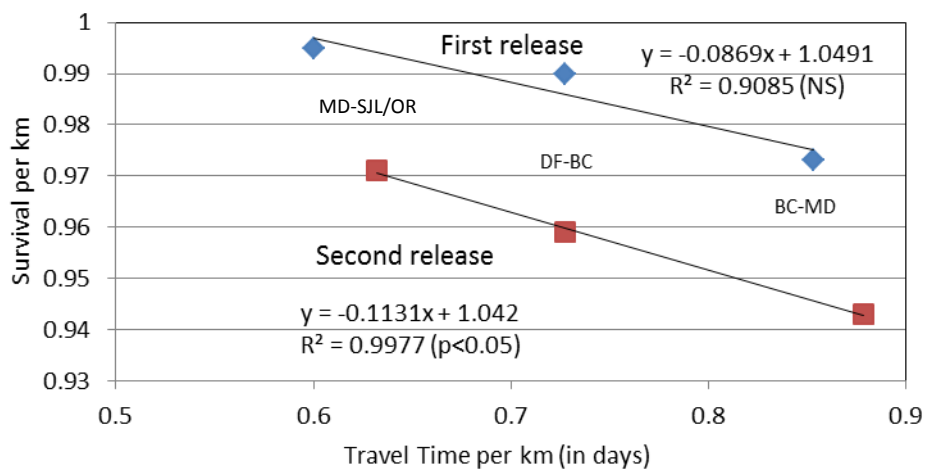


Figure 11: Travel time per km (in days) versus survival per km for river reaches, upstream of Mossdale in release group 1 and release group 2. Survival and travel time were without predator-type detections. Refer to Table 22 for data used.

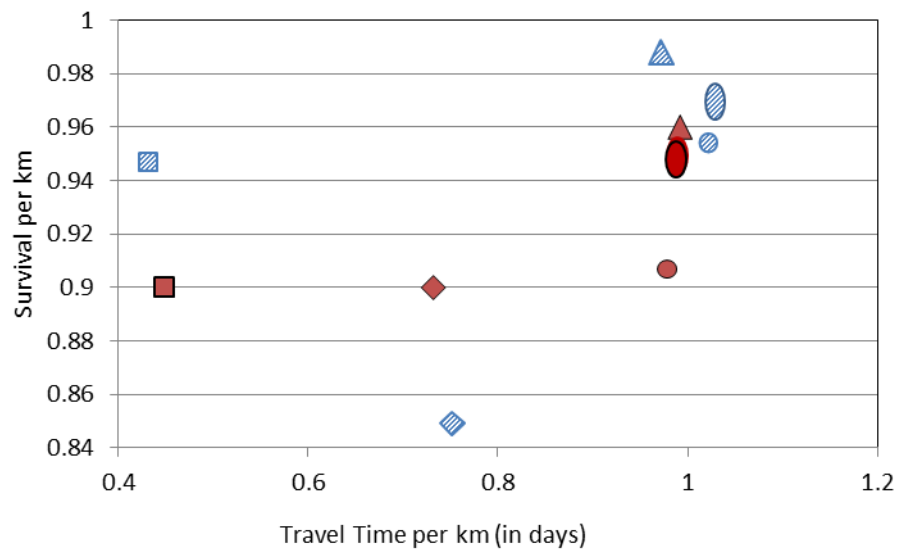


Figure 12: Travel time per km (in days) versus survival per km for reaches in the San Joaquin Delta for release group 1 (blue diagonal) and release group 2 (red solid). From Upstream to Downstream, reaches in order are: Lathrop to Garwood Bridge (triangles), Garwood Bridge to Navy Bridge Drive (squares), Navy Bridge to Turner Cut Junction (circles), MacDonald Island to Medford Island (diamonds) and Medford Island to Jersey Point (ovals). No recoveries were made at Chipps Island for the second release group to estimate travel time from Jersey Point to Chipps Island.

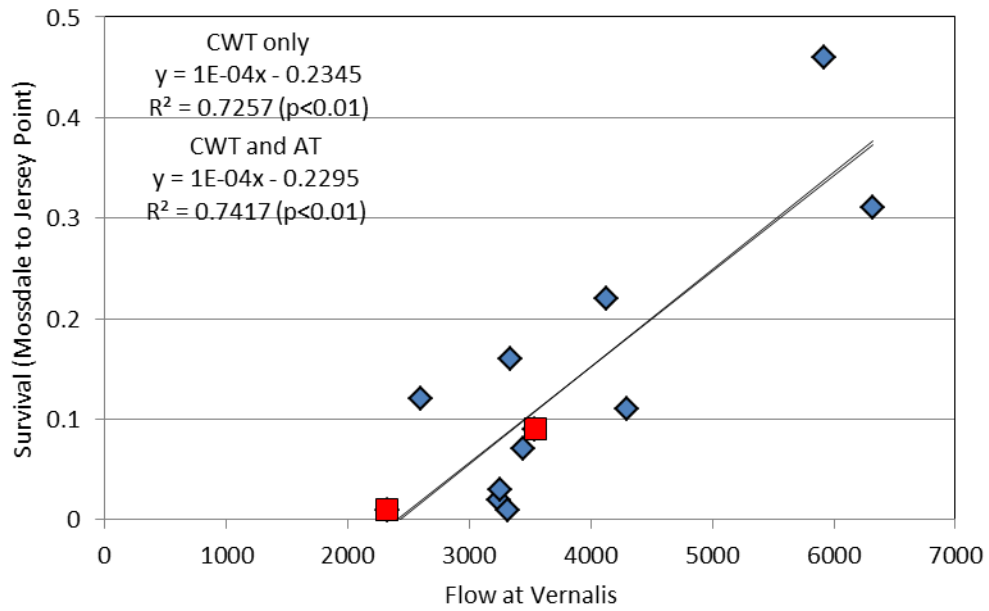


Figure 13: Estimates of survival between Mossdale and Jersey Point for CWT salmon (blue diamonds) and acoustic tag fish in 2012 (red squares) with the physical head of Old River barrier installed. Linear regression lines are plotted for both sets of data but overlap.

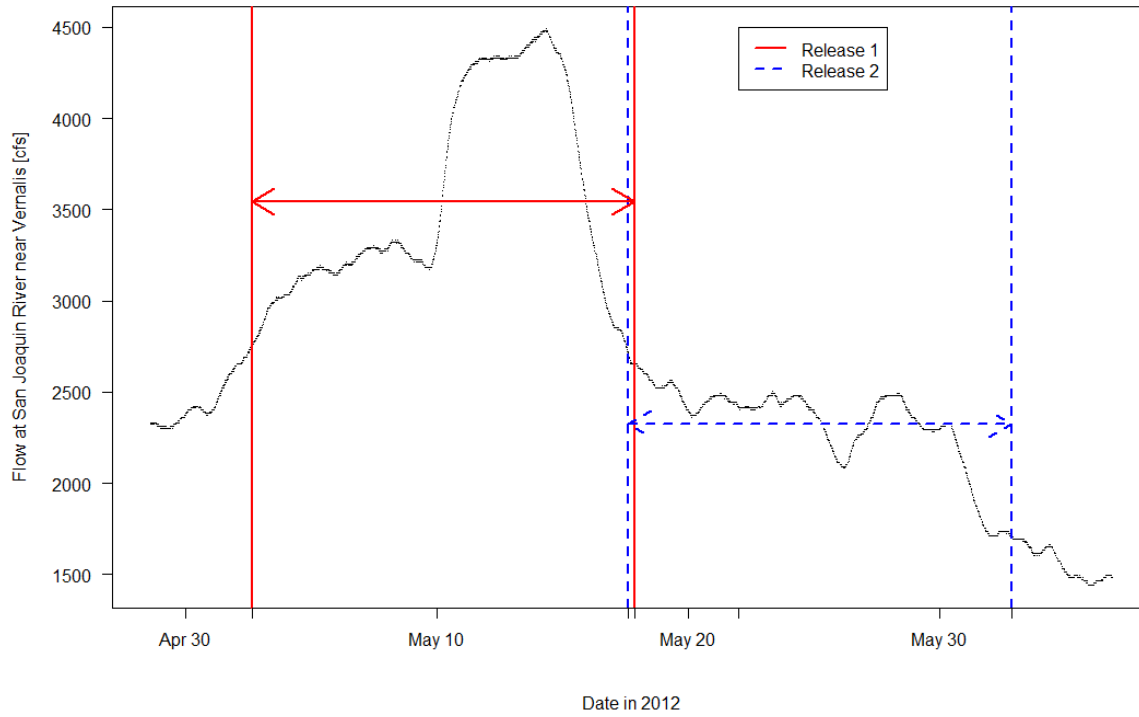


Figure 14. River discharge (flow) at Vernalis during 2012 study. Vertical lines represent expected period of travel from initial release at Durham Ferry to Chipps Island, based on release dates and maximum observed travel time over both releases. Arrow heights indicates mean flow during travel period.

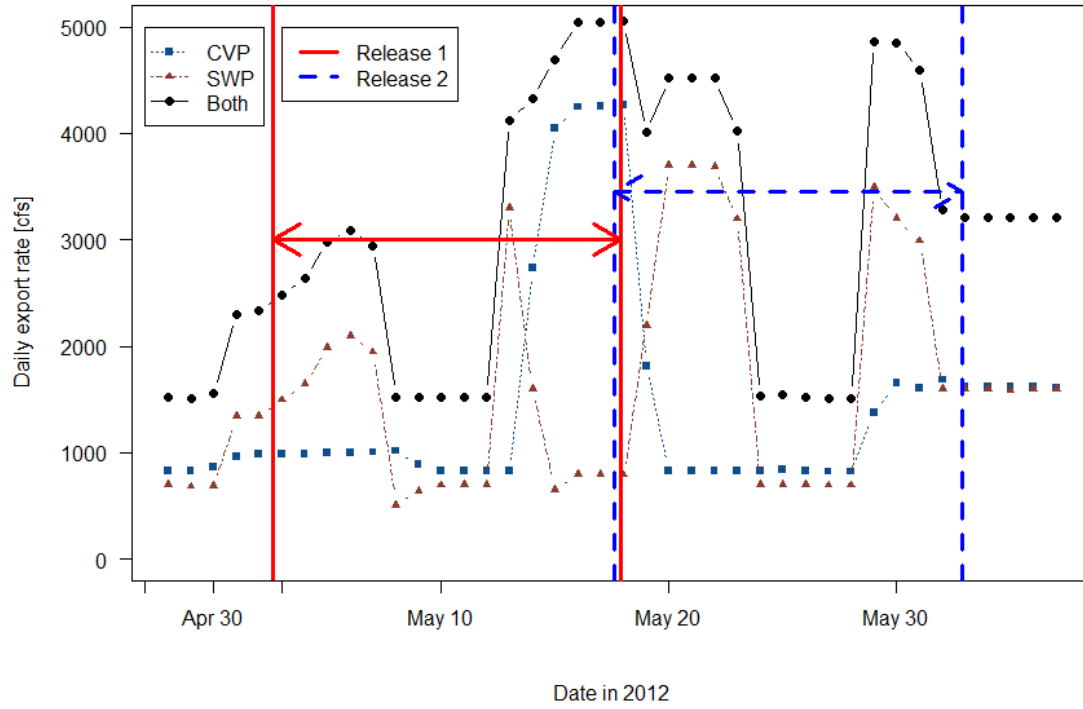


Figure 15. Daily export rate (cfs) at CVP and SWP during 2012 study. Vertical lines represent expected period of travel from initial release at Durham Ferry to Chipps Island, based on release dates and maximum observed travel time over both releases. Arrow height indicates mean combined export rate during travel period.

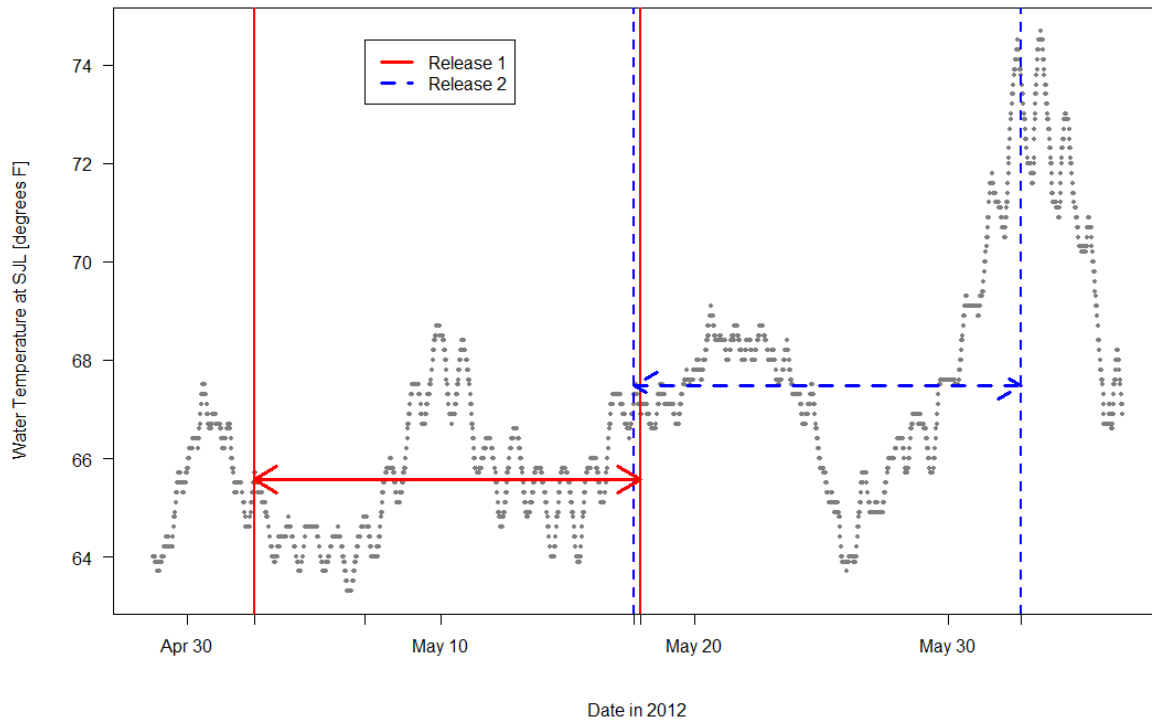


Figure 16. Temperature (°F) at the San Joaquin River gaging station near Lathrop during 2012 study. Vertical lines represent expected period of travel from initial release at Durham Ferry to Chipps Island, based on release dates and maximum observed travel time over both releases. Arrow height indicates mean temperature during travel period.

Tables

Table 1. Tagging, transport and holding date and times, and the number released (N) for Chinook Salmon as part of 2012 Chinook Salmon Study. Numbers of tagged fish use the format: [Number of Vemco-tagged fish]: [Number of HTI-tagged fish].

				Release A		Release B		Release C		Release D		Release E		Release F		Dummy tagged	Start Holding Date; Time	Total released (A – F)
Tagging Date	Transport Date/ Time	Number transported	Transport Tank #	Date; Time	N	Date; time	N	Date; Time	N									
5/1/12	5/1/12; 1352-1435	60: 15	1	5/2; 1505, 1506	24: 6	5/2; 1900, 1901	24: 6	5/2; 2256	12: 3							6	5/1; 1538	160: 42
		20: 6	2					5/2; 2257, 2306	20: 6							1		
	5/1/12; 1850-1930	60:15	1							5/3; 0300, 0301	24: 6	5/3; 0703, 0704	36: 9			0	5/1; 2020	
		20: 6	2									5/3; 1100,	20: 6		8			
5/3/12	5/3/12; 1237-1322	60: 15	1	5/4; 1500, 1503	24: 6	5/4; 1855, 1856	24: 6	5/4; 2256	12: 3							3	5/3; 1415	160: 42
		20: 6	2					5/4; 2256, 2304	20: 6							5		
	5/3/12; 1640-1725	60: 15	1							5/5; 0300	24: 6	5/5; 0702, 0703	24: 6	5/5; 1102	12: 3	3	5/3; 1808	
		20: 6	2									5/5; 1101, 1103	20: 6		4			
5/5/12	5/5/12; 1235 - 1320	60: 15	1	5/6; 1502, 1503	24: 6	5/6; 1856; 1857	24: 6	5/6; 2255	12: 3							9	5/5; 1356	160: 42
		20: 6	2					5/6; 2254, 2255	20: 6							6		
	5/5/12; 1717 - 1756	60: 15	1							5/7; 0300,	24: 6	5/7; 0700, 0701, 0702	36: 9			5	5/5; 1839	
		20: 6	2									5/7; 1100,	20: 6		9			

Table 1: (Continued)

				Release A		Release B		Release C		Release D		Release E		Release F				
Tagging Date	Transport Date/ Time	Number transported	Transport Tank #	Date; Time	N	Date; Time	N	Date; Time	N	Date; Time	N	Date; time	N	Date; Time	N	Dummy tagged	Start Holding Date; Time	Total released (A – F)
5/16/12	5/16; 1238 - 1323	60: 15	1	5/17; 1455, 1500	24 ¹ : 6	5/17; 1858, 1859 ²	24: 6	5/17; 2302	12: 3							1	5/16; 1449	160 ¹ : 45
		20: 8	2					5/17; 2301	20: 8							6		
	5/16; 1640 - 1731	60: 16	1							5/18; 0300	24: 6	5/18; 0701	36: 10			2	5/16; 1810	
		20: 6	2										5/18; 1100	20: 6	6			
5/18/12	5/18; 1246 - 1330	60: 16	1	5/19; 1458, 1459	24: 6	5/19; 1904, 1906	24: 6	5/19; 2259	12: 4							2	5/18; 1400	160: 46
		20: 8	2					5/19; 2258, 2259	20: 8							6		
	5/18; 1619 - 1709	60:16	1							5/19; 0303, 0305 ²	24: 6	5/19; 0700 ²	36: 10			1	5/18; 1736	
		20: 6	2										5/19; 1100 ²	20: 6	6			
5/20/12	5/20; 1206 - 1249	59: 15	1	5/21; 1505, 1506	23: 6	5/21; 1902, 1903	24: 6	5/21; 2259	12: 3							6	5/20; 1324	160: 44
		21: 8	2	5/21; 1506	1: 0			5/21; 2258, 2259	20: 8							9		
	5/20; 1557 - 1638	60: 15	1							5/22; 0300	24: 6	5/22; 0701, 0702	24: 6	5/22; 1100	12: 3	6	5/20; 1712	
		20: 6	2											20: 6	9			

¹ one tag not used in analyses; tag looked odd, ² released from shore due to high winds or dead battery in boat.

Table 2. Characteristics assessed for Chinook Salmon smolt condition and short-term survival

Characteristic	Normal	Abnormal
Percent Scale Loss	Lower relative numbers based on 0-100%	Higher relative numbers based on 0-100%
Body Color	High contrast dark dorsal surfaces and light sides	Low contrast dorsal surfaces and coppery colored sides
Fin Hemorrhaging	No bleeding at base of fins	Blood present at base of fins
Eyes	Normally shaped	Bulging or with hemorrhaging
Gill Color	Dark beet red to cherry red colored gill filaments	Grey to light red colored gill filaments
Vigor	Active swimming (prior to anesthesia)	Lethargic or motionless (prior to anesthesia)

Table 3. Names and descriptions of receivers and hydrophones used in the 2012 Chinook Salmon tagging study, with receiver codes used in Figure 2, the survival model (Figures 2 – 5), and in data processing by the United States Geological Survey (USGS). The release site was located at Durham Ferry.

Individual Receiver Name and Description	Hydrophone Location		Receiver Code	Survival Model Code	Data Processing Code
	Latitude (°N)	Longitude (°W)			
San Joaquin River near Durham Ferry upstream of the release site, upstream node	37.685806	121.256500	DFU1	A0a	300856
San Joaquin River near Durham Ferry upstream of the release site, downstream node	37.686444	121.256806	DFU2	A0b	300857
San Joaquin River near Durham Ferry; release site (no acoustic hydrophone located here)	37.687011	121.263448	DF	A1	
San Joaquin River near Durham Ferry downstream of the release site, upstream node	37.688222	121.276139	DFD1	A2a	300858
San Joaquin River near Durham Ferry downstream of the release site, downstream node	37.688333	121.276139	DFD2	A2b	300859
San Joaquin River near Banta Carbona	37.727722	121.298917	BCA	A3	300860
San Joaquin River near Mossdale Bridge, upstream node	37.792194	121.307278	MOSU	A4a	300861
San Joaquin River near Mossdale Bridge, downstream node	37.792356	121.307369	MOSD	A4b	300862
San Joaquin River upstream of Head of Old River, upstream node (not used in survival model)	37.805528	121.320000	HORU	B0a	300863
San Joaquin River upstream of Head of Old River, downstream node (not used in survival model)	37.805000	121.321306	HORD	B0b	300864
San Joaquin River near Lathrop, upstream	37.810875 ^a	121.322500 ^a	SJLU	A5a	300869/300870
San Joaquin River near Lathrop, downstream	37.810807 ^a	121.321269 ^a	SJLD	A5b	300871/300872
San Joaquin River near Garwood Bridge, upstream	37.934972	121.329333	SJGU	A6a	300877
San Joaquin River near Garwood Bridge, downstream	37.935194	121.329833	SJGD	A6b	300878
San Joaquin River at Stockton Navy Drive Bridge	37.946806	121.339583	SJNB	A7	300879
San Joaquin River at MacDonald Island, upstream	38.018022 ^a	121.462758 ^a	MACU	A8a	300899/300901
San Joaquin River at MacDonald Island, downstream	38.023877 ^a	121.465916 ^a	MACD	A8b	300900/300902
San Joaquin River near Medford Island, east	38.053134 ^a	121.510815 ^a	MFE	A9a	300903/300904
San Joaquin River near Medford Island, west	38.053773 ^a	121.513315 ^a	MFW	A9b	300905/300906
Old River East, near junction with San Joaquin, upstream	37.811653 ^a	121.335486 ^a	OREU	B1a	300865/300866

a = Average latitude and longitude given for sites with multiple hydrophones or for sites with multiple locations throughout the study

Table 3. (Continued)

Individual Receiver Name and Description	Hydrophone Location		Receiver Code	Survival Model Code	Data Processing Code
	Latitude (°N)	Longitude (°W)			
Old River East, near junction with San Joaquin, downstream	37.812284 ^a	121.335558 ^a	ORED	B1b	300867/300868
Old River South, upstream	37.819583	121.378111	ORSU	B2a	300873
Old River South, downstream	37.820028	121.378889	ORSU	B2b	300874
Old River at Highway 4, upstream	37.893864 ^a	121.567083 ^a	OR4U	B3a	300882/300883
Old River at Highway 4, downstream	37.895125 ^a	121.566403 ^a	OR4D	B3b	300884/300885
Old River North of Empire Cut, upstream receiver (not used in survival model)	37.967125 ^a	121.574514 ^a	OLDU	B4a	450022
Old River North of Empire Cut, downstream receiver (not used in survival model)	37.967375 ^a	121.574389 ^a	OLDD	B4b	450023
Middle River Head, upstream	37.824744	121.380056	MRHU	C1a	300875
Middle River Head, downstream	37.824889	121.380417	MRHD	C1b	300876
Middle River at Highway 4, upstream	37.895750	121.493861	MR4U	C2a	300881
Middle River at Highway 4, downstream	37.896222	121.492417	MR4D	C2b	300880
Middle River at Empire Cut, upstream receiver (not used in survival model)	37.941685 ^a	121.533250 ^a	MREU	C3a	300898/450021
Middle River at Empire Cut, downstream receiver (not used in survival model)	37.942861 ^a	121.532370 ^a	MRED	C3b	300897/450030
Radial Gate at Clifton Court Forebay, upstream (in entrance channel to forebay), array 1	37.830086	121.556594	RGU1	D1a	300888
Radial Gate at Clifton Court Forebay, upstream, array 2	37.829606	121.556989	RGU2	D1b	300889
Radial Gate at Clifton Court Forebay, downstream (inside forebay), array 1 in dual array	37.830147 ^a	121.557528 ^a	RGD1	D2a	300890/300892/ 460009/460011
Radial Gate at Clifton Court Forebay, downstream, array 2 in dual array	37.829822 ^a	121.557900 ^a	RGD2	D2b	300891/460010
Central Valley Project trashracks, upstream	37.816900 ^a	121.558459 ^a	CVPU	E1a	300894/460012
Central Valley Project trashracks, downstream	37.816647	121.558981	CVPD	E1b	300895
Central Valley Project holding tank (all holding tanks pooled)	37.815844	121.559128	CVPtank	E2	300896
Turner Cut, east (closer to San Joaquin)	37.991694	121.455389	TCE	F1a	300887
Turner Cut, west (farther from San Joaquin)	37.990472	121.456278	TCW	F1b	300886
San Joaquin River at Jersey Point, east (upstream)	38.056351 ^a	121.686535 ^a	JPE	G1a	300915 - 300922
San Joaquin River at Jersey Point, west (downstream)	38.055167 ^a	121.688070 ^a	JPW	G1b	300923 - 300930

a = Average latitude and longitude given for sites with multiple hydrophones or for sites with multiple locations throughout the study

Table 3. (Continued)

Individual Receiver Name and Description	Hydrophone Location		Receiver Code	Survival Model Code	Data Processing Code
	Latitude (°N)	Longitude (°W)			
False River, west (closer to San Joaquin)	38.056834 ^a	121.671403 ^a	FRW	H1a	300913/300914
False River, east (farther from San Joaquin)	38.057118 ^a	121.669673 ^a	FRE	H1b	300911/300912
Chipps Island (aka Mallard Island), east (upstream)	38.048772 ^a	121.931198 ^a	MAE	G2a	300931 - 300942
Chipps Island (aka Mallard Island), west (downstream)	38.049275 ^a	121.933839 ^a	MAW	G2b	300943, 300979 - 300983, 300985 - 300990
Threemile Slough, south (not used in survival model)	38.107771 ^a	121.684042 ^a	TMS	T1a	300909/300910
Threemile Slough, north (not used in survival model)	38.111556 ^a	121.682826 ^a	TMN	T1b	300907/300908

a = Average latitude and longitude given for sites with multiple hydrophones or for sites with multiple locations throughout the study

Table 4. Environmental monitoring sites used in predator decision rule and route entrainment analysis. Database = CDEC (<http://cdec.water.ca.gov/>) or Water Library (<http://www.water.ca.gov/waterdatalibrary/>).

Environmental Monitoring Site			Detection Site	Data Available					Database
Site Name	Latitude (°N)	Longitude (°W)		River Flow	Water Velocity	River Stage	Pumping	Reservoir Inflow	
CLC	37.8298	121.5574	RGU, RGD	No	No	No	No	Yes	CDEC
FAL	38.0555	121.6672	FRE/FRW	Yes	Yes	Yes	No	No	CDEC
GLC	37.8201	121.4497	ORS	Yes	Yes	Yes	No	No	CDEC
MAL	38.0428	121.9201	MAE/MAW	No	No	Yes	No	No	CDEC
MDM	37.9425	121.534	MR4, MRE	Yes	Yes	Yes	No	No	CDEC ^a
MSD	37.7860	121.3060	HOR, MOS	Yes	Yes	Yes	No	No	Water Library
ODM	37.8101	121.5419	CVP	Yes	Yes	Yes	No	No	CDEC
OH1	37.8080	121.3290	ORE	Yes	Yes	Yes	No	No	CDEC
OH4	37.8900	121.5697	OR4	Yes	Yes	Yes	No	No	CDEC
ORI	37.8280	121.5526	RGU, RGD	Yes	Yes	No	No	No	Water Library
PRI	38.0593	121.5575	MAC, MFE/MFW	Yes	Yes	Yes	No	No	CDEC
RMID040	37.8350	121.3838	MRH	No	No	Yes	No	No	Water Library
ROLD040	37.8286	121.5531	RGU, RGD	No	No	Yes	No	No	Water Library
SJG	37.9351	121.3295	SJG, SJNB	Yes	Yes	Yes	No	No	CDEC
SJJ	38.0520	121.6891	JPE/JPW	Yes	Yes	Yes	No	No	CDEC
SJL	37.8100	121.3230	SJL	Yes	Yes	Yes	No	No	Water Library
TRN	37.9927	121.4541	TCE/TCW	Yes	Yes	Yes	No	No	CDEC
TRP	37.8165	121.5596	CVP	No	No	No	Yes	No	CDEC
TSL	38.1004	121.6866	TMS/TMN	Yes	Yes	Yes	No	No	CDEC
VNS	37.6670	121.2670	DFU, DFD, BCA	Yes	No	Yes	No	No	CDEC
WCI	37.8316	121.5541	RGU, RGD	Yes	Yes	No	No	No	Water Library

a = California Water Library was used for river stage

Table 5a. Cutoff values used in predator filter in 2012. Observed values past cutoff or unmet conditions indicate a predator. Only transitions observed in 2012 are represented here. No detections were observed at MRH, RGU, or RGD in 2012. See Table 5b for Flow, Water Velocity, Extra Conditions, and Comment. Footnotes refer to both this table and Table 5b.

Detection Site	Previous Site	Residence Time ^a (hr)		Migration Rate ^{b,c} (km/hr)		BLPS (Absolute value)	No. of Visits	No. of Cumulative Upstream Forays
		Maximum	Maximum	Minimum	Maximum	Maximum	Maximum	Maximum
DFU	DF, DFD	0.5	1	0.2 (0.6 ^f)			1	1
	DFU	0.5	1				2	0
DFD	DF, DFU	4	8	0.05			1	0
	DFD	2	49				2	0
	BCA	2	4	0.1			0	0
BCA	DF, DFU	5	10	0.1			1	0
	BCA	0.1	168				2	0
	MOS	0.1	0.2	0.1			0	0
MOS	DF, DFD, BCA	10	20	0.2		8	1	0
	MOS	2	261				2	1
	HOR	1	2	0.2		8	2	1
SJL	MOS, HOR	5	15	0.2		8	2	0
	SJL	1	293				3	1
SJG	HOR, SJL	12	24	0.2		8	1	0
	SJG	6	360				1	1
	SJNB	3	6	0.2		8	2	2
SJNB	SJG	15 (6 ^f)	30 (12 ^f)	0.2		8	2	0
	SJNB	4	360				2	3
MAC	SJG, SJNB	30	60	0.2		8	1	0
	MAC	30	360				2	3
	MFE/MFW	15	30	0.2		8	2	3

a = Near-field residence time includes up to 12 hours missing between detections, while mid-field residence time includes entire time lag between first and last detections without intervening detections elsewhere

b = Approximate migration rate calculated on most direct pathway

c = Missing values for transitions to and from same site: travel times must be 12 to 24 hours, unless otherwise specified under "Extra conditions"

f = See comments for alternate criteria

Table 5a. (Continued)

Detection Site	Previous Site	Residence Time ^a (hr)		Migration Rate ^{b,c} (km/hr)		BLPS (Absolute value)	No. of Visits	No. of Cumulative Upstream Forays
		Near Field Maximum	Mid-field Maximum	Minimum	Maximum	Maximum	Maximum	Maximum
MFE/MFW	MAC	30	60	0.2	5.5	8	2	0
	MFE/MFW	15	360				3	3
HOR	DF, MOS	10	20	0.2	5.5	8	1 (2 ^f)	0
	HOR	3	288				2	1
	SJL	3 (4 ^f)	6 (8 ^f)	0.2 (0.1 ^f)	5.5 (6 ^f)	8	2	1
ORE	HOR	5	15	0.2	5.5	8	1	0
	ORE	1	287				1	0
ORS	ORE	12	24	0.2	5.5	8	1	0
	ORS	4	360				2	1
OR4	ORS	40	80	0.2	5.5	8	1	0
	MR4	40	80	0.1	5.5		2	3
	OR4	25	129				2	2
OLD	OR4	40	80	0.2	5.5	8	2	0
	MRE	40	80	0.1	5.5		1	0
MR4	MRE	10	20	0.2	5.5	8	1	2
MRE	SJNB, MAC	20	40	0.1	5.5		1	0
	TCE/TCW	20	40	0.1	5.5		1	0
CVP	DF, ORS	10	20	0.2	5.5	8	1	1
	CVP	10	390				3	3
	OR4	10	20	0.5	5.5	8	2	3
CVPtank	CVP	20	360				2	3

a = Near-field residence time includes up to 12 hours missing between detections, while mid-field residence time includes entire time lag between first and last detections without intervening detections elsewhere

b = Approximate migration rate calculated on most direct pathway

c = Missing values for transitions to and from same site: travel times must be 12 to 24 hours, unless otherwise specified under "Extra conditions"

f = See comments for alternate criteria

Table 5a. (Continued)

Detection Site	Previous Site	Residence Time ^a (hr)		Migration Rate ^{b, c} (km/hr)		BLPS (Absolute value)	No. of Visits	No. of Cumulative Upstream Forays
		Maximum	Maximum	Minimum	Maximum	Maximum	Maximum	Maximum
TCE/TCW	SJG, SJNB	12	24	0.2	5.5	8	1	0
	MAC	12	24	0.2	5.5	8	2	3
	TCE/TCW	3	360				1	3
JPE/JPW	MAC, MFE/MFW, TMN/TMS	40	80	0.1	5.5	8	1	0
	FRE/FRW	30	360	0.1	5.5		3	3
	JPE/JPW	30	360				3	0
MAE/MAW	MFE/MFW, CVPtank	40	80	0.1	5.5	8	1	0
	TMN/TMS, JPE/JPW, FRE/FRW	40	80	0.1	5.5	8	2	0
FRE/FRW	MAC, MFE/MFW, OLD	40	80	0.1	5.5	8	1	0
	JPE/JPW	30	360	0.1			3	3
TMN/TMS	MAC, MFE/MFW	10	20	0.2	3	8	1	0
	JPE/JPW	10	20	0.5	3	8	1	3

a = Near-field residence time includes up to 12 hours missing between detections, while mid-field residence time includes entire time lag between first and last detections without intervening detections elsewhere

b = Approximate migration rate calculated on most direct pathway

c = Missing values for transitions to and from same site: travel times must be 12 to 24 hours, unless otherwise specified under "Extra conditions"

Table 5b. Cutoff values used in predator filter in 2012. Observed values past cutoff or unmet conditions indicate a predator. Only transitions observed in 2012 are represented here. No detections were observed at MRH, RGU, or RGD in 2012. Footnotes, Extra Conditions and Comment refer to both this table and Table 5a.

Detection Site	Previous Site	Flow ^d (cfs)		Water Velocity ^d (ft/sec)			Extra Conditions	Comment
		At arrival	At departure ^e	At arrival	At departure ^e	Average during transition		
DFU	DF, DFD							Alternate value if coming from DFD
	DFU						Not allowed	
DFD	DF, DFU						Not allowed	
	DFD						Not allowed	
	BCA						Not allowed	
BCA	DF, DFU						Travel time < 25	
	BCA						Not allowed	
	MOS						Travel time < 20	
MOS	DF, DFD, BCA						Travel time < 20	
	MOS							
	HOR					< 0.1		
SJL	MOS, HOR						Travel time < 20	
	SJL							
SJG	HOR, SJL							
	SJG							
	SJNB	< 1700	< 4000	< 0.5	< 1	< 0.5	Change in river stage at arrival: -0.1 to 0.1	
SJNB	SJG			< 2 (> 2 ^f)				Alternate values for change in river stage at arrival: < -0.1 or > 0.1
	SJNB	< 600 (> -250) ^g	> -250 (< 600) ^g	< 0.2 (> -0.1) ^g	> -0.1 (< 0.2) ^g	< 1.5		
MAC	SJG, SJNB							
	MAC			< 0.2 (> -0.1) ^g	> -0.1 (< 0.2) ^g			

d = Classified as predator if flow or velocity condition, if any, is violated

e = Condition at departure from previous site

f = See comments for alternate criteria

g = High flow/velocity on departure requires low values on arrival (and vice versa)

Table 5b. (Continued)

Detection Site	Previous Site	Flow ^d (cfs)		Water Velocity ^d (ft/sec)			Extra Conditions	Comment
		At arrival	At departure ^e	At arrival	At departure ^e	Average during transition		
MAC	MFE/MFW			< -0.4	< 0.2	< 0.2		
MFE/MFW	MAC							
	MFE/MFW			< 0.2 (> -0.1) ^g	> -0.1 (< 0.2) ^g			
	SJG	<100 (>-300) ^g	>-300 (<100) ^g	<0.1 (>-0.5) ^g	>-0.5 (<0.1) ^g	<0.5		
HOR	DF, MOS							Alternate value if coming from MOS
	HOR						Travel time < 20	
	SJL			< 1.5	< 0.15 (0.25) ^f	< 1 (1.1) ^f		Alternate value if next transition is downstream
ORE	HOR							
	ORE						Not allowed	
ORS	ORE	> -2500		> -0.5				
	ORS	< 2500 (> -2500) ^g	> -2500 (< 2500) ^g	< 0.5 (> -0.5) ^g	> -0.5 (< 0.5) ^g			
OR4	ORS	> -700		> -0.3				
	MR4							
	OR4	< 700 (> -700) ^g	> -700 (< 700) ^g	< 0.3 (> -0.3) ^g	> -0.3 (< 0.3) ^g			
OLD	OR4	> -2000	> -1000	> -0.1	> -0.05			
	MRE							
MR4	MRE	< 2500	< 1000	< 0.25	< 0.1	< 0.1		
MRE	SJNB, MAC	< 1000		< 0.1				
	TCE/TCW	< 1000	< 200	< 0.1	< 0.05			

d = Classified as predator if flow or velocity condition, if any, is violated

e = Condition at departure from previous site

f = See comments for alternate criteria

g = High flow/velocity on departure requires low values on arrival (and vice versa)

Table 5b. (Continued)

Detection Site	Previous Site	Flow ^d (cfs)		Water Velocity ^d (ft/sec)		Average during transition	Extra Conditions	Comment
		At arrival	At departure ^e	At arrival	At departure ^e			
CVP	DF, ORS							
	CVP							CVP pumping > 1500 cfs on arrival, < 1500 cfs on departure
	OR4	< 3000	< 2000	< 1.5	< 0.8	< 0.1		CVP pumping > 1500 cfs on arrival Travel time < 100
CVPtank	CVP							
TCE/TCW	SJG, SJNB	< 1200		< 0.2				
	MAC	< 1200		< 0.2	< 0.2	< 0.2		
	TCE/TCW	< 500 (> 500) ^g	> 500 (< 500) ^g	< 0.1 (> 0.1) ^g	> 0.1 (< 0.1) ^g	-0.2 to 0.2		Travel time < 13
JPE/JPW	MAC, MFE/MFW, TMN/TMS FRE/FRW JPE/JPW							Travel time < 50
MAE/MAW	MFE/MFW, CVPtank TMN/TMS, JPE/JPW, FRE/FRW			> -2.5				
				> -2.5				
FRE/FRW	MAC, MFE/MFW, OLD							
FRE/FRW	MAC, MFE/MFW, OLD JPE/JPW							
TMN/TMS	MAC, MFE/MFW JPE/JPW					> -0.4		

d = Classified as predator if flow or velocity condition, if any, is violated

e = Condition at departure from previous site

g = High flow/velocity on departure requires low values on arrival (and vice versa)

Table 6: Water temperature and dissolved oxygen in the transport tank after loading prior to transport, after transport, and in the river at Durham Ferry release site, just prior to placing fish in holding containers; the number of mortalities after transport and prior to release.

Transport		Tank #1						Tank #2						River		
		After loading		After transport		# morts after transport	After loading		After transport		# morts after transport	Temp (°C)	DO (mg/L)	Mortalities just prior to release		
Date	Loading time	Ice Added	Temp (°C)	DO (mg/L)	Temp (°C)		DO (mg/L)	Ice Added	Temp (°C)	DO (mg/L)					Temp (°C)	DO (mg/L)
5/1/2012	1331	Yes	18.4	8.73	18.5	11.7	0	Yes	18.6	8.22	18.5	9.94	0	19.3	10.54	0
5/1/2012	1810	No	16.8	9.68	16.5	9.83	0	No	17.1	8.57	16.7	9.12	0	18.8	10.91	0
5/3/2012	1219	No	18.8	9.64	19.1	9.76	0	No	18.5	9.07	18.7	9.41	0	18.0	9.22	0
5/3/2012	1616	Yes	18.2	10.04	18.1	10.67	0	Yes	18.1	10.01	17.8	10.22	0	18.4	9.55	0
5/5/2012	1208	Yes	18.9	10.44	19.1	11.76	0	Yes	18.9	10.23	18.8	10.57	0	17.5	9.66	0
5/5/2012	1652	Yes	18.4	10.36	18.5	11.89	0	Yes	18.3	10.47	18.1	10.63	0	18.0	10.14	0
													Average	18.3		
5/16/2012	1222	Yes	19.3	9.37	19.7	9.38	0	Yes	19.4	9.46	19.7	9.42	0	19.1	11.45	0
5/16/2012	1617	Yes	19.4	9.35	19.7	10.25	0	Yes	19.5	9.38	19.5	9.51	0	19.9	9.59	0
5/18/2012	1228	Yes	19.0	9.71	19.8	10.86	0	Yes	18.9	9.64	19.3	9.74	0	19.0	8.4	0
5/18/2012	1556	Yes	19.5	9.66	19.6	10.74	0	Yes	19.6	9.67	19.8	9.73	0	19.8	8.56	0
5/20/2012	1143	Yes	19.4	10.05	19.6	10.97	0	Yes	19.0	9.67	19.3	9.81	0	19.6	9.40	0
5/20/2012	1537	Yes	20.0	10.16	20.3	11.38	0	Yes	20.3	9.61	20.5	9.84	0	20.7	10.38	0
													Average	19.7		

Table 7. Results of dummy tagged Chinook Salmon evaluated after being held for 48 hours at the release sites as part of the 2012 Chinook Salmon Study.

Holding Site	Examination Date, Time	Mean (sd) Fork Length (mm)	Mortality	Mean (sd) Scale Loss %	Normal Body Color	No Fin Hemorrhaging	Normal Eye Quality	Normal Gill Color
Durham Ferry	5/3/12, 1100	108.2 (5.6)	0/15	5.5 (2.9)	15/15	15/15	15/15	15/15
Durham Ferry	5/5/12, 1100	108.3 (3.7)	0/15	3.3 (1.0)	15/15	15/15	15/15	15/15
Durham Ferry	5/18/12, 1100	111.3 (5.4)	0/15	2.3 (1.0)	15/15	15/15	15/15	15/15
Durham Ferry	5/20/12, 1100	112.0 (4.8)	0/15	2.7 (1.5)	15/15	15/15	15/15	12/15

Table 8. Number of tags from each release group that were detected after release in 2012, including predator-type detections and detections omitted from the survival analysis.

Release Group	1	2	Total
Number Released	480	479	959
Number Detected	355	358	713
Number Detected Downstream	354	353	707
Number Detected Upstream of Study Area	196	339	535
Number Detected in Study Area	301	181	482
Number Detected in San Joaquin River Route	288	161	449
Number Detected in Old River Route	8	3	11
Number Assigned to San Joaquin River Route	286	160	446
Number Assigned to Old River Route	7	3	10

Table 9. Number of tags observed from each release group at each detection site in 2012, including predator-type detections. Routes (SJR = San Joaquin River, OR = Old River) represent route assignment at the head of Old River. Pooled counts are summed over all receivers in array and all routes. Route could not be identified for some tags.

Detection Site	Site Code	Survival Model Code	Release Group		Total
			1	2	
Release site at Durham Ferry			480	479	959
Durham Ferry Upstream	DFU	A0	1	10	11
Durham Ferry Downstream	DFD	A2	101	168	269
Banta Carbona	BCA	A3	120	244	364
Mossdale	MOS	A4	299	181	480
Head of Old River	HOR	B0	297	172	469
Lathrop	SJL	A5	288	161	449
Garwood Bridge	SJG	A6	232	78	310
Navy Drive Bridge	SJNB	A7	187	54	241
MacDonald Island Upstream	MACU	A8a	88	12	100
MacDonald Island Downstream	MACD	A8b	84	9	93
MacDonald Island (Pooled)	MAC	A8	88	12	100
Medford Island East	MFE	A9a	41	6	47
Medford Island West	MFW	A9b	41	6	47
Medford Island (Pooled)	MFE/MFW	A9	41	6	47
Turner Cut East	TCE	F1a	10	2	12
Turner Cut West	TCW	F1b	8	2	10
Turner Cut (Pooled)	TCE/TCW	F1	11	2	13
Old River East	ORE	B1	6	3	9
Old River South Upstream	ORSU	B2a	6	3	9
Old River South Downstream	ORSU	B2b	5	0	5
Old River South (Pooled)	ORS	B2	6	3	9
Old River at Highway 4, Upstream	OR4U	B3a	2	0	2
Old River at Highway 4, Downstream	OR4D	B3b	2	0	2
Old River at Highway 4, SJR Route	OR4	B3	1	0	1
Old River at Highway 4, OR Route	OR4	B3	1	0	1
Old River at Highway 4 (Pooled)	OR4	B3	2	0	2
Old River near Empire Cut, Upstream	OLDU	B4a	2	0	2
Old River near Empire Cut, Downstream	OLDD	B4b	0	0	0
Old River near Empire Cut, SJR Route	OLD	B4	1	0	1
Old River near Empire Cut, OR Route	OLD	B4	1	0	1
Old River near Empire Cut (Pooled)	OLD	B4	2	0	2
Middle River Head	MRH	C1	0	0	0
Middle River at Highway 4, Upstream	MR4U	C2a	1	0	1
Middle River at Highway 4, Downstream	MR4D	C2b	1	0	1
Middle River at Highway 4, SJR Route	MR4	C2	1	0	1
Middle River at Highway 4, OR Route	MR4	C2	0	0	0
Middle River at Highway 4 (Pooled)	MR4	C2	1	0	1

Table 9. (Continued)

Detection Site	Site Code	Survival Model Code	Release Group		Total
			1	2	
Middle River near Empire Cut, Upstream	MREU	C3a	3	0	3
Middle River near Empire Cut, Downstream	MRED	C3b	3	0	3
Middle River near Empire Cut, SJR Route	MRE	C3	3	0	3
Middle River near Empire Cut, OR Route	MRE	C3	0	0	0
Middle River near Empire Cut (Pooled)	MRE	C3	3	0	3
Radial Gates Upstream (Pooled)	RGU	D1	0	0	0
Radial Gates Downstream (Pooled)	RGD	D2	0	0	0
Central Valley Project Trashrack	CVP	E1	4	1	5
CVP Trashrack: SJR Route	CVP	E1	1	0	1
CVP Trashrack: OR Route	CVP	E1	3	1	4
Central Valley Project Holding Tank	CVPtank	E2	1	0	1
CVP tank: SJR Route	CVPtank	E2	0	0	0
CVP tank: OR Route	CVPtank	E2	1	0	1
Threemile Slough South	TMS	T1a	6	0	6
Threemile Slough North	TMN	T1b	4	0	4
Threemile Slough (Pooled)	TMS/TMN	T1	6	0	6
Jersey Point East	JPE	G1a	26	2	28
Jersey Point West	JPW	G1b	25	2	27
Jersey Point: SJR Route	JPE/JPW	G1	26	2	28
Jersey Point: OR Route	JPE/JPW	G1	0	0	0
Jersey Point (Pooled)	JPE/JPW	G1	26	2	28
False River West	FRW	H1a	7	0	7
False River East	FRE	H1b	6	0	6
False River: SJR Route	FRE/FRW	H1	7	0	7
False River: OR Route	FRE/FRW	H1	0	0	0
False River (Pooled)	FRE/FRW	H1	7	0	7
Chipps Island East	MAE	G2a	15	0	15
Chipps Island West	MAW	G2b	15	0	15
Chipps Island: SJR Route	MAE/MAW	G2	14	0	14
Chipps Island: OR Route	MAE/MAW	G2	1	0	1
Chipps Island (Pooled)	MAE/MAW	G2	15	0	15

Table 10. Number of tags observed from each release group at each detection site in 2012 and used in the survival analysis, including predator-type detections. Pooled counts are summed over all receivers in array. Route could not be identified for some tags. * = site was included in full survival model but omitted from reduced model used for analysis.

Detection Site	Site Code	Survival Model Code	Release Group		Total
			1	2	
Release site at Durham Ferry			480	479	959
Durham Ferry Upstream*	DFU	A0	1	7	8
Durham Ferry Downstream	DFD	A2	101	166	267
Banta Carbona	BCA	A3	120	243	363
Mossdale	MOS	A4	297	181	478
Lathrop	SJL	A5	286	160	446
Garwood Bridge	SJG	A6	232	78	310
Navy Drive Bridge	SJNB	A7	186	53	239
MacDonald Island Upstream	MACU	A8a	80	11	91
MacDonald Island Downstream	MACD	A8b	74	8	82
MacDonald Island (Pooled)	MAC	A8	86	12	98
Medford Island East	MFE	A9a	38	6	44
Medford Island West	MFW	A9b	38	6	44
Medford Island (Pooled)	MFE/MFW	A9	38	6	44
Turner Cut East	TCE	F1a	10	2	12
Turner Cut West	TCW	F1b	7	2	9
Turner Cut (Pooled)	TCE/TCW	F1	11	2	13
Old River East	ORE	B1	6	3	9
Old River South Upstream	ORSU	B2a	6	3	9
Old River South Downstream	ORSU	B2b	5	0	5
Old River South (Pooled)	ORS	B2	6	3	9
Old River at Highway 4, Upstream*	OR4U	B3a	2	0	2
Old River at Highway 4, Downstream*	OR4D	B3b	2	0	2
Old River at Highway 4, SJR Route*	OR4	B3	1	0	1
Old River at Highway 4, OR Route*	OR4	B3	1	0	1
Old River at Highway 4 (Pooled)*	OR4	B3	2	0	2
Middle River Head*	MRH	C1	0	0	0
Middle River at Highway 4, Upstream*	MR4U	C2a	0	0	0
Middle River at Highway 4, Downstream*	MR4D	C2b	0	0	0
Middle River at Highway 4, SJR Route*	MR4	C2	0	0	0
Middle River at Highway 4, OR Route*	MR4	C2	0	0	0
Middle River at Highway 4 (Pooled)*	MR4	C2	0	0	0
Radial Gates Upstream (Pooled)*	RGU	D1	0	0	0
Radial Gates Downstream (Pooled)*	RGD	D2	0	0	0
Central Valley Project Trashrack*	CVP	E1	4	1	5
CVP Trashrack: SJR Route*	CVP	E1	1	0	1
CVP Trashrack: OR Route*	CVP	E1	3	1	4

Table 10. (Continued)

Detection Site	Site Code	Survival Model Code	Release Group		Total
			1	2	
Central Valley Project Holding Tank*	CVPtank	E2	1	0	1
CVP tank: SJR Route*	CVPtank	E2	0	0	0
CVP tank: OR Route*	CVPtank	E2	1	0	1
Jersey Point East	JPE	G1a	24	2	26
Jersey Point West	JPW	G1b	23	2	25
Jersey Point: SJR Route	JPE/JPW	G1	24	2	26
Jersey Point: OR Route	JPE/JPW	G1	0	0	0
Jersey Point (Pooled)	JPE/JPW	G1	24	2	26
False River West	FRW	H1a	0	0	0
False River East	FRE	H1b	0	0	0
False River: SJR Route	FRE/FRW	H1	0	0	0
False River: OR Route	FRE/FRW	H1	0	0	0
False River (Pooled)	FRE/FRW	H1	0	0	0
Chippis Island East	MAE	G2a	15	0	15
Chippis Island West	MAW	G2b	15	0	15
Chippis Island: SJR Route	MAE/MAW	G2	14	0	14
Chippis Island: OR Route	MAE/MAW	G2	1	0	1
Chippis Island (Pooled)	MAE/MAW	G2	15	0	15

Table 11. Number of tags from each release group in 2012 first classified as in a predator at each detection site, based on the predator filter.

Detection Site and Code			Durham Ferry Release Groups					
			Classified as Predator on Arrival at Site			Classified as Predator on Departure from Site		
Detection Site	Site Code	Survival Model Code	1	2	Total	1	2	Total
Durham Ferry Upstream	DFU	A0	0	8	8	0	0	0
Durham Ferry Downstream	DFD	A2	4	7	11	0	10	10
Banta Carbona	BCA	A3	0	2	2	1	4	5
Mossdale	MOS	A4	1	2	3	0	3	3
Head of Old River	HOR	B0	1	4	5	0	1	1
Lathrop	SJL	A5	1	1	2	6	6	12
Garwood Bridge	SJG	A6	3	1	4	9	5	14
Navy Drive Bridge	SJNB	A7	1	2	3	11	9	20
MacDonald Island	MAC	A8	2	1	3	15	0	15
Medford Island	MFE/MFW	A9	0	0	0	0	0	0
Old River East	ORE	B1	0	1	1	0	0	0
Old River South	ORS	B2	0	0	0	0	1	1
Old River at Highway 4	OR4	B3	0	0	0	0	0	0
Old River near Empire Cut	OLD	B4	1	0	1	0	0	0
Middle River Head	MRH	C1	0	0	0	0	0	0
Middle River at Highway 4	MR4	C2	0	0	0	0	0	0
Middle River near Empire Cut	MRE	C3	0	0	0	0	0	0
Radial Gates Upstream	RGU	D1	0	0	0	0	0	0
Radial Gates Downstream	RGD	D2	0	0	0	0	0	0
Central Valley Project Trashrack	CVP	E1	0	0	0	0	1	1
Central Valley Project Holding Tank	CVPtank	E2	0	0	0	0	0	0
Turner Cut	TCE/TCW	F1	3	0	3	2	0	2
Jersey Point	JPE/JPW	G1	0	0	0	0	0	0
Chippis Island	MAE/MAW	G2	0	0	0	0	0	0
False River	FRE/FRW	H1	0	0	0	0	0	0
Threemile Slough	TMS/TMN	T1	0	0	0	0	0	0
Total Tags			17	29	46	44	40	84

Table 12. Number of tags from each release group that were detected after release in 2012, excluding predator-type detections, and including detections omitted from the survival analysis.

Release Group	1	2	Total
Number Released	480	479	959
Total Number Detected	351	346	697
Total Number Detected Downstream	350	345	695
Total Number Detected Upstream of Study Area	191	327	518
Total Number Detected in Study Area	301	179	480
Number Detected in San Joaquin River Route	287	157	444
Number Detected in Old River Route	8	3	11
Number Assigned to San Joaquin River Route	287	157	444
Number Assigned to Old River Route	7	3	10

Table 13. Number of tags observed from each release group at each detection site in 2012, excluding predator-type detections. Routes (SJR = San Joaquin River, OR = Old River) represent route assignment at the head of Old River. Pooled counts are summed over all receivers in array and all routes. Route could not be identified for some tags.

Detection Site	Site Code	Survival Model Code	Release Group		Total
			1	2	
Release site at Durham Ferry			480	479	959
Durham Ferry Upstream	DFU	A0	1	1	2
Durham Ferry Downstream	DFD	A2	97	159	256
Banta Carbona	BCA	A3	119	242	361
Mosssdale	MOS	A4	299	179	478
Head of Old River	HOR	B0	297	169	466
Lathrop	SJL	A5	287	157	444
Garwood Bridge	SJG	A6	231	75	306
Navy Drive Bridge	SJNB	A7	186	51	237
MacDonald Island Upstream	MACU	A8a	88	10	98
MacDonald Island Downstream	MACD	A8b	84	8	92
MacDonald Island (Pooled)	MAC	A8	88	10	98
Medford Island East	MFE	A9a	41	6	47
Medford Island West	MFW	A9b	41	6	47
Medford Island (Pooled)	MFE/MFW	A9	41	6	47
Turner Cut East	TCE	F1a	9	2	11
Turner Cut West	TCW	F1b	8	2	10
Turner Cut (Pooled)	TCE/TCW	F1	10	2	12
Old River East	ORE	B1	6	3	9
Old River South Upstream	ORSU	B2a	6	2	8
Old River South Downstream	ORSU	B2b	5	0	5
Old River South (Pooled)	ORS	B2	6	2	8
Old River at Highway 4, Upstream	OR4U	B3a	2	0	2
Old River at Highway 4, Downstream	OR4D	B3b	2	0	2
Old River at Highway 4, SJR Route	OR4	B3	1	0	1
Old River at Highway 4, OR Route	OR4	B3	1	0	1
Old River at Highway 4 (Pooled)	OR4	B3	2	0	2
Old River near Empire Cut, Upstream	OLDU	B4a	1	0	1
Old River near Empire Cut, Downstream	OLDD	B4b	0	0	0
Old River near Empire Cut, SJR Route	OLD	B4	1	0	1
Old River near Empire Cut, OR Route	OLD	B4	0	0	0
Old River near Empire Cut (Pooled)	OLD	B4	1	0	1
Middle River Head	MRH	C1	0	0	0
Middle River at Highway 4, Upstream	MR4U	C2a	1	0	1
Middle River at Highway 4, Downstream	MR4D	C2b	1	0	1
Middle River at Highway 4, SJR Route	MR4	C2	1	0	1
Middle River at Highway 4, OR Route	MR4	C2	0	0	0
Middle River at Highway 4 (Pooled)	MR4	C2	1	0	1

Table 13. (Continued)

Detection Site	Site Code	Survival Model Code	Release Group		Total
			1	2	
Middle River near Empire Cut, Upstream	MREU	C3a	3	0	3
Middle River near Empire Cut, Downstream	MRED	C3b	3	0	3
Middle River near Empire Cut, SJR Route	MRE	C3	3	0	3
Middle River near Empire Cut, OR Route	MRE	C3	0	0	0
Middle River near Empire Cut (Pooled)	MRE	C3	3	0	3
Radial Gates Upstream (Pooled)	RGU	D1	0	0	0
Radial Gates Downstream (Pooled)	RGD	D2	0	0	0
Central Valley Project Trashrack	CVP	E1	4	1	5
CVP Trashrack: SJR Route	CVP	E1	1	0	1
CVP Trashrack: OR Route	CVP	E1	3	1	4
Central Valley Project Holding Tank	CVPtank	E2	1	0	1
CVP tank: SJR Route	CVPtank	E2	0	0	0
CVP tank: OR Route	CVPtank	E2	1	0	1
Threemile Slough South	TMS	T1a	6	0	6
Threemile Slough North	TMN	T1b	4	0	4
Threemile Slough (Pooled)	TMS/TMN	T1	6	0	6
Jersey Point East	JPE	G1a	26	2	28
Jersey Point West	JPW	G1b	25	2	27
Jersey Point: SJR Route	JPE/JPW	G1	26	2	28
Jersey Point: OR Route	JPE/JPW	G1	0	0	0
Jersey Point (Pooled)	JPE/JPW	G1	26	2	28
False River West	FRW	H1a	7	0	7
False River East	FRE	H1b	6	0	6
False River: SJR Route	FRE/FRW	H1	7	0	7
False River: OR Route	FRE/FRW	H1	0	0	0
False River (Pooled)	FRE/FRW	H1	7	0	7
Chipps Island East	MAE	G2a	15	0	15
Chipps Island West	MAW	G2b	15	0	15
Chipps Island: SJR Route	MAE/MAW	G2	14	0	14
Chipps Island: OR Route	MAE/MAW	G2	1	0	1
Chipps Island (Pooled)	MAE/MAW	G2	15	0	15

Table 14. Number of tags observed from each release group at each detection site in 2012 and used in the survival analysis, excluding predator-type detections. Pooled counts are summed over all receivers in array. Route could not be identified for some tags. * = site was included in full survival model but omitted from reduced model used for analysis.

Detection Site	Site Code	Survival Model Code	Release Group		Total
			1	2	
Release site at Durham Ferry			480	479	959
Durham Ferry Upstream*	DFU	A0	1	1	2
Durham Ferry Downstream	DFD	A2	97	159	256
Banta Carbona	BCA	A3	119	242	361
Mossdale	MOS	A4	299	179	478
Lathrop	SJL	A5	287	157	444
Garwood Bridge	SJG	A6	231	75	306
Navy Drive Bridge	SJNB	A7	185	50	235
MacDonald Island Upstream	MACU	A8a	83	9	92
MacDonald Island Downstream	MACD	A8b	80	8	88
MacDonald Island (Pooled)	MAC	A8	87	10	97
Medford Island East	MFE	A9a	38	6	44
Medford Island West	MFW	A9b	38	6	44
Medford Island (Pooled)	MFE/MFW	A9	38	6	44
Turner Cut East	TCE	F1a	9	2	11
Turner Cut West	TCW	F1b	8	2	10
Turner Cut (Pooled)	TCE/TCW	F1	10	2	12
Old River East	ORE	B1	6	3	9
Old River South Upstream	ORSU	B2a	6	2	8
Old River South Downstream	ORSU	B2b	5	0	5
Old River South (Pooled)	ORS	B2	6	2	8
Old River at Highway 4, Upstream*	OR4U	B3a	2	0	2
Old River at Highway 4, Downstream*	OR4D	B3b	2	0	2
Old River at Highway 4, SJR Route*	OR4	B3	1	0	1
Old River at Highway 4, OR Route*	OR4	B3	1	0	1
Old River at Highway 4 (Pooled)*	OR4	B3	2	0	2
Middle River Head*	MRH	C1	0	0	0
Middle River at Highway 4, Upstream*	MR4U	C2a	0	0	0
Middle River at Highway 4, Downstream*	MR4D	C2b	0	0	0
Middle River at Highway 4, SJR Route*	MR4	C2	0	0	0
Middle River at Highway 4, OR Route*	MR4	C2	0	0	0
Middle River at Highway 4 (Pooled)*	MR4	C2	0	0	0
Radial Gates Upstream (Pooled)*	RGU	D1	0	0	0
Radial Gates Downstream (Pooled)*	RGD	D2	0	0	0
Central Valley Project Trashrack*	CVP	E1	4	1	5
CVP Trashrack: SJR Route*	CVP	E1	1	0	1
CVP Trashrack: OR Route*	CVP	E1	3	1	4

Table 14. (Continued)

Detection Site	Site Code	Survival Model Code	Release Group		Total
			1	2	
Central Valley Project Holding Tank*	CVPtank	E2	1	0	1
CVP tank: SJR Route*	CVPtank	E2	0	0	0
CVP tank: OR Route*	CVPtank	E2	1	0	1
Jersey Point East	JPE	G1a	24	2	26
Jersey Point West	JPW	G1b	23	2	25
Jersey Point: SJR Route	JPE/JPW	G1	24	2	26
Jersey Point: OR Route	JPE/JPW	G1	0	0	0
Jersey Point (Pooled)	JPE/JPW	G1	24	2	26
False River West	FRW	H1a	0	0	0
False River East	FRE	H1b	0	0	0
False River: SJR Route	FRE/FRW	H1	0	0	0
False River: OR Route	FRE/FRW	H1	0	0	0
False River (Pooled)	FRE/FRW	H1	0	0	0
Chipps Island East	MAE	G2a	15	0	15
Chipps Island West	MAW	G2b	15	0	15
Chipps Island: SJR Route	MAE/MAW	G2	14	0	14
Chipps Island: OR Route	MAE/MAW	G2	1	0	1
Chipps Island (Pooled)	MAE/MAW	G2	15	0	15

Table 15. Number of juvenile Chinook Salmon tagged by each tagger in each release group during the 2012 tagging study. OK with updated numbers

Tagger	Release Group		Total Tags
	1	2	
A	119	120	239
B	118	119	237
C	120	119	239
D	123	121	244
Total Tags	480	479	959

Table 16. Release size and counts of tag detections at key detection sites by tagger in 2012, excluding predator-type detections. * = used in chi-square test of independence.

Detection Site	Tagger			
	A	B	C	D
Release at Durham Ferry*	239	237	239	244
Mossdale (MOS)*	118	112	126	122
Lathrop (SJL)*	108	102	120	114
MacDonald Island (MAC)	27	13	29	28
Turner Cut (TCE/TCW)	4	1	3	4
Medford Island (MFE/MFW)	13	8	9	14
MacDonald Island, Medford Island, or Turner Cut (pooled)*	31	14	32	32
Old River East (ORE)*	1	4	2	2
Old River South (ORS)	1	3	2	2
Old River at Highway 4 (OR4)	1	0	0	1
Middle River at Highway 4 (MR4)	0	0	0	0
Clifton Court Forebay Interior (RGD)	0	0	0	0
Central Valley Project Holding Tank (CVPtank)	0	0	0	1
Jersey Point (JPE/JPW)*	10	3	6	7
Chipps Island (MAE/MAW)*	5	1	4	5

Table 17. Performance metric estimates (standard error in parentheses) for tagged juvenile Chinook Salmon released in the 2012 tagging study, excluding predator-type detections. South Delta ("SD") survival extended to MacDonald Island and Turner Cut in Route A. Population-level estimates were from pooled release groups.

Parameter	Release Occasion		Population Estimate
	1	2	
Ψ_{AA}	0.88 (0.03)	0.82 (0.10)	0.87 (0.03)
Ψ_{AF}	0.10 (0.03)	0.16 (0.10)	0.11 (0.03)
S_{AA}	0.05 ^d (0.01)	0 ^d (0)	0.03 (0.01)
S_{AF}	0 (0)	0 (0)	0 (0)
Ψ_A^a	0.98 (0.01)	0.98 (0.01)	0.98 (0.01)
Ψ_B^a	0.02 (0.01)	0.02 (0.01)	0.02 (0.01)
Ψ_{F2}	0.11 (0.03)	0.16 (0.11)	0.11 (0.03)
S_A	0.05 ^{cd} (0.01)	0 ^d (0)	0.03 ^c (0.01)
S_B^b	0.16 ^c (0.15)	0 (0)	0.11 ^c (0.10)
S_{Total}	0.05 ^d (0.01)	0 ^d (0)	0.03 (0.01)
$S_{A(MD)}$	0.09 ^d (0.02)	0.01 ^d (0.01)	0.06 (0.01)
$S_{A(SD)}$	0.33 ^d (0.03)	0.07 ^d (0.02)	0.23 (0.02)
ϕ_{A1A4}	0.63 ^d (0.02)	0.37 ^d (0.02)	0.50 (0.02)

a = Significant preference for route A (San Joaquin Route) ($\alpha = 0.05$) for all release occasions and for population estimate.

b = No tags were detected in subroute C; survival estimate used $\phi_{B1,B2} = S_{B1} * \Psi_{B2}$ under assumption $\Psi_{B2} = 1$.

c = No significant difference between route A and route B estimate ($P \geq 0.19$).

d = Release group 1 had significantly higher survival than release group 2 ($P < 0.0001$).

Table 18. Performance metric estimates (standard error in parentheses) for tagged juvenile Chinook Salmon released in the 2012 tagging study, including predator-type detections. South Delta ("SD") survival extended to MacDonald Island and Turner Cut in Route A. Population-level estimates were from pooled release groups.

Parameter	Release Occasion		Population Estimate
	1	2	
Ψ_{AA}	0.86 (0.03)	0.85 (0.09)	0.86 (0.03)
Ψ_{AF}	0.12 (0.03)	0.13 (0.09)	0.12 (0.03)
S_{AA}	0.05 ^d (0.01)	0 ^d (0)	0.03 (0.01)
S_{AF}	0 (0)	0 (0)	0 (0)
Ψ_A^a	0.98 (0.01)	0.98 (0.01)	0.98 (0.01)
Ψ_B^a	0.02 (0.01)	0.02 (0.01)	0.02 (0.01)
Ψ_{F2}	0.12 (0.03)	0.14 (0.09)	0.12 (0.03)
S_A	0.05 ^{cd} (0.01)	0 ^d (0)	0.03 ^c (0.01)
S_B^b	0.16 ^c (0.15)	0 (0)	0.11 ^c (0.10)
S_{Total}	0.05 ^d (0.01)	0 ^d (0)	0.03 (0.01)
$S_{A(MD)}$	0.09 ^d (0.02)	0.01 ^d (0.01)	0.06 (0.01)
$S_{A(SD)}$	0.34 ^d (0.03)	0.08 ^d (0.02)	0.24 (0.02)
ϕ_{A1A4}	0.62 ^d (0.02)	0.38 ^d (0.02)	0.50 (0.02)

a = Significant preference for route A (San Joaquin Route) ($\alpha = 0.05$) for all release occasions and for population estimate.

b = No tags were detected in subroute C; survival estimate used $\phi_{B1,B2} = S_{B1} * \Psi_{B2}$ under assumption $\Psi_{B2} = 1$.

c = No significant difference between route A and route B estimate ($P \geq 0.19$).

d = Release group 1 had significantly higher survival than release group 2 ($P < 0.0001$).

Table 19. Estimates (standard errors in parentheses) of model survival and transition parameters by release group, and of the difference (Δ) between release group estimates: Δ = Release group 1 - Release group 2. P = P-value from one-sided z-test of $\Delta > 1$. Estimates were based on data that excluded predator-type detections. * = significant (positive) difference between release groups for family-wise $\alpha=0.10$.

Parameter	Release 1	Release 2	Δ	P
S_{A2}	0.90 (0.06)	0.63 (0.04)	0.27 (0.07)	0.0001*
S_{A3}	0.78 (0.04)	0.59 (0.03)	0.19 (0.05)	0.0001*
S_{A4}	0.98 (0.01)	0.89 (0.02)	0.08 (0.02)	0.0004*
S_{A5}	0.81 (0.02)	0.48 (0.04)	0.33 (0.05)	<0.0001*
S_{A6}	0.85 (0.03)	0.73 (0.08)	0.13 (0.08)	0.0594
S_{A7}	0.49 (0.04)	0.23 (0.06)	0.27 (0.07)	0.0001*
$S_{B2,G2}^a$	0.17 (0.15)	0	0.17 (0.15)	0.1367
$\phi_{A1,A2}$	0.89 (0.05)	1.00 (0.06)	-0.11 (0.07)	0.9407
$\phi_{A8,A9}$	0.44 (0.05)	0.59 (0.16)	-0.16 (0.16)	0.8309
$\phi_{A8,G1}$	0.08 (0.03)	0	0.08 (0.03)	0.0030*
$\phi_{A9,G1}$	0.49 (0.09)	0.33 (0.19)	0.16 (0.21)	0.2265
$\phi_{B1,B2}^a$	1	0.67 (0.27)	0.33 (0.27)	0.1106
$\phi_{F1,G1}$	0	0	0	NA
$\phi_{G1,G2(A)}$	0.54 (0.10)	0	0.54 (0.10)	<0.0001*

^aThese reaches are in the Old River route

Table 20a. Average travel time in days (harmonic mean) of acoustic-tagged juvenile Chinook Salmon from release at Durham Ferry during the 2012 tagging study, without predator-type detections (see Table 20b for travel time from release with predator-type detections). Standard errors are in parentheses. There were no detections at the MRH, RGU, or RGD sites; all tags detected at FRE/FRW or MR4 were later detected at competing receivers, so those sites are omitted here.

Detection Site and Route	Without Predator-Type Detections					
	All Releases		Release 1		Release 2	
	N	Travel Time	N	Travel Time	N	Travel Time
Durham Ferry Upstream (DFU)	2	0.06 (0.02)	1	0.10 (NA)	1	0.04 (NA)
Durham Ferry Downstream (DFD)	251	0.03 (<0.01)	92	0.03 (<0.01)	159	0.03 (<0.01)
Banta Carbona (BCA)	353	0.27 (0.01)	111	0.25 (0.01)	242	0.29 (0.01)
Mossdale (MOS)	464	0.53 (0.01)	285	0.48 (0.01)	179	0.61 (0.02)
Lathrop (SJL)	430	0.71 (0.01)	273	0.65 (0.01)	157	0.85 (0.03)
Garwood Bridge (SJG)	293	1.41 (0.03)	218	1.31 (0.02)	75	1.85 (0.08)
Navy Drive Bridge (SJNB)	226	1.48 (0.03)	176	1.39 (0.02)	50	1.96 (0.10)
MacDonald Island (MAC)	89	2.83 (0.10)	79	2.74 (0.10)	10	3.88 (0.44)
Turner Cut (TCE/TCW)	12	2.84 (0.16)	10	2.91 (0.19)	2	2.57 (0.19)
Medford Island (MFE/MFW)	44	3.39 (0.25)	38	3.32 (0.27)	6	3.88 (0.55)
Old River East (ORE)	9	0.70 (0.06)	6	0.66 (0.04)	3	0.80 (0.19)
Old River South (ORS)	8	1.01 (0.07)	6	0.97 (0.04)	2	1.16 (0.43)
Old River at Highway 4 (OR4), SJR Route	1	5.08 (NA)	1	5.08 (NA)	0	NA
Old River at Highway 4 (OR4), OR Route	1	4.29 (NA)	1	4.29 (NA)	0	NA
Central Valley Project Trashrack (CVP), SJR Route	1	5.62 (NA)	1	5.62 (NA)	0	NA
Central Valley Project Trashrack (CVP), OR Route	4	2.52 (0.57)	3	2.41 (0.72)	1	2.92 (NA)
Central Valley Project Holding Tank (CVPtank), SJR Route	0	NA	0	NA	0	NA
Central Valley Project Holding Tank (CVPtank), OR Route	1	2.15 (NA)	1	2.15 (NA)	0	NA
Jersey Point (JPE/JPW), SJR Route	26	5.98 (0.63)	24	6.91 (0.69)	2	4.26 (1.26)
Jersey Point (JPE/JPW), OR Route	0	NA	0	NA	0	NA
Chippis Island (MAE/MAW), SJR Route	10	5.99 (0.41)	10	5.99 (0.41)	0	NA
Chippis Island (MAE/MAW), OR Route	1	4.12 (NA)	1	4.12 (NA)	0	NA
Chippis Island (MAE/MAW)	11	5.75 (0.41)	11	5.75 (0.41)	0	NA

Table 20b. Average travel time in days (harmonic mean) of acoustic-tagged juvenile Chinook Salmon from release at Durham Ferry during the 2012 tagging study, with predator-type detections (see Table 20a for travel time from release without predator-type detections). Standard errors are in parentheses. There were no detections at the MRH, RGU, or RGD sites; all tags detected at FRE/FRW or MR4 were later detected at competing receivers, so those sites are omitted here.

Detection Site and Route	With Predator-Type Detections					
	All Releases		Release 1		Release 2	
	N	Travel Time	N	Travel Time	N	Travel Time
Durham Ferry Upstream (DFU)	8	0.20 (0.11)	1	0.10 (NA)	7	0.23 (0.16)
Durham Ferry Downstream (DFD)	262	0.03 (<0.01)	96	0.03 (<0.01)	166	0.04 (<0.01)
Banta Carbona (BCA)	355	0.28 (0.01)	112	0.25 (0.01)	243	0.29 (0.01)
Mossdale (MOS)	464	0.53 (0.01)	283	0.48 (0.01)	181	0.63 (0.02)
Lathrop (SJL)	432	0.72 (0.01)	272	0.65 (0.01)	160	0.89 (0.03)
Garwood Bridge (SJG)	297	1.44 (0.03)	219	1.33 (0.02)	78	1.93 (0.09)
Navy Drive Bridge (SJNB)	230	1.56 (0.04)	177	1.44 (0.03)	53	2.19 (0.13)
MacDonald Island (MAC)	90	3.21 (0.17)	78	3.07 (0.17)	12	4.55 (0.72)
Turner Cut (TCE/TCW)	13	3.11 (0.26)	11	3.23 (0.31)	2	2.57 (0.19)
Medford Island (MFE/MFW)	44	3.39 (0.25)	38	3.32 (0.27)	6	3.88 (0.55)
Old River East (ORE)	9	0.77 (0.09)	6	0.66 (0.04)	3	1.18 (0.46)
Old River South (ORS)	9	1.11 (0.13)	6	0.97 (0.04)	3	1.52 (0.64)
Old River at Highway 4 (OR4), SJR Route	1	5.08 (NA)	1	5.08 (NA)	0	NA
Old River at Highway 4 (OR4), OR Route	1	4.29 (NA)	1	4.29 (NA)	0	NA
Central Valley Project Trashrack (CVP), SJR Route	1	5.62 (NA)	1	5.62 (NA)	0	NA
Central Valley Project Trashrack (CVP), OR Route	4	2.52 (0.57)	3	2.41 (0.72)	1	2.92 (NA)
Central Valley Project Holding Tank (CVPtank), SJR Route	0	NA	0	NA	0	NA
Central Valley Project Holding Tank (CVPtank), OR Route	1	2.15 (NA)	1	2.15 (NA)	0	NA
Jersey Point (JPE/JPW), SJR Route	26	5.98 (0.63)	24	6.19 (0.69)	2	4.26 (1.26)
Jersey Point (JPE/JPW), OR Route	0	NA	0	NA	0	NA
Chippis Island (MAE/MAW), SJR Route	10	5.99 (0.41)	10	5.99 (0.41)	0	NA
Chippis Island (MAE/MAW), OR Route	1	4.12 (NA)	1	4.12 (NA)	0	NA
Chippis Island (MAE/MAW)	11	5.75 (0.41)	11	5.75 (0.41)	0	NA

Table 21a. Average travel time in days (harmonic mean) of acoustic-tagged juvenile Chinook Salmon through the San Joaquin River Delta river reaches during the 2012 tagging study, without predator-type detections (see Table 21b for travel time through reaches with predator-type detections). Standard errors are in parentheses. Reaches beginning at sites with no detections are not shown (i.e., reaches that start at MRH, MR4, RGU, RGD, and FRE/FRW).

Reach		Without Predator-Type Detections					
		All Releases		Release 1		Release 2	
Upstream Boundary	Downstream Boundary	N	Travel Time	N	Travel Time	N	Travel Time
Durham Ferry (Release)	BCA	251	0.03 (<0.01)	92	0.03 (<0.01)	159	0.03 (<0.01)
	BCA	230	0.28 (0.01)	87	0.24 (0.01)	143	0.31 (0.01)
	MOS	429	0.14 (<0.01)	272	0.13 (<0.01)	157	0.16 (0.01)
	ORE	9	0.25 (0.04)	6	0.23 (0.04)	3	0.32 (0.09)
	SJL	293	0.65 (0.02)	218	0.60 (0.02)	75	0.86 (0.05)
	SJG	226	0.08 (<0.01)	176	0.08 (<0.01)	50	0.09 (0.01)
	SJNB	84	1.25 (0.07)	75	1.21 (0.07)	9	1.72 (0.37)
	TCE/TCW	12	1.19 (0.18)	10	1.37 (0.15)	2	0.72 (0.31)
	MAC	39	0.23 (0.03)	33	0.24 (0.03)	6	0.21 (0.07)
	JPE/JPW/FRE/FRW	22	2.20 (0.26)	20	2.47 (0.27)	2	1.05 (0.13)
	OR4	0	NA	0	NA	0	NA
	MR4	0	NA	0	NA	0	NA
	JPE/JPW/FRE/FRW	17	1.54 (0.21)	15	1.80 (0.19)	2	0.74 (0.20)
	OR4	0	NA	0	NA	0	NA
	MR4	0	NA	0	NA	0	NA
	JPE/JPW/FRE/FRW	0	NA	0	NA	0	NA
	OR4	1	2.25 (NA)	1	2.25 (NA)	0	NA
	MR4	0	NA	0	NA	0	NA
	ORS	8	0.27 (0.03)	6	0.29 (0.03)	2	0.22 (0.05)
	MRH	0	NA	0	NA	0	NA
	OR4	1	3.25 (NA)	1	3.25 (NA)	0	NA
	MR4	0	NA	0	NA	0	NA
	RGU	0	NA	0	NA	0	NA
	CVP	3	0.95 (0.12)	2	0.90 (0.16)	1	1.09 (NA)

Table 21a. (Continued)

Reach		Without Predator-Type Detections					
		All Releases		Release 1		Release 2	
Upstream Boundary	Downstream Boundary	N	Travel Time	N	Travel Time	N	Travel Time
OR4 via OR	JPE/JPW/FRE/FRW	0	NA	0	NA	0	NA
OR4 via SJR	JPE/JPW/FRE/FRW	0	NA	0	NA	0	NA
	RGU	0	NA	0	NA	0	NA
	CVP	1	0.55 (NA)	1	0.55 (NA)	0	NA
CVP via OR	CVPtank	1	0.01 (NA)	1	0.01 (NA)	0	NA
CVP via SJR	CVPtank	0	NA	0	NA	0	NA
JPE/JPW	MAE/MAW (Chippis Island)	9	1.21 (0.14)	9	1.21 (0.14)	0	NA
MAC		10	3.54 (0.34)	10	3.54 (0.34)	0	NA
MFE/MFW		8	3.04 (0.25)	8	3.04 (0.259)	0	NA
TCE/TCW		0	NA	0	NA	0	NA
OR4		0	NA	0	NA	0	NA
CVPtank		1	1.97 (NA)	1	1.97 (NA)	0	NA

Table 21b. Average travel time in days (harmonic mean) of acoustic-tagged juvenile Chinook Salmon through the San Joaquin River Delta river reaches during the 2012 tagging study, with predator-type detections (see Table 21a for travel time through reaches without predator-type detections). Standard errors are in parentheses. Reaches beginning at sites with no detections are not shown (i.e., reaches that start at MRH, MR4, RGU, RGD, and FRE/FRW).

Reach		With Predator-Type Detections					
		All Releases		Release 1		Release 2	
Upstream Boundary	Downstream Boundary	N	Travel Time	N	Travel Time	N	Travel Time
Durham Ferry (Release)	BCA	262	0.03 (<0.01)	96	0.03 (<0.01)	166	0.04 (<0.01)
	MOS	231	0.28 (0.01)	86	0.24 (0.01)	145	0.31 (0.01)
	SJL	431	0.14 (<0.01)	271	0.13 (<0.01)	160	0.17 (0.01)
	ORE	9	0.28 (0.06)	6	0.23 (0.04)	3	0.52 (0.27)
	SJG	297	0.67 (0.02)	219	0.62 (0.02)	78	0.90 (0.05)
	SJNB	230	0.08 (<0.01)	177	0.08 (<0.01)	53	0.09 (0.01)
	MAC	85	1.38 (0.10)	74	1.32 (0.10)	11	2.04 (0.49)
	TCE/TCW	13	1.33 (0.23)	11	1.57 (0.24)	2	0.72 (0.31)
	MFE/MFW	39	0.23 (0.03)	33	0.24 (0.03)	6	0.21 (0.07)
	JPE/JPW/FRE/FRW	22	2.20 (0.26)	20	2.47 (0.27)	2	1.05 (0.13)
	OR4	0	NA	0	NA	0	NA
	MR4	0	NA	0	NA	0	NA
	JPE/JPW/FRE/FRW	17	1.54 (0.21)	15	1.80 (0.19)	2	0.74 (0.20)
	OR4	0	NA	0	NA	0	NA
	MR4	0	NA	0	NA	0	NA
	JPE/JPW/FRE/FRW	0	NA	0	NA	0	NA
	OR4	1	2.25 (NA)	1	2.25 (NA)	0	NA
	MR4	0	NA	0	NA	0	NA
	ORS	9	0.29 (0.04)	6	0.29 (0.03)	3	0.31 (0.14)
	MRH	0	NA	0	NA	0	NA
	OR4	1	3.25 (NA)	1	3.25 (NA)	0	NA
	MR4	0	NA	0	NA	0	NA
	RGU	0	NA	0	NA	0	NA
	CVP	3	0.95 (0.12)	2	0.90 (0.16)	1	1.09 (NA)

Table 21b. (Continued)

Reach		With Predator-Type Detections					
		All Releases		Release 1		Release 2	
Upstream Boundary	Downstream Boundary	N	Travel Time	N	Travel Time	N	Travel Time
OR4 via OR	JPE/JPW/FRE/FRW	0	NA	0	NA	0	NA
OR4 via SJR	JPE/JPW/FRE/FRW	0	NA	0	NA	0	NA
	RGU	0	NA	0	NA	0	NA
	CVP	1	0.55 (NA)	1	0.55 (NA)	0	NA
CVP via OR	CVPtank	1	0.01 (NA)	1	0.01 (NA)	0	NA
CVP via SJR	CVPtank	0	NA	0	NA	0	NA
JPE/JPW	MAE/MAW (Chipps Island)	9	1.21 (0.14)	9	1.21 (0.14)	0	NA
MAC		10	3.54 (0.34)	10	3.54 (0.34)	0	NA
MFE/MFW		8	3.04 (0.225)	8	3.04 (0.25)	0	NA
TCE/TCW		0	NA	0	NA	0	NA
OR4		0	NA	0	NA	0	NA
CVPtank		1	1.97 (NA)	1	1.97 (NA)	0	NA

Table 22: Distance in km, estimated survival and survival rate per km ($S^{(1/km)}$), travel time in days, and travel time in days per km ($TT^{(1/km)}$), for the first (1st) and second (2nd) release groups of Chinook Salmon in 2012. Survival and travel time data were obtained from tables Table A5-2, and Table 21a. Distance was estimated using the shortest distance between the two points calculated from Google Earth. Data were used to generate Figure 12.

Reach	Distance in km	Survival		Survival per km		Travel time		Travel time per km	
		1st	2nd	1st	2nd	1st	2nd	1st	2nd
Durham Ferry (Release) to Banta Carbona	11	0.90	0.63	0.990	0.959	0.03	0.03	0.727	0.727
Banta Carbona to Mossdale	9	0.78	0.59	0.973	0.943	0.24	0.31	0.853	0.878
Mossdale to Lathrop/Old River	4	0.98	0.89	0.995	0.971	0.13	0.16	0.600	0.632
Lathrop to Stockton South (Garwood Bridge)	18	0.81	0.48	0.988	0.960	0.60	0.86	0.972	0.992
Stockton South to Stockton Navy Bridge	3	0.85	0.73	0.947	0.900	0.08	0.09	0.431	0.448
Navy Bridge to Turner Cut Junction	15	0.49	0.23	0.954	0.907	1.37	0.72	1.021	0.978
MacDonald Island to Medford Island	5	0.44	0.59	0.849	0.900	0.24	0.21	0.752	0.732
Medford Island to Jersey Point	21	0.49	0.33	0.967	0.949	1.80	0.74	1.028	0.986
Jersey Point to Chipps Island	22	0.54	0.00	0.972	0.000	1.21		1.009	

Table 23. Results of single-variate analyses of route entrainment at the Turner Cut Junction (all release groups). The values df_1 , df_2 are degrees of freedom for the F-test.

Covariate ^a	F-test			
	<i>F</i>	<i>df</i> ₁	<i>df</i> ₂	<i>P</i>
Change in flow at TRN	0.6896	1	8	0.4304
Change in velocity at TRN	0.6470	1	8	0.4444
Exports at CVP	0.3355	1	9	0.5766
Change in stage at TRN	0.2824	1	8	0.6095
Flow during transition from SJG	0.1864	1	9	0.6761
Stage at TRN	0.1696	1	9	0.6901
Velocity during transition from SJG	0.1311	1	9	0.7256
Release Group	0.0730	1	9	0.7931
Arrive during day at junction	0.0558	1	9	0.8185
Fork Length	0.0331	1	9	0.8597
Exports at SWP	0.0286	1	9	0.8694
Negative flow at TRN	0.0063	1	9	0.9385
Flow at TRN	0.0031	1	9	0.9568
Velocity at TRN	0.0024	1	9	0.9623

a = No covariate was significant at 5% level

Table 24. Summary statistics from multiple regression of flow at Vernalis and tag type to explain survival from Mossdale to Jersey Point with the physical head of Old River barrier. Tag type (CWT or Acoustic) was not significant (p value = 0.992775).

SUMMARY OUTPUT		Mossdale data only						
<i>Regression Statistics</i>								
Multiple R	0.86119676							
R Square	0.74165986							
Adjusted R Square	0.69468892							
Standard Error	0.07221227							
Observations	14							
<i>ANOVA</i>								
	<i>df</i>	<i>SS</i>	<i>MS</i>	<i>F</i>	<i>Significance F</i>			
Regression	2	0.164674977	0.082337	15.78976	0.000584865			
Residual	11	0.057360738	0.005215					
Total	13	0.222035714						
	<i>Coefficients</i>	<i>Standard Error</i>	<i>t Stat</i>	<i>P-value</i>	<i>Lower 95%</i>	<i>Upper 95%</i>	<i>Lower 95.0%</i>	<i>Upper 95.0%</i>
Intercept	-0.2287319	0.10572806	-2.1634	0.053388	-0.461437753	0.00397403	-0.46143775	0.003974031
X Variable 1 (tag)	-0.0005306	0.057279985	-0.00926	0.992775	-0.126603014	0.12554178	-0.12660301	0.125541781
X Variable 2 (flow)	9.533E-05	1.76263E-05	5.408389	0.000214	5.65346E-05	0.00013413	5.6535E-05	0.000134125

Appendices 1-5:

Appendix 1. Analyses of CWT salmon released in the south Delta by Ken Newman as part of the VAMP peer review in 2010.

Analyses of Salmon CWT Releases into the San Joaquin System
 Ken B. Newman, USFWS
 2 March 2010



1. Overview

- Objectives: to understand how different factors (flows, exports, barrier at head of Old River, HORE) affect survival of juvenile salmon outmigrating from San Joaquin system
- Data Generation: CWT Release-Recovery "sets", 4-5 release locations and 2-3 recovery locations
- Data Analysis: (Bayesian) Hierarchical Models
- Key Results: Usually higher survival if stay in San Joaquin River than if go down Old River BUT lots of Environmental Variation, i.e., low Signal:Noise Ratio!

2. Data Generation

- (a) Between 1985 and 2006, 35 Release-Recovery sets.
- (b) Within a set, at most 3 release locations (e.g., Mossdale, Dos Reis, and Jersey Point).
- (c) At most 3 recovery locations: Chipps Island, Ocean fisheries, and since 2000, Antioch
- (d) \Rightarrow 212 observations

3. Data Analysis

- (a) BHMs (Bayesian Hierarchical Models)
- (b) Key idea: 2 or more levels of modeling
- (c) Separate modeling of Observation (Sampling) noise from Survival (and capture) variation
- (d) Level 1: Observation Models $y^i_s \sim$ Probability Distribution(R_i , S_i and p_i)
- (e) Level 2, Random effects: S_i , $p_i \sim$ Probability Distribution(η_i , Covariates)
- (f) Level 3, Hyperparameters: $\eta_i \sim$ Prior Probability Distribution
- (g)
- (h) Focus on Models for Survival down San Joaquin and Survival down Old River

$$\begin{aligned} E[\text{logit}(S_{DR \rightarrow JP})] &= \xi_0 + \xi_1 \text{Flow}_{\text{Dos Reis}} + \xi_2 \text{Exports}_{\text{Dos Reis}} \\ E[\text{logit}(S_{OR \rightarrow JP})] &= \zeta_0 + \zeta_1 \text{Flow}_{\text{Old River}} + \zeta_2 \text{Exports}_{\text{Mossdale}} \end{aligned}$$

- (i) Fitting Details: WinBUGS with Reversible Jump model selection

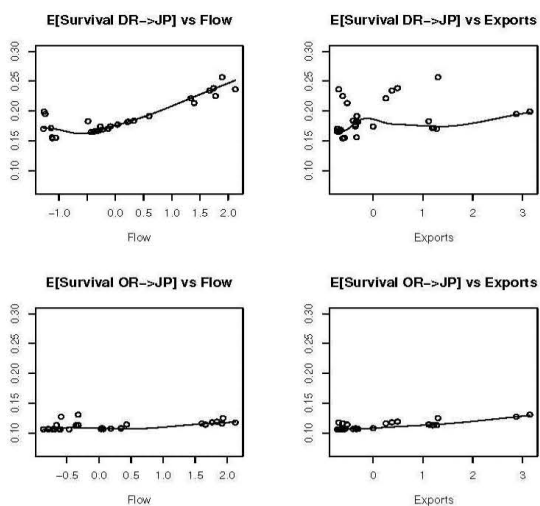
4. Results

(a) Posterior Probabilities

Models	$S_{MD \rightarrow JP}$	$S_{OR \rightarrow JP}$
Constant	0.38	0.45
Flow	0.29	0.23
Exports	0.17	0.21
Both	0.16	0.11

(b) Coefficients

Covariate	Average	SD	2.5%	median	97.5%
SJ-flow	0.16	0.25	-0.09	0.0	0.77
SJ-exports	0.07	0.19	-0.17	0.0	0.61
OR-flow	0.04	0.22	-0.42	0.0	0.62
OR-exports	0.04	0.20	-0.32	0.0	0.60



5. Caveats and Comments

- Priors *do* matter, especially with Hierarchical Models
- More to wring out of CWTs? Using time of capture? Add arrival time/travel time model?
- Acoustic tags far preferable?
- Value in probing extreme values for flows and exports

Some references:

- Clark, J.S. 2005. "Why environmental scientists are becoming Bayesians." *Ecology Letters*, **8**: 2-14.
- Clark, J.S., and Gelfand, A.E. 2006. "A future for models and data in environmental science." *Trends in Ecology and Evolution*, **21**: 375-380.
- Newman, K.B., and Brandes, P.L. 2010. Hierarchical modeling of juvenile Chinook salmon survival as a function of Sacramento-San Joaquin Delta water exports. *North American Journal of Fisheries Management*, **30**: 157-169.

Appendix 2: Standard Operating Procedure

Acoustic Tagging for Salmon 2012 South Delta Studies 4/10/12 (file dated 4/23/12)

Equipment Set Up:

- Fill surgical instrument disinfection trays with chlorhexidine (brand name Nolvasan)
 - Autoclave instruments such that each tagging event begins with sterile instruments
- Activate transmitters and confirm operational status
 - Position the transmitter in an isolated compartment to enable tracking of the transmitter ID through the implantation process
- Disinfect transmitters in chlorhexidine
 - Ensure at least 20 minutes of contact time with chlorhexidine
 - Following disinfection, thoroughly rinse transmitters in distilled or de-ionized water prior to implantation
 - Following disinfection, transmitters should only be handled by gloved hands or clean surgical instruments such as forceps
- Fill rinse tray with de-ionized or distilled water
- Set up scale, measuring board, and surgical platform or foam
 - Apply stress coat to weigh boat, measuring board, and platform to reduce damage to fish skin or mucus layer
- Fill gravity feed carboys. Add 2 ml of the MS-222 stock solution and 2 ml of the sodium bicarbonate stock solution to the 10 L of water in the MS-222 carboy. Concentration may be increased upon group consensus and in consultation with coordinator.
- Fill anesthesia container to indicated volume line. Set the initial concentration in collaboration with the tagging coordinator. Suggested starting concentration is 70 mg/ L. Concentration may be adjusted upon group consensus and in consultation with coordinator. Concentration changes should be executed for all taggers simultaneously and recorded on the tagging datasheet.
- Prepare recovery containers by filling with water, adding stress coat, and supersaturating with oxygen
 - Immediately following surgery fish will be held in recovery containers that provide 130% to 150% DO for a minimum of 10 minutes
 - Holding time in recovery containers begins when the last fish is added to the container and will be monitored using a timer
- Prepare a reject container for fish that cannot be tagged by filling with water and equipping with a bubbler . These fish will be returned to a separate holding tank.
- Start tagging data sheets. Note the time the tagging session was started and complete all appropriate data fields. Start a Daily Fish Reject Tally datasheet to account for fish that are handled but not tagged.
- The tagger should wear medical-grade exam gloves during all fish handling and tagging procedures
- Prepare the transport truck to accept containers of tagged fish.
- Prepare transport containers and lids to receive tagged fish

Surgery

- Food should be withheld from fish for ~24 h prior to surgical implantation of the transmitter.
- Anesthetize fish
 - Net one fish from source tank/raceway and place directly into an anesthesia container. Immediately start a timer to monitor anesthesia exposure time and place a lid on the container.
 - Remove the lid after about 1 minute to observe the fish for loss of equilibrium. Keep the fish in the water for an additional 30-60 seconds after it has lost equilibrium. Time to sedation should normally be 2-4 minutes, with an average of about 3 minutes. If loss of equilibrium takes less than 1 minute or if a fish is exposed to anesthesia for more than 5 minutes, reject that fish. If after anesthetizing a few fish they are consistently losing equilibrium in more or less time than typical, the anesthesia concentration may need to

be adjusted. Anesthesia concentration should only be adjusted in coordination with all study taggers and the tagging coordinator.

- Changes to anesthesia concentration should be done at 5 mg/L increments. For example, if the initial dosage was 70 mg/L, an adjusted dose should be 65 mg/L or 75 mg/L.
 - When an anesthesia change is agreed upon, all taggers should drain their anesthesia containers, refill with 10 L of water, and re-mix to the new anesthesia concentration
 - If a fish is unacceptable for tagging due to issues with anesthesia, place the fish in the “Reject” container and log it on the reject tally datasheet.
 - The anesthesia container should be emptied and remixed at regular intervals throughout the tagging operation to ensure the appropriate concentration and to avoid warming
 - The gravity feed containers should be monitored for volume and temperature and changed as needed to avoid inadequate volume to complete a surgery and significant warming
- Recording fish length, weight, and condition
 - Start a timer when a fish is removed from the anesthesia container to record the time the fish is out of water (recorded as “air time”).
 - Transfer the fish to the scale and record the weight to the nearest 0.1g
 - Scales should be calibrated regularly to ensure accuracy
 - Fish must weigh at least 13 g to be selected for tagging so that tag burden does not exceed 5% of the weight of the fish. Transmitters used for this study are Vemco brand V5 models, weighing 0.65 g in air.
 - Transfer the fish to the measuring board and determine forklength to the nearest mm.
 - Check for any abnormalities and descaling. If the fish is abnormal or grossly descaled, note this on the datasheet and place the fish in the reject container.
 - Scale condition is noted as Normal (N), Partial (P), or Descaled (D) and is assessed on the most compromised side of each fish. The normal scale condition is defined as loss of less than 5% of scales on one side of the fish. Partial descaling is defined as loss of 6-19% of scales on one side of the fish. Fish are classified as descaled if they have lost 20% or more of the scales on one side of the fish, and should not be tagged due to compromised osmoregulatory ability.
 - Data must be vocally relayed to the recorder, and the recorder should repeat the information back to the tagger to avoid miscommunication.
 - Any fish dropped on the floor should be rejected.
- Transmitter Implantation
 - Anesthesia should be administered through the gravity feed irrigation system as soon as the fish is on the surgical platform. Use the flow control valves to adjust the flow rate as needed so that the opercular rate of the fish is steady.
 - Note that low-flow or inconsistent irrigation can mimic shallow anesthesia
 - Using a scalpel, make an incision approximately 3-5 mm in length beginning a few mm in front of the pelvic girdle. The incision should be about 3 mm away from and parallel to the mid-ventral line, and just deep enough to penetrate the peritoneum, avoiding the internal organs. The spleen is generally near the incision point so the depth and placement of the incision are critical.
 - There is no exact specification for the selection of a micro scalpel for steelhead. A general recommendation is to use a 5 mm blade for fish larger than about 50 g.
 - The incision should only be long enough to allow entry of the tag.
 - Forceps may be used to open the incision to check for potential organ damage. If you observe damage or note excessive bleeding, reject the fish.
 - Scalpel blades can be used on several fish, but if the scalpel is pulling roughly or making jagged incisions, it should be changed prior to tagging the next fish.

- Gently insert the tag into the body cavity and position it so that it lies directly beneath the incision and the ceramic head is facing forward. This positioning will provide a barrier between the suture needle and internal organs.
- Close the incision with two simple interrupted stitches.
 - Vicryl Plus sutures are recommended
 - 5-0 suture size is appropriate for juvenile Chinook Salmon or similar fish with weights less than~ 50 g
 - If the incision cannot effectively be closed with two stitches, a third stitch may be added. The presence of a third suture should be noted on the datasheet.
- Ideally the gravity feed irrigation system should be switched to fresh water or a combination of sedation and freshwater during the final stages of surgery to begin recovery from anesthesia. Typically a good time to switch to freshwater is when the second suture is initiated.
- Transfer the fish from the surgical platform to a recovery container and stop the timer recording air time
 - Avoid excessive handling of fish during transfer. Ideally the fish will be moved to the recovery container on the surgical platform to reduce handling.
- Once a recovery container has been fully stocked, start a timer to monitor the 10 min of exposure to high DO concentrations for recovery.
- Between surgeries the tagger should place surgical instruments and any partially consumed suture material into the chlorhexidine bath. Multiple sets of surgical instruments should be rotated to ensure 10 min of contact time with chlorhexidine. Once disinfected, instruments should be rinsed in distilled or de-ionized water. Organic debris in the disinfectant bath reduces effectiveness, so be sure to change the bath regularly.

Tag Validation

- Filled recovery containers will be moved to the tag validation station.
 - Recovery containers may be moved from the tagging location to the tag validation station during the 10 min recovery time, but they must not be established on flow-through water exchange. The flow-through exchange will immediately reduce the DO saturation.
- Use the appropriate receiving system to confirm the identity and function of the transmitters in the recovery container. Record validation on the datasheet.
- Following tag validation, recovery containers are held in a flow-through tank until the tagging session is complete, at which time they are loaded onto a truck for transport to the holding and release location.

Cleanup

- Both the tagger and assistant must review the full complement of tagging datasheets and initial each sheet to confirm that the set of transmitters they were assigned to implant have been implanted. Use the list of transmitters provided by the tag coordinator to ensure that all transmitters supplied to you were implanted and recorded. Both the tagger and the assistant must initial the header of each of the datasheets. This review step is completed for each tagging session (that is, for each transport truck that is loaded).
- Return tag tray and datasheets to coordinator at end of each tagging session.
- Complete the reject fish tally datasheet and return to the tag coordinator.
- Use a spray disinfectant to disinfect tagging surfaces and supplies, and position them to dry.
- Return any rejected fish to the appropriate raceway where they cannot be selected for future tagging efforts.
- At the completion of the tagging effort each day, package surgical instruments for the autoclave so they can be sterilized prior to the next tagging session.

Important things to remember:

- Water containers used for tagging should be filled just prior to tagging to avoid temperature changes and should be changed frequently.
- Fish cannot be transferred between water sources until the difference between the water temperatures of the two sources is less than two degrees Celsius.
- No water sources used in the tagging operation should be more than two degrees different in water temperature from the source water temperature.
- All containers holding fish should have lids in place.
- If a tag is dropped bring it to the tagging coordinator to confirm that it is still functioning before it is implanted. The transmitter may also require disinfection if it fell onto a dirty surface.
- Carefully handle all fish containers to minimize disturbances to fish.
- Containers used to transport fish to the release site cannot be used for tagging operations until they have been held in the freezer for 24 h.

Appendix 3: Water temperature (every 15 minutes) in transport tanks during transport of tagged fish from the Tracy Fish Collection Facility to the release site (Durham Ferry)

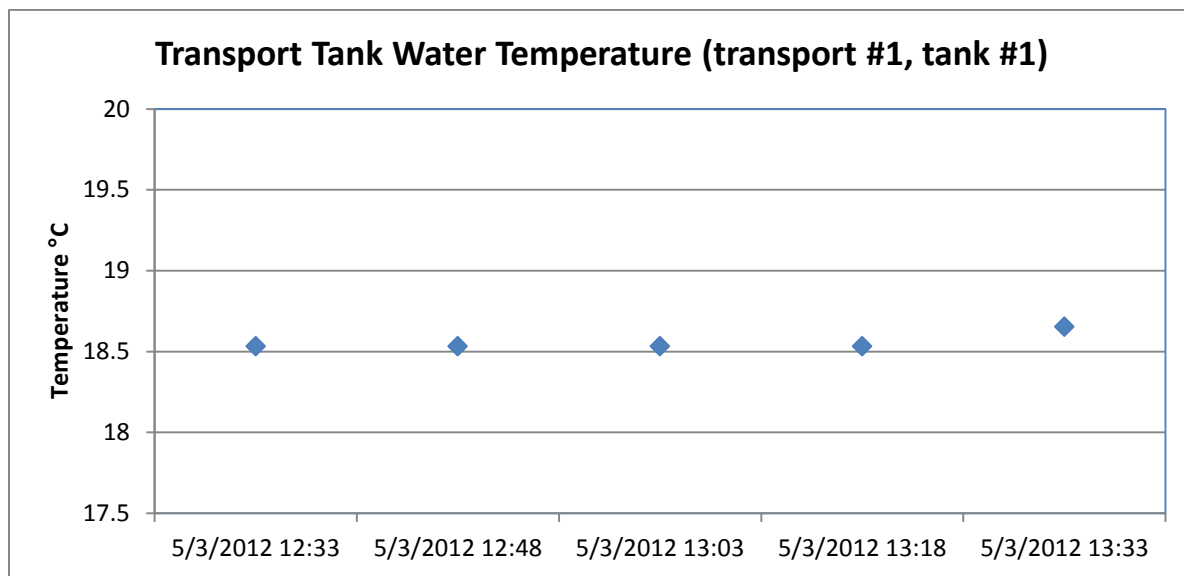


Figure A3-1. Transport tank water temperature during transport #1, tank #1 on May 3, 2012.

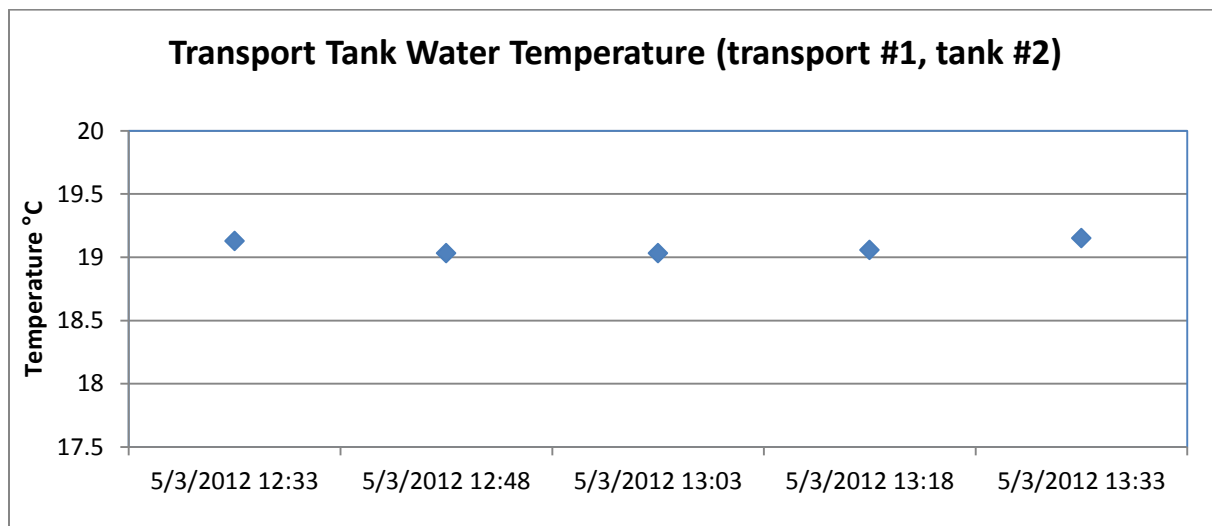


Figure A3-2. Transport tank water temperature during transport #1, tank #2 on May 3, 2012.

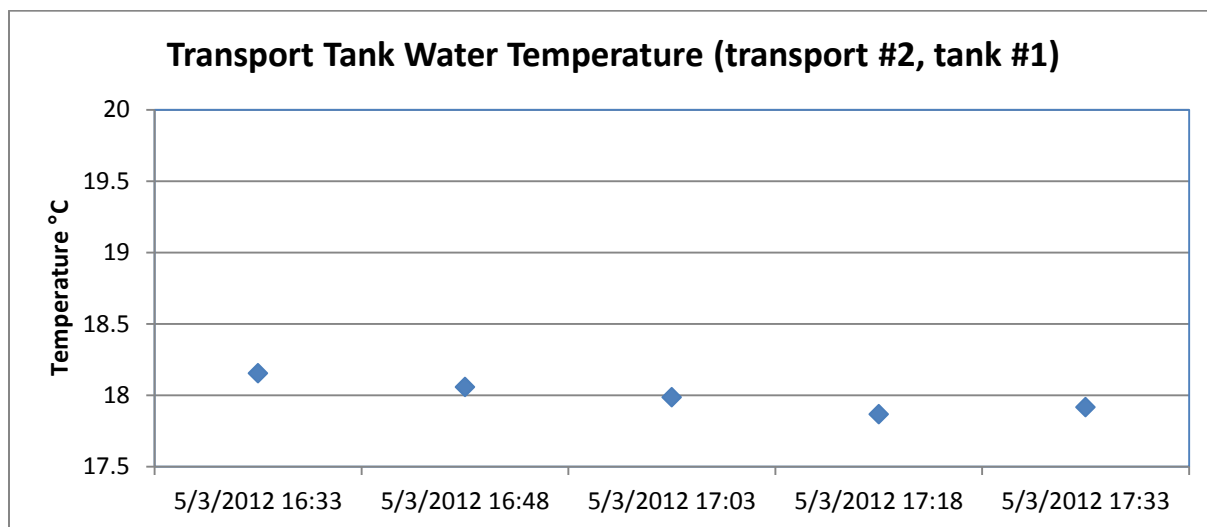


Figure A3-3. Transport tank water temperature during transport #2, tank #1 on May 3, 2012.

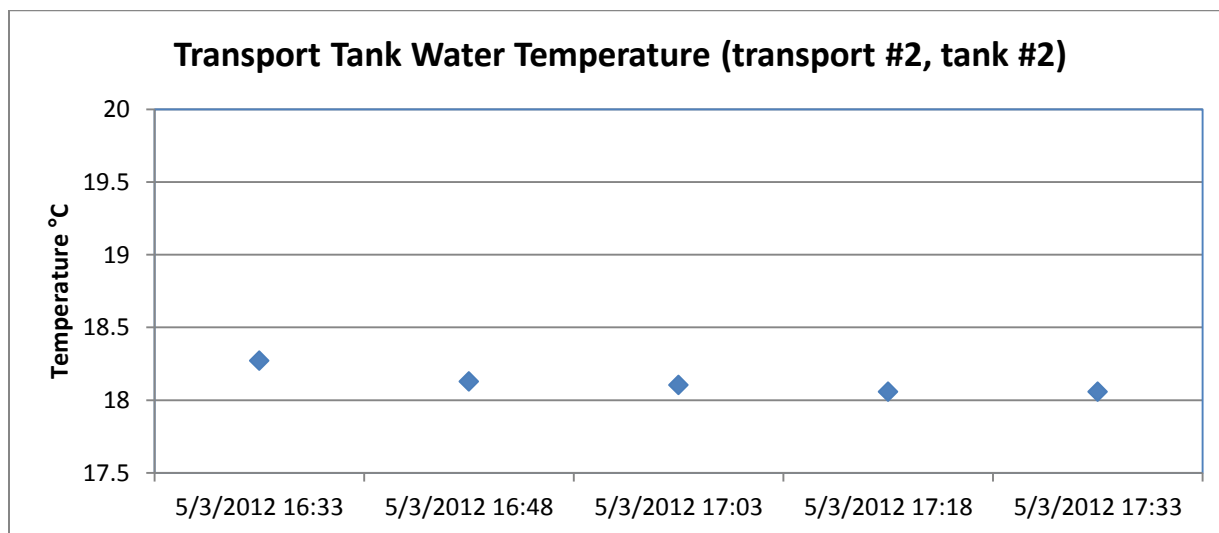


Figure A3-4. Transport tank water temperature during transport #2, tank #2 on May 3, 2012.

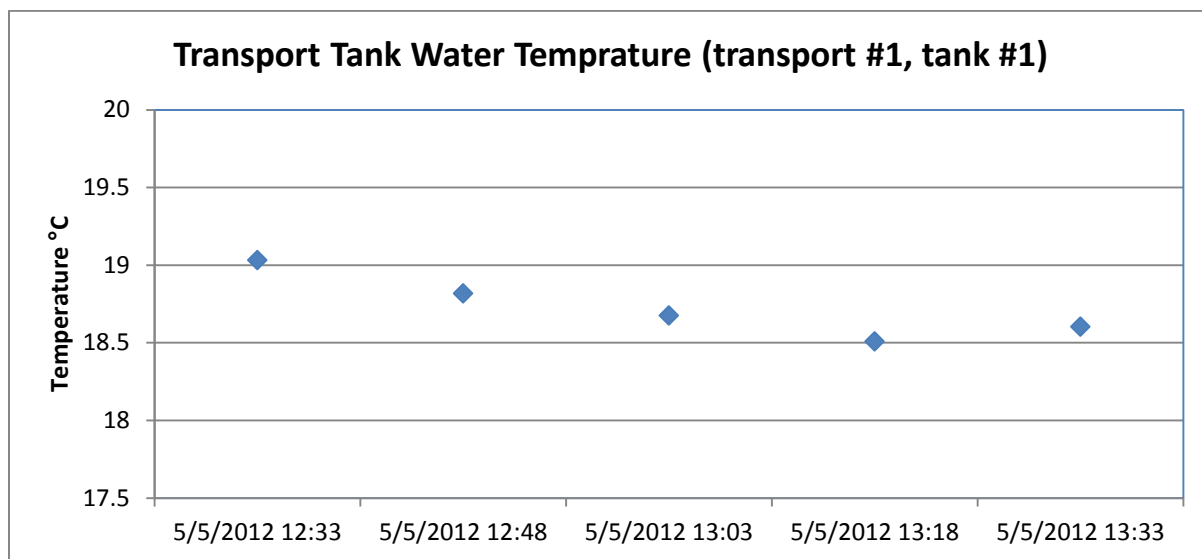


Figure A3-5. Transport tank water temperature during transport #1, tank #1 on May 5, 2012.

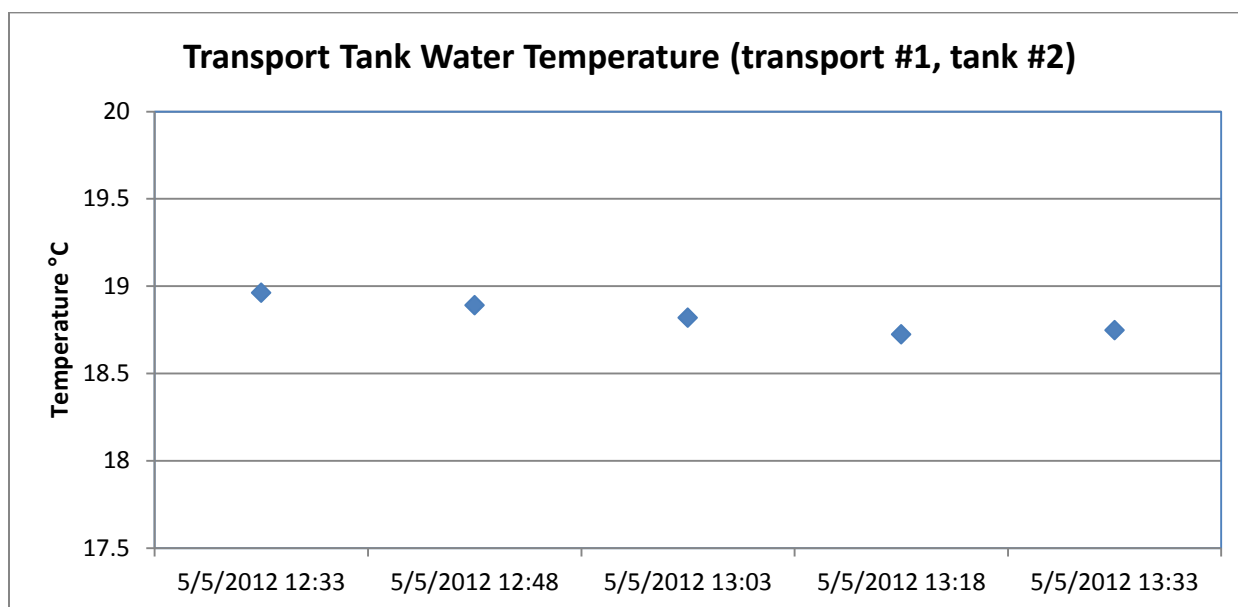


Figure A3-6. Transport tank water temperature during transport #1, tank #2 on May 5, 2012.

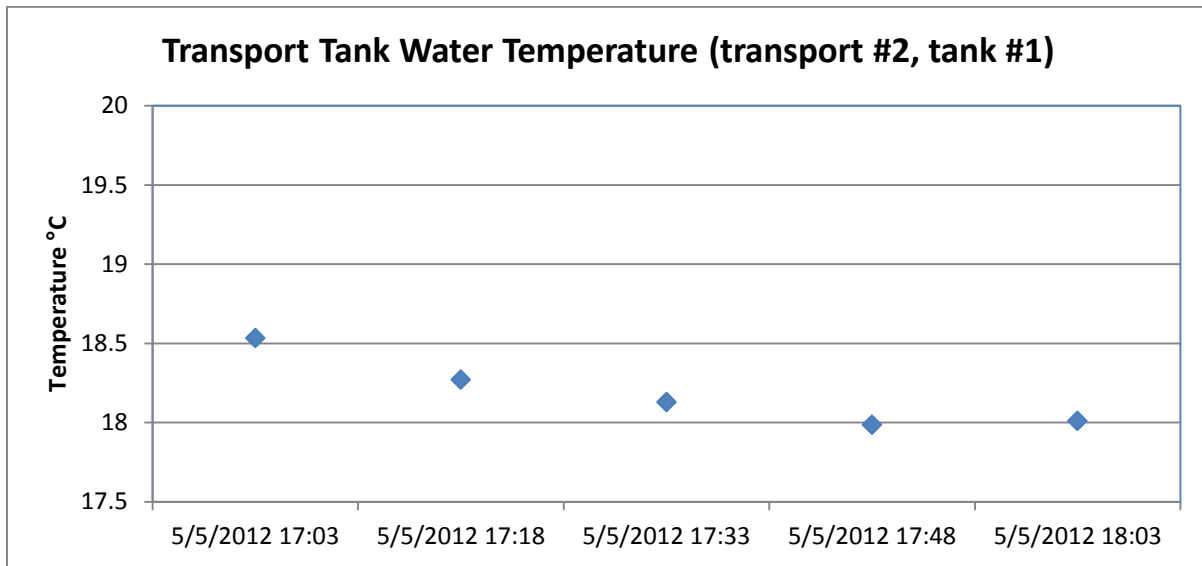


Figure A3-7. Transport tank water temperature during transport #2, tank #1 on May 5, 2012.

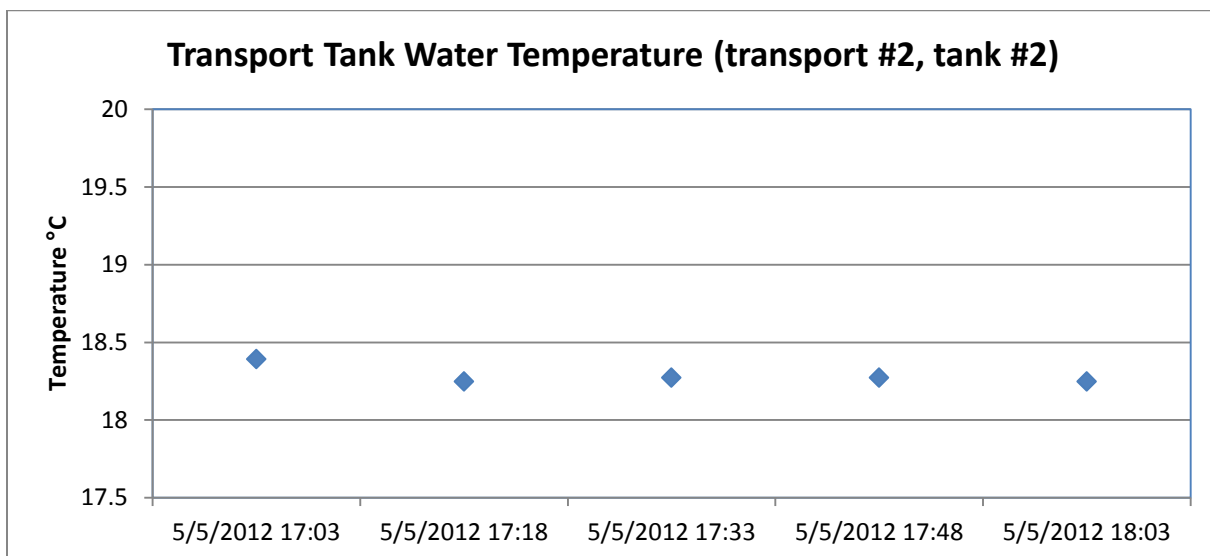


Figure A3-8. Transport tank water temperature during transport #2, tank #2 on May 5, 2012.

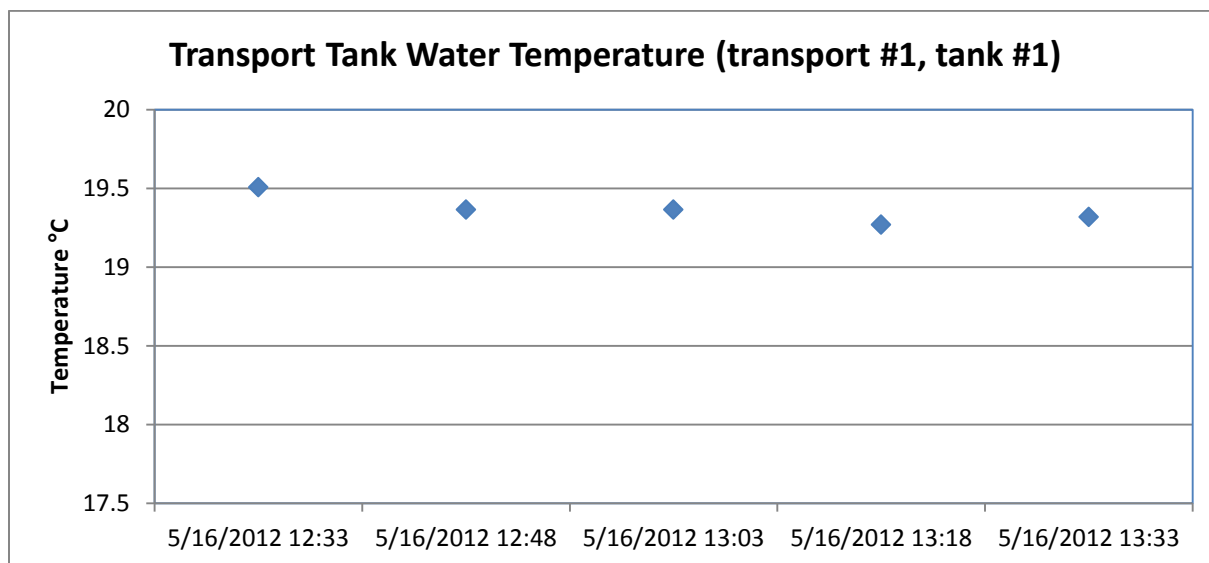


Figure A3-9. Transport tank water temperature during transport #1, tank #1 on May 16, 2012.

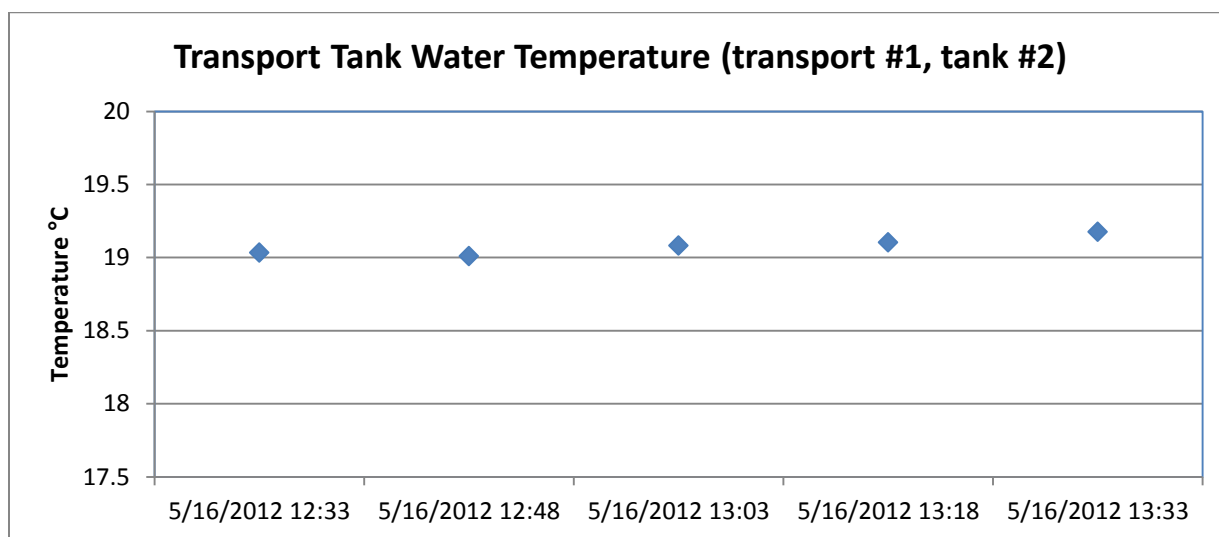


Figure A3-10. Transport tank water temperature during transport #1, tank #2 on May 16, 2012.

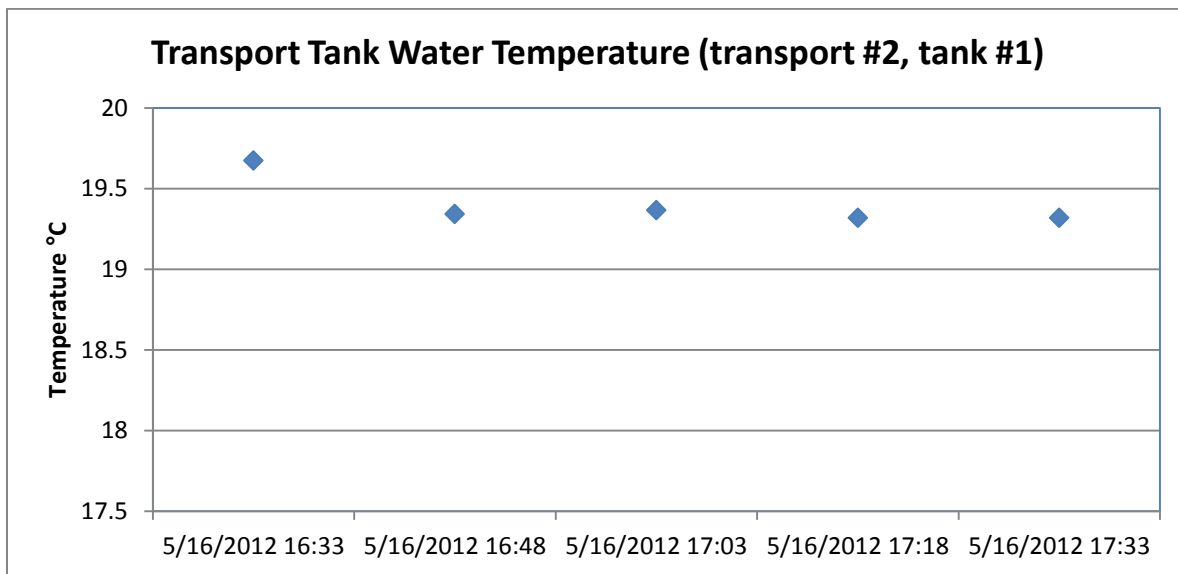


Figure A3-11. Transport tank water temperature during transport #2, tank #1 on May 16, 2012.

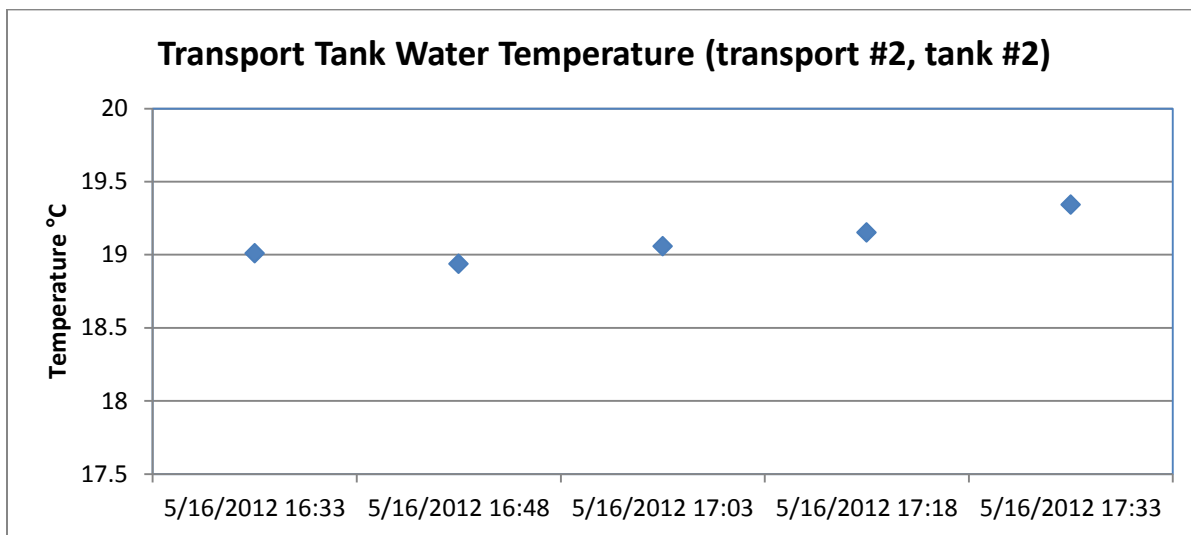


Figure A3-12. Transport tank water temperature during transport #2, tank#2 on May 16, 2012.

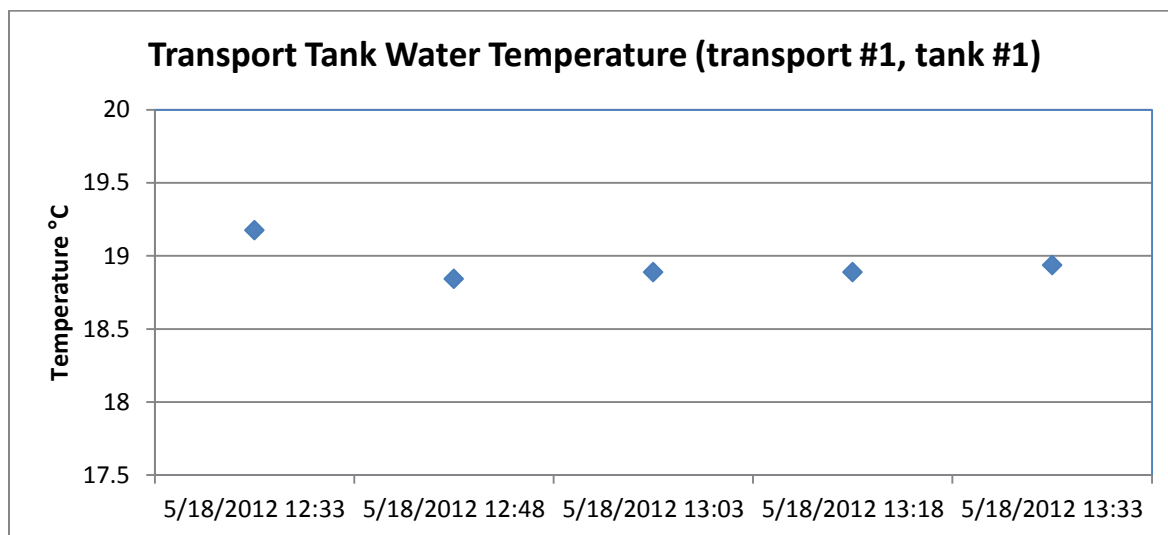


Figure A3-13. Transport tank water temperature during transport #1, tank #1 on May 18, 2012.

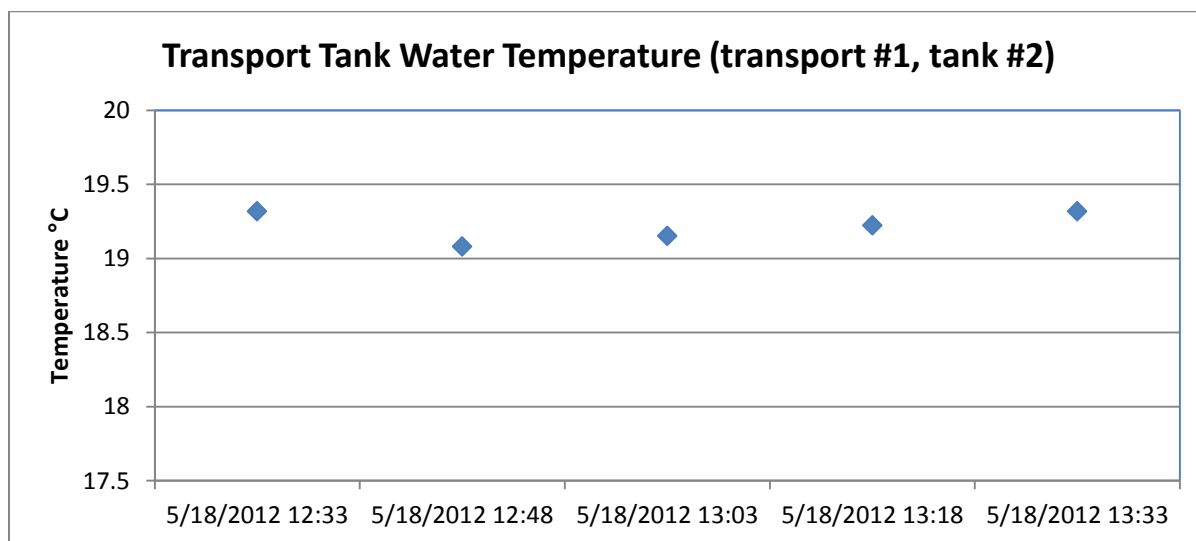


Figure A3-14. Transport tank water temperature during transport #1, tank #2 on May 18, 2012.

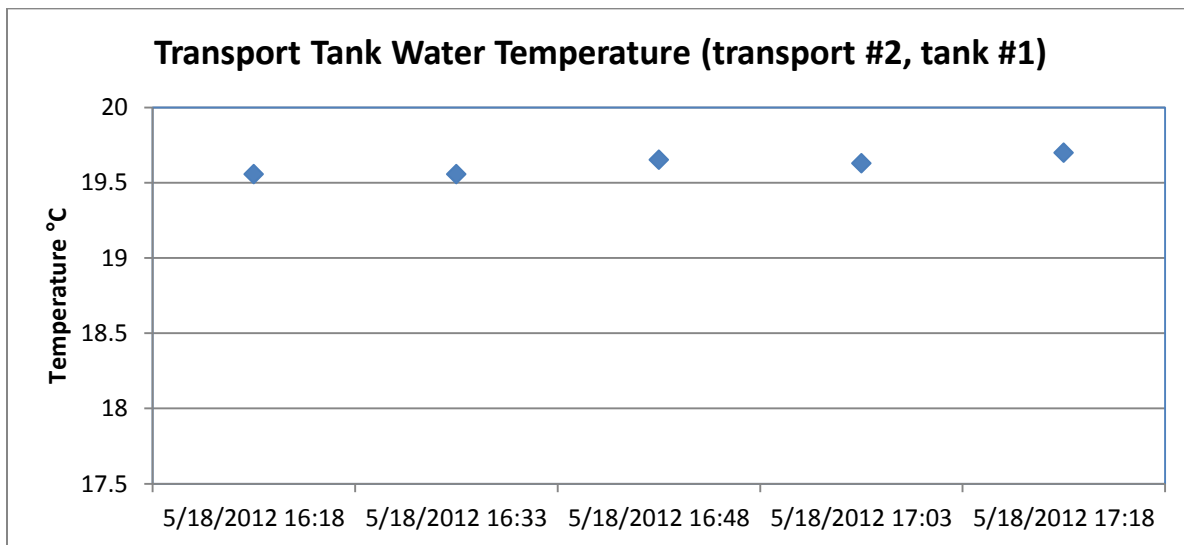


Figure A3-15. Transport tank water temperature during transport #1, tank #1 on May 18, 2012.

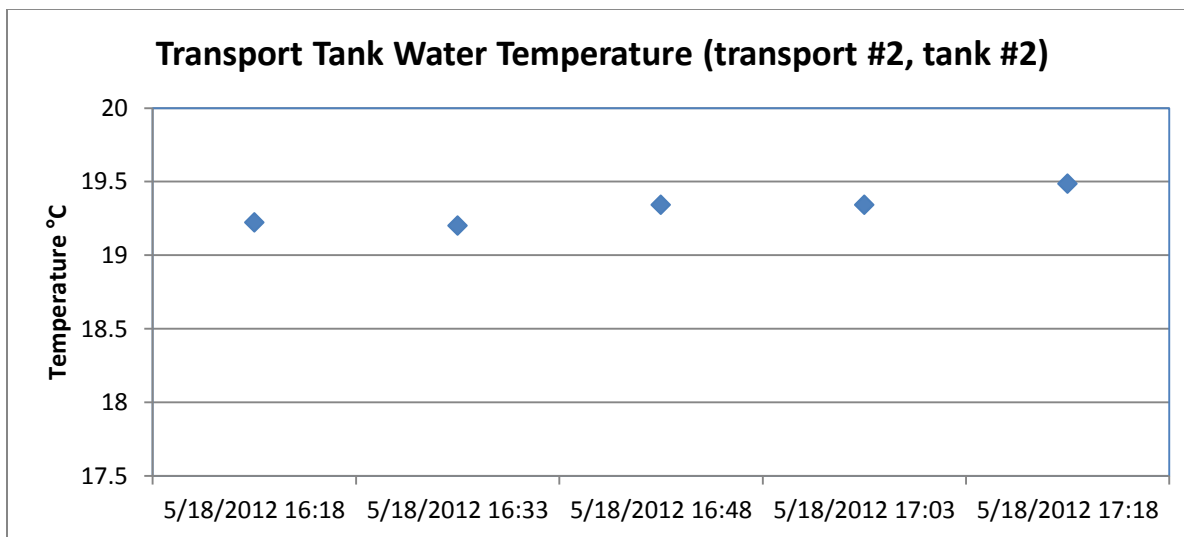


Figure A3-16. Transport tank water temperature during transport #2, tank #2 on May 18, 2012.

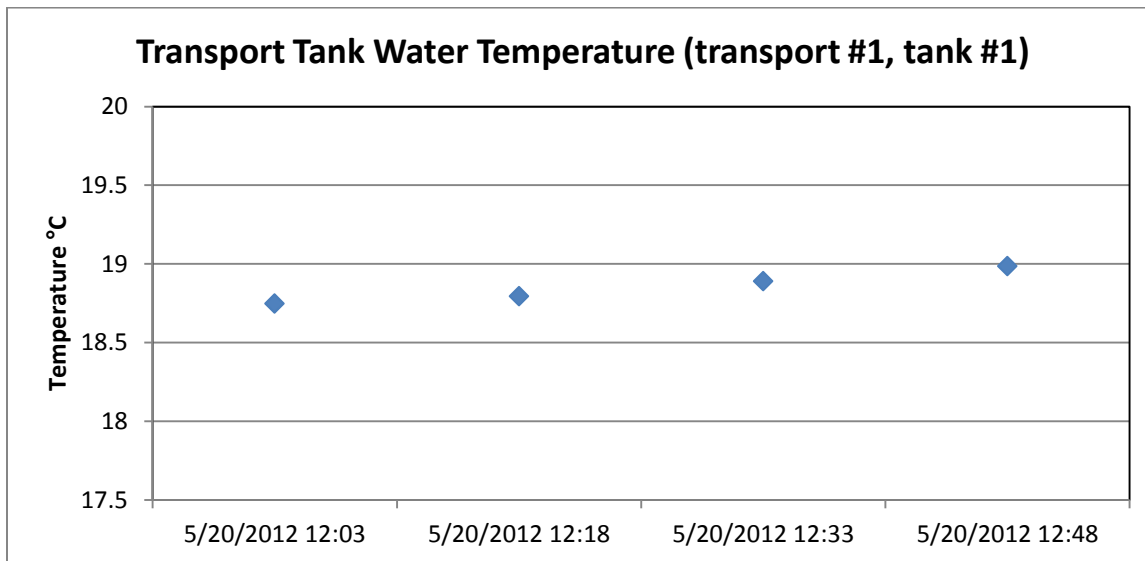


Figure A3-17. Transport tank water temperature during transport #1, tank #1 on May 20, 2012.

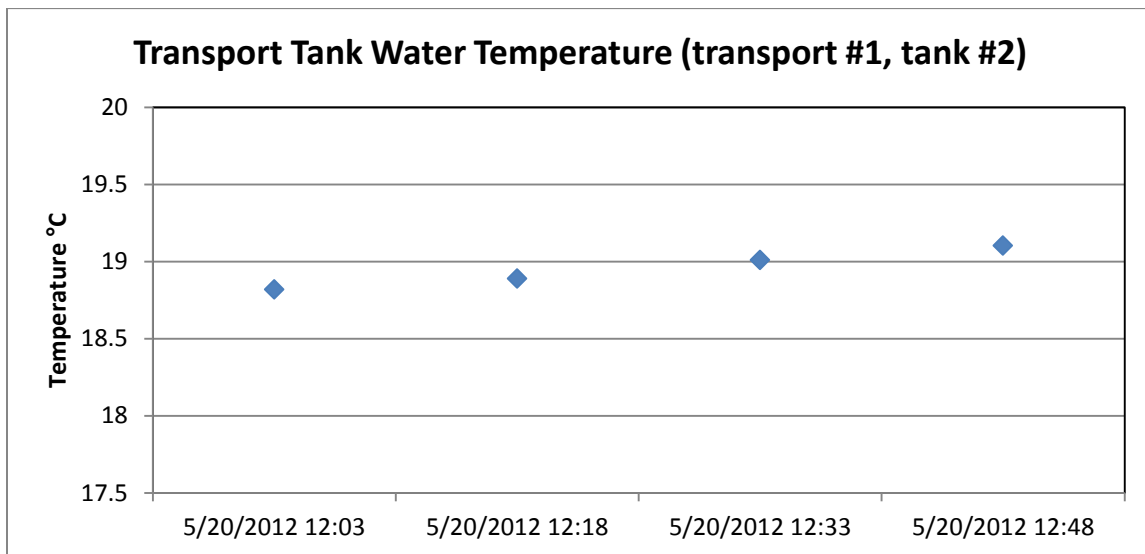


Figure A3-18. Transport tank water temperature during transport #1, tank #2 on May 20, 2012.

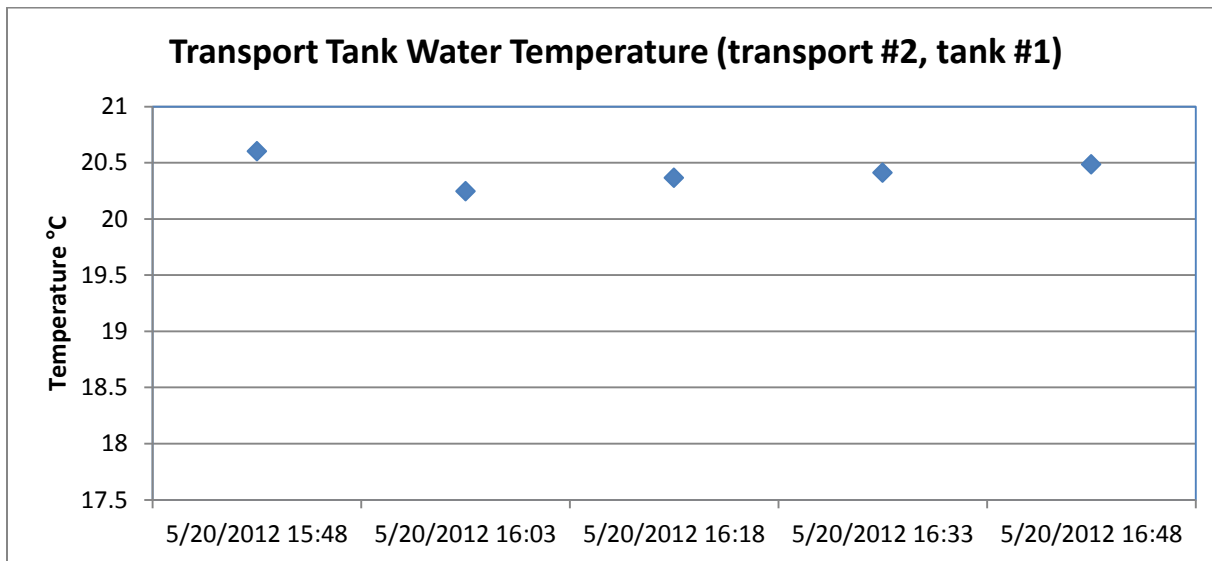


Figure A3-19. Transport tank water temperature during transport #2, tank #1 on May 20, 2012.

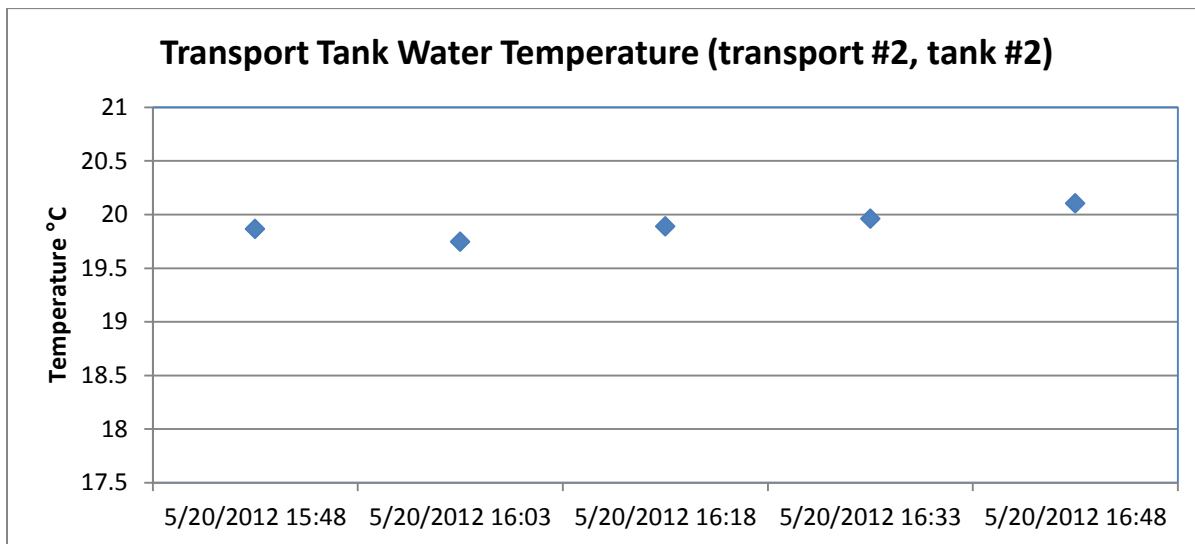


Figure A3-20. Transport tank water temperature during transport #2, tank #2 on May 20, 2012.

Appendix 4:

U.S. Fish & Wildlife Service

FY2012 Technical Report:
Pathogen screening and gill Na-K-ATPase assessment of juvenile Chinook salmon used in south delta acoustic tag studies.

J. Scott Foott



September 2012



US Fish and Wildlife Service
California-Nevada Fish Health Center
24411 Coleman Fish Hatchery Rd
Anderson, CA 96007

SUMMARY:

Pathogen testing was conducted on dummy-tag cohorts of acoustic tagged Merced River Hatchery juvenile Chinook salmon used in studies corresponding to 7 May and 23 May releases. No virus or *Renibacterium salmoninarum* infection was detected in the fish. The 23 May group had 37% prevalence of both suture abnormalities and *Aeromonas* – *Pseudomonas* sp. infection however there was little correlation between the 2 findings. As in the past, *Tetracapsuloides bryosalmonae* infection was highly prevalent ($\geq 97\%$) and the associated Proliferative Kidney Disease became more pronounced in the 23 May sample. No mortality occurred in the live cage populations at either sample date. Gill Na-K-ATPase data is not reported due to a problem with a key assay reagent. The combination of kidney impairment and poor suture condition of the 23 May salmon indicates that health of the two release groups was not equivalent.

Recommended citation for this report is:

Foott JS. 2012. FY2012 Technical Report: Pathogen screening and gill Na-K-ATPase assessment of juvenile Chinook salmon used in south delta acoustic tag studies. U.S. Fish & Wildlife Service California-Nevada Fish Health Center, Anderson, CA. Available: <http://www.fws.gov/canvfhc/reports.asp>.

Notice:

The mention of trade names or commercial products in this report does not constitute endorsement or recommendation for use by the Federal government. The findings and conclusions in this report are those of the author and do not necessarily represent the views of the US Fish and Wildlife Service.

INTRODUCTION

As a component of the 2012 Chinook salmon survival studies on reach-specific survival and distribution of migrating Chinook salmon in the San Joaquin River and delta, the CA-NV Fish Health Center conducted a general pathogen screening and smolt physiological assessment. The health and physiological condition of the study fish can help explain their performance and survival during the studies. Pathogen screenings during past VAMP studies using Merced River Hatchery (MRH) Chinook have regularly found infection with the myxozoan parasite *Tetracapsuloides bryosalmonae*, the causative agent of Proliferative Kidney Disease (PKD). This parasite has been shown to cause mortality in Chinook salmon with increased mortality and faster disease progression in fish at higher water temperatures (Ferguson 1981; Foott et al. 2007). The objectives of this project were to survey the juvenile Chinook salmon used for the studies for specific fish pathogens including *Tetracapsuloides bryosalmonae* and assess smolt development from gill $\text{Na}^+ - \text{K}^+$ -ATPase activity.

METHODS

Prior to the 7 May and 23 May sample, 30 juvenile salmon were held within live cages for approximately 48h in the San Joaquin River at Durham Ferry. These fish were surgically-implanted with a dummy tag similar in size to the acoustic tag of release cohorts. Fish were evaluated for gill and skin condition (including suture) and tissues collected for assays. A grading scale ranging 0-3 was used to score inflammation or ulceration of tissue at the suture location and openness of the surgical incision (based on training session by Cramer Fish Sciences attended by J. Day).

- 0: Clean, completely closed and healed incision with taut suture. No external indication of pulling of tissue or inflammation.
- 1: Mostly closed, but not healed incision. Minor petechial hemorrhage.
- 2: Incision more than half open, and not healed. Inflammation present over more than half the suture area.
- 3: Incision completely open. Severely inflamed tissue surrounding and/or pushing out from incision site. Severe hemorrhaging extending equal to or greater than the length of the incision site. Suture may be lost entirely or embedded within inflamed tissue. Necrotic tissue visible.

Gill lamellae were collected first into SEI buffer and frozen on dry ice. Gill Na^+/K^+ -Adenosine Triphosphatase (ATPase) activity was assayed by the method of McCormick (1993). Kidney was collected aseptically and inoculated onto brain-heart infusion agar. Bacterial isolates were screened by standard microscopic and biochemical tests (USFWS and AFS-FHS 2010). *Renibacterium salmoninarum* (bacteria that causes bacterial kidney disease) was screened by fluorescent antibody test (FAT) of kidney imprints. Three fish pooled samples of kidney and spleen were inoculated onto EPC and CHSE-214 cell lines held at 15°C for 21 d (USFWS and AFS-FHS 2010). The gill, liver, intestine and posterior kidney were rapidly removed from the fish and immediately fixed in Davidson's fixative, processed for 5 μm paraffin sections and stained with

hematoxylin and eosin (Humason 1979). Infections of the myxozoan parasite, *T. bryosalmonae*, were rated for intensity of parasite infection and associated tissue inflammation (Proliferative Kidney Disease). Intensity of infection was rated as none (zero), low (<10), moderate (11-30) or high (>30) based on number of *T. bryosalmonae* trophozoites observed in the kidney section. Severity of kidney inflammation (PKD) was rated as normal, focal, multifocal or diffuse.

RESULTS AND DISCUSSION

All salmon were alive at the time of sample collection for both dates. Suture condition of 23 May fish was judged to be poor (11 of 30 fish with #2 or 3 ratings). Several sutures were observed on the pelvic girdle. All sutures in the 7 May group were intact and showed no hemorrhage.

The prevalence of systemic bacterial infection (*Aeromonas* – *Pseudomonas* sp. (aquatic bacteria clade) was also 37% in the 23 May group however there was little association with suture hemorrhage (only 4 of 11 fish with hemorrhaged sutures had bacterial infections). No virus or *Renibacterium salmoninarum* infection was detected in the fish (Table 1). *Tetracapsuloides bryosalmonae* was seen in $\geq 97\%$ of the kidney sections from both sample groups (Table 1).

Table A4-1. Prevalence of infection (number positive / total sample) for systemic bacteria (AP= *Aeromonas* or *Pseudomonas* sp.), *R. salmoninarum* by direct fluorescent antibody test (Rsal-DFAT), virus, and *T. bryosalmonae* observed in kidney sections.

<u>Sample date</u>	<u>Bacteria</u>	<u>Rsal - DFAT</u>	<u>Virus</u>	<u><i>T.bryosalmonae</i></u>
7 May	1 / 30 (3) AP	0 / 29	0 / 10 (3p)	29 / 30 (97)
23 May	11 / 30 (37) AP	0 / 30	0 / 10 (3p)	30 / 30 (100)

The *T. bryosalmonae* infection was judged to be at an early state in the 7 May sample fish. High numbers of the parasites were seen in both groups however kidney inflammation was markedly worse in the 23 May fish (Fig. 1 and 2). Swollen kidneys and spleens were also observed in the 23 May group. Overt anemia (pale gills) was not seen in any salmon on either collection date. The systemic nature of the infection was reflected in the occurrence of the parasite in multiple tissues (spleen, visceral adipose capillaries, liver sinuses, and kidney) including blood vessels within the gill (Fig. 3). One 7 May gill section contained two *Ichthyophthirius multifilii* trophozoites however there was little tissue response. Liver hepatocytes showed little glycogen or fat content in both sample groups possibly reflective of low feed rate. No gill Na-K-ATPase data is reported due to abnormal kinetic profiles. The ADP standard curve was normal which indicates that the majority of enzymes and co-factors were functional. The pH and magnesium conditions were also normal for the assay. We suspect that the recently purchased Sigma Chemical Adenosine TriPhosphate was faulty as this nucleotide is the substrate for the ouabain-sensitive gill Na-K-ATPase enzyme.

The advanced proliferative kidney disease, increased prevalence of systemic bacteria, and hemorrhaged sutures observed in the 23 May salmon suggests that the two release groups were not equivalent in health condition. The impact on immediate (1-3 days) post-release survival of these impairments on 23 May salmon is likely to be limited however longer term survival and swimming performance could be reduced. Past work on PKD effects on smolt performance have shown that severe kidney inflammation and anemia are associated with impaired swimming and saltwater adaptation (Foott et al. 2007 and 2008).

Figure A4-1. Prevalence of *T. byrosalmonae* intensity ratings for Chinook salmon sampled on 7 and 23 May. Intensity of *T. byrosalmonae* infection observed in kidney section rated as none (0), low (<10), moderate (11-30), and high (>30). Numbers over ratings are prevalence data. Majority of parasites observed in the 7 May kidneys were found in the sinuses indicating an early stage of infection.

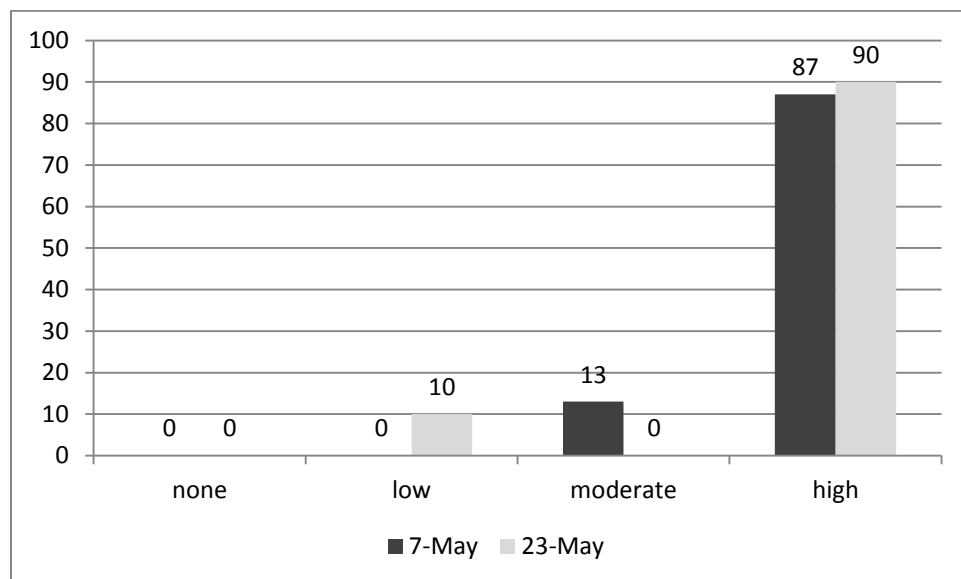


Figure A4-2. Prevalence of proliferative kidney disease ratings for Chinook salmon sampled on 7 and 23 May. Severity of kidney inflammation rated as normal, focal, multifocal, or diffuse. Numbers over ratings are prevalence data.

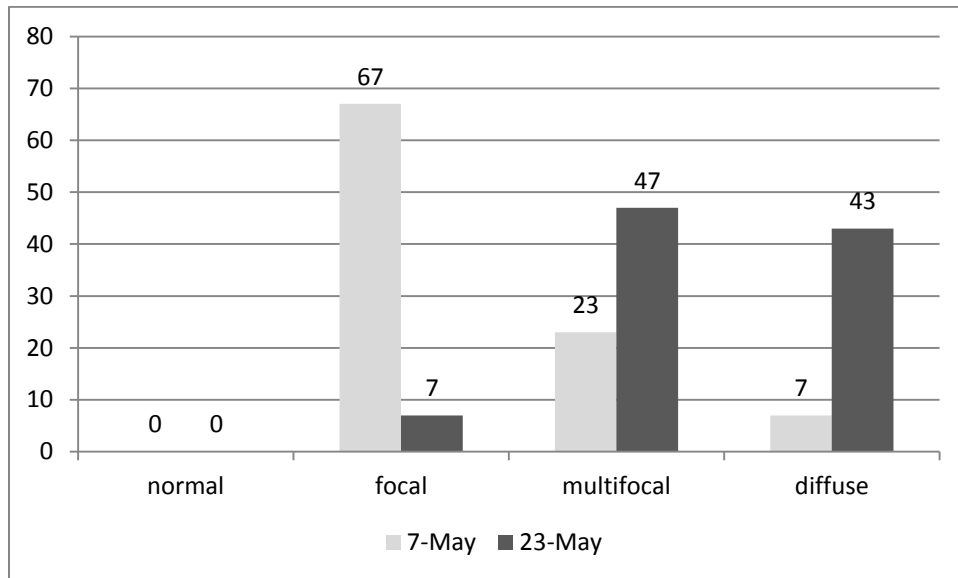


Figure A4-3. Micrograph of *T. byosalmonae* (arrow) within gill blood vessel.

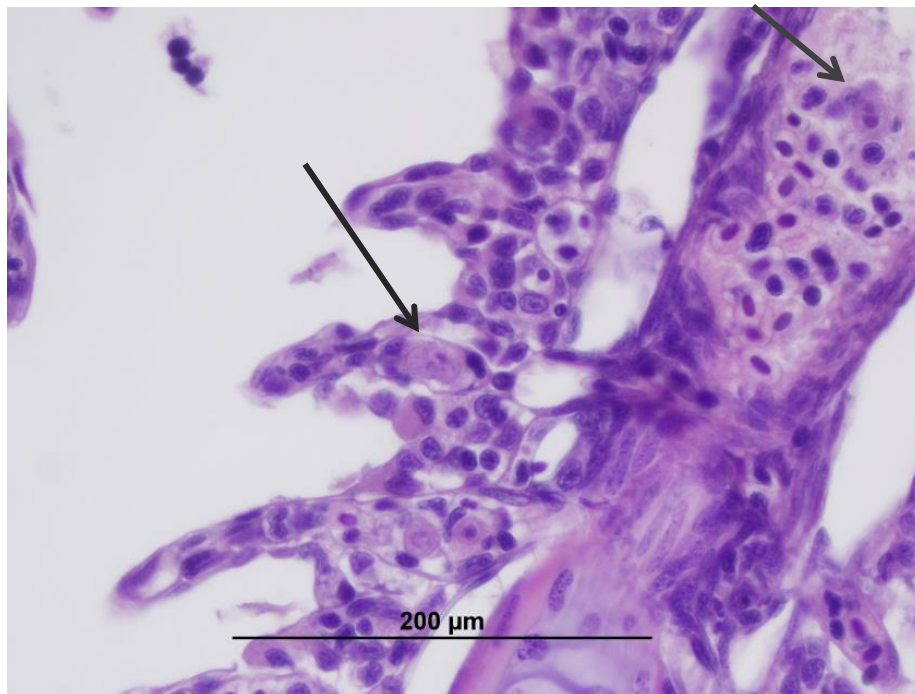


Figure A4-4. Suture condition rating 2 (exposed edge with hemorrhage) in 23 May salmon.



ACKNOWLEDGEMENTS

Ken Nichols, Anne Bolick, Kim True, and Julie Day with the FHC performed both field and laboratory work on this project and biologists with the USFWS Stockton FWO provided access to the live cages at Durham Ferry.

REFERENCES

- Foott JS and R Stone. 2008. FY 2008 Investigational report: Evaluation of sonic tagged Chinook juveniles used in the 2008 VAMP study for delayed mortality and saltwater survival – effects of Proliferative Kidney Disease. US Fish and Wildlife Service, California-Nevada Fish Health Center, Anderson, CA. Available: <http://www.fws.gov/canvfhc/reports.asp> (September 2010).
- Foott JS, R Stone and K Nichols. 2007. Proliferative Kidney Disease (*Tetracapsuloides bryosalmonae*) in Merced River Hatchery juvenile Chinook salmon: mortality and performance impairment in 2005 smolts. *California Fish and Game* 93: 57-76.
- Ferguson, HW. 1981. The effects of water temperature on the development of Proliferative Kidney Disease in rainbow trout, *Salmo gairdneri* Richardson. *Journal of Fish Disease* 4: 175-177.
- Humason GL. 1979. *Animal Tissue Techniques*, 4th edition. W H Freeman and Co., San Francisco.
- McCormick SD. 1993. Methods for Nonlethal Gill Biopsy and Measurement of Na⁺, K⁺-ATPase Activity. *Canadian Journal of Fisheries and Aquatic Sciences*. 50: 656-658.
- USFWS and AFS-FHS (U.S. Fish and Wildlife Service and American Fisheries Society-Fish Health Section). 2010. Standard procedures for aquatic animal health inspections. *In* AFS-FHS. FHS blue book: suggested procedures for the detection and identification of certain finfish and shellfish pathogens, 2010 edition. AFS-FHS, Bethesda, Maryland.

Appendix 5. Survival Model Parameters

Table A5-1. Definitions of parameters used in the release-recapture survival model; full or reduced model, or both, is specified. Parameters used only in particular submodels are noted.

Parameter	Model	Definition
S_{A2}	Both	Probability of survival from Durham Ferry Downstream (DFD) to Banta Carbona (BCA)
S_{A3}	Both	Probability of survival from Banta Carbona (BCA) to Mossdale (MOS)
S_{A4}	Both	Probability of survival from Mossdale (MOS) to Lathrop (SJL) or Old River East (ORE)
S_{A5}	Both	Probability of survival from Lathrop (SJL) to Garwood Bridge (SJG)
S_{A6}	Both	Probability of survival from Garwood Bridge (SJG) to Navy Drive Bridge (SJNB)
S_{A7}	Both	Probability of survival from Navy Drive Bridge (SJNB) to MacDonald Island (MAC) or Turner Cut (TCE/TCW)
$S_{A7,G2}$	Both	Overall survival from Navy Drive Bridge (SJNB) to Chipps Island (MAE/MAW) (derived from Submodel I)
$S_{A8,G2}$	Both	Overall survival from MacDonald Island (MAC) to Chipps Island (MAE/MAW) (Submodel I)
S_{B1}	Full	Probability of survival from Old River East (ORE) to Old River South (ORS)
$S_{B2,G2}$	Reduced	Overall survival from Old River South (ORS) to Chipps Island (MAE/MAW) (derived from Submodel I)
$S_{F1,G2}$	Both	Overall survival from Turner Cut (TCE/TCW) to Chipps Island (MAE/MAW) (Submodel I)
$\phi_{A1,A0}$	Full	Joint probability of moving from Durham Ferry release site upstream toward DFU, and surviving to DFU
$\phi_{A1,A2}$	Both	Joint probability of moving from Durham Ferry release site downstream toward DFD, and surviving to DFD
$\phi_{A1,A3}$	Both	Joint probability of moving from Durham Ferry release site downstream toward BCA, and surviving to BCA; = $\phi_{A1,A2} S_{A2}$
$\phi_{A8,A9}$	Both	Joint probability of moving from MAC toward MFE/MFW, and surviving from MAC to MFE/MFW (Submodel II)
$\phi_{A8,B3}$	Full	Joint probability of moving from MAC toward OR4, and surviving from MAC to OR4 (Submodel II)
$\phi_{A8,C2}$	Full	Joint probability of moving from MAC toward MR4, and surviving from MAC to MR4 (Submodel II)
$\phi_{A8,GH}$	Full	Joint probability of moving from MAC directly toward Jersey Point (JPE/JPW) or False River (FRE/FRW) without passing Highway 4 sites, and surviving JPE/JPW or FRE/FRW (Submodel II)
$\phi_{A8,G1}$	Reduced	Joint probability of moving from MAC toward Jersey Point (JPE/JPW) and surviving to JPE/JPW (Submodel II); = $\phi_{A8,GH} \psi_{G1(A)}$
$\phi_{A9,B3}$	Full	Joint probability of moving from MFE/MFW toward OR4, and surviving from MFE/MFW to OR4 (Submodel II)
$\phi_{A9,C2}$	Full	Joint probability of moving from MFE/MFW toward MR4, and surviving from MFE/MFW to MR4 (Submodel II)
$\phi_{A9,GH}$	Full	Joint probability of moving from MFE/MFW directly toward Jersey Point (JPE/JPW) or False River (FRE/FRW) without passing Highway 4 sites, and surviving to JPE/JPW or FRE/FRW (Submodel II)
$\phi_{A9,G1}$	Reduced	Joint probability of moving from MFE/MFW toward Jersey Point (JPE/JPW) and surviving to JPE/JPW (Submodel II); = $\phi_{A9,GH} \psi_{G1(A)}$
$\phi_{B1,B2}$	Reduced	Joint probability of moving from ORE toward ORS, and surviving from ORE to ORS; = $S_{B1} \psi_{B2}$
$\phi_{B2,B3}$	Full	Joint probability of moving from ORS toward OR4, and surviving from ORS to OR4
$\phi_{B2,C2}$	Full	Joint probability of moving from ORS toward MR4, and surviving from ORS to MR4
$\phi_{B2,D1}$	Full	Joint probability of moving from ORS toward RGU, and surviving from ORS to RGU
$\phi_{B2,E1}$	Full	Joint probability of moving from ORS toward CVP, and surviving from ORS to CVP
$\phi_{B3,D1}$	Full	Joint probability of moving from OR4 toward RGU and surviving from OR4 to RGU conditional on coming from lower San Joaquin River (Submodel II)

Table A5-1. (Continued)

Parameter	Model	Definition
$\phi_{B3,E1}$	Full	Joint probability of moving from OR4 toward CVP, and surviving from OR4 to CVP, conditional on coming from lower San Joaquin River (Submodel II)
$\phi_{B3,GH(A)}$	Full	Joint probability of moving from OR4 toward Jersey Point (JPE/JPW) or False River (FRE/FRW), and surviving from OR4 to JPE/JPW or FRE/FRW (Submodel II [route A])
$\phi_{B3,GH(B)}$	Full	Joint probability of moving from OR4 toward Jersey Point (JPE/JPW) or False River (FRE/FRW), and surviving from OR4 to JPE/JPW or FRE/FRW (Submodel I [route B])
$\phi_{C1,B3}$	Full	Joint probability of moving from MRH toward OR4, and surviving from MRH to OR4
$\phi_{C1,C2}$	Full	Joint probability of moving from MRH toward MR4, and surviving from MRH to MR4
$\phi_{C1,D1}$	Full	Joint probability of moving from MRH toward RGU, and surviving from MRH to RGU
$\phi_{C1,E1}$	Full	Joint probability of moving from MRH toward CVP, and surviving from MRH to CVP
$\phi_{C2,D1}$	Full	Joint probability of moving from MR4 toward RGU and surviving from MR4 to RGU conditional on coming from lower San Joaquin River (Submodel II)
$\phi_{C2,E1}$	Full	Joint probability of moving from MR4 toward CVP, and surviving from MR4 to CVP, conditional on coming from lower San Joaquin River (Submodel II)
$\phi_{C2,GH(A)}$	Full	Joint probability of moving from MR4 toward Jersey Point (JPE/JPW) or False River (FRE/FRW), and surviving from MR4 to JPE/JPW or FRE/FRW (Submodel II [route A])
$\phi_{C2,GH(B)}$	Full	Joint probability of moving from MR4 toward Jersey Point (JPE/JPW) or False River (FRE/FRW), and surviving from MR4 to JPE/JPW or FRE/FRW (Submodel I [route B])
$\phi_{D1,D2}$	Full	Joint probability of moving from RGU toward RGD, and surviving from RGU to RGD (equated between submodels I and II)
$\phi_{D2,G2}$	Full	Joint probability of moving from RGD toward Chipps Island (MAE/MAW) and surviving from RGU to MAE/MAW (equated between submodels I and II)
$\phi_{E1,E2}$	Full	Joint probability of moving from CVP toward CVPtank, and surviving from CVP to CVPtank (equated between submodels I and II)
$\phi_{E2,G2}$	Full	Joint probability of moving from CVPtank toward Chipps Island (MAE/MAW) and surviving from CVPtank to MAE/MAW (equated between submodels I and II)
$\phi_{F1,B3}$	Full	Joint probability of moving from TCE/TCW toward OR4, and surviving from TCE/TCW to OR4 (Submodel II)
$\phi_{F1,C2}$	Full	Joint probability of moving from TCE/TCW toward MR4, and surviving from TCE/TCW to MR4 (Submodel II)
$\phi_{F1,GH}$	Full	Joint probability of moving from TCE/TCW directly toward Jersey Point (JPE/JPW) or False River (FRE/FRW) without passing Highway 4 sites, and surviving to JPE/JPW or FRE/FRW (Submodel II)
$\phi_{F1,G1}$	Reduced	Joint probability of moving from TCE/TCW toward Jersey Point (JPE/JPW) and surviving to JPE/JPW (Submodel II); = $\phi_{F1,GH}\psi_{G1(A)}$
$\phi_{G1,G2(A)}$	Both	Joint probability of moving from JPE/JPW toward Chipps Island (MAE/MAW), and surviving to MAE/MAW (Submodel II [route A])
$\phi_{G1,G2(B)}$	Full	Joint probability of moving from JPE/JPW toward Chipps Island (MAE/MAW), and surviving to MAE/MAW (Submodel I [route B])
ψ_{A1}	Both	Probability of remaining in the San Joaquin River at the head of Old River; = $1 - \psi_{B1}$
ψ_{A2}	Both	Probability of remaining in the San Joaquin River at the junction with Turner Cut; = $1 - \psi_{F2}$
ψ_{B1}	Both	Probability of entering Old River at the head of Old River; = $1 - \psi_{A1}$
ψ_{B2}	Full	Probability of remaining in Old River at the head of Middle River; = $1 - \psi_{C2}$
ψ_{C2}	Full	Probability of entering Middle River at the head of Middle River; = $1 - \psi_{B2}$
ψ_{F2}	Both	Probability of entering Turner Cut at the junction with the San Joaquin River; = $1 - \psi_{A2}$
$\psi_{G1(A)}$	Full	Probability of moving downriver in the San Joaquin River at the Jersey Point/False River junction (Submodel II [route A]); = $1 - \psi_{H1(A)}$
$\psi_{G1(B)}$	Full	Probability of moving downriver in the San Joaquin River at the Jersey Point/False River junction (Submodel I [route B]); = $1 - \psi_{H1(B)}$

Table A5-1. (Continued)

Parameter	Model	Definition
$\Psi_{H1(A)}$	Full	Probability of entering False River at the Jersey Point/False River junction (Submodel II [route A]); = $1 - \Psi_{G1(A)}$
$\Psi_{H1(B)}$	Full	Probability of entering False River at the Jersey Point/False River junction (Submodel I [route B]); = $1 - \Psi_{G1(B)}$
P_{A0a}	Full	Conditional probability of detection at DFU1
P_{A0b}	Full	Conditional probability of detection at DFU2
P_{A2a}	Both	Conditional probability of detection at DFD1
P_{A2b}	Both	Conditional probability of detection at DFD2
P_{A2}	Both	Conditional probability of detection at DFD (either DFD1 or DFD2)
P_{A3}	Both	Conditional probability of detection at BCA
P_{A4}	Both	Conditional probability of detection at MOS
P_{A5}	Both	Conditional probability of detection at SJL
P_{A6}	Both	Conditional probability of detection at SJG
P_{A7}	Both	Conditional probability of detection at SJNB
P_{A8a}	Both	Conditional probability of detection at MACU
P_{A8b}	Both	Conditional probability of detection at MACD
P_{A8}	Both	Conditional probability of detection at MAC (either MACU or MACD)
P_{A9a}	Both	Conditional probability of detection at MFE
P_{A9b}	Both	Conditional probability of detection at MFW
P_{A9}	Both	Conditional probability of detection at MFE or MFW
P_{B1}	Both	Conditional probability of detection at ORE
P_{B2a}	Both	Conditional probability of detection at ORSU
P_{B2b}	Both	Conditional probability of detection at ORSD
P_{B2}	Both	Conditional probability of detection at ORS (either ORSU or ORSD)
P_{B3a}	Full	Conditional probability of detection at OR4U
P_{B3b}	Full	Conditional probability of detection at OR4D
P_{C1}	Full	Conditional probability of detection at MRH
P_{C2a}	Full	Conditional probability of detection at MR4U
P_{C2b}	Full	Conditional probability of detection at MR4D
P_{D1}	Full	Conditional probability of detection at RGU (either RGU1 or RGU2)
P_{D2a}	Full	Conditional probability of detection at RGD1
P_{D2b}	Full	Conditional probability of detection at RGD2
P_{E1}	Full	Conditional probability of detection at CVP
P_{E2}	Full	Conditional probability of detection at CVPtank
P_{F1a}	Both	Conditional probability of detection at TCE
P_{F1b}	Both	Conditional probability of detection at TCW
P_{F1}	Both	Conditional probability of detection at TCE/TCW
P_{G1a}	Both	Conditional probability of detection at JPE
P_{G1b}	Both	Conditional probability of detection at JPW

Table A5-1. (Continued)

Parameter	Model	Definition
P_{G1}	Both	Conditional probability of detection at JPE/JPW
P_{G2a}	Both	Conditional probability of detection at MAE
P_{G2b}	Both	Conditional probability of detection at MAW
P_{G2}	Both	Conditional probability of detection at MAE/MAW
P_{H1a}	Full	Conditional probability of detection at FRW
P_{H1b}	Full	Conditional probability of detection at FRE

Table A5-2. Parameter estimates (standard errors in parentheses) from reduced survival model for tagged juvenile Chinook Salmon released in 2012, excluding predator-type detections. Parameters without standard errors were estimated at fixed values in the model. Population-level estimates are from pooled release groups. Some parameters were not estimable because of sparse data.

Parameter	Release Occasion		Population Estimate
	1	2	
S_{A2}	0.90 (0.06)	0.63 (0.04)	0.79 (0.04)
S_{A3}	0.78 (0.04)	0.59 (0.03)	0.65 (0.03)
S_{A4}	0.98 (0.01)	0.89 (0.02)	0.95 (0.01)
S_{A5}	0.81 (0.02)	0.48 (0.04)	0.69 (0.02)
S_{A6}	0.85 (0.03)	0.73 (0.08)	0.82 (0.03)
S_{A7}	0.49 (0.04)	0.23 (0.06)	0.44 (0.03)
$S_{A7,G2}$	0.07 (0.02)	0	0.06 (0.01)
$S_{A8,G2}$	0.16 (0.04)	0	0.14 (0.04)
$S_{B2,G2}$	0.17 (0.15)	0	0.13 (0.12)
$S_{F1,G2}$	0	0	0
$\phi_{A1,A2}$	0.89 (0.05)	1.00 (0.06)	0.97 (0.04)
$\phi_{A1,A3}$	0.80 (0.04)	0.63 (0.03)	0.76 (0.02)
$\phi_{A8,A9}$	0.44 (0.05)	0.59 (0.16)	0.45 (0.05)
$\phi_{A8,G1}$	0.08 (0.03)	0	0.07 (0.03)
$\phi_{A9,G1}$	0.49 (0.09)	0.33 (0.19)	0.46 (0.08)
$\phi_{B1,B2}$	1	0.67 (0.27)	0.89 (0.10)
$\phi_{F1,G1}$	0	0	0
$\phi_{G1,G2(A)}$	0.54 (0.10)	0	0.52 (0.01)
ψ_{A1}	0.98 (0.01)	0.98 (0.01)	0.98 (0.01)
ψ_{A2}	0.89 (0.03)	0.84 (0.11)	0.89 (0.03)
ψ_{B1}	0.02 (0.01)	0.02 (0.01)	0.02 (0.01)
ψ_{F2}	0.11 (0.03)	0.16 (0.11)	0.11 (0.03)
P_{A2a}	[pooled]	[pooled]	[pooled]
P_{A2b}	[pooled]	[pooled]	[pooled]
P_{A2}	0.23 (0.02)	0.33 (0.03)	0.27 (0.02)
P_{A3}	0.31 (0.03)	0.80 (0.03)	0.49 (0.02)
P_{A4}	1.00 (< 0.01)	1	1.00 (< 0.01)
P_{A5}	1	1	1
P_{A6}	1	1	1
P_{A7}	0.94 (0.02)	0.92 (0.08)	0.94 (0.02)
P_{A8a}	[pooled]	0.88 (0.12)	0.94 (0.02)
P_{A8b}	[pooled]	0.78 (0.14)	0.90 (0.03)
P_{A8}	1	0.97 (0.03)	0.99 (< 0.01)
P_{A9a}	1	1	1
P_{A9b}	1	1	1
P_{A9}	1	1	1
P_{B1}	1	1	1

Table A5-2. (Continued)

Parameter	Release Occasion		Population Estimate
	1	2	
P _{B2a}	1	[pooled]	1
P _{B2b}	0.83 (0.15)	[pooled]	1.00 (< 0.01)
P _{B2}	1	1	1
P _{F1a}	0.88 (0.12)	1	0.90 (0.09)
P _{F1b}	0.78 (0.14)	1	0.82 (0.12)
P _{F1}	0.97 (0.03)	1	0.98 (0.02)
P _{G1a}	[pooled]	1	0.96 (0.04)
P _{G1b}	[pooled]	1	0.92 (0.05)
P _{G1}	0.93 (0.07)	1	1.00 (< 0.01)
P _{G2a}	1		1
P _{G2b}	1		1
P _{G2}	1		1

Table A5-3. Parameter estimates (standard errors in parentheses) from reduced survival model for tagged juvenile Chinook Salmon released in 2012, including predator-type detections. Parameters without standard errors were estimated at fixed values in the model. Population-level estimates are from pooled release groups. Some parameters were not estimable because of sparse data.

Parameter	Release Occasion		Population Estimate
	1	2	
S_{A2}	0.87 (0.06)	0.62 (0.04)	0.77 (0.04)
S_{A3}	0.77 (0.04)	0.59 (0.03)	0.65 (0.02)
S_{A4}	0.98 (0.01)	0.90 (0.02)	0.95 (0.01)
S_{A5}	0.81 (0.02)	0.49 (0.04)	0.70 (0.02)
S_{A6}	0.86 (0.03)	0.73 (0.07)	0.82 (0.03)
S_{A7}	0.50 (0.04)	0.26 (0.06)	0.44 (0.03)
$S_{A7,G2}$	0.07 (0.02)	0	0.06 (0.01)
$S_{A8,G2}$	0.16 (0.04)	0	0.14 (0.03)
$S_{B2,G2}$	0.17 (0.15)	0	0.11 (0.11)
$S_{F1,G2}$	0	0	0
$\phi_{A1,A2}$	0.93 (0.05)	1.03 (0.06)	1.00 (0.04)
$\phi_{A1,A3}$	0.81 (0.04)	0.64 (0.03)	0.77 (0.03)
$\phi_{A8,A9}$	0.43 (0.05)	0.49 (0.14)	0.44 (0.05)
$\phi_{A8,G1}$	0.08 (0.03)	0	0.07 (0.03)
$\phi_{A9,G1}$	0.49 (0.09)	0.33 (0.19)	0.46 (0.08)
$\phi_{B1,B2}$	1	1	1
$\phi_{F1,G1}$	0	0	0
$\phi_{G1,G2(A)}$	0.54 (0.10)	0	0.52 (0.10)
ψ_{A1}	0.98 (0.01)	0.98 (0.01)	0.98 (0.01)
ψ_{A2}	0.88 (0.03)	0.86 (0.09)	0.88 (0.03)
ψ_{B1}	0.02 (0.01)	0.02 (0.01)	0.02 (0.01)
ψ_{F2}	0.12 (0.03)	0.14 (0.09)	0.12 (0.03)
P_{A2a}	[pooled]	[pooled]	[pooled]
P_{A2b}	[pooled]	[pooled]	[pooled]
P_{A2}	0.23 (0.02)	0.34 (0.03)	0.28 (0.02)
P_{A3}	0.31 (0.03)	0.80 (0.03)	0.49 (0.02)
P_{A4}	1.00 (< 0.01)	1	1.00 (< 0.01)
P_{A5}	1	1	1
P_{A6}	1	1	1
P_{A7}	0.94 (0.02)	0.93 (0.07)	0.94 (0.02)
P_{A8a}	[pooled]	0.87 (0.12)	[pooled]
P_{A8b}	[pooled]	0.64 (0.15)	[pooled]
P_{A8}	1	0.95 (0.05)	1
P_{A9a}	1	1	1
P_{A9b}	1	1	1
P_{A9}	1	1	1
P_{B1}	1	1	1

Table A5-3. (Continued)

Parameter	Release Occasion		Population Estimate
	1	2	
P _{B2a}	1	[pooled]	1
P _{B2b}	0.83 (0.15)	[pooled]	0.56 (0.17)
P _{B2}	1	1	1
P _{F1a}	0.86 (0.13)	1	0.89 (0.10)
P _{F1b}	0.60 (0.15)	1	0.67 (0.14)
P _{F1}	0.94 (0.06)	1	0.96 (0.04)
P _{G1a}	[pooled]	1	0.96 (0.04)
P _{G1b}	[pooled]	1	0.92 (0.05)
P _{G1}	0.93 (0.07)	1	1.00 (< 0.01)
P _{G2a}	1		1
P _{G2b}	1		1
P _{G2}	1		1

Appendix B. Errata from 2011 VAMP Report

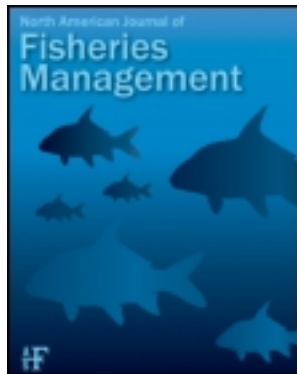
In Table H-2 (page 283) of the 2011 VAMP report (SJRG 2013), the definition for parameter $\phi_{A8,G2}$ should read “Overall survival from STN to Chipps Island (CHPE/CHPW).”

This article was downloaded by: [University of California Davis]

On: 26 November 2013, At: 15:20

Publisher: Taylor & Francis

Informa Ltd Registered in England and Wales Registered Number: 1072954 Registered office: Mortimer House, 37-41 Mortimer Street, London W1T 3JH, UK



North American Journal of Fisheries Management

Publication details, including instructions for authors and subscription information:

<http://www.tandfonline.com/loi/ujfm20>

Route Use and Survival of Juvenile Chinook Salmon through the San Joaquin River Delta

Rebecca A. Buchanan^a, John R. Skalski^a, Patricia L. Brandes^b & Andrea Fuller^c

^a Columbia Basin Research, School of Aquatic and Fishery Sciences, University of Washington, 1325 4th Avenue, Suite 1820, Seattle, Washington, 98101-2509, USA

^b U.S. Fish and Wildlife Service, 850 Guild Avenue, Suite 105, Lodi, California, 96240, USA

^c FISHBIO Environmental, LLC, 1617 South Yosemite Avenue, Oakdale, California, 95361, USA

Published online: 01 Feb 2013.

To cite this article: Rebecca A. Buchanan, John R. Skalski, Patricia L. Brandes & Andrea Fuller (2013) Route Use and Survival of Juvenile Chinook Salmon through the San Joaquin River Delta, North American Journal of Fisheries Management, 33:1, 216-229, DOI: [10.1080/02755947.2012.728178](https://doi.org/10.1080/02755947.2012.728178)

To link to this article: <http://dx.doi.org/10.1080/02755947.2012.728178>

PLEASE SCROLL DOWN FOR ARTICLE

Taylor & Francis makes every effort to ensure the accuracy of all the information (the "Content") contained in the publications on our platform. However, Taylor & Francis, our agents, and our licensors make no representations or warranties whatsoever as to the accuracy, completeness, or suitability for any purpose of the Content. Any opinions and views expressed in this publication are the opinions and views of the authors, and are not the views of or endorsed by Taylor & Francis. The accuracy of the Content should not be relied upon and should be independently verified with primary sources of information. Taylor and Francis shall not be liable for any losses, actions, claims, proceedings, demands, costs, expenses, damages, and other liabilities whatsoever or howsoever caused arising directly or indirectly in connection with, in relation to or arising out of the use of the Content.

This article may be used for research, teaching, and private study purposes. Any substantial or systematic reproduction, redistribution, reselling, loan, sub-licensing, systematic supply, or distribution in any form to anyone is expressly forbidden. Terms & Conditions of access and use can be found at <http://www.tandfonline.com/page/terms-and-conditions>

ARTICLE

Route Use and Survival of Juvenile Chinook Salmon through the San Joaquin River Delta

Rebecca A. Buchanan* and John R. Skalski

Columbia Basin Research, School of Aquatic and Fishery Sciences, University of Washington, 1325 4th Avenue, Suite 1820, Seattle, Washington 98101-2509, USA

Patricia L. Brandes

U.S. Fish and Wildlife Service, 850 Guild Avenue, Suite 105, Lodi, California 96240, USA

Andrea Fuller

FISHBIO Environmental, LLC, 1617 South Yosemite Avenue, Oakdale, California 95361, USA

Abstract

The survival of juvenile Chinook Salmon through the lower San Joaquin River and Sacramento–San Joaquin River Delta in California was estimated using acoustic tags in the spring of 2009 and 2010. The focus was on route use and survival within two major routes through the Delta: the San Joaquin River, which skirts most of the interior Delta to the east, and the Old River, a tributary of the San Joaquin River leading to federal and state water export facilities that pump water out of the Delta. The estimated probability of using the Old River route was 0.47 in both 2009 and 2010. Survival through the southern (i.e., upstream) portion of the Delta was very low in 2009, estimated at 0.06, and there was no significant difference between the Old River and San Joaquin River routes. Estimated survival through the Southern Delta was considerably higher in 2010 (0.56), being higher in the Old River route than in the San Joaquin route. Total estimated survival through the entire Delta (estimated only in 2010) was low (0.05); again, survival was higher through the Old River. Most fish in the Old River that survived to the end of the Delta had been salvaged from the federal water export facility on the Old River and trucked around the remainder of the Delta. The very low survival estimates reported here are considerably lower than observed salmon survival through comparable reaches of other large West Coast river systems and are unlikely to be sustainable for this salmon population. More research into mortality factors in the Delta and new management actions will be necessary to recover this population.

The Central Valley of California marks the southern limit of Chinook Salmon *Oncorhynchus tshawytscha* in North America (Healey 1991). Chinook Salmon population abundances in this region have been much reduced from the 19th century in response to a number of factors, including habitat loss, hatcheries, and water development (e.g., pumping water out of the basin; Healey 1991; Fisher 1994). Today, the Sacramento–San Joaquin River Delta is a highly modified environment with levees and drained fields replacing tidal wetlands, and riprap replacing natural shoreline. Demand for Delta waters is high. State and federal water export facilities

extract water from the southern portion of the Delta (Figure 1) for agricultural, industrial, and municipal use throughout California. The Delta provides drinking water for approximately 27 million Californians and irrigation water for more than 1,800 agricultural users, and 4.6–6.3 million acre-feet of water are exported from the Delta annually (DSC 2011). This intense exporting combined with tidal fluctuations can sometimes cause net flows in the Delta to be directed upstream rather than downstream (Brandes and McLain 2001). Pollution from industry, agricultural and urban runoff, and erosion are also concerns (DSC 2011). Both native and nonnative species of

*Corresponding author: rabuchan@u.washington.edu
Received March 28, 2012; accepted September 5, 2012
Published online February 1, 2013

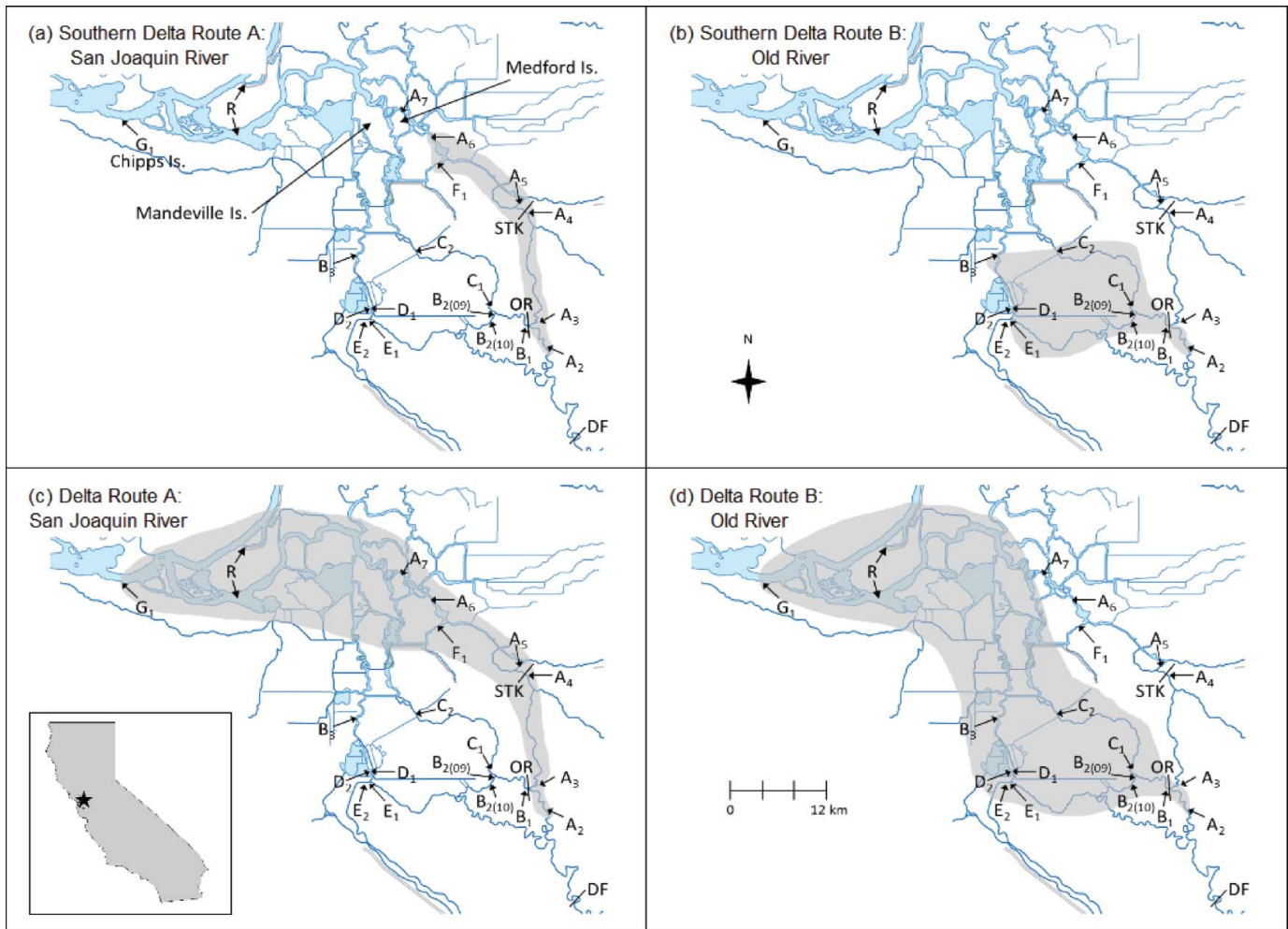


FIGURE 1. Acoustic telemetry receiver sites throughout the San Joaquin River Delta for the juvenile Chinook Salmon tagging studies in 2009 and 2010. The region included in each major route through the study area is shaded for the Southern Delta for the (a) San Joaquin River and (b) Old River routes and through the entire Delta for the (c) San Joaquin River and (d) Old River routes. Sites in the San Joaquin, Old, and Middle rivers are labeled A, B, and C, respectively. The label for site B2 includes the study years 2009 (09) and 2010 (10). Sites A7, C1, and G1 were used only in 2010. Mossdale is denoted by A2, Chipps Island at river kilometer 0 by G1, the federal water export facilities by E1 and E2, and state water export facilities by D1 and D2. The city of Stockton is near sites A5 and A6. Sites B3 and C2 are located near California Highway 4. Release sites are designated as follows: DF = Durham Ferry (2009, 2010), OR = Old River (2010), STK = Stockton (2010), and R = release after salvage and trucking. Route-specific survival and route entrainment probability were estimated for the Southern Delta in 2009 and 2010 and for the entire Delta in 2010. [Figure available in color online.]

predatory fish (e.g., Striped Bass *Morone saxatilis*, Largemouth Bass *Micropterus salmoides*, White Catfish *Ameiurus catus*) inhabit these areas and feed on migrating smolts, as do avian predators including double-crested cormorants *Phalacrocorax auritus* and white pelicans *Pelecanus erythrorhynchos*. All of these factors lower survival of migrating salmon smolts relative to historical conditions.

The Vernalis Adaptive Management Plan (VAMP) is a large-scale, long-term (12-year) experimental management program begun in 2000 that was designed to protect juvenile Chinook Salmon as they migrate from the San Joaquin River through the Sacramento–San Joaquin River Delta (Figure 1; SJRGA 2005, 2007, 2010, 2011). Part of the VAMP is a multiyear tagging study to monitor juvenile salmon survival through the Delta; the

long-term goal is to relate Delta survival to changes in river flow (discharge) and water export levels in the presence of a temporary barrier at the head of the Old River, which was designed to prevent salmon from entering the Old River (Figure 1). Prior to 2006, VAMP tagging studies relied on coded wire tags (CWTs), which provided information on salmon survival on a large spatial scale using 100,000–300,000 study fish each year (Newman 2008). Starting in 2006, the tagging studies began using micro-acoustic tags, which provide more precise survival information on a smaller spatial scale with much smaller releases groups (e.g., about 1,000 fish). Coded wire tags were discontinued in 2007. Study years 2006 and 2007 were pilot studies providing feedback on design and implementation of the acoustic tag studies. The 2008 study deployed an extensive array of acoustic

hydrophones throughout the Delta but suffered from a high degree of premature tag failure (Holbrook et al. 2013). Thus, 2009 and 2010 were the first years that provided sufficient information to estimate salmon survival through portions of the Delta on a relatively detailed spatial scale, yielding the first estimates of how fish distribute across various migration routes. Further, these 2 years represent different hydrologic conditions—very low flows in 2009 and above normal flows in 2010—thus providing preliminary information needed to identify a relationship between survival and flow. Survival through the southern portion of the Delta was estimated in both 2009 and 2010, and survival through the entire Delta was estimated in 2010 (described below; Figure 1). In both years, survival estimates were compared through two major migration routes: the San Joaquin River route and the Old River route. We present here the first spatially detailed estimates of survival and route use by juvenile Chinook Salmon through the lower San Joaquin River into the Delta.

STUDY AREA

Historically, focus has been on the survival of fish through the Delta to Chipps Island, located in Suisan Bay at the confluence of the San Joaquin and Sacramento rivers near Pittsburg, California, at river kilometer (rkm) 0 (Figure 1). Fish moving through the Delta toward Chipps Island may use any of several routes. The simplest route follows the San Joaquin River until it joins the Sacramento River near Chipps Island (Figure 1a, c; route A). An alternative route uses the Old River from its head on the San Joaquin River to Chipps Island, either via its confluence with the San Joaquin River just west of Mandeville Island, or through Middle River or the state and federal water export facilities (Figure 1b, d; route B). Additional subroutes were monitored for fish use but were contained within either route A or route B. Subroute C consists of the Middle River from the Old River to the San Joaquin downstream of Medford Island. Two other subroutes were the water export facilities off the Old River: fish entering either the State Water Project (subroute D) or the Central Valley Project (subroute E) had the possibility of being trucked from those sites and released upstream of Chipps Island. Subroutes C, D, and E were all contained in route B (Old River). Finally, fish that remained in the San Joaquin River past Stockton may have entered Turner Cut and maneuvered to Chipps Island through the interior of the Delta (subroute F). Fish in routes B, C, and F all had multiple unmonitored pathways available for passing through the Delta toward Chipps Island.

Survival through the study area was estimated on two spatial scales: (1) the southern portion of the Delta, which is bounded downstream by the federal and state water export facilities, California Highway 4, and the Turner Cut junction with the San Joaquin River (the “Southern Delta”; Figure 1a, b) and (2) the entire Delta, which is bounded downstream by Chipps Island (the “Delta”; Figure 1c, d). Both the Southern Delta and Delta regions were bounded upstream by the acoustic receiver (site A2) located near Mossdale Bridge, upstream of the Old River

junction with the San Joaquin River. The Southern Delta region was entirely contained within the Delta region (Figure 1). In 2009, no acoustic receivers were deployed at Chipps Island, so the study area was limited to the Southern Delta. In 2010, a more extensive detection field was installed, including dual receivers at Chipps Island (G1) (Figure 1). Thus, in 2010, the study area included the entire migration path through the Delta region. Two migration routes were monitored through both the Southern Delta and Delta regions: the San Joaquin Route (route A in Figure 1a, c) and the Old River route (route B in Figure 1b, d).

Since the 1990s, a temporary physical or nonphysical barrier (sound, strobe lights, and a bubble curtain) has often been installed at the head of the Old River with the aim of preventing migrating smolts from entering that river. In 2009 and 2010, a nonphysical barrier was installed there, and its smolt-guidance effectiveness was evaluated in studies concurrent with the VAMP studies (Bowen et al. 2009; Bowen and Bark 2012). The nonphysical barrier was operated during passage of approximately half of each VAMP release group in 2009 or 2010. No physical barrier was installed.

METHODS

Tagging and release methods.—Both study years used the Hydroacoustic Technology, Inc. (HTI) Model 795 microacoustic tag (diameter = 6.7 mm, length = 16.3–16.4 mm, average weight in air = 0.65 g). In 2009 a total of 933 juvenile Chinook Salmon (fall–spring-run hybrids) originating from the Feather River Fish Hatchery were tagged and released between 22 April and 13 May (fork length = 85.0–110.0 mm, mean = 94.8 mm; Table 1). Difficulties in rearing fish to size resulted in an average tag burden (i.e., the ratio of tag weight to body weight) of 7.1% (range = 4.4–10.2%), which was higher than desired ($\leq 5.5\%$; Brown et al. 2006). Six fish died in 2009 between tagging and release. In 2010, a total of 993 juvenile fall-run Chinook Salmon originating from the Merced River Fish Hatchery were tagged and released between 27 April and 20 May (fork length = 99.0–121.0 mm, mean = 110.5 mm). Tag burden in 2010 was 2.8–5.8% (mean = 4.2%; Table 1). Four fish died in 2010 between tagging and release.

In both years, tagging was performed at the Tracy Fish Facility located in the Delta approximately 30–45 km from the release site(s). Tagging procedures followed those outlined in Adams et al. (1998) and Martinelli et al. (1998). Fish were anesthetized in a 70-mg/L tricaine methanesulfonate solution, buffered with an equal concentration of sodium bicarbonate, and surgically implanted with programmed acoustic transmitters. Typical surgery times were less than 3 min. Nonfunctioning tags were removed from the study. After surgery, fish were placed in 19-L containers with high dissolved oxygen (DO) concentrations (110–130%) for recovery. Each holding container was perforated to allow partial water transfer and held no more than three tagged fish. After initial recovery from surgery, tagged fish were transported in buckets to the release site in transport

TABLE 1. Release data for groups of Chinook salmon smolts used in the 2009 and 2010 Vernalis Adaptive Management Plan studies, where DF = Durham Ferry, STK = Stockton, and OR = Old River. In 2009, releases were pooled into strata for analysis; in 2010, releases from separate locations were jointly analyzed for a single release occasion.

Release location	Release date	Release number	Mean (range) fork length (mm)	Tag burden (%)	Release stratum/occasion
Study year 2009					
DF	Apr 22	133	96.1 (86–108)	6.9 (5.2–9.0)	1
	Apr 25	134	93.4 (88–105)	7.3 (5.2–9.6)	1
	Apr 29	134	97.1 (87–110)	6.8 (4.5–3.6)	2
	May 2	134	96.6 (87–108)	6.6 (4.4–9.3)	2
	May 6	132	92.6 (85–102)	7.7 (5.5–10.2)	2
	May 9	133	93.9 (88–100)	7.3 (5.4–9.1)	2
	May 13	133	93.8 (90–104)	7.2 (5.3–8.8)	3
Study year 2010					
DF	Apr 27–28	74	108.0 (102–110)	4.4 (3.5–5.7)	1
	Apr 30–May 1	74	109.1 (103–115)	4.3 (3.1–5.4)	2
	May 4–5	73	109.4 (102–118)	4.3 (3.4–5.6)	3
	May 7–8	70	111.1 (101–119)	4.1 (3.1–5.4)	4
	May 11–12	70	112.0 (99–121)	4.1 (3.1–5.4)	5
	May 14–15	73	112.6 (101–119)	4.0 (3.1–5.3)	6
	May 18–19	70	112.1 (103–119)	3.9 (2.8–5.3)	7
STK	Apr 28–29	35	107.5 (100–115)	4.5 (3.5–5.6)	1
	May 1–2	36	108.5 (100–115)	4.4 (3.4–5.4)	2
	May 5–6	35	110.3 (104–118)	4.2 (3.4–5.0)	3
	May 8–9	36	109.6 (102–117)	4.3 (3.5–5.6)	4
	May 12–13	35	111.2 (105–119)	4.2 (3.3–5.4)	5
	May 15–16	34	112.9 (102–119)	4.0 (3.0–5.2)	6
	May 19–20	31	113.4 (108–119)	3.9 (3.1–5.0)	7
OR	Apr 28–29	36	108.2 (102–117)	4.5 (3.6–5.3)	1
	May 1–2	36	108.5 (102–115)	4.5 (3.5–5.6)	2
	May 5–6	36	108.6 (100–118)	4.5 (3.4–5.6)	3
	May 8–9	36	110.4 (104–118)	4.2 (3.5–5.1)	4
	May 12–13	36	111.8 (104–120)	4.2 (2.9–5.8)	5
	May 15–16	35	113.3 (105–119)	4.0 (3.0–5.2)	6
	May 19–20	32	112.3 (101–119)	3.9 (3.2–5.3)	7

tanks designed to guard against fluctuations in water temperature and DO. Transport to the release site took approximately 45–60 min. At the release site, tagged fish were held in either 1-m³ net pens (3-mm mesh; first release in 2009) or in perforated 121.1-L plastic garbage cans (2010) for a minimum of 24 h before release.

In 2009, all fish were released on the San Joaquin River at Durham Ferry, located at approximately rkm 110 (measured from the river mouth at Chipps Island) approximately 20 km upstream of the boundary of the study area (Mossdale Bridge; Figure 1). The release site was located upstream of the study area to allow fish to recover from handling and distribute naturally in the river channel before entering the study area. In 2010, each of seven release occasions consisted of an initial release at Durham Ferry and two supplemental releases, one located in the Old River near the junction with the San Joaquin River

and the other located in the San Joaquin River near the city of Stockton (Figure 1). The supplemental releases were designed to provide enough tagged fish in the lower reaches of the study area to estimate survival all the way to Chipps Island, even if survival was low from Durham Ferry.

For each study year, an in-tank tag life study was performed to measure the rate of tag failure under the tag operating parameters (i.e., encoding, range, and pulse width) used in the study. Stratified random sampling of tags across manufacturing lots and tag codes was used to ensure that tags in the tag-life study represented the population of tags released in study fish.

In both study years, tag effects on short-term (48-h) survival were assessed using dummy (i.e., inactive)-tagged and untagged fish that were handled using the same procedures as fish with active transmitters. No significant difference in survival was observed between dummy-tagged and untagged fish over the

48-h period (SRJGA 2010, 2011). Tag effects on longer-term (≤ 21 d) survival and predator avoidance were expected to be small based on existing studies on effects of acoustic tags on juvenile Chinook Salmon with comparable tag burden (e.g., Anglea et al. 2004).

Water temperatures at the release locations were $< 20^{\circ}\text{C}$ during most releases, ranging from 16.1°C to 21.1°C in 2009 and from 14.2°C to 18.8°C in 2010. Temperature increased as a function of distance downstream from Durham Ferry in both the San Joaquin River main stem and the Delta and increased throughout the season. Temperatures in the study area exceeded 20°C starting in mid-May in 2009 and in early June in 2010.

Hydrophone placement.—An extensive array of acoustic hydrophones and receivers was deployed throughout the Delta in each study year, with 19 receivers and hydrophones being deployed in 2009 and 32 receivers (35 hydrophones) in 2010 (Figure 1). Acoustic receivers were named according to migration route (A–G). Chippis Island, the final destination of all routes in 2010, was assigned its own route name (G). At each location, one to four hydrophones were deployed to achieve full cross-sectional coverage of the channel.

Acoustic receivers were located at the Delta entrance (Mosssdale, site A2) in both 2009 and 2010, at the Delta exit (Chippis Island, G1) in 2010, and at key points in between in both years (Figure 1). The Mosssdale site was moved 1.4 km downstream in 2010 to an acoustically quieter site. All available migration routes were monitored at the Old River (sites A3 and B1) and Turner Cut (A6 and F1) diversions from the San Joaquin River (Figure 1). Receivers were located on the San Joaquin River in Stockton near the Stockton Waste Water Treatment Facility (A4) and near the Navy Drive Bridge just upstream of the Stockton Deep Water Ship Channel (A5) because of concern about salmon survival past the water treatment plant. Receivers were also located at the entrance to the state and federal water export facilities on the Old River (Figure 1). At the federal facility (Central Valley Project, CVP), receivers were placed just upstream and downstream of the trash racks (E1) and in the holding tank (E2), where salvaged fish were held before transportation by truck to release sites in the lower Delta on the San Joaquin and Sacramento rivers (R). At the state facility, receivers were placed both outside (D1) and inside (D2) the radial entrance gates to the Clifton Court Forebay (CCF), the reservoir from which the State Water Project draws water. Both the CVP trash racks and the CCF radial gates are known feeding areas for piscine predators (Vogel 2010, 2011). Receivers were also located downstream in the Old (B3) and Middle (C2) rivers near the Highway 4 bridge. Dual receiver arrays were placed at some sites to provide data to estimate detection probabilities, typically at the downstream boundary of the study area and at sites just downstream of river junctions. Both acoustic lines within each dual array (average 0.3 km apart) were designed for full coverage of the channel. The nonphysical barrier located at the head of the Old River was evaluated via a separate network of hydrophones that were not used in the VAMP study (Bowen et al. 2009; Bowen and Bark 2012).

The locations of the hydrophones were dictated by the possible migration routes (San Joaquin [A], and Old River [B]) and subroutes, and by the two spatial scales on which inference was to be made (Southern Delta and Delta). The acoustic receivers located in Turner Cut (F1) and at the channel markers in the San Joaquin River near the Turner Cut junction (A6) monitored the exit of the San Joaquin route through the Southern Delta region in both 2009 and 2010 (Figure 1a). Likewise, the exit of the Old River route through the Southern Delta region was monitored by receivers at the state and federal water facilities and near Highway 4 in both 2009 and 2010 (Figure 1b). In 2010, the exit of both the San Joaquin route (Figure 1c) and the Old River route (Figure 1d) through the entire Delta region was monitored by dual receivers at Chippis Island.

Signal processing.—The raw tag detection data generated by the acoustic telemetry receivers were processed by identifying the date and time of each tag detection. Unique tags were identified by the period ($1/\text{frequency}$) of the acoustic signal. The 2009 data were processed manually using the HTI proprietary software *MarkTags*. The 2010 data were processed using a combination of automatic and manual processing, manual processing being limited to key detection sites (SJRGGA 2011).

The San Joaquin River Delta is home to several populations of predatory fish that are large enough to feed on juvenile salmonids, including Striped Bass, Largemouth Bass, and White Catfish. A predatory fish that has eaten an acoustic-tagged juvenile salmon and then moves past a hydrophone may introduce misleading tag detections into the data. Thus, it was necessary to identify and remove those detections that came from predators. Likely predator detections were identified in a decision process that used up to three levels of spatial–temporal analysis, based on the methods of Vogel (2010, 2011): near-field, mid-field, and far-field. Near-field analysis required manual processing of the raw acoustic telemetry data, and interpreted the pattern of the acoustic signal during detection as an indicator of fish movement near the receiver. Mid-field analysis focused on residence time within the detection field of each receiver, and transitions between neighboring receivers. Far-field analysis examined transitions on the scale of the study area. All available detection data were considered in identifying likely predator detections, as well as environmental data such as river flow and tidal stage, measured at several gaging stations throughout the Delta (downloaded from the California Data Exchange Center Web site: <http://cdec.water.ca.gov>). The predator decision process was based on the assumptions that Chinook Salmon smolts were emigrating and so were directed downstream, and that they were unlikely to move between acoustic receivers (≥ 2 km) against river flow. Movements directed upstream against the flow were considered evidence of predation, although short-term upstream movements under reverse flow or slack tide conditions were deemed consistent with a salmon smolt. Unusually fast or slow transitions between detection sites or particularly long residence time at a detection site were also considered evidence of predation. In 2009, the near-field analysis comprised the majority of the predation decision process. In 2010, more emphasis

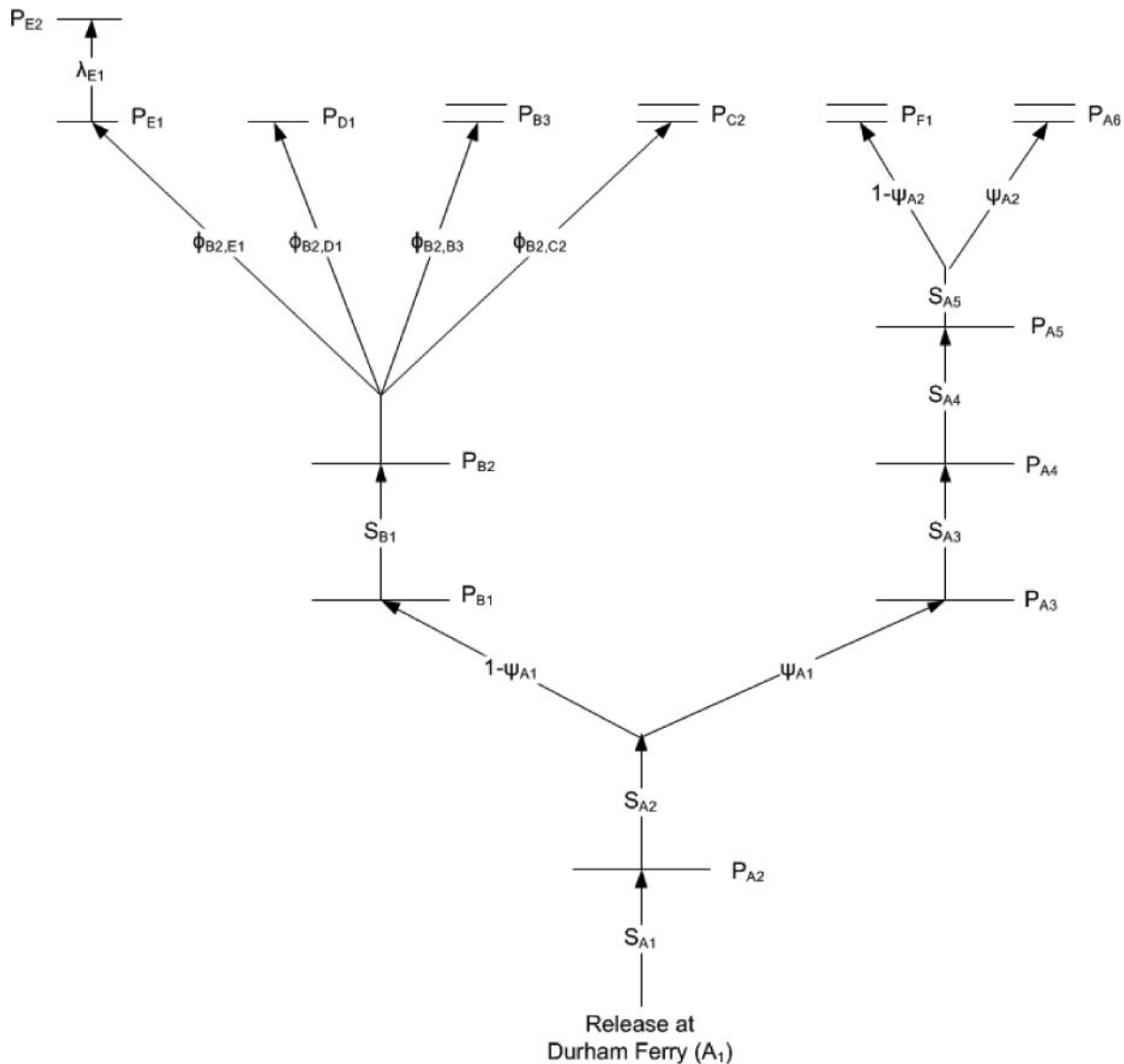


FIGURE 2. Model schematic for the 2009 Chinook Salmon smolt tagging study. Horizontal lines indicate acoustic receivers; parallel lines indicate dual receiver arrays. Model parameters are salmon reach survival (S), detection probabilities (P), route entrainment probabilities (ψ), transition probabilities ($\phi = \psi S$), and "last reach" parameters ($\lambda = \phi P$).

was placed on travel time, residence time, and movements in relation to river flow (mid-field and far-field analysis).

After removing the suspected predator detections, the processed data were converted to individual detection histories for each tagged fish. The detection history identified the chronological sequence of sites where the tag was detected. In the event that a tag was detected at a site or river junction multiple times, the last path past the site or river junction was used in the detection history as the best depiction of the final fate of the fish in the region.

Statistical survival and migration model.—A multistate statistical release–recapture model (Buchanan and Skalski 2010) was developed and used to estimate salmon smolt survival, de-

tection probabilities, and route-use ("entrainment") probabilities (Figures 2, 3). The release–recapture model was similar to the model developed by Perry et al. (2010), with states representing the various routes through the Delta. Detection sites (acoustic receivers) were named according to route.

The release–recapture models used for both study years used parameters that denoted the probability of detection (P_{hi}), route entrainment probability (ψ_{hl}), salmon reach survival (S_{hi}), and transition probabilities ($\phi_{kj,hi}$) equivalent to the joint probability of movement and survival, where h and k represent route, i and j represent detection sites within a route, and l represents junctions within a route (Figures 2, 3). The transition probability $\phi_{kj,hi}$ from site j in route k to site i in route h included all

possible routes between the two sites and was used when it was not possible to separately estimate the route entrainment and survival probabilities. Unique transition parameters were estimated at receiver D1 located outside the radial gates of the Clifton Court Forebay depending on gate status at the time of fish arrival (open or closed) in the 2010 study. Gate status data were unavailable for the 2009 study.

In some cases, it was not possible to separately estimate the transition probability to a site and the detection probability at the site. This occurred primarily at the entrances to the water export facilities (E1 = CVP trash racks, and D1 = first CCF receiver) due to sparse data. In these cases, the joint probability of survival from the previous receiver to receiver i in route h was estimated as $\lambda_{hi} = \phi_{kj,hi} P_{hi}$. We assumed that the detection probability was 100% at the radial gate receivers inside Clifton Court Forebay and in the holding tank at the Central Valley Project. These assumptions, necessary in the absence of receivers located downstream of those detection sites and unique to those routes, were reasonable as long as the receivers were operating.

A multinomial likelihood model was constructed based on possible capture histories under the assumptions of common survival, route entrainment, and detection probabilities and independent detections among the tagged fish in each release group. The likelihood model was fit using maximum likelihood in the software Program USER (Lady and Skalski 2008), providing point estimates and standard errors of model parameters and derived performance measures.

In addition to the model parameters, performance at the migration route level was estimated as functions of the model parameters. The probability of a smolt taking the San Joaquin River route (route A) was ψ_{A1} , while the probability of using the Old River route (route B) was $1 - \psi_{A1}$. Regional passage survival (S_R for region R) was estimated on two spatial scales: the southern Delta ($R = SD$; 2009 and 2010) and the entire San Joaquin River delta ($R = D$) from Mossdale Bridge to Chipps Island (2010) (Figure 1). Regional passage survival for region R ($R = SD$ or D) was defined in terms of both the route entrainment probability (ψ_{A1}) and the route-specific survival probabilities:

$$S_R = \psi_{A1} S_{A(R)} + (1 - \psi_{A1}) S_{B(R)}.$$

The route-specific survival probabilities through region R (i.e., $S_{A(R)}$ and $S_{B(R)}$ for $R = SD$ or D) were defined as

$$S_{A(R)} = S_{A2} S_{A3} S_{A4} S_{A5(R)}$$

and

$$S_{B(R)} = S_{A2} S_{B1} S_{B2(R)}.$$

The survival probabilities through the final reaches of each route (i.e., $S_{A5(R)}$ and $S_{B2(R)}$) were defined as

$$S_{A5(R)} = \begin{cases} S_{A5}, & \text{for } R = SD \\ S_{A5}(\psi_{A2}\phi_{A6,A7}\phi_{A7,G1} + [1 - \psi_{A2}]\phi_{F1,G1}), & \text{for } R = D \end{cases}$$

and

$$S_{B2(R)} = \begin{cases} \phi_{B2,B3} + \phi_{B2,C2} + \phi_{B2,D1} + \phi_{B2,E1}, & \text{for } R = SD \\ \phi_{B2,B3}\phi_{B3,G1} + \phi_{B2,C2}\phi_{C2,G1} \\ \quad + \phi_{B2,D1}\phi_{D1,D2}\phi_{D2,G1} \\ \quad + \phi_{B2,E1}\phi_{E1,E2}\phi_{E2,G1}, & \text{for } R = D. \end{cases}$$

For fish that reached the interior receivers at the Clifton Court Forebay or CVP in 2010, the parameters $\phi_{D2,G1}$ and $\phi_{E2,G1}$ included survival during and after collection and transport. Although a subroute of the Old River route to Chipps Island, through Middle River from the junction with the Old River (subroute C) was monitored in 2010, no salmon were observed leaving the Old River at that junction (site C1). Thus, the probability of a smolt taking the Middle River route to Chipps Island was estimated to be zero.

In 2009, release groups were pooled into three strata based on release timing, common environmental conditions, and monitoring equipment status: stratum 1 = releases 1–2, stratum 2 = releases 3–6, and stratum 3 = release 7 (Table 1). Malfunctioning acoustic receivers meant that some parameters could not be estimated for some strata. Model selection was used to assess the effect of stratum on model parameters common to multiple strata. In 2010, data from each of the seven release occasions (initial release at Durham Ferry combined with supplemental releases) were analyzed separately. For each release occasion, several alternative survival models were fit, differing in whether the initial (Durham Ferry) and supplemental release groups shared common detection, route entrainment, and survival parameters over common reaches. Model selection was used to find the most parsimonious model that fit all the data, following the general approach described in Burnham et al. (1987) for comparing treatment groups. Detection probabilities were parameterized first, with survival, transition, and route entrainment probabilities parameterized next. Backwards selection was used to identify the farthest reach upstream for which parameters from the initial and supplemental releases could be equated without reducing model fit. The most general models were considered first, with unique parameters for each release group for all reaches, and tested against simpler models with common parameters across the initial and supplemental release groups for the downstream reaches. All models used unique survival and transition probabilities in the first reach downstream of the supplemental release sites. Model selection was performed using the Akaike Information Criterion (AIC) as described in Burnham and Anderson (2002). Final parameter estimates were weighted averages of the release-specific estimates from the selected model, with weights equal to the

number of fish from the release group present at the supplemental release site (estimated for the initial release group). Goodness of fit was assessed using Anscombe residuals (McCullagh and Nelder 1989: p. 38).

RESULTS

2009 Results

None of the 50 tags in the 2009 tag-life study failed before day 21. Because all detections of tagged salmon smolts occurred well before day 21 after tag activation, no adjustment for tag failure was made to the survival estimates from the release-recapture model.

Initial survival after release was low in 2009, with estimates of survival from Durham Ferry to the Mossdale Bridge (site A2, approximately 20 rkm) averaging 0.47 ($SE = 0.02$). The majority of the acoustic-tag detections downstream of Durham Ferry were at the upstream sites in the San Joaquin (A2, A3) and in the Old River (B1). Very few tagged salmon smolts were detected at the exit points of the Southern Delta region in either the San Joaquin River route or the Old River route. No tagged salmon were detected at the Turner Cut receivers (F1), the Middle River receivers at Highway 4 (C2), or the interior receivers at Clifton Court Forebay (D2).

Total salmon survival through the Southern Delta region (S_{SD}) was estimable only for stratum 2 (releases 3–6) because the failure of certain acoustic receivers resulted in missing data from the three other release groups. Estimated route-specific survival through the Southern Delta was $\hat{S}_{A(SD)} = 0.05$ ($SE = 0.02$) in the San Joaquin route and $\hat{S}_{B(SD)} = 0.08$ ($SE = 0.02$) in the Old River route (Table 2). Survival estimates through the Southern

Delta in the two routes were not significantly different (Z -test, $P = 0.4788$). The route entrainment probabilities at the junction of the Old River with the San Joaquin River were estimated at $\hat{\psi}_{A1} = 0.47$ ($SE = 0.03$) for the San Joaquin River, and $1 - \hat{\psi}_{A1} = 0.53$ ($SE = 0.03$) for the Old River. Consequently, overall survival through the Southern Delta in 2009 was estimated as $\hat{S}_{SD} = 0.06$ ($SE = 0.01$; Table 2).

The first two release groups in 2009 (stratum 1) showed a higher probability of entering the Old River ($1 - \hat{\psi}_{A1} = 0.64$; $SE = 0.04$) than remaining in the San Joaquin ($P = 0.0002$). Release groups 3–6 (stratum 2) showed no preference for either route ($P > 0.05$), with $1 - \hat{\psi}_{A1} = 0.48$ ($SE = 0.04$) for the Old River route entrainment probability. No estimates of the route entrainment probabilities were available for group 7 (stratum 3) because of equipment malfunction.

Median travel time through the Southern Delta reaches ranged from 0.2 d ($SE = 0.2$) from the Stockton USGS gauge (A4) to the Navy Drive Bridge in Stockton (A5; approximately 3 km), to 2.1 d ($SE = 0.3$) from Lathrop (A3) to the Stockton USGS gauge (A4; approximately 15 km).

2010 Results

Failure times of the 48 tags in the tag-life study ranged from 10 to 36 d. The early failure of several tags in the tag-life study made it necessary to incorporate tag-life adjustments into survival estimates (Townsend et al. 2006). The estimated probability of tag survival to the time of arrival at each detection site ranged from 0.987 to Chippis Island (G1) to 0.995 to Mossdale (A2). Tag survival estimates for the supplemental releases at the Old River and Stockton were generally higher than for the initial releases at Durham Ferry.

TABLE 2. Estimates of route-specific survival (S ; standard errors in parentheses) of Chinook Salmon smolts through the Southern Delta (SD) and the entire Delta to Chippis Island (D) in the San Joaquin River (A) and Old River (B) and route entrainment probability into the San Joaquin River (A) at the head of the Old River for study years 2009 and 2010. Estimates of survival through the entire Delta are not available for 2009.

Release date	Route entrainment $\hat{\psi}_{A1}$	Southern Delta survival			Entire Delta survival		
		$\hat{S}_{A(SD)}$	$\hat{S}_{B(SD)}$	\hat{S}_{SD}	$\hat{S}_{A(D)}$	$\hat{S}_{B(D)}$	\hat{S}_D
Study year 2009							
Apr 22–25	0.36 (0.04)						
Apr 29–May 9	0.52 (0.04)	0.05 (0.02)	0.08 (0.02)	0.06 (0.02)			
May 13				0.05 (0.03)			
Average	0.47 (0.03)	0.05 (0.02)	0.08 (0.02)	0.06 (0.01)			
Study year 2010							
Apr 27–29	0.48 (0.06)	0.47 (0.07)	0.78 (0.06)	0.63 (0.05)	0.07 (0.03)	0.00 (0.00)	0.03 (0.02)
Apr 30–May 2	0.44 (0.06)	0.40 (0.06)	0.90 (0.04)	0.68 (0.05)	0.01 (0.01)	0.03 (0.02)	0.02 (0.01)
May 4–6	0.39 (0.06)	0.16 (0.04)	0.75 (0.06)	0.52 (0.06)	0.01 (0.01)	0.01 (0.01)	0.01 (0.01)
May 7–9	0.52 (0.07)	0.24 (0.05)	0.56 (0.09)	0.39 (0.06)	0.04 (0.02)	0.10 (0.03)	0.06 (0.02)
May 11–13	0.45 (0.06)	0.49 (0.06)	0.88 (0.08)	0.71 (0.06)	0.06 (0.03)	0.13 (0.04)	0.10 (0.03)
May 14–16	0.43 (0.06)	0.11 (0.04)	0.68 (0.29)	0.43 (0.17)	0.01 (0.01)	0.07 (0.02)	0.05 (0.02)
May 18–20	0.59 (0.07)	0.35 (0.06)	0.83 (0.21)	0.55 (0.10)	0.07 (0.03)	0.15 (0.05)	0.10 (0.03)
Average	0.47 (0.02)	0.32 (0.02)	0.77 (0.06)	0.56 (0.03)	0.04 (0.01)	0.07 (0.01)	0.05 (0.01)

All releases in the 2010 study had high initial survival, with estimates of survival from Durham Ferry to the Mossdale Bridge receiver (site A2; approximately 21 km) averaging 0.94 (range = 0.86–1.00). The Old River supplemental release groups had an average estimated survival to the head of Middle River (sites B2, C1) of 0.89 (range = 0.84–0.97). The Stockton supplemental release groups had an average estimated survival to the Navy Bridge in Stockton (site A5) of 0.82–1.07 (average = 0.95). Only a single tag released at either Durham Ferry or the Old River was detected in Middle River, so Middle River was omitted from the survival model. None of the 14 tags detected at Turner Cut were subsequently detected at Chipps Island.

Estimates of the probability of fish remaining in the San Joaquin River at the head of the Old River in 2010 ranged from 0.39 to 0.59 across the seven release groups (average = 0.47; $SE = 0.02$; Table 2). Only for release 3 did fish show a statistically significant ($\alpha = 0.05$) preference for the Old River over the San Joaquin River ($P = 0.0443$; one-sided Z-test).

Route-specific survival through the Southern Delta region in 2010 had an average estimate of $\hat{S}_{A(SD)} = 0.32$ ($SE = 0.02$) in the San Joaquin route and $\hat{S}_{B(SD)} = 0.77$ ($SE = 0.05$) in the Old River route. For each release occasion, survival through the Southern Delta was significantly higher in the Old River route ($P \leq 0.003$; one-sided Z-test on the lognormal scale), which ended at the water export facilities and Highway 4. Combined salmon survival through the Southern Delta region in 2010 was estimated at $\hat{S}_{SD} = 0.56$ ($SE = 0.03$), averaged over all seven release groups (Table 2).

Survival through the entire San Joaquin River Delta region (from Mossdale to Chipps Island, approximately 89 km) was considerably lower than through only the Southern Delta region in 2010, the average overall estimate being $\hat{S}_D = 0.05$ ($SE = 0.01$; Table 2). Estimated survival from Mossdale to Chipps Island averaged $\hat{S}_{A(D)} = 0.04$ ($SE = 0.01$) in the San Joaquin route, and $\hat{S}_{B(D)} = 0.07$ ($SE = 0.01$) in the Old River route. Only the first release group showed a significant difference in survival to Chipps Island between the two routes, survival through the San Joaquin route ($\hat{S}_{A(D)} = 0.07$, $SE = 0.31$) being higher than through the Old River route ($\hat{S}_{B(D)} = 0.00$, $SE = 0$; $P = 0.0100$; Table 2). Lack of significance for other release groups may have been a result of low statistical power. Pooled over release groups, however, estimated survival to Chipps Island was significantly higher through the Old River route than through the San Joaquin River route ($P = 0.0133$).

For tags released at Durham Ferry, the median travel time through the reaches ranged from 0.1 d ($SE = 0.01$) between the two Stockton receivers (A4 to A5; approximately 3 km) to 3.2 d ($SE = 0.5$) from Medford Island (A7) to Chipps Island (G1); of the multiple paths between A7 and G1, the path that used only the San Joaquin River was approximately 46 km long. No tags were observed to move from Turner Cut to Chipps Island, and the median transition from Old River South (B2) to the CVP trash racks (E1) was 0.9 d ($SE = 0.1$).

Among the 29 salmon released at Durham Ferry in 2010 that were subsequently detected at Chipps Island, 31% (9 fish) used the San Joaquin route and 69% used the Old River route. The median travel time from the head of the Old River to Chipps Island was 5.7 d (migration rate = 14.0 km/d) through the San Joaquin route, compared with 7.2 d (7 km/d) for the single fish in the Old River route that migrated in-river past Highway 4, and 2.6 d for the 19 fish in the Old River route that passed through the Central Valley Project. Travel time for the CVP fish included time spent in holding tanks and truck transport to release sites just upstream of Chipps Island, as part of the salvage operation at the facility. It appears that the fastest route through the San Joaquin River Delta to Chipps Island in 2010 was through the Old River and the CVP.

DISCUSSION

The results of 2 years of acoustic-tagging studies reported here shed light on the survival of juvenile fall Chinook Salmon in the San Joaquin River Delta. Although estimated survival was considerably higher in 2010 than in 2009, overall survival was low in both years, and survival and migration rates tended to be higher upstream and lower downstream. This pattern was observed throughout the Southern Delta in both 2009 and 2010 and throughout the entire Delta in 2010. Some reduction in migration rate is expected as fish move downstream because the cyclic tidal environment may reverse the direction of river flow and temporarily push smolts upstream. Slower migration rates, in turn, may lead to lower survival in downstream reaches, with slower-moving smolts being less able to evade predators (Anderson et al. 2005).

When survival estimates were adjusted for reach length (i.e., survival rate = $\hat{S}(km^{-1})$), two regions displayed consistently low survival rates. The San Joaquin River reach from the receiver near the Navy Drive Bridge in Stockton to the Turner Cut junction had an estimated survival rate of 0.85 in 2009 and 0.94 in 2010. The reaches in the southwestern portion of the Old River route (i.e., from the head of Middle River to the entrances of the CVP and Clifton Court Forebay and to the Old River at Highway 4) had comparable survival rate estimates in both years, ranging from 0.83 to 0.90 in 2009 and 0.94–0.95 in 2010. All other Southern Delta reaches had higher estimated survival rates, while the only reach in the full Delta study area with lower survival rate was the San Joaquin River reach from the Turner Cut junction to Medford Island (0.86 in 2010). The San Joaquin River reaches from Stockton to the Turner Cut junction and Medford Island and the western portions of the Old River route warrant further investigation into mortality factors.

The estimated probability of survival throughout the Southern Delta region was generally higher in 2010 than in 2009 in both the San Joaquin River route and the Old River route. In particular, survival in the Old River from the junction with Middle River to the entrance of the water export facilities and Highway 4 appeared considerably higher in 2010 (average estimate = 0.92)

than in 2009 (average = 0.16). Overall, the survival estimates through the Southern Delta region in 2009 (average = 0.06) were comparable to the survival estimates through the entire Delta region in 2010 (average = 0.05). Although no direct estimates of survival through the entire Delta were available in 2009, we can conclude that total survival was <0.06 . The drop in survival in 2010 from the Southern Delta (0.56) to the entire Delta (0.05) suggests that total survival through the entire Delta in 2009 may have been as low as 0.005. Even considering the uncertainty inherent in the predator decision process, we can conclude that survival through the Delta was very low in 2009. If the survival probability estimated in 2009 was similar to survival in other low-flow years, current recovery efforts for San Joaquin River Chinook Salmon may be inadequate during dry years.

Despite interannual survival differences, the average estimated probability of fish entering the Old River from the San Joaquin (0.53) did not differ between 2009 and 2010. This route's entrainment probability was estimated in the presence of the nonphysical barrier operated at the head of the Old River. The barrier was found to be effective at deterring smolts from entering the Old River in 2010, but not in 2009 (Bowen et al. 2009; Bowen and Bark 2012, "protection efficiency"). Nevertheless, the effect of the barrier on the overall VAMP study results was limited because the barrier was operated only for approximately half of each release group, and estimates of the Old River route entrainment probability probably decreased by <0.1 because of the barrier study.

The 2009 and 2010 survival estimates reported here depend partly on the decision process used to identify and remove possible predator detections. Without removing any suspect detections, overall survival through the Southern Delta region would be estimated at 0.34 in 2009 and 0.79 in 2010 and at 0.11 through the entire Delta region in 2010. Thus, estimated survival would be higher in both years, but the comparisons between 2009 and 2010 and between the Southern Delta and the entire Delta would remain. However, many of the detections producing these higher survival estimates came from tags with considerably longer residence times (e.g., up to 810 h) or longer travel times than expected for emigrating juvenile salmonids (e.g., average residence time of approximately 0.5 h at most detection sites). Additionally, the fit of the statistical survival model declined when the presumed predator detections were included, suggesting that they were unlikely to have come from emigrating salmonids. The results presented here are based on our current understanding of behavior differences between juvenile salmon and predators such as striped bass. Nevertheless, more work needs to be done to develop methods for distinguishing between detections of salmon and detections of predators, especially for acoustic tagging studies in highly complex environments such as the Delta.

There are several possible explanations for the differences in Southern Delta survival observed between 2009 and 2010. River flows in 2009 were very low, whereas 2010 had considerably higher flows (Figure 4). Water exports from the federal and state

export facilities occurred at a slightly higher and more variable rate in 2009, the combined average export level being $56.4 \text{ m}^3/\text{s}$ (range = $38.2\text{--}73.3 \text{ m}^3/\text{s}$; SJRGA 2010). In 2010, the combined average export level was $43.0 \text{ m}^3/\text{s}$ (range = $37.4\text{--}44.2 \text{ m}^3/\text{s}$) (SJRGA 2011). Both lower flows and higher exports may have contributed to the lower survival observed in 2009, although the difference in average export level between 2009 and 2010 is small compared with possible daily variation in export levels ($42.5\text{--}322.8 \text{ m}^3/\text{s}$). Differences in the source and condition of the study fish may also have contributed to performance differences between the 2 years. The 2009 study fish were hybrids of spring and fall-run Chinook Salmon from the Feather River Fish Hatchery (FRH), located in the Sacramento River basin. These hybrid fish tended to be smaller than the 2010 study fish, which were fall-run Chinook Salmon from the Merced River Fish Hatchery (MRH; located in the San Joaquin River basin). Historically, experiments in the San Joaquin Delta have used MRH fish. In 2009, however, low numbers of MRH fish prompted the switch to the FRH for that year's tagging study, despite concern that FRH fish (genetically from the Sacramento River) may not adequately represent survival of San Joaquin fall-run Chinook Salmon (Brandes and McLain 2001). In 2010, rebounding numbers at the MRH allowed us to return to MRH fish for that year's tagging study.

The smaller size of the 2009 fish resulted in an average tag burden that was higher than in 2010, and also higher than desired ($\leq 5.5\%$; Brown et al. 2006). The higher tag burden in 2009 may have contributed to the high mortality in the first reach after release (Durham Ferry to Mossdale Bridge), where an estimated 53% of study fish died in 2009. However, differences in river conditions and predator distribution may also have contributed to differences in estimated mortality in this reach between the 2 years. Dry conditions and low flows in 2009 may have concentrated predators and prey (smolts) in a smaller volume of water. Higher water temperatures in 2009 may have kept the predators more active (e.g., Niimi and Beamish 1974), and also more likely to reside in the San Joaquin River between Durham Ferry and Mossdale Bridge, where water temperatures tend to be cooler than in the Delta.

Despite the differences in survival between the 2009 and 2010 study years, both studies found that juvenile fall run Chinook Salmon have very low survival through the San Joaquin River Delta, well under 0.10. Our 2010 estimates were similar to the lower range of previous survival estimates of San Joaquin smolts based on CWT data (Brandes and McLain 2001). However, the extremely low survival potentially experienced through the Delta in 2009 would have been lower than the lowest CWT estimates. Even the higher survival observed in 2010 was considerably lower than survival estimates of juvenile late fall-run Chinook Salmon from the Sacramento River through the Delta, which ranged from 0.35 to 0.54 in the winter of 2007 (Perry et al. 2010). The Perry study used comparable methods, with similar study design, tagging, and analysis. However, the late fall run Chinook Salmon used in

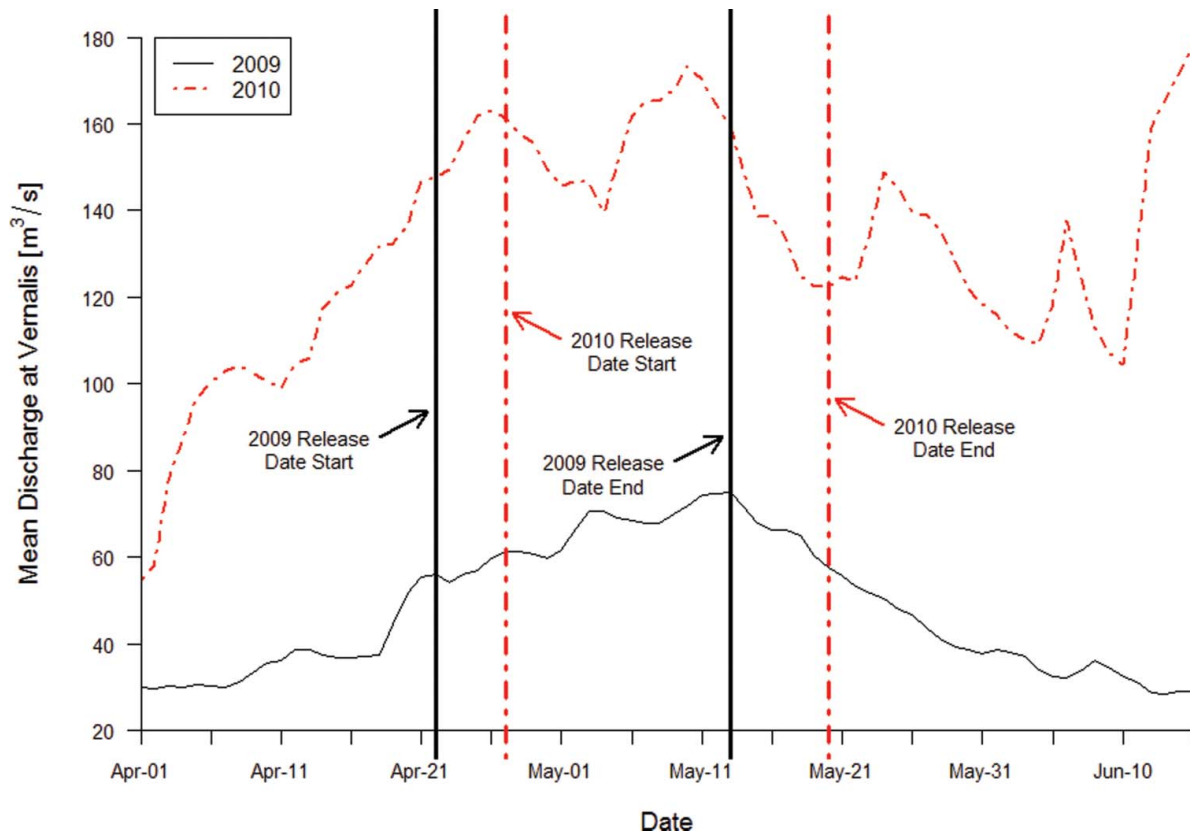


FIGURE 4. Mean daily discharge of the San Joaquin River at the U.S. Geological Survey gauge near Vernalis, California (rkm 113 from Chipps Island), during Chinook Salmon tagging studies in 2009 and 2010. [Figure available in color online.]

the Perry study migrate in winter, whereas the fall-run Chinook Salmon used in the VAMP study migrate months earlier in spring. Thus, not only were the VAMP fish smaller than the Perry study fish, they also migrated when higher predator activity is expected because of warmer temperatures and the striped bass spring spawning migration (Radtke 1966). Thus, there are several possible explanations why the VAMP study may be expected to estimate lower survival than the Perry study.

Estimates of juvenile Chinook Salmon survival through comparable environments in other basins tend to be higher than those observed in the 2009 and 2010 VAMP studies. McMichael et al. (2010) used acoustic tags to estimate survival of Chinook salmon smolts through the lower 192 rkm of the Columbia River to the river mouth; scaled by distance, the survival rate estimates ($\hat{S}^{(km^{-1})}$) were 0.999 for yearlings and 0.998 for subyearlings. Acoustic-tagged spring Chinook Salmon from the Thompson–Fraser river system had estimated survival rates of 0.989–0.997 (average = 0.995) through more than 330 rkm to the Fraser River mouth in 2004–2006 (Welch et al. 2008). These survival rates are considerably higher than both the VAMP-estimated Southern Delta survival rate of 0.92 in 2009 and the estimated entire Delta survival rate of 0.97 in 2010. Even the lowest survival rate estimate reported by Welch et al. (2008) for the Fraser River (0.989 in 2004) corresponds to much higher total survival

over a distance comparable to the VAMP study area (approximately 89 rkm). Over this distance, a population with a survival rate of 0.989/km would have an overall survival probability of 0.37, as opposed to the 2010 estimate of 0.05. Although direct comparison with other basins is difficult, it appears that the salmon smolts used in the 2009 and 2010 VAMP studies are not surviving as well on their seaward migration as other salmon population on the western coast of North America.

Part of the VAMP is a management plan based on the assumption that salmon survival to Chipps Island is higher through the San Joaquin River route than through the Old River route. This assumption is based on CWT studies between 1985 and 1990 that consistently found higher (but not statistically significant) point estimates of survival for smolts released in the San Joaquin River downstream of the Old River than for those released in the Old River (Brandes and McLain, 2001). Modeling of these data and other CWT data indicated that keeping salmon out of the Old River improved their survival (Newman 2008). The 2008 VAMP acoustic tag study results, although hampered by a high degree of premature tag failure, suggest that survival to Chipps Island was also higher through the San Joaquin River than through the Old River route in 2008 (Holbrook et al. 2009). Furthermore, there is evidence that salmon from the Sacramento River have a higher probability of reaching Chipps Island if they

remain in the Sacramento River rather than entering the central Delta (Newman and Brandes 2010, Perry et al. 2010). Since the 1990s, management has experimented with efforts to keep fish in the San Joaquin River and out of the Old River by installing a barrier (physical or nonphysical) at the head of the Old River. Our results suggest that prevailing ideas about relative survival in the two routes may be too simple, given that we found no conclusive evidence that survival was higher in the San Joaquin River route than in the Old River route. One difference between the 2009 and 2010 study years and previous years was the switch from a physical barrier to testing a nonphysical barrier at the head of the Old River in 2009 and 2010. Historically, the physical barrier at the Old River routed both fish and river flow into the San Joaquin River (SJRG 2005). In contrast, the nonphysical barrier used in 2009 and 2010 routed fish but not flow into the San Joaquin (Bowen et al. 2009; Bowen and Bark 2012). With salmon smolt survival in the San Joaquin River thought to increase with flow (SJRG 2007), it is possible that the nonphysical barrier deprived smolts routed to the San Joaquin River of the increased flows necessary for improved survival (Perry et al. 2013). There is also a concern that the larger in-water structure associated with the nonphysical barrier may create habitat for increased predation at the site. More study is needed.

The San Joaquin River Delta represents just a small portion of the entire juvenile out-migration of San Joaquin Chinook Salmon and in recent years has typically been traversed in <2 weeks (SJRG 2011; Holbrook et al. 2013). With survival through only a portion of the juvenile migration estimated at <0.10, management efforts in the lower San Joaquin River and Delta must be more protective if salmon populations are to persist in this region. However, effective management must be based on a better understanding of the factors influencing mortality than is currently available. More research into salmon use of and survival in the Delta is needed, especially in dry years that may represent future conditions under climate change. In light of increasing human demands for Central Valley water, it is unlikely that salmon survival will improve on its own. If the survival estimates observed in these two studies are representative of the future, only extreme measures have a chance of saving San Joaquin River Chinook Salmon.

ACKNOWLEDGMENTS

Many people and groups were involved in designing and implementing the VAMP study. We thank Natural Resource Scientists, Inc., California Department of Fish and Game, California Department of Water Resources, the U.S. Fish and Wildlife Service (Stockton office), the U.S. Bureau of Reclamation, Normandeau and Associates (Stevenson, Washington), and the U.S. Geological Survey (Columbia River Research Lab and Sacramento office) for their contributions to the study. We also thank Mark Bowen from the U.S. Bureau of Reclamation for access to detection data from the nonphysical barrier study at the head of the Old River, and three anonymous reviewers

for their helpful suggestions. Funding for the VAMP study was provided by the signatories to the San Joaquin River Agreement, and funding for analysis and manuscript preparation was provided by the San Joaquin River Group Authority.

REFERENCES

- Adams, N. S., D. W. Rondorf, S. D. Evans, and J. E. Kelly. 1998. Effects of surgically and gastrically implanted radio transmitters on growth and feeding behavior of juvenile Chinook Salmon. *Transactions of the American Fisheries Society* 127:128–136.
- Anderson, J. J., E. Gurarie, and R. W. Zabel. 2005. Mean free-path length theory of predator–prey interactions: application to juvenile salmon migration. *Ecological Modelling* 186:196–211.
- Anglea, S. M., D. R. Geist, R. S. Brown, K. A. Deters, and R. D. McDonald. 2004. Effects of acoustic transmitters on swimming performance and predator avoidance of juvenile Chinook Salmon. *North American Journal of Fisheries Management* 24:162–170.
- Bowen, M. D., and R. Bark. 2012. 2010 effectiveness of a non-physical fish barrier at the divergence of the Old and San Joaquin rivers (CA). U.S. Department of the Interior, Bureau of Reclamation, Technical Memorandum 86-68290-10-07, Denver.
- Bowen, M. D., S. Hiebert, C. Hueth, and V. Maisonneuve. 2009. 2009 effectiveness of a non-physical fish barrier at the divergence of the Old and San Joaquin rivers (CA). U.S. Department of the Interior, Bureau of Reclamation, Technical Memorandum 86-68290-09-05, Denver.
- Brandes, P. L., and J. S. McLain. 2001. Juvenile Chinook Salmon abundance, distribution, and survival in the Sacramento–San Joaquin Estuary. Pages 39–138 in R. L. Brown, editor. *Contributions to the biology of Central Valley salmonids*, volume 2. California Department of Fish and Game, Fish Bulletin 179, Sacramento.
- Brown, R. S., D. R. Geist, K. A. Deters, and A. Grassell. 2006. Effects of surgically implanted acoustic transmitters >2% of body mass on the swimming performance, survival and growth of juvenile Sockeye and Chinook Salmon. *Journal of Fish Biology* 69:1626–1638.
- Buchanan, R. A., and J. R. Skalski. 2010. Using multistate mark–recapture methods to model adult salmonid migration in an industrialized river. *Ecological Modelling* 221:582–589.
- Burnham, K. P., and D. R. Anderson. 2002. *Model selection and multimodel inference: a practical information-theoretic approach*, 2nd edition. Springer, New York.
- Burnham, K. P., D. R. Anderson, G. C. White, C. Brownie, and K. H. Pollock. 1987. *Design and analysis methods for fish survival experiments based on release-recapture*. American Fisheries Society, Monograph 5, Bethesda, Maryland.
- DSC (Delta Stewardship Council). 2011. Available: <http://www.deltacouncil.ca.gov/>. (13 December 2011).
- Fisher, F. W. 1994. Past and present status of Central Valley Chinook Salmon. *Conservation Biology* 8:870–873.
- Healey, M. C. 1991. Life history of Chinook Salmon (*Oncorhynchus tshawytscha*). Pages 311–393 in C. Groot and L. Margolis, editors. *Pacific salmon life histories*. University of British Columbia Press, Vancouver.
- Holbrook, C. M., R. W. Perry, and N. S. Adams. 2009. Distribution and joint fish-tag survival of juvenile Chinook Salmon migrating through the Sacramento–San Joaquin River Delta, California, 2008. U.S. Geological Survey, Open-File Report 2009-1204, Reston, Virginia. Available: pubs.usgs.gov/. (November 2011).
- Holbrook, C. M., R. W. Perry, P. L. Brandes, and N. S. Adams. 2013. Adjusting survival estimates for premature transmitter failure: a case study from the Sacramento–San Joaquin Delta. *Environmental Biology of Fishes* 96:165–173.
- Lady, J. M., and J. R. Skalski. 2008. USER 4: user-specified estimation routine. School of Aquatic and Fishery Sciences, University of Washington, Seattle. Available: www.cbr.washington.edu/paramest. (July 2012).

- Martinelli, T. L., H. C. Hansel, and R. S. Shively. 1998. Growth and physiological responses to surgical and gastric radio transmitter implantation techniques in subyearling Chinook Salmon (*Oncorhynchus tshawytscha*). *Hydrobiologia* 371/372:79–87.
- McCullagh, P., and J. A. Nelder. 1989. *Generalized linear models*, 2nd edition. Chapman and Hall/CRC Press, Boca Raton, Florida.
- McMichael, G. A., R. A. Harnish, B. J. Bellgraph, J. A. Carter, K. D. Ham, P. S. Titzler, and M. S. Hughes. 2010. Migratory behavior and survival of juvenile salmonids in the lower Columbia River and estuary in 2009. Pacific Northwest National Laboratory, PNNL-19545, Richland, Washington.
- Newman, K. B. 2008. An evaluation of four Sacramento–San Joaquin River Delta juvenile salmon survival studies. CALFED Bay-Delta Program, Project SCI-06-G06-299, Sacramento, California. Available: www.science.calwater.ca.gov/ (November 2011).
- Newman, K. B., and P. L. Brandes. 2010. Hierarchical modeling of juvenile Chinook Salmon survival as a function of Sacramento–San Joaquin Delta water exports. *North American Journal of Fisheries Management* 30:157–169.
- Niimi, A. J., and F. W. H. Beamish. 1974. Bioenergetics and growth of Large-mouth Bass (*Micropterus salmoides*) in relation to body weight and temperature. *Canadian Journal of Zoology* 52:447–456.
- Perry, R. W., P. L. Brandes, J. R. Burau, A. P. Klimley, B. MacFarlane, C. Michel, and J. R. Skalski. 2013. Sensitivity of survival to migration routes used by juvenile Chinook Salmon to negotiate the Sacramento–San Joaquin River Delta. *Environmental Biology of Fishes* 96:381–392.
- Perry, R. W., J. R. Skalski, P. L. Brandes, P. T. Sandstrom, A. P. Klimley, A. Ammann, and B. MacFarlane. 2010. Estimating survival and migration route probabilities of juvenile Chinook Salmon in the Sacramento–San Joaquin River Delta. *North American Journal of Fisheries Management* 30:142–156.
- Radtke, L. D. 1966. Distribution of adult and subadult Striped Bass, *Roccus saxatilis*, in the Sacramento–San Joaquin Delta. Pages 15–27 in J. L. Turner and D. W. Kelley, editors. *Ecological studies of the Sacramento–San Joaquin Delta, part II: fishes of the Delta*. California Department of Fish and Game, Fish Bulletin 136, Sacramento.
- SJRGA (San Joaquin River Group Authority). 2005. 2004 annual technical report: on implementation and monitoring of the San Joaquin River agreement and the Vernalis Adaptive Management Plan. SJRGA, Report to the California Water Resources Control Board, Davis, California. Available: www.sjrg.org/technicalreport. (February 2012).
- SJRGA (San Joaquin River Group Authority). 2007. 2006 annual technical report: on implementation and monitoring of the San Joaquin River agreement and the Vernalis Adaptive Management Plan. SJRGA, Report to the California Water Resources Control Board, Davis, California. Available: www.sjrg.org/technicalreport. (February 2012).
- SJRGA (San Joaquin River Group Authority). 2010. 2009 annual technical report: on implementation and monitoring of the San Joaquin River agreement and the Vernalis Adaptive Management Plan. SJRGA, Report to the California Water Resources Control Board, Davis, California. Available: www.sjrg.org/technicalreport. (February 2012).
- SJRGA (San Joaquin River Group Authority). 2011. 2010 annual technical report: on implementation and monitoring of the San Joaquin River agreement and the Vernalis Adaptive Management Plan. SJRGA, Report to the California Water Resources Control Board, Davis, California. Available: www.sjrg.org/technicalreport. (February 2012).
- Townsend, R. L., J. R. Skalski, P. Dillingham, and T. W. Steig. 2006. Correcting bias in survival estimation resulting from tag failure in acoustic and radiotelemetry studies. *Journal of Agricultural, Biological, and Environmental Statistics* 11:183–196.
- Vogel, D. A. 2010. Evaluation of acoustic-tagged juvenile Chinook Salmon movements in the Sacramento–San Joaquin Delta during the 2009 Vernalis Adaptive Management Program. San Joaquin River Group Authority, Technical Report to the California Water Resources Control Board, Davis, California. Available: www.sjrg.org/technicalreport/. (July 2012).
- Vogel, D. A. 2011. Evaluation of acoustic-tagged juvenile Chinook Salmon and predatory fish movements in the Sacramento–San Joaquin Delta during the 2010 Vernalis Adaptive Management Program. San Joaquin River Group Authority, Technical Report to the California Water Resources Control Board, Davis, California. Available: www.sjrg.org/technicalreport/. (July 2012).
- Welch, D. W., E. L. Rechisky, M. C. Melnychuk, A. D. Porter, C. J. Walters, S. Clements, B. J. Clemens, R. S. McKinley, and C. Schreck. 2008. Survival of migrating salmon smolts in large rivers with and without dams. *PLoS (Public Library of Science) Biology* [online serial] 6(10):e265. DOI: 10.1371/journal.pbio.0060265.

A cold phase of the East Pacific triggers new phytoplankton blooms in San Francisco Bay

James E. Cloern^{*†}, Alan D. Jassby[‡], Janet K. Thompson^{*}, and Kathryn A. Hieb[§]

^{*}United States Geological Survey, MS496, 345 Middlefield Road, Menlo Park, CA 94025; [‡]Department of Environmental Science and Policy, University of California, Davis, CA 95616; and [§]California Department of Fish and Game, 4001 North Wilson Way, Stockton, CA 95205

Edited by George N. Somero, Stanford University, Pacific Grove, CA, and approved October 3, 2007 (received for review June 29, 2007)

Ecological observations sustained over decades often reveal abrupt changes in biological communities that signal altered ecosystem states. We report a large shift in the biological communities of San Francisco Bay, first detected as increasing phytoplankton biomass and occurrences of new seasonal blooms that began in 1999. This phytoplankton increase is paradoxical because it occurred in an era of decreasing wastewater nutrient inputs and reduced nitrogen and phosphorus concentrations, contrary to the guiding paradigm that algal biomass in estuaries increases in proportion to nutrient inputs from their watersheds. Coincidental changes included sharp declines in the abundance of bivalve mollusks, the key phytoplankton consumers in this estuary, and record high abundances of several bivalve predators: Bay shrimp, English sole, and Dungeness crab. The phytoplankton increase is consistent with a trophic cascade resulting from heightened predation on bivalves and suppression of their filtration control on phytoplankton growth. These community changes in San Francisco Bay across three trophic levels followed a state change in the California Current System characterized by increased upwelling intensity, amplified primary production, and strengthened southerly flows. These diagnostic features of the East Pacific “cold phase” lead to strong recruitment and immigration of juvenile flatfish and crustaceans into estuaries where they feed and develop. This study, built from three decades of observation, reveals a previously unrecognized mechanism of ocean–estuary connectivity. Interdecadal oceanic regime changes can propagate into estuaries, altering their community structure and efficiency of transforming land-derived nutrients into algal biomass.

climate variability | coastal eutrophication | ocean–estuary connectivity | regime shift | trophic cascade

Ecosystem observations sustained over decades often produce surprises, revealing novel processes that regulate abundance, composition, and productivity of biological communities. In 1999, we were surprised by an October phytoplankton bloom in San Francisco Bay (SFB), a departure from the seasonal pattern observed over two preceding decades. This event signaled a large biological change manifesting over subsequent years as increasing phytoplankton biomass and new seasonal blooms. This change is puzzling because it occurred in an era of decreasing nutrient inputs. Phytoplankton increase is a well documented response to nutrient enrichment from fertilizer runoff and wastewater discharge to coastal ecosystems (1). Nutrient enrichment has promoted excessive algal production and severely degraded habitat quality in the Chesapeake Bay, northern Gulf of Mexico, and Baltic and Adriatic seas. The SFB “paradox” presented here is contrary to these experiences elsewhere and provides strong evidence that additional processes, beyond nutrient supply, can cause sustained increases in algal biomass. We use data from the United States Geological Survey (USGS) long-term study of SFB to describe the patterns of phytoplankton increase and then present evidence from other studies that the underlying process is a trophic cascade having origins in the Pacific Ocean.

Long-term research has been sustained in SFB, which exemplifies a large ecosystem at the land–sea interface influenced by natural processes of variability and multiple modes of human disturbance (2). SFB receives large inputs of nitrogen and phosphorus from its 153,000-km² agricultural watershed and its densely populated urban watershed. Nutrient inputs are comparable to those delivered to Chesapeake Bay, but SFB is a low-productivity estuary with no recurrent problems of hypoxia or harmful algal blooms (1). This eutrophication resistance has manifested over 20 years of observation as persistent low phytoplankton biomass and high nutrient concentrations. Median summer–autumn concentrations of dissolved inorganic nitrogen and phosphorus were 32.3 and 2.3 μM , respectively, in South SFB over the period 1977–1998. These values are 10 times higher than nutrient concentrations that limit phytoplankton growth, and they represent large stocks of unutilized nitrogen and phosphorus. Resistance mechanisms include tidal- and wind-driven mixing that prevent stratification, large sediment inputs and high turbidity that limits light penetration and phytoplankton photosynthesis, and fast filtration removal of phytoplankton cells by bivalve mollusks (3). Here, we report recent phytoplankton increases that signal a weakened resistance to nutrient pollution, and propose a top-down mechanism induced by a state change in the northeast Pacific Ocean. This study reveals how the expression of eutrophication from land runoff to estuaries can fluctuate with ocean-derived changes in biological community structure, a previously unrecognized mechanism of ocean–estuary connectivity with implications for how we study and manage nearshore coastal ecosystems.

Results

We have measured phytoplankton biomass as chlorophyll *a* (Chl-*a*) concentration at least monthly in SFB since 1978. Observations from 1978–1998 showed a recurrent annual pattern of low phytoplankton biomass punctuated by short-lived spring blooms. This pattern changed abruptly in 1999 with the first record of an autumn bloom, detected as elevated Chl-*a* at concentrations never observed during autumn sampling the previous 22 years (Fig. 1*A*). Autumn–winter blooms in subsequent years included unprecedented occurrences of dinoflagellate red tides (4). New seasonal blooms, coupled with increasing baseline Chl-*a*, have led to increased overall phytoplankton biomass (Fig. 1*B*). Trends over time (Theil–Sen slopes of decadal Chl-*a* series) revealed statistically significant ($P < 0.05$) phytoplankton increases beginning after 1999 (Fig. 1*C*). These changes

Author contributions: J.E.C. and A.D.J. designed research; J.E.C., J.K.T., and K.A.H. performed research; J.E.C., A.D.J., J.K.T., and K.A.H. analyzed data; and J.E.C., A.D.J., and J.K.T. wrote the paper.

The authors declare no conflict of interest.

This article is a PNAS Direct Submission.

Freely available online through the PNAS open access option.

[†]To whom correspondence should be addressed. E-mail: jecloern@usgs.gov.

This article contains supporting information online at www.pnas.org/cgi/content/full/0706151104/DC1.

© 2007 by The National Academy of Sciences of the USA

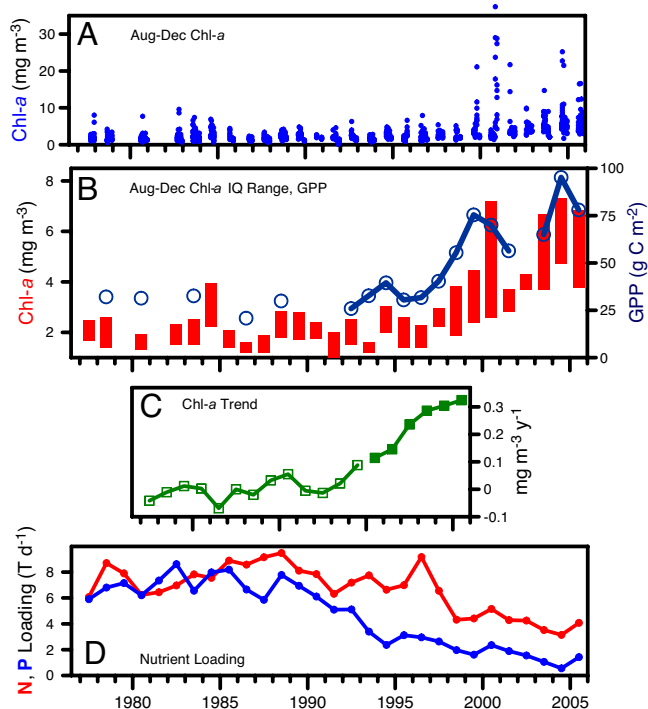


Fig. 1. Indicators of phytoplankton change in South SFB. (A) Occurrences of autumn blooms (August through December Chl-a >10) since 1999. (B) Increases in August through December Chl-a (interquartile ranges are shown as bars) and gross primary production (GPP) (open circles). (C) Ten-year windowed trends showing statistically significant ($P < 0.05$; filled squares) Chl-a increases after 1999. (D) Annual inputs of dissolved inorganic nitrogen and phosphorus from the San Jose–Santa Clara Wastewater Treatment Plant [N. Van Keuren (City of San Jose), personal communication], the largest municipal discharger to South SFB.

are also ecologically significant: estimated August through December primary production [supporting information (SI) Text] more than doubled (Fig. 1B), from 32 g C m^{-2} (pre-1998 mean) to 73 g C m^{-2} (post-1998 mean). Seasonal analysis of the 1978–2005 series detected positive Chl-a trends every month, of

which eight were statistically significant (Fig. 2E). These observations are compelling evidence of phytoplankton increase at a magnitude observed in other estuaries as a response to increasing nutrient input.

Water quality and biological communities of estuaries are strongly influenced by freshwater inputs that deliver sediments, nutrients, and contaminants from land runoff and wastewater discharge. South SFB is situated in a densely populated urban watershed, and 98% of its nitrogen input (see table 8 of ref. 5) is from municipal wastewater treatment plants (North SFB is more strongly influenced by agricultural inputs from the Sacramento and San Joaquin rivers). We explored water-quality data for indicators that the phytoplankton increase in SFB was caused by changing inputs from the surrounding landscape that could increase algal growth rate. Phytoplankton biomass grows as algal cells divide at rates regulated by macronutrient (nitrogen, phosphorus) concentrations, water temperature, and light energy. But monthly trends of dissolved inorganic nitrogen (DIN) and dissolved reactive phosphorus (DRP) concentrations in SFB were negative for each month, approaching maximum trends of $-10\% \text{ y}^{-1}$ (Fig. 2A and B). These large nutrient declines are consistent with progressive improvements in municipal wastewater treatment leading to decreasing N and P input from the urban watershed (Fig. 1D) and expectations of a corresponding reduction in algal biomass.

Monthly trends of water temperature in SFB over the period 1978–2005 were small and not statistically significant (Fig. 2D). SFB has high concentrations of suspended sediments that limit light penetration and photosynthesis, a primary factor in this estuary’s low productivity and low nutrient assimilation efficiency (1). But monthly trends of suspended particulate matter (SPM) were positive for each month (Fig. 2F), so turbidity and light limitation have not diminished over time. Algal blooms can be triggered by salinity stratification that creates a shallow high-light surface layer of fast phytoplankton growth (3). Salinity stratification of estuaries is strongest during years of high river flow and low surface salinity. Trends of surface salinity in SFB varied across months, but none were statistically significant (Fig. 2C), and there were no significant trends of stratification intensity (difference between bottom and surface salinity). We conclude that the phytoplankton increase in SFB was not caused by secular increases in the phytoplankton growth rate because nutrients have declined, turbidity has (weakly) increased, stratification has not strengthened, and water temperature has not changed inside the estuary.

We next explored biological monitoring data to consider an alternative, top-down explanation for the phytoplankton increase in SFB as a result of reduced consumption by herbivores. A large fraction of phytoplankton primary production in SFB is consumed by bivalve mollusks, and high bivalve biomass and filtration rates are keys to the low phytoplankton–high nutrient state. Summer–autumn rates of phytoplankton growth and bivalve consumption have historically been balanced (3), and simulations with a numerical model demonstrate a high sensitivity of phytoplankton biomass to changes in bivalve grazing intensity (6). The mean biomass of suspension-feeding bivalves (e.g., *Corbula amurensis*, *Venerupis japonica*, *Musculista senhousia*, and *Mya arenaria*) was 7.9 g m^{-2} (ash-free dry weight) in samples collected across shallow habitats in South SFB from 1987 through 1998. However, six surveys conducted after 1998 revealed surprisingly small populations (Fig. 3A and SI Table 1) and complete absence of these bivalves at many sampling sites, with a mean biomass of only 0.4 g m^{-2} . The ≈ 20 -fold bivalve decline after 1998 and its coincidence with a positive Chl-a trend suggests that the phytoplankton increase in SFB was a response to decreased bivalve abundance and phytoplankton consumption.

Surveys by the California Department of Fish and Game provide evidence that the bivalve population collapse was, at

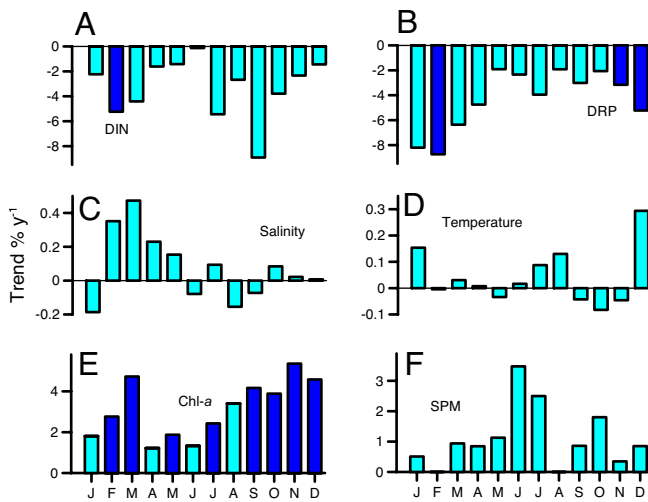


Fig. 2. Monthly trends of water quality in South SFB based on USGS measurements of DIN and DRP for the years 1990–2005, and surface salinity, water temperature, Chl-a, and SPM for the years 1978–2005. Units are percent change y^{-1} . Darker bars indicate statistically significant trends ($P < 0.05$).

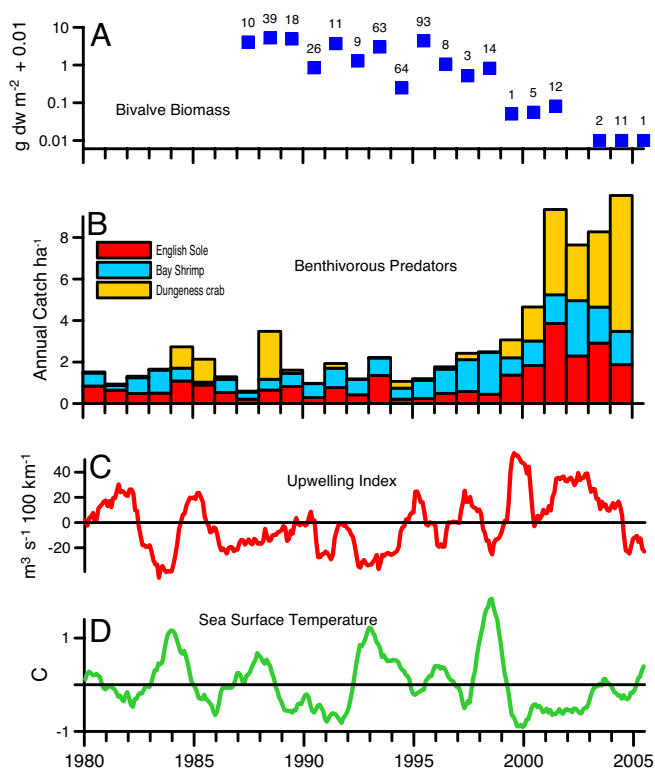


Fig. 3. Indices of biological community change within SFB and physical changes in the adjacent California Current. (A) Annual median biomass of filter-feeding bivalves across shallow habitats in South SFB; numbers above filter-squares indicate sample number per year. (B) Mean annual catch ha^{-1} , normalized to 1980–2005 averages, of English sole, Bay shrimp, and Dungeness crab, from monthly sampling across the marine domains of SFB. (C) Anomalies in upwelling intensity computed by the National Oceanic and Atmospheric Administration from atmospheric pressure fields. (D) Sea surface temperature measured at the Farallon Islands. The bottom series (C and D) are 12-mo running averages of deviations from 1977–2005 monthly means.

least partly, a result of increased predation. Cumulative abundance of *Crangon* shrimp and juvenile Dungeness crab (*Cancer magister*) and English sole (*Parophrys vetulus*) increased to record levels in SFB after 1999 and persisted at high stock densities (Fig. 3B). These species are widespread predators in SFB that feed on benthic invertebrates including bivalve mollusks. The sum of their mean abundances (normalized to 1980–2005 means) was 7.1 from 2000 through 2004 compared with 1.8 over the preceding 20 years. Fluctuations of bivalve biomass are strongly associated with interannual and decadal changes in the abundances of their predators: bivalve recruitment has failed in other estuaries during years of high predator (*Crangon* spp.) abundance (7), and collapse of bay scallop stocks in the coastal Atlantic coincided with increased abundances of bottom-feeding skates and rays (8).

Discussion

The unexpected phytoplankton increase in SFB was one component of a broad suite of biological community changes that began after 1998 and appear to be linked through a trophic cascade (9). Abundance records suggest that heightened predation by fish and crustaceans reduced bivalve abundance and phytoplankton consumption, allowing algal biomass to grow and episodic blooms to develop after spring. Such trophic cascades have been induced through experimental additions of predatory fish in lakes (10), and large-scale community changes cascade across trophic levels in marine ecosystems when apex predators

are removed by fishing (8, 11). Trophic cascades induced by human activities can exacerbate the harmful consequences of nutrient enrichment: harvest of oysters and removal of their filtration function has contributed to the large buildup of phytoplankton biomass and associated water-quality degradation of Chesapeake Bay (12). Our observations highlight again the powerful top-down control of phytoplankton biomass by bivalve suspension feeders in shallow marine ecosystems, manifested elsewhere as abrupt phytoplankton decreases after bivalve invasions from introductions of alien species (13) or hydrologic manipulations (14).

The trophic cascade described here was not associated with changes in fishing intensity, species introductions, or other human interventions. However, it coincided with pronounced physical changes in the California Current System (CCS), suggesting that it might be linked to coupled physical and biological changes in the northeast Pacific Ocean. The 1997–1998 El Niño was the strongest on record (15), and it was followed by an equally strong La Niña in 1999. This abrupt El Niño–La Niña transition across the Pacific basin initiated a multiyear period of strong upwelling and enhanced southerly flow in the California Current that transported subarctic waters along the coast (16). At the latitude of SFB, these changes were seen as sustained positive upwelling anomalies and low surface temperature at the Farallon Islands from 1999 through 2004 (Fig. 3C and D). Current measurements and drifter studies also documented unusually strong southward advection off Oregon, producing an equatorward displacement anomaly of 2,000 km during 2001–2002 and a source of cold water from northern latitudes (17). This “cold phase” of the East Pacific induced a suite of ecological changes along the North American coast, including southerly displacement of pelagic species and increased primary production, zooplankton biomass, and populations of cold-water pelagic fish (18).

The coincidental timing of phytoplankton increase in SFB with altered coastal currents suggests a coupling between SFB and the CCS through high annual variability in the recruitment of marine species whose juvenile stages immigrate into estuaries. This variability may occur through multiple mechanisms. Distributions of adult Dungeness crab and English sole are normally centered above the latitude of SFB, so cooling of the CCS may lead to southerly displacement of adult stocks whose distributions shift with changes in coastal temperature (19). Annual recruitment of Dungeness crab is strongest during cool years in the CCS as a result of reduced egg mortality, enhanced transport of pelagic larvae to settlement areas, or high primary production and food supply rates characteristic of La Niña-type conditions (20). The specific mechanisms of recruitment variability are unknown and likely vary among species. However, the coherent physical changes in the CCS and increased immigration of juvenile flatfish and crustaceans inside SFB are strong evidence that atmospherically driven changes in ocean boundary currents can induce large biological changes within estuaries (21). These changes can include trophic cascades leading to increased primary production and more efficient transformation of land-derived nutrients into algal biomass.

We suspect that there are subtle but important secondary manifestations of the trophic cascade outlined above. For example, the coastal Pacific is a source of phytoplankton biomass to SFB when blooms develop offshore and cells are transported into the Bay by tidal pumping (22). The new seasonal blooms after 1998 were dominated by large diatom species (e.g., *Thalassiosira punctigera*) characteristic of CCS communities during upwelling events, or dinoflagellates (e.g., *Akashiwo sanguinea*) after upwelling relaxation (4). Amplified cycles of upwelling and relaxation during cold phases of the East Pacific can provide either a significant amount of coastal-produced phytoplankton biomass (21, 23) or resting stages or vegetative cells to seed subsequent blooms within estuaries

(24). Much of the imported biomass to SFB was presumably consumed by bivalves when they were abundant (pre-1999), just as imported phytoplankton are rapidly consumed by oysters in the upwelling-influenced Willapa Bay (23). Conversely, ocean-derived phytoplankton biomass can persist or grow in SFB when bivalve abundance is low. Thus, although the steady increase in phytoplankton biomass after 1998 (Fig. 1B) seems to reflect growth within SFB, the new seasonal blooms (Fig. 1A) may be supplied at least in part by coastal phytoplankton species. Nonetheless, the appearance of these new seasonal blooms is ultimately conditional on the trophic cascade that enhances algal population growth within the SFB.

The guiding paradigm of estuarine ecology is that runoff from land is the essential driver of biological and water-quality variability. We illustrate how the coastal ocean can be an equally powerful driver of estuarine change. Oceanographers and atmospheric scientists have learned how redistributions of major atmospheric pressure systems over ocean basins can alter winds, coastal currents, water temperature, and productivity, leading to regime changes in the abundance and distribution of fish, birds, and mammals (25). Our observations in SFB began in 1977, coincidentally the last regime change of the Pacific Decadal Oscillation (PDO) (26) when the East Pacific entered a “warm phase” of weak coastal upwelling and reduced southerly transport by the California Current. Unprecedented biological changes across three trophic levels occurred in SFB after the East Pacific returned to a state approximating the cold phase of the PDO. More than two decades of observation were required to discover how an oceanic regime change can induce an altered ecological state of a large estuary.

Long-term observations of SFB reveal a previously unrecognized mode of ecosystem variability that has implications for the way we study and manage estuaries. Estuaries are the most degraded marine ecosystems (12), and recent assessments highlight the growing environmental and societal costs of this degradation (27), motivating a sense of urgency to implement strategies of ecosystem-based rehabilitation and sustainability (28). Our study suggests that programs to rehabilitate damaged estuaries should build from a broadened geographic reference that includes the interplay between processes occurring over ocean basins and within watersheds, and an expanded temporal reference that includes natural cycles and trends of ocean-atmosphere variability operating over multiple decades.

Data and Methods

Hydrography and Water Quality. We analyzed results of near-surface measurements at eight stations in South SFB where the 1978–2005 data record contains few gaps and trend tests can be applied (USGS stations 21, 22, 24, 25, 27, 29, 30, and 32; see SI Fig. 4). Chl-*a* was measured from *in vivo* fluorescence with calibration of fluorometers (Turner Designs Model 10 before 1987, and Sea Tech or Turner Designs SCUFA since 1987) using 10–20 discrete measures of extracted Chl-*a* from filtered samples each cruise (29). Daily calibrations were necessary because of significant fluctuations in the fluorescence:Chl-*a* ratio. Water samples were preserved in acid Lugol's solution and examined by light microscopy to identify, measure, and count phytoplankton cells (30).

From 1978 to 1987, salinity, temperature, and SPM concentration were measured by pumping bay water to a shipboard salinometer, thermistor, and nephelometer. Since 1987, these constituents have been measured by using a Seabird SBE 9/11 CTD and optical backscatter sensor (OBS). The nephelometer and OBS were calibrated each cruise with discrete measures of SPM determined as dry mass retained on 0.4- μm polycarbonate filters. Nutrient samples were filtered through 0.4- μm polycarbonate filters and frozen until analyzed for DIN ($\text{DIN} = \text{NH}_4^+ + \text{NO}_3^- + \text{NO}_2^-$) and DRP by using modifications of standard colorimetric methods (31). The light attenuation coefficient k

(m^{-1}) was computed from vertical irradiance profiles measured with a LI-COR 192S quantum sensor. We used a linear model to estimate k from SPM ($k = 0.567 + 0.0586 \times \text{SPM}$; adjusted $R^2 = 0.863$) when light profiles were not measured. All data are available online (<http://sfbay.wr.usgs.gov/access/wqdata>).

Primary Production. Direct measurements of gross primary production were used to build an empirical model (SI Fig. 5) for calculating primary production over the full record of Chl-*a* and turbidity measurements. For each day and station, we first calculated the median SPM and Chl-*a* concentrations for depths ≤ 3 m. Under the assumptions that vertical attenuation of photosynthetically available radiation (PAR) does not change with depth, Chl-*a* is vertically homogeneous, and primary production is proportional to light absorbed by photosynthetic pigments, gross primary production (GPP) for a given location and day can be estimated from

$$\text{GPP} = \frac{4.6\Psi BI_0}{k}, \quad [1]$$

where Ψ ($\text{mg C} [\text{mg Chl-}a]^{-1} [\text{mol m}^{-2}]^{-1}$) is the water column light utilization efficiency, B (mg m^{-3}) is the median Chl-*a* in the upper 3 m, and I_0 [$\text{E} (\text{einstein} = 1 \text{ mol of photons}) \text{m}^{-2} \text{d}^{-1}$] is the photosynthetically active radiation. This approach has been verified in many estuarine systems when Ψ is calibrated for local conditions. The value used here ($\Psi = 0.82$) is based on 60 ^{14}C -uptake assays conducted in SFB between 1993 and 1998 (SI Fig. 5).

The longest period of relevant solar irradiance data were provided by an annually calibrated LI-COR 192 quantum sensor mounted on the USGS R/V *Polaris* during 1980–1994. The nearest sensor covering the entire period of interest is located at Davis, California, but irradiance at the latter location averages $\approx 10\%$ higher due to a lower incidence of fog. The Davis time series did allow us to verify that there was no secular trend in irradiance during the entire period. We computed GPP from an average annual cycle (SI Fig. 6) calculated from the 1980–1994 quantum sensor data and then smoothed using a spline with 30 d.f. (<http://finzi.psych.upenn.edu/R/library/stats/html/smooth.spline.html>).

Daily GPP estimates were linearly interpolated to provide a continuous record at each station. UTM coordinates were used to determine the straight-line distances between adjacent stations: L_1, \dots, L_7 . The transect-average GPP for any time period was calculated as

$$\text{GPP}_{\text{bay}} = \frac{\sum_{i=1}^7 L_i \frac{(\text{GPP}_i + \text{GPP}_{i+1})}{2}}{\sum_{i=1}^7 L_i}, \quad [2]$$

where GPP_{bay} is the transect average and GPP_i is the value for station i . Estimates were made only for those years in which data were available for at least 75% of the month \times station data matrix.

Estimation of Monthly Water Quality Trends. Long-term trends for Chl-*a*, salinity, temperature, and SPM (Fig. 2) were calculated by using USGS data collected at stations 21, 22, 24, 25, 27, 29, 30, and 32 from January 1978 through December 2005. All samples from the upper 3 m were aggregated by their median for each sampling time and location. The spatially weighted average of each water quality variable for each transect was then calculated as

$$C_{\text{bay}} = \frac{\sum_{i=1}^7 L_i \frac{(C_i + C_{i+1})}{2}}{\sum_{i=1}^7 L_i}, \quad [3]$$

where C_{bay} is the transect average and C_i is the value for station i . The long-term trend for each water quality variable by month was then calculated as the Theil–Sen slope, which is the median slope of the lines joining all pairs of points in the same month but in different years. The statistical significance of the slope for each month was determined by the Mann–Kendall test (32).

Long-term trends for DIN and DRP (Fig. 2 A and B) were calculated by using data collected from January 1990 through December 2005 (earlier records are too sparse to include in trend tests). All samples within 0–3 m from the surface were aggregated by their median for each sampling time and location. Transects for each sampling day were summarized by the median value of all available data, rather than weighted averages, because of missing data. The long-term trends and their statistical significance were then calculated as above.

Estimation of Windowed Chlorophyll Trends. Windowed (decadal) trends for Chl-*a* used the same data as for the long-term monthly trends. Trends were determined for each successive decade ending in the years 1987–2005. Trends were calculated by the overall Theil–Sen slope; i.e., using lines joining all pairs of data points in the same month but in different years. The statistical significance of each trend was determined by the seasonal Kendall test, corrected for serial correlation (32). All calculations and tests, unless otherwise specified, were carried out in the R software environment (33). The *USGS Library for S-Plus* was used for the seasonal Kendall tests (34).

Bivalve Filter Feeders. Several independent research or monitoring surveys sampled benthic macrofauna across shallow habitats in the southernmost regions of South SFB from 1987 through 2005. From results of these surveys, we estimated the biomass (ash-free dry tissue weight) of filter-feeding bivalves using abundances, size distributions, and length–weight relationships determined for individual species. Sampling protocols varied

among studies, and general length–weight relationships were applied when these were not measured (SI Table 1).

Demersal Fish, Crabs, and Bay Shrimp. The California Department of Fish and Game has sampled fish, crabs, and shrimp in open-water habitats of SFB since 1980 (www.delta.dfg.ca.gov/baydelta/monitoring/baystudy.asp). Demersal species were sampled with an otter trawl having a 2.5-cm stretch mesh body and a 1.3-cm stretch mesh cod end. We present the annual mean catch per unit effort (CPUE, number ha^{-1}) from monthly (February through October) sampling at 24 stations in the marine domains of SFB (South SFB, Central SFB, and San Pablo Bay). CPUE was calculated for each species as total catch divided by area swept during a 5-min trawl at each station ($n = 5,486$). We present the mean annual CPUE, normalized to 1980–2005 means, for three benthivorous predators: juvenile English sole (*Parophrys vetulus*), juvenile Dungeness crab (*Cancer magister*), and Bay shrimp (*Crangon franciscorum*, *Crangon nigricauda*, and *Crangon nigromaculata*).

Oceanographic Data. We used the monthly Upwelling Index computed by the National Oceanic and Atmospheric Administration Pacific Fisheries Environmental Laboratory from surface atmospheric pressure fields (www.pfeg.noaa.gov/products/PFEL/modeled/indices/upwelling/NA/upwell_menu_NA.html). We report the mean of upwelling indices computed at 36°N and 39°N, stations that bound the entrance to SFB. Sea surface temperature (SST) was measured at the Farallon Islands by the Point Reyes Bird Observatory (http://shorestation.ucsd.edu/active/index_active.html). The series presented here (Fig. 3 C and D) are 12-mo running averages of monthly deviations from 1977–2005 monthly means to remove seasonal effects and highlight departures from normal patterns of upwelling and SST in the California Current.

We thank our colleague Jim Kuwabara for sharing bivalve data, PRBO Conservation Science for providing sea surface temperature data, and N. Van Keuren (City of San Jose) for annual nutrient loadings from the San Jose–Santa Clara Wastewater treatment plant. Long-term observations and research in San Francisco Bay are supported by the United States Geological Survey (USGS) Office of Hydrologic Research, the USGS Toxic Substances Hydrology Program, the USGS Priority Ecosystems Science Program, the San Francisco Bay Regional Monitoring Program through the San Francisco Estuary Institute, and the Interagency Ecological Program for the San Francisco Estuary through the California Department of Fish and Game San Francisco Bay Study.

- Cloern JE (2001) *Mar Ecol Prog Ser* 210:223–253.
- Nichols FH, Cloern JE, Luoma SN, Peterson DH (1986) *Science* 231:567–573.
- Cloern JE (1996) *Rev Geophys* 34:127–168.
- Cloern JE, Schraga TS, Lopez CB, Knowles N, Labiosa RG, Dugdale R (2005) *Geophys Res Lett* 32:L14608.
- Smith SV, Hollibaugh JT (2006) *Limnol Oceanogr* 51:504–517.
- Lucas LV, Koseff JR, Cloern JE, Monismith SG, Thompson JK (1999) *Mar Ecol Prog Ser* 187:1–15.
- Beukema JJ, Dekker R (2005) *Mar Ecol Prog Ser* 287:149–167.
- Myers RA, Baum JK, Shepherd TD, Powers SP, Peterson CH (2007) *Science* 315:1846–1850.
- Pace ML, Cole JJ, Carpenter SR, Kitchell JF (1999) *TREE* 14:483–488.
- Carpenter SR, Cole JJ, Hodgson JR, Kitchell JF, Pace ML, Bade D, Cottingham KL, Essington TE, Houser JN, Schindler DE (2001) *Ecol Monogr* 71:163–186.
- Daskalov GM, Grishin AN, Rodionov S, Mihneva V (2007) *Proc Natl Acad Sci USA* 104:10518–10523.
- Jackson JBC, Kirby MX, Berger WH, Bjorndal KA, Botsford LW, Bourque BJ, Bradbury RH, Cooke R, Eerlandson J, Estes JA, et al. (2001) *Science* 293:629–638.
- Alpine AE, Cloern JE (1992) *Limnol Oceanogr* 37:946–955.
- Petersen JK, Hansen JW, Laursen MB, Clausen P, Carstensen J, Conley DJ, *Ecol Appl*, in press.
- McPhaden MJ (1999) *Science* 283:950–954.
- Freeland HJ, Gatién G, Huyer A, Smith RL (2003) *Geophys Res Lett* 30:1141.
- Kosro PM (2003) *Geophys Res Lett* 30:8023.
- Peterson WT, Schwing FB (2003) *Geophys Res Lett* 30:1896.
- Perry AL, Low PJ, Ellis JR, Reynolds JD (2005) *Science* 308:1912–1915.
- Botsford LW, Lawrence CA (2002) *Prog Oceanogr* 53:283–305.
- Roegner GC, Shanks AL (2001) *Estuaries* 24:244–256.
- Martin MA, Fram JP, Stacey MT (2007) *Mar Ecol Prog Ser* 337:51–61.
- Banas NS, Hickey BM, Newton JA, Ruesink JL (2007) *Mar Ecol Prog Ser* 341:123–139.
- Smayda TJ (2002) *Harmful Algae* 1:95–112.
- McGowan JA, Cayan DR, Dorman LM (1998) *Science* 281:210–217.
- Mantua NJ, Hare SR, Zhang Y, Wallace JM, Francis RC (1997) *Bull Am Meteorol Soc* 78:1069–1079.
- Worm B, Barbier EB, Beaumont N, Duffy JE, Folke C, Halpern BS, Jackson JBC, Lotze HK, Micheli F, Palumbi SR, et al. (2006) *Science* 314:787–790.
- Lotze HK, Lenihan HS, Bourque BJ, Bradbury RH, Cooke RG, Kay MC, Kidwell SM, Kirby MX, Peterson CH, Jackson JBC (2006) *Science* 312:1806–1809.
- Cloern JE (1991) *J Mar Res* 49:203–221.
- Cloern JE, Dufford R (2005) *Mar Ecol Prog Ser* 285:11–28.
- Hager SW, Schemel LE (1997) *Dissolved Nutrient Data for the San Francisco Bay Estuary California, January Through November 1995* (US Geological Survey, Menlo Park, CA), US Geological Survey Open-File Report 97-359.
- Helsel DR, Hirsch RM (1992) *Statistical Methods in Water Resources* (Elsevier, New York).
- R Development Core Team (2005) *R: A Language and Environment for Statistical Computing* (R Foundation for Statistical Computing, Vienna).
- Slack JR, Lorenz DL, et al. (2003) *USGS Library for S-PLUS for Windows, Release 2.1*, US Geological Survey Open-File Report 03-357.

Turbidity as a control on phytoplankton biomass and productivity in estuaries

JAMES E. CLOERN*

(Received 5 September 1986; in revised form 21 May 1987; accepted 22 May 1987)

Abstract—In many coastal plain estuaries light attenuation by suspended sediments confines the photic zone to a small fraction of the water column, such that light limitation is a major control on phytoplankton production and turnover rate. For a variety of estuarine systems (e.g. San Francisco Bay, Puget Sound, Delaware Bay, Hudson River plume), photic-zone productivity can be estimated as a function of phytoplankton biomass times mean irradiance of the photic zone. Net water column productivity also varies with light availability, and in San Francisco Bay net productivity is zero (estimated respiratory loss of phytoplankton balances photosynthesis) when the ratio of photic depth (Z_p) to mixed depth (Z_m) is less than about 0.2. Thus whenever $Z_p:Z_m < 0.2$, the water column is a sink for phytoplankton production.

Much of the spatial and temporal variability of phytoplankton biomass or productivity in estuaries is explained by variations in the ratio of photic depth to mixed depth. For example, phytoplankton blooms often coincide with stratification events that reduce the depth of the surface mixed layer (increase $Z_p:Z_m$). Shallow estuarine embayments (high $Z_p:Z_m$) are often characterized by high phytoplankton biomass relative to adjacent channels (low $Z_p:Z_m$). Many estuaries have longitudinal gradients in productivity that mirror the distribution of suspended sediments: productivity is low near the riverine source of sediments (low $Z_p:Z_m$) and increases toward the estuary mouth where turbidity decreases. Some of these generalizations are qualitative in nature, and detailed understanding of the interaction between turbidity and estuarine phytoplankton dynamics requires improved understanding of vertical mixing rates and phytoplankton respiration.

INTRODUCTION

Estuaries are perceived as highly productive ecosystems because they are often nutrient-rich and have multiple sources of organic carbon to sustain populations of heterotrophs, including riverine and waste inputs and autochthonous primary production by vascular plants, macroalgae, phytoplankton, and benthic microalgae. However, the perception of high productivity should not necessarily extend to the open water column of estuaries where annual phytoplankton production can be less than that of other marine environments. In their review, BOYNTON *et al.* (1982) calculated a mean annual phytoplankton productivity of 190 g C m^{-2} for 45 estuaries. Although this mean value is higher than productivity of the open ocean, it may not exceed phytoplankton productivity in the nearshore coastal ocean. In those few geographic areas where annual phytoplankton production has been measured in an estuary and in the adjacent coastal zone, productivity generally appears to be highest in the coastal ocean (e.g. Table 1).

Phytoplankton production can be very low in coastal plain and river-dominated estuaries, environments with high turbidity caused by river inputs of suspended particu-

* U.S. Geological Survey, 345 Middlefield Rd., Menlo Park, CA 93025, U.S.A.

Table 1. Annual phytoplankton production (g C m^{-2}) in five estuaries and in the adjacent coastal ocean

Estuary	Coastal ocean
Ems-Dollard (middle) = 100–140 ^a	North Sea coastal zone = 160–240 ^b
Hudson River (lower) \cong 180 ^c	New York Bight = 370 ^d
Wassaw Sound = 90 ^e	Shelf waters off Georgia = 285 ^f
	Altamaha River plume = 600 ^f
Fraser River = 120 ^g	Strait of Georgia = 300 ^h
Columbia River = 90 ⁱ	Columbia River plume = 125 ⁱ

^aCOLIJN (1983), ^bGIESKES and KRAAY (1975), ^cCOLIJN's (1983) estimate from data of MALONE (1977), ^dMALONE (1976), ^eFURNER *et al.* (1979), ^freported in YODER *et al.* (1983), ^gPARSONS *et al.* (1970), ^hSTOCKNER *et al.* (1979), ⁱSMALL and FREY (1984). ¹ANDERSON (1972)

late matter (SPM) and/or resuspension of bottom sediments. SPM concentrations in these estuaries often exceed 50 mg l^{-1} , such that light is attenuated rapidly in the water column and phytoplankton photosynthesis is confined to a shallow photic zone. As a consequence, phytoplankton dynamics (including productivity and spatial/temporal changes in biomass) are largely controlled by light availability. This conclusion is consistent with results from both theoretical studies and field investigations. For example, WOFSY'S (1983) model indicates that phytoplankton biomass is an inverse function of SPM concentration, and that light limitation prevents phytoplankton blooms when SPM concentration exceeds 50 mg l^{-1} . PETERSON and FESTA (1984) have used numerical simulation experiments to explore the relations between SPM concentration and phytoplankton biomass and productivity. They conclude that estuarine productivity becomes strongly depressed as SPM concentration increases from 10 to 100 mg l^{-1} . In the past two decades there have been numerous studies of individual estuaries supporting the conclusion that light limitation is the major environmental control on primary production. Examples include the Bristol Channel (JOINT and POMROY, 1981), Ems-Dollard (COLIJN, 1983), Wadden Sea (CADÉE and HEGEMAN, 1979), Delaware Bay (PENNOCK and SHARP, 1986), upper Chesapeake Bay (HARDING *et al.*, 1986), and the Hudson (MALONE, 1976) and Columbia River (SMALL and FREY, 1984) estuaries.

The purpose of this paper is to review some concepts of how turbidity (SPM) influences estuarine phytoplankton, using results from an ongoing study of San Francisco Bay. Although there are direct interactions between phytoplankton and suspended mineral particles (e.g. adhesion and aggregation; AVNIMELECH *et al.*, 1982), I consider here only the indirect effects of SPM through light attenuation. Most concepts that apply to San Francisco Bay also apply to other turbid estuaries, and results from other studies are used to demonstrate how light availability can regulate estuarine phytoplankton dynamics.

SAN FRANCISCO BAY

San Francisco Bay as a representative estuary

San Francisco Bay has been the site of multidisciplinary research in the past decade, much of which is summarized or referenced in CONOMOS (1979), CLOERN and NICHOLS (1985), and NICHOLS *et al.* (1986). This large estuary of the Sacramento and San Joaquin rivers has a number of features that typify shallow and coastal plain estuaries, including: (1) morphology characterized by a central channel of 10–20 m depth flanked by subtidal

shoals <3 m deep; (2) suspended and consolidated sediments composed primarily of lithogenous materials, mostly silt and clay (CONOMOS and PETERSON, 1977); (3) large seasonal variations in the riverine input of suspended sediments, with maxima during winter storms; and (4) a large spatial gradient in turbidity with highest SPM concentrations in the upper estuary, and lowest SPM concentration at the estuary mouth. Further, San Francisco Bay comprises two distinct estuaries. The northern reach (including San Pablo and Suisun Bays, Fig. 1) is representative of partially mixed estuaries with well-developed gravitational circulation (PETERSON *et al.*, 1975) and a turbidity maximum during summer (CONOMOS and PETERSON, 1977). In contrast, the South Bay (Fig. 1) is a lagoon-type estuary with no large, direct source of freshwater. The South Bay is typically well mixed and has substantially lower SPM concentrations than the upper estuary. Results presented here are from several related studies begun in 1980 and utilizing a network of sample sites (Fig. 1) representing (1) the river-ocean gradients of SPM concentration and phytoplankton biomass, and (2) the transverse gradients between the channel and shallows.

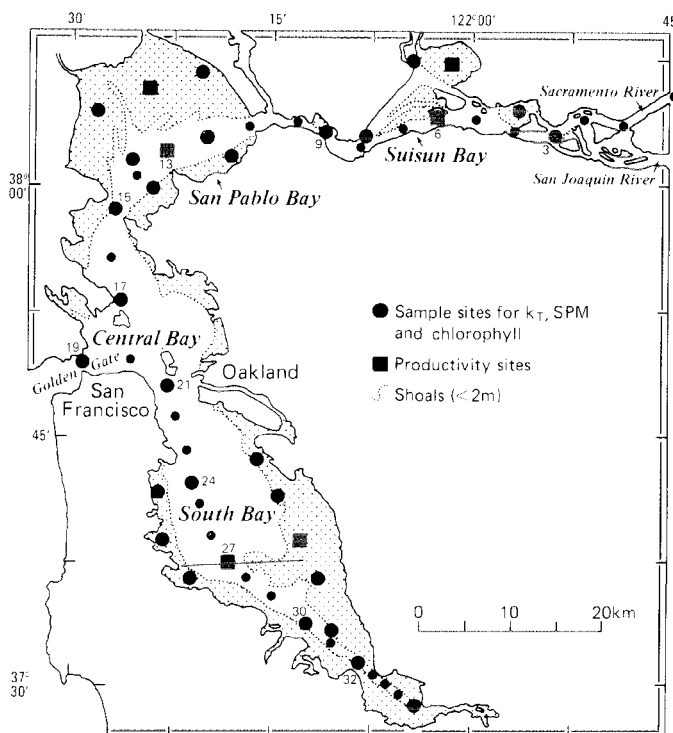


Fig. 1. Map of San Francisco Bay showing sampling sites (large symbols) for biweekly measurement of SPM, k_T , and chlorophyll *a* during 1980. Small circles represent sites where k_T and chlorophyll *a* were estimated from turbidity (nephelometry) and *in vivo* fluorescence. Squares represent sites where primary productivity was measured during 1980 and 1982 (all methods are detailed in CLOERN *et al.*, 1985). Solid line across the South Bay represents the surface transect for continuous measurement of chlorophyll *a* shown in Fig. 7.

TURBIDITY OF ESTUARIES

Turbidity of San Francisco Bay was mapped over an annual cycle by measuring the downwelling light extinction coefficient k_T and SPM concentration, at about 30 fixed sites (Fig. 1) twice monthly during 1980. Regression analysis showed a linear relation between k_T and SPM concentration (Fig. 2). The intercept of this regression (0.77 m^{-1}) represents a mean value for the "background" extinction coefficient due to light attenuation by water, dissolved constituents and the seston uncorrelated with SPM (e.g. phytoplankton). The slope of this regression is a measure of the specific attenuation coefficient (k'_s) of suspended sediments in San Francisco Bay. Although the magnitude of k'_s varies among water bodies depending on the nature of their suspensoids (KIRK, 1985), the mean value for San Francisco Bay ($0.06 \text{ m}^2 \text{ g}^{-1}$) is identical to that measured in the New York Bight with comparable methods (MALONE, 1976), and is similar to k'_s measured in the Ems-Dollard Estuary ($0.03 \text{ m}^2 \text{ g}^{-1}$; COLIJN, 1982) and in Delaware Bay ($0.075 \text{ m}^2 \text{ g}^{-1}$; PENNOCK, 1985).

Strong correlations between k_T and SPM (e.g. Fig. 2) imply that light attenuation in estuaries is primarily a function of suspended sediment concentration. This is an important distinction between estuaries and the open ocean where SPM concentration is low and k_T is more strongly correlated with phytoplankton biomass (SMJIH and BAKER, 1978). Data in Fig. 2 demonstrate the turbidity range commonly observed in estuaries. In San Francisco Bay, k_T ranges between about 1 m^{-1} in the outer estuary to $>10 \text{ m}^{-1}$ in the shallows of the inner estuary. Assuming that the photic depth (Z_p) for algal photosynthesis is the depth of 1% surface irradiance (i.e. $Z_p = 4.61/k_T$), this range of k_T is equivalent to photic depths between about 5 and $<0.5 \text{ m}$. The photic depth of large rivers and river-dominated estuaries is typically $<5 \text{ m}$, and often $<1 \text{ m}$ during peaks in river discharge, or in the estuarine turbidity maximum, or in shallow embayments where resuspension increases the SPM concentration.

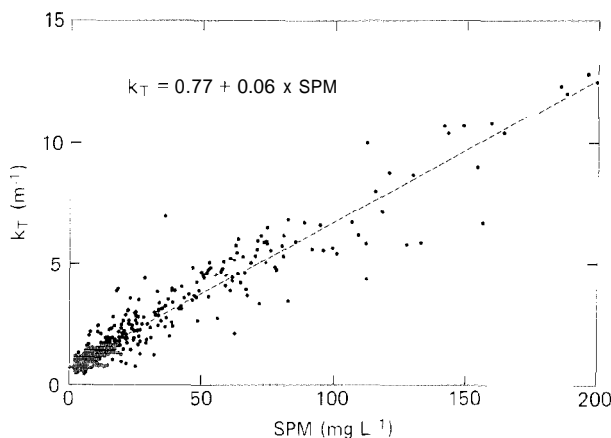


Fig. 2. Linear regression of extinction coefficient k_T against SPM concentration, for measurements made throughout San Francisco Bay during 1980 ($n = 417$; $r^2 = 0.91$). SPM concentration was measured gravimetrically and k_T was calculated from depth profiles of irradiance measured with a LiCor 192S quantum sensor [see HAGER and HARMON (1984) and CLOERN *et al.* (1985) for detailed methods].

Figure 3 summarizes the range of photic depths measured in a variety of estuaries, and compares these with Z_p for some fjords, neritic waters, and the open ocean. The contrast in light penetration between estuaries and other marine systems is obvious, and the extreme shallowness of the photic zone is another fundamental distinction that separates estuaries from coastal and oceanic waters. As a consequence, phytoplankton populations in shallow, turbid estuaries reside in a very different environment than those in deeper, clearer waters of the coastal and open ocean. This distinction has important implications for primary productivity.

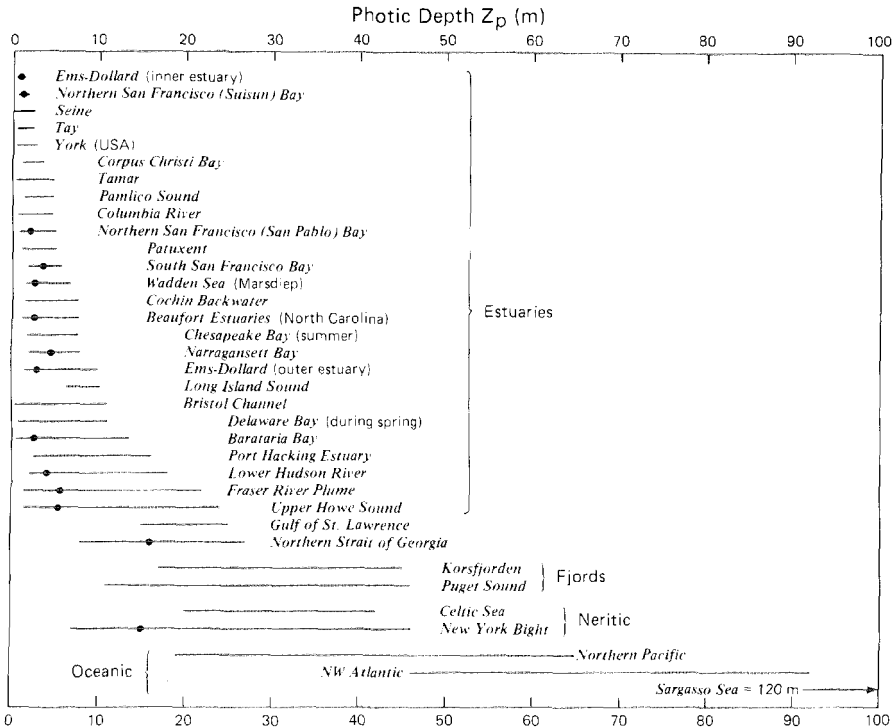


Fig. 3. Photic depths (means shown as circles and ranges shown as horizontal lines) in a variety of estuaries, compared to other marine waters. Photic depths were calculated as $4.61/k_T$ where k_T was either (1) measured directly, (2) estimated as $1.7/\text{Secchi depth}$, or (3) estimated as $0.06 \times \text{SPM}$ where SPM was measured. Data are from the following: Ems-Dollard (COLLIN, 1982), San Francisco Bay (CLOERN *et al.*, 1985), Seine (ROMANA, 1979), Tay (SHOLKOVITZ, 1979), York (MEADE, 1972), Corpus Christi Bay (FLINT, 1984), Tamar (OWENS, 1985), Pamlico (KUENZLER *et al.*, 1979), Columbia River (SMALL and FREY, 1984), Patuxent (STROSS and STOTILEMEYER, 1965), Wadden Sea (CADÉE and HEGEMAN, 1979), Cochin Backwater (QASIM, 1979), Beaufort estuaries (THAYER, 1971), Chesapeake Bay (CHAMP *et al.*, 1980), Narragansett Bay (OVIATT *et al.*, 1981), Long Island Sound and northwest Atlantic (reported by RYHER and YENTSCH, 1957), Bristol Channel (JOINT and POMROY, 1981), Delaware Bay (PENNOCK, 1985), Barataria Bay (SKLAR and TURNER, 1981), Port Hacking Estuary (SCOTT, 1978), Hudson River and New York Bight (MALONE, 1980), Fraser River and Strait of Georgia (STOCKNER *et al.*, 1979), Howe Sound (STOCKNER *et al.*, 1977), Gulf of St. Lawrence (SEVIGNY *et al.*, 1979), Korsfjorden (ERGA and HEIMDAL, 1984), Puget Sound (WINTER *et al.*, 1975), Celtic Sea (PINGREE *et al.*, 1976), North Pacific (OTOBE *et al.*, 1977), Sargasso Sea (STEEMANN NIELSEN, 1975).

ESTUARINE PRIMARY PRODUCTIVITY

Most of the spatial and temporal variability of phytoplankton productivity within San Francisco Bay is correlated with variations in biomass B (mg m^{-3} of chlorophyll a) and an index of light availability $Z_p I_0$ (I_0 = surface irradiance in units of $\text{Ein m}^{-2} \text{d}^{-1}$, where $1 \text{ Ein} = 1 \text{ mole of photons}$). For South Bay and northern San Francisco Bay, daily primary productivity in the photic zone ($\text{mg C m}^{-2} \text{d}^{-1}$) can be estimated with linear functions of $BZ_p I_0$ (COLE and CLOERN, 1984):

$$\text{South Bay: } P_p = 94 + 0.88[BZ_p I_0], n = 29, r^2 = 0.88 \quad (1)$$

$$\text{North Bay: } P_p = 63 + 0.67[BZ_p I_0], n = 53, r^2 = 0.72. \quad (2)$$

Similar analysis of productivity measurements for other estuaries suggests that such relations may apply universally (COLE and CLOERN, 1987). For example, in four estuarine/coastal environments where methods were comparable (Puget Sound, New York Bight, South and North San Francisco Bay), measures of daily productivity fit one linear function:

$$P_p = 146 + 0.73[BZ_p I_0], n = 210, r^2 = 0.82. \quad (3)$$

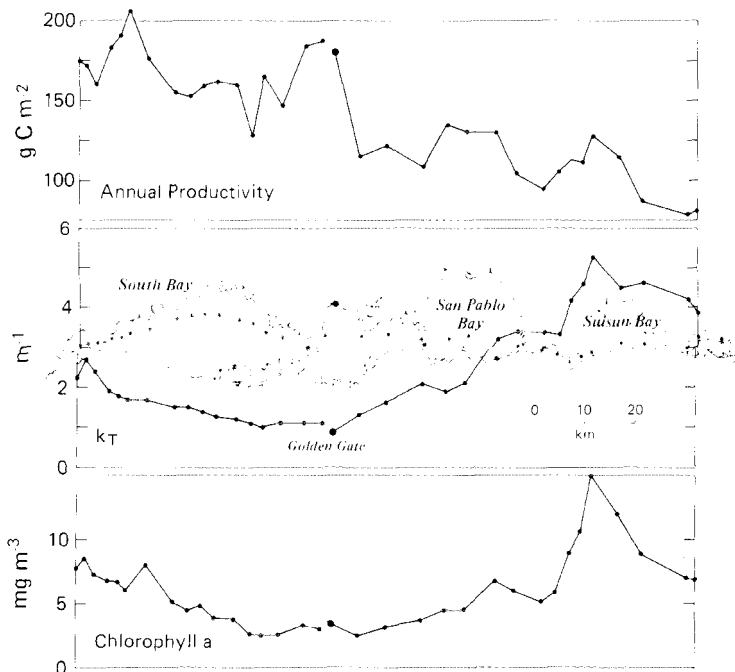


Fig. 4. Longitudinal profiles of estimated annual primary productivity, mean extinction coefficient k_T , and mean chlorophyll a concentration in San Francisco Bay during 1980. Overlay map shows the location of sampling stations. Daily productivity (P_p) was estimated at each sampling site in the channel using equations (1)–(2), surface B determined from *in vivo* fluorescence, Z_p from estimates of k_T by nephelometry, and I_0 measured with LiCor 190S quantum sensors placed in mid-South Bay and in San Pablo Bay throughout 1980. Interpolated values of B and Z_p were used between the biweekly sampling dates. For each site, daily P_p estimates were then summed to yield annual photic zone productivity.

This relation implies that biomass-specific productivity in estuaries is controlled primarily by light availability. Although it is premature to suggest that one empirical model describes P_p for all estuaries, we do know that biomass-specific productivity (P_p/B) is a linear function of light availability in a wide range of estuarine environments including the Ems-Dollard (COLIJN, 1983), western Wadden Sea (CADÉE and HEGEMAN, 1979), Delaware Bay (PENNOCK and SHARP, 1986), Peconic Bay (BRUNO *et al.*, 1983), Great South Bay (LIVELY *et al.*, 1983), and the lower Hudson River Estuary (MALONE, 1977).

Empirical functions such as equations (1)–(3) can be used to estimate primary productivity whenever B , Z_p , and I_0 are known. This approach was used to map predicted annual production along the main axis of San Francisco Bay from the Sacramento River to the estuary mouth at Golden Gate and into the South Bay (Fig. 4). Estimated annual production ranged from about 80 g C m^{-2} in Suisun Bay near the

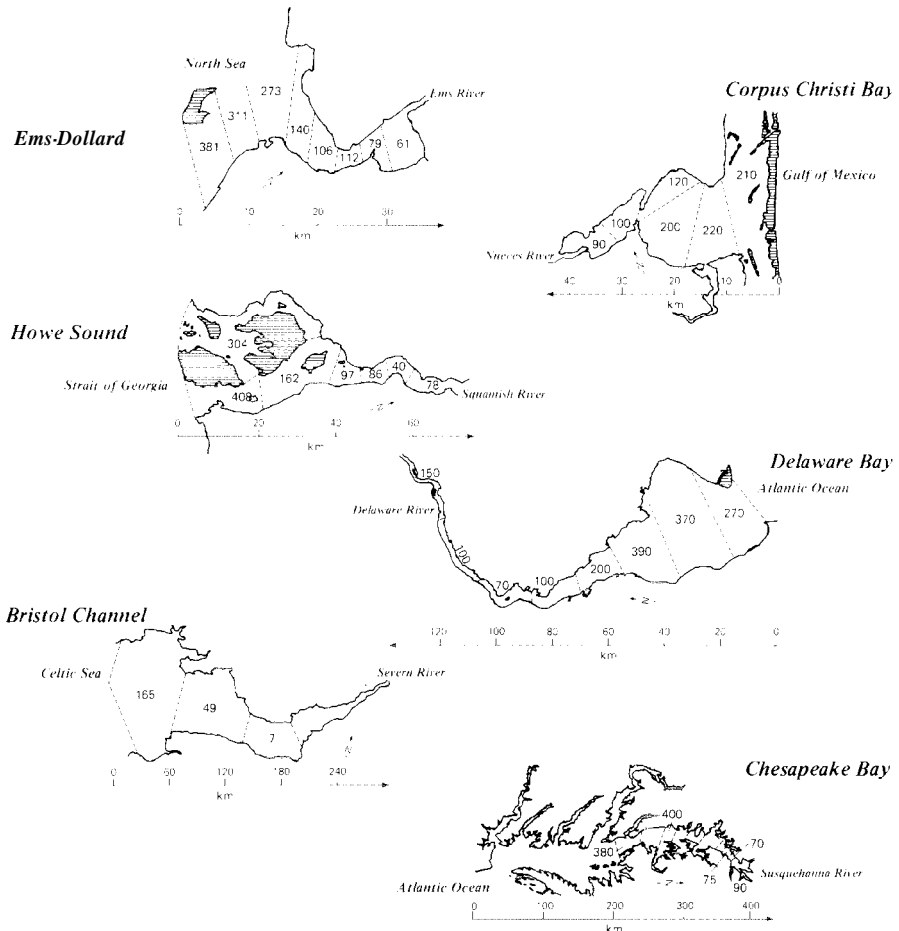


Fig. 5. Horizontal distributions of annual primary productivity in six estuaries, showing spatial gradients between the river and coastal ocean. Data are from COLIJN (1983), FLINI (1984), STOCKNER *et al.* (1977), PENNOCK and SHARP (1986), JOINT and POMROY (1981), and FLEMER (1970).

Sacramento River, to about 210 g C m^{-2} in the lower South Bay (Fig. 4). Hence the large-scale spatial variability in San Francisco Bay is characterized by increasing productivity away from the riverine source of suspended sediments. This distribution of annual production differs from that of phytoplankton biomass, which is highest in the upper estuary (Fig. 4). However, the spatial variability of annual production is related to photic depth, and generally mirrors the distribution of turbidity measured as k_T . Mean values of k_T decrease from the turbidity maximum in Suisun Bay toward the estuary mouth, and are lower in South Bay than in the upper estuary (Fig. 4).

Distributions shown in Fig. 4 indicate that San Francisco Bay is characterized by a longitudinal gradient in primary productivity, that productivity (unlike biomass) increases seaward, and that the overriding control on the distribution of annual production is the longitudinal gradient of photic depth (i.e. k_T) which reflects the distribution of river-derived suspended sediments. These features were observed over 20 years ago in the Patuxent River Estuary (STROSS and STOTFLEMEYER, 1965), and recent investigations have demonstrated similar spatial patterns in other estuaries. Figure 5 shows the large-scale horizontal distribution of annual phytoplankton production in six estuaries. In all cases, production is highest near the estuary mouth, lowest in the upper estuary (or in the turbidity maximum), and mirrors the distribution of k_T . This spatial pattern apparently continues into the coastal zone, where productivity can increase further. For example, annual production in the adjacent coastal ocean exceeds that of the Ems-Dollard, Wassaw Sound, and Hudson, Fraser, and Columbia River estuaries (Table 1). Hence our perception of estuaries as highly productive ecosystems should be qualified with the observation that phytoplankton productivity can be higher in nearby coastal waters where the photic zone is deeper and nutrient concentrations are still sufficient to sustain algal growth.

SIGNIFICANCE OF THE PHOTIC DEPTH: MIXED DEPTH

Net water column productivity

Because the photic depth (Z_p) can be a small fraction of the water column (or surface mixed layer depth, Z_m) in estuaries, measures of photic zone productivity (P_p) do not necessarily reflect the importance of phytoplankton production as a food resource for herbivores. Net production in the water column or mixed layer ($P_{,,}$) is a more useful measure for understanding carbon or energy flow to grazers, and $P_{,,}$ is less than P_p whenever $Z_p < Z_m$. The difference between P_p and $P_{,,}$ is the respiratory loss of assimilated carbon by phytoplankton in the aphotic zone, which can be substantial. The measurement of phytoplankton respiration persists as a difficult problem, but from laboratory studies of algal cultures we can infer bounds on this loss to illustrate the distinction between net production in the photic zone (P_p) and water column ($P_{,,}$).

Photosynthetic rate p ($\text{mg C m}^{-3} \text{ d}^{-1}$) is described by several empirical functions of irradiance I , including the formulation of PLATI and JASSBY (1976):

$$p = p_{\max}[\tanh(al) - rp_{\max}], \quad (4)$$

where p_{\max} is maximum gross photosynthetic rate, a defines photosynthetic efficiency at low irradiance, and r is the respiratory loss rate as a fraction of p_{\max} . Equation (4) can be used to calculate relative productivity (p/p_{\max}) at any depth z in the water column:

$$p' = p/p_{\max} = \tanh(al_z) - r \quad (5)$$

$$p' = \tanh[aI_0 \exp(-k_T z)] - r. \quad (6)$$

Integration of equation (6) over the mixed depth Z_m yields a relative productivity in the water column:

$$P'_m = \int_0^{Z_m} [\tanh(aI_0 \exp\{-k_T z\}) - r] dz. \quad (7)$$

To illustrate the significance of respiratory losses when $Z_p < Z_m$, equation (7) was solved numerically using different values for k_T (i.e. Z_p) and fixed values for a ($= 0.1 \text{ m}^2 \text{ d Ein}^{-1}$), I_0 ($= 40 \text{ Ein m}^{-2} \text{ d}^{-1}$), and Z_m ($= 10 \text{ m}$) representing the San Francisco Bay channel during summer. Relative productivity was then plotted against the ratio of photic depth to mixed depth in Fig. 6, comparing solutions for three values of the specific phytoplankton respiration rate r . This figure shows that net water column production decreases rapidly when $Z_p:Z_m < 1$, and it approaches zero as $Z_p:Z_m$ approaches a critical ratio of between 0.1 and 0.5 (depending on r). Physiological studies suggest that r can range between about 0.05 and 0.25 (e.g. VERITY, 1982), and that a representative value may be around 0.1.

The functions shown in Fig. 6 demonstrate a fundamental property of estuaries and other turbid environments. Regardless of phytoplankton biomass, net water column production is negative whenever the photic depth is less than about 20% of the mixed depth (as in the ocean; SVERDRUP, 1953). This situation occurs, for example, in upper San Francisco Bay during summer. The mean value of $Z_p:Z_m$ in the channel of Suisun Bay is about 0.1 (CLOEKN *et al.*, 1985), indicating that this part of the estuary is a net respiratory sink for phytoplankton production. Hence the biomass maximum in San Francisco Bay (Fig. 4) occurs in a region where net production may be less than zero. The distinction between water column (or mixed layer) production and photic-zone production is therefore critical in turbid estuaries, and measures confined to the photic zone (e.g. Fig. 4) can grossly misrepresent the net production of organic matter that is available to support populations of heterotrophs.

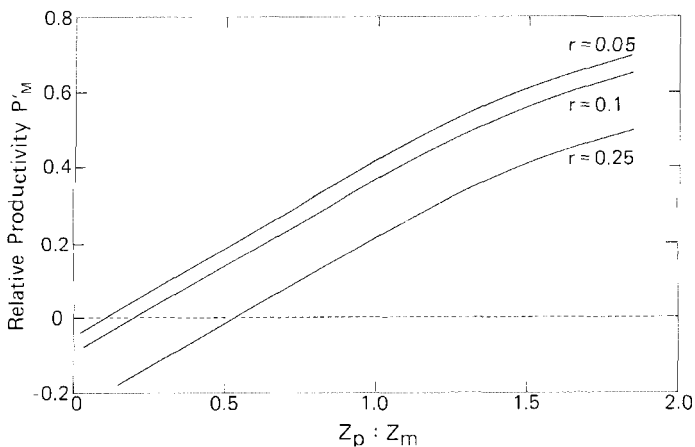


Fig. 6. Relative primary productivity P'_m (equation 7) vs the ratio of photic depth:mixed depth, for three values of the specific respiration rate r .

Spatial distribution of phytoplankton biomass

Because light availability controls productivity it must also play a major role in determining the population growth rate of estuarine phytoplankton, and we expect that biomass should vary across spatial gradients in the ratio of photic depth to mixed depth. For example, in well-mixed estuaries the ratio $Z_p:Z_m$ follows contours of bathymetry and highest phytoplankton biomass is expected to occur over subtidal shoals where Z_m is small and light availability is maximal. To demonstrate this, phytoplankton biomass (calculated chlorophyll *a* from *in-vivo* fluorescence) was measured continuously along transects between the deep channel and subtidal shoals of South San Francisco Bay during March 1985, when the water column was well mixed. A representative profile is given in Fig. 7 showing that biomass increased almost exponentially between the channel and eastern shoals. Biomass was low in the channel where calculated $Z_p:Z_m$ was less than 0.5, and it increased five-fold across the shoals where $Z_p:Z_m$ approached 1.

This horizontal distribution of biomass is consistent with spatial patterns inferred from point samples collected previously. During 1980, mean annual biomass in the shallow embayments of San Francisco Bay was 2–3 times higher than in the nearby channel (CLOERN *et al.*, 1985). During the 1980 summer bloom in Suisun Bay, high resolution mapping by remote sensing showed that chlorophyll *a* concentration consistently exceeded 60 mg m^{-3} in the shoals, and was $<30 \text{ mg m}^{-3}$ in the adjacent channel (CAIS *et al.*, 1985). Hence, in San Francisco Bay, the large-scale spatial variability of phytoplankton biomass is characterized by large transverse gradients, and this variability is caused at least partly by horizontal gradients in light availability and phytoplankton growth rate. Similar spatial patterns have been observed in other estuaries such as Delaware Bay (PENNOCK, 1985), Chesapeake Bay (MALONE *et al.*, 1986), and the Hudson Estuary (SIROIS and FREDERICK, 1978), and are predicted from WOFSY'S (1083) model of phytoplankton growth as a function of k_T and Z_m .

Temporal variability of phytoplankton biomass

Much of the temporal variability of estuarine phytoplankton biomass is also related to variations in light availability. For example, HITCHCOCK and SMAYDA (1977) attribute

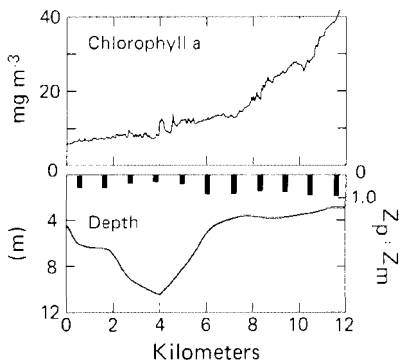


Fig. 7. Profile of near-surface chlorophyll *a*, calculated $Z_p:Z_m$ (vertical bars), and bathymetry along a transverse transect in mid-South San Francisco Bay (see Fig. 1), 21 March 1985. Chlorophyll *a* was estimated from *in vivo* fluorescence [see POWELL *et al.* (1986) for methods]. Water depth (Z_m) was recorded at 11 positions along the transect with a fathometer, and photic depth (Z_p) was estimated at these sites from values of k_T derived from nephelometry.

annual variations in the timing of the Narragansett Bay winter bloom to annual variations in mean water column irradiance \bar{I} ; the winter bloom commences only when \bar{I} exceeds about 40 langley's d^{-1} (19 W m^{-2}). Seasonal variations in SPM concentration can also influence light penetration and phytoplankton dynamics. In San Francisco Bay, bottom resuspension intensifies during mid-summer when wind speed and mean tidal current speed are both rapid. As a consequence, SPM concentration increases, Z_p decreases, growth rates (P_m/B) are near zero, and phytoplankton biomass is low in the upper estuary during mid-summer (CLOERN *et al.*, 1985).

Another important mechanism of temporal variability in $Z_p:Z_m$ is the establishment of density stratification which reduces the mixed layer depth (Z_m) and increases light availability to phytoplankton retained above the pycnocline. Density stratification in estuaries is maintained primarily by buoyancy input from freshwater inflow and is eroded by tidal stirring. Hence stratification events can follow pulsed inputs of freshwater and can respond to changes in tidal current speed (HAAS, 1977; CLOERN, 1984). In South San Francisco Bay, the spring phytoplankton bloom is usually associated with salinity stratification. Two mechanisms may support the spring bloom during stratification events: (1) reduced grazing losses to benthic suspension feeders (CLOERN, 1982), and (2) increased growth rates of phytoplankton in the surface layer as Z_m decreases. For example, an extreme stratification event occurred in early April 1983 when phytoplankton biomass increased rapidly in the surface layer (big. 8). On 29 March 1983 (during a spring tide), the water column of lower South Bay was well mixed and phytoplankton biomass was low. By 8 April 1983 (during a neap tide), a sharp pycnocline had formed at about 6 m and phytoplankton biomass increased four-fold in the surface layer. Similar phytoplankton blooms accompany stratification events in other estuarine systems, including the York River (HAAS *et al.*, 1981), St. Lawrence River (SINCLAIR, 1978), Delaware Bay (PENNOCK, 1985), the Strait of Georgia (STOCKNER *et al.*, 1979), the Korsfjorden (ERGA and HEIMDAL, 1984), and Puget Sound (WINTER *et al.*, 1975). Because estuarine phytoplankton are light-limited, temporal variability in vertical mixing (i.e. Z_m) is a primary mechanism of temporal variability in biomass.

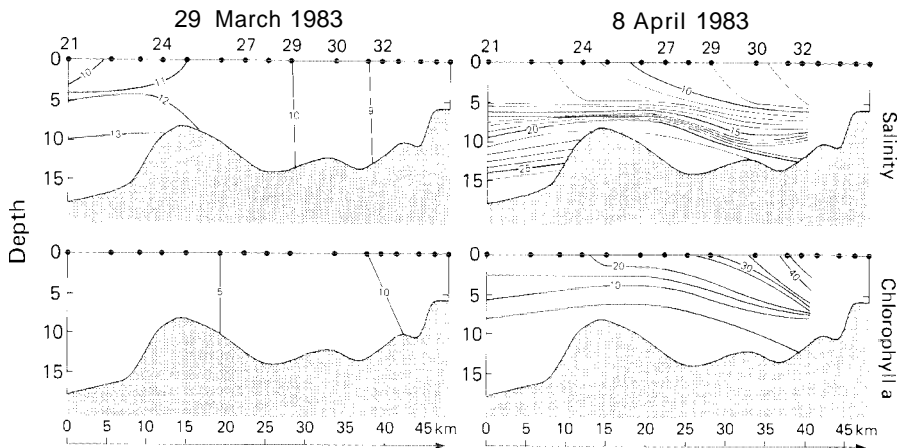


Fig. 8. Salinity and chlorophyll a contours along the South San Francisco Bay channel on 29 March and 8 April 1983. Sample sites correspond to those shown in Fig. 1.

CONCLUSIONS

Results from San Francisco Bay and other estuaries support the generalization that light availability is the critical environmental control on estuarine phytoplankton dynamics. Photic-zone productivity is strongly correlated with light availability, and in many estuaries the spatial distribution of phytoplankton production mirrors the distribution of suspended sediments, i.e. production is highest at the estuary mouth. The growth rate of phytoplankton populations is presumably also a function of light availability, and much of the spatial and temporal variability in biomass can be explained by variations in light exposure. Large-scale horizontal variability of phytoplankton biomass follows distributions of the photic depth: mixed depth ratio ($Z_p:Z_m$), and phytoplankton blooms occur when $Z_p:Z_m$ increases (e.g. through reduction of Z_m by salinity stratification).

Studies of estuarine productivity also suggest, but cannot yet confirm, two important hypotheses. First, depth profiles of algal photosynthesis indicate that the water column of turbid estuaries can be a respiratory sink ($P < 0$), even when phytoplankton biomass is high. This conclusion is based upon assumptions concerning the rates of two processes: vertical mixing (to define Z_m), and phytoplankton dark respiration. Neither process has been studied rigorously in estuaries, and our estimates of net water column production will remain tenuous until simultaneous measures of vertical mixing and respiratory loss are done across a spectrum of estuary types. Second, horizontal profiles suggest that phytoplankton productivity in estuaries may be less than in the adjacent coastal ocean. Our perception of estuaries as highly productive ecosystems should be placed in a broader geographic context, and this requires measurement of production along the continuum from rivers into the coastal ocean. Both hypotheses form a basis for the future research that is needed to better define the role of estuaries as sources of organic matter for consumer organisms.

Acknowledgements—I thank my colleagues Jan Thompson, Brian Cole, Dave Peterson, and Fred Nichols for their thoughtful comments and suggestions that contributed to the production of this paper.

REFERENCES

- ANDERSON G. C. (1972) Aspects of marine phytoplankton studies near the Columbia River, with special reference to a subsurface chlorophyll maximum. In: *The Columbia River estuary and adjacent ocean waters*, A. T. PRUTER and D. L. ALVERSON, editors, University of Washington, Seattle.
- AVNIMELECH Y., B. W. TROEGER and L. W. REED (1982) Mutual flocculation of algae and clay: Evidence and implications. *Science*, **216**, 63–65.
- BOYNTON W. R., W. M. KEMP and C. W. KEEFE (1982) A comparative analysis of nutrients and other factors influencing estuarine phytoplankton production. In: *Estuarine comparisons*, V. S. KENNEDY, editor, Academic Press, New York, pp. 69–90.
- BRUNO S. F., R. D. STAKER, G. M. SHARMA and J. T. TURNER (1983) Primary productivity and phytoplankton size fraction dominance in a temperate north Atlantic estuary. *Estuaries*, **6**, 200–211.
- CADÉE G. C. and J. HEGEMAN (1979) Phytoplankton primary production, chlorophyll and composition in an inlet of the western Wadden Sea (Marsdiep). *Netherlands Journal of Sea Research*, **13**, 224–241.
- CATTS G. P., S. KHORRAM, J. E. CLOERN, A. W. KNIGHT and S. D. DEGLORIA (1985) Remote sensing of tidal chlorophyll *a* variations in estuaries. *International Journal of Remote Sensing*, **6**, 1685–1706.
- CHAMP M. A., G. A. GOULD III, W. E. BOZZO, S. E. ACKLESON and K. C. VIERRA (1980) Characterization of light extinction and attenuation in Chesapeake Bay, August, 1977. In: *Estuarine perspectives*, V. S. KENNEDY, editor, Academic Press, New York, pp. 262–277.
- CLOERN J. E. (1982) Does the benthos control phytoplankton biomass in South San Francisco Bay (USA)? *Marine Ecology Progress Series*, **9**, 191–202.
- CLOERN J. E. (1984) Temporal dynamics and ecological significance of salinity stratification in an estuary (South San Francisco Bay, USA). *Oceanologica Acta*, **7**, 137–141.

- CLOERN J. E. and F. H. NICHOLS, editors (1985) *Temporal dynamics of an estuary: San Francisco Bay*. Dr. W. Junk Publishers, Dordrecht, 237 pp.
- CLOERN J. E., B. E. COLE, R. L. J. WONG and A. E. ALPINF (1985) Temporal dynamics of estuarine phytoplankton. A case study of San Francisco Bay. *Hydrobiologia*, **129**, 153-176.
- COLE B. E. and J. E. CLOERN (1984) Significance of biomass and light availability to phytoplankton productivity in San Francisco Bay. *Marine Ecology Progress Series*, **17**, 15-24.
- COLE B. E. and J. E. CLOERN (1987) An empirical model for estimating phytoplankton productivity in estuaries. *Marine Ecology Progress Series*, **36**, 299-305.
- COLLIN F. (1982) Light absorption in the waters of the Ems-Dollard Estuary and its consequences for the growth of phytoplankton and microphytobenthos. *Netherlands Journal of Sea Research*, **15**, 196-216.
- COLLIN F. (1983) Primary production of phytoplankton in the Ems-Dollard Estuary. Ph.D thesis. University of Groningen, BOEDE-Publicaties en Verslagen, 123 pp.
- CONOMOS T. J., editor (1979) *San Francisco Bay: The urbanized estuary*, Pacific Division American Association for the Advancement of Science, San Francisco, 413 pp.
- CONOMOS T. J. and D. H. PETERSON (1977) Suspended-particle transport and circulation in San Francisco Bay: An overview. In: *Estuarine processes*. M. WILEY, editor, Academic Press, New York, pp. 82-97.
- ERGA S. R. and B. R. HEIMDAL (1984) Ecological studies on the phytoplankton of Korsfjorden, western Norway. The dynamics of a spring bloom seen in relation to hydrographical conditions and light regime. *Journal of Plankton Research*, **6**, 67-90.
- FLEMER D. A. (1970) Primary production in the Chesapeake Bay. *Chesapeake Science*, **11**, 117-129.
- FLINI R. W. (1984) Phytoplankton production in the Corpus Christi Bay Estuary. *Contributions in Marine Science*, **27**, 65-83.
- GIESKES W. W. C. and G. W. KRAAY (1975) The phytoplankton spring bloom in Dutch coastal waters of the North Sea. *Netherlands Journal of Sea Research*, **9**, 166-196.
- HAAS L. W. (1977) The effect of the spring-neap tidal cycle on the vertical salinity structure of the James, York and Rappahannock Rivers, Virginia, USA. *Estuarine, Coastal and Marine Science*, **5**, 485-496.
- HAAS L. W., S. J. HASTINGS and K. L. WEBB (1981) Phytoplankton response to a stratification-mixing cycle in the York River Estuary during late summer. In: *Nutrients and estuaries*. B. J. NIELSON and L. E. CRONIN, editors, Humana Press, pp. 619-636.
- HAGER S. W. and D. D. HARMON (1984) Chemical determination of particulate nitrogen in San Francisco Bay. A comparison of two estimates. *Estuarine, Coastal and Shelf Science*, **19**, 181-191.
- HARDING L. W. JR. B. W. MEESON and T. R. FISHER JR (1986) Phytoplankton production in two East coast estuaries: Photosynthesis-light functions and patterns of carbon assimilation in Chesapeake and Delaware Bays. *Estuarine, Coastal and Shelf Science*, **23**, 737-806.
- HITCHCOCK G. L. and T. J. SMAYDA (1977) The importance of light in the initiation of the 1972-1973 winter-spring diatom bloom in Narragansett Bay. *Limnology and Oceanography*, **22**, 126-131.
- JOINT I. R. and A. J. POMROY (1981) Primary production in a turbid estuary. *Estuarine, Coastal and Shelf Science*, **13**, 303-316.
- KIRK J. T. O. (1985) Effect of suspensoids (turbidity) on penetration of solar radiation in aquatic ecosystems. *Hydrobiologia*, **125**, 195-208.
- KUENZLER E. J., D. W. STANLEY and J. P. KOENINGS (1979) *Nutrient kinetics of phytoplankton in the Pamlico River, North Carolina*. University of North Carolina Water Resources Research Institute Report No. 139, 163 pp.
- LIVELY J. S., Z. KAUFMAN and E. J. CARPENTER (1983) Phytoplankton ecology of a barrier island estuary: Great South Bay, New York. *Estuarine, Coastal and Shelf Science*, **16**, 51-68.
- MALONE T. C. (1976) Phytoplankton productivity in the apex of the New York Bight: Environmental regulation of productivity/chlorophyll *a*. In: *The middle Atlantic Shelf and New York Bight*, M. G. GROSS, editor, Limnology and Oceanography Special Symposium **2**, 260-272.
- MALONE T. C. (1977) Environmental regulation of phytoplankton productivity in the lower Hudson Estuary. *Estuarine, Coastal and Marine Science*, **5**, 157-171.
- MALONE T. C. (1980) Size-fractionated primary productivity of marine phytoplankton. In: *Primary productivity in the sea*, P. G. FAIKOWSKI, editor, Plenum Press, New York, pp. 301-319.
- MALONE T. C., W. M. KEMP, H. W. DUCKLOW, W. R. BOYNTON, J. H. TUTTLE and R. B. JONAS (1986) Lateral variation in the production and fate of phytoplankton in a partially stratified estuary. *Marine Ecology Progress Series*, **32**, 149-160.
- MEADE R. H. (1972) Transport and deposition of sediments in estuaries. In: *Environmental framework of coastal plain estuaries*, B. W. NELSON, editor, Geological Society of America Memoirs, **133**, pp. 91-120.
- NICHOLS F. H., J. E. CLOERN, S. N. LUOMA and D. H. PETERSON (1986) The modification of an estuary. *Science*, **231**, 567-573.
- OTOBE H., T. NAKAI and A. HATTORI (1977) Underwater irradiance and Secchi disk depth in the Bering Sea and the northern North Pacific in summer. *Marine Science Communications*, **3**, 255-270.
- OVIATI C., B. BUCKLEY and S. NIXON (1981) Annual phytoplankton metabolism in Narragansett Bay calculated from survey field measurements and microcosm observations. *Estuaries*, **4**, 167-175.

- OWENS N. J. P. (1985) Variations in the natural abundance of ^{15}N in estuarine suspended particulate matter: A specific indicator of biological processing. *Estuarine, Coastal and Shelf Science*, **20**, 505–510.
- PARSONS T. R., R. J. LEBRASSEUR and W. E. BARRACLOUGH (1970) Levels of production in the pelagic environment of the Strait of Georgia, British Columbia: A review. *Journal of the Fisheries Research Board of Canada*, **27**, 1251–1264.
- PENNOCK J. R. (1985) Chlorophyll distributions in the Delaware Estuary: Regulation by light-limitation. *Estuarine, Coastal and Shelf Science*, **21**, 711–725.
- PENNOCK J. R. and J. H. SHARP (1986) Phytoplankton production in the Delaware Estuary: Temporal and spatial variability. *Marine Ecology Progress Series*, **34**, 143–155.
- PETERSON D. H. and J. P. FESTA (1984) Numerical simulation of phytoplankton productivity in partially mixed estuaries. *Estuarine, Coastal and Shelf Science*, **19**, 563–589.
- PETERSON D. H., T. J. CONOMOS, W. W. BROENKOW and P. C. DOHERTY (1975) Location of the non-tidal current null zone in northern San Francisco Bay. *Estuarine and Coastal Marine Science*, **3**, 1–11.
- PINGREE R. D., P. M. HOLLIGAN, G. T. MARDELL and R. N. HEAD (1976) The influence of physical stability on spring, summer and autumn phytoplankton blooms in the Celtic Sea. *Journal of the Marine Biological Association of the United Kingdom*, **56**, 845–873.
- PLATT T. and A. D. JASSBY (1976) The relationship between photosynthesis and light to natural assemblages of coastal marine phytoplankton. *Journal of Phycology*, **12**, 421–430.
- POWELL T. M., J. E. CLOERN and R. A. WALTERS (1986) Phytoplankton spatial distribution in South San Francisco Bay: Mesoscale and small-scale variability. In: *Estuarine variability*, D. A. WOLFE, editor, Academic Press, New York, pp. 369–383.
- QASIM S. Z. (1979) Primary production in some tropical environments. In: *Marine production mechanisms*. M. J. DUNBAR, editor, Cambridge University Press, Cambridge, pp. 31–70.
- ROMANA L. A. (1979) Role du bouchon vaseux dans un ecosystème estuarien. *2es Journées de la thermoeologie*, Institut Scientifique et Technique des Pêches Maritimes, pp. 121–140.
- RYTHER J. H. and C. S. YEYNTSCH (1957) The estimation of phytoplankton production in the ocean from chlorophyll and light data. *Limnology and Oceanography*, **2**, 281–286.
- SCOTT B. D. (1978) Phytoplankton distribution and light attenuation in Port Hacking Estuary. *Australian Journal of Marine and Freshwater Research*, **29**, 31–44.
- SEVIGNY J.-M., M. SINCLAIR, M. I. EL-SABH, S. POULEY and A. COOTE (1979) Summer plankton distributions associated with the physical and nutrient properties of the northwestern Gulf of St. Lawrence. *Journal of the Fisheries Research Board of Canada*, **36**, 187–203.
- SHOLKOVITZ E. R. (1979) Chemical and physical processes controlling the chemical composition of suspended material in the River Tay Estuary. *Estuarine and Coastal Marine Science*, **8**, 523–545.
- SINCLAIR M. (1978) Summer phytoplankton variability in the lower St. Lawrence Estuary. *Journal of the Fisheries Research Board of Canada*, **35**, 1171–1185.
- SIROIS D. L. and S. W. FREDRICK (1978) Phytoplankton and primary production in the lower Hudson River Estuary. *Estuarine and Coastal Marine Science*, **7**, 413–423.
- SKLAR F. H. and R. E. TURNER (1981) Characteristics of phytoplankton production off Barataria Bay in an area influenced by the Mississippi River. *Contributions in Marine Science*, **24**, 43–106.
- SMALL L. F. and B. E. FREY (1984) Water column primary production in the Columbia River Estuary. Final Report, Columbia River Estuary Data Development program, Astoria, Oregon, 133 pp.
- SMITH R. C. and K. S. BAKEK (1978) The bio-optical state of ocean waters and remote sensing. *Limnology and Oceanography*, **23**, 247–259.
- STEEMANN NIELSEN E. (1975) *Marine photosynthesis with special emphasis on the ecological aspects*, Elsevier, Amsterdam, 141 pp.
- STOCKNER J. G., D. D. CLIFF and D. B. BUCHANON (1977) Phytoplankton production and distribution in Howe Sound, British Columbia: A coastal marine embayment-fjord under stress. *Journal of the Fisheries Research Board of Canada*, **34**, 907–917.
- STOCKNER J. G., D. D. CLIFF and K. R. S. SHORTREED (1979) Phytoplankton ecology of the Strait of Georgia, British Columbia. *Journal of the Fisheries Research Board of Canada*, **36**, 657–666.
- STROSS R. G. and J. R. STOTLEMEYER (1965) Primary production in the Patuxent River. *Chesapeake Science*, **6**, 125–140.
- SVERDRUP H. U. (1953) On conditions for the vernal blooming of phytoplankton. *Journal du Conseil, Conseil International pour l'Exploration de la Mer*, **18**, 287–295.
- THAYER G. W. (1981) Phytoplankton production and the distribution of nutrients in a shallow unstratified estuarine system near Beaufort, N.C. *Chesapeake Science*, **12**, 240–253.
- TURNER R. E., S. W. WOO and H. R. JIITS (1979) Phytoplankton production in a turbid, temperate salt-marsh estuary. *Estuarine and Coastal Marine Science*, **9**, 603–613.
- VERITY P. G. (1982) Effects of temperature, irradiance, and daylength on the marine diatom *Leptocylindricus danicus* Cleve. III, Dark respiration. *Journal of Experimental Marine Biology and Ecology*, **60**, 197–207.
- WINTER D. F., K. BANSE and G. C. ANDERSON (1975) The dynamics of phytoplankton blooms in Puget Sound, a fjord in the northwestern United States. *Marine Biology*, **29**, 139–176.

- WOFSY S C (1983) A simple model to predict extinction coefficients and phytoplankton biomass in eutrophic waters *Limnology and Oceanography*, **28**, 1144-1155.
- YODER J A, L P ATKINSON, S S BISHOP, E E HOWMANN and T N LES (1983) Effect of upwelling on phytoplankton productivity of the outer southeastern United States continental shelf *Continental Shelf Research*, **1**, 385-404

Significance of biomass and light availability to phytoplankton productivity in San Francisco Bay

Brian E. Cole and James E. Cloern

US Geological Survey, 345 Middlefield Road, MS 96, Menlo Park, California 94025, USA

ABSTRACT: Primary productivity was measured monthly at 6 sites within San Francisco Bay, USA, throughout 1980. The 6 sites were chosen to represent a range of estuarine environments with respect to salinity, phytoplankton community composition, turbidity, and water depth. Annual net production over the photic zone ranged from 95 to 150 g C m⁻², and was highest in regions of lowest turbidity. Daily photic zone net productivity PN_{pd} ranged from 0.05 to 2.2 g C m⁻² d⁻¹, and was significantly correlated with the composite parameter B I₀/ε (where B = phytoplankton biomass; I₀ = daily surface insolation; ε = attenuation coefficient). Linear regression of PN_{pd} against B I₀/ε indicated that most (82 %) of the spatio-temporal variability in primary productivity within this estuary is explained by variations in light availability and phytoplankton biomass. We also calculated annual water-column net productivity PN_{wy} as a fraction of annual gross productivity PG_y. The ratio PN_{wy} : PG_y was inversely related to the ratio of water depth H to annual mean photic depth \bar{Z}_p . This linear relation indicates that the water column of San Francisco Bay is a net photosynthetic source of organic carbon only when the ratio H : \bar{Z}_p < 6. In deep turbid habitats, where H : \bar{Z}_p > 6, respiratory loss exceeds productivity. Thus, 2 empirical formulations allow us to estimate productivity over the photic zone and water column from simple properties that are easily measured.

INTRODUCTION

Estimates of annual phytoplankton productivity in estuaries range between 6.8 g C m⁻² (Joint and Pomroy, 1981) in very turbid water to 530 g C m⁻² (Stockner and Cliff, 1979) in a clearer system. However, the study of production by estuarine phytoplankton is in its infancy, and although annual rates of phytoplankton production have been reported for a number of estuaries (Boynton et al., 1982), the processes that control primary and secondary productivity in estuaries are poorly understood. In a review of factors controlling phytoplankton production in 63 estuarine systems, Boynton et al. (1982) note that environmental data are poor predictors of primary productivity. They conclude that in a broad spectrum of estuaries algal production is high in warm periods and that the ratio of nitrogen to phosphorus is low during algal blooms. Otherwise, they find that generalities regarding primary productivity cannot be made when all estuarine systems are considered together.

Spatial and seasonal changes in phytoplankton productivity are described for numerous estuaries (e.g. Williams, 1966; Williams and Murdoch, 1966; Flemer,

1970; Cadée and Hegeman, 1974; Malone, 1977; Cadée, 1978; Colijn, 1978; Stockner and Cliff, 1979; Stockner et al., 1979; Joint and Pomroy, 1981). From such studies we know that productivity in a nutrient replete estuary can vary with phytoplankton biomass, turbidity, daylength, or temperature, but the findings from specific locations cannot be easily related to other estuarine systems. Except for Boynton et al. (1982), there has been little effort in developing a unified theory of what factors control primary productivity in diverse estuarine systems. In simplest terms, primary productivity in nutrient-rich waters is a function of 3 basic variables: phytoplankton biomass, biomass-specific carbon assimilation rate, and light availability. Although these may vary due to changes in phytoplankton community composition, light adaptation, grazing, settling, transport processes, temperature, daylength, or turbulence, if appropriately expressed, productivity should be predictable in terms of the 3 basic variables.

In this paper we present the results of an annual study of phytoplankton production in San Francisco Bay, USA. We show that seasonal variations in productivity differ among geographic regions within the estu-

ary, but that daily net productivity in the photic zone is highly correlated with a simple composite parameter composed of phytoplankton biomass and light availability. We also show that the concept of critical depth : mixed depth ratio, which has become a paradigm of phytoplankton ecology in oceans and lakes (Parsons and Takahashi, 1973; Harris, 1978), has relevance to turbid estuaries such as San Francisco Bay. Using the water depth : photic depth ratio we predict the fraction of gross primary production that is lost to respiration and the fraction that remains for potential consumption by herbivores.

San Francisco Bay (Fig. 1) offers a variety of subenvironments for studying the regulation of primary pro-

(1979). Each major embayment (South Bay, San Pablo Bay, Suisun Bay) is composed of a central, relatively deep (≈ 10 to 15 m) channel where the photic zone is about 10 % of the water depth, bounded by broad expanses of shoals (≈ 2 m depth) where the photic zone is 50 to 100 % of water depth. Typically, nutrient levels throughout the Bay exceed $10 \mu\text{M}$ dissolved inorganic nitrogen, $2 \mu\text{M}$ phosphate, and $50 \mu\text{M}$ silicate (Conomos et al., 1979). Phytoplankton community composition differs in the three major embayments. The South Bay population is usually dominated by microflagellates ($< 15 \mu\text{m}$ length) and small ($< 10 \mu\text{m}$ diameter) centric diatoms, although *Skeletonema costatum* and larger ($> 70 \mu\text{m}$ diameter) diatoms *Thalassiosira* spp. and *Coscinodiscus* spp. are occasionally abundant. In San Pablo Bay the population comprises marine-brackish diatoms and microflagellates, whereas in Suisun Bay freshwater diatoms usually predominate in winter and *S. costatum* and *T. eccentrica* are dominant during the summer bloom (Wong and Cloern, 1982).

METHODS

Between January 1980 and February 1981 light attenuation, chlorophyll *a*, and phytoplankton production were measured monthly at a deep-water and shallow-water site in each of the 3 major embayments in San Francisco Bay (Fig. 1). Light attenuation coefficient ϵ (all symbols and units are given in Table 1) was measured using a LiCor model 185 quantum meter coupled to a 192S sensor. Total ambient insolation I_0 (photosynthetically active radiation) during the course of an incubation experiment was measured using a LiCor 190 quantum sensor and a recording integrator. Photic depth Z_p (depth of 1 % ambient light energy) was estimated as $\ln(100)/\epsilon$.

Triplicate chlorophyll *a* samples from each site were prescreened through $59 \mu\text{m}$ Nitex screen (see below), then filtered onto Gelman type A/E glass-fiber filters. Chlorophyll *a* concentration B , corrected for phaeopigments, was determined by fluorometry (Strickland and Parsons, 1972). Although prescreening with a $59 \mu\text{m}$ mesh may remove large algal cells or chains, there was never a measurable difference in *in vivo* fluorescence between whole and screened samples, except at Station 318 on May 8 and at Stations 13 and 318 on June 5.

Productivity samples were collected from a single depth, 2 m in the channel and 1 m in the shoals, and also prescreened through a $59 \mu\text{m}$ Nitex screen. The small mesh was used to eliminate grazing by copepod nauplii and tintinnid ciliates which at times constituted a substantial fraction of zooplankton biomass (Hutchinson, 1981; 1982a, b). Following inoculation with carbon 14 ($5 \mu\text{Ci}$ in a 150 ml bottle), 24 h simu-

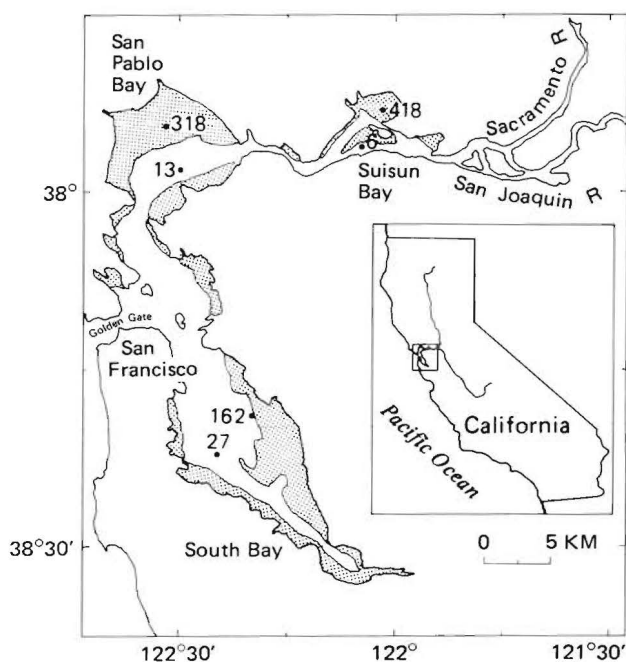


Fig. 1. Map of San Francisco Bay showing locations of incubation sampling sites. Shaded portions: areas where water depths (MLLW) are less than 2 m

duction in nutrient-rich, turbid waters. The northern reach, which includes San Pablo Bay and Suisun Bay, is a river-dominated estuary. It is partially or well mixed (depending on discharge from the Sacramento and San Joaquin Rivers), turbid, and characterized by a large horizontal salinity gradient. In contrast, the southern reach (South Bay) is a brackish embayment that has no large direct riverine source of freshwater, is usually vertically mixed (although salinity stratification occurs in winter–spring; Cloern, 1984), is less turbid than the northern reach, and usually has a small horizontal salinity gradient. Detailed descriptions of the hydrographic, nutrient, and biological character of the San Francisco Bay system are given in Conomos

Table 1. Definitions of variables (and their units)

Variable	Definition	Units
ϵ	Light attenuation coefficient	m^{-1}
I_o	Ambient photosynthetically active radiation	Einsteins $(m^2 d)^{-1}$
Z_p	Photic-zone depth	m
B	Chlorophyll <i>a</i> concentration	mg chl <i>a</i> m^{-3}
P_m^B	Maximum carbon assimilation rate	mg C (mg chl <i>a</i> d) $^{-1}$
PN_{pd}	Daily photic zone net productivity	g C $(m^2 d)^{-1}$
PN_{py}	Annual photic zone net productivity	g C $(m^2 yr)^{-1}$
R^B	Biomass-specific respiration rate	mg C (mg chl <i>a</i> d) $^{-1}$
PG_y	Annual gross productivity	g C $(m^2 yr)^{-1}$
\bar{Z}_p	Annual mean photic depth	m
H	Water-column depth	m
PN_{wy}	Annual water column net productivity	g C $(m^2 yr)^{-1}$
R_{wy}	Annual water-column respiration	g C $(m^2 yr)^{-1}$
R_{py}	Annual photic-zone respiration	g C $(m^2 yr)^{-1}$

lated *in situ* incubations were done in a deck incubator. Samples were exposed to natural sunlight of 8 intensities: 100, 55, 30, 15, 8, 3, 1, and 0 % of ambient irradiance. On clear days, light entering the deck incubator was attenuated by an additional 25 to 40 % with a neutral density Plexiglas filter positioned over the samples. Hence, photoinhibition, which is unlikely to occur in turbid well-mixed environments (Marra, 1978; Joint and Pomroy, 1981), was never observed. Irradiance within the incubator was continuously recorded with a submersible quantum sensor.

Following incubation, subsamples from each bottle were filtered by gravity or low pressure (< 110 mm Hg) through Gelman type A/E glass-fiber filters. A 3 ml aliquot of each filtrate and duplicate unfiltered 3 ml aliquots from each bottle were placed in scintillation vials. After adding 0.1 ml of 0.2 N HCl, each aliquot was bubbled under vacuum for 15 min while $^{14}CO_2$ was stripped from the sample (Schindler et al., 1972). The residual activity of the sample was measured using a liquid scintillation spectrometer. All carbon uptake rates were corrected for activity of the filtrate (excretion) and dark-bottle uptake.

Maximum daily carbon assimilation rates P_m^B were derived from chlorophyll *a* normalized photosynthesis-irradiance (P-I) curves. The Gauss-Newton nonlinear least squares technique was used to obtain the best fit of the data to the hyperbolic tangent function (Platt and Jassby, 1976):

$$P^B = P_m^B \tanh(\alpha I / P_m^B) - R^B \quad (1)$$

Simulated incubation depths were calculated as $-\ln(I_i/I_o)/\epsilon$, where I_i/I_o is the fraction of daily surface insolation received by bottle *i*. Daily photic zone net productivity PN_{pd} was calculated by integrating (trapezoidal quadrature) measured rates of carbon uptake [mg C $(m^3 d)^{-1}$] over the photic depth. Annual

photic zone net productivity PN_{py} was estimated for each site by integrating PN_{pd} over the year. Baywide the specific respiration rate R^B , as the intercept of the P-I curves (Steemann Nielsen and Hansen, 1959), averaged 4.5 % of P_m^B over the year. Since even after a 24 h incubation it is unlikely that samples held at low-light had reached a net productivity rate (Hobson et al., 1976), the intercepts were probably underestimates of the true specific respiration rate (Peterson, 1980). In previous studies in San Francisco Bay (Peterson et al., in press) a typical respiration rate was found to be about 10 % of P_m^B using oxygen light-dark bottle techniques in 24 h incubations. In the analysis presented below, we assumed that R^B was constant and equal to 0.1 P_m^B , and calculated annual gross productivity PG_y as the sum of annual net productivity and integral respiration over the photic zone.

RESULTS

Ambient insolation during the course of the experiments (Fig. 2a, 3a, 4a) was similar for all sites and ranged from 8 to 55 Einsteins $(m^2 d)^{-1}$. Attenuation coefficients varied substantially between embayments and at times between channel and shoal sites within embayments (Fig. 2b, 3b, 4b). Photic depths in South Bay were fairly constant throughout the year and averaged about 3.2 m. In San Pablo Bay large variations in attenuation coefficient resulted in fluctuations of photic depth that ranged from about 0.3 to 6.6 m. Photic depths at both sites in Suisun Bay remained < 1 m throughout most of the year. The annual range of attenuation coefficients was large at most sites, but based on annual mean attenuation coefficients (Table 2) turbidity in South Bay was less than in San Pablo Bay which was less than in Suisun Bay. In

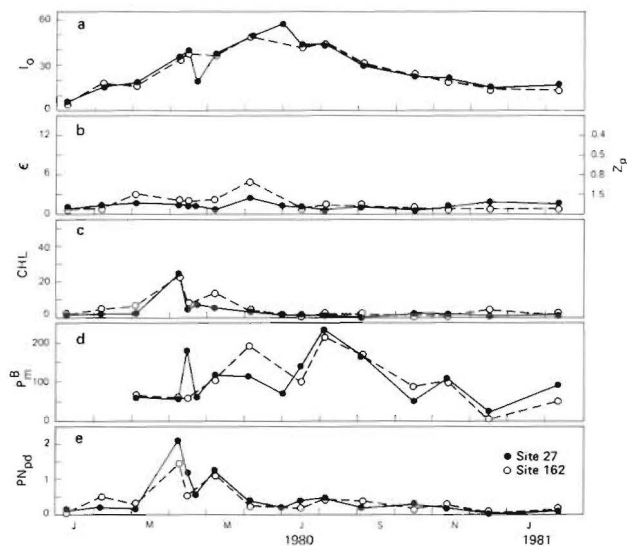


Fig. 2. South Bay. Seasonal variation of (a) ambient irradiance I_0 ($E m^{-2} d^{-1}$); (b) attenuation coefficient ϵ (m^{-1}) and photic depth Z_p (m); (c) chlorophyll a CHL ($mg m^{-3}$); (d) maximum carbon assimilation rate P_m^B [$mg C (mg chl a d)^{-1}$]; (e) daily net productivity PN_{pd} [$mg C (m^2 d)^{-1}$] for Incubation Sites 27 (●) and 162 (○)

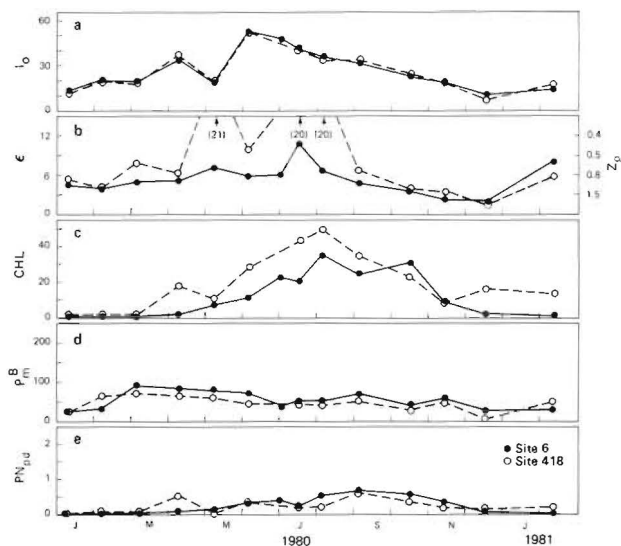


Fig. 4. Suisun Bay. Seasonal variation of (a) ambient irradiance I_0 ($E m^{-2} d^{-1}$); (b) attenuation coefficient ϵ (m^{-1}) and photic depth Z_p (m); (c) chlorophyll a CHL ($mg m^{-3}$); (d) maximum carbon assimilation rate P_m^B [$mg C (mg chl a d)^{-1}$]; (e) daily net productivity PN_{pd} [$mg C (m^2 d)^{-1}$] for Incubation Sites 6 (●) and 418 (○)

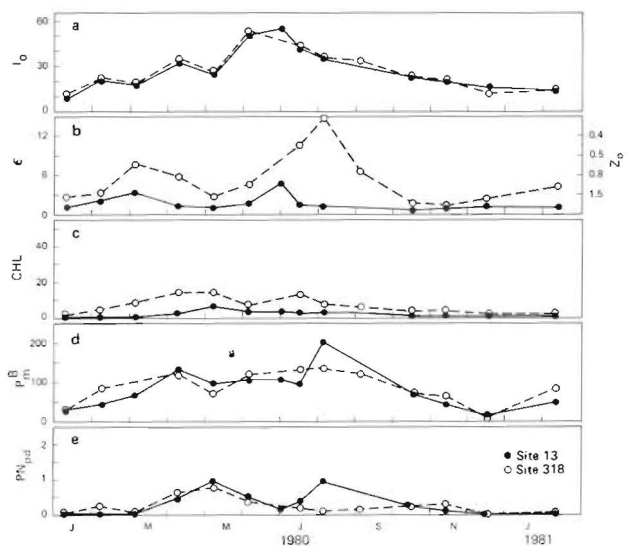


Fig. 3. San Pablo Bay. Seasonal variation of (a) ambient irradiance I_0 ($E m^{-2} d^{-1}$); (b) attenuation coefficient ϵ (m^{-1}) and photic depth Z_p (m); (c) chlorophyll a CHL ($mg m^{-3}$); (d) maximum carbon assimilation rate P_m^B [$mg C (mg chl a d)^{-1}$]; (e) daily net productivity PN_{pd} [$mg C (m^2 d)^{-1}$] for Incubation Sites 13 (●) and 318 (○)

addition, attenuation coefficients were consistently greater in the shoals than the channel of San Pablo Bay and Suisun Bay.

Although the absolute chlorophyll *a* level for a given date was typically higher at the shallow water incubation site than at the adjacent channel site, the seasonality of chlorophyll *a* was similar for the 2 incubation

sites within each embayment and distinct from the seasonality in the other two embayments (Fig. 2c, 3c, 4c). In South Bay (Fig. 2c) there was a late winter-early spring chlorophyll *a* maximum of approximately $24 mg m^{-3}$ after which chlorophyll *a* levels remained less than about $2 mg m^{-3}$. Maximum chlorophyll *a* levels in San Pablo Bay (Fig. 3c) were observed in spring. The increase and decline in biomass occurred over a longer period at the shoal site than at the deep-water location. Chlorophyll *a* concentrations at San Pablo Bay sites ranged from 0.7 to $6.4 mg m^{-3}$ at Station 13 and from 1.5 to $14.4 mg m^{-3}$ at Station 318. Maximum concentrations of chlorophyll *a* at the Suisun Bay incubation sites (Fig. 4c) exceeded those from the other 2 embayments. Winter lows of $< 1 mg chl a m^{-3}$ were followed by a gradual increase to summer maxima of 35 and $50 mg chl a m^{-3}$ at the deep-water and shallow-water sites respectively.

Daily carbon assimilation rates were usually similar at both incubation sites within each embayment (Fig. 2d, 3d, 4d). Although seasonality in P_m^B was similar at Sites 27, 162, and 13, it differed among the other sampling sites. In South Bay and San Pablo Bay, P_m^B generally increased from winter lows (P_m^B rates in South Bay were not attained in January or February) to maximum rates in midsummer. Low winter P_m^B rates in Suisun Bay were followed by annual maximum values in March after which there was a gradual decline in P_m^B over the year. Baywide, winter minimum P_m^B rates were 25 to $30 mg C (mg chl a d)^{-1}$, whereas maximum rates ranged from $230 mg C (mg chl a d)^{-1}$ in South Bay to

Table 2. Annual mean and range of attenuation coefficient (ϵ), photic depth (\bar{Z}_p), water depth (H) [MLLW water depth + 1 m], and H/\bar{Z}_p ratio for the 6 incubation sites

Station		ϵ (m^{-1})	Range	\bar{Z}_p (m)	H (m)	H/\bar{Z}_p
South Bay	27	1.3	0.7– 2.5	3.5	12	3.4
	162	1.7	0.8– 5.1	2.7	3.0	1.1
San Pablo Bay	13	1.8	0.7– 4.7	2.6	11	4.2
	318	5.6	1.4–15	0.8	2.2	2.8
Suisun Bay	6	5.7	2.4–11	0.8	10	12.5
	418	9.6	3.6–21	0.5	1.6	3.2

approximately 170 in San Pablo Bay and 83 mg C ($mg\ chl\ a\ d$) $^{-1}$ in Suisun Bay.

Although seasonality in daily net productivity (Fig. 2e, 3e, 4e) was generally similar to the pattern observed for chlorophyll *a* at each of the 6 incubation sites, baywide the levels of productivity had little relation to chlorophyll *a* concentration. At both sites in South Bay (Fig. 2e) the annual pattern in PN_{pd} was dominated by 2 peaks in early spring of 1.2 to 2.2 g C ($m^2\ d$) $^{-1}$. At all other times during the year productivity was low, not exceeding 0.5 g C ($m^2\ d$) $^{-1}$. In San Pablo Bay low [$< 0.05\ g\ C\ (m^2\ d)^{-1}$] levels of productivity in winter (Fig. 3e) were followed by a peak in spring at both the channel and shoal sites coincident with peaks in chlorophyll *a*. At the channel site a second peak in productivity, of similar magnitude to the spring peak, occurred simultaneously with a marked increase in P_m^B (Fig. 3d) and decreased turbidity (Fig. 3b). In Suisun Bay extremely low productivity during winter (Fig. 4e) preceded increased PN_{pd} that was coincident with the summer increase of chlorophyll *a*. Even though biomass in Suisun Bay was the highest observed throughout the San Francisco Bay system, maximum levels of phytoplankton productivity at Stations 6 and 418 did not exceed 0.55 g C ($m^2\ d$) $^{-1}$. Annual net productivity PN_{py} over the photic zone was 150, 110 to 130, and 95 g C m^{-2} for the South Bay, San Pablo Bay, and Suisun Bay sites respectively.

DISCUSSION

Predicting daily productivity

Although the seasonality of parameters that potentially control phytoplankton productivity in San Francisco Bay was diverse, PN_{pd} was primarily a function of phytoplankton biomass and light availability. Falkowski (1981) has also derived an empirical function that relates integral productivity to B and I_o in the New York Bight. Gieskes and Kraay (1977) similarly conclude that the productivity of surface-water samples in

the Southern North Sea can be estimated well from chlorophyll *a* concentration and incident light. When all measured values of PN_{pd} were regressed against the simple composite parameter $B I_o/\epsilon$ (Table 3; Fig. 5), we found that, both within individual embayments and baywide, about 80 % of the seasonal variability in PN_{pd} was correlated with this simple parameter. Therefore, nutrient availability, temperature, and physiological state of the phytoplankton play only minor roles in regulating productivity. All linear regressions were highly significant ($r = 0.88$ to 0.97 , $P < 0.001$) and indicated that this relation held over a wide range of I_o , ϵ , B , P_m^B , and phytoplankton communities.

PN_{pd} was consistently predicted well using this composite parameter, whereas correlations between PN_{pd} and either I_o/ϵ , I_o , ϵ , or P_m^B were weak (Table 3). Because carbon uptake is dependent on phytoplankton biomass, it is common practice to normalize productivity by the chlorophyll *a* content of the sample. Within a localized area, even normalizing integral productivity to photic zone chlorophyll *a* at times during the year (Malone, 1977; Bruno et al., 1983) aids in determining the factors regulating phytoplankton production. In San Francisco Bay there was a significant correlation ($P < 0.05$) between PN_{pd} and phytoplankton biomass (B) at 5 of the 6 incubation sites (Table 3). In each embayment the seasonal pattern in productivity was generally reflective of the seasonality in biomass (Fig. 2c, e; 3c, e; 4c, e). Except at Site 418, variations solely in chlorophyll *a* accounted for more than 50 % of the variation in observed PN_{pd} (Table 3). Within a restricted environmental setting (i.e. separate embayments), changes in chlorophyll *a* concentration accounted for most of the variation in productivity. However, only 12 % of the baywide annual variation in productivity was correlated with changes in biomass. Because there was a wide range in slopes (6.5 to 156; data not shown) for regressions between productivity and chlorophyll *a* at the 6 sites, the single regression of PN_{pd} and B data from all sites accounted for only a small fraction (12 %) of the variation in PN_{pd} baywide (Table 3). Thus, although at a given location phyto-

plankton biomass was indicative of photic-zone productivity, our results suggest that the use of chlorophyll *a* alone is of little value in predicting PN_{pd} among diverse areas. This is consistent with the conclusions of Cadée and Hegeman (1974) and Boynton et al. (1982) that over a wide range of environmental conditions or aquatic environments productivity cannot be estimated from measures of chlorophyll *a* alone.

late well with changes in P_m^B (Table 3). The poor correlation between primary productivity and P_m^B probably results from the fact that productivity is largely determined by biomass, and that spatio-temporal variations in biomass within San Francisco Bay are not controlled by the same processes that regulate growth rate (i.e. P_m^B). For example, the summer biomass maximum in Suisun Bay results from the physical accumulation of

Table 3. Coefficients of determination (r^2) from linear regressions of photic zone productivity (PN_{pd}) against $B I_0/\epsilon$, chlorophyll *a* (B), I_0/ϵ , ambient irradiance (I_0), attenuation coefficient (ϵ), and carbon assimilation rate (P_m^B)

Station	n	$B I_0/\epsilon$	B	I_0/ϵ	I_0	ϵ	P_m^B
Baywide	77	0.82**	0.12*	0.14*	0.15*	0.03	0.08*
South Bay	15	0.90**	0.77**	0.08	0.10	0.00	0.01
	162	0.89**	0.84**	0.00	0.15	0.06	0.00
San Pablo	12	0.78**	0.66**	0.43*	0.17	0.07	0.66**
	318	0.94**	0.51*	0.19	0.16	0.03	0.08
Suisun Bay	6	0.89**	0.82**	0.36*	0.26	0.00	0.01
	418	0.82**	0.29	0.39*	0.37*	0.01	0.01

** $P < 0.001$; * $P < 0.05$

In addition to phytoplankton biomass, productivity in estuaries is commonly believed to be a function of photic-zone irradiance because there is decreased productivity in turbid regions relative to clearer waters (Flemer, 1970; Cadée and Hegeman, 1974; Malone, 1977; Cadée, 1978; Colijn, 1978; Stockner et al., 1979; Joint and Pomroy, 1981). However, the most appropriate means of quantifying the light available to phytoplankton in a photic zone is not obvious. Photosynthetically available light must be related to both ambient light (I_0) and the depth of the photic zone, a measure derived from the attenuation coefficient (ϵ). We assumed that ϵ , I_0 , and I_0/ϵ , as indices of light availability, might be useful predictors of daily productivity. At some sites the use of I_0 and I_0/ϵ increased the predictability of PN_{pd} (Table 3). But neither ϵ , I_0 , or I_0/ϵ individually accounted for more than 43 % of the variation in daily productivity. The poor relationship between PN_{pd} and ϵ was surprising because there was a significant relationship between PN_{py} and annual mean photic depth \bar{Z}_p , which was calculated from ϵ (Fig. 6).

Positive correlations are reported between photic zone productivity and P_m^B in some estuaries (Williams and Murdoch, 1966; Malone, 1977), but in San Francisco Bay changes in PN_{pd} were poorly correlated with P_m^B (Table 3). In South Bay and San Pablo Bay, P_m^B generally increased until midsummer, whereas PN_{pd} was maximum in spring. In contrast, maximum PN_{pd} in Suisun Bay was observed in summer, whereas maximum P_m^B was seen in late winter. Over the year-long study, only at Station 13 did variations in PN_{pd} corre-

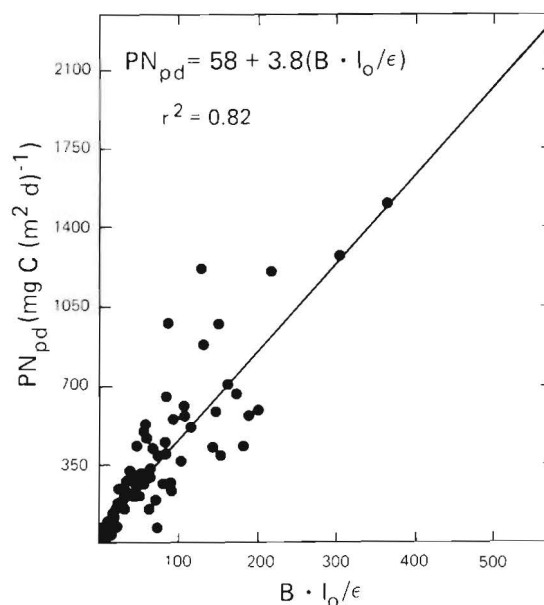


Fig. 5. Regression of daily net productivity PN_{pd} against composite parameter $B I_0/\epsilon$

phytoplankton by estuarine circulation, rather than from rapid growth rates (Cloern et al., 1983), and the spring bloom in South Bay results partly from decreased benthic grazing pressure when the water column is stratified (Cloern, 1982). Only in estuaries where biomass and carbon assimilation rates are controlled by the same processes (e.g. specific growth rate)

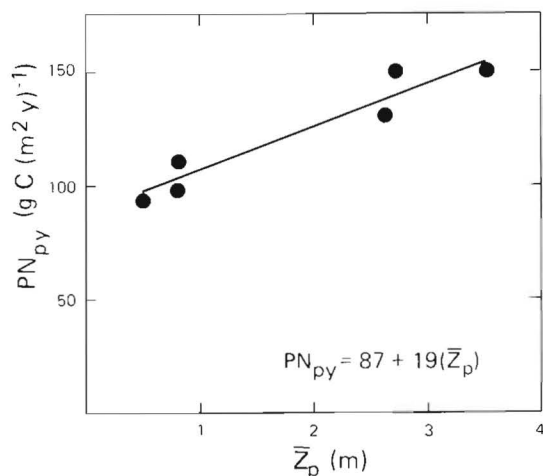


Fig. 6. Annual net productivity PN_{py} as a function of annual mean photic depth \bar{Z}_p at the 6 incubation sites

would a strong correlation between productivity and P_m^B be expected.

Predicting net water-column productivity

The high turbidity of estuaries has a profound impact not only on gross production but also upon the fraction of gross production available to higher trophic levels. Estuaries are generally shallow, but a large portion of the water column is aphotic or exposed to low irradiance. Because photosynthesis is restricted to the photic zone (Z_p), respiratory losses, which occur over the entire water-column depth (H), can greatly reduce net productivity when the ratio H/Z_p becomes large. The importance of the interaction between surface irradiance, mixed depth, photic depth, and production : respiration ratios in regulating productivity was first noted by Gran and Braarud (1935). Their concepts were developed into mathematical models (Sverdrup, 1953; Patten, 1968) to define the 'critical depth' for integral production (i.e. the depth at which respiration in the water column equals carbon production in the photic zone). By examining the mixed depth : photic depth ratio and making assumptions regarding the constancy of the production : respiration ratio (Harris, 1978), one can define conditions which control the seasonality of phytoplankton blooms in marine and freshwater environments (Parsons and Takahashi, 1973; Harris, 1978). Although H/Z_p ratios vary widely in estuaries, the concept of critical depth has not been proposed as an explanation for the differences in productivity observed in different estuaries or the temporal changes in productivity or biomass within an estuarine system. Our data suggest that the concept of critical depth is applicable to estuarine systems and

that the fraction of gross primary production which is potentially available for higher trophic levels can be estimated from the ratio H/Z_p . In these calculations we assume that mixed depth is equal to water depth, a condition which is typical in San Francisco Bay.

Assuming vertical homogeneity and that respiration rate equals $0.1 P_m^B$, annual water column respiration R_{wy} can be calculated as:

$$R_{wy} = \int_1^{365} (0.1 P_m^B B H) dt \quad (2)$$

Similarly, annual respiratory losses in the photic zone R_{py} can be estimated by substituting \bar{Z}_p for H in equation 2. We estimate that annual gross phytoplankton productivity ($PG_y = PN_{py} + R_{py}$) at the 6 sites ranged from 110 to 190 $g\ C\ m^{-2}$ and over the year respiration throughout the water column ranged from 49 to 250 $g\ C\ m^{-2}$ (Table 4).

Because \bar{Z}_p may be small relative to H , respiratory loss can cause some locations to be a net sink rather than a source of phytoplankton carbon (compare PG_y and R_{wy} for Site 6 in Table 4). The fraction of PG_y remaining after R_{wy} is accounted for is:

$$PN_{wy}/PG_y = (PG_y - R_{wy})/PG_y \quad (3)$$

The ratio PN_{wy}/PG_y (net productivity : gross productivity) was small or negative at deep (large H) and turbid (small \bar{Z}_p) sites (Table 4), which suggests that PN_{wy}/PG_y may be a simple function of the ratio H/\bar{Z}_p . Given the constraint that the limit of $PN_{wy}/PG_y = 1$ as R_{wy} (i.e. H) approaches zero (Eq. 3), values of PN_{wy}/PG_y for the 6 sites were, in fact, linearly related to H/\bar{Z}_p (Fig. 7):

$$PN_{wy}/PG_y = 1 - 0.166 (H/\bar{Z}_p) \quad (4)$$

The intercept of this function defines that critical ratio H/\bar{Z}_p above which net production becomes negative. On an annual basis for San Francisco Bay, this critical value was $H/\bar{Z}_p = 6$ (Fig. 7). Sverdrup (1953), in describing the conditions necessary for the onset of a spring bloom in the Norwegian Sea, concludes that when the mixed depth exceeds the production zone depth by 5 times the population decreases. In Lake Windermere values of mixed depth : photic depth between 3 and 4 are typical during low chlorophyll *a* periods, and chlorophyll *a* levels rise when the ratio decreases (Talling, 1971).

The need for reliable estimates of specific respiration rate has been noted by numerous researchers. Estimates of respiration in the literature range from 4 % (Platt and Jassby, 1976) to 50 % (Eppley and Sharp, 1975) of maximum assimilation rate. In San Francisco Bay R^B is generally 8 to 30 % of P_m^B (Peterson et al., in press). The 10 % respiration value used in these calcu-

Table 4. Annual gross productivity in the photic zone (PG_y), net productivity in the photic zone (PN_{py}), water column respiration (R_{wy}), and ratio of water column net productivity to gross productivity (PN_{wy}/PG_y)

Station		PG_y (g C m ⁻²)	PN_{py} (g C m ⁻²)	R_{wy} (g C m ⁻²)	PN_{wy}/PG_y
South Bay	27	190	150	120	.34
	162	180	150	49	.72
San Pablo	13	160	130	98	.39
	318	140	110	62	.56
Suisun Bay	6	120	98	250	-1.1
	418	110	93	54	.51

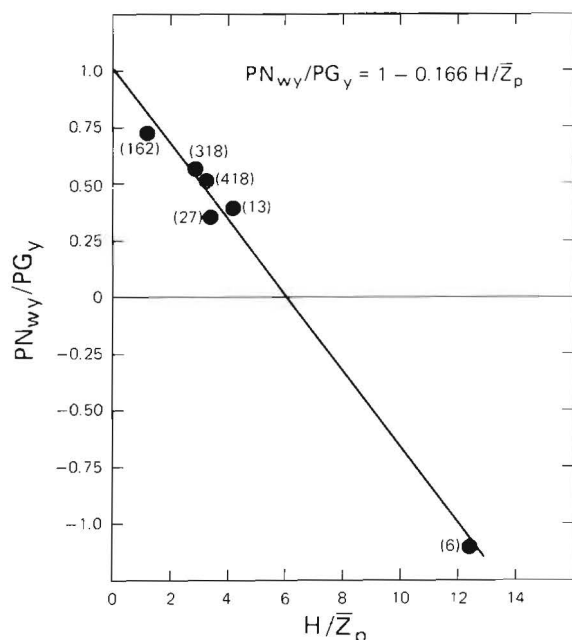


Fig. 7. Ratio of water-column net productivity to gross productivity PN_{wy}/PG_y as a function of H/Z_p

lations is probably reasonable or conservative. If respiration rates are actually higher, say 25% of P_m^B (Falkowski and Owens, 1978), then water column respiration would be 2.5 times greater and an even smaller fraction of phytoplankton production would be available to grazers (see below).

Carbon available to higher trophic levels

Implications of the critical depth concept also lead to the conclusion that not only do variations in H/Z_p ratios have profound consequences for phytoplankton population dynamics, but also that the availability of phytoplankton carbon to higher trophic levels varies with changes in this ratio. From Equation 4 and as shown in Fig. 7, the fraction of gross phytoplankton production available to herbivores can be estimated from the ratio H/Z_p . High standing stocks of phytoplankton (chloro-

phyll a) are often considered to be indicative of abundant food for higher trophic levels. As shown by our results, such a presumption may be misleading. For example, Site 6 in Suisun Bay had the highest concentrations of chlorophyll a, but because the photic zone was only a small fraction of the water-column depth (Table 2), respiratory losses exceeded gross primary production (Table 4). Baywide, there was a greater fraction of production available for herbivores at the shallow-water sites (162, 318, 418), where the ratio H/Z_p was smaller (Fig. 7), than at the deep-water sites (27, 13, 6). The extensive shallow areas of San Francisco Bay in general, and Suisun Bay in particular, must be largely responsible for maintaining the system's capacity to support herbivore populations. An estuary's capability to support higher trophic levels should thus depend in part on the size and relative proportion of areas with low and high ratios of H/Z_p rather than solely depend on phytoplankton biomass.

These findings imply 2 general conclusions. First, in deep turbid channels (e.g. Suisun Bay) the requirements for cell maintenance (respiration) are such that phytoplankton populations cannot be maintained by *in situ* growth. Rather, as postulated by Cloern and Cheng (1981) and Cloern et al. (1983), the populations found in these areas must be advected in from areas with conditions more favorable for growth (i.e. lower H/Z_p ratios). Second, the nutritional mode of herbivores might vary with turbidity. Areal productivity decreases with increasing turbidity (Fig. 6, this paper; Cadée and Hegeman, 1974; Malone, 1977; Cadée, 1978; Colijn, 1978; Joint and Pomroy, 1981), and a large fraction of phytoplankton carbon is lost through respiration in deep, turbid environments. Therefore, either the biomass of herbivores should decline in turbid environments or higher trophic levels in such environments must depend to a large degree on suspended detritus or particulate organic carbon in the sediments. Consumers in a turbid environment may therefore be less dependent upon phytoplankton production as a food source than consumers in clearer waters. Because the nutritional value of detritus is

lower than that of phytoplankton (Kirby-Smith, 1976; Heinle et al., 1977) and there is a negative relation between the percentage of detritus in the diet and growth of copepods (Heinle et al., 1977; Chervin, 1978; Chervin et al., 1981) and scallops (Kirby-Smith, 1976), one might expect to see lower macrofauna biomass in areas where there is a greater dependence on detrital carbon than phytoplankton carbon for food.

The diet for the individual species has not been studied, but distributions of zooplankton and benthic animals in San Francisco Bay support these hypotheses. In the 3 major embayments, biomass of zooplankton and benthic infauna are greater where turbidity is low, the ratio H/\bar{Z}_p is low, and there is a large proportion of phytoplankton carbon available for consumers. The average fraction of gross phytoplankton production available for consumption by herbivores in South Bay, San Pablo Bay, and Suisun Bay was 53, 48, and -29% respectively (mean PN_{wy}/PG_y ratio of channel and shoal sites from Table 4). Mean annual zooplankton biomass during 1980 was 21, 16, and 9.9 mg C m⁻³ in these same embayments (Hutchinson 1982a, b). Similarly, Thompson and Nichols (1981) report that, based on data collected in 1973, wet weight biomass of benthic macrofauna is greatest in South Bay (4800 g m⁻²) and least in Suisun Bay (100 g m⁻²) with levels in San Pablo Bay (520 g m⁻²) being intermediate between the two.

The results of our study show that daily photic zone net primary productivity in San Francisco Bay can be estimated from a simple function: $PN_{pd} = 58 + 3.8 (B I_o/\epsilon)$. Moreover, the fraction of phytoplankton carbon production available for higher trophic levels can be estimated from the ratio H/\bar{Z}_p . Thus, the capability of this complex ecosystem to support secondary production can be predicted from simple, easily measured parameters. However, it should be noted that the accuracy of calculated net water-column productivity is dependent upon accurate measures of phytoplankton respiration, a process which is not easily measured and which may be variable.

Acknowledgements. We thank Andrea Alpine for supplying the chlorophyll *a* data, assisting in collecting the productivity data, and for many helpful discussions and criticisms during field work and manuscript preparation. We also appreciate the assistance of Anne Hutchinson, Peter Alexander, Sally Wienke, and Suzanne Cartegana in collecting and analyzing the data. Valuable ideas and criticisms were provided by Janet Thompson, Steven Hager, and Frank Triska during analysis of the results and writing of the paper.

LITERATURE CITED

Boynton, W. R., Kemp, W. M., Keefe, C. W. (1982). A comparative analysis of nutrients and other factors influencing

- estuarine phytoplankton production. In: Kennedy, V. S. (ed.) Estuarine comparisons. Academic Press, New York.
- Bruno, S. G., Staker, R. D., Sharma, G. M., Turner, J. T. (1983). Primary productivity and phytoplankton size fraction dominance in a temperate North Atlantic estuary. *Estuaries* 6: 200-211
- Cadée, G. C. (1978). Primary production and chlorophyll in the Zaire River, estuary and plume. *Neth. J. Sea Res.* 12: 368-381
- Cadée, G. C., Hegeman, J. (1974). Primary production of phytoplankton in the Dutch Wadden Sea. *Neth. J. Sea Res.* 8: 240-259
- Chervin, M. B. (1978). Assimilation of particulate organic carbon by estuarine and coastal copepods. *Mar. Biol.* 49: 265-275
- Chervin, M. B., Malone, T. C., Neale, P. J. (1981). Interactions between suspended organic matter and copepod grazing in the plume of the Hudson River. *Estuar. coast. Shelf Sci.* 13: 169-183
- Cloern, J. E. (1982). Does the benthos control phytoplankton biomass in South San Francisco Bay? *Mar. Ecol. Prog. Ser.* 9: 191-202
- Cloern, J. E. (1984). Temporal dynamics and ecological significance of salinity stratification in an estuary (South San Francisco Bay, USA). *Oceanol. Acta* (in press)
- Cloern, J. E., Cheng, R. T. (1981). Simulation model of *Skeletonema costatum* population dynamics in Northern San Francisco Bay, California. *Estuar. coast. Shelf Sci.* 12: 83-100
- Cloern, J. E., Alpine, A. E., Cole, B. E., Wong, R. L. J., Arthur, J. F., Ball, M. D. (1983). River discharge controls phytoplankton dynamics in the northern San Francisco Bay estuary. *Estuar. coast. Shelf Sci.* 16: 415-429
- Colijn, F. (1978). Primary production measurements in the Ems-Dollard estuary during 1975 and 1976. *Publikaties en Verslagen Biologisch Onderzoek Eems-Dollard Estuarium* 1: 1-14
- Conomos, T. J. (1979). Properties and circulation of San Francisco Bay waters. In: Conomos, T. J. (ed.) San Francisco Bay: the urbanized estuary. Pacific Division, AAAS, San Francisco, p. 47-84
- Conomos, T. J., Smith, R. E., Peterson, D. H., Hager, S. W., Schemel, L. E. (1979). Processes affecting seasonal distributions of water properties in the San Francisco Bay estuarine system. In: Conomos, T. J. (ed.) San Francisco Bay: the urbanized estuary. Pacific Division, AAAS, San Francisco, p. 115-142
- Eppley, R. W., Sharp, J. (1975). Photosynthetic measurements in the central north Pacific: the dark loss of carbon in 24-h incubations. *Limnol. Oceanogr.* 20: 981-987
- Falkowski, P. G. (1981). Light-shade adaptation and assimilation numbers. *J. Plankton Res.* 3: 203-216
- Falkowski, P. G., Owens, T. G. (1978). Effects of light intensity on photosynthesis and dark respiration in six species of marine phytoplankton. *Mar. Biol.* 45: 289-295
- Flemer, D. (1970). Primary production in Chesapeake Bay. *Chesapeake Sci.* 11: 117-129
- Gieskes, W. W. C., Kraay, G. W. (1977). Primary production and consumption of organic matter in the southern North Sea during the spring bloom of 1975. *Neth. J. Sea Res.* 11: 146-167
- Gran, H. H., Braarud, T. (1935). A quantitative study of the phytoplankton in the Bay of Fundy and the Gulf of Maine (including observations of hydrography, chemistry, and turbidity). *J. Biol. Bd Can.* 1: 279-467
- Harris, G. P. (1978). Photosynthesis, productivity, and growth:

- the physiological ecology of phytoplankton. *Arch. Hydrobiol.* 10: 1–171
- Heinle, D. R., Harris, R. P., Ustach, J. F., Flemer, D. A. (1977). Detritus as food for estuarine copepods. *Mar. Biol.* 40: 341–353
- Hobson, L. A., Morris, W. J., Pirquet, K. T. (1976). Theoretical and experimental analysis of the ^{14}C technique and its use in studies of primary production. *J. Fish. Res. Bd Can.* 33: 1715–1721
- Hutchinson, A. (1981). Plankton studies in San Francisco Bay. III. Zooplankton species composition and abundance in the South Bay, 1978–1979. U.S. Geological Survey, Open-File Report 81–132
- Hutchinson, A. (1982a). Plankton studies in San Francisco Bay. V. Zooplankton species composition and abundance in the South Bay, 1980–1981. U.S. Geological Survey, Open-File Report 82–1002
- Hutchinson, A. (1982b). Plankton studies in San Francisco Bay. VI. Zooplankton species composition and abundance in the North Bay, 1979–1980. U.S. Geological Survey, Open-File Report 82–1003
- Joint, I. R., Pomroy, A. J. (1981). Primary production in a turbid estuary. *Estuar. coast. Shelf Sci.* 13: 303–316
- Kirby-Smith, W. (1976). The detritus problem and the feeding and digestion of an estuarine organism. In: Wiley, M. (ed.) *Estuarine processes*, Vol. 1, Uses, stresses, and adaptation to the estuary. Academic Press, New York, p. 469–479
- Malone, T. C. (1977). Environmental regulation of phytoplankton productivity in the lower Hudson Estuary. *Estuar. coast. mar. Sci.* 5: 157–171
- Marra, J. (1978). Phytoplankton photosynthetic response to vertical movement in a mixed layer. *Mar. Biol.* 46: 203–208
- Parsons, T. J., Takahashi, M. (1973). *Biological oceanographic processes*. Pergamon Press, New York
- Patten, B. C. (1968). Mathematical models of plankton production. *Int. Revue ges. Hydrobiol.* 53: 357–408
- Peterson, B. J. (1980). Aquatic primary productivity and the ^{14}C - CO_2 method: a history of the productivity problem. *Ann. Rev. Ecol. Syst.* 11: 359–385
- Peterson, D. H., Schemel, L. E., Alpine, A. E., Cole, B. E., Hager, S. W., Harmon, D. D., Hutchinson, A., Smith, R. E., Wienke, S. M. (in press). Phytoplankton photosynthesis, nitrogen assimilation and light intensity in a partially mixed estuary. *Estuar. coast. Shelf Sci.*
- Platt, T., Jassby, A. D. (1976). The relationship between photosynthesis and light for natural assemblages of coastal marine phytoplankton. *J. Phycol.* 12: 421–430
- Schindler, D. W. R., Schmidt, R. V., Reid, R. A. (1972). Acidification and bubbling as an alternative to filtration in determining phytoplankton production by the C^{14} method. *J. Fish. Res. Bd Can.* 29: 1627–1631
- Stemann Nielsen, E., Hansen, V. (1959). Measurements with the carbon-14 technique of the respiration rates in natural populations of phytoplankton. *Deep Sea Res.* 5: 222–233
- Stockner, J. G., Cliff, D. D. (1979). Phytoplankton ecology of Vancouver Harbor. *J. Fish. Res. Bd Can.* 36: 1–10
- Stockner, J. G., Cliff, D. D., Shortreed, K. R. (1979). Phytoplankton ecology of the Strait of Georgia, British Columbia. *J. Fish. Res. Bd Can.* 36: 657–666
- Strickland, J. D. H., Parsons, T. R. (1972). *A practical handbook of seawater analysis*. *Bull. Fish. Res. Bd Can.* 167
- Sverdrup, H. U. (1953). On conditions for the vernal blooming of phytoplankton. *J. Cons. int. Explor. Mer* 18: 287–295
- Talling, J. F. (1971). The underwater light climate as a controlling factor in the production ecology of freshwater phytoplankton. *Mitt. int. Verein. Limnol.* 19: 214–243
- Thompson, J. K., Nichols, F. H. (1981). Benthic macrofaunal biomass of San Francisco Bay, California: January/February and August 1973. U.S. Geological Survey, Open-File Report 81–1331
- Williams, R. B. (1966). Annual phytoplanktonic production in a system of shallow temperate estuaries. In: Barnes, H. (ed.) *Some contemporary studies in marine science*. Hafner, New York, p. 699–716
- Williams, R. B., Murdoch, M. B. (1966). Phytoplankton production and chlorophyll concentration in the Beaufort Channel, North Carolina. *Limnol. Oceanogr.* 11: 73–82
- Wong, R. L. J., Cloern, J. E. (1982). Plankton studies in San Francisco Bay. IV. Phytoplankton abundance and species composition, January 1980–February 1981. U.S. Geological Survey, Open-File Report 82–443

This paper was submitted to the editor; it was accepted for printing on January 5, 1984

Delta Chinook Final Report

Curry Cunningham, Noble Hendrix, Eva Dusek-Jennings, Robert Lessard and Ray Hilborn

EXECUTIVE SUMMARY

This project developed a stage-structured life history model of summer, spring and winter run Chinook salmon, fitted this model to available data on salmon stock abundance and environmental conditions, and estimated the impact of the environmental conditions on survival of the different stocks of Chinook salmon. This model was then used to forecast how differences in future climate change, marine conditions or productivity, and water exports would affect the survival of the different stocks of Chinook salmon.

We used several statistical techniques to evaluate the relative importance of environmental variables on the survival including both information theoretic approaches and Bayesian approaches. Due to the large number of potential explanatory covariates (59) and the inability to fit all combinations of these covariates, we used Akaike Information Criterion for small sample size (AICc) and a novel method for exploring the model space. The approach used a forward stepwise model building with AICc as the selection criteria. The steps were: 1) fit a null model without any covariate effects to the available data; 2) construct a proposal model by selecting a covariate at random from amongst the set of 59 possible covariates; 3) fit the proposed model to the data; 4) compare the proposal model to the null model; 5) keep proposal model if reduction in AICc value is greater than 2 units; 6) repeat sampling covariates without replacement, fitting the model to data, and evaluating AICc i.e. until all covariates have been tested.

Using the information theoretic approaches we found support for environmental impacts of 14 variables including flow, temperature, sediment concentration, export inflow ratios, exports, ocean upwelling, curl and PDO. The top three environmental drivers affecting fall run were export to inflow ratio, spring upwelling south of the Farallon Islands, and the delta gross channel depletion. The top three drivers affecting spring run were size at Chipps Island, export levels, and sediment concentration at Freemont. The three main factors affecting winter-run were minimum flow during fry rearing, temperatures during egg incubation, and spring upwelling south of the Farallon Islands. We then conducted a Bayesian analysis using these 14 variables to calculate the posterior distribution of the impact of these variables on survival.

We conducted forward simulations under four different export regimes to understand how management of exports would affect each of the races. Furthermore, we evaluated export management under two different climate scenarios and two ocean productivity scenarios to understand how climate variability and ocean productivity may act in concert with management of exports to affect the three Chinook runs. We developed a harvest model that reflected current management of the Central Valley Chinook stocks in which low levels of winter run escapement can reduce fall run harvest.

39 We found that both climate and exports affected projected survival and the potential
40 recruits per spawner for wild populations. Under current export levels all stocks of spring run
41 would increase across all climate scenarios tested. Winter run would increase except under the
42 most pessimistic of the four climate conditions we evaluated. Mainstem Fall run would have
43 recruits per spawner greater than 1 under the two optimistic climate scenarios and less than 1
44 under the two pessimistic climate scenarios although the future trend in mainstem fall chinook
45 could be heavily influenced by straying from hatcheries and thus hard to predict. A 30%
46 increase in exports decreased spring and fall stock survival to the point where they would all
47 decline regardless of the climate scenario. A 30% decrease in exports improved survival and
48 recruits per spawner for all stocks.

49 We found spring Chinook stocks to be most sensitive to exports and less sensitive to
50 climate conditions, whereas winter Chinook were more sensitive to climate conditions than
51 exports.

52 We did not evaluate alternative ocean harvest scenarios, although reduction or
53 elimination of ocean harvest would increase survival to spawning and thus contribute to
54 rebuilding in the same way as better climate or reduced exports.

55 INTRODUCTION

56 Salmon populations in the Sacramento River are far below historical numbers. Fisheries
57 closures have been implemented to protect spring-run Chinook (SRC), winter-run Chinook
58 (WRC), and even fall-run Chinook (FRC), which until 2005, had been considered a healthy
59 stock. The FRC was the staple of the California salmon fishery, has been closed in several years.
60 The FRC have been the most heavily subsidized with hatchery fish. The impact on commercial
61 and recreational fisheries has been dramatic. A variety of reasons in both freshwater and marine
62 environments have been cited as causes of the decline, but it appears that salmon have been
63 subjected to something of a “perfect storm” of deleterious effects, both natural and
64 anthropogenic in origin.

65 Historically both WRC and SRC used the upstream, higher altitude tributaries of the
66 Sacramento River, but the current extent of accessible freshwater habitat differs greatly and their
67 lower abundances have led to concern and listing by both state and federal agencies (Yoshiyama
68 et al. 1998, 2000, Lindley et al. 2004). WRC and SRC were separated both temporally and
69 geographically in their spawning habitat. Winter-run historically used the headwater springs,
70 spawned in the early summer, emerged from the gravel in late summer, emigrated over the
71 winter, and entered the ocean the following spring (Lindley et al. 2004). Development of eggs
72 was dependent on relatively constant flow and cool temperatures of the spring fed streams.
73 Currently, WRC are confined to spawning in the Sacramento River. SRC used the high spring
74 flows to reach the upper tributaries of the Sacramento in summer and waited out the summer in
75 high elevation pools. Spawning commenced in the fall and juveniles emerged the following
76 spring. Stream residency varied and could last over a year. Out-migration occurred in both
77 spring and fall depending upon time of residency. There are currently several extant
78 subpopulations of SRC. Lindley et al. (2004) suggest that there are four principle groupings that
79 might form the basis of a meta-population structure: 1. Winter-run, 2. Butte Creek spring-run, 3.

80 Deer and Mill Creek spring-run, 4. Fall-run, late fall-run and Feather/Yuba spring-run. Since
81 several of these runs overlap in their usage of stream and mainstem habitat, it is reasonable to
82 consider that they may compete for resources and therefore a modeling approach that accounts
83 for these overlaps could improve the precision of population predictions. Additionally, variation
84 in survival of one population can provide additional statistical ability to the estimation of
85 environmental effects that influence both populations.

86 Over the past several decades, substantial resources have been devoted to the
87 management of water resources, fisheries, and habitat in the San Francisco Bay-Sacramento
88 River Delta (Bay-Delta) ecosystem in general, with particular attention being given to resident
89 Chinook salmon runs. There has been increasing concern for species in decline, with the listing
90 of WRC and SRC in the Central Valley (CV) under both federal (Endangered Species Act, ESA)
91 and state laws. The exceedingly low return of FRC in 2008 led to a complete closure of salmon
92 fisheries. Many studies have been conducted in an attempt to explain sources of mortality in
93 freshwater and in the ocean. Tagging studies have shown extremely low survival in freshwater.
94 Wells et al. (2007) showed strong associations between survival and ocean climate indices,
95 providing evidence for a linkage between survival and primary productivity during the marine
96 portion of the life cycle.

97 Fish interact with natural and anthropogenic aspects of their environment and there can
98 be significant variation in such externalities. Decisions regarding fisheries management, water
99 management and research direction should account for all significant and predictable sources of
100 variation in those externalities where they have a measurable effect on survival. What is lacking
101 is an integrative model that can provide a level of detail in water resource management and
102 fishery management that accounts for interactions between salmon populations, both in the wild
103 as well implicitly captured in the mechanics of fisheries policy.

104 Although mathematical models of salmon species have been developed both at the
105 individual (e.g., Kimmerer 2001, Jager and Rose 2003) and the population (e.g., Botsford and
106 Brittnacher 1998) level, management and research direction have been based primarily on
107 qualitative compilations of what is known about individual salmon runs. Management would
108 benefit from models that more closely link environmental conditions to biological response.
109 Lessard et al. (*submitted manuscript*) built upon the general principle that survival could be
110 broken down into life history stages so that the relevant environmental factors in each stage
111 could be factored into the estimation of the productivity and capacity parameters that predict
112 density dependence in survival rates. A series of competing models were compared using a
113 statistical modeling and population dynamics platform (OBAN), each reconstructing population
114 dynamics and estimating the relative effects of environmental conditions in freshwater and ocean
115 stages. The study found that temperature, flow and exports explained most of the variation in
116 freshwater. Historically, gate positions of bypasses and cross channels have explained some of
117 the variation in survival, however, water management agencies have responded to biological
118 needs and have in recent years adjusted the timing and magnitude of water redirection activities
119 to mitigate negative effects on salmon. Wind stress curl, a primary productivity surrogate (Wells
120 et al. 2008), was the leading factor explaining variation in ocean survival, although indices such
121 as the Pacific Decadal Oscillation (Mantua et al. 1997) and sea surface temperature also
122 explained variation in ocean survival, although not throughout enough of the timeframe of the
123 study to be statistically competitive in model selection.

124 For the population dynamics portion of the project, we developed a multi-stock model of
125 the three Central Valley Chinook salmon species-at-risk (WRC, SRC and FRC) that incorporates
126 mortality in all phases of salmon life history, and includes the effects of uncertainty in assessing
127 population status. The approach involves several categories of models: (1) the population
128 dynamics models, (2) the parameter estimation model, (3) the growth model, and (4) the fisheries
129 management model that calibrates fishing effort to the predicted runs of the individual
130 populations.

131 **PART I FITTING A STATISTICAL MODEL**

132 *METHODS; MODEL DESCRIPTION*

133 The goal of this project was evaluate the environmental drivers of survival for Chinook
134 salmon populations spawning in the Sacramento River, CA watershed, in a statistically rigorous
135 manner. More generally, our purpose was to test a range of hypotheses describing the putative
136 factors facilitating or limiting survival, factors both natural and anthropogenic in origin and
137 describing both biotic and abiotic processes. To achieve this goal we have created a stage-
138 structured population dynamics model, which estimates the direction and magnitude of influence
139 that a range of these factors, or environmental covariates, have on survival through specific
140 portions of the Chinook life cycle, when fit to available juvenile and adult spawning abundance
141 data. The population dynamics model is currently used to explore the environmental drivers of
142 survival for four fall-run populations including: 1) Mainstem Sacramento wild-spawning
143 Chinook, 2) Battle Creek Coleman National Fish Hatchery produced Chinook, 3) Feather River
144 Hatchery produced Chinook, and 4) American River Nimbus Hatchery produced Chinook, as
145 well as three spring-run populations including: 1) Deer Creek, 2) Mill Creek, and 3) Butte Creek,
146 wild-spawning Chinook.

147 The stage-structured population dynamics model described in this document compliments
148 and expands upon previous analyses of interactions between environmental factors and survival
149 of Chinook salmon populations of the Sacramento River watershed in several ways. First, while
150 many previous analyses have modeled the survival or productivity of single components of the
151 Sacramento River Chinook stock complex (i.e. (Newman and Rice 2002, Lindley and Mohr
152 2003, Newman and Brandes 2010, Zeug et al. 2012), fall-run (Newman and Rice 2002), late-fall-
153 run (Newman and Brandes 2010), winter-run (Lindley and Mohr 2003, Zeug et al. 2012)) in
154 isolation, the current population dynamics model is applied to multiple populations of both
155 spring-run and fall-run Chinook and evaluates interactions between these populations at points in
156 the life cycle where co-rearing and co-migration occurs. Second, the current population
157 dynamics model approximates both wild and hatchery type life histories, utilizing historical
158 records of hatchery releases from the Coleman National Fish Hatchery on Battle Creek, the
159 Feather River Hatchery, and the Nimbus Fish Hatchery on the American River compiled by
160 Huber and Carlson (in review). Third, we have utilized estimates of stray rates between
161 hatcheries and wild populations of fall-run Chinook available from the proportional coded wire
162 tagging program (Kormos et al. 2012, Palmer-Zwahlen and Kormos 2013), to reconstruct
163 spawning abundance data in the presence of straying, prior to fitting the estimation model.
164 Fourth, while previous analyses have primarily evaluated survival variation in either the

165 freshwater or marine portions of the Chinook life cycle, we have created a population dynamics
 166 model with both marine and freshwater stages, permitting the testing of competing hypotheses
 167 for putative survival influences in all habitats utilized by Sacramento River Chinook. Fifth, while
 168 previous stage-structured population dynamics models used to evaluate the interaction between
 169 environmental factors and the survival of Sacramento Chinook including Zeug et al. (2012) have
 170 defined these interactions based upon a priori information or findings from other systems or
 171 laboratory experimentation, the population dynamics model we have created is statistical in
 172 nature, estimating the effect of the hypothesized environmental drivers of survival based upon
 173 historical variation observed in adult and juvenile abundance. The result is a flexible multi-stock,
 174 stage-structured, statistical, population dynamics model that estimates the influence of natural
 175 and anthropogenic environmental factors on survival of Chinook salmon throughout their life
 176 cycle, using both Bayesian and Maximum Likelihood methods.

177 *The Data*

178 In order to estimate the effect of various environmental covariates as well as basal
 179 productivity and capacity for the seven populations in specific life stages, the estimation model is
 180 conditioned on different types of data available for the Sacramento River system. The first type
 181 of data that are required by the estimation model are time-series of explanatory environmental
 182 covariates. For each environmental covariate being evaluated for its influence on Chinook
 183 survival, it is necessary to provide, a historical record of its value over time as a model input.
 184 Covariate data are z-standardized (Zar 2010) based upon the mean and standard deviation of the
 185 time-series (Eq. I.1).

$$186 \quad (I.1) \quad X_{t,i} = \frac{x_{t,i} - \sum_{t=1}^{Nt} x_{t,i} / Nt}{\sigma_i}$$

187 In this way, the *i*th covariate at time *t* ($x_{t,i}$) is transformed into units of standard deviations
 188 from the time-series mean, rather than untransformed values that span many orders of magnitude
 189 among covariates. By transforming covariate data into the same units, the magnitude of
 190 subsequently estimated coefficients describing the influence of individual covariates are more
 191 readily comparable and estimable.

192 Potential covariates were chosen for evaluation within the estimation model based upon
 193 first principals and a valid biological rationale for why each might be expected to influence
 194 either survival rate or stage-specific capacity. Covariates were developed came from a wide
 195 range of sources, including a review of the pertinent literature and expert opinion, and were
 196 created using data from the period of time throughout the year over which they were expected to
 197 exhibit the greatest influence (Table I.1).
 198

199
200

TABLE I.1. Environmental covariates

Hypothesis Number	Covariate	Covariate Description	Location	Populations
1	fall.sac.mainstem - sacAirTemp.summer	Sacramento air temperature during summer (July - September) of the brood year	Sacramento, CA	Fall Sacramento Mainstem Wild
2	fall.sac.mainstem - sacAirTemp.spring	Sacramento air temperature during spring (January - March) emergence year	Sacramento, CA	Fall Sacramento Mainstem Wild
3	fall.sac.mainstem - keswick.discharge	Average January - March water discharge (cfs) at Keswick Dam	Keswick Dam	Fall Sacramento Mainstem Wild Fall Sacramento Mainstem Wild
4	.1.2.3.4-verona.peak.streamflow	Peak (maximum) streamflow on the Sacramento River mainstem at Verona, CA (January - May)	Verona, Sacramento River	Fall Battle Creek (CNFH) Hatchery Fall Feather River Hatchery Fall American River (Nimbus) Hatchery
5	.1.2.3.4-yolo.wood.peak.streamflow	Peak (maximum) streamflow into Yolo Bypass at Woodland, CA (January - May)	Into Yolo Bypass at Woodland, CA	Fall Sacramento Mainstem Wild Fall Battle Creek (CNFH) Hatchery Fall Feather River Hatchery Fall American River (Nimbus) Hatchery
6	.1.2.3.4-freeport.sed.conc	Average February - April monthly sediment concentration (mg/L)	Freeport, Sacramento River	Fall Sacramento Mainstem Wild Fall Battle Creek (CNFH) Hatchery Fall Feather River Hatchery Fall American River (Nimbus) Hatchery
7	.1.2.3.4-bass.cpue	Index of Striped Bass abundance as number of striped bass kept	Sacramento - San Joaquin Delta	Fall Sacramento Mainstem Wild Fall Battle Creek (CNFH) Hatchery Fall Feather River Hatchery Fall American River (Nimbus) Hatchery
8	.1.2.3.4-fall.dayflow.geo	Dayflow: Delta Cross Channel and Georgiana Slough Flow Estimate (QXGEO). February - March average	Sacramento - San Joaquin Delta at the Delta Cross Channel and Georgiana Slough	Fall Sacramento Mainstem Wild Fall Battle Creek (CNFH) Hatchery Fall Feather River Hatchery Fall American River (Nimbus) Hatchery
9	.1.2.3.4-fall.dayflow.export	Dayflow: Total Delta Exports and Diversions/Transfers (QEXPORTS). March - May average	Sacramento - San Joaquin Delta	Fall Sacramento Mainstem Wild Fall Battle Creek (CNFH) Hatchery Fall Feather River Hatchery Fall American River (Nimbus) Hatchery
10	.1.2.3.4-fall.dayflow.expin	Dayflow: Export/Inflow Ratio (EXPIN). March - May average	Sacramento - San Joaquin Delta	Fall Sacramento Mainstem Wild Fall Battle Creek (CNFH) Hatchery Fall Feather River Hatchery Fall American River (Nimbus) Hatchery
11	.1.2.3.4-fall.dayflow.cd	Dayflow: Net Channel Depletion (QCD). March - May average	Sacramento - San Joaquin Delta	Fall Sacramento Mainstem Wild Fall Battle Creek (CNFH) Hatchery Fall Feather River Hatchery Fall American River (Nimbus) Hatchery
12	.1.2.3.4-fall.size.chipps	Average size of fall-run Chinook at ocean entry from Chipps Island Trawl	Chipps Island Trawl	Fall Sacramento Mainstem Wild Fall Battle Creek (CNFH) Hatchery Fall Feather River Hatchery Fall American River (Nimbus) Hatchery
13	.1.2.3.4-fall.farallon.temp.early	Average temperature at the Farallon Islands, CA (37° 41.8' N, 122° 59.9' W) during the SPRING months (February - April) BEFORE Chinook ocean entry	Nearshore Region, Farallon Islands, CA	Fall Sacramento Mainstem Wild Fall Battle Creek (CNFH) Hatchery Fall Feather River Hatchery Fall American River (Nimbus) Hatchery
14	.1.2.3.4-fall.farallon.temp.late	Average temperature at the Farallon Islands, CA (37° 41.8' N, 122° 59.9' W) during the SUMMER months (May - July) AFTER Chinook ocean entry	Nearshore Region, Farallon Islands, CA	Fall Sacramento Mainstem Wild Fall Battle Creek (CNFH) Hatchery Fall Feather River Hatchery Fall American River (Nimbus) Hatchery
15	.1.2.3.4-upwelling.north.early	NOAA Index for upwelling at Northern Location (39 N, 125 W), average of SPRING months (April - June)	Nearshore Region	Fall Sacramento Mainstem Wild Fall Battle Creek (CNFH) Hatchery Fall Feather River Hatchery Fall American River (Nimbus) Hatchery
16	.1.2.3.4-upwelling.north.late	NOAA Index for upwelling at Northern Location (39 N, 125 W), average of FALL months (July - December)	Nearshore Region	Fall Sacramento Mainstem Wild Fall Battle Creek (CNFH) Hatchery Fall Feather River Hatchery Fall American River (Nimbus) Hatchery
17	.1.2.3.4-upwelling.south.early	NOAA Index for upwelling at Southern Location (36 N, 122 W), average of SPRING months (April - June)	Nearshore Region	Fall Sacramento Mainstem Wild Fall Battle Creek (CNFH) Hatchery Fall Feather River Hatchery Fall American River (Nimbus) Hatchery
18	.1.2.3.4-upwelling.south.late	NOAA Index for upwelling at Southern Location (36 N, 122 W), average of FALL months (July - December)	Nearshore Region	Fall Sacramento Mainstem Wild Fall Battle Creek (CNFH) Hatchery Fall Feather River Hatchery Fall American River (Nimbus) Hatchery
19	.1.2.3.4.5.6.7-curl.early	NOAA Wind Stress Curl Index for upwelling at Northern Location (39 N, 125 W), average of SUMMER months (April - June)	Nearshore Region	Fall Sacramento Mainstem Wild Fall Battle Creek (CNFH) Hatchery Fall Feather River Hatchery Fall American River (Nimbus) Hatchery Spring Deer Creek Spring Mill Creek Spring Butte Creek
20	.1.2.3.4.5.6.7-curl.late	NOAA Wind Stress Curl for upwelling at Northern Location (39 N, 125 W), average of FALL months (July - December)	Nearshore Region	Fall Sacramento Mainstem Wild Fall Battle Creek (CNFH) Hatchery Fall Feather River Hatchery Fall American River (Nimbus) Hatchery Spring Deer Creek Spring Mill Creek Spring Butte Creek
21	.1.2.3.4.5.6.7-pdo.early	Pacific Decadal Oscillation (PDO), average of January - May monthly indices during first year of marine residence	Ocean	Fall Sacramento Mainstem Wild Fall Battle Creek (CNFH) Hatchery Fall Feather River Hatchery Fall American River (Nimbus) Hatchery Spring Deer Creek Spring Mill Creek Spring Butte Creek
22	.1.2.3.4.5.6.7-pdo.late	Pacific Decadal Oscillation (PDO), average of October - December monthly indices during first year of marine residence	Ocean	Fall Sacramento Mainstem Wild Fall Battle Creek (CNFH) Hatchery Fall Feather River Hatchery Fall American River (Nimbus) Hatchery Spring Deer Creek Spring Mill Creek Spring Butte Creek

201

Hypothesis Number	Covariate	Covariate Description	Location	Populations
23	fall.battle.creek - sacAirTemp.summer	Sacramento air temperature during summer (July - September) of the brood year	Sacramento, CA	Fall Battle Creek (CNFH) Hatchery
24	fall.battle.creek - sacAirTemp.spring	Sacramento air temperature during spring (January - March) emergence year	Sacramento, CA	Fall Battle Creek (CNFH) Hatchery
25	fall.battle.creek - keswick.discharge	Average January - March water discharge (cfs) at Keswick Dam	Keswick Dam	Fall Battle Creek (CNFH) Hatchery
26	fall.battle.creek - battle.discharge	Average January - March water discharge (cfs) on Battle Creek	Cottonwood, Battle Creek	Fall Battle Creek (CNFH) Hatchery
27	fall.battle.creek - battle.peak.gage.ht	Battle Creek peak gauge height November - December of brood year	Cottonwood, Battle Creek	Fall Battle Creek (CNFH) Hatchery
28	fall.feather - sacAirTemp.summer	Sacramento air temperature during summer (July - September) of the brood year	Sacramento, CA	Fall Feather River Hatchery
29	fall.feather - sacAirTemp.spring	Sacramento air temperature during spring (January - March) emergence year	Sacramento, CA	Fall Feather River Hatchery
30	fall.feather - keswick.discharge	Average January - March water discharge (cfs) at Keswick Dam	Keswick Dam	Fall Feather River Hatchery
31	fall.feather - feather.ornville.discharge	Average January - March water discharge (cfs) on the Feather River	Oronville, Feather River	Fall Feather River Hatchery
32	fall.american - sacAirTemp.summer	Sacramento air temperature during summer (July - September) of the brood year	Sacramento, CA	Fall American River (Nimbus) Hatchery
33	fall.american - sacAirTemp.spring	Sacramento air temperature during spring (January - March) emergence year	Sacramento, CA	Fall American River (Nimbus) Hatchery
34	fall.american - keswick.discharge	Average January - March water discharge (cfs) at Keswick Dam	Keswick Dam	Fall American River (Nimbus) Hatchery
35	fall.american - american.discharge	Average January - March water discharge (cfs) on the American River	Fair Oaks, American River	Fall American River (Nimbus) Hatchery
36	spring.deer - sacAirTemp.summer	Sacramento air temperature during summer (July - September) of the brood year	Sacramento, CA	Spring Deer Creek
37	spring.deer - sacAirTemp.spring	Sacramento air temperature during spring (January - March) emergence year	Sacramento, CA	Spring Deer Creek
38	.5.6.7-verona.peak.streamflow	Peak (maximum) streamflow on the Sacramento River mainstem at Verona, CA (January - May)	Verona, Sacramento River	Spring Deer Creek Spring Mill Creek Spring Butte Creek
39	.5.6.7-yolo.wood.peak.streamflow	Peak (maximum) streamflow into Yolo Bypass at Woodland, CA (January - May)	Into Yolo Bypass at Woodland, CA	Spring Deer Creek Spring Mill Creek Spring Butte Creek
40	.5.6.7-freeport.sed.conc	Average February - April monthly sediment concentration (mg/L)	Freeport, Sacramento River	Spring Deer Creek Spring Mill Creek Spring Butte Creek
41	.5.6.7-bass.cpue	Index of Striped Bass abundance as number of striped bass kept	Sacramento - San Joaquin Delta	Spring Deer Creek Spring Mill Creek Spring Butte Creek
42	.5.6.7-upwelling.north.early	NOAA Index for upwelling at Northern Location (39 N, 125 W), average of SPRING months (April - June)	Nearshore Region	Spring Deer Creek Spring Mill Creek Spring Butte Creek
43	.5.6.7-upwelling.north.late	NOAA Index for upwelling at Northern Location (39 N, 125 W), average of FALL months (July - December)	Nearshore Region	Spring Deer Creek Spring Mill Creek Spring Butte Creek
44	.5.6.7-upwelling.south.early	NOAA Index for upwelling at Southern Location (36 N, 122 W), average of SPRING months (April - June)	Nearshore Region	Spring Deer Creek Spring Mill Creek Spring Butte Creek
45	.5.6.7-upwelling.south.late	NOAA Index for upwelling at Southern Location (36 N, 122 W), average of FALL months (July - December)	Nearshore Region	Spring Deer Creek Spring Mill Creek Spring Butte Creek
46	spring.deer - deer.discharge	Average October - December water discharge (cfs) at Deer Creek	Vinna, Deer Creek	Spring Deer Creek
47	.5.6.7-spring.dayflow.geo	Dayflow: Delta Cross Channel and Georgiana Slough Flow Estimate (QXGEO). January - March average	Sacramento - San Joaquin Delta at the Delta Cross Channel and Georgiana Slough	Spring Deer Creek Spring Mill Creek Spring Butte Creek
48	.5.6.7-spring.dayflow.export	Dayflow: Total Delta Exports and Diversions/Transfers (QEXPORTS). February - April average	Sacramento - San Joaquin Delta	Spring Deer Creek Spring Mill Creek Spring Butte Creek
49	.5.6.7-spring.dayflow.expin	Dayflow: Export/Inflow Ratio (EXPIN). February - April average	Sacramento - San Joaquin Delta	Spring Deer Creek Spring Mill Creek Spring Butte Creek
50	.5.6.7-spring.dayflow.cd	Dayflow: Net Channel Depletion (QCD). February - April average	Sacramento - San Joaquin Delta	Spring Deer Creek Spring Mill Creek Spring Butte Creek
51	.5.6.7-spring.size.chipps	Average size of spring-run Chinook at ocean entry from Chipps Island Trawl	Chipps Island Trawl	Spring Deer Creek Spring Mill Creek Spring Butte Creek
52	.5.6.7-spring.farallon.temp.early	Temperature at the Farallon Islands, CA (37° 41.8' N, 122° 59.9' W) during the SPRING months (January - March) BEFORE Chinook ocean entry	Nearshore Region	Spring Deer Creek Spring Mill Creek Spring Butte Creek
53	.5.6.7-spring.farallon.temp.late	Temperature at the Farallon Islands, CA (37° 41.8' N, 122° 59.9' W) during the SUMMER months (April - June) AFTER Chinook ocean entry	Nearshore Region, Farallon Islands, CA	Spring Deer Creek Spring Mill Creek Spring Butte Creek
54	spring.mill - sacAirTemp.summer	Sacramento air temperature during summer (July - September) of the brood year	Sacramento, CA	Spring Mill Creek
55	spring.mill - sacAirTemp.spring	Sacramento air temperature during spring (January - March) emergence year	Sacramento, CA	Spring Mill Creek
56	spring.mill - mill.discharge	Average October - December water discharge (cfs) on Mill Creek	Molinos, Mill Creek	Spring Mill Creek
57	spring.butte - sacAirTemp.summer	Sacramento air temperature during summer (July - September) of the brood year	Sacramento, CA	Spring Butte Creek
58	spring.butte - sacAirTemp.spring	Sacramento air temperature during spring (January - March) emergence year	Sacramento, CA	Spring Butte Creek
59	spring.butte - butte.discharge	Average October - December water discharge (cfs) on Butte Creek	Chico, Butte Creek	Spring Butte Creek

202

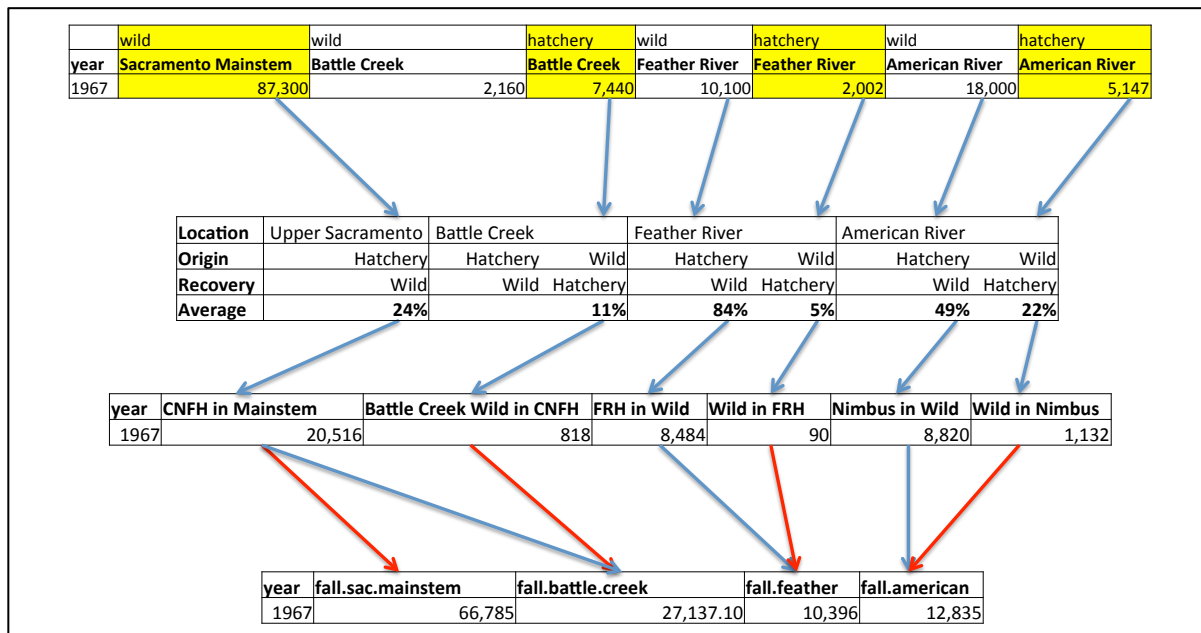
203 The second type of data required are time-series of abundance data for the populations
 204 included in the multi-stock population dynamics model. Estimates of the number of adult
 205 Chinook returning to natural spawning grounds and hatcheries are available from the GrandTab
 206 database (CDF&W 2014) for all seven populations evaluated as part of this study. However,
 207 since the Central Valley Constant Fractional Marking Program (CFM) was initiated in 2007, it
 208 has been possible to estimate the contribution of hatchery-origin Chinook to the spawning
 209 abundance observed on wild spawning grounds and the contribution of wild-origin Chinook

210 production to observed returns to regional hatcheries (Kormos et al. 2012). Historical
 211 abundances for the seven Chinook populations were reconstructed to account for straying
 212 between hatcheries and natural spawning grounds, using the average of the estimated proportion
 213 of observed adult Chinook straying in 2010 (Kormos et al. 2012) and 2011 (Palmer-Zwahlen and
 214 Kormos 2013). Average (2010-2011) proportions of observed adult abundance that were
 215 comprised of hatchery and wild individuals in each population (Table I.2), were used to
 216 reconstruct historical abundances for the fall-run spawning populations.

Location	Origin	Recovery	2010	2011	Average
Upper Sacramento	Hatchery	Wild	20%	27%	24%
Battle Creek	Hatchery	Wild			
	Wild	Hatchery	11%	11%	11%
Feather River	Hatchery	Wild	78%	90%	84%
	Wild	Hatchery	5%	4%	5%
American River	Hatchery	Wild	32%	66%	49%
	Wild	Hatchery	21%	23%	22%

217
 218 **Table I.2. Proportion of observed adult abundance by location estimated from CWT**
 219 **recoveries to be of wild or hatchery origin in 2010 and 2011, and the average used to**
 220 **reconstruct historical abundances.**

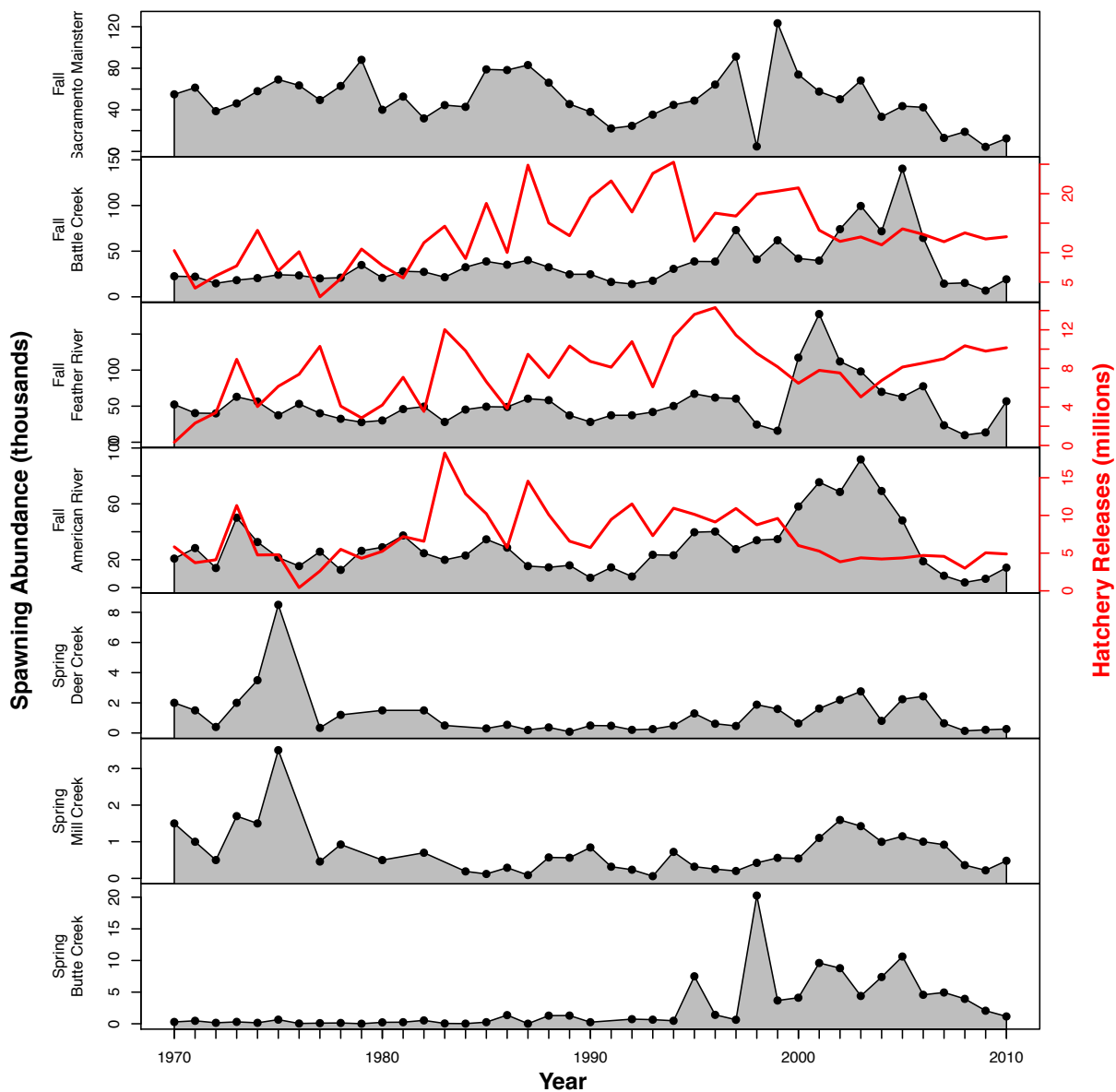
221 For example, in order to reconstruct the fall-run wild Sacramento mainstem spawning
 222 abundance, each year 24% of the observed spawning abundance was remove and reallocated to
 223 the Coleman National Fish Hatchery (Battle Creek) adult abundance, while 11% of the observed
 224 Battle Creek hatchery (CNFH) abundance was removed as wild migrants into the hatchery (Fig.
 225 I.1).



226
 227 **Figure I.1. Empirical schematic showing how the historical abundance of the 1967**
 228 **population for the four fall-run Chinook populations were reconstructed through**
 229 **additional or removal of the abundance of other stocks.**

230 Adult abundances for the four fall-run Chinook populations were reconstructed using the
 231 methods detailed above for years 1967 – 2010 (Fig. I.2). Existing adult abundance estimates
 232 reported by CDF&W (2014) for the spring-run populations included in our analyses (i.e. Deer,
 233 Mill, and Butte Creeks) were assumed to be minimally impacted by hatchery straying and
 234 therefore unaltered (Fig. I.2).

235



236 **Figure I.2. Adult abundance (grey area plot) and hatchery release (red line) data for**
 237 **Sacramento River Chinook. Fall-run abundances are reconstructed based upon hatchery-**
 238 **wild stray rate estimates, while spring-run abundances are as reported in GrandTab 2014.**
 239

240 Estimates of juvenile Chinook abundance in Sacramento River system were also used to
 241 inform estimates of model parameters. The inclusion of additional abundance indices to which

242 the estimation model is fit, confers a greater ability to partition mortality between life stages and
 243 more precise estimation of the strength and magnitude of influence from environmental
 244 covariates. Poytress et al. (2014) have used available trap efficiency information to calculate
 245 absolute abundance indices for juvenile Chinook passing Red Bluff Diversion Dam, partitioned
 246 by race. Fall-run juvenile Chinook abundance estimates from 2002 forward were assumed to be
 247 comprised predominantly of two populations, the wild Sacramento Mainstem population and the
 248 Battle Creek (CNFH) Hatchery population. Therefore, model estimates of the combined
 249 abundance of these two populations were compared to the estimates provided by Poytress et al.
 250 (2014) in likelihood calculations.

251 The third type of data required by the estimation model are historical hatchery releases.
 252 As constructed, the estimation model allows for specification of the wild or hatchery life-history
 253 type for each population. Three of the seven populations currently included in our analysis are
 254 of hatchery origin, therefore annual hatchery release numbers were required for the Battle Creek
 255 (CNFH) Hatchery, Feather River Hatchery, and American River (Nimbus) Hatchery populations.
 256 Huber and Carlson (in review) have expended significant time and effort to digitize and render
 257 historical hatchery reports in an easily accessible and usable format. For the three hatchery
 258 population included in our analysis, we have used these hatchery release data to in place of the
 259 functional relationship between spawning abundance and fecundity assumed for the wild
 260 spawning populations. Figure I.2 shows hatchery release numbers from Huber and Carlson (in
 261 review) for each of the three fall-run hatchery populations.

262 Hatchery release practices have historically differed amongst facilities and over time,
 263 with on-sight releases, releases in the Sacramento-San Joaquin delta, releases in San Francisco
 264 Bay, and many locations in between (Huber and Carlson in review). At this time, hatchery
 265 release location was not specifically considered. However, for populations whose release
 266 strategies allow fish to bypass the mortality incurred in the upriver stage, this should manifest as
 267 a reduction in the estimated influence of covariates linked to the upriver stage. In this way,
 268 although we do not specifically adjust the model stage pathway depending on hatchery release
 269 location in each year, this should not be expected to introduce any significant bias in our
 270 estimates of coefficients describing the influence of environmental covariates.

271 The fourth type of data required for these analyses were annual estimates of harvest rate
 272 by population. Harvest rate estimates are available from the U.S. Fish and Wildlife Chinookprod
 273 database. For each population of interest, this database uses both the abundance estimates from
 274 the Grandtab (CDF&W 2014) database and ocean harvest numbers from the Pacific Fishery
 275 Management Council (PFMC) to calculate harvest rates in the marine and in-river regions. For
 276 our purposes, we have calculated the total harvest rate by stock and year as the sum of ocean (
 277 $C_{t,p}^{ocean}$) and in-river catch ($C_{t,p}^{in-river}$), divided by the total abundance including observed
 278 escapement ($E_{t,p}$) and catches for that population (p) in that year (t) (Eq. I.2).

$$279 \quad (I.2) \quad hr_{t,p} = \frac{C_{t,p}^{ocean} + C_{t,p}^{in-river}}{E_{t,p} + C_{t,p}^{ocean} + C_{t,p}^{in-river}}$$

280 *Estimation model structure*

281 The purpose of our analysis is to test the various hypotheses regarding what natural and
282 anthropogenic factors have influenced Sacramento River Chinook salmon survival historically,
283 during both the freshwater and marine portions of the Chinook life cycle. Furthermore, we wish
284 to use estimates of the drivers of Chinook survival to generate robust predictions for future
285 abundance under a range of alternative climate change, oceanographic, and water management
286 scenarios. In order to achieve this objective we have created a population dynamics model that
287 estimates the influence of environmental covariates as well as population-specific basal
288 productivity (maximum survival) rates and rearing capacities for different stages in the life cycle.

289 The statistical population dynamics model is stage-structured, simulating the entire
290 Chinook life cycle from egg to spawning adult, and partitioning mortality events between those
291 separate spatio-temporal stages. For the freshwater portion of the life cycle, these stages are
292 defined by the migration pathways exhibited by the various Chinook populations and the
293 availability of two data types. First, freshwater life stages are defined in accordance with the
294 availability of environmental covariate data, so as to accurately reflect the point in time and
295 location within Sacramento River network where the Chinook have the most substantial
296 exposure to the environmental covariates. Second, model stages are structured to correspond
297 with juvenile indices of abundance at Red Bluff, CA (Poytress et al. 2014). The estimation model
298 contains six stages, three associated with juvenile rearing in freshwater and nearshore regions,
299 and three associated with the marine component of the life cycle (Fig. I.3). The first stage
300 represents rearing of juveniles in tributaries and upper reaches of the Sacramento River
301 mainstem. The second model stage represents the area within the Sacramento River watershed
302 including the Sacramento-San Joaquin Delta through Chipps Island. The third stage represents
303 juvenile rearing in the nearshore region from San Francisco Bay and the Gulf of Farallones.
304 Stages 4-6 represent the years spent in the marine environment, with associated probability of
305 maturation and potential for ocean harvest.



306
307 **Figure I.3. Map of estimation model stage structure.**

308 The population dynamics model tracks cohorts of Chinook from specific brood years
309 forward in time across sequential model stages. Chinook abundance is represented by $N_{y,s,p}$ or
310 the number of individuals from brood year y , surviving to stage s , of population p . The
311 abundance of Chinook of brood year y and population p , surviving to the end of the current stage
312 (s) is dependent upon the year, stage, and population specific survival rate $SR_{y,s,p}$ in Equation
313 I.3.

314 (I.3)
$$N_{y,s,p} = N_{y,s-1,p} * SR_{y,s,p}$$

315 Survival through the spatio-temporally explicit life stages is described by a Beverton-Holt
316 transition function (Moussalli and Hilborn 1986). The Beverton-Holt equation, while
317 traditionally used in the evaluation of spawner-recruit data (Beverton and Holt 1957), provides a
318 useful approximation for survival of individuals from one model stage to the next, as influenced
319 by two factors: 1) the productivity rate $p_{y,s,p}$, and 2) the rearing capacity $K_{y,s,p}$ of each stage (Eq.
320 I.4).

321 (I.4)
$$SR_{y,s,p} = \frac{p_{y,s,p}}{1 + \frac{p_{y,s,p} * \sum_{i=1}^{Npop} \alpha_{p,i,s} * N_{y,s-1,i}}{K_{y,s,p}}}$$

322 In this formulation (Eq. I.4) the year, stage, and population-specific productivity ($p_{y,s,p}$)
323 represents the maximum survival rate in the absence of density-dependent compensation.

324 Conversely, the year, stage, and population-specific capacity ($K_{y,s,p}$) describes the total number
 325 of individuals that can potential survive through the model stage. However, given that we are
 326 evaluating multiple co-migrating and co-rearing populations, equation I.4 also includes an
 327 interaction effect ($\alpha_{p,i,s}$) which describes how many individuals of the focal population p are
 328 displaced with respect to the stage capacity ($K_{y,s,p}$) for each individual of population i . In this
 329 way no interaction effect for a stage may be specified with a zero value for all elements of $\alpha_{p,i,s}$
 330 except $\alpha_{p,i=p,s}$. Positive, non-zero values indicate that the abundance of other populations (i)
 331 results in a reduction in overall rearing capacity for the focal population (p), and therefore
 332 reduced survival at high abundance levels which approach the stage-specific capacity ($K_{y,s,p}$).
 333 Specifying $\alpha_{p,i,s}$ elements equal to one create a situation where capacity is shared across
 334 populations with symmetric impacts on capacity.

335 In our current analysis we have identified the Sacramento-San Joaquin Delta stage (2nd)
 336 and nearshore stage (3rd) as points of possible competition and therefore capacity interactions
 337 within the model. Fall-run and spring-run juvenile Chinook are assumed to compete with
 338 members of their own race within these two stages of the life cycle and therefore shared
 339 capacities are assumed, with symmetric interactions (i.e. $\alpha_{p,i,s}$ elements equal to 1).

340 The productivity ($p_{y,s,p}$) capacity ($K_{y,s,p}$) parameters in the population dynamics model
 341 are time varying and assumed to change in response to inter-annual variation in the
 342 environmental covariates under evaluation. The productivity parameter for population p , of
 343 brood year y , in stage s is a function of the basal productivity $\beta_{s,p,0}$, or the average survival for
 344 members of that population in the current stage, as well as the sum of environmental covariate c
 345 values at time t ($X_{t,c}$) multiplied by their respective coefficients ($\beta_{s,p,c}$) which describe the
 346 influence of each covariate on stage and population-specific productivity $p_{y,s,p}$ (Eq. I.5).

$$347 \quad (I.5) \quad p_{y,s,p} = \frac{1}{1 + \exp\left(-\beta_{s,p,0} - \sum_{c=1}^{Nc_{s,p}} \beta_{s,p,c} * X_{t,c}\right)}$$

$$t = y + \delta_c$$

348 δ_c is the covariate-specific temporal reference which is the difference between the brood
 349 year y and the year in which the cohort will interact with that covariate, and is used as a pointer
 350 to ensure that the covariate value for the correct year is used when tracking each cohort forward
 351 in time, and $Nc_{s,p}$ is the number of productivity covariates linked to each population in each
 352 stage. The overall productivity parameter value ($p_{y,s,p}$) is a logit transformation of the additive
 353 effects of the basal productivity rate and covariate effects, which ensures that its value is
 354 smoothly scaled between 0 and 1 (Eq. I.5).

355 The capacity parameter for each population's brood year specific cohort in each stage
 356 ($K_{y,s,p}$) is likewise a function of a basal, or average, stage and population specific capacity across
 357 years ($\gamma_{s,p,0}$) and the additive effects of capacity-related covariates ($Y_{t,k}$) and the population-
 358 specific coefficients ($\gamma_{s,p,k}$) describing the magnitude and direction of influence each holds (Eq.
 359 I.6).

360 (I.6)
$$K_{y,s,p} = \exp\left(\gamma_{s,p,0} + \sum_{k=1}^{Nk_{s,p}} \gamma_{s,p,k} * Y_{t,k}\right)$$

361
$$t = y + \delta_k$$

361 The capacity parameter ($K_{y,s,p}$) is described in natural log space for ease of estimation
 362 and to ensure it is bounded within the set of positive values, where k is the covariate reference
 363 number and δ_k is the temporal reference for the offset from the brood year for each covariate,
 364 indicating when the population interacts with each specific covariate in the life cycle.

365 However, for populations of Chinook occupying the same habitats and subject to the
 366 same environmental covariates, it may be reasonable to assume that a common response in
 367 survival to a particular covariate is exhibited. For this reason we have further allowed for a
 368 coefficient describing the effect of a particular covariate to be shared across populations. In this
 369 way several productivity ($\beta_{s,c}$) capacity ($\gamma_{s,k}$) coefficients may be common across a subset of
 370 populations. This reduces model complexity, increases parsimony, and improves the ability to
 371 estimate of coefficient values for which a common survival response is biologically defensible.

372 The basal capacity parameters for a population ($\gamma_{s,p,0}$, see Eq. I.6), or group of interacting
 373 populations for which $\alpha_{p,i,s} > 0$ (see Eq. I.4), represent the maximum rearing capacity for that
 374 population in that stage over time in the absence of influence from environmental covariates. For
 375 populations that are currently well below historical abundance levels, or for populations without
 376 subsequent juvenile abundance estimates, it is often difficult to estimate these basal stage
 377 capacity values. However, auxiliary information may be used to inform these stage-specific
 378 capacities. Recent work by Noble Hendrix, in collaboration with researchers at NOAA, has
 379 resulted in monthly juvenile Chinook salmon capacity estimates for the Sacramento River
 380 mainstem and the Sacramento-San Joaquin Delta (Hendrix et al. 2014). In place of estimating
 381 stage capacities for: 1) Sacramento River mainstem-spawning wild fall-run Chinook in the
 382 upstream stage (1st), 2) mainstem-spawning wild, Battle Creek (CNFH) hatchery, Feather River
 383 Hatchery, and American River (Nimbus) Hatchery, populations in the Sacramento-San Joaquin
 384 Delta stage (2nd), and 3) Deer, Mill, and Butte Creek populations in the Sacramento-San Joaquin
 385 Delta stage (2nd), we have used capacity estimates available from NOAA in-stream Chinook
 386 capacity modelling (see Appendix A - Delta Submodel). The average of estimated monthly
 387 capacities in the Sacramento Mainstem for the period between January and April in each year,
 388 was used for as the input capacity for mainstem-spawning wild fall-run population. The average
 389 of estimated monthly Sacramento – San Joaquin Delta rearing capacities for the March – May
 390 and February – April periods, were used as the input capacities for the fall-run and spring-run
 391 populations in that stage, respectively.

392 Capacity estimates for the Sacramento-San Joaquin Delta from NOAA in-stream
 393 Chinook habitat capacity modelling were only available after 1980 (Hendrix et al. 2014). Given
 394 that our population dynamics model begins in year 1967, it was necessary to assume a fixed
 395 capacity for the period prior to 1980. NOAA Delta capacity estimates correlate most directly
 396 with water year type, therefore the average of estimated capacities for the fall-run and spring-run
 397 populations by water year type were calculated and used in place of actual capacity estimates

398 prior to 1980. These average capacities by water year type and Chinook run type were used in
399 years prior to 1980 based on the reported water year.

400 Survival for cohorts of Chinook is tracked forward in time across spatio-temporal model
401 stages in the same manner (Eq. I.4, I.5, I.6) independent of whether the stage is in the freshwater
402 or marine portion of the life cycle and independent of the ontogenetic status of individuals.
403 However, for the final three model stages representing the 1st, 2nd, and 3rd year in the ocean, it is
404 necessary to account for both the maturation process and marine harvest when tracking the
405 number of individuals entering the next stage. Harvest mortality is assumed to occur after the
406 annual mortality event, but prior to maturation. Catch by year, population, and stage ($C_{t,p,s}$) is
407 the number of surviving individuals multiplied by the population specific harvest rate observed
408 in each year ($hr_{t,p}$), scaled by the stage (i.e. ocean age) specific catchability coefficient (ϵ_s) (Eq.
409 I.7).

$$C_{t,p,s} = N_{y,s,p} * SR_{y,s,p} * (hr_{t,p} / \epsilon_s)$$

410 (I.7) $t = y + \rho_s$
 $\epsilon_s = \{0, 0, 0, 0, 1.54, 1.0\}$

411 In equation I.7, ρ_s is the temporal offset for model stages that indicates the difference
412 between the brood year and the calendar year, so that the proper annual harvest rate may be
413 referenced. Annual harvest rate estimates were obtained from the Pacific Fishery Management
414 Council (PFMC).

415 For the three ocean life-stages, the number of individuals of a cohort moving to the next
416 stage is governed by the survival rate ($SR_{y,s,p}$), annual catch estimate ($C_{t,p,s}$), and the maturation
417 probability (ϕ_s) (Eq. I.8).

$$N_{y,s+1,p} = (N_{y,s,p} * SR_{y,s,p} - C_{t,p,s}) * (1 - \phi_s)$$

418 (I.8) $\phi_s = \{0, 0, 0, 0.1, 0.942, 1\}$
 $t = y + \rho_s$

419 While the cohort specific survival rate varies over time, the maturation probability (ϕ_s) is
420 assumed to be temporally invariant. So then, the number of individuals of a cohort advancing to
421 the next ocean stage is the number in the previous stage ($N_{y,s,p}$) that have survived, less the
422 proportion that matures and begins homeward migration (Eq. I.8). The return abundance ($R_{y,s,p}$)
423 is the number of individuals from a cohort that survived marine and harvest mortality, and have
424 initiated the maturation process and return to freshwater to spawn (Eq. I.9).

425 (I.9) $R_{y,s,p} = (N_{y,s,p} * SR_{y,s,p} - C_{t,p,s}) * \phi_s$

426 The predicted number of spawning adults of each population in each year ($\hat{A}_{t,p}$) is the
427 sum of returning individuals ($R_{y,s,p}$) across stages or equivalently ocean age classes (Eq. I.10).

428 (I.10)
$$\hat{A}_{t,p} = \sum_{s=1}^{Nstage} R_{y,s,p}$$

$$t = y + \rho_s$$

429 Depending on whether a wild-type or hatchery-type life history is assumed for each
 430 population the next cohort ($N_{y,s=1,p}$) will be created either based on the predicted number of
 431 spawning adults and an assumed fecundity value of 2000 eggs/individuals (Eq. I.11) or based
 432 upon recorded releases from hatchery facilities (Eq. I.12).

433 (I.11)
$$N_{y,s=1,p} = \hat{A}_{t=y,p} * fec$$

434 (I.12)
$$N_{y,s=1,p} = RH_{t=y,p}$$

435 In order to estimate the value for model parameters including basal productivities ($\beta_{s,p,0}$)
 436 and capacities ($\gamma_{s,p,0}$) for each population in each stage, and coefficients describing the direction
 437 and magnitude of influence each environmental covariate has on either productivity ($\beta_{s,p,c}$) or
 438 capacity ($\gamma_{s,p,k}$) for individual populations or shared amongst populations ($\beta_{s,c}$ and $\gamma_{s,k}$), the
 439 model must be fit to available abundance data. We employ a maximum likelihood approach to
 440 compare abundance predictions with available data and estimate model parameter values
 441 (Hilborn and Mangel 1997). Predicted adult spawning abundances are calculated (Eq. I.10) as
 442 part of the population dynamics model. Absolute abundance estimates for juveniles are available
 443 for Chinook passing Red Bluff Diversion Dam (Poytress et al. 2014), and we assume that the
 444 mainstem Sacramento wild population and Battle Creek hatchery (CNFH) population comprise
 445 the majority of the juvenile fall-run Chinook sampled at this location, so the juvenile abundance
 446 estimate is calculated as the sum of these two populations (Eq. I.13)

447 (I.13)
$$\hat{J}_t = \sum_{p=1}^2 N_{y,s=1,p}$$

$$t = y + \rho_{s=1}$$

448 Model predicted adult spawning abundances are compared to empirical data, and model
 449 parameters are estimated by minimizing the negative log-likelihood of the model given the
 450 observed data (Eq. I.14).

451 (I.14)
$$L_A(\Theta | A_{t,p}) = \prod_{t=1}^n \frac{1}{\hat{\sigma}_p \sqrt{2\pi}} \exp \left[-\frac{(\ln(A_{t,p}) - \ln(\hat{A}_{t,p}))^2}{2\hat{\sigma}_p^2} \right]$$

452 The likelihood of the model parameters, given the spawning abundance data, assume a
 453 that observation error in log transformed abundances are normally distributed, with the standard
 454 deviation of the observation error distribution ($\hat{\sigma}_p$) equal to the maximum likelihood estimate
 455 (Eq. I.15).

456 (I.15)
$$\hat{\sigma}_p = \sqrt{\sum_{t=1}^n \frac{(\ln(A_{t,p}) - \ln(\hat{A}_{t,p}))^2}{n}}$$

457 Under the same assumptions the observation error likelihood of the model parameters
458 given juvenile abundance data (Eq. I.13) was calculated (Eq. I.16)

459 (I.16)
$$L_J(\Theta | J_t) = \prod_{t=1}^n \frac{1}{\hat{\sigma}_J \sqrt{2\pi}} \exp\left[-\frac{(\ln(J_t) - \ln(\hat{J}_t))^2}{2\hat{\sigma}_J^2}\right]$$

460 using the maximum likelihood estimate for the standard deviation of the normal
461 observation error distribution from the juvenile data (Eq. I.17).

462 (I.17)
$$\hat{\sigma}_J = \sqrt{\sum_{t=1}^n \frac{(\ln(J_t) - \ln(\hat{J}_t))^2}{n}}$$

463 The total data likelihood (Eq. I.18) is the sum of the negative log of the likelihood from
464 the juvenile and adult abundance data.

465 (I.18)
$$LL_T = -\ln(L_A) - \ln(L_J)$$

466 Model parameter values that minimized the total negative log likelihood (LL_T) were
467 found using AD Model Builder (Fournier et al. 2012). AD Model Builder (ADMB) is a software
468 platform allowing complex non-linear minimizations for models containing a large number of
469 parameters while also permitting profile likelihoods or posterior distributions for parameters of
470 interest to be estimated. ADMB was selected as the software design platform for this project
471 because of its flexibility, computational efficiency and ability to reliably sample a complex
472 multivariate likelihood surface. In addition to its benefits as a fast and stable optimization tool
473 for fitting statistical models to data, ADMB also estimates uncertainty in and correlations
474 between model parameters based on their derivative structure.

475 When fit to available abundance data the ADMB stage-structured population dynamics
476 model provides estimates of model parameters, uncertainty in those parameter estimates, and the
477 hessian matrix for model parameters from which the parameter covariance matrix may be
478 derived. However, with 37 separate environmental covariates to be tested as competing
479 hypotheses it was necessary to define metrics for model fit and parsimony. We use the Akaike
480 Information Criterion corrected for small sample sizes (AICc) (Burnham and Anderson 2002) as
481 a metric for model parsimony (Eq. I.19).

482 (I.19)
$$AICc = 2LL_T + 2p + \frac{2p(p+1)}{n-p-1}$$

483 AICc balances the degree to which a model is able to explain the variability in data (LL_T)
 484 against the number of parameters estimated (p) and number of data used in estimation (n), and
 485 provides a basis for model selection. The second statistic used to evaluate model fit is the mean
 486 absolute percent error in model predictions (Eq. I.20).

$$487 \quad (I.20) \quad MAPE_p = \frac{\sum_{t=1}^n \left| \frac{\hat{A}_{t,p} - A_{t,p}}{A_{t,p}} \right|}{n}$$

488 The method we have employed in the Sacramento for modelling the anadromous
 489 salmonid life cycle as a series of sequential, spatially-explicit, stage-specific Beverton-Holt
 490 transition functions that relate density-dependent survival to habitat covariates is similar to those
 491 successfully used to address conservation questions regarding other Chinook salmon populations
 492 along the West Coast. The Shiraz model developed by Scheuerell et al. (2006), employed to
 493 evaluate anthropogenic and habitat effects on production of Chinook in the Snohomish River
 494 basin of Puget Sound, Washington, was one of the first to specify interactions between habitat
 495 variables and the productivity and capacity parameters of the Beverton-Holt functions describing
 496 survival through life stages. Subsequently, Battin et al. (2007) and Honea et al. (2009) employed
 497 stage-structured models governed by linked Beverton-Holt transition functions to evaluate the
 498 influence of climate change, hydrologic variability, and habitat restoration on populations of
 499 Chinook salmon in the Columbia River basin. All three of these analyses used a Shiraz-type
 500 approach by linking habitat and climate covariates to stage-specific survival.

501 However, the model we have designed for evaluating the environmental drivers of
 502 survival for Chinook salmon in the Sacramento River differs from the Shiraz-type models
 503 described above (Scheuerell et al. 2006, Battin et al. 2007, Honea et al. 2009) in several
 504 fundamental ways. First, the model used in these analyses is statistical in nature. Whereas
 505 Scheuerell et al. (2006), Honea et al. (2009), and Battin et al. (2007), all specify the relationships
 506 between environmental covariates and the productivity and capacity parameters of the Beverton-
 507 Holt function for each stage, based upon *in situ* observations, laboratory experiments, or expert
 508 opinion, the estimation framework we have created for the analysis of the drivers of Sacramento
 509 River Chinook survival estimates these relationships directly from the abundance data. Second,
 510 estimation of the relationships between environmental covariates and the Beverton-Holt
 511 productivity and capacity parameters, will not only provide point estimates of the effect of each
 512 covariate, but also estimates of uncertainty. By estimating both the value for coefficients
 513 describing covariate effects, as well as their uncertainty, we are not only be able to discern which
 514 covariates have the largest influence, but also which covariates have had a consistent influence
 515 historically. Finally, by estimating the value of coefficients describing the magnitude and
 516 direction of influence each environmental covariate has on stage-specific productivity or
 517 capacity, our method allows for the propagation of estimation uncertainty in those relationships
 518 forward when those model parameters are used to predict future abundance trends under
 519 alternative climate, marine productivity, or water use scenarios.

520 *METHODS UNCERTAINTY – AICc SELECTIONS AND MCMC METHODS*

521 In order to test a range of hypotheses regarding which environmental covariates influence
 522 the survival of seven populations of Sacramento River Chinook, we constructed a stage-
 523 structured statistical population dynamics model. When fit to available adult and juvenile
 524 abundance data, this model estimates the magnitude and direction of influence that a set of
 525 environmental covariates has on two components of Chinook survival, namely life-stage specific
 526 productivity (maximum survival) rates and capacities. In the process of fitting population
 527 dynamics models to data as part of our analysis, there were two sources of uncertainty that we
 528 considered directly. The first was structural uncertainty, or uncertainty in the subset of
 529 environmental covariates that best represent the processes driving changes in abundance over
 530 time. The second is estimation uncertainty, or uncertainty in our ability to identify the true
 531 direction and magnitude of the effect each environmental covariate imposes on Chinook
 532 survival. To address structural uncertainty in our analysis, we used a process of forward stepwise
 533 model building, based upon an AICc criteria, with replication to ensure complete evaluation of
 534 model space, or the range of potential models that may be used to describe trends in abundance
 535 over time. This process allowed us to define the “best” model or subset of potential
 536 environmental covariates (hypotheses) for describing observed population dynamics. To address
 537 the second type of uncertainty in our analysis, estimation uncertainty, we employed Markov
 538 Chain Monte-Carlo estimation methods to quantify the probability distributions for the
 539 coefficients describing the effect of each environmental covariate on survival.

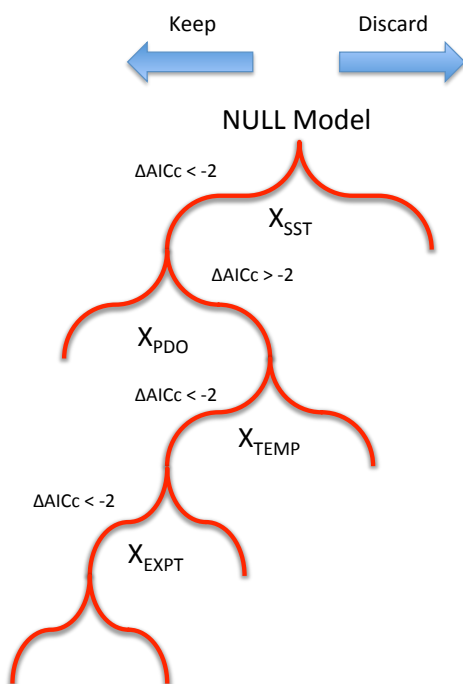
540 *Stepwise AICc Model Selection*

541 In total 37 separate environmental covariates were identified by the study team as
 542 potential drivers of interannual variation in Sacramento Chinook survival. Describing the effects
 543 of these 37 environmental covariates on separate populations in the form of either population-
 544 specific effects or common influences on groups of populations, resulted in a total 59 covariate-
 545 by-population effects, whose influence on survival may be estimated based on their ability to
 546 explain observed Chinook abundance data. Each of these 59 covariate-by-population effects
 547 represents an alternative hypothesis to be tested in our analysis.

548 Hypotheses for covariate-by-population effects on Chinook survival may be compared to
 549 a “null” model that attempts to explain variation in the time-series’ of observed juvenile and
 550 adult abundance data based on only observed ocean harvest rates, hatchery release numbers,
 551 estimated productivities (maximum survival rates) for populations in the first life-stage, and
 552 annual capacities specified by the juvenile capacity modelling (Hendrix et al. 2014). The null
 553 model represents the base case, without any influence from environmental covariates. However,
 554 in order to define the model with the best potential to provide accurate predictions for population
 555 responses to future environmental, climate, and water management scenarios it was necessary to
 556 find the most parsimonious model, or subset of explanatory covariates. Model parsimony is
 557 defined by the balance between the ability to accurately explain variation in observed data, while
 558 estimating the fewest parameters possible. The Akaike information criterion, corrected for small
 559 sample sizes (AICc, Eq. I.19), quantifies model parsimony and provides a metric for selecting
 560 amongst competing models (Burnham and Anderson 2002). Competing models incorporating

561 alternative combinations of covariate effects were compared based on their AICc values in order
 562 to define a “best-fit” model for generating predictions for future abundance trends.

563 With a total of 59 independent covariate-by-population effects to be tested for their
 564 ability to explain variation in historical Sacramento Chinook survival, the number of possible
 565 combinations of these effects, or potential models, is quite large. It becomes unrealistic to fit
 566 every possible model permutation to the available data and compare AICc values. Therefore we
 567 used a method for exploring the model space, or the range of potential models incorporating
 568 different combinations of these effects, which involved a forward stepwise model building with
 569 AICc as the selection criteria. Forward stepwise model building begins first by fitting the null
 570 model, without any covariate effects, to the available data. Second, a covariate is selected at
 571 random from amongst the set of 59 possible covariate-by-population effects and included in the
 572 model, and this model is subsequently fit to the data. Third, the AICc value for this new model is
 573 compared to that of the null model. If a reduction in AICc value for the model including the
 574 additional covariate of greater than 2 units is observed ($\Delta AICc \leq 2$), when the old model is
 575 compared to the model incorporating the new covariate, that covariate is kept, otherwise it is
 576 removed from the model. Moving forward, this process of randomly sampling covariates without
 577 replacement, fitting the model to data, and evaluating $\Delta AICc$, (i.e. steps two and three) are
 578 repeated until all covariates have been tested for their ability to improve model parsimony (see
 579 Fig. I.4).



580
 581 **Figure I.4. Diagram of forward stepwise AICc model building process. Starting from the**
 582 **null model, covariates (X_{TEMP} , X_{PDO} etc.) are sampled at random without replacement from**
 583 **the set of 59 possible hypotheses and included in the statistical model. The model is then fit**
 584 **to abundance data and the difference in AICc values between the old and new models**
 585 **dictates whether that covariate is kept or discarded, and the next iteration begins.**

586 The result of one round of forward stepwise AICc model building, or fitting the null
 587 model and 59 alternative models sequentially, is one realization of a best-fit model based upon
 588 the AICc criteria. However, experience indicates that given even small correlations among some
 589 environmental covariates, the order in which covariates are introduced has a subtle influence on
 590 the resulting model. Therefore, in order to more fully explore the uncertainty in model selection,
 591 we repeated the forward stepwise AICc process 1,000 times. By evaluating the frequency with
 592 which specific covariates appear in best-fit models across these 1,000 realizations, it is possible
 593 to determine which covariates are most important in explaining historical variation in Chinook
 594 survival. Furthermore, by repeating the stepwise AICc process 1,000 times, we are thoroughly
 595 exploring the model space and among these independently built models can determine the single
 596 model that has the lowest AICc among the candidate best-fit models.

597 *Markov Chain Monte-Carlo Estimation Methods*

598 The second critical piece of uncertainty in our analysis is estimation uncertainty.
 599 Estimation uncertainty describes variation in the estimated value of model parameters, and is a
 600 function of how well model parameters are informed by the available data. In order to quantify
 601 the level of estimation uncertainty in our analyses, particularly as it pertains to estimates of the
 602 coefficients describing the influence of environmental covariates on Chinook survival, we
 603 employed Bayesian estimation methods in addition to the maximum likelihood approach
 604 described above. Bayes' Theorem (Eq. I.21) describes the probability of a hypothesis θ , in our
 605 case a set of parameter values, given the data, which in our case are both adult spawning
 606 abundance ($A_{t,p}$) and juvenile abundance (J_t) observations.

$$607 \quad (I.21) \quad P(\theta | data) = \frac{P(data | \theta)P(\theta)}{\int P(data | \theta)P(\theta)}$$

608 The prior probability on logit transformed coefficients was normal with a mean of zero
 609 and standard deviation equal to 2.5, as per recommendations by King et al. (2010). Bounded
 610 uniform priors were assumed for all other estimated model parameters. Estimated initial (log)
 611 abundances 1967-1969 were bounded on the (0, 100) interval, basal stage productivities ($\beta_{s,p,0}$)
 612 were bounded on the (-25, 25) interval, and basal stage capacities ($\gamma_{s,p,0}$) bounded on the (-100,
 613 100) interval. Bayesian estimation methods allow the posterior probability distribution for
 614 derived and estimated parameters to be calculated, and from it the full range of parameter
 615 uncertainty. The posterior probability distribution for model parameter i (θ_i) describes the
 616 probability that the true value of that parameter is equal to a specific value. Based upon the
 617 posterior probability distributions for model parameters, we are able to calculate the expected
 618 values for model parameters as well the uncertainty in those parameter estimates.

619 Markov Chain Monte-Carlo (MCMC) methods are commonly used numerical algorithms
 620 employed to draw samples from the posterior distributions for parameters in Bayesian models
 621 (Gelman et al. 2004). We employed the Random Walk Metropolis-Hastings (RW-MH) MCMC
 622 algorithm implemented in AD Model Builder (Fournier et al. 2012) to draw samples from
 623 posterior distributions of parameters in population dynamics model. The RW-MH MCMC
 624 algorithm is a widely applicable MCMC algorithm that accounts for correlations among model

625 parameters. As implemented in ADMB, the RW-MH MCMC algorithm begins by finding the
626 parameter values that maximize the complete data likelihood, or posterior modes, and then uses
627 the estimated covariance matrix for model parameters to create a multivariate proposal
628 distribution. Based upon this multivariate proposal distribution randomly drawn parameter sets,
629 or MCMC jumps, are proposed and either accepted or rejected based upon comparison of the
630 ratio of the proposed posterior density to that of the current state, with a random uniform (0,1)
631 deviate. In this way, the RW-MH MCMC algorithm in ADMB begins as the posterior mode and
632 samples the joint posterior.

633 MCMC chains were run for 5,000,000 iterations with a thinning rate of 1/1,000 to reduce
634 posterior correlation. The first 30% of the chain was removed as a burn-in period, during which
635 the chain approached the stationary distribution for model parameters. To ensure MCMC results
636 converged to their stationary distribution, three independent chains were run simultaneously.
637 Model convergence was tested in three separate ways. First, traceplots of MCMC samples were
638 evaluated for the presence of discernable trends that would indicate a lack of convergence to the
639 true stationary distribution. Second, posterior correlations at differing lags were calculated,
640 wherein significant correlation would indicate a lack of convergence. Finally, Gelman and
641 Rubin's convergence diagnostic (Gelman and Rubin 1992, Brooks and Gelman 1998) was used
642 to compare within and among chain variance to determine if all three chains had indeed
643 converged to the same stationary distribution.

644 *RESULTS MODEL FITS*

645 *Model Selection Results*

646 In order to define the set of environmental covariates that best explains historical patterns
647 in abundance for the seven populations of Sacramento Chinook, we employed a process of
648 iterative forward stepwise AICc model selection. This process was meant to test the full range of
649 alternative hypotheses for drivers of Sacramento Chinook survival, and define the most coherent
650 set of covariates with the greatest explanatory power and predictive potential. Each iteration of
651 model selection results in a candidate best-fit model, however in order to fully explore model
652 space it was necessary to repeat this process many times with a randomized order of covariate
653 proposal in each iteration. By comparing the percent of times any particular covariate appeared
654 across the 1,000 candidate best-fit models, we are able to determine which covariates or
655 hypotheses have the greatest support from the data. Table I.3, describes the percentage of
656 candidate best-fit models that incorporated each specific covariate.

657

Hypothesis	Covariate	Sum	Percent	Hypothesis	Covariate	Sum	Percent	Hypothesis	Covariate	Sum	Percent
58	spring.butte - sacAirTemp.spring	998	100%	37	spring.deer - sacAirTemp.spring	186	19%	22	.1.2.3.4.5.6.7-pdo.late	11	1%
51	.5.6.7-spring.size.chipps	945	95%	40	.5.6.7-freeport.sed.conc	185	19%	24	fall.battle.creek - sacAirTemp.spring	11	1%
17	.1.2.3.4-upwelling.south.early	783	78%	11	.1.2.3.4-fall.dayflow.cd	182	18%	14	.1.2.3.4-fall.farallon.temp.late	9	1%
21	.1.2.3.4.5.6.7-pdo.early	657	66%	15	.1.2.3.4-upwelling.north.early	169	17%	31	fall.feather - feather.oronville.discharge	9	1%
57	spring.butte - sacAirTemp.summer	571	57%	6	.1.2.3.4-freeport.sed.conc	159	16%	59	spring.butte - butte.discharge	8	1%
48	.5.6.7-spring.dayflow.export	541	54%	56	spring.mill - mill.discharge	131	13%	13	.1.2.3.4-fall.farallon.temp.early	7	1%
9	.1.2.3.4-fall.dayflow.export	484	48%	7	.1.2.3.4-bass.cpue	107	11%	5	.1.2.3.4-yolo.wood.peak.streamflow	3	0%
10	.1.2.3.4-fall.dayflow.expin	374	37%	38	.5.6.7-verona.peak.streamflow	96	10%	16	.1.2.3.4-upwelling.north.late	2	0%
41	.5.6.7-bass.cpue	362	36%	49	.5.6.7-spring.dayflow.expin	95	10%	23	fall.battle.creek - sacAirTemp.summer	2	0%
36	spring.deer - sacAirTemp.summer	359	36%	43	.5.6.7-upwelling.north.late	94	9%	54	spring.mill - sacAirTemp.summer	2	0%
55	spring.mill - sacAirTemp.spring	316	32%	4	.1.2.3.4-verona.peak.streamflow	87	9%	25	fall.battle.creek - keswick.discharge	1	0%
46	spring.deer - deer.discharge	282	28%	3	fall.sac.mainstem - keswick.discharge	85	9%	26	fall.battle.creek - battle.discharge	1	0%
20	.1.2.3.4.5.6.7-curl.late	275	28%	2	fall.sac.mainstem - sacAirTemp.spring	83	8%	27	fall.battle.creek - battle.peak.gage.ht	0	0%
44	.5.6.7-upwelling.south.early	222	22%	29	fall.feather - sacAirTemp.spring	77	8%	28	fall.feather - sacAirTemp.summer	0	0%
50	.5.6.7-spring.dayflow.cd	220	22%	52	.5.6.7-spring.farallon.temp.early	62	6%	30	fall.feather - keswick.discharge	0	0%
18	.1.2.3.4-upwelling.south.late	205	21%	45	.5.6.7-upwelling.south.late	48	5%	32	fall.american - sacAirTemp.summer	0	0%
53	.5.6.7-spring.farallon.temp.late	202	20%	39	.5.6.7-yolo.wood.peak.streamflow	46	5%	33	fall.american - sacAirTemp.spring	0	0%
42	.5.6.7-upwelling.north.early	199	20%	1	fall.sac.mainstem - sacAirTemp.summer	45	5%	34	fall.american - keswick.discharge	0	0%
47	.5.6.7-spring.dayflow.geo	194	19%	12	.1.2.3.4-fall.size.chipps	36	4%	35	fall.american - american.discharge	0	0%
19	.1.2.3.4.5.6.7-curl.early	193	19%	8	.1.2.3.4-fall.dayflow.geo	17	2%				

658

659

660

661

662

663

664

Table I.3. Model selection results. Percent inclusion rate for environmental covariate effects across 1,000 candidate best-fit models, each resulting from one round of forward stepwise-AICc model building. Note the covariate name includes the single population name, or the numbers for multiple populations upon whose survival the effect of the environmental covariate is shared. For reference population numbers are: 1) fall-run mainstem Sacramento wild-run Chinook, 2) fall-run Battle Creek Coleman National Fish Hatchery produced Chinook, 3) fall-run Feather River Hatchery produced Chinook, 4) fall-run American River Nimbus Hatchery produced Chinook, 5) spring-run Deer Creek wild Chinook, 6) spring-run Mill Creek wild Chinook, and 7) spring-run Butte Creek wild Chinook.

665 Results of the iterative forward stepwise-AICc model selection (Table I.3) indicate
 666 that the set of environmental covariates (hypotheses) which best describe historical variation
 667 in Sacramento Chinook abundance encompass a wide range of locations within the life cycle,
 668 populations, and ecological processes. A higher inclusion rate across best-fit models for a
 669 specific covariate by population(s) effect may be interpreted as greater weight of evidence
 670 from the data that this covariate explains variation in survival and therefore may be of
 671 ecological importance (Table I.3). Foremost, it should be noted that the influence of spring
 672 air temperature at the city of Sacramento on survival of the Butte Creek population
 673 (spring.butte – sacAirTemp.spring) was included as an AICc-selected covariate in 998 of
 674 1,000 best-fit models. This covariate represents air temperature during juvenile rearing
 675 (January – March) at the city of Sacramento, and is included as a surrogate for Butte Creek
 676 stream temperature. Additional covariates which were represented in 60% or greater of
 677 iteratively built models include: 1) the combined influence of the size of out-migrating
 678 spring-run juveniles on the survival of Deer, Mill and Butte Creek spring-run populations
 679 (.5.6.7-spring.size.chipps), 2) the combined influence of near-shore upwelling during the
 680 period of ocean entry (April – June) upon the survival of the four fall-run populations
 681 (.1.2.3.4-upwelling.south.early), and 3) the combined influence of the Pacific Decadal
 682 Oscillation during winter (January – May average) of the first year of marine residence
 683 (.1.2.3.4.5.6.7-pdo.early) on the survival of all four fall-run and three spring-run populations.
 684 The 5th most frequently included covariate was the effect of summer (July – September) air
 685 temperature at Sacramento during the brood year, on survival of Butte Creek spring-run
 686 Chinook (spring.butte-sacAirTemp.summer). This covariate was included to test hypothesis
 687 that high over-summer water temperatures may have a negative impact on the survival and
 688 successful spawning of adult spring-run Chinook holding in tributaries.

689 With respect to the representation of anthropogenic drivers of Chinook survival across
 690 the 1,000 forward-AICc built models, covariates describing the influence of water exports on
 691 spring and fall-run survival were the 6th, 7th, and 8th most often included. The combined effect
 692 of average water exports from the Sacramento – San Joaquin Delta between February and
 693 April quantified by the Dayflow QEXPORTS metric on survival of spring-run Chinook
 694 (.5.6.7-spring.dayflow.export), appeared in 54% of forward stepwise-AICc built models.
 695 Similarly, the covariate representing the combined effect of March – May average
 696 Sacramento – San Joaquin water exports on the survival of the four fall-run Chinook
 697 populations (.1.2.3.4-fall.dayflow.export) was included in 48% of stepwise-AICc built
 698 models, with the ratio of water exports to total Delta water inflow (Dayflow: EXPIN) during
 699 this same period (.1.2.3.4-fall.dayflow.expin) following closely with a 37% inclusion rate.
 700 Other covariates highlighting the influence of water routing and supply in the Sacramento –
 701 San Joaquin Delta were included in a smaller subset of stepwise-AICc built models. The
 702 influence of average net channel depletion (Dayflow: QCD) between February and April on
 703 the grouped spring-run Chinook populations (.5.6.7-spring.dayflow.cd) was included in 22%
 704 of the 1,000 stepwise-AICc built models. In addition, the combined influence of the average
 705 flow into Georgiana Slough and the Delta Cross Channel (Dayflow: QXGEO) February –
 706 April on the spring-run populations (.5.6.7-spring.dayflow.geo) was included in 19% of
 707 candidate best-fit models.

708 While the inclusion rate of specific covariate-by-population effects across the 1,000
 709 stepwise-AICc built models provides an indication of the relative weight of evidence from
 710 the data, that each covariate holds some ability to explain historical patterns in survival, we
 711 consider the model with the lowest AICc value to have the best predictive ability. The single

712 model with the lowest AICc value represents the most parsimonious fit to the data, explaining
 713 the greatest amount of observed variation in adult and juvenile abundance, while estimating
 714 the fewest parameters. This lowest AICc or “final” model provides the best basis for
 715 predicting future trends in abundance under alternative climate, marine production, and water
 716 management scenarios. The final model included 14 covariate-by-population effects,
 717 spanning both the freshwater and marine portions of the life cycle (Table I.4). In addition, the
 718 effects incorporated in the final model include both single-population effects as well as
 719 shared effects of environmental covariates across multiple populations. In total five of the
 720 covariates included in the final (lowest AICc) model were related to survival in the 1st
 721 (upriver) stage, six were related to the 2nd stage representing environmental effects on
 722 survival through the Sacramento – San Joaquin Delta, two were related to the 3rd stage
 723 influencing survival in the nearshore environment, and only one covariate was related to
 724 survival during subsequent years of marine residence.

Hypothesis Number	Covariate	Covariate Description	Model Stage	Populations
3	fall.sac.mainstem - keswick.discharge	Average January - March water discharge (cfs) at Keswick Dam	Upstream	Fall Sacramento Mainstem Wild
24	fall.battle.creek - sacAirTemp.spring	Sacramento air temperature during spring (January - March) emergence year	Upstream	Fall Battle Creek (CNFH) Hatchery
46	spring.deer - deer.discharge	Average October - December water discharge (cfs) at Deer Creek	Upstream	SpringDeer Creek
57	spring.butte - sacAirTemp.summer	Sacramento air temperature during summer (July - September) of the brood year	Upstream	Spring Butte Creek
58	spring.butte - sacAirTemp.spring	Sacramento air temperature during spring (January - March) emergence year	Upstream	Spring Butte Creek
40	.5.6.7-freeport.sed.conc	Average February - April monthly sediment concentration (mg/L)	Sacramento - San Joaquin Delta	Spring Deer Creek Spring Mill Creek Spring Butte Creek
48	.5.6.7-spring.dayflow.export	Dayflow: Total Delta Exports and Diversions/Transfers (QEXPORTS). February - April average	Sacramento - San Joaquin Delta	Spring Deer Creek Spring Mill Creek Spring Butte Creek
51	.5.6.7-spring.size.chipps	Average size of spring-run Chinook at ocean entry from Chipps Island Trawl	Sacramento - San Joaquin Delta	Spring Deer Creek Spring Mill Creek Spring Butte Creek
6	.1.2.3.4-freeport.sed.conc	Average February - April monthly sediment concentration (mg/L)	Sacramento - San Joaquin Delta	Fall Sacramento Mainstem Wild Fall Battle Creek (CNFH) Hatchery Fall Feather River Hatchery Fall American River (Nimbus) Hatchery
10	.1.2.3.4-fall.dayflow.expin	Dayflow: Export/Inflow Ratio (EXPIN). March - May average	Sacramento - San Joaquin Delta	Fall Sacramento Mainstem Wild Fall Battle Creek (CNFH) Hatchery Fall Feather River Hatchery Fall American River (Nimbus) Hatchery
11	.1.2.3.4-fall.dayflow.cd	Dayflow: Net Channel Depletion (QCD). March - May average	Sacramento - San Joaquin Delta	Fall Sacramento Mainstem Wild Fall Battle Creek (CNFH) Hatchery Fall Feather River Hatchery Fall American River (Nimbus) Hatchery
17	.1.2.3.4-upwelling.south.early	NOAA Index for upwelling at Southern Location (36 N, 122 W), average of SPRING months (April - June)	Nearshore Region	Fall Sacramento Mainstem Wild Fall Battle Creek (CNFH) Hatchery Fall Feather River Hatchery Fall American River (Nimbus) Hatchery
20	.1.2.3.4.5.6.7-curl.early	NOAA Wind Stress Curl for upwelling at Northern Location (39 N, 125 W), average of FALL months (July - December)	Nearshore Region	Fall Sacramento Mainstem Wild Fall Battle Creek (CNFH) Hatchery Fall Feather River Hatchery Fall American River (Nimbus) Hatchery
21	.1.2.3.4.5.6.7-pdo.early	Pacific Decadal Oscillation (PDO), average of January - May monthly indices during first year of marine residence	1st Ocean Year	Spring Deer Creek Spring Mill Creek Spring Butte Creek

725
 726 **Table I.4. Fourteen covariate-by-population effects included in the final AICc-**
 727 **selected model.**

728 Of the covariate-by-population effects on upstream survival incorporated in the final
 729 model three were related to atmospheric temperature, used as a proxy for tributary-specific
 730 water temperatures, and two were related to water flow conditions. The three temperature-
 731 related covariate-by-population effects were all based on air temperature at Sacramento, CA
 732 and included: 1) the effect of average spring air temperature (January - March) on survival of
 733 the fall-run Battle Creek population in the year of emergence (fall.battle.creek -
 734 sacAirTemp.spring), 2) the effect of average summer air temperature (July – September)
 735 during the brood year on offspring production and oocyte through juvenile survival for the
 736 Butte Creek spring-run population (spring.butte - sacAirTemp.summer), and 3) the effect of
 737 average spring air temperature (January – March) in the year of emergence on survival of
 738 Butte Creek spring-run Chinook (spring.butte - sacAirTemp.spring). The two upstream
 739 covariate effects related to water flow conditions included, the influence of average water

740 discharge rates (cfs^{-1}) at Keswick Dam during the period between January and March on the
 741 survival of Sacramento mainstem spawning wild fall-run Chinook (fall.sac.mainstem -
 742 keswick.discharge), and the effect of average water discharge in Deer Creek between October
 743 and December on the brood year survival of spring-run Chinook spawning in that tributary
 744 (spring.deer - deer.discharge).

745 The range of covariates which best describe historical patterns in juvenile Chinook
 746 survival through the Sacramento – San Joaquin Delta stage included factors both
 747 anthropogenic and natural in origin. Interestingly, the winter (February-April) concentration
 748 of sediment (mg/L) measured at Freeport, CA was selected based upon the AICc criteria as
 749 an important explanatory covariate for both grouped fall-run (.1.2.3.4-freeport.sed.conc) and
 750 spring-run (.5.6.7-freeport.sed.conc) populations. Two other covariate effects on the
 751 combined survival of fall-run Chinook populations which relate to water flow and
 752 management in the Sacramento – San Joaquin Delta were also identified in the final model,
 753 including average March – May Dayflow metrics for: 1) QCD or net channel depletion for in-
 754 delta consumptive use (.1.2.3.4-fall.dayflow.cd), and 2) EXPIN or the ratio of total delta
 755 exports to freshwater inflows (.1.2.3.4-fall.dayflow.expin) (CDWR 2014). In addition to
 756 sediment concentration, two other covariate effects on the combined survival of the Deer,
 757 Mill, and Butte Creek spring-run populations in the Sacramento – San Joaquin Delta were
 758 present in the AICc-selected final model. These included the influence of average monthly
 759 water exports and diversions from the delta (February – April) as quantified by the Dayflow
 760 metric QEXPORTS (CDWR 2014), which represents the sum of Central Valley Project
 761 exports, State Water Project exports, Contra Costa Water District diversions, and North Bay
 762 Aqueduct exports (.5.6.7-spring.dayflow.export), and the average size of juvenile spring-run
 763 Chinook caught in the Chipps Island Trawl (.5.6.7-spring.size.chipps).

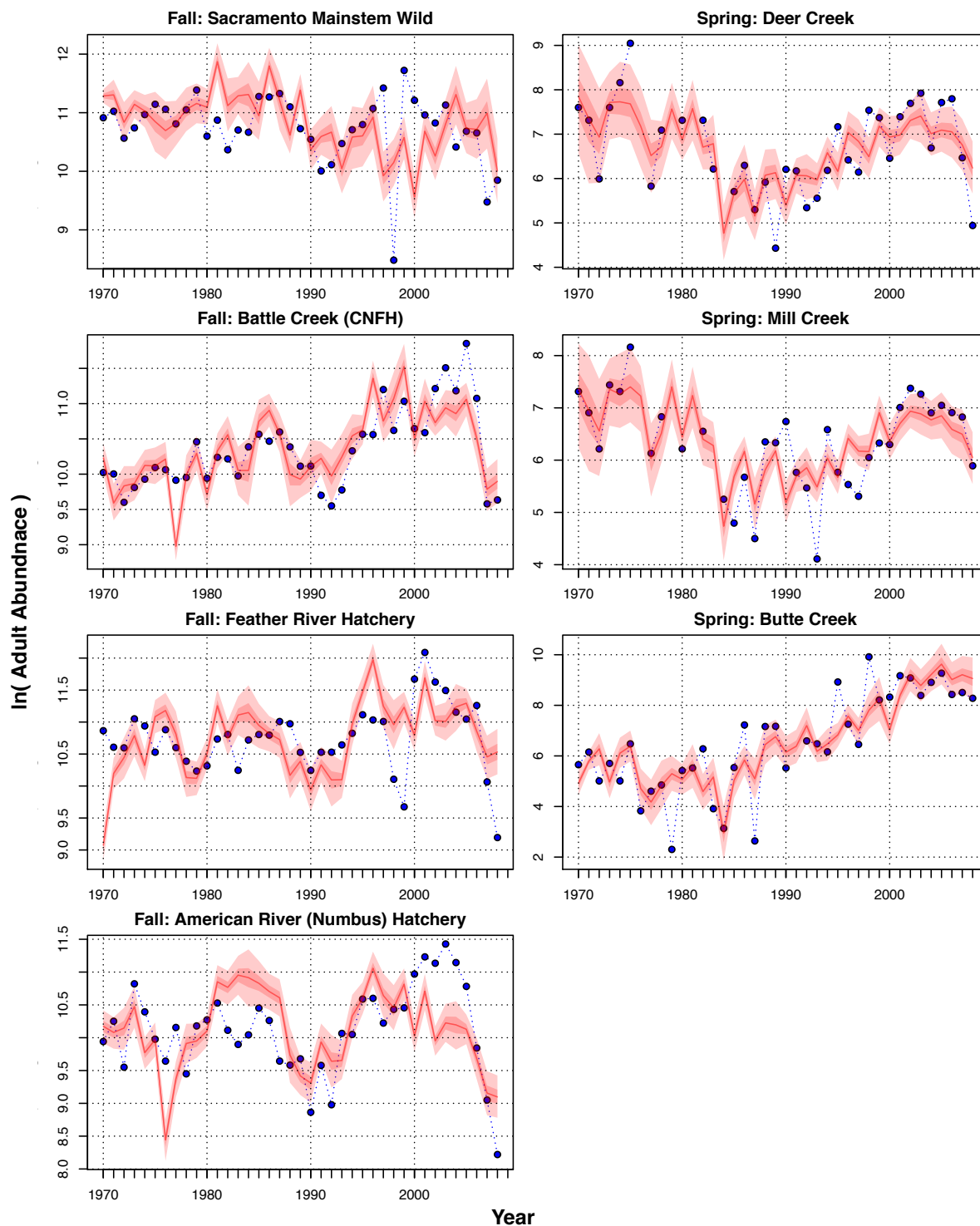
764 Based on the AICc criteria and thorough exploration of model space using replicate
 765 stepwise model building, the final model identified three covariates able to explain some of
 766 variance in Chinook survival in the nearshore region following ocean entry and survival
 767 during subsequent years of marine residency. Survival for the four fall-run Chinook
 768 populations in the nearshore region was explained in part by upwelling patterns during the
 769 spring months (April – June) at the southern NOAA/PFEL monitoring site located at 36°N
 770 latitude and 122°W longitude (.1.2.3.4-upwelling.south.early). Additionally, the effect of
 771 average wind stress curl during July – December of the year of ocean entry on the survival of
 772 all seven combined spring and fall-run populations was included in the final model
 773 (.1.2.3.4.5.6.7-curl.late). The last covariate present in the final model linked to broad-scale
 774 marine climate patterns was the effect of the average Pacific Decadal Oscillation Index
 775 during the winter of the first year at sea (January – May) on the combined survival of all
 776 seven populations (.1.2.3.4.5.6.7-pdo.early).

777 These fourteen population-by-covariate effects, spanning freshwater and marine
 778 portions of the Chinook life cycle and all seven analyzed Chinook populations, represent the
 779 most parsimonious explanation for historical patterns in Chinook survival and observed
 780 juvenile and adult abundance. This final model was used as the basis for the subsequent
 781 Bayesian analysis of the effect of each of these covariates and their realized survival
 782 influence, and used for predicting future trends in abundance under alternative water
 783 management scenarios, predictions for future climate change, and marine production patterns.

784 *Estimation Results*

785 In order to estimate the direction and magnitude of the 14 covariate effects identified
786 by AICc selection criteria across 1,000 stepwise-AICc built models (Table I.4), we have
787 employed Bayesian methods with a MCMC sampler. Separate stage-structured models were
788 used to represent each of the seven populations, however common effects across populations
789 for specific covariates were estimated, and shared capacity constraints in the Sacramento –
790 San Joaquin Delta were assumed for the four fall-run and three spring-run populations
791 separately. Estimation of model parameters was informed by juvenile and adult abundance
792 data, reconstructed to account for observed stray rates between hatchery and wild
793 populations. Figure I.6 displays observed adult abundance data for the four fall-run Chinook
794 populations and three spring-run populations as well as the posterior predictive distribution
795 from the Bayesian population dynamics model. The posterior predictive distribution
796 represented by the red line and shaded regions, describe the median, 50% and 95% credible
797 intervals for the predicted adult spawning abundance or hatchery returns for each population
798 in each year.

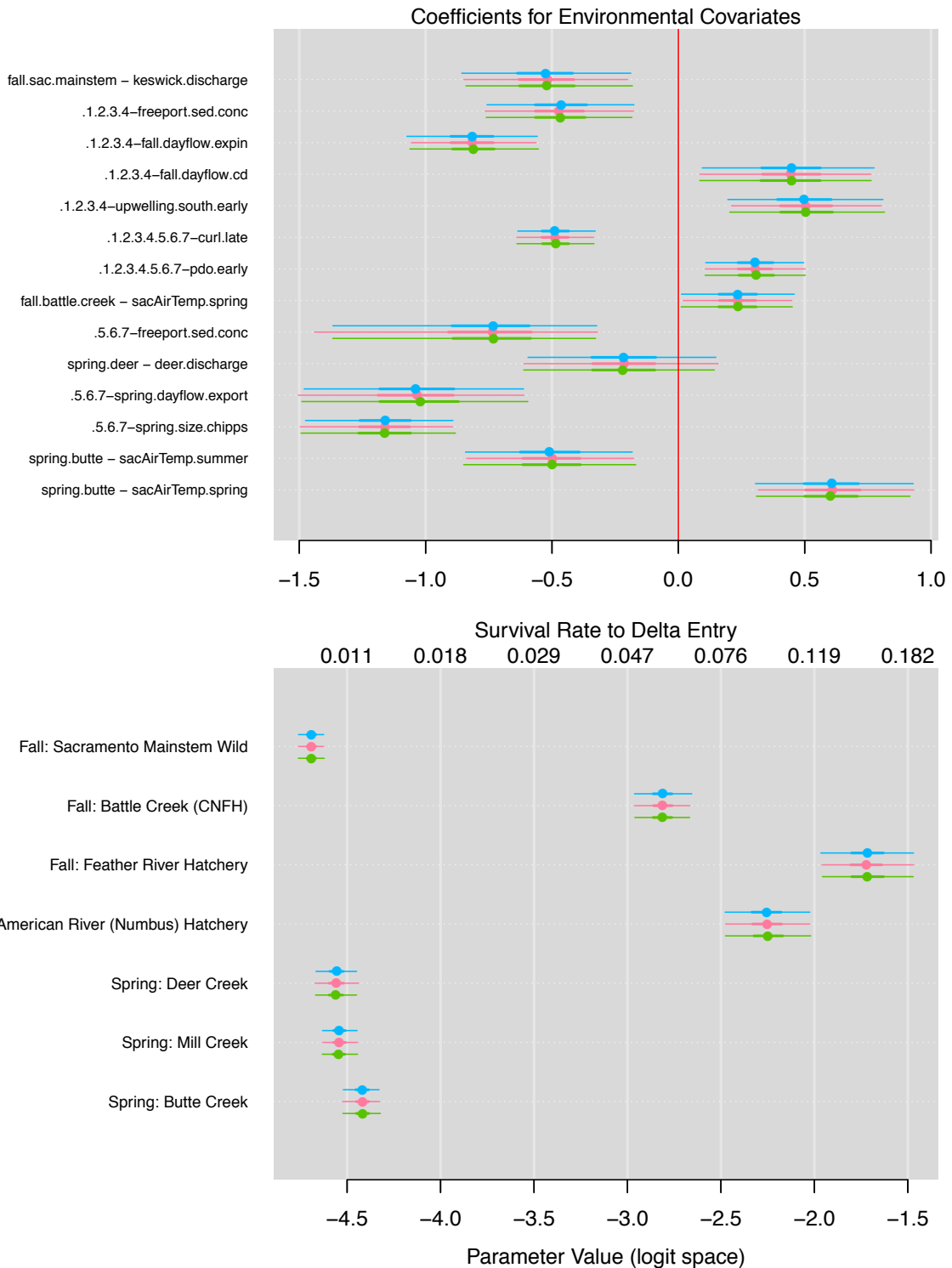
799 Results indicate that the model predicts the pattern for Deer and Mill Creek spring-run
800 populations which exhibit higher adult abundances, relative to the time series, through 1984
801 followed by a period of lower adult abundance through the mid-1990s, followed by higher
802 relative abundances through 2006 (Fig. I.5). Similarly for the Butte Creek spring-run
803 population, the model captures the period of lower spawning abundance prior 1985 followed
804 by a pronounced increase in abundance, ending with a relative plateau in the early 2000's
805 (Fig. I.5). Model predictions for Sacramento Mainstem spawning wild fall-run Chinook and
806 Feather River hatchery fall Chinook both fail to capture the low returns in 1998 – 1999, but
807 capture the reduction in abundance observed in 2007 – 2008. In general for all seven
808 populations of spring and fall-run Chinook included in the analysis, model predictions do not
809 explicitly capture interannual variation, but explain much of the general trend in abundance
810 across the time series (Fig. I.5).
811



812
 813 **Figure I.5.** Bayesian population dynamics model fit to adult abundance data. Blue
 814 points and dashed lines indicate the observed adult abundance in each year on the
 815 spawning grounds or at the hatchery, reconstructed to account for average stray rates
 816 observed from coded wire tagging data (Kormos et al. 2012, Palmer-Zwahlen and
 817 Kormos 2013). Red shaded regions are the 95% and 50% credible intervals for the
 818 model predicted abundance in each year, and the red line describes the median of the
 819 posterior predictions for abundance in each year. Observed and predicted abundances
 820 are presented in natural log space.

821 Posterior distributions for coefficients describing the direction and magnitude of
822 influence each environmental covariate has on a specific population or group of populations
823 were sampled, along with those for other model parameters including survival rate during the
824 first (upstream) life-stage. Bayesian posterior distributions describe the estimated probability
825 that a particular estimated or derived model parameter has a specific value. Figure I.6
826 displays posterior distributions for coefficients describing the influence of environmental
827 covariates on survival, as well as those for parameters describing the base survival rate to
828 Sacramento – San Joaquin Delta entry. In this figure, samples from posterior distributions
829 arising from the three separate MCMC chains are drawn in different colors. Each parameter
830 estimate is illustrated as a caterpillar plot whose median is described by a point, 50% credible
831 interval by a thick line, and 95% credible interval by a thin line. The concordance of the
832 parameter medians and credible intervals across the three MCMC chains, along with Gelman-
833 Rubin test statistic values for all parameters ≤ 1.05 , provide evidence that all three chains
834 have converged to the same stationary distribution.

835 The bottom panel of figure I.6 displays model predictions for the value of the basal
836 productivity parameter ($\beta_{s,p,0}$) in the upstream stage (Eq. I.5), or maximum survival rate to
837 Sacramento – San Joaquin Delta entry. It should be noted that for the four wild-spawning
838 populations (i.e. Mainstem Sacramento fall-run, and Deer, Mill, and Butte Creek spring runs),
839 this parameter represents the maximum survival rate from egg to Delta entry, while for the
840 three hatchery produced populations (Battle Creek (CNFH), Feather River, and American
841 River (Nimbus) fall-run) this parameter represents the maximum survival rate from hatchery
842 release to Delta entry. Parameter values in logit space are listed on the x-axis below the lower
843 panel, while back transformed maximum survival rate values appear above the lower panel.
844 Several things are clear from this figure I.6. First, the similarity in posterior distributions
845 from each of the three chains again indicates that all three have converged to the same
846 stationary distribution despite differing random walk trajectories through parameter space.
847 Second, basal productivity or maximum survival rate for the upstream stage is both
848 significantly higher and more variable for the three hatchery-reared populations. Higher
849 maximum survival rates for these populations are to be expected given that they only
850 represent mortality incurred after release, not mortality from fertilization to the date of
851 release. However, the greater variance in maximum survival rate for the hatchery populations
852 is easily discernable.
853



854
855
856
857
858
859
860

Figure I.6. Posterior probability distributions for coefficients describing the influence of environmental covariates on survival (top) and the maximum survival rate from egg (or hatchery release) to Sacramento – San Joaquin Delta entry. Caterpillar plots describe the median (dot), 50% credible interval (thick line), and 95% credible interval (thin line) of each posterior. Posteriors from each of the independent MCMC chains are depicted with different colours.

861 Posterior estimates for the value of the coefficients ($\beta_{s,p,c}$) describing the influence of
 862 each environmental covariate on a specified population, or group of populations, provide an
 863 indication of whether each covariate has a positive or negative influence on survival (Fig. 6,
 864 top panel). Table I.5 shows the estimated value for each of the coefficients along with their
 865 variance, and quantile range for each posterior distribution. These results indicate that of the
 866 14 covariates included in the final model, 8 covariates were estimated to have a negative
 867 impact on stage-specific productivity (maximum survival rate), 5 were estimated to have a
 868 positive influence, and 1 was estimated to have a negative influence on average but with a
 869 95% credible interval range overlapping zero. The covariates whose survival impact is
 870 estimated to be negative include the effect of: 1) water discharge (cfs-1) from Keswick Dam
 871 on Mainstem Sacramento spawning fall-run Chinook (fall.sac.mainstem - keswick.discharge),
 872 2) sediment concentration at Freeport, CA (mg/L) on the combined survival of the four fall-
 873 run populations (.1.2.3.4-freeport.sed.conc), 3) the export to inflow ratio in the Sacramento –
 874 San Joaquin Delta on combine survival of the fall-run populations (.1.2.3.4-
 875 fall.dayflow.expin), 4) wind stress curl on the combined survival of all seven populations of
 876 spring and fall-run Chinook (.1.2.3.4.5.6.7-curl.late), 5) spring Freeport, CA sediment
 877 concentrations on the combined survival of the three spring-run Chinook populations (.5.6.7-
 878 freeport.sed.conc), 6) water exports from the Sacramento – San Joaquin Delta on the
 879 combined survival of the three spring-run populations (.5.6.7-spring.dayflow.export), 7) the
 880 average size of juvenile spring-run Chinook on combined spring-run survival (.5.6.7-
 881 spring.size.chipps), and 8) Sacramento air temperature during summer months of the brood
 882 year on survival of Butte Creek spring-run Chinook (spring.butte - sacAirTemp.summer).

883

Covariate	Mean	sd	CV	2.50%	25%	50%	75%	97.50%
fall.sac.mainstem - keswick.discharge	-0.52	0.17	0.32	-0.85	-0.63	-0.52	-0.41	-0.19
.1.2.3.4-freeport.sed.conc	-0.47	0.15	0.32	-0.76	-0.57	-0.47	-0.37	-0.18
.1.2.3.4-fall.dayflow.expin	-0.81	0.13	0.16	-1.06	-0.90	-0.81	-0.73	-0.56
.1.2.3.4-fall.dayflow.cd	0.44	0.17	0.39	0.09	0.33	0.45	0.56	0.77
.1.2.3.4-upwelling.south.early	0.50	0.15	0.31	0.20	0.40	0.50	0.61	0.81
.1.2.3.4.5.6.7-curl.late	-0.49	0.08	0.16	-0.64	-0.54	-0.49	-0.43	-0.33
.1.2.3.4.5.6.7-pdo.early	0.30	0.10	0.33	0.11	0.24	0.31	0.37	0.50
fall.battle.creek - sacAirTemp.spring	0.23	0.11	0.47	0.01	0.16	0.24	0.31	0.45
.5.6.7-freeport.sed.conc	-0.76	0.27	0.35	-1.38	-0.90	-0.73	-0.59	-0.32
spring.deer - deer.discharge	-0.22	0.19	0.87	-0.61	-0.34	-0.22	-0.09	0.15
.5.6.7-spring.dayflow.export	-1.04	0.23	0.22	-1.49	-1.18	-1.03	-0.88	-0.61
.5.6.7-spring.size.chipps	-1.17	0.15	0.13	-1.49	-1.26	-1.16	-1.06	-0.89
spring.butte - sacAirTemp.summer	-0.51	0.17	0.34	-0.84	-0.62	-0.50	-0.39	-0.17
spring.butte - sacAirTemp.spring	0.61	0.16	0.26	0.31	0.50	0.61	0.71	0.93

884

885 **Table I.5. Values for the posterior probability distributions for coefficients**
 886 **describing the influence of environmental covariates ($\beta_{s,p,c}$) on productivity (maximum**
 887 **survival rate).**

888 Five of the coefficient values were estimated to be positive (Table I.5), indicating that
 889 an increase in the value of those covariates leads to an increase in the maximum survival rate
 890 for the associated population or group of populations. These covariates which are estimated
 891 to positively influence survival include the effect of: 1) upwelling in the nearshore region
 892 during spring of the ocean entry year on the combined survival of the fall-run Chinook
 893 populations (.1.2.3.4-upwelling.south.early), 2) spring air temperature at Sacramento, CA on
 894 the survival of fall-run Battle Creek (CNFH) Chinook (fall.battle.creek - sacAirTemp.spring),
 895 3) spring air temperature at Sacramento, CA on the survival of Butte Creek spring-run
 896 Chinook (spring.butte - sacAirTemp.spring), 4) net channel depletion in the Sacramento –
 897 San Joaquin Delta resulting from within-delta consumptive use as quantified by the Dayflow

898 metric QCD on the combined survival of the four fall-run Chinook populations (.1.2.3.4-
 899 fall.dayflow.cd), and 5) the magnitude of the Pacific Decadal Oscillation during winter
 900 (January – May) of the first year at in the ocean on the combined survival of all seven spring
 901 and fall-run Chinook populations (.1.2.3.4.5.6.7-pdo.early). For the 13 covariates classified
 902 above as having either a distinct positive or negative effect on survival, the posterior
 903 distribution describing the probability of the true value for each coefficient had a 95%
 904 credible interval that was completely above or below zero. Although the estimated median
 905 value for the coefficient describing the effect of Deer Creek discharge (cfs⁻¹) on Deer Creek
 906 spring-run Chinook survival (spring.deer - deer.discharge) is less than zero (i.e. -0.22, Table
 907 I.5) indicating an negative influence on survival, the 95% credible interval overlaps with zero
 908 indicating a significant probability (p=0.121) of the covariate having either no influence or a
 909 positive influence on survival.

910 While posterior probability distributions for coefficients representing the influence of
 911 each environmental covariate on stage and population-specific productivity ($\beta_{s,p,c}$) describe
 912 the model estimate for how much an increase or decrease in the value of that covariate is
 913 expected to change stage-specific productivity parameter of the Beverton-Holt equation (Eq.
 914 I.4), it is difficult to directly compare these estimated coefficient values for several reasons.
 915 First, the basal productivity rate ($\beta_{s,p,0}$) for each stage is population-specific, meaning that
 916 the magnitude of estimated coefficients ($\beta_{s,p,c}$) is always relative to the to the basal
 917 productivity rate for the population of interest. Second, coefficient values and basal
 918 productivity rates are estimated in logit space to ensure the resultant productivity value is
 919 smoothly scaled between 0 and 1 (Eq. I.5), and comparing coefficients and basal productivity
 920 rates in logit space may be difficult to interpret. Therefore, we have endeavored to translate
 921 the magnitude of the estimated environmental covariate effects into more easily interpretable
 922 changes in survival.

923 In order to translate the value of estimated coefficients describing the influence of
 924 environmental covariates into predictions for realized changes in survival, we calculated the
 925 survival rate for the seven populations from egg, or hatchery release, through adults returning
 926 to freshwater under a range of scenarios. Survival rates for each population were calculated
 927 by tracking a set number of individuals forward in time across life-stages, assuming no
 928 harvest mortality, and using parameter values sampled from the joint posterior for the
 929 estimation model. One thousand independent sets of model parameter values were sampled
 930 from their joint posterior in order to preserve posterior correlation, and used to quantify the
 931 variation in predictions for the influence of each environmental covariate on survival, arising
 932 from estimation uncertainty. Survival rate was calculated as the sum of spawning adults
 933 across return years, divided by the number of eggs or hatchery releases. The spawning
 934 abundance, used as the basis for calculating survival rates, was the 1970 – 2010 average for
 935 the wild-spawning populations (i.e. mainstem Sacramento fall-run, as well as Deer, Mill, and
 936 Butte Creek spring-run) and the average release numbers for the most recent 10 years for the
 937 Battle Creek (CNFH), Feather River, and American River (Nimbus) hatchery populations.
 938 Likewise, the most recent 10-year average was used for capacity of wild juvenile fall-run
 939 Chinook in the Sacramento mainstem and for the total capacity for spring-run and fall-run
 940 Chinook rearing in the Sacramento – San Joaquin Delta.

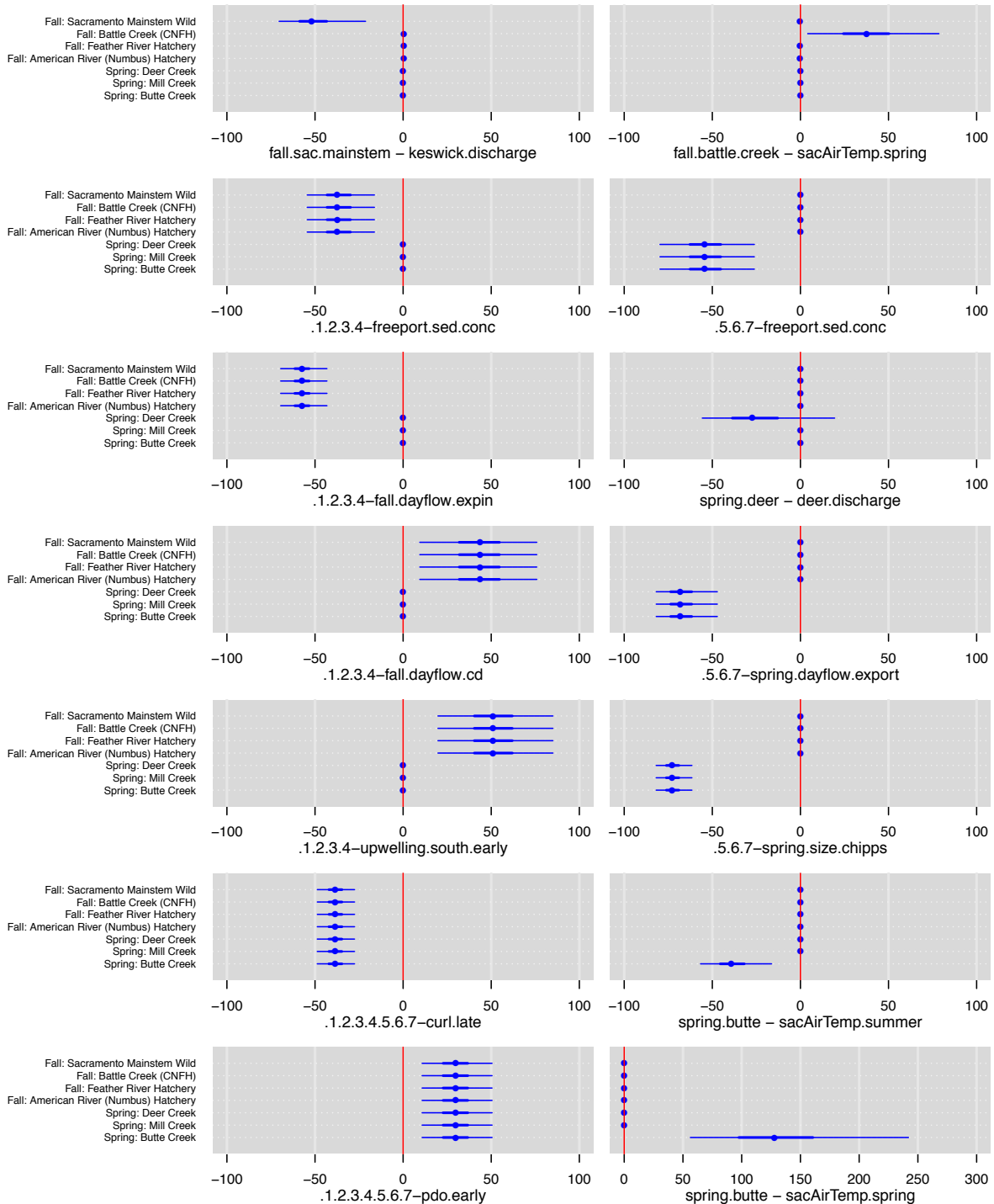
941 The distribution of survival rate predictions for each population (p), across the 1,000
 942 independent sets of parameter values (i), was first calculated for a base case ($S_{base,p,i}$).
 943 Under the base case the value for all environmental covariates was set at zero, which for z-
 944 standardized covariates is equal to the long-term average. Subsequently the covariate-specific

945 survival ($Scov_{p,i,c}$) of each population across the 1,000 parameter sets was determined, as
 946 each covariate (c) was sequentially changed to have a value of 1. Covariate-specific survival
 947 ($Scov_{p,i,c}$) thus represents the population (p) and sample (i) specific survival rate when
 948 covariate c is increased in value to 1 standard deviation above the long-term mean. From this,
 949 the percentage difference in survival for each population resulting from an increase in the
 950 value of an environmental covariate was calculated as: % *difference in Survival* $_{p,i,c} =$
 951 $\frac{(Scov_{p,i,c} - Sbase_{p,i})}{Sbase_{p,i}} * 100$. Table I.6 displays the mean and standard deviation for the expected
 952 percentage change in survival for each population across the sampled parameter sets, when
 953 each covariate is increased in value by 1 SD from the mean.

Covariate	Fall:	Fall:	Fall:	Fall:	Spring: Deer Creek	Spring: Mill Creek	Spring: Butte Creek
	Mainstem Wild	Battle Creek (CNFH)	Feather River Hatchery	American River (Numbus) Hatchery			
fall.sac.mainstem - keswick.discharge	-50.2 (12.5)	0.5 (0.1)	0.5 (0.1)	0.5 (0.1)	0 (0)	0 (0)	0 (0)
.1.2.3.4-freeport.sed.conc	-36.5 (10)	-36.5 (10)	-36.5 (10)	-36.5 (10)	0 (0)	0 (0)	0 (0)
.1.2.3.4-fall.dayflow.expin	-57 (6.6)	-57 (6.6)	-57 (6.6)	-57.1 (6.6)	0 (0)	0 (0)	0 (0)
.1.2.3.4-fall.dayflow.cd	43.3 (17.5)	43.3 (17.5)	43.3 (17.5)	43.3 (17.5)	0 (0)	0 (0)	0 (0)
.1.2.3.4-upwelling.south.early	51.1 (16.7)	51.1 (16.7)	51.1 (16.7)	51.1 (16.7)	0 (0)	0 (0)	0 (0)
.1.2.3.4.5.6.7-curl.late	-38.5 (5.4)	-38.5 (5.4)	-38.5 (5.4)	-38.5 (5.4)	-38.5 (5.4)	-38.5 (5.4)	-38.5 (5.4)
.1.2.3.4.5.6.7-pdo.early	29.8 (10.4)	29.8 (10.4)	29.8 (10.4)	29.8 (10.4)	29.8 (10.5)	29.8 (10.5)	29.8 (10.5)
fall.battle.creek - sacAirTemp.spring	-0.2 (0.1)	38.2 (19.4)	-0.2 (0.1)	-0.2 (0.1)	0 (0)	0 (0)	0 (0)
.5.6.7-freeport.sed.conc	0 (0)	0 (0)	0 (0)	0 (0)	-53.8 (13.3)	-53.8 (13.3)	-53.8 (13.3)
spring.deer - deer.discharge	0 (0)	0 (0)	0 (0)	0 (0)	-24.4 (20)	0 (0)	0 (0)
.5.6.7-spring.dayflow.export	0 (0)	0 (0)	0 (0)	0 (0)	-67.2 (9.1)	-67.2 (9.1)	-67.2 (9.1)
.5.6.7-spring.size.chipps	0 (0)	0 (0)	0 (0)	0 (0)	-72.5 (5.3)	-72.5 (5.3)	-72.5 (5.3)
spring.butte - sacAirTemp.summer	0 (0)	0 (0)	0 (0)	0 (0)	0 (0)	0 (0)	-38.4 (10.2)
spring.butte - sacAirTemp.spring	0 (0)	0 (0)	0 (0)	0 (0)	-0.1 (0)	-0.1 (0)	132.8 (47.6)

954
 955
 956 **Table I.6. Percentage change in egg (or hatchery release) to adult survival resulting**
 957 **from covariate variation. Values in the table are the mean (sd) differences in survival**
 958 **between the base case and a scenario where the value of a specific covariate (row) is**
 959 **increased by 1 standard deviation from the long-term mean.**
 960

961 Figure I.7 displays the effect of each environmental covariate on each Chinook
 962 population, as the distribution of percentage change in egg (or hatchery release) to adult
 963 survival, expected when the value of a specific covariate is 1 SD above the long-term mean.
 964 Each panel in figure I.7 describes the influence of a single covariate, while each row within a
 965 panel is the survival change expected for a specific population. Within each panel the seven
 966 population-specific caterpillar plots describe the distribution of expected survival difference,
 967 with the point demarking the median, and the thick and thin lines defining the 50% and 95%
 968 credible intervals for the prediction. Two aspects of this analysis are important to consider.
 969 First, the figure describes the difference in survival between the base case (all covariates at
 970 the mean) and that when a single covariate value is changed, and although the survival
 971 differences may be the same across populations, this should not be not be taken as evidence
 972 that population-specific survival rates are also estimated to be the same. Second, an estimated
 973 survival difference at or near zero does not imply there is no survival effect, only that this
 974 interaction was not included in the final AICc-selected model. Any small, but non-zero
 975 survival effects are the result of changes in the survival of another population in response to
 976 the covariate, with which the focal population shares a capacity constraint at some point in
 977 the life cycle.
 978



% Difference in Survival when Covariate Increased by 1 StDev

979
980

981 **Figure I.7. Percentage change in egg (or hatchery release) to adult survival resulting**
 982 **from a 1 standard deviation increase in covariate values. Each panel represents the**
 983 **outcome of increasing the value of a specific covariate (listed below the x-axis), with**
 984 **each caterpillar plot describing the effect on each population (y-axis). Plotted values are**
 985 **the difference in survival between a scenario where the covariate value is increased and**
 986 **a base case where all covariates are equal to their long-term mean. Caterpillar plots**
 987 **describe the median (dot), 50% interval (thick line), and 95% interval (thin line) for**
 988 **each survival difference accounting for estimation uncertainty.**

989 Results of this analysis of the environmental drivers of survival for Sacramento River
 990 fall and spring-run Chinook salmon indicate that several factors have the potential to
 991 significantly influence survival in the upstream portion of juvenile migration. Keswick Dam
 992 discharge is predicted to reduce egg to adult survival by 52.2%, for each increase in discharge
 993 rate of 1 SD. Increased air temperatures in the spring months following emergence are
 994 expected to increase the survival of Battle Creek (CNFH) fall-run Chinook by 37.5%,
 995 although the 95% credible interval for this predictions ranges from a moderate a modest 4.4%
 996 increase to a 79.8% increase indicating significant uncertainty in this prediction. Spring time
 997 air temperatures are expected to influence the early juvenile survival of Butte Creek spring-
 998 run Chinook in a similar direction but to a much greater extent with a predicted 124.7%
 999 increase. Conversely, increased summertime air temperatures during the period of adult
 1000 upstream holding and egg development are expected to reduce survival by 39.4%, indicating
 1001 that summertime temperatures may be reaching lethal levels or affecting adult fertility. The
 1002 final environmental variable linked to the upstream stage and early juvenile survival is water
 1003 discharge in Deer Creek, which is expected to reduce survival for Deer Creek spring-run
 1004 Chinook by a modest 26.2%. However, it is important to note that there is significant
 1005 uncertainty in this prediction with an increase in Deer Creek discharge by 1 SD predicted to
 1006 have result in anywhere between a 59.4% reduction in survival and a 27% increase in
 1007 survival 95% of the time.

1008 Later in the life cycle for Sacramento River Chinook, several factors are expected to
 1009 significantly influence juvenile survival in the Sacramento – San Joaquin Delta. A 1 SD
 1010 increase in the concentration of sediment (mg/L) at Freeport, CA is expected to result in a
 1011 37.1% reduction in the survival of the four fall-run Chinook populations. Sediment
 1012 concentration is predicted to have a slightly larger influence on survival of the three spring-
 1013 run populations, with a 54.3% reduction in egg to adult survival. Water exports from the
 1014 Sacramento – San Joaquin Delta, although quantified through different metrics, are expected
 1015 to reduce survival of both spring and fall-run juvenile Chinook. An increase in total exports
 1016 of 1 SD from the 1967-2010 average is predicted to result in a 68.1% reduction in the
 1017 survival of Deer, Mill, and Butte Creek spring-run Chinook. Similarly, an increase in the ratio
 1018 of Delta water exports to Delta inflow of 1 SD is expected to reduce survival of the four fall-
 1019 run populations by 57.8%. Interestingly however, net channel depletion or the quantity of
 1020 water removed from Delta channels to meet consumptive needs (Dayflow: QCD) is predicted
 1021 to increase the survival of fall-run Chinook by 43.7%. The final covariate linked to survival
 1022 of spring-run Chinook in the Sacramento – San Joaquin Delta is the average size of spring-
 1023 run Chinook in the Chipps Island Trawl survey. Each increase in the average size of juvenile
 1024 Chinook by 1 SD from the mean (1967-2010) is predicted to reduce survival by 72.9%.

1025 Environmental conditions in the nearshore and marine portions of the Chinook life
 1026 cycle were also found to have a significant impact on survival to adulthood. An increase in
 1027 average nearshore upwelling during late spring (April – June) in the region south of San
 1028 Francisco Bay of 1 SD above the mean, is expected to increase survival to adulthood by
 1029 51.2% for the four wild and hatchery-reared fall-run Chinook populations. Also related to
 1030 marine patterns of nutrient transport and productivity, an increase average wind stress curl
 1031 during the fall (July – December) of the first year of marine residency was estimated to
 1032 reduce survival for the seven populations of spring and fall-run Chinook by 39%. The final
 1033 covariate linked to Chinook survival in the marine environment was the Pacific Decadal
 1034 Oscillation index during winter (January – May) of the first year of marine residence. An
 1035 increase in PDO value of 1 SD above the 1967 – 2010 mean is predicted to increase survival
 1036 of the seven populations of spring and fall-run Chinook by 30%, however there exists

1037 significant uncertainty in this prediction with the 95% credible interval ranging from 10.1 -
 1038 51% increase in egg or hatchery release to adult survival.

1039 *PART I DISCUSSION*

1040 This evaluation of the putative environmental drivers of survival for seven
 1041 populations of spring and fall-run Chinook spawning within the Sacramento River watershed
 1042 was comprised of two essential components. The first component was model selection or the
 1043 process of determining the weight of evidence from the data for which subset of the 59
 1044 hypothesized covariate-by-population effects were able to best explain historical variation in
 1045 Chinook salmon survival, and are therefore informative for predicting future trends in
 1046 abundance. One thousand potential best-fit models were built using forward stepwise based
 1047 upon AICc as the selection criteria. The percentage of the 1,000 best-fit models resulting
 1048 from stepwise-AICc building which included a specific covariate provide a good indication
 1049 of the relative amount of support each of these competing hypotheses had from the adult and
 1050 juvenile abundance data (Table I.3). The fact that a range of covariates influencing both
 1051 grouped and single Chinook populations at all points in the life cycle were present amongst
 1052 those with a high inclusion rate provide evidence that there not exist a single population
 1053 bottleneck within the life cycle. This indicates that variation in environmental factors a
 1054 multiple points within the life cycle play a role in determining interannual survival to
 1055 adulthood. Of further importance is the observation that both natural covariates, including
 1056 temperature, water flow, and marine productivity patters, as well as those of anthropogenic
 1057 origin (i.e. water exports, export/inflow ratio, and water routing) appear amongst the set with
 1058 the highest inclusion rate. This finding indicates that variation in survival of Sacramento
 1059 River Chinook population in not driven by natural or anthropogenic processes in isolation.
 1060 The final model (Table I.4), chosen based on having the lowest AICc value amongst the
 1061 1,000 candidate best-fit models, likewise includes a range of covariates throughout the life
 1062 cycle representing both natural and anthropogenic processes are statistically important
 1063 predictors of survival.

1064 The influence of striped bass (*Morone saxatilis*) on survival of spring-run Chinook
 1065 was of particular interest given findings by Lindley and Mohr (2003), which indicated that
 1066 higher future abundances of striped bass were likely to lead to greater extinction potential for
 1067 winter-run Chinook. While the effect of striped bass on survival on spring-run Chinook was
 1068 included in 36% candidate best-fit models, it did not appear in the final (lowest AICc) model.
 1069 When included alongside other covariates in the final model, the estimated effect of striped
 1070 bass abundance was centered near zero, indicating an inability to estimate a distinctly
 1071 negative impact on grouped survival of spring-run Chinook. This result indicates that while
 1072 striped bass abundance does explain some of the variation in spring-run Chinook survival,
 1073 other explanatory covariates provide a better alternative explanation for historical abundance
 1074 observations.

1075 The estimated effect that water exports from the Sacramento – San Joaquin Delta on
 1076 juvenile Chinook survival through this region was also of importance. While the effect of
 1077 average water export levels on spring-run Chinook survival and the influence of
 1078 export/inflow ratio on fall-run Chinook survival both appear in the final model, these two
 1079 covariate effects have a 54% and 37% inclusion rates across the 1,000 candidate best-fit
 1080 models. The fact that these export-related covariate effects do not appear at the top of the list
 1081 of most often included covariates, indicates that while they have substantial potential to

1082 explain historical patterns in spring and fall-run Chinook survival, as indicated by distinctly
 1083 negative survival effects whose 95% credible intervals do not overlap zero (Figure I.7 and
 1084 Table I.6), there are other environmental covariate which explain a greater proportion of
 1085 variation in historical abundance.

1086 The second component of this evaluation was to estimate the direction and magnitude
 1087 of change in survival rates resulting from variation in each of the covariates in the final model
 1088 using Bayesian methods. When evaluating population dynamics model estimates for the
 1089 effect of environmental covariates on survival, it is important to place each result in the
 1090 proper biological context and determine if there exists a rational mechanistic explanation.
 1091 The effect of Sacramento air temperatures on several populations appeared as AICc-selected
 1092 explanatory covariates for several populations. Sacramento air temperature was employed as
 1093 a proxy for water temperatures in upstream regions of the Sacramento River watershed for
 1094 two reasons. First, significant and often linear relationships exist for between stream
 1095 temperatures and air temperatures in most regions. Second, stream temperature data were not
 1096 available continuously for the requisite time series (1967 – 2010) for all locations, resulting
 1097 in the necessity for interpolation based on the relationship with air temperature. Therefore,
 1098 for consistency in the covariate time-series and to reduce the risk of introducing additional
 1099 uncertainty into the estimation process, we elected to use air temperatures as covariates in
 1100 place of interpolated water temperatures. Results indicate a positive influence of increased
 1101 spring (January - March) air temperatures on the survival of Battle Creek (CNFH) fall-run
 1102 Chinook and Butte Creek spring-run Chinook. This temperature metric coincides with the
 1103 period prior to and during which juvenile Chinook are rearing. The estimated positive
 1104 influence of spring temperatures on Chinook survival could result indirectly from the increase
 1105 in primary production fostered by increased water temperatures and subsequent effects on
 1106 food availability. In this way growth potential for juvenile Chinook in freshwater depends
 1107 indirectly on temperature in the rearing environment through food availability, and directly
 1108 through effects on metabolism as warmer conditions allow juveniles to approach their
 1109 bioenergetic optimum. Finally, there is some evidence that acclimation to higher
 1110 temperatures early in life may facilitate higher thermal tolerance later in life, although research
 1111 in this area has primarily focused on Great Lakes rainbow trout and has not been explicitly
 1112 evaluated in Chinook (Myrick and Chech 1998). While spring time temperatures were
 1113 estimated to have a positive influence at this point in the lifecycle, it is important to note that
 1114 higher temperatures experienced later in the lifecycle during summer months may approach
 1115 upper tolerance limits, resulting in negative survival impacts. However, the effect of
 1116 increased summertime temperatures on juvenile survival was not evaluated as part of this
 1117 analysis.

1118 Contrary to the estimated positive effect of spring temperatures, air temperature
 1119 during the summer months (July - September) of the brood year were found to have a
 1120 negative impact on the survival of Butte Creek spring-run Chinook (Table I.6). For Butte
 1121 Creek spring-run Chinook this time period coincides with the point in the life-cycle when
 1122 adults are holding in freshwater prior to spawning. Prior to the creation of impassable barriers
 1123 to upstream migration, the life history of spring-run Chinook was adapted to make use of
 1124 high spring runoff events from snowmelt to migrate upstream into high elevation streams
 1125 with tolerable temperature regimes where they could successfully mature during the summer
 1126 months and await spawning when waters cooled to below 14 – 15°C (Williams 2006).
 1127 However, in Butte Creek mortality rates during the holding period were observed to exceed
 1128 20-30% in 2002 and 65% in 2003 during high temperature events (Ward et al. 2003). This is
 1129 likely the result of the increased metabolic demands for adult spring-run Chinook while

1130 holding in freshwater during high temperature events, and the increased rate of disease onset
 1131 and parasite load observed in other members of the *Oncorhynchus* genus exposed to high
 1132 temperatures (Kocan et al. 2009).

1133 Water flow conditions during juvenile rearing were also found to be important
 1134 predictors of Chinook survival. Water discharge rates at Keswick Dam were found to
 1135 negatively influence survival of mainstem spawning wild fall-run Chinook, and water
 1136 discharge in Deer Creek was found to reduce survival of the Deer Creek spring-run
 1137 population although to a lesser extent (Table I.6). While it is reasonable to assume that higher
 1138 discharge rates could lead to greater access to valuable off-channel rearing habitat, water flow
 1139 conditions additionally have the potential to influence foraging ability by juveniles through
 1140 the availability of drifting food sources (Neuswanger et al. 2014). None the less the finding
 1141 that fall-run Chinook survival was negatively influenced by increased water flow contradicts
 1142 findings by Stevens and Miller (1983) and Newman and Rice (2002). With respect to the
 1143 influence of water discharge on the survival of Deer Creek spring-run Chinook, this tributary
 1144 is prone to concentrated high flow events due to flood control levees and a lack of riparian
 1145 vegetation in its lower reaches (Tompkins 2006). For Deer Creek this may indicate that high
 1146 water flow rates reduce foraging opportunities for juvenile Chinook, rather than enhancing
 1147 them, as would be the case in a system with greater floodplain connectivity.

1148 Findings related to the influence of environmental covariates on survival of fall and
 1149 spring-run Chinook in the Sacramento – San Joaquin Delta are of particular interest in this
 1150 study. First, the effect of sediment concentration in waters at Freeport, California appeared in
 1151 the final AICc-selected model, and increases in sediment concentration were estimated to
 1152 have a substantial negative influence on the survival of both spring and fall-run populations.
 1153 This finding is contrary to a priori expectations that increased sediment concentrations might
 1154 provide a survival benefit, if they limit the efficacy of visual predators such as striped bass.
 1155 We remain limited in our ability to explain the estimated negative effect of sediment
 1156 concentrations save for the fact that increased sediment influx might be linked to production
 1157 potential for phytoplankton and the benthic periphyton which form the basis for the aquatic
 1158 food web. Similarly, the estimated negative influence of average juvenile spring-run
 1159 Chinook size on the common survival of the three spring-run populations appears contrary to
 1160 a priori expectations. In the review of size selective mortality in teleost fishes Sogard (1997)
 1161 found general support for the “bigger is better” hypothesis across taxa. Claiborne et al. (2011)
 1162 also found that juvenile to adult survival of yearling Chinook from the Willamette River
 1163 Hatchery increased with size at ocean entry. However, in an evaluation of the effect of size
 1164 on survival from analysis of scale samples from Chinook returning to the same hatchery,
 1165 Ewing and Ewing (2002) found either no significant size difference between juveniles at the
 1166 hatchery and those at ocean entry, or in the case of the 1989 – 1990 brood years evidence for
 1167 greater survival of smaller individuals. It is important to note that spring-run juvenile size
 1168 data was unavailable until 1976. As a result we were forced to assume the long-term average
 1169 for this covariate prior that year which may have influenced results related to this particular
 1170 covariate.

1171 Results of this analysis related to the influence of water exports from the Sacramento
 1172 – San Joaquin Delta indicate a negative influence of the export/inflow ratio on the combined
 1173 survival of the four fall-run Chinook populations and a negative influence increased total
 1174 Delta exports on the combined survival of spring-run Chinook populations (Table I.6). These
 1175 findings indicate that higher export rates lead to reduced survival for Sacramento River
 1176 Chinook on average, however a mechanistic explanation remains elusive. Direct entrainment

1177 mortality seems an unlikely mechanism given the success of reclamation and transport
1178 procedures, even given increased predation potential at the release site. Changes to water
1179 routing may provide a more reasonable explanation for the estimated survival influence of
1180 Delta water exports. Higher exports, or export/inflow ratio, result in greater water diversion
1181 into the interior delta where survival has been observed to be substantially lower than that in
1182 the Sacramento River mainstem (Perry et al. 2010), potentially resulting from an increased
1183 encounter rate with predators or prolonged residence in areas with suboptimal feeding
1184 opportunities or dissolved oxygen concentrations.

1185 In conjunction with freshwater drivers of survival for spring and fall-run Chinook
1186 populations of the Sacramento River watershed, results of this analysis indicate that several
1187 attributes of the marine environment have a significant influence on survival. Two covariates
1188 related to nearshore and offshore ocean current patterns and resultant nutrient movement
1189 within the water column were included as part of the final AICc-selected model. These
1190 covariates were the strength of nearshore upwelling and wind stress curl. Nearshore
1191 upwelling results in deep, cooler, and nutrient rich waters moving toward limnetic zone, with
1192 onshore transport and convergence fostering higher nearshore productivity during spring and
1193 summer. Conversely, wind stress curl is associated with offshore divergent transport (Wells
1194 et al. 2008). Our results indicate that increased nearshore upwelling during April – June of
1195 the year of ocean entry results in an increase in the combined survival of the four fall-run
1196 Chinook populations. Four alternative covariates quantifying upwelling patterns were
1197 evaluated as competing hypotheses for fall-run Chinook survival at different locations and
1198 quantifying time periods. Covariates were constructed using information from PFEL/NOAA
1199 monitoring sites both north and south of San Francisco Bay and for both the spring (April –
1200 June) and fall (July – December) periods. The AICc-selected covariate that appeared in the
1201 final model used the upwelling index data for spring time-period and at the southern location.
1202 Interestingly, although the effect of upwelling at the southern location in the spring months
1203 on the combined survival of spring-run Chinook appeared in 22% of candidate best-fit
1204 models, it did not appear in the final (lowest AICc) model, indicating that while upwelling
1205 may also be an important predictor of spring-run Chinook survival it appears to explain more
1206 variation in fall-run Chinook survival.

1207 Wind stress curl was found to have a negative influence on the combined survival of
1208 all seven spring and fall-run Chinook populations. These results are not unexpected given
1209 findings by Wells et al. (2007) that indicate greater Chinook growth in the first year of life
1210 with increased nearshore upwelling and decreased wind stress curl. Wells et al. (2008)
1211 likewise found that reductions in wind stress curl were linked to increased production of
1212 rockfish species although they note this may be more related to dispersal of juvenile rockfish.
1213 The estimated reduction in survival for Chinook associated with greater wind stress curl is
1214 likely explained by trophic interactions, with findings by Macias et al. (2012) indicating that
1215 biomass concentrations for phytoplankton and zooplankton are likely to be substantially
1216 higher with coastal upwelling as opposed to wind stress curl driven upwelling offshore.

1217 The Pacific Decadal Oscillation (PDO) describes a persisting periodicity in sea
1218 surface temperature, mixed layer depth, and strength and direction of ocean currents (Mantua
1219 and Hare 2002). Estimates for the influence of the PDO during January – May of the first
1220 year at sea indicating for the seven spring and fall-run Chinook populations, indicate
1221 increased survival is likely to be observed in during positive PDO events. This result is
1222 contrary to findings by Hare et al. (1999) which indicate positive PDO conditions favor
1223 production in Alaskan salmon stocks and disfavor the productivity of West Coast stocks, as

1224 well as findings by Wells et al. (2006) which highlight the negative covariation between size
1225 of Columbia River Chinook size and PDO values.

1226 **PART II SIMULATION OF FUTURE ABUNDANCE UNDER ALTERNATIVE** 1227 **CLIMATE, OCEANOGRAPHIC, AND WATER USE SCENARIOS**

1228 *INTRODUCTION*

1229 The purpose of conducting forward population projections was to simulate future
1230 survival for Sacramento River Chinook under alternative climate, oceanographic, and water
1231 management scenarios. Simulating the four populations of fall-run and three populations of
1232 spring-run Chinook forward in time, provides a means for weighing differences in future
1233 survival under alternative water export levels, relative to the uncertainty in future climate
1234 change and ocean productivity. In order to generate predictions for future survival, we
1235 integrated results from the Bayesian estimation model with expectations for future
1236 environmental conditions under two alternative future ocean production trends, two
1237 predictions for future climate change, and at four potential levels of future water exports (see
1238 Appendix B). In addition to differences in future Chinook survival arising from natural and
1239 anthropogenic environmental factors, we have also propagated both estimation and process
1240 uncertainty forward in our predictions for future abundance and realized survival rates.

1241 Future climate scenarios were based upon the U.S. Bureau of Reclamation's (USBR)
1242 Operations and Criteria Plan (OCAP) Study (USBR 2008). Two alternative scenarios for
1243 overland climate change were evaluated, the OCAP Study 9.2 and 9.5. The OCAP Study 9.2
1244 (referenced as: **cc92**) describes a wetter and cooler prediction for future climate change, with
1245 a mean increase in temperature of 0.42° C and an increase in precipitation of 12.5%.
1246 Conversely, the OCAP Study 9.5 (referenced as: **cc95**) describes a dryer and warmer outlook
1247 for future climate change in the Central Valley, with a mean increase in temperature of 1.56°
1248 C and a decrease in precipitation of 12%. In addition to differing scenarios regarding climate
1249 change, two alternative predictions for future ocean conditions were explored. These two
1250 scenarios, one representing traditional perceptions of positive growth conditions for Chinook
1251 (referenced as **oceanUP**) and the other representing negative growth conditions (referenced
1252 as **oceanDOWN**), describe alternative patterns in nearshore upwelling and temperature, and
1253 future trends in broad-scale ocean currents.

1254 Paired with these alternative scenarios for future climate change and ocean
1255 production, were four scenarios related to the magnitude of future water exports from the
1256 Sacramento-San Joaquin Delta. The four future scenarios for total water exports included: 1.
1257 **expAVG** (future exports equal to the 1967 – 2010 average), 2. **expZERO** (zero future water
1258 exports), 3. **expUP30** (an increase in future exports to 30% above the historical average), and
1259 4. **expDOWN30** (a decrease in future exports to 30% below the historical average). While it
1260 is clear that some of these water export scenarios are economically infeasible (i.e. expZERO)
1261 they were included as part of the population projections to bound the range of potential
1262 biological outcomes from management actions. All export scenarios are based upon the
1263 historical export values calculated as the average of March – May Dayflow (QEXPORT)
1264 values for fall-run Chinook, and the average of February – April values for spring-run
1265 Chinook.

1266 In total, these 2 onshore climate change scenarios, 2 ocean production scenarios, and
 1267 4 water export scenarios, resulted in 16 different realizations of the future environment for
 1268 Chinook populations of the Sacramento River watershed. These sixteen environmental
 1269 scenarios were subsequently translated into future covariate values (see Appendix B), for use
 1270 as inputs in projecting the populations forward in time and determining realized future
 1271 survival rates.

1272 *SIMULATION METHODS*

1273 Realized future survival rates were simulated by projecting all seven populations of
 1274 Sacramento River Chinook forward in time for 50 years (2007 – 2057). The structure of the
 1275 population dynamics model utilized to estimate stage-specific survival rates and the direction
 1276 and magnitude of response by populations (or groups of populations) to environmental
 1277 covariates, formed the basis for these forward population projections. Population and brood
 1278 year specific cohorts of Chinook were tracked forward in time through the same six spatio-
 1279 temporal life-stages (i.e. upstream/tributaries, Sacramento-San Joaquin Delta, nearshore, and
 1280 the 1st, 2nd, and 3rd years in the ocean). In the same way as the estimation model, both the
 1281 wild-spawning and hatchery production life cycles were represented in population
 1282 projections, with wild-spawning populations linked to future cohort production through a
 1283 fixed fecundity per individual, and hatchery production fixed at the population-specific
 1284 average of releases from the most recent 10-year period. Stage-specific capacities for
 1285 Sacramento mainstem-spawning fall-run Chinook in the upstream stage, and the grouped
 1286 spring-run and fall-run populations in the Sacramento-San Joaquin Delta, were fixed at the
 1287 average of estimates from Hendrix et al. (2014) for the most recent 10-year period. Estimated
 1288 values for population dynamics model parameters including stage and population-specific
 1289 productivity rates, and coefficients describing the direction and magnitude of influence that
 1290 environmental covariates have on stage-specific productivity (maximum survival) rates, were
 1291 used when simulating future trends in abundance.

1292 When simulating future trends in Chinook abundance in order to evaluate differences
 1293 in realized survival, it was necessary to account the two major sources of uncertainty in our
 1294 analysis and propagate this uncertainty forward into predictions under alternative
 1295 environmental and export scenarios. The first source of uncertainty in generating robust
 1296 predictions for future abundance is uncertainty in the estimates of population dynamics model
 1297 parameters. This includes uncertainty in the estimated value of life-stage and population
 1298 specific basal productivity rates, as well as coefficients describing the influence of
 1299 environmental covariates on survival. Estimation uncertainty arises when estimated values
 1300 for model parameters are poorly informed by the available data, leading to broad posterior
 1301 probability distributions indicating a broad range of parameter values with similar
 1302 probabilities of being correct given the data. To account for estimation uncertainty in model
 1303 parameters, we drew 1,000 independent sets of model parameter values from the joint
 1304 posterior sampled by the Bayesian estimation model. By drawing parameter sets from the
 1305 joint posterior, and repeating the 50-year forward projection of the seven populations using
 1306 each of the independent parameter sets, we are able to capture the influence of both the true
 1307 uncertainty in parameter values and posterior correlations between estimated parameters.

1308 The second source of uncertainty that was integrated into forward projects was
 1309 process uncertainty, or temporal variation in the state of future population dynamics. For each

1310 of the 1,000 replicate forward simulations, a random process deviate was introduced in the
 1311 calculation for initial abundance in the first model stage (Eq. II.2, II.3).

$$1312 \quad (II.2) \quad N_{y,s=1,p,e,i} = A_{t=y,p,a,e,i} * fec * \exp\left(\varepsilon_{y,p,i} - \frac{\sigma_p^2}{2}\right)$$

$$\varepsilon_{y,p,i} \sim N\left(0, \sigma_p\right)$$

1313 Equation II.2 describes how process uncertainty is introduced into the wild-spawning
 1314 life cycle used to represent the Sacramento mainstem fall-run, and Deer, Mill, and Butte
 1315 Creek spring-run Chinook populations. The number of individuals entering the upstream (1st)
 1316 model stage ($N_{y,s=1,p,e,i}$), of brood year y , population p , in simulation i of environmental
 1317 scenario e , is a function of the number of spawning adults returning in calendar year $t = y$ of
 1318 population p ($A_{t=y,p,e,i}$), the fixed fecundity rate of 2,000 eggs/individual ($fec = 2,000$), and
 1319 the exponentiated brood year y , population p , and simulation i specific process deviate
 1320 ($\varepsilon_{y,p,i}$). Conversely, equation II.3 describes how initial abundance in the first model stage was
 1321 calculated with process errors for the three populations of hatchery-produced fall-run
 1322 Chinook, where RH_p is the fixed level of hatchery releases for each population.

$$1323 \quad (II.3) \quad N_{y,s=1,p,e,i} = RH_p * \exp\left(\varepsilon_{y,p,i} - \frac{\sigma_p^2}{2}\right)$$

$$\varepsilon_{y,p,i} \sim N\left(0, \sigma_p\right)$$

1324 Process deviates ($\varepsilon_{y,p,i}$) for each brood year y , population p , and replicate simulation
 1325 i , were generated as random draws from a normal distribution with mean equal to 0, and
 1326 population-specific standard deviations (σ_p). The standard deviations for the process error
 1327 distributions (σ_p) were the maximum likelihood estimates for the residual observation
 1328 uncertainty from fitting the original population dynamics model to historical abundance data.
 1329 In total 1,000 randomly drawn process deviates, corresponding to the replicate simulations
 1330 using parameter sets drawn from the joint posterior, were generated for each population in
 1331 each of the 50 years of the forward simulation. To ensure comparability, the same set sets of
 1332 brood year and population specific process deviates were used across environmental
 1333 scenarios.

1334 When simulating future trends in Sacramento Chinook abundance and evaluating
 1335 realized survival rates, it was necessary to incorporate the likely impact of future fishery
 1336 removals. Fishing mortality was simulated based upon the current Reasonable and Prudent
 1337 Alternative (RPA) management scheme for Central Valley Chinook (see “Simulation of
 1338 Harvest Rates” below). Annual allowable harvest rates for fall-run Chinook are established
 1339 based upon the Sacramento Index (SI), however maximum harvest rates are further
 1340 contingent upon minimum abundance requirements for ESA listed winter-run Chinook.
 1341 When projecting populations forward in time, it was necessary to simultaneously model the
 1342 future dynamics of winter-run Chinook in response to the 16 environmental scenarios under
 1343 evaluation. Results from the evaluation of Sacramento River winter-run Chinook using the
 1344 OBAN model (see Appendix D) which was run in parallel with the spring and fall run model,
 1345 were used to simulate the future abundance of Sacramento River winter-run Chinook across
 1346 the same 50-year time-series in response to differences in future climate change, marine

1347 production, and water exports across scenarios. Moving forward in time, future harvest rates
 1348 depended on the model-predicted abundance of fall-run Chinook and winter-run Chinook
 1349 (see “Simulation of Harvest Rates”). Spring-run harvest rates were scaled at 95% of fall-run
 1350 harvest rates.

1351 *SIMULATION OF FUTURE HARVEST RATES*

1352 *Background*

1353 The Pacific Fisheries Management Council (Council) manages the harvest of salmon
 1354 on the coasts of California, Oregon, and Washington. The ocean salmon fishery targets
 1355 Chinook, coho, and pink salmon species, which include Sacramento River Chinook salmon.
 1356 The Sacramento River Chinook stocks overlap with Klamath River Chinook salmon in a
 1357 mixed stock fishery. Furthermore, the Sacramento River fall Chinook (SRFC) is an indicator
 1358 stock for the Central Valley Fall complex and Klamath River fall Chinook (KRFC) is an
 1359 indicator stock for the Oregon/Northern California Chinook complex. As indicator stocks,
 1360 the Council calculates both acceptable biological catches (ABC) and annual catch limits
 1361 (ACL) for the SRFC and KRFC.

1362 Both Sacramento River and Klamath River Chinook are composed of stocks
 1363 supported by hatchery production and stocks that are listed as a conservation concern under
 1364 the Endangered Species Act (ESA). In the Sacramento River and Klamath River mixed
 1365 fishery, the Sacramento winter-run (federally listed as threatened in 1990 and as endangered
 1366 in 1994 under ESA), Central Valley spring-run (listed as threatened under ESA in 1999) and
 1367 the California coastal (listed in 1999) may limit harvest rates. Target harvest rates for the
 1368 Sacramento fall run are determined annually via a forecast of abundance indexes of Chinook
 1369 salmon to both rivers. Management of the fishery occurs through a series of spatially explicit
 1370 openings and closures to structure the harvest effort in such a manner to ensure conservation
 1371 of portions of the stocks that may be at low abundances while allowing harvest of those
 1372 stocks that are healthy. There are a series of Council meetings to review the forecasted
 1373 abundance and possible management alternatives.

1374 NMFS developed a Biological Opinion in 2010 (2010 Opinion) to evaluate the effects
 1375 of the ocean salmon fishery on winter run stock (Biological Opinion on the Authorization of
 1376 Ocean Salmon Fisheries Pursuant to the Pacific Coast Salmon Fishery Management Plan and
 1377 Additional Protective Measures as it affects the Sacramento River Winter Chinook Salmon
 1378 (winter-run) Evolutionary Significant Unit (NMFS 2010)). In the 2010 Opinion, NMFS
 1379 identified that winter-run cohorts could be reduced (i.e., decrease in the number of spawners
 1380 relative to the number of spawners in the absence of the fishery) by 10 to 25% due to the
 1381 ocean salmon harvest with an average rate of 20%. Most of the impacts occur south of Point
 1382 Arena, CA from contacts with the recreational fishery (O’Farrell 2012).

1383 To avoid a jeopardy conclusion on the operation of the ocean salmon fishery, NMFS
 1384 developed a Reasonable and Prudent Alternative (RPA) to allow explicit control of the
 1385 management process to reduce impacts when extinction risk of winter run increases (e.g., due
 1386 to low stock size or periods of decline). After the issuance of the 2010 Opinion, the Council
 1387 was given options to either increase size limits or enact seasonal closures to reduce the
 1388 fishery impacts on winter-run in 2010 and 2011.

1389 In 2012, NMFS performed a Management Strategy Evaluation (MSE) for different
 1390 control rules based on the abundance of winter-run Chinook for setting the allowable harvest
 1391 rate on the mixed stock fishery (Winship et al. 2012). The control rules set allowable impacts
 1392 of age-3 winter-run south of point Arena as: 1) 0 impact (a closed fishery south of Point
 1393 Arena); 2) 25% impact, which is the historical estimate of impact rate; 3) 20% impact, which
 1394 is the current rate; and four alternatives (4-7) that reduce impact rates at certain winter-run
 1395 thresholds. These MSE compared the impact rate under each of the control rules relative to
 1396 the potential for increasing extinction risk of winter-run Chinook.

1397 *Management of Sacramento River Chinook*

1398 ***Fall-run***

1399 The fishery impact rate for SRFC is set by evaluating the Sacramento Index (SI) in
 1400 each year. The SI is calculated as the sum of a) harvest south of Cape Falcon, OR; b) SRFC
 1401 impacts due to non-retention in ocean fisheries; c) harvest in the recreational fishery in the
 1402 Sacramento River basin; and d) SRFC spawner escapement. The SI is forecasted each year
 1403 using a regression model with an autocorrelated error term that uses the number of SRFC
 1404 jacks from the previous year as the dependent variable.

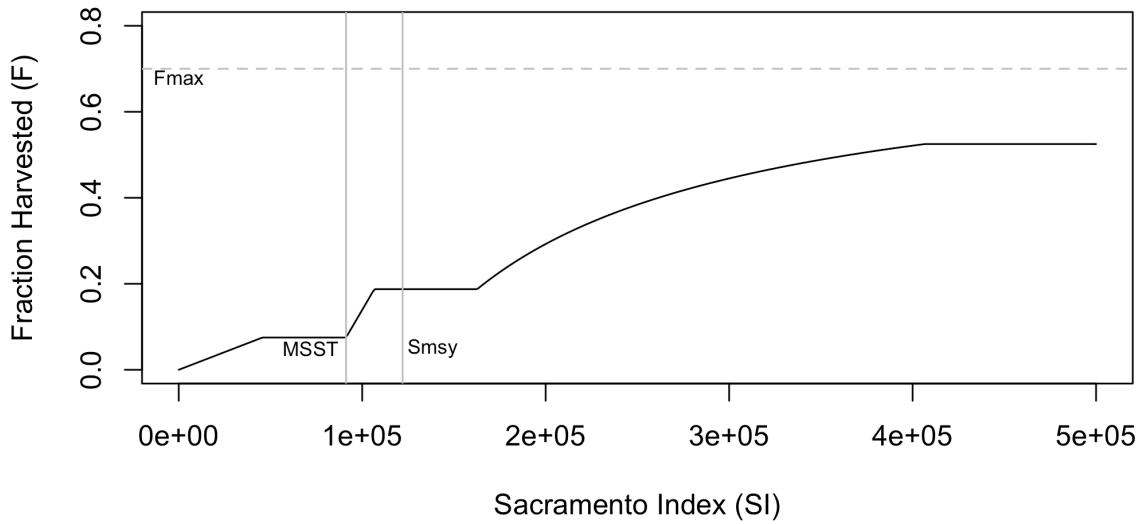
1405 The estimates of the SI are subsequently used to determine the status of the fishery as
 1406 overfished, approaching overfished, rebuilding, or rebuilt. The important metrics for
 1407 determining the status are the minimum stock size threshold (MSST) (91,500 for SRFC) and
 1408 the stock size at maximum sustainable yield (122,000). Given the status of the fishery, the
 1409 allowable biological catch, annual catch limit, and the overfished limit can then be calculated.

1410 The determination of the fishing rate is described as follows (PFMC 2014). The
 1411 discrete fishing rate (F) at the overfishing limit, F_{OFL} , is defined as being equal to F_{MSY} (or the
 1412 maximum fishery mortality threshold) and the spawner size (S) at the overfishing limit, S_{OFL}
 1413 $= N \times (1 - F_{MSY})$. Because, SRFC is a Tier-2 fishery, the fishing rate consistent with the
 1414 allowable biological catch $F_{ABC} = F_{MSY} \times 0.90$ and $S_{ABC} = N \times (1 - F_{ABC})$, where N is the
 1415 spawner equivalent units. Finally, the fishing rate consistent with the allowable catch limits,
 1416 F_{ACL} , is equivalent to F_{ABC} and $S_{ACL} = N \times (1 - F_{ACL})$, which results in $S_{ACL} = S_{ABC}$. The impact
 1417 rate is determined by the SRFC control rule as a function of the potential spawner abundance
 1418 (in this case the spawner abundance is the Sacramento Index = SI) (Figure II.1).

1419 ***Winter-run***

1420 The current RPA (NMFS 2012) uses a fishery control rule with a reduction in fishery
 1421 impact as a function of 3-year geometric average of winter-run escapement. The escapement
 1422 is defined as the total male and female, natural-origin and hatchery-origin escapement as
 1423 estimated by an annual carcass survey (USFWS 2011). The fishery control rule has the
 1424 following threshold definitions (Figure II.1): A) from escapement of 0 to 500, the allowable
 1425 impact rate south of Point Arena is 0; B) from escapement of 501 to 4000, the impact rate is
 1426 linearly increasing from 0.1 to 0.2; C) from escapement of 4000 to 5000, the impact rate is
 1427 0.2. The impact rate for escapement > 5000 is undefined. For purposes of the MSE, NMFS
 1428 assumed that the impact rate would be 0.2 for any 3-year geometric mean of escapement $>$
 1429 4000 as described on pg. 57 of Winship et al. (2012). We assumed the same upper bound of
 1430 0.2 for age-3 impact when the 3-year geometric average escapement was > 5000 .

1431

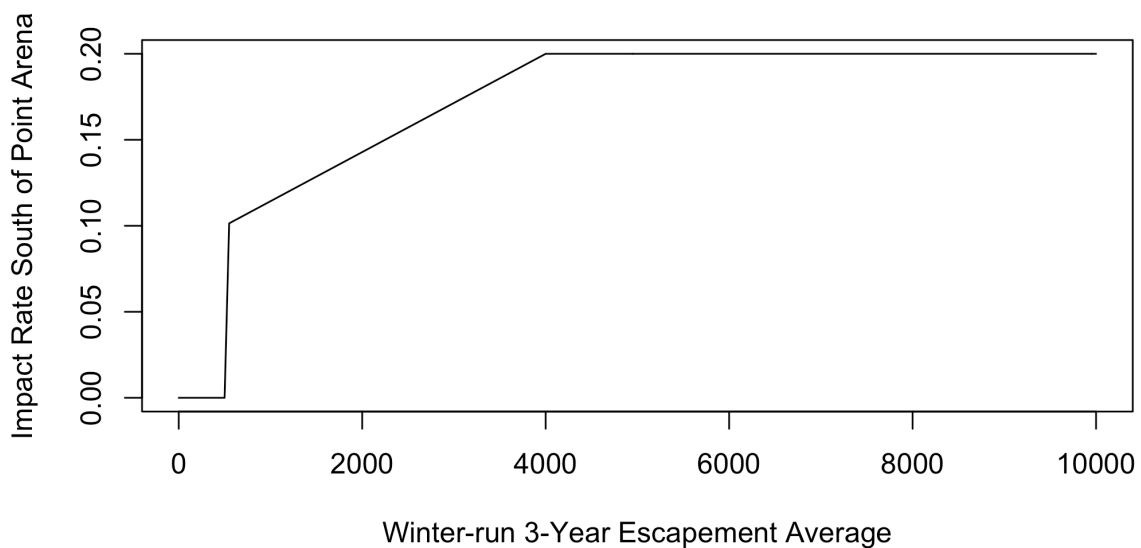


1432
1433
1434
1435

Figure II.1. Fishery control rule as a function of the potential spawner abundance (Sacramento Index) used for setting impact rates for Sacramento River fall-run Chinook.

1436
1437
1438
1439

The fishery control rule defines the impact rates south of Point Arena, which largely encompasses the winter-run marine distribution. Fall-run Chinook are found north of Point Arena, and the fishery control rule for those areas is dependent upon the abundance index for fall run.



1440
1441
1442

Figure II.2. Fishery control rule as a function of the trailing 3-year geometric average of winter-run abundance.

1443 For example, the SI forecast in 2014 was 634,650 (PFMC 2014). The spawner
 1444 escapement associated with overfishing in 2014 is 139,623, which is calculated as a function
 1445 of F_{MSY} (0.78) and the SI abundance forecast of 634,650. The SRFC is a Tier 2 stock, so the
 1446 $F_{ABC} = F_{MSY} * 0.90 = 0.70$, and the spawner escapement associated the allowable biological
 1447 catch was forecasted to be $S_{ABC} = N(1 - F_{ABC}) = 190,395$.

1448 In 2014, the 3-year geometric mean of winter-run abundance was 2,380, which
 1449 resulted in a maximum forecasted impact rate on age-3 winter-run of 15.4% (in comparison it
 1450 was 13.7% in 2012 and 12.9% in 2013).

1451 Reducing the maximum impact rate on age-3 winter-run may have important
 1452 consequences for the actual harvest rates on SRFC. Recently, Satterthwaite et al. (2013)
 1453 compared the ocean distribution of fall-run, winter-run, and spring-run during the summer
 1454 and fall, which provides some understanding of the spatial differences in the relative contacts
 1455 per unit effort of the fishery, which is a proxy for the spatial distribution of each run.
 1456 Sacramento River fall-run have relative contacts per unit effort of approximately 0.2 for
 1457 management areas located south Latitude 42 N at the CA OR border, and 0.1 north of
 1458 Latitude 42 N and Cape Falcon at the OR WA border. These results suggest that the closing
 1459 of fishing south of Point Arena, as would be required for winter-run 3-year average
 1460 escapement of less than 500, can have potential consequences for the total fall-run impact
 1461 rate. For more information, please see PFMC (2014).

1462 *Spring Run*

1463 There are no explicit fishery management rules for spring run, though it has been
 1464 noted in past NMFS Biological Opinions (e.g., NMFS 2010) that protections for winter run
 1465 are likely to be beneficial for spring run. Comparisons of ocean and river impact rates of
 1466 spring-run relative to SRFC by US Fish and Wildlife Service for the purposes of meeting the
 1467 goals of the Central Valley Project Improvement Act (CVPIA) indicated equivalent ocean
 1468 fishery rates were assumed for spring-run and fall-run, whereas river impact rates were
 1469 consistently lower for spring-run (Chinookprod_032011.xlsx obtained from
 1470 <http://www.fws.gov/stockton/afpr/>). Overall, total fishing impact rates for spring-run were
 1471 approximately 0.95 of fall-run.

1472 *Harvest Model*

1473 The management of SRFC requires annual management rules to optimize the fishery
 1474 due to changing abundances of winter-run and Klamath River stock sizes in addition to the
 1475 status of other stocks (e.g., PFMC 2014). The management process can be simplified by
 1476 making several assumptions about the fishery management dynamics:

- 1477 • Klamath River Fall Chinook do not limit the values of F_{ABC} calculated annually for
 1478 SRFC.
- 1479 • The Klamath River fall age 4 harvest rate limits, intended to protect California
 1480 Coastal Chinook, do not limit the values of F_{ABC} calculated annually for SRFC.
- 1481 • Abundance of age-3 SRFC and winter-run are obtained from the spring-run & fall-run
 1482 life cycle model and the winter-run models, respectively. In the actual management
 1483 of SRFC, estimates of an adult (age 3-5) abundance index in year t are calculated
 1484 from regressions to age-2 abundances in year $t-1$.

1485 • The fishery acts without error; thus, management overfishing (i.e., total annual
 1486 exploitation rate exceeds the maximum fishing mortality threshold of 0.78) cannot
 1487 occur.

1488 The following steps were developed for calculating the annual impact rate for SRFC
 1489 (F_{FR}), and Sacramento winter-run Chinook (F_{WR}).

- 1490 1. Calculate an estimate of the Sacramento Index as the sum of the four components
 1491 identified previously.
- 1492 2. Determine the fall-run impact rate F_{FR} based on the fishery control rule for SRFC
 1493 (Figure II.1). The control rule specifies that even if the stock is approaching an
 1494 overfished condition (the SRFC stock has a 3 year geometric average (t-2, t-1, current
 1495 year) that is below the threshold of 91,500), a *de minimis* fishery will occur at the rate
 1496 defined by the fisheries control rule.
- 1497 3. Calculate the trailing 3-year geometric average of winter-run abundance.
- 1498 4. Depending upon the 3-year geometric value, set the fishery impact rate for winter-run
 1499 (Figure II.2). If the winter-run impact rate is 0, reduce F_{FR} by 25% to account for lost
 1500 fishing opportunities south of Point Arena.
- 1501 5. Set the impact rate for spring-run $F_{SR} = 0.95F_{FR}$ to reflect reduced river impact rates.
 1502

1503 *RESULTS*

1504 Future trends in abundance for seven populations of fall and spring-run Chinook
 1505 spawning in tributaries of the Sacramento River watershed were simulated under different
 1506 scenarios for future climate change and ocean productivity, and alternative levels of water
 1507 export from the Sacramento-San Joaquin Delta. Results from a Bayesian multi-stock
 1508 population dynamics model, fit to historical abundance data, were used to parameterize
 1509 forward simulations. In addition, future trends in abundance for Sacramento winter-run
 1510 Chinook were also simulated to allow for implementation of the current fishery management
 1511 process. All eight populations were simulated forward in time for 50 years in response to the
 1512 16 alternative environmental scenarios (combinations of future climate, ocean productivity,
 1513 and water exports), subject to capacity interactions arising from juvenile competition, and
 1514 accounting for estimation uncertainty and process error in future predictions. The forward
 1515 simulation for each environmental scenario was replicated 1,000 times with randomly drawn
 1516 process deviates and model parameter values.

1517 Differences in future outcomes for these populations in response to the 16 scenarios
 1518 are best quantified through comparison of realized survival rates within populations and
 1519 across scenarios. Realized survival rate was calculated in two ways depending on the life
 1520 history of the individual populations. First, for wild-spawning Chinook stocks (mainstem
 1521 Sacramento fall-run, and Deer, Mill and Butte Creek spring-run), realized survival was
 1522 calculated as the survival rate from egg to spawning adult, or the sum of spawning
 1523 adults from a brood year across return years, divided by the spawning abundance producing
 1524 that cohort multiplied by the assumed fecundity (Eq. II.4).

$$1525 \quad (II.4) \quad RS_{y,p,e,i} = \frac{\sum_{a=1}^{Nages} A_{t,p,a,e,i}}{E_{y,p,e,i}}$$

$$t = y + \tau_a$$

1526 In equation II.4, realized survival ($RS_{y,p,e,i}$) from brood year y , of population p , for
 1527 environmental scenario e , and simulation i , is a function of the adult abundance surviving
 1528 both natural and fishing mortality and returning to spawn ($A_{t,p,a,e,i}$) in calendar year t , of
 1529 population p and age a , resulting from simulation i of environmental scenario e , and the
 1530 number of eggs ($E_{y,p,e,i}$) resulting from brood year y for that population, scenario and
 1531 simulation. τ_a represents the difference between brood year y and the calendar year of return
 1532 t , for individuals returning at each age a .

1533 Realized survival for the hatchery-produced populations (Battle Creek (CNFH),
 1534 Feather River, and American River (Nimbus) fall-run) is determined by the ratio of returning
 1535 adult spawners ($A_{t,p,a,e,i}$) to the number of hatchery for that population (RH_p), which is
 1536 assumed constant in the future (Eq. II.5)

$$1537 \quad (II.5) \quad RS_{y,p,e,i} = \frac{\sum_{a=1}^{Nages} A_{t,p,a,e,i}}{RH_p}$$

$$t = y + \tau_a$$

1538 Predictions for future realized survival rates for the three spring-run (Fig. II.3) and
 1539 four fall-run (Fig. II.4) populations across years and replicate scenarios, accounting for future
 1540 fishing mortality, across environmental and export scenarios show some consistent patterns.
 1541 As expected, survival rates for the hatchery-produced Chinook populations were much higher
 1542 than those predicted for the wild-spawning populations, given that realized survival was
 1543 measured as survival from release to spawning adult, as opposed to egg to adult survival
 1544 (Table II.1). For the fall-run Chinook populations, the final model estimated a net positive
 1545 impact of nearshore upwelling on survival, as a result these four populations show higher
 1546 average survival rates for scenarios which included a 10% increase in upwelling (oceanUP)
 1547 across both future climate change and water export scenarios. Across fall-run populations,
 1548 simulated positive upwelling conditions in the future resulted in an average increase in
 1549 realized survival of between 12% and 67% (mean: + 44%) across export scenarios, when
 1550 compared with those scenarios incorporating a 20% reduction in nearshore upwelling
 1551 (oceanDOWN, Table II.1). With respect to the spring-run Chinook populations, substantially
 1552 smaller differences in realized survival rates in response to the oceanUP scenarios were
 1553 observed, with 5 – 17% decreases in average realized egg to adult survival (Fig. II.3). Winter-
 1554 run Chinook on the other hand, were predicted to exhibit higher survival in response to the
 1555 increased upwelling under the oceanUP scenario, with 7 – 36% higher survival (Table II.1)

1556 Predictions for differences in realized survival rate across water export scenarios
 1557 indicated similar general trends across both populations and potential differences in future
 1558 climate change. For all populations realized survival rates were predicted to be highest under
 1559 the zero export scenario, followed by scenarios simulating a 30% reduction in exports,
 1560 average exports, and a 30% increase in water exports (Fig. II.3, II.4). When compared to
 1561 scenarios simulating future survival in response to water export levels at the 1967 – 2010
 1562 average, spring-run Chinook populations are expected to exhibit a higher average realized
 1563 survival in response to a 30% reduction in export volumes, with survival 27 – 48% higher for
 1564 Deer Creek, 29 – 51% higher for Mill Creek, and 19 – 38% higher for Butte Creek Chinook,
 1565 across environmental scenarios. Fall-run Chinook populations are predicted to exhibit
 1566 somewhat smaller increases in survival under a 30% export reduction (expDOWN30) relative
 1567 to average water exports in the future (expAVG), with realized survival higher by 12 – 26%
 1568 for Sacramento mainstem wild-spawning Chinook, and between 14% and 27% for the three
 1569 hatchery-produced fall-run Chinook populations across environmental scenarios (Table II.2).
 1570 Winter-run Chinook are predicted to respond to a 30% reduction in future water exports, with
 1571 only a 3 – 9% increase in survival relative to the average export scenario (Table II.2).

1572 When future dynamics of Sacramento Chinook populations were simulated with a
 1573 30% increase in water exports (expUP30), compared to the average export scenario the
 1574 mainstem Sacramento wild-spawning Chinook were predicted to experience 16 – 28% lower
 1575 median realized survival rates from egg to spawning adult, while the three hatchery-produced
 1576 populations were predicted to exhibit a 14 – 25% reduction in future survival from release to
 1577 adulthood, depending on the climate change and ocean production scenario (Fig II.4, Table
 1578 II.2). Simulation of future Deer, Mill, and Butte Creek survival indicated that, relative to the
 1579 average water export scenario, average realized egg to adult survival was predicted to be 39 –
 1580 53% lower in the presence of a 30% increase in future water exports (Fig. II.3, Table II.2).
 1581 The simulation results again indicate that the response by winter-run Chinook to altered
 1582 export levels is minimal, with a 0 – 3% reduction in average realized egg to adult survival,
 1583 across environmental scenarios.

1584 Predictions for realized survival under the zero future export scenario (expZERO)
 1585 were higher for all populations, however the magnitude of the difference in survival between
 1586 this and the average export scenario (expAVG) was largely contingent upon the climate
 1587 change scenario and population of interest. The Deer and Mill Creek spring-run populations
 1588 exhibited the largest difference in realized survival between the zero and average export
 1589 scenarios, under the OCAP 9.2 climate change prediction and positive ocean conditions
 1590 (cc92.oceanUP) (Fig. II.3). Predicted survival in the absence of exports was 79% higher for
 1591 Deer Creek, 85% higher for Mill Creek, and 59% higher for Butte Creek Chinook, compared
 1592 to average exports (Table II.2). Interestingly, the Butte Creek spring-run Chinook population
 1593 also showed one of the smallest responses to the zero export scenario across populations,
 1594 with only 27% higher survival compared to the average export scenarios under the OCAP 9.5
 1595 climate change and lower ocean production environmental scenario (cc95.oceanDOWN).
 1596 This increase in predicted survival is quite minimal when compared to the 62 – 83% higher
 1597 survival predicted for the fall-run Chinook populations with zero exports, under the same
 1598 environmental scenario (Table II.2). In general however, average realized survival for fall-run
 1599 Chinook under the zero export scenario is expected to be 28 – 62% higher for the mainstem
 1600 Sacramento wild-spawning population and 44 – 83% higher for the hatchery-produced
 1601 populations, when compared to expectations under the average export scenario. While results
 1602 indicated that realized winter-run Chinook survival would be minimally influenced by a 30%
 1603 increase or reduction in future exports, the zero export scenario is predicted to increase
 1604 survival by 28 – 91%, most appreciably when combined with a cooler and wetter future
 1605 climate change scenario and positive future marine conditions (cc92.oceanUP).

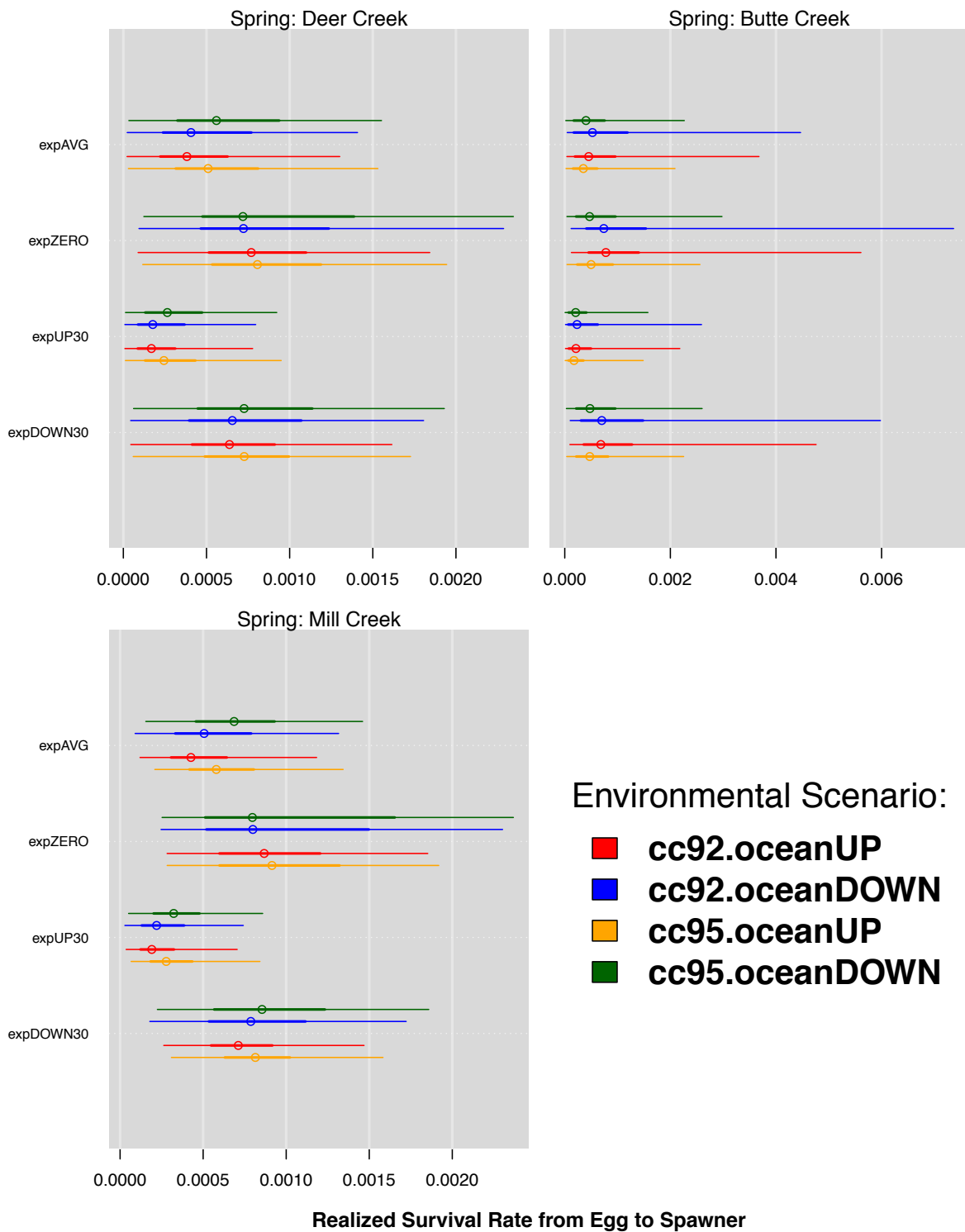
1606 In addition to higher median realized survival rates, the zero export scenario is also
 1607 predict to also produce more variable survival in the future. While most pronounced for the
 1608 spring-run Chinook populations, when the variability in realized survival is compared across
 1609 export scenarios it is consistently higher for the zero export case, across all populations (Fig.
 1610 II.3, Fig. II.4). The Butte Creek population exhibits the greatest variation in future survival,
 1611 specifically under the zero export scenario, and for the OCAP 9.2 climate change pathway
 1612 across export scenarios (Fig. II.3).

1613 While these forward simulation results suggest that higher and more variable realized
 1614 survival can be expected under the zero export scenario, across populations, climate change
 1615 trajectories, and ocean productivity patterns, it is also evident that a 30% reduction in water
 1616 exports (expDOWN30) is likely to achieve an increase in realized survival of a substantial
 1617 magnitude in many cases. For example, on average across environmental scenarios the Butte
 1618 Creek population is expected to exhibit a 41% increase in average realized survival under the
 1619 zero export scenario, and a similarly large increase of 27%, with a 30% reduction in spring
 1620 export volumes (Fig. II.3, Table II.2). This amounts to a difference of only a 14 percentage
 1621 points in the predicted survival rate increase; between the zero export and 30% export
 1622 reduction scenarios. Results are similar for the other spring-run populations, with a difference
 1623 of 25 percentage points for Mill and Deer Creek spring-run Chinook. Improvements in
 1624 survival under the zero export scenario, relative to the 30% export reduction scenario
 1625 (expDOWN30), are on average greater for the hatchery-produced fall-run Chinook
 1626 populations, but likewise suggest that on average across environmental scenarios, a
 1627 difference in survival of only 26 – 43 percentage points is likely to be observed (Table II.2).

1628 The percentage difference in realized survival increase, for the zero export and 30%
 1629 reduction scenarios, relative to the average export scenario, is most variable for the winter-
 1630 run Chinook population. The percentage increase in survival difference between expZERO

1631 and expDOWN30 is smallest under cc95.oceanDOWN scenario at 25, and greatest under the
1632 cc92.oceanUP scenario. This indicates that under a cooler and wetter future climate with
1633 greater upwelling (cc92.oceanUP), the ceasing all exports (expZERO) is likely to have a
1634 substantially higher survival benefit relative to reducing exports by 30% (expDOWN30).
1635 While, in the face of a hotter and drier future climate with reduced nearshore upwelling
1636 (cc95.oceanDOWN) where survival is severely limited by natural processes, both before and
1637 after the delta, the benefits of a 30% reduction and zero exports are more similar (Table II.2).
1638 This same pattern is predicted for the spring-run Chinook populations, but not the fall-run
1639 populations.

1640 With respect to the influence of climate change on predictions for future realized
1641 survival, differences in outcomes amongst climate change scenarios differed across
1642 populations and were smaller on average when compared differences resulting from
1643 alternative export scenarios. The Butte Creek spring-run Chinook population is predicted to
1644 have consistently higher realized survival under the OCAP 9.2 climate change forecast,
1645 which represents a slightly slower rate of warming paired with increased precipitation (Fig.
1646 II.3). Conversely, both the spring-run Deer Creek and fall-run Sacramento mainstem wild-
1647 spawning populations show slightly, but consistently, higher survival under the OCAP 9.2
1648 climate change trajectory which describes a greater increase in temperature paired with lower
1649 levels of future precipitation (Table II.1).
1650



1651

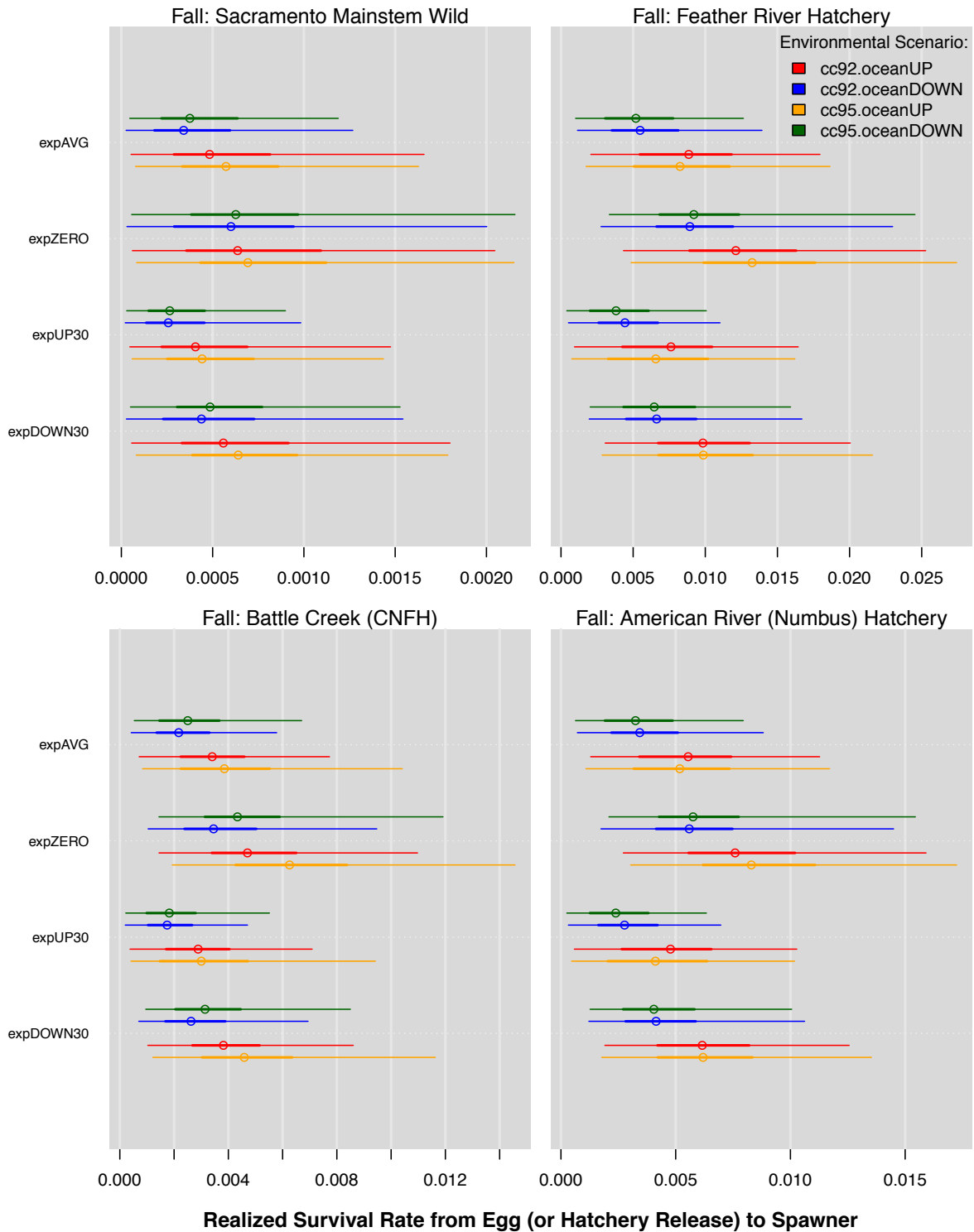
1652

1653

1654

1655

Figure II.3. Caterpillar plots describing the predicted distribution of realized survival to return, across years and simulations, for spring-run Chinook populations. The circle, thick line, and thin line describe the median, 50% credible interval and 95% credible interval for the predictions.



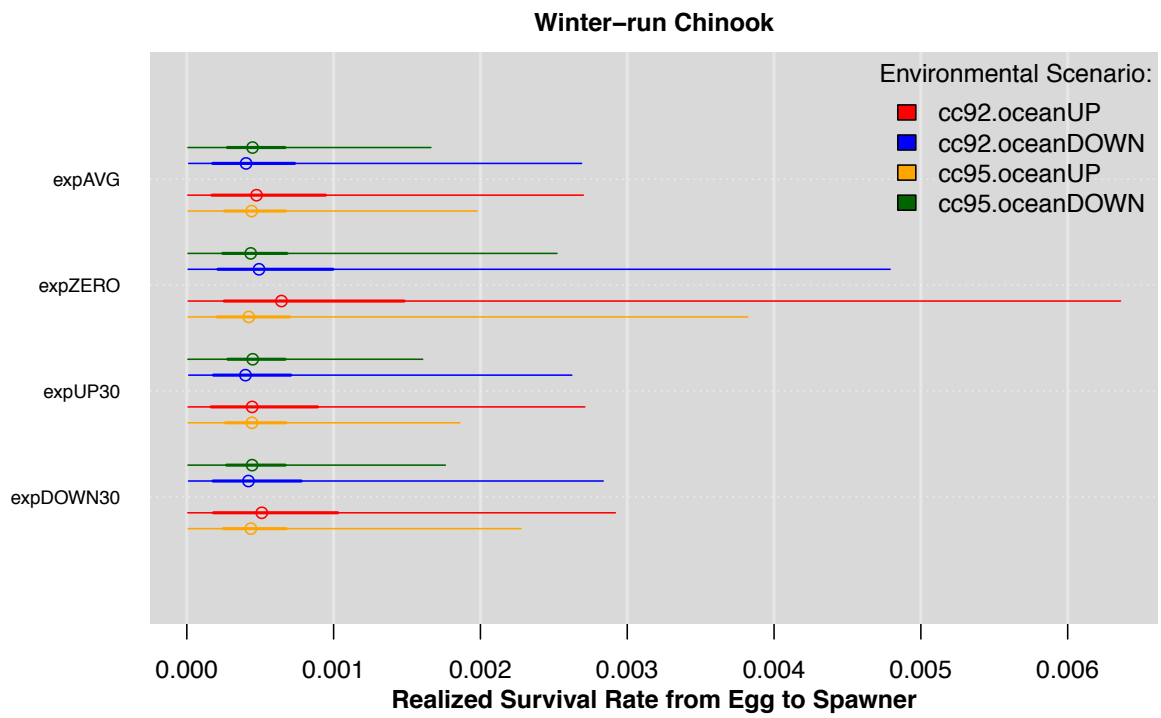
1656

1657 **Figure II.4. Caterpillar plots describing the predicted distribution of realized survival to return, across**
 1658 **years and simulations, for four fall-run Chinook populations. The circle, thick line, and thin line describe**
 1659 **the median, 50% credible interval and 95% credible interval for the predictions.**

1660

1661

1662



1663

1664 **Figure II.5. Caterpillar plots describing the predicted distribution of realized survival to return, across**
 1665 **years and simulations, for winter run Chinook populations. The circle, thick line, and thin line describe**
 1666 **the median, 50% credible interval and 95% credible interval for the predictions.**

1667

1668

1669

Population	Export Scenario	cc92.oceanUP	cc92.oceanDOWN	cc95.oceanUP	cc95.oceanDOWN
Fall: Sacramento Mainstem Wild	expAVG	0.060%	0.043%	0.064%	0.046%
	expZERO	0.077%	0.068%	0.083%	0.074%
	expUP30	0.050%	0.033%	0.053%	0.033%
	expDOWN30	0.067%	0.052%	0.072%	0.058%
Fall: Battle Creek (CNFH)	expAVG	0.355%	0.245%	0.420%	0.274%
	expZERO	0.513%	0.394%	0.665%	0.484%
	expUP30	0.303%	0.195%	0.342%	0.205%
	expDOWN30	0.406%	0.295%	0.500%	0.346%
Fall: Feather River Hatchery	expAVG	0.894%	0.605%	0.867%	0.562%
	expZERO	1.292%	0.983%	1.411%	1.026%
	expUP30	0.764%	0.483%	0.700%	0.420%
	expDOWN30	1.019%	0.731%	1.040%	0.713%
Fall: American River (Nimbus) Hatchery	expAVG	0.560%	0.380%	0.543%	0.352%
	expZERO	0.810%	0.617%	0.885%	0.643%
	expUP30	0.479%	0.303%	0.439%	0.263%
	expDOWN30	0.639%	0.459%	0.652%	0.447%
Spring: Deer Creek	expAVG	0.047%	0.052%	0.059%	0.065%
	expZERO	0.083%	0.090%	0.089%	0.095%
	expUP30	0.023%	0.025%	0.031%	0.033%
	expDOWN30	0.069%	0.075%	0.077%	0.082%
Spring: Mill Creek	expAVG	0.050%	0.058%	0.064%	0.071%
	expZERO	0.092%	0.100%	0.098%	0.105%
	expUP30	0.024%	0.027%	0.033%	0.036%
	expDOWN30	0.075%	0.084%	0.085%	0.092%
Spring: Butte Creek	expAVG	0.077%	0.092%	0.051%	0.058%
	expZERO	0.122%	0.136%	0.068%	0.074%
	expUP30	0.041%	0.049%	0.031%	0.034%
	expDOWN30	0.106%	0.121%	0.062%	0.069%
Winter-run Chinook	expAVG	0.069%	0.061%	0.059%	0.055%
	expZERO	0.133%	0.098%	0.085%	0.070%
	expUP30	0.067%	0.060%	0.058%	0.055%
	expDOWN30	0.076%	0.064%	0.062%	0.056%

1670

1671

1672

1673

1674

Table II.1. Median of simulations for the predicted percent realized survival from egg or hatchery release to spawning adult, across water export and future environmental scenarios. Matrix of scenario-specific realized survival predictions for each population are shaded from red (low) to green (high) for ease of interpretation.

1675

Population	Export Scenario	cc92.oceanUP	cc92.oceanDOWN	cc95.oceanUP	cc95.oceanDOWN
Fall: Sacramento Mainstem Wild	expZERO	30%	59%	28%	62%
	expUP30	-16%	-23%	-18%	-28%
	expDOWN30	12%	23%	12%	26%
Fall: Battle Creek (CNFH)	expZERO	44%	61%	58%	77%
	expUP30	-15%	-20%	-18%	-25%
	expDOWN30	14%	21%	19%	26%
Fall: Feather River Hatchery	expZERO	45%	62%	63%	83%
	expUP30	-14%	-20%	-19%	-25%
	expDOWN30	14%	21%	20%	27%
Fall: American River (Nimbus) Hatchery	expZERO	45%	63%	63%	83%
	expUP30	-15%	-20%	-19%	-25%
	expDOWN30	14%	21%	20%	27%
Spring: Deer Creek	expZERO	79%	72%	50%	46%
	expUP30	-50%	-52%	-47%	-49%
	expDOWN30	48%	44%	29%	27%
Spring: Mill Creek	expZERO	85%	74%	53%	47%
	expUP30	-51%	-53%	-49%	-50%
	expDOWN30	51%	46%	32%	29%
Spring: Butte Creek	expZERO	59%	47%	32%	27%
	expUP30	-46%	-47%	-39%	-41%
	expDOWN30	38%	31%	21%	19%
Winter-run Chinook	expZERO	91%	60%	44%	28%
	expUP30	-3%	-2%	-1%	0%
	expDOWN30	9%	5%	5%	3%

1676

1677

1678

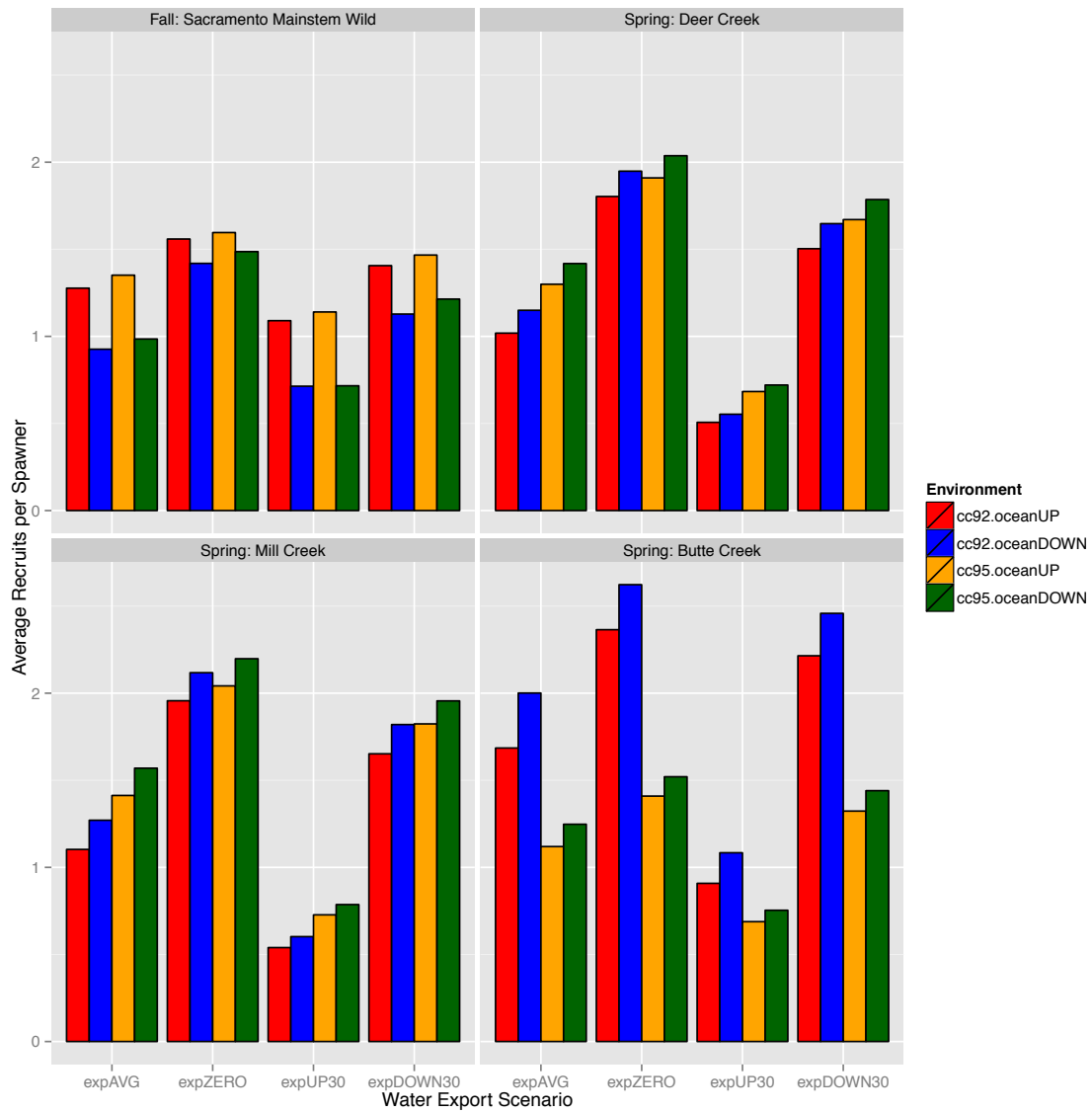
1679

Table II.2. Percent difference in median realized survival from average export (expAVG) scenario, across environmental scenarios. Values shaded from red (low) to green (high) for ease of interpretation.

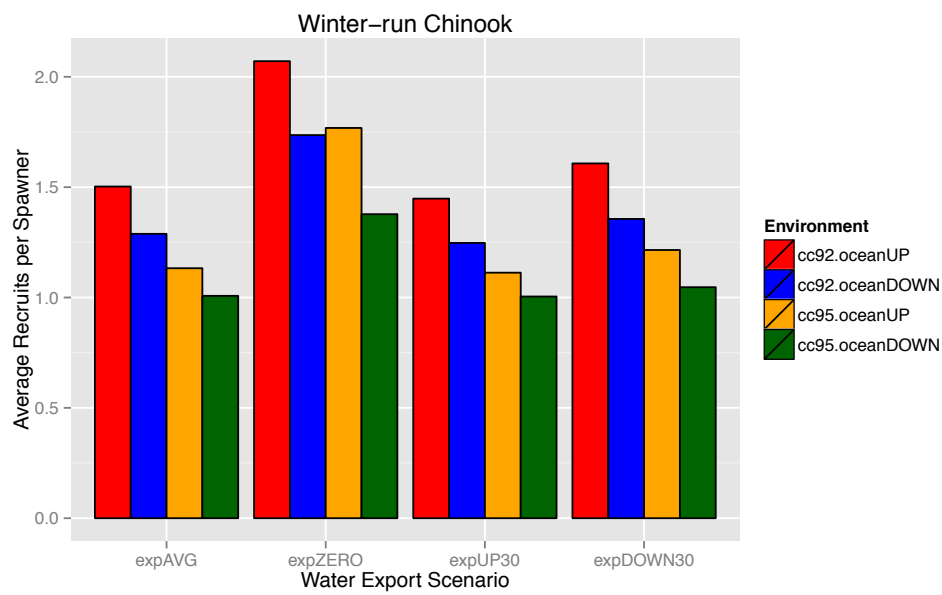
1680 In addition to estimates for future realized survival rates, for wild-spawning
1681 populations the average productivity of populations across years and replicate scenarios was
1682 also evaluated. Figure II.6, displays the average number of recruits per spawner for the
1683 Sacramento mainstem wild-spawning fall-run Chinook population, and the Deer, Mill, and
1684 Butte Creek spring-run populations and winter run, under alternative water export scenarios
1685 and environmental conditions. Scenarios that predict average productivity of less than 1
1686 recruit-per-spawner, indicate that those populations are unlikely to remain viable in the future
1687 and will tend toward extinction in the presence of environmental stochasticity. Forward
1688 simulation results for the mainstem Sacramento fall-run Chinook population indicate that
1689 under the average (expAVG) and 30% increase (expUP30) water export scenarios, average
1690 productivity in the face unfavorable ocean conditions producing a 20% reduction in future
1691 upwelling (oceanDOWN) is expected to be less than one recruit-per-spawner (Fig. II.6).
1692 However, under both of these future export scenarios average recruits-per-spawner is
1693 expected to expected to exceed one under favorable future ocean conditions (oceanUP).

1694 Predicted future realized productivity (recruits-per-spawner) for the Deer, Mill, and
1695 Butte Creek spring-run populations is predicted to be significantly lower under the scenario
1696 representing a 30% increase in future exports (expUP30). For both the Deer Creek and Mill
1697 Creek populations, average realized productivity (recruits-per-spawner) is predicted to be less
1698 than one with a 30% increase in water exports (expUP30), across all four combinations of
1699 future climate change and marine conditions (Fig. II.6). Predictions for future productivity of
1700 the Butte Creek population indicate that with the more gradual climate warming and greater
1701 future precipitation under the OCAP 9.2 scenario indicate that even with a 30% increase in
1702 water exports (expUP30) the population may be expected to produce at or near 1 recruit-per-
1703 spawner, and therefore remain viable.

1704 Average future productivity (recruits-per-spawner) is expected to be highest across
1705 environmental scenarios under the zero export (expZERO) and 30% reduction in future
1706 exports (expDOWN30). However, realized productivity is predicted to vary across
1707 populations in response to future climate change and ocean production scenarios. For the
1708 mainstem Sacramento wild-spawning fall-run population, future productivity in the face of
1709 positive ocean conditions and specifically increased nearshore upwelling (oceanUP) is
1710 predicted to be highest and exceed one recruit-per-spawner, independent of the climate
1711 change or export scenario. The form of future climate change is predicted to have the greatest
1712 impact on the Butte Creek spring-run Chinook population, with higher productivity, in terms
1713 of recruits-per-spawner, under the OCAP 9.2 scenario (Fig. II.6). This results from the fact
1714 that this population was found to be particularly sensitive to summertime temperatures, which
1715 are predicted to increase more precipitously under the OCAP 9.5 climate change scenario
1716 leading to reduced over-summer survival of adults holding prior to spawning. Spring run
1717 stocks are much more sensitive to exports than fall and winter run, but both fall and winter do
1718 see slight improvement under export restrictions.
1719



1720



1721

1722
1723

Figure II.6. Average number of realized recruits per spawner, across populations, environmental and export scenarios

1724 *PART II DISCUSSION*

1725 Results from a Bayesian population dynamics model estimating the stage and
1726 population specific maximum survival rates and changes in survival in response to natural
1727 and anthropogenic environmental covariates were used to parameterize simulations for future
1728 trends in population-specific abundance under alternative water export, climate change, and
1729 ocean production scenarios. Both estimation and process uncertainty were incorporated into
1730 future predictions by, first sampling model parameter values from the joint posterior, and
1731 second incorporating stochastic process deviations into the first modeled life-stage. One
1732 thousand replicate simulations of the 50-year future time series were used to fully quantify
1733 the influence of these two sources of uncertainty. The likely impact from future ocean harvest
1734 of Chinook was incorporated by simultaneously modeling the future trends in abundance for
1735 winter-run Chinook in the Sacramento system and replicating the current fishery management
1736 decision rules. We did not explore the impacts of modifying the harvest regime, but
1737 obviously any change in the fraction of fish harvested would have an analogous impact to
1738 increasing survival via changing exports or other environmental factors.

1739 Results from these forward simulations in the form of estimates for future realized
1740 survival rates from egg, or hatchery release, to spawning adult, and estimates for realized
1741 productivity (recruits-per-spawner) indicate that while all populations are sensitive to
1742 differences in future water exports from the Sacramento-San Joaquin Delta, differences in the
1743 future environment are likely to have substantial population-specific impacts. The
1744 observation that predicted realized survival and productivity are generally higher for the fall-
1745 run populations and equal or lower for the spring-run populations under the oceanUP
1746 scenario results from several characteristics of the forward simulation model. The oceanUP
1747 scenario represents a 10% increase in future nearshore upwelling, paired with a smaller
1748 increase in future water temperatures at the Farallon Islands. While nearshore upwelling was
1749 found by the estimation model to significantly increase survival in the nearshore region for
1750 fall-run Chinook populations, this covariate was not AICc-selected for the spring-run
1751 populations. As a result, predictions for future realized survival for the fall-run Chinook
1752 populations show as consistently higher survival and productivity patterns in response to the
1753 oceanUP scenario. This prediction for higher realized survival for fall-run Chinook
1754 populations agrees with insights by Lindley et al. (2009) pointing to unusually low nearshore
1755 upwelling patterns as one of the proximate causes of the failure of the 2004 – 2005 fall-run
1756 brood years. In addition, the grouped survival of all seven Chinook populations was found to
1757 have a positive relationship with the Pacific Decadal Oscillation. The oceanUP scenario
1758 described an initial negative PDO phase, followed by a positive PDO phase, resulting in
1759 lower marine survival initially followed by higher marine survival in later years for the
1760 populations. The opposite pattern in marine survival was observed for the seven Chinook
1761 populations under the oceanDOWN scenario in response to the PDO pattern simulated in the
1762 opposite direction.

1763 Future climate change scenarios had mixed impacts across populations as a result of
1764 the estimated response by populations to the environmental covariates impacted by the OCAP
1765 9.2 and 9.5 predictions. The cooler and wetter OCAP 9.2 scenario had a particularly strong
1766 influence on the Butte Creek population, because a strong negative influence of high
1767 summertime temperatures was predicted for this population. However, the increase in water
1768 flow associated with the OCAP 9.2 scenario resulted in increased sediment concentration at
1769 Freeport, CA. Given the negative relationship between sediment concentration at this location

1770 and survival for both fall and spring-run Chinook, this aspect of the OCAP 9.2 scenario did
1771 result in some reduction in survival for all populations, although in some cases this effect was
1772 outweighed by the interaction with temperature.

1773 Across all combinations of future export and environmental scenarios predictions for
1774 both realized survival and productivity (recruits-per-spawner) were highly variable. While we
1775 have focused on predicted differences in median survival and average productivity, the 95%
1776 credible intervals for these predictions overlap in almost all cases. This indicates that the
1777 combination of both estimation and process uncertainty introduced in the forward simulation
1778 process leads to significant variability in future abundance and our quantified metrics. This is
1779 particularly pronounced in future predictions of realized survival for the Butte Creek
1780 population, which are extremely right skewed (Fig. II.3).

1781 Quantifying results of forward simulations for wild-spawning Chinook populations in
1782 terms of average productivity (recruits-per-spawner) provided an efficient means for
1783 determining under what water export scenarios and environmental conditions specific
1784 populations are expected to persist (recruits-per-spawner > 1), or decline toward extinction
1785 (Fig. II.5). For several of the populations under the 30% increase in future water export
1786 scenario (expUP30), and for the fall-run mainstem Sacramento wild-spawning population
1787 under the average export scenario paired with decreased future upwelling (oceanDOWN),
1788 average productivity was predicted at less than one. While this result suggests that under
1789 those conditions specific populations may be expected to decline in abundance, it is important
1790 to fully understand the assumptions involved in this prediction. First, the forward simulations
1791 assume that future fishing mortality rates will vary in accordance with current management
1792 practices, as influenced by the Sacramento Index and harvest limitations based upon the
1793 abundance of winter-run Chinook. A reduction in future fishing mortality rate may be
1794 sufficient to increase the productivity of these populations above 1 recruit-per-spawner and
1795 facilitate persistence. Second, predictions for future productivity do not account for the stray
1796 rates amongst hatchery and wild populations leading to source-sink dynamics (Johnson et al.
1797 2012). These effects may be most important for the Sacramento mainstem wild-spawning
1798 fall-run Chinook population, which was found in 2010 and 2011 to have 20 – 27% of its
1799 observed spawning abundance resulting from hatchery-reared strays (Kormos et al. 2012,
1800 Palmer-Zwahlen and Kormos 2013). Whether the contribution of straying individuals may be
1801 enough to facilitate persistence of populations under environmental and export scenarios that
1802 are predicted by these analysis to lead to decline (recruits-per-spawner < 1), remains
1803 unknown.

1804

1805 **REFERENCES**

- 1806 Battin, J., M. W. Wiley, M. H. Ruckelshaus, R. N. Palmer, E. Korb, K. K. Bartz, and H. Imaki.
1807 2007. Projected impacts of climate change on salmon habitat restoration. Proc
1808 Natl Acad Sci U S A **104**:6720-6725.
- 1809 Beverton, R. J. H., and S. J. Holt. 1957. On the dynamics of exploited fish populations.
- 1810 Brooks, S. P., and A. Gelman. 1998. General methods for monitoring convergence of
1811 iterative simulations. Journal of Computational and Graphical Statistics **7**:434-
1812 455.
- 1813 Burnham, K. P., and D. R. Anderson. 2002. Model selection and multimodel inference : a
1814 practical information-theoretic approach. 2nd edition. Springer, New York.
- 1815 CDF&W. 2014. GrandTab 2014.04.22: California Central Valley Chinook population
1816 report. California Department of Fish and Wildlife.
- 1817 CDWR. 2014. DAYFLOW Data.*in* C. D. o. W. Resources, editor.
- 1818 Claiborne, A. M., J. P. Fisher, S. A. Hayes, and R. L. Emmett. 2011. Size at release, size-
1819 selective mortality, and age of maturity of Willamette River Hatchery yearling
1820 Chinook salmon. Transactions of the American Fisheries Society **140**:1135-1144.
- 1821 Ewing, R. D., and G. S. Ewing. 2002. Bimodal length distributions of cultured chinook
1822 salmon and the relationship of length modes to adult survival. Aquaculture
1823 **209**:139-155.
- 1824 Fournier, D. A., H. J. Skaug, J. Ancheta, J. Ianelli, A. Magnusson, M. N. Maunder, A. Nielsen,
1825 and J. Sibert. 2012. AD Model Builder: using automatic differentiation for
1826 statistical inference of highly parameterized complex nonlinear models.
1827 Optimization Methods and Software **27**:233-249.
- 1828 Gelman, A., J. B. Carlin, H. S. Stern, and D. B. Rubin. 2004. Bayesian data analysis. 2nd
1829 edition. Chapman & Hall/CRC, Boca Raton, Fla.
- 1830 Gelman, A., and D. B. Rubin. 1992. Inference from iterative simulation using multiple
1831 sequences. Statistical Science **7**:457-511.
- 1832 Hare, S. R., N. J. Mantua, and R. C. Francis. 1999. Inverse production regimes: Alaska and
1833 West Coast Pacific salmon. Fisheries **24**:6-14.
- 1834 Hendrix, N., E. Danner, C. M. Greene, H. Imaki, and S. T. Lindley. 2014. Life cycle
1835 modeling framework for Sacramento River Winter-run Chinook salmon. NOAA
1836 Technical Memorandum.
- 1837 Hilborn, R., and M. Mangel. 1997. The ecological detective: confronting models with
1838 data. Princeton University Press, Princeton, NJ.

- 1839 Honea, J. M., J. C. Jorgensen, M. M. McClure, T. D. Cooney, K. Engie, D. M. Holzer, and R.
1840 Hilborn. 2009. Evaluating habitat effects on population status: influence of
1841 habitat restoration on spring-run Chinook salmon. *Freshwater Biology* **54**:1576-
1842 1592.
- 1843 Huber, E. R., and S. M. Carlson. in review. Temporal trends of California Central Valley
1844 fall run Chinook salmon hatchery release practices.
- 1845 Johnson, R. C., P. K. Weber, J. D. Wikert, M. L. Workman, R. B. MacFarlane, M. J. Grove,
1846 and A. K. Schmitt. 2012. Managed metapopulations: do salmon hatchery 'sources'
1847 lead to in-river 'sinks' in conservation? *PLoS ONE* **7**:e28880.
- 1848 King, R., B. Morgan, O. Gimenez, and S. Brooks. 2010. Bayesian analysis for population
1849 ecology. CRC Press.
- 1850 Kocan, R., P. Hershberger, G. Sanders, and J. Winton. 2009. Effects of temperature on
1851 disease progression and swimming stamina in Ichthyophonus-infected rainbow
1852 trout, *Oncorhynchus mykiss* (Walbaum). *Journal of Fish Diseases* **32**:835-843.
- 1853 Kormos, B., M. Palmer-Zwahlen, and A. Low. 2012. Recover of coded-wire tags from
1854 Chinook salmon in California's Central Valley escapement and ocean harvest
1855 2010. California Department of Fish and Game, Sacramento, California.
- 1856 Lindley, S. T., C. B. Grimes, M. S. Mohr, W. Peterson, J. Stein, J. T. Anderson, L. W.
1857 Botsford, D. L. Bottom, C. A. Busack, T. K. Collier, J. Ferguson, J. C. Garza, A. M.
1858 Grover, D. G. Hankin, R. G. Kope, P. W. Lawson, A. Low, R. B. Macfarlane, K. Moore,
1859 M. Palmer-Zwahlen, F. B. Schwing, J. Smith, C. Tracy, R. Webb, B. K. Wells, and T.
1860 H. Williams. 2009. What caused the Sacramento River fall Chinook stock
1861 collapse?
- 1862 Lindley, S. T., and M. S. Mohr. 2003. Modeling the effect of striped bass (*Morone saxatilis*)
1863 on the population viability of Sacramento River winter-run chinook salmon
1864 (*Oncorhynchus tshawytscha*). *FISHERY BULLETIN* **101**:321-331.
- 1865 Macias, D., P. J. S. Franks, M. D. Ohman, and M. R. Landry. 2012. Modeling the effects of
1866 coastal wind- and wind-stress curl-driven upwellings on plankton dynamics in
1867 the Southern California current system. *Journal of Marine Systems* **94**:107-119.
- 1868 Mantua, N. J., and S. R. Hare. 2002. The Pacific decadal oscillation. *Journal of*
1869 *Oceanography* **58**:35-44.
- 1870 Moussalli, E., and R. Hilborn. 1986. Optimal Stock Size and Harvest Rate in Multistage
1871 Life-History Models. *Canadian Journal of Fisheries and Aquatic Sciences* **43**:135-
1872 141.
- 1873 Myrick, C. A., and J. J. Chech. 1998. Temperature effects on Chinook salmon and
1874 Steelhead: a review focusing on California's Central Valley populations. *Bay-Delta*
1875 *Modeling Forum*.

- 1876 Neuswanger, J., M. S. Wipfli, A. E. Rosenberger, and N. F. Hughes. 2014. Mechanisms of
1877 drift-feeding behavior in juvenile Chinook salmon and the role of inedible debris
1878 in a clear-water Alaskan stream. *Environmental Biology of Fishes* **97**:489-503.
- 1879 Newman, K. B., and P. L. Brandes. 2010. Hierarchical Modeling of Juvenile Chinook
1880 Salmon Survival as a Function of Sacramento-San Joaquin Delta Water Exports.
1881 *North American Journal of Fisheries Management* **30**:157-169.
- 1882 Newman, K. B., and J. Rice. 2002. Modeling the survival of Chinook salmon smolts out-
1883 migrating through the lower Sacramento River system. *Journal of the American*
1884 *Statistical Association* **97**:983-993.
- 1885 Palmer-Zwahlen, M., and B. Kormos. 2013. Recovery of coded-wire tags from Chinook
1886 salmon in California's Central Valley escapement and ocean harvest in 2011.
1887 California Department of Fish and Wildlife, Sacramento, California.
- 1888 Perry, R. W., J. R. Skalski, P. L. Brandes, P. T. Sandstrom, A. P. Klimley, A. Ammann, and B.
1889 MacFarlane. 2010. Estimating survival and migration route probabilities of
1890 juvenile Chinook salmon in the Sacramento-San Joaquin River Delta. *North*
1891 *American Journal of Fisheries Management* **30**:142-156.
- 1892 Poytress, W. R., J. J. Gruber, F. D. Carrillo, and S. D. Voss. 2014. Compendium report of
1893 Red Bluff Diversion Dam rotary trap juvenile anadromous fish production
1894 indices for years 2002-2012. Report of U.S. Fish and Wildlife Service to California
1895 Department of Fish and Wildlife and US Bureau of Reclamation.
- 1896 Scheuerell, M. D., R. Hilborn, M. H. Ruckelshaus, K. K. Bartz, K. M. Lagueux, A. D. Haas,
1897 and K. Rawson. 2006. The Shiraz model: a tool for incorporating anthropogenic
1898 effects and fish-habitat relationships in conservation planning. *Canadian Journal*
1899 *of Fisheries and Aquatic Sciences* **63**:1596-1607.
- 1900 Sogard, S. M. 1997. Size-selective mortality in the juvenile stage of teleost fishes: A
1901 review. *Bulletin of Marine Science* **60**:1129-1157.
- 1902 Stevens, D. E., and L. W. Miller. 1983. Effects of river flow on abundance of young
1903 Chinook salmon, American Shad, Longfin Smelt, and Delta Smelt in the
1904 Sacramento-San Joaquin River system. *North American Journal of Fisheries*
1905 *Management* **3**:425-437.
- 1906 Tompkins, M. R. 2006. Floodplain connectivity and river corridor complexity:
1907 Implications for river restoration and planning for floodplain management.
1908 University of California, Berkeley.
- 1909 USBR. 2008. Central Valley Project and State Water Project Operations Criteria and Plan
1910 Biological Assessment. U.S. Department of the Interior, Bureau of Reclamation,
1911 Mid-Pacific Region, Sacramento, California.
- 1912 Ward, P. D., T. R. McReynolds, and C. E. Garman. 2003. Butte Creek spring-run Chinook
1913 salmon, *Oncorhynchus tshawytscha* pre-spawn mortality evaluation, 2003.
1914 California Department of Fish and Game, Chico, California.

- 1915 Wells, B. K., J. C. Field, J. A. Thayer, C. B. Grimes, S. J. Bograd, W. J. Sydeman, F. B. Schwing,
 1916 and R. Hewitt. 2008. Untangling the relationships among climate, prey and top
 1917 predators in an ocean ecosystem. *Marine Ecology-Progress Series* **364**:15-29.
- 1918 Wells, B. K., C. B. Grimes, J. C. Field, and C. S. Reiss. 2006. Covariation between the
 1919 average lengths of mature coho (*Oncorhynchus kisutch*) and Chinook salmon (*O.*
 1920 *tshawytscha*) and the ocean environment. *Fisheries Oceanography* **15**:67-79.
- 1921 Wells, B. K., C. B. Grimes, and J. B. Waldvogel. 2007. Quantifying the effects of wind,
 1922 upwelling, curl, sea surface temperature and sea level height on growth and
 1923 maturation of a California Chinook salmon (*Oncorhynchus tshawytscha*)
 1924 population. *Fisheries Oceanography* **16**:363-382.
- 1925 Williams, J. G. 2006. Central valley salmon: a perspective on Chinook and steelhead in
 1926 the Central Valley of California. *San Francisco Estuary & Watershed Science* **4**.
- 1927 Zar, J. H. 2010. *Biostatistical analysis*. 5th edition. Prentice-Hall/Pearson, Upper Saddle
 1928 River, N.J.
- 1929 Zeug, S. C., P. S. Bergman, B. J. Cavallo, and K. S. Jones. 2012. Application of a Life Cycle
 1930 Simulation Model to Evaluate Impacts of Water Management and Conservation
 1931 Actions on an Endangered Population of Chinook Salmon. *Environmental*
 1932 *Modeling & Assessment* **17**:455-467.
- 1933
- 1934

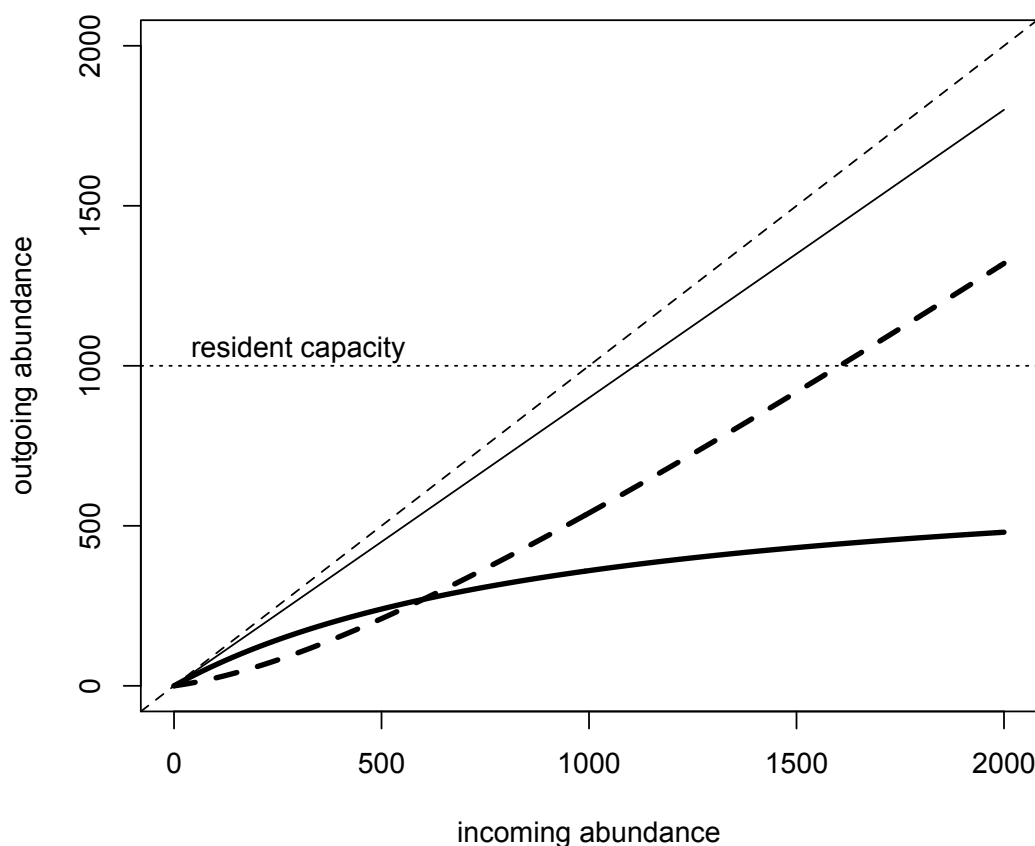
1935 **APPENDIX A LINKAGES TO THE CENTRAL VALLEY LIFE CYCLE MODEL**

1936 *BACKGROUND*

1937 The National Marine Fisheries Service (NMFS) Southwest Fisheries Science Center
 1938 (SWFSC) initiated a project to develop life-cycle models of salmon populations in the
 1939 Central Valley. The project objective is to build a framework to quantitatively evaluate how
 1940 the management and operation of the Federal Central Valley Project (CVP) and California
 1941 State Water Project (SWP) affect Central Valley salmon populations. The modeling
 1942 framework will evaluate the current operations of the CVP and SWP, i.e., Operational Plan
 1943 and Criteria (OCAP), and evaluate future water conveyance structures as proposed in the Bay
 1944 Delta Conservation Plan (BDCP). The NMFS Central Valley Life Cycle Model (CVCLCM)
 1945 targeted winter-run as the first race of Chinook for model development (Hendrix et al. 2014).

1946 The CVCLCM framework is a stage-structured model. Stages in the model were
 1947 based on developmental state as well as geographic location (e.g., smolts in the delta, smolts
 1948 in the mainstem river, or smolts in a floodplain). State transitions among life-history stages
 1949 are defined by a modified Beverton-Holt (Beverton 1957) that allows individuals exceeding
 1950 the capacity of a habitat to move to a different geographic location rather than die in that
 1951 habitat (Greene and Beechie 2004). The Beverton-Holt with movement function is defined
 1952 by a survival rate, capacity, and movement rate (Figure A.1). Each of these parameters can
 1953 be modeled as a function of environmental or anthropogenic factors that may be influenced
 1954 by management (e.g., spatial extent of floodplain habitat as it affects capacity) and
 1955 operational actions (e.g., flow as it affects movement or water temperature as it affects
 1956 survival).

1957 Capacity estimates for the river and delta habitats from the CVCLCM were used in
 1958 the current fall-run and spring-run model. In addition, there are several products from the
 1959 current model that will be useful to the CVCLCM, which is developing fall-run and spring-
 1960 run life cycle models.



1961
 1962 **Figure A.1. Beverton-Holt with movement transition function. Outgoing abundance**
 1963 **(thin solid line) is composed of migrants (thick dashed line) and residents (thick solid**
 1964 **line), which are affected by the resident capacity (dotted horizontal line). Those fish**
 1965 **that are not residents leave as migrants. The 1:1 line (thin dashed) is also plotted for**
 1966 **reference.**

1967

1968 *PRODUCTS FROM THE CVCLCM USED IN THE FALL-RUN AND SPRING-RUN MODEL*

1969 *Capacities*

1970 The CVCLCM developed estimates of monthly capacities for use in the Beverton-
 1971 Holt transition function. The capacities were estimated in four habitats/geographic areas: 1)
 1972 Sacramento River from headwaters to the city of Sacramento (river), 2) Yolo bypass
 1973 (floodplain), 3) delta (city of Sacramento to Chipps Island) and 4) Chipps Island to the
 1974 Golden Gate Bridge (bay). Two of these areas were used in the current fall-run and spring-
 1975 run life-cycle model. The Sacramento River monthly capacity estimates were used for the
 1976 Sacramento River mainstem spawning fall-run population in Stage 1 and the delta capacity
 1977 estimates were used in fall-run (average delta capacity March to May) and spring-run
 1978 (average delta capacity February to April) capacities for Stage 2.

1979 Capacities for the river, floodplain, delta, and bay habitats were calculated in the
 1980 CVCLCM as a function of habitat-specific capacity models (Hendrix et al. 2014). We
 1981 provide details on the river and delta calculations and habitat capacity estimates, because they
 1982 were included in the fall-run and spring-run model. In particular, the calculation of River
 1983 capacity was modified since the publishing of the methods in Hendrix et al. (2014).
 1984 Although the initial model development in the CVCLCM was focused on winter-run, the
 1985 estimates of capacity are applicable to all races of Chinook in the Central Valley.

1986 ***River Capacities***

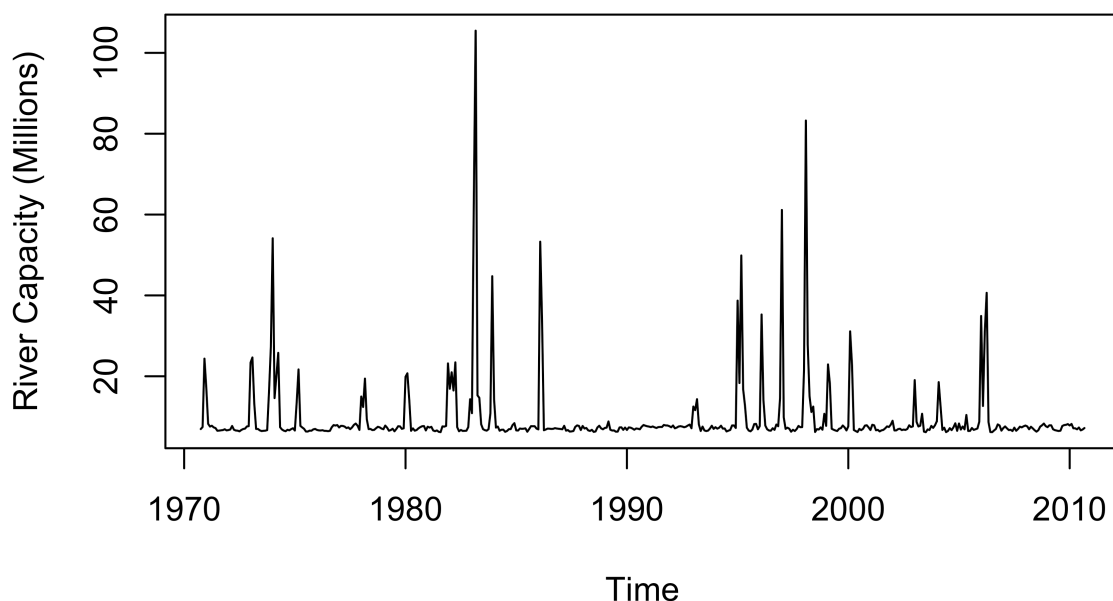
1987 The River capacities were defined as a function of velocity and depth. For each
 1988 variable preferred versus not-preferred categories were defined (Table A.1). The possible
 1989 combinations of the 2 levels of 2 variables provided 4 categories of habitat quality for rearing
 1990 Chinook salmon. The Central Valley is primarily a hatchery-dominated system with fish
 1991 released at smolt size for rapid migration to the ocean, and natural stocks are at historically
 1992 low levels; therefore, current estimates of fish density from the Central Valley may not be
 1993 indicative of densities at capacity. As a result, densities from the Skagit River, WA were
 1994 used to inform the maximum density estimates for each category (Greene et al. 2005). Two
 1995 densities were used to calculate capacities: the 90th percentile and the 95th percentile of the
 1996 distribution of densities by habitat category in the Skagit River.

1997

1998 **Table A.1. Habitat variables used to define the River capacity.**

Variable	Preferred or Not-preferred	Range
Velocity	Preferred	≤ 0.15 m/s
	Not preferred	> 0.15 m/s
Depth	Preferred	> 0.2 m and ≤ 1 m
	Not preferred	≤ 0.2 m or > 1 m

1999 Areas of habitat under each of the 4 categories were calculated by running the HEC-
 2000 RAS model on a series of Sacramento River cross-sections that define cells. Each cell in the
 2001 cross-section has a depth and velocity, and altering the flow changes the depth and velocity of
 2002 a particular cell. The area of each cell that corresponded to a specific combination of
 2003 velocity and depth category was tabulated for each monthly flow associated with a cross-
 2004 section. The appropriate density of Chinook salmon for each of the 4 categories was applied
 2005 to arrive at a density estimate for the Sacramento River in each month (Figure A.2).

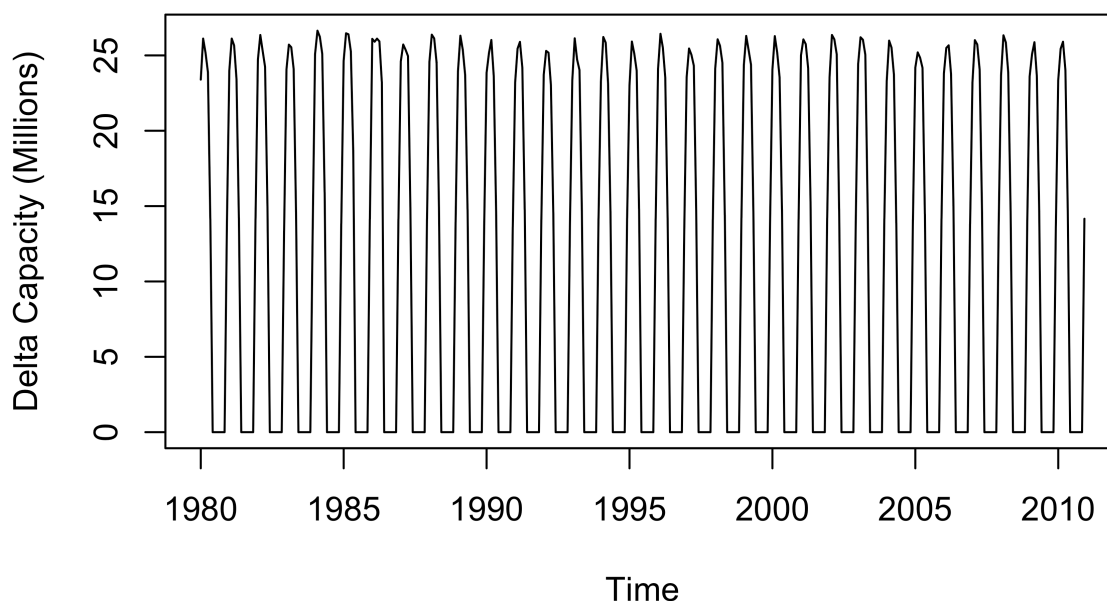


2006
2007
2008
2009

Figure A.2. Monthly capacity of Chinook salmon in the Sacramento River using a 90th percentile estimate of fish density.

2010 *Delta Capacities*

2011 The monthly capacities in the delta were defined as a function of several habitat
2012 attributes including: channel type, cover, shoreline type, blind channel area, salinity and
2013 vegetated cover along riverbanks. Analysis was conducted by using Geographic Information
2014 System (GIS) data layers. Habitat quality was determined by defining binary High/Low
2015 ranges for each axis of habitat quality, similar to the Preferred and Not-preferred approach
2016 used in the river habitat. In the delta, 8 categories of habitat quality were defined, each with
2017 an associated maximum density. Because not all habitats are accessible by rearing Chinook,
2018 a subsequent analysis was conducted to restrict habitat areas based on connectivity. Using
2019 beach seine data collected by US Fish and Wildlife Service (Speegle et al. 2013), a
2020 generalized linear model was used to estimate the probability of juvenile habitat use by
2021 seining location. This model was subsequently used to restrict habitat use by juvenile
2022 salmonids throughout the delta. Monthly estimates of capacity in the delta reflected the
2023 restricted access to particular areas of the delta and the seasonal absence of juvenile
2024 salmonids during the summer months (Figure A.3). Additional details on the capacity
2025 calculations can be found in Hendrix et al. (2014).



2026
2027 **Figure A.3. Monthly capacities of Chinook salmon in the delta using a 90th percentile**
2028 **estimate of fish density.**

2029 *PRODUCTS FROM THE FALL-RUN AND SPRING-RUN MODEL THAT COULD BENEFIT THE*
2030 *CVCLCM*

2031 In the current project, we are using a model for fall and spring-run that incorporates
2032 competition through density dependence via a Beverton-Holt transition. This interaction
2033 effectively removes some capacity for each of the interacting races. Initial model evaluations
2034 indicated that an external capacity value improves the ability to estimate an interaction effect
2035 e.g., between fall-run and spring-run or between hatchery and natural. Although the
2036 Beverton-Holt function in the CVCLCM incorporates a movement component, understanding
2037 the importance of both of these interactions is important in the context of the CVCLCM
2038 models for fall-run and spring-run Chinook.

2039 The NMFS scientists developing the fall-run and spring-run CVCLCM models will
2040 benefit from interacting with the current fall-run and spring-run model. The current model
2041 uses the CVCLCM capacities for certain stages, but these can also be modeled as functions of
2042 covariates to allow further hypothesis evaluation. In addition, the time series of observations
2043 is greater for the current model than the CVCLCM, which is restricted to 1980 to 2010. Thus
2044 earlier escapement data can be used to help parameterize the CVCLCM. Finally, the speed
2045 with which alternative hypotheses can be developed and fit to the fall-run and spring-run
2046 escapement data provides a useful tool for model construction in the CVCLCM. Hypotheses
2047 can be developed and tested on the order of minutes to hours, whereas running the full
2048 CVCLCM under a new set of environmental drivers can take on the order of days.

2049 *REFERENCES*

- 2050 Beverton, R. J. H., and S. J. Holt. 1957. On the dynamics of exploited fish populations.
- 2051 Greene, C. M. and T. J. Beechie. 2004. Consequences of potential density-dependent
2052 mechanisms on recovery of ocean-type Chinook salmon (*Oncorhynchus*
2053 *tshawytscha*). Canadian Journal of Fisheries and Aquatic Sciences 61(4):590-602.
- 2054 Greene, C. M., D. W. Jensen, G. R. Pess, E. A. Steel, and E. Beamer. 2005. Effects of
2055 environmental conditions during stream, estuary, and ocean residency on Chinook
2056 salmon return rates in the Skagit River, Washington. Transactions of the American
2057 Fisheries Society 134(6):1562-1581.
- 2058 Hendrix, N., Danner, E., Greene, C. M., Imaki, H., & Lindley, S. T. 2014. Life cycle
2059 modeling framework for Sacramento River Winter-run Chinook salmon. NOAA
2060 Technical Memorandum NOAA -TM-NMFS-SWFSC-530.
- 2061 Speegle, J., Kirsch, J., & Ingram, J. 2013. Annual Report: Juvenile fish monitoring during the
2062 2010 and 2011 field seasons within the San Francisco Estuary, California.
- 2063
- 2064

2065 **APPENDIX B CLIMATE CHANGE SCENARIO PROJECTIONS**

2066 Climate change scenario projections were used to explore the level of impact that
 2067 California's Central Valley Project (CVP) and State Water Project (SWP) operations can
 2068 have on spring, fall and winter run Chinook under favorable and unfavorable climate
 2069 forecasts. Model covariates were divided into three categories: overland covariates (river
 2070 flows, river temperatures, air temperatures), nearshore ocean covariates (upwelling, PDO,
 2071 wind stress curl, Farallon ocean temperatures), and anthropogenic water use covariates
 2072 (exports, export/inflow ratios). Overland model covariates reflected two climate change
 2073 scenarios: a warmer/drier scenario, and a cooler/wetter scenario. Nearshore ocean covariates
 2074 explored two situations: favorable nearshore conditions for Chinook at ocean entry (increases
 2075 in upwelling, PDO in negative phase, less warming of nearshore oceans), and unfavorable
 2076 conditions (decreases in upwelling, PDO in positive phase, greater warming of nearshore
 2077 oceans). Anthropogenic water use levels were modified with regard to exports to create four
 2078 options: 1. future exports=mean historical exports; 2. future exports=mean historical exports
 2079 +30%; 3. future exports=mean historical exports – 30%, and 4. future exports=0. A total of
 2080 16 climate change scenarios were generated using all combinations of overland covariates,
 2081 nearshore ocean covariates and anthropogenic water use covariates (Table B.1).

2082 *METHODS*

2083 As the basis for our climate change scenarios, we used the United States Bureau of
 2084 Reclamation's (USBR) Operations Criteria and Plan (OCAP) Study 9.2 and 9.5 (USBR
 2085 2008). OCAP Study 9.2 reflects a mean increase in temperature of 0.75° F (=0.42° C) and an
 2086 increase of 12.5% in precipitation. OCAP Study 9.5 reflects a mean increase in temperature
 2087 of 2.8° F (=1.56° C) and a decrease in precipitation of 12%. These temperature and
 2088 precipitation changes represent a mean 30-year change between 1971-2000 and projected
 2089 2011-2040 levels. Study 9.2 and 9.5 are the extreme corners of a bounding box that captures
 2090 the 10th and 90th percentiles for temperature increase and precipitation change that were
 2091 predicted by 112 climate projections from a variety of climate models and greenhouse gas
 2092 emission levels (USBR 2008). USBR used the following methodology to generate OCAP
 2093 Study 9.2 and 9.5:

- 2094 1. Plot temperature change (ΔT) vs. precipitation change (ΔP) over central California for
 2095 each of 112 archived Downscaled CMIP3 Climate Projections (Downscaled CMIP3
 2096 Climate Projections Archive website).
- 2097 2. Determine the 10th and 90th percentiles for predicted temperature and precipitation
 2098 change.
- 2099 3. Identify the levels of ΔT and ΔP associated with the 10th and 90th percentiles in the
 2100 climate projections. The intersection of the 10th and 90th percentiles for ΔT with the
 2101 10th and 90th percentiles for ΔP form a bounding box with four corners.
- 2102 4. Choose climate projections that most closely reflect the four corners of the bounding
 2103 box. OCAP Study 9.2 reflects the mildest climate change conditions over central
 2104 California (less warming/ wetter), while OCAP Study 9.5 reflects the most dramatic
 2105 climate change conditions over central California (more warming/ drier).
- 2106 5. Modify CalSim-II hydrology inputs and Sacramento River Water Quality Model
 2107 (SRWQM) inputs based on temperature and precipitation values generated by the
 2108 climate projections.

2109 6. Run CalSim-II and SRWQM models using historical data that has been modified to
2110 reflect climate change, but is still run retrospectively.

2111 We used CalSim-II and SRWQM outputs for OCAP Study 9.2 and 9.5 (USBR 2008
2112 Appendix R zipped data), but projected the hindcast covariate values from 1946-2002 onto
2113 years 2007-2063 to obtain a forward projection, while retaining year-to-year variability in
2114 covariate values and the covariance structures present in the natural system. OCAP Study 9.2
2115 and 9.5 provided two types of scenario outputs:

- 2116 1. Streamflows and controlled discharges from dams and weirs: The CalSim-II model
2117 predicts mean monthly streamflows and discharges at various points throughout the
2118 Sacramento River system and the Delta, including the following covariates from the
2119 spring, fall and winter run Chinook models:
 - 2120 a. **Keswick Dam discharge** (fall run): CalSim-II channel flows at C5 from
2121 OCAP Study 9.2 and 9.5 were used for years 1946-2002, averaged over
2122 January-March. Averaged values were then projected forward to become
2123 scenario values for 2007-2063 (Fig. B.1, Table B.2D).
 - 2124 b. **Deer Creek discharge** (spring run): CalSim-II channel flows for Deer Creek
2125 were not available in OCAP Study 9.2 and 9.5. Instead, CalSim-II channel
2126 flows at C11305 (just past the confluence of Mill Creek, Deer Creek, Antelope
2127 Creek and discharge point D11305) from OCAP Study 9.2 and 9.5 were used
2128 for years 1946-2002, averaged over October-December. Deer Creek was
2129 separated from the other constituents of C11305 using the following
2130 methodology:
 - 2131 i. CalSim-II channel flows at C11309 (Deer Creek), C11305 and D11305
2132 were obtained from OCAP scenario NAA_Existing (no action
2133 alternative) for years 1946-2002, averaged over October-December.
2134 Deer Creek flow C11309 was divided by the sum of D11305 and
2135 C11305 to determine which proportion of Deer + Mill + Antelope
2136 Creek flows should be attributed to Deer Creek.
 - 2137 ii. CalSim-II values C11305 + D11305 from OCAP Study 9.2 and 9.5
2138 were multiplied by the vector of proportions for Deer Creek, one for
2139 each year (mean over all years=0.42, sd=0.05). These values were
2140 then projected forward to become scenario values for 2007-2063 (Fig.
2141 B.2, Table B.2D).
 - 2142 c. **Exports / Inflow Ratio** (fall run): CalSim-II delta inflows (INFLOW-
2143 DELTA parameter) from OCAP Study 9.2 and 9.5 for 1946-2002, averaged
2144 over March-May, were used as the denominator in the Exports/Inflow ratio,
2145 while the four export scenarios (see 8. *CVP and SWP Dayflow Exports*; and
2146 8b. *Mean Daily Exports March-May*, below) formed the numerator (Fig. B.3,
2147 Table B.2E).
 - 2148 d. **Bend Bridge minimum monthly flow** (winter run): CalSim-II channel flows
2149 at C109 from OCAP Study 9.2 and 9.5 were used over years 1946-2002,
2150 selecting the minimum monthly flow between August-November. Minimum
2151 flow values were then projected forward to become scenario values for 2007-
2152 2063 (Fig. B.4, Table B.3A).
 - 2153 e. **Freeport sediment concentration as a function of Freeport flow** (spring
2154 and fall run): Sediment concentrations at Freeport, averaged annually over
2155 February-April, were modelled as a linear function of Freeport flows (also
2156 averaged annually over February-April) from CalSim-II scenario

2157 NAA_Existing at C169. The linear model equation, with intercept set to zero,
2158 is:

$$2159 \text{ Freeport sediment conc.} = \text{CalSim-II flow at Freeport} * 0.0022487$$

2160

2161 The R-squared value for the regression is 0.834 (Fig. B.5). Freeport flows
2162 from OCAP Study 9.2 and 9.5 for years 1946-2002, averaged over February-
2163 April, were then used in conjunction with the linear model to generate
2164 sediment concentrations. These were projected forward to years 2007-2063
2165 (Fig. B.6, Table B.2D).

2166 2. River temperatures: SRWQM generates mean monthly river temperatures at various
2167 nodes along major rivers in the Sacramento River system (USBR 2008 Appendix R
2168 zipped data)

2169 a. **Sacramento River temperature at Bend Bridge** (winter run): SRWQM
2170 outputs for OCAP Study 9.2 and 9.5 were extracted along the Sacramento
2171 River at Bend Bridge for 1946-2002. Model predictions were averaged for
2172 months July-September and projected onto years 2007-2063 (Fig. B.7, Table
2173 B.3B).

2174 In addition to the OCAP Study 9.2 and 9.5 scenario outputs, we also used several
2175 other sources of data to generate scenario covariates:

2176

2177 3. Nearshore ocean upwelling estimates: Upwelling indices were obtained from
2178 NOAA's Pacific Fisheries Environmental Laboratory (PFEL Upwelling website). We
2179 increased and decreased historic values (1946-2002) of upwelling by +10% and -20%
2180 to account for a range of changes to upwelling that might occur under climate change
2181 (N. Mantua pers. comm., 12/8/14). These altered historic values were then projected
2182 onto years 2007-2063.

2183 a. **Upwelling at 36° N, 122° W** (spring and winter run): NOAA upwelling index
2184 values at 36° N, 122° W (southwest of Monterey, CA) were averaged over
2185 April-June for years 1946-2002, and adjusted up or down before being
2186 projected onto 2007-2063 (Fig. B.8, Tables B.2B & B.3A).

2187 4. Pacific Decadal Oscillation (PDO) index: PDO indices were obtained from the Joint
2188 Institute for the Study of the Atmosphere and Oceans (Mantua and Hare). Over the
2189 last century, the PDO has displayed a 20-30 year autocorrelation pattern (Mantua et
2190 al. 1997). To capture the future impact of positive (warm) and negative (cold) PDO
2191 cycles on Chinook populations, we used two ranges of historic PDO data and
2192 projected them forward to years 2007-2063: one was a sequence that began with a
2193 positive PDO phase before flipping to a negative PDO phase, while the other began
2194 with a negative PDO phase and then flipped to a positive PDO phase. Pacific
2195 Northwest and West coast salmon production is enhanced during the negative phase
2196 of the PDO, and tends to decline during positive phases of the PDO (Mantua et al.
2197 1997, Hare et al. 1999).

2198 a. **PDO** (spring and fall run): PDO values between 1900 and 2013 were
2199 averaged annually over January-May, and two sequences with opposite
2200 patterns were selected for future scenarios (Fig. B.9). The sequence of years
2201 between 1922-1978 began with a positive PDO phase, flipping to a negative
2202 phase around 1947. The sequence of years between 1946-2002 began with a
2203 negative PDO phase, flipping to a positive phase around 1977 (Fig. B.10,
2204 Table B.2B).

- 2205 5. Wind Stress Curl Index: Calculated values for NOAA wind stress curl index for
 2206 upwelling at Northern Location (39° N, 125° W) were obtained from NOAA's Pacific
 2207 Fisheries Environmental Laboratory (PFEL Derived Winds website).
 2208 a. **Curl Index** (spring and fall run): Historic curl index values from 1946-2002
 2209 averaged over July-December were increased or decreased by 20% and plotted
 2210 as forward projections for 2007-2063 (Fig. B.11). Curl trajectories from 1967-
 2211 2063 suggested a long-term autocorrelation pattern (Fig. B.11). Because we
 2212 did not have compelling reasons to believe that future curl values would
 2213 follow the same pattern as historic values, we set the future scenario curl index
 2214 equal to mean curl from 1967-2010 (standardized curl index = 0) (Table
 2215 B.2B).
 2216 6. Farallon Islands ocean temperature: Water temperature data at the Farallon Islands
 2217 (37° 41.8' N, 122° 59.9' W) were not available for all years between 1946 and 2002,
 2218 so the methodology of projecting covariate values from 1946-2002 under climate
 2219 change onto years 2007-2063 could not be used. Instead, we calculated the mean
 2220 water temperature over February-April for 1967-2012, and increased it by 0.42° C
 2221 (=0.75° F) to correspond with OCAP Study 9.2, and by 1.56° C (=2.8° F) to
 2222 correspond with OCAP Study 9.5.
 2223 a. **Farallon Islands ocean temperature** (winter run): Mean water temperature
 2224 from February-April during years 1967-2012 was 11.8° C. This was increased
 2225 to 12.3° C and 13.4° C to match with OCAP Study 9.2 and 9.5, respectively
 2226 (Fig. B.12, Table B.3B).
 2227 7. Sacramento air temperatures: Sacramento air temperature projections for 2007-2063
 2228 were obtained from the Downscaled CMIP3 Climate Projections archive (Downscaled
 2229 CMIP3 Climate Projections Archive website) for the same climate projections that
 2230 were used to generate OCAP Study 9.2 and 9.5. Air temperatures were obtained for
 2231 the modelled grid cell containing Sacramento's latitude/ longitude (38.5556° N,
 2232 121.4689° W). OCAP Study 9.2 was based on climate model mri cgcm2.3.2a with
 2233 A2 emissions, simulation #5, and OCAP Study 9.5 was based on climate model ukmo
 2234 hadcm3 with A2 emissions, simulation #1.
 2235 a. **Sacramento air temperature - spring** (spring and fall run): Climate
 2236 projections for the modelled cell over Sacramento were averaged annually
 2237 over January-March and adjusted up by 4.55 °F to spatially downscale climate
 2238 projections to match with historic Sacramento air temperature data. The
 2239 adjustment factor was obtained for each climate projection by subtracting
 2240 mean projected air temperature between 1960-2010 (averaged over January-
 2241 March) from mean historical Sacramento air temperature over the same
 2242 period. Resulting differences were averaged for the two scenarios to obtain an
 2243 adjusting value of 4.55 °F (Fig. B.13, Table B.2A).
 2244 b. **Sacramento air temperature - summer** (fall run): Climate projections for
 2245 the modelled cell over Sacramento for July-September were adjusted up by
 2246 8.82° F to spatially downscale climate projections to match with historic
 2247 Sacramento air temperature data. Methodology for obtaining the adjustment
 2248 factor was the same as for spring Sacramento air temperatures (see above)
 2249 (Fig. B.13, Table B.2A).
 2250 8. CVP and SWP Dayflow Exports: Dayflow data for exports from the Delta were
 2251 obtained from California's Department of Water Resources (CA DWR Dayflow
 2252 website). Average daily exports were calculated for 1967-2010 and modified to
 2253 generate four future export scenarios: 1. future exports = mean historical exports; 2.

- 2254 future exports = mean historical exports +30%; 3. future exports = mean historical
 2255 exports – 30%; and 4. future exports = 0.
- 2256 a. **Mean daily exports February-April** (spring run): Dayflow exports were
 2257 averaged annually over February-April for years 1967-2010 to form the
 2258 historical export level, which was then modified for scenarios (Fig. B.14,
 2259 Table B.2C).
- 2260 b. **Mean daily exports March-May, for Export/Inflow ratio** (fall run):
 2261 Dayflow exports were averaged annually over March-May for years 1967-
 2262 2010 to form the historical export level for the Export/Inflow ratio (see Fig.
 2263 B.3 and Table B.2E for the Export/Inflow ratio).
- 2264 c. **Total daily exports December-June** (winter run): Dayflow exports were
 2265 summed over all days between December and June, then averaged over 1967-
 2266 2007 to form the mean historical export level, which was then modified for
 2267 scenarios (Fig. B.15, Table B.3A).
- 2268 9. Daily stream flows: Streamflow data are collected daily at select locations by USGS
 2269 (USGS National Water Information System website). In order to generate future
 2270 predictions for OCAP Study 9.2 and 9.5, the daily stream flow data had to be
 2271 correlated to an appropriate CalSim-II output using linear models.
- 2272 a. **Number of days Sacramento River flow at Verona > 56,000 cfs** (winter
 2273 run): A linear model was generated to relate CalSim-II monthly flows at
 2274 Verona (C160 from OCAP scenario NAA_Existing) for 1967-2003 averaged
 2275 over December-March, to the total number of days between December and
 2276 March that Sacramento River flow at Verona exceeded 56,000 cfs (data from
 2277 USGS National Water Information System website). The linear model is:
- 2278
$$\# \text{ Days flow} > 56,000 = -25.19 + \text{CalSim-II flow at Verona} * 0.001646$$
- 2279 with R-squared = 0.9285. This relationship was used in conjunction with
 2280 CalSim-II flows at Verona (C160) for December 1946-March 2003, averaged
 2281 over December-March, to generate future scenario values (projected onto
 2282 2007-2063) for number of days that Sacramento River flow at Verona exceeds
 2283 56,000 cfs (Fig. B.16, Table B.3B)
- 2284 10. Water management operations: Discharges from dams, weirs and gates are managed
 2285 in California to optimize diverse interests, including efforts to increase winter run
 2286 Chinook populations.
- 2287 a. **Proportion of time Delta Cross Channel gate is open, December-March**
 2288 (winter run): The current operations plan is to close the Delta Cross Channel
 2289 (DCC) gate while winter run Chinook are out-migrating. As a result, future
 2290 scenarios assume that the proportion of time that the DCC gate is open
 2291 between December and March is zero (Table B.3B).
- 2292 11. Parameters for which no future conditions could be generated:
- 2293 a. **Channel Depletion** (fall run): The net channel depletion is the quantity of
 2294 water removed from the Delta channels to meet consumptive use, averaged
 2295 over March-May. Since future population growth may be countered by water-
 2296 saving technologies and measures, we set the future value of channel depletion
 2297 equal to the mean value over 1967-2010 (or a standardized value of 0) (Table
 2298 B.2A).
- 2299 b. **Smolt Size at Chipps Island** (spring run): For this parameter, we assumed
 2300 that size of out-migrating smolt caught at Chipps Island will not change over

2301 future years, so smolt size for the scenario projections was set equal to mean
2302 size over 1967-2010 (standardized value of 0) (Table B.2A).
2303

2304 *ACKNOWLEDGEMENTS*

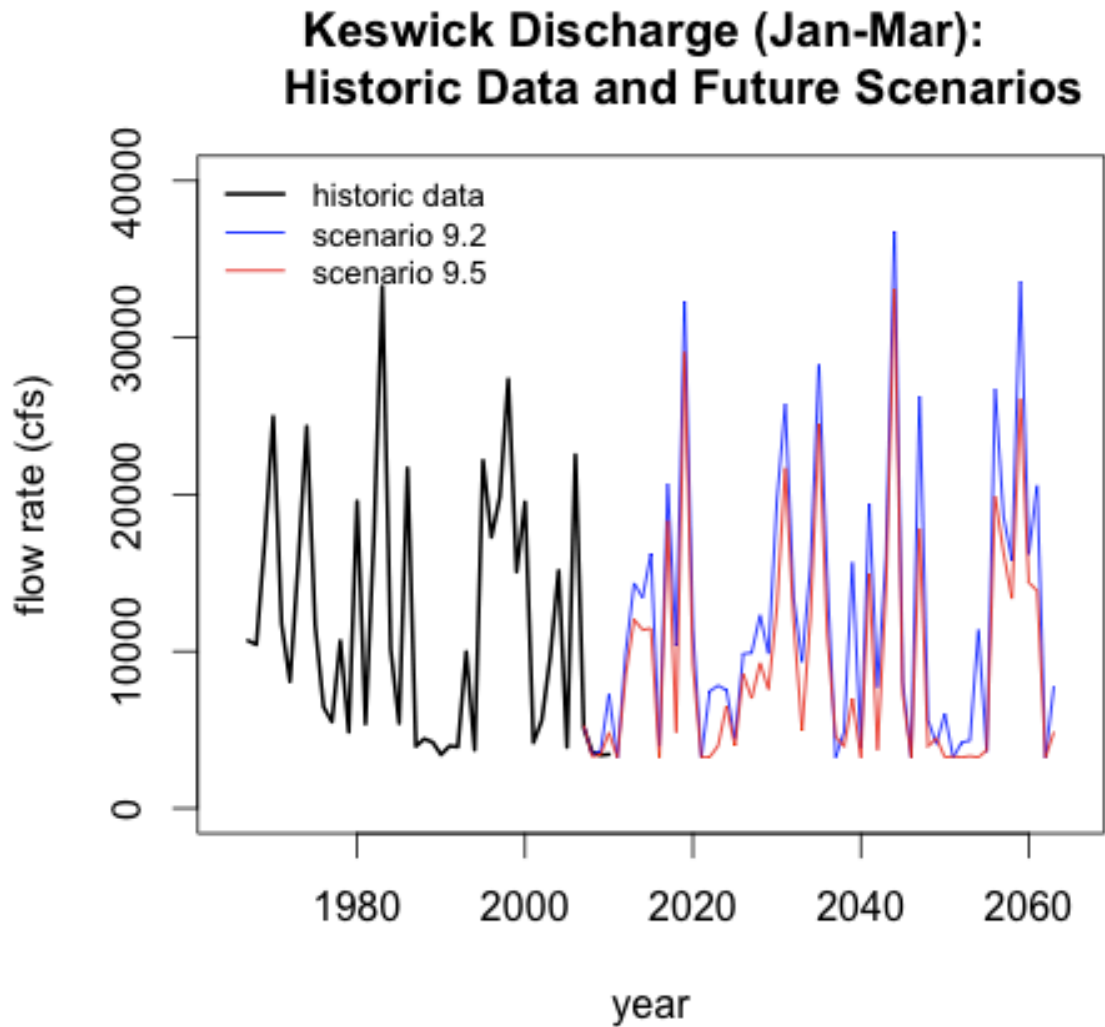
2305 We would like to thank Nate Mantua (NMFS – SWFSC) for advice on climate change
2306 impacts to physical characteristics of oceans, and Andrew Pike (NMFS – SWFSC) for his
2307 assistance with understanding and obtaining CalSim-II and SRWQM OCAP model outputs.
2308 For climate projection outputs that were used for scenario covariates, we acknowledge the
2309 modeling groups, the Program for Climate Model Diagnosis and Intercomparison (PCMDI)
2310 and the WCRP's Working Group on Coupled Modelling (WGCM) for their roles in making
2311 available the WCRP CMIP3 multi-model dataset. Support of the CMIP3 dataset is provided
2312 by the Office of Science, U.S. Department of Energy. Lastly, we thank Nate Mantua and
2313 Steve Hare for access to their historic PDO index values.

2314 CITATIONS

- 2315 California Department of Water Resources Dayflow Data. Accessed online Dec. 20, 2014.
2316 <http://www.water.ca.gov/dayflow/output/Output.cfm>
- 2317 Downscaled CMIP3 Climate Projections Archive. Accessed online Dec. 15, 2014.
2318 <http://gdo->
2319 [dcp.ucllnl.org/downscaled_cmip_projections/dcpInterface.html#Projections:%20Subs](http://dcp.ucllnl.org/downscaled_cmip_projections/dcpInterface.html#Projections:%20Subset%20Request)
2320 [et%20Request](http://dcp.ucllnl.org/downscaled_cmip_projections/dcpInterface.html#Projections:%20Subset%20Request)
- 2321 Hare, S.R., Mantua, N.J., Francis, R.C. (1999). Inverse production regimes: Alaska and West
2322 Coast Salmon. *Fisheries* 24(1): 6-14.
- 2323 Mantua, N., Hare, S.R., Zhang, Y., Wallace, J.M., Francis, R.C. (1997). A Pacific
2324 interdecadal climate oscillation with impacts on salmon production. *Bulletin of the*
2325 *American Meteorological Society* 78: 1069-1079.
- 2326 Mantua, N. and Hare, S.R., PDO Index Monthly Values: January 1900-present. Joint
2327 Institute for the Study of the Atmosphere and Ocean (University of Washington).
2328 Accessed online Dec. 30, 2014. <http://jisao.washington.edu/pdo/PDO.latest>
- 2329 Pacific Fisheries Environmental Laboratory (NOAA) Coastal Upwelling Indices. Accessed
2330 online Dec. 20, 2014.
2331 http://www.pfeg.noaa.gov/products/PFEL/modeled/indices/upwelling/NA/upwell_men_u_NA.html
2332 [nu_NA.html](http://www.pfeg.noaa.gov/products/PFEL/modeled/indices/upwelling/NA/upwell_men_u_NA.html)
- 2333 Pacific Fisheries Environmental Laboratory (NOAA) Derived Winds and Ocean Transports.
2334 Accessed online Dec. 30, 2014.
2335 <http://www.pfeg.noaa.gov/products/PFEL/modeled/indices/transports/transports.html>
- 2336 U.S. Bureau of Reclamation, 2008. Central Valley Project and State Water Project Operations
2337 Criteria and Plan Biological Assessment. U.S. Department of the Interior, Bureau of
2338 Reclamation, Mid-Pacific Region. Sacramento, California. Chapter 9 and Appendix
2339 R. http://www.usbr.gov/mp/cvo/OCAP/docs/OCAP_BA_2008.pdf
- 2340 U.S. Bureau of Reclamation, 2008. Central Valley Project and State Water Project
2341 Operations Criteria and Plan Biological Assessment. U.S. Department of the Interior,
2342 Bureau of Reclamation, Mid-Pacific Region. Sacramento, California. Appendix R,
2343 zipped data. Accessed online Dec. 15, 2014.
2344 http://www.usbr.gov/mp/cvo/ocap_page.html
- 2345
- 2346
- 2347
- 2348
- 2349

2350 FIGURES

2351



2352

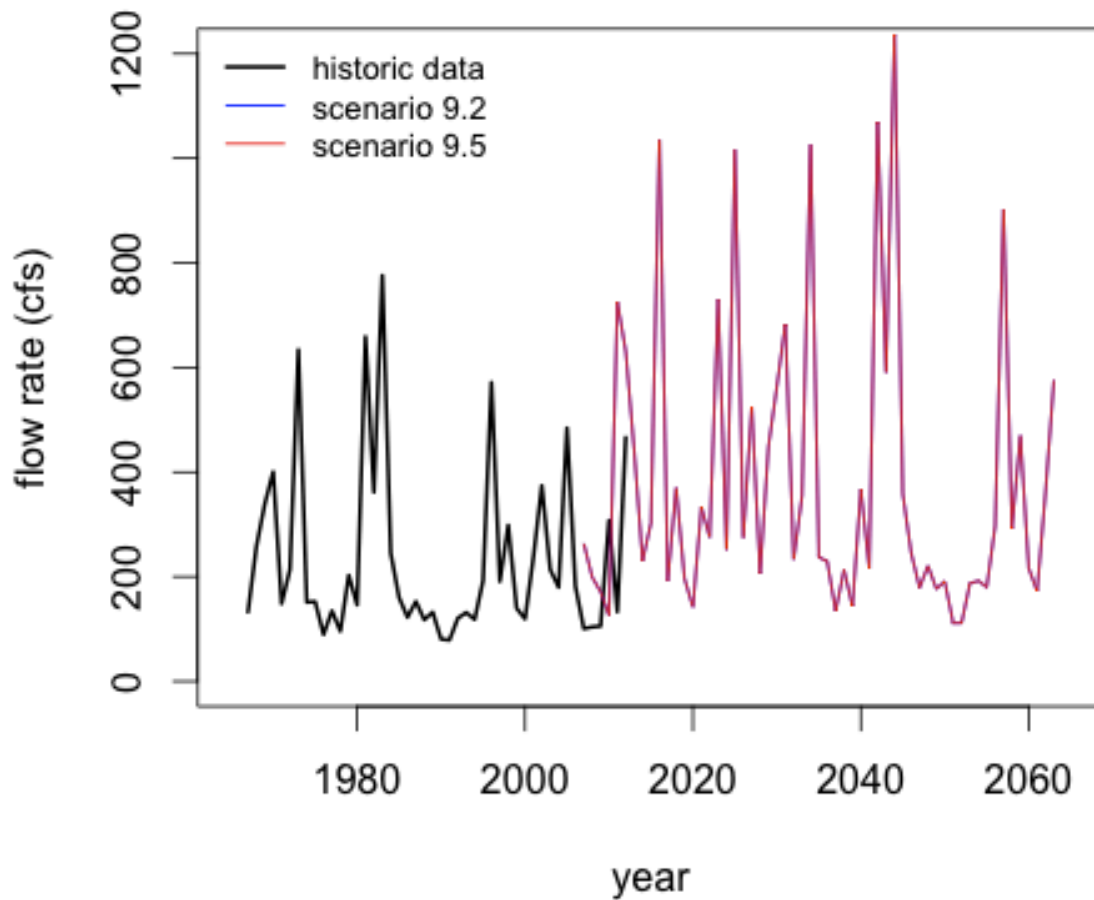
2353 **Figure B.1.** Mean annual discharge (cubic feet per second, cfs) from Keswick Dam for
 2354 January-March: historic data from 1967-2010 and climate change scenarios 9.2 and 9.5.
 2355 Climate change scenarios were based on CalSim-II OCAP Study 9.2 and 9.5 values from
 2356 1946-2002, which were projected forward to 2007-2063.

2357

2358

2359

Deer Creek Discharge (Oct-Dec): Historic Data and Future Scenarios



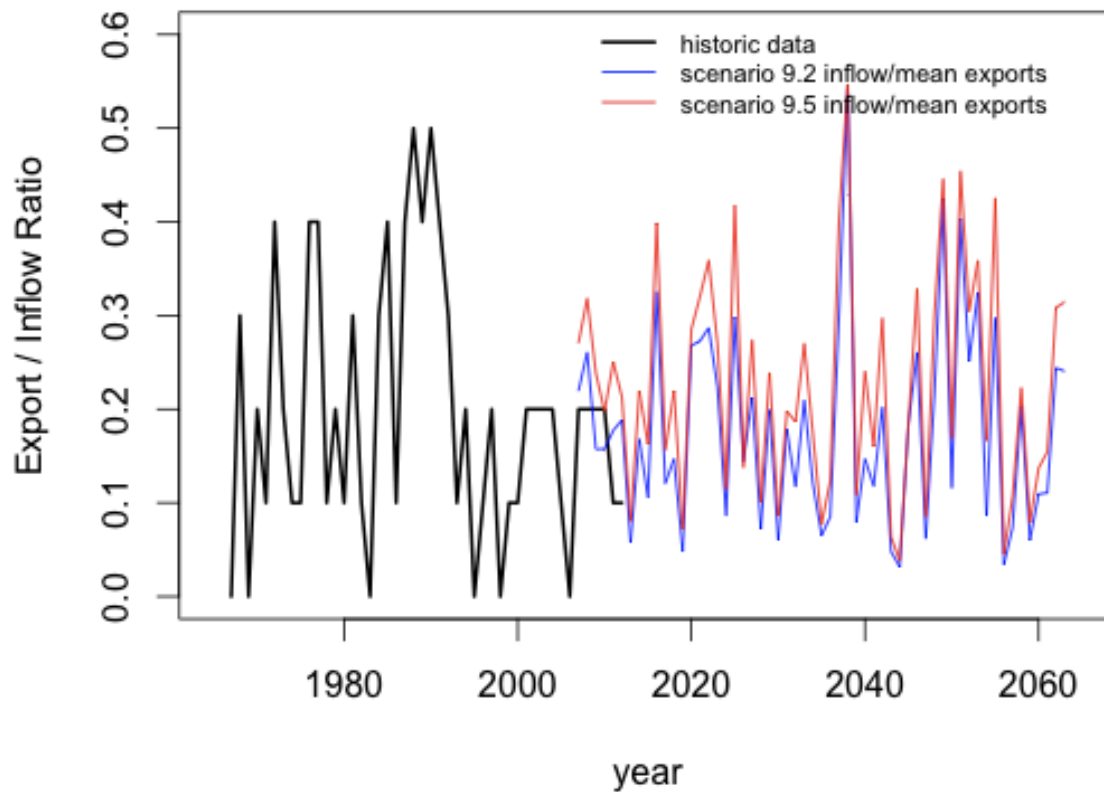
2360

2361 **Figure B.2.** Mean annual discharge (cfs) from Deer Creek for October-December: historic
 2362 data from 1967-2012 and climate change scenarios 9.2 and 9.5. Climate change scenarios
 2363 were based on CalSim-II OCAP Study 9.2 and 9.5 values from 1946-2002, which were
 2364 projected forward to 2007-2063. Note that there is no difference in projection values
 2365 between scenarios 9.2 and 9.5.

2366

2367

Ratio of Exports to Delta Inflow (Mar-May): Historic Data and Future Scenarios (Mean Exports)



2368

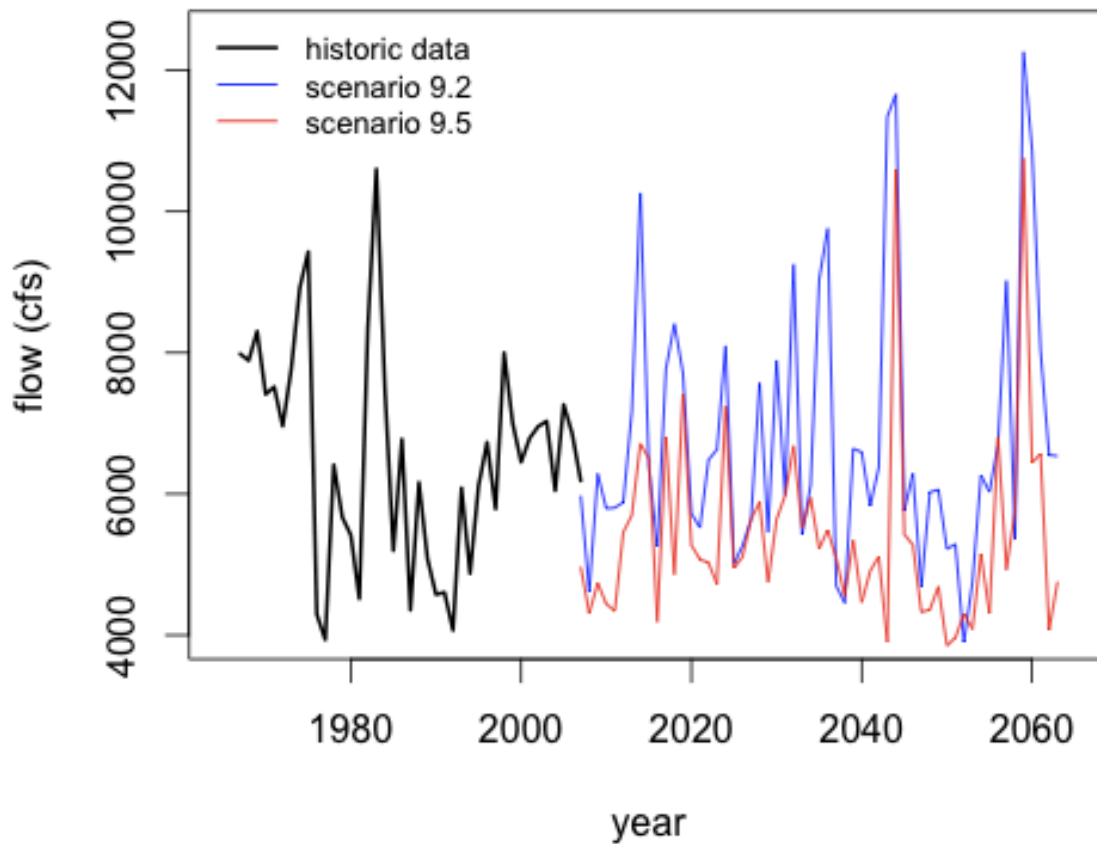
2369 **Figure B.3.** Exports to inflow ratio for the Delta, averaged over March-May: historic data
 2370 from 1967-2012 and climate change scenarios 9.2 and 9.5. Historic values are based on
 2371 Dayflow data $((QCVP + QSWP - BBID) / QTOT)$. Climate change scenarios use mean
 2372 exports from 1967-2010 for the numerator, and CalSim-II Delta inflow values from OCAP
 2373 Study 9.2 and 9.5 for the denominator. The CalSim-II Delta inflow values were from years
 2374 1946-2002, projected forward to 2007-2063.

2375

2376

2377

Bend Bridge Minimum Monthly Flow (Aug-Nov): Historic Data with Future Scenarios

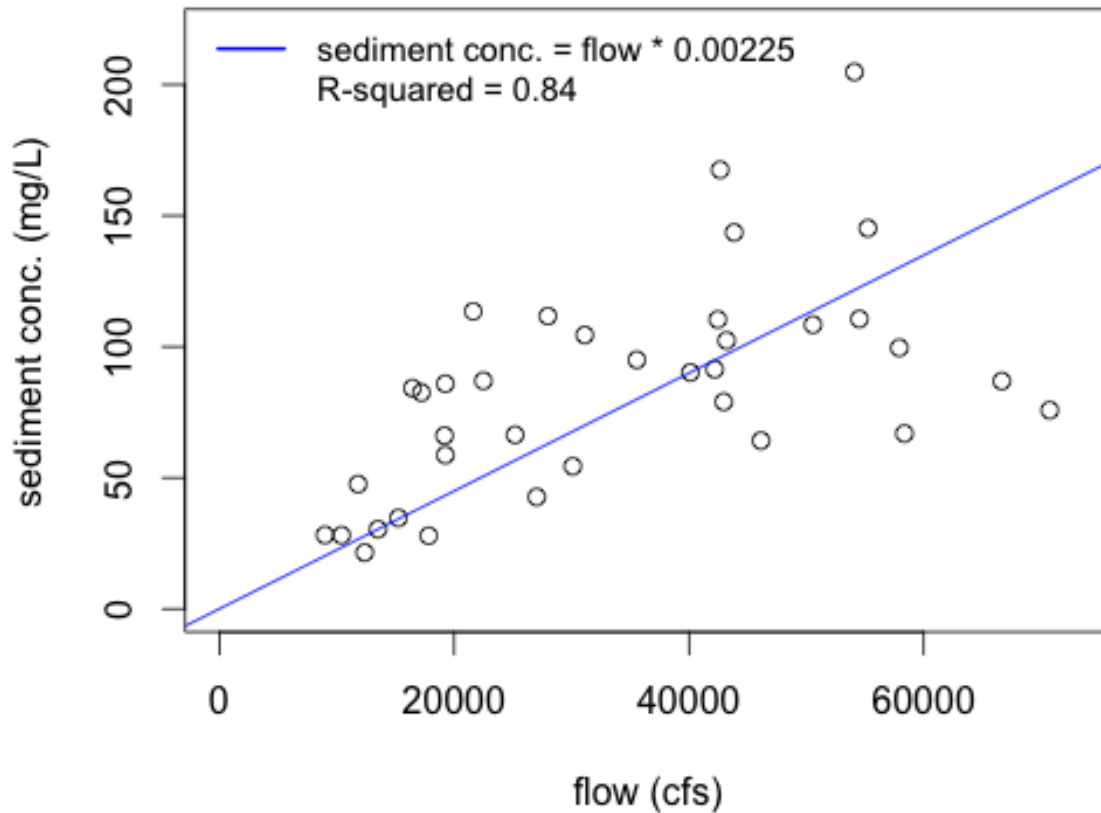


2378

2379 **Figure B.4.** Minimum monthly flow (cfs) at Bend Bridge for August-November: historic
 2380 data from 1967-2007 and climate change scenarios 9.2 and 9.5. Climate change scenarios
 2381 were based on CalSim-II OCAP Study 9.2 and 9.5 values from 1946-2002, which were
 2382 projected forward to 2007-2063.

2383

Freeport Monthly Sediment Concentration vs. Freeport Flow (Feb-Apr)



2384

2385

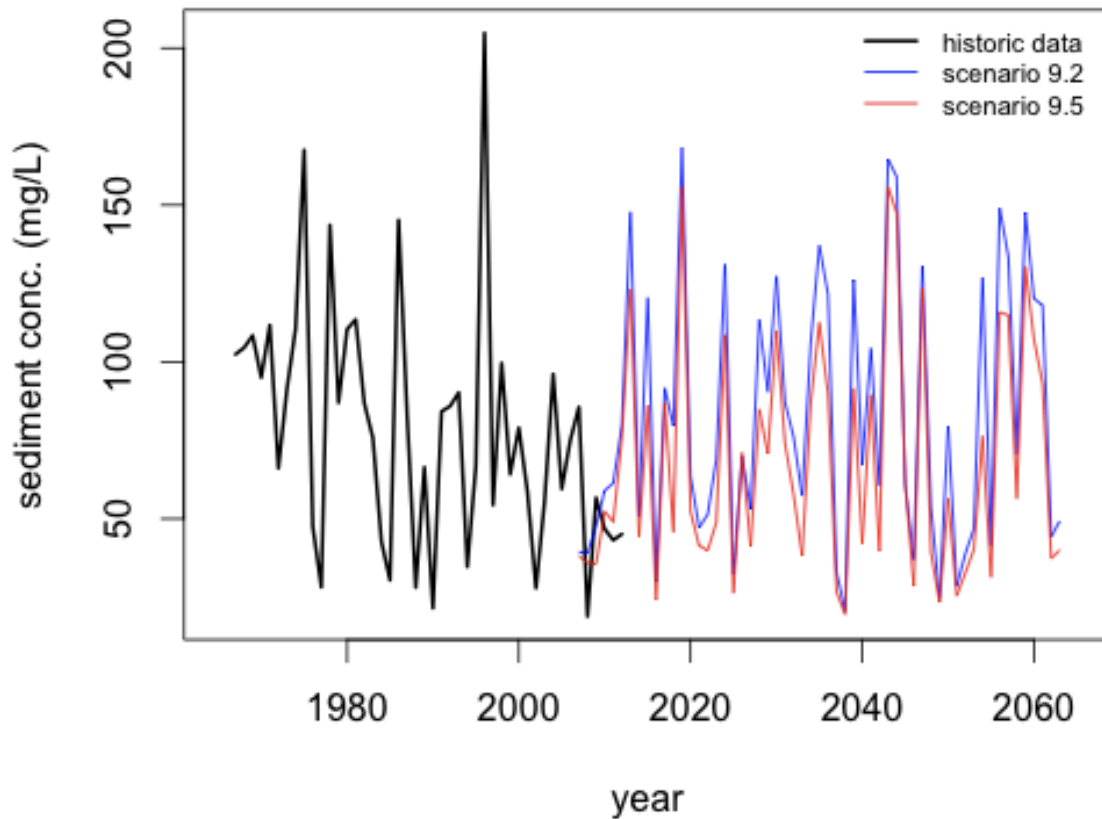
2386 **Figure B.5.** Average monthly sediment concentration (mg/L) at Freeport for years 1967-
 2387 2002, as a function of modelled Freeport flows (cfs) from CalSim-II OCAP scenario
 2388 NAA_Existing at node C169. Each point represents one year of data, averaged over months
 2389 February-April. A linear model was fit to the points, with a specified intercept of 0 (blue
 2390 line):

2391 $\text{Freeport sediment concentration} = \text{Freeport flow} * 0.0022487$

2392 The adjusted R-squared for the linear model is 0.84.

2393

Freeport Sediment Concentration (Feb-Apr): Historic Data and Future Scenarios



2394

2395 **Figure B.6.** Freeport sediment concentrations (mg/L) averaged over February-April: historic
 2396 data from 1967-2012 and climate change scenarios 9.2 and 9.5. Climate change scenario
 2397 values were obtained using Freeport flow predictions (at C169) from CalSim-II OCAP Study
 2398 9.2 and 9.5 for 1946-2002, and multiplying these values by 0.0022487 to correlate them to
 2399 sediment concentrations (see Fig. B.5). The 1946-2002 climate change scenario sediment
 2400 predictions were then projected forward to 2007-2063.

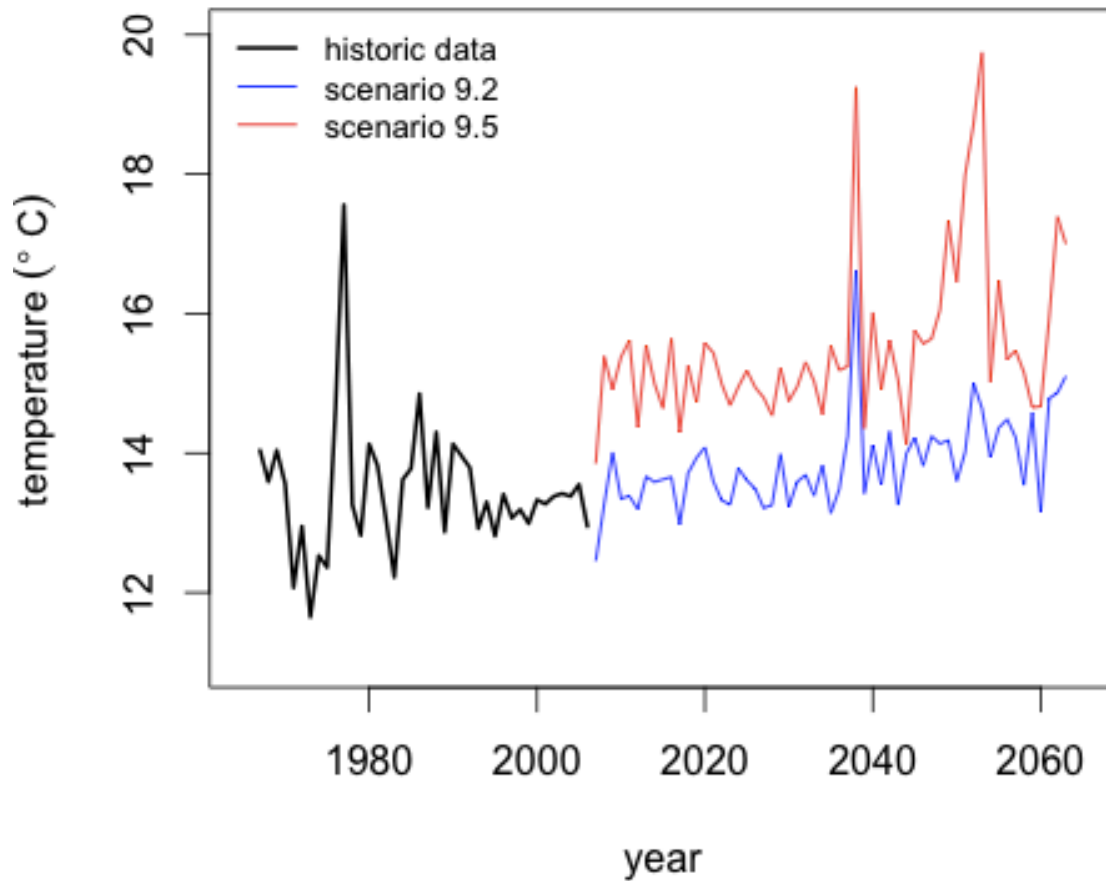
2401

2402

2403

2404

Bend Bridge Temperature (Jul-Sep): Historic Data with Future Scenarios

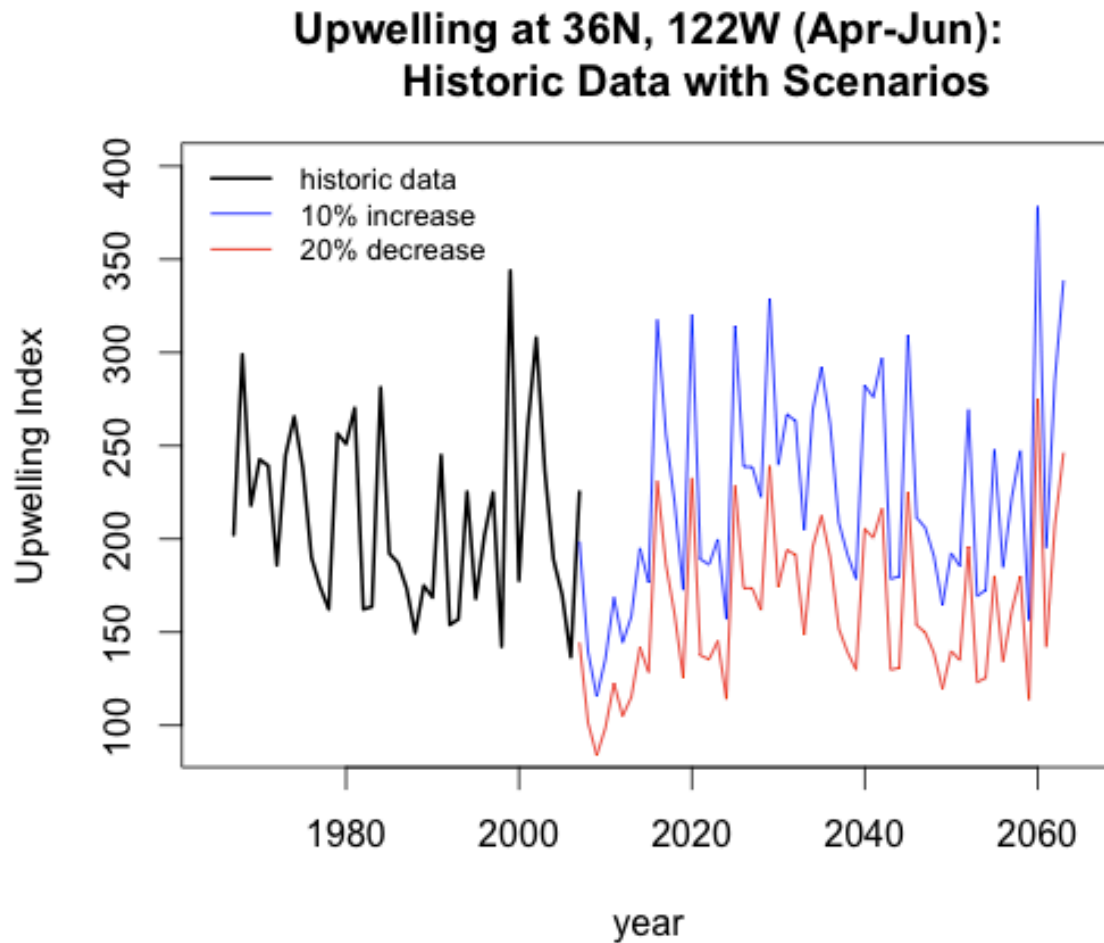


2405

2406 **Figure B.7.** Sacramento River average water temperature (° C) at Bend Bridge, averaged
 2407 over July-September: historic data from 1967-2006 and climate change scenarios 9.2 and 9.5.
 2408 Climate change scenarios were based on the SRWQM OCAP Study 9.2 and 9.5 values from
 2409 1946-2002, which were projected forward to 2007-2063.

2410

2411

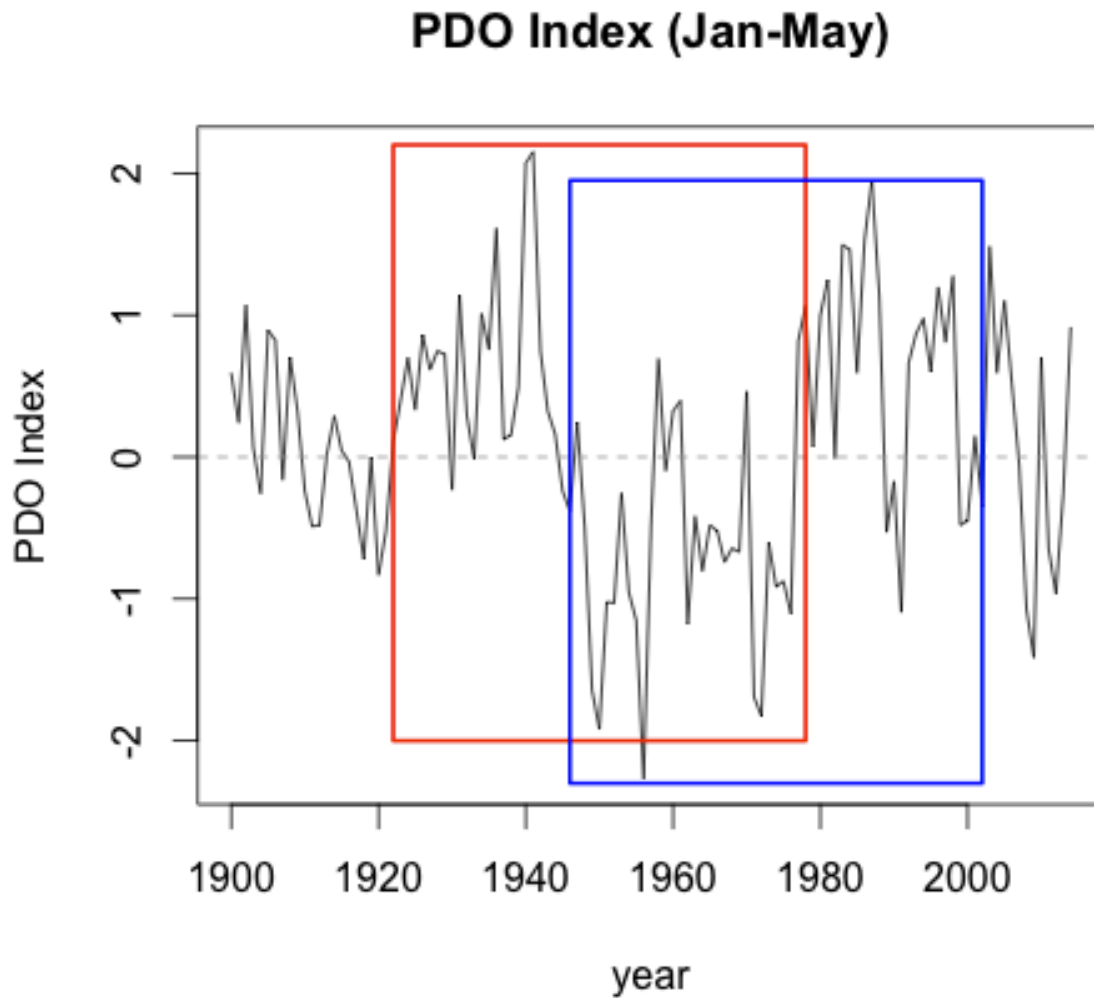


2412

2413 **Figure B.8.** NOAA upwelling index at station 36° N, 122° W averaged over April-June:
 2414 historic data from 1967-2007 and two climate change scenarios. Climate change scenarios
 2415 were based on historic upwelling values from 1946-2002, which were adjusted up (+20%) or
 2416 down (-10%) and projected forward to 2007-2063.

2417

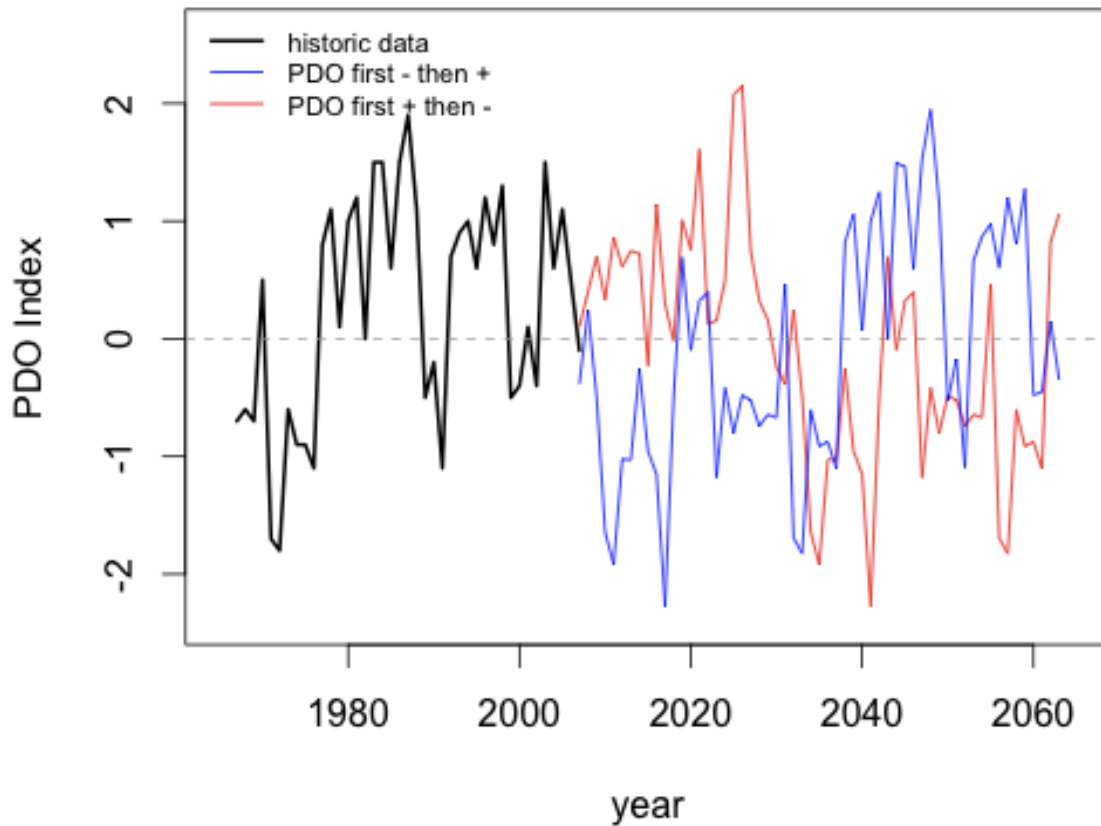
2418



2419

2420 **Figure B.9.** Historic values of the PDO index, averaged annually over January-May. West
 2421 coast salmon stocks have higher productivity during negative (cool) phases of the PDO, and
 2422 lower productivity during positive (warm) phases. The sequence of years from 1922-1978
 2423 (red box) was projected forward to 2007-2063 to represent a scenario where the PDO begins
 2424 in a positive cycle, while the sequence of years from 1946-2002 (blue box) was projected
 2425 forward to represent a scenario where the PDO begins in a negative cycle.

PDO Index (Jan-May): Historic Data and Future Scenarios

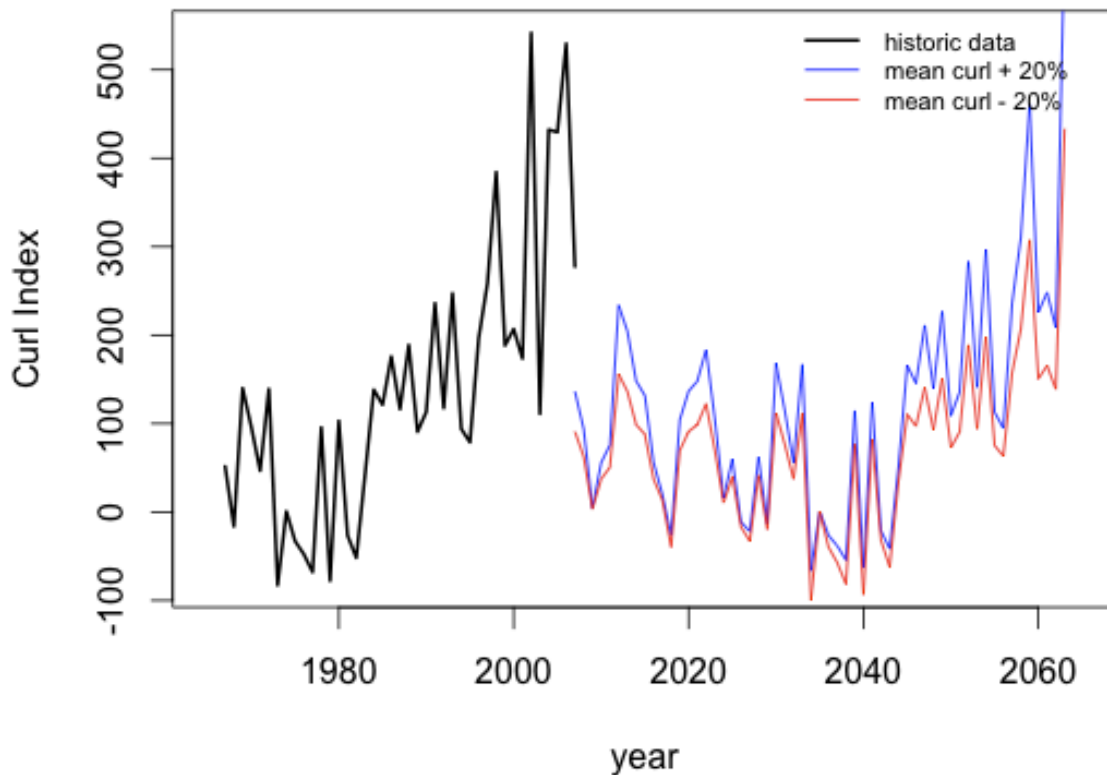


2426

2427 **Figure B.10.** PDO index averaged annually over January-May: historic data from 1967-2007
 2428 and two future scenarios. Future scenarios were projected onto 2007-2063 and consist of: 1.)
 2429 a historic sequence that begins with a negative PDO index, then flips to a positive PDO index
 2430 halfway through the time series (blue line: historic values from 1922-1978); and 2.) a historic
 2431 sequence that begins with a positive PDO index, then flips to a negative PDO index (red line:
 2432 historic values from 1946-2002).

2433

NOAA Wind Stress Curl Index (Jul-Dec): Historic Data and Potential Future Scenarios



2434

2435 **Figure B.11.** NOAA wind stress curl index averaged over July-December: historic data for
 2436 1967-2007 and potential scenario values. Potential scenario values were generated by
 2437 increasing (+20%) or decreasing (-20%) curl data from 1946-2002 according to the equations
 2438 below, then projecting the values onto 2007-2063:

2439
$$\text{Curl} + 20\% = \text{historic curl} + \text{abs value}(\text{historic curl}) * 0.2$$

2440
$$\text{Curl} - 20\% = \text{historic curl} - \text{abs value}(\text{historic curl}) * 0.2$$

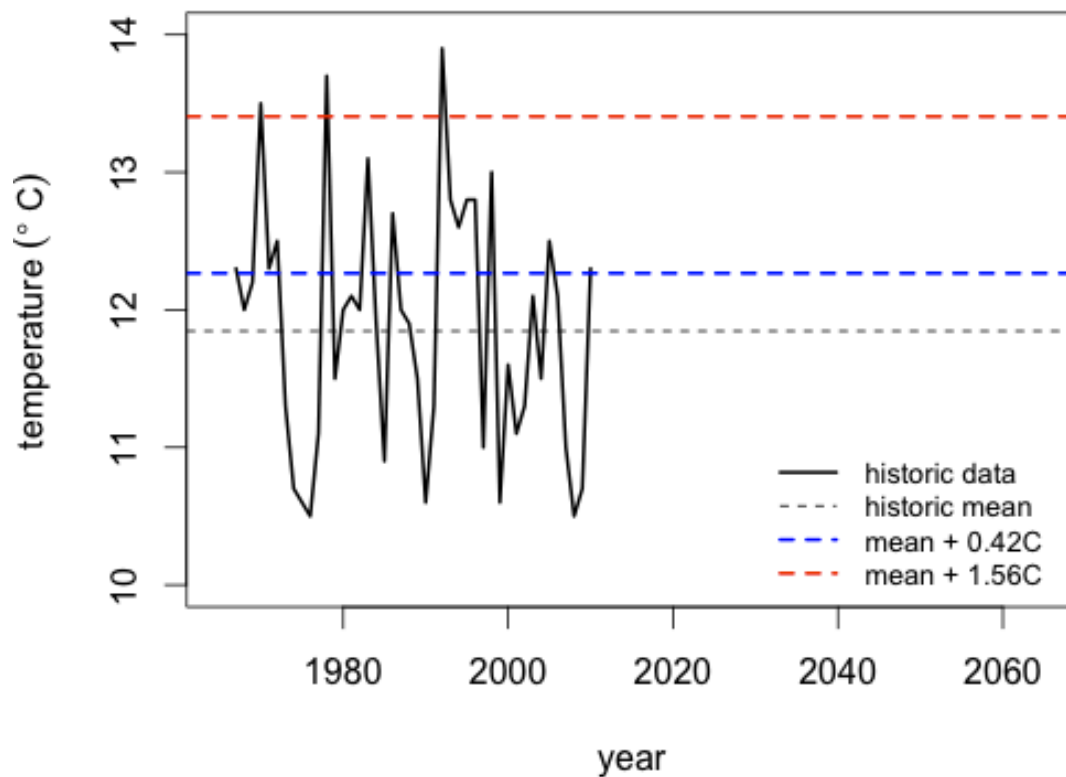
2441 Curl index trajectories from 1967-2063 suggest a long-term autocorrelation pattern. Because
 2442 we did not have compelling reasons to believe that future curl values would follow the same
 2443 pattern as historic values, we set the standardized curl projections for future scenarios to 0.

2444

2445

2446

Farallon Islands Ocean Temperature (Feb-Apr): Historic Data with Mean and Future Scenarios



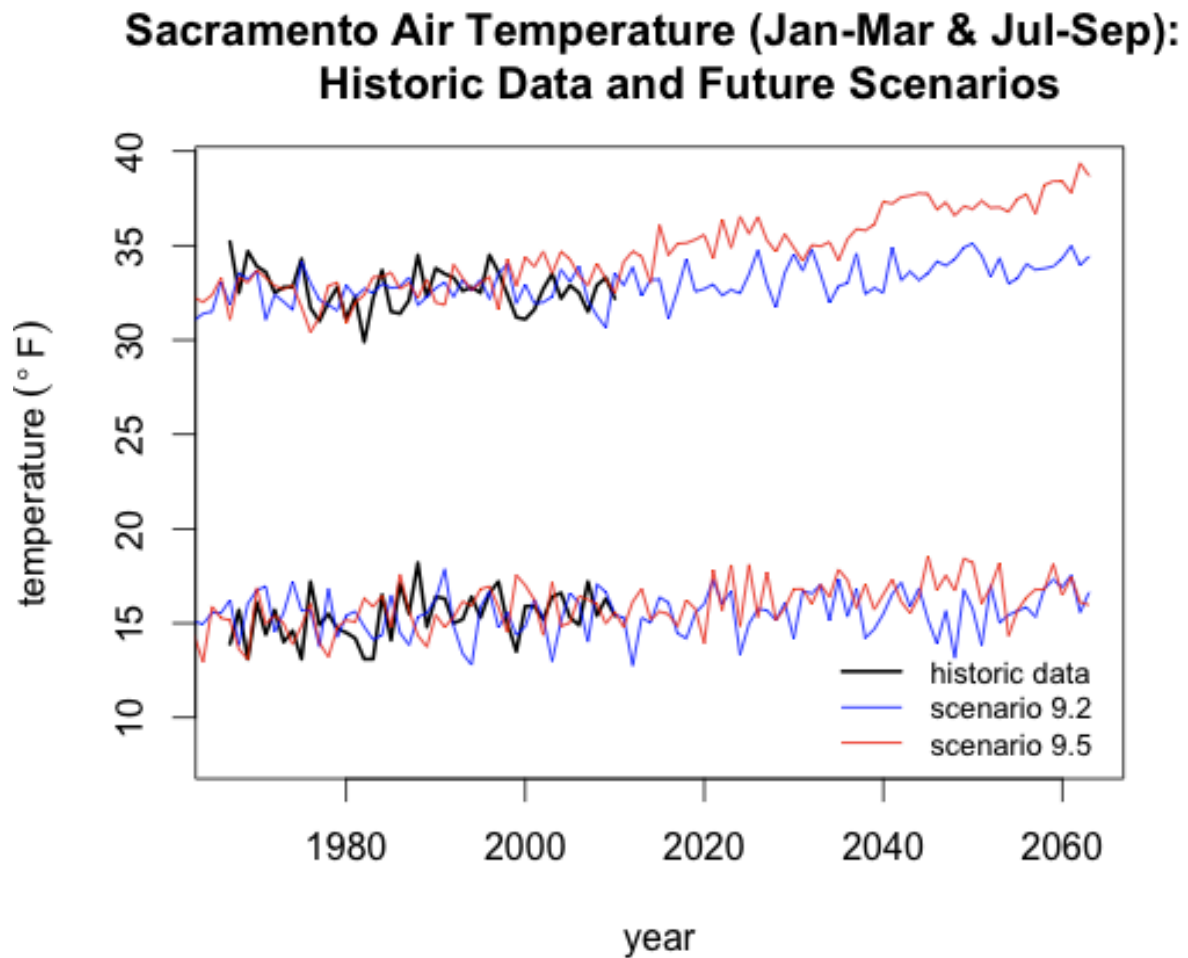
2447

2448 **Figure B.12.** Ocean temperature at the Farallon Islands averaged over February-April:
 2449 historic data with mean for 1967-2010, and two climate projections: mean +0.42° C (=0.75°
 2450 F, the average temperature increase for OCAP Study 9.2), and mean +1.56° C (=2.8° F, the
 2451 average temperature increase for OCAP Study 9.5).

2452

2453

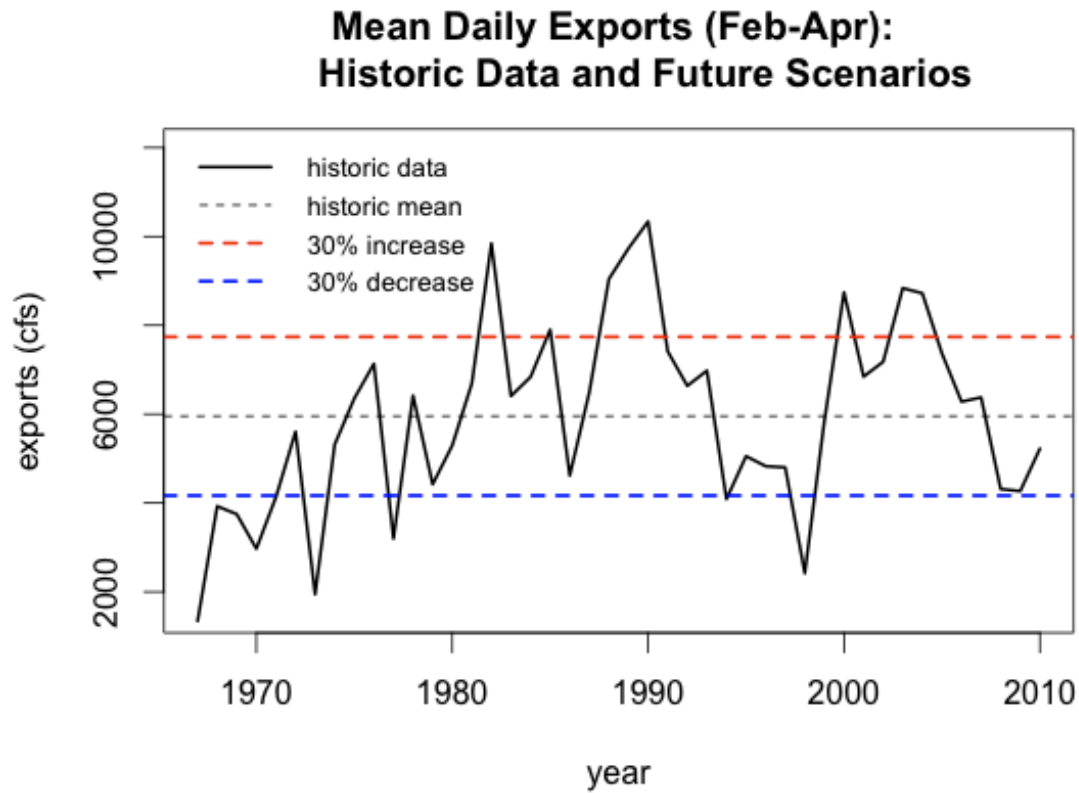
2454



2455

2456 **Figure B.13.** Sacramento air temperature averaged over spring months (January-March,
 2457 bottom lines) and summer months (July-September, top lines): historic data for 1967-2010,
 2458 and future climate change predictions based on CMIP3 climate projections. CMIP3 air
 2459 temperature predictions for the model cell over Sacramento were adjusted by + 4.55° F for
 2460 the spring, and + 8.82° F for the summer, to spatially downscale climate projections from
 2461 1967-2010 to match the range of historic Sacramento air temperature data.

2462



2463

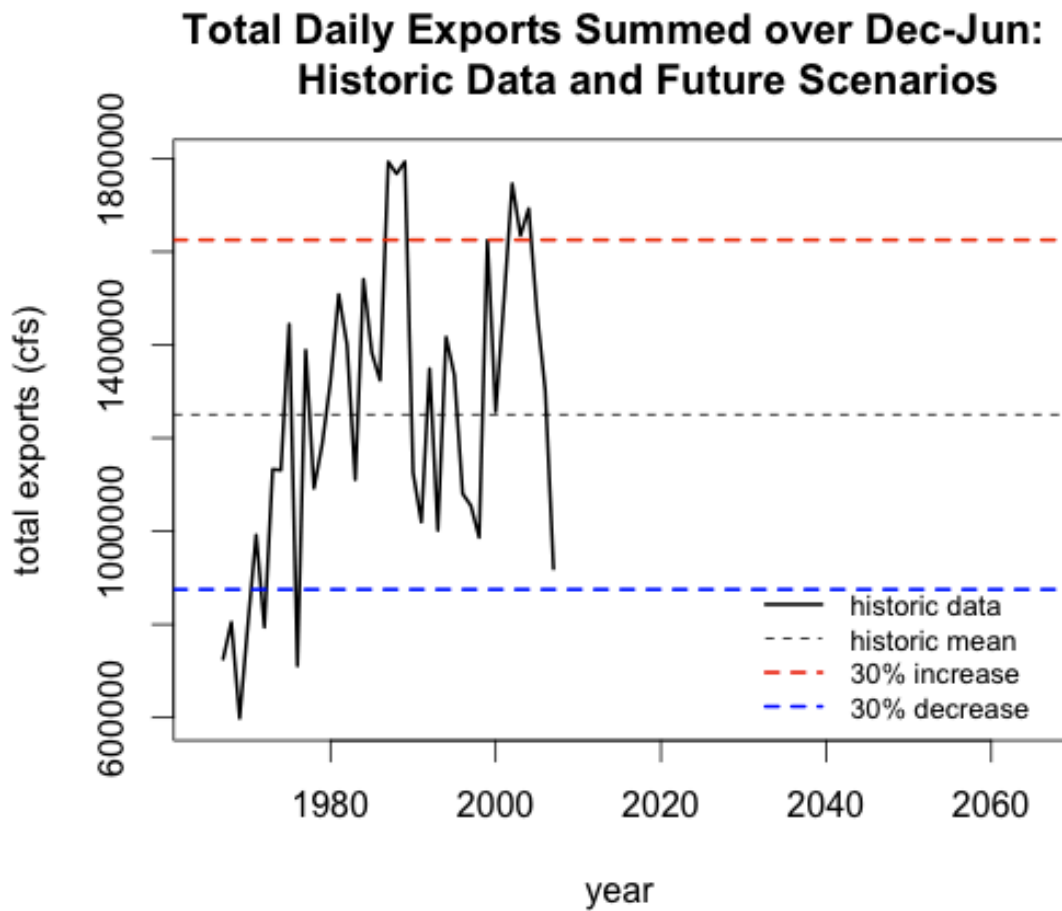
2464 **Figure B.14.** Mean daily exports (cfs) averaged annually from February-April: historic data
 2465 and future scenarios. Scenarios represent the following options: mean exports (1967-2010),
 2466 zero exports, mean exports + 30%, mean exports - 30%.

2467

2468

2469

2470

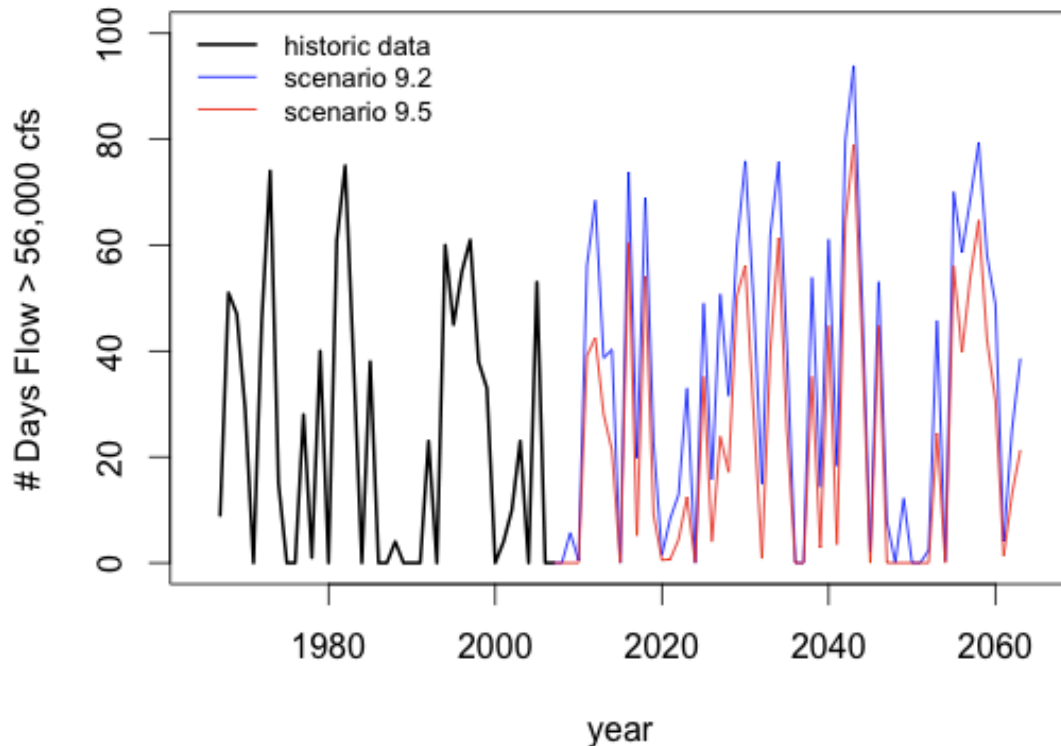


2471

2472 **Figure B.15.** Total daily exports summed over December-June: historic data and future
 2473 scenarios. Scenarios represent the following options: mean total exports (1967-2010), zero
 2474 exports, mean total exports + 30%, mean total exports - 30%.

2475

Number of Days Flow at Verona > 56,000 cfs (Dec-Mar): Historic Data with Future Scenarios



2476

2477 **Figure B.16.** Total number of days from December-March that Sacramento River flow at
 2478 Verona exceeds 56,000 cfs: historic data from 1967-2007 and climate change scenarios 9.2
 2479 and 9.5. Climate change scenario values were obtained using Verona flow predictions (at
 2480 C160) from CalSim-II OCAP Study 9.2 and 9.5 for 1946-2002 averaged over December-
 2481 March, and adjusting these values per the linear model:

2482
$$\# \text{ Days flow} > 56,000 = -25.19 + \text{CalSim-II flow at Verona} * 0.001646$$

2483 to correlate them to the number of days that flow exceeds 56,000 cfs. The 1946-2002 climate
 2484 change scenario predictions were then projected forward to 2007-2063.

2485

2486

2487

2488 **TABLES**2489 **Table B.1.** Scenario list with values drawn for each category of covariate.

2490

	OCAP Study	Upwelling	Farallon Temp	PDO Index	Exports
Scenario 1	9.2	+ 10%	+ 0.42° C	- then +	Mean Level
Scenario 2	9.2	- 20%	+ 1.56° C	+ then -	Mean Level
Scenario 3	9.2	+ 10%	+ 0.42° C	- then +	Zero
Scenario 4	9.2	- 20%	+ 1.56° C	+ then -	Zero
Scenario 5	9.2	+ 10%	+ 0.42° C	- then +	Mean + 30%
Scenario 6	9.2	- 20%	+ 1.56° C	+ then -	Mean + 30%
Scenario 7	9.2	+ 10%	+ 0.42° C	- then +	Mean - 30%
Scenario 8	9.2	- 20%	+ 1.56° C	+ then -	Mean - 30%
Scenario 9	9.5	+ 10%	+ 0.42° C	- then +	Mean Level
Scenario 10	9.5	- 20%	+ 1.56° C	+ then -	Mean Level
Scenario 11	9.5	+ 10%	+ 0.42° C	- then +	Zero
Scenario 12	9.5	- 20%	+ 1.56° C	+ then -	Zero
Scenario 13	9.5	+ 10%	+ 0.42° C	- then +	Mean + 30%
Scenario 14	9.5	- 20%	+ 1.56° C	+ then -	Mean + 30%
Scenario 15	9.5	+ 10%	+ 0.42° C	- then +	Mean - 30%
Scenario 16	9.5	- 20%	+ 1.56° C	+ then -	Mean - 30%

2491

2492

2493

2494

2495

2496 **Table B.2A.** Fall and spring covariate values for Sacramento air temperature, channel
 2497 depletion and smolt size at Chipps Island.
 2498

Year	Sacramento Air Temp (°F, Jan-Mar)		Sacramento Air Temp (°F, Jul-Sep)		Channel Depletion (cfs, Mar-May)	Size at Chipps Island (mm, Jan)
	Study 9.2	Study 9.5	Study 9.2	Study 9.5	Mean	Mean
2007	14.0	16.3	32.1	32.9	521	94.1
2008	17.1	16.0	31.3	34.1	521	94.1
2009	16.7	15.0	30.6	33.2	521	94.1
2010	15.5	15.6	33.5	32.5	521	94.1
2011	15.3	14.8	32.9	34.1	521	94.1
2012	12.8	16.1	33.9	34.7	521	94.1
2013	15.3	16.8	32.3	34.4	521	94.1
2014	15.0	15.2	33.2	33.0	521	94.1
2015	16.4	15.6	33.2	36.1	521	94.1
2016	16.1	15.5	31.1	34.5	521	94.1
2017	14.5	14.8	32.6	35.1	521	94.1
2018	14.2	16.2	34.3	35.1	521	94.1
2019	15.5	15.7	32.6	35.3	521	94.1
2020	16.0	13.9	32.7	35.6	521	94.1
2021	17.3	17.8	32.9	34.3	521	94.1
2022	16.0	15.7	32.4	36.4	521	94.1
2023	16.7	18.1	32.7	34.9	521	94.1
2024	13.3	14.8	32.5	36.5	521	94.1
2025	15.0	18.1	33.5	35.6	521	94.1
2026	15.8	15.3	34.8	36.5	521	94.1
2027	15.7	17.7	32.9	35.3	521	94.1
2028	15.2	15.2	31.7	34.7	521	94.1
2029	16.1	15.8	33.6	35.6	521	94.1
2030	14.2	16.8	34.5	34.9	521	94.1
2031	16.7	16.8	33.7	34.2	521	94.1
2032	16.6	16.0	34.8	35.0	521	94.1
2033	17.0	17.0	33.5	35.0	521	94.1
2034	15.1	16.4	32.0	35.2	521	94.1
2035	17.3	17.8	32.9	34.2	521	94.1
2036	15.4	17.3	33.0	35.3	521	94.1
2037	16.8	15.8	34.6	35.9	521	94.1
2038	14.2	17.1	32.4	35.8	521	94.1
2039	14.7	15.7	32.8	36.1	521	94.1
2040	15.5	16.5	32.5	37.3	521	94.1

2499

2500 **Table B.2A (continued).** Fall and spring covariate values for Sacramento air temperature,
 2501 channel depletion and smolt size at Chipps Island.

2502

Year	Sacramento Air Temp (°F, Jan-Mar)		Sacramento Air Temp (°F, Jul-Sep)		Channel Depletion (cfs, Mar-May)	Size at Chipps Island (mm, Jan)
	Study 9.2	Study 9.5	Study 9.2	Study 9.5	Mean	Mean
2041	16.5	17.3	34.9	37.2	521	94.1
2042	17.1	16.1	33.2	37.6	521	94.1
2043	15.9	15.5	33.6	37.6	521	94.1
2044	16.9	16.4	33.2	37.8	521	94.1
2045	15.2	18.5	33.5	37.7	521	94.1
2046	13.9	16.8	34.2	36.9	521	94.1
2047	15.7	17.5	33.9	37.3	521	94.1
2048	13.2	16.7	34.3	36.6	521	94.1
2049	16.8	18.4	34.9	37.1	521	94.1
2050	15.7	18.2	35.1	36.9	521	94.1
2051	13.8	16.0	34.5	37.4	521	94.1
2052	17.0	16.9	33.4	37.0	521	94.1
2053	15.0	18.2	34.3	37.0	521	94.1
2054	15.4	14.3	33.0	36.8	521	94.1
2055	15.6	15.7	33.3	37.5	521	94.1
2056	15.9	16.4	34.0	37.7	521	94.1
2057	15.3	16.8	33.7	36.7	521	94.1
2058	16.8	16.8	33.8	38.2	521	94.1
2059	17.3	18.1	33.9	38.4	521	94.1
2060	16.9	16.5	34.3	38.4	521	94.1
2061	17.5	17.4	35.0	37.8	521	94.1
2062	15.6	16.1	34.0	39.4	521	94.1
2063	16.6	16.0	34.4	38.7	521	94.1

2503

2504

2505 **Table B.2B.** Fall and spring covariate values for upwelling index, wind stress curl and PDO
 2506 index.

2507

Year	Upwelling Index (36N, 122W, Apr- Jun)		NOAA Wind Stress Curl Index (39N, 125W, Jul-Dec)	PDO Index (Jan-May)	
	Up 10%	Down 20%	Mean	+ then -	- then +
2007	199	145	151	0.10	-0.38
2008	139	101	151	0.40	0.24
2009	116	84	151	0.70	-0.49
2010	136	99	151	0.33	-1.64
2011	169	123	151	0.86	-1.92
2012	144	105	151	0.61	-1.02
2013	158	115	151	0.75	-1.03
2014	195	142	151	0.72	-0.26
2015	177	129	151	-0.23	-0.95
2016	318	231	151	1.14	-1.15
2017	256	186	151	0.29	-2.27
2018	220	160	151	-0.02	-0.50
2019	173	126	151	1.01	0.69
2020	320	233	151	0.76	-0.10
2021	189	138	151	1.61	0.32
2022	186	135	151	0.12	0.40
2023	200	145	151	0.16	-1.18
2024	157	114	151	0.49	-0.42
2025	314	229	151	2.07	-0.80
2026	239	174	151	2.15	-0.48
2027	239	174	151	0.74	-0.52
2028	223	162	151	0.32	-0.74
2029	329	239	151	0.16	-0.64
2030	240	174	151	-0.24	-0.67
2031	267	194	151	-0.38	0.46
2032	263	191	151	0.24	-1.69
2033	205	149	151	-0.49	-1.83
2034	270	196	151	-1.64	-0.60
2035	292	213	151	-1.92	-0.91
2036	262	190	151	-1.02	-0.88
2037	209	152	151	-1.03	-1.10
2038	192	139	151	-0.26	0.82
2039	179	130	151	-0.95	1.06
2040	282	205	151	-1.15	0.07

2508

2509

2510 **Table B.2B (continued).** Fall and spring covariate values for upwelling index, wind stress
 2511 curl and PDO index.

2512

Year	Upwelling Index (36N, 122W, Apr- Jun)		NOAA Wind Stress Curl Index (39N, 125W, Jul-Dec)	PDO Index (Jan-May)	
	Up 10%	Down 20%	Mean	+ then -	- then +
2041	276	201	151	-2.27	1.00
2042	297	216	151	-0.50	1.25
2043	179	130	151	0.69	-0.01
2044	180	131	151	-0.10	1.50
2045	309	225	151	0.32	1.46
2046	212	154	151	0.40	0.59
2047	206	150	151	-1.18	1.52
2048	191	139	151	-0.42	1.95
2049	165	120	151	-0.80	1.15
2050	193	140	151	-0.48	-0.53
2051	186	135	151	-0.52	-0.17
2052	270	196	151	-0.74	-1.09
2053	169	123	151	-0.64	0.66
2054	173	126	151	-0.67	0.87
2055	248	180	151	0.46	0.98
2056	185	134	151	-1.69	0.60
2057	222	161	151	-1.83	1.20
2058	248	180	151	-0.60	0.81
2059	157	114	151	-0.91	1.27
2060	378	275	151	-0.88	-0.48
2061	195	142	151	-1.10	-0.45
2062	285	207	151	0.82	0.15
2063	339	246	151	1.06	-0.35

2513

2514

2515 **Table B.2C.** Fall and spring covariate values for mean daily exports.

2516

Year	Mean Daily Exports (cfs, Feb-Apr)			
	Mean	None	Up 30%	Down 30%
2007	5954	0	7740	4168
2008	5954	0	7740	4168
2009	5954	0	7740	4168
2010	5954	0	7740	4168
2011	5954	0	7740	4168
2012	5954	0	7740	4168
2013	5954	0	7740	4168
2014	5954	0	7740	4168
2015	5954	0	7740	4168
2016	5954	0	7740	4168
2017	5954	0	7740	4168
2018	5954	0	7740	4168
2019	5954	0	7740	4168
2020	5954	0	7740	4168
2021	5954	0	7740	4168
2022	5954	0	7740	4168
2023	5954	0	7740	4168
2024	5954	0	7740	4168
2025	5954	0	7740	4168
2026	5954	0	7740	4168
2027	5954	0	7740	4168
2028	5954	0	7740	4168
2029	5954	0	7740	4168
2030	5954	0	7740	4168
2031	5954	0	7740	4168
2032	5954	0	7740	4168
2033	5954	0	7740	4168
2034	5954	0	7740	4168
2035	5954	0	7740	4168
2036	5954	0	7740	4168
2037	5954	0	7740	4168
2038	5954	0	7740	4168
2039	5954	0	7740	4168
2040	5954	0	7740	4168

2517

2518

2519

2520 **Table B.2C (continued).** Fall and spring covariate values for mean daily exports.

2521

Year	Mean Daily Exports (cfs, Feb-Apr)			
	Mean	None	Up 30%	Down 30%
2041	5954	0	7740	4168
2042	5954	0	7740	4168
2043	5954	0	7740	4168
2044	5954	0	7740	4168
2045	5954	0	7740	4168
2046	5954	0	7740	4168
2047	5954	0	7740	4168
2048	5954	0	7740	4168
2049	5954	0	7740	4168
2050	5954	0	7740	4168
2051	5954	0	7740	4168
2052	5954	0	7740	4168
2053	5954	0	7740	4168
2054	5954	0	7740	4168
2055	5954	0	7740	4168
2056	5954	0	7740	4168
2057	5954	0	7740	4168
2058	5954	0	7740	4168
2059	5954	0	7740	4168
2060	5954	0	7740	4168
2061	5954	0	7740	4168
2062	5954	0	7740	4168
2063	5954	0	7740	4168

2522

2523

2524

2525

2526 **Table B.2D.** Fall and spring covariate values for Freeport sediment concentration, Keswick
 2527 discharge and Deer Creek discharge.

2528

Year	Freeport Sediment Concentration (mg/L, Feb-Apr)		Keswick Discharge (cfs, Jan-Mar)		Deer Creek Discharge (cfs, Oct-Dec)	
	Study 9.2	Study 9.5	Study 9.2	Study 9.5	Study 9.2	Study 9.5
2007	39.4	38.0	5243	5300	263	263
2008	39.0	36.0	3434	3304	199	199
2009	47.7	35.6	3641	3428	171	171
2010	59.0	52.4	7253	4820	127	127
2011	61.4	49.0	3250	3250	725	725
2012	79.7	75.7	9926	8546	631	631
2013	147.8	123.3	14349	12033	442	442
2014	50.6	44.4	13435	11368	230	230
2015	120.5	86.0	16243	11469	303	303
2016	30.0	24.3	3953	3250	1034	1034
2017	91.6	87.0	20651	18332	192	192
2018	79.6	45.9	10356	4860	370	370
2019	168.1	155.8	32284	29055	196	196
2020	63.6	52.3	11435	9122	142	142
2021	47.2	41.4	3250	3250	333	333
2022	51.4	39.9	7469	3250	276	276
2023	69.0	48.8	7814	3994	730	730
2024	131.0	108.6	7531	6533	252	252
2025	32.2	26.3	4428	3992	1016	1016
2026	69.7	71.0	9841	8544	275	275
2027	53.1	41.2	9921	7004	525	525
2028	113.4	84.9	12309	9262	207	207
2029	90.5	70.8	9851	7587	449	449
2030	127.2	110.0	19597	12796	564	564
2031	87.1	74.1	25746	21687	683	683
2032	76.1	57.8	13406	11874	233	233
2033	57.3	38.2	9342	4974	355	355
2034	106.2	87.0	15483	12171	1025	1025
2035	137.0	112.5	28265	24483	238	238
2036	121.7	90.0	14762	11115	229	229
2037	33.0	26.7	3250	4583	135	135
2038	20.8	19.5	4865	3933	213	213
2039	126.1	91.5	15667	6976	144	144
2040	67.2	42.1	3896	3250	367	367

2529

2530

2531

2532 **Table B.2D (continued).** Fall and spring covariate values for Freeport sediment
 2533 concentration, Keswick discharge and Deer Creek discharge.

2534

Year	Freeport Sediment Concentration (mg/L, Feb-Apr)		Keswick Discharge (cfs, Jan-Mar)		Deer Creek Discharge (cfs, Oct-Dec)	
	Study 9.2	Study 9.5	Study 9.2	Study 9.5	Study 9.2	Study 9.5
2041	104.3	89.4	19408	14964	217	217
2042	60.7	39.8	7729	3740	1069	1069
2043	164.6	155.7	16139	14051	591	591
2044	159.0	147.5	36756	33072	1237	1237
2045	60.7	61.4	8095	7268	358	358
2046	37.1	28.7	3250	3250	245	245
2047	130.5	123.5	26225	17841	179	179
2048	53.8	39.3	5643	3915	221	221
2049	24.6	23.4	4105	4498	177	177
2050	79.5	56.3	6010	3250	191	191
2051	28.5	25.4	3250	3306	111	111
2052	38.8	32.7	4180	3250	111	111
2053	46.9	40.3	4337	3320	187	187
2054	126.9	76.3	11370	3250	192	192
2055	41.6	31.4	3618	3701	180	180
2056	149.1	115.9	26699	19849	297	297
2057	133.7	114.9	18602	16308	903	903
2058	70.5	56.5	15811	13367	292	292
2059	147.6	130.2	33555	26125	470	470
2060	120.2	107.2	16191	14408	216	216
2061	118.0	93.0	20572	13863	173	173
2062	44.3	37.5	3250	3250	361	361
2063	49.3	39.9	7795	4871	576	576

2535

2536

2537

2538

2539 **Table B.2E.** Fall and spring covariate values for export/inflow ratios.

2540

Year	Mean Daily Export/Inflow Ratio (Mar-May), Inflows for Study 9.2, Various Export Values				Mean Daily Export/Inflow Ratio (Mar-May), Inflows for Study 9.5, Various Export Values			
	E=Mean	Zero	Mean+30%	Mean-30%	E=Mean	Zero	Mean+30%	Mean-30%
2007	0.22	0	0.29	0.15	0.27	0	0.35	0.19
2008	0.26	0	0.34	0.18	0.32	0	0.41	0.22
2009	0.16	0	0.20	0.11	0.24	0	0.31	0.17
2010	0.16	0	0.20	0.11	0.20	0	0.26	0.14
2011	0.18	0	0.23	0.12	0.25	0	0.33	0.18
2012	0.19	0	0.24	0.13	0.21	0	0.28	0.15
2013	0.06	0	0.07	0.04	0.08	0	0.10	0.06
2014	0.17	0	0.22	0.12	0.22	0	0.29	0.15
2015	0.11	0	0.14	0.07	0.16	0	0.21	0.11
2016	0.33	0	0.42	0.23	0.40	0	0.52	0.28
2017	0.12	0	0.16	0.08	0.16	0	0.20	0.11
2018	0.15	0	0.19	0.10	0.22	0	0.29	0.15
2019	0.05	0	0.06	0.03	0.07	0	0.09	0.05
2020	0.27	0	0.35	0.19	0.29	0	0.37	0.20
2021	0.27	0	0.35	0.19	0.32	0	0.42	0.22
2022	0.29	0	0.37	0.20	0.36	0	0.47	0.25
2023	0.22	0	0.29	0.16	0.27	0	0.35	0.19
2024	0.09	0	0.11	0.06	0.11	0	0.15	0.08
2025	0.30	0	0.39	0.21	0.42	0	0.54	0.29
2026	0.14	0	0.19	0.10	0.14	0	0.18	0.10
2027	0.21	0	0.28	0.15	0.27	0	0.36	0.19
2028	0.07	0	0.09	0.05	0.10	0	0.13	0.07
2029	0.20	0	0.26	0.14	0.24	0	0.31	0.17
2030	0.06	0	0.08	0.04	0.09	0	0.11	0.06
2031	0.18	0	0.23	0.12	0.20	0	0.26	0.14
2032	0.12	0	0.15	0.08	0.19	0	0.24	0.13
2033	0.21	0	0.27	0.15	0.27	0	0.35	0.19
2034	0.12	0	0.16	0.08	0.17	0	0.23	0.12
2035	0.07	0	0.08	0.05	0.08	0	0.10	0.05
2036	0.09	0	0.11	0.06	0.12	0	0.16	0.09
2037	0.30	0	0.39	0.21	0.40	0	0.52	0.28
2038	0.55	0	0.71	0.38	0.55	0	0.71	0.38
2039	0.08	0	0.10	0.06	0.11	0	0.14	0.08
2040	0.15	0	0.19	0.10	0.24	0	0.31	0.17

2541

2542

2543

2544 **Table B.2E (continued).** Fall and spring covariate values for export/inflow ratios.

2545

Year	Mean Daily Export/Inflow Ratio (Mar-May), Inflows for Study 9.2, Various Export Values				Mean Daily Export/Inflow Ratio (Mar-May), Inflows for Study 9.5, Various Export Values			
	E=Mean	Zero	Mean+30%	Mean-30%	E=Mean	Zero	Mean+30%	Mean-30%
2041	0.12	0	0.15	0.08	0.16	0	0.21	0.11
2042	0.20	0	0.26	0.14	0.30	0	0.39	0.21
2043	0.05	0	0.06	0.03	0.06	0	0.08	0.04
2044	0.03	0	0.04	0.02	0.04	0	0.05	0.03
2045	0.18	0	0.24	0.13	0.18	0	0.24	0.13
2046	0.26	0	0.34	0.18	0.33	0	0.43	0.23
2047	0.06	0	0.08	0.04	0.09	0	0.11	0.06
2048	0.22	0	0.28	0.15	0.30	0	0.39	0.21
2049	0.42	0	0.55	0.30	0.45	0	0.58	0.31
2050	0.12	0	0.15	0.08	0.17	0	0.22	0.12
2051	0.40	0	0.52	0.28	0.45	0	0.59	0.32
2052	0.25	0	0.33	0.18	0.30	0	0.40	0.21
2053	0.32	0	0.42	0.23	0.36	0	0.47	0.25
2054	0.09	0	0.11	0.06	0.17	0	0.22	0.12
2055	0.30	0	0.39	0.21	0.43	0	0.55	0.30
2056	0.03	0	0.04	0.02	0.05	0	0.06	0.03
2057	0.07	0	0.10	0.05	0.11	0	0.14	0.07
2058	0.20	0	0.26	0.14	0.22	0	0.29	0.16
2059	0.06	0	0.08	0.04	0.08	0	0.10	0.06
2060	0.11	0	0.14	0.08	0.14	0	0.18	0.10
2061	0.11	0	0.14	0.08	0.15	0	0.20	0.11
2062	0.24	0	0.32	0.17	0.31	0	0.40	0.22
2063	0.24	0	0.31	0.17	0.31	0	0.41	0.22

2546

2547

2548

2549

2550 **Table B.3A.** Winter covariate values for total exports, upwelling index and Bend Bridge
 2551 flows.

2552

Year	Total Exports (Σ daily exports (cfs), Dec-Jun)				Upwelling Index (36N, 122W, Apr-Jun)		Bend Bridge Monthly Minimum Flow (cfs, Aug-Nov)	
	Mean	Zero	Up 30%	Down 30%	Up 10%	Down 20%	Study 9.2	Study 9.5
2007	1250154	0	1625201	875108	199	145	5975	4968
2008	1250154	0	1625201	875108	139	101	4616	4309
2009	1250154	0	1625201	875108	116	84	6284	4737
2010	1250154	0	1625201	875108	136	99	5791	4441
2011	1250154	0	1625201	875108	169	123	5804	4343
2012	1250154	0	1625201	875108	144	105	5881	5458
2013	1250154	0	1625201	875108	158	115	7166	5699
2014	1250154	0	1625201	875108	195	142	10262	6713
2015	1250154	0	1625201	875108	177	129	6383	6500
2016	1250154	0	1625201	875108	318	231	5261	4191
2017	1250154	0	1625201	875108	256	186	7764	6807
2018	1250154	0	1625201	875108	220	160	8409	4863
2019	1250154	0	1625201	875108	173	126	7717	7413
2020	1250154	0	1625201	875108	320	233	5722	5274
2021	1250154	0	1625201	875108	189	138	5521	5071
2022	1250154	0	1625201	875108	186	135	6478	5026
2023	1250154	0	1625201	875108	200	145	6631	4723
2024	1250154	0	1625201	875108	157	114	8097	7236
2025	1250154	0	1625201	875108	314	229	5008	4950
2026	1250154	0	1625201	875108	239	174	5264	5109
2027	1250154	0	1625201	875108	239	174	5638	5641
2028	1250154	0	1625201	875108	223	162	7568	5882
2029	1250154	0	1625201	875108	329	239	5454	4745
2030	1250154	0	1625201	875108	240	174	7893	5639
2031	1250154	0	1625201	875108	267	194	5985	5977
2032	1250154	0	1625201	875108	263	191	9251	6681
2033	1250154	0	1625201	875108	205	149	5422	5516
2034	1250154	0	1625201	875108	270	196	6129	5944
2035	1250154	0	1625201	875108	292	213	9035	5224
2036	1250154	0	1625201	875108	262	190	9760	5488
2037	1250154	0	1625201	875108	209	152	4699	5090
2038	1250154	0	1625201	875108	192	139	4457	4557
2039	1250154	0	1625201	875108	179	130	6642	5340
2040	1250154	0	1625201	875108	282	205	6591	4465

2553

2554

2555 **Table B.3A (continued).** Winter covariate values for total exports, upwelling index and
 2556 Bend Bridge flows.

2557

Year	Total Exports (Σ daily exports (cfs), Dec-Jun)				Upwelling Index (36N, 122W, Apr-Jun)		Bend Bridge Monthly Minimum Flow (cfs, Aug-Nov)	
	Mean	Zero	Up 30%	Down 30%	Up 10%	Down 20%	Study 9.2	Study 9.5
2041	1250154	0	1625201	875108	276	201	5831	4908
2042	1250154	0	1625201	875108	297	216	6375	5114
2043	1250154	0	1625201	875108	179	130	11342	3907
2044	1250154	0	1625201	875108	180	131	11658	10590
2045	1250154	0	1625201	875108	309	225	5762	5427
2046	1250154	0	1625201	875108	212	154	6286	5278
2047	1250154	0	1625201	875108	206	150	4686	4327
2048	1250154	0	1625201	875108	191	139	6023	4359
2049	1250154	0	1625201	875108	165	120	6061	4687
2050	1250154	0	1625201	875108	193	140	5220	3852
2051	1250154	0	1625201	875108	186	135	5289	3963
2052	1250154	0	1625201	875108	270	196	3900	4303
2053	1250154	0	1625201	875108	169	123	4743	4086
2054	1250154	0	1625201	875108	173	126	6268	5149
2055	1250154	0	1625201	875108	248	180	6027	4313
2056	1250154	0	1625201	875108	185	134	6689	6797
2057	1250154	0	1625201	875108	222	161	9018	4929
2058	1250154	0	1625201	875108	248	180	5361	5755
2059	1250154	0	1625201	875108	157	114	12261	10749
2060	1250154	0	1625201	875108	378	275	10876	6441
2061	1250154	0	1625201	875108	195	142	8025	6568
2062	1250154	0	1625201	875108	285	207	6552	4070
2063	1250154	0	1625201	875108	339	246	6536	4757

2558

2559

2560

2561 **Table B.3B.** Winter covariate values for number of days that Verona flow > 56,000 cfs,
 2562 Bend Bridge water temperatures, Farallon Island ocean temperatures, and proportion of time
 2563 that the Delta Cross Channel gates are open.
 2564

Year	# Days (Dec-Mar) that Verona Flow > 56,000 cfs		Bend Bridge Average Water Temperature (°C, Jul-Sep)		Farallon Islands Ocean Temperature (°C, Feb-Apr)		Prop. of Time Delta Cross Channel Gates are Open (Dec-Mar)
	Study 9.2	Study 9.5	Study 9.2	Study 9.5	+ 0.42° C	+ 1.56° C	Mean
2007	0	0	12.5	13.8	12.3	13.4	0
2008	0	0	13.3	15.4	12.3	13.4	0
2009	6	0	14.0	14.9	12.3	13.4	0
2010	0	0	13.3	15.4	12.3	13.4	0
2011	56	39	13.4	15.6	12.3	13.4	0
2012	68	43	13.2	14.4	12.3	13.4	0
2013	39	28	13.7	15.5	12.3	13.4	0
2014	40	21	13.6	15.0	12.3	13.4	0
2015	0	0	13.6	14.6	12.3	13.4	0
2016	74	60	13.7	15.6	12.3	13.4	0
2017	20	5	13.0	14.3	12.3	13.4	0
2018	69	54	13.7	15.3	12.3	13.4	0
2019	23	9	13.9	14.7	12.3	13.4	0
2020	2	1	14.1	15.6	12.3	13.4	0
2021	8	1	13.6	15.4	12.3	13.4	0
2022	13	4	13.3	15.0	12.3	13.4	0
2023	33	12	13.3	14.7	12.3	13.4	0
2024	0	0	13.8	15.0	12.3	13.4	0
2025	49	35	13.6	15.2	12.3	13.4	0
2026	16	4	13.5	14.9	12.3	13.4	0
2027	51	24	13.2	14.8	12.3	13.4	0
2028	32	17	13.3	14.5	12.3	13.4	0
2029	60	50	14.0	15.2	12.3	13.4	0
2030	76	56	13.2	14.7	12.3	13.4	0
2031	49	28	13.6	15.0	12.3	13.4	0
2032	15	1	13.7	15.3	12.3	13.4	0
2033	62	40	13.4	15.0	12.3	13.4	0
2034	76	61	13.8	14.6	12.3	13.4	0
2035	40	25	13.1	15.5	12.3	13.4	0
2036	0	0	13.5	15.2	12.3	13.4	0
2037	0	0	14.2	15.2	12.3	13.4	0
2038	54	35	16.6	19.2	12.3	13.4	0
2039	14	3	13.4	14.4	12.3	13.4	0
2040	61	45	14.1	16.0	12.3	13.4	0

2565

2566 **Table B.3B (continued).** Winter covariate values for number of days that Verona flow >
 2567 56,000 cfs, Bend Bridge water temperatures, Farallon Island ocean temperatures, and
 2568 proportion of time that the Delta Cross Channel gates are open.

2569

year	# Days (Dec-Mar) that Verona Flow > 56,000 cfs		Bend Bridge Average Water Temperature (°C, Jul-Sep)		Farallon Islands Ocean Temperature (°C, Feb-Apr)		Prop. of Time Delta Cross Channel Gates are Open (Dec-Mar)
	Study 9.2	Study 9.5	Study 9.2	Study 9.5	+ 0.42° C	+ 1.56° C	Mean
2041	18	4	13.6	14.9	12.3	13.4	0
2042	80	64	14.3	15.6	12.3	13.4	0
2043	94	79	13.3	15.1	12.3	13.4	0
2044	50	43	14.0	14.1	12.3	13.4	0
2045	2	0	14.2	15.8	12.3	13.4	0
2046	53	45	13.8	15.6	12.3	13.4	0
2047	8	0	14.2	15.6	12.3	13.4	0
2048	0	0	14.1	16.1	12.3	13.4	0
2049	12	0	14.2	17.3	12.3	13.4	0
2050	0	0	13.6	16.5	12.3	13.4	0
2051	0	0	14.0	18.0	12.3	13.4	0
2052	2	0	15.0	18.7	12.3	13.4	0
2053	46	24	14.6	19.7	12.3	13.4	0
2054	0	0	13.9	15.0	12.3	13.4	0
2055	70	56	14.4	16.5	12.3	13.4	0
2056	59	40	14.5	15.3	12.3	13.4	0
2057	69	54	14.2	15.5	12.3	13.4	0
2058	79	65	13.5	15.2	12.3	13.4	0
2059	58	42	14.6	14.7	12.3	13.4	0
2060	49	31	13.2	14.7	12.3	13.4	0
2061	4	1	14.8	15.9	12.3	13.4	0
2062	25	13	14.9	17.4	12.3	13.4	0
2063	39	21	15.1	17.0	12.3	13.4	0

2570

2571

2572

2573 **APPENDIX C: GROWTH ANALYSIS AND MODELLING**

2574 In this appendix we provide a description of the methods we used to collect and
 2575 analyze length information from various state and federal collection facilities in the
 2576 Sacramento drainage. We assembled time series of lengths, both upstream and downstream,
 2577 for both hatchery fish and combined hatchery and wild aggregates. Where possible, we used
 2578 upstream and downstream lengths to obtain annual growth estimates. In the absence of a
 2579 downstream growth measurement, we assembled a time series of downstream lengths. We
 2580 performed regressions on growth and length estimates, evaluating impacts of environmental
 2581 conditions on growth.

2582 *INTRODUCTION*

2583 The life-cycle modeling analysis in this project attempts to attribute variability in
 2584 survival to environmental factors during different parts of the life history. Survival can be
 2585 affected by the environment in complex ways, and can be mediated through biotic and abiotic
 2586 processes. We posit that size can play a role in predicting survival, and that growth itself can
 2587 be an indicator of survival as well. An obvious mechanism for size effects on survival would
 2588 be that larger fish are less vulnerable to predation than smaller fish. A mechanism for growth
 2589 being a predictor of survival would be that faster growing fish are likely to be experiencing
 2590 better feeding conditions and bioenergetic advantages, and therefore should survive better.

2591 In this appendix we look for relationships between environmental conditions and
 2592 growth, but because growth requires two measurements (a capture and a recapture, or a
 2593 release and recapture), we are not always able to get an estimate of a growth increment. Some
 2594 length estimates obtained from survey data cannot be connected to later surveys, and
 2595 therefore a growth estimate can't be derived from the measurements. An example of this
 2596 occurs with rotary screw traps operating in tributaries, where juvenile size samples are
 2597 obtained during rearing and migration. Those sizes are not directly comparable to later
 2598 samples obtained downstream, because the downstream samples are aggregates of all the
 2599 independent upstream sampled lengths. We might be able to document a pattern in upstream
 2600 sizes over the years, but growth to the downstream measurement can't be inferred. We
 2601 therefore treat size as a surrogate for growth, with the assumption that annual variability in
 2602 juvenile size is in actual fact a measurement of annual variability in growth since all fish must
 2603 at some point have emerged from the gravel at roughly the same sizes.

2604 *METHODS*

2605 We performed an analysis of length and growth patterns for Spring and Fall run
 2606 Chinook in the Sacramento River in relation to environmental factors. We collected size at
 2607 release and recapture data from state and federal agencies. We compiled records into average
 2608 sizes at release for several different stock aggregates that provided adequate sample sizes for
 2609 the years the data were available. In some case, it was possible to associate the length of a
 2610 downstream recaptured fish with a known upstream release size to obtain a growth increment

2611 estimate, but in other cases only the downstream size record was available. Upstream length
 2612 records were obtained from hatchery release information, from screw traps operated in
 2613 tributaries, and from seine surveys operated throughout the Sacramento drainage. The farthest
 2614 downstream sizes were obtained from Chipps Island, where mid-water trawl surveys
 2615 collected size information and recorded the race of the fish based on the presence of a CWT
 2616 or a length based estimated based on the length of the fish at the time the sample was
 2617 obtained.

2618 *Data compilation*

2619 *Length data*

2620 The Pacific States Marine Fisheries Commission manages and supports the Regional
 2621 Mark Processing Center (RMPC; <http://www.rmpc.org/>), which in turn manages the Regional
 2622 Mark Information System (RMIS). Agencies and organizations throughout the Western
 2623 United States report CWT data directly to the RMIS. The Delta Juvenile Fish Monitoring
 2624 Program (DJFMP) was initiated in the 1970s and is managed by the US Fish and Wildlife
 2625 Service (USFWS, 2014). The program has a stated objective to monitor the effects of water
 2626 projects in the Bay Delta on juvenile Chinook.

2627 The number of juvenile salmon leaving freshwater during the spring has been sampled
 2628 annually since 1978 by means of mid-water trawling in the estuary near Chipps Island
 2629 (Brandes and McLain 2001). The Trawl site in Suisun Bay is sampled three days per week
 2630 year round. It is sometimes sampled daily and at times two shifts per day for a total of 20
 2631 tows per day during May and June. During December and January, trawls occur 7 days per
 2632 week with ten 20 minute trawls conducted daily. Catch limits are imposed when Delta Smelt
 2633 catches exceed 8 individual Delta Smelt. The trawl survey records fish length at capture and
 2634 creates a record of the race, origin and release location if a coded wire tag is detected.

2635 We used data that had been collected since 1979 in mid-water boat trawls at Chipps
 2636 Island, Suisun Bay (Zone 10 S UTM, 4211218N, 595531E). Data from the DJFMP is
 2637 available online (<http://www.fws.gov/stockton/jfmp/>). USFWS tables available online
 2638 contained metrics of juvenile Chinook salmon that had been marked with CWTs, released
 2639 throughout the Sacramento - San Joaquin Basin and then recovered near Chipps Island in
 2640 Suisun Bay (*Coded Wire Tag 1978 -2011.xls* and *Coded Wire Tag 2012 -2013.xls*). Survey
 2641 records not containing CWTs can be found in the spreadsheets *Chipps Island Trawls 1976-*
 2642 *2011.xlsx* and *Chipps Island Trawls 2012-2014.xlsx*.

2643 We used the records from the Chipps Island trawls to create a database of fish lengths
 2644 and growths increments for all fish with CWTs (referred to as the CWT table). Each fish with
 2645 a CWT is of a known origin, so the race and the source (hatchery or wild stock origin) are
 2646 also known. We used the remaining records from the Chipps Island survey to construct a
 2647 database table of Chinook known to be of a given race, but where the origin is not known.
 2648 These records were assembled into a table we refer to as the TRAWL table, which only
 2649 distinguishes between Fall and Spring runs.

2650 We compiled juvenile salmon length data from the Sacramento watershed and the San
 2651 Francisco Bay Delta into a relational database in order to determine growth of hatchery Fall
 2652 Chinook and hatchery and wild juvenile Spring Chinook. Wild Spring stocks included Deer,
 2653 Mill and Butte creeks. Butte Creek fish were release and recaptured in Butte Creek, the Sutter

2654 Bypass or near Chipps Island in Suisun Bay. Release and recovery data were compiled from
 2655 three sources: California Department of Fish and Wildlife (CDFW), US Fish and Wildlife
 2656 Service's Delta Juvenile Fish Monitoring Program (DJFMP) and the Regional Mark
 2657 Processing Center (RMPC).

2658 From 1995 to 2001, the CDFW captured, measured, marked, and released wild
 2659 spring-run Chinook on Butte Creek (CDFG, 1999; CDFG, 2004-2; CDFG, 2004-3). The
 2660 purpose of the CDFW program was to estimate adult escapement, monitor timing and
 2661 abundance of juvenile outmigration, and monitor relative growth rates in the Butte Creek
 2662 system. Fish were captured and marked with adipose fin clips and coded wire tags at the
 2663 Parrot-Phelan Diversion Dam (PPDD; Zone 10 S UTM, 4396287N, 611463E). Releases
 2664 took place at three locations, but varied from year to year. Release sites were: PPDD,
 2665 Baldwin Construction Yard (approximately one mile downstream of the PPDD) and Adams
 2666 Dam (approximately 7 miles downstream of PPDD). After release, marked fish were subject
 2667 to recapture and sacrifice at downstream locations in Butte Creek, the Sutter Bypass and the
 2668 Sacramento Delta near Chipps Island. Rotary screw traps were used to recapture fish at all
 2669 locations and an off-stream fish screen outfitted with a trap box was used to collect fish at the
 2670 PPDD site. Recaptured fish were sacrificed, measured for fork length and their CWTs were
 2671 extracted and read. We received programmatic data formatted in a Microsoft Access
 2672 database directly from the CDFW (C. Garman, personal communication, 1/30/2014).

2673 We queried the RMIS database for juvenile Chinook that had been marked and
 2674 released at any location in the Sacramento drainage. The RMIS table was then related by
 2675 CWT code to Chipps Island mid-water trawl and Sacramento River recoveries. In this way,
 2676 we queried recoveries with release locations only within the Sacramento Basin.

2677 We obtained tributary measurements of juvenile lengths from rotary screw traps
 2678 (RSTs) operating in Butte creek, Mill creek and Deer creek. Rotary screw traps were operated
 2679 by the US Fish and Wildlife Service in Mill and Deer creeks, and by the California
 2680 Department of Fish and Wildlife in Butte creek. Screw trap operation spanned 1995-2010 in
 2681 the records used in this analysis. We used samples obtained from January to June of each
 2682 year to obtain estimates of tributary outmigration size.

2683 ***Environmental data***

2684 We compiled time series of environmental variables that pertain to the experiences of
 2685 downstream migration juveniles. For Spring Run, we used discharge at the three creeks
 2686 (Deer, Mill and Butte), flow, exports volumes and other export indices, and a CPUE index of
 2687 bass abundance. Flow temperature and discharge were obtained from USGS gauging stations
 2688 (<http://waterdata.usgs.gov/nwis/inventory>). Exports and other dayflow parameters were
 2689 obtained from water project data available on the California department of water resources
 2690 website (<http://www.water.ca.gov/dayflow/output/Output.cfm>). Environmental variables
 2691 were normalized by subtracting the mean and dividing by the standard deviation. The
 2692 variables are summarized in Table C.1 for Spring run and in Table C.2 for Fall run.

2693

2694 **Table C.1 Environmental variables used in length and growth analysis of Spring**
 2695 **Chinook.**

Covariate	Description	Location	Data Origin
Deer discharge	Average monthly water discharge (cfs) at Deer Creek	Vinna, Deer Creek	USGS 11383500 DEER C NR VINA CA
Mill discharge	Average monthly water discharge (cfs) on Mill Creek	Molinos, Mill Creek	USGS 11381500 MILL C NR LOS MOLINOS CA
Butte discharge	Average monthly water discharge (cfs) on Butte Creek	Chico, Butte Creek	USGS 11390000 BUTTE C NR CHICO CA
Yolo flow	Peak (maximum) streamflow into YOLO Bypass at Woodland, CA	Into Yolo at Woodland, CA	USGS 11453000 YOLO BYPASS NR WOODLAND CA
Bass	Index of Striped Bass abundance as number of striped bass kept. This is NOT effort standardized, but effort data is not available <1980	Delta	Marty Gingris personal comm.
GEO	The amount of water reaching the Mokelumne River system from the Sacramento River via the Delta Cross Channel and Georgiana Slough	Delta cross channel and Georgiana Slough	Dayflow: Delta Cross Channel and Georgiana Slough Flow Estimate (QXGEO)
EXP	Accounts for all water diverted from the Delta by the Federal and State governments to meet water agreements and contracts. These include Central Valley Project pumping at Tracy (QCVP), the Contra Costa Water District Diversions at Middle River (new for WY 2010; data begin on 01AUG2010), Rock Slough, and Old River (QCCC), the North Bay Aqueduct export (QNBAQ), and State Water Project exports (Banks Pumping Plant or Clifton Court Intake, QSWP).	South Delta	Dayflow: Total Delta Exports and Diversions/Transfers (QEXPORTS).
EXPIN	The Export/Inflow Ratio is the combined State and Federal Exports divided by the total Delta inflow (QTOT). EXPIN = (QCVP+QSWP-BBID)/QTOT (8)	Delta	Dayflow: Export/Inflow Ratio (EXPIN)

CD	The Dayflow parameter net channel depletion (QCD) is an estimate of the quantity of water removed from Delta channels to meet consumptive use (QGCD)	Delta	Dayflow: Net Channel Depletion (QCD)
CVP	Dayflow parameter for Central Valley Project pumping at Tracy (QCVP)	Delta	

2696

2697 **Table C.2 Environmental variables used in length and growth analysis of Fall Chinook**

Covariate Name	Description	Location	Data Origin
Keswick discharge	Average monthly water discharge (cfs) at Keswick Dam	Keswick Dam	USGS 11370500 SACRAMENTO R A KESWICK CA
Battle discharge	Average monthly water discharge (cfs) on Battle Creek	Cottonwood, Battle Creek	USGS 11376550 BATTLE C BL COLEMAN FISH HATCHERY NR COTTONWOOD CA
Battle height	Peak gauge height for the water year	Cottonwood, Battle Creek	USGS 11376550 BATTLE C BL COLEMAN FISH HATCHERY NR COTTONWOOD CA
Feather discharge	Average monthly water discharge (cfs) on the Feather River	Oronville, Feather River	USGS 11407000 FEATHER R A OROVILLE CA
Feather temp	Feather River average maximum temperature from USGS gage with (daily) interpolations from Sacramento, CA air temperature (1992+)	Oronville, Feather River	USGS 11407000 FEATHER R A OROVILLE CA
American temp	American River average maximum temperature from USGS gage with (daily) interpolations from Sacramento, CA air temperature (~1978-1998)	Fair Oaks, American River	USGS 11446500 AMERICAN R A FAIR OAKS CA
Yolo flow	Peak (maximum) streamflow into YOLO Bypass at Woodland, CA	Into Yolo at Woodland, CA	USGS 11453000 YOLO BYPASS NR WOODLAND

			CA
Bass	Index of Striped Bass abundance as number of striped bass kept. This is NOT effort standardized, but effort data is not available <1980	Delta	Marty Gingris personal comm.
GEO	The amount of water reaching the Mokelumne River system from the Sacramento River via the Delta Cross Channel and Georgiana Slough	Delta: DCC and Georgiana Slough	Dayflow: Delta Cross Channel and Georgiana Slough Flow Estimate (QXGEO)
EXP	Accounts for all water diverted from the Delta by the Federal and State governments to meet water agreements and contracts. These include Central Valley Project pumping at Tracy (QCVP), the Contra Costa Water District Diversions at Middle River (new for WY 2010; data begin on 01AUG2010), Rock Slough, and Old River (QCCC), the North Bay Aqueduct export (QNBAQ), and State Water Project exports (Banks Pumping Plant or Clifton Court Intake, QSWP).	South Delta	Dayflow: Total Delta Exports and Diversions/Transfers (QEXPORTS).
EXPIN	The Export/Inflow Ratio is the combined State and Federal Exports divided by the total Delta inflow (QTOT). $EXPIN = (QCVP+QSWP-BBID)/QTOT$ (8)	Delta	Dayflow: Export/Inflow Ratio (EXPIN)
CD	The Dayflow parameter net channel depletion (QCD) is an estimate of the quantity of water removed from Delta channels to meet consumptive use (QGCD)	Delta	Dayflow: Net Channel Depletion (QCD)
CVP	Dayflow parameter for Central Valley Project pumping at Tracy (QCVP)	Delta	Dayflow: Central Valley Project Pumping (QCVP)
SWP	Dayflow parameter for State Water Project exports (Banks Pumping	Delta	Dayflow: State Water Project Pumping

	Plant or Clifton Court Intake, QSWP)		(QSWP)
--	--------------------------------------	--	--------

2698 *Length and Growth analysis*

2699 We examined environmental factors affecting length at recapture at Chipps Island of
 2700 fish with known and unknown release lengths. Where length at release was known, we
 2701 examined growth rates. We associated each size and growth record with environmental
 2702 factors experienced by each race of salmon each year the sizes were recorded. We compared
 2703 fall and spring length at capture at Chipps Island from two separate surveys. The CWT table
 2704 provided an estimate of growth for fall and spring hatchery releases. The mid-water trawls
 2705 did not distinguish between wild and hatchery fish, so those analyses pertain to the race as a
 2706 whole, without distinction about release locations or wild/hatchery distinctions. We also
 2707 obtained sizes from DJFMP seines in Region 1 (upstream from the Delta) and compared
 2708 those sizes with Chipps Island size information. Since seine samples do not distinguish
 2709 between populations, growth obtained from subtracting upstream seine sizes from Chipps
 2710 Island trawl sizes provide estimates of aggregate Fall and Spring run sizes, but cannot
 2711 distinguish between release locations or between wild and hatchery releases.

2712 **SEINE/TRAWL - growth by race from mid-Sacramento to Chipps Island.**

2713 We queried the DJFMP seine database to obtain estimates of growth for Spring and
 2714 Fall runs. Region 1 of the DJFMP beach seine runs from Colusa State Park to Elkhorn. We
 2715 averaged lengths of Spring and Fall seine lengths for each year for fish collected between
 2716 January and June, and compared those to Chipps Island midwater trawl sizes. The trawl
 2717 survey assigned fish to Fall and Spring runs based on size ranges and records indicated that
 2718 all collections occurred in May and June. We calculated the growth for each race of fish each
 2719 year as the difference between the average trawl length and the average seine length. We
 2720 refer to these growth estimates as the SEINE/TRAWL dataset.

2721 We examined growth patterns in relation to environmental variables listed in Tables
 2722 C.1 and C.2. We performed stepwise linear regressions of growth in relation to each variable,
 2723 adding variables according to best p-value, and stopping when no further significant variables
 2724 were found.

2725 **CWT –growth and length by hatchery source.**

2726 When hatchery fish are released, the average size of a sample of the release batch is
 2727 used as the release length of record for fish in the batch. When recaptures occur at Chipps
 2728 Island, a record for each fish recaptured can be compared to a release length record on the
 2729 basis of CWT codes. To get reasonable sample sizes for recaptures, we were forced to
 2730 aggregate hatchery releases such that release locations were ignored. We aggregated all
 2731 release locations within the Sacramento drainage for each hatchery source. Since a release
 2732 batch contains a range of lengths, it is possible for the smallest recaptured fish to be smaller
 2733 than the average released fish. The growth record for each year was calculated as the average
 2734 of all the recapture lengths minus the average release length. The average of release length
 2735 was calculated as the weighted release length, weighted by the number released at each
 2736 location at each time of release. We refer to the length and growth estimates from this method
 2737 as the CWT dataset.

2738 We tested for statistical relationships between size at recapture and environmental
 2739 variables for Spring and Fall hatchery releases from Coleman National Fish Hatchery
 2740 (CNFH) and Feather Fish Hatchery (FFH). We examined growth and length patterns in
 2741 relation to environmental variables listed in Tables C.1 and C.2. We performed stepwise
 2742 linear regressions of growth and length in relation to each variable, adding variables
 2743 according to best p-value, and stopping when no further significant variables were found.

2744 **TRAWL – length by race at Chipps Island.**

2745 We selected records that were not limited to CWT tagged fish (the TRAWL dataset in
 2746 this analysis) from Chipps Island, and assembled all records of Spring and Fall chinook to
 2747 look at the size. By not being limited to CWT matches, the sample size was much larger than
 2748 for the CWT matched database, but for the TRAWL dataset, the origin of fish could not be
 2749 determined. The race of the fish was assigned by a length/timing criteria established by the
 2750 DJFMP (the “Race Table” found at www.fws.gov/stockton/jfmp). Using these records we
 2751 looked for temporal trends, comparisons between Spring and Fall runs, and relationships
 2752 between size at capture and environmental factors. Annual average size records for Spring
 2753 and Fall Chinook do not distinguish between hatchery and wild, and there is no growth
 2754 estimate because the size at release is not known, and there is no way to distinguish between
 2755 Butte, Mill, and Deer creeks. The TRAWL dataset provides an aggregate estimate of length
 2756 at Chipps Island by race alone.

2757 We examined growth patterns in relation to environmental variables listed in Tables
 2758 C.1 and C.2. We performed stepwise linear regressions of length in relation to each variable,
 2759 adding variables according to best p-value, and stopping when no further significant variables
 2760 were found. We treat length as a surrogate for growth on the assumption that some initial
 2761 length can be treated as a constant across and all variability can be thought of as occurring
 2762 after that initial length.

2763 **RST – Lengths in tributaries**

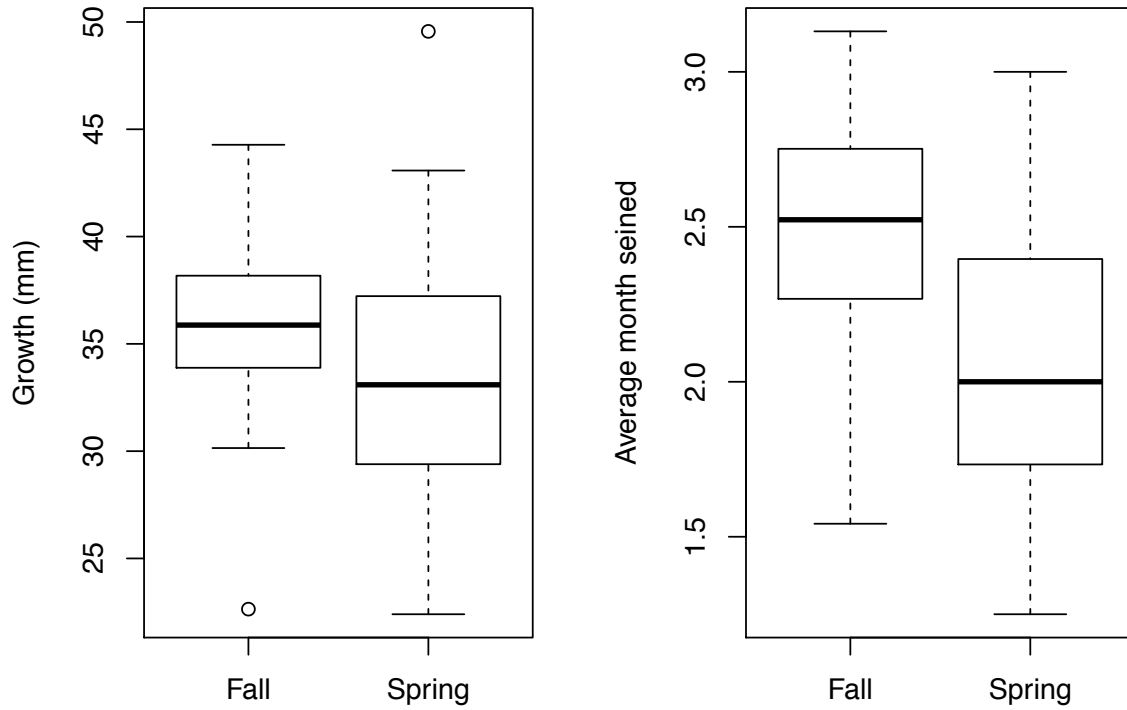
2764 Deer, Mill, and Butte creek rotary screw trap records were queried to obtain estimates
 2765 of out-migrating juvenile sizes. We took the average size of all samples obtained from the
 2766 traps between January and June of each migration year. We attempted to match CWT
 2767 releases from Butte Creek each year to recoveries within the Sacramento basin to obtain
 2768 growth estimates at various sample locations, but found that recoveries were too few to
 2769 obtain good estimates of growth. Butte Creek CWT release records with Chipps Island
 2770 recapture events began in 1996, but recaptures amounted to fewer than 10 fish per year at
 2771 Chipps Island. It was not possible to relate RST lengths to downstream lengths at Chipps
 2772 Island for a growth estimate. We therefore limited our examination of RST data to showing
 2773 temporal trends of sizes of Deer, Mill and Butte creeks.

2774 *RESULTS*

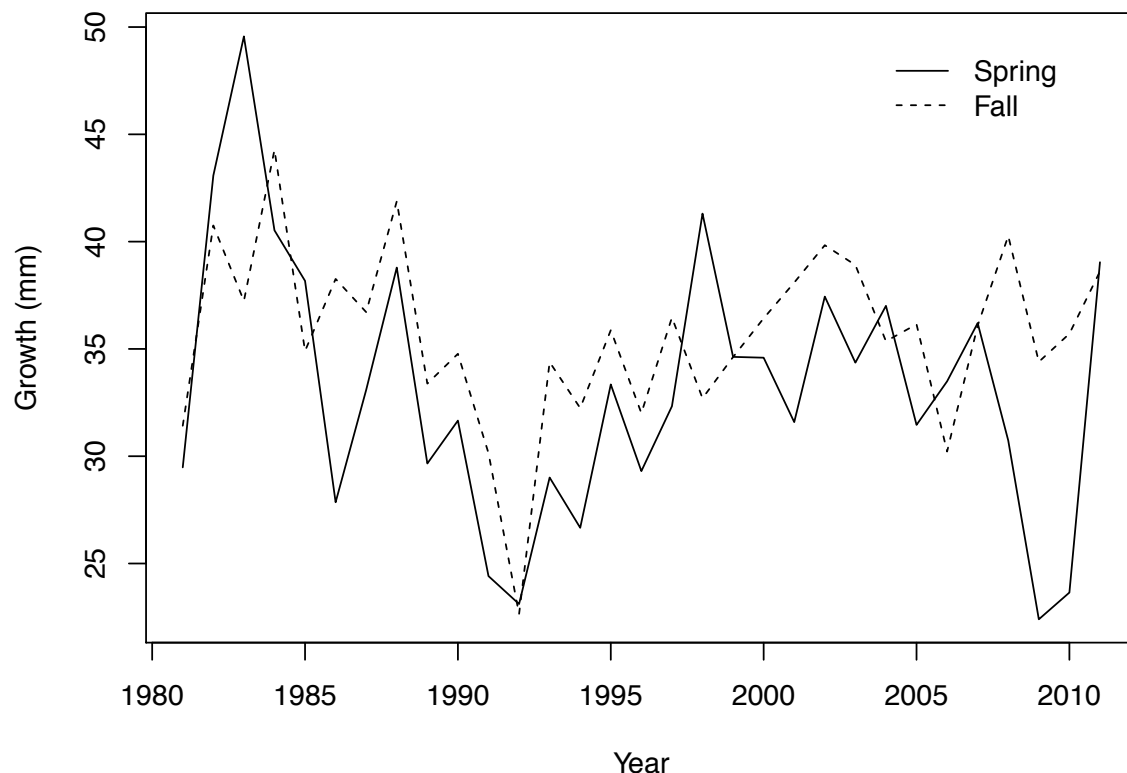
2775 **SEINE/TRAWL - growth by race from mid-Sacramento to Chipps Island.**

2776 The average growth of Spring and Fall Chinook are shown in Figure C.1 along with
 2777 the time elapsed between Seine surveys and mid-water trawls. The temporal trend in growth
 2778 is shown in Figure C.2. Fall Chinook appear to be slightly larger and on average seen in seine
 2779 surveys about half of a month later. Predominantly, Fall Chinook appear to grow slightly

2780 more between Seine and mid-water trawl surveys, which is noteworthy, since they do so in
 2781 less time as seen in the average month seined calculation.



2782 **Figure C.1 Growth between release and sampling at Chipps Island (left panel) and**
 2783 **month at which Region 1 seine was sampled (right panel).**
 2784



2785
2786 **Figure C.2 Temporal trends in Spring and Fall Chinook growth evaluated from beach**
2787 **seine and mid-water trawl surveys.**

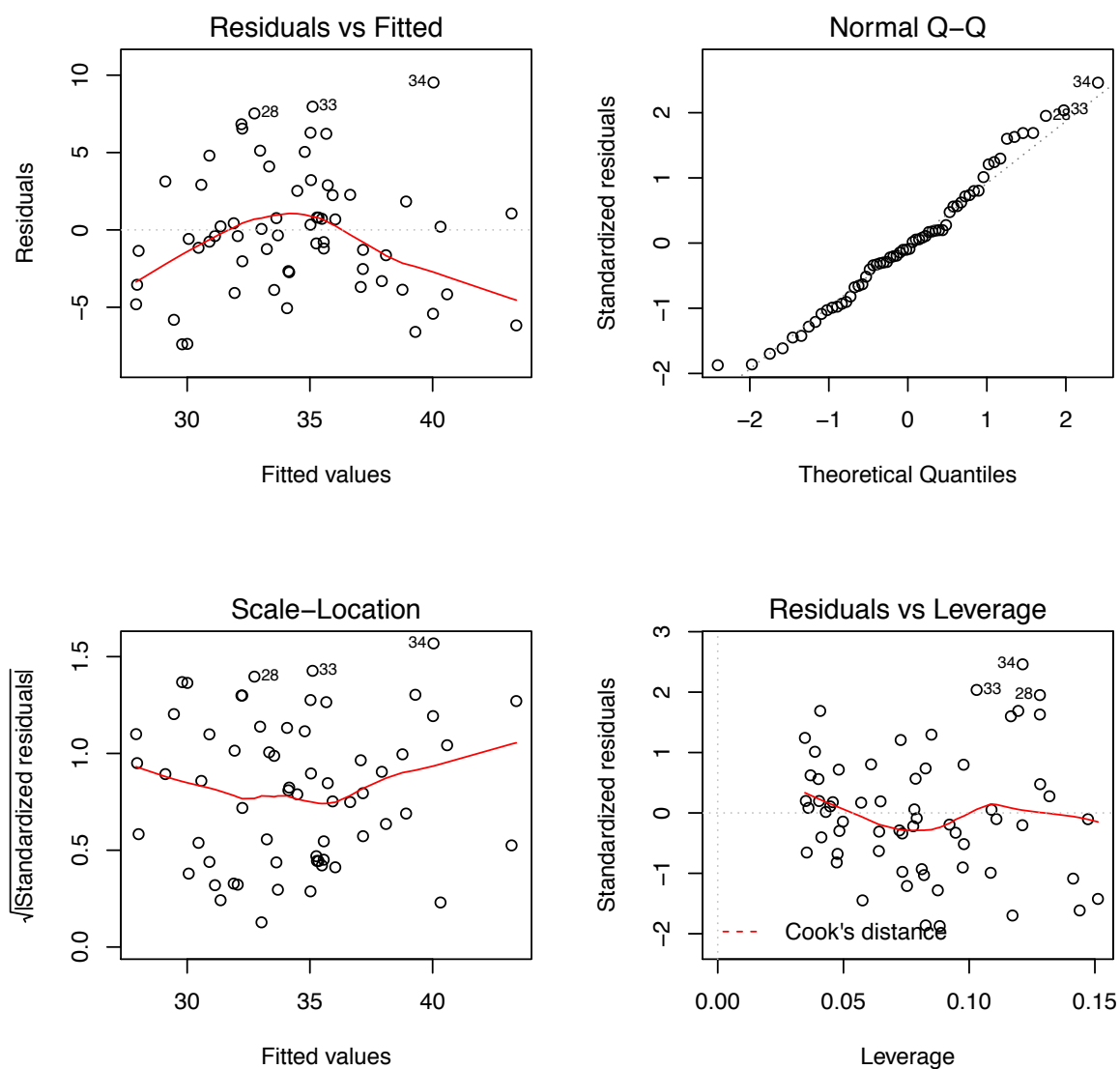
2788 Table C.3 shows the results of stepwise linear regressions. The regression results
2789 show that there are significant effects of Bass, Central Valley Project exports, race (spring or
2790 fall run), and the export to inflow ratio (EXPIN). The bass index shows a positive effect on
2791 growth. Central Valley Project exports also show a positive effect, but the export to inflow
2792 ratio shows a negative effect. The adjusted R-squared value for the fit was 0.4068. The
2793 diagnostic plot of the fit is shown in Figure C.3.

2794

2795 **Table C.3 Regression results of growth in SEINE/TRAWL data in relation to**
2796 **environmental variables. Intercept in parentheses.**

Coefficients:	Estimate	Std. Error	t value	Pr(> t)	Signif
(int-Fall)	38.3357	0.9227	41.546	<2.00E-16	***
Bass	5.4229	1.3838	3.919	0.000241	***
CVP	3.8959	0.7293	5.342	1.67E-06	***
Spring	-3.5728	1.0712	-3.335	0.001503	**
EXPIN	-1.3115	0.6071	-2.16	0.034961	*

*** p<0.001, **p<0.01, *p<0.05, . p<0.1



2797
2798 **Figure C.3 Diagnostic plot of best fitting model of seine-trawl growth of Spring and Fall**
2799 **chinook.**

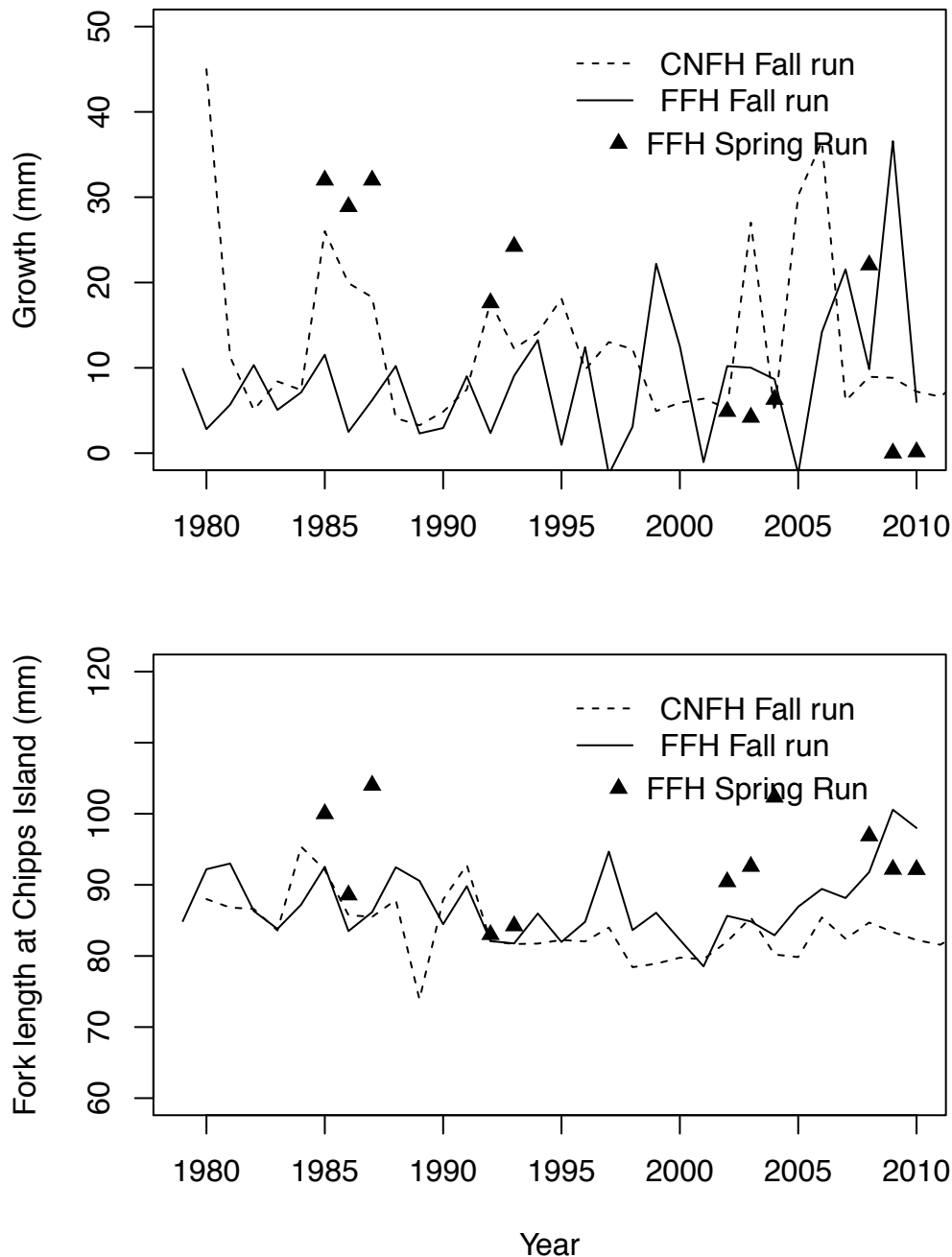
2800

2801 **CWT –growth and length by hatchery source.**

2802 Feather Fish Hatchery (FFH) spring Chinook and Coleman National Fish Hatchery
2803 (CNFH) fall Chinook growth and lengths at Chippis Island are shown in Figure C.4. We see
2804 that there is considerable variability in growth, and that Spring run fish appear to have grown
2805 faster than Fall run until the early 1990's, but are now growing less than Fall run (see Figure
2806 C.4 upper panel). Table C.4 shows the results of stepwise regressions of length against all
2807 Spring and Fall run covariates. The export to inflow ratio was the only significant predictor of
2808 catch length in the Chippis Island trawl, with EXPIN having a positive effect. The adjusted R-
2809 squared for the best fitting model shown was 0.3414. Diagnostic plots of the best fit are
2810 shown in Figure C.5, where we can see that the residuals are normal. Regressions show a

2811 hatchery effect, finding that FFH fish arrive at Chipps Island 3.5 mm larger than CNFH fish,
 2812 but FFH fish included Spring run, which were larger. Despite growth of Spring run recoveries
 2813 appearing to decline from 1985, the lengths of Spring run fish at Chipps Island appears to be
 2814 relatively constant. We found no significant relationships between growth and environmental
 2815 variables.

2816



2817
 2818 **Figure C.4 Growth of CNFH and FFH Fall runs, and FFH Spring run (upper panel)**
 2819 **and length at Chipps Island (lower panel).**

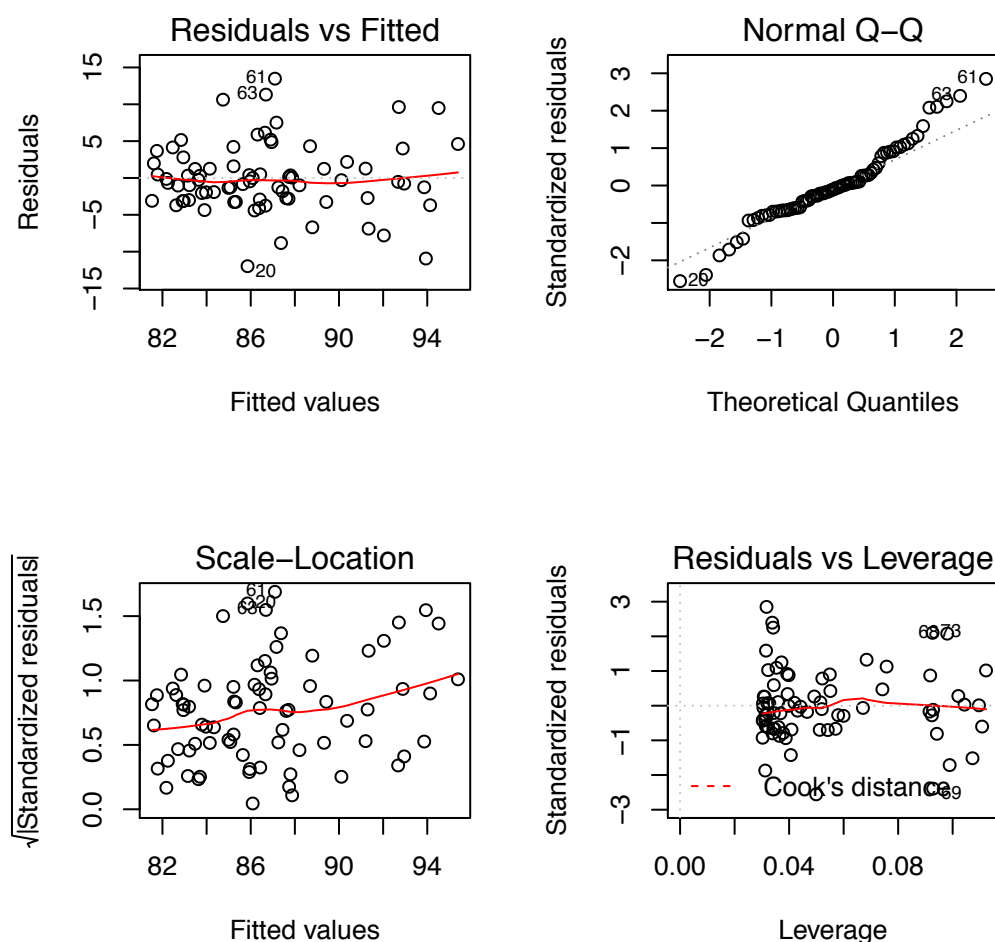
2820

2821

2822 **Table C.4 Regression results of relationship between CWT length at Chipps Island and**
 2823 **environmental variables. Intercept in parentheses for Fall CNFH.**

Coefficients:	Estimate	Std. Error	t value	Pr(> t)	Signif
(Intercept)	83.8357	0.8361	100.27	<2.00E-16	***
Race Spring	5.6019	1.6816	3.331	0.00137	**
EXPIN	1.7117	0.5764	2.969	0.00405	**
Source FFH	3.4654	1.1919	2.907	0.00484	**

*** p<0.001, **p<0.01, *p<0.05, . p<0.1

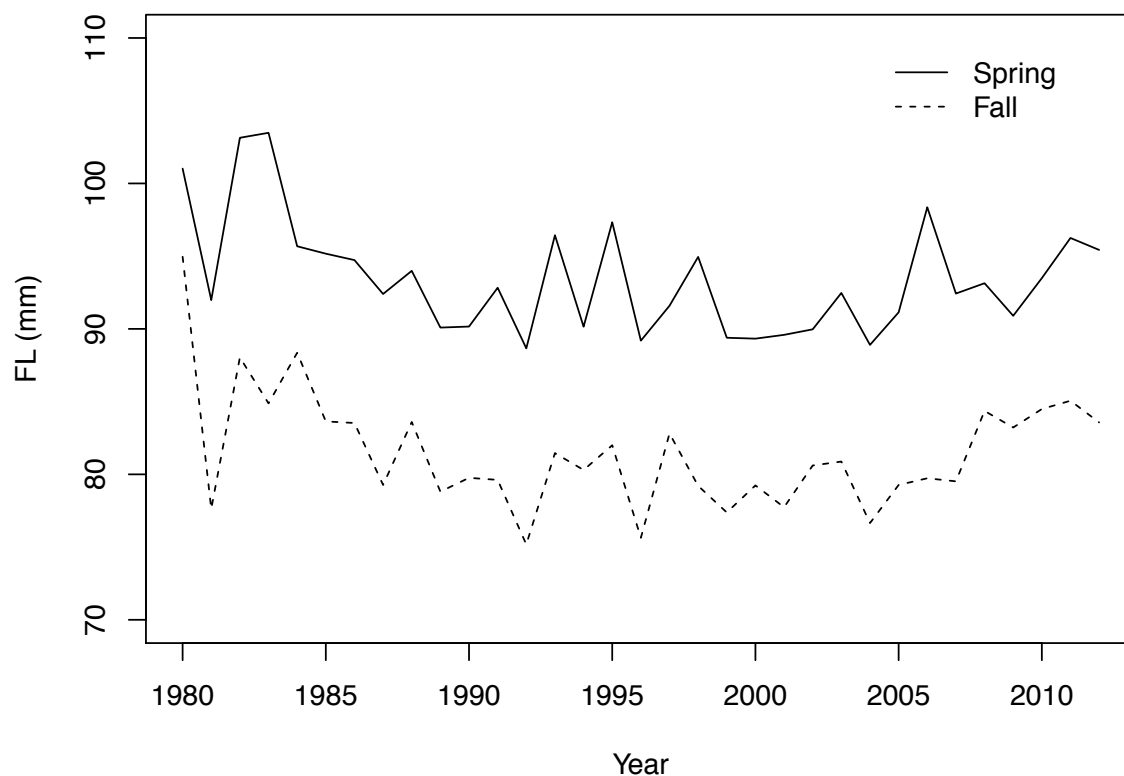


2824 **Figure C.5 Diagnostic plots of best fit of length at recapture at Chipps Island to**
 2825 **environmental variables.**
 2826

2827 **TRAWL – length by race at Chipps Island.**

2828 Unlike the CWT lengths from hatchery specific releases, the aggregated relative
 2829 Spring and Fall lengths remain consistent from the 1980's until present. Spring run appear to
 2830 be consistently larger than Fall run (see Figure C.6). Regression results are shown in Table
 2831 C.5 and indicate that Yolo flow, the Central Valley Project exports, the export to inflow ratio,
 2832 water passing via the Delta Cross Channel, and the bass index are all significant predictors of
 2833 size. The Adjusted R-squared of the best fit shown is 0.785. The diagnostic plots of the best

2834 fit is shown in Figure C.7. The TRAWL dataset had the largest samples, and despite being
 2835 aggregated wild and hatchery fish, and despite not identifying source drainages, the
 2836 regression results yield the highest R-squared. The diagnostics show normality in residuals as
 2837 well as the majority of residuals concentrated on predicted theoretical quantiles.



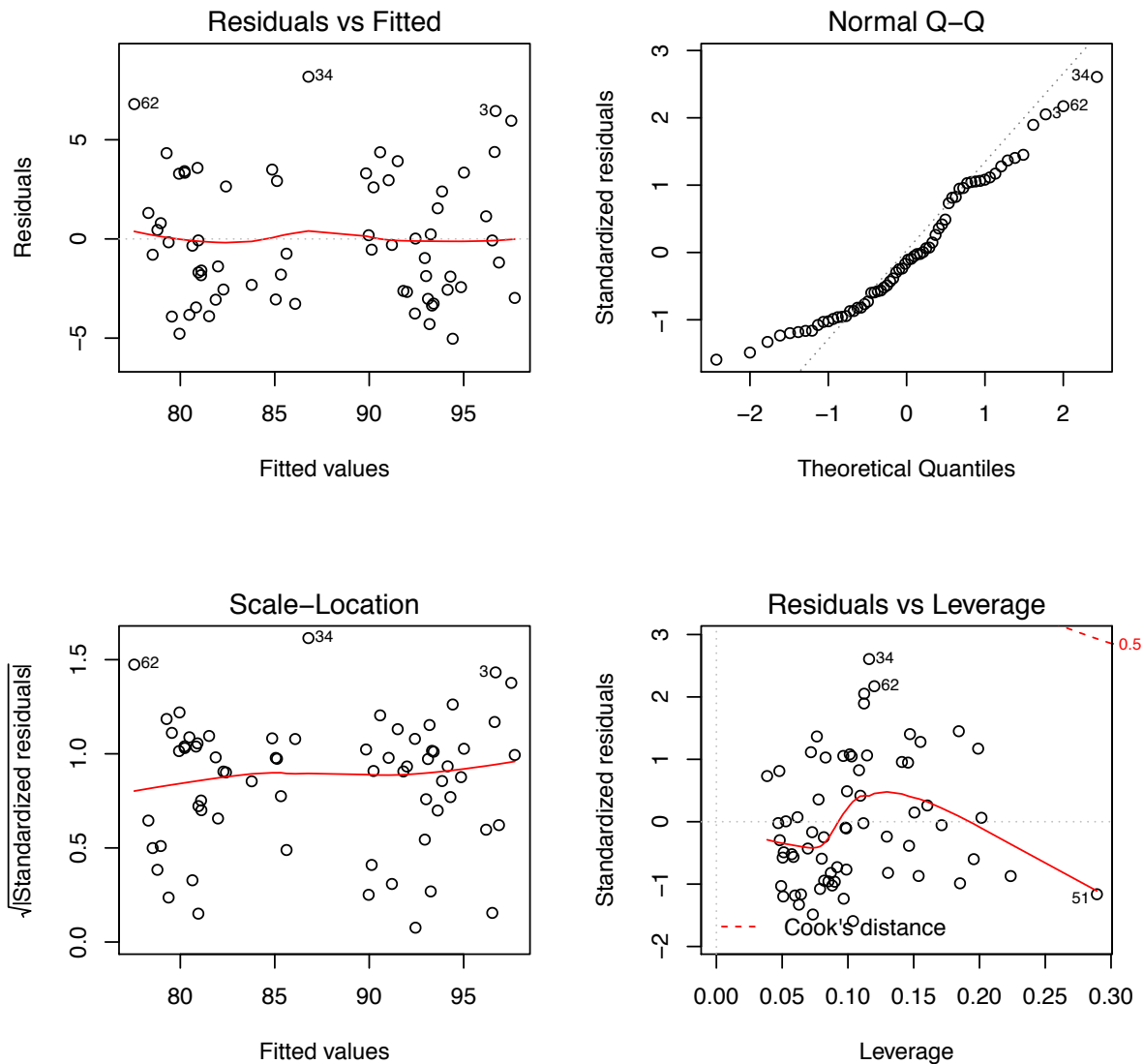
2838 **Figure C.6 Lengths of Spring and Fall aggregates at Chipps Island in TRAWL data.**
 2839

2840

2841 **Table C.5 Regression results of best fit of trawl lengths to environmental variables.**

Coefficients:	Estimate	Std. Error	t value	Pr(> t)	Signif
(Intercept)	80.9897	0.7322	110.604	<2.00E-16	***
race Spring	11.4344	0.8359	13.678	<2.00E-16	***
Yolo flow	0.99	0.5468	1.811	0.075288	.
CVP	2.6729	0.7082	3.774	0.000375	***
EXPIN	-2.5741	0.7566	-3.402	0.001206	**
GEO	-1.4716	0.6551	-2.246	0.028449	*
BASS	-1.8643	1.0438	-1.786	0.079228	.

*** p<0.001, **p<0.01, *p<0.05, . p<0.1

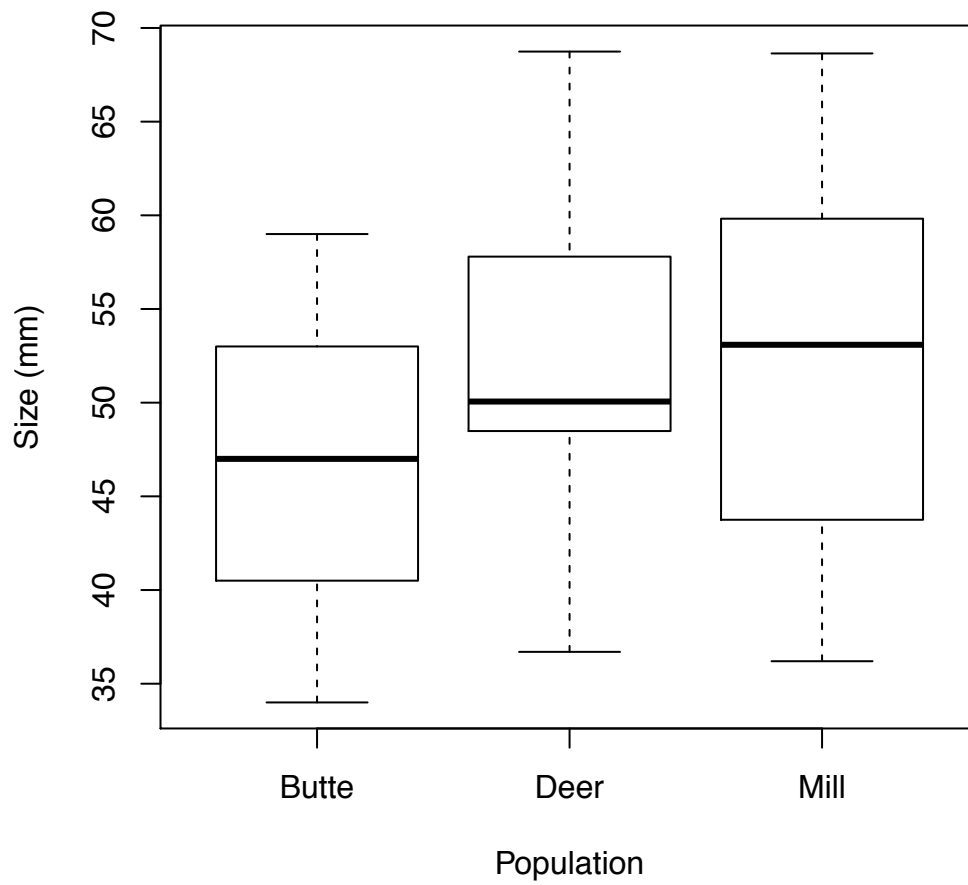


2842

2843 **Figure C.7 Diagnostic plot of best fitting model of relationship between length at Chipps**
 2844 **Island mid-water trawl and environmental variables.**

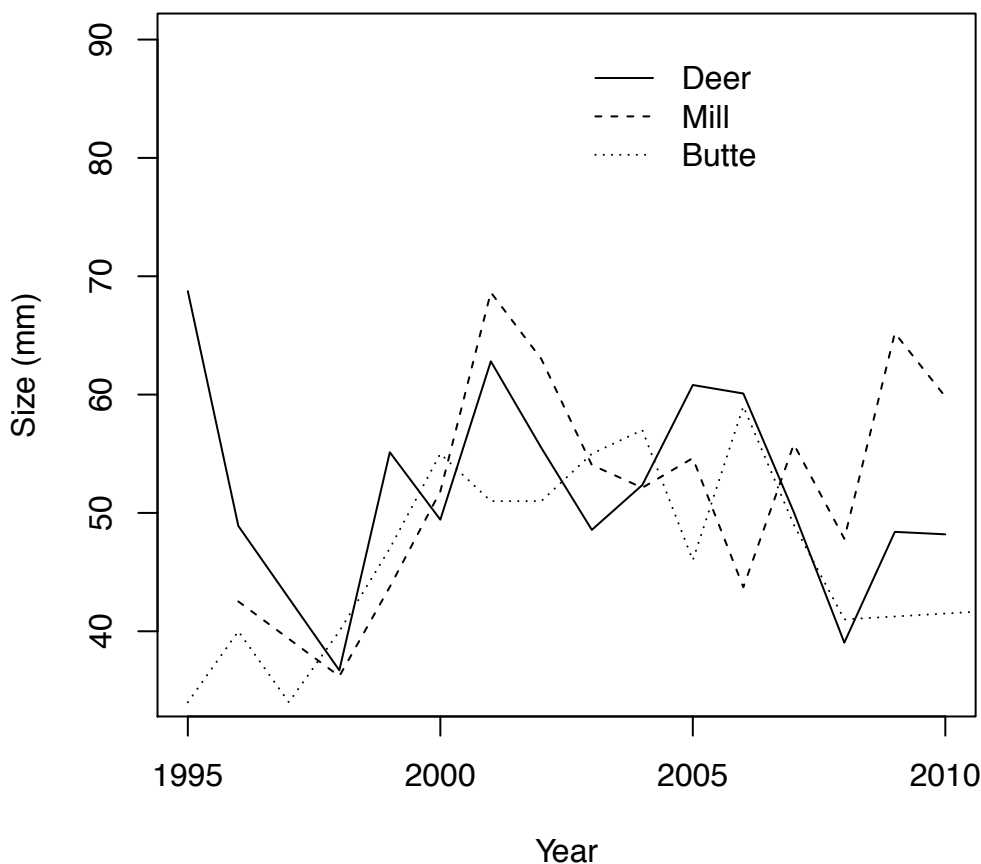
2845 **RST – Lengths in tributaries**

2846 Mill, Deer, and Butte creek Spring run average fish sizes from rotary screw trap
 2847 operations are shown in Figure C.8. We see that Mill, Deer and Butte creeks are on average
 2848 about 45-55 mm in length between January and June when records were aggregated for
 2849 outmigration estimates. The temporal pattern in sizes is shown in Figure C.9. We see no
 2850 major trend in size in tributaries between January and June, only that Butte creek fish appear
 2851 to run a bit smaller.



2852
2853
2854

Figure C.8 Average size of juveniles obtained from rotary screw traps operating in Butte, Deer and Mill creeks between January and June.



2855
 2856 **Figure C.9 Temporal trend in juvenile sizes obtained from rotary screw traps operating**
 2857 **in Deer, Butte and Mill creeks between January and June.**

2858 *DISCUSSION*

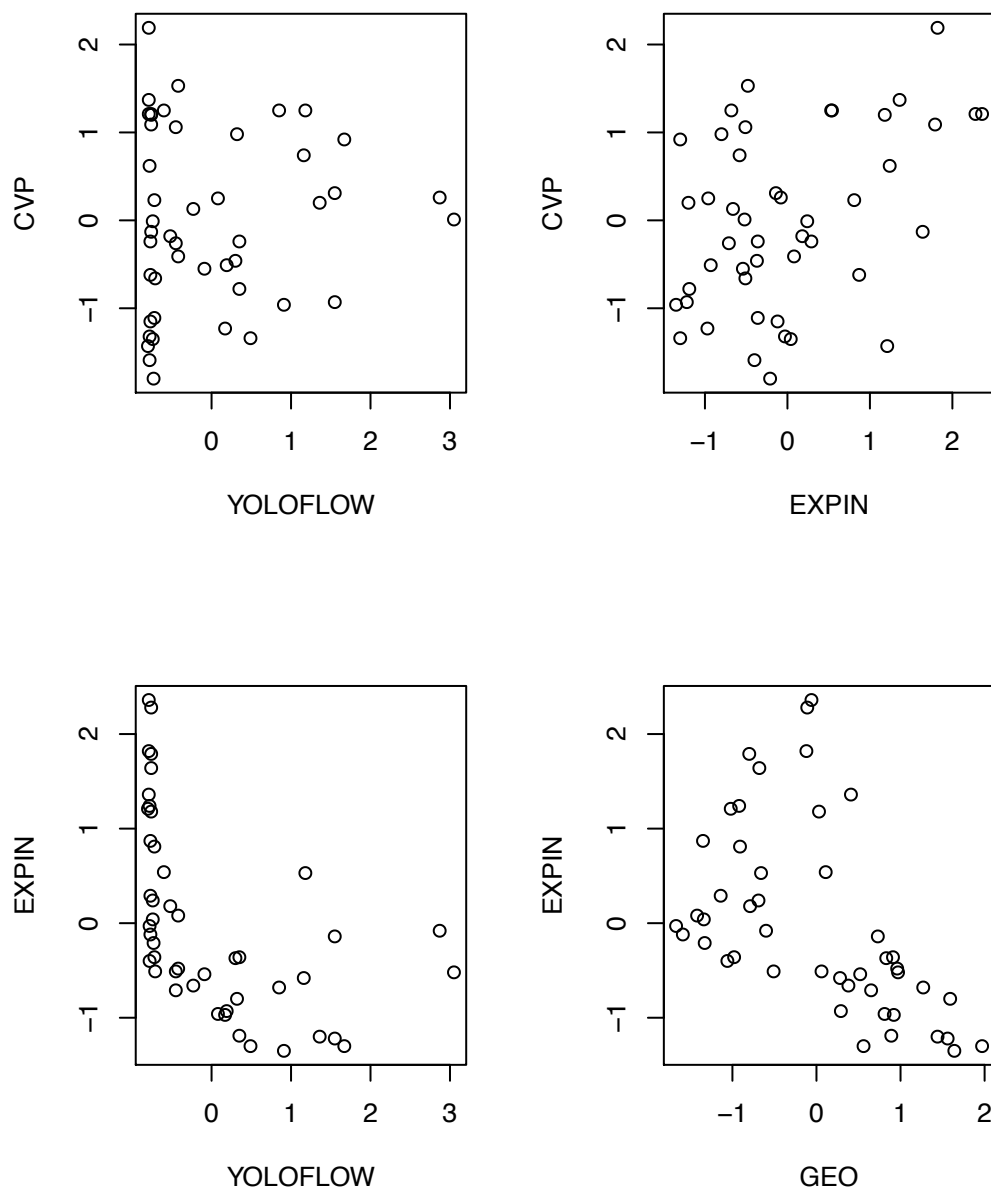
2859 This analysis drew upon varied sources of fish length information in the Sacramento
 2860 River drainage. The summary of rotary screw trap lengths indicates that Spring run out-
 2861 migrating Chinook from Deer, Mill and Butte creeks are approximately the same size, and
 2862 have been stable at approximately 55 mm in recent years. Regression analysis of recoveries
 2863 from mid-water trawl surveys at Chipps Island indicates that growth of fish from North of the
 2864 Delta to Chipps Island, as well as the length at recapture in Chipps Island trawls varied in
 2865 relation to environmental variables. Regression analyses showed that the length at Chipps
 2866 Island from the perspective of two different types of length statistics proved to be related to
 2867 environmental variables regardless of the data source of the length estimates.

2868 We used two different growth metrics. One growth metric came from lengths of CWT
 2869 recoveries and releases of hatchery fish, and the other came from seine and trawl surveys.
 2870 The CWT growth was derived from average recovery length at Chipps Island and average
 2871 release lengths at various release locations and times. The average recovery length is a
 2872 statistic based on a very small sample size relative to the release length statistic. If you

2873 consider the how many fish are released relative to recaptured, and if you consider that
2874 tagged fish are released at various locations and at different times, it is easy to see how biased
2875 the growth estimate might be. The SEINE/TRAWL growth estimate made no distinction
2876 between hatchery and non-hatchery fish and it represents an estimate of the growth of all Fall
2877 or Spring run fish between Region 1 seines and Chipps Island. In comparison to the CWT
2878 estimate, it will be more complex in it's stock composition (with hatchery and non-hatchery
2879 fish of all origins), but it is much simpler in upstream capture and release size sampling. All
2880 stocks were sampled from the same locations for sizing regardless of origin. We found a
2881 relationship between SEINE/TRAWL growth and environmental variables, but no
2882 relationship between CWT growth and environmental variables. This may be due to the
2883 complexity of how the release length was calculated for the CWT growth estimate.

2884 The environmental predictors that best explained growth were the Central Valley
2885 Project exports (CVP), the ratio of combined state and federal exports to the total Delta
2886 inflow (EXPIN), and the bass index. CVP and EXPIN are both related to flows in complex
2887 ways. CVP is related to flow because exports would tend to be less restricted at higher flows,
2888 but would have its highest impact when flows are low. We would expect that juvenile salmon
2889 growth could be high when CVP is highest under that logic. EXPIN is related to flow by a
2890 similar logic, but since EXPIN is a ratio, we would expect the largest fraction of flows to be
2891 exported when flows are low (for a given level of exports). We would expect juvenile salmon
2892 growth to be lowest when EXPIN is highest at the lowest flows.

2893 Figure C.10 illustrates some the general patterns in environmental covariation. In the
2894 upper left panel we see that CVP has the greatest degree of variability at the lowest flows
2895 (with Yolo flow being used as a surrogate for average flow at export locations). Across a
2896 range of flow values we can see that the lower bound of CVP increases. This is consistent
2897 with a general tendency of reducing exports at lower flows. The relative impact of exports at
2898 a given flow is seen with EXPIN, which we see (lower left) diminishes at higher flows. We
2899 also see that more water reaches downstream to the Mokelumne river when EXPIN is lower
2900 (lower right panel). Finally, there is a general pattern of CVP being larger when EXPIN is
2901 higher, but recall that the highest EXPIN may coincide with low flows.



2902
2903

Figure C.10 Covariation between significant environmental predictors.

2904 EXPIN was a significant predictor of length when both CWT and TRAWL datasets
 2905 were used. It was significant with $p < 0.01$ in both cases. EXPIN was also a significant
 2906 predictor ($p < 0.01$) of growth estimates of Fall and Spring aggregates obtained from the
 2907 SEINE/TRAWL dataset. The CWT length regression is in conflict with the SEINE/TRAWL
 2908 growth regression and the TRAWL length regression though. The CWT result predicts a
 2909 positive effect of EXPIN, versus a negative effect for the other two regression analyses. A
 2910 possible reason for this would be that the CWT dataset was exclusively measuring hatchery
 2911 fish (although hatchery fish would also have been present in the other two analyses). If
 2912 EXPIN has a positive effect on hatchery fish length at Chipps Island as shown in the CWT
 2913 length regression, and a negative effect on the aggregate of both hatchery and non-hatchery
 2914 fish seen in the TRAWL length and SEINE/TRAWL growth analysis, it might suggest that
 2915 that the negative effect on non-hatchery growth is even stronger than seen in the TRAWL

2916 surveys. It could also be a size related issue. If hatchery fish are smaller and more vulnerable
 2917 to entrainment, removal of the smaller fish from the out-migrating cohort would make it
 2918 appear as if they grew on average, when in fact it was just the smaller ones that did not make
 2919 it into the downstream survey sample.

2920 The relationship between flows and exports, and resulting growth and survival are
 2921 complex. We found that growth and length are negatively related to EXPIN, but positively
 2922 related to CVP. A possible mechanism, is that there is a threshold flow/export relationship
 2923 where in smaller fish become more vulnerable to entrainment. Such a mechanism would
 2924 predict that more larger fish than smaller fish make it downstream to be sampled at Chipps
 2925 Island, which has the effect of making the growth appear larger on the basis of the average
 2926 recovery size. This would appear to be favorable growth conditions despite the fact that all
 2927 individuals did not grow better on those conditions. If a relatively high CVP export year were
 2928 where to coincide with an average flow year, and if more small fish were entrained, it would
 2929 appear that fish were larger at Chipps Island.

2930 Results also indicated that Spring run were longer at Chipps Island, despite the fact
 2931 that the SEINE/TRAWL regression showed that Spring run growth was less than Fall run.
 2932 Total Central Valley Projects (combined state and federal) exports showed positive effect
 2933 on growth in the SEINE/TRAWL regression and length in the TRAWL analysis. Since there
 2934 was a negative effect from the export to inflow ratio, it may be suggest that total flows have a
 2935 positive effect, and that there may be a relationship between exports and flows that is dictated
 2936 by water extraction policies.

2937 It is interesting that regression results show that bass has a positive effect on the
 2938 growth estimates evaluated from the SEINE/TRAWL, yet has a negative effect on lengths
 2939 estimated from the TRAWL data. Since the bass index is not standardized to effort, it can't
 2940 imply a direct predation rate change on a size class of Chinook juveniles, but depending on
 2941 the relationship between the index and the size of the bass caught, it might imply a shift in the
 2942 size of Chinook vulnerable to bass predation at a given abundance of bass. It could be that
 2943 smaller fish are more vulnerable and predation biases the growth estimate by removing
 2944 smaller fish.

2945 Our examination of length/growth sensitivity to environmental variation points to a
 2946 few results. First, EXPIN is a statistically significant predictor of size and growth, with a
 2947 negative effect on both. Our samples conflate the story a bit, but if you consider that the only
 2948 positive effect was seen in the length of hatchery fish, and if you consider that the CWT
 2949 dataset had race and hatchery factors, the positive effect of EXPIN in the regression result of
 2950 the CWT data should not detract from the regression results found in both the
 2951 SEINE/TRAWL and TRAWL dataset. It should be noted however, that the highest regression
 2952 coefficient value for an environmental effect in any of our regressions was about 5, meaning
 2953 that about 5 mm per standard deviation was the maximum variability in size predicted by
 2954 variability in an environmental effect. This implies that at the extreme of 2 standard
 2955 deviations, only 10 mm of net difference in size at Chipps Island would be predicted. Still,
 2956 two standard deviations explains about 95% of the variation in environmental factors, and 10
 2957 mm explains 10-15% of the variability in length at Chipps Island (assuming 85 mm length at
 2958 Chipps Island). Since the same environmental variables explain significant variation in
 2959 rearing survival, it is feasible that length may be an instrumental in the mechanism of rearing
 2960 survival.

2961 REFERENCES

- 2962 Brandes, P.L. and J.S. McLain. 2001. Juvenile Chinook salmon abundance, distribution, and
 2963 survival in the Sacramento-San Joaquin Estuary. Pages 39 – 138 in R.L. Brown,
 2964 editor. Contributions to the Biology of Central Valley Salmonids, Volume 2, Fish
 2965 Bulletin 179. California Department of Fish and Game, Sacramento, California.
- 2966 California Department Of Fish And Game. 1998. Butte Creek Spring-Run Chinook Salmon,
 2967 *Oncorhynchus Tshawytscha*, Juvenile Outmigration And Life History 1995-1998.
 2968 Administrative Report No. 99-5.
- 2969 California Department Of Fish And Game. 2000. Butte And Big Chico Creeks Spring-Run
 2970 Chinook Salmon, *Oncoryhnchus Tshawytscha* Life History Investigation 1998-2000.
 2971 Administrative Report No. 2004-2.
- 2972 California Department Of Fish And Game. 2004. Butte And Big Chico Creeks Spring-Run
 2973 Chinook Salmon, *Oncoryhnchus Tshawytscha* Life History Investigation 2000-2001.
 2974 Administrative Report No. 2004-3.
- 2975 Garman, C.E and T. R. McReynolds. 2008. Spring-Run Chinook Salmon, *Oncoryhnchus*
 2976 *tshawytscha*, Life History Investigation. California Department of Fish and Game.
 2977 Inland Fisheries Administrative Report No. 2009-1.
- 2978 U.S. Fish and Wildlife Service – Stockton Fish and Wildlife Office. March 2014. Metadata
 2979 for the Stockton Fish and Wildlife Office’s Delta Juvenile Fish Monitoring Program.
 2980 <http://www.fws.gov/stockton/jfmp/>.

2981

2982

2983

1892

1893 **APPENDIX C: GROWTH ANALYSIS AND MODELLING**

1894 In this appendix we provide a description of the methods we used to collect and
 1895 analyze length information from various state and federal collection facilities in the
 1896 Sacramento drainage. We assembled time series of lengths, both upstream and downstream,
 1897 for both hatchery fish and combined hatchery and wild aggregates. Where possible, we used
 1898 upstream and downstream lengths to obtain annual growth estimates. In the absence of a
 1899 downstream growth measurement, we assembled a time series of downstream lengths. We
 1900 performed regressions on growth and length estimates, evaluating impacts of environmental
 1901 conditions on growth.

1902 *INTRODUCTION*

1903 The life-cycle modeling analysis in this project attempts to attribute variability in
 1904 survival to environmental factors during different parts of the life history. Survival can be
 1905 affected by the environment in complex ways, and can be mediated through biotic and abiotic
 1906 processes. We posit that size can play a role in predicting survival, and that growth itself can
 1907 be an indicator of survival as well. An obvious mechanism for size effects on survival would
 1908 be that larger fish are less vulnerable to predation than smaller fish. A mechanism for growth
 1909 being a predictor of survival would be that faster growing fish are likely to be experiencing
 1910 better feeding conditions and bioenergetic advantages, and therefore should survive better.

1911 In this appendix we look for relationships between environmental conditions and
 1912 growth, but because growth requires two measurements (a capture and a recapture, or a
 1913 release and recapture), we are not always able to get an estimate of a growth increment. Some
 1914 length estimates obtained from survey data cannot be connected to later surveys, and
 1915 therefore a growth estimate can't be derived from the measurements. An example of this
 1916 occurs with rotary screw traps operating in tributaries, where juvenile size samples are
 1917 obtained during rearing and migration. Those sizes are not directly comparable to later
 1918 samples obtained downstream, because the downstream samples are aggregates of all the
 1919 independent upstream sampled lengths. We might be able to document a pattern in upstream
 1920 sizes over the years, but growth to the downstream measurement can't be inferred. We
 1921 therefore treat size as a surrogate for growth, with the assumption that annual variability in
 1922 juvenile size is in actual fact a measurement of annual variability in growth since all fish must
 1923 at some point have emerged from the gravel at roughly the same sizes.

1924 *METHODS*

1925 We performed an analysis of length and growth patterns for Spring and Fall run
 1926 Chinook in the Sacramento River in relation to environmental factors. We collected size at
 1927 release and recapture data from state and federal agencies. We compiled records into average
 1928 sizes at release for several different stock aggregates that provided adequate sample sizes for
 1929 the years the data were available. In some case, it was possible to associate the length of a
 1930 downstream recaptured fish with a known upstream release size to obtain a growth increment

1931 estimate, but in other cases only the downstream size record was available. Upstream length
 1932 records were obtained from hatchery release information, from screw traps operated in
 1933 tributaries, and from seine surveys operated throughout the Sacramento drainage. The farthest
 1934 downstream sizes were obtained from Chipps Island, where mid-water trawl surveys
 1935 collected size information and recorded the race of the fish based on the presence of a CWT
 1936 or a length based estimated based on the length of the fish at the time the sample was
 1937 obtained.

1938 *Data compilation*

1939 *Length data*

1940 The Pacific States Marine Fisheries Commission manages and supports the Regional
 1941 Mark Processing Center (RMPC; <http://www.rmhc.org/>), which in turn manages the Regional
 1942 Mark Information System (RMIS). Agencies and organizations throughout the Western
 1943 United States report CWT data directly to the RMIS. The Delta Juvenile Fish Monitoring
 1944 Program (DJFMP) was initiated in the 1970s and is managed by the US Fish and Wildlife
 1945 Service (USFWS, 2014). The program has a stated objective to monitor the effects of water
 1946 projects in the Bay Delta on juvenile Chinook.

1947 The number of juvenile salmon leaving freshwater during the spring has been sampled
 1948 annually since 1978 by means of mid-water trawling in the estuary near Chipps Island
 1949 (Brandes and McLain 2001). The Trawl site in Suisun Bay is sampled three days per week
 1950 year round. It is sometimes sampled daily and at times two shifts per day for a total of 20
 1951 tows per day during May and June. During December and January, trawls occur 7 days per
 1952 week with ten 20 minute trawls conducted daily. Catch limits are imposed when Delta Smelt
 1953 catches exceed 8 individual Delta Smelt. The trawl survey records fish length at capture and
 1954 creates a record of the race, origin and release location if a coded wire tag is detected.

1955 We used data that had been collected since 1979 in mid-water boat trawls at Chipps
 1956 Island, Suisun Bay (Zone 10 S UTM, 4211218N, 595531E). Data from the DJFMP is
 1957 available online (<http://www.fws.gov/stockton/jfmp/>). USFWS tables available online
 1958 contained metrics of juvenile Chinook salmon that had been marked with CWTs, released
 1959 throughout the Sacramento - San Joaquin Basin and then recovered near Chipps Island in
 1960 Suisun Bay (*Coded Wire Tag 1978 -2011.xls* and *Coded Wire Tag 2012 -2013.xls*). Survey
 1961 records not containing CWTs can be found in the spreadsheets *Chipps Island Trawls 1976-*
 1962 *2011.xlsx* and *Chipps Island Trawls 2012-2014.xlsx*.

1963 We used the records from the Chipps Island trawls to create a database of fish lengths
 1964 and growths increments for all fish with CWTs (referred to as the CWT table). Each fish with
 1965 a CWT is of a known origin, so the race and the source (hatchery or wild stock origin) are
 1966 also known. We used the remaining records from the Chipps Island survey to construct a
 1967 database table of Chinook known to be of a given race, but where the origin is not known.
 1968 These records were assembled into a table we refer to as the TRAWL table, which only
 1969 distinguishes between Fall and Spring runs.

1970 We compiled juvenile salmon length data from the Sacramento watershed and the San
 1971 Francisco Bay Delta into a relational database in order to determine growth of hatchery Fall
 1972 Chinook and hatchery and wild juvenile Spring Chinook. Wild Spring stocks included Deer,
 1973 Mill and Butte creeks. Butte Creek fish were release and recaptured in Butte Creek, the Sutter

1974 Bypass or near Chipps Island in Suisun Bay. Release and recovery data were compiled from
 1975 three sources: California Department of Fish and Wildlife (CDFW), US Fish and Wildlife
 1976 Service's Delta Juvenile Fish Monitoring Program (DJFMP) and the Regional Mark
 1977 Processing Center (RMPC).

1978 From 1995 to 2001, the CDFW captured, measured, marked, and released wild
 1979 spring-run Chinook on Butte Creek (CDFG, 1999; CDFG, 2004-2; CDFG, 2004-3). The
 1980 purpose of the CDFW program was to estimate adult escapement, monitor timing and
 1981 abundance of juvenile outmigration, and monitor relative growth rates in the Butte Creek
 1982 system. Fish were captured and marked with adipose fin clips and coded wire tags at the
 1983 Parrot-Phelan Diversion Dam (PPDD; Zone 10 S UTM, 4396287N, 611463E). Releases
 1984 took place at three locations, but varied from year to year. Release sites were: PPDD,
 1985 Baldwin Construction Yard (approximately one mile downstream of the PPDD) and Adams
 1986 Dam (approximately 7 miles downstream of PPDD). After release, marked fish were subject
 1987 to recapture and sacrifice at downstream locations in Butte Creek, the Sutter Bypass and the
 1988 Sacramento Delta near Chipps Island. Rotary screw traps were used to recapture fish at all
 1989 locations and an off-stream fish screen outfitted with a trap box was used to collect fish at the
 1990 PPDD site. Recaptured fish were sacrificed, measured for fork length and their CWTs were
 1991 extracted and read. We received programmatic data formatted in a Microsoft Access
 1992 database directly from the CDFW (C. Garman, personal communication, 1/30/2014).

1993 We queried the RMIS database for juvenile Chinook that had been marked and
 1994 released at any location in the Sacramento drainage. The RMIS table was then related by
 1995 CWT code to Chipps Island mid-water trawl and Sacramento River recoveries. In this way,
 1996 we queried recoveries with release locations only within the Sacramento Basin.

1997 We obtained tributary measurements of juvenile lengths from rotary screw traps
 1998 (RSTs) operating in Butte creek, Mill creek and Deer creek. Rotary screw traps were operated
 1999 by the US Fish and Wildlife Service in Mill and Deer creeks, and by the California
 2000 Department of Fish and Wildlife in Butte creek. Screw trap operation spanned 1995-2010 in
 2001 the records used in this analysis. We used samples obtained from January to June of each
 2002 year to obtain estimates of tributary outmigration size.

2003 ***Environmental data***

2004 We compiled time series of environmental variables that pertain to the experiences of
 2005 downstream migration juveniles. For Spring Run, we used discharge at the three creeks
 2006 (Deer, Mill and Butte), flow, exports volumes and other export indices, and a CPUE index of
 2007 bass abundance. Flow temperature and discharge were obtained from USGS gauging stations
 2008 (<http://waterdata.usgs.gov/nwis/inventory>). Exports and other dayflow parameters were
 2009 obtained from water project data available on the California department of water resources
 2010 website (<http://www.water.ca.gov/dayflow/output/Output.cfm>). Environmental variables
 2011 were normalized by subtracting the mean and dividing by the standard deviation. The
 2012 variables are summarized in Table C.1 for Spring run and in Table C.2 for Fall run.

2013

2014
2015**Table C.1 Environmental variables used in length and growth analysis of Spring Chinook.**

Covariate	Description	Location	Data Origin
Deer discharge	Average monthly water discharge (cfs) at Deer Creek	Vinna, Deer Creek	USGS 11383500 DEER C NR VINA CA
Mill discharge	Average monthly water discharge (cfs) on Mill Creek	Molinos, Mill Creek	USGS 11381500 MILL C NR LOS MOLINOS CA
Butte discharge	Average monthly water discharge (cfs) on Butte Creek	Chico, Butte Creek	USGS 11390000 BUTTE C NR CHICO CA
Yolo flow	Peak (maximum) streamflow into YOLO Bypass at Woodland, CA	Into Yolo at Woodland, CA	USGS 11453000 YOLO BYPASS NR WOODLAND CA
Bass	Index of Striped Bass abundance as number of striped bass kept. This is NOT effort standardized, but effort data is not available <1980	Delta	Marty Gingris personal comm.
GEO	The amount of water reaching the Mokelumne River system from the Sacramento River via the Delta Cross Channel and Georgiana Slough	Delta cross channel and Georgiana Slough	Dayflow: Delta Cross Channel and Georgiana Slough Flow Estimate (QXGEO)
EXP	Accounts for all water diverted from the Delta by the Federal and State governments to meet water agreements and contracts. These include Central Valley Project pumping at Tracy (QCVP), the Contra Costa Water District Diversions at Middle River (new for WY 2010; data begin on 01AUG2010), Rock Slough, and Old River (QCCC), the North Bay Aqueduct export (QNBAQ), and State Water Project exports (Banks Pumping Plant or Clifton Court Intake, QSWP).	South Delta	Dayflow: Total Delta Exports and Diversions/Transfers (QEXPORTS).
EXPIN	The Export/Inflow Ratio is the combined State and Federal Exports divided by the total Delta inflow (QTOT). EXPIN = (QCVP+QSWP-BBID)/QTOT (8)	Delta	Dayflow: Export/Inflow Ratio (EXPIN)

CD	The Dayflow parameter net channel depletion (QCD) is an estimate of the quantity of water removed from Delta channels to meet consumptive use (QGCD)	Delta	Dayflow: Net Channel Depletion (QCD)
CVP	Dayflow parameter for Central Valley Project pumping at Tracy (QCVP)	Delta	

2016

2017 **Table C.2 Environmental variables used in length and growth analysis of Fall Chinook**

Covariate Name	Description	Location	Data Origin
Keswick discharge	Average monthly water discharge (cfs) at Keswick Dam	Keswick Dam	USGS 11370500 SACRAMENTO R A KESWICK CA
Battle discharge	Average monthly water discharge (cfs) on Battle Creek	Cottonwood, Battle Creek	USGS 11376550 BATTLE C BL COLEMAN FISH HATCHERY NR COTTONWOOD CA
Battle height	Peak gauge height for the water year	Cottonwood, Battle Creek	USGS 11376550 BATTLE C BL COLEMAN FISH HATCHERY NR COTTONWOOD CA
Feather discharge	Average monthly water discharge (cfs) on the Feather River	Oronville, Feather River	USGS 11407000 FEATHER R A OROVILLE CA
Feather temp	Feather River average maximum temperature from USGS gage with (daily) interpolations from Sacramento, CA air temperature (1992+)	Oronville, Feather River	USGS 11407000 FEATHER R A OROVILLE CA
American temp	American River average maximum temperature from USGS gage with (daily) interpolations from Sacramento, CA air temperature (~1978-1998)	Fair Oaks, American River	USGS 11446500 AMERICAN R A FAIR OAKS CA
Yolo flow	Peak (maximum) streamflow into YOLO Bypass at Woodland, CA	Into Yolo at Woodland, CA	USGS 11453000 YOLO BYPASS NR WOODLAND

			CA
Bass	Index of Striped Bass abundance as number of striped bass kept. This is NOT effort standardized, but effort data is not available <1980	Delta	Marty Gingris personal comm.
GEO	The amount of water reaching the Mokelumne River system from the Sacramento River via the Delta Cross Channel and Georgiana Slough	Delta: DCC and Georgiana Slough	Dayflow: Delta Cross Channel and Georgiana Slough Flow Estimate (QXGEO)
EXP	Accounts for all water diverted from the Delta by the Federal and State governments to meet water agreements and contracts. These include Central Valley Project pumping at Tracy (QCVP), the Contra Costa Water District Diversions at Middle River (new for WY 2010; data begin on 01AUG2010), Rock Slough, and Old River (QCCC), the North Bay Aqueduct export (QNBAQ), and State Water Project exports (Banks Pumping Plant or Clifton Court Intake, QSWP).	South Delta	Dayflow: Total Delta Exports and Diversions/Transfers (QEXPORTS).
EXPIN	The Export/Inflow Ratio is the combined State and Federal Exports divided by the total Delta inflow (QTOT). EXPIN = (QCVP+QSWP-BBID)/QTOT (8)	Delta	Dayflow: Export/Inflow Ratio (EXPIN)
CD	The Dayflow parameter net channel depletion (QCD) is an estimate of the quantity of water removed from Delta channels to meet consumptive use (QGCD)	Delta	Dayflow: Net Channel Depletion (QCD)
CVP	Dayflow parameter for Central Valley Project pumping at Tracy (QCVP)	Delta	Dayflow: Central Valley Project Pumping (QCVP)
SWP	Dayflow parameter for State Water Project exports (Banks Pumping	Delta	Dayflow: State Water Project Pumping

	Plant or Clifton Court Intake, QSWP)		(QSWP)
--	--------------------------------------	--	--------

2018 *Length and Growth analysis*

2019 We examined environmental factors affecting length at recapture at Chipps Island of
2020 fish with known and unknown release lengths. Where length at release was known, we
2021 examined growth rates. We associated each size and growth record with environmental
2022 factors experienced by each race of salmon each year the sizes were recorded. We compared
2023 fall and spring length at capture at Chipps Island from two separate surveys. The CWT table
2024 provided an estimate of growth for fall and spring hatchery releases. The mid-water trawls
2025 did not distinguish between wild and hatchery fish, so those analyses pertain to the race as a
2026 whole, without distinction about release locations or wild/hatchery distinctions. We also
2027 obtained sizes from DJFMP seines in Region 1 (upstream from the Delta) and compared
2028 those sizes with Chipps Island size information. Since seine samples do not distinguish
2029 between populations, growth obtained from subtracting upstream seine sizes from Chipps
2030 Island trawl sizes provide estimates of aggregate Fall and Spring run sizes, but cannot
2031 distinguish between release locations or between wild and hatchery releases.

2032 **SEINE/TRAWL - growth by race from mid-Sacramento to Chipps Island.**

2033 We queried the DJFMP seine database to obtain estimates of growth for Spring and
2034 Fall runs. Region 1 of the DJFMP beach seine runs from Colusa State Park to Elkhorn. We
2035 averaged lengths of Spring and Fall seine lengths for each year for fish collected between
2036 January and June, and compared those to Chipps Island midwater trawl sizes. The trawl
2037 survey assigned fish to Fall and Spring runs based on size ranges and records indicated that
2038 all collections occurred in May and June. We calculated the growth for each race of fish each
2039 year as the difference between the average trawl length and the average seine length. We
2040 refer to these growth estimates as the SEINE/TRAWL dataset.

2041 We examined growth patterns in relation to environmental variables listed in Tables
2042 C.1 and C.2. We performed stepwise linear regressions of growth in relation to each variable,
2043 adding variables according to best p-value, and stopping when no further significant variables
2044 were found.

2045 **CWT –growth and length by hatchery source.**

2046 When hatchery fish are released, the average size of a sample of the release batch is
2047 used as the release length of record for fish in the batch. When recaptures occur at Chipps
2048 Island, a record for each fish recaptured can be compared to a release length record on the
2049 basis of CWT codes. To get reasonable sample sizes for recaptures, we were forced to
2050 aggregate hatchery releases such that release locations were ignored. We aggregated all
2051 release locations within the Sacramento drainage for each hatchery source. Since a release
2052 batch contains a range of lengths, it is possible for the smallest recaptured fish to be smaller
2053 than the average released fish. The growth record for each year was calculated as the average
2054 of all the recapture lengths minus the average release length. The average of release length
2055 was calculated as the weighted release length, weighted by the number released at each
2056 location at each time of release. We refer to the length and growth estimates from this method
2057 as the CWT dataset.

2058 We tested for statistical relationships between size at recapture and environmental
 2059 variables for Spring and Fall hatchery releases from Coleman National Fish Hatchery
 2060 (CNFH) and Feather Fish Hatchery (FFH). We examined growth and length patterns in
 2061 relation to environmental variables listed in Tables C.1 and C.2. We performed stepwise
 2062 linear regressions of growth and length in relation to each variable, adding variables
 2063 according to best p-value, and stopping when no further significant variables were found.

2064 **TRAWL – length by race at Chipps Island.**

2065 We selected records that were not limited to CWT tagged fish (the TRAWL dataset in
 2066 this analysis) from Chipps Island, and assembled all records of Spring and Fall chinook to
 2067 look at the size. By not being limited to CWT matches, the sample size was much larger than
 2068 for the CWT matched database, but for the TRAWL dataset, the origin of fish could not be
 2069 determined. The race of the fish was assigned by a length/timing criteria established by the
 2070 DJFMP (the “Race Table” found at www.fws.gov/stockton/jfmp). Using these records we
 2071 looked for temporal trends, comparisons between Spring and Fall runs, and relationships
 2072 between size at capture and environmental factors. Annual average size records for Spring
 2073 and Fall Chinook do not distinguish between hatchery and wild, and there is no growth
 2074 estimate because the size at release is not known, and there is no way to distinguish between
 2075 Butte, Mill, and Deer creeks. The TRAWL dataset provides an aggregate estimate of length
 2076 at Chipps Island by race alone.

2077 We examined growth patterns in relation to environmental variables listed in Tables
 2078 C.1 and C.2. We performed stepwise linear regressions of length in relation to each variable,
 2079 adding variables according to best p-value, and stopping when no further significant variables
 2080 were found. We treat length as a surrogate for growth on the assumption that some initial
 2081 length can be treated as a constant across and all variability can be thought of as occurring
 2082 after that initial length.

2083 **RST – Lengths in tributaries**

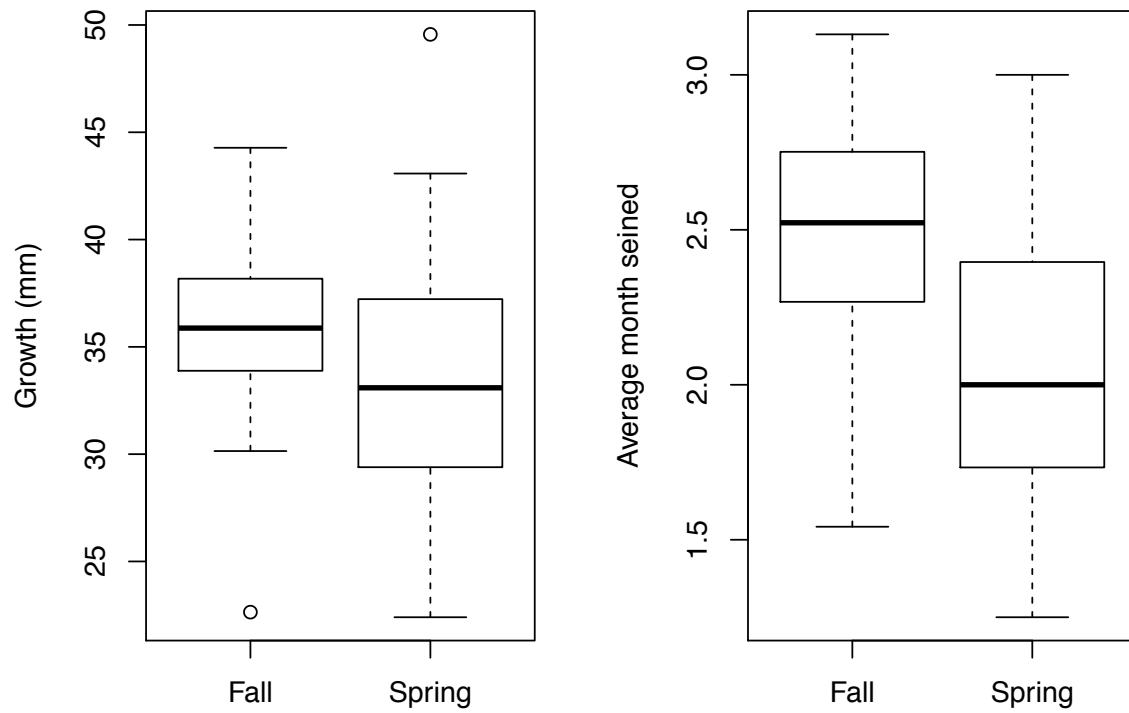
2084 Deer, Mill, and Butte creek rotary screw trap records were queried to obtain estimates
 2085 of outmigrating juvenile sizes. We took the average size of all samples obtained from the
 2086 traps between January and June of each migration year. We attempted to match CWT
 2087 releases from Butte Creek each year to recoveries within the Sacramento basin to obtain
 2088 growth estimates at various sample locations, but found that recoveries were too few to
 2089 obtain good estimates of growth. Butte Creek CWT release records with Chipps Island
 2090 recapture events began in 1996, but recaptures amounted to fewer than 10 fish per year at
 2091 Chipps Island. It was not possible to relate RST lengths to downstream lengths at Chipps
 2092 Island for a growth estimate. We therefore limited our examination of RST data to showing
 2093 temporal trends of sizes of Deer, Mill and Butte creeks.

2094 *RESULTS*

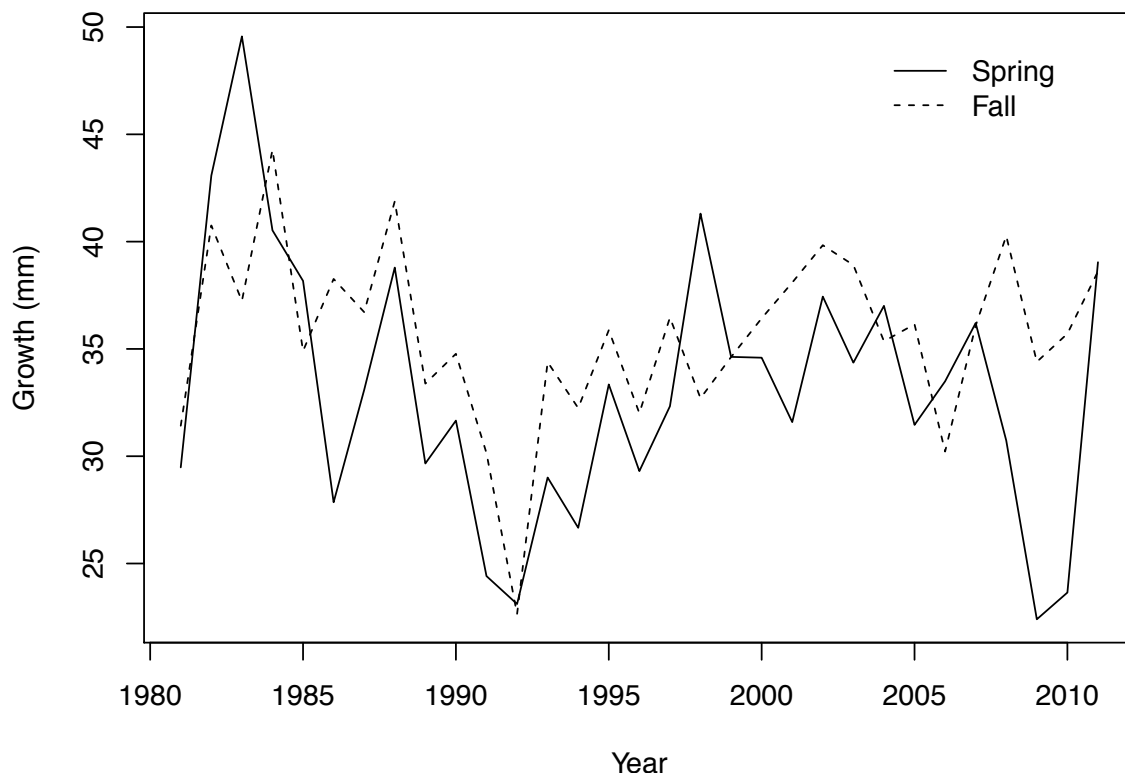
2095 **SEINE/TRAWL - growth by race from mid-Sacramento to Chipps Island.**

2096 The average growth of Spring and Fall Chinook are shown in Figure C.1 along with
 2097 the time elapsed between Seine surveys and mid-water trawls. The temporal trend in growth
 2098 is shown in Figure C.2. Fall Chinook appear to be slightly larger and on average seen in seine
 2099 surveys about half of a month later. Predominantly, Fall Chinook appear to grow slightly

2100 more between Seine and mid-water trawl surveys, which is noteworthy, since they do so in
 2101 less time as seen in the average month seined calculation.



2102 **Figure C.1 Growth between release and sampling at Chipps Island (left panel) and**
 2103 **month at which Region 1 seine was sampled (right panel).**
 2104



2105
2106 **Figure C.2 Temporal trends in Spring and Fall Chinook growth evaluated from beach**
2107 **seine and mid-water trawl surveys.**

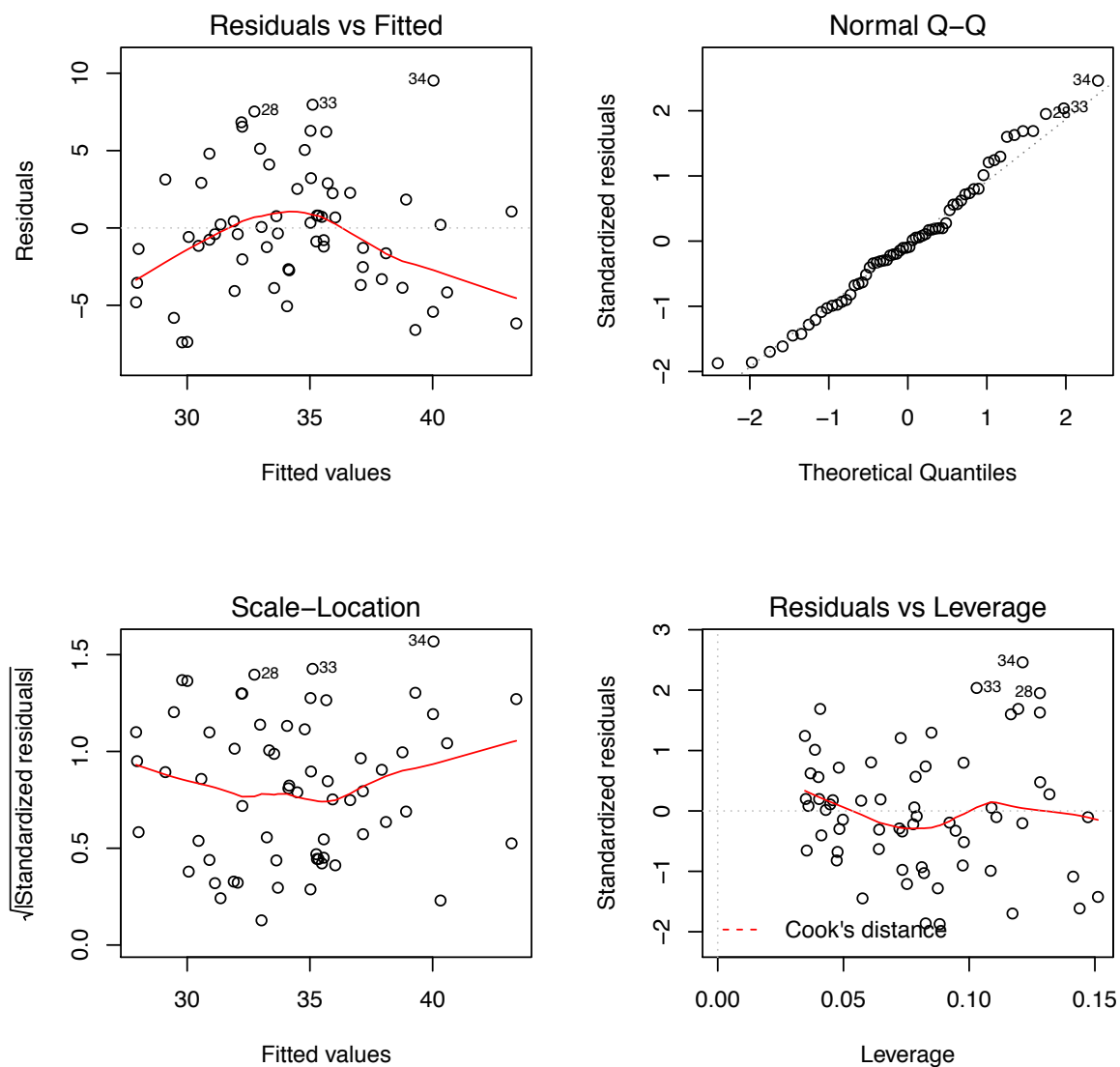
2108 Table C.3 shows the results of stepwise linear regressions. The regression results
2109 show that there are significant effects of Bass, Central Valley Project exports, race (spring or
2110 fall run), and the export to inflow ratio (EXPIN). The bass index shows a positive effect on
2111 growth. Central Valley Project exports also show a positive effect, but the export to inflow
2112 ratio shows a negative effect. The adjusted R-squared value for the fit was 0.4068. The
2113 diagnostic plot of the fit is shown in Figure C.3.

2114

2115 **Table C.3 Regression results of growth in SEINE/TRAWL data in relation to**
2116 **environmental variables. Intercept in parentheses.**

Coefficients:	Estimate	Std. Error	t value	Pr(> t)	Signif
(int-Fall)	38.3357	0.9227	41.546	<2.00E-16	***
Bass	5.4229	1.3838	3.919	0.000241	***
CVP	3.8959	0.7293	5.342	1.67E-06	***
Spring	-3.5728	1.0712	-3.335	0.001503	**
EXPIN	-1.3115	0.6071	-2.16	0.034961	*

*** p<0.001, **p<0.01, *p<0.05, . p<0.1



2117
 2118 **Figure C.3 Diagnostic plot of best fitting model of seine-trawl growth of Spring and Fall**
 2119 **chinook.**

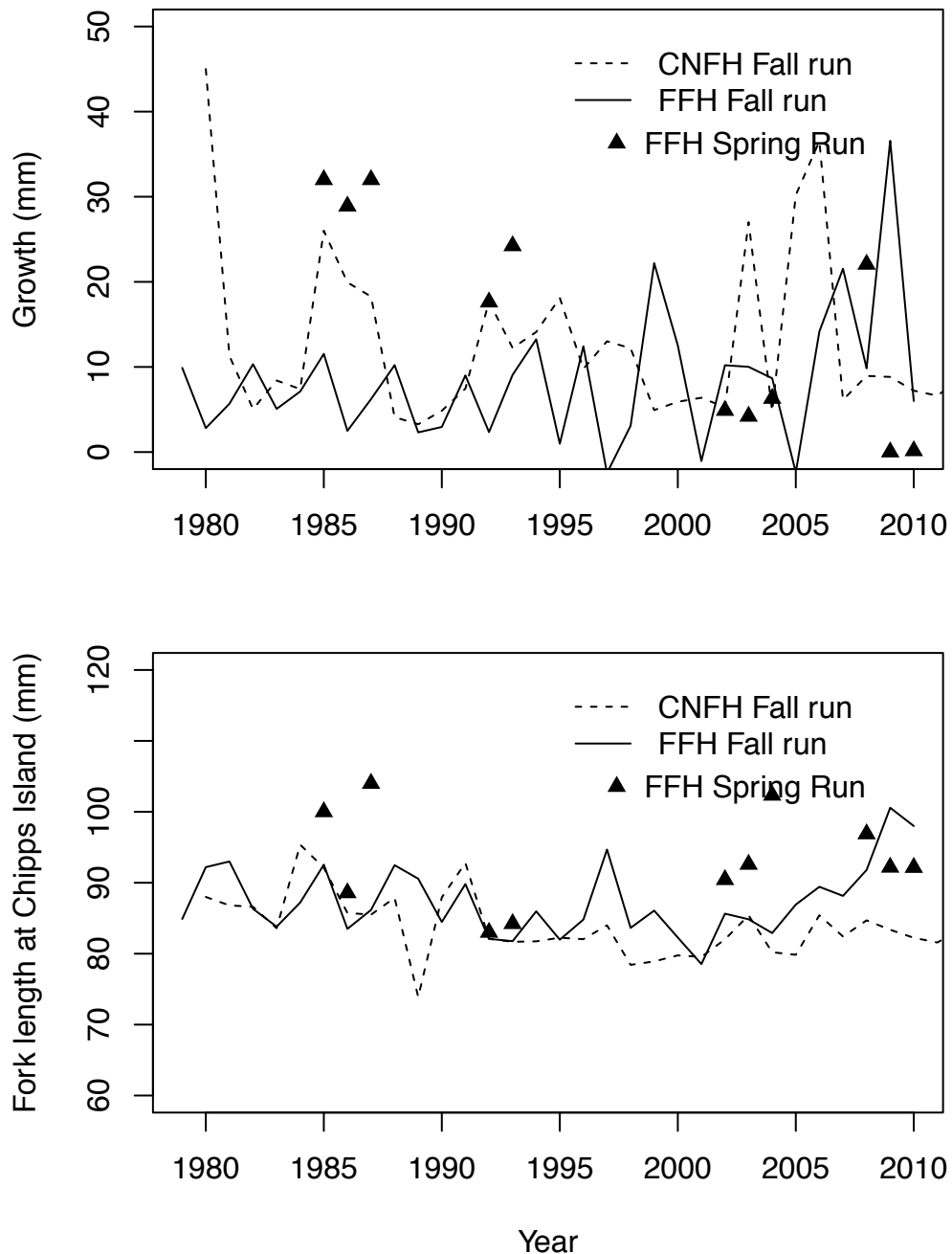
2120

2121 **CWT –growth and length by hatchery source.**

2122 Feather Fish Hatchery (FFH) spring Chinook and Coleman National Fish Hatchery
 2123 (CNFH) fall Chinook growth and lengths at Chippis Island are shown in Figure C.4. We see
 2124 that there is considerable variability in growth, and that Spring run fish appear to have grown
 2125 faster than Fall run until the early 1990's, but are now growing less than Fall run (see Figure
 2126 C.4 upper panel). Table C.4 shows the results of stepwise regressions of length against all
 2127 Spring and Fall run covariates. The export to inflow ratio was the only significant predictor of
 2128 catch length in the Chippis Island trawl, with EXPIN having a positive effect. The adjusted R-
 2129 squared for the best fitting model shown was 0.3414. Diagnostic plots of the best fit are
 2130 shown in Figure C.5, where we can see that the residuals are normal. Regressions show a

2131 hatchery effect, finding that FFH fish arrive at Chipps Island 3.5 mm larger than CNFH fish,
 2132 but FFH fish included Spring run, which were larger. Despite growth of Spring run recoveries
 2133 appearing to decline from 1985, the lengths of Spring run fish at Chipps Island appears to be
 2134 relatively constant. We found no significant relationships between growth and environmental
 2135 variables.

2136



2137
 2138 **Figure C.4 Growth of CNFH and FFH Fall runs, and FFH Spring run (upper panel)**
 2139 **and length at Chipps Island (lower panel).**

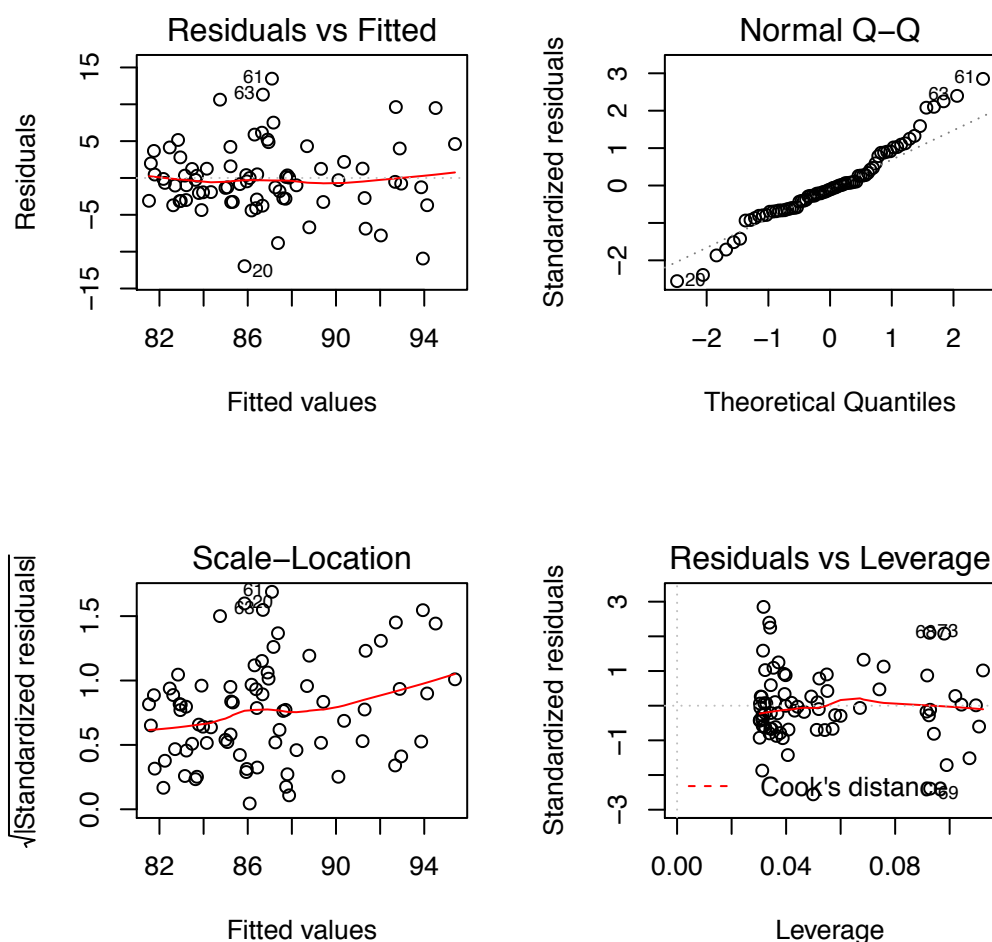
2140

2141

2142 **Table C.4 Regression results of relationship between CWT length at Chipps Island and**
 2143 **environmental variables. Intercept in parentheses for Fall CNFH.**

Coefficients:	Estimate	Std. Error	t value	Pr(> t)	Signif
(Intercept)	83.8357	0.8361	100.27	<2.00E-16	***
Race Spring	5.6019	1.6816	3.331	0.00137	**
EXPIN	1.7117	0.5764	2.969	0.00405	**
Source FFH	3.4654	1.1919	2.907	0.00484	**

*** p<0.001, **p<0.01, *p<0.05, . p<0.1

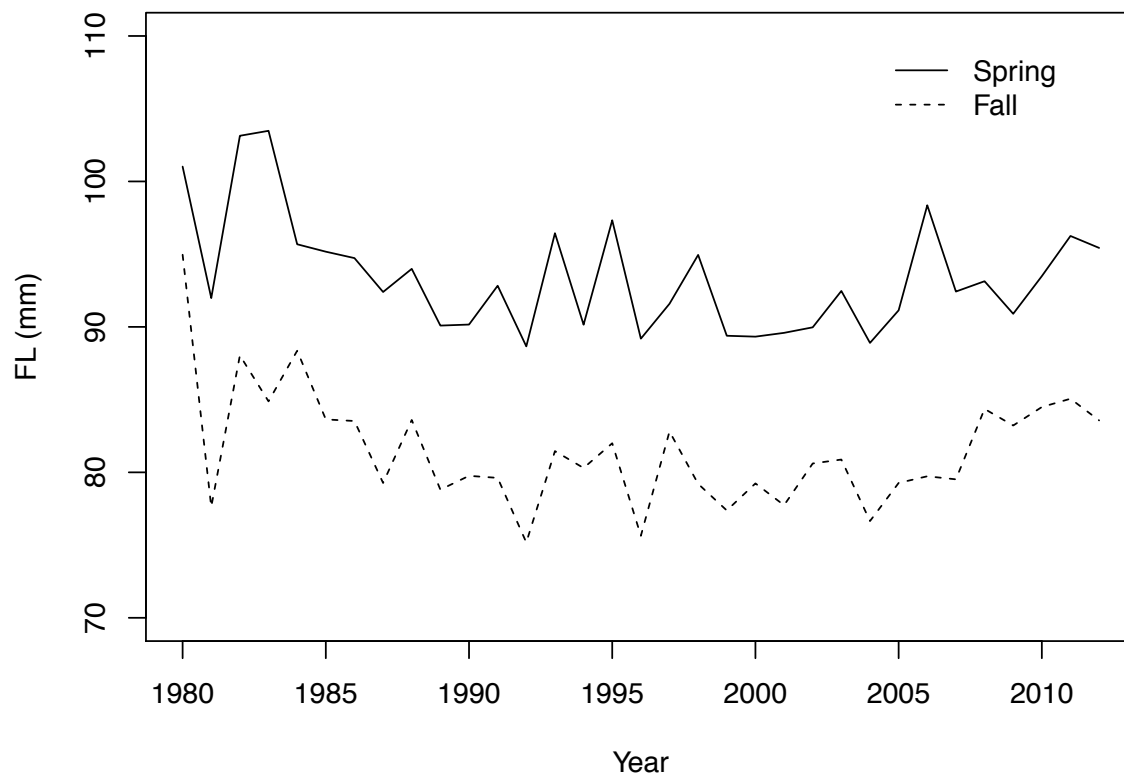


2144 **Figure C.5 Diagnostic plots of best fit of length at recapture at Chipps Island to**
 2145 **environmental variables.**
 2146

2147 **TRAWL – length by race at Chipps Island.**

2148 Unlike the CWT lengths from hatchery specific releases, the aggregated relative
 2149 Spring and Fall lengths remain consistent from the 1980's until present. Spring run appear to
 2150 be consistently larger than Fall run (see Figure C.6). Regression results are shown in Table
 2151 C.5 and indicate that Yolo flow, the Central Valley Project exports, the export to inflow ratio,
 2152 water passing via the Delta Cross Channel, and the bass index are all significant predictors of
 2153 size. The Adjusted R-squared of the best fit shown is 0.785. The diagnostic plots of the best

2154 fit is shown in Figure C.7. The TRAWL dataset had the largest samples, and despite being
 2155 aggregated wild and hatchery fish, and despite not identifying source drainages, the
 2156 regression results yield the highest R-squared. The diagnostics show normality in residuals as
 2157 well as the majority of residuals concentrated on predicted theoretical quantiles.



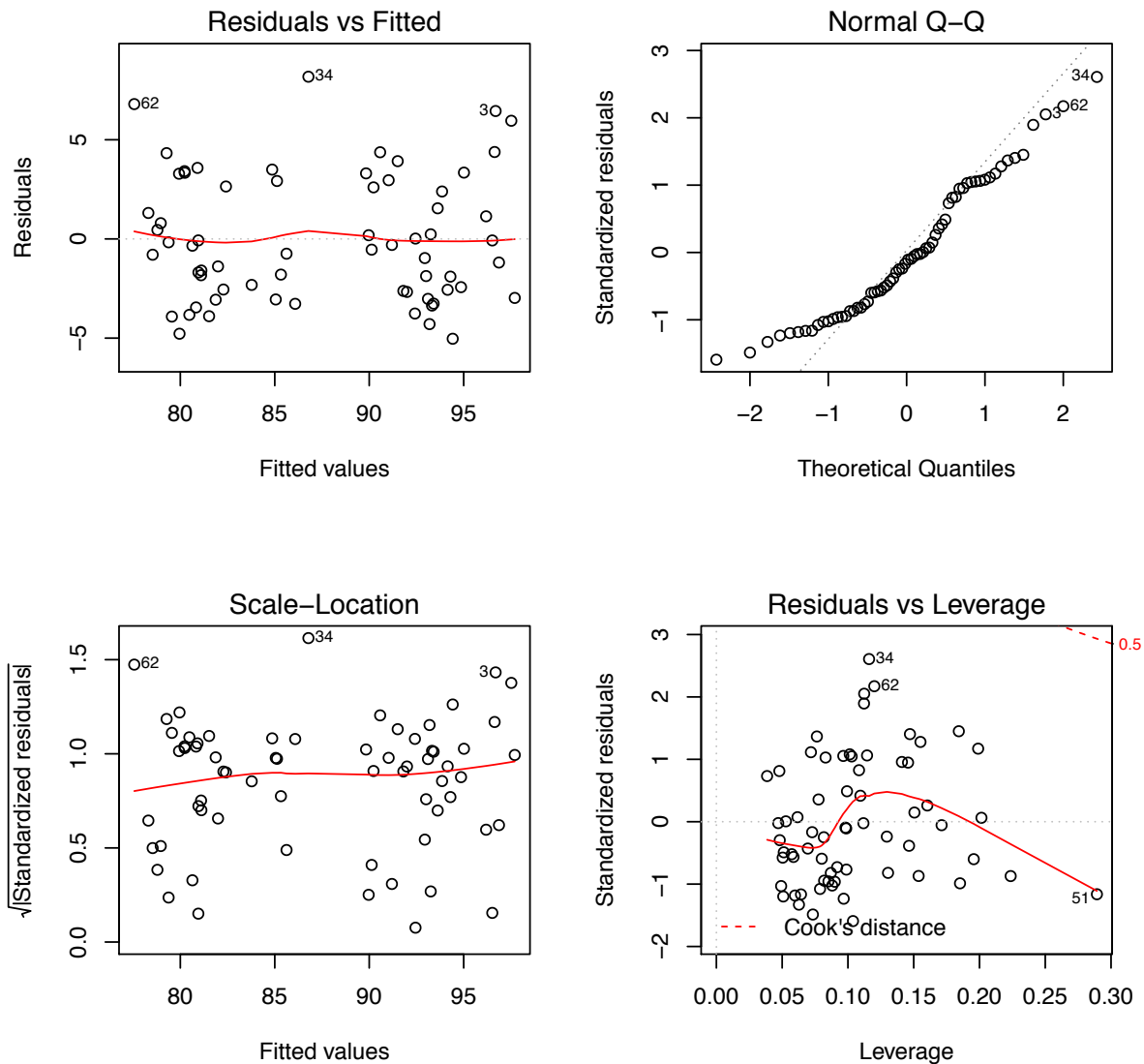
2158 **Figure C.6 Lengths of Spring and Fall aggregates at Chipps Island in TRAWL data.**
 2159

2160

2161 **Table C.5 Regression results of best fit of trawl lengths to environmental variables.**

Coefficients:	Estimate	Std. Error	t value	Pr(> t)	Signif
(Intercept)	80.9897	0.7322	110.604	<2.00E-16	***
race Spring	11.4344	0.8359	13.678	<2.00E-16	***
Yolo flow	0.99	0.5468	1.811	0.075288	.
CVP	2.6729	0.7082	3.774	0.000375	***
EXPIN	-2.5741	0.7566	-3.402	0.001206	**
GEO	-1.4716	0.6551	-2.246	0.028449	*
BASS	-1.8643	1.0438	-1.786	0.079228	.

*** p<0.001, **p<0.01, *p<0.05, . p<0.1

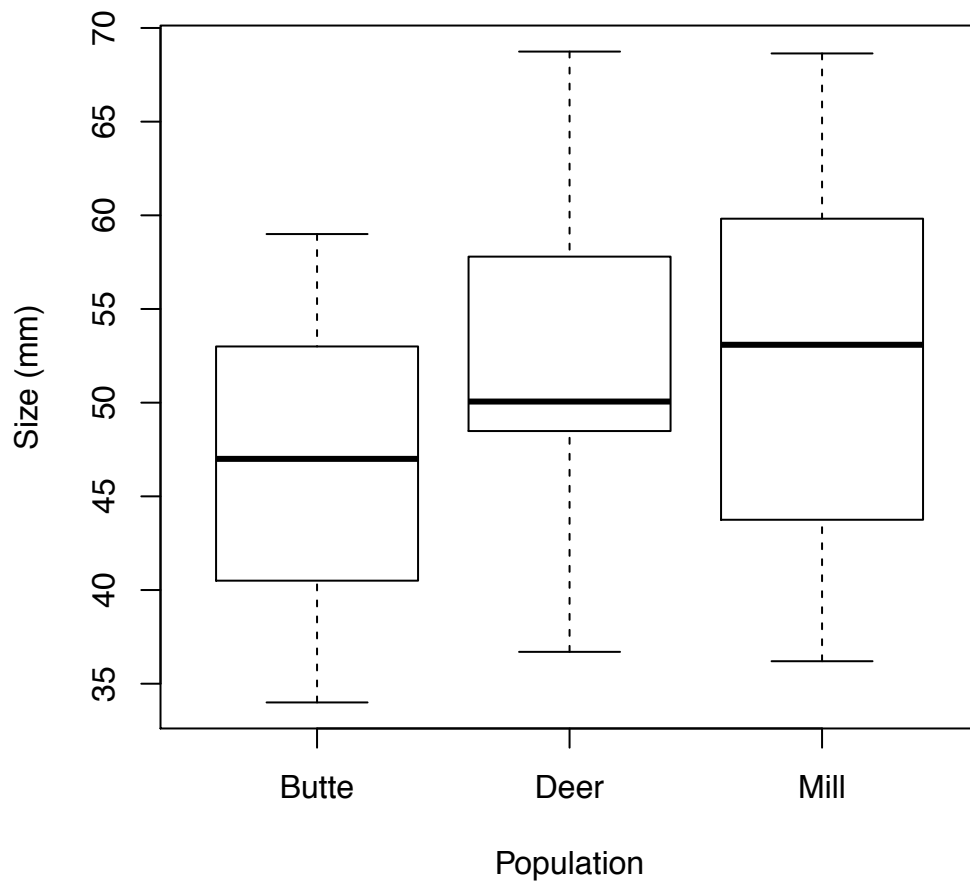


2162

2163 **Figure C.7 Diagnostic plot of best fitting model of relationship between length at Chipps**
 2164 **Island mid-water trawl and environmental variables.**

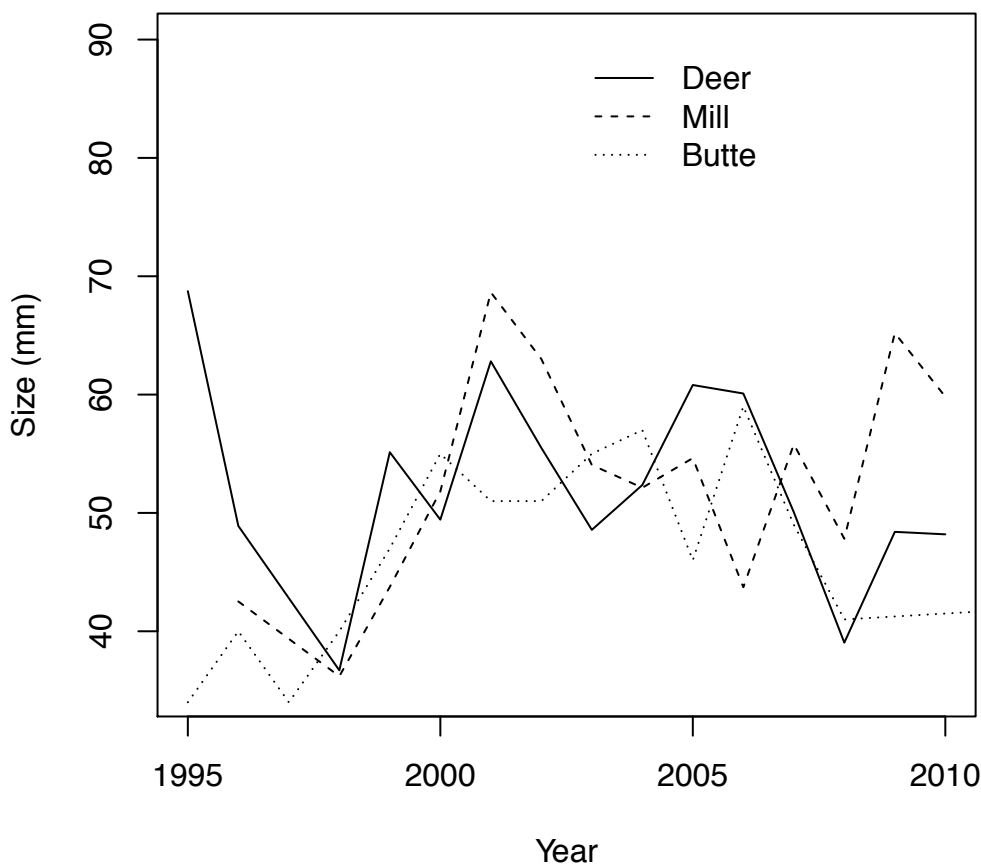
2165 **RST – Lengths in tributaries**

2166 Mill, Deer, and Butte creek Spring run average fish sizes from rotary screw trap
 2167 operations are shown in Figure C.8. We see that Mill, Deer and Butte creeks are on average
 2168 about 45-55 mm in length between January and June when records were aggregated for
 2169 outmigration estimates. The temporal pattern in sizes is shown in Figure C.9. We see no
 2170 major trend in size in tributaries between January and June, only that Butte creek fish appear
 2171 to run a bit smaller.



2172
2173
2174

Figure C.8 Average size of juveniles obtained from rotary screw traps operating in Butte, Deer and Mill creeks between January and June.



2175
 2176 **Figure C.9 Temporal trend in juvenile sizes obtained from rotary screw traps operating**
 2177 **in Deer, Butte and Mill creeks between January and June.**

2178 *DISCUSSION*

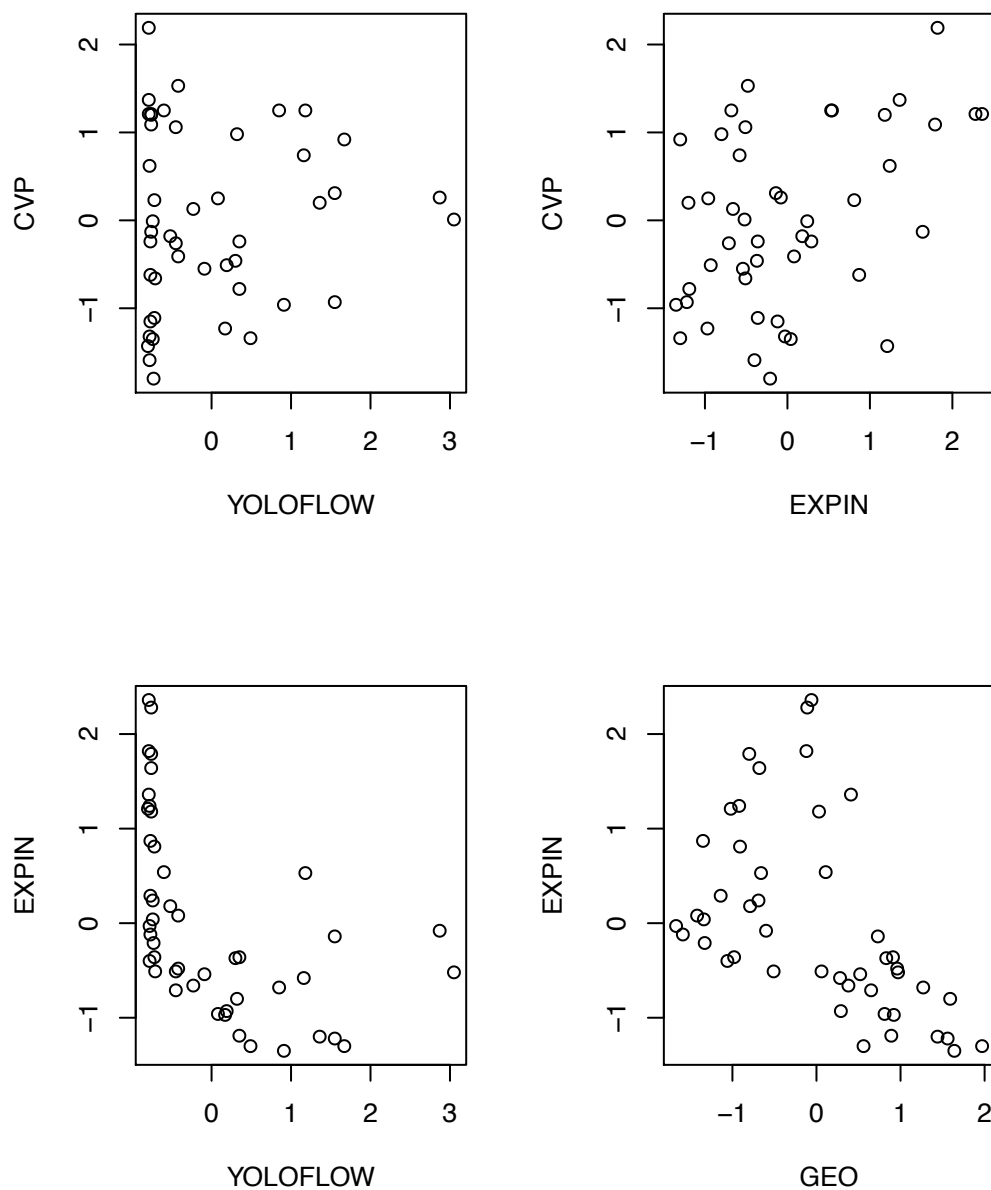
2179 This analysis drew upon varied sources of fish length information in the Sacramento
 2180 River drainage. The summary of rotary screw trap lengths indicates that Spring run out-
 2181 migrating Chinook from Deer, Mill and Butte creeks are approximately the same size, and
 2182 have been stable at approximately 55 mm in recent years. Regression analysis of recoveries
 2183 from mid-water trawl surveys at Chipps Island indicates that growth of fish from North of the
 2184 Delta to Chipps Island, as well as the length at recapture in Chipps Island trawls varied in
 2185 relation to environmental variables. Regression analyses showed that the length at Chipps
 2186 Island from the perspective of two different types of length statistics proved to be related to
 2187 environmental variables regardless of the data source of the length estimates.

2188 We used two different growth metrics. One growth metric came from lengths of CWT
 2189 recoveries and releases of hatchery fish, and the other came from seine and trawl surveys.
 2190 The CWT growth was derived from average recovery length at Chipps Island and average
 2191 release lengths at various release locations and times. The average recovery length is a
 2192 statistic based on a very small sample size relative to the release length statistic. If you

2193 consider the how many fish are released relative to recaptured, and if you consider that
2194 tagged fish are released at various locations and at different times, it is easy to see how biased
2195 the growth estimate might be. The SEINE/TRAWL growth estimate made no distinction
2196 between hatchery and non-hatchery fish and it represents an estimate of the growth of all Fall
2197 or Spring run fish between Region 1 seines and Chipps Island. In comparison to the CWT
2198 estimate, it will be more complex in it's stock composition (with hatchery and non-hatchery
2199 fish of all origins), but it is much simpler in upstream capture and release size sampling. All
2200 stocks were sampled from the same locations for sizing regardless of origin. We found a
2201 relationship between SEINE/TRAWL growth and environmental variables, but no
2202 relationship between CWT growth and environmental variables. This may be due to the
2203 complexity of how the release length was calculated for the CWT growth estimate.

2204 The environmental predictors that best explained growth were the Central Valley
2205 Project exports (CVP), the ratio of combined state and federal exports to the total Delta
2206 inflow (EXPIN), and the bass index. CVP and EXPIN are both related to flows in complex
2207 ways. CVP is related to flow because exports would tend to be less restricted at higher flows,
2208 but would have its highest impact when flows are low. We would expect that juvenile salmon
2209 growth could be high when CVP is highest under that logic. EXPIN is related to flow by a
2210 similar logic, but since EXPIN is a ratio, we would expect the largest fraction of flows to be
2211 exported when flows are low (for a given level of exports). We would expect juvenile salmon
2212 growth to be lowest when EXPIN is highest at the lowest flows.

2213 Figure C.10 illustrates some the general patterns in environmental covariation. In the
2214 upper left panel we see that CVP has the greatest degree of variability at the lowest flows
2215 (with Yolo flow being used as a surrogate for average flow at export locations). Across a
2216 range of flow values we can see that the lower bound of CVP increases. This is consistent
2217 with a general tendency of reducing exports at lower flows. The relative impact of exports at
2218 a given flow is seen with EXPIN, which we see (lower left) diminishes at higher flows. We
2219 also see that more water reaches downstream to the Mokelumne river when EXPIN is lower
2220 (lower right panel). Finally, there is a general pattern of CVP being larger when EXPIN is
2221 higher, but recall that the highest EXPIN may coincide with low flows.



2222
2223

Figure C.10 Covariation between significant environmental predictors.

2224 EXPIN was a significant predictor of length when both CWT and TRAWL datasets
 2225 were used. It was significant with $p < 0.01$ in both cases. EXPIN was also a significant
 2226 predictor ($p < 0.01$) of growth estimates of Fall and Spring aggregates obtained from the
 2227 SEINE/TRAWL dataset. The CWT length regression is in conflict with the SEINE/TRAWL
 2228 growth regression and the TRAWL length regression though. The CWT result predicts a
 2229 positive effect of EXPIN, versus a negative effect for the other two regression analyses. A
 2230 possible reason for this would be that the CWT dataset was exclusively measuring hatchery
 2231 fish (although hatchery fish would also have been present in the other two analyses). If
 2232 EXPIN has a positive effect on hatchery fish length at Chipps Island as shown in the CWT
 2233 length regression, and a negative effect on the aggregate of both hatchery and non-hatchery
 2234 fish seen in the TRAWL length and SEINE/TRAWL growth analysis, it might suggest that
 2235 that the negative effect on non-hatchery growth is even stronger than seen in the TRAWL

2236 surveys. It could also be a size related issue. If hatchery fish are smaller and more vulnerable
 2237 to entrainment, removal of the smaller fish from the outmigrating cohort would make it
 2238 appear as if they grew on average, when in fact it was just the smaller ones that did not make
 2239 it into the downstream survey sample.

2240 The relationship between flows and exports, and resulting growth and survival are
 2241 complex. We found that growth and length are negatively related to EXPIN, but positively
 2242 related to CVP. A possible mechanism, is that there is a threshold flow/export relationship
 2243 where in smaller fish become more vulnerable to entrainment. Such a mechanism would
 2244 predict that more larger fish than smaller fish make it downstream to be sampled at Chipps
 2245 Island, which has the effect of making the growth appear larger on the basis of the average
 2246 recovery size. This would appear to be favorable growth conditions despite the fact that all
 2247 individuals did not grow better on those conditions. If a relatively high CVP export year were
 2248 where to coincide with an average flow year, and if more small fish were entrained, it would
 2249 appear that fish were larger at Chipps Island.

2250 Results also indicated that Spring run were longer at Chipps Island, despite the fact
 2251 that the SEINE/TRAWL regression showed that Spring run growth was less than Fall run.
 2252 Total Central Valley Projects (combined state and federal) exports showed positive effect
 2253 on growth in the SEINE/TRAWL regression and length in the TRAWL analysis. Since there
 2254 was a negative effect from the export to inflow ratio, it may be suggest that total flows have a
 2255 positive effect, and that there may be a relationship between exports and flows that is dictated
 2256 by water extraction policies.

2257 It is interesting that regression results show that bass has a positive effect on the
 2258 growth estimates evaluated from the SEINE/TRAWL, yet has a negative effect on lengths
 2259 estimated from the TRAWL data. Since the bass index is not standardized to effort, it can't
 2260 imply a direct predation rate change on a size class of Chinook juveniles, but depending on
 2261 the relationship between the index and the size of the bass caught, it might imply a shift in the
 2262 size of Chinook vulnerable to bass predation at a given abundance of bass. It could be that
 2263 smaller fish are more vulnerable and predation biases the growth estimate by removing
 2264 smaller fish.

2265 Our examination of length/growth sensitivity to environmental variation points to a
 2266 few results. First, EXPIN is a statistically significant predictor of size and growth, with a
 2267 negative effect on both. Our samples conflate the story a bit, but if you consider that the only
 2268 positive effect was seen in the length of hatchery fish, and if you consider that the CWT
 2269 dataset had race and hatchery factors, the positive effect of EXPIN in the regression result of
 2270 the CWT data should not detract from the regression results found in both the
 2271 SEINE/TRAWL and TRAWL dataset. It should be noted however, that the highest regression
 2272 coefficient value for an environmental effect in any of our regressions was about 5, meaning
 2273 that about 5 mm per standard deviation was the maximum variability in size predicted by
 2274 variability in an environmental effect. This implies that at the extreme of 2 standard
 2275 deviations, only 10 mm of net difference in size at Chipps Island would be predicted. Still,
 2276 two standard deviations explains about 95% of the variation in environmental factors, and 10
 2277 mm explains 10-15% of the variability in length at Chipps Island (assuming 85 mm length at
 2278 Chipps Island). Since the same environmental variables explain significant variation in
 2279 rearing survival, it is feasible that length may be an instrumental in the mechanism of rearing
 2280 survival.

2281 REFERENCES

- 2282 Brandes, P.L. and J.S. McLain. 2001. Juvenile Chinook salmon abundance, distribution, and
 2283 survival in the Sacramento-San Joaquin Estuary. Pages 39 – 138 in R.L. Brown,
 2284 editor. Contributions to the Biology of Central Valley Salmonids, Volume 2, Fish
 2285 Bulletin 179. California Department of Fish and Game, Sacramento, California.
- 2286 California Department Of Fish And Game. 1998. Butte Creek Spring-Run Chinook Salmon,
 2287 *Oncorhynchus Tshawytscha*, Juvenile Outmigration And Life History 1995-1998.
 2288 Administrative Report No. 99-5.
- 2289 California Department Of Fish And Game. 2000. Butte And Big Chico Creeks Spring-Run
 2290 Chinook Salmon, *Oncoryhnchus Tshawytscha* Life History Investigation 1998-2000.
 2291 Administrative Report No. 2004-2.
- 2292 California Department Of Fish And Game. 2004. Butte And Big Chico Creeks Spring-Run
 2293 Chinook Salmon, *Oncoryhnchus Tshawytscha* Life History Investigation 2000-2001.
 2294 Administrative Report No. 2004-3.
- 2295 Garman, C.E and T. R. McReynolds. 2008. Spring-Run Chinook Salmon, *Oncoryhnchus*
 2296 *tshawytscha*, Life History Investigation. California Department of Fish and Game.
 2297 Inland Fisheries Administrative Report No. 2009-1.
- 2298 U.S. Fish and Wildlife Service – Stockton Fish and Wildlife Office. March 2014. Metadata
 2299 for the Stockton Fish and Wildlife Office’s Delta Juvenile Fish Monitoring Program.
 2300 <http://www.fws.gov/stockton/jfmp/>.

2301

2302

2303

Appendix D Modeling the influence of historical factors on population dynamics of salmon: the OBAN model

DRAFT

A.N. Hendrix¹, R. Hilborn², W. Kimmerer³, and B. Lessard⁴

¹QEDA Consulting, LLC, 4007 Densmore Ave N., Seattle, WA, 98103 noblehendrix@gmail.com

²School of Aquatic and Fishery Sciences, University of Washington, 1122 Northeast Boat Street, Seattle,
WA 98105

³Romberg Tiburon Center, San Francisco State University, 3152 Paradise Drive, Tiburon, CA 94920

⁴Columbia River Inter-Tribal Fish Commission, 700 NE Multnomah St Suite 1200, Portland, OR 97232

December 20, 2014

1 Abstract

2 We developed a general state-space modeling framework to evaluate the influence of factors on trends in
3 abundance of multiple life-history stages of salmon. The model utilizes Beverton-Holt transitions among
4 life stages, and incorporates factors into the transitions by modeling the dependence of the Beverton-Holt
5 productivity p (survival) and capacity K parameters as functions of driving factors. We estimated model
6 coefficients in a Bayesian framework to provide inference on factors hypothesized to affect the population
7 dynamics by fitting to indices of abundance. We call the modeling framework *Oncorhynchus* Bayesian
8 Analysis (OBAN), and we applied it to winter run Chinook in the Sacramento River, California, a salmon
9 run listed as endangered in 1994. Using the OBAN framework we were able to place probability statements
10 on the relationships between certain environmental and anthropogenic factors and winter-run population
11 dynamics. We found that temperatures and minimum flow in the spawning reaches and ocean productivity
12 had a high probability of affecting survival (≥ 0.8), whereas water diversions and water routing had lower

13 probabilities of affecting survival. The OBAN framework provides a means for understanding how historical
14 management of hydrology and harvest coupled with environmental variability shape the trends in abundance,
15 and thus facilitates understanding how future management actions may affect population recovery.

16 Keywords: state-space, WinBUGS, Bayesian, winter-run, California, water management

17 Introduction

18 Recovery of endangered animals requires an analysis of the factors responsible for affecting the population
19 dynamics historically and modifying those factors to facilitate recovery of the population. This is particularly
20 true of salmon populations that have seen decreases in their abundances through the majority of their range,
21 but particularly in the southerly portions of their distribution (NMFS 2014). Understanding what factors
22 have lead to the decline in abundances is an important step toward developing future management actions.
23 Incorporation of uncertainty is important when evaluating these factors to be able to identify the level of
24 confidence that one has in the relationship between historical factors and changes in population abundance.
25 An additional complication arises when abundance measurements are made with relatively poor accuracy.
26 Furthermore, natural variability in the population dynamics (i.e., spawner recruitment relationships) may
27 obfuscate the signal between causative factors and the response of the population to such factors. To address
28 these needs, we developed a state-space modeling framework that is capable of reflecting uncertainty in the
29 factors affecting salmon population dynamics.

30 The population dynamics uses stages to structure the chronology of factors affecting different portions of
31 the life cycle with density dependence among stages described by Beverton-Holt transitions (Moussalli and
32 Hilborn 1986, Scheuerell et al. 2006, Greene and Beechie 2004). The dynamics incorporate process noise
33 to reflect natural variability in the dynamics of the population and an observation process that describes
34 a state-space modeling framework (Newman et al. 2014). Although the parameters of such models can be
35 estimated using maximum likelihood methods (Maunder et al. 2011) we estimate the model parameters in a
36 Bayesian framework to allow prior knowledge and the observation process to inform the parameter estimates
37 (i.e., using posterior distributions to integrate information from these two sources). Fitting such non-linear
38 state-space models in a Bayesian context is becoming relatively commonplace (King et al. 2010, Newman
39 and Lindley 2006) and this is an extension of those methods.

40 The development of this modeling framework arises from a practical problem related to a population that

41 may have a moderate probability of extinction (Lindley et al. 2007, Botsford and Brittnacher 1998). The
42 Sacramento River winter-run Chinook (*Oncorhynchus tshawytscha*) currently listed as endangered under
43 the Federal and California Endangered Species Acts, and it has seen a decline in escapement since the
44 1970's. Like many salmon populations in decline, a list of factors that could potentially affect winter-run
45 (and other salmon transiting the Sacramento River and the San Francisco Delta) have been compiled. Some
46 of these factors include: 1) thermal mortality of eggs and alevin in the spawning reaches; 2) flow related
47 survival after emergence; 3) rearing in off-channel areas such as the Yolo bypass (Sommer et al. 2005); 4)
48 entrapment into the interior delta due to positioning of channel flow gates (Perry et al. 2010); 5) alterations
49 in the outmigration flow vectors due to exportation of water from the system (Newman and Brandes 2010;
50 Newman 2003); 6) predation from piscivorous fishes such as striped bass (*Morone saxatilis*) (Newman and
51 Lindley 2006). Salmon exiting the Bay-Delta ecosystem enter the Gulf of the Farallones and transition to a
52 near-shore environment with annual variability in productivity tied to the strength and location of upwelling
53 (Wells et al. 2007). Once winter-run attain an age of 3 years (2-ocean), they are vulnerable to the west coast
54 salmon fishery that primarily targets fall-run Chinook from the Klamath River, OR and Sacramento Rivers
55 but also catches winter-run (O'Farrell 2012); however, timing and area closures to minimize fishery impacts on
56 winter-run have been in place since the late 1990's (O'Farrell 2012). Yet, the ability to quantitatively evaluate
57 the importance of all of these factors for explaining trends in winter-run escapement has not occurred.

58 The objectives of our work is to provide a general overview of the *Onchorhynchus* Bayesian Analysis
59 (OBAN) modeling framework and to provide an analysis of the winter-run Chinook in the Sacramento River
60 as an example of how the framework was utilized.

61 **Methods**

62 **Population Dynamics Model**

63 The OBAN modelling framework provides a quantitative tool to evaluate historical patterns in salmon
64 abundance as a function of hypothesized explanatory factors. Specifically, the model: 1) estimates model
65 coefficients by fitting predictions of the population dynamics model to observed indices of abundance; 2)
66 evaluates factors that may explain dynamic vital rates; 3) accounts for mortality during all phases of the
67 salmon life history; and 4) incorporates uncertainty in the estimation of model coefficients by fitting in a
68 Bayesian framework.

69 The first step to the modeling framework is to define the life-history stages. The OBAN model structure

70 can define life-history stages based on management objectives, such as important locations of anthropogenic
 71 or environmental driving factors by the locations where indices of abundance are observed. The number of
 72 life-stages is application specific, but it has to incorporate at least two stages for freshwater (egg and juvenile
 73 stages), and an ocean stage for each age of returning adult (e.g., a stage for each of the age 2, ..., L ages of
 74 escaping adults). The OBAN model uses temporally implicit stage durations. Each freshwater stage may be
 75 defined such that it reflects the duration that the salmon are within that stage, thus stages do not need to be
 76 the same duration. As a consequence, inference on the population vital rates for that stage are predicated
 77 on its duration.

78 The OBAN framework begins with eggs as the first stage and defines the egg abundance as a function of
 79 the escapement.

$$N_{1,t} = E_t \times f_t \quad (\text{D.1})$$

80 where $N_{1,t}$ is the first stage (egg) abundance, E_t is the escapement, and f_t is the fecundity at time t . If
 81 only females are being modeled, then the fecundity reflects estimates of eggs per female. Alternatively, if
 82 escapement is not sex-specific then fecundity can be defined in terms of fecundity per adult.

83 The OBAN framework uses Beverton-Holt transitions to calculate the density-dependent transition in
 84 abundance among freshwater life stages ($1, \dots, M$) after the egg stage.

$$N_{i,t+1} = N_{i,t} \times \frac{p_{i,t}}{1 + \frac{p_{i,t}N_{i,t}}{K_{i,t}}} \quad (\text{D.2})$$

85 where $p_{i,t}$ is the productivity parameter, $K_{i,t}$ is the capacity parameter of the Beverton Holt transition and
 86 $K_{i,t}$ is the capacity parameter for stage $i = 2, \dots, Q$ in year t . Because the production of eggs is captured
 87 in equation (1), productivities are equivalent to survival rates in the absence of density dependence and are
 88 confined to the range $(0, 1)$. If density dependence is not expected to occur between two stages, the $K_{i,t}$
 89 parameter can be set to a large value to effectively remove the density-dependent portion of the equation.

90 The productivity parameter ($p_{i,t}$) and capacity parameter ($K_{i,t}$) in a given life stage i from brood year t
 91 can be modeled as 1) a constant value; 2) as a constant value with annual variation via random effects; or 3) as
 92 a dynamic rate with dependence on a set of time-varying covariates ($X_{j,t}$ for factor j in year t). By using the
 93 final formulation, the influence of anthropogenic and environmental factors on specific life history stages can
 94 be evaluated. The productivity parameter can be influenced by independent factors acting simultaneously
 95 on the life history stage to drive demographic rates, for example environmental variables that represent

96 water conditions such as temperature or flow, biotic factors such as predator abundance, food abundance,
 97 or anthropogenic factors such as diking, water diversions, and harvest.

98 The dynamic productivities are modeled as a function of various factors by using a logit transformation,
 99 which ensures that the productivities remain between 0 and 1.

$$\text{logit}(p_{i,t}) = \sum_{j=1}^F \beta_j X_{j,t} \quad (\text{D.3})$$

100 where β_j is the coefficient associated with factor $X_{j,t}$.

101 Likewise, there may be processes occurring that affect annual stage-specific capacities, such as the amount
 102 of available spawning area or the amount of flooded off-channel rearing habitat. To model the dynamic
 103 capacities, a log transformation is used, which causes the capacities to remain between 0 and ∞ , which is
 104 the appropriate parameter space for capacity.

$$\log(K_{i,t}) = \sum_{j=1}^F \gamma_j X_{j,t} \quad (\text{D.4})$$

105 where γ_j is the coefficient associated with factor $X_{j,t}$.

106 After Chinook enter the ocean, they mature and can return to spawn after a single summer or after
 107 overwintering in the ocean for multiple years (Healey 1991). When Chinook enter the ocean, we shift the
 108 notation to O_{age} to reflect the fact that some Chinook will remain in the ocean, while others will mature
 109 and migrate back to freshwater after escaping the fishery. The transition from juvenile rearing to ocean
 110 stages occurs via the following transition equation

$$O_{2,t} = N_{M,t} \times \frac{p_{M,t}}{1 + \frac{p_{M,t} O_{i,t}}{K_{M,t}}} \quad (\text{D.5})$$

Maturation of ocean stages for ages $2, \dots, L$ are calculated using the following equation:

$$M_{t+age} = O_{age,t} \phi_{age} z_{age} \quad (\text{D.6})$$

111 where M_{age} is the maturation of the adults at a specific age returning to freshwater according to the
 112 conditional maturation rate ϕ_{age} . The number of fish remaining in the ocean $O_{age,t}$ is a function of those
 113 that remain and survive to the following year. Because harvest is one of the major sources of mortality in
 114 the ocean stages, the above formulation assumes that harvest occurs before maturation; however, this order
 115 could be altered to reflect the specific dynamics of the stock of Chinook being modeled.

$$O_{age+1,t} = (1 - h_{age,t})(1 - \phi_{age})O_{age,t} \times \frac{p_{age,t}}{1 + \frac{p_{i,t}O_{age,t}}{K_{age,t}}} \quad (\text{D.7})$$

116 In the final stage, all Chinook of age L return, thus $M_{t+L} = O_{L,t}$. Survival and capacities can be modelled
 117 in the ocean stages just as in the freshwater stages to reflect the effects of localized nearshore productivity.
 118 Furthermore the conditional maturation rates may also be modeled as a function of factors using logistic
 119 regression. For example, due to differential size at ocean entry or size at release in the case of modeling a
 120 hatchery population.

$$\text{logit}(\phi_{age,t}) = \sum_{j=1}^F \delta_j X_{j,t} \quad (\text{D.8})$$

121 where δ_j is the coefficient associated with factor $X_{j,t}$.

122 Finally, the escapement in calendar year y is the sum of the mature fish returning from the ocean at ages
 123 $2, \dots, L$ from brood years $y - 2, \dots, y - L$.

$$E_y = \sum_{age=2}^L M_{age,t} \quad (\text{D.9})$$

124 Process noise can be added to the stage-specific survivals and capacities by allowing them to vary as
 125 a random effect. For example, extra variability could be incorporated through a residual error term in
 126 either equation (1) or equation (2) to add variability in the production (fecundity) relationship or in the
 127 stage transitions, respectively. To implement process noise, stage-specific random effects, e.g., $Z_{i,t} \sim N(0, \sigma_{i,p}^2)$
 128 can be added to the equation to express annual variation, where $\sigma_{i,p}^2$ reflects the variance due to process
 129 noise in stage i . The amount of process noise may require some additional structure (e.g., through prior
 130 specification), otherwise, all the observed data may ostensibly be fitted exactly by allowing the variance in
 131 the process noise to be sufficiently large.

132 Finally, the timing of the influence of factors has to be matched with the timing of the life stages such
 133 that the factors are affecting the appropriate cohort. The time subscript t refers to the brood year, thus
 134 the covariates, which are typically provided by calendar year y , are lagged appropriately for the population
 135 under study.

136 Bayesian Estimation

137 Estimation of the model parameters occurs by comparing model predictions to observed data across multiple
 138 competing "states of nature" or parameter values. This is achieved through Bayesian estimation of the
 139 likelihood of observing the data times the prior probability of the model parameter values (Gelman et al.
 140 2004). The general framework described above is used to compute predicted abundances that are then
 141 compared with observed abundances obtained through some sampling method. As a result, a sampling
 142 model is defined for each observation. The stage abundances are related to the observed indices of abundance
 143 through a sampling model $g()$. The framework is relatively flexible in that any type of sampling data can
 144 be incorporated by specifying an appropriate sampling model. Multiple types of abundance indices, $I_{i,k,y}$
 145 for stage i of index type k in year y , can be included in the modeling framework by defining the observation
 146 process $g()$ as a function of the sampling model and observation error σ_k^2 . For example, the observation
 147 process $g()$ could be defined as a lognormal for abundances or biomass, Poisson or negative binomial for
 148 counts, or Binomial for capture-recapture studies. Note that if the observation process is modeled with
 149 lognormal errors, the variance can be defined in terms of the coefficient of variation (CV = mean/standard
 150 deviation) as $\sigma_k^2 = \log(CV_k^2 + 1)$.

$$I_{i,k,t} \sim g(N_{i,t}, \sigma_k^2) \quad (\text{D.10})$$

151 Priors

152 Prior probability distributions are required for all model coefficients that are estimated within the modeling
 153 framework. For example the coefficients of the logistic regression to define stage-specific survival rates (β_j 's)
 154 and coefficients of the log-linear model (γ_j 's) to define stage-specific capacities will require prior probability
 155 distributions; normal distributions can be used to define the prior probabilities for both of these coefficients
 156 due to the transformations used in equations (3) and (4). Care should be taken in specifying the priors for
 157 the β coefficients given their inclusion into a logit() transformation, however. King et al. (2010) suggest
 158 that $N(0,2.5)$ priors may be used in the coefficients of logistic regression to ensure that excessive mass is not
 159 placed in the values near 0 and 1 (as might be the case with a more diffuse normal prior). The conditional
 160 maturation rates ϕ_{age} are required to be in the interval (0,1); therefore, Beta distributions can be used as
 161 priors for these coefficients. Finally, the variance of the measurement error on the observation process (σ_k^2)
 162 and the variance of any process noise ($\sigma_{i,p}^2$ for stage i) will also require a prior and can be specified as either

163 inverse gamma on the variance or alternatively as a uniform prior on the standard deviation of the variance
 164 (Gelman et al. 2006).

165 *Implementation of Bayesian Estimation*

166 The posterior distributions of the model parameters can be estimated by drawing samples from the full
 167 conditional distributions of each parameter given values of all other parameters through a Metropolis within
 168 Gibbs Markov Chain Monte Carlo (MCMC) approach (Gelman et al. 2004, Gilks and Spiegelhalter 1996). If
 169 conjugate priors are used, then the Gibbs sampler can be employed; however, if posterior distributions for the
 170 parameters can not be updated using the Gibbs sampler (Roberts and Polson 1994), they can instead updated
 171 by using distribution-free adaptive rejection Metropolis steps (Gilks and Spiegelhalter 1996, Spiegelhalter
 172 et al. 2003) which is the approach adopted in WinBUGS (Spiegelhalter et al. 2003).

173 To evaluate if the posterior draws were arising from a stationary target distribution, multiple chains were
 174 run from dispersed initial values for each model and the scale reduction factor (SRF, Gelman et al. 2004)
 175 was computed for all monitored quantities (model coefficients and abundance estimates). The diagnostics
 176 were implemented using the R2WinBUGS package (Sturtz et al. 2005) in R (R Core Team 2013). Monitored
 177 parameters in all models had SRF values that indicated samples were being drawn from the target distribution
 178 (i.e. $SRF \approx 1$) by 75,000 samples (Gelman and Rubin 1992). The initial 50% of the samples were used to
 179 reach the stationary target distribution and were discarded with the subsequent samples thinned to produce
 180 approximately 1,000 draws from the stationary target distributions. The 1,000 draws were used to compute
 181 the posterior mean and symmetric 95% probability intervals or credible intervals (95% CrI).

182 **Application of Model to Winter Run Chinook**

183 We defined 7 life-history stages in the winter-run OBAN model including 6 freshwater and marine transition
 184 stages and 3 annual ocean stages: 1) eggs, 2) fry 3) juveniles in the Delta (delta), 4) juveniles in the Gulf of
 185 the Farallones (gulf) 5) age 2 in the ocean, 6) age 3 in the ocean, and 7) age 4 in the ocean. The escapement
 186 was composed of mature individuals that returned at age 2, 3, and 4 (Table D.1).

187 Fecundity was assumed to vary annually, and the annual values were sampled from probability distribu-
 188 tion, i.e., $f_t \sim \log N(\mu_f, \sigma_p^2)$. This formulation allowed process noise to be incorporated into the population
 189 dynamics, but empirical information on fecundity restricted the range of process noise in the model. Multiple
 190 environmental and anthropogenic factors were incorporated into the winter-run model at different stages in
 191 the life-history based on hypotheses about factors affecting (Table D.2). The mean fecundity is calculated

192 by assuming that each adult spawner produces 2,450 eggs (Williams 2006, Winship et al. 2014).

193 *Winter Run Abundance Indices*

194 Estimates of winter-run escapement in the Central Valley have been conducted since 1967, and we used an
195 escapement abundance index from 1967 to 2008. Different methods were used to estimate escapement over
196 this period, which may affect the precision of the spawner escapement estimates (Williams 2006, Botsford
197 and Brittnacher 1998). Prior to 1987, all returning spawners passed via a counting ladder at Red Bluff
198 Diversion Dam (RBDD, Figure D.1). From 1987 onward the gates of the diversion dam have been opened
199 to enhance upstream survival of winter-run Chinook salmon, but also likely improved access to areas above
200 RBDD. The current operation of RBDD makes counts of winter-run Chinook salmon after closing the gates
201 on May 15. On average, 15% of the winter run passed RBDD by May 15, but the specific percentage in
202 a given year was as low as 3% or as high as 48% (Snider et al. 2000). Since 2001 the annual escapement
203 estimates have been calculated using a Jolly-Seber estimator derived from the carcass count data (California
204 Department of Fish and Game 2004). Juvenile production indices were calculated from rotary screw trap
205 samples and trap capture probabilities at Red Bluff Diversion Dam for 1995 through 1999 and 2002 through
206 2008 (Poytress and Carrillo 2011).

207 *Winter Run Factors*

208 Several environmental and anthropogenic factors were used to help describe variability in winter-run juvenile
209 and adult abundance indices (Table D.2). Because the abundance indices occur at RBDD, which coincides
210 with the fry stage, a basal survival rate could be estimated for the egg to fry stages and a second basal rate
211 for the fry to escapement stages. Explanatory factors were incorporated into the survival during the fry
212 stage, delta stage, and gulf stages (Table D.2). We provide a short rationale for the inclusion of each of the
213 factors here.

214 Water temperatures in the spawning reach above RBDD can sometimes reach stressful levels, thus July
215 through September mean daily water temperature (C) in the Sacramento River at Bend Bridge (TEMP)
216 was used to explain annual variability in egg to fry survival. In addition, low flow can affect survival rates of
217 alevin, so August through November minimum monthly flow in the Sacramento River at Bend Bridge was
218 also used to affect egg to fry survival. In addition, an interaction term of TEMP:FLOW was incorporated
219 into the model to determine if there was some additional mortality associated with either high temperatures
220 or low flow.

221 In the delta stage, several factors may affect winter-run survival rates. Access to the Yolo bypass, a large
 222 floodplain that provides the potential for increased survival and growth of fall-run Chinook (Sommer et al.
 223 2005), may also provide similar benefits for winter-run via bypassing the delta. The Yolo bypass floods when
 224 flows on the Sacramento River surpass 56,000 cfs; each day when flows were great enough to enter the Yolo
 225 bypass between December and March was a potential opportunity for winter-run to enter the floodplain
 226 habitat (YOLO). The Delta Cross Channel is a dual gate structure that conveys water to the interior delta,
 227 and late-fall Chinook salmon that enter the interior delta have lower survival rates relative to those that
 228 migrate down the Sacramento River (Perry et al. 2010). In the southern delta, the Central Valley Project
 229 and State Water Project export water from the delta to supply agricultural and municipal water needs.
 230 The levels of exports can vary annually and have been associated with differential survival rates of fall run
 231 Chinook (Newman and Brandes 2010, Newman 2003).

232 Finally, nearshore ocean processes can have important consequences for Chinook salmon (Wells et al.
 233 2007, Woodson et al. 2013), and here we evaluated upwelling in a region south of the entrance to San
 234 Francisco Bay (UPW) and the sea surface temperature in the Gulf of the Farallones (FARA).

235 The ocean stages were modeled as a function of maturation rates and age-3 impact rates. Information for
 236 the maturation rates were taken from an analysis of 1998, 1999, and 2000 coded wire tag (CWT) data (Grover
 237 et al. 2004) and more recent analyses of maturation rates (O'Farrell et al. 2012). Age-3 impact rates for
 238 winter-run were calculated for 1978 - 2011 from a combination of estimated impact rates from CWT returns
 239 (1998 - 2008) and from a hindcast of impact rates given spatial allocation of fishing effort (O'Farrell, M.,
 240 NMFS unpublished data). Until 1987, there was little regulation of the Central Valley Chinook salmon shery
 241 and estimates of the mortality rate on winter-run Chinook salmon in the ocean shery were approximately
 242 0.7 of the mortality rate experienced by fall-run Chinook salmon.

243 Most winter-run Chinook salmon return to spawn as 3-year-olds; however, the winter-run age-4 oceanstages
 244 are more likely to be captured in the commercial fishery because of their larger size. Grover et al. (2004)
 245 found that the harvest-related mortality of age-4 winter-run Chinook salmon was 2.5 to 3.7 times the rate
 246 of age-3. The age-4 impact rate in a calendar year y was assumed to be double the instantaneous rate of
 247 age-3 ($h_{4,y} = \exp(\log(h_{3,y}/2))$).

Results

Observed winter-run escapement was on the order of several tens of thousands in the late 1960's and early 1970's and declined to levels in the low thousands during the 1980's with a low abundance estimate of 194 in 1994. Since the mid-1990's the population has recovered to some degree with escapements in the mid 2000's on the order of several thousands. The winter-run OBAN model captured this declining trend and recovery in escapement (Figure D.2). In particular, the model was able to capture the decline in the late 1970's (along with the spike in escapement in 1980), the continued decline through the mid-1990s, and the subsequent increase through early 2000. The three different sampling methods had median estimated CV's ranging from 0.68 for the early period, 1.34 for the middle period, and 0.97 for the later period. As a result, the model was more sensitive to those sampling methods with higher precision (lower CV). In particular, the model fits to the intermediate period (in which counts were expanded assuming 15% passed RBDD by May 15) indicated that the escapement in 1990, 1991, and 1994 was underestimated relative to model predictions (Figure D.2). In contrast, the winter-OBAN model predictions of escapements during the early period (1967 - 1987) and the later period (2001-2008) fit the annual variability in escapement estimates more closely. The winter-OBAN model also fit well to patterns in the juvenile abundance index at RBDD from 1995 to 2007. The median estimated CV on the juvenile index data was 1.2, indicating that the model had intermediate sensitivity to the juvenile indices relative to escapement. The winter-run model predictions of juveniles at RBDD captured the relatively low production of fry during the late 1990's, subsequent increase in early 2000's due to higher escapements, and the decline in the index in 2007 (Figure D.3).

Annual patterns in stage-specific survivals

To predict escapement and juvenile index values, stage-specific survivals were estimated as a function of the environmental and anthropogenic factors. The estimated survival from egg to fry at RBDD averaged 0.24 95%CrI(0.11, 0.48) (Table D.3); however, survival from the 1970's to mid-1990's was highly variable. There were two years in the late 1970's where median survival was predicted to be approximately zero and periods in the early 1980's and early 1990's when survival in the alevin stage was also low (Figure D.4). Since the mid-1990's the survival rates for alevin have been more stable relative to the prior periods. Survival through the delta stage, which spans fry at RBDD to the nearshore ocean, was 0.0097 (95%CrI: 0.0041, 0.022) (Table D.3). Within the delta, annual variability was less pronounced with median survival ranging from a high of 0.017 in 1969 to a low of 0.0063 in 2004. Median delta survivals were relatively stable at approximately 0.009 through the 1980's and 1990's with slightly lower survivals during 2001 to 2004 of approximately

278 0.006 (Figure D.4). Average survival in the gulf stage was assumed to be 0.5 and variability in survival
279 among years was reflective of ocean productivity. For winter-run Chinook the mid 1980's and mid 1990's
280 were periods of poor survival, whereas 1998 and 2000 - 2001 were years of relatively good survival. Finally,
281 patterns in age-3 survival rates (which were a deterministic function of harvest rates and annual survival
282 rate of 0.8) indicated relatively low survival rates for brood years through the mid-1990's, with improving
283 ocean survival for brood years after 1995 (Figure D.4).

284 Although the magnitude of the effect from each factor cannot be evaluated directly via the magnitude
285 of the coefficient estimate (due to dependence on the stage-specific intercept), the sign of the coefficients
286 associated with factors provide an indication of the effect of the factor: positive values increase survival
287 relative to the average and negative values decrease survival. Because the winter-run OBAN model was fit
288 in a Bayesian framework, the coefficients are described by posterior distributions and the probability that
289 the coefficient value was positive was calculated (Table D.3). In the egg to fry stage, temperatures in the
290 spawning reaches (TEMP) had a consistent negative effect on survival, whereas minimum flows (FLMIN)
291 had a consistent positive effect on survival (Table D.3). A positive TEMP:FLMIN interaction term of
292 flow and temperature would exacerbate the negative effect of high temperatures and low minimum flows,
293 and the interaction term had a 0.73 probability of being positive. In the delta stage, access to the Yolo
294 bypass (YOLO) and DCC gate position open (DCC) had a positive effect on survival, whereas export levels
295 (EXPT) were negative. Finally, in the gulf stage, high temperatures in the Farallone Islands (FARA) had a
296 negative effect on winter-run survival, whereas upwelling south of the entrance to San Francisco Bay (UPW)
297 had a positive effect on survival (Table D.3). Several additional parameters were given informative priors
298 to structure the winter-run OBAN model, although if the data were informative on the coefficients, this
299 would be reflected in the posterior. The posteriors on the conditional maturation rates largely reflected the
300 informative priors. as did the CV on the process error (Table D.3).

301 The magnitude of the effect for each of the factors can not be discerned directly from the magnitude
302 of the coefficient estimate (e.g., in Table D.3), because the coefficients associated with the covariates are
303 dependent upon the intercept terms. To understand how the various factors affect the overall survival of
304 winter-run Chinook, we increased each of the covariates one at a time by 1 standard deviation (SD). The
305 survival rates under the one-at-a-time increases were compared to a baseline case, which was the survival
306 rate with all factors at their mean 1967 to 2008 level. The survival rates began at the egg stage and ended
307 at the end of age 2, prior to harvest affecting survival. To facilitate comparison, we calculated the percent
308 change relative to the baseline survival (i.e., $(alt_k - base)/base \times 100\%$), where alt_k describes a model with

309 factor k increased by 1 SD. Minimum flow had the largest effect per unit SD on winter-run survival with a
 310 median increase of 128% (Figure D.5). Temperature also had a strong effect with a negative median effect
 311 of -96.7% per unit SD. The other notable factors were exports which had a negative effect of - 12.4% per
 312 unit SD, Yolo with a median positive effect of 11.3% and upwelling with a positive effect of 42.3% per unit
 313 SD (Figure D.5). The standard deviations are not the same on a percentage basis among factors, however.
 314 For example 1 SD of TEMP is equal to 6.8% of the mean, whereas 1 SD of EXPT is equal to 25.6% of the
 315 mean. Calculations of the effects of each factor on a percent basis indicated that temperature provides the
 316 largest effect with an 11.9% decrease in survival per percent increase in temperature. Minimum flows in the
 317 spawning reach provided a median 5.73% change, temperature in the Farallones provided a median -1.55%,
 318 and upwelling provided a median 1.78% change, whereas all other factors provided a less than 1% change in
 319 survival for a 1% increase in the factor (EXPT -0.48%, YOLO 0.10%, and DCC 0.16%).

320 Correlation among coefficients was generally low with the exception of the two intercept terms β_{alevin} and
 321 β_{delta} (Pearson correlation coefficient on posterior samples = - 0.685). Despite juvenile data being present
 322 for the latter portion of the time series, some negative correlation among these two coefficients was expected
 323 due to the model structure. This correlation did not inhibit the MCMC algorithm from converging, however.
 324 All scale reduction factors on monitored parameters were approximately 1, which indicated that the 3 chains
 325 had converged to a stable distribution.

326 Discussion

327 The winter-OBAN framework provided a means to evaluate the importance of several anthropogenic and
 328 environmental factors hypothesized to affect winter-run Chinook in the Central Valley. The model results
 329 support the importance of the environmental conditions in the natal spawning and rearing area and early
 330 ocean conditions with important but more subtle effects of delta survival. Our results are comparable with
 331 previous models of winter-run Chinook, providing some justification of the overall model structure and its
 332 inference. Our estimate of delta survival can be compared with Winship et al. (2014), who estimated the fry
 333 to end of age 2 survival rate for 1996 - 2008 of 0.4%. In comparison, our delta survival rate was 0.9% times
 334 the average age 2 value of 0.5 equals a 0.45% estimate for our model from fry to the end of age 2.

335 Median egg to fry survivals were slightly lower than estimated by Winship et al. (2014), in which the
 336 median egg to fry survival was 0.30. Furthermore, they found little variability in annual egg to fry survival.
 337 Similar fry data were used for both models; however, the winter-run OBAN model was able to use the

338 1995-2008 survival relationships to improve inference on factors affecting egg to fry survival in the 1970's to
339 mid-1990's, prior to the analysis of Winship et al. (2014). We too found low variability among years in egg
340 to fry survival from 1996 to 2008, but in contrast we found that there was high variability in survival prior
341 to 1995 due to temperature and flow effects, and it played an important role in the decline of winter-run
342 Chinook during the late 1970's and 1980's.

343 The factors leading to the decline in winter-run abundance during the 1970's can be explained by several
344 periods of poor egg to fry survival tied to low flows and high water temperatures in the spawning reaches.
345 While survival through the delta did not vary dramatically, survival at early ocean entry also had several
346 periods with generally poor survival. Concurrent with this period of episodic recruitment failure and variable
347 ocean conditions, impact rates of age-3 winter-run averaged 0.38 from 1969 to 1997. The recovery of winter
348 run beginning in the late 1990's and early 2000 can be attributed to several management actions and good
349 ocean productivity from 2001 - 2003. The installation of a temperature control device in 1991 has generally
350 reduced the variability in temperature with subsequent reduction in variability of egg to fry survival since 1993
351 (Figure D.4). Concurrent with the installation of the temperature control device, harvest rate management
352 reduced the impact rates on winter-run (1998-2009 average of 0.153) (O'Farrell et al. 2012). In addition,
353 survival through the delta was generally better during the 1996 to 1998 period due to lower than average
354 exports and greater than average access to Yolo bypass.

355 *Model Critique*

356 Although the OBAN modeling framework can incorporate density dependence in the model structure, the
357 winter-run implementation here did not include it based on previous work fitting density dependence to
358 winter-run abundance indices. Estimation of the density dependence requires a signal in the data, namely
359 the reduction in survival as a function of abundance. Previous efforts to include density dependence in
360 models of winter-run population dynamics have had mixed results. Newman and Lindley (2006) included
361 density dependence in the egg to fry transition and found little support for density dependence in a model
362 without process noise, but they found strong evidence when process noise was included as a random effect in
363 each stage under a state-space formulation. The information in the data to support the density dependence
364 came from accounting for autocorrelation in the juvenile abundance state variables as well as measurement
365 errors. Winship et al. (2014) found little support for density dependence in the egg to fry stage using a
366 state-space model that estimated process noise, but fixed measurement error based on estimates of CV from
367 sampling design. Based on the similarity of our model design to Winship et al. (2014), we did not include

368 capacity in the model structure. We return to the topic of density dependence below.

369 We also did not include hatchery output explicitly in the winter-run OBAN implementation. We did,
370 however, incorporate a process noise component to the egg production stage, which was able to vary among
371 years. Hatchery supplementation should be reflected in deviations of recruitment variability, if it was in
372 fact improving the productivity of the population. Hatchery supplementation was initiated in 1991 with
373 some releases in 1994 and 1995; however, production began in earnest in 2000 with between 20 to 57 natural
374 origin females removed from the spawning population for hatchery brood stock (Winship et al. 2014). A
375 more direct approach would be to include a dummy factor in the egg production equation that identified
376 years of hatchery production. The hatchery term could be restricted to have a positive value, reflecting a
377 hypothesized expected benefit of hatchery supplementation, or allowed to be positive or negative reflecting
378 the potential for negative hatchery effects on production of natural origin juveniles.

379 *Recovery*

380 Recovery of winter-run is likely to occur through management of factors under human control while being
381 aware of the influence of uncontrollable environmental conditions (e.g., upwelling). Winter-run appear to
382 be particularly sensitive to temperatures and flows in the spawning reaches. Estimates of the temperature
383 during 1977 indicated that it was 4 standard deviations above the mean (17.6 C) during the July to September
384 period. Mortality in the egg to fry stage was similar in 1976, though, when the temperature was only 1.2
385 standard deviations (14.6 C) above the mean. The installation of a temperature control device at Shasta
386 Dam provides the ability to decouple water temperatures from flow out of the dam, and manages temperatures
387 by mixing cold hypolimnetic water with warmer surface water. While this provides a method for controlling
388 temperatures, the operations of the control device may be complicated by the multi-year climate cycles that
389 affect the reservoir storage and thus the amount of cold water available. Still, the winter-run OBAN model
390 results suggest that small deviations in temperature can have substantial impacts on survival from the egg to
391 fry stage, and managing thermal mortality can have important consequences for the population dynamics.

392 Management of factors in the delta appear to also affect winter-run, but to a lesser degree than the
393 temperature and flow effects during egg to fry survival. Within the delta, increasing access to Yolo bypass
394 and reducing exports can have a positive effect on survival. Water flows into the Yolo bypass over an
395 approximately 1.5 mile weir when flows on the Sacramento River exceed 56,000 cfs at Verona. Winter-run
396 juveniles rear above the weir location and their downstream movement is triggered by flow cues (del Rosario
397 et al. 2013). Access to the Yolo bypass occurs when these flow pulses are also substantial enough to overtop

398 the weir. Given the general lack of off-channel rearing area for salmonids in the Central Valley, improving
399 access to Yolo bypass has been identified as an important management action for recovery of Central Valley
400 salmonids, and winter-run in particular (NMFS 2014).

401 For the model with a density dependent effect in Newman and Lindley (2006), a Beverton-Holt model
402 was used and the estimated capacity was on the order of 11.5 million fry. Using these values of capacity
403 for fry, estimated fry to age-2 survival of 0.45% and ocean age 2 and age 3 survival rates of 0.5, and 0.8
404 respectively would suggest a capacity of approximately 20,500 winter-run in the absence of harvest. This
405 capacity level was exceeded every year from 1967 to 1977; thus it may not be an appropriate capacity
406 estimate for that period, but could potentially reflect more recent conditions as the Newman et al. (2006)
407 model focused on 1992 to 2003. More importantly, the existence of a carrying capacity at this level may have
408 important implications for modeling the expected responses to recovery of winter-run. Both the Newman
409 and Lindley (2006) and Winship et al. (2014) models included density dependence in the egg to fry stage,
410 presumably because spawner and juvenile data were available. Yet density dependence could more likely
411 be in the spawning stage given that winter-run are currently spawning below Keswick dam, rather than
412 in their natal tributaries surrounding Mt. Shasta (Yoshiyama et al. 2001). For evaluating the potential
413 for reconnecting winter-run populations to their natal spawning reaches, such an analysis could provide
414 information on potential population sizes under expanded habitat.

415 The state-space modeling framework has proven to be an important component to ecological modeling
416 due to its ability to reflect uncertainties in the biological processes via process noise and in the observation
417 process via measurement error. In most applications, the process noise is ascribed to random effects (e.g.
418 Newman and Lindley 2006, Winship et al. 2014), but some of the variation in process noise may be explained
419 by relationships to anthropogenic and environmental factors. Thus, the OBAN framework attempts to move
420 inference toward evaluating hypotheses by formally laying out a framework by which stage-specific variability
421 can be ascribed to explanatory factors rather than to random effects. This linkage can be particularly
422 powerful if some of the factors affecting the population dynamics can be managed for salmonid recovery.

423 **Acknowledgements**

424 We thank the School of Aquatic and Fisheries Sciences at the University of Washington for providing feedback
425 through their Quantitative Seminar series, Eva Jennings for providing help with data management, and Curry
426 Cunningham for thoughtful discussions on state-space modeling and Chinook population dynamics. Support

⁴²⁷ for this project was received under Grant Agreement 2039 from the Delta Stewardship Council.

References

- 428
- 429 Botsford, L. W. and Brittnacher, J. G. 1998. Viability of Sacramento River winter-run Chinook salmon.
430 *Conservation Biology* **12**(1): 65–79
- 431 California Department of Fish and Game. 2004. Sacramento River winter-run Chinook salmon: 2002-2003
432 biennial report. Tech. rep., California Department of Fish and Game, Native Anadromous Fish and
433 Watershed Branch
- 434 del Rosario, R. B., Redler, Y. J., Newman, K., Brandes, P. L., Sommer, T., Reece, K. and Vincik,
435 R. 2013. Migration patterns of juvenile winter-run-sized Chinook salmon (*Oncorhynchus tshawytscha*)
436 through the SacramentoSan Joaquin Delta. *San Francisco Estuary and Watershed Science* **11**(1). URL
437 <http://www.escholarship.org/uc/item/36d88128>
- 438 Gelman, A., Carlin, J., Stern, H. S. and Rubin, D. B. 2004. Bayesian Data Analysis. CRC Press
- 439 Gelman, A. and Rubin, D. B. 1992. Inference from iterative simulation using multiple sequences. *Statistical*
440 *science* 457–472
- 441 Gelman, A. et al. 2006. Prior distributions for variance parameters in hierarchical models (comment on
442 article by Browne and Draper). *Bayesian analysis* **1**(3): 515–534
- 443 Gilks, W. and Spiegelhalter, D. 1996. Markov chain Monte Carlo in practice. Chapman & Hall/CRC
- 444 Greene, C. M. and Beechie, T. J. 2004. Consequences of potential density-dependent mechanisms on recovery
445 of ocean-type Chinook salmon (*Oncorhynchus tshawytscha*). *Canadian Journal of Fisheries and Aquatic*
446 *Sciences* **61**(4): 590–602
- 447 Grover, A., Lowe, A., Ward, P., Smith, J., Mohr, M., Viele, D. and Tracy, C. 2004. Recommendations for
448 developing fishery management plan conservation objectives for Sacramento River winter Chinook and
449 Sacramento River spring Chinook. Tech. Rep. Progress Report, Sacramento River Winter and Spring
450 Chinook (SRWSC) Interagency Workgroup
- 451 Healey, M. 1991. Life history of Chinook salmon (*Oncorhynchus tshawytscha*). In C. Groot and L. Margolis,
452 eds., Pacific Salmon Life Histories, 311–393. University of British Columbia Press, Vancouver, B.C.,
453 Canada

- 454 King, R., Morgan, B., Gimenez, O. and Brooks, S. 2010. Bayesian analysis for population ecology. CRC
455 Press
- 456 Lindley, S. T., Schick, R. S., Mora, E., Adams, P., Anderson, J., Greene, S., Hanson, C., May, B., McE-
457 wan, D., MacFarlane, R. B., Swanson, C. and Williams, J. 2007. Framework for Assessing Viability of
458 Threatened and Endangered Chinook Salmon and Steelhead in the Sacramento-San Joaquin Basin. *San*
459 *Francisco Estuary and Watershed Science* **5**(1): Article 4
- 460 Maunder, M. N., Deriso, R. B. and Waters, C. 2011. A state–space multistage life cycle model to evaluate
461 population impacts in the presence of density dependence: illustrated with application to delta smelt
462 (*Hyposmesus transpacificus*). *Canadian Journal of Fisheries and Aquatic Sciences* **68**(7): 1285–1306
- 463 Moussalli, E. and Hilborn, R. 1986. Optimal stock size and harvest rate in multistage life history models.
464 *Canadian Journal of Fisheries and Aquatic Sciences* **43**(1): 135–141
- 465 Newman, K. 2003. Modelling paired release-recovery data in the presence of survival and capture hetero-
466 geneity with application to marked juvenile salmon. *Statistical Modelling* **3**(3): 157–177
- 467 Newman, K., Buckland, S., Morgan, B. J., King, R., Borchers, D., Cole, D. J., Besbeas, P., Gimenez, O.
468 and Thomas, L. 2014. Modelling Population Dynamics. Springer
- 469 Newman, K. B. and Brandes, P. L. 2010. Hierarchical Modeling of Juvenile Chinook Salmon Survival
470 as a Function of Sacramento-San Joaquin Delta Water Exports. *North American Journal of Fisheries*
471 *Management* **30**(1): 157–169
- 472 NMFS. 2014. Recovery Plan for the Evolutionarily Significant Units of Sacramento River Winter-run Chinook
473 Salmon and Central Valley Spring-run Chinook Salmon and the Distinct Population Segment of California
474 Central Valley Steelhead. Tech. rep., National Marine Fisheries Service
- 475 O’Farrell, M. R., Mohr, M. S., Grover, A. M. and Satterthwaite, W. H. 2012. Sacra-
476 mento River winter Chinook cohort reconstruction: analysis of ocean fishery impacts. URL
477 <http://swfsc.noaa.gov/publications/TM/SWFSC/NOAA-TM-NMFS-SWFSC-491.pdf>
- 478 Perry, R. W., Skalski, J. R., Brandes, P. L., Sandstrom, P. T., Klimley, A. P., Ammann, A. and
479 MacFarlane, B. 2010. Estimating survival and migration route probabilities of juvenile Chinook
480 salmon in the Sacramento-San Joaquin River Delta. *North American Journal of Fisheries Man-*

- 481 *agement* **30**(1): 142–156. doi:Doi 10.1577/M08-200.1. URL <Go to ISI>://WOS:000277113900013;
 482 <http://www.tandfonline.com/doi/full/10.1577/M08-200.1>
- 483 Poytress, W. R. and Carrillo, F. D. 2011. Brood-year 2008 and 2009 winter Chinook juvenile production
 484 indices with comparisons to juvenile production estimates derived from adult escapement. Tech. Rep.
 485 Draft Annual Report 2008 and 2009, U.S. Fish and Wildlife Service
- 486 R Core Team. 2013. R: A Language and Environment for Statistical Computing. R Foundation for Statistical
 487 Computing, Vienna, Austria. URL <http://www.R-project.org/>
- 488 Roberts, G. and Polson, N. G. 1994. On the geometric convergence of the Gibbs sampler. *J. Roy. Stat. Soc.*
 489 *B* **56**: 377–384
- 490 Scheuerell, M. D., Hilborn, R., Ruckelshaus, M. H., Bartz, K. K., Lagueux, K. M., Haas, A. D. and Rawson,
 491 K. 2006. The Shiraz model: a tool for incorporating anthropogenic effects and fish-habitat relationships
 492 in conservation planning. *Canadian Journal of Fisheries and Aquatic Sciences* **63**(7): 1596–1607
- 493 Snider, B., Reavis, B. and Hill, S. 2000. 1999 Upper Sacramento River winter-run Chinook salmon escapement
 494 survey, May - August 1999. Tech. Rep. Technical Report No. 00-1, California Department of Fish and
 495 Game, Stream Evaluation Program
- 496 Sommer, T. R., Harrell, W. C. and Nobriga, M. L. 2005. Habitat use and stranding risk of juvenile Chinook
 497 salmon on a seasonal floodplain. *North American Journal of Fisheries Management* **25**(4): 1493–1504
- 498 Spiegelhalter, D., Thomas, A., Best, N. and Lunn, D. 2003. WinBUGS version 1.4 user manual. Tech. rep.,
 499 MRC Biostatistics Unit, Cambridge, UK
- 500 Sturtz, S., Ligges, U. and Gelman, A. 2005. R2WinBUGS: A Package for Running WinBUGS from R.
 501 *Journal of Statistical Software* **12**(3): 1–16. URL <http://www.jstatsoft.org>
- 502 Wells, B. K., Grimes, C. B. and Waldvogel, J. B. 2007. Quantifying the effects of wind, up-
 503 welling, curl, sea surface temperature and sea level height on growth and maturation of a Cal-
 504 ifornia Chinook salmon (*Oncorhynchus tshawytscha*) population. *Fisheries Oceanography* **16**(4):
 505 363–382. doi:DOI 10.1111/j.1365-2419.2007.00437.x. URL <Go to ISI>://WOS:000247440500005;
 506 <http://onlinelibrary.wiley.com/doi/10.1111/j.1365-2419.2007.00437.x/full>
- 507 Williams, J. G. 2006. Central Valley Salmon: A Perspective on Chinook and Steelhead in the Central Valley
 508 of California. *San Francisco Estuary and Watershed Science* **4**(3): Article 2

- 509 Winship, A. J., OFarrell, M. R. and Mohr, M. S. 2014. Fishery and Hatchery Ef-
510 fects on an Endangered Salmon Population with Low Productivity. *Transactions of the*
511 *American Fisheries Society* **143**(4): 957–971. doi:10.1080/00028487.2014.892532. URL
512 <http://www.tandfonline.com/doi/abs/10.1080/00028487.2014.892532>
- 513 Woodson, L. E., Wells, B. K., Weber, P. K., MacFarlane, R. B., Whitman, G. E. and Johnson, R. C. 2013.
514 Size, growth and origin-dependent mortality of juvenile Chinook salmon *Oncorhynchus tshawytscha* during
515 early ocean residence. *Marine Ecology Progress Series* **487**: 163–175. doi:10.3354/meps10353
- 516 Yoshiyama, R., Gerstung, E., Fisher, F. and Moyle, P. 2001. Historical and present distribution of Chinook
517 salmon in the Central Valley drainage of California. In R. Brown, ed., *Contributions to the Biology*
518 *of Central Valley Salmonids*. Fish Bulletin 179(1), 71–176. California Department of Fish and Game,
519 Sacramento, California

Table D.1: Model parameters, state variables, and observable indices of abundance for winter-run OBAN model.

Symbol	Value	Description
Indices		
i	egg, alevin, fry, delta, bay, gulf	freshwater stages
j		covariate index
k		gear type for observation process
t	1967, ..., 2004	brood year
y	1967, ..., 2008	calendar year
age	2, 3, 4	ocean age
State Variables		
$N_{i,t}$		abundance of freshwater stage
$O_{age,t}$		abundance of ocean stage
$M_{age,t}$		abundance of mature fish
Parameters		
$\beta_{i,j}$		coefficient relating factor j to survival in stage i
$\gamma_{i,j}$		coefficient relating factor j to capacity in stage i
$\delta_{age,j}$		coefficient relating factor j to maturation at age
ϕ_{age}	(0,1)	conditional maturation in age
$CV_{E,k}$		coefficient of variation for escapement observation process k
CV_J		coefficient of variation for juvenile observation process k
CV_p		coefficient of variation of process noise
f_t	2450	fecundity per spawner
$h_{age,t}$		impact rate due to harvest
$p_{i,t}$	(0, 1)	productivity in stage i and brood year t
$K_{i,t}$	(0, ∞)	capacity in stage i and brood year t
z_2	0.5	age 2 average natural survival rate
z_3	0.8	age 3 average natural survival rate
z_4	0.8	age 4 average natural survival rate
Observables		
$I_{y,E}$		Escapement 1967 - 2008
$I_{y,J}$		Juvenile abundance at Red Bluff Diversion Dam 1995 - 1999, 2002-2007

520 Figure D.1. Map of the Central Valley (black lines), Sacramento River, San Francisco Estuary, and ocean
521 habitats used by winter-run Chinook.

522 Figure D.2. Model fit to observed winter-run escapement data (squares) from three collection methods:
523 1) Red Bluff Diversion Dam (RBDD) counts, 2) expansion of RBDD counts assuming 15% passage by May
524 15, and 3) carcass mark-recapture. Vertical lines indicate 1 standard deviation. Heavy line is the mean
525 winter-run OBAN prediction, whereas thin lines are the 95% credible interval on model predictions of the

Table D.2: Covariates used in the winter-run OBAN model.

Covariate	Mean	Standard Deviation	Stage	Description
TEMP	13.4	0.9	alevin	Jul - Sept mean temperature at Bend Bridge (C) ¹
FLMIN	6605	1477	alevin	Aug - Nov minimum of monthly average flow at Bend Bridge (cfs) ²
YOLO	22.9	24.7	delta	Dec - Mar number of days where flow is greater than 56,000 on the Sacramento River at Verona ³
DCC	0.46	0.42	delta	Dec - Mar proportion of time when Delta Cross Channel gates are open ⁴
EXPT	1250154	320854	delta	Dec - Jun total exports (cfs) ³
UPW	210.5	49.8	gulf	Apr-Jun upwelling index ⁵
FARA	11.8	0.9	gulf	Feb - Apr mean temperature in the Farallon Islands (C) ⁶

¹ Temperature regressions for 1967 - 1970; modeled temperature data 1970-2005; gage data 2005-2008 CDEC-BND

² CDEC-BND station or USGS 11377100 station

³ Dayflow (<http://www.water.ca.gov/dayflow/output/Output.cfm>)

⁴ US Bureau of Reclamation (<http://www.usbr.gov/mp/cvo/vungvari/Ccgates.pdf>)

⁵ Pacific Fisheries Environmental Laboratory (<http://las.pfeg.noaa.gov/LAS/docs/upwell.nc.html>)

⁶ University of California San Diego (http://shorestation.ucsd.edu/active/index_active.html#farallonstation)

Table D.3: Prior and posterior distributions in the winter-OBAN model.

Parameter	Prior	Mean	Median	95%CrI	Pr > 0
β_{alevin}	N(0, 2.5)	-1.17	-1.21	(-2.09, -0.09)	0.21
β_{delta}	N(0, 2.5)	-4.63	-4.64	(-5.48, -3.79)	0.00
β_{TEMP}	N(0, 2.5)	-2.00	-1.99	(-3.66, -0.35)	0.004
β_{FLMIN}	N(0, 2.5)	1.48	1.42	(0.42, 2.86)	1.00
$\beta_{TEMP:FLMIN}$	N(0, 2.5)	0.52	0.53	(-0.91, 2.06)	0.73
β_{YOLO}	N(0, 2.5)	0.13	0.11	(-0.54, 0.84)	0.65
β_{DCC}	N(0, 2.5)	0.15	0.14	(-0.37, 0.78)	0.70
β_{EXPT}	N(0, 2.5)	-0.13	-0.13	(-0.95, 0.66)	0.39
β_{UPW}	N(0, 2.5)	0.94	0.90	(-0.71, 2.83)	0.83
β_{FARA}	N(0, 2.5)	-0.24	-0.23	(-1.53, 0.91)	0.35
CV_{E1}	U(0, CV_{E3})	0.71	0.68	(0.46, 1.12)	NA
CV_{E2}	U(CV_{E3} , 2)	1.36	1.34	(0.80, 1.96)	NA
CV_{E3}	U(0, 2)	1.03	0.97	(0.62, 1.79)	NA
CV_J	U(0, 2)	1.20	1.20	(0.42, 1.93)	NA
CV_p	¹ B(2, 6)	0.26	0.25	(0.02, 0.59)	NA
ϕ_2	² B(1, 10)	0.038	0.030	(0.004, 0.128)	NA
ϕ_3	³ B(10, 1)	0.907	0.928	(0.700, 0.997)	NA

¹ Informative prior with a mean of 0.25, 95% interval (0.036, 0.58)

² Informative prior with mean of 0.091, 95% interval (0.0025, 0.31)

³ Informative prior with mean of 0.91, 95% interval (0.69, 0.99)

526 state variable of escapement.

527 Figure D.3. Model fit to observed winter-run juvenile abundance index (squares) at Red Bluff Diversion
528 Dam from 1996 to 2008. Vertical lines indicate 1 standard deviation. Heavy line is the mean winter-run
529 OBAN prediction, whereas thin lines are the 95% credible interval on model predictions of the state variable
530 of fry abundance.

531 Figure D.4. Predicted survival in the egg to fry (alevin) stage above Red Bluff Diversion Dam (A), in
532 the delta (B), in the gulf (C), and as age 3 in the ocean (D). For A - C the dark line represents the median
533 model prediction, whereas thin lines are the 95% credible interval on model predictions. For D the dark line
534 represents the assumed survival rate of age-3 due to natural mortality and harvest.

535 Figure D.5. Analysis of factors affecting winter-run survival to the end of age 2. Factors were increased
536 by 1 standard deviation and the percent change in survival to the end of age 2 relative to a baseline (all
537 factors at their 1967-2008 mean levels) was calculated for each factor. Please see Table D.2 for a description
538 of each factor.



Figure D.1:

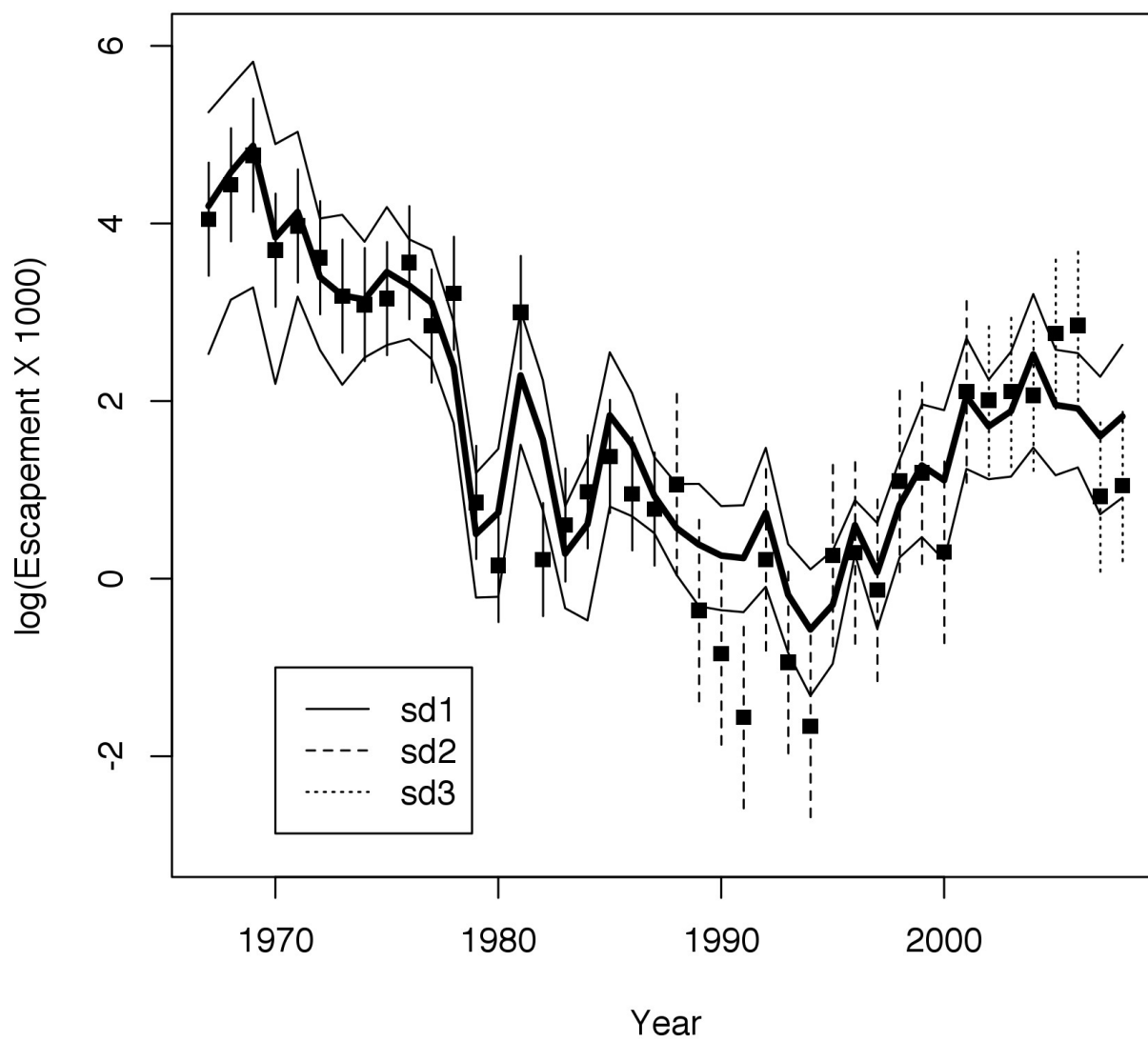


Figure D.2:

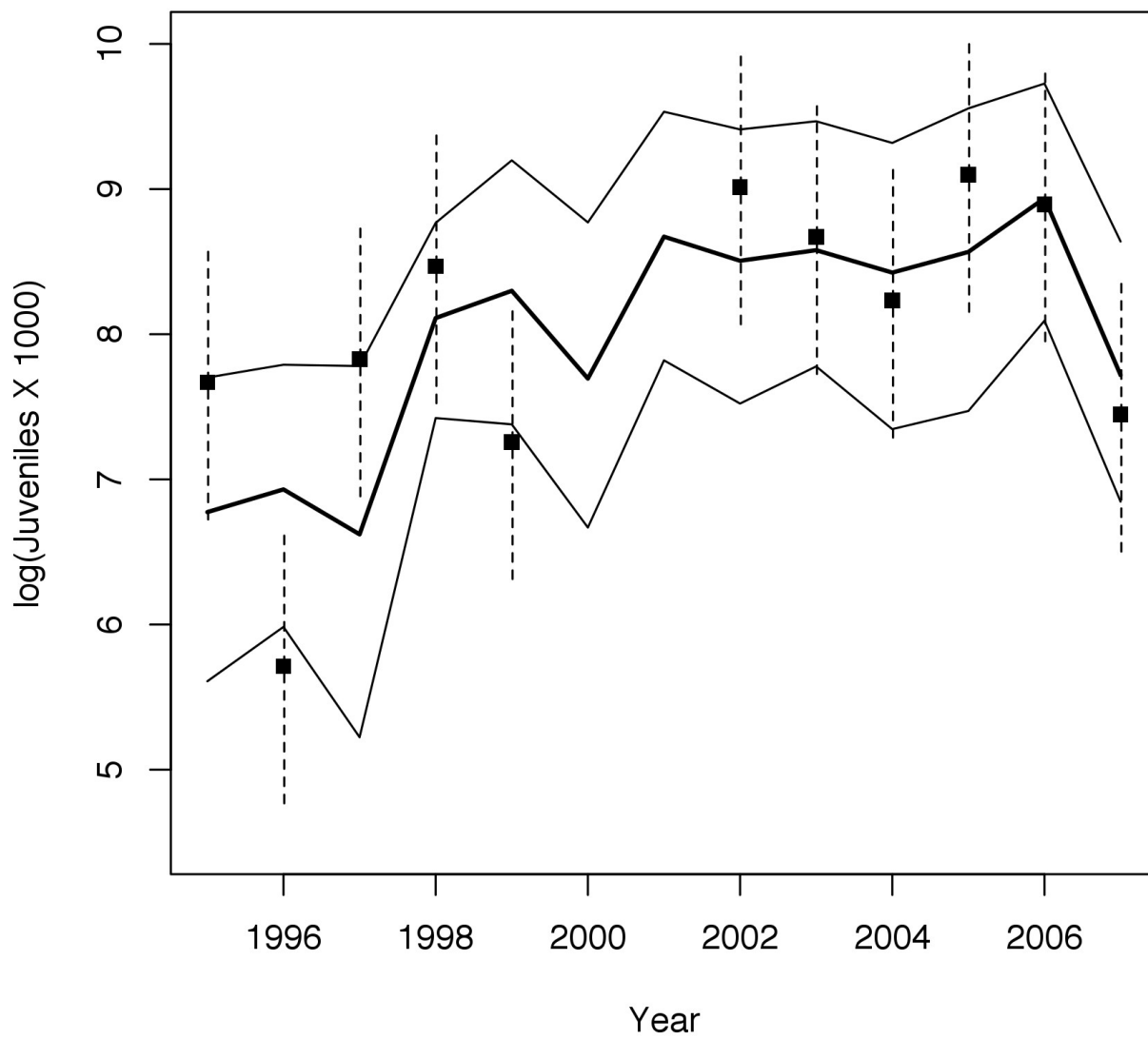


Figure D.3:

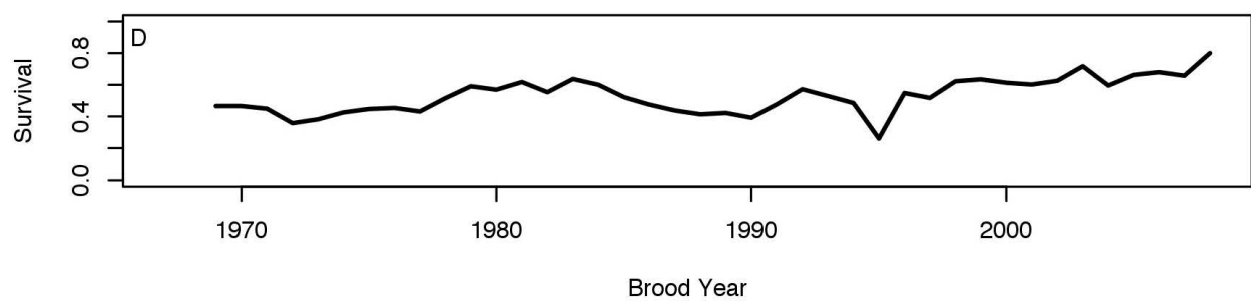
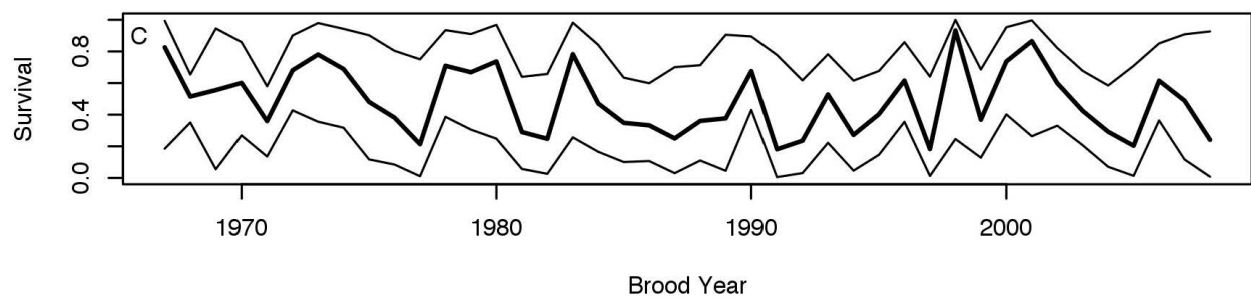
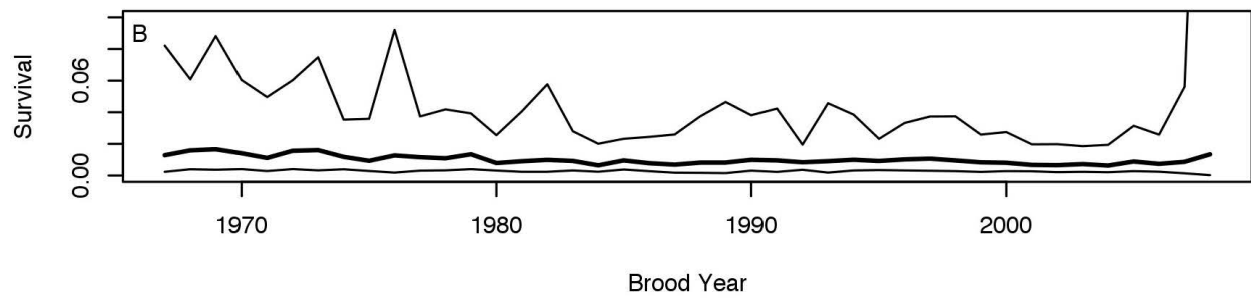
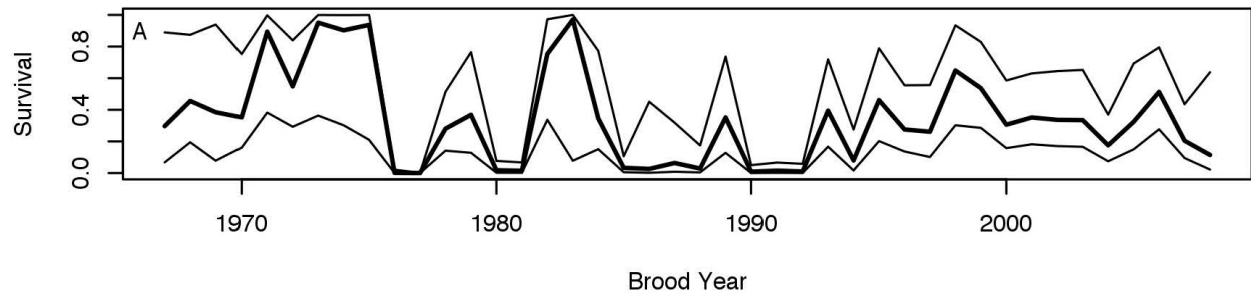


Figure D.4:

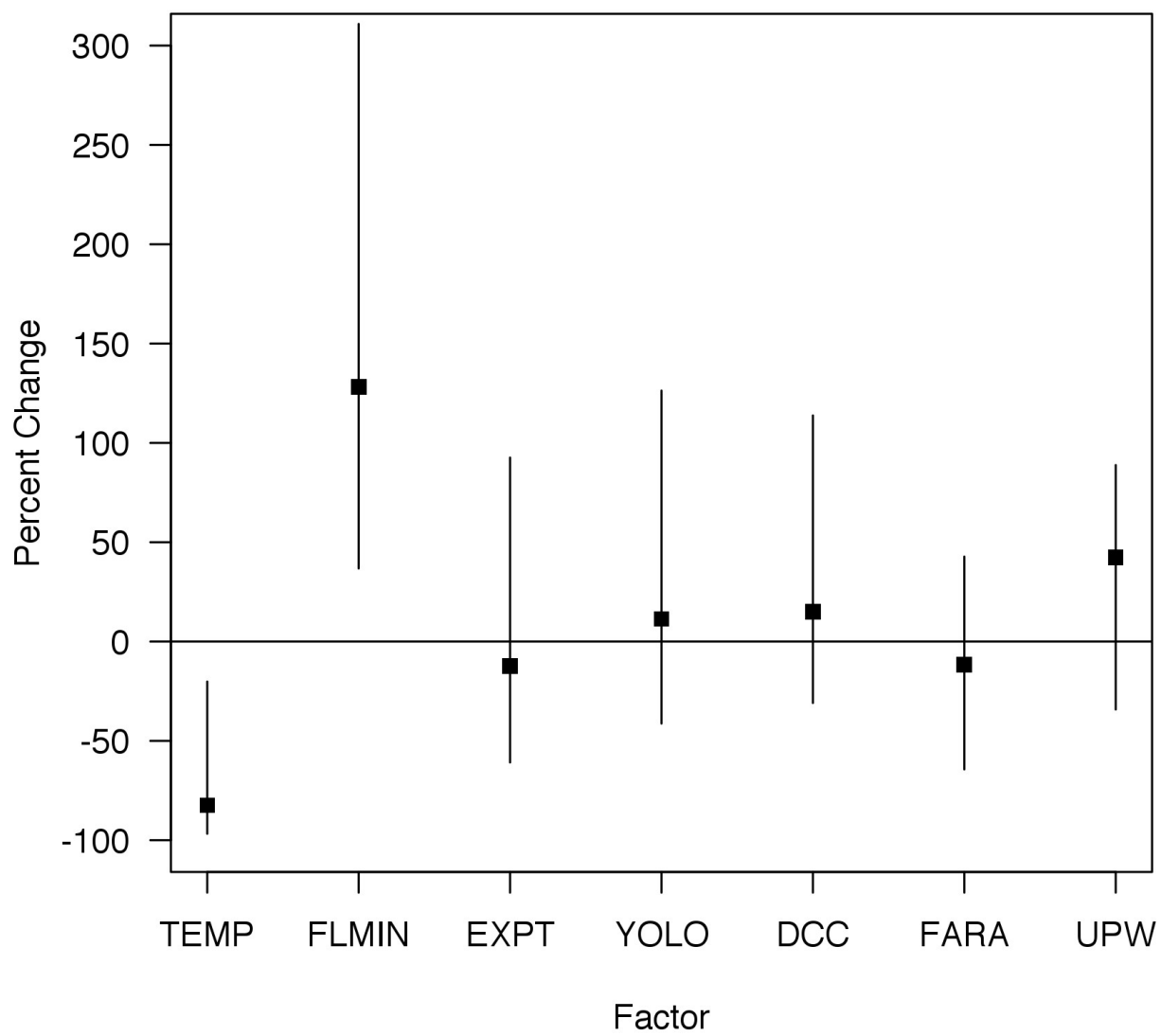


Figure D.5:



Global Seabird Response to Forage Fish Depletion—One-Third for the Birds

Philippe M. Cury, *et al.*
Science **334**, 1703 (2011);
DOI: 10.1126/science.1212928

This copy is for your personal, non-commercial use only.

If you wish to distribute this article to others, you can order high-quality copies for your colleagues, clients, or customers by [clicking here](#).

Permission to republish or repurpose articles or portions of articles can be obtained by following the guidelines [here](#).

The following resources related to this article are available online at www.sciencemag.org (this information is current as of December 22, 2011):

Updated information and services, including high-resolution figures, can be found in the online version of this article at:

<http://www.sciencemag.org/content/334/6063/1703.full.html>

Supporting Online Material can be found at:

<http://www.sciencemag.org/content/suppl/2011/12/21/334.6063.1703.DC1.html>

This article **cites 112 articles**, 23 of which can be accessed free:

<http://www.sciencemag.org/content/334/6063/1703.full.html#ref-list-1>

creasing demands of supporting and moving greater weight on land and the benefits of having more upright toe bones but directing some loads away from the toes with the predigits and fat pad, which resulted in the peculiar compromise that persists in the feet of extant elephants.

The recognition of elephant predigits as enlarged sesamoids that perform digit-like functions fuels inspiration for examining the evolution of foot function, terrestriality, and gigantism in other lineages. Sauropod dinosaurs had expansive foot pads, particularly in their pedes (24); however, no evidence of predigits has been found. Considering that the predigits form on the medial border of the feet, they would tend to be lost if digit I is lost or reduced, as it was in early perisodactyls and artiodactyls. This loss might limit foot pad expansion and thereby explain why rhinos and hippos seem to lack predigits [but see (18) for a possible rudimentary pollex in hippos] and have less expanded foot pads than elephants do (8). Regardless, the previously misunderstood and neglected predigits of elephants now deserve recognition as a remarkable case of evolutionary exaptation (4), revealing how elephants evolved their specialized foot form and function.

References and Notes

1. D. D. Davis, *Feldiana* 3, 1 (1964).
2. H. Endo *et al.*, *J. Anat.* **195**, 295 (1999).
3. S. J. Gould, *Nat. Hist.* **87**, 20 (1978).
4. S. J. Gould, E. S. Vrba, *Paleobiology* **8**, 4 (1982).

5. M. Fabrezi, *Zool. J. Linn. Soc.* **131**, 227 (2001).
6. M. R. Sánchez-Villagra, P. R. Menke, *Zoology* **108**, 3 (2005).
7. P. Blair, *Philos. Trans.* **27**, 53 (1710).
8. H. Neuville, *Arch. Mus. Natl. Hist. Nat. Paris* **13**, 6e Serie, 111 (1935).
9. K. von Bardeleben, *Proc. Zool. Soc.* **1894**, 354 (1894).
10. C. Mitgutsch *et al.* *Biol. Lett.*, 10.1098/rsbl.2011.0494 (2011).
11. Materials and methods are available as supporting material on *Science* Online.
12. G. E. Weisengruber *et al.*, *J. Anat.* **209**, 781 (2006).
13. F. Galis, J. J. M. van Alphen, J. A. J. Metz, *Trends Ecol. Evol.* **16**, 637 (2001).
14. J. Prochel, P. Vogel, M. R. Sánchez-Villagra, *J. Anat.* **205**, 99 (2004).
15. J. R. Hutchinson, C. E. Miller, G. Fritsch, T. Hildebrandt, in *Anatomical Imaging: Towards a New Morphology*, R. Frey, H. Endo, Eds. (Springer, Berlin, 2009), pp. 23–38.
16. C. E. Miller, C. Basu, G. Fritsch, T. Hildebrandt, J. R. Hutchinson, *J. R. Soc. Interface* **5**, 465 (2008).
17. D. R. Carrier, N. C. Heglund, K. D. Earls, *Science* **265**, 651 (1994).
18. A. B. Clifford, *J. Vertebr. Paleontol.* **30**, 1827 (2010).
19. N. Court, *Palaeontogr. Abt. A* **226**, 125 (1993).
20. D. E. Lieberman *et al.*, *Nature* **463**, 531 (2010).
21. F. Michilsen, P. Aerts, R. Van Damme, K. D'Août, *J. Zool. (London)* **279**, 236 (2009).
22. A. A. Biewener, *Science* **250**, 1097 (1990).
23. M. N. Scholz, M. F. Bobbert, A. J. van Soest, J. R. Clark, J. van Heerden, *J. Exp. Biol.* **211**, 3266 (2008).
24. M. F. Bonnan, in *Thunder-Lizards: the Sauropodomorph Dinosaurs*, K. Carpenter, V. Tidwell, Eds. (Indiana Univ. Press, Bloomington, IN, 2005), pp. 346–380.
25. M. M. Smuts, A. J. Bezuidenhout, *Onderstepoort J. Vet. Res.* **60**, 1 (1993).

26. M. M. Smuts, A. J. Bezuidenhout, *Onderstepoort J. Vet. Res.* **61**, 51 (1994).
27. A. Boyde, R. Travers, F. H. Glorieux, S. J. Jones, *Calcif. Tissue Int.* **64**, 185 (1999).
28. C. Delmer, *Acta Palaeontol. Pol.* **54**, 561 (2009).
29. E. Gheerbrant, *Proc. Natl. Acad. Sci. U.S.A.* **106**, 10717 (2009).
30. E. Gheerbrant, P. Tassy, *C. R. Palevol.* **8**, 281 (2009).

Acknowledgments: We thank the staff of the Structure and Motion Laboratory of the Royal Veterinary College for assistance and three anonymous reviewers for constructive criticism. Many individuals assisted with the collection of the cadaveric data; we particularly thank the European-based zoos that provided the specimens and G. Fritsch for CT scans done in Germany. O. Cosar, R. Weller, A. Wilson, and K. Jespers assisted with the ex vivo loading experiments. J. Molnar assisted with Figs. 1 to 4 and the movies. This project was funded by the Biotechnology and Biological Sciences Research Council (BBSRC) (grants BB/C516844/1 and BB/H002782/1 to J.R.H.). Additionally, A.A.P. appreciates funding from Arthritis Research UK and the BBSRC, and A.B. was supported by the Veterinary Advisory Committee of the UK Horserace Betting Levy Board. The data reported in this paper are tabulated in the SOM. The authors declare no conflicts of interest.

Supporting Online Material

www.sciencemag.org/cgi/content/full/334/6063/1699/DC1

Materials and Methods

SOM Text

Figs. S1 to S16

Tables S1 to S3

References (31–41)

Movies S1 to S4

20 July 2011; accepted 8 November 2011

10.1126/science.1211437

Global Seabird Response to Forage Fish Depletion—One-Third for the Birds

Philippe M. Cury,^{1*} Ian L. Boyd,^{2*} Sylvain Bonhommeau,³ Tycho Anker-Nilssen,⁴ Robert J. M. Crawford,⁵ Robert W. Furness,⁶ James A. Mills,⁷ Eugene J. Murphy,⁸ Henrik Österblom,⁹ Michelle Paleczny,¹⁰ John F. Piatt,¹¹ Jean-Paul Roux,^{12,13} Lynne Shannon,¹⁴ William J. Sydeman¹⁵

Determining the form of key predator-prey relationships is critical for understanding marine ecosystem dynamics. Using a comprehensive global database, we quantified the effect of fluctuations in food abundance on seabird breeding success. We identified a threshold in prey (fish and krill, termed “forage fish”) abundance below which seabirds experience consistently reduced and more variable productivity. This response was common to all seven ecosystems and 14 bird species examined within the Atlantic, Pacific, and Southern Oceans. The threshold approximated one-third of the maximum prey biomass observed in long-term studies. This provides an indicator of the minimal forage fish biomass needed to sustain seabird productivity over the long term.

Public and scientific appreciation for the role of top predators in marine ecosystems has grown considerably, yet many upper trophic level (UTL) species, including seabirds, marine mammals, and large predatory fish, remain depleted owing to human activities (1–4). Fisheries impacts include direct mortality of exploited species and the more subtle effects of altering trophic pathways and the functioning of marine ecosystems (5). Specifically, fisheries for lower trophic level (LTL) species, primarily small

coastal pelagic fish (e.g., anchovies and sardines), euphausiid crustaceans (krill), and squid (hereafter referred to as “forage fish”), threaten the future sustainability of UTL predators in marine ecosystems (6, 7). An increasing global demand for protein and marine oils contributes pressure to catch more LTL species (8). Thus, fisheries for LTL species are likely to increase even though the consequences of such activity remain largely unknown at the ecosystem level. It remains challenging, however, to assess fishing

impacts on food webs because numerical relationships between predators and prey are often unknown, even for commercially valuable fish (9, 10). Ecosystem models and ecosystem-based fisheries management, for which maintaining

¹Institut de Recherche pour le Développement, UMR EME-212, Centre de Recherche Halieutique Méditerranéenne et Tropicale, Avenue Jean Monnet, BP 171, 34203 Sète Cedex, France.

²Scottish Oceans Institute, University of St Andrews, St Andrews KY16 8LB, UK. ³Ifremer, UMR EME 212, Centre de Recherche Halieutique Méditerranéenne et Tropicale, Avenue Jean Monnet, BP 171, 34203 Sète Cedex, France.

⁴Norwegian Institute for Nature Research, Post Office Box 5685 Sluppen, NO-7485 Trondheim, Norway. ⁵Branch Oceans and Coasts, Department of Environmental Affairs, Private Bag X2, Rogge Bay 8012, South Africa.

⁶College of Medical, Veterinary and Life Sciences, University of Glasgow, Glasgow G12 8QQ, UK. ⁷15027 A Skyline Drive, Corning, NY 14830, USA. ⁸British Antarctic Survey, High Cross, Madingley Road, Cambridge CB3 0ET, UK. ⁹Baltic Nest Institute, Stockholm Resilience Centre, Stockholm University, SE-106 91 Stockholm, Sweden.

¹⁰Fisheries Centre, Aquatic Ecosystems Research Laboratory (AERL), 2202 Main Mall, The University of British Columbia, Vancouver, BC, Canada V6T 1Z4.

¹¹U.S. Geological Survey, Alaska Science Center, 4210 University Drive, Anchorage, AK 99508, USA. ¹²Ecosystem Analysis Section, Ministry of Fisheries and Marine Resources, Lüderitz Marine Research, Post Office Box 394, Lüderitz, Namibia.

¹³Animal Demography Unit, Zoology Department, University of Cape Town, Private Bag X3, Rondebosch, Cape Town 7701, South Africa. ¹⁴Marine Research Institute and Zoology Department, University of Cape Town, Private Bag X3, Rondebosch, Cape Town 7701, South Africa. ¹⁵Farallon Institute for Advanced Ecosystem Research, Post Office Box 750756 Petaluma, CA 94952, USA.

*To whom correspondence should be addressed. E-mail: philippe.cury@ird.fr (P.M.C.); ilb@st-andrews.ac.uk (I.L.B.)

predator populations is an objective (2, 11, 12), will remain controversial until these relationships are more fully quantified.

To improve our understanding of the effects of LTL fisheries on marine ecosystems, more information on predator-prey relationships across a range of species and ecosystems is required (6). Seabirds are conspicuous members of marine ecosystems globally. Many aspects of seabird ecology have been measured consistently for decades, encompassing ecosystem change at multiple scales (13). Substantial long-term data sets on seabird breeding success have been compiled for many taxa in several marine ecosystems around the world (14–16), but for relatively few has independent information on prey availability been obtained concurrently. For those where prey data are available, temporal covariance in predators and their prey suggests that seabirds can be used as indicators of forage fish population fluctuations (7, 16, 17). Here, we used data collected contemporaneously over multiple decades from seabirds and forage fish to test the hypothesis that the form of the numerical response between seabird breeding success and forage fish abundance is consistent across species and ecosystems. We used data from seabird species that have strong dietary dependencies on forage fish prey and where the time series for both the predator and the prey have high spatial and temporal congruence. We compiled data from 19 time series covering seven marine ecosystems, nine sites, and 14 seabird species and their major prey (Fig. 1 and table S1). The data set included 438 data points spanning 15 to 47 colony-years per breeding site (table S1). The abundance of principal prey for each seabird species was estimated independently of the data collected from the birds, usually as part of population assessments conducted in support of fisheries management (table S1).

To examine empirical relationships between seabird breeding success and prey abundance, we used nonparametric statistical methods that facilitate nonlinear modeling by making no a priori assumptions about the form of the relationships (generalized additive models, or GAMs). Initially, each time series (seabird breeding success and prey abundance) was normalized by expressing the measurements as the number of standard deviations from the mean; this enables robust comparisons across species and ecosystems. Once the numerical relationship was established, we used a change-point analysis (sequential *t* tests that find the most likely point at which the slope of breeding success changes in relation to prey abundance) to identify thresholds within nonlinear relationships (18) (Fig. 2A). A bootstrap analysis was used to calculate confidence intervals of the threshold, and the variance in seabird breeding success was calculated for each prey abundance class. Last, a selection of a priori parametric models ranging from linear, sigmoid, asymptotic, to hierarchical (table S2) was fitted to the general relationship. The most parsimonious

model was then used to fit the relationship between seabird breeding success and forage fish population size for each ecosystem (pooling all species) and each seabird species (pooling all ecosystems).

Seabird breeding success showed a nonlinear response to changes in prey abundance (Fig. 2A). The threshold at which breeding success began to decline from the asymptote was not significantly different from the long-term mean of prey abundance (range -0.30 and $+0.13$, standard deviation of the mean, Fig. 2A). The threshold was 34.6% (95% confidence interval 31 to 39%), or approximately one-third of the maximum observed prey abundance. The coefficient of variation between the different thresholds among species and ecosystems was 28% (table S1). All time series were of sufficient duration to identify the threshold (detection is possible after 13 years of observation, fig. S1) and the maximum biomass (detection is possible after 11 years, fig. S2). Variance in breeding success increased significantly (*F* test, $P < 10^{-4}$) below the threshold of prey abundance (Fig. 2B). Fitting parametric models to individual responses showed a similar inflection point and similar asymptotic values across ecosystems and species (Figs. 2, C and D, and 3), indicating that the functional form was a general feature of the seabird–forage fish relationship.

The asymptotic form of the relationship between seabird breeding success and forage

fish abundance has been reported previously (15, 16, 19–24), but the common scaling across species and ecosystems and the consistency of threshold values are new observations. The global pattern shows a threshold below which the numerical response declines strongly as food abundance decreases and above which it reaches a plateau and does not change even as food abundance increases. This pattern is apparently robust to the varying life-history strategies, habitat preferences, and population sizes of the seabird species considered. Nonetheless, we acknowledge that a range of factors may interact to weaken or possibly accentuate the relationship between seabird breeding performance and prey species abundance. Alternative drivers of change in breeding success include changes in habitat characteristics or predation pressures, or complex intercolony dynamics. Predators may also show more or less capacity to switch to alternative prey items, which may buffer productivity against declines in any single prey species (25).

Periods of consistently high or low breeding success, or occasional complete breeding failures, are normal in seabirds, and most species are adapted to fleeting anomalous environmental conditions. However, chronic food scarcity, as potentially defined by prey abundance below the threshold described here for seabirds, will compromise long-term breeding success, and this may affect the trajectory of their populations.

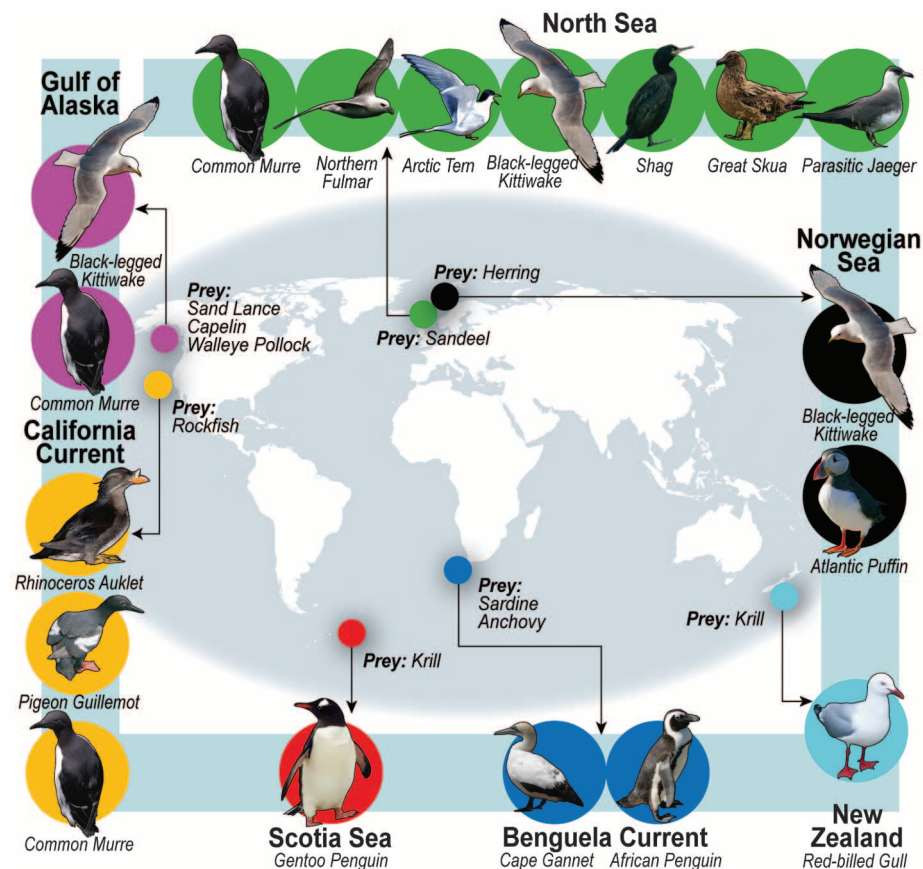


Fig. 1. Map of the distribution of seabird and prey species considered in our analysis.

Fig. 2. (A) Relationship between normalized annual breeding success of seabirds and normalized prey abundance. Each data point from all the time series was plotted with the predictions of a generalized additive model (GAM) (solid line). The gray area represents the 95% confidence interval of the fitted GAM. The threshold in the nonlinear relationship (black solid vertical line) and its 95% confidence interval (black dashed vertical lines) were detected from a change-point analysis. (B) Change in variance across the range of normalized food abundance ranging from -1.5 to 2 standard deviations in eight classes. Variance below the threshold was 1.8 times higher than above it. (C and D) Similar relationships were present when data were pooled (C) for species within ecosystems and (D) for species pooled among ecosystems using the best-fitting asymptotic model (table S2). The Arctic Tern (not shown) model fit was not significant (table S1). The colors in (A) and (C) represent the data set for each ecosystem and in (D) for each seabird species.

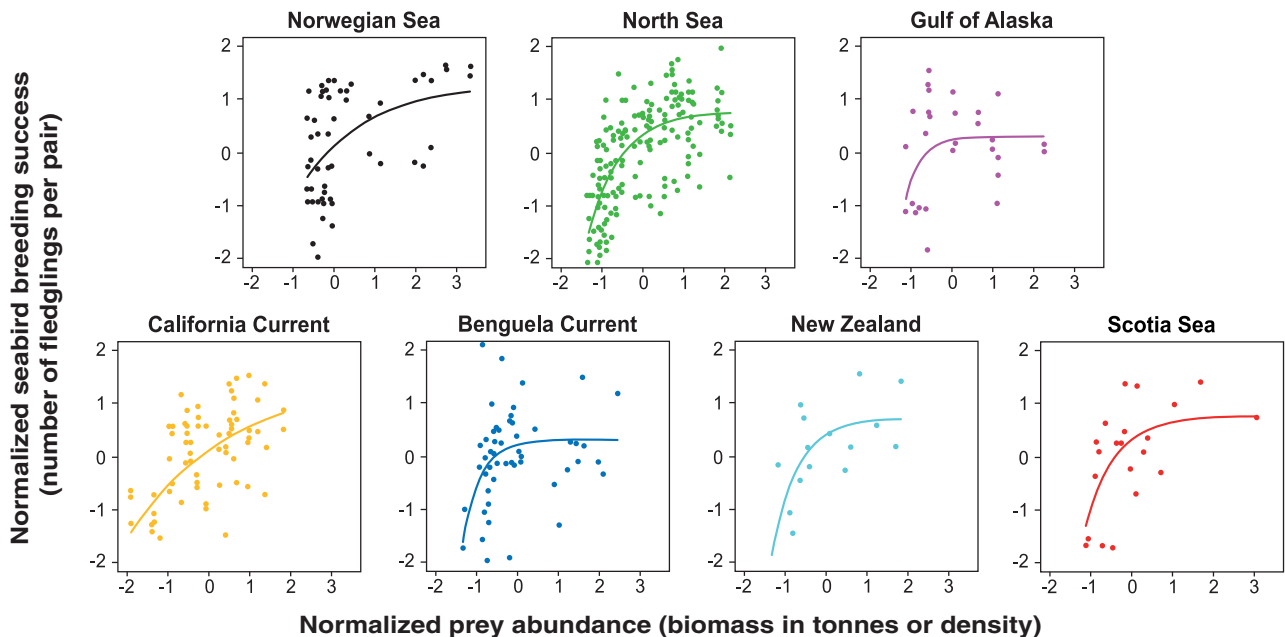
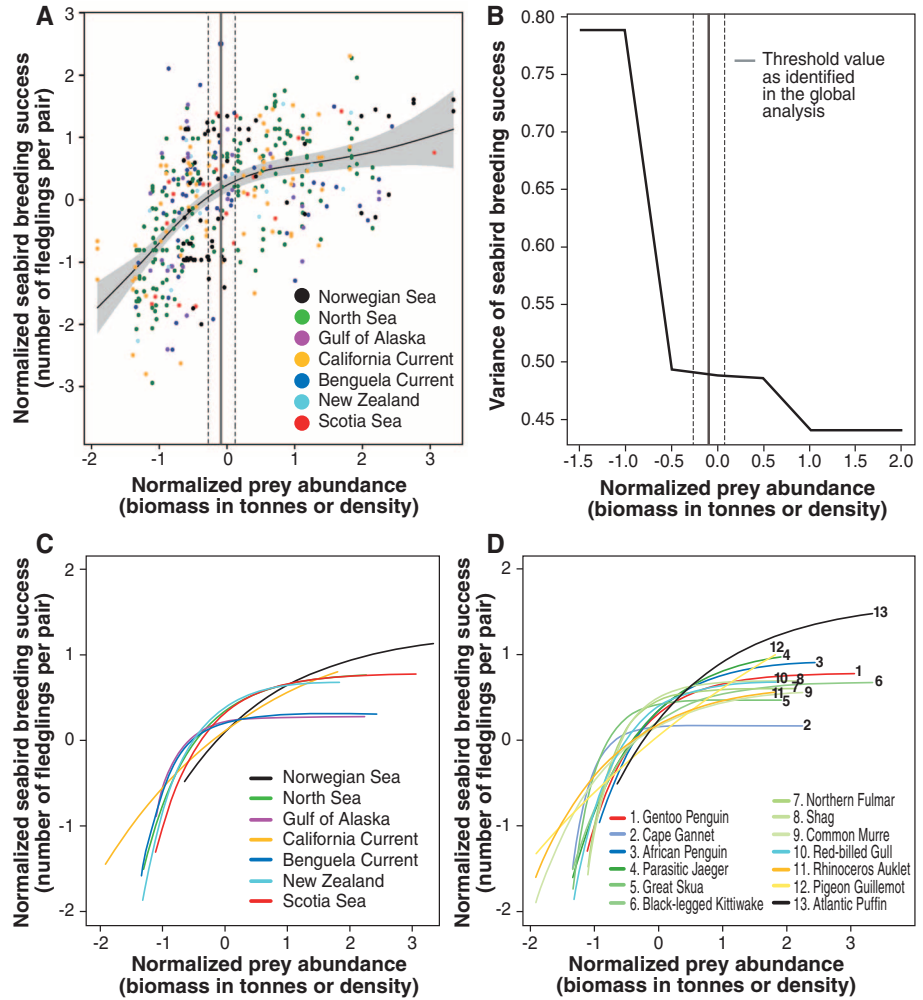


Fig. 3. Relationship between normalized annual breeding success of pooled seabird species and normalized prey abundance for the seven different ecosystems using the most parsimonious asymptotic model (table S2).

Indeed, food scarcity can also reduce adult survival in seabirds (26), with immediate population-level impacts. Whether caused by persistent overfishing, or directional or stochastic environmental change that reduces ecosystem carrying capacity, recruitment and survival will probably have thresholds of prey abundance shifted to the left of that for breeding success (15, 16). Consequently, the threshold for breeding success is likely to provide a precautionary guideline to what level of food reduction might seriously impact seabird populations.

The threshold defined by our study suggests that if management objectives include balancing predator-prey interactions to sustain healthy UTL predator populations and ecosystem functions (2), a practical indicator would be to maintain forage fish biomass above one-third of the maximum observed long-term biomass. The application of such a management guideline will depend upon local circumstances, such as the need to implement spatial management around breeding colonies or the conservation status of species (27). Although we cannot assume similarity between all taxa in the value of the predator-prey threshold, our study demonstrates consistency among a broad range of seabirds. There is also evidence that some marine mammals and predatory fish share the general form of the relationship (17, 19, 25, 28).

Tuning management goals to ensure sufficient biomass of forage fish for seabird reproduction may be a useful step toward ensuring sustainability of predator-prey interactions for other, less well-studied predators in marine ecosystems. Even for predators not showing high dependency on exploited species, this is likely to provide a precautionary step. The “one-third for the birds” guiding principle could be applied widely to help

manage forage fisheries to benefit ecosystem resilience. Indeed, predator responses of this type are already included in some specific management systems (29). Although such a guideline might be difficult to consider for new fisheries, where there are few data to determine the maximum biomass, most of the economically important coastal pelagic fish populations have sufficient data to define the threshold in many ecosystems (e.g., in the Benguela, California, and Humboldt Currents) (figs. S1 and S2).

The generality of the asymptotic form of the predator-prey relationship suggests that it is rooted in fundamental life history and ecological theory (e.g., demographic trade-offs and functional responses). In a practical context, “one-third for the birds” is a simple, empirically derived guiding principle that embraces the ecosystem approach to management aimed at sustaining the integrity of predator-prey interactions and marine food webs for the benefit of both natural predators and humans.

References and Notes

1. J. B. C. Jackson *et al.*, *Science* **293**, 629 (2001).
2. E. K. Pikitch *et al.*, *Science* **305**, 346 (2004).
3. H. K. Lotze, B. Worm, *Trends Ecol. Evol.* **24**, 254 (2009).
4. M. Hoffmann *et al.*, *Science* **330**, 1503 (2010).
5. M. Coll, S. Libralato, S. Tudela, I. Palomera, F. Pranovi, *PLoS ONE* **3**, e3881 (2008).
6. A. D. M. Smith *et al.*, *Science* **333**, 1147 (2011).
7. P. Cury *et al.*, *ICES J. Mar. Sci.* **57**, 603 (2000).
8. R. L. Naylor *et al.*, *Proc. Natl. Acad. Sci. U.S.A.* **106**, 15103 (2009).
9. P. A. Abrams, L. R. Ginzburg, *Trends Ecol. Evol.* **15**, 337 (2000).
10. L. C. Stige *et al.*, *Proc. R. Soc. Lond.* **277**, 3411 (2010).
11. H. M. Pereira *et al.*, *Science* **330**, 1496 (2010).
12. T. P. Dawson, S. T. Jackson, J. I. House, I. C. Prentice, G. M. Mace, *Science* **332**, 53 (2011).

13. R. D. Wooller, J. S. Bradley, J. P. Croxall, *Trends Ecol. Evol.* **7**, 111 (1992).
14. R. W. Furness, K. Camphuysen, *ICES J. Mar. Sci.* **54**, 726 (1997).
15. D. K. Cairns, *Biol. Oceanogr.* **5**, 261 (1987).
16. J. F. Piatt *et al.*, *Mar. Ecol. Prog. Ser.* **352**, 221 (2007).
17. I. L. Boyd, *Aquat. Conserv.* **12**, 119 (2002).
18. T. Andersen, J. Carstensen, E. Hernández-García, C. M. Duarte, *Trends Ecol. Evol.* **24**, 49 (2009).
19. I. L. Boyd, A. W. A. Murray, *J. Anim. Ecol.* **70**, 747 (2001).
20. J. M. Durant, T. Anker-Nilssen, N. C. Stenseth, *Proc. Biol. Sci.* **270**, 1461 (2003).
21. K. Reid, J. Croxall, D. Briggs, E. Murphy, *ICES J. Mar. Sci.* **62**, 366 (2005).
22. R. W. Furness, *J. Ornithol.* **148** (suppl. 2), 247 (2007).
23. J. A. Mills *et al.*, *J. Anim. Ecol.* **77**, 1129 (2008).
24. J. C. Field, A. D. MacCall, R. W. Bradley, W. J. Sydeman, *Ecol. Appl.* **20**, 2223 (2010).
25. M. E. Hunsicker *et al.*, *Ecol. Lett.* **14**, 1288 (2011).
26. A. S. Kitaysky *et al.*, *Funct. Ecol.* **24**, 625 (2010).
27. L. Pichegru, D. Grémillet, R. J. Crawford, P. G. Ryan, *Biol. Lett.* **6**, 498 (2010).
28. J. F. Piatt, D. A. Methven, *Mar. Ecol. Prog. Ser.* **84**, 205 (1992).
29. D. J. Agnew, *Antarct. Sci.* **9**, 235 (1997).

Acknowledgments: This work was partly funded by Eur-Oceans Consortium, the Institut de Recherche pour le Développement (IRD), the Lenfest Forage Fish Task Force, Mistra, the Sea Around Us Project, and the South African Research Chair Initiative. Disclaimers and acknowledgment of institutes and collaborators are provided in the SOM. Data, methods, and codes are available in the SOM.

Supporting Online Material

www.sciencemag.org/cgi/content/full/334/6063/1703/DC1
Materials and Methods
Figs. S1 to S4
Tables S1 and S2
References (30–138)
Data and Codes

19 August 2011; accepted 8 November 2011
10.1126/science.1212928

Mouse B-Type Lamins Are Required for Proper Organogenesis But Not by Embryonic Stem Cells

Youngjo Kim,^{1,2} Alexei A. Sharov,³ Katie McDole,^{1,2,4} Melody Cheng,⁵ Haiping Hao,⁶ Chen-Ming Fan,^{1,4} Nicholas Gaiano,⁵ Minoru S. H. Ko,^{3*} Yixian Zheng^{1,2,4*}

B-type lamins, the major components of the nuclear lamina, are believed to be essential for cell proliferation and survival. We found that mouse embryonic stem cells (ESCs) do not need any lamins for self-renewal and pluripotency. Although genome-wide lamin-B binding profiles correlate with reduced gene expression, such binding is not directly required for gene silencing in ESCs or trophoblast cells. However, B-type lamins are required for proper organogenesis. Defects in spindle orientation in neural progenitor cells and migration of neurons probably cause brain disorganizations found in lamin-B null mice. Thus, our studies not only disprove several prevailing views of lamin-Bs but also establish a foundation for redefining the function of the nuclear lamina in the context of tissue building and homeostasis.

The major structural components of the nuclear lamina found underneath the inner nuclear membrane in metazoan nuclei are type V intermediate filament proteins called

lamins (1). Mammals express both A- and B-type lamins encoded by three genes, *Lmna*, *Lmnb1*, and *Lmnb2*. *Lmnb1* and *Lmnb2* express lamin-B1 and -B2, respectively. *Lmnb2* also expresses

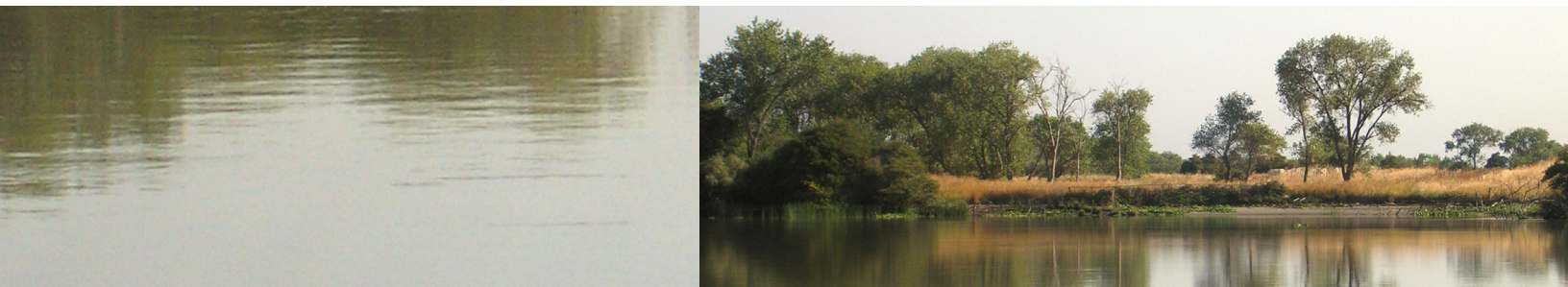
lamin-B3 through alternative splicing in testes. Mutations in lamins have been linked to a number of human diseases referred to as laminopathies (2), although the disease mechanism remains unclear. A-type lamins are expressed only in a subset of differentiated cells and are not essential for basic cell functions (3, 4). By contrast, at least one B-type lamin is found in any given cell type. Because numerous functions, including transcriptional regulation, DNA replication, and regulation of mitotic spindles, have been assigned to B-type lamins, they are thought to be essential for basic cell proliferation and survival (1, 5–8).

¹Department of Embryology, Carnegie Institution for Science, Baltimore, MD 21218, USA. ²Howard Hughes Medical Institute, Chevy Chase, MD 20815, USA. ³Developmental Genomics and Aging Section, Laboratory of Genetics, National Institute on Aging, NIH, Baltimore, MD 21224, USA. ⁴Department of Biology, Johns Hopkins University, Baltimore, MD 21218, USA. ⁵Department of Neuroscience, Johns Hopkins University School of Medicine, Baltimore, MD 21205, USA. ⁶Microarray Core Facility, Johns Hopkins University School of Medicine, Baltimore, MD 21209, USA.

*To whom correspondence should be addressed. E-mail: zheng@ciwemb.edu (Y.Z.), kom@grc.nia.nih.gov (M.S.H.K.)

INTERAGENCY ECOLOGICAL PROGRAM, MANAGEMENT, ANALYSIS, AND SYNTHESIS TEAM

An updated conceptual model
of Delta Smelt biology:
our evolving understanding of an estuarine fish



**Technical Report 90
January, 2015**

Interagency Ecological Program
for the
San Francisco Bay/Delta Estuary

A Cooperative Program of:

California Department of Water Resources
California Department of Fish and Wildlife
U.S. Bureau of Reclamation
U.S. Army Corps of Engineers

State Water Resource Control Board
U.S. Fish and Wildlife Service
U.S. Geological Survey
U.S. Environmental Protection Agency

National Marine Fisheries Service



Fall Midwater Trawl survey crew deploying net, circa 2005. Photo from CDFW.

Cover photo by Steven Culberson, USFWS

Contents

An updated conceptual model of Delta Smelt biology: our evolving understanding of an estuarine fish	xiii
Membership	xiii
Former members contributing to early drafts	xiv
Abbreviations	xiv
By Management, Analysis, and Synthesis Team	1
Executive Summary	1
Chapter 1: Introduction	5
The San Francisco Estuary	5
Pelagic fish declines	8
Changes in Delta Smelt distribution and abundance	11
Protecting Delta Smelt	12
Report Purpose and Organization	15
Chapter 2: Conceptual Models	16
Overview	16
Recent Conceptual Models for the San Francisco Estuary	18
Chapter 3: Approach	21
General Approach	21
Framework for the Delta Smelt Conceptual Model	22
Data Sources	24
Data Analysis	30
Chapter 4: Environmental Drivers and Habitat Attributes	31
Water Temperature	32
Salinity and the Size and Location of the Low Salinity Zone	39
Turbidity	49
Entrainment and Transport	55
Predation Risk	63
Contaminants	65
Pesticides	66
Ammonia and Ammonium	67
Metals and Other Elements of Concern	67
Contaminants of Emerging Concern	68
Polycyclic Aromatic Hydrocarbons (PAHs) and Polychlorinated Biphenyls (PCBs)	68
Contaminant Mixtures	68
Food and Feeding	69
Harmful algal blooms	85
Chapter 5: Updated Conceptual Models for Delta Smelt	86
Chapter 6: Delta Smelt Population Biology	91
Population Biology	91
Adults	99

Life History.....	99
Population Trends	101
Larvae	102
Life History.....	102
Population Trends	105
Juveniles.....	106
Life History.....	106
Population Trends	106
Subadults.....	106
Life History.....	106
Population Trends	107
Chapter 7: Using the Conceptual Model—Why did Delta Smelt abundance increase in 2011?	109
Comparative Approach	109
Hydrological Conditions	110
Hypotheses.....	112
Adult Hypotheses.....	112
Hypothesis 1: Hydrology and water exports interact to influence entrainment risk for adult Delta Smelt.	112
Hypothesis 2: Hydrology interacting with turbidity affects predation risk for adult Delta Smelt.	116
Hypothesis 3: Predator distribution affects predation risk of adult Delta Smelt	118
Hypothesis 4: Variability in prey availability during winter and spring affects growth and fecundity (eggs per clutch and number of clutches) of female Delta Smelt.....	118
Larval Hypotheses	120
Hypothesis 1: Delta Smelt larvae numbers are positively affected by increased duration of the temperature spawning window	120
Hypothesis 2: Increased food availability results in increased larval abundance and survival.	122
Hypothesis 3: Distributional overlap of Mississippi Silverside with Delta Smelt and high abundance of Mississippi Silverside increases predation risk/rate on larval Delta Smelt, whereas, increased turbidity, decreases predation risk/rate on larval Delta Smelt.	123
Hypothesis 4: Hydrology and water exports interact with one another to influence direction of transport and risk of entrainment for larval Delta Smelt.	127
Juvenile Hypotheses.....	132
Hypothesis 1: High water temperatures reduce juvenile Delta Smelt growth and survival through lethal and sublethal (bioenergetic stress; reduced distribution) effects.....	132
Hypothesis 2. Distribution and abundance of Striped Bass, temperature, and turbidity influence predation risk/rate on juvenile Delta Smelt.....	132
Hypothesis 3. Juvenile Delta Smelt growth and survival is affected by food availability. ..	135
Hypothesis 4. Juvenile Delta Smelt survival and growth is reduced by harmful algal blooms (HAB) because of direct (habitat quality and toxic effects) and indirect (food quality and quantity) effects.	139

Subadult Hypotheses.....	140
Hypothesis 1. Subadult Delta Smelt abundance, growth, and survival is affected by food availability.....	140
Hypothesis 2. Distribution and abundance of Striped Bass, temperature, and turbidity influence predation risk/rate on subadult Delta Smelt.....	140
Hypothesis 3. Subadult Delta Smelt abundance, survival and growth are reduced by harmful algal blooms (HAB) because of direct (habitat quality and toxic effects) and indirect (food quality and quantity) effects.	141
Hypothesis 4. Subadult Delta Smelt abundance, survival and growth are affected by the size and position of the low salinity zone during fall.	141
Chapter 8: Conclusions	142
Chapter 9: Recommendations for Future Work and Management Applications ...	147
Critical Data and Information Gaps	148
Contaminants and Toxicity	148
Predation Risk.....	149
Delta Smelt Responses	150
Mathematical Modeling.....	150
Qualitative Models.....	152
Multivariate Statistical Modeling	153
Numerical Simulation Modeling	162
Applications to Support Delta Smelt Management	164
Recommendations for future analysis and synthesis	167
References Cited	170
Appendix A: How the Delta Smelt MAST Report was Written	190
Delta Smelt MAST Report Guidelines	190
Report Purpose and Approach	190
Appendix B: Calculation of Annual Abundance Indices	196
Spring Kodiak Trawl.....	197
20 mm Survey.....	197
Summer Townet Survey.....	199
Fall Midwater Trawl Survey.....	200

Figures

- Figure 1.** Map of the San Francisco estuary. The inset shows various values of X2, the distance in kilometers from the Golden Gate to the near bottom salinity 2 isohaline. 6
- Figure 2.** Map of the upper San Francisco estuary. The upper estuary includes the Suisun Bay region and the Sacramento-San Joaquin Delta, which are west and east of Chipps Island respectively. The area from approximately Chipps Island to the west end of Sherman Island is referred to as the “confluence.” 7
- Figure 3.** Delta Smelt abundance index for life stages of Delta Smelt including the larvae-juveniles (20 mm Survey), juveniles (Summer Towntnet Survey), subadults (Fall Midwater Trawl), and adults (Spring Kodiak Trawl). The initiation of each individual survey is indicated by the initial bar with subsequent missing bars indicating when an index could not be calculated. See Chapter 3 for details of sampling programs, including geographic coverage, and Appendix B for details of calculationg abundance indices..... 9
- Figure 4.** Abundance indices from Fall Midwater Trawl for Delta Smelt, Longfin Smelt, age-0 Striped Bass, and Threadfin Shad. Missing bars indicate when an index could not be calculated. See Chapter 3 for details of sampling programs, including geographic coverage, and Appendix B for details of calculationg abundance indices..... 10
- Figure 5.** Simplified life cycle of Delta Smelt (modified from Bennett 2005). Colors correspond to different seasons with the low salinity zone changing position with season..... 12
- Figure 6.** The basic conceptual model for the pelagic organism decline (Baxter et al. 2010). 19
- Figure 7.** Species-specific conceptual model for Delta Smelt. This is one of four species-specific conceptual models developed as part of the conceptual framework for the pelagic organism decline (Baxter et al. 2010). The low salinity zone (LSZ) is defined as salinity 1-6. The Vernalis Adaptive Management Plan (VAMP) included reductions in spring exports with possible effects on Delta Smelt. 20
- Figure 8.** A new conceptual model for Delta Smelt showing Delta Smelt responses (dark blue box) to habitat attributes (light blue box), which are influenced by environmental drivers (purple box) in four “life stage seasons” (green box). Environmental drivers are influenced by landscape attributes (grey box). 24
- Figure 9.** Spatial and temporal scales of the component tiers in the general life cycle conceptual model framework for Delta Smelt. 25
- Figure 10.** Framework for the Delta Smelt life stage season conceptual models. 26
- Figure 11.** Map of Spring-Kodiak Trawl Survey sampling stations..... 27
- Figure 12.** Map of 20 mm Survey sampling stations. 28
- Figure 13.** Map of Summer Towntnet Survey sampling stations. 29
- Figure 14.** Map of Fall Midwater Trawl Survey sampling stations. 30
- Figure 15.** Map of active and historic IEP Environmental Monitoring Program (EMP) sampling stations. 33
- Figure 16.** Average monthly water temperature for stations monitored by the Environmental Monitoring Program from 1975-2012. 34
- Figure 17.** Individual female fork lengths by calendar day for mature female Delta Smelt collected in the Spring Kodiak Trawl Survey, January through May, 2005, 2006, 2010 and 2011. These data include both monthly distribution survey fish and directed survey fish.

- The directed survey (which targeted smelt spawning areas) was discontinued after January 2010. 38
- Figure 18.** Salinity distribution at low outflow. The upper panel shows the area of the low-salinity zone (4,262 hectares) at $X_2 = 85$ km, when positioned mostly between Antioch and Pittsburg. Connections to Suisun Bay and Suisun Marsh are minimal. The lower panel shows the percentage of day that the low-salinity zone occupies different areas. 41
- Figure 19.** Salinity distribution at intermediate outflow. The upper panel shows the area of the low-salinity zone (9,140 hectares) at $X_2 = 74$ km (at Chipps Island). The lower panel shows the percentage of day that the low-salinity zone occupies different areas. 42
- Figure 20.** Modeled volume, area, and depth of the low salinity zone (salinity 0.5 to 6 at various values of X_2 for 9 steady state values of outflow using bottom salinity (green diamonds) and depth-averaged salinity (black diamonds) and for daily values based on variable values from April 1994 through March 1997 (blue circles) (modified from Kimmerer et al. 2013). The top axis gives the Delta outflow corresponding to the 9 steady state scenarios. 43
- Figure 21.** Plot of monthly X_2 (km) values calculated from mean monthly unimpaired Delta outflows from 1921-2003. X_2 values are categorized by water year type for the Sacramento Valley. Also shown are the median X_2 values from 1921-2003 across all water year types (grey circles) C, red dots: critically dry; D, orange dots: dry; BN, yellow dots: below normal; AN, light blue dots: above normal; W, dark blue dots: wet. Water year type data from <http://cdec.water.ca.gov/cgi-progs/iodir/WSIHIST>. Unimpaired flow data from DWR 2007 (available at http://www.waterboards.ca.gov/waterrights/water_issues/programs/bay_delta/bay_delta_plan/water_quality_control_planning/docs/sjrf_sprrinfo/dwr_2007a.pdf). X_2 equation from Jassby et al. 2005. 44
- Figure 22.** Plots of monthly X_2 as a function of the Sacramento River Water Year Index (a measure of runoff) for the years 1956 to 1999 and 2000 to 2013 for: a, winter/spring; b, summer; and c, fall. The regression equation for each set of points is also shown. The index is calculated as: $0.4 * \text{Current April to July Runoff Forecast (in millions of acre feet, maf)} + 0.3 * \text{Current October to March Runoff in (maf)} + 0.3 * \text{Previous Water Year's Index}$ (if the Previous Water Year's Index exceeds 10.0, then 10.0 is used) (see <http://cdec.water.ca.gov/cgi-progs/iodir/WSIHIST> for further detail). 45
- Figure 23.** Plots of the log transformed a) Delta Smelt Summer Towntnet Survey abundance index and b) Delta Smelt Fall Midwater Trawl Survey abundance index, in relation to monthly averaged daily X_2 position from February to June. Lines are either simple linear least squares regression (lines) or quadratic regression (curves). 47
- Figure 24.** Secchi depth data collected during the 20 mm Survey. Surveys are conducted biweekly March-July. See Chapter 3: Data Analyses for explanation of boxplots. 52
- Figure 25.** Average and median Secchi depth in cm from monthly sampling at IEP Environmental Monitoring Program stations. Data are shown for the time period up to the pelagic organism decline (1975-2002) and after the decline (2003-2012). 54
- Figure 26.** A: Total reported October-March salvage for adult Delta Smelt and the corresponding mean salvage density based on the total monthly salvage and water volume exported by CVP and SWP. B: Both salvage and salvage density standardized by the Fall Midwater Trawl (FMWT) index for the previous year. 57

- Figure 27.** Annual time series of Largemouth Bass (top graph) and Bluegill (bottom graph) salvage at the CVP (blue bars) and SWP (green bars) fish protection facilities. Also shown are the annual San Joaquin Valley Water Year Index (SJWY Index) (blue line) and the combined annual (water year) SWP and CVP water export volume (purple line; MAF, million acre feet). 58
- Figure 28.** A: Total reported May-June salvage for juvenile Delta Smelt and the corresponding mean salvage density based on the total monthly salvage and water volume exported by CVP and SWP. B: Both salvage and salvage density standardized by the Fall Midwater Trawl (FMWT) index for the previous year..... 59
- Figure 29.** A: Total reported July-August salvage for juvenile Delta Smelt and the corresponding mean salvage density based on the total monthly salvage and water volume exported by CVP and SWP. B: Both salvage and salvage density standardized by the Fall Midwater Trawl (FMWT) index for the previous year..... 60
- Figure 30.** A: Total reported July-August salvage for sub-adult Delta Smelt and the corresponding mean salvage density based on the total monthly salvage and water volume exported by CVP and SWP. B: Both salvage and salvage density standardized by the Fall Midwater Trawl (FMWT) index for the same year..... 61
- Figure 31.** Flows in cubic feet per second for Qwest (positive values are seaward), Old and Middle River (OMR) (positive values are seaward), and total exports for years since the beginning of the pelagic organism decline (POD). Maximum monthly average Qwest values in 2006 and 2011 omitted to improve graph display, values are 50,086 cfs in April 2006, 35,477 in May 2006, and 32,884 cfs in April 2011 (Qwest and Export data are from 2013 Dayflow, OMR data are from USGS). 64
- Figure 32.** Interquartile ranges (boxes) and medians (lines) for chlorophyll-*a* measured monthly at all IEP EMP stations from 1975-2002 (blue) and 2003-2012 (red). Data from <http://www.water.ca.gov/bdma/>..... 70
- Figure 33.** Density (number/m³) of adult *Eurytemora affinis* (*E. affinis*) by month for three salinity ranges. Each month 16 stations were sampled across all salinity ranges. Horizontal lines represent single samples within a salinity range and boxes without whiskers indicate 2 samples within a salinity range. Data from the IEP Zooplankton Study index stations. See Chapter 3: Data Analyses for explanation of boxplots. 73
- Figure 34.** Density (number/m³) of adult *Pseudodiaptomus forbesi* (*P. forbesi*) by month for three salinity ranges. Each month 16 stations were sampled across all salinity ranges. Horizontal lines represent single samples within a salinity range and boxes without whiskers indicate 2 samples within a salinity range. Data from the IEP Zooplankton Study index stations. See Chapter 3: Data Analyses for explanation of boxplots. 74
- Figure 35.** Density (number/m³) of adult *Acartiella sinensis* (*A. sinensis*) by month. Each month 16 stations were sampled across all salinity ranges. Horizontal lines represent single samples within a salinity range and boxes without whiskers indicate 2 samples within a salinity range. Data from the IEP Zooplankton Study index stations. See Chapter 3: Data Analyses for explanation of boxplots. 75
- Figure 36.** Density (number/m³) of adult *Sinocalanus doerrii* (*S. doerrii*) by month. Each month 16 stations were sampled across all salinity ranges. Horizontal lines represent single

- samples within a salinity range and boxes without whiskers indicate 2 samples within a salinity range. Data from the IEP Zooplankton Study index stations. See Chapter 3: Data Analyses for explanation of boxplots. 75
- Figure 37.** Density (number/m³) of all cladoceran taxa by month. Each month 16 stations were sampled across all salinity ranges. Horizontal lines represent single samples within a salinity range and boxes without whiskers indicate 2 samples within a salinity range. Data from the IEP Zooplankton Study index stations. See Chapter 3: Data Analyses for explanation of boxplots. 76
- Figure 38.** Density (number/m³) of all mysid shrimp taxa by month. Each month 16 stations were sampled across all salinity ranges. Horizontal lines represent single samples within a salinity range and boxes without whiskers indicate 2 samples within a salinity range. Data from the IEP Zooplankton Study index stations. See Chapter 3: Data Analyses for explanation of boxplots. 76
- Figure 39.** Percentage by weight of prey types found in the digestive tracts of larval and young juvenile Delta Smelt (≤ 20 mm fork length) collected from 1-6 ppt, < 1 ppt, and Cache Slough-Sacramento River Deepwater Ship Channel (CS-SRDWSC) in A) 2005, B) 2006, C) 2010, and D) 2011. Number of digestive tracts examined are shown above the columns. Mean fork length (mm) of Delta Smelt is also shown. 78
- Figure 40.** Percentage by weight of prey types found in stomachs of age-0 Delta Smelt collected from > 6 ppt during April through December in A) 2005, B) 2006, C) 2010, and D) 2011. Number of stomachs examined are shown above the columns. One fish examined in August 2006 had an empty stomach. Mean fork length (mm) of Delta Smelt is also shown. 79
- Figure 41.** Percentage by weight of prey types found in stomachs of age-0 Delta Smelt collected from 1-6 ppt during April through December in A) 2005, B) 2006, C) 2010, and D) 2011. Number of stomachs examined are shown above the columns. Mean fork length (mm) of Delta Smelt is also shown. 80
- Figure 42.** Percentage by weight of prey types found in stomachs of age-0 Delta Smelt collected from < 1 ppt during April through December in A) 2005, B) 2006, C) 2010, and D) 2011. Number of stomachs examined are shown above the columns. Mean fork length (mm) of Delta Smelt is also shown. 81
- Figure 43.** Percentage by weight of prey types found in stomachs of age-0 Delta Smelt collected from Cache Slough-Sacramento River Deepwater Ship Channel (CS-SRDWSC) during April through December in A) 2005, B) 2006, C) 2010, and D) 2011. Number of stomachs examined are shown above the columns. Mean fork length (mm) of Delta Smelt is also shown. 82
- Figure 44.** Percentage by weight of prey types found in stomachs of adult Delta Smelt collected in 2012 during January through May from A) > 6 ppt, B) 1-6 ppt, C) < 1 ppt, and D) Cache Slough-Sacramento River Deepwater Ship Channel (CS-SRDWSC). Number of stomachs examined are shown above the columns. One fish examined from 1-6 ppt in May had an empty stomach. Mean fork length (mm) of Delta Smelt is also shown. 83
- Figure 45.** Delta Smelt general life cycle conceptual model. 87

Figure 46. Conceptual model of drivers affecting the transition from Delta Smelt adults to larvae. Hypotheses addressed in Chapter 7 are indicated by the “H-number” combinations.	87
Figure 47. Conceptual model of drivers affecting the transition from Delta Smelt larvae to juveniles. Hypotheses addressed in Chapter 7 are indicated by the “H-number” combinations.	88
Figure 48. Conceptual model of drivers affecting the transition from Delta Smelt juveniles to subadults. Hypotheses addressed in Chapter 7 are indicated by the “H-number” combinations.	88
Figure 49. Conceptual model of drivers affecting the transition from Delta Smelt subadults to adults. Hypotheses addressed in Chapter 7 are indicated by the “H-number” combinations.	89
Figure 50. Scatterplots and LOWESS splines depicting the relationship of the Fall Midwater Trawl index of Delta Smelt relative abundance (FMWT) (1968-2012) and Summer Towntnet Survey (TNS) (1969-2012) with the FMWT in the previous year.	94
Figure 51. Stage to stage survival indices based on data from Summer Towntnet Survey (TNS), Fall Midwater Trawl (FMWT), and Spring Kodiak Trawl (SKT).	95
Figure 52. Delta Smelt recruitment indices based on the annual adult, larval, juvenile, and subadult abundance indices provided by the Spring Kodiak Trawl (SKT, adults), 20 mm Survey (20 mm, larvae), Summer Towntnet Survey (TNS, juveniles), and Fall Midwater Trawl (FMWT, subadults).	96
Figure 53. Relationship of annual indices of Delta Smelt abundance from the Spring Kodiak Trawl (SKT) and Fall Widwater Trawl (FMWT) from the previous year. Year labels correspond to the year of the SKT. The linear regression with all index values log-transformed to address non-normal distributions in the raw data is: $\text{Log SKT Index} = 0.4997 + 0.6381(\text{Log FMWT Index Year}^{-1})$, $n = 11$, $p < 0.001$, $R^2 = 0.79$	103
Figure 54. Plot of the Spring Kodiak Trawl (SKT) adult abundance index against the 20 mm Survey larval abundance index 2003-2012. The comparison years of 2005, 2006, 2010, and 2011 are labeled.	104
Figure 55. Median fork length (mm) of Delta Smelt collected in January and February by the Spring Kodiak Trawl by year, 2002-2012. See Chapter 3: Data Analyses for explanation of boxplots.	105
Figure 56. Relationship of annual index of Delta Smelt abundance from the 20 mm survey (20 mm) with the annual indices from the summer townet survey (TNS) and fall midwater trawl survey (FMWT). Year labels correspond to the comparison years of interest. The linear regressions with all index values log-transformed to address non-normal distributions in the raw data are: $\text{Log 20 mm index} = 0.57 + 0.87(\text{Log TNS index})$, $n = 19$, $p < 0.05$, $R^2 = 0.44$ and $\text{Log 20 mm index} = 1.30 + 0.81(\text{Log FMWT index})$, $n = 19$, $p < 0.05$, $R^2 = 0.27$	107
Figure 57. Plots of fall midwater trawl (FMWT) abundance index as a function of summer townet survey (TNS) abundance index for 1982-2013 and 2003-2013. Note the very different scales for both axes. Lines are LOWESS smooths.	108

- Figure 58.** Annual water year indices for the a) Sacramento and b) San Joaquin Valleys since the initiation of the Summer Towntnet Survey in 1959. Horizontal dashed lines: threshold levels for water year type classifications as wet (W), above normal (AN), below normal (BN), dry (D) and critically dry (C). Darker grey bars indicate the four study years (2005, 2006, 2010, 2011) examined in Chapter 7 of this report. (Data are from <http://cdec.water.ca.gov/cgi-progs/iodir/WSIHIST>). 111
- Figure 59.** Net daily flows in cubic feet per second for a) Delta inflow from all tributaries, b) Delta outflow into Suisun Bay, and d) total freshwater exports from the Delta. Also shown are daily values for c) X2 (see Chapter 4 for explanation). Flow data are from Dayflow (<http://www.water.ca.gov/dayflow/>). X2 values are calculated from daily Delta outflow with the equation in Jassby et al. (1995.)..... 113
- Figure 60.** Daily X2 values in January to December for each of the four study years. Seasonal X2 averages are indicated by horizontal lines for spring X2 (February to June), summer X2 (July and August), and fall X2 (September to December). See Fig. 15 for seasonal X2 in other years. 114
- Figure 61.** Annual adult (December-March) Delta Smelt salvage at the CVP (blue bars) and SWP (green bars) fish protection facilities for 2005-2012..... 115
- Figure 62.** Annual combined adult (December-March) Delta Smelt salvage at the CVP and SWP fish protection facilities by month for 2005-2012..... 116
- Figure 63.** Annual average daily net flows for December through March in cubic feet per second (cfs) in Old and Middle River (OMR), past Jersey Point on the lower San Joaquin River (QWEST) and total exports in millions of acre feet (MAF), 2005-2013. Error bars are 1 standard deviation. 117
- Figure 64.** Secchi depth data collected during the Spring Kodiak Trawl Survey. Surveys are conducted monthly January-May. See Chapter 3: Data Analyses for explanation of boxplots..... 119
- Figure 65.** Mean daily temperatures (°C) at Rio Vista from February 1 through June 30, 2005, 2006, 2010, 2011. The green lines enclose the spawning window, which represents temperatures at which successful spawning is expected to occur..... 122
- Figure 66.** Trends in chlorophyll-*a* concentrations (µg/L) in samples collected by the IEP Environmental Monitoring Program during each the four study years (2005, 2006, 2010, and 2011). Sample site locations shown in figure 15. See Chapter 3: Data Analyses for explanation of boxplots. 124
- Figure 67.** Catch per unit effort (CPUE) of adult *Eurytemora affinis* and *Pseudodiaptomus forbesi* (Zoo; number individuals/m³ sampled) and Delta Smelt (DS; number individuals/10,000 m³ sampled) by calendar week from mesozooplankton sampling and Delta Smelt catch by the 20 mm and Summer Towntnet surveys, 2005 (top) and 2006 (bottom) 125
- Figure 68.** Catch per unit effort (CPUE) of adult *Eurytemora affinis* and *Pseudodiaptomus forbesi* (Zoo; number individuals/m³ sampled) and Delta Smelt (DS; number individuals/10,000 m³ sampled) by calendar week from mesozooplankton sampling and Delta Smelt catch by the 20 mm and Summer Towntnet surveys, 2010 (top) and 2011 (bottom)..... 126

- Figure 69.** Scatter plot of Mississippi Silverside catch plotted on Secchi depth (cm) at location of capture from the Spring Kodiak Trawl Survey, 2005, 2006, 2010 and 2011..... 128
- Figure 70.** Monthly length frequency of Mississippi Silversides captured by the Spring Kodiak Trawl during distribution sampling March – May in the Sacramento River and Cache Slough sampling stations only, 2002-2012. The months and geographic range were selected to overlap with that of Delta Smelt larvae as they hatch and begin to grow..... 129
- Figure 71.** Water surface temperature data collected during the Spring Kodiak Trawl Survey for three salinity regions and the Cache Slough-Sacramento River Deepwater Ship Channel (CS-SRDWSC). Surveys are conducted monthly January-May. See Chapter 3: Data Analyses for explanation of boxplots. 133
- Figure 72.** Water temperature data collected during the Summer Townt Survey for three salinity regions and the Cache Slough-Sacramento River Deepwater Ship Channel (CS-SRDWSC). Surveys are conducted biweekly June-August. See Chapter 3: Data Analyses for explanation of boxplots. 134
- Figure 73.** Turbidity data collected during the Summer Townt Survey. Surveys are conducted biweekly June-August. Note different scales among salinity regions. See Chapter 3: Data Analyses for explanation of boxplots. 135
- Figure 74.** Secchi depth data collected during the Summer Townt Survey. Surveys are conducted biweekly June-August. See Chapter 3: Data Analyses for explanation of boxplots..... 136
- Figure 75.** Trends in calanoid copepods (number/m³ for all taxa combined) collected by the IEP Environmental Monitoring Program (EMP) during each the four study years (2005, 2006, 2010, and 2011)..... 137
- Figure 76.** Trends in calanoid copepods (number/m³ for all types combined) collected by the IEP Environmental Monitoring Program (EMP) in three salinity ranges (> 6 ppt; 1-6 ppt; < 1 ppt) during each the four study years (2005, 2006, 2010, and 2011). See Chapter 3: Data Analyses for explanation of boxplots. 138
- Figure 77.** Summer Townt Survey mean visual rank of *Microcystis* spp. (ranks 1-5 possible; 1 = absent) observed at all stations during biweekly surveys (1-6) in various salinity regions (> 6, 1-6, and < 1 ppt) and in the CS-SRDWSC during June through August 2010 and 2011. Observations were not made in Cache Slough-Sacramento River Deepwater Ship Channel (CS-SRDWSC) during 2010. 139
- Figure 78.** Fall Midwater Trawl mean visual rank of *Microcystis* spp. (ranks 1-5 possible; 1 = absent) observed at all stations during monthly surveys in various salinity regions (> 6, 1-6, and < 1 ppt) and in the CS-SRDWSC during September through December 2010 and 2011..... 142
- Figure 79.** Plots of the Delta Smelt 20 mm survey abundance index as a function of a) spring (February-June) X2, b) previous year fall (September-December) X2, and c) Delta Smelt fall midwater-trawl abundance index in the previous year. Details of general linear models (GLM) used to fit the lines are in Table 7. 157
- Figure 80.** Plots of partial residuals for the relationships of the 20 mm index with the combinations of spring X2, prior fall X2, and prior FMWT abundance index summarized in Table 1 (panels a, b, d, and e). The plots shown here also include partial fit lines and

their 95% confidence intervals. Values for the time period of analysis are shown for: c, X2; and f, the fall midwater trawl abundance index from the previous year..... 158

Figure 81. Plots of the Delta Smelt 20 mm survey abundance index as a function of a) spring (February-June) X2, and b) previous year fall (September-December) X2. Lines are either simple linear least squares regression (lines) or quadratic regression (curves). Details of linear models (LM) used to fit the 1995-2013 lines are in Table 8. 159

Figure 82. Adult (panel a, SKT) and subadult (panel b, FMWT the previous year) to larvae (20 mm Survey) recruitment indices (abundance index ratios) as a function of spring X2 (February-June). For 20 mm/SKT a linear regression was calculated with and without 2013, which appears to be an outlier. For 20 mm/FMWT the previous year separate regressions were calculated for the POD period (2003-2013), the period before the POD (1995-2002), and the entire data record (not shown). See Table 9 for regression results. 161

Figure 83. Simulated output from a STELLA model for assessing sensitivity of the model to variation in model variables. 165

Figure 84. Map of Spring Kodiak Trawl Survey stations showing all currently sampled stations. Data from all stations except 719 are used in abundance index calculation. 198

Figure 85. Map of 20 mm survey stations showing all currently sampled stations. Data from all core stations are used in abundance index calculation. 199

Figure 86. Map of summer townet survey stations showing all currently sampled stations. Data from all core stations are used in abundance index calculation. 201

Figure 87. Map of fall midwater trawl survey stations showing all currently sampled stations. Data from core stations are used in abundance index calculation. 203

Tables

Table 1. Summary of relationships between log-transformed annual abundance indices for four Delta Smelt life stages (response variable) and spring X2 (February-June, see text): Survey: see description of monitoring surveys in Chapter 3; Regression: least squares linear or quadratic regression: n, number of observations (years); P, statistical significance level for the model; R², coefficient of determination; adjusted R², R² adjusted for the number of predictor terms in the regression model. Bold font indicates statistically significant relationships. 49

Table 2. Percent of age-1 Delta Smelt captured during the Spring Kodiak Trawl Survey with food present in the stomach collected January through May 2012 for three salinity regions and the freshwater Cache Slough-Sacramento River Deepwater Ship Channel (CS-SRDWSC). 120

Table 3. Delta Smelt spawning window (12 to 20 °C inclusive) and optimal hatching period (12 to 17 °C inclusive) for 2005, 2006, 2010, and 2011, defined as number of days of water temperatures, based on mean daily water temperatures measured at Rio Vista. Data are calendar day when water temperature achieved 12, 17, and 20 °C and the duration (days) between those calendar days. The upper limit in 2011 was not reached until July 4, outside the spring season. 122

Table 4. Mississippi Silverside catch by region (monthly sample number in parentheses) and year by the Spring Kodiak Trawl Survey sampling monthly March through May (months when

Delta Smelt larvae are present), 2005, 2006, 2010 and 2011; distribution survey data only. Annual sampling effort summarized consisted of 3 surveys and 37 stations. Tow volume varied substantially, but averaged 6,300 m ³ per tow for the 4 years.....	127
Table 5. Mean monthly catch of Delta Smelt per 10,000 m ³ by station for stations in the south and central Delta for the 20 mm Survey, 2005, 2006, 2010, 2011. Non-zero values are bolded.....	130
Table 6. Mean and standard deviation (SD) for X2, surface area of low salinity zone (M. McWilliams, Delta Modeling Associates, unpublished data), and values of the Fall Midwater Trawl index (FMWT) for abundance of subadult Delta Smelt.	143
Table 7. Summary of relationships between the 20 mm abundance index for Delta Smelt (response variable) and one or more predictor variables: n, number of observations (years); SE/Mean, model standard error (square root of mean squared residual) as proportion of mean response, P, statistical significance level for the model; R ² , coefficient of determination; adjusted R ² , R ² adjusted for the number of predictors in the model; AIC, Akaike information criterion; Δ AIC, AIC differences; w (AIC), AIC weights. All relationships modeled with generalized linear models (GLM) with a Poisson error distribution, log link function, and a natural cubic spline with two degrees of freedom as a smoother for all predictor variables except “Step.”	156
Table 8. Summary of relationships between the log-transformed 20 mm abundance index for Delta Smelt (response variable) and one or more predictor variables. All relationships modeled with simple least-squares linear models (LM). For explanation of column headings see Table 6.	160
Table 9. Summary of relationships of larval recruitment indices (abundance index ratios) for Delta Smelt (response variable) and spring X2 (predictor variable; spring: February-June): n, number of observations (years); SE/Mean, model standard error (square root of mean squared residual) as proportion of mean response, P, statistical significance level for the model; R ² , coefficient of determination. All relationships modeled with least-squares linear models (LM).	162
Table 10. Example tool-box for applying the conceptual model to Delta Smelt management. ...	166
Table A1. Numerical summary of review comments for the July 2013 draft MAST report.....	194
Table B1. Station weighting factors for stations used in calculations of the summer townet survey annual abundance indexes. Regions are geographic areas designated by the California Department of Fish and Wildlife. See fig. 86 for station locations.....	202
Table B2. Area-regions, weighting factor for each area-region, and stations included within each area-region. Bolded station numbers indicate the current 100 core stations used in calculation of annual abundance indexes. Underlined station numbers indicate stations previously included in calculations but subsequently dropped.....	204

An updated conceptual model of Delta Smelt biology: our evolving understanding of an estuarine fish

Membership

Randy Baxter, California Department of Fish and Wildlife

Larry R. Brown, U.S. Geological Survey

Gonzalo Castillo, U.S. Fish and Wildlife Service

Louise Conrad, California Department of Water Resources

Steven Culberson, U.S. Fish and Wildlife Service

Matthew Dekar, U.S. Fish and Wildlife Service

Melissa Dekar, Central Valley Regional Water Quality Control Board

Frederick Feyrer, U.S. Bureau of Reclamation (currently U.S. Geological Survey)

Thaddeus Hunt, California State Water Resources Control Board

Kristopher Jones, California Department of Water Resources

Joseph Kirsch, U.S. Fish and Wildlife Service

Anke Mueller-Solger, Delta Stewardship Council (currently U.S. Geological Survey)

Matthew Nobriga, U.S. Fish and Wildlife Service

Steven B. Slater, California Department of Fish and Wildlife

Ted Sommer, California Department of Water Resources

Kelly Souza, California Department of Fish and Wildlife

Former members contributing to early drafts

Gregg Erickson, California Department of Fish and Wildlife

Stephanie Fong, formerly Central Valley Regional Water Quality Control Board (currently State and Federal Contractors Water Agency)

Karen Gehrts, California Department of Water Resources

Lenny Grimaldo, formerly U.S. Bureau of Reclamation (currently ICF International)

Bruce Herbold, retired from U.S. Environmental Protection Agency

Abbreviations

CCF	Clifton Court Forebay
CVP	Central Valley Project
Delta	Sacramento-San Joaquin River Delta
DRERIP	Delta Regional Ecosystem Restoration Implementation Program
DSC	Delta Stewardship Council
EMP	Environmental Monitoring Program
FLaSH	Fall Low Salinity Habitat
FMWT	Fall Midwater Trawl Survey
IEP	Interagency Ecological Program
LSZ	low salinity zone
MAST	Management, Analysis, and Synthesis Team
NRC	National Research Council
OMR	Old and Middle River
POD	Pelagic organism decline
SFE	San Francisco Estuary
SKT	Spring Kodiak Trawl Survey

SFPF	Skinner Fish Protection Facility
SRWTP	Sacramento Regional Water Treatment Plant
SSC	suspended sediment concentration
SWP	State Water Project
TFCF	Tracy Fish Collection Facility
TNS	Summer Tow Net Survey

An updated conceptual model of Delta Smelt biology: our evolving understanding of an estuarine fish

By Management, Analysis, and Synthesis Team

Executive Summary

The main purpose of this report is to provide an up-to-date assessment and conceptual model of factors affecting Delta Smelt (*Hypomesus transpacificus*) throughout its primarily annual life cycle and to demonstrate how this conceptual model can be used for scientific and management purposes. The Delta Smelt is a small estuarine fish that only occurs in the San Francisco Estuary. Once abundant, it is now rare and has been protected under the federal and California Endangered Species Acts since 1993. The Delta Smelt listing was related to a steep decline in the early 1980s; however, population abundance decreased even further with the onset of the “pelagic organism decline” (POD) around 2002. A substantial, albeit short-lived, increase in abundance of all life stages in 2011 showed that the Delta Smelt population can still rebound when conditions are favorable for spawning, growth, and survival. In this report, we update previous conceptual models for Delta Smelt to reflect new data and information since the release of the last synthesis report about the POD by the Interagency Ecological Program for the San Francisco Estuary (IEP) in 2010. Specific objectives include:

1. Provide decision makers with a practical tool for evaluating difficult trade-offs associated with management and policy decisions.
2. Provide scientists with a framework from which they can formulate and evaluate hypotheses using qualitative or quantitative models.
3. Provide the general public with a new way of learning about Delta Smelt and their habitat.

Our updated conceptual model describes the habitat conditions and ecosystem drivers affecting each Delta Smelt life stage, across seasons and how the seasonal effects contribute to the annual success of the species. The conceptual model consists of two nested and linked levels of increasing specificity. The *general life cycle conceptual model* for four Delta Smelt life stages (adults, eggs and larvae, juveniles, and subadults) includes stationary ecosystem components and dynamic environmental drivers, habitat attributes, and Delta Smelt responses. The more detailed *life stage transition conceptual models* for each of the four Delta Smelt life stages describe relationships between environmental drivers, key habitat attributes, and the responses of Delta Smelt to habitat attributes as they transition from one life stage to the next.

Our analyses and conceptual model show that good larval recruitment is essential for setting the stage for a strong year class; however, increased growth and survival through subsequent life stages are also needed to achieve and sustain higher population abundance. We used our conceptual model to generate 16 hypotheses about the factors that may have contributed to the 2011 increase in Delta Smelt relative abundance. We then evaluated these hypotheses by comparing habitat conditions and Delta Smelt responses in the wet year 2011 to those in the

prior wet year 2006 and in the drier years 2005 and 2010. Larval recruitment was similarly high in both wet years and lower in the drier antecedent years, but juvenile and adult abundance increased only in 2011. In 2005 and 2006, the population was limited by very poor survival from the larval to the juvenile life stage. We found that in 2011, Delta Smelt may have benefitted from a combination of favorable habitat conditions throughout the year, including:

1. Adults and larvae benefitted from prolonged cool spring water temperatures, high 2011 winter and spring outflows which reduced entrainment risk and possibly improved other habitat conditions, and possibly enhanced food availability in late spring.
2. Juveniles benefitted from cool water temperatures in late spring and early summer as well as from improved food availability and low levels of harmful *Microcystis*.
3. Subadults also benefitted from improved food availability and from favorable habitat conditions in the large, low salinity zone (salinity 1-6) located more toward Suisun Bay in 2005-2006 and 2010.

Our comparisons of other habitat attributes either produced inconclusive results or were limited by a lack of suitable data or other necessary information. This was especially true for predation risk and toxicity, and other contaminant effects. Clearly more monitoring and studies are needed on these two topics, but we also found many other data and information gaps. Overall, we did not entirely reject any of our hypotheses. Together with the large amount of published information used to construct our conceptual model, this gives us some confidence that the majority of the elements and linkages of our conceptual model are relevant and (qualitatively) correct. However, the mechanisms they describe are likely variable in the degree to which they drive population outcomes, depending on the conditions in any given year and prior Delta Smelt abundance levels. In addition, the scientific merit of some linkages for which data are sparse (e.g., predation and contaminants effects) is impossible to evaluate without additional information.

Importantly, while this report identifies many data and information gaps that must be filled before some hypotheses can be objectively evaluated, the report includes a very large amount of pertinent data and information that is currently available. The San Francisco Estuary is clearly an intensely monitored and studied ecosystem and Delta Smelt may well be one of the most thoroughly studied endangered fish species in the world. The most critical data for this report came from four long-term Interagency Ecological Program fish monitoring surveys. These surveys provide sound, high-quality data about the annual distribution and relative abundance of Delta Smelt for time periods ranging from one to more than five decades. These four surveys, other monitoring surveys, and numerous research studies provide data about many habitat attributes and ecosystem drivers.

The report ends with key conclusions, a discussion of our hypothesis testing approach, and recommendations for future work and adaptive management applications. The final report Chapter contains many concrete examples of studies, modeling approaches, and management applications that are directly derived from the conceptual model. These examples are not meant to be exhaustive lists. Rather, they are primarily intended to illustrate science and management applications of our conceptual model.

We strongly recommend that analysis, synthesis and modeling efforts, such as this report, be a high priority for the management and science organizations that oversee monitoring and research in the estuary. Without these types of integrative efforts, ongoing and proposed adaptive

management processes must conduct such efforts in an *ad hoc* manner, often driven by unrealistic schedules that are unlikely to be fulfilled. Such adaptive management processes in the estuary include the ongoing adaptive management of fall outflow for Delta Smelt, the new “Collaborative Science and Adaptive Management Program,” the California Delta Stewardship Council’s Delta Plan, and the multi-agency Bay Delta Conservation Plan. On a more basic level, such synthesis efforts identify data gaps that serve to focus research and management efforts on scientifically relevant topics rather than the “crisis of the day.”

The 2011 increase in the Delta Smelt abundance index demonstrated that the species still has the ability to rebound to higher abundance levels. Delta Smelt has often been called an indicator – or canary in the coalmine – for overall ecosystem conditions in the estuary. The 2011 increase suggests that the system has not yet irreversibly shifted into an altered state that will no longer support native species. Given the profound habitat alterations in the San Francisco Estuary, continued study of the environmental drivers and habitat attributes and the subsequent responses of the Delta Smelt population seem critical to the wise management of the species. Some possible topics for future synthesis groups include:

1. Reviews and updates to existing conceptual and mathematical models.
2. Further development of mathematical models of Delta Smelt population abundance drawn specifically from the conceptual models described in this report; applications and extensions of recently published models to help make management decisions and guide new modeling efforts; additional modeling efforts and future research projects to improve resolution and understanding of the particular factors identified as critical to reproduction, recruitment, survival, and growth.
3. Review and refinement of new models such as the emerging comprehensive state-space population model (K. Newman, U.S. Fish and Wildlife Service, personal communication); development of additional models or modules of models specifically aimed at estimating effects of inadequately monitored or difficult to measure and evaluate habitat attributes such as predation risk and toxicity; development of new “nested” and/or “linked” mathematical modeling approaches that can accommodate multiple drivers and their interactive effects across temporal and spatial scales.
4. Interdisciplinary collaboration among scientists, managers, and stakeholders to develop and model management scenarios and strategies based on principles of integrative ecosystem and landscape-based management rather than relatively crude distinctions among categorical “water year types.”

Continued growth of California’s human population, climate change, new species invasions, and other changes will increase management challenges. Science and management have to go hand in hand to constantly identify, implement, evaluate, and refine the best management options for this ever-changing system. We hope that the conceptual model and information in this report will be useful for achieving these goals.

Chapter 1: Introduction

The San Francisco Estuary

Estuarine ecosystems are among the most complex ecosystems on earth (Wilson 1998). They are constantly changing ecosystems that respond to dynamic “drivers” of change (Healey et al. 2008, Baxter et al. 2010). Natural drivers include the geological and geographic setting, climatic and oceanic variability, dynamic hydrological and nutrient regimes, weather and disturbance regimes, biogeochemical processes, species assemblages, and many other biotic and abiotic features. Estuaries also respond to a broad range of human activities. Some of these “human drivers” have negative impacts on ecosystems. These negative human drivers are often called “stressors.” Human stressors on estuarine ecosystems include water and land use, pollutant discharges, species introductions, and fishing (Townend 2004, Lotze et al. 2006, Cloern and Jassby 2012). The interplay of natural and human drivers and their effects on the San Francisco Estuary and in particular on the Delta Smelt (*Hypomesus transpacificus*), an endemic fish species, is the subject of this report.

The San Francisco Estuary (SFE; Fig. 1) is comprised of an upstream region consisting of channels and islands associated with the confluence of the Sacramento and San Joaquin Rivers known as the “Delta” and a series of downstream bays and marshes that are separated from the Pacific Ocean by the “Golden Gate,” the sea passage between the San Francisco and Marin peninsulas. Because of California’s Mediterranean climate, the SFE experiences large interannual and seasonal flow variations, which are modulated by tides and human management of the rivers within the Delta watershed (Moyle et al. 2010). These hydrological variations lead to a dynamic estuarine salinity gradient. In the winter and spring fresh water often extends into San Pablo Bay, while in the summer and fall brackish water can intrude into the western Delta. These seasonal differences are exacerbated by pronounced interannual differences in precipitation in the watershed. Extremely dry years with little precipitation and very wet years with widespread flooding do not occur in predictable patterns (Dettinger 2011).

The SFE has undergone dramatic morphological, hydrological, chemical, and biological alterations since the onset of the California Gold Rush in the middle of the 19th century (Nichols et al. 1986, Arthur et al. 1996, Baxter et al. 2010, Brooks et al. 2012, NRC 2012, Whipple et al. 2012, Cloern and Jassby 2012). These alterations include five human activities that have changed ecological functions and habitats in many riverine and estuarine systems with increasingly dense human populations: diking, draining, dredging, diverting, and discharging. Specifically, diking and draining have reduced the vast wetlands that once covered and surrounded the SFE to small remnants. There has been an 80-fold decrease in the ratio of wetland to open water area in the Delta, from a historical ratio of 14:1 to a current ratio of 1:6 (Whipple et al. 2012, Herbold et al. 2014). Diking and dredging have led to a substantial reconfiguration of the bays, sloughs, and channels, while large-scale water diversions, and discharge of contaminants have altered water quantity and quality. Small water diversions occur throughout the freshwater portion of the estuary, but the largest water diversions are at the pumping facilities of the federal Central Valley Project (CVP) and the State Water Project (SWP) that export water from the southwestern Delta to agricultural and urban areas to the south (Fig. 2). In addition, a wide variety of non-native plants and animals have been introduced and have become established in the SFE (Cohen and Carlton 1998, Light et al. 2005, Winder et al. 2011).

Figure 1. Map of the San Francisco estuary. The inset shows various values of X2, the distance in kilometers from the Golden Gate to the near bottom salinity 2 isohaline.

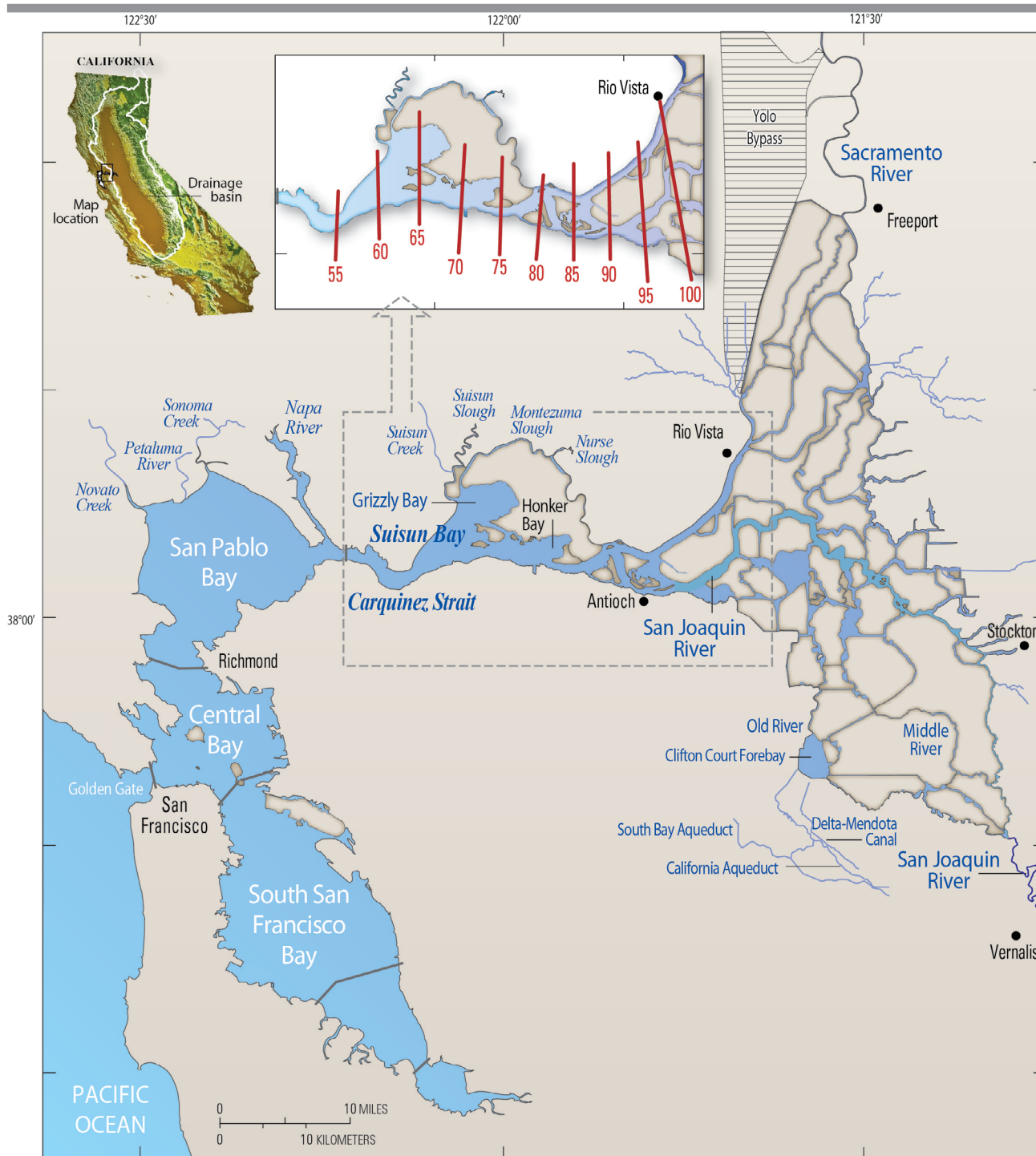
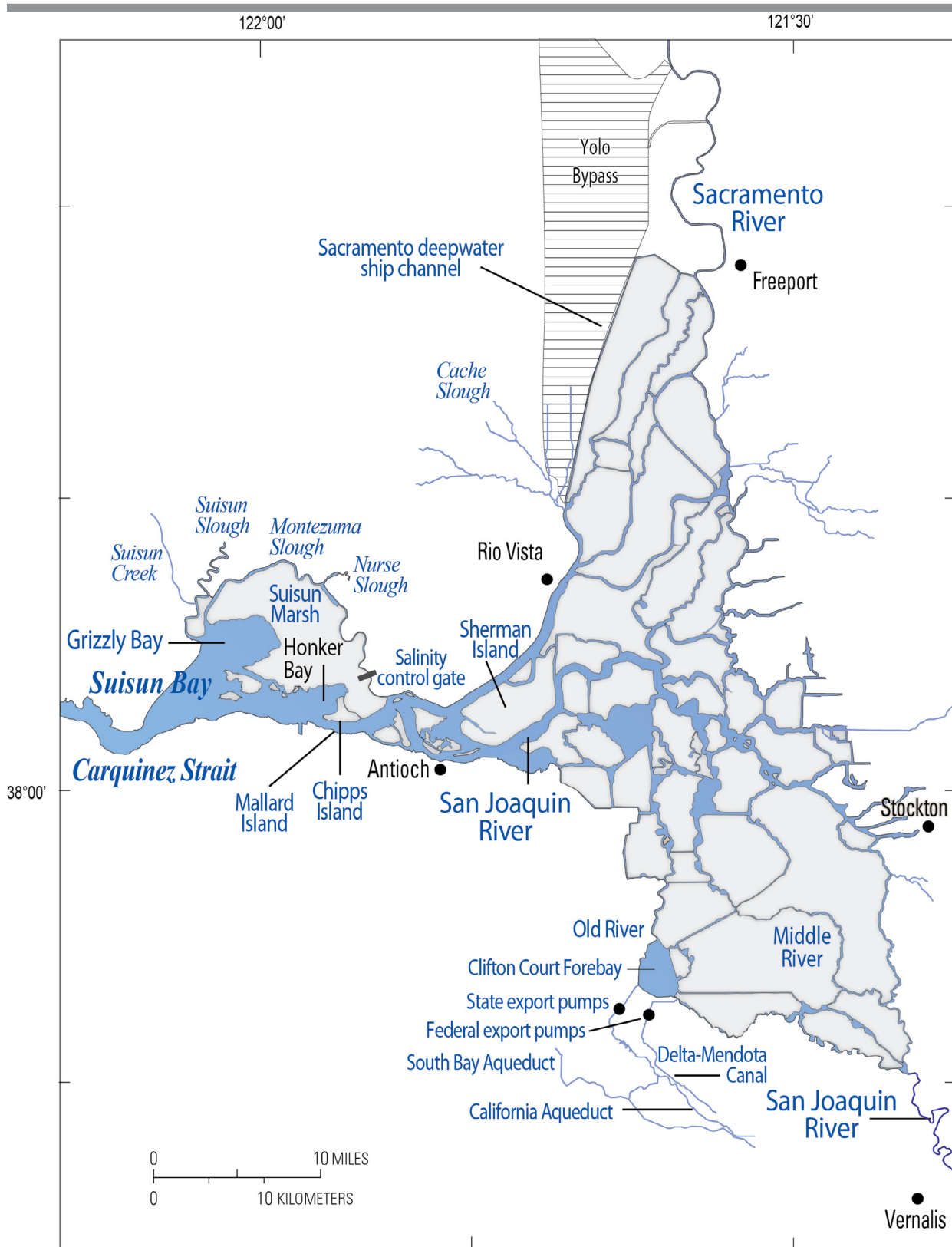


Figure 2. Map of the upper San Francisco estuary. The upper estuary includes the Suisun Bay region and the Sacramento-San Joaquin Delta, which are west and east of Chipps Island respectively. The area from approximately Chipps Island to the west end of Sherman Island is referred to as the “confluence.”



Many of the more recent ecological changes in the SFE have been documented by long-term monitoring surveys. Most of these surveys are conducted under the auspices of the Interagency Ecological Program (IEP), an interagency science consortium with three State and six federal member agencies (<http://www.water.ca.gov/iep/>). Together with monitoring conducted by others, these monitoring surveys provide one of the longest and most comprehensive environmental and biological data records in a U.S. coastal ecosystem. With each additional year of monitoring, this data record serves as an increasingly valuable tool for observing gradual changes or abrupt shifts in ecological conditions and for identifying their underlying causes (Cloern and Jassby 2012).

The modern SFE continues to be a dynamic and complex ecosystem that supports many important ecosystem services (Millennium Ecosystem Assessment 2005), including the provision of fresh water, agricultural crops, commercial and recreational fisheries, and other recreational opportunities. However, it no longer provides adequate habitat for many of its native species as evidenced by severe declines in several of its native fish populations (e.g., Bennett and Moyle 1996, Brown and Moyle 2005, Sommer et al. 2007).

Pelagic fish declines

Among the native fishes of the upper SFE (Fig. 2), the endemic Delta Smelt is of high management concern because of a decline of its annual abundance indices (see Chapter 3 for details of fish surveys and indices), particularly longer term indices for juveniles and subadults, to persistent low levels (Fig. 3). This decline led to its listing under the federal Endangered Species Act in 1993. The Delta Smelt is a slender-bodied pelagic fish with a maximum size of about 120 mm standard length (length from snout to end of vertebral column) and a maximum age of two years. It is the most estuary-dependent of the native fish species in the SFE (Moyle et al. 1992, Bennett 2005). The continued existence of the species is dependent upon its ability to successfully grow, develop, and survive in the SFE.

Delta Smelt is not the only fish species currently in decline in the Delta. Abundance indices of Longfin Smelt (*Spirinchus thaleichthys*), age-0 Striped Bass (*Morone saxatilis*), and Threadfin Shad (*Dorosoma petenense*) declined simultaneously with those of Delta Smelt in about 2002. This simultaneous decline has become known as the pelagic organism decline (POD) (Sommer et al. 2007, Baxter et al. 2008, 2010) (Fig. 4). Given the very different life histories of these four pelagic species, it is unlikely that a single environmental variable could account for the POD declines. In general, researchers have suggested that the POD declines were likely multi-causal (Sommer et al. 2007, Baxter et al. 2008, 2010, Mac Nally et al. 2010, Cloern and Jassby 2012, NRC 2012). Several researchers have suggested that the SFE has undergone an ecological regime shift (Moyle and Bennett 2008, Baxter et al. 2010, Glibert et al. 2011, Cloern and Jassby 2012). In the present system, an invasive aquatic macrophyte (*Egeria densa*) dominates the littoral zone of many areas of the Delta and provides favorable habitat for many invasive fishes (e.g., Largemouth Bass *Micropterus salmoides*; Brown and Michniuk 2007); invasive clams (*Potamocorbula amurensis* and *Corbicula fluminea*) consume a large portion of the available pelagic phytoplankton (Alpine and Cloern 1992, Lopez et al. 2006, Lucas et al. 2002, Lucas and Thompson 2012); agricultural, industrial, and urban discharges transport large quantities of nutrients and a plethora of contaminants into many regions of the estuary; and current management of water for agricultural, industrial and urban purposes is focused on optimizing the reliability of water exports by the CVP and SWP.

Figure 3. Delta Smelt abundance index for life stages of Delta Smelt including the larvae-juveniles (20 mm Survey), juveniles (Summer Townet Survey), subadults (Fall Midwater Trawl), and adults (Spring Kodiak Trawl). The initiation of each individual survey is indicated by the initial bar with subsequent missing bars indicating when an index could not be calculated. See Chapter 3 for details of sampling programs, including geographic coverage, and Appendix B for details of calculating abundance indices.

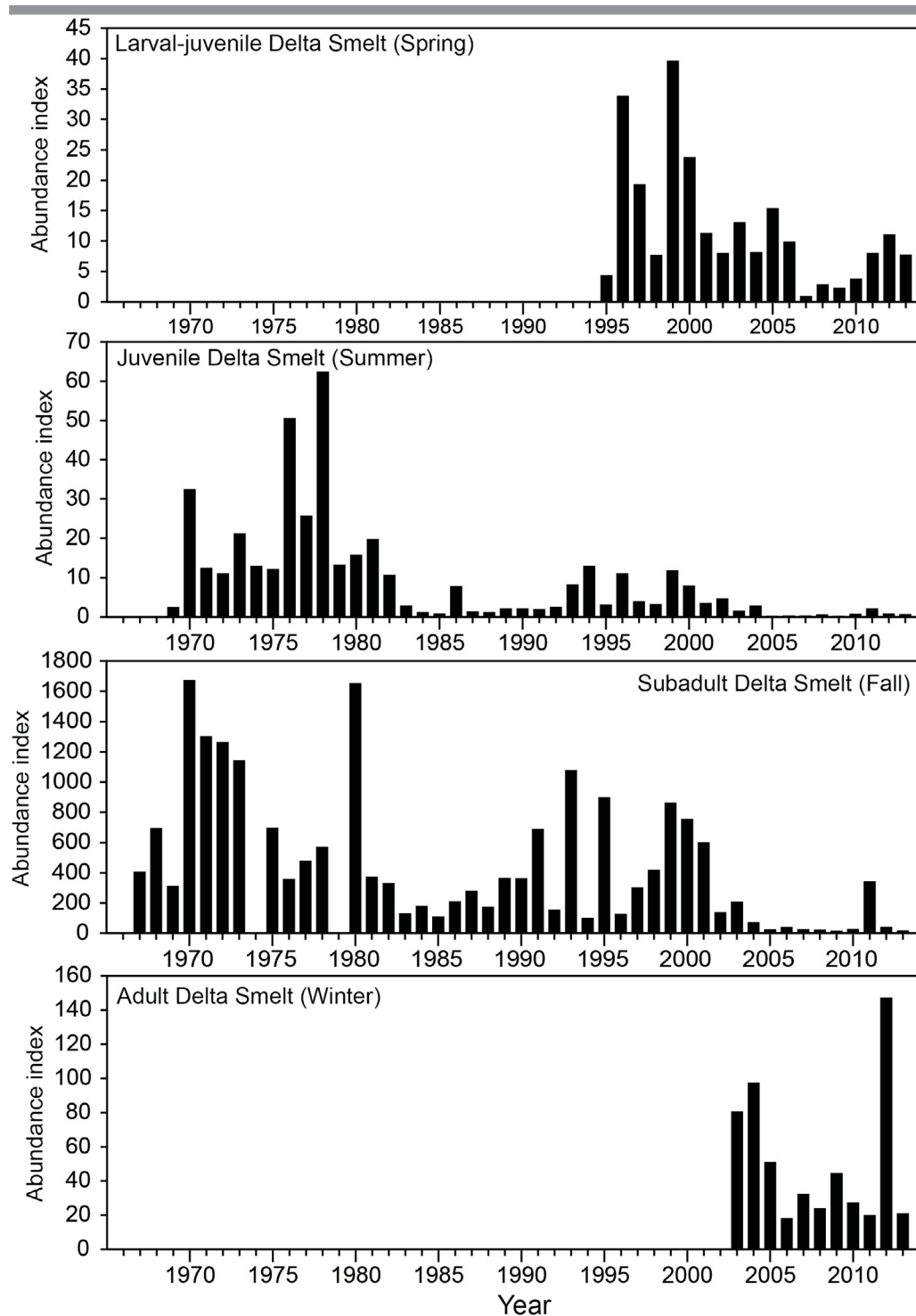
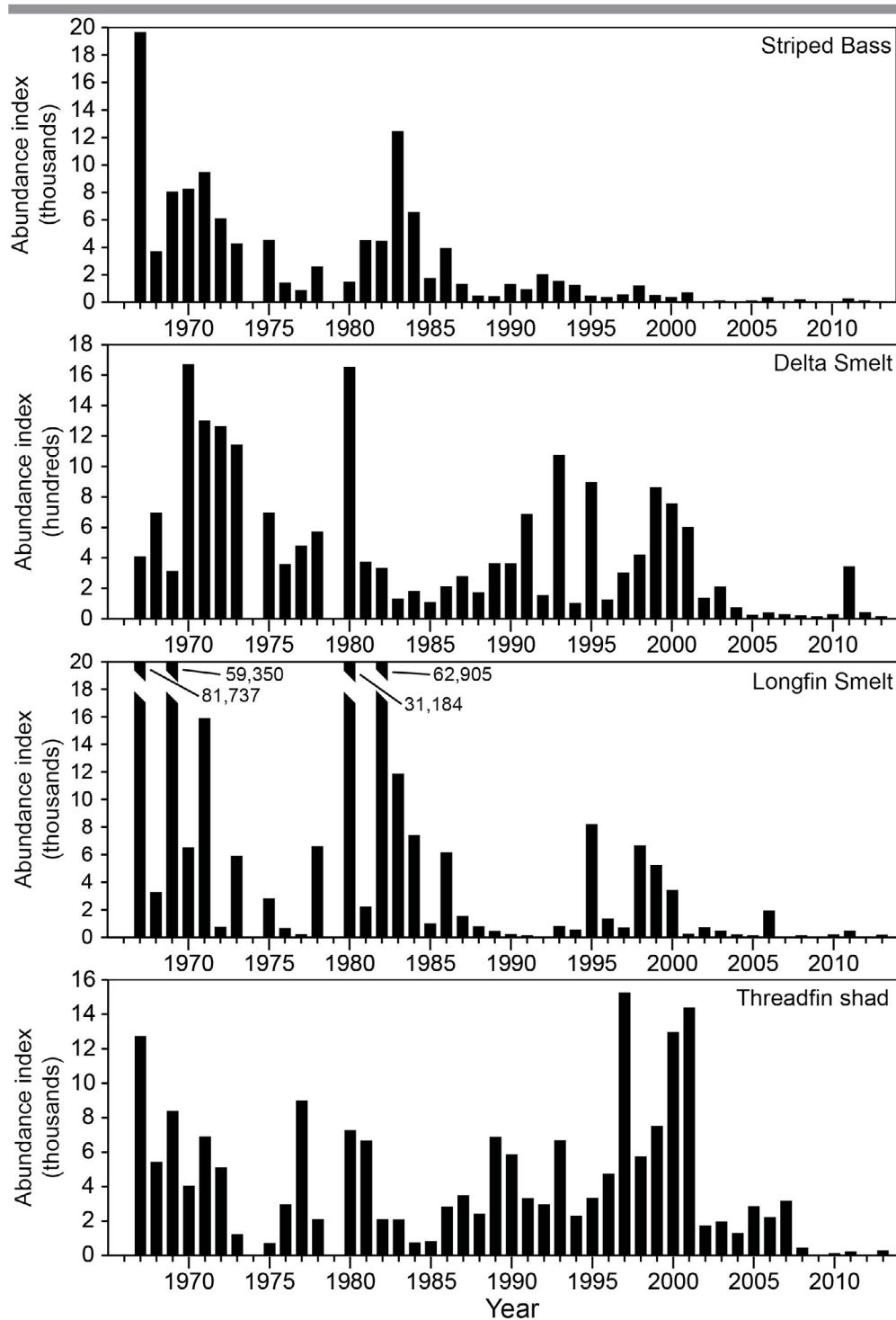


Figure 4. Abundance indices from Fall Midwater Trawl for Delta Smelt, Longfin Smelt, age-0 Striped Bass, and Threadfin Shad. Missing bars indicate when an index could not be calculated. See Chapter 3 for details of sampling programs, including geographic coverage, and Appendix B for details of calculating abundance indices.



Changes in Delta Smelt distribution and abundance

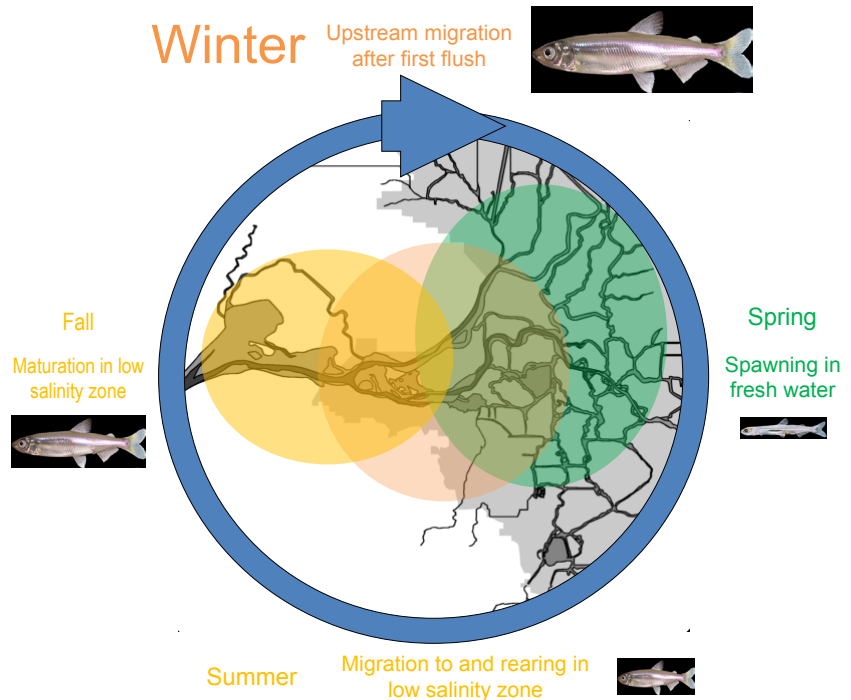
Long-term monitoring surveys conducted by the IEP have documented substantial changes in the distribution and abundance of Delta Smelt in its small native geographic range which extends from the upstream boundaries of tidal influence in the northern, eastern and southern Delta region of the estuary to Suisun and San Pablo Bays in the north-western region of the estuary. The geographic range of Delta Smelt also includes some of the larger tidal sloughs and tributaries adjacent to Suisun and San Pablo Bays, including some Suisun Marsh sloughs and the lower Napa River (Bennett 2005, Hobbs et al. 2007, Sommer et al. 2011, Merz et al. 2011, Sommer and Mejia 2013, Murphy and Hamilton 2013). Delta Smelt are generally considered a pelagic species. While they are commonly found in shallow shoal areas such as Honker and Grizzly Bays in the Suisun Bay region of the estuary and larger marsh sloughs such as Suisun and Montezuma Sloughs in Suisun Marsh and the lower reaches of Cache and Lindsey Sloughs in the northern Delta, they are less commonly encountered in near-shore areas and only rarely in smaller marsh sloughs (Bennett 2005, Merz et al. 2011, Sommer and Mejia 2013).

The Delta Smelt has been characterized as a “semi-anadromous” fish species that spawns in fresh water and rears in fresh to brackish water (Fig. 5; Dege and Brown 2004, Bennett 2005, Sommer et al. 2011, Merz et al. 2011). While Delta Smelt have been documented throughout their geographic range during most months of the year (Sommer et al. 2011, Merz et al. 2011, Murphy and Hamilton 2013), their distribution varies seasonally in response to dynamic abiotic and biotic habitat attributes such as salinity, temperature, turbidity, and presumably food supplies (Bennett et al. 2005, Sommer et al. 2013, Brown et al. 2014). In years with high freshwater discharge in winter and spring, spawning and rearing of larval and early post-larval fish can temporarily extend seaward into San Pablo Bay, while in years with less discharge it usually occurs in the Delta, Suisun Bay and Suisun Marsh. Juveniles and adults are distributed across a broader salinity range (0 to about 18) than larval and post-larval fishes which tend to be most abundant in the low salinity zone (salinity 1-6). Dege and Brown (2004) and Sommer et al. (2011) found that the center of the Delta Smelt distribution is associated with salinities of about 2 during most months and moves with the estuarine salinity gradient as the salinity gradient responds to flow.

Historically, Delta Smelt were commonly observed throughout the fresh and low salinity portions of their geographic range (Erkkila et al. 1950, Radke 1966). Over the last two decades, their geographic distribution has become more constricted during the summer and fall. At present, Delta Smelt are less commonly found in the southern and eastern Delta during the winter and spring and are largely absent from this region in the summer and fall (Nobriga et al. 2008, Sommer et al. 2011). While Delta Smelt continue to be found in the northern Delta year-round and individual catches in this region are sometimes large, particularly during winter and spring, the majority of the population is usually observed in the region near to and west of the Sacramento-San Joaquin River confluence, especially in the summer and fall (Sweetnam 1999, Feyrer et al. 2007, Nobriga et al. 2008, Merz et al. 2011, Sommer et al. 2011, Sommer and Mejia 2013).

In addition to documenting changes in distribution, long-term IEP surveys also reveal that the annual abundance indices of Delta Smelt have greatly declined since the first long-term pelagic fish monitoring survey began in summer 1959 (Fig. 3). Both a gradual, long-term decline and step changes, most recently around 2002, have been described using a variety of qualitative and statistical approaches for subadult Delta Smelt caught in the fall (e.g., Bennett and Moyle 1996, Bennett 2005, Manly and Chotkowski 2006, Thomson et al. 2010). These declines have not been smooth or entirely unidirectional and also include a great deal of interannual variability (Fig. 3).

Figure 5. Simplified life cycle of Delta Smelt (modified from Bennett 2005). Colors correspond to different seasons with the low salinity zone changing position with season.



Since the beginning of the POD in 2002, the Delta Smelt abundance indices have often been at record low levels, leading to concerns about declines in effective population size (Fisch et al. 2011) and a loss of population-level resilience, meaning the ability of the population to recover to higher population abundances when conditions are suitable. For example, population sizes might become too small to produce enough eggs or larvae to outpace predation on eggs and larvae.

Delta Smelt had previously rebounded from low population abundances, most recently in the wet years of the late 1990s (Fig. 3). The lack of increase in Delta Smelt in the wet year of 2006 combined with new evidence for genetic bottlenecks and a significant decline in effective population size from 2003 to 2007 (Fisch et al. 2011) were thus a source of great concern. However, during 2011, the next wet year after 2006, the species did increase in abundance (Fig. 3). Unfortunately, the increase in Delta Smelt abundance was short-lived and did not carry over into the following year-class in 2012, a drier year. Nevertheless, the temporary increase gave some cause for renewed optimism about the resilience of the species and its potential recovery. In addition, the contrasts between habitat conditions and Delta Smelt responses in 2006 and 2011 provided an opportunity to gain new insights into the Delta Smelt habitat requirements that might help better manage this species and its habitat.

Protecting Delta Smelt

Delta Smelt are currently protected under both California and federal endangered species legislation. The protection and recovery of Delta Smelt and its estuarine habitat in the SFE will

likely require the human population of California to reduce its dependence on some of the natural resources provided by the SFE. This will become even more challenging in the future because of climate change and the continued growth of California's human population. California's population has increased by approximately 38 million people compared to the population when California became a state in 1850 and has increased by about 22.5 million compared to 1959 when Delta Smelt monitoring started 55 years ago (U.S. Census Bureau data). More than three quarters of today's 38 million Californians live south of the SFE, and the majority of these Californians and millions of acres of farmland rely on fresh water diverted from the Delta for all or part of their water supply. The conflicts and trade-offs between species protection measures and actions to provide water and other natural resources to California's growing human population have resulted in repeated attempts to reconcile these seemingly irreconcilable objectives through regulatory requirements, new institutional arrangements, and management plans.

Among the regulatory requirements are the State water right decisions issued by the California State Water Resources Control Board, which grant SWP and CVP water rights permits, but also include requirements to protect fish. State regulations also include increasingly more stringent waste discharge permits. For example, the new permit recently issued to the Sacramento Regional County Wastewater Treatment Plant includes new requirements for major treatment upgrades to better protect downstream water uses and the health of the estuary. Federal regulations include water quality requirements under the Clean Water Act and Biological Opinions (BiOps) issued under the federal Endangered Species Act. Two BiOps assess the effects of the coordinated operations of the SWP and CVP on Delta Smelt, Green Sturgeon, and salmonid fish populations, and their designated critical habitat. These BiOps include "reasonable and prudent alternatives" to lessen negative impacts of SWP and CVP operations and avoid jeopardy to the species, while at the same time trying to avoid major reductions in water exports from the Delta.

Recent institutional reconciliation attempts include the multiagency, State and federal CALFED Bay-Delta Program and Authority (CALFED) and the California Delta Stewardship Council (DSC), a new State agency. From 1994 to 2010, CALFED attempted to reconcile water allocation and ecosystem restoration efforts in the estuary in a way that would allow them to "get better together" (Doremus 2009). After the demise of CALFED, the State of California created the DSC to address what the legislature termed the "co-equal goals" of providing a more reliable water supply for California and protecting, restoring, and enhancing the Delta ecosystem (CA Water Code §85054, <http://deltacouncil.ca.gov/>).

Among the many management plans aimed at reconciling species protection and human water and land use objectives are plans by the DSC, SWRCB, and new groupings of multiple agencies and stakeholders. The DSC recently completed and is now starting to implement its comprehensive "Delta Plan" (<http://deltacouncil.ca.gov/delta-plan-0>) to achieve the co-equal goals, while the SWRCB is on track to complete a major update to its "Bay-Delta Plan" which may result in changes to water right permits (http://www.waterboards.ca.gov/waterrights/water_issues/programs/bay_delta/). Three California State agencies recently completed a new California Water Action Plan that includes actions to help achieve the co-equal goals (http://resources.ca.gov/california_water_action_plan/). A multi-agency planning effort that includes State and federal agencies as well as local Public Water Agencies (water contractors) is working to complete the "Bay-Delta Conservation Plan" (BDCP, <http://baydeltaconservationplan.com>). The BDCP is a proposed Habitat Conservation Plan under the federal Endangered Species Act and a Natural Community Conservation Plan under the California Natural Community Conservation Planning Act. It proposes to implement habitat restoration measures, stressor reduction activities,

improved water project operations criteria, and new water conveyance infrastructure. If approved by the regulatory agencies, this plan would provide long-term permits for the various projects and water operations to proceed over a 50-year time frame.

Management actions, regulatory requirements, and institutional arrangements in the SFE have undergone substantial and complex changes over the last 150 years. Hanak et al. (2011) describe a progression from an early disorganized “laissez-faire” era of California and SFE water management followed by increasingly organized and large-scale management schemes, from local water use to state-wide water projects, which led to a current “era of conflict” and the hope for a new “era of reconciliation.” A complete review of these changes is outside the scope of this report and the reader is referred to Hanak et al. (2011) and other existing reports on this topic. It is important to note, however, that increasingly, these changes have been “adaptations” based on the results of monitoring, studies, and other scientific activities in the SFE. Many of these scientific activities have been conducted under the auspices of the IEP (Herrgesell 2013). It can be argued that some of the activities preceding and ultimately leading to the creation of the IEP in 1970 ushered in an era of increasingly intense and formalized “adaptive management” before the term itself was coined.

Adaptive management is a formal approach to natural resource management that closely connects science with management to devise, track, and improve management outcomes. This connection started to become an important aspect of fisheries management in the 1950s (e.g., Beverton and Holt 1957), although the term itself was not coined until 1978 when Holling (1978) and Walters and Hilborn (1978) provided a conceptual framework for adaptive resources management. This framework was later refined to distinguish between “passive” and “active” adaptive management. According to Williams (2011), “active adaptive management actively pursues the reduction of uncertainty through management interventions, whereas passive adaptive management focuses on resource objectives, with learning a useful but unintended byproduct of decision making [...]. In practice this means that a key difference between passive and active adaptive management is the degree to which the objectives that guide decision making emphasize the reduction of uncertainty.” In active adaptive management, management actions are designed as “experimental treatments” with clear hypotheses about outcomes that are tested through rigorous data collection and analyses. This accelerates learning, but can come at the expense of achieving resource objectives because potentially less effective management actions may be included in the experimental design. Moreover, the more intense science efforts needed for active adaptive management can be costly over the short term (Williams 2011). This may explain why passive adaptive management, while not always referred to by this name or implemented in the formal and rigorous way now advocated by the DSC’s Delta Plan (DSC 2013), has been and continues to be common in the SFE, but active adaptive management – viewed by some as the only “real” adaptive management – is still rare.

Of all current management actions and requirements affecting Delta Smelt, the actions required in the 2005 and 2008 BiOps issued by the U.S. Fish and Wildlife Service (FWS) are most directly aimed at the protection of Delta Smelt. The 2008 BiOp takes a life cycle approach to protecting Delta Smelt and includes an explicit requirement for adaptive management of fall outflow. After initial steps to design a passive adaptive management program, the U.S. Bureau of Reclamation (Reclamation) decided to take a more active approach aimed at more rapidly reducing uncertainties about the underlying mechanisms and effects of fall outflow management on Delta Smelt (Reclamation 2011, 2012, Brown et al. 2014). The study component of the fall outflow adaptive management plan, also known as the “fall low salinity habitat” (FLaSH) studies, was developed with the help of a new conceptual model (FLaSH conceptual model, Brown et

al. 2014) and has been implemented by the IEP starting in 2011. The FLaSH studies provided an opportunity to intensely study the increase in the Delta Smelt abundance index observed in 2011. At this initial stage of the adaptive management program and the FLaSH studies, the 2011 data were compared to data gathered in the previous wet year, 2006, during which fall outflow was lower. The initial data analysis effort also considered antecedent conditions in 2010 and 2005, resulting in a simple comparative approach focusing on four years (Brown et al. 2014).

Report Purpose and Organization

It is clear that the recovery of Delta Smelt and other listed and unlisted native species will be a key requirement of any plan to manage the resources of the SFE. Understanding the factors driving Delta Smelt population dynamics is a major goal of resource management agencies. The main purpose of this report is to provide an up to date assessment of factors affecting Delta Smelt throughout its primarily annual life cycle. Specific goals are to provide decision makers with scientific information for evaluating difficult trade-offs associated with management and policy decisions, provide scientists with a resource for formulating and testing hypotheses and mathematical models, and provide the general public with a new way for learning about Delta Smelt and their habitat.

We address these goals through a synthesis of scientific information about Delta Smelt with an emphasis on new information since the release of the last POD synthesis report in 2010 (Baxter et al. 2010). As in previous reports, conceptual models play a key role in this report. Conceptual models are useful tools for organizing and synthesizing information, designing research and modeling studies, and for evaluating potential outcomes of management actions. Here, we revisit previously developed conceptual models for Delta Smelt, and synthesize new information about factors affecting Delta Smelt and Delta Smelt responses to those factors. This comprehensive body of information is then used to construct and populate a Delta Smelt conceptual model, within a new framework.

Numerous conceptual models have been developed to describe the relationships and linkages among environmental drivers of ecosystem change, ecosystem and habitat attributes, and Delta Smelt responses. In Chapter 2 of this report, we provide a brief introduction to conceptual models and review some of the conceptual models developed for the SFE and for Delta Smelt. In Chapter 3, we introduce a new conceptual model framework for Delta Smelt and describe our approach to updating the previously developed Delta Smelt conceptual models. We also describe the data sources and analytical approaches used in this report. In Chapter 4, we review and synthesize recent information about drivers and habitat attributes affecting Delta Smelt and Delta Smelt responses to habitat attributes. In Chapter 5, we present an updated conceptual model for Delta Smelt that include key drivers, habitat attributes, interactions between them, and Delta Smelt responses discussed in Chapter 4. In Chapter 6, we review and synthesize recent information about Delta Smelt population dynamics, life history, and population trends. In Chapter 7, we use the updated conceptual model to formulate hypotheses about Delta Smelt responses and changing habitat conditions and test them using a simple comparative approach similar to the FLaSH approach (Brown et al. 2014), but for all life stages of Delta Smelt. The purpose of Chapter 7 is to put the new conceptual model along with the comparative approach to an immediate test that is of high relevance to the management of Delta Smelt. Chapter 8 presents key results and conclusions from the preceding Chapters. In Chapter 9, we discuss next steps for future conceptual, qualitative, and quantitative modeling as well as the science and management implications of the information contained in this report.

Chapter 2: Conceptual Models

Overview

We learn and think about the world we live in through mental models of how the world looks and how it works. Our mental models guide all our conscious decisions and actions. They are never static; we constantly update them with new information gained by observing the world around us and by assessing the outcomes of our decisions and actions. In our minds, we compare the new information against our existing mental models. Observations that agree with our mental models strengthen them, observations that don't agree with our mental models force us to modify, adjust, and update them.

Conceptual models are formalized versions of mental models that are communicated to others verbally and graphically. Ecologists and environmental managers use them to communicate hypotheses about “how ecosystems work” and to explore how human actions and other drivers change ecosystems. They usually use a combination of narrative text and graphical illustrations about ecosystem components and the relationships among them. More informal narrative conceptual models verbally describe cause-effect relationships, while more formal conceptual models may express them through scientific hypotheses or mathematical equations.

Conceptual model illustrations often take the form of pictures, plots, schematic images or diagrams, matrices, or tables (Fischenich 2008). For example, the IEP Estuarine Ecology Team used elaborate matrices to illustrate and assess the likely mechanisms underlying the statistically determined relationships between SFE fishes and “X2,” an indicator of estuarine salinity dynamics (Estuarine Ecology Team 1997), while Reclamation (2011, 2012) used a table format to illustrate how fall outflow interacts with other features of Delta Smelt habitat and affects Delta Smelt. Schoellhamer et al. (2012) used a series of conceptual X-Y plots to illustrate a conceptual model of sediment supply reduction and downstream propagation in the SFE. Glibert (2012) and Glibert et al. (2011) used schematic images to conceptualize changes in nutrients, flows, biogeochemical processes, and the food web of the SFE. Many schematic conceptual model diagrams use boxes to depict ecosystem components and arrows to illustrate the relationships, flows, and interactions among them. The conceptual models developed by the IEP for its POD investigations (see below) include examples of schematic conceptual model depictions with few boxes and arrows, while some of the conceptual models developed for the “Delta Regional Ecosystem Restoration Implementation Plan” (DiGennaro et al. 2012, see below) and the “effects hierarchy” of factors affecting Delta Smelt abundance developed by Miller et al. (2012) provide examples of more complex schematics with a large number of boxes and arrows.

Conceptual models have become essential tools for summarizing, synthesizing, and communicating scientific understanding of ecosystem structure and functioning. They are also key to successful planning and implementation of ecological research and mathematical modeling as well as to adaptive management, restoration and recovery of ecosystems, and environmental science education (e.g., Thom 2000, Ogden et al. 2005, Fortuin et al. 2011). Conceptual models are also essential tools for identifying management and science priorities and for the selection of key ecological attributes to be used to evaluate the performance of management actions (i.e., performance measures) and assess the present relative to a desired state of an ecosystem (i.e., indicators) (Washington State Academy of Sciences 2012).

Conceptual models have clear limitations. For example, even the most complex conceptual models are highly simplified descriptions of a small part of an ecosystem – they can never tell the “whole” story. Just like our every-day mental models, they are also never final. To remain relevant, ecological conceptual models must evolve and change with the evolution of our knowledge about ecosystems. Furthermore, conceptual models identify key ecosystem components and relationships, but they do not quantify them and unless they are coupled with mathematical models, conceptual models cannot be used to make quantitative predictions.

Conceptual models can be used to make qualitative predictions about changes in ecosystem components and their relationships. These qualitative predictions can serve as testable hypotheses that help design scientific analyses and studies. The creation or revision of the conceptual models themselves usually forces the formulation of hypotheses and their testing with available data and information, as will be demonstrated in the later Chapters of this report. Qualitative predictions and testable hypotheses are also at the heart of active adaptive management. They are needed to design experimental adaptive management actions and the studies and monitoring needed to assess the outcomes from such actions. The fall outflow adaptive management plan (Reclamation 2011, 2012) provides an example of how a conceptual model was used to make qualitative predictions and design a comprehensive set of studies, the FLaSH studies. Finally, the formulation of conceptual models is usually the essential first step for constructing quantitative models. Mathematical models are sets of mathematical expressions that quantify the components and relationships in the conceptual models and can be used to make quantitative predictions about the state of ecosystem components and linkages under specific circumstances (Jackson et al. 2000). The (few) quantitative predictions in the fall outflow adaptive management plan (Reclamation 2011, 2012) are based on such mathematical models.

Ecological conceptual models generally link ecological “drivers” with ecological effects or “outcomes.” Drivers are physical, chemical, or biological factors of human or natural origin (for example, nutrients from natural soils and applied fertilizers). Outcomes can be physical, chemical or biological responses to the drivers (for example, phytoplankton growth and biomass), but can also be social and economic impacts on human components of the ecosystem (for example, harmful algal blooms that affect recreational use or costs of water treatment for drinking water supply). Drivers and outcomes are the components of the system under consideration. They are linked by mechanistic cause-effect relationships. Conceptual models can also be nested within each other, for example, to accommodate different temporal or spatial scales, or conceptual models can be coupled so that the outcome of one conceptual model becomes a driver in the next one. Drivers are often categorized in various ways, including their causal proximity to specific outcomes, whether they are natural or anthropogenic, and whether they can be altered by human management strategies and actions. Graphically, drivers are often arranged in hierarchical tiers that reflect these categories.

For example, Gentile et al (2001) describe a basic three-tiered approach that links environmental outcomes (tier 1) to proximal anthropogenic drivers termed “stressors” (tier 2) and the natural and anthropogenic drivers that act on these stressors (tier 3). Davis et al. (2010) show how different ecological regimes in Australian lakes (outcomes, tier 1) arise from the interplay of stressors (tier 2) and hydrological changes (tier 3) acting on the original ecological regime (tier 4). Carr et al. (2007) review a widely used five-tiered “Driver–Pressure–State–Impact–Response” (DPSIR) framework that focuses on identifying human-caused environmental problems and solutions. In this framework, the ultimate drivers (D) are social processes that result in specific human activities that manifest as proximal “pressures” (P) that change the “state” (S), or condition, of the environment. This can have “impacts” (I) on human well-being that are recognized as

problems. Some impacts are so severe that they require a human response (R), usually in the form of institutional solutions aimed at reducing high-priority impacts. The Puget Sound Partnership Science Panel (2012) recently used the DPSIR framework to develop a conceptual model that links management strategies (i.e., responses; e.g., reduce pollution) to anthropogenic drivers (e.g., human population growth) and pressures (e.g., pollution) that affect the state of ecosystem components (e.g., habitats and species) and impact the provisioning of ecosystem services (e.g., fishing). This model helped identify scientific knowledge gaps and decision-critical issues and questions that needed to be answered in response to management priorities.

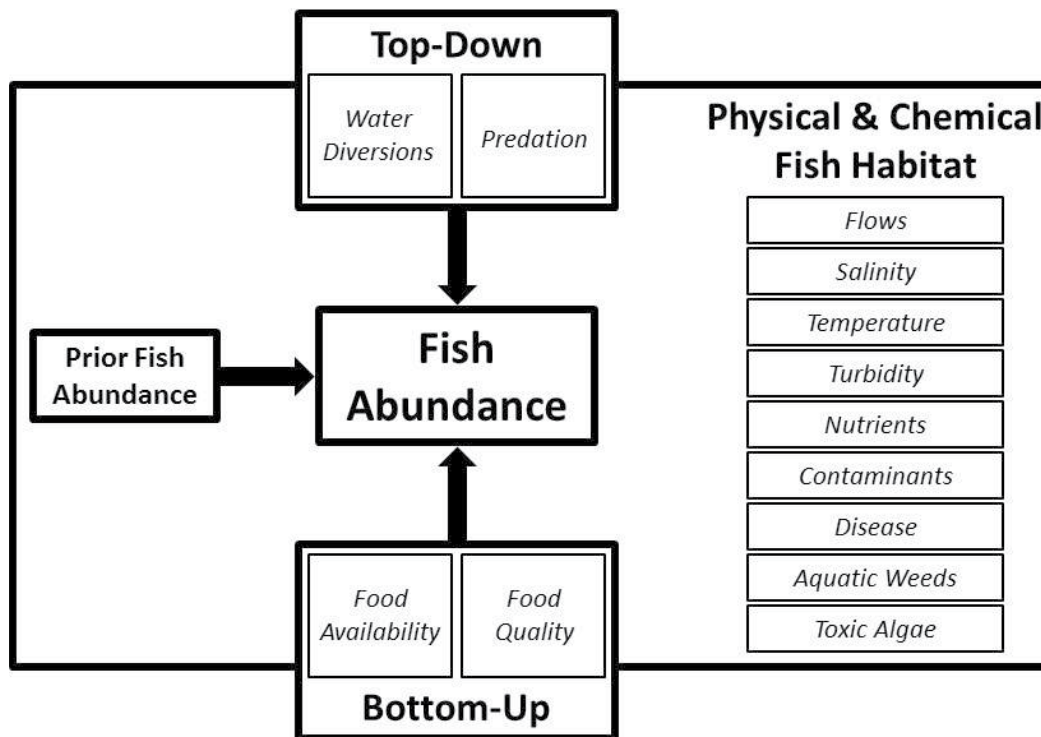
Recent Conceptual Models for the San Francisco Estuary

Over the last decade, two integrated sets of conceptual models have been developed for portions of the SFE. The first conceptual model set was developed by the Ecosystem Restoration Program (<http://www.dfg.ca.gov/ERP/>) to evaluate restoration actions in the Delta under the “Delta Regional Ecosystem Restoration Implementation Plan” (DRERIP; DiGennaro et al. 2012). DRERIP conceptual models were developed for ecological processes, habitats, specific species, and stressors. The DRERIP conceptual models were built around environmental drivers, their expected effects termed “outcomes,” and cause-and-effect relationships between the two shown as one-way arrows termed “linkages.” In the graphical depiction of the DRERIP conceptual models, different arrow widths, colors, and styles denote the importance, degree of understanding, and predictability, respectively, of the driver-linkage-outcome relationships, while symbols next to the arrows denote the direction and nature of the effect (positive, negative, or non-linear) (DiGennaro 2012, Opperman 2012). The DRERIP species conceptual models include “transition matrix” diagrams depicting how environmental drivers affect the probability of one life stage successfully transitioning to the next.

The second set of conceptual models was developed by the IEP as a comprehensive conceptual framework intended to guide investigations of the POD and to synthesize and communicate results (Sommer et al. 2007, Baxter et al. 2010). This framework includes a “basic” POD conceptual model about key drivers of change affecting pelagic fish and their habitat (Fig. 6), more narrowly focused “species-specific” conceptual models about drivers affecting the different life stages of each of the four POD fish species (e.g., Fig. 7), and a broader “ecological regime shift” conceptual model that placed the POD decline in a longer-term historical context (not shown; see Baxter et al. 2010). The basic POD conceptual model placed the four fish species in the center of interacting drivers affecting the quantity and quality of their habitat (Fig. 6), while the species-specific models identified key seasonal drivers in red, with proximal causes and effects in yellow (Fig. 7).

The National Research Council Committee on Sustainable Water and Environmental Management in the California Bay-Delta (NRC Committee) (NRC 2012) called the POD conceptual model framework “an important example of supporting science. This framework identifies and links, in the context of both ecosystem structure and functioning, the key stressors that help to explain the decline of pelagic organisms.” The NRC Committee further noted that the “drivers of change” identified in the POD conceptual models “are quantifiable” and “suitable for model evaluation” and that the:

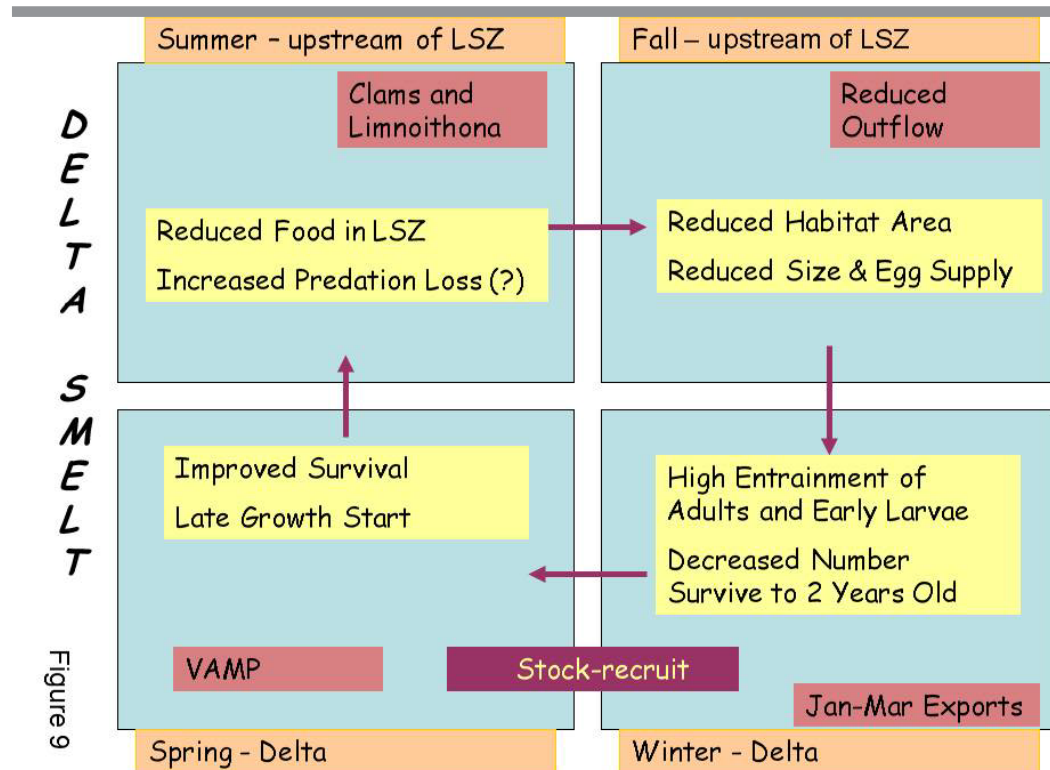
Figure 6. The basic conceptual model for the pelagic organism decline (Baxter et al. 2010).



“types of stressors identified are integrative, reflecting co-occurring physical, chemical, and biotic changes. They also apply to multiple structural (food web structure, biodiversity) and functional (food transfer changes, biogeochemical cycling) changes taking place in the Delta. The framework and associated detail are both comprehensive and useful in terms of linking these drivers to changes taking place at multiple levels of the food web. This type of conceptual approach will also be useful for examining other drivers and impacts of ecological change, including observed changes in fish community structure and production; specifically, how these changes are affected and influenced by changes in physico-chemical factors (e.g., salinity, temperature, turbidity, nutrients/contaminants) and at lower trophic levels (phytoplankton, invertebrate grazers, and prey)” (NRC 2012, p. 34-35).

Since the release of the 2012 NRC report, the POD conceptual model framework has been used as the basis for additional conceptual models developed to aid planning and quantifying the ecological effects of active adaptive management of Delta outflow to improve fall low salinity habitat for Delta Smelt and to guide the associated fall low salinity habitat (FLaSH) studies (Reclamation 2011, 2012). A more complete summary of the POD and FLASH conceptual models along with additional information about related conceptual and quantitative models in the SFE can be found in the initial FLASH report (Brown et al. 2014, see also <http://deltacouncil.ca.gov/science-program/fall-low-salinity-habitat-flash-studies-and-adaptive-management-plan-review-0>).

Figure 7. Species-specific conceptual model for Delta Smelt. This is one of four species-specific conceptual models developed as part of the conceptual framework for the pelagic organism decline (Baxter et al. 2010). The low salinity zone (LSZ) is defined as salinity 1-6. The Vernalis Adaptive Management Plan (VAMP) included reductions in spring exports with possible effects on Delta Smelt.



One important new feature of the conceptual model developed for the fall outflow adaptive management plan and the FLASH studies was the explicit consideration of interacting dynamic and relatively more stationary (geographically and temporally fixed) habitat components that was based on a conceptual model of environment-habitat-production linkages in tidal river estuaries developed by Peterson (2003). In the FLASH conceptual model, the interactions among dynamic and stationary habitat components determine the characteristics of Delta Smelt habitat in the fall and lead to varying Delta Smelt outcomes. In essence, the dynamic flow and salinity regimes of the SFE move water, particles, and organisms across the estuary's stationary topography, which has distinct physical features that modulate the dynamic habitat components. Together, these stationary and dynamic habitat components are hypothesized to control the survival, health, growth, fecundity, and, ultimately, the reproductive success of estuarine pelagic species, such as Delta Smelt. The interplay between stationary and dynamic habitat components also helps explain the distribution and movement of Delta Smelt across its range which cannot be understood – or managed – based on geography alone.

Numerous other conceptual and quantitative models have been developed for the SFE. Kimmerer (2004) summarized many of the earlier conceptual models. More recent conceptual model examples include those by Glibert (2012) and Glibert et al. (2011) as well as the five-tiered effects hierarchy by Miller et al. (2012). Recent examples of mathematical models of habitat use and population dynamics of Delta Smelt include models based on statistical approaches (e.g.,

Manly and Chotkowski 2006, Feyrer et al. 2007, Nobriga et al. 2008, Feyrer et al. 2010, Thomson et al. 2010, Mac Nally et al. 2010, Miller et al. 2012). There is also a rapidly developing body of life cycle models for Delta Smelt and other SFE fish species that use statistical and numerical simulation approaches (e.g. Blumberg et al., 2010, Maunder and Deriso 2011, Massoudieh et al. 2011, Rose et al. 2011, Rose et al. 2013a,b).

Chapter 3: Approach

This report is the result of a team effort by the IEP Management, Analysis, and Synthesis Team (MAST, often referred to as “we” in this report). Appendix A briefly describes the MAST and the report development process and schedule which included a public and independent expert peer review step that led to major revisions to the draft report.

General Approach

Our general approach in this report was to develop a new conceptual model framework for Delta Smelt and to use this framework to synthesize new scientific information and update and integrate existing conceptual models including the “basic” and “species-specific” POD conceptual models, the DRERIP “transition matrix” models, the tabular FLaSH conceptual model and the hierarchical conceptual model in Miller et al. (2012) described in Chapter 2.

The development of the new conceptual model framework was guided by the conceptual model literature (see Chapter 2) and by recommendations from the independent “FLaSH Panel” of national experts convened by the Delta Science Program. The FLaSH Panel recommended to:

“develop a schematic version of the [FLaSH] conceptual model that matches the revised, written version of the conceptual model in the draft 2012 FLaSH study report. The conceptual model in written and schematic form should continue to emphasize processes and their interactions over simple correlations, should ensure Delta Smelt vital rates remain central to thinking, and should be designed for routine use by scientists as an organizational tool and for testing hypotheses associated with the AMP [adaptive management plan]; it should be as complex as necessary to achieve these purposes. The conceptual model should also be able to encompass processes and interactions that extend before and after Fall Outflow Action periods, including areas both upstream and downstream of the LSZ” (FLaSH Panel 2012, page ii).

The conceptual modeling approach in this report is intended to provide a basis, not a substitute for the development or use of mathematical models. While mathematical models are outside of the scope of this report, we briefly discuss the promise and challenges of mathematical models for Delta Smelt, summarize some of the highlights of existing mathematical modeling efforts for Delta Smelt, and offer a brief description of two additional proposed mathematical modeling efforts — one qualitative and the other quantitative — we think are natural outgrowths of the information in this report (see Chapter 8). Development of a variety of flexible working tools to facilitate discussion of elements of the conceptual model is one intended outcome of the MAST effort. Even simple quantitative and qualitative models based on our revised conceptual model

will serve to further organize thinking and characterize weaknesses in current data collection and analysis efforts.

In this Chapter, we introduce the new conceptual model framework for Delta Smelt. This framework consists of a series of nested and tiered conceptual models: a general life cycle conceptual model and more detailed life stage transition conceptual models. It was developed following recommendations by the FLaSH Panel (FLaSH Panel 2012) and extensive reviews of a draft version of this report (see <http://www.water.ca.gov/iep/pod/mast.cfm> and Appendix A). In Chapter 4 we review and synthesize existing information about drivers, habitat attributes, and Delta Smelt responses with a focus on new information since 2010. We use the drivers in the basic POD conceptual model as the basis for this synthesis. This information is then used to populate the nested conceptual models in the new conceptual model framework with key drivers and their linkages to Delta Smelt responses. The fully populated nested conceptual models are presented in Chapter 5. Chapter 6 focuses on Delta Smelt life history and population dynamics and trends. Chapters 4 and 6 include some new analyses of long-term monitoring data, but are largely based on a review and synthesis of the existing published literature. In Chapter 7, we compare data pertaining to ecosystem drivers (drivers), habitat attributes (drivers or outcomes) and Delta Smelt responses (outcomes) in four recent years with moderate to wet hydrology: the two most recent wet years (2006 and 2011) and the two drier years immediately before them (2005 and 2010). The intent is to assess the utility of the conceptual model for formulating and testing hypotheses that expand the comparative FLaSH approach (Brown et al. 2014) that focused on the fall to a more comprehensive year-round investigation of why Delta Smelt abundance increased in the wet year of 2011, but failed to respond to wet conditions in 2006. In each of the sections in Chapter 7 covering a specific life stage, the hypotheses inherent in the conceptual model are stated and the reasoning for including each hypothesis is explained. Although we attempted to develop independent hypotheses, this was not always possible because many drivers were related and important habitat attributes were influenced by multiple drivers and their interactions, as shown in the conceptual model diagrams and explored in Chapter 4.

Key insights from Chapters 4–7 are summarized in Chapter 8. In Chapter 8, we also discuss limitations of the analytical approaches in this report. In Chapter 9, we describe additional data and analyses needed to test hypotheses that could not be conclusively tested with the available data and our simple comparative analysis approach. We also present some ongoing or possible next steps for future years, including some recommendations for future synthesis and mathematical lifecycle modeling efforts aimed at Delta Smelt and other species and for future adaptive management, including the fall outflow adaptive management and FLaSH studies effort.

Framework for the Delta Smelt Conceptual Model

The updated Delta Smelt conceptual model framework in this report integrates and modifies features of the “basic” and “species specific” POD conceptual models (Baxter et al 2010), the FLaSH conceptual model (Brown et al. 2014), the DRERIP “transition matrix” conceptual models (DiGennaro et al. 2012), and the hierarchical conceptual model in Miller et al. (2012). It consists of two nested and linked conceptual models of increasing specificity:

1. *A general life cycle conceptual model* for the four Delta Smelt life stages (adults, eggs and larvae, juveniles, and subadults) that includes stationary landscape attributes and dynamic environmental drivers, habitat attributes, and Delta Smelt responses; and

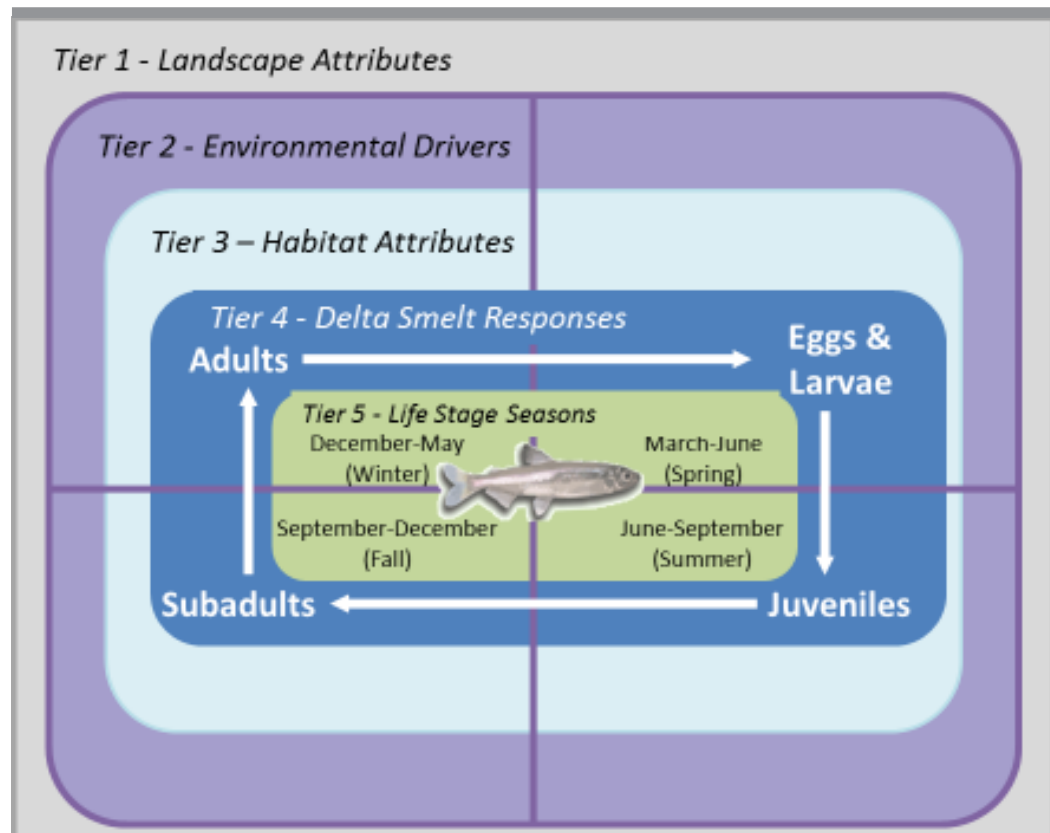
2. More detailed *life stage transition conceptual models* for each of the four Delta Smelt life stages that describe relationships between environmental drivers, key habitat attributes, and the population-level probability of successfully transitioning from one life stage to the next. This probability is dependent on the effects of environmental drivers and habitat attributes on the growth, survival, reproduction, and movements of Delta Smelt but data are currently inadequate to provide causal links for most of these processes individually.

General Life Cycle Conceptual Model

The updated general life cycle conceptual model for Delta Smelt (Fig. 8) follows the FLaSH Panels (2012) recommendation to “ensure Delta Smelt vital rates remain central to thinking” and is structurally similar to the basic POD conceptual model (Fig. 6). The general life cycle conceptual model is divided vertically and horizontally into four sections representing four Delta Smelt life stages from eggs and larvae to adults occurring in four “life stage seasons” indicated in the center of the diagram (Fig. 8; tier 5 box, green shading). This is similar to the four seasonal compartments of the species-specific conceptual model diagram in Baxter et al. (2010). Importantly, these life stage seasons are not exactly the same as calendar-based seasons. Instead, they have somewhat variable duration and overlapping months. This is because life stage transitions from eggs to adults are gradual and different life stages of Delta Smelt often overlap for a period of one to three months. Delta Smelt responses (Fig. 8; tier 4 box with dark blue shading) to important habitat attributes throughout their usually annual life cycle are placed within a box representing habitat attributes important to their growth and survival, which conveys the idea that biotic and abiotic habitat elements drive Delta Smelt responses (Peterson 2003; Fig. 8; tier 3 box with light blue shading). For each life stage season, there are a set of natural and anthropogenic environmental drivers associated with the estuarine environment (Fig. 8; tier 2 box with purple shading) that generate the habitat attributes important to Delta Smelt growth and survival. Surrounding the environmental drivers box is a fourth, outer box that represents the stationary (geographically and temporally fixed) landscape attributes of the estuarine ecosystem associated with its physical geometry and the orientation and connections of its component waterbodies (Fig. 8; tier 1 box with grey shading). In contrast to this outer box, the components and processes described in the inner boxes of this conceptual model are dynamic in space and time. Note that the fixed landscape attributes are considered fixed in the context of Delta Smelt population biology in any particular year rather than across longer time scales. The different spatial and temporal scales for each tier of the conceptual model are shown in Figure 9.

The tiered components of the general life cycle conceptual model for Delta Smelt can vary over a wide range of spatial and temporal scales (Fig. 9). Landscape attributes of the San Francisco Estuary (tier 1) encompass local to estuarine-wide features and change slowly over decades or longer periods. Environmental drivers (tier 2) that affect Delta Smelt habitat attributes vary and manifest over the broadest range of spatial and temporal scales, from local variations over tidal or daily cycles to long-term changes at the watershed or even larger geographic scales. Similar to environmental drivers, habitat attributes of Delta Smelt (tier 3) can be highly dynamic at small spatial and temporal scales or change gradually over many years, but they don’t extend beyond the geographic range of the species, which in the case of Delta Smelt is the SFE. Delta Smelt responses (tier 4) vary in response to changing habitat attributes within subregions of the estuary. In this small fish species with its maximum age of two years and extremely small geographic range, population-level responses can range from rapid (e.g., in response to toxic spills) to more

Figure 8. A new conceptual model for Delta Smelt showing Delta Smelt responses (dark blue box) to habitat attributes (light blue box), which are influenced by environmental drivers (purple box) in four “life stage seasons” (green box). Environmental drivers are influenced by landscape attributes (grey box).



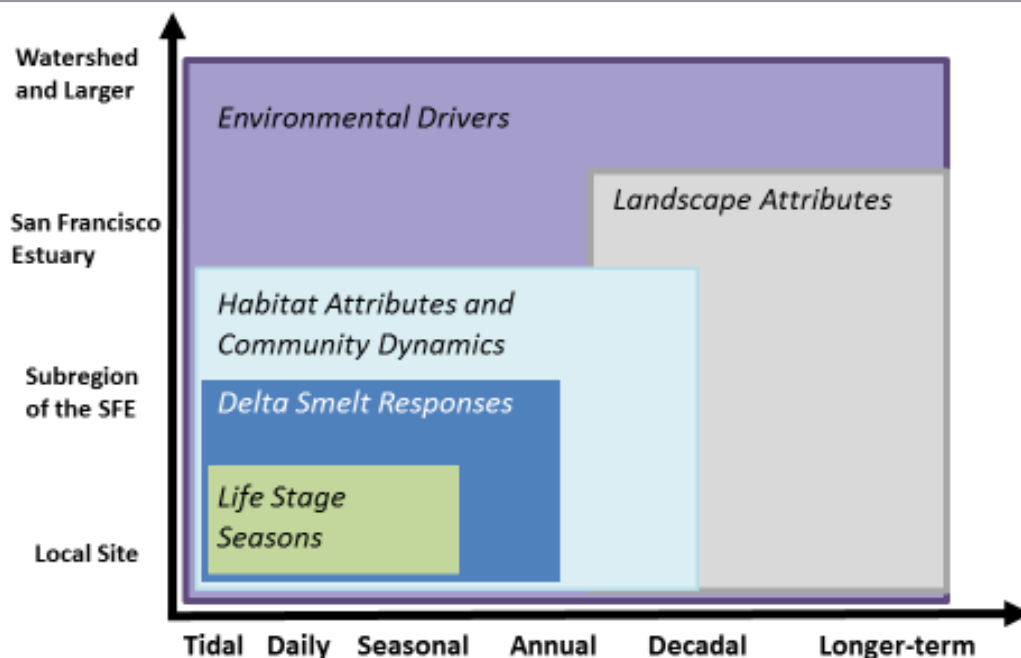
slowly over the course of one or more years. Life stage seasons (tier 5) occur over the course of a year in seasonally occupied areas of the estuary.

Similar to the POD and DRERIP conceptual models, the updated Delta Smelt life cycle conceptual model includes only those landscape attributes and environmental drivers with plausible mechanistic linkages to outcomes, which in this case are changes in habitat attributes and resulting Delta Smelt responses in the four life stage seasons. These mechanistic linkages are depicted as arrows in a series of four new conceptual models for each life stage season (Fig. 10). These life stage season conceptual models are nested components of the general life cycle conceptual model as shown in Fig. 8. They will be described in detail in Chapter 5.

Data Sources

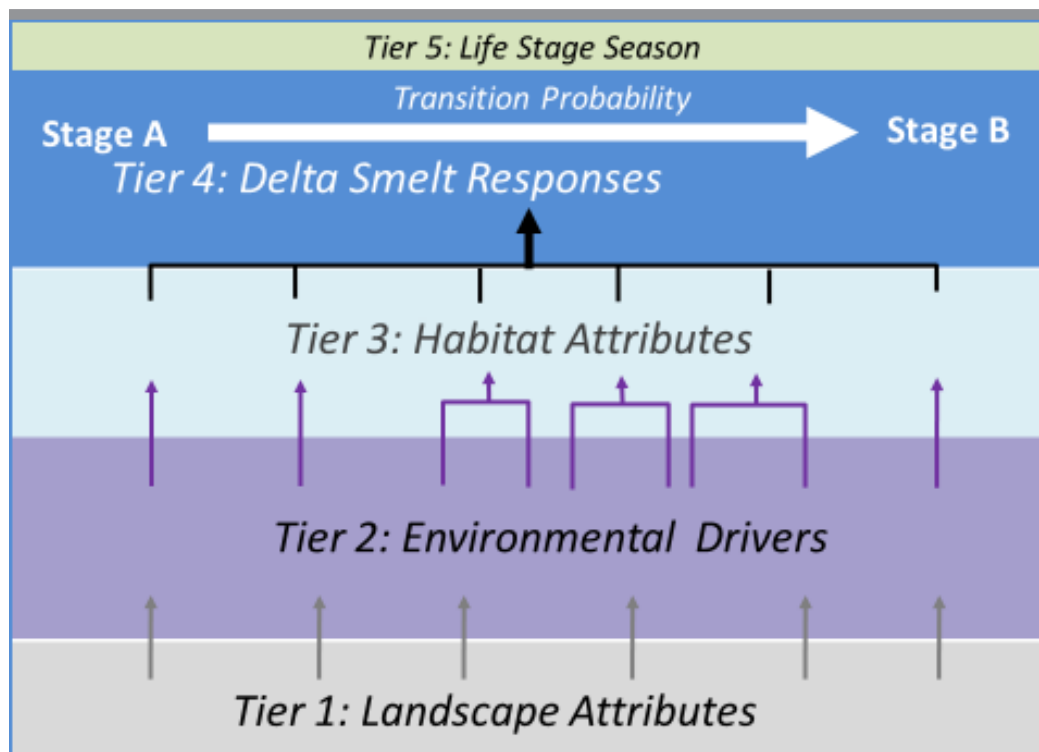
Our examination of environmental drivers in Chapter 4, Delta Smelt life history and population dynamics and trends in Chapter 6, and the evaluation of hypotheses about Delta Smelt responses to changing habitat attributes in Chapter 7 rely largely on results of previously published data and analyses, but in several cases we update these analyses with more recent data. We also include some additional analyses (described below). All these analyses depend largely on environmental monitoring data collected by IEP agencies during routine, long-term monitoring surveys

Figure 9. Spatial and temporal scales of the component tiers in the general life cycle conceptual model framework for Delta Smelt.



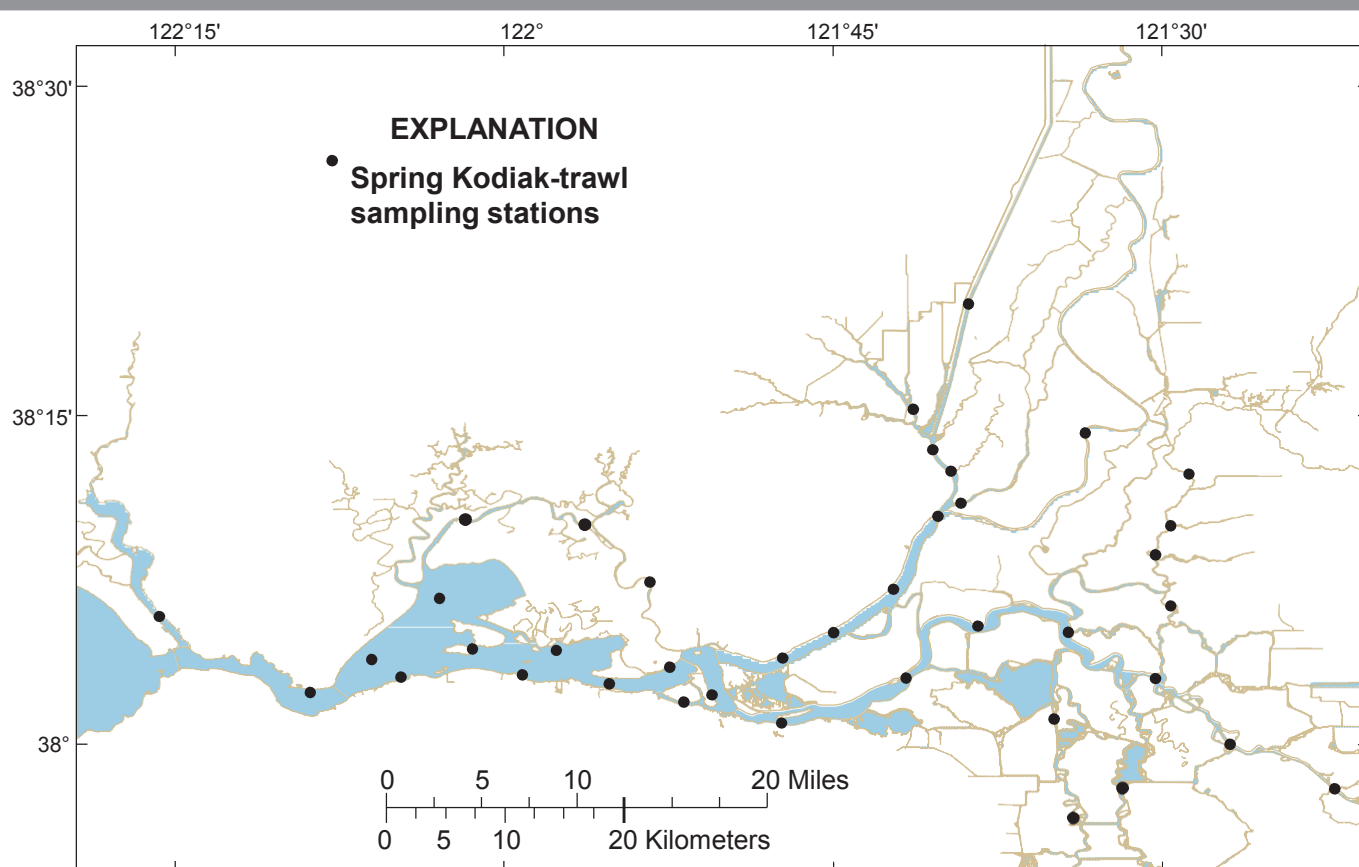
(<http://www.water.ca.gov/iep/products/data.cfm>). These surveys provide the long-term records and geographic coverage necessary and the data collected by these surveys are publicly available. Available data includes data on fish, invertebrates, phytoplankton, water quality variables, and flow. Use of these particular data sources does not reflect any preference for those data. Results from other ongoing research efforts were included as appropriate.

For the purposes of this report, we consider each stage, larvae through adults, of the Delta Smelt life cycle in the context of the monitoring programs that provide data on the Delta Smelt population. Delta Smelt eggs are not monitored and have in fact never been found in the wild. Monitoring surveys in the late winter and spring include the spring Kodiak trawl (SKT, Fig. 11), which samples maturing, spawning and post-spawning adults. The SKT is conducted monthly from January through May. Spring also includes the 20 mm survey (20 mm, Fig. 12), which samples larval and post-larval Delta Smelt and is conducted every two weeks from mid-March through mid-July. Summer includes the summer townet survey (TNS, Fig. 13); which samples juvenile fish and currently runs every two weeks from June through August. The Fall Midwater Trawl (FMWT, Fig. 14) survey samples subadult Delta Smelt monthly from September through mid-December. Each of these surveys samples fishes broadly within the upper SFE and generally covers the geographic habitat range used by Delta Smelt (Merz et al. 2011). Exceptions to complete coverage occur in some high outflow years when Delta Smelt can temporarily inhabit San Pablo Bay in association with decreased salinities caused by increased Delta outflows (Moyle 2002) and in other years when some adult fish move upstream of the geographic range of these surveys (probably to spawn) in the Yolo Bypass and Sacramento River (e.g., Feyrer et al. 2006, Merz et al. 2011). Also, FMWT and TNS sampling in the Cache Slough complex was instituted over several years starting in the 1990s for FMWT and 2000s for TNS. The current sampling locations have been in place since 2011. These exceptions to complete spatial coverage are believed to reflect small fractions of the population. Additional geographic coverage along

Figure 10. Framework for the Delta Smelt life stage season conceptual models.

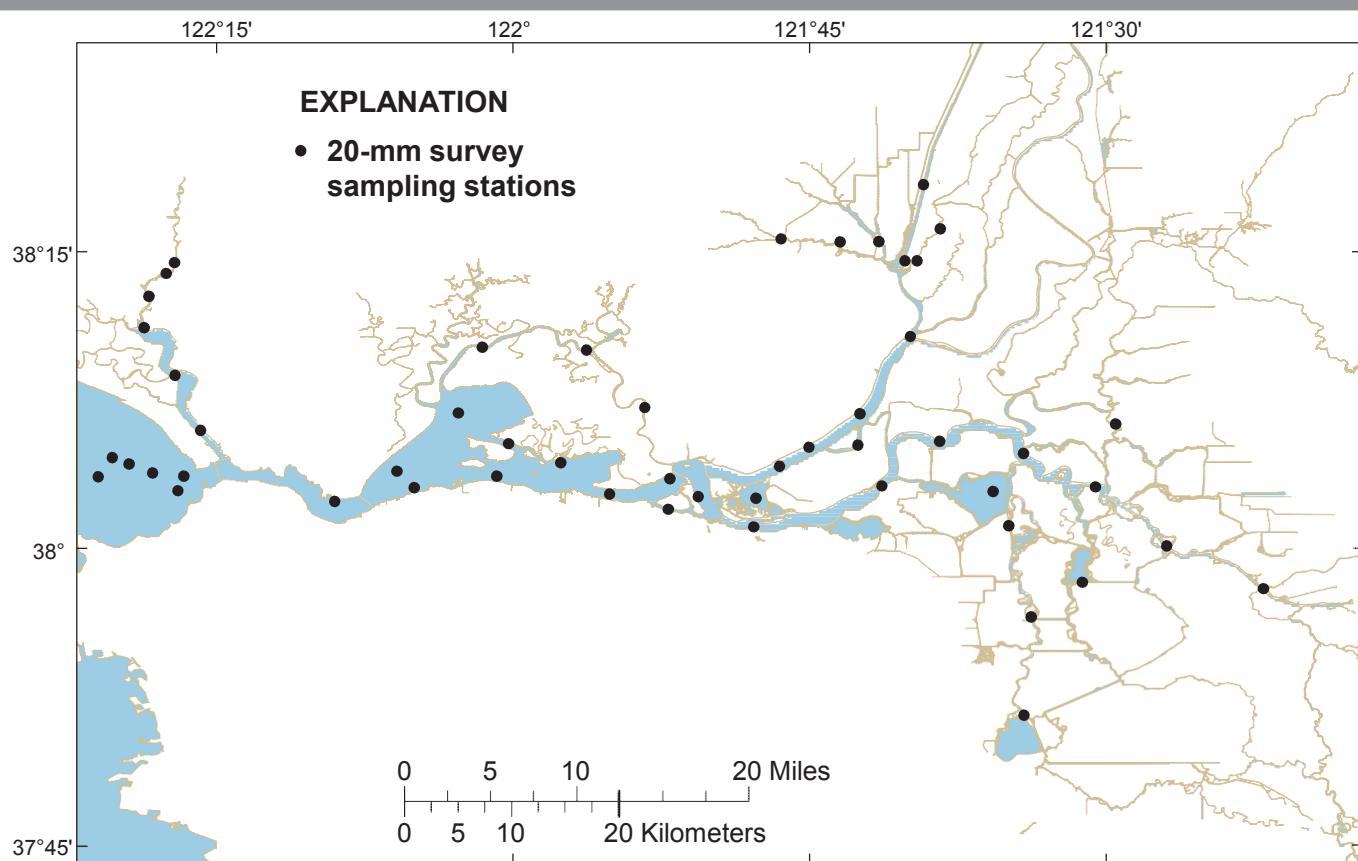
or outside of the margins of the other four monitoring surveys is provided by other IEP fish monitoring surveys such as the San Francisco Bay Study, trawling and seining conducted by the Delta Juvenile Fish Monitoring Program in the Sacramento River and the north Delta, as well as the fish salvage monitoring at the fish protection facilities associated with the SWP and CVP export pumps in the south Delta. All Delta Smelt life stages (larvae-adult) are also commonly collected from nearshore habitats and in shallow open water where trawls cannot be used effectively (e.g., Aasen 1999, Nobriga et al. 2005, Brown and May 2006); however, there are no data indicating these are preferred habitats, that these fish represent different populations (see Fisch et al. 2011), or that their abundance varies differently than data from the aforementioned trawl surveys would suggest.

Annual abundance indices for Delta Smelt life stages are calculated from the catch data provided by each of the four surveys (See Appendix B for details). Together, they provide a comprehensive account of long-term changes in the relative abundance of Delta Smelt (Fig. 3). The long series of abundance index records for the summer and fall have provided the basis for many data analyses and modeling studies (e.g., Jassby et al. 1995, Kimmerer 2002a,b, Bennett 2005, Manly and Chotkowski 2006, Thomson et al. 2010, MacNally et al. 2010, Maunder and Deriso 2011, Miller et al. 2012) and for regulatory actions (USFWS 2008). They have also been used to estimate absolute population abundance (Newman 2008). The Delta Smelt and other SFE fish abundance indices are generally considered useful indicators of the status and trends of the Delta Smelt population as well as of the status of other resident fishes in the SFE in general and serve as performance metrics for the success of management actions. All monitoring surveys have strengths and weaknesses, and the long-term fish monitoring programs in the SFE are no exception (Honey et al. 2004). In the case of Delta Smelt, strengths include reasonably good coverage of the geographic extent of Delta Smelt habitat and coverage of all life stages except

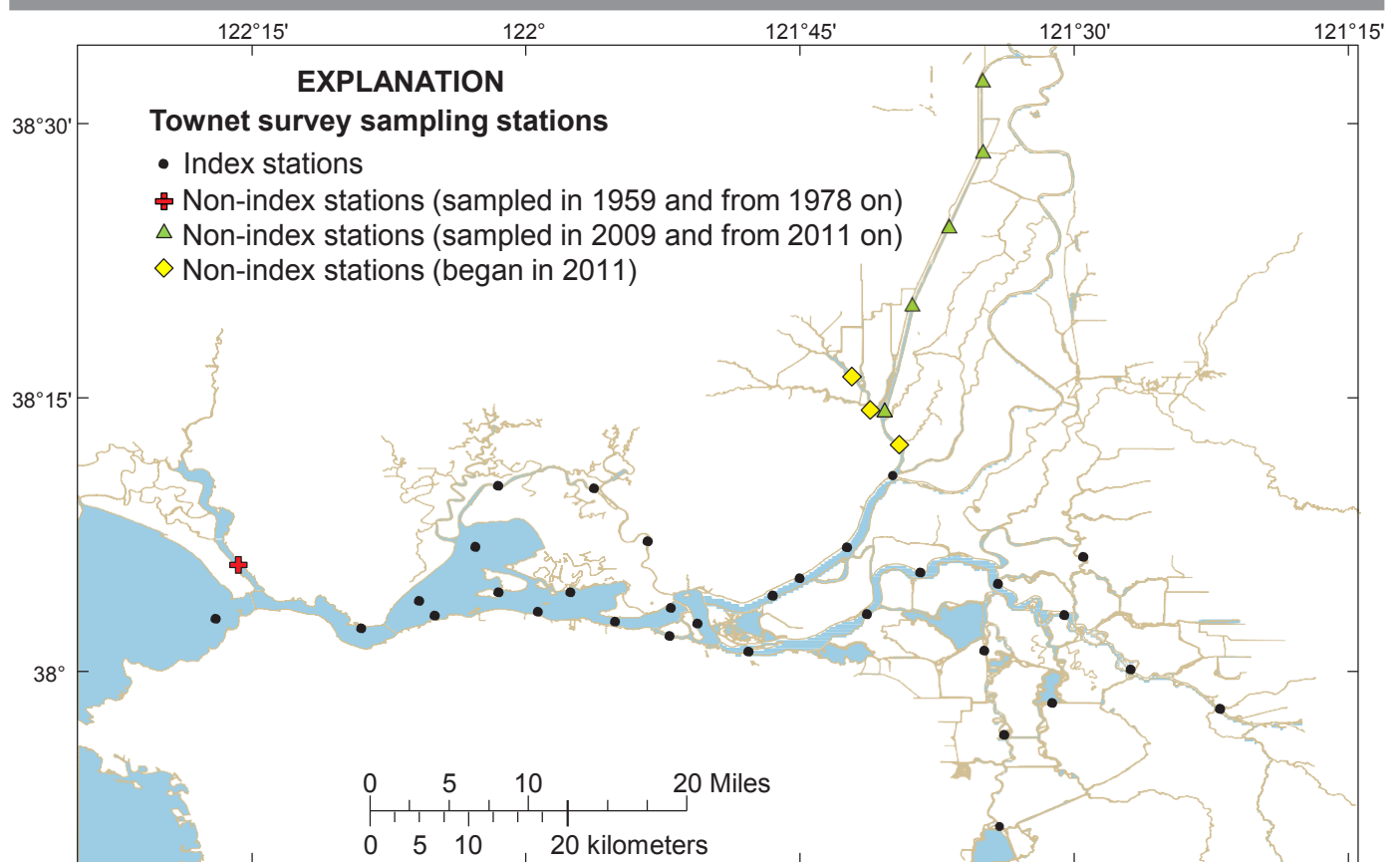
Figure 11. Map of Spring-Kodiak Trawl Survey sampling stations.

eggs (Gaines et al. 2006). They also include exceptionally long and consistent data records going back to 1959 in the case of the TNS, the oldest of the four surveys described here. There is a large amount of ancillary data (covariates), including data collected during the fish surveys, additional fish data from other monitoring surveys (Honey et al. 2004) as well as invertebrate, phytoplankton, water quality and hydrological data. Possible weaknesses include no measure of precision of abundance indices and imprecise estimates due to a high frequency of zero catches of Delta Smelt. These problems combine with survey design issues such as differences in Delta Smelt catchability with different nets and trawl regimes under changing environmental conditions, behavioral changes in distribution (Newman 2008) and the current low abundance of the species. For example, several studies have shown that Delta Smelt can exhibit lateral and vertical movements associated with tide and time of day (Bennett et al. 2002, Feyrer et al. 2013, Bennett and Burau 2014) but the overall frequency or effects of such local movements on abundance indices are unclear. Studies to further evaluate and address these issues are currently underway.

Two of the four fish monitoring surveys described here specifically target Delta Smelt; the other two do not. The SKT was designed and implemented specifically to improve detection of maturing adult Delta Smelt moving upstream in the winter and spring, particularly into the central and south Delta (Souza 2002). The 20 mm survey was designed and implemented specifically to capture late-stage larval Delta Smelt of about 20 mm in length; the SKT and 20 mm survey data help managers assess the risk of entrainment of these life stages by south Delta

Figure 12. Map of 20 mm Survey sampling stations.

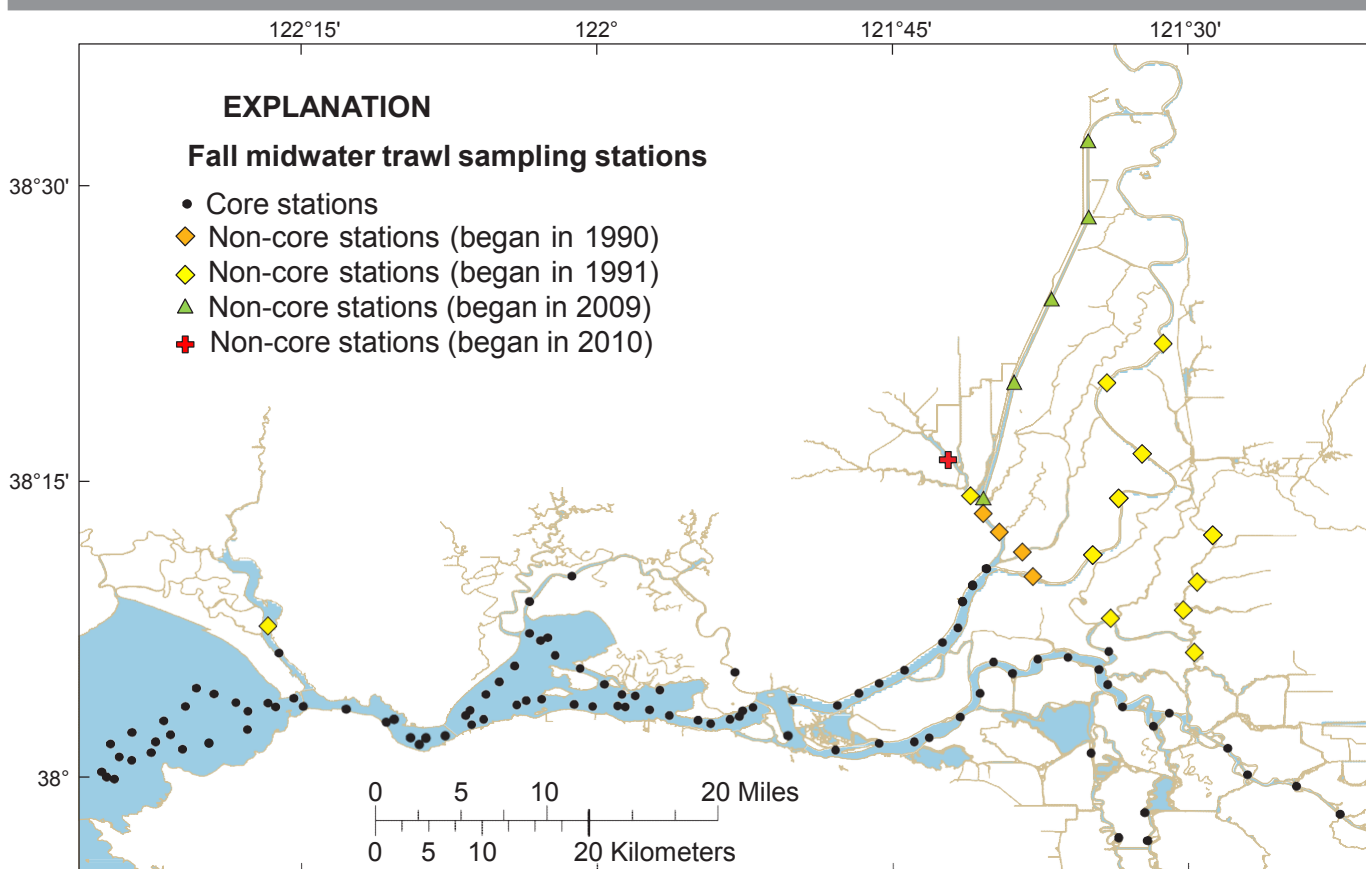
export pumps (Dege and Brown 2004). The TNS was designed to target small juvenile Striped Bass of about 17-50 mm fork length (the distance from the snout to the indentation of the tail fin) (Stevens 1977, Turner and Chadwick 1972); however, Delta Smelt tend to be of appropriate size for capture by the TNS net during the survey period. This occurs because Delta Smelt (see below) and Striped Bass spawning overlaps in time and growth of both are linked to water temperature, such that peak larval abundance occurs in April or May in most years. The TNS traditionally started and ended based on mean length of Striped Bass; however, young Delta Smelt attain sizes vulnerable to the TNS net during the same time period Striped Bass are vulnerable (Miller 2000). The survey ends when young Striped Bass surpassed 38 mm fork length (Miller 2000). Thus, regardless of the particular number of sampling surveys in a year or the index calculation method, Delta Smelt juveniles are generally vulnerable to the TNS whenever it samples. Similarly, the FMWT survey was designed to capture young-of-the-year Striped Bass, but in the 60-140 mm fork length size range (Stevens 1977). Although the survey and gear is generally effective for small pelagic fishes, the cod-end mesh (1.3 mm stretch mesh) on the net is large enough to allow some smaller sub-adult Delta Smelt to escape during the first couple survey months (see Newman 2008 for an approach to correct this effect). Even though the gear is not completely effective at retaining all sub-adult Delta Smelt, FMWT provides a reasonable relative measure of sub-adult abundance through time (Kimmerer and Nobriga 2005), albeit with low precision at the current low catch levels and given additional variation related to changes in growth, and thus changes in retention in the net from year to year. With the aforementioned caveats, we believe these surveys provide useful and valid relative abundance measures to examine the various life stage transition

Figure 13. Map of Summer Townet Survey sampling stations.

relationships described in this report as well as in many of the previously published studies cited in this report.

In addition to the annual abundance indices for Delta Smelt provided by the monitoring surveys described above, we also present annual indices of recruitment and survival. In this report, a survival index is simply the ratio of an abundance index for a particular life stage divided by the abundance index for a preceding life stage of the same Delta Smelt cohort. A recruitment index is the ratio of an abundance index for a particular life stage divided by an abundance index for a life stage of the preceding Delta Smelt year-class. These types of indices have been used in previous analyses (e.g. Miller et al. 2012), but it is important to note that they may compound the observation errors inherent in the annual abundance indices in complicated ways. This is likely more problematic for survival and recruitment indices that use the TNS and FMWT abundance indices because these surveys were not specifically designed to target Delta Smelt. It may be less problematic for the recruitment index calculated by dividing the 20 mm abundance index for larval and post-larval Delta Smelt by the preceding SKT abundance index for adult Delta Smelt because both surveys specifically target Delta Smelt. We use this recruitment index in some additional analyses included in this report. All other survival and recruitment indices are only used as a rough approximation and illustration of differences in recruitment and survival rates among different annual cohorts and life stages; they are not used for additional analyses.

Figure 14. Map of Fall Midwater Trawl Survey sampling stations.



Data Analysis

As noted previously, we review long-term trends in this report using published results, but in some cases include some additional analyses of long-term monitoring data (Chapters 4 and 7). These analyses are kept deliberately simple, for example, simple graphical explorations of time series, examinations of simple statistics such as medians and arithmetic means, and investigation of univariate relationships using simple correlation and least squares regression analyses. Such analyses are readily reproducible with the publicly available data described above. The purpose of presenting the results of these new analyses is to update previously published information with the most recent data. In many cases, the data presented in this report are summarized using boxplots. The center horizontal line in each box represents the median of the data. The upper and lower ends of the box represent the upper and lower quartiles of the data. These are also known as “hinges.” The “whiskers” are the lines extending above and below the box. The whiskers show the range of values falling within 1.5 times the inter-quartile distance from the nearest hinge. Values outside this range are shown as individual symbols. Asterisks denote values within 1.5 to 3.0 times the inter-quartile distance and circles denote values greater than 3.0 times the inter-quartile distance. Other types of plots are explicitly identified in the figure caption.

Some graphs and analyses refer specifically to the POD period. Analyses suggest the POD period started as early as 2002 or as late as 2004 (Thomson et al. 2010). We somewhat arbitrarily selected 2003-present as the POD period for this report. This period is not being recommended

as the baseline for management agencies to use when considering recovery of Delta Smelt. The time period simply reflects the consistently low level of Delta Smelt abundance in recent years and a useful baseline for identifying years with improved Delta Smelt abundance indices, which would indicate improved environmental conditions for Delta Smelt. Similarly, we also consider the 1982-2001 period between the two major step declines in Delta Smelt abundance identified by Thomson et al. (2010) separately in some graphs and analyses. Finally, some graphs and analyses refer to calendar years while others refer to water years. In California, a water year starts on October 1 and ends on September 30 of the next calendar year. California water year classifications are based on calculations of annual unimpaired runoff, which represents the natural water production of a river basin, unaltered by upstream diversions, storage, and export of water to or import of water from other basins.

In Chapter 7, we explore a series of hypothesized driver-outcome linkages using a comparative approach. The purpose is to demonstrate the utility of our conceptual model framework for generating hypotheses about the factors that may have contributed to the 2011 increase in Delta Smelt abundance. Specifically, we compare Delta Smelt responses to habitat conditions in four recent years with moderate to wet hydrology: the two most recent wet years (2006 and 2011) and the two drier years immediately before them (2005 and 2010). This comparative approach and data sources (described in Chapter 4) are deliberately similar to the comparative approach used in the FLaSH investigation (Brown et al. 2014). This approach allows us to place the results of the FLaSH investigation in a year-round, life cycle context and to more comprehensively evaluate factors that may have been responsible for the strong Delta Smelt abundance and survival response in 2011, including any possible relevant antecedent conditions from 2010. We attempt to draw comparisons with a similar set of data collected during 2005 and 2006. Our working assumption is that different Delta Smelt abundances in 2006 and 2011 should be attributable to differing environmental conditions, in some cases attributable to management actions, and subsequent ecological processes affecting the Delta Smelt population.

In Chapter 9 we briefly describe three examples of additional mathematical modeling approaches that can be used to further explore some of the linkages and interactions in our conceptual models and complement previously published and other ongoing mathematical modeling efforts for Delta Smelt. Importantly, results from the three modeling examples in Chapter 9 are included for illustrative purposes only; peer-reviewed publications of these analyses need to be completed before they can be used to draw firm conclusions.

Chapter 4: Environmental Drivers and Habitat Attributes

The general approach of this Chapter is to focus on how environmental drivers and interactions among them create habitat attributes of importance to Delta Smelt. Specifically, we review and synthesize existing information about drivers and habitat attributes and Delta Smelt responses to habitat attributes with a focus on new information since Baxter et al. (2010). We use the drivers and habitat attributes depicted in the basic POD conceptual model (Fig. 6) as the basis for this synthesis. We consider habitat attributes important when there are published studies suggesting ecological responses by Delta Smelt. Each section focuses on a habitat attribute that can be the outcome of one or more environmental drivers. Physical habitat attributes are presented first,

followed by biological habitat attributes. The order of presentation does not imply any kind of ranking of relative importance. For simplicity, we consider all habitat attributes discussed here as equally important because, as noted in Chapter 2, habitat arises from the combination of *all* physical and biological attributes affecting a species. We fully acknowledge that as Delta Smelt research proceeds and the system continues to change, additional habitat attributes may need to be added to the conceptual model, while others may be deemphasized or even deleted.

Each section starts with the general importance of a specific habitat attribute for estuarine biota followed by a brief discussion of its linkages with environmental drivers and its dynamics in space and time. Each habitat attribute is then placed in the context of Delta Smelt biology.

Water Temperature

Water temperature is fundamental to aquatic ecosystem health and function. It directly influences biological, physical, and chemical properties such as metabolic rates and life histories of aquatic organisms, dissolved oxygen levels, primary productivity, and cycling of nutrients and other chemicals (Vannote and Sweeney 1980, Poole and Berman 2001, Null et al. 2013). Water temperature is an important variable for ectothermic (“cold-blooded”) animals, including all fishes and invertebrates in the SFE. In the most extreme case, when water temperature exceeds the thermal tolerance of an organism, it will die. Temperatures within the thermal tolerance of an organism control the rate and efficiency of many physiological processes, including activity, digestion, growth, reproductive development, and reproductive output. We return to these processes after giving an overview of water temperature variability and its drivers in the Delta.

Long term temperature records from selected sites in the SFE show substantial seasonal and daily fluctuations in water temperature (Kimmerer 2004). While daily variations are evident and likely important to organisms, seasonal variations are much greater (Wagner et al. 2011). Median water surface temperatures across all stations monitored by the IEP Environmental Monitoring Program (EMP) (Fig. 15) from 1975-2012 range from 9 °C in January (minimum: 6 °C) to 22 °C in July (maximum: 28 °C). There are also clear regional variations in water temperature (Fig. 16). In July and August, the hottest summer months, water temperatures are usually highest at monitoring stations in the south Delta (average 23-26 °C, maximum 28 °C), lower at stations in the northern and western Delta (average 21-23 °C, maximum 25 °C) and lowest at stations in Suisun and San Pablo Bays (average 19-21 °C, maximum 24 °C). In January, the coldest winter month, average water temperatures are uniformly below 10 °C in the entire Delta, but above 10 °C in San Pablo Bay.

There is currently little evidence for increasing water temperatures in the Delta, although with climate change such increases are expected over the course of the century (Cloern et al. 2011, Wagner et al. 2011, Brown et al. 2013). In Spring (March-June) water temperature at IEP EMP water quality monitoring stations in the Delta increased during 1996–2005 by about 0.2 °C per year, but a similar trend was not apparent for the longer-term data record from 1975-2005 or for stations in Suisun Bay (Jassby 2008). These findings are similar to the results of Nobriga et al. (2008) who found no long-term (1970-2004) trends in temperature data collected during summer fish monitoring surveys in the Delta. Nobriga et al. (2008) also noted that the long-term (1970-2004) mean July water temperature at TNS fish monitoring stations in the southern region of the Delta is 24 °C, with current mid-summer temperatures often exceeding 25 °C. This agrees with average monthly EMP data from 1975-2012 which shows July and August water temperatures at

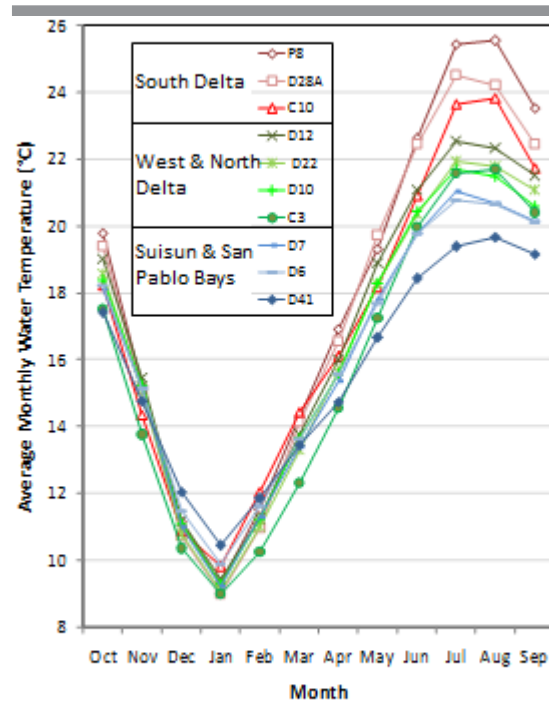
Figure 15. Map of active and historic IEP Environmental Monitoring Program (EMP) sampling stations.



a monitoring station located in Old River (station D28A) and in the San Joaquin River near the Port of Stockton (station P8) of more than 24 °C and 25 °C, respectively (Fig. 16).

In tidal systems, water temperature at a particular location is determined by the interaction between atmospheric forcing (e.g., air temperature and wind), tidal dispersion and riverine flows across the estuarine landscape (Monismith et al. 2009). In particular, estuarine water temperature is driven by heat exchange at the air–water interface and mediated by tidal and riverine flow dynamics and estuarine geomorphology (Enright et al. 2013). Wagner et al. (2011) found that regional weather patterns including air temperature and insolation (sunlight), are the primary drivers of water temperature variations in the SFE. Water flow and interaction with the stationary topography of the system also affects water temperature in the SFE, especially over shorter time scales and at smaller spatial scales. For example, Enright et al. (2013) showed that interaction

Figure 16. Average monthly water temperature for stations monitored by the Environmental Monitoring Program from 1975-2012.



of tides with tidal marsh topography can have a mediating effect on water temperature in tidal sloughs and on thermal variability at smaller spatial scales. Wagner et al. (2011) showed that high winter and spring flows can temporarily lower water temperatures. Greenberg et al. (2012) found that the present riparian vegetation on Delta levees lowers insolation by about 9% compared to a hypothetical situation without vegetation and suggested that riparian vegetation thus contributes to locally cooler water temperatures. This suggests that at least to some degree, water temperature can be managed locally and for short periods. Over larger scales, however, these types of locally mediated effects are overwhelmed by the effects of air temperature and insolation.

Air temperature and insolation in the SFE are correlated with each other (Wagner 2012) and vary strongly with

proximity to the Pacific Ocean because of the contrasting climate regimes prevailing in inland central California and the central California coast. While inland central California has a large annual air temperature range with hot, dry, sunny summers and cool, wet, and often foggy winters, the central California coast has a smaller annual air temperature range with cooler and often foggy summers and milder winters (Conomos et al. 1985). The SFE has a transitional climate with greater spatial and temporal variability in air temperature than either the coastal or the inland regions (Whipple et al. 2012). This is due to the interplay of the dynamic air masses from these regions across the stationary estuarine topography. In the summer, this interplay often results in strong afternoon winds from the ocean locally known as the “Delta breeze.” These onshore winds usually advance into the western and central Delta and, depending on the depth of the marine layer, often also into its marginal areas. In the Delta, these southwest to northeast winds can persist throughout the night and into the next morning and produce a marked decline in daily temperature. In the morning, this low is often followed by rapid warming once the winds subside and the high temperature inland air masses return to dominance (National Weather Service 2003). In the winter, ocean winds are weak and, during calm periods, cold air flows from the mountains into the estuary. This results in the formation of dense, overnight, near-surface fog locally known as “tule fog.” These calm and foggy periods are interrupted by winter storms. Many of these storms arrive from the south and southeast as “atmospheric rivers” that can often produce gale force winds and heavy rains lasting several days (Conomos et al. 1985, Dettinger and Ingram 2013).

The large variability in air temperature in the Delta is reflected by the larger annual variability in water temperature measured from 1998-2002 at continuous monitoring stations in the interior Delta compared to stations further upstream or downstream (Wagner et al. 2011). This high variability is also apparent in monthly water temperature data collected by the IEP Environmental

Monitoring Program since 1975 (Fig. 11). From 1975 to 2012, annual fluctuations in average monthly water temperature were greatest at stations in the south Delta (14-16 °C), smaller at stations in the northern and western Delta (12-13 °C), and lowest at stations in Suisun and San Pablo Bays (9-12 °C). Jassby (2008) reported that maximum daily air temperature could explain almost half the variability in maximum daily water temperature at the continuous monitoring station at Antioch during the summer months. The relationship between air and water temperature was also strong in all other months except January.

Wagner et al. (2011) and Wagner (2012) developed simple regression models for predicting water temperature at fixed temperature monitoring stations in the SFE using only air temperature and insolation on the day of interest and the water temperature from the previous day. Water temperature from the previous day accounts for both previous air temperature and the sources of water to the site, including advective flow from rivers or dispersive flow from more downstream reaches of the SFE. Each model had a different set of coefficients because of the differing influences of incoming river water or tidal exchange with San Francisco Bay. For stations with greater than 1 year of calibration data, model R^2 for daily average temperature exceeded 0.93, indicating that water temperature was highly predictable within the limits of the calibration data sets. High winter and spring flows were responsible for the largest divergences of the model outputs from measured temperatures.

The simple statistical models for water temperature developed by Wagner et al. (2011) and Wagner (2012) should be used with caution because they only predict temperature at the site of the recording instrument and do not explicitly account for mechanistic heat exchange. The analyses therefore do not incorporate the possible effect of site-specific features such as shading by riparian vegetation (Greenberg et al. 2012). Similarly, there are lateral and vertical variations in temperature on daily time scales (Wagner 2012) that could be important to organisms. For example, such variation might include substantial heterogeneity and formation of thermal refugia, which may be important to Delta Smelt.

In contrast to statistical modeling, which produces site-specific results, water temperature across regions is commonly modeled with computation-intensive deterministic simulation models. Such models use energy budgets to predict water temperature. Simple stochastic models are also possible. Like most statistical models, these stochastic models generally rely on the relationship between air and water temperature (Caissie 2006, Null et al. 2013). We are not aware that these types of models have been developed for the San Francisco Estuary.

Upper temperature limits for juvenile Delta Smelt survival are based on laboratory studies and corroborated by field data. Interpretation of the laboratory results is somewhat complicated as temperature tolerances can be affected by various factors including acclimation temperature, salinity, turbidity, and feeding status. Based on the critical thermal maximum, CT_{max} , juvenile Delta Smelt acclimated to 17 °C could not tolerate temperatures higher than 25.4 °C (Swanson et al. 2000). However, for juvenile Delta Smelt acclimated to 11.9, 15.7 and 19.7 °C, consistently higher CT_{max} were estimated (27.1, 28.2 and 28.9 °C, respectively; Komoroske et al. 2014), which corresponded closely to the maximum water temperatures recorded in the TNS and FMWT surveys. Swanson et al. (2000) used wild-caught fish, while Komoroske et al. (2014) used hatchery-reared fish, which may have contributed to the differences in results. Based on the TNS (Nobriga et al. 2008) and the 20 mm Survey (Sommer and Mejia 2013), most juvenile Delta Smelt were predicted to occur in field samples when water temperature was below 25 °C. In a multivariate autoregressive modeling analysis with 16 independent variables, MacNally et al. (2010) found that high summer (June – September) water temperature had a negative effect

on Delta Smelt subadult abundance in the fall. Water temperature was also one of several factors affecting Delta Smelt life stage dynamics in the state-space model of Maunder and Deriso (2011) and in an individual-based Delta Smelt life-cycle model (Rose et al. 2013a,b).

In addition to lethal effects, water temperature also has direct effects on the bioenergetics (interaction of metabolism and prey density) of Delta Smelt (Bennett et al. 2008) and it may affect their tolerance to other habitat attributes, such as toxicity (Brooks et al. 2012) and predation risk. Responses of different life stages of Delta Smelt to various temperature, salinity, and turbidity conditions are currently being further assessed as part of a larger UC Davis laboratory study about the “fundamental niche” of Delta Smelt (Komoroske et al. 2014, R. Connon et al., U.C. Davis, unpublished data).

The topic of bioenergetics is an important consideration in much of the remainder of this report, so we address it in more detail here. In general, the total metabolic rate of a fish will increase with temperature to an optimum temperature at which, given unlimited food, there is the maximum ability to grow and develop reproductive products (eggs or sperm) in addition to maintaining the basal metabolic rate required for survival, which also increases with temperature (Houde 1989, Hartman and Brandt 1995). As temperature increases beyond the optimum, metabolic rate continues to increase but physiological processes become less and less efficient and more energy is required just to meet the basal metabolic rate of the organism. Eventually, the metabolic rate begins to decline as temperatures approach the physiological limits of the organism and the basal metabolic rate can no longer be maintained.

At temperatures beyond the optimum, the ability to grow and mature becomes increasingly impaired. Long-term exposure to such stressful temperatures can eventually be lethal. In addition, resistance to disease and contaminants can also be affected (Brooks et al. 2012). The responses to contaminants can vary depending on the type of contaminant. For example, low temperatures can decrease the toxicity of organophosphate insecticides, but increase the toxicity of pyrethroid and organochlorine insecticides (Harwood et al. 2009), a characteristic that has been used in toxicity identification and evaluation (Weston and Lydy 2010). The previous discussion assumes unlimited food, which is unlikely to be the case for Delta Smelt or any organism in nature. Even at the optimum temperature, growth and reproductive development will depend on the quantity and quality (energy and nutrient content) of the food consumed. If the fish is unable to ingest enough food to meet its nutrient and energetic requirements, including the energy expended to capture and digest prey, it will starve, after first depleting any available energy stores (fat or muscle). Given an array of food items, fish will generally choose larger prey items. This is because the energy required to detect, chase, and capture multiple smaller prey that are equivalent in nutritional value to a single large prey item will, in many cases, exceed the energy required to capture the single prey item. Note that these same ideas apply to predatory fish that might consume Delta Smelt.

Water temperature is also thought to affect the number of eggs produced by female Delta Smelt. Egg production (i.e., fecundity) of the population is influenced not only by individual female size and number (Bennett 2005, DFW unpublished), but also by the duration of a temperature “spawning window” (Bennett 2005, Mac Nally et al. 2010), variously defined as: 15-20 °C by Bennett (2005); 7-15 °C by Wang (1986); and 12-15 °C by Baskerville-Bridges et al. (2004b). Bennett (2005) further stated that during cool springs this spawning window persists longer, allowing more cohorts to recruit. Given a sufficiently long spawning window, individual females may also repeat-spawn during the spawning season. This has been documented in culture (see Bennett 2005; J. Lindberg, U.C. Davis, personal communication 2013) and appears to occur

in the wild as well (L. Damon, CDFW, written communication 2012). Lindberg (U.C. Davis, personal communication 2013) observed that most females in culture spawned twice, some spawned three times and a very small number spawned four times. Each spawning was separated by a 4-5 week refractory period during February through June when water temperatures remained within the spawning window. Though laboratory conditions may not necessarily be representative of conditions in the wild, ripe females ready to release their second complete batch of eggs and developing a third batch have been detected in the wild during March and April (i.e., mid-season) suggesting that three spawns are possible (L. Damon, CDFW, written communication 2012). Thus, a longer spawning window would allow more females to repeat spawn adding both additional cohorts hatching under different conditions, and multiplying the fecundity of each repeat spawner (i.e., increasing the total fecundity of the individual), and thus, the total fecundity of the population. Moreover, in culture, individual females continued to grow through the spawning season and become more fecund with each batch of eggs (J. Lindberg, U.C. Davis, personal communication 2013). In the wild, the size of mature females generally increases month to month through the spawning season (Fig. 17), suggesting a potential increase in fecundity with each batch, but this has yet to be confirmed for wild fish. However, in culture, fish hatched later in the spawning season (mid-May to mid-June) grew up to be smaller-sized adults that started spawning later and had progeny with lower survival than the progeny of fish hatched earlier in the season (Lindberg et al. 2013). These observations are consistent with the reproductive patterns suggested for the wild Delta Smelt population (Bennett 2011). Overall, the effect of a prolonged spawning season on Delta Smelt population size and dynamics would seem to be positive; however, there is some uncertainty.

In the culture experiments reported by Bennett (2005), temperature strongly influenced hatching success of eggs. Specifically, Bennett (2005) reported that optimal hatching success and larval survival were estimated to occur at 15–17 °C based on studies conducted at 10, 15, and 20 °C. The data indicated that as incubation and early rearing temperatures increased, size at hatching and size at first feeding linearly decreased, possibly because basal metabolism of the developing embryo used more energy leaving less for growth. Fish that hatch relatively late in the season may experience high temperatures at a small size, which may reduce larval survival by several possible mechanisms. First, small size would limit the size of food items that the larvae could ingest because of smaller mouth size (see Nobriga 2002). Temperature may also affect food type and availability as discussed below. Second, small larvae are likely vulnerable to a larger range of predators for a longer period compared to larger larvae (e.g., “stage duration hypothesis;” Anderson 1988). Third, these fish could be potentially more vulnerable to transport toward the CVP and SWP export facilities, when Old and Middle River (OMR) flow restrictions are lifted. Restrictions are lifted when the 3-day mean water temperatures in Clifton Court Forebay (CCF) reach 25 °C or by the end of June.

As explained above, higher water temperatures increase energetic requirements and thus the food requirements of fish. To meet the increased need for food, it is possible that Delta Smelt spend more time foraging during the day. Since greater foraging time during the day increases visibility to predators, and those predators would also increase their foraging rates at higher temperatures, the encounter rate of predator and prey would likely increase at higher water temperatures. The net effect could be an increase in Delta Smelt predation risk (e.g., Walters and Juanes 1993). High temperatures can also decrease antipredator behavior, as described for Sacramento River Chinook Salmon (*Oncorhynchus tshawytscha*) (Marine and Cech 2004). In other words, the fish may make a behavioral choice to feed, grow, and become less vulnerable to predators as rapidly as possible, even though the short-term predation risk might increase. Water temperatures in the upper SFE are usually highest from June to September and decline rapidly between October and December

Figure 17. Individual female fork lengths by calendar day for mature female Delta Smelt collected in the Spring Kodiak Trawl Survey, January through May, 2005, 2006, 2010 and 2011. These data include both monthly distribution survey fish and directed survey fish. The directed survey (which targeted smelt spawning areas) was discontinued after January 2010.

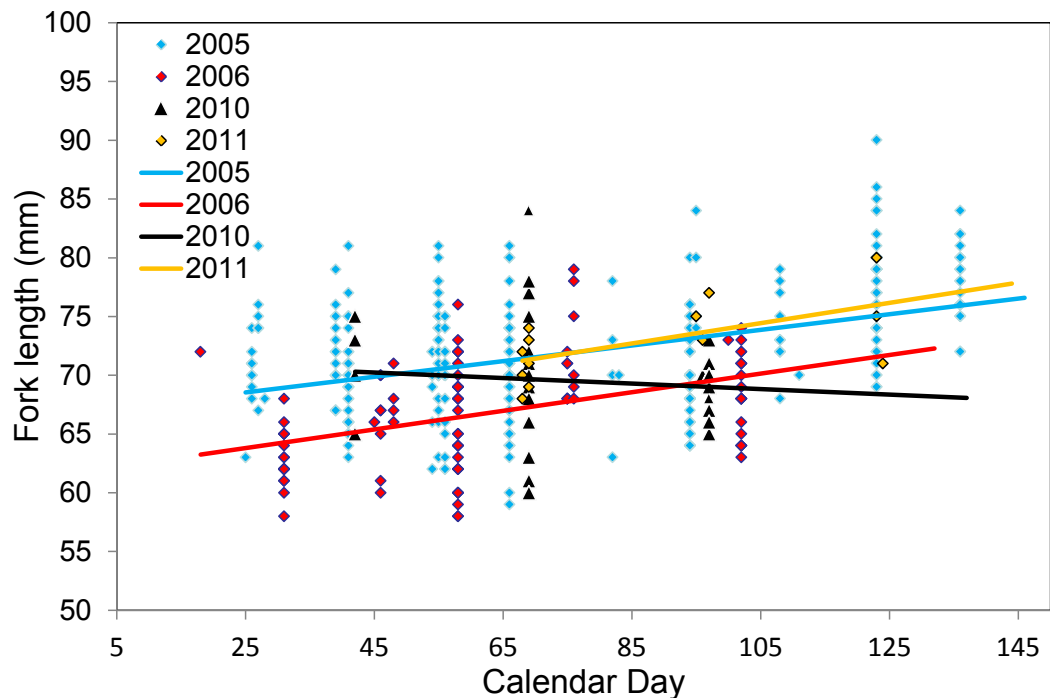


(Fig. 16). The reported optimal culture temperatures for Delta Smelt larvae and late-larvae are 16.4 ± 0.25 °C (Komoroske et al 2014). Moreover, the chronic lethal thermal maximum for Delta Smelt varies by life stage (Komoroske et al. 2014). Juvenile and subadult Delta Smelt are observed in the field most commonly at temperature near or below 20 °C (Bennett et al. 2008, Nobriga et al. 2008), a temperature which is often exceeded beginning in May or June and continuing through September and more rarely in October (see Chapter 7). Thus, we suggest that the same tradeoffs between feeding and predation risk may persist through the warmer months and into early fall, but become less likely as the season progresses into late fall and winter. Note, however, that predation risk is also influenced by a complex suite of other factors such as turbidity, life stage, and proximity to predator habitat, so the level of risk to Delta Smelt can't be determined.

Another possible indirect effect of higher water temperatures is that they may promote harmful algal blooms (HAB) (Lehman et al. 2005), which may degrade Delta Smelt habitat quality in the summer and early fall (Baxter et al. 2010). In the Delta, Lehman et al. (2013) found that blooms of the harmful cyanobacteria (blue-green algae) *Microcystis aeruginosa* required a water temperature of at least 19 °C for initiation. Other drivers of HABs and the possible effects of HABs are discussed more fully in a separate section of this Chapter. The combination of large seasonal and regional water temperature variability in the SFE and substantial direct and indirect effects of water temperature for all life stages of Delta Smelt means that this variable should be considered one of the most important habitat attributes for Delta Smelt. Differences in water

temperature between regions or time periods may have important effects on the Delta Smelt population (Rose et al. 2013b).

Salinity and the Size and Location of the Low Salinity Zone

A dynamic salinity gradient from fresh water to salt water is one of the most characteristic features of an estuary (Kimmerer 2004). It originates from the mixing of fresh inland water with salty ocean water through tidal dispersion and gravitational circulation (Monismith et al. 2002). Many estuarine-dependent organisms occur in distinct salinity ranges (e.g., Kimmerer 2002a) and the extent and location of water with suitable salinities is thus an important habitat attribute for estuarine organisms. Over the time period of available monitoring data, there is no clear long-term trend in salinity levels and distributions in the estuary. Significant increases and decreases linked to changing flow patterns have been detected for various stations and months (e.g., Jassby et al. 1995, Enright and Culbertson 2009, Shellenbarger and Schoellhamer 2011, Cloern and Jassby 2012).

The brackish (oligohaline) “low salinity zone” (LSZ) is an important region for retention of organisms and particles and for nutrient cycling. In the SFE, the LSZ provides important habitat for numerous organisms including Delta Smelt (Turner and Chadwick 1972, Kimmerer 2004, Bennett 2005). In this report we define the LSZ as salinity 1-6; however, other salinity ranges have been used by others, such 0.5-6 (Kimmerer et al. 2013) or 0.5-5 (Jassby 2008).

In the SFE, the position of the LSZ is commonly expressed in terms of X2, which is the distance from the Golden Gate in km along the axis of the estuary to the salinity 2 isohaline measured near the bottom of the water column (Jassby et al. 1995). X2 represents the approximate center of the LSZ (Kimmerer et al. 2013).

X2 is an index of the physical response of the estuary to freshwater outflow from the Delta; it decreases with increasing outflow because increasing freshwater outflow prevents seawater from moving landward. The X2 index was developed two decades ago as an easily-measured, policy-relevant “habitat indicator.” Its ecological significance for multiple species and processes was established through statistical analyses of biological responses to seasonally or annually averaged X2 values (Jassby et al. 1995) and has since been reaffirmed in additional studies (e.g., Kimmerer et al. 2002a,b, 2009, 2013, Thomson et al. 2010, Mac Nally et al. 2010). There is, however, still much uncertainty regarding the causal mechanisms for the observed biological responses of biota to X2. As with all statistically derived functional relationships, biological responses to X2 do not necessarily reflect direct causal relationships and it is generally recognized that some of the causal mechanisms may not be directly linked to the size and location of the LSZ.

Most of the scientific and management attention has focused on the LSZ and X2 from late winter to early summer (hereafter “spring X2”) depending on the species of interest, but in recent years the LSZ and X2 during the fall months (“fall X2”) has also received considerable scientific and policy attention. Annual abundance indices of several estuarine fish and invertebrate species have a negative relationship with spring X2, meaning that abundance indices increase when X2 and the LSZ are more westward and Delta outflow is higher in the late winter and spring months (Jassby et al. 1995, Kimmerer 2002a, Kimmerer et al. 2009). Delta Smelt summer abundance indices have a significant relationship with prior fall X2 and fall abundance (USFWS 2008, Mount et al.

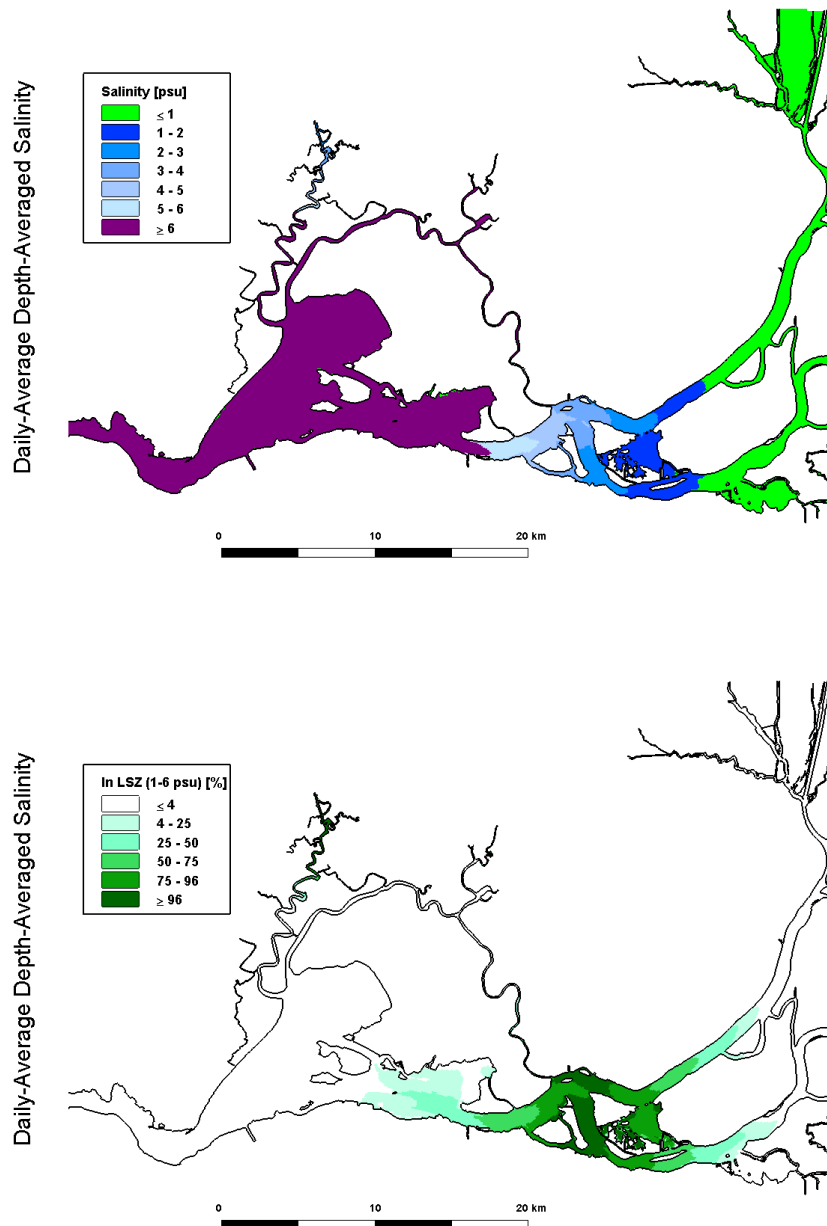
2013). Changes in spring and fall X2 have also been linked to long-term fish declines in the SFE (Thomson et al. 2010, Mac Nally et al. 2010).

The size and location of the LSZ are considered key factors determining the quantity and quality of low salinity rearing habitat available to Delta Smelt and other estuarine species. LSZ size and location are determined by the interaction of dynamic tidal and river flows with the stationary topography of the region (Reclamation 2011, 2012, Kimmerer et al. 2013). In a recent study, Kimmerer et al. (2013) used the three-dimensional hydrodynamic “UnTRIM” model which has an unstructured grid (Casulli and Zanolli 2002, 2005) to produce detailed maps of the distribution of salinity in the SFE under different outflow conditions. These maps (figure 2 in Kimmerer et al. 2013 and Fig. 18 and 19 in this report) show that under low outflow conditions typical of summer and fall months (outflow = $140 \text{ m}^3 \text{ s}^{-1}$, X2 = 85 km), the LSZ is in the western Delta confluence region, including the Sacramento and San Joaquin Rivers upstream of Chipps Island (Fig. 18), while under high outflow conditions typical of wet winter months (outflow = $1,440 \text{ m}^3 \text{ s}^{-1}$, X2 = 51 km), the LSZ is much further west in San Pablo Bay. At intermediate outflows (intermediate X2 = 74 km), it is located east of Carquinez Strait and covers Suisun Bay and parts of Suisun Marsh (Fig. 19).

Kimmerer et al. (2013) also examined the relationships between X2 and the area, average depth, and volume of the LSZ. They found that these relationships were bimodal, with the largest volumes and areas and shallowest depths at X2 values below 50 km when the LSZ is located in the large San Pablo Bay, and secondary peaks at X2 values between 60 and 75 km when the LSZ overlays the smaller Suisun Bay (Fig. 20). Area and volume were smallest and depth greatest when the LSZ was constricted in Carquinez Strait (X2~50-60 km) and in the confluence region of the Sacramento and San Joaquin Rivers (X2~80-85 km).

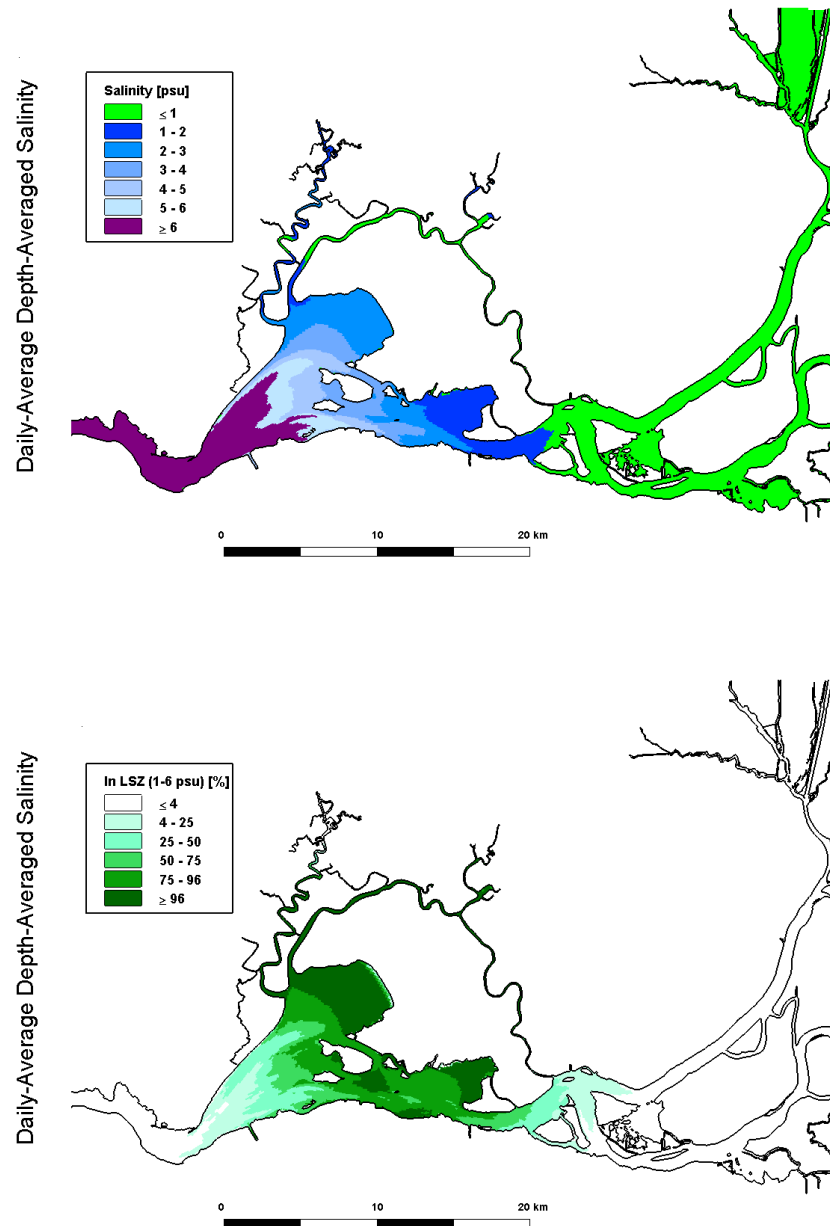
Paleosalinity investigations going back several thousand years indicate that the Delta has historically been largely fresh, while the Suisun region has alternated between brackish (oligohaline) and fresh (Ingram and Malamud-Roam 2013, Drexler et al. 2014). The LSZ and X2 likely moved according to predictable annual and interannual rhythms. Interannually, X2 was most variable in the higher-flow winter and spring months and least variable in the low-flow fall months. Seasonally X2 moved from the west in winter and spring to the east in summer and fall. CDWR (CDWR 2007) computes monthly “unimpaired” outflows which remove the effects of dam operations and water diversions. Annual X2 dynamics based on these unimpaired flows may give a sense of these historical fluctuations (Fig. 21). It is important to note, however, that unimpaired flows are not the same as historical “natural” flows because they do not take into account upstream water losses (e.g., consumption and evaporation) or physical water body alterations such as channelization, groundwater depletion, draining of wetlands, and disconnection of floodplains. The historical wetlands, floodplains, and groundwater basins would have naturally retained and released water (Whipple et al. 2012) and likely affected flows and the LSZ in different ways than today’s man-made reservoirs. Work is currently underway at UC Davis, the San Francisco Estuary Institute, and elsewhere to explore these issues, but results have not yet been published (W. Fleenor, U.C. Davis, personal communication). At this time, considerable uncertainty remains regarding the natural ranges in the timing and volume of the historical seasonal and interannual freshwater flows and how they caused the LSZ to spread out and contract across the estuary’s historical landscape. There is, however, little doubt that interannual variations in precipitation and hence river flows caused a high degree of interannual variability in the size and location of the low-salinity zone (Dettinger 2011).

Figure 18. Salinity distribution at low outflow. The upper panel shows the area of the low-salinity zone (4,262 hectares) at X2 = 85 km, when positioned mostly between Antioch and Pittsburg. Connections to Suisun Bay and Suisun Marsh are minimal. The lower panel shows the percentage of day that the low-salinity zone occupies different areas.



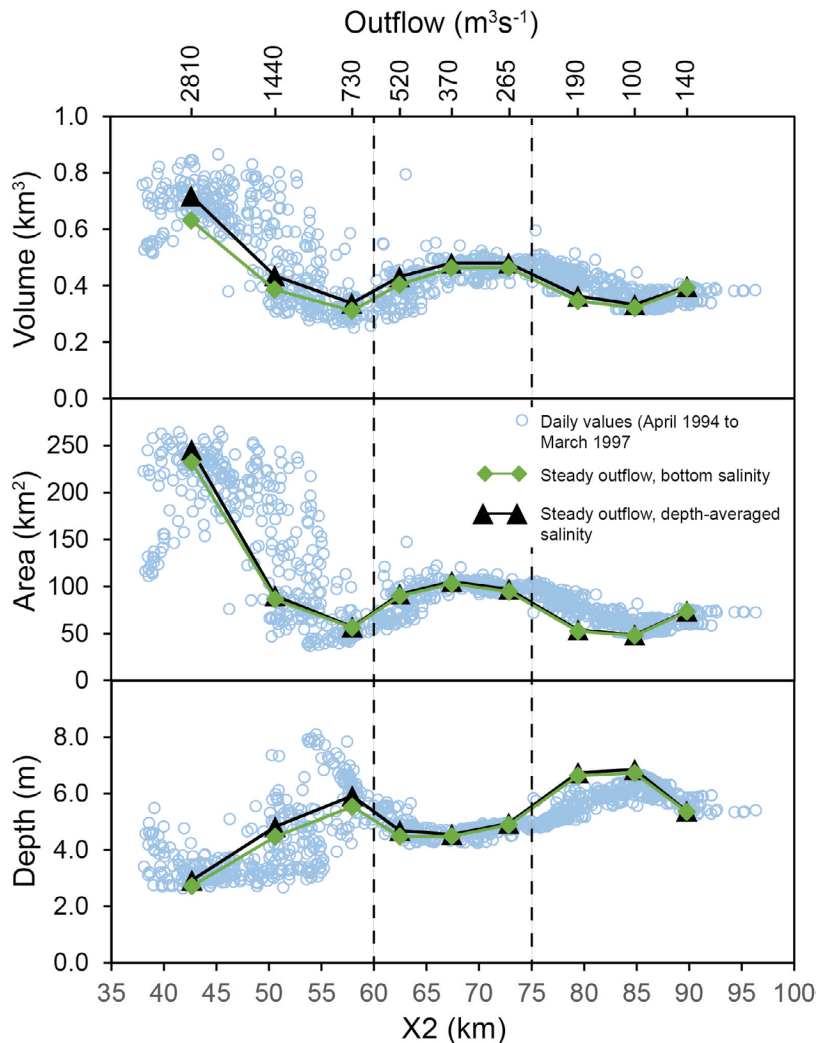
There is also no doubt that human water use and landscape alterations have changed flows into and out of the Delta and, consequently, salinity dynamics in the SFE, though changing precipitation patterns also play a role (Enright and Culberson 2009). Before the construction of today's major reservoirs, upstream water diversions coupled with the isolation of floodplains and wetlands, which had naturally stored runoff, from river channels by levees exacerbated salinity intrusions into the Delta in dry years. This was especially evident during the severe drought from

Figure 19. Salinity distribution at intermediate outflow. The upper panel shows the area of the low-salinity zone (9,140 hectares) at X2 = 74 km (at Chipps Island). The lower panel shows the percentage of day that the low-salinity zone occupies different areas.



1929 to 1934 when salinities of 2 were observed at Paintersville Bridge which is located on the Sacramento River at a distance of about 136 km from the Golden Gate (Mathew 1931). Operation of the large CVP and SWP reservoirs that were constructed after this drought has prevented such severe salinity intrusions since then and X2 has remained west of Rio Vista located on the Sacramento River 100 km upstream of the Golden Gate. Beginning with the salinity requirements in SWRCB water right decision D-1275 of 1967, salinity and the position of the LSZ have also

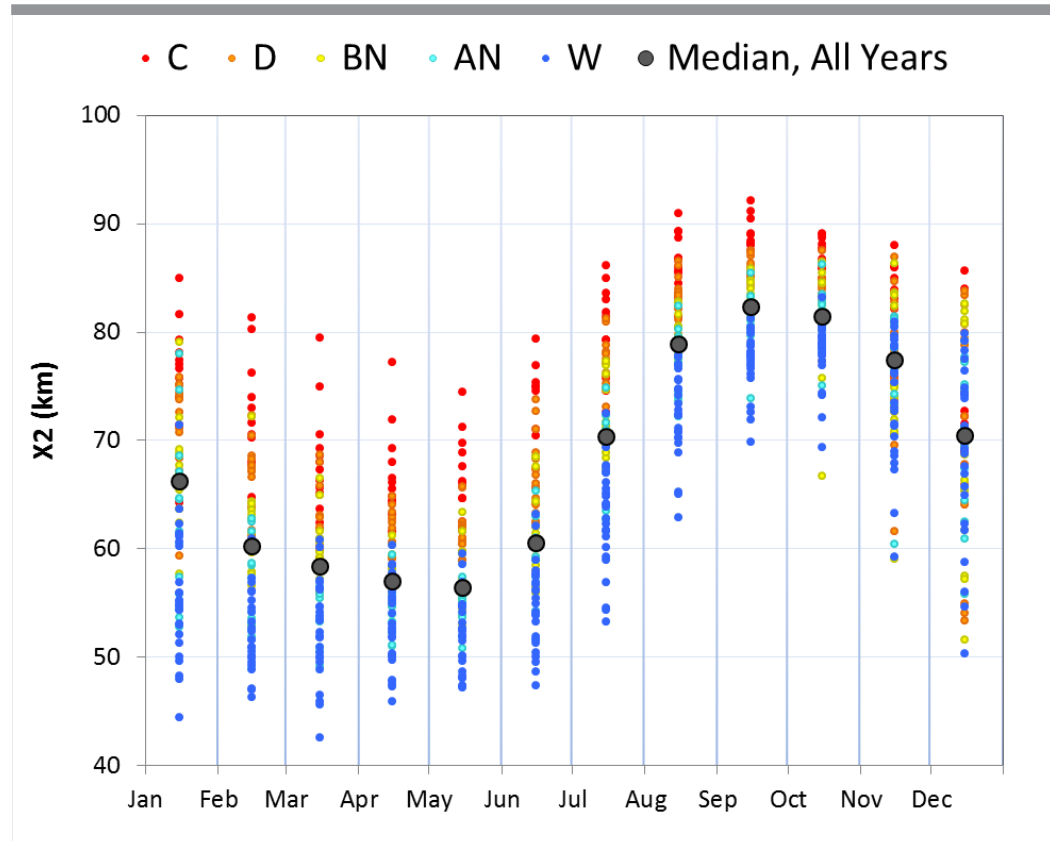
Figure 20. Modeled volume, area, and depth of the low salinity zone (salinity 0.5 to 6) at various values of X2 for 9 steady state values of outflow using bottom salinity (green diamonds) and depth-averaged salinity (black diamonds and for daily values based on variable values from April 1994 through March 1997 (blue circles) (modified from Kimmerer et al. 2013). The top axis gives the Delta outflow corresponding to the 9 steady state scenarios.



been increasingly regulated to protect “beneficial uses,” including habitat and fish protections (see Chapter 1).

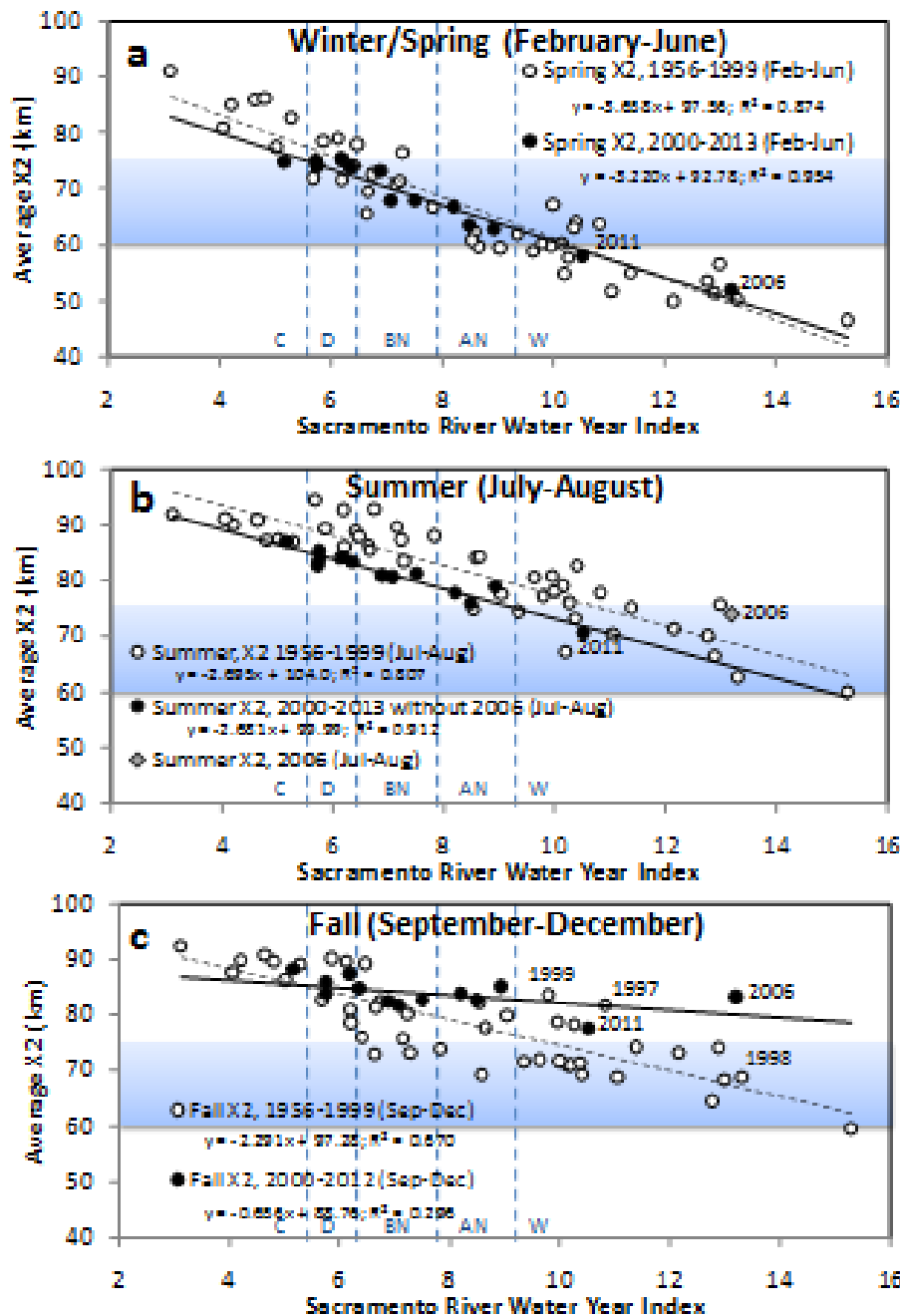
CVP and SWP water exports from the Delta began in the early 1950s with the completion of the CVP C.W. Bill Jones Pumping Plant (formerly known as the Tracy Pumping Plant) in 1951 and then increased with the completion of SWP’s Harvey O. Banks Pumping Plant in 1968. Long-term variability in the trend of Delta outflow has been reduced seasonally for the period 1921–2006, in part due to water project operations (Enright and Culberson 2009), but also due to overriding climate changes. Analyzing data from 1956–2010, Cloern and Jassby (2012) found significant increases in water exports from the Delta in all months of the year except May, but in the first half of the year, these increases in exports did not significantly affect Delta outflow. We

Figure 21. Plot of monthly X2 (km) values calculated from mean monthly unimpaired Delta outflows from 1921-2003. X2 values are categorized by water year type for the Sacramento Valley. Also shown are the median X2 values from 1921-2003 across all water year types (grey circles) C, red dots: critically dry; D, orange dots: dry; BN, yellow dots: below normal; AN, light blue dots: above normal; W, dark blue dots: wet. Water year type data from <http://cdec.water.ca.gov/cgi-progs/iodir/WSIHIST>. Unimpaired flow data from DWR 2007 (available at http://www.waterboards.ca.gov/waterrights/water_issues/programs/bay_delta/bay_delta_plan/water_quality_control_planning/docs/sjrf_sprinfo/dwr_2007a.pdf). X2 equation from Jassby et al. 2005.



show this by plotting the relationship between the Sacramento River Water Year Index, a measure of runoff, and average spring X2 (February-June) for two periods before (1956 to 1999) and after (2000-2013) the current flow and salinity requirements in SWRCB water right decision D-1641 became mandatory. The relationship appeared to remain essentially unchanged when the two time periods were compared (Fig. 22a). Cloern and Jassby (2012) further found that inflow to the Delta significantly increased in July and August, but these increases in inflow did not translate into significant increases in Delta outflow due to concurrent increases in exports during these months. Nevertheless, plots of recent data show that July and August outflows increased and the relationship between the Sacramento River Water Year Index and summer-time X2 (July-August) shifted downward in the years since the SWRCB water right decision 1641 went into effect in 2000 relative to previous years (Fig. 22b). The wet year 2006 did not fit this pattern because it had high summer X2 in spite of a high water year index. This means that with the exception of 2006, the LSZ has generally been located somewhat more westward in July and August since 2000 than from 1956 to 1999 under similar runoff conditions.

Figure 22. Plots of monthly X2 as a function of the Sacramento River Water Year Index (a measure of runoff) for the years 1956 to 1999 and 2000 to 2013 for: a, winter/spring; b, summer; and c, fall. The regression equation for each set of points is also shown. The index is calculated as: $0.4 * \text{Current April to July Runoff Forecast (in millions of acre feet, maf)} + 0.3 * \text{Current October to March Runoff in (maf)} + 0.3 * \text{Previous Water Year's Index (if the Previous Water Year's Index exceeds 10.0, then 10.0 is used)}$ (see <http://cdec.water.ca.gov/cgi-progs/iidir/WSIHIST> for further detail).



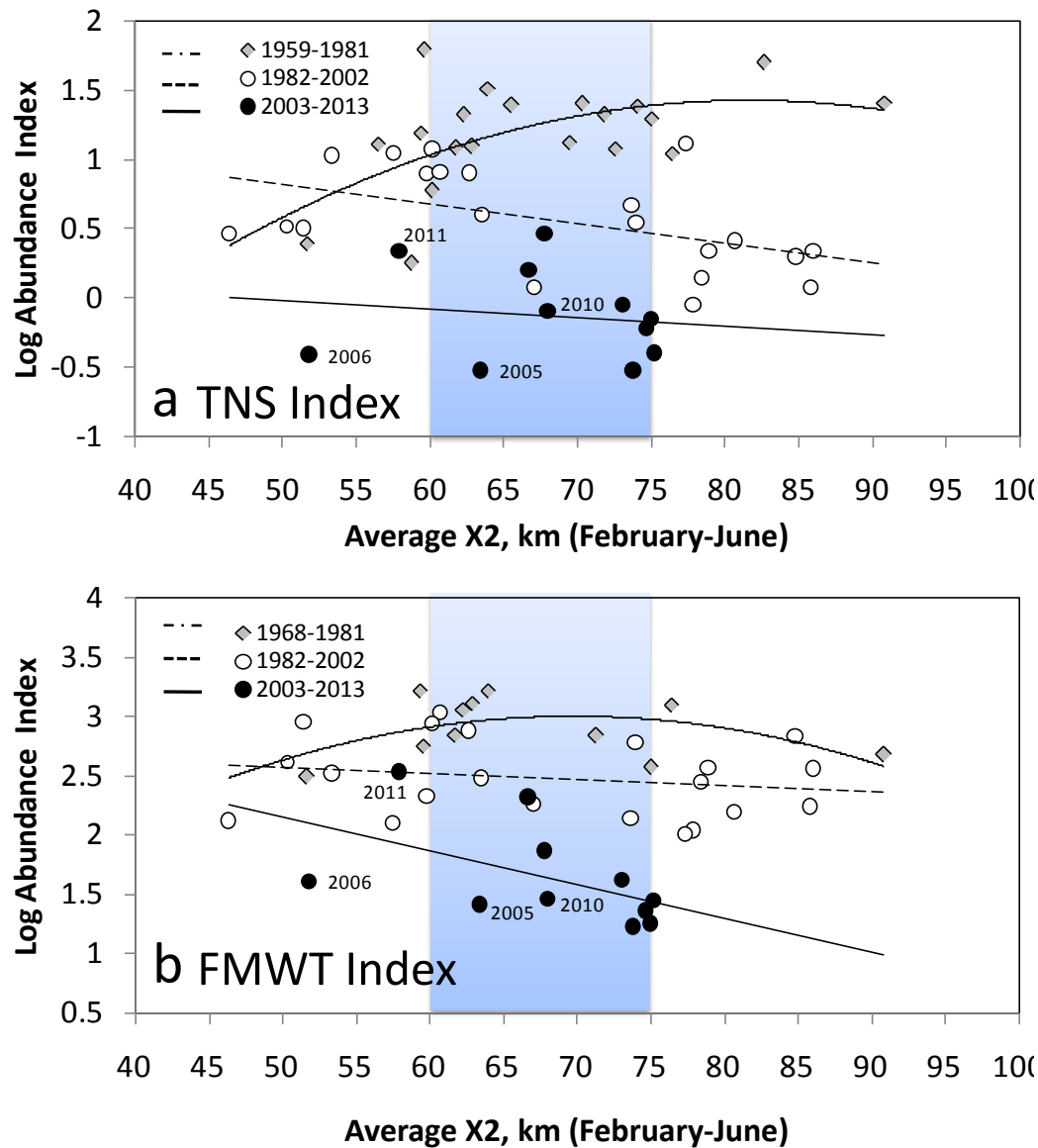
Cloern and Jassby (2012) also showed that significantly increasing exports combined with declining inflows led to significant declines in Delta outflow in each month from September to December. In plots of recent data, this led to a shallower slope of the relationship between the Sacramento River Water Year Index and fall X2 (September-December) and a more eastward LSZ location in the fall months of wetter years (below normal, above normal, and wet water year types) during 2000-2012 compared to 1956-1999, with the exception of two wet years at the end of the time series, 1997 and 1999, which fall on the 2000-2012 line (Fig. 16c, see also Feyrer et al. 2007, 2010). The areas with light blue shading in the three plots shown in Figure 16 show the range of X2 that places the LSZ over Suisun Bay and are associated with a high LSZ volume, area, and shallow LSZ depths (Kimmerer et al. 2013, Fig. 14). Fall X2 commonly fell into this range from 1956-1999 (in 18 of 44 years; Fig. 22c), but never after 2000. In 2011, the most recent wet year, fall X2 was lower than in the preceding wet years of 2006, 1997, and 1999, but still elevated relative to the majority of previous wet years. Overall, the changes in flows in the summer and fall months described by Cloern and Jassby (2012) have resulted in more muted seasonal and interannual variations in X2 and in the size and location of the LSZ in more recent years and possibly also relative to historical variability (Fig. 21).

Delta Smelt are found in the estuary at salinities up to 18 (Bennett 2005), but are most common in the in the LSZ (< 6) (Moyle et al. 1992, Sommer and Mejia 2013, Kimmerer et al. 2013). Sommer et al. (2011a) described Delta Smelt as a “diadromous species that is a seasonal reproductive migrant.” In the winter, adult Delta Smelt move upstream into fresh water for spawning. In the spring and summer, young Delta Smelt are transported or swim downstream into the LSZ (Dege and Brown 2004). Delta Smelt usually rear in low salinity habitat in the summer (Nobriga et al. 2008) and fall (Feyrer et al. 2007), although some Delta Smelt remain year-round in fresh water (Sommer et al. 2011a, Merz et al. 2011, Sommer and Mejia 2013).

The recruitment success of Longfin Smelt and age-0 Striped Bass increases linearly with more westward positions of the LSZ during spring (Jassby et al. 1995, Kimmerer 2002a). In contrast, the relationships of annual Delta Smelt indices with spring X2 are more complex because they have not been consistent over the period of record (Fig. 23). Jassby et al. (1995) found that from 1968-1991, the highest fall abundance indices for Delta Smelt coincided with intermediate values of average April-July X2 when the LSZ was positioned in Suisun Bay. Low fall abundances were, however, also observed at these intermediate X2 values. The analyses by Jassby et al. (1995) were later updated and augmented with an analysis of the relationship between Delta Smelt summer abundance and spring X2 (Kimmerer 2002a, Kimmerer et al. 2009).

We updated the analyses by Jassby et al. (1995) with more recent data and data from additional monitoring surveys to examine the hypothesis that during periods of relatively stable abundance (i.e. without step changes, Thomson et al. 2010), the abundance of different Delta Smelt life stages is related to spring outflow and the position of the LSZ as expressed by spring X2. To obtain spring X2, we first calculated mean monthly X2 values calculated from daily X2 values. We then averaged the mean monthly X2 values for February to June. This is different from the April-July period used by Jassby et al. (1995) for their Delta Smelt analyses, but similar to the spring X2 averaging period used by Kimmerer (2002a). Note that different averaging methods for calculating seasonal X2 values account for the small quantitative differences between results presented here and those of previously published analyses that used the same data, but this does not affect the overall patterns. We partitioned the data into the periods before, between, and after the 1981 and 2002 step declines in Delta Smelt abundance identified by Thomson et al. (2010). The 1981-1982 partition, but not the 2002-2003 partition, has been previously applied by Kimmerer (2002a) and Kimmerer et al. (2009).

Figure 23. Plots of the log transformed a) Delta Smelt Summer Townet Survey abundance index and b) Delta Smelt Fall Midwater Trawl Survey abundance index, in relation to monthly averaged daily X2 position from February to June. Lines are either simple linear least squares regression (lines) or quadratic regression (curves).



Kimmerer (2002a) and Kimmerer et al. (2009) found that the relationship between spring X2 and Delta Smelt juvenile abundance indices was positive before the step decline in Delta Smelt abundance that started in 1981 (Thomson et al. 2010), suggesting that historically, Delta Smelt population recruitment may have benefitted from lower outflows and a more upstream LSZ in the late winter and spring. In our analysis, we found that the relationship was perhaps more unimodal than linear (Table 1, Fig. 23a) because a model that included a quadratic spring X2 term explained more of the variation in the data than a linear model that did not, although the statistical significance of the linear model was slightly higher than that of the quadratic model because of the loss of a degree of freedom due to the additional quadratic term included in

the quadratic model. Similar to Kimmerer (2002a) and Kimmerer et al. (2009), we found that in the period after the 1981 step change and also in the period after the 2002 step change, the relationship of log-transformed summer abundance with spring X2 shifted downward and became more clearly negative than unimodal (Fig. 23a). The relationship remained statistically significant at the $P < 0.05$ level in the period after the 1981 step decline, but is no longer statistically significant after 2001. Similarly, the relationship is also not significant across the entire 52-year time series (Table 1).

Kimmerer et al. (2009) found a non-significant and essentially flat relationship between spring X2 and the entire log-transformed sub-adult abundance time series for Delta Smelt; this remains the case when data from the five most recent years is included in the analysis (Table 1). Similar to Jassby et al. (1995), we found a weakly unimodal relationship between spring X2 and log-transformed Delta Smelt subadult abundance indices before the first step change, but this relationship was not statistically significant at the $P < 0.05$ level (Table 1, Fig. 23b). Similar to juvenile abundance, the relationship of log-transformed subadult abundance with spring X2 shifted downward in the periods after each of the two step changes and became more negative than unimodal (Fig. 23b), but again these relationships were not statistically significant at the $P < 0.05$ level (Table 1).

Taken together, these findings are generally consistent with previous conclusions that moderate hydrological conditions in the late winter and spring and a large LSZ located in the Suisun region can be beneficial to Delta Smelt population abundance (Jassby et al. 1995). Historically, this may have been the case for several life stages. At present, however, juvenile and subadult Delta Smelt seem to barely respond to spring X2. As Jassby et al. (1995) point out, this does not mean that there is no longer an effect of spring X2 on juveniles and subadults; the spring X2 effect may just be masked or weakened by changes in other habitat attributes. The relationships between these life stages and spring X2 clearly underwent downward shifts after each step decline. These persistent downward shifts indicate that occasional years with beneficial spring X2 conditions continue to have a positive effect on Delta Smelt, but they are by themselves not enough to overcome the depressed abundance levels and recover the population.

The downward shifts and changes in shape of the spring X2-Delta Smelt abundance index relationships (Fig. 23) also illustrate the difficulties of determining and understanding functional responses of biota to dynamic physical habitat attributes in changing ecosystems; the species of interest, other habitat attributes, and their interactions may all change as much or more than the habitat attribute under consideration. Further, these changes may not always be gradual, but can take the form of sudden step changes that may be associated with system-wide regime shifts (Davis et al. 2010, Baxter et al. 2010, Cloern and Jassby 2012). Moreover, prior conditions and prior abundance may also influence outcomes. In Chapter 9 of this report we give a relatively simple example of additional multivariate analyses aimed at exploring the effects of hydrology and prior abundance on the abundance and recruitment of Delta Smelt larvae. More sophisticated multivariate life cycle modeling that greatly exceeds the scope of this report is needed to account for these simultaneous changes and interactive effects on all life stages.

Changes in the size, location, and dynamics of the LSZ likely also interact in complex ways with other changes, such as changes in sediment and nutrient loadings and resulting turbidity and nutrient dynamics and their effects on Delta Smelt and the food web. For example, LSZ position affects recruitment of the invasive clam *Potamocorbula amurensis*, which may in turn affect phytoplankton and zooplankton biomass, size, and production (Thompson 2005, Winder and Jassby 2011), and has likely affected fish-X2 relationships (Kimmerer et al. 2002a).

Table 1. Summary of relationships between log-transformed annual abundance indices for four Delta Smelt life stages (response variable) and spring X2 (February-June, see text): Survey: see description of monitoring surveys in Chapter 3; Regression: least squares linear or quadratic regression; n, number of observations (years); P, statistical significance level for the model; R², coefficient of determination; adjusted R², R² adjusted for the number of predictor terms in the regression model. Bold font indicates statistically significant relationships.

Life Stage	Season	Survey	Period	Regression	n	P	R ²	Adjusted R ²
Juvenile	Summer	TNS	1959-2013	Linear	52	0.614	0.005	
Juvenile	Summer	TNS	1959-1981	Linear	20	0.033	0.230	0.187
Juvenile	Summer	TNS	1959-1981	Quadratic	20	0.052	0.295	0.212
Juvenile	Summer	TNS	1982-2002	Linear	21	0.023	0.243	0.203
Juvenile	Summer	TNS	2002-2013	Linear	11	0.689	0.019	
Subadult	Fall	FMWT	1968-2013	Linear	43	0.290	0.027	0.003
Subadult	Fall	FMWT	1968-1981	Linear	11	0.699	0.017	
Subadult	Fall	FMWT	1968-1981	Quadratic	11	0.295	0.263	0.079
Subadult	Fall	FMWT	1982-2002	Linear	21	0.394	0.038	
Subadult	Fall	FMWT	2002-2013	Linear	11	0.107	0.263	0.181

Ongoing studies coordinated by the IEP as part of the POD and FLASH studies focus on the processes that link physics, chemistry, and biology in the LSZ and its habitat value for Delta Smelt and other native and non-native species. Similar to Monismith et al. (2002), preliminary results indicate that the strength of physical mixing (lateral dispersion) in the LSZ changes with the volume of freshwater outflow, underscoring the importance of variable hydrodynamics on not just the location of the LSZ, but how ecological services (nutrient mixing, organism dispersal) are influenced by variable estuarine outflow (Monismith, U.C. Berkeley, personal communication).

Turbidity

In this report, turbidity is considered an environmental driver that interacts with other environmental drivers, resulting in habitat attributes that directly affect Delta Smelt responses, rather than a stand-alone habitat attribute. Clearly, studies have shown that distribution of Delta Smelt is correlated with turbidity (e.g., Feyrer et al. 2007, Nobriga et al. 2008, Grimaldo et al. 2009, Sommer and Mejia 2013). In the conceptual model we chose to incorporate turbidity as a modifier of several important linkages between environmental drivers and habitat attributes that are important to Delta Smelt, primarily food visibility for small larvae and predation risk for all life stages. If we had incorporated turbidity as a habitat attribute and, for example, predation risk

was discussed separately from turbidity, there would have been a great deal of overlapping text between the two sections because turbidity interacts with the presence of predators to determine predation risk. Our approach is not ideal but should reduce redundant text and contribute to clarity of presentation. Nonetheless, we recognize that turbidity by itself could reasonably be considered as a habitat attribute. For example, it is possible that Delta Smelt experience stress in low turbidity habitat, which would in turn affect survival (likely through predation) but also in other direct ways such as lower growth and reduced egg production. However, we do not have evidence at this point to support that hypothesis.

In addition to salinity gradients, estuaries often have turbidity gradients. Turbidity is an optical property of water, which is the loss of transparency due to scattering of light by suspended particles. Typically, the upper reaches of estuaries have areas with high levels of suspended particles known as “estuarine turbidity maxima.” In many estuaries, these areas are located in or near the low salinity zone and are associated with higher numbers and enhanced growth for larvae of some species (Sirois and Dodson 2000a, b, Shoji et al. 2005). In the SFE, turbidity is largely determined by the amount of suspended inorganic sediment in the water (Cloern 1987, Ganju et al. 2007, Schoellhamer et al. 2012), although organic components can also play a role (USGS 2008). Sediment particles are constantly deposited, eroded, and resuspended, and are transported into, within, and out of the estuary. The amount of sediment that is suspended in the water column depends on the available hydrodynamic energy, which determines transport capacity, and on the supply of erodible sediment in the estuary and suspended sediments from the watershed.

In the upper SFE there are two main physical processes controlling turbidity. Suspended sediment is transported from the tributary watersheds into the system during high flows associated with winter and spring storm runoff (Schoellhamer et al. 2012). The first large storm of the rainy season often carries the highest concentrations of suspended sediment. Some portion of the transported sediment moves through the system to San Pablo and San Francisco Bay and the remainder is stored within the system as bottom sediment. During the remainder of the year, turbidity is primarily caused by interactions of this stored sediment with other environmental drivers (Schoellhamer et al. 2012). Water moving with the tides can resuspend fine sediments because of turbulence resulting from interactions between the bottom and water moving at high tidal velocities. At a larger scale, irregularities in the bottom topography may define geographic regions of greater turbulence and greater turbidity. In the upper estuary, such regions occur at a large bathymetric sill between Carquinez Strait and Suisun Bay and at another location within Suisun Bay (Schoellhamer 2001). Sediments may also be resuspended by turbulence related to wind waves. This process is mainly limited to areas with fine sediments on relatively shallow shoals where wind wave turbulence reaches the bottom. This process is most important in the shallows of Suisun, Grizzly, and Honker Bays and Liberty Island (Ruhl and Schoellhamer 2004, Warner et al. 2004, Morgan-King and Schoellhamer 2013). Thus, turbidity at any particular location is the result of several environmental drivers, including hydrology (transport from the watershed) and weather (wind and precipitation) interacting with the physical configuration of the upper SFE. Further, annual variation in these factors may have important effects. For example, during a drought there is little transport of suspended sediment and the same wind patterns during the summer may result in less turbidity than would occur after a wet year because less sediment was stored as benthic sediment during the winter. There is also evidence of longer term changes in turbidity (Schoellhamer et al. 2011, Hestir et al. 2013), along with regional differences.

In addition to the inorganic component of turbidity, organic matter (e.g., phytoplankton) also contributes to both suspended solids and the sediment load on the bed that is re-suspended with

wind and wave action (McGann et al. 2013). In the SFE, phytoplankton concentration varies spatially, seasonally, and on an inter-annual scale (Cloern et al. 1985, Jassby 2008, Cloern and Jassby 2012), and is controlled by multiple factors, including benthic grazing, climate, river inflows (Jassby et al. 2002), and nutrient dynamics (Glibert et al. 2011, Parker et al. 2012, Dugdale et al. 2013), which in turn are likely to affect the organic component of turbidity. Phytoplankton dynamics are discussed in detail in the ‘Food and Feeding’ section (below), but it is important to note here that plankton concentration comprises part of the SFE turbidity and is significant as it relates to productivity at higher trophic levels.

Among the geographic regions of the upper SFE, the Suisun region is one of the most turbid, when the system is not being influenced by storm flows. This results from strong turbulent hydrodynamics in the Suisun region caused by strongly interacting tidal and riverine flows, bathymetric complexity, and high wind speeds, which create waves that resuspend erodible benthic sediment in the large and open shallow bays of the Suisun region. The North Delta, especially the large open expanse of Liberty Island (flooded since 1998) and the adjacent Cache Slough region are also relatively turbid. Recent evidence suggests that Liberty Island acts as a sediment sink in the winter and a sediment source for the surrounding Cache Slough complex in the summer (Morgan-King and Schoellhamer 2013).

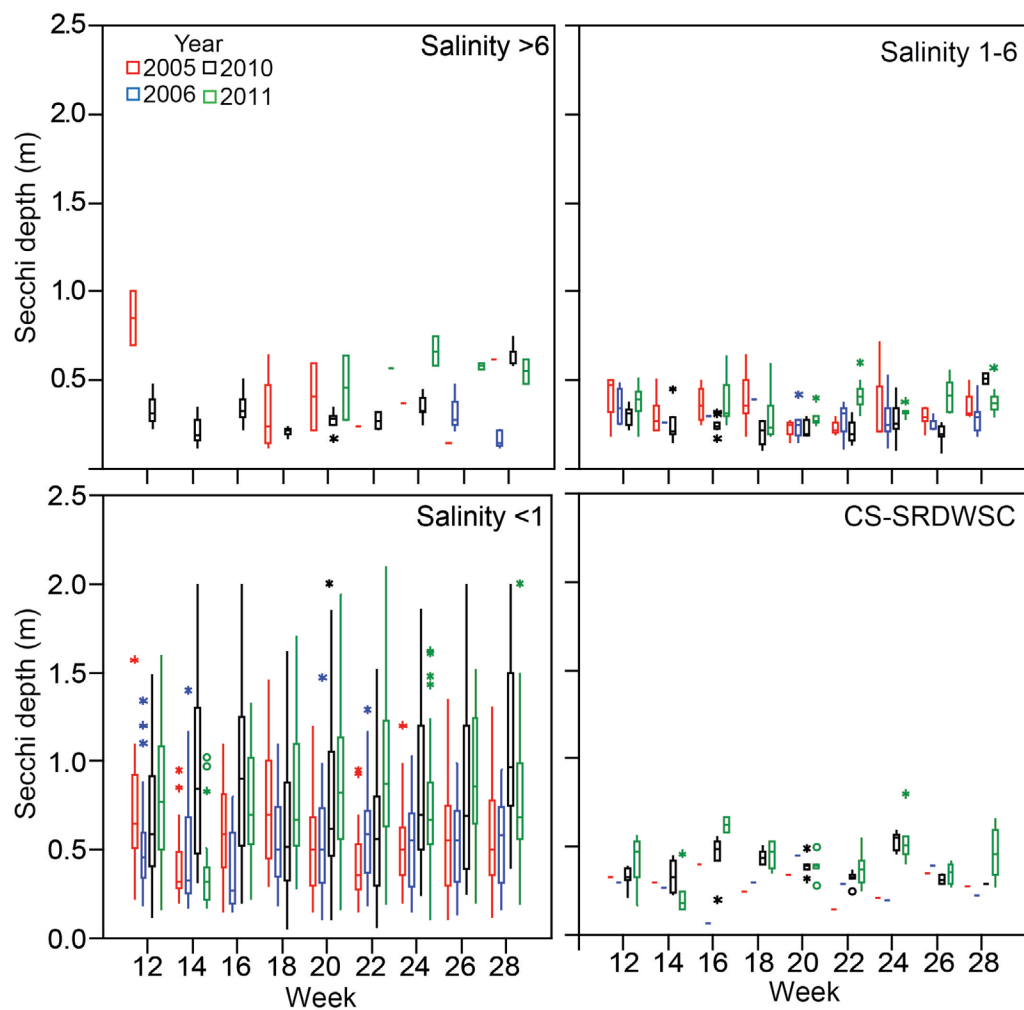
Turbidity is usually lower in the channels of the confluence of the Sacramento and San Joaquin Rivers compared to the Suisun region and North Delta region. Turbidity dynamics in the deep channels of the river confluence are driven more by riverine and tidal processes while high wind and associated sediment resuspension has little if any effect (Ruhl and Schoellhamer 2004). Turbidity is generally lowest in the south Delta (Nobriga et al. 2008). This may in part be due to sediment trapping by large, dense beds of *Egeria densa*, an invasive species of submerged aquatic vegetation (Hestir 2010). In winter/spring during the comparison years the highest Secchi disc depths (lowest turbidity) were found in the freshwater regions of the estuary (< 1 salinity), except for the Cache Slough region in the north Delta which was as turbid as the saltier regions of the estuary (Fig. 24).

There is strong evidence for an initial increase followed by a more recent long-term decline in sediment transport into the upper estuary, likely due to anthropogenic activities during the last century and a half (Schoellhamer et al. 2013, Wright and Schoellhamer 2004). Schoellhamer et al. (2013) presented a conceptual model of the effects of human activities on the sediment supplies in the SFE with four successive regimes:

1. The natural state.
2. Increasing sediment supplies due to mining, deforestation, agricultural expansion, etc.
3. Decreasing sediment supply due to sediment flushing during high flow events and sediment trapping behind dams and dikes.
4. A new altered state of low sediment supplies. The pulse of increased sediment inputs during and after the California gold rush and the more recent decline in these inputs is apparent in isotopic data from sediment cores taken in the estuary (Drexler et al. 2014).

The recent declines in sediment supplies have led to a long-term increase in water clarity in the upper Estuary (Jassby et al. 2002, Feyrer et al. 2007, Jassby 2008). Jassby et al. (2002) documented a 50% decrease in total suspended-solids concentration (TSS, a laboratory measurement of total suspended solids), approximated by suspended sediment concentration

Figure 24. Secchi depth data collected during the 20 mm Survey. Surveys are conducted biweekly March–July. See Chapter 3: Data Analyses for explanation of boxplots.



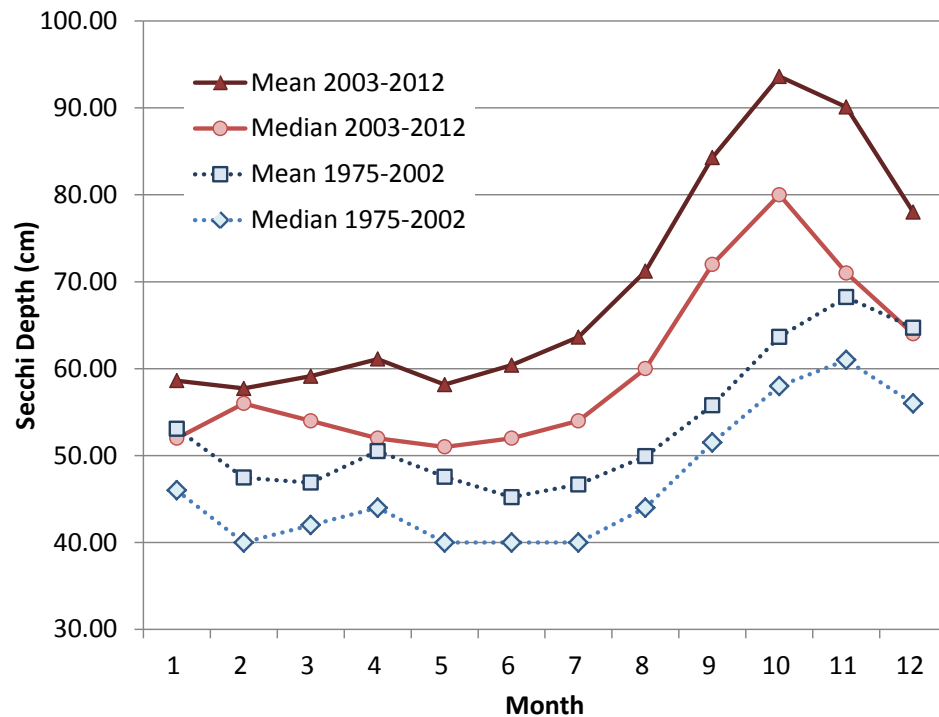
(SSC, an optical measurement done in the field for these data) in the Delta from 1975–1995. Jassby (2008) found that the downward trend continued in the decade after 1995, although at a slower pace than over the entire 1975–2005. From 1975–2005, there were significant declines in SSC of up to 6% per year at 8 of 10 Delta stations (Jassby 2008). Jassby et al. (2005) showed that TSS concentrations in the north Delta dropped sharply toward the end of the 1982–1983 El Niño–Southern Oscillation (ENSO) event, which was associated with extremely high outflows, and did not recover afterward. This step decrease after 1983 has been corroborated by further trend analyses of TSS (Hestir 2013). Following the El Niño event of 1997–1998, there was a 36% step decrease in SSC in San Francisco Bay as the threshold from transport to supply regulation was crossed as an anthropogenic erodible sediment pool was depleted (Schoellhamer 2011). Sediment trapping by dense beds of *Egeria densa* may be further reducing available sediment in the Delta (Hestir 2010). While other anthropogenic factors may have also contributed to long-term changes in turbidity (e.g., export operations; Arthur et al. 1996), quantitative analyses of the effects of these factors have not been conducted.

Before the step decline in SSC and the onset of the pelagic organism decline in the late 1990s and early 2000s (i.e. the “pre-POD” period), water transparency (roughly the opposite of turbidity) measured with a Secchi disc at all IEP EMP stations was usually highest in November and lowest in June (Fig. 25). From 2003-2012 (i.e. the “POD” period), average water transparency was not only higher (by an average of 16 cm Secchi depth) than in the previous period, but the annual dynamics also shifted forward by a month, to greatest transparency (i.e. lowest turbidity) in October and lowest transparency in May. The greatest differences in average water transparency between the pre-POD and POD periods occurred in September and October (28 and 30 cm difference between monthly averages, respectively) and the smallest differences in January-May (10 cm). While the EMP has collected turbidity data (nephelometric turbidity (NTU) measurements) since 1975, long-term fish monitoring surveys have traditionally collected Secchi disc data and only in recent years have incorporated turbidity. Therefore, Secchi disc data are presented in the majority of this report when relating Delta Smelt abundance to water clarity conditions.

Multiple field and modeling studies have established the association between elevated turbidity and the occurrence and abundance of Delta Smelt. The abundance of larval/postlarval Delta Smelt larvae was well explained by salinity and Secchi depth, a proxy for turbidity (Kimmerer et al. 2009). Sommer and Mejia (2013) and Nobriga et al. (2008) found that late-larval and juvenile Delta Smelt are strongly associated with turbid water, a pattern that continues through fall (Feyrer et al. 2007). Long term declines in turbidity may also be a key reason that juvenile Delta Smelt now rarely occur in the south Delta during summer (Nobriga et al. 2008). Thomson et al. (2010) found that turbidity (water clarity) was the only significant predictor variable that was shared by three of the four POD species; all other significant predictor variables were unique to each species. Grimaldo et al. (2009) found that the occurrence of adult Delta Smelt at the fish salvage facilities was linked, in part, with high turbidity associated with winter “first flush” events. Turbidity may also serve as a behavioral cue for small-scale (lateral and vertical movements in the water column) and larger-scale (migratory) Delta Smelt movements (Bennett and Burau 2014).

Delta Smelt are visual feeders, and feed primarily between dawn and dusk (Hobbs et al. 2006, Slater and Baxter 2014). As for all visual feeders, visual range and prey density determine feeding success of Delta Smelt. Visual range depends on size, contrast and mobility of the prey, retinal sensitivity and eye size of the visual feeder, and on the optical habitat attributes such as light scattering, absorption, and intensity (Aksnes and Giske 1993). Optical habitat attributes are affected by turbidity from suspended organic particles, such as algae and detritus, and inorganic particles, such as sand and silt. Somewhat counterintuitively, some level of turbidity appears important to the feeding success of larval Delta Smelt. Baskerville-Bridges et al. (2004a) conducted laboratory experiments in which alga densities (0, 0.5×10^6 cell/mL, and 2×10^6 cell/mL or 1, 3, and 11 NTU) and light levels (range tested: $0.01 \mu\text{moles/s} \times \text{m}^2$, $0.3 \mu\text{moles/s} \times \text{m}^2$, $1.9 \mu\text{moles/s} \times \text{m}^2$) were manipulated and first-feeding success of larval Delta Smelt was quantified. They found that maximum feeding response occurred at the highest alga concentrations and light levels tested. In a subsequent experiment, when algae were removed entirely, the feeding response was very low. The addition of algae or some other form of suspended particle is standard practice for successfully rearing Delta Smelt larvae in culture facilities (Mager et al. 2004, Baskerville-Bridges et al. 2005, Werner et al. 2010b, Lindberg et al. 2013). Presumably the suspended particles provide a background of stationary particles that helps the larvae detect moving prey. Sufficient turbidity also appears to be important to reduce overall environmental stress and increase survival of larval Delta Smelt (Lindberg et al. 2013). Thus, it seems likely that turbidity is important to the feeding success and survival of larval Delta

Figure 25. Average and median Secchi depth in cm from monthly sampling at IEP Environmental Monitoring Program stations. Data are shown for the time period up to the pelagic organism decline (1975-2002) and after the decline (2003-2012).



Smelt in the wild. Recent research on juvenile Delta Smelt, however, suggests that influence of turbidity on feeding success may vary across life stages and field conditions. Hasenbein et al. (2013) exposed juveniles to varying turbidities (5-250 NTU) and observed a negative relationship between turbidity and feeding rates, with a marked decline in feeding at 250 NTU. However, feeding rates were highest at 12 NTU and stable in the 12-120 NTU turbidity range, which is likely within the range experienced by juvenile Delta Smelt in typical summer conditions in the Delta. Turbidity values of 250 NTU are generally not observed during the summer; therefore, the typical summer turbidity range in the Delta likely does not limit juvenile feeding success.

In addition to its effects on feeding, turbidity may also reduce predation risk. Based on the general recognition that fish assemblages are often partitioned between turbid-water and clear-water assemblages (Rodríguez and Lewis 1997, Whitfield 1999, Quist et al. 2004), and that turbidity can influence the predation rate on turbid-adapted fishes (Rodríguez and Lewis 1997, Gregory and Levings 1998, Quist et al. 2004), it has generally been assumed that juvenile and adult Delta Smelt are closely associated with turbidity in order to minimize their risk of predation in their generally open-water habitat. There may also be complex interactions between feeding and predation risk that are mediated by turbidity. Recent laboratory work has shown that in light (as opposed to dark) conditions, the vertical distribution of larval Delta Smelt shifts upward in the water column when turbidity is increased from clear (< 2 NTU) to 24 NTU (L. Sullivan, San Francisco State University, unpublished data), suggesting that larval Delta Smelt may use turbidity to safely forage in surface waters that may be more food-rich. Interestingly, when a predator cue (water, after containing juvenile Striped Bass for 1 hr) is added to clear water, the distribution of larval Delta Smelt becomes bimodal, with increased densities near the surface and

closer to the bottom (L. Sullivan, San Francisco State University, unpublished data). Thus, while laboratory studies have demonstrated that larvae have improved feeding success at higher (but not too high, see above) turbidities, in natural settings, turbidity and predation risk may interact (e.g., Miner and Stein 1996) to affect Delta Smelt habitat choice and feeding success.

Turbidity may also be a migration cue for Delta Smelt. A recent field study investigated behavioral responses of Delta Smelt to winter “first flush” events in the Sacramento and San Joaquin Rivers near their confluence (W. Bennett, U.C. Davis, unpublished data). A first flush is defined as an increase in flow and turbidity associated with the onset of winter rain. This study found lateral turbidity gradients that changed with the tides and before and after first flush events and coincided with lateral Delta Smelt movements toward the channel during flood tides and toward the shoreline during ebb tides. The researchers concluded that this behavior likely facilitates maintaining channel position or moving upriver and cross-channel gradients in water turbidity may act as a behavioral cue. Feyrer et al. (2013) also found small-scale lateral and vertical gradients in turbidity in the lower Sacramento River just prior to a winter-time first flush event. In their study, turbidity and salinity were highest in the lower half of the water column and during flood tides and lowest during ebb tides in the center of the channel in the upper half of the water column. This coincided with observations of Delta Smelt which were more frequently caught throughout the water column during flood tides than during ebb tides when they were observed only in the lower half of the water column and sides of the channel. Feyrer et al. (2013) concluded that Delta Smelt may actively move in the water column by keying in on turbidity and salinity gradients or because of the physics underlying them.

Entrainment and Transport

The egg, larval, and juvenile stages of estuarine fishes and invertebrates along with small and weakly swimming adult stages are subject to involuntary transport (advection) by riverine and tidal flows. Entrainment is a specific case of involuntary transport. It refers to situations when altered flows misdirect and transport fish and other organisms in directions in which they would not normally travel or where they will encounter unfavorable conditions and increased risk of mortality. In this report, we use the term entrainment to specifically refer to the incidental removal of fishes and other organisms in water diverted from the estuary, primarily by CVP and SWP export pumping (Arthur et al. 1996, Grimaldo et al. 2009, Castillo et al. 2012).

Ultimately, watershed hydrology determines how much water can flow into and through the Delta; however, water flows into, within, and out of the Delta are manipulated in many ways. Water is: routed through and around artificial channels, gates, and barriers; stored in and released from reservoirs; discharged from agricultural and urban drains; and diverted with large and small pumps. Perhaps the greatest flow alterations in the Delta have taken place in Old and Middle Rivers (collectively referred to as “OMR”) in the central Delta (Fig. 2). Historically, these river channels were part of the tidal distributary channel network of the San Joaquin River (Whipple et al. 2012). Today, they are a central component of the CVP and SWP water conveyance system through the Delta. Water from the Sacramento River in the north now flows through the northern Delta (down Georgiana Slough, through Three-Mile Slough and around Sherman Island) and eastern Delta (via the artificial “Delta cross-channel” and down the forks of the Mokelumne River) to OMR in the central Delta, then to the SWP and CVP. The SWP and CVP pumps are capable of pumping water at rates sufficient to cause the loss of ebb tide flows and to cause negative net flows (the advective component of flow after removal of the diffusive tidal flow component) through OMR toward the pumps (see Grimaldo et al. 2009), thus greatly altering regional hydrodynamics and water quality (Monsen et al. 2007). Under these conditions, fish

and other aquatic species in the Delta may be transported toward the pumps (Arthur et al 1996, Brown et al. 1996, Moyle et al. 2010), may swim toward the pumps if they are behaviorally inclined to follow net flow (Grimaldo et al. 2009), or may move toward the pumps if they are employing tidal surfing behavior (Sommer et al. 2011).

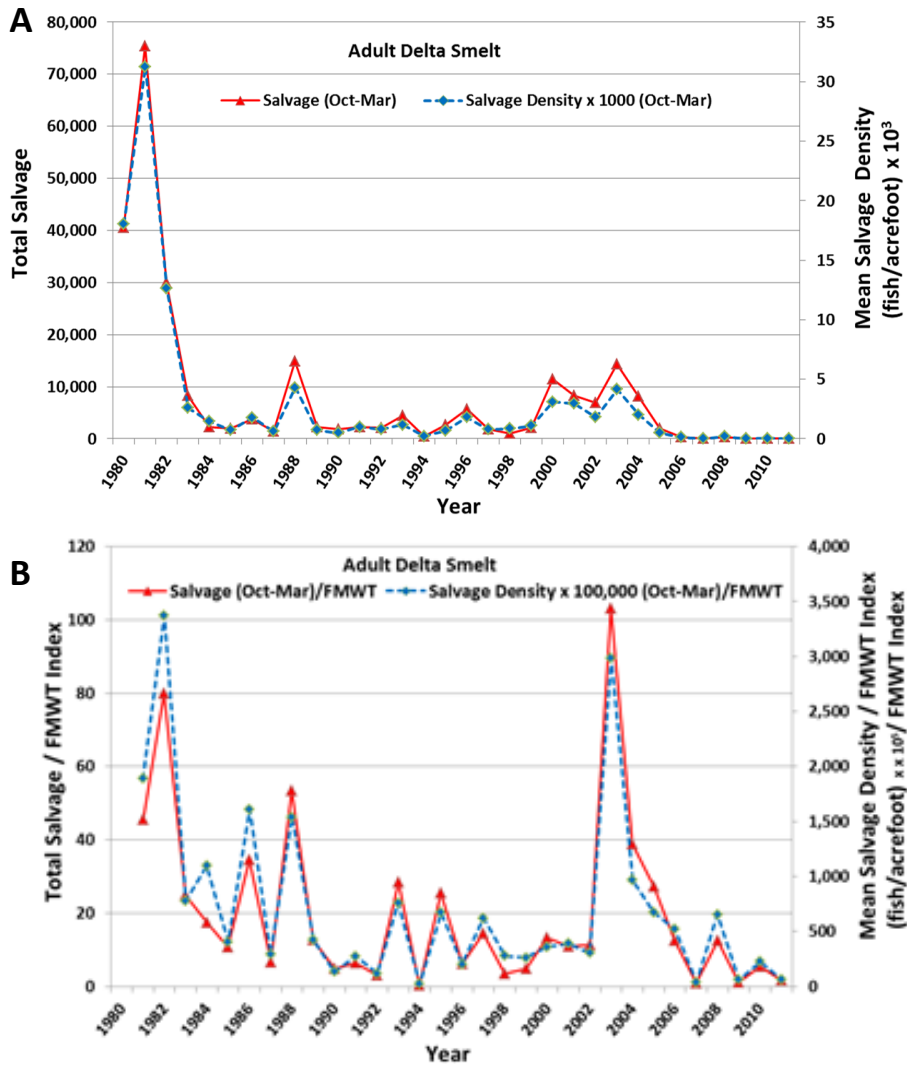
The SWP and CVP have large fish salvage facilities intended to reduce fish loss from the system due to entrainment - the State Skinner Fish Protective Facility (SFPP) and the federal Tracy Fish Collection Facility (TFCF). The SFPP and TFCF are located at the intakes to the State and federal export pumps on Old River in the southwestern Delta (Fig. 2). Both facilities have fish directing louvers and collecting screens that are used to capture and collect fish before they reach the pumps. The “salvaged” fish are then trucked to and released back into the western Delta. A variable fraction of these fish survive the capture, handling, trucking and release process (Miranda et al. 2010a,b, Aasen 2013, Afentoulis et al. 2013, Morinaka 2013a). The number of salvaged fish is monitored and reported as an index of SWP and CVP salvage and entrainment losses (Morinaka 2013b, more information and data available at <http://www.dfg.ca.gov/delta/apps/salvage/Default.aspx>). The SWP differs from the CVP in having a regulating reservoir, Clifton Court Forebay that temporarily stores water from Old River to improve operations of the SWP pumps. A change in the location of SWP water diversion from Italian Slough to Old River through CCF in 1969 may have led to a substantial increase in pre-screen losses at the SWP (Heubach ca. 1973, Kano 1990).

Fish have been salvaged since 1958 at the TFCF and since 1968 at SFPP, and the quality of the historical salvage data has improved over time. Delta Smelt salvage data is available since May 1979 for both the TFCF and SFPP (<ftp://ftp.delta.dfg.ca.gov/salvage/>). Juveniles less than 30 mm fork length are less efficiently captured in the salvage facilities (Kimmerer 2008, Morinaka 2013a) and Delta Smelt larvae less than 20 mm fork length have not been reported in the salvage data, although entrainment losses of Delta Smelt larvae have been calculated to be substantial under some circumstances (Kimmerer 2008). Development of a quantitative monitoring methodology for entrained Delta Smelt larvae at the CVP and SWP was recognized as necessary to refine triggers for protective actions (USFWS 2008). The current methodology for monitoring larval Delta Smelt at the TFCF and SFPP has provided presence-absence data since 2008 (Morinaka 2013b). Improved methods for sampling fish larvae have been reported at the TFCF (Reyes et al. 2012).

Despite these caveats salvage of Delta Smelt has been used as a rough index of entrainment losses. Delta Smelt salvage data since 1993 is considered more reliable than salvage data from earlier years. The difference in reliability is due to a change in count frequency from twice a day (0100 and 1300) from July 1978 to July 1992 to every two hours thereafter and an increased focus on proper identification of Delta Smelt following its State and federal listings as threatened (Morinaka 2013b).

Similar to the TNS and FMWT results for Delta Smelt, Delta Smelt salvage has declined dramatically since the beginning of this time series (Fig. 26). This is similar to trends for Chinook Salmon and Striped Bass salvage (not shown), but opposite to trends for Largemouth Bass and Bluegill (*Lepomis macrochirus*) salvage (Fig. 27), two species that may be benefiting from conditions resulting from an apparent ecological regime shift (Baxter et al. 2010). The ratio of Delta Smelt salvage divided by the previous year’s FMWT index has been used as a simple indicator of relative interannual entrainment losses. For adult (December-March) salvage, this ratio has been variable over time, but particularly high in the first three years of this time series (1980-1982, with 1982 being a wet year) and again during the beginning of a series of drought years in 1989 and in the fairly dry “POD” years 2003-2005 (Fig. 26). Current management

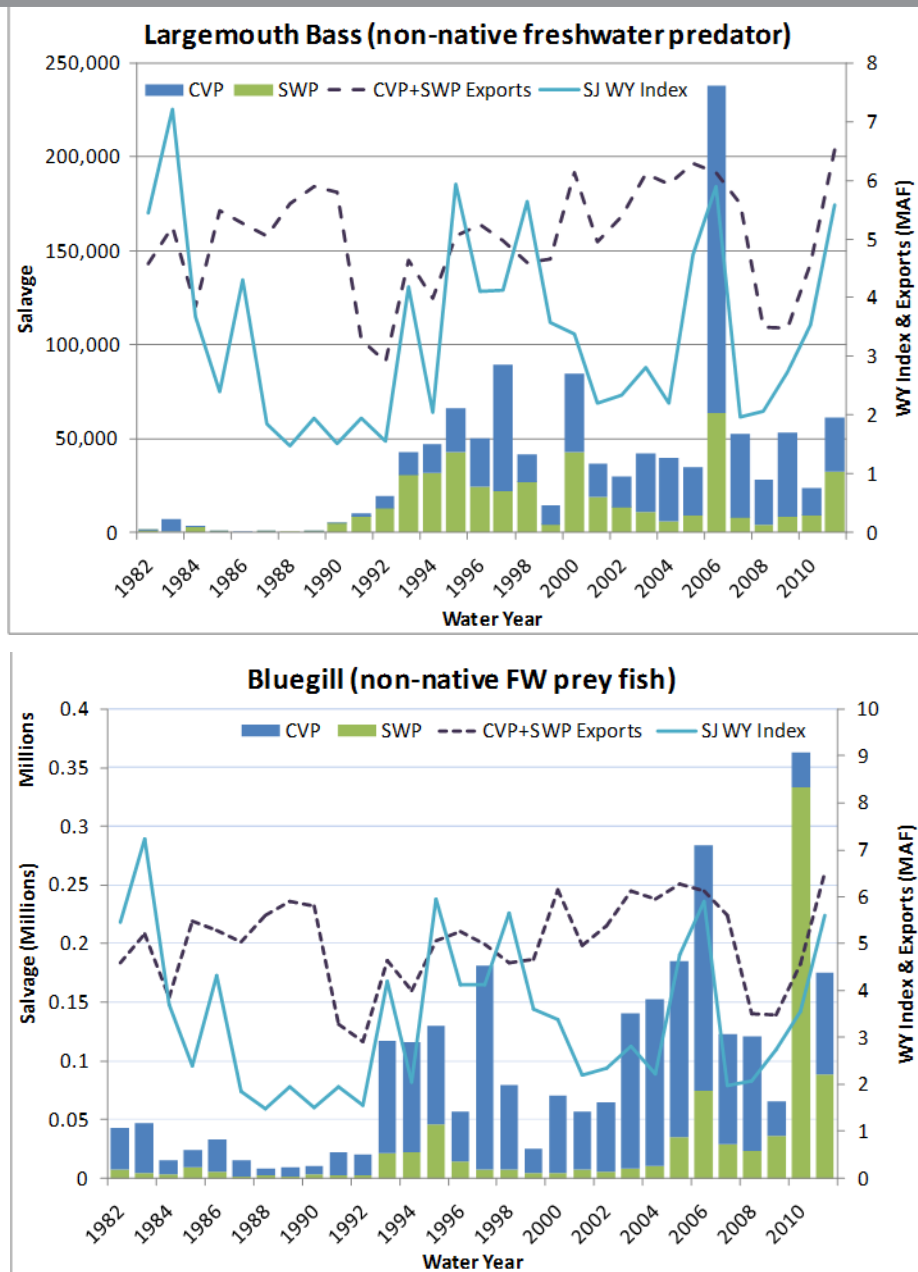
Figure 26. A: Total reported October-March salvage for adult Delta Smelt and the corresponding mean salvage density based on the total monthly salvage and water volume exported by CVP and SWP. **B:** Both salvage and salvage density standardized by the Fall Midwater Trawl (FMWT) index for the previous year.



provisions to protect Delta Smelt (USFWS 2008) are aimed at keeping this ratio at no more than the average during the period of 2006-2008.

Delta Smelt were salvaged nearly year-round in the beginning of this time series. Delta Smelt salvage since 2005 has occurred mostly from January through June, with substantial decline of May-June juvenile salvage since the mid 2000s (Fig. 28) and virtual disappearance of older juveniles from July-August salvage since the year 2000 (Fig. 29) and subadults since the early 1990s (Fig. 30). These patterns coincide with the near disappearance of Delta Smelt from the central and southern Delta in the summer (Nobriga et al 2008) and in the south Delta in the fall (Feyrer et al. 2007). Historically, adult and larval-juvenile (> 20 mm FL) Delta Smelt salvaged were not separately recorded and reported, but based on length measurements of a subset of salvaged fish, adults were predominantly salvaged between December and March or April

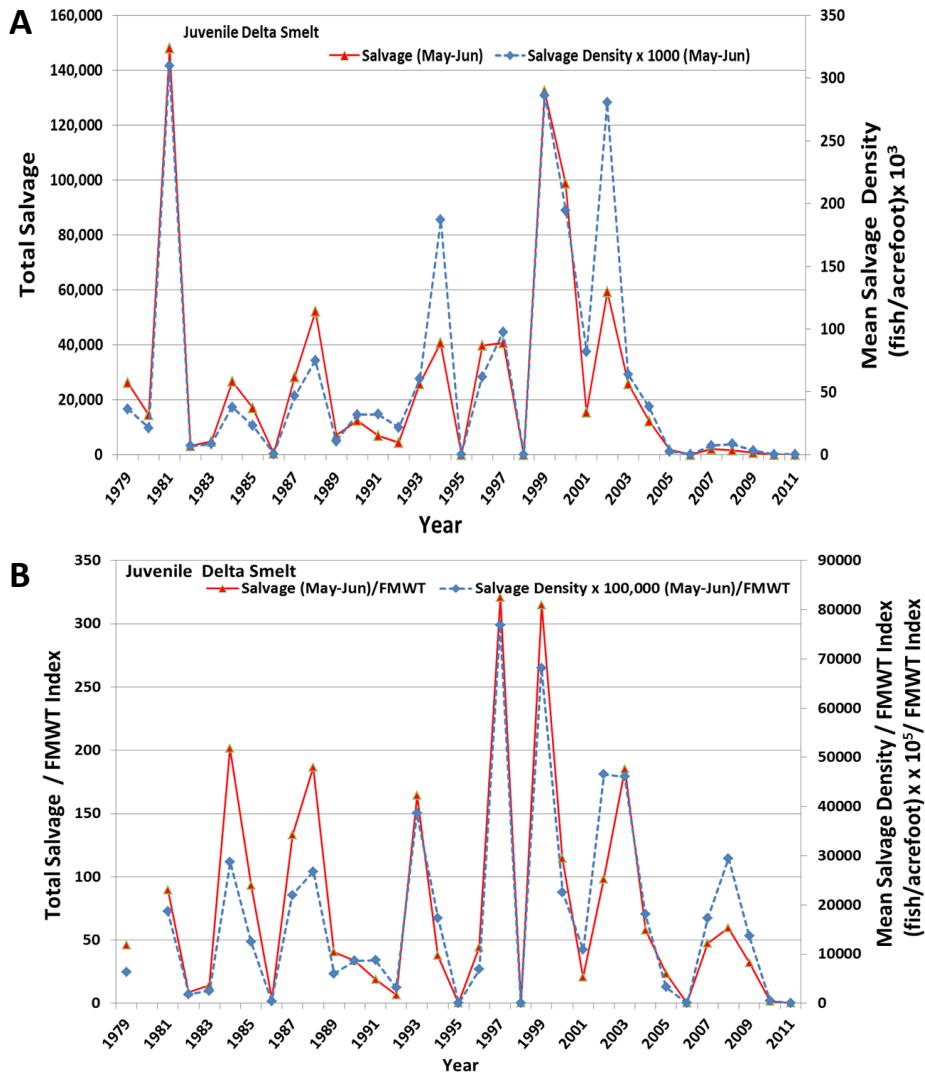
Figure 27. Annual time series of Largemouth Bass (top graph) and Bluegill (bottom graph) salvage at the CVP (blue bars) and SWP (green bars) fish protection facilities. Also shown are the annual San Joaquin Valley Water Year Index (SJWY Index) (blue line) and the combined annual (water year) SWP and CVP water export volume (purple line; MAF, million acre feet).



and most Delta Smelt larvae and juveniles were historically salvaged from April through July (Kimmerer 2008, Grimaldo et al. 2009).

Salvage data are routinely used to track and manage incidental take at the SWP and CVP and have been used to explore factors affecting entrainment and to estimate the effects of the SWP and CVP on Delta fishes. For example, Grimaldo et al. (2009) found that OMR flows and

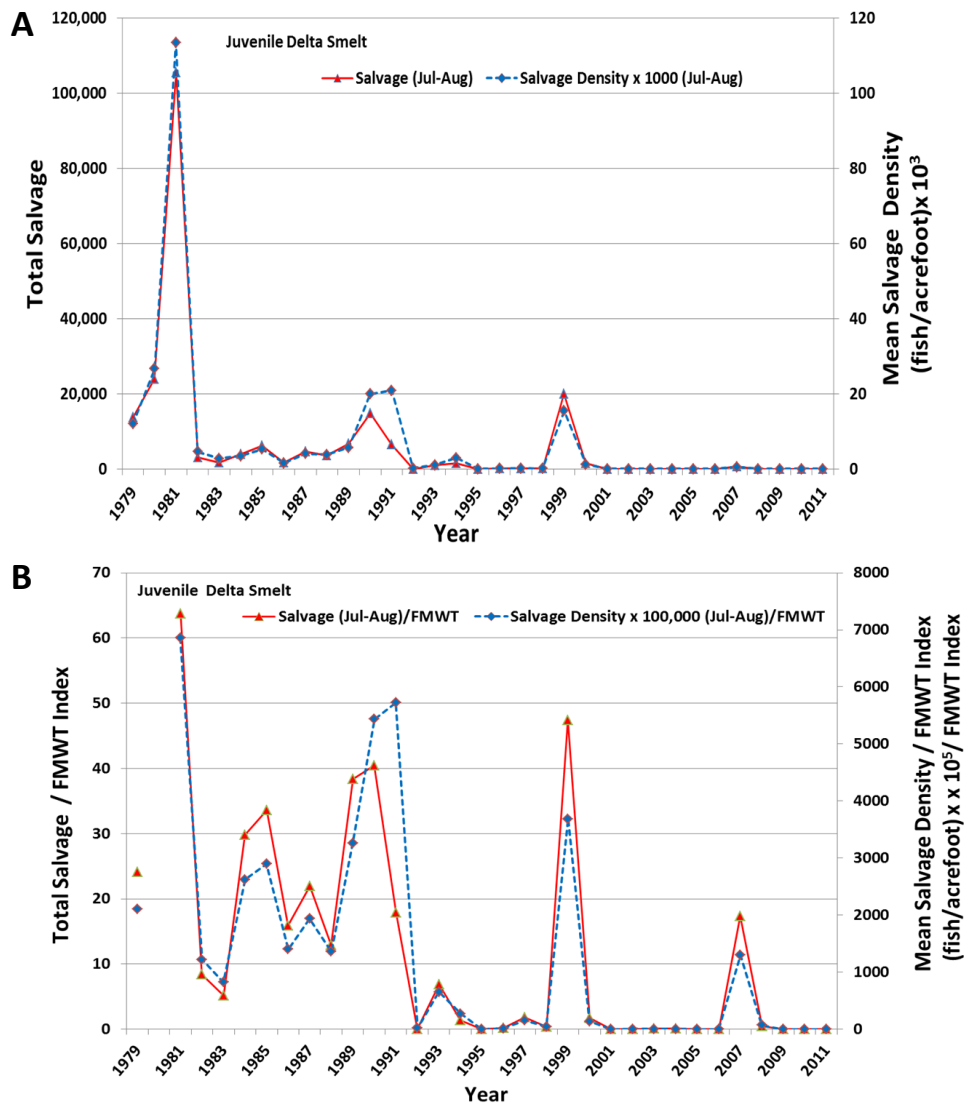
Figure 28. A: Total reported May-June salvage for juvenile Delta Smelt and the corresponding mean salvage density based on the total monthly salvage and water volume exported by CVP and SWP. **B:** Both salvage and salvage density standardized by the Fall Midwater Trawl (FMWT) index for the previous year.



turbidity account for much of the intra-annual variability in the salvage for juvenile and adult Delta Smelt.

It is important to remember, however, that salvage is only a very rough indicator of Delta Smelt entrainment. Based on mark-recapture experiments using cultured Delta Smelt, salvage was a very small fraction of total entrainment losses because of major pre-screen losses and low fish facility efficiency (Castillo et al. 2012). Experimental studies with cultured Chinook Salmon, Steelhead (*Oncorhynchus mykiss*), and Striped Bass have consistently shown that a large fraction (63% to 100%) of the entrained fish are not salvaged due to pre-screen losses and capture inefficiencies at the SWP fish facility (Brown et al. 1996, Gingras 1997, Clark et al. 2009). In addition, a mark-recapture test using field collected juvenile Chinook Salmon in CCF resulted in only 0.32% of the fish being salvaged (see Castillo et al. 2012). Pre-screen losses are generally

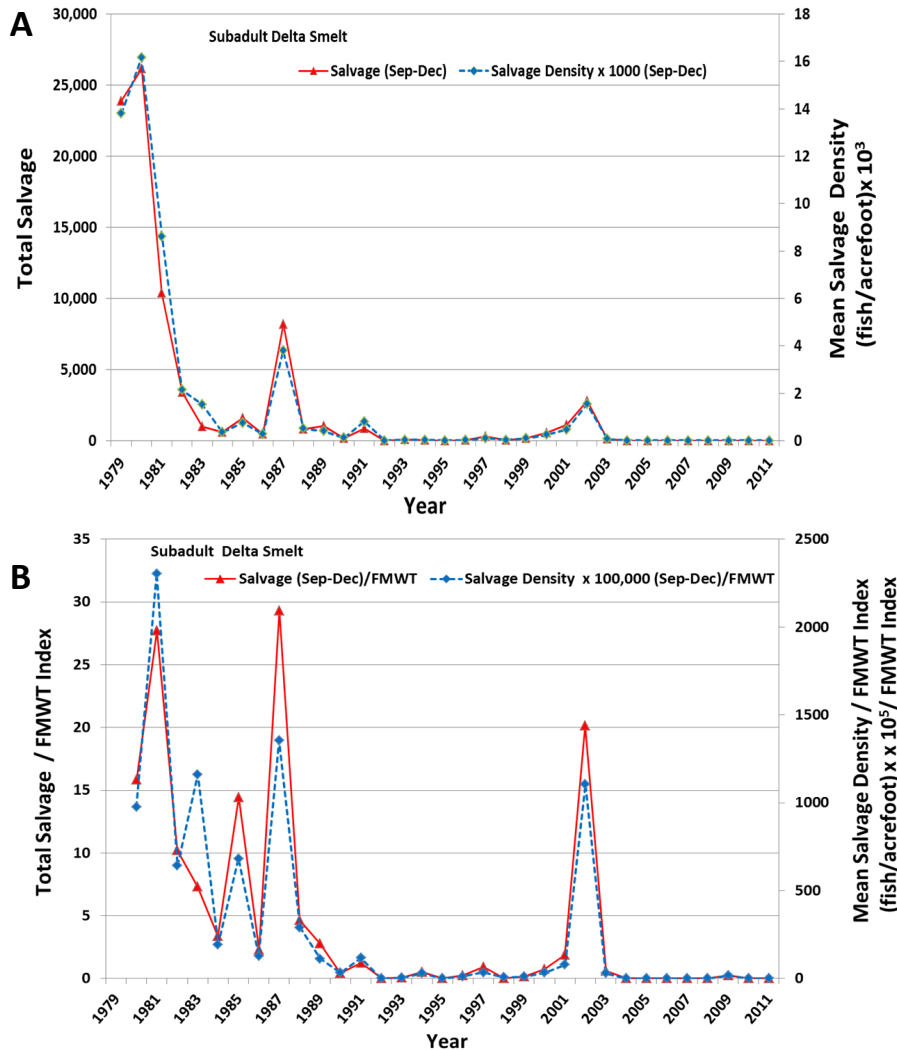
Figure 29. A: Total reported July-August salvage for juvenile Delta Smelt and the corresponding mean salvage density based on the total monthly salvage and water volume exported by CVP and SWP. **B:** Both salvage and salvage density standardized by the Fall Midwater Trawl (FMWT) index for the previous year.



attributed to increased predation and other unfavorable habitat conditions near the SWP and CVP pumps (e.g. Kano 1990, Brown et al. 1996, Gringas and McGee 1997, Clark et al. 2009, Castillo et al. 2012). For juvenile and adult Delta Smelt, Castillo et al. (2012) found that 94.3% to 100% of marked fish groups released into the SWP CCF were never salvaged and that salvage of marked fish decreased as the distance from the release site to SFPF increased and as residence time in CCF increased.

Large pre-screen losses of Delta Smelt in CCF are likely due to increased predation, especially when Delta Smelt spend a relatively long time in the reservoir in the presence of predators. MacWilliams and Gross (2013) used a particle tracking model to estimate residence time of passive particles, which can be considered surrogates for weakly swimming Delta Smelt. In 21-

Figure 30. A: Total reported July-August salvage for sub-adult Delta Smelt and the corresponding mean salvage density based on the total monthly salvage and water volume exported by CVP and SWP. **B:** Both salvage and salvage density standardized by the Fall Midwater Trawl (FMWT) index for the same year.



day simulations with the three-dimensional (3D) hydrodynamic model UnTRIM, MacWilliams and Gross (2013) found that the time particles spend in CCF varies greatly with wind and SWP operating conditions. They estimated transit times for passive particles (e.g., larval Delta Smelt) from the radial gates to the SFPF of 4.3 days under moderate export conditions (average daily SWP export rate of 2,351 cfs) and 9.1 days under low export conditions (689 cfs). The CVP does not have a regulating reservoir in the Delta and CVP pre-screen losses in the river channels leading to the TFCF are likely different from SWP pre-screen losses, but there are no studies quantifying these differences.

In general, Delta Smelt salvage increases with increasing net OMR flow reversal (i.e., more negative net OMR flows) and when turbidity exceeds 10-12 NTU (USFWS 2008, Grimaldo et al. 2009). Based on field and salvage data, Kimmerer (2008) calculated that from near 0% to 25% of larval-juvenile and 0% to 50% of the adult Delta Smelt population can be entrained at

the CVP and SWP annually, in years with periods of high exports. Although methods to calculate proportional loss estimates have since been debated (Kimmerer 2011, Miller 2011), a number of modeling efforts suggest that entrainment losses can adversely affect the Delta Smelt population (Kimmerer 2011, Maunder and Deriso 2011, Rose et al. 2013a, b).

High winter entrainment of Delta Smelt has been suspected as a contributing cause of both the early 1980s (Moyle et al. 1992) and the POD-era declines of Delta Smelt (Baxter et al. 2010). In addition to entraining Delta Smelt, water exports may likely also have indirect effects on Delta Smelt by contributing to adverse alterations of their habitat, for example, by changing Delta outflow and the size and location of the LSZ (see above) or by entraining food organisms (Jassby et al. 2002). The magnitude of these indirect effects of water exports on the Delta Smelt population has, however, not yet been quantified.

Delta Smelt are most vulnerable to entrainment when, as adults, they move from brackish water into fresh water, or as larvae, when they move from freshwater in the southern and central Delta into the brackish water of Suisun Bay. While some Delta Smelt live year-round in fresh water far from the CVP and SWP, most rear in the low-salinity regions of the estuary, also at a relatively safe distance from the SWP and CVP pumps. The timing, direction and geographic extent of the spawning movements of adult Delta Smelt affect their entrainment risk (Sweetnam 1999, Sommer et al. 2011a). Unlike the years prior to the 1990s, when high salvage of adult and juvenile Delta Smelt occurred at high, intermediate or low export levels, the risk of entrainment for fish that move into the central and south Delta is currently highest when net Delta outflow is at intermediate levels (~20,000 to 75,000 cfs) and OMR flow is more negative than -5000 cfs (USFWS 2008). In contrast, when adult Delta Smelt move upstream to the Sacramento River and into the Cache Slough region or do not move upstream at all, entrainment risk is appreciably lower. As explained later in this report, adult Delta Smelt may not move very far upstream during extreme wet years because the region of low salinity habitat becomes fresh and suitable for spawning (e.g., Suisun Bay or Napa River).

Transport mechanisms are most relevant to larval fishes, which have comparatively little ability to swim or otherwise affect their location. Dispersal from hatching areas to favorable nursery areas with sufficient food and low predation is generally considered one of the most important factors affecting the mortality of fish larvae (Hjort 1914, Hunter 1980, Anderson 1988, Leggett and Deblois 1994). Larvae of various smelt species exhibit diverse behaviors to reach and maintain favorable position within estuaries (Laprise and Dodson 1989, Bennett et al. 2002). Such nursery areas provide increased feeding success, growth rates and survival (Laprise and Dodson 1989, Sirois and Dodson 2000a, b, Peterson 2003, Hobbs et al. 2006). Until recently it was thought that larval Delta Smelt were transported from upstream hatching areas to downstream rearing areas, particularly the shallow productive waters of Suisun Bay (Moyle et al. 1992). Spring distributions of post-larval and small juvenile Delta Smelt support this view (Dege and Brown 2004). The distributions of these life stages were centered upstream of X2, but approached X2 as fish aged. These distributions could be displaced, and shifted up or down estuary with outflow and the shifting position of X2 (Dege and Brown 2004). More recent evidence suggests, however, that the timing and extent of downstream movement by young Delta Smelt is more variable than previously thought and that some may remain in upstream areas throughout the year (Sommer et al. 2011a, Contreras et al. 2011, Merz et al. 2011, Sommer and Mejia 2013).

Adult spawning site selection affects the potential importance of transport and entrainment to larvae. The risk of larval entrainment appears to increase with proximity to the south Delta export pumps (Kimmerer and Nobriga 2008). Larvae hatching in the San Joaquin River channel from

Big Break upstream to the city of Stockton and tidal channels south of these locations, can be affected by several interacting processes. Flows from the San Joaquin, Calaveras, Mokelumne and Cosumnes rivers act to cause net downstream flow, whereas export levels at the south Delta pumps act to reverse net flows in the lower San Joaquin River. High export rates can create negative flows past Jersey Point on the lower San Joaquin River (“Qwest,” see Dayflow documentation: <http://www.water.ca.gov/dayflow/output/Output.cfm>) and negative OMR flows (Fig. 31). Since the onset of the POD in 2002, positive average monthly OMR flows have only occurred in 9 months (6%) during the wettest years and average monthly Qwest flows were negative in just under half (49%) of all months (Fig. 31). Tidal conditions can also act in favor of downstream transport or entrainment depending upon whether the Delta is filling or draining in response to the fortnightly spring-neap cycle (Arthur et al. 1996). The combination of high export and low inflow can create very asymmetrical tides in OMR that covary with net negative flow resulting in stronger floods compared to ebbs, which may also contribute to fish entrainment.

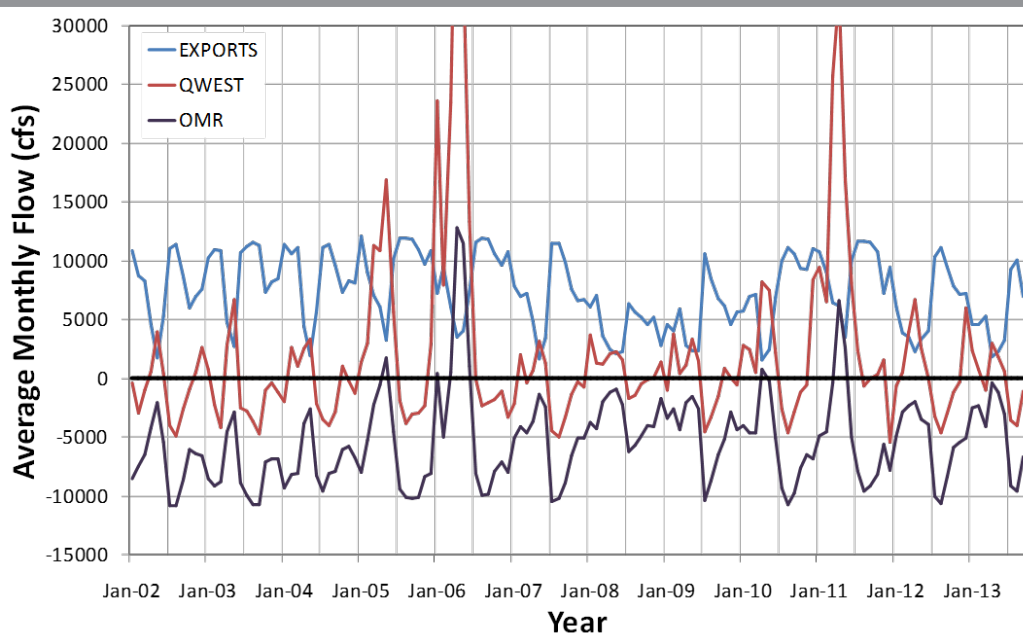
Predation Risk

Small planktivorous fishes, including osmerids, serve as prey for larger fishes, birds and mammals. As prey, they have the critically important trophic function of transferring energy to higher trophic levels. Consequently, they are often subjected to intense predation pressure (Gleason and Bengsten 1996, Jung and Houde 2004, Hallfredsson and Pedersen 2009). Prey fish populations compensate for high mortality through high reproductive rates, including strategies such as repeat spawning by individuals and rapid maturation (Winemiller and Rose 1992, Rose et al. 2001). Predation can be a dominant source of mortality for fish larvae, along with starvation and dispersion to inhospitable habitats (Hjort 1914, Hunter 1980, Anderson 1988, Leggett and Deblois 1994).

Since predation is a natural part of functional aquatic ecosystems, predators are likely not responsible for long-term declines in populations of prey fishes, such as Delta Smelt, without some additional sources of stress that disrupt the predator-prey relationship (Nobriga et al. 2013). Predation may become an issue when established predator-prey relationships are disrupted by habitat change or species invasions (Kitchell et al. 1994). As described in Chapter 1, the SFE has been extensively modified (Nichols et al. 1986, Cohen and Carlton 1998, Whipple et al. 2012, Cloern and Jassby 2012) so disrupted relationships between predators and prey are certainly plausible. For example, prey may be more susceptible to predation if they are weakened by disease, contaminants, poor water quality, or starvation. Similarly, the creation of more “ambush habitat” (e.g. structures, weed beds), declines in turbidity levels, or the introduction of a novel piscivore also may dramatically shift the existing predator-prey relationships (Ferrari et al. 2014). All of these changes have in fact taken place in the estuary, especially in the central and south Delta (Feyrer and Healey 2003, Nobriga et al. 2005, Brown and Michniuk 2007).

Virtually all fishes of appropriate size will feed on fish larvae when available and predation is theoretically maximal when larvae lengths are 10% of the length of the predator (Paradis et al. 1996). Presently, Mississippi Silverside (*Menidia audens*) is thought to be the most substantial predator of Delta Smelt larvae (Bennett and Moyle 1996, Bennett 2005, Baerwald et al. 2012). Juvenile and adult Delta Smelt have also been reported from the stomach contents of Striped Bass (Stevens 1963, Stevens 1966, Thomas 1967), White Catfish (*Ictalurus catus*) and Black Crappie (*Pomoxis nigromaculatus*) (Turner 1966a,b). Stevens (1963) reported “freshwater smelt” to be a very common component of Striped Bass stomach contents (nearly 100% frequency of occurrence in fifteen stomachs with food) on the Sacramento River near Paintersville Bridge

Figure 31. Flows in cubic feet per second for Qwest (positive values are seaward), Old and Middle River (OMR) (positive values are seaward), and total exports for years since the beginning of the pelagic organism decline (POD). Maximum monthly average Qwest values in 2006 and 2011 omitted to improve graph display, values are 50,086 cfs in April 2006, 35,477 in May 2006, and 32,884 cfs in April 2011 (Qwest and Export data are from 2013 Dayflow, OMR data are from USGS).



during March-April 1963. During 1963-1964, Stevens (1966) also evaluated seasonal variation in the diets of juvenile Striped Bass throughout the Delta; only age 2 and age 3 Striped Bass contained more than trace amounts of Delta Smelt. The highest reported predation on Delta Smelt was 8% of the age 2 Striped Bass diet by volume during the summer. Thomas (1967) reported on spatial variation in Striped Bass diet composition based on collections throughout the SFE and the Sacramento River above tidal influence. The field collections occurred from 1957-1961; data were collected on age 1 and older Striped Bass but data were only summarized as all ages combined. Delta Smelt accounted for 8% of the spring diet composition and about 16% of the summer diet composition in the Delta.

Several authors tested hypotheses about inverse correlations between estimates of adult and juvenile Striped Bass abundance and indices of Delta Smelt relative abundance or survival (Mac Nally et al. 2010, Thomson et al. 2010, Maunder and Deriso 2011, Miller et al. 2012, Nobriga et al. 2013). None of these statistical analyses has found evidence for the expected inverse correlation. Modeling studies indicate that Striped Bass predation rates on prey are affected by temperature and predator abundance (mostly the latter; Loboschewsky et al. 2012). However, the links between prey abundance and predator abundance vary from strong to non-existent, depending on the strength of their interaction in the food web (Essington and Hansson 2004). It is not currently known if changes in juvenile Striped Bass abundance correspond with changes in population-level or per capita Striped Bass predation rate on Delta Smelt (Nobriga et al. 2013).

Recent modeling efforts show that Delta Smelt declines are negatively associated with metrics assumed to reflect the abundance of predators in the estuary (Maunder and Deriso 2011, Miller

et al. 2012). These metrics are composites of the relative abundance of Mississippi Silverside, Largemouth Bass and other centrarchids; species that are potential predators of concern because of their increasing abundance (Fig. 27; Bennett and Moyle 1996, Brown and Michniuk 2007, Thomson et al. 2010), and because of inverse correlations between Largemouth Bass abundance and Delta Smelt abundance (Nobriga and Feyrer 2007, Thomson et al. 2010, Maunder and Deriso 2011). These correlations could represent predation on Delta Smelt by Largemouth Bass, or alternatively, the very different responses of the two species to changing habitat within the Delta (Moyle and Bennett 2008). Current data suggest that Largemouth Bass populations have expanded as the SAV *Egeria densa* has expanded and have come to dominate parts of the Delta (Brown and Michniuk 2007). *E. densa* and Largemouth Bass are particularly prevalent in the central and southern Delta (Brown and Michniuk 2007) and Largemouth Bass may contribute to the pre-screen losses of Delta Smelt entrained into the SWP and CVP export pumps (see above). Largemouth Bass will readily eat Delta Smelt when the opportunity exists (Ferrari et al. 2014). However, there is little evidence that Largemouth Bass are major consumers of Delta Smelt due to low spatial co-occurrence (Nobriga et al. 2005, Baxter et al. 2010; L. Conrad, California Department of Water Resources, unpublished data). Thus, the inverse correlations between these species may not be mechanistic. Rather, they may reflect adaptation to, and selection for, different environmental conditions.

As noted above, predation on fish larvae can also be an important source of mortality. Juvenile and small adult fishes of many species will consume fish larvae when they are available. Major predators of the eggs and larvae of nearshore coastal and pelagic estuarine forage fishes can include invertebrates (DeBlois and Leggett 1993) and numerous small fishes not typically thought of as “piscivorous” (Johnson and Dropkin 1992), including adults of their own species (Takasuka et al. 2003). Bennett and Moyle (1996) and Bennett (2005) noted this and specifically identified Mississippi Silversides (hereafter, Silversides) as potential predators on Delta Smelt larvae. These authors also documented increases in the Silverside population from the mid-1970s through 2002. Consumption of Delta Smelt larvae by Silversides in the Delta was recently verified using DNA techniques (Baerwald et al. 2012). Larval predation is discussed in more detail in the next Chapter.

Contaminants

Fish are particularly sensitive to alterations in the chemical composition of the natural aquatic environment, as these changes can have significant impacts on their behavioral and physiological systems (Radhaiah et al. 1987). Chemical alterations can be the result of natural processes, for example the changes in local water quality associated with tidal water movements or natural biogeochemical processes, or they can be caused by pollution from watershed- or land-based sources of nutrients, such as nitrogen compounds, and contaminants, such as pesticides, metals, and contaminants of emerging concerns (CECs). The movement of contaminants through aquatic ecosystems is complex and dynamic, and many contaminants are difficult to detect and expensive to monitor (Scholz et al. 2012).

Portions of the SFE are listed as “impaired” on California’s 303(d) list of Impaired Water Bodies due to metals, pesticides, legacy pollutants, and nutrients that exceed established water quality objectives (SWRCB 2010). In particular, the entire SFE has been listed as impaired due to pollution with metals, such as mercury and selenium, and pesticides such as chlorpyrifos, DDT (Dichlorodiphenyltrichloroethane), and diazinon. The entire Delta, but not the bays of the SFE, is also listed for observed toxicity to aquatic organisms. In addition, the Stockton Ship Channel

in the southeastern Delta is listed for enrichment with nutrients, organic compounds, and low dissolved oxygen levels; Old River in the south-central Delta is listed for elevated salinity (electrical conductivity; EC) and total dissolved solids (TDS). Delta Smelt are likely exposed to a variety of these contaminants throughout their life cycle; however, the frequency and magnitude of the effects of contaminants on Delta Smelt health and reproduction are not very well understood in the SFE (Johnson et al. 2010, Brooks et al. 2012). The following sections describe the potential effects of key contaminants on Delta Smelt.

Pesticides

Pesticides produce many physiological and biochemical changes in freshwater organisms through their influence on the activities of several enzymes (Khan and Law 2005). Specifically, pesticides can have an adverse effect on hormones or other chemical messengers important to the health of an individual. Previous work has shown that chronic exposure to low levels of pesticides may even have a more adverse effect on fish than a single acute exposure to high levels. Chronic exposures were associated with changes in behavior and physiology that could influence survival and reproduction of wild fish (Ewing 1999). Biochemical and physiological stresses induced by exposure to pesticides can result in metabolic disturbances, retardation of growth, as well as reduction in longevity and fecundity (Murty 1986).

Pesticides are among the key contaminants believed to have contributed to the Delta Smelt decline (Johnson et al. 2010, Brooks et al. 2012, NRC 2012). Because pesticide concentrations in surface water are typically highest during the winter and spring, pesticides are most likely to affect the adult and larval life stages; however, effects may occur during any life stage as pesticides are seasonally and geographically widespread (Kuivila and Hladik 2008). Kuivila and Moon (2004) found that peak densities of larval and juvenile Delta Smelt sometimes coincided in time and space with elevated concentrations of dissolved pesticides in the spring. These periods of co-occurrence lasted for up to 2–3 weeks. While concentrations of individual pesticides were lower than would be expected to cause acute mortality, little is known of the sublethal effects of pesticides on Delta Smelt. Although little evidence exists for acute effects of pesticides on fish or invertebrates, several studies have documented sublethal effects on fish health (Werner et al. 2008, Werner et al. 2010a, Werner et al. 2010b).

Herbicides and fungicides were among the most commonly detected classes of pesticides observed in water and sediment in the Delta and are also found in fish tissue (Orlando et al. 2013, Smalling et al. 2013). Herbicides are known to affect primary producers, while insecticides can affect invertebrate prey species (e.g., Brander et al. 2009, Weston et al. 2012), which could lead to contaminant-mediated food limitation for Delta Smelt. Fungicides have been found to cause endocrine disruption in fish, including reduced fecundity (Ankley et al. 2005). Recent work has shown that the insecticide esfenvalerate affects swimming behavior of exposed larval Delta Smelt (Connon et al. 2009). It was also found to alter the expression of genes involved in neuromuscular activity and immune response, detoxification, and growth and development (Connon et al. 2009). Additionally, insecticides are known to affect predator-prey relationships for fish, as well as lead to endocrine disruptions (Scholz et al. 2000, Junges et al. 2010, Relyea and Edwards 2010, Riar et al. 2013, Forsgren et al. 2013). Contamination of aquatic systems by pyrethroid insecticides was recently found to lead to genetic point mutations in the nontarget, aquatic amphipod *Hyalella azteca*, resulting in differences in pyrethroid sensitivity. Wild populations of *H. azteca* collected from areas with high sediment concentrations of pyrethroids exhibited remarkable resistance to pyrethroids compared to laboratory cultures and the observed

resistance was highly coupled to the presence of a genetic mutation. The LC50s (concentration that is lethal to 50% of the exposed population) of previously-exposed wild populations were up to two orders of magnitude greater than LC50s of laboratory cultures. Moreover, the presence of a genetic mutation was detected in 100% of *H. azteca* that survived exposure to high pyrethroid concentrations. The development of such resistance can result in costs to genetic and biological diversity, including reduced fitness, and may lead to impacts to the food web (Weston et al. 2013). The presence of such resistance and genetic mutations in Delta Smelt as a result of pyrethroids or other pesticide exposure has not been investigated

It is also important to note that environmental factors such as temperature and salinity affect pesticide toxicity in fish (Coats et al. 1989, Lavado et al. 2009). For that reason, seasonal variation in environmental factors may result in greater risk to certain life stages. The results above are for dissolved pesticides; pesticides may also be bound to sediments, representing another possible mechanism of exposure. Pesticides, such as pyrethroids and organochlorines, that strongly bind to sediment may be particularly important to the adult and larval life stage of Delta Smelt as these life stages occur during the winter and spring, when rain events (including the “first flush”) transport sediment and associated contaminants into the Delta; however, as the mechanisms that influence the desorption rates of pesticides are complex (e.g., temperature, contact time, pesticide) (e.g., Xu et al. 2008, Cornelissen et al. 1998), exposure rates for Delta Smelt life stages are likely multifaceted and difficult to predict.

Ammonia and Ammonium

Agricultural operations, wastewater treatment plant effluent, and other sources contribute to the accumulation of nutrients in the Delta. Nutrients, such as ammonium (a cation) and ammonia (its toxic, unionized form) are of particular concern in the Delta, as they can have significant negative effects on Delta Smelt and their habitat. Ammonium is increasingly converted into ammonia as pH rises. Delta Smelt spawning and larval nursery areas in the northern Delta are at particular risk to exposure to ammonia/um, mainly due to discharge by the Sacramento Regional Wastewater Treatment Plant (SRWTP) into the lower Sacramento River (Connon et al. 2011a). However, effects of nutrients such as ammonia/um are likely at all Delta Smelt life stages, as nutrients are discharged throughout the Delta year-round.

Recent work demonstrated that Delta Smelt exposed to ammonia exhibited membrane destabilization, which may lead to increased membrane permeability as well as increased susceptibility to synergistic effects of multi-contaminant exposures (Connon et al. 2011a, Hasenbein et al. 2013b); however, the concentrations of ammonia used in these studies were higher than the concentrations typically experienced by Delta Smelt in the wild. In other fish species, sublethal concentrations of ammonia/um have also led to histological effects such as gill lamellae fusions and deformities (Benli et al. 2008). Other work has also shown that neurological and muscular impacts of ammonia/um resulted in slowed escape response and subsequent mortality (McKenzie et al. 2008).

Metals and Other Elements of Concern

Historic mining sites, industrial and domestic wastewater discharges, and agricultural runoff are largely responsible for the presence of metals and other elements of concern in the Delta. Metals of particular importance in the Delta include copper and mercury; selenium is a trace element

of concern. Delta Smelt exposed to copper exhibited reduced swimming velocities and suffered digestive and neurological effects (Connon et al. 2011b). Other sublethal effects on fish caused by exposure to these elements include reduced fertility and growth, impaired neurological and endocrine functions, and skeletal deformities that affect swimming performance (Boening 2000, Chapman et al. 2010). These elements are often associated with sediment and may be particularly important to the adult and larval life stages, since sediment is transported with significant rain events, including the “first flush.”

Contaminants of Emerging Concern

Contaminants of emerging concern (CECs) such as pharmaceuticals, hormones, personal care products, and industrial chemicals are of increasing concern because they are widespread in the aquatic environment, biologically active, and are relatively unregulated (Kolpin et al. 2002, Pal et al. 2010). The California State Water Resources Control Board is currently investigating CECs in the Delta (<http://www.sccwrp.org/ResearchAreas/Contaminants/ContaminantsOfEmergingConcern/EcosystemsAdvisoryPanel.aspx>). CECs originate from many sources including industrial and domestic wastewater. They are responsible for a myriad of sublethal effects in fish including endocrine disruption, changes in gene transcription and protein expression, and morphological and behavioral changes (Brander 2013). Though the effects of CECs have been well studied in other fish species, the extent to which they influence Delta Smelt remains unclear.

Polycyclic Aromatic Hydrocarbons (PAHs) and Polychlorinated Biphenyls (PCBs)

The PAHs and PCBs found in the Delta are largely from urban and industrial sources. PAHs are formed during the incomplete burning of coal, oil, gas, garbage, and other organic substances. PCBs are synthetic organic chemicals that were used in many industrial and commercial applications. PCBs were banned in 1979, but continue to persist in the environment. PAHs and PCBs bind strongly to sediment and therefore are likely to be associated with the “first flush” and may be particularly important to the adult and larval life stages of Delta Smelt. Almost all sediments sampled in the Delta in 2006 contained PAHs (mean concentration of 0.3 parts per million in Suisun Bay) and PCBs (mean concentration of 0.8 parts per million in Suisun Bay) (SFEI 2007). Studies have found PAHs and PCBs in surface water, with concentrations in excess of established water quality objectives (Thomson et al. 2000, Oros et al. 2006). Both PCBs and PAHs can cause endocrine disruption in fish (Brar et al. 2010, Nicolas, 1999); however, specific impacts on Delta Smelt have not been documented.

Contaminant Mixtures

While the individual effects of the aforementioned contaminants can be severe, recent work has demonstrated that the interaction of the contaminants within mixtures can have both synergistic and antagonistic effects, exacerbating potential impacts on fish physiology (e.g., Jordan et al. 2012). There is increasing evidence that compounds in mixtures show adverse effects at concentrations at which no effects were observed for single toxicants (e.g., Baas et al. 2009, Silva et al. 2002, Walter et al. 2002). For example, recent work on Mississippi Silversides has demonstrated that contaminant mixtures resulted in endocrine disruptions such as varied

expression of mRNA levels for estrogen-responsive genes, reduced mean gonadal somatic indices (GSI), testicular necrosis, and biased sex ratios (Brander et al. 2013). Studies have also shown that mixtures can affect predator-prey interactions (Relyea and Edwards 2010) and cause liver abnormalities (Sacramento Splittail, *Pogonichthys macrolepidotus*; Greenfield et al. 2008). Other work on Striped Bass has demonstrated that contaminant mixtures can be maternally-transferred to fish eggs, resulting in larvae with impaired growth and abnormal brain and liver development (Ostrach et al. 2008).

Due to the unpredictability of their effects on organisms, the synergistic effects of contaminant mixtures have received a great deal of attention both within pharmacology and environmental sciences (Arnold et al. 1996, Ashby et al. 1997, Berenbaum 1989, Greco et al. 1995, Liang and Lichtenstein 1974). Currently, one of the greatest challenges in chemical mixture research is how to deal with the infinite number of combinations of chemicals and other stressors, as well as their interactive effects, on organisms (Baas et al. 2010). Additional challenges also exist trying to relate lab-based findings to wild populations for studies examining the effects of individual contaminants and contaminant mixtures on organisms using exposure concentrations that are environmentally representative. Therefore, while the potential for exposure to contaminant mixtures in all Delta Smelt life stages is highly probable, any specific effects of such interactions on Delta Smelt remain unknown.

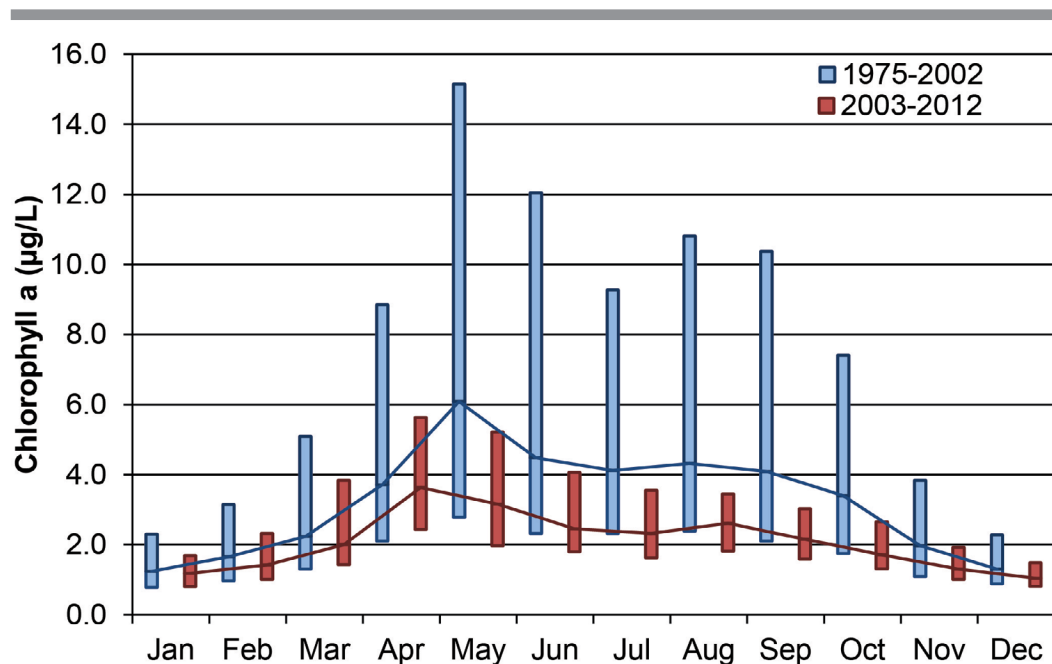
Food and Feeding

The presence of food is, obviously, a critical habitat attribute for any organism; however, the factors determining the quantity and quality of available food can be quite complex. In this section, we begin with a brief review of information about trophic processes in the upper SFE. We then discuss the available data on prey consumed by Delta Smelt. Finally, we provide a review of information on factors possibly affecting abundance and quality of food organisms.

Estuaries are commonly characterized as highly productive nursery areas for a suite of organisms. Productivity of estuarine ecosystems is often fueled by detritus-based food webs. In the SFE, much of the community metabolism in pelagic waters does result from microbial consumption of organic detritus. However, evidence suggests that metazoan production in pelagic waters is primarily driven by phytoplankton production (Sobczak et al. 2002, 2005, Mueller-Solger et al. 2002, 2006, Kimmerer et al. 2005). Protists (flagellates and ciliates) consume both microbial and phytoplankton prey (Murrell and Hollibaugh 1998, York et al. 2010) and are an additional important food source for many copepod species in the estuary (Rollwagen-Bollens and Penry 2003, Bouley and Kimmerer 2006, Gifford et al. 2007, McManus et al. 2008). However, the conversion of dissolved and particulate organic matter to microbial biomass and then to zooplankton is a relatively slow and inefficient process. Shifts in phytoplankton and microbial food resources for zooplankton might favor different zooplankton species. Moreover, phytoplankton production and biomass in the SFE is low compared to many other estuaries (e.g., Jassby et al. 2002, Kimmerer et al. 2005, Wilkerson et al. 2006, Cloern and Jassby 2012). The recognition that phytoplankton production might impose limits on pelagic fishes, such as Delta Smelt, through food availability has led to intense interest in factors affecting phytoplankton production and species composition and in management actions aimed at enhancing high-quality phytoplankton production. In addition, there is a major need to understand other trophic pathways given the observation that larger Delta Smelt periodically can take advantage of epibenthic prey (see below).

Phytoplankton biomass (measured as chlorophyll-*a*) has been routinely monitored in the estuary since the 1970s. The 1975-2012 median chlorophyll-*a* concentration across all IEP EMP stations is 2.8 $\mu\text{g/L}$ ($n = 13482$, interquartile range (IQR) = 5 $\mu\text{g/L}$). Seasonally, the highest chlorophyll-*a* concentrations tend to be observed in May and June and the lowest concentrations in December and January (Fig. 32). Regionally, monitoring stations in the South Delta/San Joaquin River usually have the highest chlorophyll-*a* concentrations. There has been a well-documented long-term decline in phytoplankton biomass (chlorophyll-*a*) and primary productivity (estimated from measurements of chlorophyll-*a* and of water column light utilization efficiency) to very low levels in the Suisun Bay region and the lower Delta (Jassby et al. 2002). Jassby et al. (2002) detected a 47% decline in June–November chlorophyll-*a* and a 36% decline in June–November primary production between the periods 1975–1985 and 1986–1995. Jassby (2008) updated the phytoplankton analysis to include the more recent data (1996–2005) from the Delta and Suisun Bay. Jassby (2008) confirmed a long-term decline in chlorophyll-*a* from 1975 to 2005 but also found that March–September chlorophyll-*a* had an increasing trend in the Delta from 1996 to 2005. Suisun Bay did not exhibit any trend during 1996–2005. A similar pattern was noted for primary production in the Delta. These chlorophyll-*a* patterns continued to hold through 2008 according to a more recent study by Winder and Jassby (2011). In the most recent decade (2003–2012), the median chlorophyll-*a* concentration across all IEP EMP stations was 2 $\mu\text{g/L}$ ($n = 2620$, IQR = 2 $\mu\text{g/L}$), compared to the 1975-2002 median chlorophyll-*a* concentration of 3 $\mu\text{g/L}$ ($n = 10862$, IQR = 6 $\mu\text{g/L}$) (Fig. 32). Most of the decrease was due to declines during May–October and especially the near-elimination of the formerly common “spring bloom” of phytoplankton in May (Fig. 32). In summary, phytoplankton biomass and production in the Delta and Suisun Bay seem to have reached a low point by the end of the 1987–1994 drought. While they recovered somewhat in the Delta, chlorophyll-*a* stayed consistently low in Suisun Bay through the POD years.

Figure 32. Interquartile ranges (boxes) and medians (lines) for chlorophyll-*a* measured monthly at all IEP EMP stations from 1975-2002 (blue) and 2003-2012 (red). Data from <http://www.water.ca.gov/bdma/>.



A major reason for the long-term phytoplankton reduction in the upper SFE after 1985 is benthic grazing by the invasive overbite clam (*Potamocorbula amurensis* also known as *Corbula amurensis*) (Alpine and Cloern 1992), which became abundant by the late 1980s (Kimmerer 2002). The overbite clam was first reported from San Francisco Estuary in 1986 and it was well established by 1987 (Carlton et al. 1990). Prior to the overbite clam invasion, the invasive Asiatic freshwater clam (*Corbicula fluminea*) (introduced in the 1940s) colonized Suisun Bay during high flow periods and the estuarine clam *Mya arenaria* (also known as *Macoma balthica*, an earlier introduction) colonized Suisun Bay during prolonged (> 14 month) low flow periods (Nichols et al. 1990). Thus, there were periods of relatively low clam grazing rates while one species was dying back and the other was colonizing, resulting in neither reaching high abundances. The *P. amurensis* invasion changed this formerly dynamic clam assemblage because *P. amurensis*, which is tolerant of a wide range of salinity, can maintain large, permanent populations in the brackish water regions of the estuary. *P. amurensis* biomass and grazing usually increase from spring to fall which contributes to the reduction in phytoplankton biomass from May to October relative to historical levels. In addition, the grazing influence of *P. amurensis* extends into the freshwater Delta beyond the clam's typical brackish salinity range, presumably due to tidal dispersion of phytoplankton-depleted water between regions of brackish water and fresh water (Kimmerer and Orsi 1996, Jassby et al. 2002).

Phytoplankton production in the SFE has been considered primarily light-limited because nutrient concentrations commonly exceed concentrations limiting primary production. According to some recent work, shifts in nutrient concentrations and ratios may, however, also contribute to the phytoplankton reduction and changes in algal species composition in the SFE. Nutrients may also play a larger role in regulating phytoplankton dynamics in the estuary as the estuary clears and light availability increases (see turbidity section above).

While phosphorus (total phosphorous and soluble reactive phosphorous) concentrations declined in the Delta and Suisun Bay region over the last few decades, nitrogen (total nitrogen and ammonium) concentrations increased. These changes have been attributed to the operation of the Sacramento Regional Wastewater Treatment Plant (SRWTP), a large secondary treatment facility that was completed in 1984 (VanNieuwenhuysen 2007, Jassby 2008). As stated previously, ammonia has two forms, un-ionized ammonia (NH_3) which is toxic to aquatic organisms and the ammonium ion (NH_4^+) which is considerably less toxic to animals and an important nutrient for plants and algae (Thurston et al. 1981). Ammonia exists in equilibrium between the two forms dependent primarily on the pH of the water, but also temperature, with increases in pH and temperature favoring the un-ionized form (Thurston et al. 1981). Dugdale et al. (2007) and Wilkerson et al. (2006) found that high ammonium concentrations prevented the formation of diatom blooms but stimulated flagellate blooms in the lower estuary. They propose that this occurs because diatoms preferentially utilize ammonium in their physiological processes even though it is used less efficiently and at high concentrations ammonium can prevent uptake of nitrate (Dugdale et al. 2007). Thus, diatom populations must consume available ammonium before nitrate, which supports higher growth rates, can be utilized or concentrations of ammonium need to be diluted. A recent independent review panel (Reed et al. 2014) found that there is good evidence for preferential uptake of ammonium and sequential uptake of first ammonium and then nitrate, but that a large amount of uncertainty remains regarding the growth rates on ammonium relative to nitrate and the role of ammonium in suppressing spring blooms.

Glibert (2012) analyzed long-term data (from 1975 or 1979 to 2006 depending on the variable considered) from the Delta and Suisun Bay and related changing forms and ratios of nutrients, particularly changes in ammonium, to declines in diatoms and increases in flagellates and

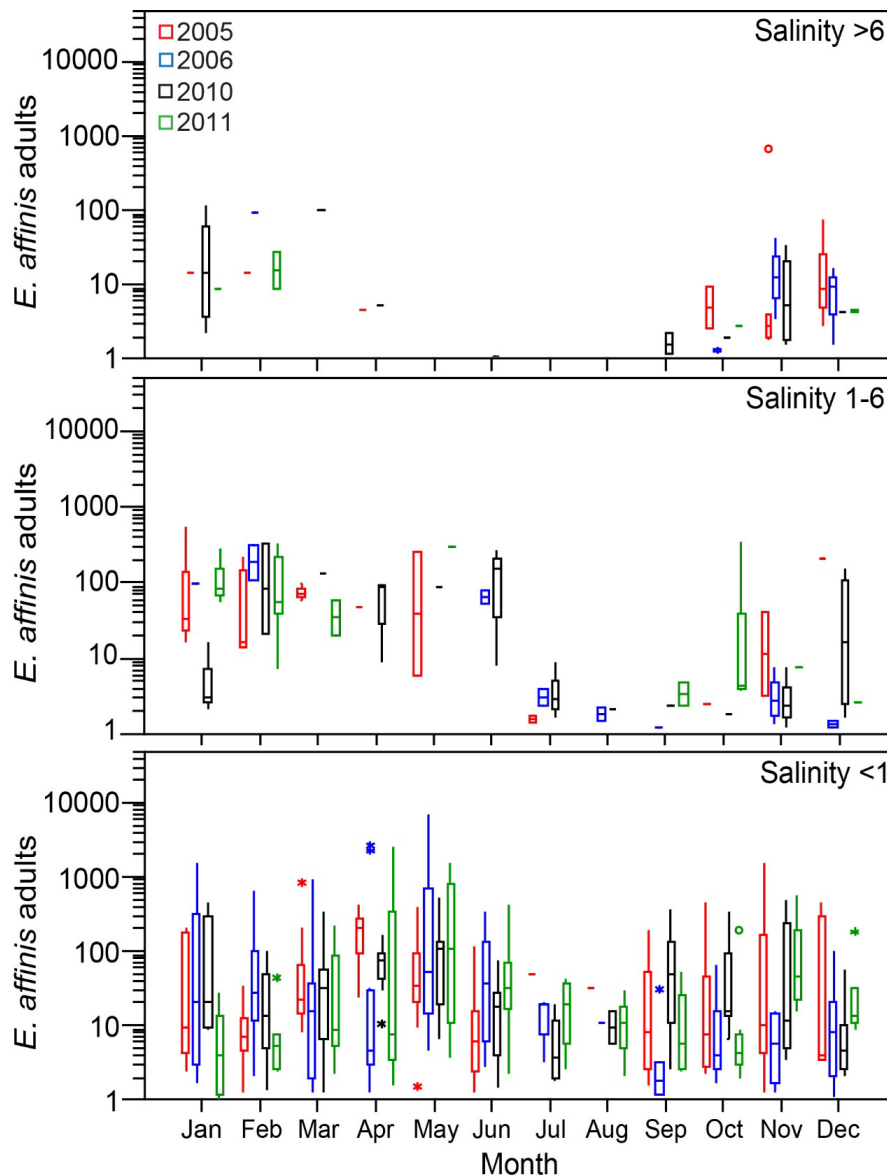
cyanobacteria. Similar shifts in species composition were noted by Brown (2009), with loss of diatom species, such as *Thalassiosira sp.*, an important food for calanoid copepods, including *Eurytemora affinis* and *Sinocalanus doerri* (Orsi 1995). More recently, Parker et al. (2012) found that the region where blooms are suppressed extends upstream into the Sacramento River to the SRWTP, the source of the majority of the ammonium in the river (Jassby 2008). Parker et al. (2012) found that at high ambient ammonium concentrations, river phytoplankton cannot efficiently take up any form of nitrogen including ammonium, leading to often extremely low biomass in the river. A study using multiple stable isotope tracers (Lehman et al. 2014) found that the cyanobacteria *M. aeruginosa* utilized ammonium, not nitrate, as the primary source of nitrogen in the central and western Delta. In 2009, the ammonia concentration in effluent from SRWTP was reduced by approximately 10%, due to changes in operation (K. Ohlinger, Sacramento Regional County Sanitation District, personal communication). In spring 2010 unusually strong spring diatom blooms were observed in Suisun Bay that co-occurred with low ammonia concentrations (Dugdale et al. 2013).

Jassby (2008) suggested the following comprehensive explanation for his observations. Phytoplankton production in the lower Delta is associated with flow and residence time; however, other factors introduce a substantial degree of interannual variability. Benthic grazing by *C. fluminea* is likely a major factor as grazing can exceed rates of primary production (Lucas et al. 2002, Lopez et al. 2006) and are abundant year round at some locations in the Delta (Fuller 2012). Current data are inadequate to estimate the overall magnitude of the grazing effect of *C. fluminea*. In Suisun Bay, benthic grazing by *P. amurensis* is a controlling factor that keeps phytoplankton at low levels. Thus, metazoan populations in Suisun Bay are dependent on importation of phytoplankton production from the upstream portions of the Delta. Upstream Delta phytoplankton can be lost via exports and within-Delta depletion; Cloern and Jassby (2012) reported phytoplankton losses equivalent to 30% of the primary production in the Delta. Ammonium concentrations and water clarity have increased; however, these two factors should have opposing effects on phytoplankton production. These factors likely also contribute to variability in the interannual pattern but the relative importance of each is unknown. The interactions among primary production, grazing, and transport time can be complex (Lucas et al. 2002, 2009a,b, Lucas and Thompson 2012).

The changes in phytoplankton production and invasion and establishment of the overbite clam *P. amurensis* were also accompanied by a series of major changes in consumers (Winder and Jassby 2011). Many of these changes likely negatively influenced pelagic fish production, including Delta Smelt. The quantity of food available to Delta Smelt is a function of several factors, including but not limited to seasonal trends in prey abundance and prey species specific salinity tolerances, which influence distribution (Kimmerer and Orsi 1996, Hennessy and Enderlein 2013). Seasonal peaks in abundance vary among calanoid copepods consumed as prey by Delta Smelt, *E. affinis* in April-May (Fig. 33), *P. forbesi* in July (Fig. 34), and *A. sinensis* in Sep-Oct (Fig. 35). Upstream, the calanoid copepod *S. doerrii* is most abundant May-June (Fig. 36). The seasonal trend in cladocerans (Fig. 37) and mysid (Fig. 38) prey are similar, being most abundant in summer.

From March through June, larval Delta Smelt rely heavily on first juvenile, then adult stages of the calanoid copepods *Eurytemora affinis* and *Pseudodiaptomus forbesi*, as well as cladocerans (Nobriga 2002, Hobbs et al. 2006, Slater and Baxter 2014), and *Sinocalanus doerrii* (Fig. 39). Nobriga (2002) found that Delta Smelt larvae expressed positive selection for *E. affinis* and *P. forbesi*, consuming these prey species in greater proportion than available in the environment. Such selection was not noted for other zooplankton prey. Regional differences in food use occur,

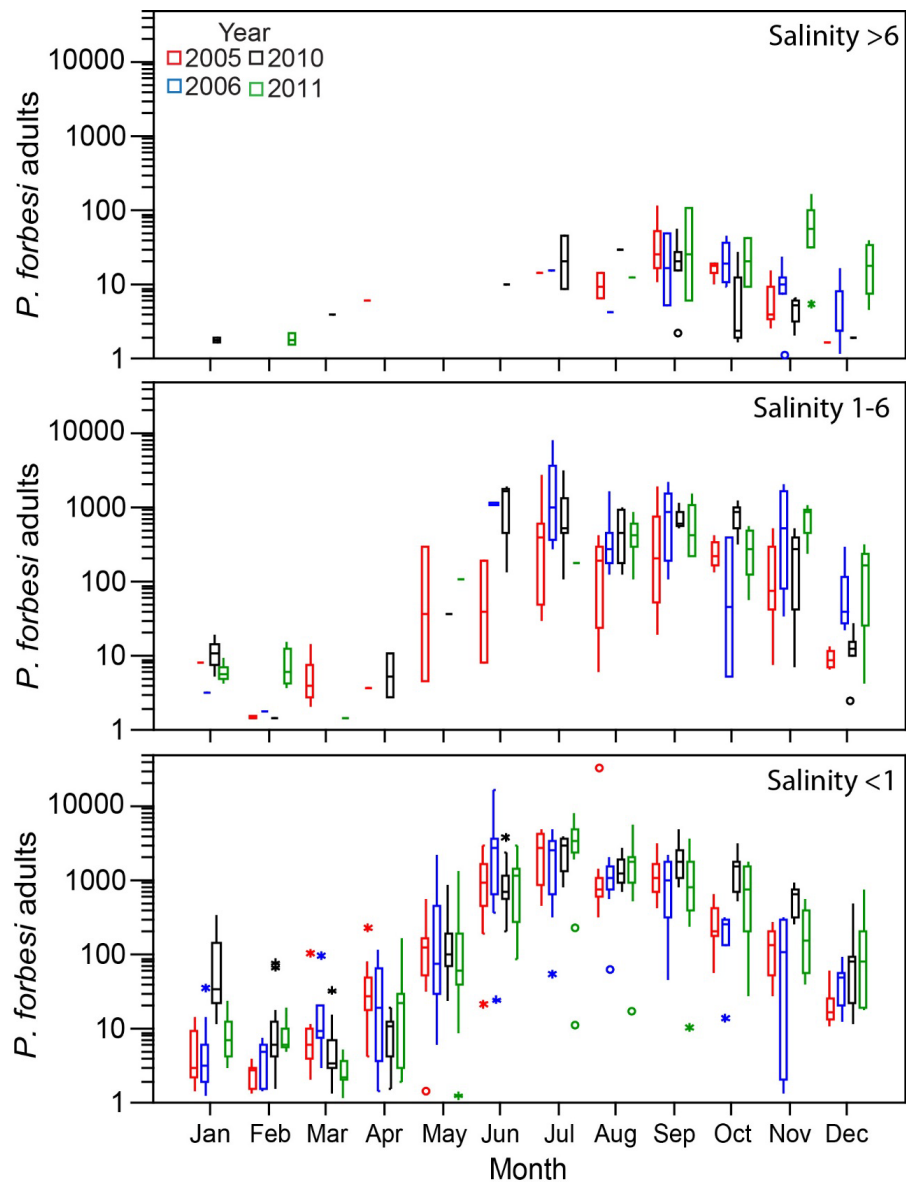
Figure 33. Density (number/m³) of adult *Eurytemora affinis* (*E. affinis*) by month for three salinity ranges. Each month 16 stations were sampled across all salinity ranges. Horizontal lines represent single samples within a salinity range and boxes without whiskers indicate 2 samples within a salinity range. Data from the IEP Zooplankton Study index stations. See Chapter 3: Data Analyses for explanation of boxplots.



with *E. affinis* and *P. forbesi* being major prey items downstream in the LSZ with a transition to *S. doerrii* and cyclopoid copepods as major prey items upstream into the Cache Slough-Sacramento River Deepwater Ship Channel (CS-SRDWSC) (Fig. 39).

Juvenile Delta Smelt (June-September) rely extensively on calanoid copepods such as *E. affinis* and *P. forbesi*, especially in freshwater (salinity < 1) and CS-SRDWSC but there is great variability among regions (figs. 40-43). Larger fish are also able to take advantage of mysids,

Figure 34. Density (number/m³) of adult *Pseudodiaptomus forbesi* (*P. forbesi*) by month for three salinity ranges. Each month 16 stations were sampled across all salinity ranges. Horizontal lines represent single samples within a salinity range and boxes without whiskers indicate 2 samples within a salinity range. Data from the IEP Zooplankton Study index stations. See Chapter 3: Data Analyses for explanation of boxplots.



cladocerans, and amphipods (Moyle et al. 1992, Lott 1998, Feyrer et al. 2003, Steven Slater, California Department of Fish and Wildlife, unpublished data) (Figs. 34-37). The presence of several epibenthic species in diets therefore indicates that food sources for this species are not confined to pelagic pathways. Such food sources may be especially important in regions of the estuary where there is extensive shoal habitat such as Liberty Island (Steven Slater, California Department of Fish and Wildlife, unpublished data).

Figure 35. Density (number/m³) of adult *Acartiella sinensis* (*A. sinensis*) by month. Each month 16 stations were sampled across all salinity ranges. Horizontal lines represent single samples within a salinity range and boxes without whiskers indicate 2 samples within a salinity range. Data from the IEP Zooplankton Study index stations. See Chapter 3: Data Analyses for explanation of boxplots.

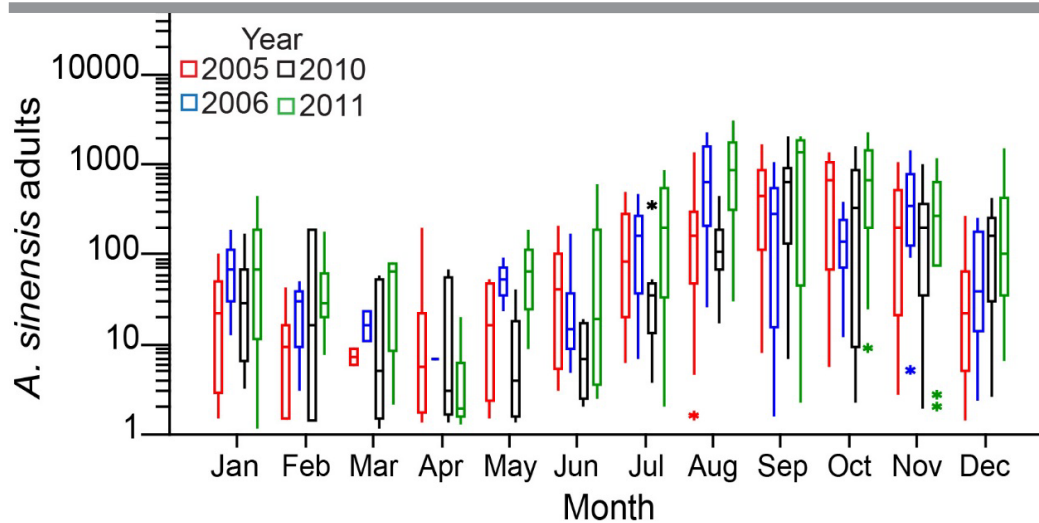
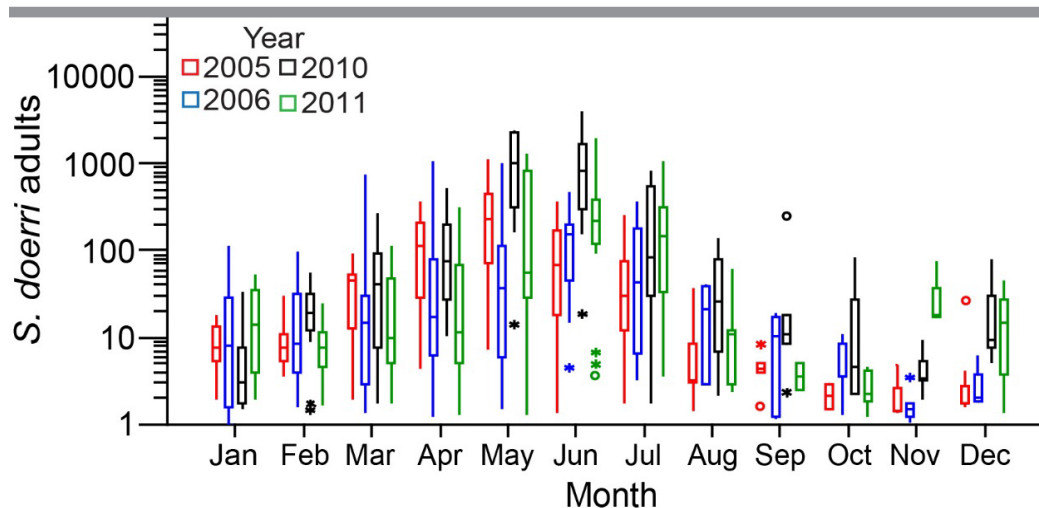


Figure 36. Density (number/m³) of adult *Sinocalanus doerrii* (*S. doerrii*) by month. Each month 16 stations were sampled across all salinity ranges. Horizontal lines represent single samples within a salinity range and boxes without whiskers indicate 2 samples within a salinity range. Data from the IEP Zooplankton Study index stations. See Chapter 3: Data Analyses for explanation of boxplots.



Subadult Delta Smelt (September through December) prey items are very similar to those of juvenile Delta Smelt but with increased variability in diet composition (Moyle et al. 1992, Lott 1998, Steven Slater, California Department of Fish and Wildlife, unpublished data) (Figs. 40-43) coinciding with the seasonal decline in pelagic zooplankton, such as *P. forbesi* (Fig. 34) and mysids (Fig. 38). Food habits of adult Delta Smelt during the winter and spring (January-May) have been less well documented (Moyle et al. 1992). In 2012, diet of adults in the LSZ and

Figure 37. Density (number/m³) of all cladoceran taxa by month. Each month 16 stations were sampled across all salinity ranges. Horizontal lines represent single samples within a salinity range and boxes without whiskers indicate 2 samples within a salinity range. Data from the IEP Zooplankton Study index stations. See Chapter 3: Data Analyses for explanation of boxplots.

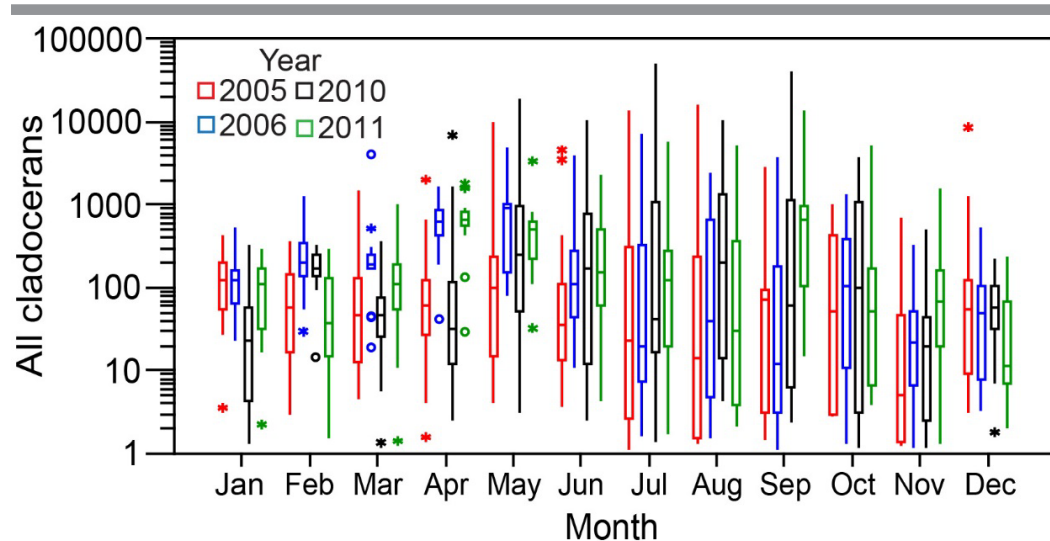
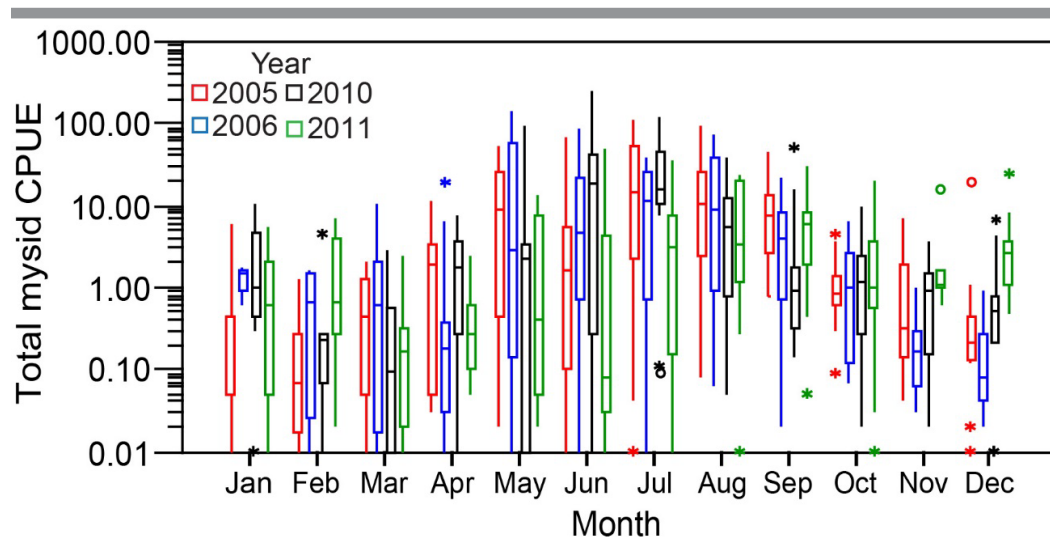


Figure 38. Density (number/m³) of all mysid shrimp taxa by month. Each month 16 stations were sampled across all salinity ranges. Horizontal lines represent single samples within a salinity range and boxes without whiskers indicate 2 samples within a salinity range. Data from the IEP Zooplankton Study index stations. See Chapter 3: Data Analyses for explanation of boxplots.



< 1 ppt were found to include cyclopoid copepods, other than *Limnoithona* spp., with a mix of larger prey types, amphipods, cladocerans, cumaceans, and larval fish and in CS-SRDWSC the calanoid copepod *S. doerrii* continued to be a large portion of the diet (Steven Slater, California Department of Fish and Wildlife, unpublished data) (Fig. 44). Larval fish found in stomachs of Delta Smelt in the higher salinity areas were primarily Pacific Herring (*Clupea pallasii*), with

some Longfin Smelt, and Prickly Sculpin (*Cottus asper*) in the Sacramento River and CS-SRDWSC region; no Delta Smelt larvae were found in the stomachs of adults (Steven Slater, California Department of Fish and Wildlife, unpublished data).

The large proportion of benthic amphipods, cumaceans, and some cladocerans (*Camptocercus* spp.) in the diet is a notable change from Delta Smelt diet in the 1970s. Delta Smelt diets historically did include amphipods, notably *Corophium* spp. (Moyle et al. 1992), yet it was a small fraction of a mostly pelagic based diet. The considerable use of benthic invertebrates for food in recent years is believed to be in large part due to food limitation associated with the long-term decline and changes in composition of the pelagic food web (Slater and Baxter 2014). The quality of benthic invertebrates as food is not currently understood, but amphipods are lower in energy (calories per gram) than copepods (Cummins and Wuychek 1971, Davis 1993) and mysids (Davis 1993).

As noted previously, the changes in phytoplankton production and phytoplankton species abundances observed and the invasion of *P. amurensis* may have had important consequences for consumer species preyed upon by Delta Smelt. For example, there has been a decrease in mean zooplankton size (Winder and Jassby 2011) and a long-term decline in calanoid copepods, including a major step-decline in the abundance of the copepod *E. affinis*. These changes are possibly due to predation by the overbite clam (Kimmerer et al. 1994) or indirect effects of clam grazing on copepod food supply. Predation by *P. amurensis* may also have been important for other zooplankton species (Kimmerer 2008). Northern Anchovy *Engraulis mordax* abandoned the low salinity zone coincident with the *P. amurensis* invasion, presumably because the clam reduced planktonic food abundance to the point that occupation of the low-salinity waters was no longer energetically efficient for this marine fish (Kimmerer 2006). Similarly, Longfin Smelt *Spirinchus thaleichthys* shifted its distribution toward higher salinity in the early 1990s, also presumably because of reduced pelagic food in the upper estuary (Fish et al. 2009). There was also a decline in mysid shrimp (Winder and Jassby 2011), including a major step-decline in 1987–1988, likely due to competition with the overbite clam for phytoplankton (Orsi and Mecum 1996). Mysid shrimp had been an extremely important food item for larger fishes like Longfin Smelt and juvenile Striped Bass (Orsi and Mecum 1996), and may be consumed by larger Delta Smelt (Moyle et al. 1992). The decline in mysids was associated with substantial changes in the diet composition of these and other fishes, including Delta Smelt (Feyrer et al. 2003, Bryant and Arnold 2007). The population responses of Longfin Smelt and juvenile Striped Bass to winter–spring outflows changed after the *P. amurensis* invasion. Longfin Smelt relative abundance was lower per unit outflow after the overbite clam became established (Kimmerer 2002b). Age-0 Striped Bass relative abundance stopped responding to outflow altogether (Sommer et al. 2007). One hypothesis to explain these changes in fish population dynamics is that lower prey abundance reduced the system carrying capacity (Kimmerer et al. 2000, Sommer et al. 2007).

In addition to a long-term decline in calanoid copepods and mysids in the upper Estuary, there have been numerous copepod species introductions (Winder and Jassby 2011). *P. forbesi*, a calanoid copepod that was first observed in the estuary in the late 1980s, has replaced *E. affinis* as the most common Delta Smelt prey during the summer. It may have a competitive advantage over *E. affinis* due to its more selective feeding ability. Selective feeding may allow *P. forbesi* to utilize the remaining high-quality algae in the system while avoiding increasingly more prevalent low-quality and potentially toxic food items such as *M. aeruginosa* (Mueller-Solger et al. 2006, Ger et al. 2010a). After an initial rapid increase in abundance, *P. forbesi* declined somewhat in abundance from the early 1990s in the Suisun Bay and Suisun Marsh regions but maintained its abundance, with some variability, in the central and southern Delta (Winder and Jassby 2011).

Figure 39. Percentage by weight of prey types found in the digestive tracts of larval and young juvenile Delta Smelt (≤ 20 mm fork length) collected from 1-6 ppt, < 1 ppt, and Cache Slough-Sacramento River Deepwater Ship Channel (CS-SRDWSC) in A) 2005, B) 2006, C) 2010, and D) 2011. Number of digestive tracts examined are shown above the columns. Mean fork length (mm) of Delta Smelt is also shown.

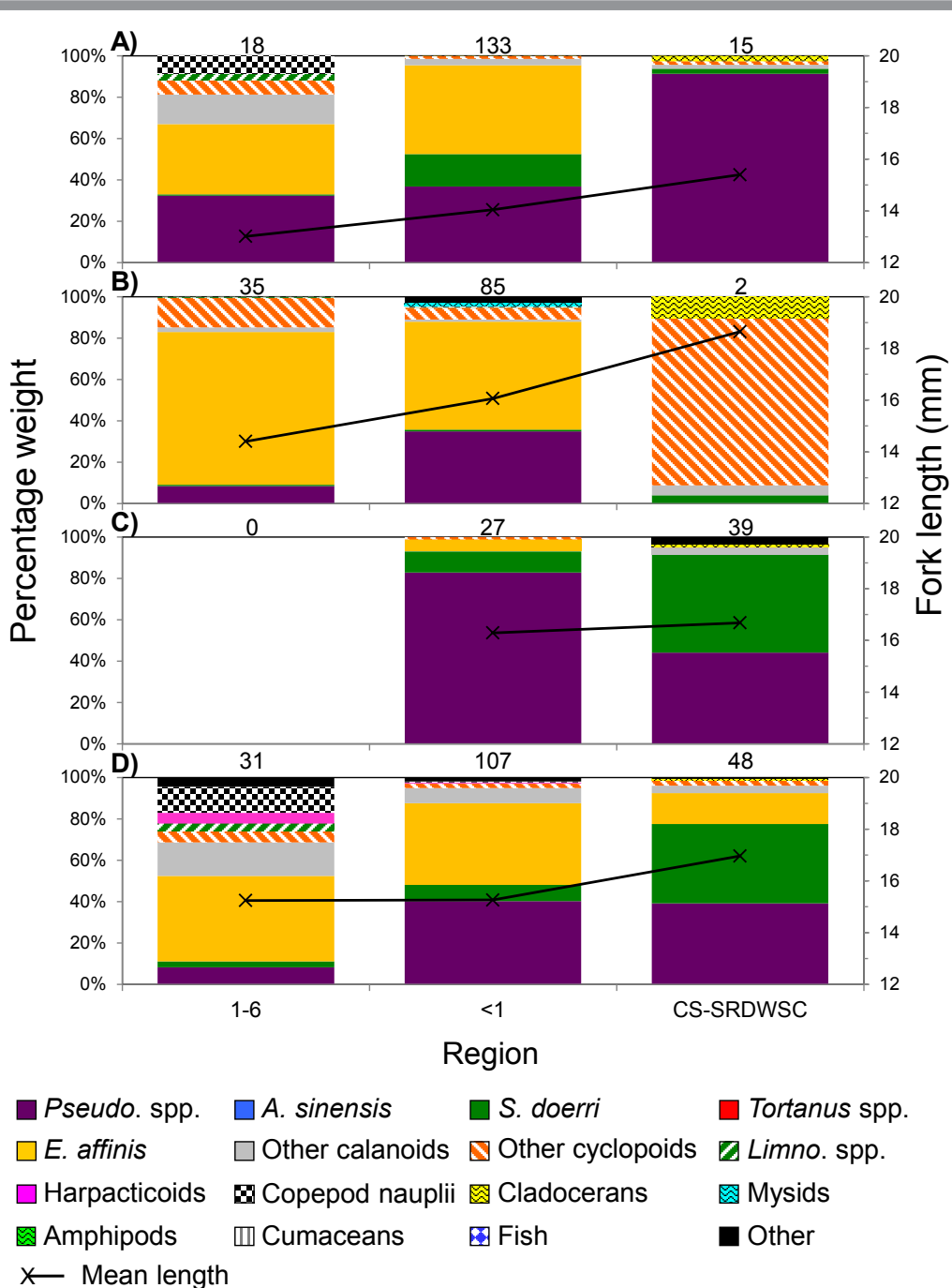
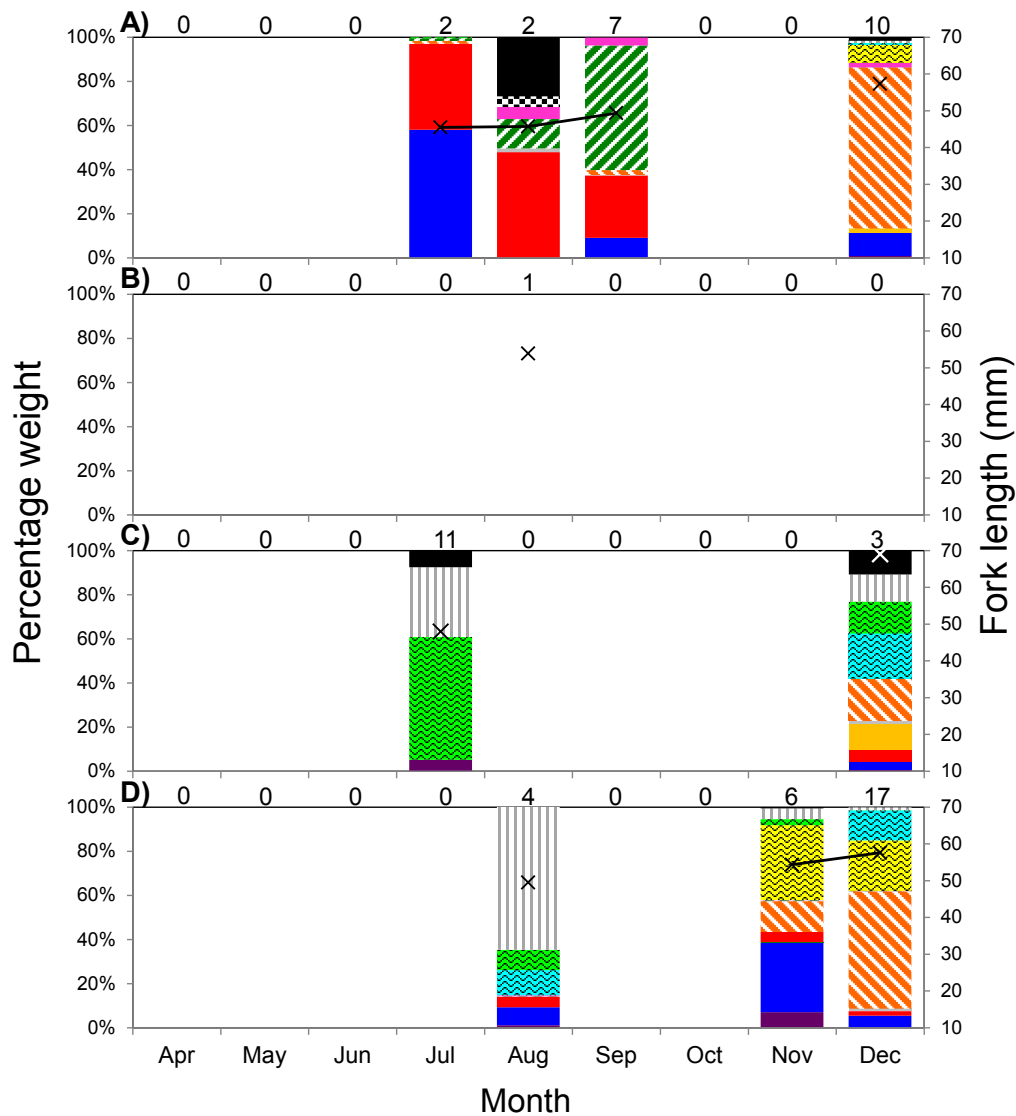


Figure 40. Percentage by weight of prey types found in stomachs of age-0 Delta Smelt collected from > 6 ppt during April through December in A) 2005, B) 2006, C) 2010, and D) 2011. Number of stomachs examined are shown above the columns. One fish examined in August 2006 had an empty stomach. Mean fork length (mm) of Delta Smelt is also shown.



- Pseudo. spp.*
 A. sinensis
 S. doerri
 Tortanus spp.
 - E. affinis*
 Other calanoids
 Other cyclopoids
 Limno. spp.
 - Harpacticoids
 Copepod nauplii
 Cladocerans
 Mysids
 - Amphipods
 Cumaceans
 Fish
 Other
- x — Mean length

Figure 41. Percentage by weight of prey types found in stomachs of age-0 Delta Smelt collected from 1-6 ppt during April through December in A) 2005, B) 2006, C) 2010, and D) 2011. Number of stomachs examined are shown above the columns. Mean fork length (mm) of Delta Smelt is also shown.

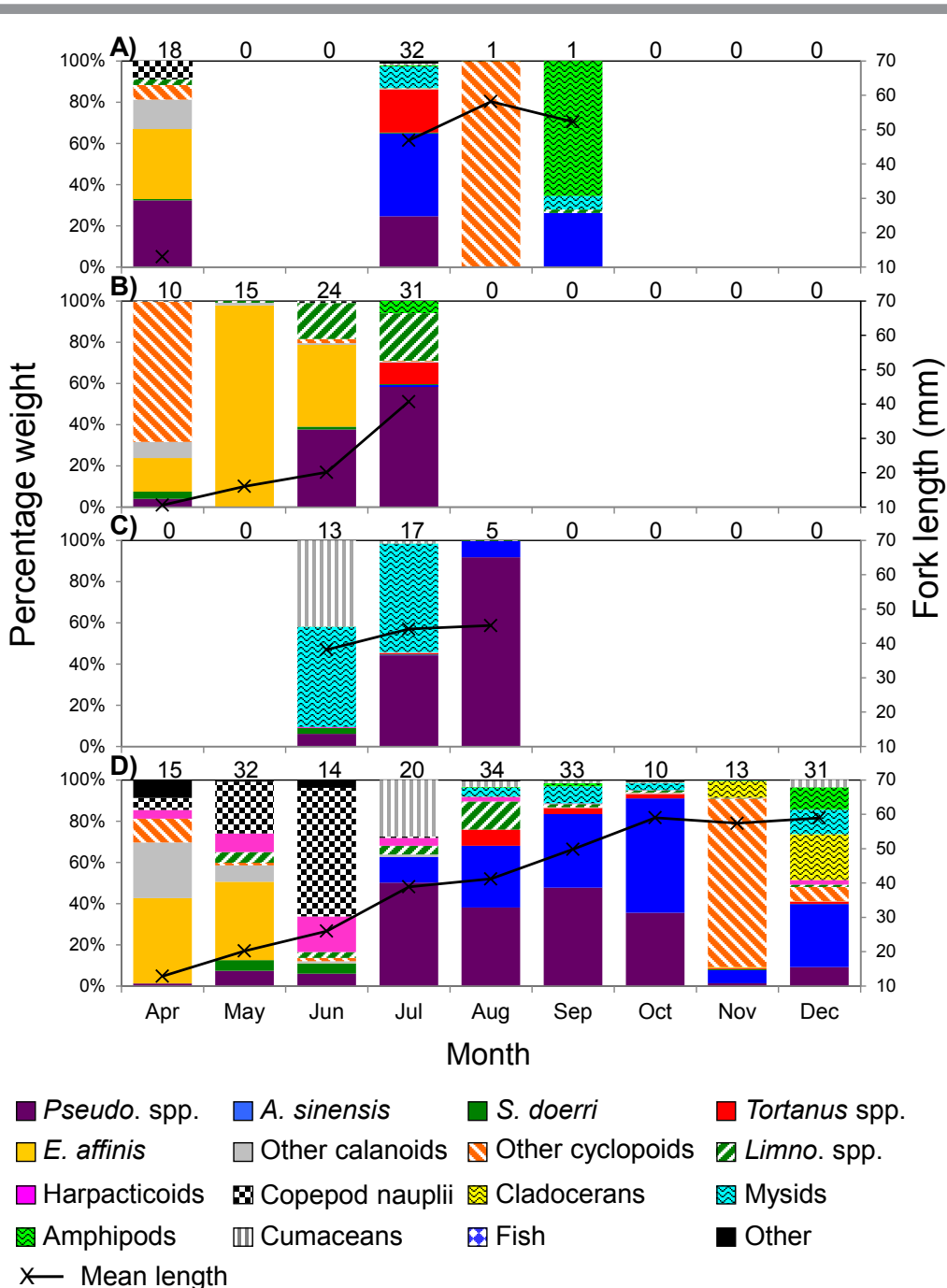
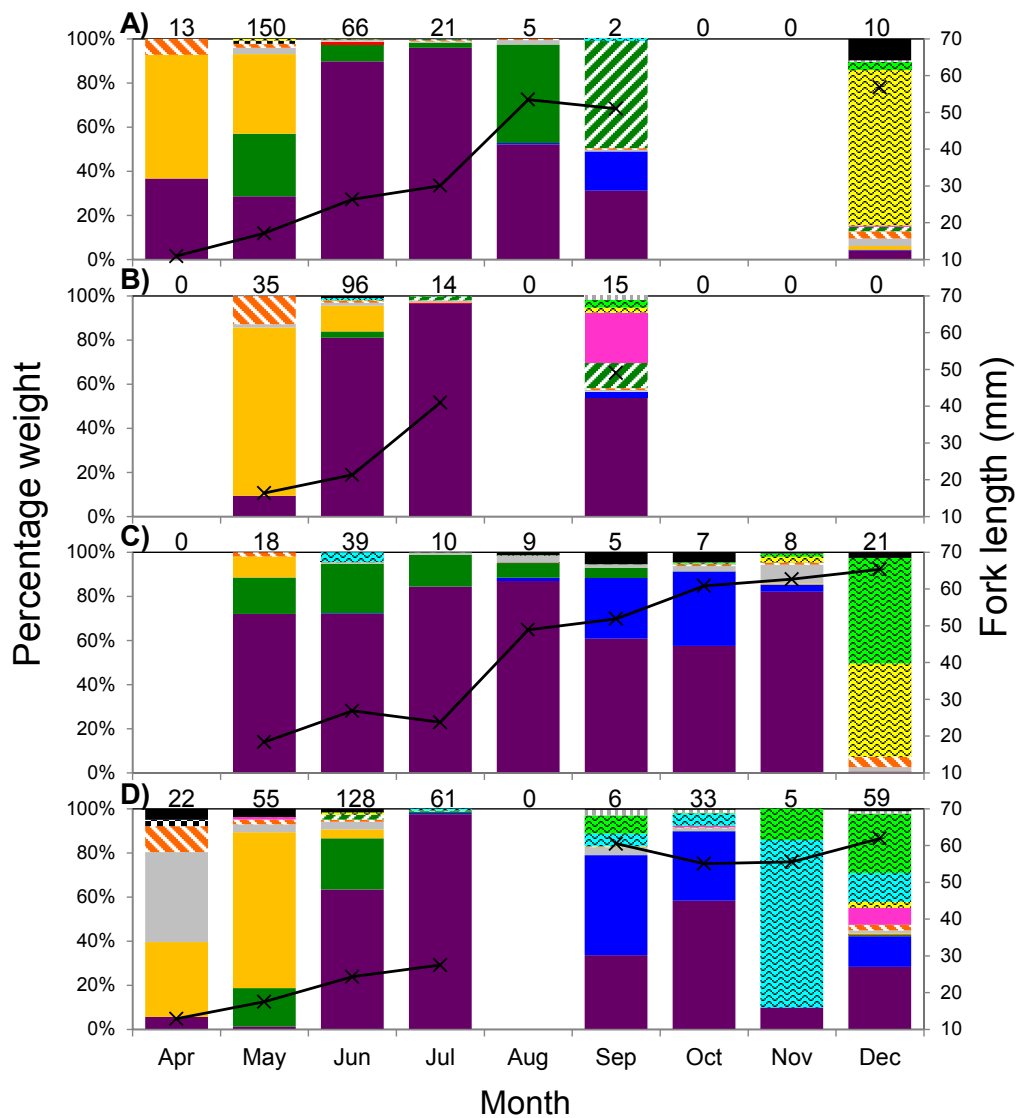


Figure 42. Percentage by weight of prey types found in stomachs of age-0 Delta Smelt collected from < 1 ppt during April through December in A) 2005, B) 2006, C) 2010, and D) 2011. Number of stomachs examined are shown above the columns. Mean fork length (mm) of Delta Smelt is also shown.



- Pseudo. spp.*
- A. sinensis*
- S. doerri*
- Tortanus spp.*
- E. affinis*
- Other calanoids
- Other cyclopoids
- Limno. spp.*
- Harpacticoids
- Copepod nauplii
- Cladocerans
- Mysids
- Amphipods
- Cumaceans
- Fish
- Other
- × — Mean length

Figure 43. Percentage by weight of prey types found in stomachs of age-0 Delta Smelt collected from Cache Slough-Sacramento River Deepwater Ship Channel (CS-SRDWSC) during April through December in A) 2005, B) 2006, C) 2010, and D) 2011. Number of stomachs examined are shown above the columns. Mean fork length (mm) of Delta Smelt is also shown.

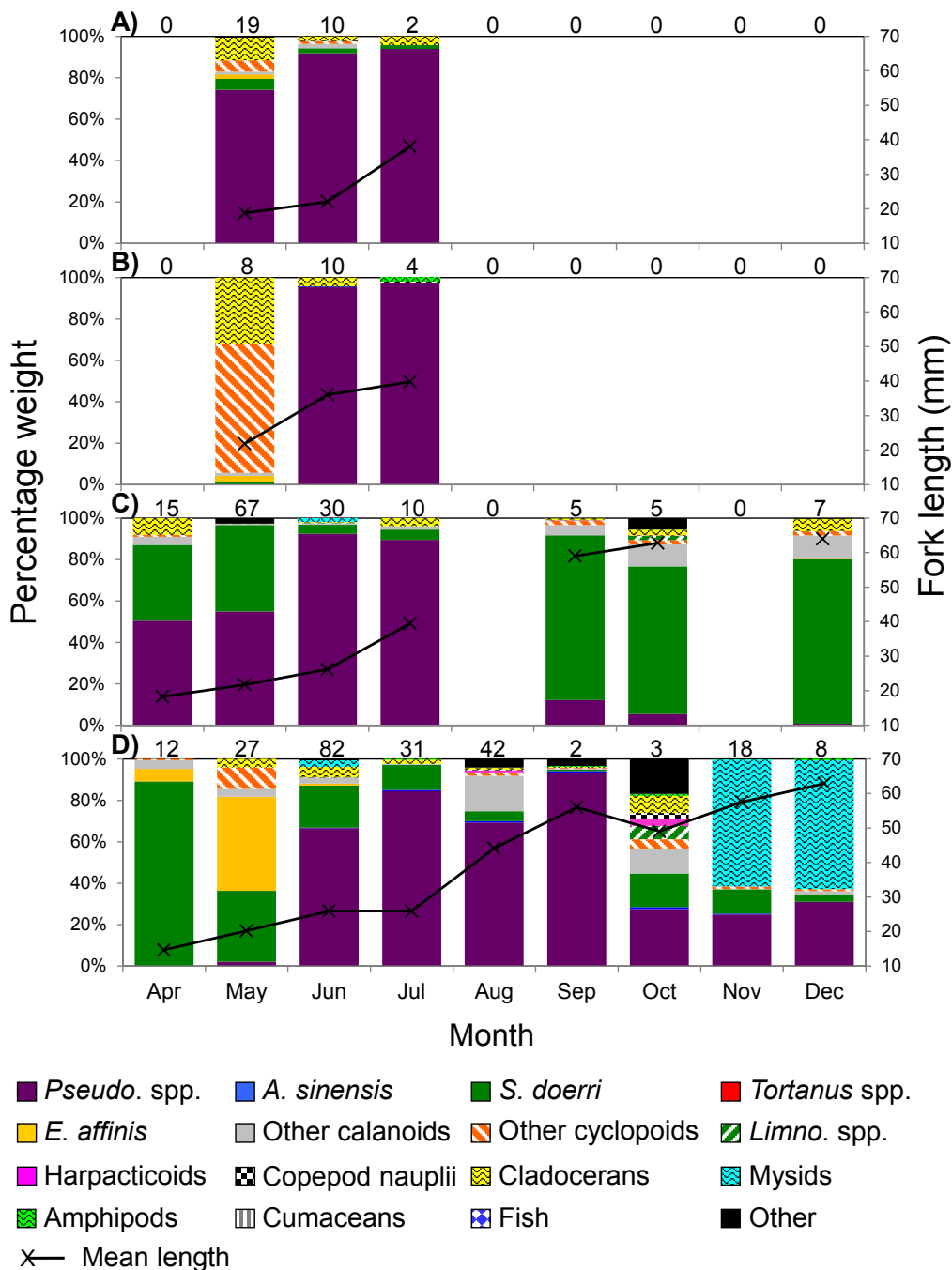
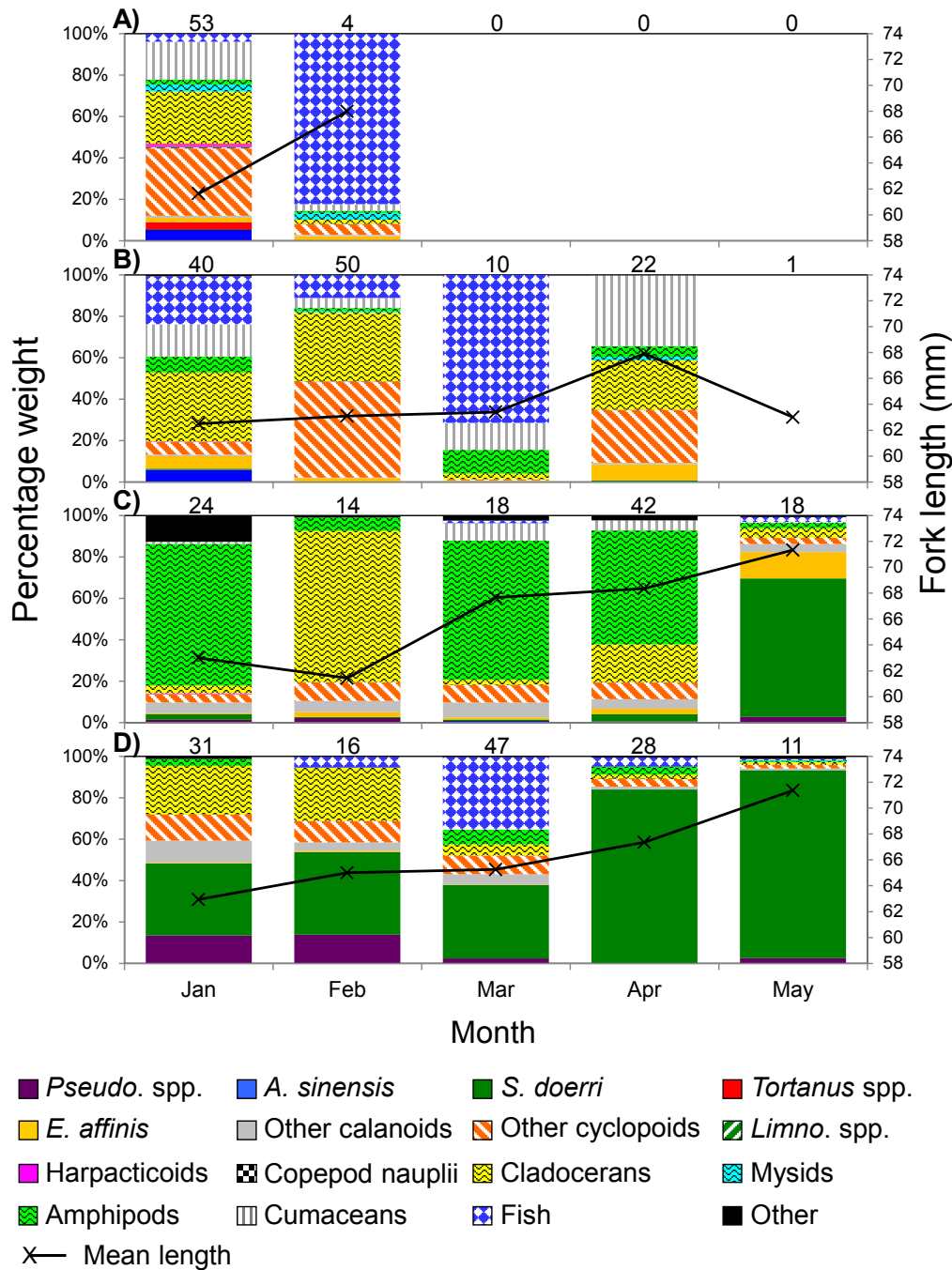


Figure 44. Percentage by weight of prey types found in stomachs of adult Delta Smelt collected in 2012 during January through May from A) > 6 ppt, B) 1-6 ppt, C) < 1 ppt, and D) Cache Slough-Sacramento River Deepwater Ship Channel (CS-SRDWSC). Number of stomachs examined are shown above the columns. One fish examined from 1-6 ppt in May had an empty stomach. Mean fork length (mm) of Delta Smelt is also shown.



Although substantial uncertainties about mechanisms remain, the decline of *P. forbesi* in the Suisun region may be related to increasing recruitment failure and mortality in this region due to competition and predation by *P. amurensis*, contaminant exposures, and entrainment of source populations in the Delta (Mueller-Solger et al. 2006, Winder and Jassby 2011, Durand 2010).

The abundance of a more recent invader, the cyclopoid copepod *Limnoithona tetraspina*, significantly increased in the Suisun Bay region beginning in the mid-1990s. It is now the most abundant copepod species in the Suisun Bay and confluence region of the estuary (Bouley and Kimmerer 2006, Winder and Jassby 2011). Gould and Kimmerer (2010) found that it grows slowly and has low fecundity. Based on these findings they concluded that the population success of *L. tetraspina* must be due to low mortality and that this small copepod may be able to avoid visual predation to which larger copepods are more susceptible. It has been hypothesized that *L. tetraspina* is an inferior food for pelagic fishes including Delta Smelt because of its small size, generally sedentary behavior, and ability to detect and avoid predators (Bouley and Kimmerer 2006, Gould and Kimmerer 2010). Nevertheless, this copepod has been found in the guts of Delta Smelt when *Limnoithona* spp. occurs at extremely high densities relative to other zooplankton (Slater and Baxter 2014). Recent experimental studies addressing this issue suggest that larval Delta Smelt will consume and grow on *L. tetraspina*, but growth is slower than with *P. forbesi* (Kimmerer et al. 2011). It remains unclear if consuming this small prey is energetically beneficial for Delta Smelt at all sizes or if there is a breakpoint above which larger Delta Smelt receive little benefit from such prey. *Acartiella sinensis*, a calanoid copepod species that invaded at the same time as *L. tetraspina*, also reached considerable densities in Suisun Bay and the western Delta over the last decade (Hennessy 2010), although its suitability as food for pelagic fish species remains unclear.

Preliminary information from studies on pelagic fish growth, condition, and histology provide additional evidence for food limitation in pelagic fishes in the estuary (IEP 2005). In 1999 and 2004, Delta Smelt growth was low from the Sacramento-San Joaquin confluence through Suisun Bay relative to other parts of the system. Delta Smelt collected in 2005 from the Sacramento-San Joaquin confluence and Suisun Bay also had high incidence of liver glycogen depletion, a possible indicator of food limitation (Bennett et al. 2008). As previously noted, warm water temperatures during the summer period may have exacerbated lack of food by raising the metabolic rate of Delta Smelt. Based on data for histopathology, date of birth from otoliths, and growth rates from otoliths of Delta Smelt in 2005, Bennett et al. (2008) proposed a novel strategy for Delta Smelt survival in 2005. Natural selection appeared to favor individuals with a specific set of characters, including relatively slow larval development, but faster than average juvenile growth in July. Water temperatures in July typically include the annual maximum (Fig. 16). The salinity field can also change rapidly as freshwater flow out of the Delta changes. Many of these fish surviving into the pre-adult stage had also hatched earlier in the spawning season (i.e., before May).

For many fishes, success at first feeding is believed to be critical to larval survival and a major cause of year-class variability (e.g., “critical period hypothesis,” Hjort 1914, Leggett and DeBlois 1994). In Rainbow Smelt *Osmerus mordax* a related smelt species, calculated larva mortality rates were related to feeding conditions at first feeding that varied on a predictable cycle of 15 days associated with tide and photoperiod (Sirois and Dodson 2000b). In feeding experiments, copepod evasion behavior affected capture by larval Striped Bass, and *E. affinis* was among the more easily captured species (Meng and Orsi 1991). There has been a long-term decline in calanoid copepods in the upper estuary, particularly in the Suisun Region (Winder and Jassby 2011), potentially reducing feeding success, growth and thereby survival. Currently, *E. affinis*

abundance peaks in spring (Hennessy 2010, 2011) coincident with hatching of Delta Smelt. *E. affinis* abundance has been negatively related to X2 since the overbite clam invasion (Kimmerer 2002b). When X2 is “high” outflow is low and *E. affinis* densities are low. These lines of evidence suggest that the first feeding conditions may improve in springs with higher outflow.

Changes in the quality and quantity of available prey may have contributed to the observed reduction in the mean size of Delta Smelt in fall since the early 1990s (Sweetnam 1999, Bennett 2005); however, mean size subsequently increased. The importance of food resources as a driver is supported by Kimmerer (2008), who showed that Delta Smelt survival from summer to fall is correlated with biomass of copepods in the low salinity zone, the central 50% of the summer Delta Smelt distribution. Other variations of this correlation were shown by Maunder and Deriso (2011) and Miller et al. (2012). Miller et al. (2012) have tested for an explicit influence of prey density during the fall. Miller et al. (2012) found a stronger correlation between Delta Smelt abundance during the fall and prey density during the fall than for prey density during the summer.

Harmful algal blooms

Periodic blooms of the toxic blue-green alga *Microcystis aeruginosa* during late summer, most commonly August and September are an emerging concern for Delta Smelt (Lehman et al. 2005, Lehman et al. 2013). Although this harmful algal bloom (HAB) typically occurs in the San Joaquin River away from the core summer distribution of Delta Smelt, some overlap is apparent during blooms and as cells and toxins are dispersed downstream after blooms (Baxter et al. 2010). Density rankings of *Microcystis* at TNS stations were highest in the south Delta, east Delta and lower San Joaquin River regions; yet *Microcystis* distribution may be expanding north over time (Morris 2013). Moreover, studies by Lehman et al. (2010) suggest that Delta Smelt likely are exposed to microcystins, which may degrade their habitat and perhaps affect the distribution of Delta Smelt (Baxter et al. 2010). For example, these HABs are known to be toxic to another native fish of the region, Sacramento Splittail (Acuña et al. 2012a) and the alien Threadfin Shad (Acuña et al. 2012b). Histopathology evidence from Lehman et al. (2010) suggested the health of two common fish in the estuary, Striped Bass, and Mississippi Silversides, was worse at locations where microcystin concentrations were elevated.

Indirect effects are also likely as *Microcystis* blooms are toxic to copepods that serve as the primary food resources of Delta Smelt (Ger et al. 2009, 2010a,b). Ger et al. (2009) determined toxicity of one form of microcystin (LR) to two species of calanoid copepods, *E. affinis* and *P. forbesi*, which are important as food to Delta Smelt. They found that, although the copepods tested were relatively sensitive to microcystin-LR compared to other types of zooplankton, ambient concentrations in the Delta were unlikely to be acutely toxic. However, chronic effects were not determined and Lehman et al. (2010) found that *Microcystis* may indeed contribute to changes in phytoplankton, zooplankton and fish populations in the Delta.

Factors that are thought to cause more intensive *Microcystis* blooms include warmer temperatures, lower flows, high nitrogen levels, and relatively clear water (Lehman et al. 2005, Baxter et al. 2010, Lehman et al. 2013, Morris 2013). These conditions occur during dry years in the SFE. Both *Microcystis* abundance and microcystin concentrations have been greater in recent years with dry year conditions (Lehman et al. 2013). These factors can also interact. For example, low flows can provide less dilution of ammonium from wastewater treatment plants (Jassby and Van Nieuwenhuysse 2005, Dugdale et al. 2012, Dugdale et al. 2013) and *Microcystis* can

readily utilize ammonium as a primary nitrogen source during blooms (Lehman et al. 2013). The intensity and duration of *Microcystis* blooms are expected to increase over the long-term, along with any negative impact on aquatic organisms, due to increased frequency of drought conditions associated with climate change (Lehman et al. 2013).

Chapter 5: Updated Conceptual Models for Delta Smelt

In this Chapter we transfer the information on drivers and Delta Smelt responses reviewed and presented in Chapter 4 into the conceptual model framework established in Chapter 3. The Delta Smelt general life cycle conceptual model recognizes the pervasive, year-round importance of the tier 1 landscape attributes and the seasonal importance of the various tier 2 environmental drivers and tier 3 habitat attributes to the tier 4 life stage transitions of Delta Smelt in the four tier 5 “transition seasons” (Fig. 45). Some habitat attributes – food, toxicity, and predation – affect life stage transitions in all seasons, while other habitat attributes – temperature, entrainment and transport, size and location of the low salinity zone, and harmful algal blooms – affect some life stage transition more than others. Clearly, adequate food must be available at all life stages for Delta Smelt to survive. Toxicity is included during all seasons because we know that contaminants of various types are present throughout the year; however, little is known about the direct or indirect effects of contaminants at ambient concentrations on individual Delta Smelt or the population as a whole. Predation is included in all seasons because we recognize that predation is likely the ultimate cause of mortality for most individual fish; however, responses of Delta Smelt to other habitat attributes and environmental drivers such as food availability and turbidity can modify predation risk.

The mechanistic linkages between landscape attributes, environmental drivers, habitat attributes and Delta Smelt responses in the four life stage seasons are depicted as one-way arrows in four new “life stage transition” conceptual models (Figs. 46-49). As mentioned in Chapter 3, the life stage transition conceptual models are nested components of the general life cycle conceptual model (Fig. 8). Each life stage transition conceptual model (Figs. 46-49) includes the habitat attributes hypothesized to affect the transition of Delta Smelt from one life-stage to the next. Hypotheses selected for detailed consideration in Chapter 7 are indicated by “H” in the diagrams. The models also show the landscape attributes and environmental drivers. While the models include many linkages among individual landscape attributes, environmental drivers, and habitat attributes, they do not include linkages between individual habitat attributes and the specific biological processes (growth, survival, reproduction) underlying the life stage transitions. The primary reason for this simplification is that the available data are generally inadequate to fully describe and differentiate among specific functional relationships and mathematical modeling that could help estimate them is beyond the scope of this report. Instead, the combined effects of all habitat attributes on the life stage transition probability are depicted by one upward arrow in each life stage transition conceptual model. This does not imply, however, that all habitat attributes have an equal role in determining life stage transition probability and population success or that the role of each habitat attribute remains constant from year to year.

In the remainder of this Chapter we briefly describe the linkages and associated hypotheses depicted in each of the life stage transition conceptual model diagrams (figs. 46-49). These

Figure 45. Delta Smelt general life cycle conceptual model.

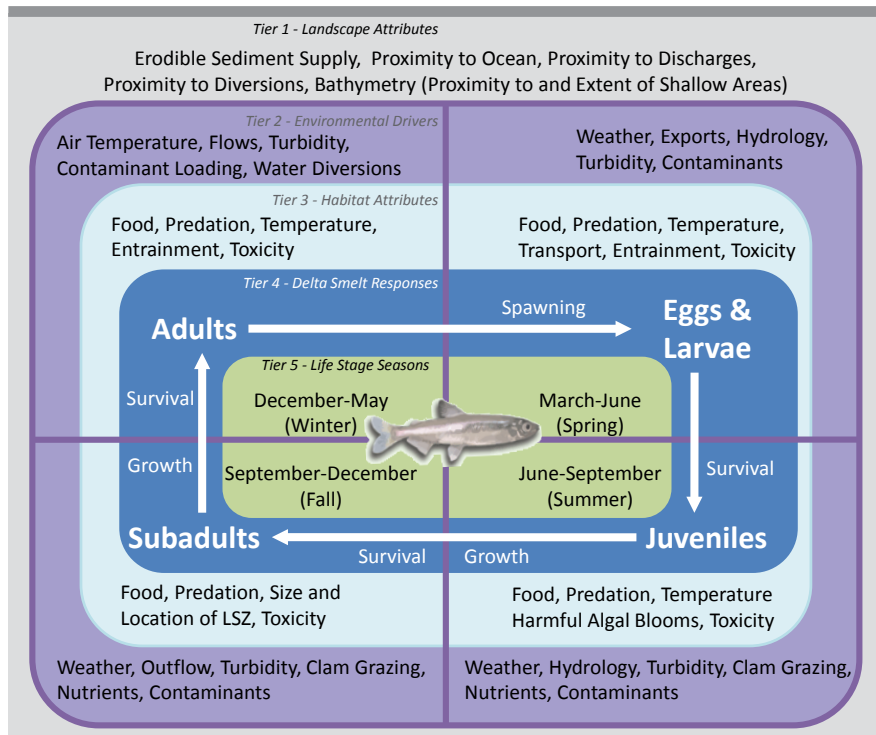


Figure 46. Conceptual model of drivers affecting the transition from Delta Smelt adults to larvae. Hypotheses addressed in Chapter 7 are indicated by the “H-number” combinations.

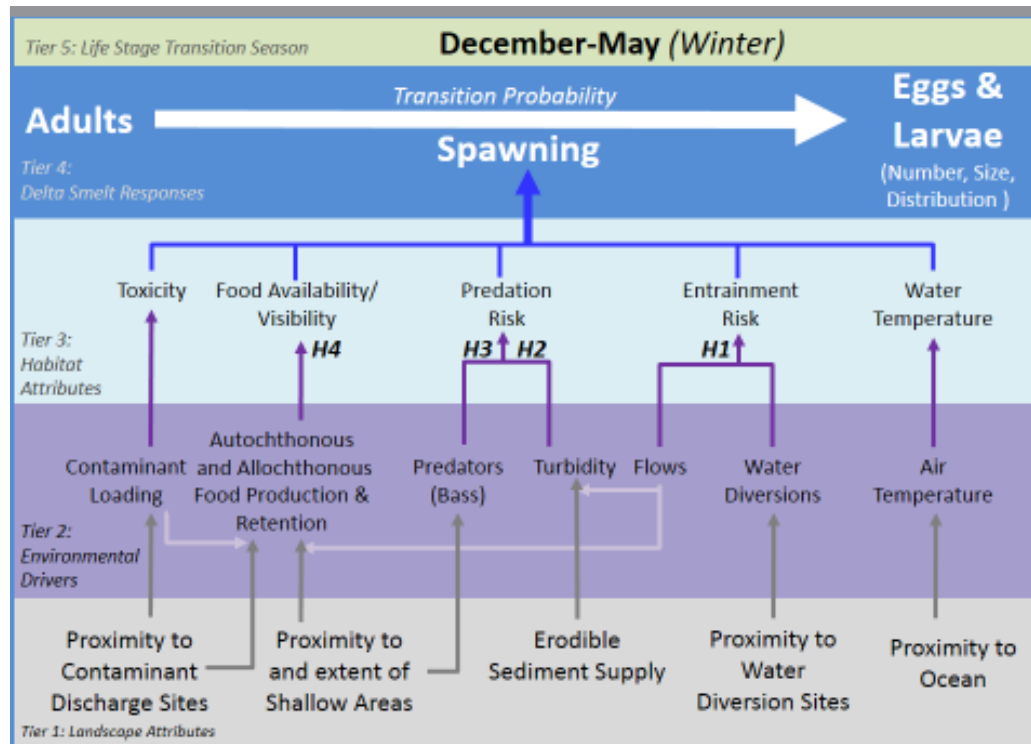


Figure 47. Conceptual model of drivers affecting the transition from Delta Smelt larvae to juveniles. Hypotheses addressed in Chapter 7 are indicated by the “H-number” combinations.

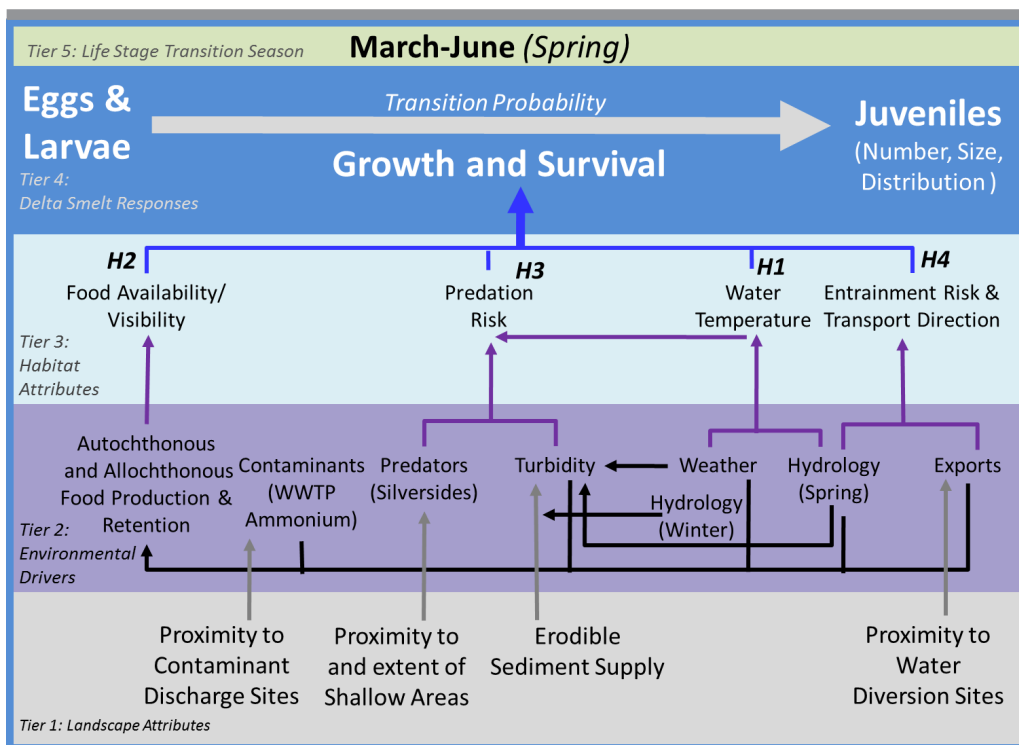


Figure 48. Conceptual model of drivers affecting the transition from Delta Smelt juveniles to subadults. Hypotheses addressed in Chapter 7 are indicated by the “H-number” combinations.

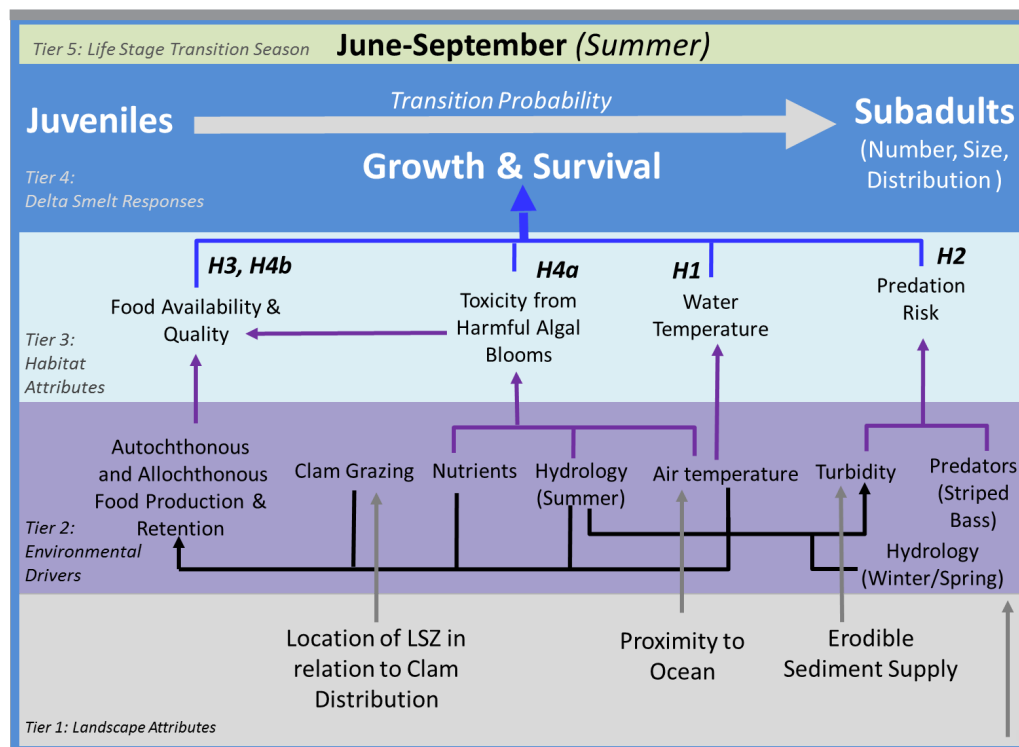
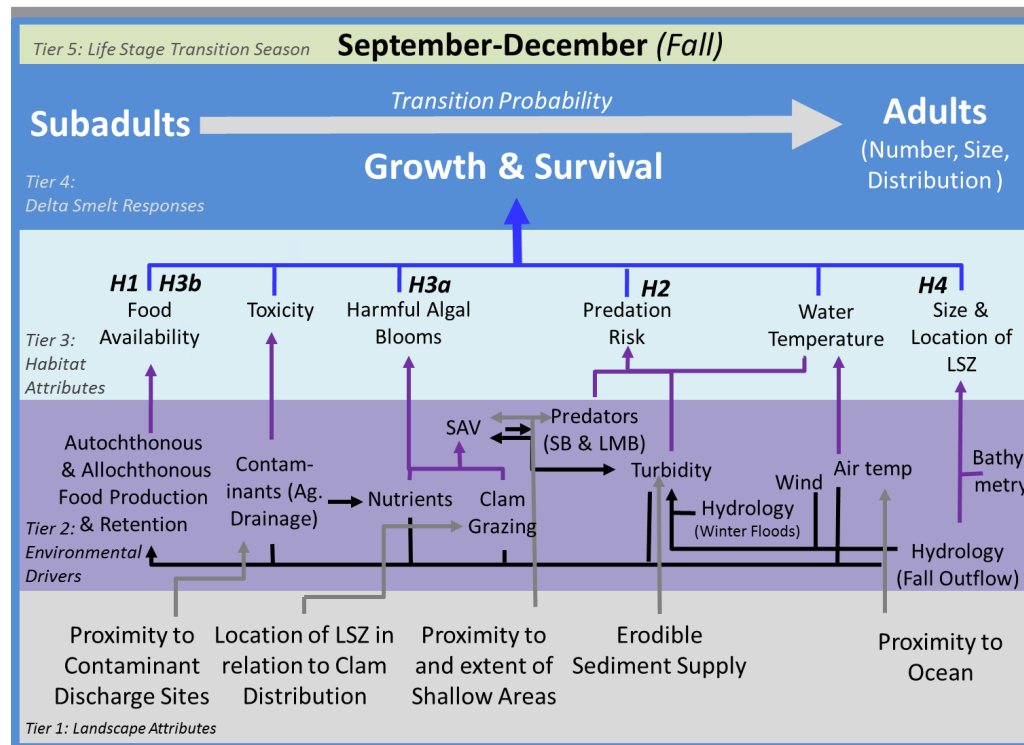


Figure 49. Conceptual model of drivers affecting the transition from Delta Smelt subadults to adults. Hypotheses addressed in Chapter 7 are indicated by the “H-number” combinations.



hypotheses are stated and addressed in more detail in Chapter 7. All hypotheses focus on the life stage that is transitioning to (i.e. occurs prior to) the next life stage, for example, adults but not eggs and larvae, larvae and post-larvae but not juveniles, and so on. That said, it is important to remember that all life stages overlap and all transitions except for the transitions from adults to eggs and from eggs to freshly hatched larvae are gradual, not abrupt, and delineations of life stages are somewhat arbitrary (see Chapter 3).

The life stage conceptual model for the transition of adult Delta Smelt to eggs and larvae (Fig. 46) includes 5 habitat attributes. Because of the lack of information about specific contaminant effects on Delta Smelt noted above, there are no specific hypotheses regarding the effects of contaminants and possible direct or indirect toxicity on Delta Smelt, but based on the information discussed in Chapter 4, the model does recognize that effects on Delta Smelt or its food supply may be occurring. Food availability and visibility are hypothesized to be important with respect to providing nutrition that allows Delta Smelt to grow into healthy, large adults that can produce a large numbers of high quality eggs as well as multiple clutches of eggs over the spawning season. The availability of food is considered dependent on both food production and the availability of such food to the fish. There are two hypotheses related to predation risk. The first is that turbidity, created by the interaction of high winter and spring flows with the erodible sediment supply in the watershed and within the Delta, influences the vulnerability of Delta Smelt to predators that co-occur with them. The second is that Delta Smelt behaviors that bring Delta Smelt close to channel edges may increase their vulnerability to Largemouth Bass, which generally occupy nearshore and vegetated habitats such as SAV beds. Entrainment risk in this life stage transition conceptual model is focused on adults. Entrainment of adults would reduce the reproductive

potential of the population. Entrainment risk depends on the distribution of the adult Delta Smelt in relation to water diversions, and the magnitudes of water diversions and flows. Delta water temperature determines the beginning and duration of the spawning season (hereafter “spawning window”).

The life stage conceptual model for the transition of Delta Smelt eggs and larvae to juveniles includes 4 habitat attributes (Fig. 47). Food production and availability is important for the survival of larvae to juveniles. Food quantity is dependent on multiple interacting factors. Turbidity is important for early feeding by delta smelt larvae. Predation risk focuses on predation of Mississippi Silversides on Delta Smelt larvae because of recent evidence that such predation occurs. Predation risk is hypothesized to depend on co-occurrence of the two species, with Mississippi Silverside generally being associated with shallower waters, turbidity, which decreases the effectiveness of predators, and water temperature, which affects energy requirements of predators (hunger level). In addition to its effect on predator bioenergetics, water temperature is hypothesized to affect the length of the spawning season (spawning window). If food availability is sufficient, then a longer spawning window may allow the adult population to produce multiple clutches of eggs, resulting in more young. This hypothesis could arguably be included in the previous life stage transition conceptual model, but considering it here allows for consideration of predation on larvae in the context of the time period over which larvae are being produced. Larvae are also at risk of entrainment or transport to unfavorable areas. The magnitude of this risk is hypothesized to depend on an interaction of spring hydrology and water exports. As indicated by numerous arrows, winter and spring hydrology affect Delta Smelt spawning and larval rearing habitat in many ways. We thus also include a more general hypothesis about the hydrological effects on Delta Smelt larval abundance and recruitment.

The life stage conceptual model for the transition of Delta Smelt juveniles to subadults includes 4 habitat attributes (Fig. 48). In addition, there is a stand-alone hypothesis dealing with population dynamics. Juvenile growth and survival is hypothesized to depend on availability and quantity of food. Food production during this summer period is hypothesized to involve complex interactions of clam grazing, nutrients, hydrology and harmful algal blooms. The probability of observing a harmful algal bloom is hypothesized to be a function of the same factors but with temperature playing an important role. Harmful algal blooms may also affect Delta Smelt directly through production of toxic microcystins. Summer water temperatures are hypothesized to have a very direct effect on juvenile Delta Smelt with water temperatures hypothesized to reach stressful levels, affecting their bioenergetics and the area of suitable habitat. The transition probability hypothesis is that at the currently small population sizes, survival from juvenile to subadult is density independent, meaning independent of the number of individuals present (see Chapter 6 for details).

The life stage conceptual model for the transition of Delta Smelt subadults to adults includes 6 habitat attributes (Fig. 49). As for the previous conceptual model, there is a stand-alone hypothesis dealing with population dynamics. As in the previous conceptual model, growth and survival are hypothesized to depend on food availability and food production and availability depends on interactions of a variety of landscape attributes and environmental drivers. Toxicity is recognized as potentially important but no specific hypotheses have been tested. Harmful algal blooms may still be present with hypothesized direct effects on Delta Smelt subadults and indirect effects on their food. Predation risk on subadult Delta Smelt is hypothesized to depend on co-occurrence of Delta Smelt with the two most likely predators, Largemouth Bass and Striped Bass. Largemouth Bass occurrence is linked with that of SAV and the vulnerability of prey to both predators is affected by turbidity and bioenergetics. Water temperature is mainly

hypothesized to have an effect through bioenergetics because water temperature becomes less stressful than in the summer. In this conceptual model the size and location of the LSZ is considered both a landscape attribute and a habitat attribute. In the earlier conceptual models, the LSZ was mainly viewed as a landscape attribute that interacted with other landscape attributes and environmental drivers to create habitat attributes. In this conceptual model the size and position of the LSZ is hypothesized to have certain characteristics that directly determine habitat quantity and quality for Delta Smelt. The transition probability hypothesis is that at the currently small population sizes, survival from subadult to adult is density independent, meaning independent of the number of individuals present (see Chapter 6 for details).

Chapter 6: Delta Smelt Population Biology

This Chapter consists of two main parts. In the first part, we introduce general concepts in population biology that are utilized in the following sections of this Chapter and to generally describe Delta Smelt population dynamics. Explaining these concepts and population trends now is intended to reduce repetitive text in the remaining sections and to reduce possible confusion for readers unfamiliar with the concepts. The concepts are discussed specifically in the context of Delta Smelt.

In the second part of this Chapter, we review information about the life history and population trends of each Delta Smelt life stage represented in our conceptual models, starting with adults. While we describe trends over the entire available time series for each life stage, we pay particular attention to differences in Delta Smelt abundance and life stage transitions between the two most recent wet years, 2006 and 2011. Our working assumption is that these differences should be attributable to differing habitat conditions and, in some cases, management actions. Differences in habitat conditions between these two years will be further explored in Chapter 7.

Population Biology

Recruitment is the addition of new individuals to a population through reproduction or immigration. In fisheries science, the term recruitment was first used by Ricker (1954) to describe the addition of fish of a new generation to a fish population, in other words, the number of young surviving to a particular age or life stage. We use the term recruitment to refer to production of larvae, juveniles, subadults, or adults by adults of the previous generation. Relationships between numbers of spawning fish or other measures of potential spawning stock (e.g., numbers of subadult or mature prespawning fish) and the numbers of fish of a given age or life stage in the subsequent generation are known as stock-recruitment relationships.

Stock-recruitment relationships have been described for many species and are a central part of the management of commercially and recreationally fished species (Myers et al. 1995, Touzeau and Gouze 1998). Different forms of stock-recruitment relationships are possible, including density-independent, density-dependent, and density-vague types. The density-independent type occurs when the current size of the population has little or no effect on the number of recruits (except possibly when stock size is extremely low). This type of population growth is rare in fish

populations and occurs when environmental factors largely determine the survival and number of recruits (e.g., the Longfin Smelt outflow abundance relationship; see Myers 1998). Density dependence occurs when the current population size affects survival and abundance of recruits and thus population growth. In such populations, within the lower range of stock size, the number of recruits is strongly and positively related to stock size. At some point as stock size increases, competition for food (or some other limiting factor) between the adult population and recruits affects survival and abundance of recruits; cannibalism is another means by which recruitment can be affected by stock size. Thus, the growth and survival of the recruit population strongly depends on the density of the stock population. In reality it's difficult to determine which type of response is occurring (e.g., Myers and Barrowman 1996). Moreover, a predominantly annual fish, such as Delta Smelt, is predicted to conform poorly to models that assume density-dependent recruitment (Winemiller 2005), which appears to be the case (e.g., Rose et al. 2013).

The idea of density dependence is related to the idea of carrying capacity. The carrying capacity of an ecosystem is the number of individuals of all species that can be supported by the available resources. In reality it can be very difficult to apply this idea to a single species in an ecosystem because of the complex relationships among species and the seasonal, annual, and other changes in resource availability. The density vague type of population growth refers to situations where there is not a statistically demonstrable stock-recruitment relationship observable in available data.

In density-dependent stock-recruitment relationships, the factors causing the density dependence can operate at various points in the life cycle of the new generation. For some species, the concept of density dependence is separated into two concepts. In this formulation, density-dependent stock recruitment is limited to the direct effects of the adult stock on recruitment of the next generation, as described above. For example, if a large spawning stock has a limited spawning area, as in the case of salmonids, then successive waves of female spawners are known to re-excavate previous nests while building their own, substantially increasing mortality of the eggs. Density dependence could also occur at the larval or juvenile stage if adults are predatory and feed on young, or if adults are in direct competition for food or space with young. The second concept of density-dependent survival is often inextricably linked to density-dependent stock-recruit relationships because the mechanisms causing declines in recruits at high stock levels are unknown. In density-dependent survival, the abundance of young affects their own survival.

In the case of Delta Smelt, density dependent survival could occur if many of the larvae starved because of insufficient food supplies due to competition with other Delta Smelt larvae, or other species. Because many Delta Smelt die after their first spawning, density-dependent survival is certainly the dominant mechanism for the species and for the remainder of this report the direct effects of adults on survival of eggs and larvae are assumed to be minimal. If resources were sufficient for larvae and juvenile fish to survive in large numbers, the surviving subadults might overwhelm food sources (i.e., surpass carrying capacity), resulting in low survival and poor reproductive output. Thus, it is important to understand species ecology and survival between life stages to understand how density dependence is affecting a population. This is particularly important for fishes in estuaries where environmental factors can create large variation in habitat size and food web productivity from season to season and year to year, thus affecting carrying capacity and the potential for density-dependent survival.

Density-independence is more straightforward. In this case, the population is controlled by factors unrelated to the density of the population. For example, high water temperatures will affect individual fish, whether the population is large or small. In reality, populations can be

affected by both density-dependent and density-independent factors at different times. This interaction is the basis for the idea of compensatory density dependence. In this formulation, a population is governed by density independent factors when population size is small. As the population increases and approaches the carrying capacity, density-dependent factors become important and the population growth rate declines. Fluctuations in carrying capacity, as noted above, are an added complication. Again, it is essential to understand the ecology of the species and survival between life stages to understand the relative importance of density dependent and density independent factors.

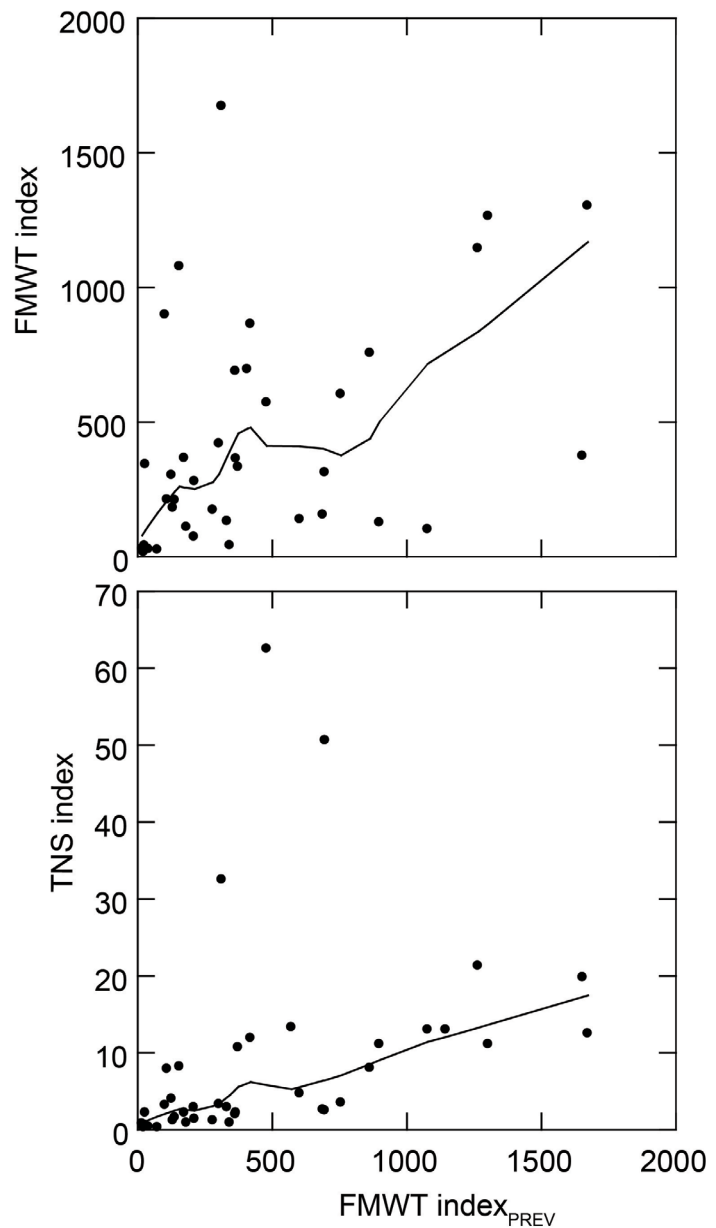
Unfortunately, Delta Smelt were never of sufficient interest as a commercial or recreational species to warrant development of stock-recruitment models until they were listed. Data now used to develop stock-recruitment models for Delta Smelt started becoming available after the initiation of fisheries studies and monitoring surveys in the late 1950s (TNS initiated 1959; FMWT initiated 1967) in association with the planning and operation of the CVP and SWP. These IEP fish monitoring surveys were designed to produce relative abundance indices or catch-per-unit-effort (CPUE, e.g., number per trawl) that could be used to monitor trends in abundance over time. More recently, annual abundance indices based on these surveys have also been incorporated into stock-recruit relationships (e.g., Moyle et al. 1992, Sweetnam and Stevens 1993, Miller 2000, Bennett 2005, Maunder and Deriso 2011). Neither of these early IEP fish monitoring surveys (TNS, FMWT) were specifically designed to monitor Delta Smelt, but instead targeted primarily the commercially and recreationally more important Striped Bass. As researchers began using TNS and FMWT indices for Delta Smelt analyses, they began investigating how the indices performed and means to improve them (see Wadsworth and Sommer 1996, Miller 2000, Newman 2008). This work is ongoing and also includes similar investigations for the newer SKT (initiated in 2002) and 20 mm survey (initiated in 1995) monitoring surveys.

The two stock-recruitment relations based on the longest data records include the relationship of the FMWT abundance index with the FMWT abundance index in the previous year and the relationship of the TNS abundance index with the FMWT abundance index in the previous year (Fig. 50). Because of the large changes that have occurred in the Delta ecosystem, including the invasion by *P. amurensis* and the POD, these plots can be difficult to interpret because carrying capacity is assumed to have changed (Bennett 2005, Kimmerer et al. 2000, Sommer et al. 2007). It does appear that there is much more variability associated with the FMWT relationship compared to the TNS relationship. This might indicate variable survival between the juvenile and subadult life stage.

In any form of a stock-recruitment model, there is a point at which low adult stock will result in low juvenile abundance and subsequent low recruitment to future adult stocks. This can occur even under favorable environmental conditions while the stock “rebuilds” itself. From a stock-recruitment perspective, the recent low abundance of Delta Smelt is of particular concern. Since about 2002, the current population is smaller than at any time previously in the record, with the exception of the 2011 year class. This strong year class suggests that Delta Smelt have yet to reach low levels where the stock will need years to rebuild, at least to pre-POD levels (Fig. 3).

In addition to their use in exploring stock-recruitment relationships, ratios of annual Delta Smelt abundance indices can also be used to obtain rough estimates of relative annual recruitment and survival rates (figs. 51 and 52). As for the stock-recruitment relationships these recruitment and survival indices should be interpreted with caution given the large changes that have taken place in the Delta and the absence of estimates of variability for the indices. The main utility of these

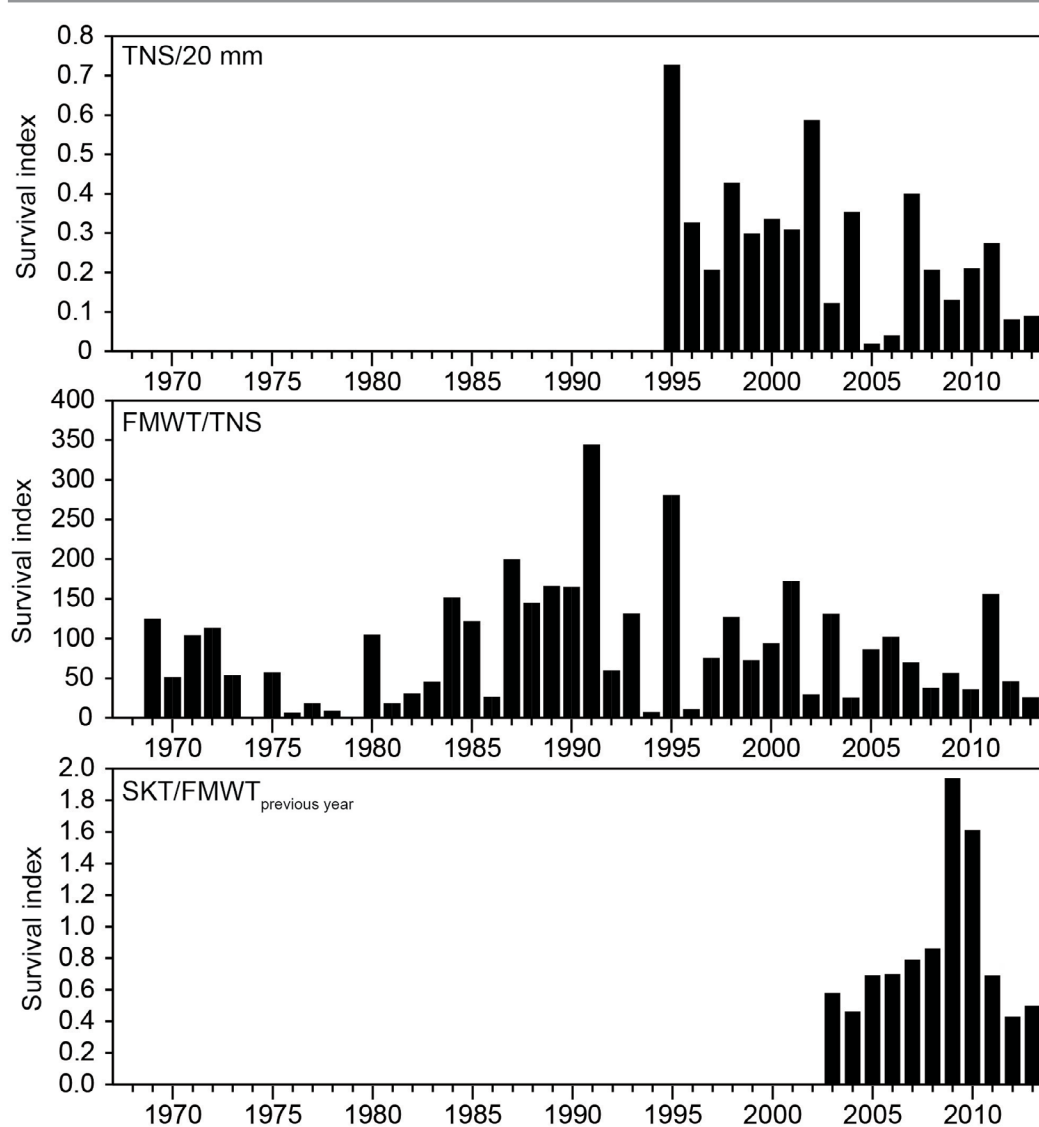
Figure 50. Scatterplots and LOWESS splines depicting the relationship of the Fall Midwater Trawl index of Delta Smelt relative abundance (FMWT) (1968-2012) and Summer Towntnet Survey (TNS) (1969-2012) with the FMWT in the previous year.



indices is identifying years with relatively high or low survival for a specific life stage transition or life stage transitions with differences in annual variability.

Here, we use the ratios of abundance indices for different life stages of the same generation as indices of survival (survival indices, Fig. 51) and the ratios of current to preceding year abundance indices as indices of recruitment (recruitment indices, Fig. 52). For the density-independent case, recruitment rate is independent of the size of the adult population. The number

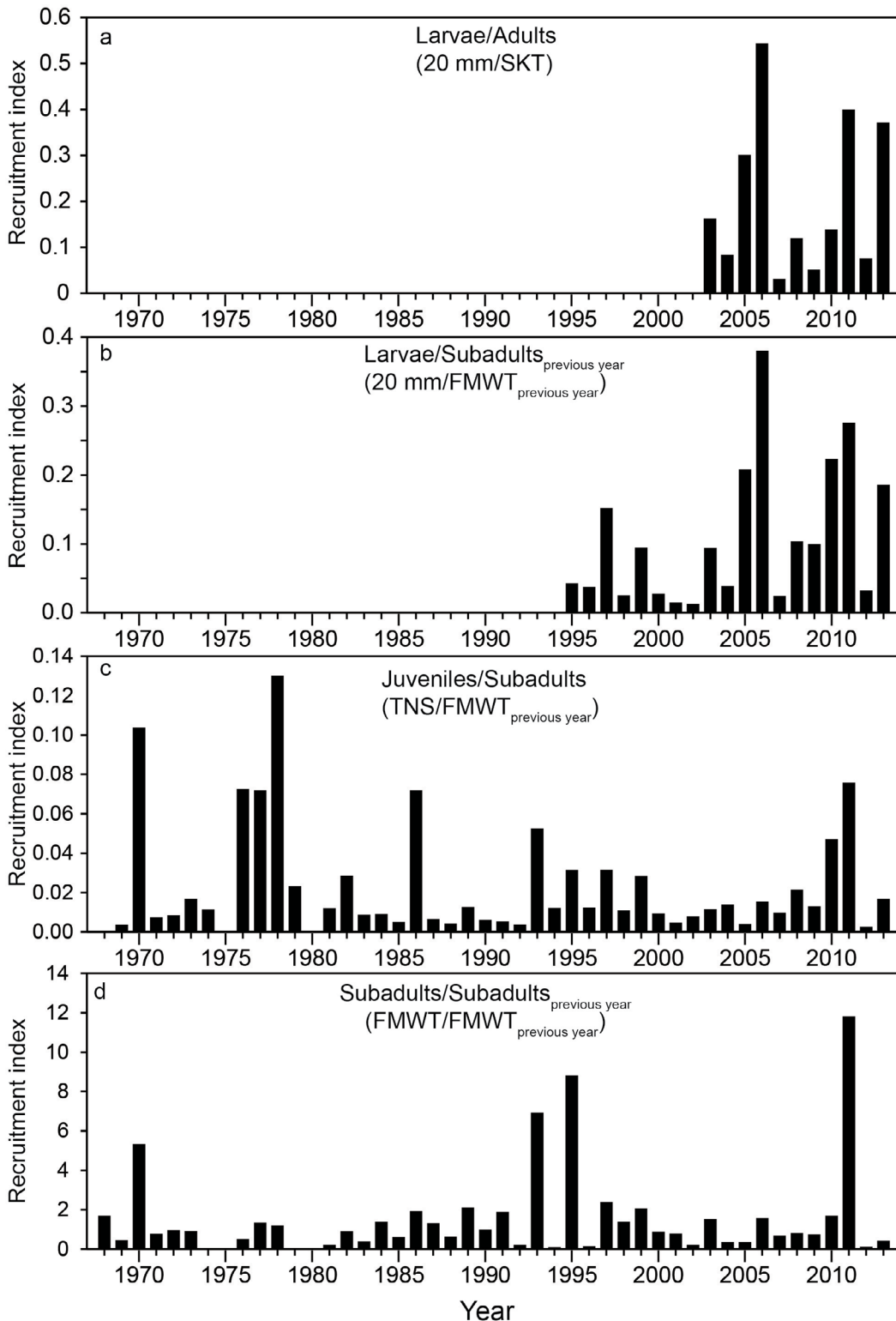
Figure 51. Stage to stage survival indices based on data from Summer Townet Survey (TNS), Fall Midwater Trawl (FMWT), and Spring Kodiak Trawl (SKT).



of recruits produced is the product of recruitment rate and the size of the adult population. For this report, we assume that the estimates have sufficiently low and comparable uncertainty to provide worthwhile interpretations, as long as caution is exercised. It is also important to remember that abundance, survival, and recruitment index values are only meaningful in a relative, not in an absolute sense.

The annual stage to stage survival indices from larvae to juveniles, subadults, and adults are shown in Figure 51. The relative recruitment rates from adults and subadults in one year to larvae, juveniles, and subadults the next year are shown in Figure 52. We recognize that a life cycle model with environmental covariates is needed to fully assess the combined effects of stock-recruitment and stage-to-stage survival indices on Delta Smelt population dynamics. Nevertheless, examination of the recruitment and survival index data sets reveal several interesting patterns for the POD period (2003-2013).

Figure 52. Delta Smelt recruitment indices based on the annual adult, larval, juvenile, and subadult abundance indices provided by the Spring Kodiak Trawl (SKT, adults), 20 mm Survey (20 mm, larvae), Summer Townet Survey (TNS, juveniles), and Fall Midwater Trawl (FMWT, subadults).



First, interannual variability in these stock and survival indices declines from larval recruitment (coefficient of variation (CV): 92%), to subsequent larvae to juvenile survival (CV: 67%), juvenile to subadult survival (CV: 43%), to subadult to adult survival (CV: 38%). This result is consistent with expected highly dynamic patterns of recruitment and survival for an annual opportunistic species such as Delta Smelt. The pattern of reduced variability in survival for larger fish suggests that older fish may no longer be vulnerable to some forms of mortality affecting earlier life stages either because a factor is no longer important when larger fish are present (e.g., effect of summer high water temperatures on juveniles) or that larger fish escape some forms of mortality (e.g., larger fish are no longer eaten by the large variety of predators able to consume larvae).

Second, the patterns of adult and larval abundance (Fig. 3) and adult to larvae recruitment (Fig. 52a) suggest: (1) even a small adult Delta Smelt stock can produce a large number of larvae under the right habitat conditions; but (2) larval recruitment is not a good predictor of juvenile survival and subsequent adult stock size. In other words, good larval recruitment sets the stage for population recovery, but good survival through subsequent life stage transitions is needed to realize its potential.

Third, there are clear contrasts in Delta Smelt responses between the two wet years 2006 and 2011 (the years of particular interest in this report) (Figs. 51 and 52). Since the initiation of the SKT survey for adult Delta Smelt in 2002 (indices calculated beginning in 2003), the recruitment of larvae from adults was greatest in the two wet years 2006 and 2011 (Fig. 52a) compared to the other, drier years in the time series, but in 2006 very strong adult to larvae recruitment was followed by very poor larvae to juvenile survival in the summer (Fig. 51a) and only average survival in the fall (Fig. 51b) and winter (Fig. 51c). This led to low abundance of the subsequent life stages of the 2006 cohort. Survival from larvae to juveniles and subadults was much better in 2011 and, along with good recruitment, led to the highest juvenile and adult abundance indices since the onset of the POD (Fig. 3). In other words, good recruitment set the stage for population recovery in both recent wet years, but a substantial abundance increase was realized only in 2011. Unfortunately the 2011 abundance increase was short-lived; it was immediately followed by poor recruitment and survival in 2012 and abundance indices for the 2012 and 2013 cohorts were once again at the low levels typical for the POD period (Fig. 3). Several consecutive years of good recruitment and survival are likely needed for a more sustained increase of the Delta Smelt population abundance to pre-POD abundance levels. Population declines such as the decline experienced by Delta Smelt do not only reduce the number of individuals, but can also reduce the genetic diversity present in the population. While the 2011-2012 data suggest that recovery of Delta Smelt abundance can still be fairly rapid via high larval recruitment followed by good survival (Figs. 51 and 52) recovery of genetic diversity is a much slower process which is an important conservation concern (Fisch et al. 2011).

Small Delta Smelt population size affects the effective population size (N_e), a measure of the genetic properties of a population and the abundance at which significant genetic diversity is lost due to inbreeding (Falconer and Mackay 1996, Schwartz et al. 2007, Antao et al. 2010). In many species N_e may be orders of magnitude smaller than the census population size (N) and low N_e/N ratios indicate the population may be in danger of losing genetic variability, potentially resulting in reduced adaptability, population persistence, and productivity (Hauser et al. 2002). For Delta Smelt, Fisch et al. (2011) detected a genetic bottleneck in each of four sampling years (2003, 2005, 2007 and 2009) and observed a significant decline in effective population size between sampling years 2003 and 2007 (Fisch et al. 2011). The genetic signal of the decline in N_e is corroborated by the observed abundance index declines and support the hypothesis that decreases

in N_e and allelic richness have likely occurred over the last few decades (Fisch et al. 2011). Genetic changes within the Delta Smelt population deserve continued evaluation with respect to changes in population size.

In addition, Delta Smelt recruitment and the fecundity of adult Delta Smelt likely vary substantially from year to year (Rose et al. 2013b). Delta Smelt fecundity is a function of female size (Bennett 2005, Lindberg et al. 2013). The mean size of adult Delta Smelt declined in the early 1990s (Sweetnam 1999), possibly due to changes in the food web (see Chapter 4), but substantially recovered in the late 2000s. Another possible reason is that in some recent years, there may have been selection for smaller, late-spawned larvae as a result of export pumping schedules (Bennett 2011). For example, Bennett (2011) proposed that high export pumping in late winter may have resulted in high entrainment mortality of offspring from larger, fitter, early spawning females, which produced larger, fitter offspring (Bennett 2011). Further, Bennett et al. (2008) and Bennett (2011) posited that curtailment of export pumping in mid-April related to the Vernalis Adaptive Management Program (VAMP), allowed for greater survival of later-spawned, smaller larvae. The major concern is that these smaller later-spawned larvae have less opportunity to grow to large adult size, especially when food is scarce. If correct, the combined effects of export pumping and food supply on Delta Smelt growth and size could have a nonlinear impact on overall fecundity and population success. This is corroborated by the results from individual-based modeling which showed that growth in fall-winter and the subsequent number of eggs produced per adult were the most important factor determining the success of the next generation (Rose et al. 2013b). Moreover, repeated losses of early-spawned larvae could potentially have a negative effect on expression of this important phenotype and result in eventual loss of genetic variability in the population, and contribute to the genetic bottlenecks reported by Fisch et al. (2011).

Given the unprecedented low abundance of Delta Smelt since 2002 (Fig. 3, summer and fall), serious consideration should be given to evaluation of Allee effects. Allee effects occur when reproductive output per fish declines at low population levels (Berec et al. 2006). In other words, below a certain threshold the individuals in a population can no longer reproduce rapidly enough to replace themselves and the population, exhibiting inverse density dependence, spirals to extinction. For Delta Smelt, possible mechanisms for Allee effects include processes directly related to reproduction and genetic fitness such as difficulty finding mates, genetic drift, and inbreeding (Gascoigne et al. 2009), although none of these effects have been documented yet in Delta Smelt (Fisch et al. 2011). Other mechanisms related to survival such as increased vulnerability to predation (Gascoigne and Lipcius 2004) are also possible. While theoretical work suggests that Allee effects might be common in nature, empirical evidence for Allee effects in natural populations of fishes remains relatively sparse (Myers et al. 1995, Liermann and Hillborn 1997), possibly because they are often masked by measurement errors (Gregory et al. 2010). Recent meta-analytical work by Keith and Hutchings (2012) suggests that Allee effects in marine fish species might be more common than previously thought. But even in the absence of “true” Allee mechanisms, small population size (Hutchings 2013) can produce an emergent Allee effect and prevent recovery of collapsed fish populations even when threats are reduced (Kuparinen et al. 2012). This may be one of the reasons why recovery of many collapsed fish populations remains slow despite large reductions in fishing (Pauly et al. 1998, Hutchings et al. 2010). This finding challenges the traditional fisheries management view that depleted populations will grow and recover rapidly when fishing pressure is relaxed (Hilborn and Walters 1992). In addition, the interactive effects of multiple Allee effects may have important implications for species conservation, but have not yet been well explored in ecology (Berec et al. 2006).

Compensatory density dependence predicts that a fish's population growth or survival rates can increase when abundance is low and decrease if abundance increases beyond a carrying capacity (Rose et al. 2001). If compensatory density dependence occurred in 2011, Delta Smelt survival would be expected to increase as long as the carrying capacity of the environment was not exceeded. Therefore, the sudden increase in subadult abundance in 2011 is consistent with the higher survival predicted by compensatory density dependence at low population abundance coupled with widespread availability of good habitat conditions throughout the year. Among the remaining comparison years, both 2005 and 2006 show evidence of compensatory recruitment to larvae (Fig. 52a). Adult abundance was moderately high in 2005, but low in 2006 and 2010 (Fig. 3). As predicted by compensatory density dependence processes, the recruitment index to larvae was higher in 2006 than in 2005. However, low adult abundance in 2010 did not give way to a similarly high recruitment index (Fig. 52a). In addition, the relatively high recruitment index in 2006 did not result in a higher larval abundance index compared to 2005 (Fig. 3). These inconsistencies, combined with a small number of comparison years, prevent any firm conclusion regarding compensatory recruitment or survival.

Similarly, if compensatory density-dependent survival was important we might expect larva to juvenile survival to be lower when larva production per adult was higher assuming similar adult populations. This was not the case for 2006, 2010, and 2011, which had relatively similar values for the SKT abundance index (figs. 3). In 2006, larval survival was low with high larval production per adult, and 2010 and 2011 had very similar larval survivals with similar adult abundances. Finally, in 2011, the highest population of juveniles led to the highest population of subadults and adults (2012 SKT), which argues against compensatory density-dependent survival. These comparisons argue against strict compensatory density dependence operating within the POD years. It seems more likely that population dynamics are driven by density independent relationships with factors such as summer water temperatures and resource availability (fluctuations in carrying capacity); however, the evidence is not conclusive. In particular, we do not understand how carrying capacity fluctuates over seasons and years or how other factors, such as predation, affect carrying capacity (Walters and Juanes 1993; Walters and Korman 1999).

Adults

Life History

The Delta Smelt is generally considered a diadromous seasonal reproductive migrant, and in the winter, many adult Delta Smelt move upstream into fresh water for spawning (Moyle et al. 1992, Bennett 2005, Sommer et al. 2011). These movements may be a specific change in behavior in response to one or more environmental cues, for example, to the rapid and often dramatic environmental changes during winter first flush periods (Sommer et al. 2011, Bennett and Burau 2014). Focused, fixed-station sampling in the winters of 2009-10 and 2010-11 revealed higher catch of Delta Smelt at higher turbidity levels, as well as an asymmetry in probability of catch with respect to tidal phase; catch was highest in the channels during flood tide, but highest near the shoreline during ebb tides (Bennett and Burau 2014). This change in horizontal channel position with respect to tidal direction has recently been confirmed by a second study in the fall of 2012 that used the "SmeltCam," an underwater video camera attached to the cod-end of the FMWT net to detect Delta Smelt (Feyrer et al. 2013). This study demonstrated that during flood tides, Delta Smelt were relatively abundant throughout the water column, but less abundant during ebb tides, and found only in the lower portion of the water column and closer

to shorelines. This asymmetry in catch supports the idea of a “tidal surfing” behavior during migration that may minimize energetic costs of upstream movement and allow Delta Smelt to follow favorable conditions with respect to turbidity and salinity (Feyrer et al. 2013). Variations of this behavior would allow fish to maintain position in the channel (stay on the edge during flood or ebb tide) or move downstream (move into the channel on ebb tide).

It is also possible that Delta Smelt movements do not represent a change in behavior; rather, fish are simply expanding their foraging or refuge distribution to habitat upstream when it becomes turbid or otherwise more suitable during and after the first flush period (Murphy and Hamilton 2013). The specific mechanism for the seasonal change in distribution, however, may be more a matter of terminology than of ecological relevance for a fish with as small a home range as Delta Smelt. Here, we acknowledge the existence of both possibilities, but will use the term “spawning migration” to simply refer to a directed movement upstream or downstream occurring prior to and during the spawning season. Using this definition, this seasonal change counts as a migration since it represents a relatively predictable and substantial change in distribution that has adaptive value including potential spawning, foraging and refuge functions (Lucas and Bara 2001).

The Delta Smelt spawning migration from their low-salinity rearing habitat into freshwater usually occurs between late December and late February, typically during first flush periods when inflow and turbidity increase on the Sacramento and San Joaquin Rivers (Grimaldo et al. 2009, Sommer et al. 2011a). Increased catches of Delta Smelt in the Delta Juvenile Fish Monitoring Program’s Chipps Island Trawl Survey and at the south Delta salvage facilities are unimodal in most years and occur within a couple of weeks of first flush events, suggesting that adult Delta Smelt are responding to environmental changes and migrating rapidly upstream once the first flush occurs (Grimaldo et al. 2009, Sommer et al. 2011a). However, spawning migrations are not always upstream. During occasional periods of very high river flows that spread freshwater habitat throughout much of the estuary, some Delta Smelt “migrate downstream” from rearing habitats in Suisun Bay and the Delta to freshwater spawning habitats as far west as the Napa River (Hobbs et al. 2007). Also under high flow conditions, it is possible that some Delta Smelt may not migrate in any direction; if their brackish-water rearing habitat becomes fresh, they can presumably spawn in suitable areas nearby. In addition, there is a small subset of the population that appears to remain in the Cache Slough complex year around; these fish presumably stay in the region for spawning (Sommer et al. 2011).

Osmerids generally spawn in shallow waters (Moulton 1974, Murawski et al. 1980, Hirose and Kawaguchi 1998, Martin and Swiderski 2001, Bennett 2005). It is believed that Delta Smelt spawn over sandy substrates in shallow areas based on the observation that first hatch larvae are collected in high concentrations in areas near expansive sandy shoals (Bennett 2005, L. Grimaldo, U.S. Bureau of Reclamation, unpublished data); confirmation of this hypothesis has not been verified through egg collections or observations of spawning adults, except in mesocosm studies (J. Lindberg, U.C. Davis, unpublished data). Pilot studies to identify egg deposition areas have been conducted by the IEP but these efforts were unsuccessful; it is unknown whether it was due to the method used, locations selected, or because of the low probability of detecting eggs from a relatively rare species.

The Delta Smelt is an opportunistic strategist (Nobriga et al. 2005). Opportunistic strategists are characterized by their short life spans, but high intrinsic rates of population increase driven by rapid maturation and repeat spawns over a protracted spawning season (Winemiller and Rose 1992). The importance of per capita fecundity to the success of the Delta Smelt population was recently highlighted in an individual-based modeling study (Rose et al. 2013a,b). In culture,

Delta Smelt can spawn up to four times per year depending on water temperature (J. Lindberg, U.C. Davis, unpublished data). Recent evidence indicates that Delta Smelt can spawn multiple times in the wild if water temperatures stay cool in the later winter and early spring (Wang 2007, L. Damon, CDFW, written comm. 2013). The ability of Delta Smelt to spawn multiple times in the wild could substantially increase per capita fecundity over previous estimates for individuals of a specific size. It could also be a contributing factor to the large interannual variability in adult to larvae recruitment (Fig. 52a).

Population Trends

Adult Delta Smelt are monitored by the Spring Kodiak Trawl (SKT) survey which was initiated by CDFW (then CDFG) in 2002 and runs from January to May each year (Honey et al 2004). An indexing method was recently developed by CDFW for the SKT survey, allowing for year to year comparisons as well as comparisons with the abundance indices for other life stages (Fig. 3). The SKT index time series used in this report comprises 11 annual indices, from 2003 to 2013; no index is available for 2002. Each index represents the abundance of adult fish hatched in the previous calendar year that survive to spawn at the beginning of the next calendar year. The highest SKT index on record occurred in 2012 (147), as a result of the high 2011 abundance of younger fish, and the lowest in 2006 (18). Of the four comparison years, 2005 had the highest SKT index (51), followed by 2010 (27) and 2011 (20) and then 2006 (18). While the SKT index was thus lower in the two wet years than in the two drier years, the SKT index increased substantially in each of the years following the two wet years; however it increased only 2-fold from 2006 to 2007 while it increased 7-fold from 2011 to 2012 (Fig. 3). It is also possible that the SKT is less effective during very high flow events. Delta outflow at times exceeded 200,000 cfs in winter 2011 and 300,000 cfs in winter 2006. These high flow events might have contributed to the low SKT indices in these two wet years, if Delta Smelt remained near shore to avoid displacement or moved into San Pablo Bay with the LSZ. In both cases they would be outside of SKT sampling range. Further evaluations are needed, however, to investigate and quantify this hypothesized effect.

The annual adult Delta Smelt abundance indices track the annual abundance indices of subadults calculated from the previous years' FMWT survey closely (Fig. 53; see also Kimmerer 2008). The relationship is particularly strong at higher fall abundance indices (FMWT index > 50), with more variability at lower abundance indices. Before the POD decline in 2002, all Delta Smelt FMWT indices were greater than 50 (Fig. 3). Thus, the FMWT might provide a useful surrogate for estimating long-term abundance trends in the adult Delta Smelt population prior to the initiation of the SKT survey in 2002, but great caution is warranted with the approach because this hindcasting would rest on only four data points with high leverage (2003-2005, 2012) and assume stable subadult to adult survival relationships and habitat conditions, neither of which is likely true. Moreover, the Kodiak trawl more efficiently captures Delta Smelt than the FMWT net. The SKT survey was set up to target Delta Smelt, while the FMWT survey was designed to monitor young Striped Bass, which tend to be larger than Delta Smelt during fall; however, there is no reason to expect the difference in capture efficiency to affect the relationship, unless such differences were a function of population size (i.e., efficiency was different above and below FMWT = 50). The utility of the FMWT as a descriptor of long-term adult population trends in the absence of long-term data from the SKT will benefit from ongoing IEP efforts to quantitatively estimate the efficiency of the FMWT and to compare efficiencies of different trawling gear and protocols. While survival from subadults in the fall (FMWT) to adults in the winter and spring (SKT) (Fig. 53) has been more stable than adult to larvae recruitment and survival between other

life stages (Figs. 51 and 52), it nevertheless shows some variability, especially when abundance is low. These data suggest that at least in the POD decade, adult numbers appear largely driven by juvenile abundance and the influence of changes in winter-time habitat attributes is less important and relatively stable from year to year.

The number of adult spawners affects population dynamics through production of eggs. Potential reproductive output is proportional to the number of adult female spawners, the clutch size for females of a specific size, and the number of egg clutches produced by each female. Although egg production in the wild has not yet been documented, we can evaluate the relationship of the SKT adult population index to the 20 mm Survey abundance index (Fig. 54). This relationship does not appear to be strong during the POD period (linear regression, $P > 0.05$). This suggests that egg production or subsequent hatching of eggs and survival of larvae and thus overall recruitment of larvae from the previous generation's adults is affected by other factors than adult population size. Hypotheses about the effects of habitat attributes in our conceptual model on adult growth and fecundity and recruitment of young are explored in Chapter 7.

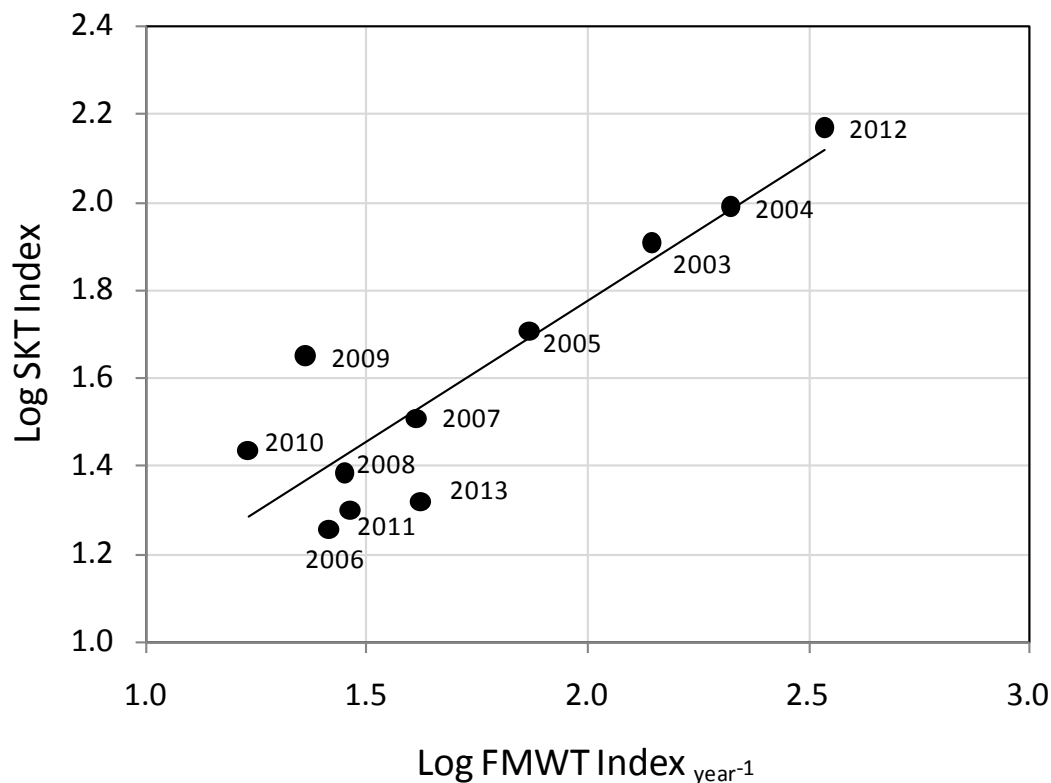
Clutch sizes of fish collected in the SKT were not measured, but annual fork lengths of Delta Smelt collected in the SKT did not vary greatly (Fig. 55). It does not appear that clutch size should have varied much in the POD years, including the four comparison years 2005-6 and 2010-11, with 2003 as the exception where the median length was greater than 70 mm standard length (Fig. 55). For Delta Smelt, which are now considered seasonal indeterminate spawners (i.e., they spawn multiple times), total reproductive output of an individual female should vary with: 1) size at the onset of the spawning window because batch fecundity is a function of size (Bennett 2005, CDFW unpublished data), 2) length of the spawning window, which is the number of days with suitable water temperatures for spawning (see larvae section below) and determines the number of batches possible; and 3) growth during the spawning window, which can potentially improve batch fecundity over time (see larval section below). Obviously, reproductive output will be higher in years when adult females are larger, abundances are higher, and the spawning window is prolonged such that multiple clutches are produced. Note that maximum reproductive output of the adult population at the beginning of spawning is not often realized due to mortality arising from density-dependent (e.g., food limitation or predation) or density-independent (e.g., entrainment, contaminants) mechanisms. According to Bennett (2011), larvae from bigger, early-spawning females may be disproportionately lost to CVP and SWP entrainment. In this report, we consider years when there are bigger females and/or a higher spawning stock size to be better in terms of reproductive potential than years when adult female size and spawning stock are smaller.

Larvae

Life History

Adult Delta Smelt, through their selection of spawning sites and spawn timing, largely determine the early rearing habitat and environmental conditions encountered by larvae. Given the Delta Smelt's annual life cycle, small size at maturity, relatively low fecundity, and small egg size compared to other fishes, life history theory suggests that parental care, here limited to selection of spawning sites and spawn timing, should be an important factor in reproductive success (Winemiller and Rose 1992). Since eggs have not been detected routinely in the wild, spawning and early rearing habitat locations are inferred from collection of ripe adults and early stage

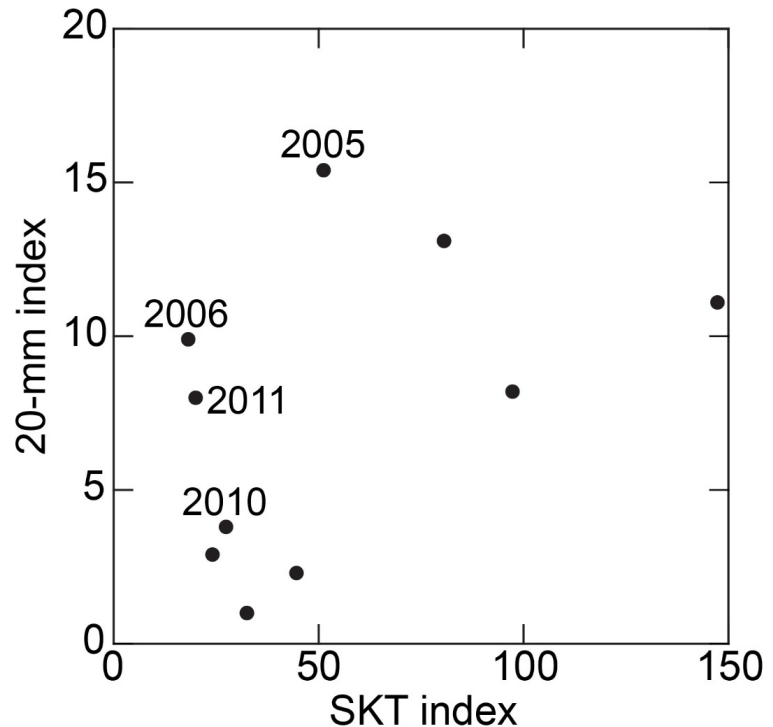
Figure 53. Relationship of annual indices of Delta Smelt abundance from the Spring Kodiak Trawl (SKT) and Fall Widwater Trawl (FMWT) from the previous year. Year labels correspond to the year of the SKT. The linear regression with all index values log-transformed to address non-normal distributions in the raw data is: $\text{Log SKT Index} = 0.4997 + 0.6381(\text{Log FMWT Index Year}^{-1})$, $n = 11$, $p < 0.001$, $R^2 = 0.79$.



larvae, which occur from the Delta margins through eastern Suisun Bay (see: <http://www.dfg.ca.gov/delta/projects.asp?ProjectID=SKT>; Wang 1986, 1991, 2007). In culture, Delta Smelt begin spawning as water temperatures increase to 10-12 °C, at which time individual females accompanied by several males select appropriate water velocities and release gametes close to the substrate from dusk to dawn (Baskerville-Bridges et al. 2004b). In lab experiments, females deposited significantly more eggs on sand and gravel substrates as compared to other substrates offered for egg deposition (J. Lindberg, U.C. Davis, unpublished data). Based on periodicity in egg deposition in culture, Bennett (2005) proposed that spawning likely coincides with peak tidal currents (i.e., spring tides), which would result in hatching near neap tides. Such a strategy would limit the initial tidal dispersal of larvae.

In culture, larvae hatch after an 11-13 day incubation period at 14.8-16.0 °C and begin a short period of buoyancy (or positive phototaxis; Baskerville-Bridges et al. 2004b) prior to slowly settling to the bottom (Mager et al. 2004). After this buoyant period, Mager et al. (2004) found that larvae were demersal unless actively swimming to feed, which occurred only during daylight hours. Exogenous feeding begins at 5-6 days post-hatch as the last of the yolk sac is absorbed; the lipid globule is absorbed at 10 days (Mager et al. 2004) providing some nutritional reserve if feeding conditions are poor. Larvae probably remain somewhat bottom oriented until swim

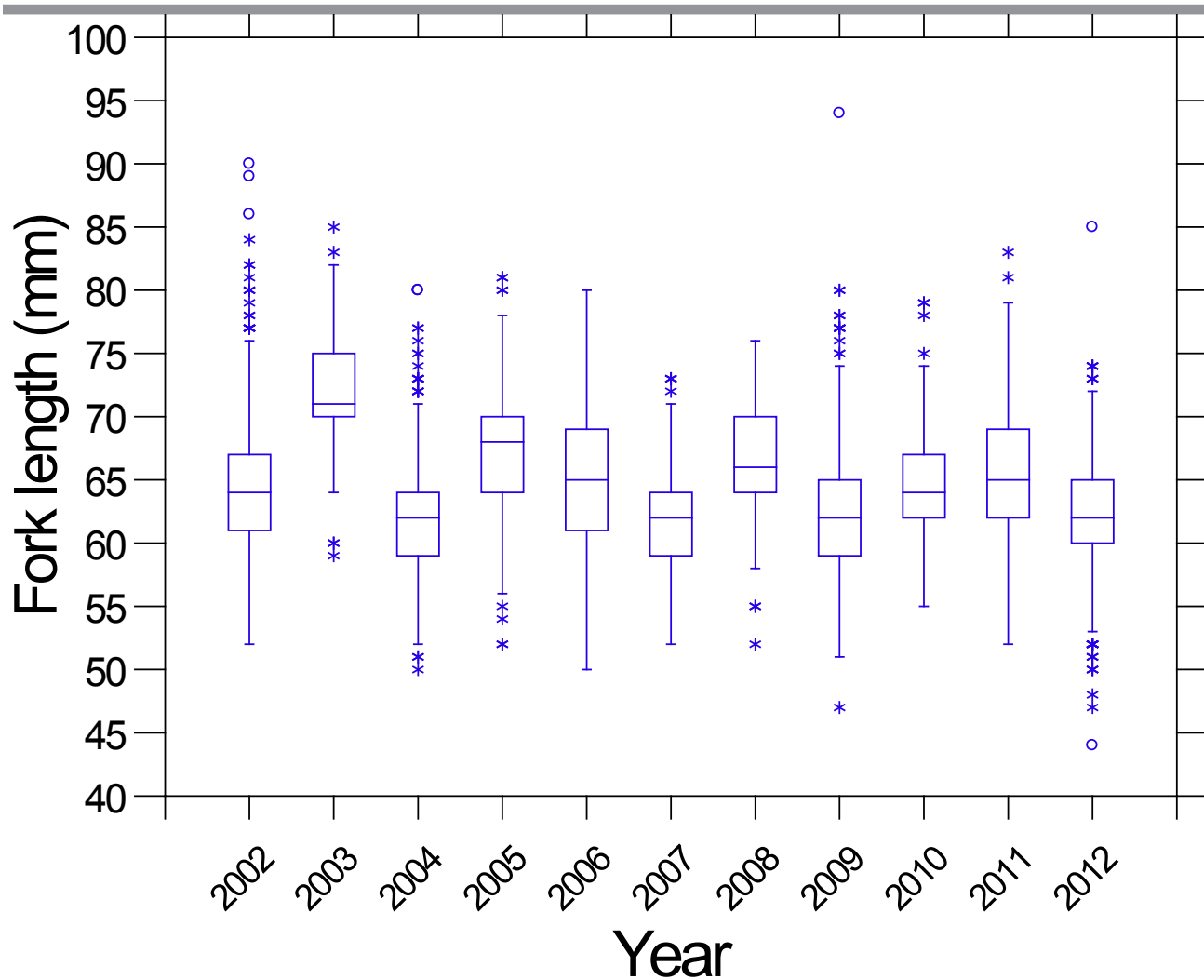
Figure 54. Plot of the Spring Kodiak Trawl (SKT) adult abundance index against the 20 mm Survey larval abundance index 2003-2012. The comparison years of 2005, 2006, 2010, and 2011 are labeled.



bladder and fin development are complete at about 65 days of age and about 20 mm TL (Mager et al. 2004, Baskerville-Bridges et al. 2004b), at which time they can fully control their buoyancy and efficiently use tidal and river currents to migrate. The center of distribution for Delta Smelt larvae and young juveniles is generally downstream of the spawning habitat, but upstream of and varying in association with X2 during spring (Dege and Brown 2004).

Early larval stages of Delta Smelt (4-15 mm) tended to be poorly collected by gear previously used in historical SFE egg and larval surveys (Striped Bass Egg and Larva Survey; sled-mounted 500 micron mesh net with 0.38 m² mouth area), but with growth and development greater proportions of the population become vulnerable. This observation led to a sampling gear change in the mid-1990s from the historical egg and larval gear to new gear targeting more vulnerable post-larvae and early juvenile Delta Smelt (i.e., 20 mm Survey). The improved catch and distribution information resulting from this change has since proven valuable to the management of Delta Smelt, and the 20 mm Survey results are now considered essential information (USFWS 2008). In the mid-2000s, an abundance index was developed from 20 mm data (Gleason and Adib-Samii 2007) that has since been used to index abundance trends of larvae in spring (e.g., Hieb et al. 2005, Contreras et al. 2011). We use 20 mm Survey abundance indices as one Delta Smelt end-point to evaluate the support for our hypotheses concerning the environmental drivers and habitat attributes responsible for abundance and survival of larvae.

Figure 55. Median fork length (mm) of Delta Smelt collected in January and February by the Spring Kodiak Trawl by year, 2002-2012. See Chapter 3: Data Analyses for explanation of boxplots.



Population Trends

The highest larval abundance indices on record occurred in the late 1990s, shortly after the initiation of the 20 mm survey in 1995. The lowest larval abundances were observed in 2007-2010 (Fig. 3). In 2011, larval abundance improved substantially from the recent minimum in 2007, and achieved levels comparable to those earlier in the 2000s (Fig. 3). Although 2011 larval abundance compared favorably to that of 2010, it remained below levels of 2005 and 2006. Thus, the modest larva abundance in 2011 did not appear sufficient to explain the high FMWT index observed in 2011 (Fig. 3). As explained above, larval abundance does not track the abundance of the parent generation very well (Fig. 54). In contrast, subsequent life stages of the same cohort track larval abundance and abundance relationships of larvae (log 20 mm index) with juveniles (log TNS index) and subadults (log FMWT index) in the same year are statistically significant (Fig. 56). However, the linear regression based on the FMWT explains less variance than the linear regression based on the TNS suggesting more variability in the abundance of the older life stages. This suggests that factors affecting juvenile mortality rates also play an important role in eventual recruitment.

Juveniles

Life History

During summer, juvenile Delta Smelt primarily rear in the west Delta, Suisun Bay, and Cache Slough complex (Moyle 2002, Bennett 2005, Merz et al. 2011, Sommer and Mejia 2013). As in late spring and fall, the center of distribution of the fish occurs in the low salinity zone, with the exception of the Cache Slough complex. The degree to which the fish use particular geographic areas depends on salinity, temperature, and turbidity (Nobriga et al. 2008); other factors that may affect their summer distribution include *Microcystis* distribution, and possibly prey density, bathymetric features, or other water quality constituents. As noted previously, Delta Smelt used to be common in the central and south Delta during the summer months, but this is no longer the case (Nobriga et al. 2008).

Population Trends

Relative abundance of juvenile Delta Smelt is presently indexed by the Summer Towntnet Survey (TNS). The survey was not designed specifically to measure Delta Smelt abundance and catches are low (Honey et al. 2004). Nonetheless, patterns in the annual abundance index provide a useful basic measure of population trends.

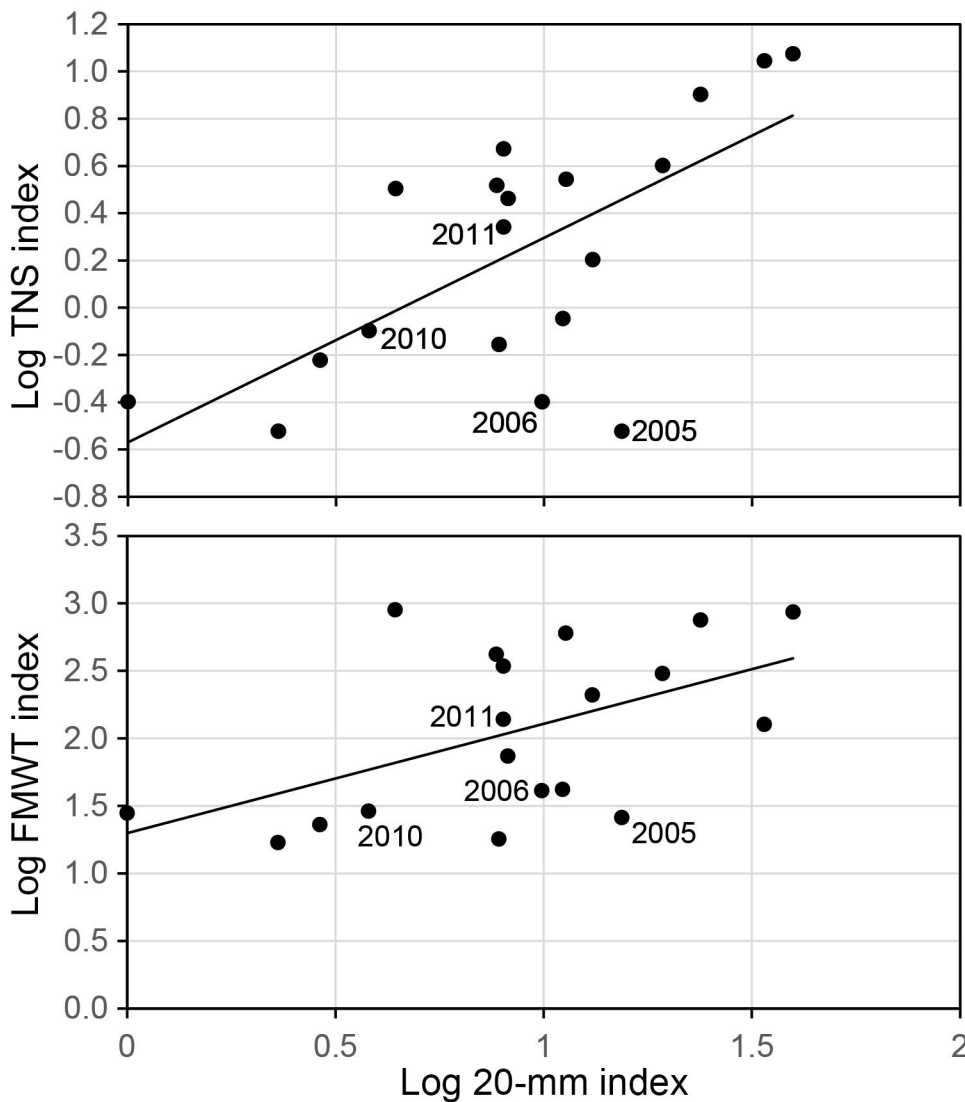
The TNS index rebounded substantially in 2011, but declined to a value consistent with low recent year indices in 2012 (Fig. 3). This pattern of persistently low abundance is consistent with the POD, which began over a decade ago (Sommer et al. 2007, Thomson et al. 2010). During the last decade, TNS abundance indices were especially low from 2005-2009 (Fig. 3). The onset of the 2005-2009 period of low juvenile abundance was characterized by extremely low larvae to juvenile survival in 2005 and 2006 (Fig. 51). Larval survival to juveniles recovered somewhat in the following years, but TNS indices stayed low (Fig. 3). Historically (e.g., early 1970s), high levels of Delta Smelt abundance during summer apparently allowed density dependent effects to occur between summer and fall in some years; this conclusion was still supported after the species declined in the early 1980s, but the apparent carrying capacity was lower (Bennett 2005). The available trawl data suggest that this trend of declining carrying capacity has continued as suggested by the very low Fall Midwater Trawl indices produced by a range of juvenile TNS abundance levels, during the POD years (Fig. 57).

Subadults

Life History

During fall, subadult Delta Smelt primarily rear in the western Delta, Suisun Bay, and Cache Slough complex (Moyle 2002, Bennett 2005, Sommer and Mejia 2013). The center of distribution is in the low-salinity zone (Sommer et al. 2011), with the exception of the Cache Slough complex. The degree to which the fish use particular geographic areas depends on salinity and turbidity (Feyrer et al. 2007). Other factors that may affect their distribution during the fall include *Microcystis* distribution and water temperature in the early fall (September-October), and possibly prey density.

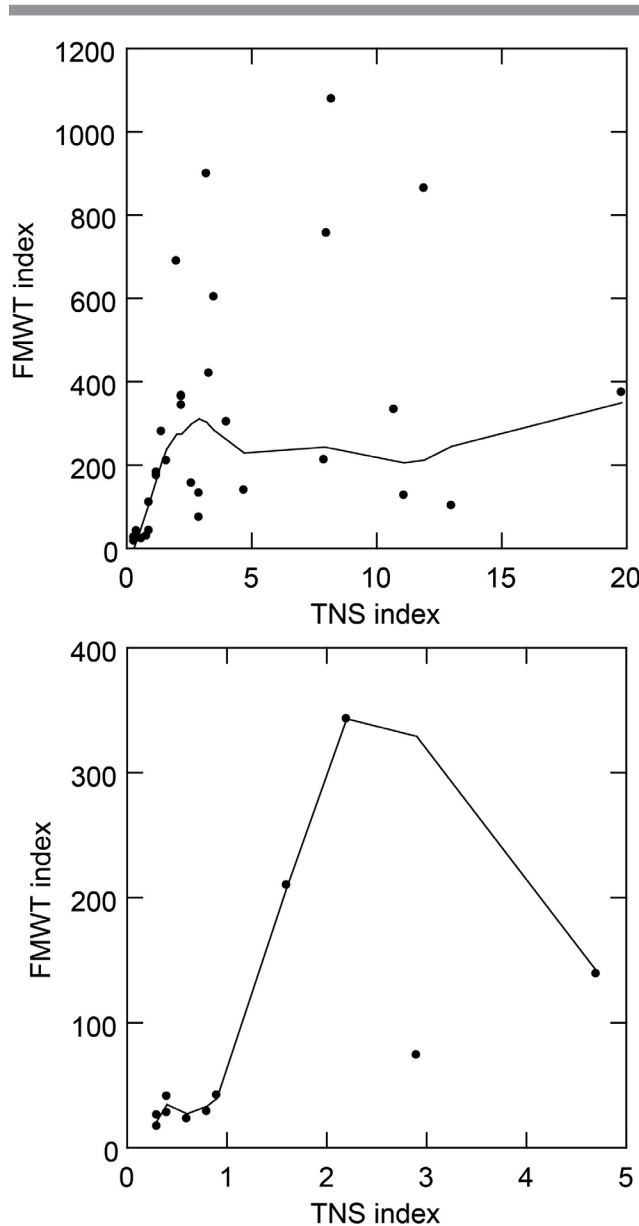
Figure 56. Relationship of annual index of Delta Smelt abundance from the 20 mm survey (20 mm) with the annual indices from the summer tonet survey (TNS) and fall midwater trawl survey (FMWT). Year labels correspond to the comparison years of interest. The linear regressions with all index values log-transformed to address non-normal distributions in the raw data are: $\text{Log 20 mm index} = 0.57 + 0.87(\text{Log TNS index})$, $n = 19$, $p < 0.05$, $R^2 = 0.44$ and $\text{Log 20 mm index} = 1.30 + 0.81(\text{Log FMWT index})$, $n = 19$, $p < 0.05$, $R^2 = 0.27$.



Population Trends

Population trends for subadult Delta Smelt are presently indexed by the FMWT. Like the TNS, the FMWT was not designed specifically to measure Delta Smelt relative abundance and catches are low (Honey et al. 2004, Newman 2008). The data are nonetheless a useful basic measure of population trends, except perhaps at very low abundance (i.e., FMWT index values less than about 50; Fig. 53). However, the general agreement between the FMWT and subsequent Spring Kodiak Trawl (SKT) sampling (Fig. 53), suggests that FMWT results are a reasonable indicator

Figure 57. Plots of fall midwater trawl (FMWT) abundance index as a function of summer townet survey (TNS) abundance index for 1982-2013 and 2003-2013. Note the very different scales for both axes. Lines are LOWESS smooths.



of general trends in abundance of adult Delta Smelt.

The FMWT index rebounded substantially in 2011, but declined to a value consistent with low recent-year indices in 2012 (Fig. 3). During the last decade, FMWT indices were especially low from 2005-2010 (Fig. 3). After the rebound in 2011, the index went back to a lower level similar to the 2005-2010 period. Since 2003, the juvenile to subadult survival index was lowest in 2004. During the four comparison years, the juvenile to subadult survival index was lowest in 2010, but relatively high in the other three years and highest in 2011 (Fig. 51).

Historically, high levels of Delta Smelt abundance during summer apparently resulted in density-dependent mortality between summer and fall in some years (Bennett 2005). This conclusion was still supported after the species declined in the early 1980s, but the apparent carrying capacity, meaning the magnitude of the FMWT index relative to the TNS index, was lower (Fig. 57). The available FMWT data suggest that these trends of density-dependent mortality during the summer-fall and declining carrying capacity have continued (Fig. 57). The close correlation of the FMWT and SKT (Fig. 53) indicates that the

factors likely affecting survival of Delta Smelt to the adult spawning population operate earlier in the life cycle (i.e., between the egg and subadult life stages). Additional mortality certainly occurs between the FMWT and SKT but the lack of variability around the regression line suggests there is not a lot of variability in the rate of that mortality. Thus, the relative annual spawning stock appears to be largely determined by fall of the birth year.

Chapter 7: Using the Conceptual Model—Why did Delta Smelt abundance increase in 2011?

In this Chapter, we further explore Delta Smelt responses and habitat attributes as depicted in the driver and life stage transition conceptual model diagrams presented in Chapter 5. The purpose is to demonstrate the utility of our conceptual model framework for generating hypotheses about the factors that may have contributed to the 2011 increase in Delta Smelt abundance. For each life stage transition, we explore a series of hypothesized linkages among ecosystem drivers, habitat attributes, and Delta Smelt responses. We evaluate these hypotheses by comparing habitat conditions and Delta Smelt responses in the wet year 2011 to those in the prior wet year 2006 and in the drier years 2005 and 2010.

In this Chapter we briefly describe the comparative approach and the hydrological conditions during the four years that are the focus of our comparisons. We then state and explore each hypothesis for the adult, larval, juvenile, and subadult life stages of Delta Smelt using data sources described in Chapter 3. Key points from these evaluations, as well as previous report Chapters, along with benefits and limitations of the comparative approach are summarized and discussed in Chapter 8. In several cases, we lacked suitable data or other necessary information to evaluate our hypotheses; these data and information gaps are described in Chapter 9. Chapter 9 also includes a brief review of some of the more complex mathematical analyses used in recent peer-reviewed publications, such approaches currently being used by others, and three examples of additional mathematical modeling approaches that can be used to further explore some of the linkages and interactions in our conceptual model and complement previously published and other ongoing mathematical modeling efforts for Delta Smelt.

Comparative Approach

The comparative approach used for evaluating the hypotheses stated in this Chapter is similar to the approach taken in the FLaSH investigation (Brown et al. 2014, see also <http://deltacouncil.ca.gov/science-program/fall-low-salinity-habitat-flash-studies-and-adaptive-management-plan-review-0>). This allowed us to place the results of the FLaSH investigation in a year-round, life cycle context as recommended by the FLaSH Panel (FLaSH Panel 2012). Specifically, we compared data from the two most recent wet years, 2006 and 2011, and the two years that immediately preceded them, 2005 and 2010. To conduct our comparisons, we determined how Delta Smelt responses or habitat attributes would be expected to respond in the different years and then compared the expected response to the observed response. If the expected and observed responses were similar, the hypothesis was considered to be supported.

Moderate to wet hydrological conditions tend to benefit many estuarine organisms, including Delta Smelt (Sommer et al. 2007). But low recruitment or low survival at any point in the predominantly annual Delta Smelt life cycle can lead to low abundance even in a wet year. Identifying the reason(s) for low abundance in a wet year may give important insights into key habitat attributes and environmental drivers that could be managed in a way that would improve the likelihood of abundance increases in all wet years.

The two wettest years after the onset of the POD were 2006 and 2011 (Fig. 58). Delta Smelt abundance increased substantially in 2011, but not in 2006 (Fig. 3). The failure of the Delta Smelt population to increase in the wet year 2006 and the increase of Delta Smelt in the wet year 2011 provides an opportunity to compare and contrast habitat attributes in these two years and possibly identify new options for management actions. As stated in Chapter 3, our working assumption is that different Delta Smelt abundances in 2006 and 2011 should be attributable to differing environmental conditions, in some cases attributable to management actions, and subsequent ecological processes influencing the Delta Smelt population.

Preceding habitat conditions may have important implications for the response of a population to the environmental conditions present during a wet year; therefore, we also consider data from 2005 and 2010. Further, we also consider adult and larval abundance in 2012 following the wet year of 2011. We did not include any years predating the POD period in this analysis. This was done to prevent the possibly more subtle, but management-relevant, environmental changes occurring during the POD period from being overwhelmed by effects of the strong POD step changes in the early 2000s as well as similarly strong changes that occurred before the POD (e.g., after the invasion of the clam *Potamocorbula amurensis*).

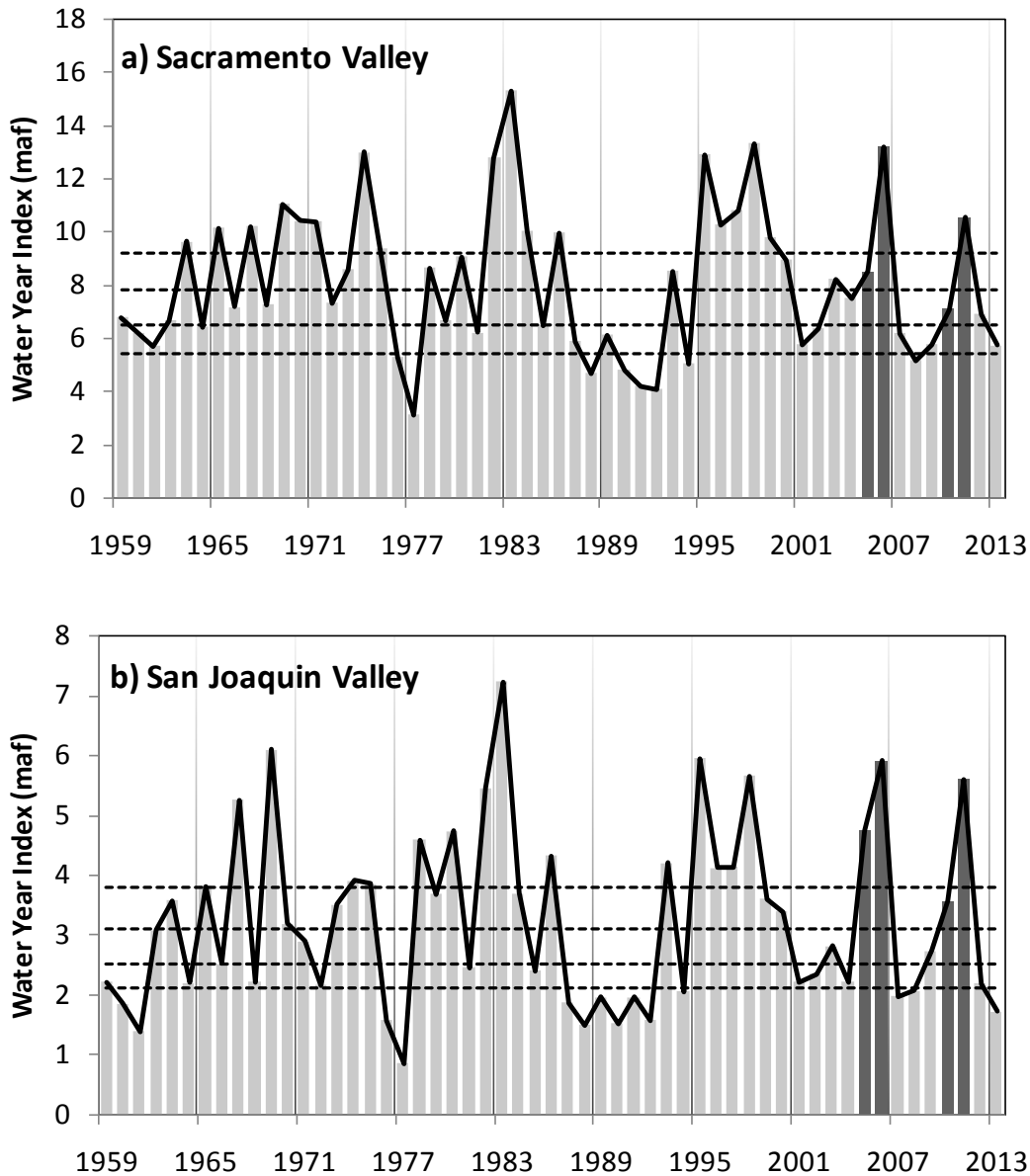
For the purpose of this report, we call 2005, 2006, 2010, and 2011 our “study years.” We use “year” rather loosely because the Delta Smelt life cycle does not follow the calendar year. As already explained, life stages can overlap and can be observed during different months in different years. Mature adults of a cohort produced in one year are generally not observed until the following year. Similarly, the life cycle does not strictly follow the water year type. We do our best to explain these mismatches when they occur and keep the presentation focused on the life cycle and the conceptual models.

Note that we do not examine the complex interactions that may occur when more than one hypothesis is true (or false), nor do we rule out that a hypothesis may be true in some years and false in others. Therefore, it is important to recognize that data contrary to a hypothesis may indicate that the habitat attribute was not controlling in the selected years, or that complex interactions among multiple habitat attributes (and corresponding hypotheses) contributed to the observed effects. Addressing such complexities is more appropriate for quantitative models as discussed in Chapter 9.

Hydrological Conditions

According to annual water year indices and classifications for overall hydrological conditions in the Sacramento and San Joaquin Valleys that provide the freshwater inflow into the Delta, 2005, 2006 and 2011 were the wettest years of the POD period (Fig. 58, see also <http://cdec.water.ca.gov/cgi-progs/iodir/WSIHIST>). In the San Joaquin Valley, 2010 was the fourth wettest year of this period. In the Sacramento Valley, 2003 and 2004 were wetter than 2010. Specifically, water year 2010 was classified as “below normal” in the Sacramento Valley and “above normal” in the San Joaquin Valley and 2011 was classified as wet in both areas, according to the water year index classifications. Water year 2005 was classified as “above normal” in the Sacramento Valley and “wet” in the San Joaquin Valley and 2006 was classified as wet in both areas. (Fig. 58). Water year 2012 was classified as “below normal” in the Sacramento Valley and “dry” in the San Joaquin Valley.

Figure 58. Annual water year indices for the a) Sacramento and b) San Joaquin Valleys since the initiation of the Summer Towntnet Survey in 1959. Horizontal dashed lines: threshold levels for water year type classifications as wet (W), above normal (AN), below normal (BN), dry (D) and critically dry (C). Darker grey bars indicate the four study years (2005, 2006, 2010, 2011) examined in Chapter 7 of this report. (Data are from <http://cdec.water.ca.gov/cgi-progs/iodir/WSIHIST>).



The overall wet hydrological conditions in the Sacramento and San Joaquin Valleys in 2005-6 and 2010-11 resulted in relatively prolonged periods of high Delta inflow and outflow and low X2 values in the winter and spring months of the four study years (Fig. 59). In the first half of the year, 2006 had the highest outflow and lowest X2 values followed by 2011, 2005, and 2010. In the second half of 2011, outflow was higher and X2 values were lower than in the second half of 2006 and of all other years during the POD period. In spite of having the lowest spring X2, 2006

had the highest fall X2 (September to October) of all study years, followed by 2005, 2010, and 2011 (Fig. 60).

The overall high flows during these four years allowed for periods of very high fresh water exports from the Delta (Fig. 59). This led to record high volumes of fresh water exported in water year 2011 (6.7 maf) and in water year 2005 (6.5 maf) and a somewhat lower export volume in water year 2006 (6.3 maf). The total water export volume was substantially lower in water year 2010 (4.8 maf) because 2010 immediately followed a three-year drought and the below normal hydrological conditions in the Sacramento Valley (Fig. 58) were not sufficient to rapidly replenish reservoirs and allow for greater exports.

Hypotheses

Individual hypotheses are indicated in the life stage transition conceptual model diagrams next to the arrows depicting each hypothesized linkage or outcome (figs. 46-49). While all linkages are considered important, we only developed hypotheses for selected linkages. We developed hypotheses for linkages with sufficient data for quantitative assessments and where there is disagreement or uncertainty regarding the outcome resulting from a driver. We also developed hypotheses for linkages considered important but where we found critical information was missing; thus, highlighting topics where new work is needed. For each of these hypotheses, we then considered the available data to examine whether the Delta Smelt response expected under the hypothesis was consistent with the observed trends in habitat attributes or population dynamics. While we would have liked to test hypotheses about the linkages between habitat attributes and the specific life stage transition processes shown in the life stage transition conceptual model diagrams, the available data often only allowed us to test “lower tier” hypotheses about the linkages between ecosystem drivers and habitat attributes.

Note that we have not examined the complex interactions that may have occurred when more than one hypothesis was true (or false), nor have we ruled out that a hypothesis may be true in some years and false in others. Therefore, it is important to recognize that data contrary to a hypothesis may indicate that the habitat attribute was not controlling in the selected years, or that complex interactions among multiple habitat attributes (and corresponding hypotheses) contributed to the observed effects. Addressing such complexities is likely more appropriate for quantitative models as discussed in Chapter 9. Our overall objective in this Chapter is to provide a demonstration of how the conceptual model can be used to generate and test hypotheses and highlight data gaps while addressing a specific topic of management interest—the increased Delta Smelt abundance index in 2011.

Adult Hypotheses

Hypothesis 1: Hydrology and water exports interact to influence entrainment risk for adult Delta Smelt.

As discussed earlier, we do not currently have a reliable measure of actual entrainment of fishes by the SWP and CVP export pumps. We also do not have actual population abundance estimates for Delta Smelt. As discussed by Kimmerer (2008, 2011) and Miller (2011), it is thus difficult to estimate proportional population losses due to entrainment. We consider the published

Figure 59. Net daily flows in cubic feet per second for a) Delta inflow from all tributaries, b) Delta outflow into Suisun Bay, and d) total freshwater exports from the Delta. Also shown are daily values for c) X2 (see Chapter 4 for explanation). Flow data are from Dayflow (<http://www.water.ca.gov/dayflow/>). X2 values are calculated from daily Delta outflow with the equation in Jassby et al. (1995.)

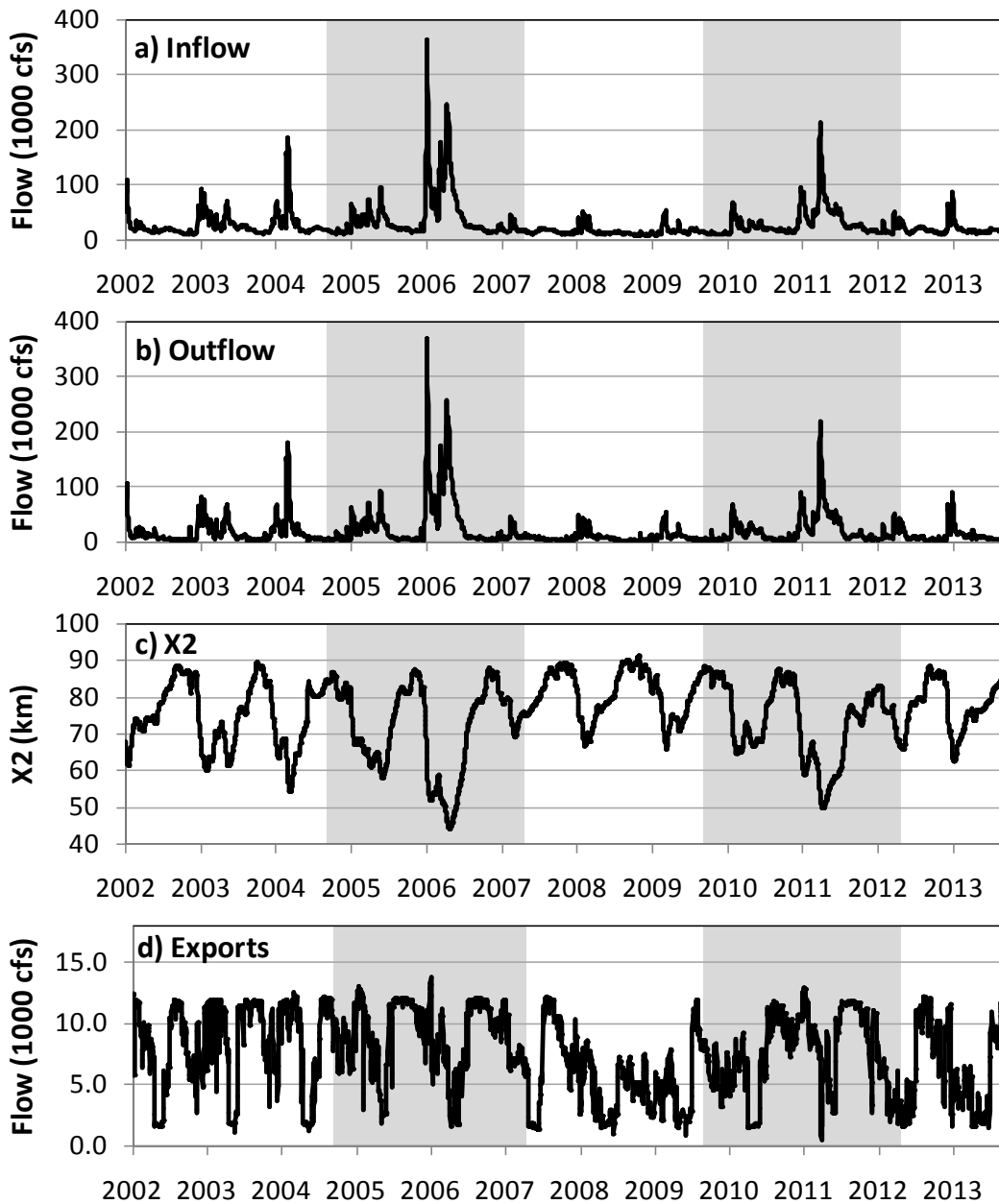
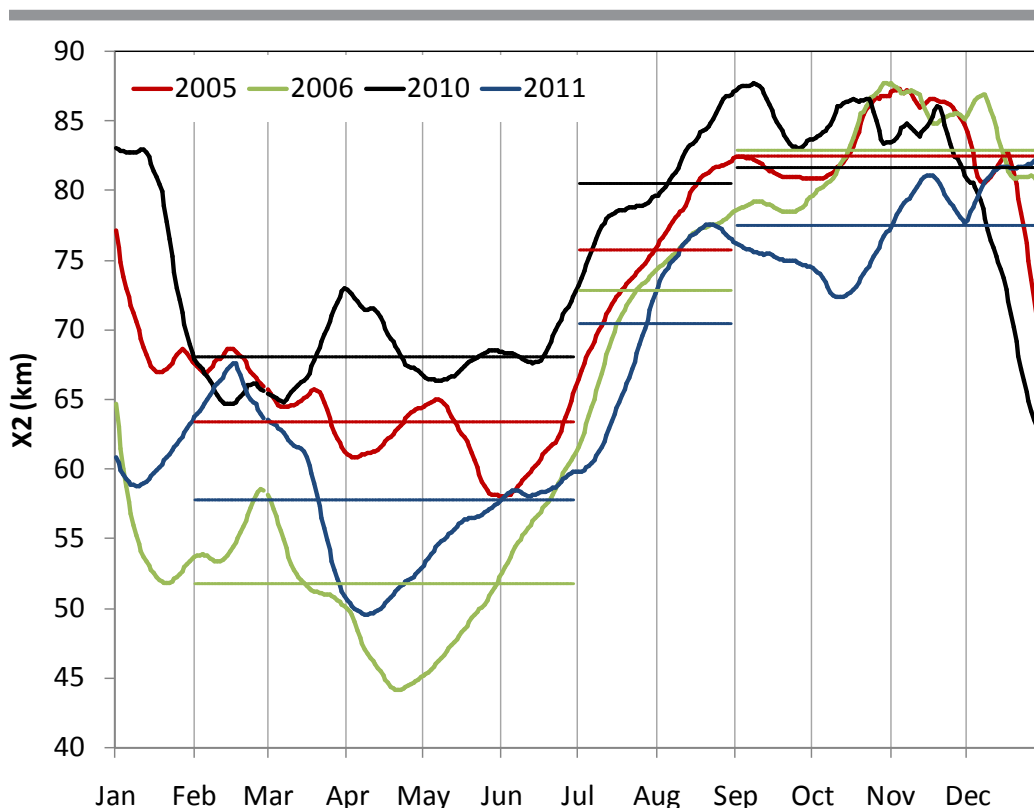


Figure 60. Daily X2 values in January to December for each of the four study years. Seasonal X2 averages are indicated by horizontal lines for spring X2 (February to June), summer X2 (July and August), and fall X2 (September to December). See Fig. 15 for seasonal X2 in other years.



proportional loss estimates for adult Delta Smelt entrainment losses for the two years for which they are available (2005 and 2006; Kimmerer 2008). However, we otherwise restrict our analysis – and this hypothesis – to an assessment of entrainment risk based on salvage and OMR flow data. Note that high entrainment risk for an individual fish does not automatically lead to a high proportion of the population lost to entrainment mortality. For example, in wetter years when large numbers of fish are present but most of the population is distributed farther away from the pumps, a large number of fish can be entrained but only a small percentage of the entire population.

Adult (December-March) Delta Smelt salvage was highest in 2005 followed by 2006 and 2010 and lowest in 2011 (Fig. 61). In 2005, most salvage occurred in January, while in the other three years it occurred in February and March (Fig. 62). Overall, adult Delta Smelt salvage in the four comparison years was on the very low end of the historical time series starting in 1980 (Fig. 26). On the other hand, the ratio of adult salvage divided by the previous year's FMWT index was high in 2005 (6th highest on record since 1979), but much lower in 2006 and 2010, and lowest in 2011 (Fig. 26).

Low salvage levels in these years and especially in 2010 and 2011 were not particularly surprising due to the low FMWT levels of the POD years along with more active management of OMR flows for Delta Smelt and salmonid protection after 2008 in accordance with the USFWS (2008) and NMFS (2009) BioOps. For management purposes, the onset of increased

adult Delta Smelt entrainment risk is inferred from distributional patterns of Delta Smelt detected by the SKT survey, Delta Smelt salvage and, more recently, consideration of Delta conditions, including turbidity patterns. Since 2009, net OMR flows during periods of increased adult Delta Smelt entrainment risk are now always less negative than they were in years prior to the BioOps. Prior to 2008, net OMR flows often reached -8,000 to -10,000 cfs (see Fig. 31, Kimmerer 2008, Grimaldo et al. 2009), when outflow was low. An exception to these strongly negative flows occurred during April-May export curtailments associated with the Vernalis Adaptive Management Program (VAMP, 2000-2012). These curtailments were especially pronounced in the first half of the VAMP period (2000-2005). During the four comparison years, winter (December-March) net OMR flows were least negative in 2006 followed by 2011 and 2010 with the most negative net OMR flows in 2005 (Fig. 63). High inflows particularly from the San Joaquin River during 2005, 2006 and 2011 moderated effects of negative OMR flows, while export pumping generally remained high. In 2010 at the end of a three-year drought, there was little water in storage to provide for Delta exports prior to the first substantial inflows in mid-January. Subsequently, export levels had to be curtailed to achieve the desired OMR flows. Average winter-time net flows past Jersey Point on the San Joaquin River were positive in all four study years and greatest in 2006 followed by 2011, 2005, and 2010 (Fig. 63).

Kimmerer (2008) used salvage, OMR flows, and fish survey data to estimate proportional population losses due to entrainment for the years 1995-2006. The years 2005 and 2006 represent some of the lower loss estimates in the years examined by Kimmerer (2008); mean population losses reached up to 22% of the adult population in some years when OMR flows were more negative than -5000 cfs (Kimmerer 2008). Even if Kimmerer's estimation method provides a potential overestimate of loss (Miller 2011), proportional losses of the adult population were less than 10% in the two years that coincide with our comparison years (2005 \approx 3% , 2006 \approx 9%; from Fig. 12 in Kimmerer 2008). These types of proportional loss estimates are not available for

Figure 61. Annual adult (December-March) Delta Smelt salvage at the CVP (blue bars) and SWP (green bars) fish protection facilities for 2005-2012.

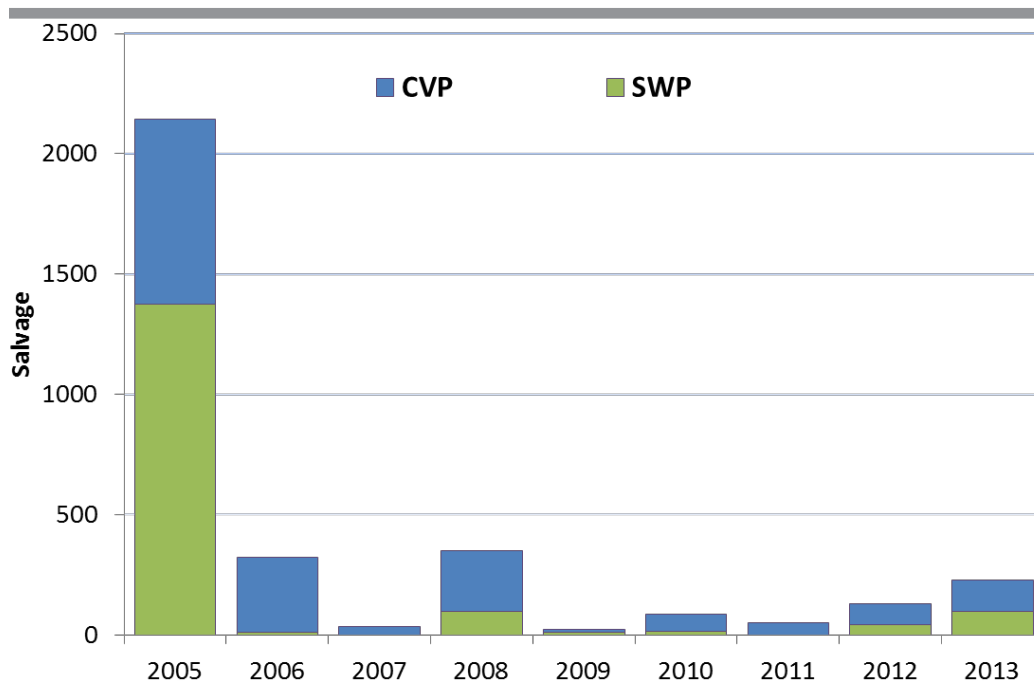
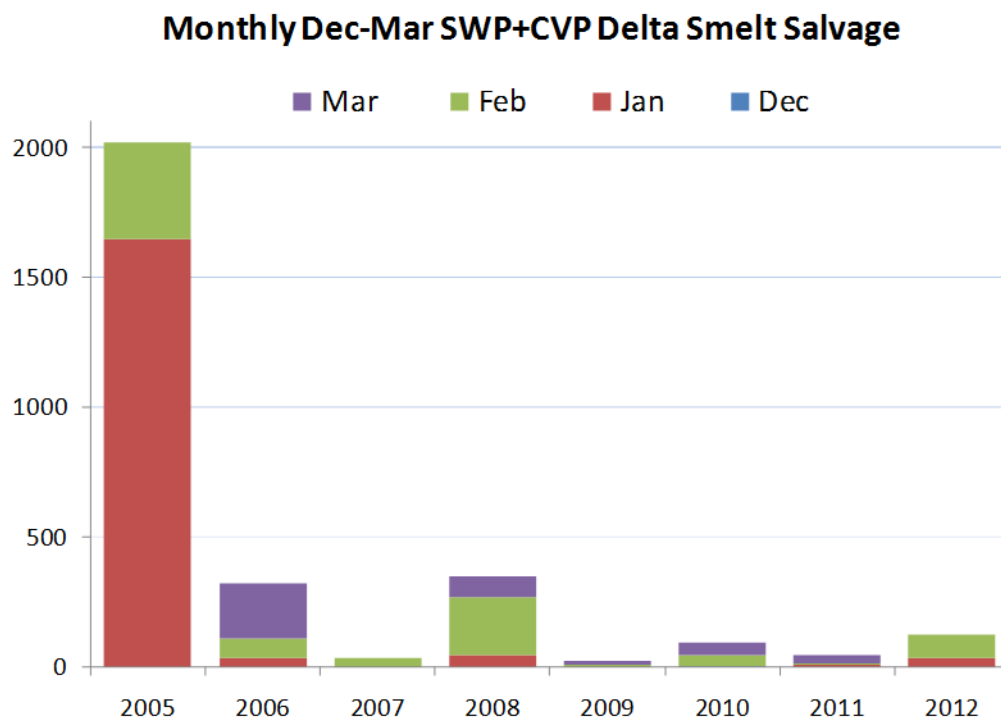


Figure 62. Annual combined adult (December-March) Delta Smelt salvage at the CVP and SWP fish protection facilities by month for 2005-2012.



2010 and 2011, but would likely be even smaller than for 2005 due to less negative OMR flows and fish distributions away from the CVP and SWP pumps. Salvage was also lower in these two years than in 2005 and 2006.

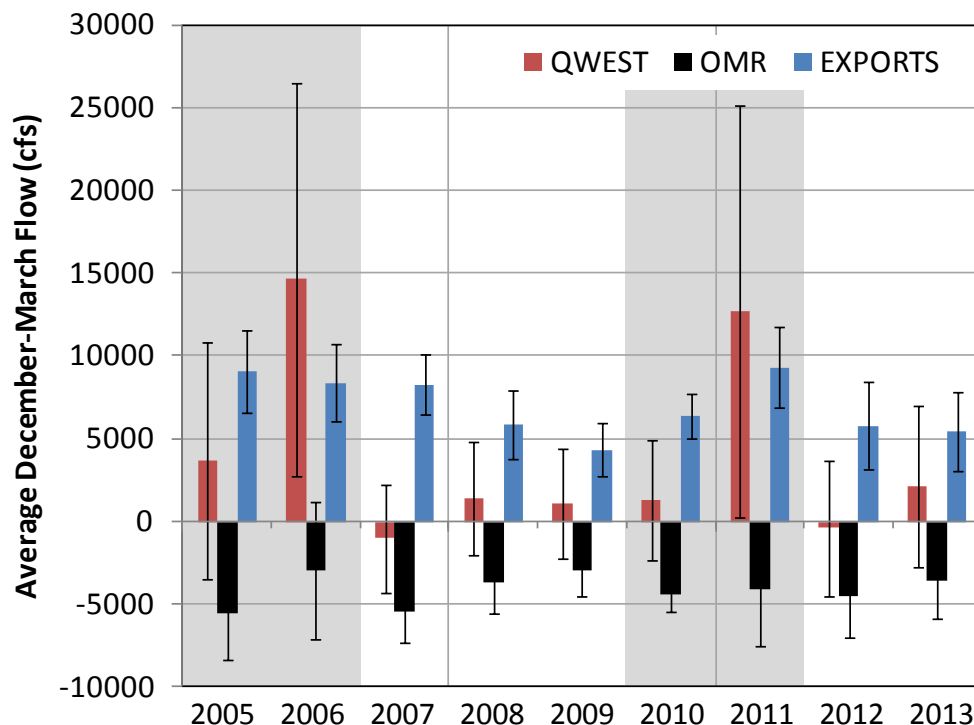
In summary, we conclude that hydrology and water exports do interact to influence entrainment risk for adult Delta Smelt and that adult Delta Smelt entrainment risk during the four comparison years was perhaps higher in 2005 than in the other years, but was low relative to historical levels in all four years.

Hypothesis 2: Hydrology interacting with turbidity affects predation risk for adult Delta Smelt.

At present, we do not have information about differences in actual predation mortality between the comparison years. As with entrainment, we thus limit this hypothesis and our analysis to to a general discussion of predation risk. Fully characterizing predation risk is exceptionally complicated, making it difficult to generate simple hypotheses that describe associated losses of all life stages of Delta Smelt. We thus limit our hypotheses about predation risk to a few factors for each life stage. For adults, we consider hydrology and turbidity as well as overlap with predators (next hypothesis).

Because Delta Smelt migrate during higher flow conditions when the water is generally turbid, it is assumed that losses to visual predators are lower or at least not substantially higher during the migration period than during other periods. First flush studies led by the USGS and UC Davis

Figure 63. Annual average daily net flows for December through March in cubic feet per second (cfs) in Old and Middle River (OMR), past Jersey Point on the lower San Joaquin River (QWEST) and total exports in millions of acre feet (MAF), 2005-2013. Error bars are 1 standard deviation.



suggest that Delta Smelt aggregate in the water column away from channel edges during daytime flood tides during upstream migration events (Bennett and Burau 2014), but it is not known if Striped Bass or Sacramento Pikeminnow *Ptychocheilus grandis*, the most likely predators of Delta Smelt in the water column, can detect and exploit these aggregations.

In the winters of 2005, 2006, 2010, and 2011 the highest Secchi depths (lowest turbidity) were found in the freshwater regions of the estuary (< 1 salinity), except for the Cache Slough region in the north Delta which was as turbid as the saltier regions of the estuary (Fig. 64). Winter-time Secchi depths in the freshwater region recorded during the SKT surveys (Fig. 64) were often higher (water clearer) than the average Secchi depths across all IEP EMP monitoring sites during these months since 2003 (about 60 cm) and especially when compared to pre-POD winter Secchi depths (around 50 cm on average) recorded by the EMP (Fig. 25). Winter-time Secchi depths in the other salinity regions were generally lower (water more turbid) than the EMP Secchi depth averages for the POD years and more similar to historical averages. In all four comparison years, predation risk associated with turbidity levels was thus likely not different from the historical risk in the more saline regions and the Cache Slough complex, but possibly higher in the freshwater regions, except for the Cache Slough region.

The salinity region differences were much more pronounced than the interannual differences between the four comparison years. Based on these data, it is not clear that higher flows in 2006 and 2011 contributed to higher turbidity in the winter months. The exception might be near the end of the Delta Smelt spawning season in early April when Secchi depths in the freshwater

region were often substantially lower in the two wetter years 2006 and 2011 than in the two drier years 2005 and 2010 (Fig. 64). This will be discussed further in the report section about larval Delta Smelt. For adults, we conclude that interannual differences in turbidity between the wetter and drier of the four comparison years did not likely contribute substantially to reduced predation risk and increased survival in the two wetter years.

Hypothesis 3: Predator distribution affects predation risk of adult Delta Smelt

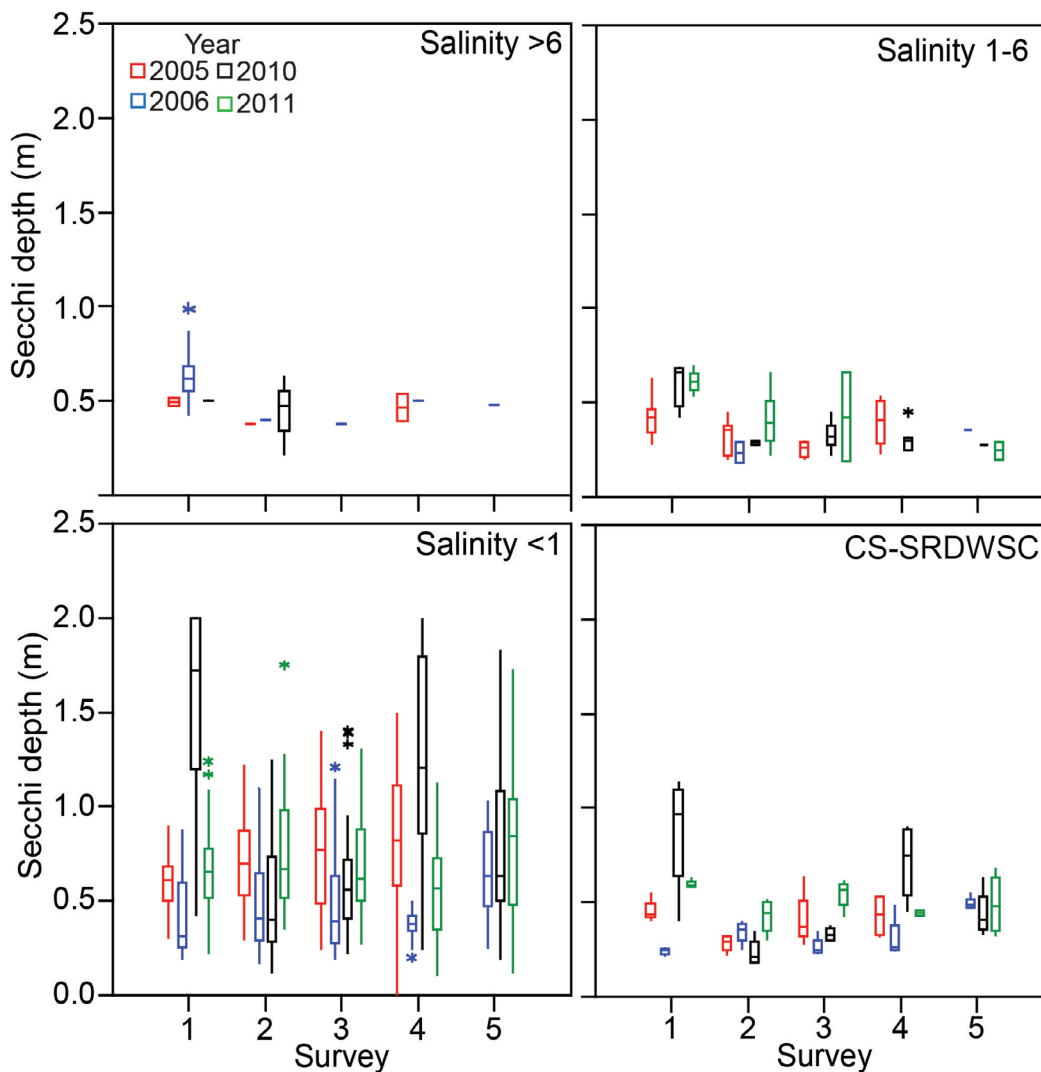
Spatial and temporal overlap with predators is a likely factor contributing to predation risk for all life stages. At present, we do not have information about how predator distribution varied between our comparison years but it is recognized that adult Delta Smelt could be vulnerable to predation if the distributions of predators and Delta Smelt populations overlapped. As already mentioned, Striped Bass and Sacramento Pikeminnow are the most likely open-water predators of adult Delta Smelt. If Delta Smelt utilize littoral habitats to a greater extent than presently assumed, then increased overlap with the distributions of Largemouth Bass and other centrarchid populations is possible. Results of field studies (Feyrer et al. 2013, Bennett and Burau 2014), described for Adult Hypothesis 2, found that adult Delta Smelt did move nearshore on a tidal basis to avoid displacement or move upstream during the “first flush.” Such movements would increase proximity to shoreline predators like Largemouth Bass, albeit during periods of increased turbidity when such visual predators would be at a disadvantage. Clearly, Hypothesis 2 and Hypothesis 3 are closely linked because predation risk is a function of predator presence and prey vulnerability. More information about predator presence is needed to evaluate this aspect of predation risk.

Hypothesis 4: Variability in prey availability during winter and spring affects growth and fecundity (eggs per clutch and number of clutches) of female Delta Smelt.

The hypothesis is that increased food availability leads to not only increased adult survivorship, but also growth, which in turn increases reproductive output (number of eggs per female increases with size; Bennett 2005). In addition, with cooler temperatures and lower metabolic rates, sufficient food resources during winter can contribute to energetically demanding multiple spawning events (three spawns possible in wild fish; L. Damon, CDFW, written communication 2012).

For adult females, the ability to meet the bioenergetic demands of reproductive development with sufficient food consumption may be particularly important for fish that spawn multiple times in a year. Preliminary findings from January through April 2012 indicated that adult Delta Smelt are indeed consuming large prey items, such as amphipods, mysids, and larval fish during their spawning period (Fig. 44) with feeding incidence near 98% for the period (Table 2). For this report, we cannot address whether food limitation is a relevant factor during the late winter-spring spawning period because we do not have sufficient data about adult Delta Smelt feeding, but we hypothesize that it may be a critical issue for spawners that need energy for multiple egg clutches. Evidence in support of this hypothesis comes from the modeling simulation experiment by Rose et al. (2013b) who found that food availability along with water temperature affected fall and winter growth and egg production prior to spawning and ultimately population success.

Figure 64. Secchi depth data collected during the Spring Kodiak Trawl Survey. Surveys are conducted monthly January-May. See Chapter 3: Data Analyses for explanation of boxplots.



Based on trajectories in adult fork lengths, it appears that adult growth may have been somewhat higher in 2005 and 2011 than in 2006 and 2010, although differences were not pronounced (Fig. 17) and as noted in Chapter 6, annual fork lengths of Delta Smelt collected in the SKT were similar in the four study years (Fig. 55). From these data we infer that environmental conditions were generally good, supporting both continued growth in length and maturation of eggs, except perhaps in 2010. In 2011, only 13 mature females were collected, so growth estimates are uncertain. In general, the number of mature females collected each year reflected year-class strength as measured by the SKT (Fig. 3), except in 2011 when only 13 ripe or ripening females were collected. Adults may use more energy for egg production than for continued somatic growth, but we do not have data on clutch sizes to evaluate this for the four study years.

Data on prey availability for current IEP sampling locations is also limited. Adult Delta Smelt diet is varied (Fig. 44) and includes pelagic and demersal invertebrates, as well as larval fish. Current mesozooplankton (copepod and cladoceran) and mysid sampling by the EMP

Table 2. Percent of age-1 Delta Smelt captured during the Spring Kodiak Trawl Survey with food present in the stomach collected January through May 2012 for three salinity regions and the freshwater Cache Slough-Sacramento River Deepwater Ship Channel (CS-SRDWSC).

		Month						
YEAR	REGION	JAN	FEB	MAR	APR	MAY	GRAND TOTAL	
2012	> 6	100%	100%				100%	
	1 - 6	100%	100%	100%	100%	0%	99%	
	< 1	100%	93%	100%	90%	89%	94%	
	CS-SRDWSC	100%	100%	100%	96%	100%	99%	
GRAND TOTAL	100%	99%	100%	95%	90%	98%		

Zooplankton Study and invertebrate sampling by the EMP Benthic Monitoring Study does not sample the full geographic range occupied by adult Delta Smelt, including Cache Slough and the Sacramento River Deep Water Ship Channel. In addition, epibenthic cumaceans and amphipods consumed by Delta Smelt might not be effectively sampled with current methods (substrate grabs using a Ponar dredge), which are more suited to sampling organisms in or attached to the substrate. Amphipods found in stomachs of adult Delta Smelt collected January 2012-May 2012 (Fig. 44) were 95% *Corophium* spp., and of those, 90% were juveniles ranging 0.8 to 1.3 mm in body length. These amphipods are believed to be mostly juvenile *Americorophium spinicorne* and *A. stimpsoni*, which as adults are tube building amphipods (Hazel and Kelley 1966). Dirt, substrate debris, and tube pieces were not found in Delta Smelt stomachs with the amphipods, so it is possible these juveniles amphipods are epibenthic or pelagic prior to settling and building tubes. Size distribution of amphipods collected by the DWR EMP Benthic Monitoring Study is not currently available. The IEP Smelt Larva Survey does collect larval fish data during winter (January-March) over a wide section of the estuary, but comparisons with larval fish consumption by adult Delta Smelt are limited because this survey is still new; it was initiated in 2009.

Data were insufficient to conclusively test the hypothesis that variability in prey availability affects growth and fecundity of adult Delta Smelt. More data are needed on growth, clutch number and size, and prey availability.

Larval Hypotheses

Hypothesis 1: Delta Smelt larvae numbers are positively affected by increased duration of the temperature spawning window

To evaluate this hypothesis, we developed two water temperature measures. The first is the number of days in the temperature spawning window as indexed by mean daily water temperatures at Rio Vista between 12 and 20 °C. This temperature range was selected as representing a reasonable balance between the various temperature ranges observed in laboratory

and field studies (Wang 1986, Baskerville-Bridges et al. 2004b, Bennett 2005) and reviewed in earlier sections of this report. Presumably, a longer duration spawning window would result in more repeat spawning for individual females and greater total fecundity. The second water temperature measure is the number of days in the optimal temperature for egg survival to hatch. We referred to Fig. 10a in Bennett (2005) and selected the temperature range of 12-17 °C as optimal for egg survival. As explained in previous sections, adult abundance, based on SKT sampling, peaked in 2012 as the 2011 year-class of Delta Smelt reached maturity (Fig. 3). In contrast, the spawning stock (i.e., 2011 SKT) that produced the 2011 year-class ranked second lowest to 2006 (Fig. 3, Adults). Despite this low level, the 2011 spawning stock produced the highest adult abundance observed to date in 2012. This suggests that adult stock size has not limited subsequent adult recruitment from rebounding to levels comparable to those of immediate pre-POD years (see Fig. 3, Subadult). As mentioned in Chapter 6, this suggests that even a severely depleted adult stock can still produce a substantial number of larvae and a rebound in the Delta Smelt population, albeit with potentially lower genetic variability than before (Fisch et al. 2011). It also suggests that factors acting on the survival of larval, juvenile and later stages have a substantial effect on recruitment of adults, because relatively low larval abundance in 2011, was associated with the high 2012 adult abundance (Fig. 3).

As mentioned in the adult section, mature adult female Delta Smelt appeared to grow throughout the spawning seasons of the years compared, except 2010 (Fig. 17). We used water temperatures at the Rio Vista Bridge as a surrogate for temperatures experienced by spawning Delta Smelt (Fig. 65) and calculated the duration of the spawning window and of optimal temperatures to hatch. We calculated each as the number of days between the date of first achieving the lower temperature and the date of first achieving the upper temperature. The onset of the spawning window occurred earliest in 2010, followed by 2005 and 2011 (Fig. 65; Table 3). The spawning window occurred latest in 2006 (Fig. 65; Table 3). The spawning window was broad in both 2005 and 2010 at 128-129 days, intermediate in 2011 at 113 days (20 °C not achieved until July 4, not shown), and was shortest in 2006 at 85 days (Fig. 65; Table 3). Assuming that female Delta Smelt undergo a 35-day refractory period, based on a 4-5 week refractory period (J. Lindberg, U.C. Davis, personal communication, 2013) between each spawning, even in 2006 three spawning events were possible, assuming fish were mature and ready to spawn at the initiation of the spawning window. In all other years, four spawning events were possible, so this measure does not discriminate among years well. The duration of optimal hatch temperature was also lowest in 2006, but other durations ranked differently across years than did spawning window duration (Table 3).

The data for the four study years do not provide conclusive support for the hypothesis that the duration of the spawning window or duration of optimal hatching temperature affected larval production. Relatively high larval abundance in 2005 was consistent with a long spawning window and moderate duration of optimal hatch temperatures (129 days and 68 days, respectively; not shown). However, 2006 with the shortest spawning window (85 days) and shortest optimal hatch duration among the 4 study years also had relatively good larva abundance (Fig. 3). In contrast, larval abundance was low in 2010 although the spawning window and optimal hatch duration were both relatively long. Other factors likely contributed to poor larval abundance in 2010, because ripening and ripe females were not detected after early April 2010 and female growth through the winter was poor (Fig. 17). Finally, both the spawning window and optimal hatch duration were fairly long in 2011 as compared to 2006, so slightly lower larval production in 2011 is inconsistent with these durations. This hypothesis was not supported.

Figure 65. Mean daily temperatures (°C) at Rio Vista from February 1 through June 30, 2005, 2006, 2010, 2011. The green lines enclose the spawning window, which represents temperatures at which successful spawning is expected to occur.

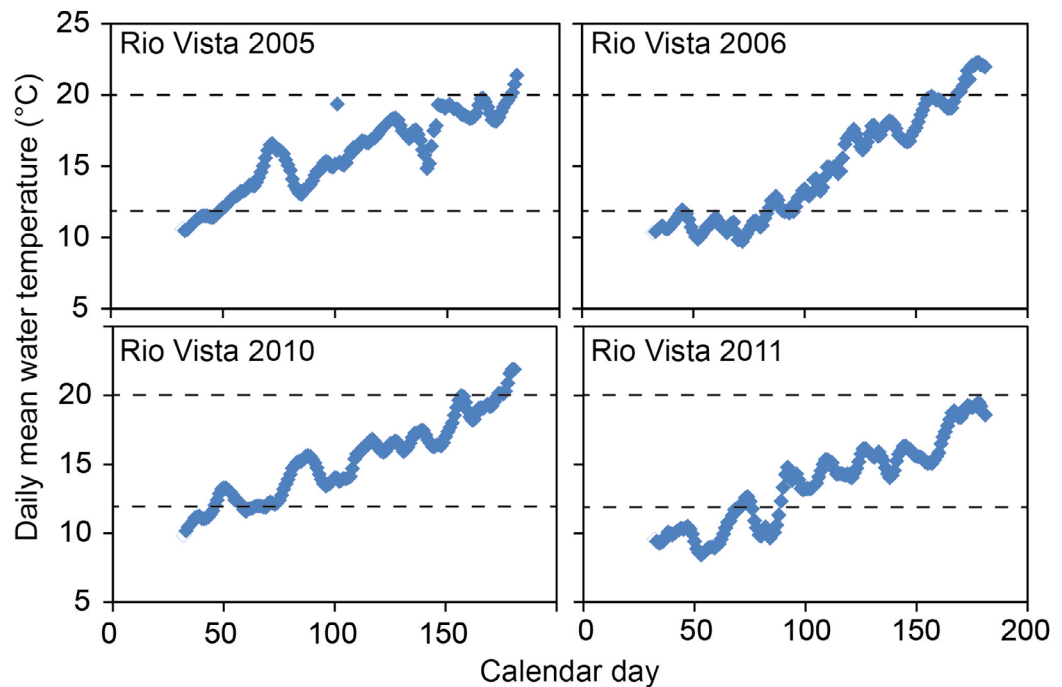


Table 3. Delta Smelt spawning window (12 to 20 °C inclusive) and optimal hatching period (12 to 17 °C inclusive) for 2005, 2006, 2010, and 2011, defined as number of days of water temperatures, based on mean daily water temperatures measured at Rio Vista. Data are calendar day when water temperature achieved 12, 17, and 20 °C and the duration (days) between those calendar days. The upper limit in 2011 was not reached until July 4, outside the spring season.

Year	Day 12 °C Achieved	Day 17 °C Achieved	Day 20 °C Surpassed	Duration 12-20	Duration 12-17	Duration 17-20
2005	50	118	179	129	68	61
2006	84	120	169	85	36	49
2010	46	136	174	128	90	38
2011	72	163	185	113	91	22

Hypothesis 2: Increased food availability results in increased larval abundance and survival.

This hypothesis focuses on seasonal changes in phytoplankton biomass and the zooplankton community and resulting changes in abundances of food items most often consumed by Delta Smelt larvae. Phytoplankton biomass data (chlorophyll-*a*) collected at 10 stations by the IEP

EMP show that the highest spring biomass levels were observed in May of 2010 and 2011 (Fig. 66). Median biomass levels were lower in April and May of 2005 and 2006 than in April and May of 2010 and 2011. This suggests that more food was available for zooplankton growth in the spring of 2010 and 2011 than in 2005 and 2006. In all four years, however, chlorophyll concentrations were lower than 10 ug/L at almost all stations, suggesting that zooplankton may have generally been food limited in these years (see Chapter 4). Nevertheless, greater phytoplankton biomass in late spring of 2010 and 2011 may have contributed to overall greater food availability and better survival of late larvae and early juveniles in these years.

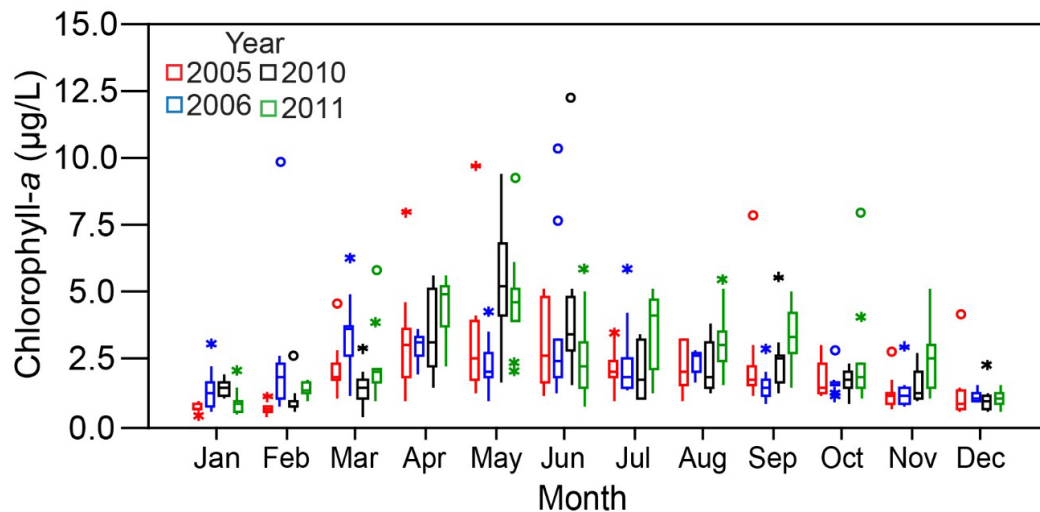
Juvenile and adult calanoid copepods, particularly *E. affinis* and *P. forbesi*, comprise most of the larval diet through June (Nobriga 2002, Slater and Baxter 2014). *E. affinis* is moderately abundant only during winter and spring and rare in summer and fall, whereas *P. forbesi* is abundant only in summer and fall (Durand 2010, Hennessy 2010, 2011, Winder and Jassby 2011). It is not clear whether the seasonal decline in abundance of *E. affinis* is related to temperature, potential competitive interactions with *P. forbesi*, differences between the species in vulnerability to consumption by *P. amurensis* (Miller and Stillman 2013), or a combination of such factors. The transition between high abundances of the two species, may create a seasonal “food gap” during late spring or early summer. This food gap has been hypothesized to be an important period for Delta Smelt larval survival (Bennett 2005, Miller et al. 2012).

To assess whether a gap in prey availability existed between periods of high abundance of *E. affinis* and *P. forbesi*, we evaluated abundance patterns in 20 mm Survey copepod data for stations with and without Delta Smelt. The food gap hypothesis was only weakly supported by the data. The density of *E. affinis* (in the presence of Delta Smelt larvae) typically reached 100 m³ by week 16 (Figs. 67 and 68). Assuming 100 m³ as a baseline density for *E. affinis*, this baseline was generally maintained until about week 22, when they declined at about the same time that *P. forbesi* densities increased to 100 m³ (Figs. 67 and 68). After combining the densities of both *E. affinis* and *P. forbesi* and tracking them through time, we detected a gap in food during week 22 (late May – early June) of 2005 (Fig. 67), which is inconsistent with 2005 exhibiting the highest larva abundance among our comparison years (Fig. 3). Such density gaps were not observed in the other three comparison years (Figs. 67 and 68), which exhibited lower abundance than 2005 (Fig. 3). Survival of larvae to juveniles was very low in 2005, but was also low in 2006 (Fig. 51) with no evidence for a food gap in 2006. Survival of larvae to juveniles was relatively high in 2010 and 2011 (Fig. 51). This analysis does not support the hypothesis that differences in zooplankton availability affected larval abundance and survival in the four study years, but higher phytoplankton biomass in April and May of 2010 and 2011 could have contributed to overall greater food availability and better survival of late larvae and early juveniles in these years.

Hypothesis 3: Distributional overlap of Mississippi Silverside with Delta Smelt and high abundance of Mississippi Silverside increases predation risk/rate on larval Delta Smelt, whereas, increased turbidity, decreases predation risk/rate on larval Delta Smelt.

Silversides are ubiquitous within the Delta (Brown and May 2006) and have long been proposed (Bennett 1995) and more recently confirmed as a predator of Delta Smelt larvae (Baerwald et al. 2012). We do not have estimates of predation losses to Silversides during the four study years and thus focus on assessing predation risk by evaluating fish distributions, predator and prey sizes, and prey growth, which is related to temperature.

Figure 66. Trends in chlorophyll-a concentrations ($\mu\text{g/L}$) in samples collected by the IEP Environmental Monitoring Program during each the four study years (2005, 2006, 2010, and 2011). Sample site locations shown in figure 15. See Chapter 3: Data Analyses for explanation of boxplots.

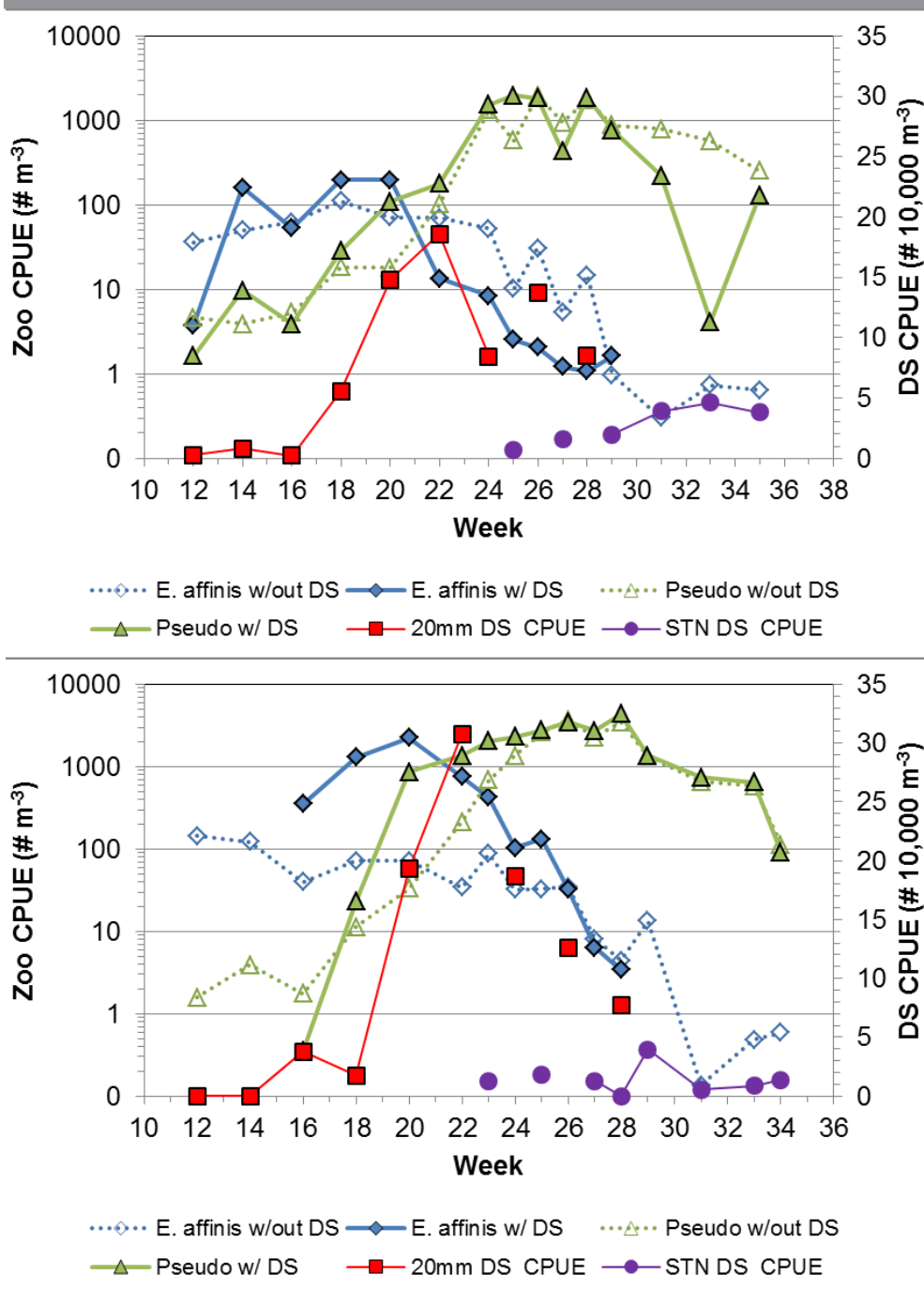


Silversides large enough to consume fish larvae are present in the Delta during spring and are likely to prey upon Delta Smelt larvae. Silverside habitat has been characterized as open water shoals and shoreline (Brown and May 2006, Grimaldo et al. 2012); however, the species also occurs in low density in deep open water primarily in summer (Grimaldo et al. 2012). Catches in the SKT confirm silverside presence in open water in spring as well, though catches tended to be low. However, SKT sampling does not occur at night when offshore Silverside densities may be higher, if foraging patterns follow those observed in Clear Lake, California (see Wurtsbaugh and Li 1985). Compared to the open embayments, SKT Silverside catches were higher in channels such as Montezuma Slough, Cache Slough, the San Joaquin River, and especially the Sacramento Deepwater Ship Channel (Table 4). This Silverside distribution matched higher March through May regional catches of Delta Smelt larvae (Table 4, see http://www.dfg.ca.gov/delta/data/20mm/CPUE_map.asp), except that larvae catches in Suisun Bay and the lower Sacramento River were occasionally high and Silversides catches were usually low. Delta Smelt larvae were found in significantly higher densities in offshore-open water habitats (Grimaldo et al. 2004), which corresponds to the habitat where Silversides consuming Delta Smelt larvae were captured (Baerwald et al. 2012). As discussed above, the relatively large-sized silversides present in the Spring Kodiak Trawl indicates some offshore movement and overlap of predator-sized foraging silversides with Delta Smelt larval habitat.

The frequency and magnitude of Silverside catches by the Spring Kodiak Trawl increased as Secchi depths approached and dropped below 50 cm (Fig. 69), suggesting that Silversides may venture offshore more frequently and in higher numbers in turbid water. This might also represent a displacement effect resulting from high flows, but high catches were most common in Montezuma Slough and the Sacramento Deepwater Ship Channel (Table 4) where displacement by flow should not have been a factor.

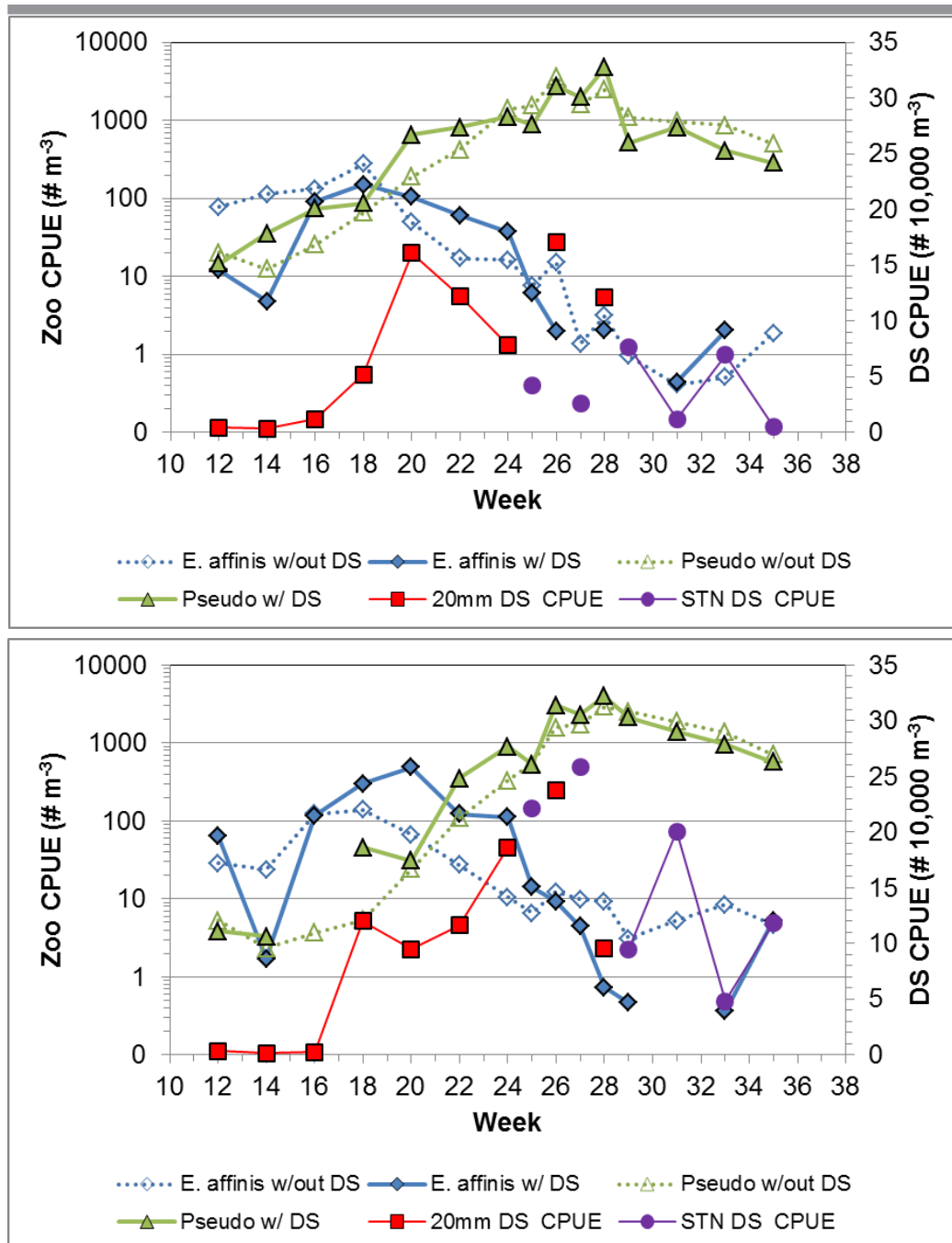
The hypothesis is somewhat supported in that: 1) Silversides are captured in Spring Kodiak Trawl in March and April (Fig. 70), when early stage Delta Smelt larvae are common; 2) Silverside

Figure 67. Catch per unit effort (CPUE) of adult *Eurytemora affinis* and *Pseudodiaptomus forbesi* (Zoo; number individuals/m³ sampled) and Delta Smelt (DS; number individuals/10,000 m³ sampled) by calendar week from mesozooplankton sampling and Delta Smelt catch by the 20 mm and Summer Towntet surveys, 2005 (top) and 2006 (bottom)



catches offshore increase with increased turbidity (i.e., declining Secchi depth; Fig. 69), and 3) there is regional overlap in Cache Slough and the Sacramento Deepwater Ship Channel, and some in Montezuma Slough (cf. Table 4 and http://www.dfg.ca.gov/delta/data/20mm/CPUE_

Figure 68. Catch per unit effort (CPUE) of adult *Eurytemora affinis* and *Pseudodiaptomus forbesi* (Zoo; number individuals/m³ sampled) and Delta Smelt (DS; number individuals/10,000 m³ sampled) by calendar week from mesozooplankton sampling and Delta Smelt catch by the 20 mm and Summer Townet surveys, 2010 (top) and 2011 (bottom).



map.asp), known larval rearing regions. It is also possible the nighttime offshore foraging by silversides is a more common strategy (Wurtsbaugh and Li 1985), but one that goes undetected by current sampling. Silverside catch per trawl (Table 4) indicates low offshore densities and the same turbidity that facilitates offshore movement may also inhibit predation effectiveness.

Table 4. Mississippi Silverside catch by region (monthly sample number in parentheses) and year by the Spring Kodiak Trawl Survey sampling monthly March through May (months when Delta Smelt larvae are present), 2005, 2006, 2010 and 2011; distribution survey data only. Annual sampling effort summarized consisted of 3 surveys and 37 stations. Tow volume varied substantially, but averaged 6,300 m³ per tow for the 4 years.

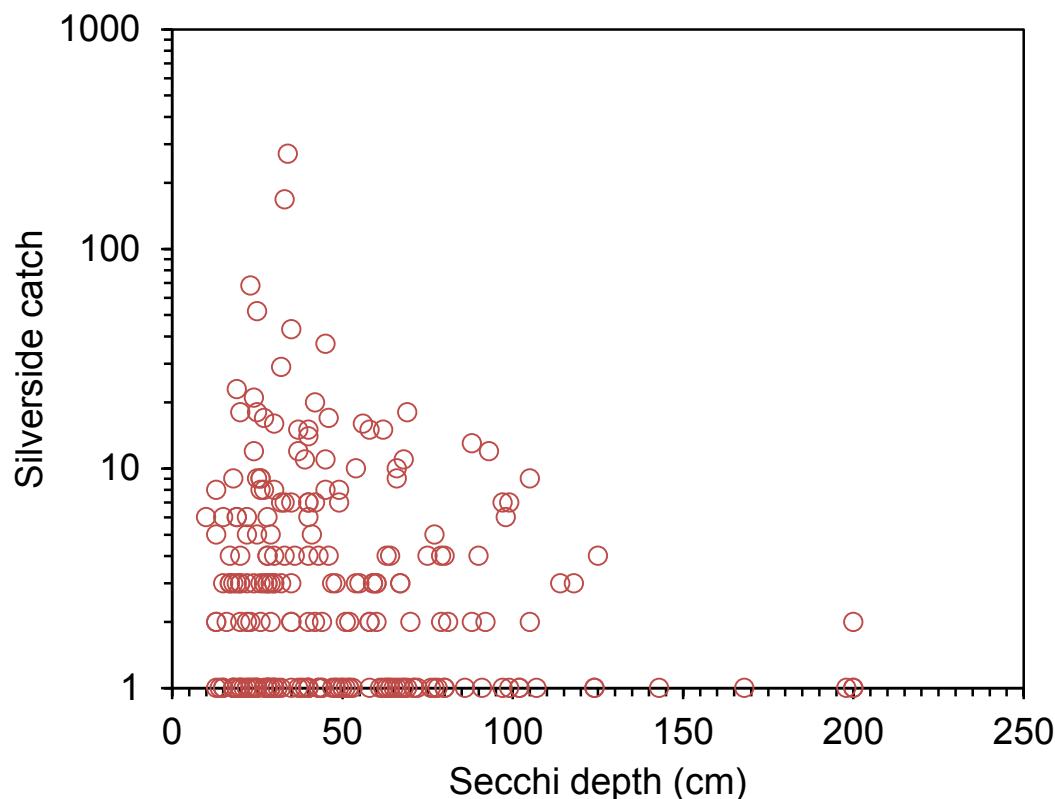
Region	2005	2006	2010	2011	Total Catch	Total Catch per Trawl
SUISUN BAY (N=10)	1	1	2	1	5	0.04
MONTEZUMA SL (N=3)	51	4	17	22	94	2.61
LOWER SACRAMENTO R (N=4)	10	1	1	3	15	0.31
CACHE SL (N=3)	9	2	4	2	17	0.47
SAC DEEPWATER SHIP CHANNEL (N=1)	14	20	45	22	101	8.42
SAN JOAQUIN R (N=8)	39	9	11	14	73	0.76
MOKLEMNE R. (N=5)	1	1	1	8	11	0.18
SOUTH DELTA (N=3)	1	0	1	1	3	0.08
ANNUAL TOTAL FOR REGIONS	126	38	82	73	319	

Overall, the conclusion regarding the effects of species distributions and abundances on predation risk is unclear. If there is an effect, it is most likely to occur in smaller channels, such as Montezuma Slough and those in the Cache Slough and the Sacramento Deepwater Ship Channel where Silversides are present in high numbers along the shoreline and larval Delta Smelt occur offshore.

Hypothesis 4: Hydrology and water exports interact with one another to influence direction of transport and risk of entrainment for larval Delta Smelt.

As for adults, we do not have proportional entrainment estimates for all four study years, so the entrainment portion of this hypothesis cannot be directly evaluated. Also, larvae (< 20 mm fork length) entrained in the State and federal water export systems are generally not quantified. To test this hypothesis we use data for the distribution and density of larvae (\geq 20 mm fork length)

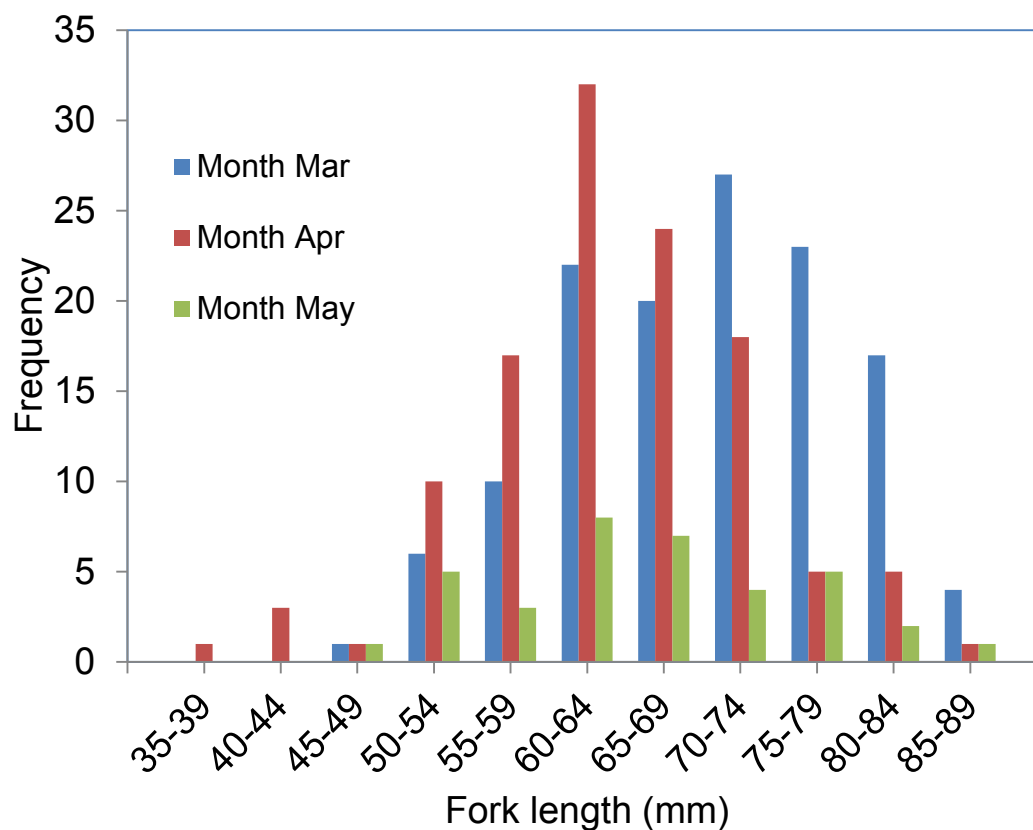
Figure 69. Scatter plot of Mississippi Silverside catch plotted on Secchi depth (cm) at location of capture from the Spring Kodiak Trawl Survey, 2005, 2006, 2010 and 2011.



in the central and south Delta and estimates of channel flows to infer risk of entrainment. Among the study years only 2005 larval entrainment was estimated by Kimmerer (2008), and loss to the population was relatively low. However, Delta Smelt density and distribution in the central and south Delta were greater in 2005 than in the three other study years (Table 5). This simple analysis suggests that in our 4-year comparison, entrainment risk for larval Delta Smelt may have been highest in 2005. Hardly any larval Delta Smelt were caught in this region in the two wet years, 2006 and 2011.

As for adults, we also used OMR flows (Fig. 31) to assess larval entrainment risk. Mean March through May OMR flows were positive during the two wet years 2006 and 2011 (8,221 cfs and 3,560 cfs respectively) and negative during the two dry years 2005 and 2010 (-417 cfs and -1,302 cfs, respectively). These OMR values suggest little if any risk during 2006 and 2011, and at most moderate risk in 2005 and 2010. Grimaldo et al. (2009) found that juvenile salvage was a function of abundance in the 20 mm Survey (positive) and OMR flows (negative). Looking more closely at various net daily flows from March to June of 2005, we find that OMR flows were moderately negative (i.e., toward the export pumps) only in March, and were zero to weakly positive in April and May, except for a brief period in mid-April (Fig. 31); also in 2005, Qwest was strongly positive from late March through early June, promoting downstream transport in the San Joaquin River, and exports were low from late April through late May (Fig. 31). The other dry year, 2010 exhibited a similar pattern, but lower inflows resulted in the magnitude of exports more directly influencing OMR flows (Fig. 31), and leading to moderately negative OMR flows

Figure 70. Monthly length frequency of Mississippi Silversides captured by the Spring Kodiak Trawl during distribution sampling March – May in the Sacramento River and Cache Slough sampling stations only, 2002-2012. The months and geographic range were selected to overlap with that of Delta Smelt larvae as they hatch and begin to grow.



in March and again in June, but only weakly negative flows in April and most of May coincident with positive Qwest. In the high outflow years 2006 and 2011, few larvae were detected in the central or south Delta (Table 5) and Qwest flows were strongly positive from March through at least early June, while OMR flows were near zero or weakly negative in March and positive to strongly positive by April and continuing to early June of both years (Fig. 31). Thus, for our comparison years, it appears that the available data generally support our hypothesis, but entrainment of larvae was unlikely to be an important factor during either wet year and was probably not a substantial factor in either dry year.

Table 5. Mean monthly catch of Delta Smelt per 10,000 m³ by station for stations in the south and central Delta for the 20 mm Survey, 2005, 2006, 2010, 2011. Non-zero values are bolded.

Year = 2005	Months				
STATION	MARCH	APRIL	MAY	JUNE	JULY
809	0.00	0.00	3.14	5.17	0.00
812	0.00	0.00	3.14	6.66	0.00
815	0.00	3.06	3.39	0.00	0.00
901	0.00	0.00	3.21	0.00	3.61
902	0.00	0.00	0.00	0.00	0.00
906	1.65	2.93	3.22	0.00	0.00
910	0.00	0.00	0.00	0.00	0.00
912	0.00	0.00	0.00	0.00	0.00
914	3.18	1.49	1.56	0.00	0.00
915	0.00	0.00	0.00	0.00	0.00
918	1.52	1.41	0.00	0.00	0.00
919	0.00	0.00	0.00	0.00	0.00
Year = 2006	Months				
STATION	MARCH	APRIL	MAY	JUNE	JULY
809	0.00	0.00	0.00	0.00	0.00
812	0.00	0.00	0.00	0.00	0.00
815	0.00	0.00	1.24	0.00	0.00
901	0.00	0.00	0.00	0.00	0.00
902	0.00	0.00	0.00	0.00	0.00
906	0.00	0.00	0.00	0.00	0.00
910	0.00	0.00	0.00	0.00	0.00
912	0.00	0.00	0.00	0.00	0.00
914	0.00	0.00	0.00	0.00	0.00
915	0.00	0.00	0.00	0.00	0.00
918	0.00	0.00	0.00	0.00	0.00
919		0.00	0.00	0.00	0.00

Year = 2010	Months				
STATION	MARCH	APRIL	MAY	JUNE	JULY
809	0.00	0.00	1.62	0.00	0.00
812	0.00	0.00	0.00	0.00	0.00
815	0.00	1.77	1.72	0.00	0.00
901	0.00	0.00	0.00	0.00	0.00
902	0.00	0.00	0.00	0.00	0.00
906	0.00	3.36	0.00	1.64	0.00
910	0.00	5.24	0.00	0.00	0.00
912	0.00	0.00	0.00	0.00	0.00
914	0.00	0.00	0.00	0.00	0.00
915	0.00	0.00	0.00	0.00	0.00
918	0.00	0.00	0.00	0.00	0.00
919	0.00	0.00	0.00	0.00	0.00
Year = 2011	Months				
STATION	MARCH	APRIL	MAY	JUNE	JULY
809	0.00	0.00	0.00	1.73	0.00
812	0.00	0.00	0.00	0.00	0.00
815	0.00	0.00	0.00	0.00	0.00
901	0.00	0.00	3.69	0.00	0.00
902	0.00	0.00	0.00	0.00	0.00
906	0.00	0.00	0.00	0.00	0.00
910	0.00	0.00	0.00	0.00	0.00
912	0.00	0.00	0.00	0.00	0.00
914	0.00	0.00	0.00	0.00	0.00
915	0.00	0.00	0.00	0.00	0.00
918	0.00	0.00	0.00	0.00	0.00
919	0.00	0.00	0.00	0.00	0.00

Juvenile Hypotheses

Hypothesis 1: High water temperatures reduce juvenile Delta Smelt growth and survival through lethal and sublethal (bioenergetic stress; reduced distribution) effects.

High water temperatures have a strong effect on juvenile Delta Smelt survival (Swanson et al. 2000, Komoroske et al. 2014). In addition to the obvious potential for lethal effects, temperature can have sub-lethal effects such as reduced habitat area, higher food requirements, increased susceptibility to disease and contaminants, and increased predation. The potential for increased prey requirements and increased predation is described below for other hypotheses.

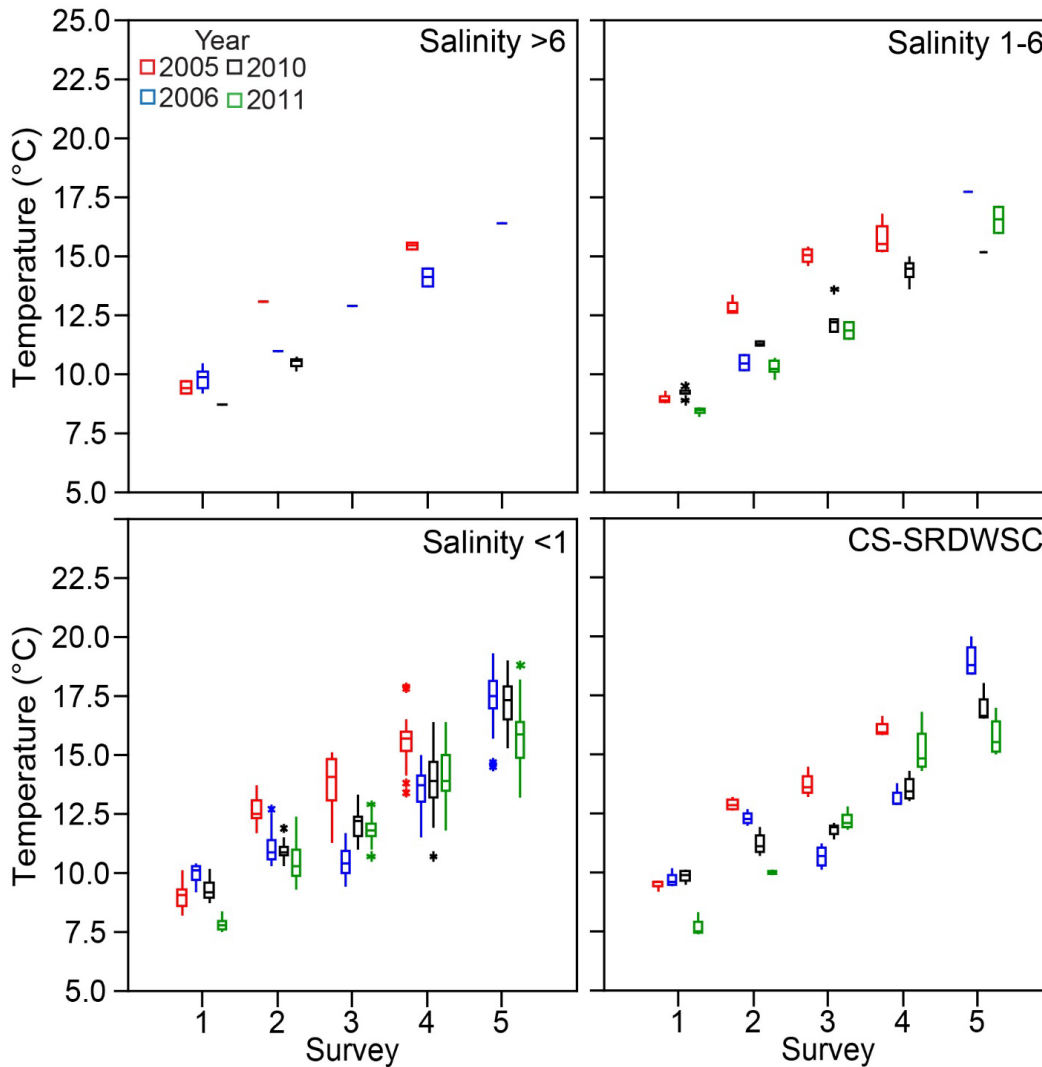
As noted in the adult section, spring water temperature was generally coolest in 2006 and 2011, but warmed up more rapidly toward the end of spring 2006 (May) than in spring 2011. Spring water temperature was overall warmest in 2005 (Fig. 71). Following the high late-spring water temperatures in 2005 and 2006, summer temperatures in 2005 and 2006 tended to be higher than in 2010 and 2011 during July and August (e.g. TNS surveys 3-5; Fig. 72). Temperatures during surveys 4 and 5 may have been particularly important as they exceeded lethal levels in freshwater at some sites, suggesting the potential for mortality. Note that this does not mean that temperatures were universally cooler in 2010 and 2011 than in 2005 and 2006; for example the region around Cache Slough had relatively high temperatures in August 2011. Larval to juvenile survival (ratio of TNS index to 20 mm index) was highest in 2011 followed by 2010, 2006, and 2005, suggesting that the cooler late spring and summer temperatures in 2011 and 2010 may have been beneficial for Delta Smelt. However, juvenile to subadult survival (ratio of FMWT index to TNS index) was highest in 2011 and lowest in 2010 (Fig. 51). While relatively high water temperature in late spring and early to mid summer of 2005 and 2006 may thus have contributed to low survival of late-stage larvae and early juveniles, water temperature may have been less important to survival in the late summer and early fall. Overall, the results of this analysis of temperature and survival data support our hypothesis that high water temperatures reduce juvenile Delta Smelt growth and survival.

At this point, our data and analyses are inadequate to address temperature effects on juvenile Delta Smelt growth. Although there are some data for Delta Smelt growth during several of the target years, it is difficult to separate the relative effects of improved bioenergetics (see below) versus simple ontogenetic changes in fish size. Juvenile fish growth rates are typically not constant and change with size (“allometric effects;” Fuiman 1983). Specifically, daily growth rates (e.g., mm/day) are often faster for smaller fish and slower for older fish. Hence, cooler years may delay Delta Smelt transitions from faster to slower growth phases, yielding a relatively fast measured growth rate at a specific point in time (e.g., September) because at that specific time the fish are still relatively young and still on the “steepest” part of an idealized growth curve.

Hypothesis 2. Distribution and abundance of Striped Bass, temperature, and turbidity influence predation risk/rate on juvenile Delta Smelt

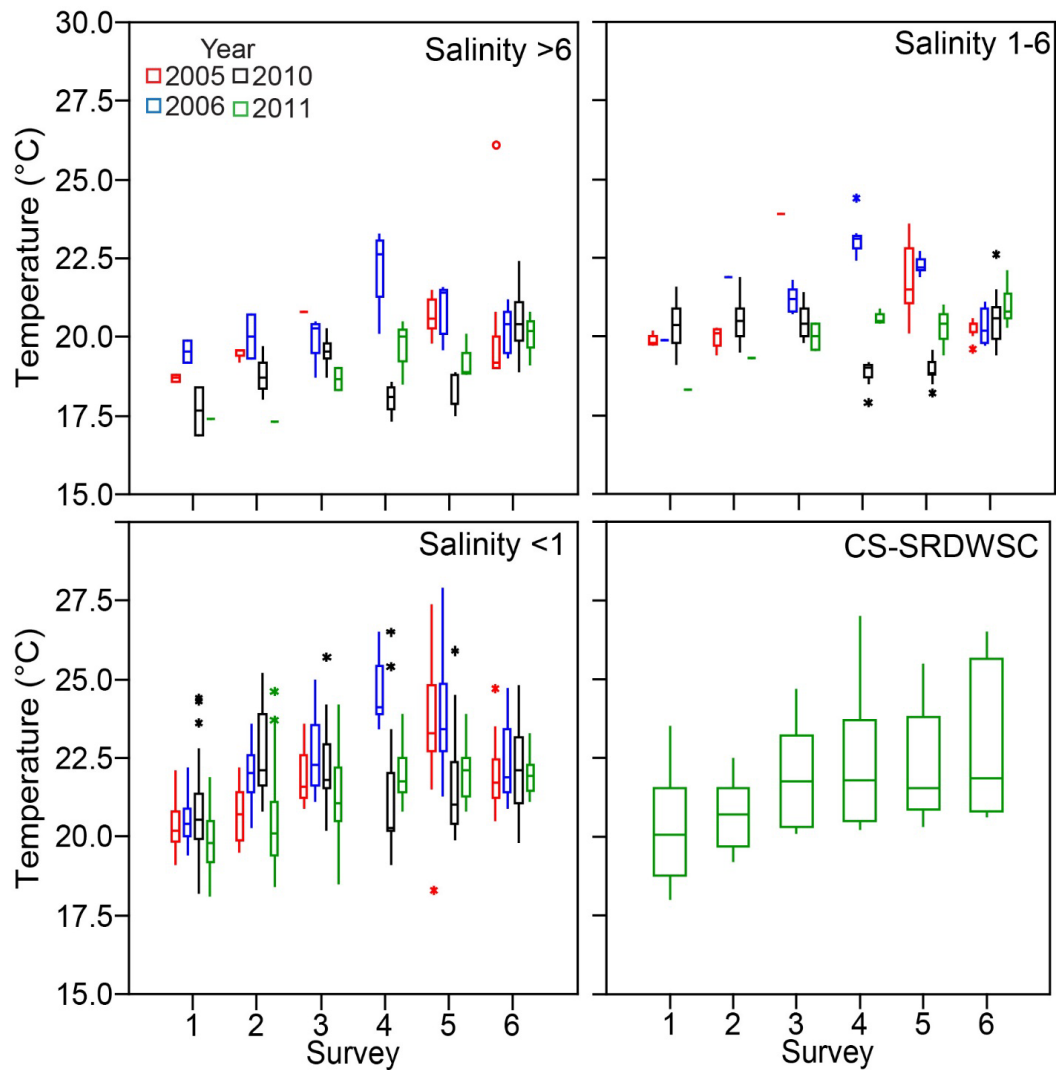
We hypothesize that subadult (age 1-3) Striped Bass are the major predator on juvenile Delta Smelt and that losses are likely affected by temperature and turbidity patterns. However, other factors likely affect predation risk (e.g., other predators such as centrarchids) and several factors

Figure 71. Water surface temperature data collected during the Spring Kodiak Trawl Survey for three salinity regions and the Cache Slough-Sacramento River Deepwater Ship Channel (CS-SRDWSC). Surveys are conducted monthly January-May. See Chapter 3: Data Analyses for explanation of boxplots.



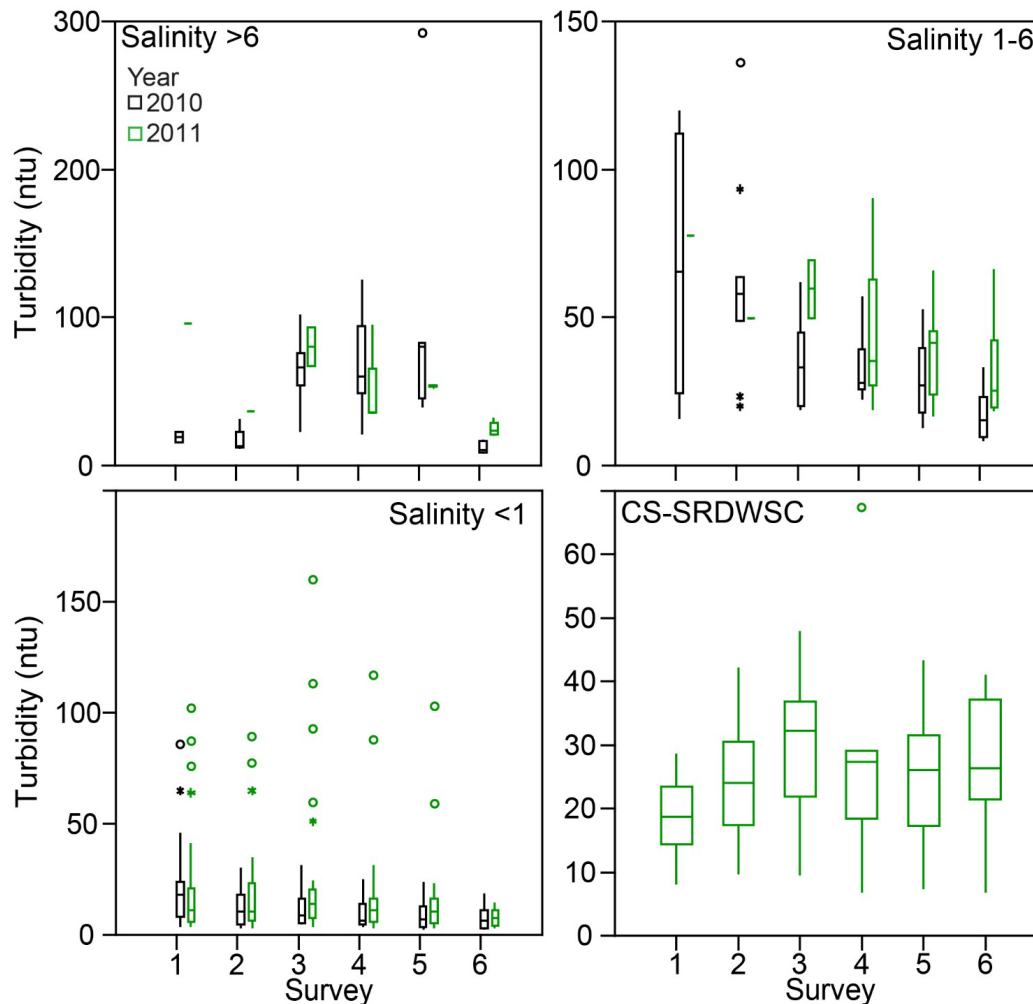
may interact. As noted above for temperature and below for food, high temperatures and low prey density likely lead to bioenergetics problems and increased foraging activity, which might reduce predator avoidance behavior (e.g., Marine and Cech 2004) in Delta Smelt. These effects may be compounded by low turbidity, which makes Delta Smelt more visible to predators in their habitat. Although higher Striped Bass abundance could theoretically result in greater consumption of prey including Delta Smelt (Lobschefsky et al. 2012), changes in habitat variables for both species such as food, temperature, and turbidity mean that predation rates on Delta Smelt periodically may be independent of predator abundance. Although there has been substantial progress in modeling (Lobschefsky et al. 2012, Nobriga et al. 2013) and genetic methods (Baerwald et al. 2012), there is not yet a standardized way to assess the effects of predation on Delta Smelt. Moreover, there are no effective surveys to assess age 1-3 Striped Bass abundance or distribution. Therefore, we are unable to directly evaluate this hypothesis. Lacking this information, we can

Figure 72. Water temperature data collected during the Summer Towntnet Survey for three salinity regions and the Cache Slough-Sacramento River Deepwater Ship Channel (CS-SRDWSC). Surveys are conducted biweekly June-August. See Chapter 3: Data Analyses for explanation of boxplots.



at least examine turbidity and temperature patterns for the four years. Temperature responses were described for Hypothesis 2. In general, summer 2005 and 2006 temperatures were relatively higher than 2010 and 2011 during key summer months (e.g. TNS surveys 3-5; Fig. 72). We expect that cooler temperatures in 2010 and 2011 may have contributed to reduced predation on Delta Smelt. Turbidity data are limited to 2010 and 2011 (Fig. 73). There were no consistent differences between the two years. Secchi depth data did not suggest major differences among the 4 years except at salinities > 6 when 2005-2006 had higher values in some months (Fig. 74).

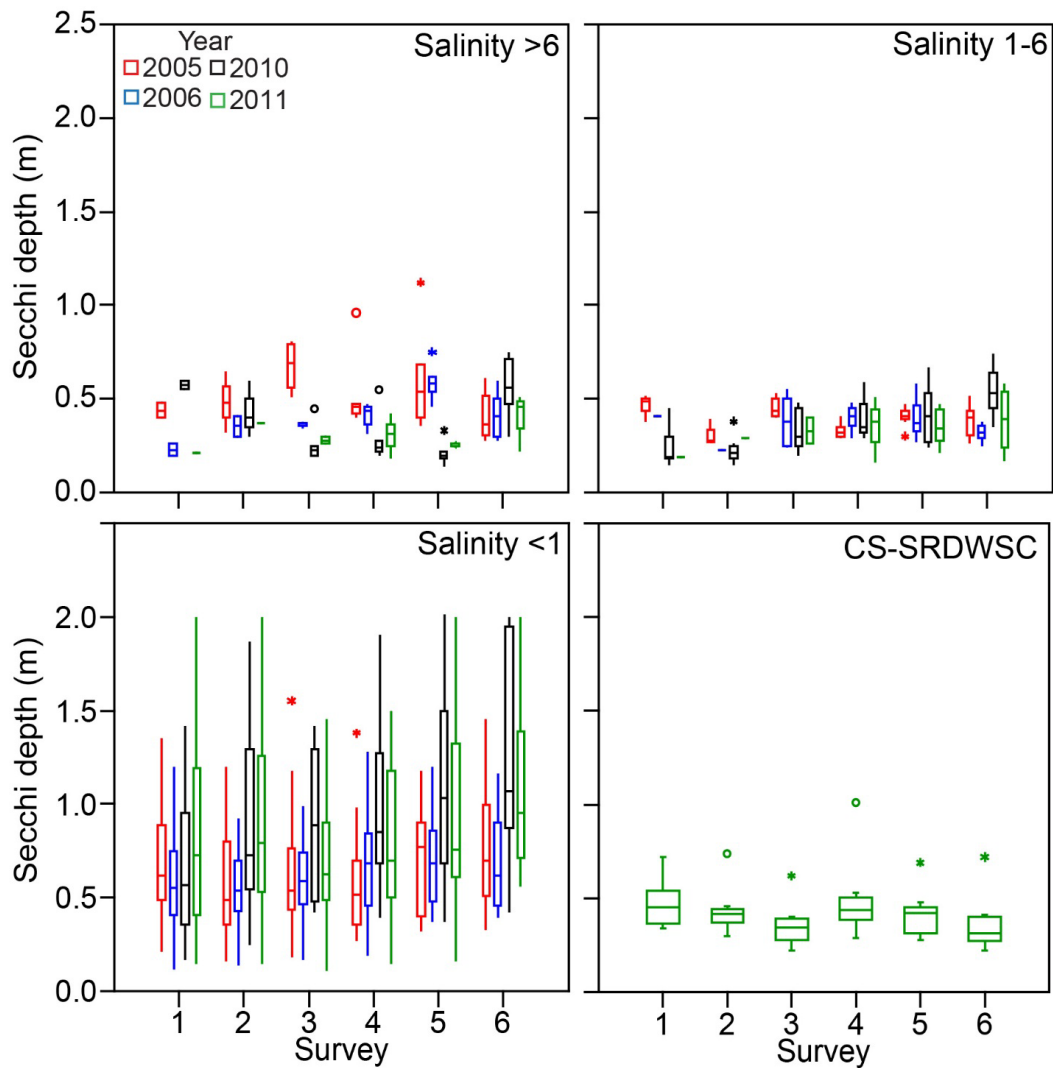
Figure 73. Turbidity data collected during the Summer Townet Survey. Surveys are conducted biweekly June-August. Note different scales among salinity regions. See Chapter 3: Data Analyses for explanation of boxplots.



Hypothesis 3. Juvenile Delta Smelt growth and survival is affected by food availability.

As for Hypothesis 1, we are currently unable to evaluate the growth data because water temperature affects development time, and because growth curves are complicated by allometric effects. The general conceptual model is that higher food abundance results in faster growth rates and larger, healthier fish. In addition, larger, healthier Delta Smelt are presumably less vulnerable to predators because of increased size making them difficult for smaller predators to capture and consume. In general, the median abundance of some of the key prey for juvenile Delta Smelt such as calanoid copepods is highest in summer months (Fig. 75), when juvenile Delta Smelt are present; however, the range of observed densities is broad in all months. As noted previously, Kimmerer (2008) found that Delta Smelt survival from summer to fall was positively associated with calanoid copepod biomass in the low salinity zone.

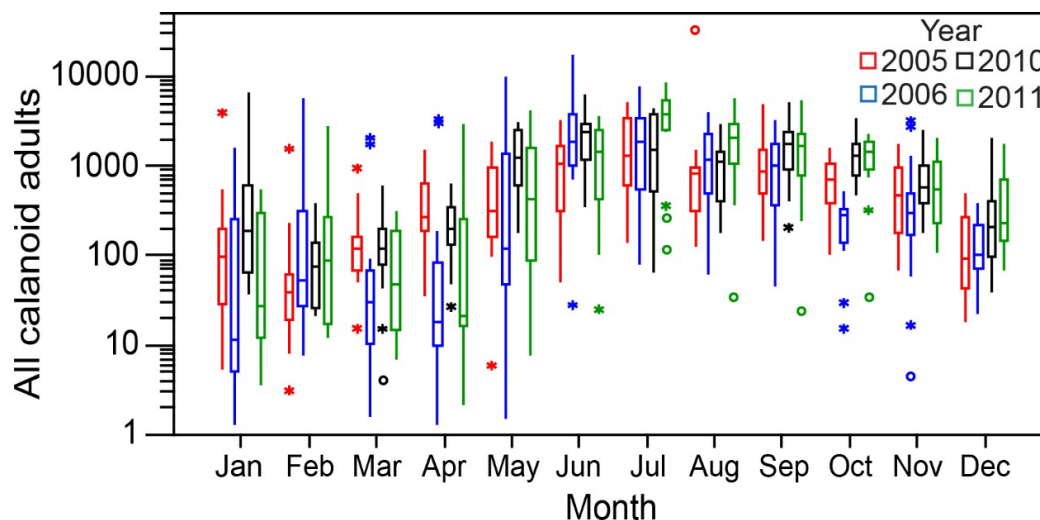
Figure 74. Secchi depth data collected during the Summer Townet Survey. Surveys are conducted biweekly June-August. See Chapter 3: Data Analyses for explanation of boxplots.



Interpretation of the field data is complicated because there are no long-term IEP EMP study stations located in some of the core habitats for Delta Smelt, for example, Cache Slough and the Sacramento River Deep Water Ship Channel. Moreover, densities of calanoid copepods vary among regions based on differing habitat (temperature and salinity) requirements of each species (Fig. 76).

Summer-time phytoplankton data (chlorophyll-*a*) suggest that the base of the food web was most enhanced in July and August 2011 and relatively depleted in 2005 (Fig. 66). There is some evidence that these changes may have affected zooplankton abundance. For example, summer densities of calanoid copepods in the LSZ and <1 ppt regions also tended to be highest in 2011 as compared to the other years (Fig. 76). This pattern generally held when individual taxa are considered including two of the most important food sources for Delta Smelt, *Eurytemora affinis* (Fig. 33) and *Pseudodiaptomus forbesi* (Fig. 34).

Figure 75. Trends in calanoid copepods (number/m³ for all taxa combined) collected by the IEP Environmental Monitoring Program (EMP) during each the four study years (2005, 2006, 2010, and 2011).

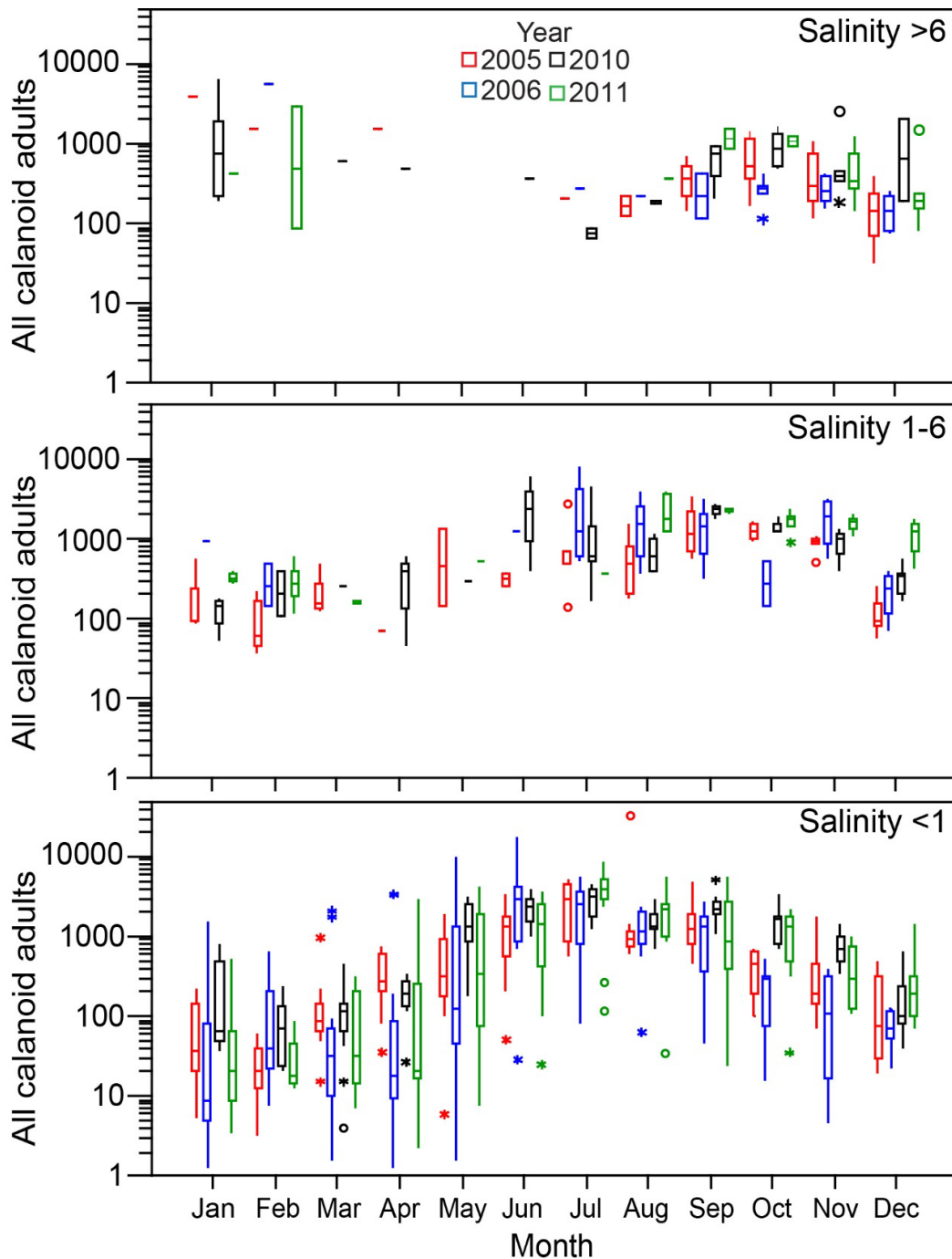


As mentioned above (Hypothesis 1), juvenile to subadult survival was highest in 2011 followed by 2006 and 2005 and lowest in 2010 (Fig. 51). If food availability was the primary habitat attribute driving juvenile survival, our expectation was that summer prey abundance would have been higher in 2011 than 2010. Figure 69 suggests that while differences were not very pronounced, prey levels were indeed somewhat higher in July and August of 2011 than 2010. Calanoid copepod levels varied across the different salinity ranges, but generally followed the same pattern (Fig. 76). In addition, calanoid copepod densities in June and August were higher in 2006 than in 2005 (Fig. 75), which may have contributed to higher juvenile to subadult survival in 2006 compared to 2005 (Fig. 51).

Fish bioenergetics are affected by both food and temperature. As mentioned above, both summer 2010 and 2011 had relatively cool temperatures as compared to 2005 and 2006, which may have affected bioenergetics. In addition, recent studies (S. Slater, CDFW, unpublished data) indicate that Delta Smelt consumption was not just limited to calanoid copepods, so our assessment does not reflect the full dietary range.

In conclusion, our analyses provide some support for the hypothesis that juvenile Delta Smelt growth and survival is affected by food availability; greater food availability may have contributed to greater juvenile survival in 2011 and 2006 compared to 2010 and 2005. However, differences in prey availability among years were not very pronounced and our analyses were limited to calanoid copepods; other species may also be important prey items for Delta Smelt.

Figure 76. Trends in calanoid copepods (number/m³ for all types combined) collected by the IEP Environmental Monitoring Program (EMP) in three salinity ranges (> 6 ppt; 1-6 ppt; < 1 ppt) during each the four study years (2005, 2006, 2010, and 2011). See Chapter 3: Data Analyses for explanation of boxplots.



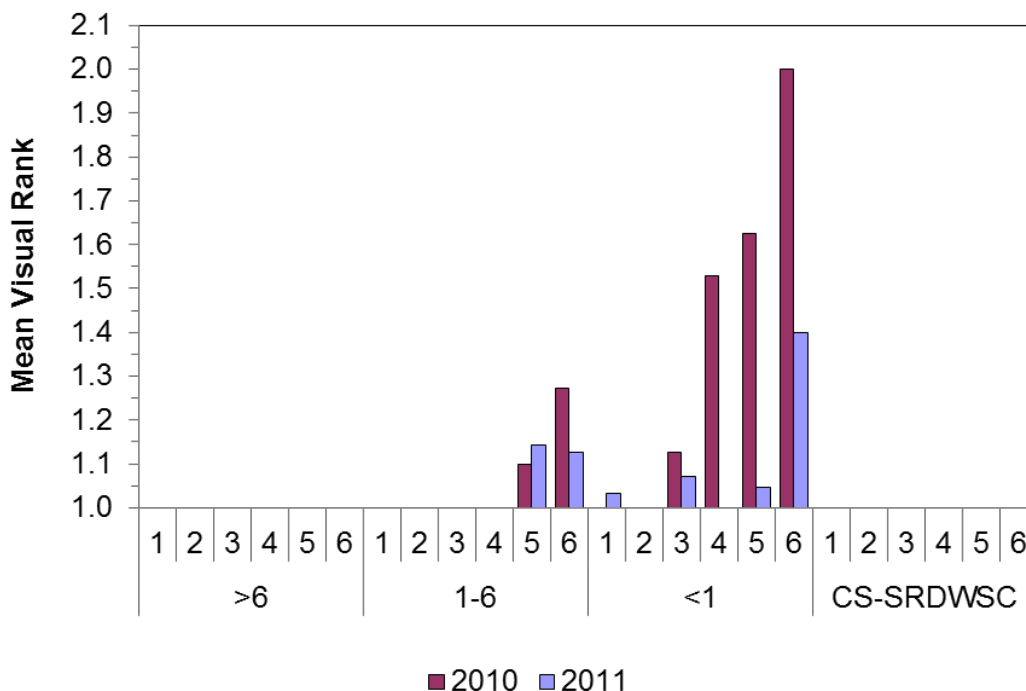
Hypothesis 4. Juvenile Delta Smelt survival and growth is reduced by harmful algal blooms (HAB) because of direct (habitat quality and toxic effects) and indirect (food quality and quantity) effects.

The appearance of late-summer HAB, especially *Microcystis*, is thought to be another component of the decline in habitat quality for Delta Smelt (Baxter et al. 2010, Lehman et al. 2010). Direct effects may include toxicity to Delta Smelt and a reduced area of suitable habitat. There also may be indirect effects on food quantity and quality, particularly with respect to their zooplankton prey (Ger et al. 2009, 2010a,b, Lehman et al. 2010).

The growth responses of Delta Smelt during the four target years are still unclear (see below), but there is evidence that Delta Smelt juvenile to subadult survival was highest in 2011 and lowest in 2010 (Fig. 51). If HABs have a negative effect on survival, we would expect that lower *Microcystis* (or other HAB) abundance would be associated with higher survival in 2011. This seems to have been the case for 2010 and 2011. Densities of *Microcystis* near the water surface were qualitatively assessed (visually ranked) at all TNS stations in these years. In agreement with our expectation, observed levels were low during the TNS in 2011 as compared to 2010 across a range of salinities (Fig. 77).

Unfortunately, we do not have data about other HAB species and more quantitative estimates, nor is similar data available for 2005 and 2006. In general, our expectation is that 2006

Figure 77. Summer Townet Survey mean visual rank of *Microcystis* spp. (ranks 1-5 possible; 1 = absent) observed at all stations during biweekly surveys (1-6) in various salinity regions (> 6, 1-6, and < 1 ppt) and in the CS-SRDWSC during June through August 2010 and 2011. Observations were not made in Cache Slough-Sacramento River Deepwater Ship Channel (CS-SRDWSC) during 2010.



Microcystis levels would have been relatively low as a result of higher flow levels that discourage blooms (Lehman et al. 2005). Based on the available qualitative data for 2010 and 2011, this analysis supports the hypothesis that juvenile Delta Smelt survival and growth is better when *Microcystis* does not bloom as intensely, but more data is needed to more conclusively assess this relationship.

Subadult Hypotheses

Hypothesis 1. Subadult Delta Smelt abundance, growth, and survival is affected by food availability.

Similar to juveniles, the general conceptual model is that higher food abundance results in faster growth rates and subsequently, lower predation loss and greater survival (e.g., Houde 1987, Sogard 1997, Takasuka et al. 2003); however the opposite situation in which the fastest growing fishes are most vulnerable to predators has also been observed in at least one east coast estuary (Gleason and Bengston 1996). Fall abundance of Delta Smelt was highest in 2011 followed by 2006, 2010, and 2005 (Fig. 3) while survival of subadults to adults was highest in 2010 followed by 2006 and equal in 2011 and 2005 (Fig. 45). In spite of the lower subadult survival in 2011, the relatively large number of subadults in 2011 gave rise to the highest adult abundance on record in 2012.

In general, fall calanoid copepod abundance and cladocera abundance were higher in 2011 in freshwater and the low-salinity zone compared to the other years, particularly 2005 and 2006 (Fig. 71). However, these data are highly variable, so this conclusion does not apply to each region in every month. With that caveat, the data generally support the hypothesis that food availability affects Delta Smelt abundance and survival; on average, prey density was higher for subadult Delta Smelt in 2011. This may have contributed to the high FMWT abundance index in 2011, although it did not contribute to an equally high survival to adults relative to the other three years. Nevertheless, it seems likely that the relatively good food availability in 2011 also contributed to the high number of adults in 2012. As noted above, we are currently unable to evaluate whether Delta Smelt grew faster in 2011 because water temperature affects spawning and hatch dates, which complicates the interpretation of growth rates.

Hypothesis 2. Distribution and abundance of Striped Bass, temperature, and turbidity influence predation risk/rate on subadult Delta Smelt

As already described for other life stages, predation risk is exceptionally complicated, making it difficult to generate simple hypotheses that describe associated losses of Delta Smelt. The data are not currently available to test this hypothesis (Nobriga et al. 2013). Thus, no firm conclusion can be made.

Hypothesis 3. Subadult Delta Smelt abundance, survival and growth are reduced by harmful algal blooms (HAB) because of direct (habitat quality and toxic effects) and indirect (food quality and quantity) effects.

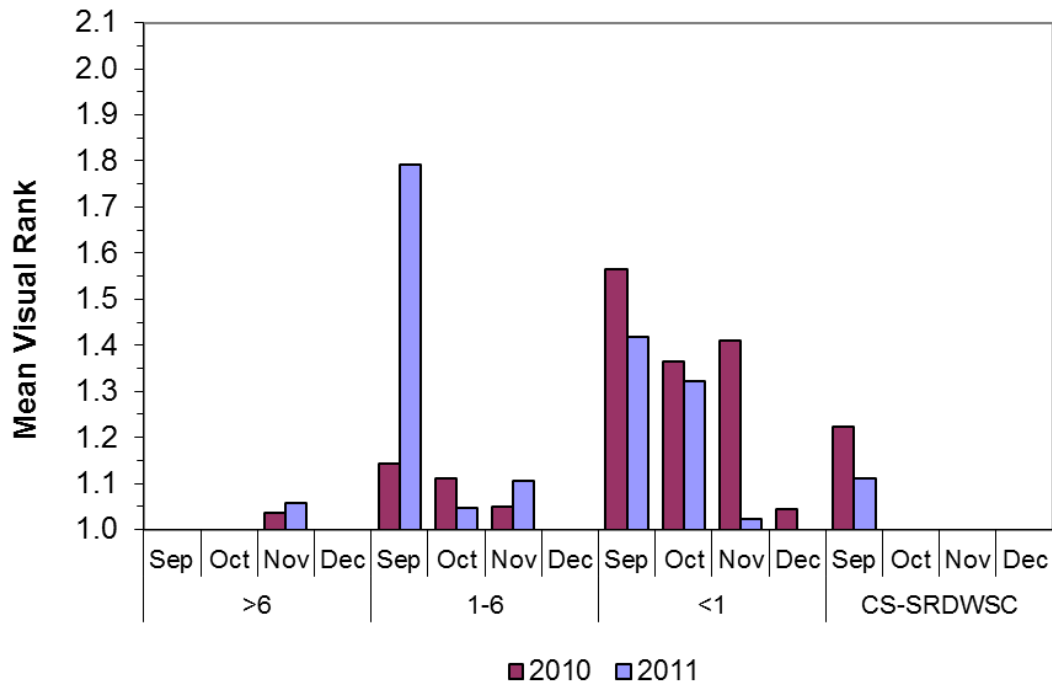
The appearance of late-summer harmful algal blooms (HAB), especially *Microcystis*, is thought to be another detriment to habitat quality for Delta Smelt (Baxter et al. 2010, Lehman et al. 2010). Direct effects may include toxicity to Delta Smelt and a reduced distribution if the fish try to limit their overlap with the bloom. There also may be indirect effects on food quantity and quality, particularly with respect to their zooplankton prey (Ger et al. 2009; 2010a,b, Lehman et al. 2010).

The growth responses of Delta Smelt during the four target years are still unclear (see above), but there is evidence that summer juvenile to subadult survival was highest in 2011, while juvenile survival to adults was highest in 2010 (Fig. 45). Our expectation is therefore that HAB were less prevalent in the summer of 2011 compared to 2010, but more prevalent in fall 2011. As already described for juveniles, the hypothesis that summer *Microcystis* bloom would be less intense in 2011 compared to 2010 was generally supported (Fig. 77). In fall, *Microcystis* levels were also overall lower in 2011 than in 2010, except in September 2011 when a high level of *Microcystis* was observed in the LSZ (Fig. 78). This may be an indication that the higher outflow in September-October 2011 displaced *Microcystis* produced in the Delta seaward into the LSZ. The comparatively high 2011 Delta Smelt FMWT index that coincided with this shift in *Microcystis* distribution is not consistent with the hypothesis; however, the occurrence of fairly high levels of *Microcystis* in the LSZ in 2011 may help explain the lower subadult to adult survival in 2011 compared to 2010. It is also important to remember that the visual survey results presented here are only qualitative and do not necessarily reflect the potential for differences in actual toxicity among years. Overall, these results are inconclusive, although they may provide limited support for the hypothesis that high *Microcystis* levels may have a negative effect on subadult to adult survival; this may help explain the lower subadult survival in 2011 compared to 2010.

Hypothesis 4. Subadult Delta Smelt abundance, survival and growth are affected by the size and position of the low salinity zone during fall.

We do not address this hypothesis in detail because it is the subject of an adaptive management experiment (FLaSH) described earlier (Reclamation 2011, 2012; see also Brown et al. 2014, <http://deltacouncil.ca.gov/science-program/fall-low-salinity-habitat-flash-studies-and-adaptive-management-plan-review-0>). According to the FLASH conceptual model, conditions are supposed to be favorable for Delta Smelt when fall X2 is approximately 74 km or less, unfavorable when X2 is approximately 85 km or greater, and intermediate in between (Reclamation 2011, 2012). Surface area for the LSZ at X2s of 74 km and 85 km were predicted to be 4000 and 9000 hectares, respectively (Reclamation 2011, 2012). The data generally supported the idea that lower X2 and greater area of the LSZ would support more subadult Delta Smelt (Table 6). The greatest LSZ area and lowest X2 occurred in September and October 2011 and were associated with a high FMWT index which was followed by the highest SKT index on record, although survival from subadults to adults was actually lower in 2011 than in 2010 and 2006. There was little separation between the other years on the basis of X2, LSZ area, or FMWT index (Table 6). The position and area of the LSZ is a key factor determining the quantity and quality of low salinity rearing habitat available to Delta Smelt and other estuarine species (see Chapter 4 for more detail

Figure 78. Fall Midwater Trawl mean visual rank of *Microcystis* spp. (ranks 1-5 possible; 1 = absent) observed at all stations during monthly surveys in various salinity regions (> 6, 1-6, and < 1 ppt) and in the CS-SRDWSC during September through December 2010 and 2011.



and Chapter 8 for additional analysis results). In addition, the complex hydrodynamics produced during higher outflows may alter the lateral mixing environment of the Estuary (especially in shallower areas like Suisun Bay) in ways that improve the quality of Delta Smelt habitat in general (Monismith, personal communication). The limited amount of available data provides some evidence in support of this hypothesis, but additional years of data and investigations are needed.

Chapter 8: Conclusions

As with all reports focusing on conceptual models, this report is intended as a working document, not as the final word on Delta Smelt ecology, because our knowledge will continue to increase. We intend the conceptual model to be used as a framework and tool to further improve our understanding of Delta Smelt ecology and to explore and test management options for improving conditions for the Delta Smelt population. In essence, the updated conceptual model represents a synthesis of our current thinking on the factors affecting vital rates of the Delta Smelt population. We fully expect a wide range of opinion about the relevance of the conceptual models presented here and about the degree of certainty regarding many of its component dynamics and linkages. We have clearly acknowledged that we lack information on many important factors and processes that likely affect Delta Smelt, such as predation and toxicity and their functional relationships

Table 6. Mean and standard deviation (SD) for X2, surface area of low salinity zone (M. McWilliams, Delta Modeling Associates, unpublished data), and values of the Fall Midwater Trawl index (FMWT) for abundance of subadult Delta Smelt.

	X2 (km)		Surface area LSZ (hectares)		FMWT index
YEAR	MEAN	SD	MEAN	SD	
2005	83	2	4889	252	26
2006	82	3	4978	320	41
2010	85	2	4635	226	29
2011	75	1	8366	133	343

with survival and growth. The conceptual model incorporates many hypotheses that should be tested via new research, modeling, and ongoing analysis and synthesis of new and previously collected data. This is how science advances.

Conceptual models are increasingly used as tools to develop questions or hypotheses about specific mechanisms through which stressors or other environmental factors drive ecological outcomes. Conceptual models can be used as a basis for communication among managers and scientists to plan research activities and assess outcomes of management actions (Ogden et al. 2005). Because of their broad utility, conceptual models are viewed as a critical element of adaptive management programs (Thom 2000). In the SFE, conceptual models have become common and even required as the community moves toward adaptive management and collaborative science. A primary outcome of conceptual models is the identification of key areas of uncertainty due to lack of information, or areas of disagreement due to different interpretations of the available data and information. Careful examination of these areas often identifies critical data and information gaps, which if filled, would allow a more robust evaluation of the major hypotheses derived from conceptual models. In this way, conceptual models can guide the research community to the topics critical for understanding Delta Smelt biology and formulating effective management actions.

The development of our conceptual model, based on assessment of recent information, identified some key points about conceptual models that are worth highlighting, including the following:

1. Nested and linked conceptual models of increasing specificity provide a useful framework for capturing the dynamics of ecosystem drivers and habitat attributes over a large range of temporal and spatial scales and for providing a comprehensive picture about their effects.
2. Our knowledge about Delta Smelt and the SFE is constantly growing and conceptual models about them have to be regularly updated and revised to properly reflect this knowledge.
3. Construction of our conceptual model and the formulation and evaluation of hypotheses greatly benefitted from the large amount of high-quality ecological data and information available about Delta Smelt and the SFE. The most critical data about Delta Smelt dynamics came from four long-term IEP fish monitoring surveys. Other monitoring

and studies provided key data and information about habitat attributes and ecosystem drivers.

4. Our conceptual model is also useful for identifying important data and information gaps. More data and information is especially needed about predation risk and toxicity, two potentially important attributes of Delta Smelt habitat.

Conceptual models are meant to be useful tools for scientists, managers, and others. But just how useful are the new conceptual models in this report? To find out, we used them to generate and test hypotheses and highlight data gaps while addressing a specific topic of high management interest—the increased Delta Smelt abundance index in 2011.

We found that our conceptual model allowed us to formulate a variety of testable hypotheses about individual components and the linkages among them. Our hypotheses and the analyses we conducted to test them had some clear limitations (discussed below), but highlighted some key points about Delta Smelt and their habitat. In many respects, the points about Delta Smelt seem self-evident from basic biology and earlier conceptual models, but they warrant reinforcement because they are crucial to understanding Delta Smelt and to developing and assessing habitat management actions. Key points about Delta Smelt include the following:

1. Environmental conditions occurring in all four seasons contribute to year-class strength of Delta Smelt - “it takes a year to make a mature Delta Smelt.”
2. Survival and recruitment are affected by many factors that interact in complex ways and the importance of these factors and interactions varies from season to season and year to year.
3. Recovery of Delta Smelt depends on better than average larval production (recruitment) and survival in all seasons. The number of eggs and larvae sets an upper limit for the production of mature adults. Low survival between any two life stages can substantially reduce the actual production of mature adults. Success of Delta Smelt in 2011 was related to a high level of larval production (recruitment) followed by moderate to high stage-to-stage survival over the entire year. In contrast, the high level of larval production (recruitment) in 2006 was followed by very low survival from larvae to juveniles which led to low abundance of mature adults.
4. Throughout 2011, Delta Smelt may have benefitted from a combination of favorable habitat conditions: 1) adults and larvae benefitted from high winter 2010 and spring 2011 outflows which reduced entrainment risk and possibly improved other habitat conditions, prolonged cool spring water temperatures, and possibly good food availability in late spring; 2) juveniles benefitted from cool water temperatures in late spring and early summer as well as from relatively good food availability and low levels of harmful *Microcystis*; 3) subadults also benefitted from good food availability and from favorable habitat conditions in the large, westward low salinity zone.

Our hypothesis tests were carried out with the simple comparative approach used in the FLaSH investigations (Brown et al. 2014). Specifically, we compared differences in Delta Smelt responses and in individual habitat attributes during the two most recent wet years and the two years immediately preceding the two wet years. Using this approach allowed us to put the FLaSH results into a year-round context as recommended by the FLaSH Panel (FLaSH Panel 2012).

It also provided an opportunity to further assess the utility of this approach for evaluating the outcome of adaptive management actions such as the fall outflow action.

As with the FLaSH investigations (Brown et al. 2014), we restricted our analyses to simple comparisons among four recent years after the 2002 POD decline for several reasons including the following:

1. Using a comparative approach similar to that in the FLaSH investigation allowed us to place the results of the FLaSH investigation in a year-round, life cycle context as recommended by the FLaSH Panel (FLaSH Panel 2012).
2. This report is intended for a broad audience. Simple comparisons are easily replicated and understood by all.
3. More pertinent data is available for recent years than for earlier years. For example, adult Delta Smelt monitoring began in 2002 with abundance index values available starting in 2003.
4. The POD regime shift (Baxter et al. 2010) changed ecological relationships and the strong pre-POD signals would have likely overwhelmed more subtle, yet meaningful, signals in the period after the POD. For example, it appears that high larval recruitment may now be positively associated with wet hydrology, but that this may not have been the case before the onset of the POD.
5. Clear differences in habitat conditions among years might point to new or refined management strategies aimed at improving specific habitat conditions.
6. More complex modeling approaches take much more time and effort than was available to produce this report. A complex life cycle modeling effort is currently underway (see Chapter 9).

As noted above, our analytical approach yielded some interesting results, but it also raised more questions than it could answer. In many cases this was due to critical data and information gaps; these will be described in more detail in Chapter 9. It also illustrates, however, several limitations of our simple comparative approach as well as difficulties associated with posing and testing hypotheses about ecological phenomena in general. Examples of specific limitations and difficulties include the following:

1. Our hypotheses focused on individual habitat attributes and were tested with a series of separate univariate analyses even though we know that Delta Smelt are affected by multiple interacting habitat attributes. We did not conduct multivariate tests or examine the complex interactions that may have occurred when more than one hypothesis was true (or false), nor did we consider or rule out that a hypothesis may be true in some years and false in others.
2. Our simple comparisons of differences in individual habitat attributes among different years cannot conclusively establish whether these differences are indeed mechanistically linked to the observed differences in Delta Smelt dynamics. In addition, an absence of observed differences does not prove that there is really no effect because actual effects can be masked or counteracted by interactions with other causal factors that differ among years. For example predation in the South Delta may mask actual entrainment

effects and toxicity of anthropogenic contaminants may counteract the effects of abundant food in some years, but not in others.

3. Results contrary to our observations may simply indicate different outcomes in other years or that complex interactions among multiple habitat attributes (and corresponding hypotheses) contributed to the observed effects.
4. We restricted our analyses to observational data collected in a small number of moderately and very wet years during the POD period; including data from additional, more historical, and drier years may have provided more conclusive results.
5. Data available for our analyses were not necessarily collected to test hypotheses similar to the ones in this report; targeted data collections are needed in addition to routine status and trends monitoring.

Many of these difficulties and limitations were expected because hypothesis testing in an ecological context is nearly always problematic. For example, Quinn and Dunham (1983) warned that attempts to follow a strictly hypothetico-deductive scheme (Popper 1959, Platt 1964) to draw “strong inference” from a series of univariate tests aiming to falsify hypotheses about the ecological effects of individual causal factors often lead to inconclusive or even erroneous results. One reason for this is that by design, they generally do not consider non-additive interactions among causal factors. While we did not necessarily set out to strictly follow such a scheme, we nevertheless treated habitat attributes as largely independent from each other and formulated a series of distinct hypotheses about their univariate effects on Delta Smelt. But habitat attributes are not necessarily additive and habitat is indeed more than the “sum of its parts.” A more inductive, multivariate modeling approach with hypotheses about interactive effects and evaluations of the relative contributions of multiple interacting habitat attributes to these effects would have likely been more appropriate, but would have required analyses beyond the scope of this report.

We give some examples of multivariate approaches in Chapter 9, but note that even with the most sophisticated modeling techniques, ecological responses to management manipulations and other changes of the SFE have been notoriously difficult to assess and interpret. Reasons for this persistent difficulty include limited opportunities for experimental control, multiple interacting causal factors, multiple ecological response pathways, and changing environmental conditions due to species invasions, species declines, and the many physical and chemical changes and management manipulations described in this report. In other words, the signal to noise ratio of management actions to environmental variation tends to be low in the SFE because of its size and complexity. The fact that Delta Smelt is now a rare species adds another considerable difficulty. Together, these difficulties are part of the reason why adaptive management actions such as those described in the ongoing Fall Outflow Adaptive Management Plan (Reclamation 2011, 2012) and the now concluded Vernalis Adaptive Management Plan (VAMP, San Joaquin River Group Authority 2013) are planned for a minimum of 10 years, allowing accumulation of data, development of appropriate interpretation of these data, and comparison of observations across as broad a range of conditions as is possible given a 10-year time frame. But even after such a relatively long period of manipulation and observation, questions will likely remain about how some factors interact to affect Delta Smelt abundance.

In summary, we conclude that our new conceptual models can be used successfully to derive testable hypotheses about Delta Smelt responses to changing habitat conditions. Our hypotheses

and the analyses we conducted to test them highlighted some key points as well as critical data gaps and the challenges associated with formulating and testing hypotheses in complex ecological contexts. The key points about Delta Smelt and their habitat generally agree with basic biological principles and earlier conceptual models, but warrant reinforcement because they are crucial to understanding Delta Smelt and to developing and assessing habitat management actions. Other results are less conclusive because of data limitations and the shortcomings of our largely univariate hypotheses and simple comparative analysis approach. Next steps should include addressing critical data gaps, modeling that more fully considers the effects of interacting factors on Delta Smelt, and applications of the information in this report in support of management actions. Examples of such efforts are provided in Chapter 9.

Chapter 9: Recommendations for Future Work and Management Applications

The conceptual model in this report can be viewed as a collection of hypotheses. These hypotheses are not limited to the hypotheses posed in Chapter 7 of this report; essentially, each component and linkage in the conceptual models can give rise to meaningful questions and hypotheses by itself or together with other components and linkages. This is one of the main functions of conceptual models.

Some of the hypotheses that can be derived from our conceptual model have already been addressed in the published research reviewed in Chapter 4 of this report. These results provide the knowledge base used to construct our conceptual model as well as previous conceptual models. They also provide the knowledge base for current Delta Smelt management efforts. The results and conclusions in this report add to this knowledge, but they also emphasize the need for additional monitoring, focused studies, and/or additional analysis and synthesis of existing data. These are the information gaps that can be used to guide future research activities to enhance our understanding of how factors interact to control Delta Smelt abundance.

Filling these information gaps is critically important for improving management strategies for Delta Smelt and for constantly adapting them to expected and unexpected future changes. It is clear that ecological changes due to continued growth of California's human population, climate change, new species invasions, and other natural and anthropogenic factors will increase the challenges associated with Delta Smelt management. Moreover, as discussed in the previous Chapter, we will likely never be able to correctly detect or predict all effects of management actions and other changes in an ecosystem as complex and constantly changing as the San Francisco estuary. Science and management have to go hand in hand to constantly identify, implement, evaluate, and refine the best management options for this ever-changing system. In this Chapter, we provide examples of next steps in three major areas where additional work is needed: 1) filling critical data and information gaps; 2) mathematical modeling; and 3) applications to support adaptive management actions. We conclude this report with recommendations for future analysis and synthesis efforts.

Critical Data and Information Gaps

A short list of the most critical data and information gaps identified by the updated conceptual model is given below. It is important to note that this is not an exhaustive list of the potentially productive research questions that could be addressed for Delta Smelt. Instead, these are primary research topics that emerge as major data and information gaps in multiple places within the updated conceptual model. This indicates that additional monitoring and research on these topics may be particularly urgently needed and filling these gaps would provide immediately useful results. The list of critical data and information gaps is organized around the environmental drivers and habitat attributes identified in our conceptual models.

Contaminants and Toxicity

There is a general awareness that exposure to contaminants can impair the health of Delta Smelt and other fishes. A few studies have documented adverse effects, but little is known regarding the thresholds at which most contaminants would be toxic to or otherwise adversely affect Delta Smelt (or their prey). Even less is known about how various contaminants may interact when they co-occur, or how their effects may be enhanced or suppressed by these interactions or by other environmental factors.

1. Focused laboratory studies may provide the most efficient way to assess effects of metals, pesticides, pharmaceutical products, or mixtures of contaminants as long as field-relevant concentrations are used. However, translating results of laboratory tests to the field remains a challenging problem (Scholz et al. 2012).
2. Significant work to understand the effect of nutrient loading from municipal sources on the food web has been done (Weston et al. 2014) (e.g., Sacramento Wastewater Treatment Plant, Parker et al. 2012). A logical next step is to conduct manipulative experiments in which effluent is reduced or shut off. This type of work has recently begun (T. Kraus, USGS, personal communication), but may require multiple iterations during a variety of seasons and environmental conditions in order to understand how such manipulations or future treatment upgrades could be used to provide desired food web responses. Monitoring should continue after any such upgrades to determine if they have the expected outcomes.

Entrainment and Transport

Evaluation of differences in entrainment among years could not be critically evaluated from salvage data; better ways to estimate, monitor, and evaluate entrainment losses due to south Delta exports are needed. Such improved estimates could be derived from experimental research on Delta Smelt and other species along with hydrodynamic modeling. Besides the need to improve the estimates of direct proportional population losses due to entrainment, similarly relevant or more important needs include assessing the influence of entrainment on key population attributes (e.g., genetics, demographics, population dynamics and viability effects).

Predation Risk

The majority of the hypotheses regarding predation risk could not be fully evaluated due to a lack of data regarding co-occurring predator and prey biomass and predation rates of predators on Delta Smelt.

1. The distribution and diet of major predators with respect to the distribution of Delta Smelt needs further investigation. For some predator species, data may already be available that describe distributions over multiple years and one data synthesis effort has already begun (Mississippi Silversides, USFWS Beach Seine Survey; analysis initiated by B. Schreier, DWR). However, data are lacking for several Striped Bass and Largemouth Bass life stages and focused studies are necessary to understand how these species' distributions overlap with the distribution of larval, juvenile, sub-adult, and adult Delta Smelt.
2. The distributional overlaps of Delta Smelt with their predators need to be described over varying conditions of turbidity, salinity, temperature, and hydrology. Linking predation risk to key environmental drivers and habitat attributes will shed light on how Delta Smelt may experience varying degrees of predation across seasons and years.

Food

Food availability is a critical aspect of Delta Smelt habitat throughout the conceptual model. However, many of the hypotheses about effects of food availability in the conceptual model could not be fully evaluated with available observational data due to incomplete information on prey densities and Delta Smelt feeding behavior throughout Delta Smelt habitat.

1. An extension of the IEP EMP into the Cache Slough complex and possibly other areas around the margins of the estuary would allow a fuller regional comparison of prey densities.
2. Another option is to make concurrent zooplankton sampling a routine part of the four major surveys monitoring Delta Smelt (SKT, 20 mm, TNS, FMWT). To varying degrees, this has been ongoing since 2005, but lack of trained staff has resulted in delayed processing of many samples and concurrent zooplankton samples have never been collected during the SKT survey. Adding appropriate zooplankton sampling and sample processing capacity to the fish monitoring surveys would allow for broader and more timely comparisons of pelagic food availability between monitoring stations with and without Delta Smelt present, similar to the analysis conducted in this report for the larvae collected during the 20mm survey (Larval Hypothesis #2).
3. Studies of Delta Smelt growth (from otoliths) and feeding habits (from stomach contents) concurrent with zooplankton sampling would maximize the utility of the concurrent prey sampling by allowing the refinement of functional response models.
4. Studies of Delta Smelt feeding behavior and prey availability with regard to amphipods and other prey that are not well sampled by any of the existing monitoring surveys could help determine the importance of these types of prey to the Delta Smelt population.

Harmful Algal Blooms

While recent research has resulted in improved understanding of the factors influencing the quantity, toxicity and location of HABs, there are still many uncertainties about their direct and indirect effects on Delta Smelt relative to other factors and about what can be done to prevent them. Furthermore and in spite of their importance to ecosystem and human health, there is still no routine quantitative monitoring program in place that specifically targets harmful algae. The TNS and FMWT surveys now include qualitative, visual assessment of *Microcystis*, but more quantitative techniques and techniques that detect additional harmful species and their toxicity would likely provide greater insights. Such techniques are increasingly available (e.g., solid phase adsorption tracking; Wood et al. 2011) and some focused studies that quantify and provide distributions of HABs have been conducted or are underway. These studies should be continued in order to address hypotheses related to the effects of HABs in the conceptual model and evaluate the utility of these techniques for routine monitoring applications.

Delta Smelt Responses

To fully evaluate the interactions of various stressors on Delta Smelt population biology, a quantitative life cycle population model is needed. While such models exist, they can be refined based on research into important aspects of Delta Smelt reproductive biology, including the reproductive output of individual Delta Smelt and the population as a whole, and how it varies with environmental conditions.

In particular, fecundity data on adult female Delta Smelt caught in the SKT have only recently been collected. This is a critical parameter, necessary to assess the reproductive potential of the population in any given year. Continued collection of fecundity data over multiple years and hydrological conditions is crucial to understanding the population response to environmental conditions in the seasons preceding reproduction. In addition, an understanding of variables controlling the number of spawning events in a year for wild Delta Smelt is necessary to understand the full reproductive potential of the population. An exploration of whether spawning events are discernible on otoliths is ongoing (Hobbs group, UC Davis); if so, retrospective analyses relating multiple spawning events to concurrent conditions (e.g., tidal phase, food availability, water temperature) may be possible.

Finally, efforts to better characterize spawning habitat and habitat attributes needed for successful egg hatching should also continue. This is needed to more fully evaluate and understand linkages between environmental drivers such as hydrology and larval recruitment. Of all the life stages of Delta Smelt, we know the least about the egg stage; Delta Smelt eggs have never been found in the wild. Because of this, we were not able to construct a life stage transition conceptual model that specifically focused on eggs. More information about spawning and egg hatching habitat is needed to fill this gap in our conceptual models and to identify management actions that would promote beneficial habitat attributes.

Mathematical Modeling

As demonstrated in this report and by others, conceptual models are useful tools for identifying and understanding key ecosystem components and relationships, but they do not quantify them and cannot be used to quantitatively define functional responses to environmental drivers or make

quantitative predictions. Furthermore, as discussed above, the simple univariate and comparative analysis approaches employed throughout this report cannot capture the effects of multiple and often interacting drivers on the Delta Smelt population as a whole and on specific processes such as growth, mortality, and reproduction. The influences of interspecific interactions and abiotic forcing factors on populations and communities in complex ecosystems such as estuaries are also difficult to directly measure in any practical way. Only mathematical models can deal with such complexities and provide quantitative assessments and predictions.

Fortunately, the number of scientific publications about Delta Smelt that include various types of increasingly sophisticated mathematical models is growing rapidly. Recent examples include mathematical models based on statistical approaches (e.g., Bennett 2005, Manly and Chotkowski 2006, Feyrer et al. 2007, Nobriga et al. 2008, Kimmerer 2008, Kimmerer et al. 2009, Feyrer et al. 2010, Thomson et al. 2010, Mac Nally et al. 2010, Miller et al. 2012, Sommer and Mejia 2013, Kimmerer et al. 2013). These efforts generally focused on habitat associations using presence/absence data from the various monitoring surveys or on changes in Delta Smelt abundance based on abundance indices generated by the monitoring surveys and the effects of multiple habitat attributes (covariates) on these changes.

There is also a rapidly developing body of population life cycle models for Delta Smelt and other SFE fish species (e.g., Blumberg et al. 2010, Maunder and Deriso 2011, Massoudieh et al. 2011, Rose et al. 2011, Rose et al. 2013a, b). These models use either a statistically-based “state–space” multistage life cycle modeling approach or a spatially explicit, individual-based simulation modeling approach. Both approaches allow for analysis of the importance of drivers that affect different life stages of Delta Smelt and vary in space and time.

Not surprisingly, results of mathematical modeling efforts to date agree strongly that no single factor can explain the observed Delta Smelt population dynamics and long-term changes in abundance. There is less agreement, however, about which factors are most important (see for example Rose et al. 2013b) and about the exact sequence and nature of their interactions that led to the 2002-3 Delta Smelt POD decline. It is possible, perhaps even likely, that the natural complexity of the estuarine ecosystem coupled with multiple human impacts will prevent definitive answers to these types of questions, especially when they are sought through overly rigid application of formal hypothetico-deductive reasoning and methods (Quinn and Dunham 1983). We agree with Rose et al. (2013b) that the inherent complexity of the system and the challenges it presents for scientists and managers alike “is perhaps the best reason to develop and compare alternative modeling approaches.” Even the most sophisticated modeling oversimplifies complex systems and includes many assumptions. This means that instead of a single modeling approach, multiple alternative conceptual and mathematical modeling approaches, from the simple to the complex, are needed to understand how complex systems work and to predict future changes with sufficient confidence to allow for effective management interventions. The following sections give a brief overview of some of the alternative mathematical modeling efforts currently underway or proposed for the future.

A comprehensive state-space modeling effort that takes advantage of available Delta Smelt abundance data from all monitoring surveys and the even larger monitoring data set about habitat attributes is currently underway (Ken Newman, FWS, personal communication) and future analyses using the individual-based model developed by Rose et al. (2013a) have been proposed (Rose et al. 2013b). As mentioned above, a full description or application of mathematical models is outside of the scope of this report, but to illustrate the utility of additional alternative approaches and further explore some of the linkages and interactions in our conceptual model,

we give three additional examples of alternative mathematical modeling approaches that may be used to further test some of the hypotheses in the conceptual models in this report. The first is a qualitative modeling approach, the second a multivariate statistical modeling approach, and the third a numerical simulation modeling approach. Each of these approaches was explored by one of the co-authors of this report. Importantly, these approaches are meant to complement, not replace state-space, individual-based, and other modeling approaches for Delta Smelt.

Furthermore, results are preliminary and included for illustrative purposes only; peer-reviewed publications of these analyses need to be completed before they can be used to draw any conclusions.

Qualitative Models

Qualitative modeling provides a theoretical foundation for understanding system behavior by minimizing the loss of generality and realism at the expense of model precision (Levins 1974, Levins 1975, Puccia and Levins 1991). Qualitative modeling is based on a mathematically rigorous approach that can be used to gain insight on community level process and to examine the consequences of intended or inadvertent human-induced perturbations in managed systems. Questions often addressed through qualitative modeling include the resilience and stability of the system and the direction of population change (Puccia and Levins 1991), the role of system structure on stability (Dambacher et al. 2003, Fox 2006) and the degree of predictability in the response of populations to perturbations (Montaño-Moctezuma et al. 2007, Hosack et al. 2009). Such questions have strong implications in terms of stability-complexity relations (May 1972, Pimm 1984, Haydon 1994) and the persistence of populations and communities following regime shifts (Baxter et al. 2010, Brook and Carpenter 2010, Capitán and Cuesta 2010, Cloern and Jassby 2012).

The increased ecological understanding of the upper SFE and the potential drivers and mechanisms underlying the interannual population responses of Delta Smelt reviewed by the FLaSH and MAST syntheses provide a strong rationale to further refine and integrate our knowledge on community level interactions and ecological drivers in this highly altered system. Towards that goal, we envision qualitative modeling as a complementary approach to other types of models to evaluate the response of Delta Smelt and other populations in the upper SFE over several temporal and spatial scales. Qualitative modeling for Delta Smelt can address some relevant system-level knowledge gaps which are usually less amenable to analyses using other modeling approaches, namely, the influence of species interactions and multiple feedback levels on community stability and population changes in response to perturbations on one or more species. For example, understanding the mechanisms leading to Delta Smelt population responses under different hydrological conditions is an area of significant interest.

Signed-digraphs are a useful representation of the structure of a system, as defined by the community matrix, and have been used in qualitative models exploring food webs (Liu et al. 2010), extinction events in communities (Vandermeer 2013), and other ecological topics of theoretical and conservation relevance. Castillo (unpublished data) used this approach to evaluate the predicted response of Delta Smelt to a sustained change in fall outflow as required in the 2008 FWS Biological Opinion. Recognizing that outflows can control X2 and the size and location of the LSZ (see Chapter 4), and affect other segments of the aquatic community supporting Delta Smelt, Castillo (unpublished data) modeled the response of subadult Delta Smelt to low (5,000 cfs; X2 = 85 km), intermediate (8,000 cfs; X2 = 81 km) and high (11,400 cfs; X2 = 74 km) fall outflow scenarios. Community composition for each outflow scenario was determined relative

to the geographical distribution of species expected to occupy the LSZ. The high outflow model included six community components: phytoplankton, zooplankton, Delta Smelt, predators of Delta Smelt, the overbite clam *Potamocorbula amurensis*, and outflow. The intermediate outflow scenario included two additional community components: the Asian clam *Corbicula fluminea* and the cyanobacteria *Microcystis aeruginosa*. The low outflow scenario included the same variables as in the intermediate flow scenario, except that the overbite clam was excluded and the Brazilian waterweed, *Egeria densa* was added. For each of these communities, community components could exhibit positive or negative feedbacks and positive or negative interactions with other community components. For each of the assumed flow conditions, the four alternative types of community interactions were assumed and each met the stability criteria, as defined by Puccia and Levins (1991). The predicted response of the Delta Smelt population was: 1) predominantly positive under the high outflow community scenario, 2) ambiguous under the intermediate outflow community scenario and 3) very ambiguous under the low outflow community scenario. According to these preliminary results, both outflow and outflow-induced changes in community composition and structure seem to play a critical role in determining the population response of Delta Smelt. These model predictions supported the hypothesis that a shift in the LSZ towards $X2 = 74$ km is a necessary condition for the fall outflow action to exert a positive influence on the Delta Smelt population. Qualitative models like these can provide useful assessments when the general direction of community interactions are understood but the data are insufficient to support a quantitative model.

Multivariate Statistical Modeling

In this report we reviewed results from many multivariate statistical modeling efforts such as the multivariate autoregressive modeling (MAR) conducted by MacNally et al (2010) to discern the main factors responsible for the POD declines and the hierarchical log-linear trend modeling by Thomson et al. (2010) that used Bayesian model selection to identify habitat attributes (covariates) with the strongest associations with abundances of the four POD fish species and determine change points in abundance and trends. The state-space life cycle modeling by Maunder and Deriso (2011) is also based on multivariate statistical modeling; an extension of this work is currently underway by Newman and others (Ken Newman, USFWS, unpublished data).

We anticipate that insight from the current conceptual model may be used to facilitate additional multivariate statistical models. As an example, we present preliminary results (Mueller-Solger, USGS, unpublished data) of univariate and multivariate statistical analyses of $X2$ relationships with annual Delta Smelt abundance indices that follow the approach in Jassby et al. (1995). The purpose is to further explore some of the hypotheses related to hydrology and the size and position of the LSZ included in our conceptual model and to illustrate the importance of considering more than one factor when trying to understand Delta Smelt dynamics. We include this brief exploration in this report because it serves as a useful and relevant example, but as noted above, we advise readers that these are preliminary results from an analysis that has not yet undergone peer review and should be viewed with caution. Moreover, individual and interactive effects of additional factors were not considered in this analysis, but are likely also important (see Chapter 8). As noted in Chapter 7, we recognize that “hydrology” by itself does not affect Delta Smelt, nor does the “ $X2$ ” index which is used in this analysis as an index of general hydrological (outflow) conditions in the estuary. As shown in our conceptual model (Fig. 38), hydrology affects Delta Smelt through the combined effects of its interactions with other dynamic drivers and stationary landscape attributes (tier 1) on habitat attributes (tier 3). Many of

these interactions have been described in this report; others should be explored further in future studies.

This analysis is intended to evaluate the effects of prior abundance, step changes, and concurrent and prior hydrological conditions in the estuary on the relative abundance of larval to early juvenile Delta Smelt (20 mm index, Fig. 3; hereafter referred to as “larval” Delta Smelt). It also considers prior hydrological conditions and the entire available abundance index time series for larval Delta Smelt provided by the 20 mm survey. The 20 mm survey, one of the newest IEP monitoring surveys, was started in 1995. Delta Smelt distribution data from this survey is heavily used to assess and manage entrainment risk. Similar to prior analyses of TNS and FMWT data (Feyrer et al. 2007, Nobriga et al. 2008), Kimmerer et al. (2009, 2013) and Sommer and Mejia (2013) used a generalized additive modeling (GAM) approach to examine the associations between Delta Smelt occurrence or catch per trawl at 20 mm survey stations and habitat attributes (salinity, temperature, turbidity, and calanoid copepod density) measured concurrently at the same stations. There have, however, been few analyses of annual abundance data from this survey. After 19 years, the 20 mm survey now provides barely enough annual abundance data points (indices) to conduct multiple regression analyses with up to two predictor variables. Clearly more years of data collection and more in-depth analyses are needed and the analyses presented here are merely a starting point.

This analysis uses annual abundance indices for larval Delta Smelt (20 mm survey, 1995-2013), adult Delta Smelt (SKT survey, 2003-2013), and subadult Delta Smelt during the previous year (FMWT survey, 1995-2013) (Fig. 3). It also uses larval recruitment indices calculated from the annual abundance indices (20 mm to SKT ratio and 20 mm to $FMWT_{Year-1}$ ratio, Fig. 46; see previous chapters for caveats regarding index ratios). Data from the SKT survey was only used for univariate analyses because the SKT index time series only has 11 data points at this time. Spring and fall X2 values were obtained by first calculating mean monthly X2 values calculated from daily X2 values provided by the DWR Dayflow database and then averaging the mean monthly X2 values for the “spring” months February to June and the “fall” months September to December. The 2002-2003 step decline in Delta Smelt abundance (Thomson et al. 2010) was introduced as a before/after factor (“Step”). Details about the data sources are provided in Chapter 3 of this report.

The multivariate analyses presented here were conducted with generalized linear modeling (GLM) following the approach of Jassby et al. (1995) and followed with a classical linear modeling (LM) approach guided by the GLM results. For the GLM, model parameters were estimated with a Poisson error distribution, a log link function describing the relationship between the predictor variable(s) and the mean, and a natural spline to represent non-linearities. The degrees of freedom for the splines were restricted to only 2 (i.e. one interior knot) because of the low number of available data points. Models requiring estimation of more than two independent parameters (aside from the intercept) were not considered for the same reason. Applying the GLM approach avoids the need for log-transforming the abundance data and using natural (quadratic) splines as smoothers allows a more natural representation of non-linearities than using polynomials.

The responses predicted by these models have a fairly high degree of precision as indicated by low values of SE/Mean and residuals were consistent with model assumptions. The results show significant univariate relationships at the $P < 0.05$ level (Table 7) between the 20 mm abundance index and spring X2, prior fall X2, and prior FMWT abundance index. The relationship is strongest with prior fall X2, followed by spring X2 and prior FMWT abundance index (Table

7). The relationship with spring X2 appears unimodal with maximum 20 mm indices associated with spring X2 values between about 55 and 70 km (Fig. 79a). The relationship with prior fall X2 appears negative (Fig. 79b), and the relationship with the prior FMWT abundance index (Fig. 79c) appears positive. Each of these univariate relationships was improved by the inclusion of one of the other predictor variables (Table 7). Relationships with spring and prior fall X2 were also improved by including the 2002-3 step change. As mentioned above, multivariate analyses with more than two predictor variables were not conducted because of the relatively small amount of available data ($n = 19$, Table 7). Based on AIC comparisons (Table 7), including the 2002 step change (introduced as a before/after factor, “Step”) somewhat improved the relationship of the 20 mm index with spring X2 (Fig. 73a) and with prior Fall X2 (Fig. 79b), but not with the prior FMWT index because that index was the basis for the analyses that detected the step change and thus already includes the step change in the actual data (Fig. 79c, model not included in Table 7). Including the prior FMWT abundance index improved the relationships with spring and fall X2 more substantially, but the model combining the effects of spring and fall X2 fit the 20 mm index data nearly as well as the model combining the effects of spring X2 and prior FMWT (Table 7).

It is interesting to note that while prior fall X2 by itself was a stronger predictor of the 20 mm index than spring X2, spring X2 was the stronger predictor when the step change or previous fall abundance were taken into account. Baxter et al. (2010) hypothesized that the shift toward higher prior fall X2 values (Fig. 17) may have contributed to an ecological “regime shift” associated with the step decline in Delta Smelt and other species. This means that prior fall X2 and the “step” factor and FMWT decline in this analysis may be related, which could explain the very similar outcomes for the two models combining spring X2 with either prior fall X2 or the prior FMWT index.

Partial residual plots show the relationship between a predictor variable and the response variable given that other independent variables are also in the model; in other words, they show the effect of one predictor variable given the effect of one or more additional predictor variables. Partial residual plots for the relationships of the 20 mm index with the combinations of spring X2 and prior fall X2 (Fig. 80 a and b) and spring X2 and prior FMWT abundance index (Fig 80 c and d) show that the general shape and direction of the relationships of the 20 mm index with each of the individual predictor variables (Fig. 79) remains intact in the models with combined predictors, but the partial residuals do not closely follow the fitted lines. This indicates that while each variable has its own, distinct effect on the 20 mm index that is maintained in the presence of the other variables, interactive effects among these variables are quite strong. In summary, low values of prior fall X2, high prior FMWT abundance, and intermediate values of spring X2 have positive associations with the abundance of larval/postlarval Delta Smelt, but the effects of individual variables are mediated by the presence of the other variables.

Because the spline degrees of freedom were strongly restricted in this GLM analysis, the results are quite similar to the results of classical linear models (LM) with log-transformed abundance data and a quadratic term to represent the unimodal non-linearity in the relationship between the 20 mm index and spring X2 (Fig. 81). We include these models here because they are more easily reproducible than the GLM models and offer simple equations for making predictions about larval abundance that can be used in adaptive management applications. As for the GLM analysis (Table 7), the best fits overall were achieved by combining spring X2 with either the step change or the prior FMWT abundance index (Table 8). All predictor combinations improved the models compared to the univariate relationships (Table 8). Based on a comparison of regression

Table 7. Summary of relationships between the 20 mm abundance index for Delta Smelt (response variable) and one or more predictor variables: n, number of observations (years); SE/Mean, model standard error (square root of mean squared residual) as proportion of mean response, P, statistical significance level for the model; R², coefficient of determination; adjusted R², R² adjusted for the number of predictors in the model; AIC, Akaike information criterion; Δ AIC, AIC differences; w (AIC), AIC weights. All relationships modeled with generalized linear models (GLM) with a Poisson error distribution, log link function, and a natural cubic spline with two degrees of freedom as a smoother for all predictor variables except “Step.”

Predictor Variable(s)	n	SE/ Mean	P	R ²	Adjusted R ²	AIC	Δ AIC	w (AIC)
Spring X2, FMWT _{year-1}	19	0.119	<0.001	0.791	0.731	39.5	0.00	0.53
Spring X2, Fall X2 _{year-1}	19	0.120	<0.001	0.787	0.726	40.1	0.60	0.39
Fall X2 _{year-1} , FMWT _{year-1}	19	0.126	<0.001	0.764	0.697	43.2	3.78	0.08
Spring X2, Step (Factor)	19	0.143	<0.001	0.677	0.612	53.6	14.12	0.00
Fall X2 _{year-1} , Step (Factor)	19	0.135	<0.001	0.712	0.655	55.8	16.35	0.00
Fall X2 _{year-1}	19	0.145	<0.001	0.646	0.601	56.0	16.53	0.00
Spring X2	19	0.176	0.006	0.476	0.411	79.9	40.43	0.00
FMWT _{year-1}	19	0.187	0.015	0.408	0.334	89.4	49.98	0.00

coefficients and P-values, the LM relationships were statistically weaker (Table 8) than in the GLM analysis (Table 7).

Another way of including prior abundance in statistical relationships of abundance with habitat attributes and environmental drivers is to use abundance indices that are proportional to prior abundance indices, in other words, ratios of present to prior abundance indices. In this report, we used the ratios of 20 mm to SKT and 20 mm to FMWT_{Year-1} abundance indices (Fig. 46; see also caveats about these indices in Chapter 3) as larval recruitment indices from adults and subadults, respectively. We found that recruitment of larvae from adults was linearly related to spring X2 for the entire available time series (2003-2013, Fig. 82a and Table 9). The recruitment index for 2013 was higher than expected based on the other data points. The relationship of the recruitment index from subadults to next year's larvae with winter-spring X2 was also linear for the POD period after the abundance step decline in 2002 (Thomson et al. 2010), but with more scatter at higher X2 values. Interestingly, no relationship was apparent at all before the 2002 step decline when the proportional larval recruitment from then more abundant subadults was generally low (Fig. 82b and Table 9). In the current POD regime, larval recruitment from parental stock appears to be highest when flows through and out of the Delta are high and the interface between fresh and brackish water is located to the west (i.e. low X2), although it can occasionally also be high at lower flows, as was the case in 2013.

In late winter and spring 2013, CVP and SWP exports were reduced to comply with OMR flow requirements in the 2008 USFWS Biological Opinion aimed at reducing the risk of adult and

Figure 79. Plots of the Delta Smelt 20 mm survey abundance index as a function of a) spring (February-June) X2, b) previous year fall (September-December) X2, and c) Delta Smelt fall midwater-trawl abundance index in the previous year. Details of general linear models (GLM) used to fit the lines are in Table 7.

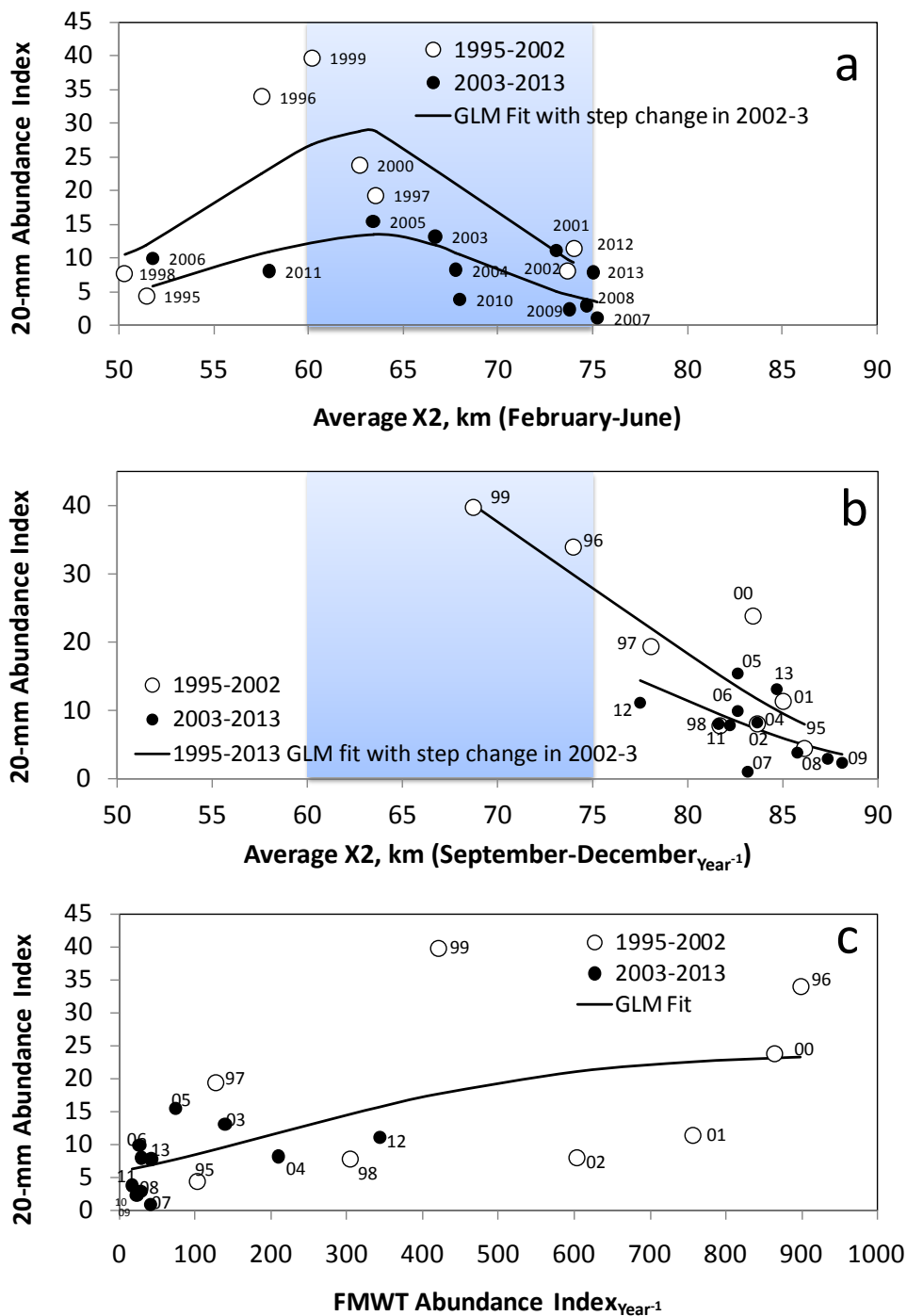


Figure 80. Plots of partial residuals for the relationships of the 20 mm index with the combinations of spring X2, prior fall X2, and prior FMWT abundance index summarized in Table 1 (panels a, b, d, and e). The plots shown here also include partial fit lines and their 95% confidence intervals. Values for the time period of analysis are shown for: c, X2; and f, the fall midwater trawl abundance index from the previous year

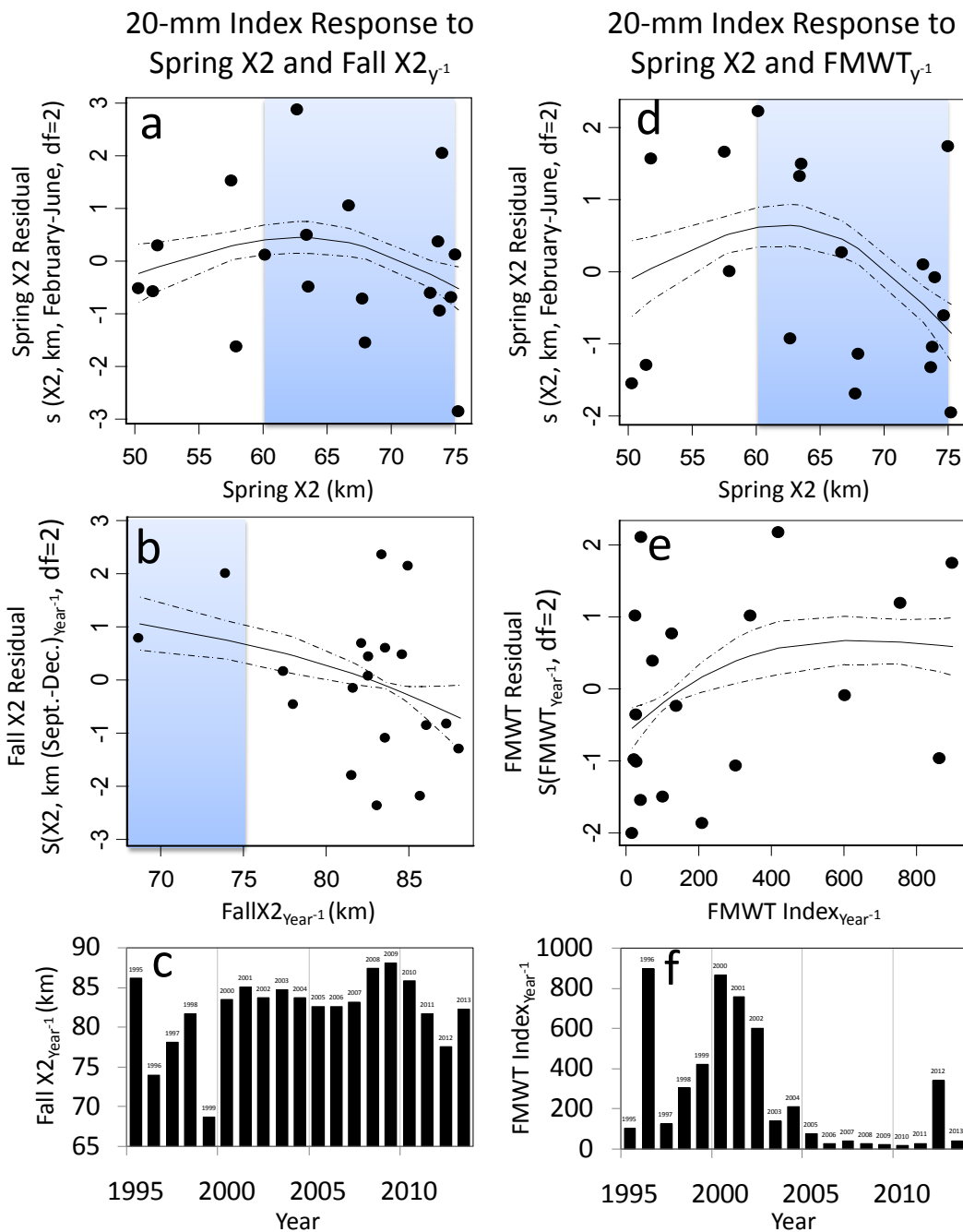
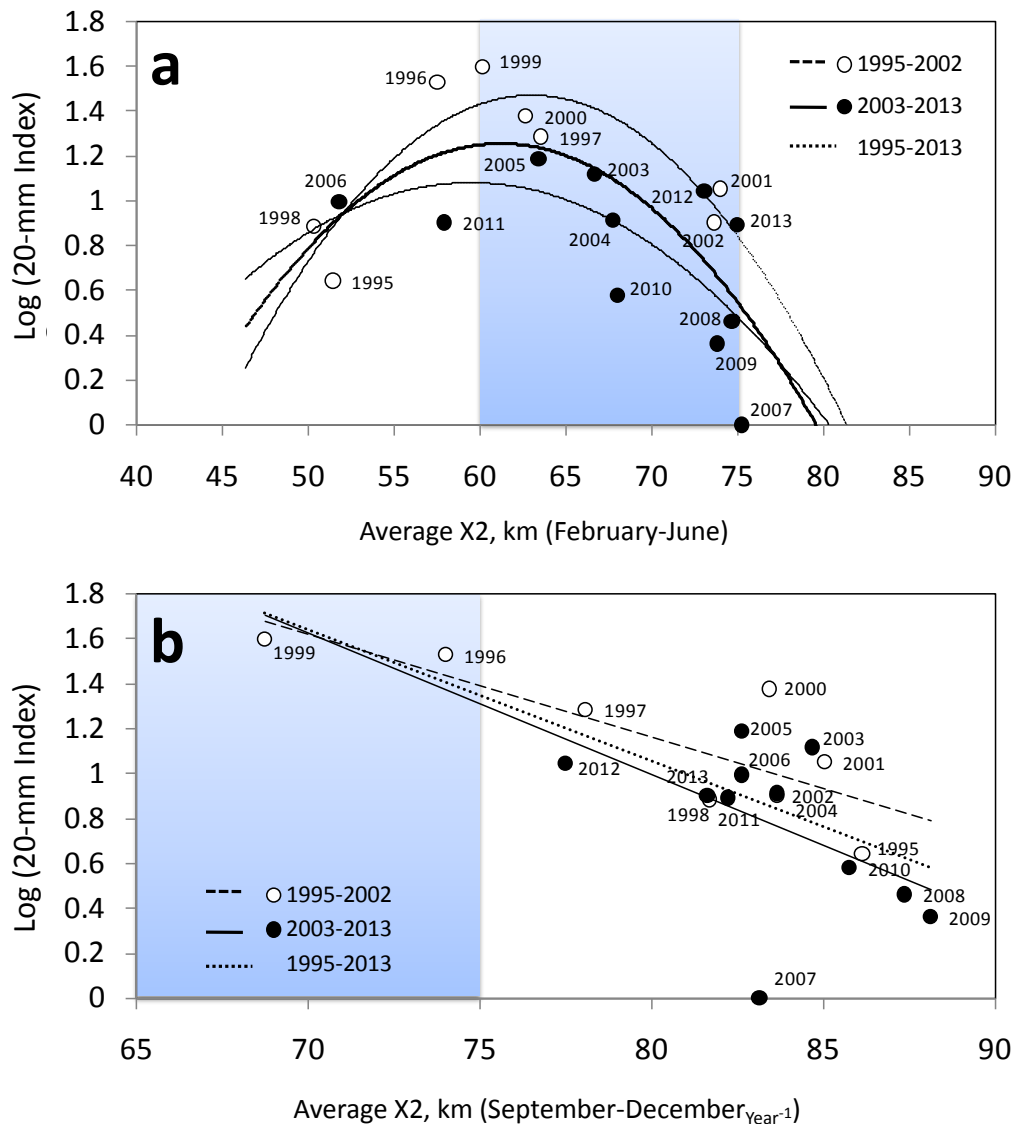


Figure 81. Plots of the Delta Smelt 20 mm survey abundance index as a function of a) spring (February-June) X2, and b) previous year fall (September-December) X2. Lines are either simple linear least squares regression (lines) or quadratic regression (curves). Details of linear models (LM) used to fit the 1995-2013 lines are in Table 8.



larval Delta Smelt entrainment into the water export pumps. This was the first time since the 2008 USFWS Biological Opinion was issued that exports were specifically reduced to lower Delta Smelt entrainment risk. In other years, flows were high enough to allow for higher export levels or export reductions to protect salmon were deemed sufficiently protective for Delta Smelt. It is possible that the intentional reduction in Delta Smelt entrainment risk in 2013 contributed to the high larval recruitment from adults during relatively low flow conditions, but additional years with similar conditions and targeted management actions as well as better estimates of entrainment and more in-depth analyses with other flow variables and flow averaging periods

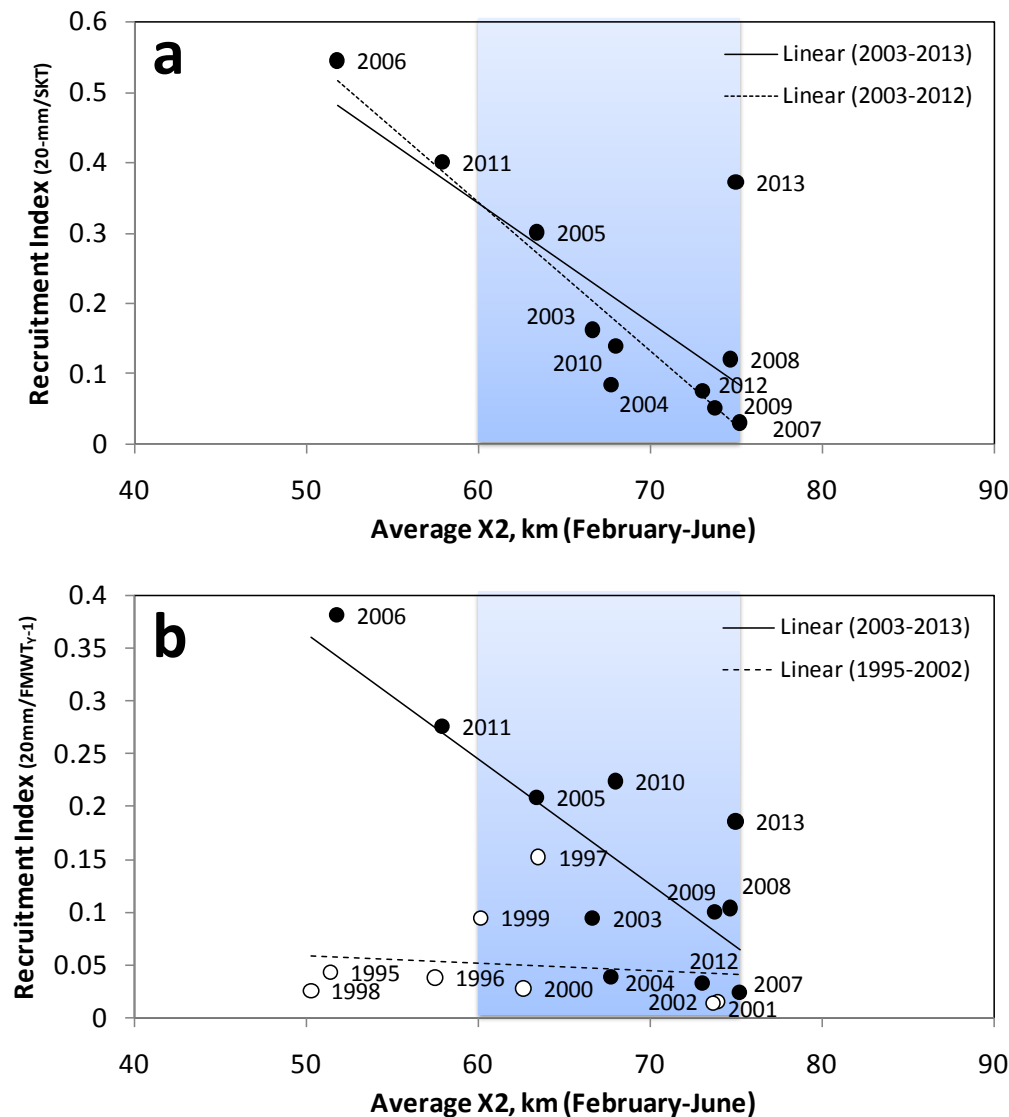
Table 8. Summary of relationships between the log-transformed 20 mm abundance index for Delta Smelt (response variable) and one or more predictor variables. All relationships modeled with simple least-squares linear models (LM). For explanation of column headings see Table 6.

Predictor Variable(s)	n	SE/ Mean	P	R ²	Adjusted R ²	AIC	Δ (AIC)	w (AIC)
Spring X2, (Spring X2) ² , log FMWT _{year-1}	19	0.237	0.000	0.745	0.694	2.1	0.00	0.85
Spring X2, (Spring X2) ² , Fall X2 _{year-1}	19	0.274	0.001	0.661	0.593	7.5	5.42	0.06
Fall X2 _{year-1} , log FMWT _{year-1}	19	0.280	0.000	0.621	0.574	7.7	5.54	0.05
Spring X2, (Spring X2) ² , Step (Factor)	19	0.292	0.002	0.616	0.540	9.9	7.78	0.02
Fall X2 _{year-1} , Step (Factor)	19	0.307	0.002	0.544	0.487	11.2	9.06	
Fall X2 _{year-1}	19	0.318	0.001	0.479	0.449	11.7	9.58	0.01
Spring X2, (Spring X2) ²	19	0.329	0.006	0.473	0.407	13.9	11.83	0.00
log FMWT _{year-1}	19	0.333	0.002	0.430	0.397	13.4	11.29	0.00

are needed to test this hypothesis and obtain a better understanding of flow effects on larval recruitment.

Overall, these preliminary findings suggest that abundance of the larval to early juvenile life stages of Delta Smelt may respond quite strongly to spring and prior fall outflow conditions. The relationships of the 20 mm index with spring X2 shown in this analysis were much stronger than relationships of the TNS and FMWT indices with spring X2 (Table 1, Fig. 17). Similarly, hydrological conditions in the fall seem to have a greater impact on subsequent abundance of larvae than on subsequent juvenile abundance (TNS index; Mount et al. 2013). This is consistent with the findings by Kimmerer et al. (2009) who noted more pronounced relationships of spring X2 with earlier than with later life stages of Delta Smelt and explained that this was “probably because the earlier life stages occupy areas that are fresher and therefore more responsive to changing flow than the more brackish regions.” While the size and location of the LSZ itself may be important for maturing adults in the fall, its interface with fresh water may be important to larvae and spawning adults. A more westward interface means a larger freshwater habitat for spawning and larval rearing that reaches into the shallow eastern region of Suisun Bay and is well connected with Suisun Marsh sloughs and, in wetter years, the Napa River. It also means a larger distance to the export pumps in the southern Delta and thus a reduced risk of entrainment for spawning adults and larvae. Interactions of flow with other drivers and habitat attributes as shown in the conceptual models in this report are likely also important. This suggests that at least

Figure 82. Adult (panel a, SKT) and subadult (panel b, FMWT the previous year) to larvae (20 mm Survey) recruitment indices (abundance index ratios) as a function of spring X2 (February-June). For 20 mm/SKT a linear regression was calculated with and without 2013, which appears to be an outlier. For 20 mm/FMWT the previous year separate regressions were calculated for the POD period (2003-2013), the period before the POD (1995-2002), and the entire data record (not shown). See Table 9 for regression results.



at present, increased Delta outflow and a more westward LSZ in fall, winter, and spring may have important beneficial effects on early life stages of Delta Smelt, but other factors (possibly including summer flows which were not included in this analysis) may be more important for their survival to adults.

Finally, similar to previously published analyses, this analysis strongly suggests that previous life stage abundance should always be taken into account in statistical explorations of habitat effects

Table 9. Summary of relationships of larval recruitment indices (abundance index ratios) for Delta Smelt (response variable) and spring X2 (predictor variable; spring: February-June): n, number of observations (years); SE/Mean, model standard error (square root of mean squared residual) as proportion of mean response, P, statistical significance level for the model; R², coefficient of determination. All relationships modeled with least-squares linear models (LM).

Index Ratio	Period	n	SE/Mean	P	R ²
20-mm/ SKT	2003- 2013	11	0.556	0.006	0.588
20-mm/ SKT	2003- 2012	10	0.270	0.000	0.918
20-mm/ FMWT _{Year-1}	2003- 2013	11	0.469	0.003	0.648
20-mm/ FMWT _{Year-1}	1995- 2002	8	1.012	0.771	0.015
20-mm/ FMWT _{Year-1}	1995- 2013	19	0.981	0.321	0.058

on Delta Smelt. Prior abundance can be introduced into these relationships as actual abundance data (e.g. abundance indices or catch per trawl data), periods of relatively constant abundance (here introduced as a “step” factor), or by combining it with present abundance in proportional abundance indices such as the index ratios used here as recruitment indices. Similar to the relationships of juveniles with spring X2 discussed in Chapter 4, the overall depressed abundance of larval Delta Smelt during the POD period that started in 2002 leads to less substantial larval abundance increases with increasing outflows and decreasing X2 values than before the onset of the POD. However, the association of high larval recruitment with high spring outflow suggests that winter and spring hydrology, through its effects on habitat attributes, may be an important driver of larval recruitment during the current POD period, although it may be less important at higher abundance levels.

In summary, this preliminary analysis provides an example of how relatively simple multivariate modeling can yield interesting insights, in this case about how prior conditions (prior fall X2), prior abundance (prior FMWT), step changes in abundance, and concurrent environmental conditions (spring X2) may all have important effects on Delta Smelt abundance in the spring. While further analyses, more sophisticated life cycle modeling, and publication in a peer-reviewed journal are needed to draw firm conclusions, these preliminary results support the idea discussed throughout this report that neither scientific understanding nor management effectiveness can be improved by only considering a single effect, or a single season or life stage. High larval recruitment is essential for setting the stage for a strong year class, but higher growth and survival through subsequent life stages are also needed to achieve and sustain higher population abundance levels.

Numerical Simulation Modeling

Quantitative simulations of the multiple factors and processes that affect Delta Smelt life stage transitions in our conceptual model are an obvious next step in the exploration and synthesis

of the information presented in this report. The purpose of simulation modeling is to represent a phenomenon or process in a way that allows users to learn more about it by interacting with the simulation (Alessi and Trollip 2001). In particular, simulations allow users to easily control experimental variables and test hypotheses. Guidance from simulation model “dry runs” can make actual laboratory and field experimentation much more efficient and effective. Simulations are also valuable in visualizing outcomes, thus further promoting learning and understanding.

The individual-based Delta Smelt model by Rose et al. (2013a, b) is an example of a complex simulation model specifically created for Delta Smelt. Another simulation modeling option is to utilize “off-the-shelf” simulation software such as the “STELLA” (Structural Thinking and Experiential Learning Laboratory) simulation construction kit (<http://www.iseesystems.com/softwares/Education/StellaSoftware.aspx>). STELLA is designed to let users easily create their own simulations using system dynamics including positive and negative causal loops, and flows, accumulations and conversions of materials.

Culberson (USFWS, unpublished data) created a simple quantitative simulation model in STELLA that includes several life stages of Delta Smelt and is based on seasonal environmental conditions and stage to stage estimates of survival. While this simulation modeling approach appears to be feasible, it remains to be seen how such an approach will approximate actual population dynamics encountered in the field and how results compare to those of other simulation models such as the individual-based life cycle model by Rose et al. (2013a,b). A user-friendly STELLA-based model can be useful in the interim, however, to explore the relative contribution of lifecycle stage and environmental covariates to the overall status of Delta Smelt abundance from year to year and to test hypotheses derived from the conceptual model. In its fullest expression, this MAST-associated lifecycle model will be useful for illustrating how multiple suites of plausible co-variates can allow for different Delta Smelt abundance outcomes. For example, it may be possible to find high abundance under degraded conditions given low entrainment losses across successive winters and springs. Conversely, it is possible to encounter low Delta Smelt abundance given otherwise good environmental and outflow conditions with significantly warmer temperatures during fall pre-adult maturation periods. Moreover, simulated changes in survival can provide a useful frame of reference to evaluate alternative outcomes of cohort size or population size attained at different life stages. For example, given the reported levels of larva, juvenile and sub-adult Delta Smelt in IEP surveys, what levels of daily survival between life stages would be required to attain the relative abundances corresponding to each of the four years being compared? Could the small anticipated differences in assumed daily survival among those four years be attributed to some combination of habitat attributes? Or, could stage-to-stage survival (e.g., percent of individuals surviving from one stage to the next) provide a more useful frame of reference to address that question? Our proposed STELLA simulation model and associated modeling exercises will comfortably allow exploration of these questions and related ideas.

This type of modeling will best be used iteratively with emerging data and within synthesis reports to identify where important gaps exist in the Delta Smelt lifecycle understanding and demonstrate how disparate information sources might be brought together to inform our smelt population estimates through time. Importantly, our model can be used in combination with the narrative description of “a year in the life” of the Delta Smelt population from the conceptual model to more effectively describe environmental and management effects on population status in the SFE. We are especially interested in using such a model to avoid single-factor outcome discussions where smelt populations are seen as the result of “one versus another” environmental

or management-related trade off, particularly when single factor analysis is aggregated over decades of data collection efforts in what we know is a constantly-changing estuary.

Figure 83 shows how output from such a model might be useful for keeping track of the variable influence of factors on overall Delta Smelt abundance across seasons within three hypothetical years. Six factors are plotted according to their sensitivity rank (their relative influence on simulated population outcomes). Specific sensitivity levels can then be identified according to the combinations of factors that emerge as important across succeeding seasons and years. Models built to simulate these influences can then be closely examined to discern how different years, year types, or management practices influence simulated abundance, and to detect where potential data gaps or inconsistencies are among the alternative conceptual models or model modes. The basis for using such an approach is a comparative one, and an absolute resolution of the size or behavior of the real Delta Smelt population is not anticipated – but remains the overall objective. Of real interest here is providing a way to interpret our emerging conceptual model within potential regime-shifts, and to capitalize on previous specifications of this model to organize our ever-improving understanding. Of additional benefit is the ability to use these models easily in “learning sessions,” where users interact with the modelers and species experts to deepen understanding of Delta Smelt biology and its relationship to Delta ecology and management.

Applications to Support Delta Smelt Management

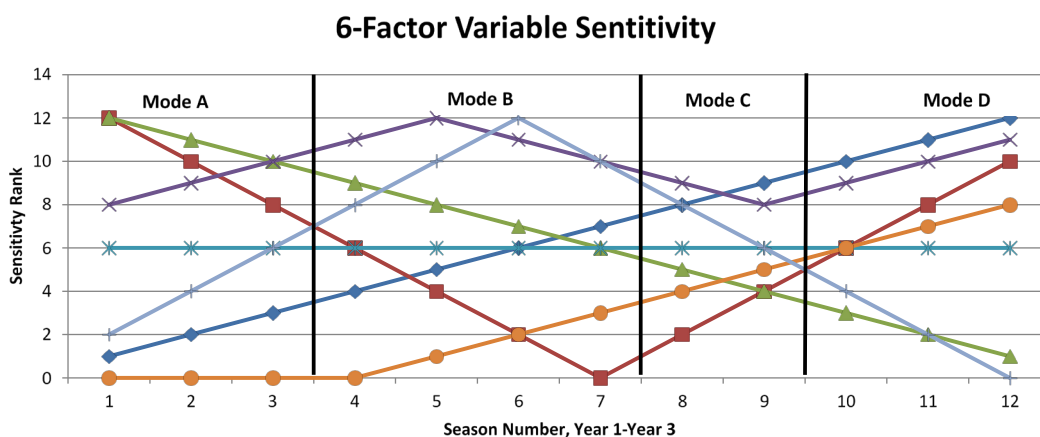
We have shown that the conceptual models in this report provide a reasonable and up to date conceptual framework that can be used to analyze and synthesize existing data and knowledge about Delta Smelt, identify critical data and information gaps, and guide new field and laboratory studies as well as mathematical modeling efforts. We have also discussed many challenges that limit our ability to reach firm conclusions and make highly confident predictions about the effects of management actions and other changes on Delta Smelt. And we have noted that science and management have to go hand in hand to constantly identify, implement, evaluate, and refine the best management options for Delta Smelt in the highly altered and ever-changing estuarine ecosystem that represents the entire range of this species.

Adaptive management is a well-established approach for systematically integrating science and management. As mentioned earlier in this report, it is increasingly required in plans for management of the San Francisco estuary, but to date, the Vernalis Adaptive Management Program (VAMP) and the Fall Outflow Adaptive Management Plan are among the few clear examples of systematically planned and implemented adaptive management in the estuary.

We end our report with examples of how our conceptual models can be used to adaptively manage and improve Delta Smelt habitat. We conclude with several recommendations for the next analysis, synthesis, and modeling efforts. These efforts are a key ingredient for the more widespread adoption and success of adaptive management strategies; without the conceptual and mathematical models provided by these efforts adaptive management of ecosystems simply cannot proceed.

Table 10 gives examples of adaptive management goals and associated uncertainties to address habitat deficiencies (“habitat problems”) identified and discussed in this report. This table is intended as an illustration of how our conceptual models can be used to inform the first three steps of the nine-step adaptive management framework developed by the DSC Delta Science Program (DSP 2013). These three steps are: 1) definition of the problem; 2) establishment of

Figure 83. Simulated output from a STELLA model for assessing sensitivity of the model to variation in model variables.



management goals and actions to address the problem; and 3) modeling of linkages between management goals and actions. The third step specifically requires conceptual or quantitative models for the purpose of evaluating outcomes of alternative management actions and identification of uncertainties and data gaps. Conceptual models are also important in the other six adaptive management steps, for example to design effective adaptive management experiments and appropriate monitoring and to analyze, synthesize and evaluate results.

Table 10 is organized around the habitat attributes identified in the conceptual models. For each habitat attribute, we describe some example categories of management actions that could be considered to improve the status of Delta Smelt. In essence, these actions represent an example “tool box” for the management of Delta Smelt.

Note that the tool box identified in Table 10 is not meant to be exhaustive. Rather, the list is intended as an example set of adaptive management actions suggested by the conceptual models. As such, the list provides no insight into the cost-effectiveness or feasibility of any of the potential actions. Moreover, we acknowledge that there is substantial uncertainty about the potential benefits of actions in the tool box. As mentioned above, identification of uncertainties about the feasibility and benefits of proposed management actions is an important step in adaptive management that can only be accomplished with the help of conceptual or quantitative models. A key point is that these studies are somewhat different than the critical data and information gaps presented earlier in this Chapter. Specifically, Table 10 emphasizes information gaps that are most relevant to specific management questions, while the earlier list focuses on needs to improve the overall scientific understanding that provides the basis for our conceptual models for Delta Smelt. Clearly, efforts to resolve uncertainties and gaps in understanding are needed in both categories. Overlapping uncertainties may highlight especially urgent data and information needs. For Delta Smelt, this includes uncertainties related to contaminants, predation, and entrainment along with interactions of physical habitat attributes with other factors.

Table 10. Example tool-box for applying the conceptual model to Delta Smelt management.

Habitat Attribute	Management Actions	Example Study Efforts
Physical Features	Increase habitat area & quality	<ul style="list-style-type: none"> -Identification of key microhabitats for each life stage and attributes. -Effects of flow/LSZ position on habitat quality, particularly key biotic habitat elements (access to prey, evasion of predators). -Approaches to maintain & expand high turbidity habitat (e.g. supply, habitat design, SAV management). -Approaches to maintain and expand habitat with moderate temperatures (e.g. channel configuration, water depth and velocity). -Evaluation of whether targeted restoration meets habitat needs (e.g. temperature, substrate, turbidity)
Chemical Features	Reduce toxicity	<ul style="list-style-type: none"> -Identification of chronic effects of contaminants. -Identification of effects of Harmful Algal Blooms. -Approaches to reduce toxicity from contaminants and HABs
Food	<ul style="list-style-type: none"> Increase pelagic production Increase access to alternative foods (e.g. epibenthic). Reduce sources of loss Manage towards higher quality foods Prevention and control of non-native species 	<ul style="list-style-type: none"> -Role of tidal wetlands as subsidy habitats (not necessarily occupied by smelt) -Ammonia-bivalve interactive effects on diatom, copepod, mysid, amphipod production. -Relative importance (contribution to smelt growth) of epibenthic foods (e.g., mysids, amphipods, aquatic insects). -Effect of bathymetry, vegetation type (and density) on access to epibenthic and pelagic foods. -Role of tidal wetlands and wetland/open-water complexes. -Approaches to reduce losses to benthic grazing (e.g. invasive clams) and/or to the suppression of bivalve populations -Value of different food types to Delta Smelt nutrition. -Effects of habitat conditions (e.g. ammonia, flow) on food quality. -Identification of nutrient sources and sinks. -Improved detection methods for invasive species -Studies to evaluate alternative control methods.
Entrainment	<ul style="list-style-type: none"> Avoid entrainment region Adjustments to timing and magnitude of exports 	<ul style="list-style-type: none"> -Identification of factors that lead to increased occupancy of South Delta. -Improved measurement of entrainment and its environmental correlates -Effects of exports and entrainment on viability (e.g. abundance, genetics, demographics). -Approaches to reduce entrainment and enhance emigration success.
Predation risk	<ul style="list-style-type: none"> Reduction of predator population Reduction of predation rate 	<ul style="list-style-type: none"> -Studies on delta smelt responses (behavior, distribution, abundance) to variation in predator abundance. -Identify habitat features that reduce predation rate (e.g. depth, turbidity, food, lower water temperatures).

Recommendations for future analysis and synthesis

Efforts to resolve the management issues listed in Table 10 or carry out the modeling and fill the critical science gaps discussed earlier in this Chapter will not succeed without an organizational commitment to continued systematic and long-term collection, synthesis and evaluation of data and information about Delta Smelt, its habitat, and important drivers of habitat and abundance changes. The importance of Delta Smelt for ecosystem and water supply management in and far beyond the SFE is widely recognized. The impressive rate at which we are learning about Delta Smelt and the estuarine ecosystem and the large amount of existing information about them is less widely recognized by many managers and even by many scientists. Part of the reason for this is that it is difficult to track the large quantity of new (since 2010) information documented in this report and even more difficult to integrate it with the previously existing information in a meaningful way. But without this integration, identification of priorities for additional scientific investigations is ad hoc and piecemeal at best and the value of new information cannot be fully realized in management applications such as those listed in Table 10.

Moreover, comprehensive adaptive management efforts simply cannot succeed without adequate conceptual and mathematical models and important science and management opportunities will be missed. Such efforts currently include the ongoing fall outflow adaptive management for Delta Smelt and new efforts called for by the new “Collaborative Science and Adaptive Management Program” (CSAMP), the California Delta Stewardship Council’s Delta Plan, and the multi-agency Bay Delta Conservation Plan (BDCP). The fact that even the incomplete draft version of our report released for public review in June 2013 already played a central role in CSAMP work planning, court documents, and elsewhere bears clear testimony to the fact that there is a great and urgent policy and management need for analysis, synthesis and conceptual models such as those provided in this report.

In consequence, we strongly recommend that there be a continued management, analysis, and synthesis effort, whether carried out by the IEP, the Delta Science Program, or some other scientist, group or agency. While it is possible for individual scientists to take on such efforts (e.g., Bennett 2005), the amount, diversity, and rapid growth of pertinent data and information suggests that team efforts may usually be a more feasible and possibly also a more effective option. Collaborative, multidisciplinary analysis and synthesis teams are also at the core of the National Center for Ecological Analysis and Synthesis in Santa Barbara, CA (NCEAS, <http://www.nceas.ucsb.edu/>), the newer National Socio-Environmental Synthesis Center in Annapolis, MD (SESYNC, <http://www.sesync.org/>) and the Delta Collaborative Analysis and Synthesis (DCAS) approach promoted by the Delta Science Program’s Delta Science Plan (DSP 2013). Important IEP POD and MAST lessons for future synthesis teams are that the role and responsibilities of all team members need to be very clear, that lines of communication need to always be open and available to all, and that there needs to be strong and fully engaged team leadership with a clearly dedicated lead author and/or lead editor for all major team products. In addition, to complete analyses and reports on schedule, it is necessary for team members to prioritize synthesis efforts for sustained periods of time, without being tasked with additional projects that may be urgent for short-term needs.

Another consideration is the type of publication that results from analysis and synthesis efforts. The IEP MAST and POD teams have written comprehensive agency reports, but would have preferred writing peer-reviewed books or monographs (e.g., published by the American Fisheries Society or by U.C. Press) had the time and resources been available to do so. Such books would be considered better scientific products with greater scientific standing and a longer life span

and would reach a much larger audience. Another approach would be to write a series of shorter articles that could be published in a special issue of a peer-reviewed scientific journal. This too would take more time and effort and would also somewhat restrict the types of topics that could be covered. Journal articles are, however, the main target for national analysis and synthesis centers such as NCEAS and SESYNC because they have the greatest scientific standing and are the most widely accepted and well established method of written science communication.

Regardless of which analysis, synthesis, and communication approach is chosen, none of these efforts can succeed without commitment of adequate funding, staffing, and other resources. The IEP MAST team that developed and wrote this report was formed in 2012 for IEP science synthesis and work planning, but it has remained a pilot-level effort that was never adequately supported. MAST work remained a part-time effort for all co-authors of this report, and for most it was an “on the side” task compared to their “regular” agency duties. There is no doubt that completion of this report could have proceeded much more rapidly with greater allocation of resources. Public and independent peer reviews of a draft version of this report (see <http://www.water.ca.gov/iep/pod/mast.cfm>) greatly improved the structure and content, but were not an original part of the MAST planning. Preparing and conducting the reviews as well as responding to the 355 specific and many more general review comments took considerable time (see also Appendix A). Other MAST tasks also added to the delays. In addition to this report, the MAST completed a synthesis report for the Fall Low Salinity Habitat (FLaSH) investigation component of the Fall Outflow Adaptive Management Program (Brown et al. 2014) and prepared a solicitation package for research proposals, which it then also reviewed.

We strongly recommend that adequate, long-term support for these types of efforts be among the highest science and adaptive management priorities for the region and the entire State of California. Given its pivotal role in adaptive management and the increasingly large amounts of new scientific data and information that are produced every year, the authors of this report, individually and as a team, cannot think of any science activity that is more urgently in need of greater support than analysis, synthesis, and communication of scientific results.

For additional analysis and synthesis efforts about Delta Smelt, we recommend that the next individual or team to take this on should:

- Build on this report by evaluating the conceptual model with more rigorous analyses that include more years of data, developing lifecycle and numerical models as discussed above, and/or using the conceptual model to develop a comprehensive list of data and information gaps and approaches to addressing these gaps in order to inform management strategies;
- Early in the process, make clear decisions about the analytical/modeling approaches to be used, the scope of the synthesis to be done, and approaches for review and communication of results;
- Evaluate additional data and information needs concerning Delta Smelt;
- Consider approaches to understand the effects of the wide variety of management actions targeting Delta Smelt, including adaptive management of fall outflow, entrainment, habitat restoration, etc (e.g., Table 10);
- Develop key “indicator” variables that can be used to track and predict the status of Delta Smelt and its habitat and serve as “performance metrics” to evaluate the success of management actions. Such variables, and a “report card” to summarize them, were considered for this report, but the MAST decided that developing them was beyond the scope of

this report and would require a fairly substantial effort that could be the main focus of an additional effort.

An additional recommendation is that an ultimate goal of these efforts should be the integration of conceptual and mathematical models such as those described in the previous section of this Chapter and the routine use of both types of models in adaptive management. Neither the recently published mathematical models nor existing conceptual models for Delta Smelt have been applied to management issues in a consistent manner. This is likely at least partially due to unfamiliarity of managers with the models and the need for specialists (model developers) to apply the mathematical and in some cases even the conceptual models to management issues in the absence of easy to use and understandable model interfaces and specifications. We also recommend a comprehensive biological modeling forum and/or more specific biological modeling teams and “summits” as recommended by the IEP Science Advisory Group (2010, available at <http://www.water.ca.gov/iep/docs/IEPModelWorkshopReview.pdf>) and, more recently, the Delta Science Plan (DSP 2013). Such groups would not only facilitate communication among modelers, but could also help make the connection from model development to model applications of interest to managers and policy makers. They would complement and could (and likely should) be integrated with the existing, California Water and Environmental Modeling Forum (CWEMF, see <http://www.cwemf.org>), which tends to focus on modeling physical processes. As with the overall analysis and synthesis teams, these groups could be implemented by the IEP, The Delta Science Program, CWEMF, or others. The chosen organizational umbrella is less important than actual implementation and involvement of appropriate local and outside scientific and management expertise. Some possible topics for these groups include:

1. Reviews and updates to existing conceptual and mathematical models
2. Further development of mathematical models of Delta Smelt population abundance drawn specifically from the conceptual models described in this report; applications and extensions of recently published models to help make management decisions and guide new modeling efforts; additional modeling efforts and future research projects to improve resolution and understanding of the particular factors identified as critical to reproduction, recruitment, survival, and growth.
3. Review and refinement of new models such as the emerging comprehensive state-space population model (Newman, personal communication); development of additional models or modules of models specifically aimed at estimating effects of inadequately monitored or difficult to measure and evaluate habitat attributes such as predation risk and toxicity; development of new “nested” and/or “linked” mathematical modeling approaches that can accommodate multiple drivers and their interactive effects across temporal and spatial scales.
4. Collaboration among physical and biological modelers, experimental and other scientists, managers, and stakeholders to develop and model management scenarios and strategies that move beyond the current focus on relatively crude distinctions among “water year types” toward a more integrative ecosystem and landscape-based management approach.

We end this report with the hope that the conceptual models and information presented will be used for achieving better management outcomes for Delta Smelt and the estuarine ecosystem on which it depends. These precious natural resources are owned by no one, but are held in public

trust by the California and U.S. governments for the benefit of all the people. We are grateful for the opportunity to serve our State and nation in the collaborative manner afforded by working under the interagency umbrella of the Interagency Ecological Program for the San Francisco Estuary.

References Cited

- Aasen, G.A. 1999. Juvenile delta smelt use of shallow-water and channel habitats in California's Sacramento-San Joaquin Estuary. *California Fish and Game* 8(4):161–169.
- Aasen, G.A. 2013. Predation on salvaged fish during the collection, handling, transport, and release phase of the State Water Project's John E. Skinner Delta Fish Protective Facility. Interagency Ecological Program of the Sacramento-San Joaquin Estuary, Technical Report 86.
- Acuña, S., D.F. Deng, P. Lehman, and S. Teh. 2012a. Sublethal dietary effects of *Microcystis* on Sacramento splittail, *Pogonichthys macrolepidotus*. *Aquatic Toxicology* 110–111:1–8.
- Acuña S., D. Baxa, and S. Teh. 2012b. Sublethal dietary effects of microcystin producing *Microcystis* on threadfin shad, *Dorosoma petenense*. *Toxicol* 60:1191–1202.
- Afentoulis V., J. Dubois, and R. Fujimura. 2013. Stress response of delta smelt, *Hypomesus transpacificus*, in the collection, handling, transport and release phase of fish salvage at the John E. Skinner Delta Fish Protective Facility. Interagency Ecological Program of the Sacramento-San Joaquin Estuary, Technical Report 87.
- Aksnes, D.L., and J. Giske. 1993. A theoretical model of aquatic visual feeding. *Ecological Modeling* 67:233–250.
- Alessi, S.M., and S.R. Trollip. 2001. Multimedia for learning. Allyn and Bacon, Boston, MA.
- Alpine, A.E., and J.E. Cloern. 1992. Trophic interactions and direct physical effects control phytoplankton biomass and production in an estuary. *Limnology and Oceanography* 37:946–955.
- Anderson, J.T. 1988. A review of size dependent survival during pre-recruit stages of fishes in relation to recruitment. *Journal of Northwest Atlantic Fish Society* 8:55–66.
- Ankley G.T., K.M. Jenson, E.J. Hurhan, E.A. Makynen, B.C. Butterworth, M.D. Kahl, D. L. Villeneuve, A. Linnum, L.E. Gray, M. Cardon, and V.S. Wilson. 2005. Effects of two fungicides with multiple modes of action on reproductive endocrine function in the fat head minnow (*Pimephales promelas*). *Toxicological Sciences* 86:300-308.
- Antao, T., A. Perez-Figueroa, and G. Luikart. 2010. Early detection of population declines: high power of genetic monitoring using effective population size estimators. *Evolutionary Applications* 4:144–154.
- Arnold S.F., D.M. Klotz, B.M. Collins, P.M. Vonier, L.J. Guilette, and J.A. McLachlan. 1996. Synergistic activation of estrogen receptor with combinations of environmental chemicals. *Science* 276:1489–1492.
- Arthur, J.F., M.D. Ball, and S.Y. Baughman. 1996. Summary of federal and state water project environmental impacts in the San Francisco Bay-Delta estuary, California. Pages 445-495 in Hollibaugh, J.T., editor. *San Francisco Bay: the ecosystem*. Pacific Division American Association for the Advancement of Science, San Francisco, California.
- Ashby J., P.A. Lefevre, J. Odum, C.A. Harris, E.J. Routledge, and J.P. Sumpter. 1997. Synergy between synthetic oestrogens. *Nature* 385:494.
- Baas, J., T. Jager, and B. Kooijman. 2009. A model to analyze effects of complex mixtures on survival. *Ecotoxicology and Environmental Safety* 72:669–76.
- Baas, J., T. Jager, and B. Kooijman. 2010. A review of DEB theory in assessing toxic effects of mixtures. *Science of the Total Environment* 408:3740-3745.
- Baerwald, M.R., B.M. Schreier, G. Schumer, and B. May. 2012. Detection of threatened delta smelt in the gut contents of the invasive Mississippi silverside in the San Francisco Estuary using TaqMan Assays. *Transactions of the American Fisheries Society* 141:1600–1607.

- Baskerville-Bridges, B, J.C. Lindberg, and S.I. Doroshov. 2004a. The effect of light intensity, alga concentration, and prey density on the feeding behavior of delta smelt larvae. *American Fisheries Society Symposium* 39:219–228.
- Baskerville-Bridges, B., J.C. Lindberg, J.V. Eenennaam, and S.I. Doroshov. 2004b. Delta smelt research and culture program 5-year summary, 1998-2003. University of California, Davis, California.
- Baskerville-Bridges, B., J.C. Lindberg, and S.I. Doroshov. 2005. Manual for the intensive culture of delta smelt (*Hypomesus transpacificus*). University of California Davis, Department of Animal Science, Davis, CA.
- Baxter, R., R. Breuer, L. Brown, M. Chotkowski, F. Feyrer, M. Gingras, B. Herbold, A. Mueller- Solger, M. Nobriga, T. Sommer, and K. Souza. 2008. Pelagic organism decline progress report: 2007 synthesis of results. Interagency Ecological Program for the San Francisco Estuary, Technical Report 227, 86 p. Available at: http://www.water.ca.gov/iep/docs/pod/synthesis_report_031408.pdf.
- Baxter, R., R. Breuer, L. Brown, L. Conrad, F. Feyrer, S. Fong, K. Gehrts, L. Grimaldo, B. Herbold, P. Hrodey, A. Mueller-Solger, T. Sommer, and K. Souza. 2010. Interagency Ecological Program 2010 Pelagic Organism Decline work plan and synthesis of results. Interagency Ecological Program for the San Francisco Estuary. 259 p. Available at: <http://www.water.ca.gov/iep/docs/FinalPOD2010Workplan12610.pdf>.
- Benli, A.C. K., G. Köksal, A. Özkul. 2008. Sublethal ammonia exposure of Nile tilapia (*Oreochromis niloticus* L.): Effects on gill, liver and kidney histology. *Chemosphere* 72:1355–1358.
- Bennett, W.A. 1995. Potential effects of exotic inland silversides on delta smelt. *IEP Newsletter* 8(1):4–6.
- Bennett, W.A. 2005. Critical assessment of the delta smelt population in the San Francisco Estuary, California: San Francisco Estuary and Watershed Science 3(2). Available at: <http://escholarship.org/uc/item/0725n5vk>.
- Bennett, W. A. 2011. The “big-mama” hypothesis: evaluating a subtle link between water export operations and the decline of delta smelt. Final Report submitted to: Mark Gowdy, State Water Resources Control Board, Sacramento, California. 11 p.
- Bennett, W. A., and J. R. Burau. 2014. Riders on the Storm: selective tidal movements facilitate the spawning migration of threatened Delta Smelt in the San Francisco Estuary. *Estuaries and Coasts* DOI 10.1007/s12237-014-9877-3: 10 pages.
- Bennett, W.A., and P.B. Moyle. 1996. Where have all the fishes gone? Interactive factors producing fish declines in the Sacramento San Joaquin Estuary. Pages 519–542, In: J.T. Hollibaugh, editor. *San Francisco Bay: the ecosystem: Pacific Division American Association for the Advancement of Science*, San Francisco, California.
- Bennett, W.A., J.A. Hobbs, and S.J. Teh. 2008. Interplay of environmental forcing and growth-selective mortality in the poor year-class success of delta smelt in 2005. Final report: “fish otolith and condition study 2005”. Prepared for the POD Management Team of the Interagency Ecological Program for the San Francisco Estuary.
- Bennett, W.A., W.J. Kimmerer, and J.R. Burau. 2002. Plasticity in vertical migration by native and exotic estuarine fishes in a dynamic low-salinity zone. *Limnology and Oceanography* 47:1496-1507.
- Berec, L., E. Angulo, and F. Courchamp. 2006. Multiple Allee effects and population management. *Trends in Ecology and Evolution* 22:185–191.
- Berenbaum, M.C. 1989. What is synergy? *Pharmacological Reviews* 41:93–141.
- Beverton, R.J.H., and S.J. Holt. 1957. On the dynamics of exploited fish populations. Her Majesty’s Stationery Office, London.
- Blumberg, A., P. Goodwin, E. Houde, S. Monismith, T. M. Powell, and C. Simenstad. 2010. Review of IEP and other Bay-Delta modeling focused on hydrodynamics and fish. Report by the IEP Science Advisory Group. Available at <http://www.water.ca.gov/iep/docs/IEPModelWorkshopReview.pdf>.
- Boening, D.W. 2000. Ecological effects, transport, and fate of mercury: a general review. *Chemosphere* 40:1335–1351.
- Bouley, P. and W.J. Kimmerer. 2006. Ecology of a highly abundant, introduced cyclopoid copepod in a temperate estuary. *Marine Ecology Progress Series* 324:219–228.
- Brander, S.M. 2013. Chapter 5: Thinking outside the box: Assessing endocrine disruption in aquatic life. Pages 103-147 in S. Ahuja, editor. *Monitoring Water Quality: Pollution assessment, analysis, and remediation*. Elsevier B.V.

- Brander, S.M., R.E. Connon, G. He, J.A. Hobbs, K.L. Smalling, S.J. The, J.W. White, I. Werner, M.S. Denison, and G.N. Cherr. 2013. From 'omics to otoliths: Responses of an estuarine fish to endocrine disrupting compounds across biological scales. *Plos One* 8(9):1–15.
- Brander, S.M., I. Werner, J.W. White, and L.A. Deanovic. 2009. Toxicity of a dissolved pyrethroid mixture to *Hyaella azteca* at environmentally relevant concentrations. *Environmental Toxicology and Chemistry* 28:1493–1499.
- Brar, N.K., C. Waggoner, J.A. Reyes, R. Fairey, and K.M. Kelley. 2010. Evidence for thyroid endocrine disruption in wild fish in San Francisco Bay, California, USA. Relationships to contaminant exposures. *Aquatic Toxicology* 96:203–215.
- Brook, W.A. and S.R. Carpenter. 2010. Interacting regime shifts in ecosystems: implication for early warnings. *Ecological Monographs* 80:353–367.
- Brooks, M.L., E. Fleishman, L.R. Brown, P.W. Lehman, I. Werner, N. Scholz, C. Mitchelmore, J.R. Lovvorn, M.L. Johnson, D. Schlenk, S. van Drunick, J.I. Drever, D.M. Stoms, A.E. Parker, and R. Dugdale. 2012. Life histories, salinity zones, and sublethal contributions of contaminants to pelagic fish declines illustrated with a case study of San Francisco Estuary, California, USA. *Estuaries and Coasts* 35:603–621.
- Brown, L., and J. May. 2006. Variation in spring nearshore resident fish species composition and life histories in the lower Sacramento-San Joaquin watershed and delta. *San Francisco Estuary and Watershed Science* 4(2). Available at: <http://www.escholarship.org/uc/item/09j597dn>.
- Brown, L.R., and D. Michniuk. 2007. Littoral fish assemblages of the alien-dominated Sacramento–San Joaquin Delta, California, 1980–1983 and 2001–2003. *Estuaries and Coasts* 30:186–200.
- Brown, L.R., and P.B. Moyle. 2005. Native fish communities of the Sacramento-San Joaquin watershed, California: a history of decline. *American Fisheries Society Symposium* 45:75–98.
- Brown, L.R., R. Baxter, G. Castillo, L. Conrad, S. Culberson, G. Erickson, F. Feyrer, S. Fong, K. Gehrts, L. Grimaldo, B. Herbold, J. Kirsch, A. Mueller-Solger, S. Slater, K. Souza, and E. Van Nieuwenhuysse. 2014. Synthesis of studies in the fall low-salinity zone of the San Francisco Estuary, September–December 2011. U.S. Geological Survey Scientific Investigations Report 2014–5041. 136 p.
- Brown, L.R., W.A. Bennett, R.W. Wagner, T. Morgan-King, N. Knowles, F. Feyrer, D.H. Schoellhamer, M.T. Stacey, M. Dettinger. 2013. Implications for future survival of delta smelt from four climate change scenarios for the Sacramento-San Joaquin Delta, California. *Estuaries and Coasts* 36:754–774.
- Brown, R., S. Greene, P. Coulston and S. Barrow. 1996. An evaluation of the effectiveness of fish salvage operations at the intake to the California aqueduct, 1979–1993. Pages 497–518 in J.T. Hollibaugh, editor. *San Francisco Bay: the ecosystem*. Pacific Division of the American Association for the Advancement of Science, San Francisco, CA.
- Brown, T. 2009. Phytoplankton community composition: the rise of the flagellates. *IEP Newsletter* 22(3):20–28.
- Bryant, M.E. and J.D. Arnold. 2007. Diets of age-0 striped bass in the San Francisco Estuary, 1973–2002. *California Fish and Game* 93(1):1–22.
- Caissie, D. 2006. The thermal regime of rivers: a review. *Freshwater Biology* 51:1389–1406.
- Capitán, J.A. and J.A. Cuesta. 2010. Catastrophic regime shifts in model ecological communities are true phase transitions. *Journal of Statistical Mechanics: Theory and Experiment* 2010:1–19.
- Carlton, J.T., J.K. Thompson, L.E. Schemel, and F.H. Nichols. 1990. Remarkable invasion of San Francisco Bay (California, USA) by the Asian clam *Potamocorbula amurensis* I. Introduction and dispersal. *Marine Ecology Progress Series* 66:81–94.
- Carr, E.R., P.M. Wingard, S.C. Yorty, M.C. Thompson, N.K. Jensen, and J. Roberson. 2007. Applying DPSIR to sustainable development. *International Journal of Sustainable Development and World Ecology* 14:543–555.
- Castillo, G., J. Morinaka, J., Lindberg, R. Fujimura, B. Baskerville-Bridges, J. Hobbs, G. Tigan, and L. Ellison. 2012. Pre-screen loss and fish facility efficiency for delta smelt at the south Delta's State Water Project, California. *San Francisco Estuary and Watershed Science* 10(4):1–23.
- Casulli, V. and P. Zanolì. 2005. High resolution methods for multidimensional advection–diffusion problems in free-surface hydrodynamics. *Ocean Modelling* 10:137–151.

- Casulli, V. and P. Zanolli. 2002. Semi-implicit numerical modeling of nonhydrostatic free-surface flows for environmental problems. *Mathematical and Computer Modelling* 36:1131–1149.
- CDWR (California Department of Water Resources). 2007. California Central Valley unimpaired flow data Fourth Edition. Bay-Delta Office, California Department of Water Resources, Sacramento, CA. Available at: http://www.waterboards.ca.gov/waterrights/water_issues/programs/bay_delta/bay_delta_plan/water_quality_control_planning/docs/sjrf_spprtinfo/dwr_2007a.pdf.
- Chapman, P.M., W.J. Adams, M.L. Brooks, C.G. Delos, S.N. Luoma, W.A. Maher, H.M. Ohlendorf, T.S. Presser and D.P. Shaw 2010. Ecological assessment of selenium in the aquatic environment. SETAC Press, Pensacola.
- Clark, K.W., M.D. Bowen, R.B. Mayfield, K.P. Zehfuss, J.D. Taplin, and C.H. Hanson. 2009. Quantification of pre-screen loss of juvenile steelhead in Clifton Court Forebay. State of California. The California Natural Resources Agency. Department of Water Resources. Fishery Improvements Section Bay-Delta Office. 119 pp.
- Cloern, J.E., B.E. Cole, R.L.J. Wong, and A.A. Alpine. 1985. Temporal dynamics of estuarine phytoplankton: a case study of San Francisco Bay. *Hydrobiologia* 129:153-176.
- Cloern, J.E. 1987. Turbidity as a control on phytoplankton biomass and productivity in estuaries. *Continental Shelf Research* 7:1367-1381.
- Cloern, J.E., and A.D. Jassby. 2012. Drivers of change in estuarine-coastal ecosystems: Discoveries from four decades of study in San Francisco Bay. *Reviews of Geophysics*, 50, RG4001, doi:10.1029/2012RG000397.
- Cloern, J.E., N. Knowles, L.R. Brown, D. Cayan, M.D. Dettinger, T.L. Morgan, D.H. Schoellhamer, M.T. Stacey, M. van der Wegen, R.W. Wagner, A.D. Jassby. 2011. Projected Evolution of California's San Francisco Bay-Delta-River System in a Century of Climate Change. *PlosONE* 6(9):e24465.
- Coats, J.R., D.M. Symonik, S.P. Bradbury, S.D. Dyer, L.K. Timson, and G.J. Atchison. 1989. Toxicology of synthetic pyrethroids in aquatic systems: An overview. *Environmental Toxicology and Chemistry* 8:671–680.
- Cohen, A.N. and J.T. Carlton. 1998. Accelerating invasion rate in a highly invaded estuary. *Science* 279:555-558.
- Connon, R., J. Geist, J. Pfeiff, A.V. Loguinov, L.S. D'Abronzio, H. Wintz, C.D. Vulpe, and I. Werner. 2009. Linking mechanistic and behavioral responses to sublethal esfenvalerate exposure in the endangered delta smelt; *Hypomesus transpacificus* (Fam. Osmeridae). *BMC Genomics* 10:608.
- Connon, R., L.A. Deanovic, E.B. Fritsch, L.S. D'Abronzio, I. Werner. 2011a. Sublethal responses to ammonia exposure in the endangered delta smelt; *Hypomesus transpacificus* (Fam Osmeridae). *Aquatic Toxicology* 105:369-377.
- Connon, R.E., S. Beggel, L.S. D'Abronzio, J.P. Geist, J. Pfeiff, A.V. Loguinov, C.D. Vulpe, and I. Werner. 2011b. Linking molecular biomarkers with higher level condition indicators to identify effects of copper exposures on the endangered delta smelt (*Hypomesus transpacificus*). *Environmental Toxicology and Chemistry* 30:290-300.
- Conomos, T.J., R.E. Smith, and J.W. Gartner. 1985. Environmental setting of San Francisco Bay. *Hydrobiologia* 129:1–12.
- Contreras, D., V. Afentoulis, K. Hieb, R. Baxter, and S. Slater. 2011. 2010. Status and trends report for pelagic fishes of the upper San Francisco Estuary. *IEP Newsletter* 24(2):27-38.
- Cornelissen, G., P.C.M. van Noort, and H.A.J. Govers. 1998. Mechanism of slow desorption of organic compounds from sediments: a study using model sorbents. *Environmental Science and Technology* 32:3124-3131.
- Cummins, K.W., and J.C. Wuycheck. 1971. Caloric equivalents for investigations in ecological energetics. *Mitteilungen-Internationale Vereinigung für Theoretische und Angewandte Limnologie* 18:1-158.
- Dambacher, J.M., H-K. Luh, H.W. Li and P.A. Rossignol. 2003. Qualitative stability and ambiguity in model ecosystems. *American Naturalist* 161:876-888.
- Davis, N. D. 1993. Caloric content of oceanic zooplankton and fishes for studies of salmonid food habits and their ecologically related species. (NPAFC Doc.) FRI-UW-9312. Fisheries Research Institute, University of Washington, Seattle. 10 p.
- Davis, J.A., L. Sim, and J.M. Chambers. 2010. Multiple stressors and regime shifts in shallow aquatic ecosystems in antipodean landscapes. *Freshwater Biology* 55:5-18.

- Deblois, E.M. and W.C. Leggett. 1993. Impact of amphipod predation on the benthic eggs of marine fish: an analysis of *Calliopius laeviusculus* bioenergetic demands and predation on the eggs of a beach spawning osmeriid (*Mallous villosus*). *Marine Ecology Progress Series* 93:205-216.
- Dege, M., and L.R. Brown. 2004. Effect of outflow on spring and summertime distribution and abundance of larval and juvenile fishes in the upper San Francisco Estuary. *American Fisheries Society Symposium* 39:49–65.
- Dettinger, M.D., 2011. Climate change, atmospheric rivers and floods in California—A multimodel analysis of storm frequency and magnitude changes. *Journal of American Water Resources Association* 47:514–523.
- Dettinger, M.D. and B.L. Ingram. 2013. The coming megastorms. *Scientific American* 308:64–71.
- DiGennaro, B., D. Reed, C. Swanson, L. Hastings, Z. Hymanson, M. Healey, et al., 2012. Using conceptual models in ecosystem restoration decision making: An example from the Sacramento-San Joaquin River Delta, California. *San Francisco Estuary and Watershed Science*, 10(3). Retrieved from: <http://www.escholarship.org/uc/item/3j95x7vt>.
- Doremus, H. 2009. CALFED and the quest for optimal institutional fragmentation. *Environmental Science and Policy* 12:729–732.
- Drexler, J.Z., J.B. Paces, C.N. Alpers, L. Windham-Meyers, L. Neymark, and H.E. Taylor. 2014. $^{234}\text{U}/^{238}\text{U}$ and $\delta^{87}\text{Sr}$ in peat as tracers of paleosalinity in the Sacramento-San Joaquin Delta of California, USA. *Applied Geochemistry* 40:164–179.
- DSC (Delta Stewardship Council). 2013. The Delta Plan. Delta Stewardship Council, Sacramento, CA. Available at: <http://deltacouncil.ca.gov/delta-plan-0>.
- DSP (Delta Science Program). 2013. Delta Science Plan. Delta Science Program, Delta Stewardship Council, Sacramento, CA. Available at: <http://deltacouncil.ca.gov/sites/default/files/documents/files/Delta-Science-Plan-12-30-2013.pdf>.
- Dugdale, R.C., F.P. Wilkerson, and A.E. Parker. 2013. A biogeochemical model of phytoplankton productivity in an urban estuary: The importance of ammonium and freshwater flow. *Ecological Modelling* 263:291–307.
- Dugdale, R.C., F.P. Wilkerson, V.E. Hogue, and A. Marchi. 2007. The role of ammonium and nitrate in spring bloom development in San Francisco Bay. *Estuarine, Coastal, and Shelf Science* 73:17–29.
- Dugdale, R., F. Wilkerson, A. Parker, A. Marchi, and K. Taberski. 2012. River flow and ammonium discharge determine spring phytoplankton blooms in an urbanized estuary. *Estuarine, Coastal and Shelf Science* 115:187–199.
- Durand, J.R. 2010. Determinants of seasonal abundance of key zooplankton of the San Francisco Estuary. M.S. Ecology and Systematics, San Francisco State University, San Francisco. 55 pp.
- Enright, C., and S. Culberson. 2009. Salinity trends, variability, and control in the northern reach of the San Francisco Estuary. *San Francisco Estuary and Watershed Science* 7(2). Available at: <http://escholarship.org/uc/item/0d52737t>
- Enright, C., S.D. Culberson, and J.R. Burau. 2013. Broad timescale forcing and geomorphic mediation of tidal marsh flow and temperature dynamics. *Estuaries and Coasts* 36:1319–1339.
- Erkkila, L.F., J.W. Moffett, O.B. Cope, B.R. Smith and R.S. Nielson. 1950. Sacramento-San Joaquin Delta fishery resources: Effects of Tracy pumping plant and Delta cross channel. U.S. Fish and Wildlife Service Special Scientific Report, Fisheries 56:1–109.
- Essington, T.E., and S. Hansson. 2004. Predator-dependent functional responses and interaction strengths in a natural food web. *Canadian Journal of Fisheries and Aquatic Sciences* 61:2215-2226.
- Estuarine Ecology Team. 1997. Assessment of the likely mechanisms underlying the “Fish-X2” relationships. Interagency Ecological Program of the Sacramento-San Joaquin Estuary, Technical Report 52.
- Ewing, R.D. 1999. Diminishing returns: Salmon decline and pesticides. Funded by the Oregon Pesticide Education Network, Biotech Research and Consulting, Inc., Corvallis, OR. 55 pp.
- Falconer, D.S., and T.F.C. Mackay. 1996. Introduction to quantitative genetics. 4th ed. New York, Longman.
- Ferrari, M.C.O., L. Ranåker, K.L. Weinersmith, M.J. Young, A. Sih, and J.L. Conrad. 2014. Effects of turbidity and an invasive waterweed on predation by introduced largemouth bass. *Environmental Biology of Fishes* 97:79-90.

- Feyrer, F. and M. Healey. 2003. Fish community structure and environmental correlates in the highly altered southern Sacramento-San Joaquin Delta. *Environmental Biology of Fishes* 66:123-132.
- Feyrer, F., B. Herbold, S.A. Matern, and P.B. Moyle. 2003. Dietary shifts in a stressed fish assemblage: Consequences of a bivalve invasion in the San Francisco Estuary. *Environmental Biology of Fishes* 67:277-288.
- Feyrer, F., K. Newman, M. Nobriga, and T. Sommer. 2010. Modeling the effects of future freshwater flow on the abiotic habitat of an imperiled estuarine fish. *Estuaries and Coasts* 34:120-128.
- Feyrer, F., M.L. Nobriga, and T.R. Sommer. 2007. Multi-decadal trends for three declining fish species: habitat patterns and mechanisms in the San Francisco Estuary, California, USA. *Canadian Journal of Fisheries and Aquatic Sciences* 64:723-734.
- Feyrer F., D. Portz, D. Odum, K.B. Newman, T. Sommer, D. Contreras, R. Baxter, S.B. Slater, D. Sereno, and E. Van Nieuwenhuyse. 2013. SmeltCam: Underwater video codend for trawled nets with an application to the distribution of the imperiled Delta Smelt. *PLoS ONE* 8(7): e67829. doi: 10.1371/journal.pone.0067829
- Feyrer, F, T. Sommer, and W. Harrell. 2006. Importance of flood dynamics versus intrinsic physical habitat in structuring fish communities: evidence from two adjacent engineered floodplains on the Sacramento River, California. *North American Journal of Fisheries Management* 26:408-417.
- Fisch, K.M., J.M. Henderson, R.S. Burton, and B. May. 2011. Population genetics and conservation implications for the endangered delta smelt in the San Francisco Bay-Delta. *Conservation Genetics* 12:1421-1434.
- Fischenich, C. 2008. The application of conceptual models to ecosystem restoration. EBA Technical Notes Collection, ERDC/EBA TN-08-1. U.S. Army Engineer Research and Development Center, Vicksburg, MS. www.wes.army.mil/el/emrrp.
- Fish, M., D. Contreras, V. Afentoulis, J. Messineo, and K. Hieb. 2009. 2008 Fishes annual status and trends report for the San Francisco Estuary. IEP Newsletter 22(2):17-36. FLASH Panel (Fall Low Salinity Habitat (FLaSH) Study Review Panel). 2012. Fall low salinity habitat (FLaSH) study synthesis – Year one of the Delta Fall Outflow Adaptive Management Plan, review panel summary report. Delta Science Program, Sacramento, CA. available at: http://deltacouncil.ca.gov/sites/default/files/documents/files/FallOutflowReviewPanelSummaryReport_Final_9_11.pdf.
- Forsgren, K. L., N. Riar, D. Schlenk. 2013. The effects of the pyrethroid insecticide, bifenthrin, on steroid hormone levels and gonadal development of steelhead (*Oncorhynchus mykiss*) under hyper saline conditions. *General and Comparative Endocrinology* 186:101-107.
- Fortuin, K.P.J., C.S.A. (Kris) van Koppen and R. Leemans. 2011. The value of conceptual models in coping with complexity and interdisciplinarity in environmental sciences education. *BioScience* 61:802-814.
- Fox, J.W. 2006. Current food web models cannot explain the overall topological structure of observed food webs. *Oikos* 115:97-109.
- Fuiman, L.A. 1983. Growth gradients in fish larvae. *Journal of Fish Biology* 23:117-123.
- Fuller, H. 2012. Benthic monitoring, 2011. IEP Newsletter 25(2):5-10.
- Gaines, S., S. Luoma, S. Monismith, S. Simenstad, and S. Sogard. 2006. IEP Delta Smelt review - Science Advisory Group Report. IEP Science Advisory Group, Sacramento, CA. Available at: http://www.water.ca.gov/iep/docs/SAG_Report-IEP_Delta_Smelt_Review.pdf.
- Ganju, N.K., D.H. Schoellhamer, M.C. Murrell, J.W. Gartner, and S.A. Wright. 2007. Constancy of the relation between floc size and density in San Francisco Bay. Pages 75-91 in J.P.-Y. Maa, L.P. Sanford, and D.H. Schoellhamer, editors. *Estuarine and Coastal Fine Sediments Dynamics*. Elsevier Science B.V.
- Gascoigne, J.C. and R.N. Lipcius. 2004. Allee effects driven by predation. *Journal of Applied Ecology* 41:801-810.
- Gascoigne, J., L. Berec, S. Gregory, and F. Courchamp. 2009. Dangerously few liaisons: a review of mate-finding Allee effects. *Population Ecology* 51:355-372.
- Gentile, J.H., M.A. Harwell, W. Cropper Jr., C.C. Harwell, D. DeAngelis, S. Davis, J.C. Ogden, and D. Lirman. 2001. Ecological conceptual models: a framework and case study on ecosystem management for South Florida sustainability. *The Science of the Total Environment* 274:231-253.

- Ger, K.A., P. Arneson, C.R. Goldman, and S.J. The. 2010b. Species specific differences in the ingestion of *Microcystis* cells by the calanoid copepods *Eurytemora affinis* and *Pseudodiaptomus forbesi*: Journal of Plankton Research 32:1479–1484.
- Ger, K.A., S.J. Teh, D.V. Baxa, S. Lesmeister, and C.R. Goldman. 2010a. The effects of dietary *Microcystis aeruginosa* and microcystin on the copepods of the upper San Francisco Estuary: Freshwater Biology 55:1548–1559.
- Ger, K.A., S.J. Teh, and C.R. Goldman. 2009. Microcystin-LR toxicity on dominant copepods *Eurytemora affinis* and *Pseudodiaptomus forbesi* of the upper San Francisco Estuary: Science of the Total Environment 407:4852–4857.
- Gifford, S.M., G. Rollwagen-Bollens, S.M. Bollens. 2007. Mesozooplankton omnivory in the upper San Francisco Estuary. Marine Ecological Progress Series 348:33–46.
- Gingras, M. 1997. Mark/recapture experiments at Clifton Court Forebay to estimate pre-screening loss to juvenile fishes: 1976–1993. Interagency Ecological Program of the Sacramento-San Joaquin Estuary, Technical Report 55.
- Gingras, M., and M. McGee. 1997. A telemetry study of striped bass emigration from Clifton Court Forebay: Implications for predator enumeration and control. Interagency Ecological Program of the Sacramento-San Joaquin Estuary, Technical Report 54.
- Gleason, E.C. and J. Adib-Samii. 2007. 20mm Metadata. Available at: <ftp://ftp.dfg.ca.gov/>.
- Gleason, T.R., and D.A. Bengtson. 1996. Growth, survival and size-selective predation mortality of larval and juvenile inland silversides, *Menidia beryllina*. Journal of Experimental Marine Biology and Ecology 199:165–177.
- Glibert, P.M. 2012. Ecological stoichiometry and its implications for aquatic ecosystem sustainability: Current Opinion in Environmental Sustainability 4:272–277.
- Glibert, P.M., D. Fullerton, J.M. Burkholder, J.C. Cornwell, and T.M. Kana. 2011. Ecological stoichiometry, biogeochemical cycling, invasive species, and aquatic food webs: San Francisco Estuary and comparative systems. Reviews in Fisheries Science 19:358–417.
- Gould, A.L. and W.J. Kimmerer. 2010. Development, growth, and reproduction of the cyclopoid copepod *Limnoithona tetraspina* in the upper San Francisco Estuary. Marine Ecology Progress Series 412:163–177.
- Greco, W.R., G. Bravo, and J.C. Parsons. 1995. The search for synergy: a critical review from a response surface perspective. Pharmacological Reviews 47:332–385.
- Greenberg, J.A., E.L. Hestir, D. Riano, G.J. Scheer, and S.L. Ustin. 2012. Using LiDAR data analysis to estimate changes in insolation under large-scale riparian deforestation. Journal of the American Water Resources Association 48:939–948.
- Greenfield, B.K., S.J. The, J.R.M. Ross, J. Hunt, G. Zhang, J. A. Davis, G. Ichikawa, D. Crane, S.S.O. Hung, D. Deng, F. Teh, and P.G. Green. 2008. Contaminant concentrations and histopathological effects in Sacramento Splittail (*Pogonichthys macrolepidotus*). Archives of Environmental Contaminants and Toxicology 55:270–281.
- Gregory, R.S., and C.D. Levings. 1998. Turbidity reduces predation on migrating juvenile Pacific salmon. Transactions of the American Fisheries Society 127:275–285.
- Gregory, S.D., C.J.A. Bradshaw, B.W. Brook, and F. Courchamp. 2010. Limited evidence for the demographic Allee effect from numerous species across taxa. Ecology 91:2151–2161.
- Grimaldo, L.F., R.E. Miller, C.M. Peregrin, and Z.P. Hymanson. 2004. Spatial and temporal distribution of native and alien ichthyoplankton in three habitat types of the Sacramento-San Joaquin Delta. American Fisheries Society Symposium 39:81–96.
- Grimaldo, L., R.E. Miller, C.M. Peregrin, and Z. Hymanson. 2012. Fish assemblages in reference and restored tidal freshwater marshes of the San Francisco Estuary. San Francisco Estuary and Watershed Science, 10(1). Available at: <http://escholarship.org/uc/item/52t3x0hq>.
- Grimaldo, L.F., T. Sommer, N. Van Ark, G. Jones, E. Holland, P. Moyle, B. Herbold, and P. Smith. 2009. Factors affecting fish entrainment into massive water diversions in a tidal freshwater estuary: Can fish losses be managed? North American Journal of Fisheries Management 29:1253–1270.
- Hallfredsson, E., and T. Pedersen. 2009. Effects of predation from juvenile herring (*Clupea harengus*) on mortality rates of capelin (*Mallotus villosus*) larvae. Canadian Journal of Fisheries and Aquatic Sciences 66:1693–1706.

- Hanak, E., J. Lund, A. Dinar, B. Gray, R. Howitt, J. Mount, P. Moyle, and B. Thompson. 2011. Managing California's water: From conflict to reconciliation. Public Policy Institute of California. <http://www.ppic.org/main/publication.asp?i=944>.
- Hartman, K.J. and S.B. Brandt. 1995. Comparative energetics and the development of bioenergetics models for sympatric estuarine piscivores. *Canadian Journal of Fisheries and Aquatic Science* 52:1647–1666.
- Harwood, A.D., J. You, and M.J. Lydy. 2009. Temperature as a toxicity identification evaluation tool for pyrethroid insecticides: Toxicokinetic confirmation. *Environmental Toxicology and Chemistry* 28:1051–1058.
- Hasenbein, M., L.M. Komoroske, R.E. Connon, J. Geist, and N.A. Fangué. 2013. Turbidity and salinity affect feeding performance and physiological stress in the endangered delta smelt. *Integrative Comparative Biology* 53:620–634.
- Hasenbein, M. I. Werner, L.A. Deanovic, J. Geist, E.B. Fritsch, A. Javidmehr, C. Foe, N.A. Fangué, and R.E. Connon. 2013. Transcriptomic profiling permits the identification of pollutant sources and effects in ambient water samples. *Science of the Total Environment* 468–469:668–698.
- Hauser, L., G.J. Adcock, P.J. Smith, J.H. Bernal Ramirez, and G.R. Carvalho. 2002. Loss of microsatellite diversity and low effective population size in an overexploited population of New Zealand snapper (*Pagrus auratus*). *Proceedings of the National Academy of Sciences of the United States of America* 99:11742–11747.
- Haydon, D. 1994. Pivotal assumptions determining the relationship between stability and complexity: an analytical synthesis of the stability-complexity debate. *The American Naturalist* 144:14–29.
- Hazel, C.R. and D.W. Kelley. 1966. Zoobenthos of the Sacramento-San Joaquin Delta. Pages 113–133 in D.W. Kelley, editor, *Ecological studies of the Sacramento-San Joaquin Estuary*. California Fish and Game, Fish Bulletin 133.
- Healey, M.C., M.D. Dettinger, and R.B. Norgaard, editors. 2008. *The state of Bay-Delta science, 2008*. CALFED Science Program, Sacramento, CA. 174 pp.
- Herbold, B., D.M. Baltz, L. Brown, R. Grossinger, W. Kimmerer, P. Lehman, C.S. Simenstad, C. Wilcox, and M. Nobriga. 2014. The role of tidal marsh restoration in fish management in the San Francisco Estuary. *San Francisco Estuary and Watershed Science* 12(1). Available at: <http://escholarship.org/uc/item/1147j4nz>.
- Herrgesell, P.A. 2013. A historical perspective of the Interagency Ecological Program: Bridging multi-agency studies into ecological understanding of the Sacramento-San Joaquin Delta and Estuary for 40 years. Report to IEP. 184 pp. Available at: http://www.water.ca.gov/iep/docs/Herrgesell_IEP_Report_FINAL.pdf.
- Heubach W. [ca. 1973]. Further observation of the densities of king salmon, striped bass, and white catfish collected at the federal and State Fish Facilities. California Department of Fish and Game, Stockton (CA). 11 p.
- Hirose, T., and K. Kawaguchi. 1998. Spawning ecology of Japanese surf smelt, *Hypomesus pretiosus japonicus* (Osmeridae), in Otsuchi Bay, northeastern Japan. *Environmental Biology of Fishes* 52:213–223.
- Houde, E.D. 1987. Fish early life dynamics and recruitment variability. *American Fisheries Society Symposium* 2:17–29.
- Houde, E.D. 1989. Comparative growth, mortality, and energetics of marine fish larvae: temperature and implied latitudinal effects. *Fishery Bulletin* 87:471–495.
- Hennessy, A. 2010. Zooplankton monitoring 2009. *IEP Newsletter* 23(2):15–22.
- Hennessy, A. 2011. Zooplankton monitoring 2010. *IEP Newsletter* 24(2):20–27.
- Hennessy, A., and T. Enderlein. 2013. Zooplankton monitoring 2011. *IEP Newsletter* 26(1):23–30.
- Hestir, E.L. 2010. Trends in estuarine water quality and submerged aquatic vegetation invasion. Ph.D. Dissertation. University of California, Davis, CA
- Hestir, E.L., D.H. Schoellhamer, T. Morgan-King, S.L. Ustin. 2013. A step decrease in sediment concentration in a highly modified tidal river delta following the 1983 El Niño floods. *Marine Geology* 345:304–313.
- Hieb, K., M. Bryant, M. Dege, T. Greiner, K. Souza and S. Slater. 2005. Fishes in the San Francisco Estuary, 2004 Status and Trends. *IEP Newsletter* 18(2):19–36.
- Hilborn, R., and C. Walters. 1992. *Quantitative fisheries stock assessment: choice, dynamics and uncertainty*, 1st edition. Chapman and Hall, New York.

- Hjort, J. 1914. Fluctuations in the great fisheries of northern Europe viewed in light of biological research. *Rapports et Procès-verbaux des Réunions Conseil international pour l'Exploration de la Mer* 19:1-228
- Hobbs, J.A., W.A. Bennett, and J.E. Burton. 2006. Assessing nursery habitat quality for native smelts (Osmeridae) in the low-salinity zone of the San Francisco estuary. *Journal of Fish Biology* 69:907-922.
- Hobbs, J.A., W.A. Bennett, J. Burton, and M. Gras. 2007. Classification of larval and adult delta smelt to nursery areas by use of trace elemental fingerprinting. *Transactions of the American Fisheries Society* 136:518-527.
- Holling, C.S. 1978. *Adaptive environmental assessment and management*. Wiley, Chichester, UK.
- Honey, K., R. Baxter, Z. Hymanson, T. Sommer, M. Gingras, and P. Cadrett. 2004. IEP long-term fish monitoring program element review. Interagency Ecological Program of the Sacramento-San Joaquin Estuary, Technical Report 78.
- Hosack, G.R., H.W. Li and P.A. Rossignol. 2009. Sensitivity to model structure. *Ecological Modeling* 220:1054-1062.
- Hunter, J. R. 1980. The feeding behavior and ecology of marine fish larvae. Pages 287-330 in J.E. Bardach, J.J. Magnuson, R.C. May, and J.M. Reinhart, editors. *Fish behavior and its use in the capture and culture of fishes*, volume ICLARM Conference Proceedings 5. International Center for Living Aquatic Resources Management, Manila, Philippines. 512 p.
- Hutchings, J.A. 2013. Renaissance of a caveat: Allee effects in marine fish. *ICES Journal of Marine Science*, doi:10.1093/icesjms/fst179.
- Hutchings, J.A., C. Minto, D. Ricard, J.K. Baum, and O.P. Jensen. 2010. Trends in the abundance of marine fishes. *Canadian Journal of Fisheries and Aquatic Sciences* 67:1205-1210.
- IEP (Interagency Ecological Program for the San Francisco Estuary). 2005. Interagency Ecological Program 2005 Work plan to evaluate the decline of pelagic species in the upper San Francisco Estuary. Available at: http://www.science.calwater.ca.gov/pdf/workshops/POD/2005_IEP-POD_Workplan_070105.pdf.
- Ingram, B.L. and F. Malamud-Roam. 2012. *The West without water*. University of California Press. 289 p.
- Jackson, L.J., A.S. Trebitz, K.L. Cottingham. 2000. An introduction to the practice of ecological modeling. *BioScience* 50:694-706.
- Jassby, A.D. 2008. Phytoplankton in the upper San Francisco Estuary: recent biomass trends, their causes and their trophic significance. *San Francisco Estuary and Watershed Science* 6(1). Available at <http://www.escholarship.org/uc/item/71h077r1>.
- Jassby, A.D., and E.E. Van Nieuwenhuysse. 2005. Low dissolved oxygen in an estuarine channel (San Joaquin River, California): Mechanisms and models based on long-term time Series. *San Francisco Estuary and Watershed Science* 3(2). Available at: <http://escholarship.org/uc/item/0tb0f19p>.
- Jassby, A.D., J.E. Cloern, and B.E. Cole. 2002. Annual primary production: patterns and mechanisms of change in a nutrient-rich tidal ecosystem. *Limnology and Oceanography* 47:698-712.
- Jassby, A.D., W.J. Kimmerer, S.G. Monismith, C. Armor, J.E. Cloern, T.M. Powell, J.R. Schubel, and T.J. Vendlinski. 1995. Isohaline position as a habitat indicator for estuarine populations. *Ecological Applications* 5:272-289.
- Jassby, A.D., A.B. Muller-Solger, and M. Vayssières. 2005. Subregions of the Sacramento-San Joaquin Delta: Identification and use. *IEP Newsletter* 18(2):46-55.
- Johnson, M.L., I. Werner, S. Teh, and F. Loge 2010. Evaluation of chemical, toxicological, and histopathological data to determine their role in the pelagic organism decline. University of California, Davis, Final report to the California State Water Resources Control Board and Central Valley Regional Water Quality Control Board.
- Johnson, J.H. and D.S. Dropkin. 1992. Predation on recently released larval American Shad in the Susquehanna River Basin. *North American Journal of Fisheries Management* 12:504-508.
- Jordan, J., A. Zare, L.J. Jackson, H.R. Habibi, and A.M. Weljie. 2012. Environmental contaminant mixtures at ambient concentrations invoke a metabolic stress response in goldfish not predicted from exposure to individual compounds alone. *Journal of Proteome Research* 11:1133-1143.
- Jung, S. and E.D. Houde. 2004. Recruitment and spawning-stock biomass distribution of bay anchovy (*Anchoa mitchilli*) in Chesapeake Bay. *Fishery Bulletin* 102:63-77.

- Junges C.M., R.C. Lajmanovich, P.M. Peltzer, A.M. Attademo, and A. Basso. 2010. Predator-prey interactions between *Synbranchus marmoratus* (Teleostei: Synbranchidae) and *Hypsiboas pulchellus* tadpoles (Amphibia: Hylidae): importance of lateral line in nocturnal predation and effects of fenitrothion exposure. *Chemosphere* 81:1233–1238.
- Kano, R.M. 1990. Occurrence and abundance of predator fish in Clifton Court Forebay, California. Interagency Ecological Program of the Sacramento-San Joaquin Estuary, Technical Report 24.
- Keith, D.M. and J.A. Hutchings. 2012. Population dynamics of marine fishes at low abundance. *Canadian Journal of Fisheries and Aquatic Sciences* 69:1150–1163.
- Khan, M.Z. and F.C.P. Law. 2005. Adverse effects of pesticides and related chemicals on enzyme and hormone systems of fish, amphibians and reptiles: a review. *Proceedings of the Pakistan Academy of Science* 42:315–323.
- Kimmerer, W. J. 2002a. Physical, biological, and management responses to variable freshwater flow into the San Francisco Estuary. *Estuaries* 25:1275–1290.
- Kimmerer, W.J. 2002b. Effects of freshwater flow on abundance of estuarine organisms: physical effects or trophic linkages. *Marine Ecology Progress Series* 243:39–55.
- Kimmerer, W.J. 2004. Open-water processes of the San Francisco Estuary: from physical forcing to biological responses. *San Francisco Estuary and Watershed Science* 2. Available at: <http://escholarship.org/uc/item/9bp499mv>.
- Kimmerer, W.J. 2006. Response of anchovies dampens effects of the invasive bivalve *Corbula amurensis* on the San Francisco Estuary foodweb. *Marine Ecology Progress Series* 324:207–218.
- Kimmerer, W.J. 2008. Losses of Sacramento River Chinook salmon and delta smelt to entrainment in water diversions in the Sacramento-San Joaquin Delta. *San Francisco Estuary and Watershed Science*. 6(2). Available at: <http://www.escholarship.org/uc/item/7v92h6fs>.
- Kimmerer, W.J. 2011. Modeling delta smelt losses at the South Delta Export Facilities. *San Francisco Estuary and Watershed Science*, 9(1). Available at: <http://www.escholarship.org/uc/item/0rd2n5vb>.
- Kimmerer, W. and M. Nobriga. 2005. Development and evaluation of bootstrapped confidence intervals for the IEP fish abundance indices. *IEP Newsletter* 18(2):68–75.
- Kimmerer, W.J., and M.L. Nobriga. 2008. Investigating particle transport and fate in the Sacramento-San Joaquin Delta using particle tracking model. *San Francisco Estuary and Watershed Science* 6(1). Available at: <http://escholarship.org/uc/item/547917gn>.
- Kimmerer, W.J., and J.J. Orsi. 1996. Changes in the zooplankton of the San Francisco Bay estuary since the introduction of the clam *Potamocorbula amurensis*. Pages 403–423 in J.T. Hollibaugh, editor. *San Francisco Bay: the ecosystem*: Pacific Division American Association for the Advancement of Science, San Francisco, California.
- Kimmerer, W.J., J.H. Cowan, Jr., L.W. Miller, and K.A. Rose. 2000. Analysis of an estuarine striped bass (*Morone saxatilis*) population: influence of density-dependent mortality between metamorphosis and recruitment. *Canadian Journal of Fisheries and Aquatic Sciences* 57:478–486.
- Kimmerer, W.J., N. Ferm, M.H. Nicolini, and C. Penalva. 2005. Chronic food limitation of egg production in populations of copepods of the genus *Acartia* in the San Francisco Estuary. *Estuaries* 28:541–550.
- Kimmerer, W.J., E. Gartside, and J.J. Orsi. 1994. Predation by an introduced clam as the likely cause of substantial declines in zooplankton of San Francisco Bay. *Marine Ecology Progress Series* 113:81–93.
- Kimmerer, W.J., E.S. Gross, and M.L. MacWilliams. 2009. Is the response of estuarine nekton to freshwater flow in the San Francisco Estuary explained by variation in habitat volume? *Estuaries and Coasts* 32:375–389.
- Kimmerer, W.J. M.L. MacWilliams, and E. Gross. 2013. Variation of fish habitat and extent of the low-salinity zone with freshwater flow in the San Francisco Estuary. *San Francisco Estuary and Watershed Science*, 11(4). Available at: <http://escholarship.org/uc/item/3pz7x1x8>.
- Kimmerer, W., J. Stillman, and L. Sullivan. 2011. Zooplankton and clam analyses in support of the Interagency Ecological Program's Work Plan on Pelagic Organism Declines (POD). Final report to the POD management team. Romberg Tiburon Center for Environmental Studies, San Francisco State University.

- Kitchell, J.F., L.A. Eby, X. He, D.E. Schindler, and R. A. Wright. 1994. Predator-prey dynamics in an ecosystem context. *Journal of Fish Biology* 45, Issue Supplement sA:209–226.
- Kolpin, D.W., E.T. Furlong, M.T. Meyer, E.M. Thurman, S.D. Zaugg, L.B. Barber, and H.T. Buxton. 2002. Pharmaceuticals, hormones, and other organic wastewater contaminants in U.S. Streams 1999-2000: A national reconnaissance. *Environmental Science and Toxicology* 36:1201-1211.
- Komoroske, L.M., R.E. Connon, J. Lindberg, B.S. Cheng, G. Castillo, M. Hasenbein, N.A. Fangue. 2014. Ontogeny influences sensitivity to climate change stressors in an endangered fish. *Conservation Physiology* 2: doi:10.1093/conphys/cou008.
- Kuivila, K. M., and C.G. Foe. 1995. Concentrations, transport and biological effects of dormant spray pesticides in the San Francisco Estuary, California. *Environmental Toxicology and Chemistry* 14:1141–1150.
- Kuivila, K.M., and M. Hladik. 2008. Understanding the occurrence and transport of current-use pesticides in the San Francisco Estuary Watershed. *San Francisco Estuary and Watershed Science* 6(3). Available at: <http://www.escholarship.org/uc/item/06n8b36k>.
- Kuivila, K. and G.E. Moon. 2004. Potential exposure of larval and juvenile delta smelt to dissolved pesticides in the Sacramento–San Joaquin Delta, California. *American Fisheries Society Symposium* 39:229–241.
- Kuparinen, A., D.M. Keith and J.A. Hutchings. 2014. Allee effect and the uncertainty of population recovery. *Conservation Biology* 28:790-798.
- Laprise, R., and J.J. Dodson. 1989. Ontogeny and importance of tidal vertical migrations in the retention of larval smelt *Osmerus mordax* in a well-mixed estuary. *Marine Ecology Progress Series* 55:101-111.
- Lavado, R., J.M Rimoldi, and D. Schlenk. 2009. Mechanisms of fenthion activation in rainbow trout (*Oncorhynchus mykiss*) acclimated to hypersaline environments. *Toxicology and Applied Pharmacology* 235: 143-152.
- Leggett, W. C., and E. Deblois. 1994. Recruitment in marine fishes: is it regulated by starvation and predation in the egg and larval stages? *Netherlands Journal of Sea Research* 32:119-134.
- Lehman, P.W., G. Boyer, C. Hall, S. Waller, and K. Gehrts. 2005. Distribution and toxicity of a new colonial *Microcystis aeruginosa* bloom in the San Francisco Bay Estuary, California. *Hydrobiologia* 541:87–99.
- Lehman, P.W., C. Kendall, M. A. Guerin, M. B. Young, S. R. Silva, G. L. Boyer, and S. J. Teh. 2014. Characterization of the *Microcystis* bloom and its nitrogen supply in San Francisco Estuary using stable isotopes. *Estuaries and Coasts*. DOI: 10.1007/s12237-014-9811-8
- Lehman, P.W., K. Marr, G.L. Boyer, S. Acuna, and S J. Teh. 2013. Long-term trends and causal factors associated with *Microcystis* abundance and toxicity in San Francisco Estuary and implications for climate change impacts. *Hydrobiologia* 718:141-158.
- Lehman, P.W., S.J. Teh, G.L. Boyer, M.L. Nobriga, E. Bass, and C. Hogle. 2010. Initial impacts of *Microcystis aeruginosa* blooms on the aquatic food web in the San Francisco Estuary. *Hydrobiologia* 637:229–248.
- Levins, R. 1974. The qualitative analysis of partially specified systems. *Annals of the New York Academy of Sciences* 231:123-138.
- Levins, R. 1975. Evolution in communities near equilibrium. Pages 16-50 in M. L. Cody and J. M. Diamond, editors. *Ecology and Evolution of Communities*. The Belknap Press of Harvard University Press, Cambridge, Massachusetts.
- Liang, T.T., and E.P. Lichtenstein. 1974. Synergism of insecticides by herbicides: effect of environmental factors. *Science* 4169:1128–1130.
- Liermann, M., and R. Hilborn. 1997. Depensation in fish stocks: a hierarchic Bayesian meta-analysis. *Canadian Journal Fisheries and Aquatic Sciences* 54:1976-1984.
- Light, T., T. Grosholz, and P. Moyle. 2005. Delta ecological survey (Phase I): Non-indigenous aquatic species in the Sacramento–San Joaquin Delta, a literature review. Final Report for Agreement # DCN #113322J011 submitted to U.S. Fish and Wildlife Service. Stockton, CA, 35 p.
- Lindberg, J.C., G. Tigan, L. Ellison, T. Rettinghouse, M.M. Nagel and K.M. Fisch. 2013. Aquaculture methods for a genetically managed population of endangered delta smelt. *North American Journal of Aquaculture* 75:186-196.

- Liu, W.-C., H.-W. Chen, F. Jordan, W.H. Lin, and C.W. Liu. 2010. Quantifying the interaction structure and the topological importance of species in food webs: A signed digraph approach. *Journal of Theoretical Biology* 267:355–362.
- Loboschefskey, E., G. Benigno, T. Sommer, K. Rose, T. Ginn, and A. Massoudieh. 2012. Individual-level and population-level historical prey demand of San Francisco Estuary striped bass using a bioenergetics model. *San Francisco Estuary and Watershed Science* 10(1). Available at: <http://escholarship.org/uc/item/1c788451>.
- Lopez, C.B., J.E. Cloern, T.S. Schraga, A.J. Little, L.V. Lucas, J.K. Thompson, and J.R. Burau. 2006. Ecological values of shallow-water habitats: Implications for restoration of disturbed ecosystems. *Ecosystems* 9:422–440.
- Lott, J. 1998. Feeding habits of juvenile and adult delta smelt from the Sacramento-San Joaquin River Estuary. *IEP Newsletter* 11(1):14–19.
- Lotze, H.K., H.S. Lenihan, B.J. Bourque, R.H. Bradbury, R.G. Cooke, M.C. Kay, S.M. Kidwell, M.X. Kirby, C.H. Peterson, and J.B.C. Jackson. 2006. Depletion, degradation, and recovery potential of estuaries and coastal seas. *Science* 312:1806–1809.
- Lucas, L.V., and J.K. Thompson. 2012. Changing restoration rules: Exotic bivalves interact with residence time and depth to control phytoplankton productivity. *Ecosphere* 3:117. Available at <http://dx.doi.org/10.1890/ES12-00251.1>.
- Lucas, L.V., J.E. Cloern, J.K. Thompson, and N.E. Monsen. 2002. Functional variability of habitats within the Sacramento-San Joaquin Delta: Restoration implications. *Ecological Applications* 12:1528–1547.
- Lucas, L.V., J.R. Koseff, S.G. Monismith, and J.K. Thompson. 2009a. Shallow water processes govern system-wide phytoplankton bloom dynamics - A modeling study. *Journal of Marine Systems* 75:70–86.
- Lucas, L.V., J.K. Thompson, and L.R. Brown. 2009b. Why are diverse relationships observed between phytoplankton biomass and transport time? *Limnology and Oceanography* 54:381–390.
- Lucas, M.C. and E. Bara 2001 *Migration of freshwater fishes*. Iowa State Press, Ames.
- Mac Nally, R., J.R. Thompson, W.J. Kimmerer, F. Feyrer, K.B. Newman, A. Sih, W.A. Bennett, L. Brown, E. Fleishman, S.D. Culberson, G. Castillo. 2010. An analysis of pelagic species decline in the upper San Francisco Estuary using multivariate autoregressive modeling (MAR). *Ecological Applications* 20:1417–1430.
- MacWilliams, M.L., and E.S. Gross. 2013. Hydrodynamic simulation of circulation and residence time in Clifton Court Forebay. *San Francisco Estuary and Watershed Science*, 11(2). Available at: <http://www.escholarship.org/uc/item/4q82g2bz>.
- Mager, R.C., S.I. Doroshov, J.P. Van Eenennaam, and R.L. Brown. 2004. Early life stages of delta smelt. *American Fisheries Society Symposium* 39:169-180.
- Manly, B.J.F. and M.A. Chotkowski. 2006. Two new methods for regime change analysis. *Archiv für Hydrobiologie* 167:593–607.
- Marine, K.R., and J.J. Cech, Jr. 2004. Effects of high water temperature on growth, smoltification, and predator avoidance in juvenile Sacramento River Chinook salmon. *North American Journal of Fisheries Management* 24:198-210.
- Martin, K.L.M. and D.L. Swiderski. 2001. Beach spawning in fishes: phylogenetic test of hypotheses. *American Zoology* 41:526-537.
- Massoudieh A., E. Loboschefskey, T. Sommer, T. Ginn, K. Rose, F. J. Loge. 2011. Spatio-temporal modeling of Striped-Bass egg and larvae movement and fate in Sacramento River Delta. *Ecological Modeling* 222:3513-3523.
- Maunder, M.N., and R.B. Deriso. 2011. A state-space multistage life cycle model to evaluate population impacts in the presence of density dependence: illustrated with application to delta smelt (*Hypomesus transpacificus*). *Canadian Journal of Fisheries and Aquatic Sciences* 68:1285–1306.
- May, R.M. 1972. Will a large complex system be stable? *Nature* 238:413-414.
- McKenzie, D.J., A. Shingles, G. Claireaux, P. Domenici. 2008. Sublethal concentrations of ammonia impair performance of the teleost fast-start escape response. *Physiological and Biochemical Zoology* 82:353-362.

- McGann M, L. Erikson, E. Wan, C. Powell II, and R.F. Maddocks. 2013. Distribution of biologic, anthropogenic, and volcanic constituents as a proxy for sediment transport in the San Francisco Bay coastal system. *Marine Geology* 345:113–142.
- McManus, G.B., J.K. York and W.J. Kimmerer. 2008. Microzooplankton dynamics in the low salinity zone of the San Francisco Estuary. *Verhandlungen des Internationalen Verein Limnologie* 30:198–202.
- Meng, L. and J.J. Orsi. 1991. Selective predation by larval striped bass on native and introduced copepods. *Transactions of the American Fisheries Society* 120:187–192.
- Merz, J.E., S. Hamilton, P.S. Bergman, and B. Cavallo. 2011. Spatial perspective for delta smelt: a summary of contemporary survey data. *California Fish and Game* 97(4):164–189.
- Millennium Ecosystem Assessment. 2005. *Ecosystems and human well-being: Synthesis*. Island Press, Washington. 155pp.
- Miller, L.W. 2000. The tow-net survey abundance index for delta smelt revisited. *IEP Newsletter* 13(1):37-44.
- Miller N.A. and J.H. Stillman. 2013. Seasonal and spatial variation in the energetics of the invasive clam *Corbula amurensis* in the upper San Francisco Estuary. *Marine Ecology Progress Series* 476:129-139.
- Miller, W.J. 2011. Revisiting assumptions that underlie estimates of proportional entrainment of delta smelt by State and federal water diversions from the Sacramento-San Joaquin Delta. *San Francisco Estuary and Watershed Science*, 9(1). Available at: <http://escholarship.ucop.edu/uc/item/5941x1h8>.
- Miller, W.J., B.F.J. Manly, D.D. Murphy, D. Fullerton, and R.R. Ramey. 2012. An investigation of factors affecting the decline of delta smelt (*Hypomesus transpacificus*) in the Sacramento-San Joaquin Estuary. *Reviews in Fisheries Science* 20:1–19.
- Miller N.A. and J.H. Stillman. 2013. Seasonal and spatial variation in the energetics of the invasive clam *Corbula amurensis* in the upper San Francisco Estuary. *Marine Ecology Progress Series* 476:129-139.
- Miner, J.G., and R.A. Stein. 1996. Detection of predators and habitat choice by small bluegills: effects of turbidity and alternative prey. *Transactions of the American Fisheries Society* 125:97-103.
- Miranda, J., R. Padilla, J. Morinaka, J. DuBois and M. Horn. 2010a. Release site predation study. Fishery Improvements Section Bay-Delta Office, California Department of Water Resources. Sacramento, CA.
- Miranda, J., R. Padilla, G. Aasen, B. Mefford, D. Sisneros and J. Boutwell. 2010b. Valuation of mortality and injury in a fish release pipe. Fishery Improvements Section Bay-Delta Office, California Department of Water Resources. Sacramento, CA.
- Monismith, S.G., J.L. Hench, D.A. Fong, N.J. Nidzieko, W.E. Fleenor, L.P. Doyle, and S.G. Schladow. 2009. Thermal variability in a tidal river. *Estuaries and Coasts* 32:100–110.
- Monismith, S.G., W. Kimmerer, J.R. Burau, M.T. Stacey. 2002. Structure and flow-induced variability of the subtidal salinity field in northern San Francisco Bay. *Journal of Physical Oceanography* 32:3003–3019.
- Monsen, N. E., J.E. Cloern, and J.R. Burau. 2007. Effects of flow diversions on water and habitat quality: examples from California's highly manipulated Sacramento-San Joaquin Delta. *San Francisco Estuary and Watershed Science* 5(3). Available at: <http://escholarship.org/uc/item/04822861>.
- Montaño-Moctezuma, G., H.W. Li and P.A. Rossignol. 2007. Alternative community structures in kelp –urchin community: A qualitative modeling approach. *Ecological Modeling* 205:343-354.
- Morgan-King, T.L., and D.H. Schoellhamer. 2013. Suspended-sediment flux and retention in a backwater tidal slough complex near the landward boundary of an estuary. *Estuaries and Coasts* 36:300-318.
- Morinaka J. 2014a. Acute mortality and injury of delta smelt associated with collection, handling, transport, and release at State Water Project fish salvage facility. Interagency Ecological Program of the Sacramento-San Joaquin Estuary, Technical Report 89.
- Morinaka J. 2013b. A history of the operational and structural changes to the John E. Skinner Delta Fish Protective Facility from 1968 to 2010. Interagency Ecological Program of the Sacramento-San Joaquin Estuary, Technical Report 85.

- Morris, T. 2013. *Microcystis aeruginosa* status and trends during the Summer Towntnet Survey. IEP Newsletter 26(2):28-32.
- Moulton, L.L. 1974. Abundance, growth, and spawning of the longfin smelt in Lake Washington. Transactions of the American Fisheries Society 103:46–52.
- Mount J., W. Fleenor, B. Gray, B. Herbold, W. Kimmerer. 2013. Panel review of the draft Bay Delta Conservation Plan. Report to American Rivers and The Nature Conservancy. Available at: <https://watershed.ucdavis.edu/files/biblio/FINAL-BDCP-REVIEW-for-TNC-and-AR-Sept-2013.pdf>.
- Moyle, P.B. 2002. Inland fishes of California, 2nd edition. University of California Press, Berkeley, CA.
- Moyle, P.B., and W.A. Bennett. 2008. The future of the Delta ecosystem and its fish. Technical Appendix D in J. Lund, E. Hanak, W. Fleenor, W. Bennett, R. Howitt, J. Mount, and P. Moyle, editors. Comparing Futures for the Sacramento-San Joaquin Delta. Public Policy Institute of California, San Francisco, California.
- Moyle, P.B., W.A. Bennett, W.E. Fleenor, and J.R. Lund. 2010. Habitat variability and complexity in the upper San Francisco Estuary. San Francisco Estuary and Watershed Science 8(3). Available at: <http://escholarship.org/uc/item/0kf0d32x>.
- Moyle, P.B., B. Herbold, D.E. Stevens, and L.W. Miller. 1992. Life history and status of delta smelt in the Sacramento-San Joaquin Estuary, California. Transactions of the American Fisheries Society 121:67–77.
- Mueller-Solger, A.B., C.J. Hall, A.D. Jassby, and C.R. Goldman. 2006. Food resources for zooplankton in the Sacramento-San Joaquin Delta. Final Report to the Calfed Ecosystem Restoration Program.
- Mueller-Solger, A.B., A.D. Jassby, and D.C. Mueller-Navarra. 2002. Nutritional quality of food resources for zooplankton (*Daphnia*) in a tidal freshwater system (Sacramento-San Joaquin River Delta). Limnology and Oceanography 47:1468–1476.
- Murawski, S.A., G.R. Clayton, R.J. Reed, and C.F. Cole. 1980. Movements of spawning rainbow smelt, *Osmerus mordax*, in a Massachusetts estuary. Estuaries 3:308-314.
- Murphy, D.D., and S.A. Hamilton. 2013. Eastward migration or marshward dispersal: understanding seasonal movements by Delta Smelt. San Francisco Estuary and Watershed Science 11(3). Available at: <http://escholarship.org/uc/item/4jf862qz>.
- Murrell, M.C. and J.T. Hollibaugh. 1998. Microzooplankton grazing in northern San Francisco Bay measured by the dilution method. Aquatic Microbial Ecology 15:53–63.
- Murty, A.S. 1986. Toxicity of pesticides to fish. Vols. I and II. C.R.C Press Inc. 483 and 355pp.
- Myers, R.A. 1998. When do environment-recruitment correlations work? Reviews in Fish Biology and Fisheries 8:285-305.
- Myers, R.A., and N.J. Barrowman. 1996. Is fish recruitment related to spawner abundance? Fishery Bulletin 94:707-724.
- Myers R.A., N.J. Barrowman, J.A. Hutchings, and A.A. Rosenberg. 1995. Population dynamics of exploited fish stocks at low population levels. Science 269:1106-1108.
- National Weather Service. 2003. WFO Sacramento County Warning Area Meteorology. Available at: <http://www.wrh.noaa.gov/sto/CWA.php>. Accessed: December 29, 2013.
- Newman, K.B. 2008. Sample design-based methodology for estimating delta smelt abundance. San Francisco Estuary and Watershed Science 6. Available at: <http://escholarship.org/uc/item/99p428z6>.
- Nichols, F.H., J.E. Cloern, S.N. Luoma, and D.H. Peterson. 1986. The modification of an estuary, Science 231:567-573.
- Nichols, F.H., J.K. Thompson, and L.E. Schemel. 1990. Remarkable invasion of San Francisco Bay (California, USA) by the Asian clam *Potamocorbula amurensis*. II. Displacement of a former community. Marine Ecology Progress Series 66:95–101.
- Nicolas, J. 1999. Vitellogenesis in fish and the effects of polycyclic aromatic hydrocarbon contaminants. Aquatic Toxicology 45:77–90.

- NMFS (National Marine Fisheries Service). 2009. Biological opinion and conference opinion on the long-term operations of the Central Valley Project and State Water Project. National Marine Fisheries Service, Southwest Region, Long Beach, CA.
- Nobriga, M. 2002. Larval delta smelt composition and feeding incidence: environmental and ontogenetic influences. *California Fish and Game* 88:149–164.
- Nobriga, M. and F. Feyrer. 2007. Shallow-water piscivore-prey dynamics in the Sacramento-San Joaquin Delta. *San Francisco Estuary and Watershed Science* 5(2). Available at: <http://escholarship.org/uc/item/387603c0>.
- Nobriga, M., F. Feyrer, R. Baxter, and M. Chotkowski. 2005. Fish community ecology in an altered river delta: spatial patterns in species composition, life history strategies, and biomass. *Estuaries* 28:776–785.
- Nobriga, M.L., E. Loboschefskey, F. Feyrer. 2013. Common predator, rare prey: exploring juvenile striped bass predation on delta smelt in California's San Francisco Estuary. *Transactions of the American Fisheries Society* 142:1563–1575.
- Nobriga, M.L., T.R. Sommer, F. Feyrer, K. Fleming. 2008. Long-term trends in summertime habitat suitability for delta smelt, *Hypomesus transpacificus*. *San Francisco Estuary and Watershed Science* 6(1). Available at <http://escholarship.org/uc/item/5xd3q8tx>.
- NRC (National Research Council), 2012, Sustainable water and environmental management in the California Bay-Delta: National Research Council, The National Academies Press, Washington, DC.
- Null, S.E., J.H. Viers, M.L. Deas, S.K. Tanaka, and J.F. Mount. 2013. Stream temperature sensitivity to climate warming in California's Sierra Nevada: impacts to coldwater habitat. *Climatic Change* 116:149–170.
- Ogden, J.C., S.M. Davis, K.J. Jacobs, T. Barnes, and H.E. Fling. 2005. The use of conceptual ecological models to guide ecosystem restoration in South Florida. *Wetlands* 25:279–809.
- Opperman, J.J. 2012. A conceptual model for floodplains in the Sacramento-San Joaquin Delta. *San Francisco Estuary and Watershed Science* 10(3). Available at: <http://escholarship.org/uc/item/2kj52593>.
- Orlando, J.L., M. McWayne, C. Sanders, and M. Hladik. 2013. Dissolved pesticide concentrations in the Sacramento – San Joaquin Delta and Grizzly Bay, California, 2011-12. United States Geological Survey Data Series 779. 24 p.
- Oros, D.R., J.R.M. Ross, R.B. Spies, T. Mumley. 2006. Polycyclic aromatic hydrocarbon (PAH) contamination in San Francisco Bay: A 10-year retrospective of monitoring in an urbanized estuary. *Environmental Research* 105:101–118.
- Orsi, J.J. 1995. Food habits of several abundant zooplankton species in the Sacramento-San Joaquin Estuary. Interagency Ecological Program of the Sacramento-San Joaquin Estuary, Technical Report 41.
- Orsi, J.J. and W.L. Mecum. 1996. Food limitation as the probable cause of a long-term decline in the abundance of *Neomysis mercedis* the opossum shrimp in the Sacramento-San Joaquin estuary. Pages 375–401 in J.T. Hollibaugh, editor. *San Francisco Bay: the ecosystem*. American Association for the Advancement of Science. San Francisco, CA.
- Ostrach, D.J., J.M. Low-Marchelli, K.J. Eder, S.J. Whiteman, and J.G. Zinkl. 2008. Maternal transfer of xenobiotics and effects on larval striped bass in the San Francisco Estuary. *Proceedings of the National Academy of Sciences of the United States of America* 105:19354–19359.
- Pal, A., K.Y.-H. Gin, A.-Y. Lin, and M. Reinhard. 2010. Impacts of emerging organic contaminants on freshwater resources: Review of recent occurrences, sources, fate and effects. *Science of the Total Environment* 408:6062–6069.
- Paradis, A.R., P. Pepin, and J.A. Brown. 1996. Vulnerability of fish eggs and larvae to predation: review of the influence of the relative size of prey and predator. *Canadian Journal Fisheries and Aquatic Sciences* 53:1226–1235.
- Parker, A.E., R.C. Dugdale, and F. P. Wilkerson. 2012. Elevated ammonium concentrations from wastewater discharge depress primary productivity in the Sacramento River and the Northern San Francisco Estuary. *Marine Pollution Bulletin* 64:574–586.
- Pauly, D., V. Christensen, J. Dalsgaard, R. Froese, and F. Torres Jr. 1998. Fishing down marine food webs. *Science* 279:860–863.

- Peterson, M.S. 2003. Conceptual view of the environment-habitat-production linkages in tidal river estuaries: Reviews in Fisheries Science 11:291–313.
- Pimm, S.L. 1984. The complexity and stability of ecosystems. Nature 307:321–326.
- Platt, J.R. 1964. Strong inference. Science 146:347–353.
- Poole, G.C. and C.H. Berman. 2001. An ecological perspective on in-stream temperature: natural heat dynamics and mechanisms of human-caused thermal degradation. Environmental Management 27:787–802.
- Popper, K. 1959. The logic of scientific discovery, English edition, Hutchinson & Co.
- Puccia, C.J. and R. Levins. 1991. Qualitative modeling in ecology: Loop analysis, signed digraphs and time averaging. Pages 119–143 in P.A. Fishwick and P.A. Luker, editors. Qualitative simulation modeling and analysis. Springer-Verlag, New York.
- Puget Sound Partnership Science Panel 2012. Priority science for restoring and protecting Puget Sound: A biennial science work plan for 2011–2013. Puget Sound Partnership, Tacoma WA. Available at: http://www.psp.wa.gov/SP_biennium_work_plan_download.php.
- Quinn, J.F. and A.E. Dunham. 1983. On hypothesis testing in ecology and evolution. American Naturalist 122:602–617.
- Quist, M.C., W.A. Hubert, and F.J. Rahel. 2004. Relations among habitat characteristics, exotic species, and turbid-river cyprinids in the Missouri River drainage of Wyoming. Transactions of the American Fisheries Society 133:727–742.
- Radhaiah, V., M. Girija, and K.J. Rao. 1987. Changes in selected biochemical parameters in the kidney and blood of the fish, *Tilapia mossambica* (Peters), exposed to heptachlor. Bulletin of Environmental Contamination and Toxicology 39:1006–1011.
- Radke, L.D. 1966. Distribution of smelt, juvenile sturgeon, and starry flounder in the Sacramento-San Joaquin Delta with observations of food of sturgeon. Pages 115–129 in J.L. Turner and D.W. Kelley, editors. Ecological Studies of the Sacramento-San Joaquin Delta Part II: Fishes of The Delta, Fish Bulletin 136.
- Reclamation (U.S. Bureau of Reclamation). 2011. Adaptive management of fall outflow for delta smelt protection and water supply reliability. U.S. Bureau of Reclamation, Sacramento, CA. Available at: <http://www.usbr.gov/mp/BayDeltaOffice/docs/Adaptive%20Management%20of%20Fall%20Outflow%20for%20Delta%20Smelt%20Protection%20and%20Water%20Supply%20Reliability.pdf>.
- Reclamation (U.S. Bureau of Reclamation). 2012. Adaptive management of fall outflow for delta smelt protection and water supply reliability. U.S. Bureau of Reclamation, Sacramento, CA. Available at: http://deltacouncil.ca.gov/sites/default/files/documents/files/Revised_Fall_X2_Adaptive_MgmtPlan_EVN_06_29_2012_final.pdf.
- Reed, D., J.T. Hollibaugh, J. Korman, E. Peebles, K. Rose, P. Smith, P. Montagna. Workshop on Delta outflows and related stressors: panel summary report. Report to the Delta Science Program, Sacramento, CA. Available at: <http://deltacouncil.ca.gov/sites/default/files/documents/files/Delta-Outflows-Report-Final-2014-05-05.pdf>.
- Relyea, R.A. and K. Edwards. 2010. What doesn't kill you makes you sluggish: How sublethal pesticides alter predator-prey interactions. Copeia 2010:558–567.
- Reyes, R., Z. Sutphin, and B. Bridges. 2012. Effectiveness of fine mesh screening a holding tank in retaining larval and juvenile fish at the Tracy Fish Collection Facility. Tracy Fish Collection Facility Studies. Tracy Technical Bulletin 2012-1. U.S. Bureau of Reclamation, Mid-Pacific Region and Denver Technical Service Center. 20 pp.
- Riar, N., J. Crago, W. Jiang, L.A. Maryoung, J. Gan, D. Schlenk. 2013. Effects of salinity acclimation on the endocrine disruption and acute toxicity of bifenthrin in freshwater and euryhaline strains of *Oncorhynchus mykiss*. Environmental Toxicology and Chemistry 32:2779–2785.
- Ricker, W.E. 1954. Stock and recruitment. Journal of the Fisheries Board of Canada, 11(5), 559–623.
- Ricker, W.E. 1975. Computation and interpretation of biological statistics of fish populations. Bulletin of the Fisheries Research Board of Canada 191:1–382.
- Rodriguez, M.A. and W.M. Lewis. 1997. Structure of fish assemblages along environmental gradients in floodplain lakes of the Orinoco River. Ecological Monographs 67:109–128.

- Rollwagen-Bollens, G.C. and D.L. Penry. 2003. Feeding dynamics of *Acartia* spp. copepods in a large, temperate estuary (San Francisco Bay, CA). *Marine Ecology Progress Series* 257:139–158.
- Rose, K., J. Anderson, M. McClure, G. Ruggerone. 2011. Salmonid integrated life cycle models workshop report of the Independent Workshop Panel. Delta Science Program. Available at http://deltacouncil.ca.gov/sites/default/files/documents/files/Salmonid_ILCM_workshop_final_report.pdf.
- Rose, K.A., J.H. Cowan, K.O. Winemiller, R.A. Myers, and R. Hilborn. 2001. Compensatory density-dependence in fish populations: importance, controversy, understanding, and prognosis. *Fish and Fisheries* 2:293-327.
- Rose, K.A., W.J. Kimmerer, K.P. Edwards, and W.A. Bennett. 2013a. Individual-based modeling of delta smelt population dynamics in the upper San Francisco Estuary: I. Model description and baseline results. *Transactions of the American Fisheries Society* 142:1238–1259.
- Rose, K.A., W.J. Kimmerer, K.P. Edwards, and W. A. Bennett. 2013b. Individual-based modeling of delta smelt population dynamics in the upper San Francisco Estuary: II. Alternative baselines and good versus bad years: *Transactions of the American Fisheries Society* 142:1260–1272.
- Ruhl, C.A., and D.H. Schoellhamer. 2004. Spatial and temporal variability of suspended-sediment concentrations in a shallow estuarine environment. *San Francisco Estuary and Watershed Science* 2(2). Available at <http://escholarship.org/uc/item/1g1756dw>.
- San Joaquin River Group Authority. 2013. 2011 Annual technical report: On implementation and monitoring of the San Joaquin River Agreement and the Vernalis Adaptive Management Plan (VAMP). Prepared by San Joaquin River Group Authority for the California State Water Resource Control Board in compliance with D-1641. 188 p. Available at: <http://www.sjrg.org/technicalreport/default.htm>.
- Schoellhamer, D.H. 2001. Influence of salinity, bottom topography, and tides on locations of estuarine turbidity maxima in northern San Francisco Bay. Pages 343–357 in W.H. McAnally, and A.J. Mehta, editors. *Coastal and Estuarine Fine Sediment Transport Processes*. Elsevier Science B.V. Available at: <http://ca.water.usgs.gov/abstract/sfbay/elsevier0102.pdf>.
- Schoellhamer, D.H. 2011. Sudden clearing of estuarine waters upon crossing the threshold from transport to supply regulation of sediment transport as an erodible sediment pool is depleted: San Francisco Bay, 1999. *Estuaries and Coasts* 34:885–899.
- Schoellhamer, D.H., S.A. Wright, and J.Z. Drexler. 2012. Conceptual model of sedimentation in the Sacramento – San Joaquin River Delta. *San Francisco Estuary and Watershed Science* 10(3). Available at: <http://www.escholarship.org/uc/item/2652z8sq>.
- Schoellhamer, D.H., S.A. Wright, J.Z. Drexler. 2013. Adjustment of the San Francisco estuary and watershed to decreasing sediment supply in the 20th century. *Marine Geology* 345:63–71. <http://dx.doi.org/10.1016/j.margeo.2013.04.007>.
- Scholz, N.L., E. Fleishman, L. Brown, I. Werner, M.L. Johnson, M.L. Brooks, C.L. Mitchelmore, and D. Schlenk. 2012. A perspective on modern pesticides, pelagic fish declines, and unknown ecological resilience in highly managed ecosystems. *Bioscience* 62:428–434.
- Schwartz, M., G. Luikart, and R. Waples. 2007. Genetic monitoring as a promising tool for conservation and management. *Trends in Ecology and Evolution* 22:25–33
- SFEI. 2007. *The pulse of the estuary: Monitoring and management water quality in the San Francisco Estuary*. San Francisco Estuary Institute, Oakland, CA.
- Shellenbarger, G.G., and D.H. Schoellhamer. 2011. Continuous salinity and temperature data from San Francisco Bay, California, 1982-2002: Trends and the freshwater-inflow relationship. *Journal of Coastal Research* 27:1191–1201.
- Shoji, J., E.W. North, and E.D. Houde. 2005. The feeding ecology of *Morone americana* larvae in the Chesapeake Bay estuarine turbidity maximum: the influence of physical conditions and prey concentrations. *Journal of Fish Biology* 66:1328–1341.
- Silva, E., N. Rajapakse, and A. Kortenkamp. 2002. Something from “nothing”— eight weak estrogenic chemicals combined at concentrations below NOECs produce significant mixture effects. *Environmental Science and Technology* 36:1751–1756.

- Sirois, P., and J.J. Dodson. 2000a. Influence of turbidity, food density and parasites on the ingestion and growth of larval rainbow smelt *Osmerus mordax* in an estuary turbidity maximum. *Marine Ecological Progress Series* 193:167–179.
- Sirois, P., and J.J. Dodson. 2000b. Critical periods and growth-dependent survival of larvae of an estuarine fish, the rainbow smelt *Osmerus mordax*. *Marine Ecological Progress Series* 203:233–245.
- Slater, S. B., and R. D. Baxter. 2014. Diet, prey selection and body condition of age-0 Delta Smelt, *Hypomesus transpacificus*, in the upper San Francisco Estuary. *San Francisco Estuary and Watershed Science* 12(3):23.
- Smalling, K.L., K.M. Kuivila, J.L. Orlando, B.M. Phillips, B.S. Anderson, K. Siegler, J.W. Hunt, and M. Hamilton. 2013. Environmental fate of fungicides and other current-use pesticides in a central California estuary. *Marine Pollution Bulletin* 73:114–153.
- Sobczak, W.V., J.E. Cloern, A.D. Jassby, B.E. Cole, T.S. Schraga, and A. Arnsberg. 2005. Detritus fuels ecosystem metabolism but not metazoan food webs in San Francisco estuary's freshwater Delta. *Estuaries* 28:124–137.
- Sobczak, W.V., J.E. Cloern, A.D. Jassby, and A.B. Muller-Solger. 2002. Bioavailability of organic matter in a highly disturbed estuary: The role of detrital and algal resources. *Proceedings of the National Academy of Sciences of the United States of America* 99:8101–8105.
- Sogard, S.M. 1997. Size-selective mortality in the juvenile stage of teleost fishes: A review. *Bulletin of Marine Science* 60:1129–1157.
- Sommer, T., and F. Mejia. 2013. A place to call home: a synthesis of delta smelt habitat in the upper San Francisco Estuary. *San Francisco Estuary and Watershed Science* 11(2). Available at: <http://www.escholarship.org/uc/item/32c8t244>.
- Sommer, T., C. Armor, R. Baxter, R. Breuer, L. Brown, M. Chotkowski, S. Culberson, F. Feyrer, M. Gingras, B. Herbold, W. Kimmerer, A. Mueller-Solger, M. Nobriga, and K. Souza. 2007. The collapse of pelagic fishes in the upper San Francisco Estuary. *Fisheries* 32(6):270–277.
- Sommer, T., F. Mejia, M. Nobriga, F. Feyrer, and L. Grimaldo. 2011. The spawning migration of delta smelt in the upper San Francisco Estuary. *San Francisco Estuary and Watershed Science* 9(2). Available at: <http://www.escholarship.org/uc/item/86m0g5sz>.
- Souza, K. 2002. Revision of California Department of Fish and Game's Spring midwater trawl and results of the 2002 Spring Kodiak trawl. *IEP Newsletter* 15(3):44–47.
- Stevens, D.E. 1963. Food habits of striped bass, *Roccus saxatilis* (Walbaum) in the Sacramento-Rio Vista area of the Sacramento River. Master's Thesis. University of California, Berkeley, CA.
- Stevens, D.E. 1966. Food habits of striped bass, *Roccus saxatilis*, in the Sacramento-San Joaquin Delta. Pages 97–103 in J.T. Turner and D.W. Kelley, editors. *Ecological studies of the Sacramento-San Joaquin Delta, part II, fishes of the delta*. California Department of Fish and Game Fish Bulletin 136.
- Stevens, D.E. 1977. Striped bass (*Morone saxatilis*) monitoring techniques in the Sacramento-San Joaquin Estuary. Pages 91–109 in W. Van Winkle, editor. *Assessing the effects of power-plant-induced mortality on fish populations*. Pergamon Press, Gatlinburg, Tennessee.
- Swanson, C., T. Reid, P.S. Young, and J.J. Cech, Jr. 2000. Comparative environmental tolerances of threatened delta smelt (*Hypomesus transpacificus*) and introduced wakasagi (*H. nipponensis*) in an altered California estuary. *Oecologia* 123:384–390.
- Sweetnam, D.A. 1999. Status of delta smelt in the Sacramento-San Joaquin Estuary. *California Fish and Game* 85:22–27.
- Sweetnam, D.A., and D.E. Stevens. 1993. Report to the Fish and Game Commission: a status review of the delta smelt (*Hypomesus transpacificus*) in California. 68 p. plus appendices.
- SWRCB. 2010. Final 2008–2010 Clean Water Act Section 303(d) List of Water Quality Limited Segments (Region 5). State Water Resources Control Board (SWRCB). Sacramento, California. Available at: http://www.waterboards.ca.gov/water_issues/programs/tmdl/integrated2010.shtml.
- Takasuka, A., I. Aoki, and I. Mitani. 2003. Evidence of growth-selective predation on larval Japanese anchovy *Engraulis japonicus* in Sagami Bay. *Marine Ecology Progress Series* 252:223–238.

- Thom, R. 2000. Adaptive management of coastal ecosystem restoration projects. *Ecological Engineering* 15:365–372.
- Thomas, J.L. 1967. The diet of juvenile and adult striped bass, *Morone saxatilis*, in the Sacramento-San Joaquin River system. *California Fish and Game* 53(1):49–62.
- Thompson, J.K. 2005. One estuary, one invasion, two responses: phytoplankton and benthic community dynamics determine the effect of an estuarine invasive suspension feeder. Pages 291–316 in S. Olenin and R. Dame, editors. *The comparative roles of suspension feeders in ecosystems*. Springer, Amsterdam.
- Thomson, B., R. Hoenicke, J.A. Davis, and A. Gunther. 2000. An overview of contaminant – related issues identified by monitoring in San Francisco Bay. *Environmental Monitoring and Assessment* 64:409–419.
- Thomson, J.R., W.J. Kimmerer, L.R. Brown, K.B. Newman, R. Mac Nally, W.A. Bennett, F. Feyrer, and E. Fleishman. 2010. Bayesian change-point analysis of abundance trends for pelagic fishes in the upper San Francisco Estuary. *Ecological Applications* 20:1431–1448.
- Thurston, R.V., R.C. Russo, and G.A. Vinogradov. 1981. Ammonia toxicity to fishes. Effect of pH on the toxicity of the un-ionized ammonia species. *Environmental Science and Technology* 15:837–840.
- Touzeau, S., and G.L. Gouze. 1998. On the stock-recruitment relationships in fish population models. *Environmental Modeling and Assessment* 3:87–93.
- Townend, I.H. 2004. Identifying change in estuaries. *Journal of Coastal Conservation* 10:5–12.
- Turner, J.L. 1966a. Distribution and food habits of centrarchid fishes in the Sacramento-San Joaquin Delta. Pages 144–153 in J.L. Turner and D.W. Kelley, editors. *Ecological studies of the Sacramento-San Joaquin Delta Part II: Fishes of the Delta*, Fish Bulletin 136.
- Turner, J.L. 1966b. Distribution and food habits of ictalurid fishes in the Sacramento-San Joaquin Delta. Pages 130–143 in J.L. Turner and D.W. Kelley, editors. *Ecological studies of the Sacramento-San Joaquin Delta Part II: Fishes of The Delta*, Fish Bulletin 136.
- Turner, J.L. and H.K. Chadwick. 1972. Distribution and abundance of young-of-the-year striped bass, *Morone saxatilis*, in relation to river flow in the Sacramento-San Joaquin Estuary. *Transactions of the American Fisheries Society* 101:442–452.
- USFWS (United States Fish and Wildlife Service). 2008. Formal Endangered Species Act consultation on the proposed coordinated operations of the Central Valley Project (CVP) and State Water Project (SWP). U.S. Fish and Wildlife Service, Sacramento, CA.
- USGS (U.S. Geological Survey). 2008. Tracking organic matter in Delta drinking water. Science action: News from the CALFED Science Program. CALFED Science Program Sacramento, CA.
- Van Nieuwenhuysse, E. 2007. Response of summer chlorophyll concentration to reduced total phosphorus concentration in the Rhine River (Netherlands) and the Sacramento–San Joaquin Delta (California, USA). *Canadian Journal of Fisheries and Aquatic Sciences* 64:1529–1542.
- Vandermeer, J. 2013. Forcing by rare species and intransitive loops creates distinct bouts of extinction events conditioned by spatial pattern in competition communities. *Theoretical Ecology* 6:395–404.
- Vannote, R.L. and B.W. Sweeney. 1980. Geographic analysis of thermal equilibria: a conceptual model for evaluating the effect of natural and modified thermal regimes on aquatic insect communities. *The American Naturalist* 115:667–695.
- Wadsworth, K., and T. Sommer. 1996. Should the delta smelt summer tow-net index be size-standardized? *IEP Newsletter* 8(2):24–26.
- Wagner, R.W. 2012. Temperature and tidal dynamics in a branching estuarine system. Ph.D. dissertation. University of California, Berkeley, CA.
- Wagner, R.W., M. Stacey, L.R. Brown, and M. Dettinger. 2011. Statistical models of temperature in the Sacramento–San Joaquin Delta under climate-change scenarios and ecological implications. *Estuaries and Coasts* 34:544–556.
- Walter, H., F. Consolaro, P. Gramatica, and M. Altenburger. 2002. Mixture toxicity of priority pollutants at no observed effect concentrations (NOECs). *Ecotoxicology* 11:299–310.

- Walters, C.J., and R. Hilborn, R. 1978. Ecological optimization and adaptive management. *Annual Review of Ecology and Systematics* 9:157–188.
- Walters, C.J., and F. Juanes. 1993. Recruitment limitation as a consequence of natural selection for use of restricted feeding habitats and predation risk taking by juvenile fishes. *Canadian Journal of Fisheries and Aquatic Sciences* 50:2058–2070.
- Wang, J.C.S. 1986. Fishes of the Sacramento-San Joaquin Estuary and adjacent waters, California: A guide to the early life histories. Interagency Ecological Program of the Sacramento-San Joaquin Estuary, Technical Report 9.
- Wang, J.C.S. 1991. Early life stages and early life history of the delta smelt, *Hypomesus transpacificus*, in the Sacramento-San Joaquin estuary with comparison of early life stages of the longfin smelt, *Spirinchus thaleichthys*. U.S. Army Corps of Engineers, Technical Report FS/BIO-IATR/91-28.
- Wang, J.C.S. 2007. Spawning, early life stages and early life histories of the Osmerids found in the Sacramento-San Joaquin Delta of California. U.S. Department of the Interior, Bureau of Reclamation, Mid-Pacific Region, Byron, California. Tracy Fish Facilities Studies, Volume 38, 72 p. plus appendices.
- Warner, J.C., D.H. Schoellhamer, C.A. Ruhl, and J.R. Burau. 2004. Floodtide pulses after low tides in shallow subembayments adjacent to deep channels. *Estuarine, Coastal and Shelf Science* 60:213–228.
- Washington State Academy of Sciences. Committee on Puget Sound Indicators. 2012. Sound indicators: A review for the Puget Sound Partnership. Washington State Academy of Sciences, Olympia, WA. Available at: http://www.washacad.org/about/files/WSAS_Sound_Indicators_wv1.pdf.
- Walters, C., & Korman, J. (1999). Linking recruitment to trophic factors: revisiting the Beverton–Holt recruitment model from a life history and multispecies perspective. *Reviews in Fish Biology and Fisheries*, 9(2), 187–202.
- Werner, I., L. Deanovic, D. Markiewicz, M. Stillway, N. Offer, R. Connon, and S. Brander. 2008. Pelagic Organism Decline (POD): Acute and chronic invertebrate and fish toxicity testing in the Sacramento-San Joaquin Delta 2006–2007. Final Report. U.C. Davis–Aquatic Toxicology Laboratory, Davis, California.
- Werner, I., L.A. Deanovic, D. Markiewicz, J. Khamphanh, C.K. Reece, M. Stillway, and C. Reece. 2010a. Monitoring acute and chronic water column toxicity in the northern Sacramento-San Joaquin Estuary, California, USA, using the euryhaline amphipod, *Hyalella azteca*: 2006–2007. *Environmental Toxicology and Chemistry* 29:2190–2199.
- Werner, I., D. Markiewicz, L. Deanovic, R. Connon, S. Beggel, S. Teh, M. Stillway, C. Reece. 2010b. Pelagic Organism Decline (POD): Acute and chronic invertebrate and fish toxicity testing in the Sacramento-San Joaquin Delta 2008–2010, Final Report. U.C. Davis–Aquatic Toxicology Laboratory, Davis, California.
- Weston, D., A.M. Asbell, S.A. Lesmeister, S.J. Teh, and M.J. Lydy. 2014. Urban and agricultural pesticide inputs to a critical habitat for the threatened Delta Smelt (*Hypomesus transpacificus*). *Environmental Toxicology and Chemistry* 33: 920–929.
- Weston, D.P. and M.J. Lydy. 2010. Urban and agricultural sources of pyrethroid insecticides to the Sacramento-San Joaquin Delta of California. *Environmental Science and Technology* 44:1833–1840.
- Weston, D.P., A.M. Asbell, S.A. Lesmeister, S.J. Teh, and M.J. Lydy. 2012. Urban and agricultural pesticide inputs to a critical habitat for the threatened delta smelt (*Hypomesus transpacificus*). Final report to the POD Management Team of the Interagency Ecological Program for the San Francisco Estuary.
- Weston, D.P., H.C. Poynton, G.A. Wellborn, M.J. Lydy, B.J. Blalock, M.S. Sepulveda, and J.K. Colbourne. 2013. Multiple origins of pyrethroid insecticide resistance across the species complex of a nontarget aquatic crustacean, *Hyalella azteca*. *Proceedings of the National Academy of Sciences of the United States of America*. 110:16532–16537
- Whipple, A.A., R.M. Grossinger, D. Rankin, B. Stanford, and R. Askevold. 2012. Sacramento-San Joaquin Delta historical ecology investigation: Exploring pattern and process. San Francisco Estuary Institute, Richmond, CA.
- Whitfield, A.K. 1999. Ichthyofaunal assemblages in estuaries: A South African case study. *Reviews in Fish Biology and Fisheries* 9:151–186.
- Wilkerson F.P., R.C. Dugdale, V.E. Hogue, and A. Marchi. 2006. Phytoplankton blooms and nitrogen productivity in San Francisco Bay. *Estuaries and Coasts* 29:401–416.

- Williams, B.K. 2011. Passive and active adaptive management: Approaches and an example. *Journal of Environmental Management* 92:1371–1378.
- Wilson E.O. 1998. *Consilience: The unity of knowledge*. Alfred A. Knopf. 322 p.
- Winder, M., and A.D. Jassby. 2011. Shifts in zooplankton community structure: Implications for food-web processes in the upper San Francisco Estuary. *Estuaries and Coasts* 34:675–690
- Winder, M., A. Jassby and R. McNally. 2011. Synergies between climate anomalies and hydrological modifications facilitate estuarine biotic invasions. *Ecology Letters* 14:749–757.
- Winemiller, K.O. and K.A. Rose. 1992. Patterns of life-history diversification in North-American fishes implications for population regulation *Canadian Journal of Fisheries and Aquatic Sciences* 49:2196–2218.
- Wood, S.A., P.T. Holland, L. MacKenzie. 2011. Development of solid phase adsorption toxin tracking (SPATT) for monitoring anatoxin-a and homoanatoxin-a in river water. *Chemosphere* 82:888–894.
- Wright, S.A., and D.H. Schoellhamer. 2004. Trends in the sediment yield of the Sacramento River, California, 1957-2001. *San Francisco Estuary and Watershed Science* 2(2). Available at: <http://escholarship.org/uc/item/891144f4>.
- Wurtsbaugh, W., and H. Li. 1985. Diel migrations of a zooplanktivorous fish (*Menidia beryllina*) in relation to the distribution of its prey in a large eutrophic lake. *Limnology and Oceanography* 30:565–576.
- Xu, Y., J. Gan, and F. Spurlock. 2008. Effect of aging on desorption kinetics of sediment-associated pyrethroids. *Environmental Toxicology and Chemistry* 27:1293–1301.
- York, J.K., B.A. Costas and G.B. McManus. 2010. Microzooplankton grazing in green water—results from two contrasting estuaries. *Estuaries and Coasts* 34:373–385.

Appendix A: How the Delta Smelt MAST Report was Written

The report titled “An updated conceptual model for Delta Smelt: our evolving understanding of an estuarine fish” (hereafter referred to as Delta Smelt MAST report) was written in 2013-2014 by the IEP Management, Analysis, and Synthesis Team (MAST). The Delta Smelt MAST report was developed through a series of report drafts and a public technical review and followed a set of general report guidelines. This report appendix describes the Delta Smelt MAST report guidelines, the report review and revisions, and report milestones.

Delta Smelt MAST Report Guidelines

Report Purpose and Approach

The Delta Smelt MAST report is a technical report intended to synthesize the latest scientific data and information on Delta Smelt, a topic of particularly high relevance to agency managers and decision makers in California. Specifically, it provides an up to date assessment and conceptual model of factors affecting Delta Smelt throughout its primarily annual life cycle and demonstrates how the conceptual model can be used in science and management. The Delta Smelt MAST report updates and redesigns previous conceptual models for Delta Smelt with new data and information since the release of the last synthesis report about the “Pelagic Organism Decline” (POD) by the Interagency Ecological Program (IEP) in 2010. It then uses the conceptual model to generate hypotheses about the factors that may have contributed to the 2011 increase in

Delta Smelt abundance and evaluate them using a simple comparative approach. The Delta Smelt MAST report ends with key conclusions, a discussion of our hypothesis testing approach, and recommendations for future work and adaptive management applications, with examples.

1. **Report Development.** The 2014 MAST report is a synthesis report developed and written by the IEP Management, Analysis, and Synthesis Team (MAST). The MAST is co-chaired by the IEP Lead Scientist and IEP Program Manager and includes senior scientists from IEP member agencies tasked with data analysis, synthesis, and work planning. The MAST report is the collective product of a dynamic and collaborative interagency team process involving focused team discussions at monthly MAST meetings, intensive conceptual model and report development at additional multi-day off-site meetings, presentations and discussions with other scientists, stakeholders, and the public (e.g., at the annual IEP workshop, meetings of the IEP Stakeholder Group and IEP Project Work Teams), and data analysis and synthesis as well as writing, integration, and revisions of report sections by MAST members with written communication via email and the MAST wiki. MAST report authors were expected to follow the MAST report guidelines described here. They were also expected to consider all internal review comments by other MAST members and members of the IEP Management and Coordinators teams as well as external technical review comments received during a 40-day public review period. Details about the public review process are given in II.
2. **Report Authorship.** The “author of record” for the 2013 MAST report is the entire IEP MAST, and the responsibility for authorship lies with the entire MAST as well. Individual authorship of report sections is not credited; the report is a product of the IEP MAST and not of any individual author or an individual IEP member agency. All current MAST members are MAST report authors and are listed alphabetically in the initial pages of the report (see III. below). Former MAST members will not be listed as authors, but will be noted as contributors. Each report section had a lead author who had primary responsibility for writing and revising the section. One designated MAST member (Larry Brown, USGS) functioned as report lead editor who compiled and integrated all sections and sent full draft report versions to the MAST for review by all MAST members. All MAST members sent their edits and comments back to Larry Brown and the section authors for revisions. The report went through multiple draft versions before its finalization.
3. **Report Organization.** The 2014 MAST report is an IEP technical report and follows the same basic organization as other IEP technical reports, including a title page, list of all authors, acknowledgements, table of contents, executive summary, an introductory section with background information and report objectives, and concise sections detailing the analysis and synthesis approach, models and hypotheses, findings, and conclusions as well as illustrative tables, figures, and full references for all citations. In response to reviewer recommendations received during the public technical review (see II.), the report was restructured and expanded from originally six to nine Chapters.
4. **Supporting Evidence.** The 2014 MAST report follows the conventions of IEP and other technical reports regarding supporting evidence, which includes the following. The rationale for any findings, conclusions, and recommendations should be fully explained in the report. Whenever possible, conceptual models and hypotheses should be evaluated through analysis of the available data. Additional supporting information should be obtained from the peer-reviewed literature or from publicly accessible reports. Related or competing hypotheses and models that have been previously published in the peer-

reviewed literature should be acknowledged and discussed in the report and conclusions should be based on even-handed, dispassionate consideration of all available evidence. Sources for all supporting data and information should be clearly identified and cited. Citation of personally communicated unpublished results (e.g. emails, memos) is permissible, but should be used sparingly.

Delta Smelt MAST Report Review and Revisions

1. **What was the purpose of the review?** The purpose of the public technical review of the draft Delta Smelt MAST report was to ensure its scientific credibility, relevance to managers and decision makers, and a transparent and legitimate process that welcomed and considered input and recommendations from other scientists, managers, stakeholders, and the public.
2. **What was expected of draft Delta Smelt MAST report reviewers?** MAST report reviewers were asked to provide written comments on any and all technical aspects of the draft report, but to pay particular attention to review criteria outlined in the MAST report review guidelines.¹
3. **Who reviewed the draft Delta Smelt MAST report?** The draft Delta Smelt MAST report released for public review on July 23, 2014, was reviewed by invited IEP staff and colleagues as well as by invited external peer reviewers and other scientists who submitted comments during the 40-day public review period, as follows.
 - a. IEP Coordinators (1 Reviewer, IEP management review)
 - b. Former MAST Members (2 Reviewers, IEP colleague scientific peer review)
 - c. Invited Subject Area Expert (1 Reviewer, IEP colleague review of contaminants sections)
 - d. Independent Scientific Peer Reviewers (3 Reviewers, external independent scientific peer review facilitated by the Delta Science Program)
 - e. Other Scientists, Stakeholders and the Public (7 Reviewers, external public review)

In addition, the IEP Coordinators were asked to review the revised, near-final version of the Delta Smelt MAST report and the executive summary and to approve the final version. The IEP Directors were briefed and invited to comment on the direction and progress of the Delta Smelt MAST report on a quarterly basis.

4. **How were external draft Delta Smelt MAST report reviewers identified, invited, and informed?** Independent Scientific Peer Reviewers for the draft Delta Smelt MAST report were identified by the Delta Stewardship Council's Delta Science Program (DSP) and Delta Lead Scientist. In accordance with the DSP "Procedures for Independent Scientific Peer Review,"² the Delta Lead Scientist determined and invited the independent scientific peer reviewers using the following selection criteria: standing in the scientific community, expertise relevant to the documents being reviewed, and free of conflict of interest.

¹ http://www.water.ca.gov/iep/docs/mast_report_process_july2013.pdf

² <http://deltacouncil.ca.gov/docs/2012-11-06/delta-science-program-procedures-conducting-independent-scientific-peer-review>

All other review was invited by email and in a notice posted on the IEP website.³ A draft of the 2013 MAST report, associated figures, and MAST report review guidelines were posted on July 23, 2013, for public technical review. The draft report release for review did not include an executive summary and conclusions. The public review period closed on August 31, 2013.

5. **How many review comments were received and where can they be accessed?** The MAST received 14 sets of review comments on the July 2013 draft MAST report. They included many general comments as well as 355 comments that referred to specific lines in the report, see table A1. All comments by external reviewers (public review comments and the review comments by the three independent scientific peer reviewers) were posted on the IEP website.⁴

6. **How were the review comments addressed?** All review comments received during the 40-day review period were compiled in an Excel spreadsheet and summarized numerically (Table A1). Review comments and procedures for addressing them were discussed by the MAST at its regular monthly meetings and during a one-day offsite meeting in November 2013. The process for addressing review comments included the following:
 - a. The lead author for each report section had the primary responsibility for addressing review comments pertaining to that section and for revising the section.
 - b. Secondary revision leads were also assigned and assisted the primary revision lead.
 - c. For each review comment in the Excel spreadsheet, it was noted whether the comment: (1) Did not suggest a revision and no revision was made; (2) Suggested a revision and a revision was made; or (3) Suggested a revision, but no revision was made, for example because it was outside of the report scope, explained elsewhere, or the lead author did not agree with the recommended revision.
 - d. Revised sections and the annotated excel spreadsheet were sent by email to the entire MAST. MAST members were alerted to all major revisions.
 - e. Major revisions were discussed with all MAST members during MAST meetings and via email.
 - f. Decisions about major revisions were made by the whole MAST; no comment implied consent.
 - g. Decisions about more minor revisions were made by the section revision leads and the report lead editor, often in consultation with some or all other MAST members.
 - h. The report lead editor (Larry Brown, USGS) compiled, further revised, and integrated all revised report sections and sent full draft report versions to the MAST for review by all MAST members. The final draft versions of the report and executive summary were also sent to the IEP coordinators for their review and approval.

³ <http://www.water.ca.gov/iep/pod/mast.cfm>

⁴ <http://www.water.ca.gov/iep/pod/mast.cfm>

Table A1. Numerical summary of review comments for the July 2013 draft MAST report.

2013 Draft MAST Report Review Comment Set #	Total Number of Comment Pages	Total Number of References and Attachment Pages	Total Number of Pages	Total Number of Specific Comments (by Line)
1-Public: Academia	3		3	19
2-Public: Academia	2		2	10
3-Public: Waste Discharge	4		4	11
4-Public: Fishing	27	27	54	29
5-Public: Water Supply	39	188	227	43
6-Public: Water Supply	2		2	7
7-Public: Water Supply	10	1	11	30
<i>All Public Reviews</i>	87	216	303	149
8-Former MAST member	6		6	58
9-Former MAST member	1	286	287	57
10-Subject Area Expert	4		4	24
11-IEP Coordinator	2		2	21
12-Academic (DSP)	4		4	0
13-Academic (DSP)	5		5	24
14-Academic (DSP)	7		7	22
<i>All Other Reviews To Date</i>	29	286	315	206
<i>All Reviews To Date</i>	116	502	618	355

7. **What major changes were made to the draft report in response to review comments?** The draft Delta Smelt MAST report underwent several major changes in response to review comments. Changes include the following:
- a. The report purpose and goals were reconsidered, clarified, and somewhat expanded. Specifically, the four-year comparison of factors that may have contributed to the Delta Smelt abundance increase in 2011 was deemphasized in favor of a broader assessment and conceptual model of factors affecting Delta Smelt throughout its primarily annual life cycle and demonstrations of how the conceptual model can be used in science and management.
 - b. The report structure was substantially changed to better fit the revised report purpose and goals and to improve the organization of the large amount of information included in the report. Four new Chapters were added to describe the updated conceptual model (Chapter 5), provide a more thorough overview of Delta Smelt life history and population dynamics (Chapter 6), summarize and discuss findings and conclusions (Chapter 8), and provide recommendations and examples of future work and management applications (Chapter 9). An executive summary was also added, along with this appendix.
 - c. The content of the report was expanded to accomplish the somewhat expanded report purpose and goals, reflect previously missing information pointed out by reviewers as well as new information from the latest scientific publications, and provide conclusions and recommendations for future work and management applications.
 - d. Several reviewers commented that the simple four-year comparative approach that was used to evaluate factors that may have contributed to the Delta Smelt abundance increase in 2011 was too limited and that more years of data and more in-depth analyses and modeling were needed for this evaluation. The MAST agreed, but decided that these types of analyses would require additional

time and resources and were outside the scope of this report which emphasized synthesis of existing information over new data analyses. Instead, the MAST decided to discuss some of the benefits and limitations of analysis and synthesis approaches used in the report in Chapter 8 and existing and ongoing analyses and modeling efforts along with additional, analysis, synthesis, modeling, and other science needs and potential management applications in Chapter 9. Three examples of additional mathematical modeling approaches are also included in Chapter 9. These approaches were explored by individual co-authors of this report. Preliminary results of these analyses are given for illustrative purposes only; peer-reviewed publications of these analyses need to be completed before they can be used to draw firm conclusions.

Delta Smelt MAST Report Milestones

Note: The time line for the development, review, revision and completion of the Delta Smelt MAST report had to be adjusted repeatedly because of numerous new work assignments for individual MAST members, the large number and depth of review comments, the federal government shut-down, personnel changes, etc.

2012

March 13-16 Initial MAST off-site meeting (Marconi Center, CA) to discuss MAST products and direction and start MAST work on the 2012 IEP proposal solicitation⁵, the “FLaSH” report⁶, and the Delta Smelt MAST report (hereafter MAST report)

Sep 13-14 MAST off-site meeting (Yolo Wildlife Area, CA)

Dec 4-5 MAST off-site meeting (Clarksburg, CA)

2013

March 29 First draft MAST report completed

April 24 MAST presentation (talk) at annual IEP Workshop (Larry Brown, USGS)

May 20 Second draft MAST report completed

June 6 Third draft MAST report completed

July 23 – Aug 31 Fourth draft MAST report completed and posted on the IEP website for a 40-day review period

August 14 Draft MAST report discussion with IEP Stakeholder Group

Sep 11 Special IEP Stakeholder Group meeting about the draft MAST report

Oct 30 MAST report poster presentation at 2013 State of the Estuary Conference

Nov 14 MAST off-site meeting (UC Davis, CA)

Dec 8 Fifth draft MAST report completed

⁵ <http://www.water.ca.gov/iep/archive/2012/solicitations.cfm>

⁶ <http://deltacouncil.ca.gov/science-program/fall-low-salinity-habitat-flash-studies-and-adaptive-management-plan-review-0>

2014

Feb 3	Sixth draft MAST report completed
Feb 11	MAST presentation (talk) at DSP-SWRCB “Delta Outflows” workshop (Larry Brown, USGS)
Feb 20	MAST presentation (talk) at a meeting of the IEP Resident Fishes Project Work Team (Larry Brown, USGS)
Feb 26	MAST presentation (talk) at annual IEP Workshop (Larry Brown, USGS)
April 16	Seventh draft MAST report completed
April 17	First draft MAST report executive summary completed
April 24	Second draft MAST report executive summary completed and sent to IEP Coordinators for review
May 15	Eight draft MAST report completed and sent to IEP Coordinators for a one-week “red flag” review. This draft includes the executive summary and a description of how the MAST report was written and revised with a list of major report revisions in response to review comments (Appendix A)
June 2	Ninth draft MAST report completed and sent to IEP Coordinators for review and IEP Directors briefings
June 11	IEP Coordinators briefed on MAST report including a review of the major changes.
June 17	Agencies and stakeholders of the CAMT Delta Smelt Scoping Team briefed about the MAST report including major findings and changes since 2013.
July 2	IEP Stakeholder Group meeting to discuss MAST report revisions and completion
July 3	Coordinators approve the final draft MAST report for publication as an IEP Technical Report; when ready the draft final report will be posted on the MAST webpage ⁷ until the IEP Technical Report publication is completed and report is posted on the IEP Technical Reports webpage ⁸
July 14	MAST model presented to IEP Wetlands Conceptual Model Team.
July 29	IEP Directors meeting with presentation and discussion of final MAST report
July 30	MAST model presented to IEP Wetlands Project Work Team.
August 6	MAST briefing to Drought Operations Plan Team

Appendix B: Calculation of Annual Abundance Indices

This Appendix describes the data and methods used by 4 long-term fish monitoring surveys for calculating annual abundance indices for Delta Smelt (*Hypomesus transpacificus*). Descriptions are arranged sequentially beginning with the Spring Kodiak Trawl, which calculates an index of abundance for adult Delta Smelt, followed by the 20 mm Survey, which calculates an index

⁷ <http://www.water.ca.gov/iep/pod/mast.cfm>

⁸ <http://www.water.ca.gov/iep/products/technicalrpts.cfm>

for late-stage larvae and small juveniles; the Summer Townet Survey calculates an index for juveniles and the Fall Midwater Trawl Survey calculates an index for sub-adults. As mentioned in the main document, abundance indices are not population estimates, but they are believed to increase monotonically with increases in true population size.

Spring Kodiak Trawl

The Department of Fish and Wildlife (DFW) initiated the Spring Kodiak Trawl Survey (SKT) in 2002. The SKT replaced the Spring Midwater Trawl and provided a more effective means to monitor the distribution and reproductive status of adult Delta Smelt. Survey results provide near real-time information on the proximity of adult Delta Smelt to south Delta export facilities and can provide an indication of likely spawning areas.

The SKT includes 5 monthly Delta-wide surveys, January through May (Figure 84). Only the first 4 surveys contribute to the annual abundance index. No index exists for 2002, when only 3 surveys were conducted. The index is calculated after all data have been verified for accuracy.

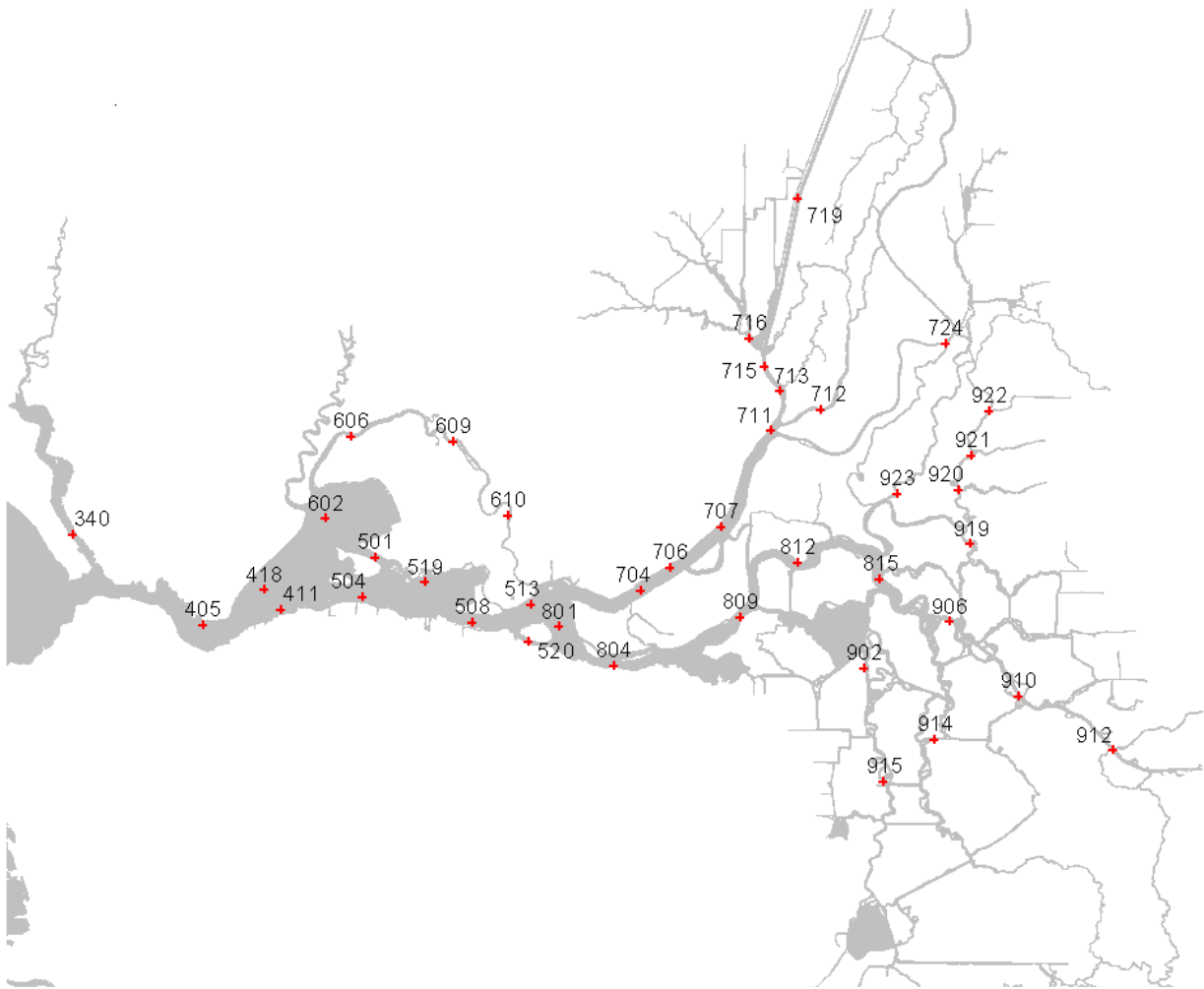
Field crews tow the net at the surface between 2 boats once for 10-min at each station per survey; 5-min surface tows are used at stations with historically high catch to limit excessive Delta Smelt take; a second 5-min surface tow is completed if Delta Smelt catch in the first tow did not exceed 50. A flow meter deployed at the start of the tow and retrieved at the end provides information on distance towed through the water. To calculate fish density, survey personnel assume that the SKT net fishes with the mouth fully opened, an area of 13.95 m² (7.62 m wide by 1.83 m deep). Volume filtered is the product of distance towed and mouth area. Volume filtered varies and by convention researchers expand catch per volume filtered (number per m³) for juvenile and adult fish to catch per 10,000 m³.

Annual abundance index calculations use adult Delta Smelt data from 39 of the 40 stations (Fig. 84). For each of the first 4 monthly surveys, adult catch per 10,000 m³ values from each station are grouped into 3 distinct regions based on geographic location: 1) the confluence and Suisun region (sites 340, 405, 411, 418, 501, 504, 508, 513, 519, 520, 602, 606, 609, 610, 801); 2) the Sacramento River and Cache Slough region (sites 704, 706, 707, 711, 712, 713, 715, 716, 719, 724); and 3) the San Joaquin River and Delta region (804, 809, 812, 815, 902, 906, 910, 912, 914, 915, 919, 920, 921, 922, 923). A monthly mean is calculated for each region and the sum of the regional means is the monthly or survey index. The sum of the 4 survey indices is the annual index.

20 mm Survey

DFW initiated the 20 mm Survey in 1995 to monitor the distribution and relative abundance of larval and juvenile Delta Smelt throughout their historical spring range in the upper San Francisco Estuary (Fig. 85), and provide near real-time information on the relative densities and proximities of these young fish to south Delta export pumps. The 20 mm Survey includes sampling on alternate weeks from mid-March through early July, typically resulting in 9 surveys per year. During each survey, field crews complete 3 oblique tows at each of the 47 stations (Fig. 85). The 20 mm Survey added stations over time, but not all contribute to annual abundance index calculation. The survey added 5 Napa River stations in 1996 for a total of 41 core stations, which are included in the annual abundance index calculations (Fig. 85, circles). In 2008, 6 non-

Figure 84. Map of Spring Kodiak Trawl Survey stations showing all currently sampled stations. Data from all stations except 719 are used in abundance index calculation.

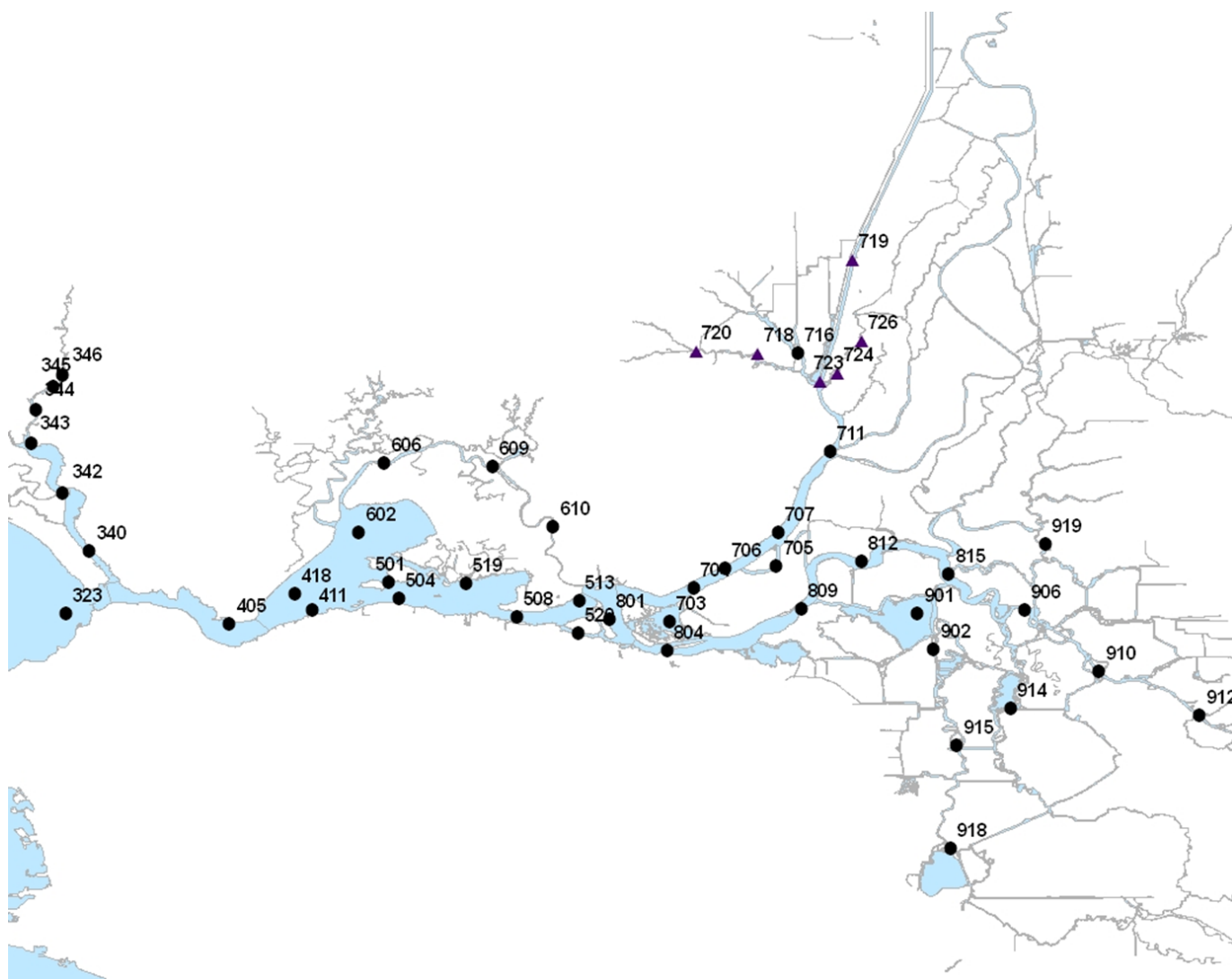


core stations were added, which are not included in the annual abundance index calculations, including Barker Slough (site 720), Lindsey Slough (site 718), Miner Slough (sites 724 and 726), and the Sacramento Deep Water Shipping Channel (n = 2; sites 719 and 723) (Fig. 85, triangles).

The 20 mm net includes a flow meter located within the mouth of the net to measure distance traveled by the net during the tow. This value is then multiplied by the fixed mouth area of the net (1.51 m²) to provide total volume filtered. The tows are then standardized to catch of Delta Smelt per 10,000 m³.

As already noted, the annual abundance index calculation uses only catch per 10,000 m³ values from the 41 index stations. For each survey, the mean fork length of Delta Smelt is calculated from measurements of the fish captured during each survey. The two surveys just before the average fork length reached 20 mm and the 2 surveys just after the average fork length reached 20 mm are included in the annual abundance index calculation. For these 4 surveys the geometric

Figure 85. Map of 20 mm survey stations showing all currently sampled stations. Data from all core stations are used in abundance index calculation.



mean of the catch of Delta Smelt per 10,000 m³ is calculated across the 41 core stations. The geometric mean for each survey is calculated as the arithmetic mean of $\log_{10}(x+1)$ -transformed values of Delta Smelt catch per 10,000 m³ across the 41 core stations. The resulting value is then back-transformed (including subtraction of 1) for the calculation of the annual abundance index. The annual abundance index is calculated as the sum of the geometric means of the 4 selected surveys.

Summer Townet Survey

The Summer Townet Survey (TNS) was started by DFW in 1959 to produce an annual index of summer abundance for age-0 Striped Bass (*Morone saxatilis*). In the mid-1990s, DFW staff developed an abundance index calculation for Delta Smelt. Annual abundance indices for Delta Smelt have been calculated for the period 1959 through the present, except for 1966-1968. The

TNS Survey samples 32 historic stations, 31 of which contribute to index calculation (labeled as “core stations,” Fig. 86). Currently sampled TNS stations range from eastern San Pablo Bay to Rio Vista on the Sacramento River and to Stockton on the San Joaquin River (Fig. 86). In 2011, TNS added 8 supplemental stations in the Cache Slough and the Sacramento River Deepwater Ship Channel region to increase spatial coverage and better describe Delta Smelt range and habitat (Fig. 86). Historically, TNS sampling began when age-0 Striped Bass achieved a mean fork length of 20 mm based on larval sampling, typically in mid-June to early July, and ended when age-0 Striped Bass surpassed a mean size of 38.1 mm fork length. Since 2003, TNS has consistently included 6 surveys annually, running on alternate weeks from early June through mid- to late August.

Field crews perform at least two 10-min oblique tows at most stations. A third tow is conducted when any fish were caught during either of the first 2 tows. At least 1 tow is completed at each of the new Cache Slough and Sacramento River Deepwater Ship Channel stations. To reduce Delta Smelt take, field crews only perform a second tow at these stations if Delta Smelt catch from the first tow is less than 10. Delta Smelt catch per tow data are used for index calculation.

The annual abundance index for Delta Smelt is the arithmetic mean of the abundance indices from the first 2 surveys conducted each year. Delta Smelt abundance indices for each biweekly survey are calculated by summing catch across all tows for each index station, multiplying the summed catch by a station weighting factor representing the water volume of that station (Table B1); then the volume-weighted catches are summed across all 31 index stations and the sum divided by 1000.

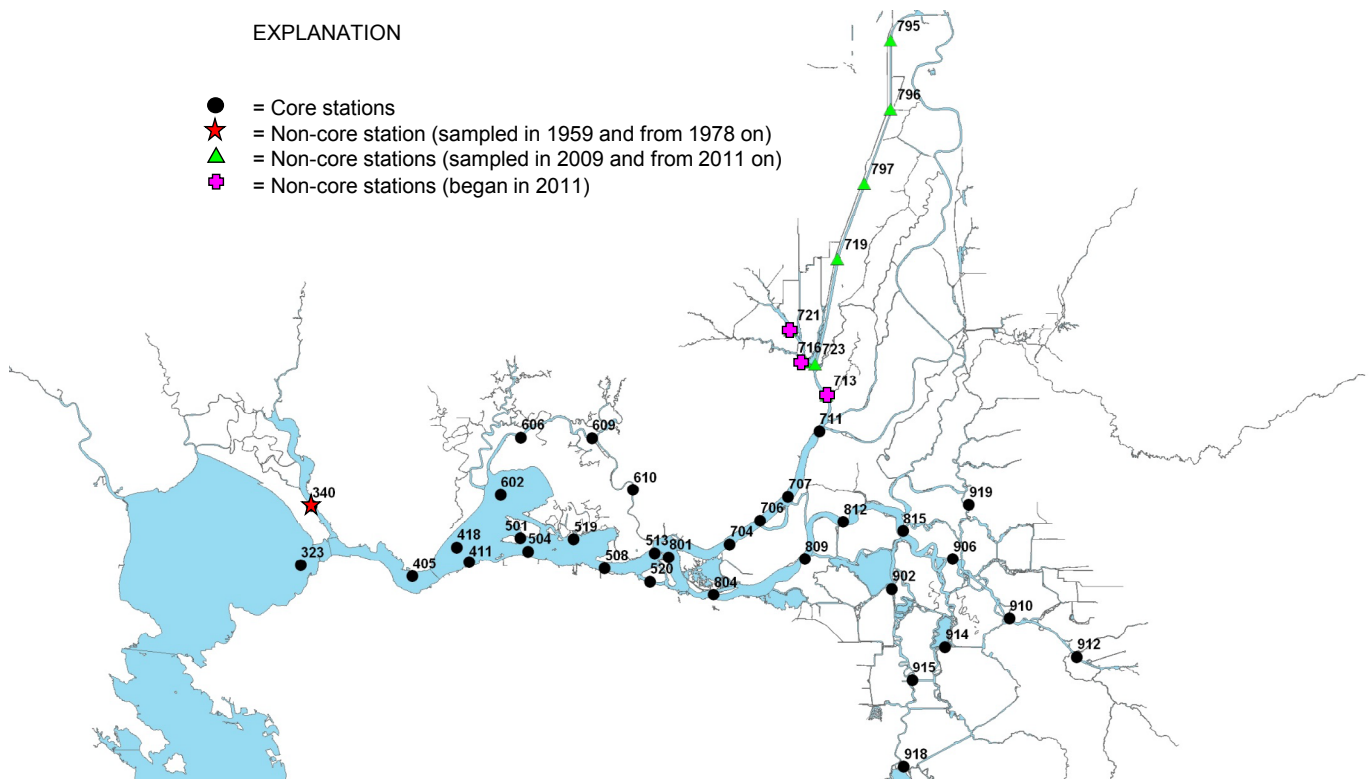
The annual abundance index for age-0 Striped Bass is calculated using similar methods, except the first two surveys are not used. Instead, abundance indices from the 2 surveys that bound the date when the fish reach a mean fork length of 38.1 mm are used; this frequently occurs after several surveys have been completed in a field season.

Fall Midwater Trawl Survey

DFW began the Fall Midwater Trawl Survey (FMWT) in 1967 to provide an annual index of relative abundance and information on the distribution of age-0 Striped Bass for the fall period. Later, DFW staff developed abundance and distribution information for other upper-estuary pelagic fishes, including Delta Smelt. Surveys have been conducted in all years from 1967 to present, except 1974 and 1979. The FMWT survey currently samples 122 stations monthly (Fig. 87), from September through December. Station locations range from San Pablo Bay to Hood on the Sacramento River, and from Sherman Lake to Stockton on the San Joaquin River (Fig. 87). Currently, annual abundance index calculations use catch data from 100 of the 122 stations sampled monthly, but the number of stations used for the index has varied through time. Table 12 contains the complete list of stations used for abundance index calculation for FMWT ($n = 117$), including historical stations (underlined) that must be included for proper calculation of past indices, but are not included in calculations for recent years. The remaining 22 stations were added in 1990, 1991, 2009, and 2010 to improve our understanding of Delta Smelt habitat use (Fig. 87). At each sampling station, field crews perform a single, 12-min oblique tow monthly.

Delta Smelt catch per tow data are used for calculation of the annual abundance index. Individual survey indices are calculated by first grouping the 100 core stations (Fig. 87) into 14 regions based on their location (Table 12). Survey indices are calculated by averaging Delta Smelt catch

Figure 86. Map of summer townet survey stations showing all currently sampled stations. Data from all core stations are used in abundance index calculation.

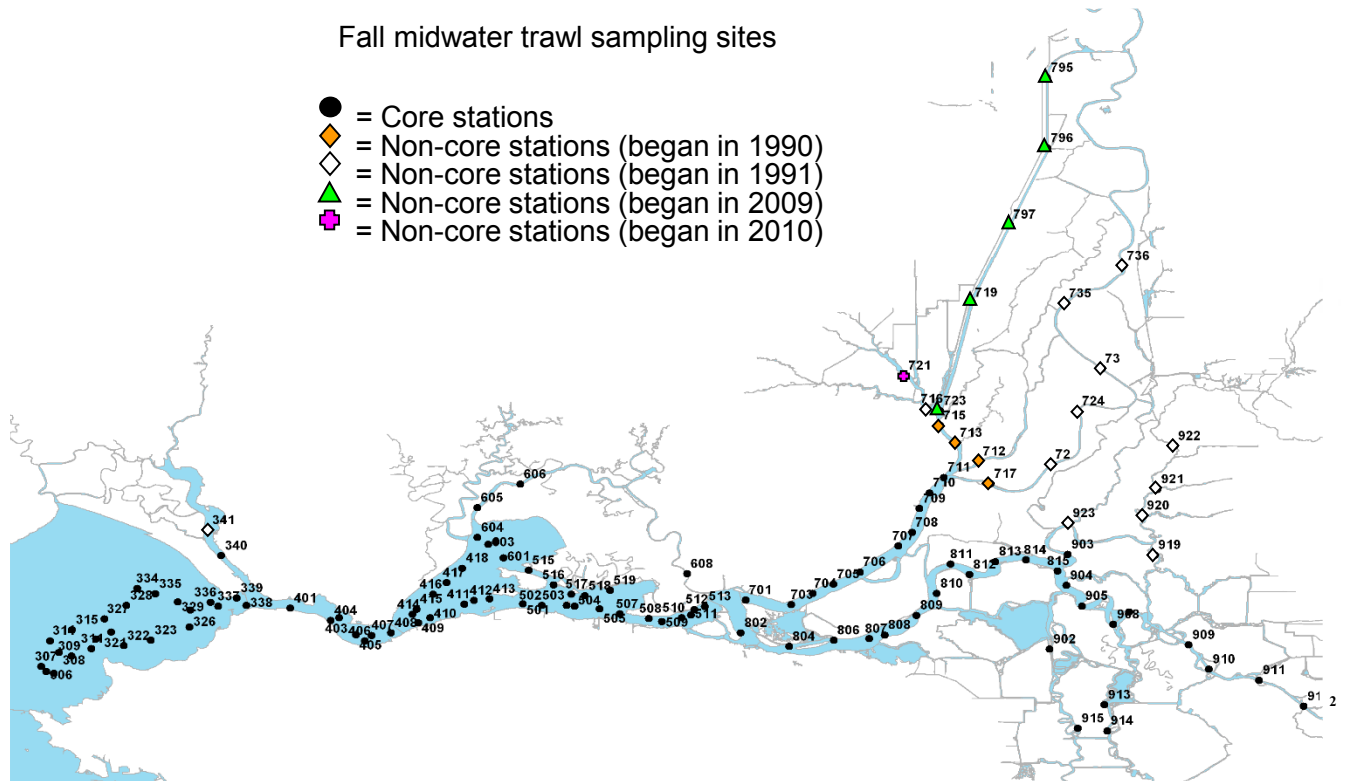


across index stations within each region, multiplying these regional means by their respective weighting factors (i.e. a scalar based on water volume; Table 12), and summing the weighted values. Annual abundance indices are calculated as the sum of the 4 survey abundance indices (i.e. September through December).

Table B1. Station weighting factors for stations used in calculations of the summer townet survey annual abundance indexes. Regions are geographic areas designated by the California Department of Fish and Wildlife. See fig. 86 for station locations.

Region	Station	Station weighting factor
MONTEZUMA SLOUGH	606	20
	609	15
	610	4
SAN PABLO BAY	323	213
SUISUN BAY	405	13
	411	46
	418	70
	501	49
	504	60
	508	31
	513	43
	519	15
	520	9
	602	44
SACRAMENTO RIVER	704	53
	706	27
	707	35
	711	32
SAN JOAQUIN RIVER	801	26
	804	52
	809	56
	812	22
EAST DELTA	815	40
	906	21
	910	11
	912	8
	919	10
SOUTH DELTA	902	23
	914	15
	915	15
	918	11

Figure 87. Map of fall midwater trawl survey stations showing all currently sampled stations. Data from core stations are used in abundance index calculation.



Interagency Ecological Program: Management, Analysis, and Synthesis Team

Table B2. Area-regions, weighting factor for each area-region, and stations included within each area-region. **Bolded station numbers indicate the current 100 core stations used in calculation of annual abundance indexes. Underlined station numbers indicate stations previously included in calculations but subsequently dropped.**

Area-region	Weighting factor	Stations included			
			8-San Pablo Bay	18.5	<u>303</u>
					<u>304</u>
1-San Pablo Bay	8.1	336			305
		337			306
		338			307
		339			308
3-San Pablo Bay	11.3	321			309
		322			310
		323			311
		<u>324</u>			
		325	10-Napa River	4.8	340
		326			
4-San Pablo Bay	6.5	327	11-Carquinez Strait	16.0	401
		328			403
		329			<u>402</u>
					404
5-San Pablo Bay	12.2	<u>330</u>			405
		<u>331</u>			406
		<u>332</u>			407
		<u>333</u>			408
		334			
		335	12-Suisun Bay	14.0	409
7-San Pablo Bay	10.2	<u>312</u>			410
		<u>313</u>			411
		314			412
		315			413
		<u>316</u>			414
					415
					416
					417
					418

13-Suisun and Honker bays	18.0	501	15-Sacramento River	12.0	701		
		502			<u>702</u>		
		503			703		
		504			704		
		505			705		
		<u>506</u>			706		
		507			707		
	18.0	508			708		
		509			709		
		510			710		
		511			711		
		512			16-San Joaquin River	14.0	802
		513	804				
		<u>514</u>	806				
		515	807				
		516	808				
		517	809				
		518	810				
		519	811				
601	812						
14-Grizzly Bay and Montezuma Slough	5.0	602			813		
		603			814		
		604			815		
		605			17-South Delta	20.0	<u>901</u>
		606					902
		<u>607</u>	903				
		608	904				
			905				
	906						
	<u>907</u>						
	908						
	909						

Franks, Sierra
NOAA -NMFS
November, 2012
Updated June 2014

Possibility of natural producing spring-run Chinook salmon in the Stanislaus and Tuolumne Rivers

Currently Central Valley spring-run Chinook salmon are listed as threatened under the Endangered Species Act (ESA). This species was first listed in 1999. Historically in the San Joaquin River system spring-run Chinook are thought to have been one of the most viable runs, but were not listed under the original ESA listing as it was presumed by 1950, that the entire run of spring-run Chinook salmon was extirpated from the San Joaquin River (Fry 1961). The former spring run of the San Joaquin River has been described as “one of the largest Chinook salmon runs anywhere on the Pacific Coast” and numbering “possibly in the range of 200,000-500,000 spawners annually” (CDFG 1990).

Analyzing the historic data and information provided specifically on the Tuolumne and Stanislaus rivers, there is high probability based on records coupled with current data that natural (fish that naturally spawned in river systems and whose parents did as well) occurring spring-run Chinook are still present in small numbers. Here it is discussed where spring-run originally used these river systems.

On the Tuolumne River, Clavey Falls (10-15 ft. high) at the confluence of the Clavey River, may have obstructed the salmon at certain flows, but spring-run salmon in some numbers undoubtedly ascended the mainstem a considerable distance. The spring-run salmon were most likely stopped by the formidable Preston Falls at the boundary of Yosemite National Park (~50 mi upstream of present New Don Pedro Dam), which is the upstream limit of native fish distribution (CDFG 1955 unpublished data).

Spring run Chinook also originally occurred in the Stanislaus River. Spring-run probably went up the system considerable distances because there are few natural obstacles (Yoshiyama et al. 1998). Much of the spawning occurred on the extensive gravel beds in the 23-mi. stretch from

Riverbank upstream to Knights Ferry, which is essentially on the Valley floor at approximately 213 feet in elevation. Upstream of Knights Ferry, where the river flows through a canyon, spawning was (historic observations of spring-run) and is (fall-run) concentrated at Two-mile Bar (~1 mi above Knights Ferry) but also occurs in scattered pockets of gravel (Yoshiyama et al. 1998). Historically, the spring run was the primary salmon run in the Stanislaus River, but after the construction of dams which regulated the stream flows (i.e., Goodwin Dam and, later, Melones and Tulloch dams); the fall run became predominant (CDFG 1972 unpublished report).

Recent information suggests that perhaps a self-sustaining (capable of reproducing without hatchery influence) population of spring-run Chinook is occurring in some of the San Joaquin River tributaries, most notably the Stanislaus and the Tuolumne Rivers. Snorkel surveys (Kennedy T. and T. Cannon 2005) conducted between October 2002 to October 2004 on the Stanislaus River identified adults in June 2003 and June 2004 between Goodwin and Lovers Leap. Additionally on the Stanislaus, snorkel surveys also observed Chinook fry in December 2003 at Goodwin Dam, Two Mile Bar, and Knights Ferry, which they interpreted as an indication of spawning occurring in September, which is earlier than when fall-run Chinook salmon would be spawning in the river.

FISHBIO a fisheries consultant has operated a resistance board weir coupled with a Vaki RiverWatcher video monitoring system on the Stanislaus since 2003 and on the Tuolumne since 2009. Information obtained from this monitoring indicates that adult Chinook salmon are passing upstream of these weirs at a time period that would historically indicate a spring-run timing. Looking specifically at the months from February to June almost annually since observation began, some adult Chinook are migrating upstream (Table 1). It should be noted that the weir has not always operated past December due to study design or non-conductive river conditions. For example in 2007, 11 phenotypic spring-run Chinook were observed passing the weir between May and June on the Stanislaus. Future monitoring will determine if these fish are a typical occurrence or an anomaly (Anderson et al. 2007). Further personal observations by fisheries biologist from other agencies (CDFG & USFWS) that are familiar with these systems have accounts of seeing adult Chinook holding in these river systems in summer months (CDFG & USFWS, Personal comm.). If this is the case then genetic testing would be needed to confirm that these fish are in fact naturally producing spring-run Chinook and not hatchery strays, *i.e.*

Feather River. Otolith analysis may be the best way to confirm this by matching chemical signatures specific to each river system. Additionally there is no segregation barrier in place for spring-run and fall-run and it is likely that fall-run are superimposing on spring-run redds (Wikert, Personal Comm.). A further analysis looking at these tributaries rotary screw trap (RST) data helps support the suggestion of self-sustaining spring-run by looking at length at date criteria and comparing it to known spring-run Chinook populations on Sacramento River tributaries. RST data provided by Stockton United State Fish and Wildlife Service (USFWS) corroborates with the adult timing, by indicating that there are a small number of fry migrating out of the Stanislaus and Tuolumne at a period that would coincide with spring-run juvenile emigration (Tables 2 & 3).

Additionally during snorkel and kayak surveys in April, May and June of 2013 with CDFW, USFWS and NMFS staff the author observed a large number of adult Chinook in the upper reaches of the Stanislaus River below Goodwin Dam.

References:

Anderson, J.T, C.B. Watry and A. Gray. 2007. Upstream Fish Passage at a Resistance Board Weir Using Infrared and Digital Technology in the Lower Stanislaus River, California 2006–2007 Annual Data Report. 40pp.

California Department of Fish and Game (CDFG). 1955. Fish and game water problems of the Upper San Joaquin River. Potential values and needs. Statement submitted to the Division of Water Resources at hearings on the San Joaquin River water applications, Fresno, California. 5 April 1955. 51 pp. (Unpublished)

California Department of Fish and Game (CDFG). 1972. Report to the California State Water Resources Control Board on effects of the New Melones Project on fish and wildlife resources of the Stanislaus River and Sacramento-San Joaquin Delta. Region 4, Anadromous Fisheries Branch, Bay-Delta Research Study, and Environmental Services Branch, Sacramento. October 1972.

California Department of Fish and Game (CDFG). 1990. Status and management of spring-run Chinook salmon. Report by the Inland Fisheries Division to the California Fish and Game Commission, Sacramento. May 1990. 33 pp.

Fry, D.H., Jr. 1961. King salmon spawning stocks of the California Central Valley, 1940-1959. California Fish and Game 47: 55-71.

Kennedy, T., and T. Cannon. 2005. Stanislaus River salmonid density and distribution survey report. Fishery Foundation of California.

Tsao, S. 2012. CDFG. Personal communication with Sierra Franks at NMFS.

Wilkert, J.D. 2012. USFWS. Personal communication with Sierra Franks at NMFS.

Yoshiyama, R. M., F. W. Fisher, and P. B. Moyle. 1998. Historical abundance and decline of Chinook salmon in the Central Valley region of California. *North American Journal of Fisheries Management* 18: 487–521.

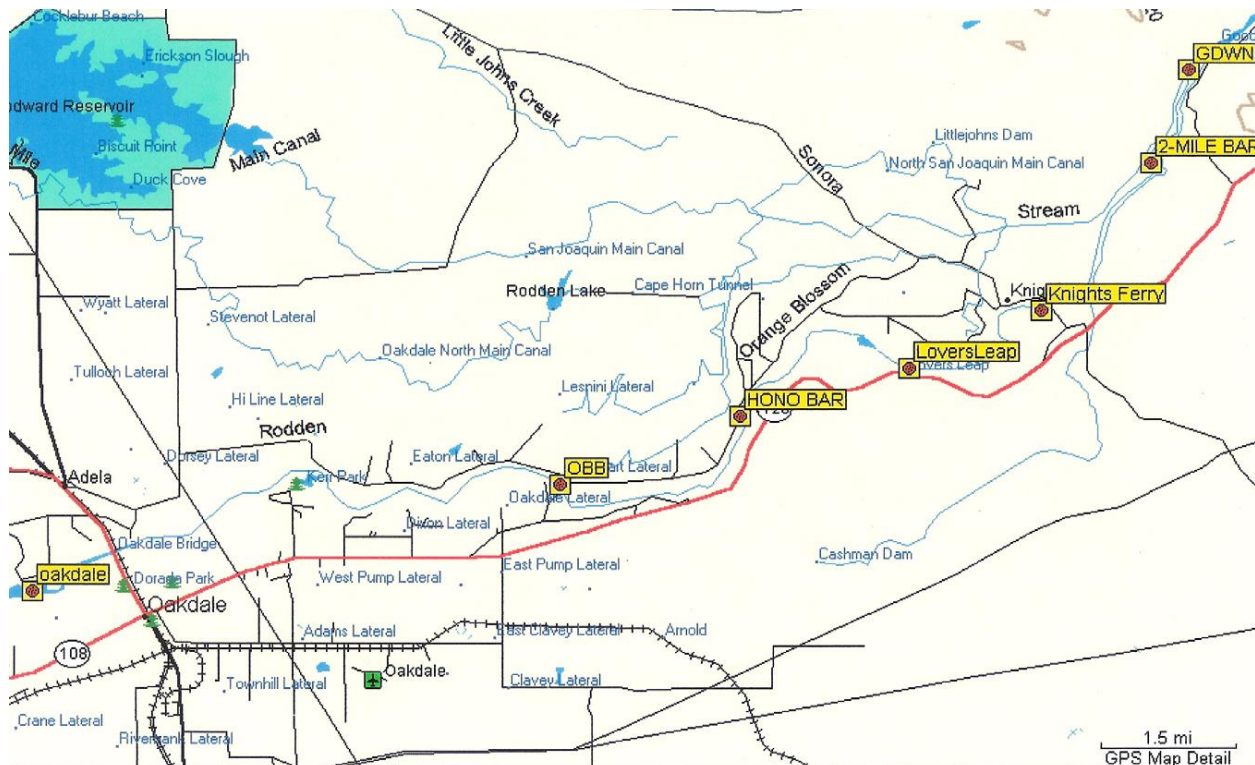


Figure 1. Displaying specific points mentioned in the text on the Stanislaus River, such as Goodwin Dam, 2-Mile Bar and Knights Ferry.

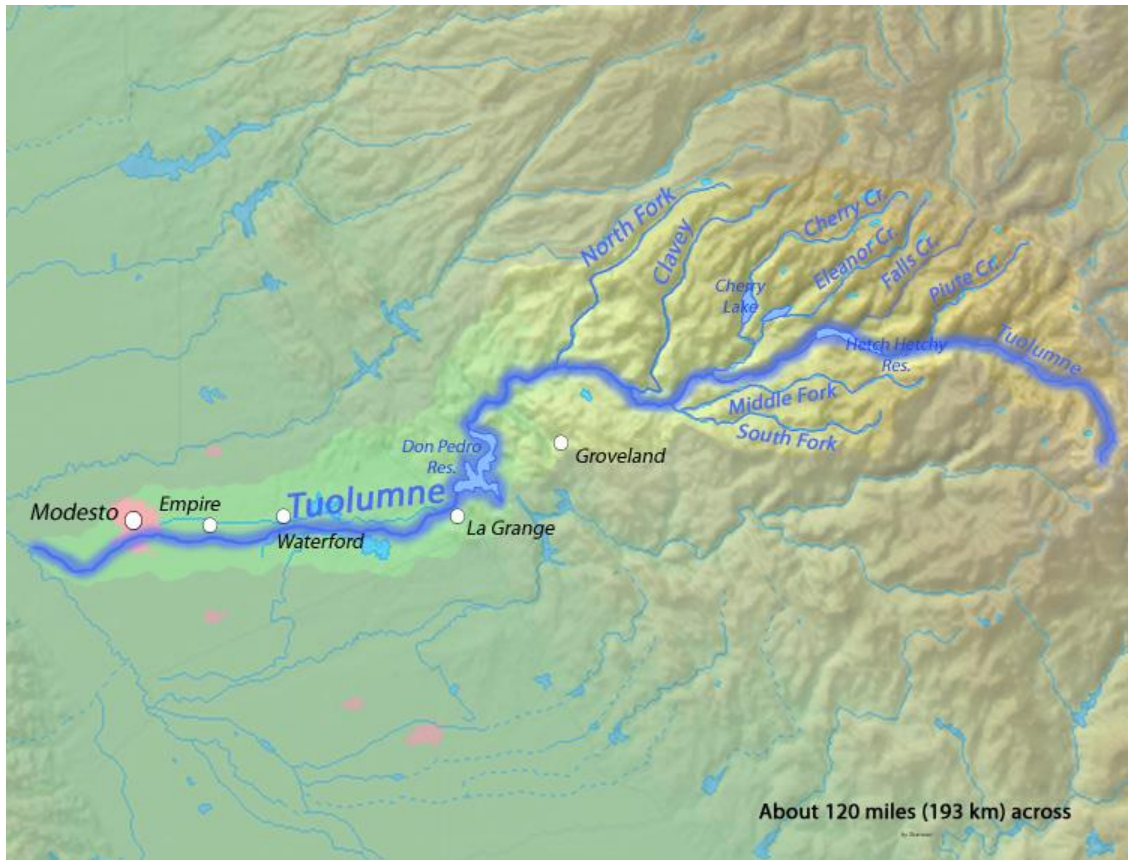


Figure 2. The Tuolumne River

Table 1. **Adult** adipose intact Chinook migrating upstream on the Tuolumne and Stanislaus Rivers (viewed by VAKI RiverWatcher weir: FISHBIO)

Tuolumne (2010, 2012)	Stanislaus (2007, 2009, 2010, 2012)
12 Confirmed adipose intact (*55 total passed)	51 confirmed adipose intact (*68 total passed)

* In 2011 the Stanislaus weir was pulled in mid-March due to flood control releases. The Tuolumne weir was not operating

* 2012 adipose clipped information not available at this time (this includes 38 total fish for the Tuolumne)

Table 2. Tuolumne RST cumulative catch 2000-2011 – matching USFWS length at date criteria for spring-run fry at Mossdale

March	245 Chinook fry -6% of TC
April	761 Chinook fry – 26% of TC
May	736 Chinook fry – 25% of TC
June	7 Chinook fry – 2% of TC

Table 3. Stanislaus (Caswell) RST cumulative catch 2000-2011 - matching USFWS length at date criteria for spring-run fry at Mossdale

March	636 Chinook fry - 9% of TC
April	911 Chinook fry - 12% of TC
May	363 Chinook fry – 6% of TC
June	4 Chinook fry - < 1% of TC

Table 4. Official Water Year Hydrologic Classification Indices from CDWR

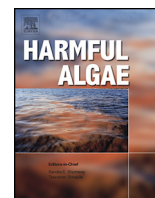
	Year Type
2000	Above Normal
2001	Dry
2002	Dry
2003	Below Normal
2004	Dry
2005	Wet
2006	Wet
2007	Critical Dry
2008	Critical Dry
2009	Dry
2010	Above Normal
2011	Wet
2012	Dry

Table 5. Rotary Screw Trap Data on the Tuolumne, cumulative from 2000 – 2011. Data courtesy of Kes Ben, USFWS.

Chinook Salmon Length Range (5 mm intervals) by Month, Tuolumne Rotary Screw Trap Data, 2000-2011.							
Length Range (mm)	January	February	March	April	May	June	December
25.1 - 30	41	60	9				2
30.1 - 35	1,835	2,336	1,473	74	17		135
35.1 - 40	2,462	2,900	1,541	37	9		39
40.1 - 45	15	67	38	2	1		
45.1 - 50	1	59	59	6	1		
50.1 - 55	4	58	144	14	1		
55.1 - 60	3	50	179	19	3		
60.1 - 65	3	35	226	58	5	2	
65.1 - 70	3	27	230	144	14	1	
70.1 - 75	7	34	199	333	61	6	
75.1 - 80	15	15	130	605	214	12	
80.1 - 85	22	8	72	658	488	25	
85.1 - 90	26	12	43	495	615	47	
90.1 - 95	12	5	20	266	679	77	
95.1 - 100	6	9	12	126	492	94	
100.1 - 105	4	16	8	26	244	47	
105.1 - 110	5	12	3	16	104	19	
110.1 - 115	2	5	2	6	33	5	
115.1 - 120		4	3	2	10	1	
120.1 - 125	2	4	3			1	
125.1 - 130	4	5	2				
130.1 - 135		3	5				
135.1 - 140	1	4	3				
140.1 - 145							
145.1 - 150			2				
150.1 - 155			1				
155.1 - 160							
160.1 - 165							
165.1 - 170		1					
175.1 - 180							
190.1 - 195							

Table 6. Rotary Screw Trap Data on the Stanislaus, cumulative from 2000 – 2011. Data courtesy of Kes Ben, USFWS.

Chinook Salmon Length Range (5 mm intervals) by Month, Stanislaus Rotary Screw Trap Data at Caswell, 2000-2011.								
Length Range (mm)	January	February	March	April	May	June	July	December
20.1 - 25			2					
25.1 - 30	53	105	29					
30.1 - 35	496	967	496	4				4
35.1 - 40	413	1,227	555	6	1			3
40.1 - 45	18	395	507	2	2			
45.1 - 50	4	298	734	21	2			
50.1 - 55		181	924	109	3			
55.1 - 60		110	965	381	10			
60.1 - 65		52	928	799	69	1		
65.1 - 70		14	761	1,280	282	5		
70.1 - 75		2	602	1,509	828	22		
75.1 - 80			358	1,480	1,305	105		
80.1 - 85		1	193	1,040	1,510	162		
85.1 - 90			85	635	1,147	256		
90.1 - 95	1		26	276	677	213	2	
95.1 - 100			11	104	274	100		
100.1 - 105			1	41	89	46		
105.1 - 110				18	24	5		
110.1 - 115		1	1	7	3	2		
115.1 - 120			1		1			
120.1 - 125			3			2		
125.1 - 130			3					
130.1 - 135		1						
135.1 - 140			2					
140.1 - 145		1	1	1				
145.1 - 150	1	1	1	1				
150.1 - 155		1	2					
155.1 - 160			1					
160.1 - 165			4					
165.1 - 170								
170.1 - 175								
175.1 - 180								
180.1 - 185								
185.1 - 190			1					



Detection of persistent microcystin toxins at the land–sea interface in Monterey Bay, California



Corinne M. Gibble*, Raphael M. Kudela

Ocean Sciences Department, 1156 High Street, University of California, Santa Cruz, CA 95064, USA

ARTICLE INFO

Article history:

Received 25 March 2014

Received in revised form 29 June 2014

Accepted 8 July 2014

Available online 31 July 2014

Keywords:

Microcystis aeruginosa

Microcystin

Monterey Bay

CyanoHAB

Harmful algal bloom

Solid Phase Adsorption Toxin Tracking

(SPATT)

ABSTRACT

Blooms of toxin-producing *Microcystis aeruginosa* occur regularly in freshwater systems throughout California, but until recently potential impacts in the coastal ocean have been largely ignored. Twenty-one sites in and around Monterey Bay were surveyed for evidence of microcystin toxin (2010–2011) at the land–sea interface. Following this initial survey four major watersheds in the Monterey Bay area were surveyed (2011–2013) for microcystin concentration, nutrients, alkalinity and water temperature to identify potential environmental factors correlated with the abundance of microcystin at the land–sea interface. During the first year microcystin was detected in 15 of 21 sites. Data from years two and three were analyzed by principal components analysis and mixed effects model. Results indicated that coastal nutrient loading (nitrate, phosphate silicate, ammonium, urea), were statistically significant predictors of the microcystin concentrations in the watersheds with clear evidence for seasonality at some sites. Microcystin was frequently at highest concentration in the autumn; however, at some locations high levels of toxin were measured during spring. Because this toxin has the ability to biomagnify and persist within food webs, elevated levels within the watershed may decrease potential for health and survival of wildlife and humans exposed to freshwater and marine waters. The widespread occurrence of microcystin at low to moderate levels throughout the year and throughout the sampled watersheds demonstrates the potential difficulty for management.

© 2014 The Authors. Published by Elsevier B.V. This is an open access article under the CC BY-NC-ND license (<http://creativecommons.org/licenses/by-nc-nd/3.0/>).

1. Introduction

Harmful algal blooms (HABs) are a global problem in both freshwater and marine ecosystems. The prevalence of HABs and subsequent toxic events may be intensified by a warming climate in tandem with increases in environmental degradation and eutrophication (Zehnder and Gorham, 1960; Welker and Steinburg, 2000; Guo, 2007; Paerl and Huisman, 2008; Davis et al., 2009; Kudela, 2011). Production of the toxin microcystin by the cyanobacterium *Microcystis aeruginosa*, was originally recognized by Ashworth and Mason (1946) in American waters in the 1940s. *M. aeruginosa* blooms are now common in lakes and rivers throughout North America, including California (Chen et al., 1993; Lehman et al., 2005). *M. aeruginosa* bloom formation and consequent toxin generation increases with environmental variables such as: high nutrient supply, elevated light levels, and warm temperatures (Zehnder and Gorham, 1960; Tsuji et al., 1994;

Jacoby et al., 2000; Welker and Steinburg, 2000; Paerl and Huisman, 2008; Davis et al., 2009; Paerl and Otten, 2013a, 2013b).

Recently toxins associated with the ostensibly freshwater cyanobacterium *Microcystis aeruginosa* have been detected in the near-shore marine ecosystem of central California, and have been confirmed as a danger to the health of sea otters feeding near ocean outflows of freshwater systems (Miller et al., 2010). *M. aeruginosa* is fairly salt-tolerant and microcystin toxins can be stable and environmentally persistent in both saltwater and freshwater habitats (Robson and Hamilton, 2003; Ross et al., 2006; Tonk et al., 2007; Miller et al., 2010). In addition to direct toxic effects, exposure of aquatic organisms to elevated concentrations of microcystins may negatively affect all levels of the food web (Demott and Moxter, 1991; Malbrouck and Kestemont, 2006; Richardson et al., 2007; Miller et al., 2010).

In 2007, numerous sea otters were found dead in Monterey Bay with signs of liver failure (Miller et al., 2010). Biochemical testing confirmed the presence of microcystin toxin with associated lesions in the livers of 21 otters. Because the occurrence of phytoplankton derived biotoxins are a common phenomenon in Monterey Bay, the otters were evaluated for domoic acid, okadaic acid, nodularin, yessotoxin and anatoxin-A. Otters that were found

* Corresponding author. Tel.: +1 831 459 4298.

E-mail addresses: cgibble@ucsc.edu (C.M. Gibble), kudela@ucsc.edu (R.M. Kudela).

positive for microcystin toxin were negative for all other toxins in the tissues. A few of the microcystin positive otters were also found to have low levels of domoic acid in the urine. However, this is a common finding during necropsy of stranded sea otters from this region, due to domoic acid being broadly dispersed in the sediments of Monterey Bay (Goldberg, 2003; Miller et al., 2010). Freshwater to marine transfer of microcystins was confirmed in areas where sea otters had been recovered, and uptake of microcystins by marine invertebrates and environmental persistence in seawater were demonstrated experimentally (Miller et al., 2010). At this time, potential population-level impacts of these biotoxins on otters and other coastal wildlife remains undetermined. The freshwater to marine transfer of microcystin to the Monterey Bay National Marine Sanctuary waters described by Miller et al. (2010) has the potential to cause major environmental harm. The stability of microcystin allows it to accumulate (van der Oost et al., 2003), and microcystin toxin has been shown to biomagnify and persist in the environment and the food web (Sivonen and Jones, 1999; Dionisio Pires et al., 2004; Kozłowski-Suzuki et al., 2012; Poste and Ozersky, 2013). Despite the confirmation of microcystin poisoning in marine mammals, the source of these toxins is unclear. Pinto Lake, California was identified as a “hotspot” for toxin production and subsequent transfer to the coastal ocean but this source was not consistent with the location of many of the otters (Miller et al., 2010), which were distributed throughout Monterey Bay, suggesting other, less obvious, sources of toxin to the coastal environment.

We took a wide ranging watershed-based approach to identify the potential pathways leading to microcystin contamination in coastal ecosystems in and around Monterey Bay, CA. Since initial surveys of other potential “hotspots” for toxin production were unsuccessful (Miller et al., 2010) via grab sampling, we deployed Solid Phase Adsorption Toxin Tracking (SPATT) samplers throughout the Monterey Bay area to provide a temporally integrated assessment of potential freshwater sources (Kudela, 2011). Because toxin frequency of occurrence, persistence, and associated environmental drivers may potentially be propelling this freshwater toxin into a sensitive and protected marine sanctuary, our overarching goals were to identify the freshwater sources of microcystin to the Monterey Bay ecosystem, and to identify the

underlying environmental drivers influencing toxin production in this area.

2. Materials and Methods

2.1. Initial survey

We surveyed 21 freshwater, estuarine, and marine locations in and around the Monterey Bay area at the land–sea interface (June 2010–July 2011) for microcystin toxin presence and concentration (Fig. 1A). Sites included small and large rivers, estuaries, and near-shore marine locations traversing the six watersheds that surround Monterey Bay (Fig. 1A). Each site was sampled monthly using SPATT (Kudela, 2011). SPATT bags were constructed using 3 g DIAION® HP-20 resin (Sorbert Technologies Inc., Georgia, USA) placed between two 3 inch × 3 inch squares of 100 μM Nitex bolting cloth (Wildlife Supply Company, Product No. 24-C34), and secured in a Caron Westex 2.5 in flex embroidery hoop (Caron International, Ontario, Canada). SPATT was activated by soaking each bag in 100% MeOH, for 48 h, and then rinsed with de-ionized water (Milli-Q), and stored in fresh Milli-Q until deployment (Mackenzie et al., 2004; Lane et al., 2010). When deployed at the beginning of each month, SPATT bags were suspended below the surface of the water, and secured with twine to a stake near the edge of the water. This allowed each bag to be suspended in the water, while being weighed down by the ring so that it remained below the surface. Toxin concentration values are reported as nanogram toxin per gram resin. SPATT toxin concentration levels are not directly comparable to grab sample values (ppb, or μg/L), but previous studies suggest a rough correspondence of 10:1 for SPATT to grab samples (Kudela, 2011), i.e. 10 ng/g SPATT is equivalent to an average concentration of 1 ppb microcystin during SPATT deployment.

2.2. Time-series

In years two and three (August 2011–August 2013) sampling locations were reduced to four major affected watersheds in the Monterey Bay area: the Big Basin watershed, Pajaro River watershed, Salinas River watershed, and the Carmel River

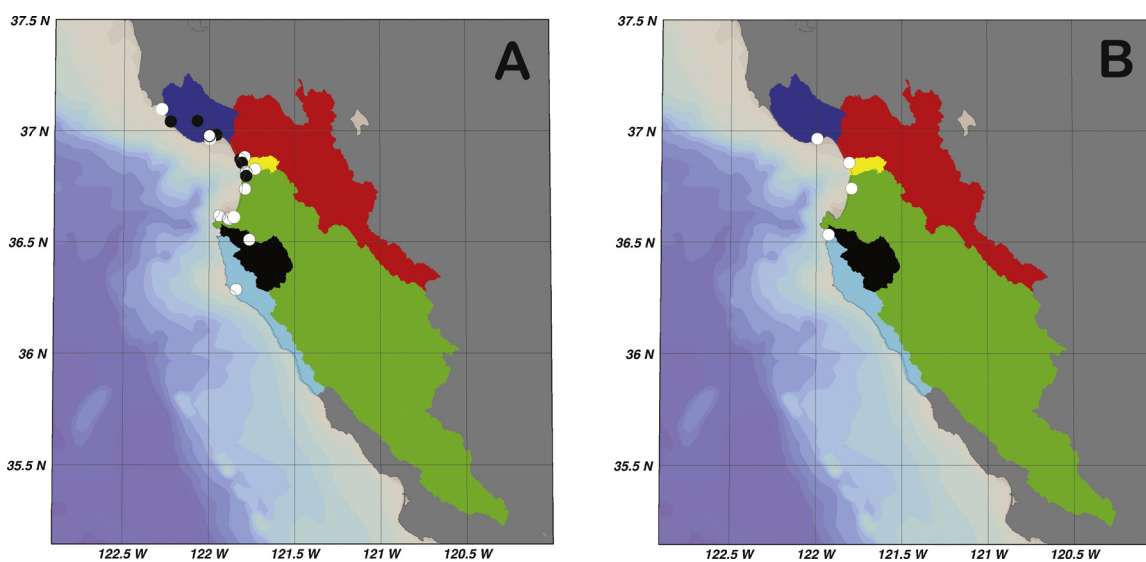


Fig. 1. Map of Monterey Bay, California, USA. (A) Sampling locations in year one (2010–2011) and sampling locations affected by microcystin toxin in year one. White symbols represent sites that were positive for microcystin, black symbols represents sites that were sampled but negative for microcystin toxin. (B) Sampling locations in year two (2011–2013). The watersheds, from north to south, are: Big Basin (dark blue), Pajaro River (red), Bolsa Nueva (yellow), Salinas River (green), Carmel River (black), Santa Lucia (light blue). Ocean bathymetry is indicated with shading. Maps created using Ocean Data View (ODV) and Exelis Visual Information Solutions (ENVI).

watershed. These four sampling locations were determined by the initial year one survey to be highly impacted by microcystin toxin. SPATT was deployed weekly at each site and whole water was collected and analyzed for temperature, ammonium, urea, nitrate, phosphate, silicate, and total toxin, with the whole water samples corresponding to the deployment and recovery dates for SPATT. With the exception of alkalinity, which was monitored only in year three (August 2012–August 2013), all other variables were measured in both years two and three. Temperature was monitored using Hobo Pendant[®] Temperature/Light Data Loggers (8K-UA-002-08; Onset Computer Corporation, Massachusetts, USA). When data loggers were unavailable for use due to theft or loss, field thermometers were employed in situ ($-10/110$ °C; Enviro-safe[®]; HB Instrument Company, Pennsylvania, USA). Ammonium, urea, nitrate, phosphate and silicate samples were collected in the field, immediately filtered ($0.7 \mu\text{M}$ GF/F filter), into 25 mL Falcon[™] centrifuge tubes, and were stored frozen until processing. The average time until processing was less than one month. Ammonium was analyzed using the OPA method and RFU values were obtained via fluorometer (TD-700; Turner Designs, California, USA) as described by Holmes et al. (1999). Urea was analyzed using a Varian Cary 50 Bio UV/Visible Spectrophotometer (Varian Medical Systems, California, USA) following methods described by Mulvenna and Savidge (1992). Nitrate, phosphate, and silicate were analyzed using a Lachat QuikChem 8500 Flow Injection Analyst System and Omnion 3.0 software (Lachat Instruments; Hach Company, Colorado, USA). Alkalinity was determined using Total Alkalinity Test Strips, 0–240 mg/L (Hach Company, Colorado, USA) in the field. Whole water was also collected in the field.

2.3. Toxin analysis

Microcystin-LR, RR, YR, LA was analyzed by liquid chromatography/mass spectrometry (LCMS) with electrospray ionization (ESI) with selected ion monitoring (SIM) on an Agilent 6130 with a Phenomenex Kinetix (100×2.10) C18 column. The method was adapted from Mekebri et al., 2009 with minor modifications to account for the choice of column and LCMS/SIM instead of tandem mass spectrometry (Kudela, 2011). Briefly, a gradient-elution method was used with HPLC water (solvent A) and LCMS acetonitrile (solvent B), both acidified with 0.1% formic acid, as the mobile phase. The gradient was as described in Mekebri et al. (2009), starting with 95:5 solvent A:B and ending with 25:75 at 19 min, held for 1 min, then followed by a 5 min equilibration at initial conditions prior to injection of the next sample. Samples were calibrated with standard curves (for each batch of samples) using pure standards (Fluka 33578 and Sigma–Aldrich M4194). Standards were run again at the end of the run for sample runs lasting more than 8 h.

Whole water was collected in the field, returned to the lab, where 3 mL of whole water was mixed with 3 mL of 10% methanol. Samples were then sonicated using a sonic dismembrator (Model 100; Thermo Fisher Scientific, Massachusetts, USA) for 30 s at ~ 10 W, filtered ($0.2 \mu\text{M}$ nylon syringe filter), and analyzed by direct injection of $50 \mu\text{L}$ onto the LCMS. SPATT samples were processed as described by Kudela (2011). Briefly, SPATT were recovered from the field and stored frozen until processing. The resin was transferred to a disposable chromatography column and sequentially extracted with 10, 20, 20 mL 50% methanol. Each extract ($50 \mu\text{L}$) was analyzed by LCMS and total toxin was determined by summing the individual extracts. Values are reported as $\mu\text{g/L}$ (=ppb) for whole water and ng/g resin for SPATT. The Minimum Detection Limit (MDL) was 0.05 ng/g for SPATT and 0.10 ng/mL (ppb) for whole water. Values <MDL were considered non-detect (zero) for statistical analysis. While it is

possible that compound other than microcystins could be falsely identified, it would require the compounds to exhibit the same mass and retention time as the standards making false positives unlikely.

2.4. Statistics

Microcystin toxin presence, concentration, and persistence were evaluated at each sampling location in year one, and for each watershed during years two and three. Data for both the discrete grab samples and the SPATT toxin concentrations were pooled for the analysis. The relationship between environmental variables (date, temperature, nitrate, phosphate, silicate, ammonium, urea) and microcystin were evaluated graphically and statistically. Because there was multicollinearity within the data from years two to three, a PCA was run to account for this, and the variables were grouped into components for further analysis (Zar, 1999; Quinn and Keough, 2002). A mixed effects model was chosen to account for autocorrelation caused by the seasonality component. Because of this autocorrelation the components (date and temperature) that comprised seasonality were removed from the PCA and added back into the model independently. When the model was run, components from the PCA (PC1 and PC2), and temperature were run against microcystin toxin. Date was added back into the model and was set as the random effect, with microcystin toxin concentration set as the fixed effect. This model is appropriate due to the nature of the flexibility it provides for correlated data (Quinn and Keough, 2002; Seltman, 2013). Variables used in the model were transformed via square root transformation to meet assumptions of normality, and $\alpha = 0.05$. From the results of the model, both negative and positive relationships between environmental variables and microcystin concentration were examined, and statistical significance was obtained. PCA and mixed effect model statistical tests were conducted using Systat 13.1 (Systat Software Inc., Chicago, Illinois, USA). The relationship between microcystin concentration and alkalinity was investigated via simple bivariate correlation using IBM SPSS Statistics 21 (IBM Corporation, Armonk, New York, USA).

To investigate any statistical relationship between river discharge and toxin presence, microcystin toxin concentration was compared to river discharge data (USGS, 2014) for each of the four watersheds. Data for the comparison were obtained from the United States Geological Survey (USGS) National Water Information System Web Interface database, and river discharge data were reported in cubic feet per second. Data were analyzed via simple bivariate correlations using IBM SPSS Statistics 21 and the significance was set at $p = 0.05$. Cross correlation function analysis (CCF) was evaluated using Systat 13.1 for effectiveness of introducing temporal lags into the data.

3. Results

3.1. Survey results (2010–2011)

In year one, 15 out of 21 locations surveyed in the Monterey Bay area were positive for microcystin toxin concentration (Fig. 1A; Table 1). There were noticeably high levels of toxin in the autumn season, and at some sites, such as the Carmel River and Salinas River, there were also noticeable spring season peaks in toxin concentration (Fig. 2). From our first year of data, four watersheds (Big Basin, Pajaro River, Salinas River, Carmel River) were identified as persistently toxic; this directed our sampling in years two and three. Toxin concentration values varied from undetectable to 20 ng/g.

Table 1

Survey data for microcystin toxin from 21 locations in and around the Monterey Bay area in year one (2010–2011).

Location	OBS	POS	Range	Mean	SD
Waddell Creek	8	1	0–1.800	0.138	0.499
Scott Creek	12	0	0	0	0
San Lorenzo River	13	0	0	0	0
Santa Cruz Harbor	10	4	0–4.025	0.495	1.147
Twin Lakes State Beach	12	3	0–0.990	0.142	0.311
Soquel Creek	13	0	0	0	0
Pajaro River	13	1	0–2.930	0.225	0.813
Pajaro Lagoon	13	0	0	0	0
Watsonville Slough	13	0	0	0	0
Bennet Slough	12	1	0–0.58	0.045	0.161
Moss Landing Harbor	11	3	0–7.097	0.987	2.315
Strawberry Pond	13	3	0–2.960	0.403	0.892
Moro Cojo	13	0	0	0	0
Salinas River	13	3	0–4.700	0.472	1.298
Laguna Grande	13	1	0–0.165	0.013	0.046
Lake El Estero	12	1	0–0.414	0.032	0.115
Monterey Coast Guard Pier	11	2	0–8.109	0.867	2.345
Fisherman's Wharf	10	2	0–5.382	0.500	1.548
Asilomar Creek	11	2	0–0.0810	0.115	0.281
Carmel River	12	7	0–19.564	2.905	5.517
Big Sur River	11	1	0–0.1837	0.014	0.051

The number of observations where SPATT was deployed and also recovered, is represented by OBS, the number of months positive for microcystin toxin is measured in ng/g and is represented by POS. The range, mean, and standard deviation represented by SD, are also provided.

3.2. Time series (2011–2013)

In year two, all four watersheds (Fig. 1B) exhibited an increase in microcystin toxin presence compared to year one (Table 2). In year three, all watersheds again exhibited similar or increased occurrences of microcystin toxin. As was seen in year one, high values of microcystin toxin concentration were observed in both autumn and spring seasons (Fig. 3), but in years two and three this seasonal pattern was evident in all four watersheds.

The PCA produced three significant principal components (Table 3). Principal component one (PC1) was comprised of ammonium and urea (21.02% variance explained), principal component two (PC2) was comprised of temperature and date (19.97% variance explained), and principal component three (PC3) was comprised of nitrate, phosphate and silicate (19.83% variance explained). All of the variables loaded positively with the exception of silicate. These PCA components were used in place of direct environmental variables to account for multicollinearity within the data. The seasonality component (date and temperature) produced an autocorrelation within the data. Seasonality was therefore removed and the PCA was re-run; two significant components were produced and grouped similarly. PC1 was comprised of ammonium and urea (29.36% variance explained), and PC2 was comprised of nitrate, phosphate, and silicate (27.25% variance explained). PC1, PC2 and temperature were then run in a mixed effects model against the presence and amount of microcystin toxin with date set as the random effect. The model showed that microcystin toxin concentration had a statistically significant relationship to all tested variables ($p < 0.05$; Table 3). Nitrate, phosphate, ammonium and urea were negatively associated with microcystin concentration within the model. Because silicate loaded negatively in the PCA, it was considered positively associated with microcystin in the model, while temperature was negatively associated with microcystin in the model (Table 3). The results of a CCF analysis indicated significant correlations between toxin concentration and individual environmental factors with temporal lags of three weeks. However, when the data were lagged, the overall model was greatly weakened. Microcystin

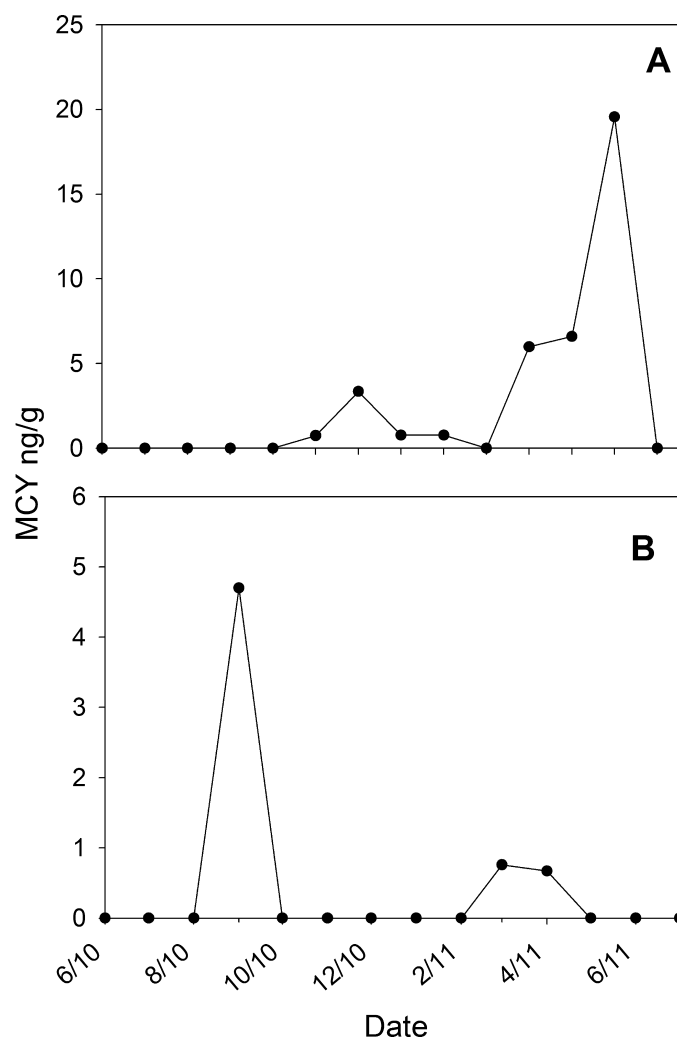


Fig. 2. Microcystin toxin (MCY) time series from SPATT samplers (ng toxin per gram resin) for two locations (A). Carmel River (B). Salinas River, during year one (June 2010–July 2011).

toxin concentration remained significantly related to all tested variables ($p < 0.05$). For this reason we present the statistical results without lags.

Bivariate correlations showed negative correlation with alkalinity and positive correlation with river flow. Alkalinity had a significant negative correlation ($p < 0.05$) with microcystin concentration (Fig. 4). River discharge and microcystin toxin concentration were significantly positively correlated for Big Basin, Pajaro River, and Carmel River watersheds ($p < 0.05$). Salinas River exhibited a weak, non-significant ($p > 0.05$) correlation. The results of CCF analysis indicated that a lag of four weeks may better align the data and increase the strength of the correlation. When the data were lagged all watersheds again were positively correlated; however, only the Pajaro River and Carmel River watersheds exhibited statistically significant correlations ($p < 0.05$).

4. Discussion

The results from this study show a serious condition at the near-shore interface in the Monterey Bay area, consistent with previous reports (Miller et al., 2010). In year one, approximately half of all tested locations were positive for microcystin toxins at some time during the year. We believe these toxins are being produced by

Table 2
Survey data for microcystin toxin and environmental variables from four watershed locations at the land–sea interface in Monterey Bay in years two and three (2011–2013).

Location	Variable	Range	Mean	SD
Big Basin Watershed	Microcystin SPATT	0–8.22	0.749	1.61
	Microcystin water	0–12.85	0.17	1.31
	Ammonium	0.07–30.37	5.56	7.13
	Urea	0.13–18.42	1.98	2.77
	Nitrate	0–92.37	11.14	19.25
	Phosphate	0.30–51.91	11.224	10.273
	Silicate	0.91–543.23	143.37	125.33
	Alkalinity	40–240	117.29	46.46
	Temperature	6.21–21.92	15.35	4.27
	Pajaro River Watershed	Microcystin SPATT	0–8.97	0.59
Microcystin water		0–1.09	0.03	0.14
Ammonium		0.05–32.1	3.06	4.33
Urea		0.15–8.28	0.94	0.96
Nitrate		1.75–1257.10	318.96	199.36
Phosphate		0–66.16	4.54	8.46
Silicate		10.37–668.72	129.38	102.30
Alkalinity		120–240	231.86	26.03
Temperature		7.75–22.00	15.72	4.09
Salinas River Watershed		Microcystin SPATT	0–62.71	1.12
	Microcystin water	0–1.02	0.02	0.12
	Ammonium	0.03–93.95	3.79	12.01
	Urea	0.10–4.47	0.93	0.77
	Nitrate	0.74–1311.12	504.22	287.47
	Phosphate	0.11–56.16	11.93	8.92
	Silicate	13.45–805.44	196.88	108.86
	Alkalinity	180–240	211.77	30.25
	Temperature	7.50–25.00	15.82	4.62
	Carmel River Watershed	Microcystin	0–62.71	1.11
Microcystin SPATT		0–104.31	7.91	16.70
Microcystin water		0–0.90	0.04	0.16
Ammonium		0–2.93	0.28	0.42
Urea		0–3.52	0.40	0.57
Nitrate		0.40–28.65	4.03	3.53
Phosphate		0.01–3.59	0.46	0.45
Silicate		27.00–856.00	292.79	106.53
Alkalinity		40–240	131.19	73.52
Temperature		7.00–20.66	13.41	2.98
	Microcystin	0–104.31	7.78	16.69

Microcystin toxin found in SPATT is measured in ng/g, microcystin toxin found in water samples is measured in ppb. The measured environmental variables: ammonium (μM), urea (μM), nitrate (μM), phosphate (μM), silicate (μM), alkalinity (mg/L), temperature ($^{\circ}\text{C}$) are shown. The range, mean, and standard deviation represented by SD, are also provided.

Microcystis aeruginosa in the nearshore freshwater environment and have the potential to be subsequently transported to the marine environment. Miller et al. (2010) found that cells lysed in seawater after 48 h; there is also possibility for some cells to be carried to the marine environment, lyse, and then release toxin. Monterey Bay is at high risk for this type of problem due to the nature of the surrounding land which is highly populated and widely used for agriculture. However, we believe this may be a phenomenon in other near-shore marine systems that have not been monitored for this particular toxin, and therefore, have gone unnoticed.

The use of SPATT technology allowed us to access time integrative toxin survey data simultaneously at many different locations, thus providing more than a “snapshot” of information such as would be obtained with intensive surveying. While SPATT was originally developed to mimic shellfish toxicity, its use has proven to be more beneficial and easy to use for toxin monitoring as compared to other popular monitoring methods like the use of shellfish testing, rote phytoplankton surveys, and whole water sampling (Mackenzie et al., 2004; Lane et al., 2010; Mackenzie, 2010; Kudela, 2011).

The occurrence of two dominant peaks, in spring and autumn, indicate an unexpected seasonal pattern of microcystin toxin for all primary watersheds in the Monterey Bay area. It is widely accepted that bloom formation is largely driven by light and nutrient availability, and often water stagnation (Zehnder and Gorham,

1960; Webb and Walling, 1992; Tsuji et al., 1994; Jacoby et al., 2000; Welker and Steinburg, 2000; Jeong et al., 2003; Paerl and Huisman, 2008; Davis et al., 2009; Paerl and Otten, 2013a). This often leads to a seasonal pattern, with optimal conditions for bloom formation occurring in summer and autumn seasons. (Reynolds et al., 1981; Paerl, 1988; Lehman et al., 2008; Moisander et al., 2009). This seasonal characteristic has similarly been identified in nearby waterways like the San Francisco Estuary (Lehman et al., 2005, 2008; Moisander et al., 2009). Additionally, Miller et al. (2010) reported that the Monterey Bay area generally experiences increases in microcystin presence and concentration in freshwater lakes and rivers during autumn. The patterns of microcystin presence and concentration observed during this study suggest that microcystins are likely present throughout the year. In years two and three microcystin toxin increased or remained elevated at all locations and the spring/autumn peaks persisted. While only three years in duration, these results suggest that microcystin production and subsequent transfer to the coastal environment has the potential to be a persistent issue in the Monterey Bay area.

The statistical analysis exhibited a distinct delineation between variables. Ammonium, urea, nitrate, and phosphate all exhibited a negative association with toxin in the model. We infer that the negative relationship was caused by biological drawdown of nutrients; toxin is produced by cells which are stimulated by the high nutrient levels, but toxin concentrations can become

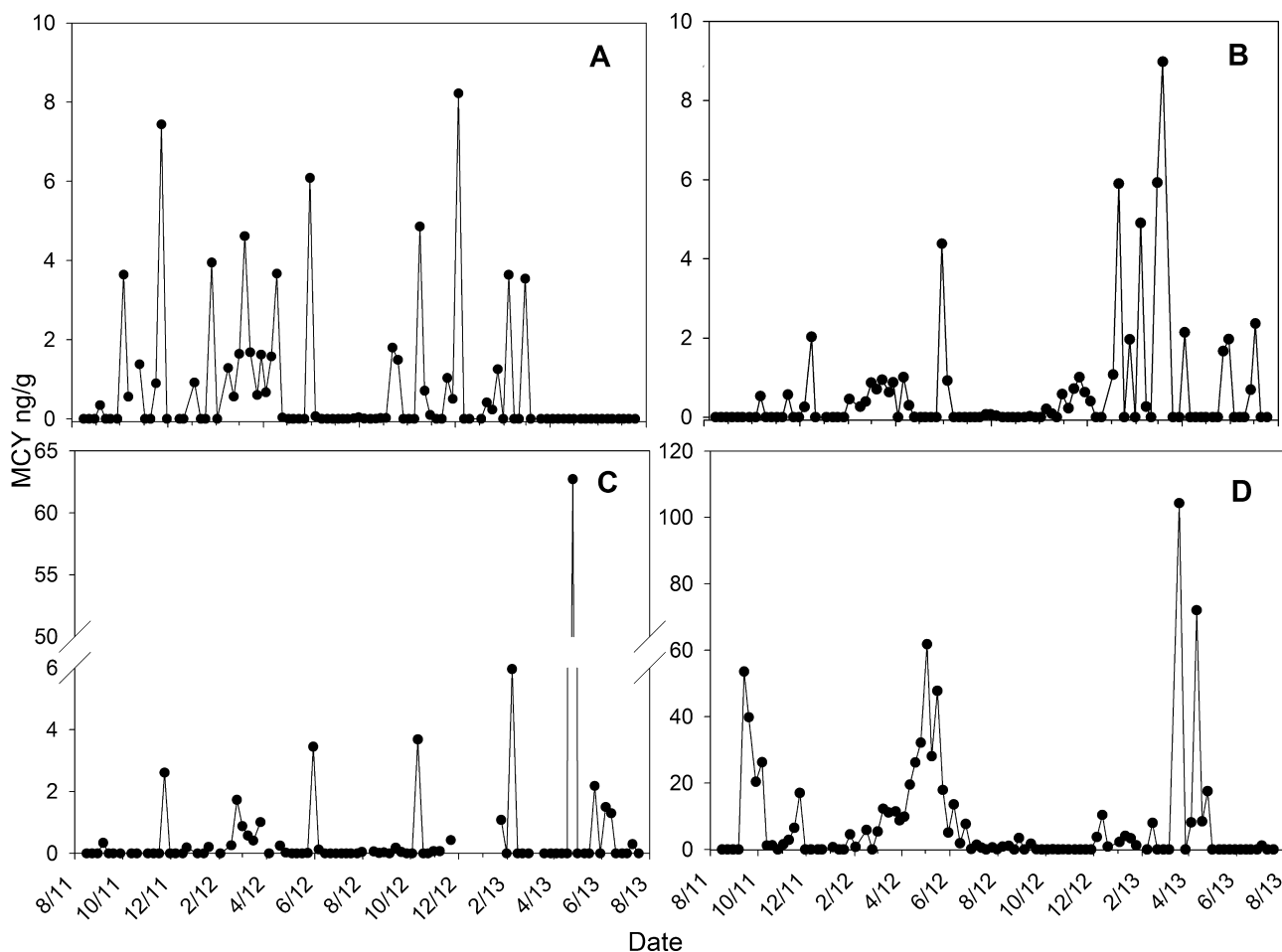


Fig. 3. Microcystin toxin from SPATT (MCY; ng/g) time series from August 2011 to August 2013. (A) Big Basin watershed; (B) Pajaro River watershed; (C) Salinas River watershed; (D) Carmel River watershed.

uncoupled from cell growth and nutrient concentrations due to cell lysis and differences between cell toxin quota and cell growth. Given the likely disconnect between toxin production and detection (SPATT were deployed for one week to one month), there is consistency with nutrient enrichment leading to increased algal biomass, with subsequent toxin production. Low nutrient levels would then be correlated with elevated toxins due to the time lag. This theory could be tested by identifying lagged correlations between nutrients and toxins, but our toxin data are integrative (SPATT) while the nutrients were collected at the time of SPATT recovery (with a coarse time scale relative to nutrient dynamics), precluding such an analysis. The assertion we present is

Table 3

Results from the mixed effects model evaluating principal components, and temperature versus microcystin toxin.

Variable	Estimate number	<i>p</i> -value
PC1		
Urea	−0.1240	0.0520
Ammonium		
PC2		
Nitrate	−0.9200	0.0060
Phosphate		
Silicate		
Temperature	−0.0480	0.0020

The first principle component is represented by PC1 and contains the variables urea and ammonium. The second principal component is represented by PC2 and contains variables nitrate, phosphate and silicate. The associated estimate numbers and *p*-values from the model are provided.

consistent with the relationship between microcystin concentrations and silicate concentrations identified in the model. Silicate was positively associated with microcystin. Silicate is not utilized by *Microcystis aeruginosa* and consequently remained in the environment while other nutrients were presumably biologically drawn down in the absence of diatom blooms. The link between

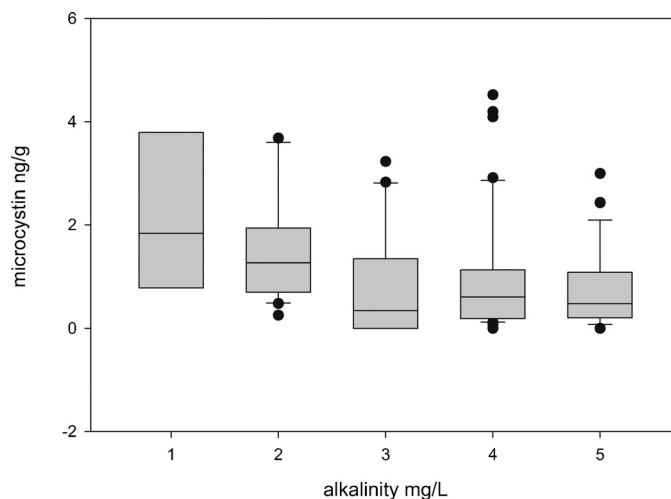


Fig. 4. Alkalinity versus microcystin toxin box plots. Data for all locations from August 2012 to August 2013 was pooled, zeros were removed and microcystin toxin data was square root transformed.

macronutrients, particularly ammonium and urea, and toxin concentrations, and the relatively high nutrient concentrations point to anthropogenic loading as a significant driver of toxin accumulation in these watersheds (Kudela et al., 2008), consistent with other studies (Paerl et al., 2001; Paerl, 2008; Schindler and Vallentyne, 2008; Wilhelm et al., 2011).

Temperature, unexpectedly, exhibited a negative association with microcystin toxin within the model. Several studies have demonstrated the link between elevated and increasing temperature and the frequency of toxic blooms (Butterwick et al., 2005; Reynolds, 2006; Paerl and Huisman, 2008, 2009). However, the phenomenon of a non-correlative relationship between microcystin toxin and temperature has been seen previously, where elevated toxin concentrations have been associated with a range of temperatures (van der Westhuizen and Eloff, 1985; Amé and Wunderlin, 2005; Davis et al., 2009; Kudela, 2011). This may be indicative of a non-linear relationship between the two variables, possibly driven by different growth–temperature responses for different toxigenic cyanobacteria (Paerl and Otten, 2013a, 2013b).

The inverse relationship between alkalinity and microcystin was expected. This dynamic has been documented previously (Aboal et al., 2005); additionally alkalinity has been correlated with shifts in algal groups when ammonium is available to provide the source of nitrogen (Brewer and Goldman, 1976). River flow had positive correlations with microcystin toxin before and after time lags. Before the data were lagged there were more significant positive correlations; after lags, all sites were positively correlated, but fewer were significant. Many studies have highlighted that stagnancy of water is associated with increased cell density of *Microcystis* (Christian et al., 1986; Reynolds, 1992; Jeong et al., 2006; Lehman et al., 2008). Lehman et al. (2008) also found that *Microcystis* cell density was positively correlated with flow at some locations in the San Francisco Estuary. Cell density was highest during periods of lowest river flow, and toxin was potentially produced during subsequent stagnant, long retention-time periods. The weak positive correlations identified in this study suggest that while river flow has an effect on toxin concentration, it is not be the dominant effect. Other contributors to toxin abundance with stronger relationships, such as nutrient loading, appear to have a greater influence on toxin levels.

Presence of microcystin toxins is often indicative of an unhealthy ecosystem (Miller et al., 2012). Within the Monterey Bay region, toxins are present and persistent in the four major watersheds flowing into the Monterey Bay National Marine Sanctuary. Despite the persistence of this toxin in California watersheds and the potential negative impacts to humans and wildlife, microcystins are not routinely monitored by federal, state or local management agencies. Because this toxin has the capacity for accumulation, biomagnification, and persistence within food webs, elevated levels within the watershed may increase the possibility for morbidity and mortality of wildlife and humans in terrestrial, estuarine, and marine waters. Additionally there is increasing evidence to support chronic exposure to microcystins as a significant threat to wildlife and humans (Bury et al., 1995; Wiegand et al., 1999; Jacquet et al., 2004; de Figueiredo et al., 2004; Malbrouck and Kestemont, 2006; Wang et al., 2010). Thus, even the low but detectable levels identified in this study may be indicative of a potentially unhealthy ecosystem. It is possible that low levels of microcystins are endemic to California and therefore a natural component of the ecosystem. The lack of baseline studies makes this assertion difficult to test, but this study provides a reasonable baseline for assessing future changes in toxins within the Monterey Bay watersheds.

Cyanobacterial harmful algal bloom events are often intensified by anthropogenic activities such as discharge of sewage, as well as both urban and agricultural practices that cause nutrient rich

runoff to flow into local watersheds (Zehnder and Gorham, 1960; Fogg, 1969; Reynolds, 1987; Paerl, 1988; Davis et al., 2009; Paerl et al., 2011). Because cyanobacteria have the capacity to thrive in water with both low and high nutrient concentrations, these organisms have the potential to outcompete other algal groups and dominate affected watersheds (Falconer and Humpage, 2005). The combined effect of high growth response to nutrient input and the ability to outcompete other organisms creates the potential for microcystin toxin to overwhelm affected ecosystems.

The extensive manifestation of microcystin at low to moderate levels throughout the year and throughout all major watersheds in the Monterey Bay area exhibits the potential complication of managing environmental impacts, and ecosystem disruptions. Management agencies have long grappled with the problem of microcystin toxins in inland watersheds. However, the ubiquity of microcystin at the land–sea interface in the Monterey Bay area represents a new management obstacle. Decisions made at the terrestrial level in the proximity of the marine environment may now impact freshwater, estuarine, and marine ecosystems, particularly given the demonstrated capacity for bio-accumulation in commercially harvested shellfish (Miller et al., 2010). New management plans and implementations may now have to regard this freshwater epidemic as an expanding and pervasive problem.

Acknowledgments

We would like to thank Dr. Melissa Miller and the Marine Wildlife Veterinary Care and Research Center (MWVCRC) for volunteer support for the first six months of sampling. We thank Kendra Negrey for methodological guidance, Rob Franks for laboratory support, and Dr. Pete Raimondi for statistical advice. This work was completed with salary and tuition assistance from the NOAA Nancy Foster Scholarship program (CMG)NOAA award number: NA10SEC4810031 and with partial support from the Central and Northern California Ocean Observing System (CeN-COOS), funded by NOAA. NOAA award number: NA11NOS0120032.

References

- Aboal, M., Angeles Puig, M., Asencio, A.D., 2005. Production of microcystins in calcareous Mediterranean streams: the Alharabe River, Segura River basin in south-east Spain. *J. Appl. Phycol.* 17, 231–243.
- Amé, M.V., Wunderlin, D.A., 2005. Effects of iron, ammonium and temperature on microcystin content by a natural concentrated *Microcystis aeruginosa* population. *Water Air Soil Pollut.* 168 (1–4) 235–248.
- Ashworth, C.T., Mason, M.F., 1946. Observations on the pathological changes produced by a toxic substance present in blue-green algae (*Microcystis aeruginosa*). *Am. J. Pathol.* 22, 369–383.
- Brewer, P.G., Goldman, J.C., 1976. Alkalinity changes generated by phytoplankton growth. *Limnol. Oceanogr.* 21, 108–117.
- Bury, N.R., Eddy, F.B., Codd, G.A., 1995. The effects of the cyanobacterium *Microcystis aeruginosa*, the cyanobacterial hepatotoxin microcystin-LR, and ammonia on growth rate and ionic regulation of brown trout. *J. Fish Biol.* 46 (6) 1042–1054.
- Butterwick, C., Heaney, S.I., Talling, J.F., 2005. Diversity in the influence of temperature on the growth rates of freshwater algae, and its ecological relevance. *Freshwater Biol.* 50 (2) 291–300.
- Chen, D.Z.X., Boland, M.P., Smillie, M.A., Klux, H., Ptak, C., Anderson, R.J., Holmes, C.F.B., 1993. Identification of protein phosphatase inhibitors of the microcystin class in the marine environment. *Toxicol.* 72 (5) 1407–1414.
- Christian, R.R., Bryant, W.L., Stanley, D.W., 1986. The relationship between river flow and *Microcystis aeruginosa* blooms in the Neuse River, North Carolina: Report of the Water Resources Research Institute of the University of North Carolina 223. p. 100.
- Davis, T.W., Berry, D.L., Boyer, G.L., Gobler, C.J., 2009. The effects of temperature and nutrients on the growth dynamics of toxic and non-toxic strains of *Microcystis* during cyanobacterial blooms. *Harmful Algae* 8, 715–725.
- de Figueiredo, D.R., Azeiteiro, U.M., Esteves, S.M., Gonçalves, F.J., Pereira, M.J., 2004. Microcystin-producing blooms—a serious global public health issue. *Ecotoxicol. Environ. Saf.* 59 (2) 151–163.
- Demott, W.R., Moxter, F., 1991. Foraging cyanobacteria by copepods: responses to chemical defense and resource abundance. *Ecology* 72 (5) 1820–1834.
- Dionisio Pires, L.M., Karlsson, K.M., Meriluto, J.A.O., Kardinaal, E., Visser, P.M., Siewertsena, K., Van Donka, E., Ibelings, B.W., 2004. Assimilation and

- deuration of microcystin-LR by the zebra mussel, *Dreissena polymorpha*. *Aquat. Toxicol.* 69, 385–396.
- Falconer, I.R., Humpage, A.R., 2005. Health risk assessment of cyanobacterial (blue-green algal) toxins in drinking water. *Int. J. Environ. Res. Public Health* 2 (1) 43–50.
- Fogg, G.E., 1969. The physiology of an algal nuisance. *Proc. R. Soc. B* 173, 175–189.
- Goldberg, J.D., 2003. Domoic Acid in the Benthic Food Web of Monterey Bay, California. [M.Sc Thesis] Moss Landing Marine Laboratories, California State University; Monterey Bay, p. 41
- Guo, L., 2007. Ecology: doing battle with the green monster of Taihu Lake. *Science* 317, 1166.
- Holmes, R.M., Aminot, A., K erouel, R., Hooker, B.A., Peterson, B.J., 1999. A simple and precise method for measuring ammonium in marine and freshwater ecosystems. *Can. J. Fish Aquat. Sci.* 56 (10) 1801–1808.
- Jacoby, J.M., Collier, D.C., Welch, E.B., Hardy, F.J., Crayton, M., 2000. Environmental factors associated with a toxic bloom of *Microcystis aeruginosa*. *Can. J. Fish Aquat. Sci.* 57, 231–240.
- Jacquet, C., Thermes, V., Luze, A.D., Puiseux-Dao, S., Bernard, C., Joly, J.S., Edery, M., 2004. Effects of microcystin-LR on development of medaka fish embryos (*Oryzias latipes*). *Toxicol.* 43 (2) 141–147.
- Jeong, K.S., Kim, D.K., Whigham, P., Joo, G.J., 2003. Modeling *Microcystis aeruginosa* bloom dynamics in the Nakdong River by means of evolutionary computation and statistical approach. *Ecol. Model.* 161, 67–78.
- Jeong, K.S., Recknagel, F., Joo, G.J., 2006. Prediction and elucidation of population dynamics of the blue-green algae *Microcystis aeruginosa* and the diatom *Stephanodiscus hantzschii* in the Nakdong River-Reservoir System (South Korea) by a recurrent artificial neural network. In: Recknagel, F. (Ed.), *Ecological Informatics*. Springer Berlin Heidelberg, pp. 225–273.
- Kozlowsky-Suzuki, B.A., Wilson, A.E., da Silva Ferr o-Filho, A., 2012. Biomagnification or biodilution of microcystins in aquatic foodwebs? Meta-analyses of laboratory and field studies. *Harmful Algae* 18, 47–55.
- Kudela, R.M., 2011. Characterization and deployment of Solid Phase Adsorption Toxin Tracking (SPATT) resin for monitoring of microcystins in fresh and saltwater. *Harmful Algae* 11, 117–125.
- Kudela, R.M., Ryan, J.P., Blakely, M.D., Lane, J.Q., Peterson, T.D., 2008. Linking the physiology and ecology of *Cochlodinium* to better understand harmful algal bloom events: a comparative approach. *Harmful Algae* 7 (3) 278–292.
- Lane, J.Q., Roddam, C.M., Langlois, G.W., Kudela, R.M., 2010. Application of Solid Phase Adsorption Toxin Tracking (SPATT) for field detection of domoic acid and saxitoxin in coastal California. *Limnol. Oceanogr. Methods* 8, 645–660.
- Lehman, P.W., Boyer, G., Hall, C., Waller, S., Gerhrts, K., 2005. Distribution and toxicity of a new colonial *Microcystis aeruginosa* bloom in the San Francisco Bay Estuary, California. *Hydrobiologia* 541, 87–99.
- Lehman, P.W., Boyer, G., Satchwell, M., Waller, S., 2008. The influence of environmental conditions on the seasonal variation of *Microcystis* cell density and microcystins concentration in San Francisco Estuary. *Hydrobiologia* 600, 187–204.
- Mackenzie, L., 2010. In situ passive solid-phase adsorption of micro-algal biotoxins as a monitoring tool. *Curr. Opin. Biotechnol.* 21, 326–331.
- Mackenzie, L., Beuzenberg, V., Holland, P., McNabb, P., Selwood, A., 2004. Solid Phase Adsorption Toxin Tracking (SPATT): a new monitoring tool that simulates the biotoxin contamination of filter feeding bivalves. *Toxicol.* 44, 901–918.
- Malbrouck, C., Kestemont, P., 2006. Effects of microcystins on fish. *Environ. Toxicol. Chem.* 25 (1) 72–86.
- Mekebri, A., Blondina, G.J., Crane, D.B., 2009. Method validation of microcystins in water and tissue by enhanced liquid chromatography tandem mass spectrometry. *J. Chromatogr. A* 1216, 3147–3155.
- Miller, M.A., Kudela, R.M., Mekebri, A., Crane, D., Oates, S.C., Tinker, M.T., Staedler, M., Miller, W.A., Toy-Choutka, S., Dominik, C., Hardin, D., Langlois, G., Murray, M., Ward, K., Jessup, D.A., 2010. Evidence for a novel marine harmful algal bloom: cyanotoxin (microcystin) transfer from land to sea otters. *PLoS ONE* 5, e12576.
- Miller, M.A., Kudela, R.M., Jessup, D.A., 2012. When marine ecosystems fall ill. *The Wildlife Professional Spring* 2012, pp. 44–48.
- Moisander, P.H., Ochiai, M., Lincoff, A., 2009. Nutrient limitation of *Microcystis aeruginosa* in northern California Klamath River reservoirs. *Harmful Algae* 8, 889–897.
- Mulvenna, P.F., Savidge, G., 1992. A modified manual method for the determination of urea in seawater using diacetylmonoxime reagent. *Est. Coast. Shelf Sci.* 34, 429–438.
- Paerl, H.W., 1988. Nuisance phytoplankton blooms in coastal, estuarine, and inland waters. *Limnol. Oceanogr.* 33, 823–847.
- Paerl, H.W., 2008. Nutrient and other environmental controls of harmful cyanobacterial blooms along the freshwater–marine continuum. In: Hudnell, K.H. (Ed.), *Cyanobacterial Harmful Algal Blooms: State of the Science and Research Needs Advances in Experimental Medicine and Biology*, 619. Springer Science + Business Media, New York, pp. 217–237.
- Paerl, H.W., Bales, J.D., Ausley, L.W., Buzzelli, C.P., Crowder, L.B., Eby, L.A., Fear, J.M., Go, M., Peierls, B.L., Richardson, T.L., Ramus, J.S., 2001. Ecosystem impacts of 3 sequential hurricanes (Dennis, Floyd and Irene) on the US's largest lagoonal estuary, Pamlico Sound, NC. *Proc. Natl. Acad. Sci.* 98, 5655–5660.
- Paerl, H.W., Huisman, J., 2008. Climate: blooms like it hot. *Science* 320, 57–58.
- Paerl, H.W., Huisman, J., 2009. Climate change: a catalyst for global expansion of harmful cyanobacterial blooms. *Environ. Microbiol. Rep.* 1, 27–37.
- Paerl, H.W., Hall, N.S., Calandrino, E.S., 2011. Controlling harmful cyanobacterial blooms in a world experiencing anthropogenic and climatic-induced change. *Sci Total Environ.* 409, 1739–1745.
- Paerl, H.W., Otten, T.G., 2013a. Harmful cyanobacterial blooms: causes, consequences, and controls. *Microb. Ecol.* 65, 995–1010.
- Paerl, H.W., Otten, T.G., 2013b. Blooms bite the hand that feeds them. *Science* 342, 433–434.
- Poste, A.E., Ozersky, T., 2013. Invasive dreissenid mussels and round gobies: a benthic pathway for the trophic transfer of microcystin. *Environ. Toxicol. Chem.* 32 (9) 2159–2164.
- Quinn, G.P., Keough, M.J., 2002. *Experimental Design and Data Analysis for Biologists*. Cambridge University Press, New York, pp. 443–444.
- Reynolds, C.S., 1987. Cyanobacterial water blooms. *Adv. Bot. Res.* 13, 67–143.
- Reynolds, C.S., 1992. *Algae*. In: Calow, P., Petts, G.E. (Eds.), *The River Handbook: Hydrological and Ecological Principles*, Vol.1. Blackwell Scientific Publication, Oxford, pp. 526.
- Reynolds, C.S., 2006. *Ecology of Phytoplankton*. Cambridge University Press, Cambridge.
- Reynolds, C.S., Jaworski, G.H.M., Cmiech, H.A., Leedale, G.F., 1981. On the annual cycle of the blue-green alga *Microcystis aeruginosa* K tz. Emend. Elenkin. *Philos. Trans. R. Soc. Lond. B* 293, 419–477.
- Richardson, L.L., Sekar, R., Myers, J.L., Gantar, M., Voss, J.D., Kaczmarek, L., Remily, E.R., Boyer, G.L., Zimba, P., 2007. The presence of the cyanobacterial toxin microcystin in black band disease in corals. *FEMS Microbiol. Lett.* 272, 182–187.
- Robson, B.J., Hamilton, D.P., 2003. Summer flow event induces a cyanobacterial bloom in a seasonal Western Australian estuary. *Mar. Freshwater Res.* 54, 139–151.
- Ross, C., Santiago-Vazquez, L., Paul, V., 2006. Toxin release in response to oxidative stress and programmed cell death in the cyanobacterium *Microcystis aeruginosa*. *Aquat. Toxicol.* 78, 66–73.
- Schindler, D.W., Vallentyne, J.R., 2008. The Algal Bowl: overfertilization of the world's freshwaters and estuaries. University of Alberta Press, Canada, p. 348.
- Seltman, H., 2013. *Experimental Design and Data Analysis*. Carnegie Mellon University E-book. <http://www.stat.cmu.edu/~hseltman/309/Book/Book.pdf>.
- Sivonen, K., Jones, G., 1999. Cyanobacterial toxins. In: Chorus, I., Bartram, J. (Eds.), *Toxic Cyanobacteria in Water*. The World Health Organization, E. and F.N. Spon, London, UK, pp. 41–111.
- Tonk, L., Bosch, K., Visser, P.M., Huisman, J., 2007. Salt tolerance of the harmful cyanobacterium *Microcystis aeruginosa*. *Aquat. Microb. Ecol.* 46, 117–123.
- Tsuji, K., Nalto, S., Kondo, F., Ishikawa, N., Watanabe, M.F., Suzuki, M., Harada, K.I., 1994. Stability of microcystins from cyanobacteria: effect of light on decomposition and isomerization. *Environ. Sci. Technol.* 1094 (28) 173–177.
- [USGS] United States Geological Survey, 2014. 2014. USGS Surface-Water Historical Instantaneous Data for the Nation. U.S. Dept. of Interior and U.S. Geological Survey. (accessed 01.04.14) <http://waterdata.usgs.gov/nwis/uv/>
- van der Oost, R., Beyer, J., Vermeulen, N.P., 2003. Fish bioaccumulation and biomarkers in environmental risk assessment: a review. *Environ. Toxicol. Pharmacol.* 13, 57–149.
- van der Westhuizen, A.J., Eloff, J.N., 1985. Effect of temperature and light on the toxicity and growth of the blue-green alga *Microcystis aeruginosa* (UV-006). *Planta* 163, 55–59.
- Wang, M., Chan, L.L., Si, M., Hong, H., Wang, D., 2010. Proteomic analysis of hepatic tissue of zebrafish (*Danio rerio*) experimentally exposed to chronic microcystin-LR. *Toxicol. Sci.* 113 (1) 60–69.
- Webb, B.W., Walling, D.E., 1992. Water quality, II. Chemical characteristics. In: Calow, P., Petts, G.E. (Eds.), *The River Handbook: Hydrological and Ecological Principles*, vol. 1. Blackwell Science Publications, Oxford, pp. 73–100.
- Welker, M., Steinburg, C., 2000. Rates of humic substance photosensitized degradation of microcystin-LR in natural waters. *Environ. Sci. Technol.* 34, 3415–3419.
- Wiegand, C., Pflugmacher, S., Oberemm, A., Meems, N., Beattie, K.A., Steinberg, C.E., Codd, G.A., 1999. Uptake and effects of microcystin-LR on detoxication enzymes of early life stages of the zebrafish (*Danio rerio*). *Environ. Toxicol.* 14 (1) 89–95.
- Wilhelm, S.W., Farnsley, S.E., LeClerc, G.R., Layton, A.C., Satchwell, M.F., DeBruyn, J.M., Boyer, G.L., Zhu, G., Paerl, H.W., 2010. The relationships between nutrients, cyanobacterial toxins and the microbial community in Taihu (Lake Tai), China. *Harmful Algae* 20, 207–215.
- Zehnder, A., Gorham, P.R., 1960. Factors influencing the growth of *Microcystis aeruginosa*. *Can. J. Microbiol.* 6, 645–660.
- Zar, J.H., 1999. *Biostatistical Analysis*, Fourth Edition. Prentice-Hall, Inc, Upper Saddle River, NJ, p. 425.

Factors Affecting Fish Entrainment into Massive Water Diversions in a Tidal Freshwater Estuary: Can Fish Losses be Managed?

LENNY F. GRIMALDO*¹

California Department of Water Resources, Division of Environmental Services, Aquatic Ecology Section,
 901 P Street, Sacramento, California 95814, USA, and Department of Fish, Wildlife, and Conservation
 Biology, University of California at Davis, One Shields Avenue, Davis, California 95616, USA

TED SOMMER, NICK VAN ARK, GARDNER JONES, AND ERIKA HOLLAND

California Department of Water Resources, Division of Environmental Services, Aquatic Ecology Section,
 901 P Street, Sacramento, California 95814, USA

PETER B. MOYLE

Department of Fish, Wildlife, and Conservation Biology, University of California at Davis,
 One Shields Avenue, Davis, California 95616, USA

BRUCE HERBOLD

U.S. Environmental Protection Agency, 75 Hawthorne Street, San Francisco, California 94105, USA

PETE SMITH

U.S. Geological Survey, 6000 J Street, Placer Hall, Sacramento, California 95819, USA

Abstract.—We examined factors affecting fish entrainment at California's State Water Project and Central Valley Project, two of the largest water diversions in the world. Combined, these diversions from the upper San Francisco Estuary support a large component of the municipal and agricultural infrastructure for California. However, precipitous declines in the abundance of several estuarine fish species, notably the threatened delta smelt *Hypomesus transpacificus*, have generated major concern about entrainment as a possible cause of the declines. We examined a 13-year data set of export pumping operations and environmental characteristics to determine factors affecting entrainment (as indexed by salvage at fish screens) and the potential for manipulation of these factors to improve conditions for fish. Entrainment of three migratory pelagic species—delta smelt, longfin smelt *Spirinchus thaleichthys*, and striped bass *Morone saxatilis*—was primarily determined by the seasonal occurrence of particular life stages close to the export facilities. We also found that the direction and magnitude of flows through the estuary and to the export facilities were reasonable predictors of pelagic fish entrainment. Entrainment of resident demersal species (prickly sculpin *Cottus asper* and white catfish *Ameiurus catus*) and littoral species (Mississippi silverside *Menidia audens* and largemouth bass *Micropterus salmoides*) was not explained by diversion flows, although large numbers of individuals from these species were collected. Our study suggests that entrainment of pelagic species can be effectively reduced by manipulating system hydrodynamics.

Worldwide, more than 50% of freshwater runoff is diverted from natural waterways, producing substantial impacts on aquatic resources (Postel 1992, 2000, 2005; Kingsford 2000). Estuaries are particularly sensitive to water diversions because reduced freshwater inflows can alter sediment budgets (Wright and Schoellhamer 2005), water quality (Lane et al. 1999; Monsen et al.

2007), biological productivity (Jassby and Cloern 2000; Jassby 2005), and distribution of invertebrates (Stora and Arnoux 1983; Rodriguez et al. 2001; Kimmerer 2002a; Massengill 2004) and fishes (Kimmerer 2002a; Feyrer et al. 2007). Natural mortality for young fishes is very high (Houde 1987); entrainment adds additional mortality that can compromise population resilience (Barnthouse et al. 1983; Stevens et al. 1985; Boreman and Goodyear 1988; Pawson and Eaton 1999; Bennett 2005; Kimmerer 2008). A better understanding of how the timing and magnitude of water diversions influence fish entrainment can help managers reduce entrainment of fish and any impacts

* Corresponding author: lgrimaldo@usbr.gov

¹ Present address: U.S. Bureau of Reclamation, 2800 Cottage Way, Sacramento, California 95825, USA.

Received March 19, 2008; accepted March 31, 2009

Published online September 3, 2009

diversions may have on fish populations (Barnthouse et al. 1988).

The tidal freshwater region of the San Francisco Estuary, the Sacramento–San Joaquin Delta (hereafter, the Delta), is a key nursery area for many resident and migratory fishes. The Delta also contains two of the largest water diversions in the world: the pumps of the State Water Project (SWP) and the federally operated Central Valley Project (CVP), which can jointly export $28 \times 10^6 \text{ m}^3$ of water/d from the Delta and up to $8 \times 10^9 \text{ m}^3$ of water/year. The SWP provides drinking water for over 23 million Californians. Water exports from the Delta also help fuel an estimated US\$25 billion annual agricultural economy, the largest agricultural economy in North America and one of the largest in the world.

Water demands often exceed supplies in California, resulting in conflicts over the allocation of freshwater among beneficial uses (Mount 1995; Service 2007). In recent years, these conflicts have increased because many pelagic fishes in the estuary have dropped to record low abundances while demands for water have increased (Sommer et al. 2007). Historically, many fishes in the estuary responded favorably to wetter years because high inflows usually improved spawning and rearing conditions in the estuary (Stevens and Miller 1983; Sommer et al. 1997; Kimmerer et al. 2001; Bennett 2005; Feyrer et al. 2007; Rosenfield and Baxter 2007). The strength of these relationships has diminished during the last few years for several possible reasons, including habitat changes, water diversions, food web alterations, and stock–recruitment effects (Sommer et al. 2007). As a consequence of declining pelagic fish populations and the resulting conflicts over water use, resource managers face a major crisis in the upper San Francisco Estuary (Service 2007).

The biological focus of water conflicts in the estuary is the native delta smelt *Hypomesus transpacificus*, a small, near-annual fish (Family Osmeridae) that is listed as threatened under the California Endangered Species Act (CESA) and the federal Endangered Species Act (ESA). Although many factors have been identified as stressors for delta smelt in the estuary (Bennett and Moyle 1996; Bennett 2005; Sommer et al. 2007), water diversions are perhaps the most readily “manageable” because export operations can be altered to reduce losses of fish or improve habitat conditions. For example, freshwater flow to the estuary is managed so that salinity is less than 2 practical salinity units at three control points in the estuary (Jassby et al. 1995) for a varying number of days between February and June (Kimmerer 2002b). This salinity standard, known as X_2 , was implemented because many species show

increased abundance, survival, or other positive responses to freshwater flows (Jassby et al. 1995; Kimmerer 2002a; Dege and Brown 2004; Feyrer et al. 2007).

There is considerable concern about the number of fish entrained at the export facilities. Unlike the X_2 –fish relationships, there is no direct evidence that entrainment affects population-level responses of fish. However, reductions in entrainment are obviously desirable given the status of pelagic fishes in the estuary; better information is needed about the factors that influence the timing, duration, and magnitude of entrainment losses. Because there are excellent long-term data sets on fish abundance, water quality, and hydrology in the Delta, we reasoned that it should be possible to identify the factors that have a strong influence on fish losses. In this paper, we compare long-term trends of hydrology, biological variables, and water quality with trends in the collection of several kinds of fishes counted at large fish facility louvers situated in front of the large export pumps. To develop a broader understanding of the effects of water diversions, we examined fishes from several representative groups: (1) pelagic fishes (delta smelt, longfin smelt *Spirinchus thaleichthys*, and striped bass *Morone saxatilis*); (2) littoral fishes (largemouth bass *Micropterus salmoides* and Mississippi silverside *Menidia audens*); and (3) demersal fishes (prickly sculpin *Cottus asper* and white catfish *Ameiurus catus*). These species are particularly important for protection (e.g., delta smelt and longfin smelt), for supporting recreational fisheries (e.g., largemouth bass and striped bass), or because they are numerically dominant species in their communities (e.g., prickly sculpin and Mississippi silverside). Our questions were (1) what are the long-term patterns in entrainment at the SWP and CVP; and (2) what factors influence entrainment of these fishes from the estuary on interannual and intra-annual scales? We hypothesized that pelagic fishes would show strong patterns in entrainment related to water project operations, while patterns in littoral and demersal fishes would be less evident. Our intent was to develop information that would provide insight into potential management actions that can be implemented at the SWP and CVP and perhaps at water diversions in other regions.

Study Area and Background

The Sacramento and San Joaquin rivers drain into the San Francisco Bay through the Delta (Figure 1). The Delta has been transformed over the last century from a large, contiguous marsh ecosystem into a channelized, armored-levee network of dredged sloughs (Conomos et al. 1985) that is unstable in structure and subject to dramatic change (Moyle 2008).

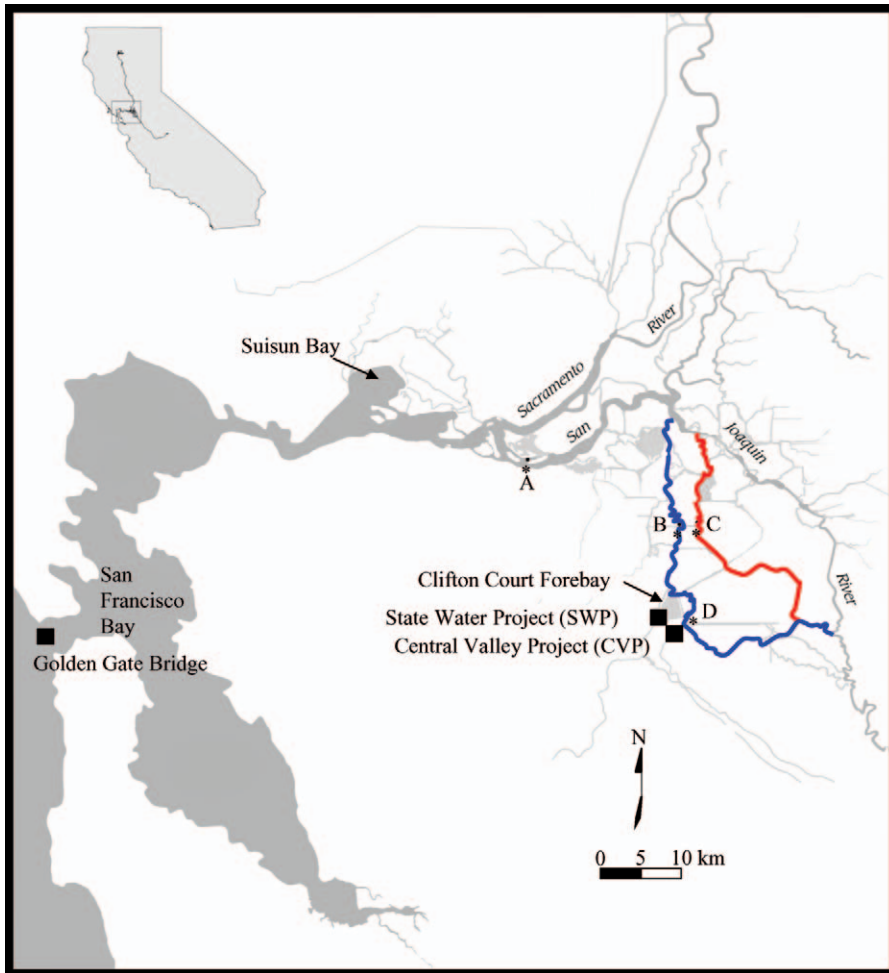


FIGURE 1.—Map of the San Francisco Estuary and the Sacramento–San Joaquin Delta, California. The State Water Project (SWP) and Central Valley Project (CVP) export and fish facilities are located in the southern Delta. The SWP and CVP water exports are best measured by combined daily tidal net flow of the Old River (blue line) and the Middle River (red line). Continuous monitoring stations for water temperature and specific conductance (A), Old River flow (B), Middle River flow (C), and turbidity (D) are indicated.

Upstream dams and diversions have substantially altered the hydrograph. Spring flows are approximately one-tenth of what they would be without the operation of upstream reservoirs (Knowles 2002). In contrast, late-summer and fall flows are now higher than what they were historically (Knowles 2002) because reservoir releases are made to fulfill export demands and to maximize storage capacity in upstream reservoirs for flood control. Releases are also made to produce suitable habitat for Chinook salmon *Oncorhynchus tshawytscha* below the reservoirs (National Marine Fisheries Service 2004).

The SWP Harvey O. Banks Pumping Plant is

operated by the California Department of Water Resources (CDWR), and the CVP Jones Pumping Plant is operated by the U.S. Bureau of Reclamation. The CVP and SWP both divert water from Old River, a tidal slough that intersects the lower San Joaquin River. Even at minimal exports, SWP and CVP operations can cause the tidally averaged flow in the Old River, Middle River, and other adjacent channels in the southern Delta to reverse and flow landward towards the diversions (Arthur et al. 1996; Monsen et al. 2007). The SWP can export water from the Delta at a rate of up to 292 m³/s, and the CVP can export water at up to 130 m³/s. At the entrance of the SWP are five gates

(6.1 × 6.1 m) that are opened and closed on a tidal basis (Le 2004). Behind the gates is Clifton Court Forebay, a relatively shallow (average depth ~ 2 m), 9.2-km² staging reservoir for SWP exports and the California Aqueduct (Kano 1990).

In front of the CVP and SWP pumps are fish salvage facilities designed to capture entrained fishes (Arthur et al. 1996; Brown et al. 1996; Bowen et al. 1998). The Tracy Fish Collection Facility on the CVP and the Skinner Fish Facility on the SWP use large behavioral louvers to steer fish into bypass structures, where the fish are counted and identified (Brown et al. 1996; Bowen et al. 1998). Daily salvage counts for each species at each facility are calculated by the following:

$$N_{di} = \sum_{p=1}^{P_{di}} \frac{N_{dpi}M_{dpi}}{m_{dpi}}, \quad (1)$$

where N_{di} is the total daily salvage at facility i (SWP or CVP), P_{di} is the number of time periods sampled during day d at facility i , N_{dpi} is the number of fish counted at facility i during time period p (min) on day d , M_{dpi} is the duration (min) of a fish salvage period p on day d for facility i , and m_{dpi} is the duration (min) of the subsampling interval during a fish salvage period p on day d for facility i . Typically, there are 12 sample periods/d. From each species, 20 individuals greater than 20 mm fork length (FL) are measured. Captured or "salvaged" fish are put into aerated tanks on trucks and then released back into the Delta downstream of the facilities. The term "salvage" is used by convention because the targeted Chinook salmon and striped bass are assumed to be saved from entrainment and released unharmed downstream (Brown et al. 1996). Other fish, particularly delta smelt, are likely to have low survival rates in the handling process (Swanson et al. 1996); therefore, under the federal ESA such fish are considered to be lost from the population upon collection (U.S. Fish and Wildlife Service 2005).

In this paper, we use salvage as an index of entrainment. Actual entrainment losses at the SWP and CVP are unknown because fish are not sampled continuously and because the louvers are less than 100% effective (Brown et al. 1996; Puckett et al. 1996; Bowen et al. 1998). Louver efficiency varies by species, life stage, and probably facility (Bowen et al. 1998, 2004), but for the purposes of this paper we assume that louver efficiencies are constant within and among years. The SWP salvage data also do not include additional fish losses in the Clifton Court Forebay as a result of predation before reaching the louvers (Gingras 1997) or within the holding tanks themselves (Liston et al. 1994). We assume that

relative predation losses in the forebay have remained constant among years in the absence of monitoring of predator numbers. Finally, prior to 1993, identification of fishes by technicians was focused on striped bass and Chinook salmon, with little consistency in the identification and counting of other fishes (Brown et al. 1996). In 1993, the California Department of Fish and Game (CDFG) emphasized accurate identification of all species. We only analyzed data collected since 1993.

Life History Traits of the Fishes Examined

The delta smelt is a near-annual species that resides in brackish waters around the western Delta and Suisun Bay region of the estuary (Moyle 2002). In the winter (December to April), prespawning delta smelt migrate to tidal freshwater habitats for spawning, and larvae rear in these areas before emigrating down to brackish water (Bennett 2005). Adult longfin smelt may also migrate into the Delta during the winter for spawning, generally moving up from San Francisco Bay or the Pacific Ocean (Rosenfield and Baxter 2007). Longfin smelt are native to the Pacific coast and generally spawn in brackish and freshwater of the estuary when 2 years old (Rosenfield and Baxter 2007), although some will live for up to 3 years (Moyle 2002). Longfin smelt were recently proposed for listing under CESA and the federal ESA (Bay Institute et al. 2007).

Striped bass, introduced to the San Francisco Estuary in 1879, generally migrate during the spring from saltwater (ocean or bay waters) to freshwater for spawning. Some age-1 and adult striped bass will return upstream during the fall (Stevens 1979). Age-0 striped bass generally rear in the Delta and Suisun Bay during the late spring and summer, and most then migrate to the San Francisco Bay or Pacific Ocean during the fall (Stevens 1979).

Resident fishes selected for analyses included the most abundant littoral and demersal fish species in the Delta (Feyrer and Healey 2003; Grimaldo et al. 2004; Nobriga et al. 2005; Brown and Michniuk 2007). The littoral species we chose were largemouth bass (introduced to California in 1891), which are strongly associated with submerged aquatic vegetation (Grimaldo et al. 2004; Nobriga et al. 2005), and Mississippi silversides (introduced to California in 1967), which are most often found in open-shoal areas. The demersal species analyzed were prickly sculpin (native), the larvae of which commonly occur in the water column (Grimaldo et al. 2004), and white catfish (introduced to California in 1874), the most abundant demersal species recorded in the salvage during the last two decades (Brown et al. 1996).

TABLE 1.—Summary of model inputs used to examine salvage of pelagic, demersal, and littoral species at the State Water Project and Central Valley Project fish facilities in the Sacramento–San Joaquin Delta, California. Life stage was determined from the length files in the salvage database. Mean fork lengths (FL; with SD) of life stages are also provided. Analyses were performed at interannual (inter) and intra-annual (intra) time scales depending on available monitoring data (na = no available data). Variables are combined Old and Middle River flows (OMR; m³/s) water temperature (WT; °C), turbidity (T; nephelometric turbidity units), zooplankton abundance (ZA), position of the 2-*psu* (practical salinity units) isohaline (X_2), and California Department of Fish and Game survey indices (FMWT = fall midwater trawl; TNS = tow-net survey; 20 mm = survey for juvenile fish \geq 20 mm FL).

Species	Life stage	FL (mm)	Inter	Intra	Period	Years	Variables
Delta smelt	Age 0	29 (5)	Yes	Yes	May–Jun	1995–2005	OMR, WT, T, ZA, 20 mm
	Adult	67 (7)	Yes	Yes	Dec–Mar	1993–2005	OMR, WT, T, ZA, X_2 , FMWT
Longfin smelt	Age 0	30 (6)	Yes	Yes	Apr–May	1995–2005	OMR, WT, T, ZA, X_2 , 20 mm
	Adult	89 (24)	Yes	Yes	Dec–Feb	1993–2005	OMR, WT, T, ZA, X_2 , FMWT
Striped bass	Age 0	43 (35)	Yes	Yes	Jun–Aug	1995–2005	OMR, WT, T, ZA, X_2 , TNS
	Age 1	114 (47)	Yes	na	Jan–Mar	1993–2005	OMR, WT, T, ZA, X_2 , TNS
Prickly sculpin	Age 0	31 (8)	Yes	Yes	May–Jul	1995–2005	OMR, WT, T, ZA, X_2 , 20 mm
	Adult	80 (20)	Yes	na	Jan–Mar	1995–2005	OMR, WT, T, ZA, X_2
White catfish	Age 0	47 (17)	Yes	Yes	Jun–Aug	1995–2005	OMR, WT, T, ZA, X_2 , 20 mm
	Age 1, adult	136 (69)	Yes	na	Jan–Mar	1993–2005	OMR, WT, T, ZA, X_2
Mississippi silverside	Age 0	34 (11)	Yes	Yes	Jun–Aug	1995–2005	OMR, WT, T, ZA, X_2 , 20 mm
	Adult	69 (17)	Yes	na	Jan–Mar	1993–2005	OMR, WT, T, ZA, X_2
Largemouth bass	Age 0	36 (21)	Yes	Yes	Jun–Aug	1995–2005	OMR, WT, T, ZA, X_2 , 20 mm
	Age 1, adult	116 (79)	Yes	na	Jan–Mar	1993–2005	OMR, WT, T, ZA, X_2

Methods

Data Sources

For each species, adult and age-0 life stages were estimated from length measurements that were made between December 1992 and 2005 and that were reported in the salvage database. Because not all of the fish counted on each day were measured, we estimated the total number of age-0 fish and age-1 and older fish in the daily counts by extrapolating the proportion of each life stage in the fish measured to the expanded counts for each day. We omitted one data point for longfin smelt from April 7, 1998, when 616 longfin smelt were recorded during the salvage count at 0400 hours (California Fish and Game 2007). We doubt the accuracy of this record because it occurred during a high-flow period (e.g., San Joaquin River, >594 m³/s; Old and Middle rivers, >288 m³/s), when salvage is generally low and when fish dispersion should be high, resulting in a catch that is spread out over a few days or hours. The highest upstream observation of larval longfin smelt in the CDFG 20-mm survey (sampling of young fish between March and July) that year was in San Pablo Bay (Dege and Brown 2004), corroborating our logic that longfin smelt salvage should have been very low.

The daily salvage data for each species (SWP and CVP combined) were plotted to show general recruitment patterns. Inspection of these plots allowed us to identify the primary months when each species was salvaged (Table 1). For example, the historical data showed that more than 90% of the total adult delta smelt collections occurred between December and

March ($>99\%$ in 8 of 13 years) and that over 90% of the longfin smelt collections occurred from December to February, so we used these winter months to define the peak adult entrainment period for these species.

Factors that May Affect Entrainment

To determine factors that influence salvage of fishes at the CVP and SWP, we compiled data on hydrodynamics, water quality, and biological factors (Table 1). The data sources that we used for pelagic fishes were somewhat more extensive than for other species because these fish are of special management significance in the estuary (Service 2007; Sommer et al. 2007). These data sets are described below.

Hydrodynamic and water quality variables.—Combined Old and Middle River daily net flows (nontidally averaged) were used instead of actual SWP and CVP water diversions to determine entrainment effects because these daily net flows reasonably measure the hydrodynamic “pull” of the exports (Arthur et al. 1996; Monsen et al. 2007) when used at the time scale applied in our analyses. Old and Middle River flow integrates a complex set of factors, including flows from the large and small tributaries, daily and neap-spring tidal variation, local agricultural diversions, and wind. Old and Middle River flows are measured daily using acoustical velocity meters (installed by the U.S. Geological Survey) located near Bacon Island (Figure 1; Arthur et al. 1996). Total inflow (m³/s) is the sum of the Sacramento River, San Joaquin River, and Yolo Bypass inflows and several smaller tributary inflows that enter the Delta (Interagency Ecological Program 2007).

Continuous water temperature and specific conductance data were compiled from a gaging station located on the lower San Joaquin River near Antioch (State Water Resources Control Board 1978). Turbidity data were obtained from a continuous monitoring sensor located in the Old River at the entrance to the SWP.

Abundance and distribution.—Abundance of fish in the vicinity of the diversions can have a major effect on entrainment (Sommer et al. 1997). Hence, we included estimates of abundance near the diversions in our analyses of factors that may affect salvage rates. The data differed depending on life stage and number of years of survey data. For age-0 fishes, we used mean annual abundances from the Delta locations in the CDFG 20-mm survey during concurrent salvage periods for all species except striped bass. The CDFG 20-mm survey, which began in 1995, typically samples young fish during each neap tide between March and July (Dege and Brown 2004). For age-0 striped bass, we evaluated the number of young fish near the diversions using the Delta index from the CDFG tow-net survey (TNS), which is used to quantify abundance of age-0 striped bass (38 mm FL; Turner and Chadwick 1972; Kimmerer et al. 2001). For striped bass, our data set included all years between 1993 and 2005 except for 1995 and 2002, when indices were not calculated for this species.

We used X_2 to test whether the distribution of adult delta smelt, longfin smelt, and striped bass during the month prior to their salvage period influenced annual salvage or intra-annual salvage numbers. X_2 is an effective measure of pelagic fish distribution in the estuary (Jassby et al. 1995; Kimmerer 2002b; Dege and Brown 2004; Feyrer et al. 2007). The effect of year-class strength was examined using the CDFG fall midwater trawl survey index (Moyle et al. 1992; Kimmerer et al. 2001) for the pelagic fishes. Similar analyses were not conducted on adult demersal and littoral species because there is currently no reliable monitoring program for these fishes in the estuary.

Prey abundance.—Zooplankton abundance from the CDFG 20-mm survey (Delta stations only) was assumed to reflect favorable habitat conditions that either promoted greater residence times or survival of age-0 fishes in the Delta, thereby resulting in greater entrainment risk and salvage. This assumption is probably valid for delta smelt, whose summer–fall survival is linked to zooplankton abundance between July and October (Kimmerer 2008). Only calanoid copepodids and copepods were used from the zooplankton data since these are the dominant prey consumed by delta smelt (Nobriga 2002). For the other fishes, we used total zooplankton abundance

(Delta stations only) because they are known to have more diverse diets (Feyrer et al. 2003).

Data Analysis

Relationships between water quality and hydrodynamic variables were identified using locally weighted scatterplot smoothers (i.e., LOWESS; Venables and Ripley 2002) and visual inspection of bivariate plots. A reduced set of environmental parameters was then selected to compare with salvage data. To remove the effect of autocorrelation within each variable and the large number of zeros in the salvage database, analyses were focused on intra-annual and interannual trends by averaging independent and dependent variables into bimonthly or monthly and annual time periods. Intra-annual models were limited to life stages and species for which data were available (Table 1).

We used ordinary least-squares regression to test whether intra-annual and interannual salvage patterns were influenced by physical and biological factors. Statistically significant models were identified using best-subset procedures. Combined Old and Middle River flows constituted the export effect in each model because this variable has been shown to be a good index of diversion flow when examined at the time scales (i.e., intra- and interannual) explored here (Monsen et al. 2007). If inclusion of this variable did not contribute significantly to the model, it was omitted and the remaining variables were examined using the best-subset procedure. The best subsets were determined using Akaike's information criterion (AIC) values; AIC penalizes for increasing the number of free parameters but rewards goodness of model fit (Venables and Ripley 2002). Where the data failed to meet assumptions of normality (Anderson–Darling test: $P < 0.05$), the data were log transformed. Nonlinear least-squares regression was used for cases in which a linear relationship was deemed unsuitable based on visual inspection of the regression plots (i.e., curvilinear fits) and AIC values.

For adult delta smelt and longfin smelt, the intra-annual salvage data were partitioned into monthly averages to determine which factors might influence the timing of salvage. The interaction of Old and Middle River flows and X_2 position in the month prior was examined for adult smelt to see whether their salvage was influenced by their proximity (i.e., distribution) to the SWP and CVP before they migrated upstream. We expected that X_2 would have little or no effect on adult smelt salvage during periods when Old and Middle River flows were strongly seaward. Turbidity was used in the model to test whether salvage followed large precipitation in the basin, otherwise known as “first flush” events. Turbidity

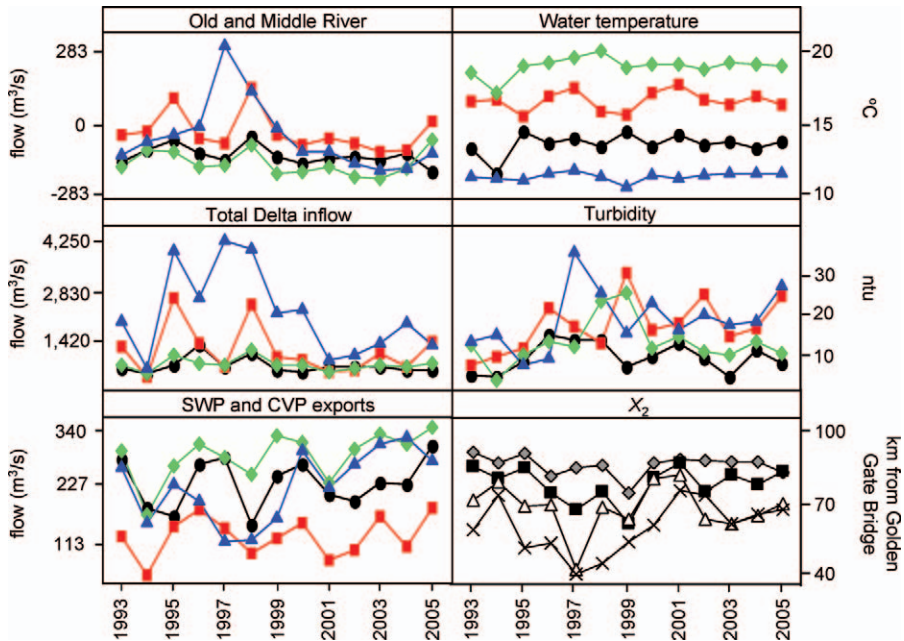


FIGURE 2.—Physical variables used to examine State Water Project (SWP) and Central Valley Project (CVP) fish salvage dynamics in the Sacramento–San Joaquin Delta, California, by season and year (blue triangles = winter, January–March; red squares = spring, April–June; green diamonds = summer, July–September; black circles = fall, October–December; ntu = nephelometric turbidity units). Mean monthly position of the 2-psu (practical salinity units) isohaline (X_2 ; km from the Golden Gate Bridge; Jassby et al. 1995) by year is also shown (gray diamonds = November; black squares = December; white triangles = January; × symbols = February).

was used in lieu of total river inflow since these variables were significantly correlated with each other at the monthly level (averaged daily data) during our study period ($r = 0.32$, $df = 142$, slope = 0.003, $P < 0.001$; excluding 9 months of missing turbidity data). For age-0 fishes, the intra-annual analyses were conducted on data divided into bi-monthly periods coincident with the CDFG 20-mm survey to test the factors influencing when age-0 fish (≥ 20 mm FL) show up in the salvage.

Results

Environmental Factors and Salvage Data

Combined Old and Middle River flows were negative or “reverse” during 47 of the 52 seasons examined (Figure 2). The most notable trend was a decrease in Old and Middle River flows during winter months corresponding to increased exports during the same period. Temperatures were generally consistent among years. Overall, the indices of adult pelagic fish abundance from CDFG monitoring surveys declined during the study period, but indices for age-0 fishes and zooplankton abundances were variable, with no obvious trend (Figure 3).

Between December 1992 and July 2005, the SWP and CVP salvaged 590,310 delta smelt, 122,747 longfin smelt, and over 32 million striped bass (Figure 4). Large numbers of littoral and demersal fishes were salvaged: 1,385,880 prickly sculpin, 3,214,687 Mississippi silversides, 596,827 largemouth bass, and 5,060,035 white catfish. Beginning in 1999, salvage of adult delta smelt and longfin smelt increased, with their highest salvage years being 2003 and 2002, respectively. Adult Mississippi silverside and largemouth bass numbers increased between 1999 and 2005, but these numbers are generally lower than numbers recorded in the early 1990s.

Salvage of age-0 native fishes (delta smelt, longfin smelt, and prickly sculpin) was highest during the spring, whereas salvage numbers of introduced species were higher in summer months (Figure 5). First salvage of adult delta smelt occurred within days of “first flush” events marked by sudden increases in river inflows and turbidity (Figure 6).

Statistical Approach

Old and Middle River flows, turbidity, and water temperature were selected as the predictor variables in

the salvage, following no obvious trends between them in the bivariate plots except for turbidity and combined Old and Middle River flows. Monthly averaged turbidity and combined Old and Middle River flows were moderately correlated during the study period ($r = 0.33$, $df = 142$, $slope = 0.018$, $P < 0.001$) but this relationship is driven during periods when Old and Middle River flows are extremely positive, which only occurred in a handful of months during periods of extreme high inflow. Therefore, turbidity was left in the models because it is a good indicator of pelagic habitat (Feyrer et al. 2007) and of seasonal river inflow. Specific conductance was significantly correlated with the combined Old and Middle River flows ($r = 0.32$, $df = 146$, $slope = -3.84$, $P < 0.001$) and therefore was eliminated from regression analyses to avoid confounding interpretations deriving from multicollinearity.

Factors Affecting Age-0 Salvage

The only model that explained interannual age-0 delta smelt salvage was that incorporating zooplankton (calanoid adults and copepods) abundance from the CDFG 20-mm survey (Figure 7). For age-0 longfin smelt, the Old and Middle River flow variable was the only parameter that explained interannual salvage abundance. Year-class strength was the only predictor of age-0 striped bass salvage. Prickly sculpin salvage was positively correlated with water temperature, and white catfish salvage was positively correlated with seaward Old and Middle River flows (Figure 7), but otherwise there were no significant predictors of salvage for age-0 resident fish. At the intra-annual scale, the best model that explained age-0 delta smelt salvage included Old and Middle River flows, turbidity, and CDFG 20-mm survey abundance (Table 2). For longfin smelt, Old and Middle River flows and 20-mm survey abundance were important predictors.

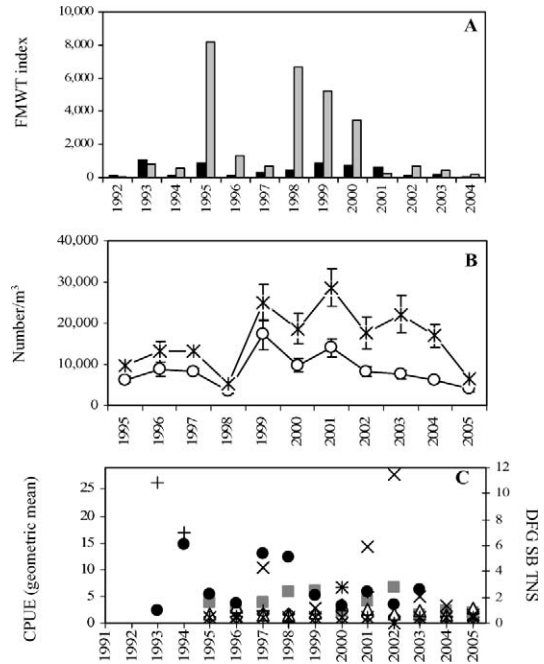


FIGURE 3.—Biological variables used to examine salvage dynamics in the State Water Project and Central Valley Project, California, by year: (A) annual delta smelt (black bars) and longfin smelt (gray bars) index values from the California Department of Fish and Game (CDFG) fall midwater trawl (FMWT) survey, 1992–2004; (B) mean abundance of calanoid copepods (open circles) and all zooplankton (stars) in the CDFG 20-mm survey; and (C) annual abundances (geometric mean of catch per unit effort, CPUE) of delta smelt (black circles), longfin smelt (× symbols), prickly sculpin (open triangles), largemouth bass (stars), Mississippi silversides (open diamonds), and white catfish (gray squares) from the CDFG 20-mm survey (primary y-axis) and Delta index for striped bass (SB) from the CDFG tow-net survey (TNS; plus symbols; secondary y-axis).

TABLE 2.—Regression coefficients and statistics for models that best explained intra-annual salvage (\log_{10} transformed) of age-0 delta smelt and longfin smelt at the State Water Project and Central Valley Project, California, between 1993 and 2005. See Table 1 for averaging periods and summary of all factors examined (OMR = combined Old and Middle River flows, m^3/s ; T = turbidity, nephelometric turbidity units; 20-mm survey = index from the California Department of Fish and Game survey of young fishes). The best models, as determined by the lowest value of Akaike’s information criterion (AIC), are highlighted in bold. Not all significant models are shown.

Species	OMR	T	20-mm survey	Intercept	df	r^2	AIC	P
Delta smelt	-0.008	—	—	2.47	42	0.36	147	<0.001
	-0.007	—	0.02	1.91	41	0.47	139	<0.001
	-0.006	0.07	—	1.30	41	0.50	137	<0.001
	-0.005	0.07	0.02	0.88	40	0.62	128	<0.001
Longfin smelt	-0.005	—	—	1.02	42	0.31	110	<0.001
	—	—	0.03	0.79	41	0.32	107	<0.001
	-0.003	—	0.02	0.82	40	0.42	101	<0.001

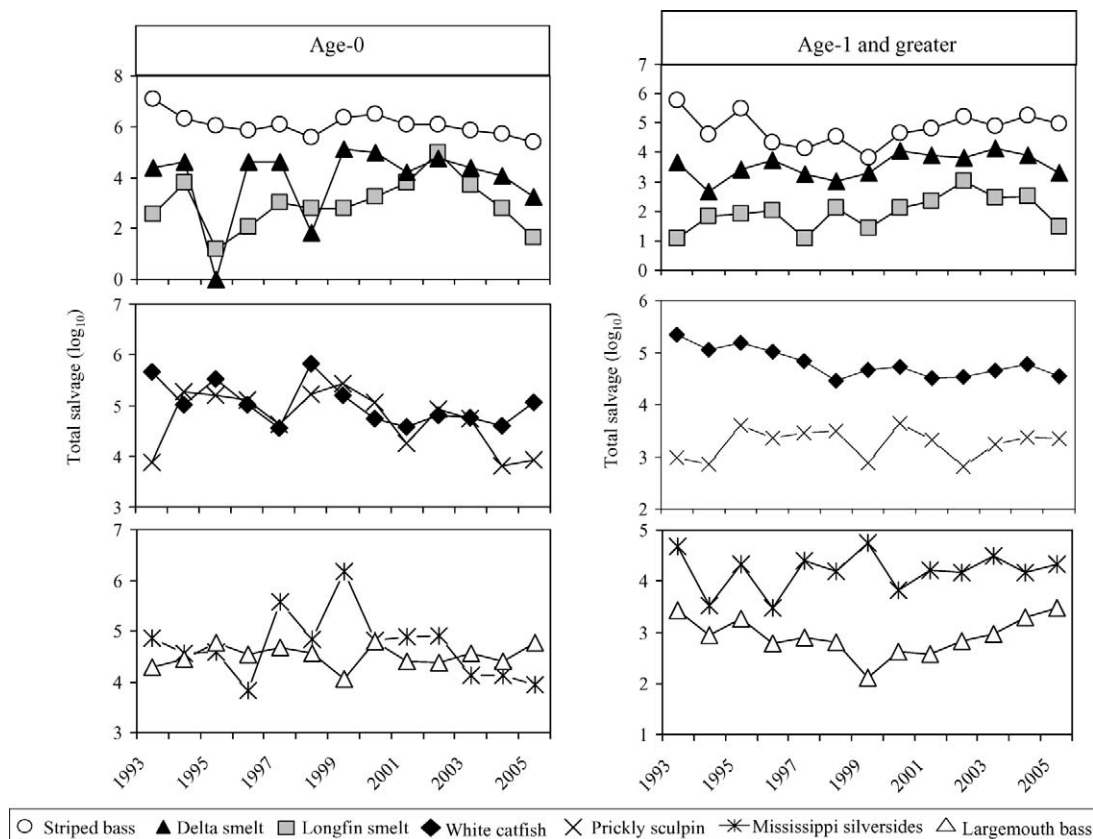


FIGURE 4.—Annual State Water Project and Central Valley Project (California) salvage numbers (\log_{10} transformed) by fish life stage (age 0, age 1 and older). See text for averaging periods.

Factors Affecting Age-1 and Adult Salvage

For the pelagic fishes, the best models of interannual salvage were based on Old and Middle River flows (Figure 8). We found no significant models for age-1 and older demersal and littoral fishes. At the intra-annual time scale, the interaction between the previous month's X_2 and the combined Old and Middle River flows was significant for explaining delta smelt salvage (Table 3). We found no significant model for longfin smelt at the intra-annual time scale.

Discussion

Understanding factors that influence the entrainment of fishes in the estuary is essential for developing management alternatives to protect fishes of concern. Few studies have examined patterns and mechanisms explaining fish losses at the CVP and SWP over the years (Stevens and Miller 1983; Stevens et al. 1985; Brown et al. 1996; Sommer et al. 1997; Bennett 2005; Kimmerer 2008), despite the fact that they are two of

the largest continuous fish sampling devices in the world. There have also been relatively few studies of the direct effects of water diversions from riverine and tidal ecosystems (Nobriga et al. 2004; Moyle and Israel 2005). Valuable information has been obtained about power plant entrainment impacts (Kelso and Millburn 1979; Boreman and Goodyear 1981, 1988; Hadderingh et al. 1983; Henderson et al. 1984); in some cases, power plant studies have revealed broader patterns of fish community dynamics (Love et al. 1998; Maes et al. 1998). Here, we show that fish losses are influenced by both biological and physical factors and provide insights into the seasonal behavior of fish in the Delta.

Life Stage

The most obvious trend in the salvage data is that far more age-0 fishes are entrained than age-1 and older fishes. This result was expected since there are simply more age-0 fishes than older age-classes and because smaller fishes are often more vulnerable to entrainment flows (Hadderingh et al. 1983; Henderson et al. 1984;

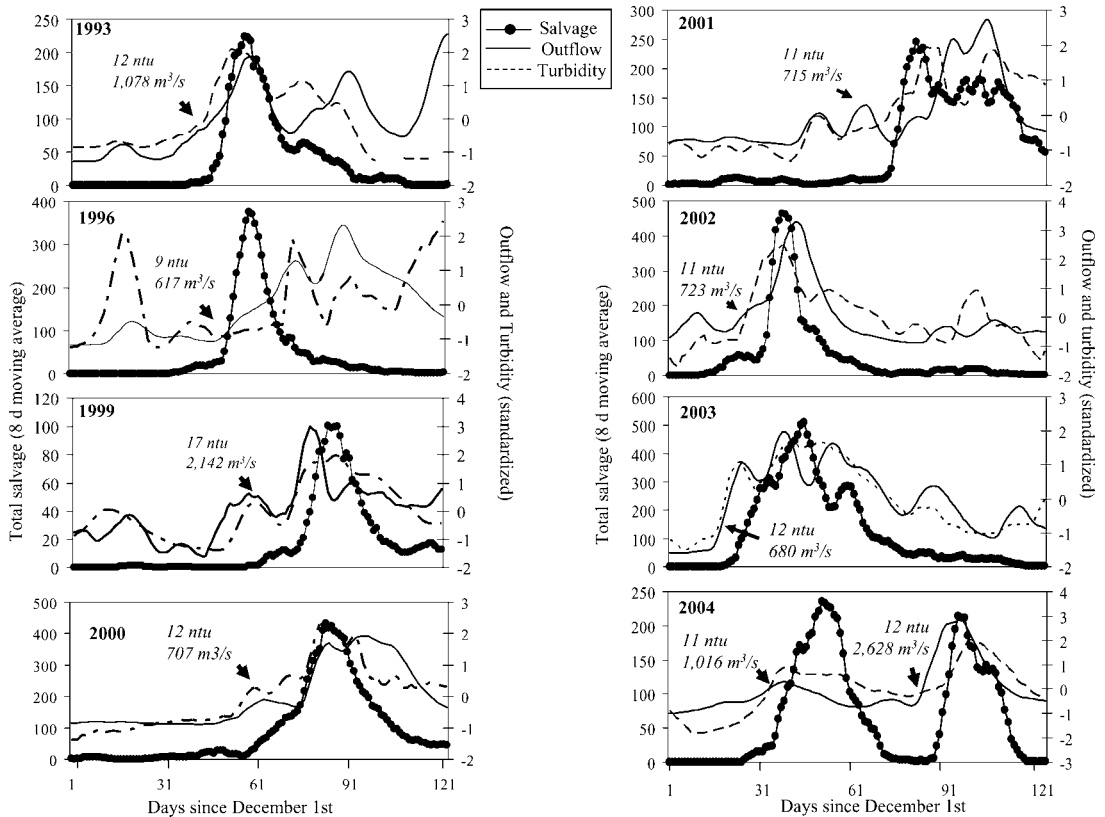


FIGURE 6.—Eight-day running averages of adult delta smelt salvage, total outflow (m^3/s), and turbidity (nephelometric turbidity units, ntu) for the eight most abundant delta smelt salvage years between December 1992 and April 2005 at the State Water Project and Central Valley Project, California. Total outflow and turbidity were standardized to a mean of zero.

sions. Though nearshore and demersal fishes can account for a large percentage of the numbers and biomass entrained in water diversions (Nobriga et al. 2004) or cooling water withdrawals (Hadderingh et al. 1983; Boreman and Goodyear 1988; Love et al. 1998), vulnerability is often highest during pelagic life stages or during periods of increased activity (e.g., feeding). Each group showed strong seasonality in entrainment (salvage), but there were major differences in the apparent effect of environmental conditions, including water exports. Specifically, exports as indexed by Old and Middle River flows play a major role in the salvage of pelagic fishes, but no similar pattern was observed in the littoral and demersal fishes. This is consistent with our hypothesis that the usual behaviors (i.e., strong habitat fidelity) of these fish limit their susceptibility to export flow effects. This result was somewhat surprising given that millions of age-0 littoral and demersal fishes are salvaged each year. Better sampling in these habitats may reveal mechanisms underlying entrainment of these fishes or mechanisms that show

why the abundance of these species has increased in recent years (Brown and Michniuk 2007) despite large removal by the water diversions.

Seasonal Patterns

Seasonal variation in entrainment is a common pattern observed at water diversions, often reflecting adult migrations (Jensen et al. 1982), age-0 recruitment (Love et al. 1998) or shifts in habitat use in relation to diversion intakes (Turnpenney 1988; Maes et al. 1998). Our investigation reveals that native fishes (delta smelt, longfin smelt, and prickly sculpin) are more vulnerable to exports during winter and spring months, whereas introduced fishes (striped bass, Mississippi silverside, largemouth bass, and white catfish) are more often salvaged during late spring and summer. The seasonal entrainment patterns observed here are consistent with patterns in the Delta; native species mostly spawn and recruit earlier in the year when temperatures are cooler ($\sim 8\text{--}16^\circ\text{C}$), whereas introduced species typically recruit during the summer when temperatures are warmer

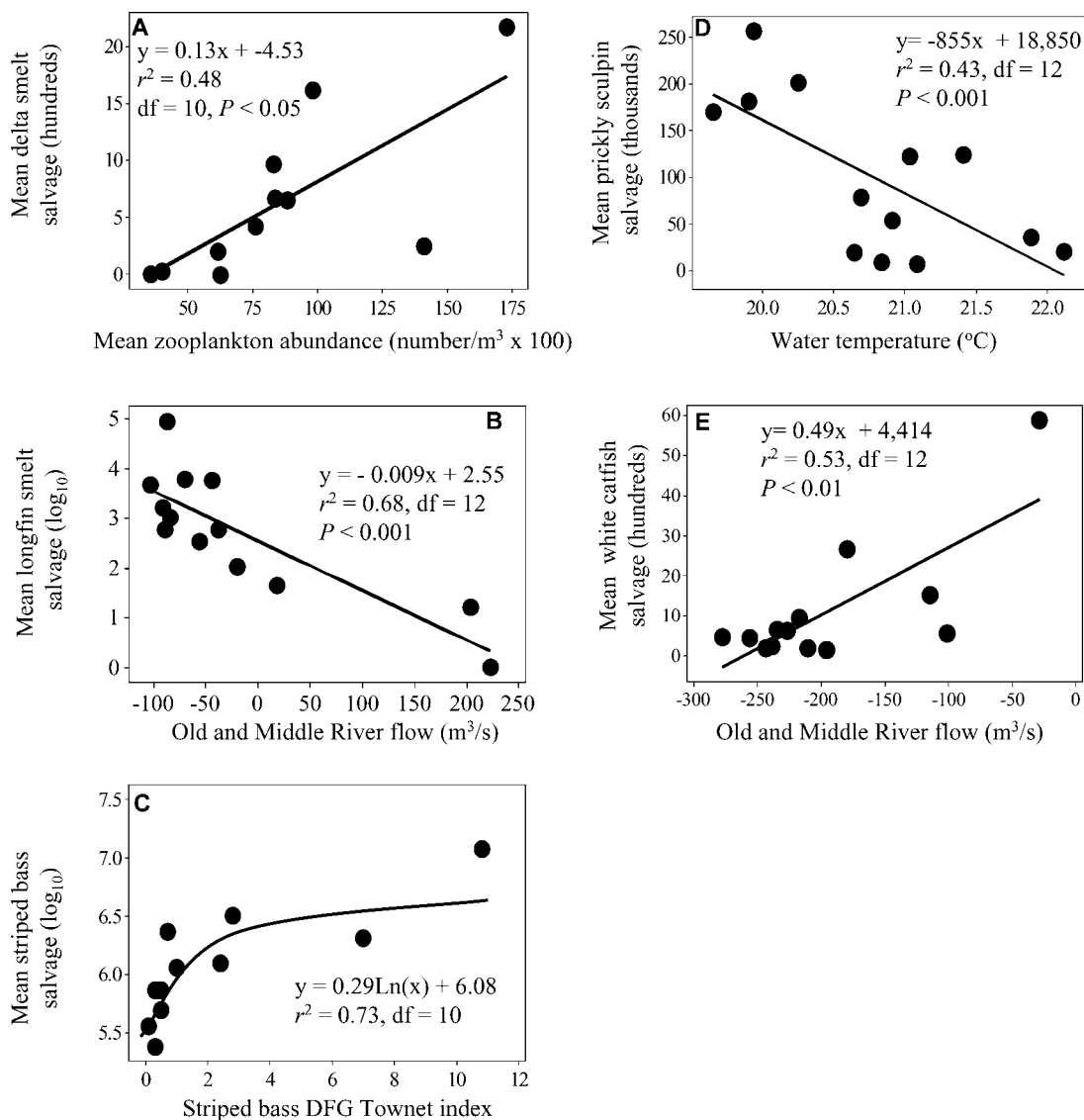


FIGURE 7.—Relationships between (A) age-0 delta smelt annual salvage in the State Water Project and Central Valley Project, California, and zooplankton abundance; (B) longfin smelt salvage and combined flow of the Old and Middle rivers; (C) striped bass salvage and the California Department of Fish and Game (DFG) tow-net survey index; (D) prickly sculpin salvage and water temperature; and (E) white catfish salvage and Old and Middle River flow. No other parameters explained the salvage of these species. See Table 1 for averaging periods.

(>15°C; Moyle 2002; Feyrer and Healey 2003; Feyrer 2004; Grimaldo et al. 2004; Bennett 2005). For the smelts, the salvage data indicate that few fish were entrained between July and November (Figure 5), mostly because the smelts' distribution shifts seaward during this period (Dege and Brown 2004; Noriga et al. 2008), whereas for resident species the seasonality in entrainment is more likely explained by habitat use.

Prey Availability

Prey availability may play a role in losses of fish at the export facilities. Annual salvage of age-0 delta smelt was best predicted by zooplankton (calanoid copepod) abundance. Kimmerer (2008) showed that survival of delta smelt between summer and fall was explained by zooplankton biomass. High zooplankton abundance may increase the survival and residence

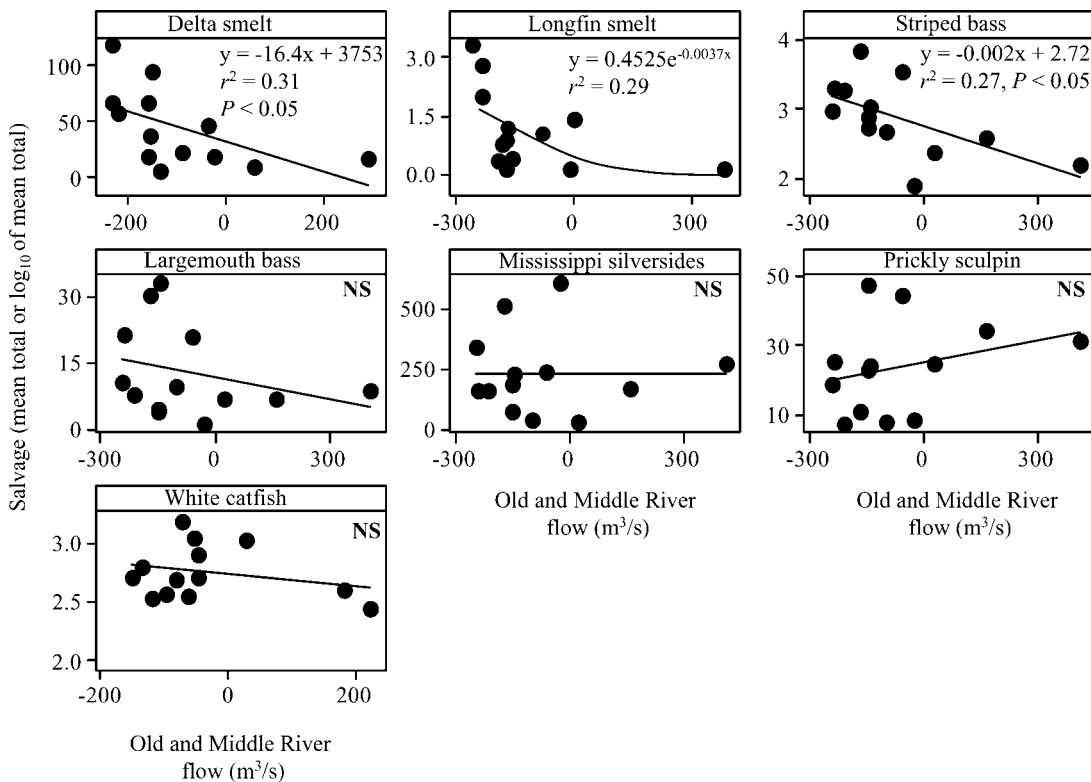


FIGURE 8.—Relationships between annual salvage of age-1 and older fishes in the State Water Project and Central Valley Project, California, and the combined flow of the Old and Middle rivers. For pelagic fishes (delta smelt, longfin smelt, and striped bass), Old and Middle River flow was the only variable that explained salvage. Regression models were not significant (NS, $P > 0.05$) for littoral (Mississippi silverside and largemouth bass) or demersal (white catfish and prickly sculpin) species.

time of age-0 delta smelt in the Delta, thereby increasing their entrainment risk in the southern portion of the Delta. Our study does not address whether entrainment represents a large source of mortality for delta smelt, but Kimmerer (2008) showed that high entrainment during dry years can result in large population losses for delta smelt.

Year-Class Strength

Similar to Sommer et al. (1997), our salvage analyses suggest that entrainment patterns may be affected by year-class strength. Specifically, we found that the number of age-0 striped bass salvaged was well predicted ($r = 0.81$) by their numbers in the TNS (Delta stations only) conducted by CDFG. Because Old and Middle River flows were not found to be a significant predictor of age-0 striped bass, we believe the relationship between striped bass salvage and year-class strength highlights the importance of localized effects (Stevens et al. 1985). In the case of age-0 striped bass, fish losses are probably episodic when large aggregations become entrained over short

intervals. The longer averaging period used in our study may obscure these sorts of short-term relationships with environmental conditions responsible for movements of schools or changes in behavior. For example, in recent years, water exports have been managed at low levels in April and May to protect delta smelt and emigrating Chinook salmon, but the exports quickly increase in June (Figure 2; see Old and Middle River flow panel) when these species move downstream. The transition in exports between May and June could be the reason why age-0 striped bass salvage increases substantially in June (Figure 5). Our study was not designed to capture such intermonthly variability, but we recognize its importance for understanding salvage patterns at daily to weekly time scales.

Age-0 delta smelt salvage at the intra-annual scale was related to the abundance of these fish in the Delta, but Old and Middle River flows and turbidity were also strong predictors. Thus, for delta smelt, the mechanisms influencing entrainment within a year is probably a measure of the degree to which their

physical habitat overlaps with the hydrodynamic "footprint" of the Old and Middle River flows. A similar result was found for age-0 longfin smelt, where Old and Middle River flows and year-class strength (from the CDFG 20-mm survey) were found to be significant predictors (Table 2) of salvage. Although spring represents a low-export period during which Old and Middle River flows are typically slightly negative (Figure 2), entrainment risk for age-0 smelts is likely to be high when they often spawn and rear in the Delta, which happens frequently for delta smelt (Nobriga et al. 2008). For adult delta smelt and longfin smelt, year-class strength did not predict salvage at the interannual level, but X_2 (used as an index of their distribution) was a predictor for delta smelt salvage at the intra-annual scale when Old and Middle River flows were negative. This result suggests that the role of population size in determining the number of adult smelt salvaged is very small when Old and Middle River flows are seaward but is probably much more important when flows are in the reverse direction, as was noted by Kimmerer (2008) for delta smelt.

Hydrodynamics

A common question in studies of riverine ecosystems is whether fish move with flow. This is a difficult question to address without direct field observations using approaches such as telemetry, a relatively impractical approach for rare and fragile species like the delta smelt (Swanson et al. 1996; Bennett 2005). Moreover, flow is especially complex in estuaries, where short- and long-term variation in tidal flow dominates. Nonetheless, the relatively strong relationships between Old and Middle River flows and the annual adult delta smelt, longfin smelt, and age-1 striped bass entrainment (salvage) indicate that fish are at least partially moving with reverse net flow towards the export facilities. In contrast, juvenile white catfish exhibited a positive relationship between salvage and seaward Old and Middle River flow, suggesting that their salvage is driven by upstream recruits that become vulnerable to entrainment when advected towards the export facilities.

Management Implications

The recent sharp decline of pelagic fish populations in the estuary has increased scrutiny of water diversion impacts in the estuary (Service 2007; Sommer et al. 2007). Though many factors have been identified as candidates for the recent decline (e.g., low food web productivity, contaminants, and water quality), CVP and SWP diversions represent one of the most directly observable sources of mortality. Our study was not designed to address the most important management

issue: whether these water diversions have population-level effects. Population-level consequences have been best studied for striped bass. Striped bass larval production was historically explained by river flows and southern Delta exports (Stevens et al. 1985). However, Kimmerer et al. (2001) found that export effects were small and sporadic, primarily occurring during the first several months of life. Moreover, striped bass population dynamics is best explained by density dependence between age-1 and age-2 year-classes, a bottleneck that dampens variation from effects early in life (Kimmerer et al. 2000). However, our analyses indicate that if there are years when density dependence is relaxed, then age-0 striped bass losses could be reduced by managing export flows during periods when these fish are abundant in the Delta.

The degree to which water exports have population-level effects on delta smelt is poorly understood. However, losses of delta smelt are perhaps greatest during winter, which represents the main period of adult delta smelt migration and spawning. We observed that recent increases in winter salvage of delta smelt (Figure 4) were associated with higher exports and reverse Old and Middle River flows (Figure 2). These changes were coincident with the low numbers of pelagic fishes in 2000 (Sommer et al. 2007), so it is possible that export losses of adults and their offspring contributed to the recent decline of delta smelt. Bennett (2005) and Kimmerer (2008) provide evidence that losses of larvae produced from these spawners can be substantial; however, the extent to which entrainment losses affect delta smelt population dynamics is unclear. Modeling studies by Bennett (2005) indicate that effects of exports on delta smelt growth and survival are very difficult to detect, so this issue remains unresolved.

Even if the population-level effects of fish entrainment are not well understood, the rapid decline of pelagic fish populations in the San Francisco Estuary has resulted in a substantial interest in finding ways to reduce losses. Traditionally, water diversion impacts are mitigated with placement of diversion screens (Moyle and Israel 2005). The SWP and CVP have fish louvers for this purpose, although they were designed primarily for Chinook salmon (Brown et al. 1996) and other species and life stages have not been adequately addressed. Hence, improvements in fish louver or screen design (e.g., positive barrier screens) could reduce losses of some of the species that we studied (Moyle and Israel 2005). Approach velocity criteria are already implemented for striped bass at 0.30 m/s, but this only provides protection for fish in the vicinity of the water diversions (State Water Resources Control

Board 1978). The present study suggests that water diversion impacts can be mitigated on a larger scale by altering the timing of exports based on the biology of fishes and changes in key physical and biological variables. Such a strategy has been used on the Hudson River, New York, where export reductions at three power plants successfully reduced the number of striped bass entrained during the winter months (Barnthouse et al. 1988). Combined with other efforts to reduce mortality, this seems to have permitted a dramatic restoration of the striped bass population on the Hudson River (Daniels et al. 2005).

The present study also suggests that fish losses can be managed through careful consideration of hydrodynamics and water quality. For example, minimizing reverse flows during periods when delta smelt and longfin smelt are migrating into the Delta could substantially reduce mortality of the critical adult life stage. The relationship between salvage of adult delta smelt and combined Old and Middle River flows (Figure 8) indicates that entrainment can be managed through manipulation of exports. Because the Old and Middle River flow variable improved the models for longfin smelt and striped bass salvage, this variable has reasonably broad applications. In addition, the significant effect of turbidity on adult delta smelt salvage (Table 2) suggests that reducing exports during periods of high outflows could reduce losses of this imperiled fish. One possibility is the implementation of an export reduction during the period immediately after the first flush, when turbidities in the Delta increase to over 10 nephelometric turbidity units (Figure 6).

Similarly, monitoring of the salinity in the estuary gives a good indication of fish distribution (Kimmerer 2002a; Dege and Brown 2004; Feyrer et al. 2007) and hence the potential for fish to be affected by water diversions. As a consequence, exports during higher outflow conditions or when X_2 is downstream would be expected to result in lower pelagic fish losses, an effect noted by Sommer et al. (1997). Temperature monitoring could also assist in the management of some species. For example, if prickly sculpin losses were a concern, exports could be adjusted according to water temperature, the only variable that significantly predicted age-0 prickly sculpin salvage (Figure 7). Overall, the native fishes examined here, and presumably other early spawning native fishes in the Delta, should benefit from a reduction in water exports between December and June. However, if such an export reduction is mitigated by increased exports in fall, then delta smelt habitat could be affected (Feyrer et al. 2007). In contrast, this study illustrates how ineffective it would be to manage the exports to reduce entrainment of largemouth bass or other littoral species

because these fish occupy habitat that probably buffers them from entrainment.

In summary, long-term monitoring data from two of the world's largest water diversions show that patterns of entrainment vary substantially with life history and season and that entrainment interacts in complex ways with hydrodynamics, water quality, and biological variables. Our findings demonstrate that integrated approaches to reduce entrainment are needed as part of a broader effort to restore imperiled fishes in the San Francisco Estuary, especially in light of rapid estuarine change (Moyle 2008). Some of these observations have already been incorporated into management of the San Francisco Estuary (Kimmerer 2002b; U.S. Fish and Wildlife Service 2005). While our findings are in many respects unique to the complex hydrodynamics and exceptionally large water diversions of the San Francisco Estuary, our demonstration of the importance of factors such as seasonality, species differences, fish year-class strength, food availability, and water quality should have application to fish entrainment in other geographical areas.

Acknowledgments

We want to thank the CDWR South Delta Program, Interagency Ecological Program, and San Francisco Estuary Program for funding and support. We also thank Russ Gartz, Kelly Souza, Cathy Ruhl, Jay Simi, and Robert Duvall for assistance with data collection and handling. Matt Nobriga, Larry Brown, Bill Bennett, Fred Feyrer, and the Delta Smelt Working Group provided helpful discussions and feedback about the data analyses and interpretation. The manuscript was improved by suggestions from two anonymous reviewers.

References

- Arthur, J. F., M. D. Ball, and S. Y. Baughman. 1996. Summary of federal and state water project environmental impacts in the San Francisco Bay-Delta Estuary, California. Pages 445–495 in J. T. Hollibaugh, editor. San Francisco Bay: the Ecosystem. American Association for the Advancement of Science, Pacific Division, San Francisco.
- Barnthouse, L. W., J. Boreman, T. L. Englert, W. L. Kirk, and E. G. Horn. 1988. Pages 267–273 in L. W. Barnthouse, R. J. Klauda, D. S. Vaughan, and R. L. Kendall, editors. Science law and Hudson River power plants. American Fisheries Society Monograph 4, Bethesda, Maryland.
- Barnthouse, L. W., W. Van Winkle, and D. S. Vaughan. 1983. Impingement losses of white perch at Hudson River power plants: magnitude and biological significance. *Environmental Management* 7:355–364.
- Bay Institute, Center for Biological Diversity, and Natural Resources Defense Council. 2007. Petition to the state of California Fish and Game Commission and supporting

- information for the listing of longfin smelt (*Spirinchus thaleichthys*) as an endangered species under the California Endangered Species Act. Available: www.bay.org/LongfinSmeltState.pdf. (July 2007).
- Bennett, W. A. 2005. Critical assessment of the delta smelt population in the San Francisco Estuary, California. *San Francisco Estuary Watershed Science* 3: Volume 3, Issue 2, Article 1. Available: <http://repositories.cdlib.org>. (July 2007).
- Bennett, W. A., and P. B. Moyle. 1996. Where have all the fishes gone? Interactive factors producing fish declines in the Sacramento-San Joaquin Estuary. Pages 519–542 in J. T. Hollibaugh, editor. *San Francisco Bay: the Ecosystem*. American Association for the Advancement of Science, Pacific Division, San Francisco.
- Boreman, J., and C. P. Goodyear. 1981. An empirical methodology for estimating entrainment losses at power plants sites on estuaries. *Transactions of the American Fisheries Society* 110:255–262.
- Boreman, J., and C. P. Goodyear. 1988. Estimates of entrainment mortality for striped bass and other fish species inhabiting the Hudson River estuary. Pages 152–160 in L. W. Barnthouse, R. J. Klauda, D. S. Vaughan, and R. L. Kendall, editors. *Science law and Hudson River power plants*. American Fisheries Society, Monograph 4, Bethesda, Maryland.
- Bowen, M. D., B. B. Baskerville-Bridges, K. W. Frizell, L. Hess, C. A. Carp, S. M. Siegfried, and S. L. Wynn. 2004. Empirical and experimental analyses of secondary louver efficiency at the Tracy Fish Collection Facility, March 1996 to November 1997. *Tracy Fish Facility Studies*, Volume 11, U.S. Bureau of Reclamation, Mid-Pacific Region, Denver Technical Service Center.
- Bowen, M., S. Siegfried, C. Liston, L. Hess, and C. Karp. 1998. Fish collections and secondary louver efficiency at the Tracy Fish Collection Facility, October 1993 to September 1995. *Tracy Fish Collection Facility Studies*, Volume 7, U.S. Bureau of Reclamation, Mid-Pacific Region, Denver Technical Service Center.
- Brown, L. R., S. Greene, P. Coulston, and S. Barrow. 1996. An evaluation of the effectiveness of fish salvage operations at the intake to the California Aqueduct, 1979–1993. Pages 497–518 in J. T. Hollibaugh, editor. *San Francisco Bay: the Ecosystem*. American Association for the Advancement of Science, Pacific Division, San Francisco.
- Brown, L. R., and D. Michniuk. 2007. Littoral fish assemblages of the alien-dominated Sacramento–San Joaquin Delta, California, 1980–1983 and 2001–2003. *Estuaries and Coasts* 30:186–200.
- California Department of Fish and Game. 2007. Fish salvage monitoring. Available: [fpt://fpt.delta.dfg.ca.gov/salvage/](http://fpt.delta.dfg.ca.gov/salvage/). (August 1, 2007).
- California Department of Water Resources. 2007. California Data Exchange Center. Available: cdec.water.ca.gov. (July 1, 2007).
- Conomos, T. J., R. E. Smith, and J. W. Gartner. 1985. Environmental setting of San Francisco Bay. *Hydrobiologia* 129:1–12.
- Daniels, R. A., K. E. Limburg, R. E. Schmidt, D. L. Strayer, and R. C. Chambers. 2005. Changes in fish assemblages in the tidal Hudson River, New York. Pages 471–504 in J. N. Rinne, R. M. Hughes, and B. Calamusso, editors. *Historical changes in large river fish assemblages of the Americas*. American Fisheries Society, Symposium 45, Bethesda, Maryland.
- Dege, M., and L. R. Brown. 2004. Effect of outflow on spring and summertime distribution of larval and juvenile fishes in the upper San Francisco Estuary. Pages 49–65 in F. Feyrer, L. R. Brown, R. L. Brown, and J. J. Orsi, editors. *Early life history of fishes in the San Francisco estuary and watershed*. American Fisheries Society, Symposium 39, Bethesda, Maryland.
- Feyrer, F. 2004. Ecological segregation of native and alien larval fish assemblages in the southern Sacramento-San Joaquin Delta. Pages 67–79 in F. Feyrer, L. R. Brown, R. L. Brown, and J. J. Orsi, editors. *Early life history of fishes in the San Francisco estuary and watershed*. American Fisheries Society, Symposium 39, Bethesda, Maryland.
- Feyrer, F., and M. Healey. 2003. Fish community structure and environmental correlates in the highly altered southern Sacramento-San Joaquin Delta. *Environmental Biology of Fishes* 66:123–132.
- Feyrer, F., B. Herbold, S. A. Matern, and P. B. Moyle. 2003. Dietary shifts in a stressed fish assemblage: consequences of a bivalve invasion in the San Francisco Estuary. *Environmental Biology of Fishes* 67:277–288.
- Feyrer, F., M. L. Nobriga, and T. R. Sommer. 2007. Multi-decadal trends for three declining fish species: habitat patterns and mechanisms in the San Francisco Estuary, California, USA. *Canadian Journal of Fisheries and Aquatic Sciences* 64:723–734.
- Gingras, M. 1997. Mark/recapture experiments at Clifton Court Forebay to estimate pre-screening losses to juvenile fishes 1976–1993. *Interagency Ecological Program Technical Report* 55.
- Grimaldo, L. F., R. E. Miller, C. M. Peregrin, and Z. P. Hymanson. 2004. Spatial and temporal distribution of ichthyoplankton in three habitat types of the Sacramento-San Joaquin Delta. Pages 81–96 in F. Feyrer, L. R. Brown, R. L. Brown, and J. J. Orsi, editors. *Early life history of fishes in the San Francisco estuary and watershed*. American Fisheries Society, Symposium 39, Bethesda, Maryland.
- Haddinger, R. H., G. H. F. M. van Aerssen, L. Groeneveld, H. A. Jenner, and J. W. Van Der Stoep. 1983. Fish impingement at power stations situated along the rivers Rhine and Meuse in The Netherlands. *Aquatic Ecology* 17:129–141.
- Henderson, P. A., A. W. H. Turmpenny, and R. N. Bamber. 1984. Long-term stability of a sand smelt (*Atherina presbyter* Cuvier) population subject to power station cropping. *Journal of Applied Ecology* 21:1–10.
- Houde, E. D. 1987. Fish early life dynamics and recruitment variability. Pages 17–29 in R. D. Hoyt, editor. *Tenth annual larval fish conference*. American Fisheries Society, Symposium 2, Bethesda, Maryland.
- Interagency Ecological Program. 2007. Dayflow documentation. Available: www.iep.water.ca.gov/dayflow/documentation/index.html. (July 15, 2007).
- Jassby, A. D. 2005. Phytoplankton regulation in a eutrophic tidal river (San Joaquin River, California). *San Francisco Estuary and Watershed Science*, Volume 3, Issue 1,

- Article 3. Available: <http://repositories.cdlib.org>. (July 2007).
- Jassby, A. D., and J. E. Cloern. 2000. Organic matter sources and rehabilitation of the Sacramento-San Joaquin Delta (California, USA). *Aquatic Conservation: Marine and Freshwater Ecosystems* 10:323–352.
- Jassby, A. D., W. J. Kimmerer, S. G. Monismith, C. Armor, J. E. Cloern, T. M. Powell, J. R. Schubel, and T. J. Vendlinski. 1995. Isohaline position as a habitat indicator for estuarine populations. *Ecological Applications* 5:272–289.
- Jensen, A. L., S. A. Spigarelli, and M. M. Thommes. 1982. Use of conventional fishery models to assess entrainment and impingement of three Lake Michigan fish species. *Transactions of the American Fisheries Society* 111:21–34.
- Kano, R. M. 1990. Occurrence and abundance of predator fish in Clifton Court Forebay, California. Interagency Ecological Program Technical Report 24.
- Kelso, J. R. M., and G. S. Millburn. 1979. Entrainment and impingement of fish by power plants in the Great Lakes which use the once-through cooling process. *Journal of Great Lakes Research* 5:182:194.
- Kimmerer, W. J. 2002a. Effects of freshwater flow on abundance of estuarine organisms: physical effects or trophic linkages? *Marine Ecology Progress Series* 243:39–55.
- Kimmerer, W. J. 2002b. Physical, biological, and management responses to variable freshwater flow into the San Francisco Estuary. *Estuaries* 25:1275–1290.
- Kimmerer, W. J. 2008. Losses of Sacramento River Chinook salmon and delta smelt to entrainment in water diversions in the Sacramento-San Joaquin Delta. *San Francisco Estuary and Watershed Science Volume 6, Issue 2* (June), Article 2. Available: <http://repositories.cdlib.org>. (September 2008).
- Kimmerer, W. J., J. H. Cowan, Jr., L. W. Miller, and K. A. Rose. 2000. Analysis of an estuarine striped bass population: influence of density-dependent mortality between metamorphosis and recruitment. *Canadian Journal of Fisheries and Aquatic Sciences* 57:478–486.
- Kimmerer, W. J., J. H. Cowan, Jr., L. W. Miller, and K. A. Rose. 2001. Analysis of an estuarine striped bass population: effects of environmental conditions during early life. *Estuaries* 24:556–574.
- Kingsford, R. T. 2000. Ecological impacts of dams, water diversions and river management on floodplain wetlands in Australia. *Austral Ecology* 25:109–127.
- Knowles, N. 2002. Natural and management influences on freshwater inflows and salinity in the San Francisco Estuary at monthly to inter-annual scales. *Water Resources Research* 38:1–11.
- Lane, R. R., J. W. Day, Jr., and B. Thibodeaux. 1999. Water quality analysis of a freshwater diversion at Caernarvon, Louisiana. *Estuaries* 22:327–336.
- Le, K. 2004. Calculating Clifton Court Forebay inflow. Pages 1–12 in *Methodology for flow and salinity estimates in Sacramento-San Joaquin Delta and Suisun Marsh*. 25th Annual Progress Report.
- Liston, C., C. Karp, L. Hess, and S. Hiebert. 1994. Predator removal activities and intake channel studies, 1991–1992. *Tracy Fish Facility Studies, Volume 1*, U.S. Bureau of Reclamation, Mid-Pacific Region, Denver Technical Service Center.
- Love, M. S., J. E. Caselle, and K. Herbinson. 1998. Declines in nearshore rockfish recruitment and populations in the southern California Bight as measured by impingement rates in coastal electrical power generating stations. *U.S. National Marine Fisheries Service Fishery Bulletin* 9:492–501.
- Maes, J., A. Taillieu, P. A. Van Damme, K. Cottenie, and F. Ollevier. 1998. Seasonal patterns in the fish and crustacean community of a turbid temperate estuary. *Estuarine, Coastal, and Shelf Science* 47:143:151.
- Massengill, R. R. 2004. Entrainment of zooplankton at the Connecticut Yankee Plant. Pages 59–64 in P. M. Jacobson, D. A. Dixon, W. C. Leggett, B. C. Marcy, Jr., and R. R. Massengill, editors. *The Connecticut River Ecological Study (1965–1973) revisited: ecology of the lower Connecticut River 1973–2003*. American Fisheries Society, Monograph 9, Bethesda, Maryland.
- Monsen, N. E., J. E. Cloern, and J. R. Burau. 2007. Effects of flow diversions on water and habitat quality; examples from California's highly manipulated Sacramento-San Joaquin Delta. *San Francisco Estuary and Watershed Science* 5(3): article 2. Available: repositories.cdlib.org/jmie/sfews/vol5/1553/art2. (March 2008).
- Mount, J. F. 1995. *California Rivers and Streams*. University of California Press, Berkeley.
- Moyle, P. B. 2002. *Inland Fishes of California*. University of California Press, Berkeley.
- Moyle, P. B. 2008. The future of fish in response to large-scale change in the San Francisco Estuary, California. Pages 357–374 in K. D. McLaughlin, editor. *Mitigating impacts of natural hazards on fishery ecosystems*. American Fisheries Society, Symposium 64, Bethesda, Maryland.
- Moyle, P. B., B. Herbold, D. E. Stevens, and L. W. Miller. 1992. Life history of delta smelt in the Sacramento-San Joaquin Estuary, California. *Transactions of the American Fisheries Society* 121:67–77.
- Moyle, P. B., and J. A. Israel. 2005. Untested assumptions: effectiveness of screen diversions for conservation of fish populations. *Fisheries* 30:20–28.
- National Marine Fisheries Service. 2004. *Biological Opinion on the long-term Central Valley Project and State Water Project operations criteria and plan*. National Oceanic and Atmospheric Administration Fisheries, Southwest Region, Long Beach, California.
- Nobriga, M. 2002. Larval delta smelt diet composition and feeding incidence: environmental and ontogenetic influences. *California Fish and Game* 88:149–164.
- Nobriga, M. L., F. Feyrer, R. D. Baxter, and M. Chotkowski. 2005. Fish community ecology in an altered river delta: spatial patterns in species composition, life history strategies, and biomass. *Estuaries* 28:776–785.
- Nobriga, M. L., Z. Matica, and Z. P. Hymanson. 2004. Evaluating entrainment vulnerability to agricultural irrigation diversions: a comparison among open-water fishes. Pages 281–295 in F. Feyrer, L. R. Brown, R. L. Brown, and J. J. Orsi, editors. *Early life history of fishes in the San Francisco estuary and watershed*. American Fisheries Society, Symposium 39, Bethesda, Maryland.
- Nobriga, M. L., R. T. Sommer, F. Feyrer, and K. Fleming.

2008. Long-term trends in summertime habitat suitability for Delta smelt (*Hypomesus transpacificus*). San Francisco Estuary and Watershed Science, Volume 6, Issue 1 (February), Article 1. Available: <http://repositories.cdlib.org>. (August 2008).
- Pawson, M. G., and D. R. Eaton. 1999. The influence of a power station on the survival of juvenile sea bass in an estuarine nursery area. *Journal of Fish Biology* 54:1143–1160.
- Postel, S. 1992. Last oasis: facing water scarcity. World Watch Environmental Alert Series. Norton, New York.
- Postel, S. 2000. Entering an era of water scarcity: the challenges ahead. *Ecological Applications* 10:941–948.
- Postel, S. 2005. Liquid assets: the critical need to safeguard freshwater ecosystems. Worldwatch Paper 170.
- Puckett, K., C. Liston, C. Karp, and L. Hess. 1996. Preliminary examination of factors that influence fish salvage estimates at the Tracy Fish Collection Facility, California, 1993 and 1994. Tracy Fish Collection Facility Studies, Volume 4. U.S. Bureau of Reclamation, Mid-Pacific Region, Denver Technical Service Center.
- Rodriguez, C. A., K. W. Flessa, and D. L. Dettman. 2001. Effects of upstream diversion of Colorado River water on the estuarine bivalve mollusc *Mulinia coloradoensis*. *Conservation Biology* 15:249–258.
- Rosenfield, J. R., and R. D. Baxter. 2007. Population dynamics and distributional patterns of longfin smelt in the San Francisco Estuary. *Transactions of the American Fisheries Society* 136:1577–1592.
- Service, R. 2007. Delta blues, California-style. *Science Magazine* 317:442–445.
- Sommer, T., C. Armor, R. Baxter, R. Breuer, L. Brown, M. Chotkowski, S. Culberson, F. Feyrer, M. Gingras, B. Herbold, W. Kimmerer, A. Mueller-Solger, M. Nobriga, and K. Souza. 2007. The collapse of pelagic fishes in the upper San Francisco Estuary. *Fisheries* 32(6):270–277.
- Sommer, T., R. Baxter, and B. Herbold. 1997. The resilience of splittail in the Sacramento-San Joaquin Estuary. *Transactions of the American Fisheries Society* 126:961–976.
- State Water Resources Control Board. 1978. Water right decision 1485. State Water Resources Control Board, Sacramento, California.
- Stevens, D. E. 1979. Environmental factors affecting striped bass (*Morone saxatilis*) in the Sacramento-San Joaquin Estuary. Pages 469–478 in R. J. Conomos, editor. San Francisco Bay: the Urbanized Estuary. American Association for the Advancement of Science, Pacific Division, San Francisco.
- Stevens, D. E., D. W. Kolhorst, L. W. Miller, and D. W. Kelly. 1985. The decline of striped bass in the Sacramento-San Joaquin Estuary, California. *Transactions of the American Fisheries Society* 114:12–30.
- Stevens, D. E., and L. W. Miller. 1983. Effects of river flow on abundance of young Chinook salmon, American shad, longfin smelt, and delta smelt in the Sacramento-San Joaquin River system. *North American Journal of Fisheries Management* 3:425–437.
- Stora, G., and A. Arnoux. 1983. Effects of large freshwater diversions on benthos of a Mediterranean lagoon. *Estuaries* 6:115–125.
- Swanson, C., R. Mager, S. I. Doroshov, and J. J. Cech. 1996. Use of salts, anesthetics, and polymers to minimize handling and transport mortality in delta smelt. *Transactions of the American Fisheries Society* 125:326–329.
- Turner, J. L. 1966. Distribution and food habits of ictalurid fishes in the Sacramento-San Joaquin Delta. California Department of Fish and Game Fish Bulletin 136:130–143.
- Turner, J. L., and P. Chadwick. 1972. Distribution and abundance of young-of-the-year striped bass, *Morone saxatilis*, in relation to river flow in the Sacramento-San Joaquin Estuary. *Transactions of the American Fisheries Society* 101:442–452.
- Turnpenny, A. W. H. 1988. Fish impingement at estuarine power stations and its significance to commercial fishing. *Journal of Fish Biology* 33:103–110.
- U.S. Fish and Wildlife Service. 2005. Biological opinion on reinitiation of formal and early section 7 endangered species consultation on the coordinated operations of the Central Valley Project and State Water Project and the operational criteria and plan to address potential critical habitat issues. Service file 1-1-05-F-0044.
- Venables, W. N., and B. D. Ripley. 2002. Modern applied statistics with S, 4th edition. Springer-Verlag, New York.
- Wright, S. A., and D. H. Schoellhamer. 2005. Estimating sediment budgets at the interface between rivers and estuaries with application to the Sacramento-San Joaquin River Delta. *Water Resources Research* 41.



Anthropogenic influence on sedimentation and intertidal mudflat change in San Pablo Bay, California: 1856–1983

Bruce E. Jaffe ^{a,*}, Richard E. Smith ^{b,1}, Amy C. Foxgrover ^a

^a U.S. Geological Survey Pacific Science Center, Santa Cruz, CA 95064, USA

^b U.S. Geological Survey, Menlo Park, CA 94025, USA

Received 15 February 2007; accepted 18 February 2007

Available online 19 April 2007

Abstract

Analysis of a series of historical bathymetric surveys has revealed large changes in morphology and sedimentation from 1856 to 1983 in San Pablo Bay, California. In 1856, the morphology of the bay was complex, with a broad main channel, a major side channel connecting to the Petaluma River, and an ebb-tidal delta crossing shallow parts of the bay. In 1983, its morphology was simpler because all channels except the main channel had filled with sediment and erosion had planed the shallows creating a uniform gently sloping surface. The timing and patterns of geomorphic change and deposition and erosion of sediment were influenced by human activities that altered sediment delivery from rivers. From 1856 to 1887, high sediment delivery ($14.1 \times 10^6 \text{ m}^3/\text{yr}$) to San Francisco Bay during the hydraulic gold-mining period in the Sierra Nevada resulted in net deposition of $259 \pm 14 \times 10^6 \text{ m}^3$ in San Pablo Bay. This rapid deposition filled channels and increased intertidal mudflat area by 60% (37.4 ± 3.4 to $60.6 \pm 6.2 \text{ km}^2$). From 1951 to 1983, $23 \pm 3 \times 10^6 \text{ m}^3$ of sediment was eroded from San Pablo Bay as sediment delivery from the Sacramento and San Joaquin Rivers decreased to $2.8 \times 10^6 \text{ m}^3/\text{yr}$ because of damming of rivers, riverbank protection, and altered land use. Intertidal mudflat area in 1983 was $31.8 \pm 3.9 \text{ km}^2$, similar to that in 1856. Intertidal mudflat distribution in 1983, however, was fairly uniform whereas most of the intertidal mudflats were in the western part of San Pablo Bay in 1856. Sediment delivery, through its affect on shallow parts of the bay, was determined to be a primary control on intertidal mudflat area. San Pablo Bay has been greatly affected by human activities and will likely continue to erode in the near term in response to a diminished sediment delivery from rivers.

© 2007 Elsevier Ltd. All rights reserved.

Keywords: sedimentation; bathymetry; long-term changes; intertidal flats; tidal flats; estuary; USA; California; San Francisco Estuary; San Francisco Bay; San Pablo Bay

1. Introduction

The spatial and temporal distribution of sedimentation, including the processes of deposition, transport, and erosion, is fundamental information for making sound decisions on a wide variety of management issues for estuaries. Sedimentation changes bathymetry and therefore habitat extent and distribution. Bathymetric changes, in turn, affect flow patterns and tidal exchange, which are important in sediment, salt, larval, and nutrient transport (e.g., Uncles and Peterson, 1996;

Monismith et al., 2002). Predicting natural and anthropogenic changes to ecosystems and designing successful restoration projects require knowledge of patterns of deposition and erosion. For example, intertidal mudflat extent is controlled by sedimentation. Planning maintenance of shipping channels and disposal sites for dredged material is better done with the knowledge of the distribution of natural sediment accumulation and erosion. Contaminant transport and cycling are also influenced by sedimentation (Marvin-DiPasquale et al., 2003; Schoellhamer et al., 2003). Deposition of clean sediment can isolate contaminated sediment, or conversely, erosion may expose contaminated sediments deposited at some time in the past (Higgins et al., 2005, 2007). At a longer time scale, planning for estuarine ecosystem change requires understanding

* Corresponding author.

E-mail address: bjaffe@usgs.gov (B.E. Jaffe).

¹ Retired.

how natural changes in the environment (e.g., sea-level rise, drought periods) and human activities, such as water management, affect sedimentation.

Although knowledge of long-term trends in deposition and erosion are important for proper management of estuarine ecosystems, it is difficult to gain this knowledge from short field experiments or other traditional methods. A long-term, large-scale perspective of the sediment system is possible, however, by analyzing a long sequence of bathymetric surveys.

This paper presents a history of bathymetry, deposition, erosion, and intertidal flat change in San Pablo Bay, California from 1856 to 1983 and relates it to changes in sediment delivery to the bay. This history was developed using computer analysis and display of hydrographic and topographic surveys made by the U.S. Coast and Geodetic Survey and the National Ocean Service (NOS). This study is not the first one addressing bathymetric change in San Pablo Bay (Gilbert, 1917; Smith, 1965; Ogden Beeman and Associates and Ray Krone and Associates, 1992) but is the most comprehensive to date.

2. Setting

San Pablo Bay is a circular bay in the northern part of the San Francisco Estuary, California (Fig. 1). The bay is shallow – two-thirds of it is less than 2 m deep at mean lower low water (MLLW). The average depth of San Pablo Bay at mean tide is 3.7 m. A deep (11–24 m, average 12 m) main channel in its southern part connects Central San Francisco Bay in the west to Carquinez Strait in the east. This channel, which averages about 2.5 km in width, is an important control on San Pablo Bay's hydrodynamic regime (Gartner and Yost, 1988) and sediment-delivery pattern (Ruhl et al., 2001).

Winds are predominantly northwesterly and are strongest during the spring and summer, with average wind speeds of approximately 3 m/s on the west shore (Hayes et al., 1984). Winter storms, which occur about twice a month, cause southeasterly and southerly winds that can exceed 18 m/s in velocity

(Conomos and Peterson, 1976). Diurnal winds are strongest during the summer, with typical afternoon wind speeds of 9 m/s, which is three times faster than morning winds (Miller, 1967).

Forcing at time scales ranging from seconds to decades influences the hydrodynamic regime of San Pablo Bay. Waves generated by moderate winds have heights of 0.5 m and periods of 2 s (Klingeman and Kaufman, 1965). Because of the short wave periods, wave orbital velocities decay rapidly with depth and interact with the bottom only in the shallow parts of the bay (e.g., water depths of less than 3 m for a 2 s period wave). Winter storms can generate larger waves with periods of 5 s in the San Francisco Bay system (Putnam, 1947). Besides generating waves, winds generate mean currents that persist for hours or days. At a longer time scale, tides and tidal currents are important. Tides in San Pablo Bay are mixed semidiurnal (form numbers of 0.71–0.77; Cheng and Gartner, 1984). Tidal currents are greatest in the main channel, with spring tide velocities of more than 1 m/s, decreasing in shallower water to 0.4 m/s in 2-m water depth (Cheng and Gartner, 1984; Gartner and Yost, 1988). The average tidal range is 1.8 m (National Oceanic and Atmospheric Administration, 1986). Water level in the study area also varies at a longer time scale. Sea level, measured by a tide gauge near the entrance to the San Francisco Estuary (Golden Gate) (Lyles et al., 1988), rose at an average rate of about 1.3 mm/yr, or about 17 cm, during the period of hydrographic surveys (1856–1983).

Bottom-sediment grain size in San Pablo Bay reflects local hydrodynamics and sediment source. Median grain size ranges from 2.3 μm at a low-energy point in the center of the bay to 430 μm in the energetic main channel near Carquinez Strait (Locke, 1971). Except for the main channel and several shallow areas, sediment consists predominantly of mud – more than half of the bay contains sediment with a median grain size of less than 5 μm .

Sediment deposited in San Pablo Bay is transported from the Sacramento and San Joaquin Rivers (after passing through

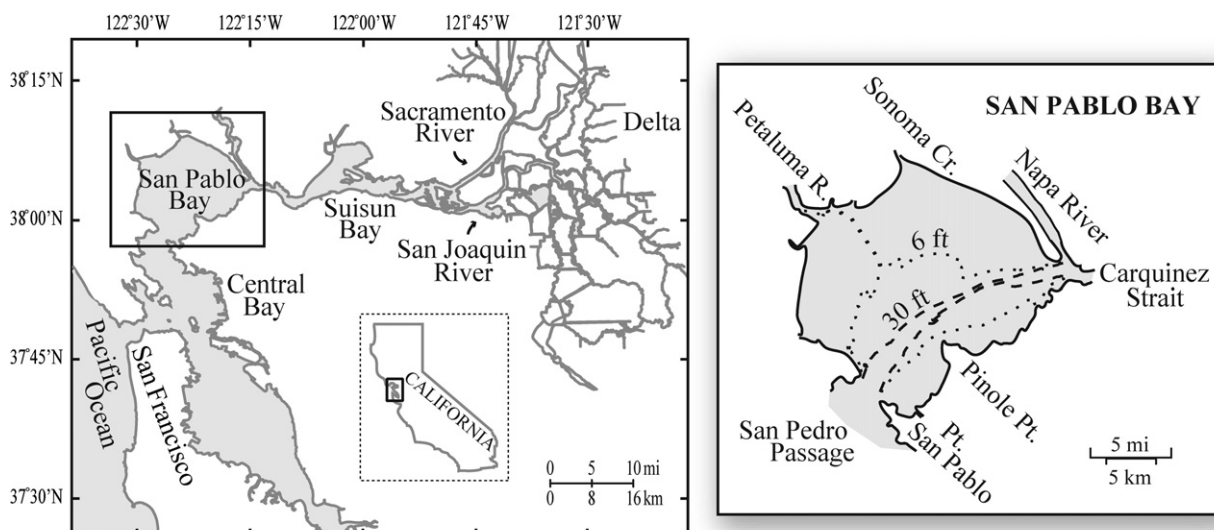


Fig. 1. Location of study area in the San Francisco Estuary, California.

Suisun Bay and Carquinez Strait), from Central San Francisco Bay, and from local streams. From 80 to 90% of the sediment reaching the San Francisco Estuary is delivered by the Sacramento and San Joaquin Rivers (Smith, 1965; Krone, 1979; Porterfield, 1980).

3. Methods

Data from six bathymetric surveys were modeled using surface modeling software with similar methods as have been reported by Sherwood et al. (1990), Hopkins et al. (1991), List et al. (1994), Jaffe et al. (1998), Cappiella et al. (1999), and Gibbs and Gelfenbaum (1999). A continuous surface representation (surface grid) of each bathymetric survey was created by using Topogrid, an ArcInfo module that utilizes a discretised thin plate spline interpolation technique (Wahba, 1990). Topogrid is designed for modeling drainage basins and represents estuarine morphology well. Input data were a combination of point soundings and hand-drawn depth contours (Jaffe et al., 1998). Topogrid uses an iterative interpolation technique where the contours are first used to establish general morphology of the surface and then both contours and point soundings are used to refine the grid. Each historical bathymetric surface is defined by more than 300,000 grid cells (each 50-m square).

Creation of accurate surface grids involved several steps (Jaffe et al., 1998). For the 1856, 1887, 1898, and 1922 surface grids, data were taken from Mylar copies of the original 1:20,000 NOS Hydrographic Sheets (H-sheets). Contours from these sheets were checked for accuracy, and additional contours were added in areas where point soundings were sparse. The annotated H-sheets were scanned and registered to a common horizontal datum (NAD27), using latitude/longitude graticules and hard shoreline features on a National Wetlands Inventory digital map (<http://wetlands.fws.gov/>). Point soundings and depth contours were digitized from the registered image. For the 1951 and 1983 surface grids, digital soundings from the NOS Geophysical Data System for Hydrographic Survey Data (National Oceanic and Atmospheric Administration, GEODAS v. 3.3) were used. For all years, input data were gridded, and the grids were compared with the input data to check for problem areas. The final step was another gridding after adding point soundings and contours so as to force grids to accurately represent historical bathymetry.

Once surface grids were revised to meet an acceptable level of error, change grids were generated by differencing surface grids and applying a vertical correction to bring surveys to a common vertical datum. The vertical correction was necessary because MLLW, the reference for soundings of each bathymetry survey, was not constant because of relative sea-level change and different averaging periods for the tidal data. In general, the averaging period was 19 years, which is the 18.6-year tidal epoch extended to an entire year to remove bias from seasonal water level fluctuation. However, tidal records in San Pablo Bay were not continuous for the entire study period, and it was necessary to use the longer tidal record at the Golden Gate tide station to determine vertical-datum corrections (Dedrick, 1983; Jaffe et al., 1991). These change grids were used to

identify patterns of change and to calculate the volumes and rates of deposition, erosion, and net sedimentation for each survey period.

4. Error analysis

4.1. Grid errors

Two types of error are associated with the grids — bias and random error. Bias enters from inaccuracies in determining the relation of MLLW datums for different surveys and from grid representation differing from the sounding values because of modeling algorithms. Random error is associated with sounding inaccuracy. Sounding errors are randomly distributed in space and independent of each other.

Uncertainty in the MLLW datum varies with the calculation method. For the last two bathymetric surveys, 1951 and 1983, MLLW datums are known (calculated from data collected for a tidal epoch at the long-term tide station near the Golden Gate). For the first bathymetric survey, in 1856, a 2-month average of MLLW measured at temporary tide staffs located in San Pablo Bay was used, and the relation of this datum to subsequent datums is more uncertain. By examining tidal records at the Golden Gate tide station, which was operational during the 1856 bathymetric survey, the relation of the 1856 datum to the datums used in later surveys can be estimated. For example, the 1887 H-sheets include notes indicating that a temporary tide station was operational in San Pablo Bay during the survey (February and March). If this 2-month-long record was used to establish the MLLW datum, and the tides behaved similarly to those at the Golden Gate, the datum would be 1.68 m (values from the Golden Gate tide staff used for reference). An alternative method for calculating the MLLW datum is to compare simultaneous measurements at the temporary tide station in San Pablo Bay with those at the Golden Gate tide station to establish a 19-year epoch (Swanson, 1974). This method yields an MLLW datum of 1.64 m referenced to the Golden Gate tide staff. The difference between the two methods is 0.040 m. To be conservative, because we do not know which method was used, we assume the error in the MLLW datum from 1856 to 1887 to be 0.040 m. Using similar reasoning, the errors in the MLLW datums for the periods 1887–1898, 1898–1922, and 1922–1951 are 0.094, 0.061, and 0.006 m, respectively.

The second source of bias, grid representation differing from the sounding values because of modeling algorithms, was estimated by comparing the modeled surface to original soundings. The average bias for all soundings during each survey period ranged from -0.07 to -0.01 m. The magnitude of this error indicates how well the grids honor the soundings. The difference between grid bias for each survey period is included in the error for net sedimentation even though it was removed.

The magnitudes of sounding errors are larger than the biases. Because sounding errors are random and have a zero mean, they do not influence estimates of net sedimentation. The sum of a large group of soundings that are both deeper and shallower than the actual depths results in cancellation of error and

a true average depth, although, each individual sounding contains some errors. The error criteria for bathymetric surveys have changed over time (Adams, 1942; Schalowitz, 1964; Sallenger et al., 1975). For example, in the early surveys, sounding error, determined by comparing independent estimates at trackline crossings, was not allowed to exceed 8 cm in water depth of less than 1.5 m. Trackline-crossing errors were examined in the field. Lines with trackline-crossing errors exceeding the error criteria were resurveyed (Schalowitz, 1964).

4.2. Intertidal mudflat area error

The error in intertidal mudflat area was estimated by assuming that MLLW (bayward edge of intertidal mudflat) could be either 0.076 m (1/4 foot) too deep or too shallow. This estimate is conservative – the actual error is probably less because of stringent sounding-error criteria for shallow soundings (Schalowitz, 1964; Sallenger et al., 1975).

5. Results

5.1. Historical bathymetric and sedimentation change in San Pablo Bay

San Pablo Bay changed markedly between 1856 and 1983. The resultant changes in morphology and sedimentation patterns are depicted in images of the bathymetry and sedimentation grids, which are based on more than 215,000 depth soundings (Fig. 2a, b).

5.1.1. Change from 1856 to 1887

In 1856, San Pablo Bay had a complex morphology with several channels and small river deltas (Figs. 2a and 3). A broad main-channel system connected the Point San Pedro pass (offshore of San Pablo Point) in the west to Carquinez Strait in the east. The main-channel system had a northern branch (average depth, approximately 8 m; maximum depth, 12 m) and a more developed southern branch (average depth, approximately 13 m; maximum depth, 27 m). The channel system had a maximum width of 5 km (Figs. 2a and 3). A well-developed channel connected the main channel to the Petaluma River in the northwest. An ebb-tidal delta offshore of Sonoma Creek restricted exchange between it and the bay (Figs. 1 and 2a). From 1856 to 1887, San Pablo Bay filled by $259 \pm 14 \times 10^6 \text{ m}^3$ (average rate of $8.3 \pm 0.4 \times 10^6 \text{ m}^3/\text{yr}$) as massive volumes of sediment released by hydraulic gold mining in the Sierra Nevada foothills entered the bay (Table 1, Fig. 2b). This influx of sediment decreased depth by an average of about 85 cm. Almost the entire bay was depositional (89%, Table 1). Parts of the main-channel margin accreted more than 4 m as it narrowed (Figs. 2a, b and 3). The primary erosional areas were the deepest part of the main channel, deeper parts of the channels in the west, and an ebb-tidal delta offshore of Sonoma Creek.

5.1.2. Change from 1887 to 1898

San Pablo Bay likely continued to fill from 1887 to 1898 (Fig. 2a, b), although the error in estimates of net sedimentation

allows for possible net erosion. The rate of net sedimentation, $1.0 \pm 3.4 \times 10^6 \text{ m}^3/\text{yr}$, decreased markedly from the earlier period (Table 1). A major factor in slowing sedimentation was the outlawing in 1884 of discharge of hydraulic-mining debris to rivers, which greatly reduced the volume of sediment entering the Sacramento–San Joaquin River Delta (hereafter referred to as the Delta) and San Francisco Bay. The main channel deepened and narrowed (Figs. 2a, b and 3). Side channels continued to fill, decreasing the connection between the bay and rivers. For example, the channel offshore of the Petaluma River decreased in width from 3.4 to 2.3 km at its bayward limit during this period as a reduced tidal prism caused by diking of tidal marshes resulted in a decreased shear-stress in the bottom of the channel, which favors deposition (see Friedrichs, 1995 for a theoretical treatment of this process). Shallows in the western part of the bay changed from depositional to either stable or erosional (Fig. 2b). Overall, about half of the bay was depositional, and half was erosional (Table 1).

5.1.3. Change from 1898 to 1922

From 1898 to 1922, a net volume of $41 \pm 20 \times 10^6 \text{ m}^3$ of sediment, an average rate of $1.7 \pm 0.9 \times 10^6 \text{ m}^3/\text{yr}$, was deposited in San Pablo Bay (Table 1). During this period, approximately two-thirds of the bay was depositional, especially in the shallow areas (<2-m depth) (Fig. 2b). The channel extending from the Petaluma River filled to a point where dredging (indicated by straight path with a dogleg cutting through intertidal mudflat, Fig. 2a) was required to allow ships to travel upriver. The primary erosional areas were the western shallows and the main channel, which continued to deepen (Figs. 2a, b and 3).

5.1.4. Change from 1922 to 1951

From 1922 to 1951, the rate of net sedimentation in San Pablo Bay was similar to the rate during the preceding 24 years. A net volume of $52 \pm 3 \times 10^6 \text{ m}^3$ of sediment, an average rate of $1.8 \pm 0.1 \times 10^6 \text{ m}^3/\text{yr}$, was deposited. The shallows were primarily depositional, and most erosion occurred in vicinity of the main channel; overall, about two-thirds of the bay was depositional. The straight section of the 30-foot contour lines in the southeast delineates an area of dredging (less than a quarter the length of the main channel). The center of the main channel continued to deepen (Figs. 2a, b and 3).

5.1.5. Change from 1951 to 1983

San Pablo Bay lost sediment overall from 1951 to 1983 in contrast to the previous ~100 years when the bay was filling with sediment. A net volume of $23 \pm 3 \times 10^6 \text{ m}^3$ of sediment, an average rate of $0.7 \pm 0.1 \times 10^6 \text{ m}^3/\text{yr}$, eroded from San Pablo Bay (Table 1). More than two-thirds of the bay (70%, Table 1) was erosional with the northern and northeastern shallows and the margins of the main channel depositional. Klingeman and Kaufman (1965) also observed deposition on the main-channel margins in a short study that used naturally occurring radioactive tracers. Dredging of the main channel near Pinole Point averaged about $0.2 \times 10^6 \text{ m}^3/\text{yr}$ from 1955 to 1983 (Ogden Beeman and Associates and Ray Krone and Associates, 1992) and is easily identified by the straight 30-foot contours in Fig. 2a. The dredged material was disposed

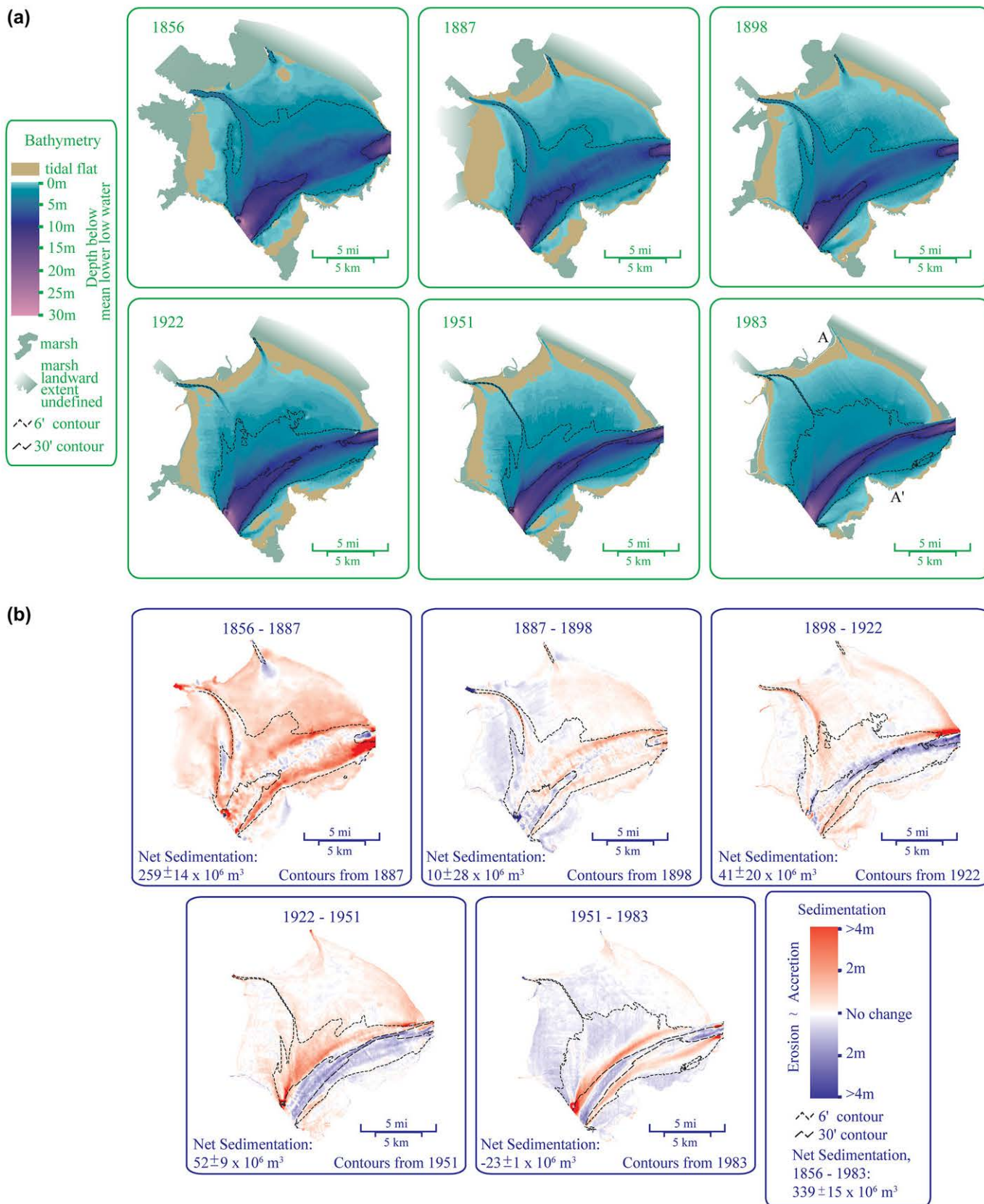


Fig. 2. (a) Color-shaded bathymetry maps of San Pablo Bay for 1856–1983, (b) color-shaded sedimentation maps of San Pablo Bay for 1856–1983. An overall decrease in depth of the bay is shown by lighter green colors in (a) and migration of the 6-foot contour bayward. The massive accretion during the hydraulic-mining period is shown in the 1856–1887 period in (b) by red shading. The erosion during the 1951–1983 period, which occurred as damming of rivers increased and land use changed, is shown by blue shading.

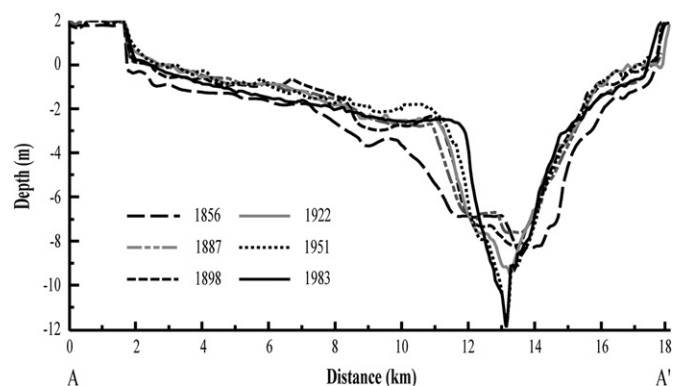


Fig. 3. Profile of San Pablo Bay floor along line A–A' (Fig. 2a) for period 1856–1983. Note that main channel has narrowed and deepened and shallows have filled over time. Most of this change occurred from 1856 to 1887 when hydraulic mining resulted in unusually high sediment delivery to San Pablo Bay.

within San Pablo Bay and did not contribute to the net loss of sediment.

5.2. A simple model for sedimentation in San Pablo Bay

Net sedimentation in San Francisco Bay results from the difference between sediment delivery from rivers, primarily through episodic flood deposition, and sediment loss from wind, wave, and tidal processes that erode the bay (Krone, 1979). A simple model for sedimentation in San Pablo Bay is that processes controlling sediment loss have not varied greatly over time and the net sedimentation reflects fluctuations in delivery rate.

The rate of sediment delivery to San Pablo Bay has changed over time in response to human activities. For instance, delivery rate increased greatly beginning in the 1850s as debris from hydraulic gold mining in the Sierra Nevada foothills was transported to the bay. Gilbert (1917, p. 67) estimated that sediment delivery before hydraulic mining “amounted to perhaps 2 million cubic yards per year” ($1.5 \times 10^6 \text{ m}^3/\text{yr}$). Approximately $1.675 \times 10^9 \text{ m}^3$ of hydraulic-mining debris was created from 1849 to 1909 (Gilbert, 1917, p. 43). Although the coarser fraction remained in the foothills, filling stream valleys by as much as 10 m (Gilbert, 1917), the finer fraction, silt and clay, was carried to the bay quickly by the Sacramento and San Joaquin Rivers. Gilbert (1917, p. 50) estimated that $1.146 \times 10^9 \text{ m}^3$ of sediment (average rate of $14.1 \times 10^6 \text{ m}^3/\text{yr}$) was transported to San Francisco Bay between 1849 and 1914. This is approximately 70% of the debris created by hydraulic mining (Gilbert, 1917, p. 46).

The California Supreme Court (Sawyer Decision) stopped discharge of mine tailings to rivers in 1884 resulting in a great decrease in the rate of sediment delivery by the early 1900s. Porterfield (1980, Table 20) estimated that the Sacramento and San Joaquin Rivers delivered an average of 5.04×10^6 metric tons/yr ($5.90 \times 10^6 \text{ m}^3/\text{yr}$, using his estimate of bulk sediment density of 53.2 lb/ft^3 [0.85 g/cm^3]) of sediment to San Francisco Bay from 1909 to 1959. Smith (1965) estimated a similar, but lower, sediment delivery to the bay for the period 1924 to 1960 of 4.04×10^6 metric tons/yr ($4.74 \times 10^6 \text{ m}^3/\text{yr}$, assuming a bulk sediment density of 0.85 g/cm^3). The delivery rate continued to decrease in the late 1900s. An average of 2.38×10^6 metric tons/yr ($2.79 \times 10^6 \text{ m}^3/\text{yr}$, assuming a bulk sediment density of 0.85 g/cm^3) of sediment was delivered to the bay from 1956 to 1990 (Ogden Beeman and Associates and Ray Krone and Associates, 1992, Table 5).

The decrease in the sediment-delivery rate during the late 1900s has multiple causes, including damming of rivers. From the 1940s to the 1970s, many dams were built to meet California's need for water (Porterfield, 1980). One consequence of dam building was a decrease in sediment delivery to the San Francisco Estuary (McKee et al., 2006; Wright and Schoellhamer, 2004). Sediment delivery is decreased not only by trapping sediment behind the dam but also by decreasing peak flows on the river, diminishing their capacity to transport sediment stored in the river system. Sediment transport is related to flow speed to the third or fourth (or higher) power (Van Rijn, 1993), and so decreasing flow speed greatly affects sediment transport and supply downstream. The volume of sediment trapped behind reservoirs on tributaries of the Sacramento River from 1940 to 2001 was greater than the decrease in suspended-sediment transport in the Sacramento River about 100 km below the dams during that same period (Wright and Schoellhamer, 2004). During this period and earlier, other human activities impacted sediment delivery to the San Francisco Estuary (Wright and Schoellhamer, 2004). Rivers were channelized, decreasing the sediment loss to flood plains and marshes, and riverbanks were stabilized, decreasing the sediment gain from riverbank erosion. Logging, urbanization, agriculture, and grazing increased sediment loads. The last two hydrographic surveys of San Pablo Bay (1951 and 1983) correspond to a period when damming and other human activities had caused a net decrease in sediment delivery to the San Francisco Estuary (Krone, 1979; Wright and Schoellhamer, 2004; McKee et al., 2006).

Comparison of net sedimentation and rate of sediment delivery in San Pablo Bay indicates similar trends (Fig. 4a).

Table 1
History of deposition, erosion, and net sedimentation in San Pablo Bay

Period	Net sedimentation (10^6 m^3)	Sedimentation rate			Surface area		
		Net ($10^6 \text{ m}^3/\text{yr}$)	Deposition ($10^6 \text{ m}^3/\text{yr}$)	Erosion ($10^6 \text{ m}^3/\text{yr}$)	Total (km^2)	Percent depositional	Percent erosional
1856–1887	259 ± 14	8.3 ± 0.4	8.8	−0.4	304	89	11
1887–1898	11 ± 36	1.0 ± 3.4	5.5	−4.5	296	54	46
1898–1922	41 ± 20	1.7 ± 0.9	3.5	−1.8	290	63	37
1922–1951	52 ± 3	1.8 ± 0.1	3.4	−1.6	280	68	32
1951–1983	$−23 \pm 3$	$−0.7 \pm 0.1$	1.7	−2.4	275	30	70

Annually, the volume of sediment deposited appears to be approximately 3×10^6 – 5×10^6 m³ less than the sediment delivery from the Sacramento and San Joaquin Rivers and local streams (local stream sediment delivery was about 0.3×10^6 m³/yr during the first part of the 20th century; Porterfield, 1980). The decrease in sediment delivery resulted in net erosion for the last time period, 1951–1983. This erosion, as well as changes in sedimentation during earlier periods, was reflected in morphologic change, including change in intertidal mudflats.

5.3. Intertidal mudflat change

The intertidal mudflat area in San Pablo Bay changed from 1856 to 1983 in response to sediment-delivery fluctuations (Fig. 4a, b). The abundant supply of sediment from hydraulic mining resulted in deposition in the shallows and a 60%

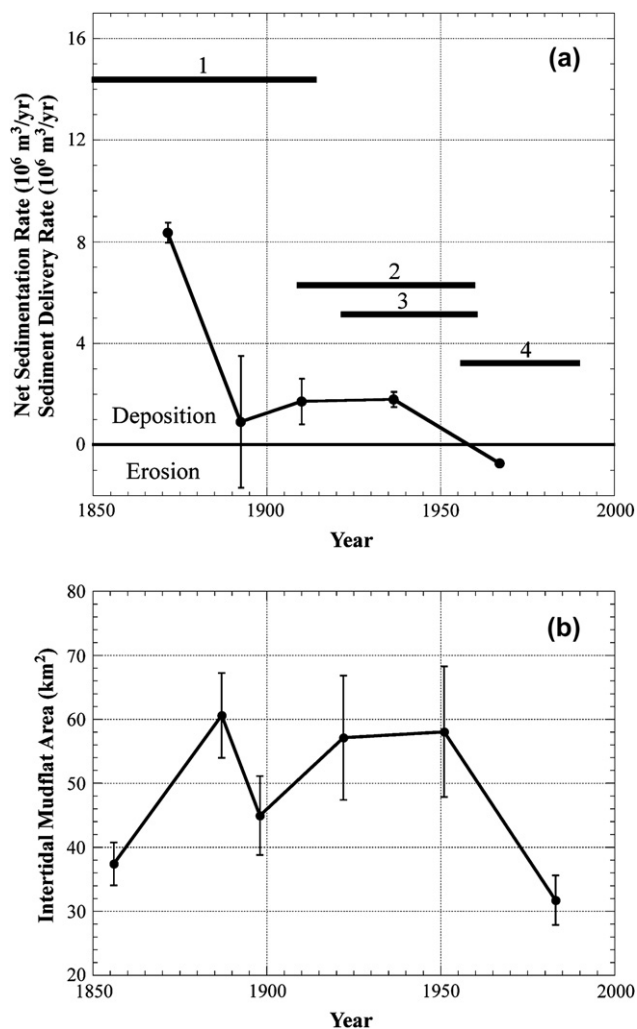


Fig. 4. (a) Net sedimentation and (b) intertidal mudflat area in San Pablo Bay from 1856 to 1983. Horizontal lines are sediment-delivery estimates: 1, Gilbert (1917) for 1850–1914; 2, Smith (1965) for 1924–1960; 3, Porterfield (1980) for 1909–1959; 4, Ogden Beeman and Associates and Ray Krone and Associates (1992) for 1956–1990. Error bars on net-sedimentation rates and intertidal mudflat area are described in Section 5. Note that San Pablo Bay was erosional for the last.

increase in intertidal mudflat area (37.4 ± 3.4 to 60.6 ± 6.6 km²) from 1856 to 1887.

The distribution of intertidal mudflats also changed significantly over time. In 1856, intertidal mudflats in the northern, eastern, and southeastern parts of the bay were narrow. These intertidal mudflats, as well as the one in the western part of the bay, widened from 1856 to 1887. From 1887 to 1898, land reclamation on the west shore of the bay and natural processes elsewhere in the bay decreased its intertidal mudflat area by about 15 ± 6 km² (Fig. 2a). Intertidal mudflat loss in the western and northern parts of the bay and gain in the eastern part of the bay resulted in a fairly uniform intertidal mudflat width in 1951 (Fig. 2a). Erosion resulted in a decrease in intertidal mudflat area from 58.0 ± 10.2 km² in 1951 to 31.7 ± 3.9 km² in 1983, an average loss of 0.82 km²/yr from 1951 to 1983.

5.4. Sedimentation in similar dynamical regions

Bay-averaged net sedimentation, though indicative of the general state of San Pablo Bay, does not describe the distribution and size of depositional and erosional areas. This information is exploited in an analysis of similar dynamical regions to assess sedimentation processes and sediment transport pathways. Here we used the patterns of deposition and erosion, and the spatial variation of tidal and wind–wave energy, to define 11 regions with coherent behavior (Fig. 5). Shallows extended to a depth of about 1.8 m and were divided into five regions, with boundaries at creeks or headlands. Boundaries of the other six regions were allowed to change over time to follow edges of large areas with either deposition or erosion.

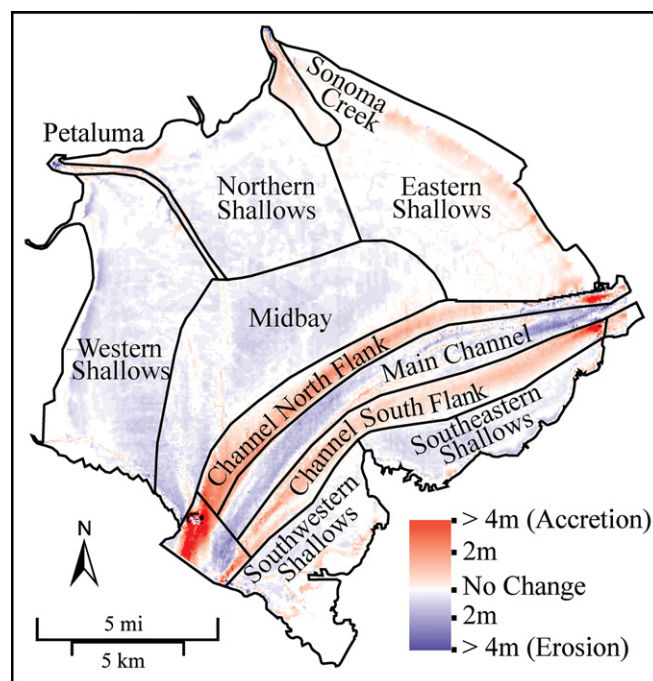


Fig. 5. Similar dynamical regions overlain on sedimentation in San Pablo Bay from 1951 to 1983. Regions were defined using the depth and patterns of erosion and deposition, which varied throughout the study.

Net-sedimentation rates in the 11 regions varied over time and, like net sedimentation for the entire bay, changed with sediment delivery to the bay. From 1856 to 1887, all regions except the Sonoma Creek ebb-tidal delta exhibited net deposition as large volumes of hydraulic-mining debris entered San Pablo Bay (Table 2). From 1951 to 1983, the most erosional period, some areas still had significant deposition (Table 2). The margins of the main channel (Channel North Flank and Channel South Flank) were depositional during all periods causing it to narrow (Figs. 2a, b and 3; Table 2). Channel deepening accompanied the narrowing during all periods except from 1856 to 1887 (Fig. 3). The eastern shallows were the only nonchannel region with net deposition during all periods. Net sedimentation in the shallows generally decreased throughout the study period (Fig. 6a).

The timing and pattern of net sedimentation in the shallows are important because of the relation between sedimentation in the shallows and intertidal mudflat area. From 1856 to 1887, the shallows exhibited net deposition (Fig. 6a) and intertidal mudflat area increased in all parts of San Pablo Bay (Fig. 6b). Net sedimentation in all the shallows decreased from 1887 to 1898, possibly because of a decrease in sediment delivery as hydraulic mining was abruptly stopped in 1884, by disequilibrium (unstable morphology), by diking of mudflats, or by a combination of these factors. Although net sedimentation decreased, the eastern shallows were still depositional.

The response of the intertidal mudflats reflected the net sedimentation in the shallows (Fig. 6a, b and 7). The intertidal mudflat area rapidly decreased after 1887 in the western part of the bay, was nearly stable in the northern and southeastern parts of the bay, and increased in the eastern part of the bay. During the last period (1951–1983), both net sedimentation and intertidal mudflat area decreased in all regions of the bay (Fig. 6a, b).

6. Discussion

6.1. Does a simple model for sedimentation work?

The simple model (presented in Section 5.2) of sediment delivery from rivers controlling net sedimentation in San Pablo

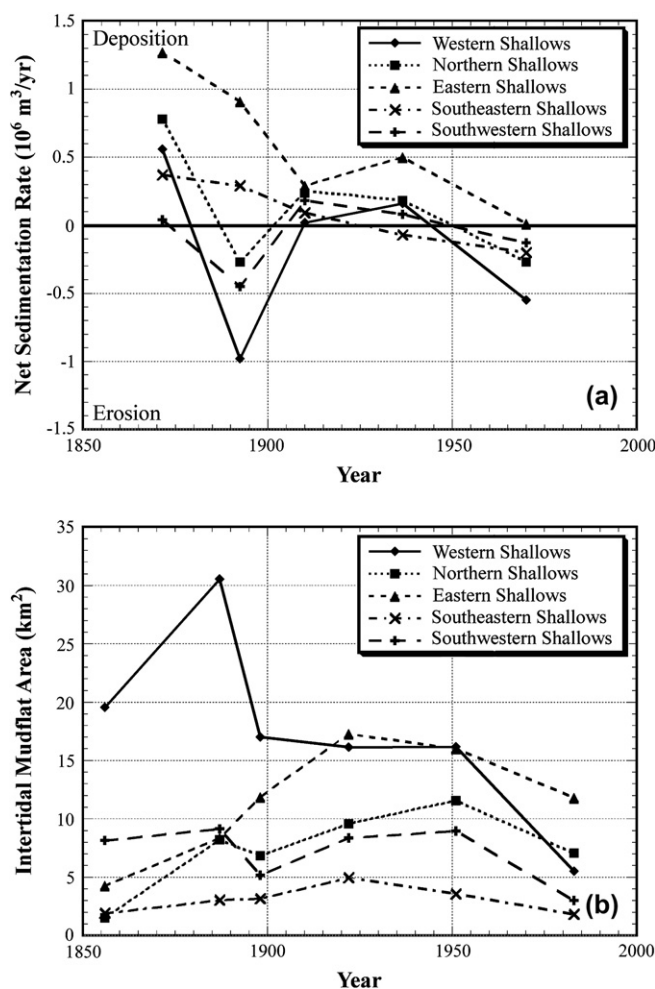


Fig. 6. Net-sedimentation rates in shallows (a) and intertidal mudflat area (b) by dynamical region.

Bay assumes that other processes that deliver and remove sediment from San Pablo Bay are constant over time. This assumption can be examined in the sediment budget for San Pablo Bay (terms and connections shown in Fig. 8). The difference between the rate of sediment delivery from rivers and the net-sedimentation rate in San Pablo Bay, S_{SPB} , is given by

Table 2
History of net-sedimentation rates for dynamically similar regions in San Pablo Bay. Regions are defined in Fig. 5

Region	Net-sedimentation rate (cm/yr)				
	1856–1887	1887–1898	1898–1922	1922–1951	1951–1983
Western Shallows	0.6	-1.0	0.0	0.2	-0.5
Petaluma Channel	0.4	0.2	0.5	0.0	0.0
Northern Shallows	0.8	-0.3	0.3	0.2	-0.3
Sonoma Creek, ETD	-0.1	0.1	0.0	0.0	0.0
Eastern Shallows	1.3	0.9	0.3	0.5	0.0
Midbay	1.3	-0.6	0.3	0.7	-0.5
Channel North Flank	1.2	1.6	0.2	1.2	0.6
Main Channel	0.1	-0.1	-1.1	-1.0	-0.3
Channel South Flank	2.2	0.7	0.3	-0.1	0.4
Southwestern Shallows	0.0	-0.5	0.2	0.1	-0.1
Southeastern Shallows	0.4	0.3	0.1	-0.1	-0.2

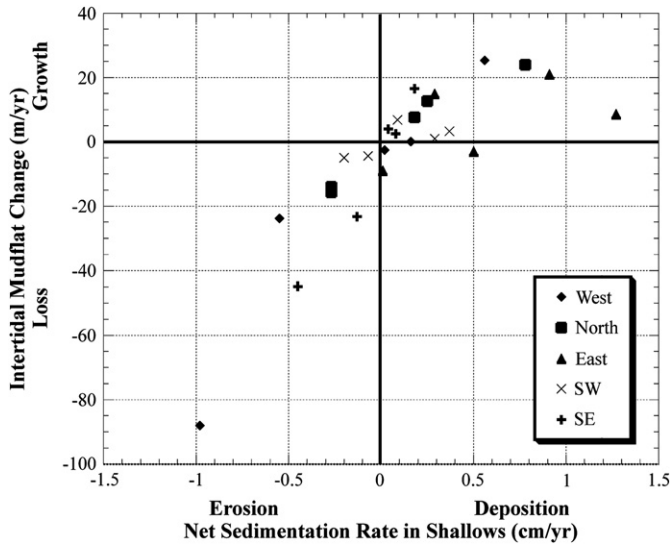


Fig. 7. Relation of net sedimentation in shallows (depth, ~ 1.8 m, Fig. 5) and average intertidal mudflat width.

$$Q_{SSJ} + Q_L - S_{SPB} = S_D + S_{SBCS} + M_D + M_{SBCS} + M_{SPB} + E_{CS} + E_{CB} + BP - Q_{CBSPB} \quad (1)$$

where Q_{SSJ} is the sediment-delivery rate from the Sacramento and San Joaquin Rivers to the Delta, Q_L is the sediment-delivery rate from local streams (primarily Napa and Sonoma Creeks and the Petaluma River), S_D is the net-sedimentation rate in Delta channels and flood plains, S_{SBCS} is the net-sedimentation rate in the Suisun Bay region and Carquinez Strait, M_D is the sediment deposition rate in tidal marshes of the Delta, M_{SBCS} is the sediment deposition rate in tidal marshes of the Suisun Bay region and Carquinez Strait, M_{SPB} is the sediment deposition rate in tidal marshes of San

Pablo Bay, E_{CS} is the rate that sediment eroded in San Pablo Bay is transported to Carquinez Strait, E_{CB} is the rate sediment eroded in San Pablo Bay is transported to Central San Francisco Bay, BP is the rate of sediment bypassing San Pablo Bay, and Q_{CBSPB} is the rate of sediment delivery from Central Bay to San Pablo Bay.

Eq. (1) can be simplified by neglecting small terms and those that are accounted for elsewhere. Assuming that marshes accrete to keep up with relative sea-level rise, the sediment deposition rates in marshes M_D , M_{SBCS} , and M_{SPB} are small relative to the other terms. For example in San Pablo Bay, the rate of deposition on marshes for 1856, when tidal-marsh extent was the largest (244 km², Van Royen and Siegel, 1959), was less than 0.4×10^6 m³/yr (244 km² marsh \times 1.4 mm/yr). Significant parts of the tidal-marsh area were reclaimed for agriculture by 1887 (Fig. 2a). Reclamation reduced tidal-marsh area in San Pablo Bay to 55 km² in 1980 (Dedrick, 1993). After 1887, M_{SPB} is a very small term in the budget, on the order of 0.1×10^6 m³/yr. Similarly, M_D and M_{SBCS} have decreased over time. Tidal-marsh area in the Suisun Bay region decreased from 265 km² in 1800 to 55 km² in 1998 (Goals Project, 1999). Marsh deposition in the Delta, which decreased over time with levee building and diking, was likely a small term in the sediment budget after the late 1800s.

Although no estimates of E_{CS} have been published, flow measurements from Burau et al. (1993) at the west end of Carquinez Strait indicate that sediment eroded from San Pablo Bay is transported upestuary during neap tides when gravitational circulation results in upestuary near-bottom flows. During spring tides, flow and sediment transport are from Carquinez Strait to San Pablo Bay throughout the water column. Ganju and Schoellhamer (2006) used Acoustic Doppler Current Profiling (ADCP) and suspended concentration data to calculate suspended-sediment flux at the east end of Carquinez Strait, approximately 10 km from San Pablo Bay. At this location,

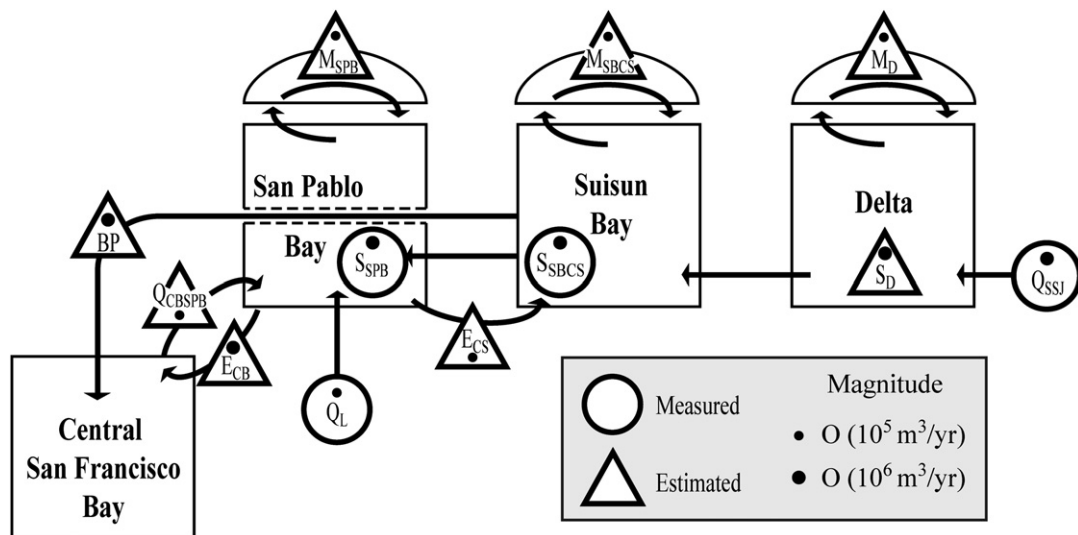


Fig. 8. San Pablo Bay sediment budget schematic. Arrows indicate direction of sediment exchange. Circles indicate measured sediment budget components. Estimated components are indicated by triangles. The order of magnitude for sediment volume rates is indicated by the size of the dot within the budget component. The notation used is Q is sediment delivery, S net sedimentation, M marsh deposition, E transport of eroded sediment, and BP is sediment bypassing.

suspended-sediment flux driven by gravitational circulation dominates during the dry months when there was a strong longitudinal salinity gradient. During the driest of years, the annual net suspended-sediment flux was upestuary. Fortunately, for balancing of the sediment budget, we need not estimate E_{CS} because it is accounted for in the net-sedimentation rates of Carquinez Strait, Suisun Bay and the Delta (if the sediment makes it that far).

Likewise, we need not account for upestuary sediment transport from Central Bay to San Pablo Bay, Q_{CBSPB} , because it is accounted for in the net-sedimentation rates of San Pablo Bay.

Neglecting small terms and those implicit in other terms and rearranging, Eq. (1) simplifies to:

$$BP + E_{CB} = Q_{SSJ} + Q_L - S_{SBCS} - S_{SPB} - S_D \quad (2)$$

To evaluate Eq. (2), we recalculated net-sedimentation rates for the same period as for river sediment-delivery estimates by weighting the rates listed in Table 1 with the percentage of time represented during each period (Table 3). The sum of the terms to the right of the equal sign, except for net sedimentation in the Delta (S_D), is well constrained by data and decrease over time (Porterfield, 1980; Cappiella et al., 1999; this analysis). S_D was accounted for in the 1850–1914 sediment-delivery estimate by Gilbert (1917) and assumed to be $1.0 \times 10^6 \text{ m}^3/\text{yr}$ thereafter based on estimates by Wright and Schoellhamer (2005) and Smith (1965).

E_{CB} is a potentially large term that can be estimated from the volumes of eroded and deposited sediment (Table 1) and the sediment delivery from rivers and the net sediment in the Delta, Suisun Bay, and Carquinez Strait (Table 3). The volume of eroded sediment is not equivalent to E_{CB} because (1) redeposition of eroded sediment in San Pablo Bay results in the volume of eroded sediment overestimating E_{CB} , and (2) new sediment replacing eroded sediment that was removed from San Pablo Bay results in the volume of eroded sediment underestimating E_{CB} . From 1956 to 1990, the minimum E_{CB} value (i.e., all eroded sediment redeposited in San Pablo Bay) is $0.7 \times 10^6 \text{ m}^3/\text{yr}$ ($2.4 \times 10^6 \text{ m}^3/\text{yr}$ eroded minus $1.7 \times 10^6 \text{ m}^3/\text{yr}$ deposited; Table 1). The maximum E_{CB} value for this period,

which occurs if all the sediment entering San Pablo Bay (from local streams, the Sacramento and San Joaquin Rivers, and net erosion from Suisun Bay and Carquinez Strait) were initially deposited, eroded, and removed from San Pablo Bay to the Central Bay is $5.1 \times 10^6 \text{ m}^3/\text{yr}$ ($3.1 \times 10^6 \text{ m}^3/\text{yr}$ from rivers and local streams plus $1.3 \times 10^6 \text{ m}^3/\text{yr}$ from erosion of Suisun Bay and Carquinez Strait plus $1.7 \times 10^6 \text{ m}^3/\text{yr}$ deposited in San Pablo Bay minus $2.4 \times 10^6 \text{ m}^3/\text{yr}$ eroded from San Pablo Bay; Tables 1, 3). These estimates neglect losses to marshes, which are relatively small. Using this approach, the ranges of E_{CB} values for 1850–1914, 1909–1959, and 1924–1960 are $0-7.7 \times 10^6$, $0-6.6 \times 10^6$, and $0-5.7 \times 10^6 \text{ m}^3/\text{yr}$; respectively. The averages of E_{CB} values during the periods 1850–1914, 1909–1959, 1924–1960, and 1956–1990 are 3.8×10^6 , 3.3×10^6 , 2.8×10^6 , and $2.9 \times 10^6 \text{ m}^3/\text{yr}$, respectively, yielding a grand average of $3.2 \times 10^6 \text{ m}^3/\text{yr}$; the average E_{CB} value for the 1900s is $3.0 \times 10^6 \text{ m}^3/\text{yr}$, an admittedly crude estimate of E_{CB} . Future research using sediment transport modeling could refine this estimate.

Assuming that $E_{CB} = 3.0 \times 10^6 \text{ m}^3/\text{yr}$ gives sediment bypassing rates of 4.9, 2.4, 1.3, and $1.1 \times 10^6 \text{ m}^3/\text{yr}$ for the periods 1850–1914, 1909–59, 1924–60, and 1956–90, respectively (Table 3). The decrease in BP during the study period is not unexpected. BP is scaled by the magnitude and frequency of floods. Larger floods transport more sediment through San Pablo Bay. This greater bypassing is caused both by stronger flows advecting sediment through the bay faster and higher sediment concentrations that commonly accompany stronger flows. More frequent floods increase cumulative sediment bypassing. Dams are designed to decrease both the magnitude and frequency of floods. With the increased damming of the Sacramento and San Joaquin Rivers and their tributaries, sediment bypassing of San Pablo Bay has likely decreased.

An additional factor to consider in sediment bypassing is that the relation between sediment concentration and flow magnitude (sediment–discharge rating curve) for rivers feeding San Pablo Bay is also changing. Wright and Schoellhamer (2004) showed that, for the same flow, the sediment concentration (and, thus, sediment transport) decreased for the Sacramento

Table 3
Major terms in sediment budget for San Pablo Bay (terms also shown in Fig. 8). Erosional loss from San Pablo Bay to Central San Francisco Bay, E_{CB} , is assumed to be constant over time and assigned a rate of $3.0 \times 10^6 \text{ m}^3/\text{yr}$. Sediment from the Sacramento and San Joaquin Rivers bypassing San Pablo Bay (primarily during floods), BP, is calculated to balance the sediment budget. When a constant rate of erosional loss of sediment from San Pablo Bay is assumed, sediment bypassing decreases as sediment delivery decreases, which is the expected relation

Period	Sediment delivery from rivers $Q_{SSJ} + Q_L$ ($10^6 \text{ m}^3/\text{yr}$)	Net sedimentation upestuary ^a $S_{SBCS} + S_D$ ($10^6 \text{ m}^3/\text{yr}$)	Net sedimentation in San Pablo Bay S_{SPB} ($10^6 \text{ m}^3/\text{yr}$)	San Pablo Bay loss ^b E_{CB} ($10^6 \text{ m}^3/\text{yr}$)	Sediment bypassing BP ($10^6 \text{ m}^3/\text{yr}$)
1850–1914	14.1	1.0	5.2	3.0	4.9
1909–1959	6.2	–0.8	1.6	3.0	2.4
1924–1960	5.0	–0.9	1.6	3.0	1.3
1956–1990	3.1	–0.3	–0.7	3.0	1.1

^a Net sedimentation in the Delta, S_D , is accounted for in the 1850–1914 sediment-delivery estimate (Gilbert, 1917) and assumed to be $1.0 \times 10^6 \text{ m}^3/\text{yr}$ thereafter based on estimates by Wright and Schoellhamer (2005) and Smith (1965).

^b E_{CB} , erosional loss from San Pablo Bay to Carquinez Straits and Suisun Bay is accounted for in S_{SBCS} ; Q_{SSJ} , sediment delivered from the Sacramento and San Joaquin Rivers at the entrance to Suisun Bay; Q_L , sediment delivered from local streams; S_{SBCS} , change in sediment storage in the Suisun Bay area and Carquinez Strait; E_{CB} , erosional loss (flux of eroded material) from San Pablo Bay to Central San Francisco Bay; BP, sediment from the Sacramento and San Joaquin Rivers that bypasses San Pablo Bay.

River from 1957 to 2001. The Sacramento River contributes 80–90% of the sediment to the bay (Porterfield, 1980). Assuming sediment concentrations are not greatly modified when traveling from the river source to San Pablo Bay, this change in the sediment–discharge rating curve also would contribute to a decrease in BP.

The magnitude and trend of sediment bypassing rates, though reasonable, are only estimates and strongly depend on estimates of the rate at which eroded sediment is removed from San Pablo Bay. If this rate has decreased (or increased) over time, the above analysis would predict a corresponding equal increase (or decrease) in sediment bypassing.

In summary, a strong correlation exists between sediment-supply and net-sedimentation rates in San Pablo Bay (Fig. 4a), complicated, however, by uncertainty in sediment bypassing and sediment removal rates, two large terms in the sediment budget that have likely changed over time. Past sediment-supply and net-sedimentation rates are consistent with a constant (at the decadal time scale) sediment removal rate and sediment bypassing that has decreased over time. However, this solution is not a unique balance of the sediment budget. To increase our ability to predict net sedimentation, we must improve our understanding of the processes that cause bypass and removal of sediment from San Pablo Bay.

6.2. Sediment transport and redistribution within San Pablo Bay

Another level of prediction desired is the response of different parts of San Pablo Bay to fluctuations in sediment delivery. To be able to predict this response, we need to understand sediment redistribution within the bay. The data presented in Section 5.4 indicate significant sediment redistribution from the western and/or northern shallows to the eastern shallows.

Spatial and temporal trends in net sedimentation in the shallows (Figs. 2b and 6a) indicate that, for all periods, net deposition in the eastern shallows is greater than in the western or northern shallows. Interestingly, all the shallows except those in southeastern part of San Pablo Bay have similar trends in net sedimentation over time, regardless of becoming more erosional or depositional, but are offset by a constant. One explanation for this offset is that sedimentation scales with sediment delivery, with an overlay of redistribution from the western or northern shallows to the eastern shallows. This combination results in net sedimentation rates that parallel each other and are offset in magnitude after accounting for redistribution from the western shallows to the eastern shallows, mimicking observed behavior (Fig. 6a). Mechanisms for sediment redistribution from west to east are asymmetric tidal currents, with stronger flood-tide currents advecting more sediment to the east (Klingeman and Kaufman, 1965, Fig. 23) and currents generated by westerly or southwesterly winds advecting sediment to the east.

6.3. Future conditions

The morphology of San Pablo Bay will not return to that of 1856. The great influx of sediment during the hydraulic-

mining period resulted in deposition that changed morphology significantly, which, in turn, changed sediment transport patterns. Adding to this perturbation to the system was diking of tidal marshes that reduced the tidal prism and resulted, for example, in filling of channels offshore of the Petaluma River (Ganju et al., 2004 presents a conceptual model for exchange of sediment between San Pablo Bay and the Petaluma River).

Generally, San Pablo Bay will continue to erode in the near term unless its sediment delivery increases. An increase in sediment delivery is not likely with damming and water projects acting to decrease sediment delivery. The eastern shallows, which are more depositional than the other shallows, will be the last area to become erosional. The effects of sea-level rise on deposition and erosion in San Pablo Bay are unknown. A decrease in bottom shear-stress from the increase in depth in the shallower portions of the bay decreasing wave orbital velocities is expected to favor deposition, but the degree that this effect will be counteracted by changes in the magnitude and pattern of tidal currents is hard to predict without the use of a coupled hydrodynamic/sediment transport model.

The main channels will likely continue to narrow and deepen. The main channel has been narrowing and deepening since 1887, and we expect this trend to continue. We speculate that the channel deepening response was initiated by channel narrowing from high sediment loads during the hydraulic-mining period. Narrowing may have sufficiently altered bottom shear-stress distributions so that deepening was easier than widening to accommodate flow. This hypothesis may be tested by applying a three-dimensional hydrodynamic and sediment transport model. Channel evolution could be modified by restoration of tidal marshes up estuary. Restoration would result in a greater tidal prism and increased flow through the main channel and could change sedimentation rates and patterns. Sea-level rise will affect channel geometry to the degree that it alters the tidal prism.

How San Pablo Bay evolves will be important to not only its health (e.g., habitat change) but that of San Francisco Bay as a whole. For example, San Pablo Bay contains more than $100 \times 10^6 \text{ m}^3$ of hydraulic-mining debris with an average mercury concentration from 0.3 to 0.6 ppm (Jaffe et al., 1999). Erosion of this sediment will release tens of thousands of grams of mercury to the water column that could be transported throughout the San Francisco Estuary. Future conditions of San Pablo Bay will also affect tidal-marsh-restoration efforts. If San Pablo Bay continues to erode, more sediment will be needed for restoration because sediment will be required not only for the creation of tidal marshes but also for the expansion of intertidal mudflats and shallows that coexist with marsh.

7. Conclusions

Quantitative analysis of historical hydrographic surveys has been used to learn how San Pablo Bay has changed since the Gold Rush and what processes were key in causing this change. It is concluded that:

- The morphology of San Pablo Bay changed drastically from 1856 to 1983. In 1856, San Pablo Bay had a complex morphology, with a broad main channel, side channels, and an ebb-tidal delta crossing the shallower parts of the bay. In 1983, all the channels except the main channel had filled, and erosive processes planed the shallows, creating uniform, gently sloping surfaces.
 - Human activities that changed sediment delivery from rivers were a primary control on sedimentation and the evolution of San Pablo Bay. From 1856 to 1887, $259 \pm 14 \times 10^6 \text{ m}^3$ of sediment was deposited in San Pablo Bay, coinciding with a high rate of sediment delivery ($14.1 \times 10^6 \text{ m}^3/\text{yr}$) to San Francisco Bay during the hydraulic-mining period. In contrast, from 1951 to 1983, $23 \pm 3 \times 10^6 \text{ m}^3$ of sediment was eroded from San Pablo Bay as the rate of sediment delivery from the Sacramento and San Joaquin Rivers decreased to about $3 \times 10^6 \text{ m}^3/\text{yr}$.
 - Intertidal mudflat area and distribution changed throughout the study period. In 1887, intertidal mudflat area was at a maximum ($60.6 \pm 6.6 \text{ km}^2$). Intertidal mudflat area had decreased to a minimum ($31.7 \pm 3.9 \text{ km}^2$) in 1983. In 1856, intertidal mudflats were largest in the western part of San Pablo Bay, but have since become more evenly distributed.
 - Intertidal mudflat area is related to sedimentation on the shallows (<1.8-m depth), reflecting sediment delivery to the bay. Intertidal mudflat area was largest after the unusually high influx of sediment from hydraulic mining resulted in building of the shallows and intertidal mudflats, and smallest in 1983 after damming decreased sediment delivery.
 - The simple model that sediment delivery controls net sedimentation explains much of the sedimentation trend in San Pablo Bay. This model predicts that erosion will increase in the future if sediment delivery continues to decrease.
- Acknowledgments**
- This research was supported by the U.S. Geological Survey's Priority Ecosystem Science study of San Francisco Bay. Laura Zink Torresan digitized historical hydrographic and topographic surveys. The manuscript was improved by reviews from Dave Schoellhamer, Noah Snyder, and three anonymous reviewers.
- References**
- Adams, K.T., 1942. Hydrographic Manual, revised ed. U.S. Department of Commerce, Coast and Geodetic Survey, Special Publication 143, 407 pp.
- Burau, J.R., Simpson, M.R., Cheng, R.T., 1993. Tidal and residual currents measured by an acoustic Doppler current profiler at the west end of Carquinez Strait, San Francisco Bay, California, March to November 1988. U.S. Geological Survey Water-Resources Investigations Report 92-4064, 76 pp.
- Cappiella, K., Malzone, C., Smith, R., Jaffe, B.E., 1999. Sedimentation and bathymetry changes in Suisun Bay: 1867–1990. U.S. Geological Survey Open-File Report 99-563. <http://geopubs.wr.usgs.gov/open-file/of99-563/>.
- Cheng, R.T., Gartner, J.W., 1984. Tides, tidal and residual currents in San Francisco Bay, California — results of measurements, 1979–1980. U.S. Geological Survey Water-Resources Investigations Report 84-4399, 368 pp.
- Conomos, T.J., Peterson, D.H., 1976. Suspended-particle transport and circulation in San Francisco Bay: An overview. In: Wiley, M. (Ed.), Estuarine Processes, vol. 2. Academic Press, New York, pp. 82–97.
- Dedrick, K.G., 1983. Use of early hydrographic surveys in studies of California estuaries. Coastal Zone '83, pp. 2296–2316.
- Dedrick, K.G., 1993. Atlas of present tidal marshlands, San Francisco Bay, California. Coastal Zone '93, pp. 2451–2463.
- Friedrichs, C.T., 1995. Stability shear stress and equilibrium cross-sectional geometry of sheltered tidal channels. Journal of Coastal Research 11, 1062–1074.
- Ganju, N.K., Schoellhamer, D.H., Warner, J.C., Barad, M.F., Schladow, S.G., 2004. Tidal oscillations of sediment between a river and a bay: a conceptual model. Estuarine, Coastal and Shelf Science 60, 81–90.
- Ganju, N.K., Schoellhamer, D.H., 2006. Annual sediment flux estimates in a tidal strait using surrogate measurements. Estuarine, Coastal and Shelf Science 69, 165–178.
- Gartner, J.W., Yost, B.T., 1988. Tides, and tidal and residual currents in Suisun and San Pablo Bays, California — results of measurements, 1986. U.S. Geological Survey Water-Resources Investigations Report 88-4027, 94 pp.
- Gibbs, A.E., Gelfenbaum, G., 1999. Bathymetric change off the Washington-Oregon coast. Proceedings of Coastal Sediments '99, Long Island, N.Y., pp. 1627–1641.
- Gilbert, G.K., 1917. Hydraulic mining debris in the Sierra Nevada. U.S. Geological Survey Professional Paper 105, 154 pp.
- Goals Project, 1999. Baylands Ecosystem Habitat Goals. A Report of Habitat Recommendations Prepared by the San Francisco Bay Area Wetlands Ecosystem Goals Project. First Reprint. U.S. Environmental Protection Agency/S.F. Regional Water Quality Control Board, San Francisco, CA/Oakland, CA.
- Hayes, T.P., Kinney, J.J., Wheeler, N.J., 1984. California Surface Wind Climatology. California Air Resources Board, Aerometric Data Division, 107 pp.
- Higgins, S.A., Jaffe, B.E., Smith, R.E., 2005. Bathychronology: Reconstructing historical sedimentation from bathymetric data in a GIS, U.S. Geological Survey Open-File Report OFR-2005-1284, 19 pp. plus appendix. <http://pubs.usgs.gov/of/2005/1273/>.
- Higgins, S.A., Jaffe, B.E., Fuller, C.C., 2007. Reconstructing sediment age profiles from historical bathymetry changes in San Pablo Bay, California. Estuarine, Coastal and Shelf Science 73 (1–2), 165–174.
- Hopkins, D., List, J.H., Jaffe, B.E., Dalziel, K.A., 1991. Cartographic production for the Louisiana Barrier Island Erosion Study: 2. Generation of surface grids. U.S. Geological Survey Open-File Report 91-615, 28 pp.
- Jaffe, B.E., List, J.H., Sallenger Jr., A.H., Holland, T., 1991. Louisiana Barrier Island Erosion Study: correction for the effect of relative sea level change on historical bathymetric survey comparisons, Isles Dernieres area, Louisiana. U.S. Geological Survey Open-File Report 91-276, 33 pp.
- Jaffe, B.E., Smith, R.E., Torresan, L., 1998. Sedimentation and bathymetric change in San Pablo Bay, 1856–1983. U.S. Geological Survey Open-File Report 98-759. <http://geopubs.wr.usgs.gov/open-file/of98-759/>.
- Jaffe, B.E., Smith, R.E., Cappiella, K., Bouse, R., Luoma, S., Hornberger, M., 1999. Mercury-Contaminated Hydraulic Mining Debris in North San Francisco Bay — A Legacy of the Gold Rush (abstract). Geological Society of America, Cordilleran Annual Section Meeting 31, no. 6, 66.
- Klingeman, P.C., Kaufman, W.J., 1965. Transport of radionuclides with suspended sediment in estuarine systems. Berkeley, University of California, Sanitation Engineering Research Laboratory Report No. 65-15, 222 pp.
- Krone, R.B., 1979. Sedimentation in the San Francisco Bay system. In: Conomos, T.J. (Ed.), San Francisco Bay, the Urbanized Estuary. Pacific Division of the American Association for the Advancement of Science, pp. 85–96.
- List, J.H., Jaffe, B.E., Sallenger Jr., A.H., Williams, S.J., McBride, R.A., Penland, S., 1994. Louisiana Barrier Island Erosion Study, Atlas of sea floor changes from 1878 to 1989. U.S. Geological Survey Miscellaneous Investigations Map I-2150-B, 62 pp.
- Locke, J.L., 1971. Sedimentation and foraminiferal aspects of the recent sediments of San Pablo Bay. M.S. thesis, San Jose State University, San Jose, CA, 100 pp.

- Lyles, S.D., Hickman, L.E., Debaugh Jr., H.A., 1988. Sea Level Variations for the United States, 1855–1986. National Oceanic and Atmospheric Administration, Washington, DC, 182 pp.
- Marvin-DiPasquale, M., Agee, J., Bouse, R., Jaffe, B., 2003. Microbial cycling of mercury in contaminated wetland and open-water sediments of San Pablo Bay, California. *Environmental Geology* 43 (3), 260–267.
- McKee, L.J., Ganju, N.K., Schoellhamer, D.H., 2006. Estimates of suspended sediment entering San Francisco Bay from the Sacramento and San Joaquin Delta, San Francisco Bay, California. *Journal of Hydrology* 323, 335–352.
- Miller, A., 1967. Smog and Weather – The Effect of the San Francisco Bay on the Bay Area Climate. San Francisco Bay Conservation and Development Commission, 40 pp.
- Monismith, S.G., Kimmerer, W., Burau, J.R., Stacey, M.T., 2002. Structure and flow-induced variability of the subtidal salinity field in Northern San Francisco Bay. *Journal of Physical Oceanography* 32, 3003–3019.
- National Oceanic and Atmospheric Administration, Geophysical Data System for Hydrographic Survey Data (GEODAS), CD, version 3.3.
- National Oceanic and Atmospheric Administration, 1986. Tide Tables, West Coast of North and South America. National Oceanic and Atmospheric Administration, Rockville, MD.
- Ogden Beeman and Associates, Ray Krone and Associates, 1992. Sediment budget study for San Francisco Bay. Final report prepared for U.S. Army Corps of Engineers, San Francisco District, under contract DACW07-89-D-0029, 25 pp.
- Porterfield, G., 1980. Sediment transport of streams tributary to San Francisco, San Pablo, and Suisun Bays, California, 1909–1966. U.S. Geological Survey Water-Resources Investigations Report 80-64, 92 pp.
- Putnam, J.A., 1947. Estimating storm-wave conditions in San Francisco Bay. *EOS (American Geophysical Union Transactions)* 28 (2), 271–278.
- Ruhl, C.A., Schoellhamer, D.H., Stumpf, R.P., Lindsay, C.L., 2001. Combined use of remote sensing and continuous monitoring to analyze the variability of suspended-sediment concentrations in San Francisco Bay, California. *Estuarine, Coastal and Shelf Science* 53, 801–812.
- Sallenger, A.H., Goldsmith, V., Sutton, C.H., 1975. Bathymetric comparisons: a manual of methodology, error criteria and techniques. Special Report in Applied Marine Science and Ocean Engineering (SRAMSOE) 66, 34 pp.
- Schalowitz, A.L., 1964. Shore and sea boundaries. U.S. Coast and Geodetic Survey Publication 10-1, 2, 749 pp.
- Schoellhamer, D.H., Schellenbarger, G.G., Ganju, N.K., Davis, J.A., McKee, L.J., 2003. Sediment dynamics drive contaminant dynamics. In: San Francisco Estuary Institute (SFEI) (Ed.), *The Pulse of the Estuary: Monitoring and Managing Water Quality in the San Francisco Estuary*. SFEI Contribution 74. San Francisco Estuary Institute, Oakland, CA, pp. 21–26.
- Sherwood, C.R., Jay, D.A., Harvey, R.B., Hamilton, P., Simenstad, C.A., 1990. Historical changes in the Columbia River Estuary. *Progress in Oceanography* 24, 299–352.
- Smith, B.J., 1965. Sedimentation in the San Francisco Bay system. In: *Proceedings of the Interagency Sedimentation Conference*, vol. 970. U.S. Department of Agriculture Miscellaneous Publication, pp. 675–708.
- Swanson, R.L., 1974. Variability of tidal datums and accuracy in determining datums from short series of observations. National Oceanic and Atmospheric Administration Technical Report 64, 41 pp.
- Uncles, R.J., Peterson, D.H., 1996. The long-term salinity field in San Francisco Bay. *Continental Shelf Research* 16, 2005–2039.
- Van Rijn, L.C., 1993. Principles of Sediment Transport in Rivers, Estuaries, and Coastal Seas. Aqua Publications, Amsterdam, 715 pp.
- Van Royen, W., Siegel, C.O., 1959. Future development of the San Francisco Bay area, 1960–2020. Report prepared for the U.S. Army Corps of Engineers, San Francisco District by Business and Defense Services Administration, U.S. Department of Commerce.
- Wahba, G., 1990. Spline models for observational data. CBMS-NSF Regional Conference Series in Applied Mathematics. Society for Industrial and Applied Mathematics, Philadelphia.
- Wright, S.A., Schoellhamer, D.H., 2004. Trends in the sediment yield of the Sacramento River, California, 1957–2001. *San Francisco Estuary and Watershed Science* (online serial) 2 (Issue 2, Article 2). <http://repositories.cdlib.org/jmie/sfews/vol2/iss2/art2>.
- Wright, S.A., Schoellhamer, D.H., 2005. Estimating sediment budgets at the interface between rivers and estuaries with application to the Sacramento–San Joaquin River Delta, *Water Resources Research* 41, W09428. doi:10.1029/2004WR003753.



Peer Reviewed

Title:

Potential Inundation Due to Rising Sea Levels in the San Francisco Bay Region

Journal Issue:

[San Francisco Estuary and Watershed Science, 8\(1\)](#)

Author:

[Knowles, Noah](#), USGS

Publication Date:

2010

Permalink:

<http://escholarship.org/uc/item/8ck5h3qn>

Additional Info:

found Jim Titus' email: titus.jim@epa.gov

Keywords:

sea level rise, climate change, estuary, wetlands, San Francisco Bay, flooding, Climate

Local Identifier:

jmie_sfews_11013

Abstract:

An increase in the rate of sea level rise is one of the primary impacts of projected global climate change. To assess potential inundation associated with a continued acceleration of sea level rise, the highest resolution elevation data available were assembled from various sources and mosaicked to cover the land surfaces of the San Francisco Bay region. Next, to quantify extreme water levels throughout the bay,

a hydrodynamic model of the San Francisco Estuary was driven by a projection of hourly water levels at the Presidio. This projection was based on a combination of climate model outputs, an empirical model, and observations, and incorporates astronomical, storm surge, El Niño, and long-term sea level rise influences.

Based on the resulting data, maps of areas vulnerable to inundation were produced, corresponding to specific amounts of sea level rise and recurrence intervals, including tidal datums. These maps portray areas where inundation will likely be an increasing

concern. In the North Bay, wetlands and some developed fill areas are at risk. In Central and South bays, a key feature is the landward periphery of developed areas that would be newly vulnerable to inundation. Nearly all municipalities adjacent to South Bay face



eScholarship
University of California

eScholarship provides open access, scholarly publishing services to the University of California and delivers a dynamic research platform to scholars worldwide.

this risk to some degree. For the bay as a whole, as early as mid-century under this scenario, the one-year peak event nearly equals the 100-year peak event in 2000. Maps of vulnerable areas are presented and some implications discussed. Results are available for interactive viewing and download at <http://cascade.wr.usgs.gov/data/Task2b-SFBay>.

Copyright Information:



Copyright 2010 by the article author(s). This work is made available under the terms of the Creative Commons Attribution 4.0 license, <http://creativecommons.org/licenses/by/4.0/>



eScholarship
University of California

eScholarship provides open access, scholarly publishing services to the University of California and delivers a dynamic research platform to scholars worldwide.

Potential Inundation Due to Rising Sea Levels in the San Francisco Bay Region

Noah Knowles¹, U.S. Geological Survey, Menlo Park, CA 94025

ABSTRACT

An increase in the rate of sea level rise is one of the primary impacts of projected global climate change. To assess potential inundation associated with a continued acceleration of sea level rise, the highest resolution elevation data available were assembled from various sources and mosaicked to cover the land surfaces of the San Francisco Bay region. Next, to quantify extreme water levels throughout the bay, a hydrodynamic model of the San Francisco Estuary was driven by a projection of hourly water levels at the Presidio. This projection was based on a combination of climate model outputs, an empirical model, and observations, and incorporates astronomical, storm surge, El Niño, and long-term sea level rise influences.

Based on the resulting data, maps of areas vulnerable to inundation were produced, corresponding to specific amounts of sea level rise and recurrence intervals, including tidal datums. These maps portray areas where inundation will likely be an increasing concern. In the North Bay, wetlands and some developed fill areas are at risk. In Central and South bays, a key feature is the landward periphery of developed areas that would be newly vulnerable to inundation. Nearly all municipalities adjacent to South Bay face

this risk to some degree. For the bay as a whole, as early as mid-century under this scenario, the one-year peak event nearly equals the 100-year peak event in 2000. Maps of vulnerable areas are presented and some implications discussed. Results are available for interactive viewing and download at <http://cascade.wr.usgs.gov/data/Task2b-SFBay>.

KEYWORDS

Sea level rise, climate change, estuary, San Francisco Bay, flooding, wetlands

INTRODUCTION

An increase in the rate of rise of mean sea level is one of the primary and potentially most troublesome aspects of projected climate change. Sea level at San Francisco's Presidio tide gauge has risen at a rate of 22 centimeters (cm) per century over the last century (Flick 2003), consistent with global average rates (Church and others 2004). In recent years, the rate of global sea level rise increased significantly over that of the previous several decades (Church and White 2006; Bindoff and others 2007). As global temperatures continue to increase, sea level will continue to rise in response, probably at a greater rate than observed historically. While it is generally accepted that global climate warming will increase

¹ Corresponding author: nknowles@usgs.gov

SAN FRANCISCO ESTUARY & WATERSHED SCIENCE

rates of sea level rise, the range in projected rates is wide, due mainly to the uncertainty in the amount of meltwater from land-based ice in Greenland and Antarctica. Recent projections (Rahmstorf 2007) estimate the range of increase of global sea level by 2100 at 50–140 cm above recent levels. Another recent study (Pfeffer and others 2008) produced a somewhat higher estimate (80–200 cm), reinforcing the opinion that sea level rise during the next several decades could exceed the estimates provided by the Intergovernmental Panel on Climate Change (IPCC) Third and Fourth Assessments (IPCC 2001, 2007). Concerning the high end of the range, Pfeffer and others (2008) concluded that sea level rise is very unlikely to exceed 200 cm by 2100. Beyond 2100, however, sea levels are expected to continue to rise for several centuries due to oceanic thermal inertia (Wigley 2005).

Pioneering studies by Williams (1985, 1987) and Gleick and Maurer (1990) were the first to estimate the impacts of sea level rise in San Francisco Bay. Williams found that a 100-cm sea level rise would result in an inland shift of the estuarine salinity field of 10 to 15 kilometers (km), potentially threatening ecosystems and freshwater supplies. In their comprehensive effort, Gleick and Maurer estimated that a 100-cm sea level rise would result in losses of residential, commercial and industrial structures bordering the bay valued at \$48 billion (1990 dollars).

A detailed assessment of what areas adjacent to the bay are vulnerable to inundation due to projected sea level rise is necessary to help avoid future risk in developing residential and commercial areas, to inform infrastructure planning (for example, water treatment outflows and roadways), and to design wetland restoration efforts with the ability to adapt to future changes, among other applications. The present study uses hydrodynamic modeling in conjunction with the most accurate elevation data available to develop high-resolution maps of areas vulnerable to periodic inundation corresponding to varying amounts of sea level rise, and to a range of inundation return intervals. The data are publicly available for use in other efforts at <http://cascade.wr.usgs.gov/data/Task2b-SFBay>.

This study addresses only the question of which areas are vulnerable to inundation, as opposed to quantifying the actual risk of inundation under a future scenario. No distinction is made between vulnerable areas already protected by levees and those that are not—at the time of this study, insufficient data on levees were available to make this distinction. Thus, potential improvements to existing levees or construction of new levees are not considered. Where levees currently exist, the results presented below indicate areas that would be flooded if these levees were to fail (due to, for example, a high-water event or an earthquake). Also, shoreline erosion and the potential accumulation of sediment and organic matter in wetlands are not accounted for here. As levee data become available and as modeling capabilities improve, future studies will address such issues and directly evaluate possible mitigation actions.

In the following sections, the elevation data set and hydrodynamic modeling approach used are described. Then some key results are presented and discussed, including maps and analysis of (1) areas vulnerable to periodic inundation by extreme high-water levels, and (2) wetlands vulnerable to changing tidal datums as sea levels rise. Finally, implications of the results and important caveats are discussed.

DATA AND METHODS

Method Overview

This study uses a hydrodynamic model to simulate water levels throughout San Francisco Bay under conditions of projected sea level rise. Statistical analysis of the projected water levels provides characterization of both long-term trends in mean sea level and high-water levels associated with short-term variability at points along the bay's shoreline. These high-water levels are then compared to nearby land-surface elevations to determine areas vulnerable to inundation around the bay. The same evaluation is also performed for high and low tidal datums. The focus here is on evaluating specific amounts of sea level rise, which can then be associated with particular future dates according to a given climate scenario, rather than focusing on specific scenarios from the

outset. Where time frames for given amounts of sea level rise to occur are considered, they are based on the range of projections by Rahmstorf (2007).

Elevation Data

To serve as the foundation of this study, the highest resolution elevation data available to date were assembled and mosaicked to cover the entire region. This new data set necessarily represents a patchwork of LiDAR (light detection and ranging) data from multiple sources, photogrammetry data, and IfSAR (interferometric synthetic aperture radar) data where no better data were available. This data set contains elevation data from six sources (Figure 1):

1. FEMA LiDAR, produced by Merrick and Company for use in FEMA's Flood Insurance Rate Maps. These data were processed to a horizontal resolution of 1 m, and the vertical 95% confidence interval is ± 30 cm.
2. Sacramento-San Joaquin Delta Region LiDAR data set, produced by the California Department of Water Resources from missions flown in 2007 and 2008. The data set's horizontal resolution is 1 meter (m), and the vertical 95% confidence interval is ± 18 cm.
3. Napa watershed LiDAR from the University of California at Berkeley Data Distribution Center for the National Center for Airborne Laser Mapping (NCALM, <http://calm.geo.berkeley.edu/ncalm>). These data are from flights in 2003, the horizontal resolution is 1 m, and the vertical 95% confidence interval is ± 30 cm.
4. South Bay salt ponds LiDAR data (Foxgrover and Jaffe 2005). These data are from flights in 2004, and the horizontal resolution is 1 m. The vertical 95% confidence interval is ± 25 cm for most of the salt-pond areas, and ± 15 cm for the hard, flat surfaces which constitute most of the area vulnerable to future inundation with sea level rise in South Bay.
5. San Francisco region photogrammetric elevation data. The U.S. Geological Survey (USGS), in cooperation with the National Geospatial-Intelligence Agency (NGA), developed ground elevation data

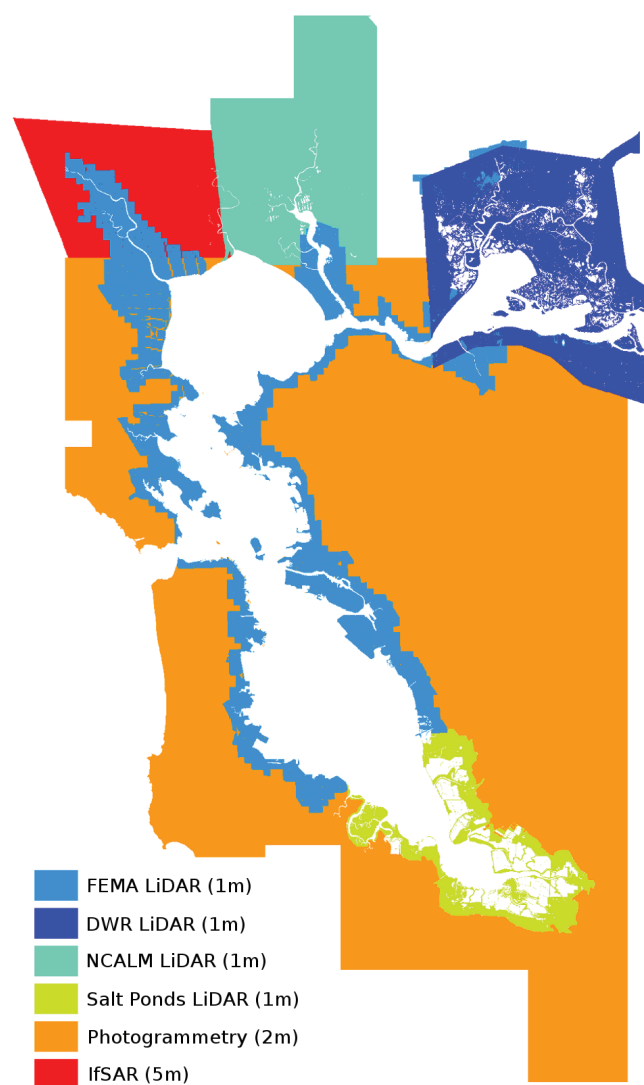


Figure 1 Sources of elevation data. Horizontal resolutions of original data are given in parentheses. All datasets were re-sampled to 2 m and merged.

from flights in 2003 at a horizontal resolution of 2 m for the purpose of producing orthorectified images. We assembled the tiles of elevation data and adjusted them to the North American Vertical Datum of 1988 (NAVD88) datum using the GEOID03 model, resulting in a data set covering the greater bay-delta region (Coons and others 2008). Vertical accuracy was not rigorously determined, but we estimate the 95% confidence interval as ± 50 cm.

SAN FRANCISCO ESTUARY & WATERSHED SCIENCE

6. Intermap IfSAR data, produced using synthetic aperture radar methods, were obtained to fill gaps in the Petaluma River and Sonoma Creek watersheds. These data are not ideal, as they have a 5-m horizontal posting and a vertical 95% confidence interval of ± 100 –200 cm. However, at the time of this writing they are the most accurate data available for the portions of that area not covered by the other data sets.

All elevation data were referenced to NAVD88 in the Universal Transverse Mercator projection (zone 10). Where necessary, the conversion to NAVD88 was made using the GEOID03 model (http://www.ngs.noaa.gov/PC_PROD/GEOID03).

These six data sets were resampled to a common horizontal resolution of 2 m using the nearest-neighbor method, then merged after comparison in areas of overlap. Agreement between all overlapping data sets was good, with slight average positive biases (10–20 cm) of the photogrammetry and IfSAR relative to the LiDAR data sets. This bias makes sense as all of the LiDAR data sets represent “bare-ground” elevations, whereas the photogrammetry and IfSAR data include the height of vegetation. As such, any estimates of inundation vulnerability in areas covered by the photogrammetry and IfSAR data sets may be considered conservative. However, of the six sources used to produce the composite elevation data set, the four LiDAR data sets, all with vertical 95% confidence intervals of less than 30 cm, together constitute 88% (at a minimum—more depending on the amount of sea level rise being evaluated) of the area vulnerable to inundation as presented in this paper.

The last step in developing the regional elevation data set was to mask out open water, as none of the measurement methods described above produce reliable results over water. First, a water mask produced by Foxgrover and Jaffe (2005) for the South Bay LiDAR data based on return characteristics was used to mask open water in the part of the bay covered by that data set. Next, two shoreline data sets representing the mean high water (MHW) tidal datum were used to mask data below this datum throughout the bay. Outside the mouth of San Francisco Bay, the shoreline was extracted from the National

Oceanic and Atmospheric Administration (NOAA) National Shoreline data set (<http://shoreline.noaa.gov/data/datasheets>). Inside the bay, another data set was available—a shoreline coverage extracted from the San Francisco Estuary Institute (SFEI) EcoAtlas (<http://www.sfei.org/ecoatlas>). The SFEI and NOAA shoreline data sets were checked against orthoimages from 2003, and it was qualitatively determined that the SFEI shoreline was more accurate. The two shorelines were clipped and joined at the Golden Gate, and used to remove all elevation data below the MHW tidal datum (due to this cutoff, the results discussed below generally exclude mud flats). As of this writing, the resulting composite data set represents the most accurate elevation data publicly available (excluding the IfSAR data which are under a restrictive license) covering the San Francisco Bay region.

Hydrodynamic Model Configuration and Validation

To assess what land elevations around the bay are vulnerable to periodic inundation, estimates of high-water levels throughout the bay must be generated. These high water excursions are the result of tides, storm surge, and other dynamic processes, requiring the use of a hydrodynamic model for this task. This model is used to produce a single 100-year projection of hourly water levels throughout the bay for use in the subsequent analysis. TRIM-2D (Cheng and others 1993) is a numerical model that uses a semi-implicit finite-difference method for solving the two-dimensional shallow water equations in San Francisco Bay. The model uses a 200 m horizontal grid with nearly 50,000 grid cells and is configured here with a six-minute time step. Note that these spatial and temporal resolutions are more than sufficient to capture the highest frequency of water-level variability addressed in this work—semi-diurnal. The model is driven solely by water-level time series at its seaward and landward boundaries, which are translated in phase and amplitude from the tide gauges with sufficiently long records nearest these boundaries, namely the Presidio and Port Chicago stations (Figure 2). Cheng and others (1993) demonstrated that the TRIM-2D hydrodynamic model accurately reproduces the historical amplitudes and phases of tidal constituents throughout the bay.

MAY 2010

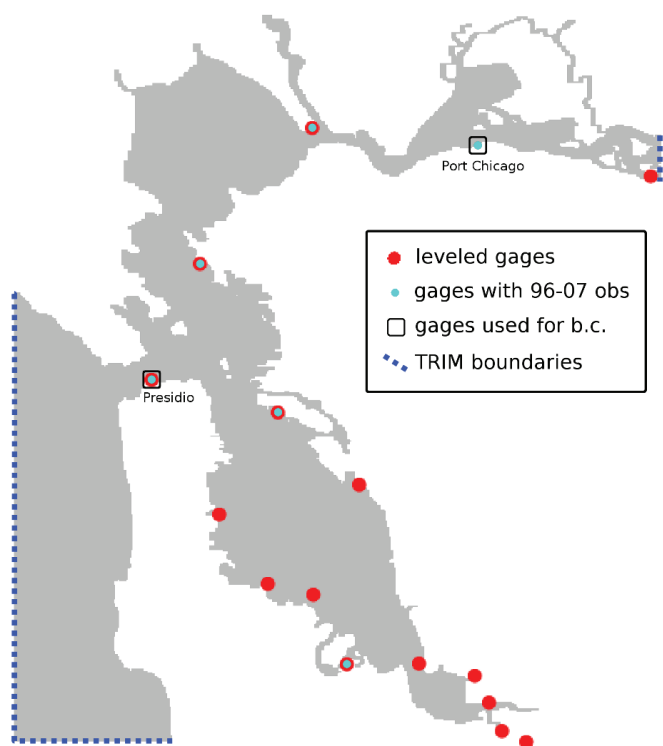


Figure 2 Key sites and features relevant to configuration and validation of TRIM-2D. The model grid is in gray. Gauge sites whose elevation relative to NAVD88 is known are in red. Gauges with data covering the validation period 1996–2007 are in bright blue. The two gauges whose data are used to derive conditions at the model boundaries (dotted blue lines) are in black squares.

The TRIM-2D model was chosen because it is capable of performing the century-long simulation needed to address the effects of long-term climate change in a reasonable amount of time. While the ideal model for this study would have a boundary condition much farther upstream than Port Chicago to avoid boundary issues and would directly simulate the hydrodynamics of inundated areas, such a model is not yet publicly available. Those proprietary models which do include such features are currently too computationally demanding to perform the needed runs in a reasonable amount of time.

The TRIM-2D model in its native configuration simulates water levels relative to mean lower-low water (MLLW), but water levels relative to NAVD88 are needed for comparison with the elevation data. The model takes as input a datum file, which was previ-

ously configured relative to the MLLW tidal datum. By adjusting this file appropriately, the model can be reconfigured to generate output water heights relative to NAVD88. To accomplish this reconfiguration, heights of MLLW relative to NAVD88 from 15 leveled tide gauges throughout the bay (Figure 2) were obtained from NOAA (<http://tidesandcurrents.noaa.gov>). These heights were then interpolated using the method of regular splines with tension (Mitasova and Hofierka 1993) to produce a MLLW adjustment grid. This grid was used in the new input datum file to TRIM-2D, and the resulting simulated water heights are referenced to NAVD88. While NOAA produces a similar datum adjustment grid for the bay region (<http://vdatum.noaa.gov>), the version available at the time of this study was deemed too inaccurate to use, as its source data did not include enough tidal stations in South Bay or near the delta, and spot checks against tidal datums from leveled tide gauges revealed inconsistencies.

With the model's datum adjusted, the calibration coefficients used to translate the boundary forcings from the nearby tide gauges to the model boundaries needed to be retuned. To this end, the model was run repeatedly over the period 1996–2007. This validation period was chosen because hourly water-level observations at six sites throughout the bay (Figure 2), including the gauges used to generate the boundary conditions, were available for the full period. The calibration coefficients were iteratively adjusted to minimize differences between simulated and observed mean sea level and average daily tidal range at these six sites.

Hydrodynamic Model Inputs

TRIM-2D requires two time series as inputs—water levels at six-minute intervals at the Presidio and Port Chicago sites—which are then mapped using calibrated coefficients to serve as the model's boundary conditions (Figure 2). A 100-year projection of mean sea level at the Presidio location was produced by Cayan and others (2009) using the method of Rahmstorf (2007), based on global mean temperatures as projected by the CCSM3 global climate model (<http://www.cesm.ucar.edu>) under the A2 greenhouse

SAN FRANCISCO ESTUARY & WATERSHED SCIENCE

gas emissions scenario (Figure 3). This model projects a $\sim 4.5^{\circ}\text{C}$ ($\sim 8.1^{\circ}\text{F}$) increase in global average surface air temperatures by 2100. This is a relatively high (but not the highest) amount of warming among the ensemble of IPCC Fourth Assessment model results (IPCC 2007). Using the Rahmstorf method, this warming corresponds to a 139-cm rise in mean sea level, which corresponds to the upper end of the range of sea level rise projections in his 2007 paper.

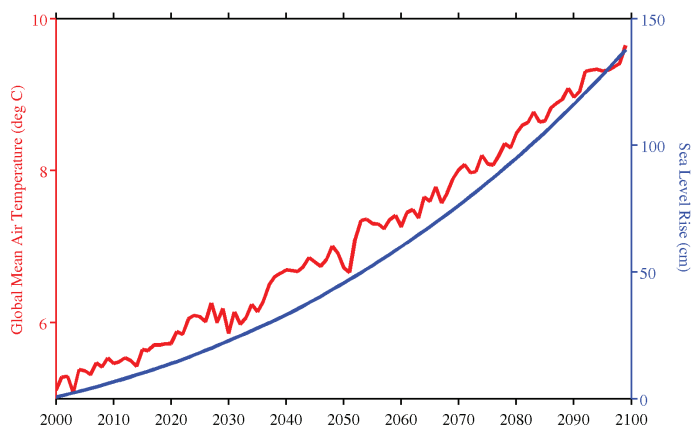


Figure 3 Annual global mean surface air temperatures (red) from the CCSM3-A2 GCM output, and corresponding relative sea level rise (blue) from the Rahmstorf model

This method provided the secular trend in water levels at the Presidio, but water levels vary under the influence of several forces over multiple time scales. Astronomical tides, storm surges, storm-related pressure drops, and El Niños are all major contributors to water-level variability. The result of these and other forces is that water levels reach successively higher peak water levels at longer time scales. Figure 4 illustrates the historical (1900–2000) average daily, monthly, and yearly high-water levels compared to hourly data for a typical year (2006) at the Presidio.

To incorporate this variability into the projected water-level time series, historical variability was superposed on the projected long-term trend in mean sea level. To do this, hourly water-level data (1900–1999) from the Presidio gauge were detrended using a least-squares linear fit to remove any historical sea level rise signal. A few small gaps in the historical data were filled using hindcast astronomical tides

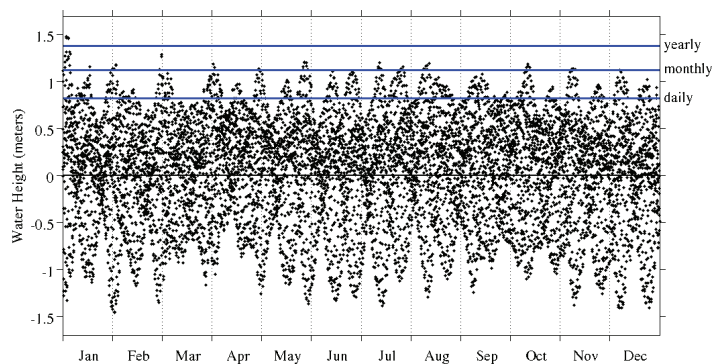


Figure 4 Hourly water levels at the Presidio for a typical year (2006), showing average historical (1900–2000) daily, monthly, and yearly high water levels

(Cheng and Gartner 1984). The resulting 100-year detrended time series, which contained variability over periods ranging from tidal to decadal scales, was added to the secular trend provided by Cayan to produce a 100-year projection of hourly water levels at the Presidio. This use of historical short-term variability (defined here as any variability other than the long-term trend) to represent future short-term variability requires two assumptions—first, that the probability distribution of short-term variability will remain unchanged under the climate change projections, and second, that these short-term variations and the secular component of the water-level time series at the Presidio site are linearly superposable. Cayan and others (2008) found the first of these assumptions to be true. The second follows as a reasonable approximation from the fact that the amplitude of both components— $O(1\text{ m})$ —is considerably smaller than the average depth near the Presidio site— $O(100\text{ m})$. This is because in sufficiently deep water, surface waves do not interact with the bottom and are thus unaffected by relatively small changes in mean depth.

With the first of the two required TRIM-2D input time series thus obtained, the Port Chicago time series was next produced. Lacking more than a few decades of data at the Port Chicago site, the approach used for the Presidio site was unworkable. The chosen solution was to map the Presidio time series to Port Chicago using a temporal version of the technique of constructed analogues (Hidalgo and others 2008). In this approach, the historical water-level time series

MAY 2010

(1996–2007) at the two stations were used to create a “map” which generates a 100-year hourly water-level projection at Port Chicago based on the Presidio projection described above. Specifically, the Presidio projection was stepped through five days at a time, with the preceding and succeeding days included to make a week of data. Each of these seven-day periods was expressed as a linear combination of the 22 best-matching (using RMS error) seven-day periods from the historical Presidio record (22 was found to be the optimal number of matches). The same coefficients in this optimal linear combination were then applied to the corresponding seven-day periods from the historical Port Chicago record to produce the estimate of Port Chicago water levels for the corresponding projected five-day period, after dropping the first and last days (which were included to minimize boundary effects in the procedure). One constraint on the method is that matching weeks were restricted to the same quarter of the year as the target week, allowing some accounting of the influence of the annual cycle of storm surges and freshwater flow.

Stepping through the 100-year Presidio projection in this manner, a corresponding 100-year projection of hourly water levels was developed for the Port Chicago station. The described procedure was applied to the non-secular component of the Presidio projection, and the Rahmstorf secular trend was then added to the resulting Port Chicago time series. A more complete description of the original method (as applied to spatial fields instead of time series) is given in Hidalgo and others (2008).

Projecting future Port Chicago water levels based on historical water levels assumes that amplitudes are unchanged as mean depth increases. Recent test runs using a Delft3D model of the bay-delta (van der Wegen, personal communication) suggest that increasing mean sea levels would result in increased tidal amplitudes at Port Chicago, meaning the results presented here are conservative, particularly in the landward reach of the estuary. These same test runs also indicate that any attenuation between the Presidio and Port Chicago sites of the long-term sea level rise signal would be negligible, justifying the method described above.

A validation run of the above procedure was performed, in which a portion of the historical Presidio record (1996–2007) was mapped to Port Chicago, with the procedure modified to exclude the target week from being selected as one of the matching patterns. The resulting “mapped” Port Chicago time series agreed well with the actual observed time series, with an RMS error of 6 cm (compared to an average daily tidal range of 148 cm) and a correlation coefficient of $r > 0.99$.

Both the Presidio and the Port Chicago 100-year hourly projections were interpolated from an hourly to a six-minute time step, and a week of hindcast astronomical tides were prepended to allow for model spin-up. A run of TRIM-2D was performed using these inputs (with a real-world run time of three weeks), resulting in a 100-year projection of six-minute gridded water heights throughout San Francisco Bay corresponding to a sea level rise of 139 cm by 2100.

ANALYSIS

Based on the projections of gridded water-level time series, water-height fields were developed corresponding to combinations of (1) specific amounts of sea level rise, and (2) specific return intervals (for example, 100-year high water with 50-cm sea level rise). This was accomplished by first separating the water-level time series of each model grid cell into a long-term trend and a detrended short-term variability time series. The long-term trend was estimated as the optimal second-degree least-squares fit to the full time series, and the residual was the short-term variability. Using the parameters of the long-term fits, the bay-wide, mean water-height field that corresponds to a specific amount of sea level rise could then be determined, providing (1) above. These fits to the long-term trends were sufficiently robust that for the subsequent analysis, it was decided they could reasonably be extended a few years beyond the end of the fitted data to represent a sea level rise of 150 cm, which would have occurred in an extended CCSM3-A2 scenario in 2105.

Return intervals represent the average period between events of a certain magnitude (corresponding to

SAN FRANCISCO ESTUARY & WATERSHED SCIENCE

“return levels”), such as floods, and are widely used for a variety of purposes, such as design and planning, regulation, and insurance requirements. High-water levels corresponding to specific return intervals associated with short-term variability were calculated next using the detrended 100-year time series at each grid cell. For periods less than a year, these series were long enough that water-level extremes could be robustly calculated simply as the corresponding mean. Mean daily higher-high water (MHHW) levels and mean daily lower-low water (MLLW) levels were calculated in this manner.

Return intervals of one year and longer were evaluated by applying the generalized extreme value (GEV) distribution, formulated by Fisher and Tippett (1928). Fisher and Tippett showed that block maxima, or a series of maxima each calculated over a specific time interval (for example, annual high-water levels), are characterized by the cumulative distribution function given in Equation 1.

Equation 1

$$F(x; \mu, \sigma, \xi) = \begin{cases} \exp\left\{-\left[1 + \xi\left(\frac{x - \mu}{\sigma}\right)\right]^{\frac{1}{\xi}}\right\}, & 1 + \xi\left(\frac{x - \mu}{\sigma}\right) > 0 \\ \exp\left\{-\exp\left[-\left(\frac{x - \mu}{\sigma}\right)\right]\right\}, & \xi = 0 \end{cases}$$

The cumulative distribution function of Equation 1 was fit to the annual maxima of the detrended time series in each grid cell throughout the bay using the maximum-likelihood method¹, also developed by Fisher (1922). This resulted in values of the parameters μ , σ , and ξ for each grid cell. The most important of these parameters, ξ , is called the shape parameter and determines the shape of the extreme tail of the probability distribution of the process being characterized—in this case water-level variability. For all points on the bay grid, $\xi < 0$, representing a short-tailed process. This indicates relatively small differences between high-water levels for progressively longer return intervals. The inverse of Equation 1 was

then used to determine water-level heights throughout the bay for a given return interval, corresponding to a specific value of the cumulative distribution function.

Finally, for a specified amount of sea level rise we can determine the gridded mean water level throughout the bay using the parameters describing the long-term trend. For a specified return interval we can determine the associated water-height field using the GEV parameters, or, in the case of tidal time scales, using the corresponding mean high water or mean low water values. Adding the projected mean water levels to those characterizing short-term events allows the water-level extremes of the bay to be characterized, both probabilistically and through time for any combination of sea level rise and return interval.

This approach assumes that the simulated 100-year, water-level time series can be separated into a long-term trend and short-term variability with the latter component being stationary (a requirement of the GEV analysis), thus extending to the entire bay the assumption that the short-term variability is independent of the long-term trend. While this assumption was clearly reasonable near the deeper waters of the Presidio site, it is not obviously so in the shallower parts of the bay where surface waves may interact with the bottom. To test this assumption, a separate hydrodynamic simulation was carried out in which the long-term sea level trend was removed from the boundary conditions, leaving only the short-term component. The last few years of the 100-year projection were simulated in this manner, and the results were compared to the detrended signal derived from the output of the original simulation. If short-term variability is indeed independent of the long-term trend in mean sea level, the two should be identical. The test run showed very slightly higher peak water levels—0(1 cm)—only in the shoals of the bay, indicating that short-term variability in those near-shore areas is dampened negligibly by the increase in mean depth with sea level rise, justifying the approach used here.

Importantly, a benefit of this approach is that the results are not limited to the particular climate scenario used (in this case, CCSM3-A2). That is, the

¹ All analysis and figures were produced using GRASS/QGIS, Matlab, and R statistical analysis software.

results are not dependent on time elapsed in the scenario but instead on the specific amount of sea level rise that has occurred. By specifying this amount along with the statistics of the short-term variability (which, being stationary through time and across scenarios, are independent of the scenario chosen), the results are completely specified. Choosing a high-end scenario for the base simulation made it possible to parameterize and subsequently evaluate a large range of potential future sea level rise.

Using the approach described above, water-level extremes were determined for different values of sea level rise and return interval for each of the nearly 50,000 points in the TRIM-2D, 200-m horizontal grid. In particular, sea level rise was evaluated in half-meter increments: 0, 50, 100, and 150 cm. In Rahmstorf's projections (2007), these amounts of sea level rise would be reached in roughly the following time frames, respectively: present-day, 2050–2100, 2080–, and 2105– (the projections do not extend far enough into the future to provide end dates for the highest two values). For each of these four cases, the inverse of Equation 1 was used to determine the water-height fields corresponding to return intervals of 1, 10, 50, 100, and 500 years. Water-height fields for the tidal datums MLLW and MHHW were also determined for the four sea level rise values. Multiple intermediate amounts of sea level rise were also evaluated, but most results presented below focus on the half-meter increments.

Finally, each water-height field was compared at all points along the bay's shoreline to the adjacent land surface elevation data to assess what areas would be inundated (at least as often as the specified return interval, on average) by water at these heights, resulting in the inundation maps and data presented in the next section. A final data set used to portray vulnerable areas in terms of land cover type was the National Land Cover Data set of 2001 (NLCD01; Homer and others 2007).

Potential sources of error in this analysis include the source elevation data, particularly errors in adjusting the LiDAR data for dense vegetation to achieve "bare earth" elevations. As mentioned earlier, the effect of present or future levees, potential accumulation of

sediment and organic matter, and shoreline erosion are not included in this study. Further, attenuation of short-term variability over inundated areas has not been accounted for; therefore, vulnerability to inundation may be overstated for areas well removed from the bay's (and the TRIM-2D model's) present-day shoreline. The estimates presented in this study have not taken into account the effect of wind waves on water levels, nor, in the long term, the possibility of tsunamis. The effect of high freshwater inflows on stage are accounted for, but only corresponding to historical climate; increased winter flood peaks associated with climate warming (for example, Knowles and Cayan 2002) would likely produce greater inundation vulnerabilities than presented here, especially in the northern part of the estuary.

Finally, subsidence of the land surface may exacerbate some of the vulnerabilities presented here; conversely, long-term uplift may do the opposite. Bürgmann and others (2006) used IfSAR data to determine that recent magnitudes of tectonic vertical deformation have been small in the bay region (<0.5 mm/yr along the bay shoreline). Changes in groundwater levels in the Santa Clara Valley caused isolated subsidence near the southern tip of the bay of up to 30 mm/yr during the last century (Poland and Ireland 1988), though improved groundwater management has led to a more stable land surface there more recently (Galloway and others 1999; Schmidt and Bürgmann 2003).

A more widespread process is the ongoing consolidation of sediments and bay mud in filled areas adjacent to the bay, resulting in subsidence of up to 17 mm/yr (Ferretti and others 2004). Also, consolidation and compaction of organic sediments is common in managed wetlands. This is particularly evident in the Suisun marsh LiDAR data in the North Bay, although ongoing subsidence rates there are not well documented. These last two processes suggest that the results presented here are likely to underestimate the possible impacts of sea level rise, as wetlands and man-made fill dominate the low lying areas around the bay.

RESULTS AND DISCUSSION

Potential Inundation Due to Extreme High-water Levels

Extreme high-water levels pose the most serious threat of overtopping or breaching levees, which would cause flooding in currently protected areas. Under sea level rise, the threat to such areas would increase. Also, low-lying areas not currently vulnerable (and therefore not yet protected by levees) would become increasingly subject to inundation. Sea level rise would bring qualitatively different types of risks for wetlands, so they are excluded from the results in this section and are discussed in the next section.

Figure 5A shows areas whose elevations are below the adjacent average 100-year high-water levels under conditions of present mean sea level in blue, and under conditions of a (high-end) 150-cm increase in mean sea level in red. For clarity, intermediate values of sea level rise are not shown in this and subsequent maps; for smaller values of sea level rise, the red areas would be smaller. An interactive, high-resolution presentation of these results, with 50-cm increments individually color-coded, is available at <http://cascade.wr.usgs.gov/data/Task2b-SFBay>.

To better understand what types of land are at risk, Figure 5B shows the areas vulnerable to 100-year

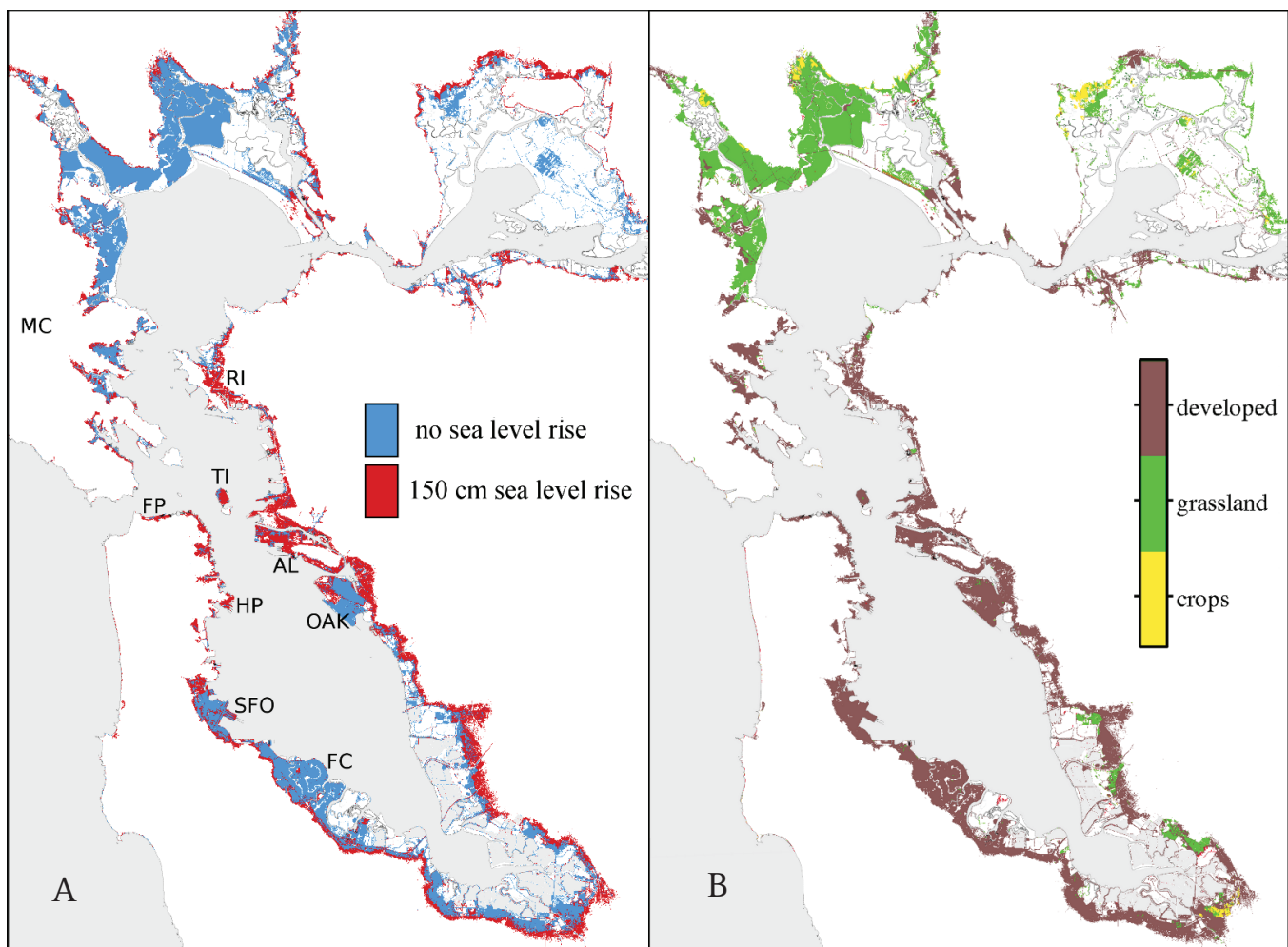


Figure 5 (A) Areas inundated or vulnerable to inundation under 100-year high-water levels for present-day (blue) and 150-cm sea level rise (red). MC=Marin County, RI=Richmond, TI=Treasure Island, FP=Fort Point, AL=Alameda, HP=Hunters Point, OAK=Oakland International Airport, SFO=San Francisco International Airport, and FC=Foster City. **(B)** Same areas as in (A), but colored according to land-use type. Wetlands are excluded from these figures.

MAY 2010

inundation, expressed in terms of land cover types based on the NLCD01 data set.

Most of the areas indicated as presently vulnerable to inundation in Figure 5A (in blue) are behind levees and would only be inundated if those levees breached or were overtopped. These areas include crops and grasslands (mostly grazed pasture) that are primarily in North Bay, San Francisco and Oakland International Airports, and developed areas based on man-made fill, such as Foster City in South Bay. A primary concern is that with sea level rise, pressure on existing levees, and thus the risk of breaches, would be greatly increased. The potential for levee overtopping would also increase. In all these locations, existing levees would need to be raised and fortified to reduce the risk of these outcomes.

Other key areas of concern evident from Figure 5 include the municipal and industrial areas that are not currently vulnerable to 100-year high-water levels but would be under this future scenario. These areas (in red) run from Hunters Point to Fort Point in San Francisco, and include portions of eastern Marin, the Richmond peninsula, much of the East Bay shoreline including the former Naval Air Station at Alameda, and virtually all of Treasure Island. These are developed areas that would require some new levees and additions to any existing protection if flooding is to be prevented.

This ring of developed areas that would be newly vulnerable to inundation extends to South Bay, here falling upland of wetlands (existing or in restoration) and in some cases, upland of other (already vulnerable) developed areas. Many of these areas are already behind levees; they simply represent lands that are not currently at risk if these levees breached but would be at risk under the future scenario. Nearly all municipalities adjacent to South Bay (or adjacent to wetlands adjacent to South Bay) would face this risk to some degree, and again, existing protection would need to be improved. Another important concern for developed areas here is the survival of existing and future restored wetlands (the South Bay Salt Pond Restoration Project), which will depend on the ability of these wetlands to accrete material quickly enough to keep pace with sea level rise (wetlands are

discussed more in the next section). If the wetlands of South Bay were submerged by rising water levels, one consequence would be that wave energy would be less attenuated and erosional forces against protective upland levees would increase.

Figure 6 quantifies the different types of land at risk for a range of sea level rise amounts in terms of total vulnerable area in each land-use category. Excluding wetlands, the dominant categories of land cover around San Francisco Bay are grasslands and developed areas. The total area of vulnerable grassland would change little with sea level rise. Most newly vulnerable areas as a result of sea level rise would be the developed areas surrounding Central and South bays (see Figure 5). These also constitute the vulnerable areas with the greatest potential economic loss.

Excluding wetlands, today, a total area of about 310 km² is inundated or vulnerable to inundation under 100-year high-water levels; this consists almost entirely of grasslands and developed areas already protected by levees. Under a 50-cm sea level rise (projected by 2053 in the CCSM3-A2 scenario), the total vulnerable area would increase by 20% to 372 km², and under a 150-cm sea level rise (2105), the total vulnerable area would increase by almost 60% to 495 km². The largest change in area of a vulnerable land cover type would occur for developed areas. Vulnerable developed area would nearly double with a 150-cm sea level rise, from 157 km² to 311 km². These estimates assume no change in land-use assign-

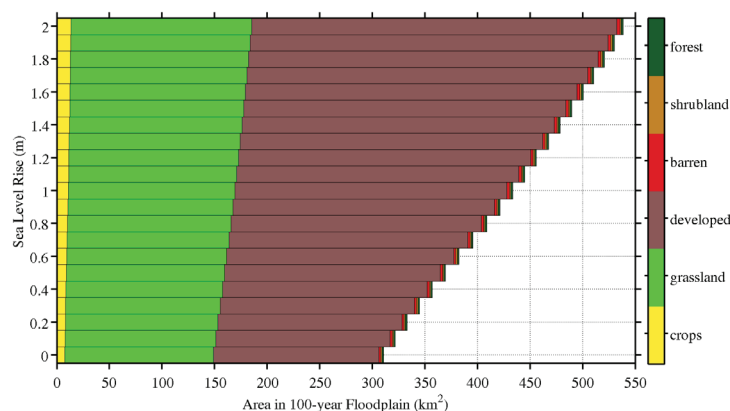


Figure 6 Total area around San Francisco Bay, excluding wetlands, vulnerable to inundation by 100-year high-water levels for a range of sea level rise, broken down into land-cover categories

SAN FRANCISCO ESTUARY & WATERSHED SCIENCE

ments over time; it is possible that some of the land currently assigned to other categories will ultimately be developed, resulting in an even greater value for total vulnerable developed area.

Figure 7 shows the bay-wide mean high-water levels and total area vulnerable to inundation for four values of sea level rise (0, 50, 100 and 150 cm) and five different return intervals (1, 10, 50, 100 and 500 years). As described earlier, water-level variability in the bay is a short-tailed process ($\xi < 0$), evidenced here by the progressively flatter response of water level and vulnerable area with increasing return interval. It should be noted that the 500-year return levels should include the effects of a potential tsunami, but the evaluation of such effects is beyond the scope of this investigation. Inclusion of tsunami effects would increase the 500-year return levels substantially. Under the high-end scenario of Rahmstorf (2007) (to which the CCSM3-A2 projection corresponds), the one-year peak event would nearly equal today's 100-year peak event by mid-century. This would not occur until 2100 under the low-end scenario (~50-cm sea level rise in 2100).

Wetlands and Changing Tidal Datums

There are about 400 km² designated in the NLCD01 as wetlands around San Francisco Bay, including the South Bay Salt Ponds, Napa Wetlands, and Suisun Marsh, among others. Figure 8 shows the amount of total wetland area, according to present-day wetland elevations, that would lie below projected future tidal datums as sea level rise progresses.

Some of the wetland area that appears as currently near the lower end of the tidal range consists of managed wetlands behind levees and other control structures. In those cases, sea level rise would threaten levee integrity and the ability to manage the wetlands for their desired uses. Wetlands not behind levees would gradually shift lower in the tidal range if elevations were to remain at their present levels. A 110-cm sea level rise would more than double the area of wetlands below local mean sea level (LMSL).

Figure 9 illustrates the spatial pattern of this shift, relative to MLLW, for the Napa and Suisun wetlands.

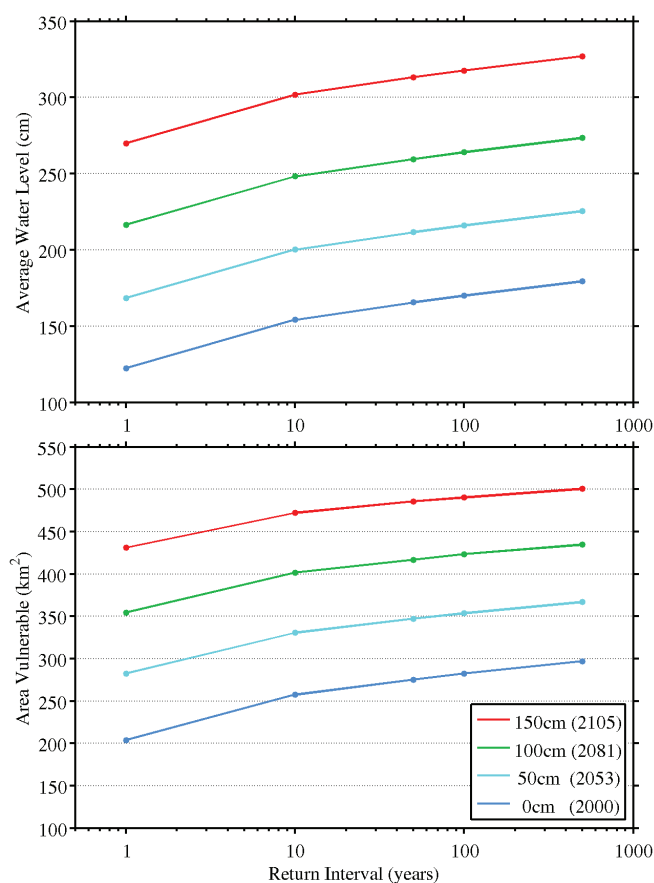


Figure 7 Bay-average water level relative to mean sea level (upper) and total area around San Francisco Bay, excluding wetlands, vulnerable to inundation (lower) versus return interval for four values of sea level rise. The earliest year in which each level is projected to be reached (using the high-end CCSM3-A2 projection) is indicated in the legend. Low-end projections do not produce a 50-cm sea level rise until around 2100.

Portions of Suisun Marsh are already subtidal. Under a 100-cm sea level rise, most of today's Suisun Marsh would be in the subtidal zone. With a 150-cm sea level rise, Napa Wetlands would be as well. Similar results are obtained for the South Bay Salt Ponds (not shown).

It is very important to note that Figures 8 and 9 ignore the dynamic nature of wetlands, particularly their ability to accrete organic and mineral sediment. The purpose here is to illustrate the magnitude of the potential changes which these processes would need to counter.

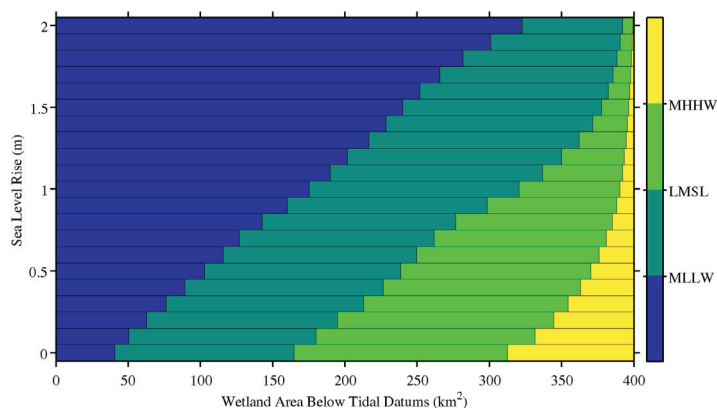


Figure 8 Total wetland area relative to fields of mean daily higher-high water levels (MHHW), local mean sea level (LMSL), and mean daily lower-low water levels (MLLW). These results are based on present-day elevations and ignore the potential for vertical accretion and lateral migration of wetlands in response to sea level rise.

The results of this study indicate that, to maintain their current positions in the tidal range, existing wetlands around San Francisco Bay would require 150, 330, or 530 million cubic meters (Mm^3) of (organic plus mineral) sediment² for respective sea level rise amounts of 50, 100, and 150 cm. Because sea-level projections over the coming century are generally quadratic in time, as typified by Figure 3, the rate of rise would increase linearly, starting at the present-day value of 20 to 30 mm/yr. The “break-even” sediment accumulation rate would also increase linearly, starting at the corresponding value of roughly $0.6 \text{ Mm}^3/\text{yr}$. Recent projections suggest that sea level could rise as little as 50 cm, or as much as 150 cm, by 2100. In the first case, the required accumulation rate would increase to $2.4 \text{ Mm}^3/\text{yr}$ by 2100 (corresponding to a sea level rise rate of 6.7 mm/yr), averaging $1.5 \text{ Mm}^3/\text{yr}$ over the century. In the second, the required rate would reach $10.1 \text{ Mm}^3/\text{yr}$ by 2100 (25.6 mm/yr), averaging $5.3 \text{ Mm}^3/\text{yr}$. If leveed wetlands remained isolated from sediment supplies despite higher sea levels, these sediment volumes would be smaller. However, those levees would require substantial

² These are estimates of the volume of accretion that would be required to maintain the vertical position within the tidal range of wetland areas already below MHHW, and to keep elevations of the remaining wetland areas just above MHHW. These values ignore depth increases in most mudflats, in subtidal shallow water habitat, and in wetland areas lacking elevation data due to the presence of open water at the time of data acquisition.

improvements to hold, and some common management practices, such as seasonal gravity draining of leveed wetlands managed as waterfowl habitat, would eventually become impossible in the absence of significant accretion.

To give the above sediment flux values some context— in recent years, inorganic sediment input to the bay from the delta and local tributaries has averaged roughly $1.9 \times 10^6 \text{ Mg/yr}$ (Schoellhamer and others 2005; McKee and others 2006), though there is evidence that the delta portion of this supply has been in decline (Wright and Schoellhamer 2004). Depending on the density estimate used (D. Schoellhamer, personal communication), this amounts to roughly 1.5 to $3.8 \text{ Mm}^3/\text{yr}$, of which only about 10% has been depositing on wetlands (Schoellhamer 2005).

Wetland deposition rates are likely to increase as presently leveed wetlands become tidally connected through restoration actions (Schoellhamer 2005) and possibly as a result of levee breaches induced by sea level rise. Nonetheless, Ganju and Schoellhamer (2010) show that even under an extremely modest rate of sea level rise, present-day inorganic sediment supply may not suffice to keep the shallowest areas of Suisun Bay from getting deeper, which may have similar implications for the adjacent wetlands.

Although the topic of sustainable wetland restoration is complex (for example, Orr and others 2003) and beyond the scope of this study, it is worth noting here some other important factors that could contribute to wetland survival in the context of rising sea levels. For instance, dredged material from the bay may come to play a greater role in augmenting wetland elevations (Johnck and others 2009). Also, Drexler and others (2009) found that in tidal freshwater marshes in the delta, vertical accretion of peat ranged from 0.3 to 4.9 mm/yr over the past 6,000 years, indicating that given suitable conditions, peat formation can play an important role in mitigating the effects of sea level rise. There is even evidence that, at least in some parts of the bay, wetlands are capable of keeping pace with even higher rates of relative sea level rise than have been discussed here. In far South Bay, rates of sedimentation and organic accumulation were sufficient to allow salt marshes

SAN FRANCISCO ESTUARY & WATERSHED SCIENCE

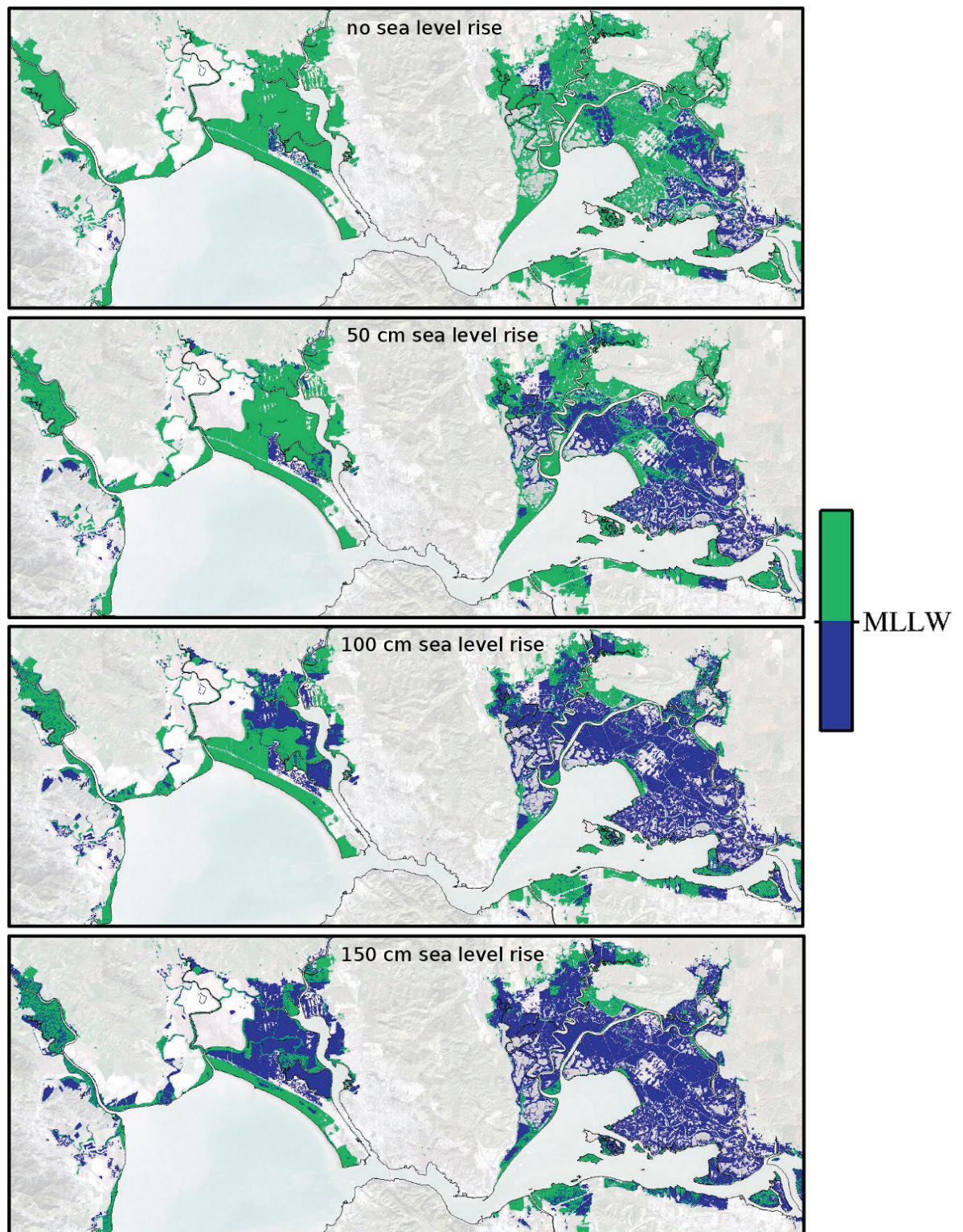


Figure 9 Wetland elevations relative to the MLLW tidal datum for four values of sea level rise. Napa wetlands are left-of-center, and Suisun Marsh is on the right. These results are based on present-day elevations and ignore the potential for vertical accretion and lateral migration of wetlands in response to sea level rise.

to compensate for an estimated one meter of subsidence due to groundwater extraction over only a few decades (Patrick and DeLaune 1990; Watson 2004). However, far South Bay has been shown to be a particularly strong depositional environment relative to other areas of San Francisco Bay (Foxgrover and others 2004; Jaffe and Foxgrover 2006). Another wetland survival mechanism not discussed above is migration to adjacent upland areas. Though this possibility is generally limited in the highly developed bay region, some promising candidate areas exist (Enright and others 2007).

CONCLUSIONS

The main features of inundation around San Francisco Bay associated with potential sea level rise have been presented here. Results for several different values of sea level rise were given, and it should be re-emphasized that these results apply regardless of when a given amount of sea level rise is reached. Some major concerns associated with sea level rise were discussed—survival of existing wetlands, inundation of currently unprotected developed areas, increased risk of failure and overtopping of existing levees, and increased consequences of such failures as more areas become vulnerable are all real dangers. However, many other complications could also occur. For example, sanitation districts around the estuary are concerned that as sea level rises, seawater could backflow into their drainage systems, causing local flooding and sanitation problems. The risks of such problems occurring will increase gradually with sea level rise, but are associated with specific events within a given year. The largest events are most likely to occur during winter storms, particularly those coinciding with a spring tide. El Niño events also lead to higher water levels and increased risk (Cayan and others 2008).

The projected changes have many implications for those living in this region. Municipal planners will need to carefully consider the increasing risks of development in low-lying areas. Changing recurrence levels will require that flood insurance maps be redrawn regularly. Local groundwater pumping will need to continue to be carefully managed to avoid

subsidence. Transportation infrastructure will be threatened. Economic and policy implications of these and other changes are discussed in reports, based in part on the results presented here, by Heberger and others (2008) and BCDC (2009).

As mentioned in the “[Data and Methods](#)” section, these results can be applied to a wide range of climate change scenarios. For example, scenarios representing higher greenhouse gas emissions in the future can result in projections of large warming and sea level rise. In such a high-end scenario, conditions in 2100 may most closely resemble the results presented here for the 150-cm sea level rise amount. Conversely, estimates of sea level rise under the most optimistic of scenarios, representing lower greenhouse gas emissions, range from 45 to 70 cm by 2100 (Moser and others 2008). In this case, the 50-cm scenario may correspond to conditions in 2100. In terms of a specific result, referring to [Figure 7](#), this means that under the most optimistic scenario, in 2100 the 1-year peak event would nearly equal today’s 100-year peak event.

It is important to note, however, that global CO₂ emissions in recent years have tracked the highest scenarios considered to date in the IPCC Assessments (TCD 2009), and the results corresponding to the high-end scenarios of sea level rise presented in this study should be seriously considered as future possibilities. Further, sea level rise is expected to continue well beyond this century. Vellinga and others (2008) estimate the high end of possible sea level rise by 2200 to be 1.5 to 3.5 m, and Schubert and others (2006) provide a mid-range estimate, corresponding to a 3°C warming, of 3 to 5 m by 2300.

Understanding and successfully adapting to these changes will require a fuller knowledge of the likely consequences and the types of actions required. An example of a gap in our current knowledge is the need for a better understanding of the adaptability of existing and restorable wetlands and the dependence of the survival of these wetlands on the bay’s sediment budget. Another very important missing piece of information is a better characterization of levee heights and their recent changes due to subsidence or uplift, and an associated regional data base.

SAN FRANCISCO ESTUARY & WATERSHED SCIENCE

Inundation data layers from this project are publicly available at <http://cascade.wr.usgs.gov/data/Task2b-SFBay> in the hope that the high-resolution regional data produced for this analysis will be useful for other regional and local studies and planning efforts.

ACKNOWLEDGMENTS

Thanks to David Schoellhamer, Chris Enright, Ralph Cheng, Bruce Jaffe, Judy Drexler, and BCDC for very helpful feedback, to Dan Cayan for providing sea level rise projections, to Mick van der Wegen of UNESCO-IHE for performing Delft 3D test runs, to Amy Foxgrover, Joel Dudas, Bill Dietrich, Ionut Iordache, and FEMA for providing elevation data, and to the reviewers for improving the manuscript. This work was funded by the California Energy Commission's Public Interest Energy Research (PIER) Program through the California Climate Change Center at Scripps Institution of Oceanography and by the CALFED Science Program CASCaDE Project. This is CASCaDE publication #19.

REFERENCES

- BCDC. 2009. Proposed Bay Plan amendment 1-08 concerning climate change. Bay Conservation and Development Commission draft report. Available from: http://www.bcdc.ca.gov/proposed_bay_plan/bp_amend_1-08.shtml
- Bindoff NL, Willebrand J, Artale V, Cazenave A, Gregory J, Gulev S, Hanawa K, Le Quere C, Levitus S, Nojiri Y, Shum CK, Talley LD, Unnikrishnan A. 2007. Observations: oceanic climate change and sea level. In: Solomon S, Qin D, Manning M, Chen Z, Marquis M, Averyt KB, Tignor M, Miller HL, editors. Climate change 2007: the physical science basis. Contribution of Working Group I to the 4th Assessment Report of the Intergovernmental Panel on Climate Change. Cambridge, UK: Cambridge University Press. Available from: <http://www.ipcc.ch/ipccreports/ar4-wg1.htm>
- Bürgmann R, Hilley G, Ferretti A, Novali F. 2006. Resolving vertical tectonics in the San Francisco Bay area from GPS and permanent scatterer InSAR analysis. *Geology* 34:221–224.
- Cayan DR, Bromirski PD, Hayhoe K, Tyree M, Dettinger MD, Flick RE. 2008. Climate change projections of sea level extremes along the California coast. *Climatic Change* 87 (Suppl 1):S57–S73.
- Cayan DR, Tyree M, Dettinger MD, Hidalgo H, Das T. 2009. California climate change scenarios and sea level rise estimates for the California 2008 Climate Change Scenarios Assessment. California Energy Commission Report No. CEC-500-2009-014-F. Available from: <http://www.energy.ca.gov/2009publications/CEC-500-2009-014/CEC-500-2009-014-F.PDF>
- Cheng RT, Casulli V, Gartner JW. 1993. Tidal, residual, intertidal mudflat (TRIM) model and its applications to San Francisco Bay, California. *Estuarine, Coastal and Shelf Science* 36:235–280.
- Cheng RT, Gartner JW. 1984. Tides, tidal and residual currents in San Francisco Bay California - results of measurements, 1979–1980. U.S. Geological Survey Water-Resources Investigations Report No. 84-4339.
- Church JA, White NJ, Coleman R, Lambeck K, Mitrovica JX. 2004. Estimates of the regional distribution of sea level rise over the 1950–2000 period. *Journal of Climate* 17:2609–2625.
- Church JA, White NJ. 2006. A 20th century acceleration in global sea-level rise. *Geophysical Research Letters* 33:L01602.
- Coons T, Souldard CE, Knowles N. 2008. High-resolution digital terrain models of the Sacramento-San Joaquin Delta region, California. U.S. Geological Survey, Data Series 359. Available from: <http://pubs.usgs.gov/ds/359>.
- Drexler JZ, de Fontaine CS, Brown TA. 2009. Peat accretion histories during the past 6,000 years in marshes of the Sacramento-San Joaquin Delta, CA, USA. *Estuaries and Coasts* 32(5):871–892.

Enright C, Wang X, Dudas J. 2007. Elevation matters: wetland restoration where it wants to be [presentation]. Interagency Ecological Program 2007 Annual Workshop; 2007 Feb 28-Mar 2; Pacific Grove (CA). Available from: <http://www.water.ca.gov/suisun/dataReports/docs/IEP2007 LiDAR-WetlandRestoration.pdf>

Ferretti A, Novali F, Bürgmann R, Hilley G, Prati C. 2004. InSAR permanent scatterer analysis reveals ups and downs in the San Francisco Bay area. EOS (Transactions, American Geophysical Union) 85:317.

Fisher RA. 1922. On the mathematical foundations of theoretical statistics. Philosophical Transactions of the Royal Society of London, Series A 222:309-368.

Fisher RA, Tippett LHC. 1928. Limiting forms of the frequency distribution of the largest or smallest member of a sample. Proceedings of Cambridge Philosophical Society 24:180-190.

Flick R. 2003. Trends in United States tidal datum statistics and tide range. Journal of Waterway, Port, Coastal and Ocean Engineering 129(4):155-164.

Foxgrover AC, Higgins SA, Ingraca MK, Jaffe BE, and Smith RE. 2004. Deposition, erosion, and bathymetric change in South San Francisco Bay: 1858-1983. U.S. Geological Survey Open-File Report 2004-1192, 25 p. Available from: <http://pubs.usgs.gov/of/2004/1192>

Foxgrover AC, Jaffe BE. 2005. South San Francisco Bay 2004 topographic LiDAR survey: data overview and preliminary quality assessment. U.S. Geological Survey Open-File Report 2005-1284, 57 p. Available from: <http://pubs.usgs.gov/of/2005/1284>

Galloway DL, Jones DR, and Ingebritsen SE. 1999. Land subsidence in the United States. U.S. Geological Survey Circular 1182, 175 p. Available from: <http://pubs.usgs.gov/circ/circ1182>

Ganju NK, Schoellhamer DH. 2010. Decadal-timescale estuarine geomorphic change under future scenarios of climate and sediment supply. Estuaries and Coasts 33:15-29.

Gleick PH, Maurer EP. 1990. Assessing the costs of adapting to sea-level rise: a case study of San Francisco Bay. Pacific Institute Report. Available from: http://www.pacinst.org/reports/sea_level_rise_sfbay

Heberger M, Cooley H, Herrera P, Gleick PH, Moore E. 2008. The impacts of sea-level rise on the California coast. California Energy Commission Report No. CEC-500-2009-024-F. Available from: <http://www.energy.ca.gov/2009publications/CEC-500-2009-024/CEC-500-2009-024-F.PDF>

Hidalgo H, Dettinger MD, Cayan DR. 2008. Downscaling with constructed analogues—Daily precipitation and temperature fields over the United States. California Energy Commission Report No. CEC-500-2007-123. Available from: http://meteora.ucsd.edu/cap/pdf/files/analog_pier_report.pdf

Homer C, Dewitz J, Fry J, Coan M, Hossain N, Larson C, Herold N, McKerrow A, VanDriel JN, Wickham J. 2007. Completion of the 2001 national land cover database for the conterminous United States. Photogrammetric Engineering and Remote Sensing 73:337-341. Available from: <http://www.epa.gov/mrlc/nlcd-2001.html>

[IPCC] Intergovernmental Panel on Climate Change. 2001. Climate change 2001, the third assessment report (AR3) of the United Nations Intergovernmental Panel on Climate Change. Available from: http://www.ipcc.ch/publications_and_data/publications_and_data_reports.htm

[IPCC] Intergovernmental Panel on Climate Change. 2007. Climate Change 2007, the fourth assessment report (AR4) of the United Nations Intergovernmental Panel on Climate Change. Available from: http://www.ipcc.ch/publications_and_data/publications_and_data_reports.htm

Jaffe BE, Foxgrover AC. 2006. Sediment deposition and erosion in South San Francisco Bay, California from 1956 to 2005. U.S. Geological Survey Open-File Report 2006-1262, 24 pp. Available from: <http://pubs.usgs.gov/of/2006/1262>

SAN FRANCISCO ESTUARY & WATERSHED SCIENCE

- Johnck E, Collins J, Dingler J, Grossinger R, Kendall T, Ross B, Werme C. 2009. Dredged sediment: from “spoils” to valued resource. In: The pulse of the estuary: monitoring and managing water quality in the San Francisco Estuary. SFEI Contribution 583. San Francisco Estuary Institute, Oakland, CA. Available from: <http://www.sfei.org/rmp/pulse/2009>
- Knowles N, Cayan D. 2002. Potential effects of global warming on the Sacramento-San Joaquin watershed and the San Francisco Estuary. Geophysical Research Letters 29:38-1-38-4. Available from: http://tenaya.ucsd.edu/~knowles/papers/knowles_grl_2002.pdf
- McKee LJ, Ganju NK, Schoellhamer DH. 2006. Estimates of suspended sediment flux entering San Francisco Bay from the Sacramento and San Joaquin Delta, San Francisco Bay, California. Journal of Hydrology 323:335-352.
- Mitasova H, Hofierka J. 1993. Interpolation by regularized spline with tension: II. Application to terrain modeling and surface geometry analysis. Mathematical Geology 25:657-667.
- Moser SC, Cayan DR, Franco G. 2008. The Future Is Now—An Update on Climate Change Science, Impacts, and Response Options for California. California Climate Change Center CEC Report No. CEC-500-2008-071. Available from: <http://www.energy.ca.gov/2008publications/CEC-500-2008-071/CEC-500-2008-071.PDF>
- Orr M, Crooks S, Williams PB. 2003. Will Restored Tidal Marshes Be Sustainable? San Francisco Estuary and Watershed Science [Internet]. Available from: <http://escholarship.org/uc/item/8hj3d20t>
- Patrick WH, Delaune RD. 1990. Subsidence, accretion, and sea level rise in South San Francisco Bay marshes. Limnology and Oceanography 35(6):1389-1395.
- Pfeffer WT, Harper JT, O’Neel S. 2008. Kinematic constraints on glacier contributions to 21st-Century sea-level rise. Science 321(5894):1340-1343.
- Poland JF, Ireland R.L. 1988. Land subsidence in the Santa Clara Valley, California, as of 1982, mechanics of aquifer systems, U.S. Geological Survey Professional Paper 497-F, 61 p. Available from: <http://pubs.er.usgs.gov/usgspubs/pp/pp497F>
- Rahmstorf S. 2007. A semi-empirical approach to projecting future sea-level rise. Science 315:368-370.
- Schmidt DA, Bürgmann R. 2003. Time-dependent land uplift and subsidence in the Santa Clara Valley, California, from a large InSAR data set. Journal of Geophysical Research 108:2416.
- Schoellhamer DH, Lionberger MA, Jaffe BE, Ganju NK, Wright SA, Shellenbarger G. 2005. Bay sediment budget: sediment accounting 101. In: The pulse of the estuary: monitoring and managing water quality in the San Francisco Estuary. SFEI Contribution 411. San Francisco Estuary Institute, Oakland, CA. Available from: <http://www.sfei.org/rmp/pulse/2005>
- Schubert R, Schellnhuber H-J, Buchmann N, Epiney A, Griebhammer R, Kulesa M, Messner D, Rahmstorf S, Schmid J. 2006. WBGU - German Advisory Council on Global Change: The Future Oceans - Warming Up, Rising High, Turning Sour. WBGU, Berlin. Available from: http://www.wbgu.de/wbgu/sn2006_en.pdf
- [TCD] The Copenhagen Diagnosis. 2009. Updating the world on the latest climate science. Allison I, Bindoff NL, Bindschadler RA, Cox PM, de Noblet N, England MH, Francis JE, Gruber N, Haywood AM, Karoly DJ, Kaser G, Le Quéré C, Lenton TM, Mann ME, McNeil BI, Pitman AJ, Rahmstorf S, Rignot E, Schellnhuber HJ, Schneider SH, Sherwood SC, Somerville RCJ, Steffen K, Steig EJ, Visbeck M, Weaver AJ. Sydney, Australia: The University of New South Wales Climate Change Research Centre (CCRC). 60 p. Available from: <http://www.copenhagendiagnosis.org>

Vellinga P, Katsman C, Sterl A, Beersma J, Hazeleger W, Church J, Kopp R, Kroon D, Oppenheimer M, Plag H-P, Rahmstorf S, Lowe J, Ridley J, von Storch H, Vaughan D, van de Wal R, Weisse R, Kwadijk J, Lammersen R, Marinova N. 2008. Exploring high-end climate change scenarios for flood protection of the Netherlands: an international scientific assessment. Wageningen, the Netherlands: KNMI. Available from: <http://www.knmi.nl/bibliotheek/knmipubWR/WR2009-05.pdf>

Watson EB. 2004. Changing elevation, accretion, and tidal marsh plant assemblages in South San Francisco Bay tidal marsh. *Estuaries* 27(4):684–698.

Wigley TML. 2005. The climate change commitment. *Science* 307:1766–1769.

Williams PB. 1985. An overview of the impact of accelerated sea level rise on San Francisco Bay. Project No. 256 for the Bay Conservation and Development Commission. San Francisco, California: Philip Williams & Associates.

Williams PB. 1987. The impacts of climate change on the salinity of San Francisco Bay. EPA Report No. EPA-230-05-89-051. San Francisco, California: Philip Williams & Associates.

Wright SA, Schoellhamer DH. 2004. Trends in the sediment yield of the Sacramento River, California, 1957–2001. *San Francisco Estuary and Watershed* [Internet]. Available from: <http://escholarship.org/uc/item/891144f4>

Primary Research Paper

Distribution and toxicity of a new colonial *Microcystis aeruginosa* bloom in the San Francisco Bay Estuary, California

P.W. Lehman^{1,*}, G. Boyer², C. Hall³, S. Waller¹ & K. Gehrts¹

¹California Department of Water Resources, 3251 S Street, Sacramento, CA 95816, USA

²College of Environmental Science and Forestry, State University of New York, Syracuse, NY 13210, USA

³Environmental Science and Policy, University of California, Davis, CA 95616, USA

(*Author for correspondence: plehman@water.ca.gov)

Received 30 June 2004; in revised form 24 September 2004; accepted 11 October 2004

Key words: *Microcystis*, cyanobacteria, toxic, estuary, harmful algal bloom

Abstract

The first distribution, biomass and toxicity study of a newly established bloom of the colonial cyanobacteria *Microcystis aeruginosa* was conducted on October 15, 2003 in the upper San Francisco Bay Estuary. *Microcystis aeruginosa* was widely distributed throughout 180 km of waterways in the upper San Francisco Bay Estuary from freshwater to brackish water environments and contained hepatotoxic microcystins at all stations. Other cyanobacteria toxins were absent or only present in trace amounts. The composition of the microcystins among stations was similar and dominated by demethyl microcystin-LR followed by microcystin-LR. *In situ* toxicity computed for the >75 μm cell diameter size fraction was well below the 1 $\mu\text{g l}^{-1}$ advisory level set by the World Health Organization for water quality, but the toxicity of the full population is unknown. The toxicity may have been greater earlier in the year when biomass was visibly higher. Toxicity was highest at low water temperature, water transparency and salinity. Microcystins from the bloom entered the food web and were present in both total zooplankton and clam tissue. Initial laboratory feeding tests suggested the cyanobacteria was not consumed by the adult copepod *Eurytemora affinis*, an important fishery food source in the estuary.

Introduction

Microcystis aeruginosa is a common freshwater cyanobacterium that blooms in eutrophic lakes and reservoirs throughout the world including the United States, Canada, Australia, New Zealand, South Africa and Japan (Paerl, 1988; Carmichael, 1995; Watanabe, 1995; Downing et al., 2001). It has also been observed in estuaries including the Neuse River estuary (Paerl, 1988) and the Potomac River estuary (Sellner et al., 1993) in the USA, the Swan River estuary in Western Australia (Robson & Hamilton, 2003) and the Patos Lagoon Estuary in Southern Brazil (Yunes et al., 1996). A bloom of the colonial form of *M. aeruginosa* has also been observed in the northern reach of San Francisco Bay Estuary (NSFE), California

between June and November since 1999 (Lehman & Waller, 2003). The single-celled form of *M. aeruginosa* is currently a common cyanobacterium in NSFE but was not identified as a dominant genus in the phytoplankton community between 1975 and 1982 (Lehman & Smith, 1991). Total cyanobacteria biomass has increased throughout the NSFE coincident with a decline in diatom biomass between 1975 and 1993 (Lehman, 2000). The highest total cyanobacteria density occurred in the spring and summer of normal and critically-dry precipitation years (Lehman, 1996).

M. aeruginosa is sometimes characterized as a harmful algal bloom (HAB) species. Blooms of these species form surface scums that impede contact recreation sports, reduce aesthetics, lower dissolved oxygen concentration and cause taste and odor

problems in drinking water (Carmichael, 1995). Some of these blooms also contain hepatotoxic microcystins that cause liver tumors and cancer in wildlife and humans (Carmichael, 1995). One surface water sample collected in the NSFE in 2000 contained microcystins concentration above the World Health Organization advisory level of $1 \mu\text{g l}^{-1}$ (World Health Organization, 1998; Lehman & Waller, 2003). No further information is available on the biomass, toxicity and distribution of the *M. aeruginosa* bloom or its potential impact to human health and ecosystem function in NSFE.

Marine and coastal HABs have occurred more frequently over the past decade worldwide (Anderson & Garrison, 1997; Horner et al., 1997) and have been observed along the coast of California since 1793 (Horner et al., 1997). Most of these blooms were associated with dinoflagellates that produced paralytic shellfish poisoning (PSP) or diatoms that produced domoic acid poisoning (DAP). It is assumed that coastal marine HABs enter estuaries along the west coast of North America although *in situ* growth was identified in Puget Sound (Horner et al., 1997). Coastally derived HABs contrast with the freshwater *M. aeruginosa* blooms that are assumed to enter estuaries from upstream during high streamflow events (Robson & Hamilton, 2003).

The colonial form of *M. aeruginosa* adds to an already extensive list of introduced species in San Francisco Estuary with adverse impacts. Approximately 212 species were introduced into the estuary since 1850 (Cohen & Carlton, 1995).

The previous dominant phytoplankton species were identified as cryptogenic, not clearly native or introduced. The potential adverse impact of this HAB on the estuary is large. Water from the northern region is used directly for drinking water and irrigation and the region is an important recreational area for sport fishing and water contact sports. The estuary is habitat for many anadromous commercial and recreational fish including striped bass and Chinook salmon and is a feeding ground for marine mammals. The estuary also contains many threatened or endangered aquatic organisms including the fish Delta smelt and winter run Chinook salmon and many of these endangered fish species are declining (Bennett & Moyle, 1996; California Bay-Delta Authority, 2000). Some of this decline may be linked to the

quantity and quality of the phytoplankton carbon available at the base of the food web (Lehman, 1992; Mueller-Solger et al., 2002; Feyrer et al., 2003; Lehman, 2004).

The purpose of this study is to develop initial information on the spatial distribution, toxicity, algal biomass and environmental conditions associated with the occurrence of the colonial *M. aeruginosa* bloom in the NSFE. Such information is needed to develop focused research and monitoring programs that evaluate the current and future impact of this bloom on estuarine processes.

Study area

The NSFE consists of an inland Delta that flows into a chain of downstream marine bays – Suisun, San Pablo and San Francisco – and creates one of the largest estuaries on the west coast of North America. The estuary stretches from the Pacific Ocean in the west to the tidal head at Greens Landing on the Sacramento River and Vernalis on the San Joaquin River. The inland Delta varies between fresh and brackish water conditions with season and water-year type and contains 200 km² of waterways formed by the Sacramento River on the north and the San Joaquin River on the south. Together these two rivers drain 47% of the runoff in California. The Sacramento River is the larger of the two rivers with an average runoff of 27 million m³ compared with 10 million m³ for the San Joaquin River. Depth varied from a few meters in the Delta to 13 m in the shipping lanes. The tide is semidiurnal and reaches 2 m throughout the region. Tidal velocities can reach 30 cm s⁻¹ in the Bay and are associated with tidal excursions of 10 km.

Materials and methods

Field and laboratory sampling

The spatial distribution of the *M. aeruginosa* bloom was identified by observation of surface waters during mid-day on September 12, 2003. *M. aeruginosa* biomass and toxicity was sampled on October 15, 2003 at 14 stations throughout the same area identified in September. Stations were selected that represented different habitat types or

use including recreational swimming (station 23), shallow water habitat (stations 41 and 42), deep river channel (stations 11–13), anadromous and native fish habitat (stations 11–43) and agricultural and drinking water (stations 43–45; Fig. 1). Colonies were sampled by horizontal surface tows of a 0.72 m diameter plankton net fitted with a 75 μm mesh screen on the cod end. Sampling a large size fraction assured that the sample primarily contained the colonial form of *M. aeruginosa*. Net tows were conducted at the center of the channel at a speed of 60 m min^{-1} and lasted 1–10 min depending on bloom biomass. Horizontal net tows were used to obtain a quantitative and integrated sample of the bloom which had a patchy distribution. Total volume of the sample

was determined from an attached General Oceanics 2030R flowmeter. Water temperature and specific conductance were also measured at each station using a freshly calibrated YSI 85 sonde. Specific conductance was converted to salinity by first converting the specific conductance values to chloride concentration (g l^{-1}) using station specific regression equations and then converting chloride concentration to salinity (ppt) using the equation: $\text{salinity} = 1.80655 \times \text{chloride}$ (Unpublished data, California Department of Water Resources; APHA et al., 1998).

Water samples containing algal biomass were stored at 4 $^{\circ}\text{C}$ and filtered within 2 h onto GF/F glass fiber filters. Filters for microcystins analysis were wrapped in aluminum foil and frozen until

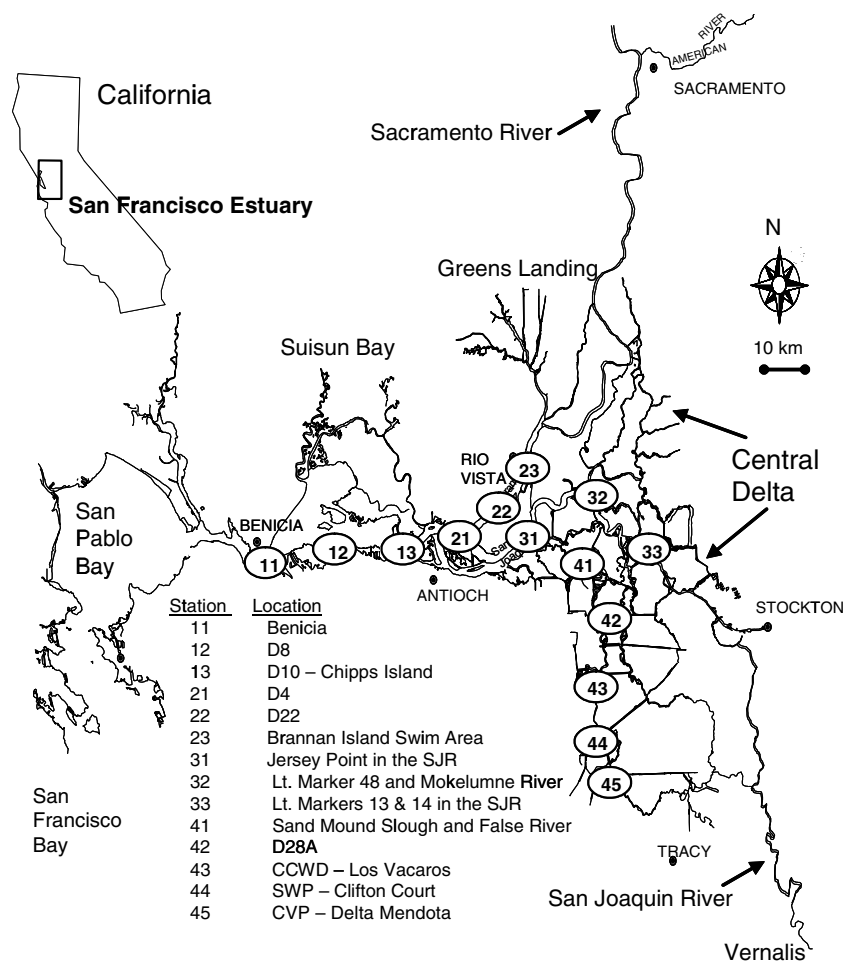


Figure 1. Map of upper San Francisco Bay Estuary with sampling station location.

laboratory analysis. Filters for chlorophyll *a* analysis were treated with magnesium carbonate as a preservative and frozen until laboratory analysis (US EPA, 1983). Sample replication was 20%. In addition, a 50 ml water sample was preserved and stained with Lugol's solution for phytoplankton cell identification with an inverted microscope (Utermohl, 1958).

The presence of microcystins in the food web was assessed by the presence of microcystins in zooplankton and clam tissue. Zooplankton were sampled at 5 stations by horizontal net tows of a 0.7 m diameter plankton net fitted with a 150 μm mesh on the cod end. Zooplankton were kept at 4 °C and were separated by hand from *M. aeruginosa* in the water sample within 48 h using a dissecting microscope. The final zooplankton sample was rinsed in distilled water and frozen until analysis. Clams were obtained using a ponar dredge. The tissue was removed from the clam shell, rinsed in distilled water and frozen until analysis.

An initial study to determine the feeding of the adult copepod *Eurytemora affinis* (Copepoda: Calanoida) on *M. aeruginosa* was evaluated by laboratory feeding tests. Six groups of 20 laboratory grown animals were each placed in a 500 ml flask containing 200 ml of 1 ppt L16 culture medium. This culture medium is a synthetic culture medium modified with vitamin B₁₂, biotin vitamins and soil extract that was useful for culturing zooplankton and algae because it had an ionic composition similar to that in many eutrophic lakes (Lindstrom, 1983). Zooplankton were held in the culture medium and not fed for 3.5 h. Previous experiments indicated a 50% reduction in gut chlorophyll *a* within 10 min of being placed in the 1 ppt L16 culture medium (Hall unpublished data). Copepods in three flasks were transferred to GFC glass fiber filters for replicate chlorophyll *a* analysis (Marker et al., 1980). An additional 150 ml of *M. aeruginosa* biomass equivalent to 146 $\mu\text{g l}^{-1}$ of chlorophyll *a* was added to the remaining three flasks. *M. aeruginosa* colonies were obtained from the Delta that day and separated from other phytoplankton by pipette with repeated washes in natural water filtered through a 0.45 μm pore size Nucleopore filter. Treatment flasks were incubated for 24 h at 20 °C and a 16:8 light:dark cycle. At the end of the incubation

period, animals were removed from the media, placed on GFC glass fiber filters and the filters were immediately frozen until analysis for chlorophyll *a* concentration.

Toxicity testing

Filters for toxin analysis were extracted by sonication with 10 ml of 50% methanol containing 1% acetic acid, clarified by centrifugation, and the extract used for analysis of the different toxins. Zooplankton were lyophilized first then extracted as above. Clams were extracted using a 50% acidified methanol in a Waring Blender. Addition of purified microcystin-LR, microcystin-YR, microcystin-RR, anatoxin-a and saxitoxin to wet filters or lyophilized zooplankton, followed by their extraction as described above recovered greater than 90% of all five toxins. To determine the recovery of microcystin from the clam samples, it was necessary to split the crude homogenate into two parts and add a known amount of microcystin spiked into one fraction. Recoveries of microcystin from these tissues ranged from 50 to 65%. This value was then used to correct the unspiked fraction for loss of microcystins during extraction.

Total microcystins concentration in plant and animal tissue was initially assessed using the protein phosphatase inhibition assay (PPIA) technique. Assays were run in 96-well plates containing 0.1 mU enzyme (recombinant protein phosphatase 1A, catalytic subunit, Roche Applied Science), 1.05 mg para-nitrophenyl phosphate (Sigma Biochemical) and 10 μl of sample or microcystin-LR (Sigma Biochemical) using the method of Carmichael & An (1999). The rate of phosphate hydrolysis was calculated from the change in absorbance at 405 nm over 1 h and compared to the control (no added microcystin-LR) and standards containing between 6 and 40 $\mu\text{g l}^{-1}$ microcystin-LR. Blanks (no enzyme, no toxin), unknowns, standards, and controls were all run in duplicate.

Samples with the highest levels of total microcystins were further analyzed by high pressure liquid chromatography (HPLC) to identify the specific microcystins in the sample. Samples were separated using a Dupont Ace 4.6 \times 250 5 μ C18 column and a two-step linear gradient of 30–70% acidified acetonitrile to acidified water at 0.8 ml/min (Harada, 1995). Detection was either

mass selective using electrospray ionization (LCMS, Agilent 1100 series MSD) and by UV absorbance using a Waters model 996 photodiode array detector (PDA) between 210 and 300 nm. For LCMS, all ions between 900 and 1250 amu were combined to form the total ion chromatograph and potential microcystins identified on the basis of their molecular ions and retention times. For PDA detection, potential microcystins were identified on the basis of having an absorbance maximum at 239 nm in their UV spectrum and on their retention times.

Anatoxin-a was determined by HPLC after derivatization with 7-fluoro-4-nitro-2,1,3-benzoxadiazole (NBD-F) (James & Sherlock, 1996). The PSP toxins (saxitoxin, neosaxitoxin, and gonyautoxins 1–4) were measured by HPLC with fluorescent detection using the electrochemical oxidation system (Boyer & Goddard, 1999) to form fluorescent derivatives.

Analysis

Because of the small sample size, differences in the means for variables among regions were determined using the Kruskal–Wallis nonparametric technique. Multiple comparisons were evaluated using least significant differences and correlation was evaluated using Spearman rank correlation coefficients. All analyses were conducted using Statistical Analysis System software (SAS Institute, Inc., 2004)

Results

Distribution

M. aeruginosa colonies >75 μm diameter were present in surface samples at all stations sampled in October (Fig. 1). The bloom distribution in October was the same as that observed in September. Sampling stations represented a wide range of habitat types from marine water habitat at the western end of Suisun Bay to freshwater habitat upstream in the Sacramento, Old and San Joaquin rivers. Chlorophyll *a* concentration in concentrated surface net tows ranged from 4 to 554 $\mu\text{g l}^{-1}$ and was significantly different among regions ($p < 0.01$; Table 1). The highest chloro-

phyll *a* concentrations ($p < 0.05$) were measured in the San Joaquin and Old rivers compared with the Sacramento River and Suisun Bay. *In situ* chlorophyll *a* concentration associated with the >75 μm diameter size fraction ranged between 0.7 and 74.6 $\text{m } \mu\text{g l}^{-1}$ based on an expansion of the net sample concentration to tow volume. How much of the surface chlorophyll *a* concentration was composed of *M. aeruginosa* is unknown but phytoplankton identification samples suggested most of the cells were *M. aeruginosa*. The chlorophyll *a* concentration of all size fractions in a Van Dorn sample taken at 1 m depth was 1–3 $\mu\text{g l}^{-1}$ throughout the region on October 15 (unpublished data, California Department of Water Resources) and probably represents the background concentration of other algae in the water column because *M. aeruginosa* was near the surface during the day.

The environmental conditions associated with the bloom varied among regions. Water temperature, salinity and Secchi disk depth were all significantly different among regions ($p < 0.01$). The high phytoplankton biomass and microcystins concentration in the San Joaquin and Old rivers were accompanied by a combination of higher ($p < 0.05$) water temperature, lower salinity ($p < 0.05$) and higher ($p < 0.05$) water transparency (Fig. 2) than the Sacramento River and Suisun Bay. Chlorophyll *a* concentration was more closely associated ($p < 0.01$) with warmer water temperature ($r = 0.66$) and higher Secchi disk depth ($r = 0.70$) and lower salinity ($r = -0.71$) than microcystins concentration ($p < 0.05$; $r = 0.54$, $r = 0.52$ and $r = -0.52$, respectively). Nutrient concentrations were high and nonlimiting throughout the area. Median dissolved inorganic nitrogen and soluble reactive phosphorus were 0.41 and 0.06 mg l^{-1} respectively (unpublished data, California Department of Water Resources).

Toxicity

Microcystins were present at all stations but concentrations differed ($p < 0.01$) among regions. Both the San Joaquin and Old rivers had higher ($p < 0.05$) microcystins concentration than the Suisun Bay region downstream. The microcystins

Table 1. Comparison of chlorophyll *a*, microcystin, anatoxin-a (ATX) and PSP concentration in concentrated net tow samples normalized to a 1 min tow for the >75 μm cell diameter size fraction of the *Microcystis aeruginosa* bloom and microcystin concentration in zooplankton and clam tissue at sampling stations in the northern San Francisco Bay Estuary

Station	Location & CA DWR code	Chlorophyll <i>a</i> ($\mu\text{g l}^{-1}$)	Microcystin tissue		ATX or PSP	Zooplankton tissue		Clam tissue	
			Microcystin-LR equivalent	CV (%)		Microcystin-LR equivalent $\mu\text{g g}^{-1}$ dwt	%CV	Microcystin-LR equivalent $\mu\text{g g}^{-1}$ dwt	%CV
<i>San Francisco Bay</i>									
11	Benicia-D6	41.6	0.02 ± 0.002	8	ND				
12	Suisun Bay-D8	9.6	0.29 ± 0.05	17	ND				
13	Chips Island-D10	5.6	0.93 ± 0.16	17	ND				
<i>Sacramento River</i>									
21	Sacramento R.-D4	26.6	4.31 ± 0.54	13	ND				
22	Horseshoe Bend-D22	3.6	5.42 ± 0.57	10	ND				
23	Brannon Island	67.1	27.54 ± 1.84	7	ND				
<i>San Joaquin River</i>									
31	Jersey Point-D16	301.0	118.60 ± 9.4	8	trace, ND				
32	Mouth of Mokelumne R.	401.0	45.30 ± 6.6	14	ND	1.02 ± 0.2	18		
33	Navigation marker 13	553.5	115.10 ± 7.95	7	trace, ND				
<i>Old River</i>									
41	San Mound Slough	194.0	42.40 ± 5.0	14	ND	2.9 ± 0.6	24	0.02	NA
42	Old River – D28A	254.0	45.00 ± 6.4	15	ND	3.3 ± 0.9	28		
43	Los Vaqueros Reservoir	89.8	19.20 ± 2.7	14	ND				
44	SWP- Clifton Court-C9	96.2	14.60 ± 2.4	16	ND	0.7 ± 0.2	22		
45	CVP-Delta Mendota Canal	107.0	12.20 ± 1.2	10	ND	3.5 ± 0.6	16		

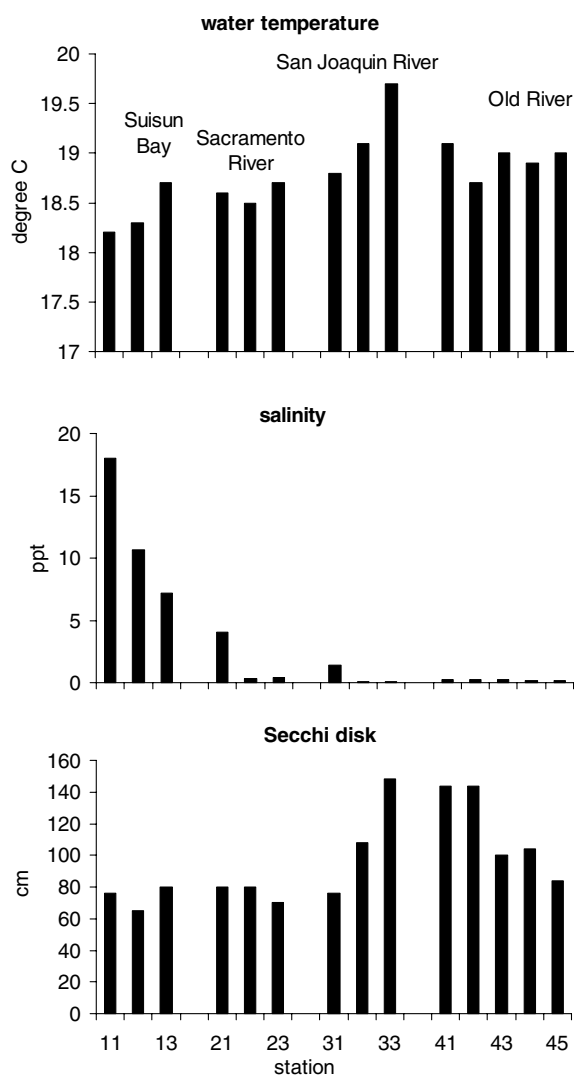


Figure 2. Environmental conditions in surface water measured at sampling stations throughout the upper San Francisco Bay Estuary on October 15, 2003.

were dominated by a demethyl microcystin-LR that comprised between 47 and 66% of the microcystins followed by microcystin-LR that comprised 9 to 23% (Table 2). *In situ* microcystins concentration based on net tow volume was much lower than the concentrated net samples (compare Fig. 3 and Table 1). Similar net tow volume computed from net size, time and tow speed and those computed from the current meter values taken during the tow suggested the volume sampled was a good estimate of total sample volume.

Toxicity generally increased with chlorophyll *a* concentration but the association was not linear (Table 1). The microcystins to chlorophyll *a* and the microcystins to total pigment ratio differed widely among stations (Fig. 4) and was high when water temperature, water transparency and salinity were comparatively low (Fig. 5). The lowest microcystins to chlorophyll *a* ratios occurred at salinities greater than 5 ppt and suggested salinity was an important factor controlling toxicity. The highest toxicity was measured near the transition zone between fresh and brackish water at station 22 on the Sacramento River (Fig. 4).

The algal tissue samples were also tested for the cyanobacterial neurotoxins, anatoxin-a and PSP toxins such as saxitoxin. PSP toxins were not detected at measurable concentrations in any of the samples. Anatoxin-a was not detected or occurred in trace amounts in concentrated 1 min net tow samples at stations 31 (0.1 g l^{-1}) and 33 ($0.4 \text{ } \mu\text{g l}^{-1}$; Table 1).

Food web impact

The animal tissue of lower food web organisms contained small amounts of microcystins. Microcystins concentration ranged from 1 to $3.5 \text{ } \mu\text{g}$ microcystins (g dry weight^{-1}) in zooplankton tissue and was $0.02 \text{ } \mu\text{g}$ microcystins (g dry weight^{-1}) in clam tissue (Table 1). The concentration in animal tissue was not a function of the microcystins concentration per unit chlorophyll *a* measured at the station (compare Table 1 and Fig. 4).

M. aeruginosa was not eaten by the adult copepod *E. affinis* in initial laboratory feeding studies. The chlorophyll *a* content of initial animals was $0.07 \pm 0.01 \text{ } \mu\text{g}$ (100 animals^{-1}) and was not different from the $0.05 \pm 0.01 \text{ } \mu\text{g}$ (100 animals^{-1}) of incubated animals. *E. affinis* was observed in the zooplankton samples used for toxicity assays.

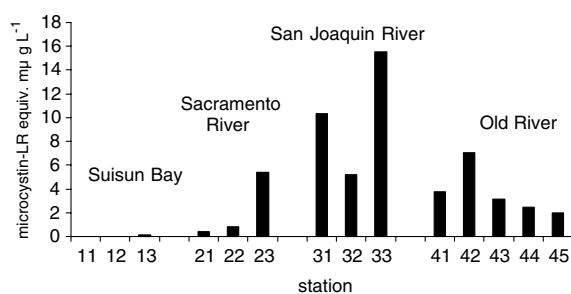
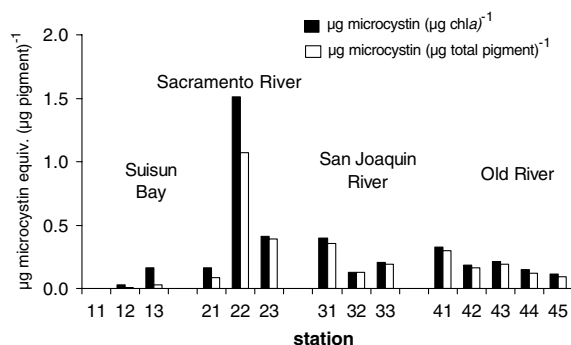
Discussion

Distribution

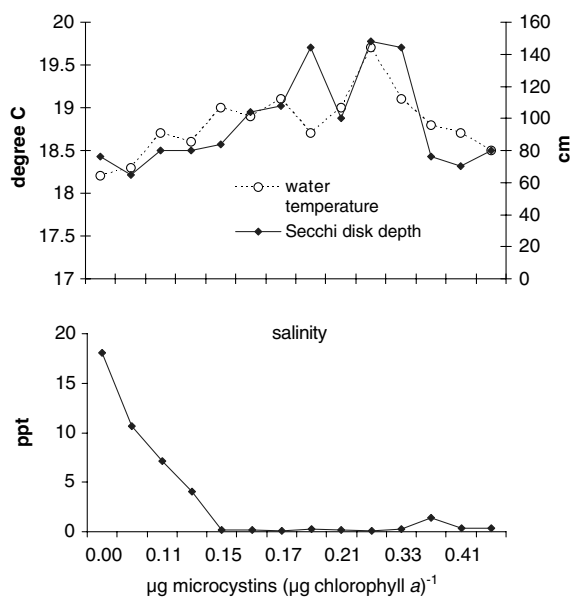
The colonial form of *M. aeruginosa* occurred throughout the NSFE at salinities from 0.1 to 18 ppt and habitats from shallow flooded islands

Table 2. Percent composition of microcystins in selected *Microcystis aeruginosa* tissue samples

Congener	Sacramento River		San Joaquin River	
	Station 23 Brannon Island %	Station 31 Jersey Point %	Station 32 Mouth of Mokelumne R. %	Station 33 Navigation marker 13 %
Demethyl	47	51	66	53
Microcystin-LR				
Microcystin-LR	20	23	9	16
Microcystin-WR	11	7	13	10
Microcystin-FR	6	5	6	8
Microcystin-RR	4	0	0	4
Unknown	12	14	6	9

Figure 3. Surface microcystins equivalent concentration in the >75 μm cell diameter size fraction.Figure 4. Concentration of total microcystin-LR equivalents per unit chlorophyll *a* and total pigment concentration in the >75 μm size fraction.

to deep shipping channels in the summer and fall of 2003. *M. aeruginosa* is a common cyanobacterium worldwide but its growth is restricted to salinity less than 7 ppt (Robson & Hamilton,

Figure 5. Variation of salinity, water temperature and Secchi disk depth with the microcystins to chlorophyll *a* ratio.

2003). Growth at low salinities may partially explain the higher biomass measured in the Delta portion of the estuary where salinity was less than 5 ppt. The absence of a visible *M. aeruginosa* bloom in the tributaries upstream suggested growth occurred within the Delta. *M. aeruginosa* blooms also developed within the estuary from cells seeded from upstream during high streamflow in the Swan Estuary in Western Australia (Robson & Hamilton, 2003). *Microcystis* spp. develop

readily from vegetative colonies in shallow water sediments (Brunberg & Blomqvist, 2003) and it is probable the bloom developed in the shallow areas of the Delta from either resident vegetative colonies or colonies seeded from upstream and spread downstream into the deep river channels with the wind and tide. Local biomass peaks in shallow water stations such as Brannon Island was probably produced by aggregation by wind and tide (Paerl, 1988).

The *M. aeruginosa* bloom was associated with high light, warm water temperature, shallow water and eutrophic conditions. This agrees with research in which water column stability, nutrient loading, light availability, water temperature, organic matter and habitat for seeding were identified as conditions needed for development and persistence of *M. aeruginosa* blooms (Paerl, 1988; Reynolds et al., 1981). Water temperature in September and October was somewhat below the optimum water temperature of 28 °C (Christian et al., 1986) but higher water temperature occurred earlier in the season when the bloom was visibly larger (unpublished data, California Department of Water Resources). Surface irradiance of 2000 $\mu\text{Em}^{-2} \text{s}^{-1}$ and Secchi disk depth of 140 cm indicated light in the water column was above the limiting level of 186 $\mu\text{Em}^{-2} \text{s}^{-1}$ (Christian et al., 1986). Median dissolved inorganic nitrogen and soluble reactive phosphorus concentrations were high and nonlimiting. *M. aeruginosa* is associated with eutrophic conditions and appeared to be more closely associated with the total nitrogen and phosphorus concentrations than the nitrogen to phosphorus ratio (Downing et al., 2001).

The colonial *M. aeruginosa* bloom in NSFE was caused by the geographic expansion of a harmful cyanobacteria bloom into a freshwater and brackish water habitat. The recent geographic expansion of harmful diatom and dinoflagellate algal bloom species through both regional spread and the occurrence of new species are well known for marine habitats (Anderson & Garrison, 1997). Many species introductions have occurred in the San Francisco Estuary since the 1850s (Cohen & Carlton, 1995). The colonial form of *M. aeruginosa* is the first recorded toxic phytoplankton bloom in the northern reach of the estuary. It may also be the first clearly known introduced phyto-

plankton bloom species in the San Francisco Estuary because the genus *Microcystis* was not observed in phytoplankton samples between 1975 and 1982 (Lehman & Smith, 1991). Previous phytoplankton bloom species were identified as cryptogenic, not clearly native or introduced (Cohen & Carlton, 1995). It is unknown if the colonial form of *M. aeruginosa* that appeared in 1999 was merely an aggregation of the single-celled form now present in the estuary or a new strain. *M. aeruginosa* colonies can congregate into larger colonies under stable conditions (O'Brien et al., 2004).

Toxicity

M. aeruginosa was a toxic cyanobacteria strain because it contained hepatotoxic microcystins at all stations. Traces of the neurotoxin anatoxin-a occurred at two stations but are usually not produced by *M. aeruginosa* (Sivonen & Jones, 1999). The trace amount of anatoxin-a at these two stations probably represent the background level in this ecosystem because these stations also contained some of the higher microcystins concentrations. It is unlikely that both the anatoxin-a and microcystins originated in the same cyanobacterium. The presence of both hepatotoxins and anatoxin-a was only reported for a *M. aeruginosa* bloom in Japan in association with the microcystins LR and RR (Park & Watanabe, 1995).

Microcystin toxicity is highly variable but the microcystin-LR found in the *M. aeruginosa* bloom in NSFE is a powerful hepatotoxin associated with both acute and chronic liver damage (Kaya, 1995). The toxicity of the demethyl microcystin-LR in NSFE is unknown. Microcystins are associated with toxicity to birds and fish and are suspected as a cause of human cancer in China and Australia (Carmichael, 1995; Kaya, 1995). The bloom probably originated from a single population of a microcystin-LR producer that spread throughout the region with the tide and wind because microcystins samples had a similar percent microcystin composition.

Acute *in situ* microcystins toxicity was probably low within the >75 μm cell diameter size fraction for humans and aquatic organisms. Total microcystins concentration in NSFE was well below the Australian and Canadian suggested water quality

standard for humans of 0.5–1 $\mu\text{g l}^{-1}$ (Carmichael, 1995) and the World Health Organization advisory level of 1 $\mu\text{g l}^{-1}$ (World Health Organization, 1998). It was also below the lower limit of the 48 h LC_{50} of 450 $\mu\text{g l}^{-1}$ for zooplankton (Hanazato, 1995). However, the *in situ* microcystins concentrations were probably conservative estimates of the bloom toxicity because net tows can underestimate the microcystins content by as much as 10-fold (J. Makarewicz, unpublished observations). This is probably a combination of cells passing through the net and the effect of the frontal boundary causing an overestimate of the amount of water that actually passed through the net. *In situ* toxicity may have been higher at locations where high water residence time, wind, channel morphology and tide aggregated biomass (Paerl, 1988). This was supported by microcystins concentration in concentrated net samples that were orders of magnitude higher than the suggested water quality advisory levels. Toxicity may also be higher earlier in the season when the bloom appears to have larger biomass (S. Waller, personal communication).

A variable microcystins to chlorophyll *a* ratio indicated chlorophyll *a* was not a reliable indicator of microcystin toxicity. The ratios of microcystins to chlorophyll *a* concentration calculated for Suisun Bay and the San Joaquin and Old rivers were within the range of 0.1–0.4 μg microcystins (μg chlorophyll *a*)⁻¹ typically measured for *Microcystis* spp. (Sivonen & Jones, 1999). The high μg microcystins (μg chlorophyll *a*)⁻¹ ratio of 1.5 measured at station 22 may be a function of the unique environmental conditions at this station where freshwater and brackish water converge. Toxicity varies with environmental conditions and was highest at intermediate water temperature and light intensity in culture experiments (van der Westhuizen & Eloff, 1985). The highest toxicity in this study occurred at relatively low water temperature, water transparency and salinity and contrasted with the lowest toxicity that occurred at relatively low water temperature and water transparency but high salinity.

Food web impact

Microcystins entered the base of the food web and were measured in both total zooplankton and

clam tissue. The maximum microcystins concentration of 3.5 μg (g dry wt)⁻¹ in zooplankton tissue was low compared with the 75–1387 μg (g dry wt)⁻¹ measured for zooplankton in Lake Kasumigaura (Watanabe et al., 1992). The direct toxicity of *M. aeruginosa* to zooplankton is reduced because it comprises only a small percentage of the zooplankton diet (Sellner et al., 1993). A combination of mechanical interference and feeding selectivity limits its use by zooplankton as a food source (Hanazato, 1995). The limited use of *M. aeruginosa* at the base of the food web in NSFE was suggested by initial laboratory feedings studies for the adult copepod *E. affinis*, but use varies by species, developmental stage, total food availability and structural form of the cyanobacteria (e.g., colonial) (DeMott et al., 1991; Reinikainen et al., 1994; Ghadouani et al., 2004). Even low microcystins concentration at the base of the food web poses a threat to the upper food web because microcystins may bioaccumulate. Tissue of the cladocera *Bosmina* spp. contained microcystins concentration that was 202% higher than in the co-occurring algal tissue (Park & Watanabe, 1995).

The impact of *M. aeruginosa* on the quantity and quality of phytoplankton biomass available to the food web may be a greater threat to the NSFE food web than toxicity. Total phytoplankton biomass is low at the base of the food web in NSFE compared with other estuaries because high turbidity limits phytoplankton growth (Jassby et al., 2002). *M. aeruginosa* blooms can reduce the growth of other phytoplankton because their surface habit limits light transmission into the water column and allows them to out compete other phytoplankton that cannot tolerate high light and water temperatures at the surface (Robarts & Zohary, 1992). Dissolved microcystins associated with the bloom may also inhibit consumption of the available desirable phytoplankton food by zooplankton (DeMott et al., 1991).

Both the quantity and quality of phytoplankton biomass appear to be important for the NSFE food web because they were correlated with long-term changes in zooplankton and *Neomysis mercedis* carbon (Lehman, 1992, 2004) and laboratory growth studies suggested local *Daphnia* grew best on phytoplankton carbon (Mueller-Solger et al., 2002). The loss of phytoplankton

food resources due to the *M. aeruginosa* bloom would add an additional impact to the phytoplankton biomass in the estuary already reduced by grazing of the clam *Potamocorbula amurensis* that was introduced into the estuary in 1987 (Jasby et al., 2002). Fish in the estuary partially adjusted to this loss of phytoplankton biomass by shifting their diet, but these shifts were not sufficient to prevent the decline in many fish species (Bennett & Moyle, 1996; Feyrer et al., 2003).

Beneficial use impact

The *M. aeruginosa* bloom is a potential threat to beneficial use in NSFE. NSFE provides agricultural and drinking water for local and upstream users. High microcystins concentration occurred in river channels used to divert water into storage reservoirs for the State Water Project and Federal Central Valley Project that supply water throughout California. Diversion of water into these reservoirs may also provide the seed needed to spread *M. aeruginosa* blooms and associated taste and odor problems into drinking water supplies. NSFE is also economically important because of its recreational use. *M. aeruginosa* blooms impact recreation through direct contact and ingestion that can cause skin and eye irritation, hay fever symptoms, dizziness, fatigue and stomach upset (Carmichael, 1995). High exposure water sports in the region include swimming, sail boarding, water skiing and wading. High microcystins concentration was measured at Brannon Island, a popular swimming beach. Sport fishing is also an important economic resource and could be impacted because of the health risk associated with ingestion of concentrated microcystins in animal tissue caused by bioaccumulation (Magalhaes et al., 2003). Wind-concentrated scums often contain microcystins concentrations that are toxic to animals and livestock, an important issue in this agricultural region. In addition, high biomass produced by blooms and the associated decomposition could eventually impact fishery production through its influence on dissolved oxygen concentration. Upstream migration of the threatened species Chinook salmon was blocked by low dissolved oxygen concentration in the San Joaquin River (Hallock et al., 1970) and low dissolved oxygen

concentration adversely impacts the health of aquatic organisms (Breitburg, 2002). High biomass can also enhance trihalomethane production, a cancer causing substance associated with chlorination of drinking water containing organic matter and an important concern in NSFE.

Because of its impact on so many beneficial uses, a regular monitoring will be needed to determine the yearly rate of expansion and toxicity of *M. aeruginosa* and the environmental factors that affect its development. The presence of microcystins in the food web suggested more information is needed on the presence of these toxins in the food web, potential pathways among trophic levels and how these change over time. Such information will be needed to assess the magnitude of the impact of *M. aeruginosa* on beneficial use in the estuary and to assess the need for a long-term management plan to control its development and toxicity.

Conclusion

This paper documents the first occurrence of a harmful algal bloom of the colonial form of *M. aeruginosa* in San Francisco Estuary. Initial surveys conducted in 2003 indicated this bloom occurred throughout the freshwater to brackish water regions of the estuary and contained hepatotoxic microcystins at all stations sampled. Microcystins were characterized by demethyl microcystin-LR followed by microcystin-LR. *M. aeruginosa* may also be the first known introduced phytoplankton species to the estuary.

The toxicity and widespread distribution of *M. aeruginosa* in NSFE demonstrated the potential of this organism to negatively impact many beneficial uses in NSFE and suggested that an active and long-term monitoring program is needed to assess the potential long-term human and ecological impacts.

Acknowledgements

This study was funded by the NOAA Coastal Ocean Program (COP) in partnership with the National Office for Marine Biotoxins and Harmful Algal Blooms at Woods Hole Oceanographic

Institution and the COP Monitoring and Event Response for Harmful Algal Blooms (MERHAB) program, the California Department of Water Resources and U.S. Bureau of Reclamation as a part of the San Francisco Bay-Delta Interagency Ecological Program. M. Satachwell at the State University of New York provided the protein phosphatase assays. E. Santos and L. Brenn assisted with monitoring.

References

- American Public Health Association, American Water Works Association and Water Environment Association. 1998. Standard Methods for the Examination of Water and Wastewater. 20th edn. American Public Health Association, Washington, DC.
- Anderson, D. M. & D. J. Garrison, 1997. The ecology and oceanography of harmful algal blooms. Special issue. *Limnology and Oceanography* 42: 1009–1305.
- Bennett, W. A. & P. B. Moyle, 1996. Where have all the fishes gone? Interactive factors producing fish declines in the Sacramento-San Joaquin Estuary. In J. T. Hollibaugh (ed.), *San Francisco Bay: The Ecosystem*. Pacific Division of the American Association for the Advancement of Science, San Francisco, California: 519–542.
- Brunberg, A. & P. Blomqvist, 2003. Recruitment of *Microcystis* (Cyanophyceae) from lake sediments: The importance of littoral inocula. *Journal of Phycology* 39: 58–63.
- Boyer, G. L. & G. D. Goddard, 1999. High performance liquid chromatography (HPLC) coupled with post-column electrochemical oxidation (ECOS) for the detection of PSP toxins. *Natural Toxins* 7: 353–359.
- Breitburg, D. 2002. Effects of hypoxia, and the balance between hypoxia and enrichment, on coastal fishes and fisheries. *Estuaries* 25: 767–781.
- California Bay-Delta Authority, 2000. Programmatic Record of Decision. Technical Report. California Bay-Delta Authority, Sacramento, CA. URL: <http://calwater.ca.gov/Archives/GeneralArchive/rod/ROD8-28-00.pdf>.
- Carmichael, W. W., 1995. Toxic microcystin in the environment. In M. F. Watanabe, K. Harada, W. W. Carmichael & H. Fujiki (eds), *Toxic Microcystis*. CRC Press, New York: 1–12.
- Carmichael, W. W. & J. An, 1999. Using an enzyme linked immunosorbent assay (ELISA) and a protein phosphatase inhibition assay (PPIA) for the detection of microcystins and nodularins. *Natural Toxins* 7: 377–385.
- Christian, R. R., W. L. Bryant Jr. & D. W. Stanley, 1986. The relationship between river flow and *Microcystis aeruginosa* blooms in the Neuse River, North Carolina. *Water Resources Research Institute Report* 223. North Carolina State University.
- Cohen, A. N. & J. T. Carlton, 1995. Indigenous aquatic species in a United States estuary: study of the biological invasions of the San Francisco Bay and Delta. United States Fish and Wildlife Service, Washington, DC and the National Sea Grant College Program, Connecticut Sea Grant.
- DeMott, W. R., Q. Zhang & W. W. Carmichael, 1991. Effects of toxic cyanobacteria and purified toxins on the survival and feeding of a copepod and three species of *Daphnia*. *Limnology and Oceanography* 36: 1346–1357.
- Downing, J. A., S. B. Watson & E. McCauley, 2001. Predicting cyanobacterial dominance in lakes. *Canadian Journal of Fisheries and Aquatic Science* 58: 1905–1908.
- Feyrer, F., B. Herbold, S. A. Matern & P. Moyle, 2003. Dietary shifts in a stressed fish assemblage: consequences of a bivalve invasion in the San Francisco Estuary. *Environmental Biology of Fishes* 67: 277–288.
- Ghadouani, A., B. Pinel-Alloul, K. Plath, G. A. Codd & W. Lampert, 2004. Effects of *Microcystis aeruginosa* and purified microcystin-LR on the feeding behavior of *Daphnia pulicaria*. *Limnology and Oceanography* 49: 666–679.
- Hallock, R. J., R. F. Elwell & D. H. Fry, 1970. Migrations of Adult King Salmon *Oncorhynchus tshawytscha* in the San Joaquin Delta, as Demonstrated by the Use of Sonic Tags. Bulletin 151. California Department of Fish and Game Fish, Sacramento, California.
- Harada, K., 1995. Chemistry and detection of microcystins. In M. F. Watanabe, K. Harada, W. W. Carmichael & H. Fujiki (eds), *Toxic Microcystis*. CRC Press, New York: 103–148.
- Hanazato, T., 1995. Toxic cyanobacteria and the zooplankton community. In M. F. Watanabe, K. Harada, W. W. Carmichael & H. Fujiki (eds), *Toxic Microcystis*. CRC Press, New York: 79–102.
- Horner, R. A., D. L. Garrison & F. G. Plumley, 1997. Harmful algal blooms and red tide problems on the US west coast. *Limnology and Oceanography* 42: 1076–1088.
- James, K. J. & I. R. Sherlock, 1996. Determination of the cyanobacterial neurotoxin, anatoxin-a, by derivatization using 7-fluoro-4-nitro-2,1,3-benzoxadiazole (NBD-F) and HPLC analysis with fluorimetric detection. *Biomedical Chromatography* 10: 46–47.
- Jassby, A. D., J. E. Cloern & B.E. Cole, 2002. Annual primary production: patterns and mechanisms of change in a nutrient-rich tidal ecosystem. *Limnology and Oceanography* 47: 698–712.
- Kaya, K., 1995. Toxicology of Microcystins. In M. F. Watanabe, K. Harada, W. W. Carmichael & H. Fujiki (eds), *Toxic Microcystis*. CRC Press, New York: 175–202.
- Lehman, P. W., 1992. Environmental factors associated with long-term changes in chlorophyll concentration in the Sacramento-San Joaquin Delta and Suisun Bay, California. *Estuaries* 15: 335–348.
- Lehman, P. W., 1996. Changes in chlorophyll *a* concentration and phytoplankton community composition with water-year type in the upper San Francisco Bay Estuary. In J. T. Hollibaugh (ed.), *San Francisco Bay: The Ecosystem*. Pacific Division of the American Association for the Advancement of Science. San Francisco, California: 351–374.
- Lehman, P. W., 2000. The influence of climate on phytoplankton community carbon in San Francisco Bay Estuary. *Limnology and Oceanography* 45: 580–590.

- Lehman, P. W., 2004. The influence of climate on mechanistic pathways that impact lower food web production in northern San Francisco Bay estuary. *Estuaries* 27: 311–324.
- Lehman, P. W. & R. W. Smith, 1991. Environmental factors associated with phytoplankton succession for the Sacramento-San Joaquin Delta and Suisun Bay Estuary, California. *Estuarine Coastal and Shelf Science* 32: 105–128.
- Lehman, P. W. & S. Waller, 2003. *Microcystis* blooms in the Delta. Interagency Ecological Program for the San Francisco Estuary Newsletter 16: 18–19.
- Lindstrom, K. 1983. Selenium as a growth factor for plankton algae in laboratory experiments and in some Swedish lakes. *Hydrobiologia* 101: 35–48.
- Magalhaes, V. F., M.M. Marinho, P. Domingos, A. C. Oliveira, S. M. Costa, L. O. Azevedo & S.M. F. O. Azevedo, 2003. Microcystins (cyanobacteria hepatotoxins) bioaccumulation in fish and crustaceans from Sepetiba Bay (Brazil, RJ). *Toxicon* 42: 289–295.
- Marker, A. F., C. A. Crowther & R. J. M. Gunn, 1980. Methanol and acetone as solvents for estimating chlorophyll *a* and phaeopigments by spectrophotometry. *Achiv fuer Hydrobiologie supplement* 14: 52–59.
- Mueller-Solger, A. B., A. D. Jassby & D. C. Mueller-Navarra, 2002. Nutritional quality for zooplankton (*Daphnia*) in a tidal freshwater system (Sacramento-San Joaquin River Delta, USA). *Limnology and Oceanography* 47: 1468–1476.
- O'Brien, K. R., D. L. Meyer, A. M. Waite, G. N. Ivey & D. P. Hamilton, 2004. Disaggregation of *Microcystis aeruginosa* colonies under turbulent mixing: laboratory experiments in a grid-stirred tank. *Hydrobiologia* 519: 143–152.
- Paerl, H. W., 1988. Nuisance phytoplankton blooms in coastal, estuarine and inland waters. *Limnology and Oceanography* 33: 823–847.
- Park, H. & M. F. Watanabe, 1995. Toxic *Microcystis* in Eutrophic lakes. In M. F. Watanabe, K. Harada, W. W. Carmichael & H. Fujiki (eds), *Toxic Microcystis*. CRC Press, New York: 57–78.
- Reinikainen, M., M. Ketola & M. Walls, 1994. Effects of the concentrations of toxic *Microcystis aeruginosa* and an alternative food on the survival of *Daphnia pulex*. *Limnology and Oceanography* 39: 424–432.
- Reynolds, C. S., G. H. M. Jaworski, H. A. Cmiech & G. F. Leedale, 1981. On the annual cycle of the blue-green alga *Microcystis aeruginosa* Kutz. Emend. Elenkin. *Philosophical Transactions of the Royal Society of London. Series B. Biological Sciences* 293: 419–477.
- Roberts, R. D. & T. Zohary, 1992. The influence of temperature and light on the upper limit of *Microcystis aeruginosa* production in a hypertrophic reservoir. *Journal of Plankton Research* 14: 235–247.
- Robson, B. J. & D. P. Hamilton, 2003. Summer flow event induces a cyanobacterial bloom in a seasonal Western Australia estuary. *Marine and Freshwater Research* 54: 139–151.
- SAS Institute, Inc., 2004. *SAS/STAT User's Guide, Version 8*. SAS Institute Inc., SAS Campus Drive, Cary, NC.
- Sellner, K. G., D. C. Brownlee, M. H. Bundy, S. G. Brownlee & K. R. Braun, 1993. Zooplankton grazing in a Potomac River cyanobacteria bloom. *Estuaries* 16: 859–872.
- Sivonen, K. & G. Jones, 1999. Cyanobacterial toxins. In I. Chorus & J. Bartram (eds), *Toxic Cyanobacteria in Water*, World Health Organization, London: 41–112.
- United States Environmental Protection Agency (US EPA), 1983. *Methods for Chemical Analysis of Water and Wastes*. Washington, DC. Technical Report EPA-600/4-79-020.
- Utermohl, H. 1958. Zur Vervollkommnung der quantitativen Phytoplankton-methodik. *Mitteilungen Internationale Vereinigung fur Theoretische und Angewandte Limnologie* 9: 1–38.
- Van der Westhuizen, A. J. & J. N. Eloff, 1985. Effect of temperature and light on the toxicity and growth of the blue-green alga *Microcystis aeruginosa* (UV-006). *Planta* 163: 55–59.
- Watanabe, M. M. 1995. Isolation, cultivation and classification of bloom-forming *Microcystis* in Japan. In M. F. Watanabe, K. Harada, W. W. Carmichael & H. Fujiki (eds), *Toxic Microcystis*. CRC Press, New York: 13–34.
- Watanabe, M. M., K. Kaya & N. Takamura, 1992. Fate of the toxic cyclic heptapeptides, the microcystins, from blooms of *Microcystis* (cyanobacteria) in a hypertrophic lake. *Journal of Phycology* 28: 761–775.
- World Health Organization, 1998. *Guidelines for Safe Recreational-Water Environments: Coastal and Freshwaters*. Draft for consultation. World Health Organization, Geneva.
- Yunes, J. S., P. S. Salomon, A. Matthiensen, K. A. Beattie, S. L. Raggett & G. A. Codd, 1996. Toxic blooms of cyanobacteria in the Patos Lagoon Estuary, Southern Brazil. *Journal of Aquatic Ecosystem Health* 5: 223–229.

See discussions, stats, and author profiles for this publication at:
<http://www.researchgate.net/publication/225403187>

The influence of environmental conditions on seasonal variation of Microcystis abundance and microcystins concentration in San Francisco Estuary

ARTICLE *in* HYDROBIOLOGIA · MARCH 2008

Impact Factor: 2.28 · DOI: 10.1007/s10750-007-9231-x

CITATIONS

49

READS

53

4 AUTHORS, INCLUDING:



P. W. Lehman

State of California

25 PUBLICATIONS 483 CITATIONS

SEE PROFILE



Gregory L Boyer

State University of New York College of...

94 PUBLICATIONS 2,355 CITATIONS

SEE PROFILE



Michael F. Satchwell

State University of New York College of...

11 PUBLICATIONS 268 CITATIONS

SEE PROFILE

The influence of environmental conditions on the seasonal variation of *Microcystis* cell density and microcystins concentration in San Francisco Estuary

P. W. Lehman · G. Boyer · M. Satchwell ·
S. Waller

Received: 9 July 2007 / Revised: 10 October 2007 / Accepted: 31 October 2007 / Published online: 28 November 2007
© Springer Science+Business Media B.V. 2007

Abstract A bloom of the cyanobacteria *Microcystis aeruginosa* was sampled over the summer and fall in order to determine if the spatial and temporal patterns in cell density, chlorophyll *a* (chl *a*) concentration, total microcystins concentration, and percent microcystins composition varied with environmental conditions in San Francisco Estuary. It was hypothesized that the seasonal variation in *Microcystis* cell density and microcystin concentration was ecologically important because it could influence the transfer of toxic microcystins into the aquatic food web. Sampling for *Microcystis* cell density, chl *a* concentration, total microcystins concentration and a suite of environmental conditions was conducted biweekly at nine stations throughout the freshwater tidal and brackish water regions of the estuary between July and November 2004. Total microcystins in zooplankton and clam tissue was also sampled in August and October. *Microcystis* cell density, chl *a* concentration and total microcystins concentration varied by an order of magnitude and peaked during August and

September when P_m^B and α^B were high. Low stream-flow and high water temperature were strongly correlated with the seasonal variation of *Microcystis* cell density, total microcystins concentration (cell^{-1}) and total microcystins concentration (chl *a*) $^{-1}$ in canonical correlation analyses. Nutrient concentrations and ratios were of secondary importance in the analysis and may be of lesser importance to seasonal variation of the bloom in this nutrient rich estuary. The seasonal variation of *Microcystis* density and biomass was potentially important for the structure and function of the estuarine aquatic food web, because total microcystins concentration was high at the base of the food web in mesozooplankton, amphipod, clam, and worm tissue during the peak of the bloom.

Keywords *Microcystis* · Estuary · Microcystins · Food web · Seasonal variation

Introduction

Microcystis aeruginosa (*Microcystis*) is a common freshwater cyanobacterium in freshwater lakes and reservoirs worldwide (Federal Environmental Agency, 2005). It also occurs in rivers that form estuaries including the Potomac River and the Neuse River in the USA, the Swan River in Australia and the Guadiana River in Spain and Portugal (Sellner et al., 1988; Pearl, 1988; Rocha et al., 2002; Orr et al., 2004).

Handling editor: D. Hamilton

P. W. Lehman (✉) · S. Waller
Division of Environmental Services, Department of Water Resources, 901 P Street, Sacramento, CA 95814, USA
e-mail: plehman@water.ca.gov

G. Boyer · M. Satchwell
Department of Environment and Forestry, State University of New York, Syracuse, NY, USA

Microcystis is considered a cyanobacterial harmful algal bloom (CHAB) species because it produces surface scums that impede recreation sports, reduce aesthetics, lower dissolved oxygen concentration and cause taste and odor problems in drinking water (Carmichael, 1995). *Microcystis* also produces toxic microcystins that are powerful hepatotoxins associated with liver cancer and tumors in humans and wildlife (Carmichael, 1995).

The toxicity of *Microcystis* blooms negatively impact phytoplankton, zooplankton, and fish production directly or indirectly through the transfer or accumulation of toxins in the food web (Kotak et al., 1996; Ibelings et al., 2005; Sedmak & Elerseck, 2005; Malbrouck & Kestemont, 2006). *Microcystis* also affects aquatic community structure and function by impacts on feeding success or food quality for zooplankton and fish (Rohrlack et al., 2005; Malbrouck & Kestemont, 2006). The abundance of cyanobacteria further affects total carbon production by causing a shift from large to small zooplankton species (Fulton & Pearl, 1987; Smith & Gilbert, 1995).

Microcystis blooms vary over the summer and fall in response to environmental factors that influence bloom initiation and those that sustain bloom growth. Since *Microcystis* does not contain heterocysts that produce nitrate from atmospheric nitrogen, both high nitrogen, and phosphorus are needed for blooms to develop (Pearl et al., 2001). Bloom initiation requires water temperature above 20°C (Jacoby et al., 2000), but accumulation of high biomass, requires long residence time for this slow growing species (Reynolds, 1997). Blooms also develop faster in vertically stable environments that allow the buoyant *Microcystis* colonies to rise to the surface of the water column where they out compete other phytoplankton for light (Huisman et al., 2004). Other factors such as high pH and turbidity or low carbon dioxide concentration enhance growth of *Microcystis* over other phytoplankton once the bloom is established, but are not required for bloom initiation or growth (Shapiro, 1990). Most of the information on the importance of environmental factors for *Microcystis* bloom development and persistence is obtained from freshwater lakes and reservoirs, less is known about the relative importance of environmental factors in estuaries, particularly nutrient-rich estuaries like San Francisco Estuary (SFE).

The cause of *Microcystis* blooms and their potential impact on estuarine productivity is an important concern for SFE where a bloom of *Microcystis* first appeared in 1999 (Lehman et al., 2005). Little is known about the seasonal variation of *Microcystis* cell density, biomass and toxic microcystin concentration, the environmental factors that affect the seasonal variation of the bloom or its impact on the structure and function of the estuarine food web. Data from a single sampling day in October 2003 indicated *Microcystis* was widely distributed across the freshwater to brackish water reaches of the estuary and contained the hepatotoxic microcystin-LR (Lehman et al., 2005). The bloom was associated with high and non-limiting nitrogen and phosphorus concentration, high water temperature and high water transparency but values from this single sampling day were not sufficient to assess the importance of these variables. The presence of total microcystins in zooplankton and clam tissue also suggested the toxins in the bloom might impact the aquatic food web.

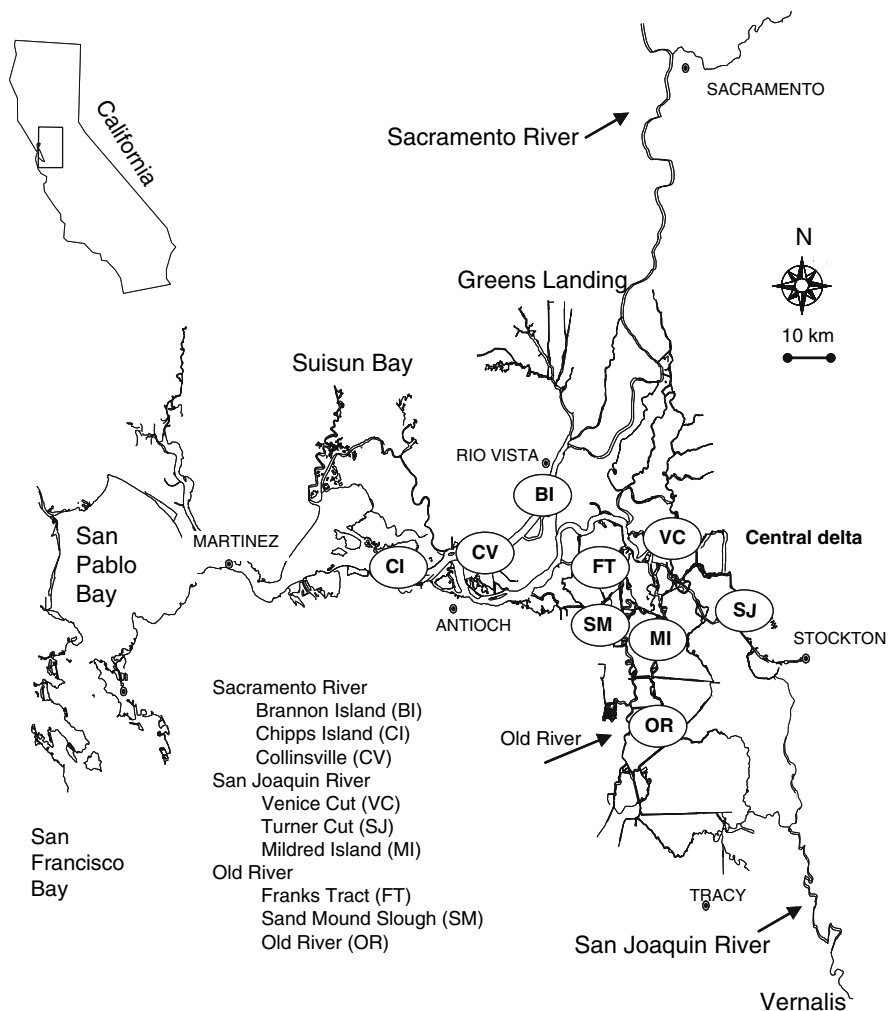
The purpose of this study was to quantify the seasonal variation of *Microcystis* cell density, chlorophyll *a* (chl *a*) concentration, microcystins concentration and the presence of microcystins in the tissues of lower aquatic food web organisms and to determine how these variables are influenced by environmental conditions in SFE. Understanding the influence of environmental conditions on the seasonal variation of the *Microcystis* bloom and its associated microcystins concentration is potentially important for management of fishery production in SFE, where the food web is dependent on phytoplankton and zooplankton production and characterized by a long-term decrease in fish, zooplankton and diatom carbon (Lehman, 2004; Sommer et al., 2007).

Materials and methods

Study area

SFE consists of an inland delta that flows into a chain of downstream marine bays—Suisun, San Pablo and San Francisco—and creates one of the largest estuaries on the west coast of North America (Fig. 1). The inland delta formed by the Sacramento River (SAC) on the north and the San Joaquin River (SJR)

Fig. 1 Map of San Francisco Estuary showing location of sampling stations



on the south contains 200 km² of waterways. SAC is the largest of the rivers with an average discharge of 4795 m³ s⁻¹ compared with 400 m³ s⁻¹ for SJR over the July through October period of this study. Other rivers influence streamflow in the delta including the Mokelumne (MOKE) and Cosumnes (CSR) Rivers with average discharge of 21 m³ s⁻¹ and 6 m³ s⁻¹, respectively. An important feature of the delta is the large amount of water removed for agriculture that causes average reverse streamflow of 1578 m³ s⁻¹ in Old River (ODR) and 1339 m³ s⁻¹ in SJR during August and September (<http://www.waterdata.usgs.gov/nwis>). Depth varies in the delta from a few meters in the flooded islands in the center of the delta to 13 m in the main river channels. Tides in the delta reach 2 m in height with tidal velocities up to 30 cm s⁻¹ and tidal excursions of 10 km.

Field and laboratory sampling

Chl *a* concentration, *Microcystis* cell density and microcystin (total and individual) concentration were sampled biweekly between July 13 and November 3, 2004 at nine stations throughout the freshwater to brackish water reaches of SFE. Selected stations represented different habitat types or beneficial use including recreational swimming (BI), shallow water habitat (MI and FT), deep river channel (CV, VC and SM), native fish habitat (SJ and CI) and agricultural and drinking water supply (OR; Fig. 1). *Microcystis* colonies were sampled by horizontal surface tows of a 0.72 m diameter plankton net fitted with a 75- μ m mesh screen (Lehman et al., 2005). Use of a smaller mesh net (40 μ m) was not possible because the net became clogged with heavy sediment. Water

temperature, specific conductance, pH, dissolved oxygen, and turbidity were also measured at each station using a Yellow Springs Instrument (YSI) 6600 sonde. Depth of the euphotic zone was estimated from Secchi disk depth. Photosynthetically active surface irradiance (PAR) was measured at 15 min intervals in Langleys at Antioch, CA using an Eppley phyroheliumeter (<http://www.iep.water.ca.gov>). Langleys were converted to mole quanta using linear correlation with LiCOR quantum sensor values ($r^2 = 0.91$; $P < 0.01$).

Surface water samples were collected by van Dorn water sampler and immediately stored at 4°C. Algal biomass was filtered within 2 h onto Millipore APFF glass fiber filters (0.7 µm pore diameter). Filters for microcystins analysis were folded, wrapped in aluminum foil and frozen at -80°C until analysis. Filters for chl *a* (corrected for phaeophytin) and phaeophytin analysis were treated with 1 ml of saturated magnesium carbonate solution as a preservative and frozen at -14°C until analysis (method 10200H, APHA et al., 1998). Phytoplankton for identification and enumeration were preserved and stained with Lugol's iodine solution and species were counted at 700X using the inverted microscope technique (Utermöhl, 1958). Sample replication was 10%.

Water samples for dissolved ammonium, nitrate-plus-nitrite, soluble reactive phosphorus, and silicate concentration were filtered through 0.45 µm pore size Millipore HATF04700 nucleopore filters. Filtered samples plus raw water samples for total phosphorus were stored at -14°C until analysis by colorimetric techniques (US EPA, 1983; USGS, 1985). Total suspended solids concentration was determined by standard methods (APHA et al., 1998). Daily average streamflow, air temperature, and water temperature were obtained from hourly data collected by the Interagency Ecological Program (<http://www.iep.water.ca.gov>).

Net primary productivity and community respiration (phytoplankton and bacteria) were measured for a single station each sampling day by 4–6 h incubations at 0.075 m depth near Antioch, CA (Fig. 1) using the dissolved oxygen light and dark bottle incubation technique (Vollenweider, 1974). Values obtained from incubating bottles in a light gradient were used to compute the photosynthetic capacity from the chl *a* specific light saturated rate of photosynthesis (P_m^B , mg C

(mg chl *a*)⁻¹ h⁻¹), the photosynthetic efficiency from the chl *a* specific initial slope (α^B ; mg C (mg chl *a*)⁻¹ (mole quanta m⁻²)⁻¹) and the photoinhibition parameter from the chl *a* specific negative slope of the P-I curve above light saturation (β^B , mg C (mg chl *a*)⁻¹ (mole quanta m⁻²)⁻¹; Lehman et al., 2007). These parameters were used to compute integrated gross (GP_{ez} , mg C m⁻² h⁻¹) and areal (GP_{ez}) primary productivity of the euphotic zone.

Zooplankton including mesozooplankton, amphipods, worms, and jellyfish were sampled at CV, SM, SJ, and MI by horizontal tows of a 0.7 m diameter plankton net fitted with a 150 µm mesh. Zooplankton tissue was kept at 4°C and separated by pipette from *Microcystis* in the water sample using a dissecting microscope within 48 h of sampling. The final zooplankton tissue sample was rinsed in distilled water and frozen at -80°C until analysis. Clams were collected using a ponar dredge. The muscle tissue was removed from the shell, rinsed in distilled water and frozen at -80°C until analysis.

Microcystin analysis

Filters and animal tissue for microcystin analysis were extracted and assessed for total microcystins using the protein phosphate inhibition assay (PPIA). Samples with high levels of total microcystins were further analyzed by high pressure liquid chromatography (HPLC) to identify the specific microcystins in the sample (Lehman et al., 2005).

Statistical analysis

Statistical analyses included correlation and single and multiple comparisons using analysis of variance. Kruskal-Wallis nonparametric analysis of variance was used when the assumptions of the analysis (normally distributed data and homogeneity of variance) were not met. Canonical correlation analysis was computed using log-transformed values in order to minimize differences in variance produced by differences in absolute size and adjust for nonhomogeneity of variance among variables. All statistical analyses were computed using Statistical Analysis System software (SAS Institute Inc., 2004).

Results

Microcystis spatial and temporal variation

Chl *a* concentration and *Microcystis* cell density in the net tow samples were greatest in SJR (Fig. 2). Average chl *a* concentration was 7-fold greater ($P < 0.05$) in SJR compared with SAC ($P < 0.05$; mean 97 ± 70 , 34 ± 36 , and 14 ± 18 ng l⁻¹ for SJR, ORD and SAC, respectively). Among stations,

chl *a* concentration was greatest ($P < 0.05$) at the shallow flooded island and slow moving river channel stations MI and SJ in SJR and lowest at the fast flowing river channels CI and CV in SAC. *Microcystis* cell density varied in a similar fashion to chl *a* concentration among rivers and was greatest ($P < 0.05$) in SJR followed by ODR and SAC (Fig. 2). Cell densities were low in the net tows and exceeded 20,000 cells ml⁻¹ only three times at MI, two times at SJ and VC in SJR and once at OR and

Fig. 2 Mean and standard deviation (vertical bar) of chlorophyll *a* concentration in the >75 μ m algal size fraction, log *Microcystis* cell density and areal gross primary productivity in the euphotic zone at stations in San Francisco Estuary between July and October 2004

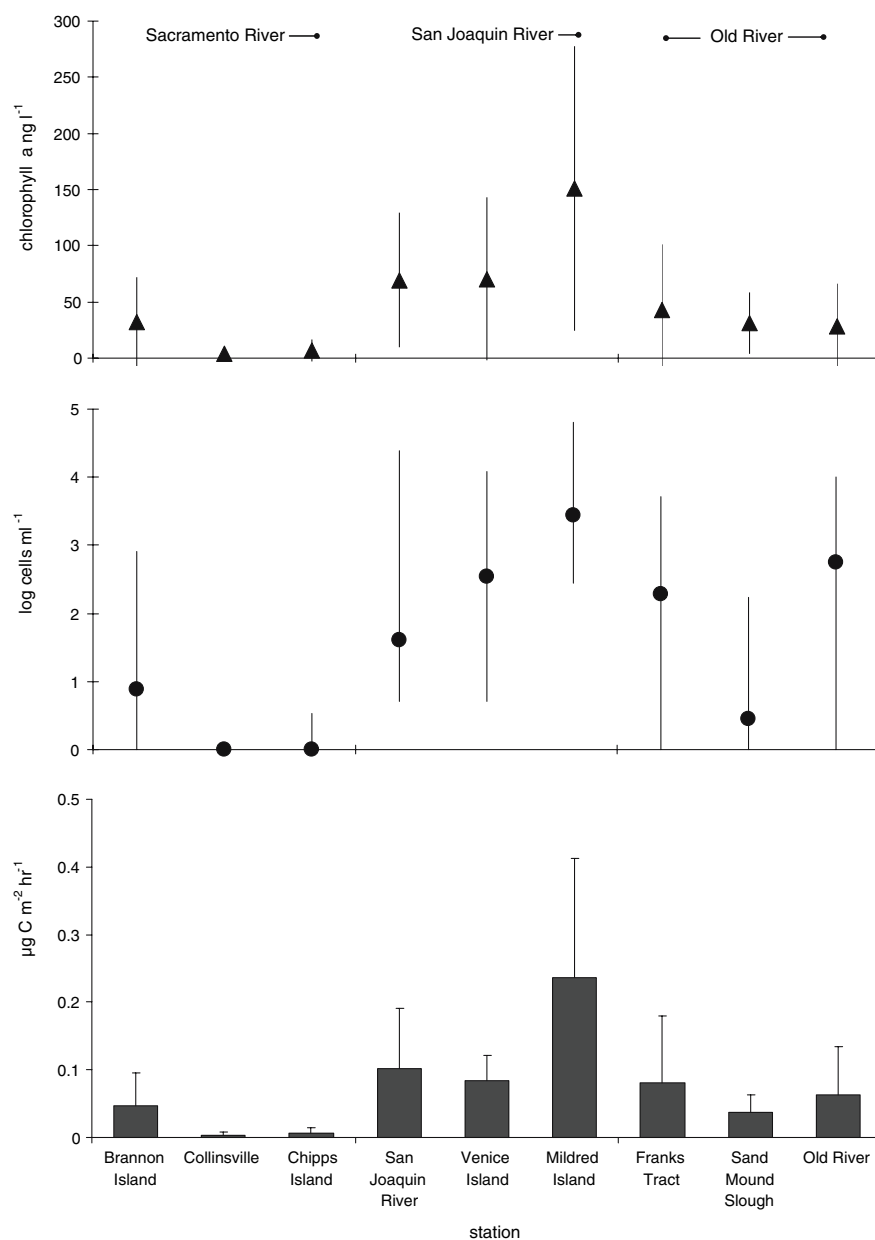
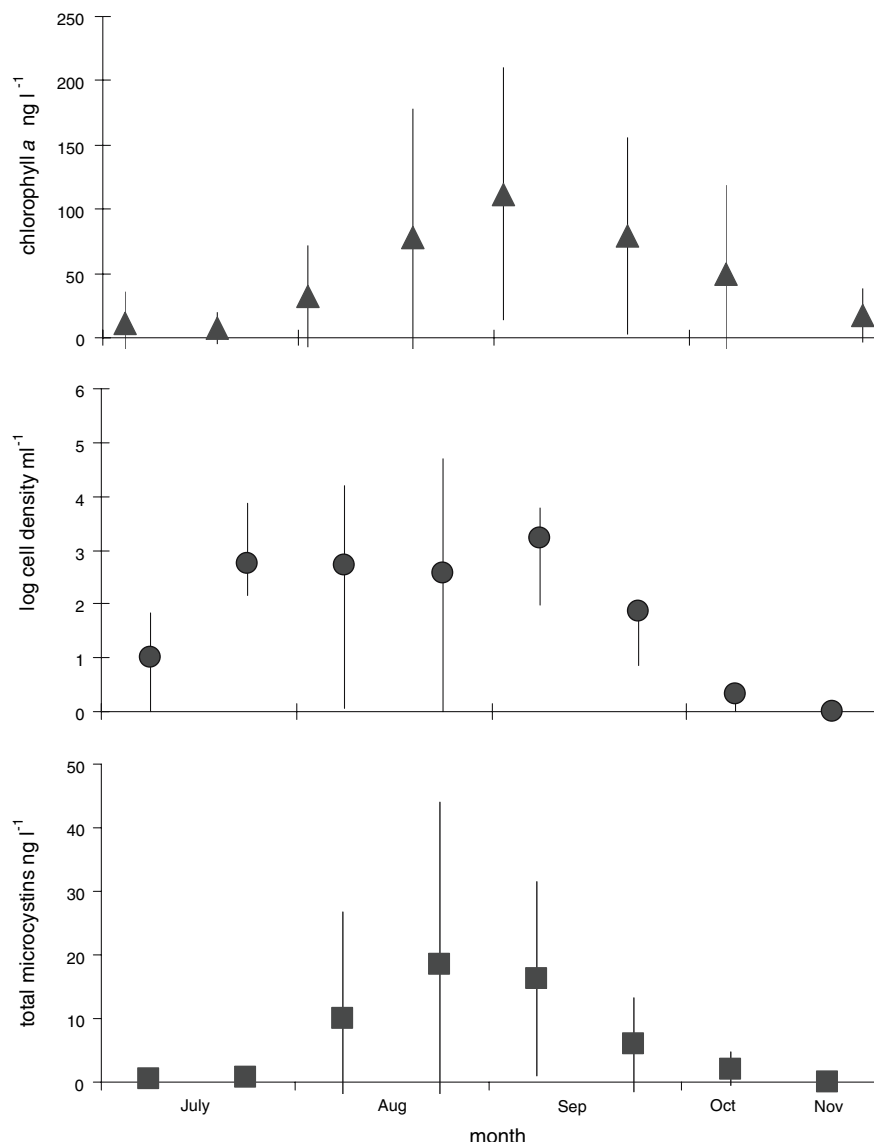


Fig. 3 Mean and standard deviation (vertical bar) of chlorophyll *a* concentration in the >75 μm algal size fraction, log *Microcystis* cell density ml^{-1} and total microcystins concentration among months between July and November 2004 in San Francisco Estuary



FT in ODR. The maximum cell density was $22,480,000 \text{ cells ml}^{-1}$ at MI.

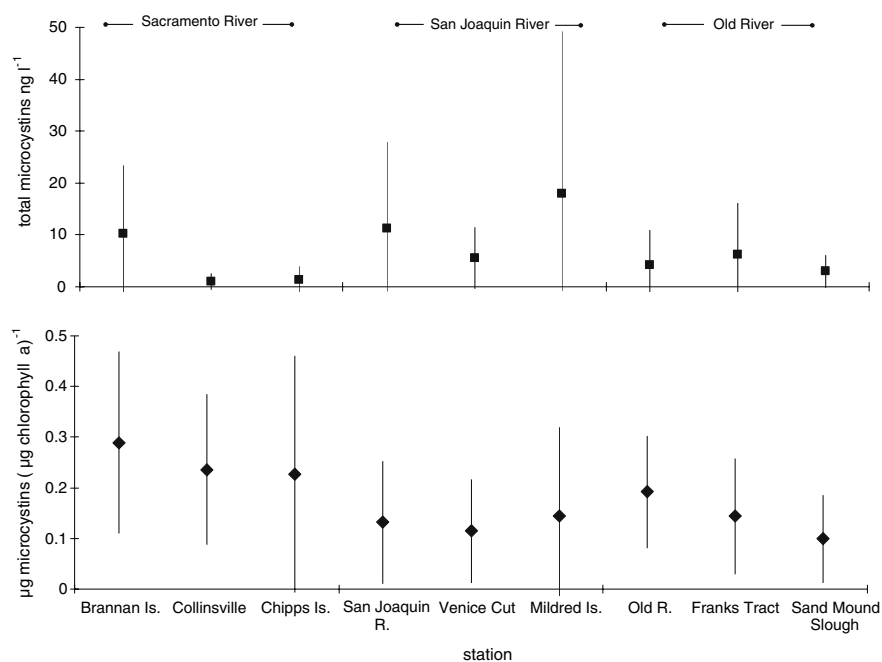
Average chl *a* concentration was 3-fold greater ($P < 0.05$) in August and September than July, October and November ($75 \pm 66 \text{ ng l}^{-1}$ and $22 \pm 29 \text{ ng l}^{-1}$, respectively; Fig. 3). This pattern differed somewhat among rivers, with peak chl *a* concentration occurring earlier ($P < 0.05$) in SJR (August) than SAC (September). Chl *a* concentration was equally high in August and September for ODR. Chl *a* concentration did not vary with *Microcystis* cell density which was consistently high ($P < 0.05$) between late July and early September (Fig. 3). *Microcystis* cell density also did

not have a strong seasonal pattern among rivers except in SJR where cell density was greatest ($P < 0.05$) in August and September.

Areal GP_{ez} was greater ($P < 0.01$) at stations in SJR and ODR than SAC (141 ± 70 , 67 ± 26 and $19 \pm 24 \text{ ng C m}^{-2} \text{ h}^{-1}$, respectively; Fig. 2) but did not differ among rivers when normalized to chl *a* concentration. Areal GP_{ez} and GP_{ez} normalized to chl *a* concentration were also greatest ($P < 0.01$) in September even though respiration ($\text{chl } a)^{-1}$ was highest that month. The seasonal variation of GP_{ez} mirrored changes in the photosynthetic parameters P_{m}^{B} , α^{B} and β^{B} which were high in August and

Table 1 Photosynthetic parameters and respiration normalized to chlorophyll *a* concentration computed from the photosynthesis-irradiance curve and light and dark bottle dissolved oxygen incubations for three stations sampled between August and October, 2004

Date	Sampling station	P_m^B mg C (mg chl <i>a</i>) ⁻¹ hr ⁻¹	α^B mg C (mg chl <i>a</i>) ⁻¹ (mole quanta m ⁻²) ⁻¹	β^B mg C (mg chl <i>a</i>) ⁻¹ (mole quanta m ⁻²) ⁻¹	Respiration mg C (mg chl <i>a</i>) ⁻¹ hr ⁻¹
August 27	Franks Tract	1.15 ± 0.12	2.52 ± 0.15	0.11 ± 0.07	-0.73 ± 0.06
September 9	Old River	2.38 ± 0.33	1.54 ± 0.26	0.11 ± 0.11	-1.76 ± 0.07
September 28	Mildred Island	2.13 ± 0.50	0.88 ± 0.37	–	-0.88 ± 0.03
October 18	Old River	0.36 ± 0.03	0.42 ± 0.10	0.06 ± 0.01	-0.10 ± 0.07

Fig. 4 Mean and standard deviation (vertical bar) of total microcystins concentration and total microcystins (chl *a*)⁻¹ for stations in the San Francisco Estuary between July and November 2004

September (Table 1). However, the seasonal variation in primary productivity and the photosynthetic parameters was large. Areal GP_{cz} varied by two orders of magnitude while P_m^B and α^B varied 6-fold (Fig. 4; Table 1). By comparison, there was a little seasonal variation in β^B which varied by a factor of 2.

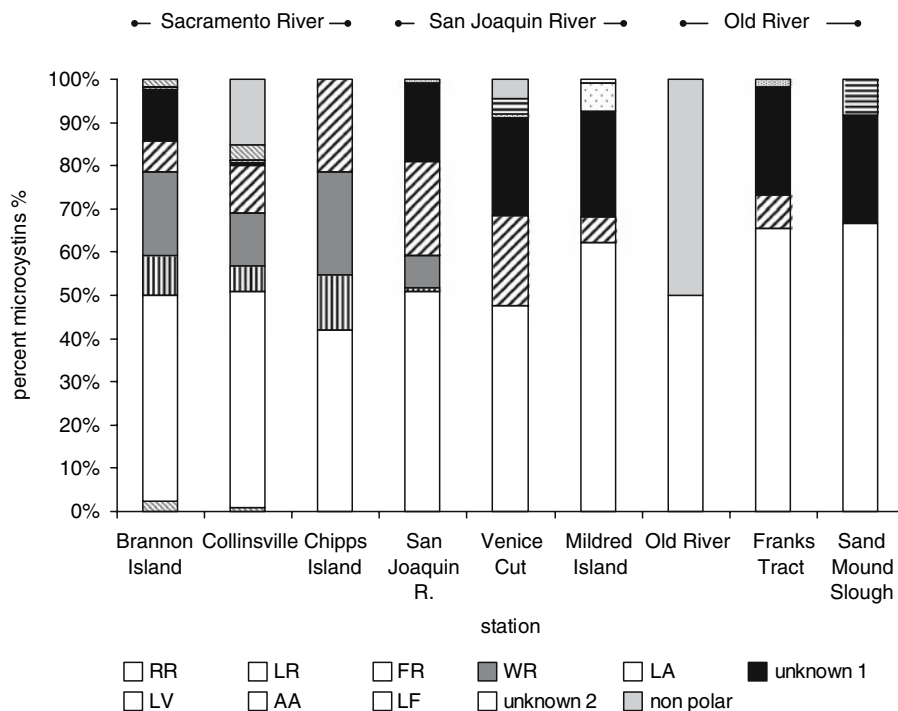
Microcystins concentration

Total microcystins concentration ranged from 0.01 ng l⁻¹ to 81 ng l⁻¹ in net tows and was 2-fold greater ($P < 0.05$) in SJR than the other rivers (Fig. 4). This contrasted with total microcystins concentration (chl *a*)⁻¹ which was 2-fold greater ($P < 0.05$) in SAC compared with SJR. Among

months, average total microcystins concentration was an order of magnitude greater ($P < 0.05$) in August and September for the whole estuary (12.64 ± 17.46 ng l⁻¹ and 0.85 ± 1.56 ng l⁻¹, respectively; Fig. 3), but the monthly pattern differed among rivers. Total microcystins concentration was greatest ($P < 0.05$) in August for SJR and September for SAC and was equally high in August and September for ODR. Total microcystins (chl *a*)⁻¹ did not differ among months for SAC and ODR but was greater ($P < 0.05$) in August for SJR.

A suite of 11 microcystins contributed to the spatial and temporal variation in total microcystins concentration (Fig. 5). Microcystin-LR comprised the greatest percent (54%) of the total microcystins at all stations followed by microcystin-unknown 1 (14%) and microcystin-LA (11%). The percent

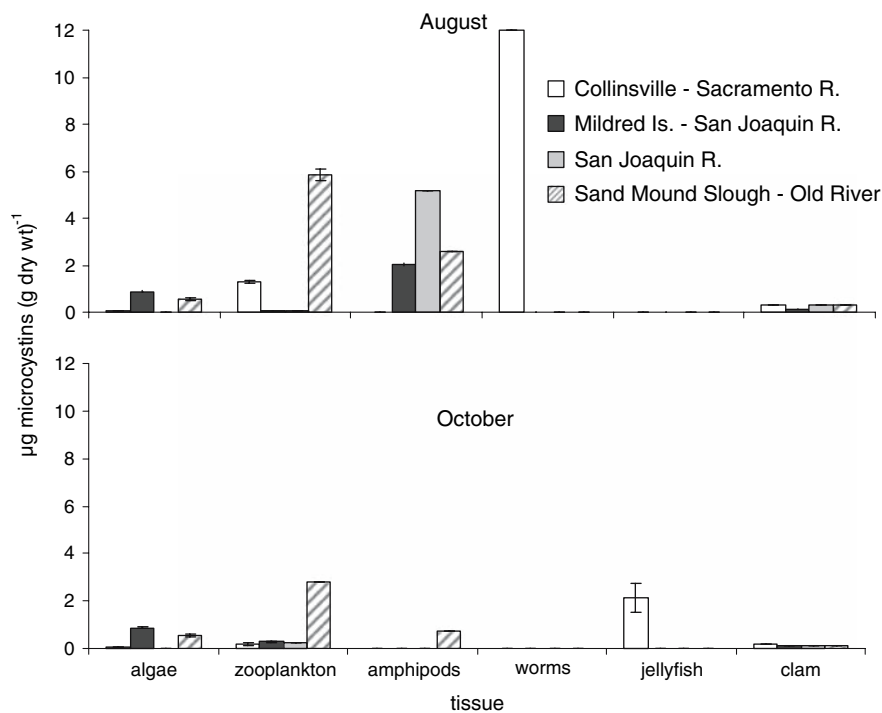
Fig. 5 Average percent composition of microcystin congeners in algal tissue between July and November 2004 in San Francisco Estuary



composition of most microcystins did not differ significantly among rivers, except for microcystin-FR and microcystin-WR which were an order of

magnitude greater ($P < 0.01$) in SAC and microcystin-LA which was at least 2-fold greater ($P < 0.05$) in SJR than ODR.

Fig. 6 Total microcystins concentration in algal and animal tissue at four stations in the San Francisco Estuary during August and October 2004



The microcystin composition was also seasonally variable among rivers. Microcystin-LA was greatest ($P < 0.05$) in July for SJR. Both microcystin-FR and microcystin-WR were greatest ($P < 0.05$) in October for SAC while microcystin-LR was greatest ($P < 0.05$) in October for SJR and ODR. Further, the number of microcystins present at the stations varied over the season with a larger average number ($P < 0.01$) of microcystins occurring between September and November (2.0 ± 1.4) than between July and August (1.3 ± 1.8).

The total microcystins in the tissues of lower food web animals was generally greater in August during the peak of the bloom and lowest in October during the decline of the bloom (Fig. 6). Total microcystins in animal tissue also varied widely among animals and was often higher in worms and amphipods than mesozooplankton (12 ± 0.00 , 2.62 ± 1.88 , 1.34 ± 2.05 μg microcystins (g dry wt.)⁻¹, respectively). However, average total microcystins concentration in mesozooplankton tissue (e.g. *Eurytemora affinis* and *Pseudodiaptomus forbesii*) was still 3–6 fold greater than in the algae (*Microcystis* and surface algae) and clam tissue (0.50 ± 0.37 and 0.21 ± 0.10 μg microcystins (g dry wt.)⁻¹, respectively). Among rivers, total microcystins concentration in mesozooplankton tissue appeared to be greater in ODR than SAC and SJR (5.8 ± 1.70 , $0.18 \pm .65$, 0.15 ± 11 μg microcystins (g dry wt.)⁻¹, respectively). A more quantitative statistical comparison of the spatial and

temporal variation in total microcystins content in animal tissue was precluded by small sample size; two samples per animal type per station.

Environmental factors

Chl *a* concentration and *Microcystis* cell density varied with physical and chemical conditions among rivers. The greatest chl *a* concentration and cell density occurred in SJR which had the lowest chloride, low total suspended solids and soluble reactive phosphorus concentration and high nitrate concentration (Table 2). The second highest chl *a* concentration and cell density occurred in ODR which like SJR had low chloride and total suspended solids concentration, but also had relatively low nitrogen and phosphorus concentration and high specific conductance. SAC with the greatest total microcystins concentration (chl *a*)⁻¹ had the highest chloride, total suspended solids and dissolved nitrogen and phosphorus concentration and the lowest specific conductance among rivers. These differences in chemical conditions were accompanied by differences in streamflow which was an order of magnitude greater ($P < 0.05$) for SAC than SJR. Water temperature was not significantly different among rivers.

Microcystis growth rate in the euphotic zone also varied with physical and chemical conditions. GP_{ez}

Table 2 Mean and standard deviation of physical and chemical variables measured for the Sacramento, San Joaquin and Old Rivers between July and November 2004

Variable	Sacramento River	San Joaquin River	Old River	Significance at $P < 0.05$ level
Chloride (mg l ⁻¹)	1259.81 ± 1175.95	34.91 ± 21.21	121.54 ± 48.64	1, 2, 3
Specific conductance (μS cm ⁻¹)	4.18 ± 3.72	66.25 ± 126.24	123.92 ± 261.17	1&2, 2&3
Secchi disk depth (cm)	60.67 ± 20.50	129.37 ± 37.66	139.73 ± 26.29	1, 2, 3
Total suspended solids (mg l ⁻¹)	20.60 ± 11.14	3.80 ± 2.06	3.79 ± 1.75	1&2, 1&3
Water temperature (°C)	19.84 ± 2.83	21.03 ± 3.68	20.95 ± 3.52	None
Nitrate (mg l ⁻¹)	0.32 ± 0.07	0.36 ± 0.22	0.19 ± 0.10	1&3, 2&3
Ammonia (mg l ⁻¹)	0.06 ± 0.03	0.05 ± 0.04	0.02 ± 0.02	1, 2, 3
Total phosphorus (mg l ⁻¹)	0.10 ± 0.02	0.08 ± 0.03	0.06 ± 0.01	1, 2, 3
Soluble reactive phosphorus (mg l ⁻¹)	0.08 ± 0.09	0.05 ± 0.01	0.05 ± 0.01	1&2, 1&3
N:P molar ratio	12.19 ± 3.63	15.97 ± 7.49	9.25 ± 4.59	1&3, 2&3
S:N molar ratio	20.76 ± 4.88	24.07 ± 10.59	35.93 ± 13.89	1&3, 2&3

Significant differences between rivers at the $P < 0.05$ level are indicated by a comma

increased with water temperature ($r = 0.56$, $P < 0.01$) and decreased with specific conductance and chloride ($r = -0.49$, $P < 0.01$ and $r = -0.68$, $P < 0.01$, respectively). GP_{ez} was also correlated with streamflow but the direction of the correlation differed among rivers with a positive correlation for SAC ($r = 0.46$, $P < 0.01$) and a negative correlation for SJR ($r = -0.51$, $P < 0.01$). The difference in these correlations may be due to the correlation between streamflow, dissolved salts, and water temperature. Streamflow was positively correlated with water temperature and negatively correlated with specific conductance and chloride ($r = 0.70$, $P < 0.01$; $r = -0.45$, $P < 0.01$; $r = -0.30$, $P < 0.01$, respectively) in SAC. In contrast, streamflow was negatively correlated with water temperature and positively correlated with specific conductance in SJR ($r = -0.74$, $P < 0.01$ and $r = 0.32$, $P < 0.01$). The streamflow pattern also differed between SAC and SJR with consistently low streamflow ($P < 0.05$) in SJR, but a gradual decrease in streamflow ($P < 0.05$) over the bloom season in SAC. GP_{ez} was also negatively correlated with total irradiance in the euphotic zone as suggested by the negative correlation between GP_{ez} and Secchi disk depth ($r = -0.24$, $P < 0.05$). This contrasted with the negative correlation between total suspended solids or dissolved solids and GP_{ez} ($r = -0.35$, $P < 0.01$ and $r = -0.67$, $P < 0.01$, respectively). GP_{ez} was also negatively correlated ($P < 0.05$) with ammonium, nitrate and soluble reactive phosphorus concentration and the N:P ratio. Nutrient concentration (Table 2) remained above limiting values for dissolved inorganic nitrogen, soluble reactive phosphorus and silica of 0.02 mg l^{-1} , 0.002 mg l^{-1} and 0.15 mg l^{-1} , respectively (Jassby, 2005). Average N:P ratios were also less than 16 between July and November and less than 10 during the peak of the bloom in August and September.

Canonical correlation analysis

Microcystis cell density was strongly correlated with streamflow and water temperature in canonical correlation analysis. Eleven water quality and seven streamflow variables that were significantly ($P < 0.05$) correlated with *Microcystis* cell density were included in the canonical correlation analysis

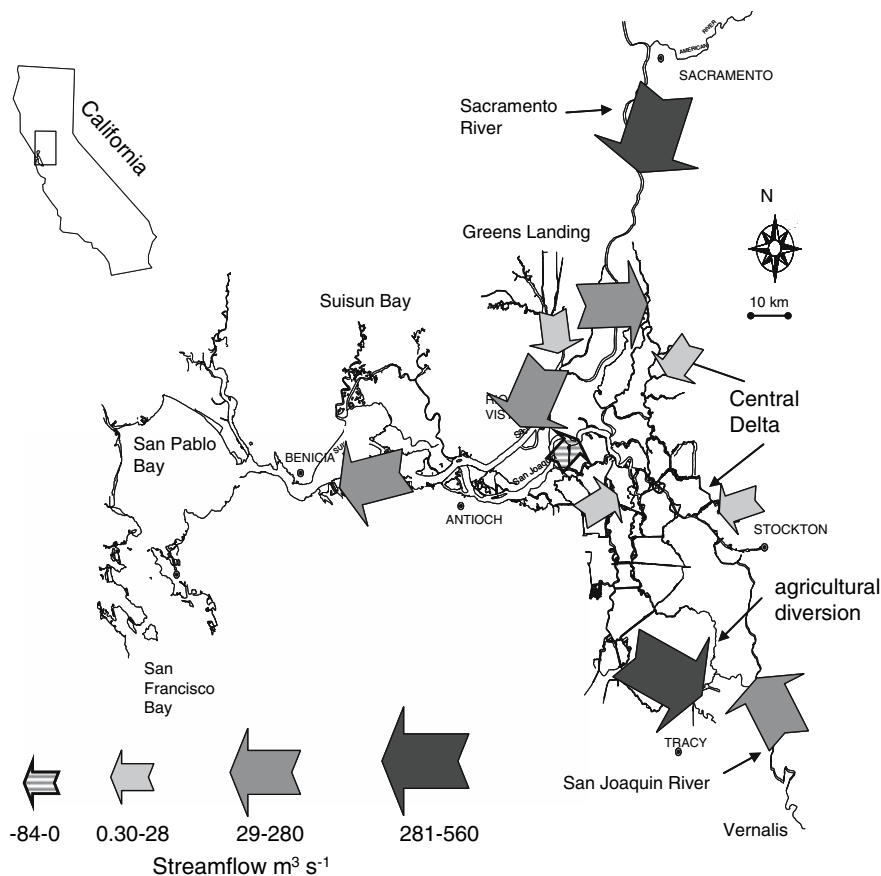
Table 3 Standardized coefficients for variables on the first significant canonical environmental variable computed by canonical correlation analysis to describe the variability of *Microcystis* cell density for data collected between July and November 2004

Variable	Standardized coefficient
<i>Microcystis cell density</i>	
East side streamflow	4.77
Contra Costa Canal pumping	1.31
Water temperature	1.04
Total dissolved solids	0.92
Silica:phosphorus molar ratio	0.48
Old River agricultural diversion	0.46
Total phosphorus	-0.05
Nitrate	-0.12
Ammonia	-0.17
Specific conductance	-0.21
N:P molar ratio	-0.43
Total suspended solids	-0.48
Miscellaneous agricultural diversions	-0.54
Chloride	-0.73
Si:N molar ratio	-0.78
Mokelumne River streamflow	-1.99
Sacramento River streamflow	-2.20
San Joaquin River streamflow	-3.03
Variance explained	59%

(Table 3). The canonical environmental variable created from these variables was significant and described 59% ($P < 0.01$) of the variation in *Microcystis* cell density between July and November. Standardized coefficients for each variable suggested high streamflow in the eastern delta, low streamflow in the SJR, SAC and MOKE, high water diversion near the city of Contra Costa and high water temperature accounted for most of the variability in cell density. However, correlation between individual environmental variables and the canonical environmental variable suggested water temperature ($r = 0.56$, $P < 0.01$), Si:N ratio ($r = -0.52$, $P < 0.01$), ammonium concentration ($r = -0.51$, $P < 0.01$) and streamflow in the MOKE and SJR ($r = -0.50$, $P < 0.01$ and $r = -0.45$, $P < 0.01$, respectively) contributed to the variance described by the canonical environmental variable.

The streamflow variables in the canonical analysis were correlated ($P < 0.05$) with a larger set of measured and computed streamflow variables

Fig. 7 Map of San Francisco Estuary indicating the mean of selected streamflow variables for August and September 2004



available for the estuary including the Sacramento, Cosumnes, Mokelumne, and San Joaquin Rivers flow, east side tributary flow, Contra Costa, State Water Project and Central Valley Project water diversion flow and streamflow past Jersey Point, and Rio Vista (<http://www.iep.water.ca.gov>). When these streamflow variables were averaged over August and September, high *Microcystis* cell density coincided with relatively low streamflow in the central delta, high streamflow in SAC, moderate streamflow in SJR and reversed (upstream arrow) streamflow in the southern delta produced by high diversion flow (Fig. 7).

The correlation between environmental conditions and *Microcystis* cell density varied among rivers. In SJR, *Microcystis* cell density was positively correlated with MOKE streamflow ($r = 0.52$, $P < 0.01$) and negatively correlated with agricultural diversion near the city of Tracy and the N:P ratio ($r = -0.67$, $P < 0.01$; $r = -0.47$, $P < 0.05$). In ODR, *Microcystis* cell density was negatively correlated with

streamflow in the MOKE ($r = -0.52$, $P < 0.01$) and SJR ($r = -0.52$, $P < 0.01$) and positively correlated with water temperature ($r = 0.52$, $P < 0.01$) and Secchi disk depth ($r = 0.42$, $P < 0.05$). In SAC, *Microcystis* cell density was positively correlated with both water temperature ($r = 0.65$, $P < 0.01$) and Secchi disk depth ($r = 0.47$, $P < 0.05$).

Microcystis also occurred within a narrow range of environmental conditions. *Microcystis* cells first appeared when water temperature reached 20°C. *Microcystis* cells were present at total suspended solids concentrations between 100 mg l⁻¹ and 500 mg l⁻¹, specific conductance between 0.1 mS cm⁻¹ and 0.3 mS cm⁻¹, Si:N ratios between 20 and 50 and ammonium concentration between 0.01 mg l⁻¹ and 0.03 mg l⁻¹. *Microcystis* cells also occurred, when streamflow was 28.32–35.40 m³ s⁻¹ in SJR and 0.85–1.13 m³ s⁻¹ in MOKE.

Total microcystins concentration (cell)⁻¹ and total microcystins (chl *a*)⁻¹ were also strongly correlated with streamflow in separate canonical correlation

Table 4 Standardized coefficients for variables on the first significant canonical environmental variable computed by canonical correlation analysis to describe the variability of total microcystins (cell^{-1}) and total microcystins (chlorophyll a) $^{-1}$ for data collected between July and November 2004

	Standardized coefficient
<i>Microcystins (cell)$^{-1}$</i>	
East side streamflow	4.77
Contra Costa Canal pumping	1.31
Water temperature	1.04
Total dissolved solids	0.92
Silica:phosphate molar ratio	0.48
Old River agricultural diversion	0.46
Total phosphorus	-0.05
Nitrate	-0.12
Ammonia	-0.17
Variance explained	59%
<i>Microcystins (chlorophyll a)$^{-1}$</i>	
Specific conductance	-0.21
Nitrogen:phosphate molar ratio	-0.43
Total suspended solids	-0.48
Miscellaneous agricultural diversions	-0.54
Chloride	-0.73
Silica:nitrogen molar ratio	-0.78
Mokelumne River streamflow	-1.99
Sacramento River streamflow	-2.20
San Joaquin River streamflow	-3.03
Variance explained	32%

analyses (Table 4). Nine water quality and streamflow variables that were significantly ($P < 0.05$) correlated with total microcystins concentration (cell^{-1}) produced a significant ($P < 0.01$) canonical environmental variable that described 32% ($P < 0.01$) of the variation in total microcystins (cell^{-1}). Large standardized coefficients within the canonical environmental variable suggested east side streamflow, municipal water diversion at the city of Contra Costa and water temperature were positively correlated with microcystins concentration (cell^{-1}). A somewhat different set of nine water quality and streamflow variables were correlated with total microcystins (chl a) $^{-1}$. These variables described 59% ($P < 0.01$) of the variance in total microcystins concentration (chl a) $^{-1}$. Large standardized coefficients on the significant canonical environmental variable indicated total microcystins concentration (chl a) $^{-1}$ was greater at low streamflow in SJR, SAC, and MOKE.

Environmental constancy

Environmental variability may further influence the seasonal variation of *Microcystis* cell density and total microcystins concentration. *Microcystis* cell density was greater in August and September when the variance in daily streamflow was low ($P < 0.05$; Table 5). The greatest number of microcystins occurred in September and October ($P < 0.01$)

Table 5 Coefficients of variation computed for daily streamflow and water temperature between July and October for locations throughout the estuary

	Coefficient of variation			
	July (%)	August (%)	September (%)	October (%)
<i>Streamflow</i>				
San Joaquin River	9	10	6	36
Sacramento River	5	6	10	18
Mokelumne River	64	16	9	23
East streamflow	8	8	6	35
Agricultural diversion	5	6	10	17
Total agricultural export	12	5	8	21
Significantly different	*			*
<i>Water temperature</i>				
San Joaquin River	2	2	5	9
Sacramento River	2	2	5	9
Significantly different			*	*

Significant difference in variance at the $P < 0.01$ level are indicated by a star (*)

during the decline of the bloom when the variance in daily water temperature was highest ($P < 0.01$). The variance in daily water temperature was influenced by daily air temperature which were correlated at Stockton on the San Joaquin River ($r = 0.50$, $P < 0.01$, $n = 96$) and Rio Vista on the Sacramento River ($r = 0.56$, $P < 0.01$, $n = 97$) between July and November 2004.

Discussion

Distribution

Microcystis occurred throughout SFE from freshwater habitats in SJR and ODR to brackish water habitats in SAC during the summer and fall of 2004. *Microcystis* was probably more widely distributed than the 2004 study suggests because *Microcystis* cells were found as far seaward as Martinez in 2003 (see Fig. 1 for location; Lehman et al., 2005). The consistently higher *Microcystis* cell density in SJR and ODR compared with SAC suggests optimum conditions for *Microcystis* growth occurred in the central delta. It is unlikely that *Microcystis* grew outside of the freshwater habitats in the central delta where salinities are commonly less than 5 ppt (Lehman et al., 2005) because *Microcystis* does not grow at salinities above 7 ppt (Robson & Hamilton, 2003). Instead, *Microcystis* cells were probably transported from the central delta with streamflow, wind and tide to more brackish water habitats downstream where they might survive, but not grow (Pickney et al., 1997). Low cell density in SAC was probably a combination of dilution and cell death at high chloride. High salinity conditions encountered during seaward transport could cause *Microcystis* colonies to lyse, aggregate, and settle to the bottom in Chesapeake Bay (Sellner et al., 1988; Orr et al., 2004).

Microcystis cell density and chl *a* concentration peaked during the summer and fall between August and September in 2004. *Microcystis* cell density and biomass commonly peak during the summer and fall when they occur in freshwater lakes and reservoirs (Watson et al., 1997). *Microcystis* also occurs during the summer and fall in the low salinity regions of some estuaries including the Swan River estuary, Australia, the Los Platos Estuary, Brazil, and the Potomac and Neuse River estuaries in the USA

(Pearl, 1988; Robson & Hamilton 2003; Sellner et al., 1993; Yunes et al., 1996). In SFE, peak *Microcystis* chl *a* concentration and cell density in August and September were associated with high GP_{ez} and characterized by high P_m^B , α^B and low β^B . Warm water temperature during August and September may have contributed to high P_m^B which is correlated with high water temperature for *Microcystis* populations in lakes (Robarts & Zachary 1987). August and September are also characterized by high streamflow in SAC and low streamflow in SJR that promote the warm water temperature, low salinity and low specific conductance conditions associated with high GP_{ez} .

Total microcystins concentration was highest in SJR during August and September when *Microcystis* cell density and chl *a* concentration were high, but was poorly correlated with either. Total microcystins concentration and chl *a* concentration were also poorly correlated for the single-day survey conducted in SFE during October 2003 (Lehman et al., 2005). The lack of a correlation between total microcystins concentration and chl *a* concentration is common because cellular microcystins content is uncoupled from growth rate (Utkilen & Gjølme, 1992). Total microcystins concentration was probably influenced by the relative growth of *Microcystis* strains or “genotypes” that contain different kinds of microcystins as well as the direct influence of environmental conditions on microcystin formation in *Microcystis* cells or “chemotypes” (Ouellette et al., 2006). Significant differences in the microcystins composition in SJR and SAC suggest there were at least two different genotypes or chemotypes contributing to the total microcystins concentration.

The variation of total microcystins concentration suggested the potential toxicity of *Microcystis* was variable. Eleven microcystins varied by eight orders of magnitude during the bloom in SFE. This level of variation might not be unusual because it was similar to the variation measured for *Microcystis* blooms in German lakes and reservoirs where 14 microcystins varied by four orders of magnitude (Fastner et al., 1999). The potential toxicity of the *Microcystis* bloom in SFE was strongly influenced by the presence of the hepatotoxic microcystin-LR which comprised about 54% of the total microcystins. However, the full toxicity of the bloom depends on the remaining 46% of the microcystins for which a

little is known (Zurawell et al., 2004). It is likely that the potential toxicity of the microcystins in SAC was higher than the other rivers because it had the highest total microcystins ($\text{chl } a$)⁻¹.

Environmental factors

Streamflow was a major factor controlling *Microcystis* cell density in SFE and probably influenced development of the *Microcystis* bloom directly and indirectly through a suite of environmental conditions. Since *Microcystis* has a relatively slow growth rate, long water residence time is needed for biomass to accumulate (Reynolds, 1997). Low streamflow in the central delta region coupled with high GP_{ez} , $\text{P}_{\text{m}}^{\text{B}}$, and α^{B} in August and September probably facilitated accumulation of *Microcystis* cells in SFE. Accumulation rather than growth was supported by the similar GP_{ez} ($\text{chl } a$)⁻¹ among rivers. Flushing rate was also a key factor affecting the seasonal variation of *Microcystis* blooms in the Swan River Estuary and in the Neuse River estuary where *Microcystis* blooms only develop when streamflow is below 13–15 $\text{m}^3 \text{s}^{-1}$ (Christian et al., 1986; Robson & Hamilton, 2003). A streamflow threshold was similarly suggested for SFE where *Microcystis* only occurred when SJR streamflow was 28–32 $\text{m}^3 \text{s}^{-1}$.

Microcystis probably grew well in the shallow-flooded island habitats in the central delta region of SFE where low streamflow helps to keep vertical mixing low (Jacoby et al., 2000). Low vertical mixing enables *Microcystis* colonies to float to the surface of the water column where they out compete other phytoplankton for light (Huisman et al., 2004). Such an adaptation was probably important in SFE, where phytoplankton growth is light limited due to high suspended sediment concentration (Jassby et al., 2002) and may partially explain the negative correlation between *Microcystis* cell density and Secchi disk depth. Low vertical mixing in the central delta region may also enhance phytoplankton metabolic activity and cell viability which are reduced at high mixing rates (Huisman et al., 2004; Regel et al., 2004). Low vertical mixing in the central delta was suggested by abundant large 2–3 cm wide colonies in MI, a shallow-flooded island in the center of the delta and small 1-cm wide colonies in the middle of the fast

flowing and turbulent river channels where *Microcystis* cell density was low (Lehman, personal observation). Large colonies were shown to rapidly break apart under turbulent conditions in laboratory tests (O'Brien et al. 2004).

Microcystis cell density was also positively correlated with water temperature in SFE. *Microcystis* growth begins in early summer, when water temperature above 20°C stimulates esterase activity in vegetative cells on the surface of the sediment and ceases in the fall when water temperature declines to below 20°C (Latour et al., 2004). Water temperature similarly contributed to the seasonal pattern in *Microcystis* cell density in SFE where *Microcystis* cells only occurred above 20°C. Maximum $\text{chl } a$ concentration occurred during mid-summer when water temperature reached 25°C, but this may not represent maximum growth rate of *Microcystis* which was higher at 29–32°C in laboratory studies (Robarts & Zohary, 1987). Water temperature probably influenced the spatial and temporal variation in *Microcystis* cell density among rivers because it reached 20°C sooner in SJR and ODR than SAC.

The importance of water temperature for microcystin development was suggested by the large coefficient for water temperature on the canonical environmental variable in canonical correlation analysis for total microcystins (cell)⁻¹. In lab studies, total microcystins concentration varied more with water temperature than irradiance and was highest at 20–24°C (Van der Wethuizen & Eloff, 1985; Wiedner et al., 2003); water temperatures similar to those measured in SFE during mid-summer. Water temperature primarily influences total microcystins concentration through its impact on growth rate, because cellular microcystins are only produced during log-phase growth (Lyck, 2004). The greater total microcystins concentration during mid-summer in SFE may be influenced by the high $\text{P}_{\text{m}}^{\text{B}}$ and α^{B} during this time.

It is possible environmental variability contributed to the seasonal variation in *Microcystis* cell density and the quantity and quality of microcystins in SFE. $\text{Chl } a$ and total microcystins concentration peaked in August and September when the variance in streamflow was low. Low daily variance in streamflow may promote the accumulation of *Microcystis* cells and the growth of relatively few *Microcystis* genotypes. In contrast, the high daily variance of water

temperature in September and October may contribute to the increased number of microcystins in these months through differential growth and survival of *Microcystis* genotypes or chemotypes (Ouellette et al. 2006). Daily water temperature is linked to seasonal changes in air temperature with streamflow dominating water temperature early in the season at high streamflow and air temperature dominating water temperature late in the season at low streamflow. This impact is supported by decadal change in water temperature in SFE that was inversely correlated with streamflow and positively correlated with air temperature in SJR and SAC (Lehman, 2004).

Nutrient concentration was not a driving force for variation of the *Microcystis* bloom in SFE. The high nutrient concentrations in SFE were a necessary condition for initiation of the *Microcystis* bloom because *Microcystis* requires both high nitrogen and phosphorus concentration for growth (Paerl et al., 2001). However, the persistence and variation of the bloom was not nutrient driven because nutrient concentrations were consistently an order of magnitude greater than limiting values throughout the water column in SFE (Jassby 2005). Nutrient ratios are generally important for cyanobacterial bloom formation (Paerl et al., 2001) with *Microcystis* blooms occurring at an N:P ratio <15 (Jacoby et al. 2000). The average N:P ratio of 10 (range 6–10) in August and September was favorable for *Microcystis* growth in SFE. The lesser influence of nutrients on *Microcystis* cell density and total microcystins concentration was supported by the low coefficients for nutrient concentration and nutrient ratios in the canonical correlation analyses.

Food web impact

The spatial and temporal variation of *Microcystis* cells might affect the presence of toxic microcystins in the estuarine food web in SFE. The high concentration of total microcystins in lower food web organisms during the peak of the *Microcystis* bloom suggested there was a direct link between microcystins in algal tissue and microcystins in the tissue of aquatic animals. Microcystins concentration was also high in the tissue of food web animals during the peak of the bloom in central Alberta Lakes, Canada

(Kotak et al., 1996). Microcystins in zooplankton and other lower food web animals can occur from active and passive ingestion of algal tissue, even though *Microcystis* may not be selectively grazed (DeBernardi & Giussani, 1990; DeMott & Moxter, 1991; Sellner et al., 1993).

The greater microcystins concentration in animal than algal tissue suggested microcystins were transferred and perhaps biomagnified through the aquatic food web in SFE. Microcystins were also transferred through food web organisms in the Alberta Lakes, Canada, Lake IJsselmeer, the Netherlands and Lakes Rotoiti and Rotoehu in the Czech Republic (Kotak et al., 1996; Ibelings et al., 2005; Wood et al., 2006). Detritus feeders may be an important transfer agent of microcystins into the SFE food web because total microcystins concentrations were high in amphipod and worm tissue. Detrital grazers were also thought to be the primary pathway for the transfer of microcystins into the food web in Alberta lakes (Kotak et al., 1996). Unexpectedly, clams which fed directly on phytoplankton may not be an important source of microcystins to the food web in SFE. Clam tissue had the lowest total microcystins content among the animals tested in 2004 and low microcystins content compared with zooplankton tissue in 2003 (Lehman et al., 2005). Mollusks could accumulate microcystins, but tissue content is often low due to the rejection of *Microcystis* colonies or rapid depuration of toxins from tissue (Prepas et al. 1997).

The *Microcystis* bloom probably did not cause acute toxicity to aquatic food web organisms in SFE. Total microcystins concentration in zooplankton tissue was below the value of 10–18 $\mu\text{g (g dry wt.)}^{-1}$ associated with acute death in *Daphnia* during laboratory feeding studies (Rohrlack et al., 2005). However, even at low concentrations, *Microcystis* can affect zooplankton community structure and function by sublethal toxicity or non-toxin related factors such as feeding inhibition or providing phytoplankton food of poor quality or low digestibility (DeMott & Mueller-Navarra, 1997; Rohrlack et al., 2005). Further, dissolved microcystins released from lysed *Microcystis* cells at the end of the bloom are toxic and can reduce feeding success for zooplankton (Pietsch et al., 2001). Large zooplankton such as *Daphnia* are sensitive to dissolved microcystins and demonstrate reduced growth and fecundity in

the presence of *Microcystis* (Reinikainen et al., 1999). More information on these potential impacts are needed for SFE.

Management strategies

The worldwide impact of *Microcystis* blooms on ecosystem structure and function and human health through drinking water and recreation suggests the potential need for management of *Microcystis* populations in SFE (White et al., 2005). Because the spatial and temporal variability of *Microcystis* cell density and total microcystins concentration is high in SFE, management might require consideration of physical, chemical, and biological factors at both large and small spatial and temporal scales (Donaghay & Osborn, 1997). Although there are many management strategies for control of *Microcystis* and its toxins (Pearl et al., 2001), regulation of streamflow may be the most important for SFE. High streamflow would prevent accumulation of *Microcystis* biomass in stable backwater sloughs or shallow-flooded islands, where residence time is long and vertical mixing is low. High streamflow would also increase vertical mixing which decreases colony viability and the competitive advantage of *Microcystis* colonies to obtain light by floating on the surface of the water column (Huisman et al., 2004). Streamflow could further be managed to influence water quality conditions such as water temperature and salinity that initiate and sustain bloom biomass and affect microcystins concentration (Jacoby et al. 2000). A decline in the density and biomass of fish, zooplankton, mysid shrimp, and diatoms has left the food web in SFE vulnerable to any adverse impact so that even a small change in the impact of *Microcystis* and its associated toxins on the food web may be important for fishery production (Lehman, 2004; Sommer et al. 2007).

Conclusion

Microcystis and its associated toxin microcystin varied spatially and temporally over the bloom season in SFE. Significant differences in cell density and chl *a* concentration were associated with the *Microcystis* bloom among months, rivers and

stations. Differences in *Microcystis* cell density and total microcystins concentration per cell⁻¹ and microcystins concentration chl *a*⁻¹ were correlated with environmental conditions, particularly streamflow and water temperature. These environmental conditions were correlated with differences in areal growth rate within the euphotic zone and probably driven by high P_m^B and α^B during the peak of the bloom. The variation of the bloom and its associated toxin concentration is potentially important ecologically because total microcystins are present in the tissues of the lower food web animals, mesozooplankton, amphipods, worms, jellyfish and clams. Although the bloom contains hepatotoxic microcystins, the present concentrations are low and probably not acutely toxicity to food web animals. However, the higher concentration of total microcystins in some animals and higher total microcystins concentration in animal than algal tissue suggests biomagnification or accumulation could increase the impact of these toxins on the aquatic community.

Acknowledgments This research was funded by a special study grant from the Sacramento-San Joaquin Delta Interagency Ecological Program. Many people assisted with the field sampling, E. Santos, M. Dempsey, K. Gehrts, S. Philippart and K. Clark and phytoplankton analysis, M. Bentencourt.

References

- American Public Health Association, American Water Works Association, & Water Environment Association, 1998. *Standard Methods for the Examination of Water and Wastewater*. 20th edn. American Public Health Association, Washington, D.C., USA.
- Carmichael, W. W., 1995. Toxic *Microcystis* in the environment. In Watanabe, M. F., K. Harada, W. W. Carmichael & H. Fujiki (eds), *Toxic Microcystis*. CRC Press: New York, 1–12.
- Christian, R. R., W. L. Bryant Jr. & D. W. Stanley, 1986. The relationship between river flow and *Microcystis aeruginosa* blooms in the Neuse River, North Carolina. Water Resources Research Institute Report 223. North Carolina State University.
- De Bernaradi, R. & G. Giussani, 1990. Are blue-green algae a suitable food for zooplankton? An overview. *Hydrobiologia* 200/201: 29–41.
- DeMott, W. R. & F. Moxter, 1991. Foraging on cyanobacteria by copepods: responses to chemical defenses and resource abundance. *Ecology* 72: 1820–1834.
- DeMott, W. R. & D. C. Muller-Navarra, 1997. The importance of highly unsaturated fatty acids in zooplankton nutrition:

- evidence from experiments with *Daphnia*, a cyanobacterium and lipid emulsions. *Freshwater Biology* 38: 649–664.
- Donaghay, P. L. & T. R. Osborn, 1997. Toward a theory of biological-physical control of harmful algal bloom dynamics and impacts. *Limnology and Oceanography* 42: 1283–1296.
- Fastner, J., U. Neumann, B. Wirsing, J. Weckesser, C. Wiedner, B. Nixdorf & I. Chorus, 1999. Microcystins (hepatotoxic heptapeptides) in German fresh water bodies. *Environmental Toxicology* 14: 13–22.
- Federal Environmental Agency, 2005. Current approaches to cyanotoxin risk assessment, risk management, regulations in different countries. In Chorus, I. (ed.), Federal Environmental Agency, Berlin.
- Fulton, R. S. III & H. W. Paerl, 1987. Effects of colonial morphology on zooplankton utilization of algal resources during blue-green algal (*Microcystis aeruginosa*) blooms. *Limnology and Oceanography* 32: 634–644.
- Huisman, J., J. Sharples, J. M. Stroom, P. M. Visser, W. E. A. Kardinaal, J. M. H. Verspagen & B. Sommeijer, 2004. Changes in turbulent mixing shift competition for light between phytoplankton species. *Ecology* 85: 2960–2970.
- Ibelings, B. W., K. Bruning, J. de Jonge, K. Wolfstein, L. M. Dionisio Pires, J. Postma & T. Burger, 2005. Distribution of microcystins in a lake foodweb: no evidence for biomagnification. *Microbial Ecology* 49: 487–500.
- Jacoby, J. M., D. C. Collier, E. B. Welch, F. J. Hardy & M. Crayton, 2000. Environmental factors associated with a toxic bloom of *Microcystis aeruginosa*. *Canadian Journal of Fisheries and Aquatic Science* 57: 231–240.
- Jassby, A. D., 2005. Phytoplankton regulation in a eutrophic tidal river (San Joaquin River, California). *San Francisco Estuaries Watershed Science* 3: 1–2.
- Jassby, A. D., J. E. Cloern & B. E. Cole, 2002. Annual primary production: patterns and mechanisms of change in a nutrient-rich tidal ecosystem. *Limnology and Oceanography* 47: 698–712.
- Kotak, B. G., R. W. Zurawell, E. E. Prepas & C. F. B. Holmes, 1996. Microcystin-LR concentration in aquatic food web compartments from lakes of varying trophic status. *Canadian Journal of Fisheries and Aquatic Sciences* 53: 1974–1985.
- Latour, D., O. Sabido, M. Salençon & H. Giraudet, 2004. Dynamics and metabolic activity of the benthic cyanobacterium *Microcystis aeruginosa* in the Grangent reservoir (France). *Journal of Plankton Research* 26: 719–726.
- Lehman, P. W., 2004. The influence of climate on mechanistic pathways that impact lower food web production in northern San Francisco Bay estuary. *Estuaries* 27: 311–324.
- Lehman, P. W., G. Boyer, C. Hall, S. Waller & K. Gehrts, 2005. Distribution and toxicity of a new colonial *Microcystis aeruginosa* bloom in the San Francisco Bay Estuary, California. *Hydrobiologia* 541: 87–99.
- Lehman, P. W., T. Sommer & L. Rivard, 2007. The influence of floodplain habitat on the quantity and quality of riverine phytoplankton carbon produced during the flood season in San Francisco Estuary. *Aquatic Ecology*. DOI 10.1007/s10452-007-9102-6.
- Lyck, S., 2004. Simultaneous changes in cell quotas of microcystin, chlorophyll *a*, protein and carbohydrate during different growth phases of a batch culture experiment with *Microcystis aeruginosa*. *Journal of Plankton Research* 26: 727–736.
- Malbrouck, C. & P. Kestemont, 2006. Effects of microcystins on fish. *Environmental Toxicology and Chemistry* 25: 72–86.
- O'Brien, K. R., D. L. Meyer, A. M. Waite, G. N. Ivey & D. P. Hamilton, 2004. Disaggregation of *Microcystis aeruginosa* colonies under turbulent mixing: laboratory experiments in a grid-stirred tank. *Hydrobiologia* 519: 143–152.
- Orr, P. T., G. J. Jones & G. B. Douglas, 2004. Response of cultured *Microcystis aeruginosa* from the Swan River, Australia, to elevated salt concentration and consequences for bloom and toxin management in estuaries. *Marine and Freshwater Research* 55: 277–283.
- Ouellette, A. J., S. M. Handy & S. W. Wilhelm, 2006. Toxic *Microcystis* is widespread in Lake Erie: PCR detection of toxin genes and molecular characterization of associated cyanobacterial communities. *Microbial Ecology* 51: 154–165.
- Paerl, H. W., 1988. Nuisance phytoplankton blooms in coastal, estuarine and inland waters. *Limnology and Oceanography* 33: 823–847.
- Pearl, H. W., R. S. Fulton III, P. H. Moisaner & J. Dyble, 2001. Harmful freshwater algal blooms, with an emphasis on cyanobacteria. *The Scientific World* 1: 76–113.
- Pickney, J. L., D. F. Millie, B. T. Vinyard & H. W. Paerl, 1997. Environmental controls of phytoplankton bloom dynamics in the Neuse River Estuary, North Carolina, USA. *Canadian Journal of Fisheries and Aquatic Science* 54: 2491–2501.
- Pietsch, C., C. Wiegand, M. V. Ame, A. Nicklisch, D. Winderlin & S. Pflugmacher, 2001. The effects of cyanobacterial crude extract on different aquatic organisms: evidence for cyanobacterial toxin modulating factors. *Environmental Toxicology* 16: 535–542.
- Prepas, E. E., B. G. Kotak, L. M. Campbell, J. C. Evans, S. E. Hruday & C. F. B. Holmes, 1997. Accumulation and elimination of cyanobacterial hepatotoxins by the freshwater clam *Anodonta grandis simpsoniana*. *Canadian Journal of Fisheries and Aquatic Sciences* 54: 41–46.
- Regel, R. H., J. D. Brookes, G. G. Ganf & R. W. Griffiths, 2004. The influence of experimentally generated turbulence on the Mash01 unicellular *Microcystis aeruginosa* strain. *Hydrobiologia* 517: 107–120.
- Reinikainen, M., J. Hietala & M. Walls, 1999. Reproductive allocation in *Daphnia* exposed to toxic cyanobacteria. *Journal of Plankton Research* 21: 1553–1564.
- Reynolds, C. S., 1997. Vegetation processes in the pelagic: a model for ecosystem theory. In O. Kinne (ed.), *Excellence in Ecology*. Ecology Institute, Germany.
- Robarts, R. D. & T. Zohary, 1987. Temperature effects on photosynthetic capacity, respiration, and growth rates of bloom-forming cyanobacteria. *New Zealand Journal of Marine and Freshwater Research* 21: 391–399.
- Robson, B. J. & D. P. Hamilton, 2003. Summer flow event induces a cyanobacterial bloom in a seasonal Western

- Australia estuary. *Marine and Freshwater Research* 54: 139–151.
- Rocha, C., H. Galvão & A. Barbosa, 2002. Role of transient silicon limitation in the development of cyanobacteria blooms in the Guadiana estuary, south-western Iberia. *Marine Ecology Progress Series* 228: 35–45.
- Rohrlack, T., K. Christoffersen, E. Dittmann, I. Nogueira, V. Vasconcelos & T. Borner, 2005. Ingestion of microcystins by *Daphnia*: intestinal uptake and toxic effects. *Limnology and Oceanography* 50: 440–448.
- SAS Institute, Inc., 2004. SAS/STAT User's Guide, Version 8. SAS Institute Inc., SAS Campus Drive, Cary, North Carolina, USA.
- Sedmak, B. & T. Elerseck, 2005. Microcystins induce morphological and physiological changes in selected representative phytoplanktons. *Microbial Ecology* 51: 508–515.
- Sellner, K. G., D. C. Brownlee, M. H. Bundy, S. G. Brownlee & K. R. Braun, 1993. Zooplankton grazing in a Potomac River cyanobacteria bloom. *Estuaries* 16: 859–872.
- Sellner, K. G., R. V. Lacouture & K. G. Parlish, 1988. Effect of increasing salinity on a cyanobacteria bloom in the Potomac River Estuary. *Journal of Plankton Research* 10: 49–61.
- Shapiro, J., 1990. Current beliefs regarding dominance of blue-greens: the case for the importance of CO₂ and pH. *Verhandlungen der Internationalen Vereinigung für Theoretische und Angewandte Limnologie* 24: 38–54.
- Smith, A. D. & J. J. Gilbert, 1995. Relative susceptibilities of rotifers and cladocerans to *Microcystis aeruginosa*. *Archiv für Hydrobiologie* 132: 309–336.
- Sommer, T. R. & others, 2007. The collapse of pelagic fishes in the upper San Francisco Estuary. *Fisheries* 32: 270–277.
- United States Environmental Protection Agency (US EPA), 1983. Methods for chemical analysis of water and wastes. Washington, DC. Technical Report EPA-600/4-79-020.
- United States Geological Survey (USGS), 1985. Methods for determination of inorganic substances in water and fluvial sediments. United States Geological Survey. Open file report 85-495.
- Utermöhl, H., 1958. Zur Vervollkommnung der quantitativen Phytoplankton-methodik. *Mitteilungen Internationale Vereinigung für Theoretische und Angewandte Limnologie* 9: 1–38.
- Utkilen, H. & N. Gjørlme, 1992. Toxin production by *Microcystis aeruginosa* as a function of light in continuous cultures and its ecological significance. *Applied and Environmental Microbiology*, 58: 1321–1325.
- Van der Westhuizen, A. J. & J. N. Eloff, 1985. Effect of temperature and light on the toxicity and growth of the blue-green alga *Microcystis aeruginosa* (UV-006)*. *Planta* 163: 55–59.
- Vollenweider, R. A., 1974. A Manual on methods for measuring primary production in aquatic environments. International Biological program handbook 12. Balckwell Scientific Publications, Oxford.
- Watson, S. B., E. McCauley & J. A. Downing, 1997. Patterns in phytoplankton taxonomic composition across temperate lakes of differing nutrient status. *Limnology and Oceanography* 42: 487–495.
- White, S. H., L. J. Duivenvoorden & L. D. Fabbro, 2005. A decision-making framework for ecological impacts associated with the accumulation of cyanotoxins (cylindrospermopsin and microcystin). *Lakes and Reservoirs: Research and Management* 10: 25–37.
- Wiedner, C., P. M. Visser, J. Fastner, J. S. Metcalf, G. A. Codd & L. R. Mur, 2003. Effects of light on the microcystin content of *Microcystis* strain PCC 7806. *Applied and Environmental Microbiology* 69: 1475–1481.
- Wood, S. A., L. R. Briggs, J. Sprosen, J. G. Ruck, R. G. Wear, P. T. Holland & M. Bloxham, 2006. Changes in concentrations of microcystins in rainbow trout, freshwater mussels and cyanobacteria in Lakes Rotoiti and Totoehu. *Environmental Toxicology* 21: 205–222.
- Yunes, J. S., P. S. Salomon, A. Matthiensen, K. A. Beattie, S. L. Raggett & G. A. Codd, 1996. Toxic blooms of cyanobacteria in the Patos Lagoon Estuary, southern Brazil. *Journal of Aquatic Ecosystem Health* 5: 223–229.
- Zurawell, R. W., H. Chen, J. M. Burke & E. E. Prepas, 2004. Hepatotoxic cyanobacteria: a review of the biological importance of microcystins in freshwater environments. *Journal of Toxicology and Environmental Health* 8: 1–37.

Initial impacts of *Microcystis aeruginosa* blooms on the aquatic food web in the San Francisco Estuary

P. W. Lehman · S. J. Teh · G. L. Boyer ·
M. L. Nobriga · E. Bass · C. Hogle

Received: 11 May 2009 / Revised: 10 November 2009 / Accepted: 16 November 2009
© The Author(s) 2009. This article is published with open access at Springerlink.com

Abstract The impact of the toxic cyanobacterium *Microcystis aeruginosa* on estuarine food web production in San Francisco Estuary is unknown. It is hypothesized that *Microcystis* contributed to a recent decline in pelagic organisms directly through its toxicity or indirectly through its impact on the food web after 1999. In order to evaluate this hypothesis, phytoplankton, cyanobacteria, zooplankton, and fish were collected biweekly at stations throughout the estuary in 2005. Concentrations of the tumor-promoting *Microcystis* toxin, microcystin, were measured in water, plankton, zooplankton, and fish by a protein phosphatase inhibition assay, and fish health was assessed by histopathology. *Microcystis* abundance

was elevated in the surface layer of the western and central delta and reached a maximum of 32×10^9 cells l^{-1} at Old River in August. Its distribution across the estuary was correlated with a suite of phytoplankton and cyanobacteria species in the surface layer and 1 m depth including *Aphanizomenon* spp., *Aulacoseira granulata*, *Bacillaria paradoxa*, *Rhodomonas* spp., and *Cryptomonas* spp. Shifts in the phytoplankton community composition coincided with a decrease in the percentage of diatom and green algal carbon and increase in the percentage of cryptophyte carbon at 1 m depth. Maximum calanoid and cyclopoid copepod carbon coincided with elevated *Microcystis* abundance, but it was accompanied by a low cladocera to calanoid copepod ratio. Total microcystins were present at all levels of the food web and the greater total microcystins concentration in striped bass than their prey suggested toxins accumulated at higher trophic levels. Histopathology of fish liver tissue suggested the health of two common fish in the estuary, striped bass (*Morone saxatilis*), and Mississippi silversides (*Menidia audens*), was impacted by tumor-promoting substances, particularly at stations where total microcystins concentration was elevated. This study suggests that even at low abundance, *Microcystis* may impact estuarine fishery production through toxic and food web impacts at multiple trophic levels.

Handling editor: D. P. Hamilton

P. W. Lehman (✉) · E. Bass · C. Hogle
Division of Environmental Services, California
Department of Water Resources, Sacramento,
CA 95691, USA
e-mail: plehman@water.ca.gov

S. J. Teh
Department of Veterinary Medicine, University
of California, Davis, CA 95616, USA

G. L. Boyer
College of Environmental Science and Forestry, State
University of New York, Syracuse, NY 13210, USA

M. L. Nobriga
Water Branch, California Department of Fish and Game,
Sacramento, CA 95811, USA

Keywords *Microcystis* · Phytoplankton
species composition · Fish histopathology ·

Food web · Microcystins · Cyanobacteria ·
Protein phosphate inhibition assay

Introduction

Microcystis aeruginosa (*Microcystis*) is a cyanobacterium species that can form harmful algal blooms (CHAB) in freshwater water bodies world wide (Chorus, 2005). Its distribution has spread into some estuaries including the Chesapeake Bay, the San Francisco Bay, and the Neuse River in the USA, the Swan River in Australia, and the Guadiana River in Spain and Portugal (Paerl, 1988; Sellner et al., 1988; Rocha et al., 2002; Robson & Hamilton, 2003, 2004; Lehman et al., 2005). *Microcystis* is considered a toxic CHAB because some species contain powerful hepatotoxins called microcystins that initiate cancer and promote tumor formation in the liver of humans and wildlife (Zegura et al., 2003; International Agency for Research on Cancer, 2006; Ibelings & Havens, 2008). It also produces a surface scum that impedes recreation, reduce aesthetics, lower dissolved oxygen concentration, and cause taste and odor problems in drinking water (Paerl et al., 2001). *Microcystis* and other freshwater cyanobacteria blooms are currently a worldwide concern because their frequency and distribution are increasing (Fristachi et al., 2008). Although the potential impact of *Microcystis* blooms on human health is known, its potential impact on the structure and function of aquatic food webs is poorly understood (Ibelings & Havens, 2008).

Microcystis can affect phytoplankton community composition through allelopathy (Legrand et al., 2003). Cyanobacteria produce a large array of metabolites including organic and amino acids, peptides, alkaloids, carbohydrates, and lipopolysaccharides that can affect higher trophic levels (Paerl et al., 2001; Smith et al., 2008). Differential response of phytoplankton and cyanobacteria (plankton) to these allelopathic substances affects plankton community composition and species diversity in laboratory cultures (Sedmak & Kosi, 1998; Suikkanen et al., 2005). In nature, the response of the plankton community is variable and probably depends on environmental conditions (Graneli et al., 2008), but the full impact of *Microcystis* on plankton communities in the field is poorly understood.

Many studies have demonstrated the effect of *Microcystis* or its toxins on zooplankton growth and survival. Microcystins either in zooplankton food or dissolved in the water column affect survival and growth rate of copepods, cladocera, and rotifers (Ghadouani et al., 2006; Federico et al., 2007). Secondary metabolites such as lipopolysaccharides in some non-toxic *Microcystis* strains can also inhibit zooplankton growth (Rohrlack et al., 2001, 2005). The greatest impact of *Microcystis* on natural zooplankton populations may be its poor food quality (Wilson et al., 2006). Low concentrations of polyunsaturated and saturated fatty acids compared with other plankton make *Microcystis* a nutritionally poor quality food (Müller-Navarra et al., 2000). The large diameter of the *Microcystis* colonies also makes them difficult to ingest, may physically clog feeding appendages and increase food rejection rate (Ghadouani et al., 2004). In addition, the presence of *Microcystis* in the water column and associated production of protease inhibitors may inhibit feeding in some zooplankton (Agrawai et al., 2001; Ferrão-Filho et al., 2002). Some or all of these factors may explain field and laboratory research which suggests *Microcystis* alters zooplankton community structure and total biomass by reducing the growth and survival of zooplankton, especially large (>1 mm) cladocerans like *Daphnia* (Ghadouani et al. 2006; Chen et al., 2007). The response of the zooplankton community to *Microcystis* is complex and depends on a variety of factors including season, length of exposure, and the *Microcystis* strain and how these interact with the fitness of each zooplankton species (Gustafsson & Hansson, 2004; Wilson & Hay, 2007).

At higher trophic levels, *Microcystis* blooms affect fish health through impacts on growth rate, histopathology, and behavior (Malbrouck & Kestemont, 2006). Microcystin enters the fish gut passively during swimming or actively through food intake, and accumulates in fish tissue (De Magalhães et al., 2001). Microcystin slows protein synthesis by inhibiting protein phosphatase 1 and 2A and promotes tumor formation and cancer in fish tissue (Fischer & Dietrich, 2000; van der Oost et al., 2003). Microcystin can increase heart rate and produce osmoregulatory imbalance by stimulating drinking in adults which makes fish more susceptible to toxins in the environment, including microcystin (Best et al., 2001, 2003). Recent research suggests microcystins also cause

oxidative stress in fish by reducing the production of antioxidants and increasing lipid peroxidation in liver, kidney, and gill tissue (Bláha et al. 2004; Prieto et al., 2007). The lipopolysaccharides in *Microcystis* cells further decrease antioxidant formation in fish and may be more toxic than microcystin (Best et al., 2002). At a population level, *Microcystis* causes effects such as mortality and delayed hatching in fish embryos or may simply affect feeding rate (Malbrouck & Kestemont, 2006; Palíková et al., 2007).

Microcystis blooms are a fairly recent occurrence in San Francisco Estuary (SFE), and were first observed in the delta region in 1999 (Lehman et al., 2005). The population level during the summer bloom period is relatively low when compared with many *Microcystis* blooms worldwide which form a dense scum on the surface of the water column (Lehman et al., 2008). It is unknown, if this bloom is still in its initial stage of establishment, or has reached maximum abundance. Recent genetic studies indicate the *Microcystis* strain in SFE is genetically different from known strains (Moisander et al., 2009). However, the coincident appearance of *Microcystis* and a decline in a number of fish and zooplankton species of concern including delta smelt (*Hypomesus transpacificus*), striped bass (*Morone saxatilis*), and threadfin shad (*Dorosoma petenense*) and their calanoid copepod prey *Eurytemora affinis* and *Pseudodiaptomus forbesii* in the freshwater regions of the estuary suggest that there is a link between the fishery decline and the presence of *Microcystis* in the estuary since 2000 (Sommer et al., 2007). Research on *Microcystis* in 2003 and 2004 confirmed the presence of toxic microcystins in plankton and zooplankton in SFE (Lehman et al., 2005, 2008). We hypothesize that *Microcystis* directly or indirectly contributed to the decline in fish and zooplankton species of concern through toxicity or impacts on the food web.

The purpose of this study was to utilize a combination of plankton, zooplankton, and fish community composition, tissue microcystins concentration, and histopathology to determine if *Microcystis* may have influenced the production or health of organisms in the estuarine food web in 2005. Such information is invaluable for developing strategies to manage future estuarine food web resources impacted by this toxic cyanobacterium. It may also assist with developing a more comprehensive understanding of the factors that contributed to the decline in pelagic organisms and

increase in *Microcystis* blooms in SFE since 2000 (Lehman et al., 2005; Sommer et al., 2007).

Materials and methods

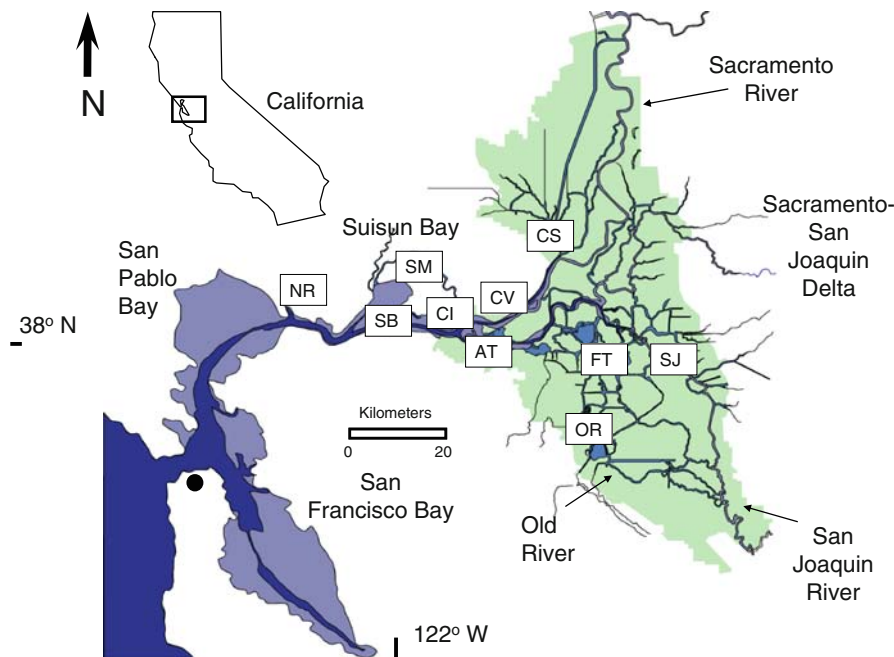
Study area

San Francisco Estuary (SFE) consists of an inland delta that flows into a chain of downstream marine bays—Suisun, San Pablo, and San Francisco—and creates one of the largest estuaries on the west coast of North America (Fig. 1). The Sacramento River on the north and the San Joaquin River on the south converge just east of Suisun Bay to form a delta that contains 200 km² of waterways. The Sacramento River is the largest of the rivers that feed the delta, and has an average discharge of $498 \pm 21 \text{ m}^3 \text{ s}^{-1}$ compared with $70 \pm 7 \text{ m}^3 \text{ s}^{-1}$ for the San Joaquin River over the August and September period of this study. The delta has many kinds of habitats from shallow flooded islands that are 2 m deep to wide and deep river channels that are 13 m deep. Flow in the delta is influenced by tides that reach 2 m in depth, tidal velocities up to 30 cm s^{-1} and tidal excursions of up to 10 km. The delta is largely rural with a population of about 500,000 people within the cities of Sacramento, Stockton, and West Sacramento. Most of the 1,300 km of sloughs and 57 islands in the delta are used for agriculture and wildlife habitat.

Field sampling

Chlorophyll *a* and total microcystins concentration plus a suite of water quality conditions were sampled biweekly at each station between August 1 and September 30, 2005 at 10 stations throughout the freshwater to brackish water reaches of SFE (Fig. 1). Stations were selected that reflected different habitats within the delta including the brackish water habitat in Suisun Bay at Chipps Island (CI) and Middle Ground (SB), saltwater marsh habitat at Montezuma Slough (SM), freshwater habitat in the Sacramento River at Cache Slough (CS), the San Joaquin River at Turner Cut (SJ) and Old River near Ranch del Rio (OR), brackish water habitat in the Sacramento River at Collinsville (CV) and the San Joaquin River at

Fig. 1 Map of San Francisco estuary showing codes for sampling stations for Napa River (NR) at the City of Napa, Suisun Bay at Middle Ground (SB), Suisun Marsh at Montezuma Slough (SM), Chipps Island (CI), Sacramento River at Collinsville (CV) and Cache Slough (CV), Old River at Franks Tract (FT) and Ranch del Rio (OR), and San Joaquin River at Turner Cut (SJ) and Antioch (AT)



Antioch (AT), and flooded island habitat in Old River at Franks Tract (FT). A station was added in the Napa River (NR) outside of the delta which did not have a *Microcystis* bloom for perspective.

Microcystis colonies in the surface layer were sampled by horizontal surface tows of a 0.5 m diameter plankton net with 75 μm mesh netting as described in Lehman et al. (2005). Water samples containing plankton biomass were stored at 4°C and filtered within 2 h onto Millipore APFF glass fiber filters. Filters for microcystins analysis were folded, wrapped in aluminum foil, frozen, and stored at -80°C until laboratory analysis for toxin content. Filters for chlorophyll *a* analysis were preserved with 1 ml of saturated magnesium carbonate solution, immediately frozen and stored at -14°C until analysis for pigment content.

Pigments were extracted from glass fiber filters in 90% acetone and analyzed for chlorophyll *a* (corrected for phaeophytin) and phaeophytin using spectrophotometry (American Public Health Association et al., 1998). Water samples for identification and enumeration of plankton were preserved and stained with Lugol's iodine solution, and phytoplankton were counted at $\times 700$ using an inverted microscope technique (Utermöhl, 1958). This magnification allowed clear identification of plankton cells $>6 \mu\text{m}$ in diameter. Phytoplankton species were identified by taxonomic

descriptions in *Freshwater Algae of North America, Ecology, and Classification* (Wehr & Sheath, 2003) and *Cyanoprokaryota 1, Teil: Chroococcales* (Komárek & Anagnostidis, 2001). *Microcystis aeruginosa* was identified as the only *Microcystis* species in each sample. Plankton cell carbon was calculated from cell volume computed from cell dimensions applied to simple geometrical shapes with correction for the small plasma volume in diatom cells (Menden-Deuer & Lessard, 2000).

Water quality conditions were determined from laboratory analysis of water collected near the surface using a van Dorn bottle sampler. Water samples for chloride, alkalinity, ammonium-N, nitrate-N plus nitrite-N, soluble reactive phosphorus, and silicate concentration were filtered through 0.45 μm pore size Millipore HATF04700 nucleopore filters. Water samples for dissolved organic carbon were filtered through Millipore APFF glass fiber filters. Filtered and raw water samples were either stored at 4°C or -14°C until analysis for nutrients (United States Environmental Protection Agency, 1983; United States Geological Survey, 1985) or dissolved microcystins analysis. Total suspended solids, total and dissolved organic carbon concentration, and alkalinity were determined by standard methods (American Public Health Association et al., 1998). Water temperature, pH, specific conductance, and dissolved oxygen were measured

near the surface using a Yellow Springs Instrument (YSI) 6600 water quality sonde.

Zooplankton were collected at each station by a 3 min diagonal tow of a 0.5 m diameter plankton net fitted with a 150 μm mesh netting. Zooplankton were kept at 4°C and separated by pipette from *Microcystis* in the water sample using a dissecting microscope within 48 h of sampling. Zooplankton tissue was rinsed in distilled water and frozen at -80°C until toxin analysis. Zooplankton for identification and enumeration were dyed and preserved in 10% buffered formalin with rose bengal dye. Species identification and enumeration were conducted using a dissecting scope.

Juvenile striped bass (*Morone saxatilis*) and Mississippi silversides (*Menidia audens*) were collected at beaches near the edge of channels adjacent to the open water sampling station. Juvenile striped bass and Mississippi silversides were selected for this study because they occur throughout the estuary and prey on mesozooplankton and amphipods that may use *Microcystis* as a food source. Fish were sampled using a 30 \times 1.8 m, 3.2 mm mesh beach seine. Sampling consisted of 2–8 hauls per station during flood tide when beaches were covered in water. Fish 30–300 mm were most vulnerable to this beach seine sampling technique (Nobriga et al., 2005). Live striped bass and Mississippi silversides were immediately placed in a cooler with river water, aerated with a stone aerator, and transported to a nearby laboratory boat for dissection. Only live fish were dissected for tissue analysis. Juvenile striped bass were not collected in sufficient quantity for analysis at FT and OR.

Fish were decapitated, and liver and muscle were surgically removed from each fish in less than 1 h after collection. The liver tissue of each fish was partitioned into two samples: one for analysis of total microcystins content and one for histopathology. For total microcystins analysis, tissue was wrapped in aluminum foil, flash frozen with liquid nitrogen and kept frozen at -80°C until analysis. Tissue samples for histopathological analysis were stored at room temperature in 10% neutral buffered formalin. Because the fish were small (typically <100 mm long), liver and muscle tissues from multiple striped bass were combined to get sufficient tissue for microcystins analysis. Mississippi silversides were so small that liver and muscle tissue could not be separated.

Microcystins analysis

Filters with plankton tissue for total microcystins analysis were extracted by sonication with 10 ml of 50% methanol containing 1% acetic acid, clarified by centrifugation, and the extract used for toxic microcystins analysis using the protein phosphatase inhibition assay (PPIA) technique, while anatoxin-a in plankton samples was measured by HPLC as described in Lehman et al. (2005). Dissolved microcystin concentration was computed as the difference between whole water and plankton tissue concentrations.

The toxic microcystins concentration in fish tissue was determined from lyophilized tissue (0.1 g dw liver or 0.6 g dw muscle) that was extracted with 50% methanol (MeOH) containing 1% acetic acid (HOAc) at a ratio of 10 ml solvent: 1 g dw tissue. The tissue was homogenized using a Biospec tissue tearor at 5,000–10,000 rpm for 1 min and then centrifuged at 3,000 rpm for 10 min. The supernatant was transferred to a glass tube, and the particulate material was re-extracted with the same volume of solvent. The pooled supernatants were taken to dryness in vacuo and resuspended in 1 ml of acidified 50% MeOH. PPIA was used to determine the total concentration of free microcystins, expressed as microcystin-LR equivalents, in the fish tissue. The PPIA method used for fish tissue was the same as that used for plankton and zooplankton tissue described above. The recovery of free microcystins in fish tissue was determined using an internal standard, [S-propyl-cys⁷] microcystin-LR, synthesized from microcystin-LR (Smith & Boyer, 2009).

Histopathology

Histopathological analysis was conducted on fish liver tissue following the methods of Teh et al. (2004). After 48 h in 10% neutral buffered formalin, tissues were dehydrated in a graded ethanol series and embedded in a paraffin block. For each tissue block, serial sections (4 μm thick) were cut and stained with hematoxylin and eosin. Tissue sections were examined under a BH-2 Olympus microscope for common and/or significant lesions.

Tissues were screened and scored on an ordinal ranking system for a variety of histopathological features and lesions (0 = none/minimal, 1 = mild, 2 = moderate, and 3 = severe; and 0 = not present or

infrequently observed, 1 = mildly affected in <10% of the tissue, 2 = moderately affected in 10–50% of the tissue, and 3 = severely affected in greater than 50% of the tissue, respectively). Due to the importance of the number of preneoplastic foci and tumors in the progression of fish hepatocarcinogenesis, basophil preneoplastic focus and hepatocellular adenoma lesions were enumerated rather than scored by severity.

Seven characteristics of the liver lesions were scored to identify toxic exposure in fish: glycogen depletion, eosinophilic protein droplets, cytoplasmic inclusions, single cell necrosis, fatty vacuolation, or lipidosis, macrophage aggregates and focal/multifocal parenchymal leukocytes or lymphocytes. Glycogen depletion was characterized by decreased hepatocyte size, loss of the 'lacy', irregular, and poorly demarcated cytoplasmic vacuolation typical of glycogen, and increased cytoplasmic basophilia (i.e., blue coloration). Eosinophilic protein droplets were characterized by the presence of proteins which appeared as refractile, eosinophilic (pink coloration), round, and well-demarcated cytoplasmic vacuoles. Cytoplasmic inclusions were characterized by the accumulation of foreign materials within the cytoplasm of hepatocytes. Single cell necrosis was characterized by cells having eosinophilic cytoplasm with nuclear pyknosis and karyorrhexis. Fatty vacuolation or lipidosis was characterized by excess lipids which appeared as clear, round, and well-demarcated cytoplasmic vacuoles. Macrophage aggregation was characterized as a cluster of macrophages packed with coarsely granular yellow–brown pigment. Focal/multifocal parenchymal leukocytes or lymphocytes were characterized by focal to multifocal aggregates of lymphocytes, occasionally mixed with other inflammatory cells. Cumulative assessment was based on the sum of the mean of individual lesion scores where higher total mean score indicated poorer fish conditions.

Statistical analysis

Due to the lack of normality in the data sets, all statistical analyses were computed using non-parametric statistics. Comparisons of physical, chemical, and biological data were computed using non-parametric statistical techniques for single and multiple comparisons, Wilcoxon and Kruskal–Wallis comparison tests (SAS, 2004). Correlation coefficients were

computed using the non-parametric Spearman rank correlation coefficient (r_s). Data were reported as the mean \pm the standard deviation.

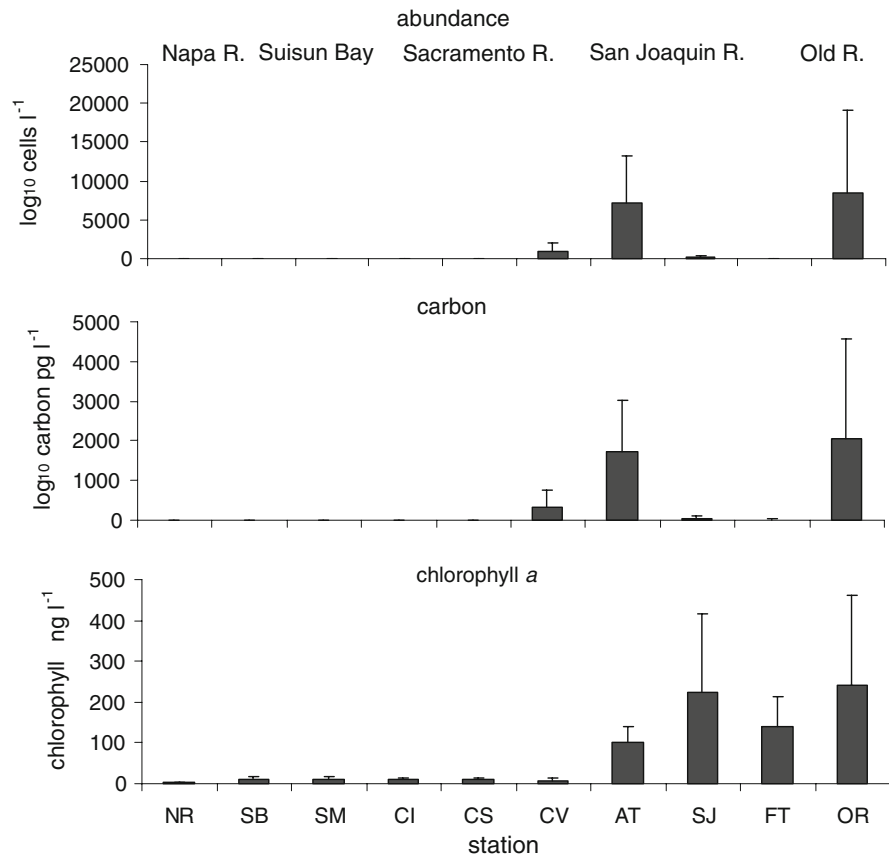
Similar patterns in plankton and zooplankton community composition or carbon and their correlation with environmental factors were evaluated with Primer-e version 6 software (Clarke, 1993; Clarke & Gorley, 2006) using a combination of multidimensional scaling (MDS), analysis of similarities among data (ANOSIM), identification of variables that best explain the data variance (BEST), and multivariate comparisons of data patterns (RELATE). These were applied to patterns in plankton species composition over space or time by visualizing the data patterns using an MDS of the Bray Curtis dissimilarity index computed from the square root of density or carbon data. Similar patterns in plankton or zooplankton community composition and carbon among stations were quantified with ANOSIM, while similarities between patterns in physical (normalized) and plankton and zooplankton community composition or carbon were quantified by Spearman rank correlation coefficients using RELATE. Species which accounted for most of the variation in the plankton, zooplankton, or environmental data were identified by Spearman rank correlation coefficients applied to groups of variables using BEST.

Results

Plankton

Microcystis abundance was greatest ($P < 0.01$, ANOSIM) in the western and central delta (stations CV, AT, FT, SJ, and OR). Average *Microcystis* abundance (9×10^6 cells l^{-1}) at these stations was nearly an order of magnitude greater than at Suisun Bay stations SB and CI (1.0×10^6 cells l^{-1}) or the outlying stations SM, CS, and NR where *Microcystis* did not occur (Fig. 2). In the western and central delta, *Microcystis* abundance was elevated at stations CV, AT, and OR and significantly greater at stations OR and AT ($P < 0.05$). Spatial variability characterized *Microcystis* in the western and central delta where abundance ranged by orders of magnitude from no cells l^{-1} at station CV in early August to 32×10^9 cells l^{-1} at station OR in mid-August.

Fig. 2 *Microcystis* abundance, carbon, and chlorophyll *a* concentration at stations throughout the estuary



Chlorophyll *a* concentration increased with *Microcystis* carbon in the surface layer (Fig. 2). *Microcystis* carbon comprised about 90% of the plankton carbon, and was correlated with both total plankton carbon ($r_s = 0.83$; $P < 0.01$) and chlorophyll *a* concentration ($r = 0.76$, $P < 0.01$) for all stations combined. *Microcystis* carbon was also positively correlated with diatom, green algae, and miscellaneous flagellate carbon ($r_s = 0.43$, $P < 0.01$; $r_s = 0.74$, $P < 0.01$, and $r_s = 0.76$, $P < 0.01$, respectively). Chlorophyll *a* concentration and total plankton carbon were also correlated ($r_s = 0.82$; $P < 0.01$).

Plankton community composition varied with *Microcystis* abundance throughout the water column. In the surface layer, plankton community composition was correlated with *Microcystis* abundance for all stations combined ($P < 0.01$, RELATE). The variation in this plankton community was primarily due to the cyanobacterium *Aphanizomenon* spp., diatoms *Aulacoseira granualata* and *Bacillaria paradoxa*,

green alga *Chlorella* sp., and miscellaneous flagellates ($r_s = 0.94$, BEST; Fig. 3). *Microcystis* comprised 5, 48, 100, 86, 100, and 95% of the total abundance at SB, CV, AT, SJ, FT, and OR, respectively, and less than 1% at the rest of the stations. *Microcystis* abundance was also significantly correlated ($P < 0.05$, RELATE) with the plankton community composition in the western and central delta where *Aphanizomenon* sp., *A. granulata* and *B. paradoxa* accounted for 92% ($r_s = 0.96$, BEST) of the variation. In addition, the abundance of cyanobacteria species including *Aphanizomenon* spp., *Planktolyngbya* spp., *Pseudodanabaena* spp., and *Merismopedia* spp. covaried ($P < 0.01$, RELATE) with *Microcystis* abundance for all stations combined (Fig. 3). The plankton community at 1 m depth was also correlated with *Microcystis* abundance in the surface layer for all stations ($P < 0.05$, RELATE; Fig. 4). About 83% of the variation in the plankton community at 1 m was associated with the abundance of the cryptophytes *Rhodomonas* spp. and *Cryptomonas* spp., the green

Fig. 3 Average percent abundance of phytoplankton and cyanobacteria genera or species among stations. Only genera or species that comprised more than 1% of the abundance for any one station were included

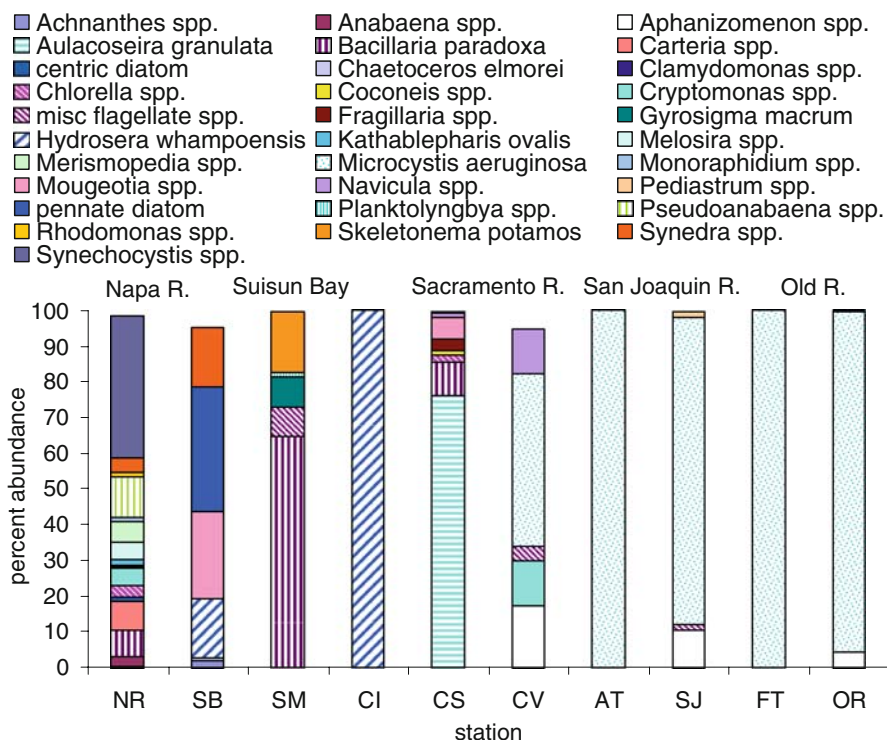
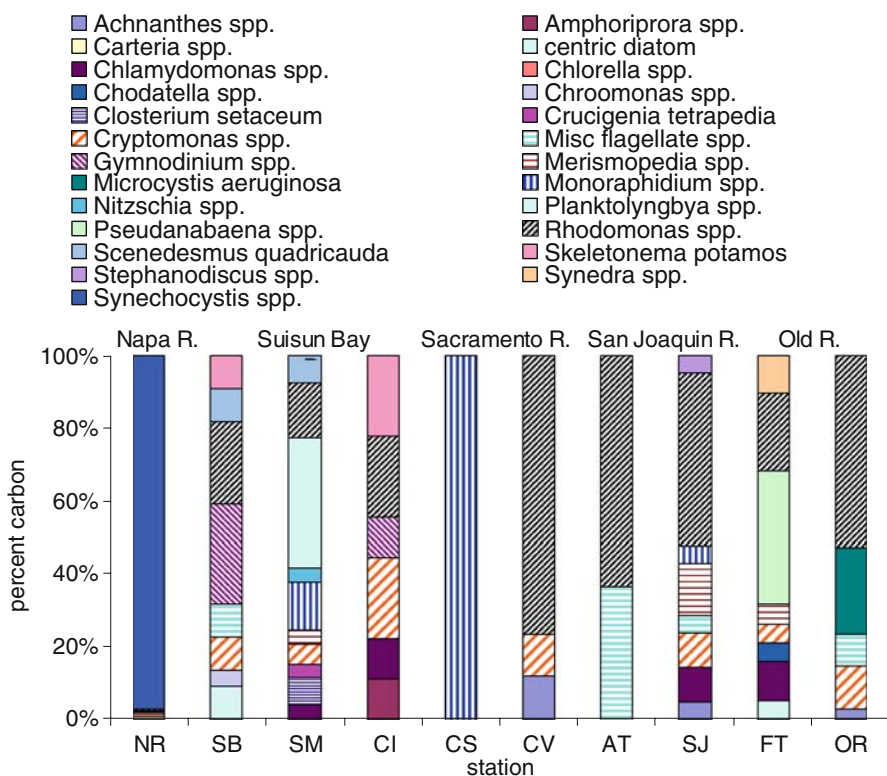


Fig. 4 Percent carbon of phytoplankton and cyanobacteria genera or species at 1 m depth. Only genera or species that composed more than 1% of the abundance for any one station were included



algae *Closterium setaceum* and *Monoraphidium* spp., and the dinoflagellate *Gymnodinium* spp. ($r_s = 0.91$, BEST) which were abundant in the western and central delta; 50% of this variation was due to *Rhodomonas* spp. alone ($r_s = 0.71$, BEST). Plankton community composition at 1 m depth was correlated with *Microcystis* abundance even on a small geographical scale. The cryptophytes *Rhodomonas* spp. and *Cryptomonas* spp., the cyanobacteria *Merismopedia* spp., and *Microcystis* and miscellaneous flagellates ($r_s = 0.86$, BEST) characterized differences in the plankton community at AT, OR, and CV compared with SJ and FT ($P < 0.05$, ANOSIM); most of this variation was due to *Rhodomonas* spp. ($r_s = 0.65$, BEST). *Microcystis* abundance was similarly greater at AT and OR compared with SJ and FT ($P < 0.05$, ANOSIM).

Differences in the plankton community composition affected the plankton carbon among groups. Plankton group carbon differed ($P < 0.05$, ANOSIM) between stations OR, CV, and AT and stations FT and SJ at 1 m (Fig. 5). Most of this difference was associated with diatom, green algae, and cryptophyte carbon ($r_s = 0.89$, BEST), and was characterized by a greater ($P < 0.05$) percentage of cryptophytes and a lower ($P < 0.05$) percentage of diatoms and green algae at stations OR, CV, and AT compared with stations SJ and FT. The difference was most striking for cryptophyte carbon which comprised 70–90% of the total carbon at OR, CV, and AT, but only 35–45% of the total carbon for nearby stations at SJ and FT. Most of the cryptophyte carbon was produced by *Rhodomonas* sp. and *Cryptomonas* sp.

Microcystis abundance was correlated with water quality conditions across regions ($P < 0.01$, RELATE). Water quality conditions differed ($P < 0.01$, ANOSIM) among the western and central delta (CV, AT, SJ, FT, and OR), Suisun Bay (SB, SM, and CI), CS and NR stations or station groups (Table 1). About 72% (BEST) of this variation was correlated with chloride, total organic carbon, and total suspended solids concentration which increased seaward. Among variables, *Microcystis* abundance was negatively correlated with chloride ($P < 0.01$, RELATE), total suspended solids ($P < 0.01$, RELATE), and total organic carbon ($P < 0.01$, RELATE), and positively correlated with nitrate-N ($P < 0.05$, RELATE), soluble phosphorus ($P < 0.05$, RELATE), and total nitrogen (nitrate-N plus ammonium-N; $P < 0.01$, RELATE) concentration.

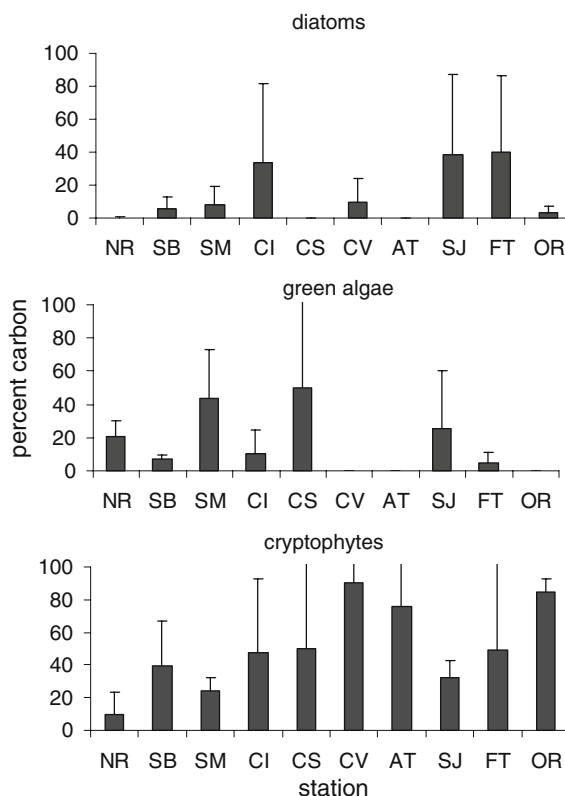


Fig. 5 Percent carbon for diatom, green algae, and cryptophyte carbon at 1 m depth

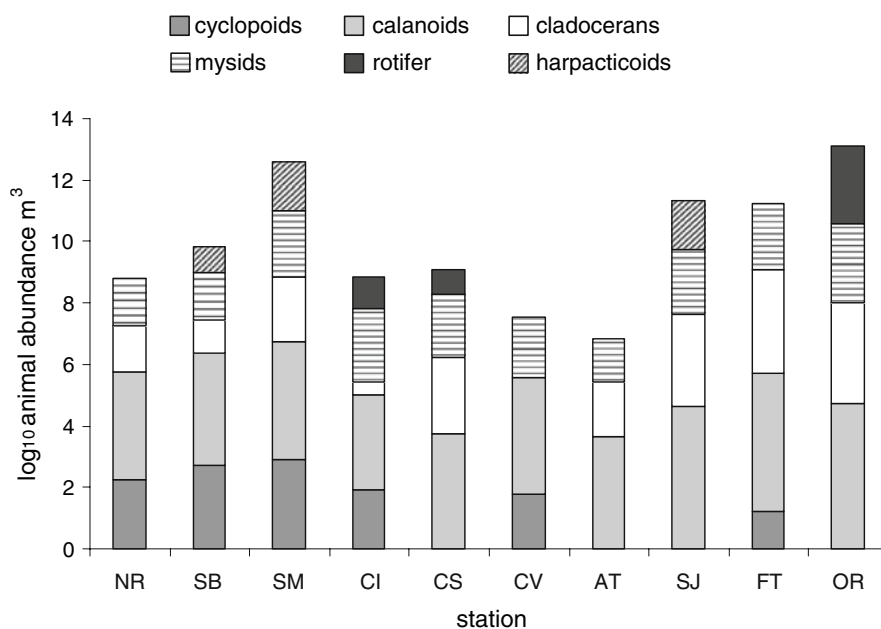
Although ammonium-N concentration was elevated at some stations in the western and central delta and the Sacramento River at stations at CS and CV, neither it nor the total nitrogen (nitrate-N and nitrite-N plus ammonium-N) to soluble phosphorus molar ratio (NP) was significantly correlated with *Microcystis* abundance across all regions or within the western and central delta separately. Plankton group carbon or plankton species abundance at 1 m was not significantly correlated with any of the water quality conditions measured, including the NP ratio.

Zooplankton

Zooplankton community composition differed ($P < 0.01$, ANOSIM) across the delta and was correlated with *Microcystis* abundance in the surface layer ($P < 0.01$, RELATE). Significant differences in the zooplankton community composition in the western and central delta and Suisun Bay ($P < 0.01$, ANOSIM)

Table 1 Average water quality conditions in the surface layer computed from biweekly data for stations sampled in the San Francisco Estuary between August and September 2005

Water quality variable	Stations									
	NR	SB	SM	CI	CS	CV	AT	SJ	FT	OR
Ammonium-N (mg l^{-1})	0.01	0.03	0.02	0.03	0.10	0.05	0.03	0.03	0.02	0.02
Chloride (mg l^{-1})	7,032.50	2,655.00	1,935.00	2,420.00	8.33	429.50	413.00	30.75	73.75	46.50
Nitrate-N (mg l^{-1})	0.01	0.31	0.22	0.32	0.20	0.28	0.24	0.22	0.11	0.17
Dissolved organic carbon (mg l^{-1})	2.93	1.65	4.30	1.71	1.90	1.72	1.82	2.09	2.00	1.89
Soluble reactive phosphorus (mg l^{-1})	0.03	0.07	0.06	0.07	0.05	0.06	0.06	0.04	0.05	0.05
Silica (mg l^{-1})	45.53	14.43	14.30	14.57	16.33	15.60	14.10	13.35	13.00	13.00
Alkalinity (mg l^{-1})	121.00	69.00	80.25	69.67	69.67	67.25	66.00	61.25	65.25	62.50
Total organic carbon (mg l^{-1})	3.20	1.71	4.65	1.99	1.85	1.90	1.86	2.05	1.85	2.13
Total phosphorus (mg l^{-1})	0.08	0.10	0.14	0.15	0.10	0.09	0.09	0.08	0.08	0.08
Total suspended solids (mg l^{-1})	10.38	23.75	41.25	61.00	20.33	34.25	9.75	3.75	2.50	2.75
Water temperature $^{\circ}\text{C}$	21.19	20.98	21.51	19.34	21.18	20.73	20.78	23.37	22.44	23.03
Dissolved oxygen (mg l^{-1})	7.23	6.70	6.78	6.77	6.73	6.70	6.70	6.63	7.00	6.70
pH	7.69	8.09	8.04	8.16	7.89	7.97	8.34	7.83	8.60	8.08
Specific conductance $\mu\text{S cm}^{-1}$	18.80	7.69	5.73	7.22	0.16	1.38	1.73	0.23	0.36	0.21

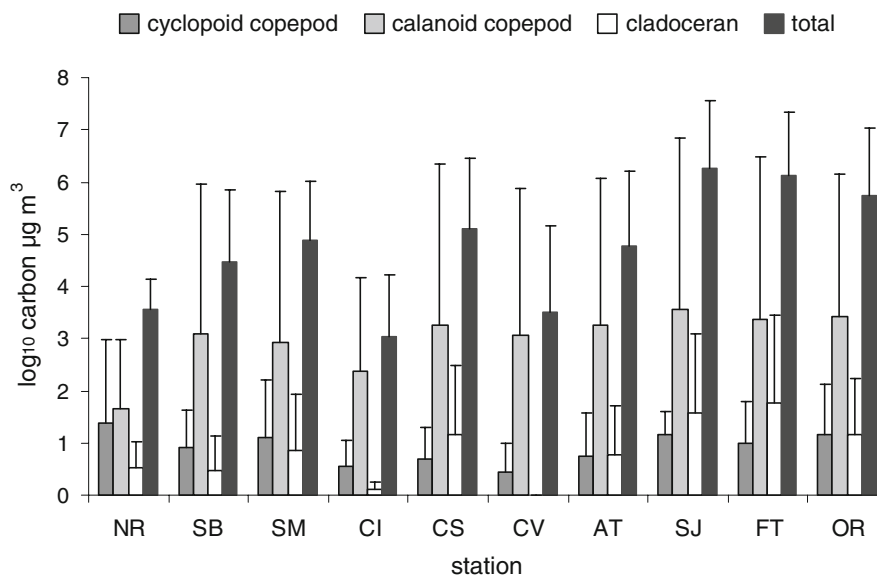
Fig. 6 Mesozooplankton abundance (\log_{10} animals l^{-1}) by taxonomic group among stations determined from diagonal net tow samples

were also correlated with *Microcystis* abundance ($P < 0.01$, RELATE). Most of the variation in the zooplankton community in the western and central delta and Suisun Bay was due to calanoid and cyclopoid copepods and cladocera ($r_s = 0.80$, BEST; Fig. 6). Calanoid copepods in the western and central delta were characterized by nauplii and the freshwater copepod *Pseudodiaptomus* spp., and were significantly

different ($P < 0.05$, ANOSIM) from Suisun Bay, where the brackish water calanoid copepod *Acartiella* spp. was abundant. Both *Pseudodiaptomus* spp. and *Acartiella* spp. accounted for 88% of the variation in the zooplankton community between the western and central delta and Suisun Bay ($r_s = 0.94$, BEST).

Microcystis carbon in the surface layer was significantly correlated with both total zooplankton carbon

Fig. 7 Log₁₀ average total and mesozooplankton group carbon ($\mu\text{g m}^{-3}$) and their standard deviation (*line*) among stations determined from diagonal net tow samples



and zooplankton group carbon for all stations ($P < 0.01$, RELATE) and for Suisun Bay and the western and central delta, separately ($P < 0.01$, RELATE). Calanoid copepod, cyclopoid copepod, rotifer, and cladocera carbon differed ($P < 0.01$, ANOSIM) between Suisun Bay, the western and central delta and the outlying stations NR and CS (Fig. 7). Nearly all of this difference in carbon among stations was due to the high biomass of the calanoid copepod *Pseudodiaptomus* sp. in the central delta ($r_s = 0.99$, BEST). Although the zooplankton group carbon differed between stations CV, SJ, and OR in the western and central delta, it was not associated with *Microcystis* abundance (Fig. 7). In contrast, *Microcystis* carbon was associated with differences in the cladocera to calanoid copepod carbon ratio among stations in the western and central delta ($P < 0.01$, RELATE). The cladocera to calanoid copepod carbon ratio was lower ($P < 0.01$) at stations OR, AT, and CV than FT and SJ (0.003 ± 0.003 and 0.02 ± 0.02 , respectively).

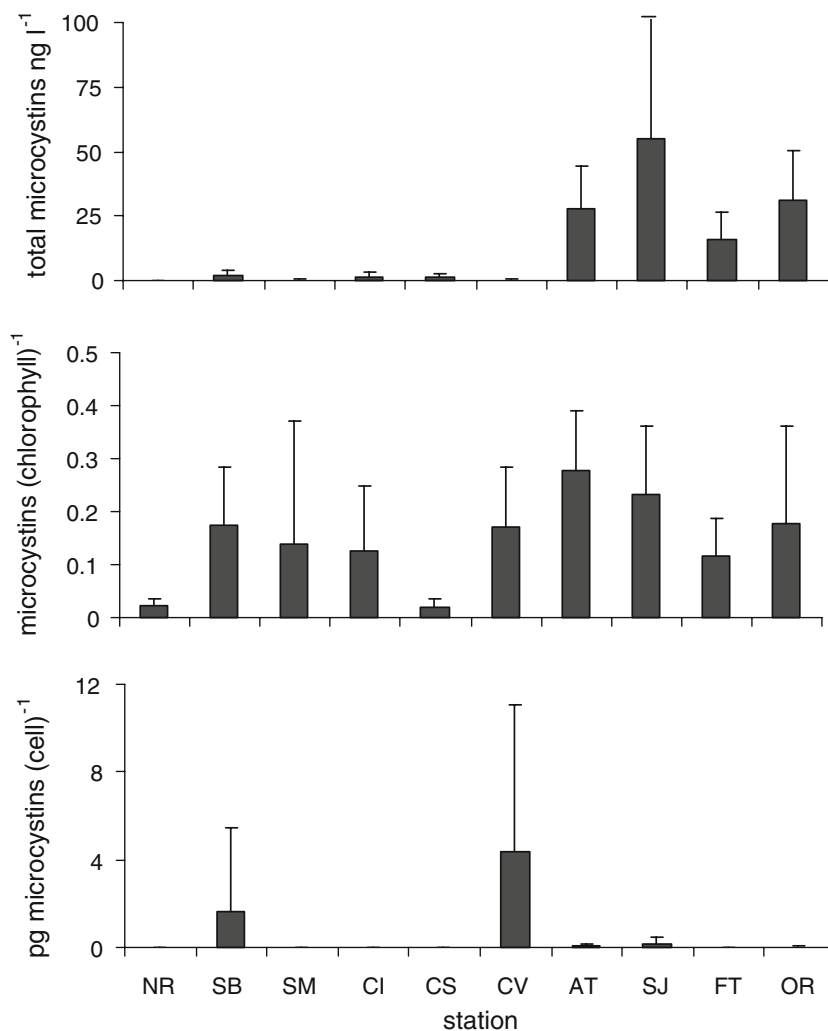
Toxins in plankton and animal tissue

Microcystins were present in the surface plankton samples throughout the estuary where *Microcystis* occurred (Fig. 8). The highest total microcystins concentration in *Microcystis* tissue ($P < 0.05$, ANOSIM) occurred in the San Joaquin and Old rivers at stations AT, SJ, FT, and OR where it reached an average of 60 ng l^{-1} . Total microcystins concentration

was correlated with both chlorophyll *a* concentration and *Microcystis* abundance for all stations ($r_s = 0.89$, $P < 0.01$; $r_s = 0.74$, $P < 0.01$), the Suisun Bay and western and central delta ($r_s = 0.87$, $P < 0.01$; $r_s = 0.68$, $P < 0.01$), and the western and central delta ($r_s = 0.79$, $P < 0.05$; $r_s = 0.45$, $P < 0.05$). The relative toxicity of *Microcystis* appeared to be uniform throughout the estuary because both total microcystins per unit chlorophyll *a* concentration and total microcystins per *Microcystis* cell were not statistically different among stations, despite large differences in average values (Fig. 8). Dissolved total microcystins concentration was above detection limits nine times during the sampling season, three times in August at CI, CS, and OR ($0.05\text{--}3.1 \text{ ng l}^{-1}$), and six times in September at SB, CV, AT, FT, and OR ($0.4\text{--}10.88 \text{ ng l}^{-1}$). Anatoxin-a concentration was low and below detection limits in plankton samples 17 times during the summer; range $2.4\text{--}143 \text{ pg l}^{-1}$.

Total microcystins were present in zooplankton and amphipod tissue throughout the estuary. Total microcystins in zooplankton and amphipod tissue ranged from 0.40 to $1.43 \mu\text{g (g dry wt)}^{-1}$, and was greatest at SJ by a factor of 2 (Table 2). Low biomass precluded absolute measurements of total microcystins in most zooplankton and amphipod tissue samples. However, detection limits suggested average total microcystins concentration in animal tissue was low, and could only have reached as high as $3.99 \mu\text{g (g dry wt)}^{-1}$ in zooplankton and $0.99 \mu\text{g}$

Fig. 8 Average (bar) and standard deviation (line) of total microcystins concentration ($\mu\text{g l}^{-1}$), total microcystins per unit chlorophyll *a* and total microcystins per *Microcystis* cell (within the $>75 \mu\text{m}$ size fraction collected in surface net tows). Total microcystins were measured by protein phosphatase inhibition assay



(g dry wt) $^{-1}$ in amphipod tissue in the central and western delta. A more thorough statistical evaluation of these trends was limited by the small sample size and qualitative nature of some of the data.

Total microcystins were present in the liver, muscle, and whole body tissues of juvenile striped bass and Mississippi silversides at all stations where fish occurred (Table 2). Total microcystins concentration in individual striped bass muscle tissue ranged by a factor of 3 from 1.03 to 3.42 $\mu\text{g (g dry wt)}^{-1}$, but averages among stations were similar (Table 2). Total microcystins concentration in striped bass liver tissue was slightly less than in muscle tissue and varied by a factor of 5 among samples (range 0.34–1.89 $\mu\text{g (g dry wt)}^{-1}$). Tissue concentrations were not statistically different among stations, but were elevated in individual samples at AT in the San Joaquin River and SM in

Suisun Bay. Mississippi silversides contained similar amounts of total microcystins in liver and muscle tissue as striped bass (Table 2). As might be expected, total microcystins concentration in the whole body tissue of Mississippi silversides was more than an order of magnitude lower than for liver and muscle tissue alone. Absolute total microcystins concentrations and differences in concentration among samples were probably lower than the actual values due to the need to composite from 2 to 10 fish tissue samples for toxin analysis from these very small fish; this was particularly true for liver samples.

Histopathology

Histopathological analysis revealed that Mississippi silversides and juvenile striped bass were likely

Table 2 Average absolute and relative total microcystins concentration (μg (g dry weight) $^{-1}$) in mesozooplankton and fish tissue measured between August and September 2005 at stations throughout the estuary

Tissue type	Stations									
	NR	SB	SM	CI	CS	CV	AT	SJ	FT	OR
Zooplankton										
Mesozooplankton	<2.91	0.40; <0.35	0.66; <1.60	<3.99	1.05; <0.43	<0.22	<1.05	1.43 \pm 0.62	<3.37	<3.14
Amphipod	<27.27	<0.99	<0.40	<0.64	<1.54	<0.24	<0.17	0.77; <0.48	<0.5	<0.42
Striped Bass										
Muscle	2.92 \pm 0.03	2.22 \pm 0.09	2.30 \pm 0.77	1.66 \pm 0.93	2.14 \pm 0.79	2.47 \pm 0.74	1.61 \pm 0.93	2.51 \pm 0.41	2.98 \pm 0.62	
Liver	1.20 \pm 0.44	1.25 \pm 0.30	1.41 \pm 0.28	1.14 \pm 0.56	0.94 \pm 0.40	1.18 \pm 0.15	1.48 \pm \pm 0.08	1.08 \pm 0.13	1.04 \pm 0.30	
Mississippi silversides										
Muscle			1.95 \pm 0.16				1.98 \pm 0.78			
Whole body	0.38 \pm 0.06	0.37 \pm 0.04	0.47 \pm 0.16	0.39 \pm 0.07	0.30 \pm 0.05	0.40 \pm 0.06	0.37 \pm 0.13	0.46 \pm 0.29	0.34 \pm 0.04	0.34 \pm 0.02
Liver			0.80				2.00 \pm 0.39			

Toxic microcystins were measured by protein phosphatase inhibition assay

exposed to toxic substances including cancer causing substances throughout the estuary. Several types of histological changes were observed in juvenile striped bass liver tissue. Mild to moderate glycogen depletion occurred in liver tissue for all stations (Fig. 9). Mild, but elevated lesion scores for cytoplasmic inclusion, single cell necrosis and lipidosis also suggested the striped bass in the Sacramento River and San Joaquin Rivers were exposed to toxic contaminants and cancer causing substances. Hepatic preneoplastic foci and the presence of tumors in liver tissue further supported the exposure of striped bass at station AT to cancer causing substances in the San Joaquin River. Importantly, elevated lesion scores for cancer causing substances and the presence of tumors in striped bass liver coincided with elevated concentrations of total microcystins at AT. Liver lesion scores for the San Joaquin River differed from those in Suisun Bay where the maximum lesion scores resulted from a different suite of biomarkers, such as eosinophilic protein droplets, macrophage aggregates, and focal parenchymal leukocytes.

The liver tissue of Mississippi silversides also demonstrated histological changes characteristic of exposure to toxic substances throughout the estuary. Like striped bass, glycogen depletion was mild to moderate at most stations (Fig. 10). Liver lesion scores characteristic of exposure to toxic substances, single cell necrosis, and cytoplasmic inclusions, occurred in liver tissue for fish in San Joaquin River and Suisun Bay, while those for hepatic lipidosis were moderately elevated in liver tissue for Suisun Bay and Old River. Maximum lesion scores in liver tissue for glycogen depletion, eosinophilic protein droplets, and cytoplasmic inclusions occurred in Suisun Bay and San Joaquin River, Sacramento River, and the San Joaquin River, respectively. All of the remaining lesion scores were highest for Mississippi silversides in Suisun Bay at station CI.

Discussion

Phytoplankton

Microcystis forms dense surface blooms that may exert a pronounced effect on the surrounding plankton through its effect on the quantity and quality of the light field in the water column in the presence of

Fig. 9 Average liver lesion scores for each biomarker quantified in juvenile striped bass collected at stations throughout the estuary. No fish were present at stations FT and OR

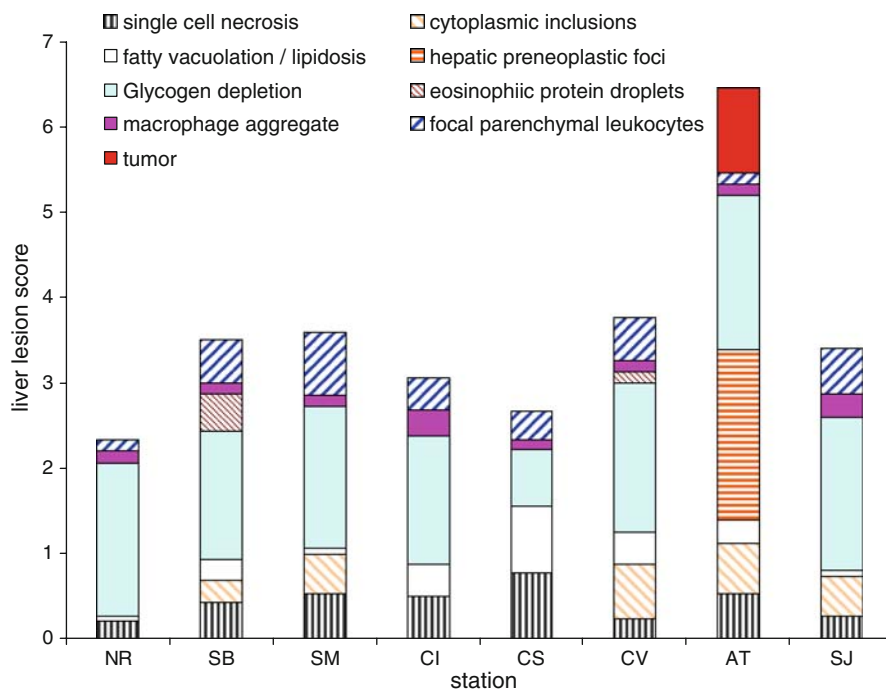
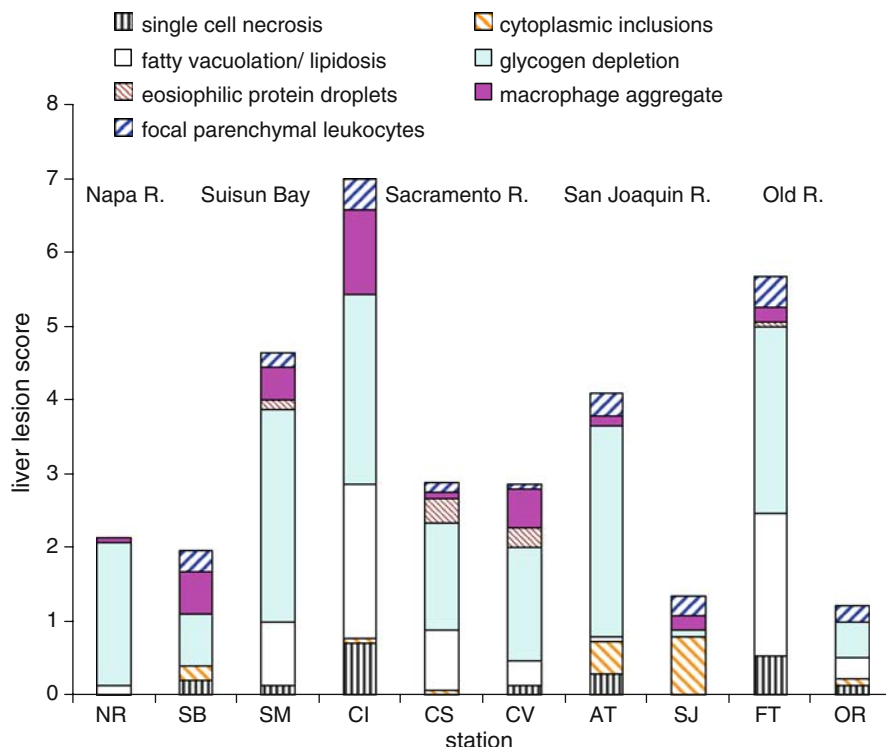


Fig. 10 Average liver lesion scores for each biomarker quantified in Mississippi silversides collected at stations throughout the estuary



carbonate concentrating mechanisms (Giordano et al., 2005) and nutrient uptake (Marinho & Azevedo, 2007). *Microcystis* contain gas vesicles that allow

them to float on the surface of the water column where they can decrease light availability and primary productivity for plankton below the surface.

This may partly explain the decreased density of diatom, green algae, and other cyanobacteria at 1 m depth compared with cryptophytes with flagella that enable them to adjust their light position in the water column. *Microcystis* can alter the pH, and hence inhibit CO₂ uptake, giving preference to cyanobacteria with their enhanced carbonate concentrating capabilities (Giordano et al., 2005). However, the pH among the stations did not differ, suggesting that differences in carbonate concentrating mechanisms were not important in SFE. *Microcystis* co-occurred with *Aphanizomenon* spp. This filamentous cyanobacterium has similar enhanced carbonate and light capturing capabilities through carboxysome and phycobilisomes as *Microcystis*, but because it has heterocysts that produce nitrogen needed for growth, it does not compete with *Microcystis* for nitrogen (Paerl et al., 2001). *Microcystis* is extremely flexible in its ability to use organic nitrogen and phosphorus and alternative forms of nutrients may provide a selective advantage for this species even though nutrients are rarely limiting in SFE (Jassby, 2005). Recent increases in ammonium concentration in the western delta may give a competitive advantage to *Microcystis* which rapidly assimilates ammonium over nitrate (Blomqvist et al., 1994; Jassby, 2005). However, recent reductions in river flow may have had a greater influence on abundance (Kuwata & Miyazaki, 2000; Lehman et al., 2008).

Microcystis may have affected plankton community composition through allelopathy by the production of microcystins or other bioactive peptides. Microcystins were associated with a decrease in diatom density and increase in the growth rate and number of cyanobacteria species in laboratory cultures (Sedmak & Kosi, 1998; Suikkanen et al., 2005). Microcystins may not have affected some phytoplankton, such as the chain diatom *Aulacoseira granulata* or the green alga *Monoraphidium contortum* in SFE, which were common in the surface layer. Laboratory studies suggest these species grow well in the presence of *Microcystis* (Sedmak & Kosi, 1998; Jia et al., 2008). *Microcystis* can inhibit photosynthesis and the growth rate of the cyanobacteria *Nostoc* spp., *Anabaena* spp., and *Synechocystis* spp. (Vassilakaki & Pflugmacher, 2008; Singh et al., 2001) and may contribute to their absence or low density in SFE. The impact of *Microcystis* on algal growth is often species specific. *Microcystis* inhibited

chlorophyll *a* synthesis in *Scenedesmus obliquus*, but increased the growth of *Scenedesmus quadricauda* in laboratory cultures (Sedmak & Kosi, 1998; Jia et al., 2008). Dissolved microcystins can also affect cell aggregation, increase cell volume, and production of photosynthetic pigments in *Scenedesmus quadricauda* (Sedmak & Eleršek, 2006). *Scenedesmus* spp. was not found in the surface or 1 m samples where *Microcystis* was abundant for this study, but has been a common species in the delta over time (www.iep.water.ca.gov). The increased abundance of the cryptophytes *Rhodomonas* spp. and *Cryptomonas* spp. in SFE may also be due to species specific responses to *Microcystis*. Although elevated *Microcystis* abundance was associated with decreased abundance of the cryptophyte *Cryptomonas arosa* (Sedmak & Kosi, 1998), cryptophyte growth varied among species when exposed to filtrates from freshwater and brackish water cyanobacteria including *Nodularia*, *Aphanizomenon*, and *Anabaena* (Suikkanen et al., 2005). The mechanisms associated with the allelopathy of *Microcystis* are poorly understood, but the growth and photosynthesis of *Peridinium gatunense* were decreased by inhibition of carbonic anhydrase activity (Sukenic et al., 2002).

The loss of diatom and green algal carbon and increase in cryptophyte carbon associated with elevated *Microcystis* abundance was sufficient to affect the quantity and quality of the phytoplankton carbon available to the food web in SFE. Diatom and green algae have some of the largest cells by volume in the phytoplankton community within SFE, therefore their loss can remove a large portion of the total carbon available to the food web (Lehman, 1996). Because cryptophytes have a relatively low average biovolume, the increase in their carbon was insufficient to compensate for the loss of diatom and green algal carbon. This was true even though most of the cryptophyte carbon was composed of two relatively large volume species, *Rhodomonas* spp. and *Cryptomonas* spp. A decrease in the diatom and green algal biovolume was also associated with an increase in cyanobacteria and cryptophyte biovolume between 1975 and 1993 in SFE, but it was attributed to long term changes in environmental conditions, particularly flow (Lehman, 2000a). Nutrient concentrations are often thought to be the primary driver of plankton blooms, particularly cyanobacteria blooms (Paerl et al., 2001). Recent research suggested haptophytes,

chlorophytes, and dinoflagellates increase with ammonium-N concentration in the Neuse River estuary (Rothenberger et al., 2009). However, nutrient concentration, including ammonium-N concentration and the NP molar ratio, did not account for the majority of the variation in *Microcystis* abundance in the surface layer or the distribution phytoplankton carbon among classes at 1 m depth for this study.

Zooplankton

Zooplankton carbon was positively correlated with *Microcystis* abundance. Most of the zooplankton carbon occurred in the western and central delta, and was composed of calanoid copepods. Copepods can actively reject toxic strains of *Microcystis*, and, therefore, are less likely to be affected by toxic blooms at low to moderate levels (DeMott & Moxter, 1991). In addition, some zooplankton can effectively use decomposed *Microcystis* as a food source (Hanazato & Yasuno, 1987). Copepod biomass was also not affected by *Microcystis* biomass in Steele Lake, Canada (Ghadouani et al., 2003). It is likely that the gradual seaward decrease in copepod carbon, dominated by the freshwater copepod *P. forbesii*, was due to other factors such as salinity or clam grazing in SFE (Kimmerer, 2004).

However, it is also possible that the presence of *Microcystis* and its toxins in the western and central delta affected the ability of calanoid copepods to reach maximum population levels. *P. forbesii* decreased in the western and central delta after 1999 and coincided with the appearance of *Microcystis* blooms (Lehman et al., 2005; Sommer et al., 2007). Although initial laboratory feeding studies indicated one of the common copepods in SFE, *Eurytemora affinis*, did not consume *Microcystis*, zooplankton tissue in SFE contained microcystins (Lehman et al., 2005, 2008). In Chesapeake Bay, zooplankton can consume some *Microcystis* even though they do not actively feed on this cyanobacterium (Sellner et al., 1993). Recent laboratory feeding studies confirmed that the survival of both *P. forbesii* and *E. affinis* was reduced when *Microcystis* exceeded 10% of the diet, and that *P. forbesii* was three times more sensitive than *E. affinis* (Ger et al., 2009). Dissolved microcystins also affect zooplankton growth and survival and can increase in the presence of zooplankton (Jang et al., 2003).

Dissolved microcystins occurred occasionally and may have contributed to the variability in zooplankton composition and biomass.

Elevated *Microcystis* biomass was associated with a low cladocera to calanoid copepod ratio. *Microcystis* blooms are often associated with low cladocera biomass because large cladocera like *Daphnia* sp. are more sensitive to *Microcystis* than small cladocera (Chen et al., 2007). *Microcystis* is a poor quality food and both toxic and non-toxic *Microcystis* adversely affect cladocera survival, growth rate, reproduction rate, clutch size, feeding rate, and nutrition (Reinikainen et al., 1999; Rohrlack et al., 2001, 2005; Wilson et al., 2006; Abrantes et al., 2006; Federico et al., 2007). *Microcystis* blooms can also affect the growth rate of cladocera by physically inhibiting feeding (Lurling, 2003). The *Microcystis* strain may also be important in SFE where DNA analysis suggested the western delta had different and more toxic *Microcystis* strains than the central delta (Moisander et al., 2009; D. Baxa, personal communication).

Fish

Toxic *Microcystis* may adversely affect fish health in the estuary when hepatotoxic microcystins cause liver damage and tumors (Malbrouck & Kestemont, 2006; Ibelings & Havens, 2008). Five of the lesion types evaluated in this study, single cell necrosis, cytoplasmic inclusions, hepatic lipidosis, hepatic preneoplastic foci, and hepatocellular adenoma (tumor) are likely pathologic responses to toxic exposure in fish (Teh et al., 1997; Malbrouck & Kestemont, 2006). The combined presence of these lesions in juvenile striped bass liver tissue suggests fish in the Sacramento and San Joaquin River were recently exposed to toxins. Low concentrations in fish tissue may indicate the rapid depuration of microcystins or toxin dilution through the food web (Ibelings & Havens, 2008). The presence of hepatic preneoplastic foci and hepatocellular adenoma in these young fish suggests the toxin was carcinogenic and affecting the fish at a very early life stage, which is atypical. We hypothesize that microcystins within the *Microcystis* colonies either contributed to or were the cause of these histopathological changes in striped bass liver tissue in the San Joaquin River, especially at station AT where the combined presence of the five lesion types

coincided with high total microcystins concentration. Ongoing research suggests *Microcystis* populations can be more toxic at AT than other stations in the estuary (D. Baxa, personal communication). Single cell necrosis and cytoplasmic inclusions in the liver tissue of Mississippi silversides further supported the contaminant exposure of fish in the lower San Joaquin River to *Microcystis* toxins. Dissolved microcystins may have contributed to the observed lesion scores, but anatoxin-a concentrations were probably too low.

Food web

Through its impact on multiple trophic levels, *Microcystis* may influence fishery production including the decline in pelagic organisms measured since 2000 in SFE (Sommer et al., 2007). The effects of *Microcystis* on food web organisms suggested by this study include direct impacts through nutrients, light, allelopathy, or toxicity on the growth and survival of phytoplankton, zooplankton, and fish or indirect impacts through the food web. The potential impact of *Microcystis* on phytoplankton group carbon maybe important for fishery production in SFE where the health and survival of key zooplankton food species like *P. forbesii* rely on the abundance of wide diameter diatom and green algae cells that provide good quality food in the optimum size range for filtering feeding (Müller-Navarra et al., 2000; Lehman, 2000b). This was supported by the strong positive correlation between total zooplankton and *Neomysis* shrimp carbon with diatom carbon between 1975 and 1993 in the estuary (Lehman, 2004), particularly after the depletion of diatoms following the invasion of the overbite clam in 1987 (Kimmerer, 2004). Although cladocera carbon was only a small percentage of the total zooplankton carbon compared with copepods, the decrease in the cladocera to calanoid copepod ratio may directly affect food availability for threadfin shad (T. Sommer, personal communication), an important forage species for piscivores in SFE (Nobriga & Feyrer, 2007). Importantly, the impact of *Microcystis* on the aquatic community may be greater than suggested by impacts on copepods and cladocera. Microcystins are commonly present throughout the food web, and in SFE were measured in clams, worms, and jellyfish that also serve as food resources for fish (Ibelings &

Havens, 2008; Lehman et al., 2005, 2008). Identifying the full impact of *Microcystis* on the SFE food web requires further information on high frequency spatial and temporal variability of the aquatic food web and body burdens across a larger suite of species and trophic levels.

Acknowledgments This project was funded by a special study grant from the San Francisco Bay Delta Interagency Ecological Program. Special thanks are due to many including E. Santos, F. Feyrer, and M. Dempsey for assistance with sampling, M. Bettencourt for phytoplankton counts and M. Satchwell (SUNY-ESF) for PPIA toxin analysis.

Open Access This article is distributed under the terms of the Creative Commons Attribution Noncommercial License which permits any noncommercial use, distribution, and reproduction in any medium, provided the original author(s) and source are credited.

References

- Abrantes, N., S. C. Antunes, M. J. Pereira & F. Goncalves, 2006. Seasonal succession of cladocerans and phytoplankton and their interactions in a shallow eutrophic lake (Lake Vela, Portugal). *Acta Oecologica* 29: 54–64.
- Agrawai, M. K., D. Bagchi & S. N. Bagchi, 2001. Acute inhibition of protease and suppression of growth in zooplankton, *Moina macrocopa*, by *Microcystis* blooms collected in Central India. *Hydrobiologia* 464: 37–44.
- American Public Health Association, American Water Works Association & Water Environment Association, 1998. Standard Methods for the Examination of Water and Wastewater, 20th edn. American Public Health Association, Washington, DC, USA.
- Best, J. H., F. B. Eddy & G. A. Codd, 2001. Effects of purified microcystin-LR and cell extracts of *Microcystis* strains PCC 7813 and CYA 43 on cardiac function in brown trout (*Salmo trutta*) alevins. *Fish Physiology and Biochemistry* 24: 171–178.
- Best, J. H., S. Pflugmacher, C. Wiegand, F. B. Eddy, J. S. Metcalf & G. A. Codd, 2002. Effects of enteric bacterial and cyanobacterial lipopolysaccharides, and of microcystin-LR, on glutathione S-transferase activities in zebra fish (*Danio rerio*). *Aquatic Toxicology* 60: 223–231.
- Best, J. H., F. B. Eddy & G. A. Codd, 2003. Effects of *Microcystis* cells, cell extracts and lipopolysaccharide on drinking and liver function in rainbow trout *Oncorhynchus mykiss* Walbaum. *Aquatic Toxicology* 64: 419–426.
- Bláha, L., R. Kopp, K. Šimková & J. Mares, 2004. Oxidative stress biomarkers are modulated in silver carp (*Hypophthalmichthys molitrix* Val.) exposed to microcystin-producing cyanobacterial water bloom. *Acta Veterinaria Brno* 73: 477–482.
- Blomqvist, P., A. Petterson & P. Hyenstrand, 1994. Ammonium-nitrogen: a key regulatory factor causing dominance

- of non-nitrogen-fixing cyanobacteria in aquatic systems. *Archiv für Hydrobiologie* 132: 141–164.
- Chen, F., P. Xie & B. Qin, 2007. Different competitive outcomes among four species of cladocerans under different alga combinations of colonial *Microcystis* spp. and green alga *Scenedesmus obliquus*. *Hydrobiologia* 581: 209–215.
- Chorus, I., 2005. Current approaches to cyanotoxin risk assessment, risk management and regulations in different countries. Federal Environmental Agency, Berlin.
- Clarke, K. R., 1993. Non-parametric multivariate analyses of changes in community structure. *Australian Journal of Ecology* 18: 117–143.
- Clarke, K. R. & R. N. Gorley, 2006. PRIMER v6: User Manual/Tutorial. PRIMER-E, Plymouth.
- De Magalhães, V. F., R. M. Soares & S. M. F. O. Azevedo, 2001. Microcystin contamination from fish in the Jacarepaquá Lagoon (Rio de Janeiro Brazil): ecological implication and human risk. *Toxicon* 39: 1077–1085.
- DeMott, W. R. & F. Moxter, 1991. Foraging cyanobacteria by copepods: responses to chemical defense and resource abundance. *Ecology* 72: 1820–1834.
- Federico, A., S. S. S. Sarma & S. Nandini, 2007. Effect of mixed diets (cyanobacteria and green algae) on the population growth of the cladocerans *Ceriodaphnia dubia* and *Moina macrocopa*. *Aquatic Ecology* 41: 579–585.
- Ferrão-Filho, A. S., S. M. F. O. Azevedo & W. R. DeMott, 2002. Effects of toxic and non-toxic cyanobacteria on the life history of tropical and temperate cladocerans. *Freshwater Biology* 45: 1–19.
- Fischer, W. J. & D. R. Dietrich, 2000. Pathological and biochemical characterization of microcystin-induced hepatopancreas and kidney damage in carp (*Cyprinus carpio*). *Toxicology and Applied Pharmacology* 164: 73–81.
- Fristachi, A., J. L. Sinclair, J. A. Hambrook-Berkman, G. Boyer, J. Burkholder, J. Burns, W. Carmichael, A. du Four, W. Frazier, S. L. Morton, E. O'Brien & S. Walker, 2008. Occurrence of Cyanobacterial Harmful Algal Blooms working group report. In Hudnell, H. K. (ed.), *Proceedings of the Interagency International Symposium on Cyanobacterial Harmful Algal Blooms*, Vol. 619. *Advances Experimental Medical Biology*. Springer, New York: 37–97.
- Ger, K. A., S. J. Teh & C. R. Goldman, 2009. Microcystin-LR toxicity on dominant copepods *Eurytemora affinis* and *Pseudodiaptomus forbesi* of the upper San Francisco Estuary. *Science of the Total Environment* 407: 4852–4857.
- Ghadouani, A., B. Pinel-Alloul & E. E. Prepas, 2003. Effects of experimentally induced cyanobacterial blooms on crustacean zooplankton communities. *Freshwater Biology* 48: 363–381.
- Ghadouani, A., B. B. Pinel-Alloul, K. Plath, G. A. Codd & W. Lampert, 2004. Effects of *Microcystis* and purified microcystin-LR on the feeding behavior of *Daphnia pulex*. *Limnology and Oceanography* 49: 666–679.
- Ghadouani, A., B. B. Pinel-Alloul & E. E. Prepas, 2006. Could increased cyanobacterial biomass following forest harvesting cause a reduction in zooplankton body size structure? *Canadian Journal of Fisheries and Aquatic Sciences* 63: 2308–2317.
- Giordano, M., J. Berdall & J. A. Raven, 2005. CO₂ concentrating mechanisms in Algae: mechanisms, environmental modulation and evolution. *Annual Review Plant Biology* 56: 99–131.
- Graneli, E., P. Salomon & G. Fistarol, 2008. The role of allelopathy for harmful algal bloom formation. In Evangelista, V., L. Barsanti, A. Frassanito, V. Passarelli & P. Gualtieri (eds), *Algal Toxins: Nature, Occurrence, Effect and Detection*. NATO Science for Peace and Security Series A: Chemistry and Biology. Springer, Netherlands: 159–178.
- Gustafsson, S. & L. Hansson, 2004. Development of tolerance against toxic cyanobacteria in *Daphnia*. *Aquatic Ecology* 38: 37–44.
- Hanazato, T. & M. Yasuno, 1987. Evaluation of *Microcystis* as food for zooplankton in a eutrophic lake. *Hydrobiologia* 144: 251–259.
- Ibelings, B. W. & K. E. Havens, 2008. Cyanobacterial toxins: a qualitative meta-analysis of concentrations, dosage and effects in freshwater estuarine and marine biota. In Hudnell H. K. (ed.), *Cyanobacterial Harmful Algal Blooms: State of the Science and Research Needs*, Vol. 619. *Advances in Experimental Medicine and Biology*. Springer, New York: 675–732.
- International Agency for Research on Cancer, 2006. Carcinogenicity of nitrate, nitrite, and cyanobacterial peptide toxins. *The Lancet Oncology* 7: 628–629.
- Jang, M., K. Ha, G. Joo & N. Takamura, 2003. Toxin production of cyanobacteria is increased by exposure to zooplankton. *Freshwater Biology* 48: 1540–1550.
- Jassby, A. D., 2005. Phytoplankton regulation in a eutrophic tidal river (San Joaquin River, California). *San Francisco Estuary and Watershed Science* 3(1), Article 3.
- Jia, X., D. Shi, R. Kang, H. Li, Y. Liu, Z. An, S. Wang, D. Song & G. Du, 2008. Allelopathic inhibition by *Scenedesmus obliquus* of photosynthesis and growth of *Microcystis aeruginosa*. In Allen, J. F., E. Gantt, J. H. Golbeck & B. Osmond (eds), *Photosynthesis. Energy from the Sun: 14th International Congress on Photosynthesis*. Springer, Heidelberg: 1339–1342.
- Kimmerer, W. J., 2004. Open water processes of San Francisco Estuary: from physical forcing to biological responses. *San Francisco Estuary and Watershed Science* 2(1), Article 1.
- Komárek, J. & K. Anagnostidis, 2001. Cyanoprokaryota 1, Teil: Chroococcales. In Ettl, H., G. Gartner, H. Heynig & D. Mollenhauer (eds), *Susswasserflora von Mitteleuropa* 19(1). Jena, Verlag von G. Fischer, Germany.
- Kuwata, A. & T. Miyazaki, 2000. Effects of ammonium supply rates on competition between *Microcystis novacekii* (Cyanobacteria) and *Scenedesmus quadricauda* (Chlorophyta): simulation study. *Ecological Modeling* 135: 81–87.
- Legrand, C., K. Rengefors, G. O. Fistarol & E. Graneli, 2003. Allelopathy in phytoplankton: biochemical, ecological and evolutionary aspects. *Phycologia* 42: 406–419.
- Lehman, P. W., 1996. Changes in chlorophyll *a* concentration and phytoplankton community composition with water-year type in the upper San Francisco Bay Estuary. In Hollibaugh, J. T. (ed.), *San Francisco Bay: The Ecosystem*. Pacific Division of the American Association for the Advancement of Science, San Francisco, CA: 351–374.

- Lehman, P. W., 2000a. The influence of climate on phytoplankton community carbon in San Francisco Bay Estuary. *Limnology and Oceanography* 45: 580–590.
- Lehman, P. W., 2000b. Phytoplankton biomass, cell diameter and species composition in the low salinity zone of northern San Francisco Bay Estuary. *Estuaries* 23: 216–230.
- Lehman, P. W., 2004. The influence of climate on mechanistic pathways that impact lower food web production in northern San Francisco Bay Estuary. *Estuaries* 27: 311–324.
- Lehman, P. W., G. Boyer, C. Hall, S. Waller & K. Gehrts, 2005. Distribution and toxicity of a new colonial *Microcystis aeruginosa* bloom in the San Francisco Bay Estuary, California. *Hydrobiologia* 541: 87–90.
- Lehman, P. W., G. Boyer, M. Satchwell & S. Waller, 2008. The influence of environmental conditions on the seasonal variation of *Microcystis* abundance and microcystins concentration in San Francisco Estuary. *Hydrobiologia* 600: 187–204.
- Lurling, M., 2003. *Daphnia* growth on microcystin-producing and microcystin-free *Microcystis aeruginosa* in different mixtures with the green alga *Scenedesmus obliquus*. *Limnology and Oceanography* 48: 2214–2220.
- Malbrouck, C. & P. Kestemont, 2006. Effects of microcystins on fish. *Environmental Toxicology and Chemistry* 25: 72–86.
- Marinho, M. M. & S. M. F. O. Azevedo, 2007. Influence of N/P ratio on competitive abilities for nitrogen and phosphorus by *Microcystis aeruginosa* and *Aulacoseira distans*. *Aquatic Ecology* 41: 525–533.
- Menden-Deuer, S. & E. J. Lessard, 2000. Carbon to volume relationships for dinoflagellates, diatoms and other protist plankton. *Limnology and Oceanography* 45: 569–579.
- Moisander, P. H., P. W. Lehman, M. Ochiai & S. Corum, 2009. Diversity of the toxic cyanobacterium *Microcystis aeruginosa* in the Klamath River and San Francisco Bay delta, California. *Aquatic Microbial Ecology* 57: 19–31.
- Müller-Navarra, D. C., M. T. Brett, A. M. Liston & C. R. Goldman, 2000. A highly unsaturated fatty acid predicts carbon transfer between primary producers and consumers. *Nature* 403: 74–77.
- Nobriga, M. L., & F. Feyrer, 2007. Shallow-water piscivore-prey dynamics in California's Sacramento-San Joaquin Delta. *San Francisco Estuary and Watershed Science* 5 [available on internet at <http://repositories.cdlib.org/jmie/sfews/vol5/iss2/art4>].
- Nobriga, M. L., F. Feyrer, R. D. Baxter & M. Chotkowski, 2005. Fish community ecology in an altered river delta: spatial patterns in species composition, life history strategies and biomass. *Estuaries* 28: 776–785.
- Paerl, H. W., 1988. Nuisance phytoplankton blooms in coastal, estuarine and inland waters. *Limnology and Oceanography* 33: 823–847.
- Paerl, H. W., R. S. Fulton, P. H. Moisander & J. Dyble, 2001. Harmful freshwater algal blooms, with an emphasis on cyanobacteria. *The ScientificWorld* 1: 76–113.
- Palíková, M., R. Krejčí, K. Hilscherová, P. Babica, S. Navrátil, R. Kopp & L. Bláha, 2007. Effect of different cyanobacterial biomasses and their fractions with variable microcystin content on embryonal development of carp (*Cyprinus carpio* L.). *Aquatic Toxicology* 81: 312–318.
- Prieto, A. I., S. Pichardo, A. Josa, I. Moreno & A. M. Cameán, 2007. Time-dependent oxidative stress responses after acute exposure to toxic cyanobacterial cells containing microcystins in tilapia fish (*Oreochromis niloticus*) under laboratory conditions. *Aquatic Toxicology* 84: 337–345.
- Reinikainen, M., J. Hietala & M. Walls, 1999. Reproductive allocation in *Daphnia* exposed to toxic cyanobacteria. *Journal of Plankton Research* 21: 1553–1564.
- Robson, B. J. & D. P. Hamilton, 2003. Summer flow event induces a cyanobacterial bloom in a seasonal Western Australia estuary. *Marine Freshwater Research* 54: 139–151.
- Rocha, C., H. Galvão & A. Barbosa, 2002. Role of transient silicon limitation in the development of cyanobacteria blooms in the Guadiana estuary, south-western Iberia. *Marine Ecology Progress Series* 228: 35–45.
- Rohrlack, T., E. Dittmann, T. Börner & K. Christoffersen, 2001. Effects of cell-bound microcystin on survival and feeding of *Daphnia* spp. *Applied Environmental Microbiology* 67: 3523–3529.
- Rohrlack, T., K. Christoffersen, E. Dittmann, I. Nogueira, V. Vasconcelos & T. Börner, 2005. Ingestion of microcystins by *Daphnia*: Intestinal uptake and toxic effects. *Limnology and Oceanography* 50: 440–448.
- Rothenberger, M. B., J. M. Burkholder & T. R. Wentworth, 2009. Use of long-term data and multivariate ordination techniques to identify environmental factors governing estuarine phytoplankton species dynamics. *Limnology and Oceanography* 54: 2107–2127.
- SAS Institute, Inc., 2004. SAS/STAT User's Guide, Version 8. SAS Institute Inc., SAS Campus Drive, Cary, NC, USA.
- Sedmak, B. & T. Eleršek, 2006. Microcystins induce morphological and physiological changes in selected representative phytoplanktons. *Microbial Ecology* 51: 508–515.
- Sedmak, B. & G. Kosi, 1998. The role of microcystins in heavy cyanobacterial bloom formation. *Journal of Plankton Research* 20: 691–708.
- Sellner, K. G., R. V. Lacouture & K. G. Parlish, 1988. Effect of increasing salinity on a cyanobacteria bloom in the Potomac River Estuary. *Journal of Plankton Research* 10: 49–61.
- Sellner, K. G., D. C. Brownlee, M. H. Bundy, S. G. Brownlee & K. R. Braun, 1993. Zooplankton grazing in a Potomac River cyanobacteria bloom. *Estuaries* 16: 859–872.
- Singh, D. P., M. B. Fyagi, A. Kumar & J. K. Thakur, 2001. Antialgal activity of a hepatotoxin-producing cyanobacterium, *Microcystis*. *World Journal of Microbiology and Biotechnology* 17: 15–22.
- Smith, J. L. & G. L. Boyer, 2009. Standardization of microcystin extraction from fish tissues: a novel internal standard as a surrogate for polar and non-polar variants. *Toxicon* 53: 238–245.
- Smith, J. L., G. L. Boyer & P. V. Zimba, 2008. A review of cyanobacterial odorous and bioactive metabolites: impacts and management alternatives in aquaculture. *Aquaculture* 280: 5–20.
- Sommer, T. R., C. Armor, R. Baxter, R. Breuer, L. Brown, M. Chotkowski, S. Culbertson, F. Feyrer, M. Gingras, B. Herbold, W. Kimmerer, A. Mueller-Solger, M. Nobriga & K. Souza, 2007. The collapse of pelagic fishes in the upper San Francisco Estuary. *Fisheries* 32: 270–277.
- Suikkanen, S., G. O. Fistarol & E. Granéli, 2005. Effects of cyanobacterial allelochemicals on a natural plankton community. *Marine Ecology Progress Series* 287: 1–9.

- Sukenik, A., R. Eshkol, A. Livne & O. Hadas, 2002. Inhibition of growth and photosynthesis of the dinoflagellates *Peridinium gatunense* by *Microcystis* sp. (cyanobacteria): a novel allelopathic mechanism. *Limnology and Oceanography* 47: 1656–1663.
- Teh, S. J., S. M. Adams & D. E. Hinton, 1997. Histopathologic biomarkers in feral fish populations exposed to different types of contaminant stress. *Aquatic Toxicology* 37: 51–70.
- Teh, S. J., X. Deng, D.-F. Deng, F. C. Teh, S. S. O. Hung, W.-M. T. Fan, J. Liu & R. Higashi, 2004. Chronic effects of dietary selenium on juvenile Sacramento splittail (*Pogonichthys macrolepidotus*). *Environmental Science and Technology* 38: 6085–6093.
- United States Environmental Protection Agency, 1983. Methods for Chemical Analysis of Water and Wastes. Technical Report EPA-600/4-79-020, Washington, DC.
- United States Geological Survey, 1985. Methods for Determination of Inorganic Substances in Water and Fluvial Sediments. Open File Report: 85–495.
- Utermöhl, H., 1958. Zur Vervollkommnung der quantitativen Phytoplankton-methodik. *Mitteilungen Internationale Vereinigung für Theoretische und Angewandte Limnologie* 9: 1–38.
- Van der Oost, R., J. Beyer & N. P. E. Vermeulen, 2003. Fish bioaccumulation and biomarkers in environmental risk assessment: a review. *Environmental Toxicology and Pharmacology* 13: 57–149.
- Vassilakaki, M. & S. Pflugmacher, 2008. Oxidative stress response of *Synechocystis* sp. (PCC 6803) due to exposure to microcystin-LR and cell-free cyanobacterial crude extract containing microcystin-LR. *Journal of Applied Phycology* 20: 219–225.
- Wehr, J. D. & R. G. Sheath, 2003. *Freshwater Algae of North America, Ecology and Classification*. Elsevier Science, San Diego, USA.
- Wilson, A. E. & M. E. Hay, 2007. A direct test of cyanobacterial chemical defense: variable effects of microcystin-treated food on two *Daphnia pulicaria* clones. *Limnology and Oceanography* 52: 1467–1479.
- Wilson, A. E., O. Sarnelle & A. R. Tillmanns, 2006. Effects of cyanobacterial toxicity and morphology on the population growth of freshwater zooplankton: meta-analysis of laboratory experiments. *Limnology and Oceanography* 51: 1915–1924.
- Zegura, B., B. Sedmak & M. Filipi, 2003. Microcystin-LR induces oxidative DNA damage in human hepatoma cell line HepG2. *Toxicol* 41: 41–48.

See discussions, stats, and author profiles for this publication at:
<http://www.researchgate.net/publication/11482807>

Increased selenium threat as a result of invasion of the exotic bivalve *Potamocorbula amurensis* into the San Francisco Bay-Delta

ARTICLE *in* AQUATIC TOXICOLOGY · MAY 2002

Impact Factor: 3.45 · DOI: 10.1016/S0166-445X(01)00265-X · Source: PubMed

CITATIONS

66

READS

26

4 AUTHORS, INCLUDING:



Samuel N Luoma

University of California, Davis

196 PUBLICATIONS 9,571 CITATIONS

[SEE PROFILE](#)



Gregory Cutter

Old Dominion University

77 PUBLICATIONS 2,276 CITATIONS

[SEE PROFILE](#)



Increased selenium threat as a result of invasion of the exotic bivalve *Potamocorbula amurensis* into the San Francisco Bay-Delta

Regina G. Linville^{a,1}, Samuel N. Luoma^{a,*}, Lynda Cutter^b,
Gregory A. Cutter^b

^a US Geological Survey, 345 Middlefield Road, Mail Stop 465, Menlo Park, CA 94025, USA

^b Department of Ocean, Earth, and Atmospheric Sciences, Old Dominion University, 4600 Elkhorn Ave., Norfolk, VA 23529-0276, USA

Received 23 February 1999; received in revised form 3 April 2001; accepted 10 October 2001

Abstract

Following the aggressive invasion of the bivalve, *Potamocorbula amurensis*, in the San Francisco Bay-Delta in 1986, selenium contamination in the benthic food web increased. Concentrations in this dominant (exotic) bivalve in North Bay were three times higher in 1995–1997 than in earlier studies, and 1990 concentrations in benthic predators (sturgeon and diving ducks) were also higher than in 1986. The contamination was widespread, varied seasonally and was greater in *P. amurensis* than in co-occurring and transplanted species. Selenium concentrations in the water column of the Bay were enriched relative to the Sacramento River but were not as high as observed in many contaminated aquatic environments. Total Se concentrations in the dissolved phase never exceeded 0.3 µg Se per l in 1995 and 1996; Se concentrations on particulate material ranged from 0.5 to 2.0 µg Se per g dry weight (dw) in the Bay. Nevertheless, concentrations in *P. amurensis* reached as high as 20 µg Se per g dw in October 1996. The enriched concentrations in bivalves (6–20 µg Se per g dw) were widespread throughout North San Francisco Bay in October 1995 and October 1996. Concentrations varied seasonally from 5 to 20 µg Se per g dw, and were highest during the periods of lowest river inflows and lowest after extended high river inflows. Transplanted bivalves (oysters, mussels or clams) were not effective indicators of either the degree of Se contamination in *P. amurensis* or the seasonal increases in contamination in the resident benthos. Se is a potent environmental toxin that threatens higher trophic level species because of its reproductive toxicity and efficient food web transfer. Bivalves concentrate selenium effectively because they bioaccumulate the element strongly and lose it slowly; and they are a direct link in the exposure of predaceous benthivore species. Biological invasions of estuaries are increasing worldwide. Changes in ecological structure and function are well known in response to invasions. This study shows that changes in processes such as cycling and effects of contaminants can accompany such invasions. © 2002 Published by Elsevier Science B.V.

* Corresponding author. Tel.: +1-650-329-4481; fax: +1-650-329-4545.

E-mail address: snluoma@usgs.gov (S.N. Luoma).

¹ Present address: University of California at Davis, Davis, CA, USA.

Keywords: *Potamocorbula amurensis*; Selenium; Exotic bivalve

1. Introduction

Selenium is an environmental toxicant that has been responsible for adverse reproductive effects and local extinctions of fish and birds in cooling reservoirs of coal-fired power plants (Lemly, 1985), wetlands receiving agricultural drainage (Presser and Ohlendorf, 1987; Skorupa, 1998) and river ecosystems draining seleniferous agricultural lands (e.g. the Colorado River and its tributaries; Hamilton, 1999). Although selenium is nutritionally essential, the window is narrow between essential concentrations in food and concentrations that cause adverse effects (Hodson and Hilton, 1983). Selenium becomes a reproductive toxin at slightly enriched concentrations because it substitutes for sulfur in the tertiary structures of proteins and thereby causes deformities in embryos or inhibition of the hatchability of eggs (e.g. Stadtman, 1974; Diplock, 1976; Skorupa, 1998).

Assessment of selenium effects in aquatic systems is complicated by the differing bioavailability of its several oxidation states (VI, selenate; IV, selenite; 0, elemental selenium; -II, selenide) and the occurrence of organic or inorganic forms within an oxidation state (Cutter and Bruland, 1984; Cutter, 1989). Biogeochemical conversion of dissolved Se to particulate forms is also complicated. Organic selenide is produced by plants (such as phytoplankton) or other primary producers (Wrench, 1978; Wrench and Measures, 1982) after uptake of selenite or selenate. Particulate elemental selenium is produced via dissimilatory reduction of selenate or selenite by bacteria (Oremland et al., 1990). Particulate selenium is a critically important phase because diet is the primary route of selenium exposure for invertebrates and other animals (Lemly, 1985; Luoma et al., 1992). Bivalves are especially effective bioaccumulators of selenium because they assimilate almost all the selenium they ingest with particulate material (e.g. from phytoplankton; Luoma et al., 1992) and they lose the element slowly (rate constants of loss are 0.01–0.03 per day; Reinfelder et al.,

1997). The selenium bioaccumulated by invertebrate consumers like bivalves is efficiently transferred to their predators upon ingestion and concentrations can be biomagnified in predator tissues. Therefore, selenium most seriously threatens upper trophic level birds and fish (Lemly, 1995).

Although predators are the species of greatest concern with regard to selenium contamination, they are mobile, impractical to sample in large numbers, and generally not especially useful for routine monitoring. Consumer species like bivalves are practical to sample (Phillips and Rainbow, 1993), and they integrate the influences of environmental concentrations, speciation and transformation of selenium. Bioaccumulated selenium in consumers is the critical link in exposure of predators. Monitoring contaminant exposure in a bioindicator is not a substitute for other types of investigations, but it can help focus more complicated studies of fate and effects (Brown and Luoma, 1995).

San Francisco Bay, the largest estuary on the west coast of North America, is formed by the confluence of the Sacramento River and the San Joaquin River. The North Bay extends from the confluence of the two rivers to the Golden Gate, and is comprised of Suisun Bay toward the rivers, an intermediate, large and shallow San Pablo Bay, and Central Bay seaward (Fig. 1). The largest water management system in the world can divert 30% of the Sacramento River during high flows and 60% during the low flow season before it reaches the Bay (for agriculture and drinking water; Nichols et al., 1986). Nearly all of the San Joaquin River is recycled southward for agricultural/urban uses by the water management system, during most months, especially in dry years. Wide seasonal and year-to-year changes in freshwater inflow are linked to precipitation and water management (Nichols et al., 1986). Seasonal and year-to-year differences in river inflows control hydraulic residence times in Suisun Bay, the salinity gradient, and distributions of dissolved and

particulate constituents like selenium (Largier, 1996; Monismith et al., 1996; Nichols et al., 1986).

San Francisco Bay is one of the few estuaries in which selenium contamination has been studied (Cutter, 1989; Johns et al., 1988). In the 1980s concentrations of selenium in birds, fish (White et al., 1988; Urquhart and Regalado, 1991) and invertebrates (Johns et al., 1988) in the Bay were high enough to be of concern (Luoma et al., 1992), despite relatively low concentrations of selenium in water (Cutter, 1989). Refineries were the predominant source of selenium during this period, especially during the season of low river discharge (Cutter and San Diego-McGlone, 1990). Saline soils rich in selenium are common in the western San Joaquin Valley (SJV). Release of selenium is accelerated by irrigation of those soils and disposal of irrigation drainage has contaminated ground water, wetlands and riverine habitats in the SJV (Presser and Ohlendorf, 1987). Selenium contamination in the San Joaquin River is well known (Presser and Ohlendorf, 1987); and San Joaquin River inputs could be a source of selenium when waters from that river reach the Bay. The selenium studies of the 1980s showed little input from this source, but those studies were conducted during a prolonged drought when

little runoff from the San Joaquin River reached the Bay.

The purpose of the present paper is to contrast Se contamination in the water column and in bivalves between the mid-1980s and 1995–1997. Two changes have occurred in the intervening period that could affect Se cycling in the Bay. First, beginning in the mid-1980s, an invading species of bivalve, *Potamocorbula amurensis*, became the predominant benthic macroinvertebrate in the Bay (Carlton et al., 1990). Biological invasions of estuaries have become an increasing problem worldwide and are known to change community structure and function (Cohen and Carlton, 1998; Carlton and Geller, 1993). *P. amurensis* is a voracious feeder that has essentially eliminated the standing stock of phytoplankton from the water column of the Suisun Bay (Cloern, 1996). The result has been an increase in energy available to the benthic food web and a decrease in energy available to the water column food web (J. Thompson, USGS, personal communication). Second, greater than normal precipitation and high river runoff occurred during this study period (May 1995–November 1997), in contrast to the periods of drought that characterized earlier study periods. This could result in more selenium

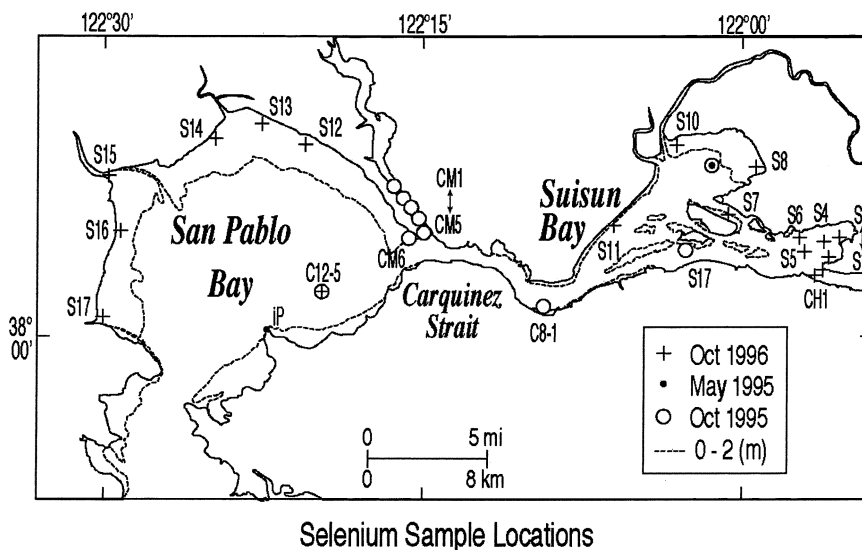


Fig. 1. Shoal (S) and Channel (C) sites sampled in North San Francisco Bay for *P. amurensis* in May 1995, October 1995 and October 1996.

entering the Bay from the agricultural runoff than occurred previously. Our study investigates several questions:

- have selenium concentrations in the predominant benthos changed after the invasion of *P. amurensis*?
- Are the seasonal and spatial patterns of selenium contamination different from those recorded earlier?
- Is selenium contamination focused in specific habitats where the element might be expected to accumulate (shallow waters vs. adjacency to marshes vs. deeper channel waters)?
- Is selenium uptake by *P. amurensis* different than in co-occurring species or experimentally transplanted species?

2. Experimental design

Four experiments were conducted to evaluate the implications of the invasion and the status of selenium contamination. To establish a reliable baseline of Se concentrations in the bivalves and evaluate seasonal variability, samples were collected near monthly from October 1995 through November 1997 at the station nearest Carquinez Strait (USGS 8.1), traditionally the most Se-contaminated reach of the Bay-Delta. Additional sites were added to resolve the spatial distribution of selenium enrichment in the bivalves. In October 1995, *P. amurensis* were collected from five locations in the tidal reaches of the Napa River and one site toward the river mouths from Carquinez Strait (USGS 6.1). The Napa River meets the Bay at Carquinez Strait, where Se concentrations have been highest. In October it is expected that the Napa River and the Bay exchange water in both directions throughout the sampling area (D. Schoelhammer, USGS, personal communication). Twenty-four sites were sampled in October 1996 to compare contamination in San Pablo and Suisun Bays and to compare deeper water sites (four stations) to shallow sites (20 stations) adjacent to different marshes. Finally, to evaluate if transplanted bivalves yielded results typical of the native community, *P. amurensis* were collected in May 1995, October 1995 and October 1996 from

three sites near those used in bivalve transplants by the San Francisco Bay Regional Monitoring Program (RMP; Fig. 1). These sites were in Grizzly Bay, Carquinez Strait (USGS 8.1) and San Pablo Bay-Pinole Point (USGS 12.5).

3. Methods

Resident clams (*P. amurensis*) were collected from the subtidal zone with a Van Veen grab and 1 or 2 mm sieves. Channel depths ranged from 8 to 20 m. The subtidal sites adjacent to marshes in Honker Bay and the Napa River (Fig. 1) were located in the shallows at an average depth of 1–3 m. Clams were also collected intertidally at low tide with a shovel, sieve and bucket. Between 60 and 120 clams of all sizes were collected at each time and each site and placed into containers of water collected at the site. The clams were kept in this ambient water in a constant temperature room at 10 °C to depurate for 48 h, as previous studies showed a residence time of material in the gut of *P. amurensis* to be approximately 24 h (Decho and Luoma, 1991). Clams from each site were separated into size classes of 1 mm difference and similar sized individuals were composited. Samples of larger numbers of individuals were necessary for smaller size classes in order to obtain enough mass for analysis. Soft tissues were dissected from the shell and tissues. Each composite was then lyophilized and homogenized. Mean concentrations characteristic of a site at a particular time were determined from analyses of three replicate composite samples each containing 20–60 individuals (each composite contained at least 250 mg dry weight (dw) soft tissue).

Selenium in the bivalves was determined by hydride atomic absorption spectrophotometry. Selenium subsamples were digested in concentrated nitric and perchloric acids at 200 °C, reconstituted in hydrochloric acid, and then stored until analysis. All glassware and field collection apparatus were acid washed, thoroughly rinsed in ultra-clean deionized water, dried in a dust-free positive pressure environment, sealed and stored in a dust free cabinet. Quality control was maintained by frequent analysis of blanks, analysis of

National Institute of Standards and Technology standard reference materials (tissues and sediments) with each analytical run, and internal comparisons with prepared quality control standards. Analyses of National Institute of Technical Standards (NITS) reference materials (oyster tissue, San Joaquin soils) were within an acceptable range of certified values reported by NITS (data in Luoma and Linville, 1996).

Water and particulate samples were collected in June 1995 and October 1996 using methodologies described earlier (Cutter, 1989). Pre-cleaned teflon Go-Flo sampling bottles were used to obtain water 1 m below the surface. The water was filtered through pre-cleaned and pre-weighed 0.45 μm Nucleopore membrane filters into 1 l linear polyethylene bottles and acidified to pH 1.5 with HCl. Filters were carefully folded, placed in polyethylene vials and immediately frozen. Total dissolved selenium was determined by boiling a 4 M HCl acidified sample with potassium persulfate solution for 1 h; then analyzing as a selenite sample by selective generation of hydrogen selenide, liquid nitrogen-cooled trapping, and atomic absorption detection (0.01 mol l⁻¹ detection limit). The standard additions method of calibration was used to ensure accuracy and all determinations were made in triplicate. Particulate selenium determinations were made using digestion procedures described by Cutter (1985) and procedures for reducing iron concentrations described by Cutter (1989). Filters were dried at 40 °C, re-weighed, then digested using a three step nitric-perchloric acid digestion. After iron removal by passage through an anion exchange resin, the digest was analyzed as a total selenium sample.

4. Results and discussion

4.1. River discharge

River discharges could influence allochthonous inputs of selenium from the San Joaquin River. Probably more important are the inflows from the Sacramento River, which has very low selenium concentrations and dilutes enriched Se inputs to

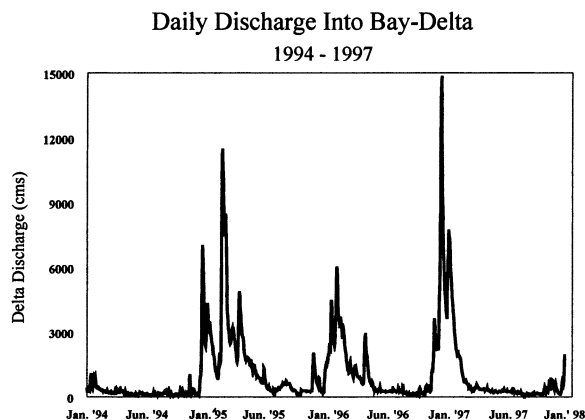


Fig. 2. Daily river discharge into San Francisco Bay, determined as net delta outflow at Chipps Island in Suisun Bay, between 1 January 1994 and 30 November 1997, as m³ s⁻¹.

the Bay (Cutter, 1989). The Mediterranean climate of the area drives a seasonal cycle in river discharge and causes large year-to-year variability in discharge. Nearly all precipitation occurs in the watershed between approximately November and April. The early flow is trapped in dams and snowfall; the highest river flows typically occur from January through approximately June, followed by low river flows through the rest of the year (Fig. 2). Interannual differences also reflect differences in precipitation. The period of record for the present study, 1995–1997, was characterized by high peak river inflows and, especially in 1995, a prolonged period of elevated river discharge. Previous studies of selenium in San Francisco Bay occurred between 1976 and 1977 and 1986 and 1990. Both were periods of prolonged drought, except for a flood in April 1986. Fig. 2 contrasts the patterns of river discharge in 1995–1997 to a typical drought year (1994) when both the magnitude and the period of high river discharges are reduced (also see hydrograph in Johns et al., 1988).

4.2. Selenium in the water column

Fig. 3(a) compares total dissolved selenium concentrations in estuarine transects from June 1995 to October 1996, with concentrations determined by the same methods in September 1986

(Cutter, 1989). All values are plotted as a function of salinity. Arrows depict the location of Carquinez Strait in each transect. Selenium concentrations in the Bay in 1995–1996 exceeded those in the Sacramento River, as in previous studies ($0.065 \pm 0.022 \mu\text{g Se per l}$; Cutter and San Diego-McGlone, 1990). The highest concentration in the Bay was $0.29 \mu\text{g l}^{-1}$. Within the Bay-Delta the concentrations at most stations followed the order June 1995 < October 1996 < September 1986, but the differences among the three transects were small, and appear to fall with the range of variation defined by Cutter and San Diego-McGlone (1990). The shape of the October 1996 transect differed from that in September 1986 because of elevated selenium concentrations at the upstream-most station, perhaps indicating some San Joaquin input. Total dissolved Se concentrations

were low compared with the USEPA water quality standard of $5 \mu\text{g Se per l}$ (Environmental Protection Agency, 1992).

Particulate selenium is the variable most likely to ultimately determine selenium bioavailability (Luoma et al., 1992). Concentrations of selenium on suspended particulate material were determined only in October 1996, during the present study. Particulate selenium was uniformly higher in Oct 1996 than in the estuarine transect conducted in September 1986 (Cutter, 1989; Fig. 3(b)). The highest concentration was observed in the river station in October 1996 (nearly $8 \mu\text{g g}^{-1}$ dw), again indicating particulate selenium inputs from the San Joaquin River were possible (subsequent studies have not found these high values, however; Cutter et al., unpublished data).

4.3. Selenium in *P. amurensis*

4.3.1. Spatial variability

Among the stations that were sampled in May 1995, selenium concentrations in soft tissues of *P. amurensis* ranged from 3.7 ± 0.7 to $7.1 \pm 0.3 \mu\text{g Se per g dw}$ (Table 1). Se concentrations were higher in *P. amurensis* from the Carquinez Strait ($7.1 \mu\text{g Se per g dw}$), than ($P < 0.01$) in the shallows of Suisun Bay ($3.9 \mu\text{g Se per g dw}$) and San Pablo Bay ($3.7 \mu\text{g Se per g dw}$). The latter two sites were not statistically different. Concentrations in October 1995 were higher than in May 1995. Se in *P. amurensis* from Carquinez Strait ($15.4 \mu\text{g Se per g dw}$) and Suisun Bay ($14.5 \mu\text{g Se per g dw}$) were not statistically different; but both were higher than Se concentrations in San Pablo Bay ($11.6 \mu\text{g Se per g dw}$; $P < 0.05$; Table 1). Concentrations were also elevated in the tidal Napa River compared with May concentrations in the North Bay.

Concentrations of Se in *P. amurensis* in October 1996 were similar to October 1995 (Table 1; Fig. 4). The range of mean Se concentrations in *P. amurensis* was 6.9 – $8.7 \mu\text{g Se per g dw}$ in San Pablo Bay, and 5.9 – $20 \mu\text{g Se per g dw}$ in Suisun Bay. The greatest enrichment was observed in the Carquinez Strait ($20.0 \mu\text{g Se per g dw}$). Higher concentrations were observed toward the rivers, at stations S1–S6, compared with other shallow water locations in Suisun Bay or San Pablo Bay

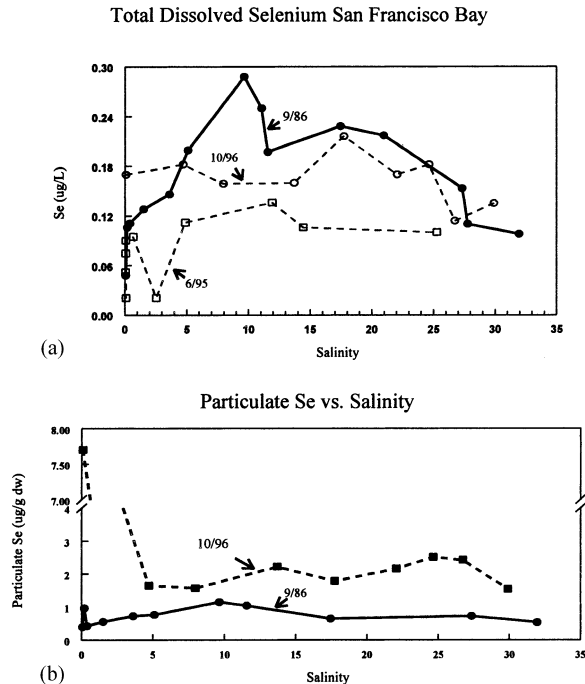


Fig. 3. (a) Dissolved Se concentrations ($\mu\text{g Se per l}$) as a function of salinity, determined in transects across the salinity gradient of North San Francisco Bay in September 1986 (Cutter, 1989), June 1995 and October 1996. (b) Concentrations of particulate Se ($\mu\text{g Se per g dw}$) as a function of salinity determined in transects across the salinity gradient of North San Francisco Bay in September 1986 (Cutter, 1989) and October 1996.

Table 1

Selenium concentrations in $\mu\text{g g}^{-1}$ dw in *P. amurensis* at 29 locations in North San Francisco Bay (Fig. 1) in May 1995, October 1995, and October 1996

Site	Se ($\mu\text{g g}^{-1}$ dry)	Standard deviation (S.D.)	Sample composites
<i>May 1995</i>			
Grizzly Bay	3.9	0.8	5
8.1 (Carq. Straits)	3.7	0.7	3
San Pablo Bay-Pinole Pt.	7.1	0.3	3
<i>October 1995</i>			
6.1	14.5	1.4	3
8.1 (Carq. Straits)	15.4	1.0	3
12.5 (San Pablo)	11.6	1.1	5
Napa 1	12.5	1.0	3
Napa 2	15.3	n/a	1
Napa 3	14.1	0.5	3
Napa 4	14.0	0.9	3
Napa 5	12.7	0.7	2
Napa 6	12.6	0.8	5
<i>October 1996</i>			
4.1	11.0	1.0	7
6.1	16.8	1.6	5
8.1 (Carq. Straits)	20.0	1.4	4
12.5 (San Pablo)	8.7	2.1	4
S1	9.6	0.2	2
S2	9.2	0.1	2
S3	7.5	0.1	2
S4	10.0	0.0	2
S5	8.9	0.4	5
S6	10.3	0.8	2
S7	5.9	1.6	4
S8	6.1	0.3	2
S9	8.2	0.7	4
S10	6.7	0.2	3
S11	7.3	0.3	4
S12	8.3	0.3	2
S13	8.1	0.5	2
S14	8.1	0.7	3
S15	6.9	1.2	3
S16	7.5	0.3	3
S17	7.9	0.7	2

Each sample composite included approximately 20–60 individual *P. amurensis*, and >250 mg dw soft tissue. Napa River stations are numbered North-to-South ascending. Stations S1–S17 are in shallow water.

($P < 0.001$; Table 1; Fig. 4). Like dissolved and particulate concentrations in October 1996, the higher concentrations toward the rivers in *P. amurensis* could have reflected inputs from the San Joaquin River.

Thus all three samplings of bivalves indicate that Se concentrations in *P. amurensis* are enriched compared with background concentrations

typical of bivalves (< 3 $\mu\text{g Se per g}$; Johns et al., 1988) and that enrichment is widespread through North San Francisco Bay. Concentrations varied nearly 4-fold among sites. The observation of the highest concentrations near Carquinez Strait is consistent with past studies (Cutter, 1989; Johns et al., 1988) and the previously identified refinery source of Se input. Dilution of contamination (i.e.

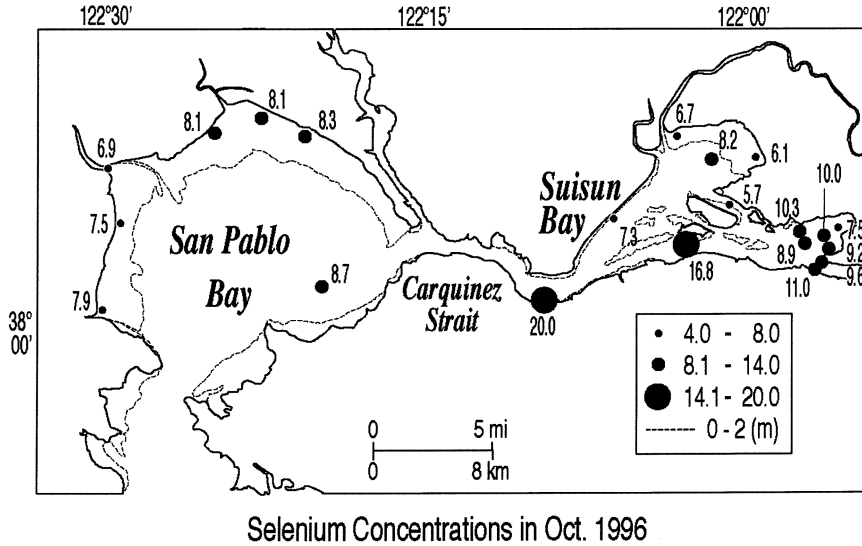


Fig. 4. Map showing distribution of mean Se concentrations in *P. amurensis* ($\mu\text{g Se per g dw}$) at 20 locations in Suisun and San Pablo Bays, in North San Francisco Bay, in October 1996. Standard deviations (S.D.) are shown in Table 1. Site codes are shown in Fig. 1.

the lowest concentrations in *P. amurensis*) near the eastward marshes in Suisun Bay and the western-most shallows of San Pablo Bay are consistent with dilution away from the refineries. Sources and mixing appeared to be more important than shallow versus deep-water habitat, despite the possibility that selenium is trapped in shallow wetlands. Some riverine input is also possible. Long residence times and complicated, tidally driven circulation patterns (Bureau et al., in prep.) probably contribute to the somewhat complicated pattern of the contamination in *P. amurensis* in Suisun and San Pablo Bay during periods of low river inflow.

4.4. Temporal variability

Selenium concentrations in *P. amurensis* from Carquinez St. varied as much as three-fold seasonally between May 1995 and November 1997 (Fig. 5). The lowest concentrations were observed in May 1995 ($7.1 \pm 0.3 \mu\text{g Se per g dw}$) and May 1997 ($6.2 \pm 0.2 \mu\text{g Se per g dw}$). Concentrations were highest in October 1995 to February 1996 ($15.4 \pm 1.0 \mu\text{g g}^{-1}$ – $18.9 \pm 0.4 \mu\text{g Se per g dw}$), October 1996 ($20 \pm 1.4 \mu\text{g Se per g dw}$), and

November 1997 ($15.3 \pm 3.4 \mu\text{g Se per g dw}$). The larger standard deviations in the four samples in late 1997 are probably the result of employing fewer individual animals per composite.

The seasonal pattern of selenium in *P. amurensis* from Carquinez Strait coincided with seasonal changes in river inflows. The lowest concentrations always occurred after episodes of highest river inflows and shortest hydraulic residence

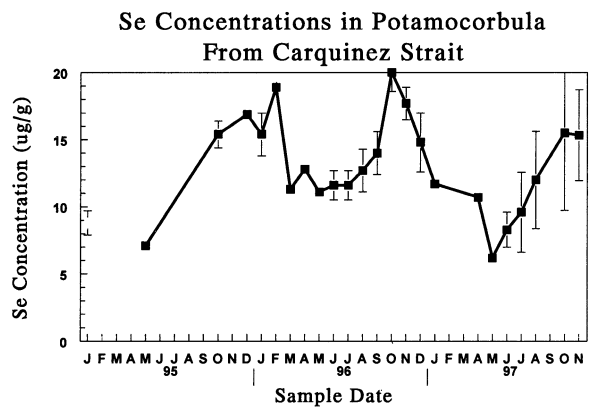


Fig. 5. Mean and S.D. of Se concentrations in *P. amurensis* ($\mu\text{g Se per g dw}$) at site C8.1 as determined at near monthly intervals between May 1995 and November 1997.

times. The greatest increase in Se occurred after prolonged periods of low flow, as hydraulic residence times increased. Increased Se bioaccumulation with increased residence times has been reported in other systems (Lemly, 1998). In contrast, Johns et al. (1988) did not observe strong seasonality in concentrations of Se in *Corbicula fluminea* in Suisun Bay, in the mid-1980s. One important difference was that that study did not include periods of river inflows as high or as prolonged as those occurring in 1995–1997.

4.5. Comparison to historic concentrations in bivalves

The selenium concentrations in *P. amurensis* in Suisun and San Pablo Bay are considerably higher than found in bivalves, in general, in uncontaminated estuaries in Northern California (1.7–3.1 μg Se per g dw, Johns et al., 1988; White et al., 1988). Data from *P. amurensis* itself is not available from uncontaminated estuaries. Concentrations in *P. amurensis* are also higher than in earlier studies from the Bay. Selenium exposures in the bivalves *Mytilus edulis* and *C. fluminea* were studied near Carquinez Strait in 1975 and 1984–1986, respectively (Risebrough, 1977; Johns et al., 1988). Risebrough et al. (1977) reported a mean concentration of 8 ± 3 μg Se per g dw in transplanted *M. edulis* from four sites near Carquinez Strait and concentrations of 10–11.4 μg Se per g dw in bivalves deployed directly in Carquinez Strait. These were some of the highest concentrations in the Bay at that time. Johns et al. (1988) sampled resident *Corbicula amurensis* at near monthly intervals from a station toward the rivers from Carquinez Strait (the most seaward population of *Corbicula* present in Suisun Bay at the time). In 67 samples they found a mean concentration of 6 ± 3 μg Se per g dw in the clams. Mean selenium concentrations in *P. amurensis* among all the samples reported above (15 ± 3 μg Se per g dw) were higher than found previously in either *M. edulis* or *C. fluminea*. The dominant bivalve in Suisun Bay changed from *C. fluminea* in 1985–86 to *P. amurensis* after the invasion of the latter species (Carlton et al., 1990; Nichols et al., 1990), so an increase in the exposure of ben-

thic predators to Se is likely if they consumed the invasive bivalve.

4.6. Comparison to monitoring with co-occurring and transplanted bivalves

Some species possess characteristics that enhance their bioaccumulation of contaminants. High assimilation efficiencies of selenium are typical of most marine organisms (Reinfelder et al., 1997; Wang and Fisher, 1999). But some species (copepods are an example) lose selenium rapidly (~ 0.15 per day) compared with other elements (Wang and Fisher, 1998), whereas loss rates from bivalves are slow (0.01–0.03 per day; Luoma et al., 1992; Reinfelder et al., 1997). Efficient assimilation and slow loss means that bivalves have generally strong capabilities to bioaccumulate selenium in their tissues (Reinfelder et al., 1997). *P. amurensis* is an unusually voracious filter feeder, it has an unusually short gut residence time (Decho and Luoma, 1991) and it utilizes a variety of food sources. All of these traits could enhance its ability to bioaccumulate Se, even compared with other bivalves.

Direct comparisons with co-occurring species are difficult with *P. amurensis*, because it tends to replace other bivalves and consumer organisms (Nichols et al., 1990). In June 1997 we found *P. amurensis* from a Carquinez Strait mudflat had 12.9 ± 1.2 μg Se per g dw and a co-occurring population of *M. balthica* contained 3.7 ± 0.1 μg Se per g dw. But this was only one coincident sampling. A comparison of *P. amurensis* with *C. fluminea* toward the rivers in Suisun Bay found similar concentrations in both species in October 1996, but sample sizes were very small. Conclusive determination of any special bioaccumulative characteristics of *P. amurensis* await further comparisons with co-occurring species and comparative kinetic studies.

An alternative approach is to compare Se bioaccumulation in *P. amurensis* with values in transplanted bivalves used to monitor the Bay. In the RMP of the San Francisco Estuarine Institute (SFEI, 1995, 1996), bivalves are transplanted for 90–100 days then contaminant uptake is compared with concentrations observed before the

Table 2

Comparison of selenium concentrations in transplant and resident species in North Bay in May 1995, October 1995 and October 1996

Site	Species transplant	Change in condition index ($T_F - T_0$)	Se ($\mu\text{g g}^{-1}$ dry) [$T_F - T_0$]	Species: resident	Se ($\mu\text{g g}^{-1}$ dry)
<i>May 1995</i>					
Grizzly Bay	<i>C. fluminea</i>	0.018	1.4 [−0.3]	<i>P. amurensis</i>	3.9 ± 0.8
Napa R. (Carquinez)	<i>C. gigas</i>	−0.022	6.2 [4.6]	<i>P. amurensis</i>	7.1 ± 0.3
San Pablo Bay-Pinole Pt.	<i>C. gigas</i>	0.006	5.4 [3.8]	<i>P. amurensis</i>	3.7 ± 0.7
<i>October 1995</i>					
Grizzly Bay	<i>C. fluminea</i>	−0.02	4.8 [0.1]	<i>P. amurensis</i>	14.5 ± 1.4
Napa R. (Carquinez)	<i>C. gigas</i>	−1.04	2.9 [−0.2]	<i>P. amurensis</i>	15.4 ± 1.0
San Pablo Bay-Pinole Pt.	<i>M. californianus</i>	−0.02	2.5 [−0.8]	<i>P. amurensis</i>	11.6 ± 1.1
<i>October 1996</i>					
Grizzly Bay	<i>C. fluminea</i>	−0.038	2.9 [1.3]	<i>P. amurensis</i>	8.2 ± 0.7
Napa R. (Carquinez)	<i>C. gigas</i>	−0.089	7.2 [2.9]	<i>P. amurensis</i>	20 ± 1.4
San Pablo Bay-Pinole Pt.	<i>M. californianus</i>	−0.039	2.7 [−2.4]	<i>P. amurensis</i>	8.7 ± 2.1

For transplanted species the final concentration is presented with the level of bioaccumulation of selenium over deployment period ($T_F - T_0$) displayed in brackets. The change in condition index over the period of deployment, a measure of growth (or lack of feeding), is also presented. 'Transplant' data from SFEI, 1995, 1996.

deployment. The RMP employs three different bivalves, due to differing salinities in the Bay, *C. fluminea* is used in Suisun Bay; the oyster *Crassostrea gigas* is used near Carquinez Strait; and the mussel *Mytilus californianus* is used in San Pablo Bay. Three of the sampling locations used for *P. amurensis* were near the above locations used by the RMP, and the 1995–1996 studies with *P. amurensis* were conducted at the same time as an RMP sampling.

Table 2 shows concentrations of Se in the transplants and the level of bioaccumulation, or lack thereof, during deployment in May 1995, October 1995 and October 1996. Changes in condition index over the deployment period are also shown; and these are compared with concentrations in the resident *P. amurensis* at the end of the deployment period of the transplanted species. Absolute concentrations of Se in tissues and patterns of bioaccumulation in time and space are compared. The differences in absolute concentrations were small in May 1995. But substantial differences were

observed between the deployed bivalves and *P. amurensis* in both October 1995 and October 1996. In October 1995, selenium concentrations in *P. amurensis* were 11.6–15.4 $\mu\text{g Se per g dw}$ among the three sites. None of the deployed species bioaccumulated Se during the deployment (concentrations were similar to the original population) and concentrations ranged from only 2.5 to 4.8 $\mu\text{g Se per g dw}$ (Table 2). A similar result occurred in October 1996. In that experiment, bioaccumulation of selenium was observed in *C. gigas* but concentrations were less than half those in *P. amurensis* at a nearby site. No significant bioaccumulation occurred in *C. fluminea*, although the concentration of Se in *P. amurensis* at that site was $8.2 \pm 0.7 \mu\text{g Se per g dw}$. Thus the seasonal pattern of greatly increased bioaccumulation in October compared with May was clear in *P. amurensis* but was not observed in the deployed animals.

The approach used to study bioaccumulation may be the cause of the differences between Se

bioaccumulation in *P. amurensis* and the transplants, *C. fluminea*, *C. gigas* or *M. californianus*. Phytoplankton blooms in Suisun Bay have essentially disappeared since the *P. amurensis* invasion, presumably due to consumption of primary production by the invasive bivalve. It is notable that condition index appeared to decline in all transplants in both October experiments (Table 2). Reduced condition index after deployment suggests that the deployed bivalves were not feeding normally in the fall. Uptake from food is the predominant route of selenium exposure (Luoma et al., 1992; Wang and Fisher, 1999). Therefore, it is possible that non-feeding deployed animals were not exposed to environmental selenium. The deployed animals gave no indication that high selenium concentrations were common in the predominant benthic species in North Bay during the season of low river inflows. Thus, the transplanted animals did not provide an accurate picture of selenium contamination in the estuary, and did not reach the level of selenium contamination found in *P. amurensis*.

4.7. Consequences of high selenium concentrations in *P. amurensis*

Bivalves are a critical link for passing selenium to benthivores because trophic transfer is the primary route of predator exposure (Lemly, 1985). The highest concentrations of Se in *P. amurensis* are especially significant in that they exceed values that other studies have shown reduce growth or cause reproductive damage when ingested in experiments by birds and fish (Hamilton et al., 1990; Heinz et al., 1989). Teratogenicity, effects on hatchability of eggs and reduced growth of young life stages have a threshold of occurrence above 3–10 $\mu\text{g Se per g dw}$ in food in various studies (Lemly, 1998; Hamilton, 1999; Heinz et al., 1989). A high frequency of adverse effects is found when concentrations in food (prey) exceed 10–11 $\mu\text{g Se per g dw}$ (Skorupa, 1998; Adams et al., 1998). The highest concentrations in *P. amurensis* exceed the latter value by two-fold.

Some of the important resource species in the North Bay/Delta eat *P. amurensis* and presumably other bivalves (sturgeon, diving ducks

such as scoter and scaup, dungeness crab; Carlton et al., 1990). Earlier studies (White et al., 1988; Urquhart and Regalado, 1991) showed that these benthivores were the predators with the highest selenium concentrations. Average yearly Se concentrations in the liver of the diving duck, surf scoter, ranged from 75 to 200 $\mu\text{g g}^{-1} \text{ dw}$ in 1986–1990, a 7- and 14-fold increase from a reference site (Humboldt Bay). White sturgeon captured between 1986 and 1990 contained annual average concentrations ranging from about 9–30 $\mu\text{g Se per g dw}$ in liver ($n = 52$); and 7–15 $\mu\text{g Se per g dw}$ in flesh ($n = 99$). In 1986, the Dungeness crab had an average soft tissue concentration of 15 $\mu\text{g Se per g dw}$, which was a three fold increase from the reference site (Humboldt Bay). Predators that fed from the water column (e.g. striped bass) seemed to have lower selenium concentrations than the benthivores.

If the susceptibility of San Francisco Bay to invasion by the exotic species *P. amurensis* (Carlton et al., 1990) caused greater Se contamination in the benthos, this effect could be passed on to benthivores. Little data is available to evaluate selenium concentrations in benthivores after 1990. But the 5-year Se Verification Study extended from 1986 through 1990 (Urquhart and Regalado, 1991). *P. amurensis* was first observed in the Bay in 1986 and became well established by 1988 (Carlton et al., 1990; Nichols et al., 1990). Annual mean selenium concentrations in bivalves and two benthivores, sturgeon and scoter, were collected simultaneously in that study and in several of the years between 1986 and 1990. Bivalve selenium concentrations (not including *P. amurensis*) and benthivore concentrations were strongly correlated in that data set (Figs. 6 and 7). The highest values in benthivores were observed in 1989 and 1990. If the mean concentration of selenium in *P. amurensis* was inserted into Fig. 7 at the 1989–1990 benthivore concentration, the added point is consistent with changing selenium exposures of predators. Thus preliminary analysis indicates that the successful invasion of this new resident of Suisun Bay could have changed the exposure of at least some predators in this system.

5. Conclusions

Invasion of San Francisco Bay by the exotic bivalve, *P. amurensis*, resulted in an increase by threefold of selenium concentrations in the predominant macrobenthic food in the estuary. Se concentrations in bivalve-consuming benthivores in the North Bay appeared to increase between the time *P. amurensis* populations were first observed (1986, Carlton et al., 1990) and when it became established as the predominant benthic species (~1988–1990; Urquhart and Regalado, 1991). This is of concern because Se is a strong reproductive toxin for such species, and Se concentrations in *P. amurensis* in fall 1995 and 1996 were in excess of the toxicologic threshold for adverse effects on such predators. Se-contaminated *P. amurensis* were widespread in Suisun and San Pablo Bays in 1995 and 1996. Seasonal variability is an important feature of selenium contamination in *P. amurensis*, with the highest concentrations occurring in fall during the period of longest hydraulic residence times. Transplanted bivalves were not good surrogate indicators for exposure and contamination of the resident bivalve.

Selenium in Benthos Carquinez Strait

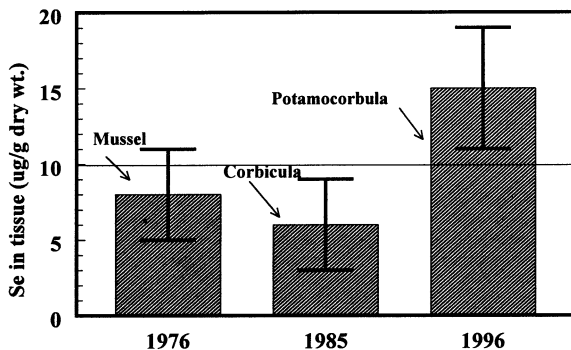
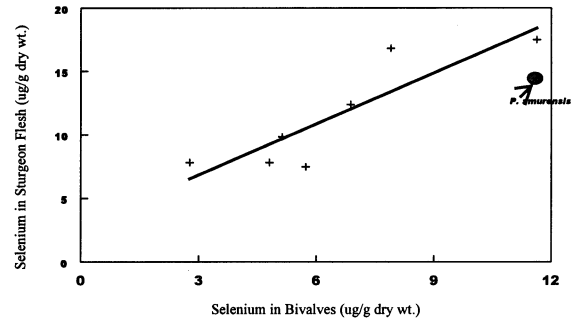


Fig. 6. Mean and S.D. of Se concentrations ($\mu\text{g Se per g dw}$) in three studies of bivalves from in or near Carquinez Strait in three different decades. 'Mussels' were studies of transplanted *M. edulis* in 1976 (Risebrough et al., 1977); 'Corbicula' represents mean of 67 samplings of the clam *C. fluminea* (Johns et al., 1988) and 'Potamocorbula' is the mean of all Carquinez samples in the present study.

Bivalves v. Sturgeon Flesh



Bivalves v. Scoter Flesh

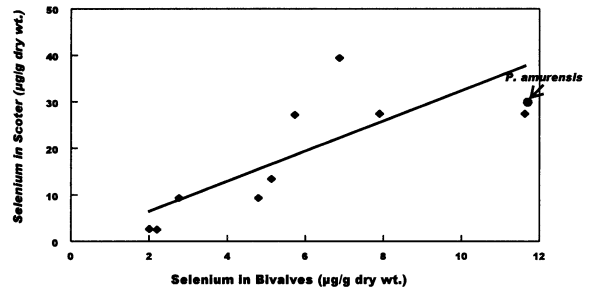


Fig. 7. Relationships between Se concentrations in resident bivalves (data from White et al., 1988; Urquhart and Regalado, 1991; Johns et al., 1988) and either sturgeon flesh or the flesh of the diving ducks (surf scoter) from North San Francisco Bay and Humboldt Bay (data from White et al., 1987, 1988, 1989; Urquhart and Regalado, 1991). Predators and prey were sampled in the same season, year and sub-bay. Mean Se concentration in *P. amurensis* at Carquinez in 1995 is superimposed on each graph to match predator data from 1989–1990, because *P. amurensis* was probably the primary food of these predators in 1989–1990.

We did not fully disprove the hypothesis that the invasive species, *P. amurensis*, is not more efficient at bioaccumulating selenium than other bivalves, although some evidence points in that direction. But this is not the only way an invasive species can affect the fate and effects of a contaminant. The efficient bioaccumulation of Se by bivalves, in general, and the efficient dietary transfer of Se from bivalves to higher trophic levels means that an invasion that shifts the structure of an estuarine community toward dominance by a bivalve-based benthic food web can enhance adverse effects of selenium in the system, by expand-

ing the availability of a contaminated food supply. Whatever the basic mechanism, it seems clear that the invasion of the non-native bivalve *P. amurensis* has resulted in increased bioavailability of a potent environmental toxin to certain benthivores in San Francisco Bay. Changes in contaminant cycling and potential effects are yet another reason to be concerned by the threat of invasive species in our estuarine ecosystems (Cohen and Carlton, 1998; Carlton and Geller, 1993).

Acknowledgement

Selenium analyses of *P. amurensis*, and quality control of those samples, were from the laboratory of A. Horowitz and K. Ehrlick, U.S. Geological Survey.

References

- Adams, W.J., Brix, K.V., Cothorn, K.A., Tear, L.M., Cardwell, R.D., Fairbrother, A., Toll, J.E., 1998. Assessment of selenium food chain transfer and critical exposure factors for avian wildlife species: need for site-specific data. In: Little, E.E., DeLonay, A.J., Greenberg, B.M. (Eds.), *Environmental Toxicology and Risk Assessment: Seventh Volume*. ASTM STP, p. 1333.
- Brown, C.L., Luoma, S.N., 1995. Use of the euryhaline bivalve *Potamocorbula amurensis* as a biosentinel species to assess trace metal contamination in San Francisco Bay. *Mar. Ecol. Prog. Ser.* 124, 129–142.
- Carlton, J.T., Geller, J.B., 1993. Ecological roulette—the global transport of nonindigenous marine organisms. *Science* 261, 78–82.
- Carlton, J.T., Thompson, J.K., Schemel, L.E., Nichols, F.H., 1990. The remarkable invasion of San Francisco Bay (California, USA) by the Asian clam *Potamocorbula amurensis*. I. Introduction and dispersal. *Marine Ecol. Prog. Ser.* 66, 81–94.
- Cloern, J.E., 1996. Phytoplankton bloom dynamics in coastal ecosystems: a review with some general lessons from sustained investigation of San Francisco Bay, California. *Rev. Geophys.* 34, 127–168.
- Cohen, A.N., Carlton, J.T., 1998. Accelerating invasion rate in a highly invaded estuary. *Science* 279, 555–558.
- Cutter, G.A., 1985. Determination of selenium speciation in biogenic particles and sediments. *Anal. Chem.* 57, 2951–2955.
- Cutter, G.A., 1989. The estuarine behaviour of selenium in San Francisco Bay: Estuarine. *Coastal Shelf Sci.* 28, 13–34.
- Cutter, G.A., Bruland, K.W., 1984. The marine biogeochemistry of selenium: a reevaluation. *Limnol. Oceanogr.* 29, 1179–1192.
- Cutter, G.A., San Diego-McGlone, M.L.C., 1990. Temporal variability of selenium fluxes in San Francisco Bay. *Sci. Total Environ.* 97/98, 235–250.
- Decho, A.W., Luoma, S.N., 1991. Time-courses in the retention of food material in the bivalves *Potamocorbula amurensis* and *Macoma balthica*: significance to the absorption of carbon and chromium. *Mar. Ecol. Prog. Ser.* 78, 303–314.
- Diplock, A.L., 1976. *Metabolic Aspects of Selenium Action and Toxicity*, CRC Critical Reviews in Toxicology.
- US Environmental Protection Agency, 1992. Rulemaking: water quality standards: establishment of numeric criteria for priority toxic pollutants: States' compliance: Final Rule. 57 Fed. Reg. 60848, 22 December 1992. Washington, DC.
- Hamilton, S.J., 1999. Hypothesis of historical effects from selenium on endangered fish in the Colorado River Basin. *Hum. Ecol. Risk Assess.* 5, 1153–1180.
- Heinz, G.H., Hoffman, D.J., Gold, L.G., 1989. Impaired reproduction of mallards fed an organic form of selenium. *J. Wildl. Manage.* 53, 418–428.
- Hodson, P.V., Hilton, J.W., 1983. The nutritional requirements and toxicity to fish of dietary and waterborne selenium. *Ecolog. Bull.* 35, 335–340.
- Johns, C., Luoma, S.N., Eldrod, V., 1988. Selenium accumulation in benthic bivalves and fine sediments of San Francisco Bay, the Sacramento-San Joaquin Delta and selected tributaries. *Estuarine Coastal Shelf Sci.* 27, 381–396.
- Largier, J.L., 1996. Hydrodynamic exchange between San Francisco Bay and the ocean: The role of ocean circulation and stratification. In: Hollibaugh, J.T., (Ed.) *San Francisco Bay The Ecosystem: Further Investigations into the Natural History of San Francisco Bay and Delta With Reference to the Influence of Man*.
- Lemly, A.D., 1985. Toxicology of selenium in a freshwater reservoir: implications for environmental hazard evaluations and safety. *Ecotoxicol. Environ. Safety* 10, 314–338.
- Lemly, A.D., 1995. A protocol for aquatic hazard assessment of selenium. *Ecotoxicol. Environ. Safety* 34, 223–227.
- Lemly, A.D., 1998. Pathology of selenium poisoning. In: Frankenberger, W., Engberg, R.A. (Eds.), *Environmental Chemistry of Selenium*. Marcel Dekker, New York, pp. 315–354 (pp. 281–296).
- Luoma, S.N., Linville, R.G., 1996. A comparison of selenium and mercury concentrations in transplanted and resident bivalves from North San Francisco Bay. *Annual Report of Regional Monitoring Program, 1995*. San Francisco Estuary Institute, pp. 160–171.
- Luoma, S.N., Johns, C., Fisher, N., Steinberg, N.A., Oremland, R.S., Reinfelder, J.R., 1992. Determination of selenium bioavailability to a benthic bivalve from particulate and solute pathways. *Environ. Sci. Tech.* 26, 485–491.
- Monismith, S.G., Burau, J.R., Stacey, M., 1996. Stratification dynamics and gravitational circulation in northern San Francisco Bay. In: Hollibaugh, J.T., (Ed.) *San Francisco*

- Bay The Ecosystem: Further Investigations into the Natural History of San Francisco Bay and Delta With Reference to the Influence of Man.
- Nichols, F.H., Cloern, J.E., Luoma, S.N., Peterson, D.H., 1986. The modification of an estuary. *Science* 231, 567–573.
- Oremland, R.S., Steinberg, N.A., Maest, A.S., Miller, L.G., Hollibaugh, J.T., 1990. Measurement of in situ rates of selenate removal by dissimilatory bacterial reduction in sediments. *Environ. Sci. Technol.* 24, 1157–1164.
- Phillips, D.J.H., Rainbow, P.S., 1993. *Biomonitoring of Trace Aquatic Contaminants*. Elsevier, London, p. 371.
- Presser, T.S., Ohlendorf, H.M., 1987. *Biogeochemical Cycling of Selenium in the San Joaquin Valley*, vol. 11. Environmental Management, California, USA, pp. 805–821.
- Reinfelder, J.R., Wang, W.X., Luoma, S.N., Fisher, N.S., 1997. Assimilation efficiencies and turnover rates of trace elements in marine bivalves: a comparison of oysters, clams and mussels. *Marine Biol.* 129, 443–452.
- Risebrough, R.W., Chapman, J.W., Okazaki, R.K., Schmidt, T.T., 1977. *Toxicants in San Francisco Bay and Estuary*. Report to the Association of Bay Area Governments, Berkeley, CA, pp. 38.
- SFEI, 1995, 1995. *The Regional Monitoring Program for Trace Substances*. San Francisco Estuary Inst, Richmond, CA, p. 385.
- SFEI, 1996, 1996. *The Regional Monitoring Program for Trace Substances*. San Francisco Estuary Inst, Richmond, CA, p. 360.
- Skorupa, J.P., 1998. Selenium poisoning of fish and wildlife in nature: lessons from twelve real-world examples. In: Frankenberger, W., Engberg, R.A. (Eds.), *Environmental Chemistry of Selenium*. Marcel Dekker, New York, pp. 315–354.
- Stadtman, T.C., 1974. Selenium biochemistry. *Science* 183 (128), 1915–1922.
- Urquhart, K.A.F., Regalado, K., 1991. *Selenium Verification Study, 1988–1990*. Water Resources Control Board Rept. 91 -2-WQ, Sacramento, CA, pp. 176.
- Wang, W.-X., Fisher, N.S., 1998. Accumulation of trace elements in a marine copepod. *Limnol. Oceanograph.* 43, 273–283.
- Wang, W.-X., Fisher, N.S., 1999. Delineating metal accumulation pathways for marine invertebrates. *Sci. Total Environ.* 237/238, 459–472.
- White, J.R., Hofmann, P.S., Hammond, D., Baumgartner, S., 1987. *Selenium Verification Study, 1986*. Water Resources Control Board Rept., Sacramento, CA, pp. 79.
- White, J.R., Hofmann, P.S., Hammond, D., Baumgartner, S., 1988. *Selenium Verification Study, 1986–1987*. Water Resources Control Board Rept., Sacramento, CA, pp. 60.
- White, J.R., Hofmann, P.S., Urquhart, K.A.F., Hammond, D., Baumgartner, S., 1989. *Selenium Verification Study, 1987–1988*. Water Resources Control Board Rept., Sacramento, CA, pp. 81.
- Wrench, J.J., 1978. Selenium metabolism in the marine phytoplankters *Tetraselmis tetraele* and *Dunaliella minuta*. *Mar. Biol.* 49, 231–236.
- Wrench, J.J., Measures, C.I., 1982. Temporal variations in dissolved selenium in a coastal ecosystem. *Nature* 299, 431–433.



Peer Reviewed

Title:

Ecosystem-scale Selenium Model for the San Francisco Bay-Delta Regional Ecosystem Restoration Implementation Plan

Journal Issue:

[San Francisco Estuary and Watershed Science, 11\(1\)](#)

Author:

[Presser, Theresa S.](#), U.S. Geological Survey
[Luoma, Samuel N.](#), John Muir Institute for the Environment, University of California, Davis

Publication Date:

2013

Permalink:

<http://escholarship.org/uc/item/2td0b99t>

Acknowledgements:

This work was supported by CALFED (in the project's earlier phases), the U.S. Geological Survey National Research and Toxics Substances Hydrology Programs, and the U.S. Environmental Protection Agency (San Francisco, California, Region 9). Jeanne DiLeo (U.S. Geological Survey, Menlo Park Publishing Service Center) prepared the outstanding graphics. We thank William Beckon and Thomas Maurer (U.S. Fish and Wildlife Service, Sacramento, California) for provision of species at risk for the Bay-Delta. We also thank William Beckon, Susan De La Cruz (U.S. Geological Survey, Vallejo, California) and Regina Linville (Office of Environmental Health Hazard Assessment, Sacramento, California) for assistance with species-specific effects models and human health considerations. Thanks also go to Mark Huebner (U.S. Geological Survey, Menlo Park, California) for exceptional assistance with manuscript preparation.

Keywords:

selenium, biodynamics, bioaccumulation, food webs, ecotoxicology, ecology, Environmental Chemistry, Environmental Health and Protection, Natural Resources Management and Policy, Environmental Science

Local Identifier:

jmie_sfews_11157

Abstract:

Environmental restoration, regulatory protections, and competing interests for water are changing the balance of selenium (Se) discharges to the San Francisco Bay-Delta Estuary (Bay-Delta). The model for Se described here as part of the Delta Regional Ecosystem Restoration Implementation



eScholarship
University of California

eScholarship provides open access, scholarly publishing services to the University of California and delivers a dynamic research platform to scholars worldwide.

Plan (DRERIP) draws both from the current state of knowledge of the Bay–Delta and of environmental Se science. It is an ecosystem-scale methodology that is a conceptual and quantitative tool to (1) evaluate implications of Se contamination; (2) better understand protection for fish and aquatic-dependent wildlife; and (3) help evaluate future restoration actions. The model builds from five basic principles that determine ecological risks from Se in aquatic environments: (1) dissolved Se transformation to particulate material Se, which is partly driven by the chemical species of dissolved Se, sets dynamics at the base of the food web; (2) diet drives bioavailability of Se to animals; (3) bioaccumulation differs widely among invertebrates, but not necessarily among fish; (4) ecological risks differ among food webs and predator species; and (5) risk for each predator is driven by a combination of exposures via their specific food web and the species' inherent sensitivity to Se toxicity. Spatially and temporally matched data sets across media (i.e., water, suspended particulate material, prey, and predator) are needed for initiating modeling and for providing ecologically consistent predictions. The methodology, applied site-specifically to the Bay–Delta, includes use of (1) salinity-specific partitioning factors based on empirical estuary data to quantify the effects of dissolved speciation and phase transformation; (2) species-specific dietary biodynamics to quantify foodweb bioaccumulation; and (3) habitat use and life-cycle data for Bay–Delta predator species to illustrate exposure. Model outcomes show that the north Bay–Delta functions as an efficient biomagnifier of Se in benthic food webs, with the greatest risks to predaceous benthivores occurring under low flow conditions. Improving the characterization of ecological risks from Se in the Bay–Delta will require modernization of the Se database and continuing integration of biogeochemical, ecological, and hydrological dynamics into the model.

Supporting material:

Appendix A

Copyright Information:

Copyright 2013 by the article author(s). This work is made available under the terms of the Creative Commons Attribution 4.0 license, <http://creativecommons.org/licenses/by/4.0/>

Ecosystem-Scale Selenium Model for the San Francisco Bay-Delta Regional Ecosystem Restoration Implementation Plan (DRERIP)

Theresa S. Presser^{1,†} and Samuel N. Luoma^{1,2}

ABSTRACT

Environmental restoration, regulatory protections, and competing interests for water are changing the balance of selenium (Se) discharges to the San Francisco Bay-Delta Estuary (Bay-Delta). The model for Se described here as part of the Delta Regional Ecosystem Restoration Implementation Plan (DRERIP) draws both from the current state of knowledge of the Bay-Delta and of environmental Se science. It is an ecosystem-scale methodology that is a conceptual and quantitative tool to (1) evaluate implications of Se contamination; (2) better understand protection for fish and aquatic-dependent wildlife; and (3) help evaluate future restoration actions. The model builds from five basic principles that determine ecological risks from Se in aquatic environments: (1) dissolved Se transformation to particulate material Se, which is partly driven by the chemical species of dissolved Se, sets dynamics at the base of the food web; (2) diet drives bioavailability of Se to animals; (3) bioaccumulation differs widely among invertebrates, but not necessarily among fish; (4) ecological risks dif-

fer among food webs and predator species; and (5) risk for each predator is driven by a combination of exposures via their specific food web and the species' inherent sensitivity to Se toxicity. Spatially and temporally matched data sets across media (i.e., water, suspended particulate material, prey, and predator) are needed for initiating modeling and for providing ecologically consistent predictions. The methodology, applied site-specifically to the Bay-Delta, includes use of (1) salinity-specific partitioning factors based on empirical estuary data to quantify the effects of dissolved speciation and phase transformation; (2) species-specific dietary biodynamics to quantify foodweb bioaccumulation; and (3) habitat use and life-cycle data for Bay-Delta predator species to illustrate exposure. Model outcomes show that the north Bay-Delta functions as an efficient biomagnifier of Se in benthic food webs, with the greatest risks to predaceous benthivores occurring under low flow conditions. Improving the characterization of ecological risks from Se in the Bay-Delta will require modernization of the Se database and continuing integration of biogeochemical, ecological, and hydrological dynamics into the model.

† Corresponding author: tpresser@usgs.gov

1 U.S. Geological Survey, 345 Middlefield Road, Menlo Park, CA 94025

2 Current affiliation: John Muir Institute of the Environment, University of California Davis, Davis, CA 95616

KEY WORDS

Selenium, biodynamics, bioaccumulation, food webs, ecotoxicology, ecology.

SAN FRANCISCO ESTUARY & WATERSHED SCIENCE

INTRODUCTION

The Delta Regional Ecosystem Restoration Implementation Plan (DRERIP) process focuses on construction of conceptual models that describe and define the relationships among the processes, habitats, species, and stressors for the Bay-Delta (DiGennaro and others 2012). The models use common elements and are designed to interconnect to achieve the goals of evaluating and informing Bay-Delta restoration actions. Selenium is recognized as an important stressor in aquatic environments because of its potency as a reproductive toxin and its ability to bioaccumulate through food webs (Chapman and others 2010; Presser and Luoma 2010a). Selenium's role is well documented in extirpation (i.e., local extinctions) of fish populations (Lemly 2002) and in occurrences of deformities of aquatic birds in affected habitats (Skorupa 1998). For Se, exposure is specific to a predator species' choice of food web and physiology, making some predators more vulnerable and, thus, more likely than others to disappear from moderately contaminated environments (Lemly 2002; Luoma and Presser 2009; Stewart and others 2004).

Concern about Se as a stressor in the Bay-Delta watershed originates from the damage to avian and fish populations that resulted when an agricultural drain to alleviate subsurface drainage conditions in the western San Joaquin Valley released Se into the Kesterson National Wildlife Refuge in the 1980s (Presser and Ohlendorf 1987). Later it was recognized that (1) some aquatic predators in the Bay-Delta were bioaccumulating sufficient Se to threaten their reproductive capabilities (SWRCB 1987, 1988, 1989, 1991) and; (2) primary Se sources included not only organic enriched sedimentary deposits in the San Joaquin Valley and elsewhere, but also their anthropogenic by-products such as oil (Cutter 1989; Presser 1994; Presser and others 2004). Proposals in 1978 and 2006 to extend an agricultural drain from the western San Joaquin Valley directly to the Bay-Delta as a way of removing Se from the valley were found both times to present substantial and broad ecological risks (e.g., USBR 1978, 2006; Presser and Luoma 2006).

Currently, Se contamination is spatially distributed from the Delta through the North Bay (Suisun Bay, Carquinez Strait, and San Pablo Bay) to the Pacific Ocean, mainly from oil-refining discharges internal to the estuary, and agricultural drainage discharges exported via the San Joaquin River. Regulatory and planning processes have intervened in the cases of both existing Se sources resulting in a decline in contamination since 1986-1992 when concentrations were maximal (SWRCB 1987, 1988, 1989, 1991; Presser and Luoma 2006; USBR 1995, 2001, 2009). However, the North Bay, the Delta, and segments of the San Joaquin River and some of its tributaries and marshes remain designated as impaired by Se (SWRCB 2011). More recently, the State initiated a Se Total Maximum Daily Load (TMDL) process to target both agricultural and oil refinery sources of Se (SFBRWQCB 2007, 2011) in coordination with development and implementation of site-specific water quality Se criteria for the protection of fish and wildlife by the U.S. Environmental Protection Agency (USEPA 2011a). The presence of a major oil-refining industry in the North Bay, and the substantial accumulated reservoir of Se in the soils and aquifers of the western San Joaquin Valley suggest that the potential for ecological risk from Se within the Bay-Delta watershed will continue into the foreseeable future as Se management and mitigation efforts take place (Presser and Luoma 2006; Presser and Schwarzbach 2008; USBR 2008; [Appendix A.1](#)).

Historic and more recent data show that certain predator species are considered most at risk from Se in the Bay-Delta (e.g., white and green sturgeon, scoter, scaup) because of high exposures obtained when they consume the estuary's dominant bivalve, *Corbula amurensis*, an efficient bioaccumulator of this metalloid (Stewart and others 2004; Presser and Luoma 2006). The latest available surveys of Se concentrations in *C. amurensis* and white sturgeon (*Acipenser transmontanus*) that were feeding (based upon isotopic evidence) in Carquinez Strait, Suisun Bay, and San Pablo Bay (Stewart and others 2004; Linares and others 2004; Kleckner and others 2010; Presser and Luoma 2010b; SFEI 2009) continue to show concentrations exceeding U.S. Fish and Wildlife Service (USFWS) dietary and tissue toxicity guide-

lines (Skorupa and others 2004; Presser and Luoma 2010b). Sturgeon contain higher concentrations of Se than any other fish species, reflecting their position as a top benthic predator (Stewart and others 2004). Surveys of surf scoter (*Melanitta perspicillata*) and greater scaup (*Aythya marila*) that feed voraciously on *C. amurensis* as they overwinter in Suisun Bay (SFEI 2005; De La Cruz and others 2008; De La Cruz 2010; Presser and Luoma 2010b) show Se has bioaccumulated to levels in muscle and liver tissue that may affect their ability to successfully migrate and breed (Heinz 1996; USDOJ 1998; Ohlendorf and Heinz 2011).

Endangered Species Act requirements led to a number of species being determined as jeopardized by Se in the Bay-Delta under a proposed chronic aquatic life Se criterion of 5 $\mu\text{g L}^{-1}$ (USFWS and NOAA Fisheries 2000), including delta smelt (*Hypomesus transpacificus*); longfin smelt (*Spirinchus thaleichthys*); Sacramento splittail (*Pogonichthys macrolepidotus*); Sacramento perch (*Archoplites interruptus*); tidewater goby (*Eucyclogobius newberryi*); green sturgeon (*Acipenser medirostris*) and its surrogate white sturgeon (*Acipenser transmontanus*); steelhead trout (*Oncorhynchus mykiss*); Chinook salmon (*Oncorhynchus tshawytscha*); California clapper rail (*Rallus longirostris obsoletus*); California least tern (*Sterna antillarum brownii*); bald eagle (*Haliaeetus leucocephalus*); California brown pelican (*Pelecanus occidentalis californicus*); marbled murrelet (*Brachyramphus marmoratus*); and giant garter snake (*Thamnophis gigas*). Recent analysis by the USFWS (2008a) of 45 species assumed the species most at risk depended on benthic food webs: greater scaup; lesser scaup (*Aythya affinis*); white-winged scoter (*Melanitta fusca*); surf scoter; black scoter (*Melanitta nigra*); California clapper rail; Sacramento splittail; green sturgeon; and white sturgeon. Not enough species-specific information is currently available for consideration of Se exposures for the giant garter snake, an endangered aquatic predator (USFWS 2006, 2009); the Dungeness crab (*Cancer magister*), an invertebrate that consumes *C. amurensis* (Stewart and others 2004); or for species that are within the Dungeness-crab food webs.

Human health advisories currently are posted for the Bay-Delta for the consumption of scoter, greater scaup, and lesser scaup based on elevated Se concentrations in their muscle and liver tissue (CDFG 2012, 2013). Selenium was found to be below the level of human health concern for consumption of edible tissue in certain species of fish, including white sturgeon, from the estuary (OEHHA 2011). White sturgeon contained the highest levels of Se among species of fish surveyed. Some individual white sturgeon sampled from North Bay locations had Se concentrations that exceeded Se advisory levels, based on specific consumption rates (see later detailed discussion under "Human Health" on page 23). Additionally, white sturgeon recreational fishing is limited, based on a decreasing species population (CDFG 2012).

It was recently suggested that the traditional regulatory approach to managing Se contamination is deeply flawed (Reiley and others 2003; Luoma and Presser 2009; Chapman and others 2010), and that a new conceptual model of the processes that control its toxicity is needed for regulatory purposes, especially in estuarine environments like the Bay-Delta. In recognition of the issues with the traditional approach to deriving a criterion for Se, the USEPA is leading a cooperative effort to develop site-specific fish and wildlife Se criteria for habitats affected by Se in California. Specifically for the Bay-Delta, the effort includes protection of Federally listed species and designated critical habitat (USFWS and NOAA Fisheries 2000; USEPA 2011a). Development of Se criteria for the Bay-Delta is proceeding first in this effort because the estuary is considered a sensitive hydrologic system and habitat in terms of Se and it was thought that protection here would elicit regulatory compliance upstream (USEPA 2011a). On the broader scale, Se is considered a general stressor of the estuary, and a constituent that should be analyzed as part of management and restoration planning and implementation (USEPA 2011b; NRC 2010, 2011, 2012).

The cooperative regulatory effort specifically recognizes that the new conceptual model must consider (1) the inaccuracies of deriving toxicity from waterborne Se concentrations; (2) the bioaccumulative nature of Se in aquatic systems; (3) Se's long-term

SAN FRANCISCO ESTUARY & WATERSHED SCIENCE

persistence in aquatic sediments and food webs; and (4) the importance of dietary pathways in determining toxicity (USEPA 1992, 2000a; USFWS and NOAA Fisheries 2000; Luoma and Presser 2009; Presser and Luoma 2006, 2010a, 2010b). Revisions by USEPA also are occurring at the national level to incorporate into the basis for regulation recent advances in the environmental science of Se. For example, a fish tissue Se criterion and implementation plan are being proposed to better integrate dietary exposure pathways into regulatory frameworks, and ensure an adequate link to toxicity (USEPA 2004, 2011b). During this transitional period when species may be jeopardized and while Se criteria are being revised, USEPA has applied the national chronic freshwater Se criterion of $5\mu\text{g L}^{-1}$ to the estuary (USEPA 1992, 2000a).

We present here an ecosystem-scale Se conceptual model for the Bay-Delta that addresses the needs of both the DRERIP process and the USEPA. Quantitative applications of the model are also possible. Quantification provides an opportunity to evaluate site-specific Se risks under different circumstances, using field data combined with a systematic quantification of each of the influential processes that link source inputs of Se to toxicity. The methodology is presented in terms of specified DRERIP components (i.e., drivers, linkages, and outcomes). As an example of how quantitative applications can be used, we calculate the dissolved ambient Se concentrations that would result in compliance with a chosen fish or bird tissue guideline under different assumptions or environmental conditions. Uncertainties and model sensitivities are illustrated by comparing outcomes of different exposure scenarios. The scenario approach could facilitate the model's use by decision-makers for quantitative evaluation of restoration alternatives for ecosystem management and protection.

MODEL OVERVIEW

The DRERIP Ecosystem-Scale Selenium Model for the Bay-Delta (Figure 1) has five interconnected modules that depict drivers (sources and hydrology), linkages (ecosystem-scale processes), concentration outcomes

(Se concentrations in water, particulates, and organisms), and food web exposure outcomes (effects on fish, wildlife, and human health). Model outcomes in Figure 1 are further refined to critical choices for modeling and species-specific risk scenarios for the Bay-Delta. Together the five modules consider the essential aspects of environmental Se exposure: biogeochemistry, food web transfer, and effects. They also take into account the estuary's ecology and hydrology as well as the functional ecology, physiology and ecotoxicology of the most vulnerable predator species. The modules define relationships that are important to conceptualizing and quantifying how Se is processed from water through diet to prey and predators, and the resulting effect on components of the food web. Thus, the DRERIP Ecosystem-Scale Selenium Model combines fundamental knowledge of Se behavior in ecosystems (Se drivers, linkages, and outcomes) with site-specific knowledge of the Bay-Delta (Bay-Delta drivers, linkages, and outcomes) to define site-specific Se risk (Figure 1).

The DRERIP Se submodels provide details for

- Sources and Hydrology (submodel A, Figure 2);
- Ecosystem-Scale Se Modeling (submodel B, Figure 3);
- Exposure: Food Webs, Seasonal Cycles, Habitat Use (submodels C, D; Figures 4, 5);
- Fish and Wildlife Health: Ecotoxicology and Effects (submodels E, F; Figures 6, 7); and
- Human Health (submodel G, Figure 8).

A human health pathway is designated, but emphasis here is on Se pathways to fish and wildlife health. The North Bay and the Delta are emphasized because the important Se sources have the potential to most affect those habitats and ecosystems (submodel A, Figure 2).

The quantitative DRERIP Ecosystem-Scale Selenium Model is based upon concepts and parameters developed elsewhere for a wide variety of aquatic systems and their food webs (submodel B, Figure 3; submodel E, Figure 6) (Luoma and Rainbow 2005; Luoma and Presser 2009; Chapman and others 2010; Presser and Luoma 2010a). To quantitatively apply the rela-

Delta Regional Ecosystem Restoration Implementation Plan Ecosystem-Scale Selenium Model

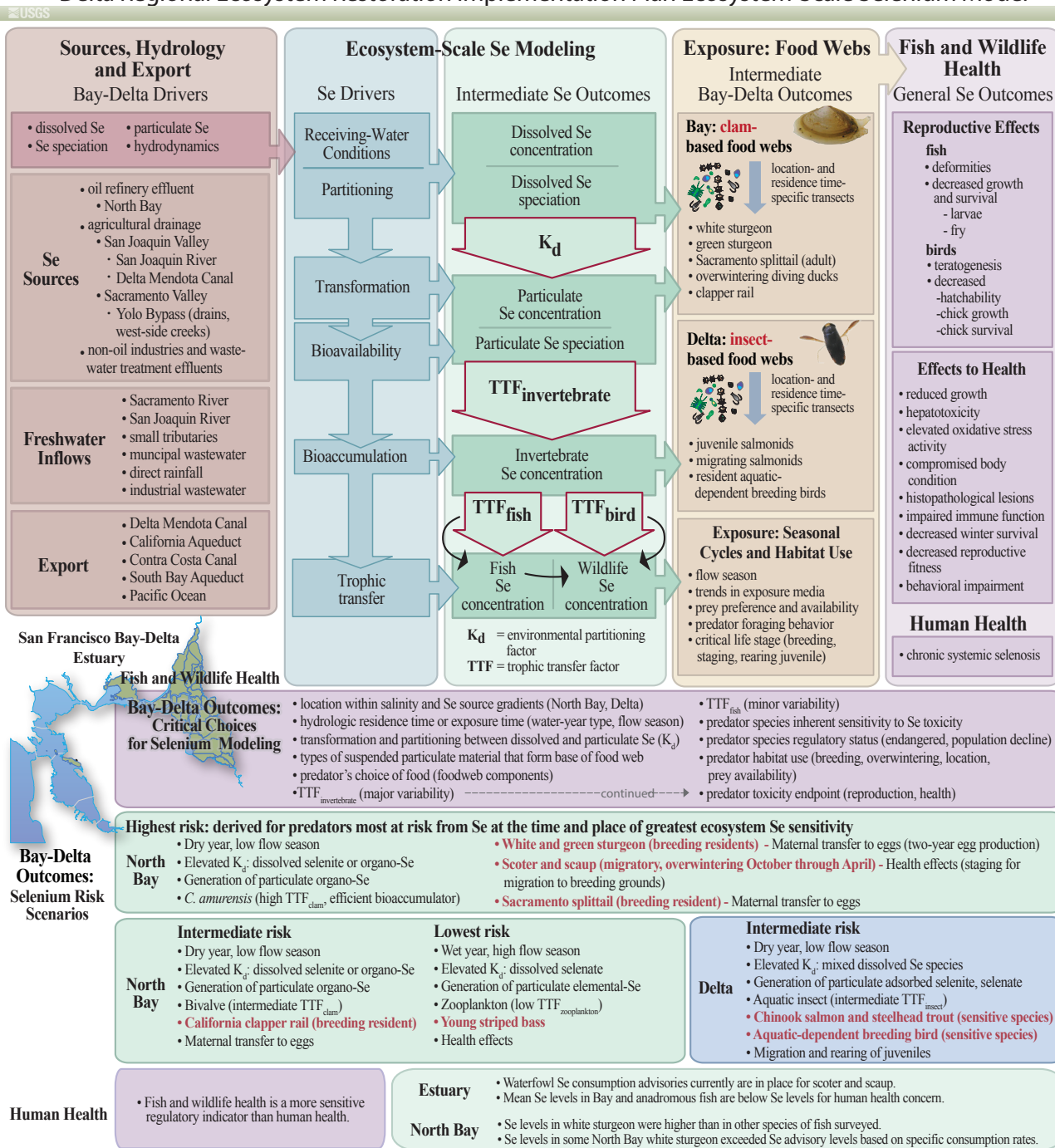


Figure 1 The DRERIP Ecosystem-Scale Selenium Model illustrates five interconnected modules that depict essential aspects of the Bay-Delta's hydrology, biochemistry, and ecology and of the exposure and ecotoxicology of predators at risk from selenium. These modules, and the detailed sub-models that follow, conceptualize (1) how selenium is processed from water through diet to predators and (2) its effects on ecosystems. Critical choices for modeling are summarized, and a quantitative application of the model for the estuary is derived for predators most at risk from Se at the time and place of greatest ecosystem Se sensitivity.

SAN FRANCISCO ESTUARY & WATERSHED SCIENCE

tionships in the conceptual model, we use empirical data from the Bay-Delta (e.g., Cutter and Cutter 2004; Presser and Luoma 2006, 2010b) to (1) help define environmental partitioning factors (K_d s) that quantify transformation of dissolved Se into particulate forms; and (2) help define biodynamic trophic transfer factors (TTFs) that quantify uptake by consumer species and their predators (submodel C, Figure 4; submodel D, Figure 5; submodel F, Figure 7). The broader, ecosystem-scale Se modeling approach was validated by comparing model forecasts with field data, across both a range of common food webs and hydrologic environments (Luoma and Rainbow 2005; Presser and Luoma 2010a) and specifically for the Bay-Delta and Newport Bay (Presser and Luoma 2006, 2009, 2010b).

The organizing principle for quantification is the progressive solution of a set of simple equations, each of which quantifies a process important in Se exposure (submodel B, Figure 3). The interaction of Se loading from different sources, hydrology, and hydrodynamics determine dissolved Se concentrations in the Bay-Delta. Transformation of Se from its dissolved form to a particulate form (represented here operationally as K_d) ultimately determines bioavailability to the food web. In a given environment, Se is taken up much faster from food than from solution by animals. Thus, the entry of Se into the food web can be estimated by a TTF for each trophic level. $TTF_{invertebrate}$ defines dietary uptake by a consumer species, which occurs when invertebrates (or herbivorous fish), feed on primary producers, detritus, microbes, or other types of particulate materials. Selenium bioaccumulation differs widely among invertebrate species because of different physiologies (Luoma and Rainbow 2005). These differences are captured by employing species-specific TTFs (Luoma and Presser 2009). Species-specific TTFs for predaceous fish and birds ($TTF_{predator}$) also are applied to the transfer of Se from invertebrate prey species to their predators (Presser and Luoma 2010a).

For the Bay-Delta, Stewart and others (2004) showed that Se concentrations differ widely among predators that live in the same environment. The main reason for those differences lies in the prey preferences of predators. For example, bass eating from the water-column food web consume invertebrates with much

lower Se concentrations than sturgeon eating benthic invertebrates, especially bivalves (Stewart and others 2004). The differences in Se uptake among predator species ($C_{predator}$) can be captured only if the correct prey species (or class of prey species) is included in the equation (submodel B, Figure 3) and the conceptualization (submodel C, Figure 4). This also means that the choice of predator species is critical in assessing risks from Se contamination.

Selenium concentrations in predators can be predicted with surprisingly strong correlation to observations from nature if particulate Se concentrations are known and an appropriate food web is used for the predator (Luoma and Presser 2009; Presser and Luoma 2010a). One use of these calculations might be to quantify the degree to which different species of birds and fish might be threatened by Se in a specified environment, for example. The correspondence between observed $C_{predator}$ and predictions of $C_{predator}$ from the series of equations that begins with dissolved concentrations (submodel B, Figure 3) depends upon how closely the partitioning between dissolved and particulate Se used in the model matches that occurring in the ecosystem of interest. One use of quantification in this instance is to run the model in the reverse direction to determine the dissolved Se concentration in a specific type of hydrologic environment and food web that would result in a specified Se concentration in the predator. Later, we present a detailed example of how the latter might be applied to real-world issues.

In the final step, effects on the reproduction and health of predaceous fish and birds are determined from bioaccumulated Se concentrations. Selenium is one of the few trace elements for which tissue concentrations have been correlated to these adverse effects in both dietary toxicity tests and field studies. The toxicity data for some of the key species in the Bay-Delta are limited or non-existent. The necessity of establishing effects thresholds from surrogate species adds some uncertainty to assessments of risk. Therefore, in our examples, we use different possible choices for such thresholds.

Additionally, modeling here is within a specified location and flow condition to provide context for

exposure and to help narrow the uncertainties in quantifying the ecological and physiological potential for bioaccumulation (Presser and Luoma 2010b).

MODULES

Sources, Hydrology, and Export

Estuary Mass Balance

The major portion of the estuary from the rivers to the Golden Gate Bridge is termed the Northern Reach, with Suisun Bay near the head of the estuary (submodel A, [Figure 2](#)). Selenium sources and their hydraulic connections within that reach have been documented in a number of publications (Cutter 1989; Cutter and San Diego-McGlone 1990; Cutter and Cutter 2004; Meseck and Cutter 2006; Presser and Luoma 2006, 2010b; SFBRQWCB 2011) ([Figure 1](#); submodel A, [Figure 2](#)). In brief, the most important regulated estuarine sources of Se are (1) internal inputs of oil refinery wastewaters from processing of crude oils at North Bay refineries; and (2) external inputs of irrigation drainage from agricultural lands of the western San Joaquin Valley conveyed mainly through the San Joaquin River. (submodel A, [Figure 2](#)). These and other potential Se sources are described in detail in [Appendix A.1](#). These details reflect the depth of history for Se management within the Bay-Delta watershed and the continuing tradeoffs that accompany their presence.

The Sacramento and San Joaquin rivers are the main sources of freshwater inflow to the Bay-Delta, with the Sacramento River being the dominant inflow under most conditions (Conomos and others 1979; Peterson and others 1985). The rivers provide 92% of the freshwater inflows to the Bay-Delta, with small tributaries and municipal wastewater providing approximately 3% each (McKee and others 2008).

In general, Se concentrations in the Sacramento River (above tidal influence, e.g., at Freeport) are low and relatively constant (1998 to 1999 average: $0.07 \mu\text{g L}^{-1}$; range 0.05 to $0.11 \mu\text{g L}^{-1}$) (Cutter and Cutter 2004). Dissolved Se concentrations in the San Joaquin River (above tidal influence, e.g., at Vernalis) were about an order-of-magnitude higher than those in the Sacramento River in 1999 (1998 to 1999 aver-

age: $0.71 \mu\text{g L}^{-1}$; range 0.4 to $1.07 \mu\text{g L}^{-1}$) (Cutter and Cutter 2004) and are much more variable. In the late 1980s and early 1990s concentrations above $5 \mu\text{g L}^{-1}$ were observed occasionally in the San Joaquin River (Presser and Luoma 2006), but in-valley source control efforts have reduced Se loads and concentrations ([Appendix A.1](#)).

In the present configuration of the Bay-Delta, the San Joaquin River is predominantly re-routed and exported back to the San Joaquin Valley (submodel A, [Figure 2](#); [Appendix A.1](#)). Hence, for the purposes of evaluating Se contamination sources, the simplest assumption is that the “baseline” Se concentrations (undisturbed by human activities) in the Delta would be close to the Se concentrations in the Sacramento River. The pre-disturbance baseline Se concentrations in the Bay or tidal reaches of the rivers would be concentrations in the Sacramento River mixed with concentrations in coastal waters, as reflected by the salinity of the sampling location. Deviations from that baseline reflect inputs of Se internal to the Bay (industrial or local streams) (Cutter and San Diego-McGlone 1990; Cutter and Cutter 2004) or input of Se to the Bay from the San Joaquin River.

The current San Joaquin River contributions to the Bay, thought to be minimal during most flow conditions, are especially difficult to measure ([Appendix A.1](#)). However, that could change. Under some proposals for modifications in water infrastructure, increased diversion of the Sacramento River through tunnels or canals would be accompanied by greater inflows from the San Joaquin River to the Delta and the Bay. In simulations available of the implications of such a change, Meseck and Cutter (2006) found that Se concentrations doubled in particulate material in the Bay.

The conceptual model described above suggests that parameters critical in determining the mass balance model for Se inputs for the Bay-Delta are (1) total river discharge (Sacramento River and San Joaquin River); (2) water diversions or exports (i.e., pumping at Tracy and Clifton Court Forebay south to the Delta-Mendota Canal and the California Aqueduct); (3) proportion of the San Joaquin River directly

Sources and Hydrology

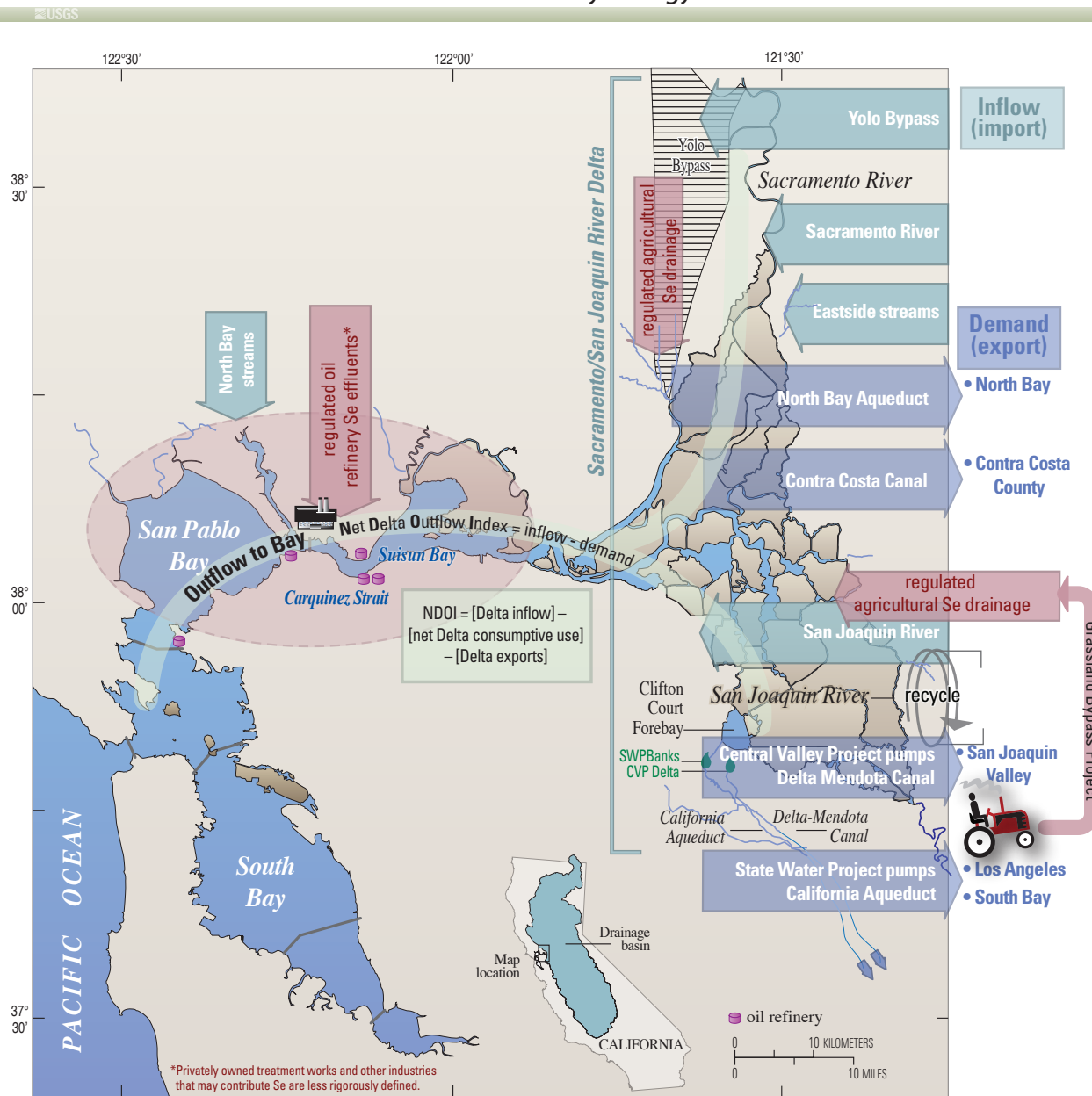


Figure 2 Submodel A. Sources and Hydrology

recycled south before it enters the Bay; 4) Se concentrations in each of the internal and external sources; and 5) total outflow of the rivers to the Bay or Net Delta Outflow Index (NDOI).

There are several uncertainties in quantification of the Se mass balance. One is the difficulty of precisely defining the contribution of the San Joaquin River to the NDOI, and hence the agricultural component of Se inputs to the Bay. Diversions and Delta hydrodynamics are sufficiently complex that every method available to determine that contribution has serious uncertainties (e.g., subtracting Sacramento River flow at Rio Vista from NDOI). Simple water accounting suggests minimal potential for flow from the San Joaquin River to enter the Bay (i.e., as measured by the percent by which river flow at Vernalis exceeds total export) during many months of the year (USBR 2012). Inputs are possible during spring months (April and May), wet and above normal years, and times of low capture efficiency (e.g., when river barriers are in-place) or when the ratio of the Sacramento River and San Joaquin River discharges is lowest in the fall.

A second uncertainty is that the strong tidal circulation in the Bay and the Delta mixes dissolved and particulate Se through the entire tidal reach, distorting spatial patterns that might otherwise help identify important sources of Se input (Ganju and others 2004). The three-dimensional nature of tidally driven hydrodynamics dissociates distributions of dissolved and particulate Se as well, adding complexity. One important outcome of this is that particulates contaminated with Se from industrial sources in Suisun Bay could feasibly be found throughout the full tidal range in both rivers, including otherwise uncontaminated segments of the Sacramento River. Riverine endmember concentrations of particulate Se, therefore, must be defined from landward of the reach of the tides, although river discharge at those locations does not necessarily represent riverine outflow to the Bay. Collecting an adequate mass of suspended particulate material for Se analysis in non-tidal freshwaters is challenging; therefore, few such data exist for the Sacramento River and even for some of the areas possibly affected by agricultural drainage. Hydrodynamic models of varying complexity are

available that can approximate water movements in this complex situation (e.g., Delta Simulation Model II). But modeling the distribution of particulate material (crucial for understanding implications of Se) is much more difficult (Ganju and others 2004).

Links Between Source Inputs and Water Inflows

Both Sacramento River and San Joaquin River discharges vary dramatically during the year depending on runoff, water management, and diversions. Residence (or retention) time is affected by river discharges (e.g., Cutter and Cutter 2004), but the strong tidal influences make that difficult to precisely define. Nevertheless, even a coarse differentiation of seasonal periods (low flow and high flow) and classification by water year (critically dry, dry, below normal, normal, above normal and wet) can be useful in evaluating influences on processes important to the fate and bioavailability of Se (Presser and Luoma 2006). Empirical data suggest processes such as dilution of local inputs and phase transformations that incorporate Se into organic particulate material appear to be affected by changes in retention time in the estuary, at least to some extent (Cutter and Cutter 2004; Doblin and others 2006; Presser and Luoma 2006, 2010a, 2010b). For example, Cutter and San Diego-McGlone (1990) found that a peak in selenite concentrations was centered around the area of inputs from oil refineries during low riverine inflows to the Bay in the 1980s; but that peak disappeared during periods of high riverine discharge. They used a one-dimensional model of the water and a Se mass balance to show that the mass of Se discharged by the refineries was the dominant source of selenite during low flows, but that it was insignificant compared to the mass of Se input from the Sacramento River during high flows. The selenite peak was reduced and replaced by a different pattern of dissolved Se speciation when Se discharges from the refineries were reduced by about half in 1999 (Cutter and Cutter 2004). Similarly, high Se concentrations in the southernmost Delta (Stockton) reflect San Joaquin River inputs, but concentrations seaward of this location decline as they are diluted by the large volumes of Se-poor Sacramento River water channeled into the Delta for export (Lucas and Stewart 2007). Local

SAN FRANCISCO ESTUARY & WATERSHED SCIENCE

tributaries could be an internal source of Se to the Bay, but these inputs occur almost entirely during high riverine inflow periods when their Se loads are insignificant compared to the large mass of Se carried into the Bay by high discharge from the Se-poor Sacramento River.

The NDOI, essentially inflow minus demand, is often used to indicate hydrologic influences on Se concentrations, including differences in retention time of a parcel of water in the Bay and Delta (Cutter and Cutter 2004). Increased exposure time (i.e., the cumulative amount of time a particle spends within a domain, taking into consideration repeated visits over multiple tidal cycles; L. Doyle, W. Fleenor, and J. Lund, University of California, Davis, pers. comms.; 2012) at the lowest inflows may explain why NDOI is a relevant indicator of the effect of flow on processes such as conversion of Se from dissolved to particulate forms.

Exports

The Delta–Mendota Canal, California Aqueduct, Contra Costa Canal, and South Bay Aqueduct all export water from the Delta. Thus, all are secondary recipients of the Se sources considered here (submodel A, Figure 2). The Delta–Mendota Canal also receives agricultural drainage directly, with that source proposed to be under regulatory control (USFWS 2009; USBR 2011). In general, however, few data are available to assess a mass balance for Se through the State Water Project, Central Valley Project, and other water-delivery systems.

In terms of export of Se to the Pacific Ocean from the Bay, some data are available for seaward locations in the Bay. Dissolved concentrations at these locations are among the lowest observed in the system when not under flood flows (Cutter 1989; Cutter and San Diego–McGlone 1990; Cutter and Cutter 2004); particulate concentrations are occasionally high, however. Under shorter residence times during high flows, increased dissolved concentrations near the Golden Gate Bridge (Cutter and Cutter 2004) suggest sources internal to the Bay affect ocean-dissolved Se concentrations. Outflows to the sea have been estimated in simple mass balance models (Cutter and San Diego–

McGlone 1990) although there are some uncertainties in such estimates. Ocean disposal was considered as one of the alternatives for comprehensive agricultural drainage management from the western San Joaquin Valley (USBR 2006). However, efficient Se recycling within productive ocean ecosystems and the opportunities for Se biomagnification in complex marine food webs suggest serious risks are likely (Cutter and Bruland 1984); hence, there are reasons for careful study before such options are considered.

Ecosystem-Scale Selenium Modeling

Dissolved Selenium Concentrations, Speciation, and Transformation

Total dissolved Se concentrations within the Bay range from 0.070 to 0.303 $\mu\text{g L}^{-1}$, with a mean of $0.128 \pm 0.035 \mu\text{g L}^{-1}$ and a median of 0.125 $\mu\text{g L}^{-1}$ across 128 samples collected since 1997 (Doblin and others 2006; Lucas and Stewart 2007). The mean concentration is only approximately two times higher than Se concentrations in the dominant freshwater endmember (the Sacramento River). In all surveys since the 1980s, Se concentrations in the tidal Bay and Delta are highest in Suisun Bay, with a downward spatial trend from Carquinez Strait toward the ocean. The latter suggests that dissolved concentrations in the ocean endmember are about the same as those in the Sacramento River.

The dissolved gradients of Se concentration are not necessarily the best indicators of the distribution of Se effects. Ecological implications depend upon the biogeochemical transformation from dissolved to particulate Se. Phase transformation of Se is of toxicological significance because particulate Se is the primary form by which Se enters food webs (Figures 1, 3 and 4) (Luoma and others 1992). Speciation of dissolved Se into its three dominant oxidation states is an important component in many conceptual models. In the Bay-Delta, speciation of dissolved Se is important because it influences the type and rate of phase transformation reaction that creates particulate Se. Examples of phase transformation reactions include (1) uptake by plants and phytoplankton of selenate, selenite, or dissolved organo-Se and transformation to particulate organo-Se by

Submodel B

Ecosystem-Scale Se Modeling

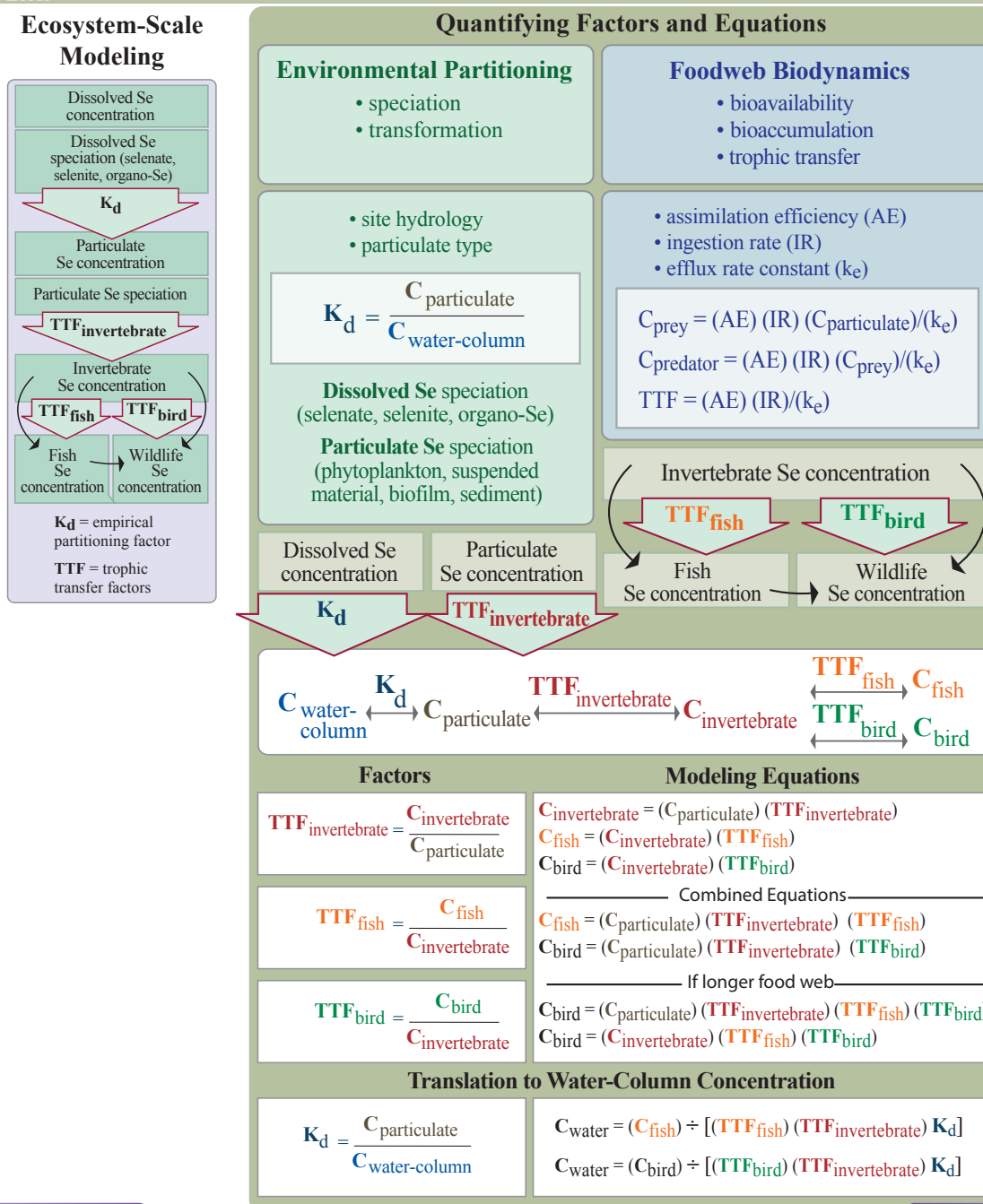


Figure 3 Submodel B. Ecosystem-Scale Se Modeling

SAN FRANCISCO ESTUARY & WATERSHED SCIENCE

assimilatory reduction, where uptake of selenate is considerably slower than uptake of the other two forms (e.g., Sandholm and others 1973; Riedel and others 1996; Wang and Dei 1999; Fournier and others 2006); (2) sequestration of selenate into sediments as particulate elemental Se by dissimilatory biogeochemical reduction (e.g., Oremland and others 1989); (3) adsorption as co-precipitated selenite through reactions with particle surfaces; and (4) recycling of particulate phases back into water as detritus or as dissolved organo-Se, after organisms die and decay (e.g., Velinsky and Cutter 1991; Reinfelder and Fisher 1991; Zhang and Moore 1996).

These different biogeochemical transformation reactions result in different forms of Se in particulate material: organo-Se, adsorbed Se, or elemental Se. Although only a few studies have determined speciation of particulate Se (e.g., Doblin and others 2006), such data can greatly aid in understanding bioavailability. Experimental studies show that particulate organo-Se is the most bioavailable form when it is eaten by a consumer species (Luoma and others 1992). Detrital or adsorbed Se is also bioavailable when ingested by animals, although to a lesser extent than organo-Se (Wang and others 1996). Non-particle associated elemental Se is not bioavailable (Schlekat and others 2000).

Concentrations of Se in particulate materials (per unit mass material) within the Bay and tidal freshwaters range widely from 0.1 to 2.2 $\mu\text{g g}^{-1}$ dry weight (dw), with a mean of $0.56 \pm 0.32 \mu\text{g g}^{-1}$ dw and a median of $0.45 \mu\text{g g}^{-1}$ dw ($n = 128$) since 1997 (Doblin and others 2006; Lucas and Stewart 2007). The 15-fold range in particulate concentrations contrasts sharply with the 4-fold range in dissolved concentrations, as do the contrasts in standard deviations. Not only are particulate concentrations much more dynamic than dissolved concentrations, but they also are about four times higher if expressed in common units. Both reflect biogeochemical transformation processes and, perhaps, inorganic adsorption. The latter is probably more important in soils than in the aquatic environment. Given the different dynamics and the variability of dissolved and particulate Se, it is not surprising that the ratio of the two also is quite variable.

Geochemical models that attempt to capture phase transformations of Se under different conditions are problematic. In fact, no models are available that can predict particulate Se concentrations based solely upon dissolved concentrations and biogeochemical conditions. One reason is that conventional thermodynamic equilibrium-partitioning models are inadequate for Se. Critical Se transformation processes are biological, and not predictable from thermodynamics. Some model approaches predict the particulate Se added on to a pre-existing particulate concentration, using a combination of phytoplankton productivity and re-suspension (Meseck and Cutter 2006; SWRCB 2011; Tetra Tech, Inc. 2010). While such models provide interesting estimates of temporal and spatial distributions of particulate Se, their major limitations lie in the basis upon which the pre-existing concentration is chosen and their inability to comprehensively account for all the processes involved in transformation.

The choice of the (pre-existing) baseline particulate Se concentration is critical to the questions models can address. Local data can be used for choosing pre-existing Se concentrations at the seaward and landward boundaries in the Bay-Delta. But the data used to date are from tidally affected reaches of the river, and are likely to be biased by redistribution of already contaminated particles from tidal pumping. As noted above, few data exist for particulate Se concentrations above the tidal reach of the Sacramento River; nor are there adequate determinations of Se concentrations on particulates from the coastal zone. In such a case, answers to questions about changing the internal Se inputs to the Bay are biased in that the boundary condition already includes such inputs (SWRCB 2011; Tetra Tech, Inc. 2010). On the other hand, this modeling approach appears to be well suited to test the influence of changing inputs from one boundary or from primary production alone (Meseck and Cutter 2006; Tetra Tech, Inc. 2010).

Observations of environmental partitioning of Se between dissolved and particulate phases can be employed to estimate transformation efficiencies in lieu of a comprehensive approach to modeling biogeochemical phase transformation for Se. Presser and Luoma (2006) first used field observations to

quantify partitioning, which they described by the somewhat controversial term K_d . Luoma and Presser (2009) were careful to emphasize that their K_d s represented conditional observations from the Bay-Delta at a specific time and place; and were not meant to be equilibrium constants. Thermodynamic equilibrium constants would be inappropriate to describe an inorganic to organic transformation. They pointed out that no single constant could be expected to apply to all environmental conditions either in the Bay-Delta or elsewhere. Site hydrology, dissolved speciation, and the type of particulate material are all influential, although specific influences were not necessarily predictable in quantitative terms. An operational approach was therefore chosen to try to estimate influences of such processes.

They defined K_d as the ratio of particulate material Se concentration (in dw) to the dissolved Se concentration observed at any instant in simultaneously collected samples. The specific equation is

$$K_d = (C_{\text{particulate material}}, \mu\text{g kg}^{-1} \text{ dw}) \div (C_{\text{water}}, \mu\text{g L}^{-1}) \quad (1)$$

Of interest here is the particulate matter at the base of the food web. As sampled in the environment that can include suspended particulate Se (which is a physically inseparable mix of phytoplankton, periphyton, detritus and inorganic suspended material), biofilm, sediment and/or attached vascular plants. Feeding characteristics of the organisms in question and data availability dictate the best choice among these. For example, for a filter-feeding bivalve in the Bay-Delta, Se concentrations determined in suspended particulate material (in $\mu\text{g g}^{-1} \text{ dw}$) are the preferred parameter for modeling because these animals filter their food from the water-column.

Some broad generalizations are possible about K_d s for Se (Presser and Luoma 2010a). For example, if all other conditions are the same, K_d will increase as selenite and dissolved organo-Se concentrations increase relative to selenate. Calculations using data from laboratory microcosms and experimental ponds show speciation-specific K_d s of 140 to 493 where selenate is the dominant form; 720 to 2,800 when an elevated proportion of selenite exists; and 12,197 to 36,300 for 100% dissolved seleno-methionine uptake

into algae or periphyton (Besser and others 1989; Graham and others 1992; Kiffney and Knight 1990). Compilations of K_d s also show different general ranges for rivers, streams, lakes, ponds, wetlands, and estuaries that are affected by Se inputs (Presser and Luoma 2010a), although with some overlap. Exposure time for phase transformation is probably an important factor driving differences among such systems. Estuaries are among the sites with the highest values (range of medians from 4,000 to 21,500) indicating efficient conversion of dissolved Se to particulate Se. Finally, although the influence of exposure time for a particle within an estuary is challenging to understand precisely, especially in the Bay-Delta because of the dominance of tidally driven circulation, K_d s seem to be higher during conditions where more time is available for transformation reactions to occur (Presser and Luoma 2010b).

The most recent transects of the Bay that provide spatially and temporally matched data for derivation of K_d s from dissolved and particulate Se concentrations were from June 1998 to November 1999 (Cutter and Cutter 2004; Doblin and others 2006). In these studies, samples were collected at 1 meter below the surface, and included dissolved Se concentrations, suspended particulate material Se concentrations, dissolved Se speciation, suspended particulate Se speciation, salinity, and total suspended material. These data were collected in four different transects across the salinity gradient in the Northern Reach under a variety of river discharge and presumed residence time conditions. The full range of dissolved Se concentrations in these transects was 0.070 to 0.303 $\mu\text{g L}^{-1}$. The suspended particulate material Se concentrations were more variable: 0.15 to 2.2 $\mu\text{g g}^{-1} \text{ dw}$. Calculated K_d s ranged from 712 to 26,912. The degree of variability across this whole data set is large. However, the largest part of the variability was driven by very high values in the landward-most and seaward-most samples, where dissolved concentrations were very low. Such ratios can be artificially inflated when values become very low in the denominator, if the numerator does not decline as rapidly. Tidal pumping of contaminated particles from the Bay upstream into the less contaminated Sacramento River water is a possible cause of such an effect.

SAN FRANCISCO ESTUARY & WATERSHED SCIENCE

Downstream transport of highly contaminated particles from the San Joaquin River into Bay or Delta water could also be a cause. Finally, seaward, where residence times are elevated in Central and San Pablo bays, biological transformation could enrich Se in particles while depleting it from the water column. If the goal is to find conditions where there is sufficient linkage between dissolved and particulate Se to be useful in forecasts of one from the other, none of these conditions would apply. Presser and Luoma (2010b) avoided such biases and thereby constrained variability by restricting K_{ds} geographically to the middle range of the salinity zone in Suisun Bay. This also focused the modeling on the most contaminated segment of the estuary.

If location is restricted to Carquinez Strait–Suisun Bay—eliminating freshwater and ocean interfaces—then the range of dissolved Se concentrations is narrowed to 0.076 to $0.215 \mu\text{g L}^{-1}$ and the range of suspended particulate material Se concentrations is narrowed to 0.15 to $1.0 \mu\text{g g}^{-1}$ dw. The variation of K_d is narrowed to a range of means of $1,180$ to $5,986$ (or of individual measurements, 712 to $7,725$). Because this data set is still large, median or mean concentrations, or a given percentile, can be used as viable indicators of partitioning in modeling scenarios.

Seasonality also is important, and restrictions to specific flow regimes also can be used to constrain variability. For example, the highest mean K_{ds} occur during periods of the lowest river inflows (and highest residence times). Constrained to Suisun Bay, the mean K_d was $1,180 \pm 936$ in June 1998. This was a high flow season wherein Cutter and Cutter (2004) estimated a residence time of 11 days. The mean K_d was $5,986 \pm 1,353$ in November 1999. This was a low flow season with an estimated residence time of 70 days. The mean K_d among all constrained samples was $3,317$, and the mean for low flow seasons was $4,710$.

Transects in the Delta were also conducted between 1998 and 2004 in different flow regimes (Doblin and others 2006; Lucas and Stewart 2007). Dissolved Se concentrations among all these samplings ranged from 0.083 to $1.0 \mu\text{g L}^{-1}$, with a mean of 0.25 ± 0.24 ($n = 72$). Particulate concentrations ranged from

0.27 to $6.3 \mu\text{g g}^{-1}$ dw, with a mean of 0.98 ± 0.94 ($n = 71$). As in the Bay transects, the range in particulate concentrations (23-fold) exceeds the range in dissolved concentrations (12-fold). Concentrations and variability, thus, were even greater in the Delta, overall, than in the Bay. In the Delta, K_{ds} ranged from 554 to $38,194$, with the range of means from $1,886 \pm 1,081$ in January 2003 (a high flow season) to $7,712 \pm 3,282$ in July 2000 (a low flow season). Sets of dissolved and particulate Se concentrations determined as part of focused research for the Delta in September 2001, the low flow season of a dry year, yielded some especially elevated K_{ds} ($>10,000$) (Lucas and Stewart 2007). In general, these elevated K_{ds} may reflect tidal pumping, or represent times and areas where Se is concentrating in particulate material because of differing hydrologic environments (e.g., slow-moving backwaters with high productivity). Constraining variability is more difficult in the Delta, hence, quantifying phase transformation from empirical data is more uncertain in this system.

Given the degree of variability in both the Bay and the Delta, modeling that requires linking dissolved Se to particulate Se should include several scenarios using different K_{ds} that are within a range of values constrained, as described above.

Uptake Into Food Webs

Kinetic bioaccumulation models (i.e., biodynamic models, Luoma and Fisher 1997; Luoma and Rainbow 2005, 2008) account for the now well-established principle that Se bioaccumulates in food webs principally through dietary exposure. Uptake attributable to dissolved exposure makes up less than 5% of bioaccumulated Se in almost all circumstances (Fowler and Benayoun 1976; Luoma and others 1992; Roditi and Fisher 1999; Wang and Fisher 1999; Wang 2002; Schlekat and others 2004; Lee and others 2006). Biodynamic modeling (submodels B and C, Figures 3 and 4) shows that Se bioaccumulation (the concentration achieved by the organism) is driven by physiological processes specific to each species (Reinfelder and others 1998; Wang 2002; Baines and others 2002; Stewart and others 2004). Biodynamic models have the further advantage of providing a basis for

deriving a simplified measure of the linkage between trophic levels: TTFs. For each species, a TTF can be derived from either experimental studies or field observations.

Experimental derivation of TTFs is based on the capability of a species to accumulate Se from dietary exposure as expressed in the biodynamic equation (Luoma and Rainbow 2005):

$$dC_{\text{species}}/dt = (AE) (IR) (C_{\text{food}}) - (k_e + k_g) (C_{\text{species}}) \quad (2)$$

where C_{species} is the contaminant concentration in the animals ($\mu\text{g g}^{-1} \text{ dw}$), t is the time of exposure in days (d), AE is the assimilation efficiency from ingested particles (%), IR is the ingestion rate of particles ($\text{g g}^{-1} \text{ d}^{-1}$), C_{food} is the contaminant concentration in ingested particles ($\mu\text{g g}^{-1} \text{ dw}$), k_e is the efflux rate constant (d^{-1}) that describes Se excretion or loss from the animal, and k_g is the growth rate constant (d^{-1}). Key determinants of Se bioaccumulation are the ingestion rate of the animal, the efficiency with which Se is assimilated from food, and the rate constant that describe Se turnover or loss from the tissues of the animal (Luoma and Rainbow 2005; Presser and Luoma 2010a). Experimental protocols for measuring such parameters as AE, IR, and k_e are now well developed for aquatic animals (Luoma and others 1992; Wang and others 1996; Luoma and Rainbow 2005). The rate constant of growth is significant only when it is comparable in magnitude to the rate constant of Se loss from the organism. Consideration of the complications of growth can usually be eliminated if the model is restricted to a long-term, averaged accumulation in adult animals (Wang and others 1996).

In the absence of rapid growth, a simplified, resolved biodynamic exposure equation for calculating a Se concentration in an invertebrate (submodel B, Figure 3) is

$$C_{\text{invertebrate}} = [(AE)(IR)(C_{\text{particulate}})] \div [k_e] \quad (3)$$

For modeling, these physiological parameters can be combined to calculate a $\text{TTF}_{\text{invertebrate}}$, which characterizes the potential for each invertebrate species to bioaccumulate Se. $\text{TTF}_{\text{invertebrate}}$ is defined as

$$\text{TTF}_{\text{invertebrate}} = [(AE)(IR)] \div k_e \quad (4)$$

Similarly, foodweb biodynamic equations for fish or birds are

$$C_{\text{fish or bird}} = [(AE) (IR) (C_{\text{invertebrate}})] \div k_e \quad (5)$$

and

$$\text{TTF}_{\text{fish or bird}} = [(AE) (IR)] \div k_e \quad (6)$$

Where laboratory data are not available, TTFs can be defined from field data, where the TTF defines the relationship between Se concentrations in an animal and in its food in dw. The field $\text{TTF}_{\text{invertebrate}}$ must be defined from spatially and temporally matched data sets (in dw or converted to dw) of particulate and invertebrate Se concentrations (submodel B, Figure 3) as

$$\text{TTF}_{\text{invertebrate}} = C_{\text{invertebrate}} \div C_{\text{particulate}} \quad (7)$$

A field derived species-specific TTF_{fish} is defined as

$$\text{TTF}_{\text{fish}} = C_{\text{fish}} \div C_{\text{invertebrate}} \quad (8)$$

where $C_{\text{invertebrate}}$ is for a known prey species, C_{fish} is reported as muscle or whole-body tissue, and both Se concentrations are reported in $\mu\text{g g}^{-1} \text{ dw}$ (submodel B, Figure 3).

Whether the TTFs are determined from the laboratory or the field, the modeling approach is sufficiently flexible to represent complexities such as mixed diets. For example, a diet that includes a mixed proportion of prey in the diet can be addressed using the equation

$$C_{\text{fish}} = (\text{TTF}_{\text{fish}}) [(C_{\text{invertebrate a}}) (\text{prey fraction}) + (C_{\text{invertebrate b}}) (\text{prey fraction}) + (C_{\text{invertebrate c}}) (\text{prey fraction})] \quad (9)$$

Equations are combined to represent step-wise bioaccumulation from particulate material through invertebrates to fish (submodel B, Figure 3) as

$$C_{\text{fish}} = (\text{TTF}_{\text{invertebrate}}) (C_{\text{particulate}}) (\text{TTF}_{\text{fish}}) \quad (10)$$

Similarly, for birds, the combined equation is

$$C_{\text{bird}} = (\text{TTF}_{\text{invertebrate}}) (C_{\text{particulate}}) (\text{TTF}_{\text{bird}}) \quad (11)$$

Modeling can accommodate longer food webs that contain more than one higher trophic level consumer (e.g., forage fish being eaten by predatory fish) by

SAN FRANCISCO ESTUARY & WATERSHED SCIENCE

incorporating additional TTFs. One equation for this type of example (submodel B, Figure 3) is

$$C_{\text{predator fish}} = \frac{(TTF_{\text{invertebrate}}) (C_{\text{particulate}})}{(TTF_{\text{forage fish}}) (TTF_{\text{predator fish}})} \quad (12)$$

Modeling for bird tissue also can represent Se transfer through longer or more complex food webs (e.g., TTFs for invertebrate to fish and fish to birds) as

$$C_{\text{bird}} = (TTF_{\text{invertebrate}}) (C_{\text{particulate}}) (TTF_{\text{fish}}) (TTF_{\text{bird}}) \quad (13)$$

Variability or uncertainty in processes that determine AEs or IRs can be directly accounted for in sensitivity analysis (Wang and others 1996). This is accomplished by considering the range in the experimental observations for the specific animal in the model. Field-derived factors require some knowledge of feeding habits, and depend on available data for that species. Laboratory and field factors for a species can be compared and refined to reduce uncertainties in modeling (Presser and Luoma 2010a).

A substantial number of species-specific TTFs are available (Luoma and Presser 2009; Presser and Luoma 2010a). These are enough data at least to begin to model important food webs. Across invertebrate species, TTFs range from 0.6 to 23. Of the 29 species studied, 27 species have TTFs > 1. Thus, most invertebrate species bioaccumulate as much as or more Se than concentrated in the trophic level below them. In other words, the concentration of Se biogeochemically transformed into algae, microbes, seston, or sediments is preserved and/or (bio)magnified as Se passes up food webs. In general, TTFs for bivalves (clams, mussels, oysters) and for barnacles are the highest among species of invertebrates (i.e., an experimentally determined TTF range of approximately 4 to 23) (Presser and Luoma 2010a).

Trophic transfer factors from the available data for fish have a median of approximately one, and vary much less than among invertebrates: from 0.5 to 1.8 (Presser and Luoma 2010a). Compilations show that TTFs derived from laboratory biodynamic experiments range from 0.51 to 1.8; TTFs for different fish species derived from field studies are similar, ranging from 0.6 to 1.7.

Trophic transfer factors for aquatic birds (diet to bird egg) are less well developed, and laboratory data are limited (Presser and Luoma 2010a). The most robust data from the laboratory relate Se concentrations in the diet (as seleno-methionine) to egg Se concentrations from controlled feeding of captive mallards (*Anas platyrhynchos*). The range of $TTF_{\text{bird egg}}$ calculated from the compilation of nominal experimental diet Se concentrations and mean egg Se data given in Ohlendorf (2003) for mallards is 1.5 to 4.5. Using the detailed data from Heinz and others (1989) narrows this range to 2.0 to 3.9, with a mean of 2.6. Field data could be used to refine $TTF_{\text{bird egg}}$ on a site-specific basis, but variability in food sources and habitat use may add uncertainty to such data, and limits applications among habitats.

Exposure: Food Webs, Seasonal Cycles, and Habitat Use

Selenium is at least conserved and usually biomagnified at every step in a food web (Presser and Luoma 2010a). Selenium toxicity is generally assumed to be observed first in specific predator species as differences in food web exposure are propagated up trophic pathways (Luoma and Rainbow 2005; Stewart and others 2004). Some invertebrate species also may be susceptible to environmentally relevant Se concentrations (Conley and others 2009, 2011). Selenium is usually not detoxified in animal tissues by conjugation with metal-specific proteins or association with non-toxic inclusions (Luoma and Rainbow 2008). Hence, general mechanisms that semi-permanently sequester metals in non-toxic forms and lead to progressive accumulation with size or age probably are less applicable to the metalloid Se than to metals in general (Luoma and Presser 2009).

Predator population distribution, feeding preference, prey availability, life stage, gender, physiology, and species sensitivity are all variables that influence how a predator is affected by Se. Field factors such as varying weather, water depth, human disturbance, and food dispersion also affect foraging energetics, and accessibility of contaminants in foods on a localized level. Despite these complexities, some generalizations are possible at the present state of

understanding. Predator species for the Bay-Delta, their food webs, and potential exposure are shown in submodels C and D (Figures 4 and 5), with further supporting information compiled in Appendix A.2 and A.3.

Based upon studies of invertebrate bioaccumulation the greatest exposures to Se will occur in predators that ingest bivalves in the Bay-Delta (Stewart and others 2004; Presser and Luoma 2006, 2010b). The estimated maximum percentages of diet that are clam-based for various benthic predators were estimated by the USFWS (2008a) (submodel C, Figure 4): lesser scaup 96%; surf scoter 86%; greater scaup 81%; black scoter 80%; white-winged scoter 75%; California clapper rail 64%; bald eagle 23%; white sturgeon (and assumed for green sturgeon) 41%; and Sacramento splittail (2-year olds) 34%. Dietary estimates are not specific to *C. amurensis*, but a bivalve component to diet in general. Bald eagles are an example of a predator with a diet wherein 23% are those waterfowl (scaups and scoters) that primarily feed on benthic mollusks (USFWS 2008a). Clapper rails feed on benthic food webs, but are littoral feeders that usually do not eat *C. amurensis*, which is mostly subtidal. Figure 4 (submodel C) also shows potential food webs for Dungeness crab. Diet component data and kinetic loss rates are not documented for life stages of this crustacean, but isotopic data indicate that clams such as *C. amurensis* would be expected to be an important food for this species (Stewart and others 2004). Selenium concentration data, in turn, indicate that predators of this crab would be subjected to elevated dietary Se concentrations (submodel C, Figure 4).

Food webs illustrated for Delta inhabitants include aquatic insects to salmonids (submodel C, Figure 4). The diets of salmon and steelhead trout are dominated by species with TTFs lower than bivalves. These species thereby incur less dietary Se exposure than molluscivores. Field data for Se concentrations are limited to 1986 to 1987 for Chinook salmon (Saiki and others 1991) and absent for steelhead trout that inhabit the estuary and migration corridors. Although their exposures are not exceptionally high, these species may be vulnerable because of their toxicological sensitivity to Se (USFWS 2008a, 2008b; Janz

2012). Delta smelt are endemic to the estuary and are included here because population numbers for the Delta smelt are alarmingly low. Thus, the USFWS (2008a) concluded that this species is particularly vulnerable to any adverse effect. It should be noted, however, that the feeding habits of Delta smelt would not suggest high exposures compared to other species, and sensitivity or bioaccumulation data are not available.

Not all predators reside in the estuary throughout their lives. When a predator is present across flow seasons and during critical life stages may influence Se exposure and effects. Predator seasonal cycle diagrams are shown for migratory birds (scoter and scaup); breeding birds (California clapper rail, bald eagle); migrating/rearing juveniles (Chinook salmon, steelhead trout); and breeding fish (green sturgeon, white sturgeon, and Sacramento splittail) (submodel D, Figure 5). The North Bay is part of the migration corridor and feeding ground for anadromous fish such as white sturgeon, Chinook salmon, and striped bass. The estuary also serves seasonally as a nursery area for species that spawn either in freshwater (e.g., Sacramento splittail) or in the ocean (e.g., Dungeness crab). Migrating diving ducks on the Pacific flyway winter and feed in the estuary as they stage for breeding in the freshwater ecosystems of the boreal forests of Canada and Alaska (De La Cruz and others 2009). As migratory waterfowl move north to breed in the spring, there is the potential for depuration of Se (USFWS 2008a; Appendix A.2 and A.3).

Some of the highest *C. amurensis* Se concentrations of the annual cycle occur when overwintering scoter and scaup actively feed in Suisun Bay and San Pablo Bay during the fall and early winter, (Linville and others 2002; Kleckner and others 2010) (submodel D, Figure 5). Long-lived white sturgeon feed predominantly on *C. amurensis* and have a two-year internal egg maturation that makes them particularly vulnerable to loading of Se in eggs and reproductive effects (Linville 2006). As an indication of this potential, Linares and others (2004) found Se concentrations as high as $47 \mu\text{g g}^{-1} \text{ dw}$ in immature gonads of 39 white sturgeon captured in the estuary. In earlier studies, Kroll and Doroshov (1991) reported that Se concentrations in developing ovaries

Submodel D

Exposure: Seasonal Cycles and Habitat Use

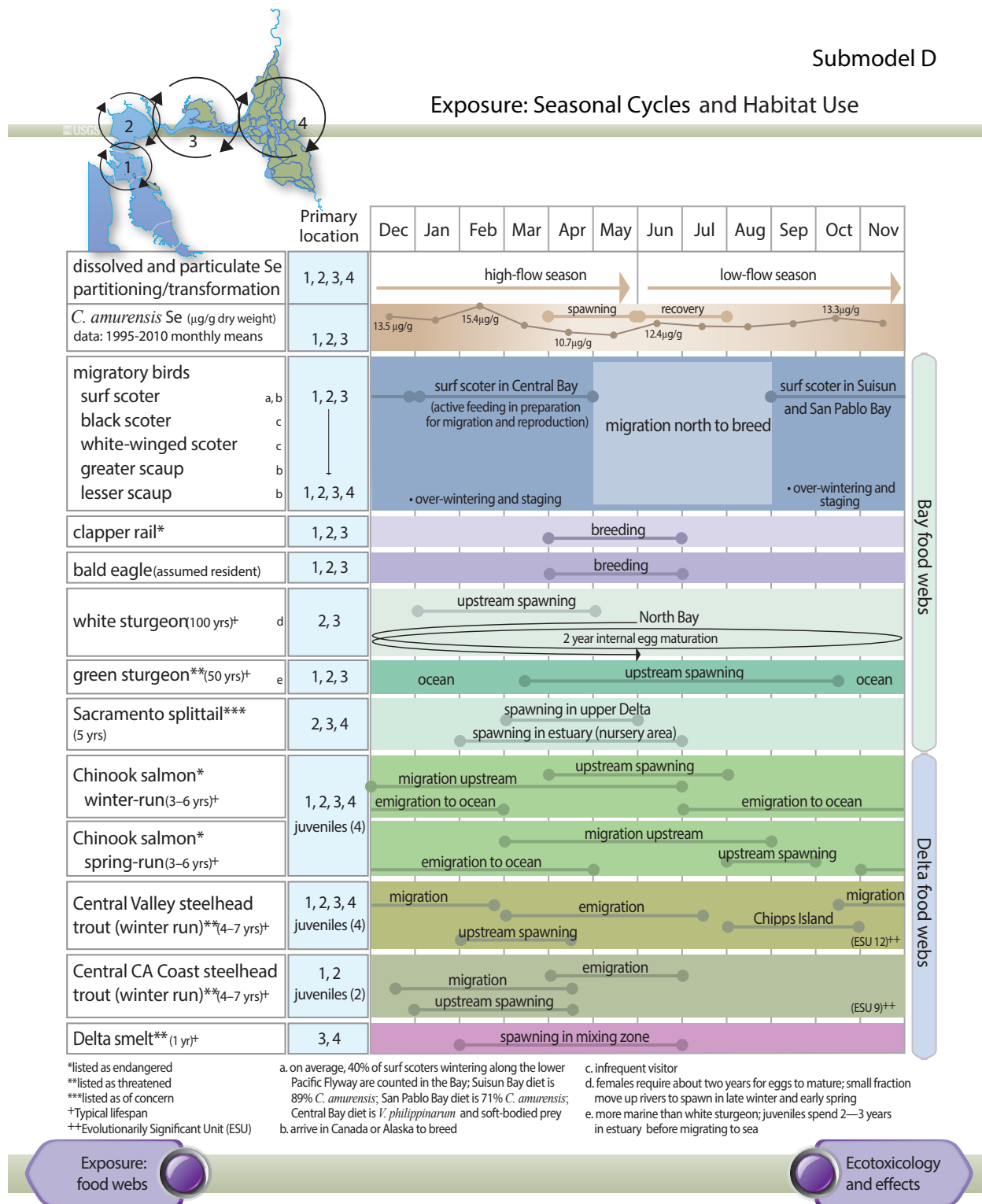


Figure 5 Submodel D. Exposure: Seasonal Cycles and Habitat Use

SAN FRANCISCO ESTUARY & WATERSHED SCIENCE

of white sturgeon from the Bay contained maxima of $72 \mu\text{g g}^{-1}$ and $29 \mu\text{g g}^{-1}$. This range of wild white sturgeon reproductive tissue Se concentrations approach or exceed levels that cause severe deformities and mortalities in newly hatched larvae (Lemly 2002; Linville 2006). Larger, older Sacramento split-tail also feed on *C. amurensis* and they are known to spawn both in the upper Delta and estuary (Stewart and others 2004). Modeling for species such as clapper rail would need specifics of diet composition (i.e., which species of clam, mussel, or crab is consumed), and whether prey species are efficient bioaccumulators of Se. Formalized, detailed knowledge such as this (submodel D, Figure 5), in turn, helps set choices in comparative modeling scenarios.

Fish and Wildlife Health: Ecotoxicology and Effects

Toxicity arises when dissolved Se is transformed to organic-Se by bacteria, algae, fungi, and plants (i.e., synthesis of Se-containing amino acids *de novo*) and then passed through food webs. It is generally thought that animals are unable to biochemically distinguish Se from sulfur, and therefore excess Se is substituted into proteins and alters their structure and function (Stadtman 1974). Other biochemical reactions also can determine and mediate toxicity (Chapman and others 2010). The effect of these reactions is recorded, most importantly in birds and fish, as failures in hatching or proper development (teratogenesis or larval deformities) (submodel E, Figure 6). Other toxicity endpoints include growth, winter survival, maintenance of body condition, reproductive fitness, and susceptibility to disease (submodel E, Figure 6; Appendix A.3). Specifically, Se can alter hepatic glutathione metabolism to cause oxidative stress (Hoffman and others 1998, 2002; Hoffman 2002) and diminished immune system function (Hoffman 2002).

Details of general ecotoxicological pathways of Se for fish and birds and effects of concern for Se are shown in submodel E (Figure 6). As represented here, birds and fish differ in how Se taken up from diet distributes among tissues (submodel E, Figure 6). Physiological pathways shown here for birds emphasize an exogenous dietary pathway and for fish an

endogenous liver pathway. Species-specific Se effect models for the Bay-Delta are shown for breeding clapper rail; migratory scoter and scaup; white sturgeon; downstream-migrating juvenile salmonids; and upstream-migrating adult salmonids (submodel F, Figure 7). Details of Se-specific toxicological information for predator species considered here are compiled in Appendix A.3.

Such health effects are important to the overall ability of birds and fish to thrive and reproduce. But the consequences of Se transfer from the mother to her progeny via each reproductive stage are the most direct and sensitive predictors of the effects on birds and fish (Heinz 1996; Lemly 2002; Chapman and others 2010). Ultimately, it would be expected that effects on reproduction, especially in slowly reproducing, demographically vulnerable species (e.g., sturgeon), could lead to effects on populations and community changes.

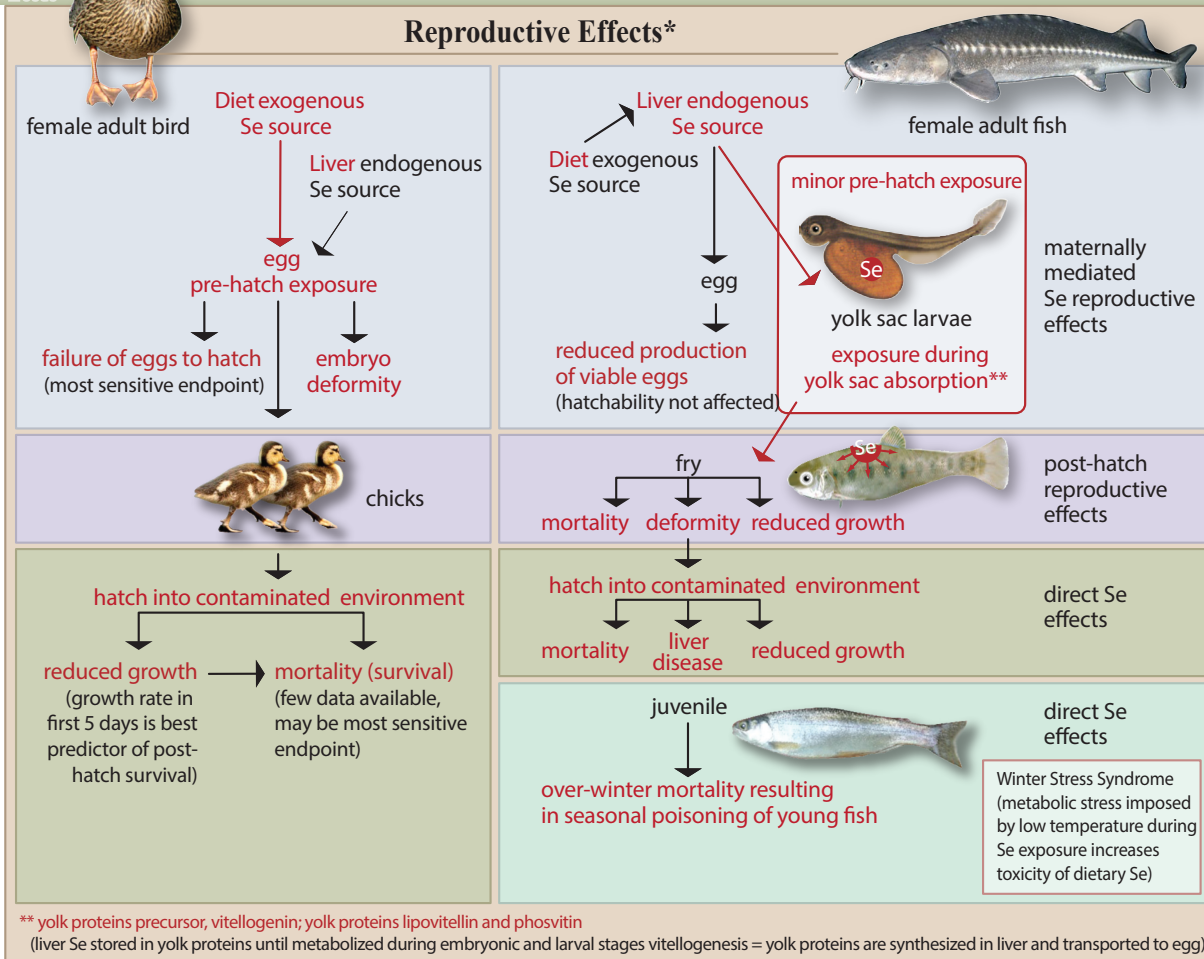
To translate exposure into toxicity, effects levels are needed for predator species. Traditionally, guidelines relate Se concentrations in water to effects. But it is increasingly recognized that the concentrations of Se bioaccumulated in fish and bird tissues are more strongly related to signs of toxicity in nature, and would provide less ambiguous guidelines (Chapman and others 2010). The best correlations occur between Se in reproductive tissue and effects on reproductive processes. To assess implications of Se contamination in water from such relationships a bioaccumulation model is, then, necessary.

Experimental determination of tissue Se concentrations at which adverse effects occur is influenced by choice of endpoint, life-stage, dietary form, route of transfer, and choice of effect concentration. Another consideration in determining the guideline is the steepness of the Se dose-response curves and the choice of mathematical models to describe the curve (Skorupa 1998; Ohlendorf 2003; Lemly 2002; Environment Canada 2005; Beckon and others 2008; Chapman and others 2010). Effect guidelines that focus on a combination of the most sensitive assessment measures might include, for example, a selenomethionine diet, parental exposure, and embryonic or larval life-stage effect (Presser and Luoma 2006).

Submodel E

Ecotoxicology and Effects

USGS



Effects to Health*

- reduced growth
- hepatotoxicity
- elevated oxidative stress activity (altered hepatic enzyme function)
- compromised body condition (edema; low body mass; low protein and fat content; loss of feathers)
- histopathological lesions
- impaired immune function
- decreased winter survival
- decreased reproductive fitness (decreased breeding propensity; reduced recruitment)
- behavioral impairment (missed breeding window, delayed timing of departure)
- lowered saline tolerance and gill effects in fish

*Reproductive endpoints measure or are related to direct effects to reproduction. Health endpoints are considered to indirectly relate to reproduction.

Food webs and seasonal cycles

Species-specific effects

Figure 6 Submodel E. Ecotoxicology and Effects

Species-Specific Effects

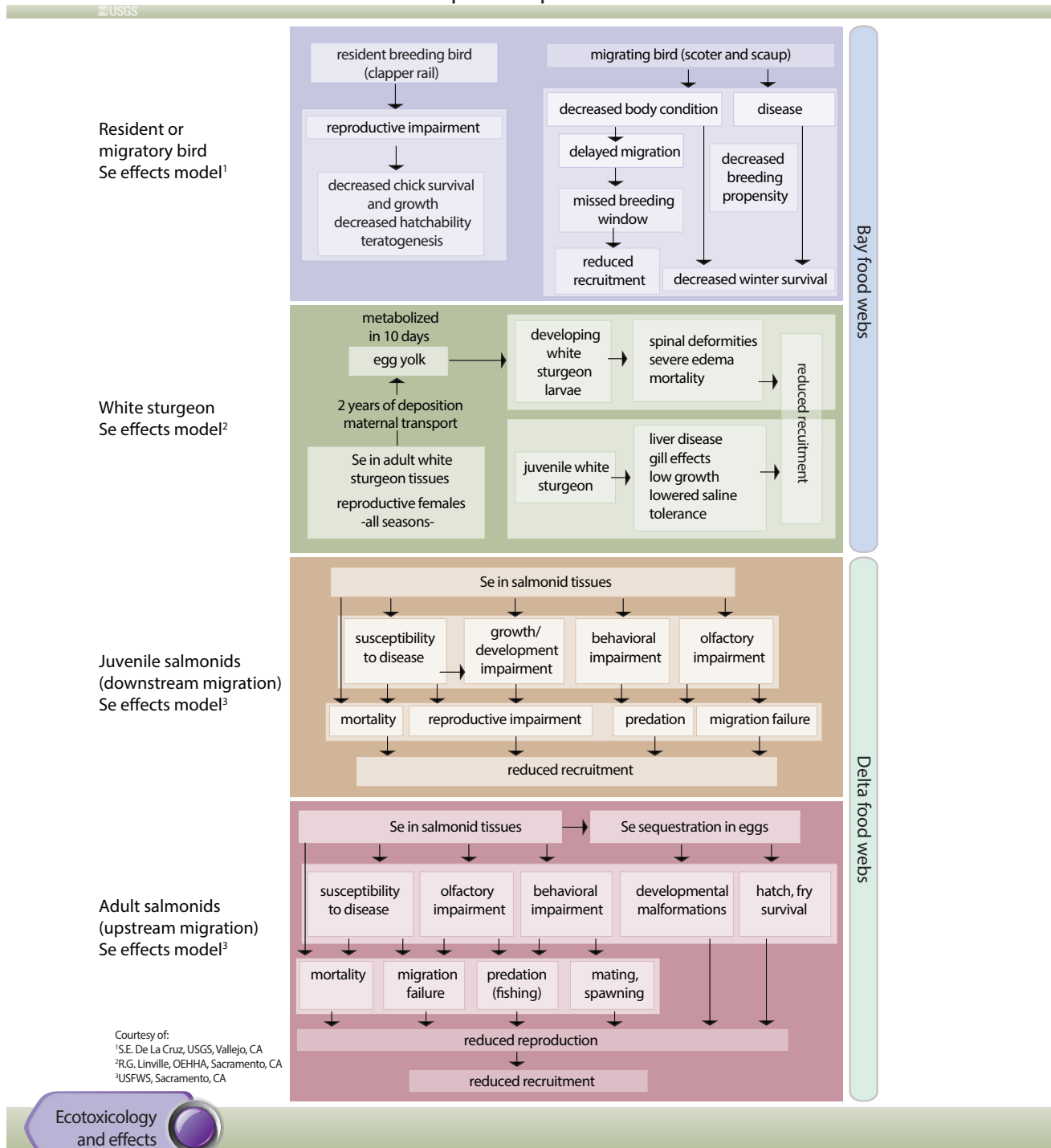


Figure 7 Submodel F. Species-Specific Effects

Even then the choice of statistical analysis and effect level can lead to disagreement about effect guidelines.

Human Health

A number of species from the Bay-Delta are consumed by humans (submodel G, [Figure 8](#)). Human health advisories against consumption of greater scaup, lesser scaup, and scoter because of elevated Se levels have been in effect since 1986 (Presser and Luoma 2006) for Suisun Bay, San Pablo Bay, Central Bay, and South Bay (CDFG 2012, 2013). The health warning states that no one should eat more than four ounces of scaup meat per week or more than four ounces of scoter meat in any two week period. Further, no one should eat the livers of ducks from these areas.

Fish consumption advisories, including for white sturgeon, exist for the Bay because of the effect of mercury and PCBs (OEHHA 2011, 2012). Pesticides, flame retardants, and Se also were tested, but a mean concentration calculated for each fish species collected from locations throughout the Bay-Delta over a range of years was found to be below that chemical's advisory tissue level (OEHHA 2011, 2012). Specifically for Se, concentrations in white sturgeon ($n = 56$ during 1997 to 2009, or 4.3 fish per year) were higher than other species of fish tested; and some Se concentrations for white sturgeon collected in North Bay locations (maximum $18.1 \mu\text{g g}^{-1} \text{ dw}$) exceeded Se advisory levels (e.g., $10.4 \mu\text{g g}^{-1} \text{ dw}$ or $2.5 \mu\text{g g}^{-1}$ wet weight based on consumption of three 8-ounce meals per week (OEHHA 2011, 2012). Length restrictions (117 to 168 cm) and a bag limit of one fish per day are in effect for legal fishing of white sturgeon in the Bay, with a mean of 134 cm measured in fish collected for advisories.

A median per angler consumption rate of 16 g d^{-1} was determined specifically for Bay fish during 1998 and 1999 (SFEI 2000). This site-specific rate can be compared to a national recreational fisher consumption rate of 17.5 g d^{-1} and a national per capita rate of 7.5 g d^{-1} (USEPA 2000b).

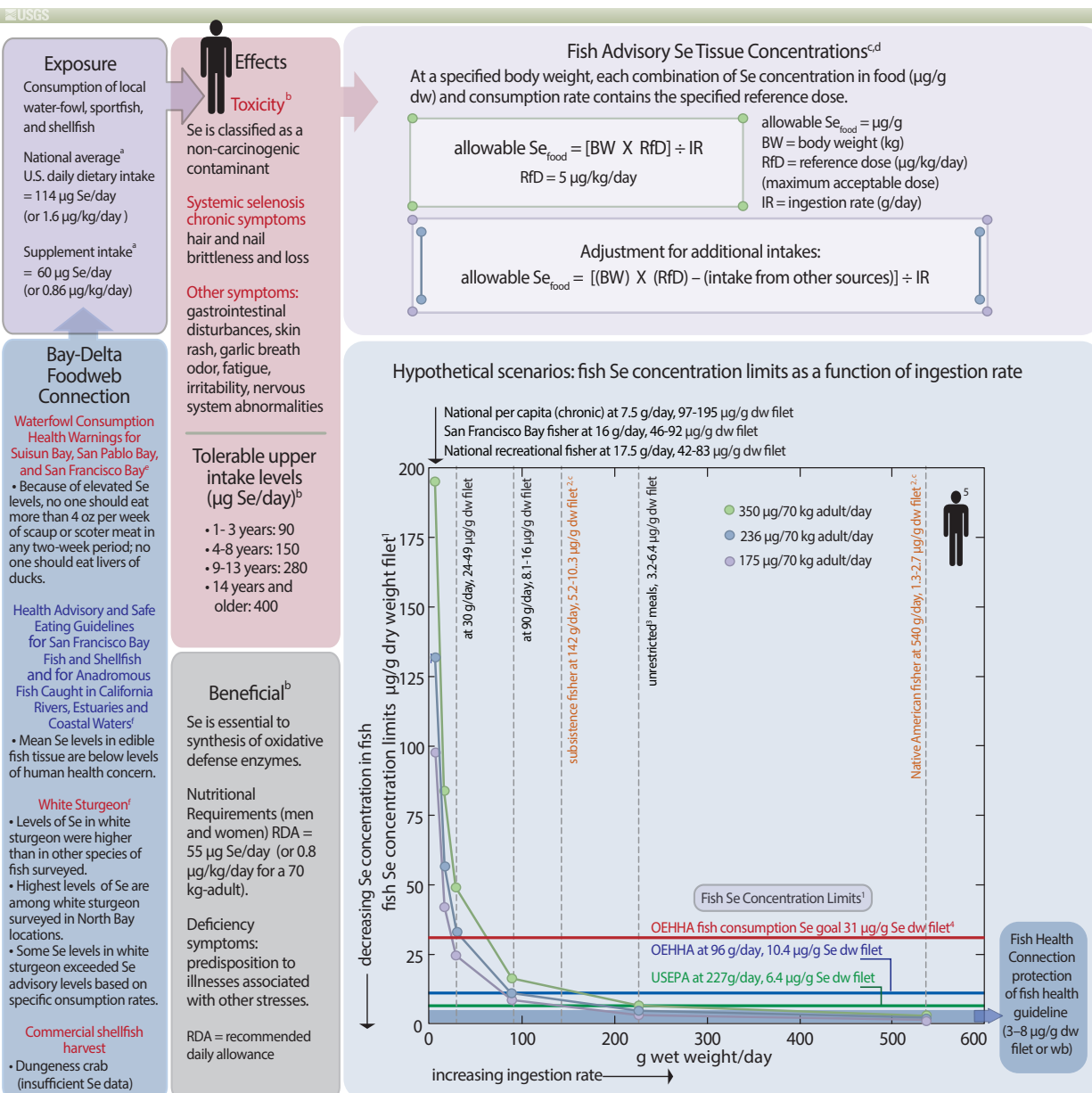
Nutritional guidelines, toxicity symptoms, and national guidance concerning human health risk for consumption of fish are shown in submodel G ([Figure 8](#)). The details of how guidelines shown in [Figure 8](#) were determined and how they might be linked to regulation of Se in wildlife and to fish health are presented in [Appendix A.4](#).

QUANTITATIVE MODELING

This section presents an example of an application of the quantitative DRERIP Ecosystem-Scale Selenium Model. The questions addressed in this example are: What are the implications for ecosystem concentrations of Se if a fish tissue and/or wildlife Se guideline is implemented (a guideline based upon Se concentrations in a predator)? More specifically, what changes in dissolved or particulate Se concentration in the Bay-Delta would be necessary to achieve the selected tissue concentrations in predators? Agencies have traditionally regulated contaminants on the basis of dissolved concentrations, and managed inputs from different sources based upon their implications for dissolved concentrations (e.g., total mass daily loadings). This example shows a methodology that ties the new concept of tissue guidelines to the traditional concept of dissolved-concentration-based management. Inherent in every regulatory guideline are assumptions about the environment being regulated. The model allows an explicit evaluation of the implications of different assumptions.

The generalized equations for prediction of a dissolved Se concentration from a tissue Se concentration are given in submodel B ([Figure 3](#)). [Table 1](#) gives the specific combinations of choices for food web, guideline, location, hydrologic condition, K_d , and TTFs used for the Bay-Delta application. In this example, several alternatives for a tissue guideline were chosen from among those that have been discussed in the regulatory context. Then, the invertebrate, particulate, and dissolved Se concentrations were calculated that would be expected if the tissue concentrations were in compliance with each choice of a guideline. Calculations also were conducted under different assumptions about K_d , food web, and TTFs. Finally, the calculated dissolved, particulate,

Human Health



^aU.S. Department of Health and Human Services (2002)
^bInstitute of Medicine (2000)
^cU.S. Environmental Protection Agency (2000b)
^dCalifornia Office of Environmental Health Hazard Assessment (California OEHHA) (2008)
^eCalifornia Department of Fish and Game (2012-2013)
^fCalifornia OEHHA (2011 and 2012)
¹Assumed conversion factors (if necessary): filet to whole-body, 1.2; wet weight to dry weight, 76% moisture
²Protection of sensitive groups through assumed increased consumption.
³Generally not to exceed 16 meals/month; one meal = 227 gms (8 oz.)
⁴No significant health risk to average consumer, 32 g/day (OEHHA, 2008)
⁵Childhood sensitivity and intake not represented here.



Figure 8 Submodel G. Human Health. See additional explanation in Appendix A.4.

Table 1 Locations, food webs, and model parameters for quantitative modeling examples

Location	Predator	Food web	Predator tissue target ($\mu\text{g g}^{-1}$ Se, dw)	TTF _{predator}	Prey	TTF _{prey}	Particulate phase as base of food web	K _d	Flow condition
San Francisco Bay (Carquinez Strait – Suisun Bay)	sturgeon	clam-based	5 or 8 whole-body	1.3	50% <i>C. amurensis</i> 50% [amphipods plus other crustaceans]	9.2	suspended particulate material	5,986	low flow (Nov 1999)
	sturgeon	clam-based	5 or 8 whole-body	1.3	50% <i>C. amurensis</i> 50% [amphipods plus other crustaceans]	9.2	suspended particulate material	3,317	average condition
	young striped bass	zooplankton-based	8 whole-body	1.1	zooplankton	2.4	suspended particulate material	3,317	average condition
	bird	clam-based	7.7, 12.5, or 16.5 egg	2	50% <i>C. amurensis</i> 50% [amphipods plus other crustaceans]	9.2	suspended particulate material	5,986	low flow (Nov 1999)
	bird	clam-based	7.7, 12.5, or 16.5 egg	2	50% <i>C. amurensis</i> 50% [amphipods plus other crustaceans]	9.2	suspended particulate material	3,317	average condition
Sacramento–San Joaquin Delta	fish	insect-based	5 or 8 whole-body	1.1	aquatic insects	2.8	suspended particulate material	3,680	average condition
	bird	insect-based	7.7, 12.5, or 16.5 egg	2	aquatic insects	2.8	suspended particulate material	3,680	average condition
San Joaquin River (main stem at Vernalis)	fish	insect-based	5 or 8 whole-body	1.1	aquatic insects	2.8	suspended particulate material	1,212	generalized (July 2000)

and invertebrate Se concentrations were compared with observations of those values from the Bay-Delta to assess how much existing conditions would be need to change to achieve compliance with the chosen guidelines (Table 2). Implicitly, comparisons of outcomes with data from nature tests how well model predictions match reality (Luoma and Rainbow 2005). Comparisons under different assumed conditions test the sensitivity of the model to changes within a few critical parameters.

The method, as indicated in the conceptual model (Figures 3 and 4, especially) includes the following steps: (1) selection of tissue guidelines to test; (2) selection of places and times of interest; (3) derivation of K_d using spatially and temporally matched dissolved and particulate Se concentrations constrained within the selected place and time; (4) selection of a food web of interest to each locality; (5)

determination of species-specific TTFs for invertebrates and their specific predators that are relevant to the place and food web; (6) prediction of invertebrate, particulate and dissolved Se concentrations; (7) comparison of predicted values to field observations of Se concentrations in these media in the Bay-Delta; and (8) conclusions about implications for compliance.

Modeling Parameters and Variables

Guidelines

The effect guidelines chosen for evaluation were 5 and 8 $\mu\text{g g}^{-1}$ dw fish whole-body; as well as 7.7, 12.5, and 16.5 $\mu\text{g g}^{-1}$ dw for bird eggs (Presser and Luoma 2010b) (Table 1). The regulatory community is debating appropriate critical tissue values that relate bioaccumulated Se concentrations and toxicity in predators (see previous discussion). We are not

SAN FRANCISCO ESTUARY & WATERSHED SCIENCE

Table 2 Predicted dissolved and particulate Se concentrations and percent exceedances for example scenarios

Location	Flow condition and tissue guideline ($\mu\text{g g}^{-1}$ Se, dw fish whole-body or bird egg)	Predicted invertebrate concentration ($\mu\text{g g}^{-1}$ Se, dw)	Predicted particulate concentration ($\mu\text{g g}^{-1}$ Se, dw)	Percent particulate Se exceedance in ecosystem	Predicted dissolved concentration ($\mu\text{g L}^{-1}$ Se)	Percent dissolved Se exceedance in ecosystem
San Francisco Bay: Carquinez Strait – Suisun Bay						
Bay sturgeon	low flow – 5.0	3.8	0.42	59	0.070	100%
	average – 5.0	3.8	0.42	59	0.126	47%
	low flow – 8.0	6.2	0.67	27	0.112	66%
	average – 8.0	6.2	0.67	27	0.202	3%
Bay striped bass	average – 8.0	7.3	3.0	0	0.914	0%
Bay birds	low flow – 7.7	3.9	0.42	59	0.070	100%
	average – 7.7	3.9	0.42	59	0.126	47%
	low flow – 12.5	6.3	0.68	25	0.113	64%
	average – 12.5	6.3	0.68	25	0.205	2%
	low flow – 16.5	8.3	0.90	11	0.150	23%
	average – 16.5	8.3	0.90	11	0.270	1%
Sacramento–San Joaquin Delta						
Delta fish	average – 5.0	4.5	1.6	7	0.441	19%
	average – 8.0	7.3	2.6	3	0.706	10%
Delta birds	average – 7.7	3.9	1.4	16	0.374	19%
	average – 12.5	6.3	2.2	3	0.607	11%
	average – 16.5	8.3	2.9	3	0.801	6%
San Joaquin River (main stem at Vernalis)						
River fish	July 2000 – 5.0	4.5	1.6	No data	1.3	16%
	July 2000 – 8.0	7.3	2.6	No data	2.1	3%

suggesting these are the best choices for guidelines; but they are within the range of those that are being discussed. In particular, the fish whole-body target of $5 \mu\text{g g}^{-1}$ and a bird egg target of $7.7 \mu\text{g g}^{-1}$ have been derived to provide additional protection for endangered species (Skorupa and others 2004; Skorupa 2008). The illustrated scenarios also considered the differences in the changes required if a bird egg-based guideline were used instead of a whole-body fish-based guideline.

Place and Time

The modeling scenarios compared two locations: a brackish-water Bay environment and a tidal freshwater Delta environment. For the Bay, we constrained

consideration to the geographic area of Carquinez Strait and Suisun Bay (Presser and Luoma 2010b) (Table 1). In terms of drivers, this location is affected by oil-refinery effluents that contain Se, and also could be influenced by inputs from the San Joaquin Valley. As noted previously, Se concentrations in at least some predators (sturgeon and diving ducks) at this location now exceed USFWS Se guidelines (Presser and Luoma 2010b). For the Delta, the area considered was from Stockton westward through the Delta, and was constrained to the freshwater environment. We also compared scenarios for average conditions across the year(s) in the Bay, to a specific example of conditions for one low flow season

(November 1999). An average condition for the Delta was modeled.

Partitioning and K_d s

The approach of Presser and Luoma (2006, 2010b) was used to select two K_d s for the scenarios from the Bay and one for the Delta (Table 1). The data for the Bay were narrowed to a Carquinez Strait–Suisun Bay location (Cutter and Cutter 2004; Doblin and others 2006; Presser and Luoma 2010b) to focus on the most contaminated area in the estuary, and to exclude the extreme K_d s at the ocean and freshwater interfaces. We selected the mean of co-collected dissolved and particulate Se concentrations from a transect for November 1999 ($K_d = 5,986$) to represent low flow conditions. Average conditions in the Bay across all seasons and several years were represented by the grand mean of all transects through the Carquinez Strait–Suisun Bay area during 1998–1999 ($K_d = 3,317$) and the freshwater Delta during 2003–2004 ($K_d = 3,680$). For comparison, the Delta grand mean K_d for low flow transects was 2,613 and for high flow transects 5,283. As discussed earlier, the value that describes transformation, even when constrained, is the most variable of any of the model parameters. The uncertainty associated with the choice of this value could be avoided if environmental guideline were based upon empirically determined particulate Se, but cannot be avoided if it is necessary to relate tissue Se to dissolved Se.

Food Webs and TTFs

For the Bay, the food web used was for suspended particulate material to *C. amurensis* to clam-eating fish or aquatic-dependent clam-eating bird (submodel C, Figure 4 and Table 1). The diet for both predators was assumed to be 50% clam and 50% benthic crustaceans. The bivalve food web is the most efficient at accumulating Se in the system, in both the field and in the quantitative model; therefore, it is the most environmentally protective to use in evaluating a tissue guideline. Different assumptions, of course, could be used for the percentage of diet that is clam-based (e.g., 75% to 96% for scoter and scaup, submodel C, Figure 4). Data on variability of benthic

assemblages with time, Bay location, and hydrologic condition also can be used to adjust dietary considerations (Peterson and Vayssieres 2010). If migrating scoter and scaup were modeled, a guideline based on body-condition endpoint, rather than a direct reproductive guideline, would be appropriate. To test the sensitivity of the choice of predator, one comparative simulation was calculated for a pelagic food web in the Bay: suspended material to zooplankton to young striped bass. The food web for the Delta was suspended particulate material to aquatic insects to juvenile salmon or steelhead trout.

Only a few recent data sets from the Bay-Delta are available that analyze Se concentrations across a reasonably complete food web (e.g., Stewart and others 2004). Some important food webs have not been assessed at all (e.g., aquatic insects and Chinook salmon or steelhead trout) (Presser and Luoma 2010b). However, studies of Se concentrations in enough individual predator and prey species are available to assess the predictions from the model and to derive, in a few instances, some critical trophic transfer relationships (e.g., Linville and others 2002; Stewart and others 2004; Schwarzbach and others 2006; Lucas and Stewart 2007; De La Cruz and others 2008; De La Cruz 2010). For the Bay, the dominant bivalve in the Carquinez Strait–Suisun Bay area is *C. amurensis*. This species strongly bioaccumulates Se (Linville and others 2002). A species-specific $TTF_{C. amurensis}$ of 17 (a range of 14 to 26 over different estuary conditions) was used here based on the field calibration that Presser and Luoma (2010b) describe. Benthic crustaceans, like amphipods and isopods, are much less efficient than clams in bioaccumulating Se; TTFs can range from 0.8 for amphipods to 2.0 for other crustaceans (Presser and Luoma 2010a). Under the assumption of a mixed diet of *C. amurensis* ($TTF_{C. amurensis} = 17$) and benthic crustaceans ($TTF_{\text{benthic crustacean}} = 0.8$ and 2.0), the combined diet TTF used here is 9.2.

An important benthic predator, white sturgeon, was chosen for the example, because the Se biomagnifier *C. amurensis* is an important food source for this species in the Bay. White sturgeon accumulate higher concentrations of Se than any other fish in the Bay (Stewart and others 2004; OEHHA 2011), making it

SAN FRANCISCO ESTUARY & WATERSHED SCIENCE

the environmentally conservative choice for evaluating a guideline. From studies in the late 1980s, field TTFs derived specifically for white sturgeon from the Bay that used bivalves as prey, showed a range from 0.6 to 1.7, with a mean of 1.3 (Presser and Luoma 2006); similar to the value of 1.1, which is the mean among all fish species studied. Calculations from more recent data sets for *C. amurensis* at Carquinez Strait, and seaward white sturgeon, showed a somewhat lower TTF of 0.8 (Presser and Luoma 2010b).

For the Delta food web, Se TTFs for freshwater aquatic insects were selected from data from literature sources (submodel C, Figure 4). For example, Presser and Luoma (2010a) derived a mean Se TTF_{insect} of 2.8 (range 2.3 to 3.2) based on matched field data sets for particulate and insect Se concentrations in freshwater environments for several species of aquatic insect larvae including mayfly, caddisfly, dragonfly, midge, and waterboatman. These values generally compare well to laboratory-derived TTFs for aquatic insect larvae (Conley and others 2009). TTFs for other potential invertebrates in Delta food webs (range 0.6 to 2.8) also are shown in submodel C, Figure 4 (Presser and Luoma 2010a).

Much less data are available to evaluate bioaccumulation in avian food webs. Data from the study of toxicity in mallards (Heinz and others 1989, 1990) are the most comprehensive studies available to use for modeling dietary exposure. From these studies, the laboratory-derived TTF_{bird egg} of 2.6 was assumed for transfer of Se from prey to bird eggs (which correlate best with toxicity). For the model, this choice of TTF for bird species was lowered to 2.0 to illustrate the possible effect of field variables on exposure factors that encompass habitat use and feeding behavior. A diet of 50% clams and 50% crustaceans was assumed for a clam-eating bird.

Implications of Model Choices and Estuary Conditions

Details of the calculations to evaluate implications of different guidelines, under different conditions, are summarized in Table 2. To compare the implications of these choices, we determined the percentage Se concentrations in dissolved and particulate form that

exceeded the value predicted to be necessary to meet the tissue guideline. All published dissolved ($n = 168$) and particulate Se ($n = 168$) data from the Bay and from the Delta, collected after 1997, are employed in this estimate. Together, the scenarios depict a Bay for which there is ecological risk from Se contamination, but the degree of risk, judged by the degree of compliance with the guidelines, depends heavily upon assumptions about toxicity (the guideline), transformation, and choice of food web.

The occurrence of $8 \mu\text{g g}^{-1}$ dw Se in sturgeon muscle from the contaminated area of San Francisco Bay (Linares and others 2004) is one of several lines of evidence that ecological risks from Se are occurring in the Bay. When this concentration was used for a predator guideline (Table 2), the model predicted Se concentrations in invertebrates and suspended particulate material and a dissolved Se concentration that were within the range typical of the Bay-Delta (Table 2). Thus, the model results appear to successfully capture the links between Se concentrations in different ecosystem components of the Bay, in general [also see Presser and Luoma (2010b) for further validation details]. This also suggests that the use of calibrated mean K_{ds} to reduce uncertainties about transformation adequately captures and constrains the variability in these processes. The agreement between ecosystem observations and the predicted Se concentrations in invertebrates and predators similarly points to the validity of the TTFs.

The most remarkable conclusion from the calculations is that fish tissue Se concentrations typical of risks to reproductive toxicity (the selected guideline examples) occur in the Bay at dissolved Se concentrations more than ten times less than the traditional water quality regulatory guideline of $5 \mu\text{g L}^{-1}$ (Table 2). At least some food webs in the Bay and the Delta are particularly vulnerable to small changes in bioavailable Se concentrations. The very high K_{ds} consistently observed in both the Bay and the Delta, compared to many other ecosystems (Presser and Luoma 2010a), may be one reason for this sensitivity. Also influential is the strong ability of invertebrates such as *C. amurensis* to bioaccumulate Se when compared to other prey species. It appears that ecosys-

tems wherein dissolved Se is efficiently transformed to particulate Se, and in which particulate Se is propagated up a food web to predators, will amplify relatively small changes in concentrations of dissolved Se concentrations to levels that could affect predators.

Under low flow conditions, 23 to 66% of dissolved Se determinations in the Bay exceeded the value predicted to be necessary to meet the higher sturgeon-based guideline or the higher bird-based guidelines (Table 2). Under guidelines chosen to protect endangered species, 100% exceedance occurs at low flow conditions. Clearly, low flow conditions, like those in November 1999, are the time of greatest ecosystem sensitivity to Se inputs (as suggested by Presser and Luoma 2006). It is notable that the example presented here does not represent the most extreme condition of a low flow season of a dry year or critically dry year.

If annual average conditions are assumed (the mean of spatially constrained K_{ds}), compliance is much more sensitive to the choice of guideline. Few if any exceedances (1 to 3%) are observed if the higher fish or bird egg guidelines are implemented under that assumption. For endangered species protection under an average condition, exceedance is approximately 47% for both the fish and bird guidelines. Of course, regulations based upon average conditions run the risk of under-protecting species sensitive to Se exposure during the protracted time in every year (especially drier years) when Se is most bioavailable.

Considering the choice of different guidelines, if a $5 \mu\text{g g}^{-1}$ guideline is implemented that uses sturgeon as the target organism, the entire Bay would be out of compliance. The model calculation suggests nearly all anthropogenic Se would have to be removed to drive sturgeon tissues to concentrations as low as $5 \mu\text{g g}^{-1}$, especially during a low flow condition. The projected dissolved Se concentration necessary to reach that level in sturgeon tissue is approximately the value for the Sacramento River, and hence the pre-disturbance baseline condition for the Bay. The modeling results suggest that if it is assumed that $5 \mu\text{g g}^{-1}$ represents the toxicity threshold for sturgeon, and if it were applied using concentrations in sturgeon from the field, then there is no room for any deviation from concentrations in the Sacramento River without risk

to the species. It is important to remember, however, that this toxicity guideline was derived for the most sensitive fish species. So, the use of the most sensitive surrogate in the toxicity guideline combined with field determinations from the fish with the greatest exposure results in an ultra-sensitive outcome.

These model results also illustrate how sensitive the implementation of a tissue guideline can be to the choice of predator. For example, many of the differences between sturgeon-based guidelines and bird egg-based guidelines are relatively small. Both appear to be sensitive indicators of ecological risks. However, the outcomes of guidance based upon striped bass, a water-column predator, are quite different from outcomes based upon bird eggs or sturgeon. The model showed that while aquatic birds and sturgeon are at risk under most assumptions, few or no exceedances of Se concentrations occur if the choice of regulatory indicator is based upon striped bass tissues. The differences are the result of the different invertebrate prey of the two species. Sturgeon eat a diet that includes strong Se bioaccumulator species (bivalves); striped bass eat from prey that live in the water-column and do not strongly bioaccumulate Se.

Selenium concentrations in the water column or particulate material of the Delta are higher and more variable than in the Bay. Average K_{ds} are similar between the Delta and the Bay. Nevertheless, few exceedances of dissolved and particulate Se concentrations (3% to 19%) are predicted in the Delta, even when the most sensitive fish guideline is used. This is consistent with the observation of low Se concentrations in the few fish that have been sampled from the Delta (e.g., Foe 2010). Use of the local food web is extremely influential in this outcome. Bioaccumulation of Se in the aquatic insect larvae (and other arthropods) that are the primary prey species of most Delta fish and birds is much lower than bioaccumulation by bivalves. As a result, it appears that the Delta food webs are easier to protect from adverse effects of Se than benthic food webs in the Bay, even if it is assumed that the most sensitive fish guideline applies. Nevertheless, the actual concentrations of dissolved Se predicted to be

SAN FRANCISCO ESTUARY & WATERSHED SCIENCE

necessary to meet the tissue guidelines range from 0.37 to 0.80 $\mu\text{g L}^{-1}$, far below the Se concentrations typical of most existing dissolved guidelines for Se (Luoma and Presser 2009). This reflects the unusually high K_d s consistently observed in this freshwater environment.

Few determinations of Se concentrations in particulate material in the incoming rivers to the Bay are available outside the tidal range. Lucas and Stewart (2007) reported matched dissolved and particulate Se concentrations from which one K_d could be calculated (a value of 1,212) for the San Joaquin River during transect sampling in 2000. The example in Table 2 shows that if that were typical of the river, and the food web was mainly based upon arthropods, then compliance with a tissue guideline could occur at dissolved Se concentrations ten times higher than would be the case in the Bay. This river simulation is based on very limited data; it is given here for comparative purposes to show the sensitivity of the model to the choice of hydrologic setting. Comprehensive modeling of the San Joaquin River system would require data collection and analysis specific to the river's settings, predator species, food webs, and habitats. Percentage exceedance (Table 2) is based on weekly sampling of total Se for the river at Vernalis from water year 1995 through water year 2010 (SWRCB 2012)

CONCLUSIONS

The DRERIP Ecosystem-Scale Selenium Model outcomes for the Bay-Delta show critical choices for Se modeling, and derived risk scenarios that illustrate varying degrees of risk, depending on those choices (Figure 1; Tables 1 and 2). In general, the conceptual model for Se shows that the focus of concern for this contaminant is the top of the food web. Quantitative model calculations show that enough is known to adequately characterize the distribution of Se through the Bay-Delta ecosystem, although the available data from which to validate the outcomes is dated and does not include conditions within a low flow season of a dry year or critically dry year. Presser and Luoma (2010b) give additional specifics for updated data collection and model refinements.

Selenium concentrations in fish or bird tissues alone appear to be good indicators of ecological risks from Se. Key invertebrates (e.g., the bivalve *C. amurensis* in the Bay) may be a more pragmatic indicator for frequent monitoring. Given that (1) suspended particulate material Se concentrations are key to accurate prediction of prey and predator Se concentrations; and (2) dissolved Se concentrations are constrained to a narrow dynamic range within the estuary, a suspended particulate material Se concentration also may be a sensitive parameter on which to assess change. Dissolved Se concentrations appear to be the variable of choice for regulatory agencies, however, because of links to total maximum daily loads.

The ability to quantitatively characterize distributions among all these ecosystem components from field determination of only one component allows great flexibility in future monitoring whatever the choice of indicator. The detailed site-specific conceptual model, and the ability to quantitatively apply that model, also provide perspective on the processes that are most influential in determining Se contamination in the predators of this Se-sensitive environment (Figure 1).

The quantitative example (Tables 1 and 2) provides some lessons for implementing regulations to manage Se in this system. First, it is notable that extremely small changes in dissolved Se concentrations, in absolute terms, have strong implications for compliance with the tissue guidelines. A regulatory program that focuses on dissolved Se would require an extremely rich data set to reliably detect the differences between compliance and non-compliance, based upon the translation from tissue to dissolved Se. This is another reason why regulation of suspended particulate material Se concentration may be a more sensitive parameter on which to assess change.

Second, if compliance is determined from tissue concentrations in a predator, the choice of that predator is crucial. Predators of bivalves in benthic food webs are much more at risk than predators from pelagic food webs. The former should be the basis of tissue monitoring in the Bay.

Third, any decision as to whether reductions in ambient concentrations of Se would be required to comply with the tissue guidelines depends upon the choice

of guideline and assumed environmental conditions. For example, the modeling suggests that a fish tissue guideline of $5 \mu\text{g g}^{-1}$ would ultimately require essentially all enriched Se inputs to the Bay to be eliminated if the guideline were applied using Se concentrations in sturgeon. According to the calculations, dissolved Se concentrations in the Bay would have to decline to nearly those in the Sacramento River to comply with such a guideline. If a guideline of $8 \mu\text{g g}^{-1}$ was used, the Bay would be near compliance under average conditions; but 66% out of compliance in a situation like November 1999 (i.e., low flow). Calculating in the opposite direction from a traditional dissolved Se concentration guideline, allowing dissolved concentrations of Se in the Bay to reach $5 \mu\text{g L}^{-1}$ (the current regulatory guideline) or even $2 \mu\text{g L}^{-1}$ would result in tissue concentrations (potentially greater than $100 \mu\text{g g}^{-1}$ in *C. amurensis*) that could threaten many of the predators in the Bay, if other conditions stay as they are.

Fourth, the current food webs in the Delta are less at risk from Se than the benthic food webs of the Bay, because of the differences in food webs. The differences between the Delta and the Bay are not the result of the freshwater versus brackish water nature of the systems of interest because, on average, transformation efficiencies are similar in the two. Where transformation processes are greatly different between two ecosystems, then a different outcome from implementing the same tissue guideline might be expected. The San Joaquin River example shows how a less efficient transformation of dissolved Se to particulate Se in the river can result in less sensitivity of the ecosystem to changes in Se concentrations.

Finally, the more specificity added to the model, the less uncertainty in predictions. If, for example, the geographic range is narrowed by using data only from Carquinez Strait–Suisun Bay, then freshwater and ocean interfaces are avoided. If the temporal range is narrowed to low flow seasons of dry years (i.e., high residence time or high exposure time), then focus can be on times when the transformative nature of the estuary is elevated. Juxtaposition of times when suspended particulate material or prey species achieve maximum Se concentrations with critical life stages of species at risk being present allows regulatory consid-

erations to focus on times that govern Se's ecological effects (i.e., ecological bottlenecks) (Figure 1).

The greatest strength of the analytical and modeling processes is that it is an orderly, ecologically consistent approach for assessing different aspects of the fate and effects of Se. Assessments such as the examples shown here can represent a starting point for initiating management decisions. Application of the DRERIP Ecosystem-Scale Selenium Model shows that management of Se requires incorporation of the complexity of dietary exposures and the systematic consideration of critical aspects of hydrology, biogeochemistry, physiology, ecology, and ecotoxicology to define ecosystem protection. Although this is complex, scenarios can be developed from specific questions that arise in the planning and implementation of restoration actions for the Bay-Delta. Quantitative evaluation of those scenarios is feasible. However, the Se database and monitoring program need to be modernized (e.g., refocused and expanded). Specifically, monitoring should include (1) representation of conditions in dry and critically dry years; and (2) collection of spatially and temporally matched data sets across media (i.e., water, suspended particulate material, prey, and predator) to ensure that derived site-specific factors are current for the ecological and hydrological dynamics of the Bay-Delta. Only then will predictions from the model remain relevant and realistic to a constantly evolving estuary.

ACKNOWLEDGEMENTS

This work was supported by CALFED (in the project's earlier phases), the U.S. Geological Survey National Research and Toxics Substances Hydrology Programs, and the U.S. Environmental Protection Agency (San Francisco, California, Region 9). Jeanne DiLeo (U.S. Geological Survey, Menlo Park Publishing Service Center) prepared the outstanding graphics. We thank William Beckon and Thomas Maurer (U.S. Fish and Wildlife Service, Sacramento, California) for provision of species at risk for the Bay-Delta. We also thank William Beckon, Susan De La Cruz (U.S. Geological Survey, Vallejo, California) and Regina Linville (Office of Environmental Health Hazard Assessment,

SAN FRANCISCO ESTUARY & WATERSHED SCIENCE

Sacramento, California) for assistance with species-specific effects models and human health considerations. Thanks also go to Mark Huebner (U.S Geological Survey, Menlo Park, California) for exceptional assistance with manuscript preparation.

REFERENCES

- Baines SB, Fisher NS, Stewart R. 2002. Assimilation and retention of selenium and other trace elements from crustacean food by juvenile striped bass (*Morone saxatilis*). *Limnology and Oceanography* 47(3):646–655.
- Beckon WN, Parkins C, Maximovich A, Beckon AV. 2008. A general approach to modeling biphasic relationships. *Environmental Science and Technology* 42(4):1308–1314.
- Besser JM, Huckins JN, Little EE, La Point TW. 1989. Distribution and bioaccumulation of selenium in aquatic microcosms. *Environmental Pollution* 62(1):1–12.
- [CDFG] California Department of Fish and Game. 2012–2013. Waterfowl and upland game hunting and other public uses on state and federal lands regulation. Sacramento (CA): California Department of Fish and Game. 80 p.
- [CDFG] California Department of Fish and Game. 2012. Current ocean fishing regulations: Pigeon Point to Point Conception: sturgeon. Sacramento (CA): California Department of Fish and Game. 6 p. Available from: <http://www.dfg.ca.gov/marine/mapregs4.asp> Accessed 11 June 2012.
- [OEHHA, California OEHHA] California Office of Environmental Health Hazard Assessment. 2008. Development of fish contaminant goals and advisory tissue levels for common contaminants in California sport fish: chlordane, DDT's, dieldrin, methylmercury, PCB's, selenium and toxaphene. Sacramento (CA): California Environmental Protection Agency. 115 p. Available from: <http://www.oehha.ca.gov/fish/gtlsx/cnr062708.html> Accessed 11 June 2012.
- [OEHHA, California OEHHA] California Office of Environmental Health Hazard Assessment. 2011. Health Advisory and safe eating guidelines for San Francisco Bay Fish and Shellfish. Sacramento (CA): California Environmental Protection Agency. 53 p. Available from: http://oehha.ca.gov/fish/nor_cal/pdf/SFBayAdvisory21May2011.pdf Accessed 11 June 2012.
- [OEHHA, California OEHHA] California Office of Environmental Health Hazard Assessment. 2012. Health Advisory and safe eating guidelines for American shad, Chinook (King) salmon, steelhead trout, striped bass, and white sturgeon caught in California rivers, estuaries, and coastal waters. Sacramento (CA): California Environmental Protection Agency. 27 p. Available from: http://www.oehha.ca.gov/fish/special_reports/pdf/AnadromousSppAdvisory.pdf Accessed 18 March 2013.
- [SFBRWQCB] California San Francisco Bay Regional Water Quality Control Board. 2007. Project plan north San Francisco Bay selenium TMDL. Oakland (CA): California San Francisco Bay Regional Water Quality Control Board. 30 p. Available from: http://www.swrcb.ca.gov/rwqcb2/water_issues/programs/TMDLs/seleniumtmdl.shtml Accessed 11 June 2012.
- [SFBRWQCB] California San Francisco Bay Regional Water Quality Control Board 2011. Total Maximum Daily Load Selenium in North San Francisco Bay, Preliminary Project Report. Oakland (CA): California San Francisco Bay Regional Water Quality Control Board. 103 p. Available from: http://www.swrcb.ca.gov/rwqcb2/water_issues/programs/TMDLs/seleniumtmdl.shtml Accessed 11 June 2012.
- [SWRCB] California State Water Resources Control Board. 1987. Selenium verification study, 1986. Sacramento (CA): California State Water Resources Control Board. 79 p + 9 appendices.
- [SWRCB] California State Water Resources Control Board. 1988. Selenium verification study, 1986–1987. Sacramento (CA): California State Water Resources Control Board. 60 p + 8 appendices.

[SWRCB] California State Water Resources Control Board. 1989. Selenium verification study, 1987–88. Sacramento (CA): California State Water Resources Control Board. 81 p + 11 appendices

[SWRCB] California State Water Resources Control Board. 1991. Selenium verification study, 1988–1990. Sacramento (CA): California State Water Resources Control Board. 79 p + 9 appendices.

[SWRCB] California State Water Resources Control Board. 2011. California Clean Water Act Section 303(d) list of Water Quality Limited Segments for 2010. Sacramento (CA): California State Water Resources Control Board. 53 p.

[SWRCB] California State Water Resources Control Board. 2012. Data retrieval, California Environmental Data Exchange Network (CEDEN). Sacramento (CA): California State Water Resources Control Board. Available from: http://ceden.org/ceden_data.shtml Accessed 18 March 2013.

Chapman PM, Adams WJ, Brooks ML, Delos CG, Luoma SN, Maher WA, Ohlendorf HM, Presser TS, Shaw DP. 2010. Ecological assessment of selenium in the aquatic environment. Pensacola (FL): SETAC Press. 358 p.

Conley JM, Funk DH, Buchwalter DB. 2009. Selenium bioaccumulation and maternal transfer in the mayfly *Centroptilum triangulifer* in a life-cycle, periphyton-biofilm trophic assay. *Environmental Science and Technology* 43(20):7952–7957.

Conley JM, Funk DH, Cariello NJ, Buchwalter DB. 2011. Food rationing affects dietary selenium bioaccumulation and life cycle performance in the mayfly *Centroptilum triangulifer*. *Ecotoxicology* 20 (8):1840–1851.

Conomos TJ, Smith RE, Peterson DH, Hager SW, Schemel LE. 1979. Processes affecting seasonal distributions of water properties in the San Francisco Bay estuarine system. In: Conomos TJ, editor. *San Francisco Bay: the urbanized estuary*. San Francisco (CA): AAAS Pacific Division. p. 115–142. Available from: http://downloads.ice.ucdavis.edu/sfestuary/conomos_1979/archive1022.PDF Accessed 12 June 2012.

Cutter GA. 1989. The estuarine behavior of selenium in San Francisco Bay. *Estuarine, Coastal, and Shelf Science* 28(1):13–34.

Cutter GA, Cutter LS. 2004. Selenium biogeochemistry in the San Francisco Bay estuary: changes in water column behavior. *Estuarine, Coastal and Shelf Science* 61(3):463–476.

Cutter GA, Bruland KW. 1984. The marine biogeochemistry of selenium a re-evaluation. *Limnology and Oceanography* 29(6):1179–1192.

Cutter GA, San Diego–McGlone MLC. 1990. Temporal variability of selenium fluxes in San Francisco Bay. *Science of the Total Environment* 97/98:235–250.

De La Cruz SE. 2010. Habitat, diet, and contaminant relationships of surf scoters wintering in San Francisco Bay: implications for conservation in urban estuaries. [Ph.D. dissertation]. Davis (CA): University of California Davis. 215 p.

De La Cruz SEW, Takekawa JY, Miles A, Eadie JM, Palm EC, Wilson MT. 2008. The influence of winter habitat use and diet on selenium risks for surf scoters (*Melanitta perspicillata*) in the San Francisco Bay Estuary [abstract]: State of the San Francisco Estuary Conference. [dates?] Oakland (CA): The San Francisco Estuary Project. 1 p.

De La Cruz SEW, Takekawa JY, Wilson MT, Nysewander DR, Evenson JR, Esler D, Boyd WS, Ward DH. 2009. Spring migration routes and chronology of surf scoters (*Melanitta perspicillata*): a synthesis of Pacific coast studies. *Canadian Journal of Zoology* 87(11):1069–1086.

DiGennaro B, Reed D, Swanson C, Hastings L, Hymanson Z, Healey M, Siegel S, Cantrell S, Herbold B. 2012. Using conceptual models and decision-support tools to guide ecosystem restoration planning and adaptive management: an example from the Sacramento–San Joaquin Delta, California. *San Francisco Estuary and Watershed Science* [Internet]. Available from: <http://www.escholarship.org/uc/item/3j95x7vt> Accessed 18 March 2013.

SAN FRANCISCO ESTUARY & WATERSHED SCIENCE

- Doblin MA, Baines SB, Cutter LS, Cutter GA. 2006. Sources and biogeochemical cycling of particulate selenium in the San Francisco Bay estuary. *Estuarine, Coastal and Shelf Science* 67(4):681–694.
- Environment Canada. 2005. Guidance document on statistical methods for environmental toxicity tests (EPS 1/RM/46)/ Method Development and Application Section. Ottawa (ON): Environmental Technology Centre, Environment Canada. 170 p. and appendices A–R, with June 2007 amendments.
- Foe C. 2010. Selenium concentrations in largemouth bass in the Sacramento–San Joaquin Delta. Sacramento (CA): Central Valley Regional Water Quality Control Board. 24 p.
- Fournier E, Adam C, Massabuau J–C, Garnier–Laplace J. 2006. Selenium bioaccumulation in *Chlamydomonas reinhardtii* and subsequent transfer to *Corbicula fluminea*: role of selenium speciation and bivalve ventilation. *Environmental Toxicology and Chemistry* 25(10):2692–2699.
- Fowler SW, Benayoun G. 1976. Influence of environmental factors on selenium flux in two marine invertebrates. *Marine Biology* 37(1):59–68.
- Ganju NK, Schoellhamer DH, Warner JC, Barad MF, Schladow GF. 2004. Tidal oscillation of sediment between a river and a bay: a conceptual model. *Estuarine Coastal and Shelf Science* 60: 81–90.
- Graham RV, Blaylock BG, Hoffman FO, Frank ML. 1992. Comparison of selenomethionine and selenite cycling in freshwater experimental ponds. *Water, Air, and Soil Pollution* 62(1–2):25–42.
- Heinz GH. 1996. Selenium in birds. In: Beyer WN, Heinz GH, Redmon–Norwood AW, editors. *Environmental contaminants in wildlife: interpreting tissue concentrations*. New York, (NY): Lewis Publishers. p. 447–458.
- Heinz GH, Hoffman DJ, Gold LG. 1989. Impaired reproduction of mallards fed an organic form of selenium. *The Journal of Wildlife Management* 53(2):418–428.
- Heinz GH, Pendleton GW, Krynitsky AJ, Gold LG. 1990. Selenium accumulation and elimination in mallards. *Archives of Environmental Contamination and Toxicology* 19(3):374–379.
- Hoffman DJ. 2002. Role of selenium and oxidative stress in aquatic birds. *Aquatic Toxicology* 57(1–2):11–26.
- Hoffman DJ, Ohlendorf HM, Marn CA, Pendleton GW. 1998. Association of mercury and selenium with altered glutathione metabolism and oxidative stress in diving ducks from the San Francisco Bay Region, USA. *Environmental Toxicology and Chemistry* 17(2):167–172.
- Hoffman, DJ, Marn C, Marois K, Sproul E, Dunne M, Skorupa JP. 2002. Sublethal effects in avocet and stilt hatchlings from selenium-contaminated sites. *Environmental Toxicology and Chemistry* 21(3):561–566.
- Institute of Medicine. 2000. *Dietary reference intakes for vitamin C, vitamin E, selenium and carotenoids*. Washington (DC): National Academy Press. 506 p.
- Janz, DM. 2012. Selenium. In: Wood CW, Farrell AP, Brauner CJ, editors. *Fish Physiology Volume 31A, Homeostasis and toxicology of essential metals*. San Diego (CA): Elsevier. p. 327–374.
- Kiffney P, Knight A. 1990. The toxicity and bioaccumulation of selenate, selenite, and seleno–L–methionine in the cyanobacterium *Anabaena flos-aquae*. *Archives of Environmental Contamination and Toxicology* 19(4):488–494.
- Kleckner AE, Stewart AR, Elrick K, Luoma SN. 2010. Selenium concentrations and stable isotopic compositions of carbon and nitrogen in the benthic clam *Corbula amurensis* from Northern San Francisco Bay, California, May 1995 to February 2010. U.S. Geological Survey Open-File Report 2010–1252. 34 p. Available from: <http://pubs.usgs.gov/of/2010/1252/> Accessed 11 June 2012.

- Kroll KJ, Doroshov SI. 1991. Vitellogenin: potential vehicle for selenium bioaccumulation in oocytes of the white sturgeon (*Acipenser transmontanus*). In: Williot P, editor. *Acipenser*: Proceedings of the 1st International Sturgeon Conference, October 3–6, 1989, Bordeaux, France. *Centre National du Machinisme Agricole du Genie Rural des Eaux et des Forets*, Bordeaux, France. p. 99–106
- Lee B–G, Lee J–S, Luoma SN. 2006. Comparison of selenium bioaccumulation in the clams *Corbicula fluminea* and *Potamocorbula amurensis*: a bioenergetic modeling approach. *Environmental Toxicology and Chemistry* 25(7):1933–40.
- Lemly AD. 2002. Selenium assessment in aquatic ecosystems: a guide for hazard evaluation and water quality criteria. New York (NY): Springer–Verlag. 180 p.
- Linares J, Linville RG, Van Eenennaam J, Doroshov S. 2004. Selenium effects on health and reproduction of white sturgeon in the Sacramento–San Joaquin Estuary. Final Report, Project No. ERP–02–P35. Davis (CA): University of California, Department of Animal Science. 56 p.
- Linville RG. 2006. Effects of excess selenium on the health and reproduction of white sturgeon (*Acipenser transmontanus*): implications for San Francisco Bay–Delta. [Ph.D. dissertation]. Davis (CA): University of California Davis. 232 p.
- Linville RG, Luoma SN, Cutter L, Cutter GA. 2002. Increased selenium threat as a result of invasion of the exotic bivalve *Potamocorbula amurensis* into the San Francisco Bay–Delta. *Aquatic Toxicology* 57(1–2):51–64.
- Lucas L, Stewart AR. 2007. Transport, transformation, and effects of selenium and carbon in the Delta of the Sacramento–San Joaquin Rivers: implications for ecosystem restoration: Final report to CALFED. Ecosystem Restoration Program Agreement No. 4600001955. Project No. ERP–01–C07. 515 p.
- Luoma SN, Fisher N. 1997. Uncertainties in assessing contaminant exposure from sediments. In: Ingersoll CG, Dillon T, Biddinger GR, editors. *Ecological risk assessment of contaminated sediments*. Pensacola (FL): SETAC Press. p. 211–237.
- Luoma SN, Presser TS. 2009. Emerging opportunities in management of selenium contamination. *Environmental Science and Technology* 43(22):8483–8487.
- Luoma SN, Rainbow PS. 2005. Why is metal bioaccumulation so variable? biodynamics as a unifying concept. *Environmental Science and Technology* 39(7):1921–1931.
- Luoma SN, Rainbow PS. 2008. Metal contamination in aquatic environments: science and lateral management. New York (NY): Cambridge University Press. 573 p.
- Luoma SN, Johns C, Fisher NS, Steinberg NA, Oremland RS, Reinfelder JR. 1992. Determination of selenium bioavailability to a benthic bivalve from particulate and solute pathways. *Environmental Science and Technology* 26(3):485–491.
- McKee L, Oram J, Yee D, Davis J, Sedlack M. 2008. Sources, pathways, and loadings workgroup five-year workplan (SFEI Contribution #657). Richmond (CA): San Francisco Estuary Institute. 35 p.
- Meseck SL, Cutter GA. 2006. Evaluating the biogeochemical cycle of selenium in San Francisco Bay through modeling. *Limnology and Oceanography* 51(5):2018–2032.
- [NRC] National Research Council. 2010. A scientific assessment of alternatives for reducing water management effects on threatened fishes in California’s Bay–Delta. Washington D.C.: National Academy Press. 93 p.
- [NRC] National Research Council. 2011. A review of the use of science and adaptive management in California’s draft Bay–Delta conservation plan. Washington D.C.: National Academy Press. 69 p.

SAN FRANCISCO ESTUARY & WATERSHED SCIENCE

- [NRC] National Research Council. 2012. Sustainable water and environmental management in the California Bay-Delta. Washington D.C.: National Academy Press. 220 p.
- Ohlendorf HM. 2003. Ecotoxicology of selenium. In: Hoffman DJ, Rattner BA, Burton Jr GA, Cairns Jr J, editors. *Handbook of Ecotoxicology*, 2nd ed. Boca Raton (FL): Lewis Publishers. p 465–500.
- Ohlendorf HM, Heinz GH. 2011. Selenium in birds. In: BeyerWN, MeadorJP, editors. *Environmental contaminants in biota: interpreting tissue concentrations*, 2nd ed. Boca Raton (FL): CRC Press. p 669–701.
- Oremland RS, Hollibaugh JT, Maest AS, Presser TS, Miller LG, Culbertson CW. 1989. Selenate reduction to elemental selenium by anaerobic bacteria in sediments and culture: biogeochemical significance of a novel, sulfate-independent respiration. *Applied and Environmental Microbiology* 55(9):2333–2343.
- Peterson DH, Smith RE, Hager SW, Harmon DD, Herndon RE, Schemel LE. 1985. Interannual variability in dissolved inorganic nutrients in northern San Francisco Bay estuary. *Hydrobiologia* 129(1):37–58.
- Peterson HA, Vayssieres M. 2010. Benthic assemblage variability in the upper San Francisco Estuary: a 27-year retrospective. *San Francisco Estuary and Watershed Science* [Internet]. Available from: <http://www.escholarship.org/uc/item/4d0616c6> 18 March 2013.
- Presser TS. 1994. The Kesterson effect. *Environmental Management* 18(3):437–454.
- Presser TS, Luoma SN. 2006. Forecasting selenium discharges to the San Francisco Bay-Delta Estuary: ecological effects of a proposed San Luis Drain extension. U.S. Geological Survey Professional Paper 1646. 196 p. Available from: <http://pubs.usgs.gov/pp/p1646/> Accessed 12 June 2012.
- Presser TS, Luoma SN. 2009. Modeling of selenium for the San Diego Creek watershed and Newport Bay, California. U.S. Geological Survey Open-File Report 2009–1114. 48 p. Available from: <http://pubs.usgs.gov/of/2009/1114> Accessed 12 June 2012.
- Presser TS, Luoma SN. 2010a. A methodology for ecosystem-scale modeling of selenium. *Integrated Environmental Assessment and Management* 6(4):685–710.
- Presser TS, Luoma SN. 2010b. Ecosystem-scale modeling in support of fish and wildlife selenium criteria development for the San Francisco Bay-Delta Estuary, California, U.S. Geological Survey Administrative Report prepared for (2010) and released by USEPA (2011), Region 9, San Francisco, California. 101 p + appendices A–D. Available from: <http://www.epa.gov/region9/water/ctr> Accessed 12 June 2012.
- Presser TS, Ohlendorf HM. 1987. Biogeochemical cycling of selenium in the San Joaquin Valley, California, USA. *Environmental Management* 11(6):805–821.
- Presser TS, Schwarzbach SE. 2008. Technical Analysis of In-Valley Drainage Management Strategies for the Western San Joaquin Valley, California: U.S. Geological Survey Open-File Report 2008–1210. 37 p. Available from: <http://pubs.usgs.gov/of/2008/1210/> Accessed 12 June 2012.
- Presser TS, Piper DZ, Bird KJ, Skorupa JP, Hamilton SJ, Detwiler SJ, Huebner MA. 2004. The Phosphoria Formation: a model for forecasting global selenium sources to the environment. In: Hein J, editor. *Life cycle of the Phosphoria Formation: from deposition to the post-mining environment*. New York (NY): Elsevier p. 299–319. Available from: http://wwwrcamnl.wr.usgs.gov/Selenium/Library_articles/chap11_global_Se-optimized.pdf Accessed 12 June 2012.
- Reiley MC, Stubblefield WA, Adams WJ, Di Toro DM, Hodson PV, Erickson RJ, Keating Jr FJ, editors. 2003. *Reevaluation of the state of the science for water-quality criteria development*. Pensacola (FL): SETAC Press. 224 p.

Reinfelder JR, Fisher NS. 1991. The assimilation of elements ingested by marine copepods. *Science* 251(4995):794–796.

Reinfelder JR, Fisher NS, Luoma SN, Nichols JW, Wang W-X. 1998. Trace element trophic transfer in aquatic organisms: a critique of the kinetic model approach. *Science of the total environment* 219(2–3):117–135.

Riedel GF, Sanders JG, Gilmour CC. 1996. Uptake, transformation, and impact of selenium in freshwater phytoplankton and bacterioplankton communities. *Aquatic Microbial Ecology* 11(1):43–51.

Roditi HA, Fisher NS. 1999. Rates and routes of trace element uptake in zebra mussels. *Limnology and Oceanography* 44(7):1730–1749.

Saiki MK, Jennings MR, Hamilton SJ. 1991 Preliminary assessment of the effects of selenium in agricultural drainage on fish in the San Joaquin Valley. In: Dinar A, Zilberman, D, editors. *The economics and management of water and drainage in agriculture*. Boston (MA): Kluwer Academic Publishers. p 369–385.

Sandholm M, Oksanen HE, Pesonen L. 1973. Uptake of selenium by aquatic organisms. *Limnology and Oceanography* 18(3):496–499.

[SFEI] San Francisco Estuary Institute. 2000. San Francisco Bay seafood consumption study. Richmond (CA): San Francisco Estuary Institute. 84 p + 1 appendix. Available from: <http://www.sfei.org/node/2022> Accessed 12 June 2012.

[SFEI] San Francisco Estuary Institute. 2005. Data retrieval, tissue, surf scoter, scaup, muscle, selenium: San Francisco Estuary Institute Regional Monitoring Program, Region-wide Science for Ecosystem Management. Oakland (CA): San Francisco Estuary Institute. Available from: <http://sfei.org/tools/wqt> Accessed 12 June 2012.

[SFEI] San Francisco Estuary Institute. 2009. Data retrieval, tissue, white sturgeon, muscle, selenium: San Francisco Estuary Institute Regional Monitoring Program, Region-wide Science for Ecosystem Management. Oakland (CA): San Francisco Estuary Institute. Available from: <http://sfei.org/tools/wqt> Accessed 12 June 2012.

Schlekat CE, Dowdle PR, Lee BG, Luoma SN, Oremland RS. 2000. Bioavailability of particle-associated Se to the bivalve *Potamocorbula amurensis*. *Environmental Science and Technology* 34(21):4504–4510.

Schlekat CE, Purkerson DG, Luoma SN. 2004. Modeling selenium bioaccumulation through arthropod food webs in San Francisco Bay, California, USA. *Environmental Toxicology and Chemistry* 23(12):3003–3010.

Schwarzbach SE, Albertson JD, Thomas CM. 2006. Impacts of predation, flooding, and contamination on the reproductive success of the California clapper rail (*Rallus longirostris obsoletus*) in San Francisco Bay. *The Auk* 123(1):45–60.

Skorupa JP. 1998. Selenium poisoning of fish and wildlife in nature: lessons from twelve real-world examples. In: Frankenberger Jr WT, Engberg RA, editors. *Environmental chemistry of Selenium*. New York (NY): Marcel Dekker Inc. p 315–354.

Skorupa JP. 2008 Great Salt Lake selenium standard: written recommendations: U.S. Fish and Wildlife Service, Division of Environmental Quality, Branch of Environmental Contaminants, Arlington, Virginia, 9 p. Available from: http://www.camnl.wr.usgs.gov/Selenium/Library_articles/Great_Salt_Lake_Selenium_Standard.pdf

Skorupa JP, Presser TS, Hamilton SJ, Lemly AD, Sample BE. 2004. EPA's draft tissue-based criterion: a technical review. U.S. Fish and Wildlife Report presented to U.S. Environmental Protection Agency, dated June 16, 2004. 35 p. http://www.camnl.wr.usgs.gov/Selenium/Library_articles/skorupa_et_al_2004.pdf Accessed 18 March 2013

Stadtman TC. 1974. Selenium biochemistry. *Science* 183(4128):915–922.

SAN FRANCISCO ESTUARY & WATERSHED SCIENCE

Stewart AR, Luoma SN, Schlekot CE, Doblin MA, Hieb KA. 2004. Food web pathway determines how selenium affects ecosystems: a San Francisco Bay case study. *Environmental Science and Technology* 38(17):4519–4526.

[Tetra Tech, Inc.] Tetra Tech Incorporated. 2010. Technical Memorandum 6: application of ECoS3 model for simulation of selenium fate and transport in North San Francisco Bay. Lafayette (CA): Tetra Tech Incorporated. 103 p. Available from: http://www.swrcb.ca.gov/rwqcb2/water_issues/programs/TMDLs/seleniumtmdl.shtml Accessed 12 June 2012.

[USBR] U.S. Bureau of Reclamation. 1978. Special task force report on the San Luis Unit as required by Public Law 94–46, Central Valley Project, California. Sacramento (CA): U.S. Bureau of Reclamation Mid-Pacific Region. 331 p + 11 maps.

[USBR] U.S. Bureau of Reclamation. 1995. Finding of no significant impact and supplement environmental assessment, Grassland Bypass Channel Project, Interim use of a portion of the San Luis Drain for conveyance of drainage water through the Grassland Water District and adjacent Grassland areas. Sacramento (CA): U.S. Bureau of Reclamation Mid-Pacific Region. 36 p + appendices.

[USBR] U.S. Bureau of Reclamation. 2001. Grassland Bypass Project environmental impact statement and environmental impact report. Sacramento (CA): U.S. Bureau of Reclamation Mid-Pacific Region. Volume I (main text; appendices A and I) and volume II (appendices B–H).

[USBR] U.S. Bureau of Reclamation. 2006. San Luis Drainage Feature Re-evaluation Environmental Impact Statement. Sacramento (CA): U.S. Bureau of Reclamation Mid-Pacific Region. Executive summary, sections 1–24, appendices A–P. 2,785 p.

[USBR] U.S. Bureau of Reclamation. 2008. San Luis Drainage Feature Re-evaluation Feasibility Report. Sacramento (CA): U.S. Bureau of Reclamation Mid-Pacific Region. 193 p + appendices A–M. 2,247 p.

[USBR] U.S. Bureau of Reclamation. 2009. Grassland Bypass Project (2010–2019) environmental impact statement and environmental impact report. Sacramento (CA): U.S. Bureau of Reclamation Mid-Pacific Region. 391 p + appendices A–H. Available from: http://www.usbr.gov/mp/nepa/documentShow.cfm?Doc_ID=4412 Accessed 12 June 2012.

[USBR] U.S. Bureau of Reclamation. 2011. Delta–Mendota Canal water quality monitoring report, quarterly report of flows, concentrations and loads of salts and selenium (on-going series). Sacramento (CA): U.S. Bureau of Reclamation Mid-Pacific Region. 39 p.

[USBR] U.S. Bureau of Reclamation. 2012. Central Valley Operations Office Water Accounting Reports. Sacramento (CA): U.S. Bureau of Reclamation Mid-Pacific Region. Available from: <http://www.usbr.gov/mp/cvo/pmdoc.html> Accessed 12 June 2012

[USDOI] U.S. Department of the Interior. 1998. Guidelines for interpretation of effects of selected constituents in biota, water, and sediment – selenium. 47 p. Available from: <http://www.usbr.gov/niwqp/guidelines/pdf/Selenium.pdf> Accessed 12 June 2012

[USDHHS] U.S. Department of Health and Human Services. 2002. Dietary intake of macronutrients, micronutrients and other dietary constituents. United States National Center for Health Statistics, 1988–1994. *Vital Health Statistics* 11(245).

[USEPA] U.S. Environmental Protection Agency. 1992. Rulemaking, water quality standards, establishment of numeric criteria for priority toxic pollutants, states' compliance (National Toxics Rule), Final Rule: *Federal Register* 57 (242) p. 60848.

[USEPA] U.S. Environmental Protection Agency. 2000a. Water Quality Standards: Establishment of Numeric Criteria for Priority Toxic Pollutants for the State of California (California Toxics Rule): *Federal Register* 65(97), p. 31681–31719. Available from: <http://regulations.vlex.com/vid/environmental-protection-agency-23304844> Accessed 12 July 2012

- [USEPA] U.S. Environmental Protection Agency. 2000b. Guidance for assessing chemical contaminant data for use in fish advisories. Volume2: risk assessment and fish consumption limits. Third edition, EPA 823-B-00-008. November 2000.
- [USEPA] U.S. Environmental Protection Agency. 2004. Notice of draft aquatic life criteria for selenium and request for scientific information, data, and views: Federal Register 69 (242):75541–75546. Available from: <http://www2.epa.gov/sites/production/files/documents/actionplan.pdf> Accessed 12 July 2012.
- [USEPA] U.S. Environmental Protection Agency. 2011a. Update on California Toxics Rule and Endangered Species Act (September, 2011): Selenium. San Francisco, (CA): U.S. Environmental Protection Agency, Region 9. Available from: <http://www.epa.gov/region9/water/ctr/> Accessed 12 June 2012.
- [USEPA] U.S. Environmental Protection Agency. 2011b. Water Quality Challenges in the San Francisco Bay/Sacramento–San Joaquin Delta Estuary. Advanced Notice of Proposed Rulemaking: Federal Register 76(35):9709–9714. Available from: <http://www2.epa.gov/sfbay-delta/bay-delta-action-plan> Accessed 18 March 2013.
- [USFWS] U.S. Fish and Wildlife Service. 2006. Giant garter snake (*Thamnophis gigas*) 5-year review: summary and evaluation. Sacramento (CA): U.S. Fish and Wildlife Service. 46 p.
- [USFWS] U.S. Fish and Wildlife Service. 2008a. Species at risk from selenium exposure in the San Francisco estuary. Sacramento (CA): U.S. Fish and Wildlife Service, Sacramento Fish and Wildlife Office, Environmental Contaminants Division March 2008. 81 p.
- [USFWS] U.S. Fish and Wildlife Service. 2008b. Potential effects of selenium contamination on federally-listed species resulting from delivery of federal water to the San Luis Unit. Sacramento (CA): U.S. Fish and Wildlife Service, Sacramento Fish and Wildlife Office, Environmental Contaminants Division. March 2008. 46 p.
- [USFWS] U.S. Fish and Wildlife Service. 2009. Endangered species consultation on the proposed continuation of the Grassland Bypass Project, 2010–2019. Sacramento (CA): U.S. Fish and Wildlife Service, Sacramento Fish and Wildlife Office. December 2009. 198 p.
- [USFWS and NOAA Fisheries] U.S. Fish and Wildlife Service and National Oceanic and Atmospheric Administration National Marine Fisheries Service. 2000. Final biological opinion on the effects of the U.S. Environmental Protection Agency’s “Final Rule for the Promulgation of Water Quality Standards: Establishment of Numeric Criteria for Priority Toxic Pollutants for the State of California. U.S. Fish and Wildlife Service and National Marine Fisheries Service. 323 p.
- Velinsky DJ, Cutter, GA. 1991. Geochemistry of selenium in a coastal salt marsh. *Geochimica et Cosmochimica Acta* 55(1):179–191.
- Wang W–X. 2002. Interactions of trace metals and different marine food chains. *Marine Ecology Progress Series* 243(1):295–309.
- Wang W–X, Dei RCH. 1999. Kinetic measurements of metal accumulation in two marine macroalgae. *Marine Biology* 135(1):11–23.
- Wang W–X, Fisher NS. 1999. Delineating metal accumulation pathways for marine invertebrates. *Science of the Total Environment* 237/238:459–472.
- Wang W–X, Fisher NS, Luoma SN. 1996. Kinetic determinations of trace element bioaccumulation in the mussel *Mytilus edulis*. *Marine Ecology Progress Series* 140(1–3):91–113.
- Zhang YQ, Moore JN. 1996. Selenium fractionation and speciation in a wetland system. *Environmental Science and Technology* 30(8):2613–2619.

Chinook salmon outmigration survival in wet and dry years in California's Sacramento River

Cyril J. Michel, Arnold J. Ammann, Steven T. Lindley, Philip T. Sandstrom, Eric D. Chapman, Michael J. Thomas, Gabriel P. Singer, A. Peter Klimley, and R. Bruce MacFarlane

Abstract: Outmigration survival of acoustic-tagged, hatchery-origin, late-fall-run Chinook salmon (*Oncorhynchus tshawytscha*) smolts from the Sacramento River was estimated for 5 years (2007–2011) using a receiver array spanning the entire outmigration corridor, from the upper river, through the estuary, and into the coastal ocean. The first 4 years of releases occurred during below-average river flows, while the fifth year (2011) occurred during above-average flows. In 2011, overall outmigration survival was two to five times higher than survival in the other 4 years. Regional survival estimates indicate that most of the improved survival seen in 2011 occurred in the riverine reaches of the outmigration corridor, while survival in the brackish portions of the estuary did not significantly differ among the 5 years. For the 4 low-flow years combined, survival rate in the river was lower in the less anthropogenically modified upper reaches; however, across all regions, survival rate was lowest in the brackish portion of the estuary. Even in the high-flow year, outmigration survival was substantially lower than yearling Chinook salmon populations in other large rivers. Potential drivers of these patterns are discussed, including channelization, water flow, and predation. Finally, management strategies are suggested to best exploit survival advantages described in this study.

Résumé : La survie durant la dévalaison de la fin de l'automne de saumoneaux quinnat (*Oncorhynchus tshawytscha*) du fleuve Sacramento issus d'écloseries et munis d'émetteurs acoustiques a été estimée sur une période de 5 ans (2007–2011) à l'aide d'un réseau de récepteurs couvrant tout le corridor de dévalaison, du cours supérieur du fleuve jusqu'au littoral océanique, en passant par l'estuaire. Les lâchers des 4 premières années ont eu lieu pendant des périodes de débits du fleuve sous la moyenne, alors que les débits étaient supérieurs à la moyenne pour les lâchers de la cinquième année (2011). En 2011, la survie globale durant la dévalaison était de deux à cinq fois supérieure à la survie durant les 4 autres années. Les estimations régionales de la survie indiquent que les meilleurs taux de survie observés en 2011 se sont produits dans des tronçons fluviaux du corridor de dévalaison, alors que la survie dans les portions saumâtres de l'estuaire n'a pas varié de manière significative durant ces 5 années. Pour les 4 années combinées de faibles débits, le taux de survie dans le fleuve était plus faible dans les tronçons supérieurs moins modifiés par l'activité humaine; cela dit, pour toutes les régions, le taux de survie était le plus faible dans la portion saumâtre de l'estuaire. Même durant l'année de débits élevés, la survie durant la dévalaison était considérablement plus faible que celle de populations de saumons quinnat d'un an dans d'autres grands cours d'eau. Les causes possibles de ces motifs, dont la canalisation, l'écoulement de l'eau et la prédation, sont abordées. Enfin, des stratégies de gestion sont suggérées pour l'exploitation optimale des avantages liés à la survie décrits dans l'étude. [Traduit par la Rédaction]

Introduction

Knowing where excessive mortality is occurring is crucial to designing effective conservation measures for salmon populations. Salmon utilize many different habitats during the different stages of their life cycle, but it is the degradation of freshwater or estuarine habitats that is commonly cited as the cause of population declines (Nehlsen et al. 1991). Of particular concern is the high mortality often experienced in these habitats during one of the most vulnerable stages in the salmon life cycle: the downstream migration of juveniles (smolts) heading to the ocean from their riverine birthplace (Healey 1991).

There has been extensive research on juvenile salmonid smolt survival in large rivers of the west coast of North America, most notably in the Columbia and Fraser rivers (McMichael et al. 2010;

Muir et al. 2001; Rechisky et al. 2013; Skalski et al. 1998; Welch et al. 2008, 2009). These studies have indicated that outmigration survival can vary widely from year to year and population to population, and further research in these rivers has shown that survival rates often correlate with environmental variables such as flow, turbidity, and temperature (Giorgi et al. 1997; Gregory and Levings 1998; Smith et al. 2003). This information has proved crucial for improving salmon survival in the Columbia River, through improvements in fish passage structures and changes in dam operations (Connor et al. 2003).

California's Sacramento River, in contrast, is critically lacking in smolt outmigration survival information. The Sacramento River, compared with the Columbia and Fraser rivers, has an order of magnitude lower discharge, exists in a warm and dry Med-

Received 26 November 2014. Accepted 13 June 2015.

Paper handled by Associate Editor Michael Bradford.

C.J. Michel. University of California, Santa Cruz, Under contract to Southwest Fisheries Science Center, National Marine Fisheries Service, National Oceanic and Atmospheric Administration, 110 Shaffer Rd., Santa Cruz, CA 95060, USA.

A.J. Ammann, S.T. Lindley, and R.B. MacFarlane. Southwest Fisheries Science Center, National Marine Fisheries Service, National Oceanic and Atmospheric Administration, 110 Shaffer Rd., Santa Cruz, CA 95060, USA.

P.T. Sandstrom,* E.D. Chapman, M.J. Thomas, G.P. Singer, and A.P. Klimley. Biotelemetry Lab, Department of Wildlife, Fish, & Conservation Biology, University of California, Davis, 1334 Academic Surge Building, Davis, CA 95616, USA.

Corresponding author: Cyril J. Michel (e-mail: cyril.michel@noaa.gov).

*Present address: Washington Department of Fish & Wildlife, Natural Resources Building, 1111 SE Washington St., Olympia, WA 98501, USA.

iterranean climate, and yet is the primary source of water to the state's industrial, domestic, and agricultural sectors. The Sacramento River and its estuary are currently the objects of intense conservation concern owing to the poor status of some of its salmon and steelhead (sea-run rainbow trout, *Oncorhynchus mykiss*) populations (among other native species) and habitats. In spite of these problems, the Sacramento River is still an important contributor to west coast Chinook salmon (*Oncorhynchus tshawytscha*) fisheries, largely because of extensive hatchery propagation efforts (O'Farrell et al. 2013). Several very large water and habitat management projects are under consideration that are expected by their proponents to contribute to the restoration of Chinook salmon populations, yet survival rates across the life cycle of these populations are poorly known. Several coded-wire and acoustic tagging studies have assessed Chinook salmon smolt survival in the Sacramento – San Joaquin Delta (the freshwater portion of the estuary), which is the hub of water infrastructure for the majority of southern California and a location where anthropogenic modifications are extensive and salmonid losses are great (Baker and Morhardt 2001; Brandes and McLain 2001; Perry et al. 2010). However, no study has assessed smolt survival through the entirety of the outmigration corridor, from the upper limit of anadromy to the Pacific Ocean.

In this study, we quantify the spatial and temporal patterns of hatchery late-fall-run Chinook salmon smolt survival in the Sacramento River system. Utilizing an extensive network of acoustic receivers, we estimated survival through the river and estuary over 5 years at a fine-scale spatial resolution previously not possible. This resolution allowed us to discern regional and temporal differences in survival that cannot be obtained using traditional tagging methods.

Methods

Study area

The Sacramento River is the longest and largest (measured by flow discharge) river that is fully contained within the state of California and is the third largest river that flows into the Pacific Ocean in the contiguous United States (Fig. 1). The headwaters are located just south of Mount Shasta in the lower Cascade Range, and the river enters the ocean through the San Francisco Estuary at the Golden Gate. The total catchment area spans approximately 70 000 km². The Sacramento River and its tributaries have been heavily dammed and otherwise impacted by human activities; it is estimated that 47% of the historic spawning, migration, and (or) rearing area is no longer accessible to Chinook salmon (Yoshiyama et al. 2001).

The Sacramento River watershed includes diverse habitats, from relatively pristine run-riffle reaches in the north, to a heavily channelized and impacted waterway further south, and finally to the San Francisco Estuary, the largest and most modified estuary on the west coast of North America (Nichols et al. 1986). The San Francisco Estuary is composed of an expansive tidally influenced freshwater delta upstream of its confluence with the San Joaquin River and a series of increasingly saline bays. The sheer size and physical differences between these two sections of the estuary merit separate consideration with respects to their influence on salmon survival; therefore, we use the terms “delta” and “bays” to differentiate between the two.

The annual mean daily discharge for the Sacramento River from 1956 to 2008 was 668 m³·s⁻¹ (California Department of Water Resources 2007). However, this water does not continue downstream unimpeded; owing to one of the world's largest water storage and water transportation infrastructures, replete with abundant dams, reservoirs, diversions, and aqueducts, it is estimated that current discharge of the Sacramento and San Joaquin rivers combined is less than 40% of the predevelopment discharge (Nichols et al. 1986). The damming and water diversions of the

Sacramento River and its tributaries have also homogenized river flows throughout the year, reducing winter high flows and flooding while increasing flows in the summer and fall (Buer et al. 1989).

The study area included approximately 92% of the current outmigration corridor of late-fall-run Chinook salmon, from release to ocean entry. Specifically, the study area's furthest upstream release site at Jelly's Ferry (518 km upstream from the Golden Gate Bridge) is only 47 km downstream from Keswick Dam, the first impassable barrier to adult salmon returning to spawn on the Sacramento River.

Central Valley late-fall-run Chinook salmon

The late-fall-run is one of the four Chinook salmon runs occurring in the Sacramento River drainage and is the only run to exhibit a predominately yearling migrant life history (Moyle 2002). Following emergence from the gravel, wild late-fall-run juveniles exhibit a river residency of 7 to 13 months, after which smolts (juvenile salmon that are actively migrating to the ocean) will migrate to the ocean between the months of October and May at a fork length of 90 to 170 mm (Fisher 1994; Snider and Titus 2000a, 2000b). In contrast, the subyearling life history demonstrated by a 4- to 7-month freshwater residency is the more common life history strategy used by the other salmon populations in the Sacramento River. Moyle et al. (1995) outlined six major threats to the late-fall-run Chinook salmon population, one of which was mortality during outmigration, potentially due to water diversions and increased predation in bank-altered areas. In 2004, the fall-late-fall-run Chinook salmon evolutionarily significant unit (ESU) was designated a “species of concern” by the United States Endangered Species Act.

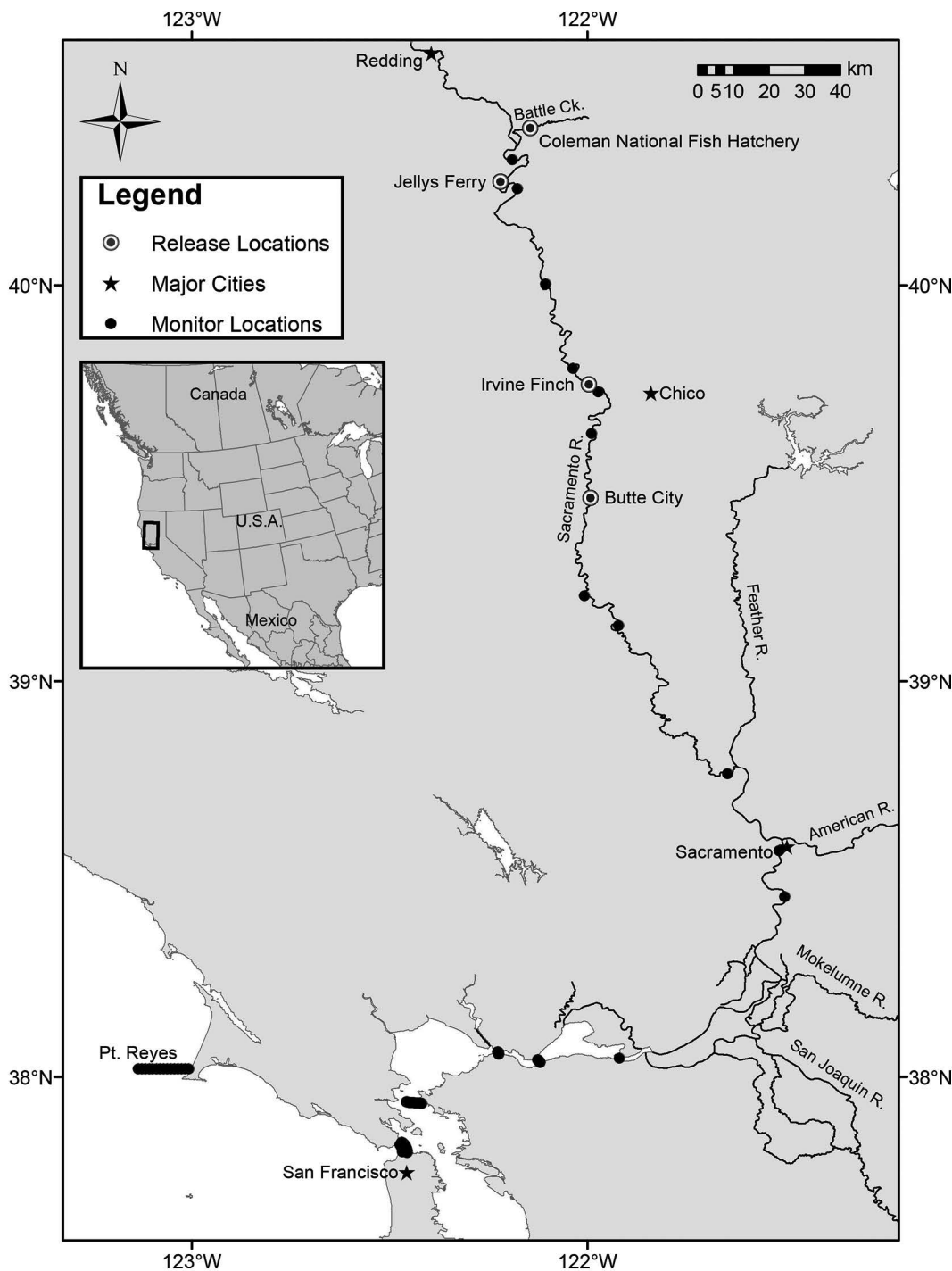
The United States Fish and Wildlife Service's (USFWS) Coleman National Fish Hatchery (Anderson, California) is the only hatchery to produce late-fall-run Chinook salmon, releasing approximately one million smolts a year between mid-December and mid-January. Annual escapement for this population can vary from just several hundred to 42 000; the mean annual escapement from the winter of 1973–1974 to the winter of 2007–2008 is 12 386 individuals (Azat 2015). Little information exists regarding what proportion of the late-fall-run adult population is of hatchery origin versus wild origin. Palmer-Zwahlen and Kormos (2013) estimated that in 2011, 100% of late-fall-run adults returning to Coleman National Fish Hatchery were hatchery fish, while 44% of late-fall adults recovered during carcass surveys on the Sacramento River were hatchery origin.

Fish tagging and releases

For five consecutive winters, from January 2007 to December 2010 – January 2011 (henceforth referred to as 2007, 2008, 2009, 2010, and 2011 seasons, based on the year during which January tagging occurred), 200 to 304 late-fall-run Chinook salmon smolts from Coleman National Fish Hatchery were implanted with acoustic tags and released into the Sacramento River. Release times were scheduled to be within a few days of the release times of the general production of hatchery fish. Only smolts 140 mm or larger were tagged to keep the tag mass to less than 6% of the fish mass. Therefore, tagged smolts were representative of the larger hatchery individuals; specifically, from 2007 to 2011, smolts at or above the 140 mm cutoff represented 23.5%, 38.4%, 50.2%, 29.6%, and 50.9%, respectively, of the total hatchery production. In the rare instance that a smolt had severe descaling, fin erosion, or other obvious injuries, the smolt was discarded and not tagged.

Acoustic tags were surgically implanted into the peritoneal cavity of anesthetized fish. The tag was inserted through a 12 mm incision anterior to the pelvic girdle and 3 mm to the side of the linea alba. The incision was then closed with two simple interrupted stitches tied with square knots of nonabsorbable nylon cable-type suture. All fish were allowed to recover for a minimum

Fig. 1. Study area map including the Sacramento River, Sacramento – San Joaquin River Delta, Suisun – San Pablo – San Francisco bays and Pacific Ocean. Bull's-eye icons signify a release location, stars symbolize a major city, and black dots symbolize a receiver location.



of 24 h before release. Additional surgery details can be found in Ammann et al. (2013). In study years 2008 and 2009, an additional group of smolts from the same hatchery were tagged with dummy acoustic transmitters to monitor tag effects and tag retention in laboratory trials. No fish shed their tags over 221 and 160 days (the entire length of the trial in both years, respectively), and tagged fish growth and survival was not significantly different than untagged fish (Ammann et al. 2013). Since fish in the field and captive studies had similar tag burdens (1.6% to 6.3% for field study, 2.6% to 5.6% for captive study), we assumed that mortality in the field study was not tag-related.

In the first year (2007), a total of 200 fish were released in small batches (13–14 fish each) every weekday afternoon for the third, fourth, and fifth weeks of January 2007 at the Coleman National Fish Hatchery into Battle Creek (river kilometre 534 — “rkm” is distance from ocean), a tributary to the Sacramento River (Table 1). In the following 4 years, fish were released in two groups. In 2008–2010, a total of approximately 300 fish were released; ~50 fish were simultaneously released at dusk at three release sites in the upper 150 km of the mainstem Sacramento River (rkm 518, 412, 363) in mid-December and early January, allowing the lower release groups to reach the lower river and estuary in larger numbers,

Table 1. Means and standard deviations (SD) for mass and fork length of acoustically tagged smolts by year and for all years combined.

Year	Sample size	Fork length \pm SD (mm)	Mass \pm SD (g)
All	1350	158.8 \pm 12.4	43.9 \pm 11.2
2007	200	164.6 \pm 10.7a	46.6 \pm 9.8a
2008	304	168.7 \pm 13.3b	52.6 \pm 13.8b
2009	300	152.1 \pm 8.5c	38.9 \pm 7.9c
2010	306	152.5 \pm 10.2c	39.3 \pm 8.8c
2011	240	158.1 \pm 7.8d	42.9 \pm 6.8d

Note: Size distributions with different letters are significantly different ($P < 0.05$).

which improved statistical precision of the survival estimation. In 2011, 240 fish were released; 120 fish were released in mid-December and early January at dusk at Jelly's Ferry (rkm 518), a site on the mainstem Sacramento River, only 7.3 km downstream of the confluence with Battle Creek. Fish were transported to the release sites by truck at low densities (~ 10 g·L⁻¹) in coolers with aerators. In years with multiple release sites, transport times were extended for closer sites to keep potential transport stress equal among all release groups.

Acoustic telemetry

Acoustic tagging technology was used to acquire high-resolution movement data and survival estimates. Uniquely coded Vemco 69 kHz V7-2L acoustic tags (mean \pm SD: 1.58 \pm 0.03 g in air, 7 mm diameter by 20 mm long; Amirix Systems, Inc., Halifax, Nova Scotia, Canada) and Vemco VR2/VR2W receivers were used to tag and track fish. The tags transmitted every 30 to 90 s (with a mean of 60 s) in the first year of the study, then transmitted every 15 to 60 s (with a mean of 45 s) in the following 4 years. Battery life tests were conducted in 2007, 2010, and 2011 with a subset of tags from the same batch used for tagging smolts. In 2007, tag life of 11 test tags ranged from 138 to 749 days, with a mean of 513 days; in 2010, tag life of 20 test tags ranged from 127 to 297 days, with a mean of 194 days; in 2011, tag life of 25 test tags ranged from 98 to 214 days, with a mean of 172 days. For the purposes of verifying that tag life was sufficient to last the entire migration of all smolts, the time elapsed from release to last known detection was calculated for each smolt for all 5 years of the study. Last known detection for smolts was either last known detection before disappearance or time of arrival to the Golden Gate receiver location (considered the end of the outmigration in this study). The longest outmigrating individual per year took 32, 89, 67, 97, and 79 days, respectively, for the years 2007–2011, with 99.2% of smolts successfully outmigrating or disappearing within the first 60 days after release. Therefore, we believe the battery life for our tags were sufficient to last the entire outmigration period of our tagged smolts.

The receiver array spanned 550 km of the Sacramento River watershed from below Keswick Dam to the entrance to the ocean (Golden Gate) and beyond to Point Reyes. This network of approximately 300 receivers at 210 receiver locations was maintained by the California Fish Tracking Consortium (<http://californiafishtracking.ucdavis.edu>), a group of academic, federal, and state institutions and private consulting firms. We selected a subset of these receiver locations for the final survival analyses, as per the selection criteria described in the Data analysis section of the Methods (see below).

The acoustic receivers automatically process all detection data and drop most false detections or incomplete codes from the detection file. All detections were then subject to standardized quality control procedures to remove any remaining false detections (see Michel et al. 2013).

Data analysis

Survival in each reach

Juvenile Chinook salmon express obligate anadromy, meaning that they will travel toward the ocean once the emigration has begun with scarce exceptions (Healey 1991). Therefore, in a linear system such as the Sacramento River, if receiver locations were capable of detecting every passing tag, then if a fish is detected at one receiver location but is never detected thereafter, we could assume that the fish has died somewhere in the reach between the receiver location where it was last detected and the next downstream receiver location.

However, receiver locations rarely operate perfectly, necessitating the estimation of detection and survival probabilities at each receiver location. We used the Cormack–Jolly–Seber (CJS) model for live recaptures (Cormack 1964; Jolly 1965; Seber 1965) within program MARK (White and Burnham 1999) using the RMark package (Laake and Rexstad 2008) within program R (version 3.0.1; R Core Team 2013). The CJS model was originally conceived to calculate survival of tagged animals over time, by resampling (recapturing) individuals and estimating survival and recapture probabilities using maximum likelihood. For species that express an obligate migratory behavior, a spatial form of the CJS model can be used, in which recaptures (i.e., tagged fish detected acoustically downstream from release) occur along a migratory corridor (Burnham 1987). The model determines if fish not detected at certain receivers were ever detected at any receiver downstream of that specific receiver, thus enabling calculation of maximum-likelihood estimates for detection probability of all receiver locations (p), survival (Φ), and 95% confidence intervals for both (Lebreton et al. 1992).

An initial run of the model with all possible river receiver locations together with the major estuary receiver locations was performed for each individual year separately, after which a subset of the river receiver locations that had consistently high tag detection probabilities through the years and that were strategically located were chosen to delimit the river reaches that were used in the spatial survival analysis. Additionally, because survival between the Battle Creek release site and Jelly's Ferry receiver location was only estimated in 2007, and because Jelly's Ferry was the furthest upstream release site for all following years, only fish known to have reached the Jelly's Ferry receiver location in 2007 were included in all survival analyses, and Jelly's Ferry was considered to be their release location. In total, 145 of the 200 smolts released in 2007 were known to have reached the Jelly's Ferry release location and were included in survival analyses. A total of 19 receiver locations were chosen, extending from just below the most upstream release site, Jelly's Ferry, to the Golden Gate (Fig. 1; Table 2). Between them, we delineated 17 reaches in which mortality can be accurately estimated (the detection probability and survival of the 18th and last reach can only be estimated jointly, as there is no detection information beyond this point in which to assess the final receiver location).

Parallel receiver lines were installed at the Golden Gate approximately 1 km apart to estimate detection probability and survival at the inner (East) Golden Gate receiver line by using the western line to assess performance of the eastern line. After the 2008 outmigration season, a coastal ocean receiver line was deployed across the continental shelf at Point Reyes, approximately 60 km north of the Golden Gate. Detections from this receiver line were included in the encounter history for the Golden Gate West line to improve accuracy in the estimation of survival and detection probability to the Golden Gate East line. However, because the Point Reyes receiver location did not exist in the 2007 or 2008 season, and few fish were detected there in subsequent years, it was not formally included as a receiver location in the survival analyses.

Survival per 10 km, regional survival, and overall survival

For each year, we used the 18 receiver locations to estimate reach survival (Φ_R) for 17 reaches, using the fully time-varying CJS

Table 2. Locations of acoustic receivers and tagged smolt release locations.

Location	rkm	Description
Battle Creek	534	Release site 2007
Jelly's Ferry	518	Receiver location and release site 2008–2011
Bend Bridge	504	Receiver location
China Rapids	492	Receiver location
Above Thomes	456	Receiver location
Below GCID	421	Receiver location
Irvine Finch	412	Receiver location and release site 2008–2010
Above Ord	389	Receiver location
Butte City Bridge	363	Receiver location and release site 2008–2010
Above Colusa Bridge	325	Receiver location
Meridian Bridge	309	Receiver location
Above Feather River	226	Receiver location
City of Sacramento	189	Receiver location
Freeport	169	Receiver location
Chipps Island	70	Receiver location
Benicia Bridge	52	Receiver location
Carquinez Bridge	41	Receiver location
Richmond Bridge	15	Receiver location
Golden Gate East	2	Receiver location
Golden Gate West	1	Receiver location
Point Reyes	-58	Receiver location

Note: Positive river kilometre (rkm) values indicate distance upstream from the Golden Gate Bridge; negative value indicates distance seaward from the Golden Gate Bridge. GCID, Glenn-Colusa Irrigation District.

model, which in this case actually varies over space; specifically, each reach has a parameter (reach model). Detection probabilities were also allowed to vary by reach. These survival estimates were then standardized by reach lengths l (giving survival per 10 km, Φ_{10}) to allow inter-reach survival comparisons. This was done by setting the time intervals (in reality, space intervals for this application) in the `process.data()` function of RMark package to a vector of reach lengths (in units of 10 km). The per 10 km survival estimates are calculated by RMark according to the following formula (eq. 1):

$$(1) \quad \Phi_{10} = \sqrt[l]{\Phi_R}$$

To account for the propagation of error, standard errors for n th root parameter estimates were calculated by the RMark package using the `delta` method (Powell 2007; Seber 1982).

Regional (river, delta, and bays) and overall (from the release site to the Golden Gate) survival was then assessed for each year. We did this by taking the product of the reach survival estimates that fall inside the spatial extent of interest, and we present this as percent survival. To account for the propagation of error, standard errors of the cumulative products of survival estimates were also calculated using the RMark package, using the `deltamethod.special()` function. When using the `delta` method for estimating the variance of the product of survival estimates, the variance-covariance matrix for the survival estimates must be included in the estimation. Confidence intervals for the product of survival estimates must be calculated on the logit scale, then back-transformed to the real probability scale. Therefore, to estimate 95% confidence intervals, we used our product of survival estimates ($\hat{\Phi}$) along with its respective standard error of the beta estimate ($\widehat{SE}_{\text{logit}(\hat{\Phi})}$) by using the following formula (eq. 2):

$$(2) \quad \text{expit}[\text{logit}(\hat{\Phi}) \pm 1.96 \times \widehat{SE}_{\text{logit}(\hat{\Phi})}]$$

The influences of different spatial and temporal factors on survival rates were assessed by modeling Φ_R as a function of the factor in question. Specifically, the influence of these factors was assessed by allowing each release group (e.g., five groups for the release year model: 2007, 2008, 2009, 2010, and 2011) within each model to have its own set of survival parameters. Each factor-specific survival model was compared with one another and with a base model (a model with no factor-specific parameters) using Akaike's information criterion corrected for small sample sizes (AIC_c). Goodness-of-fit was assessed by estimating the \hat{c} variance inflator factor of the base model. For this we used two different methods and adopted the more conservative estimate. First, we simulated \hat{c} and deviance from 100 simulations using the bootstrap procedure. Then, we estimated \hat{c} in two ways, first by dividing the deviance estimate from the original data by the mean of simulated deviances, giving a \hat{c} of 1.309, then by dividing the \hat{c} from the original data by the mean \hat{c} from the bootstraps, giving a \hat{c} of 1.494. We therefore adopted the more conservative \hat{c} of 1.494 and used it to adjust all AIC values for overdispersion (hereinafter called $QAIC_c$). As a rule of thumb, if a test model lowered $QAIC_c$ relative to the base model by a difference of more than seven, the test model was deemed substantially more parsimonious and therefore was supported over the base model.

The effects of reach ($n = 17$), release year ($n = 5$), release site ($n = 3$), and all interactions of those factors were tested (see Table 3 for models). This was done by comparing the $QAIC_c$ score of each model with the $QAIC_c$ score of a version of the "reach model" that combines data from all 5 years, which henceforth will be considering the "base model". We used the reach model as our base model under the assumption that survival must vary through space given the spatial heterogeneity of the study system. To test this assumption, a "null model" was also included for comparison. This model only allowed one parameter for survival (representing the null hypothesis: constant survival through space and time). An initial run of several models that allowed for a different parameterization of the detection probability terms while keeping the survival terms the same indicated that the model allowing for detection probability to vary by reach and year was the best supported model. Therefore, all survival models presented in Table 3 allow detection probability to vary by reach and year: $p(\text{reach} \times \text{year})$.

To better understand whether annual fluctuations in survival occurred on a regional scale, we also included three models that allowed survival to vary per reach and per year (reach \times year) in only the river, the delta (the delta being the freshwater portion of the estuary), or the bays (Suisun, San Pablo, and San Francisco bays, i.e., the brackish portion of the estuary). These models allowed survival to vary by reach in the remaining regions and are therefore also comparable with the base model.

Finally, the influence of individual covariates (fork length (mm) and mass (g)) on survival was assessed. The model selected a priori to include these covariates was the base model. The individual covariates were added both as an additive factor (different intercept per reach, but common slope) and as a factor including the interaction term (different intercept and different slope). These models were then compared using $QAIC_c$ with the base model without any individual covariates to determine whether fish size and mass affects survival.

For the purpose of considering migration rate as a potential driver for survival rates, mean successful migration movement rate (MSMMR, $\text{km}\cdot\text{day}^{-1}$; Michel et al. 2013) was calculated per year. Migration movement rate from release site to the West Golden Gate receiver line (i.e., entry to the Pacific Ocean) was calculated for every fish that was detected (i.e., successfully reached the ocean) at either of the Golden Gate receiver lines. These values were then averaged per year and compared with the overall survival for that year in Table 4.

Table 3. Survival models for different spatial and temporal factors, as well as individual covariates, ordered from lowest to highest QAIC_c, omitting 2011 data.

Survival (ϕ) treatment	Δ QAIC _c	No. of parameters
(River survival \times year) \times reach	0.0	126
(Delta survival \times year) \times reach	25.3	93
Base model (reach)	26.6	90
Reach + length	26.6	91
Reach \times year	27.9	144
Reach \times length	40.0	108
(Bays survival \times year) \times reach	49.0	105
Reach \times mass	50.0	108
Reach \times release	53.8	126
Reach \times year \times release	270.8	288
Null model (constant survival)	308.4	73

Note: The Δ QAIC_c statistic represents the QAIC_c distance from the most parsimonious model. The number of parameters includes the parameters for estimation of detection probabilities (reach- and year-specific).

Results

Overall survival of late-fall-run Chinook salmon through the entire migration corridor (rkm 518–2) per year ranged from 2.8% to 15.7%, with 2011 having the highest survival (Table 4). The MSMMR values indicate that the first 4 years of the study had relatively similar migration rates, ranging from 17.5 to 23.5 km per day, whereas 2011 had a faster migration rate of 36 km per day.

Survival rate on a reach-by-reach basis was quite variable. During the first 4 years of the study, the upper river reaches (reaches 1 through 8; rkm 518–325) had some of the lowest survival per 10 km, and the lower reaches of the river (reaches 9–12; rkm 325–169) had the highest. The delta was comparable to the upper river, and the San Francisco and Suisun bays (reaches 13–17; rkm 169–2) had the lowest survival rates (Fig. 2). During these same 4 years, detection probabilities per year and per receiver location throughout the watershed ranged from 4% to 100%, with 90% of all detection probabilities being larger than 50%. In the fifth year, river flows at the time of release were much higher than in the previous 4 years (Fig. 3), and as a result detection rates were much lower in the river, with only three of the twelve river receiver locations having a detection probability higher than 1%. Therefore, 2011 reach-specific survival in the river was not estimable.

Region-specific survival estimates were calculated using the product of all reach-specific survival estimates within the region of interest (Fig. 4; Table 4). Although reach-specific survival parameters could not be estimated for the river region in 2011, detection probability improved downstream as water velocity decreased, allowing the estimation of reach-specific and region-specific survival estimates downstream of the river region. To estimate river region survival in 2011 and to further investigate differences in survival between 2011 and the previous years, the detection data was simplified for a post hoc CJS modeling exercise that would allow the inclusion of 2011. We simplified the detection data by only including detections from four receiver locations separating the major watershed regions: Freeport at the downstream end of the river region, Chipps Island at the downstream end of the delta region, and the two parallel Golden Gate receiver lines at the downstream end of the bays region. Additionally, only fish released at the Jelly's Ferry site were included for all years, since the other release locations did not have associated receiver locations. A preliminary model that allowed survival and detection probability to vary by region and by year (region \times year) allowed us to estimate survival in the river region in 2011 (Fig. 4; Table 4). This estimate revealed that survival in the river in 2011 was much higher than in all previous years, while survival in the delta and bays was similar among all 5 years. We also constructed

Table 4. Percent overall survival to Golden Gate East receiver line (rkm 2) per year, including standard error (SE), and mean successful migration movement rate (MSMMR) with SE.

Release group	% Survival	SE	MSMMR \pm SE (km-day ⁻¹)
2007-All	2.8	1.4	23.5\pm3.6
2007-River	15.5	3.6	
2007-Delta	63.0	14.5	
2007-Bays	28.3	12.4	
2008-All	3.8	0.9	17.5\pm1.5
2008-River	24.5	3.0	
2008-Delta	59.1	4.4	
2008-Bays	26.1	4.9	
2009-All	5.9	1.2	17.5\pm1.1
2009-River	31.9	3.2	
2009-Delta	43.1	4.3	
2009-Bays	43.0	6.5	
2010-All	3.4	0.9	21.9\pm2.1
2010-River	22.7	2.5	
2010-Delta	53.6	5.6	
2010-Bays	28.1	6.4	
2011-All	15.7	2.5	36.0\pm3.0
2011-River*	63.2*	8.5*	
2011-Delta	70.6	4.8	
2011-Bays	33.1	4.7	

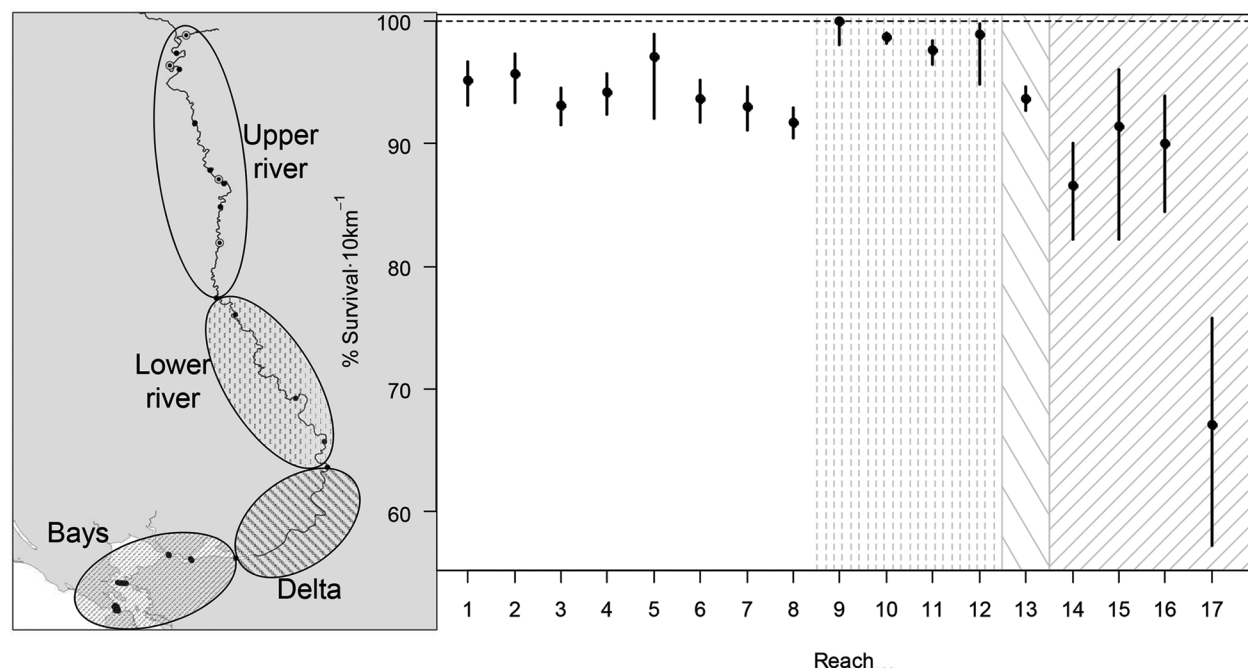
*Estimated from post hoc survival model.

a set of similar models where 1 year was given its own set of region-specific survival parameters, while the remaining 4 years shared the same region-specific survival parameters. These models allowed detection probability to vary by region and by year. Five models were constructed, each one allowing a different year to have its own survival parameters. The model allowing 2011 to have its own region-specific survival parameters while the other 4 years shared the same region-specific parameters was substantially better supported (Δ QAIC_c > 7) than all the other models of the same type, as well as the preliminary model (permitting all years to have different region-specific survival parameters).

In the analysis of the effect of different spatial and temporal factors on survival, 2011 data was omitted because of the lack of detection data available in the river portions of the watershed. The influence of reach on survival rates (base model) was found to have substantially better support (Δ QAIC_c \gg 7) than the null model (constant survival through space and time; Table 3). The reach models that included release site or year (reach \times release and reach \times year, respectively), as well as the interaction model (reach \times year \times release), did not improve their support over the base model. The year model was better supported than the release model. The only model that had substantially better support than the base model was the model that allowed for river survival to have a year effect, while delta and bays survival was held constant through time ((river survival \times year) \times reach). The model allowing only the delta reach to have a year effect ((delta survival \times year) \times reach) was marginally better supported than the base model (Δ QAIC_c < 2).

Tagged fish mass and fork length varied significantly among years ($P < 0.001$), and pairwise hypothesis testing using Bonferroni and Tukey's honestly significant difference tests both indicate that fish sizes were statistically different among all years (with the exception of the 2009–2010 pair; Table 1). However, the addition of individual covariates (mass, length) as factors to the base model did not improve parsimony in any circumstance, although the length model did fit the data better than the mass model. A model adding length as an additive factor had more support than the other covariate models and had approximately equal support with the base model (Δ QAIC_c < 0.1; Table 3). Therefore, the significant

Fig. 2. Percent survival per 10 km per reach for the 2007–2010 study years combined. Figure and map are delimited based on the regions (from upstream to downstream): upper Sacramento River, lower Sacramento River, Sacramento – San Joaquin River Delta, and Suisun – San Pablo – San Francisco bays. The Sacramento River was delimited into an upper and lower section to highlight the shift in survival rates. Error bars represent 95% confidence intervals. 2011 data was omitted owing to poor detection probabilities.



differences in mass and fork length among years did not appear to affect survival.

Discussion

This study used high resolution fish tracking and environmental data to provide the first reach-specific survival estimates of Chinook salmon smolts in the Sacramento River over the entire migration corridor. Survival was relatively high in the lower river compared with other areas, a somewhat unexpected finding given that this reach is channelized and rip-rapped. Also, and in contrast with the commonly held belief that mortality during the Central Valley smolt outmigration is greatest in the delta (Williams 2006), we observed relatively high mortality in the upper river and especially in the bays downstream of the delta. We found that survival over the entire migration route was much lower in 4 low-discharge years (2.8%–5.9%) than in 1 high-discharge year (15.9%; Fig. 3); higher survival in the high-discharge year was due mainly to increased survival in the river region. This suggests that riverine survival dynamics may be playing an underappreciated role in determining annual salmon stock abundance, as shown with Cheakamus River steelhead stock in British Columbia (Melnychuk et al. 2014).

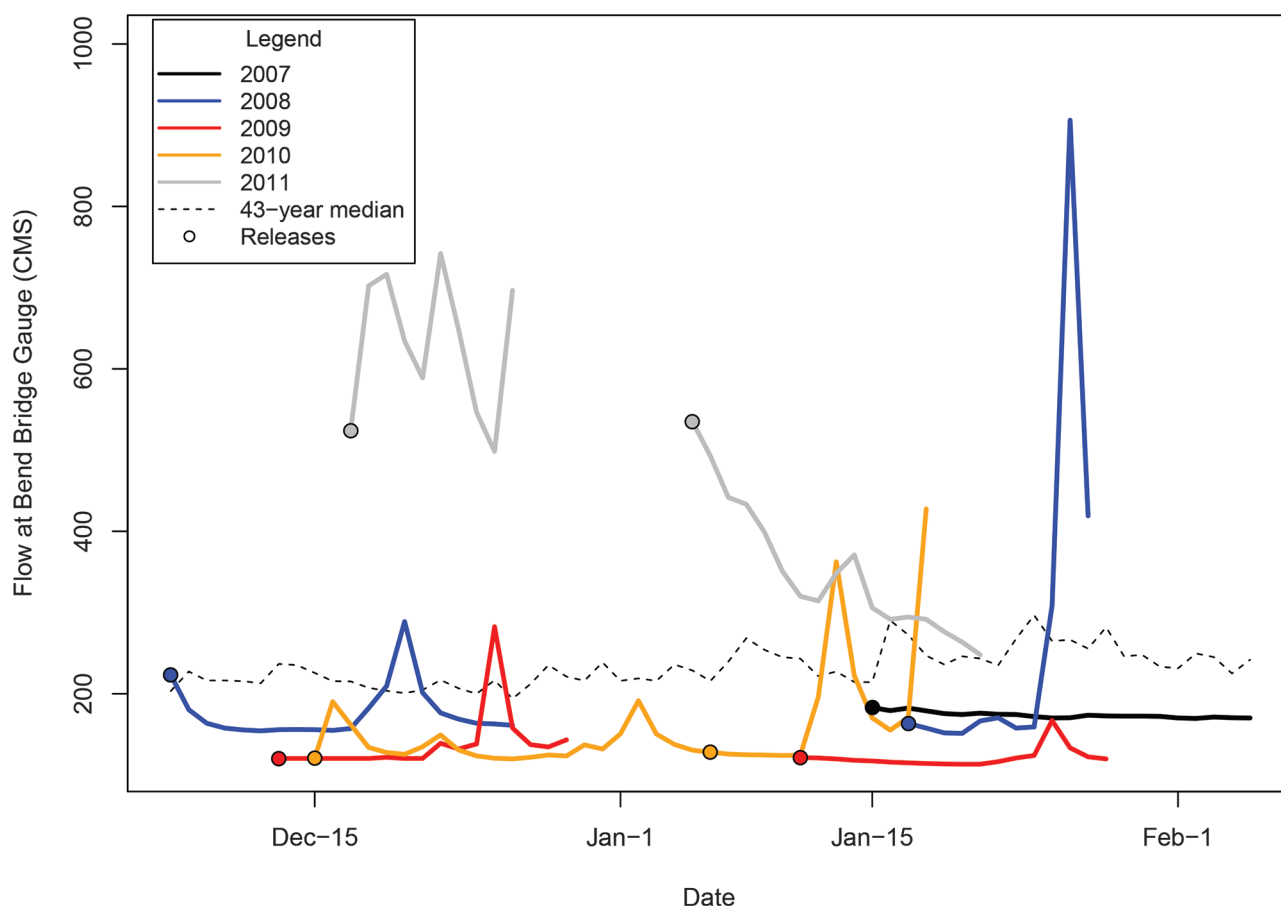
One potential reason why the lower Sacramento River had higher survival than expected may be due to channelization. Levees, riprap, and channelization have been considered detrimental for salmon populations owing to their degradation of spawning grounds (reduced input of gravel), the paucity of prey to feed upon, and an absence of cover that results in a greater frequency of predation on juveniles (Buer et al. 1989; Chapman and Knudsen 1980; Garland et al. 2002; Schmetterling et al. 2001). However, Michel (2010) found a strong positive correlation between channelized reaches and smolt survival. Given limited rearing potential, smolts likely migrate through channelized reaches, reducing the period of exposure to sources of mortality. The majority of potential predator species in the watershed are typically found associated with submerged structure and vegetation, which in the lower Sacramento River are mostly limited to the rip-rapped lit-

toral zone. A smolt travelling downstream in the lower Sacramento River only needs to avoid the channel margins to minimize exposure to predators. Outmigrating Chinook salmon smolts in the Sacramento River travel disproportionately more in the center of the channel (Sandstrom et al. 2013). Similarly, smolt survival was higher in deep impoundments compared with shallower undammed reaches of the Columbia River (Welch et al. 2008).

Previous studies of salmon survival in the Sacramento River and estuary, based primarily on coded-wire tags, suggested significantly lower mortality in the bays, but higher mortality in the river. Brandes and McLain (2001) found survival of subyearling fall-run Chinook salmon smolts from Port Chicago to the Golden Gate (roughly equal to our bays region) during the 1984–1986 years to vary between 76% and 84%, compared with a range of 26% to 43% in this study. California Department of Fish and Wildlife monitored survival rates of late-fall Chinook salmon from Battle Creek to rkm 239 (within the river region) during the 1996–2000 years using coded-wire tag recoveries at rotary screw traps. They estimated survival rates to vary between 1.1% and 2.7% (Snider and Titus 1998, 2000a, 2000b, 2000c; Vincik et al. 2006) compared with a range of 15.5% to 63.2% over a longer distance in this study. Reasons for these discrepancies could lie in the conditions during the years compared or could have to do with the difference in sampling protocol and survival estimation.

Overall survival of outmigrating late-fall-run Chinook salmon smolts in the Sacramento River is low in comparison with the Columbia and Fraser rivers, in spite of those rivers having substantially longer migration corridors. Welch et al. (2008) found that yearling Chinook salmon smolts from the Snake River (a tributary to the Columbia River) had an overall survival of 27.5% ($\pm 6.9\%$ SE) to the ocean over a distance of 910 km in 2006. That study also found that overall survival for yearling Chinook salmon smolts from various tributaries of the Fraser River to the ocean over distances ranging from 330.8 to 395.2 km had an overall survival varying from 2.0% ($\pm 3.6\%$ SE) to 32.2% ($\pm 20.7\%$ SE), with the majority of the tributary- and year-specific survival estimates

Fig. 3. Hydrograph at the Bend Bridge gauging station, 14 rkm downstream from the furthest upstream release site (Jelly's Ferry), for each of the 5 years of the study. The median daily flow values over a 43-year period (including the study years) are represented with a dotted line. Solid dots represent release date for tagged smolts in relation to the respective year's hydrograph. Hydrographs are only depicted as long as 90% of released smolts are still actively migrating in the river region; in some years, December-released fish have all died or outmigrated before January release, and therefore some yearly hydrographs are not continuous.



above 15%. Rechisky et al. (2009) found that outmigrating yearling Chinook salmon from the Yakima River (a tributary to the Columbia River) had an overall survival of 28% ($\pm 5\%$ SE) to the ocean over a distance of 655 km.

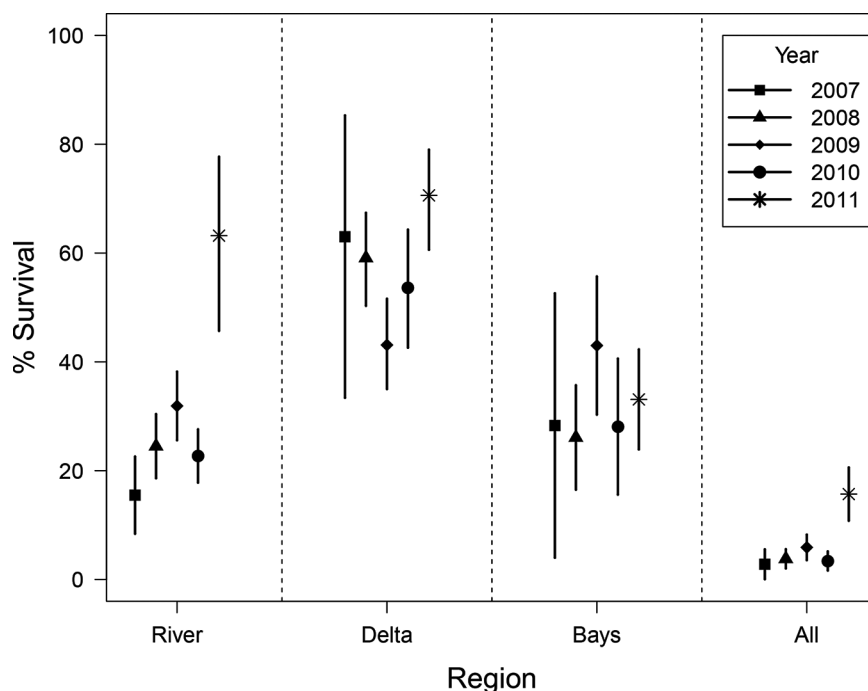
There are also striking differences in the spatial patterns of survival between the Sacramento River and the Columbia and Fraser rivers. Columbia River tagging studies have found survival for yearling Chinook salmon through the lower river and estuary to vary between 82% and 100% (or between 98.3% and 100% per 10 km), depending on the year and population (Harnish et al. 2012; Rechisky et al. 2013). Similarly sized sockeye salmon (*Oncorhynchus nerka*) smolts experienced little to no mortality during outmigration through the mainstem Fraser River (including the estuary) during the years 2010–2013 (Rechisky et al. 2014). In our study, survival through the estuary (delta and bays region combined) ranged from 15.1% to 23.4% (89.3%–91.7% per 10 km).

There are a number of possible explanations for why the survival of Chinook smolts in the Sacramento River is generally lower than that in other west coast rivers. Flows in the Sacramento River are highly regulated by large water storage dams, and peak discharge is typically much reduced in the outmigration period (Buer et al. 1989; Brown and Bauer 2010). In contrast, no dams exist on the mainstem Fraser River, and the dams on the Columbia River are used for hydropower and do not reduce or homogenize flows to the same extent as water storage dams. It is only in wet years such as 2011 that water flows are high enough for water managers to allow substantial dam releases in the Sacramento River. We

observed much higher in-river survival during 2011, and other studies have shown positive relationships between survival and river flow (Connor et al. 2003; Smith et al. 2003). Higher flows correspond to higher velocities and faster travel times, reducing the time smolts are exposed to predators (Høgåsen 1998). High flows may also be correlated to higher turbidities, which can reduce the effectiveness of visual predators (Ferrari et al. 2014; Gregory and Levings 1998).

Differences in the condition of estuaries offer another explanation. Magnusson and Hilborn (2003) found that in comparing the survival of subyearling Chinook salmon smolts in 27 different small- to medium-sized estuaries in the US Pacific Northwest, there was a significant positive relationship between survival and the percentage of the estuary that was in pristine condition. They also note that according to MacFarlane and Norton (2002), estuary use by subyearling Chinook salmon smolts was less in the brackish portion of San Francisco Estuary than other estuaries in the Pacific Northwest, potentially owing to the poor condition of the estuary. Nichols et al. (1986) posited that the San Francisco Estuary is the most modified estuary on the west coast of the United States, which suggests that the low survival estimates seen in this study are consistent with Magnusson and Hilborn's (2003) findings. Cohen and Carlton (1998) suggested that the extensive modification of the San Francisco Estuary contributes to it being perhaps the most invaded estuary in the world. Invaders include a number of piscivorous fish species that likely prey on migrating juvenile salmon. The role of predation clearly warrants study.

Fig. 4. Percent survival per major region for all 5 study years. Regions include river, delta, bays, and the percent survival for the entire watershed (All). Error bars represent 95% confidence intervals.



Survival rates during drought years observed in this study, if applicable to natural populations, suggest that populations are likely contracting. Bradford's (1995) review of Pacific salmon mortality rates suggested that typical fished Chinook salmon populations have a total mortality rate of 6.76 (based on fecundity) and a mean observed egg-to-smolt mortality rate of 2.56. Mean smolt mortality rate ($-\log_e(\text{survival})$) during the first 4 years of our study was 3.23. A stable population subject to these mortality rates would require total mortality to be no more than 0.97 (or no less than 38% survival) for the period between ocean entry and reproduction, a period of 2–4 years for late-fall Chinook subject to major ocean harvest rates.

Our results have implications for the management of Central Valley salmon hatcheries. Much of the hatchery production in the Central Valley is transported by tanker truck to the bays to avoid mortality incurred during the migration through the river and delta. Offsite release leads to undesirable levels of straying, and a recent independent review of California salmon hatchery practices recommends on-site release of hatchery production (CHSRG 2012). Salmon smolts have long been known to migrate during peak flows (Healey 1991; Høgåsen 1998; Kjelson et al. 1981). Our study has shown that fish migrating during high flows have higher survival. Hatcheries could employ a “release window” strategy during which they wait for a peak flow or coordinate their operations with releases from upstream reservoirs that could create artificial pulse flows. Reservoir releases have been shown to improve subyearling Chinook salmon smolt survival (Zeug et al. 2014), although evidence for improved yearling survival is not as clear (Giorgi et al. 1997; Young et al. 2011). The efficacy of reservoir release will depend on the degree to which survival benefits of migrating during freshets are due to decreased travel time versus higher turbidity, which may not be easily manipulated through reservoir operations.

Our study has demonstrated remarkably low survival rates for acoustically tagged hatchery-origin late-fall-run Chinook salmon smolts in the Sacramento River. The Sacramento River is also home to three other runs of Chinook salmon that migrate at smaller sizes and later in the season (Fisher 1994), when water

temperatures are higher and predators may be more active. These other runs may therefore be experiencing even lower survival. Furthermore, most mortality in this study occurred in a 1- to 2-week period for hatchery fish. This has disconcerting implications for wild fish that must spend several months to a year rearing in the watershed. As tags become smaller, the study design utilized here can be applied to document spatial and temporal patterns of survival in these other runs that are of important conservation and fishery concerns, providing resource managers with valuable information on where and when survival problems are occurring — information necessary to effective mitigation of survival problems.

Acknowledgements

Funding for the project was provided by a CALFED Bay Delta program grant, project U-05-SC-047 (A.P.K. and R.B.M. principle investigators). We are grateful for the help from many technicians and volunteers, including (but not limited to) Ian Cole, Alison Collins, Nicholas Delaney, Heidi Fish, Alex Hearn, Andrew Jones, and Ian Ralston. Special thanks are extended to Kevin Niemela, Kurtis Brown, and Scott Hamelburg of US Fish and Wildlife Service (USFWS) and the helpful staff of the Coleman National Fish Hatchery for providing late-fall-run Chinook salmon smolts and logistical support for this study. The California Fish Tracking Consortium allowed the realization of this project through the collaboration and data-sharing of several academic, federal, and state institutions. Sean Hayes, Ann-Marie Osterback, and anonymous reviewers provided valuable comments that improved the manuscript.

References

- Ammann, A.J., Michel, C.J., and MacFarlane, R.B. 2013. The effects of surgically implanted acoustic transmitters on laboratory growth, survival and tag retention in hatchery yearling Chinook salmon. *Environ. Biol. Fishes*, **96**(2–3): 135–143. doi:10.1007/s10641-011-9941-9.
- Azat, J. 2015. GrandTab 2015.04.15 California Central Valley Chinook Population Database Report. California Department of Fish and Wildlife.
- Baker, P.F., and Morhardt, J.E. 2001. Survival of Chinook Salmon Smolts in the Sacramento–San Joaquin Delta and Pacific Ocean. *In* Contributions to the

- biology of Central Valley salmonids. Edited by L.R. Brown. California Department of Fish and Game, Sacramento, Calif. pp. 163–182.
- Bradford, M.J. 1995. Comparative review of Pacific salmon survival rates. *Can. J. Fish. Aquat. Sci.* **52**(6): 1327–1338. doi:10.1139/f95-129.
- Brandes, P.L., and McLain, J.S. 2001. Juvenile Chinook salmon abundance, distribution, and survival in the Sacramento–San Joaquin Estuary. In *Contributions to the biology of Central Valley salmonids*. Edited by L.R. Brown. California Department of Fish and Game, Sacramento, Calif. pp. 39–138.
- Brown, L.R., and Bauer, M.L. 2010. Effects of hydrologic infrastructure on flow regimes of California's Central Valley rivers: implications for fish populations. *River Res. Appl.* **26**(6): 751–765. doi:10.1002/rra.1293.
- Buer, K., Forwalter, D., Kissel, M., and Stohler, B. 1989. The Middle Sacramento River: human impacts on physical and ecological processes along a meandering river. In *Proceedings of the California Riparian Systems Conference: Protection, Management, and Restoration for the 1990s*, Davis, Calif. Gen. Tech. Rep. PSW-GTR-110. 22–24 September 1988, Pacific Southwest Forest and Range Experiment Station, Forest Service, US Department of Agriculture, Berkeley, Calif. pp. 22–32.
- Burnham, K.P. 1987. Design and analysis methods for fish survival experiments based on release–recapture. American Fisheries Society, Bethesda, Md.
- California Department of Water Resources. 2007. Dayflow: an estimate of daily average Delta outflow [online]. Available from <http://www.water.ca.gov/dayflow/> [accessed 1 July 2013; modified 28 January 2011].
- CHSRG. 2012. California Hatchery Review Report. Prepared for the US Fish and Wildlife Service and Pacific States Marine Fisheries Commission. California Hatchery Scientific Review Group.
- Chapman, D.W., and Knudsen, E. 1980. Channelization and livestock impacts on salmonid habitat and biomass in western Washington. *Trans. Am. Fish. Soc.* **109**(4): 357–363. doi:10.1577/1548-8659(1980)109<357:CALIOS>2.0.CO;2.
- Cohen, A.N., and Carlton, J.T. 1998. Accelerating invasion rate in a highly invaded estuary. *Science*, **279**(5350): 555–558. doi:10.1126/science.279.5350.555. PMID:9438847.
- Connor, W.P., Burge, H.L., Yearsley, J.R., and Bjornn, T.C. 2003. Influence of flow and temperature on survival of wild subyearling fall chinook salmon in the Snake River. *N. Am. J. Fish. Manage.* **23**(2): 362–375. doi:10.1577/1548-8675(2003)023<0362:IOFATO>2.0.CO;2.
- Cormack, R.M. 1964. Estimates of survival from the sighting of marked animals. *Biometrika*, **51**(3–4): 429–438. doi:10.1093/biomet/51.3-4.429.
- Ferrari, M.C.O., Ranåker, L., Weinersmith, K.L., Young, M.J., Sih, A., and Conrad, J.L. 2014. Effects of turbidity and an invasive waterweed on predation by introduced largemouth bass. *Environ. Biol. Fishes*, **97**(1): 79–90. doi:10.1007/s10641-013-0125-7.
- Fisher, F.W. 1994. Past and present status of Central Valley chinook salmon. *Conserv. Biol.* **8**(3): 870–873. doi:10.1046/j.1523-1739.1994.08030863-5.x.
- Garland, R.D., Tiffan, K.F., Rondorf, D.W., and Clark, L.O. 2002. Comparison of subyearling fall chinook salmon's use of riprap revetments and unaltered habitats in Lake Wallula of the Columbia River. *N. Am. J. Fish. Manage.* **22**(4): 1283–1289. doi:10.1577/1548-8675(2002)022<1283:COFCS>2.0.CO;2.
- Giorgi, A.E., Hillman, T.W., Stevenson, J.R., Hays, S.G., and Peven, C.M. 1997. Factors that influence the downstream migration rates of juvenile salmon and steelhead through the hydroelectric system in the mid-Columbia River basin. *N. Am. J. Fish. Manage.* **17**(2): 268–282. doi:10.1577/1548-8675(1997)017<0268:FTTDM>2.3.CO;2.
- Gregory, R.S., and Levings, C.D. 1998. Turbidity reduces predation on migrating juvenile Pacific salmon. *Trans. Am. Fish. Soc.* **127**(2): 275–285. doi:10.1577/1548-8659(1998)127<0275:TRPOM>2.0.CO;2.
- Harnish, R.A., Johnson, G.E., McMichael, G.A., Hughes, M.S., and Ebberts, B.D. 2012. Effect of migration pathway on travel time and survival of acoustic-tagged juvenile salmonids in the Columbia River Estuary. *Trans. Am. Fish. Soc.* **141**(2): 507–519. doi:10.1080/00028487.2012.670576.
- Healey, M.C. 1991. Pacific salmon life histories. Edited by C. Groot and L. Margolis. University of British Columbia Press, Vancouver, B.C. pp. 312–230.
- Høgåsen, H.R. 1998. Physiological changes associated with the diadromous migration of salmonids. *Can. Spec. Publ. Fish. Aquat. Sci.* No. 127. pp. 1–128.
- Jolly, G.M. 1965. Explicit estimates from capture–recapture data with both death and immigration–stochastic model. *Biometrika*, **52**(1–2): 225–247. doi:10.1093/biomet/52.1-2.225. PMID:14341276.
- Kjelson, M., Raquel, P.F., and Fisher, F.W. 1981. Influences of freshwater inflow on chinook salmon (*Oncorhynchus tshawytscha*) in the Sacramento–San Joaquin Estuary. US Fish and Wildlife Service. pp. 88–108.
- Laake, J., and Rexstad, E. 2008. RMark — an alternative approach to building linear models in MARK. In *Program MARK: a gentle introduction*. Edited by E. Cooch and G.C. White.
- Lebreton, J.-D., Burnham, K.P., Clobert, J., and Anderson, D.R. 1992. Modeling survival and testing biological hypotheses using marked animals: a unified approach with case studies. *Ecol. Monogr.* **62**(1): 67–118. doi:10.2307/2937171.
- MacFarlane, R.B., and Norton, E.C. 2002. Physiological ecology of juvenile chinook salmon (*Oncorhynchus tshawytscha*) at the southern end of their distribution, the San Francisco Estuary and Gulf of the Farallones, California. *Fish. Bull.* **100**(2): 244–257.
- Magnusson, A., and Hilborn, R. 2003. Estuarine influence on survival rates of Coho (*Oncorhynchus kisutch*) and Chinook salmon (*Oncorhynchus tshawytscha*) released from hatcheries on the U.S. Pacific Coast. *Estuaries*, **26**(4B): 1094–1103. doi:10.1007/BF02803366.
- McMichael, G.A., Eppard, M.B., Carlson, T.J., Carter, J.A., Ebberts, B.D., Brown, R.S., Weiland, M., Ploskey, G.R., Harnish, R.A., and Deng, Z.D. 2010. The Juvenile salmon acoustic telemetry system: a new tool. *Fisheries*, **35**(1): 9–22. doi:10.1577/1548-8446-35.1.9.
- Melnychuk, M.C., Korman, J., Hausch, S., Welch, D.W., McCubbing, D.J.F., and Walters, C.J. 2014. Marine survival difference between wild and hatchery-reared steelhead trout determined during early downstream migration. *Can. J. Fish. Aquat. Sci.* **71**(6): 831–846. doi:10.1139/cjfas-2013-0165.
- Michel, C.J. 2010. River and estuarine survival and migration of yearling Sacramento River chinook salmon (*Oncorhynchus tshawytscha*) smolts and the influence of environment. Ecology and Evolutionary Biology, University of California – Santa Cruz, Santa Cruz, Calif.
- Michel, C.J., Ammann, A.J., Chapman, E.D., Sandstrom, P.T., Fish, H.E., Thomas, M.J., Singer, G.P., Lindley, S.T., Klimley, A.P., and MacFarlane, R.B. 2013. The effects of environmental factors on the migratory movement patterns of Sacramento River yearling late-fall run Chinook salmon (*Oncorhynchus tshawytscha*). *Environ. Biol. Fishes*, **96**(2–3): 257–271. doi:10.1007/s10641-012-9990-8.
- Moyle, P.B. 2002. Inland fishes of California. University of California Press, Berkeley, Calif.
- Moyle, P.B., Yoshiyama, R.M., Wikramanayake, E.D., and Williams, J.E. 1995. Fish species of special concern. California Department of Fish and Game, Sacramento, Calif.
- Muir, W.D., Smith, S.G., Williams, J.G., Hockersmith, E.E., and Skalski, J.R. 2001. Survival estimates for migrant yearling chinook salmon and steelhead tagged with passive integrated transponders in the Lower Snake and Lower Columbia rivers, 1993–1998. *N. Am. J. Fish. Manage.* **21**(2): 269–282. doi:10.1577/1548-8675(2001)021<0269:SEFMYC>2.0.CO;2.
- Nehlsen, W., Williams, J.E., and Lichatowich, J.A. 1991. Pacific salmon at the crossroads: stocks at risk from California, Oregon, Idaho, and Washington. *Fisheries*, **16**(2): 4–21. doi:10.1577/1548-8446(1991)016<0004:PSATCS>2.0.CO;2.
- Nichols, F.H., Cloern, J.E., Luoma, S.N., and Peterson, D.H. 1986. The modification of an estuary. *Science*, **231**(4738): 567–573. doi:10.1126/science.231.4738.567. PMID:17750968.
- O'Farrell, M.R., Mohr, M.S., Palmer-Zwahlen, M.L., and Grover, A.M. 2013. The Sacramento Index (SI). NOAA technical memorandum. US Department of Commerce.
- Palmer-Zwahlen, M., and Kormos, B. 2013. Recovery of coded-wire tags from chinook salmon in California's Central Valley Escapement and ocean harvest in 2011.
- Perry, R.W., Skalski, J.R., Brandes, P.L., Sandstrom, P.T., Klimley, A.P., Ammann, A., and MacFarlane, B. 2010. Estimating survival and migration route probabilities of juvenile chinook salmon in the Sacramento–San Joaquin River Delta. *N. Am. J. Fish. Manage.* **30**(1): 142–156. doi:10.1577/M08-200.1.
- Powell, L.A. 2007. Approximating variance of demographic parameters using the Delta Method: A reference for avian biologists. *Condor*, **109**(4): 949–954. doi:10.1650/0010-5422(2007)109[949:AVODPU]2.0.CO;2.
- R Core Team. 2013. R: a language and environment for statistical computing [online]. R Foundation for Statistical Computing, Vienna, Austria. ISBN 3-900051-07-0. Available from <http://www.R-project.org/>.
- Rechisky, E.L., Welch, D.W., Porter, A.D., Jacobs, M.C., and Ladouceur, A. 2009. Experimental measurement of hydrosystem-induced delayed mortality in juvenile Snake River spring Chinook salmon (*Oncorhynchus tshawytscha*) using a large-scale acoustic array. *Can. J. Fish. Aquat. Sci.* **66**(7): 1019–1024. doi:10.1139/F09-078.
- Rechisky, E.L., Welch, D.W., Porter, A.D., Jacobs-Scott, M.C., and Winchell, P.M. 2013. Influence of multiple dam passage on survival of juvenile Chinook salmon in the Columbia River estuary and coastal ocean. *Proc. Natl. Acad. Sci.* **110**(17): 6883–6888. doi:10.1073/pnas.1219910110.
- Rechisky, E.L., Welch, D.W., Porter, A.D., Furey, N.B., and Hinch, S.G. 2014. Telemetry-based estimates of early marine survival and residence time of juvenile Sockeye salmon in the Strait of Georgia and Discovery Passage, 2013. State of the physical, biological and selected fishery resources of Pacific Canadian marine ecosystems in 2013. Canadian Technical Report of Fisheries and Aquatic Sciences, Fisheries and Oceans Canada. pp. 123–127.
- Sandstrom, P.T., Smith, D.L., and Mulvey, B. 2013. Two-dimensional (2-D) acoustic fish tracking at River Mile 85, Sacramento River, California. US Army Corps of Engineers, Engineer Research and Development Center.
- Schmetterling, D.A., Clancy, C.G., and Brandt, T.M. 2001. Effects of riprap bank reinforcement on stream salmonids in the western United States. *Fisheries*, **26**(7): 6–13. doi:10.1577/1548-8446(2001)026<3C0006:EOBRO>3E2.0.CO;2.
- Seber, G.A.F. 1965. A note on the multiple-recapture census. *Biometrika*, **52**(1/2): 249–259. doi:10.2307/2333827. PMID:14341277.
- Seber, G.A. 1982. The estimation of animal abundance and related parameters. Chapman, London and Macmillan.
- Skalski, J.R., Smith, S.G., Iwamoto, R.N., Williams, J.G., and Hoffmann, A. 1998. Use of passive integrated transponder tags to estimate survival of migrant juvenile salmonids in the Snake and Columbia rivers. *Can. J. Fish. Aquat. Sci.* **55**(6): 1484–1493. doi:10.1139/f97-323.
- Smith, S.G., Muir, W.D., Hockersmith, E.E., Zabel, R.W., Graves, R.J., Ross, C.V., Connor, W.P., and Arnsberg, B.D. 2003. Influence of river conditions on survival and travel time of Snake River subyearling fall chinook salmon. *N. Am. J. Fish. Manage.* **23**(3): 939–961. doi:10.1577/M02-039.

- Snider, B., and Titus, R.G. 1998. Evaluation of juvenile anadromous salmonid emigration in the Sacramento River near Knights Landing, November 1995 – July 1996. Stream evaluation program technical report. California Department of Fish and Game.
- Snider, B., and Titus, R.G. 2000a. Timing, composition, and abundance of juvenile anadromous salmonid emigration in the Sacramento River near Knights Landing, October 1996 – September 1997. Stream evaluation program technical report. California Department of Fish and Game.
- Snider, B., and Titus, R.G. 2000b. Timing, composition, and abundance of juvenile anadromous salmonid emigration in the Sacramento River near Knights Landing, October 1997 – September 1998. Stream evaluation program technical report. California Department of Fish and Game.
- Snider, B., and Titus, R.G. 2000c. Timing, composition, and abundance of juvenile anadromous salmonid emigration in the Sacramento River near Knights Landing, October 1998 – September 1999. Stream Evaluation Program Technical Report. California Department of Fish and Game.
- Vincik, R.F., Titus, R.G., and Snider, B. 2006. Timing, composition, and abundance of juvenile anadromous salmonid emigration in the Sacramento River near Knights Landing, September 1999 – September 2000. Lower Sacramento River Juvenile Salmonid Emigration Program technical report. California Department of Fish and Game.
- Welch, D.W., Rechisky, E.L., Melnychuk, M.C., Porter, A.D., Walters, C.J., Clements, S., Clemens, B.J., McKinley, R.S., and Schreck, C. 2008. Survival of Migrating salmon smolts in large rivers with and without dams. *PLoS Biol.* **6**(10): e265. doi:10.1371/journal.pbio.0060265.
- Welch, D.W., Melnychuk, M.C., Rechisky, E.R., Porter, A.D., Jacobs, M.C., Ladouceur, A., McKinley, R.S., and Jackson, G.D. 2009. Freshwater and marine migration and survival of endangered Cultus Lake sockeye salmon (*Oncorhynchus nerka*) smolts using POST, a large-scale acoustic telemetry array. *Can. J. Fish. Aquat. Sci.* **66**(5): 736–750. doi:10.1139/F09-032.
- White, G.C., and Burnham, K.P. 1999. Program MARK: survival estimation from populations of marked animals. *Bird Study*, **46**(Suppl. 1): S120–S139. doi:10.1080/00063659909477239.
- Williams, J.G. 2006. Central Valley Salmon: a perspective on Chinook and Steelhead in the Central Valley of California. *San Francisco Estuary and Watershed Science*, **4**(3).
- Yoshiyama, R.M., Gerstung, E.R., Fisher, F.W., and Moyle, P.B. 2001. Historical and present distribution of chinook salmon in the Central Valley drainage of California. In *Contributions to the biology of Central Valley salmonids*. Edited by R.L. Brown. California Department of Fish and Game, Sacramento, Calif. pp. 71–176.
- Young, P.S., Cech, J.J., Jr., and Thompson, L.C. 2011. Hydropower-related pulsed-flow impacts on stream fishes: a brief review, conceptual model, knowledge gaps, and research needs. *Rev. Fish Biol. Fish.* **21**(4): 713–731. doi:10.1007/s11160-011-9211-0.
- Zeug, S.C., Sellheim, K., Watry, C., Wikert, J.D., and Merz, J. 2014. Response of juvenile Chinook salmon to managed flow: lessons learned from a population at the southern extent of their range in North America. *Fish. Manage. Ecol.* **21**(2): 155–168. doi:10.1111/fme.12063.

Evidence for a Novel Marine Harmful Algal Bloom: Cyanotoxin (Microcystin) Transfer from Land to Sea Otters

Melissa A. Miller^{1,2*}, Raphael M. Kudela², Abdu Mekebi³, Dave Crane³, Stori C. Oates¹, M. Timothy Tinker⁴, Michelle Staedler⁵, Woutrina A. Miller⁶, Sharon Toy-Choutka¹, Clare Dominik⁷, Dane Hardin⁷, Gregg Langlois⁸, Michael Murray⁵, Kim Ward⁹, David A. Jessup¹

1 Marine Wildlife Veterinary Care and Research Center, California Department of Fish and Game, Office of Spill Prevention and Response, Santa Cruz, California, United States of America, **2** Ocean Sciences Department, University of California Santa Cruz, Santa Cruz, California, United States of America, **3** Water Pollution Control Laboratory, California Department of Fish and Game, Office of Spill Prevention and Response, Rancho Cordova, California, United States of America, **4** Western Ecological Research Center, United States Geological Survey, Long Marine Laboratory, Santa Cruz, California, United States of America, **5** Monterey Bay Aquarium, Monterey, California, United States of America, **6** Department of Pathology, Microbiology and Immunology, School of Veterinary Medicine, University of California Davis, Davis, California, United States of America, **7** Applied Marine Sciences, Livermore, California, United States of America, **8** California Department of Public Health, Richmond, California, United States of America, **9** Division of Water Quality, State Water Resources Control Board, Sacramento, California, United States of America

Abstract

“Super-blooms” of cyanobacteria that produce potent and environmentally persistent biotoxins (microcystins) are an emerging global health issue in freshwater habitats. Monitoring of the marine environment for secondary impacts has been minimal, although microcystin-contaminated freshwater is known to be entering marine ecosystems. Here we confirm deaths of marine mammals from microcystin intoxication and provide evidence implicating land-sea flow with trophic transfer through marine invertebrates as the most likely route of exposure. This hypothesis was evaluated through environmental detection of potential freshwater and marine microcystin sources, sea otter necropsy with biochemical analysis of tissues and evaluation of bioaccumulation of freshwater microcystins by marine invertebrates. Ocean discharge of freshwater microcystins was confirmed for three nutrient-impaired rivers flowing into the Monterey Bay National Marine Sanctuary, and microcystin concentrations up to 2,900 ppm (2.9 million ppb) were detected in a freshwater lake and downstream tributaries to within 1 km of the ocean. Deaths of 21 southern sea otters, a federally listed threatened species, were linked to microcystin intoxication. Finally, farmed and free-living marine clams, mussels and oysters of species that are often consumed by sea otters and humans exhibited significant biomagnification (to 107 times ambient water levels) and slow depuration of freshwater cyanotoxins, suggesting a potentially serious environmental and public health threat that extends from the lowest trophic levels of nutrient-impaired freshwater habitat to apex marine predators. Microcystin-poisoned sea otters were commonly recovered near river mouths and harbors and contaminated marine bivalves were implicated as the most likely source of this potent hepatotoxin for wild otters. This is the first report of deaths of marine mammals due to cyanotoxins and confirms the existence of a novel class of marine “harmful algal bloom” in the Pacific coastal environment; that of hepatotoxic shellfish poisoning (HSP), suggesting that animals and humans are at risk from microcystin poisoning when consuming shellfish harvested at the land-sea interface.

Citation: Miller MA, Kudela RM, Mekebi A, Crane D, Oates SC, et al. (2010) Evidence for a Novel Marine Harmful Algal Bloom: Cyanotoxin (Microcystin) Transfer from Land to Sea Otters. PLoS ONE 5(9): e12576. doi:10.1371/journal.pone.0012576

Editor: Ross Thompson, Monash University, Australia

Received: April 26, 2010; **Accepted:** August 2, 2010; **Published:** September 10, 2010

Copyright: © 2010 Miller et al. This is an open-access article distributed under the terms of the Creative Commons Attribution License, which permits unrestricted use, distribution, and reproduction in any medium, provided the original author and source are credited.

Funding: Financial assistance was provided by the California Division of Water Quality, State Water Resources Control Board (SWRCB), the California Department of Fish and Game, Division of Spill Prevention and Response and the CDFG Water Pollution Control Laboratory. Co-Author Kim Ward of the SWRCB assisted with basic concepts of study design and data analysis in relation to ongoing statewide research on microcystins, but the various funding agencies had no directive or editorial role in study design, data collection and analysis, decision to publish or preparation of the manuscript.

Competing Interests: The authors have declared that no competing interests exist.

* E-mail: mmiller@ospr.dfg.ca.gov

Introduction

During 2007, 11 dead and dying southern sea otters were recovered along the shore of Monterey Bay in central California with lesions suggestive of acute liver failure. Some animals were diffusely icteric and their livers were enlarged, bloody and friable. Expected causes for this condition, such as systemic bacterial infection were excluded via microscopic examination and diagnostic testing. Livers from affected animals tested positive for cyanotoxins (microcystins) via liquid chromatography-tandem

mass spectrophotometry (LC-MS/MS) and hepatic lesions consistent with microcystin intoxication were observed microscopically. Environmental surveillance revealed that some local freshwater lakes and rivers supported *Microcystis* blooms during late summer and autumn, triggering the investigation reported here.

Cyanobacteria (formerly called “blue-green algae”) have a worldwide distribution and can form extensive blooms in freshwater and estuarine habitat. Toxin production by the cyanobacterium *Microcystis aeruginosa* was first reported in 1946 [1] and additional toxic species have been described. Exposure to environmentally

stable microcystins in food, drinking water, nutritional supplements and during medical dialysis can cause significant and sometimes fatal hepatotoxicity and possible tumor induction in humans and animals [2-6]. Microcystins are fast becoming a global health concern and recurrent blooms with toxin elaboration have been reported throughout Europe [7,8], Asia [9,10], Africa [11,12], Australia [13,14] and North and South America [15-17]. Factors that contribute to bloom formation and toxin production include warm water [18,19], nutrient enrichment [19,20] and seasonal increases in light intensity [2,21]. Rising global temperatures and eutrophication may contribute to more frequent events and cyanobacterial “super-blooms”, with enhanced risks to human health [23].

Until recently, microcystin intoxication was considered a public health issue mainly of freshwater habitat, reflected by the vast body of published literature on potential human health risks due to microcystin exposure in rivers, lakes, reservoirs and freshwater aquaculture [4,13,16,24,25,26]. In contrast, monitoring of marine water and seafood for similar risks has been limited, despite confirmation of outflows of microcystin-contaminated freshwater to the ocean [14,17,27,28], detection of impacts by microcystins on copepods, corals and fish [29-31] and identification of proteins with protein phosphatase inhibitory activity in seawater, suggesting the existence of an additional class of marine “Harmful Algal Blooms” (HAB); hepatotoxic shellfish poisoning (HSP) [15].

The ability of potent and environmentally stable cyanotoxins to magnify trophically poses additional risks: Microcystin accumulation has been demonstrated in fresh and saltwater mussels [7,32], farmed crustaceans [33,34], fish [30] and possibly humans [26]. In addition, exposure of estuarine and marine biota to microcystins may trigger behavioral adaptations, such as decreased feeding on co-occurring nutritious species, that facilitate trophic transfer [9,35-38]. Despite these concerns, worldwide shellfish sanitation and water safety programs do not typically include microcystin testing.

Along the Pacific coast of the United States, large-scale *Microcystis* blooms with toxin production occur each year in lakes and rivers throughout Washington [39], Oregon [4] and California [40,41]. In California, *Microcystis*-contaminated runoff has been documented at the marine interfaces of the Klamath River [42] and San Francisco Bay [17]. Here we extend areas of concern to include the central California coast and document numerous marine mammal deaths due to microcystin intoxication.

The potential for cyanotoxins to flow to the ocean, resulting in deaths of marine species is a newly recognized problem. Demonstration of bioaccumulation in marine invertebrates and deaths of threatened southern sea otters due to microcystin intoxication provides strong evidence for significant and recurrent marine pollution by freshwater-derived microcystins within North America’s largest national marine sanctuary. Because sea otters and humans utilize the same coastal habitat and share the same marine foods, our findings in sea otters are also likely to have important human health implications.

Materials and Methods

Performance of this research was approved by the California Department of Fish and Game, Office of Spill Prevention and Response and the University of California.

1.) Environmental testing

Chemical confirmation of microcystin exposure in tissues from southern sea otters stranding during 2007 prompted investigation of local freshwater sources flowing into Monterey Bay for any prior

history of cyanobacterial blooms. This investigation revealed that Pinto Lake, located approximately 8.5 km inland from Monterey Bay had a history of severe and recurrent *Microcystis* blooms with microcystin production. Visual examination of Pinto Lake, light microscopy and liquid chromatography-mass spectrophotometry/mass spectrophotometry (LC-MS/MS) testing in fall, 2007, confirmed the occurrence of an extensive *Microcystis* bloom with high toxin production, leading authorities to post warning signs at this location for several weeks. Stepwise sampling of water and surface bloom from Pinto Lake, its drainage into Corralitos Creek, and the Pajaro River that carries water from this region to Monterey Bay was performed during the bloom event.

Because bloom events are often ephemeral and patchy, sensitive methods are required to facilitate source tracking efforts. We investigated use of resin-based, Solid Phase Adsorption Toxin Tracking (SPATT) samplers to passively monitor fresh and salt water for microcystin contamination. SPATT was first proposed for HAB monitoring in 2004 to circumvent disadvantages associated with invertebrate bioassays [43]. To evaluate their performance under laboratory conditions, SPATT bags were placed into subsamples of concentrated water/*Microcystis* mixtures from Pinto Lake that were used for laboratory-based invertebrate exposures (section 3). Replicate SPATT samplers were also placed in each exposure tank during the invertebrate studies to assess consistency and repeatability of microcystin adsorption, and additional SPATT bags were deployed in the local marine environment and at the freshwater outflows of selected local rivers.

SPATT bags were constructed from 100 micron Nitex bolting cloth filled with 3 g (dry weight) HP20 (Diaion) resin. For activation, bags were soaked in 100% HPLC-grade methanol (MeOH) for 48 hours, rinsed thoroughly, transferred into a fresh volume of Milli-Q for MeOH residue removal by sonication and stored in Milli-Q at 4-6°C prior to use. Plastic embroidery hoops were used to fasten the bags in place during field deployment. After exposure, SPATT bags were evaluated using LC-MS for adsorption of domoic acid and microcystins as described below. In the laboratory, adsorption of environmentally-relevant concentrations of microcystins (hundreds of ppb) was observed in <24 h, following an exponential decay (adsorption) curve in a closed volume of filtered Pinto Lake water. In prior studies, 100% recovery of microcystin was achieved with simple extraction procedures (sequential 50% MeOH column extractions) (data not shown).

2.) Sea otter necropsy and microcystin testing

Sea otter carcasses were recovered by stranding network members, chilled with ice and transported to CDFG for necropsy as previously described [44]. Detailed postmortem examinations were performed by a veterinary pathologist and all major tissues were fixed in 10% neutral buffered formalin, trimmed, paraffin-embedded and 5 µm-thick, hematoxylin and eosin (H&E)-stained sections prepared and examined on a light microscope. Supplementary diagnostic testing included bacterial and fungal culture, immunofluorescence and PCR for common serovars of *Leptospira interrogans* and LC-MS/MS analysis of urine, gastrointestinal content, feces and urine for the presence of microcystin, domoic acid, okadaic acid, nodularin, yessotoxin and anatoxin-A. The primary and contributing cause(s) of death were determined based on gross lesions, histopathology and diagnostic results. Tissues, urine, serum and gastrointestinal contents were also cryoarchived at -80 C.

Analysis of water, tissue and digesta for microcystins was performed at the California Department of Fish and Game (CDFG) Water Pollution Control Laboratory or at the University

of California, Santa Cruz. The preferred method of analysis post-extraction was high performance liquid chromatography tandem mass spectrometry (LC-MS/MS), following the protocols of Mekebri et al. [45]. Prior to testing, tissue samples were first homogenized using a Buchi B-400 mixer equipped with a titanium knife assembly. Pre-weighed samples were mixed with methanol: water (90:10) using a Polytron® homogenizer for four minutes, followed by sonication for one hour. The target analytes were microcystin (MCY)-RR, -Desmethyl RR, -LR, -Desmethyl LR, -LA, -LF, -LW, -LY and -YR, domoic acid, nodularin and okadaic acid. Certified calibration solution standards purchased from Sigma Aldrich and NRC-CNRC (Certified Reference Materials Program, Institute for Marine Biosciences, National Research Council of Canada) were used for method development, analyte identification and quantitation. HPLC-grade solvents (acetonitrile, methanol, water), glass fiber filters (Type A/E, 90 mm, 1 µm), Gelman Acrodisc® CR PTFE syringe filters (13 mm, 0.45 µm), and mobile phase additives, ACS grade formic acid (98%) and trifluoroacetic acid (99%) were also used. A combined intermediate MCY standard working solution was made in methanol and used to prepare a matrix spiking solution (20 ppb), which was serially diluted to develop a seven level calibration curve ranging from 0.2 to 200 ppb.

To determine total microcystin concentration and congener type(s) in water, the cyanobacterial cell walls were ruptured by repeated freeze-thawing and sonication and a 100 ml aliquot was filtered under vacuum through a glass fiber filter. Water and filters were extracted separately and filters containing planktonic material were extracted twice with 15 mL of methanol-acidified water (90:10, v/v) by homogenizing for 1–2 minutes using a Polytron®, followed by 10 minutes of sonication in an ultrasonic bath.

For SPATT detection systems, only dissolved toxins were measured, so cell disruption was not required. Samples were analyzed using an Agilent 1200 liquid chromatograph (LC) connected to a 6130 quadrupole MS, using Selected Ion Monitoring (SIM). For all other samples, an Agilent 6410 triple quadrupole (QqQ) LC-MS was used for LC-MS/MS analysis. The following microcystin ions (m/z) were monitored: 519.8 -RR and 512.8 -desmethyl RR are both [M+2H]²⁺; 105.6 -YR, 995.7 -LR, 981.7 -desmethyl LR, 910.6 -LA, 1026.6 -LW, 987.6 -LF and 825.5 NOD-R were monitored using [M+H]⁺ using multiple reaction monitoring (MRM) mode. Full scan was also collected over the range 100–1100 amu. The MRM windows were established for microcystins using the MSMS product ions, which are the Adda fragments of m/z 135.2 and m/z 213 produced by the transition of the protonated parent ions. Agilent Mass Hunter software was used to collect and process data. The estimated method detection limits (MDL) and reporting limits (RL) for water samples were 0.02 µg/L (ppb) and 0.05 µg/L (ppb) for MCY and DA respectively, and 0.01 µg/L (ppb) and 0.02 µg/L (ppb) respectively for OA. The estimated method detection limit and reporting limit for tissues were 0.500 ng/g and 1.00 ng/g wet weight, respectively, for all toxins.

3.) Laboratory exposure of marine invertebrates

To assess microcystin uptake and retention by marine invertebrates consumed by humans and sea otters, freshwater/cyanobacterial mixtures were collected during a summer, 2009 *Microcystis* bloom at Pinto Lake. Dominance of *Microcystis* was confirmed microscopically and total microcystin concentrations were determined via LC-MS/MS. Live marine invertebrates were collected from Monterey Bay or purchased from commercial vendors, including species that are commonly farmed or harvested, such as Pacific oysters (*Crassostrea gigas*), manila clams (*Tapes semidecussatus*),

mussels (*Mytilus edulis*), snails (*Tegula* spp.), red rock crabs (*Cancer productus*) and dungeness crabs (*Cancer magister*).

Three 1,022 L, temperature-controlled seawater tanks were used to complete the invertebrate exposure studies. The tanks were designed to permit water sampling at the top, middle and bottom of each tank, so that microcystin distributions could be followed through time and compared with results from invertebrate testing. Invertebrates were divided randomly between control (Tank 1), low exposure (Tank 2) and high exposure (Tank 3) tanks and allowed to acclimatize for 3 to 7 d. Bivalves and snails were placed in wire cages or plastic mesh bags and suspended at least 20 cm below the water surface. Large crabs were placed in plastic mesh enclosures that allowed them to range from just below the tank surface to just above the bottom. Snails were fed fresh *Macrocystis* kelp fronds and crabs were provided with chopped capelin (*Mallotus villosus*) every other day. Filter-feeders were exposed to plankton in continually flowing seawater from Monterey Bay until initiation of the microcystin exposure, and then from day 4 to day 21 of the experiment. Starting 4 days post-exposure, all tanks were continually flushed with clean seawater and water and invertebrate sampling continued for 21 days to determine post-exposure depuration characteristics for freshwater microcystins.

At the start of the exposures, a less concentrated *Microcystis* mixture collected from Pinto Lake during a bloom event (2.2 ppm [2,195 ppb] aqueous microcystin-LR mixed with suspended *Microcystis*) was added to the low exposure tank (Tank 2). A more concentrated mixture (10.6 ppm [10,600 ppb] aqueous microcystin-LR mixed with suspended *Microcystis*) was added to the high exposure tank (Tank 3) at the same time, while Tank 1 (the negative control) contained only seawater. Microcystin LR concentrations were measured in invertebrates and seawater sampled from the top, middle and bottom of each tank at regular intervals (24 H, 48 H, 72 H, 7 D, 14 D, and 21 D postexposure). During the first 96 H postexposure, invertebrates in tanks 2 and 3 were continually exposed to the microcystin-contaminated inoculum, while Tank 1 contained only recirculating, clean seawater and served as a negative control. Positive controls consisted of non-exposed water and invertebrate tissues spiked with known concentrations of a commercial preparation of microcystin-LR prior to LC-MS/MS testing.

Following 96 H of continuous microcystin exposure, all 3 tanks were flushed with clean seawater and sampling continued through 21d post-exposure. Prior to seawater flushing, water was collected from tanks 2 and 3, refrigerated and sub-sampled at the same intervals as invertebrates to determine persistence of microcystin toxin in seawater. Invertebrates were washed in tapwater prior to dissection to remove any surface contamination by *Microcystis* or microcystin. Invertebrate sub-sampling techniques reflected patterns of consumption by humans or otters: For snails, the entire body and shell was homogenized and tested whole, while the soft parts of bivalves and crabs were removed and the shells and carapace were discarded. The gastrointestinal tract and/or hepatopancreas was collected and screened for the presence of microcystin-LR in addition to archiving whole bodies and muscle tissue for evaluation as funds permit. All samples were refrigerated or frozen at -80 C prior to LC-MS/MS testing.

Results

1.) Environmental testing

Analysis (LC-MS/MS) of water from Pinto Lake in fall, 2007 confirmed the occurrence of an extensive *Microcystis* bloom with high toxin production (Fig. 1). During this period, microcystin concentrations in scum from the surface of Pinto Lake exceeded

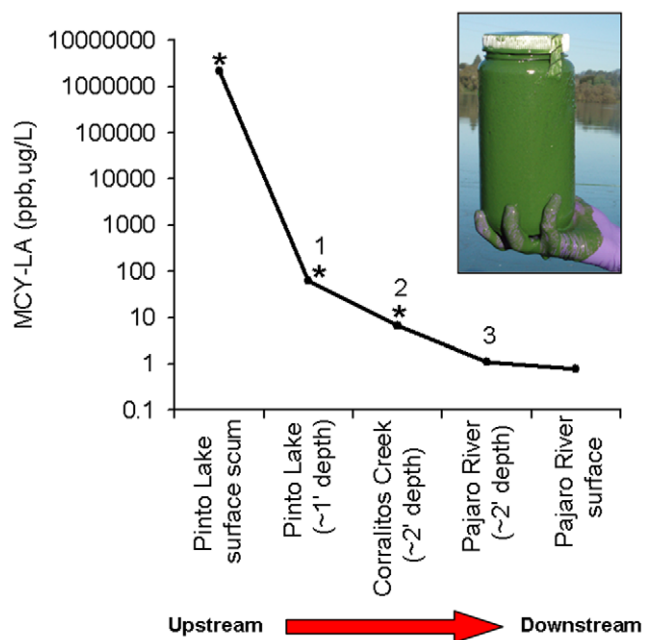


Figure 1. Tracing freshwater contamination by microcystins from land-to-sea. Inset: Sample of surface water collected during a “super-bloom” of *Microcystis* in Pinto Lake in fall, 2007 (Caution: Nitrile gloves and other appropriate personal protective equipment should be used to prevent dermal contact when collecting environmental samples of *Microcystis* and microcystins). Main figure: Time-matched microcystin-LA concentrations (ppb) in samples from Pinto Lake, just downstream in Corralitos Creek and the receiving waters of the Pajaro River within 1 km of Monterey Bay. Asterisks (*) indicate sampling locations where *Microcystis* was detected microscopically. doi:10.1371/journal.pone.0012576.g001

2,100 ppm (2.1 million ppb) MCY-LA, or approximately 2,900 ppm (2.9 million ppb) total microcystins, which is one of the highest microcystin concentrations ever reported from an environmental sample. During this same period, stepwise sampling of water and surface bloom from Pinto Lake, its drainage through Corralitos Creek and the Pajaro River confirmed the presence of *Microcystis* and microcystins from Pinto Lake to the river channel within 1 km of the ocean (Fig. 1). Recurrent *Microcystis* blooms with toxin production were also confirmed microscopically and via chemical analysis in samples from Pinto Lake and surrounding waters in 2008 and 2009 (data not shown). The most common microcystin congener that was detected in samples from Pinto Lake and the adjoining watershed during the 2007 event was MYC-LA, but MCY-RR, MCY-LR, MCY-Desmethyl-LR, MCY-LF and MCY-YR were also detected, and MCY-LR was repeatedly detected in Pinto Lake using SPATT between 2009 and 2010. No other biotoxins were detected in freshwater samples. Deployment of SPATT into microcystin/water mixtures collected from Pinto Lake demonstrated 100% adsorption of free MCY in <24 h (Fig. 2). In addition, higher sensitivity of SPATT for microcystin detection in water, when compared to intermittent “grab” samples, was also demonstrated (Fig. 3). During laboratory invertebrate studies, good agreement between duplicate SPATT bags suspended in each tank was noted for Tanks 2 and 3 (low and high microcystin exposure, respectively), while SPATT bags hung in Tank 1 (negative control) tested negative for microcystin (data not shown).

Using field-deployed SPATT, ocean water and the marine interfaces of selected coastal rivers flowing into Monterey Bay

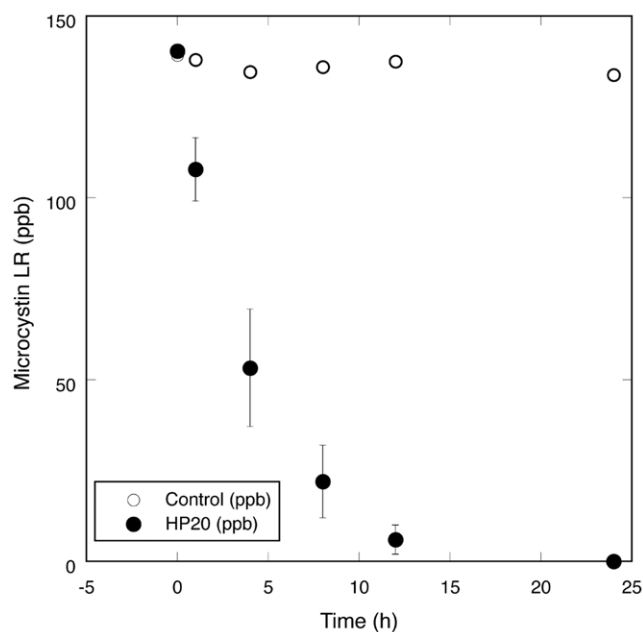


Figure 2. Evaluation of Solid Phase Adsorption Toxin Tracking (SPATT) sampler adsorption characteristics for freshwater microcystins. SPATT adsorption characteristics for microcystin were tested in the laboratory using Pinto Lake water amended with a known quantity of microcystin-LR. A control sample (open symbols) showed no change in microcystin concentration over time; In contrast, SPATT HP20 resin-based samplers (solid symbols: error bars represent standard deviation of 3 replicates) show rapid microcystin adsorption, with near-total depletion of microcystins from a controlled volume of water within <24 hours.

doi:10.1371/journal.pone.0012576.g002

tested negative for microcystins during the dry season in summer and early fall of 2009, when freshwater runoff was minimal. However, at the onset of the fall rainy season (October-November, 2009), SPATT deployed at the marine outfalls of the Pajaro and Salinas Rivers tested positive for microcystins via LC-MS (data not shown). SPATT samplers deployed weekly in the ocean at the Santa Cruz Municipal Pier (Figure 4) during 2008 and 2009 routinely tested negative for microcystins, suggesting that the main source of these toxins for sea otters was not marine in origin. However, low levels of MCY-LR were detected at the pier (located near the mouth of the San Lorenzo River), after the first major storm event of Fall, 2009. Limited testing of fresh- and seawater and invertebrates from other regions of Monterey Bay did not reveal additional sources of microcystin-contamination (data not shown). Sea otter stranding patterns suggest that similar pollution events occurred in other coastal areas, but were not detected.

2.) Sea otter necropsy and microcystin testing

Between 1999 and 2008, livers from 21 southern sea otters with gross and/or microscopic evidence of liver disease (Figs. 5 and 6) tested positive for microcystins via LC-MS/MS (Table 1). On the microscope, livers of microcystin-positive sea otters exhibited hepatocellular vacuolation, apoptosis, necrosis and hemorrhage (Fig. 6) consistent with previous descriptions of microcystin intoxication in humans and animals [1,12,13,46,13,47]. In contrast, livers from 2 captive sea otters (Table 1) and 19 wild otters without evidence of primary liver disease (data not shown) tested negative for microcystin. Carcasses of otters dying due to microcystin intoxication appeared to cluster near river mouths,

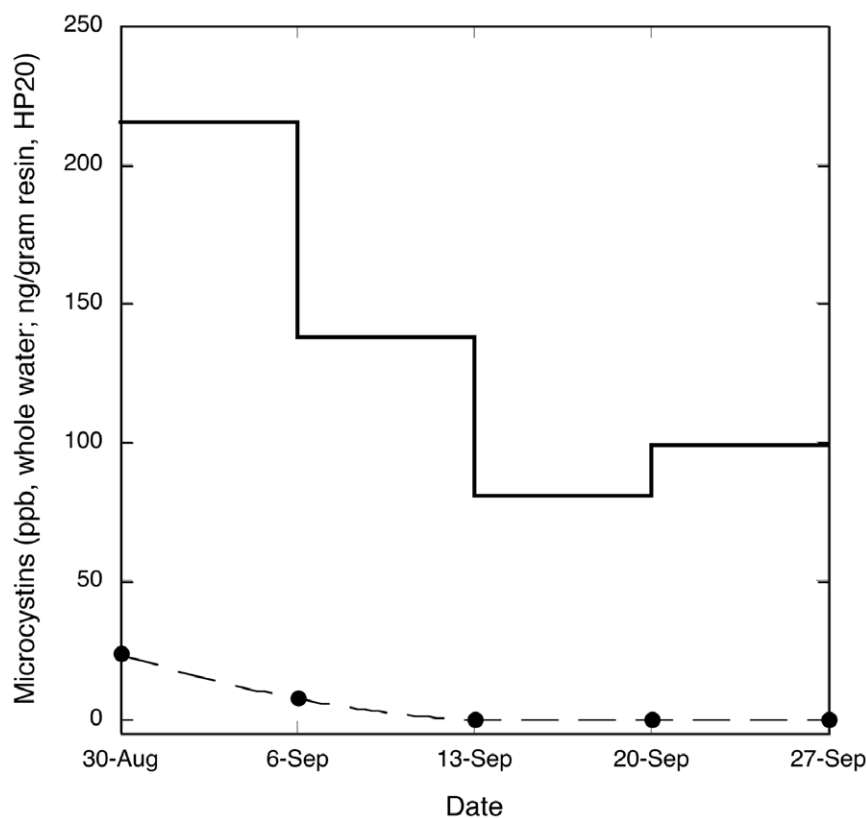


Figure 3. Variation in microcystin detection between conventional “grab” samples and Solid Phase Adsorption Toxin Tracking (SPATT). Comparison of microcystin (MCY-LR) detection in fresh water using intermittent “grab” sampling (sample periods indicated by black circles) and SPATT (solid line indicating weekly averaged toxin values) in Pinto Lake, demonstrating the higher sensitivity of SPATT for microcystin detection. Grab samples were collected at the beginning of each weekly SPATT deployment, and from the same sample location, so each 7-day integrated SPATT deployment is bracketed by two grab samples. doi:10.1371/journal.pone.0012576.g003

coastal ponds, embayments and harbors, all areas with significant potential to receive and retain plumes of contaminated fresh water (Fig. 4).

The earliest confirmed case was in 1999 (Table 1). The greatest number of cases detected/year was in 2007, with 11 LC-MS/MS-confirmed sea otter deaths due to microcystin intoxication. Based on preliminary test results, 71% of known, microcystin-associated sea otter deaths have occurred since 2005 and 81% of affected animals stranded within Monterey Bay, California. However, additional cases were detected along the Big Sur and South-central California coastline, suggesting that multiple point-sources for microcystin exposure exist along the central California coast. One additional case was suspected based on lesions observed on histopathology, but the liver tested microcystin-negative, perhaps due to near-total loss of hepatocyte mass in the liver of this animal. Pathology associated with microcystin intoxication in sea otters will be described in greater detail in a subsequent manuscript.

Hepatic microcystin concentrations varied from 1.36 to 348 ppb wet weight (ww; Table 1). Various forms of microcystin (MCY-RR, -LR and -desmethyl LR) were detected in sea otter livers, with the majority of otters (19/21) testing positive for MCY-RR, compared to 2/21 and 1/21 for MCY-LR and MCY-desmethyl-LR, respectively. One liver tested positive for both MCY-RR and -LR. Feces of one otter recovered during necropsy also tested positive for microcystin, but it is unclear whether this represents ingestion of contaminated prey or enterohepatic toxin circulation. The microcystin congener that was detected at the

highest concentration in a sea otter liver was MCY-LR (348 ppb ww). All water and tissue samples tested negative for okadaic acid, nodularin, yessotoxin and anatoxin-A. Urine from some otters with microcystin-positive livers also tested low-positive for domoic acid on LC-MS/MS; this biotoxin is widely distributed in sediments within Monterey Bay [48] and low levels of domoic acid are commonly detected in sea otter urine at necropsy (M. Miller, pers. commun.).

Four microcystin-positive otters had been previously captured and fitted with intraperitoneal VHF transmitters as part of long-term studies on habitat use, prey selection, and environmental exposure to biological pollutants. The home ranges of all four otters overlapped at the same point in south Monterey Bay (Fig. 7), suggesting a common source of microcystin exposure. Based on the spatial distribution of home ranges for radio-tagged southern sea otters [49], the likelihood of any four animals having overlapping home ranges by chance is <5.8%. Moreover, bivalve mollusks were the first or second most frequently consumed prey type for three of the four otters (for the fourth otter, no foraging data were available). This trait was shared with just 27% of all tagged animals; the majority preferentially fed on non-bivalve prey such as crabs, abalone or urchins [50]. Similar stranding clusters were identified for other microcystin-poisoned otters, leading to identification of several high-risk sites for microcystin intoxication along the shores of Monterey Bay (Fig. 4). Collectively these findings raised suspicion of bivalve prey as a possible vehicle for microcystin poisoning of sea otters.

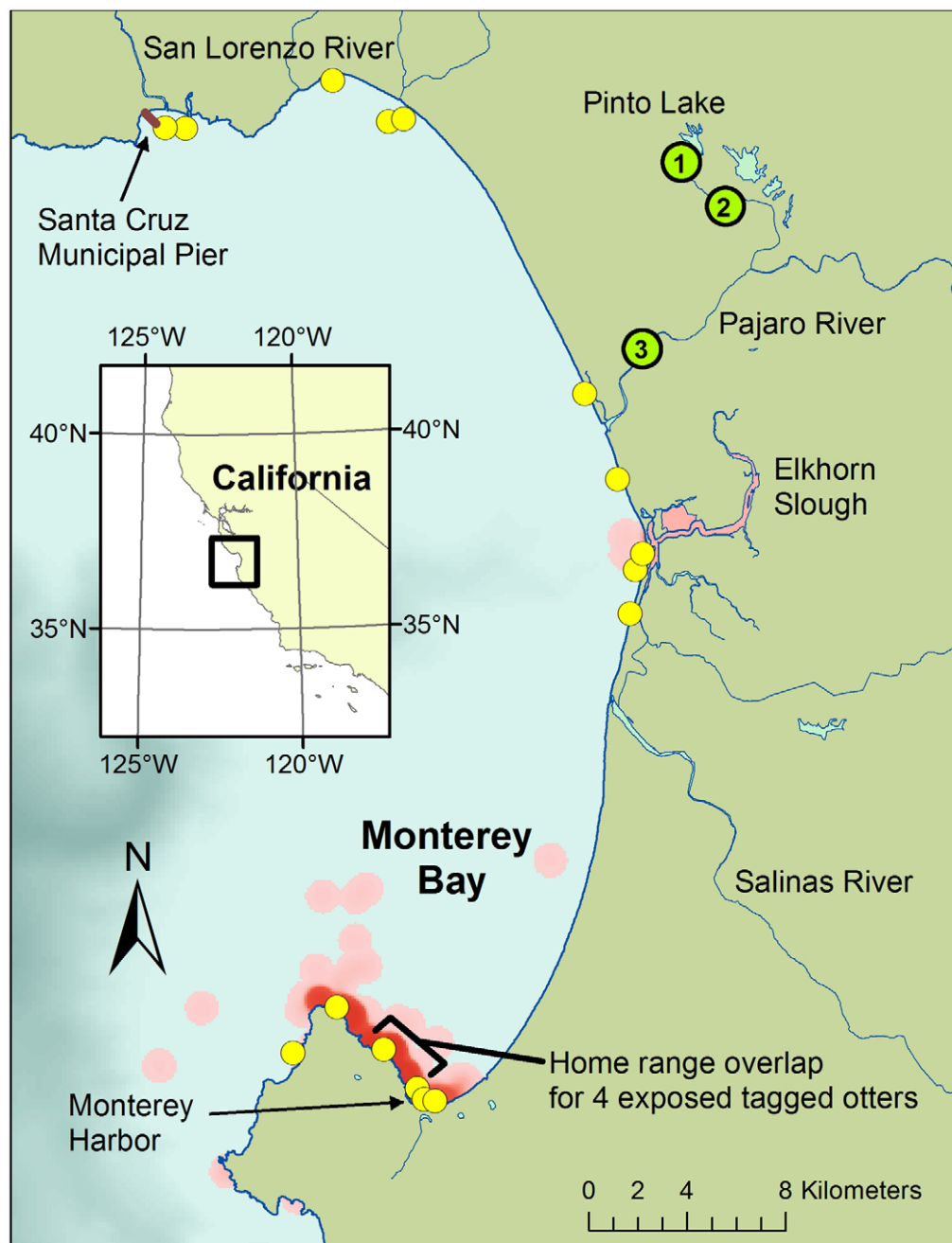


Figure 4. Map of Monterey Bay showing distribution of sea otters dying due to microcystin intoxication (yellow circles). Note spatial association of sea otter strandings with coastal locations of river mouths, harbors, coastal ponds and embayments. Habitat utilization distributions for 4 radio-tagged, microcystin-poisoned otters are plotted as kernel density distributions fit to daily re-sighting locations (red shading, with regions of most intense shading corresponding to the habitats most frequently utilized by affected animals). Locations of freshwater samples collected during a “Super-bloom” of *Microcystis* in 2007 are indicated by green circles, with numbers that correspond with the microcystin concentrations listed in Figure 1. doi:10.1371/journal.pone.0012576.g004

3.) Laboratory exposure of marine invertebrates

Intact *Microcystis* cyanobacteria initially accumulated at the top of the seawater tanks, but were almost completely lysed after 48 hours. Microcystin-LR was detectable in seawater for the duration of the study (21 days) and microcystin concentrations in refrigerated seawater had declined only 44–71% from mean one hour post-exposure levels after 3 weeks (Table 2).

Significant bioconcentration of microcystin by marine bivalves (clams, mussels and oysters) and snails, but not large marine crabs,

was documented (Table 3), with tissue concentrations of microcystin-LR up to 107 times higher in invertebrate tissues than in adjacent seawater. Microcystin concentrations in gastrointestinal tissues ranged from negative to 1,324 ppb wet weight (ww) in invertebrates, with the highest concentrations observed in clams, mussels and oysters sampled between 24 and 48 hours post-exposure.

Marine bivalves were also slow to depurate ingested microcystin; despite continuous seawater flushing beginning at 96 hours post-exposure, gastrointestinal microcystin concentrations at 14 days

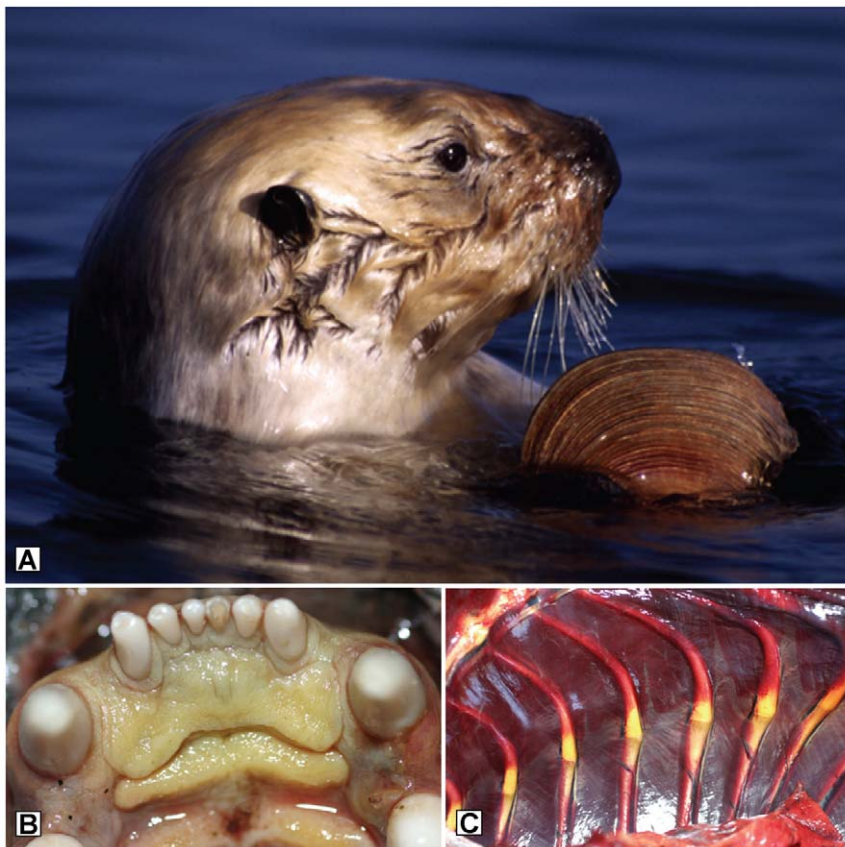


Figure 5. Microcystin detection in sea otter tissues was linked to bivalve consumption, liver damage and icterus. A.) Wild southern sea otter (*Enhydra lutris nereis*) consuming a clam in Elkhorn Slough, Monterey Bay. B.) Diffuse icterus of oral mucous membranes of an otter poisoned by microcystin, due to severe hepatic damage and elevated plasma bilirubin. C.) Severe icterus of cartilage at the costochondral junction in a sea otter that died due to microcystin intoxication.
doi:10.1371/journal.pone.0012576.g005

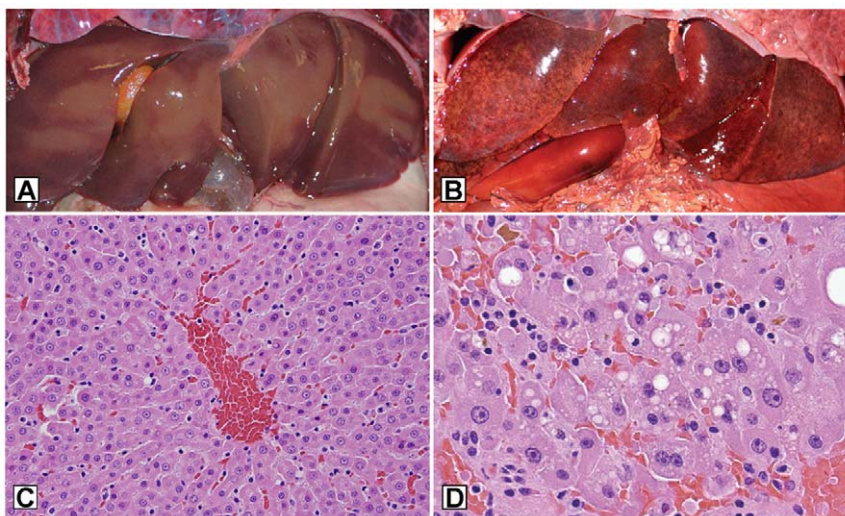


Figure 6. Gross and microscopic hepatic lesions of microcystin intoxication in sea otters, compared to control livers. A.) Gross appearance of normal sea otter liver. B.) Swollen, hemorrhagic liver from a sea otter that died due to microcystin intoxication. C.) Microscopic view of normal sea otter liver. D.) Microscopic appearance of liver from an otter that died due to microcystin intoxication, demonstrating hepatocyte swelling, cytoplasmic vacuolation, necrosis or apoptosis and parenchymal hemorrhage. Small greenish-gold accumulations of bile are apparent at the upper left and center-right portions of the photomicrograph.
doi:10.1371/journal.pone.0012576.g006

Table 1. Stranding information and microcystin (MCY) concentrations (ppb wet weight) for wild, microcystin-positive sea otters and captive controls.

Animal number	Stranding date	Stranding region	Sample tested	MCY-RR	MCY-LR	MCY-Desmethyl LR
1280-04 (Captive control)	6/27/2002	N/A	Liver	nd ¹	nd	nd
1485-06 (Captive control)	11/14/2001	N/A	Liver	nd	nd	nd
3216-99	7/28/1999	Monterey Bay	Liver	1.36	nd	nd
3377-00	6/26/2000	Monterey Bay	Liver	2.04	nd	nd
3858-03	3/17/2003	Estero Bay	Liver	nd	11.8	nd
3955-03	5/8/2003	Monterey Bay	Liver	3.19	nd	nd
4240-04	6/5/2004	Monterey Bay	Liver	nd	nd	1.53
4294-04	8/25/2004	Monterey Bay	Liver	13.13	nd	nd
3110-98	5/14/2006	Monterey Bay	Liver	9.52	nd	nd
4811-06	8/25/2006	Estero Bay	Liver	7.71	nd	nd
4844-06	9/24/2006	Monterey Bay	Liver	3.62	nd	nd
4913-07	1/30/2007	Monterey Bay	Liver	61.58	nd	nd
5020-07	6/9/2007	Monterey Bay	Liver	38.45	348	nd
5023-07	6/9/2007	Monterey Bay	Liver	104.46	nd	nd
5036-07	6/25/2007	Monterey Bay	Liver	2.69	nd	nd
5082-07	8/16/2007	Monterey Bay	Liver	5.29	nd	nd
5108-07	9/23/2007	Monterey Bay	Liver	14.39	nd	nd
5167-07	11/21/2007	Monterey Bay	Liver & feces	18.7 & 16.4	nd	nd
5174-07	11/30/2007	Monterey Bay	Liver	6.18	nd	nd
5179-07	12/1/2007	Monterey Bay	Liver	3.76	nd	nd
5182-07B	12/2/2007	Monterey Bay	Liver	4.8	nd	nd
5185-07	12/6/2007	Estero Bay	Liver	1.97	nd	nd
5416-08	11/8/2008	Big Sur	Liver	7.58	nd	nd

¹nd = microcystin concentration was below minimum detection limits on liquid chromatography-tandem mass spectrophotometry.
doi:10.1371/journal.pone.0012576.t001

post-exposure were at 120%, 14% and 6.5% of 24 hour post-exposure concentrations for oysters, clams and mussels, respectively (Table 3). Mussel digestive tract remained microcystin-positive (30.5 ppb ww) 21 days after the initial exposure period and

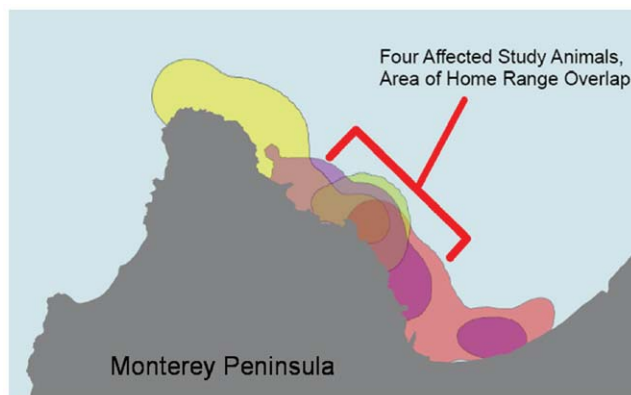


Figure 7. Overlapping home ranges of 4 tagged southern sea otters that died due to microcystin intoxication. Note the spatial overlap of all 4 home ranges on the north central Monterey Peninsula near Monterey Harbor (bracket): This harbor appears to be one of several high-risk locations for microcystin poisoning of sea otters, possibly due to prolonged retention of microcystin-contaminated water.
doi:10.1371/journal.pone.0012576.g007

following 17 days of continuous exposure to clean seawater, which was the longest post-exposure timepoint evaluated during this study

Some variation in microcystin concentration between sample periods was attributed to differences in toxin uptake by individual bivalves, similar to the approximately 4-fold individual variability noted for bioaccumulation of domoic acid and saxitoxin in individual mussels from California coastal waters (R. Kudela, pers. commun.). All non-exposed controls (ambient seawater and invertebrates) tested negative for microcystin throughout the study (data not shown), which is consistent with a proposed freshwater (not marine) source of cyanotoxin exposure for sea otters.

Discussion

Here we provide the first documentation of microcystin intoxication in a marine mammal. Our research confirms deaths of threatened southern sea otters from microcystin intoxication and incorporates 3 distinct, but interconnected lines of scientific inquiry to address the hypothesis that land-sea flow of microcystins with trophic transfer through marine invertebrates is the most likely route of sea otter exposure: 1) Time-integrative passive samplers were deployed in fresh and marine systems along the central California coast, confirming the presence of microcystins; 2) Necropsy, histopathology and chemical analysis of tissues from stranded southern sea otters and 3) Determining dynamics and persistence of freshwater microcystin uptake from contaminated seawater by marine invertebrates using controlled laboratory experiments. Although trophic transfer of biotoxins from plank-

Table 2. Microcystin-LR concentrations (ppb) at the top, middle, and bottom of seawater tanks at two exposure concentrations (Tank 2 and Tank 3¹) and varying postexposure intervals.

Inoculum 2,195 ppb	Tank 2 (low exposure) ¹					
	1 H	12 H	24 H	48 H	72 H	7 Days
Surface	2.34	0.87	5.18	0.75	1.32	Nd ²
Middle	0.756	0.71	1.37	0.87	1.03	nd
Bottom	0.500	0.650	1.90	1.32	1.01	nd
Inoculum 10,600 ppb	Tank 3 (high exposure)					
	1 H	12 H	24 H	48 H	72 H	7 Days
Surface	32.8	5.88	22.2	4.02	6.58	nd ²
Middle	5.53	5.01	7.46	6.09	4.95	nd
Bottom	5.03	5.03	7.66	3.69	6.75	nd
Mean		5.31	12.44	4.6	6.1	nd

¹All samples from Tank 1 (seawater control) tested negative for microcystin-LR. All 3 tanks were flushed with fresh seawater starting 96 H postexposure.
²nd = microcystin concentration was below minimum detection limits on liquid chromatography-tandem mass spectrophotometry.

doi:10.1371/journal.pone.0012576.t002

tonic species to higher vertebrates has been demonstrated for marine biotoxins like brevetoxin and domoic acid within estuarine and marine systems [51,52], here we provide the first documentation of putative biotoxin transfer from the lowest trophic levels of nutrient-impaired freshwater habitat to top marine predators at the land-sea interface. Our findings provide the first hint of a serious environmental and public health threat that could negatively impact marine wildlife and humans.

We confirmed that Pinto Lake, a recreational water body located just inland from Monterey Bay exhibits substantial and recurrent *Microcystis* blooms. Biochemical testing of samples from Pinto lake during fall, 2007 revealed total microcystin concentrations of almost 2,900 ppm (2.9 million ppb), one of the highest microcystin concentrations ever reported from an environmental sample; the World Health Organization limit for microcystin contamination of finished drinking water is 1 ppb (0.001 ppm) [53]. Stepwise sampling of downstream tributaries during the late dry season confirmed the presence of *Microcystis* and microcystins throughout the lower Pajaro watershed to within 1 km of the ocean. Factors that facilitate development of cyanobacterial “super-blooms” in fresh water include

elevated nutrient concentrations and salinity, warm temperatures, enhanced vertical stratification of lakes, summer droughts and increased light intensity; all factors that are exacerbated by global climate change [19,22,23,54]. Cyanobacteria can exploit these conditions by developing intracellular gas vesicles and accumulating in dense surface blooms that “shade out” nontoxic phytoplankton like diatoms and green algae. They can also increase local water temperatures through light absorption, creating a positive feedback loop that helps ensure local dominance [23]. Once formed, these biotoxins can exert their effects in areas that are remote from sites of toxin production and can bioaccumulate in invertebrates and fish, suggesting a biologically plausible route for marine mammal (and human) exposure to freshwater toxins at the land-sea interface [32,51,52].

We demonstrated the excellent adsorption characteristics of SPATT resin-based systems for microcystin detection in both fresh and salt water. These passive samplers were more sensitive than periodic grab samples for field detection of microcystins and the ability to evaluate samples for the presence of multiple biotoxins simultaneously is an additional bonus. Preliminary environmental

Table 3. Microcystin LR concentrations (ppb wet weight) in marine invertebrate gastrointestinal tissues collected from Tank 3 (high microcystin exposure tank) at various time intervals post-exposure¹.

Invertebrate Spp. ²	24 Hour	48 Hour	72 Hour	7 Days	14 Days	21 Days
Manila clam	1,324	110	125	295	183	nd ³
Mussel	979	3.13	14.3	45	64.4	30.5
Oyster	102	373	68.3	158	122	4
Dungeness crab	nd	nd	1.01	2.7	---	---
Red rock crab	nd	nd	nd	nd	nd	nd
Tegula snail	---	---	170	175	---	---
Seawater in tank ⁵	12.4	4.6	6.1	nd	nd	nd

¹All tanks were flushed continually with clean seawater beginning at 96 H post-exposure.

²n = 1 or 2 pooled invertebrates of each species at each sample point, except snails, where n=7.

³nd = microcystin concentration was below minimum detection limits on liquid chromatography-tandem mass spectrophotometry.

⁴--- = not tested.

⁵Average microcystin-LR concentration across the top, middle and bottom of Tank 3 at each time point.

doi:10.1371/journal.pone.0012576.t003

surveillance using SPATT revealed no detectable microcystin in nearshore marine waters of Monterey Bay until the fall rainy season, when the marine outfalls of the 3 most nutrient-impaired local waterways; the Salinas, the Pajaro and the San Lorenzo Rivers all tested microcystin-positive.

Because of their high metabolic rate, small home ranges and heavy reliance on nearshore-dwelling marine invertebrates as food, sea otters provide an upper trophic-level compliment to the SPATT resin for environmental detection of microcystins. Deaths due to cyanobacterial intoxication were first recognized in 2007, when 11 microcystin-poisoned sea otters were recovered along the shoreline of Monterey Bay. Microcystin intoxication appears to be an emerging health problem for southern sea otters. To date, at least 21 southern sea otters have died due to microcystin intoxication and the frequency of deaths may be increasing over time. Most microcystin-positive sea otters were recovered near embayments, harbors or river mouths. Sea otters generally do not venture into rivers to feed, so upstream exposure to microcystins is unlikely.

For radio-tagged otters that died due to microcystin intoxication, marine bivalves constituted a major portion of their diet. Sea otters routinely consume 25 to 30% of their body weight in clams, mussels, snails, crabs and other marine invertebrates daily [50,55]. Marine bivalves are highly efficient biological filters for polluted water and can bioaccumulate a wide range of terrestrial-origin pollutants, including protozoa, enteric bacteria, viruses, biotoxins and anthropogenic chemicals [32,56–58]. Embayments, harbors and river mouths are favored foraging sites, placing otters directly in the path of concentrated plumes of polluted water at the land-sea interface. A higher risk of exposure to terrestrial-origin pathogens and chemicals has been reported for sea otters residing near impaired habitats and those that feed preferentially on filter-feeding invertebrates [44,49,57,59].

Microcystin accumulation has been demonstrated in fresh- and saltwater mussels, crustaceans, corals, fish and possibly humans [7,30,31,32]. Our hypothesis that sea otters were most likely to be exposed to lethal levels of microcystins through consumption of contaminated invertebrate prey was evaluated through laboratory experiments where bioconcentration and depuration of freshwater microcystins by marine invertebrates could be assessed under defined conditions. We documented significant bioaccumulation and slow depuration of freshwater microcystins by marine oysters, clams, snails and mussels, with gastrointestinal tissue concentrations up to 107 times greater than adjacent seawater. Marine invertebrates were also slow to depurate ingested toxins, with high microcystin concentrations detected at 2 weeks post-exposure (Table 3). Freshwater microcystins were also relatively stable in seawater, with concentrations remaining at 29 to 56% of 1 hour postexposure concentrations, even after 21 days.

Collectively these data provide compelling evidence implicating land-sea flow with trophic transfer through marine invertebrates as the most likely route of biotoxin exposure. Detection of this problem initially in southern sea otters is not surprising, given the high level of scientific scrutiny of this federally-listed threatened species. Due to several unique aspects of their biology, including a

high metabolic rate, a preference to feed near the shoreline and strong reliance on filter-feeding invertebrates as prey, southern sea otters have proven to be highly sensitive indicators of health of nearshore marine ecosystems [44,49,55,60]. Southern sea otters are also a keystone species [61]; by foraging on kelp-feeding invertebrates like urchins, sea otters help maintain the complex 3 dimensional structure of the kelp forest that provides critical habitat for other marine wildlife [62].

Our data appear to strongly support the following hypotheses relevant to microcystin pollution and toxicity: H1: Significant concentrations of freshwater-derived microcystins are intermittently polluting the land-sea interface of central California. H2: These microcystins are causing mortality of threatened southern sea otters, possibly through trophic transfer to marine invertebrates feeding in contaminated freshwater plumes and H3: Wild and farmed marine bivalves consumed by sea otters and humans exhibit high microcystin uptake and slow depuration under conditions that mimic natural exposure. Monterey Bay, the region where the majority of microcystin-poisoned sea otters were recovered, forms the heart of the nation's largest marine sanctuary and is heavily utilized by humans for water contact recreation, tourism, fishing and wildlife viewing. No formal surveillance or regulatory system exists for microcystin detection in water or shellfish in most countries, including the United States. Because sea otters and humans consume many of the same marine foods, our research findings may reveal unrecognized health risks for humans when consuming invertebrates harvested at the land-sea interface.

Acknowledgments

Sincere thanks go to Bryant Austin at Studio Cosmos and Robert Ketley at the City of Watsonville for contributing photos (Part A, Figure 1 and inset of Figure 3, respectively). We thank Jack Ames, Hannah Ban-Weiss, Francesca Batac, Gloria Blondina, Wayne Carmichael, Mary Curry, Erin Dodd, Traci Fink, Corrine Gible, Dominic Gregorio, Michael Harris, Andy Johnson, Robert Ketley, Jenny Lane, Kamal Mekebri, Megan Olea, David Paradies, Meiling Roddam, Ben Weitzman and Karen Worcester for assistance with sample collection, invertebrate exposure and study design. We acknowledge the Monterey Bay Aquarium, the Marine Mammal Center, USGS-BRD, the United States Fish and Wildlife Service and CDFG for their efforts to recover and care for sick, stranded marine animals. Any use of trade, product, or firm names in this publication is for descriptive purposes only and does not imply endorsement by the U.S. Government or the State of California

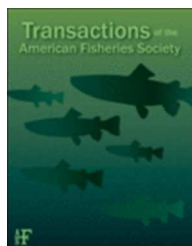
Author Contributions

Conceived and designed the experiments: MAM RMK SCO CD DH KW DAJ. Performed the experiments: MAM RMK AM DBC SCO MTT MS STC CD. Analyzed the data: MAM RMK AM DBC SCO MTT STC. Contributed reagents/materials/analysis tools: MAM RMK AM DBC MTT MS WM DH GL MM KW DAJ. Wrote the paper: MAM RMK AM DBC SCO MTT MS WM STC CD DH GL MM KW DAJ.

References

- Ashworth CT, Mason MF (1946) Observations on the pathological changes produced by a toxic substance present in blue-green algae (*Microcystis aeruginosa*). *Amer Jour Path* 22: 369–380.
- Jochimsen EM, Carmichael WW, An J, Cardo DM, Cookson ST, et al. (1998) Liver failure and death after exposure to microcystins at a hemodialysis center in Brazil. *N Engl J Med* 338: 873–878.
- Humpage AR, Falconer IR (1999) Microcystin-LR and liver tumor promotion: Effects on cytokinesis, ploidy, and apoptosis in cultured hepatocytes. *Environmental Toxicology* 14: 61–75.
- Gilroy DJ, Kauffman KW, Hall RA, Huang X, Chu FS (2000) Assessing Potential Health Risks from Microcystin Toxins in Blue-Green Algae Dietary Supplements. *Environmental Health Perspectives* 108: 435–439.
- Carmichael WW, Azevedo S, An JS, Molica RJ, Jochimsen EM, et al. (2001) Human Fatalities from Cyanobacteria: Chemical and Biological Evidence for Cyanotoxins. *Environmental Health Perspectives* 109: 663–668.
- Lankoff A, Carmichael WW, Grasman KA, Yuan M (2004) The uptake kinetics and immunotoxic effects of microcystin-LR in human and chicken peripheral blood lymphocytes in vitro. *Toxicology* 204: 23–40.

7. Amorim Á, Vasconcelos V (1999) Dynamics of microcystins in the mussel *Mytilus galloprovincialis*. *Toxicol* 37: 1041–1052.
8. Kohoutek J, Babica P, Bláha L, Maršálek B (2008) A novel approach for monitoring of cyanobacterial toxins: development and evaluation of the passive sampler for microcystins. *Analytical and Bioanalytical Chemistry* 390: 1167–1172.
9. Hanazato T, Yasuno M (1987) Evaluation of Microcystin as food for zooplankton in a eutrophic lake. *Hydrobiologia* 144: 251–260.
10. Ozawa K, Yokoyama A, Ishikawa K, Kumagai M, Watanabe MF, et al. (2003) Accumulation and depuration of microcystin produced by the cyanobacterium *Microcystis* in a freshwater snail. *Limnology* 4: 131–138.
11. Oudra B, Loudiki M, Sbiyyaa B, Martins R, Vasconcelos V, et al. (2001) Isolation, characterization and quantification of microcystins (heptapeptide hepatotoxins) in *Microcystis aeruginosa* dominated bloom of Lalla Takerkoust lake-reservoir (Morocco). *Toxicol* 39: 1375–1381.
12. Nasri H, El Hery S, Bouaicha N (2008) First reported case of turtle deaths during a toxic *Microcystis* spp. bloom in Lake Oubeira, Algeria. *Ecotoxicology and Environmental Safety* 71: 535–544.
13. Dawson RM (1998) The toxicology of microcystins. *Toxicol* 36: 953–962.
14. Robson BJ, Hamilton DP (2003) Summer flow event induces a cyanobacterial bloom in a seasonal Western Australian estuary. *Marine and Freshwater Research* 54: 139–151.
15. Chen DZX, Boland MP, Smillie MA, Klix H, Ptak C, et al. (1993) Identification of protein phosphatase inhibitors of the microcystin class in the marine environment. *Toxicol* 31: 1407–1414.
16. Domingos P, Rubim TK, Molica RJR, Azevedo SMFO, Carmichael WW (1999) First report of microcystin production by picoplanktonic cyanobacteria isolated from a northeast Brazilian drinking water supply. *Environmental Toxicology* 14: 31–35.
17. Lehman PW, Boyer G, Hall C, Waller S, Gehrts K (2005) Distribution and toxicity of a new colonial *Microcystis aeruginosa* bloom in the San Francisco Bay Estuary, California. *Hydrobiologia* 541: 87–99.
18. Zehnder A, Gorham PR (1960) Factors influencing the growth of *Microcystis aeruginosa*. *Canadian Jour Microbiol* 6: 645–660.
19. Davis TW, Berry DL, Boyer GL, Gobler CJ (2009) The effects of temperature and nutrients on the growth and dynamics of toxic and non-toxic strains of *Microcystis* during cyanobacteria blooms. *Harmful Algae* 8: 715–725.
20. Jacoby JM, Collier DC, Welch EB, Hardy EJ, Crayton M (2000) Environmental factors associated with a toxic bloom of *Microcystis aeruginosa*. *Canadian Journal of Fisheries and Aquatic Sciences* 57: 231–240.
21. Tsuji K, Naito S, Kondo F, Ishikawa N, Watanabe MF, et al. (1994) Stability of microcystins from cyanobacteria: Effect of light on decomposition and isomerization. *Environmental Science and Technology* 28: 173–177.
22. Welker M, Steinberg C (2000) Rates of Humic Substance Photosensitized Degradation of Microcystin-LR in Natural Waters. *Environmental Science & Technology* 34: 3415–3419.
23. Paerl HW, Huisman J (2008) Climate: Blooms like it hot. *Science* 320: 57–58.
24. Vasconcelos VM (1999) Cyanobacterial toxins in Portugal: Effects on aquatic animals and risk for human health. *Brazilian Journal of Medical and Biological Research* 32: 249–254.
25. Chen J, Xie P, Zhang D, Ke Z, Yang H (2006) In situ studies on the bioaccumulation of microcystins in the phytoplanktivorous silver carp (*Hypophthalmichthys molitrix*) stocked in Lake Taihu with dense toxic *Microcystis* blooms. *Aquaculture* 261: 1026–1038.
26. Backer L, Carmichael W, Kirkpatrick B, Williams C, Irvin M, et al. (2008) Recreational exposure to low concentrations of microcystins during an algal bloom in a small lake. *Marine Drugs* 6: 389–406.
27. Matthiensen A, Beattie KA, Yunes JS, Kaya K, Codd GA (2000) [D-Leu¹]Microcystin-LR, from the cyanobacterium *Microcystis* RST 9501 and from a *Microcystis* bloom in the Patos Lagoon estuary, Brazil. *Phytochemistry* 55: 383–387.
28. Tonk L, Bosch K, Visser PM, Huisman J (2007) Salt tolerance of the harmful cyanobacterium *Microcystis aeruginosa*. *Aquatic Microbial Ecology* 46: 117–123.
29. DeMott WR, Moxter F (1991) Foraging cyanobacteria by copepods: Responses to chemical defense and resource abundance. *Ecology* 72: 1820–1834.
30. Malbrouc C, Kestemont P (2006) Effects of microcystins on fish. *Environmental Toxicology and Chemistry* 25: 72–86.
31. Richardson LL, Sekar R, Myers JL, Gantar M, Voss JD, et al. (2007) The presence of the cyanobacterial toxin microcystin in black band disease of corals. *FEMS Microbiology Letters* 272: 182–187.
32. Williams DE, Dawe SC, Kent ML, Andersen RJ, Craig M, et al. (1997) Bioaccumulation and clearance of microcystins from salt water mussels, *Mytilus edulis*, and in vivo evidence for covalently bound microcystins in mussel tissues. *Toxicol* 35: 1617–1625.
33. Vasconcelos V, Oliveira S, Teles FO (2001) Impact of a toxic and a non-toxic strain of *Microcystis aeruginosa* on the crayfish *Procambarus clarkii*. *Toxicol* 39: 1461–1470.
34. Zimba PV, Camus A, Allen EH, Burkholder JM (2006) Co-occurrence of white shrimp, *Litopenaeus vannamei*, mortalities and microcystin toxin in a southeastern USA shrimp facility. *Aquaculture* 261: 1048–1055.
35. Fulton RS, III, Paerl HW (1987) Toxic and inhibitory effects of the blue-green alga *Microcystis aeruginosa* on herbivorous zooplankton. *J Plankton Res* 9: 837–855.
36. Reinikainen M, Ketola M, Walls M (1994) Effects of the concentrations of toxic *Microcystis aeruginosa* and an alternative food on the survival of *Daphnia pulex*. *Limnology and Oceanography* 39: 424–432.
37. Kotak BG, Zurawell RW, Prepas EE, Holmes CFB (1996) Microcystin-LR concentration in aquatic food web compartments from lakes of varying trophic status. *Canadian Journal of Fisheries and Aquatic Sciences* 53: 1974–1985.
38. Ger KA, Teh SJ, Goldman CR (2009) Microcystin-LR toxicity on dominant copepods *Eurytemora affinis* and *Pseudodiaptomus forbesi* of the upper San Francisco Estuary. *Science of the Total Environment* 407: 4852–4857.
39. Johnston BR, Jacoby JM (2003) Cyanobacterial toxicity and migration in a mesotrophic lake in western Washington, USA. *Hydrobiologia* 495: 79–91.
40. Moisaner PH, Lehman PW, Ochiai M, Corum S (2009a) Diversity of *Microcystis aeruginosa* in the Klamath River and San Francisco Bay delta, California, USA. *Aquatic Microbial Ecology* 57: 19–31.
41. Moisaner PH, Ochiai M, Lincoff A (2009b) Nutrient limitation of *Microcystis aeruginosa* in northern California Klamath River reservoirs. *Harmful Algae* 8: 889–897.
42. Fetcho K Final 2007 Klamath River Blue-Green Algae Summary Report. Klamath: Yurok Tribe Environmental Program. <http://www.klamathwaterquality.com/documents/2007YurokFINALBGAReport071708.pdf>.
43. MacKenzie L, Beuzenberg V, Holland P, McNabb P, Selwood A (2004) Solid phase adsorption toxin tracking (SPAT[®]): a new monitoring tool that simulates the biotoxin contamination of filter feeding bivalves. *Toxicol* 44: 901–918.
44. Miller MA, Gardner IA, Kreuder C, Paradies DM, Worcester KR, et al. (2002) Coastal freshwater runoff is a risk factor for *Toxoplasma gondii* infection of southern sea otters (*Enhydra lutris nereis*). *International Journal for Parasitology* 32: 997–1006.
45. Mekebre A, Blondina GJ, Crane DB (2009) Method validation of microcystins in water and tissue by enhanced liquid chromatography tandem mass spectrometry. *Journal of Chromatography A* 1216: 3147–3155.
46. Bishop CT, Anet EFLJ, Gorham PR (1959) Isolation and identification of the fast-death factor in *Microcystis aeruginosa* NRC-1. *Canadian Jour Biochem and Physiol* 37: 453–471.
47. Fischer WJ, Dietrich DR (2000) Pathological and biochemical characterization of microcystin-induced hepatopancreas and kidney damage in carp (*Cyprinus carpio*). *Toxicology and Applied Pharmacology* 164: 73–81.
48. Goldberg JD (2003) Domoic Acid in the Benthic Food Web of Monterey Bay, California [Master of Science]. Moss Landing: California State University Monterey Bay. 41 p.
49. Johnson CK, Tinker MT, Estes JA, Conrad PA, Staedler M, et al. (2009) Prey choice and habitat use drive sea otter pathogen exposure in a resource-limited coastal system. *Proceedings of the National Academy of Sciences* 106: 2242–2247.
50. Tinker MT, Bental G, Estes JA (2008) Food limitation leads to behavioral diversification and dietary specialization in sea otters. *Proceedings of the National Academy of Sciences* 105: 560–565.
51. Scholin CA, Gulland F, Doucette GJ, Benson S, Busman M, et al. (2000) Mortality of sea lions along the central California coast linked to a toxic diatom bloom. *Nature* 403: 80–84.
52. Flewelling IJ, Naar JP, Abbott JP, Baden DG, Barros NB, et al. (2005) Brevetoxinosis: Red tides and marine mammal mortalities. *Nature* 435: 755–756.
53. WHO (1996) Cyanobacterial toxins: Microcystin-LR in Drinking Water. Guidelines for Drinking Water Quality. 2nd ed. Geneva: World Health Organization.
54. Guo L (2007) ECOLOGY: Doing battle with the green monster of Taihu Lake. *Science* 317: 1166.
55. Estes JA (2005) Carnivory and trophic connectivity in kelp forests. In: Ray JC, Redford KH, Steneck RS, Berger J, eds. *Large Carnivores and the Conservation of Biodiversity*. Washington: Island Press. pp 61–81.
56. Miller W, Miller M, Gardner I, Atwill E, Byrne B, et al. (2006) *Salmonella* spp., *Vibrio* spp., *Clostridium perfringens*, and *Plesiomonas shigelloides* in Marine and Freshwater Invertebrates from Coastal California Ecosystems. *Microbial Ecology* 52: 198–206.
57. Miller MA, Miller WA, Conrad PA, James ER, Melli AC, et al. (2008) Type X *Toxoplasma gondii* in a wild mussel and terrestrial carnivores from coastal California: New linkages between terrestrial mammals, runoff and toxoplasmosis of sea otters. *International Journal for Parasitology* 38: 1319–1328.
58. O'Connor TP, Lauenstein GG (2006) Trends in chemical concentrations in mussels and oysters collected along the US coast: Update to 2003. *Marine Environmental Research* 62: 261–285.
59. Miller MA, Byrne BA, Jang SS, Dodd EM, Dorfmeier E, et al. (2010) Enteric bacterial pathogen detection in southern sea otters (*Enhydra lutris nereis*) is associated with coastal urbanization and freshwater runoff. *Vet Res* 41: 01.
60. Jessup DA, Miller MA, Kreuder-Johnson C, Conrad PA, Tinker MT, et al. (2007) Sea otters in a dirty ocean. *Journal of the American Veterinary Medical Association* 231: 1648–1652.
61. Estes JA, Palmisano JF (1974) Sea Otters Their Role in Structuring Nearshore Communities. *Science* 185: 1058–1060.
62. Estes JA, Danner EM, Doak DF, Konar B, Springer AM, et al. (2004) Complex trophic interactions in kelp forest ecosystems. *Bulletin of Marine Science* 74: 621–638.



Population dynamics of Longfin Smelt in the San Francisco Estuary II: disaggregating forces driving long-term decline of an estuarine forage fish

Journal:	<i>Transactions of the American Fisheries Society</i>
Manuscript ID:	TAFS-2015-0141
Manuscript Type:	Article
Keywords:	Estuarine < Ecology, Fisheries Oceanography and Recruitment, Population Dynamics
Abstract:	<p>Forage fish production has become a central concern of fisheries and ecosystem managers because populations of small fish are a critical energetic pathway between primary producers and predator populations. Management of forage fish often focuses on controlling exploitation rates, but it is also possible to manage productivity of these species in coastal ecosystems, and estuaries in particular. Like several forage fish species native to the San Francisco Estuary (California, USA), Longfin smelt <i>Spirinchus thaleichthys</i> have experienced dramatic population declines over the past few decades. Trends in the relative abundance of this population, which is not fished commercially or recreationally, have been described statistically but the mechanisms that drive population dynamics are still poorly understood. The objective of this study was to evaluate alternative conceptual models of this species' population dynamics to better understand the forces that may constrain its productivity during different phases of its life cycle. We created contrasting variants of a generalizable population model (the Ricker model) and parameterized those variants using empirical data from a long-term sampling program in this estuary. Predictions from alternative models were compared to empirical results from a second, independent data series of Longfin Smelt relative abundance to determine which population model variants best captured the empirical trend. The results indicated that freshwater flow has a positive association with recruits-per-spawner and that both recruits-per-spawner, and spawners-per-recruit, appear to be density-dependent life stage transitions. Juvenile survival may have declined to some extent, but we could not conclusively demonstrate this. By constraining the possible timing and location of mechanisms that modulate productivity in different life stages, these results improve our understanding of production for a key native forage fish in the San Francisco Estuary.</p>

SCHOLARONE™
Manuscripts

For Peer Review Only

1 **Population dynamics of Longfin Smelt in the San Francisco Estuary II: disaggregating**
2 **forces driving long-term decline of an estuarine forage fish**

3

4 Proposed running head: Longfin Smelt population dynamics

5 Longfin Smelt; *Spirinchus thaleichthys*; San Francisco Estuary; freshwater flow regime; fish
6 recruitment; forage fish; species conservation; endangered species population dynamics

7

8 Matthew L. Nobriga¹;

9 United States Fish and Wildlife Service, Dept. of Interior

10 Bay Delta Fish and Wildlife Office

11 650 Capitol Mall Suite 8-300 Sacramento, CA. 95831

12

13 Jonathan A. Rosenfield¹;

14 The Bay Institute

15 Pier 39, Box #200

16 San Francisco, CA 94133

17

18

19 ¹corresponding author: matt_nobriga@fws.gov, tel: (916) 530-5609

20

21 **Abstract:** Forage fish production has become a central concern of fisheries and
22 ecosystem managers because populations of small fish are a critical energetic pathway between
23 primary producers and predator populations. Management of forage fish often focuses on
24 controlling exploitation rates, but it is also possible to manage productivity of these species in
25 coastal ecosystems, and estuaries in particular. Like several forage fish species native to the San
26 Francisco Estuary (California, USA), Longfin smelt *Spirinchus thaleichthys* have experienced
27 dramatic population declines over the past few decades. Trends in the relative abundance of this
28 population, which is not fished commercially or recreationally, have been described statistically
29 but the mechanisms that drive population dynamics are still poorly understood. The objective of
30 this study was to evaluate alternative conceptual models of this species' population dynamics to
31 better understand the forces that may constrain its productivity during different phases of its life
32 cycle. We created contrasting variants of a generalizable population model (the Ricker model)
33 and parameterized those variants using empirical data from a long-term sampling program in this
34 estuary. Predictions from alternative models were compared to empirical results from a second,
35 independent data series of Longfin Smelt relative abundance to determine which population
36 model variants best captured the empirical trend. The results indicated that freshwater flow has a
37 positive association with recruits-per-spawner and that both recruits-per-spawner, and spawners-
38 per-recruit, appear to be density-dependent life stage transitions. Juvenile survival may have
39 declined to some extent, but we could not conclusively demonstrate this. By constraining the
40 possible timing and location of mechanisms that modulate productivity in different life stages,
41 these results improve our understanding of production for a key native forage fish in the San
42 Francisco Estuary.

43

44 Introduction

45 Forage fishes serve as energy conduits between zooplankton and higher trophic-level
46 predators (Pikitch et al. 2014). This central role in aquatic food webs means that forage fish
47 production is critical to sustainable fisheries management (Alder et al. 2008), desired ecosystem
48 functions (Hall et al. 2012), and in some cases the maintenance of biodiversity (Trathan et al.
49 2015). For instance, seabirds around the world display reduced and more variable productivity
50 when forage fish biomass drops below one-third of the maximum observed in long-term studies
51 (Cury et al. 2011). Thus, marine fisheries and ecosystem management are increasingly focusing
52 on protecting forage fishes from over-exploitation. Management may also be directed toward
53 maintaining or restoring the habitats and processes that support production of forage fish,
54 especially in estuarine ecosystems (Kennish 2002; Hughes et al. 2014).

55 A general conceptual model of forage fish productivity in coastal ecosystems, including
56 estuaries, is that recruitment is strongly influenced by the interplay of zooplankton production
57 and predation rates sustained by the forage fishes (Walters and Juanes 1993; Essington and
58 Hansson 2004). The matches and mismatches of forage fishes and their prey can be affected by
59 physical conditions such as ocean currents (Genin 2004) and upwelling (Reum et al. 2011). For
60 species that rely on low-salinity environments to complete their life-cycle, variation in
61 freshwater flow rates can also play an important role in aligning young fish with their prey and
62 protecting them from predators (Turner and Chadwick 1972; North and Houde 2003). Fish
63 behavior and physiological capacities can influence the details of this conceptual model,
64 particularly in euryhaline fishes (Kimmerer 2006; Peebles et al. 2007).

65 However, the protection of forage fish habitats can be very difficult in developed rivers
66 and their receiving estuaries because of strong competition for freshwater with human economic

67 systems (Vörösmarty et al. 2010; Cloern and Jassby 2012). Many estuarine forage fishes that are
68 tolerant of, or dependent on, low-salinity and freshwater habitats, and their supporting food
69 webs, are influenced by the timing, duration, and magnitude of freshwater flow and its effects on
70 estuarine hydrodynamics (Jassby et al. 1995; North and Houde 2003; Gillson 2011). The
71 biological productivity and accessibility of fresh water historically provided by river-estuary
72 systems have attracted considerable human settlement and exploitation that has in turn led to
73 intensive changes, including large-scale reclamation of estuarine landscapes, water pollution,
74 species introductions, modification of estuarine hydrodynamics, and declines in native biota
75 (Kennish 2002; Lotze et al. 2006; Shan et al. 2013). California's San Francisco Estuary
76 (hereafter SFE; Figure 1) is a well-known example of an estuary that has undergone tremendous
77 physical, chemical, and biological transformation (Kimmerer 2002a; Cloern and Jassby 2012).
78 The declines of once productive fisheries and the potential ongoing loss of native fish
79 biodiversity are key aquatic resource concerns in the SFE and its watershed (Moyle 2002;
80 Sommer et al. 2007; Katz et al. 2012).

81 One formerly abundant forage fish of the SFE that has undergone a substantial decline is
82 Longfin Smelt *Spirinchus thaleichthys* (Rosenfield and Baxter 2007). Longfin Smelt is a small,
83 facultatively anadromous, pelagic fish that typically reaches adult sizes of 80-150 mm in fork
84 length (Moyle 2002). Longfin Smelt inhabits lakes, coastal river estuaries, and nearshore marine
85 environments from Alaska to central California; the SFE is the southern limit of the species'
86 inland distribution along the Pacific Coast of North America. Most Longfin Smelt live for two
87 years and are semelparous. In the SFE, Longfin Smelt spawn in tidally-influenced freshwater
88 habitats, but low-salinity habitats may also provide suitable spawning areas (the microhabitat
89 requirements for Longfin Smelt spawning are not known). Spawning typically peaks in the

90 winter (December-February), when water temperatures range from about 7.0°C to 14.5°C
91 (Moyle 2002). Larvae and small juveniles aggregate in low-salinity waters during the late winter
92 through spring (Dege and Brown 2004) then move seaward into mesohaline to marine waters of
93 Central San Francisco Bay and the coastal ocean during the summer (Rosenfield and Baxter
94 2007). Juveniles and adults begin to move landward again during the fall (September-
95 December).

96 Longfin Smelt was once one of the most abundant and widespread fishes in the SFE
97 (Moyle 2002; Sommer et al. 2007). Their former abundance and broad distribution strongly
98 suggest that it once played an important role in the SFE food web; however, given an abundance
99 decline of circa 99.9%, it is likely that Longfin Smelt is currently too rare to serve as an
100 important prey to piscine, avian, or mammalian predators foraging in the estuary. Longfin Smelt
101 is one of several fish populations that play a central role in California water management because
102 in 2009 it was listed as threatened under the California Endangered Species Act (CESA), and
103 regulations developed as part of the CESA listing can limit diversions of fresh water from the
104 estuary. The United States Fish and Wildlife Service has also recently determined that the SFE
105 population of Longfin Smelt warranted protection under the U.S. Endangered Species Act
106 (Federal Register, 77 FR 19755).

107 Many details of Longfin Smelt ecology in the SFE are virtually unknown because it has
108 not been targeted by a sport or commercial fishery for many decades (Moyle 2002), though it is a
109 bycatch species in a limited bait fishery for Bay Shrimp *Crangon franciscorum*. Although
110 CDFW (2009) considered this a factor limiting Longfin Smelt recovery, we know of no evidence
111 that bycatch rates have increased substantially in recent times and until its recent listing under
112 CESA, it did not factor directly into decisions about water diversions. As a result, current

113 scientific understanding of the SFE population is largely derived from correlation-based analyses
114 of abundance indices (Stevens and Miller 1983; Jassby et al. 1995; Kimmerer 2002b),
115 evaluations of the catch data that underlie those indices (Rosenfield and Baxter 2007; Kimmerer
116 et al. 2009; La Tour 2015), and the presumption (e.g., Moyle 2002) that the SFE population is
117 fundamentally similar to the better-researched, but landlocked, population in Lake Washington,
118 Washington, USA (Chigbu 2000).

119 Longfin Smelt is also one of several fishes of the SFE that have shown a strong and
120 persistent association between juvenile production and freshwater flow variation experienced
121 early in their life cycle (Stevens and Miller 1983; Jassby et al. 1995; Kimmerer 2002b;
122 Rosenfield and Baxter 2007; Thomson et al. 2010; Maunder et al. 2015), but little attention has
123 been given to whether and how freshwater flow rates might affect Longfin Smelt production
124 beyond their first year of life. It is also well established that Longfin Smelt production per unit
125 of flow has declined (Kimmerer 2002b; Rosenfield and Baxter 2007; Thomson et al. 2010), but
126 with only one very recent exception (Maunder et al. 2015), researchers have not attempted to
127 evaluate SFE Longfin Smelt population dynamics in a classical spawner-recruit framework.

128 Food web alteration has been considered a primary factor contributing to the decline of
129 SFE Longfin Smelt, but the details of when and where prey production may limit recruitment
130 have not been determined and predation on SFE Longfin Smelt has not been studied so the role
131 of predators as a population driver can only be speculated on. The zooplankton assemblages that
132 Longfin Smelt likely prey upon began changing dramatically following the 1986 invasion of the
133 estuary by overbite clam, *Potamocorbula amurensis*. Changes included abrupt declines in
134 chlorophyll (Alpine and Cloern 1992), several crustaceans including mysid and decapod shrimps
135 (Kimmerer 2002b), and changes in the distribution (Kimmerer 2006; Sommer et al. 2011) and

136 diet composition (Feyrer et al. 2003; Nobriga and Feyrer 2008) of several fishes. In addition,
137 waste water ammonium limits the growth rate of diatoms in the SFE (Wilkerson et al. 2006),
138 which may be another, more gradually changing factor suppressing production of Longfin
139 Smelt's zooplankton prey.

140 Here we explore the population ecology of Longfin Smelt in the SFE in an attempt to
141 identify when during the life cycle (and by extension where) productivity has changed and how
142 changes through time in these productivity parameters may explain the long-term decline of this
143 Longfin Smelt population. To do this, we employ conceptually different variants of a standard
144 population modeling framework (the Ricker Model) to see which formulations of the model best
145 explain empirical trends. We did not attempt to develop a model that recreates Longfin Smelt
146 population dynamics precisely; rather, the objective of this study was to evaluate alternative
147 conceptual models of this species' population dynamics to better understand the forces that may
148 constrain its productivity during different phases of its life cycle. Specifically, we sought to (i)
149 identify factors that are correlated with productivity parameters in different life stages in order to
150 disaggregate the effect of changes in productivity at different life stages, so that (ii) future
151 research and management actions can focus on the Longfin Smelt life stages that have
152 experienced declines in productivity and the environmental variables that can be manipulated to
153 increase the production of those life stages.

154

155 Study Area

156 The SFE is formed by the confluence of two major California river systems, the
157 Sacramento and San Joaquin (Figure 1). These rivers meet in the Sacramento-San Joaquin Delta
158 (hereafter, Delta) and begin to mix with Pacific Ocean waters. This estuarine mixing intensifies

159 in a westward direction in the several embayments that comprise San Francisco Bay (Figure 1;
160 Jassby et al. 1995; Kimmerer et al. 2013). Some portion of Central San Francisco Bay, nearest
161 to the Bay's outlet to the Pacific Ocean, is usually close to marine salinity (≥ 30 psu). In the
162 northern reach of the SFE from San Pablo Bay through the Delta, average salinity decreases from
163 west to east due to the influence of the freshwater flowing from the Central Valley's rivers
164 through the Delta. The Delta is a network of tidal fresh water channels from which large
165 quantities of water are exported to more arid parts of California for agricultural and municipal
166 use. The U.S. Central Valley Project has been exporting water to the San Joaquin Valley since
167 1951 and the State Water Project has been exporting water to the San Joaquin Valley and
168 municipalities in southern California since 1968. The historical changes associated with the
169 development of California's surface water supplies and the diversion of water from the Delta
170 have been reviewed extensively (Arthur et al. 1996; Enright and Culberson 2010; Cloern and
171 Jassby 2012).

172

173

Methods

174 Overview: Fisheries population-dynamic stock assessments have long relied on spawner-recruit
175 models (e.g., Ricker 1954). These mathematical tools link the production of new cohorts of fish
176 (recruits) to the available spawning stock, and often also attempt to explain residual variation in
177 recruitment using environmental covariates (Myers 1998). Fisheries stock assessments are
178 usually applied to harvested fishes, particularly in marine ecosystems. Although Longfin Smelt
179 is not targeted for harvest in the SFE, it is nonetheless useful to construct explicit spawner-recruit
180 relationships to evaluate different conceptual models of Longfin Smelt recruitment (*see also*
181 Maunder et al. 2015).

182 Our analysis was based on alternative formulations of the Ricker (1954) model.

183

$$184 \quad R = aSe^{-BS} \quad (1)$$

185

186 In this general formulation, R is the number (or biomass) of fish recruiting to a population, S is
187 the number (or biomass) of spawners, and a and B are parameters that are solved for; a is the
188 recruits-per-spawner, in essence, the slope of the spawner-recruit relationship near the origin,
189 and B interacts with a to adjust the intensity of density dependence between generations. We
190 developed alternative conceptual models of how SFE Longfin Smelt recruitment might best be
191 modeled using the Ricker model. We used a long-term and age-specific data series of Longfin
192 Smelt relative abundance in the SFE to parameterize alternative Ricker models by (i) screening
193 variables to predict a , (ii) screening variables to predict survival from Age-0 to Age-2 in order to
194 predict S , and (iii) finding values of B that constrained predictions of R to create a contrast with
195 model variants in which we did not apply this constraint. Then we simulated time series of
196 Longfin Smelt relative abundance using each alternative Ricker model, and compared the
197 simulations to a different empirical time series of Longfin Smelt relative abundance that was
198 measured independently of the one used to parameterize the models.

199

200 Alternative Conceptual Models of Longfin Smelt Recruitment: Five alternative conceptual models
201 of Longfin Smelt recruitment were evaluated (Table 1). All models had a recruits-per-spawner
202 term (a , or “a” in the alphanumeric codes that differentiate models in Table 1). One model (1abc)
203 compared Age-0 abundance from one generation to the next (i.e., a estimated recruits-per-
204 recruit) to evaluate whether Age-0 indices were sufficient to model long-term population

205 dynamics, a hypothesis that could be inferred from the numerous published analyses of Age-0
206 Longfin Smelt abundance indices (e.g., Stevens and Miller 1983; Jassby et al. 1995; Kimmerer
207 2002b; Thomson et al. 2010). If this one-stage model performed as well as models with two-life
208 stages (the four models with “2” in their alphanumeric code in Table 1), it would indicate that
209 Age-2 Longfin Smelt abundance is more or less determined by Age-0 production (i.e., that
210 survival from Age-0 to Age-2 was relatively invariant through the data series) and that the use of
211 a traditional two life-stage spawner-recruit model is not necessary to model Longfin Smelt
212 population dynamics in the SFE.

213 The four model variants that used two life-stages incorporated a term to estimate survival
214 between Age-0 and Age-2 to estimate S from predictions of R . These models differed in their
215 combination of an explicit density-dependent term for the spawner-to-recruit life–history
216 transition (indicated by a “b” in the model alphanumeric codes in Table 1) and in whether model
217 parameters were allowed to change through time (indicated by a “c” in model alphanumeric
218 codes). The relative importance of these terms in describing empirical patterns in Longfin Smelt
219 population abundance has ecological and management implications as they suggest different
220 mechanisms constraining population dynamics.

221
222 Data sources: The California Department of Fish and Wildlife (CDFW) conducts several trawl-
223 based surveys of fisheries resources in the SFE (<https://www.wildlife.ca.gov/Regions/3>).
224 Longfin Smelt has been commonly collected in most of these surveys and CDFW generates
225 indices of Longfin Smelt relative abundance from some of the surveys (Stevens and Miller 1983;
226 Rosenfield and Baxter 2007). Here, we use data from the San Francisco Bay Study (SFBS),
227 which has been sampling since 1980, to generate spawner-recruit parameters. Then we

228 compared predictions made with these data to an estimate of Longfin Smelt relative abundance
229 from an independent data series, the Fall Midwater Trawl (FMWT). With the exceptions of
230 1974 and 1979, CDFW has generated unitless abundance indices of Longfin Smelt from the
231 FMWT data since 1967. The methodologies of these sampling programs have been reported
232 elsewhere (e.g., Stevens and Miller 1983; Rosenfield and Baxter 2007) and are not repeated here.
233 The key differences pertinent to this study are: (i) the SFBS and FMWT sampling grids overlap,
234 but the former samples further seaward and the latter samples further landward, (ii) SFBS
235 sampling occurs during all months of the year, but FMWT sampling occurs only during
236 September-December, (iii) the number of stations sampled in a month by the FMWT is
237 considerably higher than the SFBS (~ 100 versus ~ 35), (iv) the SFBS deploys both a bottom-
238 oriented otter trawl and a midwater trawl at each sampling station, whereas the FMWT uses only
239 a midwater trawl, and (v) CDFW calculates age-specific indices of Longfin Smelt relative
240 abundance from the SFBS, but only one index from the FMWT that is essentially an Age-0 index
241 (Table 2).

242 The CDFW uses February-May catch data to generate an index of Age-2 Longfin Smelt
243 relative abundance for each of the sampling gears employed by the SFBS; May-October catch
244 data are used to generate abundance indices for Age-0 Longfin Smelt. For each age-class of
245 Longfin Smelt, we averaged the midwater and otter trawl indices generated from the SFBS to
246 produce unitless annual indices for each age-class (hereafter Bay Age-0 and Bay Age-2; Table
247 2). We combined indices from the two sampling gears because the SFBS midwater trawl was
248 not deployed in some years (Rosenfield and Baxter 2007), so the Bay Age-0 and Bay Age-2
249 provided us with continuous time series of Longfin Smelt relative abundance for 1980-2013. We
250 did not attempt to estimate missing data (missing values were replaced with a zero before taking

251 the average) because it was possible that estimating missing values would be no more accurate
252 than simply treating missing data as zeroes. These choices reflect a trade-off between long-term
253 data availability and the timing of peak Longfin Smelt catches (Rosenfield and Baxter 2007).

254
255 *Selection of Environmental Covariates:* We developed one freshwater flow variable and three
256 water quality variables to use as candidate predictors of Longfin Smelt's life stage transitions.
257 Following Rosenfield and Baxter (2007), we used monthly means of the Net Delta Outflow
258 Index (hereafter Delta outflow; <http://www.water.ca.gov/dayflow/>) to represent the commonly
259 reported influence of freshwater flow on Longfin Smelt. Delta outflow is the estimated net
260 tidally-filtered river flow passing Chipps Island (Figure 1) and the freshwater flow variable that
261 most directly influences salinity distribution in the SFE's river channels and embayments (Jassby
262 et al. 1995; Kimmerer et al. 2013). These open-water habitats comprise the major larval rearing
263 areas for Longfin Smelt (Dege and Brown 2004; Hobbs et al. 2006). We calculated the monthly
264 mean outflow for December-May because these months fully overlap the spawning and larval
265 rearing phases of Longfin Smelt's life cycle in the SFE (CDFW unpublished data) and outflow in
266 these months is typically greater and more variable than in other months. As a result, outflow
267 during these months is most likely to influence the fate of Longfin Smelt (Jassby et al. 1995;
268 Kimmerer et al. 2013). Estuarine hydrodynamics are also influenced greatly during droughts,
269 which also influence the fate of Longfin Smelt (Rosenfield and Baxter 2007). The Delta outflow
270 data were available for 1956-2013 and we converted monthly means into metric units, $\text{m}^3 \cdot \text{s}^{-1}$.

271 We also used monthly means of water temperature ($^{\circ}\text{C}$) and water transparency (Secchi
272 disk depth in cm) from all available data collected by the SFBS. The water temperature data
273 provided to us by CDFW were available from 1980-2011, while the water transparency data

274 were available from 1980-2013. We calculated monthly means of these two water quality
275 variables for February-May (the indexing period for Age-2 Longfin Smelt). During February
276 through May, Age-0 Longfin Smelt are primarily in larval stages with a center of distribution
277 near the estuary's 2 psu isohaline (Dege and Brown 2004).

278 We summarized the Delta outflow, water temperature, and water transparency data
279 separately using Principal Components Analyses (PCA) on the z-scored monthly means. We
280 used PCA because sequential monthly means of flow and water quality variables can be closely
281 correlated due to California's seasonal climate and high year to year variation in precipitation.
282 This covariation makes it difficult to determine what averaging periods best reflect mechanistic
283 linkages between environmental conditions and Longfin Smelt production. We used the first
284 principal component scores from each PCA (Table 2) as candidate predictors of Longfin Smelt
285 recruits-per-spawner in the regression analyses described below.

286
287 Derivation of recruits-per-spawner (a): We represented a using either the ln-transformed ratio
288 Bay Age-0_{t=0}/Bay Age-0_{t=2} (for the one life-stage model; 1abc), or the ln-transformed ratio Bay
289 Age-0_{t=0}/Bay Age-2_{t=0} (for all four of the two life-stage models). We performed multiple linear
290 regression analyses to screen candidate predictors of a in an information-theoretic framework
291 and evaluated predictors using the corrected Akaike Information Criterion (AIC_c) to develop a
292 smaller set of statistically defensible covariates. Regression analyses were conducted separately
293 for each version of the response variable and had to be conducted separately for tests involving
294 water temperature variables due to the smaller data set mentioned above. The candidate
295 predictors and their assumed mechanistic meanings are provided in Table 3.

296 During our analyses, we discovered that the relationship between our Delta outflow
297 variable and the two life-stage version of $\ln(a)$ was not linear. We used LOESS regression to
298 depict the empirical shape of the relationship between these variables and found the LOESS
299 prediction to be very similar to a second order polynomial fit. We used AIC_c to confirm a
300 polynomial fit was better supported than a linear fit and then used the polynomial regression to
301 predict a in our model variants with two life-stages because that equation was far simpler to
302 implement than the LOESS equation.

303
304 Derivation of spawners-per-recruit (S): In models 2a, 2ab, 2ac, and 2abc, we estimated a relative
305 abundance of Age-2 Longfin Smelt to predict the relative abundance of the next generation of
306 Age-0 fish. We did this by deriving an estimator of survival from Age-0 to Age-2 ($S_{0 \rightarrow 2}$) and
307 multiplying estimates of R by this survival term to estimate the next generation of spawners (S).
308 We estimated $S_{0 \rightarrow 2}$ as the ln-transformed ratio Bay Age-2_{t=0}/Bay Age-0_{t-2} (i.e., the two SFBS
309 indices for the same cohort of fish) and tested a set of candidate predictor variables of this ratio,
310 following the same analytical approach used to predict a . For this analysis, we also included the
311 birth year FMWT index as a candidate predictor (Table 3) to evaluate whether juvenile survival
312 might be density-dependent given similar findings for several other SFE fishes (Kimmerer et al.
313 2000; Moyle et al. 2004; Bennett 2005).

314
315 Derivation of the exponent term (e^{-BS}): In order to evaluate whether density-dependence may also
316 affect R , we imposed a carrying capacity on the models identified with a “b” in their
317 alphanumeric codes (Table 1). Inclusion or exclusion of the e^{-BS} term allowed us to investigate
318 whether interannual variation in environmental conditions was sufficient to produce a natural

319 limit on the production of Age-0 Longfin Smelt (models 2a and 2ac), or conversely whether an
320 explicit carrying capacity provides for better fitting models (models 1abc, 2ab, 2abc). To do this,
321 we found values for B that reflected empirical relative abundance maxima given our estimates of
322 a . The maximum FMWT index for Longfin Smelt was 81,737 in 1967. The maximum a ,
323 indexed as Bay Age-0_{t=0}/Bay Age-0_{t=2} was 59 in 1995. We rounded these values up slightly and
324 found a value of B that, when multiplied by hypothetically increasing numbers of spawners
325 would limit the ability for our one life-stage model (model 1abc) to predict FMWT indices
326 greater than 82,000 when a was 60. Similarly for the two life-stage models, the maximum
327 observed a (indexed as Bay Age-0_{t=0}/Bay Age-2_{t=0}) for the ten years with highest Age-2
328 abundance was 168 in 1982. We rounded these values up slightly to calculate a value of B that
329 would limit the ability of simulations from these two life-stage models to predict FMWT indices
330 greater than 82,000 when a was 170.

331

332 *Evaluating changes in population model parameters assumed to result from changes in the SFE*
333 *food web*: The feeding habits of juvenile Longfin Smelt are basically undescribed in the SFE,
334 particularly for individuals foraging in mesohaline to marine waters (but see Hobbs et al. 2006
335 for data on larvae inhabiting the low-salinity zone). Hypothesized changes in Longfin Smelt
336 foraging success are either abrupt (e.g., due to the invasion of the overbite clam) or gradual and
337 continuous (e.g., due to altered nutrient concentrations or changes in water transparency). We
338 explored the predictive power of several temporal variables as surrogates for food web changes
339 in the regression analyses (Table 3). Specifically, Kimmerer (2002b) used 1987 as a change
340 point associated with invasion of the overbite clam; we used a step-decline in that year as a
341 predictor variable for a in model 1abc because fish spawned in 1987 would have been the first

342 ones to be impacted by the high density of clams detected in that year and thereafter. However,
343 Thomson et al. (2010) found that evidence for a step-decline in Longfin Smelt relative
344 abundance was strongest between 1989 and 1991. In our two-life stage models, we tested step-
345 declines in survival in 1989 and 1991; fish spawned in 1987 would have reached adulthood in
346 1989 and that is when one would first expect to see an effect of the clam on $S_{0 \rightarrow 2}$. We also
347 screened “year” as a predictor variable to test for the possibility that trends in survival were not
348 well represented as step-declines (Table 3).

349
350 Spawner-recruit simulations: Using each of the five alternative spawner-recruit models, we
351 generated 58-year time series of predicted Longfin Smelt FMWT indices (1958-2013). We
352 started each simulation by seeding 1956 and 1957 with the median observed FMWT index for
353 Longfin Smelt (798). After 1957, the simulations predicted all Longfin Smelt abundance indices
354 on their own through water year 2013. The simulations were stochastic; each year of each
355 simulation was iterated 1,000 times, using randomly drawn values of every regression parameter,
356 in which the parameter estimate was assumed to be the mean and the standard error was used to
357 scale the random variability. We restricted the simulations such that juvenile survival had to
358 remain ≤ 1 (i.e., $\leq 100\%$). This is an extremely high upper limit on survival, but it is not greatly
359 beyond the observed data; the index ratio we used to represent survival had a maximum
360 empirical value of 0.98 in 2012.

361 We evaluated model variants based on their ability to predict the empirical FMWT time
362 series and by the frequency with which they produced results that were clearly spurious. Each of
363 the resulting 5,000 simulations was compared to the empirical FMWT indices by calculating its
364 mean square error (MSE). Recall that FMWT data were available 1967-1973, 1975-1978, and

1980-2013, so we extracted those years from our simulations for this comparison. The central 95% of MSE estimates (i.e., 950 of the 1,000 iterations) were summarized using boxplots. We also evaluated the relative performance of model variants with the lowest MSEs by summarizing how frequently they had predicted Longfin Smelt quasi-extinction, which we define here as a FMWT index < 1 (the lowest empirical FMWT index was 13 in 2007). Lastly, we summarized the time series predictions from the best-performing models graphically to show more explicitly how they had performed relative to the observed FMWT abundance index time series.

Results

The first principal components (PC1s) for Delta outflow, water transparency, and water temperature had eigenvalues of 3.5, 2.0, and 1.5, respectively, and explained 58%, 50%, and 37% of the variance in the time trends of these variables. The PC1s for Delta outflow and water transparency were highly concordant with multi-month means of each year (Delta outflow Pearson $r = 0.99$, and water transparency Pearson $r = 0.98$). In contrast, the PC1 for water temperature was not correlated with mean water temperature (Pearson $r = 0.17$) and instead reflected variation within years; PC1 of temperature segregated years with relatively large temperature changes between winter and spring (i.e., cool February-March, warm April-May) from years with less seasonal variation. Therefore, we tested both the PC1 of water temperature and mean water temperature as candidate predictor variables for a and $S_{0.5}$.

Recruits-per-spawner: The linear regression analyses used to screen candidate predictor variables indicated positive effects of Delta outflow PC1 and the binary step change at 1987 as predictors of a for use in model 1abc (Table 4). The step change variable was only marginally

388 significant ($P = 0.07$) and opposite in sign to our expectation (i.e., a was predicted to increase
389 after 1987). The final model selected was $\ln(a) = 0.596 \pm 0.146(\text{Delta outflow PC1}) +$
390 $1.54 \pm 0.829(\text{Step-decline}_{1987}) - 1.39 \pm 0.748$. The analogous analyses for models 2a, 2ab, 2ac, and
391 2abc supported only the use of Delta outflow PC1 as a predictor of a ; in this case a nonlinear fit
392 was better supported than a linear fit (Table 4). The final model selected was $\ln(a) = -$
393 $0.148 \pm 0.049(\text{Delta outflow PC1})^2 + 0.954 \pm 0.152(\text{Delta outflow PC1}) + 2.94 \pm 0.303$; neither
394 linear nor nonlinear fits showed evidence of a monotonic residual time trend (Figure 2).

395
396 *Juvenile Survival:* The linear regression analyses used to screen candidate predictor variables of
397 $S_{0 \rightarrow 2}$ strongly supported the use of the birth year FMWT index (Table 5), suggesting that juvenile
398 survival is density-dependent. All of the temporal variables we tested were also statistically
399 significant (or nearly so). Interestingly, the 1989 step-decline performed poorly ($\text{AIC}_c = 103$)
400 compared to “year” ($\text{AIC}_c = 99.6$) and the 1991 step-decline ($\text{AIC}_c = 95.4$). The final model
401 selected was $\ln(S_{0 \rightarrow 2}) = -0.630 \pm 0.114(\ln\text{FMWT}) - 1.68 \pm 0.474(\text{Step-decline}_{1991}) + 3.19 \pm 1.03$.

402
403 *Model Evaluation:* The MSEs of most models overlapped at least somewhat, but two of the five
404 (models 2a and 2ac) had notably poorer fits to the FMWT data, producing higher MSEs 63% to
405 100% of the time (Figure 3). Thus, it appears that an explicit carrying capacity on R is a useful
406 model construct. The MSEs of models 1abc, 2ab, and 2abc were strongly overlapping (Figure 4)
407 suggesting that each provided a similar fit to the FMWT data. Compared to models 2ab and
408 2abc, model 1abc showed comparatively low variation in MSE among model iterations (Figure
409 4), but that low variability reflected this model’s rapid predictions of quasi-extirpation in 100%
410 of the iterations (Figure 5). Thus, although it appeared to have a comparatively good fit to the

411 FMWT data, model 1abc was clearly unreliable. By design, models 2ab and 2abc are equivalent
412 until the 1991 step-decline implemented in the latter. Thus, FMWT predictions using these
413 models were nearly equivalent from 1967-1990 (Figure 6). Median FMWT predictions using
414 model 2ab were closer to the empirical data from 1991-1994; thereafter, the median predictions
415 using model 2ab systematically overestimated the observed FMWT time series and the median
416 predictions from model 2abc were closer to the empirical data (Figure 6). As a result, the
417 median predictions of model 2abc provided a better overall representation of the empirical
418 FMWT indices (compare Figure 6D to Figure 6B); however, predictions from both models
419 strongly overlapped in each year of the simulation (Figure 6A and Figure 6C), making it
420 impossible to conclude that one outperformed the other. In addition, both models 2ab and 2abc
421 considerably underpredicted the FMWT indices and were non-linearly related to them (Figure
422 6B,D), suggesting that our e^{-BS} term was too strongly density-dependent.

423

424

425

Discussion

426

427

428

429

430

431

432

Relying on a few well-supported assumptions about Longfin Smelt life-history and ecology in the SFE, our two best-supported Ricker models both incorporated two life-stages in which productivity was density-dependent in each of the life stage transitions, and recruits-per-spawner was related to freshwater flow rates. Apparently, despite differences in geographic extent, timing, and sampling gears, the SFBS and FMWT sampling programs detect the same general patterns in Longfin Smelt population dynamics, and our Ricker model-based analyses indicated there are (at least) two important, but temporally distinct population dynamic effects;

433 an influence of fresh water flow on the production of Age-0 fish, and density-dependent and
434 possibly declining juvenile survival.

435

436 *Implications of spawner-recruit dynamics:* The influence of freshwater flow on the production
437 of Age-0 Longfin Smelt has been recognized for several decades (Stevens and Miller 1983;
438 Jassby et al. 1995; Rosenfield and Baxter 2007) albeit not with the nonlinearities that we found
439 evidence for (Table 4; Figure 2). Depending on its timing and magnitude, freshwater flow can
440 have both positive and negative effects on the recruitment of Age-0 Longfin Smelt in Lake
441 Washington (Chigbu 2000). We found no evidence that the ratio we used to depict recruits-per-
442 spawner has declined over time and thus, it does not appear that food web changes have
443 impacted this life stage transition. However, there is some suggestion of a cyclical pattern
444 among the residuals (Figure 2), which might be evidence for an ocean influence on Longfin
445 Smelt recruitment in the SFE (sensu Feyrer et al. 2015). This possibility warrants further
446 research. Improving scientific understanding of when freshwater flow modulates Longfin Smelt
447 production may help to reveal the flow-related mechanisms at work and the area where these
448 mechanisms function. Focusing on the time and place where freshwater flow is likely to have its
449 effect on recruitment may assist managers of the Central Valley hydro-system to optimize
450 freshwater flow rates to benefit Longfin Smelt production.

451

452 *Implications of Juvenile Survival:* We found no indication that freshwater flow moderated
453 the survival of Longfin Smelt between Age-0 and Age-2, a result that is consistent with
454 Kimmerer et al. (2009), but we did find evidence that survival in this life stage transition is
455 density-dependent (Table 5). In contrast to the production of Age-0 fish, there was some

456 evidence for continuous and step-declines in the survival of juvenile Longfin Smelt, which may
457 reflect food web-related impacts on this older life stage. Several other studies have detected one
458 or more step declines in overall Longfin Smelt production (Kimmerer 2002b; Thomson et al.
459 2010) and Rosenfield and Baxter (2007) noted an age-specific decline in production between
460 Age-0 and spawning-aged Longfin Smelt, which occurred sometime during the severe drought of
461 1987-1994. However, based on our spawner-recruit modeling, it was not possible to statistically
462 distinguish between the model that allowed survival rates to change (model 2abc) from one in
463 which survival did not change directionally (Model 2ab; Figures 4 and 6).

464 Constraining the timing and location of density-dependence and declining Longfin Smelt
465 survival may help to identify mechanisms controlling these parameters. The forces creating
466 density-dependent survival and possible declines in that survival are most likely to operate
467 between the timing of sampling that produces indices of Age-0 abundance (May-October in year
468 0) and Age-2 abundance (February-May). Most SFE Longfin Smelt spend most of this part of
469 their life-cycle in mesohaline or marine waters (Rosenfield and Baxter 2007), so it is more likely
470 that the mechanisms affecting juvenile survival also operate in mesohaline or marine
471 environments than mechanisms operating in fresh to low-salinity zone waters.

472
473 Implications for Forage Fish Management in the SFE: Our results support some emerging
474 generalizations about fish recruitment in the SFE. The results of the present study suggest that
475 the general life cycle model for Longfin Smelt is very similar to what has been reported for
476 Striped Bass (Kimmerer et al. 2000) and Sacramento Splittail *Pogonichthys macrolepidotus*
477 (Moyle et al. 2004). In each of these species, freshwater flow variation has been linked to
478 productivity early in the life-cycle, an effect subsequently tempered by density-dependent

479 survival in the juvenile life-stage. Density-dependent survival may seem paradoxical in a
480 declining fish species like Longfin Smelt, but fisheries recruitment theory has demonstrated how
481 density-dependent 'looking' spawner-recruit relationships can arise from food web-related
482 mechanisms that are not reflective of populations limiting their own resource base (Walters and
483 Juanes 1993).

484 The SFE population of Longfin Smelt is in the queue to potentially be listed under the
485 U.S. Endangered Species Act (Federal Register, 77 FR 19755). By disaggregating life-stage
486 specific constraints on population dynamics, this study can help inform a future ESA listing
487 decision for Longfin Smelt and development of the accompanying recovery plan if the
488 population is listed. Perhaps more importantly, this study helps to identify where in the life-
489 cycle fish productivity is limited and may be changing over time, potentially informing research
490 and monitoring efforts into Longfin Smelt recruitment limitation. The persistence of Longfin
491 Smelt and several other native forage fish species in the SFE, and potentially the predators that
492 historically relied on these populations (e.g., Striped Bass and Pacific Halibut *Paralichthys*
493 *californicus*), depends on taking steps to improve the productivity of these fishes.

494

495 **Acknowledgments**

496 This study emerged from work done by the authors for the Bay-Delta Conservation Plan. The
497 viewpoints expressed are those of the authors and do not necessarily reflect the opinions of the
498 U.S. Department of the Interior or the U.S. Fish and Wildlife Service. We thank A. Weber-
499 Stover for help assembling and reviewing an early draft of the manuscript and K. Sun for
500 generating Figure 3. R. Baxter provided the San Francisco Bay Study data. The comments of
501 three anonymous reviewers and the AE are greatly appreciated.

502

503 **Literature Cited**

504

505 Alder, J., B. Campbell, V. Karpouzi, K. Kaschner, and D. Pauly. 2008. Forage Fish: From
506 Ecosystems to Markets Annual Review of Environment and Resources. 33: 153-166.

507

508 Alpine, A. E., and J. E. Cloern. 1992. Trophic interactions and direct physical effects control
509 phytoplankton biomass and production in an estuary. *Limnology and Oceanography*
510 37:946–955.

511

512 Arthur, J. F., Ball, M. D., & Baughman, S. Y. (1996). *Summary of federal and state water*
513 *project environmental impacts in the San Francisco Bay-Delta Estuary, California*. San
514 Francisco State University.

515

516 CDFW (California Department of Fish and Wildlife). 2009. Report to the Fish and Game
517 Commission: a status review of the longfin smelt (*Spirinchus thaleichthys*) in California.
518 Available at: <http://www.dfg.ca.gov/delta/projects.asp?ProjectID=LONGFINSMELT>

519

520 Chigbu, P. 2000. Population biology of Longfin Smelt and aspects of the ecology of other major
521 planktivorous fishes in Lake Washington. *Journal of Freshwater Ecology* 15: 543-557.

522

523 Cloern, J. E., and A. D. Jassby. 2012. Drivers of change in estuarine-coastal ecosystems:
524 Discoveries from four decades of study in San Francisco Bay. *Reviews of Geophysics*
525 50.4. RG4001, doi:10.1029/2012RG000397.

526

527 Cury, P. M., and 13 co-authors. 2011. Global seabird response to forage fish depletion—one-third
528 for the birds. *Science* 334: 1703-1706.

529

530 Dege, M., and L. R. Brown. 2004. Effect of outflow on spring and summertime distribution and
531 abundance of larval and juvenile fishes in the upper San Francisco Estuary. *American*
532 *Fisheries Society Symposium* 39:49-66.

533

534 Enright, C. and S. Culberson. 2010. Salinity trends, variability, and control in the northern reach
535 of the San Francisco Estuary. *San Francisco Estuary and Watershed Science* [online
536 serial] 7: <http://escholarship.org/uc/item/0d52737t>

537

538 Essington, T. E., and S. Hansson. 2004. Predator-dependent functional responses and interaction
539 strengths in a natural food web. *Canadian Journal of Fisheries and Aquatic Sciences*
540 61:2215-2226.

541

542 Feyrer, F., J. E. Cloern, L. R. Brown, M. A. Fish, K. A. Hieb, and R. D. Baxter. 2015. Estuarine
543 fish communities respond to climate variability over both river and ocean basins. *Global*
544 *Change Biology*. In press.

545 Feyrer, F., B. Herbold, S. A. Matern, and P. B. Moyle. 2003. Dietary shifts in a stressed fish
546 assemblage: consequences of a bivalve invasion in the San Francisco Estuary.

547

548 *Environmental Biology of Fishes* 67:277-288.

- 549 Genin, A. 2004. Bio-physical coupling in the formation of zooplankton and fish aggregations
550 over abrupt topographies. *Journal of Marine Systems* 50: 3-20.
551
- 552 Gillson, J. 2011. Freshwater flow and fisheries production in estuarine and coastal systems:
553 where a drop of rain is not lost. *Reviews in Fisheries Science* 19: 168-186.
554
- 555 Hall, C.J., A. Jordaan, and M.G. Frisk. 2012. Centuries of Anadromous Forage Fish Loss:
556 Consequences for Ecosystem Connectivity and Productivity. *BioScience* 62 (8): 723-731
557
- 558 Hobbs, J. A., W. A. Bennett, and J. E. Burton. 2006. Assessing nursery habitat quality for native
559 smelts (*Osmeridae*) in the low-salinity zone of the San Francisco Estuary. *Journal of Fish*
560 *Biology* 69:907-922.
561
- 562 Hughes, B. B., M. D. Levey, J. A. Brown, M. C. Fountain, A. B. Carlisle, S. Y. Litvin, C. M.
563 Greene, W. N. Heady, and M. G. Gleason. 2014. Nursery functions of U.S. west coast
564 estuaries: the state of knowledge for juveniles of focal invertebrate and fish species. *The*
565 *Nature Conservancy*, Arlington, VA. 168pp
566
- 567 Jassby, A. D., W. J. Kimmerer, S. G. Monismith, C. Armor, J. E. Cloern, T. M. Powell, J. R.
568 Schubel, and T. J. Vendlinski. 1995. Isohaline position as a habitat indicator for estuarine
569 populations. *Ecological Applications* 5:272-289.
570
- 571 Katz, J., P. B. Moyle, R. M. Quiñones, J. Israel, and S. Purdy. 2013. Impending extinction of
572 salmon, steelhead, and trout (*Salmonidae*) in California. *Environmental Biology of Fishes*
573 96: 1169-1186.
574
- 575 Kennish, M. J. 2002. Environmental threats and environmental future of estuaries.
576 *Environmental Conservation* 29:78-107.
577
- 578 Kimmerer, W. J. 2002a. Physical, biological, and management responses to variable freshwater
579 flow into the San Francisco Estuary. *Estuaries* 25:1275-1290.
580
- 581 Kimmerer, W. J. 2002b. Effects of freshwater flow on abundance of estuarine organisms:
582 Physical effects or trophic linkages? *Marine Ecology Progress Series* 243:39-55.
583
- 584 Kimmerer, W. J. 2006. Response of anchovies dampens effects of the invasive bivalve *Corbula*
585 *amurensis* on the San Francisco Estuary food web. *Marine Ecology Progress Series* 324:
586 207-218.
587
- 588 Kimmerer, W. J., J. H. Cowan, Jr., L. W. Miller, and K. A. Rose. 2000. Analysis of an estuarine
589 striped bass population: influence of density-dependent mortality between metamorphosis
590 and recruitment. *Canadian Journal of Fisheries and Aquatic Sciences* 57: 478-486.
591
- 592 Kimmerer, W.J., E.S. Gross, and M.L. MacWilliams. 2009. Is the response of estuarine nekton to
593 freshwater flow in the San Francisco Estuary explained by variation in habitat volume?
594 *Estuaries and Coasts* 32: 375-389.

- 595
596 Kimmerer, W. J., M. L. Mac Williams, and E. S. Gross. 2013. Variation of fish habitat and
597 extent of the low-salinity zone with freshwater flow in the San Francisco Estuary. San
598 Francisco Estuary and Watershed Science [online serial] 11:
599 <http://escholarship.org/uc/item/3pz7x1x8>
600
- 601 Kratina, P., R. Mac Nally, W. J. Kimmerer, J. R. Thomson, and M. Winder. 2014. Human-
602 induced biotic invasions and changes in plankton interaction networks. Journal of
603 Applied Ecology 51: 1066-1074.
604
- 605 Lotze, H. K., H. S. Lenihan, B. J. Bourque, R. H. Bradbury, R. G. Cooke, M. C. Kay, S. M.
606 Kidwell, M. X. Kirby, C. H. Peterson, and J. B. C. Jackson. 2006. Depletion, degradation,
607 and recovery potential of estuaries and coastal seas. Science 312:1806-1809.
608
- 609 Maunder, M. N., R. B. Deriso, and C. H. Hanson. 2015. Use of state-space population dynamics
610 models in hypothesis testing: advantages over simple log-linear regressions for modeling
611 survival, illustrated with application to Longfin Smelt (*Spirinchus thaleichthys*). Fisheries
612 Research 164: 102-111.
613
- 614 Moyle, P. B. 2002. Inland Fishes of California Revised and Expanded. University of California
615 Press, Berkeley, CA.
616
- 617 Moyle, P. B., R. D. Baxter, T. Sommer, T. C. Foin, and S. A. Matern. 2004. Biology and
618 population dynamics of Sacramento splittail (*Pogonichthys macrolepidotus*) in the San
619 Francisco Estuary: a review. San Francisco Estuary and Watershed Science [online serial]
620 2: <http://escholarship.org/uc/item/61r48686>
621
- 622 Myers, R. A. 1998. When do environment-recruitment correlations work? Reviews in Fish
623 Biology and Fisheries 8:285-305.
624
- 625 Nobriga, M. L., and F. Feyrer. 2008. Diet composition in San Francisco Estuary Striped Bass:
626 does trophic adaptability have its limits? Environmental Biology of Fishes 83: 509-517.
627
- 628 North, E. W. and E. D. Houde. 2003. Linking ETM physics, zooplankton prey, and fish early
629 life-histories to striped bass *Morone saxatilis* and white perch *M. americana* recruitment.
630 Marine Ecology Progress Series 260: 219-236.
631
- 632 Peebles, E. B., S. E. Burghart, and D. J. Hollander. 2007. Causes of interestuarine variability in
633 bay anchovy (*Anchoa mitchelli*) salinity at capture. Estuaries and Coasts 30: 1060-1074.
634
- 635 Pikitch, E. K., and 19 co-authors. 2014. The global contribution of forage fish to marine fisheries
636 and ecosystems. Fish and Fisheries 15: 43-64.
637
- 638 Reum, J. C. P., T. E. Essington, C. M. Greene, C. A. Rice, and K. L. Fresh. 2011. Multiscale
639 influence of climate on estuarine populations of forage fish: the role of coastal upwelling,
640 freshwater flow and temperature. Marine Ecology Progress Series 425: 203-215.

- 641
642 Ricker, W. E. 1954. Stock and recruitment. *Journal of the Fisheries Board of Canada* 115: 559-
643 623.
- 644
645 Rosenfield, J. A. and R. D. Baxter. 2007. Population dynamics and distribution patterns of
646 Longfin Smelt in the San Francisco estuary. *Transactions of the American Fisheries*
647 *Society* 136:1577-1592.
- 648
649 Shan, X., P. Sun, X. Jin, X. Li, and F. Dai. 2013. Long-term changes in fish assemblage structure
650 in the Yellow River Estuary ecosystem, China. *Marine and Coastal Fisheries: Dynamics,*
651 *Management, and Ecosystem Science* 5: 65-78.
- 652
653 Sommer, T., F. Mejia, K. Hieb, R. Baxter, E. Loboschefskey, and F. Loge. 2011. Long-term shifts
654 in the lateral distribution of Age-0 Striped Bass in the San Francisco Estuary.
655 *Transactions of the American Fisheries Society* 140: 1451-1459.
- 656
657 Sommer, T., and 13 co-authors. 2007. The collapse of pelagic fishes in the upper San Francisco
658 Estuary (El colapso de los peces pelágicos en la cabecera del estuario San Francisco).
659 *Fisheries* 32(6): 270-277.
- 660
661 Stevens, D.E. and L.W. Miller. 1983. Effects of river flow on abundance of young Chinook
662 Salmon, American shad, Longfin Smelt, and Delta Smelt in the Sacramento-San Joaquin
663 River system. *North American Journal of Fisheries Management* 3:425-437.
- 664
665 Thomson, J. R., W. J. Kimmerer, L. R. Brown, K. B. Newman, R. Mac Nally, W. A. Bennett, F.
666 Feyrer, and E. Fleishman. 2010. Bayesian change point analysis of abundance trends for
667 pelagic fishes in the upper San Francisco Estuary. *Ecological Applications* 20:1431-1448.
- 668
669 Trathan, P. N., and 16 co-authors. 2015. Pollution, habitat loss, fishing, and climate change as
670 critical threats to penguins. *Conservation Biology*, 29: 31–41.
- 671
672 Turner, J. L., and H. K. Chadwick. 1972. Distribution and abundance of young-of-the-year
673 striped bass, *Morone saxatilis*, in relation to river flow in the Sacramento-San Joaquin
674 Estuary. *Transactions of the American Fisheries Society* 101: 442-452.
- 675
676 Vörösmarty, C. J., P. B. McIntyre, M. O. Gessner, D. Dudgeon, A. Prusevich, P. Green, S.
677 Glidden, S. E. Bunn, C. A. Sullivan, C. Reidy Liermann, and P. M. Davies. 2010. Global
678 threats to human water security and river biodiversity. *Nature* 467:555-561.
- 679
680 Walters, C. J., and F. Juanes. 1993. Recruitment limitation as a consequence of natural selection
681 for use of restricted feeding habitats and predation risk taking by juvenile fishes.
682 *Canadian Journal of Fisheries and Aquatic Sciences* 50: 2058-2070.
- 683
684 Wilkerson, F. P., Dugdale, R. C., Hogue, V. E., & Marchi, A. 2006. Phytoplankton blooms and
685 nitrogen productivity in San Francisco Bay. *Estuaries and Coasts*, 29: 401-416.
- 686

687 Table 1. Summary of five alternative Ricker models of Longfin Smelt recruitment in the San
 688 Francisco Estuary. The alphanumeric model codes are shorthand for the embedded hypotheses;
 689 the number represents the number of life stages explicitly modeled, “a” denotes that all five
 690 models include a recruits per spawner term, “b” denotes that a model has an explicit density
 691 dependent exponent (e^{-BS}), and “c” denotes that the model employs a time-dependent change in
 692 one or more parameters.

Model	Embedded Hypotheses
1abc	The trend in Age-0 relative abundance is sufficient to model long-term population dynamics; the production of Age-0 fish is density-dependent; survival has changed through time (e.g., due to changes in the estuary’s food web)
2a	Understanding the trend in Age-0 relative abundance requires explicit modeling of spawner and recruit relative abundance; the production of Age-0 fish is density independent; survival has not changed through time
2ab	Understanding the trend in Age-0 relative abundance requires explicit modeling of spawner and recruit relative abundance; the production of Age-0 fish is density dependent; survival has not changed through time
2ac	Understanding the trend in Age-0 relative abundance requires explicit modeling of spawner and recruit relative abundance; the production of Age-0 fish is density independent; survival has changed through time
2abc	Understanding the trend in Age-0 relative abundance requires explicit modeling of spawner and recruit relative abundance; the production of Age-0 fish is density dependent; survival has changed through time

693

694 Table 2. Time series of the first principal component (PC1) of principal components analyses (PCA) of available water quantity and
 695 quality variables, and Longfin Smelt indices of relative abundance used in this study. The PCAs on Delta outflow, water temperature,
 696 and water transparency were conducted on data for December-May, February-May, and February-May respectively. All abundance
 697 indices are unitless metrics of Longfin Smelt's relative abundance in the San Francisco Estuary. The Fall Midwater Trawl index is
 698 based on data collected during September-December. Bay indices are average results from the San Francisco Bay Study's two
 699 sampling gears; the Bay Age-0 index is based on data collected during May-October, and the Bay Age-2 index is based on data
 700 collected during February-May.

701

Water Year	Delta outflow PC1	Water temp PC1	Water transparency PC1	FMWT index	Bay Age-0 index	Bay Age-2 index
1956	2.77					
1957	-0.627					
1958	3.74					
1959	-1.14					
1960	-1.19					
1961	-1.29					
1962	-0.575					
1963	1.21					
1964	-1.5					
1965	1.3					
1966	-1.02					
1967	1.91			81,737		
1968	-1.12			3,279		
1969	2.68			59,350		
1970	0.928			6,515		
1971	0.152			15,903		
1972	-1.6			760		

1973	0.442			5,896		
1974	1.97			No data		
1975	-0.123			2,819		
1976	-1.93			658		
1977	-2.23			210		
1978	0.722			6,619		
1979	-1.05			No data		
1980	1.08	-1.22	-0.142	31,184	159,555	1,339
1981	-1.5	-0.651	-0.029	2,202	3,049	383
1982	3.04	-0.257	1.19	62,905	278,517	1,656
1983	5.91	-1.88	1.8	11,864	28,755	1,891
1984	0.492	-1.63	-1.56	7,408	36,774	4,924
1985	-1.67	0.222	-3.3	992	7,341	1,939
1986	1.71	-1.06	1.21	6,160	18,489	1,384
1987	-1.81	1.5	-0.68	1,520	2,428	1,785
1988	-1.97	0.335	-0.24	791	1,409	3,571
1989	-1.7	3.01	1.15	456	1,054	941
1990	-2.06	2.12	1.09	243	713	687
1991	-1.98	-1.43	2.33	134	188	351
1992	-1.88	2.18	-1.05	76	495	152
1993	0.006	-0.649	1.76	798	6,046	11
1994	-1.79	-0.06	0.379	545	1,424 ^a	414
1995	3.59	-1.57	0.885	8,205	354,186	252 ^a
1996	1.2	-0.451	-0.464	1,346	5,856	124 ^a
1997	1.6	0.627	1.25	690	7,638	1,432
1998	3.11	-2.06	3	6,654	41,729	605
1999	0.414	0.989	0.529	5,243	58,510	748
2000	0.036	-0.511	0.322	3,437	14,202	704
2001	-1.61	0.659	-0.329	247	1,460	1,158
2002	-1.35	1.37	-0.271	707	9,652	1,752
2003	-0.468	0.81	-0.229	467	2,119	739
2004	-0.514	0.852	0.268	191	2,418	686
2005	-0.235	-0.956	0.048	129	4,538	569

2006	3.79	0.371	-0.411	1,949	12,148	188
2007	-1.73	0.799	-1.56	13	2,039	447
2008	-1.67	-0.361	0.341	139	3,681	204
2009	-1.57	0.149	-0.857	65	647	272
2010	-1.17	-0.247	-0.529	191	748	197
2011	1.21	-0.996	-3.51	477	7,833	305
2012	-1.53		0.365	61	1,284	733
2013	-1.38		-2.76	164	8,495	300

702
703 ^aNo data for San Francisco Bay Study Midwater Trawl; value assumed to be zero in order to calculate the index shown in the table.

704 Table 3. Variables used as candidate covariates to predict Longfin Smelt recruits-per-spawner and survival from Age-0 to Age-2 and
 705 implied or explicit hypotheses associated with the use of each variable. SFBS indicates data from California Department of Fish and
 706 Wildlife's San Francisco Bay Study.
 707

Explanatory Variable	Data Source	Hypotheses for relationship to recruits per spawner	Hypotheses for relationship to survival from Age-0 to Age-2
PC1 for Delta outflow (m ³ ·s ⁻¹)	DAYFLOW [http://www.water.ca.gov/dayflow/]	Freshwater flow has a positive influence on survival of developing eggs, larvae, or early Age-0 fish	Freshwater flow has a positive influence on catchability of Age-2 fish or survival from Age-0 to Age-2 ^a
PC1 for water transparency (cm)	SFBS	Water transparency has a negative influence on survival of developing eggs, larvae, or early Age-0 fish	Water transparency has a negative influence on spatial distribution, catchability, or survival of Age-2 fish
PC1 for water temperature (°C)	SFBS	Intra-annual temperature change between winter and	Intra-annual temperature change between winter and spring has a

		spring has a negative influence on survival of developing eggs, larvae, or early Age-0 fish	negative influence on spatial distribution, catchability, or survival of Age-2 fish
Mean water temperature (°C)	SFBS	Temperature has a negative influence on survival of developing eggs, larvae, or early Age-0 fish	Temperature has a negative influence on spatial distribution, catchability, or survival of Age-2 fish
Year		Dummy variable to indicate an important variable with a continuous time trend had been missed (e.g., regional trends in Secchi disk depth, ammonium inhibition of phytoplankton growth rates)	Dummy variable that would indicate an important variable with a continuous time trend had been missed (e.g., regional trends in Secchi disk depth, ammonium inhibition of phytoplankton growth rates)
Step-decline		Binary variable reflecting the	Binary variable reflecting the

		discontinuous time trend	discontinuous time trend
		associated with some food web	associated with some food web
		impacts (e.g., linked to the	impacts had affected the survival
		overbite clam invasion) had	of fish older than Age-0.
		affected the survival of Age-0	
		fish.	
Fall Midwater Trawl	Fall Midwater Trawl survey	Not applicable	The abundance of Age-0 fish
index			affects subsequent survival

708 ^aThis hypothesis was tested by determining if survival from Age-0 to Age-2 could be better predicted by including flows occurring
709 during spawning, e.g., the ratio of Age-2 index in 1982/Age-0 fish in 1980 tested for an influence of the flow during 1982. The
710 influence of freshwater flow on the year in between birth and spawning was also tested, but not found to be statistically significant and
711 is not reported in this paper, for brevity.

712

713 Table 4. Results of linear regression analyses exploring candidate predictors of two versions of the Longfin Smelt recruits-per-
 714 spawner parameter in the San Francisco Estuary. In model 1abc, the response variable was the natural log of Bay-0_{t=0}/Bay-0_{t=2}. In the
 715 other models, the response variable was the natural log of Bay-0_{t=0}/Bay-2_{t=0}. The cells for each candidate predictor variable report if
 716 the variable was tested in each model step, its *p*-value when it was tested, and then whether it was dropped in subsequent steps based
 717 on its *p*-value. Note that the AIC_c from steps 1 and 2 cannot be compared to steps 3-5 due to the increase in sample size in the latter
 718 three steps.

	Step 1	Step 2	Step 3	Step 4	Step 5
1 Life-stage Model	Adj R ² = 0.26	Adj R ² = 0.26	Adj R ² = 0.31	Adj R ² = 0.32	Not applicable
(Model 1abc)	n = 30	n = 30	n = 32	n = 32	
	AIC _c = 124	AIC _c = 122	AIC _c = 127	AIC _c = 125	
Flow PC1	0.001	0.01	0.0005	0.0003	
Temperature PC1	Not tested	0.81	Dropped	Dropped	
Secchi depth PC1	Not tested	Not tested	0.56	Dropped	
Mean Temperature	0.68	Dropped	Dropped	Dropped	
Year	0.41	Dropped	Dropped	Dropped	
Step Decline 1987	Not tested	Not tested	0.06	0.07	

2 Life-stage Models	Adj R ² = 0.43	Adj R ² = 0.46	Adj R ² = 0.41	Adj R ² = 0.44	Adj R ² = 0.55
(Models 2a, 2ab,	n = 32	n = 32	n = 34	n = 34	n = 34
2ac, and 2abc)	AIC _c = 123	AIC _c = 120	AIC _c = 130	AIC _c = 126	AIC _c = 119
Flow PC1	0.00003	0.0007	0.00004	0.00001	6 · 10 ⁻⁷
Temperature PC1	Not tested	0.33	Dropped	Dropped	Dropped
Secchi depth PC1	Not tested	Not tested	0.46	Dropped	Dropped
Mean Temperature	0.66	Dropped	Dropped	Dropped	Dropped
Year	0.70	Dropped	Dropped	Dropped	Dropped
Step Decline 1987	Not tested	Not tested	0.62	Dropped	Dropped

719

720 |

721

722 Table 5. Results of linear regression analyses exploring candidate predictors of Longfin Smelt survival from Age-0 to Age-2 in the
 723 San Francisco Estuary. The response variable was the natural log of Bay-2_{t=0}/Bay-0_{t-2}. The cells for each candidate predictor variable
 724 report if the variable was tested in each model step, its *P*-value when it was tested, and then whether it was dropped in subsequent
 725 steps based on its *P*-value. Note that the AIC_c from steps 1 and 2 cannot be compared to steps 3-6 due to the increase in sample size in
 726 the latter three steps.

	Step 1	Step 2	Step 3	Step 4	Step 5	Step 6
Adjusted R ²	0.44	0.46	0.39	0.41	0.35	0.48
Sample size	n = 30	n = 30	n = 32	n = 32	n = 32	n = 32
AIC _c	94.1	91.5	102	99.6	103	95.4
ln(birth year FMWT index)	0.00009	0.00003	0.00005	0.00004	0.0002	0.000006
Flow PC1	0.38	Dropped	Dropped	Dropped	Dropped	Dropped
Temperature PC1	Not tested	0.44	Dropped	Dropped	Dropped	Dropped
Secchi depth PC1	Not tested	Not tested	0.78	Dropped	Dropped	Dropped
Mean temperature	0.99	Dropped	Dropped	Dropped	Dropped	Dropped
Year	0.005	0.004	0.01	0.01	Not tested	Not tested

Step decline at 1989	Not tested	Not tested	Not tested	Not tested	0.052	Not tested
Step decline at 1991	Not tested	0.001				

For Peer Review Only

727 Figures

- 728
- 729 1. Map of the San Francisco Estuary. The Pacific Ocean enters the estuary under the Golden Gate Bridge and
- 730 the Delta is the waterways to the east of Chipps Island. Sampling locations for California Department of
- 731 Fish and Wildlife monitoring stations are available at: <https://www.wildlife.ca.gov/Regions/3>.
- 732
- 733 2. Time series of residuals from three regression analyses of the first principal component of December-May
- 734 Delta outflow and the natural log of Longfin Smelt recruits (Age-0) per spawner (Age-2) in the San
- 735 Francisco Estuary.
- 736
- 737 3. Notched boxplots summarizing the central 95% of mean square error predictions of the Longfin Smelt Fall
- 738 Midwater Trawl index using five alternative spawner-recruit models. See Table 1 for descriptions of the
- 739 models. Where notches associated with MSE from difference models do not overlap, there is ‘strong
- 740 evidence’ their medians differ” (Quick R; <http://www.statmethods.net/graphs/boxplot.html>). The pairwise
- 741 proportions of overlapping MSE predictions from $n = 950$ model iterations are provided below the boxplot.
- 742
- 743 4. Notched boxplots summarizing the mean square error from the central 95% of predictions of the Longfin
- 744 Smelt Fall Midwater Trawl index from the two-best supported spawner-recruit models. See Table 1 for
- 745 descriptions of the models. Where notches associated with MSE from difference models do not overlap,
- 746 there is ‘strong evidence’ their medians differ” (Quick R; <http://www.statmethods.net/graphs/boxplot.html>).
- 747 The pairwise proportion of overlapping MSE predictions from $n = 950$ model iterations of models 2ab and
- 748 2abc are provided below the boxplot.
- 749
- 750 5. Time series showing the proportion of stochastic simulations of Longfin Smelt recruitment that predicted
- 751 quasi-extirpation (defined as predicted Fall Midwater Trawl index < 1.0) from three alternative spawner-
- 752 recruit models.
- 753
- 754 6. Time series of the Fall Midwater Trawl (FMWT) index for Longfin Smelt (solid line) and the two-best
- 755 supported spawner-recruit models (panel A is model 2ab, and panel C is model 2abc). Gray shading shows
- 756 the range of the central 95% of predictions and the dashed lines show the mean prediction from the $n = 950$

757 model iterations per year. Panels B and D are scatterplots of the FMWT index and the mean prediction
758 from models 2ab and 2abc, respectively.

759

For Peer Review Only

Figure 1

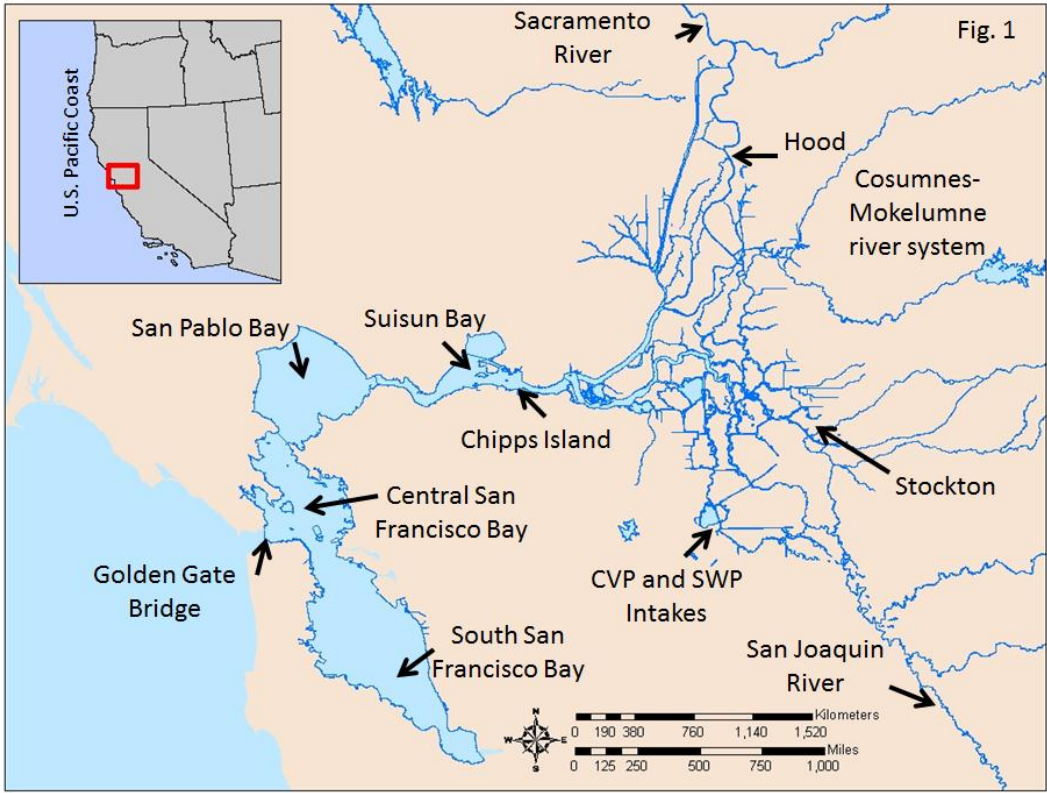


Figure 2

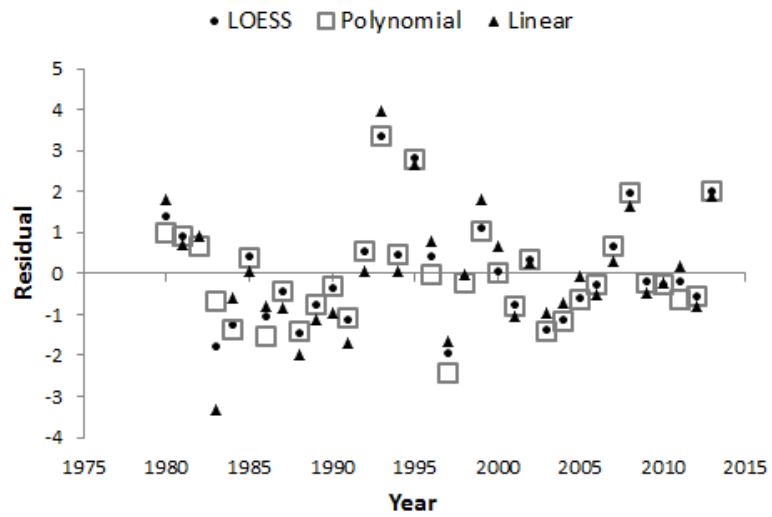


Figure 3

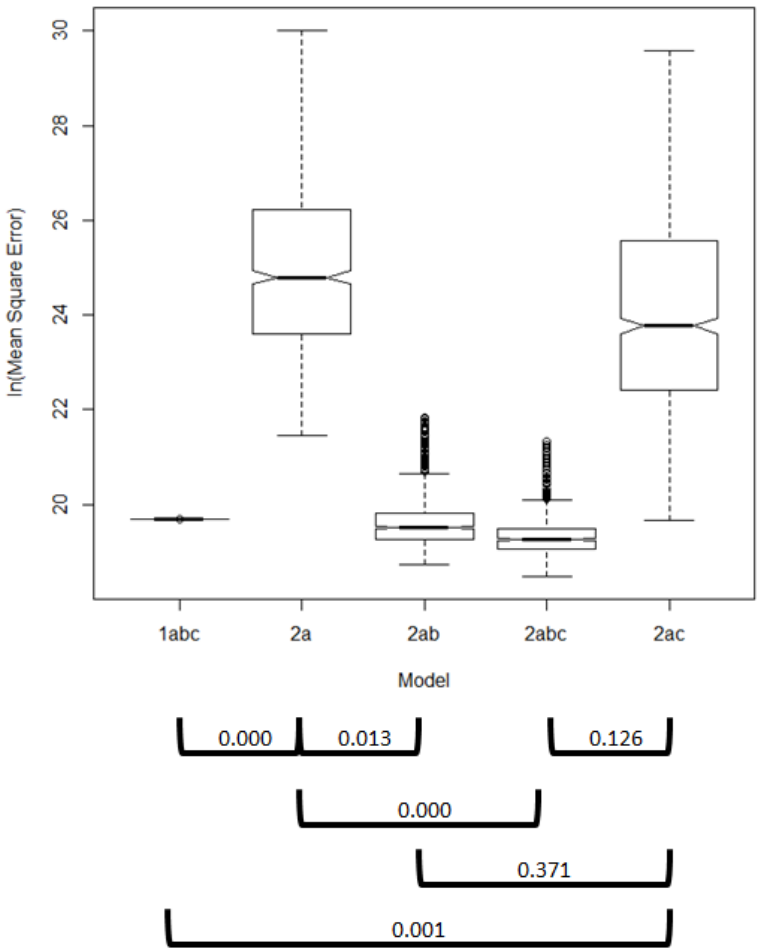


Figure 4

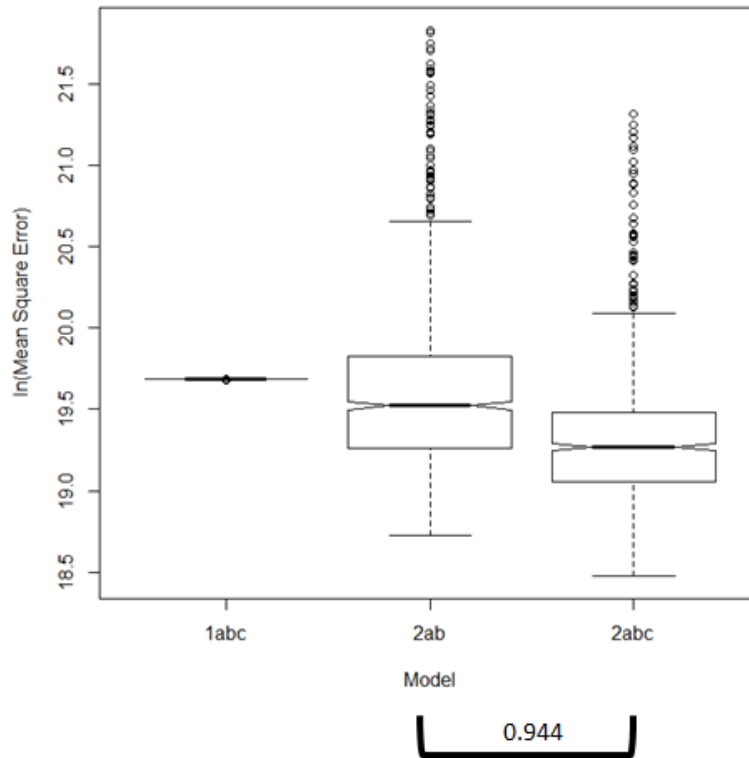


Figure 5

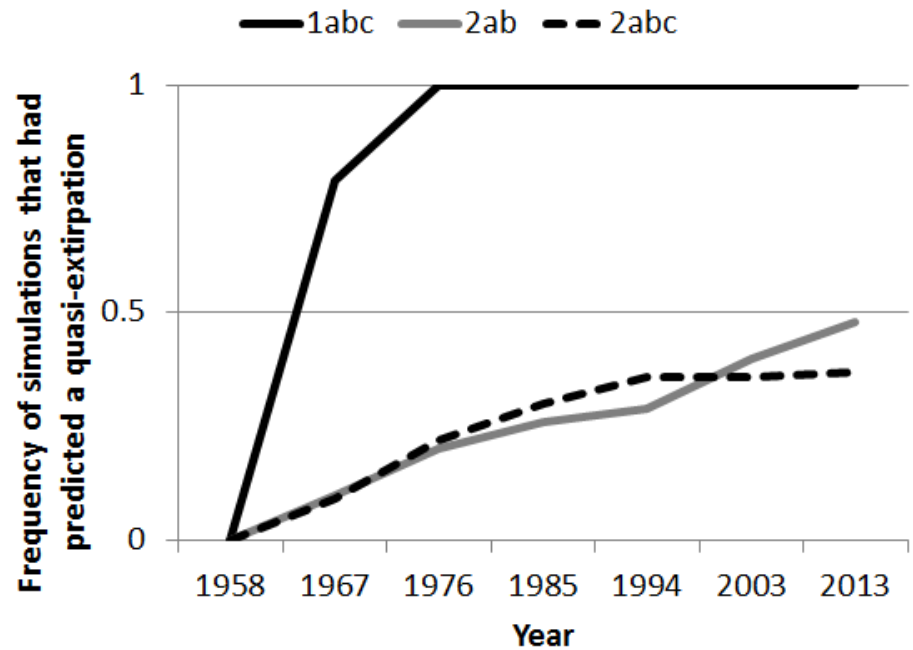
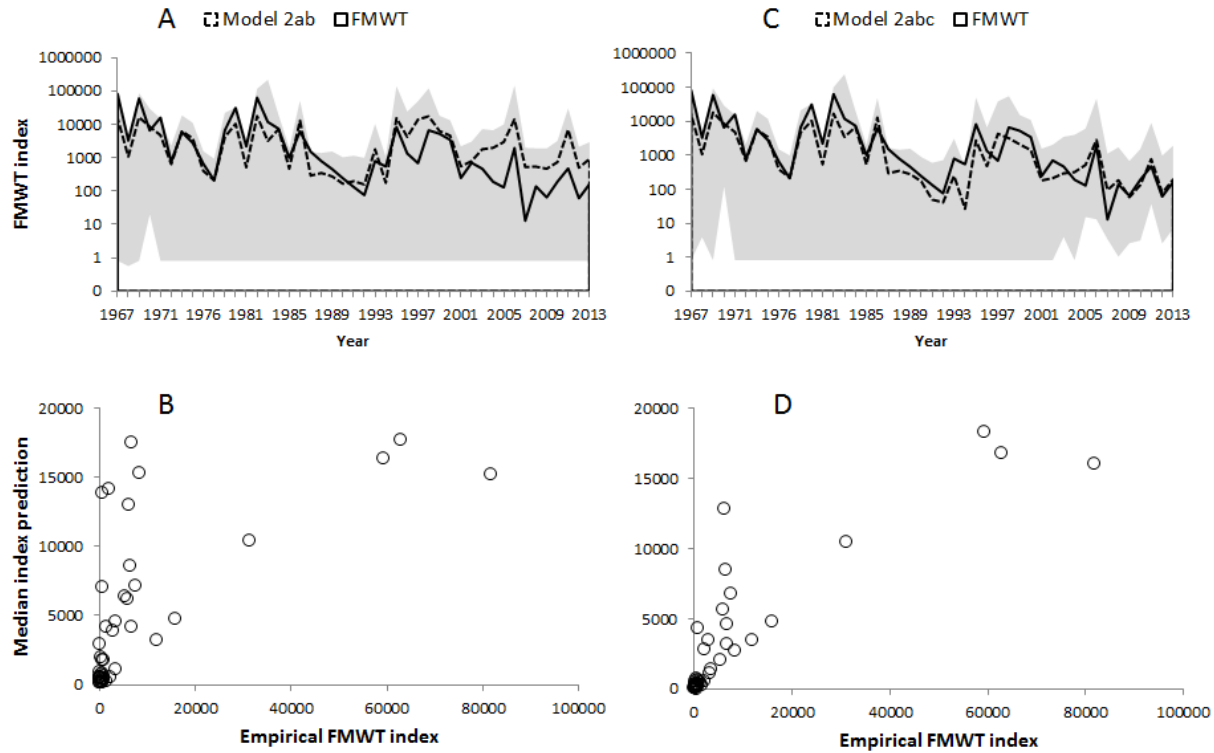


Figure 6





March 30, 2015

Rich Satkowski
 State Water Resources Control Board
 1001 I Street
 Sacramento, CA 95814

Sent via email to Rich.Satkowski@waterboards.ca.gov

RE: Protest and Objections to the TUCP filed on March 24, 2015 by the Bureau of Reclamation and Department of Water Resources

Dear Mr. Satkowski:

On behalf of the Natural Resources Defense Council and the Bay Institute, we are writing to protest and object to the Temporary Urgency Change Petition filed on March 24, 2015 by the Bureau of Reclamation and Department of Water Resources (“TUCP”).¹ The drought is causing significant hardship to rural communities, farms, and fish and wildlife across the State, and we recognize the need to conserve scarce water resources during the drought and ensure that health and safety needs for water are met. For these reasons we do not object to maintaining minimum 1,500 cfs CVP/SWP exports for health and safety purposes when the projects are otherwise failing to comply with existing water quality standards. Nor do we object to the very limited use of the midstep export exception solely for critical public health and safety purposes, consistent with the Executive Director’s prior TUCP order.

However, continued drought conditions – and the State’s management responses to the drought – are significantly increasing the risk of driving several of California’s native fisheries extinct, and of doing lasting damage to the health of the Bay-Delta estuary. As discussed in our prior protests and objections over the past year and a half, the best available science shows that continued waiver of D-1641 standards during drought conditions is likely to lead to further population declines for several species whose abundance is at some of the lowest levels ever recorded. The reduction in Delta outflow, in particular, is causing significant adverse effects on numerous fish species and the long term health of the estuary. Moreover, the water temperature modeling

¹ The petition was filed for Permits 16478, 16479, 16481, 16482 and 16483 (Applications 5630, 14443, 14445A, 17512 and 17514A, respectively) of the Department of Water Resources for the State Water Project and License 1986 and Permits 11315, 11316, 11885, 11886, 11887, 11967, 11968, 11969, 11970, 11971, 11972, 11973, 12364, 12721, 12722, 12723, 12725, 12726, 12727, 12860, 15735, 16597, 20245, and 16600 (Applications 23, 234, 1465, 5638, 13370, 13371, 5628, 15374, 15375, 15376, 16767, 16768, 17374, 17376, 5626, 9363, 9364, 9366, 9367, 9368, 15764, 22316, 14858A, 14858B, and 19304, respectively) of the United States Bureau of Reclamation for the Central Valley Project.

*NRDC and the Bay Institute Objections to and Protest of TUCP dated March 24, 2015
March 30, 2015*

recently submitted by the Bureau of Reclamation indicates that water diversions for senior contractors and other operations this year will reduce the coldwater pool in Shasta dam, and that operators are likely to again lose temperature control at Shasta Dam, which last year resulted in greater than 95% mortality of endangered winter run Chinook salmon. TUCP, Attachment A at 36 (acknowledging that temperature modeling forecasts “suggest similar impacts as described during the late summer of WY 2014”); *see* Bureau of Reclamation submittal to SWRCB related to Condition 6b of the March 5, 2015 TUCP Order (“Condition 6b Submittal”).

For these reasons, and as discussed further below, we object to and protest the following modifications of D-1641 standards proposed in the TUCP:

1. Modification of the export limit to permit exports greater than 1,500 cfs when D-1641 standards are not being met (except to meet health and safety needs);
2. Modification of the Vernalis pulse flow standard from 3,100 cfs to 710 cfs;
3. Failure to achieve reasonable temperature control to protect endangered winter run Chinook salmon below Shasta Dam in light of proposed operations, including operations for upstream deliveries in April and May.

We urge the SWRCB to deny these elements of the TUCP and to condition approval of the TUCP upon compliance with an operational plan that adequately protects endangered winter run Chinook salmon.²

1. **The SWRCB Should Deny Modification of the Export Limit to Permit Exports Greater than 1,500 cfs When D-1641 Standards are not being met (Except for Health and Safety Purposes) because the Reduction in Delta Outflow Will Cause Unreasonable Effects on Fish and Wildlife:**

The Executive Director has already concluded that approval of increased exports as proposed in the TUCP would cause unreasonable impacts to fish and wildlife. *See* Revised Order dated March 5, 2015 at 6, 27; Order dated February 3, 2015; Executive Director’s Presentation to the SWRCB on February 18, 2015. We agree with the SWRCB’s conclusion in the March 5, 2015 Order that increased exports, except as strictly necessary for health and safety uses, cause unreasonable effects on fish and wildlife.³

Not only would approval of increased exports as proposed in the TUCP increase the risk of entrainment, as discussed in that order, but more importantly, it substantially reduces Delta outflow. We renew our protests and objections filed January 27, 2015 and February 13, 2015. Further reducing Delta outflow, when the minimum D-1641 outflow and X2 standards are not being met, will cause unreasonable effects on fish and wildlife. The TUCP documents that drought conditions, including significantly reduced outflow, in the past few years are already

² In addition, TBI protests and objects to the continuing relaxation of D-1641 objectives for Delta outflow given the dire consequences for numerous resident and migratory estuarine species described in our protest of the 1/23 TUCP and objections to the 2/3 SWRCB Executive Director’s Order.

³ As the SWRCB’s prior orders explain, the fishery agencies’ concurrences under the ESA does not address the SWRCB’s legal obligations under the Water Code, and despite those agency concurrences, the SWRCB appropriately concluded that increased exports would cause unreasonable effects on fish and wildlife. *See* Revised Order dated March 5, 2015 at 5-6, 24-27.

*NRDC and the Bay Institute Objections to and Protest of TUCP dated March 24, 2015
March 30, 2015*

causing higher abundance of nonnative predators like black bass and expansion of *Corbicula* (an invasive clam species whose grazing of plankton substantially reduces important parts of the food chain for native fisheries), as well as promoting harmful algal blooms, reduced reproductive success for native fisheries, and parasitic outbreaks. TUCP, Attachment A at 69. These are many of the same concerns that we have raised in our prior protests.

Yet inexplicably, the biological analysis included in the TUCP largely ignores the impact of reduced outflow on Delta Smelt (focusing instead on entrainment) and it wholly fails to consider analysis in the recent MAST Report showing that reduced spring outflow has a significant adverse effect on delta smelt recruitment and subsequent abundance. With respect to longfin smelt, the TUCP acknowledges that because “increased outflow is one of the best predictors of Longfin Smelt year class strength, ... it is likely the proposed action will exacerbate poor Longfin Smelt recruitment and survival already expected in 2015 due to the severity of the drought.” TUCP, Attachment A at 80. The TUCP acknowledges that reduced outflow will likely reduce survival of threatened and endangered salmon and steelhead as well. *Id.* at 38-40, 46, 48. In addition, the TUCP wholly ignores the impacts of reduced Delta outflow on other species whose survival and abundance is significantly and adversely affected by reduced Delta outflow, including fall run Chinook salmon, Starry Flounder, and Crangon Shrimp. Delta outflow is one of the most dominant drivers of the health of the estuary, and the TUCP (including the proposal for increased exports) will dramatically reduce Delta outflow below the requirements of D-1641. And of course, independent scientists, the SWRCB, California Department of Fish and Wildlife, and other agencies have concluded that the existing outflow and X2 standards of D-1641 are inadequate to fully protect public trust fishery resources. *See* SWRCB 2010; CDFW 2010, 2012.

The best available science shows that the reduction in Delta outflow proposed in the TUCP will cause reduced survival and abundance of numerous fish and wildlife in the Bay-Delta estuary and upstream. This is not something that can be addressed with real time operations, but instead is a function of increased exports at the expense of Delta outflow. The TUCP unreasonably reduces Delta outflow, particularly the proposal to increase exports when D-1641 outflow and X2 standards are not being met. As in our prior protests and objections, we urge the SWRCB to maintain the existing prohibition on CVP/SWP exports in excess of 1,500 cfs when D-1641 water quality standards are not being met, except as necessary for human health and safety, and deny this element of the TUCP.

2. The SWRCB Should Deny Modification of the Vernalis Pulse Flow Standard from 3,100 cfs to 710 cfs Because it will Cause Unreasonable Effects on Fish and Wildlife:

In this TUCP, the agencies propose to reduce the Vernalis pulse flow standard from 3,100 cfs, which is the minimum pulse flow standard that applies only in Critically Dry water year types, to 710 cfs, which is the minimum base flow that applies only in Critically Dry water year types. This effectively eliminates the pulse flow and dramatically worsens conditions for salmon and steelhead in the Lower San Joaquin River and its tributaries as compared to operations approved 2014, which required 15 days of 3,300 cfs and 15 days of 1,500 cfs during the pulse flow period. *See* TUCP Order dated April 11, 2014. As the SWRCB has noted, what constitutes unreasonable effects on fish and wildlife must be considered in the context of other beneficial uses. *See* Revised Order dated March 5, 2015 at 3, 22, 24. And in contrast to Reclamation’s proposal to largely eliminate the Vernalis pulse flow, media reports indicate that the Bureau of Reclamation

*NRDC and the Bay Institute Objections to and Protest of TUCP dated March 24, 2015
March 30, 2015*

will deliver 450,000 acre feet of water to senior water rights holders on the Stanislaus River. See Steve Knell and Jeff Shields, *Irrigation Districts: State could derail delicate Stanislaus water deal*, Modesto Bee, March 28, 2015. In light of the likely impacts to salmon and other fish and wildlife by reducing the Vernalis pulse flow while delivering 450,000 acre feet of water for agricultural beneficial uses, the SWRCB should reject this element of the TUCP because it will cause unreasonable effects on fish and wildlife.

First, the dramatically reduced Vernalis pulse flow proposed in the TUCP will cause unreasonable effects on San Joaquin basin salmon and steelhead. The TUCP acknowledges that reduced flows will reduce survival of migrating steelhead in the San Joaquin River. TUCP, Attachment A at 66. However, the TUCP wholly ignores the effects on fall run Chinook salmon. As the SWRCB is well aware, the best available science demonstrates that lower flows at Vernalis are very likely to cause substantially reduced survival and subsequent abundance of salmon. *See* SWRCB 2010, 2012; CDFW 2012; NMFS 2012; NRDC and the Bay Institute 2013. The low levels are likely to have devastating effects on survival and subsequent abundance of San Joaquin basin salmon and steelhead.

Second, waiver of the Vernalis pulse flow also reduces Delta outflow by several thousand cubic feet per second during the month of April. As discussed above, and in more detail in our prior protests and objections, reduced Delta outflow significantly harms native fish and wildlife. Rejection of this element of the TUCP would likely reduce or avoid unreasonable effects on salmon and steelhead upstream, and the increased outflow benefitting salmon and pelagic species in the Delta would reduce or avoid the effects downstream. It could also result in additional conserved storage at Shasta Dam, if Keswick releases are reduced in light of increased San Joaquin inflow. For all of these reasons, the SWRCB should reject the TUCP proposal to reduce Vernalis pulse flows to 710 cfs.

3. The SWRCB Should Impose Additional Conditions on CVP/SWP to Provide Reasonable Temperature Control to Protect Endangered Winter Run Chinook Salmon Below Shasta Dam in light of Proposed Operations, Including Operations to make Upstream Deliveries in April:

We request that the SWRCB impose additional conditions on CVP/SWP operations that adequately protect winter run Chinook salmon, which likely will need to include reductions in deliveries to senior contractors. The TUCP states that the intent of the proposed modifications to D-1641 water quality standards protecting fish and wildlife is to conserve upstream storage. TUCP at 2. However, the TUCP itself acknowledges that temperature forecasts suggest a repeat of 2014's disastrous conditions for winter run Chinook salmon, *see* TUCP, Attachment A at 36, which resulted in more than 95% mortality of juvenile winter run Chinook salmon. More recent temperature and operational modeling submitted by the Bureau of Reclamation to the SWRCB indicates that operators are unlikely to maintain temperature control this year. *See* Condition 6b Submittal. It is important to recall that Reclamation's temperature model is biased and likely underestimates the resulting water temperatures this fall. *See* NMFS 2014; March 5, 2015 TUCP order at 17, 26, 32; NMFS letter to Reclamation dated January 29, 2015 at 4. The resulting water temperatures this year are likely to cause unreasonable effects to fish and wildlife, including winter run Chinook salmon and other salmon runs spawning below Keswick dam.

*NRDC and the Bay Institute Objections to and Protest of TUCP dated March 24, 2015
March 30, 2015*

That modeling also indicates that Shasta operations, including operations in April and May, are likely to result in reservoir releases that are substantially higher than that needed for temperature control, impacting end of September reservoir storage and the size of the coldwater pool for winter run and other salmonids. *See* Condition 6b Submittal. Contrary to assertions made at prior SWRCB hearings, it is clear from this modeling that reservoir releases are greater than what are necessary to meet temperature compliance. For instance, in April, the Bureau of Reclamation proposes that reservoir releases would 5,600 cfs (Scenario 6b(1) and Scenario 6b(4)), whereas the water temperature focused Scenario 6b(2) and Scenario 6b(3) would result in releases of 3,250 cfs. *Id.* at 4. Reclamation's proposed operations for April 2015 would result in substantially higher reservoir releases than in April 2014 and indicate that reservoir releases to meet senior water rights are greater than necessary to meet temperature control. The same appears to be true with respect to meeting the outdated Wilkins Slough standard under Reclamation's proposed operations, as well as the magnitude of releases in the summer months. *Id.* As a result, it is clear that CVP/SWP deliveries, including water deliveries to senior contractors, are substantially contributing to unreasonable effects on fish and wildlife below Shasta Dam. We note in this regard that the Bureau of Reclamation proposes to deliver more than 2.6 million acre feet of water to senior agricultural contractors,⁴ in addition to DWR's 20% State Water Project allocation and deliveries to DWR settlement contractors on the Feather River.

The SWRCB has a continuing obligation to protect winter run Chinook salmon and other species spawning below Shasta Dam, and the prior TUCP Order directs Reclamation "to ensure that temperature control on the Sacramento River for salmonids is maintained throughout the year and that issues encountered last year with temperature control are factored into that planning." *See* March 5, 2015 TUCP Order at 22. That TUCP Order also explicitly reserves authority of the SWRCB to require modifications to the order to protect fish and wildlife. *Id.*; *see id.* at 25-26 (acknowledging that Order WR-95 requires Reclamation to operate its facilities on the Sacramento River to achieve temperature control for salmon). In light of the temperature modeling that has been provided, the SWRCB should immediately order Reclamation to modify proposed Shasta Dam operations to ensure adequate temperature control later in the year, including the following measures:

- Limit Shasta Dam releases in April and May to minimum reservoir releases (3,250 cfs) unless necessary for temperature control or health and safety purposes;
- Reduce flows at Wilkins Slough below 3,800 cfs unless necessary for temperature control or for health and safety purposes;
- Reduce releases from Shasta in the summer months unless necessary for temperature control or for health and safety purposes, and consider increased reliance on reservoir releases from Oroville.

The SWRCB should not approve the TUCP without imposition of additional conditions that ensure Shasta operations adequately protect winter run Chinook salmon and other salmon runs spawning below Shasta Dam.

⁴ *See* Bureau of Reclamation, Central Valley Project (CVP) Water Quantities with 2015 Allocation, available online at: http://www.usbr.gov/mp/PA/water/docs/1_CVP_Water_Quantities_Allocation.pdf (last visited March 30, 2015).

*NRDC and the Bay Institute Objections to and Protest of TUCP dated March 24, 2015
March 30, 2015*

Conclusion:

California's drought, currently in its fourth year, continues to cause significant hardship and impacts to rural communities, agriculture, and the State's fish and wildlife. However, if granted in its current form, implementing the TUCP will exacerbate the impacts of four years of drought to a level that causes unreasonable effects on fish and wildlife. The SWRCB should reject those elements noted above and impose additional conditions to ensure that temperature control below Shasta Dam can be maintained.

We greatly appreciate the SWRCB's consideration of our views.

Sincerely,



Doug Obegi
Natural Resources Defense Council



Gary Bobker
The Bay Institute

cc: James Mizell, Department of Water Resources, James.Mizell@water.ca.gov;
Amy Aufdemberge, Regional Solicitor's Office, Amy.Aufdemberge@sol.doi.gov



ELSEVIER

Contents lists available at ScienceDirect

Aquatic Toxicology

journal homepage: www.elsevier.com/locate/aquatox

Effect of dietary selenomethionine on growth performance, tissue burden, and histopathology in green and white sturgeon



Nicola De Riu^{a,3}, Jang-Won Lee^{b,1,3}, Susie S.Y. Huang^{b,2},
Giuseppe Moniello^a, Silas S.O. Hung^{b,*}

^a Department of Veterinary Medicine, University of Sassari, Via Vienna 2, 07100 Sassari, Italy

^b Department of Animal Science, University of California, One Shields Avenue, Davis, CA 95616-8521, USA

ARTICLE INFO

Article history:

Received 14 October 2013

Received in revised form

27 December 2013

Accepted 29 December 2013

Keywords:

Selenomethionine

Selenium toxicity

Growth performance

Tissue burden

Histopathology

Green and white sturgeon

ABSTRACT

A comparative examination of potential differences in selenium (Se) sensitivity was conducted on two sturgeon species indigenous to the San Francisco Bay-Delta. Juvenile green (*Acipenser medirostris*), recently given a federally threatened status, and white sturgeon (*Acipenser transmontanus*) were exposed to one of four nominal concentrations of dietary L-selenomethionine (SeMet) (0 (control), 50, 100, or 200 mg SeMet/kg diet) for 8 weeks. Mortality, growth performance, whole body composition, histopathology, and Se burdens of the whole body, liver, kidneys, gills, heart, and white muscle were determined every 2 to 4 weeks. Significant ($p < 0.05$) mortality was observed in green sturgeon fed the highest SeMet diet after 2 weeks, whereas no mortality was observed in white sturgeon. Growth rates were significantly reduced in both species; however, green sturgeon was more adversely affected by the treatment. Dietary SeMet significantly affected whole body composition and most noticeably, in the decline of lipid contents in green sturgeon. Selenium accumulated significantly in all tissues relative to the control groups. After 4 and 8 weeks of exposure, marked abnormalities were observed in the kidneys and liver of both sturgeon species; however, green sturgeon was more susceptible to SeMet than white sturgeon at all dietary SeMet levels. Our results showed that a dietary Se concentration at 19.7 ± 0.6 mg Se/kg, which is in range with the reported Se concentrations of the benthic macro-vertebrate community of the San Francisco Bay, had adverse effects on both sturgeon species. However, the exposure had a more severe pathological effect on green sturgeon, suggesting that when implementing conservation measures, this federally listed threatened species should be monitored and managed independently from white sturgeon.

© 2014 Elsevier B.V. All rights reserved.

1. Introduction

Green (*Acipenser medirostris*) and white sturgeon (*Acipenser transmontanus*) are two sturgeon species native to the San Francisco Bay Delta (SFBD) and both have exceptional biological, commercial, and ecological values (Moyle, 2002). Their populations, however, have been in steady decline since the nineteenth century (Billard and Leconte, 2001). Recently, green sturgeon was listed as a species of special concern by the State of California and a threatened species by the United States Federal Government (California Natural Diversity Database (CNDDB), 2006). Elevated concentrations of chemical contaminants found in their diets are

considered one of the primary causes of their decline (National Marine Fisheries Service, 2006).

Selenium (Se) is a major water contaminant in SFBD. It is an essential micronutrient for all vertebrates (NRC, 2005), as it is a major component of glutathione peroxidase, an enzyme that protects lipid membranes from oxidative damages at the cellular and subcellular levels (Arteel and Sies, 2001). However, at a slightly higher concentration, dietary Se is toxic to many aquatic animals (Lemly, 2002, 1985; Skorupa, 1998; Steward et al., 2004). In SFBD, major Se inputs include waste discharges originating from petrochemical and industrial manufacturing operations. The most significant source, however, is from irrigated agricultural practices on the seleniferous soils of the Central Valley (Lemly, 2004).

Most field surveys on SFBD sturgeon populations have been conducted on white sturgeon due to their larger natural population. Several such reports have noted elevated tissue Se concentrations [Se]s (up to 30 $\mu\text{g/g}$ dry weight (dw) in the liver and 15 $\mu\text{g/g}$ dw in the muscle; Urquhart and Regalado, 1991; Linville et al., 2002) in these animals. Similar tissue Se levels have been reported to cause toxic effects in freshwater and anadromous fish (Lemly, 2002).

* Corresponding author. Tel.: +1 530 752 3580; fax: +1 530 752 0175.

E-mail address: sshung@ucdavis.edu (S.S.O. Hung).

¹ School of Health Sciences, Purdue University, 550 Stadium Mall Drive, West Lafayette, IN 47907, USA.

² Department of Biology, University of Ottawa, 30 Marie Curie Pvt, Ottawa, ON, Canada K1N 6N5.

³ These authors contributed equally to this work.

In contrast, very little is known about Se toxicity and tissue burden in green sturgeon. Although the two species are closely related, they exhibit different responses to environmental contaminants. Recent studies have demonstrated a higher sensitivity to dietary methylmercury (MeHg) in green sturgeon compared with white sturgeon (Lee et al., 2011, 2012). Therefore, information with regards to the physiological responses of green sturgeon to environmental contaminants, in general, should not be simply extrapolated from that of white sturgeon. The objective of our current study was to determine and compare the effects of elevated concentrations of dietary L-selenomethionine (SeMet) on the growth performance, tissue burden, and histopathology of juvenile green and white sturgeon.

2. Materials and methods

2.1. Diet preparation

Four isoenergetic and isonitrogenous purified diets were prepared according to Tashjian et al. (2006) and Lee et al. (2011). Different concentrations of L-selenomethionine (Fisher Scientific, Pittsburgh, PA) were added to a basal diet mixture to constitute the four nominal levels of 0 (control), 50, 100, and 200 mg SeMet/kg diet. These SeMet concentrations were chosen to span the range of projected dietary [Se]s in SFB (Luoma and Presser, 2000) and the selenocompound was chosen as it is the predominant Se form found in natural diets of white sturgeon (Fan et al., 2002). Furthermore, previous studies have indicated that toxic responses in animals fed SeMet were similar to those fed diets containing naturally incorporated Se compounds (Hamilton, 2004).

2.2. Animal acquisition, experimental design, and animal maintenance

The acquisition, maintenance, handling, and sampling of animals were approved by the Campus Animal Care and Use Committee at the University of California, Davis and are as described by Lee et al. (2011). Due to the different spawning and hatching times of the two sturgeon species, the two experiments were conducted consecutively, with the green sturgeon experiment conducted between June 20th and August 8th, 2007, and the white sturgeon experiment between August 29th and October 17th, 2007. In brief, 300 juvenile sturgeon (mean weight of 30 ± 2 g) were used in each of the two experiments and they were randomly distributed into twelve 90-L tanks, resulting in 4 dietary groups with 3 replicate tanks per treatment. Daily rations of 3% body weight/day (BW/d) for the first 4 weeks and 2% BW/d for the second 4 weeks (Cui and Hung, 1995) were placed in an automatic feeder (Cui et al., 1996; Hung and Lutes, 1987) which dispensed feed continuously over 24 h. Water temperature, pH, and dissolved oxygen were maintained at 18–19 °C, 7–8, and 7–9 mg/L, respectively. The effluent water was sampled weekly and [Se] was determined by a certified laboratory (BSK Analytical Laboratory, Fresno, CA, using EPA 200.8 method) and ranged from undetectable to 4.2 µg/L.

2.3. Growth performance, tissue sampling, proximate composition and selenium analysis

Fish were batch weighed on a weekly basis and feed rations were adjusted accordingly. Growth performance, tissue sampling, and diet and tissue [Se]s were determined as previously described by Lee et al. (2011) and Huang et al. (2012). For [Se] analysis, each sample was analyzed in triplicates with one replicate spiked with a sodium selenate standard to verify Se recovery. Dolt-4 (National Research Council Canada) was analyzed simultaneously

with the experimental samples and the observed concentration (6.89 mg Se/kg dw) was within the certified standard range (7.06 ± 0.48 mg Se/kg dw). The [Se]s determined in the 0, 50, 100, and 200 mg SeMet/kg diet were 2.2 ± 0.2 , 19.7 ± 0.6 , 40.1 ± 1.5 , and 77.7 ± 3.6 mg Se/kg dw, respectively. Whole body samples were lyophilized and pulverized prior to proximate composition and energy content determinations, which were determined according to AOAC, 1984, 1995, respectively.

2.4. Tissue processing and light microscopy procedures

After 4 and 8 weeks of exposure, three fish from each tank were randomly captured and euthanized with an over-dose of tricaine methanesulfonate solution (1 g/L, Argent Chemical Laboratories, Redmond, WA). Gills, heart, liver, trunk kidneys, and skeletal muscle were surgically removed, fixed, sectioned, stained, examined, and photographed according to Lee et al. (2012).

2.5. Statistical analysis

Statistical analyses were conducted using JMP 7.0 statistical software program (SAS Institute, Cary, NC). A two-way analysis of variance with interactions was used to test for significant differences among the four dietary SeMet concentrations and between the two sturgeon species. The Tukey's honestly significant difference test was used for multiple comparisons among dietary SeMet concentrations and between the two species at each time point. Statistical significance was tested at the 0.05 probability level, and all values are presented as the mean \pm standard error unless noted otherwise.

3. Results

3.1. Mortality and growth performance

Significant mortality was observed in green sturgeon fed the 200 mg SeMet/kg diet from week 2 and by week 8, mortality was also seen in the 100 SeMet/kg diet group (Table 1). At the end of the study, green sturgeon exhibited a mortality of 7.7% and 23% at the 100 and 200 mg SeMet/kg diet treatments, respectively. In contrast, no mortality was observed in the white sturgeon.

Growth rates (% BW/d) were reduced significantly in both species. After 8 weeks, green sturgeon showed depressed growth rates in all the treatment groups, when compared with the control. In contrast, white sturgeon showed depressed growth rates only at the 100 and 200 mg SeMet/kg diet treatment groups. Although growth rate was significantly higher in the control green sturgeon group, compared with that of the white sturgeon, green sturgeon was more sensitive to SeMet than white sturgeon, at all dietary SeMet levels.

Similarly, by week 8, hepatosomatic index (HSI) of green sturgeon exposed to the two upper SeMet treatments was significantly decreased compared with the control. In contrast, dietary SeMet had no significant effect on the HSI in white sturgeon.

3.2. Whole body proximate composition

Significant increases in moisture content were observed in green sturgeon fed the two highest SeMet diets. Similarly, whole body crude protein, lipid and energy contents were also significantly reduced in these treatment groups (Table 2). In white sturgeon, significant increase, compared with the control, was observed in whole body moisture content in the 200 mg SeMet/kg diet group. Significant decreases were observed in lipid contents at the 100 and 200 mg SeMet/kg diet groups. Similar decrease in energy content was also observed at the 200 mg SeMet/kg diet group.

Table 1
Growth performances of green and white sturgeon exposed to different levels of dietary selenomethionine (SeMet) for 2, 4, 6, and 8 wk.

Parameters	mg SeMet/ kg diet	2 wk		4 wk		6 wk		8 wk	
		Green	White	Green	White	Green	White	Green	White
Mortality (%)	(0) Control	0 b	0 b	0 b	0 b	0 b	0 b	0 b	0 b
	50	0 b	0 b	0 b	0 b	0 b	0 b	0 b	0 b
	100	0 b	0 b	0 b	0 b	0 b	0 b	7.7 ± 4.4 b	0 b
	200	5.3 ± 1.3 a	0 b	12.1 ± 1.5 a	0 b	16.7 ± 2.1 a	0 b	23.1 ± 4.4 a	0 b
% BWI/d ^a	(0) Control	4.5 ± 1.8 a	3.0 ± 2.1 cd	11.9 ± 6.1 a	7.1 ± 0.4 b	6.3 ± 15.9 a	3.7 ± 6.5 b	6.6 ± 14.9 a	4.2 ± 14.1 b
	50	3.8 ± 3.9 ab	3.6 ± 0.2 bc	6.8 ± 8.4 bc	7.8 ± 3.6 b	3.1 ± 14.8 bc	3.9 ± 10.5 b	2.6 ± 16.0 c	4.2 ± 22.5 b
	100	2.0 ± 3.2 ef	2.7 ± 1.2 de	3.2 ± 11.1 de	4.6 ± 4.4 cd	1.0 ± 8.7 d	2.5 ± 10.6 c	0.8 ± 4.1 de	2.8 ± 20.6 c
	200	0.7 ± 1.1 g	1.5 ± 3.2 fg	0.8 ± 7.6 f	1.9 ± 3.9 ef	-0.1 ± 3.7 d	0.9 ± 6.8 d	-0.1 ± 4.3 e	1.0 ± 11.0 d
HSI ^b	(0) Control	1.9 ± 0.1 c	3.2 ± 0.2 ab	2.0 ± 0.1 bc	3.5 ± 0.3 a	1.8 ± 0.3 c	3.0 ± 0.2 ab	2.0 ± 0.1 cd	2.6 ± 0.2 bc
	50	2.3 ± 0.2 bc	3.2 ± 0.2 ab	1.9 ± 0.2 bc	3.7 ± 0.2 a	1.4 ± 0.1 c	3.3 ± 0.3 a	1.3 ± 0.0 de	3.6 ± 0.2 a
	100	2.0 ± 0.2 c	3.4 ± 0.1 a	1.8 ± 0.3 bc	2.8 ± 0.2 ab	1.1 ± 0.2 c	3.2 ± 0.4 a	0.8 ± 0.2 e	3.0 ± 0.1 ab
	200	2.0 ± 0.4 c	3.3 ± 0.1 a	1.2 ± 0.1 c	2.7 ± 0.3 ab	0.8 ± 0.0 c	1.9 ± 0.1 bc	0.9 ± 0.1 e	2.2 ± 0.4 bc

Values represent the mean ± SE ($n = 3$), and different letters denote significant differences ($p < 0.05$) among treatments and between species within each exposure periods.

^a Percent body weight increase per day (%BWI/d) = $100 \times (\text{final body weight} - \text{initial body weight}) / (\text{initial body weight}) / \text{number of days}$. Initial body weight of the sturgeon were 30 ± 2 g (mean ± SE).

^b Hepatosomatic index (HSI) = $100 \times \text{liver weight} / \text{body weight}$.

Table 2
Whole body proximate composition (%) and selenium burden of green and white sturgeon exposed to different levels of dietary selenomethionine for 4 and 8 wk.

Parameters	mg SeMet/ kg diet	4 wk		8 wk	
		Green sturgeon	White sturgeon	Green sturgeon	White sturgeon
Moisture	(0) Control	82.9 ± 0.7 ab	78.4 ± 0.4 c	82.9 ± 0.5 b	76.7 ± 0.4 d
	50	82.4 ± 0.5 ab	77.1 ± 0.5 c	83.5 ± 0.6 b	77.5 ± 0.4 cd
	100	83.0 ± 0.7 ab	77.8 ± 0.3 c	86.5 ± 0.8 a	77.9 ± 0.1 cd
	200	85.3 ± 1.3 a	79.6 ± 1.0 bc	88.2 ± 0.2 a	79.5 ± 0.5 c
Crude Protein	(0) Control	10.2 ± 0.1 ab	11.5 ± 0.1 a	11.5 ± 0.3 a	11.6 ± 0.3 a
	50	10.6 ± 0.4 ab	11.4 ± 0.3 a	11.0 ± 0.3 a	11.4 ± 0.0 a
	100	10.5 ± 0.4 ab	11.6 ± 0.1 a	9.3 ± 0.5 b	11.7 ± 0.2 a
	200	9.4 ± 0.6 a	11.3 ± 0.4 a	7.8 ± 0.2 b	11.3 ± 0.5 a
Crude Lipid	(0) Control	2.9 ± 0.5 c	6.2 ± 0.3 ab	2.5 ± 0.4 d	7.9 ± 0.3 a
	50	2.1 ± 0.3 cd	7.7 ± 0.3 a	1.3 ± 0.1 de	6.8 ± 0.4 ab
	100	1.5 ± 0.3 cd	6.6 ± 0.3 ab	0.4 ± 0.1 e	6.1 ± 0.2 b
	200	0.7 ± 0.2 d	5.2 ± 0.9 b	0.2 ± 0.0 e	4.5 ± 0.3 c
Energy (kcal/g)	(0) Control	5.4 ± 0.1 b	6.4 ± 0.1 a	5.4 ± 0.1 c	6.6 ± 0.0 a
	50	5.1 ± 0.1 bc	6.7 ± 0.1 a	5.0 ± 0.0 d	6.5 ± 0.1 a
	100	4.9 ± 0.1 cd	6.5 ± 0.1 a	4.6 ± 0.0 e	6.4 ± 0.0 ab
	200	4.6 ± 0.1 d	6.3 ± 0.2 a	4.4 ± 0.1 e	6.1 ± 0.1 b
mg Se/kg dw	(0) Control	6.5 ± 0.9 e	7.3 ± 0.8 e	7.1 ± 0.9 d	5.6 ± 0.3 d
	50	21.7 ± 0.5 c	15.3 ± 1.6 d	22.8 ± 0.9 c	20.1 ± 0.5 c
	100	26.2 ± 1.2 bc	22.5 ± 0.9 c	27.8 ± 1.4 bc	31.8 ± 0.3 b
	200	30.6 ± 0.7 ab	34.3 ± 2.5 a	34.3 ± 0.3 b	47.1 ± 4.3 a

Values represent the mean ± SE ($n = 3$), and different letters denote significant differences ($p < 0.05$) among treatments and species within the exposure period. Initial body composition (%): Moisture 83.0 ± 0.6 and 80.2 ± 0.8 , crude protein 10.5 ± 0.3 and 9.9 ± 0.4 , lipid 1.8 ± 0.2 and 5.3 ± 0.2 , energy (kcal/g) 5.1 ± 0.1 and 6.3 ± 0.1 in green sturgeon and white sturgeon, respectively. Initial whole body Se concentrations in green and white sturgeon were 7.2 ± 0.3 and 4.8 ± 0.5 mg Se/kg dry weight (dw), respectively.

Moisture, lipid, and energy contents of green sturgeon were significantly different from those of white sturgeon at all levels of dietary SeMet. Noticeably, crude protein contents of green sturgeon fed the 100 and 200 mg SeMet/kg diets were significantly lower than those of white sturgeon in the same treatment groups. However, the most significant differences were observed in crude lipid contents between the two species.

3.3. Se burden

Different patterns in whole body Se burden were also observed between the two species (Table 2). White sturgeon accumulated Se in a dose and duration-dependent manner. In contrast, whole body Se in green sturgeon did not increase much after week 4 and there was no obvious dose-dependent Se accumulation. Pattern of Se accumulation among tissues were also different between the two species (Tables 3a and 3b). Selenium levels in the gills and kidneys of green sturgeon showed little increase after week

2 and week 4, respectively. In the white muscle, however, [Se] was found to have increased in a dose dependent manner up to the 100 mg SeMet/kg diet level. Liver [Se] increased continuously throughout the 8 weeks, except in those fed the 200 mg SeMet/kg diet, where [Se] decreased after reaching a concentration asymptote at week 6. Similarly in the heart, [Se] plateaued after reaching a maximum concentration at week 4. In contrast, tissue Se burden of white sturgeon generally increased with increasing exposure duration. In the 200 mg SeMet/kg diet group, the highest Se levels were observed at week 6. The highest tissue Se levels in green sturgeon were observed in the liver, whereas the highest Se levels in white sturgeon were seen in the kidneys.

3.4. Histopathological alteration

Histological examination showed progressions of marked lesions in the kidneys and liver of both species after each sampling period (Tables 4 and 5 and Figs. 1 and 2). Mild histological changes

Table 3a
Selenium tissue burden (mg Se/kg dw) in green and white sturgeon exposed to different levels of dietary selenomethionine (SeMet) for 2 and 4 wk.

Tissues	mg SeMet/ kg diet	2 wk		4 wk	
		Green sturgeon	White sturgeon	Green sturgeon	White sturgeon
Kidney	(0) Control	ND	8.0 ± 1.5 a	10.7 ± 0.4 d	9.1 ± 1.6 d
	50	ND	18.1 ± 0.8 b	34.2 ± 0.3 bc	29.5 ± 1.0 cd
	100	ND	36.0 ± 0.5 c	53.1 ± 10.4 ab	50.7 ± 6.0 abc
	200	ND	54.3 ± 2.4 d	50.7 ± 1.8 abc	71.2 ± 2.2 a
Liver	(0) Control	6.1 ± 1.1 c	5.8 ± 1.4 c	4.2 ± 0.4 d	4.9 ± 0.7 d
	50	14.0 ± 1.3 bc	12.4 ± 1.2 bc	23.3 ± 3.2 bc	14.2 ± 1.1 cd
	100	25.6 ± 2.9 ab	16.1 ± 0.7 bc	31.4 ± 6.9 bc	20.9 ± 1.1 bcd
	200	39.5 ± 7.1 a	23.3 ± 0.8 b	65.6 ± 6.1 a	32.3 ± 1.2 b
Gill	(0) Control	6.6 ± 0.2 f	8.0 ± 1.6 ef	6.7 ± 0.2 e	7.0 ± 1.5 e
	50	23.2 ± 1.2 cde	17.5 ± 1.9 def	26.6 ± 0.2 d	25.3 ± 0.3 d
	100	32.5 ± 2.0 bcd	34.7 ± 2.6 bc	35.5 ± 0.6 cb	40.7 ± 3.6 c
	200	44.4 ± 4.4 ab	51.6 ± 6.5 a	48.1 ± 1.5 b	60.3 ± 2.7 a
Heart	(0) Control	9.1 ± 0.7 d	7.6 ± 1.0 d	7.6 ± 0.7 f	6.7 ± 1.1 f
	50	22.7 ± 1.3 bc	17.0 ± 0.4 cd	25.2 ± 0.8 e	26.8 ± 1.0 de
	100	28.8 ± 0.8 b	29.7 ± 1.5 b	34.9 ± 1.2 cd	42.0 ± 1.1 bc
	200	43.1 ± 3.8 a	42.0 ± 4.0 a	45.6 ± 1.2 ab	53.1 ± 4.2 a
White muscle	(0) Control	8.4 ± 0.6 e	11.7 ± 0.8 de	9.0 ± 0.2 d	9.5 ± 0.3 d
	50	20.4 ± 0.1 bc	17.6 ± 0.7 cd	25.6 ± 0.1 c	25.3 ± 0.3 c
	100	26.9 ± 0.3 ab	25.9 ± 1.3 a b	32.2 ± 1.2 b	29.5 ± 0.5 bc
	200	32.2 ± 3.6 a	33.2 ± 0.8 a	34.7 ± 2.6 ab	40.4 ± 2.3 a

Values represent mean ± SE ($n = 3$) and different letters denote significant differences ($p < 0.05$) among treatments and species within each exposure period and tissue type. Initial Se concentrations (mg Se/kg dw) in green and white sturgeon were as follows: gill 6.6 ± 0.1 and 4.8 ± 0.5 ; heart 6.3 ± 0.6 and 6.5 ± 1.3 ; liver 7.0 ± 1.0 and 3.1 ± 0.3 ; kidney ND and 6.3 ± 0.9 ; and white muscle 7.6 ± 0.2 and 8.94 ± 0.2 , respectively. ND: not determined and dw: dry weight.

Table 3b
Selenium tissue burden (mg Se/kg dw) in green and white sturgeon exposed to different levels of dietary selenomethionine (SeMet) for 6 and 8 wk.

Tissue	mg SeMet/ kg diet	6 wk		8 wk	
		Green sturgeon	White sturgeon	Green sturgeon	White sturgeon
Kidney	(0) Control	9.1 ± 0.7 e	8.2 ± 1.3 e	8.5 ± 0.6 d	9.3 ± 0.9 d
	50	35.1 ± 1.0 cd	28.1 ± 1.8 de	33.3 ± 0.6 c	33.5 ± 0.3 c
	100	60.1 ± 12.6 b	54.8 ± 1.2 bc	53.0 ± 9.8 bc	54.5 ± 3.6 bc
	200	44.4 ± 1.3 bcd	127.6 ± 8.1 a	58.1 ± 2.6 b	93.3 ± 5.6 a
Liver	(0) Control	5.1 ± 0.8 c	4.7 ± 0.5 c	6.1 ± 0.3 c	4.2 ± 0.1 c
	50	32.6 ± 1.1 bc	16.0 ± 1.1 bc	34.4 ± 3.5 bc	28.0 ± 10.4 bc
	100	78.4 ± 10.5 a	26.6 ± 1.5 bc	86.1 ± 9.7 a	30.1 ± 1.0 bc
	200	106.5 ± 14.5 a	46.8 ± 2.6 b	87.0 ± 11.2 a	56.3 ± 2.6 ab
Gill	(0) Control	6.0 ± 0.2 e	6.6 ± 1.0 e	5.4 ± 0.3 e	7.6 ± 0.7 e
	50	29.3 ± 1.4 cd	20.7 ± 5.3 d	29.5 ± 0.6 d	26.7 ± 3.3 d
	100	34.1 ± 3.5 bc	45.2 ± 2.1 b	39.3 ± 0.6 c	46.4 ± 0.7 bc
	200	45.1 ± 1.6 b	60.6 ± 0.3 a	51.6 ± 1.6 b	69.5 ± 2.4 a
Heart	(0) Control	5.5 ± 0.5 d	6.4 ± 0.3 cd	5.3 ± 0.3 f	8.8 ± 0.5 f
	50	23.6 ± 0.9 bcd	26.0 ± 1.1 bcd	24.4 ± 0.3 e	28.9 ± 0.4 de
	100	29.5 ± 1.6 bc	41.0 ± 4.2 ab	33.0 ± 1.4 cd	45.8 ± 1.7 b
	200	35.5 ± 3.3 ab	58.2 ± 12.4 a	35.6 ± 2.1 c	70.6 ± 2.1 a
White muscle	(0) Control	10.0 ± 0.5 e	9.5 ± 0.3 e	8.4 ± 0.4 e	9.2 ± 0.7 e
	50	29.7 ± 1.0 cd	25.2 ± 0.6 d	31.1 ± 0.3 cd	27.0 ± 1.1 d
	100	31.4 ± 0.7 bcd	37.4 ± 3.4 ab	37.0 ± 0.3 bc	41.3 ± 0.6 b
	200	35.7 ± 1.9 abc	42.6 ± 1.1 a	36.8 ± 1.2 bc	57.9 ± 1.2 a

Note: See Table 3a.

were noted in the skeletal and heart muscles (results not shown). However, no prominent histological changes were observed in the gills of either species at all times.

3.4.1. Trunk kidney

After exposure to dietary SeMet, the kidneys of both sturgeon species exhibited marked histological changes, compared with the controls. These changes included increased tubular epithelium degeneration (TED), renal corpuscular disintegration (CD), and interstitial tissue degeneration (ITD) (Table 4 and Fig. 1c–h). Tubular epithelium degeneration was mainly characterized by hydropic degeneration, pyknosis, and cell necrosis (Fig. 1c, e, and h). Characterization of CD included the collapse of glomerular capillary loop,

hypertrophy of mesangial cells, thickening of Bowman's capsule layers, and collapse or enlargement of Bowman's space (Fig. 1c, e, and h). Lastly, ITD was identified by necrotic area and loss of tissue (Fig. 1g and h). In general, pathological alterations of the kidneys were proportional to the dose and duration of SeMet exposure.

Compared with week 4, both species displayed a more severe and higher frequency of TED, CD, and ITD in the kidneys at week 8 (Table 4). The most serious damage occurred in the tubular epithelium as TED for both species (Table 4 and Fig. 1). Although some of the lesion scores were the same between the two species, green sturgeon exhibited more severe kidney pathology in all of the SeMet treatment groups (Table 4).

Table 4
Kidney histopathological alterations of green and white sturgeon exposed to a graded levels of dietary selenomethionine (SeMet) for 4 and 8 wk.

	mg SeMet/kg diet							
	Control		50		100		200	
	Green sturgeon	White sturgeon	Green sturgeon	White sturgeon	Green sturgeon	White sturgeon	Green sturgeon	White sturgeon
	Histopathology at 4 wk							
TED	0	0	++	+	+++	++	+++	+++
CD	0	0	0	0	+	++	++	++
ITD	0	0	0	0	+	+	+	+
	Histopathology at 8 wk							
TED	0	0	+++	++	+++	+++	+++	+++
CD	0	0	++	+	++	++	++	+++
ITD	0	0	0	0	++	+	+++	++

Lesion severity scoring: 0 = absent or rarely observed, + = mild (affected less than 10%), ++ = moderate (affected greater than 10% but less than 50%), and +++ = severe (affected greater than 50%). TED, tubular epithelium degeneration; CD, renal corpuscular disintegration; ITD, interstitial tissue degeneration. N=9.

Table 5
Liver histopathological alterations of green and white sturgeon exposed to a graded levels of dietary selenomethionine (SeMet) for 4 and 8 wk.

	mg SeMet/kg diet							
	Control		50		100		200	
	Green sturgeon	White sturgeon	Green sturgeon	White sturgeon	Green sturgeon	White sturgeon	Green sturgeon	White sturgeon
	Histopathology at 4 wk							
GD	0	0	+	0	++	+	+++	+
VD	0	0	++	0	++	+	+++	+++
	Histopathology at 8 wk							
GD	0	0	++	0	+++	+	+++	++
VD	0	0	++	+	++	++	+++	++

Lesion severity scoring: 0 = absent or rarely observed, + = mild (affected less than 10%), ++ = moderate (affected greater than 10% but less than 50%), +++ = severe (affected greater than 50%). GD, glycogen depletion; VD, vacuolar degeneration including single cell necrosis. N=9.

3.4.2. Liver

After 4 weeks, the livers of both species showed marked histological alterations, including glycogen depletion (GD) and vacuolar degeneration (VD) (Table 5 and Fig. 2). In both species, the progression of the aforementioned alterations was generally proportional to the dose and duration of exposure. However, between the two species, the green sturgeon livers exhibited more severe GD and VD (Table 5 and Fig. 2c–h).

4. Discussion

4.1. Mortality and growth depression

In the current study, green sturgeon exhibited significant higher mortalities at the highest SeMet treatment, which is equivalent to a 78 mg Se/kg diet. However, similar to Tashjian et al. (2006), who reported a mean survival rate of $99 \pm 4\%$ in white sturgeon exposed to diets containing up to 191 mg Se/kg for an 8 week period, no significant mortalities were observed among white sturgeon in the current study. Although green sturgeon appeared to be more sensitive to dietary Se, the mortality rate was still lower than that of other fish species. A mean mortality of 37.5% was observed in Chinook salmon parr (*Oncorhynchus tshawytscha*) after an 8.6-week exposure to a 35.4 mg Se/kg diet (Hamilton et al., 1990). Arshad et al. (2011) reported a mean mortality of 25% in juveniles of beluga sturgeon (*Huso huso*) exposed to dietary Se at levels between 1.26 and 20.26 mg/kg for 8 weeks.

Compared with white sturgeon, the significantly higher mortality in the green sturgeon may be a consequence of their higher initial growth. Deng et al. (2002) reported faster growth rates in juvenile green sturgeon when compared with white sturgeon of similar age. As faster growth rate reflects a higher energy demand,

the green sturgeon may have been in an overall lower energy state, especially since the diets were provided in a fixed daily ration and adjusted on a weekly basis. The low HSI, whole body lipid and energy content, and glycogen storage in the hepatocytes are all indicative of the low energy reserves in the green sturgeon.

Compared with other fish species from similar studies, green sturgeon exhibited a more severe growth rate depression. At 8 weeks, green sturgeon fed the 50 and 100 mg SeMet/kg diets (equivalent to 19.7 and 40.1 mg Se/kg diet, respectively) had their average growth rates reduced to 39% and 12% of that of the controls, respectively. In contrast, growth rates of Chinook salmon parr were only reduced to 77.9% and 37.3%, when given an 18.2 and 35.4 mg Se/kg diet in the form of SeMet for 60 days (Hamilton et al., 1990). Interestingly, juvenile beluga sturgeon fed a 20.26 mg Se/kg diet, in the form of SeMet, for 8 weeks, exhibited increased growth rates (Arshad et al., 2011). The observed reduction in growth among the green sturgeon may be a combined physiological response to: (1) the higher energy demand during the rapid initial growth phase and (2) energy relocation/adaptation to chronic Se toxicity. Thus, reduced growth is likely a physiological tradeoff for achieving a comparatively lower Se-induced mortality, as to what were seen in the aforementioned studies.

4.2. Whole body proximate composition

Proximate analysis is a good indicator of the overall physiological condition of a fish (Ali et al., 2005). In the present study, changes in proximate composition, most notably the significant decreases in protein, lipid, and energy contents, indicated that both species were experiencing physiological stress induced by dietary SeMet exposure. However, the treatment effect was more severe on green sturgeon, as the white sturgeon seemed to be in an overall better

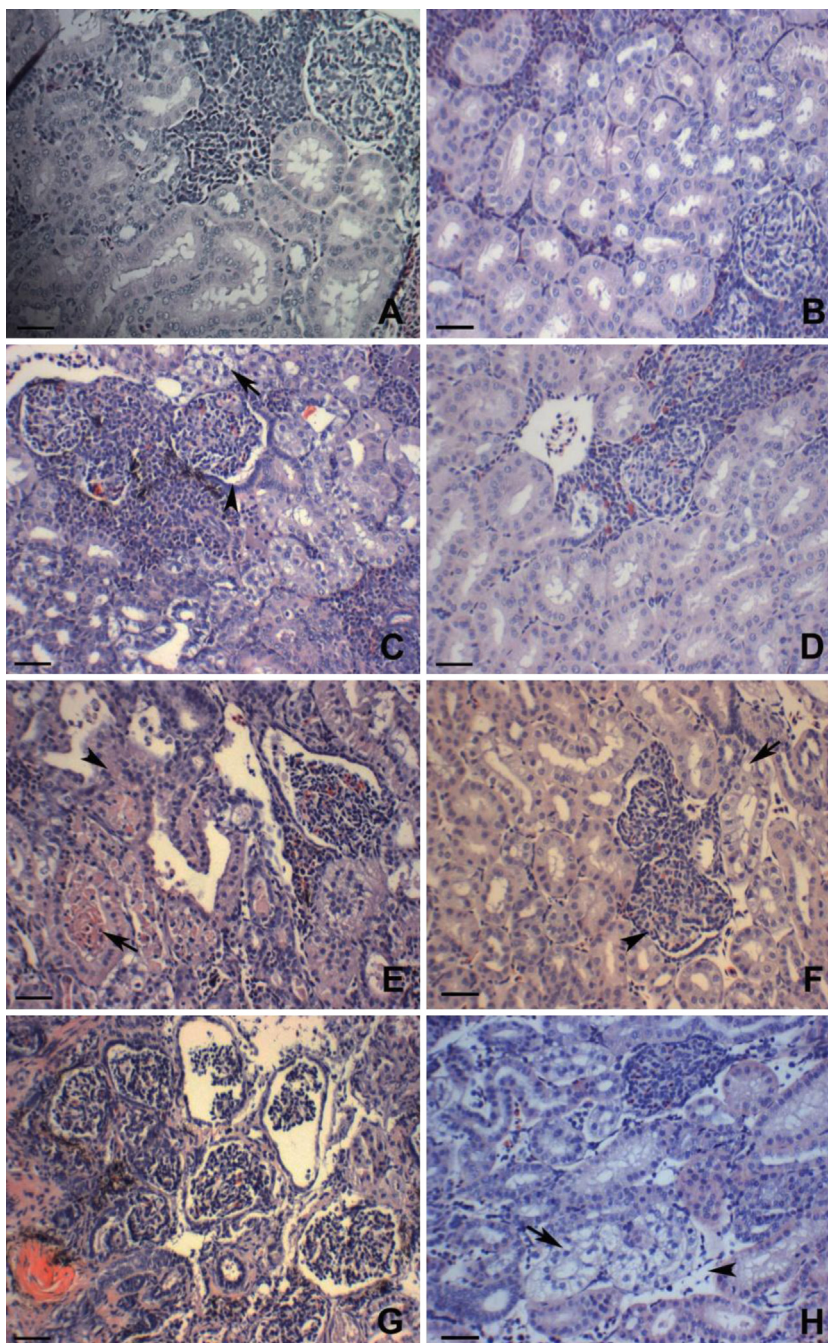


Fig. 1. The trunk kidney of *Acipenser medirostris* (left) and *A. transmontanus* (right) stained with hematoxylin/eosin: (A) and (B) kidneys of individuals from the control groups. (C) Kidney of *A. medirostris* exposed to 50 mg SeMet/kg diet for 8 weeks showing hydropic degeneration (arrow) and renal corpuscular disorganization (arrow head). (D) Kidney of *A. transmontanus* exposed to 50 mg SeMet/kg diet for 8 weeks showing slightly enlarged tubular cells. (E) Kidney of *A. medirostris* exposed to 100 mg SeMet/kg diet for 8 weeks showing severe tubular cell death (arrow head) and tubular inclusion (arrow), and renal corpuscular disintegration. (F) Kidney of *A. transmontanus* exposed to 100 mg SeMet/kg diet for 8 weeks showing moderate tubular hydropic degeneration (arrow) and collapse of glomerular capillary (arrow head). (G) Kidneys of *A. medirostris* exposed to 200 mg SeMet/kg diet for 8 weeks showing necrotic areas. (H) Kidney of *A. transmontanus* exposed to 200 mg SeMet/kg diet for 8 weeks showing severe tubular epithelium degeneration including hydropic degeneration (arrow) and loss of interstitial tissues (arrow head). All scale bars = 50 μ m.

physiological condition, given the higher lipid and energy contents of their control group.

Chemical contaminants have been shown to induce physiological stress in teleosts. [Beyers et al. \(1999\)](#) reported that largemouth bass (*Micropterus salmoides*) utilize energy relocation to compensate for the additional energetic costs associated with toxic exposures. As described in Selye's general adaptation syndrome ([Selye, 1955](#)), the authors observed a two stage energy relocation in the largemouth bass: first, an allocation of resources from somatic and reproductive growth, which have little effect on the

overall energy status of the animal; and second, the allocation of body reserves such as somatic lipid and protein, which can put the animal in an energy-deficient state. Furthermore, when the stressor persists for sufficient length of time and magnitude, the animal would inevitably enter exhaustion, the third and final stage of stress adaptation ([Selye, 1955](#)).

At the two highest dietary SeMet levels, physiological assessments indicated that green sturgeon were in the exhaustion stage. Characteristics such as glycogen depletion of hepatocytes, increased histopathology in the liver and kidneys, depressed

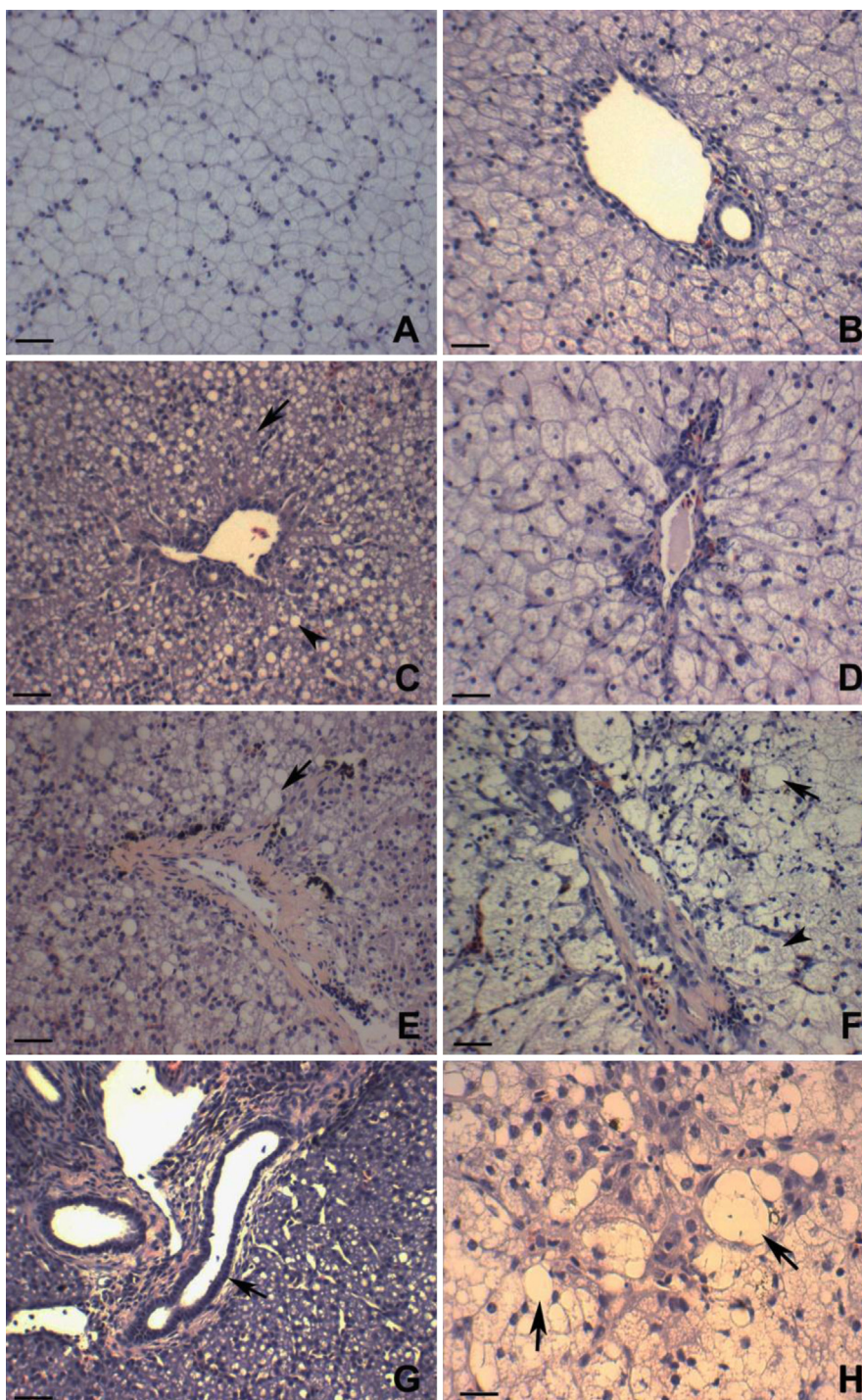


Fig. 2. The liver of *Acipenser medirostris* (left) and *A. transmontanus* (right) stained with hematoxylin/eosin: (A) and (B): Livers of individuals from control groups. (C) Liver of *A. medirostris* exposed to 50 mg SeMet/kg diet for 8 weeks showing moderate glycogen depletion (GD) (arrow) and vacuolar degeneration (VD) (arrow head). (D) Liver of *A. transmontanus* exposed to 50 mg SeMet/kg diet for 8 weeks showing slightly enlarged hepatocytes with unclear cell membranes. (E) Liver of *A. medirostris* exposed to 100 mg SeMet/kg diet for 8 weeks showing severe VD (arrow). (F) Liver of *A. transmontanus* exposed to 100 mg SeMet/kg diet for 8 weeks showing VD (arrow) and necrotic cells (arrow head). (G) Liver of *A. medirostris* exposed to 200 mg SeMet/kg diet for 8 weeks showing severe GD, VD, and dilation of bile duct (arrow). (H) Liver of *A. transmontanus* exposed to 200 mg SeMet/kg diet for 8 weeks showing VD (arrows). All scale bars = 50 μ m, except the scale bar at (H) = 25 μ m.

growth rates, and increased mortality were observed in these animals. By week 4, the animals have entered the second stage of energy mobilization, as seen in the largemouth bass (Beyers et al., 1999), in which more body constituents, such as lipid and protein, were utilized to meet the additional energy cost associated with Se toxicity. In comparison, the white sturgeon seemed to remain in the resistance state, given that their protein levels remained unaffected by SeMet. Furthermore, their body lipid contents were also

significantly higher. The species difference, again, may be due to the rapid initial growth phase of juvenile green sturgeon, in which the associated high metabolic cost led to a comparatively more energetically vulnerable status. The exact cause of the observed reduction in body lipid is unknown, however, as multiple factors such as reduced food intake due to unpalatability of SeMet enriched feed and increased energy demand for Se detoxification may be involved.

4.3. Se burden

In general, whole body Se burden increased with dietary Se level and exposure duration; however, by week 4, the extent of Se bioaccumulation have slowed down in green sturgeon (Table 2). Avoidance to Se-contaminated food has been reported in waterfowl (Heinz and Sanderson, 1990) and teleost species (Hilton et al., 1980). Unpalatability of foods containing high concentrations of Se was suggested as a factor leading to food avoidances observed in birds and fish species (Ogle and Knight, 1989). In the current study, decreased feeding was noted in green sturgeon, from week 4 onwards, in the two highest SeMet groups. However, similar observation was not made during the first 4 weeks of exposure. Other Se toxicity mechanisms, such as musculature dysfunction may have also contributed to decreased food consumption in this study. Substitution of methionine (Met) by SeMet, in the disulfide bond of muscle actin filament, can generate radical oxygen species (ROS) leading to mechanical malfunction of the organ (Dalle-Donne et al., 2001; Palace et al., 2004). Histological changes observed in the white muscle of both sturgeon species (results not shown) in this study support possible musculature malfunctioning. Similarly, SeMet substitution may have also occurred in the heart muscle, as indicated by mild histological changes in the heart tissues (results not shown), and may have compromised the cardiovascular function of these animals. Thus, it is more likely that the decrease in feeding observed in the latter 4 weeks, the starvation effect, was a secondary effect of Se toxicity, such as locomotor dysfunction, rather than unpalatability relating to the high SeMet content.

The highest Se burden was observed in the green sturgeon livers, at 6 weeks. However, the high liver [Se] may be a combined effect of decreased HSI (half the size of that of the controls), negative growth rates (%BW/d), and decreased food consumption. Lee et al. (2011) reported similar findings in juvenile green sturgeon fed various levels of dietary MeHg for 8 weeks. Regardless of the mechanisms leading to the high organ Se accumulation, extensive liver damages were observed and likely were important factors contributing to the significant growth rate decline observed in green sturgeon and their subsequent high mortality.

Urine is the primary excretion route for Se. Although mammals can also excrete excess Se via feces and exhalation, the urine plays a quantitatively greater role in whole body Se homeostasis (Ellis et al., 1997; Ivancic and Weiss, 2001). Similarly, urine is also the primary Se excretory pathway in white sturgeon (Huang et al., 2012). In the current study, the significantly higher Se burden observed in white sturgeon kidneys suggests a more active depuration of Se (compounds) relatively to that of green sturgeon. However, study on both species using oral intubation and intravenous injection methods demonstrated similar SeMet assimilation and metabolism among the sturgeon (Silas S.O. Hung, University of California at Davis, unpublished date). Thus, the Se concentration plateau observed in the green sturgeon kidneys at post week 4 was likely due to decreased feed consumption rather than decreased urinary Se.

4.4. The trunk kidney

Histological changes in the kidneys in fish have been previously studied and are reliable and sensitive biomarkers for a wide variety of chemical exposures, including SeMet (Sorensen et al., 1984; Handy and Penrice, 1993; Thophon et al., 2003). In this study, the kidneys of sturgeon exposed to SeMet showed marked abnormalities, including TED, CD, and ITD. Collapsed glomerular capillaries, mesangial cell hypertrophy, abnormally abundant matrixes, thickened Bowman's capsule layers, and collapsed or enlarged Bowman's space were also observed in the renal corpuscles of SeMet exposed sturgeon. Similar damages were reported

in green sunfish (*Lepomis cyanellus*) from Se-contaminated lakes (Sorensen et al., 1982, 1984) and in striped bass (*Morone saxatilis*) fed Se-contaminated live feed (Coughlan and Velte, 1989).

The extensive kidney lesions seen in both sturgeon species can be attributed to the primary excretory role of Se compounds (Suzuki, 2005) of the organ. The significant increase in green sturgeon whole body moisture content may be indicative of a compromised osmoregulation, given the extensive damages seen in the tubular epithelium. Other factors such as deprivation of energy and higher damages in the livers may also have contributed to the severe kidney lesions observed in green sturgeon, despite having a comparatively lower kidney Se burden compared to the white sturgeon.

4.5. Liver

The livers of both sturgeon species exposed to SeMet treatments exhibited adverse histological changes such as GD and VD, and are consistent with the histopathological lesions reported by Tashjian et al. (2006). Swollen hepatocytes and vacuolation were also reported in livers of green sunfish exposed to Se-elevated water (Sorensen et al., 1982, 1984). Reproductive failure was noted in the study and marked population decline followed suit. In the current study, the extent of the liver lesions may have also affected organ function, as seen in the decreased hepatocyte glycogen storage. Such will have an effect on glycogenesis and glycolysis, leading to an interruption of energy metabolism, as supported by the decrease in whole body energy content, growth, and the higher mortality in green sturgeon.

In addition, GD and single cell necrosis were also reported in Sacramento splittail (*Pogonichthys macrolepidotus*) fed SeMet-supplemented diets (Teh et al., 2004). Significant glycogen depletion was suggested as a result of increased liver glycogenolysis due to the excessive energy demand for repairing SeMet-induced damage and/or reduced food intake (Teh et al., 2004). Significant GD seen in the current study is thought to be an adaptation by the sturgeon to meet the high energy demand when exposed to high levels of dietary SeMet.

Laboratory studies reported hepatic oxidative stress in mallard ducks (*Anas platyrhynchos*) exposed to dietary SeMet (Hoffman, 2002). Increased dietary Se elevated plasma and hepatic GSH peroxidase activities, followed by an increased ratio of oxidized to reduced glutathione (GSSG:GSH) and hepatic lipid peroxidation. The oxidative effects were associated with teratogenesis, reduced growth, diminished immune function, and histopathological lesions. Similarly, oxidative stress is believed to have induced the histological changes observed in the current study. Deposition of dark pigments, which is thought as indicators of oxidative stress in northern pike (*Esox Lucius*; Drevnick et al., 2008), were also observed in the livers of sturgeon in the highest SeMet treatment groups and were found to be especially numerous in green sturgeon. Thus, liver damage, likely a result of Se-induced oxidative stress, may be a major factor contributing the higher susceptibility to Se toxicity by the green sturgeon in this study.

It is possible that the comparatively faster initial growth rates of juvenile green sturgeon have resulted in their energetically vulnerable states. As growth requires an increase in protein synthesis, green sturgeon may have experienced a higher frequency of Met substitution by SeMet in their functional proteins. Consequently, normal physiological functions may have been compromised by an increase in non-functional proteins, as well as the associated oxidative stress. The high energetic demands of their initial growth phase may have also compromised the species' ability to repair damages induced by Se Toxicity, leading to the stunted growth and higher mortality observed during the latter part of exposure trial.

5. Summary

The objective of this study was to compare the effects of high Se diets in the juvenile stage of two sturgeon species native to SFB. Effects on growth parameters and histopathological alterations clearly indicated that green sturgeon is more sensitive to Se-laden diets compared with white sturgeon. Furthermore, the low SeMet diet (19.7 ± 0.6 mg Se/kg dw), which caused severe adverse effects in green sturgeon, is similarly to that of the levels found in SFB benthic macro-invertebrates, which are a major dietary component of young sturgeon. As such, our results suggest that juvenile green sturgeon is more sensitive to Se toxicity and should be monitored and managed separately from white sturgeon when developing conservation measures to protect this threatened SFB population segment from Se exposure.

Acknowledgment

Funding for this study was provided by CalFed Project number SP2006–035 and partially by P.O.R. Sardegna F.S.E. 2007–2013—Axis IV—L.a. I.3.1. and Fondazione Banco di Sardegna, Italy. We are also grateful for the technical assistance provided by Paul Lutes and Eric Hallen of the Center of Aquatic Biology and Aquaculture at the University of California, Davis. The infrastructure support of the Department of Animal Science and the College of Agriculture and Environmental Sciences of the University of California, Davis was also acknowledged.

References

- Ali, M., Iqbal, F., Salam, A., Iram, S., Athar, M., 2005. Comparative study of body composition of different fish species from brackish water pond. *Int. J. Environ. Sci. Technol.* 2 (3), 229–232.
- AOAC (Association of Official Analytical Chemists), 1984. In: Williams, S. (Ed.), *Official Methods of Analysis of Association of Official Analytical Chemists*, 14th ed. Association of Analytical Chemists, VA, USA, pp. 152–160.
- AOAC (Association of Official Analytical Chemists), 1995. *Official method of analysis*, 16th ed. Association of Official Analytical Chemists, Arlington, VA, USA.
- Arshad, U., Takami, G.A., Sadeghi, M., Bai, S., Pourali, H.R., Lee, S., 2011. Influence of dietary L-selenomethionine exposure on growth and survival of juvenile *Huso huso*. *J. Ichthyol.* 27, 761–765.
- Arteel, G.E., Sies, H., 2001. The biochemistry of Selenium and the glutathione system. *Environ. Toxicol. Pharmacol.* 10, 153–158.
- Beyers, D.W., Rice, J.A., Clements, W.H., Henry, C.J., 1999. Estimating physiological cost of chemical exposure: integrating energetics and stress to quantify toxic effects in fish. *Can. J. Fish. Aquat. Sci.* 56, 814–822.
- Billard, R., Lecointre, G., 2001. Biology and conservation of sturgeon and paddlefish. *Rev. Biol. Fish.* 9, 355–392.
- California Natural Diversity Database (CNDDDB), 2006. California Department of Fish and Game, <http://www.dfg.ca.gov/whdab/html/cnddb.html>.
- Coughlan, D.J., Velte, J.S., 1989. Dietary toxicity of selenium-contaminated red shiners to striped bass. *Trans. Am. Fish. Soc.* 118, 400–408.
- Cui, Y.B., Hung, S.S.O., 1995. A prototype feeding-growth table for white sturgeon. *J. Appl. Aquac.* 5, 25–34.
- Cui, Y.B., Hung, S.S.O., Deng, D.F., Yang, Y., 1996. Growth of white sturgeon as affected by feeding regimen. *Prog. Fish-Cult.* 59, 31–35.
- Dalle-Donne, I., Rossi, R., Milzani, A., Di Simplicio, P., Columbo, R., 2001. The actin cytoskeleton response to oxidants: from small heat shock protein phosphorylation to changes in the redox state of actin itself. *Free Radical Biol. Med.* 31, 1624–1632.
- Deng, X., Van Eenennaam, J.P., Doroshov, S.I., 2002. Comparison of early life stages and growth of green and white sturgeon. *Am. Fish. Soc. Symp.* 28, 237–248.
- Drevnick, P.E., Roberts, A.P., Otter, R.R., Hammerschmidt, C.R., Klaper, R., Oris, J.T., 2008. Mercury toxicity in livers of northern pike (*Esox lucius*) from Isle Royale, USA. *Comp. Biochem. Physiol. C: Toxicol. Pharmacol.* 147, 331–338.
- Ellis, R.G., Herdt, T.H., Stowe, H.D., 1997. Physical, hematologic, biochemical, and immunologic effects of supranutritional supplementation with dietary selenium in Holstein cows. *Am. J. Vet. Res.* 58, 760–764.
- Fan, T.W.M., Teh, S.J., Hinton, D.E., Higashi, R.M., 2002. Selenium biotransformations into proteinaceous forms by foodweb organisms of selenium-laden drainage waters in California. *Aquat. Toxicol.* 57, 65–84.
- Hamilton, S.J., Buhl, K.J., Faerber, N.L., Wiedmayer, R.H., Bullard, F.A., 1990. Toxicity of organic selenium in the diet of chinook salmon. *Environ. Toxicol. Chem.* 9, 347–358.
- Hamilton, S.J., 2004. Review of selenium toxicity in the aquatic food chain. *Sci. Total Environ.* 326, 1–31.
- Handy, R.D., Penrice, W.S., 1993. The influence of high oral doses of mercuric chloride on organ toxicant concentrations and histopathology in rainbow trout, *Oncorhynchus mykiss*. *Oncorhynchus mykiss*. *Comp. Biochem. Physiol.* 106C, 717–724.
- Heinz, H.G., Sanderson, C.J., 1990. Avoidance of selenium-treated food by mallards. *Environ. Toxicol. Chem.* 9, 1155–1158.
- Hilton, J.W., Hodson, P.V., Slinger, S.J., 1980. The requirement and toxicity of selenium in rainbow trout (*Salmo gairdneri*). *J. Nutr.* 110, 2527–2535.
- Hoffman, D.J., 2002. Role of selenium toxicity and oxidative stress in aquatic birds. *Aquat. Toxicol.* 57, 11–26.
- Huang, S.S.Y., Strathe, A.B., Wang, W.F., Deng, D.F., Fadel, J.G., Hung, S.S.O., 2012. Selenocompounds in juvenile white sturgeon: evaluating blood, tissue, and urine selenium concentrations after a single oral dose. *Aquat. Toxicol.* 109, 158–165.
- Hung, S.S.O., Lutes, P.B., 1987. Optimum feeding rate of juvenile white sturgeon (*Acipenser transmontanus*): at 20° C. *Aquaculture* 65, 307–317.
- Ivancic, J., Weiss, W.P., 2001. Effect of dietary sulfur and selenium concentrations on selenium balance of lactating Holstein cows. *J. Dairy Sci.* 84, 225–232.
- Lee, J.-W., De Riu, N., Lee, S., Bai, S., Moniello, G., Hung, S.S.O., 2011. Effect of dietary methyl mercury on growth performance and tissue burden in juvenile green (*Acipenser medirostris*) and white sturgeon (*A. transmontanus*). *Aquat. Toxicol.* 105, 227–234.
- Lee, J.-W., Kim, J.W., De Riu, N., Moniello, G., Hung, S.S.O., 2012. Histopathological alterations of juvenile green (*Acipenser medirostris*) and white sturgeon (*A. transmontanus*) exposed to elevated dietary methylmercury. *Aquat. Toxicol.* 109, 90–99.
- Lemly, A.D., 1985. Toxicology of selenium in freshwater reservoir: implication for environmental hazard evaluation and safety. *Ecotoxicol. Environ. Saf.* 10, 314–338.
- Lemly, A.D., 2002. *Selenium Assessment in Aquatic Ecosystem: A guide for Hazard Evaluation on Water Quality Criteria*. Springer-Verlag, New York, NY, pp. 161.
- Lemly, A.D., 2004. Aquatic selenium pollution is a global environmental safety issue. *Ecotoxicol. Environ. Saf.* 59, 44–56.
- Linville, R.G., Luoma, S.N., Cutter, L., Cutter, G.A., 2002. Increase selenium threat as a result of exotic bivalve *Patamocorbula amurensis* into the San Francisco Bay-Delta. *Aquat. Toxicol.* 57, 51–64.
- Luoma, S.N., Presser, T.S., 2000. Forecasting selenium discharges to the San Francisco Bay-delta estuary: Ecological effects of a proposed San Luis Drain extension. U. S. Geological Survey. Open-file Report 00-416.
- Moyle, P.B., 2002. *Inland fishes of California*. University of California Press, Berkeley, CA, pp. 106–113.
- National Marine Fisheries Service, 2006. Endangered and threatened wildlife and plants: proposed threatened status for Southern distinct population segment of North American green sturgeon. Federal Register, 17757–17766.
- NRC, 2005. *Selenium, Mineral Tolerance of Animals*. National Academy Press, Washington, DC, pp. 248–261.
- Ogle, R.S., Knight, A.W., 1989. Effects of elevated foodborne selenium on growth and reproduction of the fathead minnow (*Pimephales promelas*). *Arch. Environ. Contam. Toxicol.* 18, 795–803.
- Palace, V.P., Spallholz, J.E., Holm, J., Wautier, K., Evans, R.E., Baron, C.L., 2004. Metabolism of selenomethionine by rainbow trout (*Oncorhynchus mykiss*) embryos can generate oxidative stress. *Ecotoxicol. Environ. Saf.* 58, 17–21.
- Selye, H., 1955. Stress and disease. *Science* 122, 625–631.
- Skorupa, J.P., 1998. Selenium poisoning of fish and wildlife in nature: lesson from twelve real-world experiences. In: Frankenberger Jr., W.T., Engberg, R.A. (Eds.), *In Environmental Chemistry of Selenium*. Marcel Dekker, New York, NY, pp. 315–354.
- Sorensen, E.M.B., Harlan, C.W., Bell, J.S., 1982. Renal changes in selenium-exposed fish. *Am. J. Forensic Med. Pathol.* 3 (2), 123–129.
- Sorensen, E.M.B., Cumbie, P.M., Bauer, T.L., Bell, J.S., Harlan, C.W., 1984. Histopathological, hematological, condition-factor, and organ weight changes associated with selenium accumulation in fish from Belews Lake. *North Carolina Arch. Environ. Contam. Toxicol.* 13, 153–162.
- Steward, A.R., Luoma, S.N., Schlekot, C.E., Doblin, M., Hieb, K.A., 2004. Food web pathway determines how selenium effect aquatic ecosystems: a San Francisco Bay case study. *Environ. Sci. Technol.* 38, 4519–4526.
- Suzuki, K.T., 2005. Metabolomics of selenium: Se metabolites based on speciation studies. *J. Health Sci.* 51 (2), 107–114.
- Tashjian, D.H., Teh, S.J., Sogomonnyan, A., Hung, S.S.O., 2006. Bioaccumulation and chronic toxicity of dietary L-selenomethionine in the juvenile white sturgeon (*Acipenser transmontanus*). *Aquat. Toxicol.* 79, 401–409.
- Teh, S.J., Deng, X., Deng, D.F., Teh, F.C., Hung, S.S.O., 2004. Chronic effects of dietary selenium on juvenile Sacramento splittail (*Pogonichthys macrolepidotus*). *Environ. Sci. Technol.* 38, 6085–6093.
- Thophon, S., Kruatrachue, M., Upatham, E.S., Pokethitayook, P., Sahaphong, S., Jaritkhan, S., 2003. Histopathological alterations of white seabass, *Lates calcarifer*, in acute and subchronic cadmium exposure. *Environ. Pollut.* 121, 307–320.
- Urquhart, K.A.F., Regalado, K., 1991. *Selenium Verification Study 1988–1990: California State Water Resources Control Board Report 91-2-WQWR*. Sacramento, CA, pp. 94.

This article was downloaded by: [Kenneth Rose]

On: 01 August 2013, At: 15:43

Publisher: Taylor & Francis

Informa Ltd Registered in England and Wales Registered Number: 1072954 Registered office: Mortimer House, 37-41 Mortimer Street, London W1T 3JH, UK



Transactions of the American Fisheries Society

Publication details, including instructions for authors and subscription information:

<http://www.tandfonline.com/loi/utaf20>

Individual-Based Modeling of Delta Smelt Population Dynamics in the Upper San Francisco Estuary: I. Model Description and Baseline Results

Kenneth A. Rose^a, Wim J. Kimmerer^b, Karen P. Edwards^c & William A. Bennett^d

^a Department of Oceanography and Coastal Sciences, Louisiana State University, Energy, Coast, and Environment Building, Baton Rouge, Louisiana, 70803, USA

^b Romberg Tiburon Center for Environmental Studies, San Francisco State University, 3152 Paradise Drive, Tiburon, California, 94920, USA

^c Environment Agency, Manley House, Kestrel Way, Exeter, EX2 7LQ, UK

^d Center for Watershed Sciences, John Muir Institute of the Environment, Bodega Marine Laboratory, University of California, Davis, Post Office Box 247, Bodega Bay, California, 94923, USA

Published online: 01 Aug 2013.

To cite this article: Kenneth A. Rose, Wim J. Kimmerer, Karen P. Edwards & William A. Bennett (2013) Individual-Based Modeling of Delta Smelt Population Dynamics in the Upper San Francisco Estuary: I. Model Description and Baseline Results, Transactions of the American Fisheries Society, 142:5, 1238-1259

To link to this article: <http://dx.doi.org/10.1080/00028487.2013.799518>

PLEASE SCROLL DOWN FOR ARTICLE

Taylor & Francis makes every effort to ensure the accuracy of all the information (the "Content") contained in the publications on our platform. However, Taylor & Francis, our agents, and our licensors make no representations or warranties whatsoever as to the accuracy, completeness, or suitability for any purpose of the Content. Any opinions and views expressed in this publication are the opinions and views of the authors, and are not the views of or endorsed by Taylor & Francis. The accuracy of the Content should not be relied upon and should be independently verified with primary sources of information. Taylor and Francis shall not be liable for any losses, actions, claims, proceedings, demands, costs, expenses, damages, and other liabilities whatsoever or howsoever caused arising directly or indirectly in connection with, in relation to or arising out of the use of the Content.

This article may be used for research, teaching, and private study purposes. Any substantial or systematic reproduction, redistribution, reselling, loan, sub-licensing, systematic supply, or distribution in any form to anyone is expressly forbidden. Terms & Conditions of access and use can be found at <http://www.tandfonline.com/page/terms-and-conditions>

ARTICLE

Individual-Based Modeling of Delta Smelt Population Dynamics in the Upper San Francisco Estuary: I. Model Description and Baseline Results

Kenneth A. Rose*

*Department of Oceanography and Coastal Sciences, Louisiana State University,
Energy, Coast, and Environment Building, Baton Rouge, Louisiana 70803, USA*

Wim J. Kimmerer

*Romberg Tiburon Center for Environmental Studies, San Francisco State University,
3152 Paradise Drive, Tiburon, California 94920, USA*

Karen P. Edwards

Environment Agency, Manley House, Kestrel Way, Exeter EX2 7LQ, UK

William A. Bennett

*Center for Watershed Sciences, John Muir Institute of the Environment, Bodega Marine Laboratory,
University of California, Davis, Post Office Box 247, Bodega Bay, California 94923, USA*

Abstract

Many factors have been implicated in the decline of Delta Smelt *Hypomesus transpacificus* in the upper San Francisco Estuary, and the importance of each factor is difficult to determine using field data alone. We describe a spatially explicit, individual-based population model of Delta Smelt configured for the upper estuary. The model followed the reproduction, growth, mortality, and movement of individuals over their entire life cycle on the same spatial grid of cells as the Delta Simulation Model (DSM2) hydrodynamics model. Daily values of water temperature, salinity, and densities of six zooplankton prey types were represented on the spatial grid. Reproduction was evaluated daily, and new individuals were introduced into the model as yolk sac larvae. Growth of feeding individuals was based on bioenergetics and zooplankton densities. Mortality sources included natural mortality, starvation, and entrainment in water diversion facilities. Movement of larvae was determined using a particle tracking model, while movement of juveniles and adults was based on salinity. Simulations were performed for 1995–2005. The baseline simulation was generally consistent with the available data. Predicted daily fractions of larvae entrained and annual fractions of adults entrained were similar in magnitude to data-based estimates but showed less interannual variation. Interannual differences in mean length at age 1 had large effects on maturity and subsequent egg production. Predicted and observed spatial distributions in the fall showed moderately good agreement for extremely low- and high-outflow years. As indicated by the population growth rate, 1998 was the best year and 2001 was the worst year. Water year 1998 (i.e., October 1997–September 1998) was characterized by fast growth in fall 1997, low entrainment, and high stage-specific survival rates, whereas water year 2001 had opposite conditions. Our analysis further shows how multiple factors can operate simultaneously to result in the decline in abundance of Delta Smelt.

*Corresponding author: karose@lsu.edu

Received November 9, 2012; accepted April 18, 2013

Understanding the critical drivers and environmental changes that influence the population dynamics of fish is vital for effective resource management and restoration. Most fish species live multiple years and show ontogenetic shifts in the habitats they utilize, which exposes them to multiple environmental and biological factors spread over several points in their life cycle (Rose 2000). Identification of the relative importance of these factors and how they may interact with each other is an important step toward understanding and managing fish populations. A major debate is underway about the status of many harvested marine and coastal fish populations (Myers and Worm 2003; Hilborn 2007; Worm et al. 2009), as human development of coastal areas (McGranahan et al. 2007) and demand for high-quality freshwater (Vörösmarty et al. 2000) continue to accelerate. Identification of the major factors affecting population dynamics (especially declines in population) is critical because the high economic costs of protection and restoration demand efficient and effective responses.

The need to understand mechanisms of population decline for Delta Smelt *Hypomesus transpacificus* in the San Francisco Estuary is critical. This endemic species is listed as threatened under the U.S. Endangered Species Act and is listed as endangered under the California Endangered Species Act. Delta Smelt have generally been at low abundance since the 1980s and showed an even further sharp decrease starting in about 2002 (Bennett 2005; Sommer et al. 2007; Thomson et al. 2010). Delta Smelt have also become the focus of contentious debate because of perceived conflicts between the conservation of this species and the operation of facilities that divert water from the Delta Smelt's habitat for agricultural and urban uses (Brown et al. 2009; NRC 2010). These facilities alter seasonal patterns of flow, and they entrain and kill large numbers of Delta Smelt (Kimmerer 2008).

Many factors may be involved in the decline of Delta Smelt, and quantifying the importance of each factor has proven to be elusive despite the availability of extensive long-term field data (NRC 2012). Factors examined as possible contributors to the decline include entrainment of Delta Smelt by the two large water diversion facilities in the Sacramento–San Joaquin River Delta (hereafter, “the Delta”), shifts in the composition and densities of the zooplankton (prey) community, and changes in physical habitat related to salinity and turbidity (Baxter et al. 2010). A sharp decline in four fish species (juvenile Striped Bass *Morone saxatilis*; Longfin Smelt *Spirinchus thaleichthys*; Threadfin Shad *Dorosoma petenense*; and Delta Smelt) within the upper San Francisco Estuary beginning in approximately 2000 led to a substantial effort at synthesizing existing data to determine the cause (Sommer et al. 2007). The results to date have narrowed the possible factors to some extent (e.g., contaminant effects are likely small) and have facilitated the conclusion that the recent decline in Delta Smelt was due to multiple factors acting together (Baxter et al. 2010). Two statistical analyses (Mac Nally et al. 2010; Thomson et al. 2010) examined the dynamics of the four fish species by using mon-

itoring data collected from the 1970s to 2007. Both analyses, which used similar data but different statistical methods, showed several covariates that were related to abundance of the fish, but they could not resolve the cause of the recent declines.

An alternative approach to the analysis of the effects of multiple factors on fish populations is simulation modeling of the growth, mortality, reproduction, and movement processes underlying the population dynamics. Population modeling allows the investigator to control everything and thus to perform simulation experiments for isolating the effects of individual factors and for exploring the effects of previously unobserved combinations of conditions (Rose et al. 2009). However, model results must be interpreted with caution because models are always simplifications of reality, and their predictions can be biased by decisions about which processes to include and at what temporal and spatial scales to represent those processes.

In this paper, we describe a spatially explicit, individual-based population model of Delta Smelt configured for the upper San Francisco Estuary. We chose this approach because many of the factors that are thought to contribute to the Delta Smelt's decline vary in space (Baxter et al. 2010), and simulating fish movement is more straightforward with an individual-based approach than with other modeling approaches (Tyler and Rose 1994). We first briefly describe the San Francisco Estuary and the life cycle of Delta Smelt. We then describe the spatial grid, environmental conditions, and reproduction, growth, mortality, and movement processes that are represented in the individual-based model. Hydrodynamic model output for the spatial grid and field data for temperature, salinity, and zooplankton densities were used as inputs to the population model for simulation of the period 1995–2005. The results of the baseline simulation are compared with the observed data, and we contrast the conditions between a “good year” and a “bad year” for Delta Smelt growth and survival within the baseline simulation. We conclude with a discussion of our results relative to other analyses and the strengths and weaknesses of our current model formulation. In our companion paper (Rose et al. 2013, this issue), we show that the results presented here are robust to alternative baseline assumptions, and we further explore the factors causing good and bad years by using a simulation experiment approach.

UPPER SAN FRANCISCO ESTUARY AND DELTA SMELT

The San Francisco Estuary is the largest estuary on the U.S. Pacific coast, with a watershed covering approximately 40% of California (Figure 1). The estuary connects the Sacramento and San Joaquin rivers through San Francisco Bay to the Pacific Ocean. Freshwater enters via the Sacramento River from the north and the San Joaquin River from the south; the confluence is roughly the landward limit of ocean salt penetration (Kimmerer 2004). We focus on the upper portion of the estuary (including the Delta and Suisun Bay), which encompasses the entire range of the Delta Smelt.

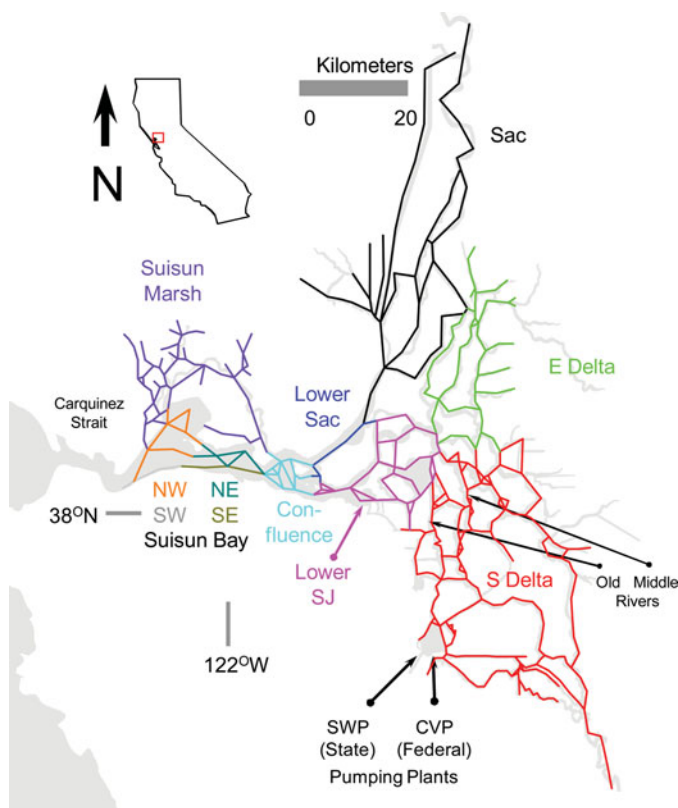


FIGURE 1. Location of the San Francisco Estuary, California, and the spatial grid and boxes used in the model. Gray represents the outline of the estuary. The 11 boxes are color coded and refer to (in numerical order): (1) Sacramento River region (Sac) of the Sacramento–San Joaquin Delta; (2) eastern Delta (E Delta); (3) southern Delta (S Delta); (4) lower Sacramento River region (Lower Sac); (5) lower San Joaquin River region (Lower SJ); (6) confluence (westernmost box in the Delta); (7) southeast Suisun Bay (SE); (8) northeast Suisun Bay (NE); (9) Suisun Marsh; (10) southwest Suisun Bay (SW); and (11) northwest Suisun Bay (NW). Additional labels show the Old River, Middle River, Carquinez Strait, and the State Water Project (SWP) and Central Valley Project (CVP) pumping plants.

The San Francisco Estuary has been described as one of the most highly altered estuarine ecosystems in the world (Nichols et al. 1986; Lund et al. 2010). Over the past 150 years, approximately 95% of the marshes surrounding the estuary have been isolated from tidal action, and numerous nonnative species have been introduced—some with substantial ecological effects (e.g., Nichols et al. 1990; Winder and Jassby 2011). The Delta, which formerly consisted of tidal marsh, is now a complex network of linked channels and sloughs surrounding islands that are protected by a constructed levee system. During the past 60 years, the upper estuary has increasingly been managed through large-scale manipulation of river flows in order to provide freshwater for agricultural, municipal, and industrial uses.

The two large water diversions in the south Delta have exported an average of 30% of the available flow into the Delta during 1960–2000, with the percentage generally increasing through time and exceeding 60% in some years and seasons

(Kimmerer 2004). The State Water Project (SWP) facility provides drinking water for over 23 million Californians, and together the two diversion facilities (the SWP and the Central Valley Project [CVP]) fuel an estimated $\$25 \times 10^9$ annual agricultural economy (Grimaldo et al. 2009). Elaborate fish recovery facilities attempt to screen fish from the diverted water but with mixed success (Kimmerer 2011). All of these changes have substantially altered both the physical and ecological aspects of the system (Nichols et al. 1986; Hollibaugh 1996; NRC 2012).

The life history of the Delta Smelt is summarized briefly here based on several sources (Moyle et al. 1992; Moyle 2002; Bennett 2005). The Delta Smelt has a relatively unusual life history strategy (Bennett 2005), as it exhibits the small size and short life span that are typical of an opportunistic life history strategy, but it has low reproductive rates that are more similar to those of an equilibrium strategist (Winemiller and Rose 1992). The Delta Smelt's life history also somewhat resembles those of salmonids (McCann and Shuter 1997) but without parental care. The geographic range of the Delta Smelt is confined to the upper San Francisco Estuary. It is primarily an annual species but with some small fraction of the population surviving a second year to spawn. Spawning takes place in freshwater during February–May at temperatures between 12°C and 20°C; spawning appears to be clustered in 2-week intervals, presumably related to the spring–neap tidal cycle. Eggs are demersal and attached; larval stages generally rear in freshwater before being transported to brackish waters, which are typically located between the confluence of the San Joaquin and Sacramento rivers and Carquinez Strait at the seaward margin of Suisun Bay (Figure 1). All life stages remain at a salinity of about 0.5–6.0 psu (the low-salinity zone) until the end of the year, when migration to freshwater begins. Delta Smelt eat primarily zooplankton throughout their lives, although adults also eat epibenthic crustaceans, such as amphipods. Delta Smelt are consumed by a variety of fish, principally visual predators.

MODEL DESCRIPTION

Overview

The model followed the reproduction, growth, mortality, and movement of individual Delta Smelt over their entire life cycle on a spatial grid of cells (Figure 1). The spatial grid was a one-dimensional network of 517 channels and 5 reservoirs used in the Delta Simulation Model (DSM2) hydrodynamic model (California Department of Water Resources [CDWR]). This one-dimensional model simulates non-steady-state hydrodynamics in a network of channels and has been widely used for analyses and water supply planning for the Delta (Kimmerer and Nobriga 2008). Simulations from DSM2 provided (1) hourly water velocities and water levels at the ends of channels and (2) hourly water flows into and out of the reservoirs. Daily water temperature, salinity, and densities of six zooplankton prey types as estimated from field data were also represented on the same spatial grid.

Each 365-d model year began on October 1, the start date for each water year. Individuals were aged on January 1 of each year. Whenever we refer to a year, it is the year that includes the summer period (e.g., model year 1996 extended from October 1, 1995, to September 30, 1996). Multiyear simulations were performed using reproduction to introduce the new individuals each year.

Reproduction was evaluated daily during the spring spawning season, and eggs developed as a daily cohort at a temperature-dependent rate. Upon hatching, new yolk sac larvae were pooled for each day and were introduced as model individuals. Individuals developed through life stages of yolk sac larva, larva, postlarva, juvenile, and adult. Growth was based on bioenergetics and zooplankton densities in the grid cells. Mortality included a stage-specific mortality rate, starvation, and mortality due to entrainment at the water diversion facilities. Movement of yolk sac larvae, larvae, and postlarvae was determined hourly by using a particle tracking model (PTM) that incorporates water velocities from the DSM2 hydrodynamic model. Movement of juveniles and adults was based entirely on a behavioral response to salinity, and the locations of individual fish on the grid were updated every 12 h.

All simulations used hydrodynamic conditions, temperature, salinity, and zooplankton densities for the period 1995–2005. This period was selected because (1) it encompasses the main period of Delta Smelt decline, (2) hydrodynamic simulations were available, and (3) field data on zooplankton and Delta Smelt were relatively complete.

Environment

A second grid of 11 coarser boxes was overlaid onto the channel grid (Figure 1) so that the more sparsely sampled field data could be used to specify daily water temperature, salinity, and zooplankton densities. The 11 boxes were determined based on previously identified regions of hydraulic similarity (e.g., Miller et al. 2012) and the availability of enough stations to ensure that at least several stations were present in each box.

Daily values of temperature, salinity, and zooplankton densities were estimated for each box and then were assigned to each channel within each box on each day (see details in Supplement A in the online version of this article). Final daily temperature and salinity values for each box are shown in Figure 2 for a year with high freshwater outflow (1998) and a year with low freshwater outflow (2001). All channels within a given box were assigned the box values. Temperature did not vary much among sampling stations within boxes, and the sampling density was too low to represent the within-box (channel-level) spatial gradients in salinity.

The food environment was represented by the biomasses of six zooplankton types: adults of *Limnoithona* spp. (calanoid copepods), calanoid copepodids, other calanoid adults, adult *Eurytemora* (calanoid copepods), adult *Acanthocyclops vernalis* (cyclopoid copepods), and adult *Pseudodiaptomus* (calanoid copepods). We included random variation when we used the

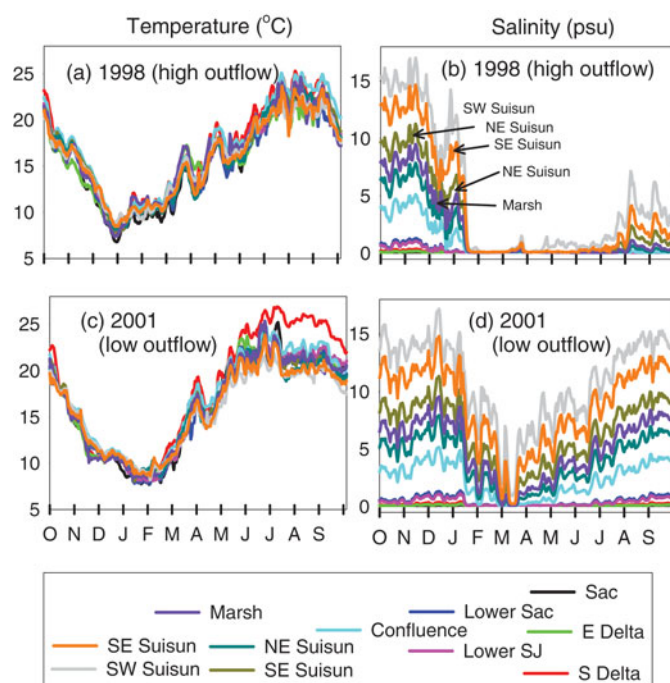


FIGURE 2. Daily temperature and salinity values in each box for (a), (b) 1998 (a year of high outflow) and (c), (d) 2001 (a year of low outflow). See Figure 1 for definition of box abbreviations. [Figure available online in color.]

boxwide mean to assign values to the channels within each box (see Supplement A). Daily zooplankton biomass densities in each box are presented for the same high-outflow (Figure 3) and low-outflow (Figure 4) years as were shown for temperature and salinity.

Spawning

Each female individual that was longer than 60 mm TL at the start of the spawning season was allowed to spawn up to two times within the spawning season. We used a simple threshold of 60 mm because it was well supported by data (Bennett 2005) and because the manner in which maturity varies around the 60-mm length was uncertain. We explore a smoother maturity function in our companion paper (Rose et al. 2013).

The earliest day of spawning was first determined each year on October 1 by looking ahead at temperatures and finding the first day on which temperature exceeded 12°C in any box. On the earliest possible day of spawning in each year, a temperature of first actual spawning was assigned to each mature individual from a uniform distribution between 12°C and 20°C. To mimic the clustering of spawning on spring–neap tidal cycles, an individual spawned at the end of the 14-d tidal cycle that followed the day when water temperature in that individual's channel exceeded its assigned spawning temperature. By the time of spawning, the migratory movement algorithm based on salinity had put adults near or into freshwater boxes.

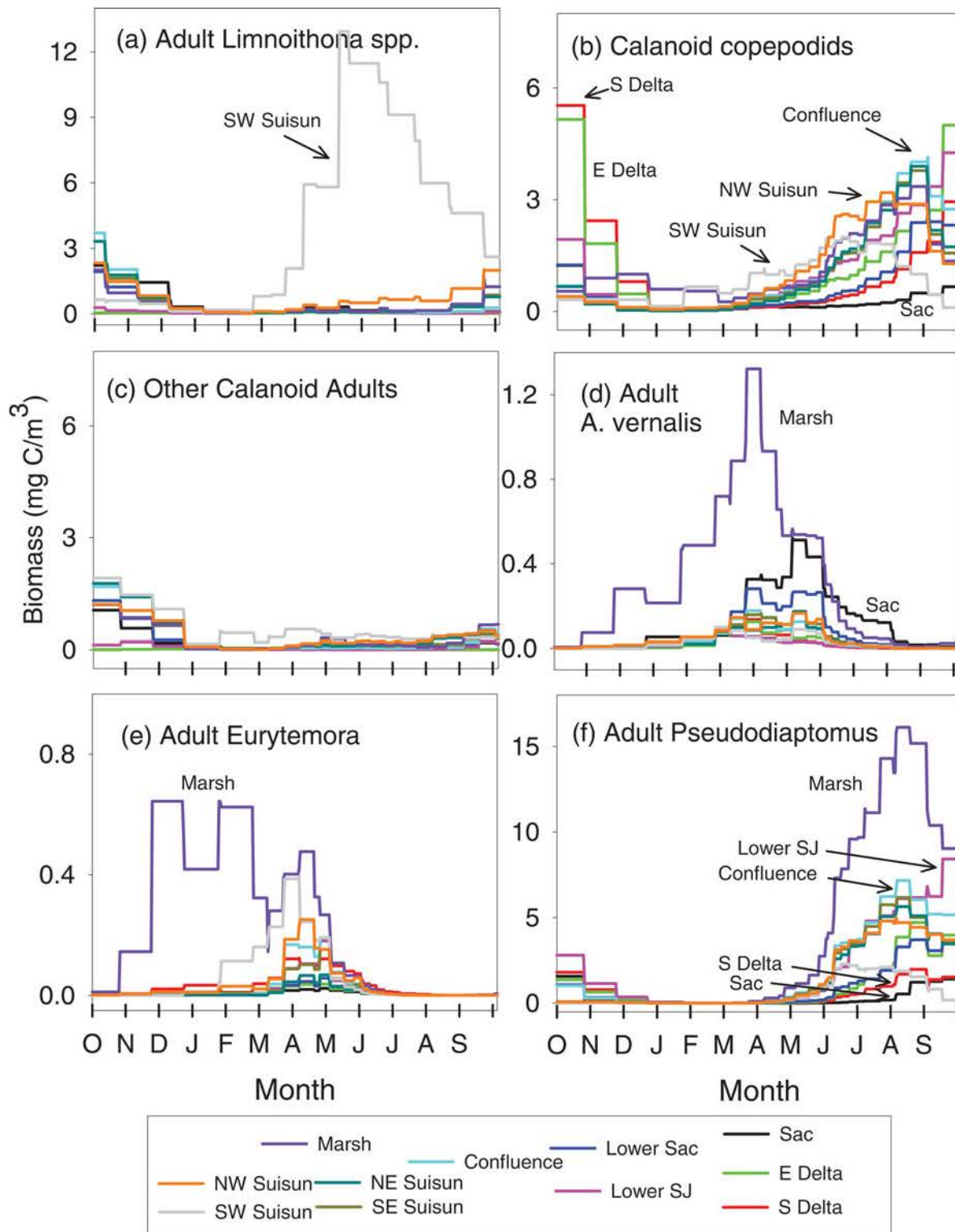


FIGURE 3. Daily biomass density values (mg C per m³ of water) for each of the six zooplankton groups in each spatial box during a year of high outflow (1998): (a) adults of *Limnoithona* spp., (b) calanoid copepodids, (c) other calanoid adults, (d) adult *Acanthocyclops vernalis*, (e) adult *Eurytemora*, and (f) adult *Pseudodiaptomus*. See Figure 1 for definition of box abbreviations. [Figure available online in color.]

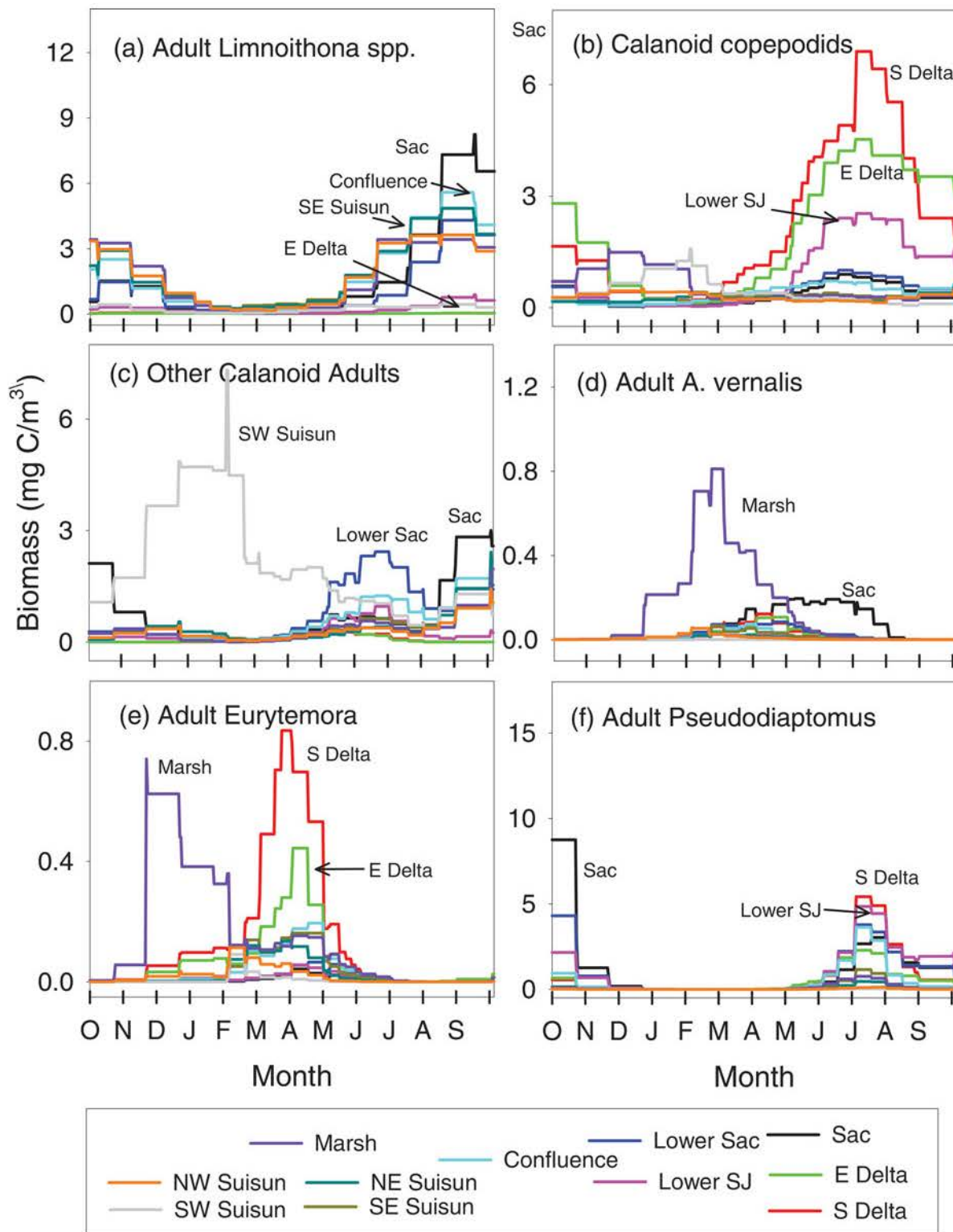


FIGURE 4. Daily biomass density values (mg C per m³ of water) for each of the six zooplankton groups in each spatial box during a year of low outflow (2001): (a) adults of *Limnoithona* spp., (b) calanoid copepodids, (c) other calanoid adults, (d) adult *Acanthocyclops vernalis*, (e) adult *Eurytemora*, and (f) adult *Pseudodiaptomus*. See Figure 1 for definition of box abbreviations. [Figure available online in color.]

Fecundity (D ; eggs/female) depended on the individual's weight on the day of spawning (Bennett 2005),

$$D = 175.4e^{\frac{L_{equiv}}{28.3}}, \quad (1)$$

where L_{equiv} (mm) is the length based on the actual weight of the fish. Upon spawning, the body weight of the individual Delta Smelt was reduced by 15%. We treated males the same as females (i.e., spawning temperatures and weight loss), but without any contribution of eggs, to produce similar weights at age.

After their first spawning event, females were evaluated daily to determine whether they would spawn a second time. Second spawning occurred if (1) the individual had regained enough weight (>95% of the weight expected from its length), (2) 14 or more days had passed since the first spawning, and (3) it was not too late (too warm) in the season for that individual to spawn in its box. The last possible day of spawning in each box was calculated as the first day after temperature exceeded 20°C plus 14 d to allow for the final tidal cycle to complete. The fecundity relationship used for the second spawning was the same as that for the first spawning, and weight was again reduced by 15%.

Eggs

Each female's first and second (if it occurred) spawns of eggs were followed separately as cohorts until hatching, when they became yolk sac larvae. Day of hatching was determined for each cohort by accumulating the daily fractional egg development (DV_e) until the degree of development exceeded 1.0. The daily fractional development towards hatching was based on temperature (Bennett 2005),

$$DV_e = \frac{1}{28.1 - 1.1 \cdot T}, \quad (2)$$

where T is the daily temperature (°C) in the box where spawning occurred. Spawning box temperature (which varied daily) was used because the eggs are attached. All eggs in each cohort that was spawned in a given box on a given day hatched on the same day. Daily egg mortality rates (M ; d^{-1}) were calculated by converting hatch rates observed at constant temperature in the hatchery to daily mortality (Bennett 2005),

$$M = \frac{-\log(s)}{DV_e} \quad (3)$$

and

$$s = -2.35 + 0.45 \cdot T - 0.016 \cdot T^2, \quad (4)$$

where s is the survival fraction through the egg stage.

Yolk Sac Larvae

Beginning with yolk sac larvae, new model individuals were created and followed for the rest of their lives. New individuals

were created from all those that hatched in each box on each day, and they were distinguished by whether they came from a first or second spawning event. Length (L ; mm) at hatch depended on the temperature on the day of hatching (Bennett 2005),

$$L = 5.92 - 0.05 \cdot T. \quad (5)$$

Weight (g wet weight) at hatch was determined from a field-based length–weight relationship (Kimmerer et al. 2005):

$$W = 0.005 \cdot L^3. \quad (6)$$

Similar to the method used for eggs, the duration of the yolk sac larval stage was determined by accumulating the daily fractional development (DV_y) of each model individual based on the temperature in its box (Bennett 2005) until the cumulative development exceeded 1.0:

$$DV_y = \frac{1}{7.53 - 0.08 \cdot T}. \quad (7)$$

Daily mortality rate of yolk sac larvae was assumed constant ($0.035 d^{-1}$) and was a key parameter adjusted as part of model calibration.

Feeding Life Stages: Development and Bioenergetics

Larvae became postlarvae at 15 mm, and postlarvae became juveniles at 25 mm; juveniles then became age-1 adults and age-1 adults from the previous year advanced to age 2 on January 1 (Bennett 2005). Age-2 adults were removed from the model just before attaining age 3. Larval to postlarval development coincided with the development of a swim bladder, and the juvenile stage marked the appearance of fin folds and an association with the low-salinity zone.

The daily growth of each feeding individual was represented by a difference form of the Wisconsin bioenergetics model (Ney 1993; Hanson et al. 1997),

$$W_t = W_{t-1} + (C - R - F - U - SDA) \cdot W_{t-1} \cdot \frac{e_p}{e_s} - Sp \cdot W_{t-1}, \quad (8)$$

where W is the weight of each individual, C is the realized consumption rate, R is the total metabolic rate, F is egestion, U is excretion, SDA is specific dynamic action, and Sp is loss due to spawning. All rates except Sp were in units of grams of prey per gram of Delta Smelt per day ($g \text{ prey} \cdot g \text{ smelt}^{-1} \cdot d^{-1}$ in wet weight); Sp was the fraction of weight lost (0.15) and occurred only on the day of spawning. The e_p and e_s terms (J/g) were used to convert grams of prey per gram of Delta Smelt to grams of smelt per gram of smelt, which was then multiplied by weight (W) to yield the weight change in grams of Delta Smelt per individual per day. The value of e_s was fixed at 4,814 J/g, while e_p was computed each day based on the fraction of *Limnoithona* in

the diet. All zooplankton groups had an energy density of 2,590 J/g; the exception was *Limnoithona*, for which energy density was assumed to be 30% lower (1,823 J/g) because Delta Smelt grow more slowly when fed *Limnoithona* (Lindsay Sullivan, San Francisco State University, personal communication).

Total length (L ; mm) was obtained from weight by using equation (6). Length was partially uncoupled from weight because length was allowed only to increase, whereas fish could lose weight. On days of weight gain, length was increased only after the individual's weight equaled that expected from its length. Thus, fish were allowed to become skinny but not fat.

Maximum consumption (C_{max}) depended on an individual's weight (W) and the water temperature (T):

$$C_{max} = a_c W^{b_c} f(T). \quad (9)$$

The temperature adjustment to maximum consumption ($f[T]$) increased from a value of CK_1 at temperature CQ to 0.98 at temperature T_O and then stayed at 0.98 until temperature reached T_M , after which the adjustment declined to CK_4 as temperature approached T_L (Table 1).

Realized consumption by the i th fish (C_i) was a functional response that depended on C_{max} and the densities of each zooplankton group j (prey density, PD_j) in the same channel as the fish:

$$C_{ij} = \frac{C_{max} W_i \left(\frac{PD_j \cdot V_{ij}}{K_{ij}} \right)}{1 + \sum_{k=1}^6 \left(\frac{PD_k \cdot V_k}{K_{ik}} \right)} \quad (10)$$

and

$$C_i = \sum_{j=1}^6 C_{ij}, \quad (11)$$

where C_{ij} is the daily rate of consumption of the j th prey type (six zooplankton groups) by individual fish i ; V_{ij} is the vulnerability of prey type j to fish i ; and K_{ik} is the half-saturation constant for fish i feeding on each prey type k . Equations (10) and (11) allowed an individual fish to consume multiple prey types without exceeding its maximum consumption. Vulnerabilities (V_{ij}) were set to 1.0 for all life stages eating all zooplankton types; the exception was Delta Smelt larvae, for which V_{ij} values of zero were used for all adult prey groups other than *Limnoithona* spp. The K -values were calibrated outside of the model to obtain diet and consumption rates that appeared realistic (Supplement B in the online version of this article).

The total metabolic rate (R) was an allometric function of weight and used an exponential relationship ($g[T]$) to adjust metabolism for temperature:

$$R = a_r W^{b_r} \cdot g(T), \quad (12)$$

where

$$g(T) = e^{(R_Q \cdot T)}. \quad (13)$$

Egestion (F) was a constant fraction of consumption, while SDA and excretion (U) were fractions of net assimilated energy

TABLE 1. Parameter values for each Delta Smelt life stage in the bioenergetics model.

Parameter	Description	Larvae	Postlarvae	Juveniles and adults
Maximum consumption (C_{max})				
a_c	Weight multiplier	0.18	0.18	0.1
b_c	Weight exponent	-0.275	-0.275	-0.54
CQ (°C)	Temperature at CK_1 of maximum	7	10	10
T_O (°C)	Temperature at 0.98 of maximum	17	20	20
T_M (°C)	Temperature at 0.98 of maximum	20	23	23
T_L (°C)	Temperature at CK_4 of maximum	28	27	27
CK_1	Effect at temperature CQ	0.4	0.4	0.4
CK_4	Effect at temperature T_L	0.01	0.01	0.01
Metabolism (R)				
a_r	Weight multiplier	0.0027	0.0027	0.0027
b_r	Weight exponent	-0.216	-0.216	-0.216
R_Q	Exponent for temperature effect	0.036	0.036	0.036
S_d	Fraction of assimilated food lost to SDA	0.175	0.175	0.175
Egestion (F) and excretion (U)				
F_a	Fraction of consumed food lost to egestion	0.16	0.16	0.16
U_a	Fraction of assimilated food lost to excretion	0.1	0.1	0.1

($C - F$; Table 1):

$$F = F_a \cdot C, \quad (14)$$

$$SDA = S_d \cdot (C - F), \quad (15)$$

and

$$U = U_a \cdot (C - F). \quad (16)$$

During calibration, we adjusted the bioenergetics parameter values developed for Rainbow Smelt *Osmerus mordax* (Lantry and Stewart 1993) until we obtained growth that was realistic for Delta Smelt. We adjusted the allometric and temperature-related parameter values of maximum consumption (a_c , b_c , CQ , T_O , T_M , and T_L in Table 1) and the temperature parameter that affected respiration (R_Q in Table 1). We determined parameter values that satisfied two conditions: (1) realistic daily growth rates and optimal temperatures for growth for mid-stage-sized larvae, juveniles, and adults; and (2) realistic weights and lengths for an individual that had grown from first feeding through age 2 under daily average temperatures and a consumption rate (C) that was equal to 0.8 of the maximum (i.e., proportion of maximum consumption [p -value] = 0.8; $C = p\text{-value} \times C_{max}$). The final bioenergetics rates for the mid-stage-sized larvae, postlarvae, juveniles, and adults are shown in Supplement B.

Mortality

Mortality occurred from stage-specific mortality rates (M), starvation, entrainment losses at the two water export pumping facilities, and old age. Stage-specific mortality rates represented predation and other causes of mortality not explicitly calculated from starvation or entrainment. Daily instantaneous mortality was temperature dependent for eggs (equations 3 and 4); M was set at 0.035 for yolk sac larvae (calibrated), 0.05 for larvae, 0.03 for postlarvae, 0.015 for juveniles, and 0.006 for adults. Starvation occurred if the weight of an individual fell below 50% of the weight expected from its length. Upon reaching age 3 (i.e., the individual's third January 1), the individual died from old age and was removed from the population.

Entrainment mortality for all life stages except eggs occurred when an individual entered Clifton Court Forebay (reservoir number 4; SWP) or arrived at node 181 (CVP; Figure 1). Yolk sac larvae, larvae, and postlarvae were transported there by the PTM, whereas juveniles and adults were unaffected by hydrodynamic conditions except through salinity. Use of only those individual juveniles and adults that arrived at the SWP and CVP by behavioral movements based on salinity resulted in underestimation of the numbers entrained by the pumping facilities. Delta Smelt are recovered at the south Delta fish facilities at higher rates when daily net flow in the southern Delta (Middle and Old rivers) is southwards toward the SWP and CVP (Grimaldo et al. 2009; Kimmerer 2011). Therefore, juveniles and adults that were located in the south Delta box (box 3) of the model were exposed to additional entrainment mortality

of 0.02 d^{-1} whenever the daily averaged flow in Middle River (downstream end of channel 90; Figure 1) was southward. The value of the added mortality (0.02 d^{-1}) was determined as part of model calibration.

Movement

Yolk sac larvae, larvae, and postlarvae were transported by water velocities on the spatial grid hourly by using a particle tracking approach, whereas juveniles and adults were moved every 12 h by using a kinesis approach to behavioral movement.

The PTM was a recoded version of the CDWR's PTM and used the same formulations (Wilbur 2000; Miller 2002). The CDWR's PTM has been used to examine entrainment impacts (e.g., Kimmerer and Nobriga 2008) and has been compared with other PTMs (Gross et al. 2010). Our recoded version used as input the hourly values of velocity at each end of each channel and the water level at each node that was generated by the DSM2 hydrodynamic model. The PTM kept track of the hourly positions of particles (the three larval stages) in three dimensions: along-channel (x = distance [m] from the upstream end of a channel), lateral (y = distance [m] from the center line of the channel), and vertical (z = distance [m] from the bottom of the channel). The y and z positions within a channel were altered by random perturbations and were used to adjust the x -direction velocity (Supplement C in the online version of this article).

Day-to-day movements and seasonal migrations of juveniles and adults were based on a kinesis approach (Humston et al. 2000, 2004), with salinity used as the cue. Salinity was used to simulate reasonable distributions of individuals within the system, but salinity did not directly affect growth or mortality. Rather, salinity was used to distribute individuals realistically, and individuals then experienced the local conditions (temperature and prey densities) in the channels.

Only the along-channel (x) position was tracked for juveniles and adults. At each 12-h time step, each individual's x position was updated, and its channel or reservoir location was determined. Kinesis represents the distance moved by each individual as the sum of an inertial component (IC) and a random component (RC), with the inertial component dominating when conditions (salinity) are good and the random component dominating when conditions are poor. The position in the x dimension (m from the upstream end of the channel) was updated every 12 h as

$$x_{t+1} = x_t + \Delta x_t \quad (17)$$

and

$$\Delta x_t = IC + RC, \quad (18)$$

where IC is the inertial component that depends on the movement velocity at the last time step (Δx_{t-1}), and RC is the random component based on fish swimming speed.

To compute IC and RC , we first computed the functions (f and g) that defined the degree to which salinity (S) in the box deviated from optimal salinity,

$$f(S) = H_1 \cdot e^{-0.5 \cdot \left(\frac{S-S_O}{\sigma_s}\right)^2} \quad (19)$$

and

$$g(S) = 1 - H_2 \cdot e^{-0.5 \cdot \left(\frac{S-S_O}{\sigma_s}\right)^2}, \quad (20)$$

where S_O is the optimal value of salinity (2.0 psu); σ_s ($= 3.0$) determines how quickly the function decreases as salinity deviates from its optimal value; and the H -values are constants (0.75 and 0.90) that define the maximum values of the functions. Inertial velocity (IC) was then computed using the distance moved in the last time step (Δx_{t-1}) and $f(S)$:

$$IC = \Delta x_{t-1} \cdot f(S), \quad (21)$$

Equation (21) results in the individual moving at the same total velocity (inertial and random combined) as in the last time step to the degree that conditions (salinity) are favorable; $f(S)$ is larger when salinity is near the optimal value (equation 19).

The random component of distance moved (RC) was computed based on $g(S)$ and a random component (r):

$$RC = r \cdot g(S). \quad (22)$$

The random component r was calculated as

$$r = N(0, 1) \cdot \frac{d}{2} + d \quad (23)$$

with

$$d = \sqrt{\frac{(0.001 \cdot L \cdot \Delta t \cdot 60 \cdot 60)^2}{2}}, \quad (24)$$

where r is a normal deviate with a mean of d and an SD of $d/2$. The numerator in equation (24) represents the distance (m) moved during one 12-h time step, assuming a swimming speed of 1.0 body length/s. The parameter d computed by equation (24) is typically about 70% of the distance to account for fish not swimming in a straight line. The probability of up-estuary movement (P_{up}) was specified as 0.50; for each individual and each time step, a random uniform number was compared with P_{up} to determine the x direction of movement (seaward or up-estuary) in a channel. The distance moved in that direction was determined by the computed velocity of the individual (Δx_i ; equation 18).

If individuals moved past the end of a channel, they then entered a node where they either continued into a new channel or entered a reservoir. The new channel or reservoir was randomly selected from all those connected to the node, regardless

of flow (Supplement C). Individuals were simply started at the beginning of a new channel. Supplement D (in the online version of this article) shows the results of testing the behavioral movement with simplified salinity patterns on the model grid.

Up-estuary migrations of adults and seaward migrations of juveniles were simulated using the above kinesis approach by changing S_O (equations 19 and 20) and P_{up} . On December 15 of each year, the spawning migration to freshwater began by changing S_O from 2 to 0 psu and by setting P_{up} to 0.85 (rather than 0.50) so that more moves were in the up-estuary direction. On May 1, the migration of adults and juveniles back to low-salinity water was simulated by setting S_O back to 2 psu and setting P_{up} to 0.15. Once individuals reached their new optimal salinity, P_{up} was switched back to 0.50.

Numerics

We used a super-individual approach (Scheffer et al. 1995) in order to accurately simulate the addition of new yolk sac larvae each year while ensuring that we did not exceed computer limitations (Supplement E in the online version of this article). Each super-individual represented some number of identical individuals in the population, which we term its "worth." Each year during spawning, the same number of super-individuals was added, but with their initial worth adjusted to reflect the yolk sac larvae produced. Mortality acted to decrement the worth of an individual, with the worth then being used to determine population-level numbers of eggs spawned and Delta Smelt densities and abundances. We used a complicated algorithm for determining how to allocate the fixed number of super-individuals each year among hatch dates and boxes (Supplement E). In all simulations, we used 150,000 super-individuals per age-class (450,000 super-individuals total) because this was sufficient for convergence (i.e., almost identical results were obtained when we followed more super-individuals). The model was coded in FORTRAN90.

Computation of Population Growth Rate

We used the individual-based model output to estimate a simple Leslie age-based matrix model for each year, which allowed us to summarize the multidimensional individual-based model results with a single variable of annual finite population growth rate (λ). The value of λ was based on the detailed dynamics of the individual-based model but allowed for easier comparison among years. A 2×2 matrix model was estimated for each year by computing the average maturity, fecundity, and age-specific survival rates (Supplement F in the online version of this article); eigenvalue analysis was then used to determine λ . The value of λ for a specific year is a measure of the conditions for Delta Smelt during that year. The λ value is also a reflection of conditions from the previous year by indicating how growth in the fall prior to spawning affected the elements related to maturity and fecundity in the matrix.

TABLE 2. Calculation of the major model output variables examined in Delta Smelt model simulations and the calculations for the data when model–data comparisons were performed. The corresponding figures for the results are noted; “text” means the results are described in the text.

Variable	Model calculations	Data calculations
(a) January adult abundance (Figure 5)	Summed worth of all individuals on January 1; includes young of the year that just became age 1 and age-1 fish that just became age 2 but does not include age-2 fish that were just removed as they became age 3.	Catch per trawl from the spring Kodiak trawl survey for 2002–2006 was averaged for January and February (first two trawls) and expanded to population size using volume sampled, 100% efficiency, and volume of Sacramento–San Joaquin Delta and Suisun Bay less than 4 m deep. November and December midwater trawl (MWT) abundance was computed the same way but by using volume of Delta and Suisun Bay less than 4 m deep. Log(Kodiak trawl abundance) was then regressed against log(MWT abundance), and the MWT values were used to estimate Kodiak trawl values for 1995–2001.
(b) Mean length of young-of-the-year, age-1, and age-2 fish (Figure 6)	Computed the weighted mean lengths on January 1 (just before their birthdays) using worth as the weighting factor in the averaging.	Mean length of fish in the December MWT samples, excluding fish greater than 100 mm, which were assumed to be age 1 or older.
(c) Annual number of adults entrained in diversion facilities (Figure 7)	Summed worth of individuals that were killed by arrival at reservoir 4 (State Water Project) or node 181 (Central Valley Project), plus the worth associated with the added mortality of all individuals in box 3 (South Delta) when Middle River flow is negative. The amount of worth (w) attributable to Middle River-related mortality (R) versus natural mortality (M) is $w(\frac{R}{M+R})(1 - e^{-M+R})$.	Methods are described by Kimmerer (2008), and results used here are shown in Figure 12a of that paper.
(d) Fraction of adults on January 1 subsequently entrained during that year	Ratio of numbers entrained (see variable c) divided by the January adult abundance (see variable a)	Methods are described by Kimmerer (2008), and results used here are shown in Figure 12c of that paper.
(e) Fraction of age-1 individuals that were mature and the number of eggs per entering age-1 individual (Figure 8)	Fraction mature was computed as the summed worth of age-1 individuals greater than 60 mm at the time of projected spawning divided by the summed worth of all age-1 individuals on the same day. The ratio of eggs to entering age-1 fish was computed as the cumulative number of eggs produced by age-1 individuals divided by the summed worth of age-1 fish on January 1 prior to spawning.	No data.
(f) Salinity weighted by densities of larvae, juveniles, and adults (Figure 9)	First, the worth of larvae (including postlarvae) was summed for each box on each day and then divided by the volume of the box to obtain number per m^3 by box on each day. Salinity in each box on each day was used to compute average salinity across boxes, weighted by the larval densities in each box. This process was repeated for juveniles and for adults. This was done for calendar years to better match following a year-class from the early spring spawning.	Number per trawl in each sample of the 20-mm, summer towntnet, fall MWT, and spring Kodiak trawl surveys was used to weight the salinity value measured with the trawls. Data values include a mix of larvae, juveniles, and adults that varied throughout the year depending on the survey.
(g) Proportion of individuals in and seaward of the confluence box for adults on December 14 and April 30, for postlarvae on June 24, and for juveniles and adults on September 1 (Figure 10)	For each stage and day, we summed the worth of individuals in each box and then divided the sum of worth in the confluence box and seaward boxes by the total summed worth over all boxes.	All of the fall MWT data from all stations during September–December were aggregated for each year, assigned to up-estuary of the confluence box (47 stations) or in or seaward of the confluence box (39 stations). The proportion in Figure 10f was computed from these two totals.

TABLE 2. Continued.

Variable	Model calculations	Data calculations
(h) Daily fraction of larvae plus postlarvae entrained in diversion facilities (Figure 11)	Summed worth of larval and postlarval individuals reaching reservoir 4 and node 181 divided by the summed worth of larvae and postlarvae at the end of the day plus the numbers lost to pumping plant entrainment during that day.	Methods are described by Kimmerer (2008), who used the 20-mm survey data, and the results are shown in Figure 14 of that paper. Note: Kimmerer's (2008) estimates included some juveniles as well as larvae and postlarvae. Also see recent papers about the estimation by Kimmerer (2011) and Miller (2011).
(i) Diets (text)	Computed averaged diets for each life stage using the biomass of zooplankton types eaten by every 500th individual on every 30th day. We first computed the proportions for each individual and then averaged the proportions over individuals. This resulted in individuals covering all life stages for the time periods during which the stages were present.	Diets reported by Lott (1998), Nobriga (2002), and Baxter et al. (2010), who summarized unpublished data from Steven Slater (California Department of Fish and Game); data were only sufficient for qualitative and general comparison.
(j) Annual finite population growth rate (λ ; Figure 12)	The λ value was computed from a 2×2 Leslie matrix model with parameter values determined from the individual-based model output each year (see Supplement F).	No data.
(k) Stage-specific survival rates (Figure 13)	Summed worth of individuals entering each life stage during the year divided by the summed worth of individuals entering the next life stage.	No data.
(l) Averaged temperature and proportion of maximum consumption (p -values; text)	Computed average temperature and average p -value for all individuals (weighted by their worth) each day and then computed seasonal averages weighting the daily values for total daily worth of age-1 individuals during February 27–June 7 (spawning) and total daily worth of juveniles during April 18–October 1 (growing season) and October 1–December 30 (fall).	

MODEL SIMULATIONS

Calibration

The model was calibrated in three steps. We first tested the movement of juveniles and adults on test grids with fixed salinity patterns to understand movement in contrived situations where we knew the correct movement patterns (Supplement D). Once the entire model had been calibrated, we again evaluated the movement patterns among years to confirm that simulated movement was realistic under dynamic salinity conditions. The results using the full model are presented below as part of the 1995–2005 historical simulation.

The second step was to determine the K -values (equation 10) for each Delta Smelt life stage and each zooplankton prey group (Supplement B). We averaged daily temperature and the biomass of each zooplankton group in each box over the periods when each life stage would be in the system. We assumed that larvae, juveniles, and adults remained in each of the 11 boxes, and we then iteratively adjusted the K -values so that the average consumption rate (i.e., with p -value = 0.8) and diets were reasonably close to the available observations.

The third and final step was to put the above two calibrated components (movement and growth) into the full model and then to simulate the period 1995–2005 by adjusting only the yolk sac larval mortality rate and the entrainment mortality multiplier based on Middle River flow. The mortality rate of yolk sac larvae was adjusted because this mortality was relatively simple (i.e., only temperature dependent and of short duration). The entrainment mortality multiplier was adjusted because the role of Middle River flow in affecting entrainment is well documented (Grimaldo et al. 2009), although the magnitude is uncertain, and we had data on adult entrainment mortality (Kimmerer 2011). We adjusted the yolk sac larval mortality rate until the predicted average January abundance for 1995–2005 was close to the data average of 2.7×10^6 ; we then adjusted the entrainment mortality multiplier until the average annual fraction of adults removed by diversions was close to the data average of 10%. We did not try to fit to individual years or to the pattern in the time series of annual abundances. Thus, any interannual differences in model output were generated by differences in temperature, salinity, entrainment, and zooplankton densities.

Historical Simulation

We report the results from the last step of the calibration: the 1995–2005 historical simulation. The calculations that were performed to obtain all reported model outputs and to summarize the field data used for model–data comparisons are shown in Table 2. The field data for Delta Smelt originate mostly from four surveys that are conducted annually by the California Department of Fish and Game (www.dfg.ca.gov/delta/): (1) the fall midwater trawl (MWT) survey began in 1967 and samples juveniles and adults monthly during September–December at 116 stations; (2) the spring Kodiak trawl survey began in 2002 and samples adults every 2–4 weeks during winter and spring at 39 stations; (3) the 20-mm survey (larval net) began in 1995 and samples larvae at 48 stations between March and July; and (4) the summer townet survey began in 1959 and samples mostly juveniles at up to 32 stations during June–August. These field data have been described and used extensively in previous analyses (e.g., Bennett 2005; Kimmerer et al. 2009; Sommer et al. 2011; Miller et al. 2012).

The model outputs and the model–data comparisons in Table 2 confirmed various aspects of the calibration or served to assess the realism of model behavior. None of the model–data comparisons can be considered as true model validation because no data were kept aside for independent comparison. Comparisons a–d in Table 2 were related to the three steps in model calibration as described above. Maturity of age-1 individuals and the number of eggs per entering age-1 individual (Table 2, comparison e) integrated the effects of growth differences (due to temperature and prey biomass) from the previous year on reproduction. Movement patterns were confirmed by using averaged salinities weighted by Delta Smelt density (comparison f) and the proportions of individuals in and seaward of the Sacramento River–San Joaquin River confluence box (comparison g). We used monthly Delta outflows (m^3/s) from DAYFLOW (www.water.ca.gov/dayflow/) to help interpret the spatial distributions in comparison g. Comparison h, the daily fraction of larvae lost to entrainment, confirmed the realism of the pumping-related mortality determined by the PTM. Overall average diets (comparison i) were examined to confirm reasonable shifts in diet from larvae to juveniles to adults. The λ values (comparison j) and stage survival rates (comparison k) provided condensed summaries of the differences among years. Finally, comparison l identified the between-year differences in temperature and food as actually experienced by the simulated fish.

MODEL RESULTS

Dynamics within the Historical Simulation

For the simulated period 1995–2005, calibration resulted in an average January adult abundance of 2.7×10^6 (compared to the data target of 2.3×10^6) and an average fraction of adults lost to the pumps of 11% (the target was 10%). The final calibrated mortality rates were 0.035 d^{-1} for yolk sac larvae and

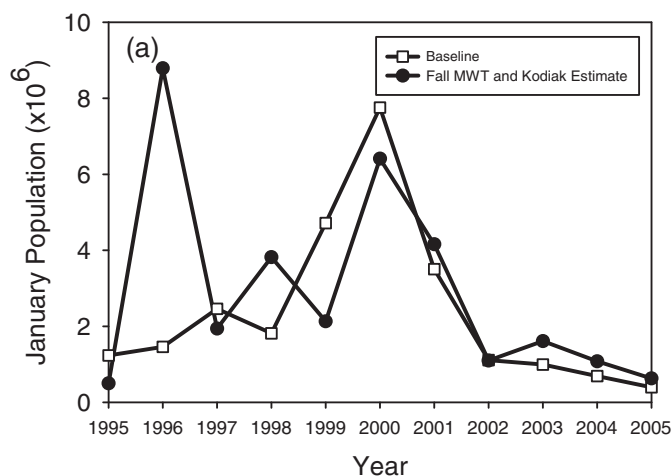


FIGURE 5. Annual abundance of adult Delta Smelt in January for 1995–2005 from the baseline simulation and as estimated from the fall midwater trawl (MWT) and spring Kodiak trawl sampling.

0.02 d^{-1} for Middle River-related pumping mortality. Annual January abundances varied from year to year in a pattern similar to that of data-based estimates, with a peak in 2000, a decline in 2001, and then low abundances in 2002–2005 (Figure 5). One exception was that the January adult abundance in 1996 had the highest data-based estimate but a relatively low simulated value.

Simulated lengths at age on January 1 were similar to data values for young of the year about to become age 1, with both model and data values varying between 55 and 65 mm (Figure 6). Faster growth was predicted for the summer and fall of 1995 (shown as the January 1996 value), 1997 (the January 1998 value), and 2001–2004. Simulated growth was slow in 1996, 1999, and 2000, resulting in shorter fish recorded during the

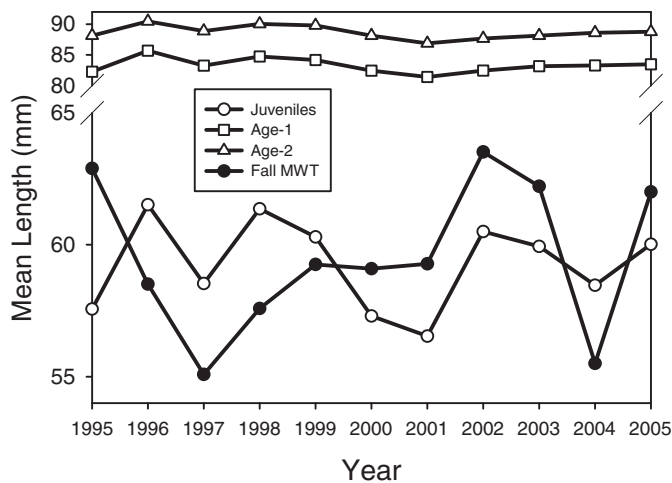


FIGURE 6. Mean total length of juvenile, age-1, and age-2 Delta Smelt on January 1 in each year (just prior to birthdays) of the 1995–2005 baseline simulation. Also included are the mean lengths of young-of-the-year fish from fall midwater trawl (MWT) sampling.

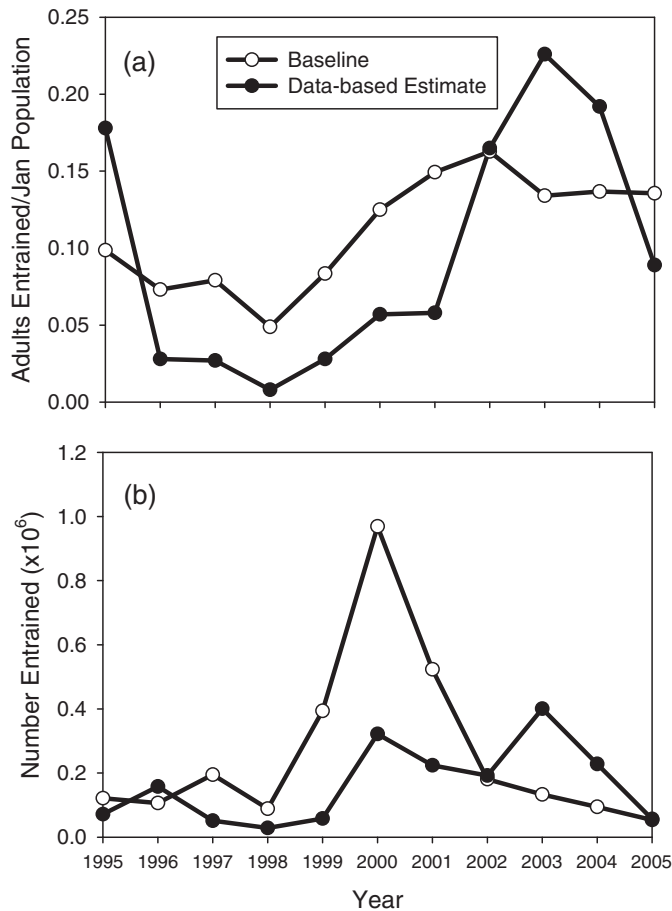


FIGURE 7. Predicted and observed annual values in 1995–2005 for (a) the fraction of adult Delta Smelt present in January that were entrained in pumping plants during the next few months (i.e., winter) and (b) the number of adults that were entrained during the same time period.

next January. Mean lengths of about 82 mm for age-1 fish (about to become age 2) and 90 mm for age-2 fish (about to become age 3) were consistent with the results of Bennett (2005).

The predicted annual fraction of adults entrained showed less interannual variation than the data-based values (Figure 7a), and the predicted numbers entrained were as much as two times the data values for 1999–2001 (Figure 7b). Predicted and estimated annual fractions entrained were low (<10%) for 1996–1999 and then increased to 15–20% for 2002–2004. Predicted fractions showed less variation and were higher than estimated values during the earlier, low-entrainment-loss years and were lower than estimated values during the latter, high-entrainment-loss years (i.e., in Figure 7a, the line connected by open circles is flatter than the line connected by black shaded circles). Substantially more model adults were entrained during 1999–2001 than were shown by the data (Figure 7b) because the fraction entrained was higher, and in two of those years the population estimate (Figure 5a) was higher than that in the data. Overestimation of the fraction entrained in early years and underestimation of the fraction entrained in later years suggested inaccuracies in the

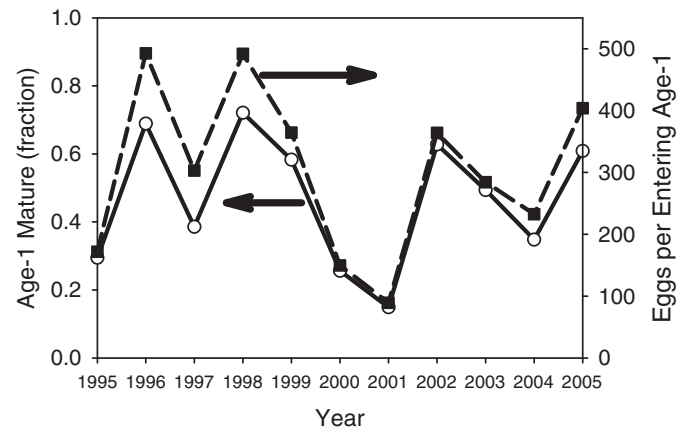


FIGURE 8. Annual fraction of age-1 individual Delta Smelt that were mature (solid line, open circles) and the number of eggs produced per entering age-1 individual (dashed line, black shaded squares) for the 1995–2005 baseline simulation.

simulated adult spatial distributions or in the use of a single value for the pumping mortality at any southward Middle River flow.

Even though the variation in mean length of age-1 adults was small (± 5 mm; Figure 6), interannual differences had large effects on maturity (Figure 8, solid line) and subsequent egg production (Figure 8, dashed line) by age-1 individuals. Age-1 individuals at the beginning of the spawning season (about 3 months into age 1) varied above and below 60 mm from year to year. This hovering around 60 mm caused the fraction of age-1 fish that were mature to range from 0.15 (in 2001) to 0.60–0.70 (in 1996, 1998, and 2002; Figure 8), tracking the slow and fast age-0 growth from the previous year (Figure 6). A greater fraction of individuals becoming mature and a higher weight of these individuals (equation 1) resulted in a fivefold difference among years in the number of eggs produced per entering age-1 individual (Figure 8). Egg production per entering age-1 fish was highest in 1998 (491.8) due to the fast growth of juveniles in 1997 and the high proportion (72%) of age-1 fish being mature at spawning; egg production per entering age-1 individual was lowest in 2001 (89.3; 15% maturity) due to slow juvenile growth in 2000. Such large variation in the fraction mature and eggs produced per entering age-1 fish seems extreme and may partially reflect the all-or-none maturity rule (100% mature if longer than 60 mm) we used. We further investigate the maturity rule in our companion paper (Rose et al. 2013).

Simulated Delta Smelt density-weighted salinities showed the up-estuary spawning migration of adults and the subsequent larval and juvenile movement seaward (Figure 9). Note that the years in Figure 9 are calendar years (i.e., they start on January 1) in order to follow a year-class. Salinity slowly rose for larvae and postlarvae during June–September as they were transported seaward (Figure 9a). Salinity also rose for juveniles during June–October (Figure 9b) after the S_0 for juveniles was changed from 0 to 2 psu on May 1. Salinity for adults went from near zero in January–May to approaching 2–6 psu beginning in June

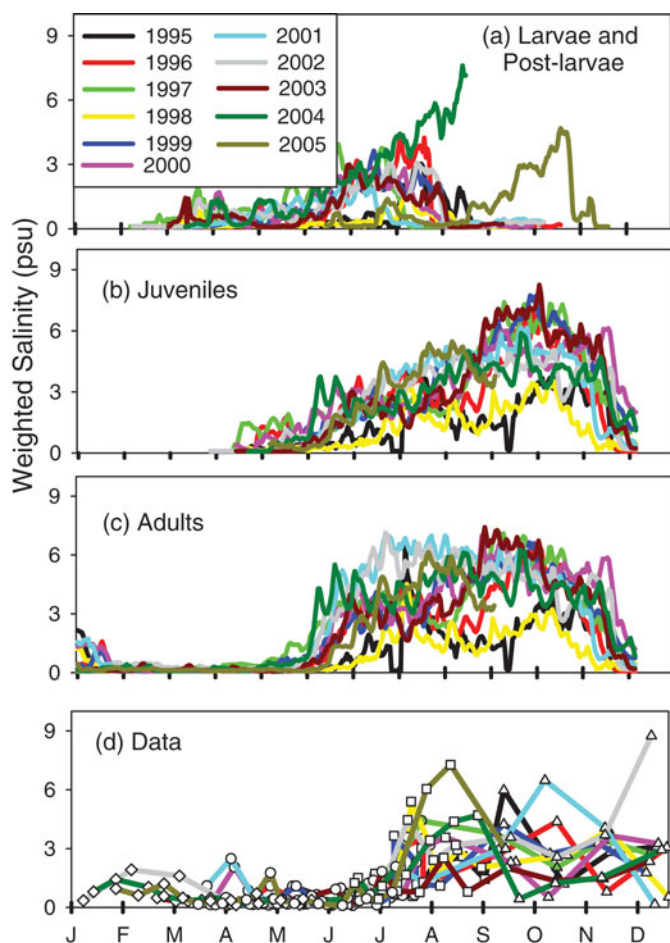


FIGURE 9. Average salinity (psu) weighted by Delta Smelt density computed daily during calendar years 1995–2005 for (a) larvae and postlarvae combined, (b) juveniles, and (c) adults in the baseline simulation. Panel (d) shows the weighted salinity values obtained by merging catch per unit effort data from the 20-mm, summer townet, fall midwater trawl (MWT), and spring Kodiak trawl surveys for 1995–2005. Years are calendar years rather than water years (e.g., 1997 refers to January–December). [Figure available online in color.]

(Figure 9c), triggered by a change in the adults' S_0 back to 2 psu on May 1. During most years, the density-weighted salinity values for juveniles and adults caused their seaward migration to occur earlier than was shown in the data (June in Figure 9c versus 9d), and they occupied water during the late summer and fall with salinities of 2–6 psu, whereas the data suggested somewhat lower-salinity waters of 1–4 psu during the late summer and fall (August–October in Figure 9c versus 9d).

The interannual influence of Delta outflow on the proportion of individuals in each spatial box is shown in Supplement G (in the online version of this article) and is summarized here by using a single metric: the proportion of fish that were within or seaward of the confluence box (Figure 10). In December, prior to their up-estuary spawning migration, adults were distributed based on salinity, which was roughly correlated with average October outflow (Figure 10a). During the high-outflow years of

1996 and 1999, more than 80% of adults were in or seaward of the confluence box, whereas during the remaining years fewer than 60% were in or seaward of the confluence box.

Spawning migration (including young-of-the-year fish that became age 1 on January 1) began in January and ended by April 30, with almost all individuals located up-estuary of the confluence box (Figure 10b). Once hatched, larvae were transported by the PTM; by June 24, when postlarvae were about to become juveniles, proportions again roughly reflected outflow conditions (Figure 10c). During 1995 and 1998, which were years of high May outflow, over 80% of postlarvae were in or seaward of the confluence box, whereas during relatively low-outflow years (2001, 2002, and 2004) only 20–30% of postlarvae were located in or seaward of the confluence box. Data for 1997 appear anomalous relative to May outflow because that year had a low May outflow but the highest June outflow over the simulation time period ($2,033 \text{ m}^3/\text{s}$ versus less than $1,327 \text{ m}^3/\text{s}$). Juvenile and adult distributions on September 1 (Figure 10d, e) resembled each other because both reflected behavioral movement towards 2-psu water. Juveniles and adults were farthest seaward during the high outflow of August 1998 and were situated up-estuary during the low-outflow years of 2001, 2002, and 2004.

Finally, the predicted and observed proportions of adults that were in or seaward of the confluence during the fall showed moderately good agreement for extremely low- and high-outflow years but not for years of intermediate flow (Figure 10f). Predicted and observed proportions showed relatively more fish in and seaward of the confluence during 1996 and 1999 and more fish being relatively up-estuary during 1995, 2004, and 2005. October outflow was highest in 1996 and 1999 and was low in 1995 and 2004 (Figure 10a); October outflow for 2005 was not low, but the summed October–December outflow in 2005 was relatively low. However, predicted proportions were flatter than observed proportions (proportions under low outflow were above the 1-to-1 line, and proportions under high outflow were below the 1-to-1 line in Figure 10f), indicating that simulated adults were generally too far seaward under low outflow and too far up-estuary under high outflow.

The simulated daily proportion of larvae and postlarvae entrained, which results from transport by the PTM, generally agreed with the data-based estimates (Figure 11). Model predictions showed less interannual variation than the data-based values. A few extreme model values of 0.2–0.3 were predicted, whereas data values never exceeded 0.1. In both the simulation and in the data, entrainment was relatively low during 1995, 1996, and 1998 and was high during 2002 and 2003. Model-predicted entrainment was also high during 2000, 2001, and 2005, which were intermediate entrainment years in the data.

Simulated diets were reasonable and consistent among years, even between the most extreme years (not shown). Larvae consumed *Limnoithona* spp. (20% of consumed biomass) and calanoid copepodids (80%) because other prey had vulnerabilities of zero. As Delta Smelt increased in size, they consumed

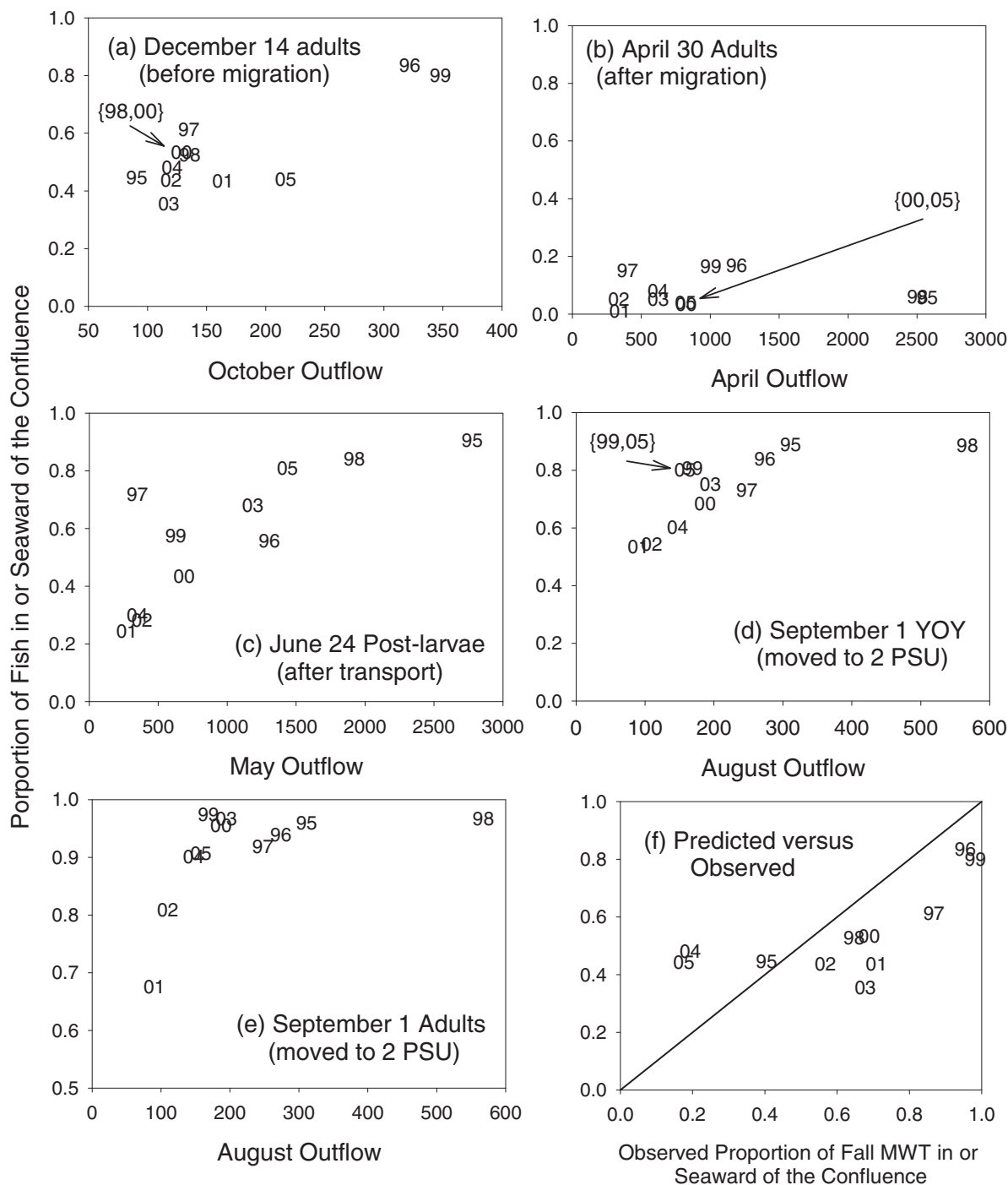


FIGURE 10. Predicted proportion of Delta Smelt individuals in the confluence and seaward boxes (see Figure 1) versus monthly Sacramento–San Joaquin Delta outflow (m³/s) in the immediately preceding months for 1995–2005 of the baseline simulation: (a) adults on December 14 (before the spawning migration), (b) adults on April 30 (after the spawning migration), (c) postlarvae on June 24 (after particle tracking model transport), (d) juveniles (young of the year) on September 1, and (e) adults on September 1. Two-digit numbers indicate water years (e.g., 96 = 1996; 02 = 2002). Panel (f) is a comparison of the predicted proportion of Delta Smelt in and seaward of the confluence box from December 14 versus the proportion estimated from the fall midwater trawl (MWT) survey. Panel (a) uses outflow from October of the previous year (e.g., October 2001 outflow for the year 2002).

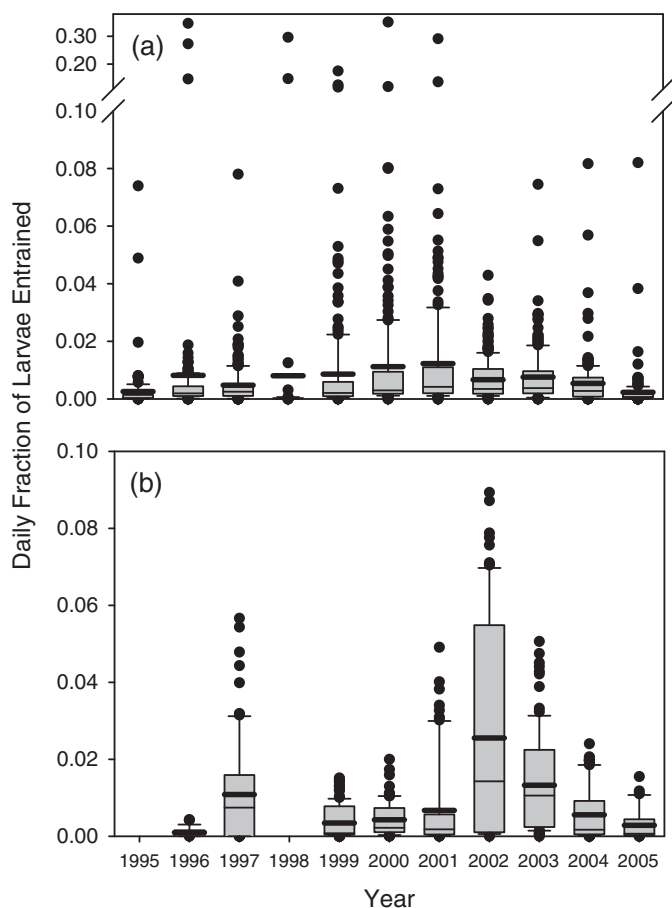


FIGURE 11. Daily entrained fraction of (a) Delta Smelt larvae and postlarvae combined as determined by the particle tracking model for 1995–2005 of the baseline simulation and (b) larvae (and some juveniles) as estimated by Kimmerer (2008). The thin line within each box is the median, the thick line is the mean, the ends of the box represent the 25th and 75th percentiles, the ends of the whiskers represent the 10th and 90th percentiles, and the black circles are points outside of the 10th and 90th percentiles.

less *Limnoithona* spp. and calanoid copepodids and more of the other four adult zooplankton types (50% [*Limnoithona* spp. and calanoid copepodids] and 50% [other types] for postlarvae; 79% and 21% for juveniles; 92% and 8% for adults). *Pseudodiaptomus* increased in the diet as fish transitioned from postlarvae to juveniles, but the *Pseudodiaptomus* contribution then decreased slightly between juvenile diets and adult diets as the biomass of this zooplankton type decreased in the fall. These results qualitatively agreed with several diet studies of Delta Smelt (Table 2), but more rigorous comparison was not attempted because of the difficulties in interpreting field diets involving rapidly digested zooplankton and without simultaneous measurement of zooplankton densities.

Best versus Worst Years in the Historical Simulation

Population growth rate (λ) from the Leslie matrix model showed that water year 1998 was the best year and water year 2001 was the worst year for the simulated Delta Smelt popula-

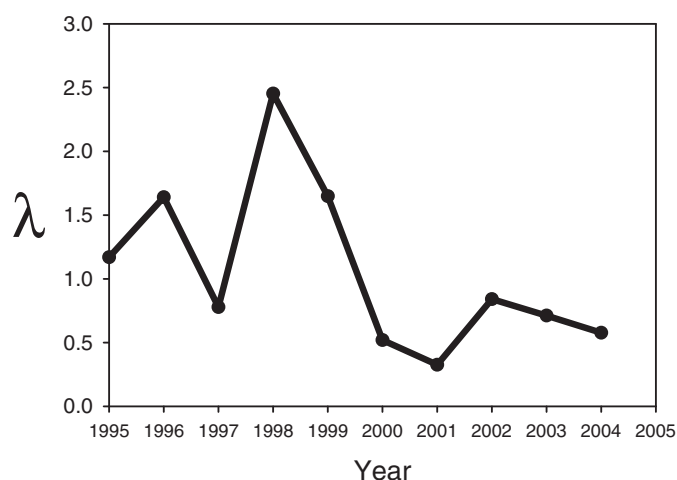


FIGURE 12. Population growth rate (λ ; fraction per year) of Delta Smelt as determined by the age-based Leslie matrix model applied to individual-based model output for each year of the 1995–2005 baseline simulation. No value for 2005 was possible because the simulations ended on September 30, 2005; information through December 31, 2005, would be needed to estimate the matrix model for 2005.

tion (Figure 12). The λ in each year resulted from a combination of (1) growth in the prior year affecting subsequent reproduction and (2) higher stage-specific survival rates in the current year for most of the life stages. Thus, water year 1998 extended from October 1997 to September 1998 and included the fall of 1997, which led up to spawning in spring 1998. Fast growth in fall 1997 resulted in large new adults at the beginning of 1998 (Figure 6) and therefore a high fraction of mature age-1 fish and a high number of eggs per entering age-1 individual (Figure 8). The year 1998 also had moderately high growth during summer (Figure 6), the lowest entrainment losses (Figure 7a, 11), and the highest stage-specific survival rates for all life stages (Figure 13). The bad year, 2001, had the second slowest growth in the prior year (2000; Figure 6) and consequently had the lowest number of eggs per entering age-1 fish (Figure 8). In addition, 2001 had moderately high entrainment losses (Figure 7) and low survival of eggs (Figure 13a), juveniles (Figure 13e), and adults (Figure 13g, h).

Compared with 2001, water year 1998 had a relatively cool and delayed warming in spring that benefited Delta Smelt larvae, but both years had similar growth conditions for juveniles during summer. Mean temperature experienced by age-1 individuals during February 27–June 7 (spawning) was 14.8°C in 1998 versus 16.4°C in 2001. Average day of spawning was April 28 in 1998 versus April 6 in 2001, and average duration of the larval stage (inversely related to growth rate) was 25.2 d (1998) versus 28.6 d (2001). Although juveniles also experienced cooler temperatures during the early summer (16.7°C versus 22.2°C for April 18–June 7), differences became smaller when viewed over the entire growing season. Average temperature experienced by juveniles during April 18–October 1 was slightly cooler during 1998 than during 2001 (20.9°C versus

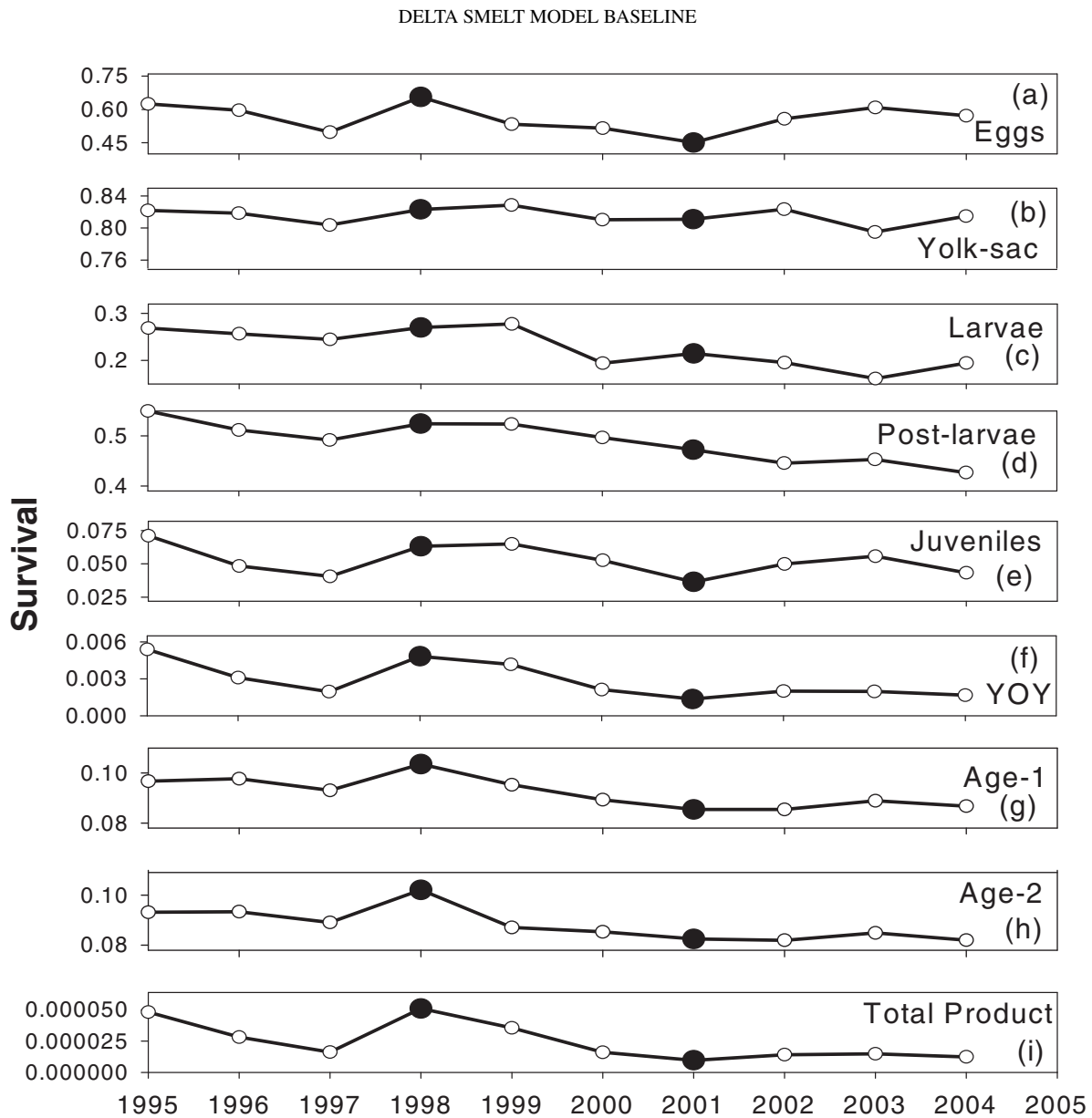


FIGURE 13. Delta Smelt stage-specific survival (fraction) from the 1995–2005 baseline simulation for (a) eggs, (b) yolk sac larvae, (c) larvae, (d) postlarvae, (e) juveniles, (f) total young of the year (product of a–e), (g) age 1, (h) age 2, and (i) total (product of f–h).

22.1°C), and the average p -value was higher in 1998 (0.89 versus 0.84). However, mean lengths of juveniles were similar between 1998 and 2001 (60.3 mm in 1999 versus 60.5 mm in 2002; Figure 6), so the difference in summer growth of juveniles between 1998 and 2001 was not a major factor.

The higher number of eggs per age-1 individual in 1998 compared with 2001 was due to faster growth during fall 1997 compared to fall 2000. Mean length of juveniles on January 1 (just before their birthday to age 1) was 61.4 mm for 1998 versus 56.5 mm for 2001. The mean p -value for October 1–December 30 was 0.76 in 1997 versus 0.68 in 2000; 1997 was also warmer than 2000 (15.9°C versus 15.0°C).

Delta outflow was generally higher in 1998 than in 2001 (Figure 10), so individuals were farther seaward, resulting in lower entrainment mortality during 1998. The PTM put 84% of post-larvae in or seaward of the confluence box on June 24 in 1998 compared with 24% on June 24 in 2001 (Figure 10c). Similarly, behavioral movement of juveniles resulted in about 88% of them occurring in or seaward of the confluence box on September 1, 1998, versus 53% on September 1, 2001 (Figure 10d). Almost no larvae were predicted to be entrained during 1998, whereas a daily average loss of 1.2% was predicted for 2001 (Figure 11a); the fraction of January adults entrained was 0.05 in 1998 versus 0.14 in 2001 (Figure 7a).

DISCUSSION

We used a detailed, individual-based approach to model the population dynamics of Delta Smelt during a time period that included a major population decline. The model was completely density independent; a density-dependent version is analyzed by Rose et al. (2013). The Delta Smelt has been declining since the 1980s and was one of four species to show a step decline around 2002 (Sommer et al. 2007). The choice of a detailed individual-based model may seem odd because of the extensive data demands of this general approach. Survey data-based modeling approaches are easier to justify in terms of calibration and in testing the degree of fit (e.g., Thomson et al. 2010; Miller et al. 2012); however, unlike our process-based approach, survey data-based approaches do not provide a means of assessing cause-and-effect relationships and so far have not helped to settle the controversy over the causes of the decline.

We opted for a spatially explicit, individual-based approach to explore the potential causes for the Delta Smelt's decline and the conditions that result in good versus bad years for Delta Smelt. The term "spatially explicit" refers to multiple, linked spatial boxes with different conditions among them. The individual-based approach allows for relatively easy simulation of movement and for local experiences to accumulate as each individual moves among the spatial boxes. A spatially explicit approach was required to enable a model that could (1) represent feeding, growth, reproduction, and movement in some detail; and (2) simulate how interannual variation in spatial distributions by life stage interacted with dynamic habitat. The chief disadvantage of such a complicated mechanistic model is that describing how it works can be difficult (Grimm et al. 2006), and many of the assumptions and parameter values must be based on judgment; thus, replication of the modeling by others is a challenge (Wilensky and Rand 2007). Indeed, the output of our model was sufficiently complicated that we chose to fit an age-structured matrix model to its output to provide a more straightforward summary of each year's condition. Our model is designed for exploring hypotheses about some of the factors affecting Delta Smelt population dynamics but is not designed for forecasting future Delta Smelt population abundances. Hypotheses about future conditions can be explored with our model but in a relative way, whereby simulated values are compared with some simulated baseline condition.

Maunder and Deriso (2011) also fitted a stage-based model of Delta Smelt by using the same extensive long-term monitoring data used here. By including covariates such as annual entrainment rate in their model, Maunder and Deriso (2011) were able to evaluate the relative importance of different factors. Their data-based modeling approach is relatively easy to describe (mathematically compact) and can be easily judged for its performance and skill (fit to data), but the approach also inherits problems with the monitoring data in terms of bias and process versus observation errors and is heavily correlation based. Clearly, the data-based approach of Maunder and Deriso (2011) and the detailed, process-based approach used here can

complement each other, and detailed comparison between the two approaches would likely allow for more insights than either approach alone can provide.

Calibration of complicated individual-based models is always a challenge. Our approach was first to adjust the movement and feeding algorithms externally under simplified conditions and then calibrate by adjusting two mortality-related parameters for the 1995–2005 historical simulation to get the averaged population abundance and averaged fraction entrained to match the data. None of the calibration steps involved adjustments to fit the model to specific years.

Model results were generally consistent with the available data and information (Table 2) about Delta Smelt. The model reasonably matched a variety of measures related to growth, mortality, and movement. Predicted growth resulted in realistic lengths at age (Figure 6). The PTM produced reasonable larval entrainment rates (Figure 11), and a simple function of Middle River flow yielded annual adult entrainment fractions that mimicked the observed values (Figure 7). Movement was confirmed both based on salinity experienced by individuals (Figure 9) and geographically (Figure 10). The fraction of individuals in the confluence box and seaward boxes during the fall agreed with estimates from fall MWT sampling. Thus, the calibrated model is a good descriptor of the 1995–2005 conditions and is useful for comparing Delta Smelt dynamics among those years. We caution that our bioenergetics model was sufficient for relating prey and temperature to growth, but it must be re-evaluated for other purposes.

There were several major discrepancies between model results and observed values. First, the model underestimated the January abundance in 1996 (Figure 5), and the reason for this is unclear. Second, the model overestimated the degree of adult entrainment in early years and underestimated the degree of adult entrainment in later years (Figure 7). This lack of sufficient interannual variation in simulated adult entrainment may be attributable to the simulated movement of adults being too similar among years (Figure 10f); the center of distribution for simulated adults was less variable across years than the center of distribution for fish caught by the fall MWT. Another possible explanation is that adult entrainment mortality was switched on or off depending on the sign of Middle River flow, whereas analyses showed that the actual entrainment rate probably increases with the magnitude of southward flow toward the diversion facilities (Kimmerer 2011).

A third discrepancy between the model and the data was that movement in the model tended to put juveniles and adults in water that was too saline during late summer to winter (Figure 9). This could reflect a conceptual difference between the data-based and modeled density-weighted salinities. Because the model tracks each individual, an individual-weighted salinity is unbiased by any sampling error. In contrast, the sampling programs catch relatively few fish and do not sample all salinities equally. However, even with the sampling issues, the results suggest that the model is contributing to this discrepancy. Two

possibilities are that (1) behavioral movement of juveniles in the model may be too slow to react to local salinity changes (Supplement D) and (2) the starting locations from the PTM were too far seaward. Some of the movement of late larval Delta Smelt in nature likely is a result of both transport (which we assumed) and behavior as the fish gain competence to direct their movements.

Finally, the model showed wide fluctuations in the fraction of age-1 individuals that were mature and the number of eggs per entering age-1 individual (Figure 8) from small changes in mean length (Figure 6). Although we lack data with which to compare these results, these differences among years seemed larger than what we would expect to see in the real population. We partially address this in Rose et al. (2013) by including length-dependent maturation as one of the alternative baselines.

We performed many comparisons of model results with the available data (Table 2), but we did not perform the classical model calibration and validation comparisons and we did not compare model predictions with commonly used abundance indices from the monitoring programs. We focused on using most of the data for calibration and often in a pattern-matching mode (Grimm et al. 2005) rather than a more traditional comparison of predicted values versus observed data (Stow et al. 2009); thus, some of the consistency between the model and the data was a result of calibration. While Delta Smelt abundance indices from the various monitoring programs have been used extensively as indicators of population abundance and survival (Bennett 2005; Maunder and Deriso 2011; Miller et al. 2012), we found the model–data comparisons using the indices to be uninformative due to the sensitivity of the indices to calculation details, such as the months included and the gear selectivity (e.g., Newman 2008).

Our analysis of model results and data for 1995–2005 clearly illustrated why it has been difficult to ascribe the Delta Smelt's decline to a single causative factor, either over the long term or as part of the recent 2002 decline. Interannual variation in λ (Figure 12) was due to a combination of the effects of temperature, salinity, larval growth, hydrodynamics, and growth of juveniles in the prior year affecting the movement, growth, mortality, and reproduction in various combinations of life stages. Small changes in mean length of young-of-the-year fish from the previous year (Figure 6) were amplified into large effects on egg production (Figure 8), and temperature affected the timing of spawning and the subsequent growth of larvae.

We did not include an explicit representation of turbidity in the final version of our model. Turbidity affects spatial distributions (Feyrer et al. 2007; Nobriga et al. 2008) and larval growth (Baskerville-Bridges et al. 2004) of Delta Smelt. We initially included turbidity (estimated from extensive Secchi depth measurements) in the same way that we included salinity and temperature (Supplement A). Turbidity showed the expected decrease during the modeled time period, which is part of a longer-term downward trend (Kimmerer 2004; Wright and Schoellhamer

2004; Nobriga et al. 2008). However, we had no basis upon which to determine relationships between turbidity and growth rate or mortality rate, and thus we could have simulated a decline in the Delta Smelt population based solely on the lower turbidity in the later years. Because we predicted the decrease in Delta Smelt without turbidity (i.e., based on hydrodynamics, temperature, salinity, and zooplankton), a turbidity effect was not included.

In the companion paper (Rose et al. 2013), we further explore Delta Smelt dynamics using the individual-based model. We configure alternative baseline simulations and perform a simulation experiment to further refine our understanding of bad versus good years for Delta Smelt. We vary salinity, temperature, zooplankton, hydrodynamics, and eggs per entering age-1 individual between the best year (1998) and the worst year (2001) to systematically quantify the effects of each factor and their combined effects on λ . We then show that these results are robust to alternative baseline configurations.

ACKNOWLEDGMENTS

This project was funded by a grant from the CALFED Science Program (SCI-05-C106). We acknowledge the many people who discussed various aspects of the model and their willingness to discuss and provide information. Stephen Monismith helped with the PTM. Rachael Miller Neilan derived the Leslie model formulation. Erik Loboschetsky provided the DSM2 output files. Lindsay Sullivan shared data on Delta Smelt feeding, and Steve Slater provided diet data. We also had discussions during model development with Rick Sitts, Joan Lindberg, and Kevin Fleming; in addition, we held a workshop in Santa Cruz, where many people provided information and advice on the modeling in its early stages. The comments of two reviewers and the Associate Editor greatly improved the clarity of the paper.

REFERENCES

- Baskerville-Bridges, B., J. C. Lindberg, and S. I. Doroshov. 2004. The effect of light intensity, alga concentration, and prey density on the feeding behavior of Delta Smelt larvae. Pages 219–227 in F. Feyrer, L. R. Brown, R. L. Brown, and J. J. Orsi, editors. Early life history of fishes in the San Francisco Estuary and watershed. American Fisheries Society, Symposium 39, Bethesda, Maryland.
- Baxter, R., R. Breuer, L. Brown, L. Conrad, F. Feyrer, S. Fong, K. Gehrts, L. Grimaldo, B. Herbold, P. Hrodey, A. Mueller-Solger, T. Sommer, and K. Souza. 2010. 2010 pelagic organism decline work plan and synthesis of results. Interagency Ecological Program for the San Francisco Estuary, California Department of Water Resources, Sacramento.
- Bennett, W. A. 2005. Critical assessment of the Delta Smelt population in the San Francisco Estuary, California. San Francisco Estuary and Watershed Science [online serial] 3(2):article 1.
- Brown, L. R., W. Kimmerer, and R. Brown. 2009. Managing water to protect fish: a review of California's environmental water account, 2001–2005. Environmental Management 43:357–368.
- Feyrer, F., M. L. Nobriga, and T. R. Sommer. 2007. Multidecadal trends for three declining fish species: habitat patterns and mechanisms in the San Francisco Estuary, California, USA. Canadian Journal of Fisheries and Aquatic Sciences 64:723–734.

- Grimaldo, L. F., T. Sommer, N. Van Ark, G. Jones, E. Holland, P. B. Moyle, B. Herbold, and P. Smith. 2009. Factors affecting fish entrainment into massive water diversions in a tidal freshwater estuary: can fish losses be managed? *North American Journal of Fisheries Management* 29:1253–1270.
- Grimm, V., U. Berger, F. Bastiansen, S. Eliassen, V. Ginot, J. Giske, J. Goss-Custard, T. Grand, S. K. Heinz, G. Huse, A. Huth, J. U. Jepsen, C. Jørgensen, W. M. Mooij, B. Müller, G. Pe'er, C. Piou, S. F. Railsback, A. M. Robbins, M. M. Robbins, E. Rossmann, N. Røger, E. Strand, S. Souissi, R. A. Stillman, R. Vabø, U. Visser, and D. L. DeAngelis. 2006. A standard protocol for describing individual-based and agent-based models. *Ecological Modelling* 198:115–126.
- Grimm, V., E. Revilla, U. Berger, F. Jeltsch, W. M. Mooij, S. F. Railsback, H. H. Thulke, J. Weiner, T. Wiegand, and D. L. DeAngelis. 2005. Pattern-oriented modeling of agent-based complex systems: lessons from ecology. *Science* 310:987–991.
- Gross, E. S., M. L. MacWilliams, C. D. Holleman, and T. A. Hervier. 2010. Particle tracking model testing and applications report. Report to the Interagency Ecological Program for the San Francisco Estuary, California Department of Water Resources, Sacramento.
- Hanson, P. C., T. B. Johnson, D. E. Schindler, and J. F. Kitchell. 1997. Fish bioenergetics 3.0 software for Windows®. University of Wisconsin, Sea Grant Institute, Technical Report WISCU-T-97-001, Madison.
- Hilborn, R. 2007. Reinterpreting the state of fisheries and their management. *Ecosystems* 10:1362–1369.
- Hollibaugh, J. T., editor. 1996. San Francisco Bay: the ecosystem. American Association for the Advancement of Science, San Francisco.
- Humston, R., J. S. Ault, M. Lutcavage, and D. B. Olson. 2000. Schooling and migration of large pelagic fishes relative to environmental cues. *Fisheries Oceanography* 9:136–146.
- Humston, R., D. B. Olson, and J. S. Ault. 2004. Behavioral assumptions in models of fish movement and their influence on population dynamics. *Transactions of the American Fisheries Society* 133:1304–1328.
- Kimmerer, W. J. 2004. Open water processes of the San Francisco Estuary: from physical forcing to biological responses. *San Francisco Estuary and Watershed Science* [online serial] 2(1):article 1.
- Kimmerer, W. J. 2008. Losses of Sacramento River Chinook Salmon and Delta Smelt to entrainment in water diversions in the Sacramento–San Joaquin Delta. *San Francisco Estuary and Watershed Science* [online serial] 6(2):article 2.
- Kimmerer, W. J. 2011. Modeling Delta Smelt losses at the south Delta export facilities. *San Francisco Estuary and Watershed Science* [online serial] 9(1):article 5.
- Kimmerer, W. J., S. R. Avent, S. M. Bollens, F. Feyrer, L. F. Grimaldo, P. B. Moyle, M. Nobriga, and T. Visintainer. 2005. Variability in length–weight relationships used to estimate biomass of estuarine fish from survey data. *Transactions of the American Fisheries Society* 134:481–495.
- Kimmerer, W. J., E. S. Gross, and M. L. MacWilliams. 2009. Is the response of estuarine nekton to freshwater flow in the San Francisco Estuary explained by variation in habitat volume? *Estuaries and Coasts* 32:375–389.
- Kimmerer, W. J., and M. L. Nobriga. 2008. Investigating particle transport and fate in the Sacramento–San Joaquin Delta using a particle tracking model. *San Francisco Estuary and Watershed Science* [online serial] 6(1):article 4.
- Lantry, B. F., and D. J. Stewart. 1993. Ecological energetics of Rainbow Smelt in the Laurentian Great Lakes: an interlake comparison. *Transactions of the American Fisheries Society* 122:951–976.
- Lott, J. 1998. Feeding habits of juvenile and adult Delta Smelt from the Sacramento–San Joaquin River Estuary. *Interagency Ecological Program Newsletter* 11(1):14–19.
- Lund, J. R., E. Hanak, W. E. Fleenor, W. A. Bennett, R. E. Howitt, J. F. Mount, and P. B. Moyle. 2010. Comparing futures for the Sacramento–San Joaquin Delta. University of California Press, Berkeley.
- Mac Nally, R., J. R. Thomson, W. J. Kimmerer, F. Feyrer, K. B. Newman, A. Sih, W. A. Bennett, L. Brown, E. Fleishman, S. D. Culbertson, and G. Castillo. 2010. Analysis of pelagic species decline in the upper San Francisco Estuary using multivariate autoregressive modeling (MAR). *Ecological Applications* 20:1417–1430.
- Maunder, M. N., and R. B. Deriso. 2011. A state–space multistage life cycle model to evaluate population impacts in the presence of density dependence: illustrated with application to Delta Smelt (*Hypomesus transpacificus*). *Canadian Journal of Fisheries and Aquatic Sciences* 68:1285–1306.
- McCann, K., and B. Shuter. 1997. Bioenergetics of life history strategies and the comparative allometry of reproduction. *Canadian Journal of Fisheries and Aquatic Sciences* 54:1289–1298.
- McGranahan, G., D. Balk, and B. Anderson. 2007. The rising tide: assessing the risks of climate change and human settlements in low elevation coastal zones. *Environment and Urbanization* 19:17–37.
- Miller, A. 2002. Particle tracking model verification and calibration. Pages 2.1–2.25 in M. Mierzwa, editor. *Methodology for flow and salinity estimates in the Sacramento–San Joaquin Delta and Suisun marsh*. California Department of Water Resources, Office of State Water Project Planning, 23rd Annual Progress Report, Sacramento. Available: modeling.water.ca.gov/delta/reports/annrpt/2002/2002Ch2.pdf. (November 2012).
- Miller, W. J. 2011. Revisiting assumptions that underlie estimates of proportional entrainment of Delta Smelt by state and federal water diversions from the Sacramento–San Joaquin Delta. *San Francisco Estuary and Watershed Science* [online serial] 9(1):article 4.
- Miller, W. J., B. F. J. Manly, D. D. Murphy, D. Fullerton, and R. R. Ramey. 2012. An investigation of factors affecting the decline of Delta Smelt (*Hypomesus transpacificus*) in the Sacramento–San Joaquin Estuary. *Reviews in Fisheries Science* 20:1–19.
- Moyle, P. B. 2002. *Inland fishes of California*, revised and expanded. University of California Press, Berkeley.
- Moyle, P. B., B. Herbold, D. E. Stevens, and L. W. Miller. 1992. Life history and status of Delta Smelt in the Sacramento–San Joaquin Estuary, California. *Transactions of the American Fisheries Society* 121:67–77.
- Myers, R. A., and B. Worm. 2003. Rapid worldwide depletion of predatory fish communities. *Nature* 423:280–283.
- Newman, K. B. 2008. Sample design-based methodology for estimating Delta Smelt abundance. *San Francisco Estuary and Watershed Science* [online serial] 6(3):article 3.
- Ney, J. J. 1993. Bioenergetics modeling today: growing pains on the cutting edge. *Transactions of the American Fisheries Society* 122:736–748.
- Nichols, F. H., J. E. Cloern, S. N. Luoma, and D. H. Peterson. 1986. The modification of an estuary. *Science* 231:567–573.
- Nichols, F. H., J. K. Thompson, and L. E. Schemel. 1990. Remarkable invasion of San Francisco Bay (California, USA) by the Asian clam *Potamocorbula amurensis*: II. displacement of a former community. *Marine Ecology Progress Series* 66:95–101.
- Nobriga, M. L. 2002. Larval Delta Smelt diet composition and feeding incidence: environmental and ontogenetic influences. *California Fish and Game* 88:149–164.
- Nobriga, M. L., T. R. Sommer, F. Feyrer, and K. Fleming. 2008. Long-term trends in summertime habitat suitability for Delta Smelt (*Hypomesus transpacificus*). *San Francisco Estuary and Watershed Science* [online serial] 6(1):article 1.
- NRC (National Research Council). 2010. A scientific assessment of alternatives for reducing water management effects on threatened and endangered fishes in California's Bay–Delta. National Academies Press, Washington, D.C.
- NRC (National Research Council). 2012. Sustainable water and environmental management in the California Bay–Delta. National Academies Press, Washington, D.C.
- Rose, K. A. 2000. Why are quantitative relationships between environmental quality and fish populations so elusive? *Ecological Applications* 10:367–385.
- Rose, K. A., A. T. Adamack, C. A. Murphy, S. E. Sable, S. E. Kolesar, J. K. Craig, D. L. Breitburg, P. Thomas, M. H. Brouwer, C. F. Cerco, and S. Diamond. 2009. Does hypoxia have population-level effects on coastal fish? musings from the virtual world. *Journal of Experimental Marine Biology and Ecology* 381(Supplement):188–203.

- Rose, K. A., W. J. Kimmerer, K. P. Edwards, and W. A. Bennett. 2013. Individual-based modeling of Delta Smelt population dynamics in the upper San Francisco Estuary: II. Alternative baselines and good versus bad years. *Transactions of the American Fisheries Society* 142:1260–1272.
- Scheffer, M., J. M. Baveco, D. L. DeAngelis, K. A. Rose, and E. H. van Nes. 1995. Super-individuals: a simple solution for modelling large populations on an individual basis. *Ecological Modelling* 80:161–170.
- Sommer, T., C. Armor, R. Baxter, R. Breuer, L. Brown, M. Chotkowski, S. Culberson, F. Feyrer, M. Gingras, B. Herbold, W. Kimmerer, A. Mueller-Solger, M. Nobriga, and K. Souza. 2007. The collapse of pelagic fishes in the upper San Francisco Estuary. *Fisheries* 32:270–277.
- Sommer, T., F. Mejia, M. Nobriga, F. Feyrer, and L. Grimaldo. 2011. The spawning migration of Delta Smelt in the upper San Francisco Estuary. *San Francisco Estuary and Watershed Science* [online serial] 9(2):article 2.
- Stow, C. A., J. Jolliff, D. J. McGillicuddy Jr., S. C. Doney, J. I. Allen, M. A. M. Friedrichs, K. A. Rose, and P. Wallhead. 2009. Skill assessment for coupled biological/physical models of marine systems. *Journal of Marine Systems* 76:4–15.
- Thomson, J. R., W. J. Kimmerer, L. R. Brown, K. B. Newman, R. Mac Nally, W. A. Bennett, F. Feyrer, and E. Fleishman. 2010. Bayesian change point analysis of abundance trends for pelagic fishes in the upper San Francisco Estuary. *Ecological Applications* 20:1431–1448.
- Tyler, J. A., and K. A. Rose. 1994. Individual variability and spatial heterogeneity in fish population models. *Reviews in Fish Biology and Fisheries* 4:91–123.
- Vörösmarty, C. J., P. Green, J. Salisbury, and R. B. Lammers. 2000. Global water resources: vulnerability from climate change and population growth. *Science* 289:284–288.
- Wilbur, R. J. 2000. Validation of dispersion using the particle tracking model in the Sacramento–San Joaquin Delta. Master's thesis. University of California, Davis. Available in condensed form: modeling.water.ca.gov/delta/reports/annrpt/2001/2001Ch4.pdf. (November 2012).
- Wilensky, U., and W. Rand. 2007. Making models match: replicating an agent-based model. *Journal of Artificial Societies and Social Simulation* [online serial] 10(4):2. Available: jasss.soc.surrey.ac.uk/10/4/2.html. (November 2012).
- Winder, M., and A. D. Jassby. 2011. Shifts in zooplankton community structure: implications for food web processes in the upper San Francisco Estuary. *Estuaries and Coasts* 34:675–690.
- Winemiller, K. O., and K. A. Rose. 1992. Patterns of life-history diversification in North American fishes: implications for population regulation. *Canadian Journal of Fisheries and Aquatic Sciences* 49:2196–2218.
- Worm, B., R. Hilborn, J. K. Baum, T. A. Branch, J. S. Collie, C. Costello, M. J. Fogarty, E. A. Fulton, J. A. Hutchings, S. Jennings, O. P. Jensen, H. K. Lotze, P. M. Mace, T. R. McClanahan, C. Minto, S. R. Palumbi, A. M. Parma, D. Ricard, A. A. Rosenberg, R. Watson, and D. Zeller. 2009. Rebuilding global fisheries. *Science* 325:578–585.
- Wright, S. A., and D. H. Schoellhamer. 2004. Trends in the sediment yield of the Sacramento River, California, 1957–2001. *San Francisco Estuary and Watershed Science* [online serial] 2(2):article 2.

This article was downloaded by: [Kenneth Rose]

On: 01 August 2013, At: 15:44

Publisher: Taylor & Francis

Informa Ltd Registered in England and Wales Registered Number: 1072954 Registered office: Mortimer House, 37-41 Mortimer Street, London W1T 3JH, UK



Transactions of the American Fisheries Society

Publication details, including instructions for authors and subscription information:

<http://www.tandfonline.com/loi/utaf20>

Individual-Based Modeling of Delta Smelt Population Dynamics in the Upper San Francisco Estuary: II. Alternative Baselines and Good versus Bad Years

Kenneth A. Rose^a, Wim J. Kimmerer^b, Karen P. Edwards^c & William A. Bennett^d

^a Department of Oceanography and Coastal Sciences, Louisiana State University, Energy, Coast, and Environment Building, Baton Rouge, Louisiana, 70803, USA

^b Romberg Tiburon Center for Environmental Studies, San Francisco State University, 3152 Paradise Drive, Tiburon, California, 94920, USA

^c Environment Agency, Manley House, Kestrel Way, Exeter, EX2 7LQ, UK

^d Center for Watershed Sciences, John Muir Institute of the Environment, Bodega Marine Laboratory, University of California, Davis, Post Office Box 247, Bodega Bay, California, 94923, USA

Published online: 01 Aug 2013.

To cite this article: Kenneth A. Rose, Wim J. Kimmerer, Karen P. Edwards & William A. Bennett (2013) Individual-Based Modeling of Delta Smelt Population Dynamics in the Upper San Francisco Estuary: II. Alternative Baselines and Good versus Bad Years, Transactions of the American Fisheries Society, 142:5, 1260-1272

To link to this article: <http://dx.doi.org/10.1080/00028487.2013.799519>

PLEASE SCROLL DOWN FOR ARTICLE

Taylor & Francis makes every effort to ensure the accuracy of all the information (the "Content") contained in the publications on our platform. However, Taylor & Francis, our agents, and our licensors make no representations or warranties whatsoever as to the accuracy, completeness, or suitability for any purpose of the Content. Any opinions and views expressed in this publication are the opinions and views of the authors, and are not the views of or endorsed by Taylor & Francis. The accuracy of the Content should not be relied upon and should be independently verified with primary sources of information. Taylor and Francis shall not be liable for any losses, actions, claims, proceedings, demands, costs, expenses, damages, and other liabilities whatsoever or howsoever caused arising directly or indirectly in connection with, in relation to or arising out of the use of the Content.

This article may be used for research, teaching, and private study purposes. Any substantial or systematic reproduction, redistribution, reselling, loan, sub-licensing, systematic supply, or distribution in any form to anyone is expressly forbidden. Terms & Conditions of access and use can be found at <http://www.tandfonline.com/page/terms-and-conditions>

ARTICLE

Individual-Based Modeling of Delta Smelt Population Dynamics in the Upper San Francisco Estuary: II. Alternative Baselines and Good versus Bad Years

Kenneth A. Rose*

Department of Oceanography and Coastal Sciences, Louisiana State University, Energy, Coast, and Environment Building, Baton Rouge, Louisiana 70803, USA

Wim J. Kimmerer

Romberg Tiburon Center for Environmental Studies, San Francisco State University, 3152 Paradise Drive, Tiburon, California 94920, USA

Karen P. Edwards

Environment Agency, Manley House, Kestrel Way, Exeter EX2 7LQ, UK

William A. Bennett

Center for Watershed Sciences, John Muir Institute of the Environment, Bodega Marine Laboratory, University of California, Davis, Post Office Box 247, Bodega Bay, California 94923, USA

Abstract

We used a previously described individual-based population model to further explore the population dynamics of Delta Smelt *Hypomesus transpacificus* in the upper San Francisco Estuary. We formulated four alternative baseline configurations of the model and used a factorial design to systematically isolate the effects of factors that determined a good versus bad year. The alternative baseline conditions were obtained by substituting different assumptions about growth, maturity, and mortality into the original baseline configuration. In the simulation experiment, we varied five factors by setting each value to its 1998 (best year) or 2001 (worst year) value: salinity, temperature, zooplankton densities, hydrodynamics, and eggs per age-1 individual at spawning. Although some of the alternative baselines resulted in lower January abundances, estimated finite population growth rates were very similar for all versions. The simulation experiment showed that juvenile growth in the winter prior to spawning (i.e., eggs per age-1 individual) was the most important single factor in making 2001 a bad year, although no single factor alone was sufficient to fully account for the poor conditions in 2001 relative to 1998. Temperature played an important secondary role, and hydrodynamics played a more minor role. The results of the simulation experiment were robust, as similar results were obtained under the four alternative baselines. We compare our results with previous modeling and statistical analyses of the long-term monitoring data; we also discuss some implications of our results for Delta Smelt management and suggest future directions for analyses.

The Delta Smelt *Hypomesus transpacificus* resides only in the San Francisco Estuary and is listed as threatened under the U.S. Endangered Species Act and as endangered under the California Endangered Species Act. Abundance of Delta Smelt

started to decline in the 1980s, and a sharp decrease starting in 2001 led to a series of management actions that were intended to benefit the species but that also involved reducing the water available to be diverted for irrigation and water supply (NRC

*Corresponding author: karose@lsu.edu

Received November 9, 2012; accepted April 19, 2013

2012). The State Water Project and the Central Valley Project have exported an average of 30% of the freshwater flowing into the estuary during 1960–2000, with the percentage generally increasing through time and exceeding 60% in some years and seasons (Kimmerer 2004). The State Water Project facility provides drinking water for over 23 million Californians; combined, the two diversion facilities fuel an estimated $\$25 \times 10^9$ annual agricultural economy (Grimaldo et al. 2009).

A suite of factors has been identified as important in contributing to the decline of Delta Smelt. These factors include entrainment by water diversion facilities (Kimmerer 2008, 2011; Miller 2011), contaminant effects (Kuivila and Moon 2004; Connon et al. 2009; Brooks et al. 2012), shifts in the zooplankton (prey) community (Nobriga 2002; Feyrer et al. 2003; Winder and Jassby 2011), and changes in physical habitat (Feyrer et al. 2007; Nobriga et al. 2008; Kimmerer et al. 2009). The role of these factors in contributing to the Delta Smelt's decline has been examined by using statistical analysis of long-term field data (Mac Nally et al. 2010; Thomson et al. 2010; Miller et al. 2012) and population dynamics modeling (Maunder and Deriso 2011). These analyses have led to what many consider to be contradictory conclusions about the relative importance of various factors in affecting Delta Smelt population dynamics (NRC 2010; Kimmerer 2011; Miller 2011).

Determining the factors that affect Delta Smelt population dynamics is critical for formulating effective remediation actions. Remediation actions under the federal Endangered Species Act are termed "reasonable and prudent alternatives" (RPAs), and specific actions were proposed as part of the recent biological opinion for Delta Smelt (USFWS 2008) and were subsequently argued in court (NRC 2010). One RPA restricts water diversions during the winter to limit losses of Delta Smelt at the diversion facilities (Grimaldo et al. 2009; Kimmerer 2011). Another controversial RPA was designed to protect fall habitat by using reservoir releases to maintain the estuarine salinity field in certain spatial regions (NRC 2010). The high economic costs of these various management actions, coupled with uncertainty about how they may affect Delta Smelt population dynamics, have led to controversy (NRC 2012).

In a companion paper (Rose et al. 2013, this issue), we described an individual-based population model of Delta Smelt and used a historical baseline simulation for 1995–2005 to identify the factors leading to good and bad years for Delta Smelt. In the present paper, we extend the analysis of Rose et al. (2013) by formulating alternative baseline configurations of the model and by using a factorial design to systematically isolate the effects of factors that determined a good year versus a bad year. We formulated four alternative baseline conditions by substituting different assumptions about growth, maturity, and mortality into the baseline configuration. The four alternative baselines were (1) fixed larval growth instead of food-dependent larval growth, (2) size-dependent mortality instead of stage-dependent mortality, (3) density-dependent mortality instead of density-independent mortality, and (4) length-dependent maturity rather than a length

threshold for maturity. Each of these assumptions was important to baseline dynamics, and each was uncertain. Our earlier identification of good and bad years was from the historical simulation, and the effects of some factors can be confounded by the autocorrelation that is inherent in a historical simulation. Here, we follow up with a designed simulation experiment in which we systematically varied the factors that are potentially important in determining good and bad years, and we further show the robustness of the simulation experiment results by repeating the experiment for each of the four alternative baseline conditions. We demonstrate that the results obtained under the original baseline conditions were similar under the four alternative baseline conditions (i.e., robust), and we further refine the role of various factors in determining good and bad years.

MODEL DESCRIPTION

Overview

The individual-based model followed the reproduction, growth, mortality, and movement of super-individuals over their entire life cycle (from eggs to age 3) on the same spatial grid as the Delta Simulation Model (DSM2) hydrodynamics model that was developed by and is widely used by the California Department of Water Resources (baydeltaoffice.water.ca.gov/modeling/deltamodeling/models/dsm2/dsm2.cfm). A model year was defined as a water year: October 1 of the previous year to September 30 (e.g., model year 2001 extends from October 1, 2000, to September 30, 2001). The model is described in detail by Rose et al. (2013) and is briefly summarized here.

The spatial grid was one-dimensional, with 517 channels and 5 reservoirs (Figure 1 in Rose et al. 2013). The DSM2 hydrodynamics model provided hourly values of water velocities and flows into and out of channels and reservoirs, which were used as inputs to a particle tracking model (PTM) that was embedded in the Delta Smelt individual-based model. A second grid of 11 coarser boxes was overlaid onto the channel grid, and values of daily temperature, salinity, and biomass densities of six zooplankton groups in each box were used to assign values to each channel.

For each super-individual, we tracked a suite of traits, including life stage, growth rate, weight, length, age, diet, location on the grid, maturity status, fecundity, and worth. Worth was the number of identical population individuals represented by the super-individual. Rather than following every individual and removing them upon death, we followed a fixed number of super-individuals and decreased their worth in each time step to account for mortality (Scheffer et al. 1995). All computations were scaled from the super-individuals to the population by multiplying by the worth of the super-individuals. Individuals were assigned to five life stages: egg, yolk sac larva, postlarva, juvenile, and adult. Advancement to the next life stage (development) was based on (1) temperature for egg to yolk sac larva

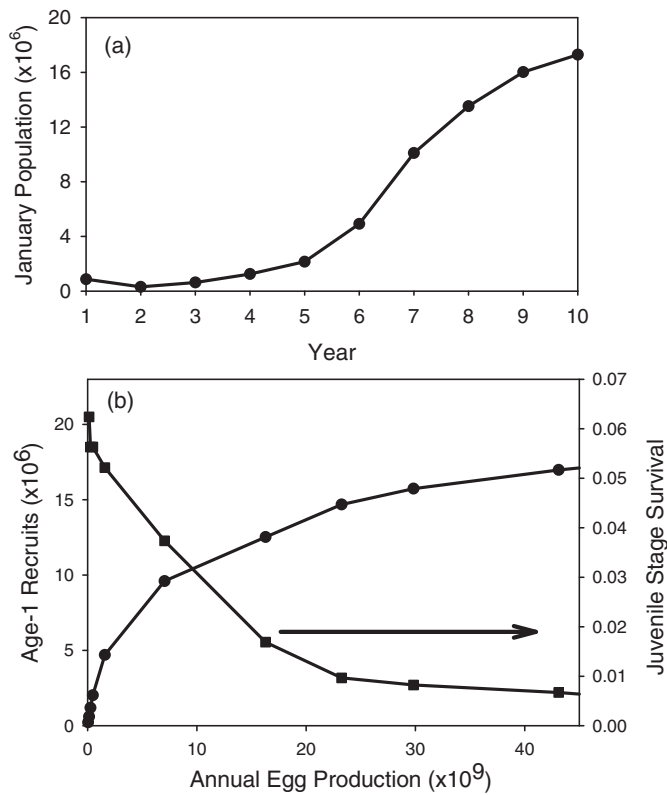


FIGURE 1. Simulated adult Delta Smelt abundance over time and juvenile survival from each year in a 15-year model run with artificially increasing egg production every year and density-dependent juvenile mortality: (a) adult abundance in January of each year and (b) age-1 recruits (circles, primary y-axis) and juvenile-stage survival (squares, secondary y-axis) versus annual egg production for each year.

to larva; (2) length for larva to postlarva to juvenile; and (3) date (January 1) for juvenile to age 1 and for age 1 to age 2.

Growth increments at each time step were determined from body weight, temperature, and the biomass densities of the six zooplankton groups (adult *Limnoithona* spp.; calanoid copepods; other calanoid adults; adult *Eurytemora*; adult *Acanthocyclops vernalis*; and adult *Pseudodiaptomus*). Length was then increased if fish weight had increased sufficiently. Mortality was a stage-specific, fixed rate plus starvation (if the weight of an individual fell below 50% of the weight expected for its length) and entrainment by the two water diversion facilities. Movement on the spatial grid was by physical transport using a PTM for yolk sac larvae, larvae, and postlarvae; movement was behavioral (in response to salinity) for juveniles and adults. Development, reproduction, growth, and mortality were updated daily, whereas movement of eggs and all larval stages was updated hourly and movement of juveniles and adults was updated every 12 h.

Model Outputs

In our companion paper (Rose et al. 2013), we presented a detailed comparison between individual-based model outputs

and data. We focus here on model predictions involving a small subset of those output variables. The major outputs presented for all simulations in this paper are the annual adult abundance in January and the annual finite population growth rate (λ). Annual adult abundance in January was computed as the summed worth of all individuals on January 1, including the young of the year that just became age 1 and the age-1 fish that just became age 2; it did not include age-2 fish that were just removed as they became age 3. We used the individual-based model output to estimate a Leslie age-based matrix model for each year to summarize the complicated individual-based model results with a single variable, λ . The value of λ was based on the detailed dynamics of the individual-based model but allowed for easier comparison among years. A 2×2 matrix model was estimated each year by computing the average maturity, fecundity, and age-specific survival rates and by using eigenvalue analysis to determine λ (see Supplement F in the online version of Rose et al. 2013).

Additional model outputs were used selectively to configure or confirm the alternative baselines and to provide some explanation for how the factors in the simulation experiment (described below) affected Delta Smelt. These outputs were defined and their calculations were described by Rose et al. (2013): stage-specific survival rates, recruitment (number of entering age-1 individuals on January 1), fraction of entering age-1 fish that were mature at the time of spawning, number of eggs per entering age-1 individual, percentage of individuals in and seaward of the Sacramento River–San Joaquin River confluence box at various times during the year (together with monthly average Sacramento–San Joaquin River Delta [hereafter, “Delta”] outflows), average daily fraction of larvae that were entrained in water diversions during a year, and annual fraction of adults that were entrained. Finally, we used a Lagrangian approach and reported the averaged values of p (proportion of maximum consumption) and temperature experienced by individuals for selected time periods in the simulations.

MODEL SIMULATIONS

Alternative Baselines

We configured four additional versions of the baseline model: fixed larval growth, size-dependent mortality, density-dependent mortality, and length-dependent maturity. We used the historical baseline simulation of 1995–2005 to help configure and calibrate the alternative baselines.

Fixed larval growth.—Model predictions of Delta Smelt abundance in the historical simulation were sensitive to larval growth rates, and we were uncertain about our formulation of larval feeding and bioenergetics. Use of a fixed duration for the larval stage eliminated variation in larval growth as a factor in year-to-year differences. Larval growth was fixed by specifying the larval duration in days rather than letting the transition from larva to juvenile be determined by length. We used the average

larval duration over years from the baseline simulation (26 d) for all simulations with the fixed larval growth rate.

Size-dependent mortality.—Mortality in the original baseline version was constant within each stage but decreased with successive stages, so penalties in survival for slow growth occurred only through the delay in transition from larvae to postlarvae and from postlarvae to juveniles. Making mortality length dependent reflected the idea that vulnerability to predation mortality decreases with increasing size (Sogard 1997; Bailey and Duffy-Anderson 2010; Gislason et al. 2010), so that faster growth would increase cumulative survival regardless of how stage transitions were triggered. We assumed that mortality rate was a function of length (M_L ; d^{-1}) for larvae through adults; we then fit the function to the constant stage-specific mortality rates from the baseline simulation, associating the rate with the midpoint length of each stage:

$$M_L = -0.034 + 0.165 \cdot L^{-0.322}. \quad (1)$$

We re-ran the 1995–2005 simulation and compared averaged annual stage-specific fractional survival rates between the baseline and the alternative with size-dependent mortality (Table 1) to confirm that this alternative produced mortality rates that were generally similar to those from the original baseline. Survival from yolk sac larva through age 2 was similar (4.4×10^{-5} in the baseline versus 3.5×10^{-5} under size-dependent mortality); juvenile survival increased (0.054 in the baseline; 0.073 under size-dependent mortality), and age-1 survival was approximately halved (0.092 in the baseline; 0.044 under size-dependent mortality).

Density-dependent mortality.—The original baseline version was set up as density independent because the recent Delta Smelt population is at such a low level that density-dependent effects seem unlikely. To allow for subsequent simulations at higher Delta Smelt densities, we included an alternative baseline with density-dependent mortality. The juvenile stage is the likely stage for density dependence based on general theory (Rothschild 1986; Cowan et al. 2000). Bennett (2005) and Maunder

and Deriso (2011) found evidence for a density-dependent relationship between summer and fall Delta Smelt indices, and this relationship occurs in our simulation for the juvenile life stage. We assumed a multiplier of the juvenile daily mortality rate based on the normalized density of juveniles in each box on each day,

$$M' = M \cdot e^{3.0 \left(\frac{D_t}{0.005} \right)}, \quad (2)$$

where D_t is the density of juveniles (number/ m^3) and 0.005 is an average juvenile density (number/ m^3).

We calibrated the value of 3.0 in equation (2) to obtain realistic maximum January adult abundances of about 20–25 million; the highest abundance estimate from the spring Kodiak trawl and fall midwater trawl (MWT) data during 1968–2006 was 24.3 million in 1981. We ran the model by repeating 1995 conditions from the historical simulation (high Delta Smelt survival) but with artificially increased egg production each year to generate a spawner–recruit curve under ever-increasing January adult abundances. We adjusted the multiplier in the exponent within equation (2) (final value = 3.0) until it generated a leveling off at high egg production that occurred roughly with about 20–25 million adults in January (Figure 1a). Juvenile-stage survival decreased with increasing population abundance from 0.06 to less than 0.01, resulting in a leveling off of age-1 recruits at about 20 million (Figure 1b). Abundance of age-1 recruits was similar to January adult abundance because most of the adults were age-1 individuals.

Length-dependent maturity.—The simple maturity rule (fish > 60 mm TL are mature) in the original baseline was substituted with a smoother, length-dependent maturity relationship (Figure 2). Model results were potentially sensitive to small

TABLE 1. Stage-specific durations (d) and survival (fraction) of Delta Smelt averaged over the 1995–2005 simulations for the original baseline and the alternative baseline that used size-dependent mortality.

Stage	Duration (d)		Survival (fraction)	
	Baseline	Size dependent	Baseline	Size dependent
Eggs	10.5	10.4	0.56	0.57
Yolk sac larvae	4.88	4.87	0.82	0.71
Larvae	26.3	26.0	0.23	0.25
Postlarvae	21.7	22.2	0.49	0.50
Juveniles	186	187	0.054	0.073
Age 1	365	365	0.092	0.044
Age 2	365	365	0.088	0.11

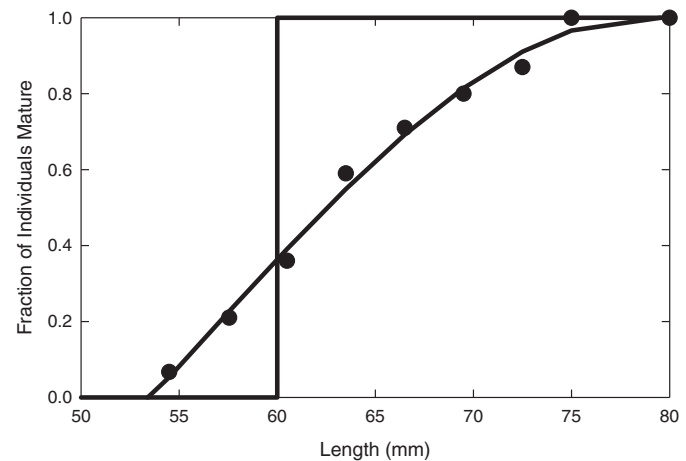


FIGURE 2. Fraction of Delta Smelt individuals that were mature as function of length for the baseline (60-mm cutoff) and the length-dependent maturity alternative. The points (circles) represent the fractions mature by length, estimated by assigning females (from the spring Kodiak trawl survey for 2002–2010) to 3-mm length bins and using ripe or spent individuals (condition codes 4–6) as mature.

changes in length of young of the year causing large changes in the mature fraction of individuals because typical lengths varied around 60 mm when maturity was determined. The relationship between fraction mature and fish length was fitted by allocating females that were sampled in the spring Kodiak trawl survey during 2002–2010 into 3-mm length bins and using ripe or spent individuals (codes 4–6) as mature. This resulted in an asymmetric relationship of fraction mature at around 60 mm (Figure 2). Use of other definitions for maturity resulted in relationships that were more symmetric at around 55–65 mm. We used the asymmetric relationship because it was justifiable based on the data and it provided a better test of model robustness.

Simulations under alternative baselines.—The 1995–2005 historical simulation with the original baseline (analyzed by Rose et al. 2013) was repeated with each of the four alternative baselines. We compared simulated January adult abundances and λ values among the original baseline and the four alternative versions. Results from a single simulation are presented. The individual-based model has stochastic aspects in assigning zooplankton biomass densities to channels and spawning temperatures to females, the y and z movements of the PTM, and the random component of behavioral movement. Because of the summing and averaging over many individuals and over time, population-level outputs (e.g., mean length at age, spatial distributions, and λ) varied by less than 5%—and often by less than 2%—among replicate simulations.

Good versus Bad Years

In this paper, we further explore the factors affecting the good year (1998) and bad year (2001) for Delta Smelt recruitment as identified in the analysis of the historical simulation (Rose et al. 2013). We performed a factorial simulation experiment to identify the conditions that caused the differences between water year 1998, which had the largest λ (2.45) within the baseline historical simulation, and water year 2001, which had the smallest λ (0.33) in the simulation. We varied five factors: salinity (S), temperature (T), zooplankton densities (Z), hydrodynamics (H), and eggs per entering age-1 individual (i.e., recruit) on January 1 (E). Each of these five factors was set to either its 1998 value or its 2001 value, resulting in a total of 32 (2^5) combinations.

Salinity.—Salinity affected the movement patterns of juveniles and adults and thus affected their spatial distribution and vulnerability to entrainment. The year 1998 was a high-outflow year, and salinities were very low for the modeled area from roughly March to August, after which salinity increased but remained below 5 psu (Figure 2b in Rose et al. 2013). Salinity in boxes down-estuary from the confluence was higher during the low-outflow year, 2001, than during 1998; this higher salinity occurred throughout 2001 except for a short period in March (Figure 2d in Rose et al. 2013). In the original baseline historical simulation, adults were located farther seaward with the salinity distribution in 1998. Average August outflow was 568 m^3/s in 1998 versus 90 m^3/s in 2001, and the percentage of adults that

were in or seaward of the confluence box on September 1 was 97% during 1998 versus 67% during 2001 of the original baseline simulation (Figure 10e in Rose et al. 2013). The fraction of January adults that were entrained was 0.05 in 1998 versus 0.14 in 2001.

Temperature.—Temperature affected the initial date and duration of the spawning period; the egg and yolk sac development and mortality rates; and the bioenergetics (growth) of larvae, postlarvae, juveniles, and adults. When viewed systemwide, differences in temperature between 1998 and 2001 were not obvious (Figure 2a, c in Rose et al. 2013). More detailed analysis of the historical simulation using the average temperature experienced by model individuals showed two major differences between 1998 and 2001: (1) warmer fall and winter at the beginning of the water year and (2) cooler and delayed warming in the spring. Fall 1997 and winter 1998 were warmer than fall 2000 and winter 2001. During October 1–December 30, juveniles experienced an average temperature of 15.9°C in 1997 versus 15.0°C in 2000. Mean temperature experienced by these individuals (which became adults after January 1) during February 27–June 7 (the spawning period) was 14.8°C in 1998 versus 16.4°C in 2001. The warming in the spring also occurred later in 1998, and the average day of spawning was April 28 in 1998 versus April 6 in 2001.

Zooplankton.—The effect of switching 1998 and 2001 zooplankton densities would seem to be the simplest to interpret because this factor only affected feeding rate and therefore growth rate; however, the use of multiple prey groups made interpretation difficult. Dominant prey groups in the annual diets of postlarval, juvenile, and adult Delta Smelt in the baseline simulation were other calanoid adults and adult *Pseudodiaptomus*. The differences between 1998 and 2001 in the biomass densities of these two key prey groups were complicated (see Figure 3c versus 4c and Figure 3f versus 4f in Rose et al. 2013). Although adult *Pseudodiaptomus* biomasses were generally higher during summer and fall in 1998 than in 2001, biomasses of other calanoid adults during summer and fall were higher in 2001 and biomass in the southwest Suisun Bay box during winter and spring was much higher in 2001. Biomass densities of the other zooplankton groups also showed complicated differences. For example, the biomass density of adult *A. vernalis* was higher (and occurred at high levels for a longer period) in the Suisun Marsh box during 1998, but adult *Eurytemora* biomass density was higher in the southern Delta and eastern Delta boxes during 2001 (see Figure 3d versus 4d and Figure 3e versus 4e in Rose et al. 2013).

We relied on the p -value from the bioenergetics model to infer prey availability. The p -value reflects prey availability scaled for maximum consumption rate, which also depends on temperature. The historical simulation using the original baseline version showed that average p -values experienced by juveniles during the faster fall–winter growth (October 1–December 30) was 0.76 in 1997–1998 versus 0.68 in 2000–2001. This difference, in combination with warmer temperatures, led to longer recruits

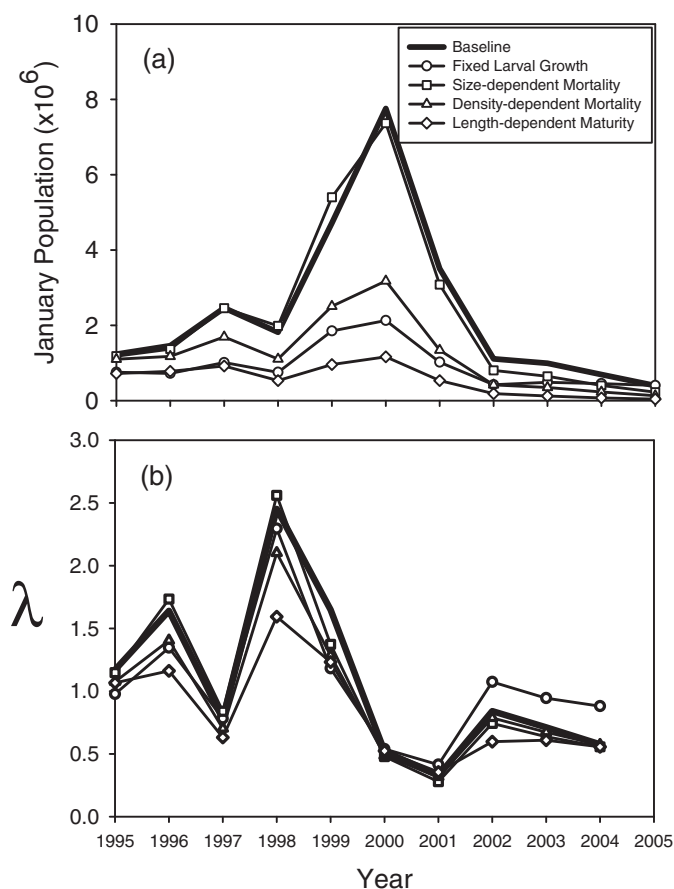


FIGURE 3. Simulated (a) annual adult Delta Smelt abundance in January and (b) finite population growth rate (λ ; fraction per year), 1995–2005, for the original baseline simulation and the four alternative baseline simulations. The values of λ were determined by using an age-based Leslie matrix model applied to individual-based model output for each year. No value for 2005 is possible because the simulations ended on September 30, 2005; information through December 31, 2005, would be needed to estimate the matrix model for 2005.

on January 1 in 1998 than in 2001 (mean TL = 61.4 mm versus 56.5 mm). Averaged p -values in 1998 were also somewhat higher during the summer growth period (April 18–October 1) for young of the year (0.89 in 1998 versus 0.84 in 2001), although by October the mean lengths of young of the year were only slightly greater in 1998 than in 2001 (54 mm versus 52 mm).

Hydrodynamics.—Hydrodynamics affected the entrainment of yolk sac larvae, larvae, and postlarvae via the PTM; the entrainment of juveniles and adults; and the starting locations of new juveniles by determining the transport of larval life stages. Average May outflow was 1,922 m³/s in 1998 versus 273 m³/s in 2001, and the percentage of postlarvae that were in or seaward of the confluence box after transport (June 24) was 84% in 1998 versus 24% in 2001. Almost no larvae were predicted to be entrained during 1998, whereas the daily average entrainment loss was 1.2% in 2001.

Eggs per age-1 individual.—Unlike the other factors, which had readily available values for 1998 and 2001, the number of eggs per age-1 individual required additional calculations in the model to achieve 1998 or 2001 values in the factorial simulation experiment. The number of eggs per age-1 fish reflected growth that occurred in the fall and winter leading up to spawning. In the original historical simulation, the mean length of young of the year on October 1 was somewhat greater in 1997 (starting value for 1998) than in 2000 (54.0 mm versus 52.0 mm) due to the more favorable summer conditions in 1997 than in 2000. This small difference was amplified by warmer temperature and higher prey densities in the fall and winter of 1997, resulting in a mean length of 61.4 mm on January 1, 1998, versus 56.5 mm on January 1, 2001. These lengths straddled the 60-mm maturity cutoff, and whereas 72% of entering age-1 individuals were mature in 1998, only 15% of entering age-1 fish were mature in 2001 of the historical baseline simulation. Thus, although there were fewer recruits on January 1, 1998, than on January 1, 2001 (0.159×10^7 versus 0.258×10^7), the number of mature age-1 female spawners was greater in 1998 (0.287×10^6 versus 0.1105×10^6) and egg production was about 1.5 times higher in 1998 (0.942×10^9 versus 0.641×10^9).

In the historical baseline simulation, the average number of eggs per age-1 individual was 491.8 for 1998 versus 89.3 for 2001. We did not explicitly simulate the previous year's conditions for the simulation experiment, in which either 1998 or 2001 conditions were repeated year after year. Rather, we adjusted the fecundity of entering age-1 individuals each year when we projected spawning so that the total projected number of eggs divided by the number of simulated entering age-1 individuals would be either 491.8 or 89.3.

Simulations in the good year versus bad year experiment.—Simulations were for 15 years, with 4 years of spin-up using 1999 conditions as in the baseline simulations, followed by 11 years of 1 of the 32 combinations of 1998 or 2001 conditions repeated every year. We used the two extreme years because they provided the best contrast for separating out the effects of multiple factors and thus for identifying which factors were most important in determining year-class strength. Eleven years of repeated conditions were simulated in order to ensure that we had the long-term (equilibrium) population responses to the specified conditions; shorter simulations could be affected by initial conditions and still reflect aspects of the transient solutions. We refer to the 32 combinations by using the letters of the factors that were set to 2001 values (i.e., S for salinity, T for temperature, Z for zooplankton, H for hydrodynamics, and E for eggs per entering age-1 individual). For example, in the simulation labeled “ EH ,” eggs per age-1 fish and hydrodynamics were set at 2001 values, while salinity, temperature, and zooplankton were set at 1998 values. We report λ averaged over years 10–14 of each 15-year simulation. As with the baseline simulations, results from a single simulation are presented because replicate simulations differed by less than 5% in their population-level outputs. Values of λ that were 25% and 50% higher than the

2001 value are shown for reference to aid in judging how close the other λ values were to the 2001 value.

Robustness

To confirm the robustness of results based on the original baseline, we also repeated all of the 32 simulation combinations under each of the four alternative baseline conditions. We only report the averaged λ for years 10–14 for four combinations (*ET*, *EH*, *ETH*, and *ETHS*) that resulted in low λ values to illustrate that the full set of combinations was robust to the alternative baselines. We focused on these four combinations because they resulted in low λ values near the 2001 value and because their robustness is particularly important, as they form the basis for identifying which factors determine how a good year differs from a bad year.

RESULTS

Alternative Baselines

The use of size-dependent mortality resulted in January adult abundances similar to those in the original baseline, while the alternative baselines with fixed larval growth, density-dependent mortality, and length-dependent maturity resulted in January abundances that were lower than those in the original baseline (Figure 3a). Lower peak abundances were expected for the density-dependent mortality version because juvenile survival was specified to decrease under high abundances. Larval growth (and therefore larval-stage survival) had an important influence on both good and bad years. Lower abundances under length-dependent maturity occurred because the maturity relationship was not symmetric around 60 mm (Figure 2) and thus would, on average, result in a lower fraction of young of the year becoming mature than was observed with the simple 60-mm rule in the original baseline.

Despite these differences in January abundances, λ values were very similar for all versions of the baseline, with the length-dependent maturity alternative differing the most from the original baseline (Figure 3b). Relatively high January adult abundance occurred in 2001 (Figure 3a), despite the lowest λ being observed in that year, because January abundance was related to conditions in the previous summer and fall and was not reflective of the spring and summer conditions in 2001. The high λ values during years prior to 2001 led to high January adult abundance in 2001. The temporal pattern in λ values for length-dependent maturity was the same as that for the original baseline, but values in all years were lower than baseline values, with the largest difference occurring in 1998 ($\lambda = 1.59$ for length-dependent maturity versus 2.45 for the original baseline). The original baseline and the four alternatives all identified 1998 as the best model year and 2001 as the worst model year for Delta Smelt.

Systematic Comparison of Best versus Worst Years

The intersimulation variability in λ values decreased and more combinations approached the 2001 value as the number of factors set to 2001 values increased (Figure 4). The percentage of combinations that resulted in λ values within 50% of the 2001 λ value increased from 0% when one factor was set to the 2001 value to 10% for two factors at 2001 values, 50% for three factors at 2001 values, and 60% for four factors at 2001 values. All but one of the combinations that generated a λ value within 50% of the 2001 value involved either eggs per age-1 individual or temperature being set at the 2001 value.

Juvenile growth in the fall prior to spawning (i.e., as reflected by the number of eggs per age-1 fish) was the most important single factor in making 2001 a bad year, although no single factor alone was sufficient to fully account for the poor conditions in 2001 relative to 1998 (Figure 4). Temperature (*T*) played an important secondary role (Figure 4, shaded circles), and hydrodynamics (*H*) played a more minor role; salinity (*S*) and zooplankton (*Z*) as single factors were unimportant. When one factor at a time was switched from 1998 to 2001 values (Figure 4, leftmost section), only eggs per age-1 fish (*E*) resulted in a λ value less than 1.0. The single factors *T* and *H* (each at the 2001 value) generated the second- and third-lowest λ values (1.1 and 1.5). As a single factor, *Z* (which determined

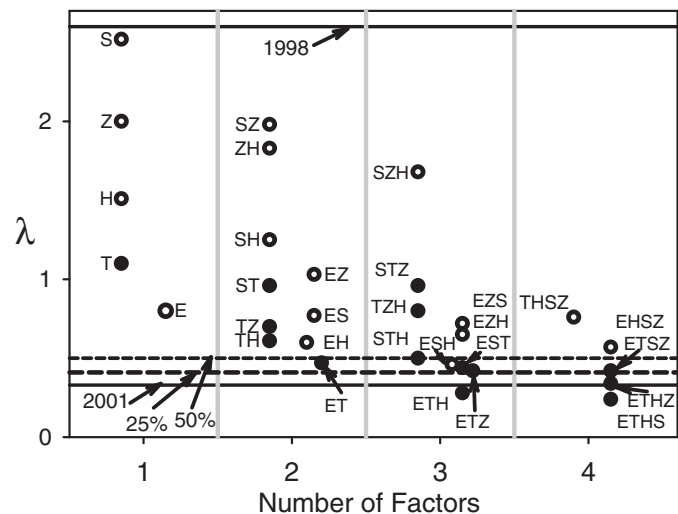


FIGURE 4. Contributions of five factors to differences between the best year (1998) and worst year (2001) for Delta Smelt. Each circle represents the mean finite population growth rate (λ) for years 10–14 of a 15-year simulation of repeated conditions for each factor (salinity [*S*], temperature [*T*], zooplankton [*Z*], hydrodynamics [*H*], and number of eggs per age-1 individual [*E*]) at either 1998 or 2001 values. Results are organized by the number of factors that were set to 2001 values (i.e., 1–4 factors; each combination code [e.g., “*STZ*”] lists the factors set at 2001 values); within each section, results with the number of eggs per age-1 individual at its 1998 value are shown on the left and results with that factor at its 2001 value are shown on the right. Shaded circles denote all combinations that included the 2001 temperature. The 1998 and 2001 values of λ are indicated by solid horizontal lines; the dotted horizontal lines represent λ values that are 25% and 50% higher than the 2001 value.

growth) generated a λ of 2.0, which was lower than the value for 1998 ($\lambda = 2.6$) but still much higher than the value for 2001 ($\lambda = 0.33$). When only S was set to the 2001 value, there was almost no effect on λ (2.52 versus 2.60).

All combinations of two factors set at 2001 values with eggs per age-1 individual at its higher 1998 value (left-side points in Figure 4, second section) generated λ values above 0.6; among these two-factor combinations, temperature and hydrodynamics at 2001 values together (*TH*) resulted in the lowest λ (0.61). The three lowest λ values all included 2001 temperature (Figure 4, shaded circles). The two-factor combinations that included the 2001 value for eggs per age-1 fish (right-side points in Figure 4, second section) resulted in λ values less than 1.0, and the *ET* and *EH* combinations produced λ values less than 0.6. Again, the lowest of these λ values was from the combination *ET* (Figure 4, shaded circle) and approached the λ value predicted for 2001 (0.47 versus 0.33).

Among the three-factor combinations set at 2001 values with eggs per age-1 individual set at the 1998 value (left-side points in Figure 4, third section), temperature and hydrodynamics were important. The highest λ (1.68) was predicted for the one combination that did not include 2001 temperature (*SZH*). The combinations with the three lowest λ values included the 2001 value for temperature (*STZ*, *TZH*, and *STH*; Figure 4, shaded circles); the two lowest of these λ values were from combinations that also included 2001 hydrodynamics ($\lambda = 0.8$ for *TZH* and 0.5 for *STH*).

When the number of eggs per age-1 fish was included as one of the three factors set at 2001 values (right-side points in Figure 4, third section), all λ values were less than 1.0. The combinations also including 2001 temperature (*ETH*, *ETZ*, and *EST*) generated the lowest λ values (0.28, 0.42, and 0.44, respectively), which were close to the λ value for 2001. The combinations that did not include 2001 temperature (Figure 4, open circles) generally had higher λ values (0.72 for *EZS* and 0.65 for *EZH*); the exception was *ESH*, which yielded a λ value (0.46) similar to those from the three combinations that included the 2001 temperature.

The number of eggs per age-1 individual and temperature continued to be very important in four-factor combinations. All four-factor combinations that included the 2001 value for eggs per age-1 fish (right-side points in Figure 4, fourth section) resulted in λ values less than 0.5, and those combinations that also included 2001 temperature (Figure 4, shaded circles) generated λ values that were close to the 2001 value. Of the four combinations that included the 2001 value for eggs per age-1 fish, the three combinations that also included 2001 temperature (*ETSZ*, *ETHZ*, and *ETHS*) all generated λ values less than 0.45, whereas the combination without temperature (*EHSZ*) generated the highest λ value (0.60). The remaining four-factor combination (*THSZ*; left-side point in Figure 4, fourth section), in which the number of eggs per age-1 individual was set at the 1998 value, generated the highest λ (0.85) observed for any four-factor combination.

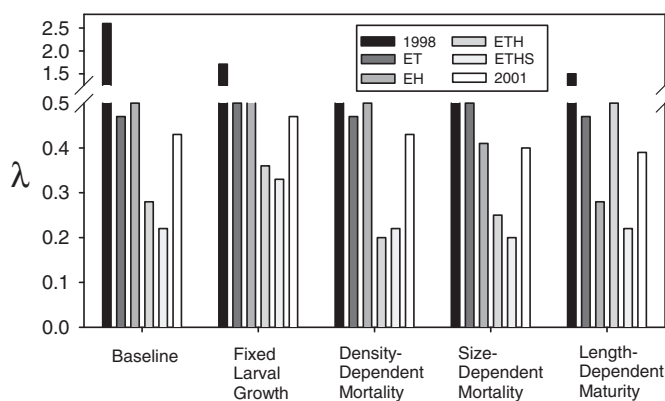


FIGURE 5. Averaged finite population growth rate (λ ; years 10–14) of Delta Smelt under the four alternative baselines and the four factor combinations that resulted in low λ values near the value for 2001. Factors are salinity (S), temperature (T), zooplankton (Z), hydrodynamics (H), and number of eggs per age-1 individual (E); each combination code (e.g., “*ETH*”) lists the factors that were set at 2001 values, and the remaining factors (i.e., with letters not shown) were set at 1998 values.

Robustness

The conditions leading to the good year (1998) were more sensitive to alternative baselines than the poor conditions leading to the bad year (2001; Figure 5). The four combinations (i.e., selected from Figure 4) that produced low λ values when set to their 2001 values under the original baseline generated similarly low λ values under the four alternative baselines. In contrast, the λ values varied more among the 1998 simulations. The alternative of density-dependent mortality produced the greatest reduction in λ for 1998 (λ decreased from 2.45 to 1.00). Larval growth and length-dependent maturity were also important in attaining the high λ predicted for 1998 in the original baseline. When larval growth was fixed at the overall average value (fixed duration), λ was reduced from 2.45 in the original baseline to 1.7; under length-based maturity, λ was reduced to 1.5. Size-dependent mortality was associated with the smallest reduction in the λ value for 1998 (λ decreased from 2.45 to 2.13).

DISCUSSION

Our analysis using a simulation experiment approach further clarified the relative influence of factors affecting Delta Smelt recruitment and population dynamics. In our companion paper (Rose et al. 2013), we compared conditions in 1998 with those in 2001 by using the 1995–2005 historical simulation. The five factors analyzed were inferred to be important in the historical simulation because their values differed, at least in some ways, between the best year and the worst year. In this paper, we systematically varied the five factors in a factorial simulation experiment to look for main and interaction effects. We moved away from the historical sequence of years and performed 15-year simulations with either 1998 or 2001 values repeated every year to allow the simulated population to reach a quasi-steady-state response. We also showed that our results, when viewed

in a comparative mode, were generally robust to alternative versions of the baseline model.

Our results demonstrated that among the factors we examined, no single factor completely accounted for the difference between the high λ in the best year (1998) and the low λ in the worst year (2001). Growth of juveniles in the fall–winter, temperature, and hydrodynamics clearly had the strongest effects, but λ could not be brought down from its 1998 value to near its 2001 value without some combination of factors. Thus, our results support the growing consensus that no single factor explains the Delta Smelt decline that occurred during 1995–2005 (Bennett and Moyle 1996; Bennett 2005; Baxter et al. 2010; Thomson et al. 2010).

Although we have shown that growth conditions in fall–winter were an important factor, there are many ways to achieve the faster growth that was predicted for 1998 relative to 2001. The growth conditions in winter affected the lengths of entering age-1 fish on January 1, with a 1998 value of 60.2 mm versus a 2001 value of 58.8 mm, and consequently affected the fraction mature (0.55 versus 0.41) and the egg production per entering age-1 fish (502.6 versus 107.6). These values for 1998 and 2001 differ from those reported in Rose et al. (2013) because the present values are averaged from the repeated years in the simulation experiment, whereas in our other paper (Rose et al. 2013) we reported values for 1998 and 2001 within the historical simulation. The difference in predicted mean lengths between 1998 and 2001 was well within the range of observed interannual values (see Figure 6 in Rose et al. 2013). Our analysis did not, however, distinguish how juveniles attained greater lengths prior to becoming age 1 and spawning. We used 1998 and 2001 conditions, but other years can also generate similar differences in growth based on combinations of zooplankton conditions and temperature; essentially, any mechanism that allows new age-1 recruits to have a greater length prior to spawning would result in a high number of eggs per age-1 fish and would set the stage for a good year. This can be achieved via warmer winter temperature (as in 1998) or by higher zooplankton densities causing faster growth at any time from the previous summer through early spring. If zooplankton conditions are better at higher salinity (seaward), then hydrodynamics (via its effect on transport) or salinity could also produce faster growth by putting individuals in boxes with higher prey biomass densities. We did not systematically examine how temperature, zooplankton, hydrodynamics, and salinity during the growing season of the year before or during the winter–spring period could potentially combine to promote faster growth and larger spawners in the spring. Rather, we used the suite of conditions for 1998 and 2001 to contrast a good year with a bad year.

A second way to increase egg production without faster growth of spawners would be to increase young-of-the-year survival prior to spawning. Total egg production was calculated as the number of eggs per entering age-1 fish times the number of age-1 fish. Our results were robust to the size-dependent mortality and length-based maturity versions of the baseline, so the

growth of adults affected the number of eggs per age-1 individual but not the abundance of age-1 fish. Higher Delta outflow at key times resulted in reduced entrainment, and hydrodynamics were consistently an important factor. Further analysis should explore spatial (box-scale) differences in mortality, which, if sufficient, could benefit the Delta Smelt via management manipulation of hydrodynamics and salinity, generating differences in starting age-1 abundances for spawning. We assumed that except for entrainment losses, mortality was stage dependent but not spatially variable.

Our results for the importance of food (zooplankton) are similar to those of Maunder and Deriso (2011), but we disagree about the roles of entrainment and density dependence. Maunder and Deriso (2011) used a stage-based life cycle model, and by introducing covariates into life stage survival (spawner–recruit) relationships, they determined that food abundance, temperature, predator abundance, and density dependence were the most important factors controlling the population dynamics of Delta Smelt. They further stated that there was some support for negative effects of water clarity and adult entrainment.

Our simulation experiment contrasting the best year versus the worst year agrees with the important role of temperature and zooplankton, but we did not examine the effects of predator abundance or water clarity. Maunder and Deriso (2011) used spring and summer zooplankton conditions: minimum *Eurytemora* and *Pseudodiaptomus* densities for April–June; average *Eurytemora* density for July; and average *Pseudodiaptomus* density for July–August. We found that fall, winter, and early spring growth was potentially important, at least for the comparison between 1998 and 2001. Maunder and Deriso (2011) examined a longer time period (1970–2006) that covered larger changes in the zooplankton community, and this could emphasize the importance of spring and summertime zooplankton relative to other factors, such as winter growth and its consequences for spring reproduction. We recommend that conditions in the winter and early spring and conditions from the year before be further evaluated for their potential to benefit Delta Smelt.

We disagree to some extent with Maunder and Deriso (2011) about the role of entrainment and density dependence. Examination of Figure 8 of Maunder and Deriso (2011) to assess the role of entrainment showed more agreement with our analysis than did their general statement of “some support for a negative relationship with . . . adult entrainment.” They showed an approximately twofold increase in adults during 2002–2006 by eliminating entrainment. This agrees with our analysis, showing higher entrainment mortality during the same years as in our simulation; however, we would term their Figure 8 results as providing more than “some” support for a negative effect of adult entrainment. The Maunder and Deriso (2011) analysis covered a longer time period (1970–2006) than our analysis (1995–2005); thus, the role of covariates can differ and density dependence likely played a larger role at the earlier, higher abundance levels (see Bennett 2005). In addition, direct comparisons between the models are somewhat confounded because our analysis and the

Maunder and Deriso (2011) analysis shared some information, such as the entrainment estimates from Kimmerer (2008) and the spawner–recruit information from long-term monitoring.

Several statistical analyses of similar monitoring and covariate data as used by Maunder and Deriso (2011) also implicated various indicators of spring and summer zooplankton food availability as being important. Thomson et al. (2010) used Bayesian change point analysis to examine variation in the fall MWT index; Mac Nally et al. (2010) used multivariate autoregressive modeling to analyze the fall MWT index in a multispecies approach; and Miller et al. (2012) used Ricker spawner–recruit relationships to analyze the ratio of indices as survival indicators. These analyses all inferred that various combinations of water temperature, water clarity, zooplankton indicators, and entrainment were correlated to various degrees with the historical pattern in the Delta Smelt abundance indices.

Other assumptions that are inherent in our modeling merit further analyses as possible alternative versions of baseline conditions. The representation of predation on Delta Smelt was partially explored by using size-dependent mortality, but there are also temporal trends and spatial patterns to the key predators of Delta Smelt that could be important. Striped Bass *Morone saxatilis* and Largemouth Bass *Micropterus salmoides* show distinct spatial distributions within the San Francisco Estuary and have also exhibited recent temporal trends, with young Striped Bass declining and Largemouth Bass increasing (Nobriga and Feyrer 2007). Furthermore, exotic Mississippi Silversides *Menidia audens* are known to readily consume larval Delta Smelt and have increased substantially in recent years (Baerwald et al. 2012).

Another assumption worthy of investigation is that the Delta Smelt population in the individual-based model consisted of individuals that all exhibit the same migratory behavior. Limited field data indicate that there is partial or divergent migration (Secor 1999; Chapman et al. 2012) within the Delta Smelt population, with some individuals possibly remaining year-round in the Cache Slough region, which is located in the southwestern portion of our Sacramento River model box (Merz et al. 2011; Sommer et al. 2011). An alternative version of the baseline individual-based model could include some proportion of individuals that remain resident in some areas. Resident individuals, or individuals with reduced or altered migrations, could exhibit different growth because of spatial variation in temperature, zooplankton, and susceptibility to entrainment.

Our detailed individual-based approach is not commonly used to simulate the population dynamics of endangered fish species, although it can be adapted for use in the more traditional population viability analysis (PVA) and risk framework. The individual-based approach is increasingly being used to simulate fish population and community dynamics for purposes of answering ecological and fisheries management questions (DeAngelis and Mooij 2005). However, although the individual-based approach is usually mentioned in reviews of PVA approaches (e.g., Akçakaya and Sjögren-Gulve 2000; Morris et al. 2002; Petersen et al. 2008), the number of examples

of its use specifically for PVA remains quite limited. Some commonly used general models apply an individual-based approach, but they employ a very simple representation of processes (e.g., Jarić et al. 2010). Examples in which a more mechanistic individual-based model approach was used include models of endangered birds (Letcher et al. 1998), turtles (Mazaris et al. 2005), and recruitment of Colorado Pikeminnow *Ptychocheilus lucius*. Using an individual-based approach very similar to our Delta Smelt modeling, Jager et al. (2001) analyzed the effects of habitat fragmentation by dams on the White Sturgeon *Acipenser transmontanus*, which is a species of concern and has been listed as endangered elsewhere. Population viability analysis usually involves many realizations of a modeled population trajectory to generate risk values. Our individual-based model cannot easily be used to perform thousands of simulations. A possible link to a PVA-type analysis of Delta Smelt would be to (1) use the individual-based model in a systematic way to create crude probability distributions for the elements of the Leslie matrix model (which can generate λ values with Monte Carlo simulation) or (2) use the coupled individual-based model and Leslie model to directly generate distributions of λ values. Once sets of λ values are obtained for a variety of environmental and biological conditions, they can be used in more traditional PVA projections of long-term persistence (see Morris et al. 2002).

Our analysis addresses several ongoing methodological issues in fish population dynamics: spatial dynamics in complex habitats, coupled biological–physical modeling, and recruitment and population dynamics at low abundances. The need for studies of long-term population dynamics to deal with spatial dynamics has recently been discussed (Giske et al. 1998; Struve et al. 2010), and approaches that deal with spatial variation explicitly are receiving greater attention (e.g., Kerr et al. 2010). Increasingly, fish-related management issues require an integrated approach that combines the physics of water with the biology of the fish and other biota (Shenton et al. 2012), and one method is the direct coupling of fine-scale hydrodynamics with long-term fish population dynamics (Buckley and Buckley 2010; Rose et al. 2010; Hinrichsen et al. 2011; Stock et al. 2011).

Our model expands on the classical particle tracking approach by simulating detailed biological processes, relatively complicated behavioral movement, and multiple generations. Our Delta Smelt model simulated growth, survival, reproduction, and movement of individual fish on the same spatial grid as the hydrodynamics, and the super-individual method allowed for 15-year simulations. Although PTMs are commonly embedded within hydrodynamics models (North et al. 2009; Hinrichsen et al. 2011), the PTMs typically do not include detailed descriptions of growth and reproduction. Rather, these studies usually invoke, at most, simple movement behavior as an addition to passive transport and are mostly used for short-term (<1 year) simulations (Miller 2007; Lett et al. 2009; Gallego 2011). However, a consequence of full life cycle modeling that includes juveniles and adults within a detailed

spatial grid is that now we must simulate behavioral movement on relatively fine scales. Modeling behavioral movement is critical to ensure that individuals experience the appropriate conditions over time, but this remains a challenge (Watkins and Rose 2013). Delta Smelt movement patterns in our simulations were generally realistic but require further refinement.

Finally, much fish population modeling has focused on the effects of harvesting from high-number populations, whereas there is an increasing need to examine dynamics of fish populations at low abundances due to overharvest and in support of recovery plans for listed species (Keith and Hutchings 2012). The focus on harvesting leads to an emphasis on density-dependent mortality, often via the spawner–recruit relationship (Rose et al. 2001). Our approach differs from this by focusing on Delta Smelt population dynamics under density-independent conditions. We emphasized how individuals were transported through or navigated through their spatially complex and temporally varying habitat. Our analysis can be viewed as part of the broader idea of multiple factors within the match–mismatch theory of controls on young-of-the-year survival and therefore recruitment (Peck et al. 2012), coupled with the idea that adult bioenergetics are important for determining maturity and annual egg production (Neil et al. 1994; Rose et al. 2001). Because our model was density independent, all of the predicted variation in stage-specific survival rates was due to variation in how spatial distributions interacted with dynamic environmental conditions. Our results showed how the spatial and temporal positioning of all life stages each year (based on physical transport and salinity), combined with the pattern in daily water temperature and the amount of Delta outflow, affected the magnitude and location of egg production and the subsequent dynamic matching of larval and juveniles with their prey types, thus affecting recruitment success. However, even our modeling results were not simple to interpret, and therefore they also illustrate how spatially and temporally dynamic habitat can create complicated match–mismatch situations.

Delta Smelt have been at the center of escalating controversy in the San Francisco Estuary region for several decades (NRC 2010; Kimmerer 2011; Miller 2011). What initially arose as a conflict between water demands for export versus for the environment (including Delta Smelt) has metastasized as the number of ostensible factors behind the decline of Delta Smelt has grown (e.g., Mac Nally et al. 2010; Maunder and Deriso 2011; Miller et al. 2012). The conflict has now evolved into a complicated situation in which multiple factors operate in interactive ways and are continually being argued over in court (Delta Smelt Consolidated Cases 2010). Our results contribute to the growing number of examples showing that multiple factors affect aquatic ecosystems (Breitburg and Riedel 2005; Ormerod et al. 2010; Cloern and Jassby 2012) and that the search for a single factor controlling fish population dynamics is unlikely to be successful (e.g., Rose 2000; Krebs 2002; Hecky et al. 2010; Lindgren et al. 2011).

Our results to date suggest that management actions to benefit Delta Smelt must deal with multiple stressors that occur at different points in the life cycle. An increase in prey would induce relatively large responses in reproduction but may not be feasible. We showed that growth leading up to spawning was important for subsequent population growth; it remains to be seen whether it is possible to promote growth of Delta Smelt or higher young-of-the-year survival prior to spawning (fall–spring) via management actions. We also showed that no single factor can alone account for the differences between good and bad years and that promoting growth should be done in combination with other actions (if feasible) to (1) ensure good temperatures for summer growth and delayed spawning and (2) ensure sufficient outflow and avoidance of high entrainment (see results in Rose et al. 2013). Our results also demonstrate that expectations should be clearly stated, as most management actions are unlikely to generate large, immediate responses because the influence of stressors varies from year to year and because the reduction in a single stressor during any one year may be moderated by the conditions in other, non-manipulated stressors occurring in that year.

We envision two other areas for future analyses using the individual-based model. First, extending the model simulations for the periods before 1995 and after 2005 would allow for more comparisons and contrasts of good versus bad years to determine other combinations of factors that may be important; climate change scenarios should be included in these simulations to allow for future-looking comparisons. This would require use of the DSM2 hydrodynamic model or another hydrodynamic model and the development of synthetic temperature, salinity, and zooplankton data. Second, a more rigorous side-by-side comparison of the Maunder and Deriso (2011) model and our individual-based model would facilitate an understanding of the relative effects of key stressors on Delta Smelt population dynamics. The population dynamics and reasons for the decline of Delta Smelt are complex. However, complexity is not a reason to avoid rigorous quantitative analyses—indeed, it is perhaps the best reason to develop and compare alternative modeling approaches.

ACKNOWLEDGMENTS

This project was funded by a grant from the CALFED Science Program (SCI-05-C106). The comments of two reviewers and the Associate Editor helped us greatly clarify the manuscript.

REFERENCES

- Akçakaya, H. R., and P. Sjögren-Gulve. 2000. Population viability analyses in conservation planning: an overview. *Ecological Bulletins* 48:9–21.
- Baerwald, M. R., B. M. Schreier, G. Schumer, and B. May. 2012. Detection of threatened Delta Smelt in the gut contents of the invasive Mississippi Silverside in the San Francisco Estuary using TaqMan assays. *Transactions of the American Fisheries Society* 141:1600–1607.

- Bailey, K. M., and J. T. Duffy-Anderson. 2010. Fish predation and mortality. Pages 322–329 in J. H. Steele, S. A. Thorpe, and K. K. Turekian, editors. *Marine biology: a derivative of the encyclopedia of ocean sciences*. Academic Press, San Diego, California.
- Baxter, R., R. Breuer, L. Brown, L. Conroy, F. Feyrer, S. Fong, K. Gehrts, L. Grimaldo, B. Herbold, P. Hrodey, A. Mueller-Solger, T. Sommer, and K. Souza. 2010. 2010 pelagic organism decline work plan and synthesis of results. Interagency Ecological Program for the San Francisco Estuary, California Department of Water Resources, Sacramento.
- Bennett, W. A. 2005. Critical assessment of the Delta Smelt population in the San Francisco Estuary, California. *San Francisco Estuary and Watershed Science* [online serial] 3(2):article 1.
- Bennett, W. A., and P. B. Moyle. 1996. Where have all the fishes gone? interactive factors producing fish declines in the Sacramento–San Joaquin Estuary. Pages 519–542 in J. T. Hollibaugh, editor. *San Francisco Bay: the ecosystem*. American Association for the Advancement of Science, San Francisco.
- Breitburg, D. L., and G. F. Riedel. 2005. Multiple stressors in marine systems. Pages 167–182 in E. A. Norse and L. B. Crowder, editors. *Marine conservation biology: the science of maintaining the sea's biodiversity*. Island Press, Washington, D.C.
- Brooks, M. L., E. Fleishman, L. R. Brown, P. W. Lehman, I. Werner, N. Scholz, C. Mitchelmore, J. R. Lovvorn, M. L. Johnson, D. Schlenk, S. van Drunick, J. I. Drever, D. M. Stoms, A. E. Parker, and R. Dugdale. 2012. Life histories, salinity zones, and sublethal contributions of contaminants to pelagic fish declines illustrated with a case study of San Francisco Estuary, California, USA. *Estuaries and Coasts* 35:603–621.
- Buckley, L. J., and L. B. Buckley. 2010. Toward linking ocean models to fish population dynamics. *Progress in Oceanography* 54:85–88.
- Chapman, B. B., K. Hulthén, J. Brodersen, P. A. Nilsson, C. Skov, L. A. Hansson, and C. Brönmark. 2012. Partial migration in fishes: causes and consequences. *Journal of Fish Biology* 81:456–478.
- Cloern, J. E., and A. D. Jassby. 2012. Drivers of change in estuarine-coastal ecosystems: discoveries from four decades of study in San Francisco Bay. *Reviews of Geophysics* 50:RG4001. DOI: 10.1029/2012RG000397.
- Connon, R. E., J. Geist, J. Pfeiff, A. V. Loguinov, L. S. D'Abronzo, H. Wintz, C. D. Vulpe, and I. Werner. 2009. Linking mechanistic and behavioral responses to sublethal esfenvalerate exposure in the endangered Delta Smelt *Hypomesus transpacificus* (fam. Osmeridae). *BMC Genomics* [online serial] 10:608. DOI: 10.1186/1471-2164-10-608.
- Cowan, J. H. Jr., K. A. Rose, and D. R. DeVries. 2000. Is density-dependent growth in young-of-the-year fishes a question of critical weight? *Reviews in Fish Biology and Fisheries* 10:61–89.
- DeAngelis, D. L., and W. M. Mooij. 2005. Individual-based modeling of ecological and evolutionary processes. *Annual Review of Ecology, Evolution, and Systematics* 36:147–168.
- Delta Smelt Consolidated Cases. 2010. F. Supp. 2d-2010 WL 2195960 at pp. 24, 26, 44. Eastern District of California.
- Feyrer, F., B. Herbold, S. A. Matern, and P. B. Moyle. 2003. Dietary shifts in a stressed fish assemblage: consequences of a bivalve invasion in the San Francisco Estuary. *Environmental Biology of Fishes* 67:277–288.
- Feyrer, F., M. L. Nobriga, and T. R. Sommer. 2007. Multidecadal trends for three declining fish species: habitat patterns and mechanisms in the San Francisco Estuary, California, USA. *Canadian Journal of Fisheries and Aquatic Sciences* 64:723–734.
- Galleo, A. 2011. Biophysical models: an evolving tool in marine ecological research. Pages 279–290 in F. Jopp, H. Reuter, and B. Breckling, editors. *Modelling complex ecological dynamics*. Springer-Verlag, Berlin.
- Giske, J., G. Huse, and Ø. Fiksen. 1998. Modelling spatial dynamics of fish. *Reviews in Fish Biology and Fisheries* 8:57–91.
- Gislason, H., N. Daan, J. C. Rice, and J. G. Pope. 2010. Size, growth, temperature and the natural mortality of marine fish. *Fish and Fisheries* 11:149–158.
- Grimaldo, L. F., T. Sommer, N. Van Ark, G. Jones, E. Holland, P. B. Moyle, B. Herbold, and P. Smith. 2009. Factors affecting fish entrainment into massive water diversions in a tidal freshwater estuary: can fish losses be managed? *North American Journal of Fisheries Management* 29:1253–1270.
- Hecky, R. E., R. Mugidde, P. S. Ramlal, M. R. Talbot, and G. W. Kling. 2010. Multiple stressors cause rapid ecosystem change in Lake Victoria. *Freshwater Biology* 55(Supplement 1):19–42.
- Hinrichsen, H. H., M. Dickey-Collas, M. Huret, M. A. Peck, and F. B. Vikebø. 2011. Evaluating the suitability of coupled biophysical models for fishery management. *ICES Journal of Marine Science* 68:1478–1487.
- Jager, H. I., J. A. Chandler, K. B. Lepla, and W. Van Winkle. 2001. A theoretical study of river fragmentation by dams and its effects on White Sturgeon populations. *Environmental Biology of Fishes* 60:347–361.
- Jarić, I., T. Ebenhard, and M. Lenhardt. 2010. Population viability analysis of the Danube sturgeon populations in a Vortex simulation model. *Reviews in Fish Biology and Fisheries* 20:219–237.
- Keith, D. M., and J. A. Hutchings. 2012. Population dynamics of marine fishes at low abundance. *Canadian Journal of Fisheries and Aquatic Sciences* 69:1150–1163.
- Kerr, L. A., S. X. Cadrin, and D. H. Secor. 2010. The role of spatial dynamics in the stability, resilience, and productivity of an estuarine fish population. *Ecological Applications* 20:497–507.
- Kimmerer, W. J. 2004. Open water processes of the San Francisco Estuary: from physical forcing to biological responses. *San Francisco Estuary and Watershed Science* [online serial] 2(1):article 1.
- Kimmerer, W. J. 2008. Losses of Sacramento River Chinook Salmon and Delta Smelt to entrainment in water diversions in the Sacramento–San Joaquin Delta. *San Francisco Estuary and Watershed Science* [online serial] 6(2): article 2.
- Kimmerer, W. J. 2011. Modeling Delta Smelt losses at the south Delta export facilities. *San Francisco Estuary and Watershed Science* [online serial] 9(1):article 5.
- Kimmerer, W. J., E. S. Gross, and M. L. MacWilliams. 2009. Is the response of estuarine nekton to freshwater flow in the San Francisco Estuary explained by variation in habitat volume? *Estuaries and Coasts* 32:375–389.
- Kimmerer, W. J., and M. L. Nobriga. 2008. Investigating particle transport and fate in the Sacramento–San Joaquin Delta using a particle tracking model. *San Francisco Estuary and Watershed Science* [online serial] 6(1):article 4.
- Krebs, C. J. 2002. Two complementary paradigms for analysing population dynamics. *Philosophical Transactions of the Royal Society of London B* 357: 1211–1219.
- Kuivila, K. M., and G. E. Moon. 2004. Potential exposure of larval and juvenile Delta Smelt to dissolved pesticides in the Sacramento–San Joaquin Delta, California. Pages 229–241 in F. Feyrer, L. R. Brown, R. L. Brown, and J. J. Orsi, editors. *Early life history of fishes in the San Francisco Estuary and watershed*. American Fisheries Society, Symposium 39, Bethesda, Maryland.
- Letcher, B. H., J. A. Priddy, J. R. Walters, and L. B. Crowder. 1998. An individual-based, spatially explicit simulation model of the population dynamics of the endangered red-cockaded woodpecker, *Picoides borealis*. *Biological Conservation* 86:1–14.
- Lett, C., K. A. Rose, and B. A. Megrey. 2009. Biophysical models. Pages 88–111 in D. Checkley, J. Alheit, Y. Oozeki, and C. Roy, editors. *Climate change and small pelagic fish*. Cambridge University Press, Cambridge, UK.
- Lindgren, M., Ö. Östman, and A. Gårdmark. 2011. Interacting trophic forcing and the population dynamics of herring. *Ecology* 92:1407–1413.
- Mac Nally, R., J. R. Thomson, W. J. Kimmerer, F. Feyrer, K. B. Newman, A. Sih, W. A. Bennett, L. Brown, E. Fleishman, S. D. Culbertson, and G. Castillo. 2010. Analysis of pelagic species decline in the upper San Francisco Estuary using multivariate autoregressive modeling (MAR). *Ecological Applications* 20:1417–1430.
- Maunder, M. N., and R. B. Deriso. 2011. A state-space multistage life cycle model to evaluate population impacts in the presence of density dependence: illustrated with application to Delta Smelt (*Hypomesus transpacificus*). *Canadian Journal of Fisheries and Aquatic Sciences* 68:1285–1306.

- Mazaris, A. D., Ø. Fiksen, and Y. G. Matsinos. 2005. Using an individual-based model for assessment of sea turtle population viability. *Population Ecology* 47:179–191.
- Merz, J. E., S. Hamilton, P. S. Bergman, and B. Cavallo. 2011. Spatial perspective for Delta Smelt: a summary of contemporary survey data. *California Fish and Game* 97:164–189.
- Miller, T. J. 2007. Contribution of individual-based coupled physical–biological models to understanding recruitment in marine fish populations. *Marine Ecology Progress Series* 347:127–138.
- Miller, W. J. 2011. Revisiting assumptions that underlie estimates of proportional entrainment of Delta Smelt by state and federal water diversions from the Sacramento–San Joaquin Delta. *San Francisco Estuary and Watershed Science* [online serial] 9(1):article 4.
- Miller, W. J., B. F. J. Manly, D. D. Murphy, D. Fullerton, and R. R. Ramey. 2012. An investigation of factors affecting the decline of Delta Smelt (*Hypomesus transpacificus*) in the Sacramento–San Joaquin Estuary. *Reviews in Fisheries Science* 20:1–19.
- Morris, W. F., P. L. Bloch, B. R. Hudgens, L. C. Moyle, and J. R. Stinchcombe. 2002. Population viability analysis in endangered species recovery plans: past use and future improvements. *Ecological Applications* 12:708–712.
- Neill, W. H., J. M. Miller, H. W. Van Der Veer, and K. O. Winemiller. 1994. Ecophysiology of marine fish recruitment: a conceptual framework for understanding interannual variability. *Netherlands Journal of Sea Research* 32:135–152.
- Nobriga, M. L. 2002. Larval Delta Smelt diet composition and feeding incidence: environmental and ontogenetic influences. *California Fish and Game* 88:149–164.
- Nobriga, M. L., and F. Feyrer. 2007. Shallow-water piscivore–prey dynamics in California’s Sacramento–San Joaquin Delta. *San Francisco Estuary and Watershed Science* [online serial] 5(2):article 4.
- Nobriga, M. L., T. R. Sommer, F. Feyrer, and K. Fleming. 2008. Long-term trends in summertime habitat suitability for Delta Smelt (*Hypomesus transpacificus*). *San Francisco Estuary and Watershed Science* [online serial] 6(1):article 1.
- North, E. W., A. Gallego, and P. Petitgas, editors. 2009. Manual of recommended practices for modelling physical–biological interactions during fish early life. ICES Cooperative Research Report 295.
- NRC (National Research Council). 2010. A scientific assessment of alternatives for reducing water management effects on threatened and endangered fishes in California’s Bay–Delta. National Academies Press, Washington, D.C.
- NRC (National Research Council). 2012. Sustainable water and environmental management in the California Bay–Delta. National Academies Press, Washington, D.C.
- Ormerod, S. J., M. Dobson, A. G. Hildrew, and C. R. Townsend. 2010. Multiple stressors in freshwater ecosystems. *Freshwater Biology* 55(Supplement 1): 1–4.
- Peck, M. A., K. B. Huebert, and J. K. Llopiz. 2012. Intrinsic and extrinsic factors driving match–mismatch dynamics during the early life history of marine fishes. *Advances in Ecological Research* 47:177–302.
- Petersen, J. H., D. L. DeAngelis, and C. P. Paukert. 2008. An overview of methods for developing bioenergetic and life history models for rare and endangered species. *Transactions of the American Fisheries Society* 137:244–253.
- Rose, K. A. 2000. Why are quantitative relationships between environmental quality and fish populations so elusive? *Ecological Applications* 10:367–385.
- Rose, K. A., J. I. Allen, Y. Artioli, M. Barange, J. Blackford, F. Carlotti, R. Cropp, U. Daewel, K. Edwards, K. Flynn, S. L. Hill, R. HilleRisLambers, G. Huse, S. Mackinson, B. Megrey, A. Moll, R. Rivkin, B. Salihoglu, C. Schrum, L. Shannon, Y.-J. Shin, S. L. Smith, C. Smith, C. Solidoro, M. St. John, and M. Zhou. 2010. End-to-end models for the analysis of marine ecosystems: challenges, issues, and next steps. *Marine and Coastal Fisheries: Dynamics, Management, and Ecosystem Science* [online serial] 2:115–130.
- Rose, K. A., J. H. Cowan Jr., K. O. Winemiller, R. A. Myers, and R. Hilborn. 2001. Compensatory density dependence in fish populations: importance, controversy, understanding and prognosis. *Fish and Fisheries* 2:293–327.
- Rose, K. A., W. J. Kimmerer, K. P. Edwards, and W. A. Bennett. 2013. Individual-based modeling of Delta Smelt population dynamics in the upper San Francisco Estuary: I. Model description and baseline results. *Transactions of the American Fisheries Society* 142:1238–1259.
- Rothschild, B. J. 1986. Dynamics of marine fish populations. Harvard University Press, Cambridge, Massachusetts.
- Scheffer, M., J. M. Baveco, D. L. DeAngelis, K. A. Rose, and E. H. van Nes. 1995. Super-individuals: a simple solution for modelling large populations on an individual basis. *Ecological Modelling* 80:161–170.
- Secor, D. H. 1999. Specifying divergent migrations in the concept of stock: the contingent hypothesis. *Fisheries Research* 43:13–34.
- Shenton, W., N. R. Bond, J. D. L. Yen, and R. Mac Nally. 2012. Putting the “ecology” into environmental flows: ecological dynamics and demographic modelling. *Environmental Management* 50:1–10.
- Sogard, S. M. 1997. Size-selective mortality in the juvenile stage of teleost fishes: a review. *Bulletin of Marine Science* 60:1129–1157.
- Sommer, T., F. Mejia, M. Nobriga, F. Feyrer, and L. Grimaldo. 2011. The spawning migration of Delta Smelt in the upper San Francisco Estuary. *San Francisco Estuary and Watershed Science* [online serial] 9(2): article 2.
- Stock, C. A., M. A. Alexander, N. A. Bond, K. Brander, W. W. L. Cheung, E. N. Curchitser, T. L. Delworth, J. P. Dunne, S. M. Griffies, M. A. Haltuch, J. A. Hare, A. B. Hollowed, P. Lehodey, S. A. Levin, J. S. Link, K. A. Rose, R. Rykaczewski, J. L. Sarmiento, R. J. Stouffer, F. B. Schwing, G. A. Vecchi, and F. E. Werner. 2011. On the use of IPCC-class models to assess the impact of climate on living marine resources. *Progress in Oceanography* 88:1–27.
- Struve, J., K. Lorenzen, J. Blanchard, L. Börger, N. Bunnefeld, C. Edwards, C. Joaquín Hortal, A. MacCall, J. Matthiopoulos, B. Van Moorter, A. Ozgul, F. Royer, N. Singh, C. Yesson, and R. Bernard. 2010. Lost in space? Searching for directions in the spatial modelling of individuals, populations and species ranges. *Biology Letters* 6:575–578.
- Thomson, J. R., W. J. Kimmerer, L. R. Brown, K. B. Newman, R. Mac Nally, W. A. Bennett, F. Feyrer, and E. Fleishman. 2010. Bayesian change point analysis of abundance trends for pelagic fishes in the upper San Francisco Estuary. *Ecological Applications* 20:1431–1448.
- USFWS (U.S. Fish and Wildlife Service). 2008. Biological opinion (BO) on the long-term operational criteria and plan (OCAP) for coordination of the Central Valley project and state water project. USFWS, California and Nevada Region, Sacramento, California.
- Watkins, K. S., and K. A. Rose. 2013. Evaluating the performance of individual-based animal movement models in novel environments. *Ecological Modelling* 250:214–234.
- Winder, M., and A. D. Jassby. 2011. Shifts in zooplankton community structure: implications for food web processes in the upper San Francisco Estuary. *Estuaries and Coasts* 34:675–690.

Sudden Clearing of Estuarine Waters upon Crossing the Threshold from Transport to Supply Regulation of Sediment Transport as an Erodible Sediment Pool is Depleted: San Francisco Bay, 1999

David H. Schoellhamer

Received: 21 June 2010 / Revised: 23 December 2010 / Accepted: 28 January 2011 / Published online: 19 February 2011
 © Coastal and Estuarine Research Federation (outside the USA) 2011

Abstract The quantity of suspended sediment in an estuary is regulated either by transport, where energy or time needed to suspend sediment is limiting, or by supply, where the quantity of erodible sediment is limiting. This paper presents a hypothesis that suspended-sediment concentration (SSC) in estuaries can suddenly decrease when the threshold from transport to supply regulation is crossed as an erodible sediment pool is depleted. This study was motivated by a statistically significant 36% step decrease in SSC in San Francisco Bay from water years 1991–1998 to 1999–2007. A quantitative conceptual model of an estuary with an erodible sediment pool and transport or supply regulation of sediment transport is developed. Model results confirm that, if the regulation threshold was crossed in 1999, SSC would decrease rapidly after water year 1999 as observed. Estuaries with a similar history of a depositional sediment pulse followed by erosion may experience sudden clearing.

Keywords Estuary · Sediment · Turbidity · Estuarine sediment transport · Suspended sediment · Sediment supply · Geomorphology · San Francisco Bay · Bed sediment · Bottom sediment · Sedimentation · Deposition · Aggradation · Degradation · Erosion · Resuspension · Erodible sediment pool · Sudden clearing · Suspended-sediment concentration

Introduction

Suspended-sediment concentration (SSC) in an estuary is commonly determined by a periodic cycle of erosion and deposition (for examples see Grabemann et al. 1997; Schoellhamer 2002; Tattersall et al. 2003; Wolanski et al. 1995). Slack tides, neap tides, and periodic stratification enable deposition on the bed, and tidal currents, spring tides, and wind waves apply shear force to the bed that resuspends sediment. At any moment, the amount of sediment that estuarine waters can suspend is regulated either by the available hydrodynamic energy (transport regulation) or by the mass of erodible sediment in the estuary (supply regulation). In addition, estuaries can be transport-regulated if the quantity of suspended sediment is limited by the duration of resuspension. For example, the duration of tidal resuspension may be limited by the time between slack tides, and the duration of wind-wave resuspension may be limited by the duration of storms, diurnal wind, or shallow depths that allow surface waves to apply sufficient shear to the bed. The concept of transport and supply regulation has been applied to riverine sediment transport (Rubin and Topping 2001).

A simple conceptual model of estuarine sedimentation is that an estuary contains an erodible sediment pool, some or all of which is suspended or resting on the bed at any given time (Fig. 1a). If all of the erodible sediment is suspended, then sediment transport is supply-regulated. If some of the erodible sediment is always on the bed, then sediment transport is transport-regulated. Outflow to the ocean and permanent deposition such as in a wetland reduce the erodible sediment pool. Supply from the watershed or ocean increases the erodible sediment pool. An estuary is in dynamic equilibrium when the erodible bed sediment

D. H. Schoellhamer (✉)
 US Geological Survey,
 6000 J Street, Placer Hall,
 Sacramento, CA 95819, USA
 e-mail: dschoell@usgs.gov

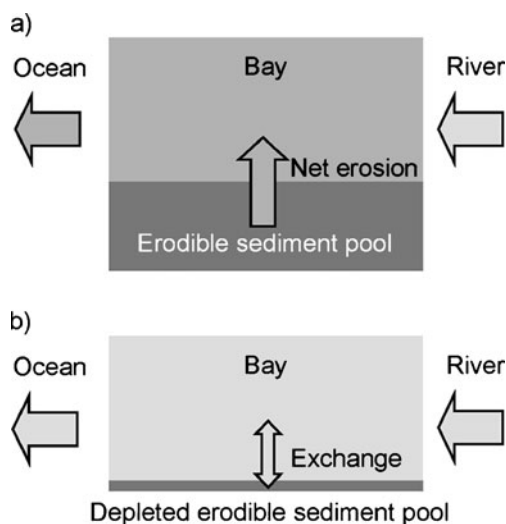


Fig. 1 Conceptual model of an erodible sediment pool (a) that becomes depleted, reducing SSC (b)

mass is constant. A time scale of perhaps decades must be considered for dynamic equilibrium because of seasonal and annual variations in watershed hydrology and oceanography.

The purpose of this paper is to demonstrate that SSC in an estuary can suddenly decrease when an erodible sediment pool becomes depleted, and this may explain a decrease in SSC in San Francisco Bay beginning in 1999. First, the motivation for this work, a decrease in SSC in San Francisco Bay beginning in 1999, is presented. Analysis of bathymetric change data supports the hypothesis that the bay contained an erodible pool of sediment that was depleted in the late 1990s. A simple quantitative conceptual model is then developed to test the plausibility of the hypothesis that depletion of an erodible sediment pool causes a step decrease in SSC. Homogeneity within the estuary is assumed as this paper focuses on the net functionality of the estuary as a component in the watershed/estuary/ocean system.

San Francisco Bay Sedimentation

San Francisco Bay is composed of four subembayments, Suisun, San Pablo, Central, and South Bays, connected to the Pacific Ocean through the Golden Gate (Fig. 2). The bottom sediments in South Bay and in the shallow water areas (less than 3–4 m) of Central, San Pablo, and Suisun Bays are composed mostly of silts and clays. Silts and sands are present in the deeper parts of Central, San Pablo, and Suisun Bays and in Carquinez Strait (Conomos and Peterson 1977). The average depth of the Bay is 2 m at mean lower low water. Tides are mixed with a range of 1 to 3 m. About 90% of freshwater inflow to the Bay comes

from the Central Valley of California and flows through the Sacramento-San Joaquin River Delta to Suisun Bay. South Bay receives much less freshwater flow than Suisun Bay. Tributaries from much smaller local watersheds provide the rest of the freshwater inflow. About 89% of SSC variability is associated with semidiurnal, fortnightly, monthly, and semiannual tidal cycles, seasonal wind, and river supply (Schoellhamer 2002). Winds and wind wave resuspension are greatest in spring and summer. There are two distinct hydrologic seasons: a wet season from late autumn to early spring with the remainder of the year being dry. Sediment from the watershed is delivered during the wet season (McKee et al. 2006). Thus, the water year (WY), which begins on October 1 and ends on September 30, is a convenient period to average water quality data such as SSC because it begins in the dry season, includes a single wet season, and ends in the dry season.

Watershed sediment supply to the bay from the Central Valley has been severely disturbed by humans since the late 1800s (Fig. 3). Hydraulic mining for gold in the late 1800s washed sediment into Central Valley rivers and the bay (Gilbert 1917). During the 1900s, many dams that trap sediment were constructed in the watershed (Wright and Schoellhamer 2004). The largest source of watershed sediment is the Sacramento River, for which 87–99% of the total load is suspended load (Porterfield 1980; Schoellhamer et al. 2005; Wright and Schoellhamer 2004). More than one half the banks of the lower Sacramento River were riprapped during the later half of the twentieth century, protecting them from erosion and decreasing sediment transport in the river (USFWS 2000). Flood control bypasses built in the Sacramento River floodplain during the early twentieth century trap sediment and reduce downstream sediment supply (Singer et al. 2008). Diminishment of the hydraulic mining sediment pulse, sediment trapping behind dams and in flood control bypasses, and bank protection all contribute to decreased sediment supply from the Central Valley to the bay. Suspended sediment supply from the Sacramento River gradually decreased by one half from 1957 to 2001 (Wright and Schoellhamer 2004). Total suspended-solid concentration in the Sacramento-San Joaquin River Delta decreased from 1975 to 1995 (Jassby et al. 2002). Canuel et al. (2009) found that sediment and carbon accumulation rates in the Sacramento-San Joaquin River Delta were 4–8 times greater before 1972 than after. At the end of the 1900s, sediment supply from the Central Valley was about equal to that from other more local bay tributaries (Schoellhamer et al. 2005).

The hydraulic mining sediment pulse deposited in Suisun, San Pablo, and Central Bay in the 1800s (Cappiella et al. 1999; Fregoso et al. 2008; Jaffe et al. 1998). In the 1900s, these subembayments became erosional.

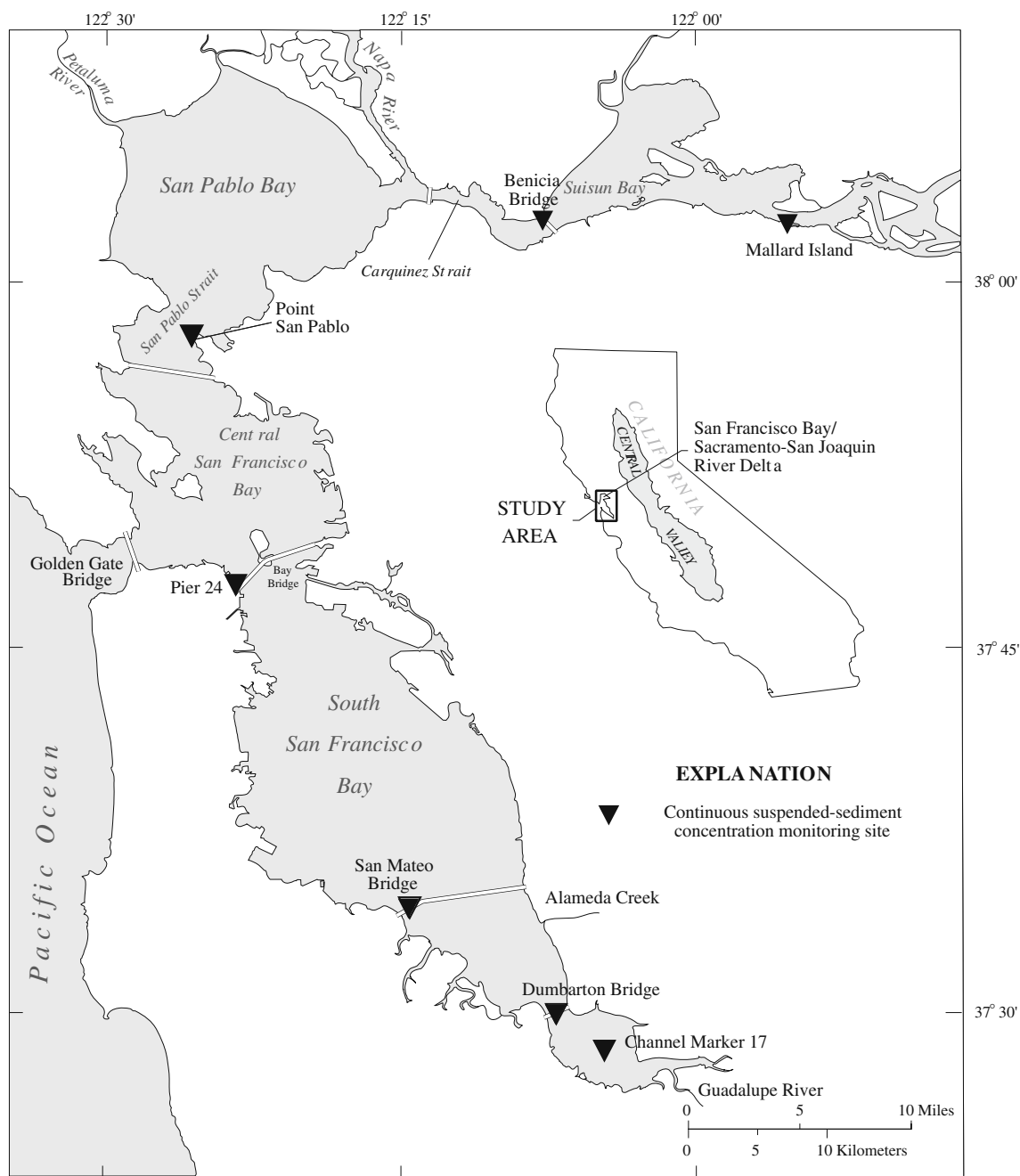


Fig. 2 San Francisco Bay study area

San Francisco Bay Suspended-Sediment Concentration Step Decrease

The US Geological Survey has used automated optical sensors to measure SSC every 15 min at several stations in San Francisco Bay beginning in December 1991 (Fig. 2, Buchanan and Lionberger 2009; Schoellhamer et al. 2007). Sensors from several manufacturers have been deployed. An optical sensor transmits a pulse of light that scatters off of suspended particles and is measured by the sensor. Every

3–4 weeks, the sensors are cleaned, data are downloaded, and calibration samples are collected. About one half of the data are invalid due to biofouling of the optical sensor, but the quantity of valid data in more recent years is approaching three quarters because self-cleaning sensors have improved.

An example time series of SSC data from mid-depth at Point San Pablo shows a decrease in SSC in the late 1990s (Fig. 4). This time series is shown because it is relatively lengthy and complete. Much of the tidal variability of the

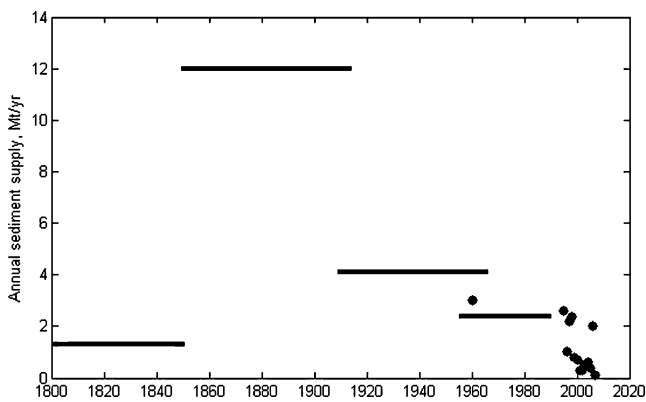


Fig. 3 Estimated annual sediment supply from the Central Valley to San Francisco Bay. Estimates from Gilbert (1917), Krone (1979), Porterfield (1980), Ogden Beeman and Associates (1992), McKee et al. (2006), and David et al. (2009). Bars indicate estimates over entire period, and points indicate yearly estimates. A bulk density of 850 kg/m³ was assumed (Porterfield 1980)

data is compressed into what appears as a solid band of data. The band is generally thickest in the spring and early summer when wind waves resuspend sediment deposited during the previous winter wet season. The band is thinnest in autumn when wind decreases and before the wet season delivers new sediment from the watershed. Maximum values of SSC were observed during floods in early 1997 and 1998.

SSC at most sites from the early 1990s to WY 1998 was almost double that from WYs 1999 to 2007 (Table 1). Mean SSC after September 30, 1997 was 36% less than before. The step change in the water year mean SSCs from WY 1998 to 1999 was significant (one-sided rank-sum test $p < 0.01$) at all sites except San Mateo Bridge. Water year mean SSC was analyzed rather than monthly mean SSC to avoid problems with variation of the timing of seasonal inflow, turbidity maxima, and seasonal wind from year to

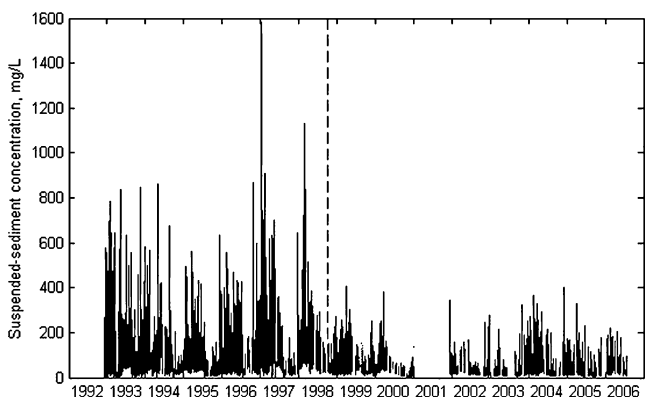


Fig. 4 Suspended-sediment concentration, mid-depth, Point San Pablo. The vertical dashed line indicates when the step decrease occurred

Table 1 Mean and median near-surface or mid-depth suspended-sediment concentrations (mg/L) during dry WY 1994, before the step decrease, after the step decrease, and during wet WY 2006

Site	Water year	Mean	Median	% valid
Mallard Island	1994–1998	45	39	67
	1999–2007	33	30	80
	2006	27	24	87
Benicia	1996–1998	73	65	69
	2002–2007	42	33	65
	2006	52	45	58
Point San Pablo	1994	99	79	66
	1992–1998	83	62	73
	1999–2006	39	31	51
	2006	37	31	38
Pier 24	1994	43	38	35
	1992–1998	33	29	43
	1999–2002	24	22	43
San Mateo Bridge	1994	63	52	36
	1992–1998	51	40	37
	1999–2005	46	39	33
Dumbarton Bridge	1994	97	86	38
	1992–1998	102	81	41
	1999–2007	62	48	48
	2006	41	28	83
Channel Marker 17	1994	166	135	66
	1991–1998	144	101	56
	1999–2005	84	56	50

year and by increased susceptibility of missing data biasing monthly means.

The SSC time series are derived by editing data from optical instruments and are subject to some interpretation, but the step change also appears in the water samples collected to calibrate the sensors. At Point San Pablo, 248 water samples were collected at mid-depth from WY 1993 to 2006, and SSC had a statistically significant step decrease (rank-sum test $p = 3.4 \times 10^{-10}$) from WYs 1993–1998 to WYs 1999–2006. The same laboratory method was used for all samples (Buchanan and Lionberger 2009).

Data from monthly water quality cruises by the US Geological Survey provide some confirmation of a step decrease despite a significantly smaller sampling frequency. At specified stations along the axis of the bay from South Bay to the Delta, vertical profiles of basic water quality properties are measured (<http://sfbay.wr.usgs.gov/access/wqdata/>). Suspended particulate matter (SPM) is measured, for which the laboratory analysis is identical to SSC measured by the continuous monitoring program (Gray et al. 2000). SPM in Suisun Bay and San Pablo Bays 1 m below the water surface had a significant step decrease

(one-sided rank-sum test $p=0.00$) from WYs 1975–1998 (median 34 mg/L) to WYs 1999–2008 (median 23 mg/L). SPM in South Bay south of the Dumbarton Bridge also had a significant step decrease (one-sided rank-sum test $p=6.2 \times 10^{-5}$) from a median of 36 to 27 mg/L. Central Bay and South Bay north of the Dumbarton Bridge did not have a significant decrease. Cloern et al. (2007) found that SPM from 1978 to 2005 in South Bay had an increasing trend that was not statistically significant. Their results differ from the analysis presented here because they tested for a trend rather than a step decrease, used a slightly smaller data set, and combined all South Bay data.

The step decrease in SSC does not appear to be due to a sudden decrease in sediment supply from rivers. In general, most measured years before the step decrease had large sediment loads, and all but 1 year after the decrease had small sediment loads (Fig. 5). The exceptions, however, indicate that SSC in a given year cannot be explained by river supply during that year. Before the step decrease, WY 1994 was a dry year (7,419 Mm³ of runoff from the Central Valley), but mean SSC was relatively large (95 mg/L, Table 1). Freshwater inflow is used here as a surrogate for sediment supply (Fig. 5) because no sediment supply data are available for WY 1994. After the step decrease, WY 2006 was a wet year (50,020 Mm³), yet mean SSC was only 39 mg/L (Table 1). If river sediment supply in a given water year is the only source of suspended sediment, then SSC would vary with river sediment supply. WYs 1994 and 2006 indicate that river supply does not directly determine SSC.

A hypothesis to explain these data is that the bay contained an erodible pool of sediment that was depleted in the late 1990s (Fig. 1b). Prior to the step decrease, bay SSC would remain high in water years with little watershed sediment supply because the erodible sediment pool supplied suspended sediment and SSC was transport-regulated. Bathymetric surveys (Cappiella et al. 1999;

Fregoso et al. 2008; Foxgrover et al. 2004; Jaffe et al. 1998) and sediment budgets prior to 1999 (Ogden Beeman and Associates 1992; Schoellhamer et al. 2005) show that the bay was eroding. WY 1998 was a wet year for which high flow persisted well into summer, probably flushing sediment from the bay to the Pacific Ocean. Despite a large sediment supply, sediment export from Suisun Bay was 8–9 times greater than sediment supply (Ganju and Schoellhamer 2006). After the step decrease in WY 1999, bay SSC is lower because the erodible pool decreased enough that sediment transport crossed the threshold from transport to supply regulation. Suspended and bed sediment exchange through erosion and deposition, but the erodible sediment pool is smaller. Not even wet years (e.g., 2006) supply enough sediment to restore the pool and transport regulation of suspended sediment, so SSC remains low. The transport capacity of bay waters exceeds the river supply and the depleted erodible pool, so sediment transport is now supply-regulated.

San Francisco Bay Erodible Sediment Pool

Analysis of historical changes in bed sediment volume supports the hypothesis that the bay contained an erodible pool of sediment that was depleted in the late 1990s. Bed sediment volume changes in the four subembayments of San Francisco Bay from the mid 1800s to late 1900s were calculated by comparing successive bathymetric surveys by Cappiella et al. (1999), Fregoso et al. (2008), Foxgrover et al. (2004), and Jaffe et al. (1998). The analyses used nearly identical methods and corrected for tidal epoch, sea level, dredging, borrow pits, and subsidence. Readers should refer to these reports for details. Systematic errors within a subembayment are less than 10 cm and typically range from one to several centimeters (Fregoso et al. 2008). In the best case, these errors would be random between subembayments, and they would cancel. In the worst case, these subembayment errors would be additive, and the maximum error for baywide sediment volume change would be 12–120 Mm³ (3–30% of the maximum bay volume change). Surveys were conducted at different times in different subembayments, and not all surveys covered an entire subembayment. From 1855 to 1990, the entire bay was surveyed five times, and for each survey, 11 to 14 years passed from surveying the first to last subembayment. Thus, the change in bed sediment volume from the first survey period (1855–1867) can be calculated for the four subsequent periods. Bed sediment volume change for incomplete surveys was estimated by multiplying the measured volume change by the ratio of total to measured surface area.

Supply of hydraulic mining sediment increased bed sediment volume by at least 260 Mm³ in the late 1800s

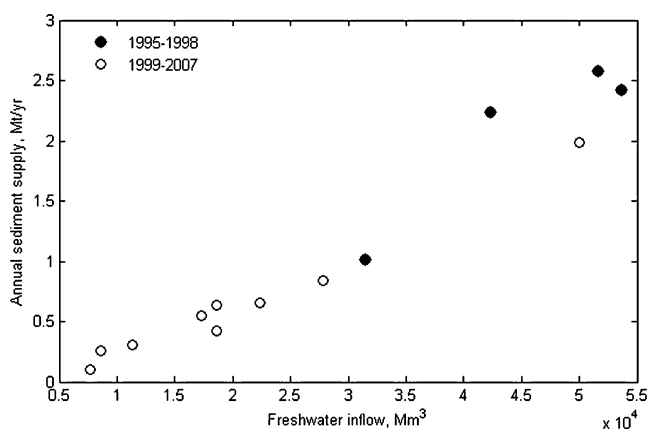


Fig. 5 Sediment supply from the Central Valley to San Francisco Bay, water years 1995–2007 (McKee et al. 2006; David et al. 2009)

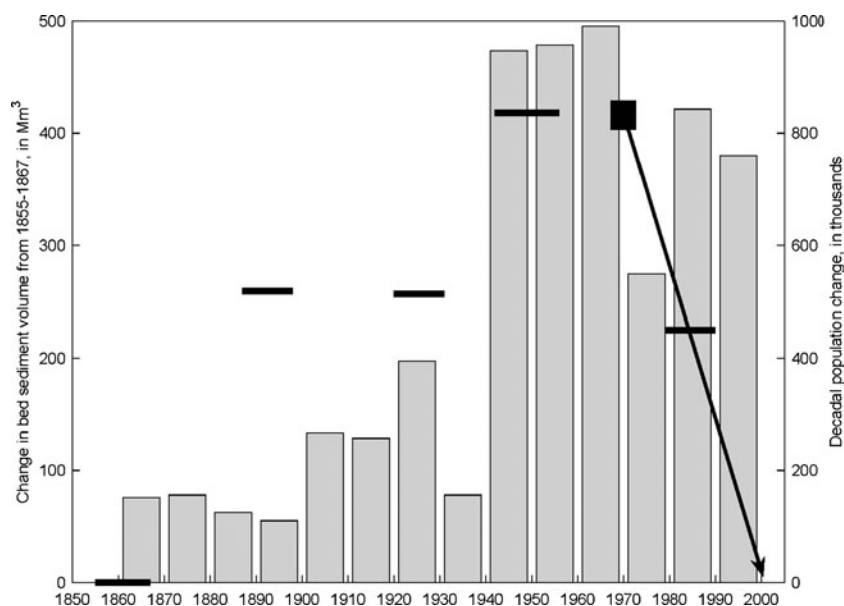


Fig. 6 San Francisco Bay sediment volume change from the 1855 to 1867 surveys (*lines*) and decadal population change (*bars*). Each subembayment was surveyed during the period shown by *each line*. Population is within the nine counties bordering San Francisco Bay (Bay Area Census 2009). Bathymetry data are from Cappiella et al. (1999), Fregoso et al. (2008), Foxgrover et al. (2004), and Jaffe et al.

(1998). Assuming that the bed sediment volume in 1970 was equal to the mid-1900s value (*square*, see text for explanation), a *line that passes through the midpoint of the late 1990s bed sediment volume measurement period* indicates that bed sediment volume would equal the 1855–1867 value in 2001

(Fig. 6), almost entirely in Suisun and San Pablo Bay. There was little change in total bed sediment volume in the early 1900s as hydraulic mining sediment continued to enter the bay at what was probably a smaller rate (Fig. 3) and the pulse of hydraulic mining sediment moved into the intertidal zone or Pacific Ocean.

From the early to mid-1900s, bay sediment volume increased by 160 Mm^3 . This second pulse of sediment was about 60% of the hydraulic mining sediment pulse and may have been caused by urbanization or increased agricultural land use. Unfortunately, there are no sediment load measurements in rivers supplying sediment to the bay during this time, so ascription of this sediment pulse is somewhat speculative. The probability that a given extremely large freshwater inflow, which are responsible for most sediment supply from the Central Valley to the bay (McKee et al. 2006), would be exceeded increased from the 1861 to 1984 (Fig. 7). Thus, freshwater inflow is an unlikely explanatory variable for the variation in bay sediment volume or the mid-1900s sediment pulse. Population of the nine county San Francisco Bay Area increased by almost one million people per decade from 1940 to 1970 (Fig. 6) as the population increased from 1.7 to 4.6 million people (Bay Area Census 2009). To accommodate this growth, land use shifted from agricultural to suburban. Population in the 18 counties of the Central Valley increased from 1.1 to 2.8 million people from 1940 to 1970 (California Department of Finance 2009). Erosion

controls for land being graded for construction increased during the 1970s (Tran et al. 1999); thus, urbanization may have produced a greater yield of sediment prior to the 1970s than after. In addition, the portion of the Central Valley used for irrigated agriculture was constant from 1922 to 1940 then approximately doubled from 1940 to 1970 to 15,000 km^2 (Nady and Larragueta 1983) and has been about 16,000 km^2 since 1980 (California Department

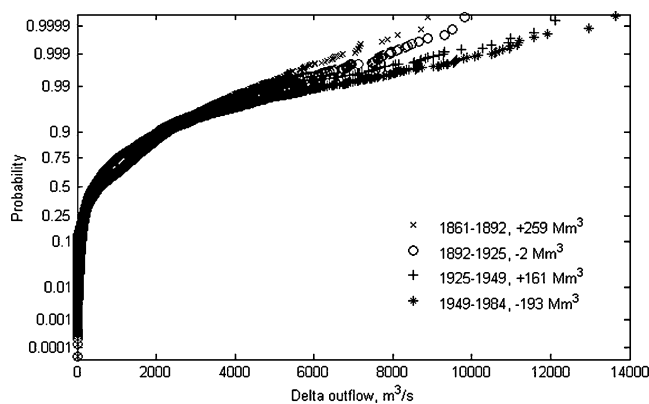


Fig. 7 Probability of flow exceedance for Delta outflow for the periods between the midpoints of San Francisco Bay bathymetric surveys. Daily flow data are from Ganju et al. (2008). Bay sediment volume change is given in the legend. The probability that a given extremely large freshwater inflow will be exceeded has increased with time. Changes in freshwater inflow cannot explain the variation in bay sediment volume

of Finance 2009). Conversion to agriculture and urban land use and overgrazing can increase sediment loads (Pasternack et al. 2001; Ruiz-Fernandez et al. 2009; Warrick and Farnsworth 2009; Wolman 1967) and thus may have supplied this second pulse of sediment. Sediment load measurements began in water year 1957, probably too late to detect the rising limb of such a pulse. Sediment yield from the Sacramento River decreased by about one half from WY 1957 to 2001 (Wright and Schoellhamer 2004). In addition, the Guadalupe River in South San Francisco Bay has a smaller (414 km²) and more urban watershed than the Sacramento River (60,900 km²), and provides evidence of an urbanization sediment pulse in the mid-1900s. Suspended sediment yield from the Guadalupe River watershed during WYs 1958–1962 was a factor of 4 to 8 greater than during WYs 2003–2005 (Schoellhamer et al. 2008).

San Francisco Bay was eroding in the late 1900s as bed sediment volume decreased (Fig. 6). As discussed previously, diminishment of the hydraulic mining and urbanization sediment pulses, sediment trapping behind dams and in flood bypasses, and bank protection all contribute to decreased sediment supply to the bay. Erosion by tides and wind waves exceed sediment supply, causing net erosion.

Prior to 1855, the San Francisco Bay and its watershed were relatively undisturbed and probably were in dynamic equilibrium with a small erodible sediment pool. In the late 1900s, however, anthropogenic sediment pulses from the late 1800s and mid-1900s were eroding and leaving the bay. Therefore, the bed sediment volume change from the 1855 to 1867 surveys can be assumed to approximate the erodible sediment pool (Fig. 6).

Changes in the erodible sediment pool caused by changes in hydrodynamic forcing, specifically decreased tidal prism due to construction fill and levees, are assumed to be negligible. Approximately 95% of tidal marsh in San Francisco Bay and the Delta was leveed or filled from 1850 to the late twentieth century, and the tidally affected surface area decreased by about two thirds (Atwater et al. 1979). Tidal marsh elevations are mostly near mean-higher-high water, however, so the fraction of lost tidal prism volume would be much smaller than the fraction of lost surface area and the decrease in tidal marsh would decrease tidal currents only during the highest of tides.

For a mean bay volume of 8,446 Mm³ (USGS 2009) and assuming the mean bay SSC equaled the mean SSC up to 1998 in Table 1 (75 mg/L) and a bed density of 850 kg/m³ (Porterfield 1980), the erodible sediment pool in the mid-1900s (420 Mm³) was about 560 times greater than the mean suspended sediment mass. Thus, the pool would have largely resided on the bed rather than in suspension, and sediment transport would have been transport-regulated.

The size of the erodible sediment pool in the mid-1900s was about 60 times greater than the mean annual sediment

supply from 1909 to 1966 (6.6 Mm³/year, Porterfield 1980). Thus, in a dry year with little watershed sediment supply, the erodible sediment pool was large enough to supply sediment to bay waters and maintain SSC without being depleted.

Linear extrapolation of the late 1900s erosion rate indicates that the bed sediment volume would return to 1855–1867 levels around 2001. If the sediment pulse observed in the mid-1900s was caused by urbanization, it likely would have continued until at least 1970 because of population growth and minimal, if any, erosion controls on suburban development. If the sediment pulse was caused by agriculturalization, it likely would have decreased around 1970 when expansion of irrigated agriculture markedly slowed. Assuming that the bed sediment volume in 1970 was equal to the mid-1900s value, a line that passes through the midpoint of the late 1990s bed sediment volume measurement period indicates that bed sediment volume would equal the 1855–1867 value in 2001 (Fig. 6). With the assumption that the bed sediment volume change equals the erodible sediment pool, the erodible sediment pool would become depleted around 2001. This rough estimate is essentially identical to when the step decrease in SSC was observed beginning in WY 1999 and thus supports the hypothesis that the SSC decrease was caused by depletion of the erodible sediment pool. A more refined model is developed in the next section.

Quantitative Conceptual Model of an Erodeable Sediment Pool

In this section, a simple numerical model of a depleting erodible sediment pool is derived and applied. The model quantifies the concepts of sediment supply, storage, and outflow in an estuary under transport and supply regulation. The model is intended to test the plausibility of the hypothesis that SSC would undergo a step decrease as an erodible sediment pool is depleted and transport-regulated sediment transport becomes supply-regulated. The model is also intended to simulate the general behavior of an erodible sediment pool. Details on bathymetry, tides, winds, and other factors that affect estuarine sediment transport are not included. This is an exploratory model designed to explain sudden clearing by simulating only the essential processes, rather than a simulation model designed to reproduce the estuary as completely as possible (Murray 2003).

Assume that the estuarine waters can be represented as a well-mixed volume with suspended sediment mass $S(t)$ that varies with time t . The maximum value of $S(t)$ due to transport regulation of suspended sediment is S_{\max} . An erodible sediment mass $M(t)$ resides in suspension and on the bed. When suspended sediment is supply-regulated, $S(t)$

is proportional to $M(t)$. Thus, $S(t)$ equals the minimum of S_{\max} and $c_s M(t)$ where c_s is a dimensionless suspension coefficient. River supply of sediment is $R(t)$ with units of mass per unit time. Outflow of sediment to the ocean $O(t)$ is proportional to $S(t)$ such that $O(t) = c_o S(t)$ where c_o is an outflow coefficient with units of time^{-1} . By conservation of mass (inflow – outflow = change in storage),

$$R(t) - O(t) = dM(t)/dt \tag{1}$$

Transport Regulation

For the case of transport regulation, suspended sediment mass $S(t) = S_{\max}$ is a constant. Then,

$$R(t) - c_o S_{\max} = dM(t)/dt \tag{2}$$

For exponentially decreasing river supply $R(t) = R(0)e^{-\alpha t}$, the solution to Eq. 2 is

$$M(t) = M_T(0) + \frac{1}{\alpha} (1 - e^{-\alpha t}) R(0) - c_o S_{\max} t \tag{3}$$

where $M_T(0)$ is the initial erodible sediment mass for transport regulation. For constant $R(t) = R_o$,

$$M(t) = (R_o - c_o S_{\max})t + M_T(0) \tag{4}$$

Supply Regulation

For the case of supply regulation, $S(t) = c_s M(t)$. Then,

$$R(t) - c_o c_s M(t) = dM(t)/dt \tag{5}$$

For declining $M(t)$, when transport regulation ends and supply regulation begins, time t is reset to zero for convenience. The initial condition for supply regulation is that the erodible sediment mass is $M_S(0)$. At the threshold where regulation changes from transport to supply, $c_s M_S(0) = S_{\max}$. For exponentially decreasing $R(t)$, the solution to Eq. 5 is

$$M(t) = \left(M_S(0) - \frac{R(0)}{c_o c_s - \alpha} \right) e^{-c_o c_s t} + \frac{R(0)}{c_o c_s - \alpha} e^{-\alpha t} \tag{6}$$

For constant R , the solution to Eq. 5 is

$$M(t) = \left(M_S(0) - \frac{R}{c_o c_s} \right) e^{-c_o c_s t} + \frac{R}{c_o c_s} \tag{7}$$

and the suspended mass is $S(t) = c_s M(t)$, so

$$S(t) = \left(c_s M_S(0) - \frac{R}{c_o} \right) e^{-c_o c_s t} + \frac{R}{c_o} \tag{8}$$

At infinite time constant inflow R equals outflow $c_o S_{\infty}$ or $S_{\infty} = R/c_o$ and $M_{\infty} = R/(c_o c_s)$.

The time scale over which suspended mass decreases in a supply-regulated estuary with a diminishing erodible sediment pool and constant sediment supply is quantified as follows. As suspended mass declines from the threshold between transport and supply regulation to a supply-regulated equilibrium, the midpoint of $S(t) = (S_{\max} + S_{\infty})/2$ occurs at $t_{1/2}$. Equation 8 then gives

$$\frac{1}{2} (S_{\max} + S_{\infty}) = (S_{\max} - S_{\infty}) e^{-c_o c_s t_{1/2}} + S_{\infty} \tag{9}$$

Solving for $t_{1/2}$ gives

$$t_{1/2} = \frac{\ln(2)}{c_o c_s} \tag{10}$$

$t_{1/2}$ is a parameter indicating the time scale over which suspended mass decreases in a supply-regulated estuary with a diminishing erodible sediment pool and constant sediment supply. The product $c_o c_s$ is the rate at which sediment mass leaves a supply-regulated estuary, so as the outflow increases, $t_{1/2}$ decreases (Fig. 8).

Application to San Francisco Bay

Application of the quantitative conceptual model to San Francisco Bay demonstrates that depletion of an erodible sediment pool in 1999 would cause a sudden decrease in SSC. The initial erodible mass is calculated from the bed volume from the 1942 to 1956 surveys when the bed volume was 418 Mm^3 greater than in 1855–1867. San Francisco Bay bed dry density varies from about 500 to 1,300 kg/m^3 (Caffrey 1995; Sternberg et al. 1986). Assuming a value of 850 kg/m^3 (Porterfield 1980) and that the change in bed sediment volume from the 1855 to 1867

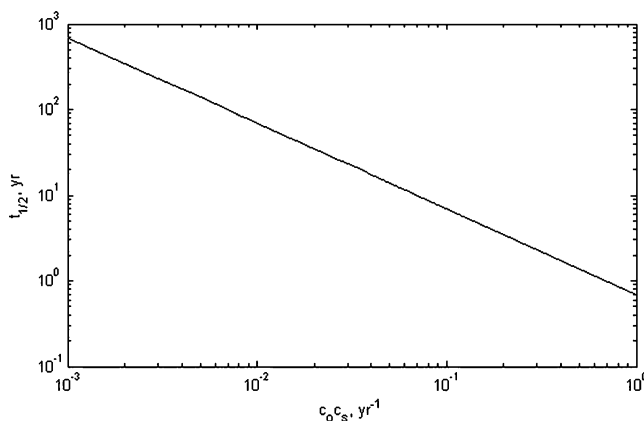


Fig. 8 $t_{1/2}$ as a function of $c_o c_s$. As suspended mass declines from the threshold between transport and supply regulation to a supply-regulated equilibrium, the midpoint of suspended mass between the two states occurs at $t_{1/2}$

Table 2 Initial year, initial river sediment supply $R(0)$, suspension coefficient c_s , outflow coefficient c_o , and resulting mean suspended mass 1999–2007 for simulations of an erodible sediment pool in San Francisco Bay

Initial year	$R(0)$, Mt/year	c_o , year ⁻¹	c_s	1999–2007 mean suspended mass (Mt)
1949	2.57	10.5	0.00529	0.53
1960	2.23	13.4	0.00668	0.48
1970	1.96	20.2	0.01875	0.26

The best estimate of mean suspended mass for WYs 1999–2007 is 0.40 Mt (Table 1)

surveys equals the erodible sediment pool, the erodible sediment pool was 355 Mt in 1949. Schoellhamer et al. (2005) estimated that the mean river sediment supply to San Francisco Bay was 1.91 Mt/year from 1955 to 1990. Hestir et al. (submitted) applied the Seasonal Kendall test to flow-adjusted SSC (Schertz et al. 1991) in the Sacramento River at Freeport and the San Joaquin River at Vernalis and found that each decreased 1.31%/year. These rivers drain the Central Valley of California and account for the majority of sediment entering San Francisco Bay (Schoellhamer et al. 2005). Suspended sediment discharge was not measured on any other tributaries to San Francisco Bay from 1974 to 1999. Suspended sediment discharge in the Guadalupe River decreased by a factor of 4–8 from 1957–1962 to 2003–2008 (Schoellhamer et al. 2008). The change in suspended sediment discharge in Alameda Creek from circa 1960 to the 2000s is ambiguous because water discharge increased but sediment yield decreased. Thus, river sediment supply is assumed to decrease at 1.31%/year ($\alpha = 0.0131 \text{ year}^{-1}$). At this decay rate, river supply would have been 2.57 Mt/year in 1949 ($R(0)$). Maximum suspended mass is assumed to equal the mean of SSC measured through WY 1998, 75 mg/L (Table 1), multiplied by the mean bay volume (8,446 Mm³, USGS 2009), which is 0.63 Mt. The outflow coefficient c_o is determined by forcing the erodible sediment mass M to equal the remaining mass for the 1979–1990 surveys, 289 Mt in 1985.

As the erodible sediment pool decreases, the time when the threshold between transport and supply regulation of suspended sediment is reached t_T is given by $S_{\max} = c_s M(t_T)$. Substitute this expression into Eq. 3, assuming t_T corresponds to the beginning of the observed SSC step decrease in WY 1999, and given α , c_o , $R(0)$, $M(t_T)$, and S_{\max} , Eq. 3 can be solved for

$$c_s = S_{\max} / (M(t_T) + \frac{1}{\alpha} (1 - e^{-\alpha t_T}) R(0) - c_o S_{\max} t_T) \quad (11)$$

These initial values and coefficients are used to solve Eq. 1 with a 1-year time step and the second order Runge–Kutta method. This approach calculates c_o such that the erodible sediment mass is correct in the 1980s and calculates c_s such that the threshold from transport to supply regulation is crossed in 1999. The initial time to start the simulation is

uncertain so initial times of 1949 (midpoint of mid-1900s surveys), 1960 (intermediate point), and 1970 (end of large urbanization period, Fig. 6) are used. For these three initial times, $R(0)$, c_s , and c_o are given in Table 2.

As the start time of the simulation gets later, the exponential decrease in suspended mass after the threshold from transport to supply regulation is passed becomes steeper and more step like (Fig. 9). Assuming the mean SSC from WY 1999 onward (48 mg/L, Table 1) applied to the entire bay volume, the mean suspended mass was 0.40 Mt. The simulation started in 1960 overpredicts this value, and the simulation started in 1970 underpredicts it (Table 2). The model is sensitive to the chosen start time because, for the same initial erodible sediment pool mass, outflow to the ocean must increase as the start time becomes later. After the threshold is crossed, a later start time causes greater outflow (c_o) and a more rapid decrease in suspended mass. Deposition rates upstream from San Francisco Bay in the Sacramento-San Joaquin River Delta were 4–8 times greater from 1944 to 1972 than from 1972

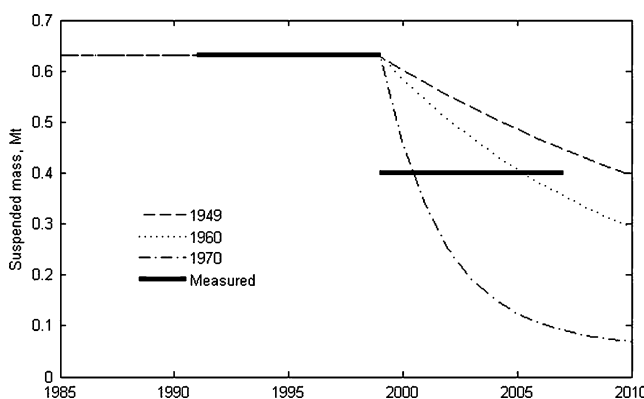


Fig. 9 Simulated and measured suspended sediment mass. Simulations specified (1) transport regulation before 1999 and supply regulation after 1999, (2) suspended mass before 1999 equals measured suspended mass (0.63 Mt), (3) initial erodible sediment mass equals the 1942–1956 estimate (355 Mt), and (4) erodible sediment mass in 1985 equals the 1979–1990 estimate (289 Mt). Dates refer to the starting time of the simulation when the initial sediment pool began to erode. The results support the hypothesis that crossing the threshold from transport to supply regulation of suspended sediment can cause the observed step decrease in suspended-sediment mass

to 2005 (Canuel et al. 2009), indicating that a downstream shift from deposition to erosion in the 1960–1970 period is reasonable.

The model is constructed to have a constant suspended mass until the threshold is reached at a specified time. These simulations demonstrate that given realistic rates of erosion, suspended mass, and river supply, if the threshold was crossed in 1999 as hypothesized, the result would be a rapid decrease in suspended mass.

If a constant river supply were used rather than an exponentially decreasing supply (not shown), then the time the threshold is crossed changes, but the suspended mass subsequently decreases rapidly in either case.

The assumption that the initial mass of the erodible sediment pool was equal to the change in sediment volume since the 1855–1867 surveys ignores the erodible sediment pool that would have existed before hydraulic mining. Prior to 1849, river supply to the bay was assumed to equal 2 million cubic yards per year (Gilbert 1917). A bulk density of 850 kg/m³ (Porterfield 1980) was used to estimate river supply $R = 1.3$ Mt/year. For the simulation started in 1960, the size of the pre-1855 equilibrium erodible sediment pool $M_{\infty} = R/(c_o c_s)$ is estimated to have been 14.5 Mt. This is only 4% of the increase in bay sediment volume from the mid-1800s to mid-1900s (355 Mt). Thus, the pre-1855 erodible sediment pool was probably much smaller than the subsequent sediment pulses and is unlikely to significantly alter these results.

To test the model, the hydraulic mining sediment pulse was hindcast with the coefficients derived for the 1949, 1960, and 1970 start times of the erosion simulations. This however is not a true validation because deposition calculated from bathymetry data was used to estimate river supply from 1849 to 1914 (Gilbert 1917), and these are the only data available to compare with the model. The three sets of coefficients in Table 2 and $R = 1.3$ Mt/year were used, and the model was run from 1700 to 1849 and established a steady state. Then, river supply from the Central Valley was increased to 18.4 million cubic yards per year for 1849–1914 (Gilbert 1917) or 12 Mt/year. This is the sum of depositional volume and outflow estimated by Gilbert (1917). The coefficients for the 1960 erosion simulation start date best match the 1880s and 1920s estimates of the erodible sediment pool from bathymetric change data (Fig. 10). Gilbert (1917) used the 1880s bathymetry data to estimate sediment supply to the bay, so that value does not offer a true validation. Deposition of the hydraulic mining pulse is too large for the 1949 coefficients and too small for the 1970 coefficients. The 1940s increase in the erodible sediment pool is not simulated because there is no corresponding quantified increase in sediment supply. Porterfield (1980) used suspended-sediment discharge measurements from the late 1950s and early 1960s to develop rating curves that were

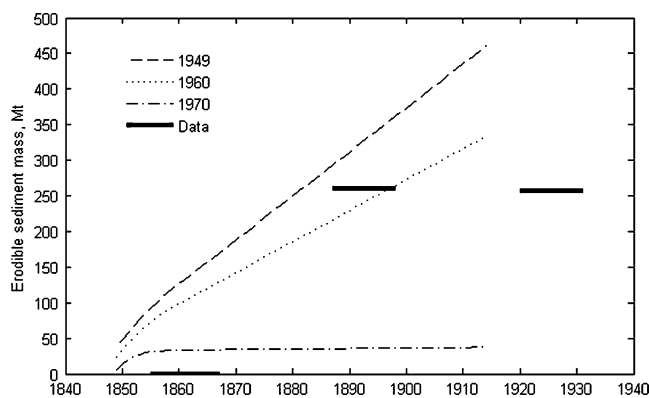


Fig. 10 Simulated and estimated mass in the erodible sediment pool during the hydraulic mining sediment pulse 1849–1914, San Francisco Bay. Simulations are for three different pairs of suspension and outflow coefficients determined by starting simulations of erosion at three different start times (1949, 1960, and 1970, Table 2). Sediment volume change from the 1855 to 1867 surveys is assumed to approximate the erodible sediment pool. A bulk density of 850 kg/m³ is also assumed (Porterfield 1980). Each subembayment was surveyed during the period shown by *each thick line*. Bathymetry data are from Capiella et al. (1999), Fregoso et al. (2008), Foxgrover et al. (2004), and Jaffe et al. (1998)

extrapolated back to 1909. Thus, there are no measurements of the second sediment pulse hypothesized to have occurred prior to the 1950s. In this simulation of the entire hydraulic mining sediment pulse, the threshold from transport to supply regulation of suspended sediment occurs in the early 1950s, and SSC decreases rapidly (not shown). Similar to the comparison with 1999–2007 suspended mass, simulation of the hydraulic mining pulse shows that the model produces reasonable results with the exception of the unquantified sediment pulse in the mid-1900s, that the coefficients for the 1960 erosion simulation start time are best, that coefficients for an erosion simulation that starts between 1960 and 1970 would be optimal, and that SSC declines rapidly once the threshold from transport to supply regulation of suspended sediment is crossed.

Discussion

The general progression of human land use has been characterized by disruptions (deforestation, mining, agricultural expansion, overgrazing, and urbanization) that create a sediment pulse to an estuary followed by dams that reduce sediment supply (Fig. 3, Hu et al. 2009; Pasternack et al. 2001; Ruiz-Fernandez et al. 2009; Syvitski et al. 2005; Warrick and Farnsworth 2009; Wolman 1967). In San Francisco Bay, hydraulic mining increased sediment discharge by a factor of 9 from the mid to late 1800s (Fig. 3, Gilbert 1917). Sedimentation rates increased 2–10-fold in other California estuaries in the nineteenth and twentieth

centuries (Warrick and Farnsworth 2009). These increases are typical of the 5–10-fold increase found in lake and marine sediment records downstream from disturbed watersheds (Dearing and Jones 2003). Sediment discharge from the primary sediment source to San Francisco Bay, the Sacramento River, decreased about 50% from 1957 to 2001 (Wright and Schoellhamer 2004). This magnitude of decrease is not uncommon; river sediment discharge to the coastal zone has decreased 45% in Southern California due to trapping behind dams (Warrick and Farnsworth 2009), 50–70% from the Mississippi River (Kesel 2003), 75% from the Trinity River in Texas (Ravens et al. 2009), and globally riverine sediment discharge to oceans has decreased $10\pm 2\%$ (Syvitski et al. 2005). Reforestation and dams have reduced the sediment discharge in the Changjiang (Yangtze River) 68% from the 1950s to 2000s, and the decrease is expected to reach 82% (Hu et al. 2009). Thus, the sequence of predevelopment equilibrium, a sediment pulse that creates an erodible sediment pool, and reduced sediment supply in San Francisco Bay is similar to that of other estuaries.

Conditions Required for Sudden Clearing

The quantitative conceptual model demonstrates that, when transport-regulated suspension becomes supply-regulated as an erodible sediment pool is depleted, suspended mass can rapidly decrease. An erodible sediment pool and crossing the regulation threshold are both necessary to have a rapid decrease in suspended mass.

Without an erodible sediment pool, annual suspended mass would be dependent on river supply and would not suddenly decrease, unless the river supply suddenly decreased. The river supply to San Francisco Bay varies annually and decreased 1.3%/year during the later half of the twentieth century (Hestir et al. submitted), which does not account for the sudden 36% decrease in suspended mass in 1999.

If sediment transport remained transport-regulated and the transport capacity does not suddenly change, then SSC would not change. Tides and seasonal winds are primarily responsible for sediment suspension in San Francisco Bay, and they are consistent from year to year, so transport capacity is likely to be constant (Schoellhamer 2002). If sediment transport were actually supply-regulated, SSC would have sharply declined from the 1950s to 1980s when the bay eroded. Data are not available for the earlier part of this period, but from 1969 to 1980, there was no significant trend ($p>0.15$) in discrete monthly SPM 2 m below the water surface at nine US Geological Survey sampling stations with enough data for analysis by the Seasonal Kendall trend test (Schertz et al. 1991). Thus, it is unlikely that there was a large decline in suspended sediment from the 1950s to 1980s and that sediment transport was supply-regulated.

For an estuary with an erodible sediment pool, decreasing river sediment supply hastens crossing the threshold from transport to supply regulation and the severity of the subsequent decrease in SSC, but decreasing river supply was not solely responsible for the SSC decrease. For San Francisco Bay, the simulation beginning in 1960 with constant sediment supply crossed the regulation threshold in 2002 (3 years later than observed) and increased the predicted 2010 suspended mass 34%. If an estuary is in equilibrium or is depositional, decreased river supply may make the estuary erosional, and if it is transport-regulated, set up the conditions required for eventual sudden clearing.

Erodible Sediment Pool

An erodible sediment pool in an estuary can be created or enlarged by a pulse of sediment from the watershed. A large flood can deliver a sediment pulse. For example, tropical storm Agnes produced 1 week of sediment discharge from the Susquehanna River to Chesapeake Bay equal to 30–50 normal years of sediment supply (Schubel 1974). Anthropogenic disturbance within the watershed can increase the quantity of erodible sediment, enabling normal runoff to deliver a pulse. Hydraulic mining increased the supply of sediment to San Francisco Bay by a factor of about 9 over several decades (Gilbert 1917). Deforestation and conversion to agricultural and urban land use are a more common anthropogenic mechanism for increasing sediment yield of a watershed (Pasternack et al. 2001; Ruiz-Fernandez et al. 2009; Wolman 1967). In general, sediment supplied from watersheds in the tropics and Indonesia in particular has increased due to deforestation (Syvitski et al. 2005).

This study applies the concept of an erodible sediment pool to an entire estuary. This is an extension of the erodible sediment pool concept used to explain tidal and fortnightly variability of SSC in some narrow estuaries and tidal rivers (Ganju et al. 2004; Grabemann and Krause 1994; Grabemann et al. 1997; Tattersall et al. 2003). At this smaller spatial scale, flood and ebb tidal currents alternately resuspend and transport the erodible sediment pool, which deposits during slack tide. The result is a tidally oscillating sediment mass that can create an estuarine turbidity maximum. The size of the oscillating sediment mass is greatest on spring tides and smallest on neap tides. The application of the erodible sediment pool concept to an entire estuary in this study differs from these previous applications in terms of spatial variability, temporal variability, and size of the erodible sediment pool.

Application of the concept to an entire estuary considers neither spatial variability in erosion, deposition, or SSC nor proximity to river inputs and the ocean. The objective of this study, however, is to understand the net functionality of the estuary as a component in the watershed/estuary/ocean system, for which the erodible sediment pool concept is applicable.

Annual to interannual time scales rather than tidal and fortnightly time scales are considered in this study. Temporal variability due to tides, wind, and river flow are not considered. At annual and interannual time scales, these forcings suspend sediment, some of which is transported from the estuary to the ocean. The quantitative conceptual model simulates this process.

At the tidal time scale, an erodible sediment pool is the quantity of sediment suspended by a particular tide. In both the Weser Estuary and Petaluma River, the size of the pool is less than the annual river supply, 4% and 82%, respectively (Ganju et al. 2004; Grabemann and Krause 1994). At the interannual time scale of this study, an erodible sediment pool is the difference between the existing sediment mass and the sediment mass of the estuary at equilibrium (no net deposition or erosion). To supply sediment during low-supply years, the pool must be larger than the average annual sediment supply. Thus, an erodible sediment pool at the interannual time scale is larger than at the tidal time scale.

Transport and Supply Regulation of Suspended Mass

As an estuarine sediment pool erodes, crossing the threshold from transport to supply regulation of suspended sediment mass can trigger a rapid decrease in SSC. In the quantitative conceptual model, the entire estuary is assumed to be either transport- or supply-regulated, and seasonal and tidal variations in regulation are neglected. In reality, some parts of an estuary may be transport-regulated while others are supply-regulated. Regulation may also vary seasonally and fortnightly. For example, in San Francisco Bay and other estuaries, there is a seasonal cycle of sediment inflow during the wet season and winnowing and redistribution of sediment by tides and waves during the dry season (Deloffre et al. 2005; Krone 1979; Lesourd et al. 2003; Ryu 2003). Thus, suspended mass may be transport-regulated after delivery of sediment from the watershed and supply-regulated at the end of the dry season. In addition, SSC in San Francisco Bay and other estuaries varies with the spring/neap tidal cycle (Brennan et al. 2002; Grabemann et al. 1997; Schoellhamer 2002; Wolanski et al. 1995), and the depth of bed sediment reworking decreases during neap tides (Brennan et al. 2002; Deloffre et al. 2005). Thus, suspended mass may be transport-regulated during neap tides and supply-regulated during spring tides. Identification and quantification of transport and supply regulation in estuaries need further research.

Ramifications of Decreased SSC

A less turbid estuary has ramifications for dredging, wetland restoration, water quality, and the ecosystem.

Smaller SSC reduces deposition, which in turn reduces maintenance dredging volumes and increases the life

expectancy of dredged-material disposal sites in an estuary. In San Francisco Bay, ocean disposal is now about equal to the average supply of sediment from the Central Valley (Schoellhamer et al. 2005). Bay disposal sites may be able to accommodate more material, reducing the need for costly ocean disposal.

Wetland restoration typically involves opening a diked area to tidal action, allowing sediment to deposit until the bed elevation is high enough for plant colonization. The rate of deposition is proportional to SSC (Krone and Hu 2001). The time required to create a wetland increases as SSC decreases. If the rate of deposition is less than the rate of sea level rise, a vegetated wetland will never form. Thus, decreased SSC affects restoration of subsided land to tidal marsh by (1) increasing the time needed to restore tidal marsh vegetation and (2) increasing the possibility that natural sedimentation cannot restore tidal marsh as sea level rises.

Many contaminants are associated with sediment (David et al. 2009; Luengen and Flegal 2009; Schoellhamer et al. 2007; Turner and Millward 2002). Smaller SSC decreases the water column concentration of sediment-associated contaminants. Water quality standards written in terms of total (dissolved and sediment-associated) concentration are more likely to be achieved because SSC is smaller. Suspended sediment moving into, within, and out of estuaries provides a pathway for the transport of sediment-associated contaminants (Bergamaschi et al. 2001; David et al. 2009; Le Roux et al. 2001; Turner and Millward 2000). Decreased SSC decreases the pelagic flux of contaminants within an estuary and from an estuary to the ocean.

In some estuaries including San Francisco Bay, suspended sediment limits light in the water column which limits phytoplankton growth (Cloern 1987). Thus, a decrease in SSC would increase phytoplankton. In San Francisco Bay beginning in 1999, chlorophyll concentrations increased, and autumn blooms occurred for the first time since at least 1978 (Cloern et al. 2007). Both SSC and chlorophyll indicate that the bay crossed a threshold and fundamentally changed in 1999. San Francisco Bay has been transformed from a low-productivity estuary to one having primary production typical of temperate-latitude estuaries. Cloern et al. (2007) also state that a shift in currents in the Pacific Ocean, improved wastewater treatment, reduced sediment inputs, and introductions of new species may be responsible for the chlorophyll increase. Larger phytoplankton blooms may also affect contaminant fate. Blooms dilute methyl mercury concentrations in phytoplankton cells, but decay of phytoplankton after a bloom increases dissolved methyl mercury (Luengen and Flegal 2009). Thus, the net effect of increased phytoplankton blooms on methyl mercury uptake into the food web is uncertain.

Reduced SSC may be one of several factors contributing to a collapse of several San Francisco Bay estuary fish

species that occurred around 2000 (Sommer et al. 2007). Abundance of some fish species increases in more turbid waters (Feyrer et al. 2007). The population collapse has had the most serious consequences for Delta smelt which require turbid water for successful feeding and predator avoidance. The relation between decreased SSC and fish decline, however, is not well established, and the concurrence of less SSC, more phytoplankton, and fewer fish merits additional study.

Conclusions

Anthropogenic disturbances in a watershed, such as mining, deforestation, and urbanization, can create a pulse of sediment that deposits in an estuary, creating an erodible sediment pool. As the erodible pool is depleted, regulation of suspended sediment can cross the threshold from transport regulation to supply regulation. A quantitative conceptual model demonstrates that upon crossing this threshold, suspended sediment mass in the estuary can decrease rapidly, suddenly clearing the estuarine waters. In San Francisco Bay, this sequence of events appears to explain a 36% step decrease in SSC beginning in WY 1999. Changes in the San Francisco Bay ecosystem in the 2000s have been symptomatic of this sudden clearing. A decreasing watershed sediment supply averaging 1.3%/year contributes to decreased SSC but cannot account for the step decrease in SSC. Human development of watersheds follows a similar pattern: disturbance creates a pulse of sediment followed by decreased sediment supply, often due to trapping behind dams. Thus, many estuaries may be susceptible to sudden clearing.

Acknowledgments I would like to thank those that have helped collect, process, and publish the continuous SSC data: Rick Adorador, Greg Brewster, Paul Buchanan, Laurie Campbell, Mike Farber, Amber Forest, Neil Ganju, Tom Hankins, Megan Lionberger, Allan Mlodnosky, Tara Morgan, Heather Ramil, Cathy Ruhl, Rob Shepline, Brad Sullivan, and Jessica Wood. Bruce Jaffe, Neil Ganju, John Oram, and two anonymous reviewers provided helpful comments on earlier versions of this article. This work was supported by the US Army Corps of Engineers, San Francisco District, as part of the Regional Monitoring Program for Water Quality in the San Francisco Estuary.

References

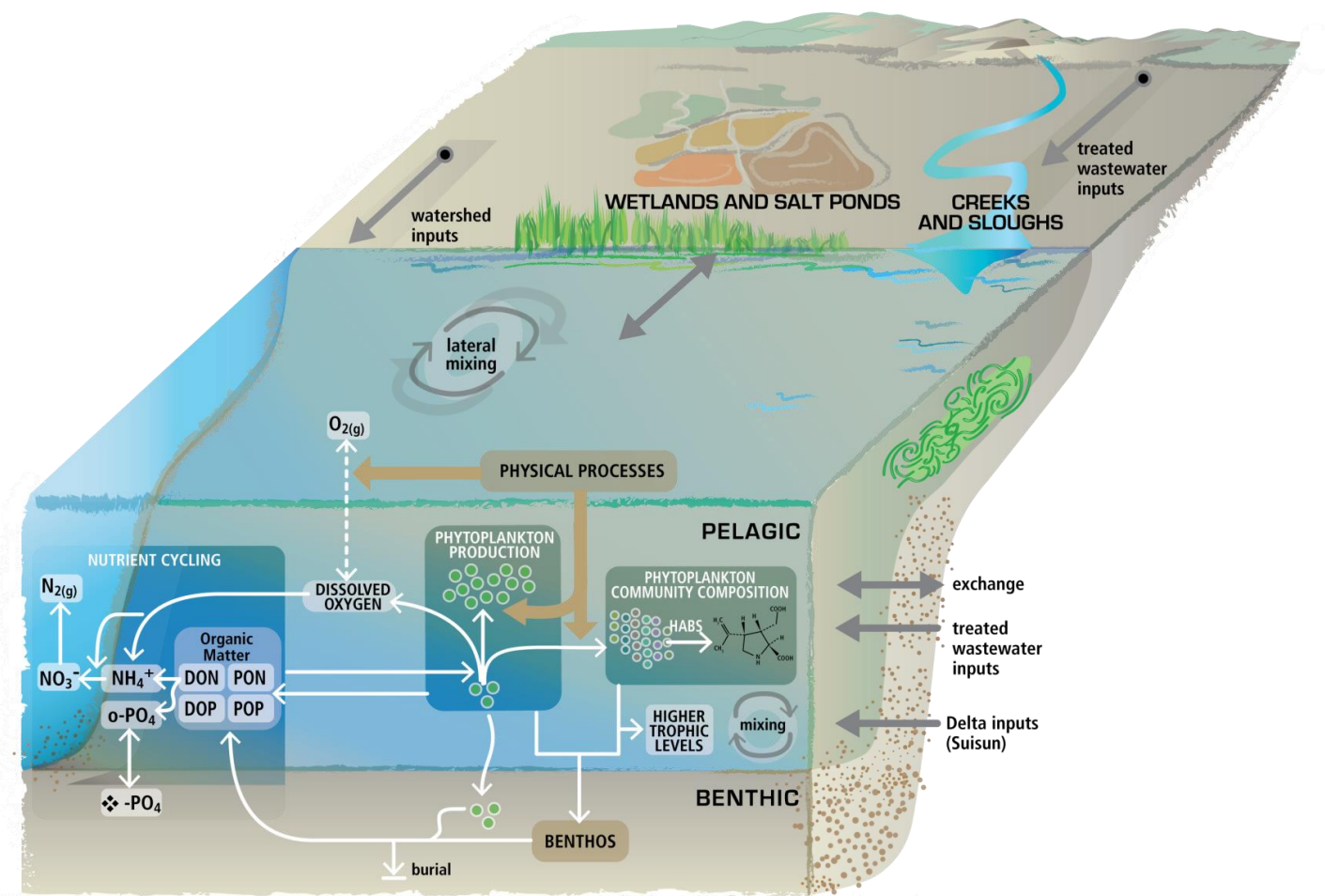
- Atwater, B.F., S.G. Conard, J.N. Dowden, C.W. Hedel, R.L. MacDonald, and W. Savage. 1979. History, landforms, and vegetation of the estuary's tidal marshes. In *San Francisco Bay, the urbanized estuary*, 347–385, ed. T.J. Conomos. San Francisco: Pacific Division of the American Association for the Advancement of Science http://www.estuaryarchive.org/archive/conomos_1979/.
- Bay Area Census, 2009, <http://www.bayareacensus.ca.gov/historical/copop18602000.htm>. Accessed 16 June 2010.
- Bergamaschi, B.A., K.M. Kuivila, and M.S. Fram. 2001. Pesticides associated with suspended sediments entering San Francisco Bay following the first major storm of WY 1996. *Estuaries* 24: 368–380.
- Brennan, M.L., D.H. Schoellhamer, J.R. Burau, and S.G. Monismith. 2002. Tidal asymmetry and variability of bed shear stress and sediment bed flux at a site in San Francisco Bay, USA. In *Fine sediment dynamics in the marine environment*, eds. J.C. Winterwerp, and C. Kranenburg, 93–108. Elsevier Science B.V.
- Buchanan, P.A., and M.A. Lionberger. 2009. *Summary of suspended-sediment concentration data, San Francisco Bay, California, Water Year 2006*. US Geological Survey Data Series Report 362, 35 <http://pubs.usgs.gov/ds/362/>
- Caffrey, J.M. 1995. Spatial and seasonal patterns in sediment nitrogen remineralization and ammonium concentrations in San Francisco Bay, California. *Estuaries* 18: 219–233.
- California Department of Finance. 2009. California Statistical Abstracts, http://www.dof.ca.gov/HTML/FS_DATA/STAT-ABS/Statistical_Abstract.php. Accessed 16 June 2010.
- Canuel, E.A., E.J. Lerberg, R.M. Dickhut, S.A. Kuehl, T.S. Bianchi, and S.G. Wakeham. 2009. Changes in sediment and organic carbon accumulation in a highly-disturbed ecosystem: The Sacramento-San Joaquin River Delta (California, USA). *Marine Pollution Bulletin* 59: 154–163.
- Cappiella, K., C. Malzone, R. Smith, and B. Jaffe. 1999. Sedimentation and bathymetry changes in Suisun Bay, 1867–1990. US Geological Survey Open-File Report 99–563. <http://pubs.er.usgs.gov/usgspubs/ofr/ofr99563>
- Cloern, J.E. 1987. Turbidity as a control on phytoplankton biomass and productivity in estuaries. *Continental Shelf Research* 7: 1367–1381.
- Cloern, J.E., A.D. Jassby, J.K. Thompson, and K.A. Heib. 2007. A cold phase of the East Pacific triggers new phytoplankton blooms in San Francisco Bay. *Proceedings of the National Academy of Science* 104: 18561–18565.
- Conomos, T.J., and D.H. Peterson. 1977. Suspended-particle transport and circulation in San Francisco Bay, an overview. *Estuarine Processes*, 2:82–97. New York, Academic Press.
- David, N., L.J. McKee, F.J. Black, A.R. Flegal, C.H. Conaway, D.H. Schoellhamer, and N.K. Ganju. 2009. Mercury concentrations and loads in a large river system tributary to San Francisco Bay, California, USA. *Environmental Toxicology and Chemistry* 28: 2091–2100.
- Dearing, J.A., and R.T. Jones. 2003. Coupling temporal and spatial dimensions of global sediment flux through lake and marine sediment records. *Global and Planetary Change* 39: 147–168.
- Deloffre, J., R. Lafite, P. Lesueur, S. Lesourd, R. Verney, and L. Guezennec. 2005. Sedimentary processes on an intertidal mudflat in the upper macrotidal Seine estuary, France. *Estuarine, Coastal and Shelf Science* 64: 710–720.
- Feyrer, F., M.L. Nobriga, and T.R. Sommer. 2007. Multidecadal trends for three declining fish species: habitat patterns, and mechanisms in the San Francisco Estuary, California, USA. *Canadian Journal of Fisheries and Aquatic Sciences* 64: 723–734.
- Foxgrover, A.C., S.A. Higgins, M.K. Ingraca, B.E. Jaffe, and R.E. Smith. 2004. Deposition, erosion, and bathymetric change in South San Francisco Bay: 1858–1983. US Geological Survey Open-File Report 2004-1192, 25 p. <http://pubs.er.usgs.gov/usgspubs/ofr/ofr20041192>
- Fregoso, T.A., A.C. Foxgrover, and B.E. Jaffe. 2008. Sediment deposition, erosion, and bathymetric change in central San Francisco Bay: 1855–1979. US Geological Survey Open-File Report 2008-1312, 41 p. <http://pubs.usgs.gov/of/2008/1312/>

- Ganju, N.K., and D.H. Schoellhamer. 2006. Annual sediment flux estimates in a tidal strait using surrogate measurements. *Estuarine, Coastal and Shelf Science* 69: 165–178.
- Ganju, N.K., D.H. Schoellhamer, J.C. Warner, M.F. Barad, and S.G. Schladow. 2004. Tidal oscillation of sediment between a river and a bay: A conceptual model. *Estuarine, Coastal and Shelf Science* 60: 81–90.
- Ganju, N.K., N. Knowles, and D.H. Schoellhamer. 2008. Temporal downscaling of decadal sediment load estimates to a daily interval for use in hindcast simulations. *Journal of Hydrology* 349: 512–523.
- Gilbert, G.K. 1917. *Hydraulic mining debris in the Sierra Nevada*. US Geological Survey Professional Paper 105.
- Grabemann, I., and G. Krause. 1994. Suspended matter fluxes in the turbidity maximum of the Weser Estuary. In *Changes in fluxes in estuaries*, ed. K.R. Dyer and R.J. Orth, 23–28. Denmark: Olsen & Olsen.
- Grabemann, I., R.J. Uncles, G. Krause, and J.A. Stephens. 1997. Behaviour of turbidity maxima in the Tamar (U.K.) and Weser (F.R.G.) estuaries. *Estuarine, Coastal and Shelf Science* 45: 235–246.
- Gray, J.R., G.D. Glysson, L.M. Turcios, and G.E. Schwarz. 2000. *Comparability of suspended-sediment concentration and total suspended-solids data*. US Geological Survey Water-Resources Investigations Report 00-4191.
- Hu, B., Z. Yang, H. Wang, X. Sun, N. Bi, and G. Li. 2009. Sedimentation in the Three Gorges Dam and the future trend of Changjiang (Yangtze River) sediment flux to the sea. *Hydrology and Earth System Sciences* 13: 2253–2264.
- Jaffe, B.E., R.E. Smith, and L.Z. Torresan. 1998. *Sedimentation and bathymetric change in San Pablo Bay, 1856–1983*. US Geological Survey Open-File Report 98-759. <http://pubs.er.usgs.gov/usgspubs/ofr/ofr98759>.
- Jassby, A.D., J.E. Cloern, and B.E. Cole. 2002. Annual primary production: Patterns and mechanisms of change in a nutrient-rich tidal ecosystem. *Limnology and Oceanography* 47: 698–712.
- Kesel, R.H. 2003. Human modifications to the sediment regime of the Lower Mississippi river flood plain. *Geomorphology* 56: 325–334.
- Krone, R.B., 1979. Sedimentation in the San Francisco Bay system. In *San Francisco Bay, the Urbanized Estuary*, ed. T.J. Conomos, 85–96. San Francisco, California: Pacific Division of the American Association for the Advancement of Science. http://www.estuaryarchive.org/archive/conomos_1979/.
- Krone, R.B., and G. Hu. 2001. Restoration of subsided sites and calculation of historic marsh elevations. *Journal of Coastal Research* 27: 162–169.
- Le Roux, S.M., A. Turner, G.E. Millward, L. Ebdon, and P. Apprion. 2001. Partitioning of mercury onto suspended sediments in estuaries. *Journal of Environmental Monitoring* 3: 37–42.
- Lesourd, S., P. Lesueur, J.C. Brun-Cottan, S. Garnaud, and N. Pupinet. 2003. Seasonal variations in the characteristics of superficial sediments in a macrotidal estuary (the Seine inlet, France). *Estuarine, Coastal and Shelf Science* 58: 3–16.
- Luengen, A.R., and A.R. Flegal. 2009. Role of phytoplankton in mercury cycling in the San Francisco Bay estuary. *Limnology and Oceanography* 54: 23–40.
- McKee, L.J., N.K. Ganju, and D.H. Schoellhamer. 2006. Estimates of suspended sediment flux entering San Francisco Bay from the Sacramento and San Joaquin Delta, San Francisco Bay, California. *Journal of Hydrology* 323: 335–352.
- Murray, A.B. 2003. Contrasting the goals, strategies, and predictions associated with simplified numerical models and detailed simulations. In *Prediction in Geomorphology*, 151–165. American Geophysical Union Geophysical Monograph 135.
- Nady, P., and L.L. Larragueta. 1983. *Development of irrigation in the Central Valley of California*. US Geological Survey Hydrologic Atlas 649.
- Ogden Beeman & Associates, Inc. 1992. Sediment budget study for San Francisco Bay. Report prepared for the San Francisco District, US Army Corps of Engineers.
- Pasternack, G.B., G.S. Brush, and W.B. Hilgartner. 2001. Impact of historic land-use change on sediment delivery to a Chesapeake Bay subestuarine delta. *Earth Surface Processes and Landforms* 26: 409–427.
- Porterfield, G. 1980. *Sediment transport of streams tributary to San Francisco, San Pablo, and Suisun Bays, California, 1909–1966*. US Geological Survey Water-Resources Investigations Report 80–64, 91.
- Ravens, T.M., R.C. Thomas, K.A. Roberts, and P.H. Santshi. 2009. Causes of salt marsh erosion in Galveston Bay, Texas. *Journal of Coastal Research* 25: 265–272.
- Rubin, D.M., and D.J. Topping. 2001. Quantifying the relative importance of flow regulation and grain-size regulation of suspended-sediment transport α , and tracking changes in bed-sediment grain size β . *Water Resources Research* 37: 133–146.
- Ruiz-Fernandez, A.C., C. Hillaire-Marcel, A. de Vernal, M.L. Machain-Castillo, L. Vasquez, B. Ghaleb, J.A. Aspiaz-Fabian, and F. Paez-Osman. 2009. Changes of coastal sedimentation in the Gulf of Tehuantepec, South Pacific Mexico, over the last 100 years from short-lived radionuclide measurements. *Estuarine, Coastal and Shelf Science* 82: 525–536.
- Ryu, S.O. 2003. Seasonal variation of sedimentary processes in a semi-enclosed bay: Hampyong Bay, Korea. *Estuarine, Coastal and Shelf Science* 56: 481–492.
- Schertz, T.L., R.B. Alexander, and D.J. Ohe. 1991. *The computer program estimate_trend (ESTREND), a system for the detection of trends in water-quality data*. US Geological Survey Water Resources Investigations Report 91-4040. <http://pubs.usgs.gov/wri/wri91-4040/>
- Schoellhamer, D.H. 2002. Variability of suspended-sediment concentration at tidal to annual time scales in San Francisco Bay, USA. *Continental Shelf Research* 22: 1857–1866.
- Schoellhamer, D.H., M.A. Lionberger, B.E. Jaffe, N.K. Ganju, S.A. Wright, and G.G. Shellenbarger. 2005. *Bay sediment budgets: Sediment accounting 101*. In *The pulse of the estuary: Monitoring and managing water quality in the San Francisco Estuary*, 58–63. Oakland: San Francisco Estuary Institute. http://www.sfei.org/rmp/pulse/2005/RMP05_PulseoftheEstuary.pdf.
- Schoellhamer, D.H., T.E. Mumley, and J.E. Leatherbarrow. 2007. Suspended sediment and sediment-associated contaminants in San Francisco Bay. *Environmental Research* 105: 119–131.
- Schoellhamer, D.H., J.L. Orlando, S.A. Wright, and L.A. Freeman. 2008. Sediment supply and demand. In *South Bay Salt Pond Restoration Project 2006 Science Symposium Presentation Synopses*, 20–22. <http://www.southbayrestoration.org/science/2006symposium/2006%20Science%20Symposium%20Synopses%20Final.pdf>
- Schubel, J.R. 1974. Effect of tropical storm Agnes on the suspended solids of the Northern Chesapeake Bay. In *Suspended solids in water*, ed. R.J. Gibbs, 4:113–132. Plenum Marine Science.
- Singer, M.B., R. Aalto, and L.A. James. 2008. Status of the lower Sacramento Valley flood-control system within the context of its natural geomorphic setting. *Natural Hazards Review* 9: 104–115.
- Sommer, T., C. Armor, R. Baxter, R. Breuer, L. Brown, M. Chotkowski, S. Culberson, F. Feyrer, M. Gingras, B. Herbold, W. Kimmerer, A. Mueller-Solger, M. Nobriga, and K. Souza. 2007. The collapse of pelagic fishes in the upper San Francisco estuary. *Fisheries* 32: 270–277.
- Sternberg, R.W., D.A. Cacchione, D.E. Drake, and K. Kranck. 1986. Suspended sediment transport in an estuarine tidal channel within San Francisco Bay, California. *Marine Geology* 71: 237–258.
- Syvitski, J.P.M., C.J. Vorosmarty, A.J. Kettner, and P. Green. 2005. Impact of humans on the flux of terrestrial sediment to the global coastal ocean. *Science* 308: 376–380.

- Tattersall, G.R., A.J. Elliot, and N.M. Lynn. 2003. Suspended sediment concentrations in the Tamar estuary. *Estuarine, Coastal and Shelf Science* 57: 679–688.
- Tran, H.N., L. Chuang, and C.L. Guss. 1999. Natural resources conservation laws. In *Erosion and sediment control laws, Ch. 3*. Natural Resources Conservation Service. <http://www.nrcs.usda.gov/technical/references/pdf/NRCLawsch3.pdf>
- Turner, A., and G.E. Millward. 2000. Particle dynamics and trace metal reactivity in estuarine plumes. *Estuarine, Coastal and Shelf Science* 50: 761–774.
- Turner, A., and G.E. Millward. 2002. Suspended particles: their role in estuarine biogeochemical cycles. *Estuarine, Coastal and Shelf Science* 55: 857–883.
- USFWS. 2000. Impacts of Riprapping to Ecosystem Functioning, Lower Sacramento River, California. http://www.fws.gov/sacramento/hc/reports/sac_river_riprap.pdf. Accessed 16 June 2010.
- USGS. 2009. San Francisco Bay bathymetry. <http://sfbay.wr.usgs.gov/sediment/sfbay/geostat.html>. Accessed 16 June 2010.
- Warrick, J.A., and K.L. Farnsworth. 2009. Sources of sediment to the coastal waters of the Southern California Bight. In *Earth science in the urban ocean: The Southern California Borderland*, eds. H. J. Lee and W.R. Normark, Special paper 454, 39–52. The Geological Society of America.
- Wolanski, E., B. King, and D. Galloway. 1995. Dynamics of the turbidity maximum in the Fly River estuary, Papua New Guinea. *Estuarine, Coastal and Shelf Science* 40: 321–337.
- Wolman, M.G. 1967. A cycle of sedimentation and erosion in urban river channels. *Geografiska Annaler A, Physical Geography* 49: 385–395.
- Wright, S.A., and D.H. Schoellhamer. 2004. Trends in the sediment yield of the Sacramento River, California, 1957–2001. *San Francisco Estuary and Watershed Science* 2. <http://repositories.cdlib.org/jmie/sfews/vol2/iss2/art2>.

Scientific Foundation for the San Francisco Bay Nutrient Management Strategy

Draft FINAL – October 2014



David B Senn, Emily Novick, and additional co-authors to be determined

*Contact: dauids@sfei.org

Summary

Dissolved inorganic nitrogen (DIN) and phosphorus (DIP) are essential nutrients for primary production that supports estuarine food webs. However DIN and DIP concentrations in San Francisco Bay (SFB) greatly exceed those in other US estuaries where water quality has been impaired by nutrient pollution. SFB receives high nutrient loads from treated wastewater effluent, agricultural runoff, and stormwater. SFB has long been recognized as a nutrient-enriched estuary, but one that has exhibited resistance to some of the classic symptoms of nutrient overenrichment, such as high phytoplankton biomass and low dissolved oxygen. SFB receives high nutrient loads from treated wastewater effluent, agricultural runoff, and stormwater. Research and monitoring in SFB over the last 40 years have identified several factors that have historically imparted resistance to the adverse effects of high nutrient loads: high turbidity, strong tidal mixing, and abundant filter-feeding clam populations, all of which tend to limit the efficiency with which DIN and DIP are converted into phytoplankton biomass. While these factors have arguably had a protective effect in many areas of SFB with respect to nutrients, they have negatively impacted the northern estuary by severely limiting food web productivity there.

However, recent observations indicate that SFB's resistance to high nutrient loads may be weakening. These observations include: a 3-fold increase in summer-fall phytoplankton biomass in South Bay since 1999; frequent detections of algal species that have been shown in other nutrient-rich estuaries to form harmful blooms; frequent detection of the toxins microcystin and domoic acid that are produced by some types of algae; an unprecedented red tide bloom in Fall 2004; low dissolved oxygen in some margin habitats, including sloughs and salt ponds; and studies suggesting that the chemical forms of nitrogen can decrease phytoplankton productivity or alter their community composition. To address growing concerns that SFB's response to nutrients is changing, the San Francisco Bay Regional Water Quality Control Board worked collaboratively with stakeholders to develop the San Francisco Bay Nutrient Management Strategy (NMS), which lays out an overall approach for building the scientific understanding to support well-informed nutrient management decisions.

Among its early priorities, the NMS recognized the need for a conceptual model to lay the scientific foundation to guide the NMS' implementation. This report targets that need and aims to achieve four main goals:

- i. Develop conceptual models connecting nutrient loads and cycling with ecosystem response in SFB;
- ii. Apply those conceptual models to identify scenarios under which nutrient-related impairment may occur in SFB's subembayments; and
- iii. Identify knowledge and data gaps that need to be addressed in order for well-informed, science-based decisions to be made about how best to manage nutrient loads to mitigate or prevent adverse impacts.
- iv. Develop an approach to prioritizing among data and knowledge gaps, and apply that approach to generate an initial recommended set of highest priority activities to inform the development of a science plan to guide NMS implementation.

This report was developed in collaboration with a team of regional scientists whose areas of expertise cover a range of relevant disciplines (see Table 1.1). Its main observations and recommendations are:

1. Changes in SFB's response to nutrient loads over the past decade, combined with the Bay's high nutrient loads and concentrations, justify growing concerns about elevated nutrients.
2. The future trajectory of SFB's response to nutrients is uncertain. One plausible trajectory is that SFB maintains its current level of resistance to the classic effects of high nutrient loads and no further degradation occurs. A second, equally plausible scenario is that SFB's resistance to nutrients continues to decline until adverse impacts become evident. The highly elevated DIN and DIP concentrations Bay-wide provide the potential for future impairment. Any major reductions in loads to SFB will take years-to-decades to implement. Thus, if future problems are to be averted, potential impairment scenarios need to be anticipated, evaluated, and, if deemed necessary, managed in advance of their onset.
3. By considering current conditions in SFB, trends of changing ecosystem response, and a conceptual model for SFB's response to nutrients, we identified the following highest priority issues:
 - a) Determine whether increasing biomass signals future impairment. This issue is most pertinent for Lower South Bay and South Bay.
 - b) Characterize/quantify the extent to which excess nutrients contribute now, or may contribute in the future, to the occurrence of HABs/NABs and phycotoxins.
 - c) Determine if low DO in shallow habitats causes adverse impacts, and quantify the contribution of excess nutrients to that condition.
 - d) Further evaluate other hypotheses for nutrient-related adverse impacts to ecosystem health, including nutrient-induced changes in phytoplankton community composition and ammonium inhibition of primary production. That evaluation – to include data analysis, additional experimentation, or modeling – should assess their potential quantitative importance, and help to determine if they should be considered among the highest priority issues.
 - e) Test future scenarios that may lead to worsening conditions through the use of numerical models.
 - f) Quantify the contributions of nutrients by sources in different areas of the Bay, considering both their transport and in situ transformations and losses.
 - g) Evaluate the potential effectiveness of various nutrient management strategies at mitigating or preventing adverse impacts.
4. Although concern related to changing ecosystem response in SFB is warranted, widespread and severe nutrient-related impacts do not currently appear to be occurring, based on existing sampling locations and parameters commonly measured. This apparent lack of current severe impacts translates into time for conducting investigations to improve understanding of SFB's response to nutrients and allows for sound, science-based management plans to be developed and implemented. That said, the considerable amount of time required to implement any management strategy raises the level of urgency such that work should move forward expeditiously.
5. Given the stakes of no action - and the time required for data collection, analysis, and modeling tools to reach a useable state - work needs to move forward in parallel on implementing multiple aspects of the Nutrient Strategy. A well-coordinated program is needed to maximize the

effectiveness and efficiency of this effort. That program needs to integrate seamlessly across what might otherwise be (or become) semi-independent program areas. Specifically, we recommend the following set of highly-integrated program areas:

- a) **Monitoring:** Develop and implement a sustainably-funded and regionally administered monitoring program that continues routine monitoring, and fills newly-identified data gaps relevant to nutrients;
 - b) **Modeling:** Develop and apply linked hydrodynamic and water quality models to integrate observations, identify critical data gaps (to be addressed through monitoring or experimental studies), quantify processes at the ecosystem scale, and evaluate future scenarios (including management alternatives);
 - c) **Observational and Experimental Studies:** Undertake special studies (field investigations, controlled experiments) to address the highest priority knowledge and data gaps identified in #3; and
 - d) **Data Synthesis and Interpretation:** Analysis of existing and newly collected data (from monitoring and experimental studies), incorporating models, to improve understanding of linkages between nutrients and ecosystem response and to inform the development of an assessment framework.
6. The Delta/Suisun boundary, while an important regulatory boundary, is not meaningful from ecological and loading standpoints. Nutrient loads to and transformations within the Delta exert considerable influence over nutrient loads to and ambient concentrations within Suisun, San Pablo, and Central Bays. Furthermore, the ecology and habitat quality of the Delta and Suisun Bay are tightly coupled. A unified approach – one that spans the Bay-Delta continuum - for evaluating the impacts of nutrients on beneficial uses will best serve both ecosystem health in the Bay-Delta and the information needs of environmental managers.

The report is lengthy, but the majority of its length comes from sections devoted to the development of a detailed conceptual model (Sections 5-9). For a higher-level read that still covers the key issues, main findings, and recommendations, we suggest reading the following sections:

- Sections 1-2: brief description of report goals and approach, and background on the NMS.
- Section 3: Overview of current conditions and a description of how nutrient-related problems would be expected to manifest in San Francisco Bay
- Section 4: Brief description of the conceptual model structure/approach
- Section 11: Identifying highest the priority scenarios, science questions, and data/knowledge gaps
- Section 12: Summary of main observations and recommendations

Acknowledgements

This report was funded by the San Francisco Bay Regional Monitoring Program. The final version of the report benefited from valuable comments from stakeholders and collaborators on earlier. Most of the water quality data presented in this report was generated by the USGS San Francisco Bay Water Quality team based in Menlo Park (<http://sfbay.wr.usgs.gov/access/wqdata/index.html>) - thanks to Tara Schraga, Charlie Martin, and Erica Kress for on-going input on all things water quality. Valuable data was also obtained from the Interagency Ecological Program Environmental Monitoring Program (<http://www.water.ca.gov/iep/activities/emp.cfm>). Thanks also to Alan Jassby for advice on using the *wq* R package.

Table of Contents

Summary	i
Acknowledgements	iv
1 Introduction	1
2. Background	4
2.1 San Francisco Bay and the Bay Area	4
2.1 San Francisco Bay Nutrient Strategy	4
3 Problem Statement	9
3.1 Recent observations in SFB	9
3.2 What would a problem look like in SFB?	20
4. Conceptual Model Overview	23
5 Physical Processes: Hydrodynamics and Sediment dynamics	26
5.1 Introduction	26
5.3 Major drivers	27
5.3.1 Tidal forcings	27
5.3.2 Wind.....	29
5.3.3 Freshwater flow	29
5.3.4 Coastal ocean exchange	30
5.4 Estuarine circulation, flushing and residence times	30
5.5 Stratification	33
5.6 Suspended Sediment	34
5.7 Summary	36
6 Nutrients	38
6.1 Introduction	38
6.2 N, P, and Si cycling	38
6.2.1 N cycling.....	38
6.2.2 P cycling	41
6.2.3 Si cycling	42
6.3 Estimated N and P Loads to SFB	42
6.4 Seasonal and spatial variation in N and P	46
6.5 Current state of knowledge	53
7 Primary Production and biomass accumulation	56
7.1 Introduction	56
7.2 Phytoplankton	56
7.2.1 Transport and Loads.....	58
7.2.2 Production and accumulation.....	58
7.2.3 Top-down biological processes that influence biomass accumulation	67
7.2.4 Spatial and temporal variations in phytoplankton biomass	72
7.3 Microphytobenthos	72

7.4 Current state of knowledge.....	73
8 Dissolved Oxygen.....	78
8.1 Introduction.....	78
8.1 General DO conceptual model.....	78
8.1.1 DO transport.....	78
8.1.2 O ₂ production and consumption.....	80
8.1.3 Spatial differences in O ₂ budgets and DO concentrations in SFB.....	81
8.2 Current state of knowledge.....	83
9. Phytoplankton Community Composition.....	85
9.1. Introduction and Background.....	85
.....	86
9.2. General Conceptual Model.....	87
9.2.1. General trends.....	88
9.2.2. Bottom-Up Controls.....	90
9.2.3 Physiological Factors: Nutrients.....	92
9.2.4 Top-Down controls.....	97
9.2.5 Interactive Effects.....	98
9.2.6 Harmful Algae.....	100
9.3 Summary of Major Conceptual or Data Gaps.....	101
10 Other proposed adverse impact pathways.....	105
11 Priority Science Questions and Knowledge/Data Gaps.....	106
11.1 Introduction.....	106
11.2 Identifying priority scenarios for further consideration.....	107
11.3 Adverse impacts.....	111
11.3 Scenarios that could prevent or mitigate adverse impacts.....	116
11.4 How would San Francisco Bay respond to changes in nutrient loads?.....	121
11.5 High priority subembayment-scenario-response combinations.....	122
11.6 Priority science questions.....	123
12 Key Observations and Recommendations.....	129
12.1 Key observations.....	129
12.2 Recommendations for Addressing Priority Knowledge Gaps.....	130
12.2.1 Recommendations.....	131
12.2.2 Grand Challenges.....	137
References.....	139

List of Figures

Figure 1.1 Report structure and approach.....	2
Figure 2.1 Habitat types of SFB and surrounding Baylands.....	5
Figure 2.2 A. Land use in watersheds that drain to SFB B. POTW locations.....	8
Figure 2.3 Location of DWR/IEP and USGS monthly sampling stations.....	6
Figure 3.1 Potential adverse impact pathways.....	9
Figure 3.2 Chl-a concentration vs. nutrient loads to SFB and other estuaries.....	10
Figure 3.3 Nutrient concentrations in South Bay compared to other estuaries.....	11
Figure 3.4 Key differences between SFB and many other estuaries.	12
Figure 3.5 Trends in Aug-Dec chl-a concentrations in South Bay, through 2005.....	11
Figure 3.6 Trends in Aug-Dec chl-a concentrations in South Bay, through 2013.....	13
Figure 3.7 Seasonal variation in chl-a concentrations near the Dumbarton Bridge	13
Figure 3.8 Phytoplankton biomass in Suisun Bay, 1975-2010.....	14
Figure 3.9 HAB toxins detected in SFB during 2011	14
Figure 3.10 Detection of potentially harmful algal species detected SFB over last 20 years.....	15
Figure 3.11 Phytoplankton biomass South and Central Bays during a red tide in September 2004 ...	15
Figure 3.12 DO in deep subtidal areas of SFB	18
Figure 3.13 Time series of DO (mg/L) at Dumbarton Bridge and Alviso Slough, Sep 5-12 2013.	19
Figure 3.14 Percentage of time DO < 5 mg/L in sloughs/salt ponds rimming Lower South Bay.....	19
Figure 3.15 Dissolved oxygen concentrations in LSB salt ponds.....	20
Figure 4.1.A Simplified nutrient conceptual model, showing major components	24
Figure 4.1.B Detailed nutrient conceptual model	25
Figure 5.1 Bathymetry in SFB	27
Figure 5.2 Physical drivers in San Francisco Bay	30
Figure 5.3 Observed salinity along main channel surveys of SFB during high and low flow	31
Figure 5.4 Time series of suspended particulate matter concentrations in San Pablo Bay.....	34
Figure 5.5 Suspended sediment concentrations in Suisun Bay (shallows and channel).....	35
Figure 5.6 Monthly average SPM (mg/L) – 2006-2011	37
Figure 6.1 Detailed nutrient cycling conceptual model	39
Figure 6.2 N and P loads to SFB subembayments.....	43
Figure 6.3 Monthly variations in NH_4^+ (μM): 2006-2011	48
Figure 6.5 Monthly variations in DIN (μM): 2006-2011	50
Figure 6.6 Monthly variations in o- PO_4 (μM): 2006-2011	51
Figure 6.7 Monthly variations in Si (μM): 2006-2011	52

Figure 7.1 Detailed phytoplankton primary production conceptual model	57
Figure 7.2 Modes of productivity in SFB, and factors influencing timing/magnitude of blooms	59
Figure 7.3 Phytoplankton Growth Rates: Light limitation vs. nutrient limitation	60
Figure 7.4 A. Phytoplankton biomass and grazing rates in South Bay (including shoals)	63
Figure 7.5 Phytoplankton biomass in LSB and South Bay during Spring 1998	64
Figure 7.6 Nutrient concentrations in SFB compared to thresholds for kinetic limitation of phytoplankton growth	66
Figure 7.7 Boxplots showing spatial distributions of DIN and DIP in surface waters of South Bay and LSB relative to characteristic K_N and K_P	66
Figure 7.8 Chl-a biomass and <i>Corbula</i> biomass in Suisun Bay	68
Figure 7.9 Grazing water column turnover rates (units of d^{-1}) in Suisun and the Delta	69
Figure 7.10 Calculated growth and grazing rates in the Low Salinity Zone	69
Figure 7.11 Phytoplankton biomass south of the Bay Bridge	71
Figure 7.12 Bivalve biomass, benthivorous predators, upwelling index, and sea surface temperature time series.	71
Figure 7.13 Monthly variations in chl-a ($\mu g L^{-1}$) 2006-2011	74
Figure 7.14 Phytoplankton biomass timeseries ($mg\ chl-a\ m^{-3}$)	75
Figure 8.1 Detailed dissolved oxygen conceptual model	79
Figure 8.2 Dissolved Oxygen in three slough habitats in Lower South Bay	83
Figure 9.1. Examples of classification of phytoplankton community structure	86
Figure 9.2 Example classification of phytoplankton community by size	86
Figure 9.3 Conceptualization of 3 scenarios of spatial variability in phytoplankton assemblage	87
Figure 9.4 Detailed phytoplankton community composition conceptual model	92
Figure 9.5. Chl-a concentration and primary production in Suisun Bay	90
Figure 9.6 Salinity and temperature ranges of selected phytoplankton species	93
Figure 9.7 Nitrogen kinetics responses reported in the literature for major algal groups,	94
Figure 9.8 Intrinsic C:P, N:P, and C:N ratios for major phytoplankton groupings	97
Figure 9.9. Shifts in phytoplankton community composition related to shifts in grazing pressure	98
Figure 9.10 Interactive effects of light, nutrient assimilation, and energetic requirements for N-metabolism on nutrient utilization	100
Figure 11.1 Changes to underlying drivers of response that could contribute to adverse impacts.	108
Figure 11.2 Pathways for changing conditions in SFB via future environmental or management scenarios	109
Figure 11.3 Prioritization of subembayment specific response to future scenarios	113

List of Tables

Table 1.1 Conceptual model technical team	3
Table 2.1 Recommended indicators within the context of the SFB NNE.....	7
Table 3.1 Potentially harmful algal species detected through USGS science program in SFB	16
Table 3.2 Plausible nutrient-related adverse impacts in SFB.....	22
Table 5.1 Subembayment area and volume, watershed area and land-use	28
Table 6.1 Typical concentrations and forms of N and P in treated wastewater effluent, by treatment level.....	44
Table 6.2 N and P loads and cycling: current state of knowledge for key processes and parameters .	54
Table 7.1 Phytoplankton productivity and biomass accumulation: current state of knowledge for key processes and parameters	76
Table 8.1 Dissolved Oxygen: current state of knowledge for key processes and parameters	84
Table 9.1 Phytoplankton community composition and HABs: current state of knowledge for key processes and parameters	103
Table 11.1 Broad Management Questions and more specific questions for SFB NMS	106
Table 11.2 Major future environmental and management scenarios considered.....	109
Table 11.3 Highest priority adverse impact scenarios, science questions, and types of studies needed to address those questions	124
Table 11.4 Highest priority mitigation scenarios, science questions, and types of studies needed to address those questions	127

1 Introduction

San Francisco Bay (SFB) has long been recognized as a nutrient-enriched estuary, but one that has exhibited resistance to some of the classic symptoms of nutrient overenrichment, such as high phytoplankton biomass and low dissolved oxygen. However, recent observations suggest that SFB's resistance to high nutrient loads is weakening. The combination of high nutrient concentrations and changes in environmental factors that regulate SFB's response to nutrients has generated concern about whether SFB is trending toward, or may already be experiencing, adverse impacts due to elevated nutrient loads. In response to these concerns, the San Francisco Bay Regional Water Quality Control Board worked collaboratively with stakeholders to develop the San Francisco Bay Nutrient Management Strategy (NMS),¹ which lays out an overall approach for building the scientific understanding to support well-informed nutrient management decisions. Among its early priorities, the NMS recognized the need for a conceptual model to lay the scientific foundation to guide the NMS' implementation. This report targets that need and aims to achieve four main goals:

- i. Develop conceptual models connecting nutrient loads and cycling with ecosystem response in SFB;
- ii. Apply those conceptual models to identify scenarios under which nutrient-related impairment may occur in SFB's subembayments; and
- iii. Identify knowledge and data gaps that need to be addressed in order for well-informed, science-based decisions to be made about how to best manage nutrient loads to mitigate or prevent adverse impacts.
- iv. Develop an approach to prioritizing among data and knowledge gaps, and apply that approach to generate an initial recommended set of highest priority activities to inform the development of a science plan to guide NMS implementation.

Audience, anticipated use, and approach

The report's approach and structure are summarized in Figure 1.1. Its primary intended audience includes technically-oriented regulators, decision makers, and other stakeholders. With that audience in mind, the report assumes a certain baseline familiarity with SFB as well as a basic understanding of the biology, nutrient cycling, biogeochemistry, and physical processes in estuaries. The report is an outgrowth of workshops and discussions over the past 2 years with a team of regional scientists whose areas of expertise cover a range of relevant disciplines and much of whose work has focused on San Francisco Bay (Table 1.1).

The report's main anticipated uses are to inform and help prioritize the types of special studies, monitoring, and modeling that are needed to inform management decisions by identifying major priority science issues and related knowledge and data gaps; and inform the development of criteria that will be used to assess ecosystem health and determine whether subembayments or specific habitats within SFB are experiencing nutrient-related impairment. Figure 1.1 summarizes the report's structure and the overall approach. The report begins by identifying what a nutrient-related problem would look like in SFB, and then summarizes recent observations that suggest SFB's response to nutrients is changing (Section 3). Focused by this problem statement, we present a the conceptual model, layed out as a series of linked modules, extending from nutrient loads and cycling to

¹http://www.waterboards.ca.gov/sanfranciscobay/water_issues/programs/planningtmdls/amendments/estuarienNE/Nutrient_Strategy%20November%202012.pdf

ecosystem response (Sections 5-10). Each module ends with a table that summarizes data availability and state of knowledge about relevant processes. The conceptual models are then used to identify scenarios under which adverse impacts may occur, and scenarios under which those impacts may be mitigated or prevented (Section 11). The report closes with a summary of major observations and recommendations (Section 12). The report draws from several decades of research and monitoring in San Francisco Bay by USGS², multiple academic institutions, and the Interagency Ecological Program³, and also builds upon other recent reports (e.g., McKee et al., 2011).

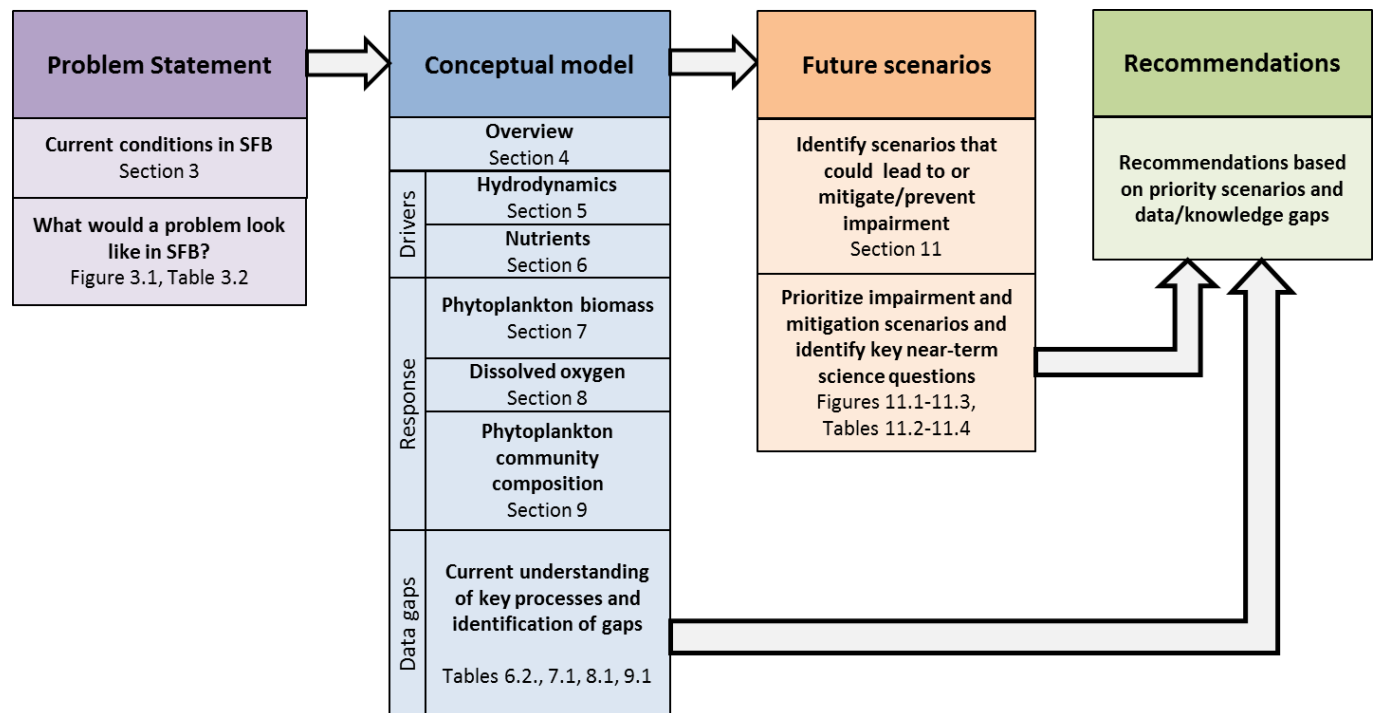


Figure 1.1 Report structure and approach

² <http://sfbay.wr.usgs.gov/access/wqdata/>

³ <http://www.water.ca.gov/iep/activities/emp.cfm>

Table 1.1 Conceptual model technical team

	Affiliation	Expertise
James Cloern, PhD	U.S. Geological Survey	Estuarine biogeochemistry and ecology
Michael Connor, PhD	East Bay Dischargers Authority	Wastewater treatment and receiving water quality issues
Richard Dugdale, PhD	San Francisco State University, Romberg Tiburon Center	Nutrient fluxes and phytoplankton productivity
James T. Hollibaugh, PhD	University of Georgia	Estuarine microbial communities and their role in biogeochemical processes
Wim Kimmerer, PhD	San Francisco State University, Romberg Tiburon Center	Zooplankton ecology
Lisa Lucas, PhD	U.S. Geological Survey	Linked hydrodynamic and biological modeling
Raphael Kudela, PhD	University of California, Santa Cruz	Phytoplankton physiology and ecology
Emily Novick, MS	San Francisco Estuary Institute	Environmental engineering, nutrient biogeochemistry
Anke Mueller-Solger, PhD	U.S. Geological Survey	Estuarine and freshwater food webs
David Senn, PhD	San Francisco Estuary Institute	Contaminant fate and transport, nutrient biogeochemistry
Mark Stacey, PhD	University of California, Berkeley	Hydrodynamics, transport and mixing in estuaries and oceans
Martha Sutula, PhD	Southern California Coastal Water Research Project (SCCWRP)	Nutrient biogeochemistry and eutrophication

2. Background

2.1 San Francisco Bay and the Bay Area

San Francisco Bay (SFB) encompasses several subembayments of the San Francisco Estuary, the largest estuary in California (Figure 2.1). SFB is surrounded by remnant tidal marshes, intertidal and subtidal habitats, tributary rivers, the freshwater “Delta” portion of the estuary, and the large mixed-land-use area known as the San Francisco Bay Area (Figure 2.2.A). San Francisco Bay hosts an array of habitat types (Figure 2.1), many of which have undergone substantial changes in their size or quality due to human activities. Urban residential and commercial land uses comprise a large portion of Bay Area watersheds, in particular those adjacent to Central Bay, South Bay and Lower South Bay (Figure 2.2.A). Open space and agricultural land uses occupy larger proportions of the watersheds draining to Suisun Bay and San Pablo Bay. The San Joaquin and Sacramento Rivers drain 40% of California, including agricultural-intensive land use areas in the Central Valley. Flows from several urban centers also enter these rivers, most notably Sacramento which is ~100 km upstream of Suisun Bay along the Sacramento River.

SFB receives high nutrient loads from 42 public owned wastewater treatment works (POTWs) servicing the Bay Area’s 7.2 million people (Figure 2.2.B). Several POTWs carry out nutrient removal before effluent discharge; however the majority perform only secondary treatment without additional N or P removal. Nutrients also enter SFB via stormwater runoff from the densely populated watersheds that surround SFB (Figure 2.2.A). Flows from the Sacramento and San Joaquin Rivers deliver large nutrient loads, and enter the northern estuary through the Sacramento/San Joaquin Delta (not shown, immediately east of the maps in Figure 2.1 and 2.2).

2.1 San Francisco Bay Nutrient Strategy

Dissolved inorganic nitrogen (DIN) and phosphorus (DIP) are essential nutrients for primary production that supports SFB food webs. However DIN and DIP concentrations in SFB greatly exceed those in other US estuaries where water quality has been impaired by nutrient pollution (Cloern and Jassby, 2012). SFB has long been considered relatively immune to its high nutrient loads. For example, the original San Francisco Bay Regional Basin Plan from 1975 stated that only limited treatment for nutrients was necessary because the system was considered to be light limited (SFBRWQCB, 1975). Research and monitoring over the last 40 years have identified several factors that impart SFB with its resistance to high nutrient loads (e.g., see Cloern and Jassby 2012; Cloern et al., 2007; Kimmerer and Thompson, 2014): high turbidity (low light), strong tidal mixing (breaks down stratification and fully mixes the water column, resulting in low light availability), and abundant filter-feeding clam populations (remove phytoplankton from the water column).

However, recent studies indicate that the response to nutrients in SFB is changing, indicate that the system is poised to potentially experience future impacts, or suggest that current nutrient levels are already causing adverse impacts. These observations include: a 3-fold increase in summer-fall phytoplankton biomass in South Bay since the late 1990s; frequent detections in SFB of algal species that have been shown in other nutrient-rich estuaries to form harmful blooms; detection of algal toxins Bay-wide; an unprecedented red tide bloom in Fall 2004; and studies suggesting that the chemical forms of nitrogen can influence phytoplankton productivity and composition. To address

growing concerns that SFB's response to nutrients is changing and that conditions may be trending toward adverse impacts due to elevated nutrient loads, the San Francisco Bay Regional Water Quality Control Board (SFBRWQCB) worked collaboratively with stakeholders to develop the San Francisco Bay Nutrient Management Strategy⁴, which lays out an approach for gathering and applying information to inform management decisions. Overall, the Nutrient Management Strategy aims to answer four fundamental questions:

1. Is SFB experiencing nutrient-related impairment, or is it likely to in the future?
2. What are the major nutrient sources?
3. What nutrient loads or concentrations are protective of ecosystem health?
4. What are efficacious and cost-efficient nutrient management options for ensuring that Bay beneficial uses are protected?

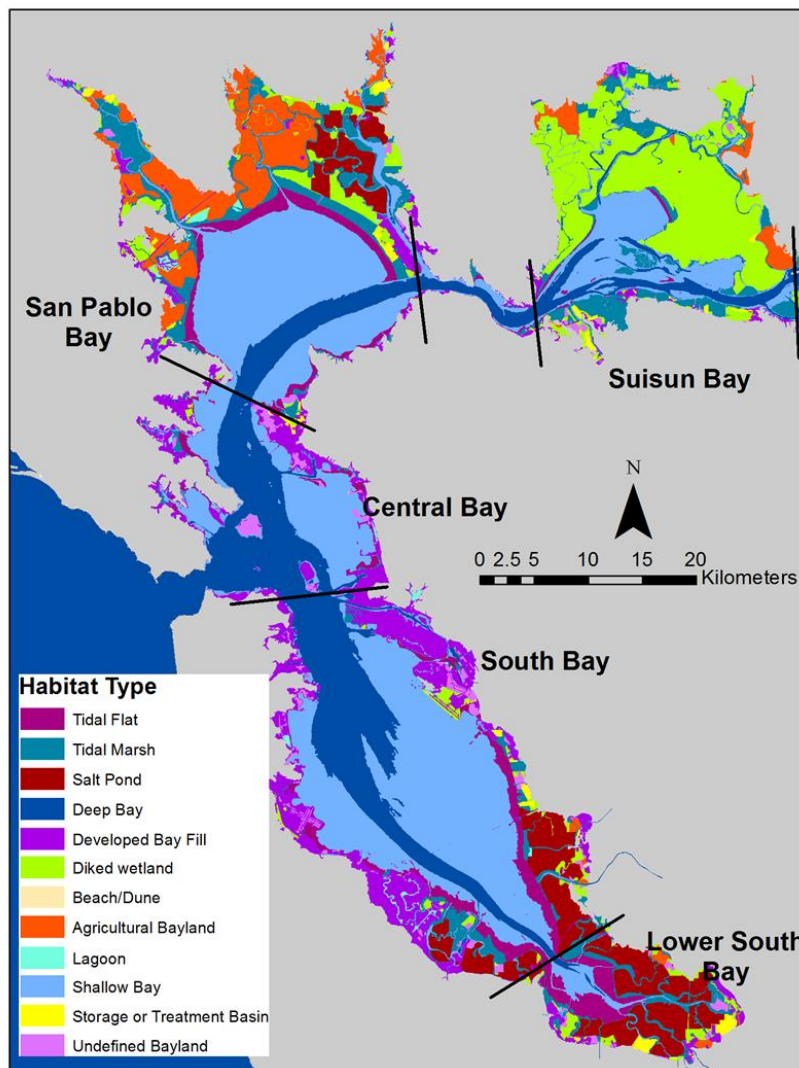


Figure 2.1 Habitat types of SFB and surrounding Baylands. Water Board subembayment boundaries are shown in black. Habitat data from CA State Lands Commission, USGS, UFWS, US NASA and local experts were compiled by SFEI.

The indications of changing SFB response to nutrients have come to the fore at a time when the availability of resources to continue assessing the Bay's condition is uncertain. Since 1969, a USGS research program has supported water-quality sampling in the San Francisco Bay. This USGS program collects monthly samples between the South Bay and the lower Sacramento River to measure salinity, temperature, turbidity, suspended sediments, nutrients, dissolved oxygen and chlorophyll a. The USGS data, along with sampling conducted by the Interagency Ecological Program (IEP), provide coverage for the entire Bay-Delta system (Figure 2.3). The San Francisco Bay

Regional Monitoring Program (RMP) has no independent nutrient-related monitoring program, but instead contributes approximately 20% of the USGS data collection cost. The Nutrient Strategy

⁴http://www.waterboards.ca.gov/sanfranciscobay/water_issues/programs/planningtmdls/amendments/estuarineNE/Nutrient_Strategy%20November%202012.pdf

highlights the need for a regionally-supported, long-term monitoring program that provides the information that is most needed to support management decisions in the Bay.

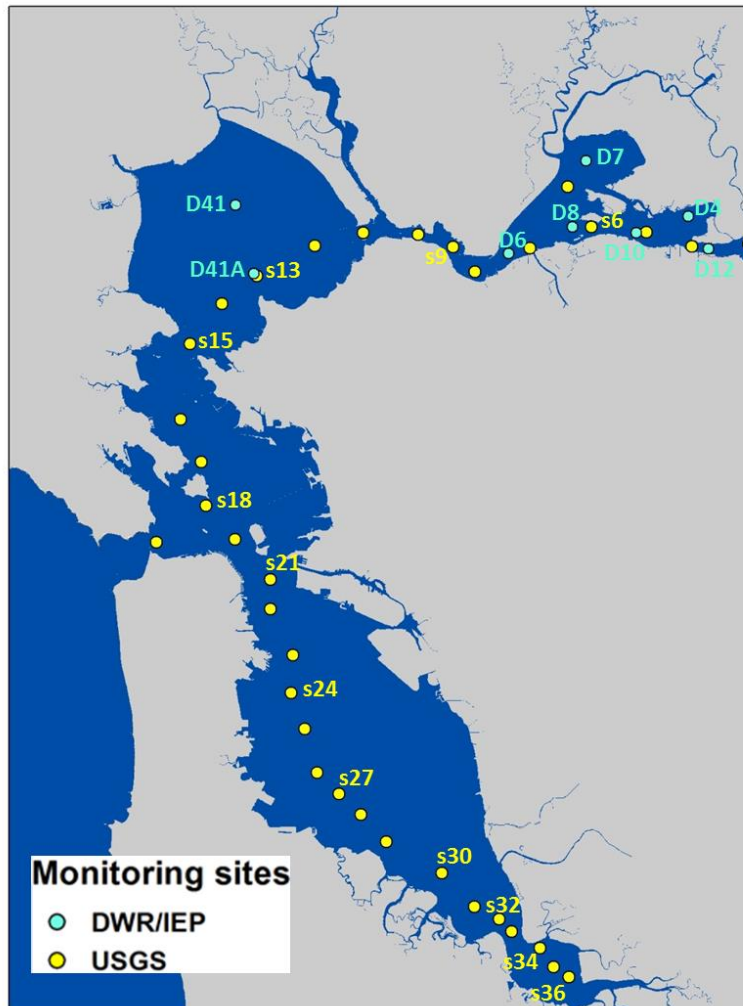


Figure 2.3 Location of DWR/IEP and USGS monthly sampling stations. Data from labeled USGS Stations (s6, s15, s18, s21, s27, s36) are used in Figures 5.7, 6.3-6.7 and 7.11.

NNE framework specific to SFB. That effort was initiated by a literature review and data gaps analysis that recommends indicators to assess eutrophication and other adverse effects of nutrient overenrichment in San Francisco Bay (McKee et al., 2011)⁵. McKee et al. (2011) evaluated a number of potential indicators of ecological condition for several habitat types based on the following criteria:

- Indicators should have well-documented links to estuarine beneficial uses
- Indicators should have a predictive relationship with nutrient and hydrodynamic drivers that can be easily observed with empirical data or a model

The timing also coincides with a major state-wide initiative, led by the California State Water Resources Control Board (State Water Board), for developing nutrient water quality objectives for the State's surface waters, using an approach known as the Nutrient Numeric Endpoint (NNE) framework. The NNE framework establishes a suite of numeric endpoints based on the ecological response of a waterbody to nutrient over-enrichment and eutrophication (e.g. excessive algal blooms, decreased dissolved oxygen). In addition to numeric endpoints for response indicators, the NNE approach includes models that link the response indicators to nutrient loads and other management controls. The NNE framework is intended to serve as numeric guidance to translate narrative water quality objectives.

Since San Francisco Bay is California's largest estuary, it is a primary focus of the state-wide effort to develop NNEs for estuaries. Through the Nutrient Strategy, the SFBRWQCB is working with regional stakeholders and with the State Water Board to develop an

⁵http://www.waterboards.ca.gov/sanfranciscobay/water_issues/programs/planningtmdls/amendments/estuarianNNE/644_SFBayNNE_LitReview%20Final.pdf

- Indicators should have a scientifically sound and practical measurement process that is reliable in a variety of habitats and at a variety of timescales
- Indicators must be able to show a trend towards increasing or/and decreasing beneficial use impairment due to nutrients

The report recommended focusing on subtidal habitats initially, and proposed the following primary indicators of beneficial use impairment by nutrients: i. phytoplankton biomass; ii. phytoplankton composition; iii. dissolved oxygen; and; iv. algal toxin concentrations. In addition, ‘supporting indicators’ and ‘co-factors’ were identified, and are summarized in Table 2.1. Supporting indicators provide additional lines of evidence to complement observations based on primary indicators, and co-factors are essential information to help interpret and analyze trends in primary or supporting indicators.

Regions of SFB behave quite differently with respect to nutrient cycling and ecosystem response due to a combination physical, chemical, and biological factors (discussed in Sections 5-9). To facilitate discussion of spatial trends in this report, SFB was divided into 5 subembayments, as depicted in Figure 2.1: Suisun Bay, San Pablo Bay, Central Bay, South Bay and Lower South Bay (LSB). These subembayment boundaries were chosen based on geographic features and not necessarily hydrodynamic features, represent one of several sets of boundaries that could be used. The boundaries illustrated in Figure 2.1 are similar to those defined by the SFBRWQCB in the San Francisco Bay Basin Plan, although we use different names for the subembayments south of the Bay Bridge.

Table 2.1 Recommended indicators within the context of the SFB NNE. Excerpted from McKee et al 2011

Habitat	Primary Indicators	Supporting Indicators	Co-Factors
All Subtidal Habitat	Phytoplankton biomass, productivity and assemblage Cyanobacteria cell counts and toxin concentration Dissolved oxygen	Water column nutrient concentrations and forms ¹ (C,N,P,Si) HAB species cell counts and toxin concentration	Water column turbidity, pH, conductivity, temperature, light attenuation Macrobenthos taxonomic composition, abundance and biomass Sediment oxygen demand Zooplankton
Seagrass Habitat	Phytoplankton biomass Macroalgal biomass & cover Dissolved oxygen	Light attenuation, suspended sediment concentration Seagrass areal distribution and cover Epiphyte load	Water column pH, temperature, conductivity Water column nutrients
Intertidal flats	Macroalgal biomass and cover	Sediment % OC, N, P and particle size Microphytobenthos biomass (benthic chl-a)	Microphytobenthos taxonomic composition
Muted Intertidal and Subtidal	Macroalgal biomass & cover Phytoplankton biomass Cyanobacteria toxin concentration	Sediment % OC, N, P and particle size Phytoplankton assemblage Harmful algal bloom toxin concentration	Water column pH, turbidity, temperature, conductivity Water column nutrients

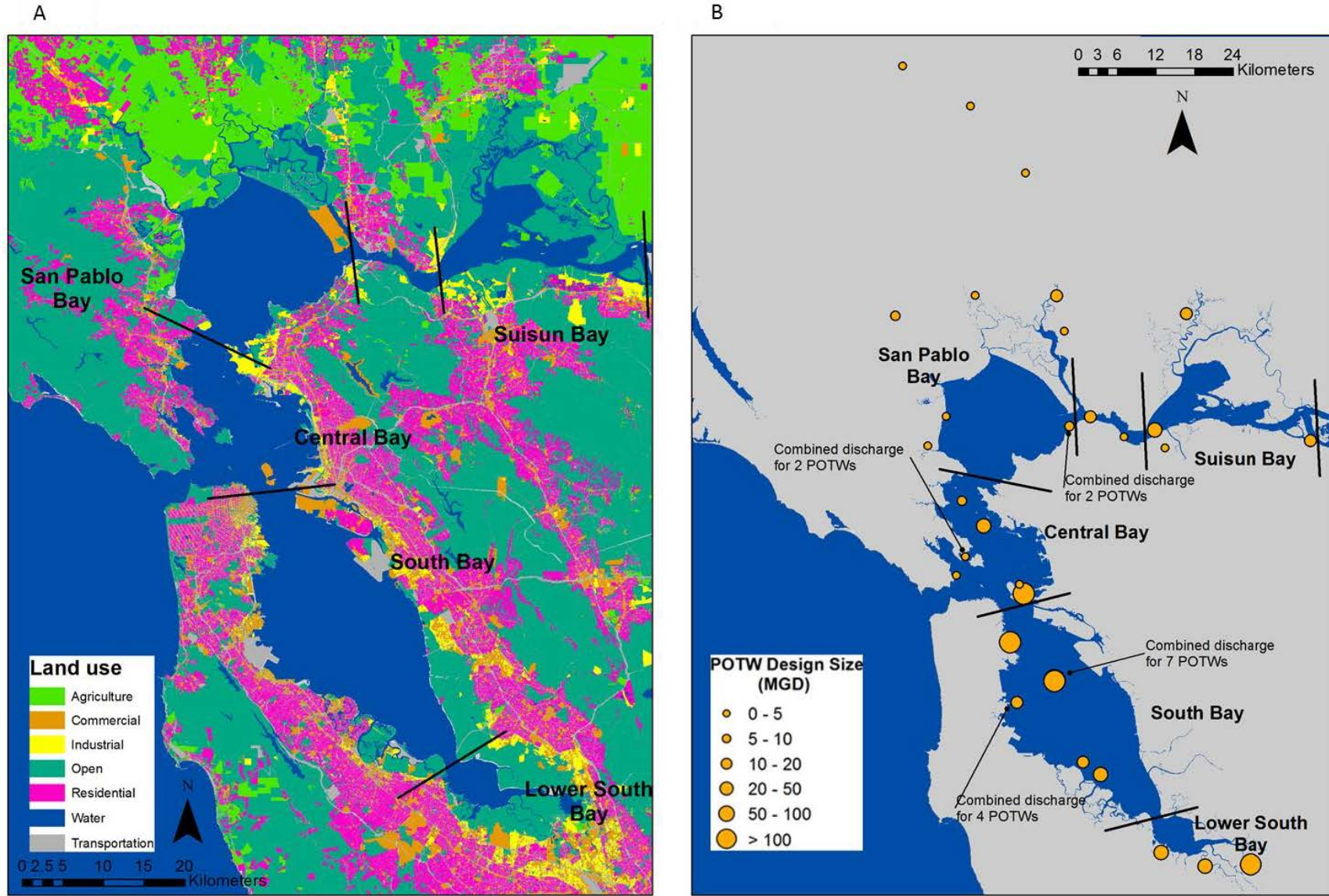


Figure 2.2 A. Land use in watersheds that drain to SFB (Data from Association of Bay Area Governments, 2000). B. Location and design size (in million gallons per day) for POTWs that discharge directly in SFB or in watersheds directly adjacent to subembayments. In both figures, Water Board subembayment boundaries are shown in black.

3 Problem Statement

3.1 Recent observations in SFB

In estuarine ecosystems in the US and worldwide, high nutrient loads and elevated nutrient concentrations are associated with multiple adverse impacts (Bricker et al. 2007). N and P are essential nutrients for the primary production that supports food webs in SFB and other estuaries. However, when nutrient loads reach excessive levels they can adversely impact ecosystem health. Individual estuaries vary in their response or sensitivity to nutrient loads, with physical and biological characteristics modulating estuarine response (e.g., Cloern 2001). As a result, some estuaries experience limited or no impairment at loads that have been shown to have substantial impacts elsewhere.

Figure 3.1 illustrates several potential pathways along which excessive nutrient loads could adversely impact ecosystem health in SFB. Each pathway is comprised of multiple linked physical, chemical, and biological processes. Some of those processes are well-understood and data are abundant data to interpret and assess condition; others are poorly understood or data are scarce. In Sections 5-9, we lay out a conceptual model describing the processes creating the pathways between loads and adverse response, and describe the current state of knowledge and data availability.

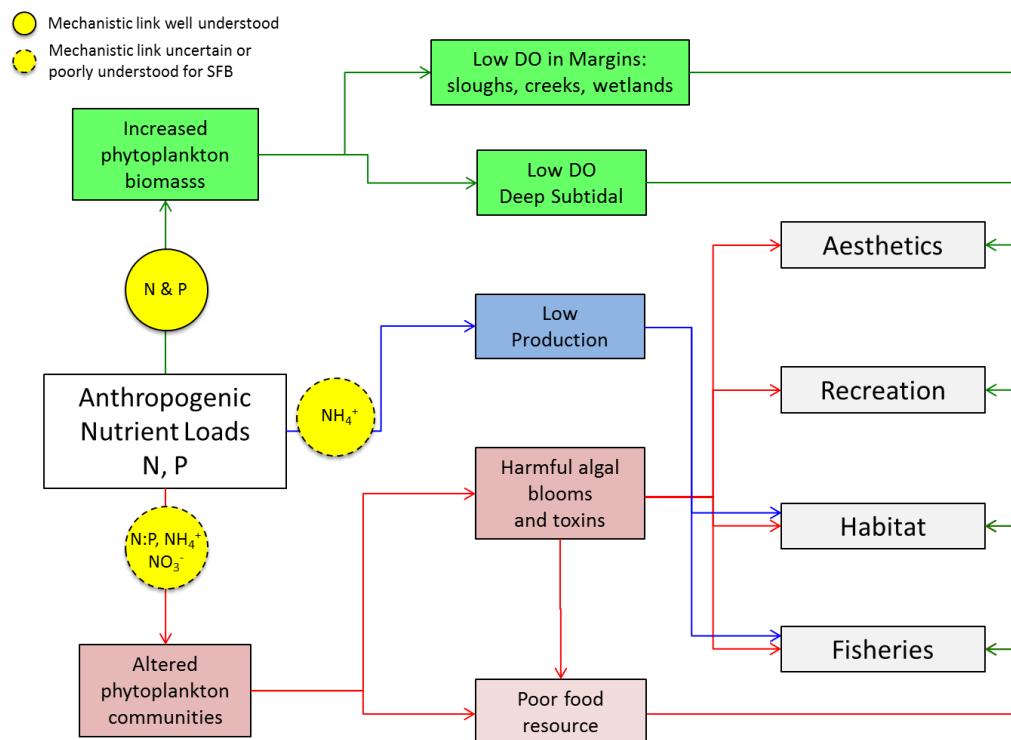


Figure 3.1 Potential adverse impact pathways: linkages between anthropogenic nutrient loads and adverse impacts on uses or attributes of SFB. The shaded rectangles represent indicators that could actual be measured along each pathway to assess condition. Grey rectangles to the right represent uses or attributes of SFB for which water quality is commonly managed. Yellow circles indicate the forms of nutrients that are relevant for each pathway

Current nutrient loads to some SFB subembayments are comparable to or much greater than those in a number of other major estuaries that experience impairment from nutrient overenrichment (Figure 3.2). Consistent with its high loads, SFB has elevated levels of dissolved inorganic nitrogen (DIN) and dissolved inorganic phosphorous (DIP) relative to other estuaries (Figure 3.3). Yet SFB does not commonly experience classic symptoms of nutrient overenrichment, such as massive and sustained phytoplankton blooms, or low dissolved oxygen over large areas in the subtidal zone. SFB has been spared the most obvious adverse impacts of high nutrient loads along these pathways due to a combination of factors that have imparted it with a degree of inherent resistance to these effects (Figure 3.4; discussed further in Sections 6 and 8). However, several recent sets of observations indicate that nutrient-related problems may already be occurring in some areas of SFB, or serve as early warnings of problems on the horizon.

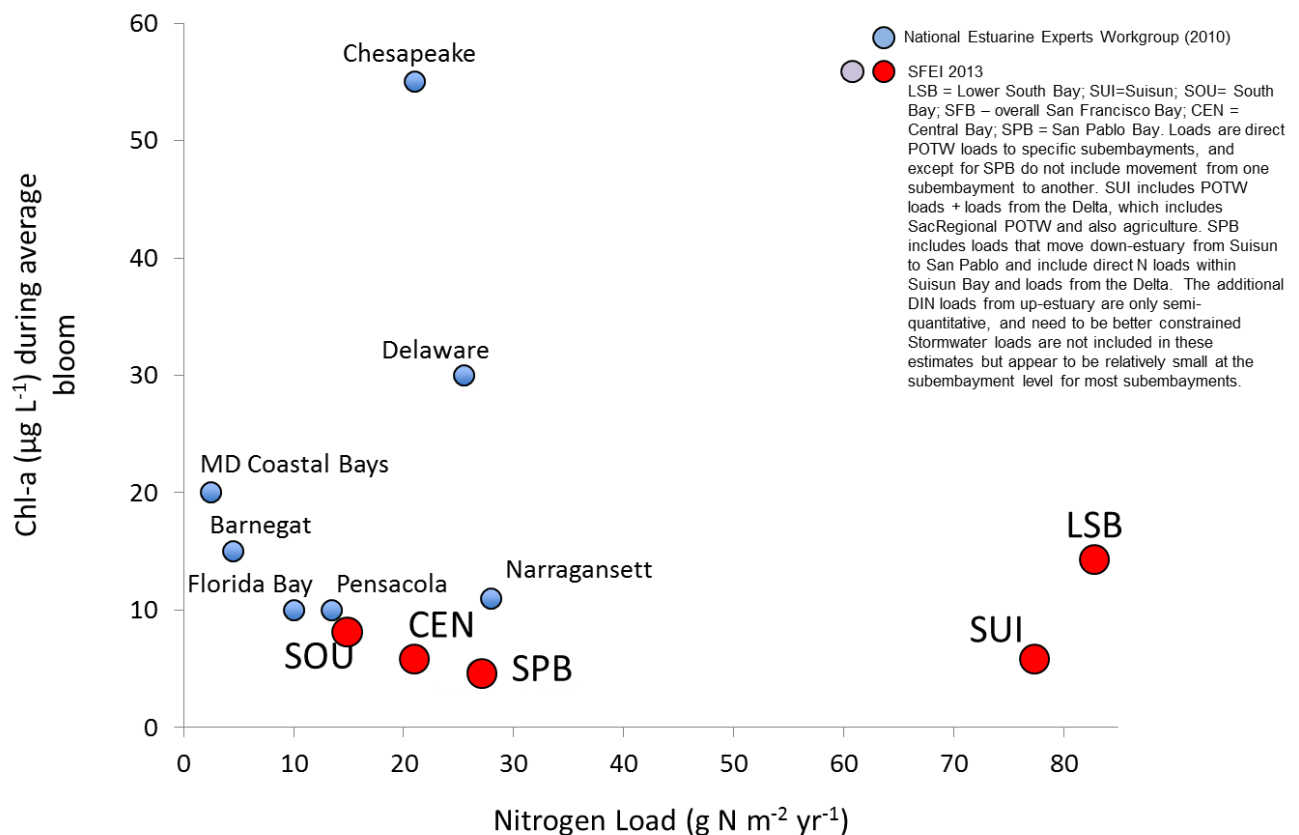


Figure 3.2 Chl-a concentration during an average bloom vs. nutrient loads to San Francisco Bay subembayments, compared to other estuaries that are considered to experience adverse impacts from nutrients. Loads considered include those from POTWs and loads entering from the Delta (which include N derived from upstream treated wastewater effluent and agriculture)

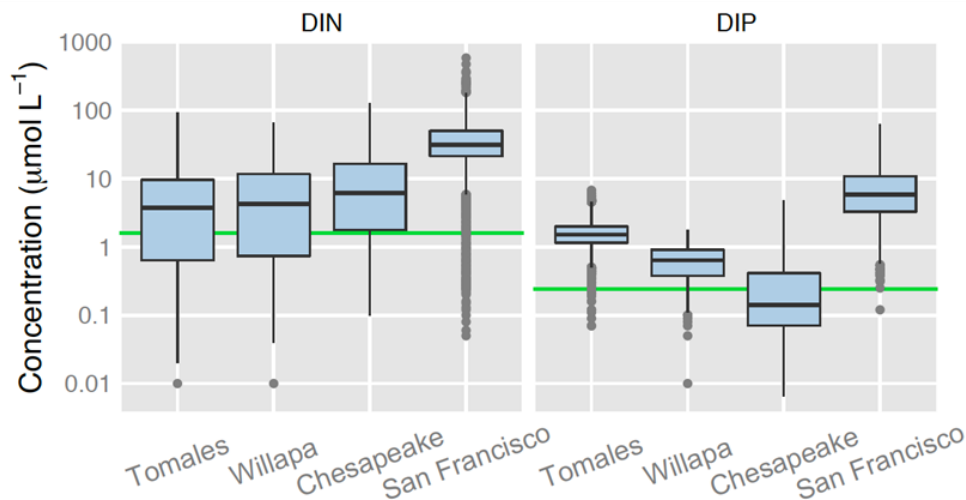


Figure 3.3 Nutrient concentrations in South Bay compared to other estuaries. Source: Cloern and Jassby (2012)

Over the past 15 years, statistically significant increases in phytoplankton biomass have been observed throughout SFB. Most notably summer/fall phytoplankton biomass tripled between the mid-1990s and the mid-2000s (Figure 3.5; Cloern et al., 2007) in South Bay and LSB, representing a shift in trophic status from oligo-mesotrophic (low to moderate productivity system) to meso-eutrophic (moderate to high productivity system) (Cloern and Jassby, 2012). More recent data from South Bay suggests that, at least presently, biomass concentrations have plateaued at a new level instead of continuing to rise (Figure 3.6; SFEI 2014a). Since the late 1990s, Fall blooms have begun occurring regularly in South Bay and LSB, areas where they seldom occurred previously (Figure 3.7 and Cloern and Jassby 2012). While the greatest magnitudes of biomass increase (i.e., in $\mu\text{g/L chl-a}$) have been observed in South Bay, other SFB subembayments have also experienced statistically significant increases in phytoplankton biomass (J Cloern, personal communication).

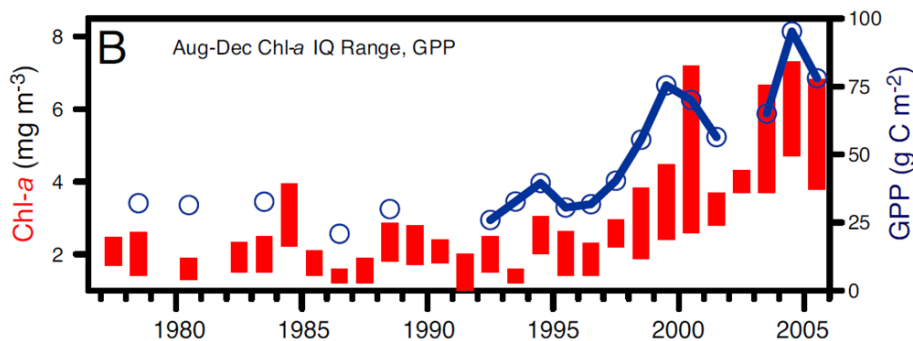
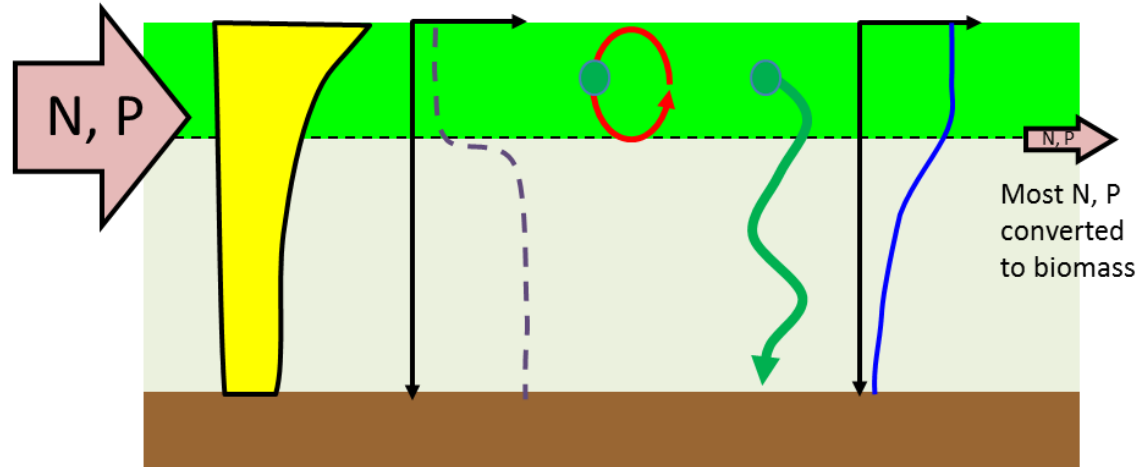


Figure 3.5 Interquartile range of Aug-Dec chl-a concentrations averaged across all USGS stations between Dumbarton Bridge and Bay Bridge, 1977-2005. Source: Cloern et al., 2007

Many other estuaries

1. Relatively high light levels over a substantial portion of the water column due limited light attenuation
2. Sustained periods of salinity- or temperature-stratification, during which phytoplankton residing in the surface layer grow rapidly on high light levels.

Nutrients are efficiently converted to phytoplankton biomass, and dissolved O_2 reaches low levels in the un-ventilated bottom waters where dead phytoplankton are respired by DO-consuming microorganisms. Discussed further in Sections 7 and 8.



San Francisco Bay

1. High turbidity, and most light attenuated within 1-2m of the surface low light
2. Strong tidal mixing, well-mixed water column
3. High abundance of filter-feeding clams that consume phytoplankton biomass

A lower proportion of nutrients is converted into biomass, benthic grazers reduces standing stock of phytoplankton which overall results in lower productivity, and less DO demand bottom waters due to lower biomass, mixing ventilates bottom waters limiting and so biomass that is respired by DO-consuming microorganisms seldom reaches low levels, prevents development of low DO.

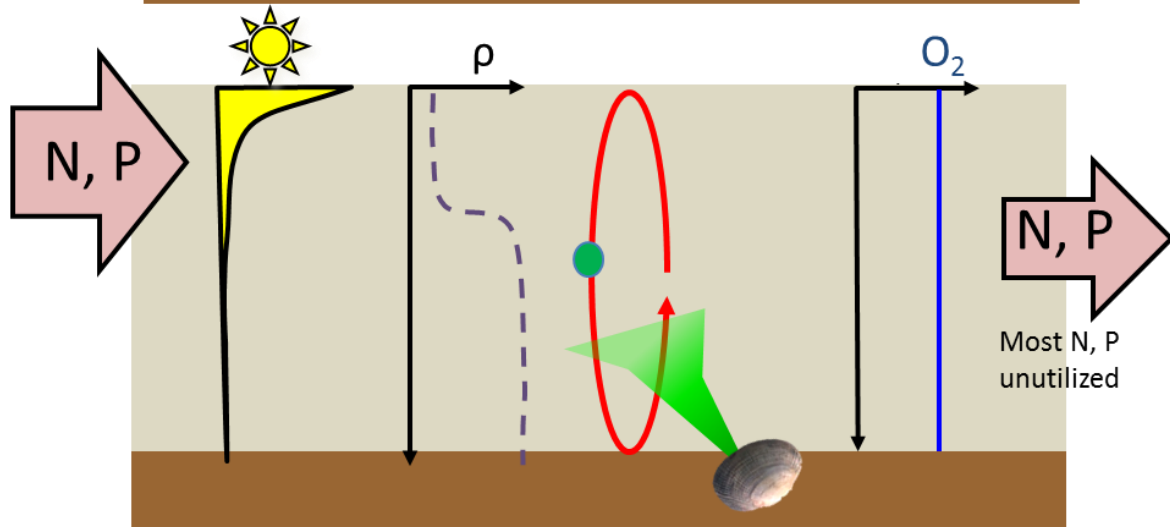


Figure 3.4 Simplified schematic illustrating key differences between SFB and many other estuaries that lead to SFB's attenuated response to nutrients in terms of phytoplankton biomass and dissolved oxygen.

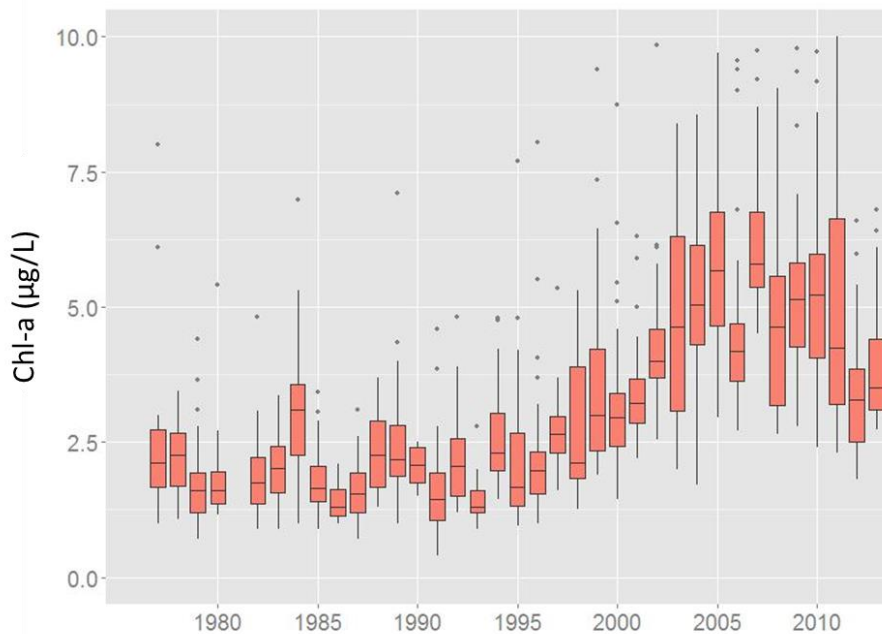


Figure 3.6 Same stations as and data as presented Figure 3.5, with data extended through 2013 (Interquartile range of Aug-Dec chl-a concentrations averaged across all USGS stations between Dumbarton Bridge and Bay Bridge, 1977-2013). Source: SFEI 2014c

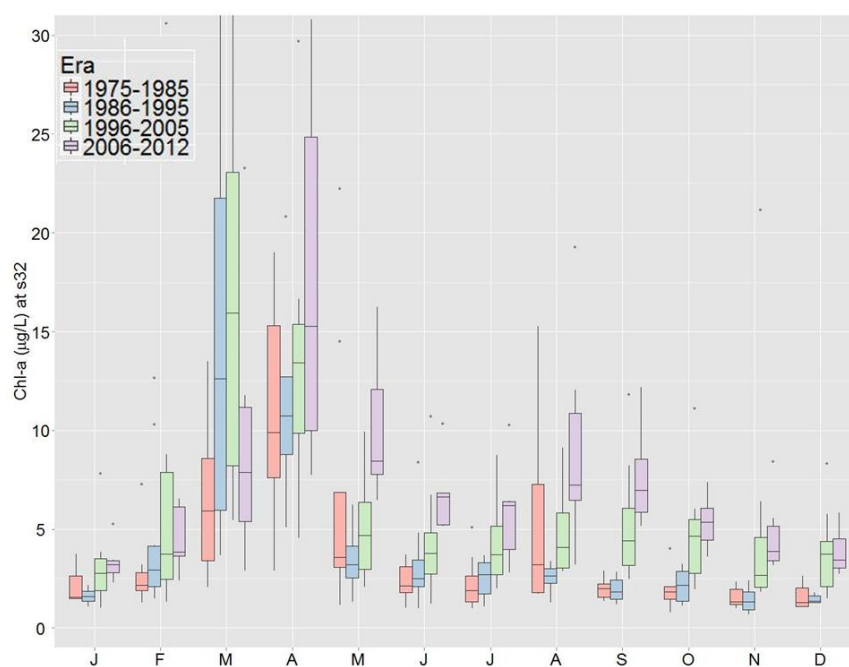


Figure 3.7 Seasonal box plot of chlorophyll-a concentrations near the Dumbarton Bridge (USGS s32), divided into ~10 year eras. Increases in summer baseline chl-a concentrations have been evident since 1996-2005. Fall blooms have also become a regular occurrence. The increases are statistically significant during all months except March and April.

In Suisun Bay, extremely low phytoplankton biomass has defined the system since 1987 (Figure 3.8), coincident in time with the invasive clam, *Potamocorbula amurensis*, becoming widely established. The extended period of low phytoplankton biomass and low rates of primary production are considered to be among the factors contributing to long-term declines in upper trophic level production in Suisun Bay and the Delta by limiting food supply (Baxter et al., 2010; NRC 2012). While the low phytoplankton biomass and productivity in Suisun Bay have generally been attributed to the impacts of *Potamocorbula* and low light levels due to high

suspended sediments (e.g., Kimmerer and Thompson, 2014), recent studies have argued that elevated ammonium (NH_4^+) concentrations in Suisun Bay also limit primary production rates and play an important role in both creating the low biomass conditions and exacerbating food limitation (Dugdale et al., 2007; Dugdale et al., 2012; Parker et al. 2012a,b). Other studies have proposed that high ambient concentrations of nitrate (NO_3^-) and NH_4^+ , and altered ratios of N:P cause shifts phytoplankton community composition toward species having poor food quality, adversely impacting Delta food webs (Glibert 2010; Glibert et al., 2011).

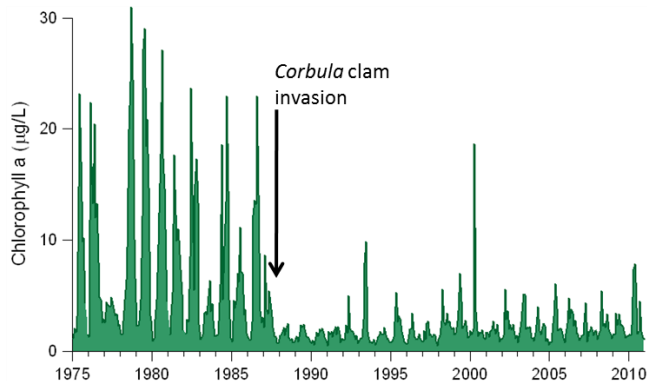


Figure 3.8 Phytoplankton biomass in Suisun Bay, 1975-2010. Source: J Cloern, USGS; Data: USGS, DWR-EMP

Harmful phytoplankton species also represent a growing concern. The harmful algae, *Microcystis spp.*, and the toxin they produce, microcystin, have been detected with increasing frequency in the Delta and Suisun Bay since ~2000 (Lehman et al., 2008). In addition, the HAB toxins microcystin and domoic acid have been detected Bay-wide (Figure 3.9). The ecological

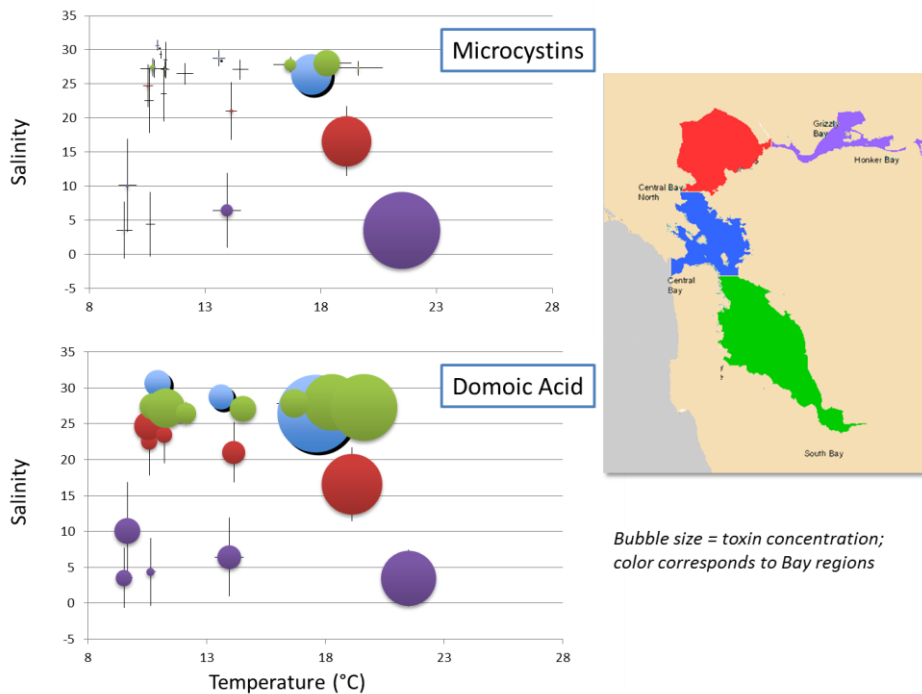
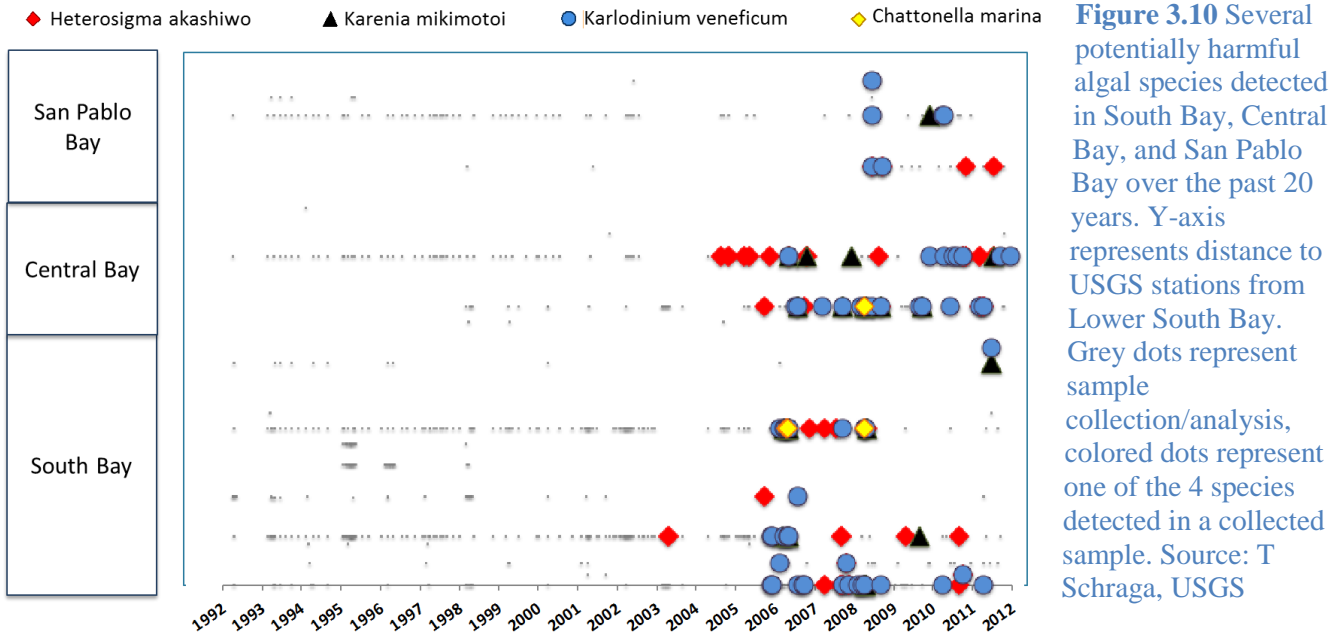


Figure 3.9 HAB toxins detected in SFB during 2011. Bars represent 1 SD for salinity and temperature Source: R. Kudela

significance of observed toxin levels in the Bay are not yet known. A number of phytoplankton species that have formed harmful algal blooms (HABs) in other systems have been detected throughout SFB (Table 3.1 and Figure 3.10). Although the abundances of HAB-forming

organisms in SFB have not reached levels that would constitute a major bloom, they do periodically exceed thresholds established for other systems (Kudela et al., in prep), and major *Microcystis spp* blooms and elevated microcystin levels have been observed with some regularity in the Delta (Lehman et al., 2008). Moreover, since HAB-forming species are present in SFB and nutrients are abundant, HABs could readily develop should appropriate physical conditions create opportunities that HABs can exploit. In fact, an unprecedented large red tide bloom



occurred in Fall 2004 following a rare series of clear calm days during which the water column was able to stratify, and chl-a levels reached nearly 100 times their typical values (Figure 3.11; Cloern et al. 2005). In addition, harmful-bloom forming species have been detected at elevated abundances in salt ponds in LSB undergoing restoration (Thebault et al., 2008), raising concerns that salt ponds could serve as incubators for harmful species that could then proliferate when introduced into the open bay.

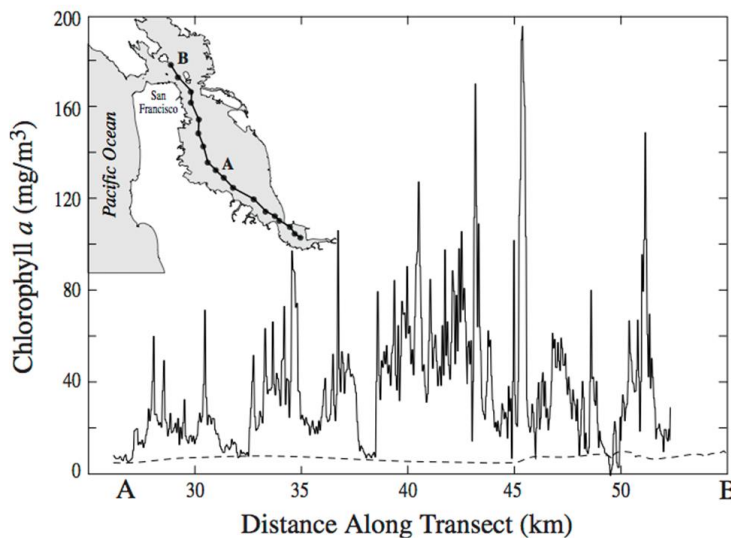


Figure 3.11 Phytoplankton biomass South and Central Bays. Measurements taken during a red tide on 8 September 2004 (solid curve). Phytoplankton biomass returned to typical seasonal levels on 14 September (dashed curve). Inset map shows location of the sampling transect A-B. Source: Cloern et al. 2005

Table 3.1 Potentially harmful algal species detected through USGS science program in SFB: 1992-2012. Source: T Schraga, USGS

Genus/Species	Division/ Phyla	1st observed	Most recent observed	# of times observed	Toxin**	Impact	Location and timing of observations
Alexandrium	Dinoflagellate	1992	2011	247	saxitoxin	neurotoxin, fish kills	South, Central, and San Pablo Bays - Spring and Fall
Amphidinium	Dinoflagellate	1996	2008	36	compounds with haemolytic and antifungal properties	fish kills	South Bay - spring bloom (March-April) and occasionally fall bloom (September-October).
Dinophysis	Dinoflagellate	1993	2011	51	okadaic acid		Central bay
Heterocapsa	Dinoflagellate	1992	2012	394		food web hab, kills shellfish	Found throughout year, but mostly seen in spring and summer, South and Central Bay, occasionally up to San Pablo Bay
Karenia mikimotoi *	Dinoflagellate	2006	2011	22	gymnocins, compounds similar to brevetoxin	kills benthic organisms, fish, birds, + mammals	South bay + Central Bay
Karlodinium veneficum *	Dinoflagellate	2005	2012	63	compounds with hemolytic, ichthyotoxic, and cytotoxic effects	kills fish, birds + mammals	South bay + Central Bay
Heterosigma akashiwo *	Raphidophyte	2003	2011	39	neurotoxin	fish kills	South bay + Central Bay
Pseudo-nitzschia	Diatom	1992	2011	132	domoic acid		Large blooms occurred in central and south Bay (stn 27) in 1990s
Anabaena	Cyanobacteria	1993	2011	24	PSTs		Sacramento River and confluence.
Aphanizomenon flos-aquae	Cyanobacteria	1995	2011	13	PSTs		Sacramento River and confluence. Low #s in South Bay

Table 3.1 continued

Genus/Species	Division/Phyla	1st observed	Most recent observed	# of times observed	Toxin**	Impact	Location and timing of observations
Aphanocapsa	Cyanobacteria	1993	2011	22			South Bay 2005+6, 2011 Delta confluence (San Joaquin source most likely)
Aphanothece sp.	Cyanobacteria	1992	2011	32			South Bay 2005+6, 1990s and 2010-11 Suisun and Sac River
Cyanobium sp.	Cyanobacteria	1999	2008	79	microcystin		South and Central Bay
Lynghya aestuarii	Cyanobacteria	2011	2011	1	saxitoxin	human health impacts (skin, digestion, respiratory, tumors) and paralytic shellfish poisoning	September 2011 - large bloom in Suisun area (stn 3)
Planktothrix	Cyanobacteria	1992	2011	23	PSTs		South Bay 2005-2007, 1990s, 2010-11 Suisun and Sac River
Synechococcus sp.	Cyanobacteria	1992	2011	66			South Bay spring (March/April)
Synechocystis	Cyanobacteria	1997	2011	224	microcystin		South Bay and San Pablo Bay, mostly in fall

All of these species have had high biomass in SFBAY. Multiple species are grouped within a genera. If it's a single species, it is listed as such

*Known as exceptionally harmful in temperate estuaries such as in Japan and Atlantic coast estuaries. All were detected for the first time in SFB in the past 10 years and have persisted

** Not all toxins are known. Genera with PST have two or more Paralytic Shellfish Toxins = microcystin, cylindrospermopsin, anatoxin, saxitoxin. All cause Paralytic Shellfish Poisoning. PSTs microcystin and cylindrospermopsin cause liver damage in mammals, anatoxin and saxitoxin damage nerve tissues in mammals (humans, dogs, etc.)

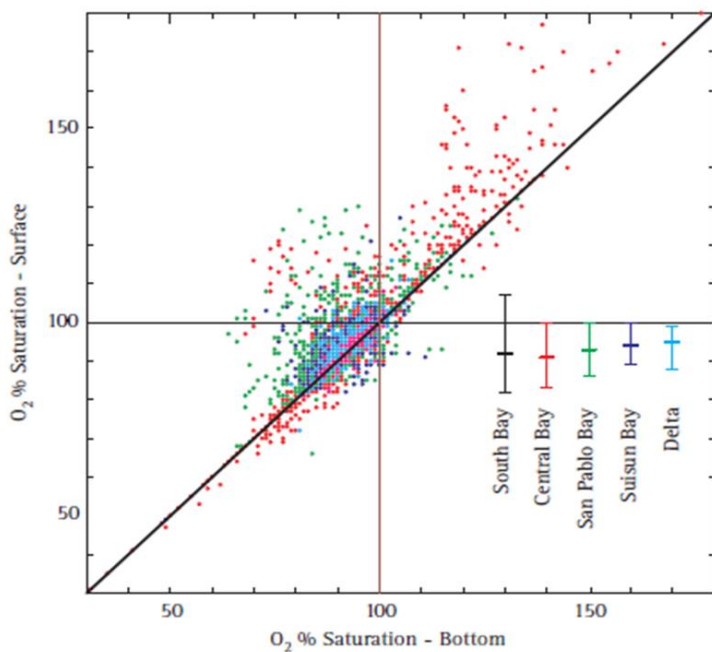


Figure 32. Oxygen concentration as percent saturation in near-surface and near-bottom samples. Color indicates region, and error bars give medians and 10th and 90th percentiles of the data. Data from USGS monitoring program, which focuses on channel stations and the portion of the Delta in the lower Sacramento River.

Figure 3.12 DO in deep subtidal areas of SFB. Source: Kimmerer 2004

DO concentrations in deep subtidal habitats throughout the Bay typically remain at levels above 5 mg L^{-1} , (Figure 3.12), the San Francisco Bay Basin Plan standard. However, in LSB, sampling has most frequently occurred at slack high tide. Recent continuous measurements at the Dumbarton Bridge indicate that DO levels at low tide are commonly $1\text{-}2 \text{ mg/L}$ lower than at high tide during summer months (e.g., Figure 3.13.A; SFEI, 2014c), and can occasionally dip below, 5 mg L^{-1} (SFEI, unpublished data). During Summer 2014, USGS sampling cruises detected $\text{DO} < 5 \text{ mg/L}$ at other deep subtidal stations south of the Dumbarton Bridge during two cruises⁶.

Low DO commonly occurs in some shallower margin habitats (Figure 3.14). For example, studies of salt ponds undergoing restoration in LSB show that they experience large diurnal DO fluctuations (Figure 3.15.A; Topping et al., 2009) and occasionally experience sustained periods of anoxia (Figure 3.15.B; Thebault et al., 2008). In some slough habitats of LSB, DO regularly dips below 5 mg L^{-1} , frequently approaches 2 mg L^{-1} (Shellenberger et al., 2008), and at a site in Alviso Slough, DO remained near or below 2 mg L^{-1} for sustained periods (up to 10-12 hours) during Summer 2012 (Figure 3.13.B) and Summer 2014 (SFEI, 2014c). Low DO has also been observed in Suisun Marsh, although whether that low DO is linked to nutrient issues in SFB is still being investigated (effluent from managed duck ponds is presumed to be a major cause; Tetra Tech 2013). Under natural conditions, shallow subtidal and tidal wetland habitats commonly experience low DO, and plants and animals native to these habitats are often well-adapted to these DO swings. However, there is a paucity of DO data in margin habitats, and the severity of low DO (frequency, duration, spatial extent, concentration), whether it is impacting biota, and the extent to which excess nutrients cause or contribute to the low DO conditions are all poorly known.

⁶ <http://sfbay.wr.usgs.gov/access/wqdata/query/easy.html>

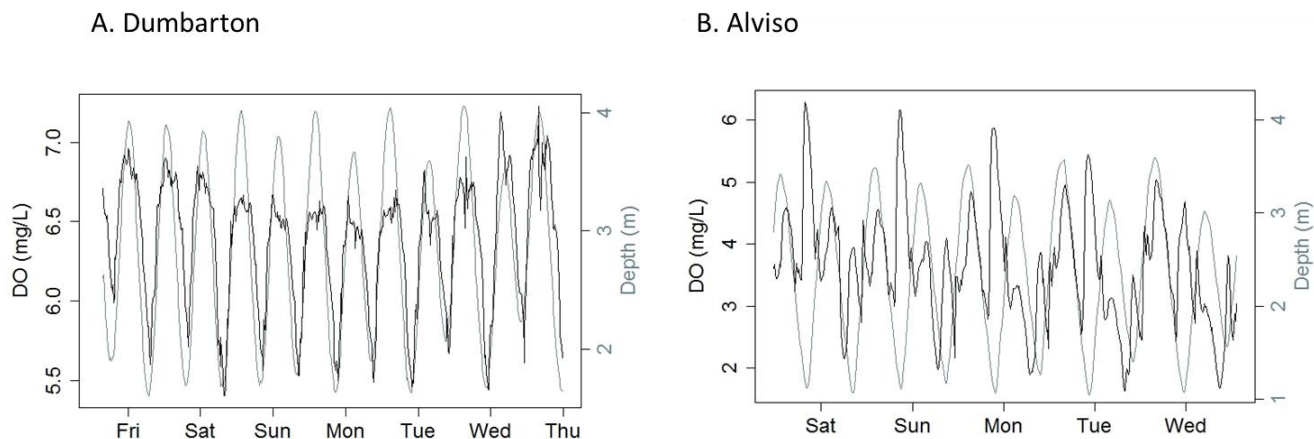


Figure 3.13 Time series of DO (mg/L) and depth at **A. Dumbarton Bridge** and **B. Alviso Slough**, Sep 5-12 2013.

In addition to characterizing and addressing any current nutrient-related problems in SFB, there is a need to anticipate potential future adverse impacts. The highly elevated DIN and DIP concentrations Bay-wide provide the potential for future impairment to develop. Any major reductions in loads to SFB will take years-to-decades to implement. Thus, if future problems are to be averted, potential impairment scenarios need to be anticipated, evaluated, and, if deemed necessary, managed in advance of their onset. A proactive approach to characterizing and managing potential problems – while they are on the somewhat-distant horizon, as opposed to imminent – will allow greater flexibility in the management options that can be pursued.

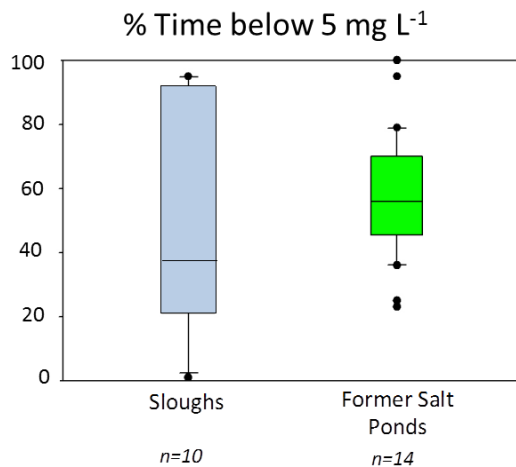


Figure 3.14 Percentage of time DO less than 5 mg/L in sloughs and salt ponds rimming Lower South Bay, based on a review of all available multi-program continuous sensor measurements. Source: SFEI 2014c

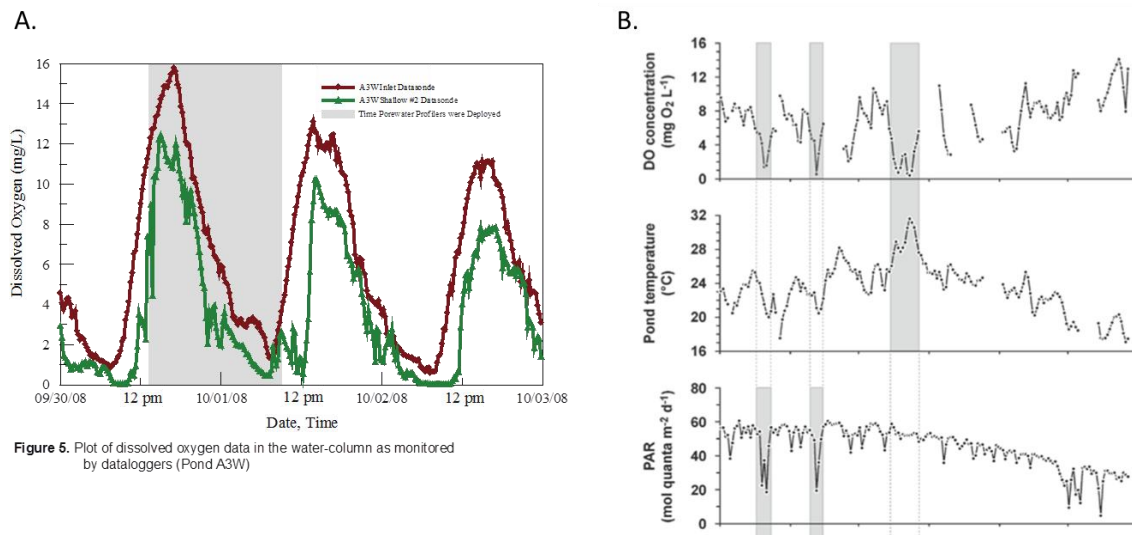


Figure 3.15 A. Dissolved oxygen concentrations in LSB salt pond A3W undergoing restoration Source: Topping et al. 2008 **B.** Dissolved oxygen concentration in LSB salt pond A18. Grey bars indicate time periods when incident light was low (clouds) or temperatures were high enough to inhibit primary production. These factors lead to sustained periods of low DO. Source: Thebault et al. 2008

3.2 What would a problem look like in SFB?

At the outset of the SFB conceptual model development, we asked the question: *What would a nutrient-related problem look like in SFB subembayments, if a problem were currently occurring, or if one was to occur in the future?*

This report does not aim to answer the question of whether SFB subembayments are currently impaired or will be in the future. Instead, we used the answers to this question to help focus the conceptual model on issues most relevant for detecting impairment and anticipating potential future impairments, and to identify meaningful and measurable indicators of ecosystem response to nutrients and ecosystem health.

Table 3.2 summarizes nutrient-related adverse impacts (AI) that were identified as plausible in San Francisco Bay, divided into eight categories. The problem categories are specific examples that extend from the more general paths depicted in Figure 3.1.

High phytoplankton biomass can have direct adverse impacts (AI.1) in SFB, through acting as a nuisance (aesthetics, odor) or through direct impacts on biota (e.g., smothering or shading aquatic macrophytes, coatings on bird wings). However, among the most common and problematic impairments due to high phytoplankton biomass is low dissolved oxygen in deep subtidal areas that develops due to degradation of phytoplankton-derived organic matter by oxygen-consuming microorganisms (AI.2). In the case of both high phytoplankton biomass and low DO, the magnitude, duration, and spatial extent are important to consider. Extremely low DO (e.g., $<2 \text{ mg L}^{-1}$), and the high phytoplankton biomass that causes it, over large areas for extended periods of time could lead to considerable impairment, whereas moderate DO deficits, or spatially-limited or short-duration events may be less problematic. In addition, low DO occurs

naturally in shallow margin habitats (e.g., sloughs, salt marshes), and native organisms are adapted to these conditions. However, elevated anthropogenic nutrient loads could exacerbate these issues by increasing the intensity of these events (i.e., even lower DO), or increasing the spatial extent, temporal frequency, or duration (AI.3). Thus, both the severity of events and whether they are entirely natural or caused or exacerbated by anthropogenic nutrients need to be considered.

Elevated nutrient concentrations, or changes in relative abundance of nutrient forms, could increase the frequency with which HABs occur, the severity of a HAB event (abundance, duration, spatial extent), and the levels of HAB-related toxins (AI.4). Phycotoxins, i.e., toxins produced by phytoplankton, bioaccumulate and can exert toxicity to consumers at all levels of the food web, including humans. Some phycotoxins also exert direct toxicity (e.g., skin contact). High nutrient loads may also increase the frequency of so-called nuisance algal blooms (NABs), which are not toxic but may degrade aesthetics due to surface scums or odors.

Several recent studies, focused in the northern Bay-Delta, have hypothesized that high NH_4^+ levels contribute to the low biomass and infrequent phytoplankton blooms in Suisun Bay by inhibiting primary production (AI.5), in particular the growth of diatoms (Dugdale et al., 2007; Parker et al., 2012a,b; Dugdale et al., 2012). Low phytoplankton biomass stands among the factors thought to contribute to ecosystem decline in Suisun Bay and the Delta. To the extent that elevated NH_4^+ contributes to lower productivity, elevated nutrient loads – and in particular NH_4^+ loads – would adversely impact ecosystem health along this pathway (Figure 3.1).

Other recent studies have hypothesized that high nutrient concentrations, elevated NH_4^+ , or altered N:P in SFB adversely impacts food webs by shifting phytoplankton community composition away from healthy assemblages and toward suboptimal compositions that do not adequately sustain organisms at higher trophic levels (AI.6; Glibert et al., 2012). Another recent study observed that high NH_4^+ concentrations can exert chronic toxicity on an important Delta/Suisun copepod at concentrations (25 μM) that approach ambient concentrations in some areas along the Sacramento River and in the Delta (Teh et al, 2011). Other studies have argued that high nutrient concentrations or altered N:P can alter individual cell composition in ways that adversely impact primary consumers (Glibert et al., 2013). The latter two examples are included under “Other nutrient-related impacts” (AI.7), along with other potential adverse impact pathways not explicitly noted.

Table 3.2 What would a problem look like in SFB? Plausible adverse impacts (AI).

	Impacted State	Rationale or Link to Beneficial Uses
AI.1	High Phytoplankton Biomass High phytoplankton biomass of sufficient magnitude (concentration), duration, and spatial extent that it impairs beneficial uses due to direct or indirect effects (IS.2). This could occur in deep subtidal or in shallow subtidal areas.	Direct impairment due to aesthetics (odors, surface scum) and potentially directly impairing biota (at very high levels, e.g., coating birds wings). Other main concern is through causing low dissolved oxygen (IS.2, IS.3)
AI.2	Dissolved Oxygen – Deep subtidal Low DO in deep subtidal areas of the Bay, over a large enough area and below some threshold for a long enough period of time that beneficial uses are impaired.	Fish kills, die-off of beneficial benthos, loss of critical habitat that result in lowered survival or spawning/reproductive success or recruitment success of fish and beneficial benthos.
AI.3	Low DO – Shallow/margin habitats: DO in shallow/margin habitats below some threshold, and beyond what would be considered “natural” for that habitat, for a period of time that it impairs beneficial uses	Fish kills, die-off of beneficial benthos, loss of critical habitat that result in lowered survival or spawning/reproductive success or recruitment success of fish and beneficial benthos
AI.4	HABs/NABs and phycotoxins Occurrence of HABs/NABs and/or related toxins at sufficient frequency or magnitude of events that habitats reach an impaired state, either in the source areas or in areas to which toxins are transported.	<i>HABs and phycotoxins:</i> Passive or active uptake of toxins, or ingestion of HAB-forming species and accumulation of toxins. Ingestion of bioaccumulated toxins by is harmful to both wildlife and humans through consumption of tainted shellfish or fish. Skin contact and inhalation can also be problematic. <i>NABs:</i> Some species are considered nuisance for reasons other than toxins (e.g., rapid biomass production leading to low DO). Impaired aesthetics, surface scums, discoloration, odors
AI.5	Low Phytoplankton Biomass Low phytoplankton biomass in Suisun Bay or other habitats due to elevated NH_4^+ , which would exacerbate food supply issues.	Suisun Bay is considered a food limited system, and low levels of phytoplankton may contribute to impairment in this highly altered system.
AI.6	Suboptimal phytoplankton assemblages Nutrient-related shifts in phytoplankton community composition, or changes in the composition of individual cells (N:P), that result in decreased food quality, and have cascading effects up the food web.	Phytoplankton primary production is the primary food resource supporting food webs in SFB. Changes in the dominant assemblages would impact food quality.
AI.7	Other nutrient-related impacts. Other direct or indirect nutrient-related effects that alter habitat or food web structure at higher trophic levels by other pathways.	Several additional nutrient-related impacts on food webs in the northern estuary have been proposed that are not captured by IS.1-IS.6, and that are not explored in detail in this report.

4. Conceptual Model Overview

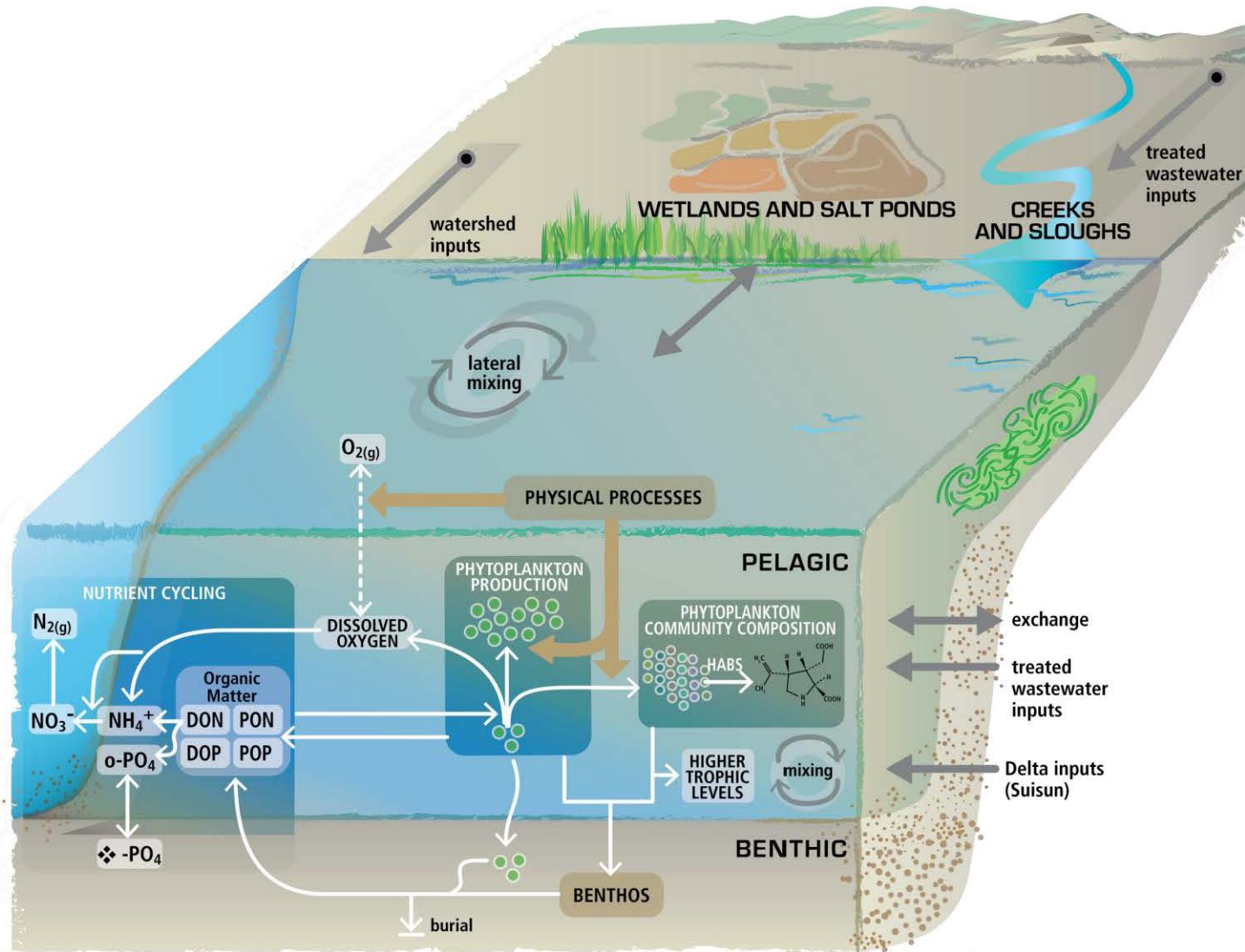
The conceptual model is described as a set of modules (Sections 5-9) that establish the mechanistic framework connecting nutrient loads with ecosystem response. Major components of the conceptual model are illustrated generally in Figure 4.1.A. The goal in developing this conceptual model was to make explicitly the multiple steps and mechanisms that fall along the path between nutrient loads and ecosystem response, and therefore views biogeochemistry, ecology, and beneficial uses in SFB through a nutrient-centric lens. In particular the conceptual model explores the pathways and mechanisms along the adverse impact pathways illustrated in Figure 3.1 and summarized in Table 3.2, and ties back to the proposed NNE indicators for assessing condition in SFB (Table 2.1).

The conceptual model is organized into five main modules:

- Section 5: Physical processes (hydrodynamics and sediments)
- Section 6: Nutrients
- Section 7: Primary production, with a major focus on phytoplankton biomass
- Section 8: Dissolved Oxygen; and
- Section 9: Phytoplankton Community Composition, HABs, and HAB toxins

The modules considered in this report extend only as far along the food web as phytoplankton biomass and community composition. Zooplankton, benthos, and fish played a central role in shaping the other modules: their habitat and food requirements were used to focus the modules for phytoplankton biomass, phytoplankton community composition, and dissolved oxygen on the most relevant processes and information needs; and the roles of primary consumers (benthic and pelagic grazers) were explicitly considered in as much as they influence phytoplankton biomass, phytoplankton community composition, and carbon flow in the system and are themselves influenced by food quality. Figure 4.1.B depicts the detailed conceptual model, with all components combined. The subsequent sections of this report focus on specific parts of this overall conceptual model. Physical processes play an important role in dictating ecosystem response to nutrients in SFB. Section 5 provides an introduction to hydrodynamic considerations, and hydrodynamic controls are woven throughout the discussions in Sections 6-9. Section 10 briefly summarizes pathways or indicators not included in the conceptual model at this time.

Although SFB's 5 subembayments have very different physical, biogeochemical, and biological characteristics that shape their individual responses to nutrients, a single set of modules was developed for all of SFB. This is appropriate since the same fundamental processes operate in each subembayment. Inter-subembayment differences in nutrient concentrations or forms and ecosystem response arise from differences in the relative importance of major drivers among subembayments, and these differences are discussed within each module.



1

Figure 4.1.A Simplified nutrient conceptual model, showing major components. Those discussed in more detail include physical processes, nutrient cycling, phytoplankton production, dissolved oxygen, and phytoplankton community composition

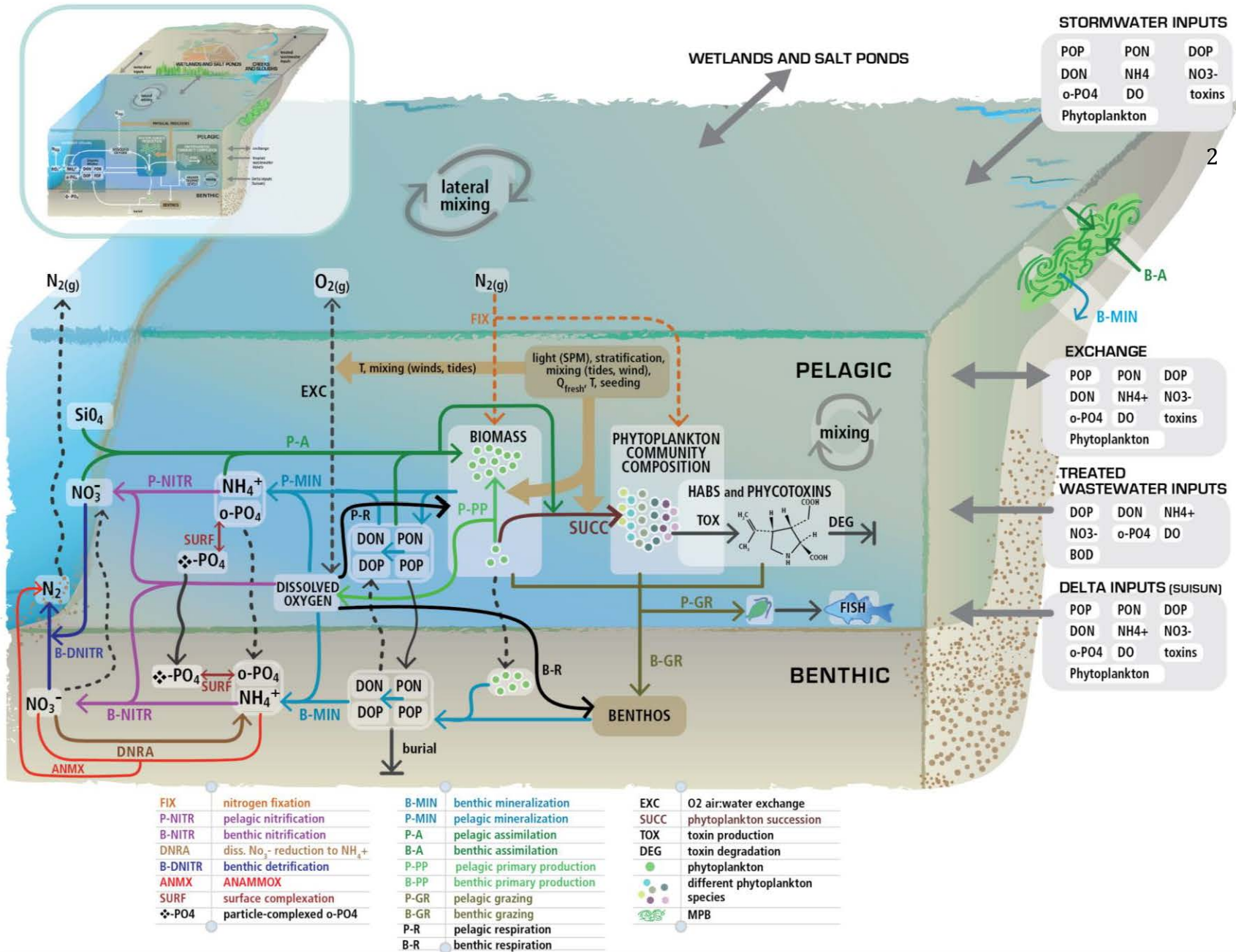


Figure 4.1.B Detailed conceptual model, all modules

5 Physical Processes: Hydrodynamics and Sediment dynamics

5.1 Introduction

Characteristics of the 5 SFB subembayments considered in this report are presented in Table 5.1. San Francisco Bay has an open water surface area of approximately 1100 km² and an average depth of approximately 7 m, resulting in a total volume of approximately 7400 km³ (Smith and Hollibaugh, 2006). Shallow shoals comprise large areas of LSB, South Bay, San Pablo Bay, and Suisun Bay (Figure 5.1; see also Figure A.1 in Appendix for higher resolution bathymetry).

The physical dynamics of San Francisco Bay are driven by the interplay of tidal, freshwater, and wind forcing with the complex topography of the Bay. In general terms, the Bay is made up of a series of subembayments: Central Bay is the deepest basin and is most strongly coupled to the Pacific. Landward from Central Bay, South Bay, Lower South Bay, and San Pablo Bay are each characterized by a single deep channel that bisects broad subtidal shoals. Upestruary from San Pablo Bay, on the landward side of Carquinez Strait, lies Suisun Bay, which is distinguished from the other embayments by its braided channels and the presence of two distinct shallow subtidal embayments: Grizzly Bay and Honker Bay. Finally, the Sacramento-San Joaquin Delta is not so much an embayment but a network of channels connecting the landward estuaries with the Bay. This complex topography sets the environment for tidal forcing, wind forcing and freshwater flows, which define the variability of tidal stage (inundation regime), salt and nutrient transport, stratification, turbulent mixing and sediment dynamics.

Freshwater inputs vary greatly among the subembayments. Suisun Bay and San Pablo Bay are river-dominated estuaries. The Sacramento and San Joaquin Rivers, enter SFB through Sacramento/San Joaquin Delta east of Suisun Bay, and 90% of the annual freshwater to SFB enters through the Delta. Additional freshwater inputs to SFB come from smaller perennial tributaries that drain the immediate surrounding watersheds, and stormwater runoff. Suisun Bay hydraulic residence times range from less than 1 day during high-flow periods to ~1 month during dry periods. Low salinity conditions generally define Suisun Bay, while San Pablo Bay is considerably more saline due to exchange with Central Bay. Compared to the northern estuary, freshwater inputs to Lower South Bay and South Bay are quite limited and consist mainly of wastewater treatment plant effluent and stormwater during the rainy season. LSB and South Bay behave more like tidal lagoons, and residence times can range from weeks to months.

Hydrodynamics and sediment dynamics play a critical role in determining San Francisco Bay's direct and indirect responses to nutrients. The intensity of vertical mixing and the length of time that a stratified water column (i.e., a surface layer and bottom layer) can be maintained strongly regulate the timing, magnitude, and duration of phytoplankton blooms in deeper sections of this turbid (light-limited) yet nutrient-rich estuary. Suspended sediment loads, tidal mixing, and wind-driven mixing maintain high levels of particles in the water column resulting in light-limiting conditions for phytoplankton growth. Exchange between the Bay's channels and broad shallow shoals – where higher average light availability allows for faster phytoplankton growth – can influence the degree to which blooms develop in the shoals and propagate to the channels. Vertical mixing rates, duration of stratification, and rates of exchange or flushing between subembayments and habitats determine the extent to which low oxygen levels can develop. A

comprehensive review of the hydrodynamics of San Francisco Bay is beyond the scope of this document. Instead, this section first describes four major physical forcings (tides, wind, freshwater flow, and coastal ocean exchange). We then focus on three issues that are particularly relevant to consideration of ecological change in response to shifting nutrient regimes: flushing times, density stratification and suspended sediment.

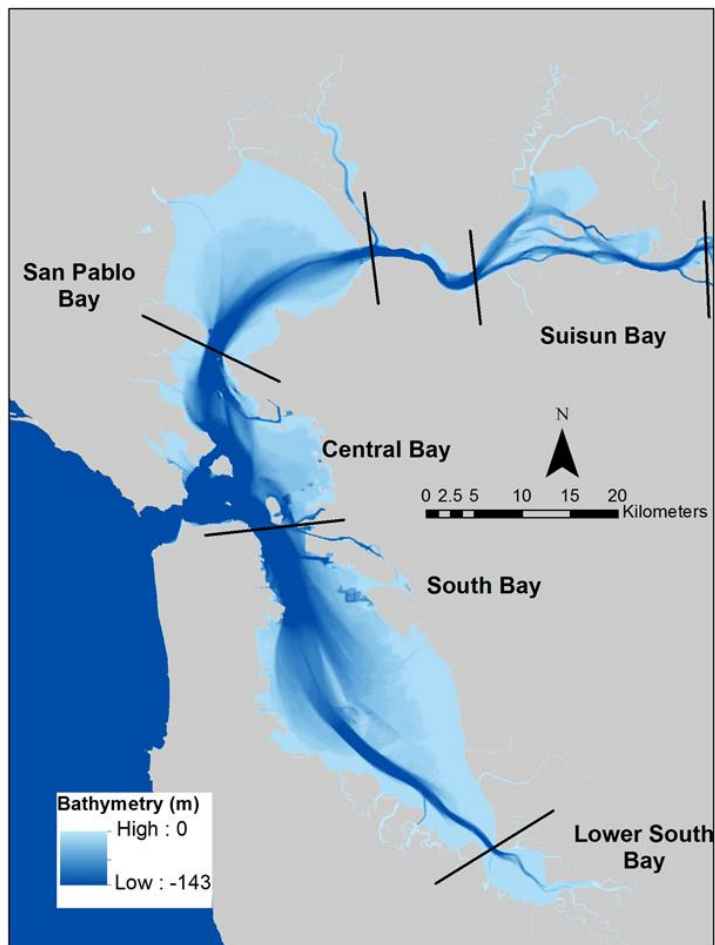


Figure 5.1 Bathymetry in SFB, shown as distance below surface (m). Water Board subembayment boundaries are shown in black. Source: NOAA bathymetry soundings

5.3 Major drivers

5.3.1 Tidal forcings

The spring-neap (~14 day) cycle in San Francisco Bay produces large diurnal asymmetries in the tides during the springs, which are characterized by one large tide and one small tide in each 24 hour cycle. The neaps, on the other hand, have more symmetric tides, which are intermediate in magnitude to the two tides seen each day during the springs. Tidal mixing energy also varies over the course of the year, with sustained highest-energy periods around the solstices (June, December), and sustained minimum energy periods around the equinoxes (March, September) (Figure 5.2)

Table 5.1 Subembayment area and volume, and watershed area and land-use

	Boundary	Bay area¹ (10 ⁶ m ²)	Bay volume¹ (10 ⁶ m ³)	Watershed area (10 ⁶ m ²)	% surface water²	% open²	% agriculture²	% commercial²	% industrial²	% residential²	% transportation²
Lower South Bay	South of Dumbarton Bridge	30	90	1320	1%	37%	2%	11%	5%	30%	14%
South Bay	Dumbarton to Bay Bridge	460	2530	1685	1%	55%	2%	8%	3%	21%	10%
Central Bay	Bay Bridge to Richmond Bridge	200	2620	255	1%	33%	0%	10%	4%	36%	16%
San Pablo Bay + Carquinez	Richmond Bridge to Benicia Bridge	310	1690	2180	3%	42%	33%	3%	2%	13%	4%
Suisun Bay	Benicia Bridge to Mallard Island	100	500	1465	4%	51%	18%	4%	2%	14%	7%

Spatially, there is an important distinction to be made between North Bay and South Bay in their response to tidal forcing. North Bay features a progressive tide, with the amplitude gradually dissipating as the tide propagates through each of the subembayments, eventually being completely dissipated upstream of the Delta. South Bay, by contrast, amplifies the tides by about 50% from the Golden Gate. This amplification is due to the specific geometry of South Bay and the nature of and position of the South Bay shorelines through a combination of reflection and funneling of the incoming tide. As a result, shoreline changes, whether development or wetland restoration, will have very different effects between North and South Bay. For example, wetland restoration in North Bay will reduce tidal energy primarily through increases in tidal dissipation due to friction. In South Bay, wetland restoration could alter the fundamental tidal dynamics in the basin, potentially reducing the tidal amplification significantly (with potential benefits for inundation, but negative effects on marsh habitat). The large areas of salt ponds slated for restoration in Lower South Bay and southern South Bay make changes in tidal dissipation a major consideration there (Figure 2.1).

5.3.2 Wind

Wind forcing is strongly diurnal during the summer months due to the afternoon sea breezes, which are from the west but modified by local topography. During the winter months, the dominant wind events are tied to storms, and they frequently are characterized by wind out of the south (on the leading edge of low pressure systems moving off of the Pacific). Winds during the fall and spring are more variable, but tend to be smaller in magnitude (Figure 5.2). The effects of the winds on transport include both direct effects on mixing and sediment resuspension and indirect effects on circulation, through the development of a surface tilt in response to sustained wind forcing.

5.3.3 Freshwater flow

Freshwater flow enters the Bay primarily through the Sacramento-San Joaquin Delta (Delta). Daily net outflow estimates from the Delta to Suisun Bay are provided in the CA Department of Water Resources “DAYFLOW”⁷ database. Daily net Delta outflow in DAYFLOW is calculated based on a combination of daily averaged inflows into the Delta, in-Delta consumptive water use, and water exports from the Delta. Other sources of freshwater flow around the perimeter of the Bay include several moderate rivers (Napa, Petaluma, Guadalupe, Alameda and Coyote Creek), small inflows from local watersheds and water treatment returns. Each of these categories of sources has its own distinct seasonal variability. The flows in the small and moderate rivers and streams entering directly into the Bay are tied to local precipitation events and peak during the winter (rainy) months. The larger inflows from the Delta are tied to Sierra snowmelt and the management of reservoirs, leading to a peak in the spring and moderate flows during the summer, decreasing into the fall (Figure 5.2). Finally, wastewater returns are much more uniform throughout the year. Spatially, the North Bay is dominated by the Delta flows, while the South Bay is influenced by a mix of local freshwater flows, wastewater returns and even Delta flows in the late Spring and early Summer months.

⁷ <http://www.water.ca.gov/dayflow/>

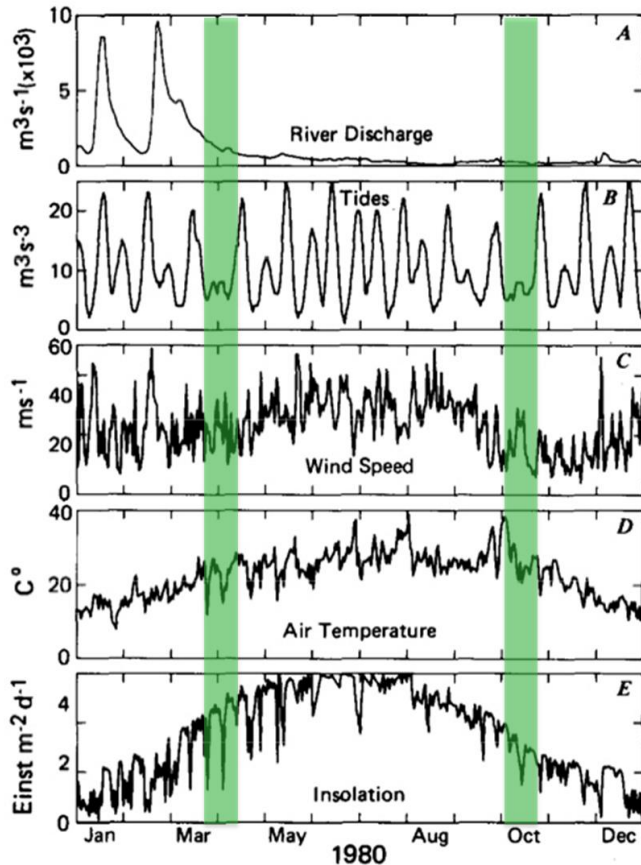


Figure 5.2 Physical drivers in San Francisco Bay. The green vertical bars illustrate the periods of minimum tidal mixing energy. In March/April, freshwater inputs and relatively low mixing energy allow the water column to stratify for ~10-14 days. In September/October, lower freshwater inputs limit the potential for salinity stratification. However, since winds are typically calm during this period, if sufficient insolation occurs (requires clear skies), surface layers will warm and the water column can be thermally stratified. Source: Cloern and Nichols, 1985

5.3.4 Coastal ocean exchange

In addition to providing tidal forcing, the oceanic boundary is also the source of salt water for the Bay. The interplay of freshwater flows and the tides leads to the intrusion of salt into the Bay, with the extent of salt intrusion, which is frequently characterized by $X2^8$ in the North Bay, being highly seasonally variable. Briefly, during high flow periods, the salt field is compressed down-estuary (Figure

5.3); when the flows relax, the salt field disperses back up-estuary. There is an asymmetry in the process for down-estuary and up-estuary movement of the salt field that is important to characterize. The down-estuary movement is advective and relatively rapid, whereas the up-estuary movement is primarily dispersive and more gradual. In South Bay, the seasonal variation of salinity is more complex: during winter, runoff events reduce the salinity locally, but it is not until late spring or early summer that the effects of Delta flows are felt south of the Bay Bridge. During winter and spring, it is possible for South Bay to have low salinities at both ends: reduced salinity in both Central Bay due to Delta flows and Lower South Bay and southern South Bay due to local flows. Finally, in the late summer and fall, evaporation in Lower South Bay can lead to hypersaline conditions and a reversed estuarine density gradient.

5.4 Estuarine circulation, flushing and residence times

The flushing (or, inversely, the residence time; see Monsen et al. 2002 for detailed discussion) of an estuary, or an embayment within an estuary, is driven by a combination of factors, including tidal forcing, density-driven circulation and, potentially, wind forcing. The combination of these influences define the “estuarine circulation”. Typical estuarine circulation has up-estuary flow in the subsurface waters due to denser saltier waters moving underneath freshwater. Less-dense

⁸ $X2$ is the distance in kilometers measured from the Golden Gate to the position along the North Bay’s axis where near-bottom salinity equals 2 psu. The position of $X2$ is strongly related to flow from the Delta, with a time lag.

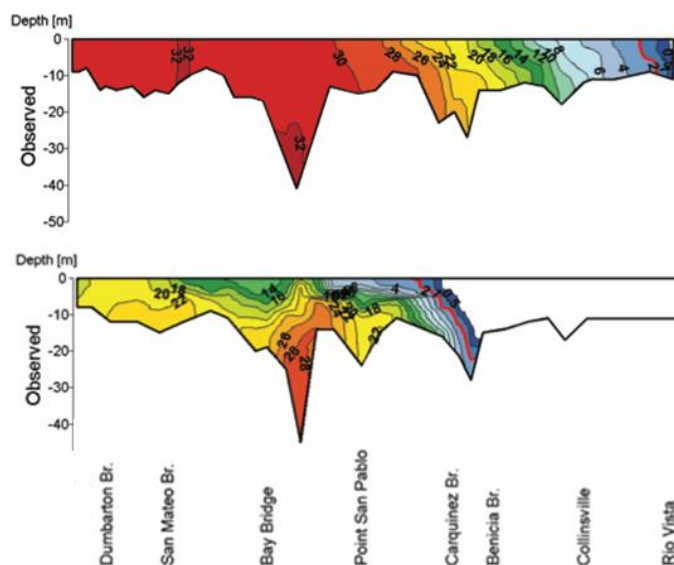


Figure 5.3 Observed salinity along main channel surveys of SFB. Top panel: Low flow period, October 26 1994. Bottom Panel: High flow period, January 18 1995. Source: Gross et al., 2009

freshier waters move down-estuary along the surface. These up-estuary salty and down-estuary exchanges occur along the axis of an estuary as well as laterally between deeper and shallower water regions. This circulation is defined both by direct forcing by the density gradient (gravitational circulation; Hansen and Rattray, 1965; Officer and Kester, 1991) and asymmetries in the tidal flows (Stacey et al., 2001; Stacey et al., 2008). The influence of wind is less established, and is likely to depend on the specific details of an estuary's geometry and a particular wind event. Supplementing the estuarine circulation, tidal dispersion processes, including tidal pumping (Fischer et al., 1979), tidal trapping (Okubo, 1973; MacVean et al., 2011) and shear dispersion (Fischer et al., 1979) will create exchanges between regions of an estuary. In many cases, these tidal processes will overwhelm the estuarine circulation and dominate flushing (Fram et al., 2007; Stacey et al., 2001; Monismith et al., 2002).

At the transition between embayments, or between the ocean and the estuary, the interplay of the tides, density-driven exchange and the topography determines the exchange. In one limiting case, pure density-driven (or gravitational) exchange determines transport between basins. In this hydraulic limit, there is no mixing in the strait and the waters of the two adjoining basins exchange under the influence of their density difference. The maximum exchange has been analyzed by Farmer and Armi (1986), and is set by the geometry of the strait and the density difference. The other limiting case is pure diffusive exchange, which results from tidal forcing interacting with the topography (see Hogg et al., 2001 for detailed discussion). The distinction between these two cases is important to the net transport: In hydraulic exchange, waters from each embayment are transported into the other in distinct layers; in diffusive exchange, net transport is directed down gradient.

At the mouth of San Francisco Bay, evidence suggests that tidal (diffusive) processes dominate the exchange, with density-driven circulation providing only about 10-15% of the total exchange (Fram et al. 2007). The implication is that the magnitude of flushing will primarily vary with the strength of the tides, which vary on the spring-neap and seasonal cycle. The Fram et al. estimate that approximately 80% of the exchange at the Bay's mouth is tidal is based on data spanning a spring-neap cycle, so spring-neap variability is aggregated in this estimate. Seasonal variability

of this result, however, is expected, with minima occurring during the spring and fall (just after the equinoxes) and maxima in the summer and winter (around the solstices). This variability was evident in the Fram et al. (2007) results, with fall dispersion coefficients reduced by about 45% relative to summer conditions. The dispersive nature of this exchange means that flushing is driven by the interaction of the tidal motions with the ocean-estuary gradient of the quantity being analyzed. In fact, the bi-directional nature of dispersive exchange means that net fluxes of individual species may be completely different from aggregate fluxes or exchanges, if their gradients are reversed (Martin et al., 2007). Similar results are to be expected at other narrow straits connecting embayments throughout San Francisco Bay.

Within individual subembayments, the residence time of subhabitats will be determined by the flushing and exchange flows along the perimeter of the subhabitat. An important distinction in much of San Francisco Bay is separating the deep channels from the broad shoals that characterize much of the Bay. In the channel, tidal and freshwater flows dominate along-channel transport, but the shoals are more strongly influenced by the interplay of tides and winds. The residence time of the shoals will be determined by the net exchange between the shoal and the adjoining channel, which has been recently examined in South Bay in a series of papers (Collignon and Stacey, 2012; Collignon and Stacey, 2013). In this work, the authors found that shoal waters were exchanged into the channel late in each ebb tide, but the nature of the exchange was a strong function of the local density gradients. Frequently, at the end of ebb the shoals are more saline than the channel (due to differential advection of the salinity gradient during the ebb), so the shoal waters that are pulled towards the channel by the tides late in the ebb tend to plunge down the slope and intrude into the channel at an intermediate depth. Although the net exchange from this transport process is not yet determined, the fact that shoal waters enter the channel at variable depths is likely to have important implications for the ecosystem through the effects on productivity. Although reversed salinity gradients were not analyzed at this site, they could develop in the early summer (due to the influence of Delta flows in northern South bay) or in the fall (due to evaporation in the Far South Bay). If the salinity gradient were reversed, then the late ebb flow of shoal waters towards the channel would lead to a surface flow in the channel, due to the shoal waters, in this case, being less saline than the channel.

At a much smaller scale, and considering local effects, recent analyses have looked at flushing of small perimeter habitats around the edge of the estuary (Hsu and Stacey, 2013). Using a combination of numerical and observational analyses, the authors found that tidal exchanges dominate the flushing of small slough-marsh complexes, but the net exchange is likely to be strongly affected by wind forcing, which is currently being analyzed. In the absence of wind, the Hsu and Stacey (2013) found that approximately half of the waters in a small slough-marsh complex in South San Francisco Bay was exchanged each tidal cycle.

Finally, small-scale features can result from local retention or convergence. The presence and maintenance of convergent fronts can lead to locally high residence times in relatively small regions. Simplified analyses of convergences and mixing (which must be in balance for the front to be maintained) can define representative timescales for retention and exchange (O'Donnell 1993; Stacey et al., 2007). Examples of these convergences are frequently associated with the

channel-shoal transition (Collignon and Stacey, 2012) or other lateral density-driven flows (Lacy et al. 2003).

5.5 Stratification

As outlined in the introduction, the Bay is characterized by large-scale salinity gradients along the Bay axes (Figure 5.3). At a large scale, the North Bay gradient is the most prominent in the estuary, defined by a transition from fresh to oceanic conditions over the length of the Bay; the gradient in South Bay is more variable and tends to be weaker than its North Bay counterpart. Moving away from the primary axis of the estuary, in other parts of the Bay salinity gradients may be comparable to or stronger than those along the North Bay axis. Specifically, the gradient along North Bay is approximately 0.5 psu/km, but salinity gradients in perimeter habitats may be 10 times that (Ralson and Stacey, 2005a,b). The presence of a horizontal salinity gradient makes the estuary susceptible to vertical stratification due to the tendency of the horizontal gradient to relax, or “lay down”, into a vertical gradient. The interaction of horizontal salinity gradients and tidal forcing, which can both create and destroy vertical stratification, leads to dynamic density stratification with important implications for vertical mixing.

In the estuarine water column, velocity shear (or vertical mixing energy) and density stratification are in competition in defining the state of the turbulence. Sheared velocity profiles act to increase the turbulent energy (and mixing), while stable density stratification acts to reduce the same (Fischer et al. 1979; Turner, 1980). The competition between shear and stratification plays a critical role in determining whether phytoplankton blooms develop (see Section 7).

The potential for stratification to develop depends on both longitudinal and lateral salinity gradients, related to the concepts of the Richardson number and Strain Induced Periodic Stratification (SIPS), whose discussion is beyond the scope of this overview. The magnitudes of these salinity gradients vary seasonally (Figure 5.3).

More recent studies of San Francisco Bay stratification dynamics (as well as other estuaries) have demonstrated the importance of lateral dynamics. If there is a lateral density gradient, as develops at the channel-shoal transition, and a lateral velocity, then lateral straining can contribute to the vertical stratification in the same way as the longitudinal does in the SIPS equation above. Examples of lateral straining’s influence on stratification come from South Bay (Collignon and Stacey, 2012); Suisun Bay (Lacy et al. 2003) as well as other estuaries.

Taken together, we expect an estuarine water column to stratify and destratify on a wide range of timescales that represent the variation of the density and tidal forcing as captured in the Simpson number. At seasonal timescales, the strength of the longitudinal density gradient varies; but just as importantly, its position changes so that the strongest density gradients may move between deep and shallow portions of the Bay (e.g., between Suisun Bay and Carquinez Strait, e.g.). As the density gradient strengthens, or moves into deeper regions, its effectiveness at creating stratification is increased and a stratified water column becomes more likely. Variations in tidal energy at the seasonal and spring-neap timescales can cause density stratification to adjust, and the strongest salinity stratification should occur during neap tides when the salinity gradient is compressed (following large freshwater flow events, e.g.). The ability of stratification to persist varies on multiple time scales due to changes in the vertical mixing energy of the tides with the spring-neap cycle: during neap tides, stratification is more persistent, but becomes periodic

during the springs (Stacey et al., 2001). The straining effects of the tidal flows lead to stratification that strengthens and weakens within the tidal cycle.

Beyond the spring-neap cycle, SFB experiences two annual minima periods in tidal energy (March/April, September/October). The green vertical bars in Figure 5.2 illustrate the periods of minimum tidal mixing energy. In March/April, freshwater inputs and relatively low mixing energy allow the water column to stratify for ~10-14 days. In September/October, lower freshwater inputs limit the potential for salinity stratification. However, it is also possible to have density stratification induced by temperature variations, although temperature induced stratification is not as commonly analyzed in estuaries (because of the dominance of salinity stratification) as in lakes or the deep ocean where it is an important factor. There are times, however, when temperature stratification may be an important factor for estuarine mixing: they result from a confluence of events involving warm, sunny days, neap (low energy) tides and low wind energy. Throughout much of the year in San Francisco Bay, this combination is unlikely, except perhaps during the fall, when the diurnal sea breeze is reduced, fog is less present, and tidal energy is at its annual minimum (Figure 5.2).

5.6 Suspended Sediment

The common paradigm for San Francisco Bay is that it is quite turbid due to high suspended sediment concentrations, or suspended particulate matter (SPM). Recent analyses (Schoellhamer 2011) have indicated that the Bay may be clearing, with Bay-wide SPM decreases of ~35% since 1998 (Figure 5.4.A), and up to 50% since 1975 in Suisun Bay (Figure 5.5). Within the Bay itself, the dynamics of the inorganic fraction of turbidity, suspended sediment concentration, is governed by its upstream supply, resuspension and deposition in the Bay, and transport throughout the Bay. The explanation for the decreased concentrations is that both external loads of suspended sediment and resuspension of material from the bed have decreased (because of a depleted erodible sediment pool; see Figure 5.4.B).

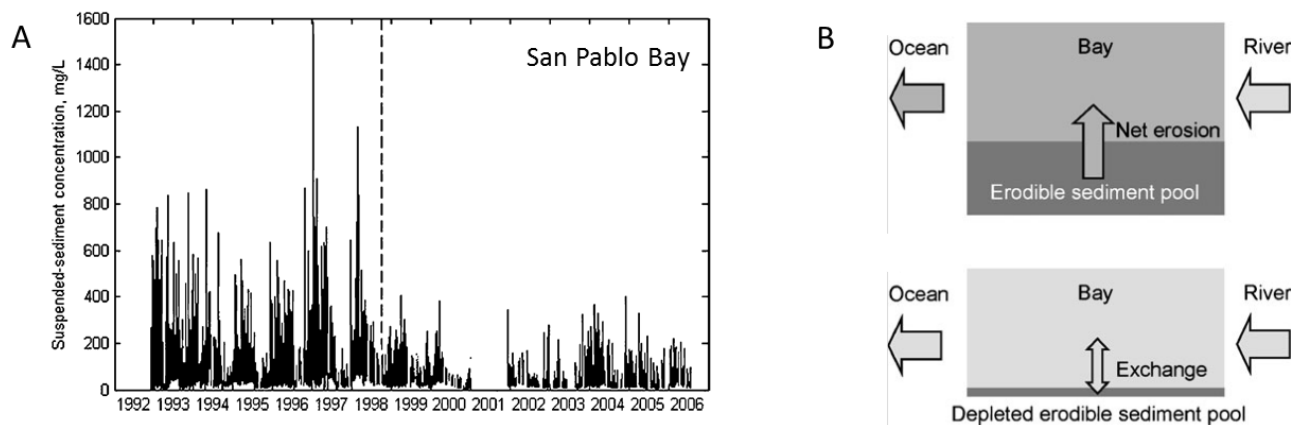


Figure 5.4 A. Time series of suspended particulate matter concentrations in San Pablo Bay measured by a continuous monitoring. **B.** Conceptualization of cause of declining sediment concentrations. Sediment inputs to SFB have declined substantially in recent years. Due to the lack of replenishment, the erodible sediment pool in the bed has been gradually depleted. As a result, less material is resuspended, resulting in lower concentrations.

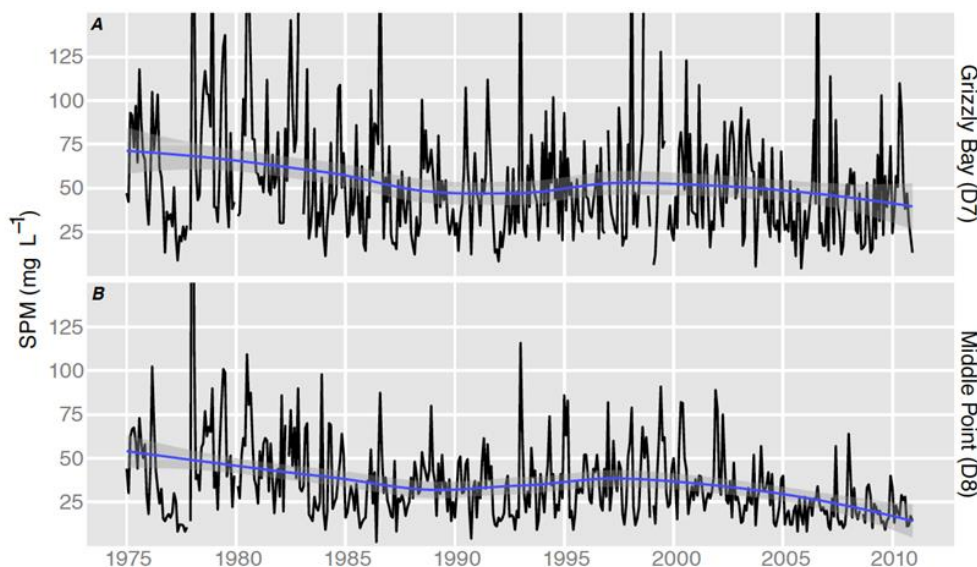


Figure 5.5 Suspended sediment concentrations in Suisun Bay: shallow Grizzly Bay (top) and in the channel (bottom). Source: Cloern and Jassby 2012

The circulation that governs sediment transport is largely the same as what governs salinity, flushing times and even stratification. The effects of supply have been considered elsewhere (Schoellhamer 2011), and we will focus here on resuspension and deposition and vertical transport. For sediment to be resuspended from the bed, the flow-induced bed stress, i.e., the frictional force at the sediment:water interface, must exceed a critical threshold (Sanford 2008; Wiberg et al. 1994). The magnitude of the critical stress will vary with the type of sediment and the degree of consolidation of the bed (Sanford 2008; Wiberg et al. 1994). Newly deposited sediments are more readily resuspended; after some time (approximately 3 days, Wiberg et al. 1994), the bed consolidates considerably and becomes more resistant to resuspension.

Both wind waves and tidal flows create stresses at the estuary bed that can act to resuspend sediments. In the deep channels, the effects of wind waves do not extend to the bed (Kundu et al. 2011), so only tidal forcing needs to be considered when analyzing resuspension. Although the tides are nearly symmetric, because of the threshold nature of sediment resuspension, even subtle asymmetries could have large impacts on the timing of sediment resuspension and net transport. The superposition of density forcing (flow in at the bed, out at the surface) with tidal flows adds to the bed stress on flood tides and reduces it on ebbs. If this asymmetry crosses the resuspension threshold, then sediment concentrations may be higher on floods than ebbs, leading to a net upstream transport of sediment. This effect is counteracted by large freshwater flow events, which add to the bed stress on ebbs and reduce it on floods. The net effect is expected to be a downstream push of sediments due to large freshwater flows events followed by tidally-driven up-estuary sediment transport once the flows reduce (Ralston and Geyer, 2009).

In the shallows, windwaves are able to reach the bed and create large oscillatory bed stresses that can resuspend sediments. The resuspended sediment from windwaves is largely contained in the wave boundary layer, which may only be a few centimeters thick, but if tidal flows coincide with this resuspension, then they can mix sediments further up into the water column. This combination of factors was found to be important to the sediment dynamics on South Bay shoals by Brand et al. (2010), who found that the highest sediment fluxes into the water column occurred on flood tides that followed wavy low water periods. The explanation was that wind

waves were able to resuspend sediments into the wave boundary layer, and then the following flood tide mixed the sediments into the water column. The importance of windwaves to resuspension mean that summer months, characterized by strong diurnal sea breezes, are likely to have the highest sediment concentrations in the shallows, even though the watershed supply is at its lowest during that period.

In the water column, settling and turbulent mixing define the evolution of the suspended sediment concentration profile. The settling velocity for the sediment depends on the particle size and density, which may be poorly defined for fine particles that form flocs. For large, dense particles, or during low energy periods, the suspended sediment is largely constrained to the near-bed region; for smaller particles, or less dense flocs, or during high energy periods, the suspended sediment is more widely distributed throughout the water column.

Figure 5.6 presents monthly-average SPM concentrations in SFB's five main subembayments. The suspended sediment concentrations in the waters of San Francisco Bay will vary tidally and diurnally (or in response to wind events), will vary between subembayments due to supply (Figure 5.6), and will vary within embayments due to spatially variable resuspension in response to the local depth. Seasonally, supply has a strong variation, with more turbid waters being brought into the Bay with winter rains, but the shoals may actually be more turbid during summer months due to resuspension of sediments from the bed.

5.7 Summary

This review is not meant as a comprehensive description of the hydrodynamics of San Francisco Bay, but is instead focused on the basics of flushing, stratification and suspended sediment. The key factors driving all three of these processes are tidal, wind and freshwater forcing. The variability of those factors, and their interactions, define the dynamics of the processes. Looking ahead several decades, the prospects for change in the Bay are extensive. Climate change and variability will bring with it warmer air temperatures and more frequent heat waves, creating the risk of more anomalous temperature stratification events. Precipitation may shift towards rain from snow, altering the timing of freshwater flows entering the Bay and the associated response in the salt field. Sea level rise will alter the tidal dynamics of the Bay, perhaps increasing the dissipation of energy due to extra inundation, or decreasing it if the Bay is made deeper (i.e. sediment accumulation does not keep pace with sea level rise). The changes the Bay faces are not limited to climate forcing, however, and anthropogenic changes may be just as pronounced. Along the Bay's shorelines, marsh restoration will alter the tidal dynamics by increasing tidal dissipation locally and, for large restoration projections, could potentially alter the tidal dynamics more broadly. The management of California's water resources through reservoir operations alters the timing and amount of freshwater flows that enter the Bay, perhaps in a more profound way than a shift in the type of precipitation would. Finally, land use practices, as well as the operation of reservoirs, alter the sediment supply that watersheds provide to the Bay. While these scenarios are all plausible, the potential magnitudes of their effects on nutrient cycling and ecosystem response remain highly uncertain.

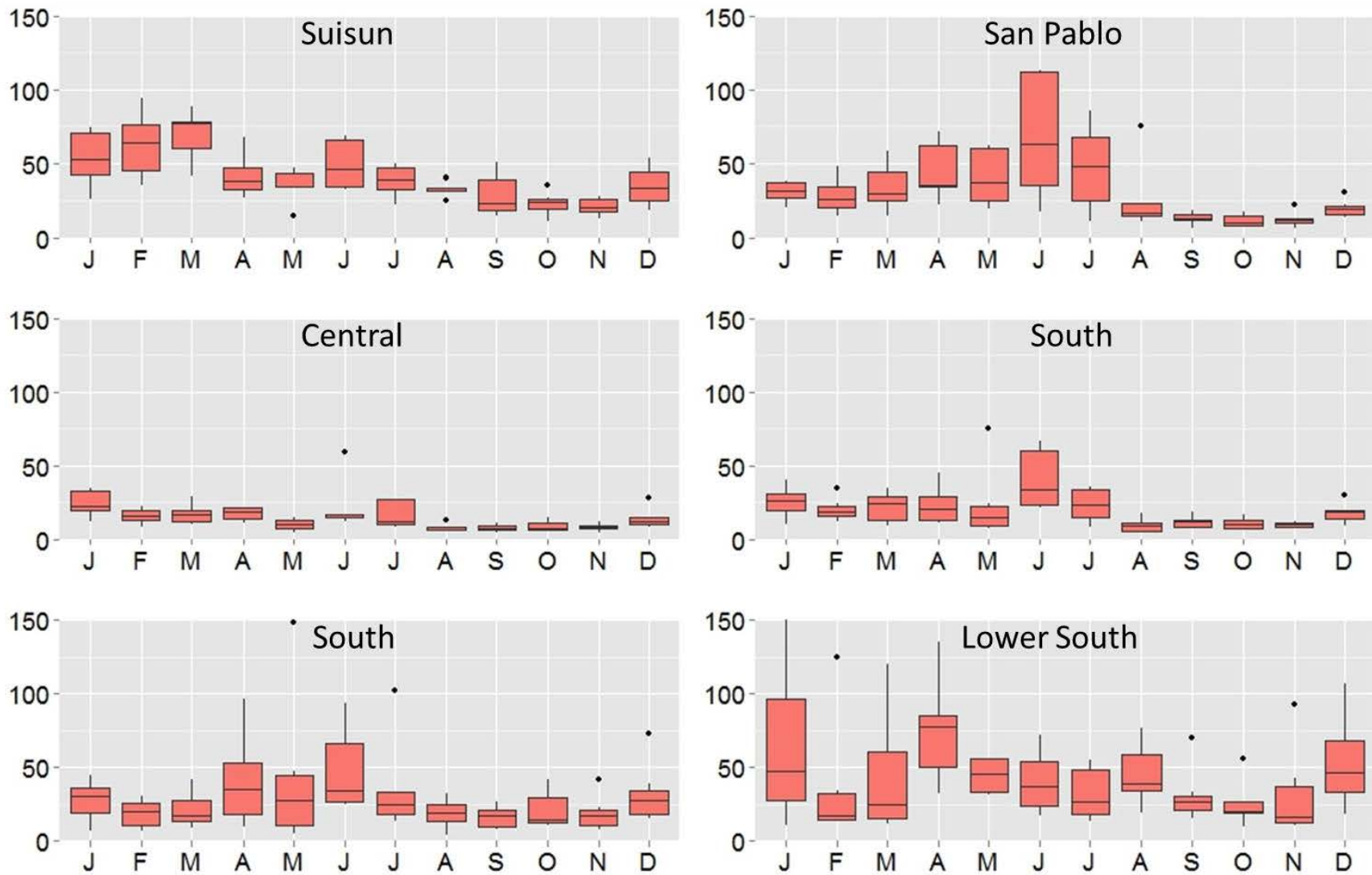


Figure 5.6 Monthly average SPM (mg/L) – 2006-2011. Data from USGS stations s6 (Suisun), s15 (San Pablo), s18 (Central), s21 (northern South Bay), s27 (southern South Bay) and s36 (Lower South) were used. Data source: <http://sfbay.wr.usgs.gov/access/wqdata/>

6 Nutrients

6.1 Introduction

The nutrient module focuses on the macro-nutrients N, P, and Si, with a greater emphasis on N and P because their loads and concentrations have been the most altered by anthropogenic activities. N, P, and Si are essential for primary production in all aquatic environments, including SFB. Cellular requirements for N, P, and Si differ among phytoplankton species, as do uptake rates. In addition, some species show a relative preference for certain forms of N. These requirements and preferences, along with the relative nutrient abundances, can influence the growth rate of phytoplankton and the magnitude (concentration) of phytoplankton blooms (Section 7). They may also influence the types of phytoplankton species that prosper under different conditions and influence the seasonal succession of the overall phytoplankton assemblage (Section 9).

The observed nutrient concentration at any given point in space and time in SFB represents a balance of multiple processes, including: input, export, mixing (vertical, lateral, longitudinal), uptake by phytoplankton, transformations, and losses. The discussion below covers the major processes that regulate nutrient cycling, with a focus on those that are important enough in SFB to be considered within a management-driven discussion, and only minimally treats some topics.

6.2 N, P, and Si cycling

6.2.1 N cycling

Nitrogen exists in several forms in aquatic systems and undergoes numerous biologically-mediated transformations between these forms (Figure 6.1). The major dissolved inorganic forms of N are the ions nitrate (NO_3^-), ammonium (NH_4^+), and nitrite (NO_2^-). Dissolved and particulate organic nitrogen (DON and PON) can comprise important fractions of N in some aquatic systems, and tend to represent lower portions of total N in systems that receive large nutrient anthropogenic inputs. Dissolved gaseous forms of N include di-nitrogen (N_2) and nitrous oxide (N_2O). N_2 is both an end-product of denitrification (discussed below) and a potential N source for a limited set of phytoplankton that perform nitrogen fixation, an energy-intensive process through which they convert N_2 into an usable organic form. Both NO_2^- and N_2O are important intermediaries in some N reactions, but typically present only at relatively low concentrations in estuarine water columns. The “bio-accessible” forms of N include NO_3^- , NH_4^+ , NO_2^- , DON, PON, and N_2O . The remainder of the N cycling description focuses primarily on NO_3^- and NH_4^+ , since they are the dominant bioaccessible N forms.

Figure 6.1 illustrates the major processes that will influence the forms and concentrations of N in SFB. Nitrogen inputs include: point-sources, primarily POTWs; large river inputs via the Sacramento-San Joaquin Delta; other freshwater inputs at the Bay margins (smaller perennial streams, along with stormwater inputs and ephemeral wet season streams); and other sources that are less readily quantified but expected to be relatively small (e.g., direct atmospheric deposition, groundwater). N is supplied to subembayments primarily in the form of NO_3^- , NH_4^+ , DON, and PON, and the relative proportions will vary by source. Atmospheric N deposition to the

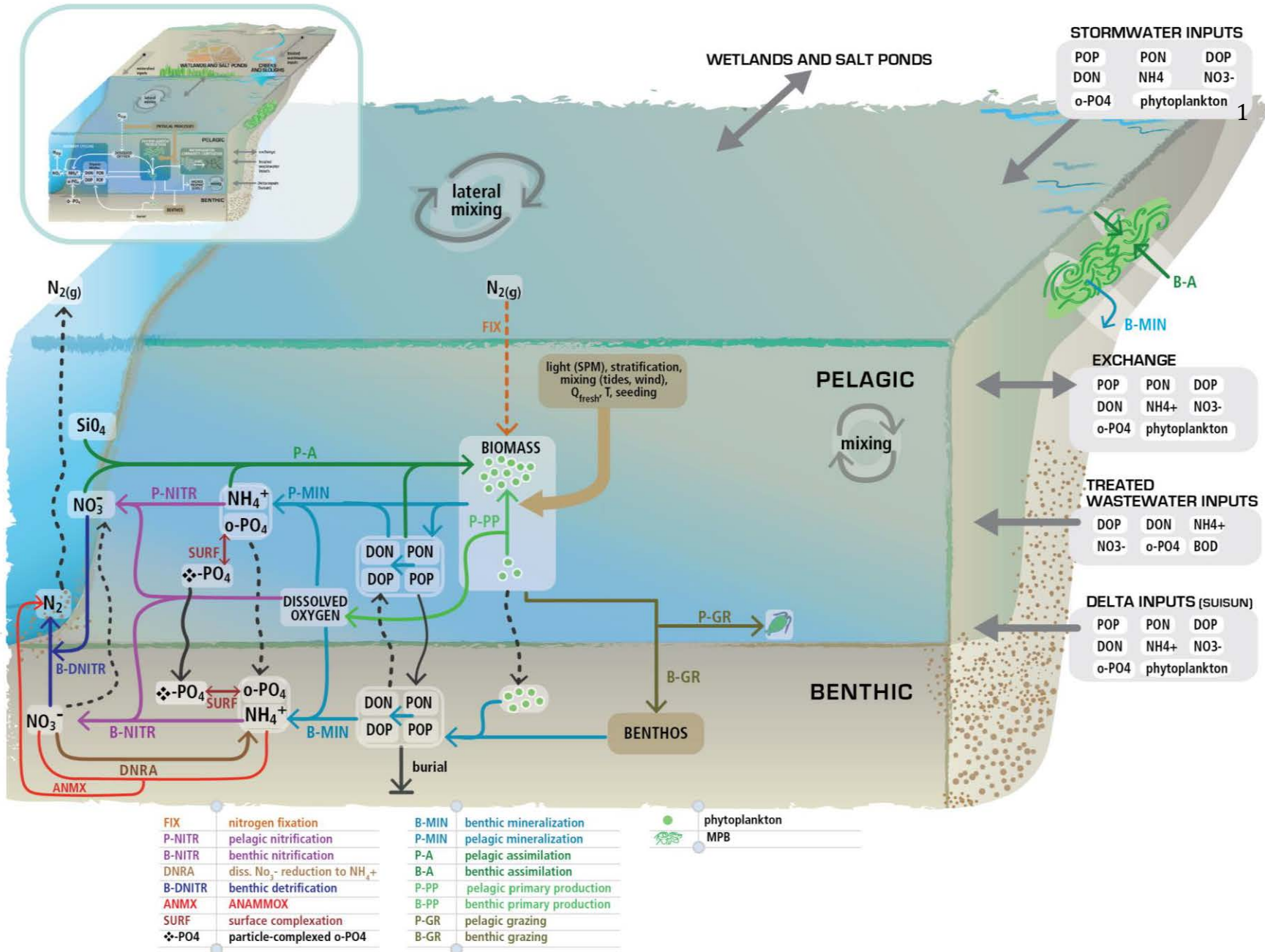


Figure 6.1 Nutrient cycling conceptual model

watersheds that drain to SFB could be an important N source; in this description, we include that source within inputs from the Delta and in freshwater inputs draining catchments that ring the Bay (N that deposited on land and was washed into rivers or streams). While N fixation can be an important source of N to some aquatic systems, it is unlikely to be an important internal source to SFB under current conditions because anthropogenic sources are so large. However, increased nitrogen fixation is a possible ecosystem-level response to nitrogen limitation should fixed N inputs from other sources decrease substantially without concomitant P decreases. Exchange with the Pacific Ocean at the Golden Gate can be either a net source or sink of N depending on coastal processes (i.e., upwelling or non-upwelling time period). Limited analysis to date suggests that SFB should be a net exporter of N throughout most of the year, except during some major upwelling events (Largier and Stacey, 2014). Hydrodynamic processes (tidal, gravitational, advective) transport N between subembayments.

Nitrogen transformations take place within the oxic water column, within the (typically) anoxic sediments, and within the narrow - but geochemically important - transition zone at the sediment:water interface. NH_4^+ and NO_3^- (and some forms of DON) can be readily taken up and assimilated into biomass by primary producers. When dead phytoplankton undergo degradation or mineralization by microbes, a portion of organic N is regenerated as NH_4^+ . Some of the regenerated NH_4^+ ammonium released is oxidized to nitrate either in the water column or at the sediment:water interface via the process of nitrification. Nitrification requires oxygen, but can proceed in environments where oxygen concentrations are low, including at the sediment-water interface. Denitrification is a form of respiration used by some heterotrophic microbes. In denitrification, NO_3^- is used instead of oxygen to oxidize organic matter, producing N_2 and carbon dioxide. Denitrification requires organic matter to proceed, and its rate can be limited by the amount and quality of organic matter, but only proceeds in anoxic environments, primarily within sediments, or biofilms, after NO_3^- diffuses from the water column into anoxic zones. Because denitrification converts NO_3^- to N_2 , it results in a true loss of N from the system. NO_3^- can also be transformed directly to NH_4^+ through a respiratory pathway used by some microbes called dissimilatory nitrate reduction to ammonium (DNRA). N can also be converted to N_2 through a microbially-mediated process called anaerobic ammonium oxidation (ANAMMOX) by which NH_4^+ and NO_2^- are converted to N_2 (Brunner et al., 2013).⁹ The coupled process of ammonium oxidation-denitrification at the sediment:water interface can be responsible for a substantial portion of the denitrification in some estuarine systems (ref). While denitrification is generally thought to be a more important pathway for NO_3^- reduction than DNRA, ANAMMOX could rival denitrification under some conditions (Kuypers et al. 2005), and does not require a labile organic matter source. A portion of the organic nitrogen produced in the Bay accumulates in the sediments where it undergoes gradual decomposition and release of NH_4^+ . N burial can take place anywhere in SFB, but burial is more likely in locations where there is net accumulation of sediments. Newly restored tidal salt marshes could be particularly important zones for denitrification because of the anoxic conditions and abundant organic matter in marsh sediments. Some of the buried PON continues to decompose, releasing ammonium into the sediment pore water, which either eventually diffuses back to the water column, or undergoes nitrification-denitrification as described above. PON is also subject to resuspension, especially

⁹ The actual expression is: $1\text{NH}_4^+ + 1.3\text{NO}_2^- \rightarrow 1\text{N}_2 + 0.3\text{NO}_3^- + 2\text{H}_2\text{O}$

in shoal environments. The fraction of sediment PON that is neither regenerated as NH_4^+ nor resuspended of the PON is buried permanently.

Nitrification, denitrification, and possibly ANAMMOX are likely to be quantitatively important processes that influence N form and fate at subembayment scales and at the full Bay scale. However, there are currently few direct measurements of these rates. Quantifying these processes and their influence on N fate will be one key component for determining the N loads that SFB subembayments can assimilate without adverse impacts. The importance of nitrification in SFB is evident, given that in some subembayments (e.g., South Bay) N is loaded as primarily NH_4^+ but is measured in the water column as primarily NO_3^- . Denitrification likely represents a substantial loss route for bioavailable N within SFB. However the magnitudes and importance of nitrification and denitrification relative to other processes (uptake by phytoplankton or microphytobenthos, transport out of the system) are currently poorly known. As a first step, the importance of denitrification and nitrification could be estimated through relatively straightforward biogeochemical modeling. At some point field studies will likely be needed to provide better rate estimates and factors that influence rates over space and time (e.g., Cornwell et al. 2013).

6.2.2 P cycling

The P cycle is also depicted in Figure 6.1. P cycling is relatively straightforward compared to N, since P only commonly occurs in two dissolved forms and does not undergo numerous transformations. P occurs as dissolved orthophosphate (o-PO_4), particle-complexed o-PO_4 , other solid mineral phases of P, and dissolved and particulate organic P (DOP and POP). o-PO_4 would generally be expected to comprise most of dissolved P in the water column. However, particle- or colloiddally-complexed P, either organic or inorganic, can also be important in the water column. o-PO_4 binds to the surfaces of iron(III)-oxide particles in both the sediments and water column. When complexed by iron(III)-oxides, o-PO_4 is essentially unavailable for uptake by primary producers; however, iron(III)-oxide particles are readily dissolved in anoxic sediments (discussed below), making this form of particle-bound o-PO_4 a temporary state. Other particulate mineral phases of P also occur, but they tend to be relatively refractory.

External P sources to SFB subembayments include: inputs from point sources, primarily POTWs; riverine inputs via the Sacramento-San Joaquin Delta of naturally-derived P (from dissolution of P-rich mineral phases) or anthropogenically-sourced P (fertilizer, livestock excrement, treated wastewater); other freshwater inputs at the Bay margins - perennial streams or rivers, stormwater inputs, and ephemeral wet-season streams; and other sources that are less readily quantified but believed to be relatively unimportant (ground water, atmospheric deposition, etc.). P has no analogous process to N-fixation. Similar to N, exchange with the Pacific Ocean at the Golden Gate can be either a net source or sink of P depending on coastal processes (i.e., upwelling or non-upwelling time period) and conditions within SFB. In addition, hydrodynamic exchange processes (tidal, gravitational, advective) transport P between subembayments.

P form and abundance are influenced by uptake and assimilation, surface reactions with particles, settling, and microbial mineralization and recycling. Within the water column, o-PO_4 can be readily taken up and assimilated by phytoplankton. During pelagic grazing on phytoplankton (by zooplankton) or mineralization of dead phytoplankton in the water column or

sediments, DOP and POP are released, a portion of which is converted to o-PO₄. Particle-complexed o-PO₄ and POP settle in the water column and eventually reach the bed sediments. Respiration using iron(III) is an important anaerobic reaction in sediments, which dissolves iron(III)-oxides and releases dissolved o-PO₄ to porewater, where it can then be transported to the water column, or undergo transformations (re-binding to particles, uptake by benthic algae or microbes). Transport back to the water column can occur slowly by diffusion, or, much more rapidly, due to burrowing by benthic organisms ('bioirrigation') or during sediment resuspension that also mixes porewater into the water column. Similar to N, burial of particulate P can take place anywhere in the bay, but is more likely in locations where there is net accumulation of sediments, like wetlands. Some of the o-PO₄ produced in sediments returns to the water column and re-enters the cycle of organic matter production and degradation.

6.2.3 Si cycling

Si cycling is also relatively straightforward compared to N cycling, since Si does not occur in multiple dissolved inorganic forms or undergo numerous transformations. However, unlike both N and P, the vast majority of Si comes from natural sources through the weathering of silicate-rich rock, and does not have major anthropogenic sources. Major sources include riverine inputs of naturally-derived Si via the Sacramento-San Joaquin Delta, and other freshwater inputs at the Bay margins. Exchange with the Pacific Ocean at the Golden Gate is a net sink for Si. Hydrodynamic exchange processes can result in net Si exchange between subembayments, although on average down-estuary exchange will be a net Si sink, since its primary source is freshwater inputs.

Si is supplied to subembayments primarily as dissolved silicate (SiO₄), solid mineral phase silicates, and reactive or refractory biogenic silicates. In the absence of biological uptake and assimilation, Si should behave conservatively in SFB, with no quantitatively important geochemical transformations other than those related to uptake/assimilation by organisms reliant on Si for growth. Although N and P requirements (C:N:P) can vary substantially among phytoplankton classes, all phytoplankton require N and P for growth. Si is distinct from N and P in this respect: among the major classes of phytoplankton, only diatoms require SiO₄ in substantial amounts. Only the growth of diatoms will influence silicate concentrations via assimilation.

The recycling of Si is slow relative to P and N. Si taken up and assimilated by diatoms is less readily regenerated during grazing or microbial degradation of cells. Instead, the silicate-rich frustules settle and accumulate as biogenic Si in the sediments, which tends to be more slowly mineralized than organic N and P. As such, compared to N and P, a larger proportion of biogenic Si that reaches the sediments is ultimately buried.

6.3 Estimated N and P Loads to SFB

Figure 6.2 presents an overview of DIN and DIP loads to SFB, broken into its five main subembayments. A separate report on N and P nutrient loads discusses loads, data gaps, and uncertainties in more detail (SFEI, 2014a). Groundwater and direct atmospheric deposition (i.e., directly to the Bay's surface) loads are expected to be small and are not discussed here. Discharge of treated wastewater effluent by publicly owned treatment works (POTWs) to SFB's subembayments is a major source of N and P. The San Francisco Bay Area has 42 POTWs (Figure 2.2.B) that service the regions 7.2 million people and discharge either directly to the Bay

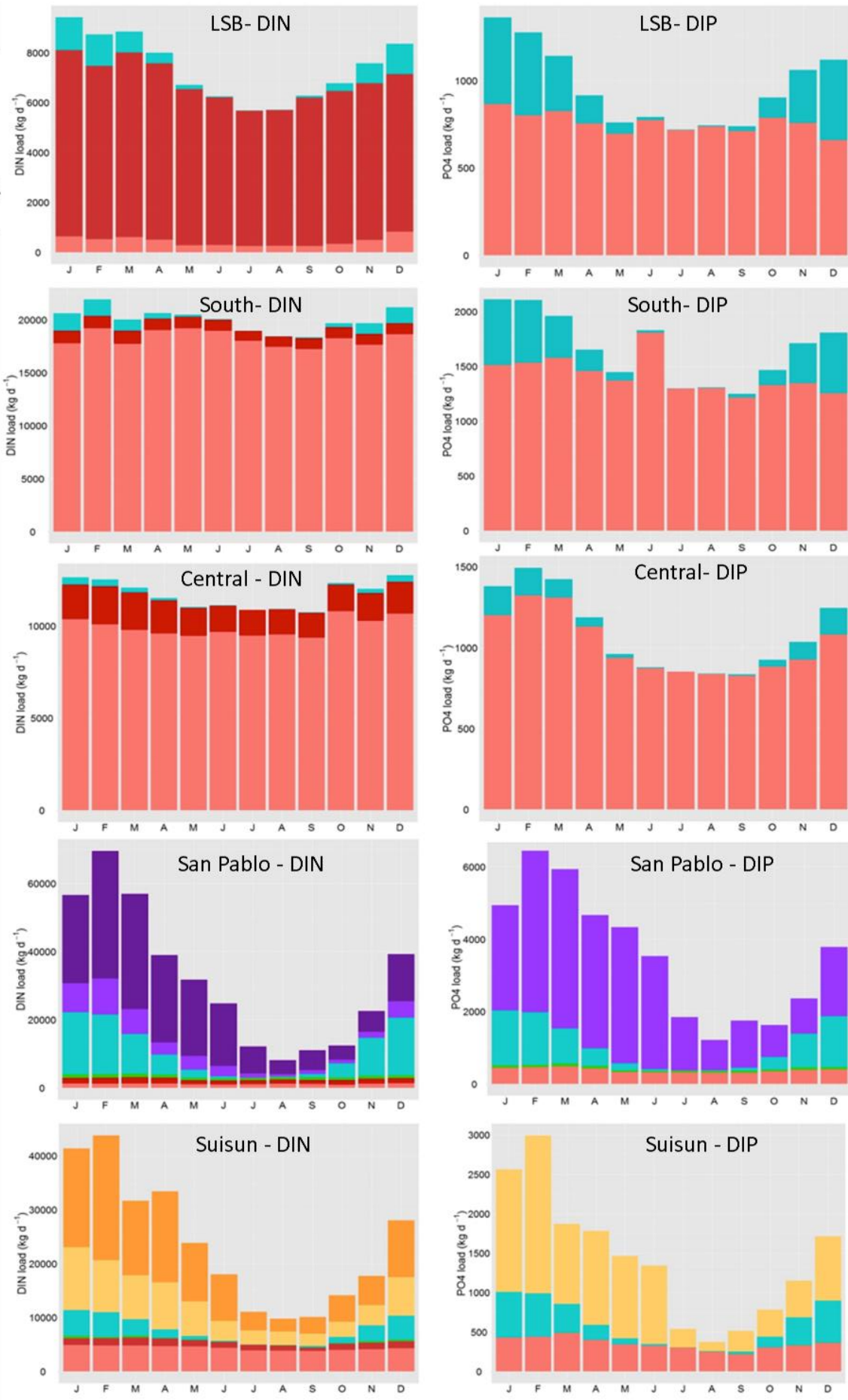
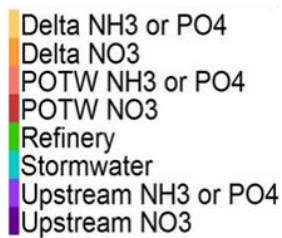


Figure 6.2 N and P loads to SFB subbays. In the cases of LSB, South Bay, and Central Bay, only direct loads to the subbays were considered and not exchange between subbays. Loads to San Pablo Bay include estimates of up-estuary loads from Suisun Bay. See SFEI 2014a for more

or to receiving waters in adjacent watersheds that drain to the Bay (note: these numbers do not include discharges east of Suisun Bay that enter through the Delta). While several of these POTWs conduct nitrification or denitrification plus some forms of advanced treatment that remove a portion of nutrients prior to discharge, most POTWs discharging to SFB carry out only secondary treatment, which transforms nutrients from organic to inorganic forms, but generally does not remove much N or P. Table 6.1 summarizes typical N and P concentrations and forms in effluent subjected to varying degrees of nutrient removal. Bay-wide, POTWs discharged (annual average) 34000 kg d⁻¹ NH₄⁺, 12000 kg d⁻¹ NO₃⁻, and 4000 kg d⁻¹ total P. Results from detailed effluent monitoring that began in July 2012 suggests ~90% of total N discharged was in the form of DIN and ~80% of total P discharged was in the form of o-PO₄ (SFEI, 2014a). Refineries also contribute N and P loads to Suisun Bay and San Pablo Bay, but their contributions appear to be relatively minor.

Table 6.1 Typical concentrations and forms of N and P in treated wastewater effluent at different treatment levels

Treatment type	NH ₄ (mg N L ⁻¹)	NO ₃ (mg N L ⁻¹)	TN (mg N L ⁻¹)	TP (mg P L ⁻¹)
Level 1: Secondary treatment	20-30	<1	25-35	4-6
Nitrification	<1	20-25	20-30	4-6
Level 2: Nitrification + biological nutrient removal	<1	8-12	10-15	0.5-1
Level 3: Nitrification + Advanced TN/TP removal	<1	3-6	4-8	0.1-0.3
Level 4: “Limit of Technology” not including Reverse Osmosis	<1	<1	<3	<0.1
Reverse Osmosis	<1	<1	<2	<0.02

¹Based on Falk, M.W., Neethling, J.B., Reardon, D.J. (2011). Striking the Balance Between Nutrient Removal in Wastewater Treatment and Sustainability, WERF research project NUTR1R06n and BACWA 2011 report

The dominant sources of N and P loads, and the form of N, vary substantially among subembayments (Figure 6.2). In LSB, South Bay, and Central Bay, POTWs are the dominant source of N and P. In LSB, NO₃⁻ is the dominant N form discharged because LSB POTWs carry out nitrification. In South Bay and Central Bay, NH₄⁺ is the dominant N form released by POTWs. In San Pablo Bay, direct POTW loads are relatively minor and primary release NH₄⁺. In Suisun Bay, NH₄⁺ is the primary form of N discharged, and the importance of those direct loads relative to other inputs varies seasonally (discussed more below).

Stormwater flows deliver seasonally-varying N and P loads to SFB. Only rough estimates of those loads have been made thus far due to data and modeling limitations. In most subembayments during most of the year, these estimates suggest that stormwater DIN and o-PO₄ loads are substantially less than POTW loads (Figure 6.2), with potential exceptions being loads

to San Pablo Bay and Suisun Bay. In this region, rain generally occurs only in the months of October-April; N and P loads from runoff are highest during this period and generally minor during the dry season, at least when considered at the subembayment scale. The relative uncertainty in the magnitude of stormwater-derived N and P loads is high. Furthermore, it is likely that the stormwater load estimates made thus far poorly represent those from perennial rivers and streams (other than the Delta). While more work is needed if more accurate stormwater N and P loads are a priority, it seems unlikely that these loads will rival POTW loads at the subcatchment scale in LSB, South Bay, and Central Bay. However, while stormwater loads may not play a dominant role at the subembayment scale in these subembayments, a more important role for stormwater-derived N and P loads in certain habitats (e.g., along the Bay's margins, including wetlands) cannot be ruled out.

N and P loads entering SFB from the Sacramento/San Joaquin Delta have the potential to be large and seasonally-dominant nutrient sources to Suisun and San Pablo Bays (Figure 6.3). Delta DIN loads far exceed those from Suisun direct POTWs for approximately half the year, and NO_3^- loads from the Delta exceed those from Suisun direct POTWs year-round. For NH_4^+ , however, direct POTW loads are comparable to or exceed Delta loads during late spring through fall. Most of the NH_4^+ entering Suisun Bay from the Delta likely comes from the Sacramento Regional County Sanitation District (Regional San) wastewater treatment plant, which currently does not nitrify and discharges ~70 km upstream of Suisun Bay. New permit requirements for Regional San require treatment upgrades over the next decade including nitrification and nitrogen removal, which will lead to both a shift in the N forms (predominantly NO_3^- instead of NH_4^+) and total N load (2-3 fold lower). Although the Delta load estimates to Suisun Bay are believed to be reasonable first approximations, they need to be further evaluated and refined using hydrodynamic and biogeochemical models for the Delta.

The load discussion thus far focused mostly on direct external loads to subembayments and not exchange between subembayments. Hydrodynamic exchange between subembayments may comprise a large proportion of loads to some subembayments. This is particularly true for San Pablo Bay, which has relatively low POTW direct loads but is down-estuary from Suisun Bay. The loads entering San Pablo Bay from Suisun Bay (which includes those that entered from the Delta) have thus far only been roughly estimated and need refinement through hydrodynamic/reactive-transport models. Nonetheless, the estimates illustrated in Figure 6.2 suggest that loads entering from Suisun could be the dominant source to San Pablo Bay for most of the year. Similarly, the southern reaches of South Bay are likely highly influenced by loads entering from LSB.

In general, SFB is a net source of nutrients to the coastal ocean throughout most of the year (Largier and Stacey, 2014). Exchange of water through the Golden Gate could conceivably act as a substantial net source of nutrients to the Bay during a limited time of the year and only under specific conditions. Freshly-upwelled coastal water contains up to $30 \mu\text{mol L}^{-1} \text{NO}_3^-$. However, the extent to which that NO_3^- -rich coastal water enters SFB depends on a complex set of hydrodynamic and climatological factors. Under maximal conditions, daily NO_3^- loads into the Bay through the GG could be substantial relative to POTW loads (Largier and Stacey, 2014), although the frequency with which the necessary hydrodynamic and climatological drivers align is unknown, and requires further investigation. The fate of the nutrient plume that leaves SFB,

and its potential impacts on biological response in coastal waters, has not received much attention to date and also warrants further investigation if coastal effects are among the issues being considered through the Nutrient Strategy.

6.4 Seasonal and spatial variation in N and P

There are large spatial and seasonal differences in nutrient forms and abundance in SFB (Figure 6.3-6.6). Yet the processes that determine the ambient forms and concentrations of N and P are the same throughout SFB. The observed seasonal and spatial differences because the importance or magnitude of those processes differ considerably within and between subembayments, as well as over a range of time scales (tidal, diurnal, seasonal), due to multiple physical factors, including morphology, freshwater inputs, proximity and magnitude of loads, and mixing (including due to tides).

The seasonal and spatial variations in NH_4^+ concentrations clearly illustrate how the time- and space-varying intensities of physical and biogeochemical processes influence nutrient form and abundance. The maximum NH_4^+ levels seen in Suisun Bay tend to be the highest concentrations observed throughout all of SFB; however Suisun NH_4^+ levels exhibit strong seasonal variability, with spring and summer concentrations being 20-30% of those observed in winter (Figure 6.3). Mass balance estimates suggest that, during spring and summer, ~75% of NH_4^+ that enters Suisun Bay is “lost”, presumably through either nitrification to NO_3^- or uptake by phytoplankton (SFEI, 2014b). This seasonality of Suisun NH_4^+ concentrations is likely due to warmer water temperatures and longer residence times in Suisun Bay and upstream of Suisun Bay in spring/summer, with the warmer temperatures favoring higher rates of nitrification, or NH_4^+ uptake by phytoplankton. Longer residence times during this time of year allow those reactions to proceed further, and longer days in May-Oct could also contribute to greater primary production and related uptake of NH_4^+ . NH_4^+ concentrations in LSB offer an interesting counter-example to Suisun Bay (Figure 6.3). A strong seasonality in NH_4^+ concentrations is also evident in LSB. Although LSB has one of the highest areal N loads of all SFB subembayments (Figure 3.1), the vast majority of N loaded directly to LSB is in the form of NO_3^- (Figure 6.3). Therefore, a sizable portion of the NH_4^+ observed in LSB is likely due to NH_4^+ regenerated from the sediments. Sediment sources of NH_4^+ may be more evident in LSB not necessarily because they are larger, but because of LSB’s morphology. LSB is quite shallow, and has a low ratio of water volume to sediment area compared to other subembayments; thus, any flux from LSB sediments would be mixed over a relatively small volume of water, causing a larger increase in concentration per unit mass of NH_4^+ . The local NH_4^+ concentration maximum in June-July is likely due in part to higher rates of mineralization of organic matter in the sediments due to higher water temperatures, and longer residence times during these months allowing the NH_4^+ to accumulate to higher levels. The NH_4^+ concentration minima in April and September coincide with periods of highest phytoplankton biomass (discussed in Section 7), and may be evidence of NH_4^+ uptake by phytoplankton.

NO_3^- concentrations also exhibit strong seasonal and spatial variability (Figure 6.4). LSB has the highest NO_3^- concentrations (40-80 $\mu\text{mol L}^{-1}$), due to several factors: all POTWs in LSB nitrify before discharging effluent; LSB’s volume is small relative to other subembayments and relative to the loads it receives; and there is limited net exchange of LSB water with the rest of the Bay, allowing NO_3^- to accumulate to higher concentrations. After LSB, NO_3^- concentrations are highest in Suisun Bay and South Bay. In Suisun Bay, the substantial NO_3^- loads entering from

the Delta likely contribute to these elevated NO_3^- concentrations. The lowest NO_3^- concentrations ($\sim 20 \mu\text{mol L}^{-1}$) are observed Central, San Pablo, and northern South Bay, all of which have greater exchange with coastal waters entering through the Golden Gate.

Nitrification and denitrification likely play quantitatively important roles in determining the observed forms of N and the seasonality in concentrations in SFB subembayments. For example, although the vast majority of N loaded to Central Bay and South Bay occurred in the form of NH_4^+ (Figure 6.2), ambient N was present primarily as NO_3^- (Figure 6.4), evidence of *in situ* nitrification's importance. Figure 6.5 presents DIN concentrations. Summer DIN concentrations in LSB were 30-40% lower than winter concentrations, with the lower concentrations likely due to a combination of denitrification at the sediment:water interface when water temperatures warm and higher uptake rates by phytoplankton during this time of year. DIN concentrations in southern South Bay (s27) exhibited similar seasonality. DIN concentrations in Suisun Bay are also lower in summer than winter. Initial box-model-derived estimates for Suisun Bay suggest that approximately $\sim 30\%$ of DIN input loads are lost via uptake or denitrification in Suisun Bay during summer months (Novick et al., 2014). These initial observations illustrate why developing accurate estimates *in situ* nitrification and denitrification rates will be important for identifying acceptable loads and apportioning observed concentrations to specific sources. LSB had the highest o-PO_4 concentrations, which were ~ 4 -fold higher than most other subembayments (Figure 6.6). In Suisun Bay, o-PO_4 does not show the same strong seasonality as NH_4^+ or NO_3^- exhibited. In the other subembayments, o-PO_4 concentrations showed more defined seasonality. Minimum o-PO_4 concentrations occur in April and May in San Pablo Bay, Central Bay, South Bay, and LSB, consistent with modest o-PO_4 drawdown occurring due to spring phytoplankton blooms. o-PO_4 concentrations then increase to relatively constant concentrations over summer and fall, before dropping to lower levels in wet season winter months (Nov-Feb).

Concentrations of organic N and organic P in SFB are uncertain, since they have not been consistently measured (except in Suisun Bay). However, because of the large anthropogenic DIN and DIP loads SFB receives, it is reasonable to hypothesize that DIN and DIP often dominate total N (TN) and total P (TP).

Dissolved SiO_4 concentrations vary both seasonally and spatially in SFB (Figure 6.7). The lowest SiO_4 concentrations are observed in Central Bay, with increasingly higher concentrations in more terrestrially-influenced areas of SFB. Suisun Bay has the highest SiO_4 concentrations, due to its large freshwater inputs, with lower concentrations observed in summer and fall, as Delta flows decrease and salinity increases. Seasonal drawdowns in SiO_4 concentrations in LSB and southern South Bay appear evident during spring, coincident with periods of high primary production rates and the dominance of diatoms (Sections 7 and 9).

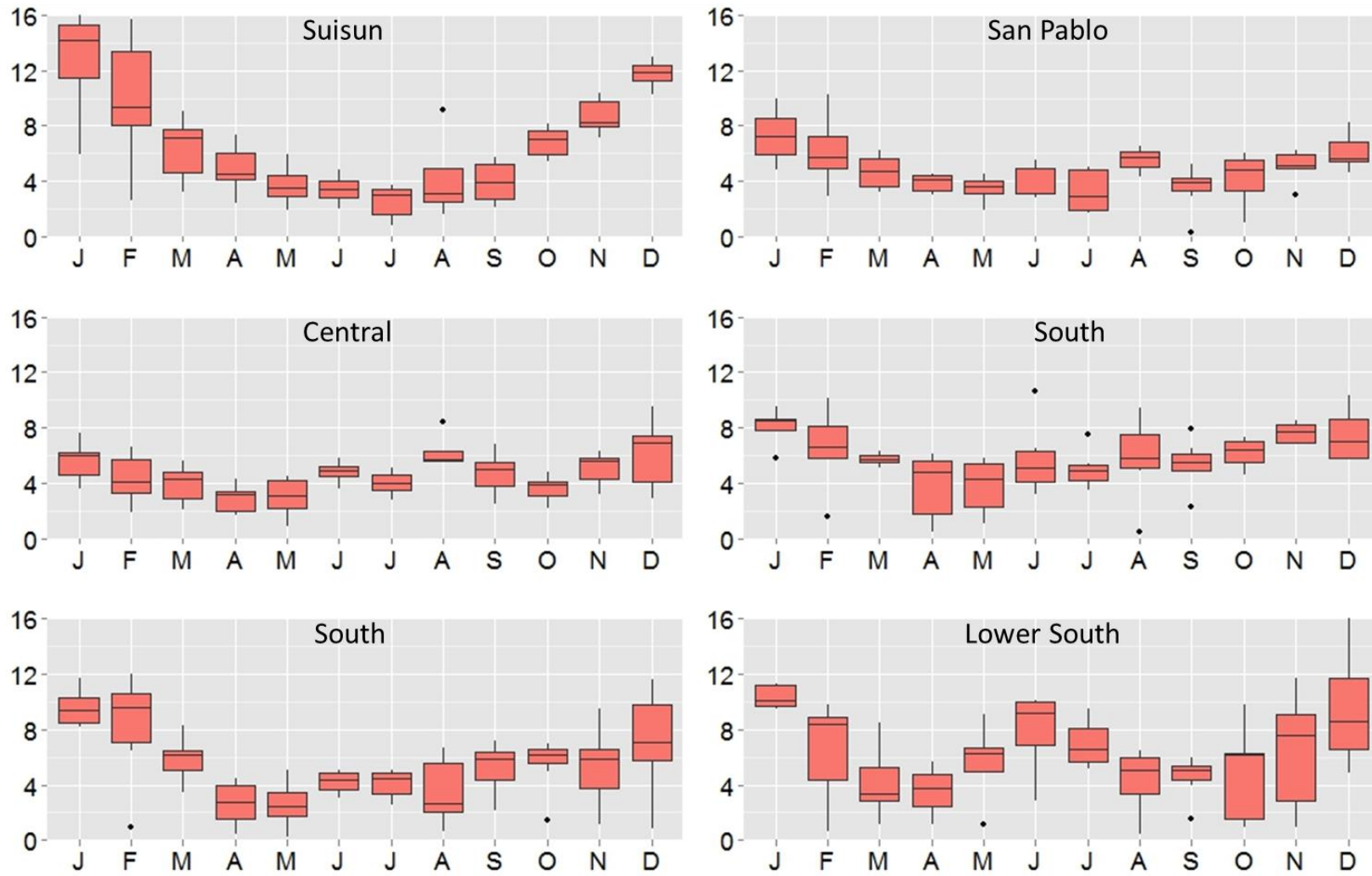


Figure 6.3 Monthly variations in NH_4^+ (μM): 2006-2011. Data from USGS stations s6 (Suisun), s15 (San Pablo), s18 (Central), s21 (northern South Bay), s27 (southern South Bay) and s36 (Lower South) were used. Data source: <http://sfbay.wr.usgs.gov/access/wqdata/>

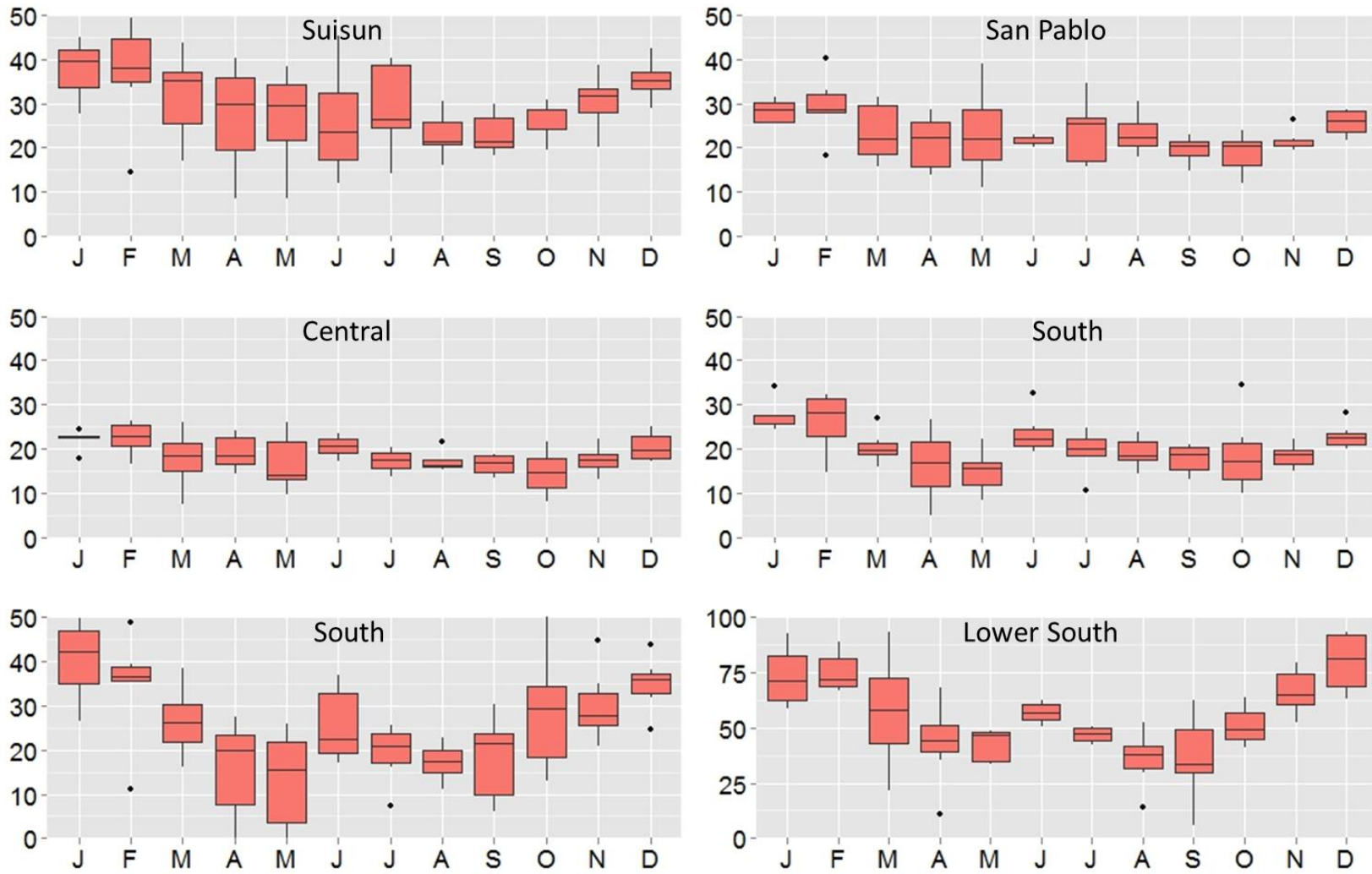


Figure 6.4 Monthly variations in NO_3^- (μM): 2006-2011. Data from USGS stations s6 (Suisun), s15 (San Pablo), s18 (Central), s21 (northern South Bay), s27 (southern South Bay) and s36 (Lower South) were used. Note the vertical different scales. Data source: <http://sfbay.wr.usgs.gov/access/wqdata/>

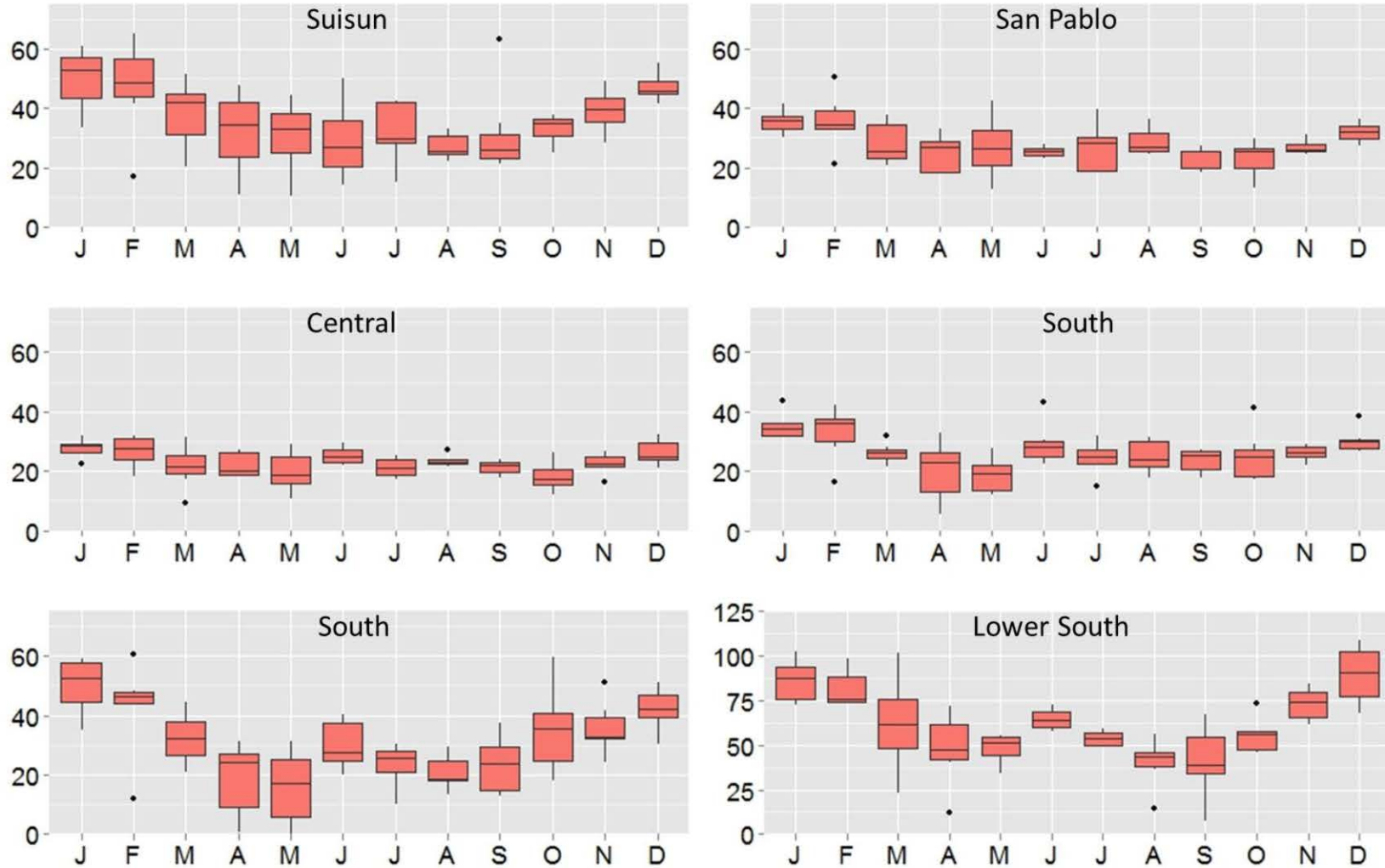


Figure 6.5 Monthly variations in DIN (μM): 2006-2011. Data from USGS stations s6 (Suisun), s15 (San Pablo), s18 (Central), s21 (northern South Bay), s27 (southern South Bay) and s36 (Lower South) were used. Note the vertical different scales. Data source:

<http://sfbay.wr.usgs.gov/access/wqdata/>

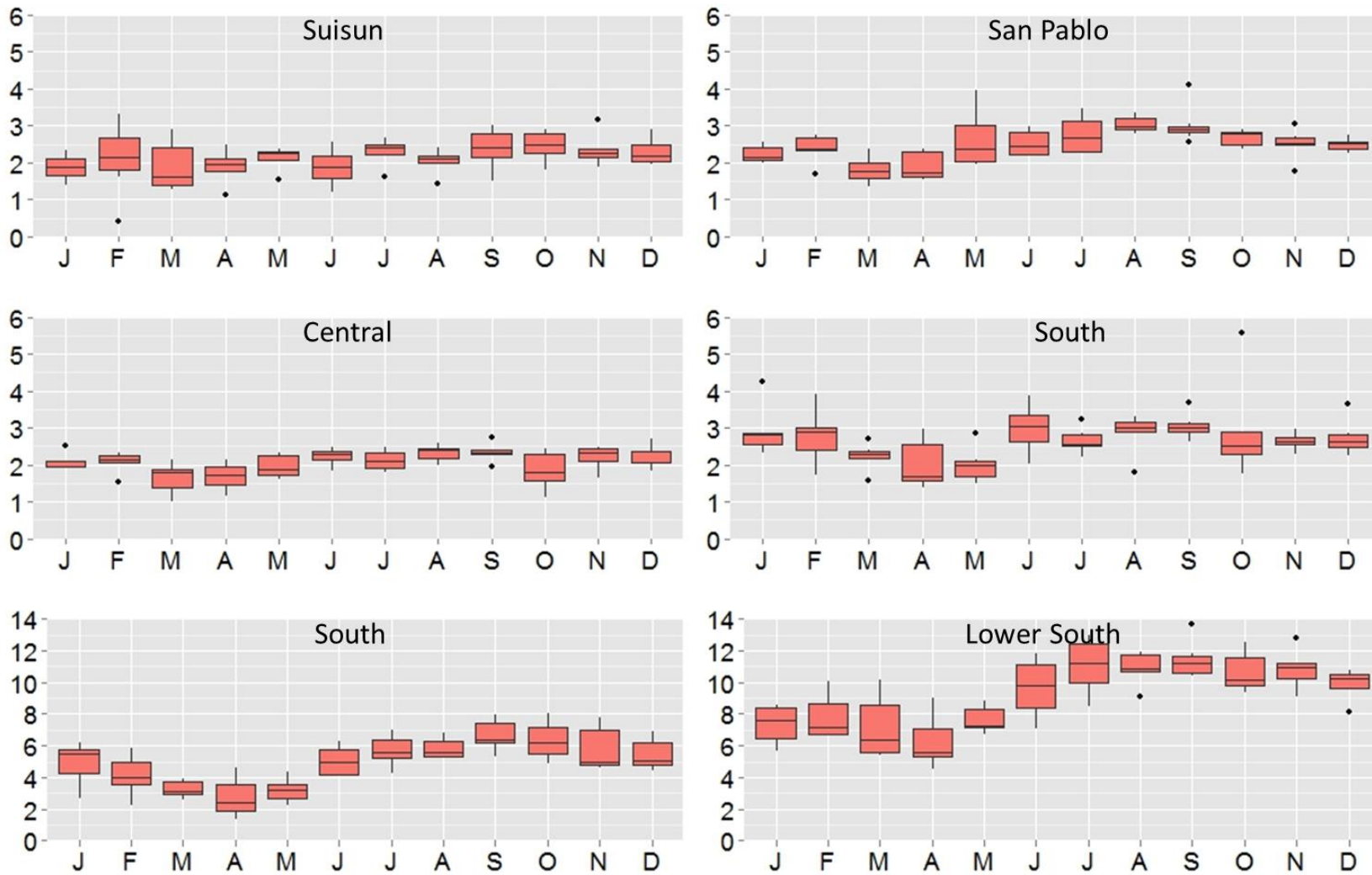


Figure 6.6 Monthly variations in o-PO₄ (µM): 2006-2011. Data from USGS stations s6 (Suisun), s15 (San Pablo), s18 (Central), s21 (northern South Bay), s27 (southern South Bay) and s36 (Lower South) were used. Note the different vertical scales. Data source: <http://sfbay.wr.usgs.gov/access/wqdata/>

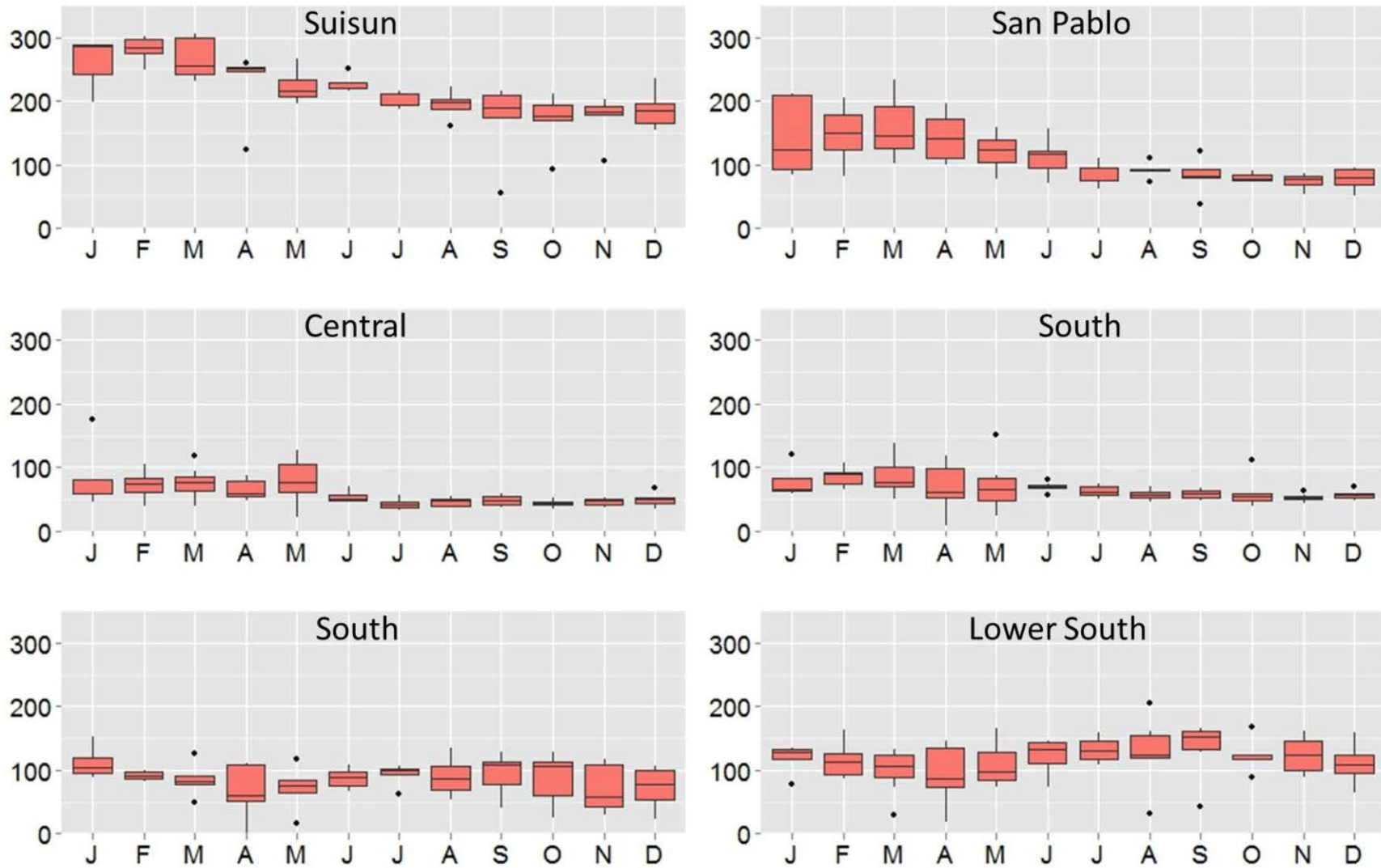


Figure 6.7 Monthly variations in Si (μM): 2006-2011. Data from USGS stations s6 (Suisun), s15 (San Pablo), s18 (Central), s21 (northern South Bay), s27 (southern South Bay) and s36 (Lower South) were used. Data source: <http://sfbay.wr.usgs.gov/access/wqdata/>

6.5 Current state of knowledge

Table 6.2 summarizes the current state of knowledge and data/knowledge gaps related to N and P in SFB. The prioritizations in the rightmost two columns are related to the discussion in Section 11. Nitrification (water column or sediment:water interface) and denitrification (sediment:water interface) likely play important roles in regulating ambient concentrations of NH_4^+ and NO_3^- in the Bay. Developing models, initially basic and gradually more sophisticated, that would allow quantification of these processes is an essential early step for informing decisions about allowable N loads to subembayments and source attribution, and about needs for additional data collection. Assuming that mass balance estimates from modeling suggest that nitrification and denitrification play important roles in N cycling in SFB, field studies will likely need to be conducted to quantify transformations rates. Some work has been conducted to characterize organic matter mineralization and NH_4^+ production in sediments at multiple locations throughout the Bay (Caffrey 1995), and more recent studies have investigated nutrient flux or transformations across the sediment:water interface in Suisun Bay and the Delta (Cornwell et al., 2013). However more work would likely be needed to assess variability in rates as function of space and season.

Limited data exists on nutrient concentrations at time scales shorter than ~1 month. Finer temporal resolution data will be needed to improve understanding about nutrient transformation rates. There is also limited information on nutrient concentrations along the shoals and in shallow margin habitats. Finally, organic N and P (PON, POP, DON, DOP) have not been routinely measured in most locations in the Bay (except at IEP sites in Suisun Bay and San Pablo Bay), and their importance and bioavailability are poorly known.

Table 6.2 N and P loads and cycling: current state of knowledge for key processes and parameters

Process or Parameters	Importance for quantitative understanding	Current Level of Knowledge about magnitude, composition, or controls	Need for <u>additional or continued</u> data collection, process studies, modeling	Priority for study in next 1-5 years
Loads				
POTWs	High	Moderate: Comprehensive effluent monitoring is currently underway. Prior to 2012, data availability varies by POTW and in general is fairly sparse for several nutrient forms (NO ₃ , o-PO ₄ , TN, TP)	Very High	Very High
Stormwater runoff	Uncertain	Low: Limited stormwater data and limited modeling effort	High	High
Delta	High	Low: Initial estimates suggest Delta loads may be a large source but they need to be validated, and time-series of loads are needed.	Very High	Very High
Groundwater	Low	Low: Poorly quantified but not expected to be major source because of relatively high loads from other sources	Low	Low
Direct atmospheric deposition	Low	Low: Poorly quantified but not expected to be major source because of relatively high loads from other sources, including from the large Central Valley watershed	Low	Low
Exchange through GG	Uncertain	Low: Has the potential to be large, but highly uncertain	High	High
Processes				
Benthic denitrification	High	Low: see OM mineralization and NH ₄ and PO ₄ release below	Very High	Very High
Pelagic denitrification	Low	Low: not expected to be important because of oxic water column	Low	Low
Benthic nitrification	High	Low: see OM mineralization and NH ₄ and PO ₄ release below. Potentially large, but limited field measurements, and need for both field and model-based estimates.	Very High	Very High
Pelagic nitrification	High	Low: Potentially large, but limited field measurements, and need for both field and model-based estimates.	Very High	Very High
N fixation	Low/Uncertain	Low	Moderate	Low

Process or Parameters	Importance for quantitative understanding	Current Level of Knowledge about magnitude, composition, or controls	Need for additional or continued data collection, process studies, modeling	Priority for study in next 1-5 years
OM mineralization and release of NH ₄ and o-PO ₄ from sediments, and in the water column	High	Low: Potentially a substantial source from the sediments to the water column. Limited data from two studies in SFB, but well-studied in other systems and at least initially may be able to use that information. Field studies aimed at exploring this issue will also inform sediment oxygen demand, benthic primary production, benthic denitrification, and benthic nitrification.	Very High	Very High
Settling/burial of N and P	High	Low/Moderate: limited field estimates to date, although could be estimated based on other sedimentation data.	Moderate	Low
Rates of NH ₄ , NO ₃ , and o-PO ₄ uptake by phytoplankton	High	Moderate: field measurements exist for NH ₄ and NO ₃ in northern estuary, limited data in South Bay and LSB. Uptake rates for P are not well-studied. Both N and P uptake rates can be partially constrained by knowing phytoplankton C:N:P and productivity	Moderate	Moderate
Other processes: DNRA, ANAMOX	Low	Low: but expected to be relatively small	Low	Low
N and P budgets for subembayments: loads, transformations, sources/sinks, export	High	Low: The ability to quantify these will provide important information on the subembayments' ability to process/assimilate N and P. Basic modeling work needed.	Very High	Very High
Ambient concentration data				
Phytoplankton C:N:P	High	Low: Currently not routinely measured during monitoring	Very High	Very High
Concentration of NO ₃ , NH ₄ , and PO ₄	High	Moderate: monthly data available at ~15 stations Bay-wide but finer spatial and temporal resolution needed to inform process level understanding and modeling	Very High	Very High
Concentrations of NO ₂ ⁻ and N ₂ O	Low/Moderate	Moderate: not needed for nutrient budgets, but informative as diagnostic of processes	Moderate	Moderate
Concentration of DON, PON, DOP, POP within and loaded to the system	Moderate/uncertain	Low: Little current data, and information is needed. Given the high DIN and DIP concentrations, abundance organic forms may be relatively low.	High	High

1 **7 Primary Production and biomass accumulation**

2 **7.1 Introduction**

3 Primary production in SFB is carried out by phytoplankton, benthic algae (microphytobenthos,
4 MPB), macrophytes, and macroalgae. In its current form, the primary production module of the
5 conceptual model focuses mostly on phytoplankton, and to a lesser degree on MPB.
6 Macrophytes and macroalgae are not considered in this report. For more on the latter topics, the
7 reader is referred to the SFB NNE Literature Review and Data Gaps Analysis (McKee et al.,
8 2011).

9
10 Phytoplankton biomass is an important indicator of ecosystem health with respect to nutrient
11 loads, and is among the potential indicator of ecosystem health and nutrient-related adverse
12 impacts for SFB (Figure 3.1; Table 2.1). Phytoplankton reside at the base of the food web, and
13 are the predominant food resource for most pelagic and benthic primary consumers in SFB
14 (Jassby et al., 1993). Phytoplankton require nutrients for growth, and in many aquatic systems
15 there is a direct link between phytoplankton biomass and nutrient loads, with nutrient abundance
16 being one of several factors that can regulate both the rate of primary production and the ultimate
17 biomass that can be generated. As noted in Section 3, excessive phytoplankton biomass is one
18 plausible impaired state in SFB. Excessive phytoplankton biomass can have direct adverse
19 impacts, such as coatings on bird wings, odor, and degraded aesthetics. High rates of primary
20 production and accumulation of high levels of phytoplankton biomass are also problematic
21 because they lead to low dissolved oxygen levels in the water column and sediments when
22 phytoplankton die, settle, and are metabolized by microbes (Section 8). By absorbing light, high
23 phytoplankton biomass can also adversely impact the production of submerged aquatic
24 vegetation (SAV), which serves as valuable habitat in some estuaries. However, impacts of high
25 phytoplankton biomass on SAV is not considered to be among the most important adverse
26 impact pathways in SFB because of already low-light conditions due to high turbidity from
27 inorganic particles.

28
29 Phytoplankton biomass is actually comprised of multiple species, with complex community
30 responses caused by natural and anthropogenic drivers. Both the biomass and the types of
31 phytoplankton present (community composition) are important for adequately supporting food
32 webs. This section focuses on phytoplankton biomass; Section 9 addresses community
33 composition. Microphytobenthos are discussed in Section 7.3.

34 **7.2 Phytoplankton**

35 Phytoplankton biomass is the concentration of living phytoplankton material in the water
36 column. Phytoplankton biomass is commonly presented in units of mg chl-a m^{-3} or $\mu\text{g chl-a L}^{-1}$,
37 although it would be more accurate to describe it in units of $\mu\text{g C L}^{-1}$. The biomass measured at
38 any given point in space and time is the net result of multiple processes (Figure 7.1): growth;
39 settling; pelagic and benthic grazing; sinking and degradation or burial; and exchange or mixing
40 between areas through the movement of water masses (lateral, longitudinal, vertical) (Cloern,
41 1996). The magnitudes of these processes vary in space and time, and this variation leads to
42 spatial and temporal differences in biomass concentrations.

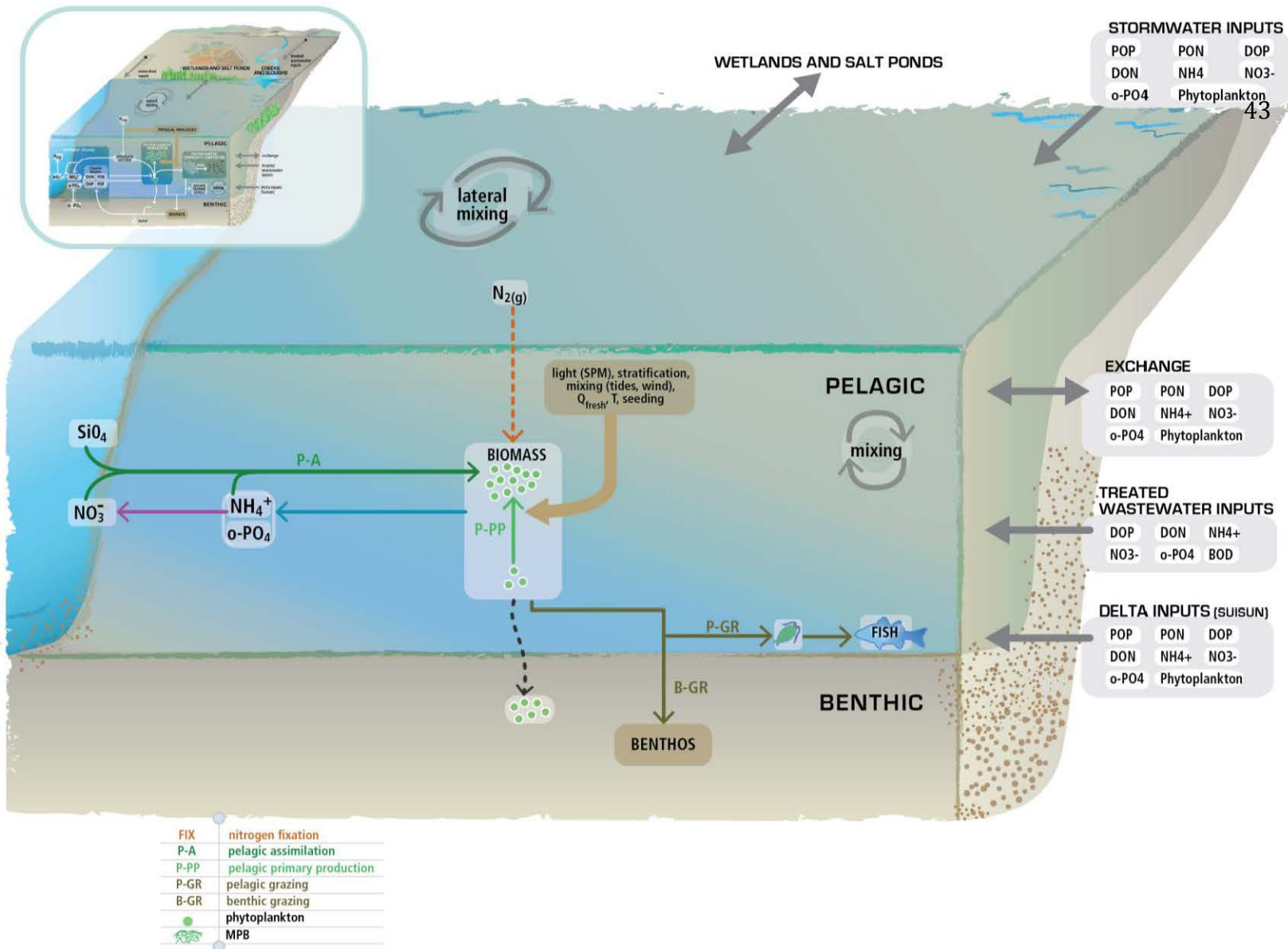


Figure 7.1 Phytoplankton primary production conceptual model. Physical processes play an important role in determining when and where phytoplankton blooms occur, their size, duration, and the concentration of biomass that accumulates. The relationship between physical processes and production are described in more detail in Figure 7.2.

7.2.1 Transport and Loads

Sources of externally-produced phytoplankton biomass to a subembayment include: flow from rivers, perennial streams, and stormwater carrying phytoplankton produced in adjacent systems; hydrodynamic exchange between adjacent subembayments or habitats (e.g., water movement between shoals and channel); and exchange with the coastal ocean. In general, the majority of phytoplankton biomass observed in SFB is produced within the Bay (Jassby et al., 1993). Suisun Bay may serve as a notable exception: Jassby et al. (1993) estimated that the load of phytoplankton-derived particulate organic carbon (POC) exported from the Delta to Suisun Bay could account for 20-80% (median ~ 50%) of Suisun's POC budget, including Suisun *in situ* production. Those estimates were based on data from 1975-1989. Considering the substantial ecosystem changes observed since the late 1980s both in the Delta and Suisun, these estimates likely need to be updated. In addition, the coastal ocean can be a non-trivial source of phytoplankton biomass to Central Bay, especially during the upwelling season (Martin et al., 2007).

7.2.2 Production and accumulation

The processes that control biomass can be divided into those that influence the rate of growth and those that influence the rate of accumulation. Typical modes of phytoplankton productivity and biomass accumulation in SFB are represented in Figure 7.2. The most common condition is low phytoplankton productivity and low biomass (Figure 7.2.A). Blooms develop when the water column becomes periodically stratified (Figure 7.2.B) or when appropriate conditions prevail in shallow areas (Figure 7.2.C and 7.2.D). Major processes and drivers are described below.

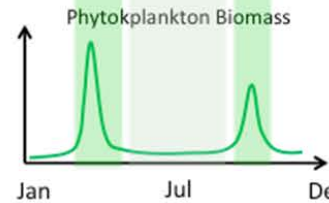
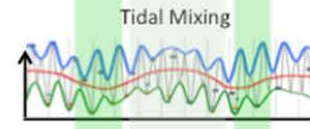
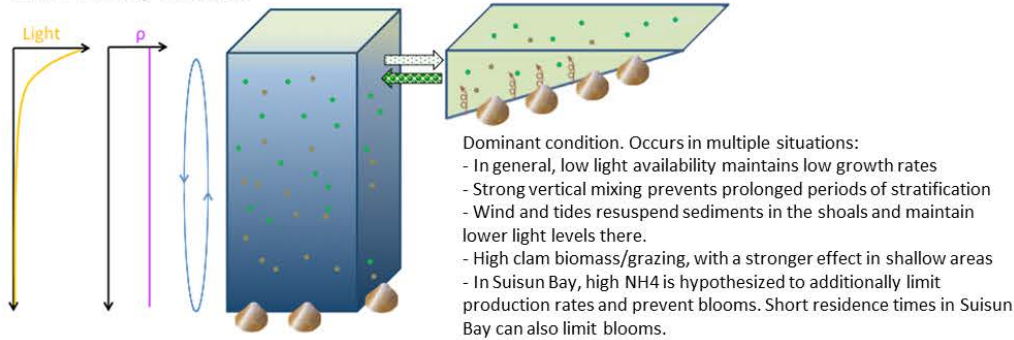
7.2.3 Factors that influence production rates

Several factors influence phytoplankton production rates, including temperature; light availability; nutrient concentrations; and potential anthropogenic factors, such as contaminants, that could inhibit or slow production rates, including pesticides or toxic metals (e.g., copper), or the hypothesized inhibition of growth by elevated NH_4^+ (e.g., Dugdale et al., 2007).

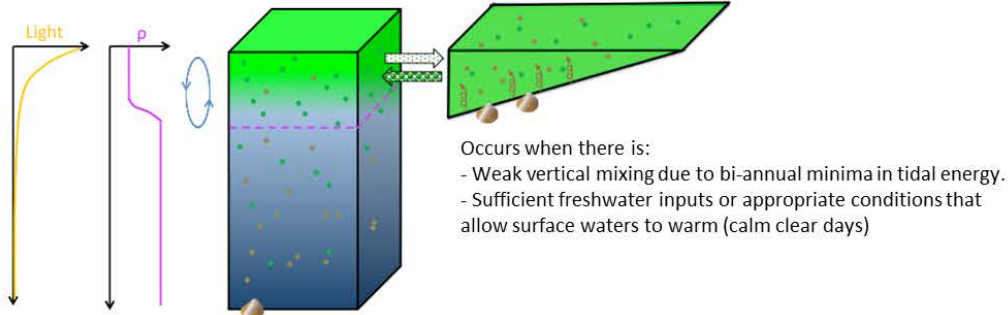
Temperature: Phytoplankton maximum growth rates vary strongly with temperature (e.g., Eppley 1972; Behrenfield and Falkowski, 1997). Bay-wide average temperatures vary seasonally from 10 °C to >20 °C, with as much as a 7 °C difference in maximum temperatures between subembayments. These temperature ranges translate into substantial differences in maximum growth rates: annual maximum growth rates could differ by up to a factor 1.4 between subembayments (LSB vs. Central), and by up to a factor of 2 seasonally (LSB summer vs. winter) (assuming $Q_{10} = 1.88$; Bissinger et al., 2008)

Light levels: Throughout much of SFB and during most of the year, light availability acts as the main limitation on phytoplankton growth rates. A number of field investigations and model-based estimates document the importance of light limitation in SFB (Cloern 1982; Cloern et al. 1985; Cole et al. 1986; Cole and Cloern 1987; Alpine and Cloern 1988; Caffrey et al. 1994; Jassby et al., 2002; Cloern et al., 2007). Phytoplankton growth rates depend primarily on the amount of time cells spend in light-rich zones (Figure 7.3) (e.g., Alpine and Cloern, 1988; Cloern et al., 1985). The amount of light reaching the water column surface (incident light or insolation) varies seasonally due to length of day, and over shorter time scales (hours-days) due to cloud cover (Figure 5.2). From the surface, light levels decrease exponentially with depth, primarily due to light scattering and absorption by suspended particulate matter (SPM).

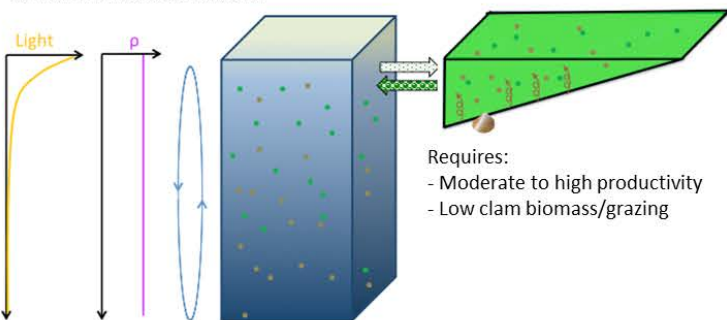
A. No bloom, baseline



B. Stratification-induced bloom



C. Shoal-induced bloom



D. Shoal-induced bloom that propagates to channel

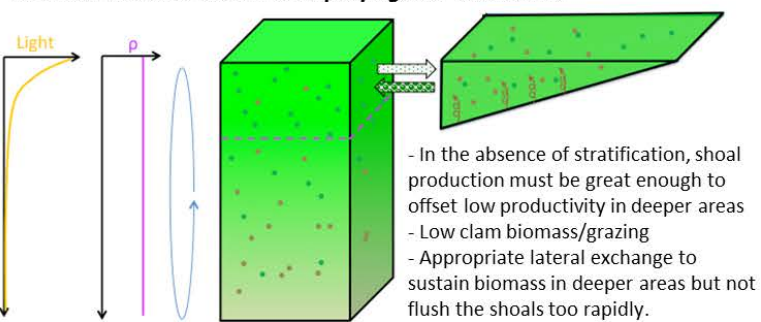


Figure 7.2 Modes of productivity in SFB, and factors influencing timing and magnitude of blooms

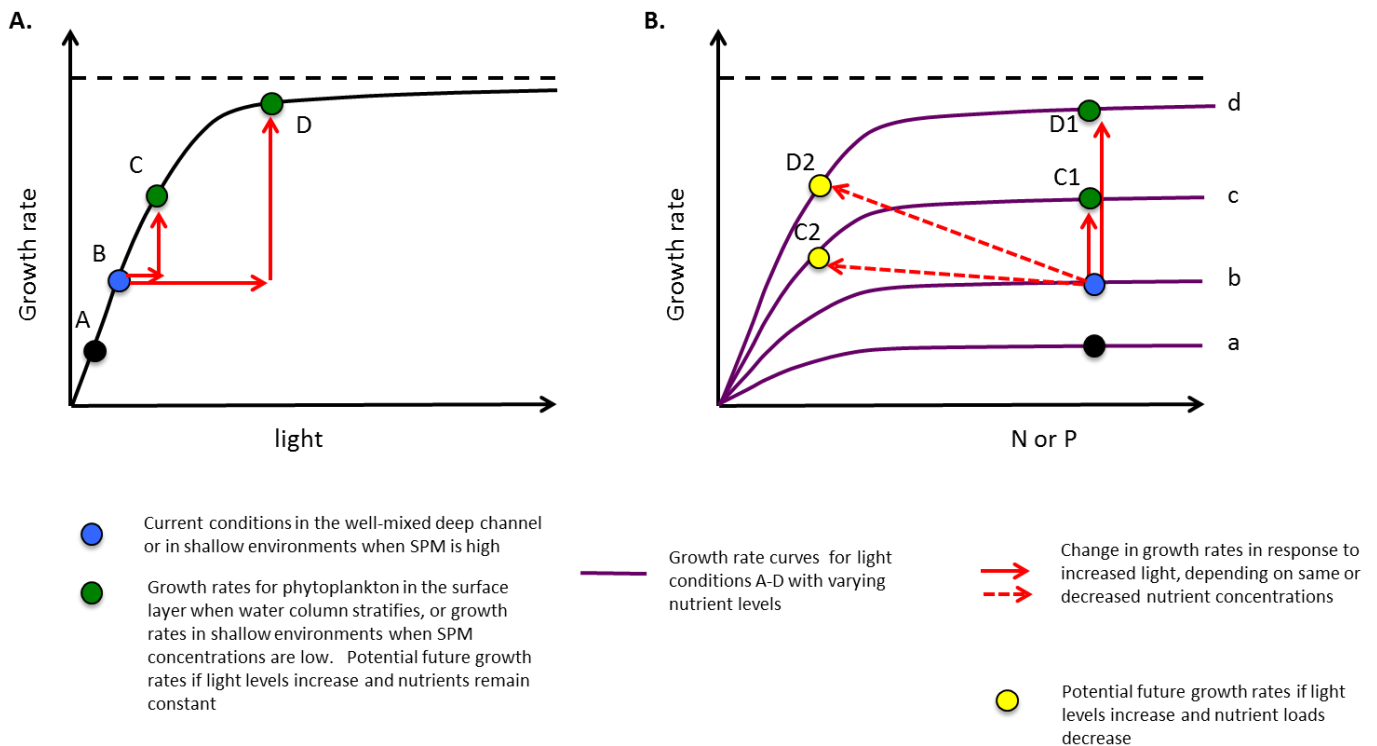


Figure 7.3 Phytoplankton Growth Rates: Light limitation vs. nutrient limitation. In general, throughout most of SFB, light limits phytoplankton growth most of the time. **A.** When nutrients are available at non-limiting levels, phytoplankton growth rate increases as a function of light to some maximum level (this maximum growth rate varies by temperature and species). Growth rates increase as light levels increase. **B.** The four curves (a-d) illustrate growth under four different light levels. At each constant light, growth rate varies as a function of nutrient concentration (x-axis). In SFB, N and P concentrations are typically high enough that growth rates are not nutrient limited. Instead, phytoplankton are thought to grow at their maximum growth rate for that specific light level (i.e., the flat part of the curves). Under current nutrient loads/concentrations, if light levels increase (shift from blue to green dots, due either to decreasing SPM, or in response to periodic stratification), growth rates and biomass accumulation will increase. However, if nutrient loads and concentrations were lower (blue to yellow dots) growth rates and biomass accumulation would not increase as much.

SFB is considered a turbid system, and the photic zone - the depth at which light levels are 1% of incident light - is typically only 1-2 m thick (Cloern et al., 1985). Unlike some other nutrient-rich systems in which phytoplankton cells can themselves contribute substantially to light attenuation, light attenuation in SFB is primarily due to non-phytoplankton SPM (Cloern, 1987).

SPM concentrations and photic zone depth vary substantially between subembayments, within subembayments, and as a function of season (Figure 5.6). SPM concentrations also increase when high winds resuspend more sediments, and show periodic increases and decreases in response to the spring-neap tide cycle (Schoellhamer, 2002). SPM and light attenuation coefficients are often higher along shallow shoals than in deeper areas, due to turbulent energy from wind and tides more readily resuspending particles from the bottom. Despite the higher SPM concentrations along shoals, though, average light levels that phytoplankton experience may still be higher there because they are mixed over a shallower depth. SPM concentrations have decreased significantly in some areas of SFB over the past several decades. For example, SPM concentrations have dropped by on-average 50% in Suisun Bay since 1975 (Figure 5.5;

Cloern and Jassby, 2012), due to decreasing loads, gradual loss of erodible bed sediments already in the Bay, and step declines in turbidity due to “washout events” (Schoellhamer, 2011). This 50% decrease in SPM translates to roughly a doubling of the photic zone depth. The Bay-wide average decrease in SPM is ~35% (Schoellhamer, 2011).

Hydrodynamic controls over phytoplankton’s access to light and production rates

The vertical and lateral movements of water masses - and the phytoplankton they contain - within SFB play an important role in regulating overall system productivity by controlling the average amount of time phytoplankton remain within the light-rich photic zone. Variability in the magnitude of vertical and lateral mixing also plays a role in determining if, when, and where phytoplankton blooms develop and terminate (Cloern 1991; Lucas et al., 1998). Thus, understanding and modeling hydrodynamics in the Bay are essential for understanding and predicting productivity and the accumulation of phytoplankton biomass.

The presence or absence of vertical stratification in the water column strongly influences productivity (Figure 7.2.A and 7.2.B). When the water column is vertically well-mixed (Figure 7.2.A), the amount of time phytoplankton spend in the photic zone decreases in proportion to water column depth. Vertical layering of the water column – stratification – develops when less dense layers of water overlay more-dense layers. These density differences arise due to differences in salinity (density increases with increasing salinity) and temperature (density decreases with temperature). The density difference limits vertical mixing and allows phytoplankton to reside in the relatively thin (e.g., 1-3 m), light-rich surface layer, as opposed to being moved over the entire water column. When confined to the surface layer, phytoplankton harvest more light, resulting in higher growth rates (Figure 7.2.B and 7.3.A). (Note: Stratification also positively influences biomass accumulation in the sense that filter-feeding benthos cannot access phytoplankton in the surface layer).

Factors that influence whether stratification occurs, and how long it persists, therefore have an important influence on productivity and biomass accumulation. SFB experiences strong tidal mixing which acts to break down stratification by vertically-mixing the water column (Cloern, 1991). Tidal mixing intensity varies periodically: two tidal cycles per day with different mixing energies; the spring/neap cycle by which tides vary in magnitude on ~14 day cycle; and twice-annual periods of lowest sustained tidal mixing energy (March, September) and maximum sustained mixing energy (December, June; Figure 5.2). Assuming there is sufficient freshwater input (or lateral or longitudinal gradients in salinity) for salinity gradients to be develop, stratification/destratification can occur with the same periodicity as tidal mixing intensity. Thus, the duration of stratification events can vary from hours (semi-diurnal to diurnal stratification) to days and weeks (during the weakest tides twice per year) depending on the strength of stratification relative to the tidal mixing energy. Cloern (1996) observed that blooms along the deep channel of South Bay generally developed in March, when periods of weak tidal mixing co-occurred with sufficient freshwater input to allow stratification to develop and persist for 10-14 days. The termination of these blooms corresponded with increased tidal energy that vertically-mixed the water column (Cloern 1996). This cycle is likely also important in other subembayments. In Suisun Bay, in the 1970s and early 1980s, IEP monitoring data indicates that phytoplankton biomass remained elevated over longer periods, i.e., throughout Spring, Summer, and Fall. Suisun receives larger freshwater inputs than other subembayments

Recently (past 10-20 years), fall blooms have been occurring with increased frequency in southern South Bay and LSB (e.g., Figure 3.7; Cloern and Jassby, 2012). The reason for these fall blooms in LSB and South Bay is unknown, but could be in part due to lower SPM (higher light levels) and lower grazing pressure (Section 7.2.3). If stratification plays a role in the increased biomass in fall, density differences during this time may have been due to surface water heating than freshwater inputs. Clear skies (greater solar insolation) and calm winds would thus be required for stratification to develop and persist. One particularly striking example of a fall bloom occurred in September 2004, when calm winds and weak tides occurred coincident with record temperatures and clear days, allowing a warm surface layer to establish (Figure 3.11). A bloom of the red tide organism *Akashiwo sanguinea* developed, with biomass levels reaching nearly 200 mg chl-a m⁻³ (Cloern et al., 2005), the highest levels observed in this region of SFB over the 40-year period of record. The bloom terminated after only 1 week, once mixing energy levels increased.

SFB's expansive shallow shoals are important zones for phytoplankton production. Large proportions of Suisun Bay, San Pablo Bay, South Bay, and Lower South Bay have water depths of <2 m. Field and modeling studies in South Bay indicate that phytoplankton blooms often originate along the shoals (Figure 7.2.C and 7.2.D), exploiting the relatively light-rich conditions of the shallow water column (Cloern et al., 1989; Huzzey et al., 1990; Lucas et al., 1999; Lucas et al., 2009 ; Thompson et al., 2008). This is well illustrated in South Bay and LSB in Figures 7.4 and 7.5. Under appropriate lateral mixing conditions, production along the shoals can lead to high biomass there, and appreciable biomass transport to the relatively unproductive channel (Figure 7.4; Thompson et al., 2009; Lucas et al., 2009). Figure 7.5 illustrates a sustained bloom (>1 month) with 60 to >100 ug/L over the entire water. Since average light levels in the deep channel, when well-mixed, are too low to support substantial growth, most of this biomass was likely produced along the shoals and subsequently mixed over the water column (i.e., Figure 7.2.D). Because sediments are more readily resuspended in shallow environments, higher turbidity, resulting from tidally- or wind-driven local resuspension of sediments, can decrease productivity on the shoals (Lucas et al., 2009). Furthermore, filter feeding by clams can more efficiently clear the shoal water column than the deep channel water column, and reign in shoal blooms (see Section 7.2.3; and Lucas and Thompson 2013). Despite the apparent importance of productivity along the shoals, there is relatively limited data available from these areas. Increased monitoring (including continuous monitoring with moored sensors, e.g, turbidity, chlorophyll, etc.) is needed to understand when shoal induced blooms (Figure 7.2.C and 7.2.D) drive overall production in subembayments.

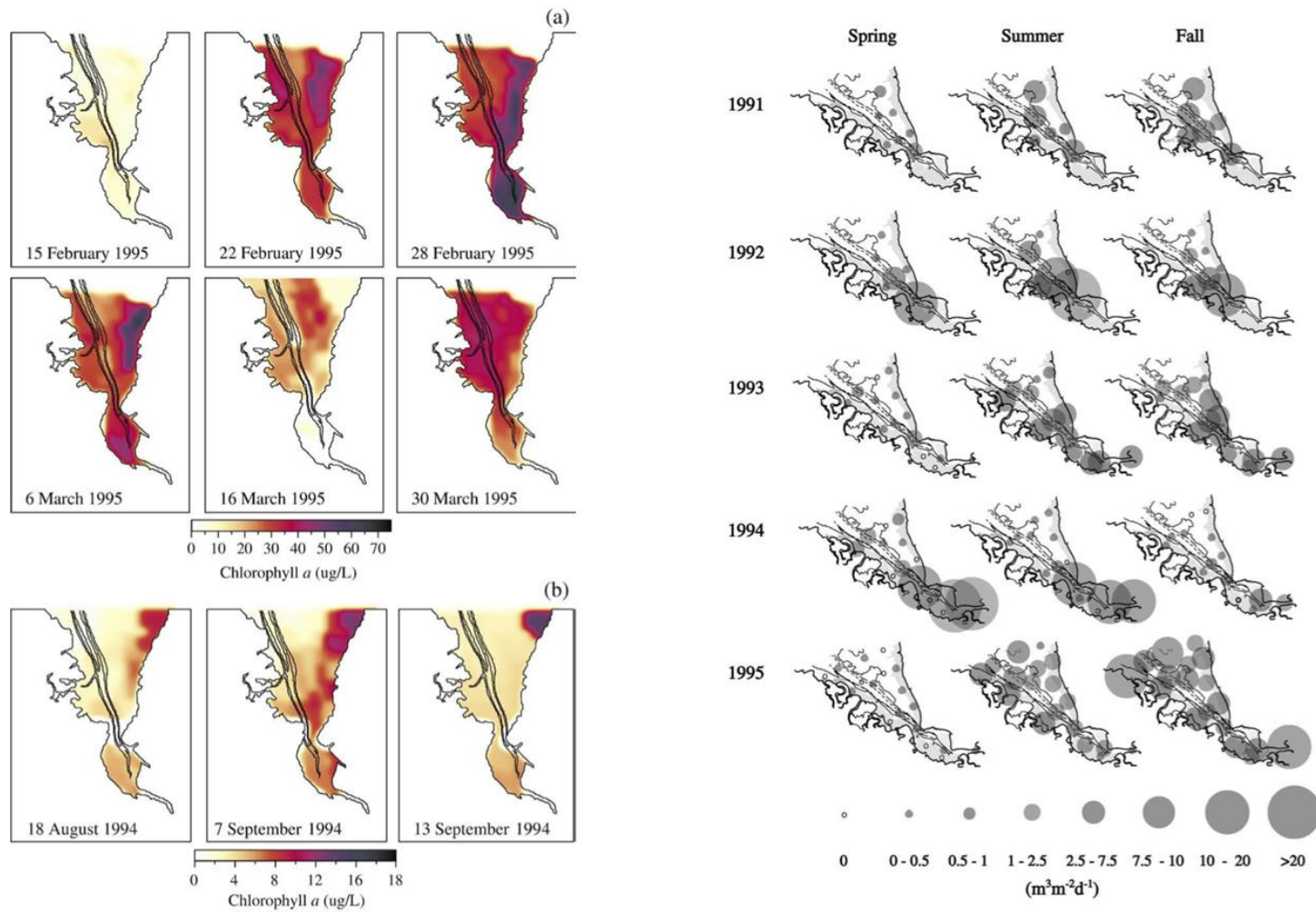


Figure 7.4 A. Phytoplankton biomass South Bay illustrating bloom initiation on shoals and propagating to the channel. **B.** Spatial, seasonal, and interannual variation in bivalve grazing rates in South Bay and LSB. Source: Thompson et al. 2008

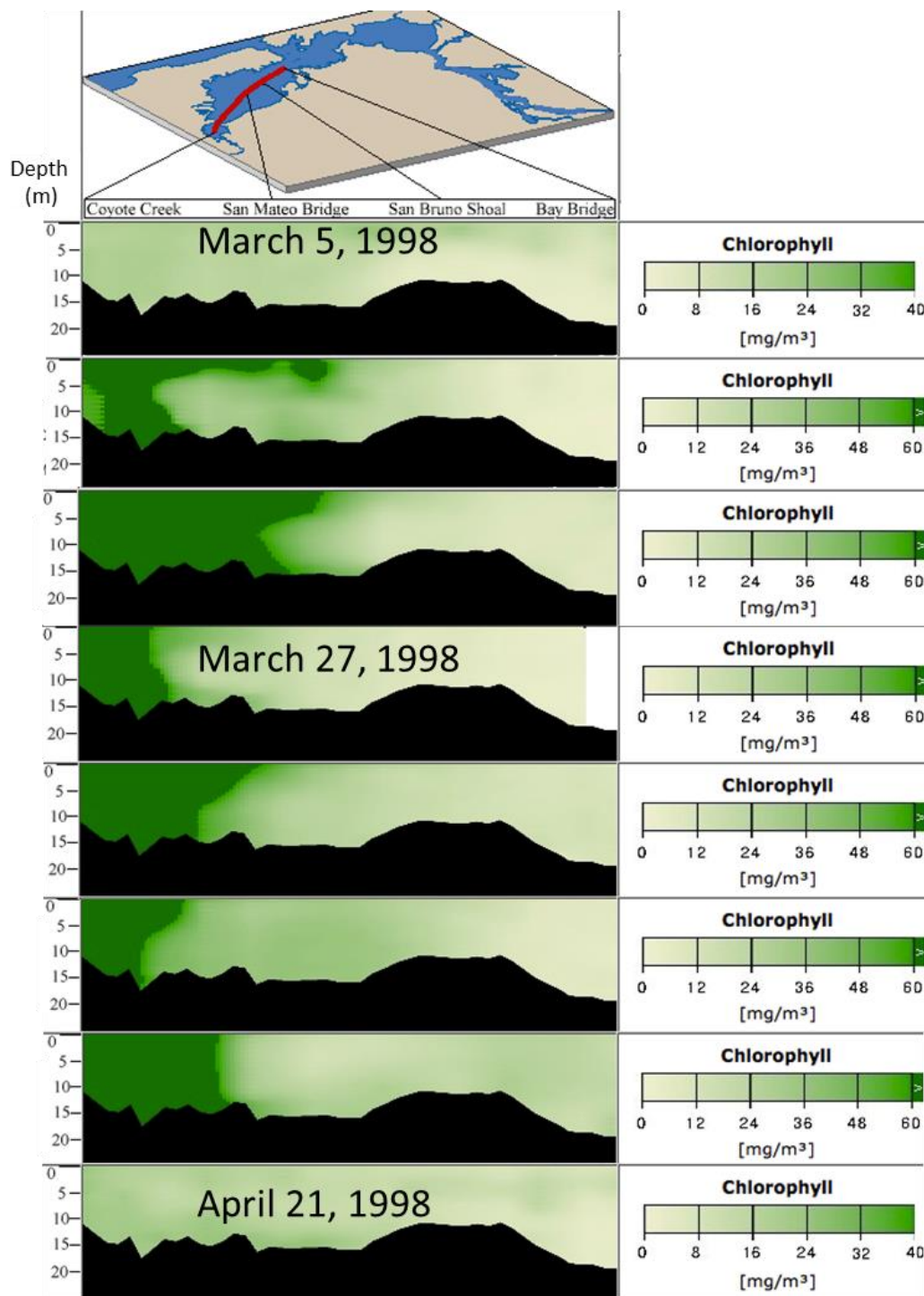


Figure 7.5 Phytoplankton biomass in LSB and South Bay during Spring 1998. Note that chl-a concentrations are constant over the full water column, illustrating the production scenario in Figure 7.2 D. Source: <http://sfbay.wr.usgs.gov/access/wqdata/archive/longterm.html>.

Cole and Cloern (1984) demonstrated that primary production rates in SFB could be reliably quantified by knowing incident light intensity, depth of the photic zone, and the concentration of phytoplankton biomass (as $\mu\text{g chl-a L}^{-1}$). This relationship is calibrated using an “efficiency factor”, ψ , for new biomass production per unit light energy (expressed in units $\text{mg chl-a [Einstein m}^{-2} \text{J}^{-1}]$), which is specific to the phytoplankton community of the system (Cole and Cloern, 1987; Jassby et al., 2002). Using this ψ -based relationship to estimate productivity is valid as long as ψ remains constant over space and time (Jassby et al., 2002 ; Kimmerer et al. 2012 ; Parker et al., 2012), and C:chl-a is reasonably well-known and constant. Recent studies focused in northern SFB have suggested that both ψ and C:chl-a may have changed considerably over the past 20 years, potentially due to large changes in phytoplankton community composition (Kimmerer et al., 2012; Parker et al., 2012). However, the analytical techniques for measuring production rate differed between Cole and Cloern (1984) and Parker et al. (2012), and some or all of the apparent difference in the calibration coefficients could be the result of these analytical differences. In either case, the overall ψ -based approach remains valid, although it may need to be periodically re-calibrated and validated, and different relationships (i.e., different values of ψ) may need to be developed to account for a range of conditions (light-inhibition, different phytoplankton communities, T).

Nutrients and phytoplankton production rates

In many estuaries nutrient concentrations both influence primary production rates and determine when a bloom terminates (due to nutrient depletion). However, in SFB, nutrients tend to be replete year-round, and thus they seldom control production rates (Figure 7.6, 7.7 and 7.3.B). Nutrient concentrations do exhibit periodic drawdowns in SFB, owing in part to phytoplankton growth (Thompson et al., 2008; Figure 3.14 in SFEI 2014b). However, at least in deep channel environments where most data is available, concentrations infrequently dip to levels that would be expected to substantially slow overall production rates (Figure 7.6 and 7.3.B). Instead, field and modeling studies in SFB suggest that phytoplankton bloom termination at the subembayment scale more commonly occurs due to other factors, especially break-down in stratification (Cloern 1991), and sometimes increase in grazing pressure (Thompson et al., 2008). The tops of the grey shaded areas in Figure 7.6 correspond to 2 times K (half-saturation constant) for N, P, or Si. A value of $10 \times K$ would be a more conservative estimate of when a concentration may begin to slow growth rates. If a value of $10 \times K$ is used, the interpretation of infrequent nutrient limitation remains generally the same, except for DIN in South Bay. Even in the case of South Bay using $10 \times K_N \sim 10 \mu\text{M}$, though, [DIN] rarely falls below that value ($\sim 15\%$ of the time). The case of South Bay and LSB are better illustrated in Figure 7.7, which presents DIN and DIP concentrations at individual stations in terms of their interquartile ranges, 95% confidence intervals and outliers. At all stations the interquartile ranges lie well above the $10 \mu\text{M}$; at stations 19-27 and 36, the 95% confidence intervals also lie above $10 \mu\text{M}$. DIP concentrations almost always exceed $\sim 2 \mu\text{M}$ ($10 \times K_P$). So, while there are windows in space/time when DIN falls below a potentially growth rate limiting concentration, DIN substantially exceeds rate-limiting concentrations the vast majority of time. Nonetheless, a closer examination chl-a, DIN, and other nutrient time series would be worthwhile for providing insights into when, where, and under what conditions DIN does reach these lower levels.

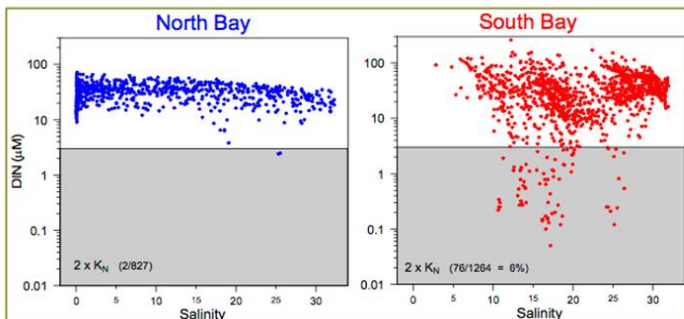


Figure 5.6.5. Near-surface DIN concentration vs. salinity in North and South Bay. Data shown are all measurements made by USGS from 1988-2000. Gray rectangle indicates potential N limitation.

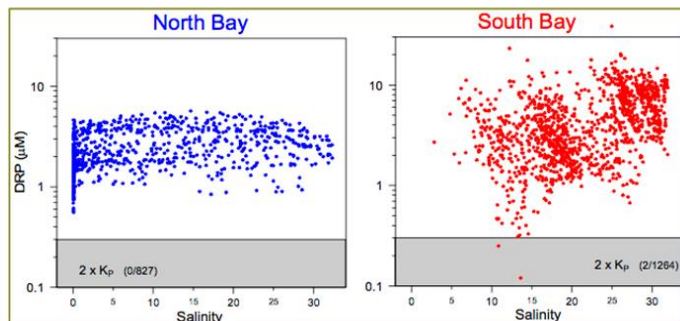


Figure 5.6.6. Near-surface DRP (PO_4^{3-}) concentration vs. salinity in North and South Bay. Data shown are all measurements made by USGS from 1988-2000. Gray rectangle indicates potential P limitation.

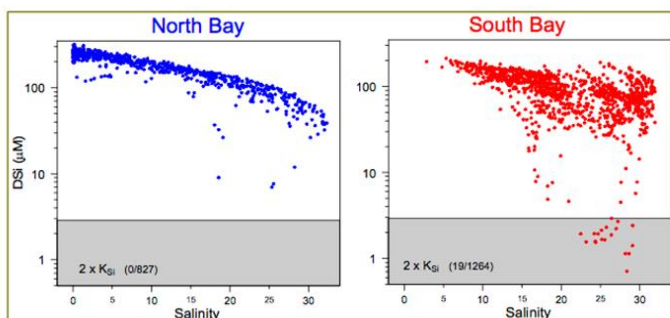


Figure 5.6.7. Near-surface $Si(OH)_4$ (DSi) concentration vs. salinity in North and South Bay. Data shown are all measurements made by USGS from 1988-2000. Gray rectangle indicates potential Si limitation.

Figure 7.6 Nutrient concentrations in SFB compared to thresholds for kinetic limitation of phytoplankton growth. Source: Cloern and Dugdale 2010.

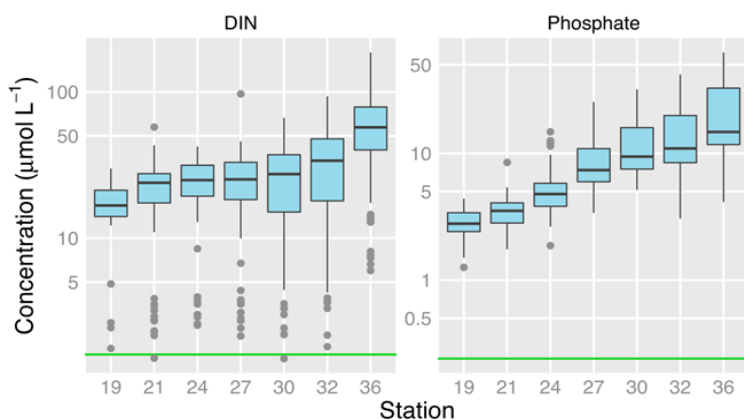


Figure 7.7 “Boxplots showing spatial distributions of DIN and DIP in surface waters (0-3m) of South Bay and LSB, 1969-2010. Green lines represent characteristic K_N and K_P to indicate nutrient concentrations that potentially limit phytoplankton growth.” Source: Cloern and Jassby 2012

Low production rates due to elevated ammonium in Suisun Bay

Recent studies in SFB and the Delta have argued that the influence of nutrients on biomass production rate may be more complex than the generally accepted idea of nutrient limitation on growth. Dugdale and colleagues argue that elevated NH_4^+ levels in Suisun Bay and the Delta slow primary production rates and can prevent blooms from developing (Dugdale et al. 2007, 2012; Parker et al., 2012a,b). These studies refer to the phenomenon as the “ NH_4^+ paradox”: the

crux of the hypothesis is that when NH_4^+ concentrations exceed 2-4 μM , phytoplankton can not access the relatively large NO_3^- pool on which these studies suggest they can grow more rapidly than NH_4^+ . The NH_4^+ paradox studies acknowledges that other factors such as light limitation, clam grazing, and residence time also exert influence over phytoplankton production or biomass accumulation. However Dugdale and colleagues hypothesize that NH_4^+ -inhibition of productivity could be a quantitatively important mechanism during critical periods, such as during spring, when clam grazing may in fact be low due to seasonal variations in clam abundance (Dugdale et al., 2007).

There remains considerable disagreement within the scientific community – including among this report’s authors – about the mechanistic interpretations of the NH_4^+ -paradox studies, and about the potential ecosystem-scale importance of the mechanism relative to other factors that regulate phytoplankton growth rates and biomass accumulation. A detailed review of these studies was recently completed, and the reader is referred to that report for more information (SFEI 2014b). Experiments to explore the NH_4^+ -paradox are continuing. More integrative studies (e.g., modeling) and controlled experiments are needed to evaluate the importance of hypothesized NH_4^+ -inhibition mechanism relative to other processes.

7.2.3 Top-down biological processes that influence biomass accumulation

Benthic grazing

Benthic grazing plays an important and sometimes dominant role in regulating the amount of biomass that accumulates in the water column of some SFB subembayments, or habitats within those embayments. (e.g., Thompson et al. 2008; Kimmerer and Thompson, 2014; Cloern et al., 2007; Lucas and Thompson, 2013). The effect of benthic grazing rates on phytoplankton biomass is dependent on the filtration rates ($\text{m}^3 \text{g}^{-1} \text{d}^{-1}$) of the species present and the abundance of grazers (g m^{-2}). Grazer abundance varies seasonally and spatially based on individual species’ life histories, predation, and habitat preference (salinity, sediment type, etc.). Grazer abundance is also tightly coupled to their food supply: i.e., the biomass of grazers at any point in is related to the amount of food available prior to that time. The influence of the filtration rate on phytoplankton concentrations in the overlying water column also depends on water column depth: at a given filtration rate (which is proportional to clam biomass), a shallow water column will be cleared of its phytoplankton faster than a deep water column. The effect of benthos on phytoplankton biomass also depends on other factors such as benthic boundary layer thickness and stratification, which are themselves influenced by turbulent mixing energy.

Potamocorbula amurensis filtration efficiency is high on relatively large phytoplankton ($>5 \mu\text{m}$ = 100%; Kimmerer and Thompson 2014) and lower for smaller phytoplankton ($<5 \mu\text{m}$ = 75%; Kimmerer and Thompson, 2014; Werner and Hollibaugh, 1993). This size-dependent filtration efficiency may allow *Potamocorbula* to disproportionately graze larger cells from the water column and potentially influence size distribution of phytoplankton biomass. However, higher settling rates of large phytoplankton classes like diatoms would tend to increase their downward transport (relative to other size classes) to zones where they can be entrained by clams, and this could be an even more important factor on the relative impacts of grazing on different phytoplankton classes.

Three sets of observations offer insights into the strong influence that benthic suspension feeders can have on phytoplankton biomass. The first example is the observation that, based on mass

balances of phytoplankton biomass in South Bay, production paradoxically exceeded losses from zooplankton grazing and transport (Cloern 1982). This implied a missing sink of phytoplankton biomass in South Bay, which Cloern (1982) hypothesized was clam grazing

The second example is the *Potamocorbula amurensis* invasion in Suisun Bay. *Potamocorbula* was which first detected in Suisun Bay in 1987, and its effect on phytoplankton biomass was almost immediate (Figure 3.8). Baseline biomass values dropped considerably, and peak biomass levels decreased by a factor of 5-10. Overall, mean annual biomass and dropped five-fold after the *Potamocorbula* invasion, and the state of chronic low annual primary production has persisted since 1987. While substantial phytoplankton biomass was observed over multiple months (May-September) during most years prior to 1987, blooms have occurred only rarely post-1987. *Potamocorbula* biomass exhibits pronounced seasonality and large interannual variability (Figure 7.8), as well as considerable spatial variability (Figure 7.9). One reason for clam loss during late summer and fall is predation by migratory waterfowl. The seasonality in *Potamocorbula* abundance may allow windows for blooms to develop before clam grazing rates are high enough to draw down phytoplankton biomass. Occasional spring blooms have been observed over the last several years (Dugdale et al, 2012; R Dugdale, pers. comm.). A large fall bloom was also observed in September 2011. *Potamocorbula* tolerate salinities that are commonly encountered in Suisun Bay (Low Salinity Zone, LSZ), and are well-established at all depths throughout Suisun and at locations in San Pablo Bay (Figure 7.9). *Potamocorbula* do, however, have a fairly clear up-estuary boundary, apparently dictated by salinity (Figure 7.9). *Potamocorbula* are voracious filter feeders, and, at their current densities in the LSZ, grazing rates typically exceed phytoplankton growth rates in the LSZ (Figure 7.10; Kimmer and Thompson, 2013).

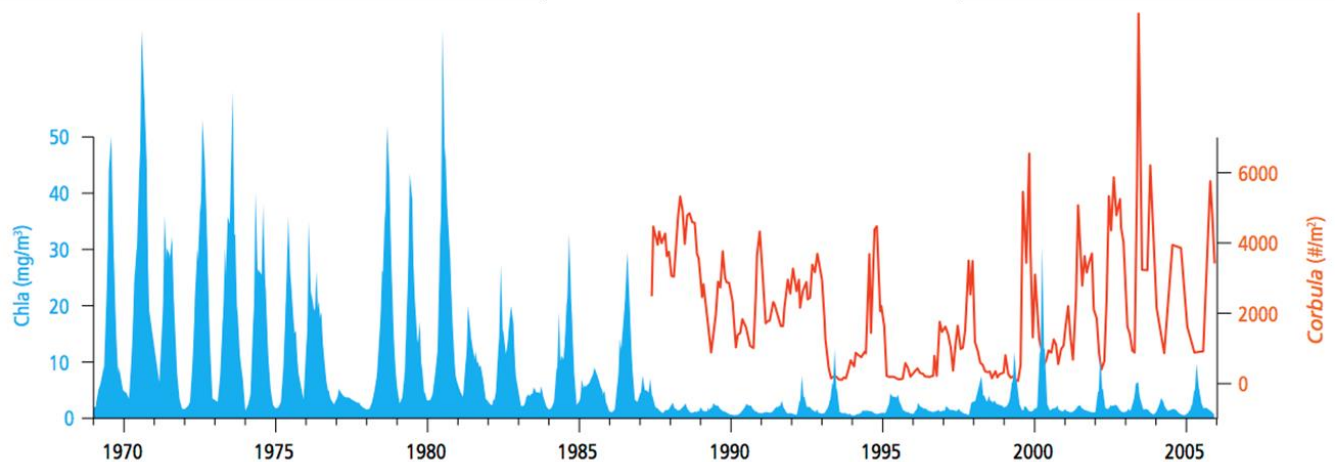


Figure 7.8 Chl-a biomass and *Corbula* biomass in Suisun Bay. Note the temporal coincidence of *Corbula* biomass minima and phytoplankton biomass maxima. Plot from Werme et al 2011. Data from IEP/DWR.

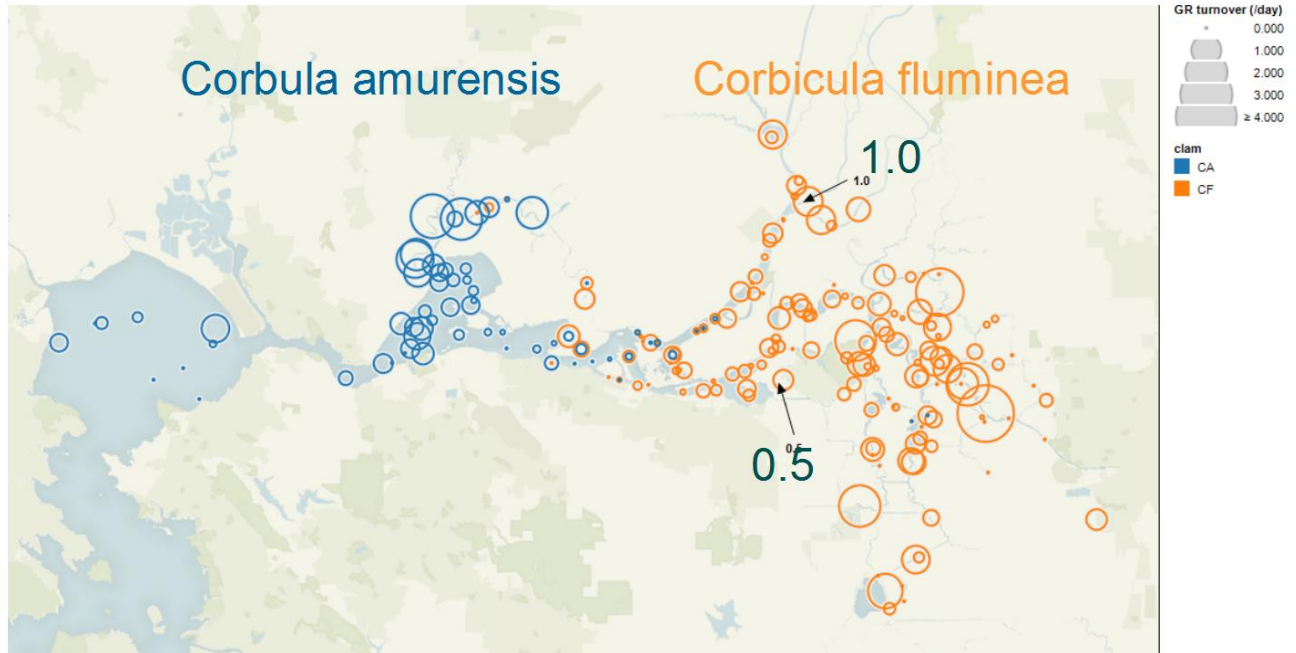


Figure 7.9 Grazing water column turnover rates (units of d^{-1}) for *Corbula* in Suisun *Corbicula fluminea* in the Delta. Source: J Thompson, pers. comm.

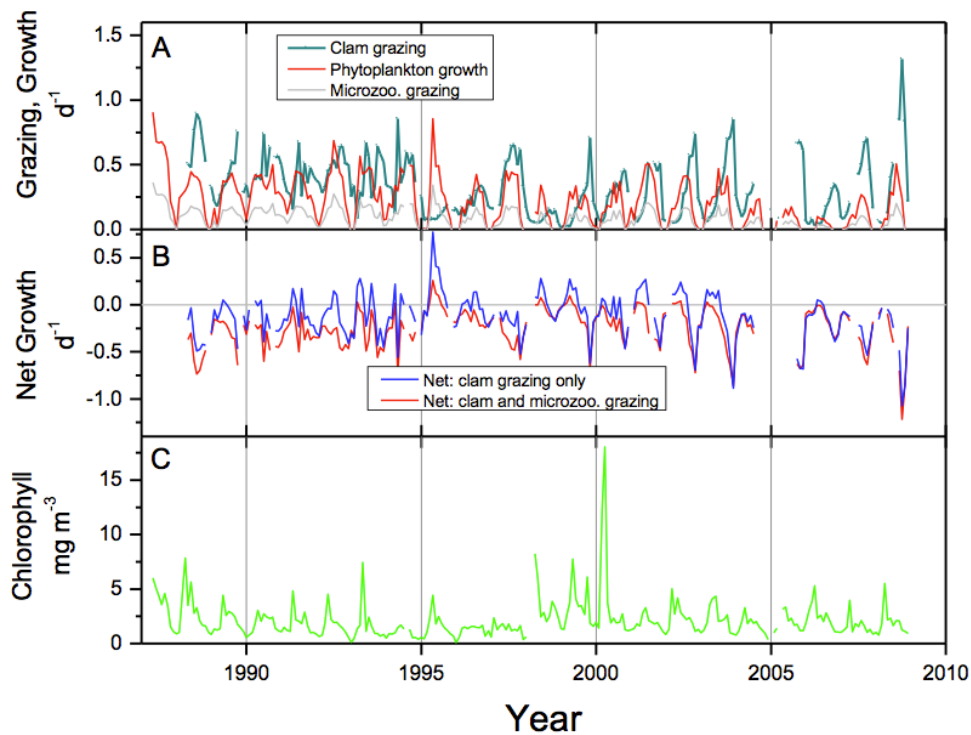


Figure 7.10 Calculated growth and grazing rates in the Low Salinity Zone (essentially Suisun Bay). Source: Kimmerer and Thompson (2014)

The third example of benthic grazer impacts on biomass is from South Bay. Through the mid-1990s, benthic filter feeding was considered to be one of the dominant controls on phytoplankton biomass accumulation and productivity in South Bay (Thompson et al., 2008 ; Lucas et al., 2009). Clams were heavily preyed upon by migrating birds in the fall. Thompson et al. (2008) observed that interannual variations in abundance and timing of spring reestablishment of benthic suspension feeders along the shoals dictated whether or not blooms could form on the shoals, and propagate from the shoals to the channel (Figure 7.4.B). In addition, Cloern et al (2007) observed sharp increases in chl-a and in gross primary production in the South Bay beginning in the late 1990s (Figure 7.11). After ruling out several potential drivers (e.g., changes in nutrient loads), they hypothesized that the increase in phytoplankton biomass was due, at least in part, to a pronounced loss of benthic suspension feeders. They argued that the decline in benthos abundance was due to an observed increase in benthivorous predators (sole, Bay shrimp, Dungeness crab; Figure 7.12), which they argued was attributable to large-scale climate forcings that resulted in increased oceanic production of juvenile predators that migrated into SFB to feed and grow (a change in the North Pacific Gyre Oscillation; Cloern et al., 2010).

The amount of historic data on benthos abundance and on-going benthos monitoring varies spatially in SFB. The IEP has several long-term monthly benthos monitoring stations in Suisun and San Pablo Bays (Peterson and Vayssières 2010). In recent years there has also been ample additional benthos monitoring by a semi-annual IEP pilot randomized monitoring program in San Pablo Bay, Suisun Bay, and the Delta; it is not yet known if this program will continue in future years. There are no sustained benthos programs in the other subembayments; however, there are multiple years during which intensive benthic sampling has taken place (e.g., Thompson et al. 2008; see Figure 7.4), and other opportunistic sampling efforts after which samples have been archived but not yet analyzed for biomass (J Thompson, personal communication). A consistent benthos monitoring program is needed in these other subembayments, most importantly Lower South Bay and South Bay, to better understand the drivers of recent change, and continue exploring cause and effect.

Pelagic grazing

Pelagic grazing rates by zooplankton are dependent on the types of zooplankton present, their abundance, and their biomass-normalized grazing rates. Copepods, mesozooplankton that are an important food resource in SFB and the Delta, derive most of their energy from phytoplankton as opposed to detrital organic matter (Mueller-Solger et al 2002; Sobczak et al 2002, 2004), and at least in Suisun Bay and the Delta are often food limited (Mueller-Solger et al 2002; Kimmerer et al 2005). Despite mesozooplankton's reliance on phytoplankton, modeling estimates by Kimmerer and Thompson (2014) suggest that they have only a limited effect on phytoplankton biomass in Suisun Bay. Cloern (1982) reached the same conclusion for South Bay. However, microzooplankton have the potential to substantially influence phytoplankton biomass in Suisun Bay (Figure 7.10; Kimmerer and Thompson, 2014). Outside of Suisun Bay there are limited data on mesozooplankton and microzooplankton biomass and feeding rates. While it may be reasonable to expect that the effect of mesozooplankton grazing on phytoplankton biomass is small Bay-wide, microzooplankton could play a substantial role, based on observations in Suisun Bay. Additional zooplankton monitoring in other subembayments is needed to better constrain pelagic grazing rates.

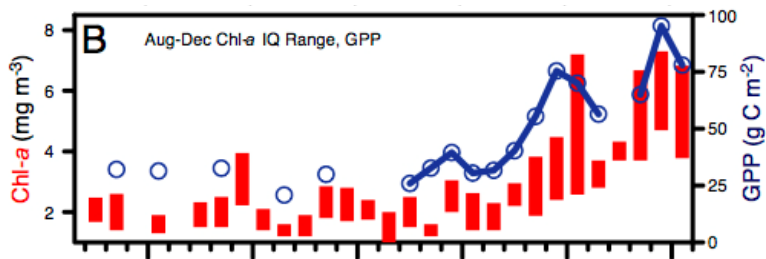


Figure 7.11 Phytoplankton biomass south of the Bay Bridge. Source: Cloern et al., 2007

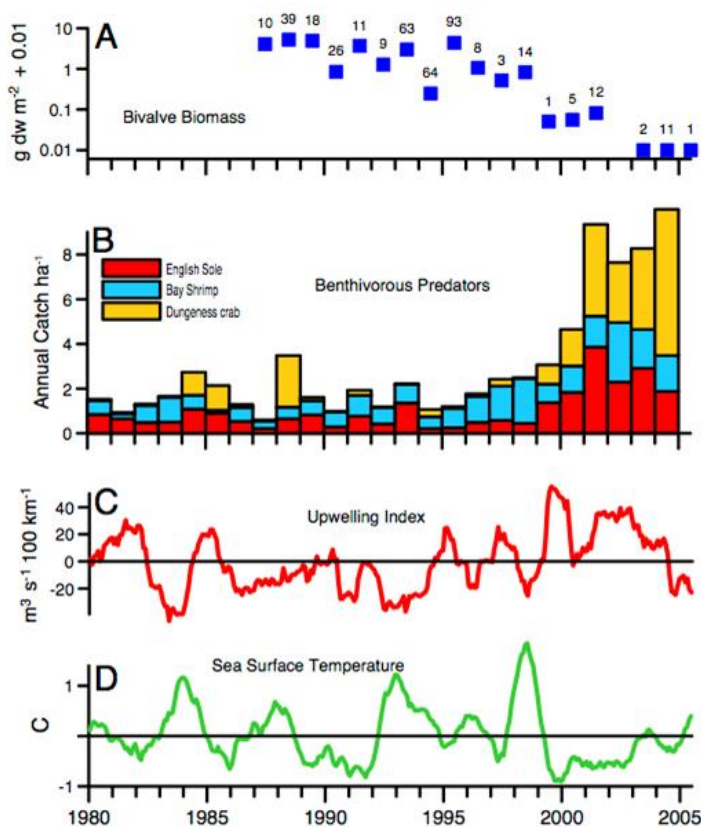


Fig. 3. Indices of biological community change within SFB and physical changes in the adjacent California Current. (A) Annual median biomass of filter-feeding bivalves across shallow habitats in South SFB; numbers above squares indicate sample number per year. (B) Mean annual catch ha^{-1} , normalized to 1980–2005 averages, of English sole, Bay shrimp, and Dungeness crab, from monthly sampling across the marine domains of SFB. (C) Anomalies in upwelling intensity computed by the National Oceanic and Atmospheric Administration from atmospheric pressure fields. (D) Sea surface temperature measured at the Farallon Islands. The bottom series (C and D) are 12-mo running averages of deviations from 1977–2005 monthly means.

Figure 7.12 Bivalve biomass, benthivorous predators, upwelling index, and sea surface temperature time series. Source: Cloern et al. 2007.

7.2.4 Spatial and temporal variations in phytoplankton biomass

Figure 7.13 presents monthly averages of phytoplankton biomass (2006-2011) broken down by subembayment; Figure 7.14 shows time series from 1975-2012. The highest phytoplankton biomass concentrations are generally observed in LSB. Bay-wide, the largest blooms typically occur in spring. Over the last ten years, however, pronounced fall blooms have also been occurring in LSB and South Bay (Figures 7.13 and 3.6). The rate of increase in chl-a concentration ($\mu\text{g L}^{-1} \text{yr}^{-1}$) is greatest in LSB and South Bay. More modest rates of increase are visually-evident in all subembayments based on rising baselines (Figure 7.14), and these increases are also statistically-significant (J Cloern, pers. comm.). Therefore, it is possible that there may be some Bay-wide common explanation that explains at least part of the increase (e.g, decreasing suspended sediment concentrations), and additional subembayment-specific explanations (e.g., decreased clam abundance).

7.3 Microphytobenthos

Microphytobenthos (MPB; i.e., benthic algae) primary production has received little attention in SFB relative phytoplankton production. However, given the large intertidal area in several of SFB's subembayments, primary production by benthic microalgae could represent a quantitatively important component of overall production. Although only roughly quantified due to limited data, Jassby et al. (1993) suggested that MPB production could account for as much as 30% of overall primary production in SFB. Thus, MPB production could have a substantial influence on food web structure (supporting organisms that utilize benthic microalgae), dissolved oxygen budgets, and nutrient cycling.

Many of the factors that influence phytoplankton growth rates will similarly influence MPB growth. These include: light availability, temperature, and nutrients (Figure 7.1). While MPB primarily occur attached to bed sediments, they are also commonly found in the water column due to physical resuspension. Benthic diatoms (mainly pennate, but some centric) have been the major MPB taxa identified in the limited studies carried out to date in SFB (Guarini et al. 2002). The standing stock of MPB biomass (often reported as mg chl-a m^{-2}) is a function of productivity rates ($\text{mg chl-a m}^{-2} \text{d}^{-1}$), grazing rates, and exchange with the water column. Light availability strongly influences MPB productivity and is a function of water column depth and light attenuation (i.e., SPM concentration), and of variations in depth due to tides. The amount of MPB resuspension depends on sediment type and consolidation, biofilm production in the sediment, and the magnitude of shear stresses (Macintyre, 1996; Underwood and Kromkamp 1999). Sediment resuspension reduces light penetration for MPB that remain at the sediment:water interface; however, MPB that are resuspended could experience increased light availability. MPB residing on intertidal mudflats experience unattenuated incident light levels during low tide, and productivity would be greatest then. Because of SFB's high turbidity, little MPB growth would occur in subtidal areas. Nutrient limitation is unlikely to be an important constraint on MPB growth, because MPB can readily access NH_4^+ and o-PO_4 diffusing out of the sediments and nutrients in the overlying water column. In sandy sediments with low organic matter content, MPB can be nutrient limited (Underwood and Kromkamp, 1999). MPB concentrations have been shown to be lower in sandy silts and sands than in finer, cohesive sediment (Cammen, 1982; Montagna et al, 1983; Cammen 1991; de Jong and de Jonge, 1995; Underwood and Smith, 1998a). Temperature will influence growth rates in way similar to

phytoplankton. CO₂ availability may also limit MPB productivity, but is likely a minor factor compared to light availability. Zoobenthos, some bottom-feeding fish, and birds would be the prime grazers on MPB. MPB biomass, however, would be generally unaffected by filter-feeding clams. Thus, MPB production may comprise a larger proportion of overall production in shallow areas with high abundance of filter-feeding clams.

While MPB production is potentially important in terms of its overall contribution to primary production in SFB, and some estimates of its magnitude have been made, little is known about how much it influences the food web, the net effect it has on dissolved oxygen budgets, or how it might respond to system perturbations (e.g, decreases in SPM). As noted above, Jassby (1993) estimated that MPB production could account for approximately 30% of overall primary production in both southern and northern SFB subembayments. Studies in other estuaries have found that MPB could account for up to 50% of total primary production (Underwood and Kromkamp, 1999). Guarini et al (2002) estimated that MPB productivity ($\text{mg C (mg chl-}a\text{)}^{-1} \text{d}^{-1}$) could be nearly 4x as large in South Bay as in Suisun Bay, due to spatial differences in MPB assemblage or bathymetry-induced differences in light exposure to intertidal areas. In a more recent study, direct measurements of sediment chl-*a* ($\text{mg chl-}a \text{ m}^{-2}$) were made in the Delta and Suisun Bay (Cornwell and Glibert 2014). Benthic chl-*a* abundance was roughly 30% greater in September 2011 than in March 2012 at both locations, which is consistent with higher expected biomass at the end of the warm season. In addition, Cornwell and Glibert (2014) found that benthic chl-*a* was approximately 4-fold higher in the Delta than in Suisun Bay, likely due in part differences in depth and light availability.

7.4 Current state of knowledge

Tables 7.1 summarizes the current state of knowledge and knowledge/data gaps related to primary production from phytoplankton biomass and MPB in SFB. The prioritizations in the rightmost two columns are related to the discussion in Section 11.

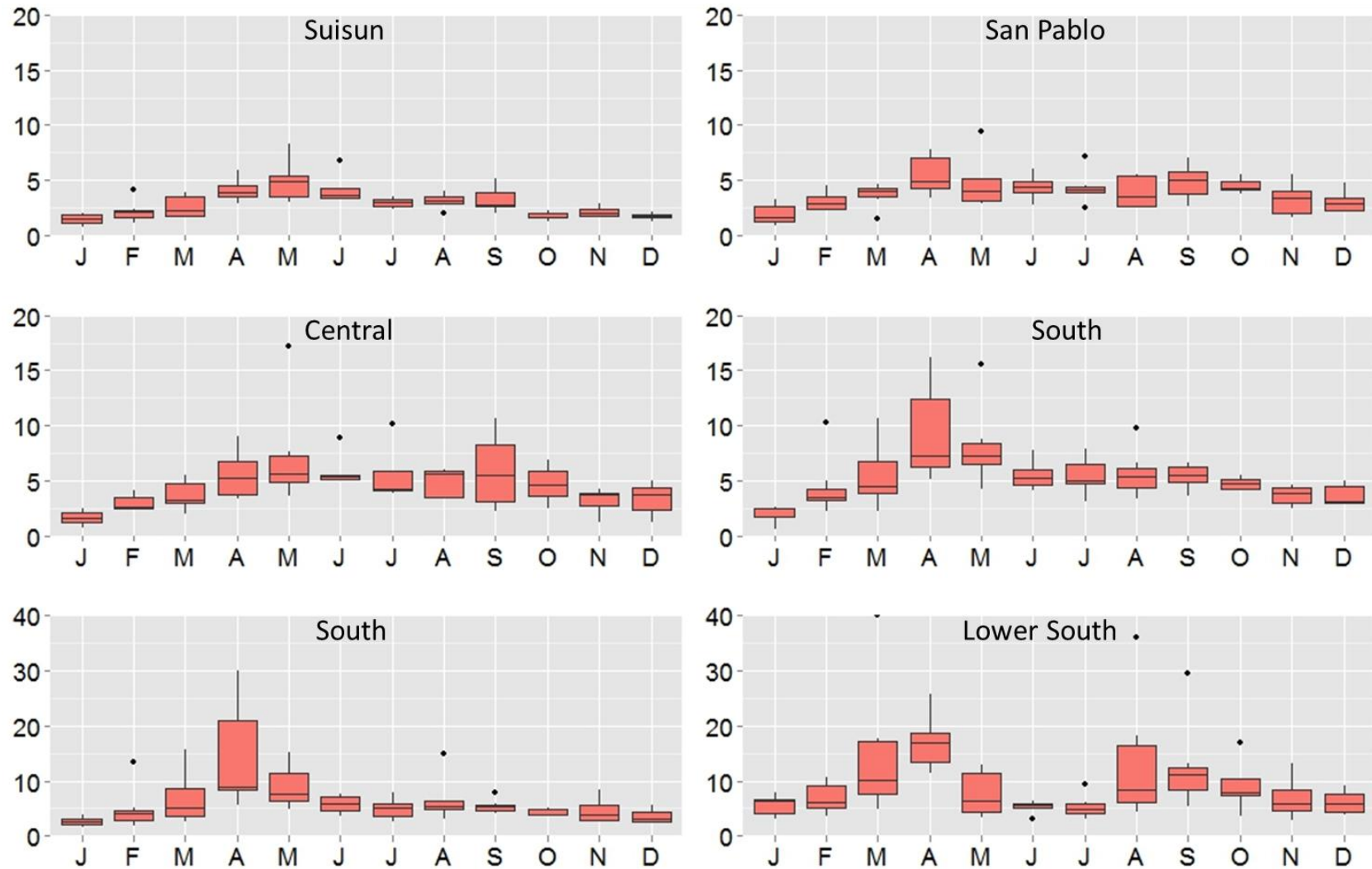


Figure 7.13 Monthly variations in chl-a ($\mu\text{g L}^{-1}$) 2006-2011. Data from USGS stations s6 (Suisun), s15 (San Pablo), s18 (Central), s21 (northern South Bay), s27 (southern South Bay) and s36 (Lower South) were used. Note the different vertical scales. Data source: <http://sfbay.wr.usgs.gov/access/wqdata/>

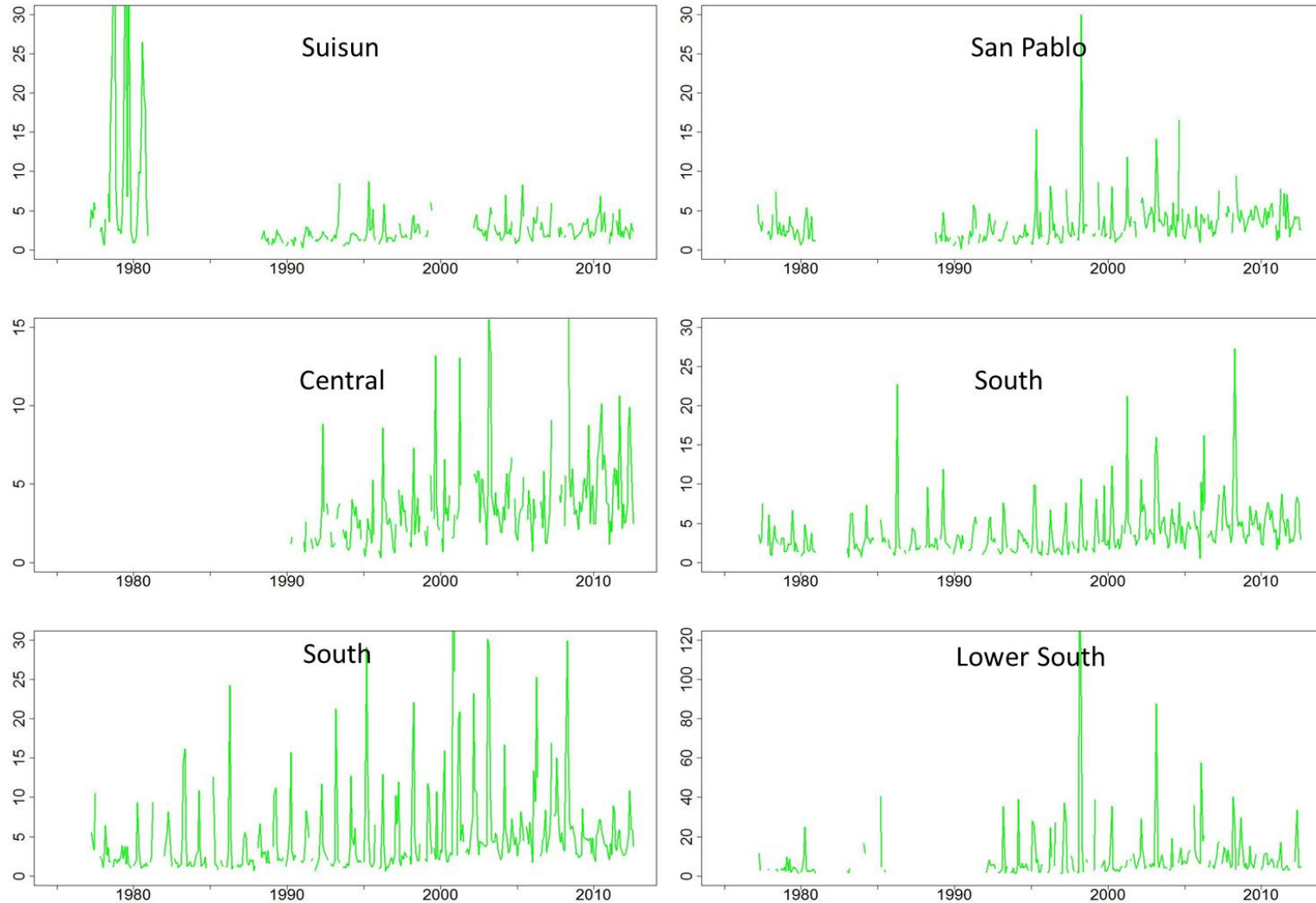


Figure 7.14 Phytoplankton biomass (mg chl-a m⁻³). Note different y-axes. Data from USGS stations s6 (Suisun), s15 (San Pablo), s18 (Central), s21 (northern South Bay), s27 (southern South Bay) and s36 (Lower South) were used. Data source: <http://sfbay.wr.usgs.gov/access/wqdata/>

2 Table 7.1 Phytoplankton and MPB productivity and biomass accumulation: current state of knowledge for key processes and parameters

Process or Parameters	Importance for quantitative understanding	Current Level of confidence about magnitude or mechanistic controls	Need for <u>additional or continued</u> data collection, process studies, modeling	Priority for study in next 1-5 years
PHYTOPLANKTON - Processes				
Primary production rates	High	Low/Moderate: Basic understanding about light limited production is well modeled. Recent studies suggest that the relationship may have shifted, and revisiting this may be important for estimating system productivity.	Very High	High
Pelagic grazing	High	Low: Long-term program in Suisun Bay/Delta for macrozooplankton, but limited micro-zooplankton data, which may be more quantitatively important in terms of overall grazing rate. No systematic zooplankton sampling in LSB, South Bay, Central Bay.	Very High	High
Benthic grazing	High	Low: good data to support estimates in Suisun Bay. Limited data in LSB South Bay. Monitoring of benthos abundance would inform this.	Very High	Very High
Sinking, respiration, burial	High	Moderate: Discussed within context of Dissolved Oxygen	Low	Low
Inhibition of primary production rates by elevated NH ₄ ⁺	High/ Uncertain	Low: Several studies have been completed and others are underway. Uncertainty remains about mechanism and relative importance of the process. Field/lab studies and modeling work can be done in parallel, with the former designed to further elucidate the mechanism and thresholds and the latter to quantify its role relative to other factors.	Very High	Very High
Production in the shoals vs. channels (during stratification), and physical or biological controls on bloom growth/propagation	High	Low: Considered to be an important process but limited data available. Data needed to better predict bloom magnitudes.	Very High	Very High
Germination of resting stages	Low	Low: Not considered among the highest priority processes to study	Low	Low
PHYTOPLANKTON - Ambient concentration data				
High frequency data in channel	High	Low: Very limited high temporal resolution (continuous) phytoplankton biomass data beyond of Suisun Bay. Needed to better predict blooms.	Very High	Very High
High temporal resolution data in shoals	High	Low: Very limited high temporal resolution (continuous) phytoplankton biomass data beyond of Suisun Bay. Needed to better predict blooms.	Very High	Very High
Biomass data along the Bay's deep channel	High	Moderate/High: USGS program has been collecting monthly data at along the channel for the past 35 years, and needs to be continued.	Very High	Very High
Phytoplankton C:N ,C:chl-a, and size-fractionated chl-a	High	Low: Valuable information to inform understanding of processes and for modeling	Very High	Very High

Process or Parameters	Importance for quantitative understanding	Current Level of confidence about magnitude or mechanistic controls	Need for <u>additional or continued</u> data collection, process studies, modeling	Priority for study in next 1-5 years
<i>Microphytobenthos - Processes</i>				
Primary production rates	Moderate	Low: may be able to predict productivity based on light levels and chl-a, although needs to be confirmed	Moderate	Moderate
Grazing	Moderate/Unknown	Low: Potentially important as a sink, but difficult to study.	Low	Low
<i>Microphytobenthos - Ambient abundance data</i>				
Basic biomass information, seasonal, spatial	High	Low: Very limited data on MPB abundance and productivity, despite the fact that MPB productivity may be comparable in magnitude to phytoplankton productivity.	High	High

8 Dissolved Oxygen

8.1 Introduction

Dissolved oxygen concentrations are a highly relevant indicator of nutrient-related impairment, both because maintaining sufficient dissolved oxygen levels is critical for sustaining aquatic life, and because low dissolved oxygen is a common ecosystem response to high nutrient loads. Oxygen is both produced and consumed within the estuary, and also transported into the water column across the air:water interface by gas exchange and by water inputs. If the oxygen loss rate exceeds the oxygen production or input rate, dissolved oxygen levels decrease and hypoxia or anoxia can develop. Persistent hypoxia or anoxia leads to aquatic organism stress or death, or, for organisms that can escape low DO areas, causes the loss of habitat. Anoxia leads to sulfide gas production, which can be toxic to aquatic organisms and causes both odor problems and infrastructure damage (corrosion, discoloration of painted exteriors). In addition, under low DO conditions NH_3 can accumulate to levels that exert direct toxicity on benthos.

Prior to the 1970s, areas of SFB, specifically LSB, did experience low DO (Cloern and Jassby, 2012). Implementation of secondary wastewater treatment addressed the issue of large-scale and persistent anoxia in deep subtidal areas. However, limited information is available about DO levels in margin habitats, including sloughs, tidal wetlands, and managed ponds, and the occurrence and potential impacts of low DO there are unknown.

8.1 General DO conceptual model

Dissolved oxygen concentration, measured at a given point in space and time in the water column, represents the concentration that results from multiple competing production and loss processes, as well as inputs, outputs, and mixing (Figure 8.1).

8.1.1 DO transport

O_2 is readily exchanged across the air:water interface, and is highly soluble in water, with the DO saturation concentration (DO_{sat} ; mg/L) varying in direct proportion to the O_2 partial pressure in the overlying air. DO_{sat} decreases with increasing water temperature and salinity. If DO concentrations in the water column are undersaturated relative to O_2 in the overlying air, atmospheric exchange will occur, with O_2 flux from the atmosphere into the water column. If DO concentration exceeds saturation (e.g., after periods of intense photosynthesis), DO flux will occur from water to the atmosphere. In both cases, exchange at a rate proportional to the magnitude of DO under- or over-saturation and the amount of mixing-energy at the air:water interface (determined largely by wind speed in open-water areas).

DO also enters (or leaves) a habitat through fluvial transport (from the Delta, perennial ephemeral streams, stormwater inputs, and treated wastewater effluent), water exchange between subembayments (advective, tidal, gravitational), and mixing or exchange between habitats within a subembayment. Exchange between adjacent subembayments or habitats can result in net increases or decreases in DO depending on whether the prevailing conditions differ substantially between the two systems. During coastal upwelling events, gravitational circulation (i.e., intrusions of denser (colder, more saline) water) has the potential to transport substantial volumes of relatively low DO water far up-estuary, displace an equal volume of relatively DO-

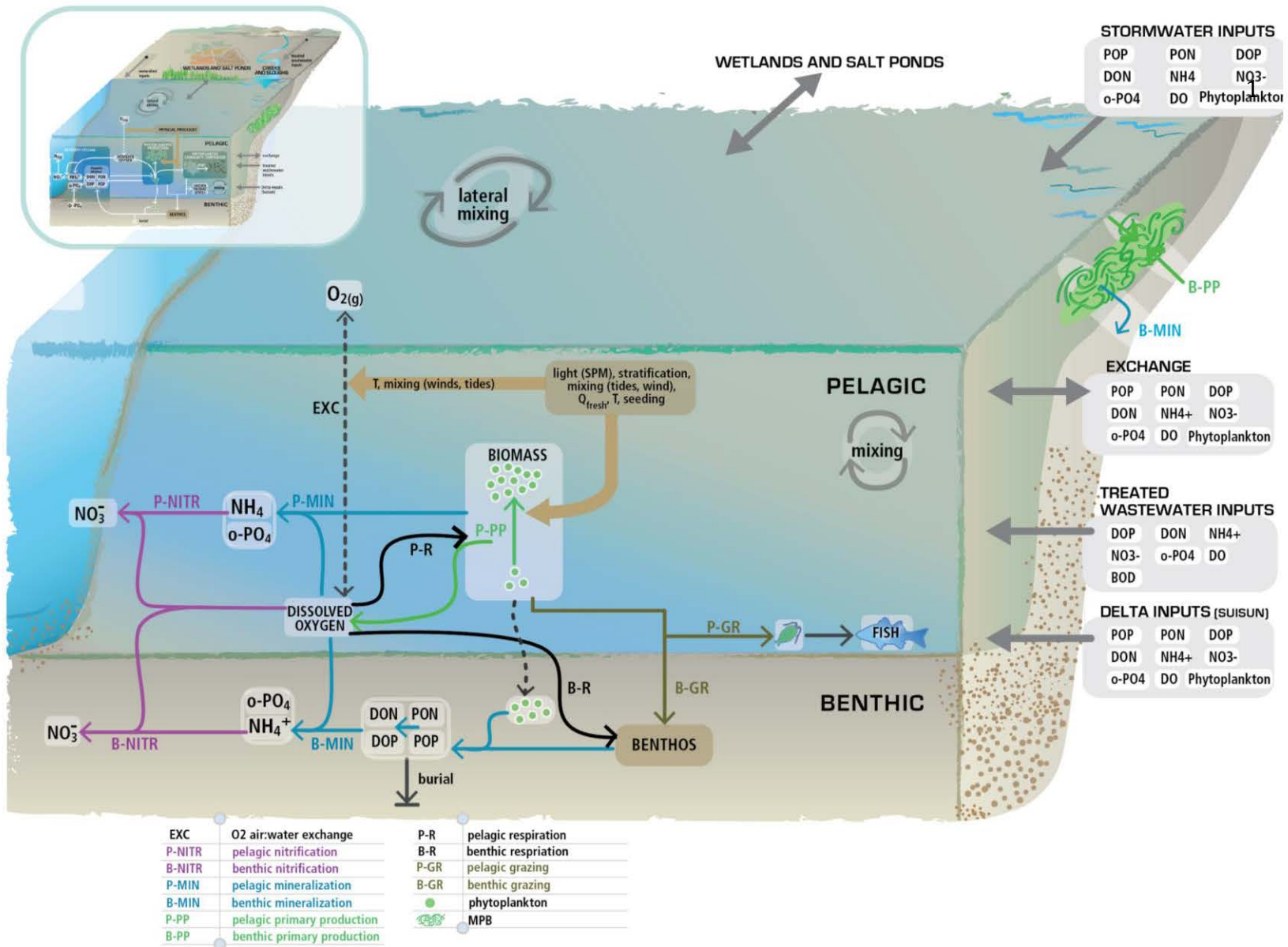


Figure 8.1 Dissolved oxygen conceptual model

rich water down-estuary, and measurably influence DO concentrations when the water column mixes. Tidal exchange between a subembayment and wetlands, salt ponds, and sloughs along its margins could be a net source or sink of DO, depending on the balance of O₂ production and consumption in those systems. This is discussed further below.

8.1.2 O₂ production and consumption

The major processes that result in DO production or consumption are illustrated in Figure 8.1 Primary production - by phytoplankton, MPB, and macrophytes – produces O₂ during daylight hours. The O₂ production rate varies in proportion to the primary production rate, which, for phytoplankton and MPB, is light-limited in most SFB habitats. Thus, analogous to primary production rates (Section 7), O₂ production rates exhibit large variability on hourly and seasonal time scales, respond to weather conditions that influence incident light (cloud cover or fog), and may vary substantially between shallow and deep habitats or in response to stratification.

Respiration by aquatic and benthic organisms consumes DO. Viable phytoplankton respire throughout the entire day, and consume oxygen in the process. During daylight hours, their O₂ production exceeds respiration, resulting in net O₂ production; however, during dark periods only respiration occurs, with net DO consumption. As a result DO levels can exhibit a diurnal sinusoidal-like cycle, with maxima and minima near mid-afternoon and sunrise, respectively. In some habitats, transport of water masses with differing DO concentrations by semi-diurnal tides whose magnitude varies on a spring-neap cycle can mask the diurnal signal generated by respiration and production (SFEI, 2014c).

The balance between O₂ production and consumption is also influenced by microbial respiration of dead organic matter (OM). Microbes consume oxygen while mineralizing or degrading OM derived from two broad source categories: biomass from during primary production by phytoplankton, MPB, and other plants within SFB (autochthonous OM); and terrestrial organic matter (allochthonous OM) carried to the Bay by freshwater inputs and treated wastewater effluent (i.e., the latter of which is commonly referred to as biochemical oxygen demand, BOD)., While BOD loads to SFB from POTWs used to be high, those loads decreased substantially once secondary treatment was implemented in the 1970s. Some OM mineralization occurs in the water column (pelagic respiration), but much of it happens in the sediments and at the sediment:water interface (benthic mineralization) where particulate OM accumulates after settling. Aerobic microbial respiration occurs continuously, although respiration rates are strongly influenced by temperature, the abundance of fresh or readily-degradable OM, and DO concentrations. In the sediments, when the DO supply is exhausted (which often occurs within a few millimeters or centimeters into the sediments), anaerobic respiration occurs using alternate electron acceptors (nitrate, manganese(IV), iron(III), sulfate). Although anaerobic respiration does not directly consume O₂, the reduced compounds produced during anaerobic respiration (Fe(II), Mn(II), sulfide) diffuse upward through the sediments into oxygenated sediment layers or into the water column, and react with and consume O₂ there.

Nitrification of NH₄⁺ to NO₃⁻ by nitrifying microbes also consumes O₂. Major NH₄⁺ sources to the Bay include the NH₄⁺ discharged in treated wastewater effluent from POTWs and NH₄⁺ produced *in situ* during OM respiration. Nitrification of NH₄⁺, and associated O₂ consumption, occur in both the water column (pelagic nitrification) and at the sediment:water interface (benthic nitrification).

Sediment oxygen demand (SOD) can play a dominant role influencing the O₂ budget of a habitat. SOD is an overarching term that includes benthic mineralization, benthic nitrification, and benthic oxidation of reduced compounds. SOD tends to exert greater influence over DO concentrations in shallow habitats, where the ratio of overlying water volume to sediment area is relatively small compared to deeper areas. While SOD includes several types of reactions, its magnitude is ultimately driven by the amount of OM loading to the sediments. That OM can be imported to the system (fluvial inputs; allochthonous OM) or produced *in situ* (autochthonous OM). As respiration proceeds, OM in the sediments is consumed. The rate and total amount of SOD depends on the rate and total amount of new OM delivery to the sediments. In SFB, a large portion of SOD likely traces back to autochthonous OM production by phytoplankton and MPB, and therefore to nutrient loads, although allochthonous inputs may contribute more substantially to SOD in margin habitats and in Suisun Bay (due to allochthonous inputs from the Delta).

8.1.3 Spatial differences in O₂ budgets and DO concentrations in SFB

An aquatic ecosystem's O₂ budget can be characterized in terms of whether it acts as a net producer or consumer of O₂, referred to as net ecosystem metabolism (NEM). If a system produces more (NEM > 0) or less (NEM < 0) oxygen than it consumes it is considered net autotrophic or net heterotrophic, respectively. NEM will vary considerably based on the time scale and location considered, because of temporal (e.g., diurnal variability in O₂ production rate) and spatial variability in the magnitudes of O₂ sources and sinks. Past studies have shown that SFB shallow shoals and intertidal areas are likely to have NEM > 0 (Caffrey et al. 2003). Atmospheric exchange, along with high rates of phytoplankton and MPB primary production (due to the shallow water column and higher average light levels), maintain high DO concentrations. While benthic mineralization, benthic nitrification, pelagic mineralization and pelagic respiration also occur in these areas, the DO inputs more than offset these O₂ sinks.

SFB's deep subtidal habitats more frequently have negative NEM (Caffrey et al. 1998), and, as a result, DO is often undersaturated in these areas. Due to light limitation, deep areas generally experience lower rates of pelagic primary production than shallow habitats, and little or no MPB primary production occurs due to insufficient light. As a result, O₂ production rates are lower. At the same time, deep channel areas receive both viable and dead/decaying phytoplankton inputs through lateral exchange with shallow subtidal areas, which exert O₂ demand. Although atmospheric flux of O₂ may occur at similar rates in shallow and deep habitats, the same O₂ flux entering the deep water column is diluted over a larger volume; thus this exchange may not keep pace with respiration losses. Primary production rates in deep channel areas can be higher when the water column stratifies (Figure 7.2.B). However, eventually this OM settles to the bottom where it is respired. During stratified periods, DO concentrations can decrease in bottom waters due to respiration, since DO cannot be replenished through vertical mixing or atmospheric exchange at the surface. Due to the relatively short duration of stratification events in SFB, DO in deep subtidal habitats seldom dip below 80% saturation (Figure 3.12). Low DO can also be observed in SFB bottom waters when plumes or "intrusions" of recently-upwelled and relatively dense (colder, more saline) coastal water containing low-DO enter through the Golden Gate and occupy the bottom layer of some subembayments. Monitoring data from USGS R/V Polaris cruises indicate that these events tend to be fairly short-lived, with the water column mixing fully over the period of days to weeks.

While ship-based measurements indicate that DO levels in deep subtidal areas generally fall above the 5 mg/L Basin Plan standard (Figure 3.12, Kimmerer, 2004), continuous monitoring data at Dumbarton bridge illustrate that DO concentrations do vary substantially. During summer and fall, DO concentrations at Dumbarton Bridge commonly vary by 1-2 mg L⁻¹, with lowest concentrations observed at low tide (Figure 3.13 A), and values occasionally dipping below 5 mg L⁻¹. The variability in DO is strongly associated with tidal stage (SFEI 2014, 2014c). One plausible hypothesis for the correspondence between low DO and low tide is that, at low tide, the water moving past sensors at Dumbarton Bridge has a higher percentage of water from margin habitats where DO may be lower. The large variability suggests that oxygen demand within LSB can be quite substantial at the subembayment scale. In LSB, USGS *Polaris* sampling has most frequently occurred at slack high tide. It is therefore possible that DO concentrations from USGS *Polaris* cruises are biased high. During Summer 2014, USGS sampling cruises detected DO < 5 mg/L at other deep subtidal stations south of the Dumbarton Bridge during two cruises (<http://sfbay.wr.usgs.gov/access/wqdata/archive/longterm.html>).

SFB's shallow margin habitats – e.g., sloughs, tidal wetlands, and restored salt ponds ringing LSB - experience large DO swings that are influenced by both temporal variability in DO production rates and tidal exchange (Thebault et al., 2008; Schellenbarger et al., 2008). Compared to the abundance of monitoring data available for deep subtidal habitats (Figure 3.12), DO data for shallow margin habitats is quite limited. However, the observations that are available suggest that DO concentrations commonly dip below 5 mg L⁻¹ in those habitats, and frequently reach much lower values (Figures 3.14 and 8.2; SFEI 2014c). Continuous DO measurements (moored sensors at a single location) in sloughs provide evidence of large DO swings occurring at a periodicity that points to a strong tidal influence (Figure 8.2). Sloughs are shallow habitats and may have higher average light levels and greater DO production during daylight hours than the open Bay during some low turbidity periods; but sloughs also frequently have elevated turbidity due to sediment resuspension, which decreases light levels. Connection of some sloughs to salt ponds or wetlands could deliver higher loads of dead organic matter to slough sediments, increasing benthic mineralization rates. At night, net O₂ production is negative, which in a non-tidal system would lead to early morning DO minima. However, the diurnal cycle in O₂ production is superposed upon semi-diurnal tidal exchange. During flood tide, relatively DO-rich water from the open areas of LSB moves into the margins and above the sensors (depending on distance upslough from the open water and tidal phase, i.e., spring or neap) and supplements the O₂ budget (Figure 8.2). In the cases illustrated in Figure 8.2, DO minima and maxima occur twice daily, with maxima sometimes occurring at night and minima during the day, suggesting that the tidal influence on DO can be as strong or stronger than the diurnal variations in DO production.

Some highly-altered habitats in SFB, such as restored salt ponds and the surrounding sloughs in LSB, have delicately balanced O₂ budgets. The ponds have extremely high primary production rates and O₂ production rates, made possible by relatively high average light levels because of the shallow environment, and high nutrient concentrations (Thebault et al., 2008). Benthic mineralization rates are also high due to the reservoir of labile OM in the sediments. As a result, large diurnal fluctuations in DO levels occur (Figure 3.15.A and 8.2). While Figure 3.15A shows a diurnal cycle of maxima and minima, DO also drops to low levels for longer periods of time. Thebault et al. (2008) observed that when primary production rates are periodically low

(e.g., during a prolonged period of summer clouds or fog), sustained periods of anoxia can occur (Figure 3.15.B). On the one hand, the high productivity in restored salt ponds supports wetland food webs, including those of migratory birds (Thebault et al. 2008). On the other hand, the extent to which the large diurnal fluctuations in DO, or the more prolonged periods of anoxia that occur on cloudy days (Thebault et al., 2008), may be having adverse impacts is not currently known.

The slough and salt pond examples discussed here were specifically for LSB. However, South Bay, San Pablo Bay, and Suisun Bay also have substantial shallow subtidal margin habitats. Shallow margin habitats commonly experience naturally-low DO concentrations. In these habitats, it will be important to explore several questions: How common is low DO? Are events more severe (frequency, duration, DO deficit, spatial extent) than would be expected under natural conditions? Are the events having adverse impacts on beneficial uses? To what extent are anthropogenic nutrients contributing to or causing these events? Well-designed experiments, monitoring, and modeling may be needed in some of these systems to assess condition, and quantify the major drivers of O₂ budgets.

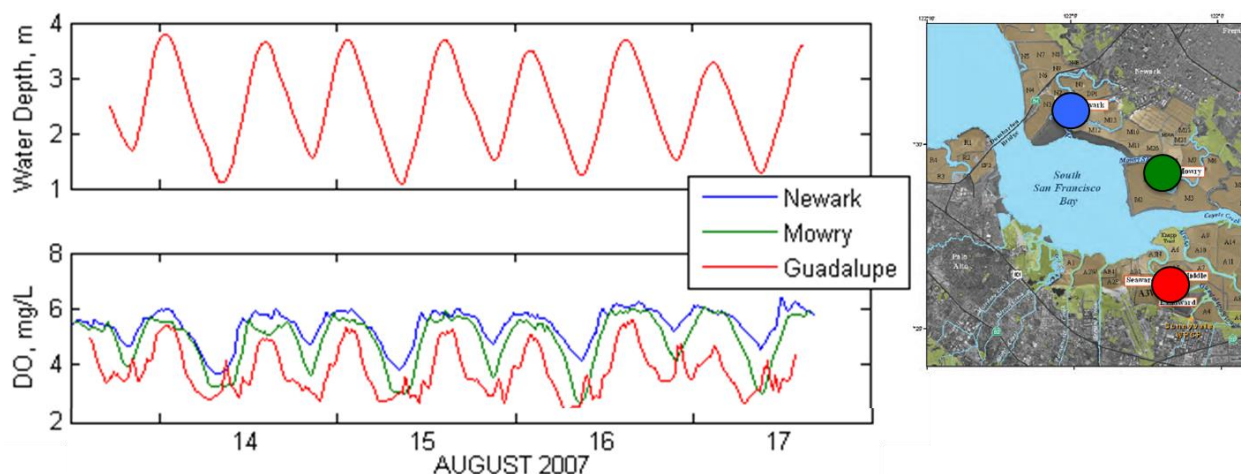


Figure 8.2 Dissolved Oxygen in three slough habitats in Lower South Bay measured using continuous monitoring sensors. Top panel shows water depth. Dissolved oxygen concentrations increase during the flood tide due to water with higher DO from LSB being tidally advected into sloughs. DO concentrations gradually decrease over the outgoing tide interval, likely caused, at least in part, by sediment oxygen demand within the sloughs, and lower DO water from up-slough moving back over the sensor. Colors of lines correspond to location denoted by circle colors in map. Source: Schellenbarger et al., 2008

8.2 Current state of knowledge

Table 8.1 summarizes major knowledge and knowledge data gaps for dissolved oxygen. The prioritizations in the rightmost two columns are related to the discussion in Section 11.

Table 8.1 Dissolved Oxygen: current state of knowledge for key processes and parameters

Process or Parameters	Importance for quantitative understanding	Current Level of confidence about magnitude or mechanistic controls	Need for <u>additional or continued</u> data collection, process studies, modeling	Priority for study in next 1-5 years
Processes or loads				
Atmospheric exchange	High	Moderate: Difficult to measure but readily modeled (albeit with substantial uncertainty)	Low	Low
Pelagic and benthic nitrification (for O ₂ budget)	Low/Moderate	Moderate: NH ₄ loads/concentrations provide an upper bound on this oxygen sink. It is not expected to be a major DO sink, or	Low	Low
Sediment oxygen demand (Benthic respiration + oxidation of reduced compounds).	High	Low: This set of processes is particularly important for understanding O ₂ budget in shallow margin environments. The mechanisms are well understood but rates are poorly constrained and likely are highly variable in space/time. Field experiments are possible. Increased (high spatial/temporal resolution) monitoring of DO will also allow “average” demand to be quantified by difference/modeling.	Very High	Very High
Pelagic and benthic primary production rates	High	Low: Benthic production rates, in particular are particularly poorly constrained and would require field surveys. Pelagic rates can be reasonably well-estimated based on phytoplankton biomass and light. As noted above, high spatial/temporal resolution monitoring of chl-a will help refine estimates	Very High	Very High
Pelagic respiration	Moderate	Moderate: In shallow areas, sediment oxygen demand will be of much greater importance than pelagic respiration. Pelagic respiration rates by viable phytoplankton can be reasonably well-estimated based on biomass. Respiration of dead OM is a function of OM abundance and quality, and water temperature. In deep channel areas of the Bay, where pelagic respiration will be more important than sediment oxygen demand, low DO does not appear to be a major issue, and thus constraining these rates are not among the highest priorities.	Low	Low
DO – Ambient concentration data				
High spatial resolution DO data in deep channel	High	Low: USGS research program provides an excellent long-term record along the Bay’s spine. This work needs to be continued.	Very High	Very High
High temporal resolution DO data in deep channel	High	Low: Limited DO data available from continuous sensors, in particular in South Bay and LSB. A network of sensors is installed in Suisun Bay and the Delta.	Very High	Very High
High temporal resolution data in shoals and shallow margin habitats	High	Low: Some special studies have been performed, and some on-going monitoring by POTWs and others (e.g., USGS studies in salt ponds). While these individual efforts have valuable information and some reports are available, a meta-analysis of this data has not been completed, and there is currently no overarching regional program.	Very High	Very High

9. Phytoplankton Community Composition

9.1. Introduction and Background

Phytoplankton community composition is highly relevant to the ecological status and function of the greater San Francisco Bay. The importance of community composition follows directly from the general conceptual model for phytoplankton biomass (Section 7), since it is the community at the level of strains, species, and functional types that in aggregate makes up the “phytoplankton biomass”. Selection pressure operates on species and has resulted in systematic phylogenetic differences between the red and green “superfamilies” (Quigg et al., 2003). These evolutionary differences in turn drive differences in nutrient assimilation, elemental composition, growth rates, and size (Irigoien et al., 2004; Irwin et al., 2006; Quigg et al., 2003). This has profound effects on ecosystem function. Phytoplankton photosynthesis drives the metazoan food webs of San Francisco Bay (Cloern et al., 2005; Jassby et al., 1993; Kimmerer et al., 2012). Changes in community composition can also alter energy flow from predominantly supporting higher trophic levels to a microbially-dominated, highly regenerating community which in turn leads to increased respiration and hypoxia (c.f. Cloern and Dufford 2005).

There are several potential ways to assess community composition (Figure 9.1). One of the simplest divisions is based on size. As a general rule, increased mean (or median) phytoplankton size is directly related to increased productivity, increased new production, and increased trophic transfer (Chisholm, 1991; Wilkerson et al., 2000). Phytoplankton size is particularly important for SFB because only phytoplankton $> \sim 5 \mu\text{m}$ equivalent spherical diameter (ESD) are available as a food source for copepods (Berggreen et al., 1988). Size-based classification is sometimes coupled with nutritional mode to separate the plankton into heterotrophs, mixotrophs, and photoautotrophs (Figure 9.2). While this is convenient conceptually, there is increasing evidence that many phytoplankton, including perhaps the majority of dinoflagellates, are facultative mixotrophs, blurring the line between these divisions (Burkholder et al., 2008).

Moving beyond size, a common approach taken when examining community composition is to group organisms into “phytoplankton functional types” (PFTs) such as diatoms, dinoflagellates, cryptophytes, etc., and/or based on trait-differentiated groupings such as high-nutrient, high light, etc. (Reynolds et al., 2002; Smayda et al., 2001). This level of analysis is often convenient for relating phytoplankton composition to ecological forcing functions (e.g. Cloern and Dufford, 2005). Continuing to a finer level of detail, community composition can also be analyzed at the species level, the basis for taxonomic classification. Finally, there is increased interest in the molecular and strain-level variability of phytoplankton. This becomes particularly important when the organism of interest is considered a harmful algal bloom (HAB) species (Burkholder et al., 2006), in part because many of the coastal HAB organisms do not fit well into classic paradigms as a function of PFT or size (Kudela et al., 2010).

For the purposes of this conceptual model, it is assumed that phytoplankton community composition can be adequately addressed using a combination of high-level metrics (size, trophic status, functional category) with the exception of HAB organisms that must be assessed at the species or strain level.

Size	Trophic Status	Functional Type	Genus/Species/Strain
Picoplankton (0.2-2.0 μm)	Heterotroph	Cyanophyte	>500 species,
		Chlorophyte	Unknown # of strains...
Nanoplankton (2-20 μm)	Mixotroph	Cryptophyte	
		Pyrrophyte	
Microplankton (20-100 μm)	Autotroph	Bacillariophyte	

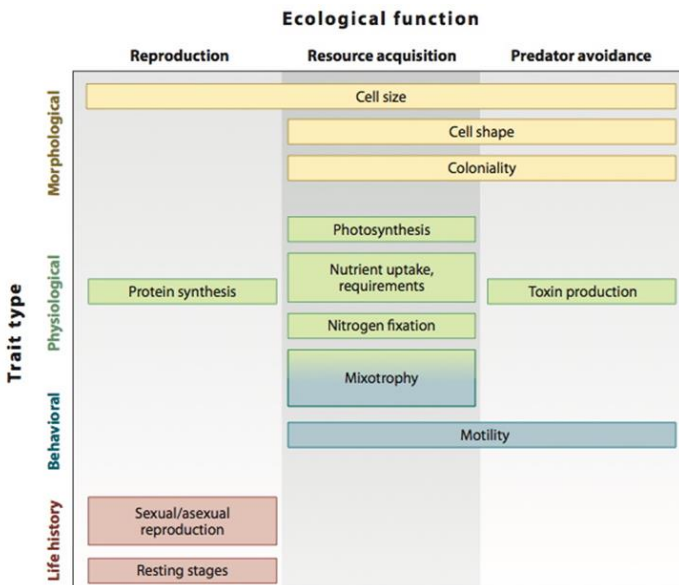


Figure 1
A typology of phytoplankton functional traits.

Figure 9.1. Examples of partitioning phytoplankton community structure. Classification can be based on phylogeny or on ecological function and traits, or some combination. Figure on right is from Litchman and Klausmeier (2008)

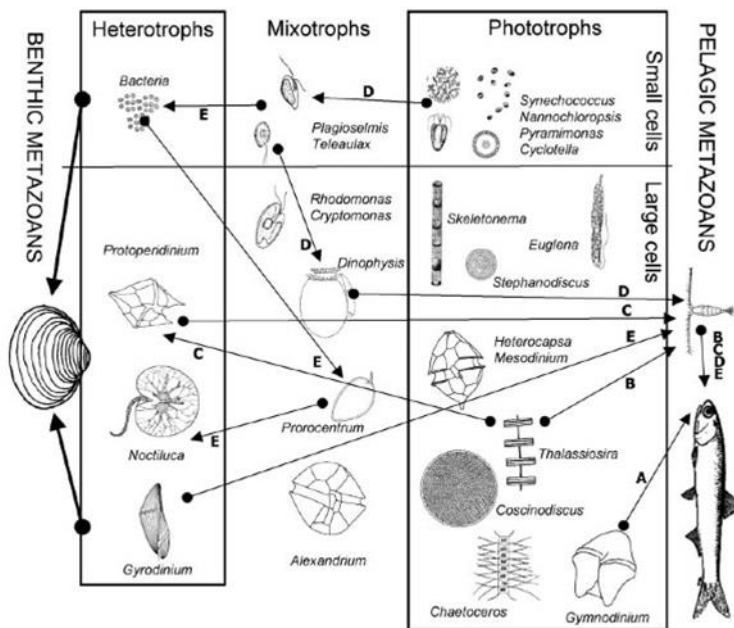


Fig. 7. Phytoplankton classification by size (small cells <15 μm) and nutritional mode that influence pathways through which energy and essential biochemicals are supplied to benthic metazoans (e.g. bivalve mollusks) and pelagic metazoans (e.g. copepods and anchovies). Trophic Pathway A is an efficient direct link from large-cell phototrophs to larval fishes. Other pathways route energy through mesozooplankton: (B) directly from large-cell phototrophs, (C) from heterotrophic algae feeding on large-cell phototrophs, or (D) from mixotrophs or (E) microheterotrophs deriving energy fixed by small-cell phototrophs and routed through the microbial loop. Some images redrawn from Tomas (1993, 1996)

1

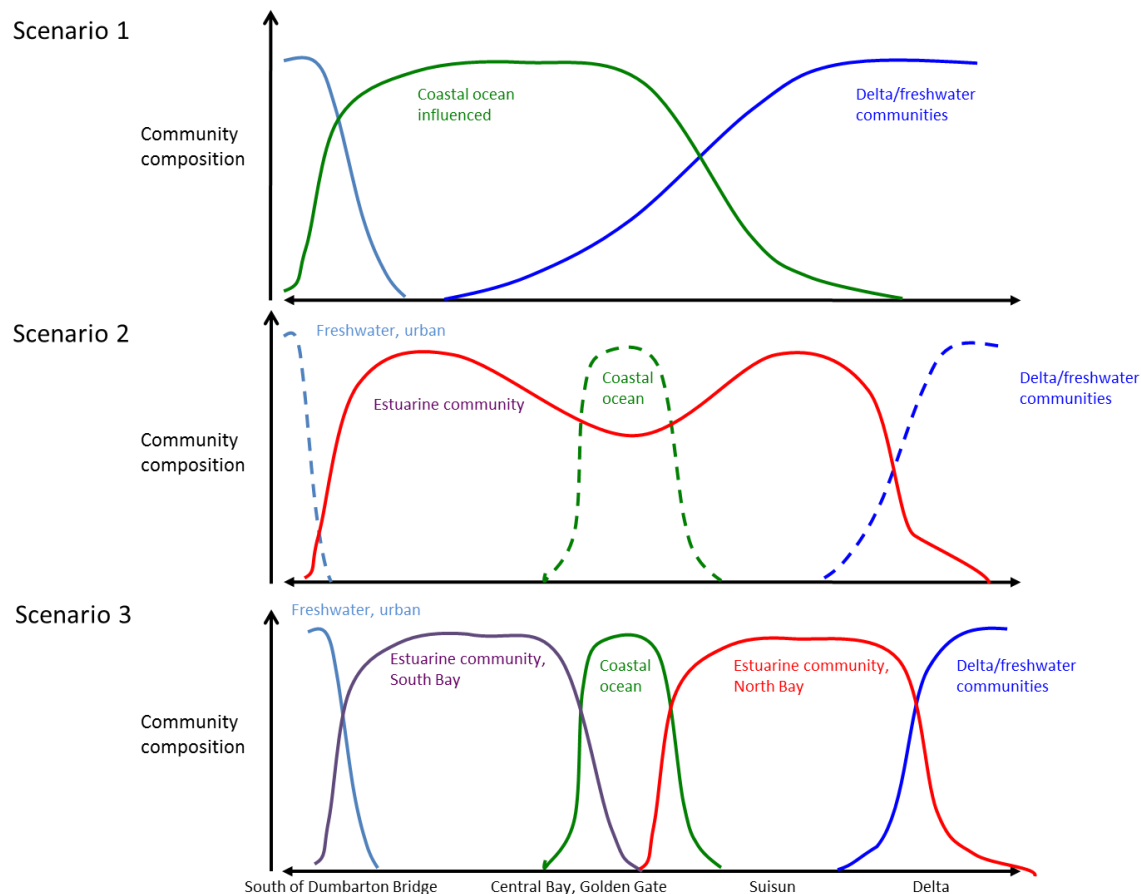
Figure 9.2. From Cloern and Dufford (2005).

2 9.2. General Conceptual Model

3 In order to use community composition as a metric for ecosystem status it is first necessary to
 4 define the spatial extent of the Bay included in the model. While the physical (geographical)
 5 boundaries are set, with the open ocean as one (external) boundary and the Sacramento/San
 6 Joaquin River and South Bay inputs as the other boundary, there are at least three potential
 7 models for describing San Francisco Bay (Figure 9.3):

- 8 1) the Bay is a mixture of the ocean and riverine end-members;
- 9 2) the Bay is a separate and distinct estuarine community, with mixing (source and sink) of
 10 oceanic and freshwater phytoplankton at the boundaries;
- 11 3) the Bay is composed of a series of basins (e.g. South Bay, Central Bay, etc.) with distinct
 12 community composition.

13
 14 Under scenario 1, community composition is largely driven by external factors that influence the
 15 oceanic and freshwater end-members. Scenario 2 assumes that the phytoplankton are dominated
 16 by a distinct estuarine community with transient “invasion” by oceanic and riverine inputs.
 17 Scenario 3 is predicated on distinct communities occupying each sub-basin, responding to
 18 location-specific forcing, such that Suisun is under fundamentally different control than South
 19 Bay (for example). These scenarios are not mutually exclusive, and could (for example) vary
 20 seasonally or interannually in response to river flow, residence time, and hydrologic
 21 modifications such as the restoration of the South Bay Salt Ponds.



22 **Figure 9.3** Conceptualization of 3 scenarios of spatial variability in phytoplankton assemblage

23 The community composition data necessary to evaluate these conceptual models do exist, and
 24 some distinct patterns have been identified between subembayments (e.g. South Bay and North
 25 Bay). However, the data are often aggregated to look at large-scale and long-term patterns
 26 (Cloern et al., 2005, 2010; Kimmerer, et al. 2012; Winder et al., 2010) unless there is an obvious
 27 end-member intrusion impacting the community composition (Cloern et al., 2005; Lehman et al.,
 28 2010). ***A first-order question that should be examined in more detail is whether a sub-basin
 29 analysis provides more or less information than the aggregate trends.*** For now, it is assumed
 30 that a simple model with oceanic, freshwater, and estuarine components is sufficient for
 31 development of a community composition conceptual model. This forms the basis for the
 32 conceptual model developed by the Phytoplankton Composition working group (Figure 9.4).
 33 Specific forcing functions are discussed in more detail below.

34 9.2.1. General trends

35 San Francisco Bay exhibits both a weak seasonal cycle and decadal trends in community
 36 composition that generally follow the trends identified for the Biomass conceptual model. Total
 37 chlorophyll in the Delta is typically high in summer (Jassby et al. 2002) while chlorophyll in
 38 south San Francisco Bay is the highest during (typically) several-week spring blooms and shorter
 39 fall blooms (Cloern et al. 2007). Like many nutrient enriched systems, San Francisco Bay is
 40 characterized by a bloom-bust cycle of larger cell species periodically dominating a more stable
 41 community of small cell species (Cloern and Dufford, 2005; Wilkerson et al., 2006; Kimmerer et
 42 al. 2012). These large-cell blooms are superimposed on a picoplankton background population
 43 composed primarily of cyanobacteria and small eukaryotes (*Nannochloropsis* sp., *Teleaulax*
 44 *amphioxeia*, *Plagioselmis prolonga*) that are found across a wide range of salinities and seasonal
 45 conditions (Ning et al., 2000; Cloern and Dufford, 2005).

46
 47 San Francisco Bay contains over 500 phytoplankton taxa. Approximately 10-20 phytoplankton
 48 species account for between 77% and >90% of the total biomass (Cloern and Dufford, 2005).
 49 Diatoms (Bacillariophyta) dominate, accounting for ~81%; dinoflagellates and cryptophytes
 50 (Pyrrophyta and Cryptophyta) made up 11% and 5% respectively (Cloern and Dufford, 2005).
 51 Picoplankton make up <15% of the Bay biomass (<2% during blooms; Ning et al., 2000; Cloern
 52 and Dufford, 2005).

53
 54 At a decadal scale several shifts in community composition are evident. Some phytoplankton
 55 taxa (*Prorocentrum aporum*, *Coscinodiscus marginatus*, *Protoperidinium depressum*, *Eucampia*
 56 *zodiacus*) have not been seen since 1996 while others (*Protoperidinium bipes*, *Pseudo-nitzschia*
 57 *delicatissima*, *Scrippsiella trochoidea*, *Thalassiosira nodulolineata*) have appeared. In addition,
 58 the benthic diatom *Entomoneis* sp. similarly was a minor component of the community from
 59 1992-2001, comprising 0.1% of the biomass and identified in about 20% of all samples (Cloern
 60 and Dufford 2005, as reported in Kimmerer 2012). Kimmerer et al 2012 suggest that, although it
 61 is not clear how much it contributes to productivity in the water column, its sudden appearance at
 62 a fairly substantial portion of phytoplankton biomass could be an indication of change in the
 63 system.

64
 65 Several studies have argued that there is also evidence for abrupt shifts in community
 66 composition from the longer time-series. Total biomass decreased substantially in 1986 (Figure
 67 9.5) as noted by many others (e.g. Lehman, 2000; Glibert, 2010; Kimmerer, 2012). Lehman
 68 (2000) described a decrease in diatom abundance from 1975-1989 and hypothesized a

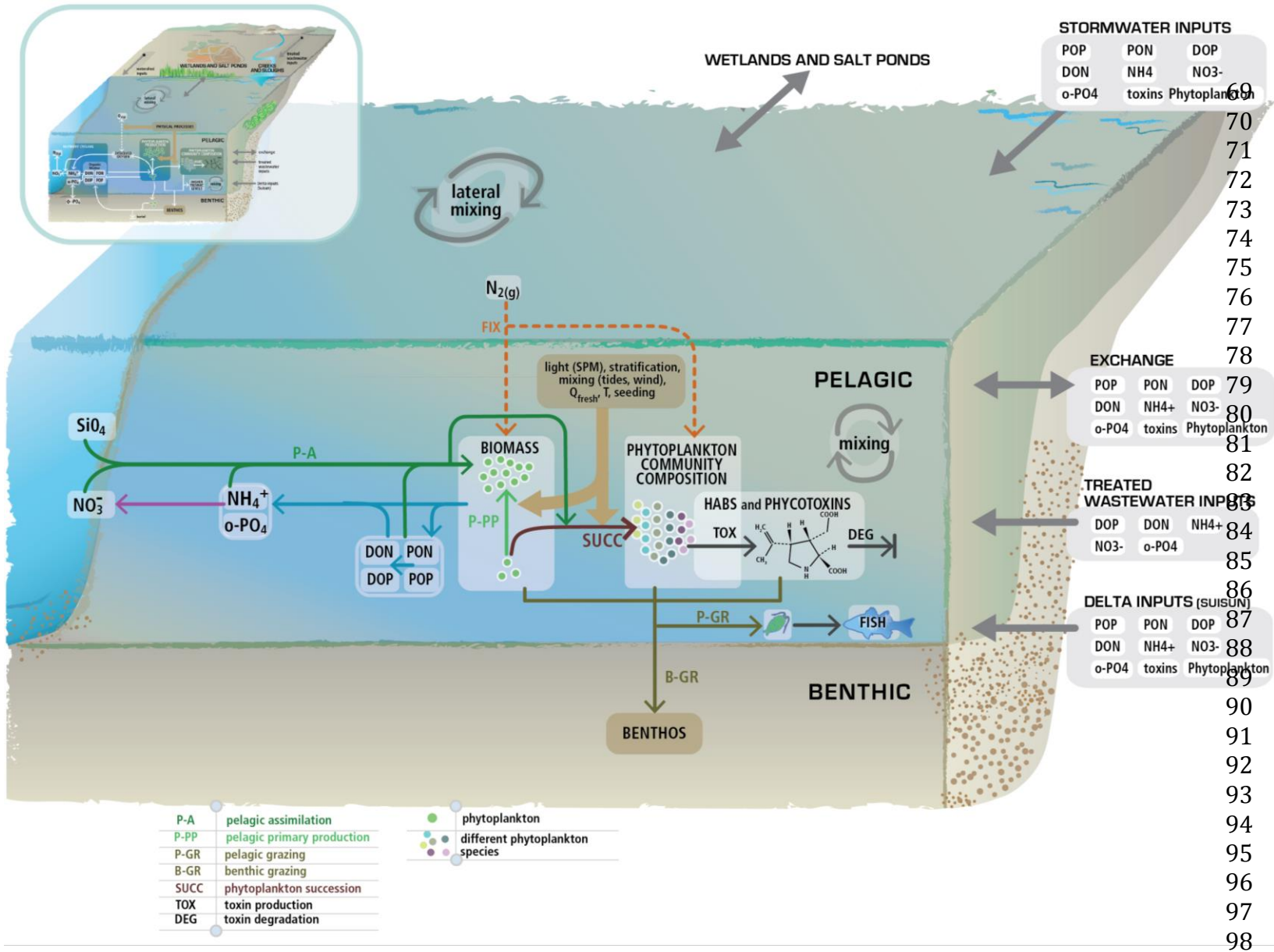


Figure 9.4 Phytoplankton community composition conceptual model

mechanistic link to the 1977 climate regime shift and El Niño, attributing the change to community shifts in high stream flow, wet years (low light, high turbulence, favoring pennate diatoms) and dry years (long residence time, favoring cryptophytes and flagellates). Using the same data, Glibert (2010) described a decline in diatoms, and increase in cryptophytes, chlorophytes, and cyanobacteria after 1986, coincident with an abrupt decline in biomass. These shifts were attributed to changes in nutrient composition and stoichiometry. The proposed phytoplankton community composition changes and hypothesized mechanisms for those trends are based on long-term monitoring data collected by DWR Environmental Monitoring Program (DWR-EMP) at multiple stations throughout Suisun Bay and the Delta from 1975-present. Considering the multi-decade and multi-station record that the EMP dataset offers and the considerable attention the nutrient-focused hypotheses have received over the past several years, the dataset has received relatively limited systematic analysis. That data is currently being reanalyzed to evaluate trends in phytoplankton assemblage and their correspondence with changes in physical, chemical, and biological drivers (Malkassian et al., in preparation; Cloern et al., in preparation).

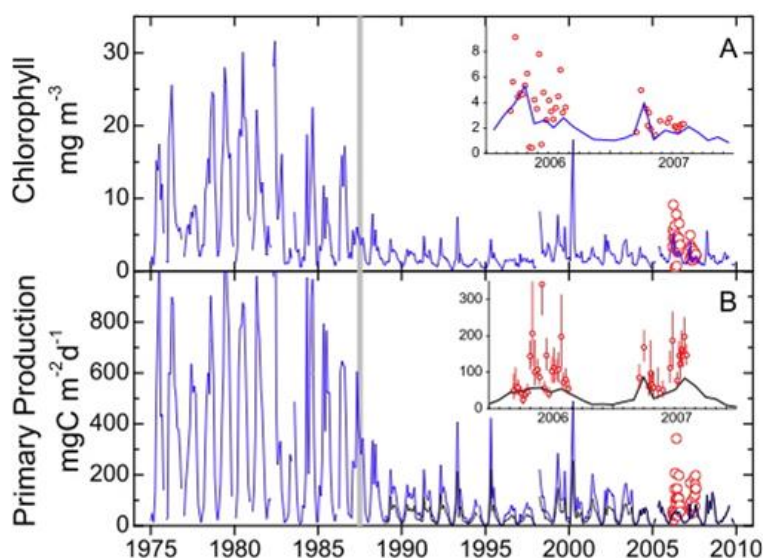


Fig. 9 Chlorophyll concentration (*A*) and estimated primary production (*B*) in this study and from a long-term monitoring program. *Insets* show data for 2006–2007 only. *A Lines* monthly means of chlorophyll from the Interagency Ecological Program environmental monitoring (Sommer et al. 2007) for stations in the western Delta to San Pablo Bay with salinity between 0.5 and 10; *open circles* means by date from all salinities in this study; *B Lines* primary production estimated from IEP

data on chlorophyll and Secchi depth and using PAR estimated as in Fig. 7; *line* from 1975 to 1988 and *upper line* to 2004 use the mean value of Ψ determined from data of Cole and Cloern (1984), and the *lower line* and that after 2004 use the mean value of Ψ from our data for 2006 and 2007 combined (Parker et al. 2012). *Error bars* in inset give 95% confidence limits

Figure 9.5. From Kimmerer et al. 2012.

9.2.2. Bottom-Up Controls

Basin-scale oscillations

There is ample evidence that San Francisco Bay community composition responds more or less uniformly (i.e. across the estuary) to both basin-scale and climate-scale trends. As described above, Lehman (2000) identified stream flow as an important indicator of community composition. Low light, turbulence, and short residence times were associated with pennate and single-celled centric diatoms. Cryptophytes and flagellates were associated with “critically dry” periods of increased residence time, light intensity, and water temperature. Cloern et al. (1983)

similarly argued that river flow can regulate community composition by selectively retaining particles (neritic diatoms) near productive shallow bays under low flow, but promotes loss of seed populations during both high and very low flow (drought) because of changes in circulation and the position of the suspended particulate maximum. Within the Delta, low streamflow has also been associated with enhanced *Microcystis* blooms (Lehman et al. 2010), attributed to reduced turbulence and prolonged retention. Basin-scale oscillations also profoundly impact the coastal plankton assemblage. Since the oceanic end-member can serve as a seed population for the estuary, San Francisco Bay is also indirectly influenced by El Niño, the Pacific Decadal Oscillation, the North Pacific Gyre Oscillation, and other mesoscale changes (Cloern et al. 2005, 2010).

While these observed patterns suggest that community composition is regulated to some degree by bottom up controls (and therefore can be to some extent predicted; Cloern et al. 2011), a larger analysis of coastal estuaries suggests that each estuarine system is unique and responds to some combination of annual forcing, regime shifts and climate trends, and the residual (or stochastic) component (Cloern and Jassby 2008, 2010), suggesting that the low-frequency basin- or climate-scale patterns must be interpreted with caution.

Temperature

Phytoplankton species composition is strongly controlled by temperature, since each species and strain exhibits an optimal growth response to a specific temperature range (Eppley, 1972). In addition to this species-level response, PFTs also exhibit some generalized temperature optima. Diatoms generally prefer colder temperatures, and are associated with cool periods both annually and interannually in San Francisco Bay (Lehman 2000). Diatoms also exhibit optimal nitrate assimilation at lower temperatures and also reduce nitrate under cold temperatures as an electron sink to maintain optimal energy balance (Lomas and Glibert, 1999). As temperature rises some PFTs respond positively. *Microcystis* and other cyanobacteria appear to be favored by warmer conditions (Lehman et al. 2010; Paerl and Huisman 2008, 2009). Less is known about the temperature-specific response for other PFTs (flagellates, cryptophytes, dinoflagellates) but community composition generally shifts towards more of these groups coincident with increased temperature (e.g. Lehman 2000). Because temperature covaries with several other environmental factors including flow, nutrients, stratification, etc. it is difficult to determine what the impact of rising temperatures would be. ***Experimental manipulations of temperature or temperature and CO₂ would provide useful information about potential shifts in phytoplankton community composition for San Francisco Bay.***

Irradiance

San Francisco Bay productivity is generally considered to be light-limited, and is well described by a “light utilization” productivity model that uses chlorophyll, PAR, and light attenuation (Cole and Cloern 1984). Parker et al. (2012) recently re-evaluated this approach and concluded that while the general model still works, there is considerable variability in the calibration coefficient, possibly due to a shift in the carbon:chlorophyll ratio of the phytoplankton assemblage. Parker et al. (2012) noted that concurrent evaluation of the phytoplankton community composition from 2006-2007 (during their study period) by Lidström (2009) are consistent with PFT-specific shifts in both the C:CHL ratio and P_m^B (light-saturated productivity). The authors conclude that seasonal, interannual, and long-term shifts in community composition from diatoms to flagellates may be linked to changes in the modeled

productivity. It should be noted, however, that the analytical techniques for measuring production rate differed between Cole and Cloer (1984) and Parker et al. (2012), and that some or all of the apparent difference in the calibration coefficients could be the result of these analytical differences. ***In either case, these observations suggest that, if bulk productivity estimates are to be used as an index of ecosystem health, the light-utilization model should be evaluated for its sensitivity to PFT-specific response functions and potentially other factors (e.g., temperature, light levels).***

Mixing/Turbulence

As summarized in Cloern and Dufford (2005), mixing and turbulence become important for phytoplankton community composition primarily through alleviation of light limitation due to runoff-induced salinity stratification, increased light penetration (decreased turbidity), and separation of phytoplankton and benthic grazers. Classically, it is also assumed that diatoms respond positively to turbulence while ephemeral dinoflagellate blooms respond to “windows of opportunity” when environmental conditions, such as reduced grazing, enhanced stratification, and warm conditions, allow these organisms to respond rapidly (e.g. Stoecker et al. 2008; Cloern et al. 2005). As noted above, there is also evidence for shifts between diatoms and flagellates/cyanobacteria linked to changes in retention and mixing (e.g. Lehman et al. 2010). It should be noted, however, that Cloern and Dufford (2005) noted niche-separation of a small number of marine and riverine species, but also noted that a large fraction of the phytoplankton community were “generalists”, doing equally well across a broad range of conditions (Figure 9.6). This suggests that canonical descriptions of PFT response to environmental conditions such as mixing are potentially useful but should not be over-interpreted.

9.2.3 Physiological Factors: Nutrients

San Francisco Bay is generally considered to be nutrient-replete. This has been corroborated several times (e.g. Mallin et al. 1993), and is supported by the lack of response between productivity and river flow (Kimmerer 2005; Kimmerer et al. 2012). While this perspective is useful for examining forcing of phytoplankton biomass, this general nutrient-replete condition can mask considerable variability at the species or PFT level of community composition. It is generally assumed that dinoflagellates exhibit low affinity for N-substrates relative to diatoms (Smayda, 1997, 2000) and that nutrient uptake kinetics scale as a function of cell size (larger size equals lower affinity; e.g. Irwin et al., 2006; Litchman et al., 2007), although Collos et al. (2005) argue that at high-nutrient concentrations, such as in upwelling systems and estuaries, multiphasic kinetics may be quite common among a diverse array of phytoplankton species. Kudela et al. (2010) summarized the measured kinetics responses for N-uptake in several algal groups, focusing on harmful algal bloom species from upwelling systems (Figure 9.7). While the general canonical pattern of lower K_s for diatoms and higher for dinoflagellates, there is considerable overlap and the number of recorded species is quite low. It is particularly striking that there appear to be no phytoplankton strains isolated from San Francisco Bay in the National Center for Marine Algae (NCMA). Again, this highlights the need to be cautious when applying canonical patterns for nutrient utilization derived from global data sets.

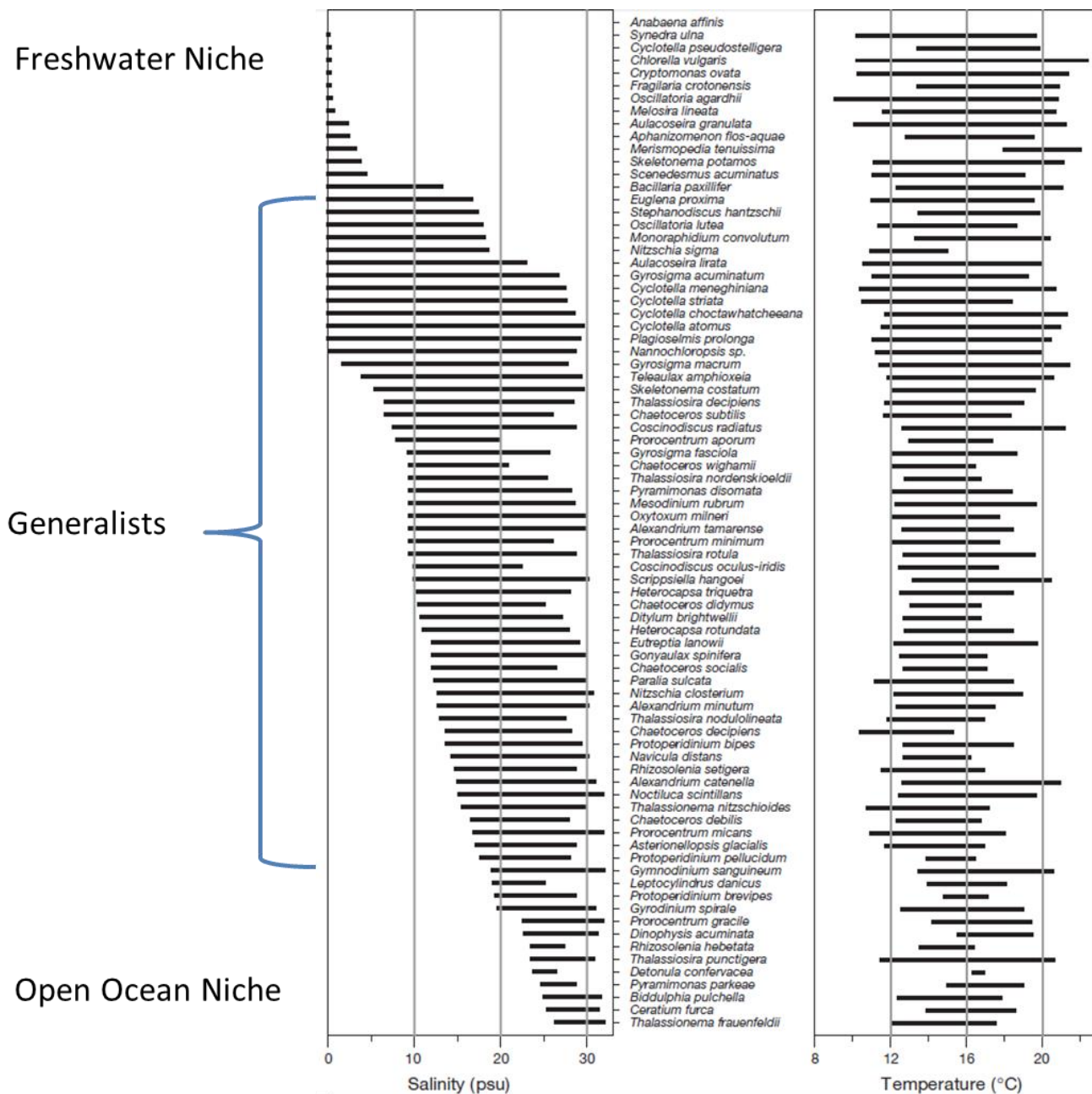


Fig. 6. Salinity and temperature ranges of selected phytoplankton species. Horizontal bars span 10th and 90th percentile salinity and temperature at which each species occurred within 599 samples distributed along salinity gradients of San Francisco Bay (Fig. 2B,C)

Figure 9.6 From Cloern and Dufford 2005.

Despite the nutrient-replete status of San Francisco Bay, several groups have proposed direct or indirect nutrient effects on phytoplankton species composition. While not specific to San Francisco Bay, vitamin B1, B7, and B12 have been implicated in controlling phytoplankton species composition in estuarine (Tang et al. 2010), coastal, and HNLC waters (Koch et al. 2011). The response is greatest in large (>2 μm ESD) cells, and in particular for dinoflagellates. There has been no published evaluation of vitamin B effects in San Francisco Bay.

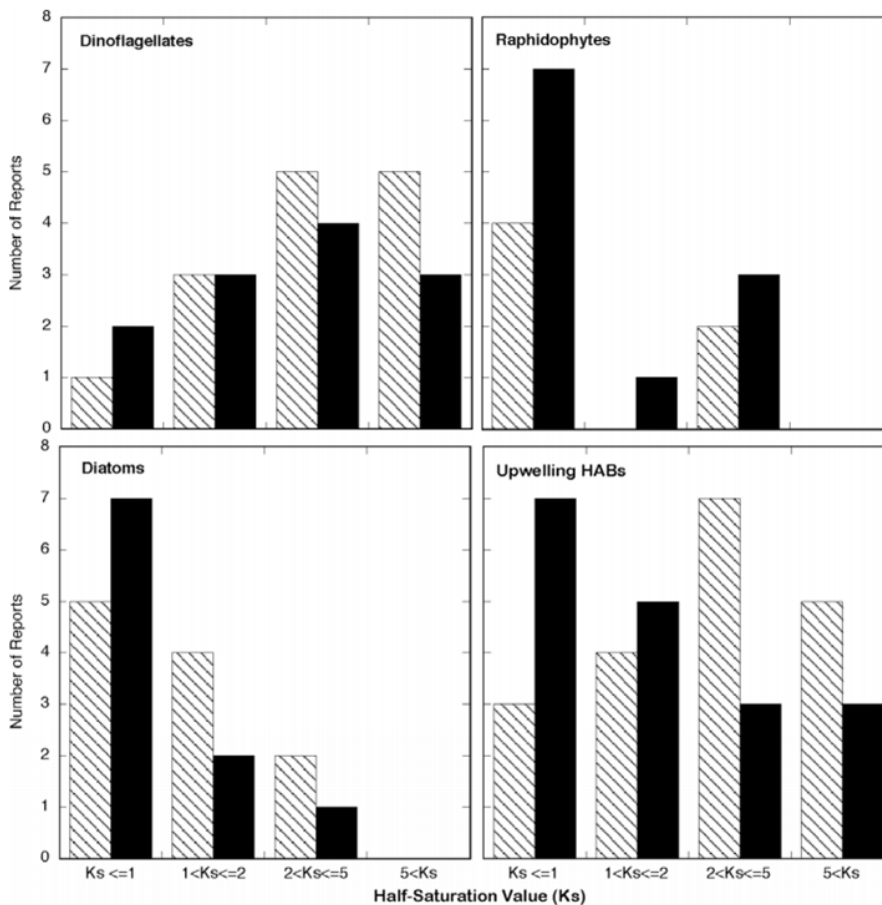


Fig. 1. Kinetics values for nitrate (solid bars) and ammonium (hashed bars) were binned based on the half-saturation (K_s) value using the same categories as Smayda (2000) for Dinoflagellates, Raphidophytes, Diatoms, and Upwelling HABs. Data were obtained from Smayda (1997, 2000), Kudela and Cochlan (2000) and Table 2. Smayda (2000) reported a general trend of low K_s values for diatoms and high K_s values for dinoflagellates, as is seen here. Note that for the Upwelling HAB group, nitrate K_s values more closely approximate the Diatom grouping, while for ammonium the pattern is similar to the Dinoflagellate grouping.

Figure 9.7 A summary of nitrogen kinetics responses reported in the literature for major algal groups, as reported in Kudela et al. 2010.

Other nutrient interactions have also been poorly defined for the estuary. For example, free copper has a strong, PFT-specific response on algae (Brand et al. 1986; Sunda and Huntsman, 1995), and elevated copper concentrations will become toxic to phytoplankton (Brand et al. 1986; Sunda et al. 1987). Brand et al. (1986) demonstrated that neritic diatoms are least sensitive, while cyanobacteria and dinoflagellates were most sensitive to copper. Copepods such as *Acartia tonsa* also exhibit more sensitivity to copper than do diatoms (Sunda et al. 1987), suggesting that copper could subtly impact both the productivity and loss terms, leading to shifts in community composition. Buck et al. (2007) recently reviewed copper trends in San Francisco Bay. They concluded that copper concentrations have declined significantly since 1993, with the North Bay declining 17% and South Bay declining 29-44%; no data were available prior to 1993, but copper concentrations were presumably elevated due to anthropogenic-driven inputs. As copper concentrations dropped, it is at least possible that inhibition of flagellates, cyanobacteria, and zooplankton has been alleviated, leading to increased competition with diatoms.

Two other nutrient relationships have been proposed as regulators of both total biomass and community composition. Dugdale et al. (2007) have proposed that elevated ammonium

concentrations from wastewater discharge is suppressing diatom productivity, while Glibert (2010) and Glibert et al. (2011) have argued that N:P ratios are indirectly controlling community composition. Dugdale et al. (2007) proposed a modified conceptual model of bloom initiation for the North Bay as follows: (1) In spring, increased irradiance and increased river flow (diluted ammonium) promote diatom growth, initially fueled by ammonium; (2) if the ammonium is drawn down to $< \sim 4 \mu\text{M}$, nitrate uptake is initiated; (3) if conditions remain suitable (increased irradiance, low ammonium, retention) a bloom develops. This hypothesis was developed primarily with direct field observations, but there are multiple ongoing projects evaluating several aspects with both field and laboratory experiments.

Elevated external NH_4^+ levels are toxic to photosynthetic organisms because the build-up of a charged molecule on one side of cell membranes results in the establishment of a high cross-membrane potential. While NH_4^+ is mostly transported into the cell via active, ATP-dependent transport (as are nearly all charged molecules) it can also passively diffuse into the cell via channels (facilitated diffusion). When external concentrations are elevated, these channels will allow a large influx of NH_4^+ as a consequence of the cross-membrane potential. The influx initiates active pumping to rid the cytosol of NH_4^+ and to prevent an intracellular pH disturbance (Bligny et al. 1997). However, the efflux of NH_4^+ maintains the cross-membrane gradient, thereby the channel influx, and necessitates continued, active efflux pumping at a great energetic cost to the cell, culminating in the cessation of growth and sometimes death of the organism (Britto et al. 2001). Some plant species have adapted to high external NH_4^+ concentrations by preventing the establishment of a cross-membrane potential, eliminating the futile NH_4^+ cycling and high respiratory cost of efflux pumping (Britto et al. 2001). Because the susceptibility to the establishment of a cross-membrane potential varies from organism to organism, susceptibility to NH_4^+ toxicity also varies greatly. For example, susceptibility to NH_4^+ toxicity is known to vary by orders of magnitude in aquatic plant species and in unicellular algae. Freshwater unicellular algae such as *Chlorella vulgaris* isolated from wastewater settling ponds can tolerate NH_4^+ concentrations up to 3 mmol/L (Berg et al. unpublished data, Perez-Garcia et al. 2011). Among marine species, diatoms also tolerate NH_4^+ concentrations in the mmol/L range (Antia et al. 1975, Lomas 2004, Hildebrand 2005, Pahl et al. 2012). In contrast, marine phytoplankton species with a large variety of NH_4^+ transport proteins encoded in their genomes, and with low half saturation constants for NH_4^+ uptake, can be susceptible to toxicity at orders of magnitude lower NH_4^+ . [update with recent papers]

While NH_4^+ toxicity at the physiological level has a response time on the order of the cell division time, it can culminate in a much greater, community-level response that builds-up over longer time scales. The community-level response is manifested through a change in phytoplankton community composition to species that are more tolerant to high NH_4^+ concentrations and to primary and secondary consumers that can feed on those species (Glibert et al. 2011). This can also lead to proliferation of Harmful Algal Blooms since many of the noxious and toxic species found in the California Current show a preference for reduced N compounds such as NH_4^+ (Kudela et al. 2010). It is this community-level response that is important for ecosystem function. But, the latter cannot occur if the former, physiological effect is not present.

To date, investigators have used a lack of chlorophyll *a* (Chl *a*) biomass or a lack of nitrate (NO_3^-) uptake as evidence of NH_4^+ stress on the phytoplankton community in Suisun Bay,

(Dugdale et al. 2007). However, both changes in Chl *a* and NO_3^- uptake may be influenced by a multitude of factors including irradiance, community composition, and season, making it difficult to use these indirect measures as evidence of NH_4^+ inhibition (e.g. Kimmerer et al. 2012). In addition, although NH_4^+ inhibition of NO_3^- uptake by phytoplankton has been widely demonstrated, there is also considerable evidence showing that phytoplankton, across the range of taxa (including diatoms), grow at comparable rates on both NH_4^+ and NO_3^- (SFEI, 2014b). Lastly, while the ammonium-inhibition hypothesis has primarily been used to explain observations from the North Bay, it remains unclear why the similar NH_4^+ concentrations found in South Bay and Lower South Bay do not inhibit blooms there. ***A direct comparison between the North and South Bay would likely help to determine whether ammonium concentrations are directly inhibiting diatoms, are indirectly shifting the community towards organisms with lower K_s and higher maximal uptake rates (Figure 9.7), or are covarying or interacting with some other variable such as irradiance, or size-selective grazing (Section 9.2.7).***

A complementary hypothesis linking nutrients and community composition has been proposed based on the stoichiometry of N and P (Glibert 2010; Glibert et al. 2011). Glibert (2010) proposed that decadal changes in phytoplankton community composition altered the food web of San Francisco Bay by favoring varying groups of organisms. Prior to 1982, the community was dominated by a nitrate-driven diatom assemblage (Figures 9.5). With the increasing ammonium loads from wastewater treatment plants the community shifted towards flagellates. As the N:P ratio continued to increase, cyanobacteria were eventually favored. This analysis is based largely on a statistical metric called cumulative sum analysis, and has been criticized by others as flawed (Cloern and Jassby et al. 2012; but also see Lancelot et al. 2012). Glibert et al. (2011) elaborated on this argument by proposing a conceptual model for how estuarine systems respond to changes in N:P ratios. They argue that even though N and P are in excess for phytoplankton growth, the ratio impacts higher trophic levels (and thus the ecological stoichiometry of the system). The authors argue that decadal changes in DIN:DIP ratios correlate with declines in diatoms and chlorophytes, and increases in dinoflagellates, because diatoms and dinoflagellates also exhibit different intrinsic N:P ratios. There are two potential issues with this argument. First, so long as N and P are saturating, the ratio should have no direct impact on species composition, other than by selecting for the organism with optimal growth. Second, Chlorophytes have a higher N:P ratio than either diatoms or dinoflagellates, suggesting that chlorophytes should be dominant under these conditions (Figure 9.8). The authors argue that this is accounted for due to the stoichiometric adjustments and feedback loops that occur between primary producers and higher consumers, and that both the Pelagic Organism Decline and the invasion of organisms such as *Potamocorbula* were triggered by bottom-up control through nutrient stoichiometry. These assertions are controversial, but the conclusion, that phytoplankton community composition is an indicator of ecosystem “health”, is nonetheless consistent with other hypotheses.

9.2.4 Top-Down controls

Grazers: *Potamocorbula*

While Glibert et al. (2011) conclude that the invasion of *Potamocorbula* was triggered by gradual shifts in ecosystem nutrient stoichiometry, others have pointed to the invasion as coincident with the rapid decline of diatoms in San Francisco Bay (Figure 9.5). The long-term shift in phytoplankton from diatoms to flagellates and cyanobacteria and the timing of declines in apparent silica uptake in Suisun Bay (Kimmerer 2005) and in abundance of anchovies in the Low Salinity Zone (Kimmerer 2006) are consistent with an influence of grazing by the clam

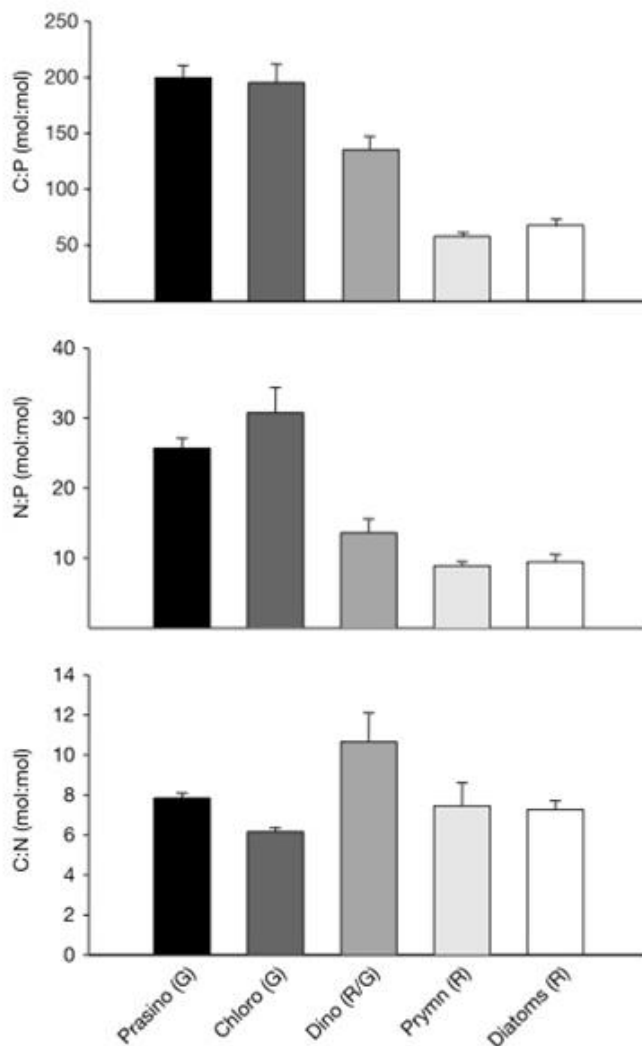


Figure 1 C:N:P composition varies between phyla and superfamilies. Phytoplankton C:P, N:P and C:N (mol:mol) ratios are grouped phylogenetically—Prasinophyceae (Prasino) and Chlorophyceae (Chloro) are members of the green (G) plastid superfamily whereas Dinophyceae (Dino), Prymnesiophyceae (Prymn) and Bacillariophyceae (Diatoms) are members of the red (R) plastid superfamily. Error bars indicate standard errors.

Figure 9.8 Intrinsic C:P, N:P, and C:N ratios for major phytoplankton groupings. From Quigg et al. 2003

shift in phytoplankton from diatoms to flagellates and cyanobacteria and the timing of declines in apparent silica uptake in Suisun Bay (Kimmerer 2005) and in abundance of anchovies in the Low Salinity Zone (Kimmerer 2006) are consistent with an influence of grazing by the clam

Potamocorbula amurensis.

Potamocorbula exhibits lower feeding rates on bacteria (typically $<1 \mu\text{m}$) than on phytoplankton (Werner and Hollibaugh 1993). Thus, the phytoplankton biomass available to many grazers is considerably lower than indicated by bulk chlorophyll values. The combination of low productivity and a high proportion of small cells offers poor support to the food web of the upper estuary, likely resulting in shifts in diet and food limitation and contributing to the poor condition of some fish species (Feyrer et al. 2003; Bennett 2005) and the general pattern of decline across species and trophic levels (Kimmerer et al., 2012). This direct modulation of phytoplankton community composition by an introduced benthic predator presents a conceptual model of trophic interactions that is strikingly different from the bottom-up, stoichiometrically driven scenario described above. As detailed below, *Potamocorbula* grazing could also have other indirect impacts on community composition in addition to the size-selective removal of PFTs.

Other grazers

Winder and Jassby (2011) document both abrupt and gradual changes in zooplankton composition, abundance, and occurrence in San Francisco Bay. Major shifts coincide with the extended drought from 1987-1994 and the invasion by *Potamocorbula*. The calanoid copepod *Limnithona tetraspina* increased rapidly in the 1990s to become the numerically abundant zooplankton, presumably due to predator avoidance, low respiration, and a dietary preference for bacteria and mixotrophic ciliates, which were in turn stimulated by the shift from diatoms to flagellates and cyanobacteria (Figure 9.9). Rollwagen-Bollens et al. (2011) also noted the importance of microzooplankton as both a consumer of small autotrophs and a link to metazoans. Microzooplankton grazing is classically assumed to differentially impact small autotrophs, suggesting that microzooplankton grazing has increased in importance as a biomass sink with the decrease in diatom abundance. This could also lead to more stochastic bloom events of other organisms as proposed by Irigoien et al. (2005) and Stoecker et al. (2008), who argued that blooms occur when a particular species of PFT exploits a “loophole” in grazing pressure. This is also consistent with Greene et al. (2011) who reported high mortality rates of microzooplankton due to *Potamocorbula* grazing, thus potentially disrupting trophic transfer and stimulating more nano- and picoplankton by removing grazing pressure on these smaller organisms, even though the nano- and picoplankton are not efficiently grazed by *Potamocorbula* directly. This highlights the potential complex interactions between top-down and bottom effects in relation to the use of phytoplankton community composition as an index of ecosystem health.

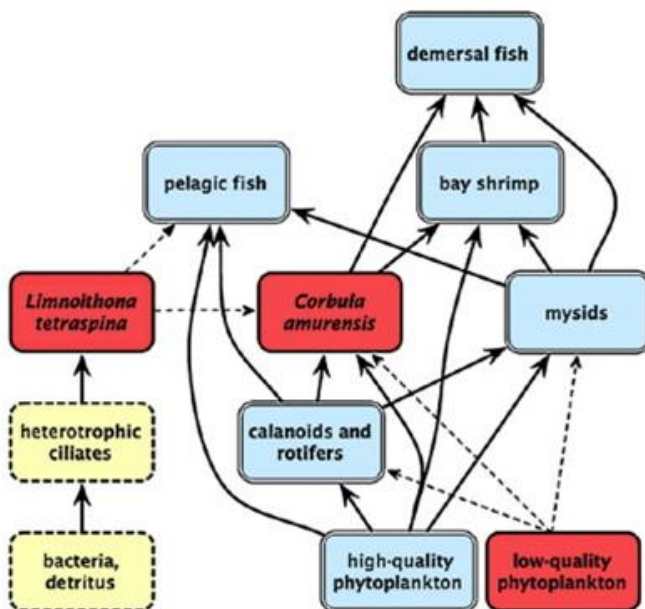


Fig. 11 Trophic interactions of the pelagic food web in the upper San Francisco Estuary at the “suisun” subregion. Arrows indicate major energy flow based on gut content analysis or literature data. Solid lines represent strong and dashed lines weak trophic interactions. Box colors reflect long-term taxa trends: red are increasing taxa, blue decreasing taxa, and yellow taxa of unknown trends over the last four decades. Phytoplankton is separated into groups of high (group I; e.g., diatoms) and low (group II; e.g., cyanobacteria, chlorophytes) food quality and/or availability for herbivorous organisms. Biomass trends

Figure 9.9. Shifts in phytoplankton community composition are associated with shifts in grazing pressure. Source: Winder and Jassby 2011

9.2.5 Interactive Effects

Several of the previous sections allude to interactive effects between multiple drivers. For example, water flow in the Northern Bay regulates turbidity, water clarity, residence time, nutrient concentrations and ratios, and benthic-pelagic coupling. Trace metals and vitamins can have subtle influences on phytoplankton community composition, leading to shifts in trophic efficiency as well as shifts in dominant phytoplankton assemblages. The ecological stoichiometry hypothesis proposed by Glibert et al. (2011) assumes a series of interactive effects, ultimately stemming from changes in nutrient forms and ratios. A conceptual model (or models) of phytoplankton community composition must be flexible enough to allow for these interactive effects, and for differential responses spatially and temporally.

A specific example of the potential for interactive effects focuses on light-nutrient-photosynthesis interactions. There is clear evidence for light limitation of phytoplankton productivity in San Francisco Bay, while it is generally accepted that macronutrients are not limiting to productivity. The interactive effects of these processes are rarely examined, but can have a direct impact on phytoplankton community composition. After carbon assimilation, nitrogen metabolism is the second largest sink for photosynthetic reductant (ATP, NADPH) in most photo-autotrophs. Under light limitation (e.g. San Francisco Bay), it is often assumed that ammonium will be a preferred N source compared to nitrate because of the large differential in energy required, since nitrate must be reduced first to nitrite and then to ammonium before being metabolized in the cell. As noted above, diatoms will also reduce nitrate as an electron sink under rapidly changing light environments (such as occurs in a turbulent estuary). Much of this N is subsequently effluxed as ammonium. This could conceivably lead to a scenario where (1) diatoms are initially light-limited in a heterogenous, rapidly mixing environment, leading to (2) efflux of ammonium, nitrite, and DON as an electron sink; as the water column stabilizes, (3) physiological energy balance is restored, ammonium efflux stops, and N is assimilated to produce more biomass, leading to (4) depletion of ammonium followed by depletion of nitrate as a diatom bloom develops. While there is no direct evidence for this occurring in San Francisco Bay, Kimmerer et al. (2012) noted that productivity was positively correlated to light availability and negatively correlated with ammonium concentrations, while Parker et al. (2012) noted a shift towards lower C:N ratios, both of which are consistent with this scenario.

These potentially complex interactions are not limited to diatoms. A previous field study of a “red tide” of the dinoflagellate *Lingulodinium polyedrum* in Southern California demonstrated that, to maintain the bloom, the dinoflagellates had to be using urea, possibly in some combination with other nitrogen sources (Kudela and Cochlan, 2000). This observation would not be evident from direct measurements of nutrients, photosynthetic carbon fixation, or ¹⁵N-labeled nitrogen uptake, but could be inferred by comparing the elemental ratio of the algae with nutrient kinetics curves, nutrient versus irradiance uptake curves, and photosynthesis versus irradiance curves (Figure 9.12). In contrast to typical paradigms, the bloom could also maintain balanced growth at very low or very high irradiances using only nitrate, while the classic Michaelis-Menten kinetics would suggest the bloom was using NO₃>NH₄>Urea. While these complex interactions are presumably common in dynamic environments, simultaneous evaluation of these interactive effects is rarely performed. Since every species (and probably strain) of algae has a potentially unique combination of light, nutrient, and carbon assimilation capabilities there is plenty of opportunity for seemingly stochastic selection of species or PFTs in the real world.

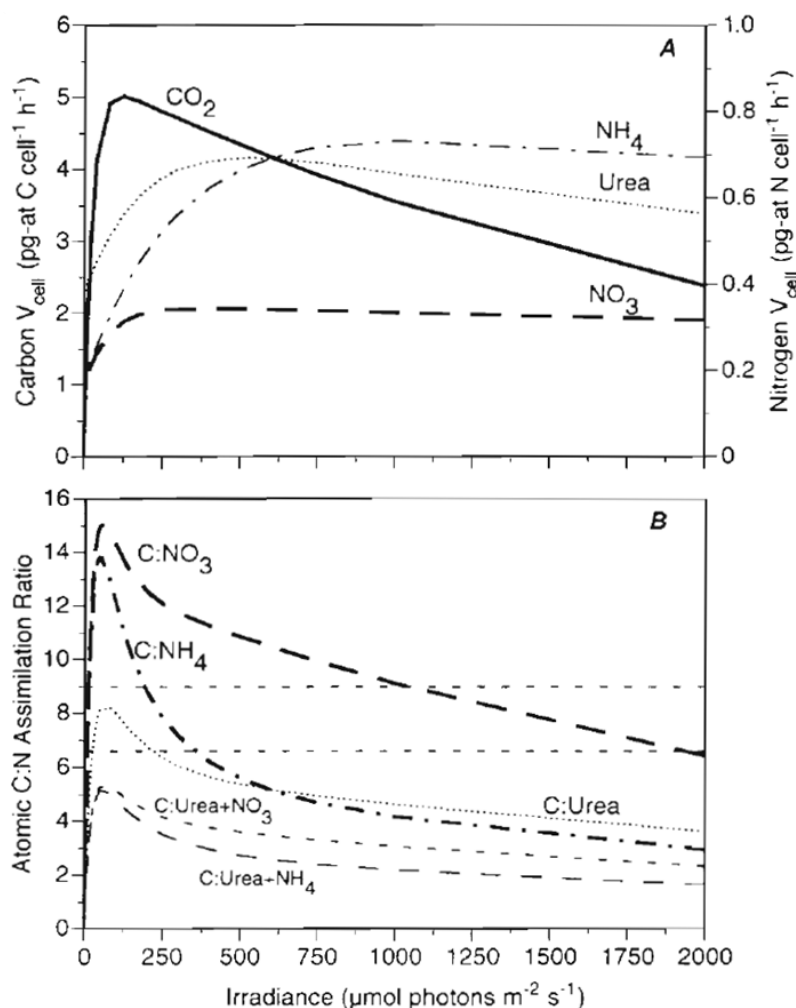


Figure 9.10 The interactive effects of light, nutrient assimilation, and the energetic requirements for N-metabolism (see Figure 9.11) can result in unexpected patterns of nutrient utilization. Panel A shows uptake versus irradiance for a red tide comprised of the dinoflagellate *Lingulodinium polyedrum*, indicating more efficient utilization of ammonium and urea compared to nitrate. Panel B shows the C:N assimilation ratio for different combinations of C and N. The lower dashed line is the Redfield ratio, the upper dashed line is the measured C:N ratio of the algae. At very low light, the observed C:N ratio could be maintained with any source of N. At moderately low light (up to 250 μmol photons m⁻² s⁻¹) urea is almost certainly utilized, and urea could sustain balanced growth (if sufficiently available) across the full range of irradiances. Note that nitrate alone could only sustain balanced growth at both extremely low and extremely high light levels. In contrast, uptake kinetics (not shown) would indicate preference as NO₃>NH₄>Urea (based on K_s values). At the time of collection, ambient nutrients were approximately at the K_s value or higher throughout the water column. From Kudela and Cochlan, 2000.

9.2.6 Harmful Algae

A special case within the larger framework of phytoplankton community composition are those organisms classified as harmful algal blooms. This provides perhaps the most direct metric of ecosystem health since sufficiently elevated numbers of these algae and their associated toxins is a clear indication of impacted ecosystem health. HAB organisms are well studied at the species level in terms of both physiological parameters and ecological patterns. Despite the persistent nutrient enriched status of San Francisco Bay, few harmful algal blooms have been reported recently for the estuary. A lack of monitoring, especially for toxins, may play a role, given the large number of potentially harmful algae present in San Francisco Bay (Cloern and Dufford, 2005; Table 3.1 and Figure 3.9). However, there have been historical occurrences (see Cloern et al., 1994 referenced in Cloern, 1996), and recently cyanobacteria and dinoflagellate blooms have been documented. For example, blooms of the cyanobacteria *Microcystis aeruginosa* have been occurring in the late summer/autumn in the northern Bay and Delta since 1999 (Lehman et al., 2005), the raphidophyte *Heterosigma akashiwo* created a red tide in the Central Bay in summer 2002 (Herndon et al., 2003), and the dinoflagellate *Akashiwo sanguinea* caused a red tide in the Central and South Bay areas during September 2004 (Cloern et al., 2005).

Microcystis aeruginosa blooms have occurred in the Delta and the North Bay during July through November of each year since 1999. The colonial form of *M. aeruginosa* is the first recorded toxic phytoplankton bloom in the northern reach of SF Bay and may have been recently introduced because it was not recorded in historic samples taken between 1975 and 1982 (Lehman et al., 2005), although sampling technique during that period may have been suboptimal for detecting *Microcystis* (samples collected at 1m depth, as opposed to surface samples/horizontal tows). *M. aeruginosa* can form surface scums and is a nuisance to recreational users; reduce aesthetics and oxygen; and produce microcystin, a hepatatoxin to humans and wildlife (Lehman et al., 2005; Lehman et al., 2008). Several surveys of *M. aeruginosa* blooms in the Delta have documented that the blooms can be widespread, often with microcystin concentrations that exceed World Health Organization guidelines for risks to humans and wildlife (e.g., Lehman et al. 2005; Lehman et al., 2008). *M. aeruginosa* may also produce cascading effects on the food web (Brooks et al. 2012).

The other well-studied HAB organisms within California waters, *Alexandrium catenella* (causes paralytic shellfish poisoning) and *Pseudo-nitzschia spp.* (causes domoic acid poisoning) are also present in the estuary. Indeed, sampling in South Bay Salt Pond A18 during 2006 (Thébault et al. 2008) revealed the presence of six phytoplankton taxa that can potentially cause harmful algal blooms (HABs): dinoflagellates *Alexandrium sp.* and *Karenia mikimotoi*, pelagophyte *Aureococcus anophagefferens*, raphidophyte *Chattonella marina*, and cyanophytes *Anabaenopsis sp.* and *Anabaena sp.* Microscopic analysis of samples collected by USGS monitoring in 2006 and 2008 revealed seven additional species of phytoplankton (e.g., Figure 3.9 and Table 3.1) that, when present at bloom abundances, have disrupted aquatic food webs, caused mortality of invertebrates, fish and birds, or human illness in other shallow marine ecosystems. In 2007 and 2008 the USGS water-quality sampling program also found HAB species in South San Francisco Bay, including *Karlodinium (Gyrodinium galatheanum) veneficum* (November 2007), *Chattonella marina* (March 2008), and *Heterosigma akashiwo* (September 2007). Appearances of these taxa are surprising because they were not detected previously in 3 decades of sampling (Cloern and Dufford 2005). These observations, all made after the first salt ponds were opened in 2004, suggest that the salt ponds might function as incubator habitats and a source of toxic phytoplankton to San Francisco Bay as they are opened to tidal exchange. Dinoflagellates, flagellates, and pelagophytes form HABs in other shallow marine ponds that are enriched in organic matter and have long hydraulic residence time (e.g. Gobler et al. 2005). Shallow, semi-isolated systems (such as the salt ponds) can also serve as “biological capacitors”, providing inocula for large-scale blooms in nearby bay and coastal waters (Vila et al., 2001). Actions to open these habitats might pose an unanticipated risk to the water quality and living resources of San Francisco Bay and to tidal-ponds created by the South Bay Salt Pond Restoration Program, particularly for water birds and fish assemblages.

Given the prevalence of HAB organisms in the Bay, the dramatic increase in blooms of Microcystis, and the potential linkages between ecosystem health and HABs (Kudela et al. 2008), it would be prudent to more closely monitor HAB organisms and associated toxins within San Francisco Bay as indicators of water quality.

9.3 Summary of Major Conceptual or Data Gaps

San Francisco Bay is somewhat unique in that it is well studied for both physical/environmental parameters, and for phytoplankton community composition. Despite this wealth of information, any attempt to develop a conceptual model of community composition runs into the fundamental

issue identified by Cloern and Dufford (2005): "...the problem is hyperdimensional, whereby communities are assembled by selective forces operating on variation in algal size, motility, behavior, life cycles, biochemical specializations, nutritional mode, chemical and physiological tolerances, and dispersal processes...our knowledge base is therefore insufficient for constructing reliable numerical models of phytoplankton population dynamics at the species level, in spite of our recognition that the functions provided by the phytoplankton vary among species." While this issue is not intractable, it is unlikely that we will be able to predict or fully understand the species-level variability in San Francisco Bay in the near future. We can, however, identify important components of a conceptual model for phytoplankton community composition at the level of traits and ecosystem function (Figure 9.4). The immediate challenge is to identify the relative importance of these sometimes conflicting conceptual relationships. A long-term goal should perhaps be the development of sophisticated numerical-biological models that incorporate "evolution" and natural selection. This approach is being increasingly applied to oceanic ecosystems with some success (Follows and Dutkiewicz 2011) and has recently been used to test fundamental questions about community assembly and stability (Barton et al. 2010a,b). Applications of such models in the near term – as synthesis tools for examining multi-dimensional parameter space – may allow us to rule in or rule out hypotheses, evaluate potential drivers of phytoplankton community shifts, and identify the highest priority experimental studies. Several gaps in our ability to develop or apply a conceptual model of phytoplankton community assembly include the following specific issues:

- It is unclear how many spatio-temporal compartments need to be included for San Francisco Bay. The estuary could be modeled as single unit, as North Bay versus South Bay, or as a series of sub-basins. While many authors recognize that algae are both imported and exported from the ocean and riverine end members, it is still very common to describe the mean patterns for the estuary or develop conceptual models based on data from particular locations. The estuary clearly responds to forcing from the oceanic and riverine end-members; any conceptual model of community assemblage for San Francisco Bay must be linked to models of the coastal ocean and the watershed.
- The estuary is generally considered to be nutrient-replete, but there is little or no information available about vitamins, trace-metals, and the influence of anthropogenic contaminants such as pesticides that may be influencing community composition. Several of these factors would likely co-vary with more easily measured parameters and could easily be overlooked.
- Very little is known about the species-specific physiological properties of the community, nor about the potential interactions between (e.g.) light, nutrients, photosynthesis, etc.
- The presence of HABs and toxins has been largely ignored in San Francisco Bay. The prevailing assumption is that the Bay is resilient to these impacts, but this may simply be a lack of monitoring and measurement. Large-scale restructuring such as the opening of the salt ponds has the potential to suddenly and dramatically alter this perspective.
- Several conceptual models have been proposed that could account for the abrupt and long-term trends in community composition, and are diametrically opposed. Similar to the classic paradigm of top-down versus bottom-up control in marine systems, reality is probably somewhere in between, and may change spatially and temporally.

Tables 9.1 summarizes the current state of knowledge and knowledge/data gaps related to phytoplankton community composition. The prioritizations in the rightmost two columns are related to the discussion in Section 11.

Table 9.1 Phytoplankton community composition and HABs: current state of knowledge for key processes and parameters

Process or Parameters	Importance for quantitative understanding	Current Level of Certainty about magnitude, composition, or controls	Need for additional or on-going data collection or process studies	Priority for study in next 1-5 years
Processes				
Pelagic grazing rates (size-selective)	High	Low: No systematic zooplankton sampling in LSB, South Bay, Central Bay. Only 1 station in San Pablo.	Moderate	Moderate
Size-selective benthic grazing rates	High	Low: Good data to support estimates in Suisun Bay. Limited data in LSB South Bay. Monitoring of benthos abundance would inform this.	Very High	Very High
Temperature, light, and nutrient (concentration, N:P, form of N) preferences of phytoplankton PFTs specific to SFB subembayments	High	Low: Limited understanding of how these factors/preferences may shape phytoplankton community composition, in particular in a light-limited nutrient-replete system.	Very High	Very High
Effects of trace metals, organics or pesticides	Moderate/Uncertain	Low: Limited information on vitamins, trace-metals, and the influence of anthropogenic contaminants such as pesticides that may be influencing community composition. competition with diatoms.	Moderate	Moderate
Effect of physical forcings, including exchange between subembayments, oceanic and terrestrial (including wetlands, salt ponds) end-member inputs, large scale climate forcings	High	Moderate: Data on community composition over the past 20 years (Bay wide) and up to 40 years (Suisun and Delta) to explore different explanations.	Very High	Very High
NH ₄ inhibition: diatom productivity	High/Uncertain	Low: Several studies completed, others underway.	Very high	Very high
Ambient composition data				
Size-fractionated chl-a	High	Low: Provides a coarse measure of in which classes phytoplankton biomass resides, which is a useful albeit coarse surrogate for food quality. Not currently being collected but could be easily added to monitoring.	High	High

Process or Parameters	Importance for quantitative understanding	Current Level of Certainty about magnitude, composition, or controls	Need for additional or on-going data collection or process studies	Priority for study in next 1-5 years
Phytoplankton community composition, monthly time-scales, at sufficiently high spatial resolution, and higher temporal/spatial resolution to test mechanisms	High	Moderate: 20 year near-monthly Bay-wide record from USGS and ~40 year record for Suisun and Delta. But few higher resolution data sets or special studies.	Very high	Very high
Frequency and magnitude of detection of HABs or HAB toxins	High	Low: Limited data on HABs and toxins, and	Very high	Very high
Phytoplankton community composition in salt ponds, particularly HAB-forming species	High	Low: Limited data to date, but of high concern.	Very High	Very High
Surrogate measures for phytoplankton composition	Low	Low: The use of phytoplankton pigments or digital image recognition approaches could be piloted that would eventually increase the amount of composition data that could be collected	Very High	Very High

10 Other proposed adverse impact pathways

While other potential nutrient-related adverse impact pathways - including those that have impacted other estuaries or have been hypothesized in SFB – are possible, this report focused on a subset considered to be most relevant or most important in SFB (Figure 3.1, Table 3.2 AI.1-AI.6). Other adverse impact pathways, listed below, may need to be considered at a later date if observations indicate that they are indeed important in some habitats of SFB.

- Loss of submerged aquatic vegetation (SAV) habitat due to shading from phytoplankton or periphyton growth
- Excessive growth of macroalgae
- Excessive macrophyte growth, in particular invasive species
- Nutrient-induced changes in the composition of individual phytoplankton cells that cause adverse outcomes on primary consumers (Glibert et al., 2013)
- Direct NH_4^+ toxicity to copepods (Teh et al., 2011)

11 Priority Science Questions and Knowledge/Data Gaps

11.1 Introduction

The overarching questions that the Nutrient Management Strategy aims to address seem straightforward at first glance (Table 11.1 Column A). But those questions barely scratch the surface. Below the surface, the number of questions, and the information needed to answer those questions, grow exponentially (Table 11.1 Column B), because:

- San Francisco Bay is a large and complex estuary, comprised of distinct habitats that receive different nutrient loads, and that process and respond differently to those loads.
- A broad array of potential adverse impacts (Table 3.2) needs to be considered, and many of those paths have unique knowledge and data gaps;
- There are numerous important physical/chemical/biological processes along the pathways between nutrient loads and response (the conceptual model presented in Sections 5-9), and considerable knowledge and data gaps.

Table 11.1 Overarching Management Questions and next-layer more specific questions for SFB NMS

A. Overarching Questions	B. Next layer of more specific questions
1. Is SFB experiencing nutrient-related impairment under current conditions, or is it likely to in the future?	1.a Which impairment pathways (Figure 3.1 and Table 3.2), and what “conditions” constitute impairment?
	1.b What subembayments?
	1.c Which habitats (deep subtidal, intertidal, margins)?
	1.d What plausible future scenarios need to be considered, how would conditions differ under those scenarios, and would impairment develop?
2. What are the major nutrient sources?	2.a What are the magnitudes of the major nutrients sources, and how do those magnitudes vary temporally: POTWs; stormwater; agriculture; upstream inputs from the Delta; other perennial streams/rivers?
	2.b How do those individual loads contribute to ambient nutrient concentrations as a function of space and time throughout the Bay, considering temporal variability in the physical, chemical, and biological factors that influence their fate and transport once entering the Bay?
3. What nutrient loads or concentrations are protective of ecosystem health?	3.a What is/are the most important or sensitive endpoint(s), which nutrient forms cause or contribute to that adverse impact, and what loads or concentrations would be protective?
	3.b After considering fate and transport, what loads, from the combination of sources, would be protective?
4. What are efficacious and cost-efficient nutrient management options for ensuring that Bay beneficial uses are protected?	4.a What management actions - load reductions and other actions - will protect ecosystem health?
	4.b What actions mitigate or prevent impairment, and do so at the most reasonable cost and/or by delivering the greatest set of multiple net benefits?

When considering both the breadth and depth of monitoring, modeling and special studies that would be needed to address all the issues, it is clear that trying to tackle it all, in-depth, and in parallel would be impossible. Some degree of prioritization is needed to focus effort on the most important issues first.

The goal of this section is to inform the direction of scientific inquiry and monitoring by taking an initial step toward identifying the highest priority issues, the related science questions, critical knowledge and data gaps, and the types of investigations that would most directly target those gap and allow well-informed nutrient management decisions to be made. In Section 3, we explored the following question: *What would nutrient-related problems look like in San Francisco Bay if they were occurring now or in the future?* In response to this question, 8 adverse impact categories were identified (Table 3.2, Figure 3.1). In this section, using the conceptual model as a guide, we identify scenarios (current conditions, future environmental change, management actions) under which those adverse impacts could occur (or may already be occurring), and examine those scenarios to identify highest priority issues warranting further exploration. Based on the set of highest priority issues related we then identify key science questions, major knowledge gaps or data gaps (based on the assessments in Tables 6.2, 7.1, 8.1, 9.1), and identify the types of studies needed to address those questions and gaps.

11.2 Identifying priority scenarios for further consideration

Scenarios were identified and explored as follows:

Current Conditions or Current Trends:

These ‘scenarios’ address the question: *Based on current observations – current conditions or current trends – are some subembayments or habitat-types already experiencing, or heading toward experiencing, adverse impacts from nutrients?*

In considering the conditions and trends, the analysis does not aim to assess whether impairment is occurring, but rather to frame and present the issue, and its priority level, for comparison with other issues. Four broad categories were encountered: i. Existing data suggest do not suggest a major problem; ii. Existing data may be suggestive of a potential problem but are currently insufficient to definitively answer this question; iii. There is currently little or no data, but adverse impacts are highly plausible based on the conceptual model; and iv. mechanistic-studies are needed to address key conceptual gaps;

Environmental change scenarios

N and P are abundant in SFB, but physical and biological drivers severely limit their conversion into phytoplankton biomass, and generally prevent SFB from experiencing exceedingly high biomass and low dissolved oxygen. Some of those same regulating factors may help prevent potentially harmful phytoplankton, which are regularly detected at low numbers in SFB, from developing into full-blown HABs/NABs. This set of scenarios focuses on uncontrollable environmental change and was developed through exploring the following questions:

What could cause a relaxation of the physical or biological controls that regulate the Bay’s response to high nutrients, and thereby contribute to, cause, or worsen adverse impacts?

Future scenarios require serious consideration for several reasons. First, SFB boasts multiple examples of unexpected and substantial environmental changes over the past 20-40 years that have had major impacts on ecosystem response and ecosystem health (see Sections 3, 7, and 9;

e.g., biomass increases in South Bay over the past 20 years; 30-50% decrease in suspended sediment concentrations Bay-wide over past 20-30 years; *Potamocorbula* invasion in Suisun in 1987; shifts in zooplankton community composition and abundance in Suisun Bay due to invasions and other drivers; decline in benthos-feeding organisms in South Bay). Second, the potential effects of climate change need to be evaluated. Third, it will take many years, even multiple decades, to implement major management actions. Taking action only once a problem arrives means years or decades of impairment before ‘the fix’ can be implemented. If future problems are to be averted, impairment scenarios need to be anticipated, evaluated, and, if deemed necessary, managed in advance of their onset. Lastly, implementing management actions while a problem is still over the horizon, as opposed to already upon us, will allow time for planning, and for a broader range of management options to be considered. Planning ahead will increase the likelihood and feasibility of implementing “the best solution” – a set of management actions that achieve multiple benefits (beyond just nutrients) and are the most cost-effective.

To identify environmental change scenarios requiring further analysis, we first used the conceptual model to identify changes to regulating factors that could lead to, or exacerbate, the adverse impacts identified in Section 3 (Table 3.2; Figure 3.1). Figure 11.1 illustrates how shifts in various regulating factors could adversely influence ecosystem responses. Next, we identified environmental change scenarios under which those shifts could occur. Those scenarios are summarized Table 11.1, and mapped to changes in regulating factors in Figure 11.2.

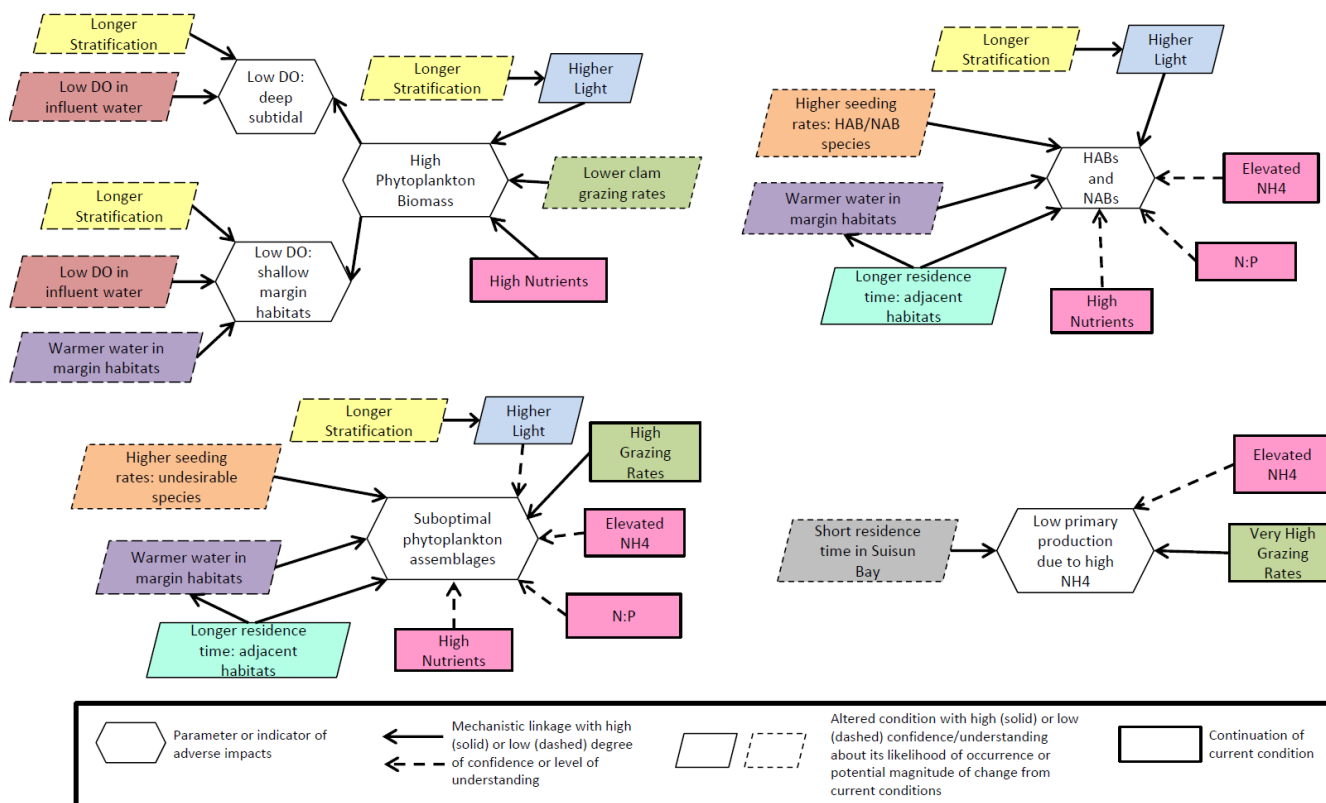


Figure 11.1 Changes to underlying drivers of response that could contribute to adverse impacts.

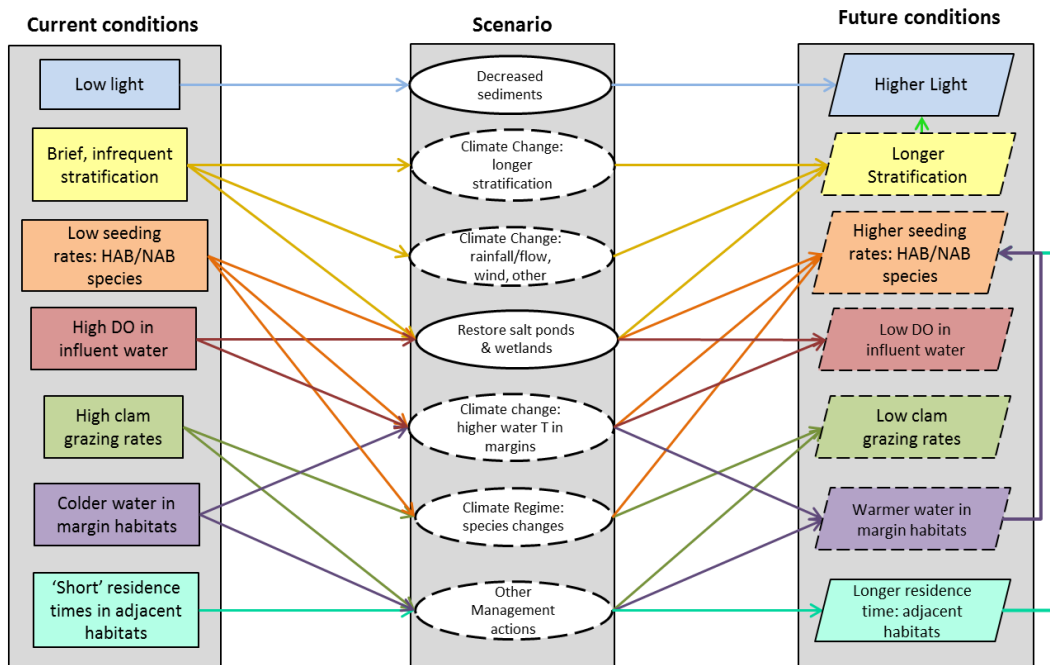


Figure 11.2 On the left, Current Conditions within SFB that have thus far provided resistance to harmful effects of high nutrient loads. In the middle, potential environmental or management scenarios that could create future conditions with weaker resistance to nutrient-related adverse impacts. Likelihood of a scenario is indicated by a solid line (more certain) or a dashed line (unknown likelihood of occurrence, or unknown magnitude or direction). Dashed lines for Future Conditions indicate uncertainty about degree to which condition would change in response to scenarios

Management action scenarios

We considered two broad categories of management actions: management actions that would specifically target nutrient-related problems; and management actions being implemented for other reasons that could have unintended (positive or negative) effects with respect to nutrients (e.g., large-scale habitat restoration projects (SBSP, Deltaplans, BEHGU); flow rerouting in the Delta (ref); shoreline redevelopment (ref)). Similar to the approach followed for environmental change scenarios, we used the conceptual model to identify junctures along the path between nutrient loads and adverse impacts where a change to regulating factor could substantially influence ecosystem response (positive or negative). We then identified specific or more general management actions that could act on those factors, which are also summarized in Table 11.2.

Subembayment-Scenario-Response matrix

To organize the numerous issues requiring consideration into a single graphic and facilitate the systematic comparison of issues and their importance, we developed the matrix in Figure 11.3. Figure 11.3 depicts subembayment-scenario-response combinations. Columns represent scenarios, organized into their three categories. Rows represent potential ecosystem responses based on the adverse impact categories in Table 3.2, grouped by subembayment. For each combination, we assessed whether it would result in worsened conditions; would result in improved conditions; or was not highly relevant with respect to nutrients.

Table 11.2 Major scenarios considered

Environmental Change (EC) or Management Scenario (MS)	Description
EC.1	Continued decreasing suspended sediment concentrations in SFB due to a continuation of lower external loads and depletion of the erodible sediment pool.
EC.2	Increased frequency or duration of stratification due to climate change, in particular thermal stratification in fall
EC.3	Climate-change related changes in precipitation patterns (timing, intensity) and timing of snow melt. Potential effects include: altered timing/intensity of freshwater flows from the Central Valley and Sierras that could change stratification duration and residence time in the Delta, Suisun, and other subembayments; changes in freshwater flows from watersheds adjacent to subembayments and influence stratification in particular in LSB and South Bay.
EC.4	Climate regime shifts (el Nino/La Nina, PDO) that cause shifts in biota, such as introducing new phytoplankton species, or changes in abundance bottom feeding macrobiota that have top down controls on food web (e.g., similar to the loss of clams in South Bay, and their eventual return)
EC.5	Climate-change related increases in water temperature in margin habitats
EC.6	Dramatically decreased <i>Corbula</i> abundance due to environmental factors (disease, increased predator abundance)
MS.1	N-P load reductions at POTWs discharging directly to SFB subembayments or adjacent watersheds (not including those east of Suisun Bay)
MS.2	Nitrification with no further nutrient removal at POTWs discharging directly to SFB subembayments or adjacent watersheds (not including those east of Suisun Bay)
MS.3	Stormwater load reductions through the use of best management practices, low impact development, etc.
MS.4	Wetland restoration around the Bay margins. Largest scale planned changes in LSB and South Bay, but large areas for potential for restoration in San Pablo Bay and Suisun Bay (See Figure 5.2)
MS.5	Salt pond restoration and reconnection. Largest scale planned changes in LSB and South Bay, but large areas for potential for restoration in San Pablo Bay and Suisun Bay (See Figure 5.2)
MS.6	Managed shellfish beds to increase water column filtration rates to maintain low phytoplankton biomass
MS.7	Sac-Regional upgrades: Nitrification, N-removal
MS.8	Other Central Valley load reductions
MS.9	Delta flow changes, due to changes in water withdrawals or flow routing, or due to restoration

We then ranked the combinations from low to high priority, in terms of the need for further investigation, based on the following factors:

- The combination was considered to be among the most plausible or probable issues to develop into a substantial problem, or among the most feasible mitigation approaches;
- Major gaps in knowledge or data exist that limit our current ability to make further assessments (in terms of determining if there is currently a problem, high likelihood of a future problem, or whether a management action would mitigate impacts), and severely limit the confidence with which science-based decisions can currently be made;
- The combination was a tractable issue to explore, and highly relevant to management decisions. In other words, resources directed toward exploring these issues (monitoring, special studies, modeling) could yield a large return on investment in terms of the knowledge/data gaps filled and scientifically-informed decision-making.

A subset of these combinations is discussed below. First, Section 11.2 explores combinations that represent adverse impacts. Next, Section 11.3 discusses combinations under which adverse impacts would be mitigated or prevented adverse impacts from nutrients. Based on a consideration of the full scenario set, Section 11.4 identifies a subset of highest priority combinations (Section 11.4) and Section 11.5 discusses the related priority science questions and knowledge/data gaps.

11.3 Adverse impacts

The discussion below is organized around the adverse impact pathways (i.e., from Table 3.1). For each pathway, current conditions/trends are discussed first, followed change scenarios that could cause or exacerbate impacts along that pathway.

High biomass and low DO in deep subtidal areas

Current Conditions or Current Trends: Phytoplankton biomass has increased in all SFB subembayments over the past 20-30 years, and small but statistically significant decreases in DO have also been noted (J Cloern, pers. comm.). Biomass increases have been greatest in LSB and South Bay. Current phytoplankton biomass levels in LSB and South Bay do not appear to be having pronounced impacts within deep subtidal areas, since DO concentrations have generally tended to remain above 5 mg/L. However, the rate of change in biomass in South Bay between the mid-1990s and 2005 was rapid (Figure 3.5). Recent data from the past several years suggest that biomass may have reached a new plateau. Nonetheless, the underlying causes of the biomass change over the 20 year, and indeed why it plateaued as opposed to continued increasing, remain highly uncertain, and therefore so does its future trajectory. When conditions are appropriate, LSB and southern South Bay can also experience large and long-lived blooms (50-100 µg/L, 1-2 months; Figure 7.5). High phytoplankton biomass and low DO in deep subtidal areas of LSB and South Bay are thus considered high priority issues based on current conditions and trends. Determining whether LSB and South Bay are trending toward experiencing adverse impacts due to high biomass and low DO in deep subtidal habitats requires identifying the causes of recent change, forecasting future biomass and DO, and comparing present and future conditions to numeric criteria (being developed separately as part of the SFB Assessment Framework).

Change scenarios: Bay-wide, several scenarios could lead to increased rates of primary production, increased biomass accumulation, and low DO in deep subtidal areas, including (see also Table 11.1 and Figure 11.3): i. continued decreases in suspended sediment concentrations;

ii. increased frequency of climatic conditions that allow stratification to occur more frequently or persist for longer periods of time; iii) changing rainfall patterns that strengthen and lengthen spring salinity stratification; iv.) wetland or salt pond restoration dampening turbulent mixing energy, which would allow stratification to persist longer during its current spring and fall periods, and also outside those times; v. wetland/salt pond restoration and reconnection to the open Bay, and elevated nutrients being more efficiently converted to biomass that is tidally-transported to deep subtidal habitats vi.) loss of benthic grazers (in Suisun Bay). Suisun Bay currently has extremely low phytoplankton biomass. High biomass and low DO would only occur in Suisun if there was an abrupt loss of the *Potamocorbula* clam (e.g., due to disease, predator introduction). Prior to the *Potamocorbula*'s establishment, Suisun was highly productive. With the substantial light level increases in Suisun Bay and its higher nutrient concentrations since pre-1987, greater biomass accumulation than pre-1987 would be expected now if *Potamocorbula* disappeared. Further declines in suspended sediment or more frequent or longer stratification would amplify this effect. Indeed, baseline phytoplankton biomass has increased in Suisun Bay over the past 15 years (Figure 3.8), although levels remain far below pre-1987 concentrations.

High Biomass and Low DO in shallow margin habitats

Current Conditions or Current Trends: LSB, South Bay, San Pablo Bay, and Suisun Bay have large shallow margin habitat areas that provide critical ecosystem services (Figure 2.1). To date, these habitats have received limited systematic monitoring. The available data that has been analyzed to date indicate that low DO occurs periodically in LSB's shallow margin habitats, i.e., as sloughs, creeks, and salt ponds undergoing restoration (Figures 3.13 from earlier in report; SFEI 2014c). Low DO is also commonly observed in Suisun Marsh (Tetra Tech 2013). However, it is unknown how the severity (spatial extent, DO concentration, duration, and frequency) of low DO compare to what would be expected under natural conditions. In addition, the impacts of this low DO on habitat quality is unknown, but would depend on both the severity of low DO and how it effects the biota utilizing (or who would otherwise utilize) that habitat. Lastly, if adverse impacts are occurring, the degree to which anthropogenic nutrient loads cause or contribute to those impacts needs to be determined. Given the severe data limitations, limited investigation to date, and the disproportionately high-value of these habitats to biota, current conditions related to low DO in margin habitats emerged as a high priority issue for all subembayments that have substantial areas of shallow margin habitat.

Change scenarios: Many of the same change scenarios that would lead to high biomass and low DO in deep subtidal habitats would similarly affect DO in margin habitats. For example, decreases in SPM concentrations would increase light levels and production rates. Any changes filter-feeding benthos abundance would have an even greater effect on phytoplankton biomass in margin habitats than in deep subtidal areas because of the shallower depth. Reconnection of wetlands and salt ponds through restoration could deliver low DO water or high BOD loads (in the form of reduced compounds or phytoplankton biomass) to sloughs.

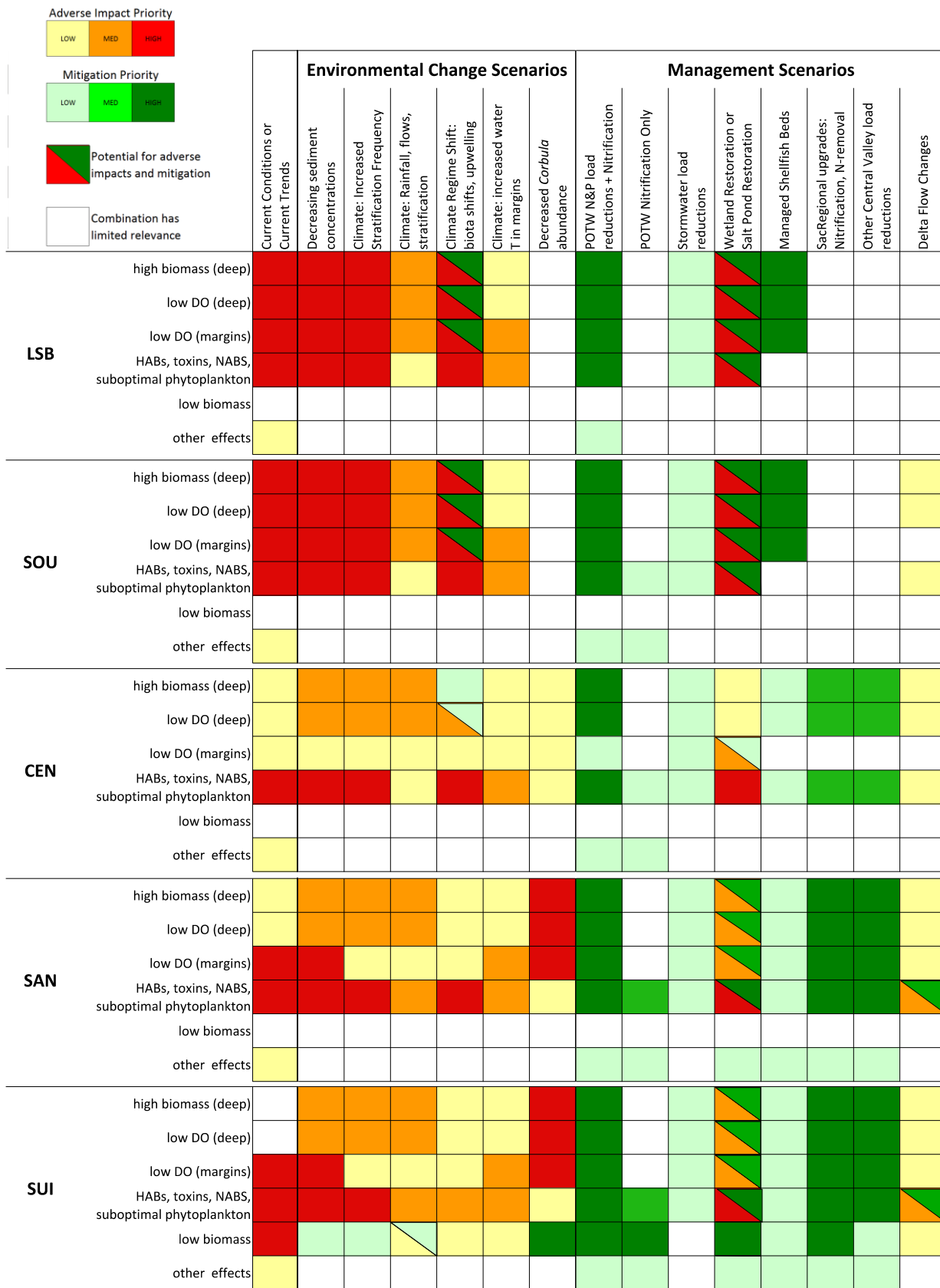


Figure 11.3 Prioritization of subembayment specific response. Columns represent scenarios and rows represent potential ecosystem responses based on the adverse impact categories in Table 3.2

HABs/NABs and phycotoxins

Current Conditions or Current Trends: Recent measurements indicate that HAB toxins, or phycotoxins, occur year-round in all SFB subembayments, plus the Delta (Figure 3.9). The current ecological significance of the observed phycotoxins in SFB is unknown. HAB-forming species are frequently detected throughout the estuary at low abundances (Table 3.1, Figure 3.10), and have been observed in salt ponds undergoing restoration (Thebault et al., 2008). The underlying mechanisms or triggers that determine when a HAB may form, when high levels of phycotoxins are produced, and the relationship with nutrients are among the most poorly understood. Yet the Fall 2004 nuisance red tide bloom in Central Bay and South Bay clearly demonstrated how an undesirable organism can readily take advantage of SFB's high nutrient concentrations when favorable physical conditions allow (Figure 3.11). That bloom was the first of its kind in nearly 40 years of observations, and it remains unknown whether it was a low-probability event that occurred by pure coincidence during that year, or if the underlying factors that contributed to its occurrence in 2004 are related to broader patterns of changing ecosystem response in SFB.

Given the potential magnitude of problems that HABs/NABs can cause when they do occur, the currently poor understanding of the mechanisms that may lead to HAB/NAB blooms and phycotoxin production, and the potential for major blooms that current high nutrient concentrations provide, HABs/NABs and phycotoxins need to be considered among the highest priority issues Bay-wide.

Change Scenarios: Future scenarios that would lead to increased light levels (lower SPM) or longer periods of stratification would favor HABs/NABs through allowing for increased growth rates and fuller utilization of abundant nutrient supplies. In addition, restored salt ponds and wetlands (LSB, South Bay, and San Pablo Bay) have the potential to be HAB and NAB incubators, due to their relatively long residence times, warm water temperatures, high light levels, and abundant nutrients. The potential linkage between large-scale salt pond restoration efforts and increased HAB frequency and elevated toxins need to be examined. Increased water temperatures in margin habitats due to climate change or longer water residence time could also favor HABs/NABs. Lastly, changes in large-scale climate forcings could change – increase or decrease - the seeding-rate of HAB-forming species from the coastal ocean to SFB.

Suboptimal phytoplankton community compositions

HABs/NABs are one category of undesirable shifts in the phytoplankton community. However, other manifestations of nutrient-driven community shifts, such as toward compositions of poor nutritional quality for supporting food webs, have also been proposed. While they are addressed separately in this section, HABs/NABs and other shifts in phytoplankton community compositions are combined in Figure 11.3, and to some degree the knowledge and data gaps related to current and future conditions are similar.

Like HABs and NABs, the combination of factors, including nutrients, that would cause undesirable compositional shifts are poorly understood in SFB. On the one hand, it can be argued that since nutrients seldom limit phytoplankton growth that – from phytoplankton succession viewpoint – nutrients are not a major determinant of which species thrive (Sections 9.2.6 and 9.2.9). On the other hand, it has been hypothesized that nutrients concentrations, forms, and ratios alter phytoplankton community composition through different mechanisms (Glibert 2010;

Glibert et al., 2011; Glibert et al., 2013). If nutrient-related suboptimal phytoplankton composition will be included among the potential adverse impacts that management decisions will aim to address, more investigation is needed into the hypothesized underlying mechanisms and the potential importance of their effects relative to other factors regulating ecosystem response. Mechanisms need to be explored in controlled experiments. Ecosystem-scale observations are also needed, requiring a well-designed and targeted program to collect high-quality data on phytoplankton taxonomy and ancillary data over a wide range of conditions (physical, chemical, and biological).

Low phytoplankton biomass caused by elevated NH_4^+

Current Conditions or Current Trends: In Suisun Bay and the Delta, phytoplankton biomass levels are extremely low and blooms rarely occur (Figure 3.8), and food limitation is considered to be among the factors contributing to fish declines (Baxter et al., 2011). Elevated NH_4^+ concentrations have been hypothesized to play an important role in preventing phytoplankton blooms and maintaining low biomass in Suisun Bay (Dugdale et al., 2007; Parker et al., 2012a,b; Dugdale et al. 2012). However, there remains uncertainty and disagreement within the scientific community, including among this report's authors, about the mechanism and its importance relative to other processes that regulate biomass accumulation (Section 7.2.3; see also SFEI 2014X). Similar to suboptimal phytoplankton community compositions, if NH_4^+ inhibition will be included among the potential adverse impacts that management decisions will aim to address, more investigation is needed into the hypothesized underlying mechanisms and the potential importance of their effects relative to other factors regulating ecosystem response. Focused experiments are needed to test key aspects of the hypothesis (see SFEI 2014b for further discussion), and modeling is needed to compare the magnitude of any NH_4^+ -related effect to other factors that regulate phytoplankton biomass accumulation (e.g., light limitation, clam grazing rate, residence time).

Change Scenarios: Only one of the future scenarios considered in this report could potentially exacerbate low productivity due to elevated NH_4^+ in Suisun Bay: shifts in rainfall patterns that cause increased flows from the Delta which in turn flush phytoplankton from the system faster at a rate faster than they can grow. This future scenario is not currently considered to be among the highest priorities.

Other food web effects

Currently there is limited field or experimental evidence that nutrients adversely affect the food web along additional pathways such as: direct toxicity to copepods (Teh et al., 2011), creating conditions that allowed *Potamocorbula* to become and thereafter remain established in Suisun Bay (Glibert et al., 2011); and changes in individual phytoplankton cell composition that adversely impact copepod populations (Glibert et al. 2013). Similar to suboptimal phytoplankton community composition and NH_4^+ inhibition, if these other nutrient-related food web effects will be included among the potential adverse impacts that management decisions will aim to address, more investigation is needed into the hypothesized underlying mechanisms and the potential importance of their effects relative to other factors regulating ecosystem response. Compared to adverse impacts, at this point were not considered to be among the current highest priorities issues.

11.3 Scenarios that could prevent or mitigate adverse impacts

Scenarios under which nutrient-related adverse impacts could be prevented or mitigated are discussed below, organized by scenarios (as opposed to Section 2's organization around adverse impact pathways)

N and P load reductions from POTWs discharging directly to SFB subembayments

Since POTWs are responsible for ~65% of the nutrients loads entering SFB (Bay-wide, annual average; Figure 6.2), reducing POTW N and P loads is an obvious management scenario to explore. Although some POTWs currently perform nitrification prior to discharge, and several carry out advanced treatment that removes a portion of N and P, most SFB POTWs do not perform nutrient removal. Substantial reductions in POTW N and P loads can be achieved with conventional, albeit still expensive, treatment upgrades (N: 2-5 fold decrease; P: >10 fold decrease; Table 6.1). If nutrient load reductions are deemed necessary, the key challenges will be to determine how much removal is necessary to protect ecosystem health, and to identify the optimal approach for achieving those reductions (including potentially through nutrient trading between POTWs), since costs could differ by billions of dollars among options.

At present, DIN and o-PO₄ seldom limit phytoplankton growth in most deep subtidal habitats of SFB and during most times of the year. Therefore, reducing POTW nutrient loads would be unlikely to result in substantially-decreased phytoplankton production - at least in deep subtidal habitats- unless the decreases are very large (e.g., 5-10 fold reduction).

Decreasing POTW nutrient loads would, however, cap phytoplankton production (and biomass) and DO deficits at levels lower than today's potential maxima by decreasing the amount of DIN and o-PO₄ available for phytoplankton growth. To the extent that HAB/NAB frequency, or suboptimal phytoplankton composition, are influenced by high nutrients or highly altered nutrient ratios, POTW load reductions would also mitigate these impacts. Direct POTW nutrient load reductions are discussed below for each subembayment. As noted in Section 6.4, this segmentation greatly oversimplifies hydrodynamics and nutrient cycling, but remains instructive for a qualitative discussion.

LSB and South Bay: POTWs are the dominant external sources of DIN and o-PO₄ to LSB and South Bay (Figure 6.2; SFEI 2014a). Reducing POTW loads would therefore substantially reduce total subembayment-scale nutrient inputs to LSB and South Bay. The San Jose wastewater treatment has already reduced its N and P loads by ~40% and ~10-fold, respectively, through treatment upgrades in the mid-1990s (SFEI 2014a,c). However, LSB has the smallest volume and slowest net flushing rate of all SFB's subembayments, allowing N and P to accumulate to higher concentrations.

The effects of load reductions may differ between deep subtidal habitats. For deep subtidal habitats in LSB and South Bay, while moderate POTW load reductions may not result in phytoplankton biomass reductions during much of the year, load reductions would create a lower-level cap on phytoplankton production and biomass. Given that the efficiency with which nutrients have been converted to biomass in South Bay and Lower South Bay has increased over the past 10-20 years (Figure 3.5 and 3.6), this may be an important consideration for preventing future potential adverse impacts. Although DO generally remains above 5 mg/L in deep subtidal habitats, recent observations suggest that DO does approaches, and occasionally dips below, 5

mg/L in LSB deep subtidal areas. If such conditions are deemed to be problematic, POTW load reductions could mitigate that impact. In addition, load reductions would presumably (depending on the decrease) have an effect on episodic major bloom events like that depicted in Figure 7.5, to the extent that such events are considered problematic. Similarly, decreased nutrient loads could help cap the magnitude of episodic HAB/NAB events. For these latter two examples, the frequency with which such events occur compared to some “acceptable frequency” (a regulatory decision) would need to be considered in determining the benefit of load reductions.

The situation may be different in shallow margin habitats. The limited data from sloughs rimming LSB indicate that DO concentrations do frequently fall well below 5 mg/L at some locations (Figure 3.14; SFEI 2014c). Based on the conceptual model, it is reasonable to hypothesize that POTW-derived nutrients contribute to low DO in shallow margin habitats, and that POTW load reductions would decrease the severity of those events (spatial extent, DO deficit, frequency, duration). At the same time, multiple factors may contribute to low DO in sloughs, including organic matter entering from adjacent watersheds, and periodic naturally-low DO; therefore, the contribution of anthropogenic nutrients to low DO still needs to be determined. The extent to which low DO in margin habitats is having adverse impacts depends to a large degree on whether it is impacting biota that utilize that habitat (other potential impacts include odor problem from sulfide production). Data on benthos and pelagic macrobiota abundances in margin habitats are extremely limited. In addition there needs to be a systematic analysis of DO tolerances of key organisms.

Suisun and San Pablo Bays: Evaluating the relative importance of direct POTW load reductions to Suisun Bay and San Pablo Bay is less straightforward than for LSB and South Bay. Suisun Bay sizable loads from POTWs discharging directly to Suisun Bay; however it also receives large, seasonally varying NH_4^+ , NO_3^- , and o-PO_4 loads from the Delta (Figure 6.3). San Pablo Bay in turn receives seasonally varying loads from Suisun Bay plus the Delta (Figure 6.3). Therefore, an evaluation of the effect that reduced direct POTW loads to Suisun Bay will have on ambient conditions within Suisun Bay needs to consider magnitudes of upstream loads. The planned ~65% N load reductions from Sacramento Regional County Sanitation District (Regional San), which should go on-line within 10 years, are expected to have a major influence on DIN loads that enter Suisun Bay from the Delta (see Figure 6.3; planned decrease at Regional San ~ 10,000 kg d⁻¹). After those reductions, direct POTW loads to Suisun Bay will represent a much larger portion of the total load, at least during low-flow months. The extent to which direct POTW loads to Suisun would mitigate adverse impacts will also depend on the time of year and the adverse impact pathway and nutrient forms that are most concerning (i.e., Figure 3.1). If, for example, the goal is to achieve reduced ambient NH_4^+ concentrations, upgraded treatment at CCCSD could be impactful, since it discharges ~4000 kg d⁻¹ NH_4^+ to Suisun, which would be the largest external NH_4^+ source once Regional San’s loads are cut. However, if cutting DIN concentrations is the goal, initial estimates suggest that Delta loads will remain a non-trivial contributor, especially during winter and spring, even after Regional San’s loads decrease (Figure 6.3; Regional San’s current DIN load is ~15000 kg/d, indicating there is a seasonally varying additional source of 5000-20000 kg/d).

Central Bay: Assessing the potential effectiveness of load reductions from Central Bay POTWs on Central Bay conditions is more complex. Central Bay receives direct POTW loads and is the

ultimate recipient of loads that enter northern and southern subembayments. A detailed modeling analysis would be needed to determine the relative contribution of loads from different sources. Coastal upwelling and exchange flows through the Golden Gate can carry oceanic-source NO_3^- and o-PO_4 into Central Bay. However, while upwelling-related loads have the potential to be large under some conditions, on average Central Bay is expected to be a net exporter of N and P to the coastal ocean (Largier and Stacey, 2014).

Nitrification of POTW effluent

Unlike reducing N and P loads from POTWs (Section 11.3.1), nitrification of POTW effluent alone does not decrease nutrient loads, but instead changes the predominant N form from NH_4^+ to NO_3^- . However, to the extent that elevated NH_4^+ concentrations favor HABs/NABs, cause shifts in phytoplankton community composition, or inhibit primary production, nitrification of POTW effluent has the potential to mitigate these adverse impacts.

South Bay and Central Bay: POTWs discharging to South Bay and Central Bay release N primarily in the form of NH_4^+ . Thus nitrifying effluent prior to discharge would substantially reduce NH_4^+ loads. The benefit of nitrification prior to discharge needs to be weighed relative to what appears to be fairly efficient *in situ* nitrification, as evidenced by NO_3^- being the major DIN form in these subembayments despite them receiving primarily NH_4^+ loads. In addition, the importance of *in situ* NH_4^+ production (release from sediments, OM matter mineralization in the water column) needs to be considered.

Lower South Bay: All POTWs in LSB have been performing nitrification since the 1980s, although nitrification efficiency at one of those POTWs (Sunnyvale) varies seasonally. So this scenario is not particularly relevant in LSB. Interestingly, though, LSB has the second highest NH_4^+ concentrations Bay-wide (Figure 6.3). Much of the observed NH_4^+ likely comes from organic matter mineralization within LSB. This suggests that nontrivial baseline NH_4^+ concentrations could continue in other subembayments after external NH_4^+ inputs cease. Note, however, that the influence of *in situ* NH_4^+ production on ambient water column concentrations may be most pronounced in LSB because of its shallow bathymetry, which causes sediment processes to have larger effects on water column concentrations.

Suisun Bay: Upgrading Suisun POTWs to include nitrification would likely have a substantial impact on ambient NH_4^+ concentrations in Suisun Bay. Suisun Bay and San Pablo Bay receive large seasonally-varying NH_4^+ loads from the Delta, much of which originates from Regional San's discharge. In evaluating the potential environmental effectiveness of upgrading Suisun POTWs to include nitrification, the seasonally-varying magnitudes of Delta NH_4^+ loads need to be considered, as do planned decreases in Regional San's NH_4^+ loads. Under current loading conditions, direct POTW discharges to Suisun Bay are the major NH_4^+ source during dry months (Figure 6.2). Regional San's NH_4^+ loads will be cut to near zero within 10 years. At that time, POTWs discharging directly to Suisun Bay would be the primary NH_4^+ source, other than NH_4^+ produced *in situ* with Suisun Bay or within the Delta and Sacramento River and transported into Suisun Bay. *In situ* nitrification appears to play an important role in shaping ambient NH_4^+ concentrations in Suisun Bay during summer/fall months (Section 6.4; SFEI, 2014b). In evaluating the benefit of upgrading POTWs to nitrification alone (i.e., no N or P removal), the incremental benefit achieved relative to *in situ* nitrification may need to be considered.

Stormwater load reductions

Stormwater and flow from perennial streams that drain directly to SFB deliver seasonally-varying N and P loads to the system. Only rough estimates of those loads are available at this point. At the subembayment scale, stormwater N and P loads have the potential to contribute substantially to total nutrient loads in Suisun Bay and San Pablo Bay during the wet season (Figure 6.2; SFEI 2014a), and are of lesser importance in other subembayments. Although more work is needed to better constrain loads from stormwater and perennial streams, it seems unlikely that stormwater N and P loads would rival POTW loads at the subcatchment scale unless the current stormwater load estimates substantially underestimate actual loads. In calculating the stormwater loads, only inorganic NH_4^+ , NO_3^- , and o-PO_4 . Recent stormwater monitoring data suggests that organic N and non-o- PO_4 forms of P commonly comprise more than 50% of total N and P (SFEI 2014d). At the same time, a portion of the organic-N and particle-complexed P pool would be less bioavailable than DIN and DIP, and would be only slowly converted to bioavailable forms. In summary, it is possible that subembayment-scale stormwater loads could be higher than initially estimated and may warrant further examination. For LSB, South Bay, Central Bay, and (to a lesser extent) Suisun Bay, even if stormwater loads were twice as large, their contribution to N loads would remain relatively small compared to POTW loads; however, stormwater P loads could prove non-trivial. Stormwater N and P cannot be discounted in San Pablo Bay.

The discussion of stormwater loads above was focused primarily on their subembayments-scale importance. Stormwater and perennial stream N and P loads have the potential to be more important in shallow margin habitats than they appear to be at the subembayment scale, and a more spatially-explicit evaluation may of their importance may be warranted.

Changes in grazer abundance due to climate forcings or other factors

In some SFB subembayments, grazing plays an important role in limiting phytoplankton biomass accumulation. Cloern et al. (2007) argue that a loss of benthic grazers due to a shift in the Pacific Decadal Oscillation (PDO) could be responsible for much of the increase in phytoplankton biomass in South Bay and LSB (Figure 7.10). A shift in the PDO back to pre-1998 conditions would presumably allow benthic grazers to repopulate South Bay and Lower South Bay, and return phytoplankton biomass to lower levels. On the other hand, a decline in *Potamocorbula* in Suisun Bay due to disease or other factors would eliminate a major sink for phytoplankton biomass, and allow for large blooms to return and better support the food web.

Wetland and salt pond restoration

Wetland and salt pond restoration efforts around the Bay's margins have the potential to reduce N (and to a lesser degree P) concentrations and potentially play a major role in an integrated nutrient management strategy. Denitrification (or annamox) converts NO_3^- to N_2 gas, thus serving as a true N sink. High denitrification rates can occur in wetlands. However, denitrification rates vary over a wide range, with strong dependence on temperature and other conditions (e.g., amount of labile organic matter in the sediments). Furthermore, sufficient hydraulic exchange needs to occur between the nitrate-replete Bay and wetlands to maximize loss by denitrification. This latter limitation could be overcome by moving deep-channel POTW outfalls to locations within wetlands so that they directly discharge effluent to wetlands. However, the issue of seasonally-varying denitrification rates would remain. Wetlands also

retain P. However, unlike N, P has no true sink other than burial, which is inherently inefficient both because of resuspension and recycling.

The largest wetland restoration efforts are currently going forward in LSB and in the southern third of South Bay (Figure 2.1). The scale of planned restoration is such that those areas could potentially serve as major nutrient sinks. Large areas that ring other subembayments are also being considered for wetland restoration. While the use of wetlands to remove nutrients holds promise, its potential to mitigate the adverse impacts of high nutrient loads would need to be carefully evaluated, initially through modeling work, and subsequently, if warranted, through pilot field studies.

Managed shellfish beds to maintain low phytoplankton biomass

Using managed shellfish beds (e.g., clams, oysters) is an alternative management option being considered in other estuaries to maintain phytoplankton biomass at acceptable levels (Rose et al., 2014). The *Potamocorbula* invasion in Suisun Bay serves as an unfortunate yet compelling example how effective shellfish can be at reducing biomass (Figure 3.8). Managed shellfish beds could be used exclusively as a phytoplankton biomass management tool, or could be a commercial venture that offsets some of the associated maintenance costs. The bed's collective filtration rates would need to be great enough to maintain baseline phytoplankton levels at acceptable levels. The beds would also need to control phytoplankton blooms, which in SFB deep subtidal habitats tend to occur during relatively short windows of time (e.g., 5-10 days). The collective filtration rate of beds would be directly related to shellfish biomass, which would in turn depend on food that had been previously available to support their growth. Pre-growing enough shellfish biomass to handle, for example, a spring bloom would require a well-coordinated program. Shellfish beds would need to be placed in appropriate locations and at appropriate densities so that they could access sufficient phytoplankton. The feasibility and effectiveness of cultivated shellfish beds as a management option could be initially evaluated through basic modeling, and explored through pilot studies thereafter. Given the large amounts of legacy bioaccumulative pollutants (e.g., methyl-Hg, PCBs) in San Francisco Bay, the suitability of shellfish for human consumption or as animal feed needs to be considered. Shellfish are primary consumers and would therefore tend to bioaccumulate lower levels of contaminants than higher trophic level organisms, especially during early life stages when they are steadily increasing their own biomass.

Load decreases from the Central Valley

To the extent that elevated nutrients are having adverse impacts in Suisun Bay along pathways other than those related to high-biomass/low-DO, reductions in the loads entering Suisun Bay from the Delta would have the potential to substantially mitigate these adverse impacts. However, there remains uncertainty and disagreement within the scientific community about several of the hypothesized mechanisms for nutrient-related adverse impacts (NH_4^+ inhibition, phytoplankton community composition, elevated NH_4^+ or N:P allowing *Potamocorbula* to become and remain established; effects on higher trophic levels of nutrient-induced changes in the N:P of individual phytoplankton cells) and their importance relative to other processes that regulate biomass accumulation. If these hypothesized mechanisms will be included among the potential adverse impacts that management decisions will aim to address, more investigation is needed into the hypothesized underlying mechanisms and the potential importance of their effects relative to other factors regulating ecosystem response.

Delta nutrient loads to SFB influence ambient concentrations most in Suisun Bay and San Pablo Bay. Initial estimates suggest that Delta loads could be the dominant nutrient source to Suisun and San Pablo Bays throughout much of the year (Figure 6.3; SFEI, 2014a,b). Delta loads would also influence ambient concentrations in Central Bay, but likely to a lesser extent than in the up-estuary subembayments. While during very high flows some freshwater from the Delta has been shown to enter South Bay and, less frequently, LSB, the Delta-derived loads likely have relatively low influence there.

Scenarios for load decreases from the Central Valley can be divided into three groups: 1. decreased loads from the Regional San POTW, which is located ~70 km upstream of Suisun Bay along the Sacramento River; 2. reductions from other POTW discharging within the Delta or in upstream watersheds; and 3. reductions in agriculturally-derived loads, originating either within the Delta or within the watersheds drained by the Sacramento or San Joaquin Rivers. As noted earlier, Regional San's current discharge of ~15000 kg d⁻¹ DIN, primarily in the form of NH₄⁺, travels along the Sacramento River's main stem, and also moves with the river into and through the Delta. During low flow periods considerable nitrification (up to 60%; Parker et al., 2012; SFEI 2014b) and likely some denitrification can occur in transit. The Sacramento River, prior to reaching Regional San's discharge, also carries a large and seasonally varying NO₃⁻ load, presumably from upstream agriculture loads (Kratzer et al. 2011). The San Joaquin River also delivers large and seasonally varying NO₃⁻ loads to the Delta (Kratzer et al., 2011), but relatively little NH₄⁺. Due to complex flow patterns within the Delta, water withdrawals that alter flow routing, and transformations, losses, and additional loads within the Delta, determining which sources contribute most to loads that eventually enter SFB will be a non-trivial undertaking. That said, it is reasonable to suggest that most of the NH₄⁺ load (and some of the NO₃⁻ due to *in situ* nitrification) appears to originate from Regional San, while other sources, including agriculture, contribute a substantial portion of the NO₃⁻ load. Recent permit requirements are requiring In response to recent permit requirements, Regional San will nitrify and carry out biological nitrogen removal before discharge, with upgrades implemented by the year 2020. Under this upgraded operation, Regional San will discharge ~5,000 kg d⁻¹ NO₃⁻ and little or no NH₄⁺, amounting to a complete shift from NH₄⁺ to NO₃⁻, and a 2/3 reduction in overall DIN load. The cessation of NH₄⁺ loads will represent a considerable reduction in overall NH₄⁺ loads to Suisun Bay during much of the year, and will also likely translate into substantial DIN loads to Suisun Bay. The feasibility and effectiveness of agricultural N and P load reductions also need to be considered. Initial estimates indicate that these loads are large during some times of the year (Figure 6.2). Any major reductions in agriculture-sourced loads could therefore have a substantial effect on nutrient concentrations in Suisun and San Pablo Bay. However, achieving those reductions is made more challenging by their nonpoint-source origins. Loads from POTWs that discharge within the Delta are relatively small at the scale of the whole Delta-Suisun system and the loads that enter Suisun. To better understand the effect that load reductions at Regional San will have on nutrient levels in Suisun Bay, nutrient fate and transport within the Delta and Suisun Bay need to be examined through modeling and field studies, since initial mass balance estimates suggest that losses of NH₄⁺ and DIN can be substantial (SFEI 2014b, Novick et al., 2014)

11.4 How would San Francisco Bay respond to changes in nutrient loads?

Carstensen et al. (2011) and Duarte et al. (2009) explored multi-decade water quality observations in 6 nutrient-impacted estuaries in Europe and North America over time courses

that included periods of eutrophication and subsequent recovery periods when nutrient loads were reduced through management actions. In all cases they found that the chl-a:nutrient relationship exhibited considerable hysteresis, and the estuaries followed markedly different and slower recovery trajectories in terms of chl-a response than than expected based on the eutrophication trajectories. Duarte et al. (2009) hypothesized that the apparent hysteresis in the chl-a response during the phase when total nitrogen decreased resulted from shifts in baseline conditions over time that made the systems more sensitive to nutrients, and/or “regime shifts” from one relatively stable system state to another. In both cases, they suggest that the altered responsiveness could have been caused or hastened by nutrients themselves or be the result of other physical or biological factors (e.g., invasive species, increased water temperature). Carstensen et al. 2011 observed that the ratio of chl-a:TN actually increased in a consistent manner across the 4 systems they studied, and argued that large-scale changes were the cause (e.g., climate change, or similar types of increased human stress on coastal ecosystems).

Based on observations in other estuaries, it is reasonable to expect that there will be hysteresis in the response:nutrient relationship (e.g., chl-a:TN, HAB-frequency:TN) in SFB during the early stages after any load reductions are implemented. That likelihood needs to be kept in mind when considering incremental management actions and adaptive management to inform next steps. It will also be important to manage expectations of regulators, managers, stakeholders, and the public by communicating the complexities of ecosystems and uncertainties, and foreshadowing the likelihood that responses to management actions may be muted or delayed. It is important to note that, although both Duarte et al (2009) and Carstensen et al. (2011) deliver discouraging news, both studies stress that nutrient load reductions were nonetheless important to have implemented: although conditions may not have improved to the degree originally expected, based on their conceptual models and empirical evidence no action would have led to worsened conditions.

11.5 High priority subembayment-scenario-response combinations

Through evaluating the full range of scenarios summarized in Figure 11.3 (Sections 11.2-11.3), a subset of scenario-subembayment-response combinations emerged as the highest priority issues to address through near-term research and monitoring (e.g., over the next 1-5 years):

Adverse Impact Combinations

1. High biomass leading to low DO or nuisance levels of phytoplankton in LSB and South Bay, based on both current trends and future conditions under several scenarios
2. Low DO, resulting from high phytoplankton biomass, in margin habitats (sloughs, creeks, wetlands, restored salt ponds), under current conditions and potentially exacerbated by several future scenarios.
3. HABs/NABs based on both current conditions/trends and on future conditions under several scenarios, including reconnection of salt ponds, longer stratification, climate regime shift, and climate change.
4. Low phytoplankton biomass in Suisun Bay under current conditions

Mitigation/Prevention Combinations

5. Reductions in nutrient loads from direct POTW discharges, and reduction in nutrient loads from the Delta
6. Reductions in stormwater nutrient loads
7. Other mitigation strategies: wetland treatment and managed shellfish beds

8. Effectiveness of nitrification (at Regional San and Suisun direct POTWs) on NH_4^+ inhibition of primary production.

11.6 Priority science questions

Based on the high priority adverse impact and management scenarios, we identified a set of high-level priority science questions and the types of investigations that are needed to address these questions (Tables 11.3 and 11.4). These questions are not necessarily intended to be an exhaustive list, but rather to serve as a starting point that can be refined as detailed science plans are developed.

Table 11.3 Highest priority adverse impact scenarios, science questions, and types of studies needed to address those questions

	Literature Review	Analysis of existing data and synthesis	Data collection and monitoring	Field or laboratory experiments	Bay Modeling: Basic	Bay Modeling: Complex or full bay	Watershed Modeling	Assessment Framework	Technology, cost-benefit analysis
1 High phytoplankton biomass and low DO in LSB and South Bay									
a. What level of phytoplankton biomass (and over what area, for what period of time) would result in adverse impacts in LSB and South Bay habitats?	x	x			x	x		x	
b. What are the relative importances of the fundamental drivers that underlie recent changes in phytoplankton biomass in LSB (decreased SPM, loss of benthic grazers, other)?		x	x		x	x			
c. What is the importance of organic matter produced in margin habitats to biomass and DO budgets in LSB and South Bay deep subtidal habitats?			x		x	x			
d. What will be the response of phytoplankton biomass and DO if suspended sediments continue decreasing at rates similar to the past 20 years? Do adverse impacts become increasingly likely at environmentally-relevant SPM values? Or are adverse impacts unlikely along this pathway under this scenario?			x		x	x			
e. What scenarios could lead to worsened conditions and adverse impacts? - Longer periods of stratification due to salt pond and wetland restoration efforts, higher production/biomass? - Changes in climate patterns, longer periods of stratification, higher T, higher production/biomass? - Salt pond and wetland restoration, greater biomass production in margin habitats that is transported to deep subtidal habitats? - Multiple changes in parallel (lower SPM, longer stratification, biomass from margins, low grazing rates)?		x	x	x	x	x			
f. Based on this analysis, what are likely future trajectories in LSB and South Bay? Will biomass concentrations level off or continue increasing? What will be the response of DO?		x	x		x	x			
g. What reductions in nutrient loads are necessary to prevent adverse impacts?			x		x	x			
2 High phytoplankton biomass and low DO in margin habitats									
a. What low DO 'severity' would cause adverse impacts: spatial extent within individual sub-habitats (e.g., %age of slough), DO deficit, frequency, duration? Individual sub-habitats vs. overall condition (e.g., individual slough(s) impacted vs. percentage of total slough kilometers impacted)?	x	x						x	
b. How common (spatially) are low DO occurrences in these habitats? What is the severity of the low DO in each sub-habitat and collectively (within individual sloughs/creeks/salt-ponds, and collectively, what is the spatial extent (e.g., small stretch vs. entire slough), frequency, duration, DO deficit, bottom layer or full water column)?		x	x						

	Literature Review	Analysis of existing data and synthesis	Data collection and monitoring	Field or laboratory experiments	Bay Modeling: Basic	Bay Modeling: Complex or full bay	Watershed Modeling	Assessment Framework	Technology, cost-benefit analysis
c. Are relevant biota adversely impacted by low DO? Field surveys, potentially controlled studies. Avoidance, stress/toxicity, death	x	x	x	x					
d. What mechanisms act to cause the periodicity of low DO, including causing it to develop and dissipate? New organic matter sources (e.g., <i>in situ</i> production within sloughs or inputs from adjacent habitats, microphytobenthos vs. phytoplankton), on-going sediment oxygen demand, residence time, stratification, freshwater inputs, tidal exchange		x	x	x	x	x			
e. To what extent do anthropogenic nutrient loads contribute to or cause increased severity (spatial extent, DO deficit, frequency, duration) of low DO?		x		x	x				
f. Based on observed (or modeled) conditions relative to conditions that have adverse impacts, are these habitats (subset or as a whole) adversely impacted by low DO?		x	x		x	x		x	
3. HABs/NABs and phycotoxins									
a. What frequency or magnitude of HABs/NABs or HAB-toxins would be considered to cause adverse impacts?	x	x			x			x	
b. How do the abundances of phycotoxins and the HAB-forming species vary in space and time within the Bay? Have there been detectable changes over time, based on existing data? What are the sources of phycotoxins (in situ production vs. transport into SFB or subembayments)?		x	x	x					
c. What causes/contributes to increased frequency or elevated abundances of HAB/NAB-forming organisms? To what extent do nutrients cause, contribute to, or enable increased abundance/blooms? Seeding rates from the coast, seeding rates from adjacent habitats (including salt ponds), role of physical drivers (T, light, mixing/stratification) and chemical conditions (nutrients) favoring higher <i>in situ</i> production specifically of <u>HAB/NAB forming organisms</u>	x		x	x	x	x			
d. What causes/contributes to production of <i>in situ</i> phycotoxins production? To what extent do nutrients cause, contribute to, or enable increased phycotoxins production? role of physical drivers (T, light, mixing/stratification) and chemical conditions (nutrients) favoring higher <i>in situ</i> production	x		x	x					
e. What future scenarios could increase the frequency or severity of HAB/NAB events or increase phycotoxin abundance? - restoration and reconnection of salt ponds/wetlands? high-light, warm, nutrient-replete incubators? - future water management practices in the Delta (withdrawals, longer residence times) ? - changes in climate patterns? How likely are those changes in the 20-30 yr time horizon?		x	x	x	x				

	Literature Review	Analysis of existing data and synthesis	Data collection and monitoring	Field or laboratory experiments	Bay Modeling: Basic	Bay Modeling: Complex or full bay	Watershed Modeling	Assessment Framework	Technology, cost-benefit analysis
h. Based on a comparison of observed conditions and conditions considered to induce adverse impacts, are regions/subembayments/habitats of SFB experiencing HAB/NAB related adverse impacts, or will they in the future?			X					X	
i. What decreases in nutrient loads or ambient nutrient concentrations would decrease adverse impacts, or the risk of adverse impacts, from HABs/NABs?					X	X			
4. Other Nutrient Impact Pathways: Low phytoplankton biomass (NH₄⁺ inhibition), Suboptimal phytoplankton community composition									
a. What is the underlying mechanism by which NH ₄ ⁺ slows or inhibits primary production? Characterize NH ₄ ⁺ concentrations and magnitude of effect. At what NH ₄ ⁺ concentrations are primary production rates substantially impacted?	X	X		X					
b. What is the relative contribution of elevated NH ₄ ⁺ compared to other factors that maintain low phytoplankton biomass in Suisun Bay (clam grazing, light limitation, flushing)?					X	X			
c. Are current NH ₄ ⁺ loads or concentrations adversely impacting biomass levels in Suisun Bay?		X	X		X	X		X	
d. What nutrient load reductions would prevent or mitigate adverse impacts due to NH ₄ ⁺ inhibition of primary production?					X	X			
e. What constitute optimal, or healthy, phytoplankton assemblages in SFB's subembayments? Conversely, what assemblages would be considered to poorly support desirable food webs?	X	X						X	
f. How have phytoplankton community compositions changed within SFB subembayments over recent years?		X	X						
g. Based on what is known from other systems or from prior experimental/field work (Bay-Delta or elsewhere), what hypothesized mechanisms are most likely to influence phytoplankton community composition in the Bay-Delta, based on ambient conditions (nutrient concentrations, light, temperature, stratification, etc.)? What controlled experiments or observations in SFB are needed to further evaluate these proposed mechanisms in SFB?	X	X							
h. What is the magnitude (or relative importance) of the role that current ambient nutrient concentrations play in shaping phytoplankton community composition?	X	X		X	X	X			
i. What changes to nutrient availability would mitigate or prevent adverse impacts of nutrients on phytoplankton community composition?	X	X		X	X	X			
i. What other adverse impact pathways may require further attention in SFB (aquatic macrophytes, macroalgae, SAV habitat)?	X	X							

Table 11.4 Highest priority mitigation scenarios, science questions, and types of studies needed to address those questions

	Literature Review	Analysis of existing data and synthesis	Data collection and monitoring	Field or laboratory experiments	Bay Modeling: Basic	Bay Modeling: Complex or full bay/Delta	Watershed Modeling:	Assessment Framework	Technology, cost-benefit analysis
5. Reductions in nutrient loads from POTWs and nutrient loads from the Delta									
a. What are the magnitudes of loads from individual POTWs?		x	x						
c. How do internal processes shape nutrient concentration within SFB, how do they vary in space/time: mixing/flushing, nitrification, denitrification, uptake/assimilation, regeneration from sediments, etc.				x	x	x			
b. What are the zones of influence and magnitude of contributions of individual POTWs and Delta loads, and how do these vary seasonally and interannually?					x	x			
d. How do Delta loads to Suisun Bay vary seasonally and interannually? What portions of the loads that enter Suisun Bay from the Delta originate from Regional San, others POTWs? What portions of the loads come from Central Valley agriculture? What are the load contributions from agriculture within the Delta?		x	x		x	x	x		
f. What will Delta loads to Suisun Bay be under future scenarios: restoration, changes to water management practices, changes in agricultural practices?					x	x			
i. Considering areas of influence, zones where impairment may be occurring, and internal processes, what combination of load reductions are needed to mitigate or prevent impairment?					x	x			
g. What is the range of options for achieving various levels of nutrient load reductions from POTWs? What are the costs and multiple benefits (nutrients + other benefits, e.g., recycled water) of individual POTW efforts, and of longer-term integrated sub-regional plans?									x
h. Given the necessary load reductions and cost-benefits, what are the best options for achieving load reductions?									x
6. Reductions in stormwater nutrient loads									
a. Are stormwater nutrient loads potentially important sources to some margin habitats in some subembayments, or at the subembayments scale, and do they warrant further consideration?		x	x		x	x	x		
b. If yes, what are the loads from priority watersheds? What is their contribution to nutrient loads, or organic matter/BOD loads, to margin habitats?		x	x				x		
c. What are the magnitudes of stormwater nutrient contributions to deep subtidal habitats in other subembayments?					x	x			

	Literature Review	Analysis of existing data and synthesis	Data collection and monitoring	Field or laboratory experiments	Bay Modeling: Basic	Bay Modeling: Complex or full bay/Delta	Watershed Modeling:	Assessment Framework	Technology, cost-benefit analysis
7. Other mitigation strategies: wetland restoration/treatment and shellfish beds									
a. What is the potential for wetland restoration/treatment to mitigate adverse impacts of nutrients?	x				x	x			
b. What is the potential for managed shellfish beds to mitigate adverse impacts of nutrients?	x				x	x			
b. If wetlands or managed shellfish beds appear to be promising nutrient management options – what do pilot studies, advanced modeling, and economic considerations suggest about their potential to be part of an integrated management program?					x	x			x
8. Influence of nitrification at Regional San and Suisun direct POTWs on NH₄⁺ inhibition of primary production or other adverse impacts									
a. What is NH ₄ ⁺ fate within the Delta and how does this change as a function of season, flow, etc.?					x	x			
b. What load reductions are necessary to reduce NH ₄ ⁺ to ambient concentrations that would not inhibit production or have other adverse impacts?					x	x			

12 Key Observations and Recommendations

12.1 Key observations

1. Changes in SFB's response to nutrient loads over the past decade, combined with the Bay's high nutrient loads and concentrations, justify growing concerns about elevated nutrients.
2. The future trajectory of SFB's response to nutrients is uncertain. One plausible trajectory is that SFB maintains its current level of resistance to the classic effects of high nutrient loads and no further degradation occurs. A second, equally plausible scenario is that SFB's resistance to nutrients continues to decline until adverse impacts become evident. The highly elevated DIN and DIP concentrations Bay-wide provide the potential for future impairment. Any major reductions in loads to SFB will take years-to-decades to implement. Thus, if future problems are to be averted, potential impairment scenarios need to be anticipated, evaluated, and, if deemed necessary, managed in advance of their onset.
3. By considering current conditions in SFB, trends of changing ecosystem response, and a conceptual model for SFB's response to nutrients, we identified the following highest priority issues:
 - a. Determine whether increasing biomass signals future impairment. This issue is most pertinent for Lower South Bay and South Bay.
 - b. Characterize/quantify the extent to which excess nutrients contribute now, or may contribute in the future, to the occurrence of HABs/NABs and phycotoxins.
 - c. Determine if low DO in shallow habitats causes adverse impacts, and quantify the contribution of excess nutrients to that condition.
 - d. Further evaluate other hypotheses for nutrient-related adverse impacts to ecosystem health, including nutrient-induced changes in phytoplankton community composition and ammonium inhibition of primary production. That evaluation – to include data analysis, additional experimentation, or modeling – should assess their potential quantitative importance, and help to determine if they should be considered among the highest priority issues.
 - e. Test future scenarios that may lead to worsening conditions through the use of numerical models.
 - f. Quantify the contributions of nutrients by sources in different areas of the Bay, considering both their transport and in situ transformations and losses.
 - g. Evaluate the potential effectiveness of various nutrient management strategies at mitigating or preventing adverse impacts.
4. Although concern related to changing ecosystem response in SFB is warranted, widespread and severe nutrient-related impacts do not currently appear to be occurring, based on existing sampling locations and parameters commonly measured. This apparent lack of current severe impacts translates into time for conducting investigations to improve understanding of SFB's response to nutrients and allows for sound, science-based management plans to be developed and implemented. That said, the considerable amount of time required to implement any management strategy raises the level of urgency such that work should move forward expeditiously.

5. Given the stakes of no action - and the time required for data collection, analysis, and modeling tools to reach a useable state - work needs to move forward in parallel on implementing multiple aspects of the Nutrient Strategy. A well-coordinated program is needed to maximize the effectiveness and efficiency of this effort. That program needs to integrate seamlessly across what might otherwise be (or become) semi-independent program areas. Specifically, we recommend the following set of highly-integrated program areas:
 - a. **Monitoring:** Develop and implement a sustainably-funded and regionally administered monitoring program that continues routine monitoring, and fills newly-identified data gaps relevant to nutrients;
 - b. **Modeling:** Develop and apply linked hydrodynamic and water quality models to integrate observations, identify critical data gaps (to be addressed through monitoring or experimental studies), quantify processes at the ecosystem scale, and evaluate future scenarios (including management alternatives);
 - c. **Observational and Experimental Studies:** Undertake special studies (field investigations, controlled experiments) to address the highest priority knowledge and data gaps identified in #3; and
 - d. **Data Synthesis and Interpretation:** Analysis of existing and newly collected data (from monitoring and experimental studies), incorporating models, to improve understanding of linkages between nutrients and ecosystem response and to inform the development of an assessment framework.
6. The Delta/Suisun boundary, while an important regulatory boundary, is not meaningful from ecological and loading standpoints. Nutrient loads to and transformations within the Delta exert considerable influence over nutrient loads to and ambient concentrations within Suisun, San Pablo, and Central Bays. Furthermore, the ecology and habitat quality of the Delta and Suisun Bay are tightly coupled. A unified approach – one that spans the Bay-Delta continuum - for evaluating the impacts of nutrients on beneficial uses will best serve both ecosystem health in the Bay-Delta and the information needs of environmental managers.

12.2 Recommendations for Addressing Priority Knowledge Gaps

Section 12.2.1 provides an overview of the recommended highest priority work efforts over the next 1-5 years to address knowledge and data gaps to, in a targeted way, inform nutrient management decisions in SFB. The process we followed (outlined in Figure 1.1) consisted of

- Identifying the highest priority scenarios (Section 11) for potential impairment along one or more pathways, and high priority science questions that need to be addressed related to those scenarios (Tables 11.3 and 11.4);
- Prioritizing data or knowledge gaps related to the key processes that control ecosystem response to nutrients along the pathways of the near-term highest priority scenarios, developed within conceptual module descriptions in Sections 6-10 and identified in Tables 6.2, 7.1, 8.1, and 9.1.

Recommendations presented in Section 12.2.1 are organized around several major themes or types of work. Not all high priority data gaps are discussed below, and the reader is also referred to Tables 6.2, 7.1, 8.1, and 9.1 and Tables 11.3-11.4. Section 12.2.2 takes a broader view, and describes knowledge gaps and data needs in terms of a set of ecological and management challenges that lie ahead.

12.2.1 Recommendations

R.1 Develop a regionally-administered and sustainably-funded nutrient monitoring program

Major research and monitoring efforts in San Francisco Bay and the Delta include the USGS research program¹⁰ and the IEP Environmental Monitoring Program (Figure 5.3).¹¹ The data generated through these programs, and the related interpretations, form much of the foundation for current understanding of SFB's response to nutrients. However, the focus and mandates of these programs are not necessarily aligned with those of a program designed to inform nutrient management decisions. Furthermore, future funding of the USGS program is uncertain.

Developing a regionally-administered and sustainably-funded nutrient monitoring program needs to be a major priority. Effort needs to be directed toward developing the institutional and funding frameworks for the program, and developing its primary science goals and activities. Several initial recommendations are presented below.

R.1.1 Program development

R.1.1.1 Develop institutional and funding agreements

Developing and implementing a regional nutrient monitoring program will be a major undertaking in terms of logistics and cost, and long-term institutional support will be needed. There are several entities currently involved in ship-based and continuous (moored sensors) monitoring (e.g., USGS, IEP, CA Department of Water Resources, CA Department of Fish and Game). To avoid unnecessary duplication of effort and maximize resources, there may be considerable advantage to achieving some monitoring program goals through fostering close coordination among on-going programs, and augmenting those efforts with additional monitoring. Activities distributed across independent programs need to be well-coordinated, especially in terms of methods, QA/QC, data management and data sharing, synthesis, and reporting.

R.1.1.2 Develop the monitoring program science plan: management questions, goals, priorities, and approaches

A nutrient monitoring program science plan needs to be developed that lays out the management questions, and the program's goals and priorities relative to those management questions. Detailed plans for achieving those goals also need to be developed. A number of the goals and data needs may differ considerably from those of the current research and monitoring activities (i.e., USGS, IEP). When evaluating the future program's needs relative to current efforts, particular attention needs to be given to the following issues:

- The optimal distribution of effort and resources among broad monitoring categories (water column vs. benthos, shoals vs. channel, open bay vs. margins, physical/hydrodynamic vs. biological vs. chemical)
- Key parameters or processes to be measured within these categories;
- Spatial and temporal resolution of sampling; and
- The distribution of monitoring effort between ship-based sampling and moored sensors for continuous monitoring.

¹⁰ <http://sfbay.wr.usgs.gov/access/wqdata/>

¹¹ <http://www.water.ca.gov/iep/activities/emp.cfm>

For some of these issues, considerable data resources already exist from long-term monitoring in SFB. A major component of the monitoring program design effort should include analyzing this data to inform decisions (e.g., about the necessary spatial and temporal density of sampling). Pilot studies should also be part of planning, to inform which parameters provide important additional information, test methods that provide less expensive approaches for essential data collection, and select moored sensor sites and parameters.

R.1.2. Initial monitoring program science recommendations

Several clear monitoring program recommendations emerged through developing the conceptual model, and identifying data/knowledge gaps related to priority scenarios (Tables 6.2, 7.1, 8.1, and 9.1).

R.1.2.1 Continue ship-based monitoring along SFB's deep channel

The long-term record provided by the USGS research program has yielded important insights into the mechanisms that shape SFB's response to nutrients, including physical and biological processes that regulate that response, and how that response has changed over time. Maintaining and building upon this program will be critical for anticipating future changes, and for assessing the effectiveness of any management actions. New parameters may be needed informative, such as size-fractionated chl-a and C:chl-a, organic forms of N and P, as well as others noted below.

R.1.2.2 Develop a moored sensor sub-program for high temporal resolution data

Data collection at higher temporal resolution for chl-a, DO, nutrients, turbidity, and other parameters is needed at multiple locations to assess condition and to improve our quantitative understanding of ecosystem response to nutrients, including the processes that influence phytoplankton blooms, influence oxygen budgets, and regulate nutrient fate. High temporal resolution data will be essential for accurately calibrating water quality models. Continuous monitoring with moored sensor systems is feasible for a wide range of water quality parameters. Techniques for some parameters are becoming increasingly well-established and reliable (e.g., salinity, T, turbidity, chl-a, DO), while others are advancing (e.g., nitrate, phosphate, ammonium, phytoplankton counts and identification). Moored sensor systems can telemeter data, allowing for near real-time assessment of conditions. The data from moored sensors are not a substitute for ship-based sampling, but rather provide strongly complementary information about physical and biological processes that influence key water quality parameters (chlorophyll, DO, T, SpC) over time-scales (hours) that are too short to effectively monitor or study through ship-based sampling. While there are currently multiple stations in Suisun Bay and the Delta that measure some nutrient-related parameters, there are only 3 newly-added stations south of the Bay Bridge for measuring chl-a or nutrients (added in September 2013), and few that measure DO and other parameters (T, SpC, turbidity).

R.1.2.3 In addition to monitoring along the channel, monitoring is needed in shoal environments, including lateral transects

Sampling along the shoals is needed for improved understanding of phytoplankton and nutrient processes, and for model calibration. Most of the water quality data available in SFB is from stations along the deep channel. The shoals are important areas for phytoplankton and MPB production, and large lateral heterogeneities in phytoplankton biomass (and SPM, which influences light availability and growth rates) are common in SFB (Thompson et al., 2008; Cloern, 1995). In addition, a substantial proportion of nutrient transformations likely take place along the shoals (benthic nitrification and denitrification). Shoal monitoring can be accomplished

both through boat/ship-based transects or with moored sensors, and the best approach will vary depending on the questions being addressed. Using autonomous underwater vehicles (AUVs) outfitted with sensors may also be a possibility. AUVs are commonly employed in research studies, and some AUV-sensor systems are already commercially-available. Pilot studies that test AUVs in SFB would be useful for assessing the feasibility and cost effectiveness of this approach, and to inform planning.

R.1.2.4 Coordinated monitoring in shallow subtidal habitats.

Some agencies (e.g., stormwater, wastewater) carry out periodic monitoring in shallow habitats, and several focused studies have been conducted in Lower South Bay systems (Thebault et al., 2008; Shellenbarger et al. 2008; Topping et al., 2009). However, there is currently no systematic monitoring in shallow margin habitats either at the subembayments scale or Bay-wide. Data collection on productivity (e.g., chl-a, light levels) and DO concentrations in select systems would help inform whether adverse impacts are occurring in these systems due to low DO, and help ascertain the causes of low DO. Before embarking on this effort, it would be worthwhile to examine existing data from current or recent studies (e.g., studies in LSB) to assess the need for monitoring and identify the best approaches to pursue.

R.1.2.5 Increased focus HAB/NAB-forming species, phycotoxins, and phytoplankton community composition in general

Given the prevalence of HAB-forming organisms in the Bay and the frequent detection of phycotoxins Bay-wide, it would be prudent to more closely monitor phytoplankton composition, the occurrence of HAB-forming organisms and phycotoxins within San Francisco Bay. Composition and biovolume data collected for HAB-related work would also support assessment and improved mechanistic understanding of other hypothesized nutrient-related shifts in phytoplankton community composition. The abundance and forms of nutrient are two among many factors that can influence phytoplankton community composition and the occurrence of HABs. The relative contributions of those factors toward causing adverse shifts in composition or HAB occurrences are poorly understood. More frequent (in space and time) analysis of phytoplankton composition and phycotoxins, in combination with special studies, (see Recommendation 4.1) will be needed to better understand these mechanisms and assess potential linkages to nutrients.

Determining taxonomy and biomass by microscopy is expensive and time consuming, which limits the amount of data that can be collected. Some amount of manual microscopy ground-truthing will always be needed. However, other techniques, in combination with microscopy, may allow for increased data collection of at lower costs. Carrying out pilot studies will help inform which techniques provide valuable and cost-effective information. Measuring phytoplankton-derived pigments is one such approach. Different classes of phytoplankton have distinct pigment fingerprints. It is possible, with sufficient calibration (relative to microscopy) and training of software to quantify phytoplankton biomass within specific classes. Flow cytometers and digital imaging tools are also available. These systems - which measure optical properties and capture images of individual cells, and employ image-recognizing software to identify and count phytoplankton down to the species level - can be deployed at moored stations for continuous monitoring, used on a monitoring vessel as it cruises along a transect, or used in the laboratory. Moored applications can telemeter data, allowing for near real-time information.

One such system provided early warning of a toxic algal bloom in the Gulf of Mexico.¹² An additional advantage of digital imaging approaches is that an archive of phytoplankton image data would be developed: if a phytoplankton species eventually becomes important, the digital archive could be mined to determine when that species first appeared.

Pilot projects have been initiated recently that are measuring phycotoxins in SFB (Figure 3.8), and an algal pigment pilot study is underway. Continuation of similar pilot studies, and testing a variety of methods, will help identify the most informative and cost-effective options, all the while establishing baseline concentration data against which future data can be compared. The feasibility of measuring algal toxins in archived benthos samples should also be considered in order to generate longer time series of algal toxins and look for changes over the past decade or more (if well preserved samples exist).

R.1.2.6 Benthos monitoring to quantify spatial, seasonal, and interannual variability in grazer abundance

Grazing by benthic filter feeders is considered to be one of the main controls on phytoplankton biomass accumulation in several subembayments. To estimate the influence of the benthic grazing, and track its changes in space and time, benthos surveys are needed on a regular basis in some subembayments, most importantly Lower South Bay, South Bay, San Pablo Bay, and Suisun Bay. In recent years there has been ample benthos monitoring in Suisun Bay and the Delta (and some in San Pablo Bay), although the fate of this program is not known. There are currently no sustained programs in the other subembayments. However, there are some years during which intensive benthic sampling has taken place (e.g., Thompson et al. 2008; see Figure 7.4.B), and along with opportunistic sampling efforts (in some cases, samples have been archived but not yet analyzed for biomass; J Thompson, personal communication). Benthos monitoring could occur less frequent than water quality monitoring, e.g., three times per year (spring, summer, fall). Sorting, counting, and weighing benthos samples is time consuming and costly. A pilot study to test the feasibility of using benthic cameras may also be worth considering (alongside traditional sample collection for calibration/validation), since its use could potentially allow for more cost-effective benthos surveys.

R.1.2.7 Zooplankton abundance/composition

Monitoring data on zooplankton are needed to quantify pelagic grazing rates. Zooplankton abundance and composition may also serve as an important indicator of food supply and quality for higher trophic levels. Long term zooplankton monitoring has been carried out in Suisun Bay and the Delta. However, zooplankton abundance and composition are not currently measured in other subembayments.

R.1.2.8 Allocate sufficient funding for data interpretation and synthesis

Data analysis and data synthesis are essential components of a monitoring program. Allocating sufficient funds for these activities will allow field results to be efficiently translated into management-relevant observations that inform decisions, and allow the monitoring program to nimbly evolve to address emerging data requirements. Annual reports will be needed that not only compile and present data, but that also evaluate and interpret trends. More detailed special studies will also be needed periodically to generate scientific synthesis reports on complex data sets (e.g., spatial and seasonal trends in phytoplankton community composition).

¹² <http://www.whoi.edu/oceanus/viewArticle.do?id=46486>

R.2. Develop and implement a science plan for SFB that targets the highest priority management and science questions

The size of SFB, and the complexity and diversity of its nutrient-response issues, create a situation in which there are numerous science questions that need to be addressed to improve our understanding of the system. Addressing the management and science questions will require a combination of field studies, controlled experiments, monitoring, and modeling across the topics of nutrient cycling, phytoplankton response (biomass and community composition), and hydrodynamics. It will not be feasible to explore all the relevant science questions – that would take longer than management decisions can wait, and would outstrip any reasonable budget. To best target science efforts, there would be considerable benefit to developing and implementing a science plan that: identifies the highest priority management issues, and associated science questions; and identifies the sets of studies and data collection/monitoring needs that efficiently target those questions. In some cases, the management issues, science questions, data gaps, and studies may be similar Bay-wide. In other cases, the science questions or data gaps may be subembayment- or habitat-specific. The science questions listed in Tables 11.3-11.4 and the recommendations in this section could serve as a starting point in what would be an iterative Science Plan development process.

Analysis of existing data from SFB, combined with broader critical literature review, would be useful early steps in science plan development, to articulate what is well-understood - in other estuaries and SFB - and focus scientific studies and monitoring on addressing the most critical knowledge and data gaps.

R.3. Develop hydrodynamic, nutrient cycling, and ecosystem response models

Tables 11.3-11.4 illustrate that modeling will play a central role in addressing a wide range of science questions. Models can also be used to prioritize data collection needs. While there are multiple hydrodynamic models available for SFB, there are currently no integrated hydrodynamic-phytoplankton-nutrient models. Considerable progress could be made toward addressing several important science questions through using “simplified-domain” models that are built upon simplified (spatially-aggregated), but still accurate, hydrodynamics. Potential applications of these simplified domain models include (not an exhaustive list):

- R.3.1* Quantitative analysis of nutrient budgets (including losses/transformations of nutrients);
- R.3.2* Quantifying the relative importance of major processes that control primary production in Suisun Bay (light, clams, flushing, NH_4^+ inhibition), and explore which factors may explain the changes in phytoplankton biomass in South Bay over the past ~20 years.
- R.3.3* Performing sensitivity/uncertainty analysis, and identifying highest priority monitoring activities, process level studies, or rate measurements to minimize model uncertainty.
- R.3.4* Forecasting ecosystem response under future scenarios, and narrowing the list of high priority scenarios;

In developing such models, there is a benefit to “starting simple”, and adding complexity as needed. LSB/South Bay and South Bay could serve as good initial focus areas for basic model development and application, because of the abundance of data for those systems and since these two subembayments are where concerns about adverse impacts from nutrients are greatest. Lessons learned through applying basic models will be useful for informing larger-scale or more complex model development.

Higher spatial resolution models, or larger spatial scale models (e.g., full Bay as opposed to individual subembayments) will be needed to explore several important issues, including:

- R.3.5 Determine the zones of influence of individual POTWs under a range of hydrodynamic forcings and estimated transformations/losses
- R.3.6 Test future scenarios under which adverse impacts may develop Bay-wide or in individual subembayments
- R.3.7 Evaluate the effectiveness of different nutrient control strategies for achieving desired reductions in ambient concentrations as a function of space and time.
- R.3.8 Quantify loads from the Delta to Suisun Bay under seasonally- and interannually-varying hydrological conditions, and the influence of these loads in Suisun and down-estuary subembayments under a range of forcings.
- R.3.9 Quantify the importance of net nutrient loads from the coastal ocean to SFB under a range of commonly-occurring forcing scenarios, and explore the fate of the nutrient-rich SFB plume leaving the Golden Gate, and the potential influence of those nutrients on coastal ecosystems.

R.4. Carry out special studies to address key knowledge gaps about mechanisms that regulate ecosystem response, and inform whether or not impairment is occurring

The draft list of priority science questions in Tables 11.3-11.4, viewed alongside the data/knowledge gap priorities in Tables 6.2, 7.1, 8.1, and 9.1, present an initial picture of the types of data collection and studies that are the most important in the near term. A number of priorities have been discussed above in the context of monitoring program development (*R.1.2.1-1.2.8*) and modeling (*R.3.1-R.3.9*). An overview of special study priorities is provided below; however, the reader is also referred to the Tables 11.3-11.4, 6.2, 7.1, 8.1, and 9.1.

Nutrient cycling

- R.4.1 Controlled field/lab experiments to measure pelagic nutrient transformations (pelagic nitrification, nutrient uptake rates)
- R.4.2 Controlled field/lab experiments to measure benthic nutrient transformations (benthic nitrification, denitrification, mineralization and N and P fluxes from sediments)
- R.4.3 Quantify the importance of internal nutrient transformations using models.

Productivity of phytoplankton and MPB

- R.4.4 Controlled experiments that further test the proposed “NH₄⁺-paradox” mechanism of lower productivity when NH₄⁺ is elevated, determine relevant thresholds, and allow its effect to be better parameterized and compared to other regulating factors in models (*R.3.2*).
- R.4.5 Through analysis of existing data or through field studies, assess the variability or uncertainty in the Cole and Cloern (1987) productivity relationship due to factors such as different phytoplankton assemblages, temperature, light levels, etc.
- R.4.6 Field measurements to quantify MPB primary production rates and biomass.
- R.4.7 Compare MPB production and biomass with phytoplankton production and biomass, consider how MPB’s relative importance would change (or already has changed) due to ecosystem change (lower suspended sediments, benthic grazers), and explore how those changes influence nutrient cycling, oxygen budgets, and food webs.

Dissolved O₂

- R.4.8 Controlled field experiments to quantify sediment oxygen demand in a range of depositional environments. These can be carried out in conjunction with the benthic nutrient transformation special studies as part of the same experimental protocol (R.4.2).
- R.4.9 Monitoring and targeted mechanistic studies of DO in shallow margin habitats to assess the severity of low DO (concentration, spatial extent, frequency, duration).
- R.4.9 In cooperation with other efforts or as special nutrient-related studies, determine the degree to which low DO in margin habitats (or in open water areas of some areas of the Bay, specifically LSB) adversely impact biota. To a certain degree, this work could be carried out based on existing data from other studies on DO tolerances of key organisms. Field surveys of fish or benthos abundance may also be warranted.
- R.4.10 Through field experiments and modeling, quantify the degree to which anthropogenic nutrients contribute to occurrences of low DO.

HABs, toxins, and phytoplankton community composition

- R.4.12 Rigorous analysis of existing phytoplankton community composition data – for HAB-forming species and composition more broadly – to test qualitative and quantitative agreement with various conceptual models, and refine those conceptual models as needed.
- R.4.13 Field studies (collecting phytoplankton composition data at higher temporal or spatial resolution) to test mechanisms of HAB development and phytoplankton community succession in response to physical, chemical, and biological drivers.
- R.4.14 Field studies to evaluate the potential importance of salt ponds as incubators of HAB-forming species.
- R.4.15 Controlled experiments, using mixed cultures and monocultures from SFB, that mechanistically explore the interactive effects of nutrient availability (including variability in concentrations and forms), light, and temperature on HAB/NAB development and phycotoxins production, or other shifts toward assemblages that poorly support food webs. The goals of such studies would be to identify conditions that favor some classes or species of phytoplankton over others under the prevailing conditions in SFB (light limitation, excess nutrients), and enable predictions about assemblage response. Such information is also essential for identifying nutrient concentrations or loads that would decrease the risk of HAB occurrences or other adverse assemblage shifts.
- R.4.16 Apply the information from R.4.1.5 within models to, among other issues, evaluate the magnitude of the nutrient component of stress, and explore potential composition responses to changing conditions, including those due to potential management actions (e.g., nutrient load reductions).

12.2.2 Grand Challenges

During the conceptual model development and identification of knowledge gaps, data gaps, and monitoring needs, four so-called “Grand Challenges” emerged related to understanding and managing SFB ecosystem health. While there is overlap between the underlying management issues that motivated the more specific recommendations above and those that motivated the Grand Challenges, the Grand Challenges represent a somewhat different, more holistic perspective or framework for considering science and data collection needs. In so doing they

highlight connections between nutrient issues and other ecosystem health concerns, and provide an additional impetus for addressing those data collection needs.

Grand Challenge 1: What do we need to know in 10-20 yrs to make improved decisions related to water quality management or ecosystem health, including those related to nutrients? 1-2 decades is approximately the time scale over which large capital improvement projects are planned and implemented. 10-20 years is also a long enough time period for trends to become evident, e.g, the changes in phytoplankton biomass in South Bay and LSB since the late 1990s (Figure 3.4). What information needs to be collected now, to serve as baseline condition data, so that changes in important indicators can be confidently identified and attributed to the correct causal agent(s), whether those changes lead to improved or worsened condition?

Grand Challenge #2: The northern estuary is poised to experience major changes due to management actions and environmental change. Anticipated changes include: nitrification and nutrient load reductions at Sac Regional wastewater treatment plant; numerous large scale restoration projects and changes in water management in the Delta; changing climate patterns altering the timing, residence time, and amount of water passing through the Delta. What do we need to be measuring now in order to determine if these changes have positive, negative, or no impacts on ecological health in SFB and the Delta? How will phytoplankton respond to changes in nutrient loads/speciation? How will the food web respond?

Grand Challenge #3: Large areas along the margins of South Bay and LSB are slated to undergo restoration. Given the size of these areas compared to the adjacent water surface area (Figure 2.1), it is reasonable to expect that proposed restorations along the margins will have measurable impacts on water quality and ecological health in the open Bay. Some of these effects may be positive, including increased habitat for fish, birds and other organisms. It will be desirable to document those changes; in order to do so, baseline data is needed for these higher trophic level indicators of ecosystem health. Those changes could also encourage more denitrification and decreased N within the Bay, which could be considered within integrated nutrient management plans. As discussed earlier, there may also be unintended and undesirable consequences, including: restored/reconnected salt ponds acting as incubators for HAB-forming phytoplankton species; exceedingly high primary production rates and high biomass, causing periodic low DO in wetlands and sloughs; and increased duration of stratification due to dampening of tidal mixing energy. What hypotheses of adverse impacts need to be tested, as part of restoration planning, so that the risks of severe unintended consequences can be minimized?

Grand Challenge #4: Similar to Grand Challenges 1-3, what baseline observational data is needed to detect climate-related changes in habitat quality in SFB and to disentangle them from other anthropogenic drivers? What types of modeling simulations should be done to anticipate effects? The CASCaDE II¹³ project is exploring these issues, largely focused in the Delta. Similar studies may be warranted in the Bay.

¹³ <http://cascade.wr.usgs.gov/>

References

- Alpine, A.E. and J.E. Cloern (1988). "Phytoplankton growth rates in a light-limited environment, San Francisco Bay". *Marine Ecology Progress Series* **44**; 167-173
- Antia, N. J., B. R. Berland, et al. (1975). "COMPARATIVE EVALUATION OF CERTAIN ORGANIC AND INORGANIC SOURCES OF NITROGEN FOR PHOTOTROPIC GROWTH OF MARINE MICROALGAE." *Journal of the Marine Biological Association of the United Kingdom* **55**(3): 519-539.
- Baxter, R., R. Breuer, L. Brown, L. Conrad, F. Feyrer, S. Fong, K. Gehrts, L. Grimaldo, B. Herbold, P. Hrodey, A. Mueller-Solger, T. Sommer, and K. Souza. 2010. Interagency Ecological Program 2010 Pelagic Organism Decline Work Plan and Synthesis of Results. Available online at: <http://www.water.ca.gov/iep/docs/FinalPOD2010Workplan12610.pdf>.
- Barton, A. D., S. Dutkiewicz, et al. (2010a). "Patterns of Diversity in Marine Phytoplankton." *Science* **327**(5972): 1509-1511.
- Barton, A. D., S. Dutkiewicz, et al. (2010b). "Response to Comment on "Patterns of Diversity in Marine Phytoplankton"." *Science* **329**(5991).
- Berggreen, U., B. Hansen and T. Kiorboe (1988). "Food Size Spectra, Ingestion and Growth of the Copepod *Acartia tonsa* During Development - Implications for Determination of Copepod Production" *Marine Biology*, **99** (3); 341-352
- Behrenfeld, M. J. and P. G. Falkowski (1997). "A consumer's guide to phytoplankton primary productivity models." *Limnology and Oceanography* **42**(7): 1479-1491.
- Bennett, W. A. (2005). "Critical assessment of the delta smelt population in the San Francisco Estuary, California." *San Francisco Estuary and Watershed Science* **3 no. 2**.
- Bissinger, J.E., D.J.S. Montagnes, J. Sharples, and D. Atkinson (2008) Predicting marine phytoplankton maximum growth rates from temperature: Improving on the Eppley curve using quantile regression *Limnology and Oceanography* **53** (2), 487
- Bligny, R., E. Gout, et al. (1997). "pH regulation in acid-stressed leaves of pea plants grown in the presence of nitrate or ammonium salts: Studies involving P-31-NMR spectroscopy and chlorophyll fluorescence." *Biochimica Et Biophysica Acta-Bioenergetics* **1320**(2): 142-152.
- Brand, A., et al. (2010) "Wind - enhanced resuspension in the shallow waters of South San Francisco Bay: Mechanisms and potential implications for cohesive sediment transport." *Journal of Geophysical Research: Oceans* (1978–2012)115.C11
- Brand, L. E., W. G. Sunda, et al. (1986). "REDUCTION OF MARINE-PHYTOPLANKTON REPRODUCTION RATES BY COPPER AND CADMIUM." *Journal of Experimental Marine Biology and Ecology* **96**(3): 225-250.
- Bricker, S. L., B., Dennison, W., Jones, A., Boicourt, K., Wicks, C., and Worner, J. (2007). "Effects of Nutrient Enrichment in the Nation's Estuaries: A Decade of Change." *NOAA coastal Ocean Program Decision Analysis Series No. 26*.
- Britto, D. T., M. Y. Siddiqi, et al. (2001). "Futile transmembrane NH₄⁺ cycling: A cellular hypothesis to explain ammonium toxicity in plants." *Proceedings of the National Academy of Sciences of the United States of America* **98**(7): 4255-4258.
- Brooks, M. L., E. Fleishman, et al. (2012). "Life Histories, Salinity Zones, and Sublethal Contributions of Contaminants to Pelagic Fish Declines Illustrated with a Case Study of San Francisco Estuary, California, USA." *Estuaries and Coasts* **35**(2): 603-621.
- Burkholder, J.M, D.A. Dickey et al. (2006) "Comprehensive Trend Analysis of Nutrients and Related Variables in a Large Eutrophic Estuary: A Decadal Study of Anthropogenic and Climatic Influences" *Limnology and Oceanography* **51** (1); 463-487
- Burkholder, J. M., P. M. Glibert, et al. (2008). "Mixotrophy, a major mode of nutrition for harmful algal species in eutrophic waters." *Harmful Algae* **8**(1): 77-93.
- Caffrey, J. M. (2003). "Production, respiration and net ecosystem metabolism in US estuaries." *Environmental Monitoring and Assessment* **81**(1-3): 207-219.
- Caffrey, J. M., J.E. Cloern, C. Grenz (1998). "Changes in production and respiration during a spring phytoplankton bloom in San Francisco Bay, California, USA: implications for net ecosystem metabolism." *MARINE ECOLOGY PROGRESS SERIES* **172**: 1-12.

- Cammen, L. M. (1982). "EFFECT OF PARTICLE-SIZE ON ORGANIC CONTENT AND MICROBIAL ABUNDANCE WITHIN 4 MARINE-SEDIMENTS." *Marine Ecology Progress Series* **9**(3): 273-280.
- Cammen, L. M. (1991). "ANNUAL BACTERIAL PRODUCTION IN RELATION TO BENTHIC MICROALGAL PRODUCTION AND SEDIMENT OXYGEN-UP TAKE IN AN INTERTIDAL SANDFLAT AND AN INTERTIDAL MUDFLAT." *Marine Ecology Progress Series* **71**(1): 13-25.
- Carstensen, J., M. Sánchez-Camacho, C.M. Duarte, D Krause-Jensen, Núria Marbà (2011) "Connecting the Dots: Responses of Coastal Ecosystems to Changing Nutrient Concentrations" *Environmental Science & Technology* 2011 45 (21), 9122-9132.
- Chisholm, S. W. (1992). "Phytoplankton size." *Primary Productivity and Biogeochemical Cycles in the Sea* PG Falkowski and AD Woodhead (eds). Plenum Press, New York.
- Cloern, J.E. (1982) "Does the benthos control phytoplankton biomass in South San Francisco Bay?" *Marine Ecology Progress Series* **9**: 191-202
- Cloern, J.E. (1987) "Turbidity as a control on phytoplankton biomass and productivity in estuaries" *Continental Shelf Research* **7** (11/12): 1367-1381
- Cloern, J. E. (1991). "Tidal stirring and phytoplankton bloom dynamics in an estuary." *Journal of Marine Research* **49**: 203-221.
- Cloern, J. E. (1996). "Phytoplankton bloom dynamics in coastal ecosystems: a review with some general lessons from sustained investigation of San Francisco Bay, California." *Reviews of Geophysics* **34**(2): 127-168.
- Cloern, J. E., A. E. Alpine, et al. (1983). "River discharge controls phytoplankton dynamics in the Northern San Francisco Bay Estuary." *Estuarine, Coastal and Shelf Science* **16**: 415-429.
- Cloern, J.E., B.E. Cole, et al. (1985) "Temporal dynamics of estuarine phytoplankton: a case study of San Francisco Bay" *Hydrobiologia* **129**: 153-176
- Cloern, J. E., B. E. Cole, et al. (1994). "Notes on a *Mesodinium rubrum* red tide in San Francisco Bay (California, USA)." *Journal of Plankton Research* **16**(9): 1269-1276.
- Cloern, J. E. and R. Dufford (2005). "Phytoplankton community ecology: principles applied in San Francisco Bay." *Marine Ecology Progress Series* **285**: 11-28.
- Cloern, J. E., K. A. Hieb, et al. (2010). "Biological communities in San Francisco Bay track large-scale climate forcing over the North Pacific." *Geophysical Research Letters* **37**.
- Cloern, J. E. and A. D. Jassby (2008). "Complex seasonal patterns of primary producers at the land-sea interface." *Ecology Letters* **11**(12): 1294-1303.
- Cloern, J. E. and A. D. Jassby (2012). "DRIVERS OF CHANGE IN ESTUARINE-COASTAL ECOSYSTEMS: DISCOVERIES FROM FOUR DECADES OF STUDY IN SAN FRANCISCO BAY." *Reviews of Geophysics* **50**.
- Cloern, J. E., A. D. Jassby, et al. (2007). "A cold phase of the East Pacific triggers new phytoplankton blooms in San Francisco Bay." *Proceedings of the National Academy of Sciences* **104**(47): 18561-18565.
- Cloern, J. E., N. Knowles, et al. (2011). "Projected Evolution of California's San Francisco Bay-Delta-River System in a Century of Climate Change." *Plos One* **6**(9).
- Cloern, J. E., T. M. Powell, et al. (1989). "Spatial and temporal variability in South San Francisco Bay (USA). II. Temporal changes in salinity, suspended sediments, and phytoplankton biomass and productivity over tidal time scales." *Estuarine, Coastal and Shelf Science* **28**: 599-613.
- Cloern, J. E., T. S. Schraga, et al. (2005). "Heat wave brings an unprecedented red tide to San Francisco Bay." *Eos Transactions of the American Geophysical Union* **86**(7): 66.
- Cloern, J.E. and R. Dugdale (2010) San Francisco Bay, in Glibert, P.M. et al., eds, *Nutrients in Estuaries: A Summary Report of the National Estuarine Experts Workgroup 2005-2007*, p. 117-126.
- Cloern, J. E., T. S. Schraga, et al. (2005). "Climate anomalies generate an exceptional dinoflagellate bloom in San Francisco Bay." *Geophysical Research Letters* **32**: 5 pp. .
- Cole, B. E. and J. E. Cloern (1984). "Significance of biomass and light availability to phytoplankton productivity in San Francisco Bay." *Marine Ecology Progress Series* **17**: 15-24.
- Cole, B. E. and J. E. Cloern (1987). "An empirical model for estimating phytoplankton productivity in estuaries." *Marine Ecology Progress Series* **36**: 299-305.
- Collignon, A. G., and M.T. Stacey (2013) "Turbulence Dynamics at the Shoal-Channel Interface in a Partially-Stratified Estuary." *Journal of Physical Oceanography* **43** (5) : 970-989
- Collignon, A. G., and M.T. Stacey (2012) "Intratidal Dynamics of Fronts and Lateral Circulation at the Shoal Channel Interface in a Partially Stratified Estuary." *Journal of Physical Oceanography* **42**(5): 869-883.
- Collos, Y., A. Vaquer, et al. (2005). "Acclimation of nitrate uptake by phytoplankton to high substrate levels." *Journal of Phycology* **41**(3): 466-478.

- Cornwell, J.C., P.M. Glibert, M.S. Owens (2014) Nutrient Fluxes from sediments in the San Francisco Bay Delta" *Estuaries and Coasts* (2014) 37:1120–1133
- Dejong, D. J. and V. N. Dejonge (1995). "DYNAMICS AND DISTRIBUTION OF MICROPHYTOBENTHIC CHLOROPHYLL-A IN THE WESTERN SCHELDT ESTUARY (SW NETHERLANDS)." *Hydrobiologia* **311**(1-3): 21-30.
- Duarte, C.M., D.J. Conley, J. Carstensen, M Sanchez-Camacho (2009) "Return to Neverland: shifting baselines affect eutrophication re-toration targets" *Estuaries and Coasts*, 32:29-36.
- Dugdale, R., F. Wilkerson, et al. (2012). "River flow and ammonium discharge determine spring phytoplankton blooms in an urbanized estuary." *Estuarine Coastal and Shelf Science* **115**: 187-199.
- Dugdale, R. C., F. P. Wilkerson, et al. (2007). "The role of ammonium and nitrate in spring bloom development in San Francisco Bay." *Estuarine, Coastal and Shelf Science* **73**: 17-29.
- Eppley, R. W. (1972). "TEMPERATURE AND PHYTOPLANKTON GROWTH IN SEA." *Fishery Bulletin* **70**(4): 1063-1085.
- Farmer, D. M., and L.Armi (1986). "Maximal two-layer exchange over a sill and through the combination of a sill and contraction with barotropic flow." *Journal of Fluid Mechanics* **164.1**: 53-76.
- Feyrer, F., B. Herbold, et al. (2003). "Dietary shifts in a stressed fish assemblage: Consequences of a bivalve invasion in the San Francisco Estuary." *Environmental Biology of Fishes* **67**(3): 277-288.
- Fischer, H.B.,E.J. List, R.C.Y. Koh, J. Imberger,and N.H. Brooks, (1979). *Mixing in Inland and Coastal Waters*. Academic Press, 302 pp.
- Follows, M. J. and S. Dutkiewicz (2011). Modeling Diverse Communities of Marine Microbes. *Annual Review of Marine Science, Vol 3*. C. A. Carlson and S. J. Giovannoni. **3**: 427-451.
- Fram, J. P.,M.A. Martin, and M.T. Stacey, (2007). "Dispersive fluxes between the coastal ocean and a semienclosed estuarine basin." *Journal of physical oceanography* **37** (6):1645-1660.
- Friedrichs, C. T., et al.(2000) "Bottom-boundary-layer processes associated with fine sediment accumulation in coastal seas and bays." *Continental Shelf Research* **20**(7): 807-841.
- Glibert, P. M. (2010). "Long-Term Changes in Nutrient Loading and Stoichiometry and Their Relationships with Changes in the Food Web and Dominant Pelagic Fish Species in the San Francisco Estuary, California." *Reviews in Fisheries Science* **18**(2): 211-232.
- Glibert, P. M. (2012). "Ecological stoichiometry and its implications for aquatic ecosystem sustainability." *Current Opinion in Environmental Sustainability* **4**(3): 272-277.
- Glibert, P. M., D. Fullerton, et al. (2011). "Ecological Stoichiometry, Biogeochemical Cycling, Invasive Species, and Aquatic Food Webs: San Francisco Estuary and Comparative Systems." *Reviews in Fisheries Science* **19**(4): 358-417.
- Glibert, P.M., T.M. Kana, K Brown (2013), "From limitation to excess: the consequences of substrate excess and stoichiometry for phytoplankton physiology, trophodynamics and biogeochemistry, and the implications for modeling", *J. Mar. Syst.*: 125:14-28, <http://dx.doi.org/10.1016/j.jmarsys.2012.10.004>
- Gobler, C. J., D. J. Lonsdale, et al. (2005). "A review of the causes, effects, and potential management of harmful brown tide blooms caused by *Aureococcus anophagefferens* (Hargraves et Sieburth)." *Estuaries* **28**(5): 726-749.
- Greene, V. E., L. J. Sullivan, et al. (2011). "Grazing impact of the invasive clam *Corbula amurensis* on the microplankton assemblage of the northern San Francisco Estuary." *Marine Ecology Progress Series* **431**: 183-193.
- Gross, E.S. (2010). Three-dimension modeling of tidal hydrodynamics in San Francisco Estuary. *San Francisco Estuary and Watershed Science*, 7(2)
- Guarini, J. M., J. E. Cloern, et al. (2002). "Microphytobenthic potential productivity estimated in three tidal embayments of the San Francisco Bay: A comparative study." *Estuaries* **25**(3): 409-417.
- Hansen, D. V., and M. Rattray (1965). "Gravitational circulation in straits and estuaries." *Journal of Marine Research* **23** (2)
- Herndon, J., W. P. Cochlan, et al. (2003). "*Heterosigma akashiwo* blooms in San Francisco Bay " *IEP Newsletter* **16**(2): 46-48.
- Hildebrand, M. (2005). "Cloning and functional characterization of ammonium transporters from the marine diatom *Cylindrotheca fusiformis* (Bacillariophyceae)." *Journal of Phycology* **41**(1): 105-113.
- Hogg, A. M., G.N. Ivey, and K.B. Winters (2001) "Hydraulics and mixing in controlled exchange flows." *Journal of Geophysical Research: Oceans (1978–2012)* 106.C1: 959-972.
- Hsu, K. and M.T. Stacey (2013). "Residence times in small perimeter habitats", accepted for publication in *Estuaries and Coasts*.

- Huzzey, L. M., J. E. Cloern, et al. (1990). "Episodic changes in lateral transport and phytoplankton distribution in South San Francisco Bay." *Limnology and Oceanography* **35**(2): 472-478.
- Irigoien, X., K. J. Flynn, et al. (2005). "Phytoplankton blooms: a 'loophole' in microzooplankton grazing impact?" *JOURNAL OF PLANKTON RESEARCH* **27**(4): 313-321.
- Irigoien, X., J. Huisman, et al. (2004). "Global biodiversity patterns of marine phytoplankton and zooplankton." *Nature* **429**(6994): 863-867.
- Irwin, A. J., Z. V. Finkel, et al. (2006). "Scaling-up from nutrient physiology to the size-structure of phytoplankton communities." *JOURNAL OF PLANKTON RESEARCH* **28**(5): 459-471.
- Jassby, A. D., J. E. Cloern, et al. (2002). "Annual primary production: patterns and mechanisms of change in a nutrient-rich tidal ecosystem." *Limnology and Oceanography* **47**(3): 698-712.
- Jassby, A. D., J. E. Cloern, et al. (1993). "Organic carbon sources and sinks in San Francisco Bay: variability induced by river flow." *Marine Ecology Progress Series* **95**: 39-54.
- Kimmerer, W. J. (2006). Response of anchovies dampens effects of the invasive bivalve *Corbula amurensis* on the San Francisco Estuary foodweb. Oldendorf, ALLEMAGNE, Inter-Research.
- Kimmerer, W. J. (2005). "Long-term changes in apparent uptake of silica in the San Francisco estuary." *Limnology and Oceanography* **50**(3): 793-798.
- Kimmerer, W. J., A. E. Parker, et al. (2012). "Short-Term and Interannual Variability in Primary Production in the Low-Salinity Zone of the San Francisco Estuary." *Estuaries and Coasts* **35**(4): 913-929.
- Kimmerer, W. J., J. K. Thompson (2014) "Phytoplankton Growth Balanced by Clam and Zooplankton Grazing and Net Transport into the Low-Salinity Zone of the San Francisco Estuary" *Estuaries and Coasts* **37** (5): 1202-1218
- Koch, F., M. A. Marcoval, et al. (2011). "The effect of vitamin B-12 on phytoplankton growth and community structure in the Gulf of Alaska." *Limnology and Oceanography* **56**(3): 1023-1034.
- Kudela, R. M. and W. P. Cochlan (2000). "Nitrogen and carbon uptake kinetics and the influence of irradiance for a red tide bloom off southern California." *Aquatic Microbial Ecology* **21**(1): 31-47.
- Kudela, R. M., J. Q. Lane, et al. (2008). "The potential role of anthropogenically derived nitrogen in the growth of harmful algae in California, USA." *Harmful Algae* **8**(1): 103-110.
- Kudela, R. M., S. Seeyave, et al. (2010). "The role of nutrients in regulation and promotion of harmful algal blooms in upwelling systems." *Progress in Oceanography* **85**(1-2): 122-135.
- Kundu, P.K., J.M. Cohen, D.R. Dowling, (2011). *Fluid Mechanics*. Academic Press, 920 pp.
- Lacy, J. R., et al. "Interaction of lateral baroclinic forcing and turbulence in an estuary." *Journal of Geophysical Research: Oceans (1978–2012)* **108**.C3 (2003).
- Lancelot, C., P. Grosjean, et al. (2012). "Rejoinder to "Perils of correlating CUSUM-transformed variables to infer ecological relationships (Breton et al. 2006; Glibert 2010)"." *Limnology and Oceanography* **57**(2): 669-670.
- Lehman, P. W. (1992). "ENVIRONMENTAL-FACTORS ASSOCIATED WITH LONG-TERM CHANGES IN CHLOROPHYLL CONCENTRATION IN THE SACRAMENTO-SAN-JOQUIN DELTA AND SUISUN BAY, CALIFORNIA." *Estuaries* **15**(3): 335-348.
- Lehman, P. W. (2000). "The influence of climate on phytoplankton community biomass in San Francisco Bay Estuary." *Limnology and Oceanography* **45**(3): 580-590.
- Lehman, P. W., G. Boyer, et al. (2005). "Distribution and toxicity of a new colonial *Microcystis aeruginosa* bloom in the San Francisco Bay Estuary, California." *Hydrobiologia* **541**: 87-99.
- Lehman, P. W., G. Boyer, et al. (2008). "The influence of environmental conditions on the seasonal variation of *Microcystis* cell density and microcystins concentration in San Francisco Estuary." *Hydrobiologia* **600**: 187-204.
- Lehman, P. W., S. J. Teh, et al. (2010). "Initial impacts of *Microcystis aeruginosa* blooms on the aquatic food web in the San Francisco Estuary." *Hydrobiologia* **637**(1): 229-248.
- Lidström, U. (2009). "Primary production, biomass and species composition of phytoplankton in the low salinity zone of the northern San Francisco Estuary." *MS thesis, San Francisco State University*.
- Litchman, E., C. A. Klausmeier, et al. (2007). "The role of functional traits and trade-offs in structuring phytoplankton communities: scaling from cellular to ecosystem level." *Ecology Letters* **10**(12): 1170-1181.
- Litchman, E., and C.A. Klausmeier. 2008. Trait-based community ecology of phytoplankton. *Annual Review of Ecology, Evolution, and Systematics* **39**: 615-639
- Lomas, M. W. (2004). "Nitrate reductase and urease enzyme activity in the marine diatom *Thalassiosira weissflogii* (Bacillariophyceae): interactions among nitrogen substrates." *Marine Biology* **144**(1): 37-44.
- Lucas, L.V., J.E. Cloern, et al. (1998) "Does the Sverdup critical depth model explain bloom dynamics in estuaries" *Journal of Marine Research* **50**: 375-415

- Lucas, L. V., J. R. Koseff, et al. (1999). "Processes governing phytoplankton blooms in estuaries. II: The role of horizontal transport." *Marine Ecology Progress Series* **187**: 17-30.
- Lucas, L. V., J. R. Koseff, et al. (2009). "Shallow water processes govern system-wide phytoplankton bloom dynamics: A modeling study." *Journal of Marine Systems* **75**(1-2): 70-86.
- Lucas, L. V. a. T., J.K. (2013). "Changing restoration rules: Exotic bivalves interact with residence time and depth to control phytoplankton productivity." *Ecosphere*, in press.
- MacIntyre, H. L., R. J. Geider, et al. (1996). "Microphytobenthos: The ecological role of the "secret garden" of unvegetated, shallow-water marine habitats .1. Distribution, abundance and primary production." *Estuaries* **19**(2A): 186-201.
- MacVean, L.J., and M.T. Stacey "Estuarine dispersion from tidal trapping: a new analytical framework." *Estuaries and Coasts* **34**.1 (2011): 45-59.
- Mallin, M. A., H. W. Paerl, et al. (1993). "REGULATION OF ESTUARINE PRIMARY PRODUCTION BY WATERSHED RAINFALL AND RIVER FLOW." *Marine Ecology Progress Series* **93**(1-2): 199-203.
- Martin, M. A., J.P. Fram, and M.T. Stacey. "Seasonal chlorophyll a fluxes between the coastal Pacific Ocean and San Francisco Bay." *Marine Ecology Progress Series* **337** (2007): 51-61.
- McKee, L. J., Sutula, M., Gilbreath, A.N., Beagle, J., Gluchowski, D., and Hunt, J. (2011). "Nutrient Numeric Endpoint Development for San Francisco Bay - Literature Review and Data Gaps Analysis." *Southern California Coastal Water Research Project Technical Report No. 644*. June 2011.
- Monismith, S.G., et al. "Structure and flow-induced variability of the subtidal salinity field innorthern San Francisco Bay." *Journal of Physical Oceanography* **32**.11 (2002): 3003-3019.
- Monsen, N. E., et al. "A comment on the use of flushing time, residence time, and age as transport time scales." *Limnology and Oceanography* **47**.5 (2002): 1545-1553.
- Montagna, P. A., B. C. Coull, et al. (1983). "THE RELATIONSHIP BETWEEN ABUNDANCES OF MEIOFAUNA AND THEIR SUSPECTED MICROBIAL FOOD (DIATOMS AND BACTERIA)." *Estuarine Coastal and Shelf Science* **17**(4): 381-394.
- Ning, X., J. E. Cloern, et al. (2000). "Spatial and temporal variability of picocyanobacteria *Synechococcus* sp. in San Francisco Bay." *Limnology and Oceanography* **45**(3): 695-702.
- Nixon, S., B. Buckley, et al. (2001). "Responses of very shallow marine ecosystems to nutrient enrichment." *Human and Ecological Risk Assessment* **7**(5): 1457-1481.
- Novick, E., D.B. Senn, J. Wu and A. Malkassian.(2014). "Characterizing Nutrient Trends, Loads and Transformations in Suisun Bay and the Delta". Poster Presented at the Interagency Ecological Program Annual Workshop. February 27-28, 2014; Folsom, CA
- NRC. 2012. Sustainable Water and Environmental Management in the California Bay-Delta. Committee on Sustainable Water and Environmental Management in the California Bay-Delta; Water Science and Technology Board; Ocean Studies Board; Division on Earth and Life Studies; National Research Council. Available at: http://www.nap.edu/catalog.php?record_id=13394.
- O'Donnell, J.. "Surface fronts in estuaries: a review." *Estuaries* **16**.1 (1993): 12-39.
- Officer, C. B., and D.B. Kester "On estimating the non-advective tidal exchanges and advective-gravitational circulation exchanges in an estuary." *Estuarine, coastal and shelf science* **32**.1(1991): 99-103.
- Okubo, A. "Effect of shoreline irregularities on streamwise dispersion in estuaries and other embayments." *Netherlands Journal of Sea Research* **6**.1 (1973): 213-224.
- Paerl, H. W. and J. Huisman (2008). "Climate - Blooms like it hot." *Science* **320**(5872): 57-58.
- Paerl, H. W. and J. Huisman (2009). "Climate change: a catalyst for global expansion of harmful cyanobacterial blooms." *Environmental Microbiology Reports* **1**(1): 27-37.
- Pahl, S. L., D. M. Lewis, et al. (2012). "Heterotrophic growth and nutritional aspects of the diatom *Cyclotella cryptica* (Bacillariophyceae): effect of nitrogen source and concentration." *Journal of Applied Phycology* **24**(2): 301-307.
- Parker, A. E., R. C. Dugdale, et al. (2012a). "Elevated ammonium concentrations from wastewater discharge depress primary productivity in the Sacramento River and the Northern San Francisco Estuary." *Marine Pollution Bulletin* **64**(3): 574-586.
- Parker, A. E., V. E. Hogue, et al. (2012b). "The effect of inorganic nitrogen speciation on primary production in the San Francisco Estuary." *Estuarine Coastal and Shelf Science* **104**: 91-101.
- Parker, A. E., Kimmerer, W.J., Lidstrom, U. (2012). "Re-evaluating the generality of empirical models for light-limited primary production in the San Francisco Estuary." *Estuaries and Coasts* **35**(4): 930-942.

- Perez-Garcia, O., Y. Bashan, et al. (2011). "ORGANIC CARBON SUPPLEMENTATION OF STERILIZED MUNICIPAL WASTEWATER IS ESSENTIAL FOR HETEROTROPHIC GROWTH AND REMOVING AMMONIUM BY THE MICROALGA CHLORELLA VULGARIS." *Journal of Phycology* **47**(1): 190-199.
- Quigg, A., Z. V. Finkel, et al. (2003). "The evolutionary inheritance of elemental stoichiometry in marine phytoplankton." *Nature* **425**(6955): 291-294.
- Ralston, D. K., and W.R. Geyer "Episodic and long-term sediment transport capacity in the Hudson River estuary." *Estuaries and coasts* **32.6** (2009): 1130-1151.
- Ralston, D. K., and M.T. Stacey "Longitudinal dispersion and lateral circulation in the intertidal zone." *Journal of Geophysical Research* **110.C7** (2005): C07015.
- Ralston, D. K., and M.T. Stacey "Stratification and turbulence in subtidal channels through intertidal mudflats." *Journal of Geophysical Research: Oceans (1978–2012)* **110.C8** (2005).
- Reynolds, C. S., V. Huszar, et al. (2002). "Towards a functional classification of the freshwater phytoplankton." *JOURNAL OF PLANKTON RESEARCH* **24**(5): 417-428.
- Rollwagen-Bollens, G., S. Gifford, et al. (2011). "The Role of Protistan Microzooplankton in the Upper San Francisco Estuary Planktonic Food Web: Source or Sink?" *Estuaries and Coasts* **34**(5): 1026-1038.
- Rose, J.M., S.B. Bricker, M.A. Tedesco, G.H. Wikfors (2014) A role for shellfish aquaculture in coastal nitrogen management *Environ. Sci. Technol.* **48**:2519-2525
- Sanford, L. P. "Modeling a dynamically varying mixed sediment bed with erosion, deposition, bioturbation, consolidation, and armoring." *Computers & Geosciences* **34.10** (2008): 1263-1283.
- Sanford, L. P., and J.P.Y. Maa, "A unified erosion formulation for fine sediments." *Marine Geology* **179.1** (2001): 9-23.
- Schoellhamer, D.H. (2002) Variability of suspended-sediment concentration at tidal to annual time scales in San Francisco Bay, USA *Continental Shelf Research* **22**: 1857-1866
- Schoellhamer, D. H. (2011). "USGS Suspended Sediment Monitoring Program." [A presentation at the Nutrient Strategy Session to Outline a Bay Monitoring Program. 30 June 2011, Richmond, CA.](#)
- SFEI (2014a). "External nutrient loads to San Francisco Bay." San Francisco Estuary Institute, Richmond, CA. Contribution No. 704
- SFEI (2014b). "Suisun Bay Ammonium Synthesis Report." San Francisco Estuary Institute, Richmond, CA. Contribution No. 706
- SFEI (2014c). "Lower South Bay Synthesis Report" San Francisco Estuary Institute, Richmond, CA. In progress.
- SFEI (2014d). " WY 2012 and WY 2013 Nutrient Stormwater Monitoring". San Francisco Estuary Institute, Richmond, CA. In progress.
- SFBRWQCB (1975). "San Francisco Bay Basin (Region 2) Water Quality Control Plan." [As amended December 2011, available at \[http://www.waterboards.ca.gov/rwqcb2/basin_planning.shtml\]\(http://www.waterboards.ca.gov/rwqcb2/basin_planning.shtml\).](#)
- Shellenbarger, G. G., Schoellhamer, D.H., Morgan, T.L., Takekawa, J.Y., Athearn, N.D., and Henderson, K.D. (2008). "Dissolved oxygen in Guadalupe Slough and Pond A3W, South San Francisco Bay, California, August and September 2007." *U.S. Geological Survey Open-File Report 2008–1097*, 26 p.
- Smayda, T. J. (1997). "Harmful algal blooms: Their ecophysiology and general relevance to phytoplankton blooms in the sea." *Limnology and Oceanography* **42**(5): 1137-1153.
- Smayda, T. J. (2000). "Ecological features of harmful algal blooms in coastal upwelling ecosystems." *South African Journal of Marine Science-Suid-Afrikaanse Tydskrif Vir Seewetenskap* **22**: 219-253.
- Smayda, T. J. and C. S. Reynolds (2001). "Community assembly in marine phytoplankton: application of recent models to harmful dinoflagellate blooms." *JOURNAL OF PLANKTON RESEARCH* **23**(5): 447-461.
- Stacey, M. T., J.B. Burau, S.G. Monismith "Creation of residual flows in a partially stratified estuary." *Journal of Geophysical Research: Oceans (1978–2012)* **106.C8** (2001): 17013-17037.
- Stacey, M. T., J.P. Fram and F.K. Chow. "Role of tidally periodic density stratification in the creation of estuarine subtidal circulation." *Journal of Geophysical Research: Oceans (1978–2012)* **113.C8** (2008).
- Stacey, M.T., M.A. McManus, J.V. Steinbeck "Convergences and divergences and thin layer formation and maintenance." *Limnology and Oceanography* **52.4** (2007): 1523.
- Stoecker, D. K., A. E. Thessen, et al. (2008). "'Windows of opportunity' for dinoflagellate blooms: Reduced microzooplankton net growth coupled to eutrophication." *Harmful Algae* **8**(1): 158-166.
- Sunda, W. G. and S. A. Huntsman (1995). "REGULATION OF COPPER CONCENTRATION IN THE OCEANIC NUTRICLINE BY PHYTOPLANKTON UPTAKE AND REGENERATION CYCLES." *Limnology and Oceanography* **40**(1): 132-137.
- Sunda, W. G., P. A. Tester, et al. (1987). "EFFECTS OF CUPRIC AND ZINC ION ACTIVITIES ON THE SURVIVAL AND REPRODUCTION OF MARINE COPEPODS." *Marine Biology* **94**(2): 203-210.

- Tang, Y. Z., F. Koch, et al. (2010). "Most harmful algal bloom species are vitamin B-1 and B-12 auxotrophs." Proceedings of the National Academy of Sciences of the United States of America **107**(48): 20756-20761.
- Teh, S., I. Flores, M. Kawaguchi, S. Lesmeister, and C. Teh. (2011). "Full Life-Cycle Bioassay Approach to Assess Chronic Exposure of *Pseudodiaptomus forbesi* to Ammonia/Ammonium." Unpublished report submitted to State Water Resources Control Board.
- Tetra Tech (2013) Suisun Marsh Conceptual Model/ Impairment Assessment Report for Organic Enrichment, Dissolved Oxygen, Mercury, Salinity, and Nutrients
- Thebault, J., T. S. Schraga, et al. (2008). "Primary production and carrying capacity of former salt ponds after reconnection to San Francisco Bay." Wetlands **28**(3): 841-851.
- Thompson, J. K., J. R. Koseff, et al. (2008). "Shallow water processes govern system-wide phytoplankton bloom dynamics: A field study." Journal of Marine Systems **74**(1-2): 153-166.
- Topping, B. R., Kuwabara, J.S., Athearn, N.D., Takekawa, J.Y., Parchaso, F., Henderson, K.D., and Piotter, S. (2009). "Benthic oxygen demand in three former salt ponds adjacent to south San Francisco Bay, California." U.S. Geological Survey Open-File Report 2009-1180, 21 p.
- Turner, J.S. 1980. Buoyancy Effects in Fluids. Cambridge University Press, 412 pp.
- Underwood, G. J. C. and J. Kromkamp (1999). Primary production by phytoplankton and microphytobenthos in estuaries. Advances in Ecological Research, Vol 29: Estuaries. D. B. Nedwell and D. G. Raffaelli. **29**: 93-153.
- Underwood, G. J. C. and D. J. Smith (1998). "Predicting epipelagic diatom exopolymer concentrations in intertidal sediments from sediment chlorophyll a." Microbial Ecology **35**(2): 116-125.
- Vila, M., J. Camp, et al. (2001). "High resolution spatio-temporal detection of potentially harmful dinoflagellates in confined waters of the NW Mediterranean." JOURNAL OF PLANKTON RESEARCH **23**(5): 497-514.
- Werme, C., Taberski, K., McKee, L., Dugdale, R., Hall, T., Connor, M. (2011). A Growing Concern: Potential Effects of Nutrients on Bay Phytoplankton. Article in *The Pulse of the Estuary*, San Francisco Estuary Institute, Richmond, CA
- Werner, I. and J. T. Hollibaugh (1993). "POTAMOCORBULA-AMURENSIS - COMPARISON OF CLEARANCE RATES AND ASSIMILATION EFFICIENCIES FOR PHYTOPLANKTON AND BACTERIOPLANKTON." Limnology and Oceanography **38**(5): 949-964.
- Wiberg, P.L., D.E. Drake, D.A. Cacchione, (1994). Sediment resuspension and bed armoring during high bottom stress events on the northern California Inner Continental-Shelf measurements and predictions. *Continental Shelf Research* **14**, 1191-1219.
- Wilkerson, F. P., R. C. Dugdale, et al. (2006). "Phytoplankton blooms and nitrogen productivity in San Francisco Bay." Estuaries and Coasts **29**(3): 401-416.
- Wilkerson, F. P., R. C. Dugdale, et al. (2000). "Biomass and productivity in Monterey Bay, California: contribution of the large phytoplankton." Deep-Sea Research Part II-Topical Studies in Oceanography **47**(5-6): 1003-1022.
- Winder, M. and J. E. Cloern (2010). "The annual cycles of phytoplankton biomass." Philosophical Transactions of the Royal Society B-Biological Sciences **365**(1555): 3215-3226.

Evaluating Tidal Marsh Sustainability in the Face of Sea-Level Rise: A Hybrid Modeling Approach Applied to San Francisco Bay

Diana Stralberg^{1,2*}, Matthew Brennan³, John C. Callaway⁴, Julian K. Wood¹, Lisa M. Schile⁵, Dennis Jongsomjit¹, Maggi Kelly⁵, V. Thomas Parker⁶, Stephen Crooks³

1 Climate Change and Informatics Group, PRBO Conservation Science, Petaluma, California, United States of America, **2** Department of Biological Sciences, University of Alberta, Edmonton, Canada, **3** Estuaries and Wetlands Team, ESA PWA, San Francisco, California, United States of America, **4** Department of Environmental Science, University of San Francisco, San Francisco, California, United States of America, **5** Department of Environmental Science, Policy and Management, University of California at Berkeley, Berkeley, California, United States of America, **6** Department of Biology, San Francisco State University, San Francisco, California, United States of America

Abstract

Background: Tidal marshes will be threatened by increasing rates of sea-level rise (SLR) over the next century. Managers seek guidance on whether existing and restored marshes will be resilient under a range of potential future conditions, and on prioritizing marsh restoration and conservation activities.

Methodology: Building upon established models, we developed a hybrid approach that involves a mechanistic treatment of marsh accretion dynamics and incorporates spatial variation at a scale relevant for conservation and restoration decision-making. We applied this model to San Francisco Bay, using best-available elevation data and estimates of sediment supply and organic matter accumulation developed for 15 Bay subregions. Accretion models were run over 100 years for 70 combinations of starting elevation, mineral sediment, organic matter, and SLR assumptions. Results were applied spatially to evaluate eight Bay-wide climate change scenarios.

Principal Findings: Model results indicated that under a high rate of SLR (1.65 m/century), short-term restoration of diked subtidal baylands to mid marsh elevations (−0.2 m MHHW) could be achieved over the next century with sediment concentrations greater than 200 mg/L. However, suspended sediment concentrations greater than 300 mg/L would be required for 100-year mid marsh sustainability (i.e., no elevation loss). Organic matter accumulation had minimal impacts on this threshold. Bay-wide projections of marsh habitat area varied substantially, depending primarily on SLR and sediment assumptions. Across all scenarios, however, the model projected a shift in the mix of intertidal habitats, with a loss of high marsh and gains in low marsh and mudflats.

Conclusions/Significance: Results suggest a bleak prognosis for long-term natural tidal marsh sustainability under a high-SLR scenario. To minimize marsh loss, we recommend conserving adjacent uplands for marsh migration, redistributing dredged sediment to raise elevations, and concentrating restoration efforts in sediment-rich areas. To assist land managers, we developed a web-based decision support tool (www.prbo.org/sfbayslr).

Citation: Stralberg D, Brennan M, Callaway JC, Wood JK, Schile LM, et al. (2011) Evaluating Tidal Marsh Sustainability in the Face of Sea-Level Rise: A Hybrid Modeling Approach Applied to San Francisco Bay. *PLoS ONE* 6(11): e27388. doi:10.1371/journal.pone.0027388

Editor: Julian Clifton, University of Western Australia, Australia

Received: June 7, 2011; **Accepted:** October 15, 2011; **Published:** November 16, 2011

Copyright: © 2011 Stralberg et al. This is an open-access article distributed under the terms of the Creative Commons Attribution License, which permits unrestricted use, distribution, and reproduction in any medium, provided the original author and source are credited.

Funding: Funding for this research was provided by the Bay Fund of the San Francisco Foundation, the California Landscape Conservation Cooperative, the California Coastal Conservancy, the California Bay-Delta Authority's CalFed program, the United States Department of Energy's National Institute for Climate Change Research, the Faucett Family Foundation, and an anonymous donor to PRBO Conservation Science. The funders had no role in study design, data collection and analysis, decision to publish, or preparation of the manuscript.

Competing Interests: The authors have declared that no competing interests exist.

* E-mail: stralber@ualberta.ca

Introduction

Projections of sea-level rise (SLR) range from 18 cm to nearly 2 m over the next century [1,2] (and recent assessments suggest that as much as 5 m could be possible [3]), making low-lying coastal zones particularly vulnerable to climate change. The primary threats of SLR are well known: exacerbated beach and shoreline erosion, and inundation of critical infrastructure and coastal wetlands [4–6]. Uncertainty about how dynamic ecosystems such as coastal and estuarine tidal marshes (hereafter “tidal

marshes”) may respond to different aspects of climate change has prompted a large body of research exploring potential tidal marsh responses to increased rates of SLR [7–9], as well as increased temperature [10], salinity [11], and CO₂ concentrations [12].

Tidal marshes provide high-value ecosystem services such as water filtration, flood abatement, protection for infrastructure, and carbon sequestration [13–15]. They also have high ecological value, supporting a large number of specialized and endemic species [16,17] and have already experienced dramatic historical declines in area and hydrologic integrity [18]. The sensitivity of

tidal marshes to increased rates of SLR will vary depending upon factors such as mineral sediment supply [19], vegetation productivity [7], rates of subsidence or uplift [20], changes in storm frequency and intensity [21], and availability of uplands suitable for marsh migration [22]. Estuarine systems with low sediment inputs and high rates of subsidence such as the Mississippi River Delta have already experienced substantial marsh loss due to relative SLR (i.e., including the influence of subsidence) [23], while sediment-rich systems such as parts of San Francisco Bay have demonstrated resilience to rapid rates of relative SLR [24,25].

Tidal marshes are dynamic ecosystems that occupy a relatively narrow band of elevation, governed primarily by vegetation tolerance of tidal inundation, along with other factors, including hydroperiod, sediment supply, and biological dynamics [7,8,26,27]. With adequate sediment supply, the marsh plain builds to an elevation high within the tidal frame, typically around mean higher high water (MHHW) under semidiurnal tides [28]. At higher elevations, reduced tidal inundation curtails building processes through reduced mineral sediment supply and oxidation of soil organic material. At lower elevations, increased flooding frequency and duration increase mineral sedimentation and therefore enhance marsh building. In addition, vegetation plays an important role in trapping sediment and contributing organic material through above- and below-ground growth [29,30], with additional potential feedbacks between elevation and plant dynamics [7].

Under conditions where rates of SLR exceed marsh building processes the marsh plain falls in elevation relative to the tidal frame. A new steady state may be achieved, reflecting increased sedimentation at lower elevations that balances increased SLR. Alternatively, if supply of sediment is inadequate to keep pace with SLR, the marsh plain will continue to fall relative to sea level, eventually to an elevation where vegetation cannot tolerate the prolonged inundation, and the marsh will transition to a mudflat [9,31]. When topographically suitable uplands are lacking or located behind levees (as in most urbanized estuaries), marshes will not be able to migrate landward as they have done historically, resulting in marsh loss.

Previous research has shown a positive relationship between local rates of relative SLR and rates of sediment accretion [24,25,32]. However, increased sediment accretion in response to SLR is limited by mineral sediment inputs as well as plant growth and organic material accumulation, which may decrease in response to increases in salinity resulting from SLR and changes in precipitation regimes [11]. Measured rates of sediment accretion in tidal marshes have varied from 1 to 15 mm/yr, with the highest rates recorded in regions with very high rates of relative SLR driven by local subsidence, e.g., parts of Chesapeake Bay, the Mississippi River Delta, and other large delta systems [33–36]. However, the likelihood that tidal marshes can keep pace with high rates of SLR appears to diminish rapidly if rates of relative SLR are more than 10 mm/yr or increase rapidly [37,38].

With hundreds of millions of dollars invested in tidal marsh restoration and conservation, management strategies need to clearly identify and integrate thresholds and sensitivities of mineral sediment supply, organic accumulation rates, and starting elevation for marsh sustainability under various climate change scenarios. The long-term persistence of these habitats also depends on our ability to identify and protect areas where marshes can move upland as sea level rises and to identify barriers to that movement, such as levees. Conservation planners need to know where in the landscape tidal marshes will have the greatest long-term sustainability and how to prioritize restoration activities. To

address these problems, spatially explicit projections of tidal marsh sustainability and restoration potential are needed at the estuary scale.

Many modeling approaches have been implemented and have improved our understanding of marsh responses to increased rates of SLR [39]. The challenge in developing models for tidal marshes is to combine realistic local processes of sediment feedbacks with broader scale (i.e., estuary-wide) spatial dynamics. Many models have accurately represented realistic local processes, focusing on mineral and/or organic material dynamics [7,31,40]. Most of these models lack spatial variability, although recently-developed geomorphic models also incorporate channel dynamics and erosion across the marsh plain surface [41,42]. Other models, such as SLAMM (sea level affecting marshes model), have focused on broad-scale spatial patterns but have not realistically modeled feedbacks of elevation on sediment dynamics or other critical local processes [43,44]. Combining high resolution process-based models with broad-scale spatial modeling that includes hydrodynamics would be ideal; however, this is very computer intensive and is subject to potential accumulation of errors across multiple time steps. Although estuary-wide mechanistic approaches are being developed, the application of this sort of model is currently not practical.

Given the increasing interest among resource managers in spatially-explicit, estuary-wide assessments of potential SLR impacts on tidal marshes, we developed a hybrid method that involves a realistic, mechanistic treatment of marsh accretion dynamics and incorporates spatial variation across an estuary. Our approach is simple, transparent, and easily transferable and updatable, such that results can be readily accessible to land managers. At the core is a process-based model of point-based mineral accumulation based on Krone's [45] model called Marsh98 [9,46], which includes feedbacks between elevation and sediment inputs and incorporates constant rates of organic accumulation. We extended the point-based predictions to develop spatially-explicit projections of marsh sustainability based on current marsh elevation at the 5-m pixel level, and characterization of mineral (suspended sediment concentrations) and organic (relative plant productivity) inputs at the level of biogeomorphic subregions. While this approach lacks the hydrodynamic component to spatially transport sediment, it still allows for the evaluation of realistic process-based accretion dynamics and is feasible to apply across an entire estuary, over long time frames, and across multiple scenarios. It is of particular interest in the San Francisco Bay, California, USA (hereafter "Bay"), where, since European settlement, more than 90% of tidal marshes across the Bay have been destroyed or altered, primarily through agricultural and urban land development [47,48]. Many of the Bay's remaining marshes are adjacent to developed urban areas with minimal or no natural upland buffer zones. The large-scale loss of Bay wetlands has caused dramatic functional changes to the region over the last 150 years, affecting endangered and endemic species. Furthermore, over \$60 billion in infrastructure is at risk of inundation under high rates of SLR [49]; some of this loss could be prevented with tidal marsh restoration. Thus, there is considerable interest to maintain the integrity of current tidal marshes and facilitate restoration of diked baylands throughout the Bay [50].

Herein, we used our modeling approach to explore the sustainability of tidal marshes under a range of SLR and sediment availability conditions, using San Francisco Bay as a case study. In doing so, we sought to answer the following key questions: (1) What are the thresholds and sensitivities for marsh sustainability in terms of mineral sediment supply, organic material contribution, SLR rates, and starting elevations? (2) How is the Bay-wide area

and composition of intertidal habitats likely to change under varying projections for SLR and sediment availability? (3) How much space exists for new marshes to form, and how much habitat may be expected under these different scenarios? Our goal was also to deliver results to land managers in an easily accessible and interactive web-based map tool, to support conservation planning and restoration activities.

Specifically, we evaluated eight scenarios for bay-wide change over the next century, intended to capture low and high levels of potential outcomes based on a combination of factors:

- Two subregion-specific levels of suspended sediment concentration (SSC)
- Two subregion-specific levels of organic material (OM) accumulation
- Two rates of SLR (0.5 and 1.65 m/century)

We evaluated these eight scenarios over the range of actual starting elevations and estimated levels of SSC and OM accumulation found throughout the Bay.

Materials and Methods

Study area

Our study area within the San Francisco Bay, which is characterized by a mixed semi-diurnal tide cycle, includes salt water and brackish tidal marshes west of the confluence of the San Joaquin and Sacramento rivers (Fig. 1). The area has a Mediterranean-type climate, with warm, dry summers and rainy, cool winters [51]. Rain and runoff from snow pack of the Sierra Nevada mountains create lower salinity conditions in the Bay during the winter and spring, with significantly reduced freshwater influx and higher salinity during the summer and fall [52]. Plant species richness and productivity are greater in lower salinity tidal marshes [28,53].

Bay tidal marshes owe their early development to changes in sea level. During the last glacial event, San Francisco Bay was a river valley. By about 5,000 years before present, sea level had risen to an elevation adequate to flood the Bay, creating conditions for fringing tidal wetlands [54,55]. These wetlands continued to build and transgress landwards over subsequent millennia. Seasonal flows of the Sacramento River, as well as from local catchments, brought sediment to the Bay, maintaining expansive marshes and mudflats. Tidal marshes and mudflats continued to expand through the 1800 s, when hydraulic mining activities in the Sierra Nevada foothills deposited considerable sediments in the Bay, estimated to be an order of magnitude larger than pre-mining conditions [55,56].

During the 20th century, filling and levee building activities reduced tidal marshes to less than 10% of their original 220,000 ha [28] although approximately 5,000 ha have since been regained through restoration efforts [57]. Upstream activities such as dams, water diversions, riverbank protection, and altered land use limited the downstream delivery of sediment and caused erosion of subtidal habitats [58]. Since 1999, a substantial decrease in suspended sediment has been observed at long-term deepwater monitoring stations [59]. This step change is attributed to the flushing of the hydraulic mining pulse from the estuary and limitations on downstream delivery [60,61].

The current Bay wetland landscape west of the Sacramento/San Joaquin River delta is an intricate mosaic of natural and restored tidal marshes intermixed with diked baylands. Tidal marshes line the bay and river margins and, in most cases, abut levees along urban and agricultural land. We defined the bayward

limits of our study area based on the mapped edge between tidal marsh and mudflat habitats according to the San Francisco Estuary Institute's EcoAtlas (<http://www.sfei.org/ecoatlas/index.html>) and used the USGS national elevation dataset (NED) to delineate upland boundaries. The upper limit was defined as the 15.2 m (50-ft.) elevation contour line plus a 100-m horizontal buffer to account for error in the NED, resulting in a total study area of just over 186,000 ha. Mapping of study area boundaries and subregions was performed in ArcGIS 9.3.1 (ESRI, Redlands, CA, USA).

Biogeomorphic subregions

Suspended sediment concentrations (SSC) differ throughout the Bay because of variations in wave conditions, proximity to mudflats, bathymetric convergence zones, and river inputs. These subregional differences help define the morphology, extent, and resilience to SLR of Bay tidal marshes. In addition, marshes with high rates of organic matter (OM) production have been observed to accrete at faster rates than marshes composed primarily of inorganic sediments [7,40]. Marshes associated with the highest OM accumulation rates are typically found in brackish and freshwater environments.

In light of this spatial variation, we separated the Bay into 15 biogeomorphic subregions (ranging in area from 2,123 to 34,605 ha) based on sediment and salinity characteristics (Fig. 1). Each subregion was categorized according to "low" and "high" estimates of SSC and OM for that subregion, based on information described in the following sections and summarized in Table S1. These subregion-specific "low" and "high" values were used to explore scenarios of high/low SSC and OM.

Accretion model

Marsh accretion (the vertical accumulation of sediment mineral and organic material) was estimated using the Marsh98 model, which has been used widely to examine marsh response to SLR across San Francisco Bay [9]. The Marsh98 model is based on the mass balance calculations described by Krone [45]. This model assumes that the elevation of a marsh surface increases at a rate that depends on the (1) availability of suspended sediment and (2) depth and periods of inundation by high tides. Marsh98 implements these processes by calculating the amount of suspended sediment that deposits during each period of tidal inundation and sums that amount of deposition over the period of record. OM was added directly to the bed elevation at each time step at a constant rate (see below for details). Marsh98 was implemented in the Fortran programming language, and multiple runs were executed using MatLab v.2010b (MathWorks Inc., Natick, MA).

Modeling was conducted relative to the tidal datum of mean lower low water (MLLW) and converted to mean higher high water (MHHW) based on a 1.8-m tide range. The tidal boundary condition used for all model runs was a repeated tidal month that has statistical characteristics representative of the observed tides at the mouth of San Francisco Bay and in the North and Central Bays. However, the tides are naturally amplified in the South Bay such that the tide range increases by approximately 50% at the far southern end of the Bay. The tide range diminishes in Suisun Bay and eastward into the Sacramento/San Joaquin Delta.

Given the spatially-varying tide range, a sensitivity analysis was conducted testing the impact of a larger tide range on the marsh accretion rates and elevation. For cases with moderate to high SSC as are typically found in the South Bay, simulations run with a tide range of 2.8 m predicted marsh surface elevations after a century that were at most 0.2 m lower relative to MHHW than simulations using a 1.8-m

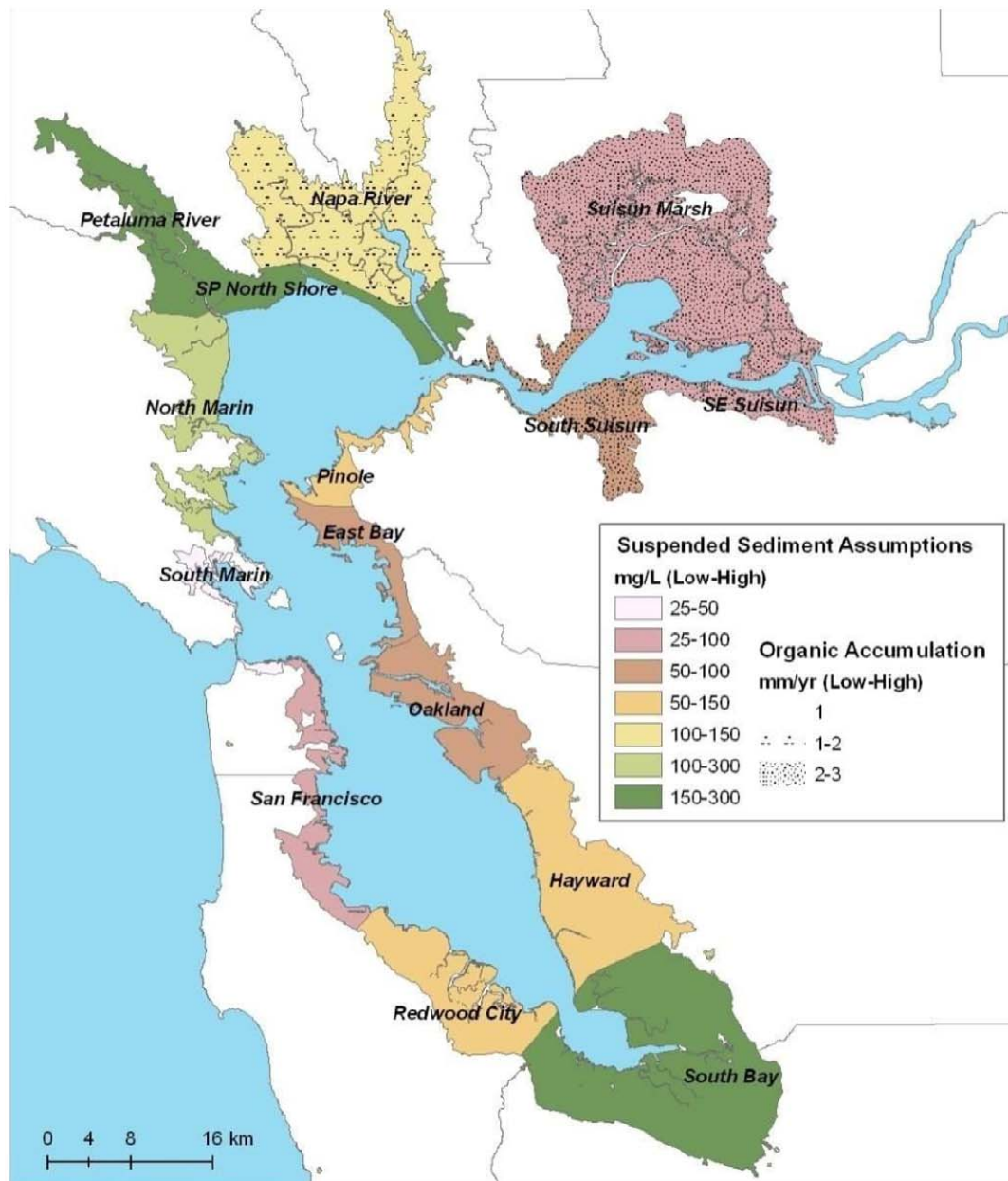


Figure 1. Biogeomorphic subregions within San Francisco Bay study area and assumptions about suspended sediment concentrations and organic matter accretion rates for climate change scenarios.

doi:10.1371/journal.pone.0027388.g001

tide range (although overall accretion was higher). In relative terms, this difference is less than 5% of the total predicted accretion for all cases. Thus, we used a single tidal range (1.8 m) to simplify the analysis.

Model input parameters

To address the range of conditions across the Bay, as well as climate change uncertainty, we considered seven SSC levels, three OM accumulation rates (except for scenarios with subtidal initial elevations, which included no OM), two rates of SLR, and three initial bed elevations, for a total of 70 model runs (90 possible—20 subtidal/OM combinations not considered). Various combinations of these 70 model runs were combined at the subregion level and interpolated to a range of starting elevations to generate six bay-wide spatial change scenarios.

Initial bed elevation. Two of the initial bed elevations evaluated span the range of regularly inundated vegetated marsh, the lower of which was based on the colonization elevation for vegetation (low marsh), assumed to be -0.5 m MHHW (mean tide level plus 0.3 m or 1.3 m MLLW) [62]. The higher initial bed elevation was based on the standard marsh plain (mid marsh) elevation around 0 m MHHW (1.8 m MLLW). The third initial bed elevation at -2.4 MHHW (0.6 m below MLLW) was used to predict the bed elevation trajectory for marsh development from subtidal conditions.

Rate of SLR

We chose two nonlinear SLR scenarios based on the guidance provided by the US Army Corps of Engineers [63], which

recommends scenarios modifying curves proposed by the National Research Council to extrapolate intermediate and high SLR scenarios (“NRC-I” and “NRC-III”, respectively). These scenarios project 0.52 m and 1.65 m of SLR over the next century (2010 to 2110) with most of this change occurring within the second half of the century (Fig. 2). The high-end rates are similar to recent estimates [1,64], and to the draft State of California planning guidelines, which recommend planning for 0.41 m of rise in the next 50 years and 1.4 m in the next 100 years [65].

Suspended sediment concentration. To represent the range of observed SSC, we modeled seven different concentrations: 25, 50, 100, 150, 200, 250, and 300 mg/L. Although observations of SSC within Bay tidal marshes are limited, several deepwater (major channel and open bay) data sources helped inform this range. The first four values are representative of observed SSC along the deepwater channel [66]. SSC at the bay-marsh boundary is thought to be higher because of wave resuspension over nearby mudflats [67]. For tributaries entering the North Bay, Ganju et al. [68] corroborate the concentrations at the high end of our range. A second line of evidence for the high SSC values comes from calibrations of the Marsh98 model to observed rates of bed elevation change at several restoration sites around the Bay [46].

Organic material. Based on data from over 30 dated sediment cores (^{137}Cs and ^{210}Pb) from multiple sites across the Bay (Callaway, unpublished data), we modeled OM accretion using constant rates of 1, 2, and 3 mm/yr for the scenarios with initial bed elevations in the vegetated marsh regime. For the scenarios with subtidal initial bed elevations, no OM accretion was included. As a sensitivity analysis, for one test run based on high SSC (150 mg/L) and high SLR, we also ran the model in two stages, adding OM from the point at which the bed elevation reached the vegetation colonization elevation; differences in final elevations were negligible.

Elevation and tidal range mapping

A seamless 5-m elevation grid for the study area was developed based on best available data sources (Figure S1). LiDAR elevation

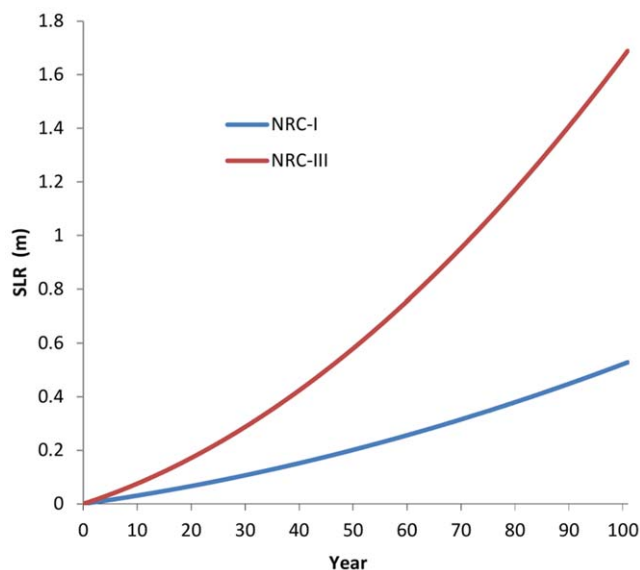


Figure 2. High (NRC-III) and low (NRC-I) sea-level rise trajectories used for climate change scenarios. Year 0 represents 2010 and year 100 represents 2110. doi:10.1371/journal.pone.0027388.g002

data were available for most of our study area and were used wherever possible. Approximately 4,300 ha of diked subtidal lands (including several former and active salt ponds) were inundated with water and thus not captured by elevation mapping efforts. All datasets were converted to the NAVD88 vertical datum (m) and resampled to a 5-m×5-m grid-cell resolution. While a comprehensive accuracy assessment was not possible, we used available real-time kinetic GPS data (horizontal accuracy: $\pm 1\text{--}2$ cm; vertical accuracy: $\pm 2\text{--}3$ cm) from four North Bay study sites to investigate potential systematic biases in the datasets. Due to obvious vegetation biases in two of these sites in Suisun Bay and the western Delta, where marsh vegetation (*Schoenoplectus* spp.) often forms particularly impenetrable mats, we used available vegetation data to develop correction factors for each general vegetation type (Table S2) and applied those correction factors throughout the relevant subregions based on available vegetation maps [69,70].

NOAA tide gauge and benchmark data (<http://tidesandcurrents.noaa.gov/>) were used to convert NAVD88 elevations to a MHHW reference more suitable for cross-bay analysis of tidal marsh habitat due to variability in tidal range across the bay. We developed a second-order inverse distance-weighted interpolation of MHHW levels (relative to mean lower low water, MLLW) across our study area ($n = 55$ tide gauges). The same procedure was repeated for NAVD88 elevations at MLLW measured for $n = 19$ benchmark locations. The two resulting grids (100-m resolution) were applied as offsets to the resulting elevation grid, corrected for vegetation bias where data were available, resulting in a bay-wide estimate of elevation (m) with respect to MHHW. Simply stated: NAVD88 elevation + MLLW offset – MHHW offset = MHHW elevation.

Spatial scenario development

Model outputs were linearly interpolated in 10-cm increments for starting elevations ranging from -3.7 to 1.7 m (relative to MHHW) such that for starting elevation x between starting elevations y and z , the future projection for a given time period t and scenario s was calculated as:

$$F(x,t,s) = F(z,t,s) - \frac{|F(z,t,s) - F(y,t,s)|}{(10 * (z-y))}$$

The lower bound for the interpolation was set at -4.0 m (MHHW), reflecting the lowest projected future elevation obtained from a model run starting at -2.4 m (MHHW). Elevations below this lower bound were assumed to remain constant (i.e., keep pace with SLR) across all scenarios and time steps. However, values are unreliable below -2.4 m due to the necessarily arbitrary lower limit for interpolation. The upper bound was set at 1.7 m (MHHW) for the high SLR scenario and 0.6 for the low SLR scenario, reflecting the area subjected to future tidal inundation. Elevations above the amount of SLR for a given scenario and time step were assumed to decrease by that amount (i.e., no accretion potential).

Interpolated model outputs were applied to a composite 5-m elevation grid for SF Bay, referenced to the MHHW tidal datum. Results for each combination of SSC, OM, and SLR assumptions were combined by geographic subregion to produce an individual scenario layer. For these scenarios, we assumed that wave- and current-induced bed shear stresses are minimal. Locations with significant wave exposure and/or tidal currents, which include much of the open bay margins, are unlikely to accrete above subtidal elevations. Thus we ignored current open bay and

outboard mudflats, and restricted our analysis to areas currently landward of the marsh-mudflat boundary. We assumed that subsided (currently diked) potential restoration sites within our study area are not large enough to be subject to erosion at levels sufficient enough to prevent vegetation colonization. Indeed, no San Francisco Bay tidal marsh restoration sites have yet failed to vegetate [71].

Analysis of marsh sustainability and restoration potential

Using the accretion model outputs for low marsh (-0.5 m MHHW) and mid marsh (0 m MHHW) starting elevations, we evaluated the potential for marsh sustainability over the next century (in 20-year increments) under each combination of SSC, OM, and SLR rate. The transition from low to mid marsh occurs approximately halfway between these elevations and mid marsh can persist at elevations lower than 0 m MHHW [62]. Thus a mid marsh area could lose elevation and still sustain marsh vegetation. However, because we were interested in the potential for a marsh to maintain its starting elevation our definition of marsh sustainability was zero elevation loss (rounded to the nearest 10 cm).

Due to the large number of planned restoration projects within subsided diked baylands, we also examined the minimum starting bed elevations required to achieve mid marsh elevations (-0.2 m to 0.1 m MHHW) over the next century in 20-year increments. This represents the potential to attain and maintain a vegetated marsh plain by restoring tidal action to currently diked (and generally subsided) areas. These calculations were based on elevation-interpolated model outputs to allow a broader range of starting elevations to be considered. Strictly speaking, we could not evaluate starting elevations lower than -2.4 m MHHW, the lowest bed elevation used in the accretion model runs. However, constantly-inundated subtidal elevations will accrete sediment very rapidly in the absence of significant erosional forces [46]. Thus, minimum starting bed elevations may be less than -2.4 m.

Area calculations for restoration scenarios

We developed a polygon GIS layer representing all diked areas within our study area to distinguish existing from potential tidal marsh habitat. Diked areas were defined as those that were separated from regular tidal inundation by dikes, levees, or roads of any height and material; additional information on levee integrity was not readily available. The layer was modified from the EcoAtlas modern baylands layer (“diked baylands” category) based on levee lines supplied by the Pacific Institute (http://www.pacinst.org/reports/sea_level_rise/data/index.htm) and manual inspection of 1-m resolution natural color and color infrared Bay-wide aerial photography flown in 2006 and 2009 by the National Agriculture Imagery Program (<http://www.fsa.usda.gov/FSA/apfoapp?area=home&subject=prog&topic=nai>). We used a 2001 urban development layer from NOAA C-CAP (<http://www.csc.noaa.gov/digitalcoast/data/ccapregional/>) to identify developed areas not available for tidal marsh restoration.

Elevation projections were classified according to marsh type and summarized by subregion, scenario, and diked/developed status. Upland was defined as >0.3 m above MHHW; high marsh was defined as 0.2 to 0.3 m above MHHW; mid marsh as -0.2 to 0.1 m MHHW; low marsh as -0.5 to -0.3 m MHHW; mudflat as -1.8 to -0.6 m MHHW; and subtidal as anything below -1.8 MHHW (i.e., 0 m MLLW). We also compared restoration potential for areas of (1) high and (2) low-intermediate sediment availability within the currently diked areas. We used results from actual study area subregions grouped as follows: (1) high sediment availability (North Bay): Petaluma River, North Marin, San Pablo

Bay North Shore; and (2) low-intermediate sediment availability (Central Bay): Redwood City, Hayward, San Francisco, Oakland, East Bay, Pinole, and South Marin (see Fig. 1 and Table S1). We selected these particular regions because they represent the range of sediment availability within the Bay, and because they have tide ranges similar to the 1.8 -m value used in our accretion models.

Web-based map viewer and decision support tool

To make our results easily accessible to land managers and decision-makers, a web-based map viewer and decision support tool was created that allows users to view projected changes in tidal marsh extent and location at varying spatial scales, over multiple time frames, and under various SLR, SSC, and OM scenarios [72]. Users can view maps of current and future marsh extent together with data overlays (diked areas, public lands, and urbanization) to assess restoration opportunities and impediments.

Results

Thresholds and sensitivities

Marsh sustainability. According to accretion model outputs, marshes in areas with very low suspended sediment concentrations (25 mg/L) would not sustain their current elevation for more than 40 years under either SLR rate (Fig. 3). However, with high OM accumulation rates (3 mm/yr) and slightly higher SSC (50 mg/L), low marsh elevations would be sustained for up to 100 years under a low rate of SLR. Under a high SLR rate, marshes with 50 mg/L SSC would not be sustainable for 20 years regardless of OM (Fig. 3).

Under a low rate of SLR and intermediate SSC (100 mg/L), low marsh elevations would be sustained for 100 years, while mid marsh would last up to 80 years with high OM accumulation rates (Fig. 3). Under a high SLR rate and intermediate SSC, low marsh elevation loss would be expected within 40 years. With 150 mg/L, mid marsh sustainability throughout the next century was projected for a low SLR rate; only low marsh with at least 2 mm/year OM accumulation would be sustainable under a high rate of SLR. At 200 , 250 , and 300 mg/L, mid marsh was sustainable under a high rate of SLR for progressively longer periods of time (up to 80 years with 300 mg/L SSC), but not over the full 100-year period. Higher OM accumulation rates (2 – 3 mm/year) would not extend sustainability for more than a 20-year period.

Restoration potential and initial elevation. Under a low rate of SLR and high SSC (≥ 150 mg/L), our models show that mid marsh restoration (i.e., establishment and maintenance of a vegetated marsh plain) could be achieved over the next century with initial bed elevations at least as low as -2.4 m MHHW (i.e., subtidal) (Fig. 4). With very high SSC (300 mg/L), mid marsh habitat could be expected within 20 years at subtidal locations, while close to 100 years would be necessary with 150 mg/L. For low-intermediate sediment concentrations (≤ 100 mg/L), successful mid marsh restoration would be expected only from marsh starting elevations. Higher rates of organic accumulation (2 – 3 mm/yr) would allow somewhat lower starting elevations, but could not (by definition) make a difference of more than 20 cm per century.

Under a high rate of SLR, however, mid marsh restoration could only be achieved over a 100-year time period given starting elevations above MHHW (current upland areas), or very high sediment concentrations (Fig. 4). With very high SSC (250 – 300 mg/L), mid marsh habitat could be restored even in areas that are currently subtidal. At lower sediment concentrations, mid marsh could initially be restored from low- and mid-marsh starting

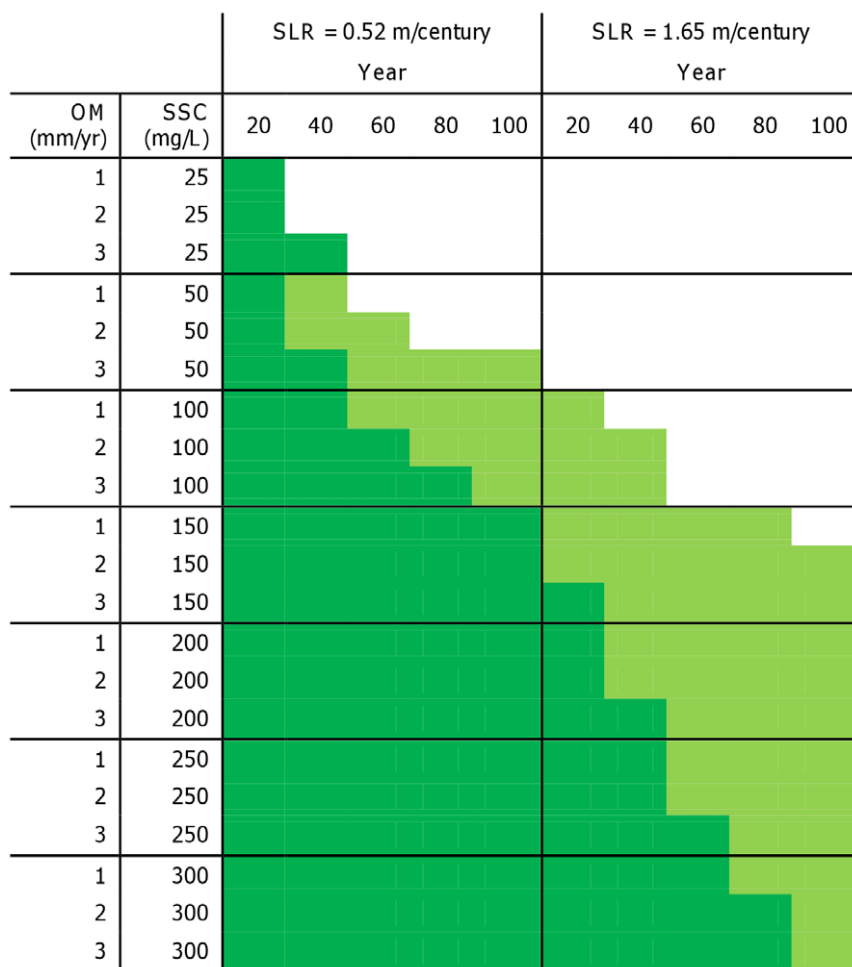


Figure 3. Sustainability (no elevation loss) of low marsh (light green) and mid marsh (dark green) areas under different sea-level rise scenarios, suspended sediment concentrations (SSC) and organic material contribution (OM). Blank cells represent no marsh sustainability.

doi:10.1371/journal.pone.0027388.g003

elevations below MHHW but would not persist more than 80 years (40 years at very low SSC).

Bay-wide habitat change

Based on mapping of current elevations and barriers to tidal inundation, there are currently ~2,500 ha of high marsh, 7,600 ha of mid marsh, and 3,000 ha of low marsh in San Francisco Bay (Table 1, Fig. 5a). An additional 7,500 ha of marsh (plus up to 4,300 ha of unmapped diked subtidal areas) could exist if existing dikes, levees, roads, and other barriers to tidal inundation were removed (Fig. 5b). 4,300 ha of potential tidal marsh are considered un-restorable due to urban development (Table 1). Below we detail projected changes over the next 100 years by habitat type. Subregional details are available in Table S3.

Habitat change trajectories. Across most scenarios examined, intertidal habitats (mudflat through high marsh elevations) were projected to increase over the next century, reflecting the combined expansion of wetlands into current upland areas and sedimentation of currently subtidal areas. Lower rates of increase, or slight decreases, were projected toward the end of the century, as topographic limitations to marsh expansion become more important and, for the most pessimistic scenario (high SLR, low SSC), subtidal elevations increase (Fig. 6). Restoration

potential for intertidal habitats (within currently diked areas) showed a similar pattern, although the area of urban development at elevations potentially subject to tidal inundation (in the absence of levees), was projected to increase even more rapidly (Fig. 6).

Only under the most optimistic scenario (low SLR, high SSC), however, was mid marsh habitat projected to continue increasing until the end of the century, both in terms of currently tidal and potential restoration areas. Under the other scenarios, mid marsh habitat was projected to increase through mid-century (2040–2080, depending on the scenario) but start declining in area thereafter. Low marsh habitats had similar projections, but would decline in existing area and increase in restoration potential under the most optimistic scenario (Fig. 6). Vegetation trajectories for potential low marsh restoration were fairly stable by the end of the century. Current areas of high marsh were projected to decrease under all scenarios, more rapidly under high rates of SLR (Fig. 6). However, restoration potential for this habitat type remained constant over time across all scenarios.

High marsh. The area of high marsh was projected to decrease dramatically over the next century across all scenarios examined – more than any other habitat type (Table 1, Fig. 7). With a high SLR rate, the area could be reduced to just over 100 ha bay-wide by 2110; with a low rate of SLR the total projected

OM (mm/yr)	SSC (mg/L)	SLR = 0.52 m/century					SLR = 1.65 m/century				
		Year					Year				
		20	40	60	80	100	20	40	60	80	100
1	25	-0.2	-0.1	0	0.1	0.2	-0.1	0.2	0.5	0.9	1.4
2	25	-0.2	-0.1	-0.1	0	0.1	-0.1	0.2	0.5	0.9	1.4
3	25	-0.2	-0.2	-0.1	-0.1	0	-0.1	0.1	0.5	0.9	1.4
1	50	-0.2	-0.1	-0.1	0	0.2	-0.1	0.2	0.5	0.9	1.4
2	50	-0.2	-0.2	-0.1	0	0.1	-0.1	0.1	0.5	0.9	1.4
3	50	-0.2	-0.2	-0.2	-0.1	-0.1	-0.1	0.1	0.4	0.9	1.3
1	100	-0.2	-0.3	-0.3	-0.3	-0.2	-0.1	0.1	0.4	0.8	1.2
2	100	-0.3	-0.3	-0.4	-0.4	-0.4	-0.1	0.0	0.3	0.7	1.2
3	100	-0.3	-0.4	-0.5	-0.5	-0.5	-0.2	0.0	0.3	0.7	1.2
1	150	-0.4	-0.7	-1.1	-1.7	-2.3	-0.3	-0.2	0.2	0.5	0.9
2	150	-0.4	-0.7	-1.2	-1.8	-2.3	-0.3	-0.2	0.1	0.4	0.9
3	150	-0.4	-0.8	-1.3	-1.8	-2.3	-0.3	-0.3	0	0.4	0.8
1	200	-0.6	-1.8	-2.4	-2.4	-2.4	-0.5	-0.9	-1.2	0.1	0.4
2	200	-0.7	-1.8	-2.4	-2.4	-2.4	-0.5	-1.0	-1.3	-0.6	0.4
3	200	-0.7	-1.8	-2.4	-2.4	-2.4	-0.5	-1.0	-1.4	-0.9	0.3
1	250	-1.1	-2.4	-2.4	-2.4	-2.5	-0.9	-2.4	-2.4	-2.4	-2.4
2	250	-1.1	-2.4	-2.4	-2.4	-2.5	-1.2	-2.4	-2.4	-2.4	-2.4
3	250	-1.2	-2.4	-2.4	-2.4	-2.5	-1.2	-2.4	-2.4	-2.4	-2.4
1	300	-2.0	-2.4	-2.4	-2.4	-2.5	-1.7	-2.4	-2.4	-2.4	-2.4
2	300	-2.0	-2.4	-2.4	-2.4	-2.5	-1.7	-2.4	-2.4	-2.4	-2.4
3	300	-2.0	-2.4	-2.4	-2.4	-2.5	-1.7	-2.4	-2.4	-2.4	-2.4

Figure 4. Minimum initial elevations with respect to MHHW needed to achieve mid marsh restoration (≥ -0.2 m MHHW). Cells are color-coded to represent classification of initial conditions as follows: blue = subtidal, brown = mudflat, light green = low marsh, dark green = mid marsh, orange = high marsh, yellow = upland.
doi:10.1371/journal.pone.0027388.g004

area was just over 500 ha under both high and low SSC scenarios. While most of the future potential for this habitat would occur in areas that are already urbanized, approximately 700–900 ha are possible in undeveloped areas that are currently behind levees, dikes or roads (hereafter “diked areas”) (Table 1, Fig. 8).

Mid marsh. Future (100-yr) spatial habitat projections for mid marsh were highly dependent upon SSC and SLR assumptions. Under all but the most pessimistic scenario (high SLR and low SSC) the total bay-wide area of mid marsh was projected to increase to between 8,300 and 18,700 ha over the next century, as sites that are newly restored or planned for restoration in the near future (primarily former salt ponds) continue to accrete sediment and build elevation (Table 1, Fig. 7). Under the most optimistic scenario (low SLR, high SSC), 25,200 ha in currently diked areas could potentially become mid marsh habitat with new restoration efforts (Table 1, Fig. 8). However, under the more pessimistic scenario (high SLR and low SSC), the total area of mid marsh was projected to decrease dramatically, to less than 600 ha bay-wide in narrow fringes along bay margins (current upland areas). Up to 2,600 ha in currently diked upland areas (also along the bay margins) could potentially be obtained through new restoration efforts (Table 1, Fig. 8). The creation of new mid marsh habitat on up to 10,700 ha of land with potentially suitable elevations under a high rate of SLR is prevented by existing urban development (Table 1).

Low marsh. Low marsh habitat was projected to increase—due to a combination of mid marsh loss in some areas and new habitat creation in others—under all scenarios except for high

SSC and low SLR (Table 1, Figs. 7 and 8). In this case, the decrease represented primarily a conversion to mid marsh, as low elevation areas would continue to accrete sediment.

Upland. The area of natural uplands projected to be reclaimed by tidal inundation (and thereby available for marsh expansion) by 2110 ranged from approximately 2,000 ha under a low rate of SLR to 3,300 ha under a high rate of SLR, as more uplands would be inundated (Table 1). Undeveloped diked uplands could provide an additional 2,300 (low SLR) to 7,000 (high SLR) ha for marsh expansion if barriers to tidal inundation were removed (Table 1). The projections for currently upland urban areas that would become tidally inundated without levee protection ranged from 2,900 (low SLR) to 13,200 (high SLR) ha.

Restoration potential. Comparing restoration potential (for currently diked areas) between regions with low-medium sediment supply (Central Bay) and regions with high sediment supply (North Bay), future habitat trajectories were dramatically different across all scenarios examined (Fig. 9). Despite higher starting elevations, the Central Bay had lower mid marsh restoration potential than the North Bay across all scenarios. Although more mid marsh habitat could initially be restored in low sediment areas due to higher elevations (in this case), models projected an overall loss of habitat by the end of the century in all but the most optimistic scenario (Fig. 9). Conversely, the North Bay was projected to experience a net gain in mid marsh habitat by the end of the century under all scenarios.

Under the most pessimistic scenario (high SLR, low SSC), models projected initial increases in marsh area, followed by

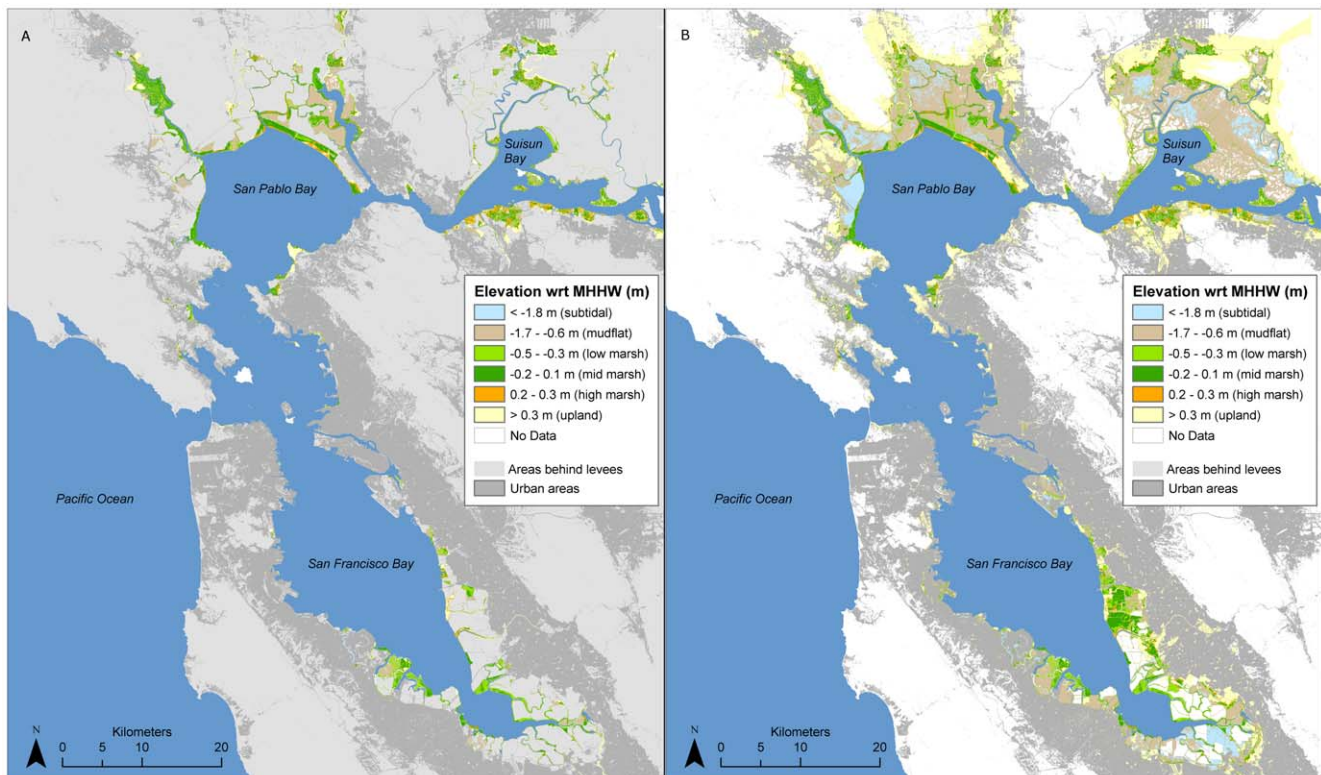


Figure 5. (A) Existing and (B) potential intertidal habitats in San Francisco Bay based on current mapped elevations. See Figure S1 for map of data sources.
doi:10.1371/journal.pone.0027388.g005

Table 1. Area (ha) of current and potential future tidal marsh habitat, and upland areas reclaimed, under different sea-level rise and sediment availability assumptions for San Francisco Bay.

Year	Scenario	Current Land Status	Low Marsh	Mid Marsh	High Marsh	Total Marsh	Uplands Reclaimed
2010	Current	Tidal	2,992	7,572	2,464	13,029	-
2110	SSC High/SLR Low	Tidal	1,013	18,714	528	20,256	2,046
2110	SSC High/SLR High	Tidal	4,752	8,274	109	13,135	3,307
2110	SSC Low/SLR Low	Tidal	3,510	12,744	528	16,782	2,046
2110	SSC Low/SLR High	Tidal	4,422	574	109	5,104	3,307
2010	Current	Diked	3,041	3,360	1,109	7,510	-
2110	SSC High/SLR Low	Diked	5759	12,971	888	19,399	6,958
2110	SSC High/SLR High	Diked	6438	25,173	670	32,499	2,301
2110	SSC Low/SLR Low	Diked	2767	2,608	888	6,045	6,958
2110	SSC Low/SLR High	Diked	6240	10,485	670	17,613	2,301
2010	Current	Urban	1,273	1,888	1,096	4,257	-
2110	SSC High/SLR Low	Urban	3,472	10,673	1,251	15,895	13,223
2110	SSC High/SLR High	Urban	518	7,511	1,749	9,280	2,941
2110	SSC Low/SLR Low	Urban	3,883	5,692	1,251	11,325	13,223
2110	SSC Low/SLR High	Urban	1,396	4,353	1,749	6,999	2,941

To demonstrate restoration potential, the potential future marsh area for currently diked lands reflects the assumption that all barriers to inundation are removed in 2010. Suspended sediment availability (SSC) high and low assumptions vary by Bay subregion. Sea-level rise (SLR) assumptions were developed by the National Research Council (low = 0.52 m/century; high = 1.65 m/century). Values for the urban category represent areas that are considered un-restorable due to urban development.

doi:10.1371/journal.pone.0027388.t001

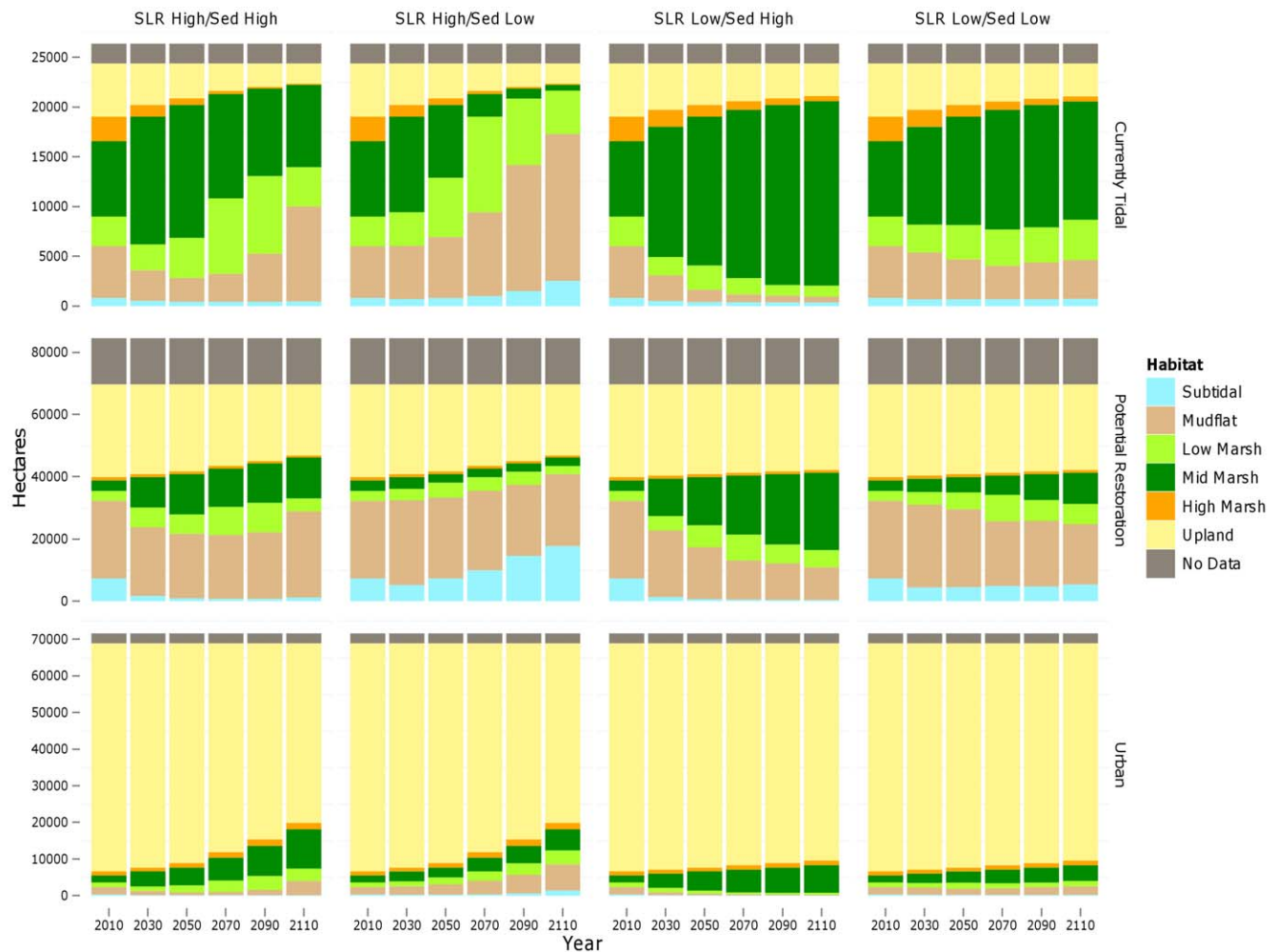


Figure 6. Area of potential future habitats within study area under different SLR and sediment (“Sed”) scenarios for three categories of habitat: currently tidal, potential restoration (currently diked), and urban (assumed non-restorable). Note different scales on each set of graphs.

doi:10.1371/journal.pone.0027388.g006

widespread marsh drowning, with the conversion of mid marsh to low marsh in high sediment areas, as shown in an example from the Petaluma River region in the North Bay (Fig. 10), and to mudflat or subtidal habitats in low sediment areas. Projections can be further explored online (www.prbo.org/sfbayslr).

Discussion

By applying results from a mechanistic accretion model [9] to spatial variation in sediment, salinity, and current elevations, we were able to develop spatially-explicit projections of marsh response to a set of plausible SLR scenarios for 15 San Francisco Bay subregions. When model runs were combined across subregions with different estimated SSC and OM values, Bay-wide projections of mid marsh habitat area varied substantially, depending primarily on SLR and SSC assumptions. Across all scenarios evaluated, however, our models projected a shift in the mix of intertidal habitats, with a loss of high marsh and gains in low marsh and mudflats within the study area. We found that the minimum SSC that would be required for 100-year mid marsh sustainability (i.e., no elevation loss) is greater than 300 mg/L for a high rate of SLR (1.65 m SLR/century), and between 100 and

150 mg/L for a low rate of SLR (0.5 m/century). High rates of OM accumulation had minimal impacts on this threshold in a SLR context because the maximum rate of OM accumulation that we evaluated (3 mm/year) was swamped by SLR.

Given that suspended sediment concentrations above 300 mg/L are rare in the Bay, and considering the projected acceleration of SLR beyond the 100-year timeframe examined here, our model suggests a bleak prognosis for long-term natural marsh sustainability under a high-SLR scenario. However, results also indicated that under a high rate of SLR (1.65 m/century), short-term restoration of diked subtidal baylands to mid marsh elevations (-0.2 m MHHW) within the next century could be achieved with SSC greater than 200 mg/L (100 mg/L under a low rate of SLR). Thus, even under a high-SLR scenario, opportunities for sustainable tidal marsh restoration and conservation within the next century may be found, but are limited to certain high-sediment regions of the Bay. Under a low-SLR scenario, the potential for long-term marsh sustainability and successful marsh restoration should remain high, depending on future sediment supplies.

The approach we have developed can theoretically be applied to any estuary to provide a rapid evaluation of future marsh sustainability and expansion potential. The model is an improve-

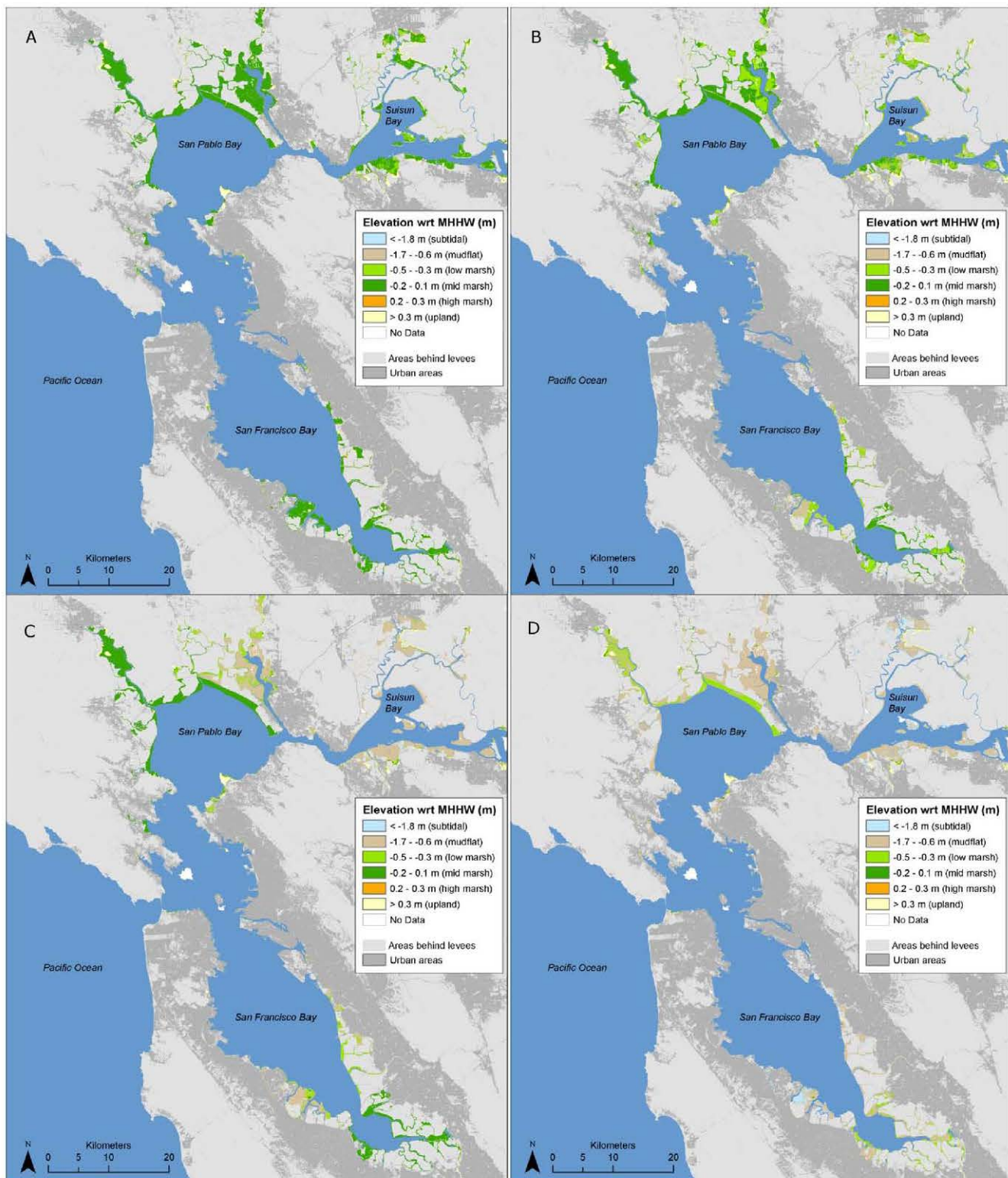


Figure 7. Potential 2110 intertidal habitats and elevations with respect to mean higher high water under different sea-level rise (SLR) and sediment availability assumptions with no removal of levees or other barriers to tidal inundation. (A) high sediment/low SLR, (B) low sediment/low SLR, (C) high sediment/high SLR, and (D) low sediment/high SLR. All scenarios shown assume low organic accumulation rates (1 mm/yr). doi:10.1371/journal.pone.0027388.g007

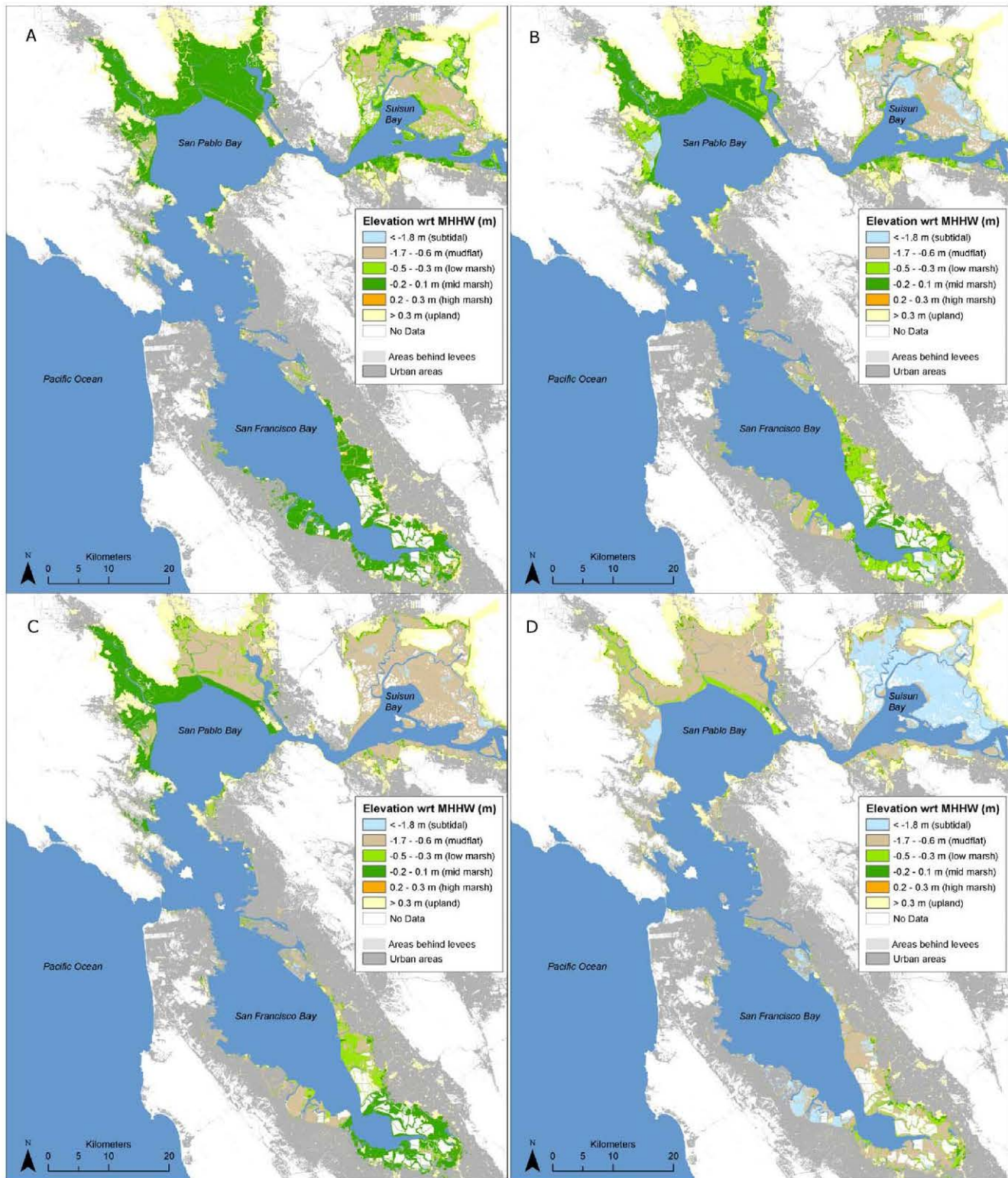


Figure 8. Potential 2110 intertidal habitats and elevations with respect to mean higher high water under different sea-level rise (SLR) and sediment availability assumptions with complete removal of all levees and other barriers to tidal inundation. (A) high sediment/low SLR, (B) low sediment/low SLR, (C) high sediment/high SLR, and (D) low sediment/high SLR. All scenarios shown assume low organic accumulation rates (1 mm/yr). doi:10.1371/journal.pone.0027388.g008

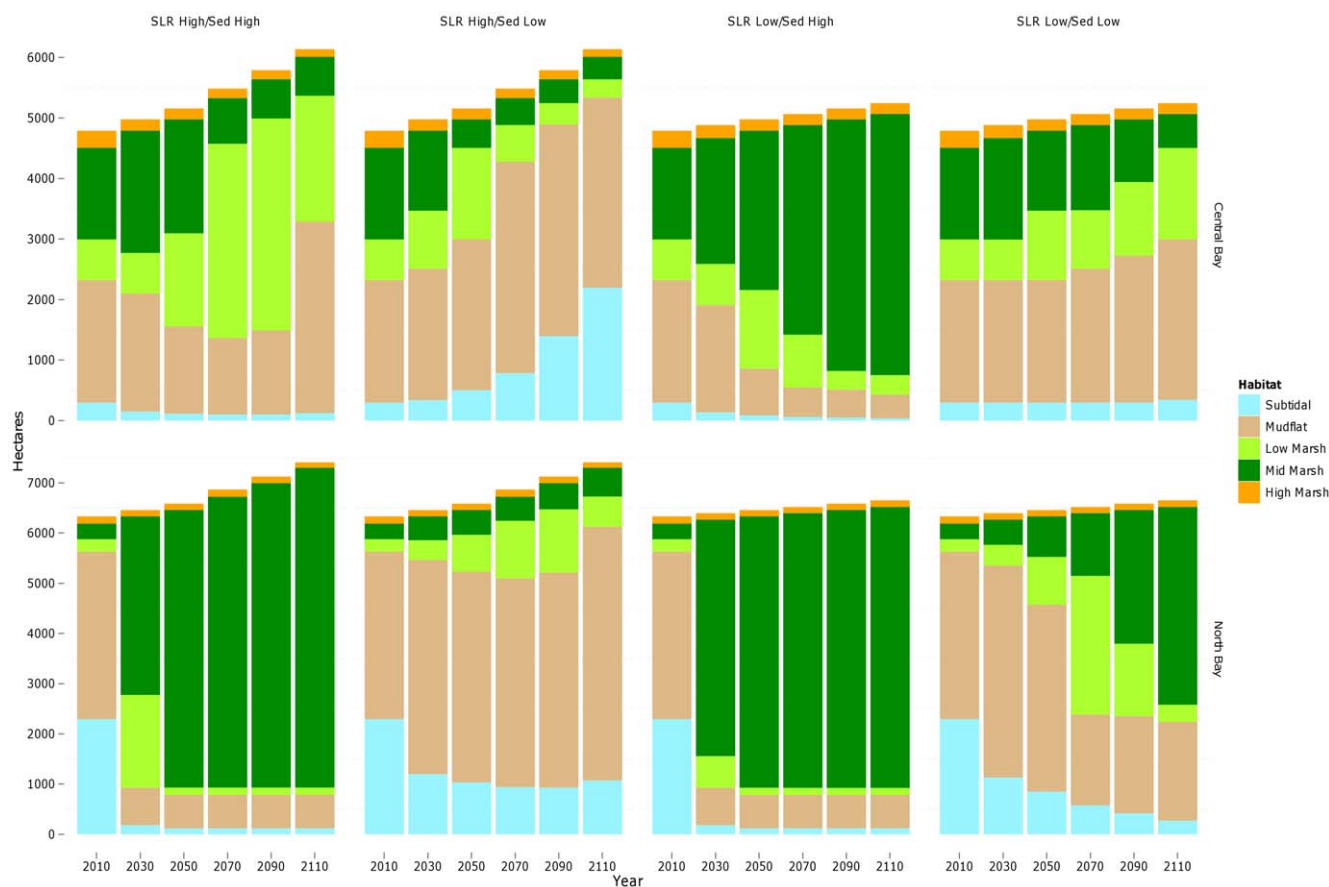


Figure 9. Area of potential future habitats within areas of high (North Bay) and low (Central Bay) sediment availability under different SLR and sediment ("Sed") scenarios. Note different scales on each set of graphs.
doi:10.1371/journal.pone.0027388.g009

ment on other available spatial models that predict wetland sustainability in the face of SLR because it incorporates a feedback between mineral sediment inputs and elevation [45]. Without this feedback, simple SLR projection models typically overestimate wetland loss because vertical accretion is constant at the relatively low rate that is found in high elevation, relatively mature tidal marshes. Evidence from field studies and process-based models indicates that vertical accretion rates are likely to increase in response to increases in inundation rates [7,32,35,40] as long as suspended sediment concentrations are sufficient. Our model incorporates this process to create more realistic projections of marsh sustainability, which may be used to assess the vulnerability to SLR and restoration potential of individual marsh sites. An additional important contribution is the development of a user-friendly web-based mapping tool to display our results [72]. This on-line tool will allow users to compare scenarios at multiple spatial scales, to evaluate the sustainability of particular locations, and to identify potential restoration sites. Managers and decision-makers can use the tool to improve the long term effectiveness of conservation strategies by maximizing the amount of tidal marsh in high-sediment regions, identifying and prioritizing key upland transitional sites, prioritizing sediment placement, and planning for future high marsh refugia.

Restoration and management implications

Importantly, even the most pessimistic scenario (low SSC, high SLR) resulted in projections of a Bay-wide increase in habitat until

nearly 2050, indicating that large-scale effects of SLR on tidal marsh may not be seen until near the end of the century. Furthermore, due to the rapidly increasing rate of SLR projected near the turn of the next century, the trajectory of marsh loss is likely to continue at accelerated rates after 2100, with anticipated severe consequences if high rates of SLR continue. This pattern, and the potential for rapid marsh plain loss once marsh drowning begins [42] indicates the importance of proactive marsh conservation planning, via the application of sediment to raise elevations at vulnerable sites before marsh loss occurs, the prioritization of more resilient (high sediment) sites for restoration, and the protection of key upland sites as future marshland. Although our results suggest that sites with low SSC may not be sustainable regardless of starting elevation, the strategic repeated delivery of sediment could potentially be used to sustain a site indefinitely. This requires a shift in sediment management strategies to capture and redistribute excess sediment, especially clean dredge materials. Collaborative efforts to maximize the beneficial reuse of dredge materials are already underway among San Francisco Bay jurisdictions and stakeholders. Because sediment contamination is a major concern [73,74], an approach using multiple lines of evidence to assessing sediment quality has been developed in part to inform sediment reuse decisions and minimize ecological impacts [75]. Due to regional variability in sediment availability, marsh resilience was projected to be much lower in some subregions (e.g., Central Bay) than others (e.g., North and South Bay systems). Thus, when restoration choices are

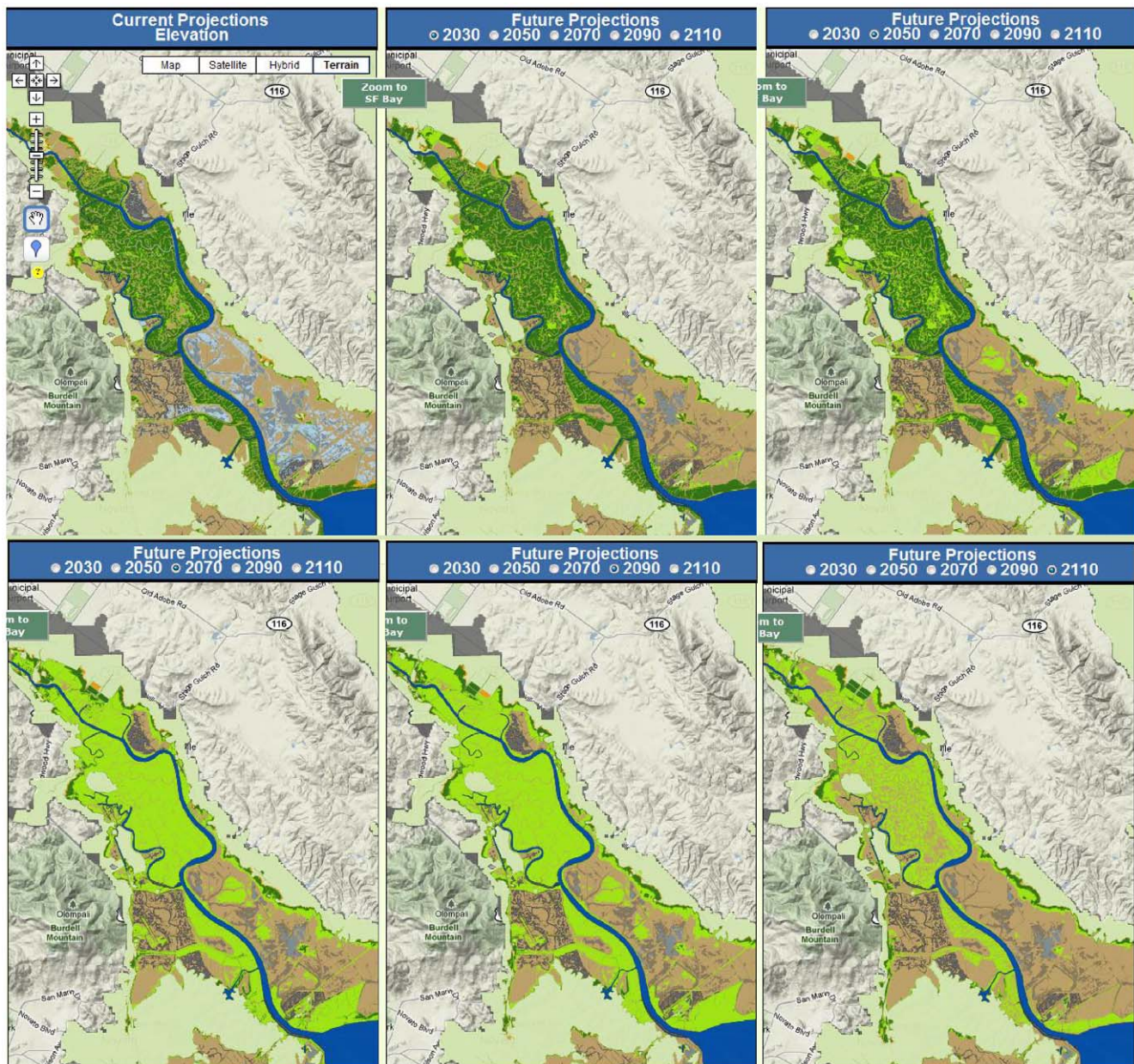


Figure 10. Projected elevation change for the most pessimistic scenario (low sediment, high SLR), using the on-line tool to zoom into the Petaluma River area. Maps assume an absence of levees, roads, and other barriers to tidal inundation. Maps demonstrate the increase in low and mid marsh through mid-century, followed by a decline as SLR accelerates and outpaces accretion rates. Note the limited amount of landward marsh expansion (See Table S3 for area summaries).
doi:10.1371/journal.pone.0027388.g010

explicit, efforts should be concentrated in sediment-rich areas with better prospects for long-term sustainability. However, high-vulnerability (low-sediment) subregions should be closely monitored and may provide early opportunities for validation of marsh sustainability projections. Although it would be easy to dismiss these areas, certain sites may be more amenable to intervention, and could be maintained either by restoring natural sources of sediment or by strategically applying dredge materials [71]. The relative viability of different sites would depend on factors such as wind-wave exposure, proximity to sediment sources, and accessibility, and may also be evaluated with respect to ecological values, e.g., presence of special status and endemic species.

Furthermore, future restoration priorities also should be informed by the availability of adjacent upland sites that are suitable for lateral marsh expansion or migration (i.e., undeveloped sites with very gradual slopes). Although our spatial analysis revealed relatively little area naturally available to accommodate future marshes (up to 3,300 ha under high SLR), we found that more than twice as much area (up to 7,000 ha) could be reclaimed by removing levees and other barriers to tidal action. In some of these areas, managed realignment of barriers to tidal inundation could be useful to facilitate marsh expansion while continuing to provide flood control benefits [76,77]. Unfortunately, the large majority of areas with elevations suitable for marsh expansion within the Bay (>13,000 ha) are already urbanized and thus

unavailable. The existing opportunities for marsh expansion into upland areas within particular subregions may be evaluated using our web-based tool.

Model limitations

While we believe that the results summarized here represent the most realistic assessment currently feasible, several limitations must be emphasized. In particular, the model does not include influence of waves, which become more important as site size increases and availability of sediment diminishes [46]. Sites that are more vulnerable to waves include those with bed elevations between vegetation colonization elevation and MLLW. At these sites, wind-wave erosion may result in marsh retreat at the bay edge, and conversion of low marsh to mudflat [42]. In this respect, the projected habitat areas are most likely an overestimate of future habitat potential, especially for low marsh habitat. Conversely, future high marsh areas are likely underestimated, as we did not consider the influence of storms or other factors that may result in the deposition of new sediment above MHHW.

In addition, we had limited data from which to estimate the relative contribution of organic material to the accretion model. The organic matter calibrations were based on data from salt marshes and rates are likely higher in slightly brackish to freshwater tidal marshes. Thus, higher rates of organic accretion may currently occur, or may occur in the future due to higher temperatures for C4 plants and higher CO₂ concentrations for C3 plants that may increase plant productivity [12,78]. Furthermore, the predicted increase in low marsh area would bring with it a shift in dominant species that may influence organic accretion rates resulting from different morphologies (e.g., volume of below-ground biomass) [7]. Thus, it is possible that we underestimated the potential future contribution of vegetation and organic matter inputs to marsh development, and thus future habitat potential. Additionally, although we considered decreased rates of organic accumulation as a proxy for increases in salinity that are projected to occur with SLR [79,80], we did not explicitly consider the adverse effects of increased salinity on plant productivity and survival, which in turn could reduce the organic contribution to accretion [11]. Similarly, effects of changing inundation on organic matter processes were not included in our model.

Finally, there is some uncertainty in the range of sediment and salinity assumptions used for each subregion, as well as spatial variability within those subregions. This is especially true for more distant future time periods, given that sediment concentrations have decreased in some parts of the Bay and are likely to continue to decrease in the future [61,80]. Although our low sediment scenario was intended to encompass such future declines, the magnitude and timing is highly uncertain. If our scenarios encompass most of this range of uncertainty, Bay-wide discrepancies are likely to be small. But for an individual site, results could change dramatically depending on actual available sediment concentrations.

Critical future uncertainties

The large disparity across scenarios highlights the importance of future sediment supply and SLR rates in determining the fate of Bay tidal marshes. Importantly, the effects of these critical variables are not linear. There are key thresholds beyond which marshes are not sustainable, with lower rates of SLR having lower thresholds for SSC requirements.

Sediment inputs to San Francisco Bay are controlled by precipitation patterns but also upstream land use decisions and water storage and diversion practices. All of these factors have high levels of future uncertainty [81–83]. With the reduced precipita-

tion that is projected for California by most general circulation models, water may become more tightly managed and thus reduce flows to the Bay, particularly during dry summer months [79,80]. Alternatively, increased precipitation, especially when delivered by high severity storms, may bring more large pulses of fresh water and sediment to the Bay, especially during winter months. Future SLR rates are also highly uncertain, but may become more precise in the near future as models and empirical data improve.

Unfortunately these key uncertainties will be difficult to address, especially over the long term, when estimates of sediment supply and SLR become increasingly variable. In the short term, however, SLR rates can be projected with a higher level of confidence, and sediment availability can be better understood through data collection and hydrodynamic modeling. Thus, by (1) collecting better data on current suspended sediment concentrations in marshes, (2) monitoring rates of marsh accretion, and (3) proactively managing sediment within an estuary, we can improve and manipulate short-term projections of marsh sustainability. In the meantime, future SLR projections may be refined, and potentially modified via societal actions to reduce greenhouse gas emissions.

Ecosystem ramifications

Across all scenarios evaluated, our model projections suggest a shift from high to low elevation marsh habitat, which will certainly affect vegetation composition, and will likely have cascading effects on ecological communities. The high marsh zone is high in plant diversity, relative to mid and low marsh, and hosts several endangered plant species, including soft birds-beak (*Chloropyron molle*, formerly *Cordylanthus mollis*), and many endemic species [84]. Much of this habitat has already been lost or degraded due to urban and agricultural development, restriction of tidal exchange, and the erection of levees, contributing to the endangered status of the plant and animal species that depend upon it [50,85].

Mid marsh comprises the majority of current vegetated tidal marsh, and the primary breeding habitat of several specialized bird species, including endangered rail species, as well three endemic subspecies of tidal marsh song sparrow (*Melospiza melodia*) [86–88] and the endemic San Francisco common yellowthroat (*Geothlypis trichas sinuosa*) [89]. While future projections for this habitat are highly variable and dependent on sediment supply and SLR rates, its large-scale loss would have wide-reaching impacts on marsh vertebrates, which generally use low marsh to a much more limited extent (or only for foraging).

Marsh drowning will result in an increase in unvegetated intertidal habitat (i.e., mudflats), as will the inevitable erosion of low marsh habitat, especially along bay margins. This may or may not counteract expected mudflat losses within the open bay [90] but should at least provide new foraging habitats for shorebirds, waterfowl, and other waterbirds. Thus, although the loss of vegetated marsh would have negative consequences for marsh-dependent species, there are likely to be benefits for other species. As a result, restoration and conservation planning in the face of SLR will necessarily involve an evaluation of ecological trade-offs, as is already the case for current restoration planning efforts [91].

Conclusions

Our model indicates at least two critical implications for tidal marsh habitat in the next century. First, the most optimistic scenarios for marsh habitat sustainability in the next century involve high availability of mineral sediment. However, sediment loads are physical inputs into the system that are largely controlled by upstream land use decisions and water storage and diversion practices and thus are very uncertain and likely to be dynamic over

the next 100 years. Second, with high SLR and SSC less than 150 mg/L, barring the significant transfer of sediment from other areas, upland habitat will have to be captured for restoration purposes in order to make up for mid marsh habitat loss. This is a challenging scenario due to the many physical barriers currently in place that prohibit wetland migration and the complexity of land ownership surrounding the Bay.

In light of these and other challenges posed by SLR for wetland managers, realistic, spatial projections must be made available quickly and clearly to inform critical conservation prioritization and restoration planning decisions. We hope the models and results presented herein and the supporting web tool (<http://www.prbo.org/sfbayslr>) provide such a contribution.

Supporting Information

Figure S1 Data sources for mapped starting elevations within San Francisco Bay study area. (PDF)

Table S1 Climate change scenario assumptions for San Francisco Bay subregions. See map in Figure 1. (PDF)

Table S2 GPS-based vegetation corrections (m) used to adjust elevations in Suisun Bay marshes (subregions 14 and 15). (PDF)

Table S3 Projected area (ha) of current and potential future marsh habitat, as well as upland areas reclaimed, under various sea-level rise (SLR) and sediment availability assumptions for the San Francisco Bay (Bay)

References

- Vermeer M, Rahmstorf S (2009) Global sea level linked to global temperature. *Proc Natl Acad Sci U S A* 106: 21527–21532.
- Intergovernmental Panel on Climate Change (IPCC) (2007) *Climate Change 2007: The Physical Science Basis*. Contribution of Working Group I to the Fourth Assessment Report of the Intergovernmental Panel on Climate Change; Solomon S, Qin D, Manning M, Chen Z, Marquis M, et al. eds. Cambridge: Cambridge University Press. pp 996.
- Hansen JE, Sato M (2011) Paleoclimate implications for human-made climate change. In: Berger A, Mesinger F, Sijači D, eds. *Climate Change at the Eve of the Second Decade of the Century: Inferences from Paleoclimate and Regional Aspects: Proceedings of the Milutin Milankovitch 130th Anniversary Symposium*. Springer. Available: <http://arxiv.org/abs/1105.0968v3>. Accessed 2011 Oct 17.
- Nicholls RJ, Hoozemans FMJ, Marchand M (1999) Increasing flood risk and wetland losses due to sea-level rise: regional and global analyses. *Global Environ Chang* 9: S69–S87.
- Dasgupta S, Laplante B, Meisner C, Wheeler D, Yan J (2009) The impact of sea level rise on developing countries: a comparative analysis. *Clim Change* 93: 379–388.
- FitzGerald DM, Fenster MS, Argow BA, Buynevich IV (2008) Coastal impacts due to sea-level rise. *Annu Rev Earth Pl Sc* 36: 601–647.
- Morris JT, Sundareshwar PV, Nietch CT, Kjerfve B, Cahoon DR (2002) Responses of coastal wetlands to rising sea level. *Ecology* 83: 2869–2877.
- Day JW, Rybczyk J, Scarton F, Rismondo A, Are D, et al. (1999) Soil accretionary dynamics, sea-level rise and the survival of wetlands in Venice Lagoon: A field and modelling approach. *Estuar Coast Shelf Sci* 49: 607–628.
- Orr M, Crooks S, Williams PB (2003) Will restored tidal marshes be sustainable? *San Francisco Estuary and Watershed Science* 1. Available: <http://escholarship.org/uc/item/8hj3d20t>. Accessed 2011 Oct 18.
- Gedan KB, Bertness MD (2009) Experimental warming causes rapid loss of plant diversity in New England salt marshes. *Ecol Lett* 12: 842–848.
- Callaway JC, Thomas Parker V, Vasey MC, Schile LM (2007) Emerging issues for the restoration of tidal marsh ecosystems in the context of predicted climate change. *Madrone* 54: 234–248.
- Langley JA, McKee KL, Cahoon DR, Cherry JA, Megonigal JP (2009) Elevated CO₂ stimulates marsh elevation gain, counterbalancing sea-level rise. *Proc Natl Acad Sci U S A* 106: 6182–6186.
- Crooks S, Herr D, Tamelander J, Laffoley D, Vandever J (2011) Mitigating Climate Change through Restoration and Management of Coastal Wetlands and Near-shore Marine Ecosystems: Challenges and Opportunities. *Environment Department Paper* 121. Washington, DC: World Bank, Available: <http://siteresources.worldbank.org/ENVIRONMENT/Resources/MtgnCCThrumGtoCoastalWetlands.pdf>. Accessed 2011 June 03.
- Zedler JB, Kercher S (2005) Wetland resources: status, trends, ecosystem services, and restorability. *Annu Rev Env Resour* 30: 39.
- Costanza R, d'Arge R, de Groot R, Farber S, Grasso M, et al. (1997) The value of the world's ecosystem services and natural capital. *Nature* 387: 253–260.
- Greenberg R, Maldonado J, Droegge S, McDonald MV (2006) Tidal marshes: a global perspective on the evolution and conservation of their terrestrial vertebrates. *BioScience* 56: 675–685.
- Chapman V (1977) *Ecosystems of the World 1: Wet Coastal Ecosystems*. New York: Elsevier Scientific Publishing Co. 428 p.
- Pennings SC, Bertness MD (2001) Salt marsh communities. In: Steven DG, Bertness MD, Hay ME, eds. *Marine Community Ecology*. Sunderland, MA, USA: Sinauer. pp 289–316.
- Allen JRL (1990) Salt-marsh growth and stratification: A numerical model with special reference to the Severn Estuary, southwest Britain. *Mar Geol* 95: 77–96.
- Nicholls RJ, Cazenave A (2010) Sea-Level Rise and Its Impact on Coastal Zones. *Science* 328: 1517–1520.
- Pethick JS, Crooks S (2000) Development of a coastal vulnerability index: a geomorphological perspective. *Environ Conserv* 27: 359–367.
- Allen JRL (2000) Morphodynamics of Holocene salt marshes: a review sketch from the Atlantic and Southern North Sea coasts of Europe. *Quaternary Sci Rev* 19: 1155–1231.
- Blum MD, Roberts HH (2009) Drowning of the Mississippi Delta due to insufficient sediment supply and global sea-level rise. *Nature Geosci* 2: 488–491.
- Patrick WH, Jr., DeLaune RD (1990) Subsidence, accretion, and sea level rise in South San Francisco Bay marshes. *Limnol Oceanogr* 35: 1389–1395.
- Watson E (2004) Changing elevation, accretion, and tidal marsh plant assemblages in a South San Francisco Bay tidal marsh. *Estuar Coast Shelf Sci* 27: 684–698.
- Reed D (1990) The impact of sea-level rise on coastal salt marshes. *Prog Phys Geog* 14: 465–481.
- Pethick JS (1981) Long-term accretion rates on tidal salt marshes. *J Sed Res* 51: 571–577.
- Atwater BF, Conrad SG, Dowden JN, Hedel CW, MacDonald RL, et al. (1979) History, landforms, and vegetation of the estuary's tidal marshes. In: Conomos TJ, ed. *San Francisco Bay: the Urbanized Estuary*. San Francisco CA: American Association for the Advancement of Science. pp 347–386.
- Nyman JA, Walters RJ, Delaune RD, Patrick JWH (2006) Marsh vertical accretion via vegetative growth. *Estuar Coast Shelf Sci* 69: 370–380.

estuary. To demonstrate restoration opportunities, the potential future marsh area for currently diked lands reflects assumption that all dikes will be removed. Urban areas are not included. Suspended sediment availability (Sed) high and low assumptions vary by Bay subregion. SLR assumptions were developed by the National Research Council (low = 0.52 m/century; high = 1.65 m/century). See Table S1 for list of subregion names and sediment assumptions, and Figure 1 for subregion map. (XLSX)

Acknowledgments

The PRBO informatics team (especially M. Fitzgibbon, D. Moody, and S. Michale) built the online application allowing users to visualize, query, and download model results. Justin Vandever and Lindsey Sheehan assisted with Marsh98 model runs. Ellen Herbert provided valuable input on organic accumulation assumptions. Noah Knowles (USGS), Kathleen Schaefer (FEMA), Tom Robinson (Sonoma County Open Space District), Stuart Siegel (Wetlands and Water Resources), Joel Dudas (DWR), and Michelle Mestrovich (County of Sonoma ISD/GIS Central) assisted with the acquisition of elevation data. Wendy Eliot, Beth Huning, Ellie Cohen, Grant Ballard, Nadav Nur, Sam Veloz, Melissa Pitkin, and John Baker were instrumental in providing feedback and support for the project. This is PRBO contribution #1816.

Author Contributions

Wrote the paper: DS JCC MB JKW. Conceptualized and initiated the project: DS SC JCC MB. Helped design the analyses: VTP LMS MK JKW. Ran models and conducted spatial analyses: MB DS DJ LMS. Provided significant written contributions to the manuscript: MK LMS VTP SC DJ.

30. McKee KL, Cahoon DR, Feller IC (2007) Caribbean mangroves adjust to rising sea level through biotic controls on change in soil elevation. *Global Ecol Biogeogr* 16: 545–556.
31. French JR (1993) Numerical simulation of vertical marsh growth and adjustment to accelerated sea-level rise. North Norfolk, UK: *Earth Surf Proc Land* 18: 63–831.
32. Stevenson JC, Ward LG, Kearney MS (1986) Vertical accretion in marshes with varying rates of sea level rise. In: Wolfe DA, ed. *Estuarine Variability*. Orlando FL: Academic Press. pp 241–259.
33. Stevenson JC, Kearney MS, Pendleton EC (1985) Sedimentation and erosion in a Chesapeake Bay brackish marsh system. *Mar Geol* 67: 213–235.
34. Kearney MS, Stevenson JC (1991) Island land loss and marsh vertical accretion rate evidence for historical sea-level changes in Chesapeake Bay. *J Coast Res* 7: 403–415.
35. Hatton RS, DeLaune RD, Patrick WH, Jr. (1983) Sedimentation, accretion, and subsidence in marshes of Barataria Basin, Louisiana. *Limnol Oceanogr* 28: 494–502.
36. Nyman JA, DeLaune RD, Patrick WH (1990) Wetland soil formation in the rapidly subsiding Mississippi River Deltaic Plain: Mineral and organic matter relationships. *Estuar Coast Shelf Sci* 31: 57–69.
37. Kirwan M, Temmerman S (2009) Coastal marsh response to historical and future sea-level acceleration. *Quaternary Sci Rev* 28: 1801–1808.
38. Kirwan ML, Guntenspergen GR, D'Alpaos A, Morris JT, Mudd SM, et al. (2010) Limits on the adaptability of coastal marshes to rising sea level. *Geophys Res Lett* 37: L23401.
39. Rybczyk JM, Callaway JC (2009) Surface elevation models. In: Perillo GME, ed. *Coastal wetlands: an integrated ecosystem approach*. Amsterdam, Boston: Elsevier. pp 835–853.
40. Callaway J, Nyman J, DeLaune R (1996) Sediment accretion in coastal wetlands: A review and a simulation model of processes. *Current Topics in Wetland Biogeochemistry* 2: 2–23.
41. Kirwan ML, Murray AB (2007) A coupled geomorphic and ecological model of tidal marsh evolution. *Proc Natl Acad Sci U S A* 104: 6118–6122.
42. Fagherazzi S, Carniello L, D'Alpaos L, Defina A (2006) Critical bifurcation of shallow microtidal landforms in tidal flats and salt marshes. *Proc Natl Acad Sci U S A* 103: 8337–8341.
43. Park R, Trehan MS, Mausel PW, Howe RC (1989) The effects of sea level rise on U.S. coastal wetlands. U.S. EPA Office of Policy, Planning, and Evaluation. Available: http://www.epa.gov/globalwarming/climatechange/effects/downloads/rtc_park_wetlands.pdf. Accessed 2011 June 03.
44. Craft C, Clough J, Ehman J, Joye S, Park R, et al. (2009) Forecasting the effects of accelerated sea-level rise on tidal marsh ecosystem services. *Front Ecol Env* 7: 73–78.
45. Krone RB (1987) A Method for Simulating Historic Marsh Elevations. Coastal Sediments '87 Proceedings of the Specialty Conference on Quantitative Approaches to Coastal Sediment Processes. May 12–14, 1987; New Orleans, LA. pp 316–323.
46. Williams P, Orr M (2002) Physical evolution of restored breached levee salt marshes in the San Francisco Bay estuary. *Restor Ecol* 10: 527–542.
47. Fretwell JD, Williams JS, Redman PJ (1996) National Water Summary on Wetland Resources. Water-Supply Paper 2425. Washington, DC: U.S. Geological Survey. Available: <http://water.usgs.gov/nwsum/WSP2425/>. Accessed 2011 June 03.
48. San Francisco Estuary Project (SFEP) (1991) San Francisco Estuary Project status and trends report on wetlands and related habitats in the San Francisco Estuary. ABAG Public report to US-EPA. Oakland CA: San Francisco Estuary Project. Available: <http://www.sfestuary.org/pages/index.php?ID=5>. Accessed 2011 June 03.
49. Heberger M, Cooley H, Herrera P, Gleick PH, Moore E (2009) The Impacts of Sea-level Rise on the California Coast. A paper from the California Climate Change Center (CEC-500-2009-024-F). Pacific Institute. Available: http://www.pacinst.org/reports/sea_level_rise/report.pdf. Accessed 2011 Aug 03.
50. Goals Project (1999) Baylands ecosystem habitat goals. A report of habitat recommendations prepared by the San Francisco Bay Area Wetlands Ecosystems Goals Project. Joint publication of the U. S. Environmental Protection Agency, San Francisco, CA, and San Francisco Bay Regional Water Quality Control Board. Available: <http://www.sfei.org/sites/default/files/sfbaygoals031799.pdf>. Accessed 2011 June 03.
51. Josselyn M (1983) The ecology of San Francisco Bay tidal marshes: a community profile. Biological Report FWS/OBS-83/23. Washington, DC: U.S. Fish and Wildlife Service, Division of Biological Services. Available: <http://www.nwrc.usgs.gov/techrpt/83-23.pdf>. Accessed 2011 June 03.
52. Conomos TJ (1979) Properties and circulation of San Francisco Bay waters. In: Conomos TJ, ed. *San Francisco Bay: the Urbanized Estuary*. San Francisco, CA: Pacific Division of the American Association for the Advancement of Science. pp 47–84.
53. Grewell BJ, Callaway JC, Ferren WR (2007) Estuarine Wetlands. In: Barbour M, Keeler-Wolf T, Schoenherr AA, eds. *Terrestrial Vegetation of California*, 3rd edition. Berkeley, CA: University of California Press. pp 124–154.
54. Fairbanks RG (1989) A 17,000-year glacio-eustatic sea level record: influence of glacial melting rates on the Younger Dryas event and deep-ocean circulation. *Nature* 342: 637–642.
55. Goman M, Malamud-Roam F, Ingram BL (2008) Holocene environmental history and evolution of a tidal salt marsh in San Francisco Bay, California. *J Coast Res* 24: 1126–1137.
56. van Geen A, Luoma SN (1999) The impact of human activities on sediments of San Francisco Bay, California: an overview. *Mar Chem* 64: 1–6.
57. Williams PB, Faber PM (2001) Salt marsh restoration experience in the San Francisco Bay Estuary. *J Coast Res* 27: 203–211.
58. Jaffe BE, Smith RE, Foxgrover A (2007) Anthropogenic influence on sedimentation and intertidal mudflat change in San Pablo Bay, California: 1856–1983. *Estuar Coast Shelf Sci* 73: 175–187.
59. Schoellhamer D (2009) Suspended sediment in the Bay: Past a tipping point. Oakland, CA: San Francisco Estuary Institute. pp 56–65. Available: http://www.sfei.org/sites/default/files/RMP_Pulse09_n0583_final4web.pdf. Accessed 2011 June 03.
60. Wright SA, Schoellhamer DH (2004) Trends in the Sediment Yield of the Sacramento River, California, 1957–2001. San Francisco Estuary and Watershed Science 2. Available: <http://escholarship.org/uc/item/891144f4>. Accessed 2011 Oct 18.
61. Schoellhamer D (2011) Sudden clearing of estuarine waters upon crossing the threshold from transport to supply regulation of sediment transport as an erodible sediment pool is depleted: San Francisco Bay, 1999. *Estuar Coast* 34: 885–899.
62. Atwater BF, Hedel CW (1976) Distribution of tidal-marsh plants with respect to elevation and water salinity in the natural tidal marshes of the Northern San Francisco Bay Estuary, California. U.S. Geological Survey Open-File Report 76-389. pp 41. Available: <http://pubs.er.usgs.gov/publication/ofr76389>. Accessed 2011 June 03.
63. ACOE (2009) Incorporating Sea-Level Change Considerations in Civil Works Programs. Engineering Circular #1165-2-211. U.S. Army Corps of Engineers. Available: <http://140.194.76.129/publications/eng-circulars/ec1165-2-211/entire.pdf>. Accessed 2011 June 03.
64. Rahmstorf S (2007) A Semi-Empirical Approach to Projecting Future Sea-Level Rise. *Science* 315: 368–370.
65. Cayan DR, Tyree M, Dettlinger MD, Hidalgo H, Das T, et al. (2009) Climate change scenarios and sea level rise estimates for the California 2008 Climate Change Scenarios Assessment. CEC-500-2009-014-D. Available: <http://www.energy.ca.gov/2009publications/CEC-500-2009-014/CEC-500-2009-014-D.PDF>. Accessed 2011 June 03.
66. Buchanan PA, Ganju NK (2005) Summary of suspended-sediment concentration data, San Francisco Bay, California, Water Year 2003. USGS Data Series Report 113. Sacramento, California: United States Geological Survey. Available: <http://pubs.usgs.gov/ds/2005/113/ds113.pdf>. Accessed 2011 June 03.
67. Ruhl CA, Schoellhamer DH (2004) Spatial and temporal variability of suspended-sediment concentration in a shallow estuarine environment. *San Francisco Estuary and Watershed Science* 2: 1.
68. Ganju NK, Schoellhamer DH, Warner JC, Barad MF, Schladow SG (2004) Tidal oscillation of sediment between a river and a bay: a conceptual model. *Estuar Coast Shelf Sci* 60: 81–90.
69. Vaghti M, Keeler-Wolf T (2004) Suisun Marsh Vegetation Mapping Change Detection 2003. Unpublished report on file at Wildlife and Habitat Data Analysis Branch. Sacramento, CA: California Department of Fish and Game. Available: <http://imaps.dfg.ca.gov/references/ds163/ds163.pdf>. Accessed 2011 June 03.
70. Tuxen K, Schile L, Stralberg D, Siegel S, Parker T, et al. (2011) Mapping changes in tidal wetland vegetation composition and pattern across a salinity gradient using high spatial resolution imagery. *Wetl Ecol Manag* 19: 141–157.
71. Philip Williams and Associates, Faber P (2004) Design Guidelines for Tidal Wetland Restoration in San Francisco Bay. San Francisco, CA: Philip Williams and Associates, prepared for the Bay Institute, Available: <http://www.wrmp.org/design/>. Accessed 2011 June 03.
72. Veloz S, Fitzgibbon M, Stralberg D, Michale S, Jongsomjit D, et al. (2011) San Francisco Bay sea level rise: Climate change scenarios for tidal marsh habitats. [web application]. Petaluma, California. Available: <http://www.prbo.org/sfbayslr>. Accessed 2011 June 03.
73. Hornberger ML, Luoma SN, van Geen A, Fuller C, Anima R (1999) Historical trends of metals in the sediments of San Francisco Bay, California. *Mar Chem* 64: 39–55.
74. Thompson B, Anderson B, Hunt J, Taberski K, Phillips B (1999) Relationships between sediment contamination and toxicity in San Francisco Bay. *Mar Environ Res* 48: 285–309.
75. San Francisco Estuary Institute (SFEI) (2009) The Pulse of the Estuary: Monitoring and Managing Water Quality in the San Francisco Estuary. Oakland, CA: San Francisco Estuary Institute, Available: <http://www.sfei.org/rmp/pulse>. Accessed 2011 June 03.
76. Andrews JE, Burgess D, Cave RR, Coombes EG, Jickells TD, et al. (2006) Biogeochemical value of managed realignment, Humber estuary, UK. *Sci Total Environ* 371: 19–30.
77. Townend I, Pethick J (2002) Estuarine flooding and managed retreat. *Philos Trans R Soc London Ser A* 360: 1477–1495.
78. Cherry JA, McKee KL, Grace JB (2009) Elevated CO₂ enhances biological contributions to elevation change in coastal wetlands by offsetting stressors associated with sea-level rise. *J Ecol* 97: 67–77.

79. Knowles N, Cayan DR (2002) Potential effects of global warming on the Sacramento/San Joaquin watershed and the San Francisco estuary. *Geophys Res Lett* 29: 1891.
80. Cloern JE, Knowles N, Brown LR, Cayan D, Dettinger MD, et al. (2011) Projected evolution of California's San Francisco Bay-Delta-River system in a century of climate change. *PLoS ONE* 6: e24465.
81. Brekke LD, Miller NL, Bashford KE, Quinn NWT, Dracup JA (2004) Climate change impacts uncertainty for water resources in the San Joaquin River Basin, California. *J Am Water Resour As* 40: 149–164.
82. Maurer EP, Duffy PB (2005) Uncertainty in projections of streamflow changes due to climate change in California. *Geophys Res Lett* 32: L03704.
83. Miller NL, Bashford KE, Strem E (2003) Potential impacts of climate change on California hydrology. *J Am Water Resour As* 39: 771–784.
84. Vasey MC, Parker VT, Callaway JC, Herbert ER, Schile LM (2011) Tidal wetland vegetation in the San Francisco Bay-Delta estuary. *San Francisco Estuary and Watershed Science*; In press.
85. Wasson K, Woolfolk A (2011) Salt marsh-upland ecotones in Central California: Vulnerability to invasions and anthropogenic stressors. *Wetlands* 31: 1–14.
86. Spautz H, Nur N (2008) Samuel's Song Sparrow, *Melospiza melodia samuelis*. In: Shuford WD, Gardali T, eds. *California Bird Species of Special Concern: A ranked assessment of species, subspecies, and distinct populations of immediate conservation concern in California*. Camarillo and Sacramento, CA: California Department of Fish and Game. pp 412–418.
87. Spautz H, Nur N (2008) Suisun Song Sparrow, *Melospiza melodia maxillaris*. In: Shuford WD, Gardali T, eds. *California Bird Species of Special Concern: A ranked assessment of species, subspecies, and distinct populations of immediate conservation concern in California*. Camarillo and Sacramento, CA: California Department of Fish and Game. pp 405–411.
88. Chan Y, Spautz H (2008) Alameda Song Sparrow, *Melospiza melodia pusillula*. In: Shuford WD, Gardali T, eds. *California Bird Species of Special Concern: A ranked assessment of species, subspecies, and distinct populations of immediate conservation concern in California*. Camarillo and Sacramento, CA: California Department of Fish and Game. pp 419–424.
89. Gardali T, Evens JG (2008) Salt Marsh Common Yellowthroat, *Geothlypis trichas sinuosa*. In: Shuford WD, Gardali T, eds. *California Bird Species of Special Concern: A ranked assessment of species, subspecies, and distinct populations of immediate conservation concern in California*. Camarillo and Sacramento, CA: California Department of Fish and Game. pp 346–350.
90. Galbraith H, Jones R, Park R, Clough J, Herrod-Julius S, et al. (2002) Global climate change and sea level rise: potential losses of intertidal habitat for shorebirds. *Waterbirds* 25: 173–183.
91. Stralberg D, Applegate DL, Phillips SJ, Herzog MP, Nur N, et al. (2009) Optimizing wetland restoration and management for avian communities using a mixed integer programming approach. *Biol Conserv* 142: 94–109.

RESEARCH ARTICLE

Reconstructing the Migratory Behavior and Long-Term Survivorship of Juvenile Chinook Salmon under Contrasting Hydrologic Regimes

Anna M. Sturrock^{1†*}, J. D. Wikert², Timothy Heyne³, Carl Mesick², Alan E. Hubbard⁴, Travis M. Hinkelman⁵, Peter K. Weber⁶, George E. Whitman⁷, Justin J. Glessner⁸, Rachel C. Johnson^{7,9}

1 Institute of Marine Sciences, University of California Santa Cruz, Santa Cruz, California, United States of America, **2** US Fish and Wildlife Service, Lodi, California, United States of America, **3** Tuolumne River Restoration Center, California Department of Fish and Wildlife, La Grange, California, United States of America, **4** School of Public Health, Division of Biostatistics, University of California, Berkeley, California, United States of America, **5** Cramer Fish Sciences, Auburn, California, United States of America, **6** Glenn T. Seaborg Institute, Lawrence Livermore National Laboratory, Livermore, California, United States of America, **7** Department of Animal Sciences, University of California Davis, Davis, California, United States of America, **8** UC Davis Interdisciplinary Center for Plasma Mass Spectrometry, Department of Geology, University of California Davis, Davis, California, United States of America, **9** National Marine Fisheries Service, Southwest Fisheries Science Center, Santa Cruz, California, United States of America

† Current address: Department of Environmental Science, Policy & Management, University of California, Berkeley, California, United States of America

* a.sturrock@berkeley.edu


 OPEN ACCESS

Citation: Sturrock AM, Wikert JD, Heyne T, Mesick C, Hubbard AE, Hinkelman TM, et al. (2015) Reconstructing the Migratory Behavior and Long-Term Survivorship of Juvenile Chinook Salmon under Contrasting Hydrologic Regimes. PLoS ONE 10(5): e0122380. doi:10.1371/journal.pone.0122380

Academic Editor: Z. Daniel Deng, Pacific Northwest National Laboratory, UNITED STATES

Received: December 17, 2014

Accepted: January 31, 2015

Published: May 20, 2015

Copyright: This is an open access article, free of all copyright, and may be freely reproduced, distributed, transmitted, modified, built upon, or otherwise used by anyone for any lawful purpose. The work is made available under the [Creative Commons CC0](https://creativecommons.org/licenses/by/4.0/) public domain dedication.

Data Availability Statement: Otolith strontium isotope data and juvenile passage estimates are available on Dryad (doi:10.5061/dryad.c56rk).

Funding: United States Fish and Wildlife Service funding under United States Bureau of Reclamation Agreement R09AC20043 was awarded to RCJ. Work at LLNL by PKW was performed under the auspices of the United States Department of Energy, Contract DE-AC52-07NA27344.

Competing Interests: The authors have declared that no competing interests exist.

Abstract

The loss of genetic and life history diversity has been documented across many taxonomic groups, and is considered a leading cause of increased extinction risk. Juvenile salmon leave their natal rivers at different sizes, ages and times of the year, and it is thought that this life history variation contributes to their population sustainability, and is thus central to many recovery efforts. However, in order to preserve and restore diversity in life history traits, it is necessary to first understand how environmental factors affect their expression and success. We used otolith ⁸⁷Sr/⁸⁶Sr in adult Chinook salmon (*Oncorhynchus tshawytscha*) returning to the Stanislaus River in the California Central Valley (USA) to reconstruct the sizes at which they outmigrated as juveniles in a wetter (2000) and drier (2003) year. We compared rotary screw trap-derived estimates of outmigrant timing, abundance and size with those reconstructed in the adults from the same cohort. This allowed us to estimate the relative survival and contribution of migratory phenotypes (fry, parr, smolts) to the adult spawning population under different flow regimes. Juvenile abundance and outmigration behavior varied with hydroclimatic regime, while downstream survival appeared to be driven by size- and time-selective mortality. Although fry survival is generally assumed to be negligible in this system, >20% of the adult spawners from outmigration year 2000 had outmigrated as fry. In both years, all three phenotypes contributed to the spawning population, however their relative proportions differed, reflecting greater fry contributions in the wetter

year (23% vs. 10%) and greater smolt contributions in the drier year (13% vs. 44%). These data demonstrate that the expression and success of migratory phenotypes vary with hydrologic regime, emphasizing the importance of maintaining diversity in a changing climate.

Introduction

Life history diversity is often cited as a crucial component of population resilience, based on theoretical and empirical evidence that asynchrony in local population dynamics reduces long-term variance and extinction risk at both regional and metapopulation scales [1]. Pacific salmon are recognized for their complex life histories, having evolved alongside the shifting topography of the Pacific Rim [2]. In the California Central Valley (CCV), four runs of imperilled Chinook salmon (*Oncorhynchus tshawytscha*) coexist, exhibiting asynchronous spatial and temporal distributions that allow them to exploit a range of ecological niches [3,4]. The maintenance of multiple and diverse salmon stocks that fluctuate independently of each other has been shown to convey a stabilizing ‘portfolio effect’ to the overall the stock-complex [5,6]. Such ‘risk spreading’ can also act at finer scales [7,8], such as within-population variation in the timing of juvenile emigration. Preserving and restoring life history diversity remains an integral goal of many salmonid conservation programs [9], yet baseline monitoring data with which to detect and respond to changes in trait expression are scarce and difficult to relate directly to population abundance.

The expression and success of certain traits can be largely driven by hydroclimatic conditions experienced during critical periods of development [10]. CCV Chinook salmon are at the southern margin of their species range, and are subjected to highly variable patterns in precipitation and ocean conditions [4,11]. It is also a highly modified system, with >70% of spawning habitat lost or degraded as a result of mining activities, dam construction, and water diversions [4,12]. The majority of salmon rivers in the CCV experience regulated flows according to ‘water year type’ (WYT). Optimization of reservoir releases presents considerable challenges, given often limited availability and multiple uses of the water resource, inability to predict annual precipitation, and uncertainty surrounding the direct and indirect effects of flow on salmon survival [13]. Such challenges are particularly critical for the more southerly San Joaquin basin, whose salmon populations fluctuate considerably with river flows experienced during juvenile rearing (Fig 1).

Juvenile Chinook salmon exhibit significant variation in the size, timing and age at which they outmigrate from their natal rivers [3,14]. Selection for one strategy over another may vary as a function of freshwater and/or marine conditions [10,15]. In the CCV, fall-run juveniles typically rear in freshwater for one to four months before smoltification prompts downstream migration toward the ocean [16]. In this system, contributions of the smaller fry and parr outmigrants to the adult population are often assumed to be negligible, as survival tends to correlate with body size [17,18] and there is little evidence for downstream rearing in the San Francisco estuary [19]. However, this has never been explicitly tested for smaller size classes. Indeed, salmon fry are frequently observed rearing in tidal marsh and estuarine habitats in other systems [3], and have been observed in non-natal habitats in the CCV, such as the mainstem Sacramento and San Joaquin Rivers, freshwater delta, and estuary [20]. Juvenile salmon that enter the ocean at a larger size and have faster freshwater growth have demonstrated a survival advantage when faced with poor ocean conditions [18]. Yet intermediate size classes can be better represented in the adult population [21,22], and size-selective mortality can be

moderated by a variety of other processes [23]. In a regulated system such as the CCV, identifying the relationships between observable traits, hydroclimatic regime and survival would be invaluable for reducing uncertainty and predicting how populations may respond to climate change and management actions related to water operations.

Quantifying the relative contribution of fry, parr and smolt outmigrants to the adult population has, until now, been largely limited by the methodological challenges associated with reconstructing early life history movements of the adults. Mark-recapture studies using acoustic and coded wire tags (CWT) have provided empirical indices of juvenile survival through stretches of the Sacramento-San Joaquin River Delta (hereafter, “the Delta”) [24,25], but are hindered by low rates of return and tend to utilize hatchery fish that may exhibit different rearing behavior and sea-readiness to their wild counterparts [26]. Furthermore, ‘fry pulses’ tend to be dominated by individuals <45mm FL, which are difficult to mark externally without causing damage or behavioral modifications. No study to date has tracked habitat use of individual salmon over an entire lifecycle to estimate the relative success of juvenile outmigration phenotypes under different flow conditions. Previous studies have tended to rely on correlations between environmental conditions (e.g. flow) experienced during outmigration and the abundance of returns (Fig 1) [27]. Recent advances in techniques using chemical markers recorded in biomineralised tissues provide rare opportunity to retrospectively “geolocate” individual fish in time and space [28]. Given their incremental growth and metabolically inert

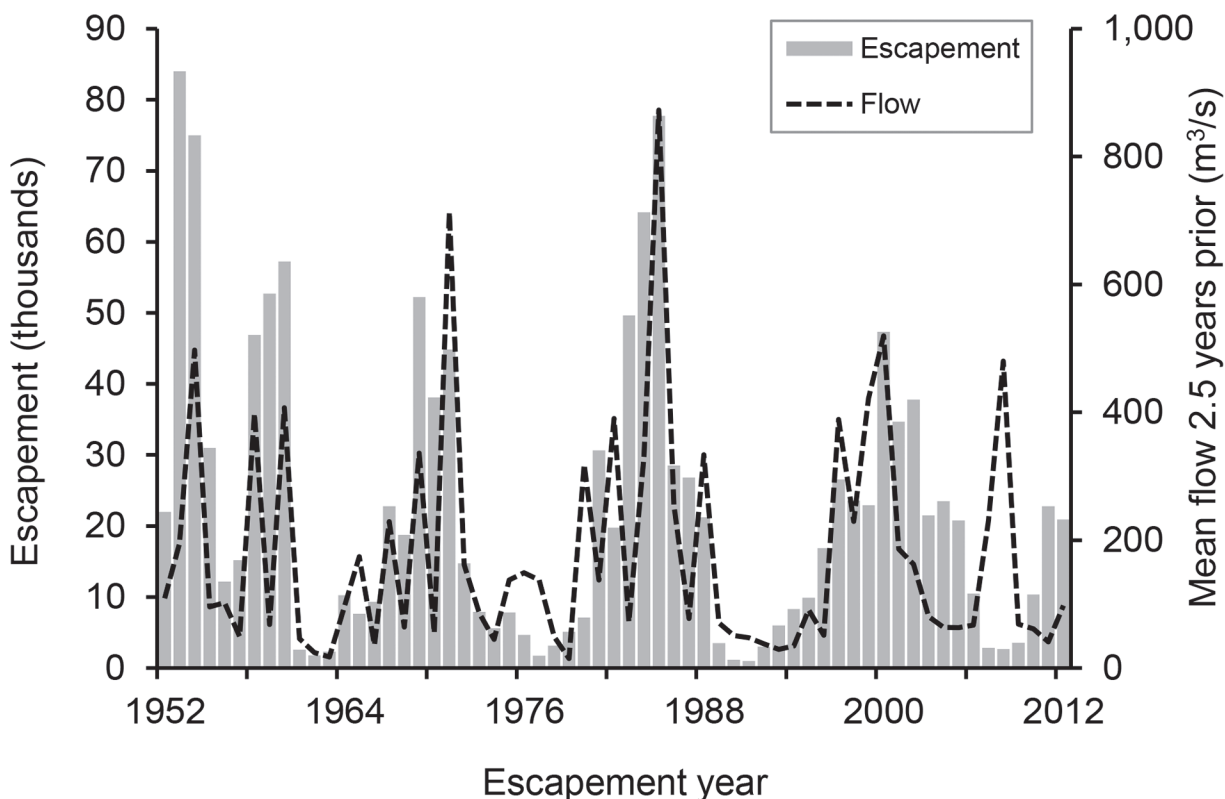


Fig 1. Relationship between adult salmon returns to the San Joaquin basin and the river flows experienced as juveniles. Fall-run Chinook salmon returns (‘escapement’) to the San Joaquin basin from 1952 to 2011 (CDFW GrandTab, www.CalFish.org) relative to mean flows at Vernalis (USGS gauge 11303500, <http://waterdata.usgs.gov/nwis>) for the January to June outmigration period they experienced 2.5 years previous. Note that adult abundance estimates have not been corrected for age distributions (we assumed that all adults returned at age 3), inter-annual variation in harvest rates or out-of-basin straying. The large deviation in 2007 reflected poor returns that were attributed to poor ocean conditions [96] and resulted in the closure of the fishery. Adapted from [97].

doi:10.1371/journal.pone.0122380.g001

nature, otoliths ('ear stones') represent a unique natural tag for reconstructing movement patterns of individual fish [29]. The technique relies on differences in the physicochemical environment producing distinct and reproducible "fingerprints" in the otolith. In the CCV, strontium isotopes ($^{87}\text{Sr}/^{86}\text{Sr}$) are ideal markers because the water composition varies among many of the rivers and is faithfully recorded in the otoliths of Chinook salmon [30–32]. Changes in otolith $^{87}\text{Sr}/^{86}\text{Sr}$ values can be used to reconstruct time- and age-resolved movements as salmon migrate through the freshwater and estuarine environments [33]. Furthermore, otolith size is significantly related to body size [34,35], allowing back-calculation of individual fork length (FL) at specific life history events [36].

Here, we document metrics of juvenile life history diversity (phenology, size, and abundance) of fall-run Chinook salmon as they outmigrated from the Stanislaus River during an 'above normal' (2000) and 'below normal' (2003) WYT. We used otolith $^{87}\text{Sr}/^{86}\text{Sr}$ and radius measurements to reconstruct the size at which returning (i.e. "successful") adults from the same cohort had outmigrated, then combined juvenile and adult datasets to estimate the relative contribution and survival of fry, parr and smolt outmigrants. Our main objectives were to determine (1) if a particular phenotype contributed disproportionately to the adult spawning population, (2) whether this could be attributed to selective mortality, and (3) if patterns in phenotype expression and success varied under contrasting flow regimes.

Study Area

The Stanislaus River (hereafter, "the Stanislaus") is the northernmost tributary of the San Joaquin River, draining 4,627 km³ on the western slope of the Sierra Nevada (Fig 2) [37]. The basin has a Mediterranean climate and receives the majority of its annual rainfall between November and April. Contrasting with the Sacramento watershed in the north, the hydrology of the San Joaquin basin is primarily snowmelt driven [4]. There are over 40 dams in the Stanislaus, which collectively have a capacity of 240% of the average annual runoff [38]. Historically, the Stanislaus contained periodically-inundated floodplain habitat and supported spring- and fall-run Chinook salmon; however, spring-run salmon were extirpated by mining and dam construction, reducing habitat quality and preventing passage to higher elevation spawning grounds [4].

Materials and Methods

Ethics statement

This research was conducted in strict accordance with protocols evaluated and approved by the University of California, Santa Cruz Institutional Animal Care and Use Committee for this specific study (permit number BARNR1409). Otolith and scale samples were collected by California Department of Fish and Wildlife (CDFW) staff from adult salmon carcasses (i.e. already expired) as part of their annual carcass survey, permitted under the State legislative mandate to perform routine management actions. No tissue collections were taken from any state- or federally-listed endangered or protected species for this study.

Juvenile sampling and hydrologic regime

Typically, fall-run Chinook salmon return to the San Joaquin basin from September to early January, and their offspring outmigrate the following January to June [16,39]. Juveniles were sampled as they left the Stanislaus using rotary screw traps (RST) at Caswell Memorial State Park (Fig 2, N 37°42'7.533", W 121°10'44.882). Sampling was terminated when no juveniles had been captured for at least seven consecutive days in June or July [40]. Here, we focused on

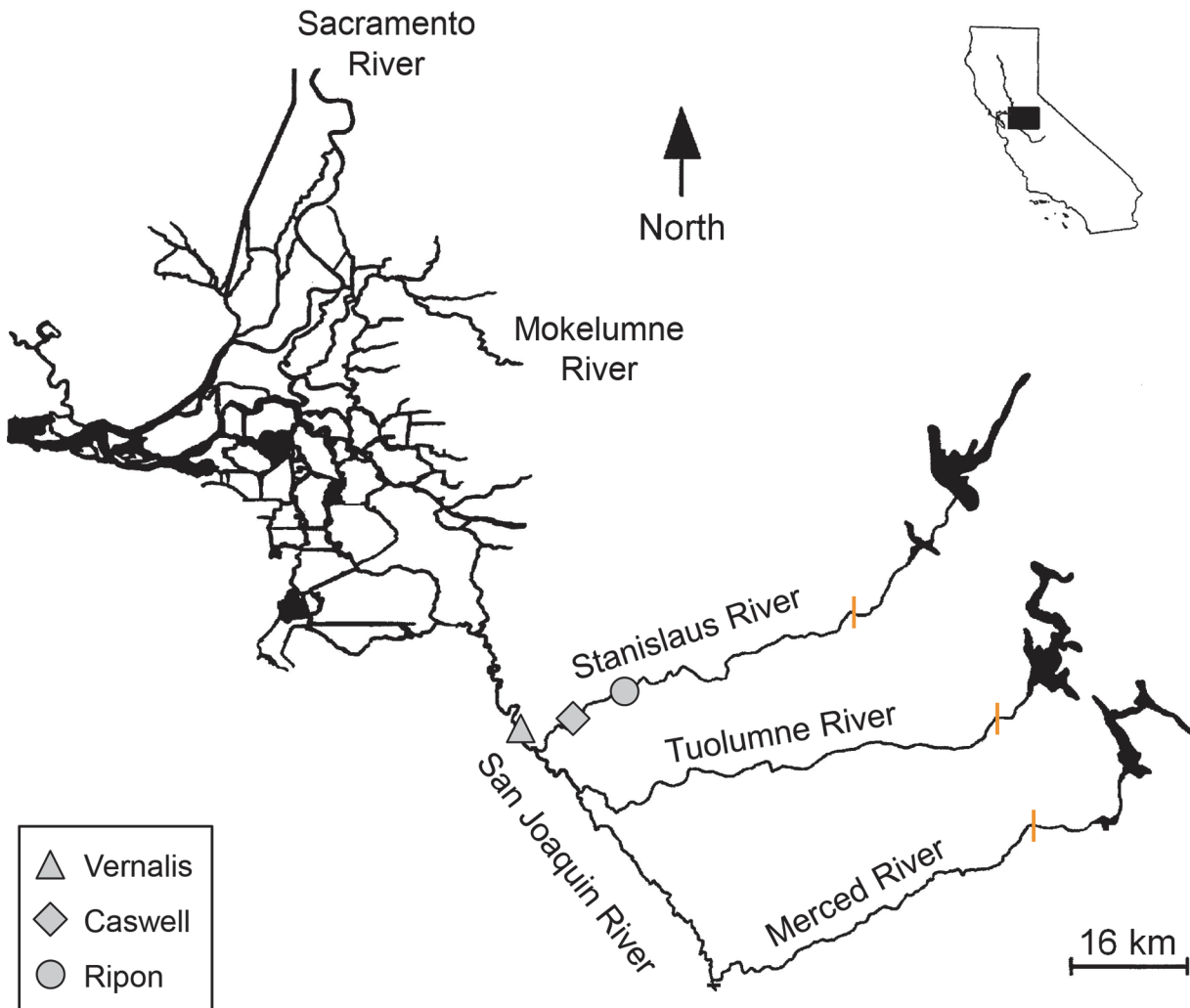


Fig 2. The San Joaquin basin of the Central Valley, California (inset). Map showing the major rivers in the San Joaquin basin, and the location of the rotary screw trap site at Caswell Memorial State Park and USGS gauges at Ripon and Vernalis. The upstream barriers to salmon migration in the three main tributaries are indicated by orange bars.

doi:10.1371/journal.pone.0122380.g002

an ‘above normal’ (2000) and ‘below normal’ (2003) WYT, and defined the outmigration period as January 1 to June 30, inclusive. When traps were checked, all fish were counted and up to 50 were randomly selected for fork length (FL) and weight measurements. Given potential subjectivity in visual staging criteria [41], we defined migratory phenotypes (fry, parr and smolt) by size: ≤ 55 mm, >55 to ≤ 75 mm, and >75 mm FL, respectively (after [21]). Unmeasured fish were assigned to phenotype using the observed proportions in the measured fish for the same date. For each phenotype, we interpolated missing catch values with a triangular weighted mean [42].

Marked fish were periodically released to develop a statistical model of trap efficiency, which was used to expand counts of fry, parr and smolt-sized outmigrants. Trap efficiency was estimated using a GLM with a quasibinomial error distribution because of overdispersion in capture probabilities. We used the same efficiency model as [42], only using phenotype (fry, parr, smolt) to characterize fish size, rather than FL. We propagated uncertainty by deriving estimated expanded counts from repeated Monte Carlo draws ($n = 2000$) from the estimated

sampling distribution of the estimated coefficients from the logistic efficiency model using R package `mvtnorm` [43]. Daily flow observations (USGS gauge no. 11303000 at Ripon, www.waterdata.usgs.gov/nwis) were used with the randomly-sampled model coefficients to simulate daily trap efficiency. Passage estimates were then simulated using daily catch and simulated trap efficiencies. We incorporated extra-binomial variation by generating simulated daily catch values from a beta-binomial distribution (based on the simulated efficiencies and passage estimates, as well as the dispersion estimated from the efficiency model). Finally, new daily passage estimates were calculated using simulated catch and trap efficiencies. Thus the final passage estimates incorporate both sampling error (catch) and estimation error (efficiency model). Annual passages estimates and confidence intervals (2.5% and 97.5% quantiles) were generated by summing daily passage estimates for the 6 month outmigration period (i.e. $n = 2000 \times 180$ days).

Measured daily size-frequency distributions were applied directly to the expanded abundance estimates, then grouped into 2mm FL bins. We attempted to produce passage estimates by FL, but the distribution used in the uncertainty propagation procedure (see above) is asymmetric at low catches, resulting in zero-inflation and the median of the resampled distribution often being lower than the observed raw catch.

Turbidity was measured at Caswell using a LaMott turbidity meter [40]; mean daily flow and maximum daily temperature were measured at Ripon (gauge details above). Daily passage estimates, turbidity, flow and temperature were \log_{10} transformed, then averaged for the 6-month outmigration period and compared among years by ANOVA, adjusting for temporal autocorrelation using the Durbin-Watson (DW) test [44]. Pearson's chi-squared test was used to identify differences in the proportion of phenotypes among years. Fry, parr and smolt phenology was summarized using three metrics associated with their date of passage past the trap: the range, interquartile range (IQR), and median (or "peak") outmigration date. Phenotype "migratory periods" were defined as the maximum IQR for both years combined.

Adult sampling and cohort reconstruction

To track outmigration cohorts 2000 and 2003 into the adult escapement, sagittal otoliths were extracted from Chinook salmon carcasses (aged 2–4 years, 45–112 cm FL) collected in the 2001–2006 CDFW Carcass Surveys (Table 1). Unmarked fish were sampled randomly, but in earlier years, known-hatchery fish with CWTs and clipped adipose fins ("adclipped") were preferentially sampled to assess the accuracy of age estimations. We utilized all otoliths collected from all unmarked fish, but included a subset of CWT fish from outmigration year 2000 ($n = 27$), which we analyzed blind to assess the accuracy of our natal assignments. Ages were estimated by counting scale annuli [45,46]. Each scale was aged by at least two independent readers and discrepancies resolved by additional reading(s).

Table 1. Adult sample sizes, age structure and collection periods.

Age	Outmigration cohort 2000 (wetter)			Outmigration cohort 2003 (drier)		
	N	%	Collection period	N	%	Collection period
2	6	7%	11/20/01–12/06/01	2	2%	11/08/04–11/12/04
3	80	87%	10/07/02–12/12/02	56	67%	11/02/05–12/15/05
4	6	7%	11/12/03–12/04/03	25	30%	11/15/06–12/06/06

Otoliths were analyzed from salmon carcasses belonging to adults that had outmigrated in 2000 and 2003, including 27 known-origin fish included as a blind test of our natal assignments.

doi:10.1371/journal.pone.0122380.t001

Otolith $^{87}\text{Sr}/^{86}\text{Sr}$ analyses

Otolith strontium isotope ratios ($^{87}\text{Sr}/^{86}\text{Sr}$) were measured along a standardized 90° transect [47] by multiple collection laser ablation inductively coupled plasma mass spectrometry (MC-LA-ICPMS; Nu plasma HR interfaced with a New Wave Research Nd:YAG 213 nm laser). Spot analyses were used to allow coupling of chemical data with discrete microstructural features, but otherwise preparation and analysis methods followed those of Barnett-Johnson et al. [32,48]. In brief, otoliths were rinsed 2–3 times with deionized water and cleaned of adhering tissue. Once dry, otoliths were mounted in Crystalbond resin and polished (600 grit, 1500 grit then 3 μm lapping film) until the primordia were exposed. Depending on sample thickness and instrument sensitivity, a 40–55 μm laser beam diameter was used with a pulse rate of 10–20 Hz, 3–7 J/cm^2 fluence, and a dwell time of 25–35 seconds, resulting in individual ablations roughly equivalent to 10–14 days of growth. Where individual ablations exhibited isotopic changes with depth (e.g. at habitat transition zones), only the start of the ablation was used (e.g. S1 Fig). Helium was used as the laser cell carrier gas (0.7–1.0 L/min) to improve sample transmission and was mixed with argon before reaching the plasma source. Krypton interference (^{86}Kr) was blank-subtracted by measuring background voltages for 30 s prior to each batch of analyses, and ^{87}Rb interferences were removed by monitoring ^{85}Rb . Isotope voltages were integrated over 0.2 s intervals then aggregated into 1 s blocks. Outliers ($>2\text{SD}$) were rejected. Marine carbonate standards ('UCD Vermeij Mollusk' and *O. tshawytscha* otoliths) were analyzed periodically to monitor instrument bias and drift, producing a mean mass-bias corrected $^{87}\text{Sr}/^{86}\text{Sr}$ ratio (normalized to $^{86}\text{Sr}/^{88}\text{Sr} = 0.1194$) within 1SD of the global marine value of 0.70918 (0.70922 ± 0.00008 2SD).

Strontium isotopes to reconstruct natal origin and size at outmigration

The baseline of natal $^{87}\text{Sr}/^{86}\text{Sr}$ signatures described in [32] was updated and expanded upon to increase sample sizes and among-year representation, resulting in an 'isoscape' that encompassed all major CCV sources, with many sampled across multiple years and hydrologic regimes. Linear discriminant function analysis (LDFA) was used to predict the natal origin of the sampled adult spawners, assuming equal prior probabilities for all sites (S1 Text). Differences in natal $^{87}\text{Sr}/^{86}\text{Sr}$ values were tested between years and sites (S1 Text, S1 Table and S2 Fig), and the performance of the LDFA was assessed using known-origin reference samples (S2 Table). Adults in this study were considered strays (not produced in the Stanislaus) when their natal $^{87}\text{Sr}/^{86}\text{Sr}$ were closer to other sources in the isoscape, and were excluded from further analysis.

For adults that had successfully returned to the Stanislaus, we monitored the change in $^{87}\text{Sr}/^{86}\text{Sr}$ across the otolith to identify the point at which they had outmigrated as juveniles. The Stanislaus has a significantly lower isotopic value (0.70660 ± 0.00008 SD) than the mainstem San Joaquin River immediately downstream from it (0.70716 ± 0.00013 SD), resulting in a clear increase and inflection point in otolith $^{87}\text{Sr}/^{86}\text{Sr}$ at natal exit (e.g. Fig 3B). If the inflection point was unclear, sequential spot analyses were analyzed by LDFA, and exit was defined as a >0.3 decrease in posterior probability of Stanislaus-assignment to a probability <0.5 . Deviation from the mean $^{87}\text{Sr}/^{86}\text{Sr}$ Stanislaus value was assumed to reflect considerable time spent in non-natal water, as (1) the Stanislaus $^{87}\text{Sr}/^{86}\text{Sr}$ signature shows minor variation in otoliths (S1 Table) and water samples collected immediately upstream of the confluence, (2) the RST location is 13.8 km upstream of the confluence (Fig 2) and (3) the length of time integrated by each laser spot is ~ 12 days. Therefore, the distance used to back-calculate exit size was from the otolith core to the last natal spot. To improve resolution and accuracy, additional ablations were performed around the transition zone, typically resulting in sub-weekly resolution.

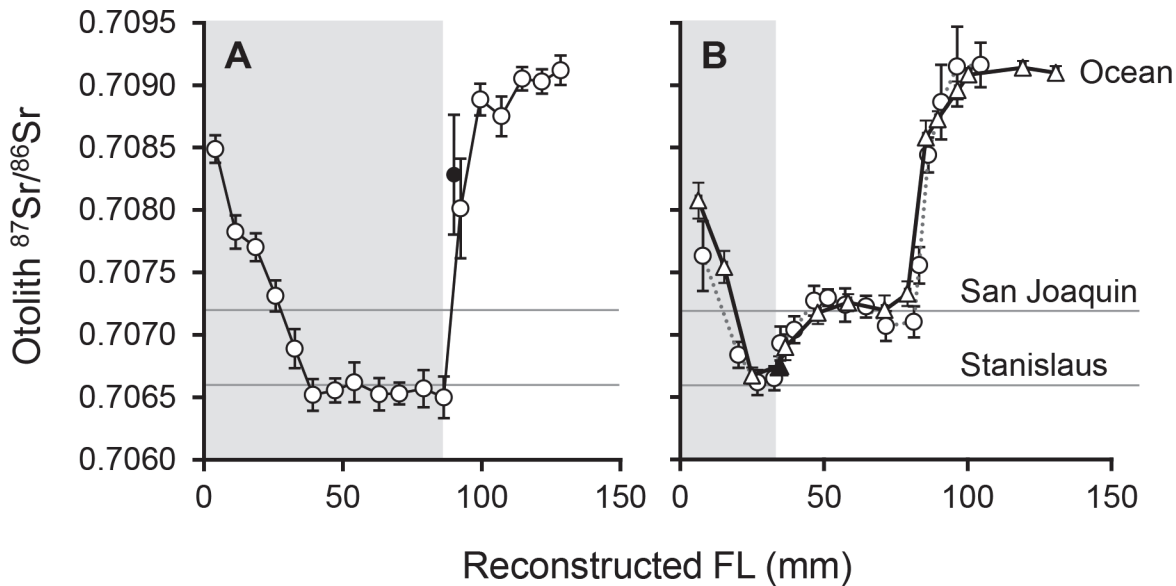


Fig 3. Otolith $^{87}\text{Sr}/^{86}\text{Sr}$ reconstructions of a smolt and fry outmigrant. Otolith $^{87}\text{Sr}/^{86}\text{Sr}$ profiles against back-calculated FL for two adult Chinook salmon that returned to the Stanislaus River having outmigrated as (A) a smolt and (B) a fry. The shaded box indicates the time spent rearing in the natal river. The fry outmigrant reared for several weeks downstream in the San Joaquin River before migrating out to the ocean, as indicated by both the left (triangles, solid line) and right (circles, dashed line) otolith (back-calculated FL = 33.3mm vs. 34.9mm). Mean $^{87}\text{Sr}/^{86}\text{Sr}$ signatures for the Stanislaus and San Joaquin Rivers, and modern-day ocean are displayed. Black filled symbols indicate 're-spots' carried out to improve sampling resolution. Error bars = 2SE.

doi:10.1371/journal.pone.0122380.g003

Reconstructed size at outmigration in the returning adults

The relationship between otolith radius (OR) and FL was first calibrated using juveniles collected from multiple sites in the CCV (S3 Table). All individuals belonged to the same Evolutionarily Significant Unit, which is critical for producing unbiased back-calculation models [49]. As there was no difference in the OR of paired otoliths from single individuals ($n = 30$, $\bar{x}\Delta = 2.5\mu\text{m}$, 95% CI = -5.6 – $10.6\mu\text{m}$), left and right otoliths were used interchangeably. OR was measured along the same 90° transect used for isotope analyses, using a Leica DM1000 microscope and Image Pro Plus (7.0.1).

Reconstructed sizes were grouped into 2mm FL bins and categorized as fry, parr or smolt outmigrants based on the criteria of [21]. Size-frequency distributions were compared between the juvenile and adult samples to identify trends indicative of size-selective mortality. The error around the OR-FL calibration line was used to estimate 95% CI around the proportions of fry, parr and smolt outmigrants using random resampling ($n = 5000$) of the residuals. This allowed us to derive the relative contribution of each phenotype to the adult spawning population.

Survival of juvenile migratory phenotypes

To generate survival indices, we normalized the contribution of each phenotype to the adult population by their abundance within each outmigration cohort based on RST sampling. To estimate spawner abundance ("natural escapement"), we removed adclipped strays from total escapement estimates (GrandTab, available at www.calfish.org) using river- and year-specific tag recovery rates (S4 Table), then separated cohorts using annual age distributions [50] and removed unmarked strays using our otolith natal assignments (see results and S4 Table). We evaluated the use of spawner abundance vs. "adult production" (after [51]). While production accounts for different harvest rates among years [52], the two metrics produced similar trends

in survival ($r^2 = 0.98$), and we found that escapement, which includes harvest, bycatch and natural mortality between outmigration and spawning, to be more intuitive to interpret.

The otolith-derived proportions ($\pm 95\%$ CI) of phenotype i in the escapement (β_i) were applied to our natural escapement estimates (E_n) to estimate the number of fry, parr and smolt spawners (E_i), then E_i was compared with the number of outmigrants of phenotype i (J_i) to estimate their relative survival (S_i):

$$E_i = E_n \beta_i \quad S_i = E_i / J_i$$

To estimate 95% CI for S_i we combined error in β_i and J_i using the delta method. The 95% CI for S_i depends on the estimate and its standard error (SE): \hat{S}_i , $SE(\hat{S}_i)$. Assuming independence of β_i and J_i , we estimated variance as $SE(\log(\hat{S}_i)) \cong \sqrt{(\frac{1}{J_i})^2 SE^2(\hat{J}_i) + (\frac{1}{\beta_i})^2 SE^2(\hat{\beta}_i)}$. From this, we derived 95% CI for S_i as $(e^{\log(\hat{S}_i) - 1.96 \times SE(\log(\hat{S}_i))}, e^{\log(\hat{S}_i) + 1.96 \times SE(\log(\hat{S}_i))})$. Note that uncertainties in adult escapement were not incorporated into these confidence intervals; however, the RST-expansions used to estimate J_i were deemed likely to introduce the largest amount of error.

Results

Juvenile outmigration relative to hydrologic regime

Mean flow and turbidity for the 6 month outmigration period were higher in 2000 than 2003 (DW-adjusted $F_{1, 361} = 7.52$, $p = 0.006$ and $F_{1, 257} = 14.53$, $p = 0.0002$, respectively) (Fig 4). In the drier year (2003) the river was warmer during the smolt migratory period (Apr 15-May 18: DW-adjusted $F_{1, 60} = 4.54$, $p = 0.037$) and peak daily temperatures first exceeded 15°C three weeks earlier (Fig 4).

Peak flows were about five times higher in 2000 than 2003, and accompanied by spikes in turbidity and juvenile migration (Fig 4). The number of outmigrants was an order of magnitude higher in 2000 (Table 2), reflecting significantly higher daily abundances of fry, parr and smolt outmigrants (DW adjusted $F_{1, 161} = 11.23$, $p < 0.001$; $F_{1, 196} = 47.99$, $p < 0.001$; $F_{1, 199} = 6.45$, $p = 0.0118$, respectively). While fry dominated in both years, phenotype contributions differed significantly between years ($X^2 = 223,683$, $p < 0.001$), with parr approximately twice as abundant as smolts in 2000, but vice versa in 2003 (Table 2). One yearling (FL = 140mm) was

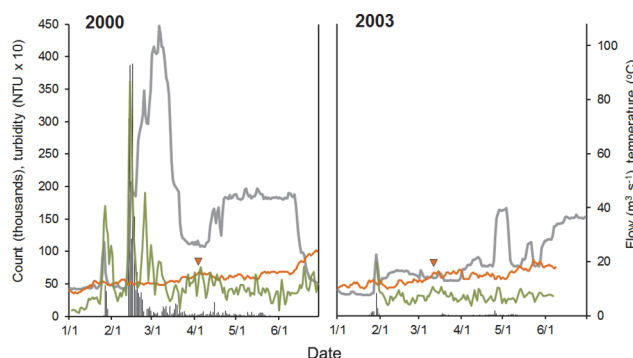


Fig 4. Daily abundance of juvenile salmon outmigrating in 2000 and 2003 relative to ambient environmental conditions. Juvenile salmon were sampled by rotary screw traps at Caswell as they outmigrated from the Stanislaus, and raw counts were expanded into daily abundance estimates (vertical bars) based on trap efficiency models. River flow (grey line) and maximum daily temperature (orange line) were measured at Ripon (data available at <http://cdec.water.ca.gov/>). Turbidity (green line) was measured at Caswell [40]. The first instance of temperatures reaching 15°C is indicated by an arrow on each plot.

doi:10.1371/journal.pone.0122380.g004

Table 2. Abundance and migration timing of juvenile migratory phenotypes.

Outmigration cohort	Migratory phenotype	N (95% CI)	Proportion of the sample	Duration of migratory period (range)	Duration of "peak" migratory period (interquartile range)	Peak migration date (median)
2000 (wetter)	Fry	1,837,656 (1,337,351– 2,495,523)	0.85	115 d (Jan 2–Apr 25)	4 d (Feb 14–Feb 17)	Feb 16
	Parr	212,042 (141,238– 310,174)	0.10	116 d (Feb 4–May 29)	29 d (Mar 18–Apr 15)	Apr 1
	Smolt	101,467 (70,181– 145,793)	0.05	110 d (Mar 8–Jun 25)	34 d (Apr 15–May 18)	May 9
	TOTAL	2,151,165 (1,577,638– 2,911,393)				
2003 (drier)	Fry	79,862 (59,795– 103,916)	0.50	80 d (Jan 23–Apr 12)	4 d (Jan 27–Jan 30)	Jan 29
	Parr	25,729 (17,889– 36,282)	0.16	118 d (Feb 5–June 2)	27 d (Mar 18–Apr 13)	Mar 21
	Smolt	55,465 (38,415– 76,289)	0.34	107 (Feb 24–Jun 10)	21 d (Apr 18–May 8)	Apr 25
	TOTAL	161,056 (119,868– 209,151)				

The abundance and proportions of fry, parr and smolt outmigrants sampled by rotary screw traps, and the timing of their outmigration from the Stanislaus River in 2000 and 2003.

doi:10.1371/journal.pone.0122380.t002

captured in the RST in 2000, but none in 2003, otherwise the size range of outmigrants was similar between years (25–115mm in 2000 vs. 27–115mm in 2003).

Phenology varied between phenotypes and years (Table 2 and Fig 5). In general, migratory windows were shorter and earlier in the drier year, with smolt outmigration ceasing 15 days earlier in 2003 than in 2000. The peak migratory periods were similar across years for fry and parr, the former exhibiting a compressed interquartile range (4 d) that was tightly correlated with the start of winter flow pulses (Fig 5).

Natal origin of unmarked adults

The unmarked adults from outmigration cohorts 2000 and 2003 comprised 18% and 51% hatchery strays, respectively, primarily from the Mokelumne, Merced, and Feather River

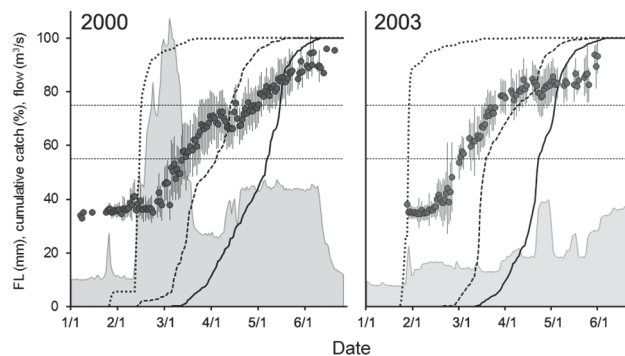


Fig 5. Size and phenology of juveniles outmigrants relative to river flow in 2000 and 2003. Mean (\pm SD) daily fork length (FL) of juveniles outmigrants, and cumulative percentage of fry (short dashed line), parr (long dashed line) and smolt (solid line) outmigrants relative to flow (filled area). Reference lines indicate the size categories used to define the migratory phenotypes: fry (\leq 55mm), parr (55–75mm) and smolts ($>$ 75mm).

doi:10.1371/journal.pone.0122380.g005

Table 3. Natal assignments of unmarked adults based on otolith $^{87}\text{Sr}/^{86}\text{Sr}$.

Natal source	Outmigration cohort 2000 (%)	Outmigration cohort 2003 (%)
Stanislaus River	82	49
Mokelumne River Hatchery	11	39
Merced River Hatchery	2	1
Feather River Hatchery	5	7
Nimbus Hatchery	2	2
Thermalito Rearing Annex ^a		1

Natal assignments of unmarked adults fish captured in the Stanislaus River between 2001 and 2006 that outmigrated in 2000 and 2003.

^a Part of the Feather River Hatchery

doi:10.1371/journal.pone.0122380.t003

Hatcheries (Table 3). These individuals were removed from subsequent analyses, ensuring that size back-calculations were calculated only for Stanislaus-origin fish that had experienced the same outmigration conditions as the RST-sampled juveniles.

Back-calculation of size at outmigration

A strong, positive relationship was observed between OR and FL ($r^2 = 0.92$, $n = 224$, $p < 0.001$; $\text{FL} = 0.171 (\pm 0.003 \text{ SE}) \times \text{OR} - 12.76 (\pm 1.54 \text{ SE})$), remaining linear across the full range of FLs reconstructed in the current study. This relationship was used to reconstruct FLs for individual $^{87}\text{Sr}/^{86}\text{Sr}$ profiles (e.g. Fig 3). The back-calculated size at which returning adults had outmigrated from the Stanislaus ranged from 31.3mm to 86.6mm in 2000, and 46.0mm to 90.5mm in 2003 (Fig 6). No yearlings were detected in the adult returns in either year.

To explore reproducibility of the method, paired left and right otoliths were analyzed from a subset of adults ($n = 3$ fry and $n = 1$ smolt outmigrant). All fish were assigned to the same migratory phenotype using either otolith, and the mean difference between back-calculated FLs was 2.3mm (e.g. Fig 3B).

Contribution and survival of juvenile migratory phenotypes

The relative abundance of the migratory phenotypes in the escapement differed significantly to the outmigrating juvenile population in both 2000 ($X^2 = 20,931$, $p < 0.0001$) and 2003 ($X^2 = 1,381$, $p < 0.0001$). The phenotype composition of the adult population also differed significantly between years ($X^2 = 749$, $p < 0.0001$), reflecting higher fry contributions in the wetter year (23% in 2000 vs. 10% in 2003) and higher smolt contributions in the drier year (44% in 2003 vs. 13% in 2000). Despite representing only 10–16% of the outmigrating juveniles (Table 2), parr were the most commonly observed phenotype in the surviving adult populations (46–64%, Table 4), although parr and smolt contributions to the escapement were near-identical in 2003 (46% vs. 44%, respectively). Conversely, fry outmigrants represented 10–23% of the adult escapement, despite representing 50–85% of the juvenile sample (Tables 2 & 4). The lowest survival was observed in individuals $< 45\text{mm}$, particularly in 2003, when the smallest outmigrant in the adult sample had left the river at 46mm FL, while the smallest individual captured in the RST was 27mm FL (Fig 6). Conversely, in 2000, 11% of the adults had left at FLs $\leq 46\text{mm}$ (the smallest at 31.3mm), compared with 80% of the original juvenile population (the smallest at 25mm; Fig 6).

In both years, fry survival downstream of the Stanislaus (S_{fry}) was significantly lower than parr or smolt survival ($p < 0.05$). S_{parr} was approximately double S_{smolt} in both years, but the confidence intervals were overlapping (Table 4). Generally, outmigrant survival downstream of

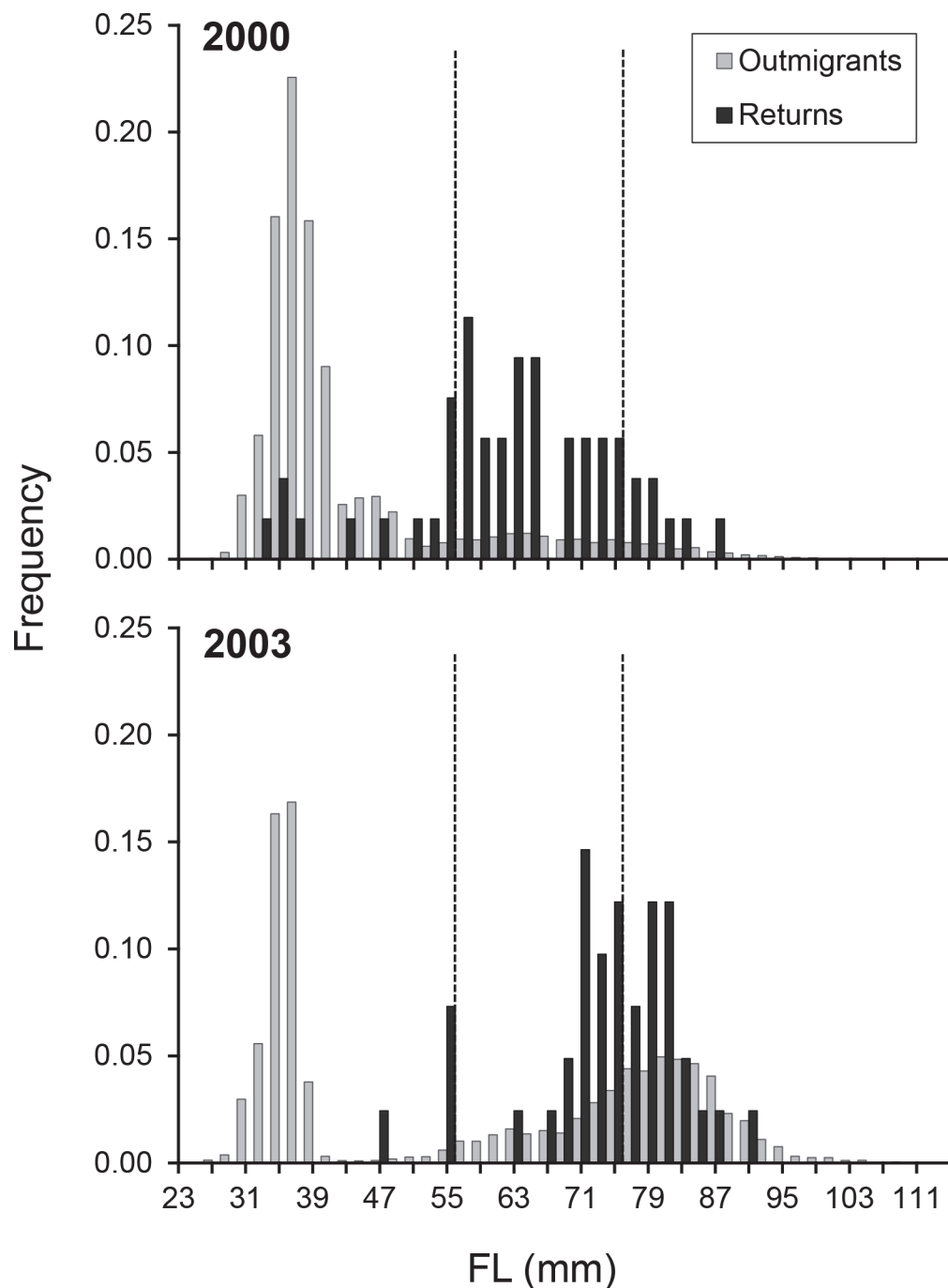


Fig 6. Size-at-outmigration of the juveniles and surviving adults that left freshwater in 2000 and 2003. Size-frequency distributions showing the fork length (FL) at which juveniles outmigrated from the Stanislaus River in 2000 and 2003 (grey bars) and the reconstructed size-at-outmigration of the returning (i.e. “successful”) adults from the same cohort (black bars). FLs given in 2mm bins (where the x-axis represents \leq that value, e.g. “55” = FL 53.01–55.0mm). Size classes used to categorize fry, parr and smolt outmigrants are indicated by dashed lines.

doi:10.1371/journal.pone.0122380.g006

the Stanislaus was slightly higher in the drier year (2003) than the wetter year (2000), but significant differences were not detected ([Table 4](#)).

Table 4. Contribution and survival of fry, parr and smolt outmigrants to the adult escapement.

Outmigration cohort	Phenotype	Contribution to the adult escapement (%) ^a	No. spawners produced ^a	Survival (%) ^b
2000 (wetter)	Fry	23 (19–36)	1,334 (1112–2113)	0.07 (0.04–0.12)
	Parr	64 (43–66)	3,781 (2557–3892)	1.78 (1.15–2.76)
	Smolt	13 (9.4–25)	778 (556–1446)	0.77 (0.39–1.52)
2003 (drier)	Fry	10 (2.4–12)	148 (37–186)	0.19 (0.1–0.33)
	Parr	46 (34–61)	705 (520–928)	2.74 (1.73–4.34)
	Smolt	44 (34–59)	668 (520–891)	1.2 (0.78–1.87)

^a 95% CI in parentheses, derived from error around the FL back-calculation model.

^b 95% CI in parentheses, derived from error around the FL back-calculation and RST efficiency models

doi:10.1371/journal.pone.0122380.t004

Discussion

In this study we document the expression of juvenile salmon migratory phenotypes under two contrasting flow regimes and provide new insights into their contribution to the adult spawning population and ultimate survival. We observed variable expression and survivorship of fry, parr and smolt life histories within and between years, yet all three phenotypes consistently contributed to the adult spawning population. This result challenges the common perception in the CCV, that smolt outmigrants are the dominant phenotype driving adult population abundance. Our key findings in the context of the salmon life cycle in order to link the datasets, methods, and processes examined in the study (Fig 7). Overall, the wetter year (2000) was characterized by higher numbers of juvenile outmigrants and adult returns, despite fewer adult spawners contributing to the cohort the previous fall. Using the number of parental spawners as a coarse proxy for juvenile production, these trends suggest higher in-river mortality in the drier year (2003). Given similar downstream (outmigration-to-return) survival rates, these data suggest that for the two focus years of the study, cohort strength was primarily determined within the natal river, prior to juvenile outmigration.

Juvenile outmigration behavior and phenotype expression

Juvenile outmigration timing in salmonids is inextricably linked to large-scale patterns in hydroclimatic regime and local-scale patterns in the magnitude, variation, and timing of flows [14,42]. In the Stanislaus, increases in flow were accompanied by pulses of outmigrants in both years, though greatly amplified during the turbid storm events of 2000. Correlations between fry migration, flow, and turbidity are commonly reported in the literature [14,53,54], and are suggested to have evolved as a result of reduced predation from visual piscivores [14,27,55,56]. The peak in migration in late January 2003 contained 85% of the year's total fry outmigrants and coincided with a managed water release that resulted in mean river flows of 28.4 m³ s⁻¹ [57]. This pulse flow appeared to stimulate fry migration, but comprised relatively clear water (~8 NTU) and contained outmigrants almost entirely <40mm FL (Fig 5). In both years, the larger parr- and smolt-sized fish also appeared to respond to instream flows, exhibiting smaller migration pulses from March through May, coincident with both natural and managed flows (Fig 4) [58,59].

The date and periods of peak migration were generally earlier and shorter in 2003, particularly for smolts. While warmer conditions can result in faster growth rates [60], smoltification in juvenile Chinook salmon is significantly impaired at temperatures above 15°C [61] and this critical temperature was reached at Ripon three weeks earlier in 2003, prior to the onset of peak parr migration. As the reduction in juvenile abundance in 2003 occurred in spite of greater

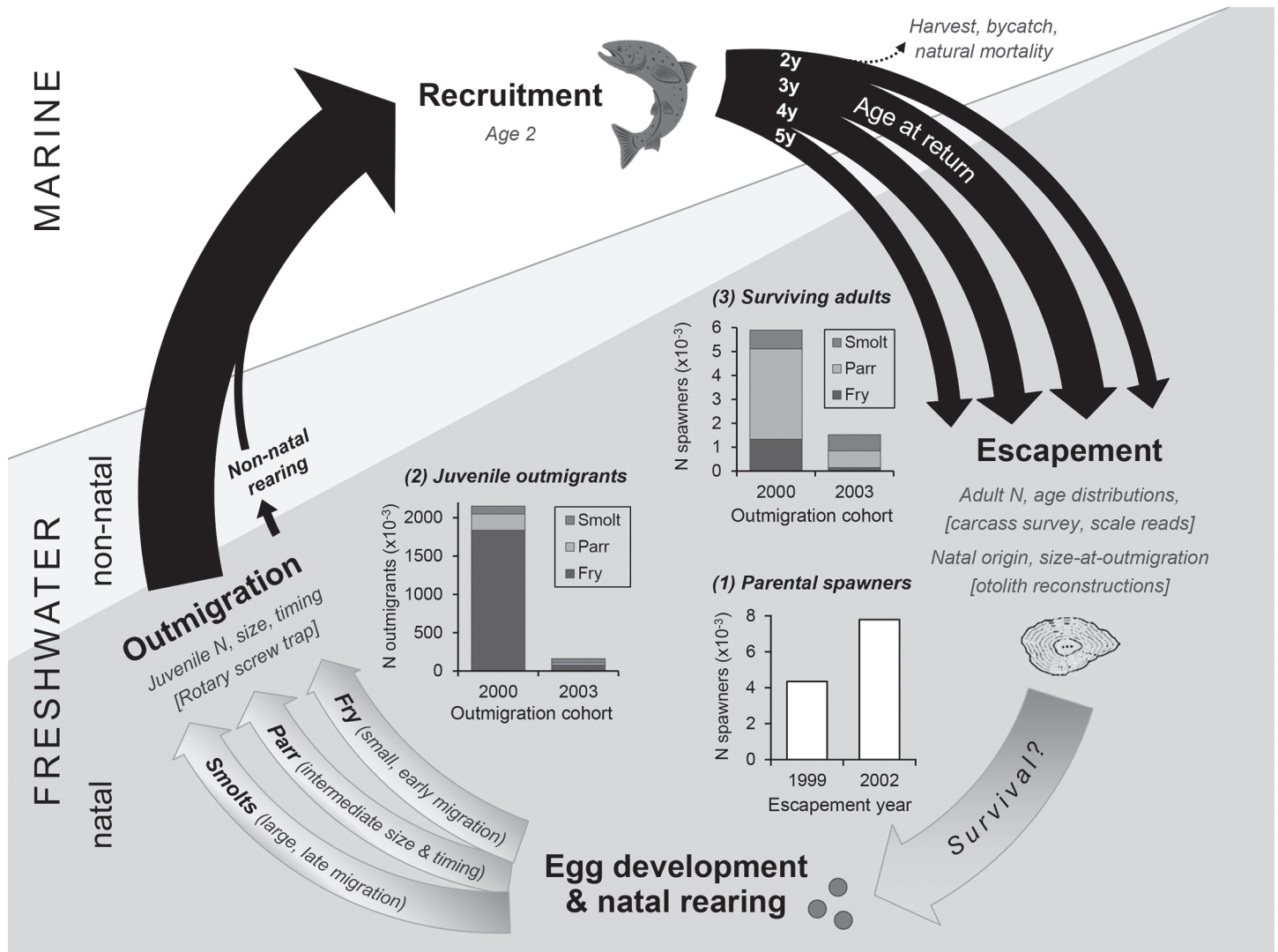


Fig 7. Schematic to conceptualize the data sources, methods and results presented in this study. This figure outlines the life cycle of fall-run Chinook salmon in the California Central Valley. Inset plot (1) demonstrates the abundance of parental spawners in the 1999 and 2002 escapement that contributed to the two focus years. Inset plots (2) and (3) illustrate the abundance and proportions of migratory phenotypes (fry, parr and smolts) observed in the juvenile sample (based on RST sampling) and in the adult escapement (based on otolith reconstructions), respectively. Arrow widths (not to scale) illustrate the typical proportions of 2, 3, 4 and 5 year olds observed in the adult escapement; note that age 5 fish tend to comprise <1% of the returns [50].

doi:10.1371/journal.pone.0122380.g007

numbers of parental spawners (Fig 7), we hypothesize that the truncation of migratory periods was driven by in-river mortality rather than altered migration timing or faster transitions between size classes. Juveniles tend to encounter less floodplain habitat, and increased predation rates and physiological stress in warmer, drier years [62], which likely resulted in a lower carrying capacity in the natal tributary [63] and increased density dependent mortality [64,65].

Survival of migratory phenotypes

Although lower flows and warmer temperatures in the Stanislaus may have contributed to the lower outmigrant production observed in 2003, our results suggest that after exiting the natal river, there was no significant difference in juvenile survival. Survival rates were, if anything, marginally higher in 2003, contradicting many tagging studies which find reduced salmon

survival through the freshwater delta during low flow conditions [24,66–68]. This discrepancy is likely due to differences in the sampling design and the time period represented by the different indices. Tagging studies generally release larger hatchery fish in similar sized batches during the later months of the outmigration season, when warmer conditions likely increase their vulnerability to predation [62]. Conversely, our survival estimates were based on variable numbers of fish over a larger size spectrum and broader migratory window, incorporating mortality events in all habitats downstream of the natal river, including the mainstem river, delta, estuary and ocean. However, we assume that differences in our survival indices would be driven by selective mortality events occurring during outmigration and early ocean residence. In support of this, there was no relationship between back-calculated size at outmigration and return FL ($r^2 < 0.01$, $p > 0.05$), implying that size-selective mortality did not vary by phenotype in the adult fish. However, marine distributions of adult salmon can be non-random [69], and if driven by timing at ocean entry, the migratory phenotypes could have been subjected to different ocean processes and mortality rates even as adults.

Parr and smolt outmigrants. Life history theory predicts selection to favor different phenotypes under different hydrologic regimes, maintaining behavioral and phenotypic diversity [70]. Yet in the current study, parr consistently exhibited the greatest contribution to the adult population and the highest survival rates. Greater representation of intermediary-sized juveniles has also been observed in some years in the ocean fisheries of Chinook [21] and Atlantic salmon [22], contradicting the expected directionality of size-selective mortality. Generally, larger or faster-growing individuals within a population are thought to have a selective advantage as a result of greater feeding opportunities, lower vulnerability to predation and greater tolerance of environmental perturbations [71]. However, the strength of size-selection in juvenile CCV Chinook salmon can vary as a function of ocean productivity [18], highlighting the importance of maintaining life history diversity in outmigration strategies. Without large-scale field experiments, it is not possible to definitively ascertain why smolts were not the most successful phenotype, however the San Joaquin basin is at the southernmost reaches of the species distribution [3] and its salmon populations are exposed to high temperatures, poor water quality, and significant water diversions [72,73]. This frequently results in river conditions that could impair growth and smoltification, and increased vulnerability to predation and disease [62], particularly at the end of the season when smolt-sized fish are most prevalent. Thus, the survival advantage of parr is likely attributable to both size and migration timing, analogous to the marine-orientated “critical size and period hypothesis” proposed by Beamish and Mahnken [74]. Furthermore, current flow practices in the San Joaquin basin include managed releases in April and May, intended to improve the survival of smolts [75]. These managed flows typically occur after most parr have left their natal tributaries, potentially selecting for this phenotype by providing downstream benefits as they migrate through (or rear in) the San Joaquin River and freshwater Delta.

Fry outmigrants. Little is known about the factors driving fry behavior or survival, yet the numbers that outmigrated during the wetter year (2000) were orders of magnitude higher, when they also contributed more than double the number of adult survivors (23% in 2000 vs. 10% in 2003). While fry consistently exhibited lower survival rates than their conspecifics (Table 4), reflecting the typical direction for size-selective mortality [71], the fact that any survived to contribute to the adult population, let alone contributing >20% of the adult returns, is a significant finding. Based on these data, their sheer abundance during high flow conditions at least partially helps to explain the increases in returns following wet outmigration conditions in the San Joaquin watershed (Fig 1). Early-migrating fry and parr may represent a significant portion of the population that can access favorable downstream rearing habitats in high flow years and survive to contribute to the adult population. Indeed, our otolith reconstructions

indicated that all of the smallest (≤ 46 mm FL) fry outmigrants in the surviving adult population ($n = 4$ in 2000, $n = 1$ in 2003) had spent several weeks rearing in the San Joaquin mainstem prior to leaving freshwater (e.g. Fig 3B). These data corroborate the extended transit times of CWT-tagged fish released in the San Joaquin basin and freshwater Delta in wetter years (averages of 16 d in 2000 vs. 6 d in 2003), although their mean size also differed (81mm vs. 87mm, respectively) [58]. Fry are observed in downstream freshwater and estuarine habitats in the CCV [20,76], and were probably more common when the Delta was a large tidal wetland [14,24,53]. This study confirms that these individuals can survive and contribute meaningfully to adult returns.

Currently there are no genetic data to support or refute a heritable component to early out-migration behavior, but it could otherwise meet the criteria of an adaptive trait, given that its expression is associated with “differential survival” and there is evidence for “a mechanism of selection” [77]. There is still some debate as to whether fry pulses during high flow events represent displacement due to reduced swimming ability or a deliberate behavior that might be considered a ‘strategy’ [3,14]. While catastrophic floods undoubtedly result in riverbed scouring and some fry displacement, not all individuals outmigrate during these events. Conversely, some fry migration is observed during periods with no pulse flows [78]. Given the frequency with which this phenotype is reported and the considerable rearing potential of downstream habitats, it is conceivable that fry dispersal is a heritable strategy, representing a ‘migratory contingent’ within the population [79,80]. Indeed, their consistent contribution to the adult population (observed here and in [21]) conclusively demonstrates that fry migration can be successful. If, however, early outmigration is purely an expression of phenotypic plasticity, it is likely that multiple factors are involved in stimulating the behavioral switch, including hydrology, intraspecific interactions [3] and density dependent mechanisms [65,81–83]. Irrespective of the underlying mechanisms, quantifying the relative success of migratory phenotypes across a broader range of hydrologic regimes is fundamental to understanding how environmental conditions and water operations contribute to salmon population dynamics.

Otolith strontium isotopes and sources of uncertainty

One of the most significant advances of the current study was the pairing of RST sampling with otolith reconstructions. This process enabled us to compare fish size at a specific time and location across life stages, and provided a unique method for generating survival estimates into adulthood. CWT studies and acoustic telemetry have provided valuable insights into survival through particular stretches of the CCV [25,75], but tend to focus on larger fish and provide no information about the long-term success of particular traits. In addition, acoustic tags have focused on understanding flow-survival relationships for smolts, which are physiologically ready for seaward migration and likely use the mainstem rivers, delta, and estuary differently than fry or parr, which may exhibit prolonged rearing. Otolith $^{87}\text{Sr}/^{86}\text{Sr}$ ratios are an ideal natural tag as they vary among many of the rivers in the CCV, resulting in high classification scores for natal assignments (S1 and S2 Tables) [30,32,84]. Sr isotopes also represent a unique and sensitive marker for reconstructing downstream movements and non-natal rearing patterns in the freshwater system (e.g. Fig 3B). While seasonal variation in $^{87}\text{Sr}/^{86}\text{Sr}$ values have been reported in certain systems [85] and interannual variations were detected for some sites (S1 Table), these were minor compared with most of the geographic differences, with the majority of sites exhibiting classification scores $>70\%$ even when pooled across years (S2 Table). Importantly, the Stanislaus exhibited a stable and distinct isotopic signature; with 96% of juveniles correctly classified using jack-knife resampling (S2 Table). Identification of natal origin represents a significant advantage of using otolith Sr isotopes over element concentrations. This was critical

for pairing RST- and otolith-derived datasets and providing confidence that our size reconstructions were not skewed by hatchery smolts.

A high occurrence of straying of fall-run Chinook salmon occurs between the San Joaquin and Sacramento basins [86–88], potentially due to the relative outflows during the return migration as well as hatchery release practices [89]. However the extent to which hatchery fish are functioning to sustain the San Joaquin salmon populations has gone largely undetected until recently [86,87]. In the current study, hatchery strays represented 18–51% of the unmarked fish, reducing the number of samples available to inform outmigration strategies of wild fish and increasing analytical costs. However, the removal of strays was vital to ensure that FL reconstructions were only performed on individuals that had experienced the same conditions as the RST-sampled juveniles. The implementation of 100% visual identification of hatchery fish [90] would increase the feasibility and efficiency of future life history diversity studies in this system.

We attempted to reduce and account for sources of uncertainty, but the low number of focus years and sample sizes, and the potential for error propagation limit the strength of our inferences. With greater representation of 2 and 4 year olds in our adult sample, a more sophisticated analysis using age-specific natal assignments could have been carried out. While no yearlings were detected in the surviving adults, their rarity in the RST-sampled outmigrant population indicate that larger sample sizes would be required to ascertain the success of this strategy with any confidence. Similarly, our approach for assigning natal origin based on otolith chemistry following yolk sac absorption means that individuals that outmigrated as yolk sac fry could have been misclassified as strays. However, yolk sac fry are rarely observed in the outmigrant population (0.1% of the 2001–2011 RST catch at Caswell), so this was deemed unlikely to significantly influence our results.

Management implications

The complex biophysical properties of freshwater systems have led to the evolution of dynamic habitat mosaics [91] and diverse salmon life histories and distributions. The observed life history diversity likely provides within-population buffering, an as yet understudied component of the portfolio effect [5,6]. These data add to the mounting evidence that managing and conserving life history diversity is necessary to support resilient salmon populations, particularly in the face of climate change and projected human population growth [9,10]. Diversity in phenotypic traits is thought to produce a more stable population complex by decoupling population dynamics and buffering variance [6]. However, population resilience does not necessarily immediately translate into population abundance. In a highly regulated system such as the CCV, there is debate as to whether environmental unpredictability dictates a need to manage salmon stocks for diversity and resilience, or whether our understanding of (and control over) the relevant processes is sufficient to manage purely for abundance. Such topics are complicated by socio-economic and ecological trade-offs, however, by improving our understanding of how juvenile life history strategies are expressed and respond to different flow regimes, we may be able to optimize both. Currently, the portfolio effect for CCV salmon stocks is weak and deteriorating [92] and San Joaquin populations face serious future challenges, given predicted 25–40% reductions in snowmelt by 2050 [93]. CCV salmon exhibit diverse outmigration timings that have evolved over geological time scales in response to the unpredictable hydroclimatic conditions characteristic of the region [11]. Yet modern-day water and hatchery management practices tend to constrain outmigration timing. For example, alterations to the natural hydrograph, such as suppression of winter pulse flows, likely to truncate migratory windows, reduce the variability in outmigration timing, and significantly suppress the fry life history type. Such

simplification and truncation of life history diversity could significantly reduce the resiliency of the stock-complex and exacerbate the risk of a temporal mismatch with favorable ocean conditions [94]. Indeed, the only clear deviation from the flow-driven relationship in Fig 1 was attributed to juveniles entering the ocean during a suboptimal period and resulted in the closure of the fishery in 2008. Perhaps with more diverse, resilient stocks, the consequences would have been less extreme. Largely without direct empirical support, hatchery and flow management practices tend to focus on optimizing the success of the largest, smolt-sized juveniles that are assumed to contribute the most to adult returns [14,21,24]. Here, we found that all phenotypes contributed to the reproductive adult population, with smolts comprising less than half of the surviving adults following two contrasting flow regimes. Without otolith reconstruction data for additional years, species, and watersheds, the broader inferences one can make regarding the influence of hydroclimatic regime on juvenile salmon survival are limited. However our data and a previous study [21] indicate that assumptions regarding size-selective mortality and smolt-focused management schemes need to be tested on a species, system and hydroclimatic basis.

This study has demonstrated the value of a combined RST and otolith geochemistry study to reconstruct patterns in the expression and survival of salmon migratory phenotypes. The results show that under paired years of low and high flow conditions, parr outmigrants comprised a significant portion of the returning adult population, while fry made smaller, but substantial contributions. Future efforts should focus on reducing the error in juvenile production estimates in order to produce more meaningful survival estimates, and understanding the demographic role that fry and parr play in salmon population dynamics. Management actions that promoted the expression and survival of fry in natal and downstream rearing habitats could result in demographic and genetic benefits to the population. Recognition of the importance of hydrodynamic regime and life history diversity should provide guidance to system managers when reassessing goals and future management strategies [5,95]. It is also important that management actions consider carefully-designed monitoring programs to detect changes in stock abundance and life history diversity at appropriate temporal and spatial scales.

Supporting Information

S1 Text. Testing the performance of the Sr isotope.

(DOCX)

S1 Fig. Time-resolved plot of a single spot ablation at a habitat transition. This plot (macro developed by C. Donohoe) shows how the isotopic composition of the otolith can change with sample depth (equivalent to analysis time). Typically we would use ~20 seconds of data per spot (A), but in cases like this we would use only the surface material (B) to avoid signal attenuation and to ensure consistency between otolith $^{87}\text{Sr}/^{86}\text{Sr}$, microstructure and distance analyses.

(DOCX)

S2 Fig. Median $^{87}\text{Sr}/^{86}\text{Sr}$ natal values for major sources of Chinook salmon in the California Central Valley. Values are based on juvenile otoliths and/or water samples. The mainstem San Joaquin River (SJR) isotopic signature is displayed, but was not included as a potential natal source. Boxes represent 25-75th percentiles, whiskers represent 5-95th percentiles. Site codes are defined in S1 Table. Isotopic signatures not significantly different ($p > 0.05$, Tukey's test) are joined by brackets. Mean ocean $^{87}\text{Sr}/^{86}\text{Sr}$ is indicated by a dashed line.

(TIF)

S1 Table. $^{87}\text{Sr}/^{86}\text{Sr}$ isoscape used to train the LDA and assign unknown adult otoliths to natal location. Data based on known-origin otolith (O) and/or water (W) samples. Interannual differences were tested by ANOVA or Welch's Test when data exhibited unequal variance. Differences among sites are shown in [S2 Fig](#) Underlined years represent water samples collected Oct 1997 to Apr 1998 that were pooled into a single water year (1998). (DOCX)

S2 Table. Natal assignments and correct classification scores of known-origin samples. Assignments based on $^{87}\text{Sr}/^{86}\text{Sr}$ values and jackknife resampling. Site codes are defined in [S1 Table](#). Equal prior probabilities were given to all sites and sites are ordered by increasing mean $^{87}\text{Sr}/^{86}\text{Sr}$ value. The training dataset ($n = 290$) comprised both juvenile otoliths and water samples. Counts are for actual rows by predicted columns. Samples from the Stanislaus River (STA) are highlighted in bold, while groups of sites with statistically overlapping $^{87}\text{Sr}/^{86}\text{Sr}$ signatures ($p > 0.05$, Tukey's test) are shown in italics and [S2 Fig](#) (DOCX)

S3 Table. Reference samples used to calibrate the fork length back-calculation model. (DOCX)

S4 Table. The number of adult spawners produced by the 2000 and 2003 outmigration cohorts ("natural escapement") (DOCX)

Acknowledgments

This study was prepared by AMS under USBR Agreement R09AC20043. Work at LLNL was performed under the auspices of the U.S. Department of Energy, Contract DE-AC52-07NA27344. The statements, findings, conclusions, and recommendations are those of the author(s) and do not necessarily reflect the views of the Bureau of Reclamation (USBR), US Fish & Wildlife Service, California Department of Fish and Wildlife (CDFW), or the US Department of the Interior. We are grateful to the staff at CDFW who collected the otoliths and read the scales, particularly C. Sinclair and G. Murphy. We are also grateful to everyone who provided juvenile otoliths, particularly C. Watry. We thank Doug Threlhoff and all the staff at Cramer Fish Sciences who have operated the Caswell RST for so many years and provided one of the most robust time-series of juvenile production in the Central Valley. Special thanks to Elizabeth Vasquez and Patricia Clinton (USBR) for their continued support of this project. We thank S. Carlson and S. Nusslé (UC Berkeley) for their insightful comments on the manuscript and statistics, respectively, C. Donohoe (UC Santa Cruz) for the use of his excellent macro, and F. Loge and M. Miller for providing laboratory space and use of equipment at UC Davis.

Author Contributions

Conceived and designed the experiments: RCJ JDW. Performed the experiments: AMS RCJ TH JJG PKW GEW. Analyzed the data: AMS RCJ TMH AEH CM. Contributed reagents/materials/analysis tools: TH. Wrote the paper: AMS RCJ.

References

1. Hanski I (1998) Metapopulation dynamics. *Nature* 396: 41–49.
2. Montgomery DR (2000) Coevolution of the Pacific salmon and Pacific Rim topography. *Geology* 28: 1107–1110.
3. Healey MC (1991) Life history of chinook salmon (*Oncorhynchus tshawytscha*). In: Groot C, Margolis L, editors. *Pacific salmon life histories*. Vancouver: UBC Press. pp. 311–394.

4. Yoshiyama RM, Gerstung ER, Fisher FW, Moyle PB (2001) Historical and Present Distribution of Chinook Salmon in the Central Valley Drainage of California. In: Brown RL, editor. Contributions to the biology of Central Valley salmonids, Vol 1 Fish Bulletin No 179. Sacramento. pp. 71–176.
5. Hilborn R, Quinn TP, Schindler DE, Rogers DE (2003) Biocomplexity and fisheries sustainability. Proceedings of the National Academy of Sciences 100: 6564–6568. PMID: [12743372](#)
6. Schindler DE, Hilborn R, Chasco B, Boatright CP, Quinn TP, Rogers LA, et al. (2010) Population diversity and the portfolio effect in an exploited species. Nature 465: 609–612. doi: [10.1038/nature09060](#) PMID: [20520713](#)
7. Greene CM, Hall JE, Guilbault KR, Quinn TP (2010) Improved viability of populations with diverse life-history portfolios. Biology Letters 6: 382–386. doi: [10.1098/rsbl.2009.0780](#) PMID: [20007162](#)
8. Bolnick DI, Amarasekare P, Araújo MS, Bürger R, Levine JM, Novak M, et al. (2011) Why intraspecific trait variation matters in community ecology. Trends in Ecology & Evolution 26: 183–192.
9. Ruckelshaus MH, Levin P, Johnson JB, Kareiva PM (2002) The Pacific Salmon Wars: What Science Brings to the Challenge of Recovering Species. Annual Review of Ecology and Systematics 33: 665–706.
10. Beechie T, Buhle E, Ruckelshaus M, Fullerton A, Holsinger L (2006) Hydrologic regime and the conservation of salmon life history diversity. Biological Conservation 130: 560–572.
11. Spence BC, Hall JD (2010) Spatiotemporal patterns in migration timing of coho salmon (*Oncorhynchus kisutch*) smolts in North America. Canadian Journal of Fisheries and Aquatic Sciences 67: 1316–1334.
12. Moyle PB (1994) The Decline of Anadromous Fishes in California. Conservation Biology 8: 869–870.
13. Jager HI, Rose KA (2003) Designing Optimal Flow Patterns for Fall Chinook Salmon in a Central Valley, California, River. North American Journal of Fisheries Management 23: 1–21.
14. Williams JG (2006) Central Valley Salmon: A Perspective on Chinook and Steelhead in the Central Valley of California. San Francisco Estuary and Watershed Science 4.
15. Wells BK, Grimes CB, Waldvogel JB (2007) Quantifying the effects of wind, upwelling, curl, sea surface temperature and sea level height on growth and maturation of a California Chinook salmon (*Oncorhynchus tshawytscha*) population. Fisheries Oceanography 16: 363–382.
16. Yoshiyama RM, Fisher FW, Moyle PB (1998) Historical Abundance and Decline of Chinook Salmon in the Central Valley Region of California. North American Journal of Fisheries Management 18: 487–521.
17. Reisenbichler RR, McIntyre JD, Hallock RJ (1982) Relation between size of chinook salmon, *Oncorhynchus tshawytscha*, released at hatcheries and returns to hatcheries and ocean fisheries 57–59 p.
18. Woodson LE, Wells BK, Johnson RC, Weber PK, MacFarlane RB, Whitman GE (2013) Using size, growth rate and rearing origin to evaluate selective mortality of juvenile Chinook salmon *Oncorhynchus tshawytscha* across years of varying ocean productivity. Marine Ecology Progress Series 487: 163–175.
19. MacFarlane RB, Norton EC (2002) Physiological ecology of juvenile chinook salmon (*Oncorhynchus tshawytscha*) at the southern end of their distribution, the San Francisco Estuary and Gulf of the Farallones, California. Fishery Bulletin 100: 244–257.
20. Kjelson M, Raquel P, Fisher F (1982) Life-history of fall run Chinook salmon, *Oncorhynchus tshawytscha*, in the Sacramento-San Joaquin estuary, California. In: Kennedy VS, editor. Estuarine Comparisons. New York, NY: Academic Press. pp. 393–411.
21. Miller JA, Gray A, Merz J (2010) Quantifying the contribution of juvenile migratory phenotypes in a population of Chinook salmon *Oncorhynchus tshawytscha*. Marine Ecology Progress Series 408: 227–240.
22. Ewing RD, Ewing GS (2002) Bimodal length distributions of cultured chinook salmon and the relationship of length modes to adult survival. Aquaculture 209: 139–155.
23. Good SP, Dodson JJ, Meekan MG, Ryan DA (2001) Annual variation in size-selective mortality of Atlantic salmon (*Salmo salar*) fry. Canadian Journal of Fisheries and Aquatic Sciences 58: 1187–1195.
24. Brandes P, McLain J (2001) Juvenile chinook salmon abundance, distribution, and survival in the Sacramento-San Joaquin estuary. In: Brown RL, editor. Contributions to the biology of Central Valley salmonids, Vol 2 Fish Bulletin No 179. Sacramento: California Department of Fish and Game. pp. 39–138.
25. Perry R, Brandes P, Burau J, Klimley AP, MacFarlane B, Michel C, et al. (2013) Sensitivity of survival to migration routes used by juvenile Chinook salmon to negotiate the Sacramento-San Joaquin River Delta. Environmental Biology of Fishes 96: 381–392.

26. Berejikian BA, Tezak EP, Schroder SL, Flagg TA, Knudsen CM (1999) Competitive differences between newly emerged offspring of captive-reared and wild Coho salmon. *Transactions of the American Fisheries Society* 128: 832–839.
27. Unwin MJ (1997) Survival of chinook salmon, *Oncorhynchus tshawytscha*, from a spawning tributary of the Rakaia Rivet. New Zealand, in relation to spring and summer mainstem flows. *Fishery Bulletin* 95: 812–825.
28. Campana SE, Thorrold SR (2001) Otoliths, increments, and elements: keys to a comprehensive understanding of fish populations? *Canadian Journal of Fisheries and Aquatic Sciences* 58: 30–38.
29. Sturrock AM, Trueman CN, Darnaude AM, Hunter E (2012) Can otolith elemental chemistry retrospectively track migrations in fully marine fishes? *Journal of Fish Biology* 81: 766–795. doi: [10.1111/j.1095-8649.2012.03372.x](https://doi.org/10.1111/j.1095-8649.2012.03372.x) PMID: [22803735](https://pubmed.ncbi.nlm.nih.gov/22803735/)
30. Ingram LB, Weber PK (1999) Salmon origin in California's Sacramento–San Joaquin river system as determined by otolith strontium isotopic composition. *Geology* 27: 851–854.
31. Kennedy B, Folt C, Blum J, Chamberlain C (1997) Natural isotope markers in salmon. *Nature* 387: 766.
32. Barnett-Johnson R, Pearson T, Ramos F, Grimes C, MacFarlane R (2008) Tracking natal origins of salmon using isotopes, otoliths, and landscape geology. *Limnology and Oceanography* 53: 1633–1642.
33. Kennedy BP, Klaue A, Blum JD, Folt C, Nislow KH (2002) Reconstructing the lives of fish using Sr isotopes in otoliths. *Canadian Journal of Fisheries and Aquatic Sciences* 59: 925–929.
34. Campana SE, Neilson JD (1985) Microstructure of fish otoliths. *Canadian Journal of Fisheries and Aquatic Sciences* 42: 1014–1032.
35. Neilson JD, Geen GH (1982) Otoliths of Chinook salmon (*Oncorhynchus tshawytscha*): daily growth increments and factors influencing their production. *Canadian Journal of Fisheries and Aquatic Sciences* 39: 1340–1347.
36. Titus RG, Volkoff MC, Snider WM (2004) Use of Otolith Microstructure to Estimate Growth Rates of Juvenile Chinook Salmon from a Central Valley, California Stock. *American Fisheries Society Symposium* 39: 181–202.
37. Kondolf GM, Falzone A, Schneider KS (2001) Reconnaissance-level assessment of channel change and spawning habitat on the Stanislaus River below Goodwin Dam. Report to U.S. Fish and Wildlife Service, Sacramento, CA.
38. Schneider KS, Kondolf GM, Falzone A (2000) Channel-floodplain disconnection on the Stanislaus River. University of California, Berkeley 94720: 165–170.
39. Fisher FW (1994) Past and Present Status of Central Valley Chinook Salmon. *Conservation Biology* 8: 870–873.
40. Cramer Fish Sciences (2012) Juvenile Salmonid Out-migration Monitoring at Caswell Memorial State Park in the Lower Stanislaus River, California. 2010–2011 Biennial Report. Grant No. 813326G008. 48pp. p.
41. PSMFC (2014) Juvenile Salmonid Emigration Monitoring in the Lower American River, California. http://www.fws.gov/sacramento/Fisheries/CAMP-Program/Documents-Reports/Documents/2014_American_River_rotary_screw_trap_annual_report.pdf. 107 p.
42. Zeug SC, Sellheim K, Watry C, Wikert JD, Merz J (2014) Response of juvenile Chinook salmon to managed flow: lessons learned from a population at the southern extent of their range in North America. *Fisheries Management and Ecology*: n/a-n/a.
43. Genz A, Bretz F, Miwa T, Mi Z, Leisch F, Scheipl F, et al. (2014) Multivariate Normal and t Distributions. In: CRAN, editor. <http://cran.r-project.org/web/packages/mvtnorm/mvtnorm.pdf>.
44. van Belle G (2008) *Statistical Rules of Thumb*, 2nd Edition. Hoboken, New Jersey: John Wiley & Sons, Inc.
45. Guignard J (2008) Addendum to the Stanislaus River fall Chinook salmon escapement survey 2006: age determination report. Report to the United States Bureau of Reclamation, contract # R0640001.
46. Guignard J (2007) Addendum to the Stanislaus River fall Chinook salmon escapement survey 2005: age determination report. Report to the United States Bureau of Reclamation, contract # R0540004.
47. Barnett-Johnson R, Grimes C, Royer C, Donohoe C (2007) Identifying the contribution of wild and hatchery Chinook salmon (*Oncorhynchus tshawytscha*) to the ocean fishery using otolith microstructure as natural tags. *Canadian Journal of Fisheries and Aquatic Sciences* 64: 1683–1692.
48. Barnett-Johnson R, Ramos F, Grimes C, MacFarlane R (2005) Validation of Sr isotopes in otoliths by laser ablation multicollector inductively coupled plasma mass spectrometry (LA-MC-ICPMS): opening avenues in fisheries science applications. *Canadian Journal of Fisheries and Aquatic Sciences* 62: 2425–2430.

49. Zabel R, Haught K, Chittaro P (2010) Variability in fish size/otolith radius relationships among populations of Chinook salmon. *Environmental Biology of Fishes* 89: 267–278.
50. Mesick C, Marston D, Heyne T (2009) Estimating recruitment for fall-run Chinook salmon populations in the Stanislaus, Tuolumne, and Merced Rivers. http://www.waterboards.ca.gov/waterrights/water_issues/programs/bay_delta/deltaflow/cspa.shtml: Instream Energy Flow Branch USFWS.
51. USFWS (2014) “Chinookprod” database. Unpublished database maintained by the Anadromous Fish Restoration Program and Comprehensive Assessment and Monitoring Program, Lodi and Sacramento, California.
52. PFMC (2014) Appendix Tables A1 & 5 from Stock Assessment and Fishery Evaluation Review of 2013 Ocean Salmon Fisheries. http://www.pcouncil.org/wp-content/uploads/salsafe2013_appdxa.pdf.
53. Williams JG (2012) Juvenile Chinook Salmon (*Oncorhynchus tshawytscha*) in and Around the San Francisco Estuary. *San Francisco Estuary and Watershed Science* 10.
54. Vasques J, Kundargi K (2001) 1999–2000 Grayson Screw Trap Report. San Joaquin Valley Southern Sierra Region (Region 4).
55. Gray A, Jones K, Watry C, Merz J (2012) Stanislaus River juvenile Chinook salmon out-migration population dynamics (1996–2009) and potential river management implications. U.S. Fish and Wildlife Service’s Comprehensive Assessment and Monitoring Program. 85 p.
56. Gregory RS, Levings CD (1998) Turbidity Reduces Predation on Migrating Juvenile Pacific Salmon. *Transactions of the American Fisheries Society* 127: 275–285.
57. Demko D (2003) Chapter 6 Complimentary Studies Related to the VAMP. Evaluation of Chinook salmon fry survival in the Stanislaus River: biological response to supplemental winter flow pulse In: SJRGA, editor. 2003 Annual Technical Report.
58. SJRGA (2003) Chapter 5 Salmon Smolt Survival Investigations.
59. SJRGA (2000) VAMP 2000 Salmon smolt survival investigations.
60. Beckman BR, Larsen DA, Lee-Pawlak B, Dickhoff WW (1998) Relation of Fish Size and Growth Rate to Migration of Spring Chinook Salmon Smolts. *North American Journal of Fisheries Management* 18: 537–546.
61. U.S. Environmental Protection Agency (2003) EPA Region 10 Guidance for Pacific Northwest State and Tribal Temperature Water Quality Standards. Seattle, WA.: Region 10 Office of Water.
62. Marine KR, Cech JJ (2004) Effects of High Water Temperature on Growth, Smoltification, and Predator Avoidance in Juvenile Sacramento River Chinook Salmon. *North American Journal of Fisheries Management* 24: 198–210.
63. Burns JW (1971) The carrying capacity for juvenile salmonids in some northern California streams. *California Fish and Game* 57: 44–57.
64. Greene CM, Beechie TJ (2004) Consequences of potential density-dependent mechanisms on recovery of ocean-type chinook salmon (*Oncorhynchus tshawytscha*). *Canadian Journal of Fisheries and Aquatic Sciences* 61: 590–602.
65. Achord S, Levin PS, Zabel RW (2003) Density-dependent mortality in Pacific salmon: the ghost of impacts past? *Ecology Letters* 6: 335–342.
66. Cavallo B, Merz J, Setka J (2013) Effects of predator and flow manipulation on Chinook salmon (*Oncorhynchus tshawytscha*) survival in an imperiled estuary. *Environmental Biology of Fishes* 96: 393–403.
67. Kjelson M, Raquel P, Fisher F (1981) Influences of freshwater inflow on Chinook salmon (*Oncorhynchus tshawytscha*) in the Sacramento-San Joaquin Estuary. In: Cross RD, Williams DL, editors. *Proceedings of the National Symposium on Freshwater Inflow to Estuaries*: U.S. Fish and Wildlife Service. pp. 88–108.
68. SJRGA (2013) Chapter 5: Salmon smolt survival investigations. In: San Joaquin River Group Authority, editor. *On implementation and monitoring of the San Joaquin River Agreement and the Vernalis Adaptive Management Plan (VAMP): 2011 Annual Technical Report*: California Water Resources Control Board in compliance with D-1641.
69. Weitkamp LA (2010) Marine Distributions of Chinook Salmon from the West Coast of North America Determined by Coded Wire Tag Recoveries. *Transactions of the American Fisheries Society* 139: 147–170.
70. Sterns SC (1992) *The evolution of life histories*. New York: Oxford University Press.
71. Sogard SM (1997) Size-Selective Mortality in the Juvenile Stage of Teleost Fishes: A Review. *Bulletin of Marine Science* 60: 1129–1157.
72. Moyle PB, Israel JA, Purdy SE (2008) Salmon, steelhead, and trout in California status of an emblematic fauna. Center for Watershed Sciences, UC Davis.

73. Myrick CA, Cech JJ (2004) Temperature effects on juvenile anadromous salmonids in California's central valley: what don't we know? *Reviews in Fish Biology and Fisheries* 14: 113–123.
74. Beamish RJ, Mahnken C (2001) A critical size and period hypothesis to explain natural regulation of salmon abundance and the linkage to climate and climate change. *Progress in Oceanography* 49: 423–437.
75. SJRGA (2011) On implementation and monitoring of the San Joaquin River Agreement and the Vernalis Adaptive Management Plan (VAMP): 2010 Annual Technical Report.
76. Speegle J, Kirsch J, Ingram J (2013) Annual Report: Juvenile fish monitoring during the 2010 and 2011 field seasons within the San Francisco Estuary, California. Lodi, California.
77. Taylor EB (1991) A review of local adaptation in Salmonidae, with particular reference to Pacific and Atlantic salmon. *Aquaculture* 98: 185–207.
78. Cramer Fish Sciences (2006) 2006 Stanislaus River Data Report—Final Data.
79. Secor D (1999) Specifying divergent migrations in the concept of stock: the contingent hypothesis. *Fisheries Research* 43: 13–34.
80. Hjort J (1914) Fluctuations in the great fisheries of Northern Europe. *Conseil Permanent International Pour L'Exploration De La Mer* 20: 1–228.
81. Via S, Gomulkiewicz R, De Jong G, Scheiner SM, Schlichting CD, Van Tienderen PH (1995) Adaptive phenotypic plasticity: consensus and controversy. *Trends in Ecology & Evolution* 10: 212–217.
82. Waples RS, Teel DJ, Myers JM, Marshall AR (2004) Life-History Divergence in Chinook Salmon: Historic Contingency and Parallel Evolution. *Evolution* 58: 386–403. PMID: [15068355](#)
83. Greene CM, Beamer EM (2011) Monitoring Population Responses to Estuary Restoration by Skagit River Chinook salmon.
84. Barnett-Johnson R, Teel D, Casillas E (2010) Genetic and otolith isotopic markers identify salmon populations in the Columbia River at broad and fine geographic scales. *Environmental Biology of Fishes* 89: 533–546.
85. Semhi K, Clauer N, Probst JL (2000) Strontium isotope compositions of river waters as records of lithology-dependent mass transfers: the Garonne river and its tributaries (SW France). *Chemical Geology* 168: 173–193.
86. Kormos B, Palmer-Zwahlen M, Low A (2012) Recovery of coded-wire tags from Chinook salmon in California's Central Valley Escapement and Ocean Harvest in 2010.
87. Johnson R, Weber P, Wikert J, Workman M, MacFarlane R, Grove M, et al. (2012) Managed Metapopulations: Do Salmon Hatchery 'Sources' Lead to In-River 'Sinks' in Conservation? *Plos One* 7.
88. Mesick C (in review) The proportion of hatchery fish in California's Central Valley fall-run Chinook salmon escapements from 1980 to 2010.
89. Marston D, Mesick C, Hubbard A, Stanton D, Fortmann-Roe S, Tsao S, et al. (2012) Delta Flow Factors Influencing Stray Rate of Escaping Adult San Joaquin River Fall-Run Chinook Salmon (*Oncorhynchus tshawytscha*). *San Francisco Estuary and Watershed Science* 10.
90. Selective Fisheries Evaluation Committee S (2012) Summary of mass marking activities and mark selective fisheries conducted by Canada and the United States, 2005–2009.
91. Hauer FR, Lorang M (2004) River regulation, decline of ecological resources, and potential for restoration in a semi-arid lands river in the western USA. *Aquatic Sciences* 66: 388–401.
92. Carlson SM, Satterthwaite WH (2011) Weakened portfolio effect in a collapsed salmon population complex. *Canadian Journal of Fisheries and Aquatic Sciences* 68: 1579–1589.
93. DWR (2010) Climate Change Characterization and Analysis in California Water Resources Planning Studies, Final Report.
94. Satterthwaite WH, Carlson SM, Allen-Moran SD, Vincenzi S, Bograd SJ, Wells BK (2014) Match-mismatch dynamics and the relationship between ocean-entry timing and relative ocean recoveries of Central Valley fall run Chinook salmon. *Marine Ecology Progress Series* 511: 237–248.
95. Wood CC, Bickham JW, John Nelson R, Foote CJ, Patton JC (2008) Recurrent evolution of life history ecotypes in sockeye salmon: implications for conservation and future evolution. *Evolutionary Applications* 1: 207–221. doi: [10.1111/j.1752-4571.2008.00028.x](#) PMID: [25567627](#)
96. Lindley ST, Grimes CB, Mohr MS, Peterson W, Stein J, Anderson JT, et al. (2009) What caused the Sacramento River fall Chinook stock collapse?: Pacific Fishery Management Council.
97. The Bay Institute (2013). <http://thebayinstitutepepadcom/my-blog/2013/01/end-the-drought-nowhtml>.

University of California Santa Cruz
Assessing SPATT in San Francisco Bay
SFEI Contract 1051

Final Report

This project involves using Solid Phase Adsorption Toxin Tracking (SPATT) to detect and quantify microcystin and other phytotoxins in San Francisco Bay, and to undertake controlled experiments using SPATT whose goal is to improve the ability to translate SPATT-derived measurements into average ambient concentrations of phytotoxins.

In **Task 1**, SPATT was deployed on San Francisco Bay cruises in a flow-through configuration and at fixed sites as part of on-going monitoring work for phycotoxins in San Francisco Bay. As discussed with SFEI, one SPATT was deployed per basin in the surface-sampling flow-through system during the monthly *Polaris* cruises. Based on adjustments to cruise schedules and cruise types, SPATT were routinely deployed on all available cruises.

In **Task 2** controlled experiments were conducted in the laboratory to better characterize partitioning of phytotoxins out of solution and into the SPATT. Experiments were designed to evaluate measurement reproducibility, and whether reproducibility can be optimized by adjusting SPATT configuration. Options include:

- a. Controlled experiments carried out in simulated flow-through systems in which SPATT will be exposed to brackish water and seawater containing concentrations of a surrogate compound for toxins, e.g., microcystin-RR or similar. Toxin will be quantified as a function of both dissolved concentration and exposure time. This “calibration” information will allow for more accurate back-calculations of average ambient concentrations in natural systems.
- b. Time-series “bottle” experiments in which SPATT will be exposed in containers holding brackish water with known concentrations of a surrogate compound for toxins (e.g., microcystin-RR). SPATT will be removed at multiple time points and toxin uptake will be measured. This information will aid in characterizing the uptake kinetics of microcystin under conditions simulating deployments at a single site.

Research priorities for Task 2 were identified collaboratively by Kudela and SFEI, and a project plan was developed that is feasible within the available budget.

Results—Task 1

We have processed 155 SPATT samples from USGS cruises, between October

2011 and November 2014. Additional samples (through April 2015) have also been obtained and processed, but were not included in a recent analysis as part of a separate SFEI effort. For convenience, data presented here are limited to the 155 SPATT, but we continue to process the samplers.

While we anticipated 60 SPATT per year, several of the USGS cruises were canceled or reduced in geographic range in 2013 due to ship issues. For each SPATT we have analyzed for domoic acid (DA) and microcystins LR, RR, YR, and LA. These four congeners are identified by OEHHA as the primary microcystin toxins in California, and are considered to be of equivalent toxicity. We therefore sum the congeners to report “total microcystin”.

Preliminary data analysis was conducted on the SPATT and USGS underway data for presentation at several meetings:

- Kudela, RM, C Mioni, M Peacock, T Schraga. San Francisco Bay acts as a reservoir and mixing bowl for both marine and freshwater toxins. Coastal and Estuarine Research Federation, 3-7 November 2013, San Diego, CA.
- Kudela, RM, C Mioni, M Peacock, T Schraga. San Francisco Bay acts as a reservoir and mixing bowl for both marine and freshwater toxins. Eastern Pacific Oceans Conference, Fallen Leaf Lake, California, September 17-19, 2013.
- Kudela, R, Peacock, M, Schraga, T, Senn D. 2014. Does San Francisco Bay have a harmful algal bloom problem? 2014 Bay-Delta Science Conference, 28-30 October 2014, Sacramento, CA.

Those presentations are used as the basis for this interim report.

Between 2011-2014, 25 Full Bay and 28 South Bay cruises were analyzed. From those samples, 71.5% were positive for microcystins and 96.5% were positive for domoic acid (Figure 1). Concentrations ranged from 0-400 ng/g domoic acid, and 0-25 ng/g microcystins (Figure 2). Peaks in both toxins were coincident in time, and appear to be related to river flow. Moderate river flow is associated with the highest toxin concentrations. Spatially, toxins were fairly uniformly distributed throughout the four basins (Figure 3). During some periods there was clear separation based on temperature-salinity (T-S) properties, with domoic acid associated with “marine” waters and microcystins associated with “fresh” waters. However at other times toxins were distributed without a clear pattern through the Bay (Figures 4, 5).

The range of toxin concentrations, range of environmental parameters, and length of the time-series (3+ full years of data) make this dataset conducive to statistical modeling to identify relationships between toxins and environmental drivers or correlates (see Recommendations below).

Results—Task 2

We have conducted several “bottle” experiments to evaluate SPATT adsorption under representative conditions. In particular, we recently expanded the SPATT methodology to include anatoxin-a. This is a potent neurotoxin also known as “sudden death factor”. While there are no reports of anatoxin-a for San Francisco

Bay, we have routinely seen elevated levels in the Eel River, and occasionally get positive hits in nearby Pinto Lake. We recently concluded a laboratory calibration for anatoxin-a, looking at adsorption and recovery efficiency, effect of different source waters, and effect of temperature on adsorption.

We can now quantify SPATT (using HP20 resin) characteristics for domoic acid, microcystins, and anatoxin-a. Excitingly, we can use a single extraction method to analyze all three toxins from the same SPATT. We can also analyze for okadaic acid (Diarrhetic Shellfish Poisoning), extending our capability to 4 toxins that cover the majority of compounds expected in San Francisco Bay.

Because SPATT and grab samples (or indicator organisms) are fundamentally different measurement methods, we do not recommend a direct calibration factor between the various toxin detection methods. Rather, we provide ranges of SPATT concentrations that correlate to management action levels. For example, OEHHA recommends an alert or action level of 0.8 ppb total microcystins. Based on the large comparative dataset, this would be equivalent to a threshold concentration of ~1-4 ng/g for SPATT (see below). Based on that criteria, San Francisco Bay appears to approach this alert level seasonally (Figure 2).

Additional Analyses

We requested an extension to the contract to more fully characterize SPATT. We proposed to complete the following:

- SPATT deployment/analysis through 2014, providing a full 3-year record
- Finish characterization of toxin uptake in a simulated flow-through system
- Prepare a peer-reviewed publication describing the presence of toxins in San Francisco Bay

We further recommended the following. These five recommendations are beyond the scope of the current contract, but could be implemented within a 12-18 month contract at a similar cost to this contract.

- 1) Continue SPATT deployment beyond the scope of this contract;
- 2) Analyze matched filter samples from the USGS cruises for particulate toxins, to further calibrate the SPATT data; this could also be compared to an existing dataset of HPLC pigments and microscopy samples;
- 3) Analyze archived mussel tissue provided by the RMP as a pilot dataset, to determine whether additional sample analysis is warranted. This would directly link toxins to trophic accumulation.
- 4) Develop a method for saxitoxins. This is the only toxin group that we know is in SFB that is not currently included in our analysis. It requires some personnel time to set up the method, and supplies costs.
- 5) Analyze archived SPATT for anatoxin-a and okadaic acid.

Results from the Contract Extension

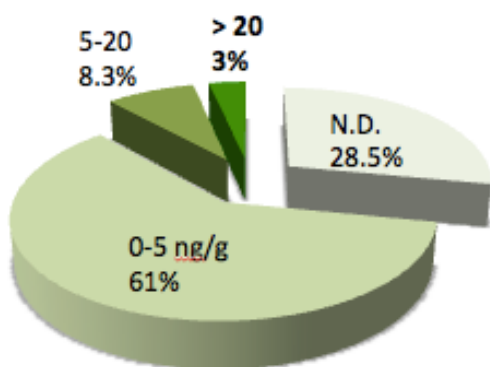
Following this document, we provide a separate write-up for the laboratory characterization (the second bullet from the proposed contract extension). Analysis of SPATT through 2014 was also completed, and an initial write-up with peer-review is ongoing as part of the following report and manuscript:

Sutula, Martha , Raphael Kudela, James Hagy, Gry Mine Berg, Suzanne Bricker, James E. Cloern, Richard Dugdale, Lawrence W. Harding, Jr., and David Senn. 2015 (in prep.). Scientific Basis for Assessment of Nutrient Impacts on San Francisco Bay.

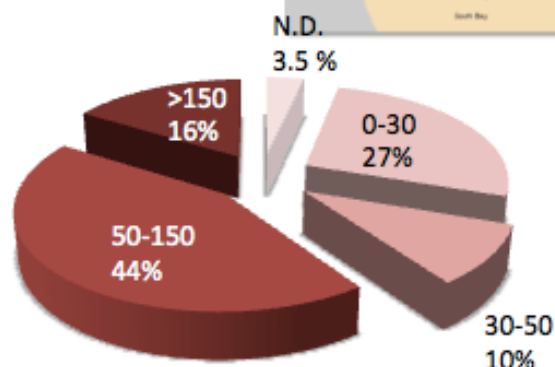
2011-2014: USGS Deployment of SPATT

October 2011 – July 2014

- 25 Full-Bay cruises
- 28 South Bay cruises



Microcystins



Domoic Acid

Figure 1. Summary results from the USGS cruises.

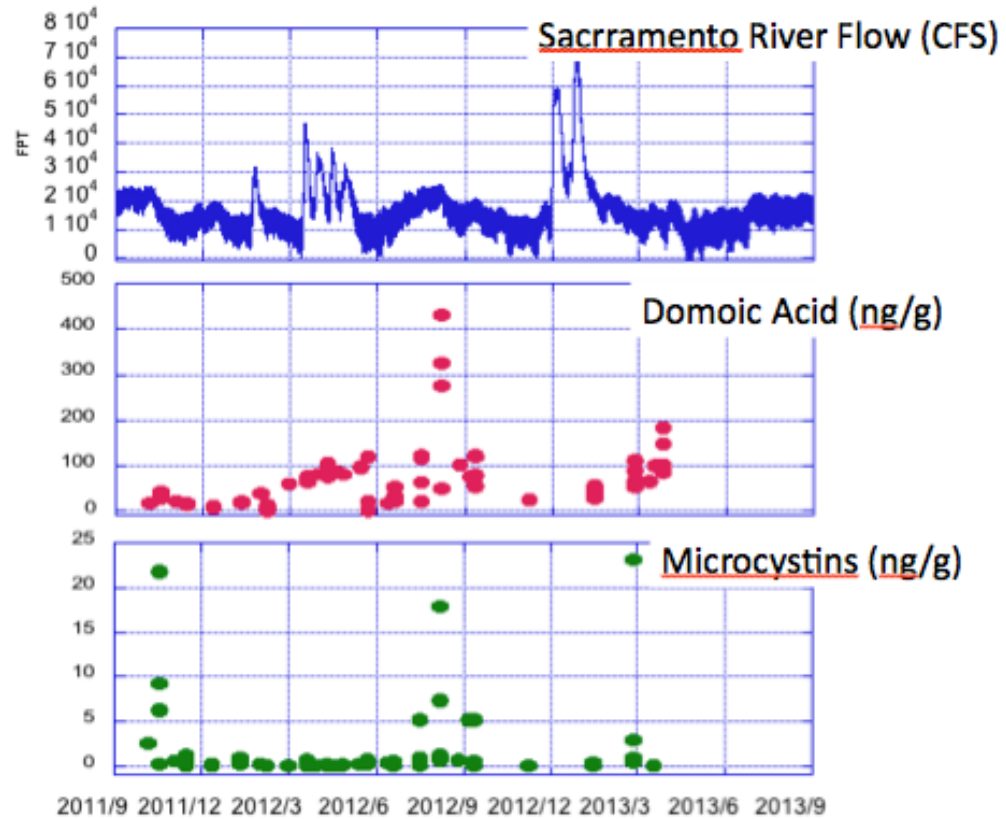


Figure 2. Toxin data shown as a time-series, with river flow (top). Toxins are generally associated with moderate flow in the autumn. The two peaks in autumn 2011 and summer 2012 are shown in more detail in Figures 4-5.

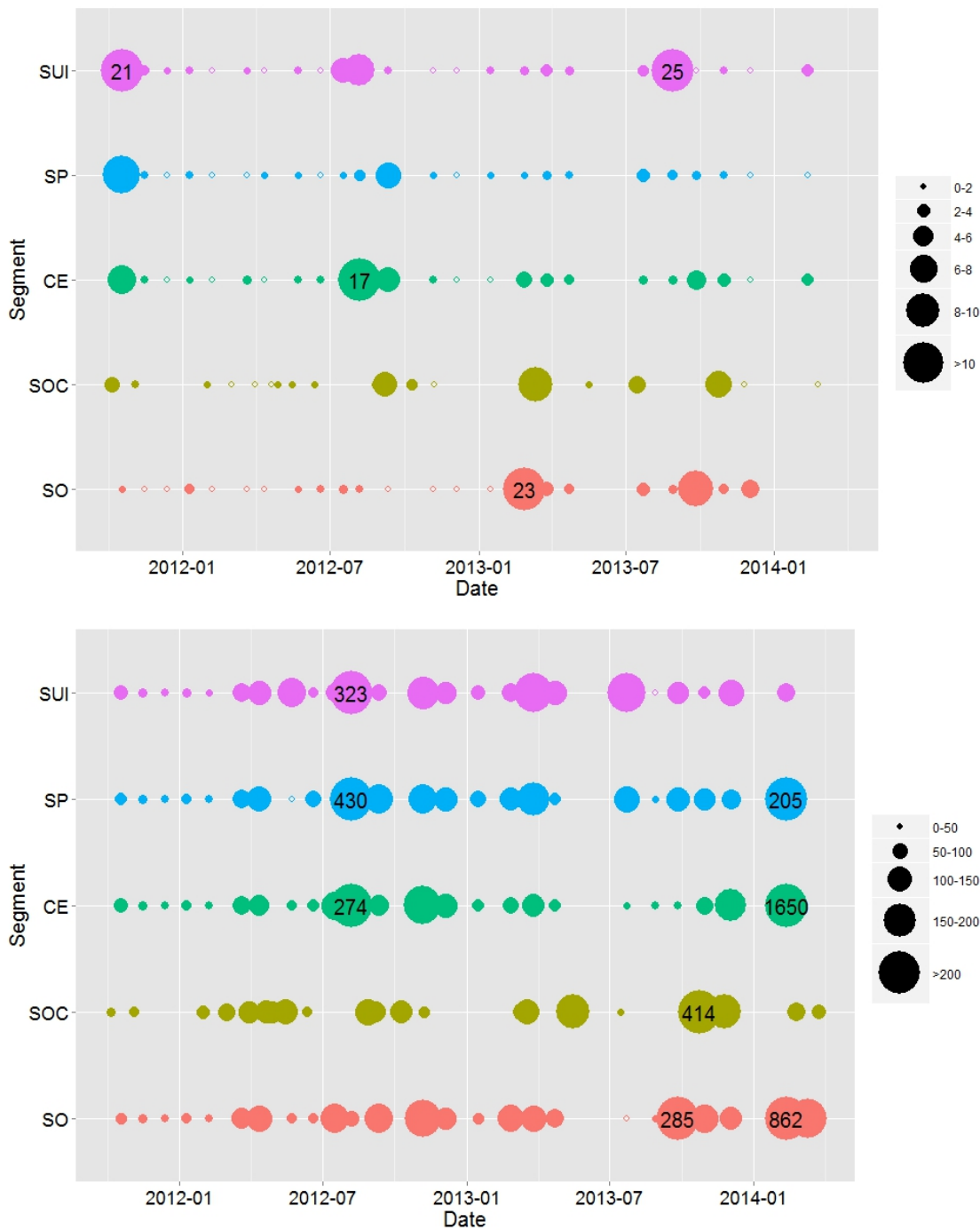


Figure 3. All of the SPATT data shown as concentration (larger circle equals more toxin). Note that microcystins are easily detectable, but fairly low. DA values are fairly high. Letter codes refer to subembayment: SO=South Bay, SOC=South Central, CE=Central, SP=San Pablo, SUI=Suisun.

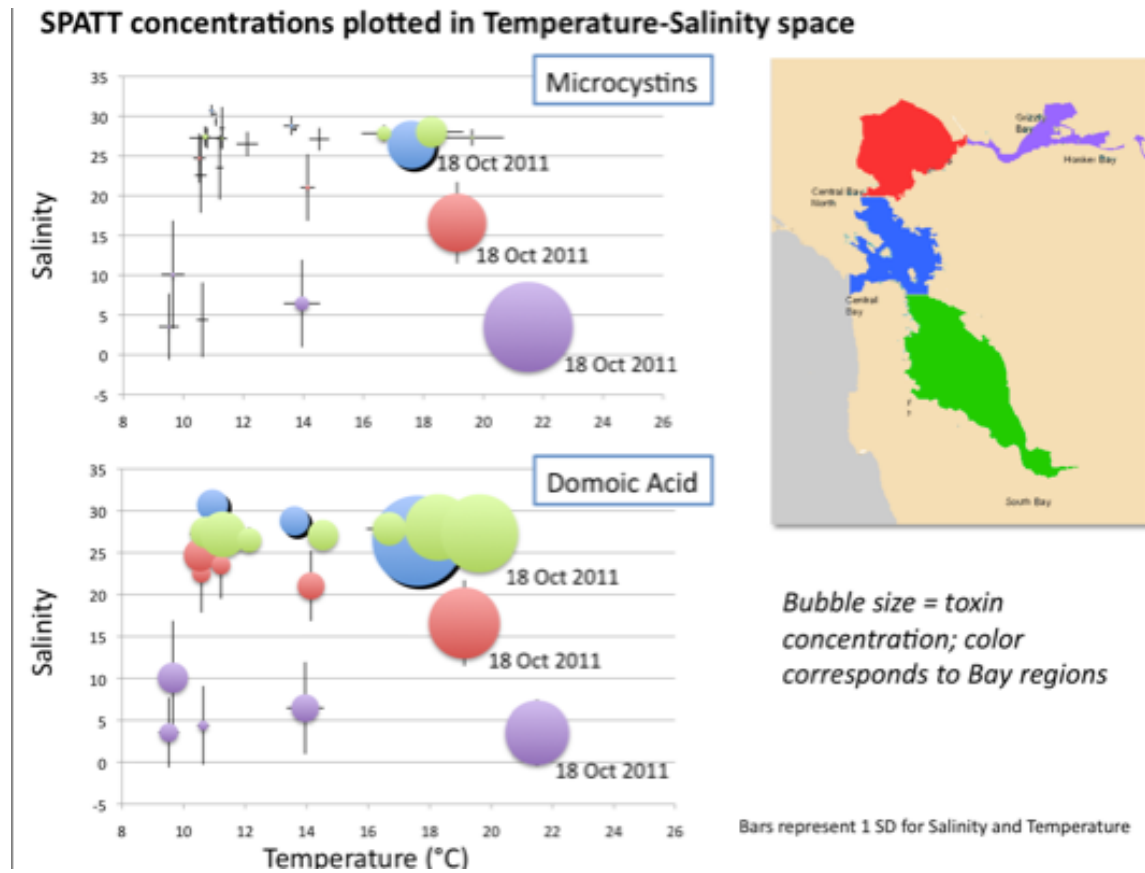


Figure 4. Toxin data plotted in T-S space. For this period, microcystins are clearly coming from the Delta, and spreading into the rest of the Bay, while DA is coming from Central Bay and spreading into the rest of the Bay, suggesting that sometimes, it's simply conservative mixing that is moving the toxins around.

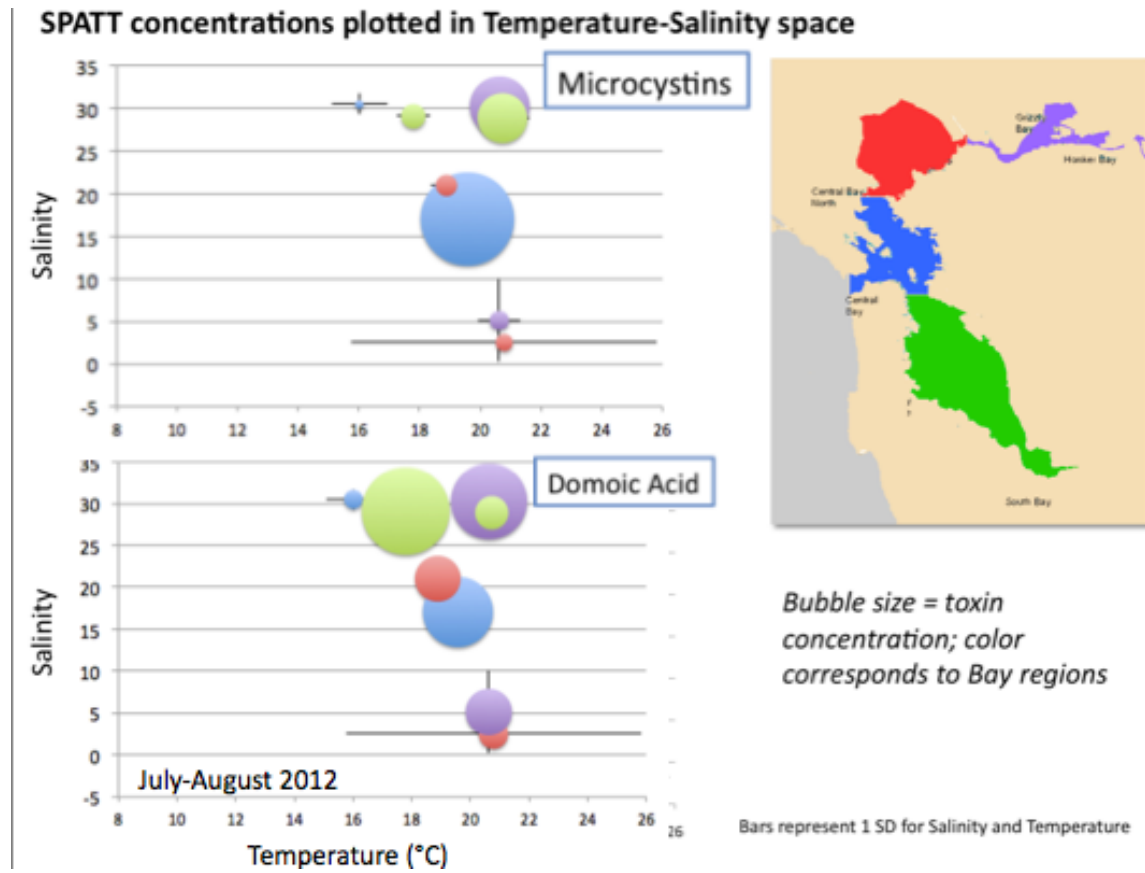


Figure 5. Another example, from July-August 2012. It is not as clear how the geographic patterns relate to environmental forcing. Highest microcystins are in Central Bay, with moderate levels in South Bay and the Delta. There is evidence (not shown) that microcystins are coming in from a separate South Bay source, possibly the sloughs and salt ponds. The DA is highest in South Bay, and pretty high in the Delta, suggesting transport of cells that eventually release toxin.

Results from Contract Extension Calibration of SPATT—Background

A primary objective of this project was to intercalibrate SPATT toxin data for microcystins and domoic acid such that data from the USGS underway mapping aboard the R/V *Polaris* can be qualitatively related to regulatory limits. OEHHA recommended 0.8 ppb for the sum of total (particulate and dissolved) microcystin LR, RR, YR, and LA. There are no formal guidelines for domoic acid, but regulatory limits for fish and shellfish is 20 ppm in tissue.

It is not possible to *directly* compare SPATT values to the regulatory guidance because (a) SPATT measures dissolved, and not total toxin; (b) SPATT toxins and grab samples for domoic acid are not equivalent to toxin levels in tissue; (c) SPATT integrates spatially and temporally. Additionally, SPATT is generally considered to be more sensitive than grab samples (Lane et al. 2010, 2012; Kudela 2011; Gobble and Kudela, 2014). Given these caveats, it is still desirable to relate SPATT concentrations to regulatory limits/guidelines.

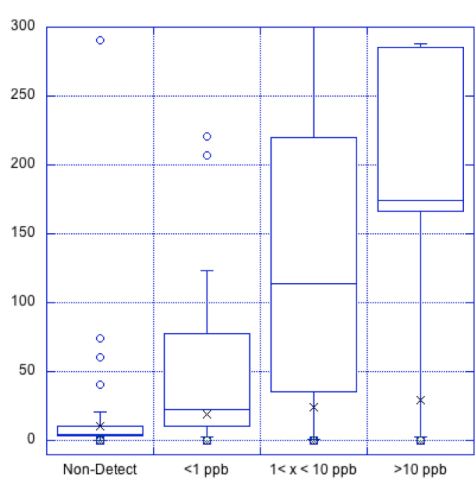


Figure 1. SPATT data from Pinto Lake, showing the correspondence between grab sample bins and SPATT values.

An initial attempt to provide an intercomparison used environmental data from long time-series at the Santa Cruz Municipal Wharf (Lane et al. 2010) and from Pinto Lake, California (Kudela 2011). For both of those programs SPATT, using the HP20 resin, are deployed weekly, with matching samples for dissolved and particulate domoic acid, and mussel tissue (SCMW), and dissolved and total microcystins (Pinto Lake). Using those data, SPATT values were binned into ranges corresponding to grab samples or mussel samples: non-detect, < 1 ppb, 1-10 ppb, and > 10 ppb for microcystins, and 0-5, 5-10, 10-20, and >20 ppm domoic acid in mussel tissue. Ranges were determined by binning the corresponding SPATT data

an calculating the median, mean, and standard deviation. These data are depicted graphically for microcystins in Figure 1 and the ranges are provided in Tables 1-2.

As part of laboratory characterization, resin capacity and equilibration times were evaluated when SPATT were developed (Lane et al. 2010; Kudela 2011). Since then, adsorption/desorption of microcystin LR was more rigorously evaluated (Zhao et al. 2013) and HP20 was again identified as the optimal resin for environmental use, with linear absorption characteristics over several days. HP20 was also identified as the best resin for use with lipophilic toxins in seawater for prolonged (days) deployment, with reasonably linear uptake and a combination of good adsorption

and desorption capabilities; other resins performed better under some circumstance, but were found not to be as universally applicable to a broad range of toxins, deployment times, and recovery methods (Zendong et al. 2014). Thus there is growing acceptance of HP20 resin as a “universal” SPATT resin, with the best overall combination of characteristics.

Table 1. SPATT concentrations corresponding to total microcystins from matching grab samples.

Microcystin Grab Sample (ppb)	SPATT (ng/g)
Non-Detect	5-13
< 1 ppb	20-50
1 < x < 10 ppb	50-200
> 10 ppb	175-275

Table 2. SPATT concentrations corresponding to mussel tissue domoic acid concentrations from matching mussel samples (SPATT were deployed weekly; mussels samples were collected weekly).

Domoic Acid Mussel (ppm)	SPATT (ng/g)
0-5 ppm	0-30
5-10 ppm	30-50
10-20 ppm	50-75
>20 ppm	>150

Calibration of R/V *Polaris* Underway Measurements

In order to translate the general characteristics of HP20 SPATT, a simulation was set up in the laboratory to mimic conditions on the R/V *Polaris* cruises. The following assumptions were made:

- 1) Transects include fresh, brackish, and marine waters;
- 2) Individual SPATT deployments are for no longer than 12 hours;
- 3) SPATT adsorption may differ when using a flow-through system compared to passive (static) water bodies such as Pinto Lake and Santa Cruz Wharf;

- 4) Temperature and salinity vary over the transects, potentially influencing toxin adsorption;
- 5) SPATT samplers are stored frozen prior to analysis.

Given these assumptions, the laboratory experiment was designed to mimic typical field conditions. A large volume (~16 L) of low-salinity water (Sacramento River water with Monterey Bay water mixed in, final salinity ~10). A recent study (Fan et al. 2014) showed HP20 adsorption varies with salinity, but not significantly so compared to other sources of variability, so it was assumed that salinity did not need to be directly tested again. The water was spiked with an initial concentration of ~34 ppb MC-LR, and 82 ppb domoic acid (a trace amount, ~3 ppb, of MC-YR was also present). The water was subsequently diluted to create a series of toxin concentrations for testing SPATT adsorption.

Adsorption kinetics should also be sensitive to temperature, since adsorption is a physical-chemical interaction between the resin and the sorbents (toxins). This was tested as part of the laboratory trial by testing adsorption at 3 temperatures (22°C, 15°C, 4°C) and three time periods (20 minutes; 1 hour; 2 hours). For each time point 2-3 SPATT were soaked in a large (~2 L) volume, with the ambient toxin concentration tested before and after each SPATT exposure to account for uptake.

For the SPATT adsorption tests (other than temperature), two methods were employed. First, SPATT were exposed for 15 minutes in a glass, 2L container with spiked water at 5 concentrations. This was designed primarily to calibrate SPATT uptake using the method employed by Peggy Lehman (DWR) in a previous field experiment. For that study, Bay and Delta water were collected into a container and SPATT were added for 15 m. Second, the large (~16L) carboy was connected to a peristaltic pump and water was recirculated through a 2L glass container (about 1.5L was in the container), using a flow rate of 2.5 L/min, which is a typical flow rate for underway mapping systems. The SPATT were prepared/deployed following the same methods as for the USGS cruises. For each time point, the SPATT were removed, allowed to drain, placed in 50 mL plastic centrifuge tubes, and frozen. The SPATT were subsequently thawed and toxin was extracted using the standard UCSC protocol (10 mL 50% MeOH, 20 mL 50% MeOH, 20 mL 50% MeOH with 1M ammonium acetate). An additional step, collection of the Milli-Q rinse water, was added to test for loss of toxin during processing. As per UCSC protocol, each eluate fraction was run separately on an Agilent 6130 LC/MS, and the total toxin per SPATT sampler was calculated based on volumes and concentrations of extract (see also Lane et al. 2010; Kudela 2011; Gobble and Kudela 2014). Pictures of the flow-through setup are provided in Figure 2.

For the flow-through experiment, replicate (2-3) SPATT were placed in the flow-through container and allowed to absorb for 20 minutes to 24 hours. The spiked water was then diluted to adjust the toxin concentration, and additional SPATT were tested. This was repeated for 4 concentrations. Additional SPATT were tested

during the transitions, to determine how quickly SPATT exposed to high toxin concentrations would equilibrate to a lower concentration.



Figure 2. Laboratory setup for the flow-through testing of SPATT. Upper photo shows the carboy, receiving container, and pump. Lower photo shows SPATT (in embroidery hoops) within the receiving container.

Calibration of SPATT--Results

Temperature: There was no significant difference (ANOVA, $p > 0.05$) for SPATT toxin concentrations of both microcystin and domoic acid as a function of temperature. This is consistent with previous laboratory experiments conducted when SPATT methodology was first developed.

Milli-Q Rinse: For standard processing of SPATT, the Milli-Q (deionized water) rinse is not tested for toxin. As part of these experiments Milli-Q volumes and toxin concentrations were measured. While toxins were detected in the rinse water, it was a few percent of the total extracted toxin (for both microcystin and domoic acid), as previously reported (Lane et al. 2010, Kudela 2011). While this lost toxin could be important for cases where very low toxin levels are of interest, SPATT is already more sensitive than grab samples so this is considered to be an acceptable loss.

Microcystins, 15 minute exposure: Adsorption of MCY-LR and MCY-YR was linear as a function of concentration. Toxins were easily detected after 15 minutes of exposure. Previous comparison of SPATT to grab samples exhibited a calibration factor of about 10-50x (SPATT is 10-50x more sensitive than grab samples), as exhibited in Table 1. Shorter exposure resulted in a calibration factor of about 5x, as seen in Figure 3. Given typical underway mapping speeds, 15 minutes would roughly correspond to spatial scales of about a kilometer, and assuming exposure to toxin occurred for 0-15 minutes at a given concentration, the SPATT factor would be 1-5x.

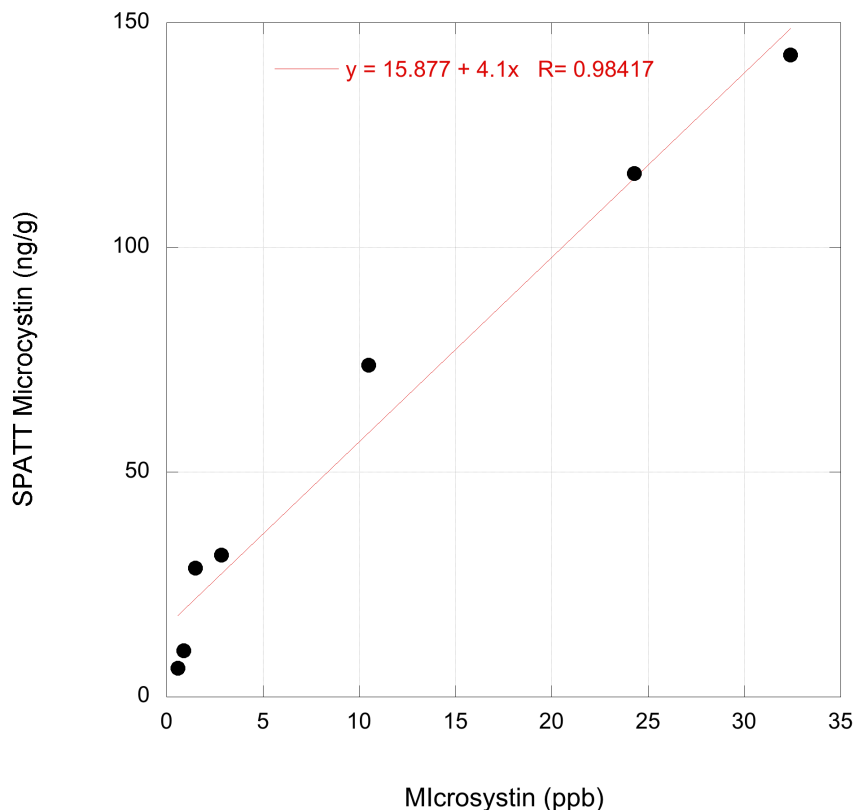


Figure 3. SPATT versus ambient water concentration for microcystins for SPATT exposed to constant concentration of toxin for 15 minutes. When forced to a zero-intercept, the calibration factor is 4.97x.

Microcystins, > 1 hour exposure: Testing of SPATT showed that microcystins equilibrate in approximately 1 hour. The calibration of toxin versus SPATT was therefore recalculated using SPATT exposed for 1-24 hours to estimate the upper-limit calibration factor. Results are presented in Figure 4. Linearity is excellent, and the calibration factor increases considerably compared to the 15 minute exposure, with a calibration factor of 271x.

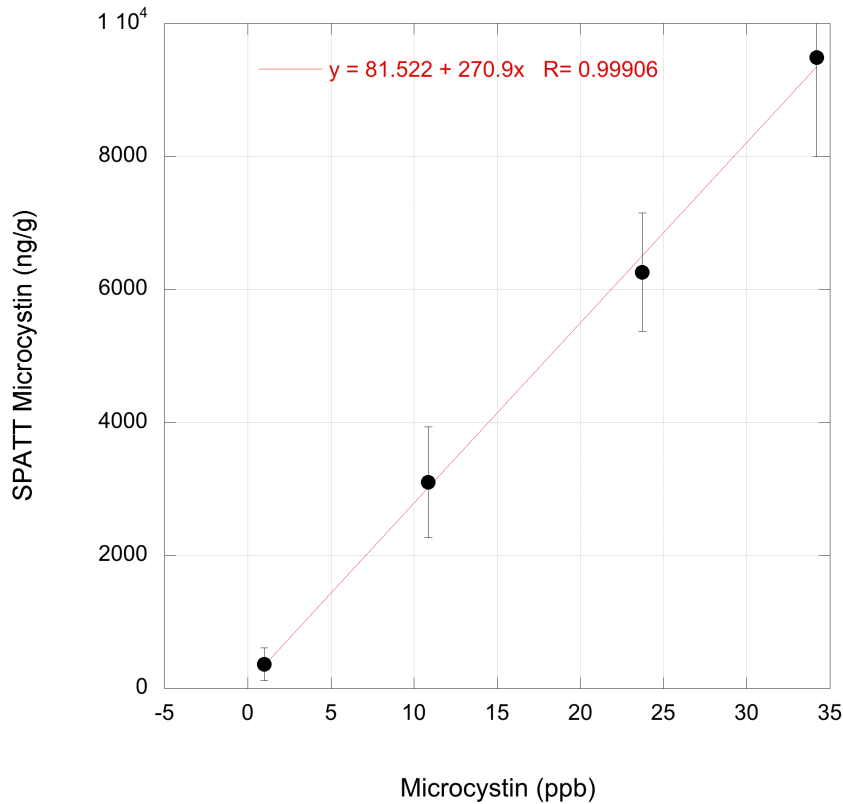


Figure 4. SPATT versus ambient water concentration for microcystins with SPATT exposed to a constant concentration for >1 hour.

Microcystins, transferred to lower concentration: When SPATT were allowed to equilibrate at a higher toxin concentration and were then exposed to water of lower concentration, similar kinetics were observed (not shown) with equilibrium occurring in ~1 hour, and a linear decrease over the first 60 minutes observed.

Field Calibration of SPATT Microcystins: the laboratory data for adsorption kinetics (time) and toxin levels (concentration) were used to develop a matrix showing the relationship between field SPATT observations and potential ambient toxin concentrations. The matrix is shown in Figure 5, together with statistics showing the total microcystin concentrations observed from October 2011- November 2014 for San Francisco Bay. The suggested “alert level” of 1 ng/g microcystins is indicated, along with the estimated non-detect limit.

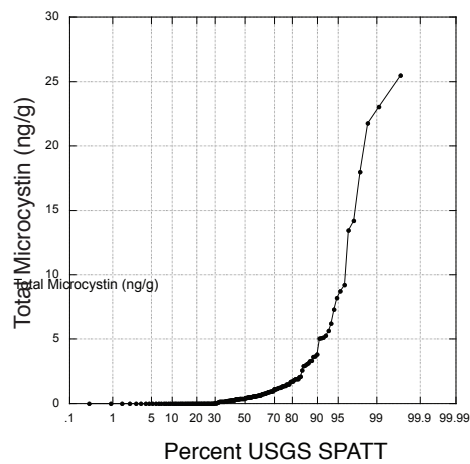
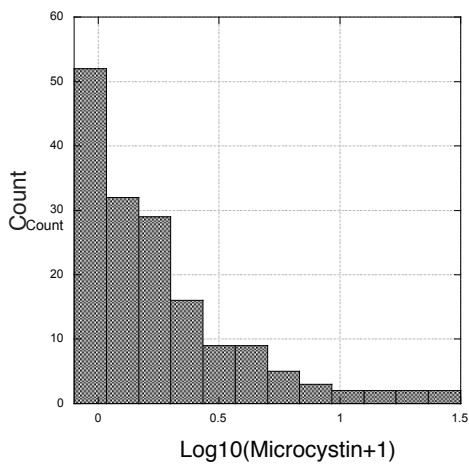
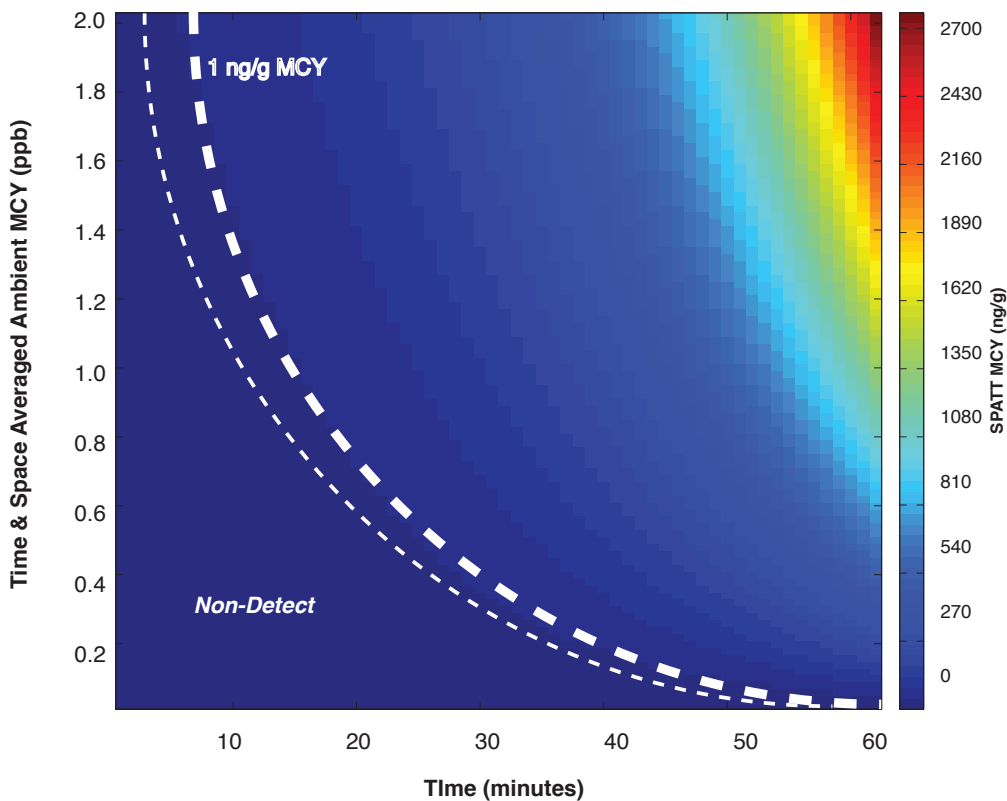


Figure 5. The top graph shows the SPATT concentrations that would be measured as a function of exposure time versus concentration. Note that toxin levels would increase/decrease in response to exposure (x-axis) to water with higher/lower concentration, with an equilibrium time of ~1 hour. The lower panels show the histogram of toxin concentrations observed in SFB (left) and cumulative percent (lower right).

Domoic Acid, 15 minute exposure: Adsorption of DA was exponential rather than linear (as seen for microcystins). Toxins were easily detected after 15 minutes of exposure. This makes calibration of SPATT more difficult, since it strongly depends on how long the SPATT are exposed. Data are presented in Figure 6.

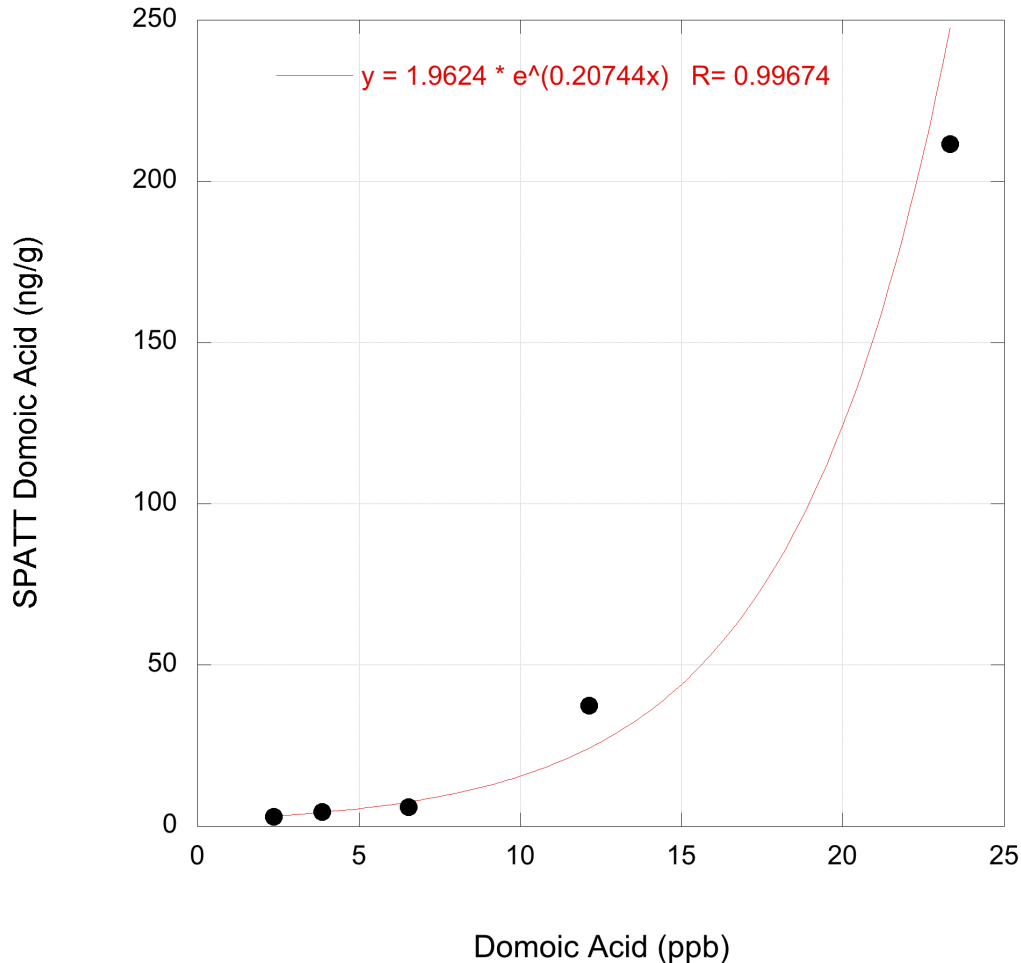


Figure 6. SPATT versus ambient water concentration for domoic acid for SPATT exposed to constant concentration of toxin for 15 minutes.

Domoic Acid, > 20 hour exposure: Testing of SPATT showed that domoic acid continues to be adsorbed for up to 24 hours, while other studies (Lane et al. 2010, Zendong et al. 2014) shows that SPATT continues to adsorb toxins for multiple days, but is quasi-linear when multiple days are included. Results for up to 24 hour exposure for varying concentrations of domoic acid are presented in Figure 7. As with 15 minute exposure the data fit an exponential curve, suggesting that SPATT concentrations of domoic acid may underestimate low values and overestimate high values, compared to what would be assume using a linear relationship.

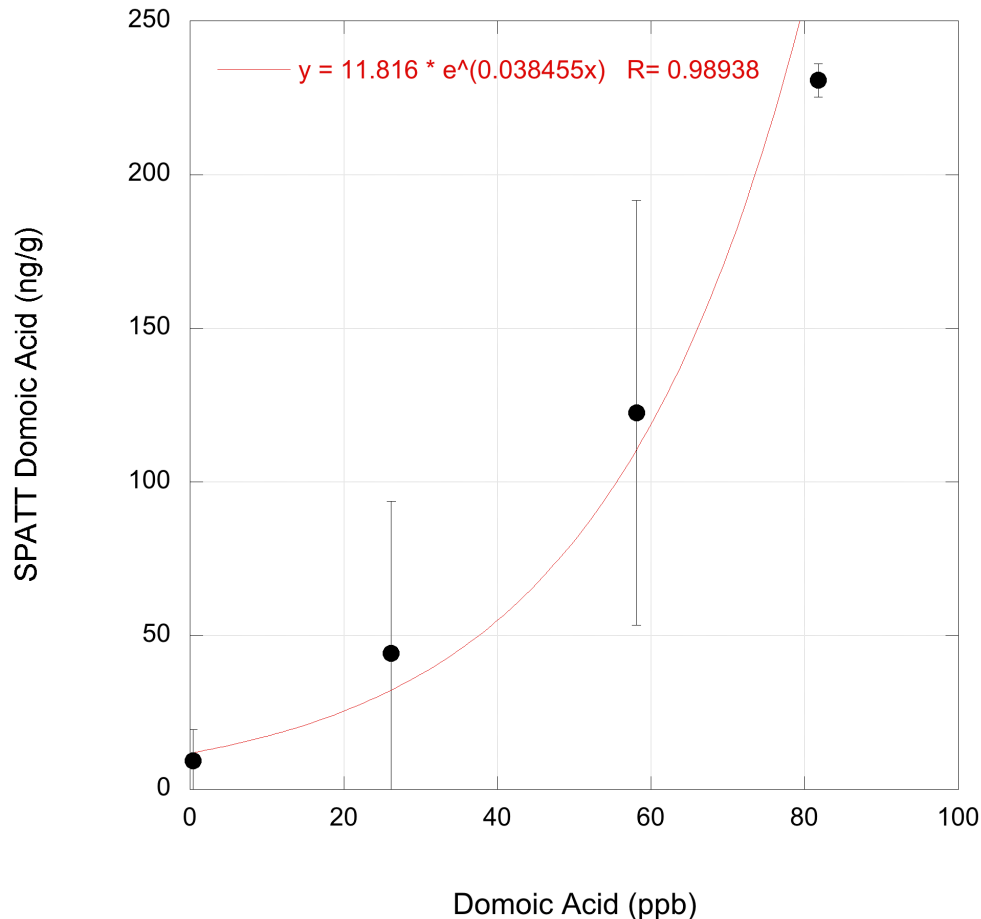


Figure 7. SPATT versus ambient water concentration for domoic acid for SPATT exposed to constant concentration of toxin for >20 hours.

Domoic Acid, transferred to lower concentration: When SPATT were allowed to equilibrate at a higher toxin concentration and were then exposed to water of lower concentration, similar kinetics were observed (not shown) with equilibrium initially fast, and then slowing down. The net result would be to (again) overestimate concentrations when exposed to high levels of domoic acid, compared to a linear response for time-averaged concentrations.

Field Calibration of SPATT Domoic Acid: the laboratory data for adsorption kinetics (time) and toxin levels (concentration) were used to develop a matrix showing the relationship between field SPATT observations and potential ambient toxin concentrations. The matrix is shown in Figure 8, together with statistics showing the total domoic acid concentrations observed from October 2011- November 2014 for San Francisco Bay. The suggested “alert level” of 75 ng/.g domoic acid is indicated, along with the estimated non-detect limit.

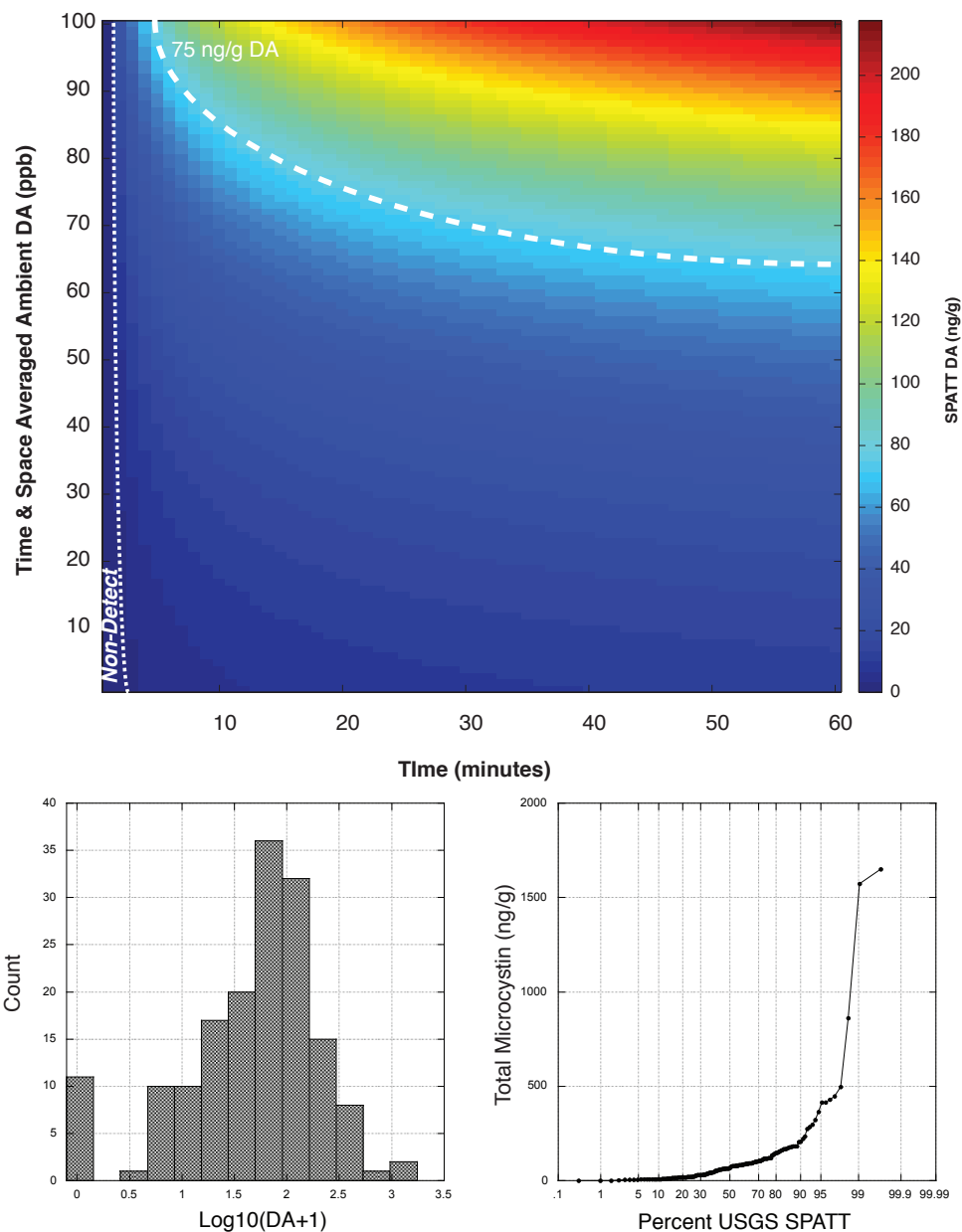


Figure 8. The top graph shows the SPATT concentrations that would be measured as a function of exposure time versus concentration. Note that toxin levels would increase/decrease in response to exposure (x-axis) to water with higher/lower concentration, with an equilibrium time of ~several days. The lower panels show the histogram of toxin concentrations observed in SFB (left) and cumulative percent (lower right).

Calibration of SPATT—Comparison to Mussels

Mussel samples were obtained from the RMP monitoring program for 2012 and 2014. This provides a direct comparison between a regulatory measurement (tissue samples) and SPATT from approximately the same time period and location, keeping in mind that the SPATT are deployed in surface water on a subembayment scale for a few hours, while mussels are deployed at depth for ~6 months.

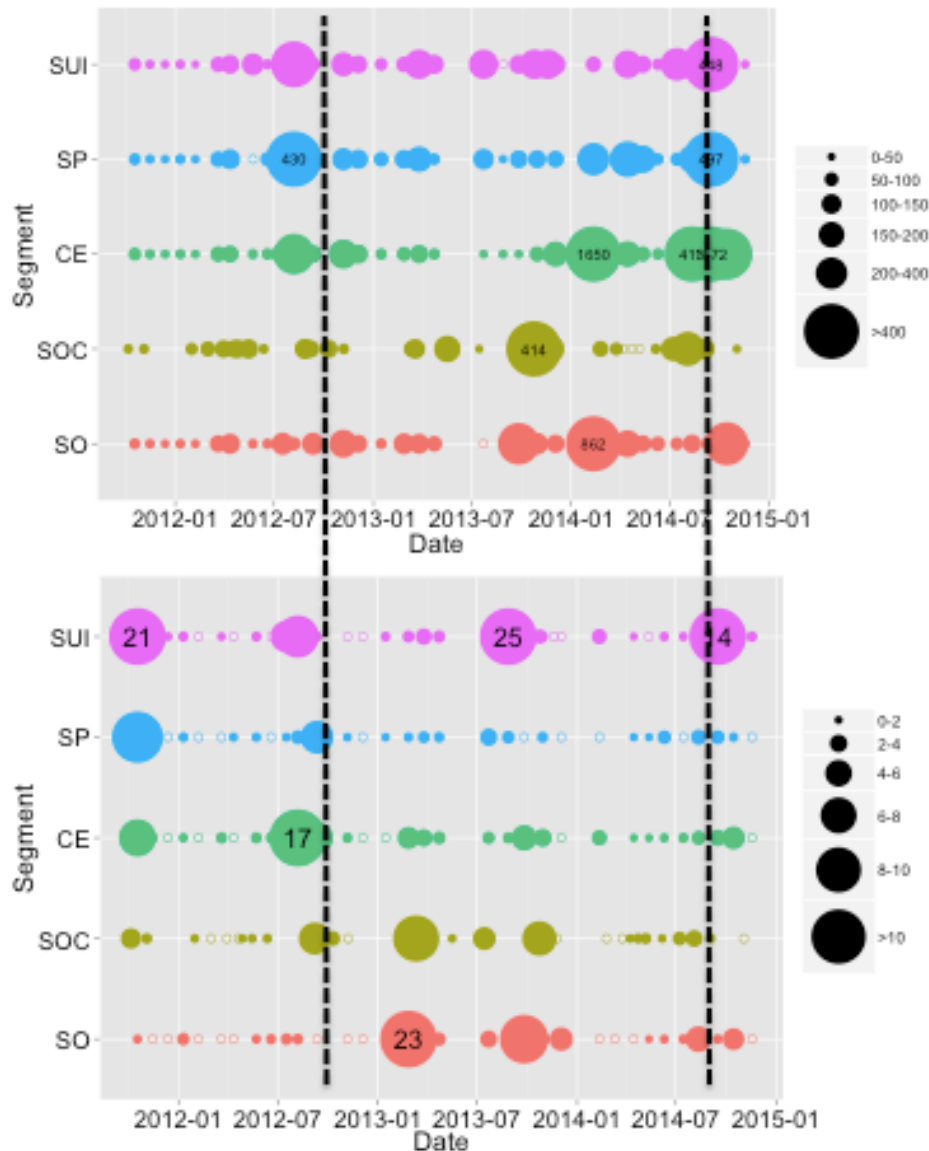


Figure 9. SPATT time-series, with bivalve retrieval dates overlaid as dashed lines. Note that bivalves were retrieved shortly after widespread toxin throughout the Bay for both DA and microcystins.

Figure 9 shows the SPATT time-series for microcystins and DA, with the mussel collection. Note that toxin was detected in mussels immediately following periods when SPATT indicated widespread presence within the Bay. For the mussel samples, 100% of sites had detectable domoic acid, while 82% (2012) and 100% (2014) of mussels had detectable microcystins. Of the two, the microcystins were closer to regulatory closure, with a maximum value of $\sim 22 \mu\text{g}/\text{kg}$ (WHO guidelines recommend closure at $24 \mu\text{g}/\text{kg}$). Comparison of SPATT with the mussel data suggest that a microcystin level of 10-20 ng/g SPATT would be too conservative, so more recent recommendations have lowered this to 1 ng/g. Similarly, presumably because of the non-linearity in uptake, DA values of 30-50 ng/g are probably too conservative, and the new recommended value is 75 ng/g (these values are reported in Sutula et al., in prep; "Scientific Basis for Assessment of Nutrient Impacts on San Francisco Bay").

Calibration of SPATT--Recommendations

Based on this initial pilot study of field-deployed SPATT and laboratory calibration, it seems clear that the SPATT time-series should be continued as part of the USGS cruises. Discussions with USGS and SFEI have explored the possibility of further dividing the Bay into subembayments consistent with the analysis performed by Sutula et al. (in prep.). This would primarily mean adding a Lower South Bay SPATT sampler, and separating Central Bay and North Central Bay. It is also recommended that, if possible, additional mussel samples be collected since this is the most unambiguous comparison between SPATT and ecosystem impairment. As part of separate SFEI funding, analysis is also underway to compare discrete filter samples with SPATT, but this will be subject to sampling variability (in previous comparisons, $>50\%$ of grab samples were negative while SPATT was positive) and to issue with limits of detection using filters due (primarily) to the heavy sediment load encountered when filtering whole water. It would also be useful to conduct a statistical analysis of SPATT relative to environmental conditions, to identify likely drivers of variability. Finally, additional laboratory testing of SPATT adsorption/desorption (for example, in response to salinity) could be carried out.

Ranking these recommendations by feasibility, cost, and impact, the following is proposed (from highest to lowest), with the recommendation followed by comments [in brackets]:

- 1) Continue SPATT time-series.

[SPATT is ongoing, primary limitation is availability of funds for both deployment and analysis of the data].

- 2) Collect additional mussel (or other invertebrate) samples for toxin analysis compared to SPATT. Ideally, deploy SPATT co-located with mussels.

[Feasible, but RMP currently conducts experiments every 2 years. So costs increase considerably if more frequent sampling is desired].

- 3) Add Lower South Bay and North Central Bay to the existing SPATT time-series.

[Minimal additional effort; would require permission from USGS, and would increase current costs by about 25%].

- 4) Collect/analyze discrete plankton samples for toxins to compare with SPATT.

[This is underway as part of separate funding; it's not clear that it will provide a direct intercalibration, given the past issues with comparing grab samples and SPATT].

- 5) Conduct retrospective analysis of SPATT versus environmental conditions to identify drivers of variability.

[This is probably a high priority, but the longer the time-series, the more valuable the analysis; analyzing now would primarily capture the drought period. Consider waiting until the drought ends, or anticipate analyzing again in the future. This could be a task for SFEI via the funded project for Blakely in 2015-16].

- 6) Conduct additional laboratory intercalibration.

[This could be done, but given the data already presented and the recent publications on SPATT, the chemistry is reasonably well-constrained. It would be a low priority compared to intercalibration with field samples].

Final Recommendation for interpreting SPATT: as documented in the Sutula et al. (in prep.) document, current recommendations based on statistical analysis, comparison with other field sites, and comparison with limited mussel samples is to consider "elevated" toxin concentrations equivalent to 1 ng/g total microcystins or 75 ng/g domoic acid for SPATT deployed by subembayment in San Francisco Bay. Values should be considered as "ranges" rather than absolute concentrations. For example, reasonable ranges, based on these updated thresholds, would be <1, 1-10, >10 for microcystins (no threat, moderate threat, high threat), and <50, 50-150, >150 for domoic acid. These ranges could be improved with additional mussel sampling, using logistic regression to define probability ranges (e.g. Lane et al. 2009; Anderson et al. 2011).

References

- Anderson, CR, RM Kudela, C Benitez-Nelson, E Sekula-Wood, CT Burrell, Y Chao, G Langlois, J Goodman, and DA Siegel. 2011. Detecting toxic diatom blooms from ocean color and a regional ocean model, *Geophysical Research Letters* 38, L04603, doi:10.1029/2010GL045858.
- Gibble, CM, RM Kudela. 2014. Detection of persistent microcystin toxins at the land-sea interface in Monterey Bay, California. *Harmful Algae*, 39: 146-153. doi:10.1016/j.hal.2014.07.004.
- Kudela, RM. 2011. Characterization and Deployment of Solid Phase Adsorption Toxin Tracking (SPATT) resin for monitoring of microcystins in fresh and salt water. *Harmful Algae*, 11: 117-125, doi: 10.1016/j.hal.2011.08.006.
- Lane, JQ, GW Langlois, and RM Kudela. 2012. Update on the application of Solid Phase Adsorption Toxin Tracking (SPATT) for field detection of domoic acid. Proceedings of the 14th International Conference on Harmful Algae, Intergovernmental Oceanographic Commission of UNESCO.
- Lane, JQ, P Raimondi, and RM Kudela. 2009. The development of a logistic regression model for the prediction of toxigenic *Pseudo-nitzschia* blooms in Monterey Bay, California. *Marine Ecology Progress Series*, 383: 37-51.
- Lane, JQ, CM Roddam, GW Langlois, and RM Kudela 2010. Application of Solid Phase Adsorption Toxin Tracking (SPATT) for field detection of domoic acid and saxitoxin in coastal California, *Limnology and Oceanography Methods*, 8:645-660.
- Lin, F., G. Sun, J. Qiu, Q. Ma, P. Hess, A. Li. 2014. Effect of seawater salinity on pore-size distribution on a poly(styrene)-based resin and its adsorption of diarrhetic shellfish toxins. *J. Chromatography A*, 1373: 1-8.
- Zendong, Z., C. Herrenknecht, E. Abadie, C. Brissard, C. Tixier, F. Mondeguer, V. Séchet, Z. Amzil, P. Hess. 2014. Extended evaluation of polymeric and lipophilic sorbents for passive sampling of marine toxins. *Toxicon*, 91:57-68.
- Zhao, H., et al. 2013. Mechanism and application of solid phase adsorption toxin tracking for monitoring microcystins. *Journal of Chromatography A* 1300: 159-164.



BUREAU OF RECLAMATION
2800 Cottage Way, E-1604
Sacramento, California 95825



DEPARTMENT OF WATER RESOURCES
1416 Ninth Street, Room 1115-1
Sacramento, California 95814

March 24, 2015

Mr. Thomas Howard
Executive Director
State Water Resources Control Board
1001 I Street
Sacramento, California 95814

Dear Mr. Howard:

The Department of Water Resources (DWR) and the U.S. Bureau of Reclamation (Reclamation) request a modification of the Revised Order that Approved a Temporary Urgency Change in License and Permit Terms and Conditions Requiring Compliance with Delta Water Quality Objectives in Response to Drought Conditions (dated March 5, 2015) (Order). The CVP and SWP Drought Contingency Plan (DCP), submitted to the State Water Resources Control Board on January 15, 2015 provides a description of the hydrologic conditions as of that date and actions proposed to balance multiple needs in a fourth consecutive dry year. The DCP serves as an initial framework to develop proposed modifications for conditions contained in Water Rights Decision 1641 (D-1641). DWR and Reclamation request the proposed modifications in the attached TUCP to be effective from April through the end of September.

Reclamation and DWR worked collaboratively with state and federal fish and wildlife agencies to prepare the DCP, as well as the Interagency Drought Strategy (Draft December 11, 2014). These documents outline the strategic goals of operations for this fourth year of drought, which serve as the context for the modifications the Projects are requesting. These overarching goals and objectives include:

1. Operating the CVP and SWP during the continuing drought to meet essential human health and safety needs and lessen critical economic losses.
2. Controlling of salt water intrusion in the Sacramento-San Joaquin Delta.
3. Preserving cold water pools in upstream reservoirs for temperature management to maintain cool water temperatures for salmon and steelhead.
4. Maintaining adequate protections for state and federally endangered and threatened species and other fish and wildlife resources.
5. Providing an overview of biological monitoring to improve water deliveries while also meeting water quality and species requirements.



BUREAU OF RECLAMATION
2800 Cottage Way, E-1604
Sacramento, California 95825



DEPARTMENT OF WATER RESOURCES
1416 Ninth Street, Room 1115-1
Sacramento, California 95814

The current Order allows Reclamation and DWR the following D-1641 modifications for CVP and SWP operations for the months of February and March:

1. The minimum daily Delta outflow of 7,100 cfs or equivalent salinity (2.64 millimhos per centimeter (mmhos/cm) at Collinsville), plus the requirement to meet higher flows of 11,400 cfs or equivalent salinity (2.64 mmhos/cm at Chipps Island) for a specified number of days depending on hydrology, was reduced to a minimum Delta outflow requirement of 4,000 cfs;
2. A minimum level of exports from the Delta when outflow is between 4,000 cfs and 7,100 cfs was approved at 1,500 cfs; authorized the use of an intermediate export rate under very limited conditions. The intermediate export rate could be increased up to 3,500 cfs when Delta outflow is between 5,500 cfs and 7,100 cfs, the DCC Gates are closed, DWR or Reclamation determined additional water is necessary to meet minimum public health and safety needs, and notifying the Executive Director of the State Water Resource Control Board;
3. The minimum San Joaquin River flow requirement at Vernalis was reduced from between 710 cfs or 1,140 cfs, depending on hydrology, to 500 cfs; and
4. The requirement to close the DCC Gates was changed to allow the gates to be open under certain circumstances.

The intent of the proposed modifications included in this letter, and the attached TUCP modification, for April to September operations is to continue the focus on conserving as much water as possible in upstream reservoirs in order to protect aquatic species, water quality, and water supplies in this fourth consecutive dry year. The conservation of storage will help meet fall Sacramento River temperature requirements and minimize potential impacts from a continuation of drought including for the benefit of Chinook salmon. The proposed suite of operational modifications from April 1 through September 30 includes continuation of provisions in the current TUC Order regarding compliance specifications for outflow requirements.

Because of the severity of drought impacts to water users south of the Delta, Reclamation and DWR are revising and resubmitting their previous request for approval of a step in intermediate export rate for the period between April, May and June. As with the previous proposal, the intermediate export is a contingency to improve south of Delta water supply in the event that hydrologic conditions remain dry and sporadic precipitation events occur. This requested Export Limit modification would only be implemented when Delta Outflow is within the range of 5,500 cfs to 7,100 cfs, and is intended to give the Projects the flexibility to capture increased natural and abandoned flows resulting from a sporadic storm event. Given the current dry hydrology and continuing dry forecast, the Projects anticipate that exercising this modification is unlikely.



BUREAU OF RECLAMATION
2800 Cottage Way, E-1604
Sacramento, California 95825



DEPARTMENT OF WATER RESOURCES
1416 Ninth Street, Room 1115-1
Sacramento, California 95814

For clarity, this is a request for regulatory flexibility. If a storm event creates hydrologic conditions that would allow for this modification to be implemented, Reclamation and DWR would consult with RTDOT to consider real-time conditions, including water quality and latest fisheries survey information. If consensus is obtained at RTDOT that any additional exports can be implemented without causing unreasonable harm to fish and wildlife, Reclamation or DWR would notify the State Water Resource Control Board Executive Director and seek final approval.

This request was conditionally approved in the revised March 5, 2015 Order, to apply only when Reclamation or DWR determines that additional water is necessary to meet minimum public health and safety needs. Due to the severity of drought conditions in the SWP and CVP south of Delta service areas and the limited amount of water that might be exported under this modification in April, May and June, Reclamation and DWR believe it would be impractical to attempt to track this increment of water separately from other project deliveries.

Specifically, and as described in more detail in the attached TUCP, Reclamation and DWR request the following modifications:

1. The minimum monthly Net Delta Outflow Index (NDOI) described in Figure 3 of D-1641 during the months of April, May and June to be no less than 4,000 cfs; for the month of July, the monthly requirement for NDOI shall be no less than 3,000 cfs. The 7-day running average shall be no less than 1,000 cfs below the monthly average.
2. The San Joaquin River at Airport Way Bridge, Vernalis river flow requirement during the 31-day pulse flow period to be no less than 710 cfs. For the period following the 31-day pulse flow through May 31st, the San Joaquin River flow at Vernalis river flow to be approximately 300 cfs. For June, the San Joaquin River flow Vernalis river flow to be approximately 200 cfs.
3. The minimum level of exports from the Delta when outflow is between 4,000 cfs and 7,100 cfs to be 1,500 cfs; and the use of an intermediate export rate under very limited conditions. The intermediate export rate could be increased up to 3,500 cfs when Delta outflow is between 5,500 cfs and 7,100 cfs under certain conditions.
4. The minimum monthly Sacramento River flow requirements measured at Rio Vista for September to be no less than 2,500 cfs, with the 7-day running average no less than 2,000 cfs.
5. The critical year D-1641 Agricultural Western Delta Salinity Standard at Emmaton (14 -day running average of 2.78 millimhos per centimeter) compliance point to be moved to Three Mile Slough from April to August 15.
6. The San Joaquin River at Vernalis Salinity requirement to be modified to 1.0 EC from April to August.



BUREAU OF RECLAMATION
2800 Cottage Way, E-1604
Sacramento, California 95825



DEPARTMENT OF WATER RESOURCES
1416 Ninth Street, Room 1115-1
Sacramento, California 95814

These proposed modifications reflect the elements included in the DCP 99% hydrology (without installation of Emergency Drought Barriers) as well as additional concepts for potential water operations. Currently DWR and Reclamation are closely monitoring and analyzing the need to install rock barriers in the Delta to protect water quality and minimize impacts on stored water supplies. If it is decided that Emergency Drought Barriers must be installed this water year, the Projects will submit a subsequent TUCP, based on most recent hydrology, to request additional modifications to D-1641 requirements. A preliminary evaluation in the DCP, as well as recent modeling, indicates the following D-1641 requirements could need modification:

1. The minimum monthly NDOI described in Figure 3 of D-1641 during the months of June through October.
2. The critical year D-1641 Agricultural Western Delta Salinity Standard at Emmaton (14-day running average of 2.78 millimhos per centimeter through August 15).
3. The mean monthly Rio Vista flow standard in September, October, and November.
4. The salinity standards for Eastern and Western Suisun Marsh beginning in May.

Urgent Need, Effects on Other Uses, Reasonable Protection of Fish and Wildlife and Protective of the Public Interest

The "urgent need" described in the previous change requests continue to exist. So far this year, the hydrology has been extremely dry with minimal precipitation events. The lack of precipitation events in 2015, combined with the past three dry year conditions have resulted in diminishing water supplies throughout the state. San Luis Reservoir and DWR's and Reclamation's reservoirs north of the Delta remain critically low. As a result, the proposed change remains urgent. This TUCP request adds additional measures to help address critically low storage levels in San Luis Reservoir and DWR's and Reclamation's reservoirs north of the Delta and associated water supply needs of those reservoirs.

This action should also not have an unreasonable impact to fish and wildlife. Reclamation and DWR have conducted a Biological Review and are seeking concurrence from National Marine Fisheries Service and U.S. Fish and Wildlife Service that these actions are consistent with the federal Endangered Species Act (Attachment A). DWR will also plan to consult with the California Department of Fish and Wildlife to determine if the existing Consistency Determination would remain in effect.

The attached analysis indicates that legal users of water will not be injured by this action (Attachment B). Delta water quality objectives protective of municipal/industrial and agricultural uses remain in place and the proposed combination of outflows and export levels are expected to continue to provide water quality adequate to meet the needs of beneficial uses. However, hydrologic conditions indicate that sufficient water may not be available in upstream reservoirs to maintain a cold water pool and also meet the Emmaton standard. Additionally, as occurs in the South Delta when water quality objectives are met, there may be an exception in achieving the agricultural objective for Old River at Tracy Road.



BUREAU OF RECLAMATION
2800 Cottage Way, E-1604
Sacramento, California 95825



DEPARTMENT OF WATER RESOURCES
1416 Ninth Street, Room 1115-1
Sacramento, California 95814

By conserving reservoir storage through the remainder of this year, providing protections for aquatic species, water quality and water supply, and thereby avoiding the severe consequences associated with depletion of reservoir capacity, the proposed changes are in the public interest. This request has been considered and is supported by the RTDOT established to recommend additional changes to the Order necessary to address risks presented by the ongoing and severe drought.

Sincerely,

David Murillo
Regional Director
Bureau of Reclamation

Mark W. Cowin
Director
Department of Water Resources

Date: 3/24/2015

Date: 3/24/2015

TUCP for April – September Draft Outline of Proposed Changes

This proposed suite of modifications includes continuation of a number of provisions in the current TUCP Order and other elements of D-1641 that could be modified.

I. Requested Changes

1. Modification of Net Delta Outflow Index

D-1641 requires a Delta outflow minimum monthly average Net Delta Outflow Index (NDOI) of 7,100 cfs 3-day average and salinity requirements during the months of April, May and June. Reclamation and DWR petition the State Water Board to adopt a Delta outflow standard of a minimum monthly NDOI during the months of April, May and June to be no less than 4,000 cfs; for the month of July, the monthly requirement for NDOI shall be no less than 3,000 cfs. The 7-day running average shall be no less than 1,000 cfs below the monthly average.

These modifications are necessary because of the extraordinarily dry conditions of the past several years in combination with the forecasts of limited future precipitation, low reservoir storage, and the competing demands on water supply of fish and wildlife protection, Delta salinity control, and critical water supply needs.

2. Modification of San Joaquin River Flow

D-1641 requires a San Joaquin River at Airport Way Bridge, Vernalis minimum monthly average flow. D-1641 also requires a 31-day pulse flow period in April and May. The Projects petition the State Water Resource Control Board to adopt the following San Joaquin River at Airport Way Bridge, Vernalis river flow requirements:

- During the Vernalis 31-day pulse flow period, the monthly average flow to be no less than 710 cfs.
- For the period following the 31-day pulse flow through May 31st, the SJ River flow at Vernalis would be no less than 300 cfs on a 30-day running average.
- In June, the SJ River flow at Vernalis would be no less than 200 cfs average for the month.

This modification is necessary because of the extraordinarily dry conditions of the past several years in combination with the forecasts of limited future precipitation, extremely low reservoir storage, high water temperatures, and the competing demands on water supply of fish and wildlife protection, Delta salinity control, and critical water supply needs.

3. Modification of Export Limit

Table 3 of D-1641 describes export limits. Generally, exports are limited to 35% of Delta inflow from February through June of each year, and 65% of Delta inflow from July through January of each year. Reclamation and DWR petition the State Water Resource Control Board to adopt the following, modified from the maximum Export Limits included in Table 3 of D-1641, for the months of April, May, and June.

- When precipitation and runoff events occur, and the DCC Gates are closed, and Footnote 10 of Table 3 of D-1641 is being met [3-day average Delta outflow of 7,100 cfs, or electrical conductivity of 2.64 millimhos per centimeter on a daily or 14-day running average at the confluence of the Sacramento and the San Joaquin Rivers (Collinsville station C2) if applicable], but any additional Delta outflow requirements contained in Table 4 of D-1641 (“Chippys days” or “Port Chicago days” requirements) are not being met, then exports of natural and abandoned flows are permitted up to Export Limits contained in Table 3 of D-1641 at the SWP Banks Pumping Plant and at the CVP Jones Pumping Plant, subject to other applicable laws and regulations including the federal Endangered Species Act (ESA) and California ESA (CESA).
- When NDOI of at least 7,100 cfs is not being met as specified above, or the DCC Gates are open, then the combined maximum exports at the SWP Banks Pumping Plant and the CVP Jones Pumping Plant shall be no greater than 1,500 cfs with one exception. DWR and Reclamation may export up to a combined 3,500 cfs of natural and abandoned flows, on a 3-day running average, provided that NDOI is greater than 5,500 cfs and the DCC Gates are closed. Before implementing this action, DWR and Reclamation will consult with RTDOT to confirm that real-time conditions are consistent with the conditions evaluated as part of this petition. If consensus is obtained at RTDOT, Reclamation or DWR would notify the SWB Executive Director for final approval.
- During the effective period of any issued Order, if precipitation events occur that enable DWR and Reclamation to fully comply with the Delta outflow, river flows, and DCC Gate Closure requirements contained in D-1641, then D-1641 requirements shall be operative, except that any SWP and CVP exports greater than 1,500 cfs shall be limited to natural or abandoned flow, or transfers as specified in condition 1e of the March 5, 2015, modified Order.

4. Modifications of DCC Gate Operations

D-1641 and the NMFS Biological Opinion require the closure of the DCC gates from February 1 through May 20. Reclamation and DWR petition the State Water Resources Control Board to modify the DCC gate operation requirements contained in Table 3 of D-1641 such that the DCC gates may be opened during April and May as necessary to

reduce intrusion of high salinity water into the Delta while preserving limited storage in upstream reservoirs and reducing impacts to migrating Chinook salmon. The DCC gate triggers matrix (as described in Appendix G of the April 2014 Drought Operations Plan and Operational Forecast) will be used by the Projects to determine operation of the DCC gates. If the Projects determine that the DCC gates must open to provide for salinity management in the Delta during a period that requires closure under D-1641 or the NMFS Biological Opinion then the Projects, through the RTDOT process, will provide at least a 5-day notice to the fish and wildlife agencies so that enhanced monitoring can begin. The Projects will implement enhanced monitoring and triggers to open and close the gates, as needed for protection of listed species.

5. Modification of Rio Vista Flow Requirement

D-1641 Table 3 dictates a minimum monthly Sacramento River flow requirement measured at Rio Vista of 3,000 cfs in the months of September (for critically dry water years). This requirement also states that the 7-day running average Sacramento River flow measured at Rio Vista shall be no lower than 2,000 cfs during this time. Reclamation and DWR petition the State Water Resource Control Board to modify the D-1641 Table 3 Sacramento River at Rio Vista flow requirements to be no less than 2,500 cfs on a monthly average in September. The 7-day running average shall not be less than 2,000 cfs.

6. Modification of Western Delta Salinity Compliance Point

In a critical year, D-1641 requires the Agricultural Western Delta Salinity Standard at Emmaton have a 14-day running average of 2.78 millimhos per centimeter from April 1 to August 15. Reclamation and DWR petition the State Water Resource Control Board to modify this requirement by moving the compliance location from Emmaton to Three Mile Slough on the Sacramento River beginning April 1.

7. Modification of San Joaquin River Salinity Requirement

In all year types, D-1641 requires a San Joaquin River at Vernalis Salinity limit of 0.7 EC from April through August. Reclamation petitions the State Water Resource Control Board to modify the San Joaquin River at Vernalis Salinity requirement from 0.7 EC to 1.0 EC from April to August.

Attachment A

Biological Review for Endangered Species Act Compliance

Attachment 2. Biological Review for Endangered Species Act Compliance with the WY 2015 Drought Contingency Plan April through September Project Description

Methods and Modeling

Conceptual models of impacts from drought management actions were presented in the Biological Review for the February-March Project Description (Figure 1, Reclamation 2015). The potential effects of the proposed April through September 2015 operational actions are considered in the context of these conceptual models. Additionally, the biological opinions (NMFS 2009, USFWS 2008) were reviewed regarding biological linkage to the considered actions.

M A N A G E M E N T L I N K A G E A S S E S S M E N T	DCC Gate Operation (Interior delta salinity)	Outflow (NDOI) (Change in Location)	Inflow (Storage impacted by DOP, seasonal depletions)	OMR (change in BiOp criteria)	Exports (E/I calculation)
	<ul style="list-style-type: none"> Route entrainment 	<ul style="list-style-type: none"> Tidal influence Migration rate Rearing period Survival rate 	<ul style="list-style-type: none"> Migration rate Rearing period Survival rate 	<ul style="list-style-type: none"> Route entrainment Migration rate Rearing period Survival rate 	<ul style="list-style-type: none"> Route entrainment Migration rate Facility survival
	<ul style="list-style-type: none"> DJFMP periodicity 	<ul style="list-style-type: none"> Changes in DSM2 velocity characteristics 	<ul style="list-style-type: none"> Changes in DSM2 velocity characteristics 	<ul style="list-style-type: none"> SD/CD DJFMP presence/absence 	<ul style="list-style-type: none"> SD/CD DJFMP presence/absence
	<ul style="list-style-type: none"> Changes in DSM2 proportion daily flow 	<ul style="list-style-type: none"> Changes in DSM2 proportion daily flow 	<ul style="list-style-type: none"> Changes in DSM2 proportion daily flow 	<ul style="list-style-type: none"> Facility salvage (Density, total, timing) 	<ul style="list-style-type: none"> Facility salvage (Density, total, timing)
	<ul style="list-style-type: none"> Delta survival information 	<ul style="list-style-type: none"> Delta survival information 	<ul style="list-style-type: none"> Delta survival information 	<ul style="list-style-type: none"> Delta survival information 	<ul style="list-style-type: none"> Delta survival information

Figure 1 Conceptual model of drought contingency plan elements and their biological linkage to salmonids and assessment information available for evaluation.

Operational Forecast Model

The February 90% Operational Forecast provides potential tributary and Delta operational conditions. In particular, this information is useful for evaluating potential Central Valley Project and State Water Project (CVP and SWP) tributary operations during April through September. The reservoir releases in this forecast include implementation of RPA actions from the NMFS Biological Opinion on the Long Term Coordinated Operations of the CVP and SWP for Clear Creek, American River, and Stanislaus River. These are described in the Project Description, which includes some modifications of these actions. When these monthly average flows assume implementation different from the RPA, a qualitative description of habitat-related impacts are described. Temperature related impacts of the forecast related to divisions of the CVP are not included at this time, since the Sacramento River Temperature Task Group (SRRTG) is actively meeting to provide advice and review of the temperature forecast modeling to support development of the seasonal Sacramento Temperature Management Plan. Temperature

Attachment 2. Biological Review for Endangered Species Act Compliance with the WY 2015 Drought Contingency Plan April through September Project Description

management for the American River Group will be considered by the American River Group (ARG).

DSM2 Model

Delta Simulation Model II (DSM2) simulations were performed and evaluated for three operational management scenarios (Table 1). These simulations were designed to evaluate potential effects of the Project Description's reduced Sacramento and San Joaquin River outflow and other operational modifications on potential Delta hydrodynamics for the months of April through May when listed salmonids are most likely to be present in the Delta and hydrology forecasts are more foreseeable. These scenarios were concatenated to look at a 31-day pulse flow period ("April") and post-pulse period ("May") to evaluate DSM2 results. The Baseline scenario (Hydrology 1) represents an unmodified set of D-1641 standards for NDOI, Vernalis flows, and Delta Cross Channel Gate operations, while a Project Description scenario (Hydrology 2) included a modified NDOI and Vernalis flows.

The April modeled Vernalis average monthly flow, which were inclusive of an Appendix 2e pulse flow volume is likely positively biased compared to the predicted Vernalis average monthly flow during the pulse flow period, which in the TUCP is proposed to be no less than 710cfs. According to the modeled flows at Channel 6 (Mosssdale, downstream of Vernalis but likely to have similar flow) summarized in Table 4 and 5, the modeled monthly average flow during April and May was 951 cfs, 241 cfs more than the 710 cfs proposed in the current TUCP order. Whether realized flows at Vernalis will more closely match the modeled flows or the proposed flows will depend on accretions and depletions during April and May. This uncertainty suggests modeled flows under the Project Description are likely greater than what will actually be observed, which influences the interpretation of any possible impacts on fishes resulting from the Project Description. Additionally, results from a hydrodynamic scenario with similar NDOI and Vernalis flows and an open DCC gate for two months are presented (Hydrology 2'). Other input values remained constant and reflected the best information available to DWR modelers when models were run on March 13, 2015. These flows do not necessarily reflect current forecast information and actual conditions have and will differ from the modeled scenarios. The modeled scenarios represent minimum values, yet provide the best evaluation approach to describing the worst conditions likely to be observed for the flow measures. These issues increase the uncertainty of assessments of impacts to all species reviewed.

Attachment 2. Biological Review for Endangered Species Act Compliance with the WY 2015 Drought Contingency Plan April through September Project Description

Table 1. DSM2 Model Input for Scenarios Evaluated in the Biological Review. DSM2 Run Name is Listed Parenthetically for Each Scenario

Scenario	NDOI		Freeport flow (cfs)		Vernalis flow (cfs)		Combined Exports (cfs)		DCC Status
	April	May	April	May	April	May	April	May	
Baseline (Hydrology 1)	7,100		7,100- (VNS +export)		710 +3100 cfs (4/1 -5/1)		1,500		Closed
Project Description – DCC Gate Closed (Hydrology 2)	4,000		4,000-(Lower VNS +export)		300+App. 2e flow (4/1 – 5/1) ¹		1,500		Closed
Project Description -- DCC Gate Open (Hydrology 2')	4,000		4,000-(Lower VNS +export)		300+App. 2e flow (4/1 – 5/1) ¹		1,500		Open for 2 months

DSM2 modeling outputs for each scenario were used to evaluate the distribution of 15-minute flow and velocity values for multiple channels, including:

- Upstream of Head of Old River on San Joaquin (Channel 6)
- Downstream of Head of Old River on San Joaquin (Channel 9)
- Upstream of Stockton Deepwater Shipping Channel (Channel 12)
- Jersey Point on San Joaquin River (Channel 49)
- Sherman Island on San Joaquin River (Channel 50)
- Downstream of Head of Old River on Old River (Channel 54)
- Old River south of Railroad Cut (Channel 94)
- Old River at San Joaquin River (Channel 124)
- Middle River north of Railroad Cut (Channel 148)
- Three Mile Slough near San Joaquin River (Channel 310)
- Sacramento River near Sherwood Harbor (Channel 412)
- Sacramento River at Sutter Slough (Channel 388)
- Sacramento River upstream of Delta Cross Channel (Channel 421)
- Sacramento River downstream of Delta Cross Channel (Channel 422)

¹ The TUCP identifies proposed modification of the average monthly flow during the Vernalis 31-day pulse flow period to be no less than 710 cfs.

Attachment 2. Biological Review for Endangered Species Act Compliance with the WY 2015 Drought Contingency Plan April through September Project Description

- Sacramento River upstream of Georgiana Slough (Channel 422)
- Sacramento river downstream of Georgiana Slough (Channel 423)
- Sacramento River near Cache Slough (Channel 429)
- Sherman Island on Sacramento River (Channel 434)

Hydrodynamic Metrics

Hydrodynamic metrics, such as daily mean velocity and flow were calculated (Tables 2-5). Additionally, mean daily proportion positive velocity, daily mean velocity, and daily mean flow were used to assess changes in the Delta at these locations. These were calculated over the separate April and May periods (Tables 6-7).

These data are also visualized spatially at both temporal steps to assess regional impacts and more complex hydrodynamics around the Delta Cross Channel and Head of Old River under each scenario. Daily proportion positive velocity is the percentage of the day that river flows have a positive velocity value (flows in downstream direction). Daily mean velocity and mean flow are the average of all values summed over the 24 hour period, which takes into account the effects of tidal stage on velocity magnitudes. These daily values are then averaged for the period of interest. The difference in the values of these hydrodynamic metrics between the Baseline and Project Description model run was calculated to assess how the metric was affected by the Project Description. We also calculated the difference in the values of these hydrodynamic metrics between the Project Description and Project Description with DCC gates open scenarios.

Density plots of DSM2 modeled 15-minute velocity data were developed for the eighteen channel nodes modeled for the two scenarios. Figures 2-23 show nodes showing variation between modeled scenarios in April and May periods for the different hydrology scenarios. These plots show low levels of change in the 15-minute velocity plots and in the lower river reaches tidal hydrodynamics and channel morphology drive channel velocities to a greater extent than the operational differences evaluated in the modeled scenarios. Figures 24-27 show spatially key channel nodes through the Delta during April and May for a few of the hydrodynamic metrics.

Differences in the river inflow between the Project Description and Baselines modeled scenarios are seen in the velocity plots at the upper extent of the tidal influence on the Sacramento near Sherwood Harbor (Figure 2-3) and San Joaquin river near Head of Old River (Figures 16-17). In the May portion of the model runs, there is a larger difference between the Baseline and Project Description modeled velocities due to reduced San Joaquin River contribution to the NDOI and thus greater flows at Freeport in May than April (Figures 2 and 3). At all other channel nodes during May and all nodes for the April portion of the model runs, the influence of these river inflows quickly dissipates as tides begin to dominate on the Sacramento (Figures 4-15). An open DCC gates during these months also impacts velocities upstream of the DCC gates (Channel node 421, Figures 6-7), and modeled results show a greater range of velocities, both negative and positive in this reach, due to increased flows rates downstream on an ebbing tide and upstream on a flooding tide. Modeled channel velocities in the Sacramento River near the DCC and Georgiana Slough differ between the Baseline and Project Description scenarios. Modeled results from the Project Description with an open DCC show a reduction in daily mean velocities in April and May downstream of the DCC (Channel node 422; Figures 8-9). At locations in the

Attachment 2. Biological Review for Endangered Species Act Compliance with the WY 2015 Drought Contingency Plan April through September Project Description

North Delta further south, tidal conditions dominate and the range and magnitude of velocities observed in the modeling are similar into the western Delta (Figures 10-15).

Difference between the Project Description and Baseline model run influence the velocity along the San Joaquin River more during the modeled April period than May period (Figures 16-21) from upstream of Head of Old River to downstream of the Stockton Deepwater Ship Channel. These differences influence the proportion of daily positive flow (Tables 6-7), daily velocities (Tables 2-3), and daily flows (Tables 4-5). In the South Delta along Old and Middle River corridor, these changes are less significant due to the low export levels in the Baseline and Project Description model run. The modeled daily average hydrodynamic changes resulting from the proposed operations for both the April and May periods are small (Tables 4-5, approximately 62cfs for channel 148 in April and 152cfs in May) and do not show substantive differences in daily average velocities (Tables 2-3, Figure 22-23) between Baseline period at channel node 148 (Middle River north of Railroad Cut).

Attachment 2. Biological Review for Endangered Species Act Compliance with the WY 2015 Drought Contingency Plan April through September
Project Description

Table 2. Daily Mean Velocities (ft/sec) between Base and Project Description Model Scenarios and Their Difference (Hydrology 2 minus Hydrology 1) at All Channel Nodes during April

Date	Node 6			Node 9			Node 12			Node 49			Node 50			Node 54			Node 94			Node 124			Node 148		
	Hydr #1	Hydr #2	Difference	Hydr #1	Hydr #2	Difference	Hydr #1	Hydr #2	Difference																		
1-Apr	1.20	0.26	-0.94	1.29	0.20	-1.09	1.05	0.19	-0.86	0.09	0.07	-0.03	0.10	0.08	-0.02	0.36	-0.06	-0.20	-0.01	-0.03	-0.04	-0.06	-0.06	0.01	-0.02	-0.03	-0.01
2-Apr	1.21	0.34	0.87	1.38	0.30	1.08	1.14	0.26	0.88	0.08	0.06	0.02	0.10	0.07	0.02	0.37	-0.06	0.18	-0.04	-0.03	0.02	-0.07	-0.06	-0.01	-0.03	-0.03	0.01
3-Apr	1.21	0.38	0.82	1.38	0.35	1.03	1.14	0.31	0.84	0.07	0.05	0.02	0.09	0.07	0.02	0.37	-0.06	0.16	-0.03	-0.03	0.02	-0.07	-0.06	-0.01	-0.03	-0.03	0.01
4-Apr	1.20	0.38	0.82	1.38	0.36	1.02	1.14	0.31	0.83	0.07	0.04	0.02	0.08	0.06	0.02	0.37	-0.06	0.16	-0.02	-0.03	0.02	-0.07	-0.06	-0.01	-0.02	-0.03	0.01
5-Apr	1.20	0.38	0.82	1.38	0.36	1.02	1.15	0.32	0.83	0.06	0.04	0.02	0.08	0.06	0.02	0.37	-0.06	0.16	-0.02	-0.03	0.02	-0.07	-0.06	-0.01	-0.02	-0.03	0.01
6-Apr	1.20	0.38	0.82	1.38	0.36	1.02	1.15	0.32	0.83	0.05	0.02	0.02	0.06	0.04	0.02	0.37	-0.07	0.16	-0.02	-0.03	0.02	-0.07	-0.07	-0.01	-0.03	-0.03	0.01
7-Apr	1.20	0.38	0.82	1.38	0.36	1.02	1.15	0.32	0.83	0.04	0.01	0.02	0.05	0.03	0.02	0.37	-0.07	0.16	-0.02	-0.03	0.02	-0.07	-0.07	-0.01	-0.03	-0.03	0.01
8-Apr	1.20	0.38	0.82	1.38	0.36	1.02	1.15	0.32	0.83	0.02	0.00	0.02	0.03	0.01	0.02	0.37	-0.07	0.16	-0.03	-0.04	0.02	-0.08	-0.07	-0.01	-0.03	-0.04	0.01
9-Apr	1.21	0.39	0.82	1.39	0.38	1.01	1.16	0.33	0.83	0.02	-0.01	0.02	0.03	0.00	0.02	0.37	-0.06	0.17	-0.02	-0.04	0.02	-0.07	-0.06	-0.01	-0.03	-0.04	0.01
10-Apr	1.21	0.40	0.81	1.41	0.42	0.99	1.17	0.36	0.81	0.02	0.00	0.02	0.03	0.01	0.02	0.36	-0.05	0.17	0.01	-0.02	0.02	-0.06	-0.05	-0.01	-0.02	-0.02	0.01
11-Apr	1.21	0.40	0.81	1.42	0.42	0.99	1.19	0.38	0.81	0.05	0.03	0.02	0.06	0.04	0.02	0.36	-0.04	0.17	0.04	0.00	0.02	-0.05	-0.04	-0.01	0.00	0.00	0.01
12-Apr	1.22	0.40	0.82	1.41	0.41	1.00	1.19	0.38	0.82	0.09	0.06	0.02	0.09	0.07	0.02	0.36	-0.04	0.17	0.05	0.00	0.02	-0.05	-0.04	-0.01	0.01	0.00	0.01
13-Apr	1.21	0.39	0.82	1.41	0.40	1.01	1.18	0.36	0.82	0.10	0.08	0.02	0.11	0.09	0.02	0.36	-0.04	0.17	0.05	0.00	0.02	-0.05	-0.04	-0.01	0.01	0.00	0.01
14-Apr	1.21	0.39	0.82	1.40	0.39	1.01	1.17	0.35	0.82	0.11	0.09	0.02	0.12	0.10	0.02	0.36	-0.04	0.17	0.04	0.00	0.02	-0.05	-0.04	-0.01	0.01	0.00	0.01
15-Apr	1.20	0.38	0.83	1.38	0.36	1.02	1.17	0.34	0.82	0.11	0.09	0.02	0.13	0.10	0.02	0.36	-0.05	0.16	0.03	0.00	0.02	-0.06	-0.05	-0.01	0.00	0.00	0.01
16-Apr	1.20	0.38	0.82	1.37	0.35	1.02	1.15	0.33	0.83	0.11	0.09	0.02	0.13	0.11	0.02	0.36	-0.05	0.16	0.02	-0.01	0.02	-0.06	-0.05	-0.01	0.00	-0.01	0.01
17-Apr	1.19	0.37	0.81	1.36	0.34	1.02	1.14	0.31	0.83	0.11	0.09	0.02	0.13	0.11	0.02	0.36	-0.06	0.16	0.00	-0.02	0.02	-0.07	-0.06	-0.01	-0.01	-0.02	0.01
18-Apr	1.18	0.37	0.81	1.35	0.34	1.01	1.13	0.31	0.82	0.10	0.08	0.02	0.12	0.10	0.02	0.36	-0.06	0.16	-0.02	-0.03	0.02	-0.07	-0.06	-0.01	-0.02	-0.03	0.01
19-Apr	1.18	0.37	0.81	1.35	0.35	1.00	1.13	0.31	0.82	0.08	0.05	0.02	0.10	0.08	0.02	0.36	-0.07	0.16	-0.03	-0.03	0.02	-0.08	-0.07	-0.01	-0.03	-0.03	0.01
20-Apr	1.18	0.37	0.80	1.35	0.35	1.00	1.14	0.31	0.82	0.05	0.03	0.02	0.08	0.05	0.02	0.36	-0.07	0.16	-0.03	-0.04	0.02	-0.08	-0.07	-0.01	-0.03	-0.04	0.01
21-Apr	1.18	0.38	0.81	1.36	0.35	1.01	1.14	0.32	0.83	0.03	0.01	0.02	0.05	0.03	0.02	0.36	-0.07	0.16	-0.03	-0.04	0.02	-0.08	-0.07	-0.01	-0.03	-0.04	0.01
22-Apr	1.19	0.38	0.81	1.38	0.36	1.02	1.15	0.32	0.83	0.02	0.00	0.02	0.03	0.01	0.02	0.36	-0.07	0.16	-0.03	-0.04	0.02	-0.08	-0.07	-0.01	-0.03	-0.04	0.01
23-Apr	1.20	0.40	0.81	1.40	0.40	1.00	1.16	0.34	0.82	0.02	-0.01	0.02	0.03	0.00	0.02	0.36	-0.06	0.16	-0.01	-0.03	0.02	-0.07	-0.06	-0.01	-0.03	-0.03	0.01
24-Apr	1.22	0.40	0.81	1.42	0.42	1.00	1.19	0.38	0.81	0.03	0.01	0.02	0.04	0.02	0.02	0.36	-0.05	0.17	0.03	-0.01	0.02	-0.05	-0.05	-0.01	0.00	-0.01	0.01
25-Apr	1.22	0.41	0.82	1.43	0.43	1.01	1.20	0.38	0.82	0.07	0.05	0.02	0.07	0.05	0.02	0.36	-0.04	0.17	0.05	0.00	0.02	-0.05	-0.04	-0.01	0.01	0.00	0.01
26-Apr	1.23	0.40	0.83	1.43	0.42	1.01	1.20	0.38	0.83	0.09	0.07	0.02	0.09	0.07	0.02	0.37	-0.04	0.17	0.05	0.00	0.02	-0.05	-0.04	-0.01	0.01	0.00	0.01
27-Apr	1.23	0.40	0.83	1.42	0.41	1.02	1.19	0.36	0.83	0.10	0.08	0.02	0.11	0.08	0.02	0.37	-0.04	0.18	0.04	0.00	0.02	-0.05	-0.04	-0.01	0.01	0.00	0.01
28-Apr	1.23	0.36	0.87	1.42	0.36	1.06	1.18	0.32	0.86	0.10	0.08	0.02	0.11	0.09	0.02	0.37	-0.04	0.19	0.03	-0.01	0.02	-0.05	-0.04	-0.01	0.00	-0.01	0.01
29-Apr	0.79	0.38	0.41	0.92	0.34	0.58	0.75	0.28	0.47	0.09	0.07	0.02	0.10	0.08	0.02	0.26	-0.04	0.09	0.01	-0.01	0.02	-0.05	-0.04	-0.01	-0.01	-0.01	0.01
30-Apr	0.37	0.34	0.03	0.30	0.27	0.03	0.25	0.23	0.02	0.08	0.07	0.01	0.09	0.08	0.01	0.16	-0.05	0.01	0.00	-0.01	0.00	-0.05	-0.05	0.00	-0.01	-0.01	0.00

Date	Node 310			Node 388			Node 412			Node 421			Node 422			Node 423			Node 429			Node 434		
	Hydr #1	Hydr #2	Difference																					
1-Apr	0.05	0.02	-0.03	0.52	0.46	-0.06	0.63	0.56	-0.07	0.51	0.45	-0.05	0.45	0.40	-0.05	0.36	0.32	-0.05	0.33	0.29	-0.04	0.12	0.10	-0.01
2-Apr	0.04	0.01	0.03	0.51	0.44	0.07	0.63	0.53	0.10	0.50	0.43	0.07	0.44	0.38	0.06	0.36	0.29	-0.06	0.32	0.27	-0.05	0.11	0.09	-0.01
3-Apr	0.03	0.00	0.03	0.51	0.44	0.07	0.63	0.53	0.10	0.50	0.43	0.07	0.44	0.38	0.06	0.35	0.29	-0.06	0.32	0.27	-0.05	0.10	0.09	-0.01
4-Apr	0.02	0.00	0.03	0.52	0.44	0.07	0.64	0.54	0.10	0.50	0.43	0.07	0.44	0.38	0.06	0.35	0.28	-0.06	0.31	0.26	-0.05	0.09	0.08	-0.01
5-Apr	0.01	-0.01	0.03	0.52	0.44	0.07	0.64	0.54	0.10	0.50	0.43	0.07	0.44	0.38	0.06	0.35	0.28	-0.06	0.31	0.26	-0.05	0.09	0.07	-0.01
6-Apr	0.00	-0.02	0.03	0.51	0.44	0.07	0.64	0.54	0.10	0.50	0.43	0.07	0.44	0.38	0.06	0.35	0.28	-0.06	0.30	0.25	-0.05	0.08	0.06	-0.01
7-Apr	-0.01	-0.03	0.03	0.51	0.44	0.08	0.64	0.54	0.10	0.50	0.43	0.07	0.44	0.38	0.06	0.35	0.28	-0.07	0.30	0.25	-0.05	0.06	0.05	-0.01
8-Apr	-0.02	-0.05	0.03	0.51	0.44	0.08	0.64	0.54	0.10	0.50	0.43	0.07	0.44	0.38	0.06	0.35	0.28	-0.07	0.30	0.25	-0.05	0.05	0.04	-0.01
9-Apr	-0.02	-0.05	0.03	0.51	0.44	0.08	0.65	0.55	0.10	0.51	0.44	0.07	0.45	0.38	0.06	0.35	0.29	-0.07	0.30	0.25	-0.05	0.04	0.02	-0.01
10-Apr	-0.01	-0.04	0.02	0.54	0.46	0.07	0.66	0.56	0.10	0.52	0.46	0.07	0.46	0.40	0.06	0.37	0.31	-0.06	0.31	0.26	-0.05	0.03	0.02	-0.01
11-Apr	0.03	0.00	0.02	0.58	0.50	0.07	0.67	0.57	0.10	0.54	0.47	0.07	0.48	0.42	0.06	0.40	0.34	-0.06	0.34	0.29	-0.05	0.06	0.04	-0.01
12-Apr	0.06	0.03	0.02	0.58	0.51	0.07	0.67	0.57	0.10	0.55	0.48	0.07	0.48	0.42	0.06	0.41	0.35	-0.06	0.35	0.30	-0.05	0.09	0.07	-0.01
13-Apr	0.07	0.05	0.03	0.58	0.50	0.07	0.67	0.57	0.10	0.54	0.47	0.07	0.48	0.42	0.06	0.41	0.35	-0.06	0.36	0.31	-0.05	0.11	0.09	-0.01
14-Apr	0.07	0.05	0.03	0.57	0.50	0.07	0.66	0.56	0.10	0.54	0.47	0.07	0.48	0.41	0.06	0.40	0.34	-0.06	0.36	0.31	-0.05	0.12	0.11	-0.01
15-Apr	0.07	0.05	0.03	0.56	0.49	0.07	0.65	0.55	0.10	0.53	0.46	0.07	0.47	0.41	0.06	0.39	0.33	-0.06	0.35	0.30	-0.05	0.13	0.11	-0.01
16-Apr	0.07	0.04	0.03	0.55	0.48	0.07	0.64	0.54	0.10	0.52	0.45	0.07	0.46	0.40	0.06	0.38	0.32	-0.06	0.35	0.30	-0.05	0.13	0.12	-0.01
17-Apr	0.06	0.04	0.03	0.54	0.47																			

Attachment 2. Biological Review for Endangered Species Act Compliance with the WY 2015 Drought Contingency Plan April through September Project Description

Table 3. Daily Mean Velocities (ft/sec) between Base and Project Description Model Scenarios and Their Difference (Hydrology 2 minus Hydrology 1) at All Channel Nodes during May

Date	Node 6			Node 9			Node 12			Node 49			Node 50			Node 54			Node 94			Node 124			Node 148		
	Hydr #1	Hydr #2	Difference	Hydr #1	Hydr #2	Difference	Hydr #1	Hydr #2	Difference																		
1-May	0.35	0.21	0.14	0.26	0.15	0.11	0.21	0.13	0.08	0.06	0.05	0.01	0.08	0.07	0.01	0.16	-0.06	0.04	-0.05	-0.03	0.01	-0.06	-0.06	0.00	-0.03	-0.03	0.00
2-May	0.33	0.12	0.21	0.24	0.05	0.18	0.19	0.05	0.14	0.06	0.04	0.01	0.07	0.06	0.01	0.16	-0.06	0.07	-0.08	-0.04	0.01	-0.07	-0.06	0.00	-0.04	-0.04	0.00
3-May	0.33	0.12	0.21	0.24	0.05	0.19	0.18	0.04	0.14	0.05	0.04	0.01	0.07	0.06	0.01	0.16	-0.07	0.07	-0.09	-0.05	0.01	-0.07	-0.07	0.00	-0.04	-0.05	0.00
4-May	0.33	0.12	0.21	0.24	0.05	0.19	0.18	0.04	0.14	0.05	0.04	0.01	0.07	0.06	0.01	0.16	-0.07	0.07	-0.09	-0.05	0.01	-0.07	-0.07	0.00	-0.05	-0.05	0.00
5-May	0.33	0.12	0.21	0.24	0.05	0.19	0.19	0.05	0.14	0.04	0.03	0.01	0.06	0.05	0.01	0.16	-0.07	0.07	-0.09	-0.06	0.01	-0.08	-0.07	0.00	-0.05	-0.06	0.00
6-May	0.33	0.12	0.21	0.24	0.05	0.19	0.19	0.05	0.14	0.02	0.01	0.01	0.04	0.03	0.01	0.16	-0.07	0.07	-0.10	-0.06	0.01	-0.08	-0.07	0.00	-0.05	-0.06	0.00
7-May	0.34	0.13	0.21	0.24	0.06	0.18	0.19	0.05	0.14	0.01	0.00	0.01	0.03	0.02	0.01	0.17	-0.07	0.07	-0.10	-0.06	0.01	-0.08	-0.07	0.00	-0.06	-0.06	0.00
8-May	0.35	0.15	0.20	0.27	0.09	0.18	0.20	0.07	0.13	0.00	-0.01	0.01	0.01	0.00	0.01	0.16	-0.07	0.07	-0.09	-0.06	0.01	-0.07	-0.07	0.00	-0.06	-0.06	0.00
9-May	0.36	0.15	0.21	0.30	0.12	0.19	0.23	0.09	0.14	0.00	-0.01	0.01	0.01	0.00	0.01	0.16	-0.06	0.07	-0.06	-0.05	0.01	-0.06	-0.06	0.00	-0.04	-0.05	0.00
10-May	0.37	0.15	0.22	0.31	0.12	0.19	0.24	0.11	0.14	0.01	0.00	0.01	0.02	0.01	0.01	0.16	-0.05	0.07	-0.04	-0.03	0.01	-0.06	-0.05	0.00	-0.03	-0.03	0.00
11-May	0.37	0.15	0.22	0.31	0.12	0.19	0.25	0.11	0.14	0.04	0.03	0.01	0.04	0.04	0.01	0.16	-0.05	0.07	-0.03	-0.03	0.01	-0.06	-0.05	0.00	-0.02	-0.03	0.00
12-May	0.36	0.14	0.22	0.30	0.11	0.19	0.24	0.10	0.14	0.06	0.05	0.01	0.07	0.06	0.01	0.16	-0.05	0.08	-0.03	-0.03	0.01	-0.06	-0.05	0.00	-0.02	-0.03	0.00
13-May	0.36	0.14	0.22	0.29	0.10	0.19	0.23	0.09	0.14	0.07	0.06	0.01	0.08	0.07	0.01	0.16	-0.05	0.08	-0.04	-0.03	0.01	-0.05	-0.05	0.00	-0.02	-0.03	0.00
14-May	0.35	0.14	0.22	0.28	0.09	0.19	0.22	0.08	0.14	0.08	0.07	0.01	0.09	0.08	0.01	0.16	-0.05	0.08	-0.04	-0.03	0.01	-0.06	-0.05	0.00	-0.03	-0.03	0.00
15-May	0.33	0.12	0.21	0.26	0.07	0.18	0.22	0.08	0.14	0.09	0.07	0.01	0.10	0.09	0.01	0.16	-0.05	0.07	-0.04	-0.03	0.01	-0.06	-0.05	0.00	-0.03	-0.03	0.00
16-May	0.32	0.11	0.21	0.23	0.05	0.18	0.21	0.07	0.14	0.09	0.08	0.01	0.11	0.10	0.01	0.16	-0.06	0.07	-0.05	-0.03	0.01	-0.06	-0.06	0.00	-0.03	-0.03	0.00
17-May	0.32	0.11	0.21	0.22	0.04	0.19	0.19	0.05	0.14	0.09	0.07	0.01	0.11	0.10	0.01	0.16	-0.07	0.07	-0.06	-0.04	0.01	-0.07	-0.07	0.00	-0.03	-0.04	0.00
18-May	0.32	0.11	0.21	0.23	0.04	0.18	0.18	0.04	0.14	0.07	0.06	0.01	0.10	0.09	0.01	0.16	-0.07	0.07	-0.09	-0.05	0.01	-0.08	-0.07	0.00	-0.05	-0.05	0.00
19-May	0.32	0.12	0.20	0.23	0.05	0.18	0.18	0.04	0.14	0.05	0.04	0.01	0.08	0.07	0.01	0.16	-0.08	0.07	-0.10	-0.06	0.01	-0.08	-0.08	0.00	-0.05	-0.06	0.00
20-May	0.32	0.12	0.21	0.23	0.05	0.19	0.19	0.05	0.14	0.02	0.01	0.01	0.04	0.03	0.01	0.17	-0.08	0.06	-0.10	-0.06	0.01	-0.08	-0.08	0.00	-0.06	-0.06	0.00
21-May	0.33	0.13	0.20	0.24	0.06	0.18	0.19	0.06	0.13	0.00	-0.01	0.01	0.02	0.01	0.01	0.17	-0.08	0.07	-0.09	-0.06	0.01	-0.08	-0.08	0.00	-0.06	-0.06	0.00
22-May	0.35	0.15	0.20	0.28	0.10	0.18	0.21	0.07	0.13	0.00	-0.01	0.01	0.01	0.00	0.01	0.16	-0.07	0.06	-0.08	-0.06	0.01	-0.07	-0.07	0.00	-0.06	-0.06	0.00
23-May	0.37	0.15	0.21	0.30	0.12	0.19	0.23	0.10	0.14	0.00	-0.01	0.01	0.01	0.00	0.01	0.16	-0.06	0.07	-0.06	-0.05	0.01	-0.06	-0.06	0.00	-0.04	-0.05	0.00
24-May	0.37	0.15	0.22	0.31	0.12	0.19	0.24	0.10	0.14	0.02	0.01	0.01	0.02	0.01	0.01	0.16	-0.05	0.07	-0.05	-0.03	0.01	-0.05	-0.05	0.00	-0.03	-0.03	0.00
25-May	0.37	0.15	0.22	0.31	0.12	0.19	0.24	0.10	0.14	0.04	0.03	0.01	0.04	0.03	0.01	0.16	-0.05	0.08	-0.04	-0.03	0.01	-0.05	-0.05	0.00	-0.03	-0.03	0.00
26-May	0.37	0.15	0.22	0.30	0.11	0.19	0.23	0.09	0.14	0.05	0.04	0.01	0.06	0.05	0.01	0.16	-0.05	0.08	-0.05	-0.03	0.01	-0.05	-0.05	0.00	-0.03	-0.03	0.00
27-May	0.36	0.14	0.23	0.29	0.09	0.19	0.22	0.08	0.14	0.06	0.05	0.01	0.06	0.05	0.01	0.16	-0.05	0.08	-0.06	-0.03	0.01	-0.05	-0.05	0.00	-0.03	-0.03	0.00
28-May	0.36	0.13	0.22	0.28	0.08	0.19	0.21	0.07	0.14	0.06	0.05	0.01	0.07	0.06	0.01	0.16	-0.05	0.07	-0.05	-0.03	0.01	-0.05	-0.05	0.00	-0.03	-0.03	0.00
29-May	0.35	0.13	0.22	0.27	0.07	0.19	0.21	0.06	0.14	0.06	0.05	0.01	0.07	0.06	0.01	0.16	-0.05	0.07	-0.06	-0.04	0.01	-0.06	-0.05	0.00	-0.03	-0.04	0.00
30-May	0.33	0.12	0.21	0.26	0.07	0.19	0.21	0.06	0.14	0.06	0.05	0.01	0.07	0.06	0.01	0.16	-0.06	0.07	-0.06	-0.04	0.01	-0.06	-0.06	0.00	-0.03	-0.04	0.00
31-May	0.27	0.15	0.12	0.20	0.09	0.11	0.18	0.09	0.09	0.06	0.05	0.01	0.07	0.07	0.01	0.14	-0.06	0.04	-0.06	-0.03	0.01	-0.06	-0.06	0.00	-0.03	-0.03	0.00

Date	Node 310			Node 388			Node 412			Node 421			Node 422			Node 423			Node 429			Node 434		
	Hydr #1	Hydr #2	Difference																					
1-May	0.00	0.00	0.00	0.71	0.51	0.21	0.88	0.61	0.26	0.69	0.50	0.20	0.61	0.44	0.17	0.52	0.35	-0.17	0.45	0.32	-0.13	0.12	0.09	-0.03
2-May	-0.01	-0.01	0.00	0.70	0.50	0.20	0.87	0.61	0.26	0.69	0.49	0.19	0.61	0.44	0.17	0.51	0.34	-0.17	0.44	0.31	-0.13	0.12	0.09	-0.03
3-May	-0.01	-0.01	0.00	0.70	0.50	0.20	0.87	0.62	0.26	0.68	0.49	0.19	0.60	0.44	0.17	0.50	0.34	-0.17	0.44	0.31	-0.13	0.12	0.09	-0.03
4-May	-0.01	-0.01	0.00	0.70	0.50	0.20	0.88	0.62	0.26	0.68	0.49	0.19	0.60	0.44	0.17	0.50	0.33	-0.17	0.44	0.31	-0.13	0.12	0.09	-0.03
5-May	-0.02	-0.02	0.00	0.70	0.50	0.20	0.88	0.62	0.26	0.68	0.49	0.19	0.60	0.43	0.17	0.50	0.33	-0.17	0.43	0.30	-0.13	0.11	0.09	-0.03
6-May	-0.04	-0.04	0.00	0.70	0.50	0.20	0.88	0.62	0.26	0.68	0.49	0.19	0.60	0.43	0.17	0.50	0.33	-0.17	0.43	0.29	-0.13	0.09	0.07	-0.03
7-May	-0.05	-0.05	0.00	0.70	0.50	0.20	0.88	0.62	0.26	0.69	0.50	0.19	0.61	0.44	0.17	0.50	0.33	-0.17	0.42	0.29	-0.13	0.08	0.05	-0.03
8-May	-0.06	-0.06	0.00	0.70	0.50	0.20	0.89	0.63	0.26	0.69	0.50	0.19	0.61	0.44	0.17	0.50	0.33	-0.17	0.42	0.29	-0.13	0.06	0.04	-0.03
9-May	-0.06	-0.06	0.00	0.71	0.52	0.20	0.90	0.64	0.25	0.70	0.52	0.18	0.62	0.46	0.16	0.51	0.35	-0.16	0.42	0.30	-0.13	0.05	0.03	-0.02
10-May	-0.03	-0.04	0.00	0.75	0.55	0.19	0.91	0.66	0.26	0.72	0.54	0.18	0.63	0.47	0.16	0.53	0.37	-0.16	0.44	0.31	-0.12	0.06	0.04	-0.02
11-May	-0.01	-0.01	0.00	0.77	0.57	0.20	0.92	0.67	0.26	0.73	0.55	0.18	0.65	0.48	0.16	0.56	0.39	-0.16	0.46	0.33	-0.13	0.08	0.06	-0.02
12-May	0.01	0.01	0.00	0.78	0.57	0.21	0.93	0.67	0.25	0.74	0.55	0.19	0.65	0.49	0.16	0.57	0.40	-0.17	0.48	0.34	-0.13	0.10	0.08	-0.03
13-May	0.02	0.01	0.00	0.78	0.57	0.21	0.92	0.67	0.25	0.73	0.55	0.19	0.65	0.48	0.16	0.57	0.40	-0.17	0.48	0.35	-0.13	0.12	0.10	-0.03
14-May	0.02	0.02	0.00	0.77	0.57	0.21	0.91	0.66	0.25	0.73	0.54	0.19	0.65	0.48	0.17	0.56	0.40	-0.16	0.48	0.35	-0.13	0.13	0.11	-0.03
15-May	0.02	0.02	0.00	0.77	0.56	0.20	0.90	0.65	0.25	0.73	0.54	0.19	0.64	0.48	0.17	0.55	0.39	-0.16	0.48	0.35	-0.13	0.14	0.12	-0.03
16-May	0.03	0.02																						

Attachment 2. Biological Review for Endangered Species Act Compliance with the WY 2015 Drought Contingency Plan April through September
Project Description

Table 4. Daily Mean Flows (cfs) Between Base and Project Description Model Scenarios and Their Difference (Hydrology 2 minus Hydrology 1) at All Channel Nodes During April

Date	Node 6			Node 9			Node 12			Node 49			Node 50			Node 54			Node 94			Node 124			Node 148		
	Hydr #1	Hydr #2	Difference	Hydr #1	Hydr #2	Difference	Hydr #1	Hydr #2	Difference																		
1-Apr	2984	662	2322	2235	333	1902	2165	299	1866	5024	3052	-1972	5393	3321	-2072	629	269	-360	-404	-678	-274	-2329	-2137	192	-334	-447	-113
2-Apr	3064	865	2199	2407	497	1910	2378	460	1918	4282	2379	-1903	4567	2564	-2004	637	326	-311	-563	-727	-164	-2496	-2221	276	-428	-489	-61
3-Apr	3067	973	2094	2411	594	1817	2382	561	1820	3729	1928	-1800	4023	2126	-1897	637	354	-283	-512	-651	-139	-2534	-2259	275	-413	-464	-51
4-Apr	3067	974	2093	2414	600	1814	2382	565	1818	3132	1345	-1787	3489	1605	-1884	634	347	-287	-441	-590	-149	-2578	-2306	271	-385	-442	-57
5-Apr	3069	976	2093	2419	610	1809	2387	573	1814	2498	706	-1793	2901	1014	-1886	632	342	-290	-394	-549	-156	-2583	-2319	264	-369	-429	-60
6-Apr	3071	977	2093	2420	610	1810	2388	573	1815	1556	-251	-1807	1766	-130	-1896	634	342	-291	-448	-605	-157	-2640	-2378	262	-405	-466	-62
7-Apr	3073	981	2092	2422	608	1814	2391	573	1818	736	-1081	-1817	579	-1323	-1902	636	349	-287	-454	-609	-156	-2672	-2407	265	-415	-475	-60
8-Apr	3077	982	2095	2430	615	1814	2393	574	1819	-73	-1900	-1827	-568	-2483	-1915	633	343	-290	-479	-637	-158	-2692	-2430	262	-447	-509	-61
9-Apr	3083	1000	2083	2444	644	1799	2402	596	1806	-525	-2334	-1809	-1182	-3077	-1894	631	336	-295	-396	-554	-158	-2486	-2229	257	-435	-495	-61
10-Apr	3086	1023	2063	2460	706	1754	2430	675	1755	-39	-1789	-1750	-721	-2567	-1846	627	329	-298	-169	-328	-159	-2098	-1854	245	-297	-356	-60
11-Apr	3083	1023	2060	2466	719	1747	2457	716	1742	2533	803	-1729	1734	-85	-1819	623	325	-298	76	-87	-163	-1875	-1650	225	-101	-165	-64
12-Apr	3075	1010	2066	2455	700	1755	2460	706	1754	5115	3338	-1777	4676	2811	-1864	622	326	-296	109	-53	-162	-1896	-1657	238	-64	-127	-64
13-Apr	3069	998	2071	2440	674	1766	2435	671	1764	6353	4545	-1808	6307	4403	-1904	622	328	-294	97	-62	-160	-1840	-1598	241	-71	-134	-63
14-Apr	3062	977	2085	2427	648	1779	2419	638	1781	6723	4898	-1826	6940	5019	-1921	623	334	-289	9	-145	-154	-1894	-1640	253	-116	-177	-61
15-Apr	3059	963	2096	2414	608	1806	2419	625	1794	6665	4830	-1835	7056	5127	-1929	627	342	-285	-69	-222	-154	-2087	-1820	267	-159	-220	-60
16-Apr	3059	961	2097	2404	582	1822	2395	585	1809	6353	4516	-1837	6797	4868	-1929	630	348	-282	-196	-347	-151	-2354	-2080	274	-229	-288	-58
17-Apr	3060	964	2097	2405	583	1822	2377	555	1822	6025	4191	-1834	6481	4553	-1928	631	348	-283	-304	-454	-150	-2511	-2240	271	-287	-344	-57
18-Apr	3062	965	2097	2406	584	1822	2370	544	1827	5006	3189	-1818	5392	3675	-1917	632	347	-284	-457	-609	-152	-2705	-2431	274	-393	-450	-57
19-Apr	3065	968	2097	2411	588	1822	2372	545	1828	3233	1432	-1801	4016	2111	-1905	633	348	-285	-517	-672	-155	-2864	-2594	270	-448	-508	-59
20-Apr	3069	972	2097	2417	596	1821	2381	553	1828	1173	-629	-1802	1627	-261	-1887	632	346	-286	-522	-678	-156	-2918	-2651	268	-461	-521	-60
21-Apr	3074	977	2097	2426	602	1824	2391	561	1830	-111	-1941	-1830	-376	-2291	-1915	631	346	-285	-517	-672	-155	-2939	-2670	269	-468	-528	-59
22-Apr	3081	985	2097	2438	613	1825	2396	566	1829	-816	-2643	-1827	-1493	-3408	-1915	630	346	-284	-502	-657	-155	-2843	-2577	266	-485	-545	-60
23-Apr	3089	1017	2072	2459	673	1786	2416	622	1794	-829	-2625	-1796	-1537	-3421	-1884	626	336	-290	-353	-506	-153	-2459	-2200	259	-426	-485	-59
24-Apr	3091	1030	2061	2475	722	1753	2453	705	1748	670	-1069	-1738	-66	-1904	-1838	623	330	-293	-19	-177	-158	-1967	-1730	237	-187	-248	-61
25-Apr	3086	1025	2060	2473	721	1752	2472	725	1747	3694	1951	-1743	2944	1114	-1830	624	328	-296	150	-12	-162	-1786	-1559	227	-41	-105	-64
26-Apr	3078	1012	2066	2455	702	1753	2463	710	1753	5824	4035	-1789	5550	3672	-1877	627	327	-300	162	-1	-164	-1710	-1477	233	-21	-85	-65
27-Apr	3072	1003	2069	2437	679	1759	2435	678	1757	6482	4669	-1813	6593	4686	-1907	630	329	-301	74	-89	-163	-1681	-1447	234	-72	-136	-64
28-Apr	3067	898	2169	2427	597	1830	2416	589	1827	6339	4493	-1846	6656	4713	-1943	631	314	-318	-47	-216	-169	-1767	-1525	242	-141	-207	-67
29-Apr	1712	748	964	1456	470	986	1501	466	1035	5488	3877	-1611	5849	4156	-1692	434	283	-151	-203	-329	-126	-1890	-1679	211	-214	-268	-54
30-Apr	670	616	53	398	361	37	404	366	37	4128	3417	-711	4406	3661	-745	259	246	-13	-228	-253	25	-1934	-1801	133	-220	-231	-11

Date	Node 310			Node 388			Node 412			Node 421			Node 422			Node 423			Node 429			Node 434		
	Hydr #1	Hydr #2	Difference																					
1-Apr	152	-271	-423	879	773	-105	6492	5720	-772	3956	3531	-425	3968	3543	-424	2178	1862	-315	2247	1932	-315	6978	5912	-1066
2-Apr	2	-393	-396	873	738	-134	6498	5505	-993	3923	3364	-559	3925	3367	-558	2124	1733	-390	2170	1780	-390	6140	4945	-1195
3-Apr	-90	-459	-369	872	731	-141	6501	5481	-1020	3907	3312	-595	3902	3307	-595	2094	1686	-407	2123	1716	-407	5499	4289	-1210
4-Apr	-198	-565	-367	877	736	-141	6548	5528	-1020	3920	3325	-595	3910	3315	-595	2085	1676	-408	2101	1693	-408	4954	3753	-1201
5-Apr	-327	-695	-368	877	736	-142	6556	5535	-1021	3921	3324	-597	3907	3310	-597	2078	1667	-411	2072	1662	-410	4389	3187	-1202
6-Apr	-495	-866	-371	874	731	-142	6559	5535	-1023	3918	3319	-600	3902	3302	-600	2070	1657	-413	2031	1618	-413	3469	2263	-1206
7-Apr	-621	-992	-371	869	727	-142	6556	5529	-1028	3918	3316	-601	3899	3298	-602	2072	1656	-416	2000	1583	-417	2400	1189	-1211
8-Apr	-759	-1131	-371	870	727	-143	6600	5569	-1031	3953	3350	-603	3934	3331	-603	2088	1667	-421	1998	1578	-420	1415	194	-1221
9-Apr	-824	-1192	-368	869	727	-142	6649	5631	-1018	3978	3383	-595	3959	3365	-594	2106	1690	-416	2004	1591	-413	597	-612	-1209
10-Apr	-621	-975	-354	912	779	-133	6775	5768	-1007	4106	3545	-562	4084	3522	-562	2223	1833	-391	2091	1697	-393	394	-773	-1167
11-Apr	-37	-384	-346	989	855	-134	6872	5860	-1011	4262	3696	-566	4251	3688	-563	2424	2031	-394	2316	1928	-389	2265	1111	-1154
12-Apr	416	56	-360	996	861	-135	6893	5885	-1008	4288	3714	-574	4288	3714	-573	2496	2094	-403	2448	2047	-401	4975	3796	-1179
13-Apr	586	218	-368	989	853	-136	6872	5883	-989	4262	3681	-581	4267	3685	-581	2486	2081	-405	2487	2082	-405	6662	5463	-1199
14-Apr	579	205	-373	971	834	-137	6749	5752	-997	4207	3621	-586	4213	3626	-587	2424	2019	-405	2448	2043	-405	7466	6260	-1205
15-Apr	508	131	-377	953	815	-138	6655	5644	-1011	4147	3559	-587	4153	3564	-588	2346	1945	-402	2385	1981	-404	7765	6559	-1207
16-Apr	387	9	-378	934	796	-138	6616	5598	-1018	4074	3485	-588	4086	3496	-590	2260	1860	-400	2335	1933	-402	7838	6630	-1208
17-Apr	262	-116	-379	909	769	-141	6607	5586	-1020	3998	3407	-591	4014	3423	-591	2176	1779	-397	2266	1867	-399	7741	6529	-1212
18-Apr	62	-313	-375	898	755	-143	6610	5588	-1022	3946	3350	-596	3949	3354	-595	2085	1686	-407	2172	1773	-400	6988	5782	-1206
19-Apr	-268	-636	-368	897	753	-144	6619	5596	-1023	3926	3327	-599	3913	3314	-599	2024	1620	-404	2077	1674	-403	5540	4336	-1203
20-Apr	-650	-1021	-371	893																				

Attachment 2. Biological Review for Endangered Species Act Compliance with the WY 2015 Drought Contingency Plan April through September
Project Description

Table 5. Daily Mean Flows (cfs) Between Base and Project Description Model Scenarios and Their Difference (Hydrology 2 minus Hydrology 1) at All Channel Nodes During May

Date	Node 6			Node 9			Node 12			Node 49			Node 50			Node 54			Node 94			Node 124			Node 148		
	Hydr #1	Hydr #2	Difference	Hydr #1	Hydr #2	Difference	Hydr #1	Hydr #2	Difference																		
1-May	629	374	-255	335	170	-165	317	157	-159	2967	2234	-733	3114	2348	-766	263	189	-74	-591	-626	-35	-2220	-2084	136	-396	-411	-15
2-May	610	201	-409	306	24	-282	269	-11	-280	2354	1494	-860	2419	1519	-899	264	138	-126	-819	-888	-69	-2442	-2309	133	-509	-539	-29
3-May	608	195	-414	303	14	-289	255	-34	-289	2148	1295	-853	2290	1395	-896	263	138	-125	-913	-969	-56	-2562	-2422	140	-572	-595	-23
4-May	610	197	-414	306	15	-291	253	-38	-291	1801	955	-845	2161	1268	-893	263	140	-123	-962	-1022	-61	-2662	-2522	140	-618	-643	-25
5-May	613	201	-412	309	17	-292	256	-35	-292	812	-4	-817	1326	469	-858	264	143	-120	-987	-1049	-62	-2736	-2599	137	-648	-674	-26
6-May	617	203	-415	309	16	-293	259	-31	-290	-599	-1432	-833	-398	-1263	-865	268	151	-117	-1010	-1074	-64	-2788	-2656	132	-673	-701	-28
7-May	622	215	-406	313	25	-287	262	-23	-285	-1619	-2457	-838	-1938	-2809	-872	275	157	-118	-1013	-1076	-64	-2786	-2656	131	-694	-722	-28
8-May	645	251	-394	350	76	-274	287	8	-280	-2187	-3036	-848	-2798	-3677	-880	267	152	-115	-948	-1012	-64	-2618	-2490	128	-685	-713	-28
9-May	665	261	-404	403	118	-285	352	67	-284	-2122	-2946	-824	-2821	-3681	-860	261	142	-119	-759	-824	-64	-2314	-2192	122	-576	-604	-28
10-May	668	259	-409	413	129	-284	386	103	-284	-926	-1728	-802	-1852	-2702	-850	262	136	-126	-583	-651	-68	-2062	-1949	113	-417	-447	-30
11-May	661	250	-410	407	124	-283	394	110	-283	1273	462	-811	313	-538	-851	260	132	-128	-496	-565	-69	-2025	-1913	112	-348	-378	-30
12-May	649	237	-412	390	107	-283	379	96	-283	2889	2056	-833	2267	1395	-872	260	131	-129	-492	-561	-69	-2005	-1888	117	-344	-373	-30
13-May	644	231	-413	371	89	-283	351	68	-283	3736	2884	-852	3466	2572	-894	261	130	-131	-535	-603	-69	-2004	-1882	122	-369	-398	-29
14-May	634	224	-409	358	73	-285	331	48	-284	4228	3356	-872	4270	3356	-914	264	134	-131	-577	-646	-69	-2048	-1920	128	-395	-425	-30
15-May	606	195	-411	329	47	-283	318	32	-286	4357	3476	-881	4650	3727	-924	264	135	-129	-612	-679	-69	-2193	-2056	137	-419	-449	-29
16-May	599	184	-415	293	6	-287	291	4	-287	4327	3439	-888	4747	3817	-930	260	140	-126	-664	-729	-65	-2418	-2275	142	-449	-477	-28
17-May	599	184	-415	284	-8	-292	245	-45	-290	4027	3145	-882	4475	3550	-925	267	143	-124	-822	-882	-60	-2639	-2494	144	-528	-553	-26
18-May	603	188	-415	287	-6	-293	230	-63	-293	3043	2184	-859	3680	2773	-907	268	145	-123	-986	-1048	-62	-2819	-2674	146	-641	-666	-26
19-May	608	195	-413	295	1	-294	237	-56	-291	977	1184	-821	1739	871	-868	268	149	-128	-1053	-1116	-63	-2950	-2812	139	-701	-727	-27
20-May	616	200	-415	301	7	-294	248	-41	-290	-1088	-1912	-824	-919	-1775	-856	273	158	-115	-1071	-1134	-63	-2973	-2841	131	-721	-749	-28
21-May	625	224	-401	314	30	-284	261	-22	-283	-1969	-3281	-833	-2416	-3281	-866	277	160	-117	-1021	-1085	-64	-2868	-2741	127	-712	-741	-29
22-May	656	260	-396	369	93	-276	303	23	-281	-2176	-3006	-830	-2819	-3681	-862	266	152	-114	-926	-991	-64	-2589	-2468	122	-677	-705	-28
23-May	671	266	-405	411	125	-286	366	80	-285	-1732	-2539	-807	-2398	-3243	-845	262	143	-119	-735	-799	-64	-2218	-2104	113	-546	-574	-28
24-May	669	261	-408	415	132	-283	391	108	-283	-372	-1151	-779	-1193	-2017	-825	262	135	-127	-579	-648	-69	-1922	-1819	102	-394	-423	-30
25-May	662	251	-410	408	125	-283	393	110	-283	1482	697	-784	693	-129	-822	259	130	-128	-516	-586	-71	-1842	-1741	100	-343	-373	-30
26-May	650	239	-411	392	107	-285	378	93	-285	2602	1801	-802	2121	1282	-838	257	129	-128	-541	-610	-69	-1835	-1731	104	-357	-386	-29
27-May	639	226	-413	373	87	-286	354	68	-287	2904	2085	-819	2667	1810	-858	256	128	-128	-618	-687	-69	-1896	-1788	108	-403	-432	-29
28-May	635	220	-415	361	74	-287	333	45	-288	3058	2224	-833	2976	2103	-874	255	127	-128	-554	-625	-71	-1932	-1822	110	-372	-402	-30
29-May	628	216	-413	348	58	-290	314	24	-290	2781	1945	-836	2771	1895	-876	256	131	-126	-692	-759	-67	-2105	-1988	117	-447	-475	-29
30-May	611	201	-410	337	46	-290	309	17	-291	2823	1984	-839	2892	2011	-880	258	133	-125	-711	-776	-65	-2245	-2121	123	-455	-483	-28
31-May	497	262	-235	249	71	-177	242	57	-186	2529	2053	-475	2691	2179	-512	231	158	-74	-709	-765	-56	-2230	-2198	32	-458	-483	-25

Date	Node 310			Node 388			Node 412			Node 421			Node 422			Node 423			Node 429			Node 434		
	Hydr #1	Hydr #2	Difference																					
1-May	-434	-415	19	1252	859	-393	9151	6413	-2737	5491	3887	-1604	5495	3887	-1608	3187	2106	-1081	3216	2128	-1087	7582	5325	-2257
2-May	-579	-593	-14	1234	848	-386	9140	6435	-2705	5449	3880	-1569	5451	3882	-1569	3118	2056	-1061	3149	2084	-1065	7286	5049	-2237
3-May	-634	-647	-13	1232	844	-388	9125	6478	-2706	5447	3871	-1575	5444	3870	-1574	3085	2021	-1064	3119	2053	-1066	7258	5017	-2241
4-May	-694	-705	-11	1239	850	-389	9240	6532	-2708	5462	3883	-1580	5453	3873	-1579	3067	1997	-1070	3100	2030	-1069	7089	4851	-2238
5-May	-889	-894	-5	1240	851	-389	9252	6541	-2711	5466	3881	-1585	5450	3865	-1585	3045	1970	-1075	3054	1981	-1073	6300	4084	-2215
6-May	-1150	-1158	-9	1237	849	-389	9259	6540	-2719	5472	3884	-1588	5452	3863	-1589	3036	1956	-1080	2992	1911	-1081	4832	2611	-2221
7-May	-1327	-1325	-8	1240	851	-389	9211	6585	-2726	5506	3920	-1586	5483	3898	-1586	3051	1964	-1088	2973	1886	-1086	3424	1196	-2228
8-May	-1415	-1426	-11	1236	849	-388	9338	6626	-2711	5522	3944	-1577	5498	3922	-1576	3061	1971	-1089	2957	1875	-1082	2352	134	-2218
9-May	-1314	-1329	-16	1253	877	-376	9450	6772	-2678	5587	4068	-1519	5561	4042	-1519	3122	2066	-1056	2987	1936	-1054	1701	-456	-2157
10-May	-994	-1013	-19	1313	947	-366	9536	6867	-2669	5699	4223	-1476	5673	4203	-1470	3257	2241	-1017	3112	2099	-1010	1243	118	-2125
11-May	-608	-615	-7	1353	972	-381	9625	6954	-2671	5812	4315	-1497	5797	4304	-1493	3421	2372	-1049	3306	2265	-1041	4221	2067	-2155
12-May	-368	-374	-5	1369	979	-390	9665	7007	-2657	5850	4339	-1511	5845	4335	-1511	3483	2423	-1059	3420	2362	-1058	6190	3985	-2205
13-May	-274	-283	-9	1367	973	-395	9616	6974	-2642	5831	4303	-1529	5831	4302	-1530	3461	2403	-1058	3446	2386	-1060	7507	5278	-2229
14-May	-233	-248	-15	1366	971	-394	9581	6923	-2657	5822	4277	-1545	5823	4277	-1547	3428	2376	-1052	3442	2387	-1055	8431	6195	-2236
15-May	-233	-252	-19	1352	961	-391	9513	6827	-2686	5789	4233	-1556	5793	4234	-1559	3371	2324	-1047	3407	2353	-1054	8964	6727	-2237
16-May	-261	-283	-23	1337	950	-387	9517	6815	-2703	5749	4189	-1560	5760	4195	-1565	3313	2270	-1043	3389	2339	-1050	9373	7135	-2238
17-May	-373	-395	-22	1312	921	-391	9557	6848	-2709	5697	4128	-1569	5711	4142	-1570	3238	2199	-1040	3337	2292	-1046	9465	7225	-2240
18-May	-556	-574	-18	1298	903	-395	9569	6857	-2712	5648	4068	-1580	5646	4068	-1579	3143	2093	-1050	3231	2180	-1051	8707	6474	-2233
19-May	-937	-943	-6	1301	906	-395	9626	6912	-2715	5658	4075	-1583	5641	4057	-1584	3108	2041	-1067	3138	2072	-1065	6890	4671	-2219

Attachment 2. Biological Review for Endangered Species Act Compliance with the WY 2015 Drought Contingency Plan April through September
Project Description

Table 6. DSM2 Results for Mean Daily Proportion Positive Flows, Mean Daily Flow, and Mean Daily Velocity at Each Channel Node for April. Differences are calculated as Hydrology 2 or 2¹ minus Hydrology 1

Channel Nodes		Proportion Positive Daily Flow					Average Daily Flow (cfs)					Mean Daily Velocity (ft/s)				
		Baseline	Proposed	Difference between Baseline and Proposed	Proposed (DCC Open)	Difference between Baseline and Proposed (Open)	Baseline	Proposed	Difference between Baseline and Proposed	Proposed (DCC Open)	Difference between Baseline and Proposed (Open)	Baseline	Proposed	Difference between Baseline and Proposed	Proposed (DCC Open)	Difference Between Proposed and Proposed DCC Open
6	San Joaquin	0.99	0.89	-0.10	0.89	-0.01	2943	951	-1993	951	0.0	1.16	0.38	-0.78	0.38	0.00
9	San Joaquin	0.98	0.63	-0.35	0.63	0.00	2325	608	-1717	607	-0.4	1.33	0.36	-0.97	0.36	0.00
12	South Delta	0.98	0.58	-0.39	0.58	0.00	2303	585	-1718	585	-0.4	1.11	0.32	-0.79	0.32	0.00
49	Central Delta	0.53	0.53	0.00	0.53	0.00	3344	1576	-1768	2124	547.4	0.07	0.05	-0.02	0.05	0.01
50	Central Delta	0.53	0.52	0.00	0.53	0.00	3331	1473	-1858	2050	576.3	0.08	0.06	-0.02	0.07	0.01
54	San Joaquin	1.00	0.97	-0.03	0.96	0.00	610	330	-280	331	0.4	0.35	0.19	-0.16	0.19	0.00
94	South Delta	0.52	0.52	0.00	0.52	0.00	-251	-406	-155	-404	2.0	0.00	-0.02	-0.02	-0.02	0.00
124	South Delta	0.46	0.46	0.00	0.47	0.00	-2302	-2053	249	-2209	-155.2	-0.06	-0.06	0.01	-0.06	0.00
148	South Delta	0.52	0.52	0.00	0.52	0.00	-285	-345	-60	-348	-2.3	-0.01	-0.02	-0.01	-0.02	0.00
310	Central Delta	0.52	0.52	-0.01	0.52	0.00	-110	-461	-351	-261	199.3	0.03	0.00	-0.02	0.02	0.01
388	North Delta	0.65	0.62	-0.03	0.61	-0.02	943	787	-156	683	-103.9	0.55	0.47	-0.08	0.41	-0.06
412	North Delta	0.94	0.85	-0.09	0.84	-0.01	6856	5726	-1130	5727	0.5	0.66	0.56	-0.11	0.56	0.00
421	North Delta	0.71	0.66	-0.05	0.69	0.02	4163	3515	-648	3825	310.7	0.53	0.45	-0.08	0.49	0.04
422	North Delta	0.70	0.66	-0.04	0.61	-0.05	4157	3509	-648	2636	-872.8	0.47	0.40	-0.07	0.30	-0.10
423	North Delta	0.62	0.59	-0.02	0.57	-0.02	2303	1854	-449	1376	-478.1	0.38	0.31	-0.07	0.24	-0.08
429	North Delta	0.59	0.57	-0.02	0.56	-0.01	2284	1836	-448	1359	-476.8	0.34	0.28	-0.06	0.22	-0.06
434	North Delta	0.53	0.53	0.00	0.53	0.00	4689	3418	-1271	2839	-579.0	0.09	0.07	-0.01	0.07	-0.01

Attachment 2. Biological Review for Endangered Species Act Compliance with the WY 2015 Drought Contingency Plan April through September
Project Description

Table 7. DSM2 Results for Mean Daily Proportion Positive Flows, Mean Daily Flow, and Mean Daily Velocity at Each Channel Node for May. Differences are calculated as Hydrology 2 or 2¹ minus Hydrology 1

Channel Nodes		Proportion Positive Daily Flow					Average Daily Flow (cfs)					Mean Daily Velocity (ft/s)				
		Baseline	Proposed	Difference between Baseline and Proposed	Proposed (DCC Open)	Difference between Baseline and Proposed (Open)	Baseline	Proposed	Difference between Baseline and Proposed	Proposed (DCC Open)	Difference between Baseline and Proposed (Open)	Baseline	Proposed	Difference between Baseline and Proposed	Proposed (DCC Open)	Difference Between Proposed and Proposed DCC Open
6	San Joaquin	0.72	0.57	-0.15	0.57	0	627	228	-399	228	0	0.34	0.14	-0.21	0.14	0.00
9	San Joaquin	0.59	0.55	-0.04	0.55	0	343	64	-279	64	0	0.26	0.08	-0.18	0.08	0.00
12	South Delta	0.56	0.53	-0.03	0.53	0	308	30	-279	30	0	0.21	0.07	-0.14	0.07	0.00
49	Central Delta	0.52	0.52	0	0.53	0.01	1365	545	-820	1292	747	0.04	0.03	-0.01	0.04	0.01
50	Central Delta	0.52	0.52	0	0.52	0	1231	372	-859	1157	785	0.06	0.05	-0.01	0.06	0.01
54	San Joaquin	0.9	0.78	-0.12	0.77	-0.01	263	142	-120	142	0	0.16	0.09	-0.07	0.09	0.00
94	South Delta	0.51	0.5	-0.01	0.5	0	-758	-822	-64	-819	3	-0.07	-0.07	-0.01	-0.07	0.00
124	South Delta	0.46	0.46	0	0.46	0	-2352	-2230	122	-2435	-204	-0.06	-0.06	0.00	-0.07	-0.01
148	South Delta	0.51	0.51	0	0.51	0	-512	-539	-28	-543	-3	-0.04	-0.04	0.00	-0.04	0.00
310	Central Delta	0.51	0.51	0	0.52	0.01	-734	-745	-11	-476	269	-0.02	-0.02	0.00	0.00	0.02
388	North Delta	0.73	0.65	-0.08	0.62	-0.03	1311	929	-383	791	-138	0.74	0.54	-0.20	0.47	-0.07
412	North Delta	1	0.95	-0.05	0.95	0	9525	6911	-2614	6911	0	0.91	0.66	-0.25	0.66	0.00
421	North Delta	0.86	0.72	-0.14	0.75	0.03	5686	4187	-1499	4596	409	0.71	0.53	-0.18	0.58	0.05
422	North Delta	0.84	0.71	-0.13	0.63	-0.08	5677	4178	-1499	3078	-1100	0.63	0.47	-0.16	0.35	-0.12
423	North Delta	0.68	0.62	-0.06	0.59	-0.03	3281	2247	-1034	1604	-643	0.54	0.37	-0.16	0.27	-0.10
429	North Delta	0.63	0.59	-0.04	0.57	-0.02	3253	2219	-1035	1575	-644	0.46	0.33	-0.13	0.25	-0.08
434	North Delta	0.53	0.53	0	0.53	0	5980	3805	-2175	3021	-784	0.10	0.08	-0.02	0.07	-0.01

Attachment 2. Biological Review for Endangered Species Act Compliance with the WY 2015 Drought Contingency Plan April through September Project Description

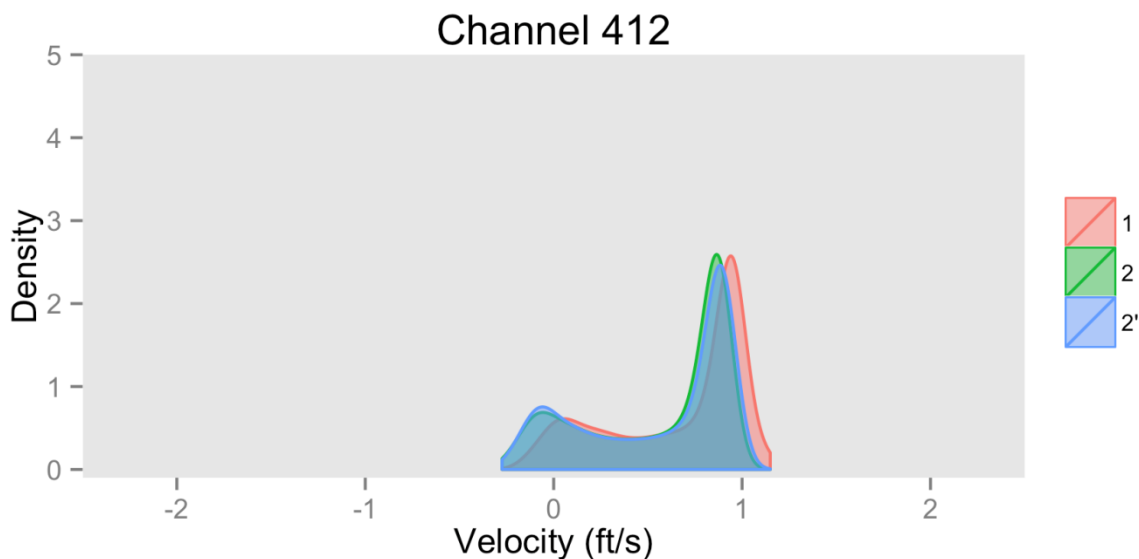


Figure 2. Density plot of velocity (ft/s) observed at DSM2 Channel Node 412 under three scenarios during the April modeled period (Sacramento River near Sherwood Harbor, North Delta)

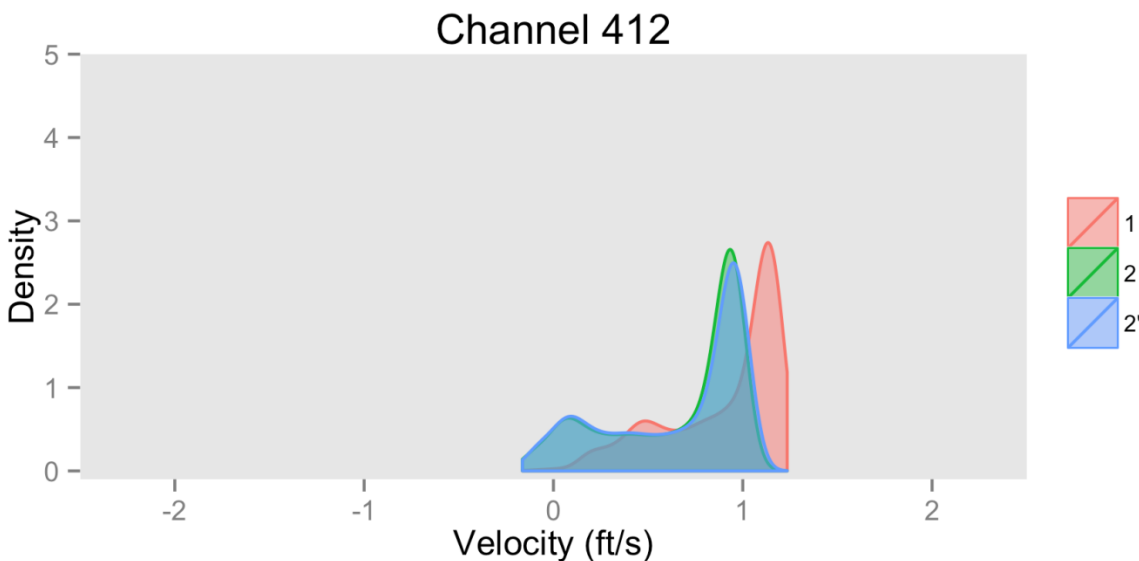


Figure 3. Density plot of velocity (ft/s) observed at DSM2 Channel Node 412 under three scenarios during the May modeled period (Sacramento River near Sherwood Harbor, North Delta)

Attachment 2. Biological Review for Endangered Species Act Compliance with the WY 2015 Drought Contingency Plan April through September Project Description

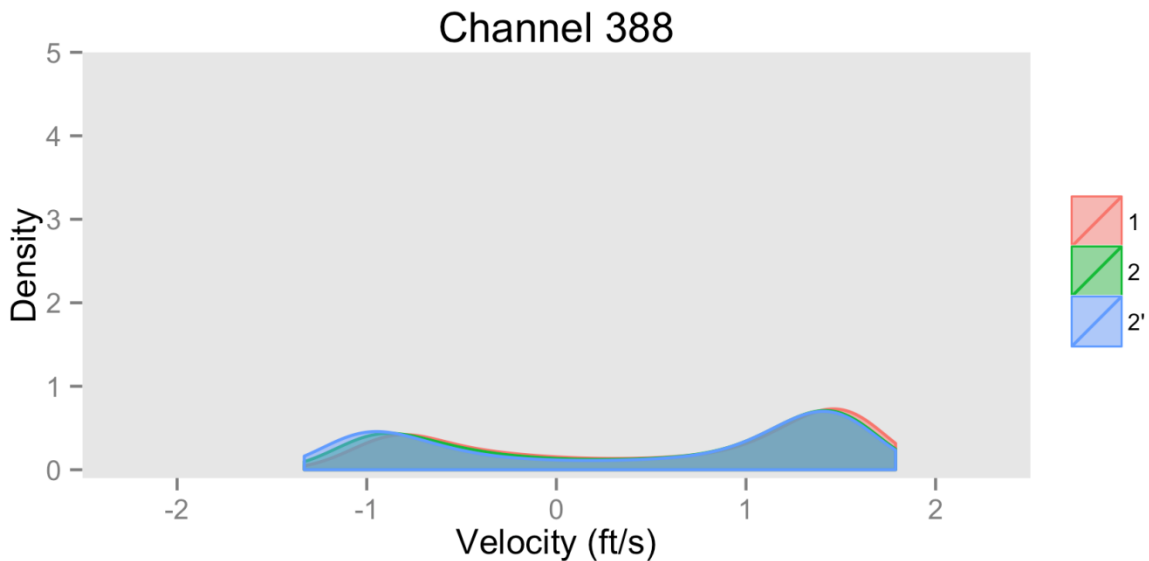


Figure 4. Density plot of velocity (ft/s) observed for DSM2 Channel 388, Sutter Slough and Sacramento River junction, in April

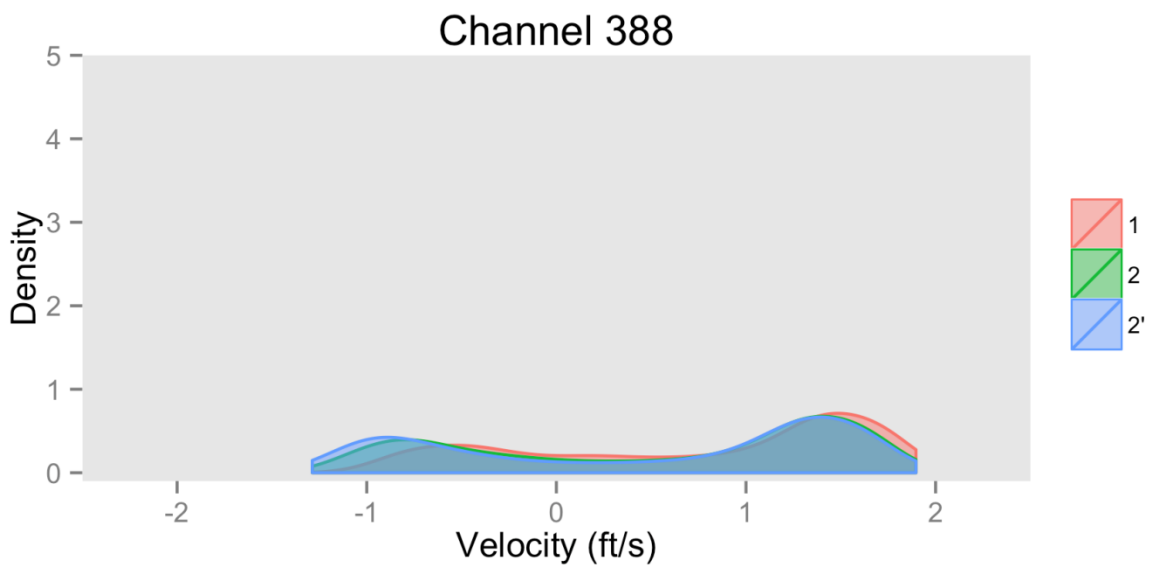


Figure 5. Density plot of velocity (ft/s) observed for DSM2 Channel 388, Sutter Slough and Sacramento River junction, in May

Attachment 2. Biological Review for Endangered Species Act Compliance with the WY 2015 Drought Contingency Plan April through September Project Description

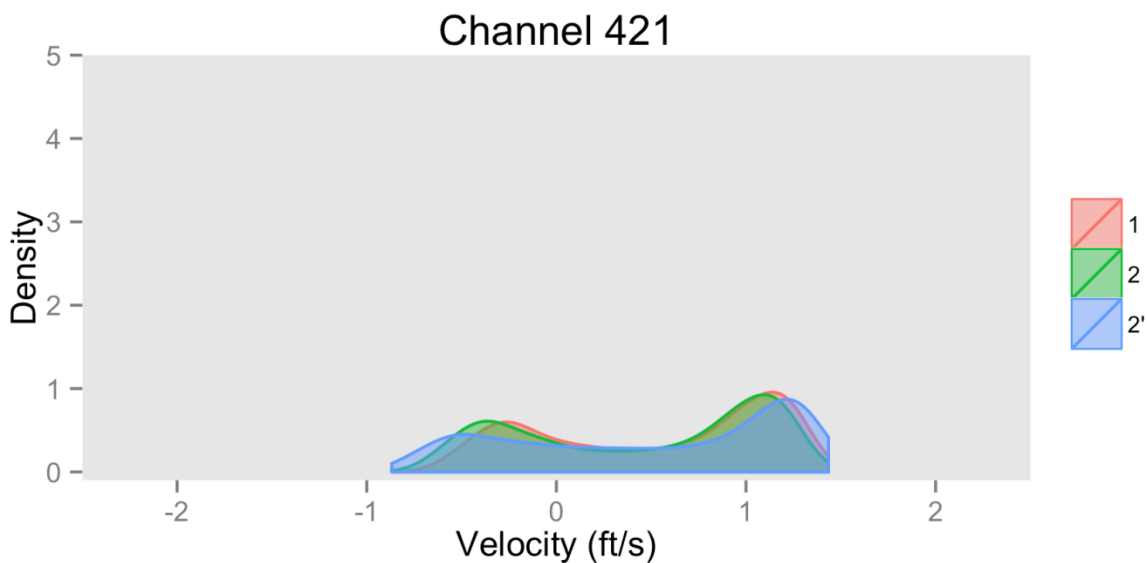


Figure 6. Density plot of velocity (ft/s) observed for DSM2 Channel 421, upstream of the DCC channel junction, in April

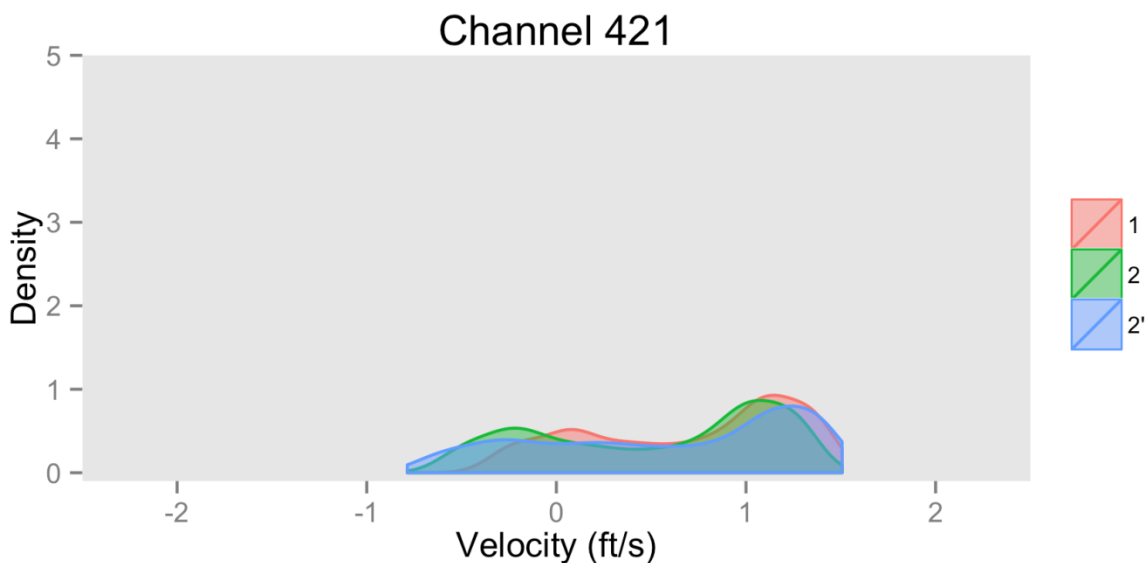


Figure 7. Density plot of velocity (ft/s) observed for DSM2 Channel 421, upstream of the DCC channel junction, in May

Attachment 2. Biological Review for Endangered Species Act Compliance with the WY 2015 Drought Contingency Plan April through September Project Description

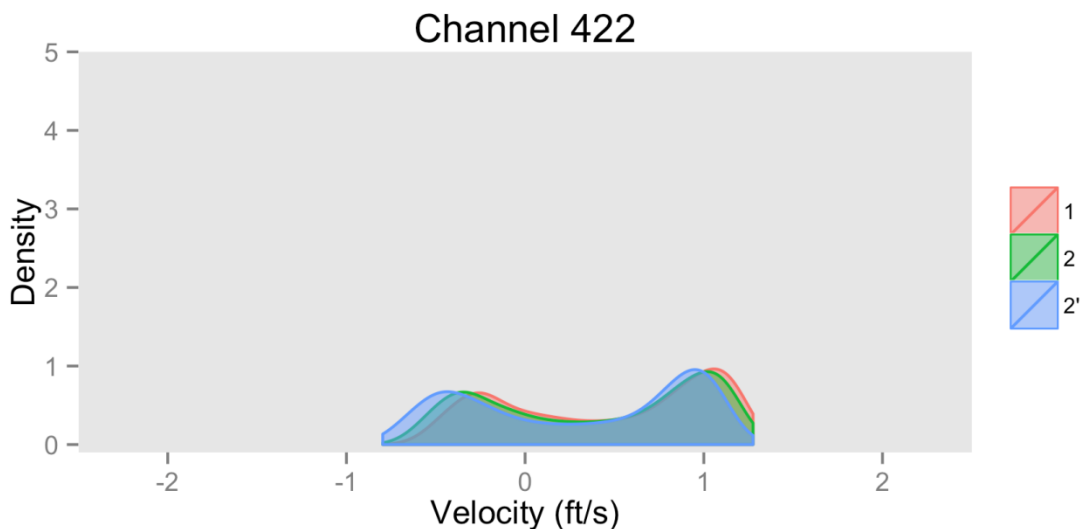


Figure 8. Density plot of velocity (ft/s) observed for DSM2 Channel 422, Sacramento River between Delta Cross Channel and Georgiana Slough in April

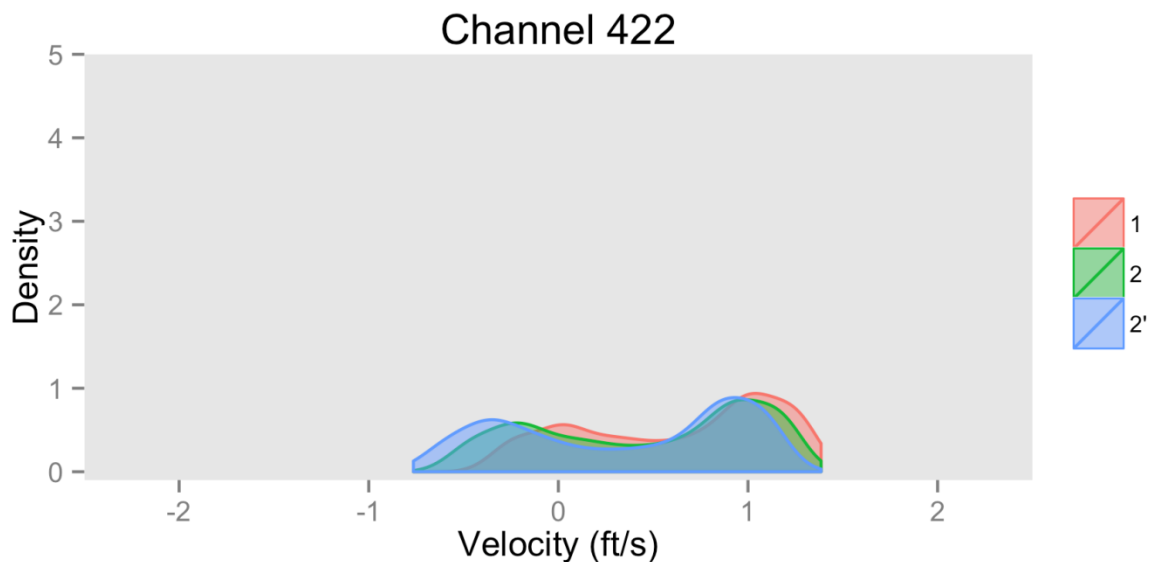


Figure 9. Density plot of velocity (ft/s) observed for DSM2 Channel 422, Sacramento River between Delta Cross Channel and Georgiana Slough in May

Attachment 2. Biological Review for Endangered Species Act Compliance with the WY 2015 Drought Contingency Plan April through September Project Description

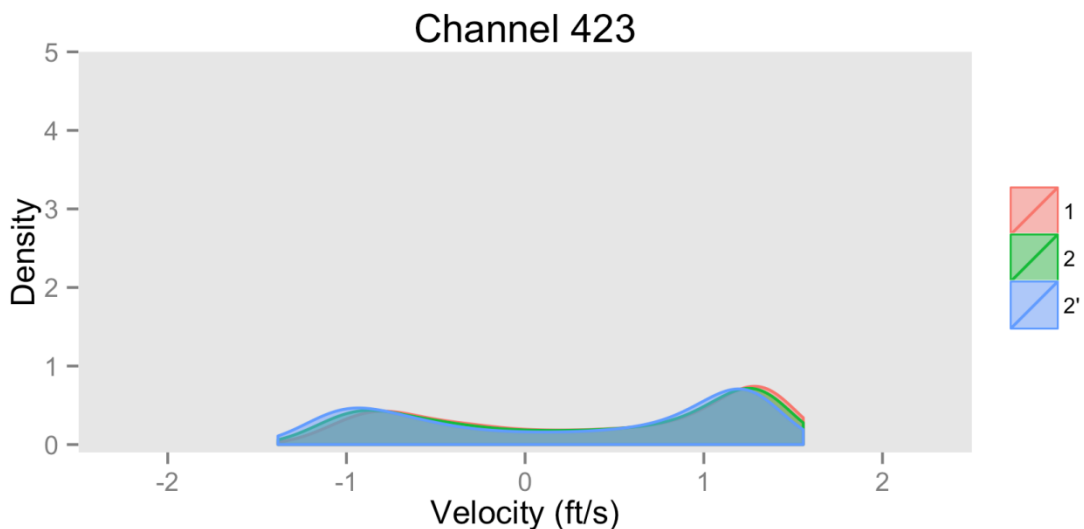


Figure 10. Density plot of velocity (ft/s) observed for DSM2 Channel 423, Sacramento River downstream of the Delta Cross Channel and Georgiana Slough in April

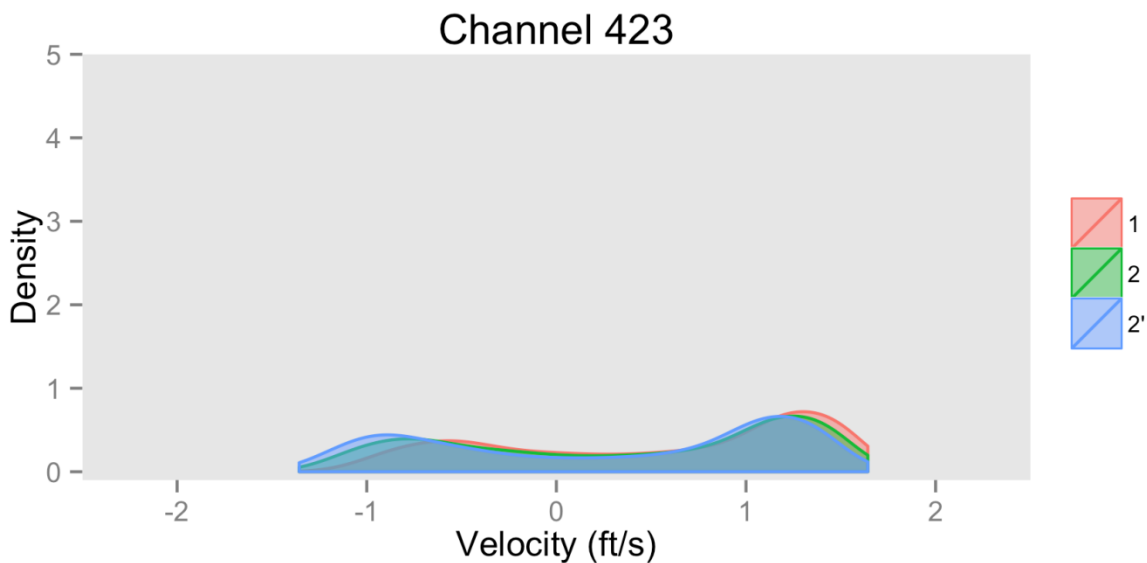


Figure 11. Density plot of velocity (ft/s) observed for DSM2 Channel 423, Sacramento River downstream of the Delta Cross Channel and Georgiana Slough in May

Attachment 2. Biological Review for Endangered Species Act Compliance with the WY 2015 Drought Contingency Plan April through September Project Description

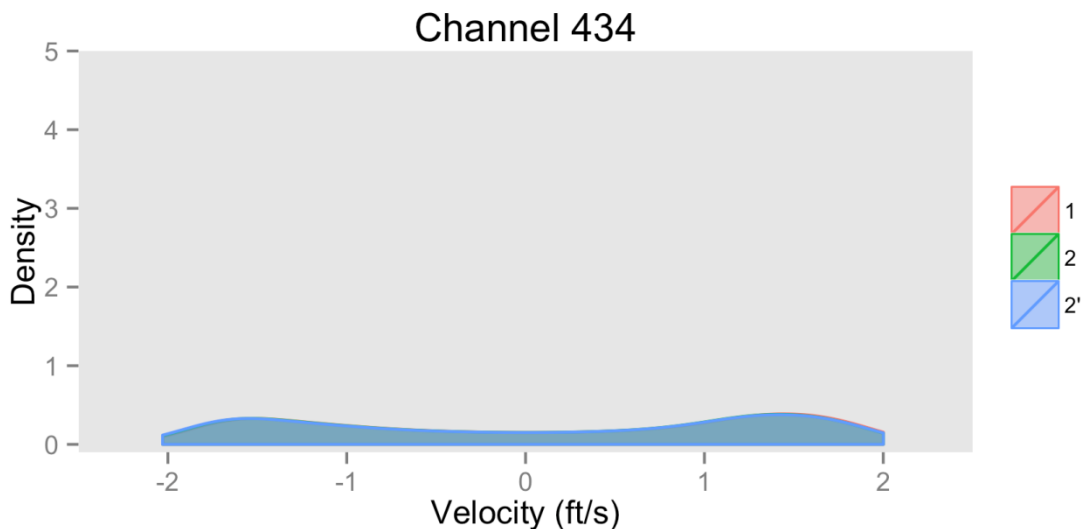


Figure 12. Density plot of velocity (ft/s) observed for DSM2 Channel 424, Sacramento River between Decker Island and Sherman Island in April

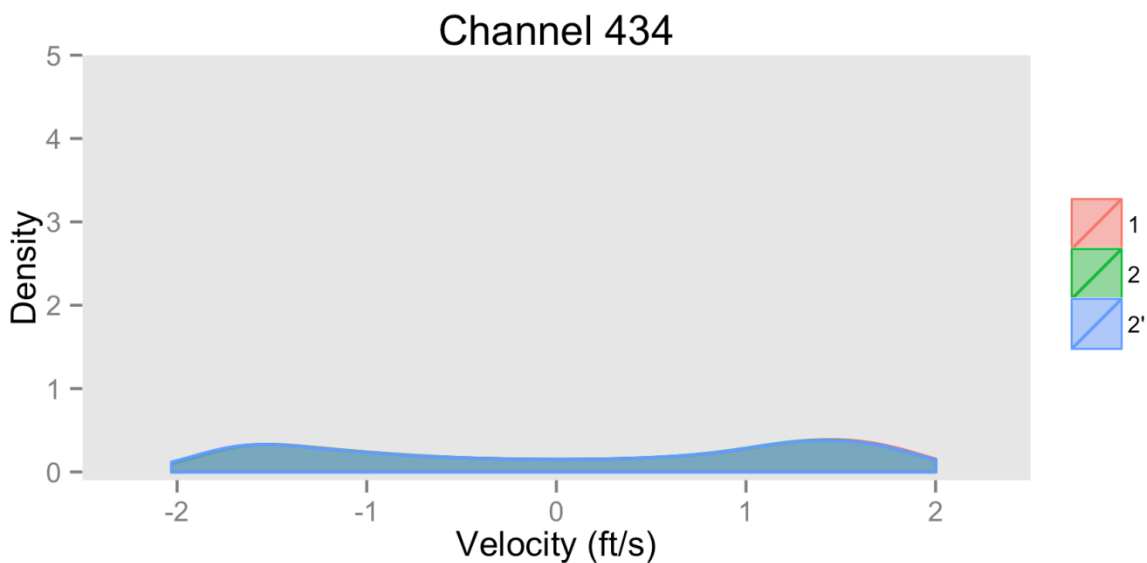


Figure 13. Density plot of velocity (ft/s) observed for DSM2 Channel 424, Sacramento River between Decker Island and Sherman Island in May

Attachment 2. Biological Review for Endangered Species Act Compliance with the WY 2015 Drought Contingency Plan April through September Project Description

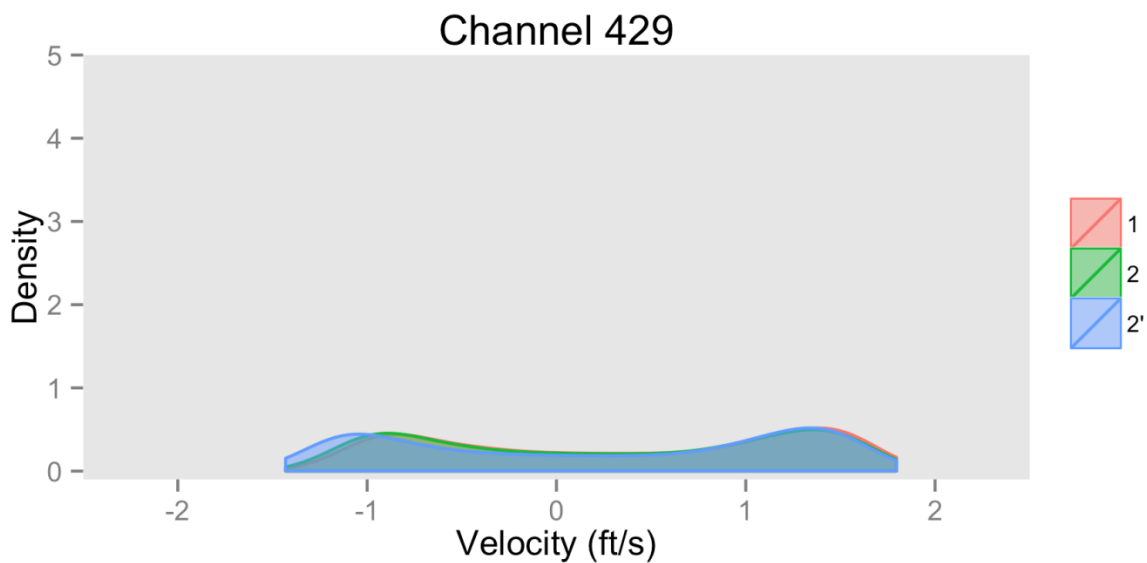


Figure 14. Density plot of velocity (ft/s) observed at DSM2 Channel Node 412 under three scenarios during the April modeled period (Sacramento River near Cache Slough, North Delta)

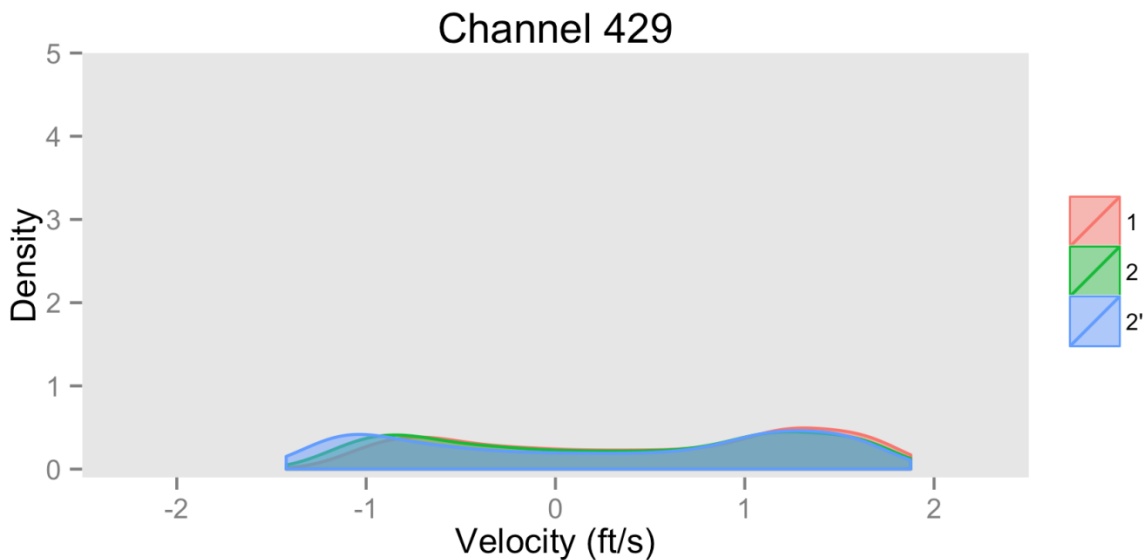


Figure 15. Density plot of velocity (ft/s) observed at DSM2 Channel Node 412 under three scenarios during the May modeled period (Sacramento River near Cache Slough, North Delta)

Attachment 2. Biological Review for Endangered Species Act Compliance with the WY 2015 Drought Contingency Plan April through September Project Description

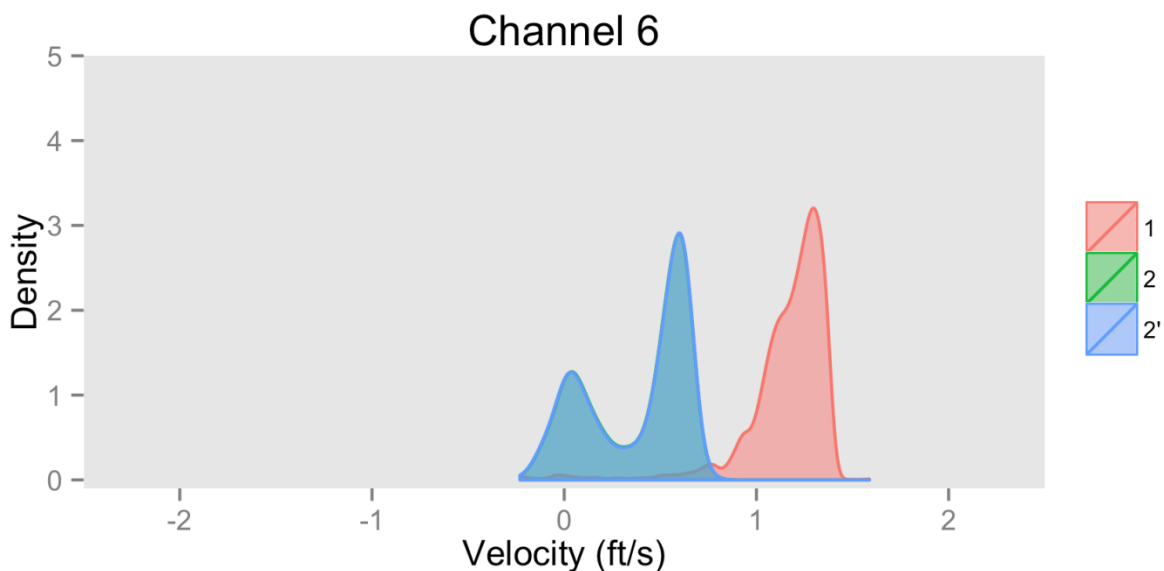


Figure 16. Density plot of velocity (ft/s) observed at DSM2 Channel Node 6 under three scenarios during the April modeled period (Upstream of Head of Old River on San Joaquin, San Joaquin)

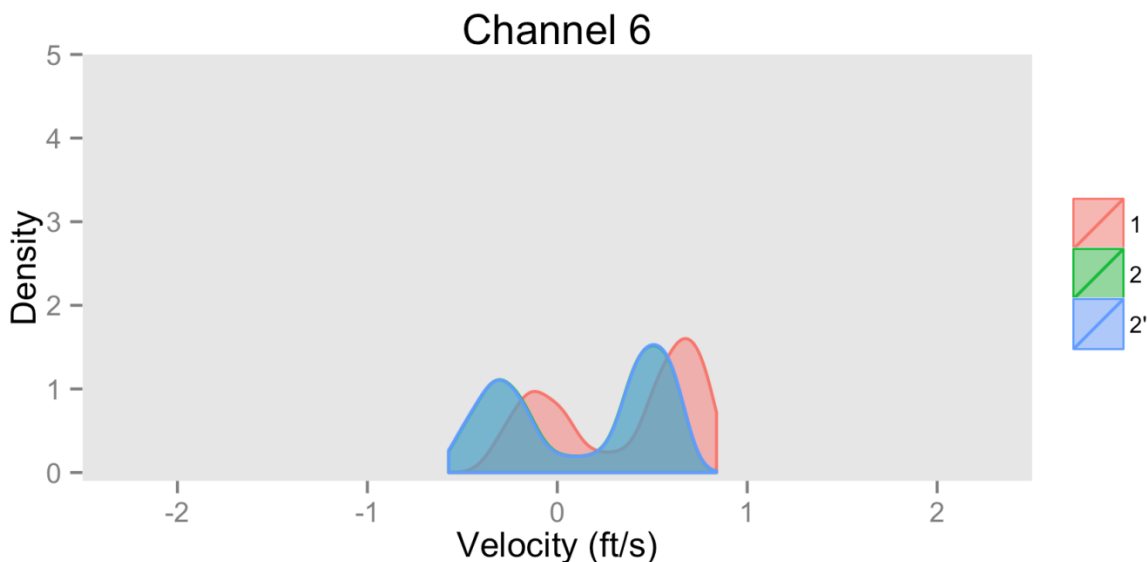


Figure 17. Density plot of velocity (ft/s) observed at DSM2 Channel Node 6 under three scenarios during the May modeled period (Upstream of Head of Old River on San Joaquin, San Joaquin)

Attachment 2. Biological Review for Endangered Species Act Compliance with the WY 2015 Drought Contingency Plan April through September Project Description

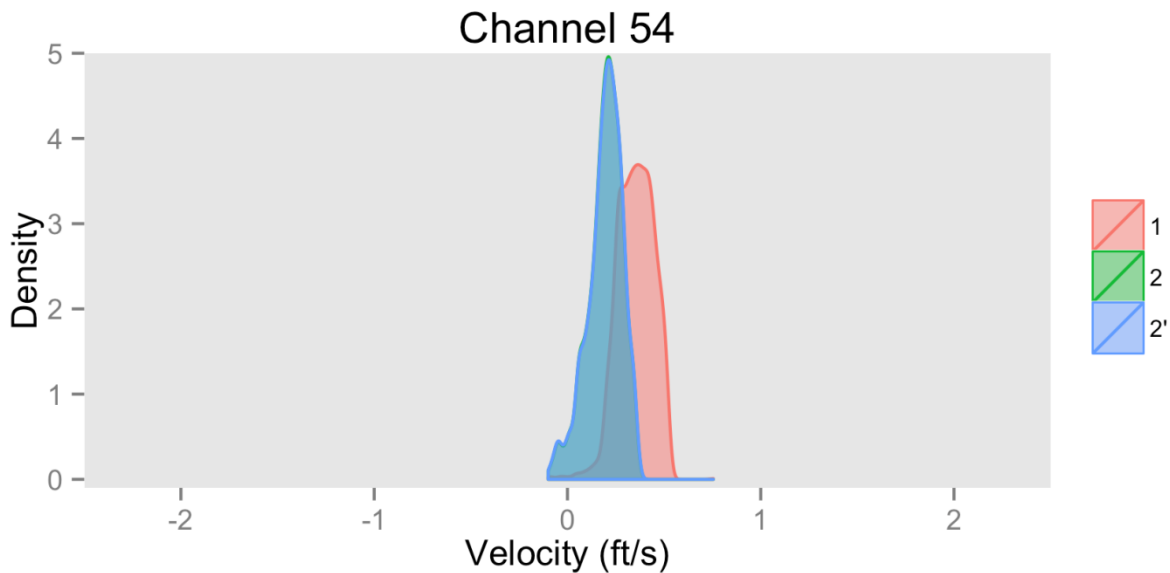


Figure 18. Density plot of velocity (ft/s) observed at DSM2 Channel Node 54 under three scenarios during the April modeled period (Downstream of Head of Old River on Old River, San Joaquin)

:

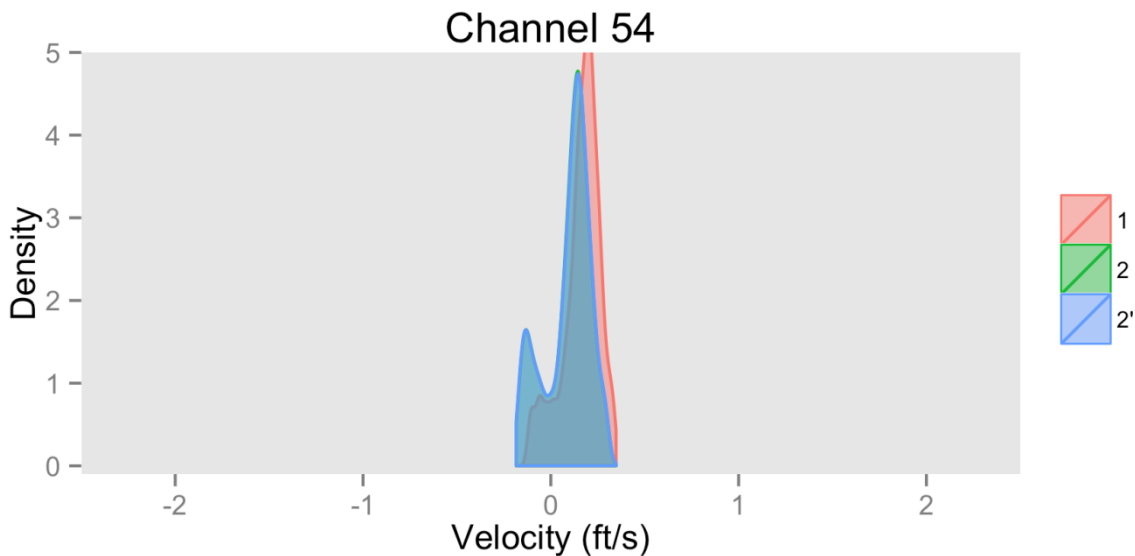


Figure 19. Density plot of velocity (ft/s) observed at DSM2 Channel Node 54 under three scenarios during the May modeled period (Downstream of Head of Old River on Old River, San Joaquin)

Attachment 2. Biological Review for Endangered Species Act Compliance with the WY 2015 Drought Contingency Plan April through September Project Description

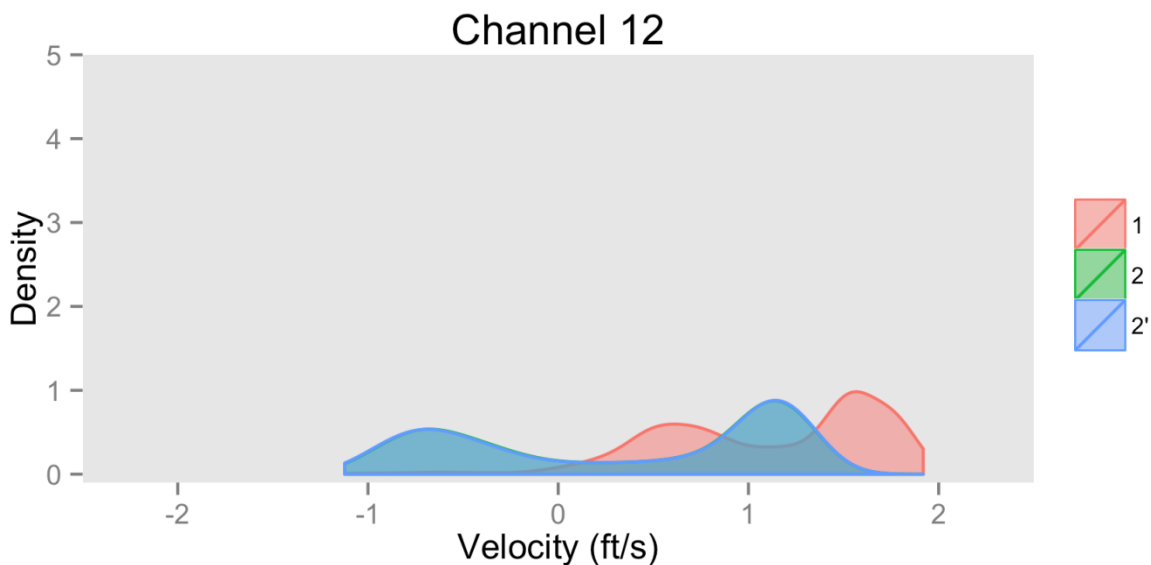


Figure 20. Density plot of velocity (ft/s) observed at DSM2 Channel Node 12 under three scenarios during the April modeled period (Upstream of Stockton Deepwater Shipping Channel , South Delta)

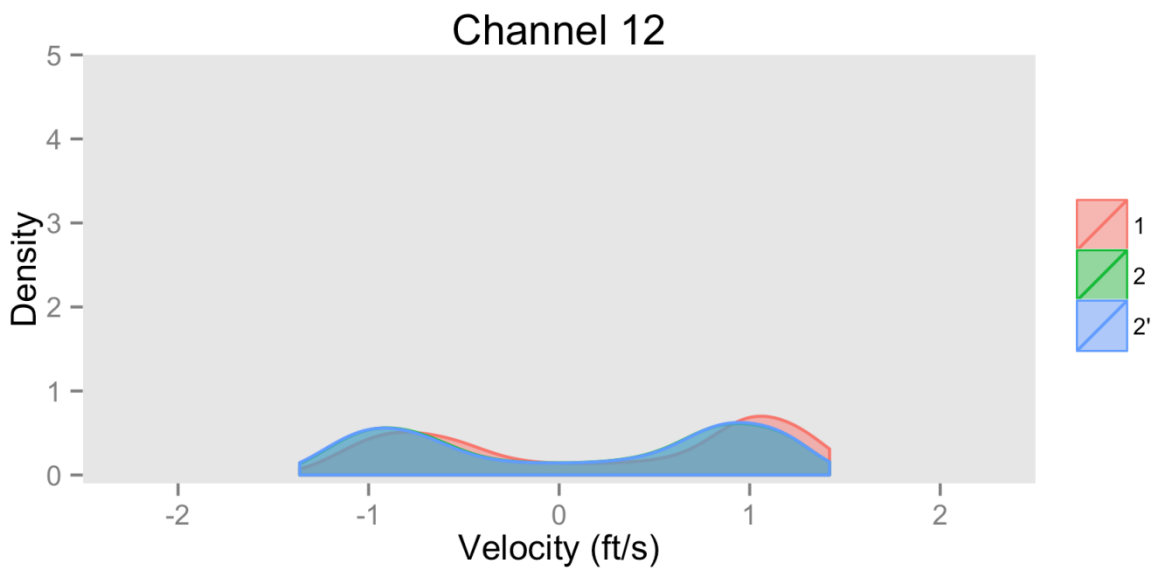


Figure 21. Density plot of velocity (ft/s) observed at DSM2 Channel Node 12 under three scenarios during the May modeled period (Upstream of Stockton Deepwater Shipping Channel , South Delta)

Attachment 2. Biological Review for Endangered Species Act Compliance with the WY 2015 Drought Contingency Plan April through September Project Description

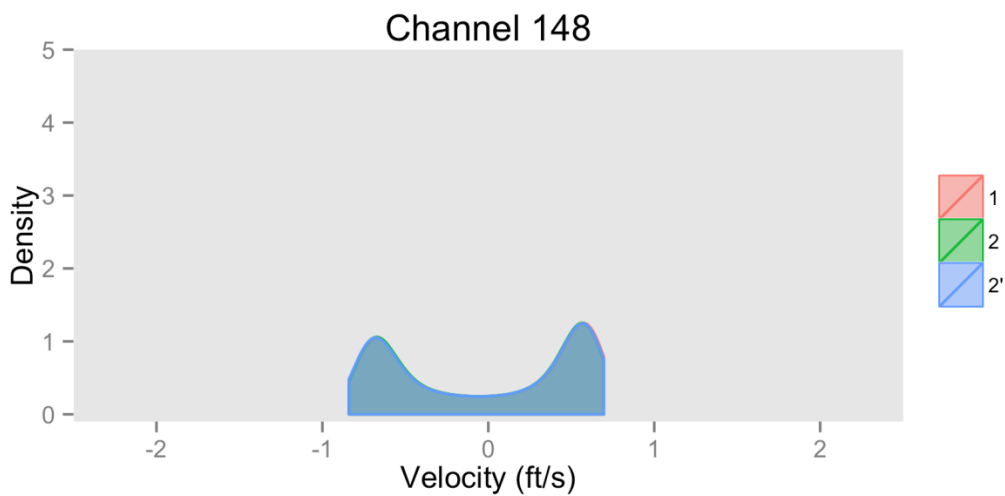


Figure 22. Density plot of velocity (ft/s) observed for DSM2 Channel 148, Middle River north of Railroad cut, in April

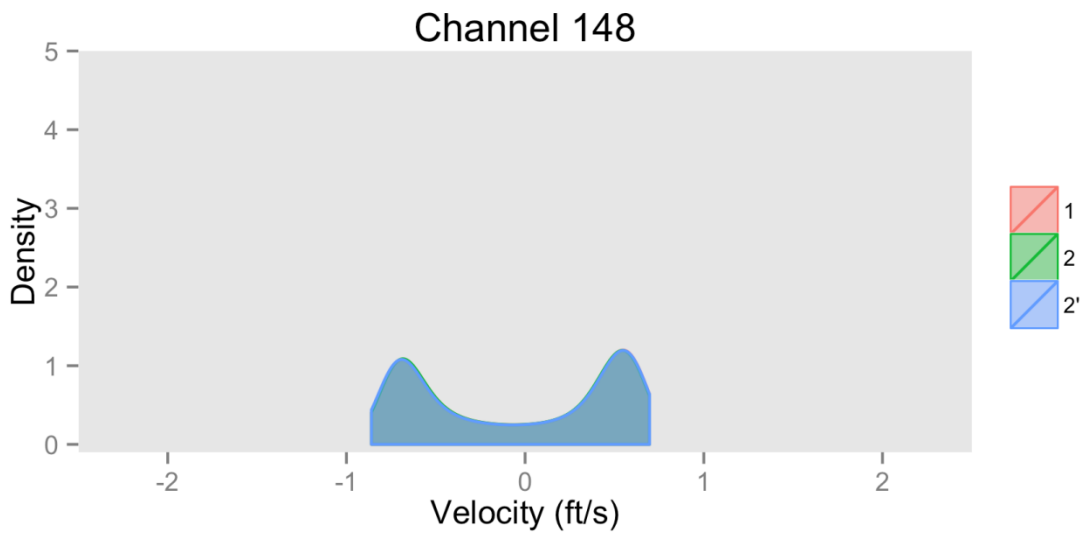


Figure 23. Density plot of velocity (ft/s) observed for DSM2 Channel 148, Middle River north of Railroad cut, in May

Attachment 2. Biological Review for Endangered Species Act Compliance with the WY 2015 Drought Contingency Plan April through September
Project Description

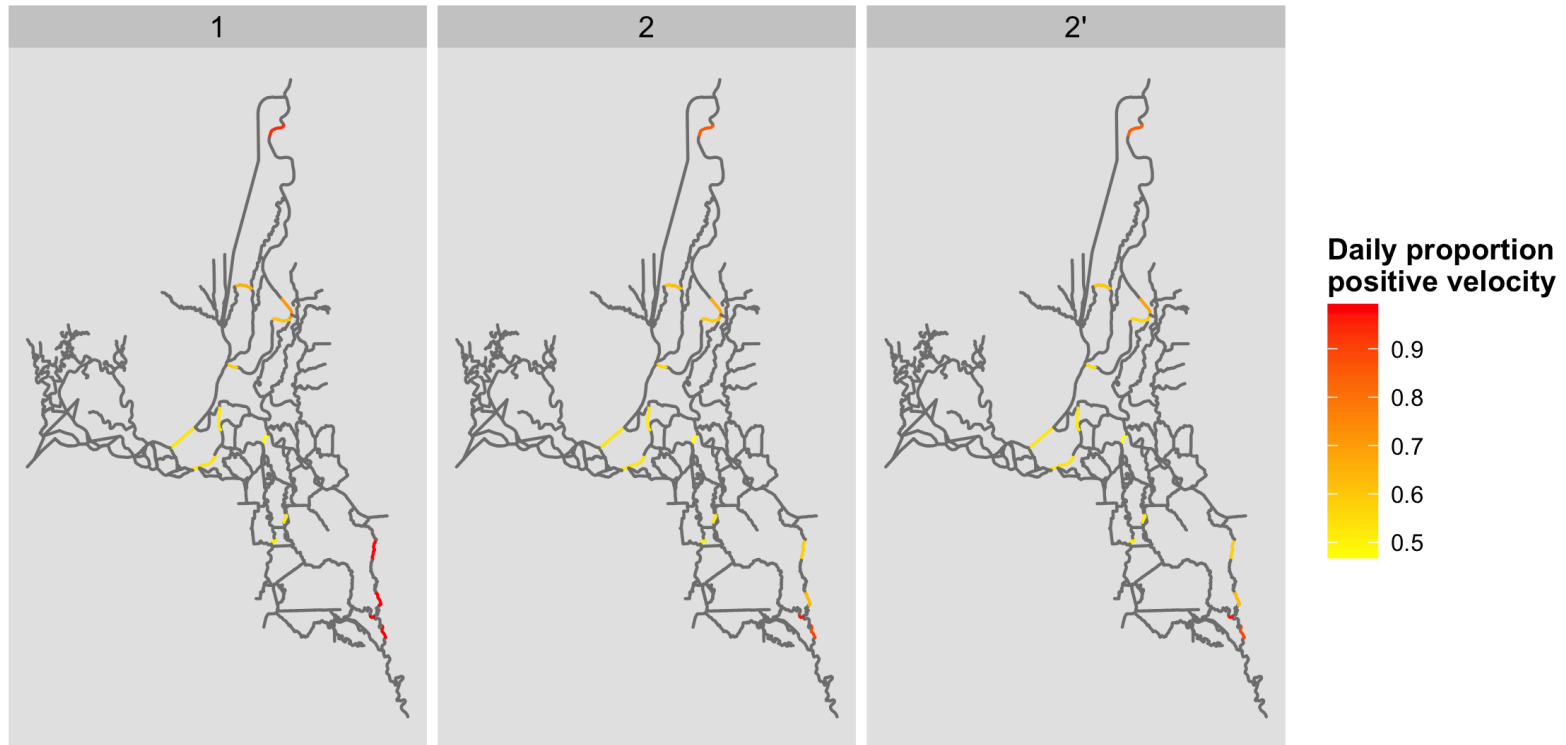


Figure 24. Maps of the Delta with Key Channels Color-Coded for Daily Proportion Positive Velocity, May 2015

Attachment 2. Biological Review for Endangered Species Act Compliance with the WY 2015 Drought Contingency Plan April through September
Project Description

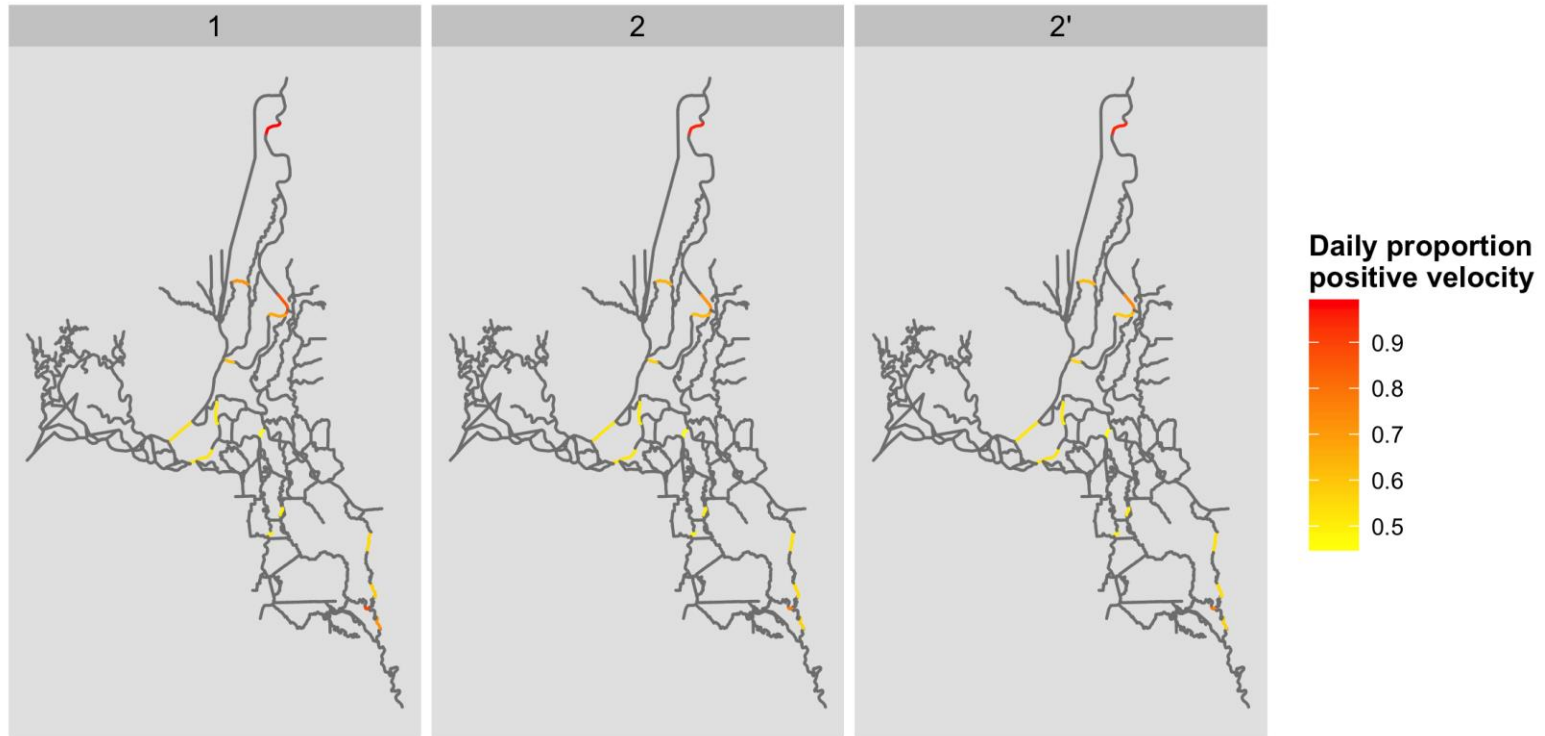


Figure 25. Maps of the Delta with Key Channels Color-Coded for Daily Proportion Positive Velocity, April 2015

Attachment 2. Biological Review for Endangered Species Act Compliance with the WY 2015 Drought Contingency Plan April through September
Project Description

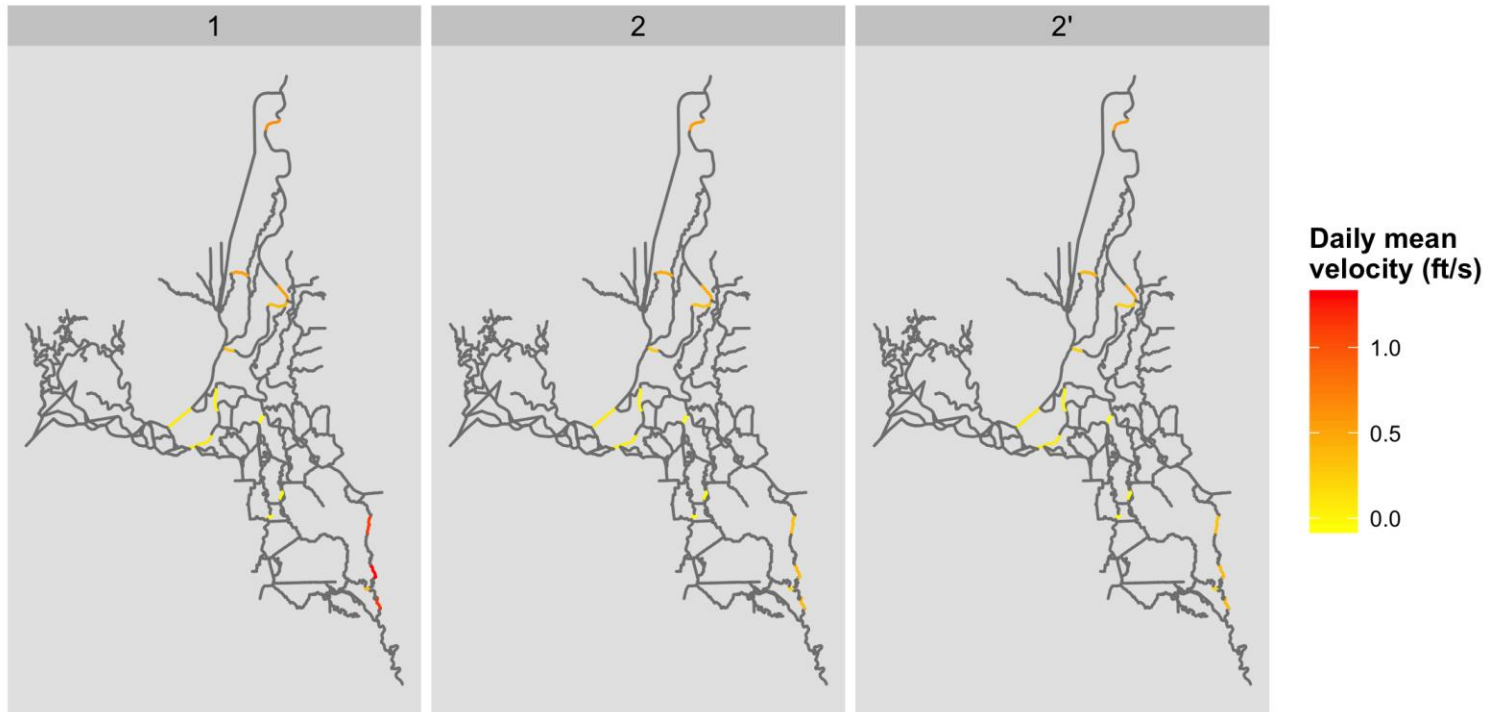


Figure 26. Maps of the Delta with Key Channels Color-Coded for Daily Mean Velocity Generated from DSM2, May 2015

Attachment 2. Biological Review for Endangered Species Act Compliance with the WY 2015 Drought Contingency Plan April through September
Project Description

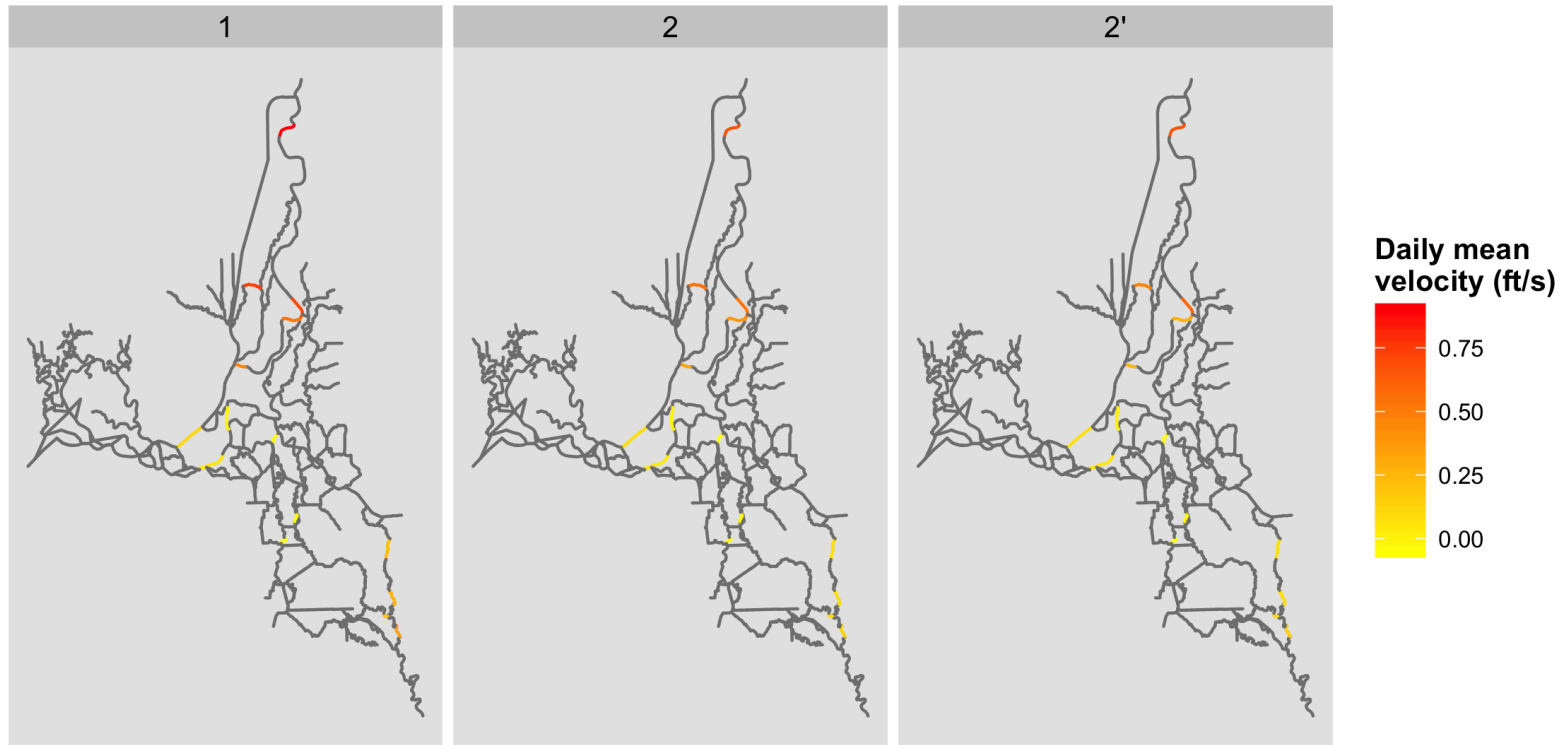


Figure 27. Maps of the Delta with Key Channels Color-Coded for Daily Mean Velocity Generated from DSM2, April 2015

Attachment 2. Biological Review for Endangered Species Act Compliance with the WY 2015 Drought Contingency Plan April through September Project Description

Particle Tracking Model

For the purposes of the biological review, particle “entrainment” was assessed for the three scenarios: Baseline, Project Description with closed DCC gates, Project Description with open DCC gates (Table 1). Although the DSM2 particle tracking model does not currently incorporate a behavioral component, particles are considered dependable proxies for the relative effect of hydrological conditions on early-stage smelt larval movement because larvae are weak swimmers and are only minimally capable of selectively maintaining a position in the water column [*i.e.*, they tend to behave a lot like neutrally buoyant particles; see Kimmerer (2008)]. Six injection locations and seven flux locations were assessed (Figure 28). Daily entrainment flux fate at the CVP/SWP projects at the end of the model period (May 31) was considered and graphed for cumulative daily flux (Figure 29). Combined entrainment at the Projects was highest in both scenarios for particles inserted at Station 815 (near Prisoners Point on the San Joaquin River). The flux of particles past Chipps Island from all injection points are shown in Figures 30 and 31 for both the modeled Baseline and Project Description scenarios.

Attachment 2. Biological Review for Endangered Species Act Compliance with the WY 2015 Drought Contingency Plan April through September Project Description

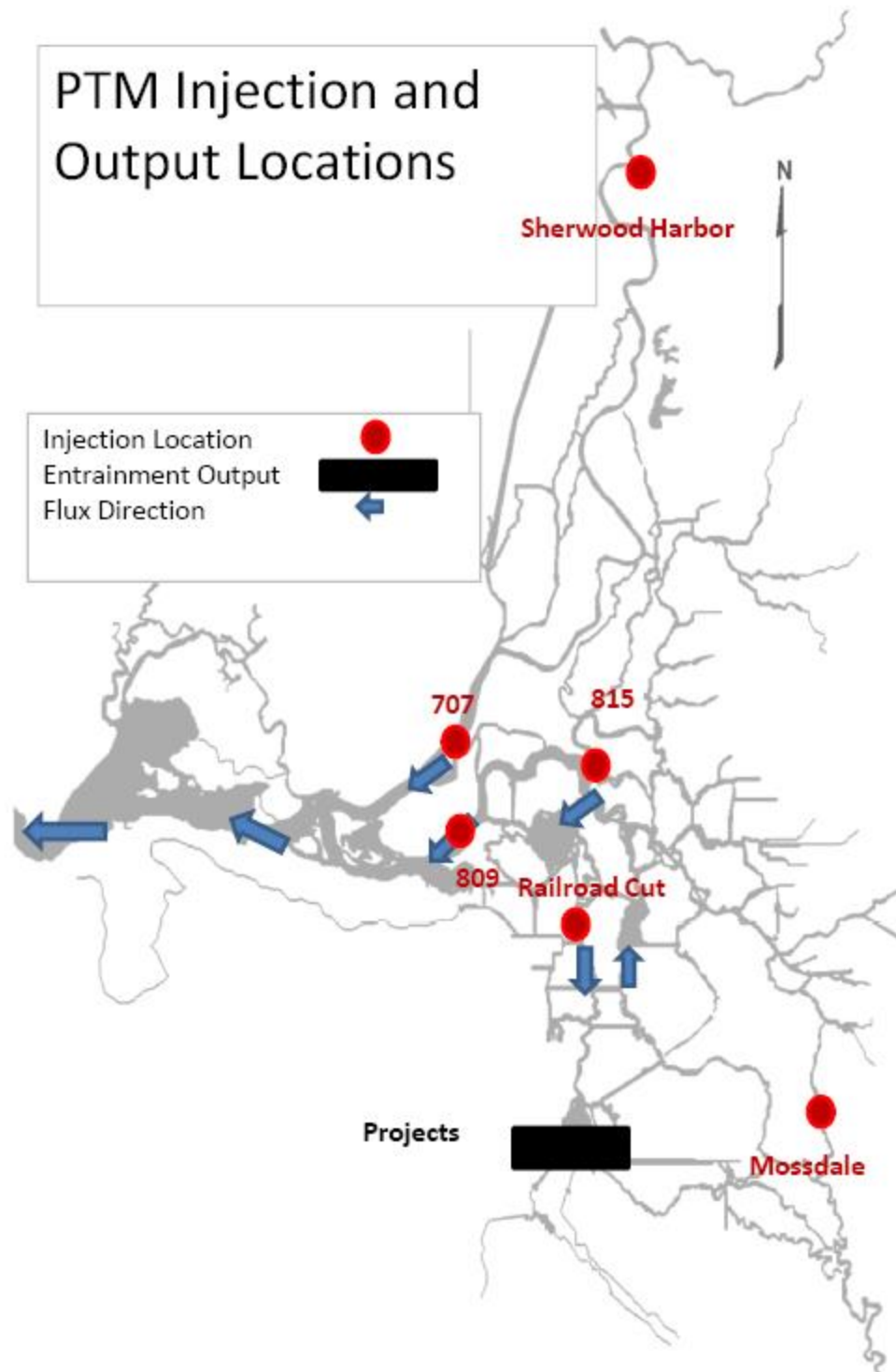


Figure 28. PTM Model injection and output locations. Six injection points are evaluated

Attachment 2. Biological Review for Endangered Species Act Compliance with the WY 2015 Drought Contingency Plan April through September Project Description

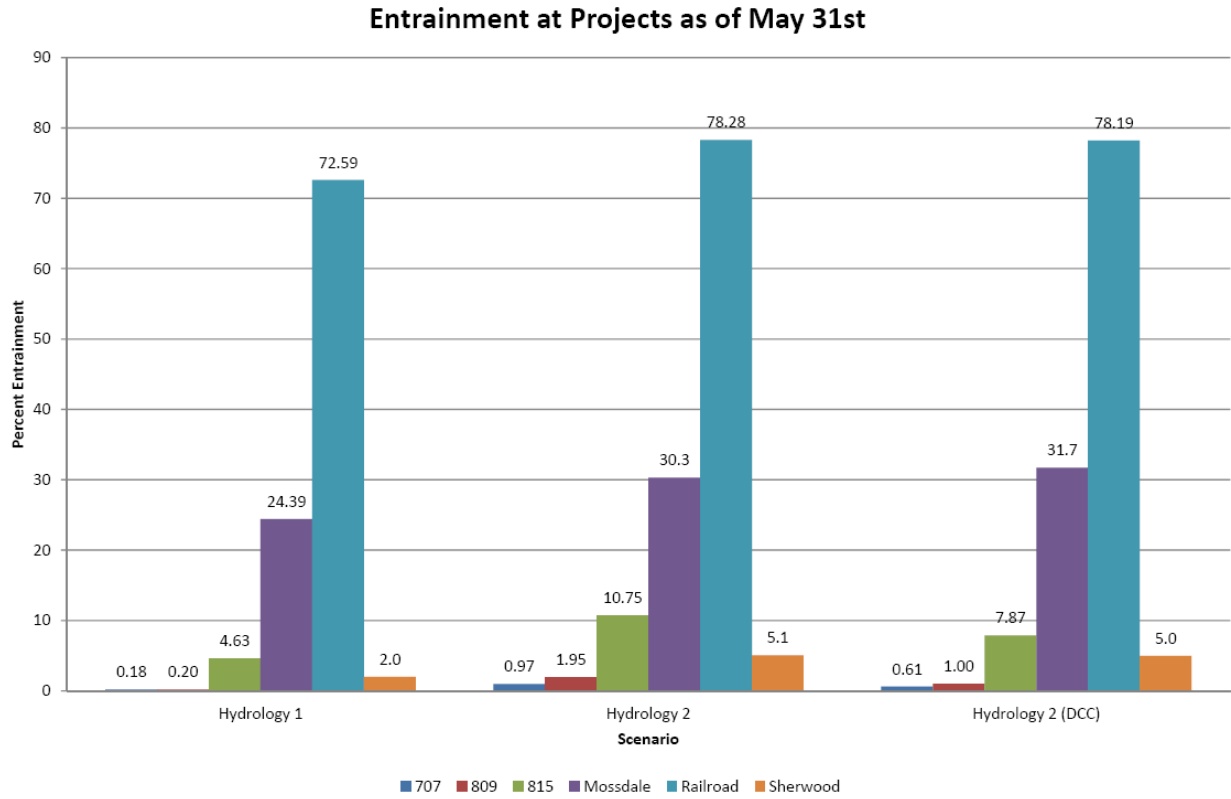


Figure 29. Entrainment at Projects from multiple injection locations under the Project Description (Hydrology 2) and Unmodified (Hydrology 1) model scenarios

Attachment 2. Biological Review for Endangered Species Act Compliance with the WY 2015 Drought Contingency Plan April through September Project Description

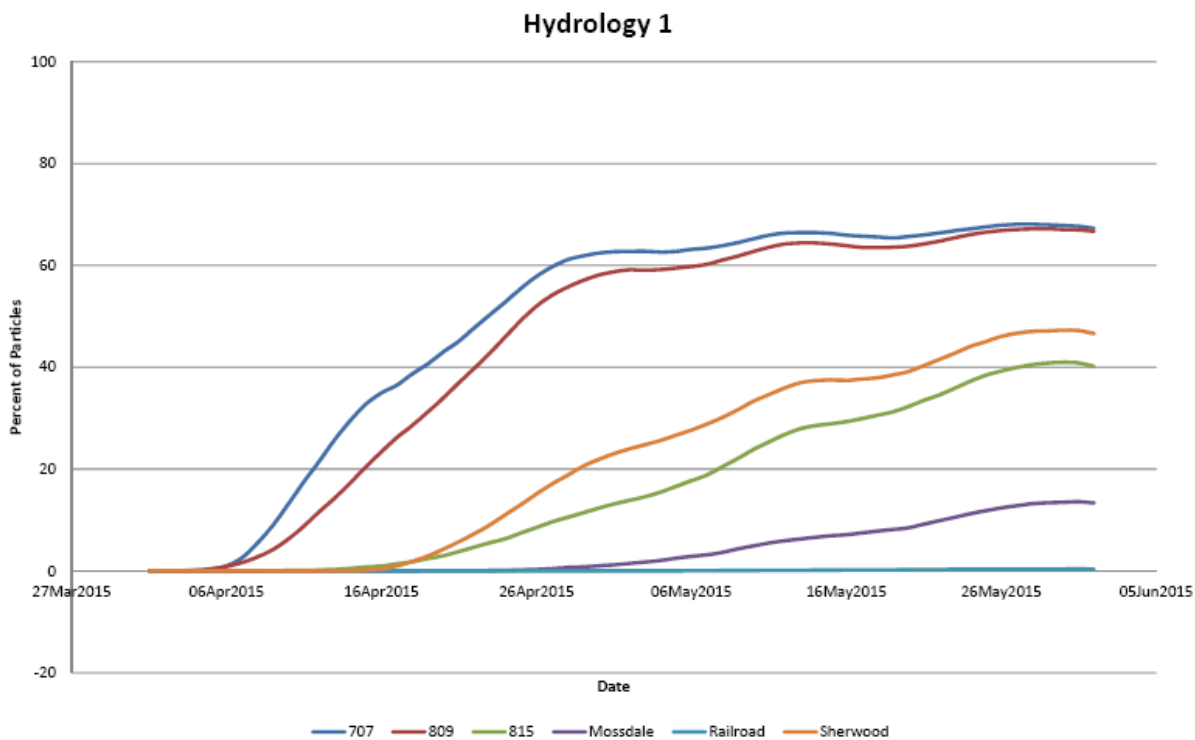


Figure 30. Flux Fate Past Chippis Island under the modeled Baseline scenario (Hydrology 1) for multiple injection locations

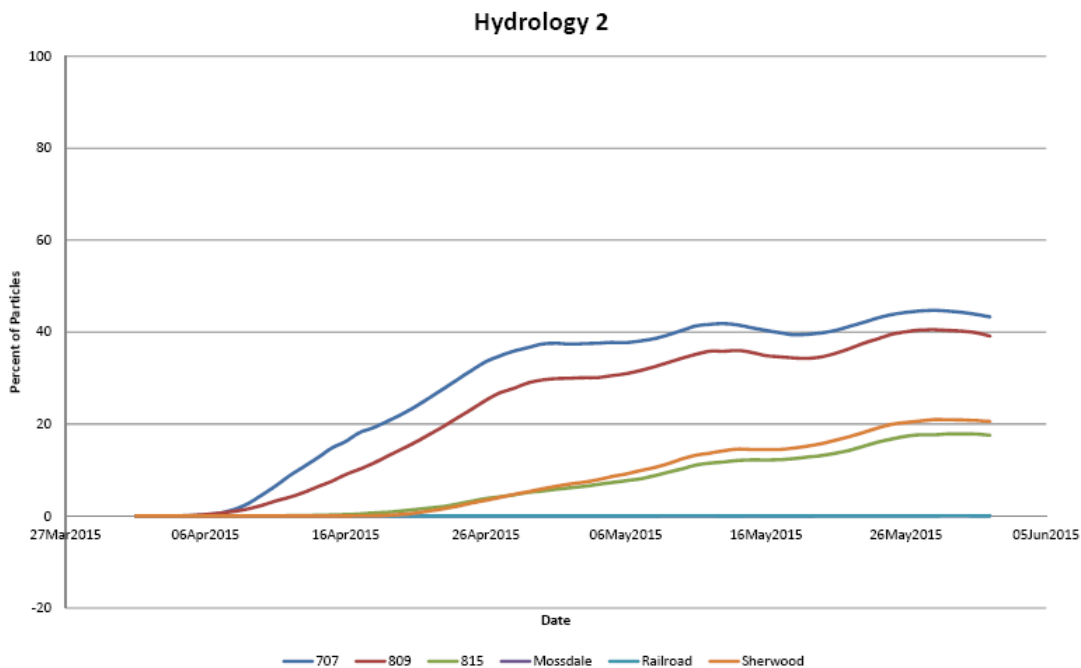


Figure 31. Flux Fate Past Chippis Island under the modeled Project Description scenario (Hydrology 2) for multiple injection locations

Status of the Species and Effects of Project Description

Status of Winter Run Chinook Salmon

A small number of winter-run Chinook Salmon (*Oncorhynchus tshawytscha*) (n=3,015; 90% CI= 2,741-3,290) returned to spawn in the upper Sacramento River in 2014. Of these 3,105 winter-run Chinook, 388 were collected at the Keswick trap for broodstock at Livingston Stone National Fish Hatchery. Assuming that 3-year old fish make up the majority of each spawning cohort, returning adults in 2014 were produced by a much smaller spawning escapement in 2011 (*i.e.*, 827 adult spawners). The effects of limited cold water storage and loss of temperature control out of Keswick Dam from mid-August through the fall of 2014 led to substantial egg and fry mortality. The mortality associated with this loss of temperature control was estimated to have affected up to 95% of the brood year 2014 eggs and fry (Doug Killam, CFDW, pers comm.). The average egg to fry mortality for brood year 2007-2012 was estimated to be 69% based on female escapement, fecundity, and the RBDD juvenile production index (Reclamation 2015).

As of March 11, 2015, approximately 408,704 juvenile winter-run Chinook Salmon were estimated to have migrated past the Red Bluff Diversion Dam (RBDD, Figures 32-33). The rotary screw traps at RBDD were operated for just 8 of 31 days during December 2014², a period when the Sacramento River flows and turbidity levels were at their highest. Very few natural-origin juvenile winter-run Chinook Salmon are hypothesized to remain upstream of the Delta and these are anticipated to migrate into the Delta and lower Sacramento River by the end of April based upon historical RBDD passage data (Tables 8-9). Monitoring data throughout the Sacramento River suggest that the majority of salmonids, including natural-origin juvenile winter-run Chinook Salmon are currently residing in the Lower Sacramento River and Delta (Figure 34, Tables 10-11). Detections of winter-run sized juveniles in the Chipps Island trawl monitoring have been low, but trending upwards, indicating that while few have migrated out of the Delta at this time, outmigration to the ocean is increasing (Figure 35). During April, the seaward migration of juvenile winter-run Chinook Salmon is likely to be completed due to changes in photoperiod and temperature, which stimulate smoltification and migratory behavior in these rearing fishes. Historical patterns indicate that the majority of out-migration typically occurs in March and is not complete until early spring (del Rosario *et al.* 2013). Discussions by the Delta Operations for Salmonids and Sturgeon (DOSS) team have estimated on March 17 that for the natural origin winter-run juveniles greater than 85% were rearing in the Delta, less than 15% had exited the Delta, and “few remaining stragglers” had yet to enter the Delta. A low level of salvage of winter-run sized juveniles has occurred during the winter, with a cumulative loss of 102 natural-origin winter-run sized juvenile Chinook as of March 20, 2015. This may be due to several factors, acting individually or in concert, including low population numbers, low exports, and low survival.

The entire production population of hatchery-origin winter-run Chinook Salmon were released into the upper Sacramento River in Redding from February 4-6, 2015. This segment of the

² Biweekly reports from RBDD are available at: http://www.fws.gov/redbluff/RBDD%20JSM%20Biweekly/2014/rbdd_jsmp_2014.html

Attachment 2. Biological Review for Endangered Species Act Compliance with the WY 2015 Drought Contingency Plan April through September Project Description

winter-run population, which was released concurrently with a storm pulse, began entering the North Delta within a week after release based on monitoring data, coded wire tag recoveries, and acoustic tag detections. Detection of acoustic tags and recoveries of CWT tags have in occurred at the Sacramento I-80 receiver, in the Knights Landing rotary screw traps (RSTs), the Sacramento regional beach seines, and the Sacramento trawls occurring near Sherwood Harbor on the Sacramento River. Discussions by the DOSS team have estimated passage into the Delta to be approximately 70-85% for the hatchery winter-run Chinook salmon. A subset of this release group from LSNFH was tagged with JSAT acoustic telemetry tags (n=500) and provided another means to track the downstream migration of the hatchery-origin winter-run juveniles, in addition to the standard river, Delta, and salvage fish monitoring efforts already in place. As of March 16, 2015, approximately 27.8% of the acoustic tagged hatchery winter-run were observed to have entered the Delta at the I-80/50 bridge in Sacramento, based on at least 2 detections of each tag by the array on the bridge abutments. If only single detections are used (which could include some false positives), the percentage of the tagged hatchery fish reaching the North Delta is 39.2%. It is worth noting that the Tisdale Weir did overtop immediately following the release of these fish and adipose fin-clipped juvenile salmonids (indicative of hatchery fish which includes both winter-run Chinook Salmon released from LSNFH and late-fall Chinook salmon concurrently released from the Coleman National Fish Hatchery [CNFH]) were rescued from the downstream apron of the weir. This observation suggests that some proportion of the hatchery release groups from both the LSNFH and CNFH releases entered the Sutter Basin and took that route downstream. As of March 20, 2015, the total observed loss of hatchery winter-run, confirmed by CWT, at the salvage facilities is 8.40. The DOSS estimates for the hatchery winter-run Chinook and the detected passage of the telemetry tagged differ considerably, which could result from, in part, detections probabilities being reduced due to high turbidity and flows, differential migration rates or holding patterns.

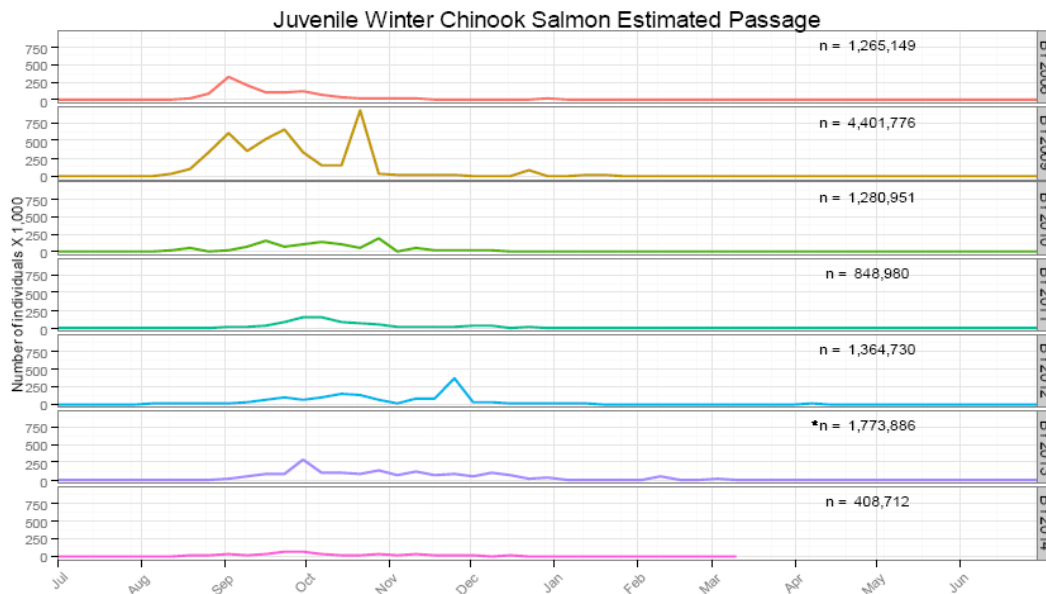


Figure 32. Weekly Estimated Passage of Juvenile Winter-run Chinook Salmon at Red Bluff Diversion Dam (RK 391) by Brood-Year (BY)³

³ Fish sampled using rotary-screw traps for the period of July1, 2008 to present. Winter-run passage value interpolated using a monthly mean for the period October 1, 2013-October 17, 2013 due to government shutdown. Figure supplied by USFWS on March 11, 2015.

Attachment 2. Biological Review for Endangered Species Act Compliance with the WY 2015 Drought Contingency Plan April through September Project Description

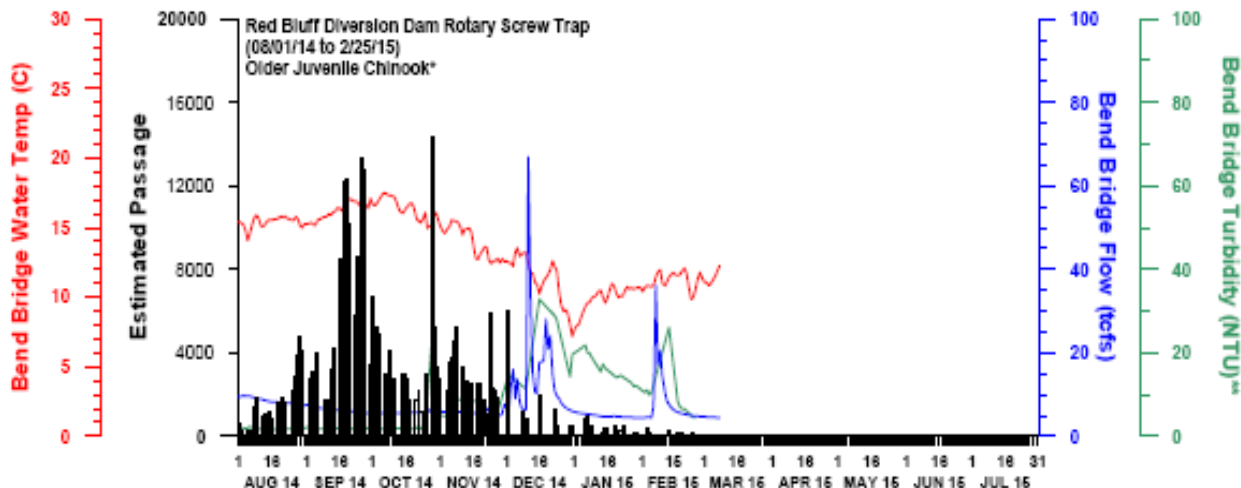


Figure 33. Red Bluff Diversion Dam Passage of Juvenile Older Chinook Salmon and Associated Environmental Data⁴

Table 8. Estimated Passage of Juvenile Winter Chinook Salmon at Red Bluff Diversion Dam (RK391) by Passage Quartile and Brood Year (BY)⁵

	Winter run Chinook Brood						
	2007	2008	2009	2010	2011	2012	2013
First	1/9/08	2/20/09	1/25/10	1/5/11	1/24/12	12/21/12	2/14/14
25%	1/25/08	3/1/09	3/3/10	3/16/11	3/22/12	3/18/13	3/5/14
50%	3/15/08	3/12/09	3/13/10	4/4/11	4/7/12	3/26/13	3/9/14
75%	3/25/08	3/26/09	3/31/10	4/15/11	4/11/12	4/4/13	3/14/14
Last	4/28/08	5/19/09	4/28/10	4/22/11	4/27/12	4/15/13	4/11/14

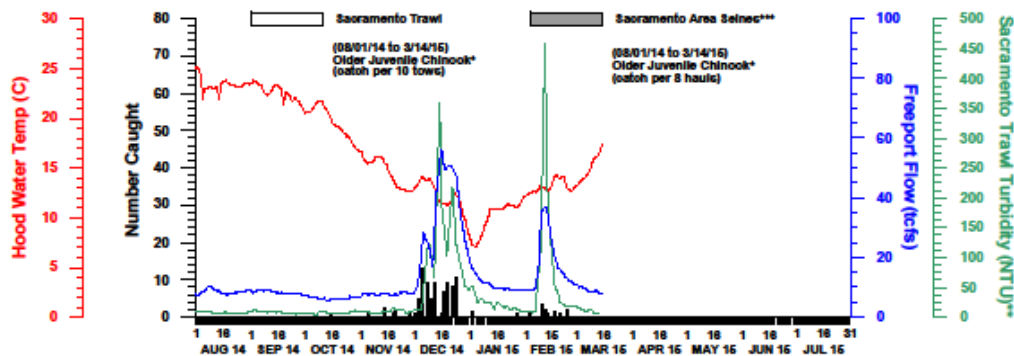


Figure 34. Sacramento Trawl and Sacramento Area Beach Seines Older Juvenile Chinook Salmon Catch Data and Associated Environmental Data⁶

⁴ Figure supplied by DWR on March 8, 2015

⁶ Figure supplied by DWR on March 18, 2015.

Attachment 2. Biological Review for Endangered Species Act Compliance with the WY 2015 Drought Contingency Plan April through September Project Description

Table 9. Weekly Catch of Juvenile Winter-run Chinook Salmon at Tisdale and Knights Landing Rotary Screw Traps for WY15 through March 13, 2015

	Tisdale								Knights Landing								
	Wild Juveniles					Ad Clipped			Weekly Total	Wild Juveniles					Ad Clipped		Weekly Total
	Fall	Spring	Winter	Late fall	Steelhead	Salmon	Steelhead	Fall		Spring	Winter	Late fall	Steelhead	Salmon	Steelhead		
10/4/2014 - 10/10/2014	0	0	0	0	0	0	0	0	0	0	1	0	0	0	0	0	1
10/11/2014 - 10/17/2014	0	0	0	0	0	0	0	0	0	0	0	0	0	0	0	0	0
10/18/2014 - 10/24/2014	0	0	0	0	0	0	0	0	0	1	0	0	0	0	0	0	1
10/25/2014 - 10/31/2014	0	2	117	2	0	0	0	121	0	1	95	4	0	0	0	100	
11/1/2014 - 11/7/2014	0	1	2	0	0	0	0	3	0	0	2	0	0	0	0	2	
11/8/2014 - 11/14/2014	0	0	1	0	0	0	1	2	0	0	2	0	0	0	0	2	
11/15/2014 - 11/21/2014	0	0	3	1	0	0	0	4	0	0	3	0	0	0	0	3	
11/22/2014 - 11/28/2014	0	0	3	0	0	0	0	3	0	0	2	0	0	0	0	2	
11/29/2014 - 12/5/2014	0	0	7	0	0	2	0	9	0	0	2	0	0	0	0	2	
12/6/2014 - 12/12/2014	10	14	10	2	0	5	0	41	17	50	32	8	0	24	0	131	
12/13/2014 - 12/19/2014	169	9	0	2	0	2	0	182	148	88	5	1	0	4	0	246	
12/20/2014 - 12/26/2014	654	35	24	5	1	6	0	725	411	112	14	4	0	8	0	549	
12/27/2014 - 1/2/2015	154	22	1	1	0	0	0	178	13	6	0	1	0	0	0	20	
1/3/2015 - 1/9/2015	91	61	6	0	2	0	0	160	15	13	0	2	0	2	0	32	
1/10/2015 - 1/16/2015	52	16	4	0	0	1	6	79	25	13	0	1	0	0	7	46	
1/17/2015 - 1/23/2015	30	7	3	0	0	0	4	44	12	6	0	0	0	0	5	23	
1/24/2015 - 1/30/2015	9	0	2	0	0	0	4	15	3	1	0	0	0	1	0	5	
1/31/2015 - 2/6/2015	2	1	1	0	0	0	0	4	1	0	0	0	0	0	0	1	
2/7/2015 - 2/13/2015	4795	43	3	0	0	193	18	5052	6118	79	22	0	3	332	80	6634	
2/14/2015 - 2/20/2015	251	11	4	0	0	40	0	306	674	21	7	0	2	102	25	831	
2/21/2015 - 2/27/2015	18	0	1	0	0	5	0	24	7	0	3	0	0	5	0	15	
2/28/2015 - 3/6/2015	2	0	3	0	0	4	0	9	0	0	0	0	0	0	0	0	
3/7/2015 - 3/13/2015	0	1	1	0	0	0	0	2	2	0	0	0	0	1	0	3	
Species Total	6237	223	196	13	3	0	258	33	6963	7446	391	190	21	5	479	117	8649

Table 10. Lower Sacramento River and Delta beach seine and trawling recoveries of salmonids during WY 2015⁷

Beach Seine Region	Wild juveniles					Ad clipped		Regional Total
	Fall	LateFall	Spring	Winter	Steelhead	Chinook	Steelhead	
Bay East	0	0	0	0	0	0	0	0
Bay West	0	0	0	0	0	0	0	0
Central Delta	36		10	1	0	0	1	48
Lower Sacramento	745	3	236	45	0	7	1	1037
North Delta	865	3	243	18	0	9	2	1140
Sacramento	216	2	55	8	2	10	0	293
South Delta					0	0	0	0
San Joaquin	2	0	0	0	0	0	0	2
Trawl								
Sacramento	116	5	17	11	0	17	0	166
Chippis				7	0	12	4	23
Jersey Point	371	1	5	2	0	0	4	383
Prisoners Pt	149	1	5	1	0	8	14	178
Species Total	2500	15	571	93	2	63	26	3270

⁷ Trawl and beach seine data updated through March 16, 2015. Provided by USFWS Delta Juvenile Fish Monitoring Program.

Attachment 2. Biological Review for Endangered Species Act Compliance with the WY 2015 Drought Contingency Plan April through September Project Description

Table 11. Salmonid presence in beach seines through different regions of the Delta during WY 2015

Week	Lower Sacramento	North Delta	Central Delta	San Joaquin	Sacramento	Grand Total
10/15/2014 - 10/21/2014	1					1
11/12/2014 - 11/18/2014		2				2
11/19/2014 - 11/25/2014		2				2
11/26/2014 - 12/2/2014	4				1	5
12/3/2014 - 12/9/2014	26	19			11	56
12/10/2014 - 12/16/2014	18	29			5	52
12/17/2014 - 12/23/2014	75	143			30	248
12/24/2014 - 12/30/2014	72	271	1		40	384
12/31/2014 - 1/6/2015	374	12			23	409
1/7/2015 - 1/13/2015	13	39	10		35	97
1/14/2015 - 1/20/2015	40	34	3		8	85
1/21/2015 - 1/27/2015	33	9				42
1/28/2015 - 2/3/2015	12	23			6	41
2/4/2015 - 2/10/2015	42	90	2		13	147
2/11/2015 - 2/17/2015	94	104			11	209
2/18/2015 - 2/24/2015	88	57	1	1	17	164
2/25/2015 - 3/3/2015	33	99	15		56	203
3/4/2015 - 3/10/2015	109	205	15		35	364
3/11/2015 - 3/13/2015	2			1		3
Grand Total	1036	1138	47	2	291	2415

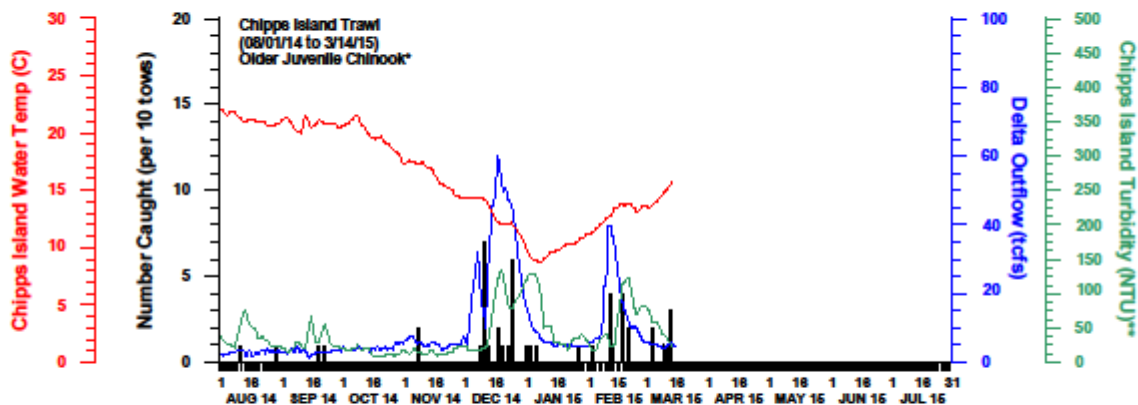


Figure 35. Chipps Island Trawl older juvenile Chinook Salmon catch data and associated environmental data⁸

Effects of Project Description on Winter-Run Chinook Salmon

The predicted distribution of winter-run Chinook Salmon during the Project Description period and a summary of potential effects is presented in Table 12, followed by more details per action type and location.

⁸ Figure supplied by DWR March 17, 2015.

Attachment 2. Biological Review for Endangered Species Act Compliance with the WY 2015 Drought Contingency Plan April through September Project Description

Table 12. Presence of Winter-run Chinook Salmon During the Project Description Period and Exposure to Potential Effects

Winter-run Chinook Salmon Life Stage	Life Stage Present	Tributary Habitat Effect	South/Central Delta Entrainment Effect	Facility Loss Effect
Egg/Alevin	This life stage will be present in the Sacramento River May through September for BY 15.			
Sacramento R	Yes	Yes ⁹	N/A	N/A
Juvenile	This life stage will be present in the Delta during April and May for BY 14 and in the Sacramento during August to September for BY 15.			
Sacramento R	Yes	Reduced Survival	N/A	N/A
Delta	Yes	N/A	Yes	Uncertain
Adults	This life stage will be present in the Sacramento River and Delta during April through July			
Sacramento R	Yes	No Change	N/A	N/A
Delta	Yes	N/A	N/A	N/A

Sacramento River Actions

Temperature operations remain under discussion by the Sacramento River Temperature Task Group (SRTTG). The recent 90% temperature forecasts provided to the SRTTG in January and February both suggest that a temperature compliance point of 56°F at the Clear Creek CDEC gaging station cannot be maintained through the winter-run Chinook Salmon egg incubation and fry rearing period. These forecasts suggest temperatures below 56°F would no longer be attainable in mid-August to early September, which would suggest no potential impact on spawning adults. These forecasts suggest similar impacts as described during the late summer of WY 2014 (Figure 36). Impacts to egg and alevin stages are more difficult to predict due to uncertainties with actual spawn timing, redd locations, and observed hydrological and temperature profiles. A temperature management plan for the upper Sacramento River continues to be developed and an appropriate biological review will be provided upon its completion. Forecasted Sacramento River flows during the Project Description do not include large weekly fluctuations, and will incorporate ramping rates, which minimize stranding and isolation of winter-run Chinook Salmon juveniles.

⁹ Temperature management and effects will be evaluated by the SRTTG.

Attachment 2. Biological Review for Endangered Species Act Compliance with the WY 2015 Drought Contingency Plan April through September Project Description

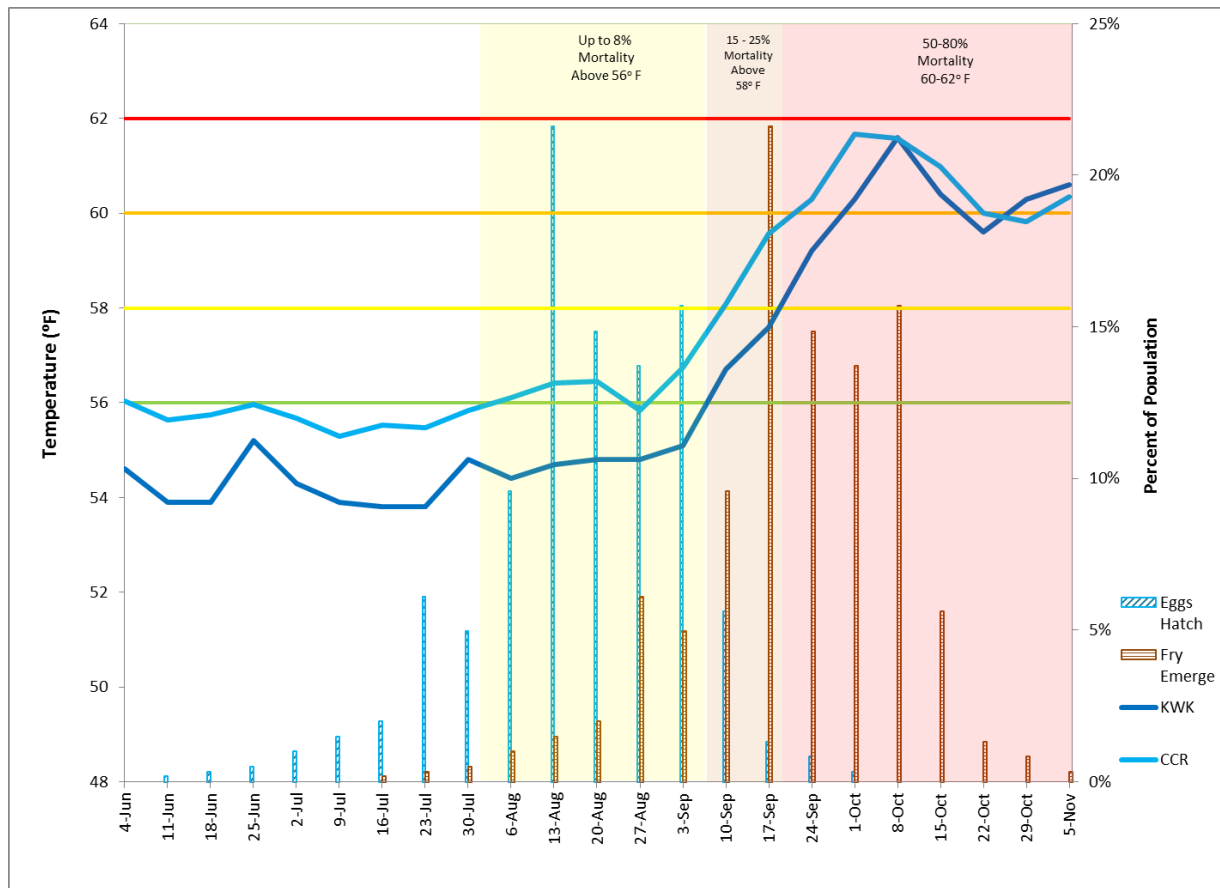


Figure 36. Water Temperatures at Keswick Dam (KWK) and Clear Creek Confluence (CCR, WY14 temperature compliance point) and Winter-run Chinook Salmon Early Life Stages between May 1 and November 6, 2014 ¹⁰

Net Delta Outflow Index and Water Quality Modifications

The Project Description during the remainder of WY 2015 is intended to preserve storage in Shasta Reservoir and increase the cold water pool available for management of temperatures for winter-run Chinook Salmon as late into the summer as feasible. Under the Project Description, the Net Delta Outflow Index (NDOI) will be modified from a minimum monthly daily average of 7,100 cfs to no less than 4,000 cfs during the months of April through June, and no less than 3,000 cfs during the month of July. This reduction in NDOI will lead to reduced Keswick releases during these months, which may affect out migrating winter-run Chinook Salmon during the remainder of spring 2015. DOSS estimated on March 17, 2015 that <5% of natural winter-run and <15% of hatchery winter-run remain in the riverine habitat affected by these releases upstream of the Delta. Approximately 85% of each of these groups is projected to be within the Delta and subject to effects resulting from any modified operations. These effects have been described previously (NMFS 2014a, USBR 2014a, USBR 2014b), but are reviewed here again since the distribution and proportion of winter-run Chinook Salmon in the Delta and Sacramento River have changed since these prior assessments. The changes in hydrodynamics in the modeled scenarios are representative of a range of conditions possible during April and May, and do not reflect the influence of potential Delta drought barriers that may be installed in the Delta.

¹⁰ Figure supplied by CDFW on January 20, 2015.

Attachment 2. Biological Review for Endangered Species Act Compliance with the WY 2015 Drought Contingency Plan April through September Project Description

Although the NMFS BiOp (2009) does not contain outflow standards, the BiOp assumed that D-1641 standards would be met, which would afford protection to listed species and their designated critical habitats. The reduction in outflow as part of the Project Description may impact juvenile salmonids migrating through the North Delta between the Sherwood Harbor and the Sutter and Steamboat slough reach, where Sacramento River flows meet the tidally-dominated western Delta. The Project Description's reduction in Delta outflow to as low as 4000 cfs may reduce survival of out migrating winter-run Chinook Salmon, migrating through the North Delta through increased predation mediated by hydrodynamic and habitat mechanisms. Once out migrating fish reach the tidally-dominated western Delta (i.e., Sutter and Steamboat slough area downstream towards Chipps Island) or San Joaquin River under the minimum outflows identified in the Project Description, they are likely to encounter daily proportion of positive velocities and mean velocity that are similar to outflow conditions observed in the Baseline modeling (see, *e.g.*, Figures 10-15). There is a moderate level of uncertainty in these conclusions.

The Project Description's reduced outflow increases tidal excursion upstream (reduced daily proportion of positive velocities) into the waterways in the North Delta region primarily in April. In April, there is a reduction in the proportion of positive daily flows passing Georgiana Slough and/or an open Delta Cross Channel compared to May in both the Baseline and Project Description DSM2 modeling (Tables 6-7). Increased reverse flows and slower mean velocities result in longer travel times for migrating fish, which has been shown to reduce outmigration survival (Singer et al. 2013, Perry 2010, and Romine et al. 2013). Georgiana Slough flows become less positive as tidal excursion causes reversal in this channel when outflow is reduced. Reducing outflow also causes a decrease in the daily proportion of positive velocities through the Sacramento River downstream of Sutter and Steamboat sloughs confluence with the Sacramento River. These increased tidal excursions may increase juvenile entrainment into Georgiana Slough and, if open, the Delta Cross Channel. When the DCC gates are open, the daily mean channel velocity becomes even less positive in these reaches (Tables 6-7, Figures 8-9). When the DCC gates are open, the daily proportion of positive velocities further decreases in the Sacramento River upstream of the DCC gates and more noticeable between the DCC gate and Georgiana Slough. When the DCC is open, there is a reduction in the daily proportion of positive flows through Georgiana Slough. There is a low level of uncertainty in this conclusion.

At low outflow, channel margin habitat becomes exposed above the surface of the water and is unavailable to juvenile salmonids present. This lack of cover may reduce juvenile survival. It is hypothesized that lower outflows may intensify the density of littoral predators into a smaller, shallower area and/or decrease the quantity of cover available to outmigrating salmonids to avoid predators. There is a high level of uncertainty in this conclusion. Decreased daily mean velocities may result in increased residence time of juvenile winter-run Chinook Salmon, which is hypothesized to result in an increased size at ocean entry if they are rearing in areas with suitable environmental metrics and food resources. There is a high level of uncertainty in this conclusion.

Attachment 2. Biological Review for Endangered Species Act Compliance with the WY 2015 Drought Contingency Plan April through September Project Description

Delta Cross Channel Gates

Under the Project Description, modified Delta Cross Channel Gates operations may occur based on water quality and fish presence. At this time, it is believed that an open DCC Gate has a low potential for entraining a substantial proportion of the juvenile winter-run Chinook Salmon population through this junction and into the Central Delta. This is because a majority of the natural (>95%) and hatchery (>70-85%) juvenile winter-run population is believed to already be in the Delta; many of those may have already passed this location and are currently residing downstream of the DCC gate location or have exited the system altogether and have emigrated to the marine environment. The remaining fraction of the natural and hatchery winter-run juvenile population that may still occur above the DCC location will be vulnerable to entrainment into an open DCC gate configuration as they emigrate downriver past the DCC gate location. Because outmigration of both natural and hatchery winter-run juveniles past Chipps Island is expected to be largely complete by mid-April, the Project Description's Modification of the DCC gate operations will affect winter-run in the North Delta compared to the Baseline scenario, but only for a short time. It is uncertain whether the increase in the likelihood of entrainment into the Central Delta will result in any change to facility loss of winter-run, both because the duration of the effect is expected to be short, and because the limited exports in the Project Description scenarios may not result in greater entrainment into the South Delta and facility loss (see discussion in "Exports" section).

If the DCC gates were open Sacramento River water will flow through the DCC and into the Mokelumne River system. This may result in some level of straying of upstream migrating adult Winter-run Chinook Salmon into the Mokelumne River system. It is expected that this may delay these adults on their upstream spawning migration. Adult winter-run Chinook Salmon which have entered the Mokelumne River system should be able to re-enter the Sacramento mainstem through the open DCC gates and continue their upstream movements. A delay in reaching the spawning grounds and an increase in energy expenditure may result. This could result in lower survival of juveniles produced from straying individuals, if temperatures in the upper river become unsuitable for egg and fry survival.

Exports

The Project Description scenario is expected to result in minimal additional entrainment of juvenile winter-run Chinook. Exports, barring a precipitation event substantial enough to produce natural and abandoned flows resulting in an NDOI greater than 5500cfs and closure of the DCC gates, if open, will be limited to combined 1500 cfs. The PTM for the Baseline and Project Description scenarios with Sherwood Harbor as the injection location (Figure 29) indicates that ~3% more particles are entrained at the export facilities in the modified scenarios (5% for Project Description (DCC Closed), 5.1% for Project Description (DCC open)) compared to the baseline (2%). The exposure to the increased risk of facility loss will occur in early April, after which the majority of juvenile winter-run Chinook are located further west and are exiting the Delta past Chipps Island. Considering that the majority of natural origin and hatchery winter-run are currently still rearing in the Delta and salvage of fish at the CVP/SWP fish collection facilities has occurred this season, concern for the entrainment risk at the projected export ranges would be a moderate risk of entrainment in early April, and low (for Winter-run) from mid-April onward.

Attachment 2. Biological Review for Endangered Species Act Compliance with the WY 2015 Drought Contingency Plan April through September Project Description

Summary of Effects on Winter Run Chinook Salmon

The proposed operational modifications to the D-1641 flow and operational criteria may reduce through-Delta survival of migrating juvenile winter-run Chinook Salmon by the reducing the transit rate for these migrating salmonids, which may increase the predation potential. The timing of Delta exit appears to be fairly consistent over time and while less than 15% have been projected to have migrated out of the Delta, the remaining portion should exit during April and possibly into May (del Rosario 2013). While salvage of listed juvenile Chinook is projected to remain moderate due in part to the migratory behavior being displayed by winter-run Chinook Salmon juvenile and the low levels of exports, if exports increased during the Project Description in April and May, a measure to reduce the risks associated with entrainment loss would occur by shifting exports from the SWP to the CVP.

Status of Spring-Run Chinook Salmon

The 2014 spawning run of spring-run Chinook Salmon returning to the upper Sacramento River Basin was lower in four of seven locations compared to the 2013 escapement, with markedly lower escapement observed in Clear Creek, Butte Creek, and Feather River Hatchery (Table 13).

Table 13. Spring-run Chinook Escapement in 2013 and 2014

Tributary	2013	2014	Percent Change	Source
Battle Creek	608	429	-29	Laurie Earley, USFWS
Clear Creek	659	95	-86	
Antelope Creek	0	7	-	Matt Johnson, DFW
Mill Creek	644	679	+5.4	
Deer Creek	708	830	+17	
Butte Creek	16783	4815	-71	Clint Garman, DFW
Feather River Hatchery	4294	2825	-34	Penny Crenshaw, DWR

Spawning of spring-run Chinook salmon in the Sacramento River Basin occurs approximately from mid-August through mid-October, peaking in September. In 2014, this peak in spawning activity corresponded with the high Sacramento River temperatures downstream of Keswick Dam resulting in an elevated potential for high egg and alevin mortality. It is believed that spring-run Chinook salmon eggs in the Sacramento River underwent significant, and potentially complete mortality due to high water temperature downstream of Keswick Dam starting in mid-August when water temperatures downstream of Keswick Dam exceeded 56°F (see water temperatures in August through October in Figure 36) in WY 2014. Spring-run Chinook

Attachment 2. Biological Review for Endangered Species Act Compliance with the WY 2015 Drought Contingency Plan April through September Project Description

Salmon eggs spawned in the tributaries to the Sacramento River may also have experienced warmer temperatures in 2014 due to low flows through late October, as well as scouring or sedimentation during rain events from late October through December.

Juvenile spring-run Chinook salmon begin emigration from Clear Creek soon after emergence, with passage near the mouth peaking in November through December and continuing to around May. Recent year passage indices are shown in Table 14. For BY 2014, extremely few juvenile Spring-run Chinook Salmon were observed migrating downstream past RBDD (Figure 37) during high winter flows, when spring-run Chinook Salmon originating from the upper Sacramento River, Clear Creek, and other northern tributaries are typically observed to outmigrate. As of March 11, 2015¹¹, only 35,435 BY 2014 spring-run Chinook Salmon were estimated to have passed Red Bluff Diversion Dam, and these low RBDD passage estimates are a concern. A second pulse of juvenile spring-run Chinook Salmon typically migrate past RBDD in the springtime (Poytress et al. 2014). However, this second pulse appears to positively bias estimates of spring-run Chinook passage due to the presence of millions of unmarked fall-run Chinook salmon hatchery fish released from the Coleman National Fish Hatchery on Battle Creek. These hatchery production fish typically overlap with the spring-run Chinook salmon category based on the length-at-date run assignments (Poytress et al. 2014).

Table 14. Passage Indices of Juvenile Spring-run Chinook Salmon with 90% and 95% Confidence Intervals for Brood Years (BY) 2003-2013 Captured by the Upper Rotary Screw Trap at River Mile (RM) 8.4 in Clear Creek, Shasta County, California, by the U.S. Fish and Wildlife Service. The Adjusted Passage Index (Proportionate to Juveniles per Redd) Includes Redds Below the Trap, yet Above the Separation Weir. For BY 2013, Confidence Intervals and Adjusted Index Have Not Been Calculated Yet

Brood year	95% LCI	90% LCI	Passage index	90% UCI	95% UCI	Adjusted index	Juveniles per redd
2003	88,817	90,113	108,338	130,960	137,672	110,422	2,083
2004	87,439	90,417	107,054	131,700	136,701	110,028	2,974
2005	87,516	89,516	104,197	122,580	128,418	106,201	2,004
2006	111,749	113,659	127,197	144,692	148,539	149,318	1,843
2007	92,728	94,472	110,224	130,585	135,069	114,914	2,345
2008	88,834	89,653	96,166	102,920	104,402	121,622	1,414
2009	62,213	63,214	68,296	74,319	75,384	74,084	1,158
2010	15,228	15,618	17,359	19,416	19,910	19,288	1,929
2011	49,247	49,893	53,896	58,238	59,007	57,265	3,369
2012	16,124	16,363	17,891	19,695	20,020	19,447	778
2013			227,912				1,767

¹¹ Fish were sampled using rotary-screw traps for the period July 1, 2008 to present. Figure supplied by USFWS on March 11, 2015.

Attachment 2. Biological Review for Endangered Species Act Compliance with the WY 2015 Drought Contingency Plan April through September Project Description

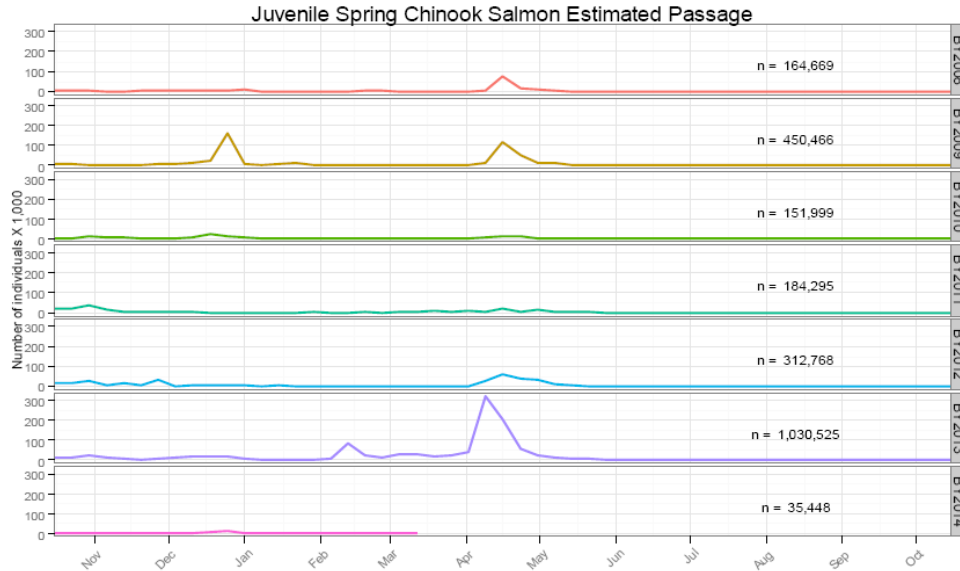


Figure 2. Weekly estimated passage of juvenile Spring Chinook Salmon at Red Bluff Diversion Dam (RK391) by brood-year (BY). Fish were sampled using rotary-screw traps for the period October 16, 2008 to present.

Figure 37. Weekly Estimated Passage of Juvenile Spring Run Chinook Salmon at Red Bluff Diversion Dam (RK 391) by brood year (BY)¹²

In fall 2014, yearling spring-run Chinook Salmon from Mill and Deer creeks experienced flow and temperature conditions typically associated with the outmigration of this life history expression from these tributaries. Although not currently monitored with RSTs, these tributaries have experienced flows (Figures 38-39) exceeding “First Alert” thresholds identified in the NMFS BiOp Action IV.1.2. Recent analyses of multiple years of RST data have determined that 99% of outmigrating yearlings are captured at flows greater than 95 cfs (Kevin Reece, DWR, pers. comm.).

Spring-run young-of-the-year (YOY) sized Chinook Salmon juveniles have been observed at the Tisdale Weir and Knights Landing RSTs since early December 2014 (Table 9). Likewise, juvenile YOY spring-run Chinook have been observed in the catch from multiple Delta beach seine regions, and in the standard trawling and special drought monitoring trawling surveys, including those in the Central Delta (Tables 10-11). Monitoring data suggest that the majority of surviving BY 2014 natural origin YOY juveniles are currently residing in the Delta, downstream of Knights Landing. No yearling spring-run Chinook Salmon have been caught in 2014 Delta monitoring, however, yearling spring-run observations are expected to be rare because of their relatively large size and strong swimming ability (associated with gear avoidance), and relatively low densities relative to YOY. The majority of YOY, yearling, and surrogate (hatchery late fall) spring-run are currently rearing in the Delta. This estimate is based on the best professional judgment of the biologists participating on the DOSS work team. No natural or hatchery origin spring-run Chinook Salmon have been salvaged at the fish collection facilities as of March 15, 2015.

¹² Fish were sampled using rotary-screw traps for the period July 1, 2008 to present. Figure supplied by USFWS on March 11, 2015.

Attachment 2. Biological Review for Endangered Species Act Compliance with the WY 2015 Drought Contingency Plan April through September Project Description

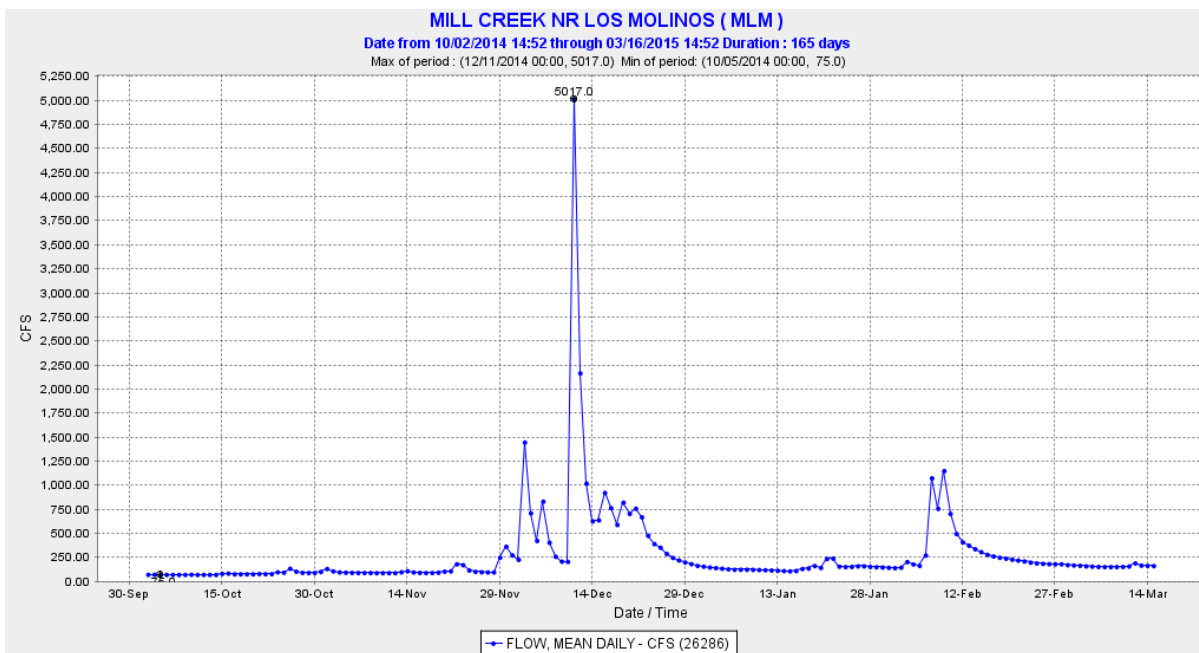


Figure 38. Mill Creek Mean Daily Flow (cubic feet per second) Measured near Los Molinos (MLM) During WY2015¹³

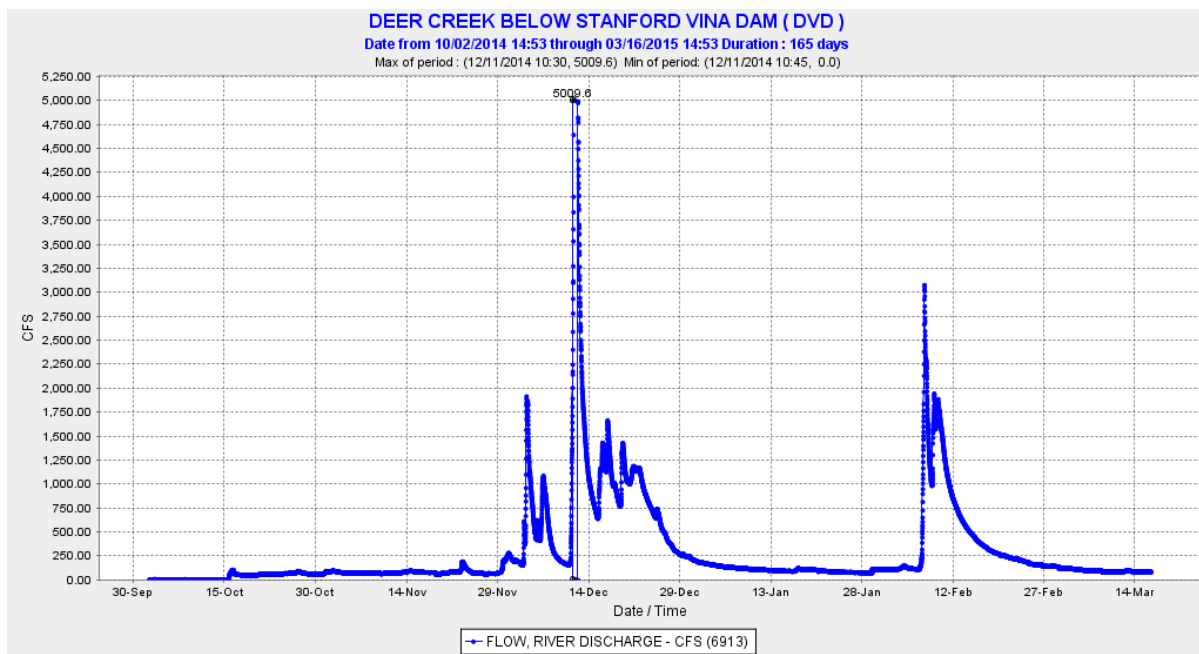


Figure 39. Deer Creek Discharge (cubic feet per second) Measured Downstream of Stanford Vina Dam (DVD) During WY2015¹⁴

¹³ Downloaded from CDEC on March 16, 2015.

¹⁴ Downloaded from CDEC on March 11, 2015.

Attachment 2. Biological Review for Endangered Species Act Compliance with the WY 2015 Drought Contingency Plan April through September Project Description

Adult spring-run Chinook salmon will be entering the upper Sacramento River and Clear Creek during spring and continue into the summer of 2015, then holding until they start spawning in mid-August, with peak spawning occurring in September and completing by mid-October. Spring-run Chinook salmon spawning in Clear Creek occurs primarily upstream of a barrier weir installed at river mile 7 that separates spring-run and fall-run Chinook salmon spawning based on timing of entry into the tributary and protects spring-run Chinook salmon eggs from superimposition by fall-run Chinook salmon spawners later in the year. Table 15 shows spring-run Chinook Salmon spawning distribution in Clear Creek. Distribution has shifted upstream somewhat through the years after removal of McCormick-Seltzer diversion dam (approximately RM 6.2) in 2000 and with repeated gravel additions.

Spring-run Chinook Salmon may spawn in the Sacramento River between RBDD and Keswick Dam in very low densities with only a total of 449 redds documented from 2001 to 2014 (average 37/year; range= 0-105; no data available for 2009 or 2011; CDFW unpublished data). Most spring-run Chinook Salmon redds (93 percent) have been documented upstream of Jelly's Ferry Bridge (river mile [RM] 265.9).

Table 15. Distribution of Spring run Chinook Salmon Redds in Clear Creek, 2003–2013. River miles (RM) Begin at the Confluence at RM 0, and End at Whiskeytown Dam at RM 18.3. Both RM 7 (0.6 miles) and RM 18 (0.3 miles) are Incomplete Miles. RM 7 was Not Available for Spring run Spawning in 2003-2005, and 2011 When the Weir Was Located at the Lower Site

Year	RM 7	RM 8	RM 9	RM 10	RM 11	RM 12	RM 13	RM 14	RM 15	RM 16	RM 17	RM 18	Total
2003	NA	4	5	9	2	3	0	15	3	4	5	3	53
2004	NA	9	1	9	2	0	2	4	3	3	4	0	37
2005	NA	4	2	11	4	0	1	4	10	3	11	2	52
2006	4	11	8	12	13	7	0	4	8	10	5	0	82
2007	0	6	1	5	0	2	1	1	7	15	11	0	49
2008	8	18	3	11	4	6	0	11	5	13	6	1	86
2009	3	8	2	15	4	1	4	6	4	4	13	0	64
2010	1	1	0	3	0	0	0	1	1	2	1	0	10
2011	NA	1	0	5	0	2	1	5	0	2	0	0	16
2012	1	2	1	7	2	1	2	5	2	2	0	0	25
2013	5	11	2	30	5	11	6	11	10	25	23	3	142
2014	1	6	3	12	1	6	2	6	4	4	10	0	55

Attachment 2. Biological Review for Endangered Species Act Compliance with the WY 2015 Drought Contingency Plan April through September Project Description

Effects of Project Description on Spring-run Chinook Salmon

The predicted distribution of spring-run Chinook Salmon during the Project Description period and a summary of potential effects is presented in Table 16, followed by more details per action type and location.

Table 16. Presence of Spring run Chinook Salmon During the Project Description Period and Exposure to Potential Effects

Spring-run Chinook Salmon Life Stage	Life Stage Present	Tributary Habitat Effect	South/Central Delta Entrainment Effect	Facility Loss Effect
Egg This life stage will be present in the Sacramento River in September				
Sacramento R	Yes	Yes	N/A	N/A
Clear Creek	Yes	Yes	N/A	N/A
Juvenile This life stage will be present in the Sacramento River and Delta during April and May				
Sacramento R	Yes	Reduced Survival	N/A	N/A
Clear Creek	Yes	No Modification in Project	N/A	N/A
Delta	Yes	N/A	Increased	Uncertain
Adults This life stage will be present in the Sacramento River and Delta during April through September				
Sacramento R	Yes	No Change	N/A	N/A
Delta	Yes	N/A	No Change	No Change

Sacramento River Actions

Temperature operations as part of the Project Description remain under discussion by the SRTTG. The 90% temperature forecasts provided to the SRTTG in January and February both forecast a temperature compliance point of 56°F at the Clear Creek CDEC gaging station cannot be maintained during September when peak spring-run Chinook salmon spawning and egg incubation occurs. Impacts to egg and alevin stages are more difficult to predict due to uncertainties with actual spawn timing, redd locations, and observed hydrological and temperature profiles. A temperature management plan for the upper Sacramento River, including Clear Creek, continues to be developed and an appropriate biological review will be provided upon its completion. Forecasted Sacramento River flows during the Project Description include

Attachment 2. Biological Review for Endangered Species Act Compliance with the WY 2015 Drought Contingency Plan April through September Project Description

reduced releases from Shasta during September, which may cause some spring-run Chinook redd dewatering. Chinook redd dewatering at multiple locations was documented during Fall 2014 when Keswick flows were reduced below 5,000 cfs.

Net Delta Outflow Index and Water Quality Modifications

Drought operational actions impacting Sacramento River outflow proposed during the remainder of WY2015 are intended to preserve storage in Shasta Reservoir and increase the potential coldwater pool available for management of temperatures for both winter-run and spring-run Chinook Salmon. Similar to winter-run Chinook Salmon, the reduction in Keswick releases to meet modified spring D-1641 NDOI standards may affect outmigrating spring-run Chinook Salmon during the remainder of spring 2015. As of March 17, 2015, DOSS estimates that the majority (80-95%) of natural-origin YOY Spring-run Chinook Salmon are rearing in the Delta, with approximately 5-20% remaining upstream of the Delta and <5% have exited the Delta. In contrast, the entire cohort of yearling spring-run Chinook Salmon are either in, or have existed the Delta (approximately 50% each), with the exception of a few possible stragglers upstream of the Delta.

Effects to individuals remaining upstream would be similar to those described above for Winter-run Chinook Salmon upstream of the Delta. To review, reductions in Delta outflow to as low as 4,000 cfs during April and May may reduce migratory survival of any YOY spring-run Chinook Salmon migrating through the Sacramento River until reaching the tidally dominated North Delta through increased predation mediated by hydrodynamic and habitat mechanisms. Increased tidal excursions are likely to increase entrainment of any downstream migrating YOY into Georgiana Slough and, if open, the Delta Cross Channel. The reduced velocities in the lower Sacramento River due to reduced inflow is evident in the DSM2 modeling and increased tidal excursion occurs in this modeling causing less positive velocities until tides reduce the force of incoming riverine flows and mute any difference observed in the modeling from the Baseline and Project Description scenarios (Figures 2-11). The possible reductions in outflow through multiple distributaries in the North Delta may increase straying and travel time of adult spring-run Chinook Salmon in this region during April and May.

Rearing juvenile spring-run Chinook Salmon within the Delta are not expected to be affected by the Project Description's modifications to NDOI and Delta water quality standard during April and May. Flows are tidally dominated in the North Delta and Central Delta areas where rearing occurs (Figures 4-15). There is low certainty in our understanding of the juvenile salmonid biological processes affected by flow in the Delta. South Delta conditions in the Project Description scenario are similar to the Baseline scenario during April and May (Figures 22 and 23). There is moderate certainty in our understanding of how hydrodynamics and suitable habitats for rearing juvenile salmonids are affected in the Delta by the Project Description .

Clear Creek Actions

Temperature management on Clear Creek attempts to achieve a temperature compliance schedule to reduce thermal stress to over-summering steelhead and to spring-run Chinook Salmon during their holding, spawning, and incubation periods. Under the 90% Operation Forecast, monthly average flows in August and September are estimated to be 85 cfs and 150 cfs, respectively, and with those lower flows, there is a potential for temperature criteria to be

Attachment 2. Biological Review for Endangered Species Act Compliance with the WY 2015 Drought Contingency Plan April through September Project Description

exceeded during these months. Adult spring-run Chinook Salmon holding when temperatures exceed 60°F may experience higher pre-spawn mortality, and those surviving may have reduced egg viability. If temperatures exceed 56°F after September 15, there will be greater mortality of incubating eggs and pre-emergent fry. There is low uncertainty in this conclusion. The temperature management for Clear Creek will be coordinated through the Sacramento River Temperature Task Group under the SWRCB 90-5 requirements and as outlined in RPA Action I.1.5.

Delta Cross Channel Gates

Under the Project Description, modified Delta Cross Channel Gates operations may occur based on water quality and fish presence as described in the Project Description. Effects to spring-run Chinook Salmon are generally similar to those discussed above for winter-run Chinook whereby an open DCC Gate has a low potential for entraining juvenile spring-run Chinook Salmon through this junction and into the Central Delta due to most juvenile (about 85-95% YOY and 95% yearling) spring-Run Chinook Salmon having already passed this location earlier this year. There is a low potential for adult straying associated with some Sacramento River water flowing through the DCC and into the Mokelumne. Additionally, there is a low potential for temporary adult migration delays and associated lower egg viability due to physiological stress from increasing energy expenditures or increasing exposure to high water temperatures.

Exports

The Project Description scenario is expected to result in minimal additional entrainment of juvenile spring-run Chinook Salmon. Exports, barring a precipitation event substantial enough to produce natural and abandoned flows resulting in an NDOI greater than 5500cfs, and closure of the DCC gates, if open, will be limited to combined 1500 cfs. These low export levels are not expected to appreciably affect survival of juvenile spring-run Chinook Salmon emigrating through the Delta. The PTM run with Sherwood Harbor as the injection location (Figure 29) indicates that ~3% more particles are entrained at the export facilities in the modified scenarios (5% for Project Description (DCC Closed), 5.1% for Project Description (DCC open)) compared to the baseline (2%). Since export levels are the same between the Project Description and Baseline scenarios, the change in the risk of loss at the export facilities is likely unchanged between scenarios for fish in the interior delta, but, due to the expected increase in entrainment of fish into the central/south Delta, more fish might reach the interior Delta under the actions in the Project Description (even if, though to a lesser extent, if the DCC is closed). Therefore, the cumulative effect of exports due to the Project Description is uncertain, since that effect will depend on distribution of outmigrating spring-run Chinook salmon. The majority of natural origin Spring run Chinook Salmon are currently rearing in the Delta, yet as of March 15, 2015, no Spring run Chinook Salmon juveniles have been salvaged at the pumping plants. This is likely due to the very low juvenile productivity. The entrainment risk at the minimum export levels described in the Project Description is similar to the Baseline scenario, and remains low-to-moderate through April and May based on their current distribution and rarity.

Summary of Effects on Spring-run Chinook Salmon

The extreme drought conditions are causing increased stress to spring-run Chinook Salmon populations, with or without water project operations, in the form of low flows reducing rearing and migratory habitats, higher water temperatures affecting survival, and likely higher than

Attachment 2. Biological Review for Endangered Species Act Compliance with the WY 2015 Drought Contingency Plan April through September Project Description

normal predation rates. Water management over the first portion of WY 2015 has focused on maintaining a level of reservoir storage which is generally higher than what would have been in place at this time without the planning that has gone into attempting to reduce adverse effects on resources. The current drought operations plan strives to continue to save some water resources for the future in the hopes of minimizing long-term adverse effects of the drought.

Cumulatively, the Project Description modification to the D-1641 flow and operational criteria may reduce through-Delta survival of juvenile migrating spring-run Chinook Salmon and may modify their designated critical habitat during April and May. Changes in Sacramento River outflow during April and May can possibly delay adult spring-run Chinook salmon migration. Drought conditions and current reservoir storage levels have forecasted to impact the ability to maintain suitable water temperatures in the Upper Sacramento River and Clear Creek. Temperature effects on Clear Creek and in the Upper Sacramento may lead to possible higher pre-spawn mortality of adult Spring-run Chinook Salmon and reduced egg viability if temperatures exceed 60°F during August and early September, as well as greater mortality of incubating eggs and pre-emergent fry if temperatures exceed 56°F after September 15.

Status of Green Sturgeon

Information on green sturgeon is extremely limited. Adult green sturgeon will migrate into the upper Sacramento River through the Delta in March and April. Last year, a review of telemetric data found 26 tagged green sturgeon entered the San Francisco Bay with only half migrating upstream of RBDD (M. Thomas, UC Davis, pers. comm.). Already in 2015, one acoustically-tagged adult was recorded migrating past Sacramento this winter and based on typical migration rates, has likely reached Red Bluff (M. Thomas, UC Davis, pers. comm.).

Adult green sturgeon have been observed to overwinter in the Sacramento River, and a number of tagged 2014 adults appeared to still be present in the upper Sacramento River as of January, 2015 (R. Chase, Reclamation, pers. comm.), but it is unknown if they remained in this area during the past two months (M. Thomas, UC Davis, pers. comm.). Also, adult green sturgeon exit through the Lower Sacramento River during the summer and fall following their spawning, then return to SF Bay throughout this period also. Green sturgeon exit the San Francisco Bay late in the summer through the winter.

Spawning typically occurs from April through July. Spawning in the upper Sacramento River was documented during 2014 and associated larval green sturgeons were observed at RBDD during the summer of 2014 (n=316). This was greater than the long-term average of 186 fishes, but less than the highest number observed (i.e., >3,500 in 2011; Figure 40). At RBDD, two juvenile green sturgeon were also observed in the fall of 2014, but no additional fish have been recorded as of March 12, 2015 (Bill Poytress, USFWS, pers. comm.). At GCID, ten juvenile green sturgeon (TL= 110-285) were observed from September through October 2014 and no additional fish have been recorded as of March 9, 2015. Based on Israel and Klimley (2009), BY 2014 juvenile green sturgeon have likely migrated downstream from their natal spawning areas and are overwintering in the Lower Sacramento River and Delta.

Green sturgeon observations are extremely rare in the Delta, primarily related to the use of monitoring gear types that are not designed to sample the benthic habitats where green sturgeon

Attachment 2. Biological Review for Endangered Species Act Compliance with the WY 2015 Drought Contingency Plan April through September Project Description

are most likely to be found if they are present. Although the lower Sacramento and Delta fish monitoring surveys do not target benthic environments, they have captured juvenile green sturgeon in the past, but none have been observed in these surveys in recent years including during 2011 when high numbers were observed migrating downstream past RBDD. One dead green sturgeon (FL= 670mm) was removed from the SWP Fish Facility on February 9, 2015. In 2011, over a thousand juvenile green sturgeons were enumerated at RBDD and none were observed in Delta or Bay fish monitoring. While this absence in the monitoring may suggest no impact from Delta Cross Channel operations or outflow operations, it may also suggest the recruitment of juveniles may be limited before the species reaches one year old due to habitat, predation, or multiple stressors; which is a phenomenon that has been observed in other North American sturgeon species. More monitoring needs to be conducted in order to reduce this uncertainty.

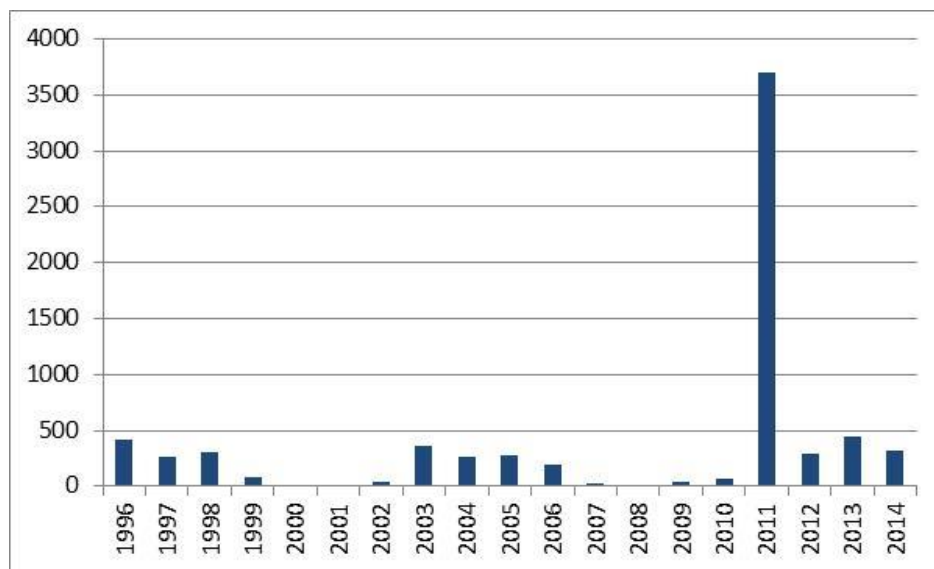


Figure 40. Larval Green sturgeon counted at Red Bluff Diversion Dam rotary screw traps¹⁵

Effects of Project Description on Green sturgeon

The predicted distribution of Green Sturgeon during the Project Description and a summary of potential effects are presented in Table 17, followed by more details per action type and location.

Sacramento River Outflow

The Project Description's reduction in upper Sacramento River CVP reservoir releases to meet modified spring and summer NDOI and Wilkin Slough standards may affect spawning green sturgeon. Although little is known about spawning habitat, these habitats do not seem limited. Adult green sturgeon spawn in specific locations presumably based on turbulent velocities, cold water temperatures, coarse substrate, presence of conspecifics, and large riverbank expansion bars likely to provide nursery habitats for larval and juveniles. The Project Description's

¹⁵ The annual average catch is 426 fish. In 2011, an egg was observed directly upstream of the rotary traps; thus, the large number of fish in 2011 represents a unique sampling of a spawning event (Josh Gruber, USFWS, pers comm.). If 2011 data is removed, the annual average of juvenile green sturgeon counted is 183 fishes.

Attachment 2. Biological Review for Endangered Species Act Compliance with the WY 2015 Drought Contingency Plan April through September Project Description

reservoir release operation, described in the 90% Forecast, is unlikely to influence habitat characteristics for larval or juvenile green sturgeon. There is low certainty in our understanding of how hydrodynamics is affected in these regions by the Project Description and suitable

Green sturgeon Life Stage	Life Stage Present	Tributary Habitat Effect	South/Central Delta Entrainment Effect	Facility Loss Effect
Egg	This life stage will be present in the Sacramento River in April-June.			

habitats for rearing and spawning.

Table 17. Presence of Green Sturgeon During the Project Description Period and Exposure to Potential Effects

Attachment 2. Biological Review for Endangered Species Act Compliance with the WY 2015 Drought Contingency Plan April through September Project Description

Sacramento	Yes	No Change	N/A	N/A
Juvenile	This life stage will be present in the Sacramento River and Delta April-September.			
Sacramento R	Yes	No Change	N/A	N/A
Delta	Yes	N/A	No Change	No Change
Subadults	This life stage may be present in the Delta April- September.			
Delta	Limited	N/A	No Change	No Change
Adults	This life stage will be present in the Sacramento River and Delta April-September.			
River	Yes	No Change	N/A	N/A
Delta	Yes	N/A	No Change	No Change

Net Delta Outflow Index and Water Quality Modifications

Juveniles and sub-adult green sturgeon rearing and utilizing the Delta are not expected to be affected by the Project Description's modifications to NDOI and Delta water quality standard from April through September. Over the course of juvenile green sturgeon rearing in the Delta (1 to 3 years), the fish are exposed to a wide variety of flows, depending on where they happen to be at a particular moment. In most of the Delta where green sturgeon are expected to be rearing, flows are tidally dominated. The 90% Operational Forecast characterizes Delta flow conditions in the Central Delta (OMR flows); North Delta (NDOI flows); and South Delta (exports) where tidal conditions occur. There is low certainty in our understanding of the juvenile and sub-adult green sturgeon biological processes affected by flow in the Delta. Delta conditions in the Project Description scenario are similar to the Baseline scenario during April and May, and the 90% without a modeled 90% Forecast of the Baseline summer hydrology, it is difficult to determine the summertime impacts of the actions in the Project Description. The minimal exports during the summertime between June and September may be assumed to be less than any other hydrology, which would cause more negative summertime flows in the South and Central Delta regions due to pumping greater than the minimum health and safety diversion. This suggests the actions in the Project Description would cause a reduced risk to entrainment into these regions and the CVP/SWP fish collection facilities. There is moderate certainty in our understanding of how hydrodynamics is affected in the Delta by the Project Description and suitable habitats for foraging juvenile and sub-adult green sturgeon.

Adult green sturgeon will be potentially present in the Delta throughout the Project Description as they migrate into and out of the Sacramento River and possibly forage in the Delta during the summer. The reductions in outflow through multiple distributaries in the North Delta in the Project Description may increase straying and travel time of green sturgeon in this region during April through September. During these months, a substantial portion of adult green sturgeon will

Attachment 2. Biological Review for Endangered Species Act Compliance with the WY 2015 Drought Contingency Plan April through September Project Description

migrate through the North Delta. Foraging green sturgeon utilize Sacramento and interior migratory routes through the Delta, and also Steamboat slough during the summer. Since these areas are normatively used by green sturgeon, the impact of increased travel time is unlikely to negatively impact adult green sturgeon.

Delta Cross Channel

The Project Description's Modification of the DCC gate operations will have a similar, but lesser, potential effect on green sturgeon, as it potentially has on salmonids in the North Delta compared to the Baseline scenario. To review, opening the DCC gates provides an alternate outmigration route through the Central Delta for juvenile, subadult, and adult green sturgeon that may pass this location during April through September. The possible effect is less since green sturgeon utilize Sacramento and interior migratory routes through the Delta, and also Sutter and Steamboat sloughs often foraging and spend summer in the Western, Interior and Central Delta regardless of the DCC gates being open. Modeling of the Baseline and Project Description scenarios show South and Central Delta condition in May to be similar with no change in this regions' proportion positive daily flow, but some negative and positive impacts on average daily flows and velocities through these regions. Thus, while the likelihood of entrainment into the Central Delta during April and May may increase, these routes are not clearly less suitable or expose green sturgeon to greater risks at the minimum level of diversions described in the Project Description. The effect of entrainment into the Central Delta is unknown since it is hypothesized that hydrodynamic and habitat characteristics in this region are similar to those in the North Delta under the Project Description's hydrodynamic scenario.

Summary of Effects on Green sturgeon

Cumulatively, the Project Description's modifications in flow and water quality criteria should not reduce riverine or through-Delta survival of juvenile green sturgeon. The Project Description's changes in Sacramento River outflow during April and May can possibly delay juvenile, sub-adult, and adult green sturgeon migration. Modification to D-1641 Municipal and Industrial and Agricultural water quality standards in the Delta from April to September will not likely affect green sturgeon.

Status of Central Valley Steelhead

Sacramento River

Adult steelhead abundance is not estimated in the mainstem of the Sacramento River or any other waterways of the Central Valley. Much of the spawning is believed to occur in the tributaries of the Central Valley rather than in the mainstem rivers. Observed levels of catches of juvenile outmigrating *O. mykiss* at Red Bluff Diversion Dam have been low in 2014-2015 in comparison with recent past years. Peaks in juvenile downstream passage generally occur in the August/September time period; however, there was no peak emigration observed this past year. Fish emigrating during the peaks are primarily YOY *O. mykiss*. For a representation of smolt production from the upstream river and tributaries, the data need to be segregated by size. Larger fish pass mostly later in the fall and winter after the peaks in passage shown in Figure 41. A slight peak occurred in March of 2014. This peak was not present in the earlier years and may indicate a smolt emigration during one of the few significant rain events in 2014.

Attachment 2. Biological Review for Endangered Species Act Compliance with the WY 2015 Drought Contingency Plan April through September Project Description

For WY2015 (as of March 9, 2015), 10 unmarked (two on 10/15/2014; five from 1/7/2015 and 1/27/2015; and three from 3/3/15-3/5/15) and 1,109 marked steelhead (from 1/7/2015 to 2/21/2015) were captured at the GCID RST. Marked fish likely originated from a Coleman Hatchery release of 688,000 brood year 2014 steelhead (100% marked with adipose clip only) in the Sacramento River at Bend Bridge (fish released in two groups: 144,700 on January 2, 2015, and 543,300 on January 5-9, 2015). For WY2015 (as of 3/8/15), three unmarked (two captured from 1/5/2015 and 1/8/2015, and one on 12/22/2014) and 33 marked steelhead (one on 11/8/14, 32 from 1/12/15-2/13/15) were observed at the Tisdale Weir RST; and five unmarked (2/10/15-2/14/15) and 117 clipped (2/8/15-2/19/15) steelhead were captured at Knights Landing RST. A low to moderate level of salvage of natural- and hatchery-origin, respectively, juvenile steelhead has occurred this winter, with a cumulative loss of 95 natural-origin and 1,754 hatchery-origin juvenile steelhead as of March 15, 2015.

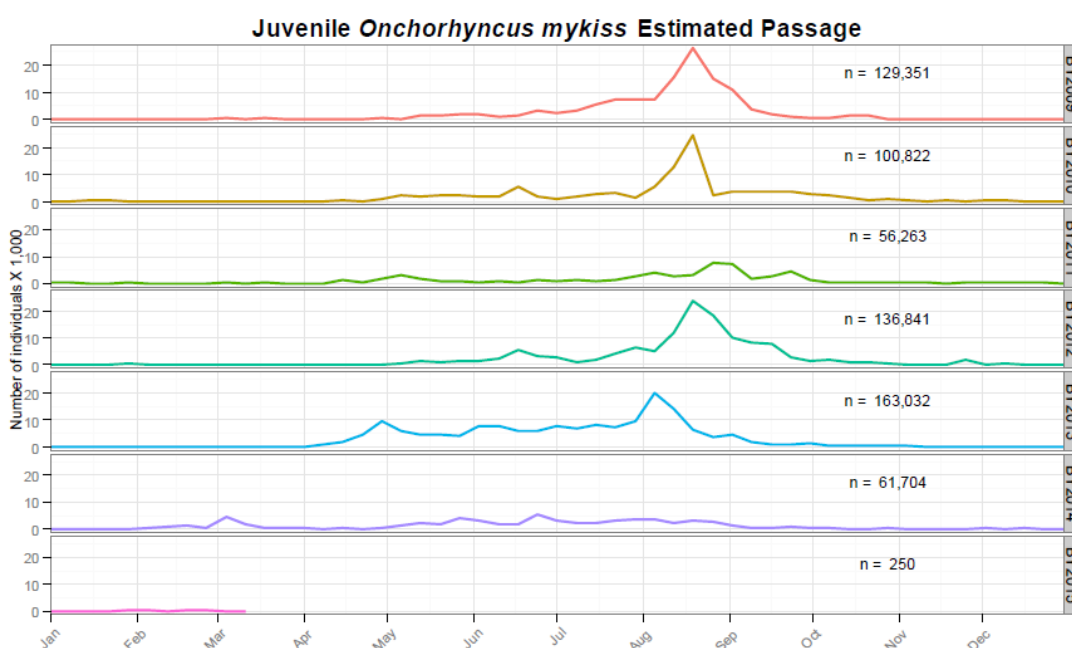


Figure 41. Weekly Estimated Passage of Juvenile Rainbow/steelhead trout at Red Bluff Diversion Dam (RK391) by Brood Year. Fish were Sampled Using Rotary-screw Traps for the Period January 1, 2009 to March 2015

Clear Creek

As of March 12, 2015, steelhead spawning surveys are underway on Clear Creek. Surveys are carried out from early December through the end of March. The preliminary steelhead redd index count for 2015 is 188 redds. Table 18 shows the redd index results through 2014. The redd index values include some mix of resident and anadromous *O. mykiss*.

The rotary screw traps on Clear Creek capture primarily YOY *O. mykiss* (not displayed here). Steelhead emigrating from Clear Creek are further monitored as they pass Red Bluff Diversion Dam in combination with other upper Sacramento River tributaries.

Attachment 2. Biological Review for Endangered Species Act Compliance with the WY 2015 Drought Contingency Plan April through September Project Description

Table 18. Clear Creek Steelhead Redd Index 2003–2014

Year	Redd index
2003	78
2004	151
2005	144
2006	43
2007	165
2008	148
2009	409
2010	233
2011	218
2012	178
2013	239 ^a
2014	313 ^a

^a In survey years 2013 and 2014, an additional survey reach was added at the downstream end of the study area. An additional 40 steelhead redds were counted in 2013, and 93 redds were counted in 2014 in this reach. USFWS is in the process of determining how to include these redds in the annual index for comparison to other years.

American River

Steelhead spawning in the American River occurs from late December to about late March or early April. Reclamation conducts bi-weekly steelhead spawning surveys throughout the spawning period. The American River in-river steelhead population consists primarily of hatchery-produced fish that spawn in the river, and the steelhead return is dominated by fish that return to the hatchery or are harvested prior to spawning in the river (Figure 42). Seining surveys conducted by CDFW throughout the summer and fall have shown that summer rearing distribution for steelhead essentially mirrors the spawning distribution. Mark and recapture of rearing steelhead has shown strong natal site fidelity. Although few recaptures of marked fish occur, the recaptures that do occur all happen within close proximity to the marking site (i.e., at the same riffle or the next riffle upstream or downstream). No thermal refugia have ever been found in the lower American River. The coolest water is essentially in the faster flowing sections of the river and the steelhead rear and feed primarily in the faster water areas (riffles predominantly) of the river through the summer.

Attachment 2. Biological Review for Endangered Species Act Compliance with the WY 2015 Drought Contingency Plan April through September Project Description

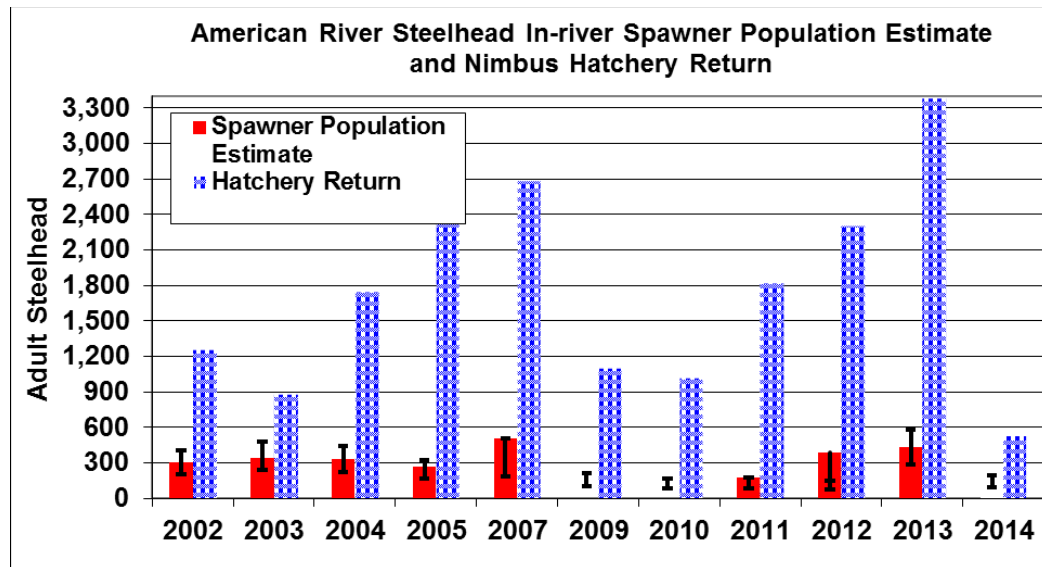


Figure 42. American River Steelhead Spawner Population Estimates Compared to Nimbus Hatchery Steelhead Return (updated from Hannon 2013). The Red Bars are Area Under the Curve Population Estimates (based on observations of adults holding on redds) and the Error Bars are the Redd Count Based Estimates. No ‘Area Under the Curve’ Based Estimates are Available for 2009, 2010, and 2014

Steelhead spawning surveys have identified few steelhead redds in the American River in 2015 from January through March 6 and hatchery returns have been near the lowest since the 1950s. The hatchery return for 2015 is 146 steelhead as of March 10 and only 46 of those were females. Nimbus flow releases have been 800–900 cfs throughout the spawning period, less than half the median flow of 2,000-3,000 cfs typically released during this time period. The majority of spawning is now complete based on the timing of spawning from past surveys (Hannon 2013). Figure 43 shows a comparison of spawning timing between the years surveys occurred. The 2015 spawning data are still draft but escapement appears to be very low. Coleman National Fish Hatchery steelhead eggs have been transferred to Nimbus Hatchery during January and February 2015 as part of a study evaluating replacing the Nimbus Hatchery steelhead broodstock with a broodstock that would be considered a part of the Central Valley steelhead distinct population segment. The low steelhead return has provided an opportunity to test an aspect of the broodstock replacement with Central Valley steelhead from Battle Creek/Coleman Hatchery. The goal of this egg transfer is to produce 150,000 steelhead smolts and evaluate their performance in the hatchery environment and in the American River following release from the hatchery.

The hatchery-produced steelhead in 2014 were all released into the river in May 2014 as YOY fish because water temperatures that supplied the hatchery raceways were anticipated to become lethal for fish reared in the hatchery over the summer.

Attachment 2. Biological Review for Endangered Species Act Compliance with the WY 2015 Drought Contingency Plan April through September Project Description

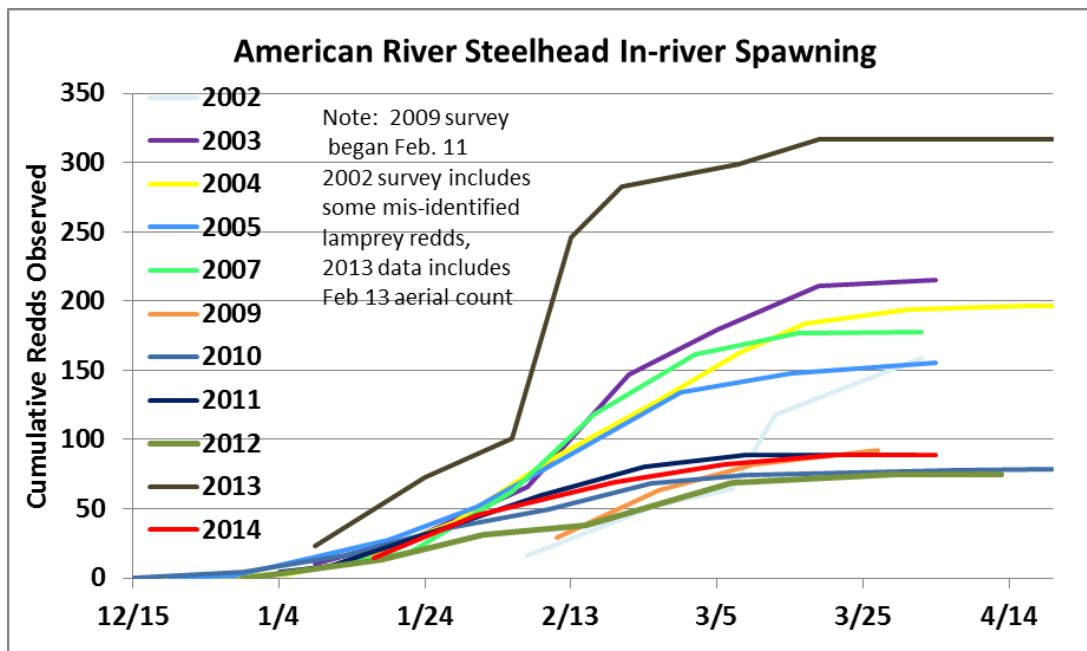


Figure 43. American River Steelhead Redd Observation Timing, 2002 - 2014

Stanislaus River

A weir on the Stanislaus River near Riverbank identifies *O. mykiss* passage using a VAKI camera. Two *O. mykiss* (> 16") and one *O. mykiss* (<16") were counted at the weir from October 2014 to December 15, 2014. Data after that have been unavailable.

Bergman et al. (2014) estimated a population of *O. mykiss* in an approximately 300 meter reach of the river immediately below Goodwin Dam to be 3,427 (SE =1,522) (95% CI = 1,492-7,873) using mark and recapture of trout identified using spot pattern recognition. This reach probably represents the highest density of trout in the river (based on snorkel survey observations) but indicates a much greater resident than anadromous component to the population. The stable cool water conditions in this tail-water area should allow at least the resident component of the population to persist through most drought conditions.

Steelhead spawn timing in the Stanislaus River is likely similar to other CVP rivers. Formal spawning surveys have not been conducted, but a trial survey was conducted by Reclamation and CDFW in February 2014 between Knights Ferry and Horseshoe Bar and near Goodwin Dam. Ten redds were found in the Knights Ferry reach and two were found in Goodwin Canyon at the cable crossing area. The redds are likely a mixture of resident and potentially anadromous *O. mykiss*. One of the redds was occupied by spawners with estimated lengths of 25 cm (10 inches) and 35 cm (14 inches). The California regulatory cutoff between steelhead and rainbow trout is 40 cm (16 inches) for anglers. The absence of abundant spawning near Goodwin Dam during this survey probably indicates mostly resident (later spawning) fish in that area.

Snorkel surveys conducted in 2003–2005 identified the first steelhead fry observations around mid-March to early April each year. Fry were observed between Goodwin Dam and Orange Blossom Bridge with observations in one year down to Valley Oak near the City of Oakdale.

Attachment 2. Biological Review for Endangered Species Act Compliance with the WY 2015 Drought Contingency Plan April through September Project Description

None were observed below Valley Oak. This indicates that spawning was limited to the area mostly upstream of Orange Blossom Bridge. Higher rearing densities were always found from Goodwin Dam down to the Lover’s Leap area. This likely coincides with the area of most spawning for both resident trout and steelhead. A majority of outmigrating steelhead smolts leave the Stanislaus River during the late winter and early spring. Based on recoveries of steelhead in the Caswell and Oakdale rotary screw traps, 50% of steelhead have emigrated by March 4 and 76% smolts have exited the Stanislaus River by the end of March (Figures 44-45).

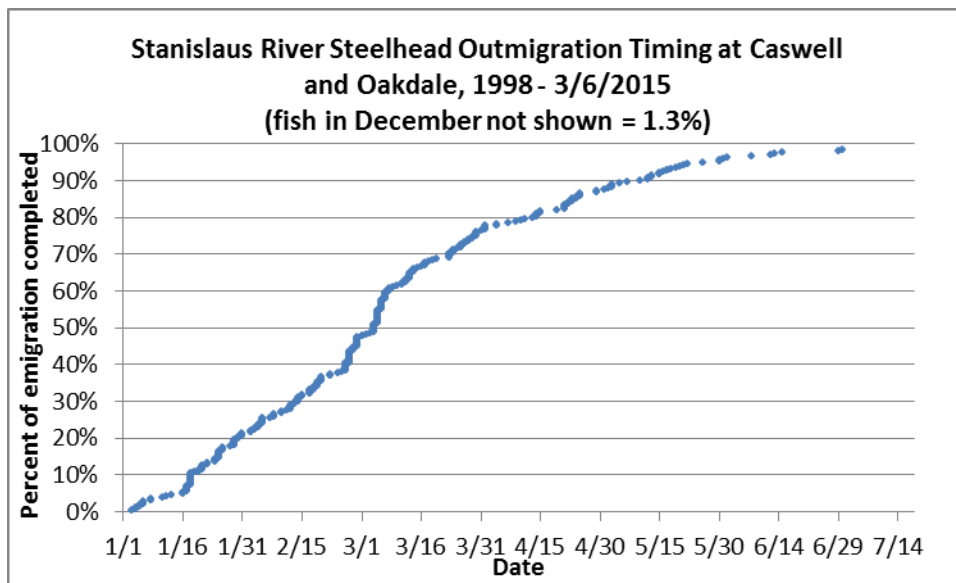


Figure 44. Stanislaus River Steelhead Outmigration Timing from Caswell Park and Oakdale Screw Traps, 1998-3/6/2015 (includes only fish rated as smolt index 5). Fish Leaving in December Constitute 1.3% of Migrants and Are Not Shown

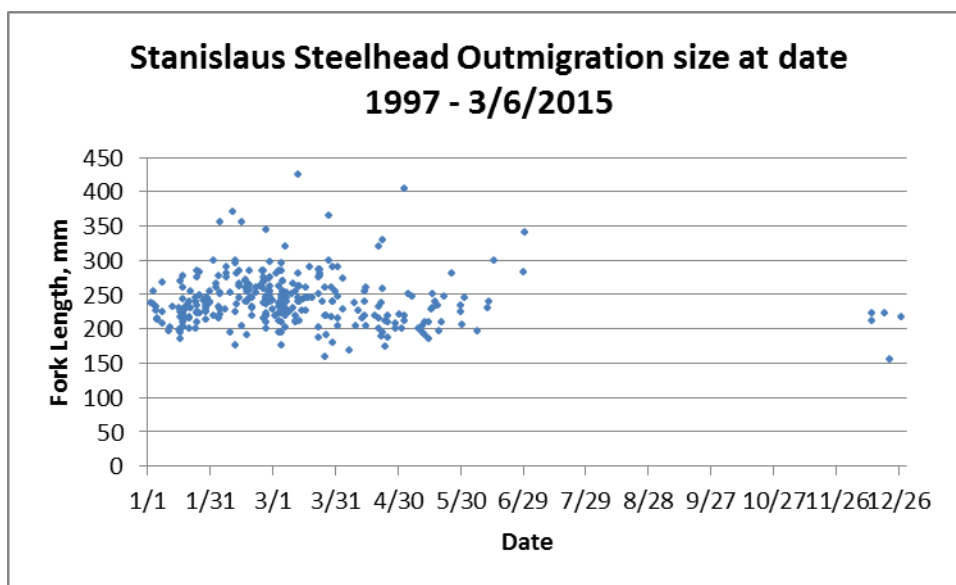


Figure 45. Stanislaus River Steelhead Outmigration Timing and Size from Oakdale and Caswell Rotary Screw Traps

Delta

Attachment 2. Biological Review for Endangered Species Act Compliance with the WY 2015 Drought Contingency Plan April through September Project Description

Information on steelhead in the Delta is extremely limited. Steelhead smolts are seldom recovered in Sacramento River and Delta fish monitoring efforts due to sampling biases related to their large size and swimming ability. False negatives (*i.e.*, zero catches when the target species is present) are more likely with steelhead smolts than smaller older juvenile Chinook Salmon, but historic data can be assessed to consider their typical periodicity in Delta monitoring efforts. From 1998 to 2011, temporal observations of wild steelhead juveniles (n=2,137) collected in Delta monitoring efforts occurred less than 10% of the time in January, >30% of the time during February, and >20% of the time during March.

The temporal occurrence of Central Valley steelhead near and within the Delta is informed by recovery of natural steelhead in various monitoring surveys (Table 19). For WY2015 (as of March 9, 2015), 36 adipose-clipped steelhead and no unmarked steelhead have been recovered in various beach seine and trawling efforts in the Delta and Lower San Joaquin River. Of these, one marked steelhead was observed in the Chipps Island mid-water trawl (228 mm clipped fish on 3/2/15) and three marked steelhead were observed (one each) at Sacramento beach seine monitoring locations: Miller Park (300 mm acoustic tagged fish on 12/8/14); Sherwood Harbor (178 mm clipped fish on 2/17/15); and Verona (203 mm clipped fish on 2/17/15). Additionally, marked steelhead were observed at three Kodiak trawling locations including: Jersey Point (four clipped fish from 2/28/15-2/20/15), Prisoner's Point (fourteen clipped fish from 2/12/15-3/3/15), and Sherwood Harbor (fourteen clipped fish; one on 1/23/15 and thirteen from 2/9/15-2/20/15). No outmigrating steelhead have been observed in the Mossdale trawl yet; however, Figure 46 indicates that most steelhead are recorded at this location during April and May. Adipose clipped steelhead from Coleman National Fish Hatchery and Feather River Hatchery, are considered ESA listed Central Valley steelhead. No steelhead have been released from Nimbus Fish Hatchery to date in 2015. These fish were released in-river in May 2014 and marked with a secondary mark of a clipped pelvic fin. Fish monitoring at Mossdale on the lower San Joaquin River also encounter steelhead entering the Delta, and based on these information it is likely steelhead may still be migrating into the Delta from the San Joaquin in April and early May (Figure 46).

An expanded salvage of 22 natural origin and 450 adipose-clipped steelhead have been estimated at the state and federal fish collection facilities at the South Delta CVP/SWP export pumps. Of these, all 22 natural origin and 382 adipose-clipped fish were salvaged at the SWP and no natural origin and 68 adipose-clipped fish were salvaged at the CVP fish collection facilities. Most steelhead have been salvaged during the past month. The high ratio of clipped to unclipped steelhead (17:1) likely indicates a low abundance of naturally-produced steelhead compared to the number of hatchery steelhead.

Attachment 2. Biological Review for Endangered Species Act Compliance with the WY 2015 Drought Contingency Plan April through September Project Description

Table 19. Percentage of Juvenile Sacramento River Steelhead Entering the Delta, as Recovered at Various Monitoring Locations by Month. Data from the DJFMP and Chipp Island Trawl Data are from the 1976-2011 dataset

Month	DJFMP Beach Seines	Chipp Island
January	25	5
February	20	10
March	30	15
April	5	30
May	10	35
June	0	5
July	>5	0
August	0	0
September	0	0
October	0	0
November	0	0
December	<5	0

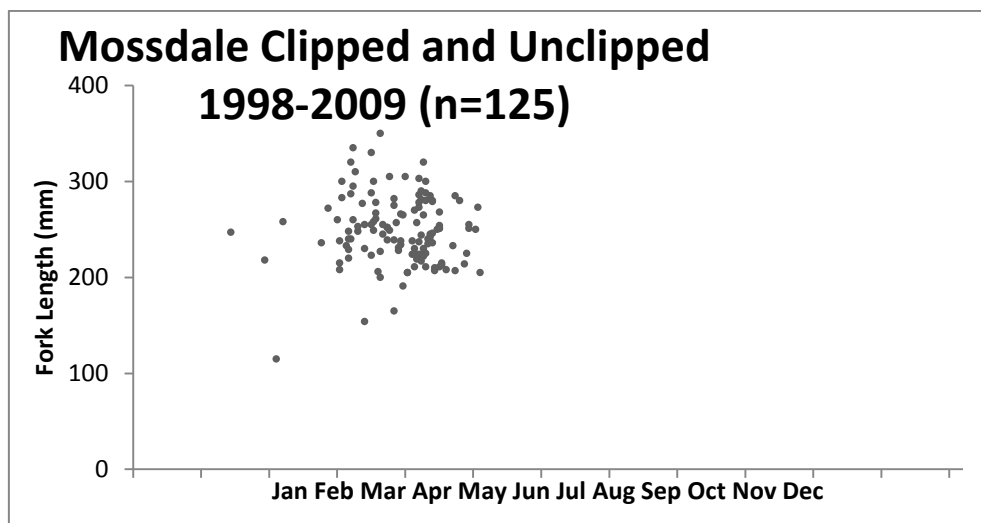


Figure 46. Fork Length by Date of Clipped and Unclipped Juvenile Steelhead Captured in the USFWS and CDFG Mossdale Trawl Fish Monitoring Study, 1998-2009

Effects of Project Description on Central Valley Steelhead

The predicted distribution of steelhead during the Project Description and a summary of potential effects is presented in Table 20, followed by more details per action type and location.

Attachment 2. Biological Review for Endangered Species Act Compliance with the WY 2015 Drought Contingency Plan April through September Project Description

Table 20. Presence of Steelhead During the Project Description Period and Potential Effects South/Central

Steelhead Life Stage	Life Stage Present	Tributary Habitat Effect	Delta Entrainment Effect	Facility Loss Effect
Egg	This life stage will be present in the Sacramento River and tributaries April through May			
Sacramento R and tributaries	Yes	Yes	No	N/A
San Joaquin R and Stanislaus R	Yes	Yes	No	N/A
Juvenile	This life stage will be present in the Sacramento River, San Joaquin River and Delta during April through September			
Sacramento R and tributaries	Yes	Potentially reduced survival	N/A	N/A
San Joaquin R and Stanislaus R	Yes	Potentially reduced survival	N/A	N/A
Delta (Sac River side)	Yes	N/A	Increased	Uncertain
Delta (SJR side)	Yes	N/A	Increased	Increased
Adults	This life stage will be present in the Sacramento and San Joaquin Rivers and Delta during April-May and August-September			
Sacramento R and tributaries	Yes	No Change	No Change	No Change
San Joaquin R and Stanislaus R	Yes	No Change	No Change	No Change
Delta	Yes	No Change	No Change	No Change

Sacramento River Actions

Monthly average flows in the Sacramento River are forecast to be at the 3,250 cfs base flow in March and then increase to a high of a monthly average of 9,594 in July and then back down to

Attachment 2. Biological Review for Endangered Species Act Compliance with the WY 2015 Drought Contingency Plan April through September Project Description

5,000 cfs in September. Rearing habitat limitations for steelhead have not been identified at the base flow. Water temperature management for Winter-run Chinook provides suitable conditions for the steelhead lifecycle throughout the year in habitat below Keswick Dam. During these drought conditions, the length of the suitable steelhead rearing habitat will be lower but rearing habitat availability is not expected to appreciably reduce the steelhead population in the mainstem Sacramento River. The end of the juvenile emigration period occurs during March through May. The base flows in the Sacramento River may potentially result in lower emigration survival than what would occur in wetter years. This effect of reduced emigration survival for steelhead originating from the Sacramento River basin is unquantified and is attributed to the persistent drought conditions continuing in WY 2015.

Water temperature conditions in the September time period for upstream migrating adult steelhead will be stressful and could result in delay of upstream migration through the lower Sacramento River until natural cooling with shorter day length occurs.

Net Delta Outflow Index and Water Quality Modifications

Similar to effects in the mainstem Sacramento River, the proposed lower outflow under drought conditions may result in lower survival of steelhead smolts emigrating to the ocean in the March through May period. This effect is unquantified and is attributed to the drought conditions necessitating modification of D-1641 Delta fish and environmental flow conditions. There is a high degree of uncertainty in this conclusion because this effect occurs largely in tidal areas so could be very slight.

Delta Cross Channel Gates

Under the Project Description, modified Delta Cross Channel Gates operations may occur based on water quality and fish presence. At this time, it is believed that an open DCC Gate has a low potential for entraining a substantial proportion of the juvenile Sacramento River steelhead. The remaining fraction of the natural and hatchery steelhead population that may still occur above the DCC location will be vulnerable to entrainment into an open DCC gate configuration as they emigrate downriver past the DCC gate location. Similar to Spring run Chinook Salmon, the Project Description's modification of the DCC gate operations will affect steelhead in the North Delta compared to the Baseline scenario, but only for a short time. It is uncertain whether the increase in the likelihood of entrainment into the Interior Delta will result in any change to facility loss of steelhead, both because the duration of the effect is expected to be short and because the limited exports in the Project Description scenarios may not result in greater entrainment into the South Delta and facility loss (see discussion in "Exports" section).

If the DCC gates were open Sacramento River water will flow through the DCC and into the Mokelumne River system. This may result in some level of straying of upstream migrating adult Winter-run Chinook Salmon into the Mokelumne River system. It is expected that this may delay these adults on their upstream spawning migration. Adult Winter-run Chinook Salmon which have entered the Mokelumne River system should be able to re-enter the Sacramento mainstem through the open DCC gates and continue their upstream movements. A delay in reaching the spawning grounds and an increase in energy expenditure may result. This could result in lower survival of juveniles produced from straying individuals, if temperatures in the upper river become unsuitable for egg and fry survival.

Attachment 2. Biological Review for Endangered Species Act Compliance with the WY 2015 Drought Contingency Plan April through September Project Description

Clear Creek Actions

Flows on Clear Creek are forecast to range between 175 cfs and 85 cfs over the summer with the exception of springtime pulse as prescribed in the RPA to attract spring Chinook into the river. Steelhead rearing over the summer occurs in the upper reaches of Clear Creek with the downstream extent of suitable juvenile rearing habitat determined by water temperature. The extreme drought conditions will likely result in below average Trinity River diversions and thus a compressed length of the river suitable for oversummer rearing steelhead. Temperatures in the upper reaches of the stream are estimated to be suitable for rearing for the juvenile steelhead produced by the close to average number of adult spawners. A lower than average number of juvenile emigrants in 2016 per adult spawner could be expected to occur with the below normal habitat availability under the extreme drought conditions.

The temperature management for Clear Creek will be coordinated through the Sacramento River Temperature Task Group under the SWRCB 90-5 requirements and as outlined in RPA Action I.1.5. The temperature criteria are based on the Spring-run Chinook requirements and are expected to be protective of steelhead rearing through the summer. If these criteria are not met, juvenile steelhead habitat will be further restricted, predation by nonnatives may reduce survival, and disease may become more prevalent. The amount of uncertainty regarding Clear Creek effects is moderate.

American River Actions

Monthly flows in the American River are forecast to be held at 500 cfs through March and April. The lower than normal flows may enable cold water releases from Folsom to be maintained as long as possible through the summer. This will also result in a higher than normal rate of heating as water moves downstream. Flows will increase starting in May up to a peak of 3,035 cfs monthly average flows in July and then drop down to around 700 cfs in September. Reclamation will submit a draft temperature management plan to NMFS by May 1 per RPA Action II.2.

Considering the low steelhead escapement in the American River in 2015 it is hypothesized that water temperatures will be the limiting factor to the survival rate for rearing steelhead in 2015. Density dependence should not be a factor. Physical habitat and food should be less limiting than temperatures at the expected low rearing densities. However, if the Nimbus Hatchery steelhead are released in the spring or summer, as occurred in 2014, then density dependence would come into play under the low flow conditions.

American River at Hazel Avenue water temperatures were used to estimate steelhead emergence timing based on spawning timing (Figure 47). Temperatures after March 18 were estimated based on the near term weather forecast and additional warming expected to occur through April and May. The spawning timing for 2015 based on the bi-weekly spawning surveys is shown in Table 21. The emergence timing estimate used 600 accumulated temperature units to emergence (degrees C). Hazel Avenue temperatures reflect the coolest temperatures in the American River, thus emergence will be slightly earlier further downstream as water temperatures increase downstream up to a limit. The difference will be around a three to four day earlier emergence at Watt Avenue for the later season redds. High mortality is likely at over 59 F. Estimated

Attachment 2. Biological Review for Endangered Species Act Compliance with the WY 2015 Drought Contingency Plan April through September Project Description

emergence of fry from current year spawners should be completed by around May 4 (Table 18). Note that redds were included on March 28 based on timing in past surveys. This March 28 survey has not occurred as of this writing so this is a guess. In addition the redd survey data are still draft and subject to change.

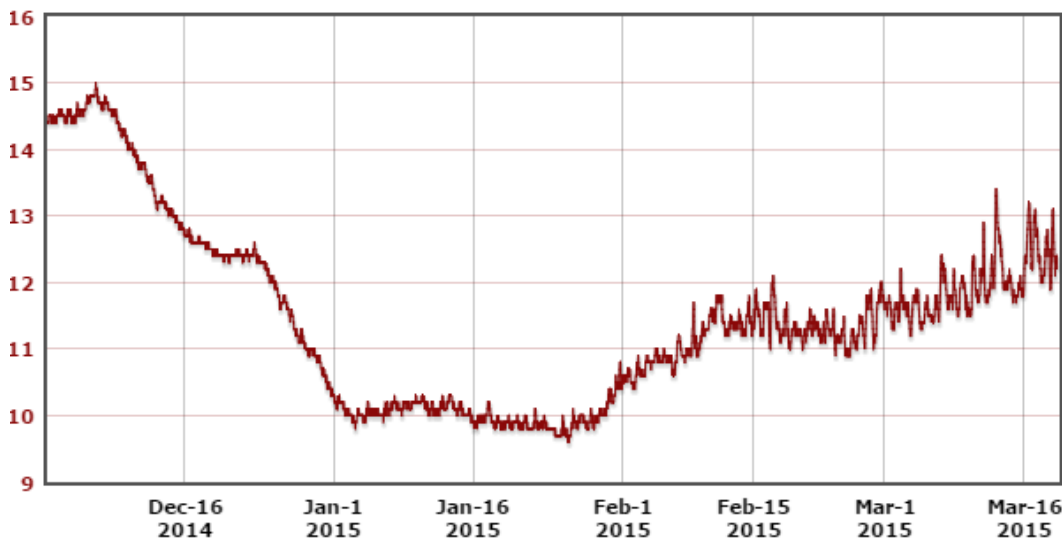


Figure 47. American River at Hazel Avenue water temperature (degrees C), December 2014 – March 19, 2015

Table 21. American River steelhead fry emergence from the gravel timing in 2015

Survey Date	Redds SH and unknown	600 ATU emergence Date	Cumulative % emerged
1/9/2015	0	3/5/2015	0%
1/23/2015	35	3/17/2015	43%
2/5/2015	35	3/27/2015	85%
2/20/2015	6	4/7/2015	93%
3/6/2015	4	4/15/2015	98%
3/28/2015 ¹	2	5/4/2015	100%

¹ The March 28 survey has not occurred so spawning on this date is a guess based on past experience.

Based on the current preliminary spawning survey results at a fecundity of 5,732 eggs/ female (based on recent past hatchery data and size of fish observed on redds in 2015) and 1.5 redds per female about 313,000 eggs would be produced by the observed redds. A 25% egg to fry survival (lower survival than typically assumed due to currently warmer water that will reach levels that will likely reduce egg to fry survival for later spawners this year) would produce about 78,250 emergent fry. Eggs from the later spawning fish may not survive to emergence. CDFW is planning to conduct juvenile steelhead monitoring during the summer. Surveys would be conducted in close proximity to spawning areas and within restoration reaches and would enable an assessment of survival in the expected stressful water temperatures over the summer.

Attachment 2. Biological Review for Endangered Species Act Compliance with the WY 2015 Drought Contingency Plan April through September Project Description

The steelhead smolts leaving the American River in spring of 2015 are expected to complete emigration by around the end of April when temperatures under these drought conditions are expected to be affecting survival for fish leaving the river later. These fish are the progeny of steelhead that spawning in 2014 when water temperatures through the summer were stressful for rearing steelhead. These fish may have suffered mortality or left early. Estimates of fry to smolt survival for naturally spawned steelhead have ranged from 4% to 11% for brood years 2002 to 2010 (Table 22). The survival rate is likely to be lower under the drought conditions.

Table 22. Estimates of American River wild smolt production and hatchery smolt survival based on adult hatchery counts, spawner surveys and hatchery yearling releases (updated from Hannon 2013)

Adult Spawning Year	2013	2012	2011	2010	2009	2008	2007	2006	2005	2004	2003	2002	2001	2000
Year smolts released or outmigrated	2011	2010	2009	2008	2007	2006	2005	2004	2003	2002	2001	2000	1999	1998
Hatchery smolts released in Jan/Feb. of above year	426,920	439,490	250,440	422,380	394,292	454,570	410,330	455,140	419,160	281,705	467,023	402,300	400,060	385,887
In-river spawning adults	437	389	172	121	155		504		266	330	343	300		
Total Hatchery Produced Adult Return ¹	4,449	3,124	2,318	1,905	1,885	853	3,613	2,660	3,472	2,425	1,386	1,745	3,392	2,057
Unclipped Adults in hatchery	57	41	34	34	58	47	116		118	17	27	69	50	
Percent return of hatchery fish (clipped adult return divided by smolts released two years prior)	1.04%	0.71%	0.93%	0.45%	0.48%	0.19%	0.88%	0.58%	0.83%	0.86%	0.30%	0.43%	0.85%	0.53%
Wild smolts that outmigrated (two years prior) ²	9,664	11,241	5,531	10,222	15,374	25,041	18,900		17,457	5,808	20,661	22,827	5,896	
Estimate of fry produced based on redd surveys ³	825,864	182,125	181,323	175,564	246,592		272,340		230,640	402,931	447,057	325,897		
Fry to smolt survival estimated	In 2016	In 2015	In 2014	6%	5%	No Estir	4%	No Estir	11%	5%	No Estir	5%		
¹ assumes 20% recreational harvest based on angler surveys in 1999 and 2001 except 2009 and 2010 use actual creel survey estimates														
² assumes same smolt to adult survival of wild smolts as for hatchery released smolts and that 10% of in-river spawners are naturally produced fish														
³ no adjustments made for potential missed redds														

Conditions in the American River have met the criteria for a conference year under the flow management standard in compliance with the RPA. Therefore, operations will be adaptively managed in partnership with the fishery agencies and the Water Forum to best meet needs under the extreme drought conditions. There is a moderate level of uncertainty in the conclusions about American River steelhead.

Stanislaus River Actions

Stanislaus River flows under Appendix 2E of the 2009 BO are being coordinated with the Stanislaus Operations Group to provide the best conditions as feasible under the current drought situation. Mean monthly flows are projected to be around 460 cfs and 380 cfs in April and May respectively and then drop to a baseflow of 150 cfs through September. The Ripon dissolved oxygen standard of 7.0 ppm, described in SWRCB D-1422, is modified in the Project Description by moving the compliance location upstream to Orange Blossom Bridge over the project period. Given the *O. mykiss* population in the Stanislaus which has been sustained under flows of 150 cfs in past years it is hypothesized that the limiting factor to oversummer survival in 2015 will be water temperatures under the extreme drought conditions affecting conditions in the Stanislaus watershed. Summer operations on the Stanislaus may not be able to meet the temperature compliance schedule described in NMFS RPA Action III.1.2. The RPA will be followed regarding notification and Stanislaus Operations Group (SOG) advice. Under the expected flows and temperatures the oversummer steelhead rearing habitat will be confined to the area upstream of Orange Blossom Bridge. The relaxation of the dissolved oxygen standard from Ripon to 7.0 at Orange Blossom Bridge could result in dissolved oxygen levels reaching lethal levels for fish at times in the Ripon area. A DO of 7.0 is considered protective of salmonids.

Attachment 2. Biological Review for Endangered Species Act Compliance with the WY 2015 Drought Contingency Plan April through September Project Description

Steelhead rearing habitat will be reduced due to temperatures and may be marginal at Orange Blossom Bridge. A dissolved oxygen level of 7.0 and greater at Orange Blossom would be protective of steelhead over the summer in the area between Orange Blossom and Goodwin as DO will be higher on average further upstream.

We expect that spawning of steelhead will be complete by the end of March based on observations in other watersheds. At a temperature of 56°F (13.3°C) emergence of steelhead fry should be completed by May 15. If water temperature becomes greater than a mean daily temperature of 56°F in the redd locations, then emergence would be completed sooner, up to a limit. Mean daily water temperatures greater than 59°F (15°C) could result in very low egg to fry survival if they occur during the incubation period. Recent water temperatures near Goodwin Dam are shown in Figure 48. Resident trout often spawn later than steelhead, so it is likely that the fry from resident fish will continue to emerge past the May 15 date. It is hypothesized that some coldwater refugia should be present, particularly in the deep pools at and upstream of Knights Ferry so that *O. mykiss* populations will persist and the resident population will continue to maintain spawner abundance and juvenile productivity of *O. mykiss* on the Stanislaus River.

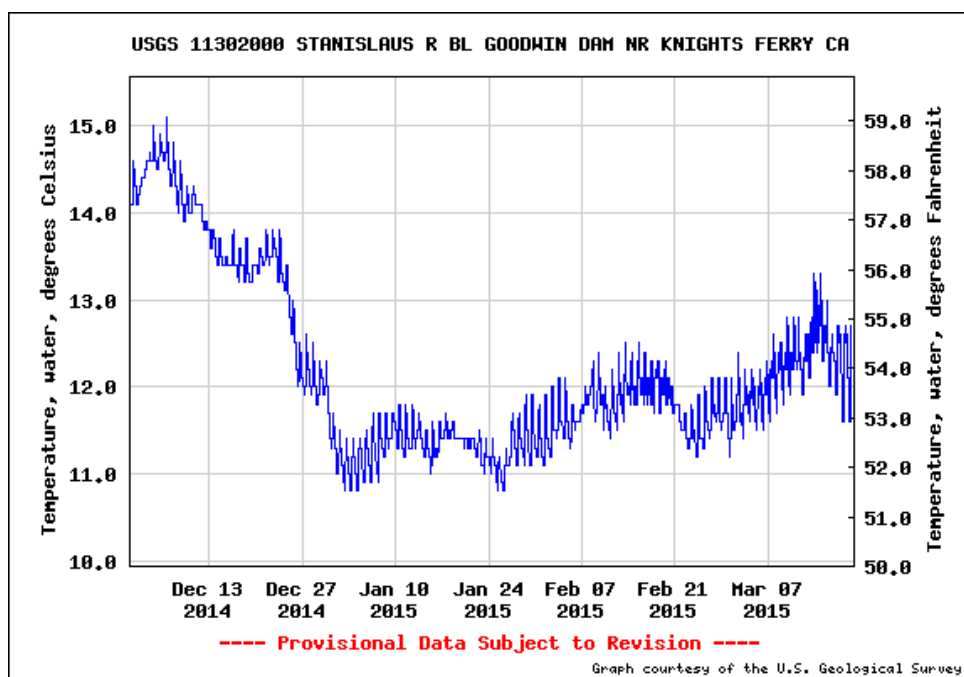


Figure 48. Stanislaus River below Goodwin Dam at the cable crossing water temperature, 12/1/2014 – 3/19/2015

Rotary screw traps in the Stanislaus at Caswell provide information on size and timing of steelhead emigrating from the Stanislaus. During late 2013 through March 6, 2015, no steelhead have been captured at Caswell. Trap calibrations are not conducted for *O. mykiss* but since capture rate is size-dependent for Chinook, larger steelhead are likely much less susceptible to capture than Chinook (Joe Merz, Cramer Fish Science, pers comm). Therefore zero steelhead captured does not represent an absence of emigration from the Stanislaus. The median date of steelhead exit from the Stanislaus based on screw trap data was March 4 for the period from 1997 to 2015.

Attachment 2. Biological Review for Endangered Species Act Compliance with the WY 2015 Drought Contingency Plan April through September Project Description

A pulse flow as specified in the NMFS RPA (2011 amendment), based on SOG advice and NMFS determination, will be scheduled to occur sometime during the late March to April time period to provide migratory cues and flows for the last of the emigrating juvenile steelhead before downstream temperatures become inhospitable. The timing is being coordinated at the SOG. Dissolved oxygen concentration varies with temperature and the warming water temperatures in the spring may also result in stressful DO levels in the lower Stanislaus River in April and May.

The low quality habitat along routes to the ocean likely results in low emigration survival, especially in extreme drought conditions such as this and is likely a large contributor to why the steelhead component of the *O. mykiss* population in the San Joaquin basin is small. It is hypothesized that steelhead escapement in two years will be lower than during previous wetter years due to lower steelhead survival through the lower San Joaquin River between Durham Ferry (near the confluence of the Stanislaus River) and Lathrop than during previous wetter years as well as along the rest of the various routes to the ocean.

Adult steelhead upstream migration generally occurs in October and later in the Stanislaus River. A few may occasionally enter the river in September but this year conditions will likely be unsuitable in the lower San Joaquin and Stanislaus in September (low flows, high temperatures, stressful dissolved oxygen levels) so any steelhead that attempt to migrate early will likely be delayed.

There is a moderate level of uncertainty in conclusions regarding Stanislaus River steelhead.

Delta Exports

Delta exports are forecast to be at a low level due to the drought conditions. The low export levels are not expected to appreciably affect survival of steelhead emigrating through the delta from the Sacramento River. This emigration should be completed by early May when water temperature is likely to be warm for emigrating steelhead. Steelhead emigrating from the San Joaquin River prior to the HORB being in place are more likely to be salvaged at the CVP facility and be trucked downstream of the Delta. Under these extreme low flow conditions the steelhead that experience this route through the fish salvage facilities are hypothesized to have a better chance of survival to the ocean than those that continue down the mainstem San Joaquin River route. The degree of uncertainty with this conclusion is moderate.

No appreciable effect of the pumping levels on the early part of the adult upstream migration in September is expected to occur.

San Joaquin River I:E ratio and San Joaquin River downstream of Stanislaus River Confluence

The Project Description flows at Vernalis are hypothesized to result in less suitable conditions for steelhead emigration than would otherwise occur in the Baseline modeling. These conditions reduce survival of outmigrating San Joaquin basin steelhead downstream of the Stanislaus River confluence until tidal conditions dominate the South Delta. San Joaquin River flow limits are being reduced during the Vernalis pulse flow period and then will be no less than 300 cfs after the pulse until the end of May. Summer Vernalis flows would be no less than 200 cfs monthly

Attachment 2. Biological Review for Endangered Species Act Compliance with the WY 2015 Drought Contingency Plan April through September Project Description

average. Water temperatures are likely to be unsuitable for steelhead emigration by early May due to the drought conditions. These conditions in the San Joaquin following the pulse period are expected to be lethal to steelhead so that later emigrants are not likely to survive.

The Vernalis salinity standard is modified in the Project Description. Additional flows from the Stanislaus River and San Joaquin River tributaries would be required to meet the existing standard. The change in salinity in the San Joaquin River would not affect steelhead as they would not be present in the summer. The result of the low flows over the summer in the Stanislaus, which are enabled to occur with the salinity relaxation, are discussed above in the Stanislaus River section.

If there is a precipitation event outside of the pulse period, then the Project Description modifies RPA Action IV.2.1 to allow pumping to capture abandoned or natural flows in the Delta up to the OMR limits. If precipitation occurs then that would be the same period that steelhead would likely to emigrate. Pumping will occur preferentially at the Jones Pumping Plant if condition permit, which should increase salvage rates and reduce loss, due to lower pre-screen mortality at the Tracy Fish Collection Facility. In a future year, Reclamation and DWR would make available an amount of water equal to half the volume of any increased exports realized over the April – May period for the fishery agencies to shape. This could benefit steelhead in future years but would not benefit fish this year. The degree of uncertainty with this conclusion is moderate.

Summary of Effects on Steelhead

The drought conditions are causing increased stress to steelhead populations, with or without water project operations, in the form of low flows reducing rearing and migratory habitats, above normal water temperatures affecting survival, and likely higher than normal predation on juvenile steelhead. The water management over the last year has focused on maintaining a level of reservoir storage which is generally higher than what would be in place at this time without the planning that has gone into attempting to reduce adverse effects on resources. The Project Description strives to balance spring and summer operations between Shasta and Folsom divisions of the CVP to minimize affects across CVP tributaries in WY 2015. Steelhead survival will be low in 2015 in all tributaries and migratory pathways and is likely to result in a smaller returning year class of steelhead from those juvenile steelhead emigrating this year.

Battle Creek/Coleman Hatchery experienced one of the highest adult steelhead returns that has been measured and eggs from some of those fish are being provided to Nimbus Hatchery on the American River where the steelhead currently do not contribute to the Central Valley steelhead DPS. Although an experiment at this point, if these fish are successful in surviving to emigration next spring then they could contribute to increasing the proportion of Central Valley steelhead returning to the American River in the future and improving genetic diversity for Central Valley steelhead.

Attachment 2. Biological Review for Endangered Species Act Compliance with the WY 2015 Drought Contingency Plan April through September Project Description

Status of Delta Smelt

As California enters a fourth year of drought, abundance of Delta Smelt has continued to decline. The 2014 Fall Midwater Trawl (FMWT) annual index for Delta Smelt was 9, which is the lowest reported fall index since the beginning of this survey in 1967, and approximately one half of the previous lowest index values of 17 (2009) and 18 (2013). These results and a detailed account of the spatial distribution of the adult population based on survey data at that time were described in the Biological Review of the Feb-Mar 2015 TUCP (Reclamation, 2015c). The third Spring Kodiak Trawl (SKT) survey for March 9 – 12, 2015 (Figure 49) yielded six adult Delta Smelt, a record low number for March (Figure 50) and a number that has only occurred over the period of record at this level once before in May surveys, when catches typically tail off because of post-spawn mortality. These winter survey results provide additional evidence that the Delta Smelt population is likely at an all-time low. The recent catch data also indicate most adult Delta Smelt may be in the Sacramento River and outside the influence of the export facilities.

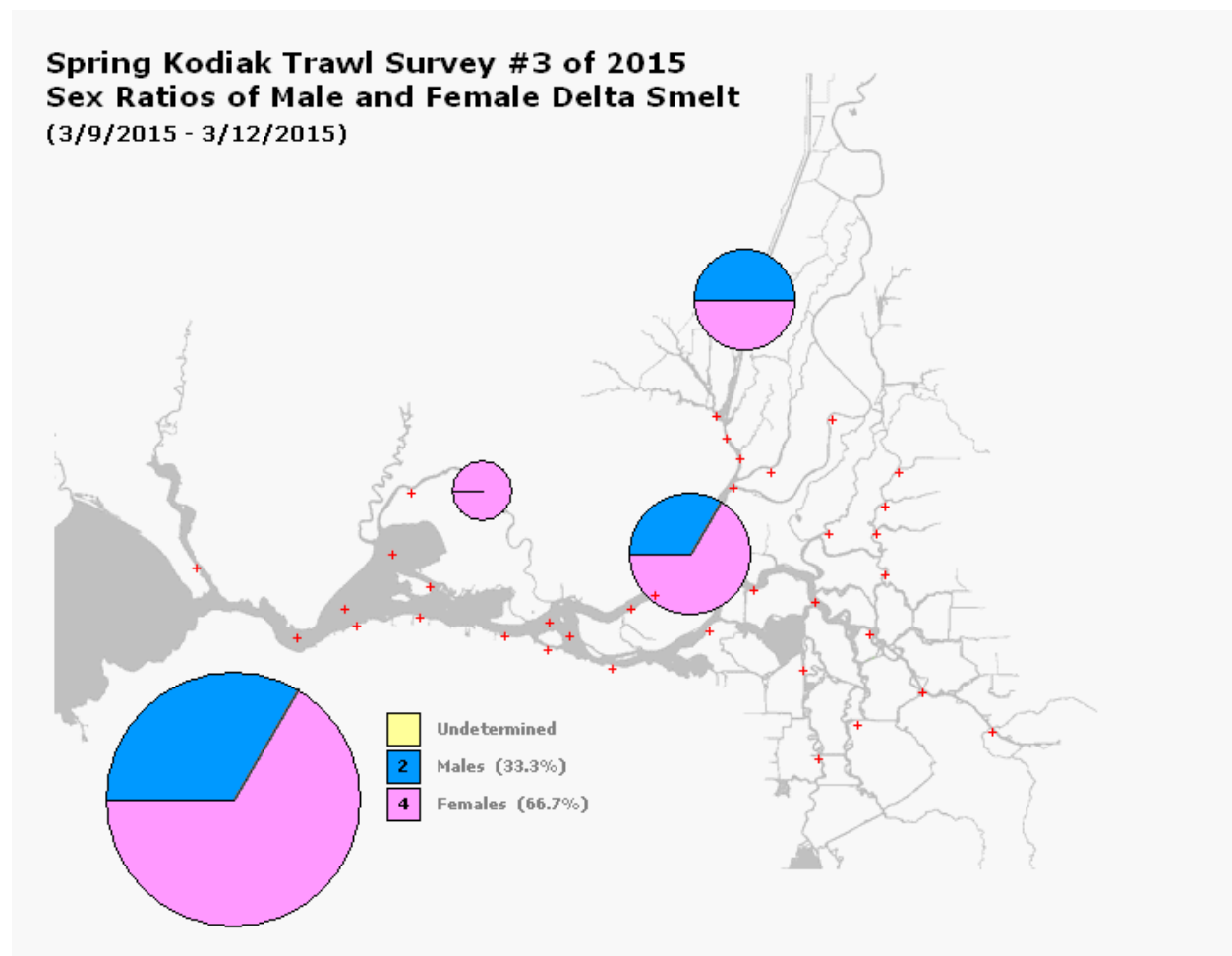


Figure 49. March distribution of adult Delta Smelt from Spring Kodiak Trawl #3

Attachment 2. Biological Review for Endangered Species Act Compliance with the WY 2015 Drought Contingency Plan April through September Project Description

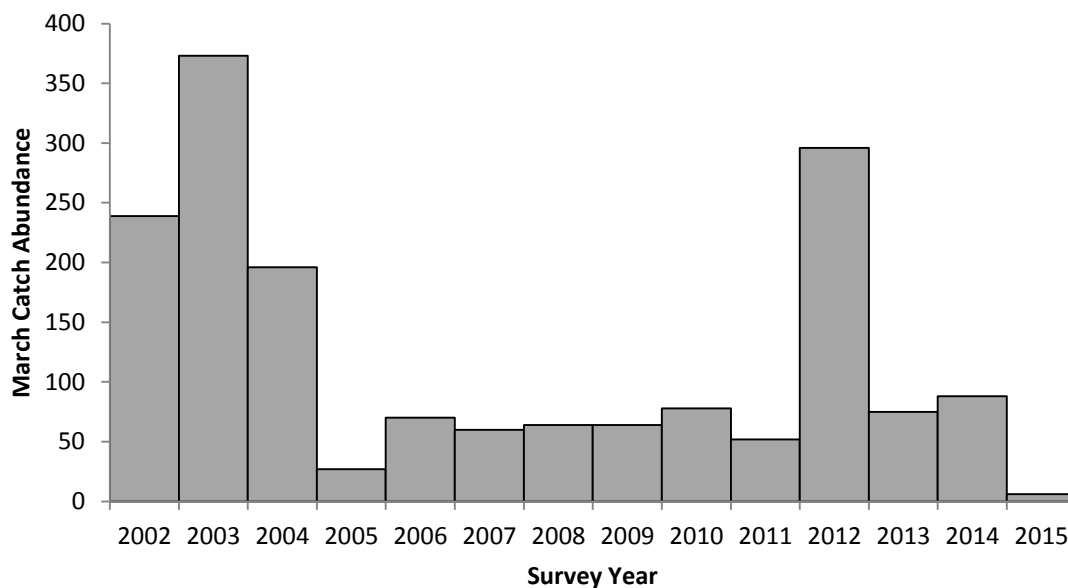


Figure 50. The number of Delta Smelt collected in March for Spring Kodiak Trawl surveys from 2002-2015

Drought Impacts

Research presented at the Interagency Ecological Program (IEP) workshop (March 18-20, 2015) showed that drought impacts Delta Smelt a number of ways. It can reduce the area of low salinity habitat to which they migrate for spawning and thereby reduce food availability for adults and for juveniles moving there to rear. Drought can indirectly impact reproductive potential by lowering the number of oocytes females produce (Hammack, 2015). This is brought about by a link between low outflow and elevated water temperature. Warming temperature shortens the spawning window, which causes fewer clutches to be produced per female (Jeffries, 2015). Both of these mechanisms combine with low adult abundance to impair population fecundity. Lower outflow also tends to reduce turbidity. Delta Smelt use turbid water to avoid predators and they also use it as foraging habitat (Hasenbein, 2015a). Otolith analysis has revealed that Delta Smelt, since 1999, experienced an 8% decline in growth between dry and wet years and spawning is more successful the north Delta during drought (Hobbs, 2015). The quality of their habitat is further compromised by concentrations of herbicides such as Diuron and Hexazinone, which increase with reduced outflow and have synergistic effects that reduce food availability for juveniles (Hasenbein, 2015b). Furthermore, warm, slow moving water characterized by drought promotes conditions in which parasites like Ich (*Ichthyophthirius multifiliis*;) and cyanobacteria like *Microcystis* thrive. Ich causes skin lesions to form on a variety of fish and has an increased prevalence among captive Delta Smelt above 17°C (Frank *et al.*, 2015). *Microcystis* is a toxic hepatotoxin that became established throughout the Delta in 2000 and also thrives in water above 17°C with low turbulence (Lehman, 2015). Because of the extended high water temperatures associated with drought, *Microcystis* blooms extended into December of 2014 (Lehman, 2015). This highly toxic cyanobacteria is known to kill phytoplankton, zooplankton and compromise fish health (Acuña *et al.*, 2012). Finally, the abundance of non-native Delta Smelt predators, such as black bass, increased in the Delta in response to the drought in 2014, mainly because it expanded their preferred habitat (Barnard, 2015). The same pattern was found for non-native

Attachment 2. Biological Review for Endangered Species Act Compliance with the WY 2015 Drought Contingency Plan April through September Project Description

competitors, such as clams like *Corbicula*, which seem to be expanding throughout the Delta despite the drought (Thompson, 2015).

Salvage

The estimated cumulative season total for adult Delta Smelt salvage is 68. No salvage has been reported since February 21st. The State Water Project (SWP) and Central Valley Project (CVP) initiated larval fish monitoring on March 2nd and February 24th, respectively. The frequency of larval fish samples at the CVP has been reduced at times due to heavy debris load in the salvage collections. Regardless, no larval Delta Smelt have been reported at either facility to date. However, pre-screen loss of all life stages (e.g., predation) may decouple entrainment at low densities so that fish entrained at low densities are not observed in salvage.

This is further supported by regular presence of adult Delta Smelt at Jersey Point and Prisoners point surveys for most of the winter indicate likely presence of larvae in the central Delta in spring. Daily “early-warning” sampling resumed during the week of February 2nd at Jersey and Prisoners Point in anticipation of storm conditions. Weekly sampling resumed the week of March 9th and no adult Delta Smelt have been caught at Jersey Point since March 16th (when one individual was caught) and no Delta Smelt have been caught at Prisoners Point since February 15th.

The 3-station average water temperature threshold of 12°C (Action 3 of the 2008 Biological Opinion (BO)) was first exceeded on February 2nd and was reported on March 15th to be 17.8°C. This suggests Delta Smelt spawning has occurred early this year. On March 16th, the Smelt Working Group (SWG) suggested the most likely reason for steep decline in catch of Delta Smelt in the SKT #3 survey (Figure 2) was fish may not have survived after a first spawn (SWG notes from 3/16/15) or they could have been avoiding the gear (Baxter). This hypothesis is partly supported by poor condition of the few mature fish caught in SKT #3. Hatching will likely continue over the next few weeks, although the peak of the spawning season has likely passed. As water temperatures rise, larvae are beginning to recruit to juvenile size, and a broader distribution in the central Delta may become evident by way of larval field surveys. Intermittent salvage of adult Delta Smelt indicates the likely presence of larvae in the central and southern Delta within the vicinity of the SWP and CVP pumps. Those larval and juvenile Delta Smelt hatching in the central and southern Delta are vulnerable to entrainment; however, exports are currently at minimum levels, resulting in favorable Old and Middle River (OMR) flows (SWG-notes from 3/16/15). A temperature off-ramp occurs when water temperature at Clifton Court Forebay reaches 25°C for three consecutive days (BO). This off-ramp typically occurs in late June or early July, although present unseasonably warm water temperatures may suggest an earlier temperature off-ramp (the calendar-based off-ramp is June 30th).

Effects of Proposed Action on Delta Smelt

The following discussion is based on DSM2 particle tracking model (PTM) simulations described earlier. When reviewing this section, it is important to remember that adult Delta Smelt do not behave as neutrally-buoyant particles so a literal translation of results into changes in entrainment or entrainment risk is not advisable. In particular, the model predictions of westward advection are not relevant. It is the changes in central/south Delta hydrodynamics that are of interest because these flow conditions may affect tide-surfing fishes seeking turbid fresh water.

Attachment 2. Biological Review for Endangered Species Act Compliance with the WY 2015 Drought Contingency Plan April through September Project Description

To estimate the effects of the Proposed Action on Delta Smelt, a PTM from April to June was compared to baseline hydrological conditions, assuming an equally distributed population between injection points (Figure 28). Only particles located between Railroad Cut and the pumping facilities experienced flux towards the pumps. Throughout the rest of the Delta, particles either remained in the Delta or eventually moved west regardless of the outflow scenario.

The Baseline scenario represents a constant North Delta Outflow Index (NDOI) of 7100 cfs, while the Project Description scenarios (Hydrology 2 and 2') reduces NDOI to 4000 cfs, and in 2' an open DCC Gates. The Project Description uses the February 90% Operational Forecast for Central Valley hydrologic and operation conditions during the remainder of the Project Description's period. March exceedance forecast is under development and appears to be trending drier than the February 90% exceedance forecast. Reclamation and DWR are petitioning the State Water Board to adopt a Delta outflow standard of a minimum monthly NDOI for April, May and June to be no less than 4000 cfs and for July to be no less than 3000 cfs with a 7 day running average no less than 1000 cfs below the monthly average. Other input values remained constant and reflected the best information available to Department of Water Resources (DWR) modelers when models were run on March 17th, but it should be noted that particles were injected on April 1st and tracked through May 31st. The modeled conditions of the proposed reduction in NDOI resulted in slight overall increase in the final fate of particles at the facilities compared to baseline conditions (Figure 29).

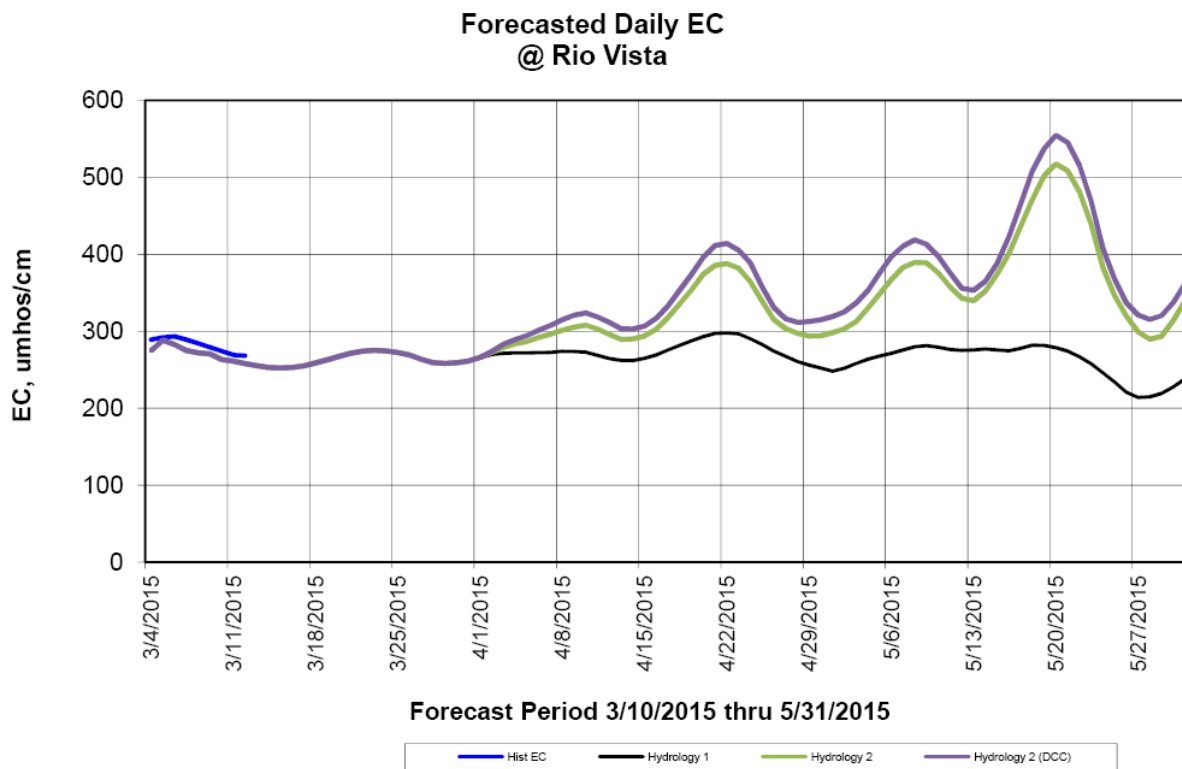


Figure 51. Forecasted electrical conductivity (EC) under different hydrologic scenarios from March – June, 2015 at Rio Vista

Attachment 2. Biological Review for Endangered Species Act Compliance with the WY 2015 Drought Contingency Plan April through September Project Description

Similar to the effects review from 2014 (Reclamation, 2014), if such changes would remain through the summer, the 2 ppt isohaline (X2) will shift upstream and, given the general decrease in habitat suitability when the low-salinity zone moves upstream of Suisun Bay, is assumed to result in higher predation rates, and greater exposure to contaminant effects, losses in irrigation diversions, water temperatures stress, etc. (Feyrer et al., 2007). Similar to the effects review from 2014 (Reclamation, 2014c), if such changes would remain through the summer, the 2 ppt isohaline (X2) will shift upstream and, given the general decrease in dynamic habitat with movement upstream of the low-salinity zone, would result in reduced spawning and rearing habitat (Feyrer et al., 2007). Further constraints on habitat for juvenile Delta Smelt towards upstream spawning areas in the lower Sacramento/San Joaquin Rivers and the Cache Slough Complex/Sacramento Deep Water Ship Channel will reduce the quantity of available habitat, but will be within the range of salinity generally occupied by Delta Smelt during the summer and fall. As Sommer and Mejia (2013) noted, Delta Smelt are not confined to a narrow salinity range and occur from fresh water to relatively high salinity, even though the center of distribution is consistently associated with X2 (Sommer et al., 2011). However, Nobriga et al. (2008) found the probability of occurrence of Delta Smelt was highest at low EC (1,000-5,000 $\mu\text{mhos/cm}$), and declines at higher EC. EC forecasts for Rio Vista and Emmaton (Figures- 51-52) and locations upstream are within this range during the period modeled. Therefore we conclude that while changes in salinity in the lower Sacramento River are within the physiological tolerances of Delta Smelt, the proposed modifications are expected to shift the Delta Smelt population further upstream. There is a relatively high level of uncertainty in these conclusions when compared to Reclamation (2014c) due to a lack of temporally projected data.

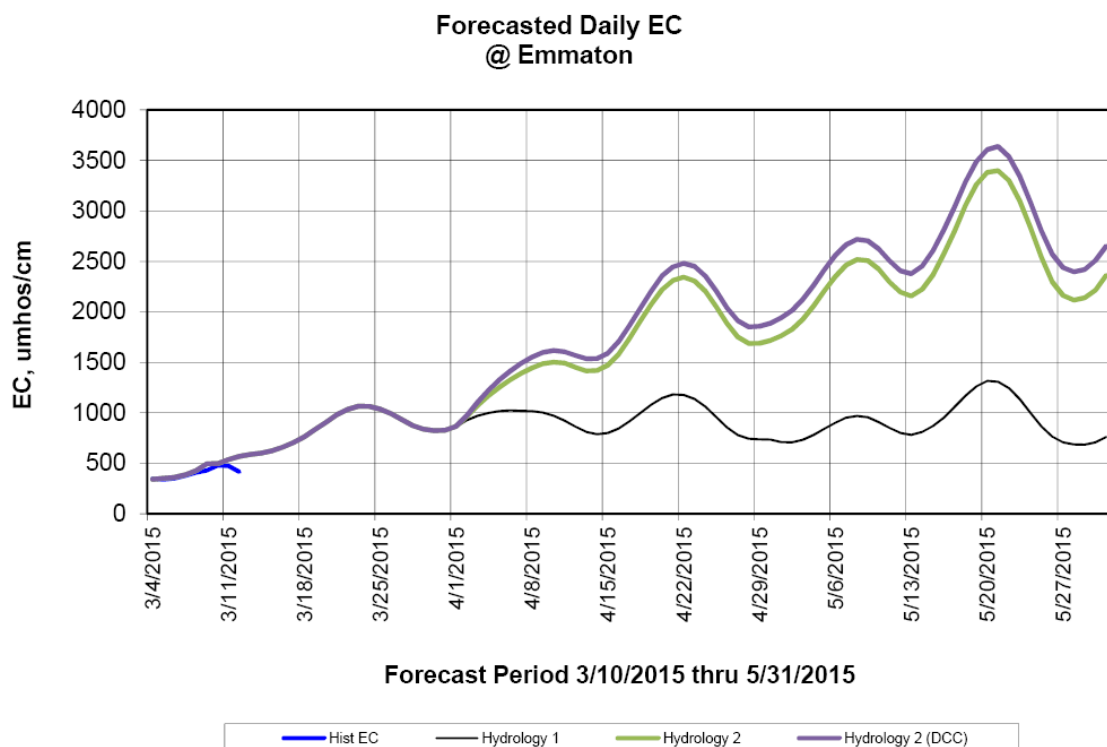


Figure 52. Forecasts of electrical conductivity (EC) under different hydrologic scenarios from March – June, 2015 at Emmaton

Attachment 2. Biological Review for Endangered Species Act Compliance with the WY 2015 Drought Contingency Plan April through September Project Description

The upstream shift of Delta Smelt distribution on the Sacramento River will increase the potential for stochastic events to exacerbate mortality and density-dependent effects on the population (Feyrer *et al.*, 2011). As an example, there may be water temperature increases during prolonged heat waves that would pose risks to Delta Smelt. In general, summer temperatures are higher in landward channels (Wagner, 2012), so reduced inflow is expected to shift the distribution of Delta Smelt into these warmer regions. In addition, with the shifting of X2 above the Sacramento-San Joaquin confluence, salinities may be too high downstream for juvenile Delta Smelt to move substantially seaward, where the maritime influence and larger water bodies maintain cooler water temperatures.

In the San Joaquin River, modeling suggests EC at Jersey Point will increase given the proposed action although it is similar to historical EC values (Figure 53). Regardless, it is inferred there would be little physiological effect on Delta Smelt from changes in salinity in the lower San Joaquin River, as ranges are well within the physiological tolerance level for the species (Nobriga *et al.*, 2008). However, the increase in salinity may alter the distribution of Delta Smelt into less favorable areas within the lower San Joaquin (*e.g.*, Franks Tract).

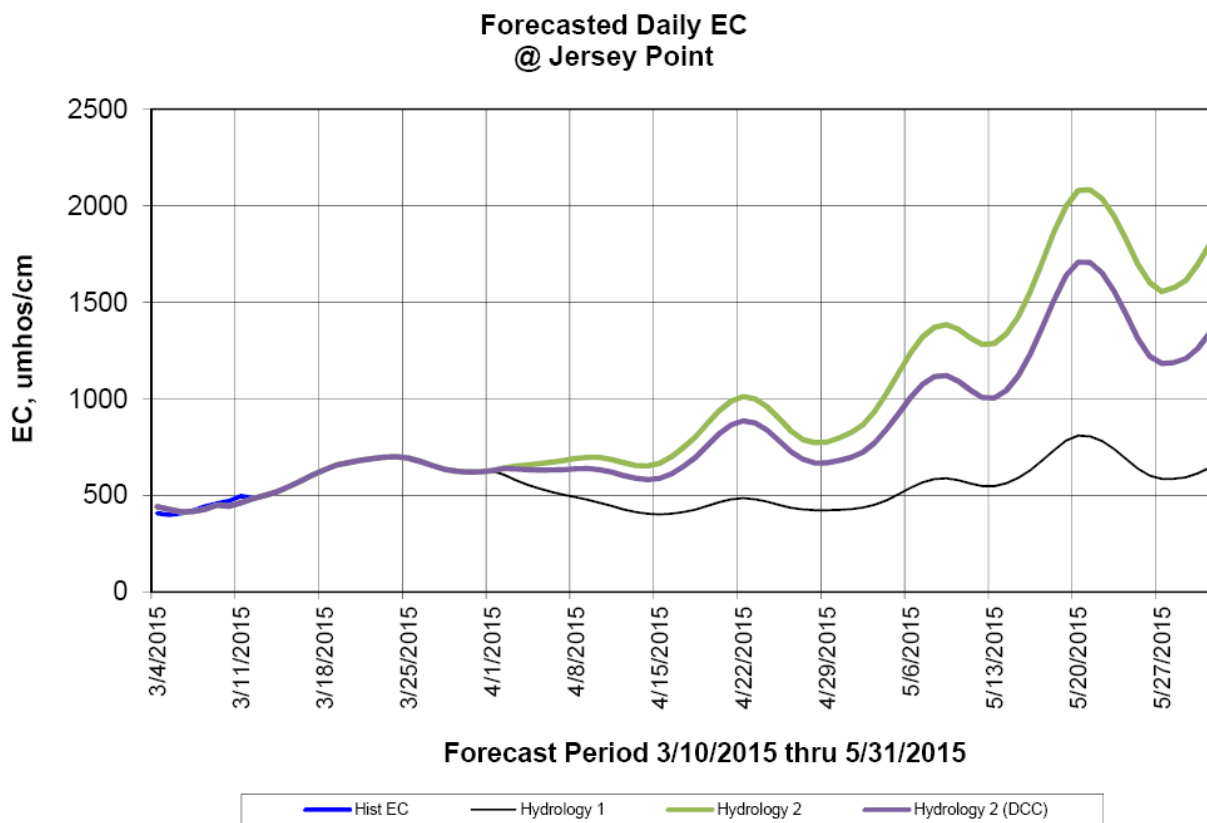


Figure 53. Forecasts of electrical conductivity (EC) under different hydrologic scenarios from March – June, 2015 at Jersey Point

Attachment 2. Biological Review for Endangered Species Act Compliance with the WY 2015 Drought Contingency Plan April through September Project Description

Hydrodynamic Effects on Entrainment

The proposed modifications will result in lower outflows that may reduce survival of migrating young-of-year Delta smelt that are currently in the Interior Delta. For example, lower flows may expose them to loss at the CVP/SWP export facilities, and increase their travel time and exposure to degraded habitats and predators described above. For Delta Smelt residing in the north Delta, reduced outflow, while limiting available habitat, is not expected to result in additional entrainment. Modeling outputs suggest effects from the actions in the Project Description by reducing outflow are negligible through the end of May (Table 23). There is a low level of uncertainty in this conclusion.

Table 23. Presence of Delta Smelt During the Project Description Period and Potential Effects, based on the most recently available survey data¹⁶

Delta Smelt	Life stage Affected	Change in Risk of Lowered Recruitment	Change in Risk of Entrainment at Facilities	Certainty
Eggs	Attached to substrate with very low risk of entrainment			
Larvae	Presence has been established based on Smelt Larva Survey #5 and 20 mm Survey #1. This life stage has not yet recruited to most sampling gear			
Juvenile	Juvenile Delta Smelt (>20mm) have not yet been detected this year			
Adults	Distribution based on February 2015 Spring Kodiak Trawl survey and salvage at SWP/CVP export facilities			
No detections in South Delta	Yes	Not Applicable	Reduced	Moderate
Present in San Joaquin River	Yes	Not Applicable	Reduced	Moderate
Present in Sacramento River	No	Not Applicable	Not Affected	Moderate
Present in Confluence and down	No	Not Applicable	Not Affected	High

Food Availability

Prey availability is constrained by habitat use, which in turn affects what types of prey are encountered. Larval Delta Smelt are visual feeders. They find and select individual prey organisms and their ability to see prey in the water is enhanced by turbidity (Baskerville-Bridges & Lindberg, 2004). Thus, Delta Smelt diets are largely comprised of small invertebrates (i.e., zooplankton) that inhabit the estuary's turbid, low-salinity, open-water habitats. Larval Delta

¹⁶ Distributions are based on monitoring data through March 16.

Attachment 2. Biological Review for Endangered Species Act Compliance with the WY 2015 Drought Contingency Plan April through September Project Description

Smelt have particularly restricted diets (Nobriga, 2002). They do not feed on the full array of zooplankton with which they co-occur; they mainly consume three copepods: *Eurytemora affinis*, *Pseudodiaptomus forbesi*, and freshwater species of the family Cyclopidae. Further, the diets of first-feeding Delta Smelt larvae are largely restricted to the larval stages of these copepods. As Delta Smelt grow larger, mouth gape and swimming ability increase, enabling them to target larger copepods.

In the laboratory, a turbid environment (>25 Nephelometric Turbidity Units (NTU)) was necessary to elicit a first-feeding response (Baskerville-Bridges & Lindberg, 2004). Successful feeding seems to depend on a high density of food organisms and turbidity, and increases with stronger light conditions (Baskerville-Bridges & Lindberg, 2004; Mager *et al.*, 2003). The most common first prey of wild Delta Smelt larvae are larval stages of several copepod species which occur in the North Delta region. The variability of shallow and deep water habitat, and the resuspension of sediment due to wind and tidal action in the North Delta, may buffer effects of the proposed modifications because much, if not most, of the habitat in this region would remain suitable. Expectations for the North Delta contrast with the lower San Joaquin River where the upstream relocation of X2 may result in a greater proportion of the available habitat encompassing areas of high surface aquatic vegetation (SAV) and associated low turbidities. This could lower prey capture efficiency for Delta Smelt and increase predation rate on juveniles. There is moderate level of uncertainty in this conclusion.

In addition to turbidity effects, changes in flow may affect residence time, which in turn may influence planktonic production. Lower flows are expected to increase hydraulic residence times, potentially resulting in improved planktonic production (Lucas *et al.*, 2009). However, the specific effect is difficult to predict because benthic grazing can offset these benefits, hence the response of the food web to the changes in flow is unclear. There is a moderate level of uncertainty about this conclusion.

Summary of Effects on Delta Smelt

Adults

Small numbers of Delta Smelt adults and larvae observed in 2015 field surveys indicates the WY 2014 drought had a significant impact on the population. Like many other species in the Delta, the Delta Smelt population is showing low recruitment again this year due to effects of continued drought. Model results indicate the Proposed Action may increase entrainment risk for Delta Smelt moving around in the San Joaquin River above baseline conditions. As indicated by forecasted daily EC results, salinity is expected to shift the centroid of the distribution associated with X2 inland. If recent SKT and USFWS Jersey Point survey results reasonably reflect the current distribution of Delta Smelt, there is a diminishing presence of adult Delta Smelt in the vicinity of Jersey Point. Entrainment of these adults is unlikely to be a management issue this year. Published analyses of a 13-year dataset of salvage records at the CVP/SWP fish collection facilities indicate that increased salvage of adult Delta Smelt at the CVP/SWP occurs when turbidities increase in the South Delta and OMR flows are highly negative (Grimaldo *et al.*, 2009). Given the present low turbidity in the South Delta, migration of remaining adults into areas of elevated entrainment risk is not expected. The salvage of adult Delta Smelt typically ends by May (Reclamation 2014c). After the onset of spawning, salvage of adult Delta Smelt

Attachment 2. Biological Review for Endangered Species Act Compliance with the WY 2015 Drought Contingency Plan April through September Project Description

diminishes, with regulatory focus shifting from protection of adults to protection of larvae/juveniles by the end of March (as determined by water temperatures or biological triggers; BO).

Larvae and Juveniles

Delta Smelt have a strong positive association with the position of X2, with more downstream positions providing higher quality habitat (Feyrer *et al.*, 2011). Under the proposed action, it is likely summer Delta Smelt distributions will not be in areas optimal for growth and survival (Nobriga *et al.*, 2008). In previous low-flow years, when water quality conditions became less tolerable for Delta Smelt in the Cache Slough Complex, the North Delta population appeared to have the capability to move quickly downstream towards the low salinity zone. It is likely, given the strongly tidal nature of the Cache Slough Complex, Delta Smelt are able to ride these tidal flows to escape unfavorable habitat conditions in the North Delta. Under the current proposal, X2 would move further upstream, reducing the potential for downstream movement beyond the limitations already anticipated from the unmodified severe drought conditions. The proportion of the total population of Delta Smelt in the North Delta in summer appears to be highly variable (Feyrer, 2015), but can be relatively substantial (Sommer & Mejia, 2013). There is a moderate level of uncertainty about the expected effects in the North Delta.

Ongoing IEP monitoring, Early Warning Monitoring, and fish salvage operations, will continue to inform management and advisory groups who will be providing input to Reclamation on a near real-time basis.

Status of Longfin Smelt

In Bay Study trawls conducted during the beginning of February, 2015, the majority of adult Longfin Smelt were detected in Suisun Bay, the Confluence area, and the lower Sacramento River (Figures 54-55; note the different scales between the figures). As of March 16, 2015, no adult or age-1 Longfin Smelt have been detected at either the CVP or SWP fish facilities. Earlier in the season (January), adult Longfin Smelt was detected in the Early Warning sampling in the lower San Joaquin River at Jersey Point, though recent surveys have not detected any in this area. This presence indicates that larval Longfin may be present in the central and south Delta, which is corroborated by the detection of larval Longfin in larval fish sampling at the salvage facilities (see below).

Attachment 2. Biological Review for Endangered Species Act Compliance with the WY 2015 Drought Contingency Plan April through September Project Description

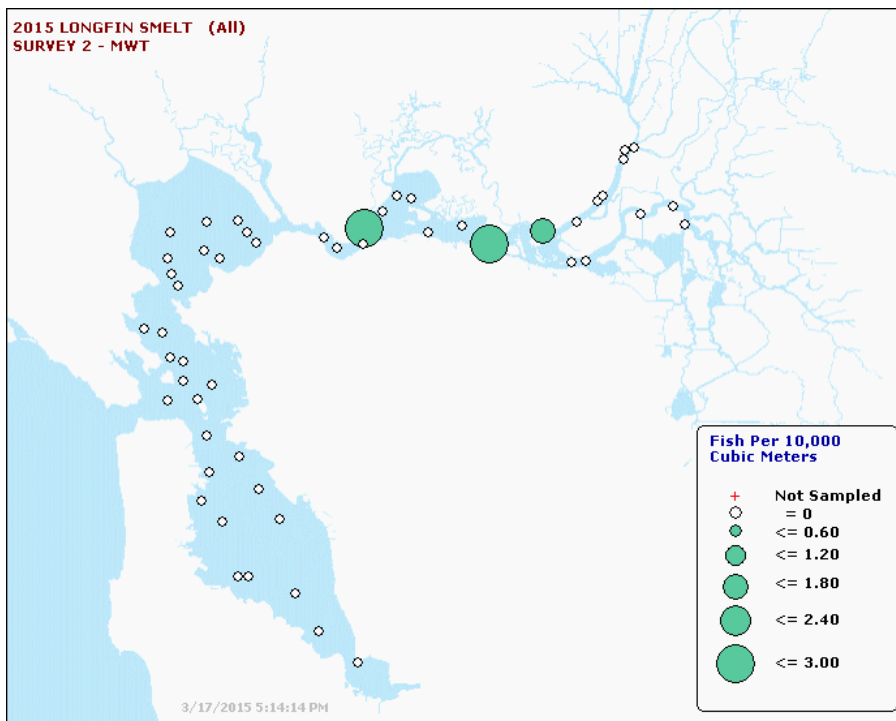


Figure 54. Distribution of adult Longfin Smelt in the Bay Study Midwater Trawl during February 2015

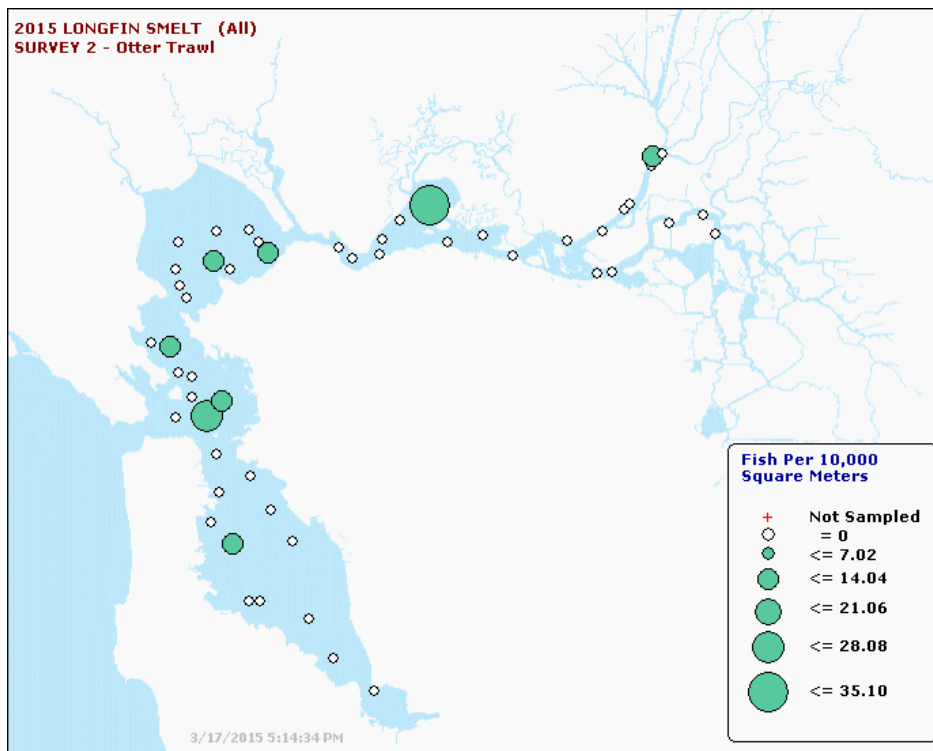


Figure 55. Distribution of adult Longfin Smelt in the Bay Study Otter Trawl during February 2015

Attachment 2. Biological Review for Endangered Species Act Compliance with the WY 2015 Drought Contingency Plan April through September Project Description

The fifth Smelt Larva Survey (SLS), conducted during the week of March 2, 2015, found larval Longfin Smelt larvae were primarily distributed in the lower Sacramento River, at the confluence, and east of the confluence in Suisun Bay (Figure 56). Several larvae were also collected in the lower San Joaquin River at Jersey Point (n=1) and Oulton Point (n=3), and one larvae was collected in the south Delta at station 914 near Mildred Island. While larvae in these southern areas will be at a low to medium risk of entrainment during operations, larvae in the south Delta represent only 1% of the total larval catch in SLS #5 east of Carquinez Straights (n=101). As of March 16, 2015, one larvae each have been collected at the CVP and SWP salvage facilities, (February 27 and March 3, respectively). Compared to previous years, it appears Longfin Smelt spawning in 2015 is substantially reduced and larval abundances are low.

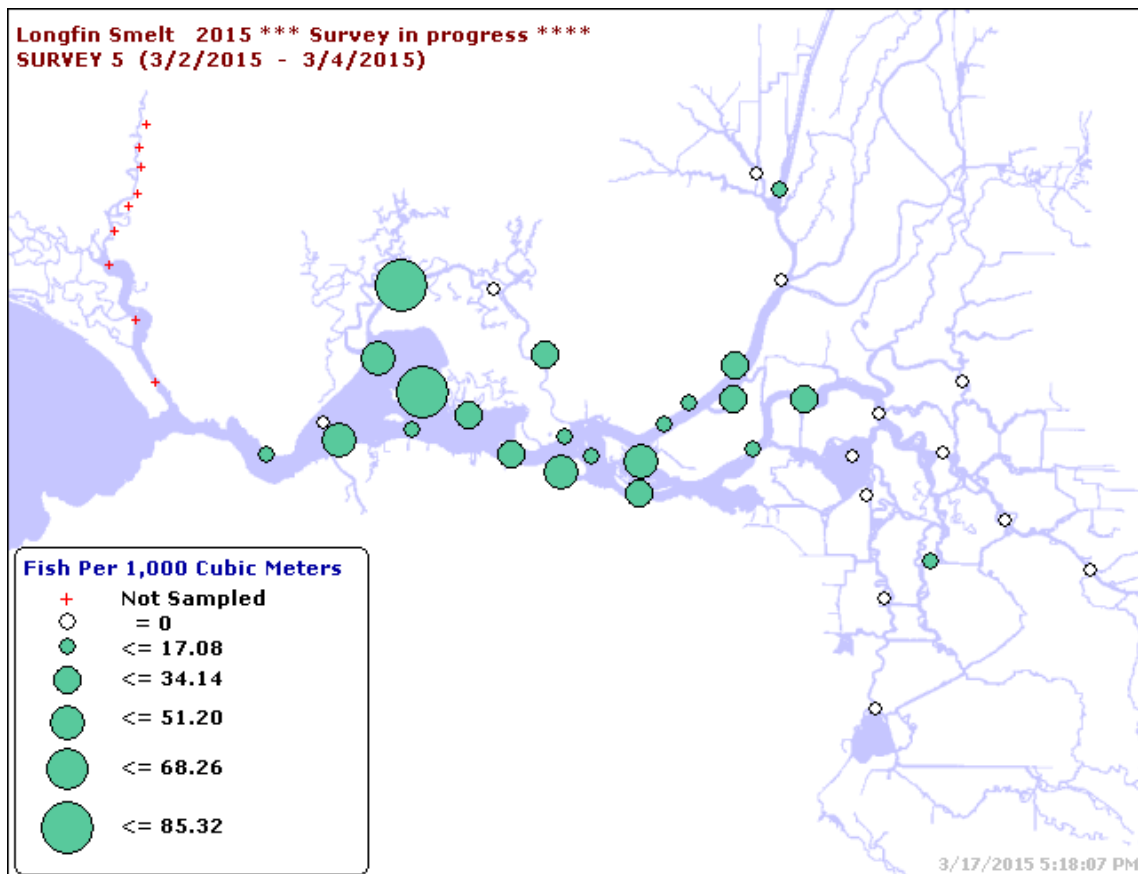


Figure 56. Distribution of larval Longfin Smelt from the Smelt Larva Survey #5 conducted in early March, 2015

It is likely that Longfin Smelt spawning is close to ending. However, the historical presence of recently-hatched larvae in sampling during March and April, indicates that spawning can continue into March (CDFG, 2009). It is possible Longfin Smelt distributed near the confluence may yet make spawning forays into the central and south Delta, which would put them at increased risk of entrainment, although these risks are inherently unquantifiable at this time due to the unprecedented circumstances of continued drought conditions (Table 24).

Attachment 2. Biological Review for Endangered Species Act Compliance with the WY 2015 Drought Contingency Plan April through September Project Description

Table 24. Presence of Longfin Smelt During the Project Description Period and Potential Effects, based on the most recently available survey data¹⁷

Longfin Smelt	Life stage Affected	Change in Risk of Lowered Recruitment	Change in Risk of Entrainment at Facilities	Certainty
Eggs	Attached to substrate with very low risk of entrainment			
Larvae	Distribution based on Smelt Larva Survey #5			
~1% South Delta	Yes	Increased	Increased	High
~11% San Joaquin River	Yes	Increased	No Change	Moderate
~22% Sacramento River	Yes	Increased	No Change	Moderate
~66% Confluence and Suisun	Yes	Increased	No Change	Moderate
Juvenile	Juvenile Longfin (>20mm) have not yet been detected this year			
Adults	Distribution based on February 2015 Bay Study survey			
0% South Delta	Not Applicable	Not Applicable	Not Applicable	Moderate
0% San Joaquin River	Not Applicable	Not Applicable	Not Applicable	Moderate
<5% Sacramento River	No	Not Affected	Not Affected	Moderate
95% Confluence, Suisun & SF Bay	No	Not Affected	Not Affected	High

Effect of Proposed Action on Longfin Smelt

To estimate the effect of the proposed decrease in outflow on Longfin Smelt, particle tracking models were run using hydrology from the proposed action and baseline conditions, assuming an equally distributed population between injection points (Figure 29). The modeled conditions of the proposed reduced outflow to 4,000 cfs resulted in small changes in the fate of the majority of particles (at the end of the modeling period) compared to baseline conditions. Under all modeled conditions, particles originating from within the south Delta (injection node Railroad Cut) had the majority of particles arriving at the state and federal pumping facilities by May 31 (Figure 29). Of these particles, 78% were entrained at the pumping facilities as of May 31 under the proposed decrease in flows, compared to 73% under baseline. For particles originating at Prisoner's Point, 11% were entrained at the export facilities versus 5% under baseline conditions. Flux past Chippis for these particles was 17% compared to 40% for baseline conditions. Of the

¹⁷ Distributions are based on monitoring data through March 16.

Attachment 2. Biological Review for Endangered Species Act Compliance with the WY 2015 Drought Contingency Plan April through September Project Description

particles injected at Jersey Point under the proposed action, the percentage that moved past Chipps Island by May 31 was 40% (vs. 68% for baseline conditions) and entrainment at the facilities was 2% (vs. 0% for baseline conditions). For particles seeded in the Sacramento River (station 707) at Three-mile Slough above Decker Island, only 1% were entrained to the export facilities versus 0% under baseline conditions. Flux past Chipps Island for these particles was 45% versus 66% under baseline conditions. As larval Longfin Smelt are distributed in the lower San Joaquin and Sacramento Rivers, the general reduction in flux past Chipps Island negatively affect downstream larval transport. However, the majority of larval Longfin detected in SLS #5 were downstream of Chipps Island, so the population level impacts of this reduced flux may not be substantial. However, it is impossible to quantify whether the differences between baseline conditions and the proposed action are truly biologically significant to the Longfin Smelt populations without knowledge of the size of the population and more detailed knowledge of their distribution. However, a qualitative prediction is possible based on the PTM results and a historical relationship between outflow and Longfin Smelt recruitment.

The proposed action will reduce outflow, and increased outflow is one of the best predictors of Longfin Smelt year class strength (CDFG 2009). Therefore, it is likely the proposed action will exacerbate poor Longfin Smelt recruitment and survival already expected in 2015 due to the severity of the drought. Given the results of the PTM model, it is likely that Longfin Smelt larvae in the San Joaquin River (Prisoner's Point and upstream) and in the south Delta will have a somewhat increased risk of entrainment into the south Delta as part of the Proposed Action, where they are not expected to survive warming water temperatures (Table 24). Longfin Smelt already located in the south Delta, near Frank's Tract and within Old and Middle Rivers will be at high risk of entrainment at the export facilities under both baseline conditions and the proposed action. Larvae in other parts of the San Joaquin River and elsewhere in the Delta will also see an increase, though slight, in export entrainment risk.

Summary of Effects on Longfin Smelt

Like other species, Longfin Smelt are likely to experience poor recruitment this year due to effects of the continuing drought. Low spawning and larval detection rates this year seem to verify these low survival rates. The reduction in outflow due to the proposed action will likely have some negative impact on Longfin spawning and recruitment, though this effect is hard to quantify given the already poor environmental conditions due to the drought. The Proposed Action is unlikely to increase entrainment of Longfin Smelt to the export facilities in any substantive manner, as recent surveys indicate that the majorities of both adult and larval Longfin Smelt are distributed outside the zone of influence of the pumps. However, larval Longfin Smelt that are in the San Joaquin River (near Prisoner's Point), and especially those in the south Delta, will be at elevated risk of entrainment into the facilities.

References

- Acuña, S., D.F. Deng, P. Lehman, and S. Teh. 2012. Sublethal dietary effects of *Microcystis* on Sacramento Splittail, *Pogonichthys macrolepidotus*. *Aquatic Toxicology* 110-111: 1-8.
- Barnard, D. 2015. Resident fish revisited: Black bass drought response. Presented at the Interagency Ecological Program 2015 Workshop, March 18-20, 2015, Folsom, CA.
- Baskerville-Bridges, B. and C. Lindberg. 2004. The effect of light intensity, alga concentration, and prey density on the feeding behavior of Delta Smelt larvae. Pages 219-228 in F. Feyrer, L.R. Brown, R.L. Brown and J.J. Orsi (eds.), *Early Life History of Fishes in the San Francisco Estuary and Watershed*. Am. Fish. Soc. Symp. 39, Bethesda, MD, USA.
- Baxter, R. Insights into Delta Smelt habitat provided by gear selectivity studies. Presented at the Interagency Ecological Program 2015 Workshop, March 18-20, 2015, Folsom, CA.
- Bergman, P., D. Delaney, J. Merz, and C. Watry. 2014. Memo: A pilot mark-recapture study using spot patterns of *Oncorhynchus mykiss* in the Stanislaus River, California. Prepared by Cramer Fish Sciences. Submitted to Erwin Van Nieuwenhuyse, U.S. Bureau of Reclamation, March 10, 2014.
- CDFG [California Department of Fish and Game]. 2009. Report to the Fish and Game Commission: A status review of the Longfin Smelt (*Spirinchus thaleichthys*) in California.
- del Rosario, R.B, Y.J. Redler, K. Newman, P.L. Brandes, T. Sommer, K. Reece, and R. Vincik. 2013. Migration patterns of juvenile winter-run-sized Chinook Salmon (*Oncorhynchus tshawytscha*) through the Sacramento-San Joaquin Delta. *San Francisco Estuary and Watershed Science* 11(1): 24p. Available at < <https://escholarship.org/uc/item/36d88128>>
- Feyrer, F. 2015. Drivers of pelagic fish distribution in the North Delta. Presented at the Interagency Ecological Program 2015 Workshop, March 18-20, 2015. Folsom, CA.
- Feyrer, F., K. Newman, M. Nobriga, and T. Sommer. 2011. Modeling the effects of future outflow on the abiotic habitat of an imperiled estuarine fish. *Estuaries and Coasts* 34:120-128.
- Feyrer, F., M.L. Nobriga, and T.R. Sommer. 2007. Multidecadal trends for three declining fish species: Habitat patterns and mechanisms in the San Francisco Estuary, California, USA. *Canadian Journal of Fisheries and Aquatic Sciences* 64:723-734.
- Frank, D., M. Hasenbein, K. Eder, J. Geist, N.A. Fangue, and R.E. Connon. 2015. Diagnosing disease state in *Hypomesus transpacificus* following infection by *Ichthyophthirius*

Attachment 2. Biological Review for Endangered Species Act Compliance with the WY 2015 Drought Contingency Plan April through September Project Description

- multifiliis*. Presented at the Interagency Ecological Program 2015 Workshop, March 18-20, 2015, Folsom, CA.
- Grimaldo, L.F., T. Sommer, N. Van Ark, G. Jones, E. Holland, P.B. Moyle, B. Herbold, and P. Smith. 2009. Factors affecting fish entrainment into massive water diversions in a tidal freshwater estuary: Can fish losses be managed? *North American Journal of Fisheries Management* 29:1253-1270.
- Hammack, B. 2015. Nutritional status and fecundity of Delta Smelt in the San Francisco Estuary. Presented at the Interagency Ecological Program 2015 Workshop, March 18-20, 2015, Folsom, CA.
- Hannon, J. 2013. American River steelhead (*Oncorhynchus mykiss*) spawning - 2013 with comparisons to prior years. U.S. Bureau of Reclamation. Sacramento, CA. 32 p.
- Hasenbein, M. 2015a. Physiological stress responses to turbidity in larval Delta Smelt. Presented at the Interagency Ecological Program 2015 Workshop, March 18-20, 2015, Folsom, CA.
- Hasenbein, S. 2015b. Direct and indirect effects of herbicide mixtures on primary and secondary productivity. Presented at the Interagency Ecological Program 2015 Workshop, March 18-20, 2015. Folsom, CA.
- Hobbs, J. 2015. Delta smelt in drought: Growth and life history. Presented at the Interagency Ecological Program 2015 Workshop, March 18-20, 2015, Folsom, CA.
- Israel, J.A. and A.P. Klimley, 2009. Life history conceptual model North American Green Sturgeon (*Acipenser medirostris*). Sacramento-San Joaquin Delta Regional Ecosystem Restoration Implementation Plan. 49 p.
- Jeffries, K. 2015. The effects of water temperature on Longfin Smelt and Delta Smelt. Presented at the Interagency Ecological Program 2015 Workshop, March 18-20, 2015, Folsom, CA.
- Kimmerer, W.J. 2008. Losses of Sacramento River Chinook Salmon and Delta Smelt to entrainment in water diversions in the Sacramento-San Joaquin Delta. *San Francisco Estuary and Watershed Science* 6(2). Available at <<https://escholarship.org/uc/item/7v92h6fs>>
- Lehman, P. 2015. Response of *Microcystis* to Drought. Presented at the Interagency Ecological Program 2015 Workshop, March 18-20, 2015. Folsom, CA.
- Lucas, L.V., J.K. Thompson, and L.R. Brown. 2009. Why are diverse relationships observed between phytoplankton biomass and transport time? *Limnology and Oceanography* 54: 381-390.
- Mager, R., S. Doroshov, J. Van Eenennaam, and R. Brown. 2003. Early life stages of Delta Smelt. *American Fisheries Society Symposium* 39:169-180.

Attachment 2. Biological Review for Endangered Species Act Compliance with the WY 2015 Drought Contingency Plan April through September Project Description

- NMFS [National Marine Fisheries Service]. 2009. Biological and Conference Opinion on the Long-Term Operations of the Central Valley Project and State Water Project. Southwest Region, Long Beach, CA. June 4.
- NMFS. 2011. Amended Biological and Conference Opinion on the Long-Term Operations of the Central Valley Project and State Water Project. Central Valley Office, Sacramento, CA.
- NMFS. 2014. Letter from Mr. William Stelle to Mr. David Murillo. Interim Contingency Plan for March pursuant to Reasonable and Prudent Alternative Action I.2.3.C of the Biological and Conference Opinion on the Coordinated Long-term Operation of the Central Valley Project and State Water Project CA.
- Nobriga, M.L. 2002. Larval Delta smelt diet composition and feeding incidence: Environmental and ontogenetic influences. *California Fish and Game* 88:149-164.
- Nobriga, M.L., T.R. Sommer, F. Feyrer, and K. Fleming. 2008. Long-term trends in summertime habitat suitability for Delta smelt. *San Francisco Estuary and Watershed Science* 6(1). Available at <<https://escholarship.org/uc/item/5xd3q8tx>>
- Perry, R.W. 2010. Survival and migration dynamics of juvenile Chinook Salmon (*Oncorhynchus tshawytscha*) in the Sacramento-San Joaquin River Delta. Dissertation. School of Aquatic and Fisheries Science, University of Washington, Seattle, WA. 237p.
- Poytress, W.R., J.J. Gruber, F.D. Carillo, and S.D. Voss. 2014. Compendium report of Red Bluff Diversion Dam rotary trap anadromous fish production indices for Years 2002-2012. Report of the U.S. Fish and Wildlife Service to California Department of Fish and Wildlife and U.S. Bureau of Reclamation. Red Bluff, CA. 138 p.
- Romine, J.G., R.W. Perry, S.J. Brewer, N.S. Adams, T.L. Liedtke, A.R. Blake, and J.R. Burau. 2013. The Regional Salmon Outmigration Study: Survival and migration routing of juvenile Chinook Salmon in the Sacramento-San Joaquin River Delta during the winter of 2008-2009. U.S. Geological Survey, Open File Report 2013-1142. 36 p.
- Reclamation. 2014a. Letter from Mr. Paul Fujitani to Mrs. Maria Rea. Re: Contingency Plan for February pursuant to Reasonable and Prudent Alternative (RPA) Action I.2.3.C of the 2009 Coordinated Long-term Operation of the Central Valley Project (CVP) and State Water Project (SWP) Biological Opinion (2009 BiOp). Mid-Pacific Region, Sacramento CA.
- Reclamation. 2014b. Attachment G- Revised DCC Gate Triggers Matrix in Central Valley Project and State Water Project Drought Operations Plan and Operational Forecast April 1, 2014 through November 15, 2014. Submitted to the State Water Resources Control Board on April 18, 2014.

Attachment 2. Biological Review for Endangered Species Act Compliance with the WY 2015 Drought Contingency Plan April through September Project Description

- Reclamation. 2014c. Update to the Delta and Longfin Smelt supporting information for Endangered Species Act compliance regarding Delta water quality. April 25, 2014. Mid-Pacific Region, Sacramento CA.
- Reclamation. 2015a. Brood Year 2013 winter-run Chinook Salmon drought operation and monitoring assessment. Report. Mid-Pacific Region, Sacramento CA. March 2015.
- Reclamation. 2015b. Letter from Mr. Ron Milligan to Mrs. Maria Rea. Re: Interim Contingency Plan for February and March pursuant to Reasonable and Prudent Alternative (RPA) Action 1.2.3.C of the 2009 Coordinated Long-term Operation of the Central Valley Project (CVP) and State Water Project (SWP) Biological Opinion. (2009 BiOp). Mid-Pacific Region, Sacramento CA. January 27.
- Reclamation. 2015c. Supporting information for Endangered Species Act compliance for Old and Middle River flow management consultation framework. Mid-Pacific Region, Sacramento CA. February 2015.
- Singer, G.P, A.R Hearn, E.D Chapman, M.L. Peterson, P.E. LaCivita, W.N. Brostoff, A. Bremmer, and A.P. Klimley. 2013. Interannual variation of reach specific migratory success for Sacramento River Hatchery yearling late fall-run Chinook Salmon (*Oncorhynchus tshawytscha*) and Steelhead Trout (*Oncorhynchus mykiss*). *Environmental Biology of Fishes* 96:363-379.
- USFWS [U.S. Fish and Wildlife Service]. 2008. Formal Endangered Species Act Consultation on the Proposed Coordinated Operations of the Central Valley Project (CVP) and State Water Project (SWP), Service File No. 81420-2008-F-1481-5. Available at <<http://www.fws.gov/sfbaydelta/ocap/>>.
- Sommer, T. and F. Mejia. 2013. A place to call home: A synthesis of Delta Smelt habitat in the upper San Francisco Estuary. *San Francisco Estuary and Watershed Science* 11(2). Available at <<https://escholarship.org/uc/item/32c8t244>>.
- Sommer, T., F.H. Mejia, M.L. Nobriga, F. Feyrer, and L. Grimaldo. 2011. The spawning migration of Delta Smelt in the upper San Francisco Estuary. *San Francisco Estuary and Watershed Science* 9(2). Available at <<https://escholarship.org/uc/item/86m0g5sz>>.
- Thompson, J. 2015. Corbicula may be 'lying in wait'; can we restore habitat around them? Presented at the Interagency Ecological Program 2015 Workshop, March 18-20, 2015, Folsom, CA.
- Wagner, R.W. 2012. Temperature and tidal dynamics in a branching estuarine system. Dissertation. University of California, Berkeley. Available at <<http://gradworks.umi.com/35/55/3555978.html>>.

Attachment B

DWR and Reclamation Request for Modifications of Revised Order that Approved a Temporary Urgency Change in License and Permit Terms and Conditions Requiring Compliance with Delta Water Quality Objectives in Response to Drought Conditions (dated March 5, 2015)

DWR and Reclamation Request for Modifications of Revised Order that Approved a Temporary Urgency Change in License and Permit Terms and Conditions Requiring Compliance with Delta Water Quality Objectives in Response to Drought Conditions (dated March 5, 2015)

Compliance with D-1641 Salinity Standards at Emmaton compared to Threemile Slough

The proposed change of the salinity compliance location from Emmaton to Threemile Slough would have very similar effects in 2015 as compared to 2014. This is because the DSM2 modeling that occurred in 2014 used the same Net Delta Outflow Index (NDOI) assumptions through the compliance season as Reclamation and DWR are requesting this year. Therefore, conclusions drawn from the 2014 request can be applied to 2015 and projected water quality results and flows will be very similar to the 2014 projections. Page 31 of the April 29, 2014 TUCP request describes the modeling assumptions used in the Delta modeling forecasts. In the DSM2 modeling simulations, a dry (90%) forecasted hydrology is used as the starting point for determining the necessary NDOI that will result in compliance with the following D-1641 water quality objectives:

- Emmaton – 2.78 mmhos/cm
Or Three Mile
- San Joaquin at Jersey Point – 2.20 mmhos/cm\
- South Fork at Terminous - 0.54 mmhos/cm
- San Joaquin at San Andreas Landing - 0.87 mmhos/cm
- West Canal at Mouth of CCFB – 1.0 mmhos/cm
- DMC at Tracy Pumping Plant – 1.0 mmhos/cm
- Rock Slough - 1.0 mmhos/cm

The forecasted hydrology is modified by adjusting the Sacramento inflow into the model. Using the minimum cost compliance tool, DSM2 is run, varying Sacramento inflow, until it just meets the salinity objectives while keeping the other inflows, exports, diversions, consumptive use and cross channel operations the same. Once the needed Sacramento flow to achieve the water quality objectives is determined, the NDOI is calculated.

Projected salinity and flow impacts for 2015 will be very similar to the 2014 impacts. The needed Net Delta Outflow for current objectives and for a movement of the Emmaton objective to Three Mile Slough will be the similar given the modeling assumptions for both forecasts. However, the needed 2015 Sacramento flow to meet the Emmaton and Three Mile objectives will be less due to lower projected exports in the summer months. A conservative comparison of salinity at Emmaton and Rio Vista is contained the 2015 Biological Review on pages 71-73, figure 51 and 52.

There may be some minor differences in salinity closer to the exports as there is not as much of a movement of Sacramento River flow upstream into Old and Middle River due to projected lower exports in 2015 (see table below). The upstream flow into Old and Middle Rivers for both 2014 and 2015 forecast will be impacted more by consumptive use in the central and south Delta.

The table below shows differences between 2014 and 2015 forecasted flows.

	2014 Forecast	2015 Forecast
Sacramento River	Adjusted to meet D-1641 Water Quality Objectives	Adjusted to meet D-1641 Water Quality Objectives
San Joaquin River	The 2014 forecast shows a flow of approximately 2000 cfs in April between 500 to 1000 cfs during the summer (p.49 of April 2014 petition)	A 2015 February forecast indicates that San Joaquin forecasted flows are approximately 1000 cfs in April falling to between 500 and 1000 cfs during the summer.
Exports (CVP and SWP)	Exports in the 2014 forecast were forecasted to be around 4000 in April falling to approximately 1500 in the summer months	Exports in the 2015 February forecast are estimated to be closer to 1000 cfs in the summer months.
Delta Cross Channel	D-1641 operation	D-1641 operation
Consumptive Use	Delta Coordinated Operations Model	Delta Coordinated Operations Model

Status of Species

Winter-run Chinook salmon

A small number of winter-run Chinook salmon (*Oncorhynchus tshawytscha*) (n=3,015; 90% CI= 2,741-3,290) returned to spawn in the upper Sacramento River in 2014. Of these 3,105 winter-run Chinook, 388 were collected for broodstock at the Keswick trap. Assuming that 3-year old fish make up the majority of each spawning cohort, returning adults in 2014 were produced by a much smaller spawning escapement in 2011 (i.e., 827 adult spawners). The effects of limited cold water storage and loss of temperature control out of Keswick Dam from early September through the fall of 2014 led to substantial egg and fry mortality (Figure 1). Typically, the peak of fry outmigration from the upper Sacramento River has occurred in early-to-mid October, with fish rearing in the middle reaches of the Sacramento River downstream of Red Bluff Diversion Dam (RBDD). However, in 2014, the winter-run Chinook salmon fry population appeared to start moving downstream past RBDD in September and no noticeable peaks in passage have been observed through the current period (Figures 2 and 3). A one-day emigration pulse event occurred in late October, which was associated with a spike in turbidity; but observation of migrating fry passed RBDD have so far remained extremely low even with large precipitation events in early and mid-December and their associated increases in turbidity and river flows.

Because of staffing issues and concerns about debris during the high flows in December, the rotary screw traps at RBDD were operated for just 8 of 31 days during December 2014¹. While this adds some uncertainty to the 2014 brood year passage estimates, historical patterns suggest that most winter-run Chinook salmon juveniles would have passed RBDD before December. Also, the seasonal passage estimates RBDD do include estimates of passage on non-sampled days based on interpolation. So, while it is possible that some of the higher passage days might not have been sampled and the estimated seasonal passage may be somewhat underestimating actual passage, the current RBDD passage estimate is less than half of the estimated passage for brood year 2011 juveniles, despite an adult escapement nearly four times the escapement observed in 2011.

Few winter-run Chinook salmon juveniles are currently being observed in the upper Sacramento River and the annual population estimates remain lower than expected. As of January 14, 2015, an estimated 402,000 winter-run Chinook salmon juveniles have migrated past RBDD (Gruber 2015). Flows from Keswick Dam were reduced during November for cold water pool conservation (Figure 4), and of 89 potential stranding sites along the Sacramento River from Tehama (Los Molinos) to Keswick Dam (about 70 river miles), only nine completely isolated sites were identified to have winter-run salmon trapped in them (Doug Killam, California

¹ Biweekly reports from RBDD are available at:
http://www.fws.gov/redbluff/RBDD%20JSM%20Biweekly/2014/rbdd_jsmp_2014.html

Salmonid and Green Sturgeon Supporting Information for Endangered Species Act Compliance for Temporary Urgency Change Petition Regarding Delta Water Quality January 27, 2015

Department of Fish and Wildlife [CDFW], pers. comm. January 20, 2015). Field biologists attribute the rarity of stranded juveniles in potential stranding locations to rarity of juveniles, not to improved avoidance of stranding relative to previous years.

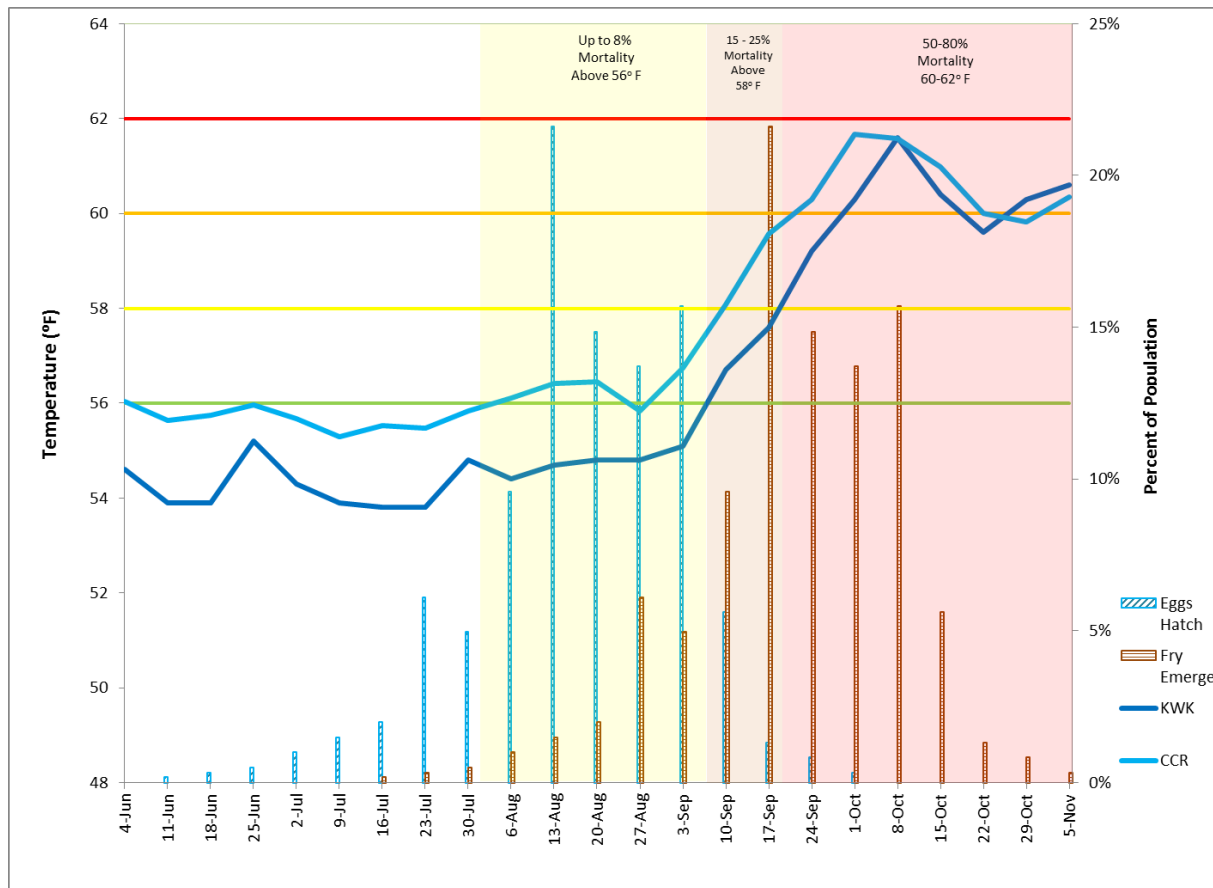


Figure 1. Water temperatures at Keswick Dam (KWK) and Clear Creek Confluence (CCR, WY14 temperature compliance point) and winter-run Chinook salmon early life history between May 1 and November 6, 2014. ²

² Figure supplied by CDFW on January 20, 2015.

Salmonid and Green Sturgeon Supporting Information for Endangered Species Act Compliance for Temporary Urgency Change Petition Regarding Delta Water Quality January 27, 2015

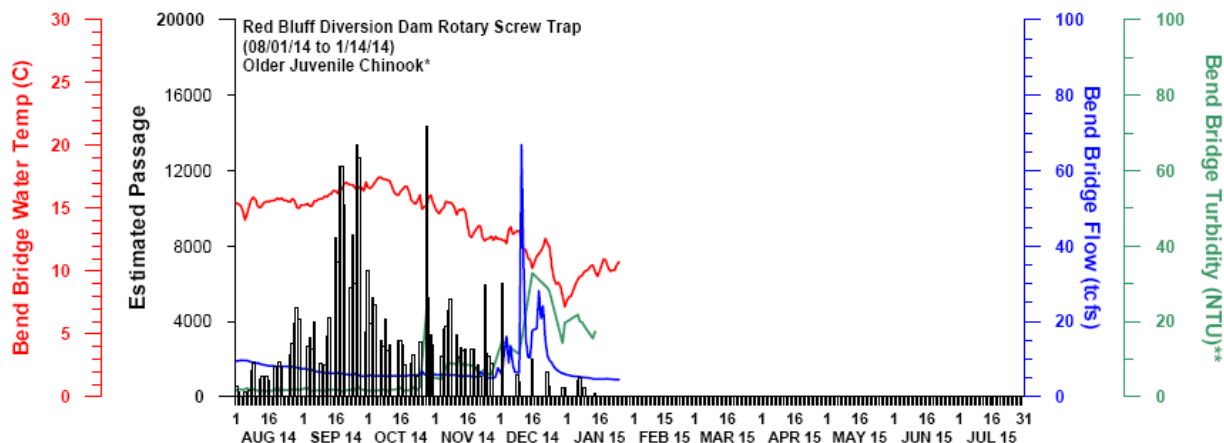


Figure 2. Daily estimated passage of Older Juvenile Chinook Salmon at Red Bluff Diversion Dam (RK 391) and associated environmental data at Bend Bridge (RK 415), BY2014. ³

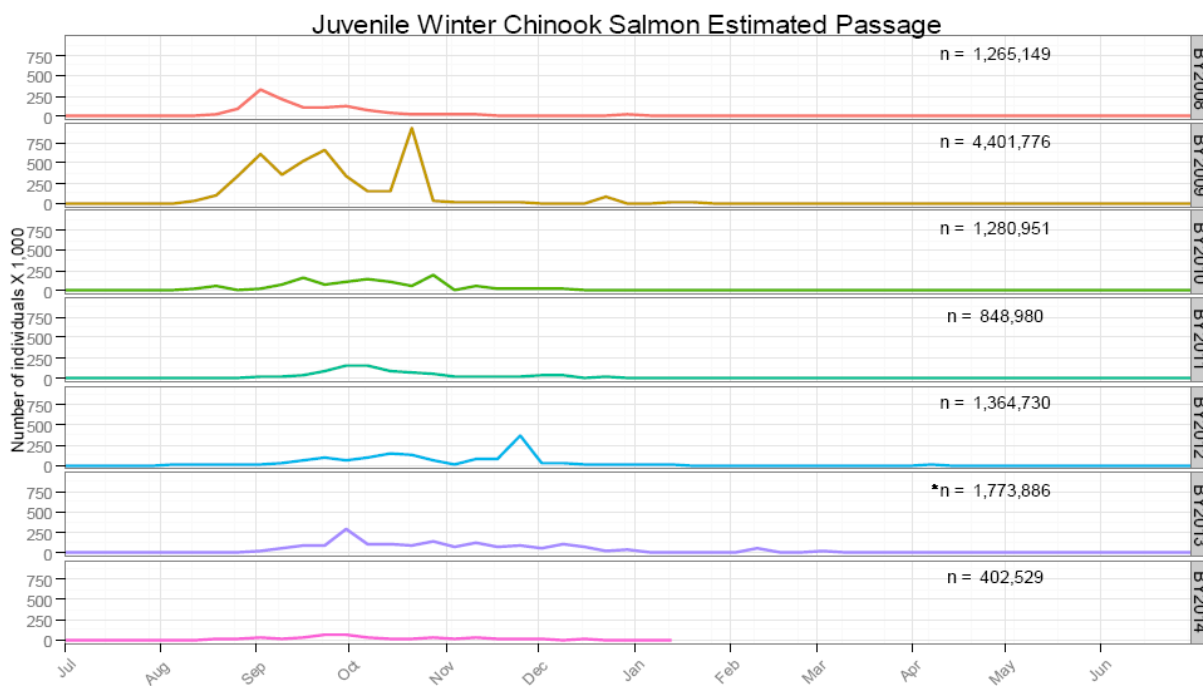


Figure 1. Weekly estimated passage of juvenile winter Chinook Salmon at Red Bluff Diversion Dam (RK391) by brood-year (BY). Fish were sampled using rotary-screw traps for the period July 1, 2008 to present.

Figure 3. Weekly estimated passage of Juvenile Winter-run Chinook Salmon at Red Bluff Diversion Dam (RK 391) by brood year (BY), BY2008-BY2014. ⁴

³ Figure supplied by DWR to DOSS on January 27, 2015.

⁴ Fish were sampled using rotary-screw traps for the period July 1, 2008 to present. Winter-run passage value interpolated using a monthly mean for the period of October 1 through October 17, 2013, due to government shutdown. Figure supplied by USFWS on January 15, 2015.

Salmonid and Green Sturgeon Supporting Information for Endangered Species Act Compliance for Temporary Urgency Change Petition Regarding Delta Water Quality January 27, 2015

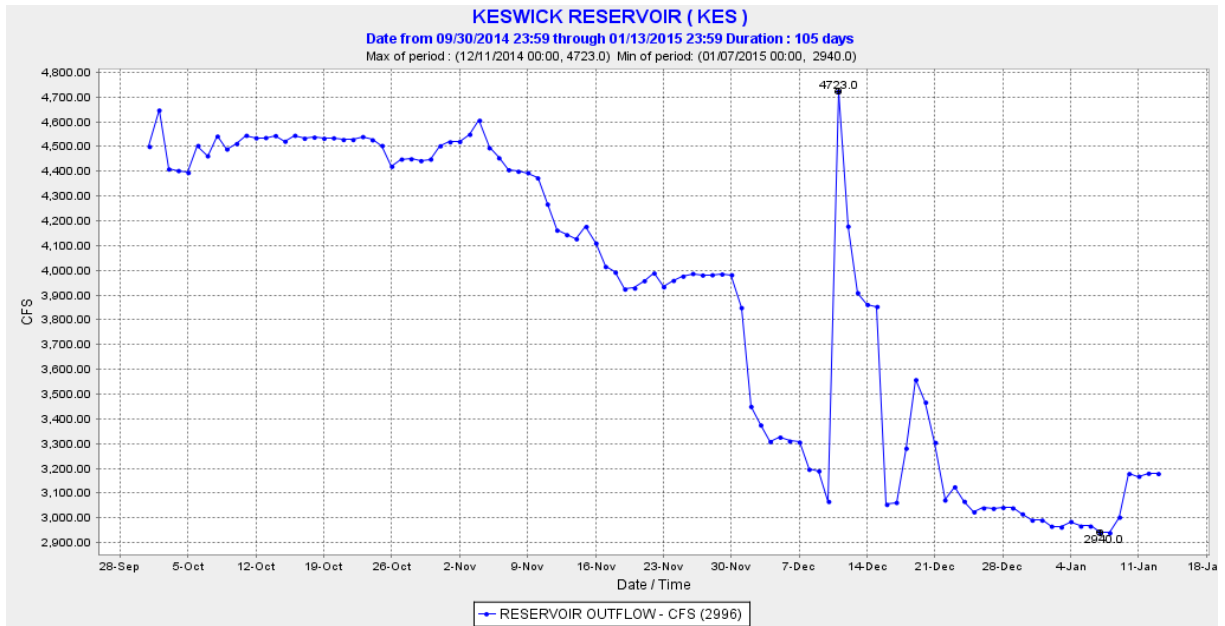


Figure 4. Keswick Reservoir outflow measured at Keswick Reservoir (KES) for water year (WY) 2015.⁵

These observations suggest that brood year (BY) 2014 winter-run Chinook salmon experienced substantial negative effects associated with drought-related environmental conditions. These effects are predicted to include significantly greater temperature mortality during the incubation of eggs and juvenile rearing stages than has previously been observed, truncation of the migration period from natal habitats due to the loss of a substantial proportion of the later portion of the incubating eggs and rearing juveniles, and significant reductions in the expression of a diversity of juvenile life history traits (parr and smolt migrants).

Del Rosario et al. (2013) described multiple pulses of distinctly different-sized juvenile winter-run Chinook salmon typically moving through the Lower Sacramento River past Knights Landing from November to January. These pulses of fish are associated with flow pulses greater than $400\text{m}^3/\text{s}$ (approximately 14,000 cfs) as measured at Wilkins Slough. For juvenile winter-run Chinook salmon BY2014 (through January 20, 2015), observations at Knights Landing and Tisdale Weir rotary screw traps (RST) indicate two migration pulses of juveniles have moved downstream into the Delta. The initial pulse emigrated during a storm event in late October that did not increase river flows on the Sacramento River substantially, but did increase turbidity in the mainstem Sacramento River. The second pulse emigrated during a large storm event in mid-December (Figure 3, Table 1). As a result, it appears that winter-run Chinook salmon juveniles

⁵ Downloaded from CDEC on January 14, 2015.

Salmonid and Green Sturgeon Supporting Information for Endangered Species Act Compliance for Temporary Urgency Change Petition Regarding Delta Water Quality January 27, 2015

emigrated from the upper Sacramento River between mid-October and mid-December, and the majority of the population (>95%) has moved out of the riverine system and entered the Delta.

Based on the 2014 adult winter-run Chinook salmon escapement (3,015 spawners, including 388 collected as hatchery broodstock), NMFS recently estimated a juvenile production estimate (JPE)⁶ for both natural-origin (124,251) and hatchery-produced (188,500) winter-run Chinook salmon entering the Delta during WY 2015. This year's JPE reflects a number of significant changes as a result of recommendations by the (1) Long Term Biological Opinion Independent Review Panel, (2) Interagency Ecological Program Winter-Run Project Work Team, and (3) internal discussions by NMFS with the NMFS-Southwest Fisheries Science Center. While NMFS presented three methods of calculating the JPE—historical NMFS JPE method, Cramer Fish Science (CFS) Model, and the Juvenile Production Index (JPI) from USFWS—NMFS decided that the JPI method was a better fit because both the NMFS JPE and CFS models inaccurately represented the extreme drought conditions and associated early life stage losses due to high temperatures that occurred in 2014 as described previously (Figure 1). On the basis of the JPE, the authorized level of incidental take under the 2009 biological opinion for the Long Term Operations for the combined CVP/SWP Delta pumping facilities from October 1, 2014 through June 30 2015 was set at 2,490 natural (non-clipped, i.e., wild) winter-run Chinook salmon juveniles. The incidental take for hatchery-produced winter-run Chinook salmon juveniles was set at 1,885.

Due to the very low estimated abundances of juvenile winter-run Chinook salmon entering the Delta, observational data from sampling programs could be negatively biased due to rarity of observing winter-run Chinook salmon in the monitoring efforts. Nonetheless, observations from the Delta Juvenile Fish Monitoring Program's beach seining and trawling surveys, and special drought monitoring surveys (i.e., trawling efforts at Jersey and Prisoners Point) to date support the conclusion that winter-run Chinook salmon have migrated downstream and are currently rearing extensively in the Lower Sacramento and Delta survey regions (Table 2). Natural origin winter-run Chinook salmon have been observed weekly in very low densities at the CVP and SWP facilities since December 14, 2014 (combined loss =110, as of January 26, 2015); this also suggests that some juveniles are also present in the south Delta waterways. Finally, few winter-run Chinook salmon juveniles have been observed at Chipps Island suggesting that the majority of the population has not yet migrated to the ocean and is currently rearing in the Delta (Table 2). This broad distribution of juvenile winter-run Chinook salmon across the Delta during the winter

⁶ http://www.westcoast.fisheries.noaa.gov/publications/Central_Valley/Water%20Operations/20150116_nmfs_winter-run_juvenile_production_estimate_nr.pdf

Salmonid and Green Sturgeon Supporting Information for Endangered Species Act Compliance for Temporary Urgency Change Petition Regarding Delta Water Quality January 27, 2015

Table 1. Raw weekly fish observation data from Tisdale and Knights Landing rotary screw traps in WY2015.⁷

	Tisdale								Knights Landing								
	Wild Juveniles					Ad clipped			Weekly total	Wild juveniles					Ad clipped		Weekly total
	Fall	Spring	Winter	Late fall	Steelhead	Salmon	Steelhead	Fall		Spring	Winter	Late fall	Steelhead	Salmon	Steelhead		
10/4/2014 - 10/10/2014	0	0	0	0	0	0	0	0	0	0	1	0	0	0	0	0	1
10/11/2014 - 10/17/2014	0	0	0	0	0	0	0	0	0	0	0	0	0	0	0	0	0
10/18/2014 - 10/24/2014	0	0	0	0	0	0	0	0	0	1	0	0	0	0	0	0	1
10/25/2014 - 10/31/2014	0	2	117	2	0	0	0	121	0	1	95	4	0	0	0	0	100
11/1/2014 - 11/7/2014	0	1	2	0	0	0	0	3	0	0	2	0	0	0	0	0	2
11/8/2014 - 11/14/2014	0	0	1	0	0	0	1	2	0	0	2	0	0	0	0	0	2
11/15/2014 - 11/21/2014	0	0	3	1	0	0	0	4	0	0	3	0	0	0	0	0	3
11/22/2014 - 11/28/2014	0	0	3	0	0	0	0	3	0	0	2	0	0	0	0	0	2
11/29/2014 - 12/5/2014	0	0	7	0	0	2	0	9	0	0	2	0	0	0	0	0	2
12/6/2014 - 12/12/2014	10	14	10	2	0	5	0	41	17	50	32	8	0	24	0	131	
12/13/2014 - 12/19/2014	169	9	0	2	0	2	0	182	148	88	5	1	0	4	0	246	
12/20/2014 - 12/26/2014	654	35	24	5	1	6	0	725	411	112	14	4	0	8	0	549	
12/27/2014 - 1/2/2015	148	22	1	1	0	0	0	172	13	6	0	1	0	0	0	20	
1/3/2015 - 1/9/2015	91	61	6	0	2	0	0	160	15	13	0	2	0	2	0	32	
Species Totals	1072	144	174	13	3	15	1		604	278	158	21	0	38	0		

⁷ Data updated through January 9, 2015. These raw catch numbers have not been expanded to account from inoperable traps, sampling period variation, and sampling cone variation.

Salmonid and Green Sturgeon Supporting Information for Endangered Species Act Compliance for Temporary Urgency Change Petition Regarding Delta Water Quality January 27, 2015

is common and was described initially by Erkkila *et al.* (1951) prior to the initiation of CVP operations in the early 1950's.

Table 2. Weekly Fish Observation Data from the Delta Juvenile Fish Monitoring Program in WY2015.⁸

Beach Seine Region	Wild juveniles					Ad clipped		Weekly Total
	Fall	LateFall	Spring	Winter	Steelhead	Chinook	Steelhead	
Bay East	0	0	0	0	0	0	0	0
Bay West	0	0	0	0	0	0	0	0
Central Delta	3	0	1	0	0	0	0	4
Lower Sacramento	22	0	3	6	0	0	0	31
North Delta	23	0	8	0	0	1	0	32
Sacramento	263	8	177	54	1	13	0	516
South Delta	0	0	0	0	0	0	0	0
San Joaquin	0	0	0	0	0	0	0	0
Trawl								
Sacramento	103	5	21	15	0	16	0	160
Chippis	2	20	0	5	0	62	0	89
Jersey Point	22	1	3		0	0	0	26
Prisoners Pt	5	1	3	1	0	0	0	10
Species Total	443	35	216	81	1	92	0	

The observations described herein (i.e., RBDD, Tisdale, and Knights Landing RSTs; Delta Juvenile Fish Monitoring Program's beach seining and trawling surveys, and special drought monitoring [i.e., trawling surveys at Jersey and Prisoner's Point]), have been reviewed by the Delta Operation for Salmon and Sturgeon (DOSS) work team to evaluate the distribution of winter-run Chinook salmon juveniles in the Central Valley. Based on the currently available data, DOSS estimates that the majority (>95%) of winter-run Chinook salmon are in the Delta, while <5% either remain upstream of Knights Landing or have already exited the Delta past Chipps Island. This estimate is based on the best professional judgment of the biologists participating on the DOSS work team.

At this time, adult winter-run Chinook salmon are starting to enter the Sacramento River system and have begun to migrate to the upper reaches of the river. These adult winter-run Chinook salmon must hold in the upper Sacramento River between the RBDD and the impassable Keswick Dam until they are ready to spawn during the summer. These fish require cold water holding habitat for several months prior to spawning to allow for maturation of their gonads, and then subsequently require cold water to ensure the proper development of their fertilized eggs, which are highly sensitive to thermal conditions during this embryo development period (i.e., embryogenesis). Adults returning to the river in 2015 are predominantly members of the cohort

⁸ Data updated through January 13, 2015.

Salmonid and Green Sturgeon Supporting Information for Endangered Species Act Compliance for Temporary Urgency Change Petition Regarding Delta Water Quality January 27, 2015

from BY2012 (assuming a 3-year cohort cycle). Based on cohort replacement rate (CRR) estimates, BY2012 had the fifth lowest CRR since 1992.

Spring-run Chinook Salmon

The 2014 spawning run of spring-run Chinook returning to the upper Sacramento River was lower in four of seven locations compared to the 2013 escapement, with considerably lower escapement observed in Butte Creek and Feather River Hatchery (Table 3).

Table 3. Spring run Chinook escapement in 2013 and 2014.

Location	2013	2014	Source
Battle Creek	608	429	Laurie Earley, USFWS
Clear Creek	659	95	
Antelope Creek	0	7	Matt Johnson, DFW
Mill Creek	644	679	
Deer Creek	708	830	
Butte Creek	16783	4815	Clint Garman, DFW
Feather River Hatchery	4294	2825	Penny Crenshaw, DWR

Spring-run Chinook salmon eggs in the Sacramento River underwent significant, and potentially complete, mortality due to high water temperature downstream of Keswick Dam starting in early September when water temperatures downstream of Keswick Dam exceeded 56°Fahrenheit (F) (see water temperatures during September and October in Figure 1). Spawning of spring-run Chinook salmon in the Sacramento River Basin occurs approximately from mid-August through mid-October, peaking in September. This peak in spawning activity corresponded with the high Sacramento River temperatures downstream of Keswick Dam throughout the fall of 2014, and illustrates the potential for high egg and alevin mortality. Spring-run Chinook salmon eggs spawned in the tributaries to the Sacramento River may also have experienced warmer temperatures this year due to low flows through late October, as well as scouring or sedimentation during rain events from late October through December. Extremely few juvenile spring-run Chinook salmon have been observed this year migrating downstream past RBDD (Figure 5) during high winter flows, when spring-run Chinook salmon originating from the upper Sacramento River, Clear Creek, and other northern tributaries are typically observed to outmigrate. While, as noted for winter-run Chinook, the rotary screw traps at RBDD were operated for just 8 of 31 days during December 2014⁹, the low RBDD passage estimates are a concern. A second pulse of juvenile spring-run Chinook salmon typically migrate past RBDD in the springtime (Poytress et al. 2014). However, this second pulse appears to positively bias

⁹ Biweekly reports from RBDD are available at: http://www.fws.gov/redbluff/RBDD%20JSM%20Biweekly/2014/rbdd_jsmp_2014.html

Salmonid and Green Sturgeon Supporting Information for Endangered Species Act Compliance for Temporary Urgency Change Petition Regarding Delta Water Quality January 27, 2015

estimates of spring Chinook passage due to the millions of unmarked fall-run Chinook salmon hatchery production fish falling into the spring-run Chinook salmon category based on the length-at-date run assignments (Poytress et al. 2014).

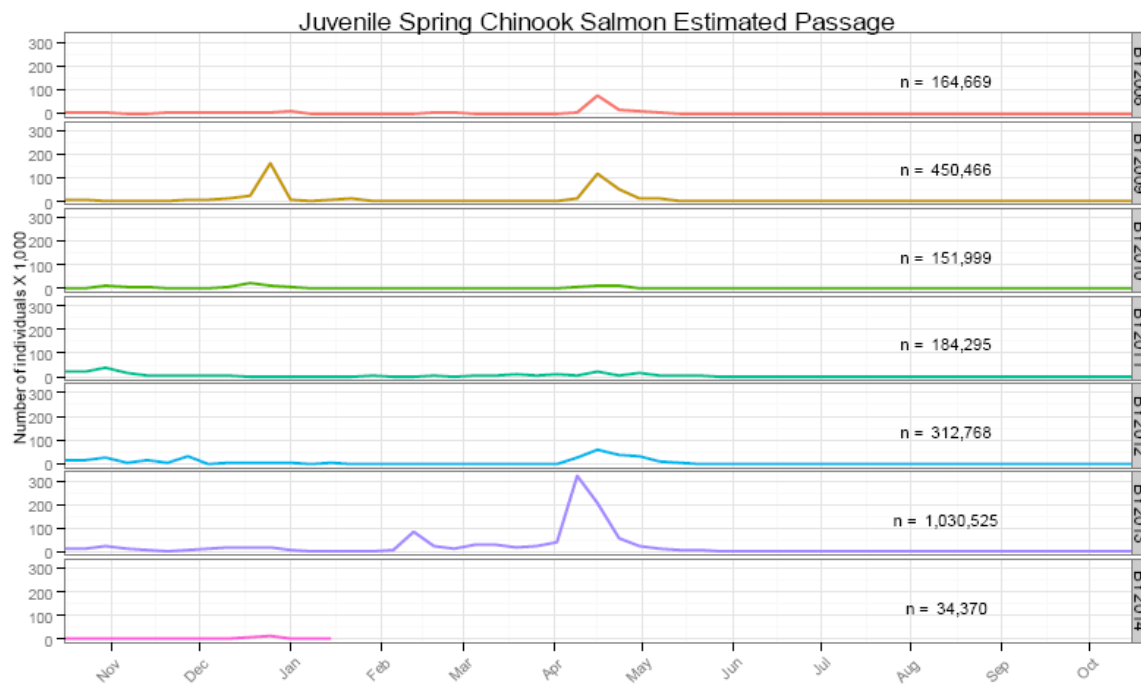


Figure 5. Weekly estimated passage of Juvenile Spring-Run Chinook Salmon at Red Bluff Diversion Dam (RK 391) by brood year (BY).¹⁰

In fall 2014, yearling spring-run Chinook salmon from Mill and Deer creeks experienced flow and temperature conditions typically associated with the outmigration of this life history expression from these tributaries. Although not currently monitored with RSTs, these tributaries have experienced flows (Figure 6-7) exceeding “First Alert” thresholds identified in the NMFS BiOp Action IV.1.2. Recent analyses of multiple years of RST data have determined that 99% of outmigrating yearlings are captured at flows greater than 95 cfs (Kevin Reece, DWR, pers. comm.). Based on the currently available data, DOSS estimates that the majority (80-90%) of yearling spring-run Chinook salmon are in the Delta, while <5% remain upstream of Knights Landing and <15% have already exited the Delta past Chipps Island. This estimate is based on the best professional judgment of the biologists participating on the DOSS work team.

Spring-run young-of-the-year (YOY) sized Chinook salmon juveniles have been observed at the Tisdale Weir and Knights Landing RSTs since early December, 2014 (Table 1). Likewise,

¹⁰ Fish were sampled using rotary-screw traps for the period July 1, 2008 to present. Figure supplied by USFWS on January 15, 2015.

Salmonid and Green Sturgeon Supporting Information for Endangered Species Act Compliance for Temporary Urgency Change Petition Regarding Delta Water Quality January 27, 2015

juvenile YOY spring-run Chinook have been observed in the catch from multiple Delta beach seine regions, and in the standard trawling and special drought monitoring trawling surveys, including those in the Central Delta. However, as of January 18, 2015, neither yearling nor YOY spring-run Chinook salmon have been observed at the state and federal fish collection facilities in the South Delta. Based on the currently available data, DOSS estimates up to half (25-50%) of YOY spring-run Chinook salmon are in the Delta, while 50-75% remain upstream of Knights Landing and <5% have already exited the Delta past Chipps Island. This estimate is based on the best professional judgment of the biologists participating on the DOSS work team.

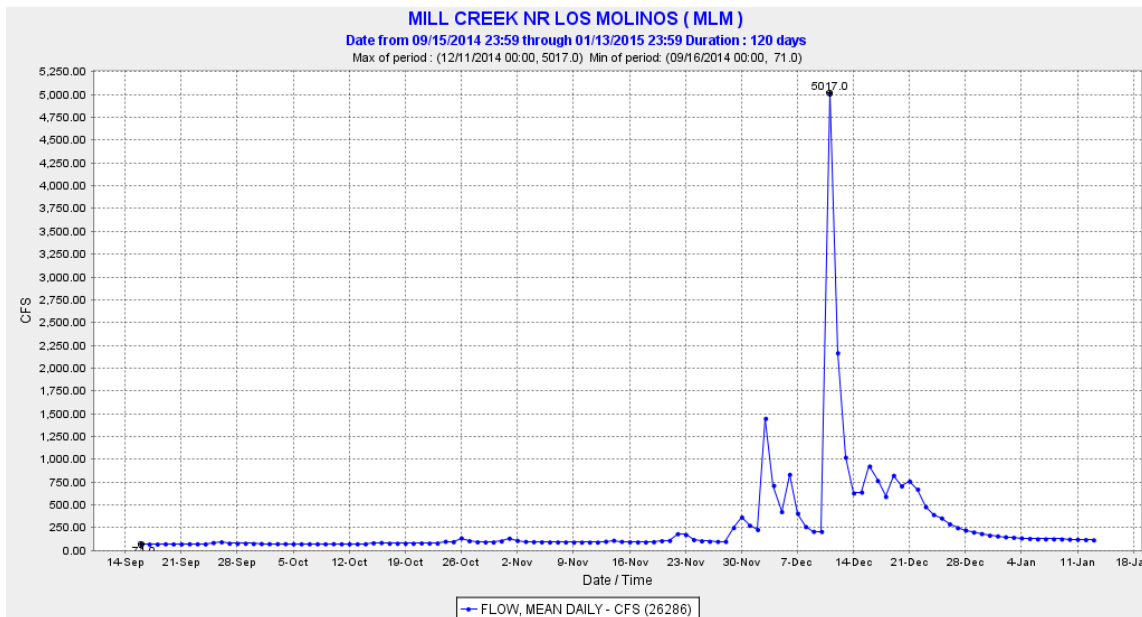


Figure 6. Mill Creek mean daily flow (cubic feet per second) measured near Los Molinos (MLM) during WY2015.¹¹

¹¹ Downloaded from CDEC on January 14, 2015.

Salmonid and Green Sturgeon Supporting Information for Endangered Species Act Compliance for Temporary Urgency Change Petition Regarding Delta Water Quality January 27, 2015

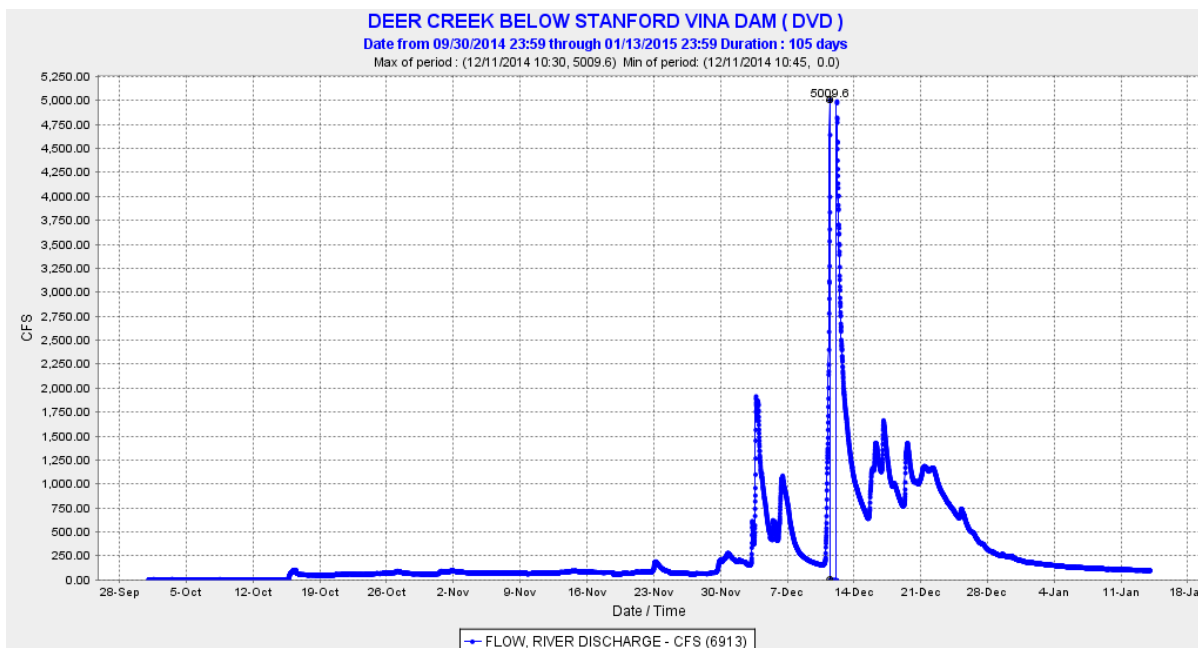


Figure 7. Deer Creek discharge (cubic feet per second) measured downstream of Stanford Vina Dam (DVD) during WY2015.¹²

Steelhead

California Central Valley steelhead (*Oncorhynchus mykiss*) smolts are seldom recovered in Sacramento River and Delta fish monitoring efforts due to sampling biases related to their larger size and enhanced swimming ability. False negatives (*i.e.*, zero catches when the target species is present) are more likely with steelhead smolts than smaller older juvenile Chinook salmon, but historic data can be assessed to consider their typical periodicity in Delta monitoring efforts. Between 1998 and 2011, temporal observations of wild steelhead juveniles (n=2,137) collected in Delta monitoring efforts occurred less than 10% of the time in January, >30% of the time during February, and >20% of the time during March.

Observed patterns of outmigrating *O. mykiss* from BY2014 at RBDD appear most similar to that of BY2011 (Figure 8); however, there was no peak migration observed in the typical August/September period. For WY2015 (as of January 12, 2015), five unmarked (two on 10/15/2014; and three between 1/7/2015 and 1/11/2015) and 828 marked steelhead (1/7/2015 to 1/12/2015) were captured at the GCID RST. The latter marked fish likely originated from a Coleman release of 688,000 brood year 2014 steelhead (100% marked with adipose clip only) in the Sacramento River at Bend Bridge (fish released in two groups: 144,700 on January 2, 2015, and 543,300 on January 5-9, 2015). For WY2015 (as of January 23, 2015), three unmarked (two captured between 1/5/2015 and 1/8/2015, and one on 12/22/2014) and 11 marked steelhead (first on 11/8/2014, 10 since 1/12/2015) were observed at the Tisdale Weir RST; and 12 clipped steelhead were captured at Knights Landing RST as of 1/22/2015.

¹² Downloaded from CDEC on January 14, 2015.

Salmonid and Green Sturgeon Supporting Information for Endangered Species Act Compliance for Temporary Urgency Change Petition Regarding Delta Water Quality January 27, 2015

For WY2015 (as of January 23, 2015), one steelhead (acoustic tagged) was observed in the Sacramento beach seine monitoring at Miller Park (300mm fish on 12/8/2014); one clipped steelhead was observed at Sherwood Harbor on 1/23/2015, but not at any of the other trawl locations (i.e, Chipps Island Trawl, Mossdale Trawl, or Jersey Point/Prisoner's Point Trawl); and three steelhead were observed at the SWP (one unmarked on 11/16/2014 for a total salvage of 4, two clipped: one each on 1/23/15 and 1/25/15 for a total salvage of 8) and none at the CVP fish collection facilities at the South Delta CVP/SWP export pumps.

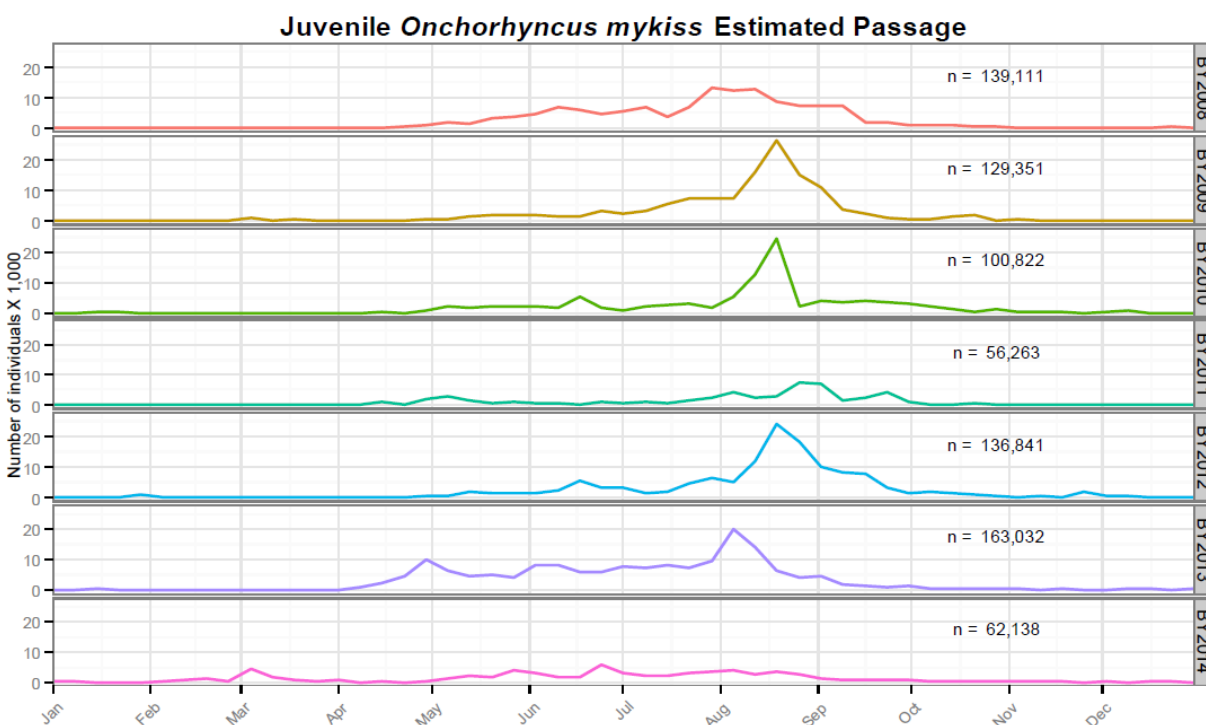


Figure 8. Weekly estimated passage of *O. mykiss* at Red Bluff Diversion Dam (RK 391) by brood year (BY).¹³

Green Sturgeon

Information on green sturgeon is extremely limited. Adult green sturgeon will migrate into the upper Sacramento River through the Delta between March and June. Spawning in the upper Sacramento River was documented during 2014. A review of telemetric data found 26 tagged green sturgeon entered the San Francisco Bay with only half migrating upstream of RBDD (M. Thomas, UC Davis, pers. comm.). Adult green sturgeon have been observed to overwinter in the Sacramento River, and a number of the tagged 2014 adults still appear to be present in the upper Sacramento River as of January 14, 2015 (R. Chase, Reclamation, pers. comm.). Larval green

¹³ Fish were sampled using rotary-screw traps for the period July 1, 2008 to present. Figure supplied by USFWS on January 15, 2015.

Salmonid and Green Sturgeon Supporting Information for Endangered Species Act Compliance for Temporary Urgency Change Petition Regarding Delta Water Quality January 27, 2015

sturgeon were observed at RBDD (n=319). This was greater than the long-term average of 186 fishes (Figure 9). At RBDD, two juvenile green sturgeon were also observed in the fall of 2014.

At GCID, ten juvenile green sturgeon (TL= 110-285) were observed from September 2014 to January 19, 2015. Green sturgeon observations are extremely rare in the Delta primarily related to the use of monitoring gear types that are not designed to sample the benthic habitats where green sturgeon are most likely to be found if they are present. Although the lower Sacramento and Delta fish monitoring surveys do not target benthic environments they have captured juvenile green sturgeon in the past, but no sturgeon have been observed in those surveys in recent years. Likewise, green sturgeon have not been observed at the state and federal fish collection facilities in the South Delta in recent years. In 2011 more than 3,000 juvenile green sturgeons were captured in the RSTs at RBDD, however no green sturgeon were observed in any of this years' river, Delta, or Bay fish monitoring surveys.

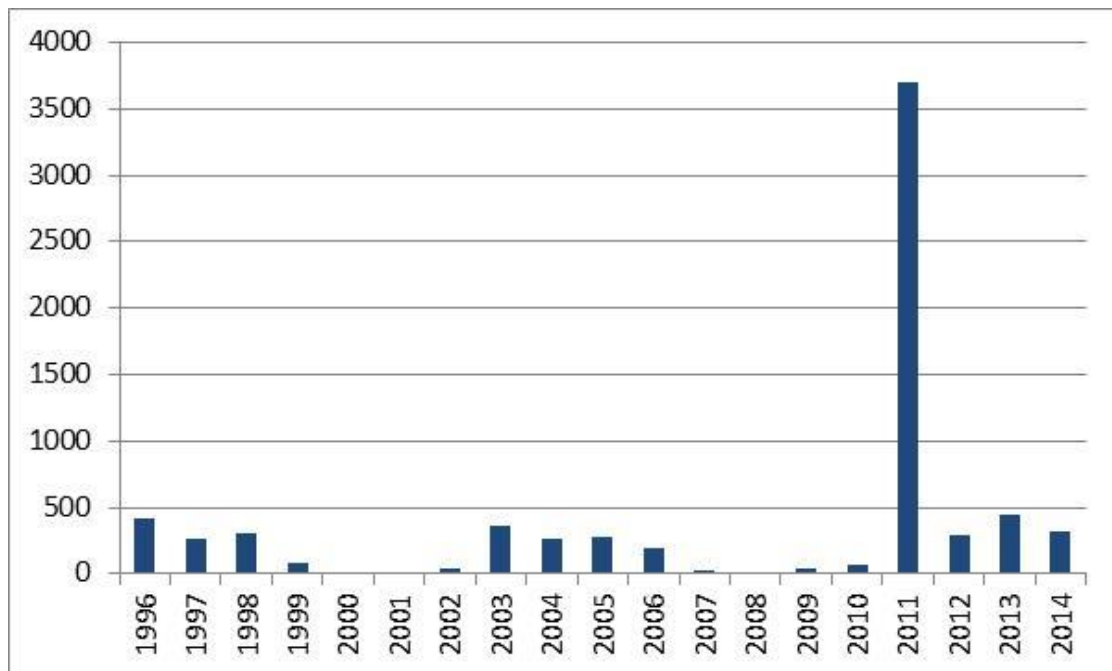


Figure 9. Larval Green sturgeon counted at Red Bluff Diversion Dam rotary screw traps.¹⁴

¹⁴ The annual average catch is 426 fish. In 2011, an egg was observed directly upstream of the rotary traps; thus, the large number of fish in 2011 represents a unique sampling of a spawning event (Josh Gruber, USFWS, pers comm.). If 2011 data is removed, the annual average of juvenile green sturgeon counted is 183 fishes.

Proposed Action

See Project Description for February – March 2015 Drought Response Actions provided to support Endangered Species Act consultation (Reclamation 2015).

Analytical Framework

Methods and Metrics

A conceptual model for impacts from drought management actions was developed as part of an interagency assessment of the WY2014 drought on winter-run Chinook salmon. The conceptual model describes freshwater behavioral responses to indicators of environmental conditions (e.g., outflow, inflow, Delta Cross Channel [DCC] gates, and exports) that are expected to be affected by the Petition’s Project Description. The NMFS BiOp (2009) was reviewed regarding biological linkage to these various actions.

This conceptual model was modified to provide a qualitative assessment of effects predicted to be linked to the four elements of this WY 2015 February and March Project Description: (1) modification to D-1641 Net Delta Outflow Index (NDOI), (2) modification to D-1641 export limits, (3) modification to the D-1641 DCC gate operation, and (4) modification of D-1641 San Joaquin River flow standard. This model highlights the biological linkages between drought management actions in the project description with predictions that can be assessed from the literature and modeling completed (Figure 10). Although OMR modifications are not proposed in the Project Description, they may be incorporated into a Temporary Urgency Change Petition (TUCP) request at a later date.

M A N A G E M E N T L I N K A G E A S S E S S M E N T	<p>DCC Gate Operation (Interior delta salinity)</p> <ul style="list-style-type: none"> Route entrainment DJFMP periodicity Changes in DSM2 proportion daily flow Delta survival information 	<p>Outflow (NDOI) (Change in Location)</p> <ul style="list-style-type: none"> Tidal influence Migration rate Rearing period Survival rate Changes in DSM2 velocity characteristics Changes in DSM2 proportion daily flow Delta survival information 	<p>Inflow (Storage impacted by DOP, seasonal depletions)</p> <ul style="list-style-type: none"> Migration rate Rearing period Survival rate Changes in DSM2 velocity characteristics Changes in DSM2 proportion daily flow Delta survival information 	<p>OMR (change in BiOp criteria)</p> <ul style="list-style-type: none"> Route entrainment Migration rate Rearing period Survival rate SD/CD DJFMP presence/absence Facility salvage (Density, total, timing) Delta survival information 	<p>Exports (E/I calculation)</p> <ul style="list-style-type: none"> Route entrainment Migration rate Facility survival SD/CD DJFMP presence/absence Facility salvage (Density, total, timing) Delta survival information
---	--	---	--	---	---

Figure 10. Conceptual model of drought contingency plan elements and their biological linkage to salmonids and assessment information available for evaluation.

Salmonid and Green Sturgeon Supporting Information for Endangered Species Act Compliance for Temporary Urgency Change Petition Regarding Delta Water Quality January 27, 2015

To evaluate February and March impacts to listed species due to Delta hydrodynamics caused by the proposed action's changes in outflow and exports, Delta Simulation Model II (DSM2) simulations were performed and evaluated for three different regulatory and operational management decision scenarios (Table 4). It is likely that actual conditions will differ somewhat from the modeled scenarios. Recent meteorological patterns appear to show a decoupled Sacramento and San Joaquin Valley storm pattern (with more rain falling in the Sacramento River basin), and if this continues, it is possible that actual Sacramento River outflow at Freeport could reach the modeled quantities, while actual San Joaquin outflow would not. In particular, if San Joaquin River flows at Vernalis remain low (<850 cfs) and pumping is increased as outflow is greater than 7,100 cfs, there may be a greater impact to San Joaquin fish than indicated in the results of the modeled scenarios. This increases the uncertainty of assessments of impacts to San Joaquin River steelhead.

Table 4. DSM2 regulatory and operational scenarios for February and March 2015 developed for biological review.

Scenario Name	Outflow (cfs)	Freeport flow (cfs)	Vernalis flow (cfs)	Combined Exports (cfs)	OMR (cfs)
4,000 Outflow	4,000	5,600	500	1,500	-1,400
5,500 Outflow	5,500	9,100	500	3,500	-3,200
99% Mod	7,100	11,700	850	6,000	-5,000
90% Least	11,400	15,300	1,400	6,400	-5,000

DSM2 modeling outputs for each scenario were used to evaluate the distribution of 15-minute flow and velocity values for multiple channels including:

- Upstream of Head of Old River (Channel 6)
- Downstream of Head of Old River (Channel 9)
- Upstream of Stockton Deepwater Shipping Channel (Channel 12)
- Downstream of Stockton Deepwater Shipping Channel (Channel 21)
- Turner Cut (Channel 173)
- Columbia Cut (Channel 160)
- Downstream of Head of Old River (Channel 54)
- Grant Line Canal (Channel 81)
- Old River at San Joaquin River (Channel 124)
- Jersey Point on San Joaquin River (Channel 49)
- Sherman Island on Sacramento River (Channel 434)
- Three Mile Slough near San Joaquin River (Channel 310)
- Sherman Island on San Joaquin River (Channel 50)

Salmonid and Green Sturgeon Supporting Information for Endangered Species Act Compliance for Temporary Urgency Change Petition Regarding Delta Water Quality January 27, 2015

- Sacramento River upstream of Delta Cross Channel (Channel 421)
- Sacramento River upstream of Georgiana Slough (Channel 422)
- Sacramento river downstream of Georgiana Slough (Channel 423)
- Sacramento River near Cache Slough (Channel 429)

Hydrodynamic metrics, such as daily proportion positive velocity and daily mean velocity, were used to assess changes in the Delta at these locations. Daily proportion positive velocity is the percentage of the day that river flows have a positive velocity value (flows in downstream direction). Daily mean velocity is the average of all velocities values summed over the 24 hour period which takes into account the effects of tidal stage on velocity magnitudes. Distributions of these hydrodynamic metrics under the different outflow and export ranges for each scenario were also examined to qualitatively describe comparisons between different operational conditions likely to occur under the Project Description.

We discuss effects within the Delta during February and March using currently available species distribution and abundance data along with expected upcoming life stage periodicity information. To evaluate impacts to listed species due to Delta outflow changes, DCC gate configuration, and Delta hydrodynamics caused by the proposed February – March 2015 drought response actions, relevant peer-reviewed literature on these factors and fish biology, behavior, and survival are reported. Results from these sources were used to describe modified operation of the DCC gates on reach-specific and through Delta survival.

Effects Analysis

January Forecasts

Current storage in Shasta and Folsom reservoirs is greater than in January 2014, yet remains low compared to long term historical conditions. Storage in Trinity, Oroville, and New Melones reservoirs remains lower than January 2014 storage levels in these reservoirs. CVP/SWP operators and fishery agencies have been attempting since fall 2014 to conserve cold water pools system-wide in these reservoirs for listed species' summer temperature and habitat requirements. The January 50%, 90%, and 99% exceedance forecasts for WY 2015 projects reservoir volumes throughout spring and summer operations that are below their historic averages for those months (Tables 5 -7). Actual January 2014 Delta conditions are between the 90% and 99% exceedance forecasts (Table 8).

End-of-April (EOA) storages, representing the end of the reservoir storage conservation period, are projected to be between approximately 3,030 TAF (90% forecast) and 4,140 TAF (50% forecast) in Shasta Reservoir. Although there remains a significant range of possible temperature management outcomes for the Sacramento River, neither forecast allows for targeting the furthest downstream temperature compliance point target of 56°F between April and September

Salmonid and Green Sturgeon Supporting Information for Endangered Species Act Compliance for Temporary Urgency Change Petition Regarding Delta Water Quality January 27, 2015

at Bend Bridge. Additionally, if the 90% forecast is realized, maximum Shasta Reservoir elevation would limit the flexibility of the Shasta Temperature Compliance Device to only the Middle, Lower, and Side gates, which is similar to temperature control condition in WY2014. Furthermore, the considerable precipitation that would be necessary to attain a 50% forecasted EOA Shasta Reservoir storage appears highly unlikely since recent meteorology has reflected less precipitation than was anticipated under even the 90% forecast.

These factors are reasonably likely to result in extremely high egg mortality or even complete failure of natural brood year 2015 spring-run Chinook and winter-run Chinook below Keswick due to water temperature exceedances above critical thresholds. Relaxation of Delta outflow standards and Vernalis flow standards, while still continuing to meet required tributary releases from Oroville, Folsom, and New Melones (Reclamation 2015), will enhance the opportunities for summertime cold water management across CVP/SWP operated reservoirs in WY2015.

Table 5. 50% Exceedance Forecast

January 1 - 50% HYDROLOGIC EXCEEDENCE

RESERVOIRS	END OF MONTH STORAGES (TAF)								
	2015								
	JANUARY	FEBRUARY	MARCH	APRIL	MAY	JUNE	JULY	AUGUST	SEPTEMBER
Trinity	917	1019	1172	1287	1199	1080	958	867	783
Shasta	2188	2843	3498	3835	3898	3611	3195	2856	2733
Folsom	491	486	587	646	878	935	825	694	642
Oroville	1463	1933	2431	2742	2900	2910	2374	1883	1523
New Melones	583	635	684	675	655	597	502	397	322

RESERVOIRS	MONTHLY AVERAGE RELEASES (CFS)								
	2015								
	JANUARY	FEBRUARY	MARCH	APRIL	MAY	JUNE	JULY	AUGUST	SEPTEMBER
Trinity	300	300	300	550	4200	2100	1100	450	450
Sacramento	3250	3250	3250	5000	7000	10700	11050	9500	6200
American	900	5000	4700	4550	2100	2300	3400	3700	2250
Feather	950	950	800	1800	1050	1050	8600	8050	6950
Stanislaus	200	200	200	650	750	500	350	350	250

	DELTA SUMMARY (CFS)								
	2015								
	JANUARY	FEBRUARY	MARCH	APRIL	MAY	JUNE	JULY	AUGUST	SEPTEMBER
Rio Vista Flows	11150	27100	22300	13950	8200	6250	10600	10100	8850
Sac River at Freeport	13250	31750	26350	17250	11450	11700	19800	18950	16600
SJ River at Vernalis	1450	3150	3000	2650	3100	1400	1100	1050	950
Computed Outflow	13000	31900	27150	17950	11400	7500	6500	5450	4450
Combined Project Pumping	3550	5100	3300	1550	1600	2400	10500	11250	11200

Salmonid and Green Sturgeon Supporting Information for Endangered Species Act Compliance for Temporary Urgency Change Petition Regarding Delta Water Quality January 27, 2015

Table 6. 90% Exceedance Forecast.

January 1 - 90% HYDROLOGIC EXCEEDENCE

END OF MONTH STORAGES (TAF)

RESERVOIRS	2015								
	JANUARY	FEBRUARY	MARCH	APRIL	MAY	JUNE	JULY	AUGUST	SEPTEMBER
Trinity	888	926	1007	1075	967	862	761	658	599
Shasta	2036	2389	2751	2889	2815	2566	2261	1994	1875
Folsom	465	537	640	642	646	488	316	229	210
Oroville	1403	1641	1926	2067	2037	1874	1682	1523	1485
New Melones	543	544	537	492	411	333	255	180	123

MONTHLY AVERAGE RELEASES (CFS)

RESERVOIRS	2015								
	JANUARY	FEBRUARY	MARCH	APRIL	MAY	JUNE	JULY	AUGUST	SEPTEMBER
Trinity	300	300	300	550	2900	800	450	450	450
Sacramento	3250	3250	3250	4500	6400	8750	8500	7750	4900
American	900	1700	1900	3150	2500	4000	3800	2550	1350
Feather	950	950	800	1050	1300	1950	1400	1300	1200
Stanislaus	200	200	300	550	500	550	400	350	250

DELTA SUMMARY (CFS)

	2015								
	JANUARY	FEBRUARY	MARCH	APRIL	MAY	JUNE	JULY	AUGUST	SEPTEMBER
Rio Vista Flows	9450	12200	9800	7400	5800	5300	2650	2600	2600
Sac River at Freeport	11300	14550	12000	9700	8600	10450	8550	8350	7800
SJ River at Vernalis	1050	1400	1600	1450	1450	1050	900	750	750
Computed Outflow	9650	12750	12250	9250	7100	7100	4250	4350	4200
Combined Project Pumping	3550	4350	1800	1150	1150	1200	1250	1400	2300

Salmonid and Green Sturgeon Supporting Information for Endangered Species Act Compliance for Temporary Urgency Change Petition Regarding Delta Water Quality January 27, 2015

Table 7. 99% Exceedance Forecast.

January 1 - 99% HYDROLOGIC EXCEEDENCE

RESERVOIRS	END OF MONTH STORAGES (TAF)								
	2015								
	JANUARY	FEBRUARY	MARCH	APRIL	MAY	JUNE	JULY	AUGUST	SEPTEMBER
Trinity	860	894	920	929	843	769	704	637	576
Shasta	1966	2173	2393	2434	2242	1843	1397	1070	936
Folsom	440	499	523	520	484	347	251	217	182
Oroville	1374	1516	1704	1762	1681	1468	1250	1027	1023
New Melones	543	544	537	491	409	331	254	178	122

RESERVOIRS	MONTHLY AVERAGE RELEASES (CFS)								
	2015								
	JANUARY	FEBRUARY	MARCH	APRIL	MAY	JUNE	JULY	AUGUST	SEPTEMBER
Trinity	300	300	300	600	1500	800	450	430	450
Sacramento	3250	3250	3250	4500	7000	10000	9850	7800	4900
American	900	800	1950	2000	1750	3050	2200	1200	1100
Feather	950	950	800	1650	1700	2700	2400	3100	950
Stanislaus	200	200	300	350	350	350	400	330	250

	DELTA SUMMARY (CFS)								
	2015								
	JANUARY	FEBRUARY	MARCH	APRIL	MAY	JUNE	JULY	AUGUST	SEPTEMBER
Rio Vista Flows	7800	7350	7050	6100	5750	5850	2900	2600	2000
Sac River at Freeport	9350	9200	8800	8200	8550	11200	8950	8400	6950
SJ River at Vernalis	1050	850	850	1750	1550	300	250	350	350
Computed Outflow	7050	7100	8050	7800	7100	7100	4200	4300	4050
Combined Project Pumping	3550	3350	1300	900	850	900	900	900	900

Footnote: These forecast numbers include adjustments to January inflows based upon observed conditions through mid-January.

Table 8. January to September 2014 Actual Reservoir Storage, Releases, and Delta Conditions¹⁵

Actual 2014 (January - September)

Reservoirs	EOM Storages (TAF)								
	2014								
	Jan	Feb	Mar	Apr	May	Jun	Jul	Aug	Sep
Trinity (Trinity Lake) CLE	1187	1306	1281	1196	1062	865	697	606	561
Shasta (Shasta Dam) SHA	1773	2198	2408	2177	1851	1575	1342	1157	1108
Folsom (Folsom Lake) FOL	304	436	546	547	470	406	381	344	304
Oroville (Oroville Dam) ORO	1406	1716	1876	1734	1511	1252	1100	1075	953
New Melones (New Melones Reservoir) NML	1060	1036	917	799	712	625	553	519	513

Reservoirs	Monthly Average Releases (CFS)								
	2014								
	Jan	Feb	Mar	Apr	May	Jun	Jul	Aug	Sep
Trinity (Trinity Lake) CLE	534	392	499	1669	1813	2366	3244	2668	1547
Sacramento (Keswick) KES	3084	3060	2766	3096	6839	8972	9203	7665	5558
American (Nimbus) NAT	745	650	614	718	1387	2107	1997	1505	1398
Feather (Oroville Dam) ORO	1624	729	641	881	3678	4930	5419	3387	1919
Stanislaus (Goodwin) GDW	295	255	403	1553	1259	270	316	232	184

	Delta Summary (CFS)								
	2014								
	Jan	Feb	Mar	Apr	May	Jun	Jul	Aug	Sep
Rio vista	4214	8144	11814	7212	3542	4524	3828	3389	3366
Sac River at Freeport	6511	10811	14815	9595	5645	8854	8853	8461	8249
SJ river at Vernalis	856	822	844	1770	1528	319	254	307	410
NDOI (outflow)	4780	11145	12721	7912	4174	5407	4085	3419	3202

¹⁵ Data from <http://cdec.water.ca.gov/reservoir.html>. Table supplied by CDFW on January 26, 2015.

Salmonid and Green Sturgeon Supporting Information for Endangered Species Act Compliance for Temporary Urgency Change Petition Regarding Delta Water Quality January 27, 2015

During February and March a continuation of Keswick minimal releases at the levels identified in the TUC Petition is hypothesized to increase the time needed for Chinook and steelhead smolts to emigrate down the Sacramento River, which will result in reduced outmigration survival (Singer et al 2013) and a reduced smoltification window (McCormick et al 1998). In contrast, any predicted increases in reservoir storage that may be realized by operating to the TUC Petition's outflow range will be critical to any measures to maintain water temperatures necessary for the biological needs of winter-run Chinook, spring-run Chinook, steelhead, and green sturgeon downstream of these reservoirs over the summer and fall of 2015. It should be noted that these January forecasts include later upstream impacts to BY 2015 fishes, including redd dewatering. Thus, this reduced outflow range in February and March is a proactive approach by Reclamation and DWR to immediately implement appropriate contingency measures that may benefit BY 2015 cold water listed species, as required in NMFS BiOp Action I.2.3.C.

Net Delta Outflow Index Modification

Although the NMFS BiOp (2009) does not contain NDOI standards, it did assume NDOI standards would be met. Based on the conceptual model, the reduction in outflow, as identified in the Petition's Project Description, may impact juvenile salmonids migrating through the North Delta between Sacramento and Rio Vista, where Sacramento River flows meet the tidally dominated western Delta. Currently, the greatest presence of salmonids in the Delta has been detected in the Lower Sacramento River and North Delta regions (DOSS 2015). The proposed reduction in minimum Delta outflow from a monthly average of 7,100 cfs to 4,000 cfs is lower than those under minimum standards to meet the D-1641 NDOI standards in February and March. This proposed reduction may reduce survival of juvenile salmonids migrating through the Lower Sacramento River and North Delta by increasing rates of predation mediated by hydrodynamic mechanisms (i.e. transit times, turbidity). However, once migrating fish reach the tidally-dominated regions in the western Delta (i.e. Rio Vista towards Chipps Island), South Delta, or Central Delta under the Petition's NDOI outflow threshold (4,000 cfs), they are likely to encounter a daily proportion of positive velocities and a mean velocity that are not substantially different from outflow conditions observed when a 7,100 cfs NDOI standard is being achieved (Table 9, Figures 11-12). This is due to the greater influence tides have in these

Salmonid and Green Sturgeon Supporting Information for Endangered Species Act Compliance for Temporary Urgency Change Petition Regarding Delta Water Quality January 27, 2015

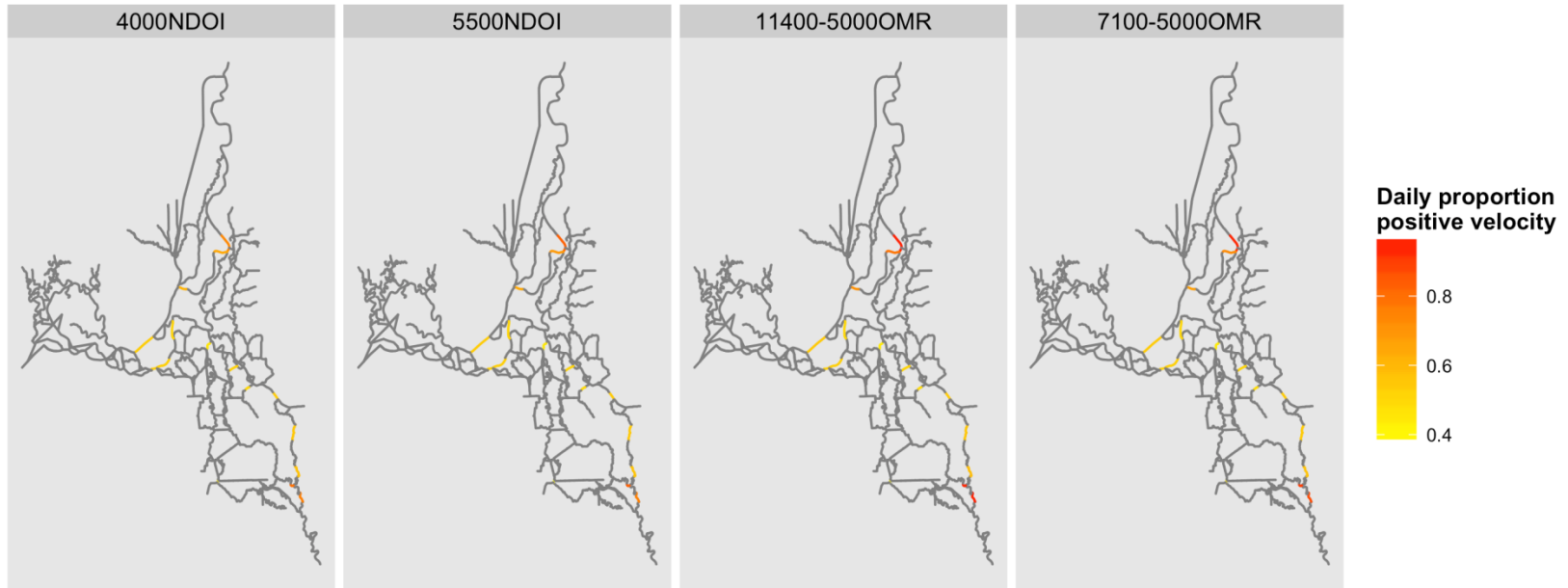
Table 9. DSM2 Results for Daily Proportion Positive Flows at Each Channel Node¹⁶. Note that Freeport and Vernalis flows are different between scenarios; see Table 4 for details. The DJFMP Seine Region Containing the Channel Node was identified from USFWS metadata.

Modeled NDOI	4000	5500	7100	Difference between NDOI 7100 and 4000	Difference between NDOI 7100 and 5500	DJFMP Seine Region
Modeled OMR	-1400	-3200	-5000			
Modeled Export	1500	3500	6400			
Channel Node						
6	0.76	0.76	0.88	-0.12	-0.12	San Joaquin
9	0.56	0.56	0.56	0.01	0.00	San Joaquin
12	0.54	0.54	0.54	0.01	0.00	South Delta
21	0.53	0.53	0.53	0.00	0.00	South Delta
49	0.52	0.52	0.52	0.00	0.00	Central Delta
50	0.52	0.52	0.51	0.00	0.00	Central Delta
54	0.79	0.83	0.90	-0.11	-0.07	San Joaquin
81	0.43	0.37	0.42	0.01	-0.05	South Delta
124	0.45	0.44	0.43	0.02	0.01	South Delta
160	0.52	0.51	0.50	0.01	0.00	South Delta
173	0.50	0.49	0.48	0.01	0.00	South Delta
310	0.51	0.50	0.50	0.01	0.01	Central Delta
421	0.73	0.84	0.94	-0.21	-0.10	North Delta
422	0.72	0.82	0.91	-0.19	-0.10	North Delta
423	0.64	0.68	0.73	-0.08	-0.04	North Delta
429	0.60	0.64	0.67	-0.06	-0.03	North Delta
434	0.53	0.53	0.53	-0.01	0.00	Central Delta

¹⁶ A map of DSM2 node locations is available at:
http://baydeltaoffice.water.ca.gov/modeling/deltamodeling/models/dsm2v6/DSM2_Grid2.0.pdf

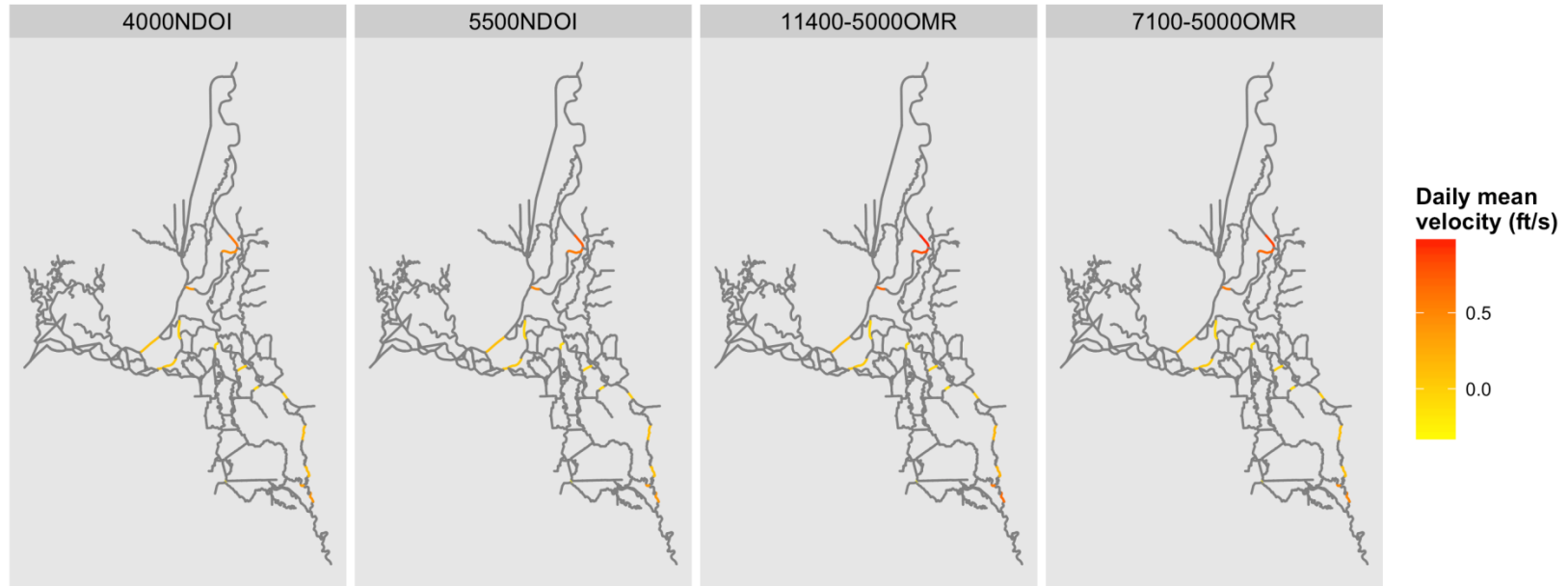
Salmonid and Green Sturgeon Supporting Information for Endangered Species Act Compliance for Temporary Urgency Change Petition Regarding Delta Water Quality January 27, 2015

Figure 11. Maps of the Delta with Key Channels Color-Coded for Daily Proportion Positive Velocity.



Salmonid and Green Sturgeon Supporting Information for Endangered Species Act Compliance for Temporary Urgency Change Petition Regarding Delta Water Quality January 27, 2015

Figure 12. Maps of the Delta with Key Channels Color-Coded for Daily Mean Velocity Generated from DSM2.



Salmonid and Green Sturgeon Supporting Information for Endangered Species Act Compliance for Temporary Urgency Change Petition Regarding Delta Water Quality January 27, 2015

regions under low Delta inflows. There is high certainty in our understanding of how hydrodynamics are affected in these regions by the Petition's Project Description.

In the North Delta, DSM2 modeling between 7,100 and 4,000 NDOI levels demonstrate a decrease in outflow, which will impact the Delta hydrodynamics in two ways that will influence Salmonid migration speed and patterns. These hydrodynamic processes influence survival by changing juvenile salmonids exposure to predators in the Lower Sacramento River and other relevant reaches (i.e. Georgiana Slough, Delta Cross Channel, Sutter and Steamboat sloughs). First, reduced outflow may increase tidal excursion in the upstream direction over a greater spatial range (reduced daily proportion of positive velocities) into the Lower Sacramento River region. These increased upstream tidal excursions appear to increase the duration of reverse flows into Georgiana Slough and/or an open DCC gates (Table 9), which likely increases entrainment into these waterways. Survival rate in the main stem Sacramento River or in one of the multiple distributary channels is decreased due to the longer duration of the downstream emigration phase resulting from reduced flows as compared to periods of greater downstream flows (greater NDOI). Also, the increased tidal excursion may increase entrainment into Sutter and Steamboat sloughs by creating greater probability of flow convergence at these junctions. However, due to the lower flows the time needed to migrate downstream through these two migratory corridors is also expected to increase, resulting in diminished survival compared to higher flows. There is high certainty in our understanding of the biological processes affected by reduced outflow along the Sacramento River salmonid migration corridor.

Second, DSM2 results show reduced NDOI will cause the daily mean channel velocity along the Sacramento River and North Delta to be less positive even at channels along the Sacramento River at Sherman Island and near Cache Slough (Figure 12). When the DCC gates are open, the daily mean channel velocity becomes even less positive in these reaches. Reducing outflow likely causes a decrease in the daily proportion of positive velocities through the Sacramento River downstream of Sutter and Steamboat sloughs confluences with the Sacramento River. A review of a similar NDOI modification (Reclamation 2014a) indicated that the impacts of reduced NDOI on the proportion of daily positive flows and mean daily velocities propagate up to Sutter and Steamboat Sloughs, although this effect was not modeled for this Petition. Additionally, Georgiana Slough flows become less positive as tidal excursion causes flow reversals in this channel when outflow is reduced. When the DCC gates are open, the daily proportion of positive velocities further decreases in the Sacramento River upstream of the DCC gates and more noticeably between the DCC gate and Georgiana slough. When the DCC is open, there is a reduction in the daily proportion of positive flows through Georgiana Slough. There is high certainty in our understanding of how hydrodynamics is affected in these regions by the Petition's Project Description.

Decreased daily proportion of positive velocities and daily mean channel velocities, due to the Petition's reduced outflow range, will increase migrating salmonids' residence time in the North

Salmonid and Green Sturgeon Supporting Information for Endangered Species Act Compliance for Temporary Urgency Change Petition Regarding Delta Water Quality January 27, 2015

Delta, which likely exposes them to increased predation and mortality rates. There are no models to quantify the increase in mortality rates due to reduced flows in this reach, however comparisons may be made. The DCC's capacity is 3500cfs, which is in range of the Petition's change to the outflow standard. Two telemetry studies reported on changes in reach-specific survival when the DCC was open and closed, which provide a comparison for survival through the North Delta reach and downstream when this quantity of daily flow is removed from the channel. The average difference in survival rates for salmonids through the North Delta from Sutter and Steamboat sloughs to Rio Vista when the DCC was open (n=7, survival ranged from 0.012-0.306) versus closed (n=3, survival ranged from 0.099-0.233) was 3.4% (Table 2 in Romine et al. 2013). Perry et al. (2010) had a single measurement of survival in this reach when the DCC gates were open vs. closed and the difference was 12.1%. Reach-specific survival showed large variations within and between studies, and factors other than travel time and flow are suggested to have contributed to variations in survival estimates including environmental conditions and temporal shifts in predators (Perry et al. 2010) and tag failure (Romine et al. 2013). A previous study of steelhead (Singer et al. 2013) did not demonstrate interior routes to have the lowest survival. In that study, steelhead smolt survival was estimated to be higher through the eastern Delta route (i.e. Georgiana Slough, Mokelumne River, and San Joaquin River routes) than the western Delta route (Sutter and Steamboat sloughs) in one of two years studied, although survival was highest along the Sacramento River mainstem route in both years. There is moderate certainty in our understanding of the survival processes affected by flow associated with the DCC and Georgiana Slough migration routes.

BY2015 adult winter-run Chinook salmon may be affected by the Petition's proposed reduction in outflow, which would reduce detectable flow signal for upriver migration and may lead to longer transit times and increased predation mortality. Juveniles and sub-adult green sturgeon rearing and utilizing the Delta are not expected to be affected by the change in inflows to the Delta during February and March. Adult green sturgeon will be present in the Delta during the month of February, and are expected to migrate through the North Delta starting in March. Over the course of juvenile rearing in the Delta (1 to 3 years) the fish are exposed to a wide variety of flows, depending on where they happen to be at a particular moment. In most of the Delta where green sturgeon are expected to be rearing, flows are tidally dominated. There is low certainty in our understanding of the adult salmonid and green sturgeon biological processes affected by flow in the Delta.

Modification of Export Limits

Action IV.2.3 in the 2009 NMFS BiOp specifies fish loss density, daily older juvenile Chinook salmon and wild steelhead loss, and loss of surrogate hatchery releases of winter-run and late-fall run Chinook salmon as triggers to reduce the vulnerability of emigrating ESA-listed salmon and steelhead to entrainment into South Delta channels and at the pumps between January 1 and June 15. A calendar-based requirement, starting on January 1, is for the 14-day OMR average flow to be no more negative than -5,000cfs. Under the Petition's Project Description, these triggers will

Salmonid and Green Sturgeon Supporting Information for Endangered Species Act Compliance for Temporary Urgency Change Petition Regarding Delta Water Quality January 27, 2015

continue to be used to manage such that the 5-day net average OMR flow is not more negative than a calculated -3,500 or -2,500cfs OMR flow until fish densities return below levels of concern.

During February and March, juvenile and adult salmonids may experience South Delta hydrodynamic conditions under the Petition's Project Description that could result in greater export rates than were observed with modified NDOI targets during similar periods in WY2014. These modified export limits (subject to a 35% Export/Inflow standard per D-1641¹⁷) may occur when NDOI is less than 7,100 cfs but greater than 5,500 cfs. These export limits allow for combined pumping of 1,500 cfs when NDOI is less than 5,500 cfs. Old and Middle River conditions under these inflow and export management scenarios are predicted to be approximately -3,200 to -1,400 cfs. If precipitation events occur that enable Reclamation to comply with D-1641 standards and DCC gate closure requirements, then export levels may increase at the CVP/SWP. OMR management per NMFS BiOp Action IV.2.3 will continue to use fish loss density, daily loss, and loss of specific hatchery releases of late-fall and Winter-run Chinook salmon as triggers to reduce the vulnerability of emigrating ESA-listed salmon, steelhead, and green sturgeon to entrainment into South Delta channels and at the pumps between February 1 and March 30. Daily flows in Old and Middle River averaged approximately -4,885 cfs in December, 2014 and approximately -4140 cfs in January 2015 (through January 22) (Figure 13).

When comparing the Petition's Project Description's modeled conditions when NDOI is 4,000 cfs and OMR is -1,400 cfs to conditions when NDOI is 7,100 and OMR is -5,000 cfs, the majority of modeled channels in the South and Central Delta regions show no change in the mean daily proportion positive velocities under the lower NDOI. The only observed change in the metrics evaluated between these runs occurred at Columbia Cut, where with the NDOI of 4,000 cfs and OMR at -1,400 cfs, the daily average velocity becomes positive (0.01), instead of remaining negative (-0.01) similar to observed when NDOI is modeled at 7,100 cfs (0.02). The intermediate modeling with NDOI of 5,500 cfs and exports of 3,500 predicted similar conditions in the South and Central Delta regions compared to the model run with NDOI of 7,100 cfs and an OMR value of -5,000 cfs. These modeling results suggest that daily proportion of positive velocities may be quite balanced (i.e. similar frequencies of positive and negative velocities) rather than more riverine (i.e. predominantly positive velocities) at the intermediate or low NDOI condition in these regions and achieve similar tidal hydrodynamics throughout the San Joaquin River and South Delta.

¹⁷ As in WY 2014, the E/I standard will be implemented using the inflow averaging period (3-day or 14-day) that allows the greatest exports.

Salmonid and Green Sturgeon Supporting Information for Endangered Species Act Compliance for Temporary Urgency Change Petition Regarding Delta Water Quality January 27, 2015

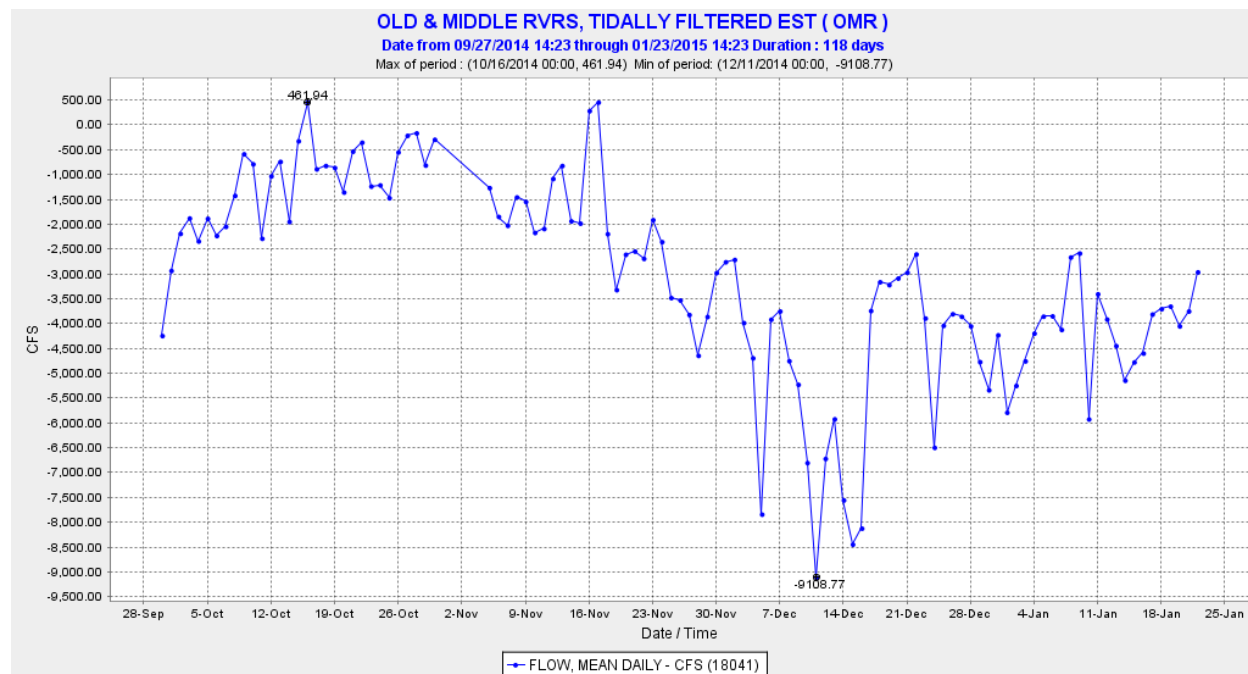


Figure 13. Old and Middle Rivers tidally-filtered daily flows (cubic feet per second) measured at Old & Middle Rivers (OMR) for WY 2015.¹⁸

The conditions may increase transit rates for salmonids, reduce dispersion of tributary turbidity input, and provide stable conditions for non-native vegetation supporting predaceous fish species, which cumulatively reduces survival rates of juvenile salmonids along the San Joaquin River migration corridor and in the South Delta region. There is low certainty in our understanding of the biological and environmental processes affected by NDOI and exports along the San Joaquin River salmonid migration corridor.

The mean daily proportion positive velocities become less frequently positive in the NDOI 5,500 cfs model than in the NDOI 4,000 cfs model run in Grant Line Canal due to higher pumping and increased San Joaquin flow reaching the facilities without increased San Joaquin River flow at Vernalis. Reduced Vernalis flows in the NDOI 4,000 cfs and NDOI 5,100 cfs models shows the same reduction in mean daily proportion positive velocities upstream of Head of Old River due to similarly modeled San Joaquin River flows at Vernalis. Under greater exports when the NDOI is 7,100 cfs and OMRs are -5,000 cfs, South Delta locations proximal to the facilities (Grant Line Canal) show greater proportions of mean daily proportion positive velocities than when NDOI was modeled at 4,000 cfs and OMRs are 1,400 cfs. This would indicate that the effect of greater exports increases the mean daily proportion of positive velocities towards the facilities in these channels. Greater positive velocities may support outmigration through the Delta; however it may increase salvage and loss of salmonids in the South Delta region if these flows are towards the facilities it may increase facility salvage and loss of salmonids. This is particularly

¹⁸ Downloaded from CDEC on January 23, 2015.

Salmonid and Green Sturgeon Supporting Information for Endangered Species Act Compliance for Temporary Urgency Change Petition Regarding Delta Water Quality January 27, 2015

the case for San Joaquin River steelhead entering the South Delta through Old River. There is moderate certainty in our understanding of the biological processes affected by exports in South Delta salmonid migration corridors and fish collection facilities at the CVP/SWP pumps.

Impacts to juvenile and subadult life stages of green sturgeon are anticipated to remain minimal. Age 1 to 3 green sturgeon are expected to be rearing in the Delta, and are typically exposed to a broad spectrum of flows over the course of the year during this life history phase and freely move throughout the Delta to find suitable conditions for their needs. There is low certainty in our understanding of the biological processes in green sturgeon affected by exports in the South Delta region and fish collection facilities at the CVP/SWP pumps.

Delta Cross Channel Gate Modification

The 2009 BiOp (NMFS 2009) and D-1641 include a calendar-based closure of the DCC Gates between February 1 and May 20 to protect winter-run, spring-run, and fall-run Chinook salmon and steelhead from entrainment into the Interior Delta. Studies have shown that the mortality rate of the fish entrained into the DCC and subsequently into the Mokelumne River system is higher than for fish that remain in the mainstem corridor (Perry and Skalski 2008; Vogel 2004, 2008). Closure of the DCC gates during periods of salmon emigration eliminates the potential for entrainment into the DCC and the Mokelumne River system with its high mortality rates. In addition, closure of the gates appears to redirect the migratory paths of emigrating fish into channels with relatively less mortality (*e.g.*, Sutter and Steamboat sloughs), due to a redistribution of river flows among the channels. The overall effect is an increase in the apparent survival rate of these salmon populations as they move through the Delta. There is high certainty in our understanding of the biological processes in salmonids affected by DCC gate operations.

A series of studies conducted by Reclamation and U.S. Geological Survey (USGS, Horn and Blake 2004) used acoustic tracking of released juvenile Chinook salmon to follow their movements in the vicinity of the DCC under different flows and tidal conditions. The study results indicate that the behavior of the Chinook salmon juveniles increased their exposure to entrainment through both the DCC and Georgiana Slough. Horizontal positioning along the east bank of the Sacramento River during both the flood and ebb tidal conditions enhanced the probability of entrainment into the two channels. Upstream movement of fish with the flood tide demonstrated that fish could pass the channel mouths on an ebb tide and still be entrained on the subsequent flood tide cycle. In addition, diel movement of fish vertically in the water column exposed more fish at night (~70%) to entrainment into the DCC than during the day (~30%; Jon Burau, pers. comm.). Perry et al. (2010) included two releases of acoustically-tagged late fall-run Chinook salmon to evaluate the impact of DCC gate opening of reach specific and total Delta survival. Mainstem survival downstream of the DCC gate was lower when they were open (0.443) than when the closed (0.564). During 2008-2009, ten releases of juvenile late fall run Chinook salmon were made by USGS (Romine et al. 2013, Table 10) and through Delta survival was greater when the DCC gates were closed (0.170) than when they were open (0.123). These

Salmonid and Green Sturgeon Supporting Information for Endangered Species Act Compliance for Temporary Urgency Change Petition Regarding Delta Water Quality January 27, 2015

values are negatively biased due to tag failure (Romine et al. 2013). Perry et al. (2010) observed through-Delta survival to be greater with the DCC closed (0.543) than open (0.351), principally due to increased survival through the Sutter and Steamboat sloughs route from 0.263 to 0.561. In addition to the Petition's effects on emigrating juvenile salmonids, the Petition's opening of the DCC may increase straying of returning winter-run Chinook adult salmon on the Sacramento River mainstem by diverting a portion of the Sacramento River flows through the forks of the Mokelumne River and Central Delta. This will lead to false attraction and hence straying into these waterways.

Table 10. Average Values for Releases Described in Romine et al. (2013). Seven releases occurred with DCC open and three releases occurred with it closed.¹⁹

DCC Position	S_A	S_B	S_C	S_D	Ψ_A	Ψ_B	Ψ_C	Ψ_D	S_{TOTAL}
Open	0.143	0.1	0.098	0.159	0.486	0.267	0.064	0.182	0.123
Closed	0.177	0.205	-	0.102	0.521	0.276	-	0.202	0.17

During the fall and early winter when juvenile listed salmonids are not typically present in the Lower Sacramento River and Delta, action triggers in the Chinook salmon Decision Tree use fish monitoring catch indices from Knights Landing and Sacramento River to detect substantial winter-run Chinook migration into the lower Sacramento River. Catch index exceedance values were based on analyses of historic screw trap, beach seine, and trawl data (Chappell 2004). Historic analyses (Chappell 2004) modified the "critical trigger" and duration of DCC gate closure in the Chinook Salmon Decision Tree. Multiple exceedance levels were identified to modify DCC operations in a manner that reduces risks due to the elevated presence of spring-run and winter-run Chinook salmon upstream of the Delta. The Knights Landing Catch Index Catch Index of 23.2 on October 31, 2014 triggered closure of the DCC gates on November 2, 2014.

Currently, the greatest presence of winter-run Chinook salmon in Delta monitoring efforts appears to be in the Lower Sacramento River and the North Delta regions, and a majority of spring-run Chinook are also in these areas (DOSS 2015), which are proximal to the DCC. When emigrating salmonids are in proximity of the DCC gates they are vulnerable to entrainment through the DCC when the gates are open. Based on the conceptual model, greater percentages of ESA-listed salmonids, including hatchery winter-run Chinook, continue to enter the Delta through February and March, there is an increasing risk of exposure as greater proportions of these populations enter the Delta through the winter and spring.

¹⁹ S= survival and Ψ =route entrainment; Routes: A=Sacramento, B=Sutter and Steamboat, C= DCC route, D= Georgiana Slough route

Salmonid and Green Sturgeon Supporting Information for Endangered Species Act Compliance for Temporary Urgency Change Petition Regarding Delta Water Quality January 27, 2015

Vernalis Flows Modification

Under D-1641, the minimum monthly average flow objective in the lower San Joaquin River (measured at Airport Way Bridge, Vernalis) during February and March is 710 cfs or 1,140 cfs²⁰ during critically dry years such as WY 2015. The Project Description reduces the Vernalis monthly average base flows to 500 cfs for February and March.

Based on the conceptual model, the Petition's Project Description to reduce flows at Vernalis to less than the Critical WY D-1641 flow objective may reduce survival of juvenile salmonids migrating through the lower San Joaquin River. This change will increase their migration travel time, which increases their exposure to degraded habitats and predators. Reduced Vernalis flows, in combination with reduced NDOI, results in a reduction in the daily proportion of positive flows along the lower San Joaquin River downstream of the Head of Old River (Table 9). Although only a limited number of Lower San Joaquin River channels were assessed there did not appear to be an increase in the daily proportion of negative flows in these channels downstream of the Stockton Deepwater Ship Channel. Along Grant Line Canal, the DSM2 run with the more negative OMR flows (NDOI 7,100, OMR -5,000) had greater positive flows towards the facilities than compared to the run with very low NDOI and OMR flows of 4,000 cfs and -1,400 cfs, respectively. This suggests that a more positive OMR leads to greater tidal conditions (i.e. more balanced daily proportion of positive velocities and daily mean channel velocities) in local waterways such as Grant Line Canal, which will likely increase migrating salmonids' residence time in these waterways, and increase their exposure to predation and mortality. Effects of increasing exports and creating more negative OMR conditions in South Delta waterways north of the CVP/SWP export facilities would likely show an increase in the magnitude of negative velocities and a reduction in the daily average magnitude of flow velocities, indicating that less water was moving downstream to the ocean (positive direction) and more water was moving towards the export facilities. This would also lead to increasing the residence time of salmonids in these waterways, with a corresponding reduction in survival. The modeling conducted for the Project Description did not include these additional waterways.

There are no models to quantify the increase in mortality due to reduced flows in this reach; however, comparisons may be made using results from recent acoustic tagging studies of juvenile San Joaquin steelhead migration and survival through the South Delta (Buchanan et al. 2014). Although there are only two years of data and these studies were conducted during the spring (late March through June) under higher flow conditions (>3,000 cfs) and variable Head of Old River Barrier (HORB) status (in or out), they provide an indication of possible relative survival and travel time differences. Average survival rates of tagged steelhead released at Durham Ferry from the lower San Joaquin River through the Delta ranged from 0.38 to 0.69

²⁰ The higher flow objective applies when the 2-ppt isohaline (measured as 2.64 mmhos/cm surface salinity) is required to be at or west of Chipps Island.

Salmonid and Green Sturgeon Supporting Information for Endangered Species Act Compliance for Temporary Urgency Change Petition Regarding Delta Water Quality January 27, 2015

($SE \leq 0.05$) in 2011 when San Joaquin River flows were high ($>15,000$ cfs at Vernalis) and no HORB was installed. Average survival rates through the Delta ranged from 0.24 to 0.32 ($SE \leq 0.03$) in 2012 when river flows were considerably lower (about 3,000 cfs) and the HORB was installed. The median travel time of tagged steelhead from Durham Ferry to the Head of Old River was 5–6 days in both years, and ranged up to 28 days in 2011 and 35 days in 2012. These results, albeit not directly comparable due to timeframes and HORB conditions, provide limited evidence that steelhead survival may be reduced by proposed Vernalis flow requirements. Additionally, it appears that median travel times of surviving migrants are generally independent of flow level; however, travel times took up to an additional seven days for some migrants under lower flow conditions. This hints at the possibility that lower survival in 2012 may be associated with increased travel times of those fish not surviving. There is low certainty in our understanding of the hydrodynamic and biological processes in steelhead affected by exports along the San Joaquin River and in the South Delta.

Although travel times may increase and survival be reduced under lower flows, only about 5% of the total number of steelhead captured in the lower San Joaquin River during Mossdale trawling surveys (1997-2003) have been collected in February and March, and most were greater than 200 mm (one 115 mm). These surveys indicate that few, if any, juvenile steelhead can be expected to migrate in the lower San Joaquin River during February and March and, those that do migrate during this period will be less susceptible to predation due to their larger size. Given the low likelihood that steelhead will be migrating during this period, but the moderate to high potential for lower flows to effect migration travel times and survival for any juvenile steelhead migrating during February and March, changes in hydrodynamic conditions under the Project Description may have a moderate effect on juvenile steelhead in the lower San Joaquin River. There is moderate uncertainty in this prediction based on the unknown number and size of juvenile steelhead attempting to migrate through the lower San Joaquin River during February and March this year, and their behavioral response to flows as low as 500 cfs in the lower San Joaquin River.

Cumulative Effects of Action

The Petition's action to: 1) Reduce the D-1641 Delta outflow standard for February and March from at least 7,100 cfs to 4,000 cfs, 2) Allow exports of up to 3,500 cfs when NDOI is between 7,100 cfs and 5,500 cfs, exports of 1,500 cfs when NDOI is below 5,500 cfs, and exports up to those achieving OMR flows no more negative than -5,000 cfs when NDOI is greater than 7,100 cfs, 3) Modify the D-1641 and NMFS BiOp DCC gate operations using the triggers matrix in Attachment G of Reclamation 2014b, and 4) Reduce the D-1641 Vernalis flow to 500 cfs, will affect the abundance and spatial distribution of juvenile winter-run and spring-run Chinook salmon, steelhead, and green sturgeon. The modifications to outflow and DCC gate operations as part of the proposed action may affect the spatial distribution and abundance of adult winter-run Chinook salmon and green sturgeon. Life history diversity of steelhead may be affected due to

Salmonid and Green Sturgeon Supporting Information for Endangered Species Act Compliance for Temporary Urgency Change Petition Regarding Delta Water Quality January 27, 2015

reduced survival through the San Joaquin River migration corridor. There is moderate certainty in these analyses due to the limited variability in the modeling and potential for actual hydrodynamic conditions to vary from modeled conditions, especially on the San Joaquin River.

The proposed Project Description's modification of outflow, exports, and Vernalis flows may reduce survival of juvenile listed salmonids, steelhead and green sturgeon, and may modify their designated critical habitat. The modification of juvenile winter-run and spring-run Chinook salmon and steelhead survival due to changes in outflow would occur primarily in migratory corridors in the North Delta due to increased entrainment into the Interior Delta. Steelhead survival may also be reduced along the mainstem San Joaquin River downstream of the Stanislaus River until tidal hydrodynamics dominate this channel upstream of the Stockton Deepwater Ship Channel. The location where tides influence outflow will move upstream of the Head of Old River, thus leading to increased entrainment of steelhead toward the CVP/SWP facilities. The Petition's action to reduce Delta outflow keeps the CVP/SWP operation proactively compliant with implementation of NMFS RPA I.2.2C and I.2.3C. The Petition's outflow action will enhance the potential to operate summer reservoir releases by potentially increasing the ability to control in-river water temperatures. This may decrease the endangerment to brood year 2015 by reducing mortality to incubating winter-run and spring-run Chinook eggs and holding adults during the summer of 2015.

Modeling of the Petition's intermediate export limits when NDOI is between 5500 and 7,100 cfs suggests that exports at intermediate values (3500 cfs) lead to greater mean daily proportion of positive velocities in the South Delta proximal to the facilities from the San Joaquin River (i.e Grant Line Canal) but not along the San Joaquin River migration route's channels. This modeling suggests hydrodynamics in this South Delta region proximal to the facilities may reduce local salmonid travel times towards the facility, while San Joaquin River hydrodynamics do not change and travel times remain similar. Although not modeled, the South Delta waterways north of the CVP/SWP export facilities are likely to have decreased daily proportion of positive velocities when exports are increased, which may increase residence time of rearing salmonids. These effects may increase unmeasured mortality in the South Delta region by increasing entrainment towards the facilities where pre-screen mortality is likely very high due to unprecedented nonnative vegetation problems and also maintain long transit times on the San Joaquin River where exposure to degraded habitat and predaceous species is constant.

Under the driest conditions, if NDOI reaches 5,500 cfs, the CVP/SWP will reduce exports to 1,500 cfs, which increases positive flows in the South and Central Delta relative to the baseline condition of NDOI 7,100 cfs and OMR no more negative than -5,000 cfs. Under these driest conditions, there will be reduced entrainment and salvage of listed species at the CVP/SWP fish collection facilities adjacent to the South Delta export facilities.

Salmonid and Green Sturgeon Supporting Information for Endangered Species Act Compliance for Temporary Urgency Change Petition Regarding Delta Water Quality January 27, 2015

The Petition's DCC gate operation will minimize the additional mortality risk to juvenile outmigrating and rearing winter-run and spring-run Chinook and juvenile steelhead, since the DCC gate operations matrix limits DCC flexibilities when migrating ESA-listed salmonids are present in the Lower Sacramento River region. During the period the gates are open, exports will be limited to 1,500 cfs. This export limit along with the implementation of the DCC gate operations matrix will minimize entrainment of existing rearing fish in the Interior and South Delta. The Petition's DCC gate operations may also cause straying of adult winter-run Chinook and green sturgeon.

References

- Buchanan, R., J. Israel, and P. Brandes. 2014. Juvenile San Joaquin steelhead migration and survival through the South Delta, 2011 and 2012. Presentation at the 8th Biennial Bay-Delta Science Conference, October 28-30, 2014, Sacramento, CA.
- Chappell, E. 2004. Are the current EWA Chinook Decision Tree numeric criteria appropriate? Presentation to the EWA Technical Review Panel Supporting Documents. Available at: http://www.science.calwater.ca.gov/events/reviews/review_ewa_archive_04.html
- Del Rosario, R.B, Y.J. Redler, K. Newman, P.L. Brandes, T. Sommer, K. Reece, and R. Vincik. 2013. Migration patterns of juvenile winter-run-sized Chinook Salmon (*Oncorhynchus tshawytscha*) through the Sacramento-San Joaquin Delta. *San Francisco Estuary and Watershed Science* 11(1): 24p.
- DOSS [Delta Operations for Salmonids and Sturgeon]. 2015. Meeting Notes: Delta Operations for Salmonids and Sturgeon (DOSS) Group Conference call, 01/06/2015 at 9:00 a.m.
- Erkkila, L.F., J.W. Moffett, and O.B. Cope. 1951. Sacramento - San Joaquin Delta Fishery Resources: Effects of Tracy Pumping Plant and Delta Cross Channel. Special Scientific Report-Fisheries, No. 56. Department of Interior, U.S. Fish and Wildlife Service. 109 p.
- Gruber, J. 2015. U.S. Fish and Wildlife Service Biweekly report (January 1, 2015 - January 14, 2015): Juvenile salmonids sampled at Red Bluff Diversion Dam. Available at <http://www.fws.gov/redbluff/RBDD%20JSM%20Biweekly/2015/Biweekly20150101-20150114.pdf>
- Horn, M.J. and A. Blake. 2004. Acoustic tracking of juvenile Chinook salmon movement in the vicinity of the Delta Cross Channel. 2001 Study results. U.S. Department of the Interior. Technical Memorandum No. 8220-04-04.

Salmonid and Green Sturgeon Supporting Information for Endangered Species Act Compliance for Temporary Urgency Change Petition Regarding Delta Water Quality January 27, 2015

McCormick, S.D., L.P. Hansen, T.P. Quinn, and R.L. Saunders. 1998. Movement, migration and smolting of Atlantic salmon (*Salmo salar*). Canadian Journal of Fisheries and Aquatic Science 55(Suppl. 1): 77-92.

National Marine Fisheries Service. 2009. Biological and Conference Opinion on the Long-Term Operations of the Central Valley Project and State Water Project. Central Valley Office, Sacramento CA.

National Marine Fisheries Service. 2014. Letter from Mrs. Maria Rea to Mr. David Murillo. Re: Contingency Plan for February Pursuant to Reasonable and Prudent Alternative (RPA) Action I.2.3.C of the 2009 Coordinated Long-term Operation of the Central Valley Project (CVP) and State Water Project (SWP) Biological Opinion (2009 BiOp). Central Valley Office, Sacramento CA.

Perry, R.W. and J.R. Skalski. 2008. Migration and survival of juvenile Chinook salmon through the Sacramento-San Joaquin River delta during the winter of 2006-2007. Report prepared for the U.S. Fish and Wildlife Service. September 2008. 32 p.

Perry, R.W., J. Skalski, P. Brandes, P. Sandstrom, A.P. Klimley, A. Amman, and R.B. MacFarlane. 2010. Estimating survival and migration route probabilities of juvenile Chinook salmon in the Sacramento-San Joaquin River Delta. North American Journal of Fisheries Management 30: 142-156.

Poytress, W.R, J.J. Gruber, F.D. Carillo, and S.D. Voss. 2014. Compendium report of Red Bluff Diversion Dam Rotary Trap Anadromous Fish Production Indices for Years 2002-2012. Report of the U.S. Fish and Wildlife Service to California Department of Fish and Wildlife and U.S. Bureau of Reclamation. Red Bluff, CA. 138 p.

Reclamation [U.S. Bureau of Reclamation]. 2008. Appendix B: Chinook Salmon Decision Tree *in* Biological Assessment on the Continued Log-term Operations of the Central Valley Project and the State Water Project. Mid-Pacific Region, Sacramento CA.

Reclamation. 2014a. Letter from Mr. Paul Fujitani to Mrs. Maria Rea. Re: Contingency Plan for February Pursuant to Reasonable and Prudent Alternative (RPA) Action I.2.3.C of the 2009 Coordinated Long-term Operation of the Central Valley Project (CVP) and State Water Project (SWP) Biological Opinion (2009 BiOp). Mid-Pacific Region, Sacramento CA.

Reclamation. 2014b. Attachment G- Revised DCC Gate Triggers Matrix in Central Valley Project and State Water Project Drought Operations Plan and Operational Forecast April 1, 2014 through November 15, 2014. Submitted to the State Water Resources Control Board on April 18, 2014.

Salmonid and Green Sturgeon Supporting Information for Endangered Species Act Compliance for Temporary Urgency Change Petition Regarding Delta Water Quality January 27, 2015

Reclamation. 2015. Central Valley Project and State Water Project Drought Contingency Plan January 15,2015- September 30, 2015.Submitted to the State Water Resources Control Board on January 15 2015.

Romine, J.G., R.W. Perry, S.J. Brewer, N.S. Adams, T.L. Liedtke, A.R. Blake, and J.R. Burau. 2013. The Regional Salmon Outmigration Study- survival and migration routing of juvenile Chinook salmon in the Sacramento-San Joaquin River Delta during the winter of 2008-2009. U.S. Geological Survey, Open File Report 2013-1142, 36 p.

Singer, G.P, A.R Hearn, E.D Chapman, M.L. Peterson, P.E. LaCivita, W.N. Brostoff, A. Bremmer, and A.P. Klimley. 2013. Interannual variation of reach specific migratory success for Sacramento River hatchery yearling late-fall run Chinook salmon (*Oncorhynchus tshawytscha*) and steelhead trout (*Oncorhynchus mykiss*). Environmental Biology of Fishes 96: 363-379.

Vogel, D.A. 2004. Juvenile Chinook salmon radio-telemetry studies in the northern and central Sacramento-San Joaquin Delta, 2002-2003. Report to the National Fish and Wildlife Foundation, Southwest Region. January. 44 p.

Vogel, D.A. 2008. Pilot study to evaluate acoustic-tagged juvenile Chinook salmon smolt migration in the Northern Sacramento-San Joaquin Delta 2006-2007. Report prepared for the California Department of Water Resources, Bay/Delta Office. Natural Resource Scientists, Inc. March. 43 p.

DEPARTMENT OF THE INTERIOR**Fish and Wildlife Service****50 CFR Part 17****[Docket No. FWS-R8-ES-2008-0045]****[4500030113]****Endangered and Threatened Wildlife and Plants; 12-month Finding on a Petition to List the San Francisco Bay-Delta Population of the Longfin Smelt as Endangered or Threatened****AGENCY:** Fish and Wildlife Service, Interior.**ACTION:** Notice of 12-month petition finding.

SUMMARY: We, the U.S. Fish and Wildlife Service (Service), announce a 12-month finding on a petition to list the San Francisco Bay-Delta distinct population segment (Bay Delta DPS) of longfin smelt as endangered or threatened and to designate critical habitat under the Endangered Species Act of 1973, as amended (Act). After review of the best available scientific and commercial information, we find that listing the longfin smelt rangewide is not warranted at this time, but that listing the Bay-Delta DPS of longfin smelt is warranted. Currently, however,

listing the Bay-Delta DPS of longfin smelt is precluded by higher priority actions to amend the Lists of Endangered and Threatened Wildlife and Plants. Upon publication of this 12-month finding, we will add the Bay-Delta DPS of longfin smelt to our candidate species list. We will develop a proposed rule to list the Bay-Delta DPS of longfin smelt as our priorities allow. We will make any determinations on critical habitat during the development of the proposed listing rule. During any interim period, we will address the status of the candidate taxon through our annual Candidate Notice of Review (CNOR).

DATES: The finding announced in this document was made on [INSERT DATE OF FEDERAL REGISTER PUBLICATION].

ADDRESSES: This finding is available on the Internet at <http://www.regulations.gov> at Docket Number [FWS-R8-ES-2008-0045]. Supporting documentation we used in preparing this finding is available for public inspection, by appointment, during normal business hours at the U.S. Fish and Wildlife Service, San Francisco Bay-Delta Fish and Wildlife Office, 650 Capitol Mall, Sacramento, CA 95814. Please submit any new information, materials, comments, or questions concerning this finding to the above street address.

FOR FURTHER INFORMATION CONTACT: Mike Chotkowski, Field Supervisor, San Francisco Bay-Delta Fish and Wildlife Office (see **ADDRESSES**); by telephone at 916-930-5603; or by facsimile at 916-930-5654. If you use a telecommunications device for the deaf (TDD), please call the Federal Information Relay Service (FIRS) at 800-877-8339.

SUPPLEMENTARY INFORMATION:

Background

Section 4(b)(3)(B) of the Endangered Species Act of 1973, as amended (Act) (16 U.S.C. 1531 *et seq.*), requires that, for any petition to revise the Federal Lists of Endangered and Threatened Wildlife and Plants that contains substantial scientific or commercial information that listing the species may be warranted, we make a finding within 12 months of the date of receipt of the petition. In this finding, we will determine that the petitioned action is: (1) Not warranted, (2) warranted, or (3) warranted, but the immediate proposal of a regulation implementing the petitioned action is precluded by other pending proposals to determine whether species are endangered or threatened, and expeditious progress is being made to add or remove qualified species from the Federal Lists of Endangered and Threatened Wildlife and Plants. Section 4(b)(3)(C) of the Act requires that we treat a petition for which the requested action is found to be warranted but precluded as though resubmitted on the date of such finding, that is, requiring a subsequent finding to be made within 12 months. We must publish these 12-month findings in the **Federal Register**.

Previous Federal Actions

On November 5, 1992, we received a petition from Mr. Gregory A. Thomas of the Natural Heritage Institute and eight co-petitioners to add the longfin smelt (*Spirinchus thaleichthys*) to the List of Endangered and Threatened Wildlife and designate critical habitat in

the Sacramento and San Joaquin Rivers and estuary. On July 6, 1993, we published a 90-day finding (58 FR 36184) in the **Federal Register** that the petition contained substantial information indicating the requested action may be warranted, and that we would proceed with a status review of the longfin smelt. On January 6, 1994, we published a notice of a 12-month finding (59 FR 869) on the petition to list the longfin smelt. We determined that the petitioned action was not warranted, based on the lack of population trend data for estuaries in Oregon and Washington, although the southernmost populations were found to be declining. Furthermore, we found the Sacramento-San Joaquin River estuary population of longfin smelt was not a distinct population segment (DPS) because we determined that the population was not biologically significant to the species as a whole, and did not appear to be sufficiently reproductively isolated.

On August 8, 2007, we received a petition from the Bay Institute, the Center for Biological Diversity, and the Natural Resources Defense Council to list the San Francisco Bay-Delta (hereafter referred to as the Bay-Delta) population of the longfin smelt as a DPS and designate critical habitat for the DPS concurrent with the listing. On May 6, 2008, we published a 90-day finding (73 FR 24911) in which we concluded that the petition provided substantial information indicating that listing the Bay-Delta population of the longfin smelt as a DPS may be warranted, and we initiated a status review. On April 9, 2009, we published a notice of a 12-month finding (74 FR 16169) on the August 8, 2007, petition. We determined that the Bay-Delta population of the longfin smelt did not meet the discreteness element of our DPS policy and, therefore, was not a valid DPS. We therefore determined that the Bay-Delta population of the longfin smelt was not a listable entity under the Act.

On November 13, 2009, the Center for Biological Diversity filed a complaint in U.S. District Court for the Northern District of California, challenging the Service on the merits of the 2009 determination. On February 2, 2011, the Service entered into a settlement agreement with the Center for Biological Diversity and agreed to conduct a rangewide status review and prepare a 12-month finding to be published by September 30, 2011. In the event that the Service determined in the course of the status review that the longfin smelt does not warrant listing as endangered or threatened over its entire range, the Service agreed to consider whether any population of longfin smelt qualifies as a DPS. In considering whether any population of longfin smelt qualifies as a DPS, the Service agreed to reconsider whether the Bay-Delta population of the longfin smelt constitutes a DPS. At the request of the Service, Department of Justice requested an extension from the Court to allow for a more comprehensive review of new information pertaining to the longfin smelt and to seek the assistance of two expert panels to assist us with that review. The plaintiffs filed a motion of non-opposition, and on October 3, 2011, the court granted an extension to March 23, 2012 for the publication of a new 12-month finding.

Species Information

Species Description and Taxonomy

Longfin smelt measure 9–11 centimeters (cm) (3.5–4.3 inches (in)) standard length, although third-year females may grow up to 15 cm (5.9 in). The sides and lining of the gut

cavity appear translucent silver, the back has an olive to iridescent pinkish hue, and mature males are usually darker in color than females. Longfin smelt can be distinguished from other smelts by their long pectoral fins, weak or absent striations on their opercular (covering the gills) bones, incomplete lateral line, low numbers of scales in the lateral series (54 to 65), long maxillary bones (in adults, these bones extend past mid-eye, just short of the posterior margin of the eye), and lower jaw extending anterior of the upper jaw (McAllister 1963, p. 10; Miller and Lea 1972, pp. 158–160; Moyle 2002, pp. 234–236).

The longfin smelt belongs to the true smelt family Osmeridae and is one of three species in the *Spirinchus* genus; the night smelt (*Spirinchus starksi*) also occurs in California, and the shishamo (*Spirinchus lanceolatus*) occurs in northern Japan (McAllister 1963, pp. 10, 15). Because of its distinctive physical characteristics, the Bay-Delta population of longfin smelt was once described as a species separate from more northern populations (Moyle 2002, p. 235). McAllister (1963, p. 12) merged the two species *S. thaleichthys* and *S. dilatatus* because the difference in morphological characters represented a gradual change along the north-south distribution rather than a discrete set. Stanley *et al.* (1995, p. 395) found that individuals from the Bay-Delta population and Lake Washington population differed significantly in allele (proteins used as genetic markers) frequencies at several loci (gene locations), although the authors also stated that the overall genetic dissimilarity was within the range of other conspecific fish species. They concluded that longfin smelt from Lake Washington and the Bay-Delta are conspecific (of the same species) despite the large geographic separation.

Delta smelt and longfin smelt hybrids have been observed in the Bay-Delta estuary,

although these offspring are not thought to be fertile because delta smelt and longfin smelt are not closely related taxonomically or genetically (California Department of Fish and Game (CDFG) 2001, p. 473).

Biology

Nearly all information available on longfin smelt biology comes from either the Bay-Delta population or the Lake Washington population. Longfin smelt generally spawn in freshwater and then move downstream to brackish water to rear. The life cycle of most longfin smelt generally requires estuarine conditions (CDFG 2009, p. 1).

Bay-Delta Population

Longfin smelt are considered pelagic and anadromous (Moyle 2002, p. 236), although anadromy in longfin smelt is poorly understood, and certain populations are not anadromous and complete their entire life cycle in freshwater lakes and streams (see *Lake Washington Population* section below). Within the Bay-Delta, the term pelagic refers to organisms that occur in open water away from the bottom of the water column and away from the shore. Juvenile and adult longfin smelt have been found throughout the year in salinities ranging from pure freshwater to pure seawater, although once past the juvenile stage, they are typically collected in waters with salinities ranging from 14 to 28 parts per thousand (ppt) (Baxter 1999, pp. 189–192). Longfin smelt are thought to be restricted by high water temperatures, generally greater than 22 degrees Celsius (°C) (71 degrees Fahrenheit (°F)) (Baxter *et. al.* 2010, p. 68), and will move down the

estuary (seaward) and into deeper water during the summer months, when water temperatures in the Bay-Delta are higher. Within the Bay-Delta, adult longfin smelt occupy water at temperatures from 16 to 20 °C (61 to 68 °F), with spawning occurring in water with temperatures from 5.6 to 14.5 °C (41 to 58 °F) (Wang 1986, pp. 6–9).

Longfin smelt usually live for 2 years, spawn, and then die, although some individuals may spawn as 1- or 3-year-old fish before dying (Moyle 2002, p. 36). In the Bay-Delta, longfin smelt are believed to spawn primarily in freshwater in the lower reaches of the Sacramento River and San Joaquin River. Longfin smelt congregate in deep waters in the vicinity of the low salinity zone (LSZ) near X2 (see definition below) during the spawning period, and it is thought that they make short runs upstream, possibly at night, to spawn from these locations (CDFG 2009, p. 12; Rosenfield 2010, p. 8). The LSZ is the area where salinities range from 0.5 to 6 practical salinity units (psu) within the Bay-Delta (Kimmerer 1998, p. 1). Salinity in psu is determined by electrical conductivity of a solution, whereas salinity in parts per thousand (ppt) is determined as the weight of salts in a solution. For use in this document, the two measurements are essentially equivalent. X2 is defined as the distance in kilometers up the axis of the estuary (to the east) from the Golden Gate Bridge to the location where the daily average near-bottom salinity is 2 psu (Jassby *et al.* 1995, p. 274; Dege and Brown 2004, p. 51)).

Longfin smelt in the Bay-Delta may spawn as early as November and as late as June, although spawning typically occurs from January to April (CDFG 2009, p. 10; Moyle 2002, p. 36). Longfin smelt have been observed in their winter and spring spawning period as far upstream as Isleton in the Sacramento River, Santa Clara shoal in the San Joaquin system, Hog

Slough off the South-Fork Mokelumne River, and in Old River south of Indian Slough (CDFG 2009a, p. 7; Radtke 1966, pp. 115–119).

Exact spawning locations in the Delta are unknown and may vary from year to year in location, depending on environmental conditions. However, it seems likely that spawning locations consist of the overlap of appropriate conditions of flow, temperature, and salinity with appropriate substrate (Rosenfield 2010, p. 8). Longfin smelt are known to spawn over sandy substrates in Lake Washington and likely prefer similar substrates for spawning in the Delta (Baxter *et. al.* 2010, p. 62; Sibley and Brocksmith 1995, pp. 32–74). Baxter found that female longfin smelt produced between 1,900 and 18,000 eggs, with fecundity greater in fish with greater lengths (CDFG 2009, p. 11). At 7°C (44.6°F), embryos hatch in 40 days (Dryfoos 1965, p. 42); however, incubation time decreases with increased water temperature. At 8–9.5°C (46.4–49.1 °F), embryos hatch at 29 days (Sibley and Brocksmith 1995, pp. 32–74).

Larval longfin smelt less than 12 millimeters (mm) (0.5 in) in length are buoyant because they have not yet developed an air bladder; as a result, they occupy the upper one-third of the water column. After hatching, they quickly make their way to the LSZ via river currents (CDFG 2009, p. 8; Baxter 2011a, pers comm.). Longfin smelt develop an air bladder at approximately 12–15 mm (0.5–0.6 in.) in length and are able to migrate vertically in the water column. At this time, they shift habitat and begin living in the bottom two-thirds of the water column (CDFG 2009, p. 8; Baxter 2008, p. 1).

Longfin smelt larvae can tolerate salinities of 2–6 psu within days of hatching, and can

tolerate salinities up to 8 psu within weeks of hatching (Baxter 2011a, pers. comm.). However, very few larvae (individuals less than 20 mm in length) are found in salinities greater than 8 psu, and it takes almost 3 months for longfin smelt to reach juvenile stage. A fraction of juvenile longfin smelt individuals are believed to tolerate full marine salinities (greater than 8 psu) (Baxter 2011a, pers. comm.).

Longfin smelt are dispersed broadly in the Bay-Delta by high flows and currents, which facilitate transport of larvae and juveniles long distances. Longfin smelt larvae are dispersed farther downstream during high freshwater flows (Dege and Brown 2004, p. 59). They spend approximately 21 months of their 24-month life cycle in brackish or marine waters (Baxter 1999, pp. 2–14; Dege and Brown 2004, pp. 58–60).

In the Bay-Delta, most longfin smelt spend their first year in Suisun Bay and Marsh, although surveys conducted by the City of San Francisco collected some first-year longfin in coastal waters (Baxter 2011c, pers. comm.; City of San Francisco 1995, no pagination). The remainder of their life is spent in the San Francisco Bay or the Gulf of Farallones (Moyle 2008, p. 366; City of San Francisco 1995, no pagination). Rosenfield and Baxter (2007, pp. 1587, 1590) inferred based on monthly survey results that the majority of longfin smelt from the Bay-Delta were migrating out of the estuary after the first winter of their life cycle and returning during late fall to winter of their second year. They noted that migration out of the estuary into nearby coastal waters is consistent with captures of longfin smelt in the coastal waters of the Gulf of Farallones. It is possible that some longfin smelt may stay in the ocean and not re-enter freshwater to spawn until the end of their third year of life (Baxter 2011d, pers. comm.). Moyle

(2010, p. 8) states that longfin smelt that migrate out of and back into the Bay-Delta estuary may primarily be feeding on the rich planktonic food supply in the Gulf of Farallones. Rosenfield and Baxter (2007, p. 1290) hypothesize that the movement of longfin smelt into the ocean or deeper water habitat in summer months is at least partly a behavioral response to warm water temperatures found during summer and early fall in the shallows of south San Francisco Bay and San Pablo Bay (Rosenfield and Baxter 2007, p. 1590).

In the Bay-Delta, calanoid copepods such as *Pseudodiaptomus forbesi* and *Eurytemora sp.*, as well as the cyclopoid copepod *Acanthocyclops vernalis* (no common names), are the primary prey of longfin smelt during the first few months of their lives (approximately January through May) (Slater 2009b, slide 45). Copepods are a type of zooplankton (organisms drifting in the water column of oceans, seas, and bodies of fresh water). The longfin smelt's diet shifts to include mysids such as opossum shrimp (*Neomysis mercedis*) and other small crustaceans (*Acanthomysis sp.*) as soon as they are large enough (20–30 mm (0.78–1.18 in)) to consume these larger prey items, sometime during the summer months of the first year of their lives (CDFG 2009, p. 12). Upstream of San Pablo Bay, mysids and amphipods form 80–95 percent or more of the juvenile longfin smelt diet by weight from July through September (Slater 2009, unpublished data). Longfin smelt occurrence is likely associated with the occurrence of their prey, and both of these invertebrate groups occur near the bottom of the water column during the day under clear water marine conditions.

Lake Washington Population

The Lake Washington population near Seattle, Washington is considered a landlocked population of longfin smelt, as are the populations of longfin smelt in Harrison and Pitt Lakes in British Columbia east of Vancouver (Chigbu and Sibley 1994, p. 1). These populations are not anadromous and complete their entire life cycle in freshwater. Young longfin smelt feed primarily on the copepods *Diaptomus*, *Diaphanosoma*, and *Epischura*, with older fish switching over to mysids (Wydoski and Whitney 2003, p. 105). Chigbu and Sibley (1994, pp. 11–14) found that mysids dominate the diets of longfin smelt in their second year of life (age-1), while amphipods, copepods, and daphnia also contributed substantially to the longfin smelt's diet. A strong spawning run of longfin smelt occurs on even years in Lake Washington, with weak runs on odd years. They spawn at night in the lower reaches of at least five streams that flow into Lake Washington. Water temperatures during spawning were 4.4° C (40° F) to 7.2° C (45° F) (Wydoski and Whitney 2003, p. 105). Chigbu and Sibley (1994, p. 9) found that female longfin smelt produced between 6,000 and 24,000 eggs, while Wydoski and Whitney (2003, p. 105) found that longfin smelt produced between 1,455 and 1,655 eggs. The reason for the large difference between the observations of these two studies is not known.

Habitat

Longfin smelt have been collected in estuaries from the Bay-Delta (33° N latitude) to Prince William Sound (62° N latitude), a distance of approximately 1,745 nautical miles (Figure 1). Mean annual water temperatures range from 2.4°C (36.3° F) in Anchorage to 14.1° C (57.3° F) in San Francisco (NOAA 2011a). The different estuary types that the longfin smelt is found in and the range of variability of environments where the species has been observed will be

discussed below.

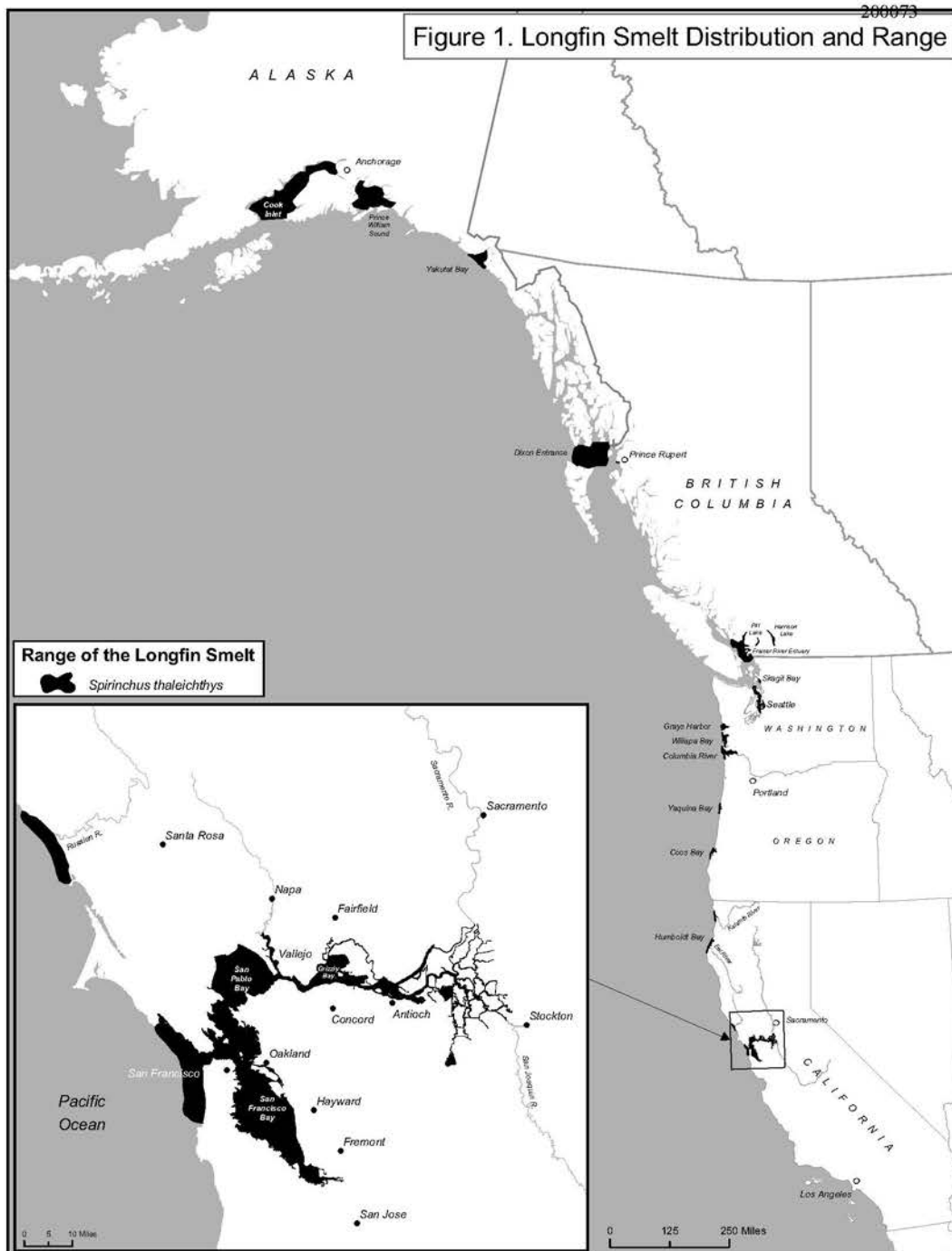


FIGURE 1. Map of coastal sites where longfin smelt are known to occur.

The origin and geomorphology of West Coast estuaries result from geologic forces driven by plate tectonics and have been modified by glaciations and sea level rise (Emmett *et al.* 2000, pp. 766–767). Major classifications of estuaries include fjord, drowned-river valley, lagoon, and bar-built. Fjords typically are long, narrow, steep-sided valleys created by glaciation, with moderately high freshwater inflow but little mixing with seawater due to the formation of a sill at the mouth (NOAA 2011b). Fjords generally have one large tributary river and numerous small streams (Emmett *et al.* 2000, p. 768). Drowned-river valleys, also termed coastal plain estuaries, are found primarily in British Columbia, Washington, and Oregon, and are the dominant type along the west coast, occurring as a result of rising sea levels following the last ice age. Lagoons, primarily found in California, occur where coastal river systems that are closed to the sea by sand spits for much of the year are breached during the winter (Emmett *et al.* 2000, p. 768). The rarest type of estuary is the bar-built, which is formed by a bar and semi-enclosed body of water (Emmett *et al.* 2000, p. 768). Estuaries have also been classified by physical or environmental variables into Northern Riverine, Southern California, Northern Estuarine, Central Marine, Fjord, and Coastal Northwest Groups (Monaco *et al.* 1992, p. 253). Longfin smelt have been collected from estuaries of all types and classifications.

The Bay-Delta is the largest estuary on the West Coast of the United States (Sommer *et al.* 2007, p. 271). The modern Bay-Delta bears only a superficial resemblance to the historical Bay-Delta. The Bay-Delta supports an estuary covering approximately 1,235 square kilometers (km²) (477 square miles (mi²)) (Rosenfield and Baxter 2007, p. 1577), which receives almost half of California's runoff (Lehman 2004, p. 313). The historical island marshes surrounded by low natural levees are now intensively farmed and protected by large, manmade structures

(Moyle 2002, p. 32). The watershed, which drains approximately 40 percent of the land area of California, has been heavily altered by dams and diversions, and nonnative species now dominate, both in terms of numbers of species and numbers of individuals (Kimmerer 2004, pp. 7–9). The Bay Institute has estimated that intertidal wetlands in the Delta have been diked and leveed so extensively that approximately 95 percent of the 141,640 hectares (ha) (350,000 acres (ac)) of tidal wetlands that existed in 1850 are gone (The Bay Institute 1998, p. 17).

The physical and biological characteristics of the estuary define longfin smelt habitat. The Bay-Delta is unique in that it contains significant amounts of tidal freshwater (34 km² (13 mi²)) and mixing zone (194 km² (75 mi²)) habitat (Monaco *et al.* 1992, pp. 254–255, 258). San Francisco Bay is relatively shallow and consists of a northern bay that receives freshwater inflow from the Sacramento-San Joaquin system and a southern bay that receives little freshwater input (Largier 1996, p. 69). Dominant fish species are highly salt-tolerant and include the commercially important Pacific sardine (*Sardinops sagax*) and rockfish (*Sebastes* spp.). Major habitat types include riverine and tidal wetlands, mud flat, and salt marsh, with substantial areas of diked wetland managed for hunting. The sandy substrates that longfin smelt are presumed to use for spawning are abundant in the Delta.

The Russian River collects water from a drainage area of approximately 3,846 km² (1,485 mi²), has an average annual discharge of 1.6 million acre-feet, and is approximately 129 km (80 mi) in length (Langridge *et al.* 2006, p. 4). Little information is available on potential spawning and rearing habitat for longfin smelt, but it is likely to be both small and ephemeral because spawning and rearing habitat is highly dependent upon freshwater inflow, and there may

be insufficient freshwater flows for spawning and rearing in some years (Moyle 2010, p. 5). A berm encloses the mouth of the Russian River during certain times of the year, essentially cutting it off from the coastal ocean. This results in a lack of connectivity with the ocean that could be important during dry years. However, in most years the berm is breached by freshwater flows, which allows longfin smelt to enter the Russian River and spawn.

The Eel River drains an area of 3,684 mi² (9,542 km²) and is the third largest river in California. Wetlands and tidal areas have been reduced 60 to 90 percent since the 1800s (Cannata and Hassler 1995, p. 1), resulting in changes in tidal influence and a reduction in channel connectivity (Downie 2010, p. 15). The estuary is characterized by a small area where freshwater and saltwater mix (Monaco *et al.* 1992, p. 258) and thus provides only limited potential longfin rearing habitat.

Humboldt Bay is located only 26 km (16 mi) north of the Eel River and is approximately 260 mi (418 km) north of the Bay-Delta. Humboldt Bay is the second largest coastal estuary in California after the Bay-Delta. However, true estuarine conditions rarely occur in Humboldt Bay because it receives limited freshwater input and experiences little mixing of freshwater and saltwater (Pequegnat and Butler 1982, p. 39).

The Klamath Basin has been extensively modified by levees, dikes, dams, and the draining of natural water bodies since the U.S. Bureau of Reclamation's Klamath Project, designed to improve the region's ability to support agriculture, began in 1905. These changes to the system have altered the biota of the basin (NRC 2008, p. 16). Over the years, loss of

thousands of acres of connected wetlands and open water in the Klamath River Basin has greatly reduced habitat value, likely depleting the ability of this area to cycle nutrients and affecting water quality (USFWS 2008, p. 55). The river drains a vast area of 10 million ac (4 million ha). Although a large river, the Klamath River estuary is characterized by small tidal freshwater and mixing zones (Monaco *et al.* 1992, p. 258) and thus provides limited potential longfin smelt rearing habitat.

Yaquina Bay is located on the mid-coastal region of Oregon, 201 km (125 mi) south of the Columbia River and 348 km (216 mi) north of the California border. Wetlands encompass 548 ha (1,353 ac), including 216 ha (534 ac) of mud flats and 331 ha (819 ac) of tidal marshes (Yaquina Bay Geographic Response Plan 2005, p. 2.1). Forty-eight percent of the estuary is intertidal (Brown *et al.* 2007, p. 6). The estuary has been modified greatly, being alternately dredged and filled at different locations as a result of development. Dredging, industrial, and residential uses have reduced fish habitat and water quality in the bay. Dredging disturbs sediment, resulting in increased turbidity and reduced sunlight penetration, which can impact native eelgrasses and the benthic species dependent eelgrass beds for breeding, spawning, and shelter (Oberrecht 2011, pp. 1–8).

On the Columbia River, dams, dikes, maintenance dredging, and urbanization have all contributed to habitat loss and alterations that have negatively affected fish and wildlife populations (Lower Columbia River Estuary Partnership 2011, p. 1). It is estimated that as much as 43 percent of estuarine tidal marshes and 77 percent of tidal swamps in the river estuary available for fish species have been lost since 1870 (Columbia River Estuary Study

Taskforce2006, pp. 1–30). Sixty square miles of peripheral tidal habitat have been lost to diking, filling, and conversion to upland habitat for industrial and agricultural use since 1870 (Columbia River Estuary Study Taskforce 2006, p. 1). Prior to construction of dams, estuary islands and much of the floodplain were inundated throughout the year, beginning in December and again in May or June. Dam operations on the Columbia River’s main stem and major tributaries have substantially reduced peak river flows. Dikes and levees have all but eliminated flooding in many low-lying areas. Dredging of shipping channels has caused loss of wetlands and altered shoreline configuration. Dredging has resulted in large sediment reductions upstream, and the dredged sediments have created islands downstream. This has likely reduced spawning habitat and sheltering sites for fish (OWJP 1991, pp. 1–24; Lower Columbia Fish Recovery Board 2004a, pp. 1–192).

Puget Sound is a large saltwater estuary of interconnected flooded glacial valleys located at the northwest corner of the State of Washington. Puget Sound is about 161 km (100 mi) long, covers about 264,179 ha (652,800 ac), and has over 2,092 km (1,300 mi) of shoreline. Fed by streams and rivers from the Olympic and Cascade Mountains, waters flow out to the Pacific Ocean through the Strait of Juan de Fuca (Lincoln 2000, p. 1). The basin consists of eight major habitat types, the largest of which is kelp and eelgrass, but also includes wetlands, mudflats, and sandflats. Puget Sound consists of five regions, each with its own physical and biological characteristics. Urban and industrial development borders the main basin, which is bounded by Port Townsend on the north and the Narrows (Tacoma) on the south. Approximately 30 percent of freshwater inflow to the main basin is from the Skagit River, which drains an area of approximately 8,011 km² (3,093 mi²). Sills at Admiralty Inlet and the Narrows influence

circulation. Puget Sound is highly productive. The fish community includes many commercially important species, such as Pacific herring, Pacific salmon, and several species of rockfish (NOAA 2011c, p. 11). There are 10 major dams and thousands of small water diversions in the Puget Sound system (Puget Sound Partnership 2008b, p. 21). Human activities in the region have resulted in the loss of 75 percent of the saltwater marsh habitat and 90 percent of the estuarine and riverine wetlands (Puget Sound Partnership 2008b, p. 21).

The coastline of British Columbia has been shaped by plate tectonics and extensive glaciations. Particularly in summer, prevailing winds drive coastal upwelling, which results in a highly productive food chain. The tidal amplitude is 3–5 meters (m) (9.8–16.4 ft) in most areas, and numerous large and small rivers provide freshwater inflow. Biological communities are diverse and highly variable, including coastal wetlands, kelp beds, and seaweed beds that support a diverse marine fauna (Dale 1997, pp. 13–15). Nearshore areas of British Columbia are characterized by steep to moderately sloping fjords, 20–50 m (65–164 ft) in depth, with salinities ranging from 18 to 28 ppt (AXYS Environmental Consulting 2001, pp. 5, 11, 20). Bar-built estuaries that are semi-enclosed by an ocean-built bar occur on the west coast of Vancouver Island and the Queen Charlotte Islands (Emmett *et al.* 2000, pp. 769–770). Oxygen depletion is common in fjords (Emmett *et al.* 2000, p. 776), but because they are anadromous, longfin smelt would presumably be able to avoid those conditions. However, if depletion were to occur during spawning or rearing, recruitment could be affected.

The Fraser River, at approximately 1,375 miles (2,213 km), is the longest river in British Columbia and the tenth longest river in Canada. The Fraser River drains an area of 220,000 km²

and flows to the Strait of Georgia at the City of Vancouver before it drains into the Pacific Ocean. Diking and drainage in the lower basin area have reduced the extent of estuarine wetlands that are important to the longfin smelt and other fishes that utilize these areas (Blomquist 2005, p. 8).

Habitat types common in Alaskan estuaries include eel grass beds, understory kelp, sand and gravel beds, and bedrock outcrops (NOAA 2011d). Shallow nearshore areas provide a mosaic of habitat types that support a variety of fishes (NOAA 2005, p. 59). In southwestern Alaska, the related osmerid species capelin (*Mallotus villosus*) was found to occur in sand-and-gravel habitats, and the surf smelt (*Hypomesus pretiosus*) was found to occur in bedrock habitats (NOAA 2005, pp. 27, 29). As in British Columbia, if oxygen depletion occurs in fjord habitats during spawning or rearing, longfin smelt recruitment could be affected.

Cook Inlet is a large mainland Alaskan estuary located in the northern Gulf of Alaska. Cook Inlet is approximately 290 km (180 miles) long. The watershed covers about 100,000 km² of southern Alaska (USACE 2011, p. 1).

Distribution

Longfin smelt are widely distributed along 3,541 km (2,200 mi) of Pacific coastline from the Bay-Delta to Cook Inlet, Alaska (Table 1). We found no evidence of range contraction; the current distribution of longfin smelt appears to be similar to its historical distribution.

TABLE 1. Known occurrences of longfin smelt.

State	Location	Reference
California	Monterey Bay	Eschmeyer 1983, p. 82; Wang 1986, pp. 6–10).
	Bay-Delta	Eschmeyer 1983, p. 82; Wang 1986, pp. 6–10
	Offshore Bay-Delta	City of San Francisco 1993, p. 5-8
	Russian River Estuary	Cook 2010, pers. comm.
	Van Duzen River	Moyle 2002, p. 235
	McNulty Slough of Eel River	CDFG 2010, unpublished data
	Offshore Humboldt Bay	Quirollo 1994, pers. comm.
	Humboldt Bay and tributaries	CDFG 2010, unpublished data
	Mad River	Moyle 2002, p. 235
	Klamath River	Kisanuki <i>et. al.</i> 1991, p. 72, CDFG 2009, p. 5
	Lake Earl	D. McLeod field note 1989 (Cannata and Downie 2009)
Oregon	Coos Bay	Veroujean 1994, p. 1
	Yaquina Bay	ODFW 2011, pp. 1-3, ANHP 2006, p. 3
	Tillamook Bay	Ellis 2002, p. 17
	Columbia River Estuary	ODFW 2011, pp. 1–3
Washington	Willapa Bay	WDFW 2011, pp. 1–3
	Grays Harbor	U.S. Army Corps of Engineers 2000, p. 2
	Puget Sound Basin	Miller and Borton 1980, p. 17.4
	Lake Washington	Chigbu and Sibley 1994, p. 1
British Columbia	Fraser River	Fishbase 2011a, p. 1; Fishbase 2011b, p. 1
	Pitt Lake	Taylor 2011, pers. comm.
	Harrison Lake	Page and Burr 1991, p. 57
	Vancouver	Hart 1973, p. 147
	Prince Rupert	Hart 1973, p. 147
	Skeena Estuary	Kelson 2011, pers. comm.
Alaska	Dixon Entrance	Alaska Natural Heritage Program 2006, p. 3
	Sitka National Historical Park	NPS 2011, p. 1
	Glacier Bay	Arimitsu 2003, pp. 35, 41
	Klondike Gold Rush National Historical Park	NPS 2011, p. 1
	Yakutat Bay	Alaska Natural Heritage Program 2006, p. 3
	Wrangell-St. Elias National Park	Arimitsu 2003, pp. 35, 41, NPS 2011, p. 1

State	Location	Reference
	Cook Inlet	NOAA 2010b, p. 4, NOAA 2010a, p. 8
	Kachemak Bay	Abookire <i>et al.</i> 2000, NPS 2011, p. 1
	Hinchinbrook Island	Alaska Natural Heritage Program 2006, p. 3
	Lake Clark National Park and Preserve	NPS 2011, p. 1
	Prince William Sound	Alaska Natural Heritage Program 2006, p. 3

California

The southernmost known population of longfin smelt is the Bay-Delta estuary, and longfin smelt occupy different habitats of the estuary at various stages in their life cycle (See Habitat section above). Eschmeyer (1983, p. 82) reported the southern extent of the range as Monterey Bay, and Wang (1986, pp. 6–10) reported that an individual longfin smelt had been captured at Moss Landing in Monterey Bay in 1980. Most sources, however, identify the Bay-Delta as the southern extent of the species' range (Moyle 2002, p. 235).

Small numbers of longfin were collected within the Russian River estuary each year between 1997 and 2000 (SCWA 2001, p. 18). No surveys were conducted in 2001 or 2002 (Cook 2011, pers. comm.). Recent surveys (since 2003) in the Russian River estuary conducted by Sonoma County Water Agency have not collected longfin smelt; however, in 2003, trawling surveys were replaced by beach seining, a type of survey less likely to capture a pelagic fish species such as the longfin smelt. Longfin smelt breeding has not been documented at the Russian River (Baxter 2011b, pers. comm.), and because of its limited size, the Russian River estuary is not believed to be capable of supporting a self-sustaining longfin smelt population

(The Bay Institute *et al.* 2007, p. ii; Moyle 2010, p. 5).

Longfin smelt were observed spawning in the Eel River estuary in 1974 (Puckett 1977, p. 19). Although longfin were observed in the Eel River in 2008 and 2009 (Cannata and Downie 2009), it is unknown whether or not they currently spawn there. Humboldt Bay is located 420 km (260 mi) north of the Bay-Delta. Longfin smelt were collected in Humboldt Bay or its tributaries every year from 2003 to 2009, with the exception of 2004 (CDFG 2010, unpublished data). Longfin smelt also have been observed in coastal waters adjacent to Humboldt Bay (Quirollo 1994, pers. comm.). The Humboldt Bay population is thought to be the nearest known breeding population to the Bay-Delta (Baxter 2011b, pers. comm.). Longfin smelt were collected consistently in the Klamath River estuary between 1979 and 1989 (Kisanuki *et al.* 1991, p. 72), and one longfin smelt was collected in the Klamath River in 2001 (CDFG 2009, p. 5).

Oregon

In Oregon, there are historical records of longfin smelt in Tillamook Bay, Columbia River, Coos Bay, and Yaquina Bay (ANHP 2006, p. 3). One individual was detected in Tillamook Bay in 2000 (Ellis 2002, p. 17). Williams *et al.* (2004, p. 30) collected 308 longfin in the Columbia River estuary in 2004. Longfin smelt were reported in the Columbia River estuary, the coastal waters adjacent to the Columbia River, and in Yaquina Bay in 2009 (Nesbit 2011, pers. comm.). In Coos Bay, longfin smelt were detected in low numbers in the early 1980s. However, longfin smelt do not appear to be common in Coos Bay and were not detected

during sampling that occurred in the 1970s and the late 1980s (Veroujean 1994, no pagination).

Washington

In Washington, within the Puget Sound Basin, longfin smelt are known to occur in the Nooksack River, Bellingham Bay, Snohomish River, Duwamish River, Skagit Bay, Strait of San Juan de Fuca, Twin River, and Pysht River (Table 1). Longfin smelt are known to occur in nearby Bellingham Bay (Penttila 2007, p. 4). Longfin smelt were collected in the Snohomish River estuary during extensive beach seine and fyke trapping in 2009 (Rice 2010, pers. comm.). Longfin smelt were captured (reported as non-target) in high-rise otter trawls in the lower Duwamish River (Anchor and King County 2007, p. 11). Longfin smelt are common in the Strait of San Juan de Fuca (Penttila 2007, p. 4). Miller *et al.* (1980, p. 28) found longfin smelt to be the second most common species in tow-net surveys conducted in the Strait of San Juan de Fuca. Most fish caught in these surveys were young of the year and were found near the Twin and Pysht Rivers, both of which may have suitable spawning grounds (Miller *et al.* 1980, p. 28). Occurrences of longfin smelt within northern Puget Sound and the Strait of Georgia may reflect the abundance and distribution of the anadromous populations from the Fraser River in British Columbia (Washington Department of Fish and Wildlife 2011, pp. 1–3). Currently, the National Park Service states that longfin smelt are probably present within Olympic National Park (NPS 2011, p. 1). Longfin smelt appear to be common in Grays Harbor (U.S. Army Corps of Engineers 2000, p. 2). Longfin smelt have been infrequently documented in the upper Chehalis estuary at Cosmopolis; however, when they do occur, they have been reported as abundant (Anderson 2011). Ocean trawls off Willapa Bay have collected longfin smelt, although no

spawning population has been identified in the basin (Anderson 2011).

A resident, freshwater population of longfin smelt occurs in Lake Washington (Chigbu and Sibley 1994, p. 1). First caught in 1959, it is believed that the longfin smelt either were introduced to the lake or became trapped during canal construction (Chigbu *et. al.* 1998, p. 180). In the 1960s, the abundance of longfin smelt in Lake Washington was low but increased to higher levels in the 1980s (Chigbu and Sibley 1994, p. 4).

British Columbia

Longfin smelt populations occur in Pitt Lake and Harrison Lake in British Columbia (Page and Burr 1991, p. 57; Taylor 2011, pers. comm.); these populations are believed to be resident fish that are not anadromous (that is, they are thought to complete their entire life cycle in freshwater). Pitt Lake is located approximately 64 river km (40 mi) up the Fraser and Pitt Rivers, and Harrison Lake is located approximately 121 river km (75 mi) up the Fraser and Harrison Rivers. Longfin smelt are known to occur within the Fraser River near Vancouver (Hart 1973, p. 147; Fishbase 2011a, p. 1; Fishbase 2011b, p. 1). Longfin smelt are also known to occur in the Skeena River estuary near Prince Rupert (Hart 1973, p. 147; Kelson 2011, pers. comm.; Gottesfeld 2002, p. 54)

Alaska

In Alaska, longfin smelt are known from Hinchinbrook Island, Prince William Sound,

Dixon Entrance, Yakutat Bay, and Cook Inlet (Alaska Natural Heritage Program 2006, p. 3). In nearly 1,000 recent beach seine surveys in Alaska, longfin smelt have only been caught off Fire Island in upper Cook Inlet in 2009 and 2010 (NOAA 2010b, p. 4; Johnson 2010, pers. comm.; Wing 2010, pers. comm.). However, as stated earlier, longfin smelt are unlikely to be caught in beach seine surveys because they are a pelagic species and do not typically occur near shore where beach seine surveys take place. Surveys in Prince William Sound did not collect longfin smelt in 2006 or 2007 (NOAA 2011, p. 1). Longfin smelt were collected in Wrangell-St. Elias National Park and Glacier Bay in 2001 and 2002 (Arimitsu 2003, pp. 35, 41). Longfin were collected in Kachemak Bay in 1996–1998 seine and trawling surveys (Abookire *et al.* 2000). The NPS was not able to confirm presence or absence in Lake Clark National Park and Preserve. The NPS concludes that presence is probable in Glacier Bay National Park and Preserve, Klondike Gold Rush National Historical Park, Sitka National Historical Park, and Wrangell-St. Elias National Park and Preserve (NPS 2011, p. 1).

Abundance

In most locations throughout their range, longfin smelt populations have not been monitored. Within the Bay-Delta, longfin smelt are consistently collected in the monitoring surveys that have been conducted by CDFG as far back as the late 1960s. We know of no similar monitoring data for other longfin smelt populations. CDFG did report catches of longfin smelt in Humboldt Bay from surveys conducted between 2003 and 2009; small numbers of longfin were collected each of the years except 2004 (CDFG 2010, unpublished data). Moyle (2002, p. 237; 2010, p. 4) noted that the longfin smelt population in Humboldt Bay appeared to

have declined between the 1970s and 2002, but survey data are not available from that time.

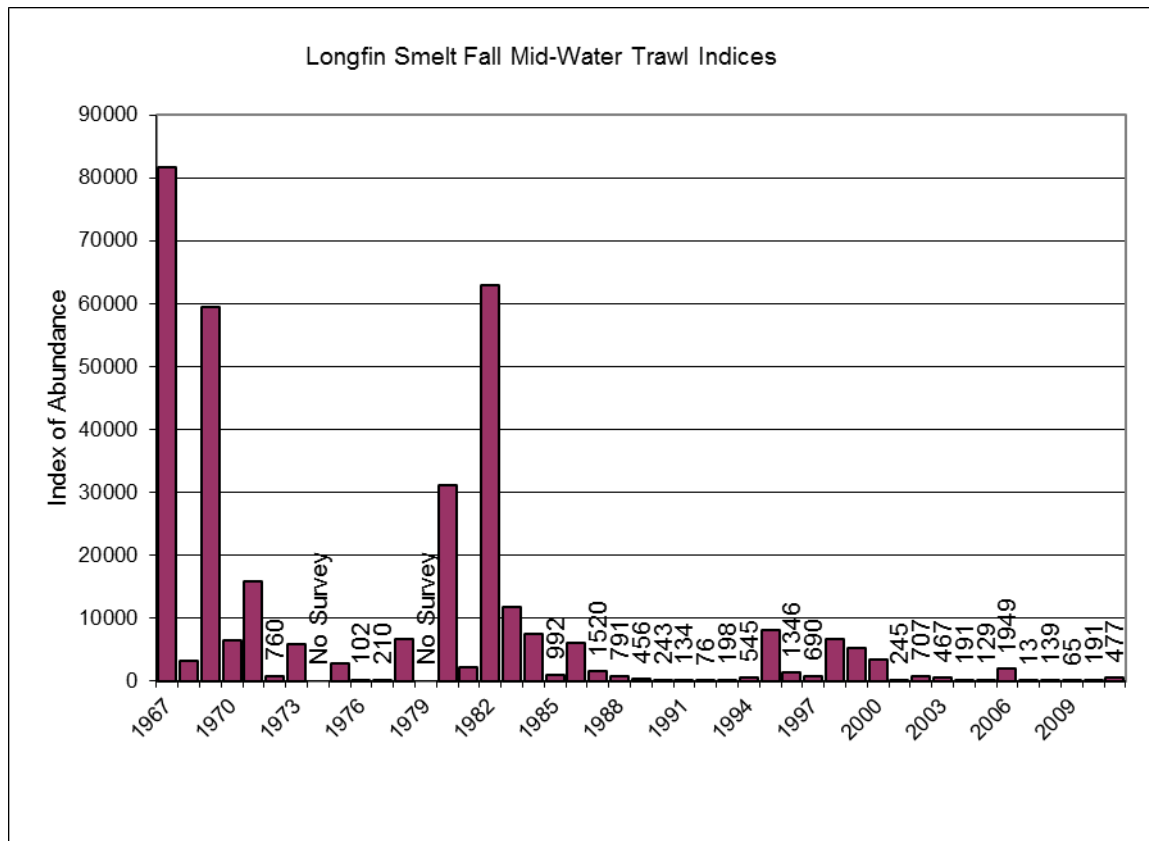
Longfin smelt numbers in the Bay-Delta have declined significantly since the 1980s (Moyle 2002, p. 237; Rosenfield and Baxter 2007, p. 1590; Baxter *et al.* 2010, pp. 61–64). Rosenfield and Baxter (2007, pp. 1577–1592) examined abundance trends in longfin smelt using three long-term data sets (1980–2004) and detected a significant decline in the Bay-Delta longfin smelt population. They confirmed the positive correlation between longfin smelt abundance and freshwater flow that had been previously documented by others (Stevens and Miller 1983, p. 432; Baxter *et al.* 1999, p. 185; Kimmerer 2002b, p. 47), noting that abundances of both adults and juveniles were significantly lower during the 1987–1994 drought than during either the pre- or post-drought periods (Rosenfield and Baxter 2007, pp. 1583–1584).

Despite the correlation between drought and low population in the 1980s and 90s, the declines in the first decade of this century appear to be caused in part by additional factors. Abundance of longfin smelt has remained very low since 2000, even though freshwater flows increased during several of these years (Baxter *et al.* 2010, p. 62). Abundance indices derived from the Fall Midwater Trawl (FMWT), Bay Study Midwater Trawl (BSMT), and Bay Study Otter Trawl (BSOT) all show marked declines in Bay-Delta longfin smelt populations from 2002 to 2009 (Messineo *et al.* 2010, p. 57). Longfin smelt abundance over the last decade is the lowest recorded in the 40-year history of CDFG's FMWT monitoring surveys. Scientists became concerned over the simultaneous population declines since the early 2000s of longfin smelt and three other Bay-Delta pelagic fish species—delta smelt (*Hypomesus transpacificus*), striped bass (*Morone saxatilis*), and threadfin shad (*Dorosoma petenense*) (Sommer *et al.* 2007,

p. 273). The declines of longfin smelt and these other pelagic fish species in the Bay-Delta since the early 2000s has come to be known as the Pelagic Organism Decline, and considerable research efforts have been initiated since 2005, to better understand causal mechanisms underlying the declines (Sommer *et al.* 2007, pp. 270–277; MacNally *et al.* 2010, pp. 1417–1430; Thomson *et al.* 2010, pp. 1431–1448). The population did increase in the 2011 FMWT index to 477 (Contreras 2011, p. 2), probably a response to an exceptionally wet year.

The FMWT index of abundance in the Bay-Delta shows great annual variation in abundance but a severe decline over the past 40 years (Figure 2). The establishment of the overbite clam (*Corbula amurensis*) in the Bay-Delta in 1987 is believed to have contributed to the population decline of longfin smelt (See Factor E: Introduced Species, below), as well as to the declining abundance of other pelagic fish species in the Bay-Delta (Sommer *et al.* 2007, p. 274). Figure 2 shows low values of the abundance index for longfin smelt during drought years (1976–1977 and 1986–1992) and low values overall since the time that the overbite clam became established in the estuary.

FIGURE 2. Longfin smelt abundance (total across year-classes) as indexed by the Fall Mid-Water Trawl of the Bay-Delta, 1967–2011.



* The survey was not conducted in 1974 or 1979.

** Index values for years of very low abundance were added.

Using data from 1975–2004 from the FMWT survey, Rosenfield and Baxter 2007 (p. 1589) found that longfin smelt exhibit a significant stock-recruitment relationship—abundance of juvenile (age-0) fish is directly related to the abundance of adult (age-1) fish from the previous year. They found that the abundance of juvenile fish declined by 90 percent during the time period analyzed. Rosenfield and Baxter (2007, p. 1589) also found a decline in age-1 individuals that was significant even after accounting for the decline in the age-0 population. If unfavorable environmental conditions persist for one or more years, recruitment into the population could be suppressed, affecting the species' ability to recover to their previous abundance. The current low abundance of adult longfin smelt within the Bay-Delta could reduce the ability of the species to

persist in the presence of various threats.

Conservation Actions

Bay-Delta

The CALFED program existed as a multi-purpose (water supply, flood protection, and conservation) program with significant ecosystem restoration and enhancement elements. Implemented by the California Bay-Delta Authority, the program brought together more than 20 State and Federal agencies to develop a long-term comprehensive plan to restore ecological health and improve water management for all beneficial uses in the Bay-Delta system. The program specifically addressed ecosystem quality, water quality, water supply, and levee system integrity. The California Bay-Delta Authority was replaced in 2009 by the Delta Stewardship Council, but many of its programs continue to be implemented and are now housed within the CALFED program's former member agencies.

The CALFED Ecosystem Restoration Program (ERP) developed a strategic plan for implementing an ecosystem-based approach for achieving conservation targets (CALFED 2000a, pp. 1–3). The CDFG is the primary implementing agency for the ERP. The goal of ERP in improving conditions for longfin smelt will carry forward, irrespective of the species Federal listing status. CALFED had an explicit goal to balance the water supply program elements with the restoration of the Bay-Delta and tributary ecosystems and recovery of the longfin smelt and other species. Because achieving the diverse goals of the program is iterative and subject to

annual funding by diverse agencies, the CALFED agencies have committed to maintaining balanced implementation of the program within an adaptive management framework. The intention of this framework is that the storage, conveyance, and levee program elements would be implemented in such a way that the longfin smelt's status would be maintained and eventually improved.

CALFED identified 54 species enhancement conservation measures for longfin smelt, more than half of which have been completed (CALFED Ecosystem Restoration Project 2011, entire). One such restoration action at Liberty Island at the southern end of the Yolo Bypass (a flood control project) has likely benefitted longfin smelt. After years of active agricultural production on Liberty Island, the levees were breached in 1997, and the island was allowed to return to a more natural state (Wilder 2010, slide 4). Wildlands Corporation has recently completed a restoration project removing several levees surrounding Liberty Island and creating 186 acres of various habitats for fish (Wildlands 2011, p. 1). Longfin smelt are utilizing the flooded island, and were collected in a number of surveys between 2003 and 2005 (Liberty Island Monitoring Program 2005, pp. 42–44; Marshall *et al.* 2006, p. 1).

The Bay-Delta Conservation Plan (BDCP), an effort to help provide restoration of the Bay-Delta ecosystem and reliable water supplies, is currently in preparation by a collaborative of water agencies, resource agencies, and environmental groups. The BDCP is intended to provide a basis for permitting take of listed species under sections 7 and 10 of the Act and the California Natural Communities Conservation Planning Act, and would provide a comprehensive habitat conservation and restoration plan for the Bay-Delta, as well as a new funding source. The BDCP

shares many of the same goals outlined in the 2000 CALFED Record of Decision (CALFED 2000) but would not specifically address all listed-species issues. The BDCP would, however, target many of the threats to current and future listed species and could contribute to species recovery. However, the BDCP, if completed, would not be initiated until at least 2013 or later. The plan's implementation is anticipated to extend through 2060.

Humboldt Bay

The Humboldt Bay Watershed Advisory Committee has completed the Humboldt Bay Salmon and Steelhead Conservation Plan with funding from CDFG, National Oceanographic Atmospheric Administration (NOAA), and the California State Coastal Conservancy with the purpose of protecting and restoring salmon habitat in Humboldt Bay through cooperative planning (Humboldt Bay Watershed Advisory Committee 2005, pp. 1–2). Many of the habitat restoration activities proposed may benefit longfin smelt, including restoration in freshwater streams and brackish sloughs. The Natural Resource Services has designed an enhancement program that is based on the Humboldt Bay Salmon and Steelhead Conservation Plan. Natural Resource Services has completed a tidal marsh enhancement project on Freshwater Creek and has other projects in the design stage (Don Allen 2011, pers. comm.). The Natural Resource Services is a division of the Redwood Community Action Agency dedicated to improving the health of northern California communities and the watersheds that they depend on (NRS 2011, p. 1). These types of restoration efforts are current and ongoing and may benefit longfin smelt by increasing access to intertidal areas within Humboldt Bay.

Puget Sound

The Puget Sound Partnership is a Washington State Agency created in 2007, to oversee the restoration and protection of Puget Sound. The Puget Sound Partnership created an Action Agenda that identifies and prioritizes work needed to protect and restore Puget Sound (Puget Sound Partnership 2008b, p. 2). Protection actions including local watershed planning, shoreline management planning, and citizen involvement through groups such as beach watchers and shore stewards are among the current restoration efforts in Puget Sound watershed (Puget Sound Partnership 2008a, pp. 1–2). These measures are expected to benefit longfin smelt by protecting and restoring habitat through legislative approval and funding for land acquisition for protection and restoration of ecologically important lands and habitats and by adding lands to State Aquatic Reserves program (Puget Sound Partnership 2008a, pp. 1–2).

Alaska

State and Federal land ownership affords protection for vast distances of shoreline within Glacier Bay and Wrangell-St. Elias National Parks, Tongass National Forest, and State landholdings. Kachemak Bay, located near the mouth of lower Cook Inlet, is a National Estuarine Research Reserve regarded as extremely important for marine biodiversity conservation (ADFG 2006, pp. 133–134). Alaska's only State wilderness park, Kachemak Bay State Park, is also located in Kachemak Bay (ADNR 2011, p. 1). Yakutat Bay lies between peninsular and mainland Alaska and is bordered by Wrangell-St. Elias National Park to the northwest and Tongass National Forest. The Federal lands surrounding Yakutat Bay protect it from the effects of development. The Tongass National Forest management plan requires that

logging activities be distanced from estuarine and riparian edges (ADFG 2006, p. 107). As a species group, the osmerids are identified in Alaska's Comprehensive Wildlife Conservation Strategy as Species of Greatest Conservation Need (ADFG 2006, pp. 140–143). The Conservation Action Plan for anadromous smelts identifies objectives, issues, and conservation actions to address information gaps. Determining life history, trophic ecology, instream flow and habitat needs, and monitoring protocols are included as measures that need to be undertaken as part of Alaska's Conservation Strategy to identify conservation status and needs of anadromous smelt including longfin.

Summary of Information Pertaining to the Five Factors

Section 4 of the Act (16 U.S.C. 1533) and implementing regulations (50 CFR part 424) set forth procedures for adding species to, removing species from, or reclassifying species on the Federal Lists of Endangered and Threatened Wildlife and Plants. Under section 4(a)(1) of the Act, a species may be determined to be endangered or threatened based on any of the following five factors:

- (A) The present or threatened destruction, modification, or curtailment of its habitat or range;
- (B) Overutilization for commercial, recreational, scientific, or educational purposes;
- (C) Disease or predation;
- (D) The inadequacy of existing regulatory mechanisms; or
- (E) Other natural or manmade factors affecting its continued existence.

In making these findings, information pertaining to each species in relation to the five factors provided in section 4(a)(1) of the Act is discussed below. In considering what factors might constitute threats to a species, we must look beyond the exposure of the species to a particular factor to evaluate whether the species may respond to the factor in a way that causes actual impacts to the species. If there is exposure to a factor and the species responds negatively, the factor may be a threat, and during the status review, we attempt to determine how significant a threat it is. The threat is significant if it drives or contributes to the risk of extinction of the species such that the species warrants listing as endangered or threatened as those terms are defined by the Act. However, the identification of factors that could impact a species negatively may not be sufficient to compel a finding that the species warrants listing. The information must include evidence sufficient to suggest that the potential threat has the capacity (i.e., it should be of sufficient magnitude and extent) to affect the species' status such that it meets the definition of endangered or threatened under the Act.

In making our 12-month finding on the petition, we considered and evaluated the best available scientific and commercial information. Much of the scientific and commercial information available on potential threats to longfin smelt comes from information on the Bay-Delta, and therefore the threats analysis is largely focused on the Bay-Delta longfin smelt population.

Factor A. The Present or Threatened Destruction, Modification, or Curtailment of Its Habitat or Range

Potential threats to longfin smelt habitat include the effects of reduced freshwater flow, climate change, and channel disturbance. Nearly all information available on Factor A threats to longfin smelt come from the Bay-Delta estuary. Therefore, our analysis below focuses on habitat impacts to the Bay-Delta population.

Reduced Freshwater Flow

Most longfin smelt populations, other than those in a few freshwater lakes in Washington and British Columbia, are known from estuaries. Estuaries are complex ecosystems with boundaries between freshwater, brackish water, and saltwater that vary in time and space. Drought and water diversions affect these boundaries by altering the amounts and timing of freshwater flow into and within the estuary. These altered freshwater flows affect the physical and biological characteristics of the estuary, and the physical and biological characteristics of the estuary define longfin smelt habitat.

Many environmental attributes respond to variance in freshwater flow into the estuary, including patterns of flooding and drought, nutrient loading, sediment loading (turbidity), concentration of organic matter and planktonic biota, physical changes in the movement and compression of the salt field, and changes in the hydrodynamic environment (Kimmerer 2002a, p. 40). The San Francisco Estuary exhibits one of the strongest and most consistent responses of biota to flow among large estuaries (Kimmerer 2004, p. 14).

Reduced freshwater flows into estuaries may affect fish and other estuarine biota in

multiple ways. Effects may include: (1) Decreased nutrient loading, resulting in decreased primary productivity; (2) decreased stratification of the salinity field, resulting in decreased primary productivity; (3) decreased organic matter loading and deposition into the estuary; (4) reduced migration cues; (5) decreased sediment loading and turbidity, which may affect both feeding efficiency and predation rates; (6) reduced dilution of contaminants; (7) impaired transport to rearing areas (e.g., low-salinity zones); and (8) reduction in physical area of, or access to, suitable spawning or rearing habitat Kimmerer (2002b, p. 1280).

Bay-Delta Population

Freshwater flow is strongly related to the natural hydrologic cycles of drought and flood. In the Bay-Delta estuary, increased Delta outflow during the winter and spring is the largest factor positively affecting longfin smelt abundance (Stevens and Miller 1983, pp. 431–432; Jassby *et al.* 1995; Sommer *et al.* 2007, p. 274; Thomson *et al.* 2010, pp. 1439–1440). During high outflow periods, larvae presumably benefit from increased transport and dispersal downstream, increased food production, reduced predation through increased turbidity, and reduced loss to entrainment due to a westward shift in the boundary of spawning habitat and strong downstream transport of larvae (CFDG 1992; Hieb and Baxter 1993; CDFG 2009a). Conversely, during low outflow periods, negative effects of reduced transport and dispersal, reduced turbidity, and potentially increased loss of larvae to predation and increased loss at the export facilities result in lower young-of-the-year recruitment. Despite numerous studies of longfin smelt abundance and flow in the Bay-Delta, the underlying causal mechanisms are still not fully understood (Baxter *et al.* 2010, p. 69; Rosenfield 2010, p. 9).

As California's population has grown, demands for reliable water supplies and flood protection have grown. In response, State and Federal agencies built dams and canals, and captured water in reservoirs, to increase capacity for water storage and conveyance resulting in one of the largest manmade water systems in the world (Nichols *et al.* 1986, p. 569). Operation of this system has altered the seasonal pattern of freshwater flows in the watershed. Storage in the upper watershed of peak runoff and release of the captured water for irrigation and urban needs during subsequent low flow periods result in a broader, flatter hydrograph with less seasonal variability in freshwater flows into the estuary (Kimmerer 2004, p. 15).

In addition to the system of dams and canals built throughout the Sacramento River-San Joaquin River basin, the Bay-Delta is unique in having a large water diversion system located within the estuary (Kimmerer 2002b, p. 1279). The State Water Project (SWP) and Central Valley Project (CVP) operate two water export facilities in the Delta (Sommer *et al.* 2007, p. 272). Project operation and management is dependent upon upstream water supply and export area demands. Despite the size of the water storage and diversion projects, much of the interannual variability in Delta hydrology is due to variability in precipitation from year to year. Annual inflow from the watershed to the Delta is strongly correlated to unimpaired flow (runoff that would hypothetically occur if upstream dams and diversions were not in existence), mainly due to the effects of high-flow events (Kimmerer 2004, p. 15). Water operations are regulated in part by the California State Water Resources Control Board (SWRCB) according to the Water Quality Control Plan (WQCP) (SWRCB 2000, entire). The WQCP limits Delta water exports in relation to Delta inflow (the Export/Inflow, or E/I ratio).

It is important to note that in the case of the Bay-Delta, freshwater flow is expressed as both Delta inflow (from the rivers into the Delta) and as Delta outflow (from the Delta into the lower estuary), which are closely correlated, but not equivalent. Freshwater flow into the Delta affects the location of the low salinity zone and X2 within the estuary. Because longfin smelt spawn in freshwater, they must migrate farther upstream to spawn as flow reductions alter the position of X2 and the low-salinity zone moves upstream (CDFG 2009, p. 17). Longer migration distances into the Bay-Delta make longfin smelt more susceptible to entrainment in the State and Federal water pumps (see Factor E: Entrainment Losses). In periods with greater freshwater flow into the Delta, X2 is pushed farther downstream (seaward); in periods with low flows, X2 is positioned farther landward (upstream) in the estuary and into the Delta. Not only is longfin smelt abundance in the Bay-Delta strongly correlated with Delta inflow and X2, but the spatial distribution of longfin smelt larvae is also strongly associated with X2 (Dege and Brown 2004, pp. 58–60; Baxter *et al.* 2010, p. 61). As longfin hatch into larvae, they move from the areas where they are spawned and orient themselves just downstream of X2 (Dege and Brown 2004, pp. 58-60). Larval (winter-spring) habitat varies with outflow and with the location of X2 (CDFG 2009, p. 12), and has been reduced since the 1990s due to a general upstream shift in the location of X2 (Hilts 2012, unpublished data). The amount of rearing habitat (salinity between 0.1 and 18 ppt) is also presumed to vary with the location of X2 (Baxter *et al.* 2010, p. 64). However, as previously stated, the location of X2 is of particular importance to the distribution of newly-hatched larvae and spawning adults. The influence of water project operations from November through April, when spawning adults and newly-hatched larvae are oriented to X2, is greater in drier years than in wetter years (Knowles 2002, p. 7).

Research on declines of longfin smelt and other pelagic fish species in the Bay-Delta since 2002 (referred to as Pelagic Organism Decline—see Abundance section, above) have most recently been summarized in the Interagency Ecological Program’s 2010 Pelagic Organism Decline Work Plan and Synthesis of Results (Baxter *et al.* 2010, pp. 61–69). While Baxter *et al.* (2010, pp. 17–19) acknowledge significant uncertainties about the causal mechanisms underlying the Pelagic Organism Decline, they have identified reduced Delta freshwater flows as one of several key factors that they believe contribute to recent declines in the abundance of longfin smelt (Baxter *et al.* 2010, pp. 61–69, Figure 5).

Other Populations

Information on effects of reduced freshwater flows on longfin smelt populations other than the Bay-Delta population are lacking. Dams and reservoirs are located in the inland water basins of most of the estuaries where longfin smelt occur. Some of these systems are large and consist of multiple dams and diversions (e.g., Klamath River basin, Columbia River basin). Water diversion systems with dams, canals, and water pipelines located upstream of the estuary may affect longfin smelt aquatic habitat by reducing freshwater flows into the estuary—especially if water is diverted out of the drainage basin—and altering the timing of freshwater flows into the estuary.

Climate Change

“Climate” refers to an area's long-term average weather statistics (typically for at least 20- or 30- year periods), including the mean and variation of surface variables such as temperature, precipitation, and wind, whereas “climate change” refers to a change in the mean and/or variability of climate properties that persists for an extended period (typically decades or longer), whether due to natural processes or human activity (Intergovernmental Panel on Climate Change (IPCC) 2007a, p. 78). Although changes in climate occur continuously over geological time, changes are now occurring at an accelerated rate. For example, at continental, regional, and ocean basin scales, recent observed changes in long-term trends include: a substantial increase in precipitation in eastern parts of North American and South America, northern Europe, and northern and central Asia, and an increase in intense tropical cyclone activity in the North Atlantic since about 1970 (IPCC 2007a, p. 30); and an increase in annual average temperature of more than 2° F (1.1°C) across the United States since 1960 (Global Climate Change Impacts in the United States (GCCIOUS) 2009, p. 27). Examples of observed changes in the physical environment include: an increase in global average sea level, and declines in mountain glaciers and average snow cover in both the northern and southern hemispheres (IPCC 2007a, p. 30); substantial and accelerating reductions in arctic sea-ice (e.g., Comiso *et al.* 2008, p. 1); and a variety of changes in ecosystem processes, the distribution of species, and the timing of seasonal events (e.g., GCCIOUS 2009, pp. 79-88).

The IPCC used Atmosphere-Ocean General Circulation Models and various greenhouse gas emissions scenarios to make projections of climate change globally and for broad regions through the 21st century (Meehl *et al.* 2007, p. 753; Randall *et al.* 2007, pp. 596–599), and reported these projections using a framework for characterizing certainty (Solomon *et al.* 2007,

pp. 22-23). Examples include: (1) It is virtually certain there will be warmer and more frequent hot days and nights over most of the earth's land areas; (2) it is very likely there will be increased frequency of warm spells and heat waves over most land areas, and the frequency of heavy precipitation events will increase over most areas; and (3) it is likely that increases will occur in the incidence of extreme high sea level (excludes tsunamis), intense tropical cyclone activity, and the area affected by droughts (IPCC 2007b, p. 8, Table SPM.2). More recent analyses using a different global model and comparing other emissions scenarios resulted in similar projections of global temperature change across the different approaches (Prinn *et al.* 2011, pp. 527, 529).

All models (not just those involving climate change) have some uncertainty associated with projections due to assumptions used, data available, and features of the models; with regard to climate change this includes factors such as assumptions related to emissions scenarios, internal climate variability, and differences among models. Despite this, however, under all global models and emissions scenarios, the overall projected trajectory of surface air temperature is one of increased warming compared to current conditions (Meehl *et al.* 2007, p. 762; Prinn *et al.* 2011, p. 527). Climate models, emissions scenarios, and associated assumptions, data, and analytical techniques will continue to be refined, as will interpretations of projections, as more information becomes available. For instance, some changes in conditions are occurring more rapidly than initially projected, such as melting of arctic sea ice (Comiso *et al.* 2008, p. 1; Polyak *et al.* 2010, p. 1797), and since 2000 the observed emissions of greenhouse gases, which are a key influence on climate change, have been occurring at the mid- to higher levels of the various emissions scenarios developed in the late 1990s and used by the IPCC for making projections

(e.g., Raupach *et al.* 2007, Figure 1, p. 10289; Manning *et al.* 2010, Figure 1, p. 377; Pielke *et al.* 2008, entire). Also, the best scientific and commercial data available indicate that average global surface air temperature is increasing and that several climate-related changes are occurring and will continue for many decades even if emissions are stabilized soon (e.g. Meehl *et al.* 2007, pp. 822-829; Church *et al.* 2010, pp. 411-412; Gillett *et al.* 2011, entire).

Changes in climate can have a variety of direct and indirect impacts on species, and can exacerbate the effects of other threats. Rather than assessing “climate change” as a single threat in and of itself, we examine the potential consequences to species and their habitats that arise from changes in environmental conditions associated with various aspects of climate change. For example, climate-related changes to habitats, predator-prey relationships, disease and disease vectors, or conditions that exceed the physiological tolerances of a species, occurring individually or in combination, may affect the status of a species. Vulnerability to climate change impacts is a function of sensitivity to those changes, exposure to those changes, and adaptive capacity (IPCC 2007, p. 89; Glick *et al.* 2011, pp. 19-22). As described above, in evaluating the status of a species, the Service uses the best scientific and commercial data available, and this includes consideration of direct and indirect effects of climate change. As is the case with all potential threats, if a species is currently affected or is expected to be affected by one or more climate-related impacts, this does not necessarily mean the species is an endangered or threatened species as defined under the Act. If a species is listed as endangered or threatened, this knowledge regarding its vulnerability to, and impacts from, climate-associated changes in environmental conditions can be used to help devise appropriate strategies for its recovery.

The effects of climate change do not act in isolation, but act in combination with existing threats to species and systems. We considered the potential effects of climate change on the longfin smelt based on projections derived from various modeling scenarios. Temperature increases are likely to lead to a continued rise in sea level, further increasing salinity within longfin smelt estuarine rearing habitat and likely shifting spawning and early rearing upstream as the boundary of fresh and brackish water moves upstream (Baxter 2011, pers. comm.). Reduced snowpack, earlier melting of the snowpack, and increased water temperatures will likely alter freshwater flows, possibly shifting and condensing the timing of longfin smelt spawning (Baxter 2011, pers. comm.).

Effects of climate change could be particularly profound for aquatic ecosystems and include increased water temperatures and altered hydrology, along with changes in the extent, frequency, and magnitude of extreme events such as droughts, floods, and wildfires (Reiman and Isaak 2010, p. 1). Numerous climate models predict changes in precipitation frequency and pattern in the western United States (IPCC 2007b, p. 8). Projections indicate that temperature and precipitation changes will diminish snowpack, changing the availability of natural water supplies (USBR 2011, p. 143). Warming may result in more precipitation falling as rain and less storage as snow. This would result in increased rain-on-snow events and increase winter runoff as spring runoff decreases (USBR 2011, p. 147). Earlier seasonal warming increases the likelihood of rain-on-snow events, which are associated with mid-winter floods. Smaller snowpacks that melt earlier in the year result in increased drought frequency and severity (Reiman and Isaak 2010, p. 6). These changes may lead to increased flood and drought risk

during the 21st century (USBR 2011, p. 149).

It is uncertain how a change in the timing and duration of freshwater flows will affect longfin smelt. The melting of the snowpack earlier in the year could result in higher flows in January and February, which are peak spawning and hatching months for longfin smelt. This would reduce adult migration distance and increase areas of freshwater spawning habitat during these months, potentially creating better spawning and larval rearing conditions. Associated higher turbidity may reduce predation on longfin smelt adults and larvae (Baxter 2011, pers. comm.). However, if high flows last only a short period, benefits may be negated by poorer conditions before and after the high flows. As the freshwater boundary moves farther inland into the Delta with increasing sea level (see below) and reduced flows, adults will need to migrate farther into the Delta to spawn, increasing the risk of predation and the potential for entrainment into water export facilities and diversions for both themselves and their progeny.

Global sea level rose at an average rate of 1.8 mm (0.07 in) per year from 1961 to 2003, and at an average rate of 3.1 mm (0.12 in) per year from 1993 to 2003 (IPCC 2007a, p. 49). The IPCC (2007b, p. 13) report estimates that sea levels could rise by 0.18 to 0.58 m (0.6 to 1.9 ft) by 2100; however, Rahmstorf (2007, p. 369) indicated that global sea level rise could increase by over 1.2 m (4 ft) in that time period (CEC 2009, p. 49). Even if emissions could be halted today, the oceans would continue to rise and expand for centuries due to their capacity to store heat (CEC 2009, pp. 49–50). In the Bay-Delta, higher tides combined with more severe drought and flooding events are likely to increase the likelihood of levee failure, possibly resulting in major alterations of the environmental conditions (Moyle 2008, pp. 362–363). It is reasonable to

conclude that more severe drought and flooding events will also occur in other estuaries where the longfin smelt occurs. Sea level rise is likely to increase the frequency and range of saltwater intrusion. Salinity within the northern San Francisco Bay is projected to rise 4.5 psu by the end of the century (Cloern *et al.* 2011, p. 7). Elevated salinity levels could push the position of X2 farther up the estuary and could result in increased distances that longfin smelt must migrate to reach spawning habitats. Elevated sea levels could result in greater sedimentation, erosion, coastal flooding, and permanent inundation of low-lying natural ecosystems (CDFG 2009, p. 30).

Typically, longfin smelt spawning in the Bay-Delta occurs at water temperatures between 7.0 and 14.5 °C (44.6–58.2 °F), although spawning has been observed at lower temperatures in other areas, such as Lake Washington (Moyle 2002, p. 236). Mean annual water temperatures within the upper Sacramento River portion of the Bay-Delta estuary are expected to approach or exceed 14 °C during the second half of this century (Cloern *et al.* 2011, p. 7). Increased water temperatures could compress the late-fall to early-spring spawning period and could result in shorter egg incubation time. Longfin smelt are adapted to hatching in cold, relatively unproductive waters where they grow slowly until ample food resources are available in spring. Warmer water during winter would likely result in increased metabolism of larvae, which may result in increased food needs for maintenance and growth and create a mismatch between food needs and availability (Baxter 2011, pers. comm.). If increased water temperatures compress the spawning period and lead to more synchronized hatching during winter, then prevailing low sunlight and low food resources could result in greater intra-specific (within species) competition (Baxter 2011, pers. comm.). Moreover, increasing water temperatures might also lead to earlier spawning and hatching of other fishes, and to greater inter-specific (between species)

competition.

Although climate change and sea level rise are projected to result in continued increases in water temperature and salinity, longfin smelt is considered euryhaline (tolerant of a wide range of salinities) (Moyle 2002, p. 236; Rosenfield and Baxter 2007 p. 1578) and is known to move between different parts of the estuary that vary greatly in temperature and salinity. Being able to move between aquatic habitats that vary greatly in water temperature and salinity may reduce the potential impacts of climate change and sea level rise to some degree.

Channel Disturbances

Dredging and other channel disturbances potentially degrade spawning habitat and cause entrainment loss of individual fish and eggs; disposal of dredge spoils also can create large sediment plumes that expose fish to gill-clogging sediments and possibly to decreased oxygen availability (Levine-Fricke 2004, p. 56). Longfin smelt is a pelagic species (living away from the bottom of the water column and shoreline), and thus less likely to be directly affected by dredging, sand and gravel mining, and other disturbances to the channel bed compared to bottom-dwelling fish species. Longfin smelt are likely most vulnerable to entrainment by dredging during spawning and egg incubation because eggs are deposited and develop on channel bottom substrates (CDFG 2009, p. 27). Egg development takes approximately 40 days (Moyle 2002, p. 236).

We have found no information documenting population impacts of dredging or sand and

gravel mining on longfin smelt. Channel maintenance dredging occurs regularly within the Bay-Delta and other estuaries that serve as shipping channels (e.g., Humboldt Bay, Coos Bay, Yaquina Bay, Columbia River). In their 2009 status review on longfin smelt, CDFG concluded that effects of regular maintenance dredging and sand mining within the Bay-Delta estuary on longfin smelt were expected to be small and localized (CDFG 2009, p. 26). They reviewed two studies on entrainment effects of channel dredging, and each study found that no longfin smelt were entrained during dredging (fish that were entrained were primarily bottom-dwelling species).

There is currently a proposal to deepen and selectively widen the Sacramento Deep Water Ship Channel and the lower portion of the Sacramento River in the Bay-Delta. This dredging project would remove between 6.1–7.6 million cubic meters (8 and 10 million cubic yards) of material from the channel and Sacramento River and extend for 74 km (45.8 mi) (USACE 2011a, entire). Potential effects of this new project to longfin smelt include mortality through loss of spawning substrate, habitat modification, and a shift in spawning and rearing habitat. The project also has potential to alter breeding and foraging behavior of the Bay-Delta longfin smelt population. However, this project is only a proposal at this time and is not certain to occur. Potential effects of the proposed project are currently under evaluation.

Summary of Factor A

Although we find that reduced freshwater flows are currently a threat to the Bay-Delta longfin smelt population, it is difficult to make inferences on the effects of reduced freshwater

flows to longfin smelt populations throughout the species range. Because the Bay-Delta system includes one of the largest man made water system in the world, it would be impractical to compare diversions and alterations in other estuaries to diversions and alterations in the Bay-Delta. The effects of water development in the Bay-Delta are unique to the physical, geologic, and hydrologic environment of the estuary. Reduced flow from diversions and dams in other estuaries is not expected to be as significant as the reduced flows that have been shown in the Bay-Delta because less water is exported from other estuaries. We have no information to show that reduced freshwater flow is a threat to longfin smelt in other estuaries. Therefore, we conclude that while reduced flow is a threat to the Bay-Delta population of longfin smelt, the best available science does not indicate that the lack of freshwater flow is a threat to the species in other parts of its range.

Climate change will likely affect longfin smelt in multiple ways, but longfin smelt are able to move between a wide range of aquatic environments that vary greatly in water temperature and salinity. These behavioral and physiological characteristics of the species may help it adapt to effects of climate change. We conclude at this time that the best available information does not indicate that climate change threatens the continued existence of longfin smelt across its range.

Channel disturbances may have localized impacts to longfin smelt habitat suitability, but the best available information does not indicate that they pose significant threats to the species throughout its range.

Based on the best available scientific information, we conclude that reduced freshwater flows, climate change, and channel disturbances are not significant current or future threats to longfin smelt across its range except in the Bay-Delta, where reduced freshwater flow is a threat.

Factor B. Overutilization for Commercial, Recreational, Scientific, or Educational Purposes

Recreational and Commercial Fishing

In California, longfin smelt was listed as a threatened species under the State's Endangered Species Act in 2009. This status makes take of longfin smelt illegal, unless authorized by an incidental take permit or other take authorization. However, longfin smelt are caught as bycatch in small bay shrimp trawl fishery and bait fishing (anchovies and sardines) operations in South San Francisco Bay, San Pablo Bay, and Carquinez Strait (CDFG 2009a, p. 1). CDFG (2009d, pp. 6, 9) estimated the total longfin smelt bycatch from shrimping in 1989 and 1990 at 15,539 fish, and in 2004 at 18,815–30,574 fish. CDFG noted in 2009 that the bay shrimp trawl fishery industry had declined since 2004 (CDFG 2009d, p. 3). No shrimp fishery currently takes place in Humboldt Bay (Mello 2011, pers. comm.).

In Oregon, smelt species may not be targeted in commercial fisheries, and if taken incidentally, smelt catch cannot exceed 1 percent of the total weight landed (ODFW 2011, p. 17). Rules limit in which estuaries bait fishing for herring, sardines, anchovies, and shad may occur. In Oregon, there is currently no known shrimping taking place within the estuaries where the longfin smelt might be found. Although a limited entry roe herring fishery is allowed in Yaquina

Bay, no landings have occurred there since 2003, because biomass estimates have generally been too low to make the fishery economically viable (Krutzikowsky 2011, pers. comm.). Anchovy fishing is allowed in Tillamook Bay, Yaquina Bay, and Coos Bay, but because there is currently no anchovy fishing occurring in these areas (Krutzikowsky 2011, pers. comm.), longfin smelt are not taken as bycatch. Records for commercial landings in Oregon show a total of 9.1 kilograms (kg) (20 pounds (lb)) landed from 2005 to 2010 for smelt species other than eulachon. Recreational fishing for smelt species is allowed only in marine waters (Oregon Sport Fishing Regulations, p. 11).

The State of Washington includes longfin smelt in a class of fish referred to as forage fish (small schooling fish that are major food items for many species of fish, birds, and marine mammals) (Bargmann 1998, p. 1). Both recreational and commercial fisheries exist for forage fish in Washington, but the recreational fishery is much smaller than the commercial fishery. A sport fishing license is not needed to catch smelt. Smelt can be harvested recreationally using a dip net or jig. Dip net fishing for longfin smelt is allowed in the Nooksack River and there are approximately two hundred trips a year made to fish for longfin smelt in this area (O'Toole 2011, pers. comm.). It is unlawful to use a herring or smelt rake. Sport and tribal commercial fisheries have been reported to occur on the Nooksack River longfin smelt stock (Bargmann 1998, p. 37). Longfin smelt may be caught incidentally in a medium-sized shore or pier-based recreational fishery for surf smelt in Puget Sound.

There is currently no commercial fishing regulation specific to longfin smelt in Washington (Paulson 2011, pers. comm.). The daily limit for smelt is 4.5 kg (10 lb) and, like

Oregon, is counted as an aggregate, which can include herring, sardines, sandlance, and anchovies (WDFW 2011, p. 27). There is a robust commercial herring fishery in Washington that takes approximately 450 metric tons (500 tons) of fish per year (for sport bait) and a commercial surf smelt fishery that takes approximately 450,000 kg (100,000 lb) of fish per year (for human consumption). Longfin smelt bycatch in both of these fisheries is low. Anchovy fishing in Washington primarily takes place in Grays Harbor and the mouth of the Columbia River (O'Toole 2011, pers. comm.).

In British Columbia, take of smelt from recreational fishing is limited to 20 kilograms (kg) (44 lb) per day and 40 kg (88 lb) of total catch in possession. The fishing season takes place from April 1 to June 14 (Department of Fisheries and Oceans Canada 2011a, p. 47). A commercial fishing industry targeting surf smelt may incidentally take longfin smelt (Department of Fisheries and Oceans Canada 2011b, p. 1). British Columbia supports a year-round shrimp fishery in Prince Rupert and Chatham Sound. Sardine and shrimp fishing occurs near Vancouver.

In Alaska, a commercial fishery for smelt, which includes eulachon, was reopened in 2005. This fishery is restricted to the brackish waters of Cook Inlet, from May 1 to June 30. The total annual harvest of eulachon and longfin smelt may not exceed 90 metric tons (100 tons) of smelt. However, longfin smelt are unlikely to be specifically targeted in this fishery due to their small numbers in relation to eulachon in the region (Shields 2005, p. 4). Sport fishing is limited to salt water, where herring and smelt may be taken (Alaska Department of Fish and Game (ADFG) 2010, p. 1). In Prince William Sound, the herring fishery has closed due to low

abundance of herring.

Monitoring Surveys

Fisheries monitoring surveys are conducted by NOAA's National Marine Fisheries Service, the Service and by State and local agencies in water bodies inhabited by longfin smelt throughout their range. Most of these surveys target other species, primarily salmonids, and rarely collect longfin smelt outside of the Bay-Delta area.

Within the Bay-Delta, longfin smelt are regularly captured in monitoring surveys. The Interagency Ecological Program (IEP) implements scientific research in the Bay-Delta. Although the focus of its studies and the level of effort have changed over time, in general, their surveys have been directed at researching the Pelagic Organism Decline in the Bay-Delta. Between the years of 1987 to 2011, combined take of longfin smelt less than 20 mm (0.8 in) in length ranged from 2,405 to 158,588 annually. All of these fish were preserved for research or assumed to die in processing. During the same time period, combined take for juveniles and adults (fish greater than or equal to 20 mm (0.8 in)) ranged from 461 to 68,974 annually (IEP 2011, no pagination). Although mortality is unknown, the majority of these fish likely do not survive. The Chipps Island survey, which is conducted by the Service, has captured an average of 2,697 longfin smelt per year during the past 10 years. Biologists attempt to release these fish unharmed, but at least 5,154 longfin smelt were known to have died during the Chipps Island survey between 2001 and 2008 (Service 2010, entire).

Survey methods have been modified recently to minimize potential impacts to delta smelt, a related species that also occurs in the Bay-Delta (75 FR 17669; April 7, 2010). These modifications are likely to result in reduced impacts to longfin smelt also. The Service conducts other surveys in the Bay-Delta to monitor salmon populations (Mosssdale trawl, Sacramento trawl, beach seine surveys), but few longfin smelt are captured during these surveys. Mortality due to monitoring surveys was not identified by the Interagency Ecological Program in its most recent synthesis of results as a factor in the decline of longfin smelt and other pelagic fish species in the Bay-Delta since the early 2000s (Baxter *et al.* 2010, pp. 19–53, 61–69).

Summary of Factor B

The species is incidentally caught in commercial shrimp and bait fishing operations throughout much of its range, but the bycatch numbers are usually low. In California, take of longfin smelt is illegal without authorization because the species is listed as threatened under the California Endangered Species Act. Because of its small size, it is not targeted by recreational angling, although it is certainly caught and used as bait for other larger recreational fish species. Monitoring surveys have resulted in high numbers of longfin smelt mortality in the Bay-Delta in the past, but efforts being made to reduce survey mortality for delta smelt, such as reductions in tow times, likely have also benefitted longfin smelt. The scientific collection surveys being conducted in the Bay-Delta are limited to research designed to benefit the species, and mortality from monitoring surveys has not been identified as a factor in the longfin smelt's recent population decline. We have no information indicating that mortality from monitoring surveys threatens any populations within the species' range. We conclude that overutilization due to

commercial, recreational, or scientific take is not a significant current or future threat to the longfin smelt throughout its range.

Factor C. Disease or Predation

Disease

All the information we found on disease in longfin populations originated from studies in the Bay-Delta. Two investigations published in 2006 and 2008 by the California-Nevada Fish Health Center detected no significant health problems in juvenile longfin smelt in the Bay-Delta (Foott and Stone 2008, pp. 15–16). The low observed rate of parasitic infection did not appear to affect the health of the fish, as indicated by the lack of associated tissue damage or inflammation (Foott and Stone 2008, p. 15). The only additional documentation of relevant wild fish disease in the Bay-Delta was a severe intestinal infection by a new species of myxozoan observed in nonnative juvenile yellowfin goby (*Acanthogobius flavimanus*) from Suisun Marsh (Baxa *et al.* in prep cited in Baxter *et al.* 2008, p. 16). The nonnative gobies could act as potential vectors of the parasite to other susceptible species in the Bay-Delta. It is unknown whether this or similar infections are affecting the health of longfin smelt.

The south Delta is fed by water from the San Joaquin River, where pesticides (e.g., chlorpyrifos, carbofuran, and diazinon), salts (e.g., sodium sulfates), trace elements (boron and selenium), and high levels of total dissolved solids are prevalent due to agricultural runoff (64 FR 5963; February 8, 1999). Pesticides and other toxic chemicals may adversely affect the

immune system of longfin smelt and other fish in the Bay-Delta and other estuaries, but we found no information documenting such effects (see Factor E: Contaminants, below).

Predation

As a forage species, longfin smelt are preyed upon by a variety of fishes, birds, and mammals (Barnhart *et al.* 1992, p. 44). However, we found little information on predation of longfin smelt other than information for the Bay-Delta population and Lake Washington population. The striped bass (*Morone saxatilis*) is a potential predator of longfin smelt in the Bay-Delta. Striped bass were introduced into the Bay-Delta in 1879 and quickly became abundant throughout the estuary. However, their numbers have declined substantially over the last 40 years (Thomson *et al.* 2010, p. 1440), and they are one of the four species studied under Pelagic Organism Decline investigations (Baxter *et al.* 2010, p. 16). Numbers of largemouth bass (*Micropterus dolomieu*), another introduced species in the Bay-Delta, have increased in the Delta over the past few decades (Brown and Michniuk 2007, p. 196). Largemouth bass, however, occur in shallow freshwater habitats, closer to shore than the pelagic longfin smelt, and do not typically co-occur with longfin smelt. Baxter *et al.* (2010, p. 40) reported that no longfin smelt have been found in largemouth bass stomachs sampled in a recent study of largemouth bass diet. Moyle (2002, p. 238) believed that inland silverside (*Menidia beryllina*), another nonnative predatory fish, may be an important predator on longfin smelt eggs, larvae, juveniles, and adults. Rosenfield (2010, p. 18) acknowledged that they are likely major predators of longfin smelt eggs and larvae but thought it unlikely that they were an important predator on juveniles and subadults because inland silversides prefer shallow water habitats whereas juvenile

and subadult longfin smelt do not.

In the Bay-Delta, predation of longfin smelt may be high in the Clifton Court Forebay, where the SWP water export pumping plant is located (Moyle 2002, p. 238; Baxter *et al.* 2010, p. 42). However, once they are entrained in the Clifton Court Forebay, longfin smelt mortality would be high anyway due to high water temperatures in the forebay (CDFG 2009b, p. 4) and entrainment into the SWP water export pumping plant. In addition to elevated predation levels in the Clifton Court Forebay, predation also is concentrated at sites where fish salvaged from the SWP and CVP export facilities are released (Moyle 2002, p. 238). However, few longfin smelt survive the salvage and transport process (see Factor E: Entrainment Losses, below) and therefore predation is not expected to be an important factor at drop-off sites. Reduced freshwater flows may result in lower turbidity and increased water clarity (see Factor A, above), which may contribute to increased risk of predation (Baxter *et al.* 2010, p. 64).

In Lake Washington, longfin are preyed upon by prickly sculpin (*Cottus asper*) (Tabor *et al.* 2007, p. 1085) and cutthroat trout (*Oncorhynchus clarki*) (Norwak *et al.* 2004, p. 632; Beauchamp *et al.* 1992, p. 156). Cutthroat trout have displaced the northern pikeminnow as the most important predator in Lake Washington and may be having an effect on other components of the ecosystem, including longfin smelt populations (Norwak *et al.* 2004, pp. 633–634).

Summary of Factor C

Similar to other threats, very little information is available about disease or predation

threats to longfin smelt populations outside of the Bay-Delta. We found no information that disease is a threat to the longfin smelt throughout its range. Longfin smelt is a small fish that is preyed upon by a wide variety of fish, birds, and mammals, but we found no information documenting predation as a threat to the species rangewide. Predation, along with mortality from entrainment (see Factor E: Entrainment Losses, below), has been identified as a top-down effect that may be contributing to recent declines of longfin smelt and other pelagic fish species in the Bay-Delta estuary (Pelagic Organism Decline) (Sommer *et al.* 2007, p. 275). However, factors contributing to the Pelagic Organism Decline are numerous and complex, and the combination of underlying causal mechanisms remains uncertain (Baxter *et al.* 2010, pp. 61–69). Therefore, based on our review of the best available scientific and commercial information, we conclude that disease or predation are not significant current or future threats to the longfin smelt throughout its range.

Factor D. The Inadequacy of Existing Regulatory Mechanisms

Federal Laws

A number of federal environmental laws and regulations exist that may provide some protection for longfin smelt: the National Environmental Policy Act, the Central Valley Project Improvement Act, and the Clean Water Act.

National Environmental Policy Act

The National Environmental Policy Act (NEPA) (42 U.S.C. 4321 *et seq.*) requires all Federal agencies to formally document, consider, and publicly disclose the environmental impacts of major Federal actions and management decisions significantly affecting the human environment. NEPA documentation is provided in an environmental impact statement, an environmental assessment, or a categorical exclusion, and may be subject to administrative or judicial appeal. However, the Federal agency is not required to select an alternative having the least significant environmental impacts, and may select an action that will adversely affect sensitive species provided that these effects are known and identified in a NEPA document. Therefore, we do not consider the NEPA process in itself is to be a regulatory mechanism that is certain to provide significant protection for the longfin smelt.

Central Valley Project Improvement Act

The Central Valley Project Improvement Act (Pub. L. 102-575) (CVPIA) amends the previous Central Valley Project authorizations to include fish and wildlife protection, restoration, and mitigation as project purposes having equal priority with irrigation and domestic uses, and fish and wildlife enhancement as having an equal priority with power generation (Pub. L. 102-575, October 30, 1992; Bureau of Reclamation 2009). Included in CVPIA section 3406 (b)(2) was a provision to dedicate 800,000 acre-feet of Central Valley Project yield annually (referred to as “(b)(2) water”) for fish, wildlife, and habitat restoration. Since 1993, (b)(2) water has been used and supplemented with acquired environmental water (Environmental Water Account and CVPIA section 3406 (b)(3) water) to increase stream flows and reduce Central Valley Project export pumping in the Delta. These management actions were taken to contribute to the CVPIA

salmonid population doubling goals and to protect Delta smelt and their habitat (Guinee 2011, pers. comm.). As discussed above, (see Biology and Factor A discussions), increased freshwater flows have been shown to be positively correlated with longfin smelt abundance; therefore, these management actions, although targeted towards other species, should also benefit longfin smelt.

Clean Water Act

Established in 1977, the Clean Water Act (33 U.S.C. 1251 *et seq.*) is the primary Federal law in the United States regulating water pollution. It employs a variety of regulatory and non-regulatory means to reduce direct water quality impacts and manage polluted runoff. The Clean Water Act provides the basis for the National Pollutant Discharge Elimination System (NPDES) and gives the Environmental Protection Agency (EPA) the authority to set effluent limits and require any entity discharging pollutants to obtain a NPDES permit. The EPA is authorized through the Clean Water Act to delegate the authority to issue NPDES permits to State governments and has done so in California. In States that have been authorized to implement Clean Water Act programs, EPA retains oversight responsibilities. Water bodies that do not meet applicable water quality standards are placed on the section 303(d) list of impaired water bodies, and the State is required to develop appropriate total maximum daily loads (TMDL) for the water body. A TMDL is a calculation of the maximum amount of a pollutant that a water body can receive and still meet water quality standards. At present, TMDLs are not in place in all impaired watersheds in which longfin smelt are known to occur. The Clean Water Act has not effectively limited ammonia input into the system, and ammonia has been shown to

negatively affect the longfin smelt's food supply.

State Laws

The State of California has a number of environmental laws and regulations which may provide some protection for longfin smelt: California Endangered Species Act, California Environmental Quality Act, California Marine Invasive Species Act, Porter-Cologne Water Quality Control Act, and regulatory prohibitions on streambed alterations.

California Endangered Species Act

Longfin smelt was listed as threatened under the California Endangered Species Act (CESA) (California Fish and Game Code 2050 et seq.) in 2009. The CESA prohibits unpermitted possession, purchase, sale, or take of listed species. However, the CESA definition of take does not include harm, which under the Act's implementing regulations includes significant modification or degradation of habitat that actually kills or injures wildlife by significantly impairing essential behavioral patterns (50 CFR 17.3). CESA allows take of species for otherwise lawful projects through use of an incidental take permit. An incidental take permit requires that impacts be minimized and fully mitigated (CESA sections 2081 (b) and (c)). Furthermore, CESA requires that the issuance of the permit will not jeopardize the continued existence of a State-listed species. The CESA does require consultation between CDFG and other State agencies to ensure that activities of State agencies will not jeopardize the continued existence of State-listed species (CERES 2009, p. 1). Longfin Smelt Incidental Take Permit No.

2081-2009-001-03 specifies that the Smelt Working Group, which was created under the Service's 2008 delta smelt biological opinion (Service 2008, p. 30), provide recommendations for export pumping reduction to CDFG if any of several criteria is reached. One of the criteria is that total salvage of adult longfin smelt (fish greater than or equal to 80 mm in length) at the State Water Project and Central Valley Project export pumps between December and February may not exceed five times the Fall Midwater Trawl longfin smelt annual abundance index. Also, if longfin abundance is low and surveys indicate that adults are distributed close to the export pumps, the Smelt Working Group may consider making recommendations for Old and Middle River Flows that would reduce pumping (CDFG 2009c, pp. 1–34; Smelt Working Group 2011, p. 4).

California Environmental Quality Act

The California Environmental Quality Act ((CEQA) (Public Resources Code section 21000 *et seq.*)) requires review of any project that is undertaken, funded, or permitted by the State of California or a local government agency. If significant effects are identified, the lead agency has the option of requiring mitigation through changes in the project or to decide that overriding considerations make mitigation infeasible (CEQA sec. 21002). In the latter case, projects may be approved that cause significant environmental damage, such as destruction of listed endangered species or their habitat. Protection of listed species through CEQA is, therefore, dependent on the discretion of the lead agency. The CEQA review process ensures that a full environmental review is undertaken prior to the permitting of any project within longfin smelt habitat.

California Marine Invasive Species Act

The California Marine Invasive Species Act (AB 433) was passed in 2003. This 2003 act requires ballast water management for all vessels that intend to discharge ballast water in California waters. All qualifying vessels coming from ports within the Pacific Coast region must conduct an exchange in waters at least 50 nautical mi offshore and 200 m (656 ft) deep or retain all ballast water and associated sediments. To determine the effectiveness of the management provisions of this 2003 act, the legislation also requires State agencies to conduct a series of biological surveys to monitor new introductions to coastal and estuarine waters. These measures should further minimize the introduction of new invasive species into California's coastal waters that could be a threat to the longfin smelt. The Coastal Ecosystems Protection Act of 2006 deleted a sunset provision of the Marine Invasive Species Act, making the program permanent.

Porter-Cologne Water Quality Control Act

The Porter-Cologne Water Quality Control Act (California Water Code 13000 *et seq.*) is a California State law that establishes the State Water Resources Control Board (SWRCB) and nine Regional Water Quality Control Boards that are responsible for the regulation of activities and factors that could degrade California water quality and for the allocation of surface water rights (California Water Code Division 7). In 1995, the SWRCB developed the Bay-Delta Water Quality Control Plan that established water quality objectives for the Delta. This plan is currently implemented by Water Rights Decision 1641, which imposes flow and water quality

standards on State and Federal water export facilities to assure protection of beneficial uses in the Delta (USFWS 2008, pp. 21–27). The various flow objectives and export restraints were designed, in part, to protect fisheries. These objectives include specific freshwater flow requirements throughout the year, specific water export restraints in the spring, and water export limits based on a percentage of estuary inflow throughout the year. The water quality objectives were designed to protect agricultural, municipal, industrial, and fishery uses; they vary throughout the year and by the wetness of the year.

In December 2010, the California Central Valley Regional Water Quality Control Board (Regional Board) adopted a new National Pollutant Discharge and Elimination System (NPDES) permit for the Sacramento Regional Wastewater Treatment Plant to address ammonia loading to the Sacramento River and the Delta. In January 2011, the Sacramento Regional County Sanitation District petitioned the Regional Board for a review of the permit, which may require a year or more. There is currently no TMDL in place for ammonia discharge into the Sacramento watershed. The EPA is currently updating freshwater ammonia criteria that will include new discharge limits on ammonia (EPA 2009, pp. 1–46). Ammonia has been shown to have negative effects on prey items that longfin smelt rely upon (see Factor E: Contaminants, below). This regulation does not adequately mitigate potential negative effects to longfin smelt from ammonia in the Bay-Delta.

Streambed Alteration

In California, section 1600 *et seq.* of the California Fish and Game Code authorizes

CDFG to regulate streambed alteration. The CDFG must be notified of and approve any work that substantially diverts, alters, or obstructs the natural flow or that substantially changes the bed, channel, or banks of any river, stream, or lake. If an existing fish or wildlife resource, including longfin smelt, may be substantially adversely affected by a project, the project proponent must submit proposals to protect the species to the CDFG at least 90 days before the start of the project. However, these proposals are subject to agreement by the project proponent. If CDFG deems proposed measures to be inadequate, a third party arbitration may be initiated. However, projects that cause significant environmental damage such as destruction of species and their habitat including longfin smelt may be approved because the CDFG has no authority to deny requests for streambed alteration.

Oregon Environmental Regulations

Oregon classifies longfin smelt as a native migratory fish under Oregon Administrative Rule (Division 412, 635-412-0005). Operators of artificial obstructions located in waters in which any native migratory fish are currently or were historically present must provide for fish passage requirements during installation, replacement, or abandonment of artificial obstructions (ODFW 2011, p. 1). This State law helps ensure passage of migratory longfin smelt between rearing and spawning habitat.

Washington Environmental Regulations

Washington's State Environmental Policy Act (RCW 43.21C) provides a process similar to CEQA and is applicable to every State and local agency in Washington State. This law requires State and local governments to consider impacts to the environment and include public participation in project planning and decision making (Washington Division of Wildlife 2011, p. 1). Project proponents must submit a proposal for their project to the appropriate city, county, or State lead agency where the project is taking place. The lead agency then makes a determination of whether or not the project will have significantly adverse environmental impacts. The lead agency then may require the applicant to change the proposal to minimize environmental impacts or in rare cases may deny the application (Washington State Department of Ecology (WSDE) 2002, pp. 1–2).

Alaska Environmental Regulations

The Anadromous Fish Act (AS 16.05.871- .901) requires that anyone desiring to alter a streambed or waterbody first obtain a permit from the Alaska Department of Fish and Game (ADFG). Regulated activities include construction, road crossings, gravel mining, water withdrawal, stream realignment, and bank stabilization. Although there are no minimization or mitigation components to this law, the ADFG commissioner has the ability to deny a permit if he or she finds the plans and specifications are insufficient for the proper protection of anadromous fish. The Fishway or Fish Passage Act (AS 15.05.841) requires that activities within or crossing a stream obtain permission from ADFG if they will impede the passage of resident or anadromous fish. This provides some degree of protection for longfin smelt, which is categorized as an anadromous fish in the State of Alaska.

Canadian Environmental Regulations

The Canadian Environmental Assessment Act (S.C. 1992, c. 37) was passed by the Canadian Parliament in 1992. The Act requires Federal departments to conduct environmental assessments for proposals where the government is the proposer or the project involves Federal funding or permitting. The Canadian Environmental Protection Act of 1999 is intended to prevent pollution, protect the environment and human health, and contribute to promoting sustainable development. Canada has the Canadian Environmental Protection Act (CEPA), which is equivalent to the United States' NEPA. It was enacted to protect Canada's natural resources through pollution prevention and sustainable development. This provides some level of protection for longfin smelt from pollution and habitat degradation. The longfin smelt is not currently a protected species under the Species at Risk Act (SARA) of 2002 (S.C. 2002 c. 29; SARA). SARA is similar to the United States' Endangered Species Act. If the longfin smelt were determined by the Canadian government to need protection in the future, it could be listed under SARA.

Summary of Factor D

We evaluate existing regulatory mechanisms that have an effect on threats that we have identified elsewhere in the threats analysis. We do not evaluate the lack of a regulatory mechanism that may address a particular threat if that regulatory mechanism does not exist. We find that the threats to the longfin smelt and its habitat on Federal, State, and private lands on a

range-wide basis are minimal (Factors A, B, C and E). Existing federal regulatory mechanisms provide a degree of protection for longfin smelt from these threats. Therefore, we find that regulatory mechanisms provide adequate protections to longfin smelt and its habitat throughout its range.

Factor E. Other Natural or Manmade Factors Affecting Its Continued Existence

Other natural or manmade factors potentially affecting the continued existence of longfin smelt include entrainment losses from water diversions, introduced species, and contaminants.

Entrainment Losses

The only information we found on entrainment losses of longfin smelt comes from the Bay-Delta population. Entrainment occurs when fish are drawn toward water diversions, where they are typically trapped or killed. In the Bay-Delta, water is diverted and fish potentially entrained at four major water export facilities within the Delta, two power plants, and numerous small water diversions throughout the Delta for agriculture and in Suisun Marsh for waterfowl habitat. In their 2009 status review of longfin smelt, CDFG (2009, pp. 19–26) summarized entrainment losses at these water diversions.

Water Export Facilities

The four State and Federal water export facilities (pumping stations) in the Delta are the State Water Project (SWP) facility in the south Delta, the Central Valley Project (CVP) in the south Delta, the Contra Costa facility in the south Delta, and the North Bay Aqueduct facility in the north Delta. The SWP and CVP facilities pump the majority of the water exported from the Delta. Average annual volumes of water exported from these facilities between 1995 and 2005 were 3.60 km³ at the SWP facility, 3.10 km³ at the CVP facility, 0.15 km³ at the Contra Costa facility, and 0.05 km³ at the North Bay Aqueduct facility (Sommer *et al.* 2007, p. 272).

Depending on upstream flow through the Delta, operation of the SWP and CVP facilities often causes reverse flows in the river channels leading to them; longfin smelt that occupy these channels during certain times of the year may be entrained by these reverse flows. The SWP and CVP water export facilities are equipped with their own fish collection facilities that divert entrained fish into holding pens using louver-bypass systems to protect them from being killed in the pumps. The fish collected at the facilities are referred to as “salvaged,” and are loaded onto tanker trucks and returned to the western Delta downstream (Aasen 2009, p. 36). The movement of fish can result in mortality due to overcrowding in the tanks, stress, moving procedures, or predation at locations where the fish are released. Salvage is an *index* of entrainment, not an estimate, and is much smaller than total entrainment (Castillo *et al.* in review). Of spawning age fish (age-1 and age-2), which contribute most to longfin smelt population dynamics in the Bay-Delta, the total number of longfin smelt salvaged at both pumps between 1993 and 2007 was 1,133 (CDFG 2009, Attachment 3, p. 2).

Fish entering the intake channel of the CVP or the radial gates of the 31,000-acre Clifton Court Forebay reservoir (SWP) are considered entrained (Fujimura 2009, p. 5; CDFG 2009b, p.

2). Most longfin smelt that become entrained in Clifton Court Forebay are unable to escape (CDFG 2009b, p. 4). The number of fish entrained at the SWP and CVP facilities has never been determined directly, but entrainment losses have been estimated indirectly using data from research and monitoring efforts. The magnitude of entrainment of larval longfin smelt is unknown because only fish greater than 20 mm in length are salvaged at the two facilities (Baxter *et al.* 2008, p. 21). In years with low freshwater flows, approximately half of the longfin smelt larvae and early juveniles may remain for weeks within the Sacramento-San Joaquin Delta (Dege and Brown 2004), where model simulations indicate they are vulnerable to entrainment into State Water Project, Central Valley Project, and other diversions (Kimmerer and Nobriga 2008, CDFG 2009a, p. 8).

Entrainment is no longer considered a major threat to longfin smelt in the Bay-Delta because of current regulations. Efforts to reduce delta smelt entrainment loss through the implementation of the 2008 delta smelt biological opinion and the listing of longfin smelt under the CESA have likely reduced longfin smelt entrainment losses. The high rate of entrainment that occurred in 2002 that threatened the Bay Delta longfin smelt population is unlikely to recur, and would no longer be allowed under today's regulations because limits on longfin smelt take due to CESA regulations (see Factor D discussion, below) would trigger reductions in the magnitude of reverse flows.

Power Plants

Two power plants located near the confluence of the Sacramento and San Joaquin Rivers, the Contra Costa Generating Station and the Pittsburg Generating Station, pose an entrainment risk to longfin smelt. Past entrainment losses of delta smelt at these two facilities were significant and considered a threat to delta smelt (75 FR 17671; April 7, 2010). Power plant operations have been substantially reduced since the late 1970s, when high entrainment and impingement were documented (CDFG 2009, p. 24); the power plants are now either kept offline or operating at very low levels, except as necessary to meet peak power needs. From 2007–2010, capacity utilization of these units averaged only 2.3 percent of maximum capacity. No longfin smelt were detected during impingement sampling conducted between May of 2010 and April of 2011 to monitor entrainment losses at the two power plants (Tenera Environmental 2011, entire). The company that owns the two power plants has committed to retiring one of the two power stations in 2013 (Contra Costa Generating Station) and has made this commitment enforceable through amendments to its Clean Air Act Title V permit (Raifsnider 2011, pers. comm.).

Agricultural Diversions

Water is diverted at numerous sites throughout the Bay-Delta for agricultural irrigation. Herren and Kawasaki (2001) reported over 2,200 such water diversions within the Delta, but CDFG (2009, p. 25) notes that number may be high because Herren and Kawasaki (2001) did not accurately distinguish intake siphons and pumps from discharge pipes. CALFED's Ecosystem Restoration Program (ERP) includes a program to screen remaining unscreened small agricultural diversions in the Delta and the Sacramento and San Joaquin Rivers. The purpose of

screening fish diversions is to prevent entrainment losses; however, very little information is available on the efficacy of screening these diversions (Moyle and Israel 2005, p. 20).

Agricultural operations begin to divert water in March and April, and many longfin smelt have begun leaving the Delta by this time. Water diversions are primarily located on the edge of channels and along river banks. Longfin smelt are a pelagic fish species and tend to occupy the middle of the channel and the middle of the water column, where they are unlikely to be vulnerable to entrainment into these diversions.

Suisun Marsh Diversions

There are 366 diversions in Suisun Marsh used to enhance waterfowl habitat (USFWS 2008, p. 172). Water is pumped at these diversions between October and May. Longfin larvae are abundant in the Marsh from February through April, while adults are abundant from October to February (Meng and Mattern 2001, p. 756; Rosenfield and Baxter 2007, p. 1588). During a 2-year study sampling 2.3 million m³ (81.2 million ft³) of water entering intakes, entrainment was found to be low, capturing only 124 adult longfin and 160 larvae (Enos *et al.* 2007, p. 16). Restrictions on pumping have been put in place to protect delta smelt and salmon. These restrictions likely also benefit longfin smelt.

Introduced Species

Nonnative introduced species (both plants and animals) are common in many of the estuaries within the range of the longfin smelt. Introduced species can significantly alter food

webs in aquatic ecosystems. Introduced animal species can adversely affect longfin smelt through predation (see Factor C discussion, above) or competition. Although introduced species are common within many of the estuaries occupied by longfin smelt, most of the information we found on effects of introduced species on longfin smelt was for the Bay-Delta population.

Bay-Delta Population

The Bay-Delta is considered one of the most highly invaded estuaries in the world (Sommer *et al.* 2007, p. 272). Longfin smelt abundance in the Bay-Delta has remained low since the mid-1980s (see Abundance section, above). This long-term decline has been at least partially attributed to effects of the introduced overbite clam (Kimmerer 2002a, p. 47; Sommer *et al.* 2007, p. 274; Rosenfield and Baxter 2007, p. 1589; Baxter *et al.* 2010, pp. 61–62). The overbite clam has impacted zooplankton abundance and species composition by grazing on the phytoplankton that comprise part of the zooplankton's food base (Orsi and Mecum 1996, pp. 384–386) and by grazing on larval stages of certain zooplankton like *Eurytemora affinis* (no common name) (Kimmerer 2002, p. 51; Sommer *et al.* 2007, pp. 274–276). Longfin smelt recruitment (replacement of individuals by the next generation) has steadily declined since 1987, even after adjusting for Delta freshwater flows (Nobriga 2010, slide 5). These data suggest that changes in the estuary's food web following introduction of the overbite clam may have had substantial and long-term impacts on longfin smelt population dynamics in the Bay-Delta.

Numerous other invasive plant and animal species have been introduced into the Bay-Delta, and ecosystem disruptions will undoubtedly continue as new species are introduced.

Sommer *et al.* (2007, p. 272) note that the quagga mussel (*Dreissna bugensis*) was discovered in southern California in late 2006, and that it could become established in the Bay-Delta and cause substantial ecosystem disruption.

Other Populations

The Eel River is undergoing a shift from native anadromous to resident introduced fish species. Of particular importance are the California roach (*Hesperoleucus symmetricus*) and the Sacramento pikeminnow (*Ptychocheilus grandis*) (Brown and Moyle 1997, p. 274). The Sacramento pikeminnow is known to cause shifts in spatial distribution of native species (Brown & Moyle 1991, p. 856). The Sacramento pikeminnow preys on native fishes, particularly emigrating juvenile salmonids (Moyle 2002, p. 156) and likely preys upon the longfin smelt when present.

In Humboldt Bay, one study recorded 73 nonnative species, with another 13 species of uncertain status (Boyd 2002, pp. 89–91). Many of the nonnative species, most of which are invertebrates, have been present in the Bay for over 100 years, although some introductions have also occurred more recently (Boyd 2002, pp. 89–91). It is possible that the presence of some of these introduced species have resulted in changes to the food web resulting in changes to longfin smelt food availability in Humboldt Bay, as has occurred in the Bay-Delta. However, there are no data with which to evaluate this hypothesis. Commercial oyster culturing in Humboldt Bay began in 1955 (Barrett 1963, p. 38). Oyster culture beds within the bay are located in areas that are favorable to eelgrass (*Zostera marina*), and the harvesting of oysters in these beds has

resulted in a reduction of and damage to native eelgrass in Humboldt Bay (Trianni 1996, p. 4; Rummrill and Poulton 2004, p. 2). Longfin smelt are known to feed on fauna found on native eelgrass, and therefore loss of eelgrass communities could result in lower levels of longfin smelt prey, possibly resulting in decreased longfin smelt survival.

Over 100 species of nonnative, invasive aquatic plants and animals have been documented in the Yaquina Bay estuary in Oregon (Oregon State University 2011, p. 1). One of the plants that has become established is *Zostera japonica*, a seagrass that was introduced to Yaquina Bay as live packing material for Japanese oysters. It poses a competitive threat to the native eelgrass (Brown *et al.* 2007, p. 9), and longfin smelt are known to feed on fauna found on native eelgrass (Phillips 1984, pp. 1–85). Invasive fish species in Yaquina Bay include American shad (*Alosa sapidissima*), common carp (*Cyprinus carpio*), bass (*Micropterus spp.*), and walleye (*Sander vitreum*).

Numerous nonnative, invasive plant and animal species have established populations within the Columbia River estuary. Nonnative, invasive plants and fish are the largest taxa to inhabit the estuary, followed by mollusks and crustaceans (Sanderson *et al.* 2009, pp. 245–256). American shad was introduced in the Columbia River soon after 1871 (Petersen *et al.* 2011, pp. 1–42). The spawning adult shad population in the Columbia River is more than 5,000,000 individuals, the largest anywhere (Petersen *et al.* 2011, pp. 1–42). Shad may have large, negative effects on Columbia River ecosystems, as adult and juvenile shad prey on zooplankton, thereby reducing the availability of prey for other fish species (Sanderson *et al.* 2009, pp. 245–256). Also present in the lower Columbia River are channel catfish (*Ictalurus punctatus*), striped

bass, smallmouth bass (*Microperterus dolomieu*), largemouth bass (*Micropterus salmoides*), and walleye (*Sander vitreus*). These nonnative fishes are aggressive predators and have likely substantially altered food webs in the Columbia River estuary (Sanderson *et al.* 2009, pp. 245–256). The Eurasian water milfoil (*Myriophyllum spicatum*) may have been introduced into the lower Columbia River by ballast water from European ships in the 1800s (Aiken *et al.* 1979, pp. 201–215). It forms dense mats of vegetation and results in reduced dissolved oxygen concentrations as the plants decompose, altering aquatic ecosystem chemistry and function (Cronin *et al.* 2006, pp. 37–43; Unmuth *et al.* 2000, pp. 497–503), which could potentially restrict longfin smelt distribution in the region.

Hundreds of invasive plants and animals have found their way into Puget Sound through importation of soils, plants, fruits, and seeds; through boat hulls and ship ballast water discharge; and through intentional human releases. Invasive tunicate species that reproduce quickly and cover docks and boat hulls are also present in the sound (Puget Sound Partnership 2008b, p. 26).

Contaminants

Bay-Delta

Similar to other potential threats to longfin smelt, most of the information available is for the Bay-Delta. In 2009, over 15 million pounds of pesticides were applied within the five-county Bay-Delta area (California Department of Pesticide Regulation 2011, p. 1). Toxicity to invertebrates has been noted in water and sediments from the Delta and associated watersheds

(e.g., Werner *et al.* 2000, pp. 218, 223). Fish exposed to agricultural drainage water from the San Joaquin River watershed can exhibit body burdens of selenium exceeding the level at which reproductive failure and increased juvenile mortality occur (Saiki *et al.* 2001, p. 629). Toxicity studies specific to longfin smelt are not available, but data do exist for other fish species such as the delta smelt, a related species. Longfin smelt could be similarly affected by contaminants as some life stages utilize similar habitat and prey resources, and longfin smelt have a physiology similar to delta smelt. Kuivila and Moon (2004, p. 239) found that peak densities of larval and juvenile delta smelt sometimes coincided in time and space with elevated concentrations of dissolved pesticides in the spring. These periods of co-occurrence lasted for up to 2 to 3 weeks. Concentrations of individual pesticides were low and much less than would be expected to cause acute mortality; however, the effects of exposure to the complex mixtures of pesticides are unknown.

Bay-Delta waters are listed as impaired for several legacy and currently used pesticides under the Clean Water Act section 303(d) (California Department of Pesticide Regulation 2011, p. 1). Concentrations of dissolved pesticides vary in the Delta both temporally and spatially (Kuivila 2000, p. 1). Several areas of the Delta, particularly the San Joaquin River and its tributaries, are impaired due to elevated levels of diazinon and chlorpyrifos, which are toxic at low concentrations to some aquatic organisms (MacCoy *et al.* 1995, pp. 21–30). Several studies have demonstrated the acute and chronic toxicity of two common dormant-spray insecticides, diazinon and esfenvalerate, in fish species (Barry *et al.* 1995, p. 273; Goodman *et al.* 1979, p. 479; Holdway *et al.*; 1994, p. 169; Scholz *et al.* 2000, p. 1911; Tanner and Knuth 1996, p. 244).

Pyrethroid pesticides are of particular concern because of their widespread use, and their tendency to be genotoxic (DNA damaging) to fishes at low doses (in the range of micrograms per liter) (Campana *et al.* 1999, p. 159). The pyrethroid esfenvalerate is associated with delayed spawning and reduced larval survival of bluegill sunfish (*Lepomis macrochirus*) (Tanner and Knuth 1996, pp. 246–250) and increased susceptibility of juvenile Chinook salmon (*Oncorhynchus tshawytscha*) to disease (Clifford *et al.* 2005, pp. 1770–1771). In addition, synthetic pyrethroids may interfere with nerve cell function, which could eventually result in paralysis (Bradbury and Coats 1989, pp. 377–378; Shafer and Meyer 2004, pp. 304–305).

Weston and Lydy (2010, p. 1835) found the largest source of pyrethroids flowing into the Delta to be coming from the Sacramento Regional Water Treatment Plant (SRWTP), where only secondary treatment occurs. Their data not only indicate the presence of these contaminants, but the concentrations found exceeded acute toxicity thresholds for the amphipod *Hyalella azteca*. This is of substantial concern because the use of insecticides in the urban environment had not before been considered the primary source of insecticides flowing into the Delta. Furthermore, this was not the case for the Stockton Waste Water Treatment facility, where tertiary treatment occurs, suggesting that the tertiary treatment that occurs at the Stockton facility could minimize or eliminate toxic effluent being dispersed from wastewater facilities (Baxter *et al.* 2010, p. 33).

Several studies were initiated in 2005 to address the possible role of contaminants and disease in the declines of Bay-Delta fish and other aquatic species. The primary study consists of twice-monthly monitoring of ambient water toxicity at 15 sites in the Bay-Delta and Suisun Bay (Baxter *et al.* 2010, pp. 16, 17, 30). Significant mortality of amphipods was observed in 5.6

percent of samples collected in 2006–2007 and 0.5 percent of samples collected in 2008–2009. Werner *et al.* (2010b, p. 3) found that larval delta smelt were between 1.8 and 11 times more sensitive than fathead minnows (*Pimephales promelas*) to copper, ammonia, and all insecticides except permethrin. Aquatic insects in which the longfin smelt relies upon for food have been shown to be sensitive to ammonia. *H. azteca* was the most sensitive to all pyrethroids tested, while *E. affinis* and *C. Dubia* were the most sensitive to ammonia (Werner *et al.* 2010b, pp. 18, 23). Pyrethroids are of particular interest because use of these insecticides has increased within the Bay-Delta watershed as use of organophosphate insecticides has declined. Longfin smelt are probably most vulnerable to the effects of toxic substances during the winter and spring, when their early life stages occur in the Delta and Suisun and San Pablo Bays, where they are closer to point and non-point inputs of contaminants from runoff.

The largest source of ammonia entering the Delta ecosystem is the Sacramento Regional Wastewater Treatment Plant (SRWTP), which accounts for 90 percent of the total ammonia load released into the Delta. Ammonia is un-ionized and has the chemical formula NH_3 . Ammonium is ionized and has the formula NH_4^+ . The major factors determining the proportion of ammonia or ammonium in water are water pH and temperature. This is important, as NH_3 ammonia is the form that can be directly toxic to aquatic organisms, and NH_4^+ ammonium is the form documented to interfere with uptake of nitrates by phytoplankton (Dugdale *et al.* 2007, p. 17; Jassby 2008, p. 3).

Effects of elevated ammonia levels on fish range from irritation of skin, gills, and eyes to reduced swimming ability and mortality (Wicks *et al.* 2002, p. 67). Delta smelt have been shown

to be directly sensitive to ammonia at the larval and juvenile stages (Werner *et al.* 2008, pp. 85–88). Longfin smelt could similarly be affected by ammonia as they utilize similar habitat and prey resources and have a physiology similar to delta smelt. Ammonia also can be toxic to several species of copepods important to larval and juvenile fishes (Werner *et al.* 2010, pp. 78–79; Teh *et al.* 2011, pp. 25–27).

In addition to direct effects on fish, ammonia in the form of ammonium has been shown to alter the food web by adversely impacting phytoplankton and zooplankton dynamics in the estuary ecosystem. Historical data show that decreases in Suisun Bay phytoplankton biomass coincide with increased ammonia discharge by the SRWTP (Parker *et al.* 2004, p. 7; Dugdale *et al.* 2011, p. 1). Phytoplankton preferentially take up ammonium over nitrate when it is present in the water. Ammonium is insufficient to provide for growth in phytoplankton, and uptake of ammonium to the exclusion of nitrate results in decreases in phytoplankton biomass (Dugdale *et al.* 2007, p. 23). Therefore, ammonium impairs primary productivity by reducing nitrate uptake in phytoplankton. Ammonium's negative effect on the food web has been documented in the longfin smelt rearing areas of San Francisco Bay and Suisun Bay (Dugdale *et al.* 2007, pp. 26–28). Decreased primary productivity results in less food available to longfin smelt and other fish in these bays.

Several streams that flow into the Bay-Delta are listed as impaired because of high concentrations of metals such as cadmium, copper, lead, and zinc. Metal concentrations have been found to be toxic to fish in the upper Sacramento River near and downstream from Redding (Alpers *et al.* 2000a, p. 4; 2000b, p. 5). Elevated levels of metals such as copper in streambed

sediment continue to occur in the upper Sacramento River Basin downstream from Redding (MacCoy and Domagalski 1999, p. 35). Copper and other metals may affect aquatic organisms in upper portions of contributing watersheds of the Delta. Mercury and its bioavailable form (methylmercury) are distributed throughout the estuary, although unevenly. Mercury has been known to bioaccumulate and cause neurological effects in some fish species, but it has not been associated with the Pelagic Organism Decline (Baxter *et al.* 2010, p. 28). No specific information is available on the effects of mercury exposures to longfin smelt. Selenium, introduced into the estuary primarily from agricultural irrigation runoff via the San Joaquin River drainage and oil refineries, has been implicated in toxic and reproductive effects in fish and wildlife (Baxter 2010 *et al.*, p. 28; Linville *et al.* 2002, p. 52). Selenium exposure has been shown to have effects on some benthic foraging species; however there is no evidence that selenium exposure is contributing to the decline of longfin smelt or other pelagic species in the Bay-Delta (Baxter *et al.* 2010, p. 28).

Large blooms of toxic *Microcystis aeruginosa* (blue-green algae) were first documented in the Bay-Delta during the summer of 1999 (Lehman *et al.* 2005, p. 87). *M. aeruginosa* forms large colonies throughout most of the Delta and increasingly down into eastern Suisun Bay (Lehman *et al.* 2005, p. 92). Blooms typically occur when water temperatures are above 20 °C (68 °F) (Lehman *et al.* 2005, p. 87). Preliminary evidence indicates that the toxins produced by local blooms are not directly toxic to fishes at current concentrations (Baxter *et al.* 2010, p. 10). However, the copepods that the related delta smelt eat are particularly susceptible to those toxins (Ger 2008, pp. 12, 13). *Microcystis* blooms may also decrease dissolved oxygen to lethal levels for fish (Lehman *et al.* 2005, p. 97). Blooms typically occur between late spring and early fall

when the majority of longfin smelt occur farther downstream, so effects are expected to be minimal.

Other Populations

As in the Bay-Delta, pesticide and metals contamination occurs in Yaquina Bay, the Columbia River, and the Fraser River (Johnson *et al.* 2007, p. 1; Lower Columbia River Estuary Partnership (LCREP) 2011, p. 1; Blomquist, 2005, p. 8). Ammonia contamination occurs in the Klamath River (Oregon Department of Environmental Quality (ODEQ) 2011, p. 1) and Cook Inlet (ADEC 2011a, p. 1), and toxic algal blooms occur in the Klamath River (California State Water Resources Control Board (CSWRCB) 2010, p. 1) and Yaquina Bay (ODEQ Water Quality Assessment Online Database 2011).

Industrial contaminants such as dioxins, polychlorinated biphenyls (PCBs), and polyaromatic hydrocarbons (PAHs) occur in Humboldt Bay (NCRWQCB 2010 pp. 3–4), Yaquina Bay (Johnson *et al.* 2007, p. 1), the Columbia River (LCREP 2011, p. 1), Puget Sound (Puget Sound Partnership 2008b, p. 21), and the Fraser River (British Columbia Ministry of Environment 2001, pp. 5–6; Blomquist, 2005, p. 8). Suspended sediment is a contaminant in the Eel River (Downie 2010, p. 10), Humboldt Bay (NCRWQCB 2010 pp. 3–4), Yaquina Bay (ODEQ Water Quality Assessment Online Database 2011), and Puget Sound (WA Department Ecology 2008, p. 1). Nutrient enrichment and low levels of dissolved oxygen occur in the Klamath River (CSWRCB 2010, p.1), Yaquina Bay (Bricker *et al.* 1999, pp. 1–71), and Fraser River (British Columbia Ministry of Environment 2001, pp. 5–6). Fecal coliform and other

forms of bacteria contaminate Yaquina Bay, Puget Sound, the Fraser River, and Cook Inlet (Brown et al 2007, pp. 16-17, WA Department Ecology 2008, p. 1, Blomquist, 2005, p. 8, ADEC 2011a, p. 1).

Oregon and Washington States have listed multiple reaches of the Lower Columbia River on their Federal Clean Water Act 303(d) lists, due to total dissolved gas levels exceeding State water quality standards. This occurs at several dams on these rivers where water flowing over the spillway of a dam creates air bubbles. When these are carried to depth in the dam's stilling basin, the higher hydrostatic pressure forces air from the bubbles into solution. The result is water supersaturated with dissolved nitrogen, oxygen, and the other constituents of air (ODEQ 2002, p. ix). High total dissolved gas levels can cause gas bubble trauma in fish, which can result in injury or mortality to fish species (ODEQ 2002, pp. 1–150).

Summary of Contaminants

Most fish including longfin smelt can be sensitive to adverse effects from contaminants in their larval or juvenile stages. Adverse effects to longfin smelt would be more likely to occur where sources of contaminants occur in close proximity to spawning and rearing habitats (brackish or fresh waters). Laboratory studies have shown certain contaminants to potentially have adverse effects on individual delta smelt, a related species. Field studies have shown that the contaminants of concern are elevated in some of the estuaries throughout the species' range, including the Bay-Delta.

Summary of Factor E

We evaluated whether entrainment losses, introduced species, and contaminants threaten the longfin smelt throughout its range. Longfin smelt is broadly distributed across a wide variety of estuaries from central California to Alaska, and there is no monitoring data documenting a population decline other than the population decline in the Bay-Delta.

Because the Bay-Delta system is one of the largest man made water systems in the world, it would be impractical to compare diversions and alterations in other estuaries to diversions and alterations in the Bay-Delta. The effects of entrainment in the Bay-Delta are unique to the estuary because of the large water diversions. Because diversions in other estuaries are much smaller, we expect that the effects from these diversions would be minimal in relation to the effects in the Bay-Delta. We have no information to show that entrainment is a threat to longfin smelt throughout its range.

Introduced species and contaminants are threats to the Bay-Delta long smelt population, but there is no information indicating that they are threats to the species in other parts of its range. Although invasive species are present in other estuaries, none have been documented to be having an effect on the longfin smelt food supply like the overbite clam has had. Similarly, although contaminants are present in other estuaries where the longfin smelt resides, none have been shown to have effects on the longfin smelt food supply like ammonia in the Bay-Delta has been shown to have.

Finding

As required by the Act, we considered the five factors in assessing whether the longfin smelt is endangered or threatened throughout all of its range. We have carefully examined the best scientific and commercial information available regarding the past, present, and future threats faced by the longfin smelt. We reviewed the petition, information available in our files, other available published and unpublished information, and we consulted with recognized longfin experts and other Federal and State agencies.

Little information is available on longfin smelt populations other than the Bay-Delta and Lake Washington populations. Smelt caught along the Pacific Coast are rarely identified to species. Therefore, information on longfin smelt distribution and abundance outside the Bay-Delta is limited. Although monitoring data indicate a significant decline in the abundance of longfin smelt in the Bay-Delta, population monitoring for other populations is not available. Estuaries are complex ecosystems, and different estuaries within the longfin smelt's range vary greatly in their environmental characteristics and in how they are managed. For example, in no estuary within the range of the longfin smelt, other than the Bay-Delta, are large volumes (up to 35 percent of freshwater inflow between February and June, and up to 65 percent of inflow between July and January) of freshwater pumped directly out of the estuary.

Under Factor A, channel disturbances may have localized impacts to longfin smelt habitat suitability. However, we conclude that these activities are not significant threats to longfin smelt throughout its range. Climate change will likely affect longfin smelt in multiple

ways, but longfin smelt are able to move between a wide range of aquatic environments that vary greatly in water temperature and salinity, and these behavioral and physiological characteristics of the species may help it adapt to the effects of climate change. We conclude that the best available information does not indicate that climate change threatens the continued existence of longfin smelt across its range. We conclude that reduced freshwater flows are a threat to the Bay-Delta longfin smelt population, but not to the species in the rest of its range. The Bay-Delta is unique among estuaries occupied by longfin smelt because large volumes of freshwater are exported away from the estuary on an annual basis. In addition, it is difficult to extrapolate from the Bay-Delta to other estuaries because the effects of water management in the Bay-Delta are likely unique to the physical, geologic, and hydrologic environment of that estuary. We conclude that the best scientific information available indicates that continued existence of the longfin smelt is not threatened in any part of its range outside of the Bay-Delta by the present or threatened destruction, modification, or curtailment of its habitat or range now or in the foreseeable future

Under Factor B, we evaluated potential threats from recreational and commercial fishing and from monitoring surveys on longfin smelt. Longfin smelt are protected from intentional take in California because the species is listed as threatened under CESA. Efforts have been made to reduce mortality of longfin smelt as bycatch in a bay shrimp trawl commercial fishery and in monitoring surveys in the Bay-Delta. Longfin smelt is caught as part of recreational or commercial fisheries in Oregon, Washington, British Columbia, and Alaska, but numbers of fish caught are considered low, and we found no evidence that fisheries harvest was causing population declines of longfin smelt. We conclude that overutilization is not a significant current

or future threat to longfin smelt across its range.

Under Factor C, we evaluated potential threats from disease and predation. We found no evidence of rangewide threats to the continued existence of the species due to disease or predation, now or in the foreseeable future.

Under Factor D, we conclude that several Federal and State laws and regulations provide varying levels of protection for the longfin smelt throughout its range. Several of these regulatory mechanisms promote protection of longfin smelt habitat and provide tools to implement these habitat protections. We conclude that longfin smelt is not threatened throughout its range by inadequate regulatory mechanisms, now or in the foreseeable future.

Under Factor E, we evaluated potential threats due to entrainment losses from water diversions, introduced species, and contaminants. Information indicates that introduced species are a threat to the Bay-Delta longfin smelt population and that ammonium may constitute a threat to the Bay-Delta longfin smelt population, but information does not indicate that entrainment losses, introduced species, or contaminants are threatening longfin smelt populations in other parts of its range, now or in the foreseeable future.

Based upon our review of the best available scientific and commercial information pertaining to the five factors, we find that the threats are not of sufficient imminence, intensity, or magnitude to indicate that the longfin smelt is in danger of extinction (endangered), or likely to become endangered within the foreseeable future (threatened), throughout all of its range.

Therefore, we find that listing the longfin smelt as an endangered or threatened species throughout all of its range is not warranted at this time.

Distinct Vertebrate Population Segment

Having found that the best available information does not indicate that the longfin smelt warrants listing rangewide, we now assess whether any distinct population segments of longfin smelt meet the definition of endangered or are likely to become endangered in the foreseeable future (threatened). Under the Services' (joint policy of the Fish and Wildlife Service and National Marine Fisheries Service) DPS policy (61 FR 4722; February 7, 1996), three elements are considered in the decision concerning the establishment and classification of a possible DPS. These are applied similarly for additions to or removal from the Federal List of Endangered and Threatened Wildlife. These elements include: (1) The discreteness of a population in relation to the remainder of the species to which it belongs; (2) the significance of the population segment to the species to which it belongs; and (3) the population segment's conservation status in relation to the Act's standards for listing, delisting, or reclassification (i.e., is the population segment endangered or threatened). We have identified one population that potentially meets all three elements of the 1996 DPS policy—the population that occurs in the Bay-Delta estuary. During the rangewide five-factor analysis, significant threats were identified only for the Bay-Delta population. Therefore, we determined that only the Bay-Delta population potentially meets the third element of the DPS.

Discreteness

Under the DPS policy, a population segment of a vertebrate taxon may be considered discrete if it satisfies either one of the following conditions:

(1) It is markedly separated from other populations of the same taxon as a consequence of physical, physiological, ecological, or behavioral factors. Quantitative measures of genetic or morphological discontinuity may provide evidence of this separation.

(2) It is delimited by international governmental boundaries within which differences in control of exploitation, management of habitat, conservation status, or regulatory mechanisms exist that are significant in light of section 4(a)(1)(D) of the Act.

Marked Separation from Other Populations as a Consequence of Physical, Physiological, Ecological, or Behavioral Factors

The limited swimming capabilities of the longfin smelt, existing ocean current patterns, and the great distances between the Bay-Delta and other known breeding populations make it unlikely that regular interchange occurs between the Bay-Delta and other longfin smelt breeding populations. Longfin smelt is a relatively short-lived species that completes its 2- to 3-year life cycle moving between freshwater spawning habitat in the Delta and brackish water rearing habitat downstream (seaward) in the estuary within Suisun Bay, San Pablo Bay, and central San Francisco Bay. At least a portion of the population also migrates into the near-coastal waters of the Gulf of Farallones (Rosenfield and Baxter 2007, p. 1590). Although its swimming

capabilities have not been studied, it is a small fish believed to have a limited swimming capacity (Moyle 2010, pp. 5–6). How longfin smelt return to the Bay-Delta from the Gulf of Farallones is not known (Rosenfield and Baxter 2007, p.1590).

The Bay-Delta population is the southernmost population of longfin smelt and is separated from other longfin smelt breeding populations by 56 km (35 mi). The nearest location to the Bay-Delta where longfin smelt have been caught is the Russian River, located north of the Bay-Delta; however, little information is available for this population (see Distribution section, above). Due to limited freshwater flow into the estuary and interannual variation in freshwater flow, it is unlikely that the estuary provides sufficient potential spawning and rearing habitat to support a regularly breeding longfin smelt population (Moyle 2010, p. 4).

The Eel River and Humboldt Bay are the next nearest locations where longfin smelt are known to occur, and they are located much farther to the north—Eel River is located 394 km (245 mi) north of the Bay-Delta, and Humboldt Bay is located 420 km (260 mi) north of the Bay-Delta. Moyle (2010, p. 4) considered Humboldt Bay to be the only other estuary in California potentially capable of supporting longfin smelt in most years.

In our April 9, 2009, longfin smelt 12-month finding (74 FR 16169), we concluded that the Bay-Delta population was not markedly separated from other populations and, therefore, did not meet the discreteness element of the 1996 DPS policy. This conclusion was based in part on the assumption that ocean currents likely facilitated dispersal of anadromous longfin smelt to and from the Bay-Delta to other estuaries in numbers that could readily sustain the Bay-Delta

population group if it was to be extirpated. Since 2009, we have obtained information relevant to assumptions that we made in the 2009 12-month finding. Additional clarifying information comes in part from a declaration submitted to the U.S. District Court for the Northern District of California on June 29, 2010, by Dr. Peter Moyle, Professor of Fisheries Biology at the University of California at Davis (Moyle 2010, pp. 1–8). Moyle (2010, pp. 5–6) notes that he believes that we overestimated the swimming capacity of longfin smelt in our 2009 12-month finding. Moyle (2010, p. 8) states that longfin smelt that migrate out of and back into the Bay-Delta estuary may primarily be feeding on the rich planktonic food supply in the Gulf of Farallones, and that this migration between the Bay-Delta and near coastal waters of the Gulf of Farallones does not indicate that longfin smelt are necessarily dispersing long distances to other estuaries to the north.

At the time of our last finding, we did not have information available assessing the ability of longfin smelt to disperse northward from the Bay-Delta or southward to the Bay-Delta using currents in the Pacific Ocean. Since the time of our previous finding (74 FR 16169; April 9, 2009), we have reviewed additional information on ocean currents in nearshore waters and over the continental shelf from approximately the Gulf of Farallones north to Coos Bay. We have evaluated the potential for longfin smelt to disperse northward from the Bay-Delta or southward to the Bay-Delta. On October 28, 2011, we convened a panel of experts to evaluate the potential of longfin smelt dispersal via ocean currents. Oceanographers on the panel were tasked with answering a series of questions on how ocean currents would affect longfin smelt potentially dispersing into or out of the Bay-Delta. Much of the following analysis was derived from that panel discussion. Our analysis relies upon ocean current information as it relates to what is

known of longfin smelt biology and life history from the Bay-Delta population.

Table 2 overlays longfin smelt life history with general ocean current patterns in central and northern California. However, the California Current System exhibits a high degree of seasonality as well as weekly variability. Currents are highly variable in fall and winter but tend to be predominately northward. Surface currents are northward during the storm season from December to March and transition to southward in March or April. Offshore of central California the surface currents remain generally southward during summer. However, despite the predominant southward surface current, northward currents are common at depths around 60 to 200 m along the continental slope at all times of the year. This deeper current is known as the California Undercurrent (Paduan 2011, pers. comm.)

TABLE 2. Summary of longfin smelt life history within the Bay-Delta, and generalized coastal ocean circulation.

Month	Dec	Jan	Feb	Mar	Apr	May	Jun	Jul	Aug	Sep	Oct	Nov
First Year		Peak Hatching-freshwater, upstream Delta										
		Larval Rearing San Pablo and San Francisco Bays-salinities <8 psu										
	Juveniles Rearing				Juvenile Rearing – Primarily San Pablo, San Francisco Bays-							
Second Year		Juvenile Rearing										
						– Juvenile Rearing -Movement to the coastal ocean begins in the summer, mass movement to coastal ocean begins in July and August						
	Spawning Migration											
	Peak Spawning-freshwater, Delta											

Coastal Current	Storm Season (Northward Flow)	Upwelling Season (Predominate Southward and Offshore Flow)	Relaxation Season (Weak Northward Flow)
-----------------	----------------------------------	--	--

Eddies (clockwise water circulation areas) exist at various points between the Bay-Delta and Humboldt Bay at landmarks such as Point Arena and Cape Mendocino. These eddies vary in their distance from shore between 10 to 100 km (6 to 62 mi) (Padaun 2011, pers. comm.). During the summer upwelling season, northerly winds drive a southward offshore flow of near-surface waters (Dever *et al.* 2006, p. 2109) and also set up a strong current over the continental shelf that is deflected offshore at capes such as Cape Mendocino, Point Arena, and Point Reyes (Magnell *et al.* 1990, p. 7; Largier 2004, p. 107; Halle and Largier 2011, pp. 1–24). Several studies have used drifters (flotation devices tracked by satellites) and pseudo-drifters (computer-simulated satellite-tracked flotation devices) to evaluate currents in the California region of the Pacific Ocean. These studies indicate that the circulation patterns located off Point Arena and Cape Mendocino limit dispersal (particularly southward) of flotation devices in the region (Sotka *et al.* 2004, p. 2150; Drake *et al.* 2011, pp. 1–51; Halle and Largier 2011, posters). This limitation is important because Cape Mendocino and Point Arena are between the Bay-Delta and the nearest likely self-sustaining population of longfin smelt in Humboldt Bay.

Longfin smelt are an euryhaline species, of which an unknown fraction of the population exhibits anadromy (Moyle 2002, p. 236; Rosenfield and Baxter 2007 p. 1578). Based on their small size and limited swimming ability, we expect that longfin smelt would be largely dependent on ocean currents to travel the large distance between the Bay-Delta and the Humboldt Bay. During wet years, newly spawned longfin smelt larvae may be flushed out to the

ocean between December and March. It is unlikely that longfin smelt larvae can survive ocean transport because larvae are not known to tolerate salinities greater than 8 ppt (Baxter 2011b, pers. comm.), and surface salinities less than 8 ppt do not exist consistently in the ocean (Bograd and Paduan 2011, pers. comm.).

A portion of the longfin smelt that spawn in the Bay-Delta make their way to the ocean once they are able to tolerate full marine salinities, sometime during the late spring or summer of their first year of life (age-0) (City of San Francisco and CH2MHill 1984 and 1985, entire), and may remain there for 18 months or longer before returning to the Bay-Delta to spawn (Baxter 2011c, pers. comm.). A larger portion of longfin smelt enter the coastal ocean during their second year of life (age-1) (City of San Francisco and CH2MHill 1984 and 1985, entire) and remain there for 3 to 7 months until they re-enter the Bay-Delta to spawn in early winter (Rosenfield and Baxter 2007, p 1590; Baxter 2011c, pers. comm.). Most of these age-1 longfin smelt move to coastal waters in July and August, possibly to escape warm water temperatures or to obtain food (Moyle 2010, p. 8; Rosenfield and Baxter 2007, p. 1290). Some longfin smelt may live to 3 years of age and may remain in the coastal ocean until they are 3 years old. However, no 3-year old longfin smelt have been observed in the coastal ocean (Baxter 2011d, pers. comm.; Service 2011, unpublished data).

It is possible that some of these juvenile or adult longfin smelt could make their way into the Russian River, Eel River, or Humboldt Bay and supplement or sustain those populations by utilizing northward ocean currents (Padaun 2011, pers. comm.; Service 2011b, pp. 1-4), but there is no documentation of such long-distance coastal movements. The northward ocean currents are

strongest and most reliable in winter, when satellite-tracked particles move between the Bay-Delta and Humboldt Bay in as little as 2 months (Service 2011, p. 3).

Opportunities for longfin smelt dispersal utilizing ocean currents from northern estuaries to the Bay-Delta are more limited. Studies have revealed that currents near Cape Mendocino and Point Arena would carry small objects to the west away from the coast (Padaun 2011b, pers. comm.; Bograd 2011, pers. comm.). It is possible that longfin smelt in nearshore waters could travel south past these eddies if they stay close enough to shore. It is even possible that some longfin smelt may be moved closer to shore by the eddies (Bograd 2011, pers. comm.; Paduan 2011, pers. comm.). However, any longfin smelt that do travel south past the Cape Mendocino and Point Arena escarpments would be unlikely to re-enter the Bay-Delta. These offshore ocean currents could displace any longfin smelt potentially moving south more than 100 km (62 mi) offshore of the Bay-Delta (Paduan 2011a, pers. comm.). Pathways that transport objects close to shore would be expected to be rare, if they exist at all (Padaun 2011b, pers. comm.; Bograd 2011, pers. comm.). So while we considered whether ocean currents may transport or facilitate movement of longfin smelt from northern estuaries to the Bay-Delta estuary, there is no information showing that such dispersal movement occurs.

Using the best scientific data available, we compared longfin smelt biology and life history with the latest available ocean current data provided by oceanographers. We conclude that longfin smelt in the Bay-Delta population do not regularly breed or interact with longfin smelt in other breeding populations to the north and are therefore markedly separated from other longfin smelt populations.

Under the 1996 DPS policy, the discreteness standard does not require absolute separation of a DPS from other members of its species, nor does the standard require absolute reproductive isolation (61 FR 4722). Because of the great distances between the Bay-Delta and known breeding populations to the north, the small size of the longfin smelt, and the low likelihood that ocean currents could facilitate longfin smelt movements between widely separated populations, we conclude that the Bay-Delta population is markedly separated from other longfin smelt populations and therefore discreet.

Quantitative Measures of Genetic or Morphological Discontinuity

The 1996 DPS policy states that quantitative measures of genetic or morphological discontinuity may provide evidence of marked separation and discreteness. Stanley *et al.* (1995, p. 395) compared allozyme variation between longfin smelt from the Bay-Delta population and the Lake Washington population using electrophoresis. They found that individuals from the populations differed significantly in allele (portions of a chromosome that code for the same trait) frequencies at several loci (gene locations). However, the authors also stated that the overall genetic dissimilarity was within the range of other conspecific (of the same species) fish species, and concluded that longfin smelt from Lake Washington and the Bay-Delta are conspecific, despite the large geographic separation (Stanley *et al.* 1995, p. 395). This study provided evidence that the Bay-Delta population of longfin smelt differed in genetic characteristics from the Lake Washington population, but did not compare other populations rangewide to the Bay-Delta population. More recently, Israel *et al.* (2011, pp. 1–10) presented

preliminary results from an ongoing study, but these results were inconclusive in providing evidence of whether the Bay-Delta population is markedly separated from other longfin smelt populations (Cope 2011, pers. comm.; Service 2011a, pp. 1-3).

We conclude that the limited quantitative genetic and morphological information available does not provide additional evidence of marked separation of the Bay-Delta longfin smelt population beyond the evidence presented above under Marked Separation from Other Populations as a Consequence of Physical, Physiological, Ecological, or Behavioral Factors.

Delimited by International Governmental Boundaries Within Which Differences in Control of Exploitation, Management of Habitat, Conservation Status, or Regulatory Mechanisms Exist that are Significant in Light of Section 4(a)(1)(D) of the Act

The Bay-Delta population of longfin smelt is not delimited by an international boundary. Therefore, we conclude that it does not meet the international governmental boundaries criterion for discreteness.

Conclusion for Discreteness

Because of its limited swimming capabilities and because of the great distances between the Bay-Delta and known breeding populations to the north, we conclude that the Bay-Delta population is markedly separated from other longfin smelt populations, and thus meets the discreteness element of the 1996 DPS policy. The best available information indicates that

longfin smelt from the Bay-Delta population complete their life cycle moving between freshwater, brackish water, and saltwater portions of the estuary and nearby coastal ocean waters in the Gulf of Farallones. The nearest known breeding population of longfin smelt is Humboldt Bay, 420 km (260 mi) north of the Bay-Delta. As a result, potential interchange between the Bay-Delta population and other longfin smelt breeding populations is limited. Although the best scientific information suggests that potential movement of longfin smelt northward from the Bay-Delta would be facilitated by ocean currents, potential movement from more northern estuaries south to the Bay-Delta would be more difficult and unlikely because of ocean currents. Based on our review of the best available scientific and commercial information available, we conclude that the Bay-Delta population of longfin smelt is markedly separated from other longfin smelt populations as a consequence of physical, physiological, ecological, or behavioral factors.

Significance

Since we have found that the Bay-Delta longfin smelt population meets the discreteness element of the 1996 DPS policy, we now consider its biological and ecological significance in light of Congressional guidance that the authority to list DPSes be used “sparingly” while encouraging the conservation of genetic diversity. In making this determination, we consider available scientific evidence of the discrete population segment’s importance to the taxon to which it belongs. As precise circumstances are likely to vary considerably from case to case, the DPS policy does not describe all the classes of information that might be used in determining the biological and ecological importance of a discrete population. However, the DPS policy describes four possible classes of information that provide evidence of a population segment’s

biological and ecological importance to the taxon to which it belongs. As specified in the DPS policy, this consideration of the population segment's significance may include, but is not limited to, the following:

(1) Persistence of the discrete population segment in an ecological setting unusual or unique to the taxon;

(2) Evidence that loss of the discrete population segment would result in a significant gap in the range of a taxon;

(3) Evidence that the discrete population segment represents the only surviving natural occurrence of a taxon that may be more abundant elsewhere as an introduced population outside its historic range; or

(4) Evidence that the discrete population segment differs markedly from other populations of the species in its genetic characteristics.

A population segment needs to satisfy only one of these conditions to be considered significant. Furthermore, other information may be used as appropriate to provide evidence for significance.

(1) Persistence of the discrete population segment in an ecological setting unusual or unique to the taxon.

The Bay-Delta population is the southernmost breeding population in the range of the species. Populations at the edge of a species' range may be important in species conservation because environmental conditions at the periphery of a species' range can be different from environmental conditions nearer the center of a species' range. Thus, populations at the edge of the taxon's range may experience different natural selection pressures that promote divergent evolutionary adaptations (Scudder 1989, entire; Fraser 2000, entire). Lomolino and Channell (1998, p. 482) hypothesized that because peripheral populations should be adapted to a greater variety of environmental conditions, they may be better suited to deal with anthropogenic (human-caused) disturbances than populations in the central part of a species' range; however, this hypothesis remains unproven. This could be especially important because of changing natural selection pressures associated with climate change.

For example, increasing ocean temperatures is an environmental change to which the Bay-Delta population of longfin smelt may be uniquely adapted. Because it is the southern-most estuary within the species' range, the Bay-Delta has warmer average water temperatures than estuaries in central and northern parts of the species' range. As a result, the Bay-Delta longfin smelt population may have behavioral or physiological adaptations for coping with higher water temperatures that may come as a result of climate change (see discussion under Factor A: Climate Change). Baxter *et al.* (2010, p. 68) conclude that high water temperatures in the Bay-Delta influence spatial distribution of longfin smelt in the estuary. Rosenfield and Baxter (2007, p. 1290) hypothesize that the partial anadromy exhibited by the population (part of the population is believed to migrate out into the cooler, nearby coastal ocean waters in the Gulf of

Farallones) and concentrations of longfin smelt in deeper water habitat in summer months is at least partly a behavioral response to warm water temperatures found during summer and early fall in the shallows of south San Francisco Bay and San Pablo Bay (Rosenfield and Baxter 2007, p. 1590).

The Bay-Delta estuary, although greatly degraded, is the largest estuary on the Pacific Coast of the United States (Sommer *et al.* 2007, p. 271). Because of its large size and diverse habitat, it is capable of supporting a large longfin smelt population. Large populations are valuable in the conservation of species because of their lower extinction risks compared to small populations. Historically, longfin smelt is believed to have been one of the more abundant pelagic fishes in the Bay-Delta. The areal extent of tidal freshwater habitat in the Bay-Delta estuary exceeds that of other California estuaries by an order of magnitude (NOAA 2007, p. 1), providing not only more available spawning habitat but also important habitat diversity should conditions at any one location become unsuitable. The Bay-Delta contains significant amounts of tidal freshwater and mixing zone habitat (Monaco *et al.* 1992, p. 255), which is crucial for spawning and rearing of juvenile longfin smelt. Other Pacific Coast estuaries where longfin smelt occur are predominately river-dominated estuaries (e.g., Russian River, Eel River, Klamath River, Columbia River), which have much smaller areas of low-salinity brackish water for longfin smelt rearing habitat.

(2) Evidence that loss of the discrete population segment would result in a significant gap in the range of a taxon.

Loss of the Bay-Delta population of longfin smelt would result in a significant gap in the range of the taxon because the nearest persistent longfin smelt breeding population to the Bay-Delta population is in Humboldt Bay, which is located approximately 420 km (260 mi) away. Loss of the Bay-Delta population would truncate the range of the species by hundreds of miles.

(3) Evidence that the discrete population segment represents the only surviving natural occurrence of a taxon that may be more abundant elsewhere as an introduced population outside its historic range.

This factor does not apply to the Bay-Delta longfin smelt population because other naturally occurring populations are found within the species' range.

(4) Evidence that the discrete population segment differs markedly from other populations of the species in its genetic characteristics.

As discussed above under Quantitative Measures of Genetic or Morphological Discontinuity, two studies have evaluated genetic characteristics of the Bay-Delta longfin smelt population. One study concluded that genetic characteristics of the Bay-Delta population differed from the Lake Washington population but did not compare any other populations (Stanley *et al.* 1995, pp. 390–396). Israel *et al.* (2011, pp. 1–10) presented preliminary results from an ongoing study, but these results are inconclusive in determining whether the Bay-Delta population differs markedly from other longfin smelt populations in its genetic characteristics. Therefore, although information indicates that the genetic characteristics of the Bay-Delta

population differs from at least one other longfin smelt population (Lake Washington), there is no other information currently available indicating that the genetic characteristics of the Bay-Delta population differ markedly from other longfin smelt populations.

Conclusion for Significance

We conclude that the Bay-Delta population is biologically significant to the longfin smelt species because the population occurs in an ecological setting unusual or unique for the species and its loss would result in a significant truncation of the range of the species. The Bay-Delta longfin smelt population occurs at the southern edge of the species' range and has likely experienced different natural selection pressures than those experienced by populations in middle portions of the species' range. The population may therefore possess unique evolutionary adaptations important to the conservation of the species. The Bay-Delta also is unique because it is the largest estuary on the Pacific Coast of the United States. Because of its large size and diverse aquatic habitats, the Bay-Delta has the potential to support a large longfin smelt population and is thus potentially important in the conservation of the species. The Bay-Delta population also is significant to the taxon because the nearest known breeding population of longfin smelt is hundreds of miles away, so loss of the Bay-Delta population would significantly truncate the range of the species and result in a significant gap in the species' range. Based on our review of the best available scientific and commercial information, we conclude that the Bay-Delta population meets the significance element of the 1996 DPS policy.

Determination of Distinct Population Segment

Because we have determined that the Bay-Delta population meets both the discreteness and significance elements of the 1996 DPS policy, we find that the Bay-Delta longfin smelt population is a valid DPS and thus is a listable entity under the Act. Therefore, we next evaluate its conservation status in relation to the Act's standards for listing (i.e., is the population segment, when treated as if it were a species, endangered or threatened?).

Distinct Population Segment Five-Factor Analysis

Because the Bay-Delta population of longfin smelt meets the criteria for a DPS, we will now evaluate its status with regard to its potential for listing as endangered or threatened under the five factors enumerated in section 4(a) of the Act. Our evaluation of the Bay-Delta DPS of longfin smelt follows.

Under **Summary of Information Pertaining to the Five Factors**, we evaluated threats to longfin smelt throughout its range. Much of this rangewide analysis focused on threats to the Bay-Delta population because so little information exists for other parts of the species' range. Although the threats of lack of freshwater flow, contaminants, and invasive species do not rise to the level of being significant threats rangewide, the best available scientific and commercial data indicates that these threats are significant to the species within the Bay-Delta. We utilized the vast amounts of research that have been conducted within the Bay-Delta by the Interagency Ecological Program and University of California at Davis to make our determinations of threats

in the Bay-Delta.

Factor A. The Present or Threatened Destruction, Modification, or Curtailment of Its Habitat or Range

Reduced Freshwater Flow

As we discussed above in the rangewide analysis, a primary threat to the Bay-Delta longfin smelt is reduced freshwater flows. In the Bay-Delta, freshwater flow is strongly related to the natural hydrologic cycles of drought and flood. Studies of Bay-Delta longfin smelt have found that increased Delta outflow during the winter and spring is the largest factor positively affecting longfin smelt abundance (Stevens and Miller 1983, pp. 431–432; Jassby *et al.* 1995, p. 285; Sommer *et al.* 2007, p. 274; Thomson *et al.* 2010, pp. 1439–1440). During high outflow periods larvae are believed to benefit from increased transport and dispersal downstream, increased food production, reduced predation through increased turbidity, and reduced loss to entrainment due to a westward shift in the boundary of spawning habitat and strong downstream transport of larvae (CFDG 1992, pp. 45-61; Hieb and Baxter 1993, pp. 106-107; CDFG 2009a, p. 18). Conversely, during low outflow periods, the negative effects of reduced transport and dispersal, reduced turbidity, and potentially increased loss of larvae to predation and increased loss at the export facilities result in lower young-of-the-year recruitment. Despite numerous studies of longfin smelt abundance and flow in the Bay-Delta, the underlying causal mechanisms are still not fully understood (Baxter *et al.* 2010, p. 69; Rosenfield 2010, p. 9).

As California's population has grown, demands for reliable water supplies and flood protection have grown. In response, State and Federal agencies built dams and canals, and captured water in reservoirs, to increase capacity for water storage and conveyance resulting in one of the largest manmade water systems in the world (Nichols *et al.* 1986, p. 569). Operation of this system has altered the seasonal pattern of freshwater flows in the watershed. Storage in the upper watershed of peak runoff and release of the captured water for irrigation and urban needs during subsequent low flow periods result in a broader, flatter hydrograph with less seasonal variability in freshwater flows into the estuary (Kimmerer 2004, p. 15).

In addition to the system of dams and canals built throughout the Sacramento River-San Joaquin River basin, the Bay-Delta is unique in having a large water diversion system located within the estuary (Kimmerer 2002b, p. 1279). The State Water Project (SWP) and Central Valley Project (CVP) operate two water export facilities in the Delta (Sommer *et al.* 2007, p. 272). Project operation and management is dependent upon upstream water supply and export area demands. Despite the size of the water storage and diversion projects, much of the interannual variability in Delta hydrology is due to variability in precipitation from year to year. Annual inflow from the watershed to the Delta is strongly correlated to unimpaired flow (runoff that would hypothetically occur if upstream dams and diversions were not in existence), mainly due to the effects of high-flow events (Kimmerer 2004, p. 15). Water operations are regulated in part by the California State Water Resources Control Board (SWRCB) according to the Water Quality Control Plan (WQCP) (SWRCB 2000, entire). The WQCP limits Delta water exports in relation to Delta inflow (the Export/Inflow, or E/I ratio).

It is important to note that in the case of the Bay-Delta, freshwater flow is expressed as both Delta inflow (from the rivers into the Delta) and as Delta outflow (from the Delta into the lower estuary), which are closely correlated, but not equivalent. Freshwater flow into the Delta affects the location of the low salinity zone and X2 within the estuary. As longfin smelt spawn in freshwater, they must migrate farther upstream to spawn as flow reductions alter the position of X2 and the low-salinity zone moves upstream (CDFG 2009, p. 17). Longer migration distances into the Bay-Delta make longfin smelt more susceptible to entrainment in the State and Federal water pumps (see Factor E: Entrainment Losses, below). In periods with greater freshwater flow into the Delta, X2 is pushed farther downstream (seaward); in periods with low flows, X2 is positioned farther landward (upstream) in the estuary and into the Delta. Not only is longfin smelt abundance in the Bay-Delta strongly correlated with Delta inflow and X2, but the spatial distribution of longfin smelt larvae is also strongly associated with X2 (Dege and Brown 2004, pp. 58–60; Baxter *et al.* 2010, p. 61). As longfin hatch into larvae, they move from the areas where they are spawned and orient themselves just downstream of X2 (Dege and Brown 2004, pp. 58-60). Larval (winter-spring) habitat varies with outflow and with the location of X2 (CDFG 2009, p. 12), and has been reduced since the 1990s due to a general upstream shift in the location of X2 (Hilts 2012, unpublished data). The amount of rearing habitat (salinity between 0.1 and 18 ppt) is also presumed to vary with the location of X2 (Baxter *et al.* 2010, p. 64). However, as previously stated, the location of X2 is of particular importance to the distribution of newly-hatched larvae and spawning adults. The influence of water project operations from November through April, when spawning adults and newly-hatched larvae are oriented to X2, is greater in drier years than in wetter years (Knowles 2002, p. 7).

In addition to the effects of reduced freshwater flow on habitat suitability for longfin smelt and other organisms in the Bay-Delta, one of the principal concerns over the biological impacts of these water export facilities has been entrainment of fish and other aquatic organisms. For a detailed discussion, see Factor E: Entrainment Losses, below.

Given the observed negative association between the reduction of freshwater outflow and longfin smelt abundance, we consider the current reductions in freshwater outflow to pose a significant threat to the Bay-Delta DPS of longfin smelt. Based on the observed associations in the Bay-Delta between freshwater outflow and longfin abundance, the lack of effective control mechanisms, and projections of freshwater outflow fluctuations, we expect the degree of this threat to continue and likely increase within the foreseeable future. We conclude that lack of freshwater flow is a significant current and future threat to the Bay-Delta DPS of longfin smelt.

Climate Change

Climate change may affect the Bay-Delta DPS of longfin smelt habitat as a result of (1) Changes in the timing and availability of freshwater flow into the estuary due to reduced snowpack and earlier melting of the snowpack; (2) sea level rise and saltwater intrusion into the estuary; (3) effects associated with increased water temperatures; and (4) effects related to changes in frequency and intensity of storms, floods, and droughts. It is difficult to evaluate effects related to changes in the timing and availability of freshwater flow into the estuary due to reduced snowpack and earlier melting of the snowpack because these potential effects will likely be impacted to some extent through decisions on water management in the intensively managed

Sacramento River-San Joaquin River water basin. Continued sea level rise will result in saltwater intrusion and landward displacement of the low-salinity zone, which would likely negatively affect longfin smelt habitat suitability. Increasing water temperatures would likely affect distribution and movement patterns of longfin smelt in the estuary; longfin smelt may be displaced to locations with deeper and cooler water temperatures. This displacement may result in decreased survival and productivity. Increased frequency and severity of storms, floods, and droughts could result in reduced longfin smelt habitat suitability, but it is difficult to estimate these effects because of uncertainty about the frequency and severity of these events. However, warming may result in more precipitation falling as rain and less storage as snow, increasing winter runoff as spring runoff decreases (USBR 2011, p. 147).

It is uncertain how a change in the timing and duration of freshwater flows will affect longfin smelt. Higher flows in January and February (peak spawning and hatching months) resulting from snow packs that melt sooner and rain-on-snow events could potentially create better spawning and larval rearing conditions. This would reduce adult migration distance and increase areas of freshwater spawning habitat during these months. In addition, the higher turbidity associated with these flows may reduce predation on longfin smelt adults and larvae (Baxter 2011, pers. comm.). However, if high flows last only a short period, benefits may be negated by poorer conditions before and after the high flows. As the freshwater boundary moves farther inland into the Delta with increasing sea level (see below) and reduced flows, adults will need to migrate farther into the Delta to spawn, increasing the risk of predation and the potential for entrainment into water export facilities and diversions for both themselves and their progeny. Because of the uncertainties surrounding climate change and the potential for increased winter

runoff that could benefit longfin smelt, we determined that there is not sufficient information to conclude that climate change threatens the continued existence of the Bay-Delta DPS of longfin smelt.

Channel Disturbances

Channel dredging in the Bay-Delta is an ongoing periodic disturbance of longfin smelt habitat, but most activity occurs in areas where longfin smelt are not likely to be present. We conclude that the effects of ongoing channel maintenance dredging are small and localized and do not rise to a level that would significantly affect the population as a whole.

There is currently a proposal to deepen and selectively widen the Sacramento Deep Water Ship Channel and the lower portion of the Sacramento River in the Bay-Delta. This dredging project would remove between 6.1–7.6 million cubic meters (8 and 10 million cubic yards) of material from the channel and Sacramento River and extend for 74 km (45.8 mi) (USACE 2011a, entire). Potential effects of this new project to longfin smelt include mortality through loss of spawning substrate, habitat modification, and a shift in spawning and rearing habitat. The project also has potential to alter breeding and foraging behavior of the Bay-Delta longfin smelt population. However, this project is only a proposal at this time and is not certain to occur. Potential effects of the proposed project are currently under evaluation.

Summary of Factor A

In summary, we conclude that the best available scientific and commercial information available indicates that the effects of reduced freshwater flows constitute a current and future threat to the Bay-Delta DPS of longfin smelt. We find that the Bay-Delta DPS of longfin smelt is currently threatened in part due to the present or threatened destruction, modification, or curtailment of its habitat or range due to reduced freshwater flow.

Factor B. Overutilization for Commercial, Recreational, Scientific, or Educational Purposes

Commercial and Recreational Take

Because of its status as a threatened species under the California Endangered Species Act, take of longfin smelt in the Bay-Delta is illegal, unless authorized by an incidental take permit or other take authorization. However, longfin smelt are caught as bycatch in a small bay shrimp trawl commercial fishery that operates in South San Francisco Bay, San Pablo Bay, and Carquinez Strait (Hieb 2009, p. 1). CDFG (Hieb 2009, pp. 6, 9) estimated the total longfin smelt bycatch from this fishery from 1989–1990 at 15,539 fish, and in 2004 at 18,815–30,574 fish. CDFG noted in 2009 that they thought the bay shrimp trawl fishery had declined since 2004 (Hieb, p. 3) and just recently reported the number of active shrimp permits at less than 10 (Hieb 2011, pers. comm.).

Scientific Take

Within the Bay-Delta, longfin smelt are regularly captured in monitoring surveys. The Interagency Ecological Program (IEP) implements scientific research in the Bay-Delta. Although the focus of its studies and the level of effort have changed over time, in general, their surveys have been directed at researching the Pelagic Organism Decline in the Bay-Delta. Between the years of 1987 to 2011, combined take of longfin smelt less than 20 mm (0.8 in) in length ranged from 2,405 to 158,588 annually. All of these fish were preserved for research or assumed to die in processing. During the same time period, combined take for juveniles and adults (fish greater than or equal to 20 mm (0.8 in)) ranged from 461 to 68,974 annually (IEP 2011). Although mortality is unknown, the majority of these fish likely do not survive. The Chipps Island survey, which is conducted by the Service, has captured an average of 2,697 longfin smelt per year during the past 10 years. Biologists attempt to release these fish unharmed, but at least 5,154 longfin smelt were known to have died during the Chipps Island survey between 2001 and 2008 (Service 2010, entire).

Incidental take from bycatch and monitoring surveys has not been identified as a possible factor related to recent longfin smelt population declines in the Bay-Delta (Baxter *et al.* 2010, pp. 61–69). CDFG (2009, p. 32) recommended adaptively managing scientific collection of longfin smelt to avoid adverse population effects, and survey methods have been modified recently to minimize potential impacts to delta smelt (75 FR 17669; April 7, 2010). These modifications likely have resulted in reduced impacts to longfin smelt. Based on the best scientific and commercial information, we conclude that the Bay-Delta DPS of longfin smelt is not currently threatened by overutilization for commercial, recreational, scientific, or educational purposes, nor do we anticipate overutilization posing a significant threat in the future.

Factor C. Disease or Predation

Disease

Little information is available on incidence of disease in the Bay-Delta longfin smelt DPS. Larval and juvenile longfin smelt were collected from the Bay-Delta in 2006 and 2007 and analyzed for signs of disease and parasites (Foott and Stone 2006, entire; Foott and Stone 2007, entire). No significant health problem was detected in either year (Foott and Stone 2007, p. 15). The south Delta is fed by water from the San Joaquin River, where pesticides (e.g., chlorpyrifos, carbofuran, and diazinon), salts (e.g., sodium sulfates), trace elements (boron and selenium), and high levels of total dissolved solids are prevalent due to agricultural runoff (64 FR 5963; February 8, 1999). Pesticides and other toxic chemicals may adversely affect the immune system of longfin smelt and other fish in the Bay-Delta and other estuaries, but we found no information documenting such effects.

Predation

Striped bass were introduced into the Bay-Delta in 1879 and quickly became abundant throughout the estuary. However, their numbers have declined substantially over the last 40 years (Thomson *et al.* 2010, p. 1440), and they are themselves one of the four species studied under Pelagic Organism Decline investigations (Baxter *et al.* 2010, p. 16). Numbers of largemouth bass, another introduced species in the Bay-Delta, have increased in the Delta over

the past few decades (Brown and Michniuk 2007, p. 195). Largemouth bass, however, occur in shallow freshwater habitats, closer to shore than the pelagic longfin smelt, and so do not tend to co-occur with longfin for much of their life history. Baxter *et al.* (2010, p. 40) reported that no longfin smelt have been found in largemouth bass stomachs sampled in a recent study of largemouth bass diet. Moyle (2002, p. 238) believed that inland silverside, another nonnative predatory fish, may be an important predator on longfin eggs and larvae, but Rosenfield *et al.* (2010, p. 18) believed that to be unlikely because inland silversides prefer shallow water habitats where juvenile and subadult longfin smelt are rare.

In the Bay-Delta, predation of longfin smelt may be high in the Clifton Court Forebay, where the SWP water export pumping plant is located (Moyle 2002, p. 238; Baxter *et al.* 2010, p. 42). However, once they are entrained in the Clifton Court Forebay, longfin smelt mortality would be high anyway due to high water temperatures in the Forebay (CDFG 2009b, p. 4) and entrainment into the SWP water export pumping plant. In addition to elevated predation levels in the Clifton Court Forebay, predation also is concentrated at sites where fish salvaged from the SWP and CVP export facilities are released (Moyle 2002, p. 238). However, few longfin smelt survive the salvage and transport process (see Factor E: Entrainment Losses, below), and therefore predation is not expected to be an important factor at drop off sites. As discussed above, reduced freshwater flows may result in lower turbidity and increased water clarity (see discussion under DPS' Factor A), which may contribute to increased risk of predation (Baxter *et al.* 2010, p. 64).

Based on a review of the best available scientific and commercial information, we conclude that disease does not constitute a threat to the Bay-Delta longfin smelt DPS. Available information indicates that Bay-Delta longfin smelt experience elevated levels of predation near the water diversions at the SWP and CVP water export facilities in the south Delta and at the salvage release sites. Reduced freshwater flows resulting from water diversions result in increased water clarity, and increased water clarity may result in increased predation risks to longfin smelt.

In summary, striped bass predation is in decline and largemouth bass predation is unlikely a threat because of the minimal overlap in time and space of largemouth bass and longfin smelt. Therefore, the current rates of predation on longfin smelt are not expected to be having a substantial effect on the overall population level. Based on the best available scientific and commercial information, we conclude that neither disease nor predation are significant current or future threats to the Bay-Delta longfin smelt DPS.

Factor D. The Inadequacy of Existing Regulatory Mechanisms

Existing Federal and State regulatory mechanisms discussed under Factor D of the rangewide analysis that provide protections or reduce threats to the Bay-Delta DPS of longfin smelt include: California Endangered Species Act, Porter-Cologne Water Quality Control Act, California Marine Invasive Species Act, Central Valley Project Improvement Act, and Clean Water Act (including the National Pollutant Discharge Elimination System). Several of these regulatory mechanisms provide important protections for the Bay-Delta DPS of longfin smelt

and act to reduce threats, such as reduction of freshwater outflow, the invasion of the overbite clam and ammonia discharges (See Factors A, above, and E, below).

The longfin smelt was listed under the California Endangered Species Act as threatened throughout its range in California on March 5, 2009 (CDFG 2009, p. V). CESA does allow take of species for otherwise lawful projects through use of an incidental take permit. A take permit requires that impacts be minimized and fully mitigated (CESA sections 2081 (b) and (c)). Furthermore, the CESA ensures through the issuance of a permit for a project that may affect longfin smelt or its habitat, that the project will not jeopardize the continued existence of a State-listed species.

The Porter-Cologne Water Quality Control Act is the California State law that establishes the State Water Resources Control Board (SWRCB) and nine Regional Water Quality Control Boards that are responsible for the regulation of activities and factors that could degrade California water quality and for the allocation of surface water rights. The State Water Resources Control Board Water Rights Decision 1641 (D-1641) imposes flow and water quality standards on the State and Federal water export facilities to assure protection of beneficial uses in the Delta (FWS 2008, pp. 21-27). The various flow objectives and export restraints are designed, in part, to protect fisheries. These objectives include specific outflow requirements throughout the year, specific water export restraints in the spring, and water export limits based on a percentage of estuary inflow throughout the year. The water quality objectives are designed to protect agricultural, municipal, industrial, and fishery uses; they vary throughout the year and by the wetness of the year. These protections have had limited effectiveness in providing

adequate freshwater flows within the Delta. Lack of freshwater outflow continues to be the primary contributing factor to the decline of the longfin smelt in the Bay-Delta (see Factor A, above, for further discussion).

The California Marine Invasive Species Act requires ballast water management for all vessels that intend to discharge ballast water in California waters. All qualifying vessels coming from ports within the Pacific Coast region must conduct an exchange in waters at least 50 nautical mi offshore and 200 m (656 ft) deep or retain all ballast water and associated sediments. To determine the effectiveness of the management provisions of the this State act, the legislation also requires State agencies to conduct a series of biological surveys to monitor new introductions to coastal and estuarine waters. These measures should further minimize the introduction of new invasive species into California's coastal waters that could be a threat to the longfin smelt.

The Central Valley Project Improvement Act amends the previous Central Valley Project authorizations to include fish and wildlife protection, restoration, and mitigation as project purposes having equal priority with irrigation and domestic uses, and fish and wildlife enhancement as having an equal priority with power generation. Included in CVPIA section 3406 (b)(2) was a provision to dedicate 800,000 acre-feet of Central Valley Project yield annually (referred to as "(b)(2) water") for fish, wildlife, and habitat restoration. Since 1993, (b)(2) water has been used and supplemented with acquired environmental water (Environmental Water Account and CVPIA section 3406 (b)(3) water) to increase stream flows and reduce Central Valley Project export pumping in the Delta. These management actions were taken to

contribute to the CVPIA salmonid population doubling goals and to protect Delta smelt and their habitat (Guinee 2011, pers. comm.). As discussed above (under Biology and Factor A), increased freshwater flows have been shown to be positively correlated with longfin smelt abundance; therefore, these management actions, although targeted towards other species, should also benefit longfin smelt.

The Clean Water Act (CWA) provides the basis for the National Pollutant Discharge Elimination System (NPDES). The CWA gives the EPA the authority to set effluent limits and requires any entity discharging pollutants to obtain a NPDES permit. The EPA is authorized through the CWA to delegate the authority to issue NPDES Permits to State governments. In States that have been authorized to implement CWA programs, the EPA still retains oversight responsibilities (EPA 2011, p. 1). California is one of these States to which the EPA has delegated CWA authority. The Porter-Cologne Water Quality Control Act established the California State Water Resources Control Board (SWRCB) and nine Regional Water Quality Control Boards that are now responsible for issuing these NPDES permits, including permits for the discharge of effluents such as ammonia. The SWRCB is responsible for regulating activities and factors that could degrade California water quality (California Water Code Division 7, section 13370-13389).

The release of ammonia into the estuary is having detrimental effects on the Delta ecosystem and food chain (see Factor E, below). The release of ammonia is controlled primarily by the CWA (Federal law) and secondarily through the Porter-Cologne Water Quality Control Act (State law). EPA is currently updating freshwater discharge criteria that will include new

limits on ammonia (EPA 2009, pp. 1-46). An NPDES permit for the Sacramento Regional Wastewater Treatment Plant, a major discharger, was prepared by the California Central Valley Regional Water Quality Control Board in the fall of 2010, with new ammonia limitations intended to reduce loadings to the Delta. The permit is currently undergoing appeal, but it is likely that the new ammonia limits will take effect in 2020. Until that time, CWA protections for longfin smelt are limited, and do not reduce the current threat to longfin smelt.

Summary of Factor D

A number of Federal and State regulatory mechanisms exist that can provide some protections for the Bay-Delta DPS of longfin smelt. However, the continued decline in longfin smelt trend indicators suggests that existing regulatory mechanisms, as currently implemented, are not adequate to reduce threats to the species. Therefore, based on a review of the best scientific information available, we conclude that existing regulatory mechanisms are not sufficient to protect the species.

Factor E. Other Natural or Manmade Factors Affecting Its Continued Existence

Other factors affecting the continued existence of the Bay-Delta DPS of longfin smelt are entrainment losses due to water diversions, introduced species, and contaminants (see Factor E of the **Summary of Information Pertaining to the Five Factors** section, above).

Entrainment Losses Due to Water Diversions

Entrainment losses at the SWP and CVP water export facilities are a known source of mortality of longfin smelt and other pelagic fish species in the Bay Delta, although the full magnitude of entrainment losses and population-level implications of these losses is still not fully understood. High entrainment losses of longfin smelt and other Bay-Delta pelagic fish between 2000 and 2005 correspond with high volumes of water exports during winter (Baxter *et al.* 2010, p. 63). Baxter *et al.* (2010, p. 62) hypothesize that entrainment is having an important effect on the longfin smelt population during winter, particularly during years with low freshwater flows when a higher proportion of the population may spawn farther upstream in the Delta. However, Baxter *et al.* (2010, p. 63) conclude that these losses have yet to be placed in a population context, and no conclusions can be drawn regarding their effects on recent longfin smelt abundance. CDFG (2009, p. 22) believes that efforts to reduce past delta smelt entrainment loss through the implementation of the 2008 delta smelt biological opinion for SWP and CVP operations may have reduced longfin smelt entrainment losses, incidentally providing a benefit to the longfin smelt. These efforts to manage entrainment losses in drier years, when entrainment risk is greater, substantially reduce the threat of entrainment for longfin smelt.

Estimates of entrainment have shown that it may have been a threat to the Bay-Delta longfin smelt DPS in the past. Fujimura (2009) estimated cumulative longfin smelt entrainment at the SWP facility between 1993 and 2008 at 1,376,432 juveniles and 11,054 adults, and estimated that 97.6 percent of juveniles and 95 percent of adults entrained were lost. Fujimura (2009) estimated cumulative longfin entrainment at the CVP facility between 1993 and 2008 at 224,606 juveniles and 1,325 adults, and estimated that 85.2 percent of the juveniles and 82.1

percent of the adults entrained were lost. These estimated losses are 4 times higher than observed salvage at the CVP and 21 times higher than the actual salvage numbers at the SWP (Fujimura 2009, p. 2). The estimated entrainment numbers were much higher than the actual salvage numbers at the SWP, due in large part to the high pre-screen losses in the Clifton Court Forebay (CDFG 2009a, p. 21). It should be noted that these estimates were calculated using equations and parameters devised for other species and may not accurately estimate longfin smelt losses. Further, estimates may be misleading because the majority of estimated losses occurred during the dry year of 2002 (1.1 million juveniles estimated at the SWP) while during all other years estimated entrainment was below 70,000 individuals.

Entrainment is no longer considered a threat to longfin in the Bay-Delta because of current regulations. Efforts to reduce delta smelt entrainment loss through the implementation of the 2008 delta smelt biological opinion and the listing of longfin smelt under the CESA have likely reduced longfin smelt entrainment losses. The high rate of entrainment that occurred in 2002 that threatened the Bay Delta longfin smelt DPS is very unlikely to recur, and would no longer be allowed under today's regulations because limits on longfin smelt take due to CESA regulations (see DPS' Factor D discussion, above) would trigger reductions in the magnitude of reverse flows.

Although larval and adult longfin smelt are lost as a result of entrainment in the water export facilities in the Delta, we conclude that the risk of entrainment is generally greatest when X2 is upstream and export volumes from the CVP and SWP pumps are high. Therefore, we have

determined that longfin smelt are not currently threatened by entrainment, nor do we anticipate longfin smelt will be threatened by entrainment in the future.

Introduced Species

In Suisun Bay, a key longfin smelt rearing area, phytoplankton biomass is influenced by the overbite or Amur River clam. A sharp decline in phytoplankton biomass occurred following the invasion of the estuary by this species, even though nutrients were not found to be limiting (Alpine and Cloern 1992, pp. 950-951). Abundance of zooplankton decreased across several taxa, and peaks that formerly occurred in time and space were absent, reduced or relocated after 1987 (Kimmerer and Orsi 1996, p. 412). The general decline in phytoplankton and zooplankton is likely affecting longfin smelt by decreasing food supply for their prey species, such as *N. mercedis* (Kimmerer and Orsi 1996, pp. 418–419). Models indicate that the longfin smelt abundance index has been on a steady linear decline since about the time of the invasion of the non-native overbite (or Amur) clam in 1987 (Rosenfield and Swanson 2010, p. 14).

Given the observed negative association between the introduction of the overbite clam and longfin smelt abundance in the Bay-Delta and the documented decline of key longfin smelt prey items, we consider the current overbite clam population to pose a significant threat to the Bay-Delta DPS of longfin smelt. Based on the observed associations in the Bay-Delta between overbite clam invasion and longfin abundance and the lack of effective control mechanisms, we expect the degree of this threat will continue into the foreseeable future. The Bay-Delta has numerous other invasive species that have disrupted ecosystem dynamics; however, only the

overbite clam has been shown to have an impact on the longfin smelt population. We consider the overbite clam to be a significant ongoing threat to the Bay-Delta longfin smelt population.

Contaminants

Extensive research on the role of contaminants in the Pelagic Organism Decline is currently being conducted (Baxter *et al.* 2010, pp. 28–36). Of potential concern are effects of high levels of mercury and other metals; high ammonium concentrations from municipal wastewater; potentially harmful cyanobacteria algal blooms; and pesticides, especially pyrethroid pesticides, which are heavily used in San Joaquin Valley agriculture. Contaminants may have direct toxic effects to longfin smelt and other pelagic fish and indirect effects as a result of impacts to prey abundance and composition. Ammonium has been shown to impact longfin smelt habitat by affecting primary production and prey abundance within the Bay-Delta (Dugdale *et al.* 2007, p. 26). While contaminants are suspected of playing a role in declines of pelagic fish species in the Bay-Delta (Baxter *et al.* 2010, p. 28), contaminant effects remain unresolved.

The largest source of ammonia entering the Delta ecosystem is the Sacramento Regional Wastewater Treatment Plant (SRWTP), which accounts for 90 percent of the total ammonia load released into the Delta. Ammonia is un-ionized and has the chemical formula NH_3 . Ammonium is ionized and has the formula NH_4^+ . The major factors determining the proportion of ammonia or ammonium in water are water pH and temperature. This is important, as NH_3 ammonia is the form that can be directly toxic to aquatic organisms, and NH_4^+ ammonium is the form

documented to interfere with uptake of nitrates by phytoplankton (Dugdale *et al.* 2007, p. 17; Jassby 2008, p. 3).

In addition to potential direct effects on fish, ammonia in the form of ammonium has been shown to alter the food web by adversely impacting phytoplankton and zooplankton dynamics in the estuary ecosystem. Historical data suggest that decreases in Suisun Bay phytoplankton biomass coincide with increased ammonia discharge by the SRWTP (Parker *et al.* 2004, p. 7; Dugdale *et al.* 2011, p. 1). Phytoplankton preferentially take up ammonium over nitrate when it is present in the water. Ammonium is insufficient to provide for growth in phytoplankton, and uptake of ammonium to the exclusion of nitrate results in decreases in phytoplankton biomass (Dugdale *et al.* 2007, p. 23). Therefore, ammonium impairs primary productivity by reducing nitrate uptake in phytoplankton. Ammonium's negative effect on the food web has been documented in the longfin smelt rearing areas of San Francisco Bay and Suisun Bay (Dugdale *et al.* 2007, pp. 27–28). Decreased primary productivity results in less food available to longfin smelt and other fish in these bays.

In summary, although no direct link has been made between contaminants and longfin smelt (Baxter *et al.* 2010, p. 68), ammonium has been shown to have a direct effect on the food supply that the Bay-Delta longfin smelt DPS relies upon. Therefore, we conclude that high ammonium concentrations may be a significant current and future threat to the Bay-Delta DPS of longfin smelt.

Summary of Factor E

The best available information indicates that introduced species constitute a threat to the Bay-Delta DPS of longfin smelt and that and contaminants (high ammonium concentrations) may constitute a threat to the Bay-Delta DPS of longfin smelt. Entrainment is a potential threat to the DPS, but information currently available does not indicate that entrainment threatens the continued existence of the Bay-Delta longfin smelt population. Although entrainment results in mortality of longfin smelt, Baxter *et al.* (2010, p. 63) concluded that these losses have yet to be placed in a population context, and no conclusions can be drawn regarding their effects on recent longfin smelt abundance. Therefore, based on the best scientific evidence available, we conclude that the Bay-Delta longfin smelt DPS is threatened in part due to other natural or manmade factors including the nonnative overbite clam and high ammonium concentrations.

Finding

This status review identified threats to the Bay-Delta DPS of longfin smelt attributable to Factors A, D, and E, as well as interactions between these threats. The primary threat to the DPS is from reduced freshwater flows. Upstream dams and water storage exacerbated by water diversions, especially from the SWP and CVP water export facilities, result in reduced freshwater flows within the estuary, and these reductions in freshwater flows result in reduced habitat suitability for longfin smelt (Factor A). Freshwater flows, especially winter-spring flows, are significantly correlated with longfin smelt abundance—longfin smelt abundance is lower when winter-spring flows are lower. While freshwater flows have been shown to be significantly correlated with longfin smelt abundance, causal mechanisms underlying this

correlation are still not fully understood and are the subject of ongoing research on the Pelagic Organism Decline.

In addition to the threat caused by reduced freshwater flow into the Bay-Delta, and alteration of natural flow regimes resulting from water storage and diversion, there appear to be other factors contributing to the Pelagic Organism Decline (Baxter 2010 *et al.*, p. 69). Models indicate a steady linear decline in abundance of longfin smelt since about the time of the invasion of the nonnative overbite clam in 1987 (Rosenfield and Swanson 2010, pp. 13–14; see Factor E: Introduced Species) in the Bay-Delta. However, not all aspects of the longfin smelt decline can be attributed to the overbite clam invasion, as a decline in abundance of pre-spawning adults in Suisun Marsh occurred before the invasion of the clam, and a partial rebound in longfin smelt abundance occurred in the early 2000s (Rosenfield and Baxter 2007, p. 1589).

The long-term decline in abundance of longfin smelt in the Bay-Delta has been partially attributed to reductions in food availability and disruptions of the Bay-Delta food web caused by establishment of the nonnative overbite clam in 1987 (Factor E) and ammonium concentrations (Factor E). Impacts of the overbite clam and ammonium on the Bay-Delta food web have been long-lasting and are ongoing. We conclude that ongoing disruptions of the food web caused by the overbite clam are a threat to the continued existence of the Bay-Delta DPS of longfin smelt. We also conclude that high ammonium concentrations in the Bay-Delta may constitute a threat to the continued existence of the overbite clam.

Multiple existing Federal and State regulatory mechanisms provide important protections

for the Bay-Delta DPS of longfin smelt and act to reduce threats to the DPS. However, the continued decline in the abundance of the Bay-Delta longfin smelt DPS indicates that existing regulatory mechanisms, as currently implemented, are not adequate to sufficiently reduce threats identified in this finding. Therefore, we find that inadequate existing regulatory mechanisms contribute to threats faced by the Bay-Delta longfin smelt DPS.

The threats identified are likely acting together to contribute to the decline of the population (Baxter *et al.* 2010, p. 69). Reduced freshwater flows result in effects to longfin smelt habitat suitability, at the same time that the food web has been altered by introduced species and ammonium concentrations. It is possible that climate change could exacerbate these threats; however, due to uncertainties of how longfin smelt will respond to climate change effects, we cannot conclude that climate change will threaten the continued existence of the Bay-Delta longfin smelt DPS. The combined effects of reduced freshwater flows, the invasive overbite clam (reduced levels of phytoplankton and zooplankton that are important to the Bay-Delta food web), and high ammonium concentrations act to significantly reduce habitat suitability for longfin smelt.

The best scientific and commercial information available indicates that the threats facing the Bay-Delta DPS of longfin smelt are of sufficient imminence, intensity and magnitude to threaten the continued existence of the species now or in the foreseeable future. Therefore, we find that listing the Bay-Delta longfin smelt DPS is warranted. We will make a determination on the status of the DPS as endangered or threatened when we prepare a proposed listing determination. However, as explained in more detail below, an immediate proposal of a

regulation implementing this action is precluded by higher priority listing actions, and progress is being made to add or remove qualified species from the Lists of Endangered and Threatened Wildlife and Plants.

We reviewed the available information to determine if the existing and foreseeable threats render the species at risk of extinction now such that issuing an emergency regulation temporarily listing the species under section 4(b)(7) of the Act is warranted. We determined that issuing an emergency regulation temporarily listing the DPS is not warranted at this time because the threats are not of sufficient magnitude and imminence to pose an immediate threat to the continued existence of the DPS. However, if at any time we determine that issuing an emergency regulation temporarily listing the Bay-Delta DPS of longfin smelt is warranted, we will initiate this action at that time.

Significant Portion of Its Range

The Act defines “endangered species” as any species which is “in danger of extinction throughout all or a significant portion of its range,” and “threatened species” as any species which is “likely to become an endangered species within the foreseeable future throughout all or a significant portion of its range.” The definition of “species” is also relevant to this discussion. The Act defines “species” as “any subspecies of fish or wildlife or plants, and any distinct population segment [DPS] of any species of vertebrate fish or wildlife which interbreeds when mature” (16 U.S.C. 1532(16)). The phrase “significant portion of its range” (SPR) is not defined by the statute, and we have never addressed in our regulations: (1) The consequences of a

determination that a species is either endangered or likely to become so throughout a significant portion of its range, but not throughout all of its range; or (2) what qualifies a portion of a range as “significant.”

Two recent district court decisions have addressed whether the SPR language allows the Service to list or protect less than all members of a defined “species”: *Defenders of Wildlife v. Salazar*, 729 F. Supp. 2d 1207 (D. Mont. 2010), concerning the Service’s delisting of the Northern Rocky Mountain gray wolf (74 FR 15123, April 2, 2009); and *WildEarth Guardians v. Salazar*, 2010 U.S. Dist. LEXIS 105253 (D. Ariz. September 30, 2010), concerning the Service’s 2008 finding on a petition to list the Gunnison’s prairie dog (73 FR 6660, February 5, 2008). The Service had asserted in both of these determinations that it had authority, in effect, to protect only some members of a “species,” as defined by the Act (i.e., species, subspecies, or DPS), under the Act. Both courts ruled that the determinations were arbitrary and capricious on the grounds that this approach violated the plain and unambiguous language of the Act. The courts concluded that reading the SPR language to allow protecting only a portion of a species’ range is inconsistent with the Act’s definition of “species.” The courts concluded that once a determination is made that a species (i.e., species, subspecies, or DPS) meets the definition of “endangered species” or “threatened species,” it must be placed on the list in its entirety and the Act’s protections applied consistently to all members of that species (subject to modification of protections through special rules under sections 4(d) and 10(j) of the Act).

Consistent with that interpretation, and for the purposes of this finding, we interpret the phrase “significant portion of its range” in the Act’s definitions of “endangered species” and

“threatened species” to provide an independent basis for listing; thus there are two situations (or factual bases) under which a species would qualify for listing: a species may be endangered or threatened throughout all of its range; or a species may be endangered or threatened in only a significant portion of its range. If a species is in danger of extinction throughout an SPR, it, the species, is an “endangered species.” The same analysis applies to “threatened species.” Based on this interpretation and supported by existing case law, the consequence of finding that a species is endangered or threatened in only a significant portion of its range is that the entire species will be listed as endangered or threatened, respectively, and the Act’s protections will be applied across the species’ entire range.

We conclude, for the purposes of this finding, that interpreting the SPR phrase as providing an independent basis for listing is the best interpretation of the Act because it is consistent with the purposes and the plain meaning of the key definitions of the Act; it does not conflict with established past agency practice (i.e., prior to the 2007 Solicitor’s Opinion), as no consistent, long-term agency practice has been established; and it is consistent with the judicial opinions that have most closely examined this issue. Having concluded that the phrase “significant portion of its range” provides an independent basis for listing and protecting the entire species, we next turn to the meaning of “significant” to determine the threshold for when such an independent basis for listing exists.

Although there are potentially many ways to determine whether a portion of a species’ range is “significant,” we conclude, for the purposes of this finding, that the significance of the portion of the range should be determined based on its biological contribution to the conservation

of the species. For this reason, we describe the threshold for “significant” in terms of an increase in the risk of extinction for the species. We conclude that a biologically based definition of “significant” best conforms to the purposes of the Act, is consistent with judicial interpretations, and best ensures species’ conservation. Thus, for the purposes of this finding, and as explained further below, a portion of the range of a species is “significant” if its contribution to the viability of the species is so important that without that portion, the species would be in danger of extinction.

We evaluate biological significance based on the principles of conservation biology using the concepts of redundancy, resiliency, and representation. *Resiliency* describes the characteristics of a species and its habitat that allow it to recover from periodic disturbance. *Redundancy* (having multiple populations distributed across the landscape) may be needed to provide a margin of safety for the species to withstand catastrophic events. *Representation* (the range of variation found in a species) ensures that the species’ adaptive capabilities are conserved. Redundancy, resiliency, and representation are not independent of each other, and some characteristic of a species or area may contribute to all three. For example, distribution across a wide variety of habitat types is an indicator of representation, but it may also indicate a broad geographic distribution contributing to redundancy (decreasing the chance that any one event affects the entire species), and the likelihood that some habitat types are less susceptible to certain threats, contributing to resiliency (the ability of the species to recover from disturbance). None of these concepts is intended to be mutually exclusive, and a portion of a species’ range may be determined to be “significant” due to its contributions under any one or more of these concepts.

For the purposes of this finding, we determine if a portion's biological contribution is so important that the portion qualifies as "significant" by asking whether *without that portion*, the representation, redundancy, or resiliency of the species would be so impaired that the species would have an increased vulnerability to threats to the point that the overall species would be in danger of extinction (i.e., would be "endangered"). Conversely, we would not consider the portion of the range at issue to be "significant" if there is sufficient resiliency, redundancy, and representation elsewhere in the species' range that the species would not be in danger of extinction throughout its range if the population in that portion of the range in question became extirpated (extinct locally).

We recognize that this definition of "significant" (a portion of the range of a species is "significant" if its contribution to the viability of the species is so important that without that portion, the species would be in danger of extinction) establishes a threshold that is relatively high. On the one hand, given that the consequences of finding a species to be endangered or threatened in an SPR would be listing the species throughout its entire range, it is important to use a threshold for "significant" that is robust. It would not be meaningful or appropriate to establish a very low threshold whereby a portion of the range can be considered "significant" even if only a negligible increase in extinction risk would result from its loss. Because nearly any portion of a species' range can be said to contribute some increment to a species' viability, use of such a low threshold would require us to impose restrictions and expend conservation resources disproportionately to conservation benefit: listing would be rangewide, even if only a portion of the range of minor conservation importance to the species is imperiled. On the other

hand, it would be inappropriate to establish a threshold for “significant” that is too high. This would be the case if the standard were, for example, that a portion of the range can be considered “significant” only if threats in that portion result in the entire species’ being currently endangered or threatened. Such a high bar would not give the SPR phrase independent meaning, as the Ninth Circuit held in *Defenders of Wildlife v. Norton*, 258 F.3d 1136 (9th Cir. 2001).

The definition of “significant” used in this finding carefully balances these concerns. By setting a relatively high threshold, we minimize the degree to which restrictions will be imposed or resources expended that do not contribute substantially to species conservation. But we have not set the threshold so high that the phrase “in a significant portion of its range” loses independent meaning. Specifically, we have not set the threshold as high as it was under the interpretation presented by the Service in the *Defenders* litigation. Under that interpretation, the portion of the range would have to be so important that current imperilment there would mean that the species would be *currently* imperiled everywhere. Under the definition of “significant” used in this finding, the portion of the range need not rise to such an exceptionally high level of biological significance. (We recognize that if the species is imperiled in a portion that rises to that level of biological significance, then we should conclude that the species is in fact imperiled throughout all of its range, and that we would not need to rely on the SPR language for such a listing.) Rather, under this interpretation we ask whether the species would be endangered everywhere without that portion, *i.e.*, if that portion were completely extirpated. In other words, the portion of the range need not be so important that even the species being in danger of extinction in that portion would be sufficient to cause the species in the remainder of the range to be endangered; rather, the *complete extirpation* (in a hypothetical future) of the species in that

portion would be required to cause the species in the remainder of the range to be endangered.

The range of a species can theoretically be divided into portions in an infinite number of ways. However, there is no purpose to analyzing portions of the range that have no reasonable potential to be significant or to analyzing portions of the range in which there is no reasonable potential for the species to be endangered or threatened. To identify only those portions that warrant further consideration, we determine whether there is substantial information indicating that: (1) The portions may be “significant,” *and* (2) the species may be in danger of extinction there or likely to become so within the foreseeable future. Depending on the biology of the species, its range, and the threats it faces, it might be more efficient for us to address the significance question first or the status question first. Thus, if we determine that a portion of the range is not “significant,” we do not need to determine whether the species is endangered or threatened there; if we determine that the species is not endangered or threatened in a portion of its range, we do not need to determine if that portion is “significant.” In practice, a key part of the determination that a species is in danger of extinction in a significant portion of its range is whether the threats are geographically concentrated in some way. If the threats to the species are essentially uniform throughout its range, no portion is likely to warrant further consideration. Moreover, if any concentration of threats to the species occurs only in portions of the species’ range that clearly would not meet the biologically based definition of “significant,” such portions will not warrant further consideration.

We have determined that the longfin smelt does not face elevated threats in most portions of its range, and we have determined that the portion of the range that has concentrated threats

(the Bay-Delta portion of the range) is a DPS. The rangewide five factor analysis for longfin smelt does not identify any portions of the species' range outside of Bay-Delta where threats are concentrated. Potential threats to the species are by and large uniform throughout its range with the exception of the Bay-Delta. Therefore, we will not further consider the Bay-Delta DPS as an SPR.

Listing Priority Number

The Service adopted guidelines on September 21, 1983 (48 FR 43098) to establish a rational system for utilizing available resources for the highest priority species when adding species to the Lists of Endangered or Threatened Wildlife and Plants or reclassifying species listed as threatened to endangered status. The system places greatest importance on the immediacy and magnitude of threats, but also factors in the level of taxonomic distinctiveness by assigning priority in descending order to monotypic genera (genus with one species), full species, and subspecies (or equivalently, distinct population segments of vertebrates (DPS)). As a result of our analysis of the best available scientific and commercial information, we assign the Bay-Delta DPS of longfin smelt a listing priority number of 3, based on the high magnitude and immediacy of threats. A number three listing priority is the highest listing allowed for a DPS under the current listing priority guidance. One or more of the threats discussed above are occurring (or we anticipate they will occur in the near future) within the range of the Bay-Delta DPS of the longfin smelt. These threats are ongoing and, in some cases (such as nonnative species), are considered irreversible. While we conclude that listing the Bay-Delta DPS of longfin smelt is warranted, an immediate proposal to list this species is precluded by other higher

priority listings, which we address below.

Preclusion and Expeditious Progress

Preclusion is a function of the listing priority of a species in relation to the resources that are available and the cost and relative priority of competing demands for those resources. Thus, in any given fiscal year (FY), multiple factors dictate whether it will be possible to undertake work on a listing proposal regulation or whether promulgation of such a proposal is precluded by higher priority listing actions.

The resources available for listing actions are determined through the annual Congressional appropriations process. The appropriation for the Listing Program is available to support work involving the following listing actions: Proposed and final listing rules; 90-day and 12-month findings on petitions to add species to the Lists of Endangered and Threatened Wildlife and Plants (Lists) or to change the status of a species from threatened to endangered; annual “resubmitted” petition findings on prior warranted-but-precluded petition findings as required under section 4(b)(3)(C)(i) of the Act; critical habitat petition findings; proposed and final rules designating critical habitat; and litigation-related, administrative, and program-management functions (including preparing and allocating budgets, responding to Congressional and public inquiries, and conducting public outreach regarding listing and critical habitat). The work involved in preparing various listing documents can be extensive and may include, but is not limited to: Gathering and assessing the best scientific and commercial data available and conducting analyses used as the basis for our decisions; writing and publishing documents; and obtaining, reviewing, and evaluating public comments and peer review comments on proposed

rules and incorporating relevant information into final rules. The number of listing actions that we can undertake in a given year also is influenced by the complexity of those listing actions; that is, more complex actions generally are more costly. The median cost for preparing and publishing a 90-day finding is \$39,276; for a 12-month finding, \$100,690; for a proposed rule with critical habitat, \$345,000; and for a final listing rule with critical habitat, \$305,000.

We cannot spend more than is appropriated for the Listing Program without violating the Anti-Deficiency Act (see 31 U.S.C. 1341(a)(1)(A)). In addition, in FY 1998 and for each fiscal year since then, Congress has placed a statutory cap on funds that may be expended for the Listing Program, equal to the amount expressly appropriated for that purpose in that fiscal year. This cap was designed to prevent funds appropriated for other functions under the Act (for example, recovery funds for removing species from the Lists), or for other Service programs, from being used for Listing Program actions (see House Report 105-163, 105th Congress, 1st Session, July 1, 1997).

Since FY 2002, the Service's budget has included a critical habitat subcap to ensure that some funds are available for other work in the Listing Program ("The critical habitat designation subcap will ensure that some funding is available to address other listing activities" (House Report No. 107 - 103, 107th Congress, 1st Session, June 19, 2001)). In FY 2002 and each year until FY 2006, the Service has had to use virtually the entire critical habitat subcap to address court-mandated designations of critical habitat, and consequently none of the critical habitat subcap funds have been available for other listing activities. In some FYs since 2006, we have been able to use some of the critical habitat subcap funds to fund proposed listing determinations for high-priority candidate species. In other FYs, while we were unable to use any of the critical

habitat subcap funds to fund proposed listing determinations, we did use some of this money to fund the critical habitat portion of some proposed listing determinations so that the proposed listing determination and proposed critical habitat designation could be combined into one rule, thereby being more efficient in our work. At this time, for FY 2012, we plan to use some of the critical habitat subcap funds to fund proposed listing determinations.

We make our determinations of preclusion on a nationwide basis to ensure that the species most in need of listing will be addressed first and also because we allocate our listing budget on a nationwide basis. Through the listing cap, the critical habitat subcap, and the amount of funds needed to address court-mandated critical habitat designations, Congress and the courts have in effect determined the amount of money available for other listing activities nationwide. Therefore, the funds in the listing cap, other than those needed to address court-mandated critical habitat for already listed species, set the limits on our determinations of preclusion and expeditious progress.

Congress identified the availability of resources as the only basis for deferring the initiation of a rulemaking that is warranted. The Conference Report accompanying Pub. L. 97-304 (Endangered Species Act Amendments of 1982), which established the current statutory deadlines and the warranted-but-precluded finding, states that the amendments were “not intended to allow the Secretary to delay commencing the rulemaking process for any reason other than that the existence of pending or imminent proposals to list species subject to a greater degree of threat would make allocation of resources to such a petition [that is, for a lower-ranking species] unwise.” Although that statement appeared to refer specifically to the “to the maximum extent practicable” limitation on the 90-day deadline for making a “substantial

information” finding, that finding is made at the point when the Service is deciding whether or not to commence a status review that will determine the degree of threats facing the species, and therefore the analysis underlying the statement is more relevant to the use of the warranted-but-precluded finding, which is made when the Service has already determined the degree of threats facing the species and is deciding whether or not to commence a rulemaking.

In FY 2011, on April 15, 2011, Congress passed the Full-Year Continuing Appropriations Act (Pub. L. 112-10), which provided funding through September 30, 2011. The Service had \$20,902,000 for the listing program. Of that, \$9,472,000 was used for determinations of critical habitat for already listed species. Also \$500,000 was appropriated for foreign species listings under the Act. The Service thus had \$10,930,000 available to fund work in the following categories: Compliance with court orders and court-approved settlement agreements requiring that petition findings or listing determinations be completed by a specific date; section 4 (of the Act) listing actions with absolute statutory deadlines; essential litigation-related, administrative, and listing program-management functions; and high-priority listing actions for some of our candidate species. In FY 2010, the Service received many new petitions and a single petition to list 404 species. The receipt of petitions for a large number of species is consuming the Service’s listing funding that is not dedicated to meeting court-ordered commitments. Absent some ability to balance effort among listing duties under existing funding levels, the Service was only able to initiate a few new listing determinations for candidate species in FY 2011. For FY 2012, on December 17, 2011, Congress passed a continuing resolution which provides funding at the FY 2011 enacted level with a 1.5 percent rescission through December 23, 2011 (Pub. L. 112-68). Until Congress appropriates funds for FY 2012,

we will fund listing work based on the FY 2011 amount minus the 1.5 percent.

In 2009, the responsibility for listing foreign species under the Act was transferred from the Division of Scientific Authority, International Affairs Program, to the Endangered Species Program. Therefore, starting in FY 2010, we used a portion of our funding to work on the actions described above for listing actions related to foreign species. In FY 2011, we anticipated using \$1,500,000 for work on listing actions for foreign species, which reduces funding available for domestic listing actions; however, only \$500,000 was allocated for this function. Although there are no foreign species issues included in our high-priority listing actions at this time, many actions have statutory or court-approved settlement deadlines, thus increasing their priority. The budget allocations for each specific listing action are identified in the Service's FY 2011 and FY 2012 Allocation Tables (part of our record).

For the above reasons, funding a proposed listing determination for the Bay-Delta DPS of longfin smelt is precluded by court-ordered and court-approved settlement agreements, listing actions with absolute statutory deadlines, and work on proposed listing determinations for those candidate species with a higher listing priority (i.e., candidate species with LPNs of 1 or 2).

Based on our September 21, 1983, guidelines for assigning an LPN for each candidate species (48 FR 43098), we have a significant number of species with a LPN of 2. Using these guidelines, we assign each candidate an LPN of 1 to 12, depending on the magnitude of threats (high or moderate to low), immediacy of threats (imminent or nonimminent), and taxonomic status of the species (in order of priority: monotypic genus (a species that is the sole member of

a genus); species; or part of a species (subspecies, or distinct population segment)). The lower the listing priority number, the higher the listing priority (that is, a species with an LPN of 1 would have the highest listing priority).

Because of the large number of high-priority species, we have further ranked the candidate species with an LPN of 2 by using the following extinction-risk type criteria: International Union for the Conservation of Nature and Natural Resources (IUCN) Red list status/rank, Heritage rank (provided by NatureServe), Heritage threat rank (provided by NatureServe), and species currently with fewer than 50 individuals, or 4 or fewer populations. Those species with the highest IUCN rank (critically endangered), the highest Heritage rank (G1), the highest Heritage threat rank (substantial, imminent threats), and currently with fewer than 50 individuals, or fewer than 4 populations, originally comprised a group of approximately 40 candidate species (“Top 40”). These 40 candidate species have had the highest priority to receive funding to work on a proposed listing determination. As we work on proposed and final listing rules for those 40 candidates, we apply the ranking criteria to the next group of candidates with LPNs of 2 and 3 to determine the next set of highest priority candidate species. Finally, proposed rules for reclassification of threatened species to endangered species are lower priority, because as listed species, they are already afforded the protections of the Act and implementing regulations. However, for efficiency reasons, we may choose to work on a proposed rule to reclassify a species to endangered if we can combine this with work that is subject to a court-determined deadline.

With our workload so much bigger than the amount of funds we have to accomplish it, it is important that we be as efficient as possible in our listing process. Therefore, as we work on proposed rules for the highest priority species in the next several years, we are preparing multi-species proposals when appropriate, and these may include species with lower priority if they overlap geographically or have the same threats as a species with an LPN of 2. In addition, we take into consideration the availability of staff resources when we determine which high-priority species will receive funding to minimize the amount of time and resources required to complete each listing action.

As explained above, a determination that listing is warranted but precluded must also demonstrate that expeditious progress is being made to add and remove qualified species to and from the Lists of Endangered and Threatened Wildlife and Plants. As with our “precluded” finding, the evaluation of whether progress in adding qualified species to the Lists has been expeditious is a function of the resources available for listing and the competing demands for those funds. (Although we do not discuss it in detail here, we are also making expeditious progress in removing species from the list under the Recovery program in light of the resource available for delisting, which is funded by a separate line item in the budget of the Endangered Species Program. During FY 2011, we completed delisting rules for three species.) Given the limited resources available for listing, we find that we made expeditious progress in FY 2011 and are making expeditious progress in FY 2012 in the Listing Program. This progress included preparing and publishing the following determinations:

FY 2011 and FY 2012 Completed Listing Actions

Publication Date	Title	Actions	FR Pages
10/6/2010	Endangered Status for the Altamaha Spiny mussel and Designation of Critical Habitat	Proposed Listing Endangered	75 FR 61664-61690
10/7/2010	12-month Finding on a Petition to list the Sacramento Splittail as Endangered or Threatened	Notice of 12-month petition finding, Not warranted	75 FR 62070-62095
10/28/2010	Endangered Status and Designation of Critical Habitat for Spikedace and Loach Minnow	Proposed Listing Endangered (uplisting)	75 FR 66481-66552
11/2/2010	90-Day Finding on a Petition to List the Bay Springs Salamander as Endangered	Notice of 90-day Petition Finding, Not substantial	75 FR 67341-67343
11/2/2010	Determination of Endangered Status for the Georgia Pigtoe Mussel, Interrupted Rocksnail, and Rough Hornsnail and Designation of Critical Habitat	Final Listing Endangered	75 FR 67511-67550
11/2/2010	Listing the Rayed Bean and Snuffbox as Endangered	Proposed Listing Endangered	75 FR 67551-67583
11/4/2010	12-Month Finding on a Petition to List <i>Cirsium wrightii</i> (Wright's Marsh Thistle) as Endangered or Threatened	Notice of 12-month petition finding, Warranted but precluded	75 FR 67925-67944
12/14/2010	Endangered Status for Dunes Sagebrush Lizard	Proposed Listing Endangered	75 FR 77801-77817
12/14/2010	12-month Finding on a Petition to List the North American Wolverine as Endangered or Threatened	Notice of 12-month petition finding, Warranted but precluded	75 FR 78029-78061
12/14/2010	12-Month Finding on a Petition to List the Sonoran Population of the Desert Tortoise as Endangered or Threatened	Notice of 12-month petition finding, Warranted but precluded	75 FR 78093-78146
12/15/2010	12-Month Finding on a Petition to List <i>Astragalus microcymbus</i> and <i>Astragalus schmollii</i> as Endangered or Threatened	Notice of 12-month petition finding, Warranted but precluded	75 FR 78513-78556
12/28/2010	Listing Seven Brazilian Bird Species as Endangered Throughout Their Range	Final Listing Endangered	75 FR 81793-81815
1/4/2011	90-Day Finding on a Petition to List the Red Knot subspecies <i>Calidris canutus roselaari</i> as Endangered	Notice of 90-day Petition Finding, Not substantial	76 FR 304-311
1/19/2011	Endangered Status for the Sheepnose and Spectaclecase Mussels	Proposed Listing Endangered	76 FR 3392-3420

2/10/2011	12-Month Finding on a Petition to List the Pacific Walrus as Endangered or Threatened	Notice of 12-month petition finding, Warranted but precluded	76 FR 7634-7679
2/17/2011	90-Day Finding on a Petition To List the Sand Verbena Moth as Endangered or Threatened	Notice of 90-day Petition Finding, Substantial	76 FR 9309-9318
2/22 /2011	Determination of Threatened Status for the New Zealand-Australia Distinct Population Segment of the Southern Rockhopper Penguin	Final Listing Threatened	76 FR 9681-9692
2/22/2011	12-Month Finding on a Petition to List <i>Solanum conocarpum</i> (marron bacora) as Endangered	Notice of 12-month petition finding, Warranted but precluded	76 FR 9722-9733
2/23/2011	12-Month Finding on a Petition to List Thorne's Hairstreak Butterfly as Endangered	Notice of 12-month petition finding, Not warranted	76 FR 9991-10003
2/23/2011	12-Month Finding on a Petition to List <i>Astragalus hamiltonii</i> , <i>Penstemon flowersii</i> , <i>Eriogonum soledium</i> , <i>Lepidium ostleri</i> , and <i>Trifolium friscanum</i> as Endangered or Threatened	Notice of 12-month petition finding, Warranted but precluded & Not Warranted	76 FR 10166-10203
2/24/2011	90-Day Finding on a Petition to List the Wild Plains Bison or Each of Four Distinct Population Segments as Threatened	Notice of 90-day Petition Finding, Not substantial	76 FR 10299-10310
2/24/2011	90-Day Finding on a Petition to List the Unsilvered Fritillary Butterfly as Threatened or Endangered	Notice of 90-day Petition Finding, Not substantial	76 FR 10310-10319
3/8/2011	12-Month Finding on a Petition to List the Mt. Charleston Blue Butterfly as Endangered or Threatened	Notice of 12-month petition finding, Warranted but precluded	76 FR 12667-12683
3/8/2011	90-Day Finding on a Petition to List the Texas Kangaroo Rat as Endangered or Threatened	Notice of 90-day Petition Finding, Substantial	76 FR 12683-12690
3/10/2011	Initiation of Status Review for Longfin Smelt	Notice of Status Review	76 FR 13121-13122
3/15/2011	Withdrawal of Proposed Rule to List the Flat-tailed Horned Lizard as Threatened	Proposed rule withdrawal	76 FR 14210-14268
3/15/2011	Proposed Threatened Status for the Chiricahua Leopard Frog and Proposed Designation of Critical Habitat	Proposed Listing Threatened; Proposed Designation of Critical Habitat	76 FR 14126-14207
3/22/2011	12-Month Finding on a Petition to List the Berry Cave Salamander as Endangered	Notice of 12-month petition finding, Warranted but precluded	76 FR 15919-15932
4/1/2011	90-Day Finding on a Petition to List the Spring Pygmy Sunfish as Endangered	Notice of 90-day Petition Finding, Substantial	76 FR 18138-18143

4/5/2011	12-Month Finding on a Petition to List the Bearmouth Mountainsnail, Byrne Resort Mountainsnail, and Meltwater Lednian Stonefly as Endangered or Threatened	Notice of 12-month petition finding, Not Warranted and Warranted but precluded	76 FR 18684-18701
4/5/2011	90-Day Finding on a Petition To List the Peary Caribou and Dolphin and Union population of the Barren-ground Caribou as Endangered or Threatened	Notice of 90-day Petition Finding, Substantial	76 FR 18701-18706
4/12/2011	Proposed Endangered Status for the Three Forks Springsnail and San Bernardino Springsnail, and Proposed Designation of Critical Habitat	Proposed Listing Endangered; Proposed Designation of Critical Habitat	76 FR 20464-20488
4/13/2011	90-Day Finding on a Petition To List Spring Mountains Acastus Checkerspot Butterfly as Endangered	Notice of 90-day Petition Finding, Substantial	76 FR 20613-20622
4/14/2011	90-Day Finding on a Petition to List the Prairie Chub as Threatened or Endangered	Notice of 90-day Petition Finding, Substantial	76 FR 20911-20918
4/14/2011	12-Month Finding on a Petition to List Hermes Copper Butterfly as Endangered or Threatened	Notice of 12-month petition finding, Warranted but precluded	76 FR 20918-20939
4/26/2011	90-Day Finding on a Petition to List the Arapahoe Snowfly as Endangered or Threatened	Notice of 90-day Petition Finding, Substantial	76 FR 23256-23265
4/26/2011	90-Day Finding on a Petition to List the Smooth-Billed Ani as Threatened or Endangered	Notice of 90-day Petition Finding, Not substantial	76 FR 23265-23271
5/12/2011	Withdrawal of the Proposed Rule to List the Mountain Plover as Threatened	Proposed Rule, Withdrawal	76 FR 27756-27799
5/25/2011	90-Day Finding on a Petition To List the Spot-tailed Earless Lizard as Endangered or Threatened	Notice of 90-day Petition Finding, Substantial	76 FR 30082-30087
5/26/2011	Listing the Salmon-Crested Cockatoo as Threatened Throughout its Range with Special Rule	Final Listing Threatened	76 FR 30758-30780
5/31/2011	12-Month Finding on a Petition to List Puerto Rican Harlequin Butterfly as Endangered	Notice of 12-month petition finding, Warranted but precluded	76 FR 31282-31294
6/2/2011	90-Day Finding on a Petition to Reclassify the Straight-Horned Markhor (<i>Capra falconeri jerdoni</i>) of Torghar Hills as Threatened	Notice of 90-day Petition Finding, Substantial	76 FR 31903-31906
6/2/2011	90-Day Finding on a Petition to List the Golden-winged Warbler as Endangered or Threatened	Notice of 90-day Petition Finding, Substantial	76 FR 31920-31926
6/7/2011	12-Month Finding on a Petition to List the Striped Newt as Threatened	Notice of 12-month petition finding, Warranted but precluded	76 FR 32911-32929

6/9/2011	12-Month Finding on a Petition to List <i>Abronia ammophila</i> , <i>Agrostis rossiae</i> , <i>Astragalus proimanthus</i> , <i>Boechea (Arabis) pusilla</i> , and <i>Penstemon gibbensii</i> as Threatened or Endangered	Notice of 12-month petition finding, Not Warranted and Warranted but precluded	76 FR 33924-33965
6/21/2011	90-Day Finding on a Petition to List the Utah Population of the Gila Monster as an Endangered or a Threatened Distinct Population Segment	Notice of 90-day Petition Finding, Not substantial	76 FR 36049-36053
6/21/2011	Revised 90-Day Finding on a Petition To Reclassify the Utah Prairie Dog From Threatened to Endangered	Notice of 90-day Petition Finding, Not substantial	76 FR 36053-36068
6/28/2011	12-Month Finding on a Petition to List <i>Castanea pumila</i> var. <i>ozarkensis</i> as Threatened or Endangered	Notice of 12-month petition finding, Not warranted	76 FR 37706-37716
6/29/2011	90-Day Finding on a Petition to List the Eastern Small-Footed Bat and the Northern Long-Eared Bat as Threatened or Endangered	Notice of 90-day Petition Finding, Substantial	76 FR 38095-38106
6/30/2011	12-Month Finding on a Petition to List a Distinct Population Segment of the Fisher in Its United States Northern Rocky Mountain Range as Endangered or Threatened with Critical Habitat	Notice of 12-month petition finding, Not warranted	76 FR 38504-38532
7/12/2011	90-Day Finding on a Petition to List the Bay Skipper as Threatened or Endangered	Notice of 90-day Petition Finding, Substantial	76 FR 40868-40871
7/19/2011	12-Month Finding on a Petition to List <i>Pinus albicaulis</i> as Endangered or Threatened with Critical Habitat	Notice of 12-month petition finding, Warranted but precluded	76 FR 42631-42654
7/19/2011	Petition To List Grand Canyon Cave Pseudoscorpion	Notice of 12-month petition finding, Not warranted	76 FR 42654-42658
7/26/2011	12-Month Finding on a Petition to List the Giant Palouse Earthworm (<i>Drilolerius americanus</i>) as Threatened or Endangered	Notice of 12-month petition finding, Not warranted	76 FR 44547-44564
7/26/2011	12-month Finding on a Petition to List the Frigid Ambersnail as Endangered	Notice of 12-month petition finding, Not warranted	76 FR 44566-44569
7/27/2011	Determination of Endangered Status for <i>Ipomopsis polyantha</i> (Pagosa Skyrocket) and Threatened Status for <i>Penstemon debilis</i> (Parachute Beardtongue) and <i>Phacelia submutica</i> (DeBeque Phacelia)	Final Listing Endangered, Threatened	76 FR 45054-45075

7/27/2011	12-Month Finding on a Petition to List the Gopher Tortoise as Threatened in the Eastern Portion of its Range	Notice of 12-month petition finding, Warranted but precluded	76 FR 45130-45162
8/2/2011	Proposed Endangered Status for the Chupadera Springsnail (<i>Pyrgulopsis chupaderae</i>) and Proposed Designation of Critical Habitat	Proposed Listing Endangered	76 FR 46218-46234
8/2/2011	90-Day Finding on a Petition to List the Straight Snowfly and Idaho Snowfly as Endangered	Notice of 90-day Petition Finding, Not substantial	76 FR 46238-46251
8/2/2011	12-Month Finding on a Petition to List the Redrock Stonefly as Endangered or Threatened	Notice of 12-month petition finding, Not warranted	76 FR 46251-46266
8/2/2011	Listing 23 Species on Oahu as Endangered and Designating Critical Habitat for 124 Species	Proposed Listing Endangered	76 FR 46362-46594
8/4/2011	90-Day Finding on a Petition To List Six Sand Dune Beetles as Endangered or Threatened	Notice of 90-day Petition Finding, Not substantial and substantial	76 FR 47123-47133
8/9/2011	Endangered Status for the Cumberland Darter, Rush Darter, Yellowcheek Darter, Chucky Madtom, and Laurel Dace	Final Listing Endangered	76 FR 48722-48741
8/9/2011	12-Month Finding on a Petition to List the Nueces River and Plateau Shiners as Threatened or Endangered	Notice of 12-month petition finding, Not warranted	76 FR 48777-48788
8/9/2011	Four Foreign Parrot Species [crimson shining parrot, white cockatoo, Philippine cockatoo, yellow-crested cockatoo]	Proposed Listing Endangered and Threatened; Notice of 12-month petition finding, Not warranted	76 FR 49202-49236
8/10/2011	Proposed Listing of the Miami Blue Butterfly as Endangered, and Proposed Listing of the Cassius Blue, Ceraunus Blue, and Nickerbean Blue Butterflies as Threatened Due to Similarity of Appearance to the Miami Blue Butterfly	Proposed Listing Endangered Similarity of Appearance	76 FR 49408-49412
8/10/2011	90-Day Finding on a Petition To List the Saltmarsh Topminnow as Threatened or Endangered Under the Endangered Species Act	Notice of 90-day Petition Finding, Substantial	76 FR 49412-49417
8/10/2011	Emergency Listing of the Miami Blue Butterfly as Endangered, and Emergency Listing of the Cassius Blue, Ceraunus Blue, and Nickerbean Blue Butterflies as Threatened Due to Similarity of Appearance to the Miami Blue	Emergency Listing Endangered and Similarity of Appearance	76 FR 49542-49567

	Butterfly		
8/11/2011	Listing Six Foreign Birds as Endangered Throughout Their Range	Final Listing Endangered	76 FR 50052-50080
8/17/2011	90-Day Finding on a Petition to List the Leona's Little Blue Butterfly as Endangered or Threatened	Notice of 90-day Petition Finding, Substantial	76 FR 50971-50979
9/01/2011	90-Day Finding on a Petition to List All Chimpanzees (<i>Pan troglodytes</i>) as Endangered	Notice of 90-day Petition Finding, Substantial	76 FR 54423-54425
9/6/2011	12-Month Finding on Five Petitions to List Seven Species of Hawaiian Yellow-faced Bees as Endangered	Notice of 12-month petition finding, Warranted but precluded	76 FR 55170-55203
9/8 /2011	12-Month Petition Finding and Proposed Listing of <i>Arctostaphylos franciscana</i> as Endangered	Notice of 12-month petition finding, Warranted; Proposed Listing Endangered	76 FR 55623-55638
9/8/2011	90-Day Finding on a Petition To List the Snowy Plover and Reclassify the Wintering Population of Piping Plover	Notice of 90-day Petition Finding, Not substantial	76 FR 55638-55641
9/13/2011	90-Day Finding on a Petition To List the Franklin's Bumble Bee as Endangered	Notice of 90-day Petition Finding, Substantial	76 FR 56381-56391
9/13/2011	90-Day Finding on a Petition to List 42 Great Basin and Mojave Desert Springsnails as Threatened or Endangered with Critical Habitat	Notice of 90-day Petition Finding, Substantial and Not substantial	76 FR 56608-56630
9/21/2011	12-Month Finding on a Petition to List Van Rossem's Gull-billed Tern as Endangered or Threatened	Notice of 12-month petition finding, Not warranted	76 FR 58650-58680
9/22/2011	Determination of Endangered Status for Casey's June Beetle and Designation of Critical Habitat	Final Listing Endangered	76 FR 58954-58998
9/27/2011	12-Month Finding on a Petition to List the Tamaulipan Agapema, <i>Sphingicampa blanchardi</i> (no common name), and <i>Ursia furtiva</i> (no common name) as Endangered or Threatened	Notice of 12-month petition finding, Not warranted	76 FR 59623-59634
9/27/2011	Partial 90-Day Finding on a Petition to List 404 Species in the Southeastern United States as Endangered or Threatened With Critical Habitat	Notice of 90-day Petition Finding, Substantial	76 FR 59836-59862
9/29 /2011	90-Day Finding on a Petition to List the American Eel as Threatened	Notice of 90-day Petition Finding, Substantial	76 FR 60431-60444

10/4/2011	12-Month Finding on a Petition to List the Lake Sammamish Kokanee Population of <i>Oncorhynchus nerka</i> as an Endangered or Threatened Distinct Population Segment	Notice of 12-month petition finding, Not warranted	76 FR 61298-61307
10/4/2011	12-Month Finding on a Petition to List <i>Calopogon oklahomensis</i> as Threatened or Endangered	Notice of 12-month petition finding, Not warranted	76 FR 61307-61321
10/4/2011	12-Month Finding on a Petition To List the Amargosa River Population of the Mojave Fringe-toed Lizard as an Endangered or Threatened Distinct Population Segment	Notice of 12-month petition finding, Not warranted	76 FR 61321-61330
10/4/2011	Endangered Status for the Alabama Pearlshell, Round Ebonyshell, Southern Sandshell, Southern Kidneyshell, and Choctaw Bean, and Threatened Status for the Tapered Pigtoe, Narrow Pigtoe, and Fuzzy Pigtoe; with Critical Habitat	Proposed Listing Endangered	76 FR 61482-61529
10/4/2011	90-Day Finding on a Petition To List 10 Subspecies of Great Basin Butterflies as Threatened or Endangered with Critical Habitat	Notice of 90-day Petition Finding, Substantial and Not substantial	76 FR 61532-61554
10/5/2011	90-Day Finding on a Petition to List 29 Mollusk Species as Threatened or Endangered With Critical Habitat	Notice of 90-day Petition Finding, Substantial and Not substantial	76 FR 61826-61853
10/5/2011	12-Month Finding on a Petition to List the Cactus Ferruginous Pygmy-Owl as Threatened or Endangered with Critical Habitat	Notice of 12-month petition finding, Not warranted	76 FR 61856-61894
10/5/2011	12-Month Finding on a Petition to List the Northern Leopard Frog in the Western United States as Threatened	Notice of 12-month petition finding, Not warranted	76 FR 61896-61931
10/6/2011	Endangered Status for the Ozark Hellbender Salamander	Final Listing Endangered	76 FR 61956-61978
10/6/2011	Red-Crowned Parrot	Notice of 12-month petition finding, Warranted but precluded	76 FR 62016-62034
10/6/2011	12-Month Finding on a Petition to List Texas Fatmucket, Golden Orb, Smooth Pimpleback, Texas Pimpleback, and Texas Fawnsfoot as Threatened or Endangered	Notice of 12-month petition finding, Warranted but precluded	76FR 62166-62212
10/6/2011	12-Month Finding on a Petition to List the Mohave Ground Squirrel as Endangered or Threatened	Notice of 12-month petition finding, Not warranted	76 FR 62214-62258
10/6/2011	Partial 90-Day Finding on a	Notice of 90-day	76 FR 62260-62280

	Petition to List 404 Species in the Southeastern United States as Threatened or Endangered With Critical Habitat	Petition Finding, Not substantial	
10/7/2011	12-Month Finding on a Petition to List the Black-footed Albatross as Endangered or Threatened	Notice of 12-month petition finding, Not warranted	76 FR 62504-62565
10/11 /2011	12-Month Finding on a Petition to List <i>Amoreuxia gonzalezii</i> , <i>Astragalus hypoxylus</i> , and <i>Erigeron piscaticus</i> as Endangered or Threatened	Notice of 12-month petition finding, Not warranted	76 FR 62722-62740
10/11/2011	12-Month Finding on a Petition and Proposed Rule to List the Yellow-Billed Parrot	Notice of 12-month petition finding, Warranted Propose Listing, threatened	76 FR 62740-62754
10/11/2011	12-Month Finding on a Petition to List the Tehachapi Slender Salamander as Endangered or Threatened	Notice of 12-month petition finding, Not warranted	76 FR 62900-62926
10/11/2011	Endangered Status for the Altamaha Spiny mussel and Designation of Critical Habitat	Final Listing Endangered	76 FR 62928-62960
10/11/2011	12-Month Finding for a Petition to List the California Golden Trout as Endangered	Notice of 12-month petition finding, Not warranted	76 FR 63094-63115
10/12/2011	12-Month Petition Finding, Proposed Listing of Coquí Llanero as Endangered, and Designation of Critical Habitat for Coquí Llanero	Notice of 12-month petition finding, Warranted; Proposed Listing Endangered	76 FR 63420-63442
10/12/2011	12-Month Finding on a Petition to List Northern Leatherside Chub as Endangered or Threatened	Notice of 12-month petition finding, Not warranted	76 FR 63444-63478
10/12/2011	12-Month Finding on a Petition to List Two South American Parrot Species	Notice of 12-month petition finding, Not warranted	76 FR 63480-63508
10/13/2011	12-Month Finding on a Petition to List a Distinct Population Segment of the Red Tree Vole as Endangered or Threatened	Notice of 12-month petition finding, Warranted but precluded	76 FR 63720-63762
12/19/2011	90-Day Finding on a Petition To List the Western Glacier Stonefly as Endangered With Critical Habitat	Notice of 90-day Petition Finding, Substantial	76 FR 78601-78609
1/3/2012	90-Day Finding on a Petition to List Sierra Nevada Red Fox as Endangered or Threatened	Notice of 90-day Petition Finding, Substantial	77 FR 45-52
1/5/2012	Listing Two Distinct Population Segments of Broad-Snouted Caiman as Endangered or Threatened and a Special Rule	Proposed Reclassification	77 FR 666-697

1/12/2012	90-Day Finding on a Petition To List the Humboldt Marten as Endangered or Threatened	Notice of 90-day Petition Finding, Substantial	77 FR 1900-1908
1/24/2012	90-Day Finding on a Petition to List the 'Iwi as Endangered or Threatened	Notice of 90-day Petition Finding, Substantial	77 FR 3423-3432
2/1/2012	90-Day Finding on a Petition to List the San Bernardino Flying Squirrel as Endangered or Threatened With Critical Habitat	Notice of 90-day Petition Finding, Substantial	77 FR 4973-4980
2/14/2012	Determination of Endangered Status for the Rayed Bean and Snuffbox Mussels Throughout Their Ranges	Final Listing Endangered	77 FR 8632-8665

Our expeditious progress also includes work on listing actions that we funded in previous fiscal years and in FY 2012 but have not yet been completed to date. These actions are listed below. Actions in the top section of the table are being conducted under a deadline set by a court. We are implementing a work plan that establishes a framework and schedule for resolving by September 30, 2016, the status of all of the species that the Service had determined to be qualified as of the 2010 Candidate Notice of Review. The Service submitted such a work plan to the U.S. District Court for the District of Columbia in *In re Endangered Species Act Section 4 Deadline Litigation*, No. 10-377 (EGS), MDL Docket No. 2165 (D. D.C. May 10, 2011), and obtained the court's approval. The Service had already begun to implement that work plan last FY and many of these initial actions in our work plan include work on proposed rules for candidate species with an LPN of 2 or 3. As discussed above, selection of these species is partially based on available staff resources, and when appropriate, include species with a lower priority if they overlap geographically or have the same threats as the species with the high priority. Including these species together in the same proposed rule results in considerable savings in time and funding, when compared to preparing separate proposed rules for each of them in the future. Actions in the lower section of the table are being conducted to meet

statutory timelines, that is, timelines required under the Act.

Actions funded in Previous FYs and in FY 2012 but not yet completed	
Species	Action
Actions Subject to Court Order/Settlement Agreement	
4 parrot species (military macaw, yellow-billed parrot, scarlet macaw) ⁵	12-month petition finding
Longfin smelt	12-month petition finding
20 Maui-Nui candidate species ² (17 plants, 3 tree snails) (14 with LPN = 2, 2 with LPN = 3, 3 with LPN = 8)	Proposed listing
Umtanum buckwheat (LPN = 2) and white bluffs bladderpod (LPN = 9) ⁴	Proposed listing
Grotto sculpin (LPN = 2) ⁴	Proposed listing
2 Arkansas mussels (Neosho mucket (LPN =2) & Rabbitsfoot (LPN = 9)) ⁴	Proposed listing
Diamond darter (LPN = 2) ⁴	Proposed listing
Gunnison sage-grouse (LPN =2) ⁴	Proposed listing
Coral Pink Sand Dunes Tiger Beetle (LPN = 2) ⁵	Proposed listing
Lesser prairie chicken (LPN = 2)	Proposed listing
4 Texas salamanders (Austin blind salamander (LPN = 2), Salado salamander (LPN = 2), Georgetown salamander (LPN = 8), Jollyville Plateau (LPN = 8)) ³	Proposed listing
West Texas aquatics (Gonzales Spring Snail (LPN = 2), Diamond Y springsnail (LPN =2), Phantom springsnail (LPN = 2), Phantom Cave snail (LPN = 2), Diminutive amphipod (LPN = 2)) ³	Proposed listing
2 Texas plants (Texas golden gladecress (<i>Leavenworthia texana</i>) (LPN = 2), Neches River rose-mallow (<i>Hibiscus dasycalyx</i>) (LPN = 2)) ³	Proposed listing
4 AZ plants (Acuna cactus (<i>Echinomastus erectocentrus</i> var. <i>acunensis</i>) (LPN = 3), Fickeisen plains cactus (<i>Pediocactus peeblesianus fickeiseniae</i>) (LPN = 3), Lemmon fleabane (<i>Erigeron lemmonii</i>) (LPN = 8), Gierisch mallow (<i>Sphaeralcea gierischii</i>) (LPN =2)) ⁵	Proposed listing
FL bonneted bat (LPN =2) ³	Proposed listing
3 Southern FL plants (Florida semaphore cactus (<i>Consolea corallicola</i>) (LPN = 2), shellmound applecactus (<i>Harrisia</i> (= <i>Cereus</i>) <i>aboriginum</i> (= <i>gracilis</i>)) (LPN = 2), Cape Sable thoroughwort (<i>Chromolaena frustrata</i>) (LPN = 2)) ⁵	Proposed listing
21 Big Island (HI) species ⁵ (includes 8 candidate species – 6 plants & 2 animals;	Proposed listing

4 with LPN = 2, 1 with LPN = 3, 1 with LPN = 4, 2 with LPN = 8)	
12 Puget Sound prairie species (9 subspecies of pocket gopher (<i>Thomomys mazama</i> ssp.) (LPN =3), streaked horned lark (LPN = 3), Taylor's checkerspot (LPN = 3), Mardon skipper (LPN = 8)) ³	Proposed listing
2 TN River mussels (fluted kidneyshell (LPN = 2), slabside pearlymussel (LPN = 2)) ⁵	Proposed listing
Jemez Mountain salamander (LPN = 2) ⁵	Proposed listing
Actions with Statutory Deadlines	
5 Bird species from Colombia and Ecuador	Final listing determination
Queen Charlotte goshawk	Final listing determination
6 Birds from Peru & Bolivia	Final listing determination
Loggerhead sea turtle (assist National Marine Fisheries Service) ⁵	Final listing determination
Platte River caddisfly (from 206 species petition) ⁵	12-month petition finding
Ashy storm-petrel ⁵	12-month petition finding
Honduran emerald	12-month petition finding
Eagle Lake trout ¹	90-day petition finding
Spring Mountains checkerspot butterfly	90-day petition finding
Aztec gilia ⁵	90-day petition finding
White-tailed ptarmigan ⁵	90-day petition finding
Bicknell's thrush ⁵	90-day petition finding
Sonoran talussnail ⁵	90-day petition finding
2 AZ Sky Island plants (<i>Graptopetalum bartrami</i> & <i>Pectis imberbis</i>) ⁵	90-day petition finding
Desert massasauga	90-day petition finding
Boreal toad (eastern or southern Rocky Mtn population) ⁵	90-day petition finding
Alexander Archipelago wolf ⁵	90-day petition finding
Eastern diamondback rattlesnake	90-day petition finding

¹ Funds for listing actions for these species were provided in previous FYs.

² Although funds for these high-priority listing actions were provided in FY 2008 or 2009, due to the complexity of these actions and competing priorities, these actions are still being developed.

³ Partially funded with FY 2010 funds and FY 2011 funds.

⁴ Funded with FY 2010 funds.

⁵ Funded with FY 2011 funds.

We have endeavored to make our listing actions as efficient and timely as possible, given the requirements of the relevant law and regulations, and constraints relating to workload and

personnel. We are continually considering ways to streamline processes or achieve economies of scale, such as by batching related actions together. Given our limited budget for implementing section 4 of the Act, these actions described above collectively constitute expeditious progress.

The Bay-Delta DPS of longfin smelt will be added to the list of candidate species upon publication of this 12-month finding. We will continue to evaluate this DPS as new information becomes available. Continuing review will determine if a change in status is warranted, including the need to make prompt use of emergency listing procedures.

We intend that any proposed listing determination for the Bay-Delta DPS of longfin smelt will be as accurate as possible. Therefore, we will continue to accept additional information and comments from all concerned governmental agencies, the scientific community, industry, or any other interested party concerning this finding.

References Cited

A complete list of references cited is available on the Internet at <http://www.regulations.gov> and upon request from the San Francisco Bay-Delta Fish and Wildlife Office (see **ADDRESSES** section).

Authors

The primary authors of this notice are the staff members of the San Francisco Bay-Delta

Fish and Wildlife Office.

Authority

The authority for this section is section 4 of the Endangered Species Act of 1973, as amended (16 U.S.C. 1531 *et seq.*).

Dated: MAR 13 2012

/s/ Gary D. Frazer

Acting Director, Fish and Wildlife Service

Billing Code 4310-55-P

**COMPENDIUM REPORT OF RED BLUFF DIVERSION DAM ROTARY TRAP
JUVENILE ANADROMOUS FISH PRODUCTION INDICES FOR YEARS
2002-2012**



Prepared by:
William R. Poytress
Joshua J. Gruber
Felipe D. Carrillo
And
Scott D. Voss

U.S. Fish and Wildlife Service
Red Bluff Fish and Wildlife Office
10950 Tyler Road
Red Bluff, CA 96080

July 2014

Disclaimer

The mention of trade names or commercial products in this report does not constitute endorsement or recommendation for use by the federal government.

The correct citation for this report is:

Poytress, W. R., J. J. Gruber, F. D. Carrillo and S. D. Voss. 2014. Compendium Report of Red Bluff Diversion Dam Rotary Trap Juvenile Anadromous Fish Production Indices for Years 2002-2012. Report of U.S. Fish and Wildlife Service to California Department of Fish and Wildlife and US Bureau of Reclamation.

Compendium Report of Red Bluff Diversion Dam Rotary Trap Juvenile Anadromous Fish Production Indices for Years 2002-2012

William R. Poytress, Joshua J. Gruber, Felipe D. Carrillo and Scott D. Voss

*U.S. Fish and Wildlife Service
Red Bluff Fish and Wildlife Office*

Abstract.— Fall, late-fall, spring, and winter-run Chinook salmon (*Oncorhynchus tshawytscha*) and Steelhead/Rainbow trout (*Oncorhynchus mykiss*) spawn in the Sacramento River and tributaries in California's Central Valley upstream of Red Bluff Diversion Dam (RBDD) throughout the year. Sampling of juvenile anadromous fish at RBDD allows for year-round quantitative production and passage estimates of all runs of Chinook and *O. mykiss*. Incidental capture of Green Sturgeon (*Acipenser medirostris*) and various Lamprey species (*Lampetra spp. and Entosphenus tridentatus*) has occurred throughout juvenile Chinook monitoring activities since 1995. This compendium report addresses, in detail, juvenile anadromous fish monitoring activities at RBDD for the period April 4, 2002 through September 30, 2013.

Sampling was conducted along a transect using four 8-foot diameter rotary-screw traps attached via aircraft cables directly to RBDD. Trap efficiency (i.e., the proportion of the juvenile salmonid population passing RBDD captured by traps) was modeled with percent of river discharge sampled (%Q) to develop a simple least-squares regression equation. Chinook and *O. mykiss* passage were estimated by employing the trap efficiency model. The ratio of fry to pre-smolt/smolt passing RBDD was variable among years. Therefore, juvenile passage was standardized to determine juvenile production by estimating a fry-equivalent Juvenile Production Index (JPI) for among-year comparisons. Catch per unit volume (CPUV) was used as an index of relative abundance for Green Sturgeon and Lamprey species. Abiotic data collected or calculated throughout sample efforts included: water temperature, flow, turbidity, and moon illuminosity (fraction of moon illuminated). The abiotic variables were analyzed to determine if relationships existed throughout the migration periods of the anadromous species.

A trap efficiency model developed in 2000 to estimate fish passage demonstrated improved correlation between 2002 and 2013 with the addition of 85 mark-recapture trials. The model's *r*-squared value improved greatly with the addition of numerous mark-recapture trials that used wild fry size-class salmon over a variety of river discharge levels. Total passage estimates including annual effort values with 90% confidence intervals (CI) are presented, by brood year, for each run of Chinook. Fry and pre-smolt/smolt Chinook passage estimates with 90% CI's are summarized annually by run in Appendix 1. Comparisons of relative variation within and between runs of Chinook were performed by calculating Coefficients of Variation (CV). Fall Chinook annual total passage estimates ranged between 6,627,261 and 27,736,868 juveniles for brood years 2002-2012 ($\bar{y} = 14,774,923$, CV = 46.2%). On average, fall Chinook passage was composed of 74% fry and 26% pre-smolt/smolt size-class fish (SD = 10.3). Late-fall

Chinook annual total passage estimates ranged between 91,995 and 2,559,519 juveniles for brood years 2002-2012 (\bar{y} = 447,711, CV = 159.9%). On average, late-fall Chinook passage was composed of 38% fry and 62% pre-smolt/smolt size-class fish (SD = 22.5). Winter Chinook annual total passage estimates ranged between 848,976 and 8,363,106 juveniles for brood years 2002-2012 (\bar{y} = 3,763,362, CV = 73.2%). On average, winter Chinook passage was composed of 80% fry and 20% pre-smolt/smolt size-class fish (SD = 11.2). Spring Chinook annual total passage estimates for spring Chinook ranged between 158,966 and 626,925 juveniles for brood years 2002-2012 (\bar{y} = 364,508, CV = 45.0%). On average, spring Chinook passage was composed of 54% fry and 46% pre-smolt/smolt size-class fish (SD = 20.0). Annual total passage estimates for *O. mykiss* ranged between 56,798 and 151,694 juveniles for calendar years 2002-2012 (\bar{y} = 116,272, CV = 25.7).

A significant relationship between the estimated number of adult females and fry-equivalent fall Chinook production estimates was detected (r^2 = 0.53, df = 10, P = 0.01). Recruits per female were calculated and ranged from 89 to 1,515 (\bar{y} = 749). Egg-to-fry survival estimates averaged 13.9% for fall Chinook. A significant relationship between estimated number of females and fry-equivalent late-fall Chinook production estimates was detected (r^2 = 0.67, df = 10, P = 0.002). Recruits per female were calculated and ranged from 47 to 243 (\bar{y} = 131). Egg-to-fry survival estimates averaged 2.8% for late-fall Chinook. A significant relationship between estimated number of females and fry-equivalent winter Chinook production estimates was detected (r^2 = 0.90, df = 10, P < 0.001). Recruits per female were calculated and ranged from 846 to 2,351 (\bar{y} = 1,349). Egg-to-fry survival estimates averaged 26.4% for winter Chinook. No significant relationship between estimated number of females and fry-equivalent spring Chinook production estimates was detected (r^2 = 0.00, df = 10, P = 0.971). Recruits per female were calculated and ranged from 1,112 to 8,592 (\bar{y} = 3,122). Egg-to-fry survival estimates averaged 61.5% for spring Chinook. Spring Chinook juvenile to adult correlation values appear unreasonable and well outside those found for other runs and from other studies.

Catch of Green Sturgeon was highly variable, not normally distributed and ranged between 0 and 3,701 per year (median = 193). Catch was primarily composed of recently emerged, post-exogenous feeding larvae. The 10-year median capture total length averaged 27.3 mm (SD = 0.8). Green Sturgeon annual CPUV was typically very low and ranged from 0.0 to 20.1 fish/ac-ft (\bar{y} = 2.5 fish/ac-ft, SD = 5.9). Data were positively skewed and median annual CPUV was 0.8 fish/ac-ft.

Lamprey species sampled included adult and juvenile Pacific Lamprey (*Entosphenus tridentatus*) and to a much lesser extent River Lamprey (*Lampetra ayresi*) and Pacific Brook Lamprey (*Lampetra pacifica*). Unidentified lamprey ammocoetes and Pacific Lamprey composed 99.8% of all captures, 24% and 75%, respectively. River Lamprey and Pacific Brook Lamprey composed the remaining 0.2%, combined. Lamprey captures occurred throughout the year between October and September. Lamprey ammocoete annual relative abundance ranged from 3.6 to 11.7 fish/ac-ft (\bar{y} = 6.8 fish/ac-ft, SD = 2.6). Overall, these data were normally distributed as median annual CPUV was 6.5 fish/ac-ft, similar to the mean value. Pacific Lamprey macrophthalmia

annual relative abundance was generally higher than ammocoete relative abundance and ranged from 2.1 to 112.8 fish/ac-ft ($\bar{y} = 41.0$ fish/ac-ft, $SD = 34.7$). Overall, Pacific Lamprey data was slightly positively skewed and median CPUV was 34.1 fish/ac-ft.

Tabular summaries of the abiotic conditions encountered during each annual capture period were summarized for each run of salmon, *O. mykiss*, Green Sturgeon and Lamprey species. The range of temperatures experienced by Chinook fry and pre-smolt/smolt in the last 11 years of passage at RBDD have been within the optimal range of temperature tolerances for juvenile Chinook survival. Green Sturgeon have likely benefitted from temperature management efforts aimed at winter Chinook spawning and production, albeit less comprehensively. Lamprey species have also likely benefitted from temperature management as temperatures for early life stages of Lamprey in the mainstem Sacramento River appear to have been, on average, optimal in the last 11 years.

The relationship between river discharge, turbidity, and fish passage are complex in the Upper Sacramento River where ocean and stream-type Chinook of various size-classes (i.e., runs, life stages and ages) migrate daily throughout the year. Fish passage increases often coincided with an increase in turbidity which were sampled more effectively than increases in river discharge. A positive bias of fish passage estimates may result if the peak turbidity event was sampled following an un-sampled peak flow event. The importance of the first storm event of the fall or winter period cannot be overstated. Smolt passage and juvenile Lamprey passage increase exponentially and fry passage can be significant during fall storm events.

Rotary trap passage data indicated fry size-class winter Chinook exhibit decreased nocturnal passage levels during and around the full moon phase in the fall. Pre-smolt/smolt winter Chinook appeared less influenced by nighttime light levels and much more influenced by changes in discharge levels. Spring, fall and late-fall Chinook fry exhibited varying degrees of decreased passage during full moon periods, albeit storms and related hydrologic influx dominated peak migration periods.

Table of Contents

Abstract.....	iii
List of Tables	viii
List of Figures	xi
Introduction	1
Study Area.....	3
Methods.....	4
Sampling Gear	4
Sampling Regimes	4
Data Collection.....	4
Trap Effort	5
Sampling Effort	5
Mark-Recapture Trials	6
Trap Efficiency Modeling	6
Daily Passage Estimates.....	6
Weekly Passage.....	7
Estimated Variance	7
Fry-Equivalent Chinook Production Estimates	8
Relative Abundance	8
Exploratory Data Analyses	9
Results.....	9
Sampling Effort	9
Mark-Recapture Trials	10
Trap Efficiency Modeling	11
Chinook Capture Fork Length Analyses	11
<i>O. mykiss</i> Capture Size Analyses.....	13
<i>O. mykiss</i> CAMP Program Life-Stage Comparisons	13
<i>O. mykiss</i> Weight-Length Analysis.....	14
Salmonid Passage	14
Fry-Equivalent Chinook Production Estimates	17
Green Sturgeon Data	19
Lamprey Species Data.....	20
Abiotic conditions	21
Discussion.....	23
Trap Efficiency Modeling	23
Chinook Capture Size Analyses	24
<i>O. mykiss</i> Life-Stage and Growth	25
Sample Effort Influence on Passage Estimates.....	25
Chinook Passage Variability	26
Fry-Equivalent Chinook Production Estimates	29
Green Sturgeon Capture Dynamics	33
Lamprey Capture Dynamics.....	35

Table of Contents continued

Water Temperature and Juvenile Fish Dynamics	36
River Discharge, Turbidity, and Juvenile Fish Dynamics	37
Moon Illuminosity and Juvenile Fish Dynamics	39
Acknowledgments.....	41
Literature Cited	42
Tables.....	53
Figures.....	78
Appendix 1	106
Appendix 1 List of Tables	107
Appendix 2	113
Appendix 2 List of Figures.....	114

List of Tables

Table	Page
1. Summary of annual RBDD rotary trap sample effort by run and species for the period April 2002 through September 2013, by brood year (BY).....	54
2. Summary of mark-recapture experiments conducted by RBDD rotary trap project between 2002 and 2013. Summaries include trap effort data, fish release and recapture group sizes (<i>N</i>) and mean fork lengths (FL), percentage of river discharge sampled (%Q), and estimated trap efficiency for each trial (%TE). Model data below each trial period indicate dates model was employed, total trials incorporated into model and linear regression values of slope, intercept, p-value, and coefficient of determination.	55
3. Annual capture fork length summary of <i>O. mykiss</i> by age and life-stage classification from the RBDD rotary trap project between April 2002 through December 2012 by calendar year (CY).....	60
4. Annual linear regression equations with 95% confidence intervals (CI) for Log ₁₀ transformed juvenile (80-200 mm) <i>O. mykiss</i> weight-length data sampled at the RBDD rotary traps from April 2002 to December 2012 by calendar year (CY).....	61
5a. RBDD rotary trap fall Chinook total annual effort and passage estimates (sum of weekly values), lower and upper 90% confidence intervals (CI), ratio of fry to pre-smolt/smolt passage and ratio of estimated passage (Est) and interpolated passage (Interp) for brood year (BY) 2002-2012.....	62
5b. RBDD rotary trap late-fall Chinook total annual effort and passage estimates (sum of weekly values), lower and upper 90% confidence intervals (CI), ratio of fry to pre-smolt/smolt passage and ratio of estimated passage (Est) and interpolated passage (Interp) for brood year (BY) 2002-2012.....	62
5c. RBDD rotary trap winter Chinook total annual effort and passage estimates (sum of weekly values), lower and upper 90% confidence intervals (CI), ratio of fry to pre-smolt/smolt passage and ratio of estimated passage (Est) and interpolated passage (Interp) for brood year (BY) 2002-2012.....	63
5d. RBDD rotary trap spring Chinook total annual effort and passage estimates (sum of weekly values), lower and upper 90% confidence intervals (CI), ratio of fry to pre-smolt/smolt passage and ratio of estimated passage (Est) and interpolated passage (Interp) for brood year (BY) 2002-2012.....	63

List of Tables Continued

Table	Page
5e. RBDD rotary trap <i>O. mykiss</i> total annual effort and passage estimates (sum of weekly values), lower and upper 90% confidence intervals (CI), and ratio of estimated passage (Est) and interpolated passage (Interp) for the for calendar year (CY) 2002-2012.	64
6a. Fall Chinook fry-equivalent production estimates, lower and upper 90% confidence intervals (CI), estimates of adults upstream of RBDD (Adult Estimate), estimated female to male sex ratios, estimated females, estimates of female fecundity, calculated juveniles per estimated female (recruits/fem) and egg-to-fry survival estimates (ETF) by brood year (BY) for Chinook sampled at RBDD rotary traps between December 2002 and September 2013.....	65
6b. Late-fall Chinook fry-equivalent production estimates, lower and upper 90% confidence intervals (CI), estimates of adults upstream of RBDD (Adult Estimate), estimated female to male sex ratios, estimated females, estimates of female fecundity, calculated juveniles per estimated female, and egg-to-fry survival estimates (ETF) by brood year (BY) for Chinook sampled at RBDD rotary traps between April 2002 and March 2013..	66
6c. Winter Chinook fry-equivalent production estimates, lower and upper 90% confidence intervals (CI), estimates of adults upstream of RBDD (Adult Estimate), estimated female to male sex ratios, estimated females, estimates of female fecundity, calculated juveniles per estimated female (recruits per female) and egg-to-fry survival estimates (ETF) by brood year (BY) for Chinook sampled at RBDD rotary traps between July 2002 and June 2013.....	67
6d. Spring Chinook fry-equivalent production estimates, lower and upper 90% confidence intervals (CI), estimates of adults upstream of RBDD (Adult Estimate), estimated female to male sex ratios, estimated females, estimates of female fecundity, calculated juveniles per estimated female (recruits per female) and egg-to-fry survival estimates (ETF) by brood year (BY) for Chinook sampled at RBDD rotary traps between October 16, 2002 and September 30, 2013.	68
7. Green Sturgeon annual capture, catch per unit volume (CPUV) and total length summaries for sturgeon captured by RBDD rotary traps between calendar year (CY) 2002 and 2012	69

List of Tables Continued

Table	Page
8a. Unidentified Lamprey ammocoetes annual capture, catch per unit volume (CPUV) and total length summaries for ammocoetes captured by RBDD rotary traps between water year (WY) 2003 and 2013.....	70
8b. Pacific Lamprey macrothalmia and adult annual capture, catch per unit volume (CPUV) and total length summaries for macrothalmia captured by RBDD rotary traps between water year (WY) 2003 and 2013.....	70
9a. Summary of fall Chinook abiotic sample conditions at RBDD rotary traps during dates of capture by brood year (BY).....	71
9b. Summary of late-fall Chinook abiotic sample conditions at RBDD rotary traps during dates of capture by brood year (BY).....	72
9c. Summary of winter Chinook abiotic sample conditions at RBDD rotary traps during dates of capture by brood year (BY).....	73
9d. Summary of spring Chinook abiotic sample conditions at RBDD rotary traps during dates of capture by brood year (BY).....	74
9e. Summary of <i>O. mykiss</i> abiotic sample conditions at RBDD rotary traps during dates of capture by calendar year (CY).....	75
9f. Summary of Green Sturgeon abiotic sample conditions at RBDD rotary traps during dates of capture by calendar year (CY).....	76
9g. Summary of Lamprey <i>spp.</i> abiotic sample conditions at RBDD rotary traps during dates of capture by water year (WY).....	77

List of Figures

Figure	Page
1. Location of Red Bluff Diversion Dam rotary trap sample site on the Sacramento River, California (RM 243).....	79
2. Rotary-screw trap sampling transect at Red Bluff Diversion Dam Complex (RM 243), Sacramento River, California	80
3. Trap efficiency model for combined 8-ft diameter rotary traps at Red Bluff Diversion Dam (RM 243), Sacramento River, CA. Mark-recapture trials ($N = 142$) were used to estimate trap efficiencies. Histogram indicates percentage of time traps sampled various levels (half percent bins) of river discharge between April 2002 and September 2013.....	81
4. Fall Chinook fork length (a) capture proportions, (b) cumulative capture size curve, and (c) average weekly median boxplots for fall Chinook sampled by rotary traps at RBDD between December 2002 and September 2013.	82
5. Late-fall Chinook fork length (a) capture proportions, (b) cumulative capture size curve, and (c) average weekly median boxplots for late-fall Chinook sampled by rotary traps at RBDD between April 2002 and March 2013.....	83
6. Winter Chinook fork length (a) capture proportions, (b) cumulative capture size curve, and (c) average weekly median boxplots for winter Chinook sampled by rotary traps at RBDD between July 2002 and June 2013	84
7. Spring Chinook fork length (a) capture proportions, (b) cumulative capture size curve, and (c) average weekly median boxplots for spring Chinook sampled by rotary traps at RBDD between October 2002 and September 2013.	85
8. <i>O. mykiss</i> fork length (a) capture proportions, (b) cumulative capture size curve, and (c) average weekly median boxplots for <i>O. mykiss</i> sampled by rotary traps at RBDD between April 2002 and December 2012.....	86
9. Predicted weight (g) for <i>O. mykiss</i> with measured fork lengths (FL) between 80 and 200 mm using annual weight-length regression equation.....	87
10. RBDD rotary trap fall Chinook annual passage estimates with 90% confidence intervals (CI) for the period December 2002 through September 2013	88

List of Figures continued

Figure	Page
11. RBDD rotary trap fall Chinook (a) boxplots of weekly passage estimates relative to annual total passage estimates and (b) cumulative weekly passage with 11-year mean passage trend line for the period December 2002 through September 2013.	89
12. RBDD rotary trap late-fall Chinook annual passage estimates with 90% confidence intervals (CI) for the period April 2002 through March 2013.....	90
13. RBDD rotary trap late-fall Chinook (a) boxplots of weekly passage estimates relative to annual total passage estimates and (b) cumulative weekly passage with 11-year mean passage trend line for the period April 2002 through March 2013	91
14. RBDD rotary trap winter Chinook annual passage estimates with 90% confidence intervals (CI) for the period July 2002 through June 2013	92
15. RBDD rotary trap winter Chinook (a) boxplots of weekly passage estimates relative to annual total passage estimates and (b) cumulative weekly passage with 11-year mean passage trend line for the period July 2002 through June 2013	93
16. RBDD rotary trap spring Chinook annual passage estimates with 90% confidence intervals (CI) for the period October 2002 through September 2013.....	94
17. RBDD rotary trap spring Chinook (a) boxplots of weekly passage estimates relative to annual total passage estimates and (b) cumulative weekly passage with 11-year mean passage trend line for the period October 2002 through September 2013. ...	95
18. RBDD rotary trap <i>O. mykiss</i> annual passage estimates with 90% confidence intervals (CI) for the period April 2002 through December 2012	96
19. RBDD rotary trap <i>O. mykiss</i> (a) boxplots of weekly passage estimates relative to annual total passage estimates and (b) cumulative weekly passage with 11-year mean passage trend line for the period April 2002 through December 2012.	97
20. Relationships between a) fall, b) late-fall, c) winter, and d) spring Chinook fry-equivalent production estimates and estimated number of female adult Chinook salmon upstream of RBDD between 2002 and 2012. Note: fall and late-fall adult females were natural log transformed due to extraordinary escapement values estimated for the year 2002	98

List of Figures continued

Figure	Page
21. Green sturgeon a) annual total length capture boxplots, b) annual cumulative capture trends with 10-year mean trend line, and c) relative abundance indices. All fish captured by rotary traps at RBDD (RM 243) on the Upper Sacramento River, CA between 2003 and 2012. Data from 2002 excluded from analysis due to limited effort and USBR Crown Flow study resulting in incomparable sampling regimes and results.....	99
22. Unidentified lamprey ammocoetes a) total length distribution box plots, b) cumulative annual capture trends, and c) relative abundance indices from rotary trap samples collected between October 1, 2002 and September 30, 2013 by water year from the Sacramento River, CA at the RBDD (RM 243).....	100
23. Pacific Lamprey (macrophthalmia and adults) a) total length distribution box plots, b) cumulative annual capture trends, and c) relative abundance indices from rotary trap samples collected between October 1, 2002 and September 30, 2013 by water year from the Sacramento River, CA at the RBDD (RM 243).....	101
24. Regression analysis results of natural log (Ln) Green Sturgeon catch per unit volume (CPUV) and a) full moon illuminosity, b) mean daily turbidity, c) peak daily discharge and d) maximum daily temperatures at RBDD. All fish captured by rotary trap at RBDD (RM 243) on the Upper Sacramento River, CA between 2003 and 2012. Data from 2002 excluded from analysis due to limited effort and USBR Crown Flow study resulting in incomparable sampling regimes and results.....	102
25. Regression analysis results of natural log (Ln) Lamprey <i>spp.</i> catch per unit volume (CPUV) and a) full moon illuminosity, b) Ln mean daily turbidity, c) peak daily discharge and d) maximum daily temperatures at RBDD. All fish captured by rotary trap at RBDD (RM 243) on the Upper Sacramento River, CA between water year 2003 and 2013.	103
26. Comparison of estimated juveniles produced per estimated number of females in relation to distribution of fall Chinook spawners in the mainstem Sacramento River (MST), Battle Creek (BC), and Clear Creek (CC) between years 2002 and 2012.....	104
27. Timing comparison of RBDD stage (i.e., discharge level) and turbidity measurements along with sample collection times for storm events on a) December 1-4, 2005 and b) November 15-25, 2012. Numerals within sample period boxes in figure b indicate rank of standardized Chinook passage totals from greatest (1) to least (7)	105

Introduction

The United States Fish and Wildlife Service (USFWS) has conducted direct monitoring of juvenile Chinook salmon (*Oncorhynchus tshawytscha*) passage at Red Bluff Diversion Dam (RBDD; RM 243) on the Sacramento River, CA since 1994 (Johnson and Martin 1997). Martin et al. (2001) developed quantitative methodologies for indexing juvenile Chinook passage using rotary-screw traps to assess the impacts of the RBDD Research Pumping Plant. Absolute abundance (production and passage) estimates were needed to determine the level of impact from the entrainment of salmonids and other fish community populations through experimental 'fish friendly' Archimedes and internal helical pumps (Borthwick and Corwin 2001). The original project objectives were met by 2000 and funding of the project was discontinued.

In 2001, funding was secured through a CALFED Bay-Delta Program grant for three years of annual monitoring operations to determine the effects of restoration activities in the Upper Sacramento River aimed primarily at winter Chinook¹ salmon. Through various amendments, extensions, and grant approvals by the CALFED Ecosystem Restoration Program, the State of California based funding source lasted until 2008. At this point, the State of California defaulted on their funding agreement and internal USFWS funding sources through the Central Valley Project Improvement Act (CVPIA) bridged the gap for a period of time until State funding was restored. The US Bureau of Reclamation, the primary proponent of the Central Valley Project (CVP) of which this project provides monitoring and abundance trend information, has funded this project since 2010 due to regulatory requirements contained within the Biological Opinion for the Operations and Criteria Plan for the CVP (NMFS 2009).

Protection, restoration, and enhancement of anadromous fish populations in the Sacramento River and its tributaries is an important element of the CVPIA Section 3402. The CVPIA has a specific goal to double populations of anadromous fishes in the Central Valley of California. Juvenile salmonid production monitoring is an important component authorized under Section 3406 (b)(16) of CVPIA and has funded many anadromous fish restoration actions which were outlined in the CVPIA Anadromous Fisheries Restoration Program (AFRP) Working Paper (USFWS 1995), and Draft Restoration Plan (USFWS 1997; finalized in 2001).

¹ The National Marine Fisheries Service first listed Winter-run Chinook salmon as threatened under the emergency listing procedures for the ESA (16 U.S.C.R. 1531-1543) on August 4, 1989 (54 FR 32085). A proposed rule to add winter Chinook salmon to the list of threatened species beyond expiration of the emergency rule was published by the NMFS on March 20, 1990 (55 FR 10260). Winter Chinook salmon were formally added to the list of federally threatened species by final rule on November 5, 1990 (55 FR 46515), and they were listed as a federally endangered species on January 4, 1994 (59 FR 440). Critical habitat for winter Chinook salmon has been designated from Keswick Dam (RM 302) to the Golden Gate Bridge (58 FR 33212; June 16, 1993). Winter Chinook salmon have been listed as endangered under the CESA since September 22, 1989 (California Code of Regulations, Title XIV, Section 670.5). Their federal endangered status was reaffirmed in June 2005 (70 FR 37160).

Since 2002, the USFWS rotary trap winter Chinook juvenile production indices (JPI's) have primarily been used in support of production estimates generated from carcass survey derived adult escapement data using the National Oceanic and Atmospheric Administration's (NOAA) Juvenile Production Estimate Model. Martin et al. (2001) stated that RBDD was an ideal location to monitor juvenile winter Chinook production because (1) the spawning grounds occur almost exclusively above RBDD (Vogel and Marine 1991; Snider et al. 1997, USFWS 2011), (2) multiple traps could be attached to the dam and sample simultaneously across a transect, and (3) operation of the dam could control channel morphology and hydrological characteristics of the sampling area providing for consistent sampling conditions for purposes of measuring juvenile fish passage.

Fall, late-fall, spring, and winter-run Chinook salmon and Steelhead/Rainbow Trout (*Oncorhynchus mykiss*) spawn in the Sacramento River and tributaries upstream of RBDD throughout the year resulting in year-round juvenile salmonid passage (Moyle 2002). Sampling of juvenile anadromous fish at RBDD allows for year-round quantitative production and passage estimates of all runs of Chinook and Steelhead/Rainbow trout. Timing and abundance data have been provided in real-time for fishery and water operations management purposes of the CVP since 2004². Since 2009, confidence intervals, indicating uncertainty in weekly passage estimates, have been included in real-time bi-weekly reports to allow better management of available water resources and to reduce impact of CVP operations on both federal Endangered Species Act (ESA) listed and non-listed salmonid stocks. Currently, Sacramento River winter Chinook are ESA listed as endangered. Central Valley spring Chinook and Central Valley Steelhead (hereafter *O. mykiss*) are listed as threatened within the Central Valley Endangered Species Unit.

Incidental capture of Green Sturgeon (*Acipenser medirostris*) and various Lamprey species (*Lampetra spp. and Entosphenus sp.*) has occurred throughout juvenile Chinook monitoring activities at RBDD since 1995 (Gaines and Martin 2002). Although rotary traps were designed to capture outmigrating salmonid smolts, data from the incidental capture of sturgeon and lamprey species has become increasingly relied upon for basic life-history information and as a measure of relative abundance and species trend data. The Southern distinct population segment of the North American Green Sturgeon was proposed for listing as threatened under the Federal ESA on April 7, 2006 (FR 17757) which then took effect June 6, 2006. Pacific Lamprey (*Entosphenus tridentatus*) are thought to be extirpated from at least 55% of their historical habitat and have been recognized by the USFWS as a species needing a comprehensive plan to conserve and restore these fish (Goodman and Reid 2012).

The objectives of this compendium report are to: (1) summarize the estimated abundance of all four runs of Chinook salmon and *O. mykiss* passing RBDD for brood

² Real-time biweekly reports located for download at: http://www.fws.gov/redbluff/rbdd_biweekly_final.html

years (BY) 2002 through 2012, (2) estimate annual relative abundance of Green Sturgeon and Lamprey species production for eleven consecutive years, (3) define temporal patterns of abundance for all anadromous species passing RBDD, (4) correlate juvenile salmon production with adult salmon escapement estimates, (5) perform exploratory data analyses of potential environmental covariates driving juvenile fish migration trends, and (6) describe various life-history attributes of anadromous juvenile fish produced in the Upper Sacramento River as determined through long-term monitoring efforts at RBDD.

This compendium report addresses, in detail, our juvenile anadromous fish monitoring activities at RBDD for the period April 4, 2002 through September 30, 2013. This report includes JPI's and relative abundance estimates for the 2002-2012 brood year emigration periods and will be submitted to the California Department of Fish and Wildlife to comply with contractual reporting requirements for Ecosystem Restoration Program Grant Agreement Number P0685507 and to the US Bureau of Reclamation who funded in part or in full the surveys from years 2008 through 2013 (Interagency Agreement No. R10PG20172).

Study Area

The Sacramento River originates in Northern California near Mt. Shasta from the springs of Mt. Eddy (Hallock et al. 1961). It flows south through 370 miles of the state draining numerous slopes of the coast, Klamath, Cascade, and Sierra Nevada ranges and eventually reaches the Pacific Ocean via San Francisco Bay (Figure 1). Shasta Dam and its associated downstream flow regulating structure, Keswick Dam, have formed a complete barrier to upstream anadromous fish passage since 1943 (Moffett 1949). The 59-river mile (RM) reach between Keswick Dam (RM 302) and RBDD (RM 243) supports areas of intact riparian vegetation and largely remains unobstructed. Within this reach, several major tributaries to the Sacramento upstream of RBDD support various Chinook salmon spawning populations. These include Clear Creek and Cottonwood Creek (including Beegum Creek) on the west side of the Sacramento River and Cow, Bear, Battle and Payne's Creek on the east side (Figure 1). Below RBDD, the river encounters greater anthropogenic impacts as it flows south to the Sacramento-San Joaquin Delta. Impacts include, but are not limited to, channelization, water diversion, agricultural and municipal run-off, and loss of associated riparian vegetation.

RBDD is located approximately 1.8 miles southeast of the city of Red Bluff, California (Figure 1). The dam is 740-feet (ft) wide and composed of eleven, 60-ft wide fixed-wheel gates. Between gates are concrete piers 8-ft in width. The USBR's dam operators were able to raise the RBDD gates allowing for run-of-the-river conditions or lower them to impound and divert river flows into the Tehama-Colusa and Corning canals. USBR operators generally raised the RBDD gates from September 16 through May 14 and lowered them May 15 through September 15 during the years 2002-2008. As of the spring of 2009, the RBDD gates were no longer lowered prior to June 15 and

were raised by the end of August or earlier (NMFS 2009) in an effort to reduce the impact to spring Chinook salmon and Green Sturgeon. Since the fall of 2011, the RBDD gates have been left in the raised position allowing unobstructed upstream and downstream passage of adult and juvenile anadromous fish. The RBDD has been replaced by a permanent pumping plant upstream of the RBDD and the facilities have been relinquished to the Tehama Colusa Canal Authority as of spring 2012. Mothballing of the RBDD infrastructure was scheduled to occur in 2014.

Methods

Sampling Gear.—Sampling was conducted along a transect using four 8-ft diameter rotary-screw traps (E.G. Solutions® Corvallis, Oregon) attached via aircraft cables directly to RBDD. The horizontal placement of rotary traps across the transect varied throughout the study but generally sampled in the river-margin (east and west river-margins) and mid-channel habitats simultaneously (Figure 2). Rotary traps were positioned within these *spatial zones* unless sampling equipment failed, river depths were insufficient (< 4-ft), or river hydrology restricted our ability to sample with all traps (water velocity < 2.0 ft/s).

Sampling Regimes.—In general, rotary traps sampled continuously throughout 24-hour periods and samples were processed once daily. During periods of high fish abundance, elevated river flows, or heavy debris loads, traps were sampled multiple times per day, continuously, or at randomly pre-selected periods to reduce incidental mortality. When abundance of Chinook was very high, sub-sampling protocols were implemented to reduce listed species take and incidental mortality in accordance with National Marine Fisheries Service (NMFS) Section 10(a)(1)(A) research permit terms and conditions. The specific sub-sampling protocol implemented was contingent upon the number of Chinook captured or the probability of successfully sampling various river conditions. Initially, rotary trap cones were structurally modified to only sample one-half of the normal volume of water entering the cones (Gaines and Poytress 2004). If further reductions in capture were needed, the number of traps sampled was reduced from four to three. During storm events and associated elevated river discharge levels, each 24-hour sampling period was divided into four or six non-overlapping strata and one or two strata was randomly selected for sampling (Martin et al 2001). Estimates were extrapolated to un-sampled strata by dividing catch by the strata-selection probability (i.e., $P = 0.25$ or 0.17). If further reductions in effort were needed or river conditions were intolerable, sampling was discontinued or not conducted. When days or weeks were unable to be sampled, mean daily passage estimates were imputed for missed days based on weekly or monthly mean daily estimates (i.e., interpolated).

Data Collection.—All fish captured were anesthetized, identified to species, and enumerated with fork lengths (FL) measured to the nearest millimeter (mm). When capture of Chinook juveniles exceeded approximately 200 fish/trap, a random sub-sample of the catch to include approximately 100 individuals was measured, with all

additional fish being enumerated and recorded. Chinook salmon race was assigned using length-at-date criteria developed by Greene³ (1992). Juvenile salmon were assigned to a fry or pre-smolt/smolt life stage based on their fork length. Individuals ≤ 45 mm were classified as fry, and individuals ≥ 46 mm were classified as pre-smolt/smolts.

O. mykiss between 80 and 200-mm fork length were weighed to the nearest gram using a digital scale with a stated accuracy of ± 0.5 grams. This size range was selected to reduce the influence of measurement error for fish lengths <80 mm (Pope and Kruse 2007). Additionally, state and federal permit regulations restricted the use of anesthetizing agents for fish that may be consumed by the public (i.e., fish >200 mm). *O. mykiss* were visually assessed and assigned a life-stage rating based on morphological features following protocols developed by the Comprehensive Assessment and Monitoring Program (CAMP; USFWS 1997). Furthermore, *O. mykiss* annual weight-length regression coefficients were generated by transforming (Log_{10}) the weight and fork length data to create a linear regression equation:

$$\text{Log}_{10}(\text{Total Weight}) = b(\text{Log}_{10}\text{Fork Length}) + a$$

Confidence interval overlap between the annual slope coefficients was used to test if the annual *O. mykiss* growth rates between years were significantly different (Pope and Kruse 2007). If the 95% confidence intervals around any two slope coefficients did not overlap they were considered significantly different.

Green Sturgeon and Lamprey species were measured for total length (TL) to the nearest mm. Identification of Green Sturgeon larvae was possible based on meristics for individuals > 46 mm TL and assumed for all individuals <46 mm⁴. Lamprey species were identified to the genus level during the ammocoete stage and described as ammocoetes. Adult and macrophthalmia (eyed juveniles) were identified to the genus and species level using dentition patterns, specifically by the number of inner lateral horny plates on the sucking disk (Moyle 2002).

Trap Effort. Data quantifying effort by each rotary trap were collected at each trap sampling and included the length of time each trap sampled (expressed as sample weight with 1440 minutes equal to 1.0 for 24-hour samples), water velocity immediately in front of the cone at a depth of 2-ft, and depth of cone “opening” submerged. Water velocity was measured using a General Oceanic® Model 2030 flowmeter. These data collectively were used to calculate the estimated volume of water sampled by traps (X_i)

³ Generated by Sheila Greene, California Department of Water Resources, Environmental Services Office, Sacramento (May 8, 1992) from a table developed by Frank Fisher, California Department of Fish and Game, Inland Fisheries Branch, Red Bluff (revised February 2, 1992). Fork lengths with overlapping run assignments were placed with the latter spawning run.

⁴ To confirm the identification of larval sturgeon, samples were transferred to UC Davis to be grown-out between 1996 and 1997 (Gaines and Martin 2002) and annual subsamples of larvae were sent to UC Davis for genetic analyses between 2003 and 2012 (Israel et al 2004, Israel and May 2010). To date, all samples have been confirmed to be Green Sturgeon.

in acre-feet (ac-ft). Trap effort data were then standardized to a sample weight of 1.0 for within- and between-day comparisons. Individual (X_i) data were summed for the number of traps operating within a 24-hour sample period to estimate daily water volume sampled (X_d). The percent river volume sampled by traps ($\%Q_d$) was estimated as the ratio of river volume sampled (X_d) to total river volume passing RBDD in acre-feet. River volume (Q_d) was obtained from the United States Geological Survey gauging station at Bend Bridge at RM 258 (USGS site no. 11377100, http://waterdata.usgs.gov/usa/nwis/uv?site_no=11377100). Daily river volume at RBDD was adjusted from Bend Bridge river flows by subtracting daily RBDD diversions, when applicable.

Sampling Effort. Annual rotary trap sampling effort was quantified by assigning a value of 1.00 to a sample consisting of four, 8-ft diameter rotary-screw traps sampling 24 hours daily, three hundred and sixty-five days a year. Annual values <1.00 represent occasions where less than four traps were sampling, traps were structurally modified to sample only one-half the normal volume of water, or when less than the entire year were sampled. Annual passage estimate effort was calculated by summing the total number of days passage was estimated, based on 3 or 4 traps sampling (minimum required to generate passage estimate; Martin et al. 2001), and divided by the sum of the annual total number of days sampled plus the number of days unsampled.

Mark-Recapture Trials. Chinook collected as part of daily samples were marked with bismark brown staining solution (Mundie and Traber 1983) prepared at a concentration of 21.0 mg/L of water. Fish were stained for a period of 45-50 minutes, removed, and allowed to recover in fresh water. Marked fish were held for 6-24 hours before being released 2.5-miles upstream from RBDD after official sunset. Recapture of marked fish was recorded for up to five days after release. Trap efficiency was calculated based on the proportion of recaptures to total fish released (i.e., mark-recapture trials). Trials were conducted as fish numbers and staffing levels allowed under a variety of river discharge levels and trap effort combinations.

Trap Efficiency Modeling. To develop a trap efficiency model, mark-recapture trials were conducted as noted above. Estimated trap efficiency (i.e., the proportion of the juvenile population passing RBDD captured by traps; \hat{T}_d) was modeled with $\%Q$ to develop a simple least-squares regression equation (eq. 5). The equation (slope and intercept) was then used to calculate daily trap efficiencies based on daily estimated river volume sampled. Each successive year of mark-recapture trials were added annually to the original trap efficiency model developed by Martin et al. (2001) on July 1 of each year.

Daily Passage Estimates (\hat{P}_d).—The following procedures and formulae were used to derive daily and weekly estimates of total numbers of unmarked Chinook and *O. mykiss* passing RBDD. We defined C_{di} as catch at trap i ($i = 1, \dots, t$) on day d ($d = 1, \dots, n$),

and X_{di} as volume sampled at trap i ($i = 1, \dots, t$) on day d ($d = 1, \dots, n$). Daily salmonid catch and water volume sampled were expressed as:

$$1. \quad C_d = \sum_{i=1}^t C_{di}$$

and,

$$2. \quad X_d = \sum_{i=1}^t X_{di}$$

The %Q was estimated from the ratio of water volume sampled (X_d) to river discharge (Q_d) on day d .

$$3. \quad \% \hat{Q}_d = \frac{X_d}{Q_d}$$

Total salmonid passage was estimated on day d ($d = 1, \dots, n$) by

$$4. \quad \hat{P}_d = \frac{C_d}{\hat{T}_d}$$

where,

$$5. \quad \hat{T}_d = (a)(\% \hat{Q}_d) + b$$

and, $\hat{T}_d =$ estimated trap efficiency on day d .

Weekly Passage (\hat{P}).—Population totals for numbers of Chinook and *O. mykiss* passing RBDD each week were derived from \hat{P}_d where there are N days within the week:

$$6. \quad \hat{P} = \frac{N}{n} \sum_{d=1}^n \hat{P}_d$$

Estimated Variance.—

$$7. \quad \text{Var}(\hat{P}) = \left(1 - \frac{n}{N}\right) \frac{N^2}{n} s_{\hat{P}_d}^2 + \frac{N}{n} \left[\sum_{d=1}^n \text{Var}(\hat{P}_d) + 2 \sum_{i \neq j}^n \text{Cov}(\hat{P}_i, \hat{P}_j) \right]$$

The first term in eq. 7 is associated with sampling of days within the week.

8.
$$s_{\hat{P}_d}^2 = \frac{\sum_{d=1}^n (\hat{P}_d - \hat{P})^2}{n-1}$$

The second term in eq. 7 is associated with estimating \hat{P}_d within the day.

9.
$$Var(\hat{P}_d) = \frac{\hat{P}_d(1-\hat{T}_d)}{\hat{T}_d} + Var(\hat{T}_d) \frac{\hat{P}_d(1-\hat{T}_d) + \hat{P}_d^2 \hat{T}_d}{\hat{T}_d^3}$$

where,

10.
$$Var(\hat{T}_d) = \text{error variance of the trap efficiency model}$$

The third term in eq. 7 is associated with estimating both \hat{P}_i and \hat{P}_j with the same trap efficiency model.

11.
$$Cov(\hat{P}_i, \hat{P}_j) = \frac{Cov(\hat{T}_i, \hat{T}_j) \hat{P}_i \hat{P}_j}{\hat{T}_i \hat{T}_j}$$

where,

12.
$$Cov(\hat{T}_i, \hat{T}_j) = Var(\hat{\alpha}) + x_i Cov(\hat{\alpha}, \hat{\beta}) + x_j Cov(\hat{\alpha}, \hat{\beta}) + x_i x_j Var(\hat{\beta})$$

for some $\hat{T}_i = \hat{\alpha} + \hat{\beta} x_i$

Confidence intervals (CI) were constructed around \hat{P} using eq. 13.

13.
$$P \pm t_{\alpha/2, n-1} \sqrt{Var(\hat{P})}$$

Annual JPI's were estimated by summing \hat{P} across weeks.

14.
$$JPI = \sum_{week=1}^{52} \hat{P}$$

Fry-Equivalent Chinook Production Estimates.—The ratio of Chinook fry (<46 mm FL) to pre-smolt/smolt (>45 mm FL) passing RBDD was variable among years. Therefore, we standardized juvenile production by estimating a fry-equivalent JPI for among-year comparisons. Fry-equivalent JPI's were estimated by the summation of fry JPI and a weighted (1.7:1) pre-smolt/smolt JPI (inverse value of 59% fry-to-presmolt/smolt survival; Hallock undated). Rotary trap JPI's could then be directly compared to determine variability in production between years.

Relative Abundance.—Catch per unit volume (CPUV; Gaines and Martin 2002) was used as an index of relative abundance (RA) for Green Sturgeon and Lamprey species at RBDD.

$$15. \quad RA_{dt} = \frac{C_{dt}}{V_{dt}}$$

RA_{dt} = relative abundance on day d by trap t (catch/acre-foot),
 C_{dt} = number of fish captured on day d by trap t , and
 V_{dt} = volume of water sampled on day d by trap t .

The volume of water sampled (V_{dt}) was estimated for each trap as the product of one-half the cross sectional area (wetted portion) of the cone, water velocity (ft/s) directly in front of the cone at a depth of 2-feet, cone modified (multiplied by 0.5) or not (multiplied by 1.0), and duration of sampling.

Exploratory Data Analyses.—The sampling of four runs of Chinook, *O. mykiss*, Green Sturgeon, and Lamprey occurred over 11 years and a variety of environmental conditions. Abiotic data collected or calculated throughout sample efforts included water temperature, flow, turbidity, and moon illuminosity (fraction of moon illuminated). The abiotic factors were analyzed to determine if patterns or trends existed throughout the migration periods of the various species. Additional statistical analyses were performed, when applicable, and additional methods are noted within the results section for species-specific data trends analyzed.

Results

Sampling Effort.—Annual sampling effort varied throughout the 11-year period of reporting. The reasons for less than 100% effort varied by time of year and run sampled due to numerous factors. These factors can be categorized as either intentional or unintentional decreases in effort. Intentional decreases in effort were primarily due to ESA Section 10(a)1(A) take and incidental mortality limits, the desire to decrease potential impacts to ESA listed fish or hatchery released production groups, or when staffing levels were not appropriate for the conditions encountered. Unintentional decreases in effort were due primarily to storm activity and related debris flows or conditions considered too dangerous to sample. Additionally, during the years RBDD was in operation (2002-2011), many days were not sampled due to operational requirements imposed by USBR operators (e.g., lowering or raising of the dam gates).

Annual sample effort was assigned a value of 1.0 based on sampling four traps 365 days a year. Annual sample effort values by salmonid species and run are described in Table 1. Overall, annual sample effort for all salmonids combined ranged from 0.53 to

0.91 ($\bar{y} = 0.80$, $SD = 0.10$) following annual juvenile salmonid brood year cycles. The lowest values corresponded to the year 2002 when sampling did not begin until mid-April of the year. The highest value corresponded to the year 2007 when flow events were mild, staffing levels were optimal, and permit restrictions did not dictate major sampling effort reductions (Table 1).

Mark-Recapture Trials.—Trap efficiency estimates were calculated by conducting mark-recapture trials (Volkhardt et al. 2007) using unmarked salmon collected from daily trap samples. Trials were conducted when trap catch values allowed the release of 1,000 fish per trial, generally, as well as when staffing and river conditions would allow. Mark-recapture trials were also employed to validate daily trap efficiency estimates by comparing actual with predicted (modeled) estimates. This was especially important during peak salmon outmigration periods.

The number of trials conducted each calendar year ranged from 0 in 2010 to 21 in 2004 ($\bar{y} = 7.7$) and totaled 85 trials between 2002 and 2013 (Table 2). Trials were conducted with four rotary traps ($N = 74$) or three traps ($N = 11$). Some trials were conducted with cones modified to sample half the volume of water ($N = 25$) or mixed ($N = 1$), but primarily unmodified and sampling full effort ($N = 59$). Trap efficiencies were tested with the RBDD gates raised ($N = 72$) and lowered ($N = 13$) during the years when RBDD was in operation (Table 2).

Trials were conducted through a variety of flow and trap effort conditions representing actual sampling conditions detected throughout various fish migration periods (Table 2). Estimates of the percentage of river water volume sampled by traps (%Q) ranged from 0.72 to 6.87% ($\bar{y} = 3.10$, $SD = 1.32$). Efficiency estimates for the 85 trials ranged from 0.34 to 5.48% ($\bar{y} = 2.37\%$, $SD = 0.01$).

Released fish groups ranged from 340 to 5,143 individuals ($\bar{y} = 1,598$) and recaptured fish numbers ranged from 7 to 119 ($\bar{y} = 36$) per trial. Trials were conducted predominantly with fry size-class (<46 mm fork length), naturally produced fall Chinook (67%) and to a lesser extent winter Chinook (22%). Trials were conducted in some years using unmarked pre-smolt/smolt (11%) following annual Coleman National Fish Hatchery Fall Chinook production releases⁵ during spring, as conditions and staffing levels allowed (Table 2).

Average fork lengths of release groups in the fry size-class had fork lengths ranging from 35.5 to 57.1 mm ($\bar{y} = 37.2$ mm). Recaptured fork lengths ranged from 34.6 to 62.4 mm ($\bar{y} = 37.3$ mm). Average fork lengths of fish released in the pre-smolt/smolt size-class ranged from 68.7 to 81.2 mm ($\bar{y} = 75.3$ mm). Recaptured fork lengths ranged from 61.3 to 80.2 mm ($\bar{y} = 75.3$ mm; Table 2). A paired t-test was performed on the average

⁵ Coleman National Fish Hatchery is located upstream of RBDD on Battle Creek a tributary to the Sacramento. Fall Chinook production fish (~12 million per year) were adipose clipped (i.e., marked) in varying proportions over the years of study between 0 and 25%. Unmarked fish were included in some efficiency trials as they could not be distinguished from naturally produced fish.

release and recaptured fish lengths for all trials and indicated no significant difference between the released and recaptured fish sizes ($P = 0.759$, $df = 83$, $t = -0.308$).

Trap Efficiency Modeling.—Between 1998 and 2000, Martin et al. (2001) developed a trap efficiency model for the RBDD rotary trapping operation by conducting 58 mark-recapture trials (one trial excluded due to zero efficiency value). These data were used as the basis of the trap efficiency model to calculate daily passage estimates. The model was further developed between 2002 and 2013 with the addition of 85 mark-recapture trials. Trap efficiency was positively correlated to (% Q), with higher efficiencies occurring as the relative percentage of discharge volume sampled by rotary traps increased. Trap efficiency was inversely related to river discharge (Q), as river discharge increased, trap efficiency decreased.

As mark-recapture trials were conducted, the trap efficiency model was typically updated one time each year. The newest model was applied on July 1 of each year, the beginning of the annual winter Chinook juvenile brood year period. Between 2002 and 2013 nine different models were utilized. The specific dates and model parameters with P -values used throughout the reporting period are listed chronologically below the groups of mark-recapture trials incorporated into the models in Table 2. The net result over the 11-year period was stabilization and improvement of the trap efficiency model with the addition of 85 mark-recapture trials. Overall, the P -values indicated a high level of significance for the parameter % Q in all years ($P < 0.001$). The model's r -squared value dropped in the first few years and then improved greatly with the addition of numerous naturally produced fry size-class mark-recapture trials over a variety of river discharge levels (Table 2; Figure 3).

Over the 11 years' data was collected a wide range of % Q values were sampled (0.44 to 6.86%, $\bar{y} = 2.90$, $SD = 0.01$). On 10 occasions, extremely low % Q values (<0.72%) were sampled outside of the range of values tested through efficiency trials (Figure 3). The net result was that trap efficiency values were extrapolated outside the range of the model on a mere 10 of 3,315 days sampled (0.3%).

Chinook Capture Fork Length Analyses.—Chinook run assignment based on length-at-date (LAD) criteria was originally developed from growth data in the Upper Sacramento River at the Tehama Colusa Fish Facility using fall Chinook production records from 1972 through 1981 (Fisher 1992). An estimate of apparent growth rate was originally developed from fall Chinook < 90 mm FL as fish migrated or were depleted from the spawning channels by this size (Fisher 1992). Johnson et al. (1992) further developed (extrapolated) the data to predict run for fish ≥ 90 mm and ≤ 250 mm FL. The data was further refined by Frank Fisher of the California Department of Fish and Game, whereby estimated growth curves were produced for all runs based on adult timing, water temperatures, and juvenile emergence timing and growth (Brown and Greene 1992). The growth curves were fitted to a table of daily growth increments (i.e., fork length at age in days) by the California Department of Water Resources in the early

1990's (Brown and Greene 1992; Greene 1992). The following fork length data encompassed fish sampled by rotary traps using the LAD tables up to 180 mm FL, as fish were rarely captured above this length (i.e., extreme outliers).

Fall Chinook sampled from brood years 2002-2012 were heavily weighted to the fry size-class category (<46mm). On average, 75.7% of all fish sampled as fall could be described as fry (SD = 6.9) with 71.0% of the fry measuring less than 40 mm FL (Figure 4a). The remaining 24.3% (SD = 6.9) were attributed to the pre-smolt/smolt category (>45 mm) with fish between 70 and 89 mm composing 71.0% of that value. Overall, fall Chinook were sampled between 30 and 134 mm annually, with trivial numbers below or above this range (Figure 4b). Fall Chinook showed little growth, on average, between December and March, followed by a significant increase in length in April, followed by more moderate and variable growth through November (Figure 4c). The growth pattern exhibited by fall Chinook appears strongly influenced by the duration of the fall Chinook spawning period and the LAD criteria. Beginning on April 1, newly emerged fry were classified as late-fall Chinook instead of fall Chinook thereby significantly increasing the median fork length of fall Chinook during the first two weeks of April.

Late-fall Chinook sampled from brood years 2002-2012 were not heavily weighted to the fry size-class category (<46mm). On average, 24.9% of all fish sampled as late-fall could be described as fry (SD = 12.8) with 96.3% of the fry measuring less than 40 mm FL (Figure 5a). The remaining 75.1% (SD = 12.8) were attributed to the pre-smolt/smolt category (>45 mm) with fish between 70 and 89 mm composing 48.3% of that value. Overall, late-fall Chinook were sampled between 26 and 180 mm annually (Figure 5b). Late-fall Chinook showed little growth, on average, between April and May, followed by a significant increase in length in June and July, followed by more moderate and variable growth between late-September and February (Figure 5c). The growth pattern exhibited by late-fall Chinook appears modestly influenced by the LAD criteria. Beginning on July 1, newly emerged fry were classified as winter Chinook instead of late-fall Chinook slightly increasing the median fork length of late-fall Chinook during the first few weeks of July. In mid-September and to a lesser extent in late-December, the overall fork length distribution for late-fall Chinook increases from one week to the next and was likely a result of decreased sampling effort due to RBDD gate operations and initial winter storms.

Winter Chinook sampled from brood years 2002-2012 were heavily weighted to the fry size-class category (<46mm). On average, 77.9% of all fish sampled as winter could be described as fry (SD = 8.8) with 92.8% of the fry measuring less than 40 mm FL (Figure 6a). The remaining 22.1% (SD = 8.8) were attributed to the pre-smolt/smolt category (>45 mm) with fish between 46 and 69 mm composing 85.3% of that value. Overall, winter Chinook were sampled between 27 and 162 mm annually (Figure 6b). Winter Chinook showed little growth, on average, between July and October, followed by a significant increase in length in mid-October, followed by more moderate growth through December. The growth pattern was then highly variable between January and

April (Figure 6c). The growth pattern exhibited by winter Chinook appears moderately influenced by the LAD criteria. Beginning on October 16, newly emerged fry were classified as spring Chinook instead of winter Chinook thereby significantly increasing the median fork length of winter Chinook during the last two weeks of October.

Spring Chinook sampled from brood years 2002-2012 were slightly weighted to the fry size-class category (<46mm). On average, 58.6% of all fish sampled as spring could be described as fry (SD = 19.6) with 90.0% of the fry measuring less than 40 mm FL (Figure 7a). The remaining 41.4% (SD = 19.6) were attributed to the pre-smolt/smolt category (>45 mm) with fish between 70 and 89 mm composing 69.2% of that value. Overall, spring Chinook were sampled between 28 and 143 mm annually (Figure 7b). Spring Chinook showed moderate growth, on average, between October and mid-December, followed by more consistent increasing growth through May (Figure 7c). Spring Chinook disappear from the catch typically by June with sporadic capture of large smolts in July of some years. The growth pattern exhibited by spring Chinook appears moderately influenced by the LAD criteria. Beginning on December 1, newly emerged fry were classified as fall Chinook instead of spring Chinook likely resulting in positive size-class bias for spring Chinook.

O. mykiss Capture Size Analyses.—Following the conventions used by Gaines and Martin (2002) size categorization for *O. mykiss* followed a slightly different pattern than Chinook and was organized by fork length as fry (<41 mm), sub-yearling (41–138 mm), and yearling (>138 mm). Moyle (2002) described Sacramento River *O. mykiss* populations as highly variable, but typically reaching 140-150 mm FL in their first year. The focus of our data reporting is age-0 and the focus of our size-class analyses was primarily < 139mm and secondarily < 200 mm for length-weight analyses.

O. mykiss sampled from calendar years 2002-2012 were heavily weighted towards the 41-80 mm size-class (79.2%; Figure 8a) which fell into the sub-yearling category (Figure 8b). On average, a modest 8.2% could be categorized as fry (Table 3). Overall, *O. mykiss* yearling and estimated age-2 fish were annually sampled at rates of 2.4% and 0.6%, respectively (Table 3). There was little variation detected within any size-class between categories, yet variance in weekly captures was high throughout the year (Figure 8c). The variable life-history strategies of *O. mykiss* resident and anadromous forms was evident from our size-class capture data. In general, newly emerged fry occurred in early-April and increased in size to early July. Thereafter, a second cohort of either resident trout or summer steelhead⁶ was sampled which demonstrated a secondary growth pattern through December (Figure 8c).

O. mykiss CAMP Program Life-Stage Comparisons.— *O. mykiss* capture patterns appeared to be different than that of Chinook salmon as relatively few *O. mykiss* were captured as fry (\bar{y} = 8.3%) and the majority were sampled as sub-yearlings (\bar{y} = 88.7%;

⁶ Summer steelhead are believed to be extirpated since the construction of dams blocked access to headwater habitat (Moyle 2002).

Table 3; Figure 8b). Fry capture was highest in 2002 and 2006 (11.2% and 17.5%) although these years sampled the first and third fewest *O. mykiss* of the 11 years, respectively. Yearling and age-2 capture was generally low averaging only 3.0%.

Life stage classification of fry was uniform throughout all years (\bar{y} = 6.8%, SD = 2.6%) and did not vary greatly in 2002 and 2006 in contrast to age classification. Parr and silvery-parr accounted for 91.5% of the *O. mykiss* handled at RBDD although there was a large difference between the two categories, 74.0% and 17.5% respectively. Annual variability in parr and silvery-parr classifications (SD = 15.5 and 16.8) seemed to change after 2005 and was likely due to a protocol change or interpretation of morphological characteristics by field staff. Juveniles showing signs of anadromy (i.e., smolts) made up only 1.6% of individuals sampled.

O. mykiss Weight-Length Analysis.—Log₁₀ transformed *O. mykiss* weight-length data showed a strong overall relationship between the two variables (r^2 = 0.942, Table 4). The annual slope coefficients for the 11-year period varied slightly, ranging from 2.858 to 3.052. The variability in growth was not considered significant as the 95% CI annual slope coefficients encompassed the slope coefficient of the overall mean (Table 4). Typical of most weight-length models (Pope and Kruse 2007), the variability about the regression increased with the overall length of the fish (Figure 9).

Salmonid Passage.—Passage estimates for the four runs of Chinook were calculated weekly as fry and pre-smolt/smolt passage. The sum of the weekly fry and pre-smolt/smolt passage values equal the weekly *total* passage values. Confidence intervals (CI) were calculated at the 90% level for all runs for weekly passage estimates. Weekly CI values were summed to obtain the annual CI's around the annual passage estimate (i.e., summed weekly passage estimates). Negative CI values were set to zero and result in some years CI's being asymmetrical around the annual passage estimate. Annual passage estimates (i.e., total passage estimates), by brood year, with CI's and annual effort values are presented for Chinook within Tables 5a-5d and graphically in Figures 10, 12, 14, and 16. Fry and pre-smolt/smolt Chinook passage estimates with 90% CI's summarized annually by run can be found in Appendix 1 (Tables A1-A8). Comparisons of relative variation within and between runs of Chinook were performed by calculating Coefficients of Variation (Sokal and Rohlf 1995) of passage estimates.

Fall Chinook annual passage estimates ranged between 6,627,261 and 27,736,868 juveniles for brood years 2002-2012 (\bar{y} = 14,774,923, CV = 46.2%; Table 5a). On average, fall Chinook passage was composed of 74% fry and 26% pre-smolt/smolt size-class fish (SD = 10.3). Proportions as low as 56% and as high as 87% fry were detected (Table 5a). Annual effort values resulted in interpolations of between 9 and 60% of annual passage estimates (\bar{y} = 28%). In general, the effect of annual effort on CI width indicated greater spread of CI's with decreasing effort (Figure 10).

On average, weekly fall passage equated to 5% of total annual fall Chinook passage between mid-January and early March (Figure 11a). Weekly passage varied considerably during this period with some weeks' passage totals accounting for >25% of annual passage values. Between BY 2002 and 2012, 75% of average annual passage occurred by the end of March, signifying January through March as the greatest period of migration. A second, albeit much diminished, mode of passage occurred between late April and May of each year due to the release of unmarked fall Chinook production fish from Coleman National Fish Hatchery. These fish could not be distinguished from wild fish due to fractional marking processes that varied over the 11-year period from 0 to 25%. Overall, fall passage was complete by the end of July each year with sporadic small pulses of smolts through November (Figure 11b).

Late-fall Chinook annual passage estimates ranged between 91,995 and 2,559,519 juveniles for brood years 2002-2012 ($\bar{y} = 447,711$, CV = 159.9%; Table 5b). On average, late-fall Chinook passage was composed of 38% fry and 62% pre-smolt/smolt size-class fish (SD = 22.5). Proportions as low as 11% and as high as 72% fry were detected (Table 5b). Annual effort values resulted in interpolations of between 9 and 56% of annual passage estimates ($\bar{y} = 31\%$). The effect of annual effort on CI width indicated greater spread of CI's with decreasing effort due to hatchery fish releases, in general (Figure 12).

On average, weekly late-fall passage started abruptly and held at $\leq 5\%$ of total annual passage between April and May (Figure 13a). Weekly passage varied considerably during this period with some weeks' passage totals accounting for >35% of annual passage values. A second, similar magnitude mode of passage occurred between July and August in most years. A third, albeit diminished, mode occurred during October and November with passage accounting for up to 35% of the annual run in some years. Between BY 2002 and 2012, 75% of average annual passage occurred by mid-September, signifying April through September as the greatest period of migration. Overall, late-fall passage was complete by the end of December each year with sporadic small pulses of smolts through February (Figure 13b).

Winter Chinook annual passage estimates ranged between 848,976 and 8,363,106 juveniles for brood years 2002-2012 ($\bar{y} = 3,763,362$, CV = 73.2%; Table 5c). On average, winter Chinook passage was composed of 80% fry and 20% pre-smolt/smolt size-class fish (SD = 11.2). Proportions as low as 53% and as high as 90% fry were detected (Table 5c). Annual effort values resulted in interpolations of between 8 and 42% of annual passage estimates ($\bar{y} = 18\%$). The effect of annual effort on CI width indicated greater spread of CI's with decreasing effort due to subsampling measures during peak migration periods (i.e., take or impact reduction), in general (Figure 14).

On average, weekly winter passage increased consistently through September to a peak into early October. Weekly passage varied considerably during August through December with some weeks' passage totals accounting for >20% of annual passage values. Between BY 2002 and 2012, 75% of average annual passage occurred by mid-

October. Weekly passage between October and December indicated wide variability over the 11-year period, yet the trend showed steady decreases followed by a second increase or mode of winter passage in November and December (Figure 15a). Overall, winter passage was 99% complete by the end of December each year with sporadic pulses of smolts through March that contributed minimally to the annual total winter passage estimate (Figure 15b).

Spring Chinook annual passage estimates ranged between 158,966 and 626,925 juveniles for brood years 2002-2012 ($\bar{y} = 364,508$, $CV = 45.0\%$; Table 5d). On average, spring Chinook passage was composed of 54% fry and 46% pre-smolt/smolt size-class fish ($SD = 20.0$). Proportions as low as 24% and as high as 91% fry were detected (Table 5d). Annual effort values resulted in interpolations of between 1 and 49% of annual passage estimates ($\bar{y} = 29\%$). The effect of annual effort on CI width indicated a slightly greater spread of CI's with decreasing effort due to subsampling during winter storm events, in general (Figure 16).

On average, weekly spring passage started abruptly and held at roughly 5% of total annual passage between mid-October and mid-November (Figure 17a). Weekly passage varied somewhat during this period with some weeks' passage totals accounting for up to 20% of annual passage values. A second, increased magnitude mode of passage occurred during December in most years with a single week accounting for nearly 50% of the annual passage estimate. Between BY 2002 and 2012, 75% of average annual passage occurred by mid-April, signifying October through April as the greatest period of migration. A third mode of similar magnitude to the second mode occurred during April and May with passage accounting for up to 45% of the annual run in some years. This could be characterized as an erroneous increase in spring passage. Unmarked fall production fish exceeded the size-class for fall run and therefore fell within the spring run category using LAD criteria. Between 2007 and 2012, on average, 4.3% of the marked fall production fish fell within the spring-run size-class using LAD criteria. Assumedly, a similar proportion of the unmarked fish were added into the spring-run passage estimates as they could not be distinguished from naturally produced fish. Overall, spring Chinook passage was complete by the end of May each year (Figure 17b).

O. mykiss passage estimates were generated using trap efficiency estimates calculated using the Chinook-based trap efficiency model. Caution should be exercised when interpreting the following results as Chinook and *O. mykiss* trap efficiency values likely differ, perhaps greatly. Irrespective of the accuracy of the magnitude of passage estimates based on Chinook efficiency trials, the trends in abundance remain plausible due to the standardization of effort and catch. Unlike Chinook, *O. mykiss* were not attributed to a fry or pre-smolt/smolt category and passage estimates with 90% CI's were calculated that included all size-classes and life-stages combined.

Annual passage estimates for *O. mykiss* ranged between 56,798 and 151,694 juveniles for calendar years 2002-2012 ($\bar{y} = 116,272$, $CV = 25.7\%$; Table 5e). Annual

effort values resulted in interpolations of between 4 and 56% of annual passage estimates ($\bar{y} = 22\%$). The effect of annual effort on CI width indicated a slightly greater spread of CI's with decreasing effort, in general (Figure 18).

On average, weekly *O. mykiss* passage was low (<5% on average) from April through July of each year with some variability. In 11 years of sampling only once did passage exceed 10% of annual passage during these months. Weekly passage between July and August increased to peak values ranging from 5% to nearly 25% (Figure 19a). Between 2002 and 2012, 75% of average annual passage occurred by mid-August. Weekly passage generally declined between September and October. Overall, *O. mykiss* passage was negligible between December and the following February each year (Figure 19b).

Fry-Equivalent Chinook Production Estimates.—Juvenile Chinook passage values were standardized to *fry-equivalent* production estimates for within- and between-year comparisons. As noted above, the various runs were sampled with oftentimes considerable variability in fry to pre-smolt/smolt ratios over the 11-year sample period (Table 5a-5d). By multiplying 1.7 to all fish sampled in the pre-smolt/smolt category (>45mm) within each run, annual Chinook production above the RBDD transect could be estimated. These standardized production estimates could then be compared to adult escapement estimates calculated from the California Central Valley Chinook Population Report (Azat 2013) or carcass survey data in the case of winter Chinook (USFWS 2006-2011 and 2013). Moreover, by comparing production to the number of adult Chinook females each year (by run) and estimating fecundity data from CNFH and Livingston Stone National Fish Hatchery (LSNFH) hatchery production records, estimated recruits per female and egg-to-fry survival estimates were generated.

Fall Chinook fry-equivalent production estimates between 2002 and 2012 ranged from 7,554,574 to 30,624,209 ($\bar{y} = 17,262,473$, CV = 43.2%). Lower and upper 90% CI's were generated for each week, summed annually, and averaged between 6,670,475 and 30,707,529 (Table 6a).

Adult fall Chinook escapement estimates above RBDD (mainstem Sacramento River plus tributaries reported) estimated escapement between 12,908 and 458,772 ($\bar{y} = 93,661$) for the same years. Fall Chinook carcass survey data collected by California Department of Fish and Wildlife (CDFW) provided annual female:male sex ratio estimates averaging 0.46:0.54 (D. Killam, unpublished data). A significant relationship between estimated number of females and fry-equivalent fall Chinook production estimates was detected ($r^2 = 0.53$, $df = 10$, $P = 0.01$; Figure 20a). Recruits per female were calculated ranging from 89 to 1,515 ($\bar{y} = 749$). Assuming an average female fecundity value of 5,407, based on fall Chinook spawning records from CNFH between 2008 and 2012 (K. Brown, unpublished data), resulted in an egg-to-fry survival estimate averaging 13.9% for fall Chinook (Table 6a).

Late-fall Chinook fry-equivalent production estimates between 2002 and 2012 ranged from 116,188 to 4,041,505 ($\bar{y} = 669,939$, $CV = 169.8\%$). Lower and upper 90% CI's were generated for each week, summed annually, and averaged between 222,044 and 1,236,432 (Table 6b).

Adult late-fall Chinook escapement estimates above RBDD estimated escapement between 2,931 and 36,220 ($\bar{y} = 9,108$) for the same years. Late-fall Chinook annual female:male sex ratio estimates relied on an assumption of the average ratio found for fall Chinook (i.e., 0.46:0.54). A significant relationship between estimated number of females and fry-equivalent late-fall Chinook production estimates was detected ($r^2 = 0.67$, $df = 10$, $P = 0.002$; Figure 20b). Recruits per female were calculated ranging from 47 to 243 ($\bar{y} = 131$). Assuming an average female fecundity value of 4,662 based on late-fall Chinook spawning records from CNFH between 2008 and 2012 (K. Brown, unpublished data) resulted in an egg-to-fry survival estimate averaging 2.8% for late-fall Chinook (Table 6b).

Winter Chinook fry-equivalent production estimates between 2002 and 2012 ranged from 996,621 to 8,943,194 ($\bar{y} = 4,152,547$, $CV = 70.1\%$). Lower and upper 90% CI's were generated for each week, summed annually, and averaged between 2,265,220 and 6,124,494 (Table 6c).

Adult winter Chinook escapement estimates above RBDD (USFWS/CDFW carcass survey data; available at http://www.fws.gov/redbluff/he_reports.aspx) estimated escapement between 824 and 17,205 ($\bar{y} = 6,532$) for the same years. Winter Chinook annual female:male sex ratio estimates were estimated during the annual carcass surveys (Table 6c). A highly significant relationship between estimated number of females and fry-equivalent winter Chinook production estimates was detected ($r^2 = 0.90$, $df = 10$, $P < 0.001$; Figure 20c). Recruits per female were calculated ranging from 846 to 2,351 ($\bar{y} = 1,349$). Annual female fecundity values were estimated based on winter Chinook spawning records from LSNFH between 2008 and 2012 (USFWS Annual Propagation Reports; available at http://www.fws.gov/redbluff/he_reports.aspx) and resulted in an egg-to-fry survival estimate averaging 26.4% for winter Chinook (Table 6c).

Spring Chinook fry-equivalent production estimates between 2002 and 2012 ranged from 207,793 to 747,026 ($\bar{y} = 471,527$, $CV = 40.9\%$). Lower and upper 90% CI's were generated for each week, summed annually, and averaged between 199,365 and 792,668 (Table 6d).

Adult spring Chinook escapement estimates above RBDD (mainstem Sacramento River plus tributaries reported) estimated escapement between 77 and 399 ($\bar{y} = 195$) for the same years. Spring Chinook annual female:male sex ratio estimates relied on an assumption of the average ratio found for fall Chinook (i.e., 0.46:0.54). No significant relationship between estimated number of females and fry-equivalent spring Chinook production estimates was detected ($r^2 = 0.00$, $df = 10$, $P = 0.971$; Figure 20d). Recruits

per female were calculated ranging from 1,112 to 8,592 ($\bar{y} = 3,122$). Assuming an average female fecundity value of 5,078, based on averaging of 5 years of fall and late-fall Chinook spawning records from CNFH and 10 years of winter Chinook spawning records from LSNFH, resulted in an egg-to-fry survival estimate averaging 61.5% for spring Chinook (Table 6d).

Green Sturgeon Data.—Capture of young of the year sturgeon occurred annually between calendar years 2002 and 2012, except in 2008. Catch was highly variable, not normally distributed, and ranged between 0 and 3,701 per year (median = 193; Table 7). Sturgeon sampled by rotary traps could be positively identified as Green Sturgeon in the field *above* total length of 46 mm. At this size, lateral scutes were fully developed and could be counted to distinguish between White (*Acipenser transmontanus*) and Green Sturgeon (Moyle 2002). Of 2,912 sturgeon measured in the field, 99.14% were less than 46 mm. In all years, except 2007 and 2008, sub-samples of larval and/or juvenile sturgeon rotary trap catch (up to 50% in some years) were supplied to UC Davis for genetic research and all were determined to be Green Sturgeon (See Israel et al. 2004; Israel and May 2010). We therefore assumed all sturgeon captured in rotary traps were Green Sturgeon based on the results of genetic analyses. Moreover, Green Sturgeon were the only confirmed spawning Acipenserids sampled at or above the RBDD transect between 2008 and 2012 during sturgeon spawning surveys (Poytress et al. 2009-2013).

Green Sturgeon catch was primarily composed of recently emerged, post-exogenous feeding larvae with a 10-year median capture total length averaging 27.3 mm (SD = 0.8; Table 7). Sturgeon were sampled between 18 and 188 mm, but those sampled above 40 mm were considered outliers (N = 51; Table 7; Figure 21a).

The temporal pattern of Green Sturgeon captures occurred, on average, between May 1 and August 28 of each year. Green Sturgeon capture trends indicated annual variability, but on average 50% were sampled by the end of June each year and nearly 100% by the end of July (Figure 21b), with outliers (i.e., juveniles) captured in August, September and as late as November (e.g., 188 mm TL) in some years.

Relative abundance of Green Sturgeon was measured as catch per estimated water volume sampled (CPUV in ac-ft) through rotary trap cones and summed daily. Daily values were summed annually to produce each year's annual index of abundance. Absolute abundance estimates, via trap efficiency trials, could not be calculated due to low numbers of sturgeon sampled on a daily basis and the fragile nature of newly emerged exogenous feeding larvae.

Green Sturgeon annual CPUV was typically low and ranged from 0.0 to 20.1 fish/ac-ft ($\bar{y} = 2.5$ fish/ac-ft, SD = 5.9). Data were positively skewed and median annual CPUV was 0.8 fish/ac-ft. Relative abundance distribution data were highly influenced by samples collected in 2011 that equated to two orders of magnitude higher

than any other year's index (Figure 21c). Overall, variability in CPUV between years was relatively high as the CV was 236% for the eleven-year period (Table 7).

Lamprey Species Data.—Capture of multiple lamprey species occurred between water year (WY; October - September) 2003 and 2013. WY 2002 was excluded from analyses as less than 50% of the entire year was sampled. Lamprey species sampled included adult and juvenile Pacific Lamprey and to a much lesser extent River Lamprey (*Lampetra ayresi*), and Pacific Brook Lamprey (*Lampetra pacifica*). Unidentified lamprey ammocoetes and Pacific Lamprey (PL) composed 99.8% of all captures, 24% and 75%, respectively. River Lamprey and Pacific Brook Lamprey combined, composed the remaining 0.2% of all captures. Annual catch, length, and relative abundance information for River and Pacific Brook Lamprey can be found in Appendix 1 (Tables A9 and A10) and are not discussed further due to very low capture rates.

Annual catch of ammocoetes was relatively stable and ranged between 385 and 1,415 individuals per year ($\bar{y} = 757$, median = 657; Table 8a). The catch coefficient of variation for ammocoetes was 38.5%. Minimum TL of lamprey ammocoetes was 14 mm and maximum TL was 191. Over the eleven complete years sampled, the average minimum and maximum TL's were 32 and 164 mm, respectively ($\bar{y} = 105$, SD = 4.7; Figure 22a).

Annual catch of PL macrophthalmia and a small fraction of adults was variable and ranged between 204 and 5,252 individuals per year ($\bar{y} = 2,335$, median = 2,747; Table 8b). The catch coefficient of variation for PL was 75.3%. Minimum TL of PL was 72 mm and maximum TL was 834. Over the eleven years sampled, the average minimum and maximum TL's were 88 and 665 mm, respectively ($\bar{y} = 150$, SD = 37.3; Figure 23a).

Lamprey captures occurred throughout the year between October and September. Ammocoete capture trends indicated annual variability, but on average 25% were sampled by the end of January, 50% were sampled by the end of March, 75% were sampled by the end of May and 100% by the end of September (Figure 22b). Transformed PL (macrophthalmia and adult) capture trends indicated a different pattern of capture and annual variability compared to ammocoetes. On average, 5% were sampled through October, 50% were sampled through December, 75% were sampled through February, 90% by the beginning of April with a 100% by the end of September (Figure 23b).

Relative abundance of ammocoetes and PL were measured as CPUV through individual rotary trap cones and summed daily. Daily values were summed annually to produce each year's annual index of abundance. Absolute abundance estimates employing mark-recapture methods could not be calculated due to the sporadic capture of adequate numbers of juveniles (e.g., > 1,000 individuals) that would be needed for mark-recapture trials. Moreover, emphasis was placed on conducting Chinook mark-recapture trials at times of pronounced lamprey abundance.

Ammocoete annual relative abundance ranged from 3.6 to 11.7 fish/ac-ft (\bar{y} = 6.8 fish/ac-ft, SD = 2.6; Figure 22c). Overall, ammocoete data were normally distributed as median CPUV was 6.5 fish/ac-ft, similar to the mean value. Variability in CPUV between years was modest and the coefficient of variation was 39% for the eleven-year period (Table 8a).

PL annual relative abundance was generally higher than ammocoete relative abundance and ranged from 2.1 to 112.8 fish/ac-ft (\bar{y} = 41.0 fish/ac-ft, SD = 34.7; Figure 23c). Overall, PL data was slightly positively skewed and median CPUV was 34.1 fish/ac-ft. Variability in CPUV between years was moderate and the coefficient of variation was 85% for the eleven-year period (Table 8b).

Abiotic Conditions.—Tabular summaries of the abiotic conditions that were encountered during each annual capture period were summarized for each run of salmon, *O. mykiss*, Green Sturgeon and Lamprey species. Tabular summaries associated with each species annual captures are located in Tables 9a-9f and include: dates of capture, peak daily water temperature, peak daily river discharge levels and mean daily turbidity values. A series of exploratory plots comparing the above daily environmental data variables plus an index of moon illuminosity were generated for fry and pre-smolt Chinook daily passage estimates for visual analyses. Winter Chinook fry and pre-smolt/smolt plots are included in Appendix 2 (Figures A1-A23) for reference.

Annual environmental covariate data for fall Chinook salmon can be found in Table 9a. Results presented below describe data averaged over 11 brood years. Fall Chinook were sampled over a period of 250 to 273 days per year (\bar{y} = 264 days, SD = 7). Water temperatures ranged from 45 to 62 °F (\bar{y} = 55°F, SD = 0.8). Sacramento River discharge ranged from 5,605 to 72,027 CFS (\bar{y} = 14,844 CFS, SD = 5,442). Turbidity values ranged from 1.5 to 298.7 NTU (\bar{y} = 14.4 NTU, SD = 6.3).

Annual environmental covariate data for late-fall Chinook salmon can be found in Table 9b. Results presented below describe data averaged over 11 brood years. Late-fall Chinook were sampled over a period of 270 to 338 days per year (\bar{y} = 300 days, SD = 24). Water temperatures ranged from 46 to 62 °F (\bar{y} = 56°F, SD = 0.7). Sacramento River discharge ranged from 5,536 to 67,520 CFS (\bar{y} = 12,580 CFS, SD = 2,829). Turbidity values ranged from 1.4 to 272.0 NTU (\bar{y} = 11.3 NTU, SD = 6.2).

Annual environmental covariate data for winter Chinook salmon can be found in Table 9c. Results presented below describe data averaged over 11 brood years. Winter Chinook were sampled over a period of 207 to 278 days per year (\bar{y} = 250 days, SD = 20). Water temperatures ranged from 46 to 61 °F (\bar{y} = 55°F, SD = 0.8). Sacramento River discharge ranged from 5,349 to 66,800 CFS (\bar{y} = 11,952 CFS, SD = 3,767). Turbidity values ranged from 1.3 to 290.2 NTU (\bar{y} = 12.5 NTU, SD = 5.1).

Annual environmental covariate data for spring Chinook salmon can be found in Table 9d. Results presented below describe data averaged over 11 brood years. Spring Chinook were sampled over a period of 221 to 250 days per year ($\bar{y} = 232$ days, $SD = 9$). Water temperatures ranged from 46 to 62 °F ($\bar{y} = 53^\circ\text{F}$, $SD = 0.6$). Sacramento River discharge ranged from 5,349 to 68,720 CFS ($\bar{y} = 13,370$ CFS, $SD = 6,116$). Turbidity values ranged from 1.4 to 305.9 NTU ($\bar{y} = 16.0$ NTU, $SD = 7.0$).

Annual environmental covariate data for *O. mykiss* can be found in Table 9e. Results presented below describe data averaged over 10 calendar years. *O. mykiss* were sampled over a period of 331 to 363 days per year ($\bar{y} = 349$ days, $SD = 12$). Water temperatures ranged from 46 to 63 °F ($\bar{y} = 56^\circ\text{F}$, $SD = 0.8$). Sacramento River discharge ranged from 5,333 to 67,610 CFS ($\bar{y} = 12,519$ CFS, $SD = 3,551$). Turbidity values ranged from 1.4 to 263.7 NTU ($\bar{y} = 11.4$ NTU, $SD = 4.1$).

Annual environmental covariate data for Green Sturgeon can be found in Table 9f. Results presented below describe data averaged over 11 calendar years. Green Sturgeon were sampled over a period of 56 to 151 days per year ($\bar{y} = 88$ days, $SD = 27$). Water temperatures ranged from 55 to 61 °F ($\bar{y} = 58^\circ\text{F}$, $SD = 0.9$). Sacramento River discharge ranged from 9,639 to 23,538 CFS ($\bar{y} = 13,483$ CFS, $SD = 2,181$). Turbidity values ranged from 2.4 to 93.9 NTU ($\bar{y} = 8.5$ NTU, $SD = 6.9$).

Due to the large amount of variability and lack of a normal distribution, all environmental covariate CPUV data analyses for Green Sturgeon were performed using natural log transformed data (Sokal and Rohlf 1995). Environmental covariates were regressed against the natural log of daily CPUV estimates for Green Sturgeon in a linear regression setting (Figure 24). Maximum daily water temperature was the only variable found to be significantly related to Green Sturgeon relative abundance, albeit the relationship explained ~5% of the variability around daily relative abundance ($r^2 = 0.045$, $df = 315$, $P < 0.001$).

Annual environmental covariate data for Lamprey *spp.* can be found in Table 9g. Results presented below describe data averaged over 11 water years. Lamprey were sampled over a period of 358 to 364 days per year ($\bar{y} = 362$ days, $SD = 2$). Water temperatures ranged from 46 to 63 °F ($\bar{y} = 56^\circ\text{F}$, $SD = 0.7$). Sacramento River discharge ranged from 5,347 to 68,873 CFS ($\bar{y} = 12,595$ CFS, $SD = 4,177$). Turbidity values ranged from 1.2 to 306.8 NTU ($\bar{y} = 11.9$ NTU, $SD = 4.4$).

Due to the variability and lack of a normal distribution, all environmental covariate CPUV data analyses for Lamprey *spp.* were performed using natural log transformed data. Environmental covariates were regressed against the natural log of daily CPUV data for Lamprey *spp.* in a linear and multiple regression setting. All four independent variables appear to contribute to predicting Lamprey *spp.* relative abundance and were significantly related to abundance levels ($r^2 = 0.223$, $df = 1999$, $P < 0.001$). Individual variable linear regression analyses indicated turbidity, water temperature, discharge,

and full moon illuminosity were correlated in descending order of magnitude (Figure 25). None of the covariates tested explained more than ~16% of the variability associated with daily CPUV data.

Discussion

Trap Efficiency Modeling.—Over the past 11 years, annual mark-recapture trials added 85 data points to the RBDD rotary trap efficiency linear regression model (Figure 3). Explanation of the variability associated with trap efficiency and %Q, in terms of the associated r-squared value, was reduced for the first few years and then steadily increased in more recent years. The reduction was due, in part, to more precise %Q calculations over the initial model when diversions from RBDD were not subtracted from daily river discharge values. Diversions were able to be removed from the total discharge (Q) passing the transect as these data became available in real-time starting in 2002.

The addition of a multitude of fry size-class trials over a variety of discharge levels greatly increased the accuracy of trap efficiency estimates. Fry size-class fish are the predominant size-class sampled at RBDD (i.e., fall and winter Chinook) thereby making them the best representatives for use in mark-recapture trials. The original trap efficiency model developed by Martin et al. (2001) employed primarily hatchery-raised smolts, as these fish were all that were available in large quantities and permitted for use in experiments to develop the initial model. However, hatchery fish weakly represented the primary fish size-class sampled by RBDD rotary traps. Roper and Scarnecchia (1996) and Whitton et al. (2008) found significant differences in trap efficiency when conducting paired mark-recapture trials using hatchery and wild caught fish. The most recent years of RBDD data support this concept.

While a simple linear regression model has worked well over the years for our real-time data output needs, analysis of the data within the model, other possible covariates, and other more advanced modeling techniques has been warranted. Analysis incorporating additional potential explanatory variables was conducted using a generalized additive model technique (GAM; Hastie and Tibshirani 1990). From this analysis, variables including turbidity, fish size and run, water temperature, weather condition, lunar phase, and river depth were explored in addition to %Q. The result was that only %Q and weather were found to be significant model explanatory variables ($r^2 = 0.68$; $df = 141$, $P < 0.01$). The weather variable needs focused testing by conducting more mark-recapture trials under a variety of weather conditions to determine the applicability or mechanism of this variable. The GAM modeling technique may be employed in the future as an improved statistical format to interpolate missed sample days.

At minimum, an update to the 142 trial linear trap efficiency model (Figure 3) needs to be implemented for future passage estimate calculations. The update will

include the removal of hatchery fish trials ($N=23$) used as surrogates for natural stocks. Removal of all RBDD “gates in” mark-recapture trials ($N=31$) due to the cessation of RBDD dam operations since 2011 (NMFS 2009) is also warranted.

The loss of annual maintenance and RBDD gate lowering operations at the rotary trap sample site (Figure 1) will allow the river channel’s geometry to change more frequently due to natural flow driven substrate transport mechanisms. RBDD operations of the past virtually “reset” the sample site to facilitate pumping during the gates-out period and improve fish passage at the fish ladders during the gates-in period. As the sample site’s channel configuration is allowed to fluctuate in the absence of dam operations, the overall effect could be differing trap efficiency values in relation to flow compared to previous years’ data. Annual mark-recapture trials will be needed to evaluate this phenomenon, which has been observed in other uncontrolled channel sampling locations (e.g., Clear Creek; Greenwald et. al. 2003). The use of a GAM model may also be of benefit in this situation as it could be constructed and employed annually to account for wide variation in annual trap efficiency values; albeit at the expense of being able to produce real-time data summaries.

A linear model that also removed the remaining pre-2002 trials ($N=16$) which estimated %Q in a less precise manner, would result in the most representative trap efficiency model. A post-RBDD wild Chinook model of this type would incorporate 72 mark-recapture trials with a high degree of significance ($N=72$, $r^2 = 0.669$, $F = 141.5$, $P < 0.001$) and be most representative of current sampling conditions in terms of fish size-class and environmental conditions.

Chinook Capture Size Analyses.—Overall capture of Chinook salmon by RBDD rotary traps was heavily weighted towards fry size-class less than 40mm in fork length. All four runs’ greatest proportion of fish were found in this size-class, albeit in a range of proportions from 24% for late-fall (Figure 5b) to over 72% for winter run (Figure 6b). The capture size-class results fit well with the migratory strategies of ‘stream’ and ‘ocean type’ as noted in Moyle (2002) for late-fall/spring and fall/winter Chinook, respectively. The question of size selectivity or capture bias of rotary traps, a passive sampling gear (Hubert 1996), comes into question when dealing with two very different migration strategies.

A two sample t-test was performed to evaluate the potential for size-class bias by comparing fry (fall and winter Chinook) size-class trap efficiency values ($N=43$) to pre-smolt/smolt (fall) trap efficiency values ($N=10$) between similar river discharge conditions. The t-test results did not indicate any significant difference between the mean efficiency values ($t = -0.398$, $df = 51$, $P = 0.624$). Interestingly, the mean efficiency and standard deviation of the values were identical ($\bar{y} = 2.1\%$, $SD = 0.01$) between groups. We recommend further study of the relationship between pre-smolt/smolt size-class and trap efficiency to determine if differences or bias may exist between or among Chinook runs. Additional sampling effort would be needed to capture

substantially more pre-smolts in the numbers required for efficiency trials in the Sacramento River to further test this potential bias. Smolting salmonids also appear to succumb to stress induced mortality at a much greater rate than fry, particularly in warmer water conditions due to relatively high respiration levels, adding to the difficulty in testing this potential bias.

O. mykiss Life-Stage and Growth.— Catch of *O. mykiss* was scattered throughout the year with multiple modes in abundance of predominately sub-yearling parr and silvery-parr occurring in early May and August. *O. mykiss* fry (<41 mm) made up 17.5% of the total *O. mykiss* catch in 2006 and was 2.4 standard deviations from the 11-year mean. In contrast, yolk-sac fry, made up only 9.4% of the *O. mykiss* catch in 2006 and varied less than 1 standard deviation from the 11-year mean (Table 3). Elevated spring discharge resulted in poor sampling conditions which reduced sampling effort, possibly scoured redds, and ultimately resulted in low overall *O. mykiss* catch in 2006. Regardless of the cause of low catch rates, it is unlikely the migration patterns of *O. mykiss* changed in 2006 and the variability in age-class distribution was likely due to our sampling effort in that year.

The small percentage of *O. mykiss* smolts that showed signs of anadromy were generally migrating during March through June which was consistent with outmigrating smolts found in Battle, Mill, and Deer Creeks (Johnson and Merrick 2012; Colby and Brown 2013). Interpretation of *O. mykiss* data collected at the RBDD was complicated as a robust resident (non-anadromous) population exists throughout the Upper Sacramento River and its' tributaries. Populations of anadromous and resident *O. mykiss* life history forms are often sympatric and may inter-breed (Zimmerman and Reeves 2000; Docker and Heath 2003), thereby reducing our abilities to separate the anadromous and non-anadromous components of this species. Donahue and Null (2013) conducted research using otolith Strontium/Calcium ratios to determine whether *O. mykiss* returning to a hatchery were progeny of anadromous or resident females. A similar analysis could be conducted using juvenile *O. mykiss* collected at the RBDD. Data from juveniles might provide incite as to whether temporal separation in spawn timing exists between anadromous and resident forms of *O. mykiss* coexisting within the Upper Sacramento River basin.

Linear regression equations developed using weight-length data obtained from *O. mykiss* showed a strong correlation between the two variables ($r^2 = 0.942$). The annual slope coefficient varied slightly between 2.858 and 3.052. Carlander (1969) suggested that slopes less than 3.0 might indicate a crowded or stunted population. However, permit restrictions may have introduced bias into our results as we were unable to anesthetize and weigh fish >200 mm thereby reducing the slope of the regression compared to that of a complete analysis of the population.

Sample Effort Influence on Passage Estimates.—Sampling effort had profound effects on the precision of passage estimates and confidence intervals (Figures 10, 12,

14, 16, and 18). In general, as sampling effort decreased, variance within weekly passage estimates increased and the width of confidence intervals subsequently increased. This effect was most prominent when effort was reduced during peak periods of outmigration or for long periods of time (> 1 week) when sharp increases or decreases in fish abundance occurred. Unfortunately, sampling of outmigrant Chinook on a large river system such as the Sacramento River is invariably subject to discharge events that are insurmountable for variable periods of time.

Logistical factors including staffing and permitting restrictions can also have significant effects on the precision of estimates. For example, a comparison of BY 2002 and BY 2005 winter Chinook passage with equivalent effort values (0.64) shows less precision of BY 2002 passage estimates over BY 2005 (Table 5c). The basis of the relatively low effort in 2002 was capture restrictions prompted by ESA Section 10(a)(1)(A) NMFS permits for endangered winter Chinook. Moreover, staff levels were initially low as the program was reinstated after a nearly two-year hiatus and substantial sub-sampling measures (i.e., standardized sub-sampling of repeated weeks) had to be taken during record abundance levels. The net effect was that sampling of fry, the predominant size-class of ocean type Chinook (Moyle 2002; Figure 6a/b), was reduced in terms of the number of days each week and hours of each night sampled during the peak emigration period. The overall net effect was 20% wider CI's about the 2002 estimate (i.e., less precision) compared to BY 2005. This was due to interpolation of 45% of the fry data which comprised 90% of the 2002 annual estimate. In contrast, BY 2005 sampled 90% of the fry data which comprised 90% of the annual estimate. Effort was reduced 36% in 2005 as a result of winter storms whereby sampling ceased for 3 straight weeks due to high river discharge levels. The effect of that lost sampling time in January did little to reduce the precision of the BY 2005 estimate as it was during a period when a mere fraction of a percent of total passage for winter Chinook typically occurs (Figure 15). The impact to the BY 2005 *fall Chinook* passage estimate, on the other hand, was very wide CI's about the estimate due to the lowest effort of all 11 years during a critical time period for that run's outmigration (Table 5a, Figure 11).

In summary, the precision of passage estimates can vary widely for numerous reasons within runs and among years. Inter-annual variability in environmental conditions will always be a factor when attempting to sample a riverine environment. Making good sampling decisions with knowledge of the species of interest and riverine conditions coupled with tenacity to sample critical periods of outmigration (Volkhardt et al. 2007) are key to generating passage estimates with an acceptable level of precision. Applying effort throughout each period of interest needs to be balanced between the value of data collected, an acceptable level of precision required of the data, the cost to attain the required precision, the impact sampling may have to a particular species, and the feasibility to appropriately sample the species of interest.

Chinook Passage Variability.—Juvenile Chinook passage by one to four runs occurs every single day of the year in varying proportions at RBDD. The sources and degree of

variability of juvenile Chinook passage are as diverse as the life-history and migration strategies of the runs they encompass. The magnitude of run-specific adult spawners appears to have the greatest influence on the overall magnitude of juvenile Chinook passage and associated variability.

In recent decades, fall Chinook adults consistently dominated the Upper Sacramento River spawning salmon populations (Williams 2006, Azat 2013). Throughout the past decade, we witnessed a ‘collapse’ of the Sacramento River fall Chinook adult population and accordingly tracked declines in juvenile passage (Figure 10). Lindley et al. (2009) analyzed the freshwater and marine components of fall Chinook outmigrants from BY 2004 and 2005 through their return as adults in 2007 and 2008. They indicated BY 2004 and 2005 juveniles encountered poor marine conditions upon ocean entry in the spring of 2005 and 2006 which resulted in the marked decline in fall Chinook adult abundance starting in 2007.

Juvenile fall Chinook had the greatest mean annual passage value (14,774,923) of the four runs sampled at RBDD (Table 5a). Fall Chinook passage also exhibited the second smallest degree of variability with a CV of 46.2%. Notably, fall Chinook annual production by the CNFH averages 12 million juveniles, a similar value to the mean passage value of unmarked fall Chinook⁷. Fall Chinook production fish from CNFH contributed heavily to the relative stability of the annual returning fall Chinook adult population (Williams 2006) and, consequently, juvenile passage estimates over the past eleven years (i.e., basis of fall Chinook population).

Temporal abundance patterns of fall Chinook indicate the primary passage of juveniles occurs between late December and March (Figure 11a/b). Over half the run passed RBDD by mid-February, yet this varied over the 11-year period by +/- one month. Fall run passage on the American River (Williams 2006), Clear Creek (Earley et al. 2013a) and Stanislaus River (Pyper and Justice 2006) in California generally subsides to low values by the end of March. This would be consistent with the ocean type migration strategy as noted by Moyle (2002). The remaining fall run smolts and subsequent ‘jump’ in abundance in April to May was a result of the unmarked proportion of the CNFH production releases. Reduced variability in weekly passage was observed in the final 20% of annual fall Chinook passage (Figure 11b).

Spring Chinook had the lowest average passage value of 364,000 juveniles and the lowest CV of 45% (Table 5d). The low value of spring Chinook passage at RBDD can be attributed to a relatively small number of adults spawning primarily in Battle and Clear Creeks (Figure 1). Some extant populations appear to inhabit Beegum Creek, a tributary to Cottonwood Creek (CDFG 2001), and in the mainstem Sacramento River (Killam 2009, Azat 2013). Of particular interest with respect to the accuracy of spring Chinook

⁷ Fall Chinook passages estimates do not include the marked proportion (0-25%) of CNFH production fish. Unmarked fish of hatchery origin are included in annual passage estimates and their occurrence is evidenced by increased passage values primarily in May through June of each calendar year (Figure 11b).

juvenile passage at RBDD is the annual spawn timing of adult spring Chinook and expected juvenile emergence timing. USFWS rotary trapping operations on Battle and Clear Creeks between 2003 and 2012 have not predicted emergence (i.e., through temperature unit analyses; Beacham and Murray 1990) nor sampled juvenile spring Chinook prior to November of each year. On average, the first spring Chinook juvenile migrants from Battle and Clear Creeks were sampled during the week of November 26th each year (USFWS, unpublished data). As a result, LAD criteria used to identify juvenile spring Chinook at RBDD are noticeably inaccurate as fish sampled prior to late November were not sampled upstream in primary production areas at that time of year.

Simulating a removal of all LAD spring run between October 16 and November 25 of each year sampled would result in *decreased* spring run passage estimates by 19%, on average (range 2.6 to 44.2%). The effects of removing incorrectly assigned fry annually did not indicate a statistically significant difference between annual estimates (paired *t*-test, $N = 11$, $P < 0.001$). When incorrectly assigned fry are removed, the slightly more accurate simulated spring Chinook annual passage values remain within the 90% CI of standard estimates.

Furthering the simulation by adding the weekly October through November spring Chinook estimated passage to the winter Chinook passage estimates (i.e., late spawning or emerging winter run most likely candidate; see USFWS 2013), had minimal effect on the magnitude of winter Chinook passage. The average *increase* to winter Chinook passage was a mere 2.6% (range 0.6 to 8.8%) and simulated passage remained within the 90% CI of the annual winter Chinook estimates in all years.

Winter Chinook average annual juvenile passage was the second highest of the four runs estimated at 3,763,362 (Table 5c). The CV of the annual estimates was 73.2%; higher than fall or spring, but moderately dispersed. Overall, passage in years 2002, 2003, 2005, and 2006 surpassed the highest previous value of winter Chinook passage since juvenile monitoring began in 1995 (Gaines and Martin 2002). Similar to fall Chinook, winter Chinook adult escapement and subsequent juvenile passage began a marked decline in 2007 (Figure 16). Juvenile winter Chinook have been determined to enter the ocean during March and April of each spring (Pyper et al. 2013). Overall, it is believed that juvenile winter Chinook suffered the same fate as juvenile fall Chinook with poor marine conditions upon ocean entry in the spring of 2005 and 2006. Winter Chinook juvenile cohort replacement rates dropped below 1.0 starting with BY 2007, similar to adult fall run as noted in Lindley et al. (2009). The lowest passage estimate between 2002 and 2012 for winter Chinook occurred in 2011 at 848,976. Not until 2014 will we know if adult or juvenile cohort replacement rates will improve to a value of 1.0 or greater. Winter Chinook passage estimates between BY 1999 to BY 2002 (Gaines and Poytress 2003) indicate that replacement rates can vary substantially and replacement rates of 3.0 or greater have been estimated between juvenile cohorts.

Late-fall Chinook passage averaged 447,711 juveniles for the 11-year period and exhibited the greatest amount of variability with a CV of 159.9%. Late-fall Chinook juvenile passage estimates are likely affected by LAD criteria similar to spring Chinook in terms of potential for overestimation. The variability associated with weekly late-fall passage shows a decrease in median abundance by the beginning of June each year which may be more representative of actual late-fall emergence. Additionally, as demonstrated by Figures 13 a/b, the late-fall migration starts abruptly unlike for fall and winter Chinook which follow a more bell-shaped pattern in abundance (See Figures 11a/b and 15 a/b). It was highly likely that early emergent late-fall fry were, in fact, late emerging fall Chinook. Run specific genetic monitoring (Banks et al. 2000, Banks and Jacobsen 2004) could assist in determining the magnitude of the error in run assignment.

Sampling effort during mid-April to mid-May, the early late-fall run emergent period, was also typically low in an effort to reduce impacts to CNFH fall Chinook production fish caught in rotary traps. Within trap predation of fry by CNFH production smolts could also negatively bias late-fall juvenile production estimates. Sub-sampling of portions of the day and night ($\leq 25\%$ of each period) were only feasible with full staffing in some years which can reduce potential bias. During all other years, multiple sample days were typically sacrificed to allow peaks in CNFH production fish to recede ultimately reducing the accuracy of late-fall passage estimates.

Fry-Equivalent Chinook Production Estimates.—Estimation and analyses of the productivity of salmon runs in the Upper Sacramento River basin can provide valuable information to a variety of interests. Management of California's complex water resources for agriculture, municipal, commercial, and ecological uses is an increasingly controversial and complex endeavor. Knowledge of the effects of manipulating water storage and river processes on the productivity of the Sacramento River fish populations can only benefit fishery and water operations managers in an attempt to balance the competing demands on the system. Reducing uncertainty associated with threatened and/or endangered fish population dynamics by employing knowledge of the abundance, migration timing, and variability of those populations over time can then inform the decision making processes guiding management of water and fishery resources into the future.

Fall Chinook fry-equivalent juvenile production indices (FEJPI; Table 6a) indicate a significant and moderate correlation with fall Chinook escapement estimates (Figure 20a). Approximately 53% of the variation associated with fall FEJPI's was attributed to the estimated number of females in the system above RBDD each year (Figure 20a). The CV of estimated fall run females was greater than 132% indicating wide dispersion of contributors to the juvenile population over the eleven-year period. Conversely, the CV of FEJPI's was relatively low valued at 43%. Furthermore, recruits per female and similarly egg-to-fry survival demonstrated moderately low average values of 749 and

13.9%, respectively, when compared to the estimated values for winter Chinook (Table 6a).

As noted in Kocik and Taylor (1987), factors limiting production are typically a combination of biotic and abiotic factors. The sources of variability relating to fall FEJPIs are directly and indirectly related to adult abundance, but abundance alone does not explain the low CV in fall run juvenile production. A simple, albeit incorrect, conclusion might be that adult escapement of fall Chinook in some years exceeds the useable spawning area of the system (Bovee 1982, Connor et al. 2001) or optimal spawning efficiency (Wales and Coots 1955). Upon closer examination of the likely origin(s) of juvenile production, the data indicate substantial variability in the distribution of fall run adults between the mainstem Sacramento River and tributaries, including Clear Creek and Battle Creek, between years. Proportions of returning adults within the mainstem and Battle Creek have demonstrated high degrees of variability (Figure 26). The overwhelming return of fall run to Battle Creek in 2002 resulted in the lowest value of fall Chinook recruits per female ($N = 89$) which was outside two standard deviations of the average (Table 6a). The number of adults returning to the CNFH clearly overwhelmed the capacity of Battle Creek to produce juveniles. Sub-optimal wetted useable spawning area (Bovee 1982), red superimposition (McNeil 1968, Heard 1978), and female stress resulting in egg retention (Neave 1953, Foerster 1968) were likely just some of the factors that reduced the overall productivity of the 2002 fall Chinook adults returning to the Upper Sacramento River.

In years when estimates of fall Chinook production were at their highest in terms of recruits/females (Table 6a), the proportions spawning in the mainstem and combined tributaries were closest to 50:50. Further examination indicates that when contributions from the Battle and Clear Creeks accounted for equal proportions (i.e., 25% each), peak values of $\sim 1,500$ recruits/females were estimated to have been produced resulting in the highest net spawning efficiency (Wales and Coots 1955). Optimal natural juvenile fall Chinook production values in the Upper Sacramento River system could result under some conditions if integration of restoration projects on Battle and Clear Creeks integrate with mitigation projects (e.g., CNFH production) for the mainstem Sacramento River. The effect of consistent hatchery fall Chinook production on Battle Creek irrespective of natural fish production in the Sacramento and Chinook-bearing tributaries should be considered for further evaluation as was noted in Williams (2006). The effects of restoration of Clear Creek appear to be providing production benefits on stream and basin wide scales. Management prerogatives and actions related to the CVP affect both factors, to varying degrees, and decisions should be prioritized to attain optimal results for both fisheries and water operations.

Late-fall Chinook FEJPIs indicated high variability (CV = 170%; Table 6b), but a strong correlation with escapement estimates ($r^2 = 0.67$; Figure 20b). The magnitude of late-fall FEJPIs were consistently an order of magnitude less than FEJPIs of fall Chinook. One exception was 2002, which increased the CV for the eleven-year period by 100%

(Table 6b). The fall and late-fall adult Chinook escapement values of 2001 and 2002 were high compared to the other 10 years of data (Azat 2013). A large run of late spawning fall run may also have contributed to the large number of juvenile fish falling within the late-fall size-class according to LAD criteria, but the adult estimate could have suffered similar inaccuracies in run assignment. Variability in CV values of anadromous fish was described by Rothchild and Dinardo (1987) as being inversely related to the number of years included within the time series analyses. While 2002 appears to be an outlier in this data set, it is likely with more years of data collection and analyses the CV associated with late-fall production would be more commensurate with other runs of Chinook.

The stream-type migration strategy noted by Moyle (2002) and our size classification method categorized the majority of late-fall outmigrants as smolts ($\bar{y} = 62\%$) which inflated the late-fall FEJPIs greatly at times (Table 5b, Table 6b). Recruits per female and similarly egg-to-fry survival had low CVs and the lowest average values of 131 and 2.8%, respectively, in comparison to other runs (Table 6b). This was unexpected as this metric does not appear to apply well to a run that was sampled primarily as smolts ($\bar{y} = 62\%$) over eleven years. Moreover, fry-equivalent calculations based on a static fry-to-smolt survival estimate of 59% (Hallock undated) was unlikely to be an accurate constant for late-fall Chinook as it was calculated from hatchery-based fall Chinook survival data. The fact that correlations with adult escapement were determined to be significant and moderately strong was unexpected given the vagaries of sampling late-fall Chinook smolts and the use of the static 59% survival estimate inversely applied to the majority of the run sampled. Additionally, difficulties with performing carcass surveys for late-fall Chinook due to low visibility, winter flow events or logistical issues (Killam 2009 and 2012) typically result in sub-optimal sampling conditions and, assumedly, would reduce the accuracy of the adult estimate.

Overall, production of late-fall Chinook appears low and the run has been characterized by some as vulnerable to extinction (Moyle et al. 2008, Katz et al. 2012). Greater attention to the relatively low abundance levels and juvenile rearing habitat needs of this genetically distinct run (Banks et al. 2000, Garza et al. 2007, Smith et al. 2009) with its unique over-summering, relatively long freshwater residency (Randall et al. 1987) and large size-at-outmigration strategy (Zabel and Achord 2004) should be afforded. The life-history strategies of late-fall Chinook have likely allowed them to persist in the Upper Sacramento River system as they occupy a distinct ecological niche. Juvenile monitoring of this run could benefit greatly if confidence in the accuracy of run assignment of juveniles was examined using non-lethal genetic techniques (Harvey and Stroble 2013).

Comparisons between winter Chinook adults and juvenile production began early using data generated by this monitoring project. Martin et al. (2001) demonstrated a strong relationship with only 5 years of data. The annual analyses of the winter FEJPI and adult estimates continually indicated a strong relationship with the addition of each

year's data (See Gaines and Poytress 2003, Poytress and Carrillo 2008, Poytress and Carrillo 2012). The analysis of the most recent 11 years of data continues to indicate a strong relationship between the two variables even as adult escapement values have varied an order of magnitude.

Winter Chinook FEJPIs indicated mild variability (CV = 67%; Table 6c) and a very strong level of significance and correlation with female adult escapement estimates ($r^2 = 0.90$; Figure 20c). Intensive adult and juvenile monitoring for this ESA listed endangered species coupled with superlative sampling conditions, in most years, appears to have resulted in very high quality information regarding the status and trends in adult and juvenile population abundance.

Egg-to-fry survival estimates generated from annual winter Chinook data indicate a range of values between 15 and 49% (Table 6c). At first glance, this appeared counterintuitive based on the highly regulated Sacramento River system (e.g., flow and water temperatures) that typically exists during the winter Chinook spawning period. The average egg-to-fry survival estimate of 26% is considerably higher than that determined from other studies on Pacific salmonids ($\bar{y} = 15\%$; e.g., Wales and Coats 1955) but was consistent with highly regulated aquatic systems (Groot and Margolis 1991). A very low CV of 38% also appeared consistent with a regulated system. Recruits per female, similarly, indicated a low CV of 36% and the second highest average value of 1,349 (Table 6c).

Natural log transformed adult female estimates influenced juvenile production and a significant relationship was determined accounting for roughly half of the variability associated with egg-to-fry survival rates ($r^2 = 0.51$, $df = 10$, $P = 0.012$). Densities of winter Chinook spawners are much lower currently than in the years estimated following the completion of Shasta Dam (USFWS 2001). Completion of the re-engineered Anderson-Cottonwood Irrigation District fish ladders in 2001 resulted in greater access and subsequently a greater concentration of spawners in the uppermost reaches accessible to anadromous fish (USFWS 2006-2011). Competition for optimal spawning habitat can result in lower juvenile production if sub-optimal wetted useable spawning area (Bovee 1982), red superimposition (McNeil 1968, Heard 1978), and female stress resulting in egg retention (Neave 1953, Foerster 1968) occur to varying degrees. Low resolution carcass recovery data (e.g., reach specific) indicate an abundance of spawners utilizing the uppermost 6 river miles of the Sacramento River (USFWS 2006-2011) even as seemingly suitable habitat has been made available for approximately 20+ river miles downstream of the terminus at Keswick Dam (RM 302). Geist et al. (2002) studied physiochemical characteristics affecting redd site selection preferences by Chinook and different growth and development rates have been attributed to different segments within the same river (Wells and McNeil 1970). High resolution redd surveys or spawning area mapping employing a GIS spatial analytical framework (Earley et al. 2013b) may shed light on the variability associated with winter Chinook spawning habitat over a variety of adult abundance levels. Analyses of these

types of data could result in less uncertainty over the annual specific density dependent mechanisms affecting juvenile production and provide direction for future restoration activities for winter Chinook.

Spring run Chinook FEJPIs were the lowest of all four runs monitored and indicated the lowest variability (CV = 41%; Table 6d). No relationship with female adult escapement estimates was detected ($r^2 = 0.00$; Figure 20d) and may be attributed substantially to measurement error (Sokal and Rohlf 1995). Estimates of recruits per female averaged 3,122 and the egg-to-fry survival value averaged 61.5%. These values appear unreasonable outside of a hatchery environment and well above those found for other runs (this report) and other studies (e.g., Wales and Coots 1955, Groot and Margolis 1991). Individual annual estimates varied moderately (CV= 70.8%) and nearly half appeared highly unlikely, with some values exceeding the number of eggs deposited by spawners (Table 6d).

Spring Chinook juvenile fish production estimates at RBDD were the least accurate and currently constitute 2.1%, on average, of total annual Chinook production above RBDD. Mainstem Sacramento River spawner estimates ranged from a low of 0 to a high of 370 between 2002 and 2012. Annual indexes of spring Chinook adult abundance above RBDD during the same years constitute 2.7% of the total escapement estimated in the Sacramento River system (Azat 2013). Given the relatively sporadic and low adult abundance levels, vagaries of using LAD criteria and annual CNFH fall Chinook production releases with fractional mark rates, no relationship could be found between adult escapement and spring Chinook FEJPIs when attempting to use methods to correct for these inaccuracies. The effects of inaccurate spring run assignment did not appear to affect the FEJPIs of other runs (e.g., winter or fall run) and therefore were not considered biologically significant. Genetic monitoring of fry in the fall after emergence from tributaries where emergence and migration data is collected (e.g., Earley et al. 2013a) may allow for more accurate estimation of the contributions of this run to the Upper Sacramento River outmigrant population.

Green Sturgeon Capture Dynamics.—Rotary traps were originally constructed to sample outmigrating salmonid smolts, but have been effective in sampling a variety of downstream migrating fish (Volkhardt et al. 2007). Rotary traps sampling at RBDD have been effective at monitoring temporal and spatial trends in relative abundance of Green Sturgeon since 1995 (Gaines and Martin 2002).

Annual adult Green Sturgeon aggregations were observed behind the RBDD when gates were lowered each spring (Brown 2007). Green sturgeon larvae were captured in 2012 (Table 7), the first year the RBDD gates were not lowered as it was replaced by a permanent pumping plant (NMFS 2009). Spawning was determined to have occurred in multiple locations as far as 20 river miles upstream of RBDD (Poytress et al. 2009-2013). The location of the RBDD rotary traps has been confirmed to be within the Green

Sturgeon spawning grounds as eggs were sampled directly below the RBDD and upstream of the RBDD traps in multiple years (Poytress et al. 2009, 2010, 2012).

Total length distribution data from Green Sturgeon collections at RBDD indicate a narrow and consistent size-class of larvae (Figure 21a). These data are consistent with laboratory-based studies conducted by Kynard et al. (2005) on the behavior of early life intervals of Klamath River Green Sturgeon. Their study determined that larvae migrated during two distinct periods (i.e., two-step migration). The first migration of newly exogenous feeding larvae was determined to be an initial dispersion from production areas. The second migration (of juveniles) to overwintering areas occurred in the fall some 180 days after hatching, on average. Our rotary trap data suggest we are sampling exclusively the initial redistribution of larvae from egg incubation and hatching areas.

Benthic D-net sampling conducted by Poytress et al. (2010-2011) targeted the lowest portion of the water column (inverse of rotary traps) and consistently captured Green Sturgeon larvae of the same size-class and temporal distribution pattern as rotary traps. D-net samples were collected between May and early-August (See Figure 21b for corresponding RST data only) downstream of spawning areas in years 2008-2011; even as no larvae were collected by rotary traps in 2008. Larvae were sampled by both methods primarily in the thalweg and in river velocities ≥ 1.3 ft/sec⁸. Conversely, zero *juveniles* were collected with benthic D-nets in a pilot study (Poytress et al. 2013) targeting this life-stage and habitat type in the benthos during the fall period. Rotary traps have collected a few sporadic juveniles (e.g., outliers; Figure 21a) over the entire sample record of the project. These data indicate that Green Sturgeon juveniles are no longer utilizing our sampling region or more likely using a different habitat type (Hayes et al. 1996). Accordingly, rotary traps appear to be a relatively ineffective gear type for sampling the secondary juvenile sturgeon migration.

Protections afforded to ESA listed southern distinct population segment of Green Sturgeon (since 2006), limited quantities of larvae, and the small size at capture have not allowed their drift distances (Auer and Baker 2002), rates (Braaten et al. 2008), or rotary trap efficiencies to be calculated for the initial dispersion migration of Sacramento River Green Sturgeon at RBDD. Relative abundance indices for Green Sturgeon were highly variable, typically low valued at <1.0 fish/ac-ft sampled (Table 7), and contained one extraordinarily strong year-class (Figure 21c). As noted by Allen and Hightower (2010), variations in recruitment by orders of magnitude between years is common among fish stocks. Moreover, strong and weak year classes greatly influence adult fish populations. Green sturgeon relative abundance indices should not be interpreted as recruitment to the adult population, but should be viewed as a production metric influencing recruitment (e.g., age-0 year class strength). Alternately,

⁸ Rotary traps generally require a minimum water velocity of 1.2 ft/sec to operate properly. D-nets sampled velocities ranging from 1.3 – 6.6 ft/sec. RST' sampled velocities ranging from 1.3 – 6.3 ft/sec.

Green Sturgeon larvae relative abundance indices could be viewed as an indirect metric for adult spawning population densities *upstream* of RBDD if genetic monitoring were conducted consistently (Israel and May 2010).

Lamprey Capture Dynamics.— Similar to Green Sturgeon, rotary trap sampling for Chinook salmon has provided the additional benefit of capturing out-migrating lamprey ammocoetes and juveniles. Greater attention to this ancestor of the earliest vertebrates (Moyle 2002) has recently been paid by the USFWS since it was petitioned for listing under the ESA in 2003 (Nawa et al. 2003). Although not listed due to inadequate data on the species' range and threats, the USFWS has engaged in a strategy to collaboratively conserve and restore Pacific Lamprey throughout their native range. Through the formation and development of the Pacific Lamprey Conservation Initiative, an assessment of Lamprey populations in California has recently been completed (Goodman and Reid 2012). The assessment noted that Lamprey species had been extirpated from at least 55% of their historical habitat north of Point Conception, CA by 1985. Long-term monitoring data sets including the RBDD rotary trap data, utilizing temporal and spatial distribution patterns as well as size-class and relative abundance levels of lamprey, can aid in the assessment and conservation of this ecologically vital species (Close et al. 2002).

Variability in annual size-class total length distributions was typically minor for both lamprey life stages sampled (Figure 22a and Figure 23a). Ammocoetes were slightly smaller than macrophthalmia and slightly more variable in their annual average length distributions valued at 110 mm TL (CV= 4.6%; Table 8a). Pacific Lamprey macrophthalmia were the dominant life stage sampled and the median size at capture was consistently near 125 mm TL (CV= 1.6%; Table 8b). Adults, typically noted as outliers, were encountered in much lower frequencies and were considered upstream migrants inadvertently captured when the RBDD gates were lowered as they sought upstream passage around the partial migration barrier.

Temporal distribution patterns indicated that ammocoetes and macrophthalmia migrate past RBDD year-round. Ammocoetes, on average, were sampled regularly throughout the year (Figure 22b), whereas macrophthalmia moved, en masse, episodically between November and March (Figure 23b). These data are consistent with studies of macrophthalmia in the Columbia River system as noted by Close et al. (1995) and Kostow (2002).

Relative abundance indices of ammocoetes (Figure 22c) varied little between years and little overall when compared with macrophthalmia (Figure 23c). Macrophthalmia abundance indices varied considerably between years (Table 8b). On average, macrophthalmia relative abundance was six times that of ammocoetes indicating metamorphosis and redistribution to different habitats from those used for rearing by ammocoetes (Goodman and Reid 2012). Differences in the relative abundance CV's of the two life stages likely indicates differences in catchability (Hubert and Fabrizio 2007)

or habitat use (Hayes et al. 1996), variable migration trigger effects, or variability in sampling effort that often occurred during periods of macrophthalmia migration.

Water Temperature and Juvenile Fish Dynamics.—Slight variation within and among salmonid runs (including *O. mykiss*) and years was noted for water temperatures found at RBDD (Tables 9a-e). Nonetheless, Upper Sacramento River salmonids were subjected to a relatively wide 20 degree range of water temperatures. Temperatures were recorded between 44 and 64 degrees with the average being 55 degrees each year. As summarized in Vogel and Marine (1991), the range of temperatures experienced by Chinook fry and pre-smolt/smolt in the last 11 years of passage at RBDD have been within the optimal range of thermal tolerances for survival.

Sacramento River water temperatures below Shasta/Keswick dams can be managed at certain times of the year under some conditions through discharge management to provide selective withdrawal at submerged intakes (USBR 1991 & 1994, Vermeyen 1997). Ambient air temperatures typically regulate river water temperatures during winter and early spring periods while storage and flood control operations are preeminent. The water temperatures recorded during the last 11 years appear to have been favorable for extant spring run spawners, and more so for fall and late-fall run Chinook and *O. mykiss* spawner and outmigrant populations.

The most vulnerable Chinook run to temperature management operations conducted by the USBR is winter Chinook (NMFS 2009). Temperature management of the Sacramento River via Shasta/Keswick releases by the USBR for winter Chinook appeared to be effective during the last 11 years as evidenced by the relatively favorable and stable egg-to-fry survival estimates (Table 6c). Moreover, temperature management of the upper 50 river miles of the Sacramento River aimed at winter Chinook resulted in benefits to over-summering late-fall Chinook pre-smolts and a relatively small proportion of fall Chinook smolts.

Temperature management during the summertime aimed at winter Chinook may have indirectly favored the resident form of *O. mykiss*. As noted by Lieberman et al. (2001), altering the thermal regime and food web structure by way of temperature management likely affects the proportion of anadromous to resident forms in large rivers. Lamprey species have likely benefitted from temperature management as temperatures for early life stages of lamprey in the mainstem Sacramento River appear to have been, on average, optimal (Meeuwig et al. 2005) in the last 11 years (Table 9g).

Green Sturgeon have likely benefitted from temperature management efforts aimed at winter Chinook spawning and production, albeit less comprehensively. Van Ennennaam et al. (2005) determined Green Sturgeon egg development temperatures to be optimal between 57.0 and 63.5° F. Mayfield and Cech (2004) determined optimal temperatures for larval development to be between 59.0 and 66.2°F. Temperatures recorded at RBDD during larval capture periods averaged 58.3°F and were generally

within sub-optimal (lower end) to optimal ranges (Table 9f). A weak negative relationship between Green Sturgeon CPUV and water temperatures was detected in our analysis indicating greater capture rates at lower water temperatures (Figure 24d). The slightly sub-optimal temperatures might result in larvae migrating from incubation areas prematurely. Conversely, the optimal thermal environment of the lab-based migration data from Kynard et al. (2005) resulted in very similar migration timing between the lab and larval captures in rotary traps in terms of days post hatch (Poytress et al. 2013). Sacramento River Green Sturgeon larvae appear to be following their natural life-history migration patterns as opposed to being coerced from their incubation areas due to sub-optimal water temperatures at RBDD. This may not be true for larvae migrating some 20 miles upstream where the effects of temperature management may have a more pronounced negative effect on Green Sturgeon larvae (Poytress et al. 2013). Temperature management for Chinook may also have the indirect negative effect of redirecting the spawning habitat of Green Sturgeon adults by 20 river miles. A habitat comparison study on the relative value of the upper 20 river miles of the Sacramento River versus 20 lower river miles of habitat currently benefitting Green Sturgeon adult spawners and eggs from temperature management efforts should be conducted.

River Discharge, Turbidity, and Juvenile Fish Dynamics.—Volkhardt et al. (2007) stated that “flow” (i.e., discharge) was a dominant factor in juvenile trapping operations. Trapping efficiency and migration rates are affected by flow and the RBDD rotary trap passage data reflect these statements well. Exploratory plots demonstrating fry (Appendix 2, Figures A1-A11) and pre-smolt/smolt winter Chinook passage (Appendix 2, Figures A12-A23) were produced to illustrate the effects of environmental variables on fish migration. Turbidity was plotted, but not included in the final plots presented as the effects could not be deciphered from discharge at the daily scale of analyses.

The effects of river discharge on turbidity and resultant fish passage are complex in the Upper Sacramento River where ocean and stream-type Chinook of various size-classes (i.e., runs, life stages and ages) migrate daily throughout the year. Decreases in discharge in the Shasta/Keswick dam regulated Sacramento River, typical of late summer to early winter periods, appear to coincide with relatively clear water conditions and low turbidity (e.g., ~ 1.5 NTU) at RBDD. Fall or early winter freshets and winter rain-driven storm events result in highly variable increases in discharge levels and turbidity measures in terms of the magnitude and duration depending upon the source(s) of run-off.

A course scale analyses of fish passage and river discharge and turbidity measurements during storm events typically indicates a pattern that fish passage increases with simultaneous increases in both variables. Inspection of Chinook passage on a daily time step typically demonstrate a reduction in fish passage a day prior to a storm or rain-event during periods of stable river discharge. As storms produced increases in run-off or discharge from tributary inputs outside of the Shasta/Keswick

dam complex, mean daily turbidity typically increased and fish passage began to increase. When storm related increases in discharge diminished, turbidity diminished, but Chinook passage often increased greatly for 24-72 hours after the peak flow event.

One problem confounding the results of storm and fish passage observations and analyses was that sampling during large storm run-off/discharge events often ceased due to safety concerns, concerns for fish impacts or simply due to the inability to sample the river when woody debris stop rotary traps from operating properly. In some years, storm events resulted in discharge levels too great to sample effectively or damaged traps which resulted in numerous days or weeks un-sampled afterwards. The results are typically negative bias in passage estimates if days following the peak discharge or concurrent turbidity events are un-sampled. Alternately, the direction of bias can be positive depending on time of year, interpolation methods, sample effort during extended storm periods, or fish developmental stage.

A fine scale, hourly analysis of fish passage, river discharge and turbidity during storm events indicated a more intricate relationship between the variables. As a comparison, two separate storm events (December 2005 and November 2012) were analyzed (Figure 27a/b). In 2005, 24-hour samples were conducted prior to and after the peak flow period which was missed due to an inability to sample the river as it more than quintupled in discharge (i.e., 7,000 CFS to ~35,000 CFS). During this storm event, sampling was conducted following the peak of river discharge as river stage decreased, but while turbidity continued to peak (Figure 27a). The planned 24-hour sample had to be cut short due to the huge influx of fry and smolt passage that occurred during the turbidity increase (i.e., from 10's to 1,000's per hour) and the need to reduce the potential impact to listed winter Chinook.

During a November 2012 storm event, a different strategy was employed to collect data more effectively throughout the storm period. For this event, we randomly sampled portions of the day and night in an attempt to manage the huge influx of fish anticipated to occur during the year's first storm event. Between 11/17/12 and 11/23/12, the project was able to collect 7-randomly selected samples that occurred throughout the first major river stage increase (Figure 27b). Samples were collected during increases and decreases in river stage. Samples were also collected prior to, during, and following a substantial increase in turbidity that lagged behind the initial stage increase by nearly 12 hours (Figure 27b). Fry and pre-smolt/smolt Chinook and juvenile lamprey fish passage increased exponentially. The peak period of fish capture occurred following the peak in river stage and during the increase and peak periods of turbidity measurements taken at RBDD. Capture rates subsided in the following days, but then increased greatly during the night-time period at the beginning of the next stage increase (Figure 27b).

Overall, it appears that flow and turbidity are important drivers for fish passage. The RBDD rotary trap data indicate that increased turbidity often results in greater fish

passage than increases in river discharge or stage alone which often occur as part of water management operations at Shasta Dam. The two variables generally increase sequentially with discharge increases followed by turbidity increases (Figure 27a/b). Fish passage increases often coincide with the increase in turbidity which can often be sampled more effectively than increases in river discharge and may result in positive bias of juvenile fish passage estimates if the peak turbidity event is sampled compared to the peak flow event.

The importance of the first storm event of the fall or winter period cannot be overstated. Chinook smolt and juvenile lamprey passage increased exponentially and fry passage can be significant if first storms occur as fall Chinook begin to emerge. Fishery and water operations managers should be aware of the importance of the first Sacramento River stage increases following the summer and fall Sacramento River flow regulation period. The redistribution of winter and over-summering fall and late-fall Chinook smolts, or more generally, all anadromous juvenile fish⁹ migrating from the Upper Sacramento River to the lower river and Sacramento San-Joaquin Delta with the first storm events of each water year should be incorporated into management plans for Delta operations.

Moon Illuminosity and Juvenile Fish Dynamics.—As noted in Hubert and Fabrizio (2007), species and life stages within species exhibit differing behaviors and therefore catchability in response to light levels. Gaines and Martin (2002) determined that Chinook passage occurred primarily during nocturnal periods except when turbidity levels and discharge increased with storm events. Further analyses of the effects of moon phase and ambient light levels in a statistical framework may be warranted for Chinook salmon as trends were detected based on observations. Rotary trap passage data indicated winter Chinook fry exhibit decreased nocturnal passage levels during and around the full moon phase in the fall (Appendix 3, Figures A1-A11). Pre-smolt/smolt winter Chinook appeared less influenced by night-time light levels and much more influenced by changes in discharge levels (Appendix 3, Figures A12-A23). A similar phenomenon was noted by Reimers (1971) for juvenile fall Chinook in Edson Creek, Oregon. Alternately, more data concerning night time cloud cover may further clarify the behavior associated with moon illuminosity as pre-smolt/smolt were more likely to encounter unclear night time weather between late October and December each year.

Spring, fall and late-fall Chinook fry exhibited varying degrees of decreased passage during full moon periods, albeit storms and related hydrologic influx dominated peak migration periods. *O. mykiss* relative abundance was not analyzed with respect to moon illuminosity. Lamprey CPUV regression analyses indicated a significant, but nearly imperceptible relationship (Figure 25a) likely due to the fact that lamprey are captured throughout the year under nearly all conditions. Green Sturgeon regression analysis

⁹ Juvenile Green Sturgeon have been captured sporadically during the first flow events along with large numbers of Pacific Lamprey juveniles and ammocoetes.

indicated no significant linear relationship between moon illuminosity and relative abundance (Figure 24a). Migration of age-0 Green Sturgeon larvae has been determined to occur during nocturnal hours (Kynard et al. 2005) primarily between 21:00 and 02:00 using D-nets (Poytress et al. 2011) and was presumed to be similar for rotary traps as periodic diel sampling events have not collected sturgeon during daytime sample periods.

Acknowledgments

The CALFED program and later California Bay-Delta Authority Ecosystem Restoration Program through a Directed Action of the California Department of Fish and Game (Grant # P0685507) provided funding for this project between 2002 and 2009. The U.S Bureau of Reclamation provided additional financial support during periods of fiscal insecurity by the State of California and for years 2010 through 2013 (Interagency Agreement No. R10PG20172). Numerous individuals over the years helped with development and implementation of this project including, but not limited to, Mark Belter, Brian Bissell, Oliver "Towns" Burgess, Michelle Casto-Yerty, David Colby, Nick Demetris, Melissa Dragan, Charles Elliott, Jessica Fischer, Sierra Franks, Phillip Gaines, Jerrad Goodell, Mike Gorman, Andrew Gross, Eric Grosvenor, Aime Gucker, Jeremy Haley, James Hoang, Matt Holt, Jess Johnson, Doug Killam, Tammy Knecht, Edwin Martin, Ryan Mertz, Josh Olsen, Erich Parizek, Andy Popper, Chad Praetorius, Adam Reimer, Ben Reining, Peter Roginski, Marie Schrecengost, Geoffrey Schroeder, Zach Sigler, Jennessy Toribio, David Trachtenbarg, Greg True, Charmayne Walker and Kara Yetifshfksy. Elizabeth Cook, Billie Jo DeMaagd, Valerie and Robert Emge, Tom Kisanuki, Christine Olsen, Harry Ostapenko, Deon Pollett, Jim Smith, Angela Taylor, and Keenan True provided programmatic support. We sincerely appreciate the support provided by the U.S. Bureau of Reclamation and former Red Bluff Diversion Dam staff, especially Jerry Sears and Paul Freeman.

Literature Cited

- Allen, M. S. and J.E. Hightower. 2010. Fish Population Dynamics: Mortality, Growth and Recruitment. Pages 43-79 in W.A. Hubert and M. C. Quist, editors. Inland Fisheries Management, 3rd edition. American Fisheries Society, Bethesda, Maryland.
- Auer, N.A., and E.A. Baker. 2002. Duration and drift of larval lake sturgeon in the Sturgeon River, Michigan. *Journal of Applied Ichthyology* 18:557-564.
- Azat, J. 2013. GrandTab 2013.04.18. California Central Valley Chinook Population Database Report. California Department of Fish and Wildlife.
<http://www.calfish.org/tabid/213/Default.aspx>
- Banks, M.A., Rashbrook, V.K., Calvaetta, M.J., Dean, C.A., and D. Hedgecock. 2000. Analysis of microsatellite DNA resolves genetic structure and diversity of chinook salmon (*Oncorhynchus tshawytscha*) in California's Central Valley. *Canadian Journal of Fisheries and Aquatic Sciences* 57:915-927.
- Banks M.A. and D.P. Jacobson. 2004. Which genetic markers and GSI methods are more appropriate for defining marine distribution and migration of salmon? North Pacific Anadromous Fish Commission Technical Note 5, 39-42.
- Beacham, T.D. and C.B. Murray. 1990. Temperature, Egg Size, and Development of Embryos and Alevins of Five Species of Pacific Salmon: A Comparative Analysis. *Transactions of the American Fisheries Society*. 119:6: 927-945.
- Borthwick, S. M. and R. R. Corwin. 2011. Fish entrainment by Archimedes lifts and an internal helical pump at Red Bluff Research Pumping Plant, Upper Sacramento River, California: February 1997 – May 2000. Red Bluff Research Pumping Plant Report Series, Volume 13. U.S. Bureau of Reclamation, Red Bluff, CA.
- Bovee KD. 1982. A guide to stream habitat analysis using the instream flow incremental methodology. Washington, DC:U.S. Fish and Wildlife Service, FWS/OBS-82/26.
- Braaten, P. J., Fuller, D.B., Holte, L.D., Lott, R.D., Viste, W., Brandt, T.F. and R.G. Legare. 2008. Drift Dynamics of Larval Pallid Sturgeon and Shovelnose Sturgeon in a Natural Side Channel of the Upper Missouri River, Montana. *North American Journal of Fisheries Management*. 28:808-826.
- Brown, K. 2007. Evidence of spawning by green sturgeon, *Acipenser medirostris*, in the Upper Sacramento River, California. *Environmental Biology of Fishes* 79:297-303.

- Brown, R. L. and S. Greene. 1992. Biological Assessment: Effects of the Central Valley Project and State Water Project Delta Operations on Winter-Run Chinook Salmon. California Department of Water Resources.
- California Department of Fish and Game (CDFG). 2001. Spring-run Chinook Salmon. Annual Report Prepared for the Fish and Game Commission. Habitat Conservation Division, Native Anadromous Fish and Watershed Branch. March, 2001.
- Carlander, K. D. 1969. Handbook of freshwater fishery biology. Volume One. The Iowa State University Press, Ames.
- Close, D. A., M. S. Fitzpatrick, H. W. Li, B. Parker, D. Hatch, and G. James. 1995. Status report of the Pacific lamprey (*Lampetra tridentata*) in the Columbia River Basin. (Project No. 94-026, Contract No. 95BI9067). Prepared for U.S. Department of Energy, Bonneville Power Administration, Portland, Oregon. 35 pp.
- Close, D. A., M. S. Fitzpatrick, and H. W. Li. 2002. The ecological and cultural importance of a species and risk of extinction, Pacific lamprey. *Fisheries* 27(7):19-25.
- Colby, D. J., and M. R. Brown. 2013. Juvenile salmonid monitoring in Battle Creek, California, November 2010 through June 2011. U.S. Fish and Wildlife Service, Red Bluff Fish and Wildlife Office, Red Bluff, California.
- Connor, W. P., Garcia, A. P., Connor, A. H., Garton, E. O., Groves, P, A, and Chandler, J.A. 2001. Estimating the carrying capacity of the Snake River for fall chinook salmon redds. *Northwest Science*. 75: 363-371.
- Docker, M. F., and D. D. Heath. 2003. Genetic comparison between sympatric anadromous steelhead and freshwater resident rainbow trout in British Columbia, Canada. *Conservation Genetics* 4:227-231.
- Donohoe, C. J., and R. Null. 2013. Migratory history and maternal origin of rainbow trout (*Oncorhynchus mykiss*) returning to Coleman National Fish Hatchery in 2008. Institute of Marine Sciences, University of California, Santa Cruz, Santa Cruz, California.
- Earley, J. T., D. J. Colby, and M. R. Brown. 2013a. Juvenile salmonid monitoring in Clear Creek, California, from October 2010 through September 2011. U.S. Fish and Wildlife Service, Red Bluff Fish and Wildlife Office, Red Bluff, California.
- Earley, L. A., S.L. Giovannetti, and M.R. Brown. 2013b. Fall Chinook Salmon Redd Mapping for the Clear Creek Restoration Project, 2008-2012. U.S. Fish and Wildlife Service, Red Bluff Fish and Wildlife Office, Red Bluff, California.

- Fisher, F.W. 1992. (DRAFT) Chinook Salmon, *Oncorhynchus Tshawytscha*, Growth and Occurrence in the Sacramento-San Joaquin River System. Inland Fisheries Division of California Department of Fish and Game. June, 1992.
- Foerster, R. E. 1968. The sockeye salmon, *Oncorhynchus nerka*, Fisheries Research Board of Canada Bulletin 162.
- Gaines, P.D. and C. D. Martin. 2002. Abundance and Seasonal, Spatial and Diel Distribution Patterns of Juvenile Salmonids Passing the Red Bluff Diversion Dam, Sacramento River. Red Bluff Research Pumping Plant Report Series, Volume 14, U.S. Fish and Wildlife Service, Red Bluff, CA.
- Gaines, P.D. and W.R. Poytress. 2003. Brood-year 2002 winter Chinook juvenile production indices with comparisons to adult escapement. U.S. Fish and Wildlife Service report to California Bay-Delta Authority. San Francisco, CA.
- Gaines, P.D. and W.R. Poytress. 2004. Brood-year 2003 winter Chinook juvenile production indices with comparisons to adult escapement. U.S. Fish and Wildlife Service report to California Bay-Delta Authority. San Francisco, CA.
- Garza, J.C., Blankenship, S.M. Lemaire, C., and G. Charrier. 2007. Genetic population structure of Chinook salmon (*Oncorhynchus tshawytscha*) in California's Central Valley. Draft Final Report for CalFed Project "Comprehensive Evaluation of Population Structure and Diversity for Central Valley Chinook Salmon". 82pp.
- Geist, D.R., T.P. Hanrahan, E.V. Arntzen, G.A. McMichael, C.J. Murray, and Y.J. Chien. 2002. Physiochemical characteristics of the hyporheic zone affect redd site selection by chum salmon and fall Chinook salmon in the Columbia River. North American Journal of Fisheries Management 22: 1077-1085.
- Goodman, D.H. and S.B. Reid. 2012. Pacific Lamprey (*Entosphenus tridentatus*) Assessment and Template for Conservation Measures in California. U.S. Fish and Wildlife Service, Arcata, California. 117 pp.
- Greene, S. 1992. Daily fork-length table from data by Frank Fisher, California Department of Fish and Game. California Department of Water Resources, Environmental Services Department, Sacramento.
- Greenwald, G. M., J.T. Earley, and M.R. Brown. 2003. Juvenile salmonid monitoring in Clear Creek, California, from July 2001 to July 2002. USFWS Report. U.S. Fish and Wildlife Service, Red Bluff Fish and Wildlife Office, Red Bluff, California.
- Groot, C. and L.Margolis. 1991. Pacific Salmon Life Histories. UBC Press, Vancouver, B.C.

- Hallock, R.J. Undated. The status of inland habitat and factors adversely impacting salmon resources. Anadromous Fisheries Program, California Department of Fish and Game, Red Bluff, CA.
- Hallock, R.J., W.F. Van Woert, and L. Shapolov. 1961. An Evaluation of Stocking Hatchery-reared Steelhead Rainbow Trout (*Salmo gairdnerii gairdnerii*) in the Sacramento River System. California Department of Fish and Game. Fish Bulletin 114. 74 p.
- Harvey, B. and C. Stroble. 2013 Comparison of genetic versus Delta Model Length-at-Daterun assignments for juvenile Chinook salmon at state and federal south Delta salvage facilities. California Department of Water Resources. Submitted to Interagency Ecological Program for the San Francisco Bay/Delta Estuary. Technical Report 88, March 2013.
- Hastie, T.J. and Tibshirani, R.J (1990) *Generalized Additive Models*, London: Chapman and Hall.
- Hayes, D. B., C. Paolo Ferreri, and W. M. Taylor. 1996. Active Fish Capture Methods. Pages 193-220 in B.R. Murphy and D. W. Willis, editors. Fisheries Techniques, 2nd edition. American Fisheries Society, Bethesda, Maryland.
- Heard, W. R. 1978. Probable case of streambed overseeding-1967 pink salmon, *Oncorhynchus gorbuscha*, spawners and survival of their progeny in Sashin Creek, southeastern Alaska. U.S. National Marine Fisheries Service Fishery Bulletin 76:569-582.
- Hubert, W. A. 1996. Passive capture techniques. Pages 157-192 in B. R. Murphy and D. W. Willis, editors. Fisheries techniques, 2nd edition. American Fisheries Society, Bethesda, Maryland.
- Hubert, W. A. and M.C. Fabrizio. 2007. Relative abundance and catch per unit effort. Pages 279-326 in C.S. Guy and M.L. Brown, editors. Analysis and interpretation of freshwater fisheries data. American Fisheries Society, Bethesda, Maryland.
- Israel, J.A., J.F. Cordes, M.A. Blumberg, and B. May. 2004. Geographic patterns of genetic differentiation among collections of green sturgeon. North American Journal of Fisheries Management 24:922-931.
- Israel, J.A. and B. May. 2010. Indirect genetic estimates of breeding population size in the polyploidy green sturgeon (*Acipenser medirostris*). Molecular Ecology 19, 1058-1070.

- Johnson, R. R. D.C. Weigand and F. W. Fisher. 1992. Use of growth data to determine the spatial and temporal distribution of four runs of juvenile chinook salmon in the Sacramento River, California. Report No. AFF1/FRO-92-15. U. S. Fish and Wildlife Service, Northern Central Valley Fishery Resource Office, Red Bluff, CA.
- Johnson, R. R. and C. D Martin. 1997. Abundance and seasonal, spatial and diel distribution patterns of juvenile salmonids passing Red Bluff Diversion Dam, Sacramento River, July 1994 - June 1995. Red Bluff Research Pumping Plant Report Series, Volume 2. U. S. Fish and Wildlife Service, Red Bluff, CA.
- Johnson M. R. and K. Merrick. 2012. Juvenile Salmonid Monitoring Using Rotary Screw Traps in Deer Creek and Mill Creek, Tehama County, California, Summary Report: 1994-2010. RBFO Technical Report No. 04-2012.
- Katz, J., Moyle, P. B., Quinones, R.M., Israel, J.A. and S.E. Purdy. 2012. Impending extinction of salmon, steelhead and trout (Salmonidae) in California. Environmental Biology of Fish. Published online January 2012.
- Killam, D. 2009. Chinook Salmon Populations for the Upper Sacramento River Basin 2008. Revised 1-11-2010. Northern Region-Department of Fish and Game, Sacramento River Salmon and Steelhead Assessment Project Technical Report No. 09-1.
- Killam, D. 2012. Chinook Salmon Populations for the Upper Sacramento River Basin 2011. Northern Region-Department of Fish and Game, Sacramento River Salmon and Steelhead Assessment Project Technical Report No. 03-2012.
- Kocik, J.F. and W.W. Taylor. 1987. Effect of Fall and Winter Instream Flow on Year-Class Strength of Pacific Salmon Evolutionarily Adapted to Early Fry Outmigration: A Great Lakes Perspective. American Fisheries Society Symposium 1 :430-440.
- Kostow, K. 2002. Oregon lamprey: natural history status and analysis of management issues. Oregon Department of Fish and Wildlife, Corvallis, Oregon. 112 pp.
- Kynard, B., E. Parker, and T. Parker. 2005. Behavior of early life intervals of Klamath River green sturgeon, *Acipenser medirostris*, with a note on body color. Environmental Biology of Fishes 72:85-97.
- Lieberman, D. M., M. J. Horn, S. Duffy. 2001. Effects of a temperature control device on nutrients, POM, and plankton in the tailwaters below Shasta Lake, California. Hydrobiologia 452:191-202.
- Lindley, S. T., C. B. Grimes, M. S. Mohr, W. Peterson, J. Stein, J. T. Anderson, L.W. Botsford, , D. L. Bottom, C. A. Busack, T. K. Collier, J. Ferguson, J. C. Garza,

- A. M. Grover, D. G. Hankin, R. G. Kope, P. W. Lawson, A. Low, R. B. MacFarlane, K. Moore, M. Palmer-Zwahlen, F. B. Schwing, J. Smith, C. Tracy, R. Webb, B. K. Wells, T. H. Williams. 2009. What caused the Sacramento River Fall Chinook stock collapse? Pre-publication report to the Pacific Fishery Management Council.
- Martin, C.D., P.D. Gaines and R.R. Johnson. 2001. Estimating the abundance of Sacramento River juvenile winter Chinook salmon with comparisons to adult escapement. Red Bluff Research Pumping Plant Report Series, Volume 5. U.S. Fish and Wildlife Service, Red Bluff, CA.
- Mayfield, R.B. and J.J. Cech. 2004. Temperature effects on green sturgeon bioenergetics. Transactions of the American Fisheries Society 133:961-970.
- McNeil, W. J. 1968. Migration and distribution of pink salmon spawners in Sashin Creek in 1965, and survival of their progeny. U.S. Fish and Wildlife Service Fishery Bulletin 66:575-586.
- Meeuwig, M. H., J. M. Bayer, and J. G. Seelye. 2005. Effects of temperature on survival and development of early life stage Pacific and western brook lamprey. Transactions of the American Fisheries Society 134:19-27.
- Moffett, J.W. 1949. The First Four Years of King Salmon Maintenance Below Shasta Dam, Sacramento River, California, California Department of Fish and Game 35(2): 77-102.
- Moyle, P. B. 2002. Inland fishes of California. University of California press. Berkeley, California.
- Moyle, P.B., J.A. Israel, and S.E. Purdy. Salmon, Steelhead, and Trout in California in California, Status of an Emblematic Fauna. Report Commissioned by California Trout, 2008. Center for Watershed Sciences, University of California, Davis. Davis, CA.
- Mundie, J.H. and R.E. Traber. 1983. Movements of coho salmon *Onchorhynchus kisutch* fingerlings in a stream following marking with a vital stain. Canadian Journal of Fisheries and Aquatic Science 40:1318-1319.
- National Marine Fisheries Service (NMFS). 2009. Biological Opinion on the Long-term Central Valley Project and State Water Project Operations Criteria and Plan. NOAA (National Oceanic and Atmospheric Administration), National Marine Fisheries Service, Southwest Fisheries Service Center, Long Beach, California.
- Nawa, R. K., J. E. Vaile, P. Lind, T. M. K. Nandananda, T. McKay, C. Elkins, B. Bakke, J. Miller, W. Wood, K. Beardslee, and D. Wales. 2003. A petition for rules to list:

Pacific lamprey (*Lampetratridentata*); river lamprey (*Lampetra ayresi*); western brook lamprey (*Lampetra richardsoni*); and Kern brook lamprey (*Lampetra hubbsi*) as threatened or endangered under the Endangered Species Act. January 23, 2003.

- Neave, F. 1953. Principles affecting the size of pink and chum salmon populations in British Columbia. *Journal of Fisheries Research Board of Canada*. 9:450-491.
- Pope, K. L., C. G. Kruse. 2007. Condition. Pages 423-471 in C. S. Guy and M. L. Brown, editors. *Analysis and interpretation of freshwater fisheries data*. American Fisheries Society, Bethesda, Maryland.
- Poytress, W.R., and F. D. Carrillo. 2008. Brood-year 2006 winter Chinook juvenile production indices with comparisons to juvenile production estimates derived from adult escapement. Report of U.S. Fish and Wildlife Service report to California Bay-Delta Authority and California Department of Fish and Game, Sacramento, CA.
- Poytress, W.R., and F. D. Carrillo. 2012. Brood-year 2010 winter Chinook juvenile production indices with comparisons to juvenile production estimates derived from adult escapement. Report of U.S. Fish and Wildlife Service report to California Department of Fish and Game and US Bureau of Reclamation.
- Poytress, W.R., J.J. Gruber, D.A. Trachtenbarg, and J.P. Van Eenennaam. 2009. 2008 Upper Sacramento River Green Sturgeon Spawning Habitat and Larval Migration Surveys. Annual Report of U.S. Fish and Wildlife Service to US Bureau of Reclamation, Red Bluff, CA.
- Poytress, W.R., J.J. Gruber, and J.P. Van Eenennaam. 2010. 2009 Upper Sacramento River Green Sturgeon Spawning Habitat and Larval Migration Surveys. Annual Report of U.S. Fish and Wildlife Service to U.S. Bureau of Reclamation, Red Bluff, CA.
- Poytress, W.R., J.J. Gruber, and J.P. Van Eenennaam. 2011. 2010 Upper Sacramento River Green Sturgeon Spawning Habitat and Larval Migration Surveys. Annual Report of U.S. Fish and Wildlife Service to U.S. Bureau of Reclamation, Red Bluff, CA.
- Poytress, W.R., and F. D. Carrillo. 2012. Brood-year 2010 winter Chinook juvenile production indices with comparisons to juvenile production estimates derived from adult escapement. Report of U.S. Fish and Wildlife Service report to California Department of Fish and Game and US Bureau of Reclamation.
- Poytress, W.R., J.J. Gruber, and J.P. Van Eenennaam. 2012. 2011 Upper Sacramento River Green Sturgeon Spawning Habitat and Larval Migration Surveys. Annual Report of U.S. Fish and Wildlife Service to U.S. Bureau of Reclamation, Red Bluff, CA.

- Poytress, W.R., J.J. Gruber, C.E. Praetorius, and J.P. Van Eenennaam. 2013. 2012 Upper Sacramento River Green Sturgeon Spawning Habitat and Young-of-the-Year Migration Surveys. Annual Report of U.S. Fish and Wildlife Service to U.S. Bureau of Reclamation, Red Bluff, CA.
- Pyper, B. and C. Justice. 2006. Analyses of rotary screw trap sampling of migrating juvenile Chinook salmon in the Stanislaus River, 1996-2005. Cramer Fish Sciences, Gresham, Oregon.
- Pyper, B., T. Garrison., S. Cramer, P.L. Brandes., D.P. Jacobsen., and M. A. Banks. 2013. Absolute abundance estimates of juvenile spring-run and winter-run Chinook salmon at Chipps Island. Cramer Fish Sciences Technical Report for U.S. Fish and Wildlife Service, Lodi, CA. 89 pp.
- Randall, R. G., Healey, M.C., and J.B. Dempson. 1987. Variability in Length of Freshwater Residence of Salmon, Trout, and Char. American Fisheries Society Symposium 1:27-41.
- Reimers, P.E. 1971. The Length of Residence of Juvenile Fall Chinook Salmon in Sixes River, Oregon. Doctoral Thesis submitted to Oregon State University.
- Roper, B and D. L. Scarnecchia. 1996. A comparison of trap efficiencies for wild and hatchery age-0 Chinook salmon. North American Journal of Fisheries Management 16:214-217.
- Rothchild, B. J. and G.T. DiNardo. 1987. Comparison of Recruitment Variability and Life History Data among Marine and Anadromous Fishes. American Fisheries Society Symposium 1 :531-546.
- Smith, C.T., LaGranve, A.R., and W. R. Ardren in Cooperation with M.A. Banks and D.P. Jacobsen. 2009. Run Composition of Chinook salmon at Red Bluff Diversion Dam during gates-in operations: A comparison of phenotypic and genetic assignment to run type. U.S. Fish and Wildlife Service, Abernathy Fish Technology Center, Longview, WA. CY 2007 Report prepared for U.S. Bureau of Reclamation-Mid Pacific Region, Red Bluff, CA.
- Snider, B., B. Reavis, and S. Hamelburg, S. Croci, S. Hill, and E. Kohler. 1997. 1996 Upper Sacramento River winter-run Chinook salmon escapement survey. California Department of Fish and Game, Environmental Services Division, Sacramento, CA.
- Sokal, R. R. and F. J. Rohlf. 1995. Biometry the principles and practice of statistics in biological research, 3rd edition. W. H. Freeman and Company.

United States Bureau of Reclamation. 1991. Planning report and final environmental statement: Shasta Outflow Temperature Control. USBR, Mid-Pacific Region. Shasta County, California.

United States Bureau of Reclamation. 1994. Sacramento Basin Fish Habitat Improvement Study – Final Environmental Assessment. USBR, Mid-Pacific Region.

United States Fish and Wildlife Service (USFWS). 1995. Working Paper on Restoration Needs. Habitat Restoration Actions to Double Natural Production of Anadromous Fish in the Central Valley of California, Vol. 2. Section 9. May, 1995. Prepared for the US Fish and Wildlife Service under the direction of the Anadromous Fish Restoration Program Core Group. Stockton, CA.

United States Fish and Wildlife Service (USFWS). 1997. Comprehensive Assessment and Monitoring Program (CAMP) Implementation Plan. March, 1997. Prepared by Central Valley Fish and Wildlife Restoration Program Office, Sacramento, CA. Prepared with technical assistance from Montgomery Watson, Jones & Stokes Associates, Inc., and CH2M Hill, Sacramento, CA.

United States Fish and Wildlife Service (USFWS). 2001. Final Restoration Plan for the Anadromous Fish Restoration Program. A plan to increase natural production of anadromous fish in the Central Valley of California. Prepared for the Secretary of the Interior by the United States Fish and Wildlife Service with the assistance from the Anadromous Fish and Restoration Program Core Group under authority of the Central Valley Project Improvement Act.

United States Fish and Wildlife Service (USFWS). 2006. Upper Sacramento River winter Chinook salmon carcass survey 2005 annual report. USFWS, Red Bluff Fish and Wildlife Office, Red Bluff, California.

United States Fish and Wildlife Service (USFWS). 2007. Upper Sacramento River winter Chinook salmon carcass survey 2006 annual report. USFWS, Red Bluff Fish and Wildlife Office, Red Bluff, California.

United States Fish and Wildlife Service (USFWS). 2008. Upper Sacramento River winter Chinook salmon carcass survey 2007 annual report. USFWS, Red Bluff Fish and Wildlife Office, Red Bluff, California.

United States Fish and Wildlife Service (USFWS). 2009. Upper Sacramento River winter Chinook salmon carcass survey 2008 annual report. USFWS, Red Bluff Fish and Wildlife Office, Red Bluff, California.

- United States Fish and Wildlife Service (USFWS). 2010. Upper Sacramento River winter Chinook salmon carcass survey 2009 annual report. USFWS, Red Bluff Fish and Wildlife Office, Red Bluff, California.
- United States Fish and Wildlife Service (USFWS). 2011. Upper Sacramento River winter Chinook salmon carcass survey 2010 annual report. USFWS, Red Bluff Fish and Wildlife Office, Red Bluff, California.
- United States Fish and Wildlife Service (USFWS). 2013. Upper Sacramento River winter Chinook salmon carcass survey 2012 annual report. USFWS, Red Bluff Fish and Wildlife Office, Red Bluff, California.
- Van Eenennaam, J.P., J. Linares-Casenave, X. Deng, and S.I. Doroshov. 2005. Effect of incubation temperature on green sturgeon embryos, *Acipenser medirostris*. *Environmental Biology of Fishes* 72:145-154.
- Vermeyn, T. B. 1997. Use of Temperature Control Curtains to Control Reservoir Release Water Temperatures. Report R-97-09, United States Department of the Interior, Bureau of Reclamation. Water Resources Research Laboratory, Technical Services Center. Denver, Colorado.
- Vogel, D.A. and K.R. Marine. 1991. Guide to Upper Sacramento River Chinook salmon life history. CH2M Hill for the U.S. Bureau of Reclamation Central Valley Project, Redding, CA.
- Volkhardt, G. C., S.L. Johnson, B.A. Miller, T.E. Nickelson, and D. E. Seiler. 2007. Rotary screw traps and inclined plane screen traps. Pages 235-266 in D. H. Johnson, B. M. Shrier, J.S. O'Neil, J. A. Knutzen, X. Augerot, T. A. O'Neil and T. N. Pearsons. *Salmonid field protocols handbook: techniques for assessing status and trends in salmon and trout populations*. American Fisheries Society, Bethesda, Maryland.
- Wales, J.H., and M. Coots. 1955. Efficiency of chinook salmon spawning in Fall Creek, California. *Transactions of American Fisheries Society*. 84:137-149.
- Wells, R. A. and W. J. McNeil. 1970. Effect of quality of spawning bed on growth and development of pink salmon embryos and alevins. U.S. Fish and Wildlife Service Special Scientific Report Fisheries 616.
- Whitton, K. S., D. J. Colby, J. M. Newton, and M. R. Brown. 2008. Juvenile salmonid monitoring in Battle Creek, California, November 2007 through June 2008. USFWS Report. U.S. Fish and Wildlife Service, Red Bluff Fish and Wildlife Office, Red Bluff, California.

- Williams, J. G. 2006. Central Valley Salmon, A Perspective on Chinook and Steelhead in the Central Valley of California. San Francisco Estuary and Watershed Science. Volume 4, Issue 3, Article 2.
- Zabel, R. W. and S. Achord. 2004. Relating size of juveniles to survival within and among populations of Chinook salmon. *Ecology*, 85 (3), pp. 795-806.
- Zimmerman C.E., and G. H., Reeves. 2000. Population structure of sympatric anadromous and nonanadromous *Oncorhynchus mykiss*: evidence from spawning surveys and otolith microchemistry. *Canadian Journal of Fisheries and Aquatic Sciences* 57:2152–2162.

Tables

Table 1. Summary of annual RBDD rotary trap sample effort by run and species for the period April 2002 through September 2013, by brood year (BY).

BY	Fall	Late-Fall	Winter	Spring	<i>O. mykiss</i>
2002	0.76	0.57	0.64	0.75	0.53
2003	0.81	0.76	0.81	0.81	0.76
2004	0.85	0.88	0.84	0.85	0.83
2005	0.56	0.73	0.64	0.57	0.83
2006	0.90	0.70	0.83	0.89	0.59
2007	0.88	0.90	0.89	0.89	0.91
2008	0.79	0.89	0.87	0.85	0.89
2009	0.84	0.72	0.75	0.79	0.76
2010	0.75	0.86	0.81	0.77	0.85
2011	0.87	0.77	0.82	0.86	0.76
2012	0.85	0.89	0.89	0.86	0.86
Min	0.56	0.57	0.64	0.57	0.53
Max	0.90	0.90	0.89	0.89	0.91
Mean	0.81	0.79	0.80	0.81	0.78
SD	0.094	0.104	0.088	0.091	0.122
CV	11.7%	13.2%	10.9%	11.3%	15.6%

Table 2. Summary of mark-recapture experiments conducted by RBDD rotary trap project between 2002 and 2013. Summaries include trap effort data, fish release and recapture group sizes (N) and mean fork lengths (FL), percentage of river discharge sampled (%Q) and estimated trap efficiency for each trial (%TE). Model data below each trial period indicate dates model was employed, total trials incorporated into model and linear regression values of slope, intercept, p -value and coefficient of determination.

Date	Run	# Traps Sampling	Traps		Release Group		Recapture Group		%Q	%TE
			Modified	RBDD Gates	N	FL (mm)	N	FL (mm)		
6/26/2002	Fall ¹	4	Yes	Lowered	805	68.7	8	61.3	1.58	0.99
8/6/2002	Fall ¹	4	Yes	Lowered	743	69.7	16	80.2	1.66	2.15
8/20/2002	Fall ¹	3	Yes	Lowered	340	76.5	7	77.7	1.41	2.06
Model	Employed	#Trials	Slope	Intercept	P	R^2				
7/1/2002 -	6/30/2003	61	0.00792	0.00003205	<0.0001	0.394				
Date	Run	# Traps Sampling	Traps		Release Group		Recapture Group		%Q	%TE
			Modified	RBDD Gates	N	FL (mm)	N	FL (mm)		
1/28/2003	Fall	4	Yes	Raised	5,143	36.8	33	37.0	0.75	0.64
2/5/2003	Fall	4	Yes	Raised	2,942	36.7	10	37.9	1.36	0.34
2/10/2003	Fall	4	Yes	Raised	3,106	37.8	29	37.9	1.59	0.93
2/21/2003	Fall	3	Yes	Raised	3,256	37.4	15	37.3	0.72	0.46
2/26/2003	Fall	4	Yes	Raised	2,019	37.0	22	37.2	1.14	1.09
3/1/2003	Fall	4	No	Raised	1,456	37.0	31	37.0	3.31	2.13
3/4/2003	Fall	4	No	Raised	1,168	37.1	28	37.4	3.76	2.40
3/7/2003	Fall	4	No	Raised	1,053	37.4	22	36.6	3.58	2.09
3/20/2003	Fall	3	No	Raised	1,067	38.2	17	38.3	2.83	1.59
9/2/2003	Winter	4	No	Lowered	1,119	37.1	14	36.1	2.03	1.25
9/5/2003	Winter	3	No	Lowered	1,283	36.7	26	37.2	2.52	2.03
9/8/2003	Winter	3	No	Lowered	1,197	37.3	30	37.1	2.57	2.51
9/23/2003	Winter	3	No	Raised	1,012	35.5	18	35.6	2.20	1.78

9/27/2003	Winter	4	No	Raised	1,017	36.9	28	36.6	2.93	2.75
10/1/2003	Winter	4	No	Raised	1,064	37.6	20	36.7	3.09	1.88
10/6/2003	Winter	4	No	Raised	999	37.2	22	36.8	2.82	2.20
10/10/2003	Winter	4	No	Raised	1,017	38.1	16	38.3	3.06	1.57
10/15/2003	Winter	4	No	Raised	1,209	38.0	26	37.6	2.98	2.15
Model	Employed	#Trials	Slope	Intercept	<i>P</i>	<i>R</i> ²				
7/1/2003 -	6/30/2004	79	0.00752	0.00046251	<0.0001	0.426				

Date	Run	# Traps Sampling	Traps Modified	RBDD Gates	Release Group		Recapture Group		%Q	%TE
					<i>N</i>	FL (mm)	<i>N</i>	FL (mm)		
1/18/2004	Fall	4	Yes	Raised	2,074	37.1	26	37.1	1.52	1.25
1/24/2004	Fall	4	Yes	Raised	2,018	38.4	36	37.4	1.79	1.78
1/31/2004	Fall	4	Yes	Raised	2,024	37.7	33	37.6	1.61	1.63
2/6/2004	Fall	4	Yes	Raised	1,999	37.9	31	38.0	1.61	1.55
2/9/2004	Fall	4	Yes	Raised	2,017	37.8	27	37.0	1.69	1.34
2/13/2004	Fall	4	Yes	Raised	2,009	37.2	31	38.3	1.87	1.54
3/14/2004	Fall	3	No	Raised	1,401	38.3	18	39.6	1.98	1.28
3/23/2004	Fall	3	No	Raised	815	38.8	15	39.1	2.50	1.84
4/28/2004	Fall ¹	4	Yes	Raised	1,304	72.9	33	71.7	1.94	2.53
5/4/2004	Fall ¹	4	No	Raised	814	75.5	18	75.1	3.35	2.21
5/18/2004	Fall ¹	4	No	Lowered	867	80.2	10	75.1	3.20	1.15
5/26/2004	Fall ¹	4	No	Lowered	1,096	81.2	27	80.2	2.83	2.46
6/2/2004	Fall ¹	4	No	Lowered	888	76.2	28	77.2	2.77	3.15
6/15/2004	Fall ¹	4	No	Lowered	691	76.4	12	79.1	2.17	1.74
8/31/2004	Winter	4	No	Lowered	1,096	36.5	41	36.0	3.00	3.74
9/3/2004	Winter	4	No	Lowered	1,153	36.6	50	35.6	3.23	4.34
9/17/2004	Winter	4	No	Raised	1,023	36.0	14	35.4	2.52	1.37

9/20/2004	Winter	4	No	Raised	1,017	35.8	21	35.4	2.48	2.06
9/23/2004	Winter	4	No	Raised	2,006	36.0	31	35.1	2.62	1.55
9/27/2004	Winter	4	No	Raised	1,918	36.1	36	36.1	2.77	1.88
10/1/2004	Winter	4	No	Raised	1,682	36.4	24	36.0	3.11	1.43
Model	Employed	#Trials	Slope	Intercept	<i>P</i>	<i>R</i> ²				
7/1/2004 -	6/30/2006	99	0.007464	0.00087452	<0.0001	0.385				

Date	Run	# Traps Sampling	Traps Modified	RBDD Gates	Release Group		Recapture Group		%Q	%TE
					<i>N</i>	FL (mm)	<i>N</i>	FL (mm)		
1/23/2005	Fall	4	No	Raised	1,283	36.6	41	37.2	4.21	3.20
2/1/2005	Fall	3	Yes	Raised	1,971	36.6	31	36.0	1.35	1.57
2/10/2005	Fall	4	No	Raised	1,763	36.6	46	36.7	4.06	2.61
3/10/2005	Fall	4	No	Raised	1,216	36.6	27	36.5	3.93	2.22
3/13/2005	Fall	4	No	Raised	1,328	36.3	43	35.6	4.06	3.24
4/1/2005	Fall	4	No	Raised	1,949	57.1	50	62.3	3.49	2.57
9/11/2005	Winter	4	No	Lowered	1,437	35.6	14	38.9	2.22	0.97
10/4/2005	Winter	4	No	Raised	1,587	35.9	14	36.1	1.83	0.88
10/13/2005	Winter	4	No	Raised	1,577	35.7	21	36.6	2.33	1.33
2/15/2006	Fall	4	No	Raised	1,610	37.4	33	36.6	3.19	2.05
2/23/2006	Fall	4	No	Raised	1,503	37.2	38	36.6	2.68	2.53
1/21/2007	Fall	4	No	Raised	1,520	0.0	33	37.8	4.02	2.17
1/28/2007	Fall	4	Yes	Raised	1,987	37.6	18	37.8	3.65	0.91
2/5/2007	Fall	3	Yes	Raised	2,909	37.5	29	37.3	1.62	1.00
2/16/2007	Fall	4	No	Raised	1,782	37.9	34	38.5	3.51	1.91
3/2/2007	Fall	4	No	Raised	1,591	38.5	54	38.6	3.68	3.39
3/15/2007	Fall	4	No	Raised	953	37.6	26	37.6	4.29	2.73
3/20/2007	Fall	4	No	Raised	835	37.6	23	38.8	4.18	2.75

3/24/2007	Fall	4	No	Raised	944	37.7	23	38.0	4.24	2.44
Model	Employed	#Trials	Slope	Intercept	<i>P</i>	<i>R</i> ²				
7/1/2006 -	6/30/2007	118	0.006653	0.00240145	<0.0001	0.420				
Date	Run	# Traps Sampling	Traps Modified	RBDD Gates	Release Group		Recapture Group		%Q	%TE
					<i>N</i>	FL (mm)	<i>N</i>	FL (mm)		
1/23/2008	Fall	4	No	Raised	2,234	38.4	50	38.2	3.99	2.24
2/7/2008	Fall	4	Yes	Raised	2,324	38.1	60	37.9	2.19	2.58
2/14/2008	Fall	4	Mixed	Raised	1,993	38.4	83	38.8	3.40	4.16
2/20/2008	Fall	4	No	Raised	1,703	37.2	48	36.8	5.29	2.82
2/28/2008	Fall	3	No	Raised	2,080	37.6	63	38.3	3.45	3.03
Model	Employed	#Trials	Slope	Intercept	<i>P</i>	<i>R</i> ²				
7/1/2007 -	6/30/2008	123	0.00645	0.00303101	<0.0001	0.414				
Date	Run	# Traps Sampling	Traps Modified	RBDD Gates	Release Group		Recapture Group		%Q	%TE
					<i>N</i>	FL (mm)	<i>N</i>	FL (mm)		
1/23/2009	Fall	4	No	Raised	1,923	36.1	54	37.1	4.53	2.81
2/5/2009	Fall	4	No	Raised	1,868	36.8	58	37.4	4.65	3.10
Model	Employed	#Trials	Slope	Intercept	<i>P</i>	<i>R</i> ²				
7/1/2008 -	6/30/2010	125	0.006332	0.00328530	<0.0001	0.425				
Date	Run	# Traps Sampling	Traps Modified	RBDD Gates	Release Group		Recapture Group		%Q	%TE
					<i>N</i>	FL (mm)	<i>N</i>	FL (mm)		
1/20/2011	Fall	4	No	Raised	1,834	36.9	79	35.9	3.92	4.31
1/26/2011	Fall	4	No	Raised	1,989	37.6	109	36.0	4.56	5.48
2/1/2011	Fall	4	No	Raised	1,593	36.4	61	36.0	5.04	3.83

2/11/2011	Fall	4	No	Raised	1,582	35.7	81	37.4	5.34	5.12
Model	Employed	#Trials	Slope	Intercept	<i>P</i>	<i>R</i> ²				
7/1/2010 -	6/30/2012	129	0.007297	0.00123101	<0.0001	0.493				
Date	Run	# Traps Sampling	Traps Modified	RBDD Gates	Release Group		Recapture Group		%Q	%TE
					<i>N</i>	FL (mm)	<i>N</i>	FL (mm)		
1/30/2012	Fall	4	No	Raised	1,319	36.3	46	36.1	4.08	3.49
2/4/2012	Fall	4	No	Raised	1,146	35.8	51	35.4	5.52	4.45
2/16/2012	Fall	4	No	Raised	1,465	35.7	73	35.0	5.36	4.98
2/28/2012	Fall	4	No	Raised	1,228	35.5	57	34.6	5.40	4.64
Model	Employed	#Trials	Slope	Intercept	<i>P</i>	<i>R</i> ²				
7/1/2012 -	6/30/2012	133	0.007676	0.00037735	<0.0001	0.561				
Date	Run	# Traps Sampling	Traps Modified	RBDD Gates	Release Group		Recapture Group		%Q	%TE
					<i>N</i>	FL (mm)	<i>N</i>	FL (mm)		
1/16/2013	Fall	4	Yes	Raised	1,991	35.6	72	35.8	2.56	3.62
1/23/2013	Fall	4	Yes	Raised	1,965	35.9	39	35.3	2.61	1.98
1/30/2013	Fall	4	Yes	Raised	1,981	36.3	44	35.6	2.57	2.22
2/3/2013	Fall	4	Yes	Raised	1,998	36.5	42	36.1	2.69	2.10
2/13/2013	Fall	4	Yes	Raised	2,079	36.3	48	36.2	2.62	2.31
2/18/2013	Fall	4	Yes	Raised	2,156	36.1	35	36.8	2.89	1.62
2/22/2013	Fall	4	No	Raised	2,439	36.7	119	36.6	6.52	4.88
2/26/2013	Fall	4	No	Raised	1,400	36.1	65	37.3	6.87	4.64
3/3/2013	Fall	4	No	Raised	899	36.5	37	36.9	6.71	4.12
Model	Employed	#Trials	Slope	Intercept	<i>P</i>	<i>R</i> ²				
7/1/2013 -	9/30/2013	142	0.007255	0.00150868	<0.0001	0.587				

¹ Denotes Coleman National Fish Hatchery Fall Chinook production fish used during trial.

Table 3. Annual capture fork length summary of *O. mykiss* by age and life-stage classification from the RBDD rotary trap project between April 2002 through December 2012 by calendar year (CY).

Age Classification (%)					Life Stage Classification (%)					
CY	Fry <41 mm	Sub-Yearling 41-138 mm	Yearling 139-280 mm	2+ >280 mm	CY	Yolk- sac Fry	Fry	Parr	Silvery- parr	Smolt
2002	11.2	86.7	1.6	0.5	2002	0.0	6.3	54.4	37.2	2.1
2003	8.1	89.5	2.3	0.0	2003	0.0	5.6	57.7	34.9	1.8
2004	9.8	89.7	0.5	0.0	2004	0.0	4.6	60.2	34.7	0.5
2005	3.5	93.2	3.1	0.2	2005	0.0	2.8	48.7	45.6	2.9
2006	17.5	75.3	5.6	1.5	2006	0.2	9.2	78.9	9.2	2.4
2007	6.5	91.2	1.7	0.6	2007	0.1	8.7	85.3	5.3	0.6
2008	6.3	92.3	0.9	0.5	2008	0.1	8.2	79.4	12.0	0.4
2009	9.0	87.7	2.1	1.2	2009	0.0	10.7	82.8	5.1	1.4
2010	7.7	89.8	1.7	0.8	2010	0.3	9.7	87.4	1.7	1.0
2011	4.6	89.7	5.0	0.6	2011	0.1	3.5	90.9	2.8	2.7
2012	6.6	90.0	2.3	1.1	2012	0.2	5.9	88.2	4.2	1.5
Mean	8.3	88.7	2.4	0.6	Mean	0.1	6.8	74.0	17.5	1.6
SD	3.8	4.8	1.6	0.5	SD	0.1	2.6	15.5	16.8	0.9

Table 4. Annual linear regression equations with 95% confidence intervals (CI) for Log_{10} transformed juvenile (80-200 mm) *O. mykiss* weight-length data sampled at the RBDD rotary traps from April 2002 through December 2012 by calendar year (CY).

CY	Weight-Length Equation	R^2	Slope	
			Lower 95% CI	Upper 95% CI
2002	$\text{Log}_{10}(\text{weight})=2.843(\text{Log}_{10}\text{FL})-4.616$	0.903	2.648	3.039
2003	$\text{Log}_{10}(\text{weight})=2.968(\text{Log}_{10}\text{FL})-4.886$	0.968	2.885	3.052
2004	$\text{Log}_{10}(\text{weight})=3.005(\text{Log}_{10}\text{FL})-4.941$	0.952	2.879	3.132
2005	$\text{Log}_{10}(\text{weight})=3.03(\text{Log}_{10}\text{FL})-5.009$	0.952	2.929	3.132
2006	$\text{Log}_{10}(\text{weight})=3.052(\text{Log}_{10}\text{FL})-5.085$	0.917	2.811	3.293
2007	$\text{Log}_{10}(\text{weight})=2.961(\text{Log}_{10}\text{FL})-4.864$	0.947	2.853	3.069
2008	$\text{Log}_{10}(\text{weight})=2.939(\text{Log}_{10}\text{FL})-4.819$	0.942	2.833	3.044
2009	$\text{Log}_{10}(\text{weight})=3.017(\text{Log}_{10}\text{FL})-4.981$	0.974	2.922	3.112
2010	$\text{Log}_{10}(\text{weight})=2.977(\text{Log}_{10}\text{FL})-4.911$	0.934	2.836	3.118
2011	$\text{Log}_{10}(\text{weight})=2.911(\text{Log}_{10}\text{FL})-4.778$	0.939	2.743	3.078
2012	$\text{Log}_{10}(\text{weight})=2.858(\text{Log}_{10}\text{FL})-4.662$	0.903	2.746	2.970
Mean	$\text{Log}_{10}(\text{weight})=2.946(\text{Log}_{10}\text{FL})-4.840$	0.942	2.913	2.979

Table 5a. RBDD rotary trap fall Chinook total annual effort and passage estimates (sum of weekly values), lower and upper 90% confidence intervals (CI), ratio of fry to pre-smolt/smolt passage and ratio of estimated passage (Est) and interpolated passage (Interp) for brood year (BY) 2002-2012.

BY	Effort	Total	Low 90%CI	Up 90% CI	Fry	Smolt	Est	Interp
2002	0.76	17,038,417	857,106	47,315,257	0.86	0.14	0.54	0.46
2003	0.81	27,736,868	8,839,840	50,653,446	0.85	0.15	0.74	0.26
2004	0.85	14,108,238	5,079,300	24,967,671	0.56	0.44	0.70	0.30
2005	0.56	18,210,294	3,500,275	39,096,017	0.64	0.36	0.40	0.60
2006	0.90	16,107,651	6,522,666	26,414,402	0.63	0.37	0.85	0.15
2007	0.88	12,131,603	6,130,892	18,170,520	0.79	0.21	0.84	0.16
2008	0.79	9,115,547	4,381,560	13,849,709	0.73	0.27	0.81	0.19
2009	0.84	8,532,377	3,064,273	14,052,588	0.81	0.19	0.56	0.44
2010	0.75	8,842,481	4,727,816	13,252,907	0.71	0.29	0.79	0.21
2011	0.87	6,271,261	3,431,940	9,125,109	0.71	0.29	0.82	0.18
2012	0.85	24,429,420	16,028,521	33,112,943	0.87	0.13	0.91	0.09
Mean	0.81	14,774,923			0.74	0.26	0.72	0.28
SD	0.09	6,825,382			0.10	0.10	0.16	0.16
CV	11.7%	46.2%			13.9%	40.3%	22.0%	57.4%

Table 5b. RBDD rotary trap late-fall Chinook total annual effort and passage estimates (sum of weekly values), lower and upper 90% confidence intervals (CI), ratio of fry to pre-smolt/smolt passage and ratio of estimated passage (Est) and interpolated passage (Interp) for brood year (BY) 2002-2012.

BY	Effort	Total	Low 90%CI	Up 90% CI	Fry	Smolt	Est	Interp
2002	0.57	2,559,519	659,986	4,953,910	0.17	0.83	0.52	0.48
2003	0.76	346,058	78,407	911,270	0.57	0.43	0.56	0.44
2004	0.88	147,160	74,930	220,231	0.17	0.83	0.91	0.09
2005	0.73	143,362	41,800	333,415	0.35	0.65	0.71	0.29
2006	0.70	460,268	125,197	902,089	0.62	0.38	0.44	0.56
2007	0.90	535,619	271,079	800,447	0.27	0.73	0.86	0.14
2008	0.89	91,995	46,660	138,310	0.11	0.89	0.89	0.11
2009	0.72	219,824	97,294	342,652	0.13	0.87	0.73	0.27
2010	0.86	183,439	61,775	305,937	0.62	0.38	0.61	0.39
2011	0.77	97,040	28,738	165,997	0.72	0.28	0.53	0.47
2012	0.89	140,534	42,673	249,500	0.48	0.52	0.80	0.20
Mean	0.79	447,711			0.38	0.62	0.69	0.31
SD	0.10	715,999			0.23	0.23	0.16	0.16
CV	13.2%	159.9%			58.8%	36.5%	23.8%	52.5%

Table 5c. RBDD rotary trap winter Chinook total annual effort and passage estimates (sum of weekly values), lower and upper 90% confidence intervals (CI), ratio of fry to pre-smolt/smolt passage and ratio of estimated passage (Est) and interpolated passage (Interp) for brood year (BY) 2002-2012.

BY	Effort	Total	Low 90%CI	Up 90% CI	Fry	Smolt	Est	Interp
2002	0.64	7,119,041	2,541,407	12,353,367	0.90	0.10	0.58	0.42
2003	0.81	5,221,016	3,202,609	7,260,798	0.85	0.15	0.86	0.14
2004	0.84	3,434,683	1,998,468	4,874,794	0.90	0.10	0.82	0.18
2005	0.64	8,363,106	4,558,069	12,277,233	0.90	0.10	0.89	0.11
2006	0.83	6,687,079	3,801,539	9,575,937	0.87	0.13	0.76	0.24
2007	0.89	1,440,563	931,113	1,953,688	0.80	0.20	0.92	0.08
2008	0.87	1,244,990	776,634	1,714,013	0.85	0.15	0.77	0.23
2009	0.75	4,402,322	2,495,734	6,311,739	0.81	0.19	0.74	0.26
2010	0.81	1,285,389	817,207	1,756,987	0.68	0.32	0.92	0.08
2011	0.82	848,976	576,177	1,122,022	0.75	0.25	0.88	0.12
2012	0.89	1,349,819	904,552	1,795,106	0.53	0.47	0.92	0.08
Mean	0.80	3,763,362			0.80	0.20	0.82	0.18
SD	0.09	2,753,256			0.11	0.11	0.11	0.11
CV	10.9%	73.2%			13.9%	57.5%	12.8%	59.6%

Table 5d. RBDD rotary trap spring Chinook total annual effort and passage estimates (sum of weekly values), lower and upper 90% confidence intervals (CI), ratio of fry to pre-smolt/smolt passage and ratio of estimated passage (Est) and interpolated passage (Interp) for brood year (BY) 2002-2012.

BY	Effort	Total	Low 90%CI	Up 90% CI	Fry	Smolt	Est	Interp
2002	0.75	277,477	110,951	494,590	0.57	0.43	0.59	0.41
2003	0.81	626,915	249,225	1,053,421	0.80	0.20	0.67	0.33
2004	0.85	430,951	174,174	710,419	0.36	0.64	0.78	0.22
2005	0.57	616,040	131,328	1,382,036	0.69	0.30	0.58	0.42
2006	0.89	421,436	239,470	603,952	0.41	0.59	0.80	0.20
2007	0.89	369,536	229,766	510,868	0.91	0.09	0.99	0.01
2008	0.85	164,673	66,515	262,959	0.24	0.76	0.62	0.38
2009	0.79	438,405	176,952	700,959	0.50	0.50	0.51	0.49
2010	0.77	158,966	62,563	261,105	0.56	0.44	0.67	0.33
2011	0.86	184,290	101,443	272,769	0.48	0.52	0.85	0.15
2012	0.86	320,897	173,312	469,137	0.42	0.58	0.74	0.26
Mean	0.81	364,508			0.54	0.46	0.71	0.29
SD	0.09	164,135			0.20	0.20	0.14	0.14
CV	11.3%	45.0%			36.4%	43.0%	19.7%	47.6%

Table 5e. RBDD rotary trap *O. mykiss* total annual effort and passage estimates (sum of weekly values), lower and upper 90% confidence intervals (CI), and ratio of estimated passage (Est) and interpolated passage (Interp) for calendar year (CY) 2002-2012.

CY	Effort	Total	Low 90%CI	Up 90% CI	Est	Interp
2002 ¹	0.53	124,436	27,224	244,701	0.53	0.47
2003	0.76	139,008	54,885	243,927	0.78	0.22
2004	0.83	151,694	86,857	218,132	0.95	0.05
2005	0.83	85,614	32,251	152,568	0.76	0.24
2006	0.59	83,801	20,603	169,712	0.44	0.56
2007	0.91	139,424	73,827	205,647	0.89	0.11
2008	0.89	131,013	69,331	193,584	0.88	0.12
2009	0.76	129,581	62,350	197,795	0.83	0.17
2010	0.85	100,997	47,050	155,692	0.74	0.26
2011	0.76	56,798	23,494	89,369	0.76	0.24
2012	0.86	136,621	78,804	194,892	0.96	0.04
Mean	0.78	116,272			0.78	0.22
SD	0.12	29,912			0.16	0.16
CV	15.6%	25.7%			20.9%	72.2%

¹ Incomplete year; sampling began in April 2002.

Table 6a. Fall Chinook fry-equivalent production estimates, lower and upper 90% confidence intervals (CI), estimates of adults upstream of RBDD (Adult Estimate), estimated female to male sex ratios, estimated females, estimates of female fecundity, calculated juveniles per estimated female (recruits per female) and egg-to-fry survival estimates (ETF) by brood year (BY) for Chinook sampled at RBDD rotary traps between December 2002 and September 2013.

BY	FRY EQ Passage	Lower 90% CI	Upper 90% CI	Adult Estimate	Sex Ratio (F: M) ¹		Estimated Females	Fecundity ²	Recruits per Female	ETF
2002	18,683,720	1,216,244	51,024,926	458,772	<i>0.46</i>	<i>0.54</i>	211,035	5,407	89	1.6%
2003	30,624,209	10,162,712	55,109,506	140,724	0.57	0.44	79,509	5,407	385	7.1%
2004	18,421,457	6,224,790	33,728,746	64,276	0.48	0.52	31,045	5,407	593	11.0%
2005	22,739,315	4,235,720	49,182,045	80,294	0.47	0.53	37,738	5,407	603	11.1%
2006	20,276,322	8,670,090	32,604,760	78,692	0.54	0.46	42,730	5,407	475	8.8%
2007	13,907,856	7,041,759	20,838,463	31,592	0.54	0.46	16,996	5,407	818	15.1%
2008	10,817,397	5,117,059	16,517,847	36,104	0.46	0.54	16,644	5,407	650	12.0%
2009	9,674,829	3,678,373	15,723,368	12,908	0.51	0.49	6,531	5,407	1,481	27.4%
2010	10,620,144	5,637,617	15,895,197	29,321	0.24	0.76	7,008	5,407	1,515	28.0%
2011	7,554,574	4,171,332	10,960,125	31,931	0.29	0.71	9,260	5,407	816	15.1%
2012	26,567,379	17,219,525	36,197,837	65,664	0.50	0.50	32,635	5,407	814	15.1%
Mean	17,262,473	6,670,475	30,707,529	93,662	0.46	0.54	44,648		749	13.9%
CV	43.2%	64.0%	51.7%	134.7%			132.4%		57.2%	57.2%

¹ Sex ratios based on RBDD fish ladder data between 2003 and 2007 and CNFH data between 2008 and 2012. Average, in italics, input for 2002 due to lack of available data.

² Female fecundity estimates based on average values from CNFH fall Chinook spawning data collected between 2008 and 2012.

Table 6b. Late-fall Chinook fry-equivalent production estimates, lower and upper 90% confidence intervals (CI), estimates of adults upstream of RBDD (Adult Estimate), estimated female to male sex ratios, estimated females, estimates of female fecundity, calculated juveniles per estimated female, and egg-to-fry survival estimates (ETF) by brood year (BY) for Chinook sampled at RBDD rotary traps between April 2002 and March 2013.

BY	FRY EQ Passage	Lower 90% CI	Upper 90% CI	Adult Estimate	Sex Ratio (F: M) ¹		Estimated Females	Fecundity ²	Recruits per Female	ETF
2002	4,041,505	1,063,720	7,808,619	36,220	0.46	0.54	16,661	4,662	243	5.2%
2003	451,230	133,225	1,067,819	5,513	0.46	0.54	2,536	4,662	178	3.8%
2004	233,106	124,245	342,837	8,924	0.46	0.54	4,105	4,662	57	1.2%
2005	209,066	70,548	441,133	9,610	0.46	0.54	4,421	4,662	47	1.0%
2006	582,956	186,984	1,086,699	7,770	0.46	0.54	3,574	4,662	163	3.5%
2007	809,272	426,272	1,192,625	13,939	0.46	0.54	6,412	4,662	126	2.7%
2008	149,049	80,500	218,597	3,747	0.46	0.54	1,724	4,662	86	1.9%
2009	353,003	159,726	546,546	3,792	0.46	0.54	1,744	4,662	202	4.3%
2010	232,279	89,343	376,286	3,961	0.46	0.54	1,822	4,662	127	2.7%
2011	116,188	38,688	194,400	3,777	0.46	0.54	1,737	4,662	67	1.4%
2012	191,672	69,229	325,189	2,931	0.46	0.54	1,348	4,662	142	3.0%
Mean	669,939	222,044	1,236,432	9,108			4,190		131	2.8%
CV	169.8%	134.4%	178.7%	105.5%			105.5%		48.1%	48.1%

¹ Sex ratio value of (0.46:0.54) is equivalent to the average ratio for fall Chinook between 2003 and 2012 used in Table 6a.

² Female fecundity estimates based on average values from CNFH late-fall Chinook spawning data collected between 2008 and 2012.

Table 6c. Winter Chinook fry-equivalent production estimates, lower and upper 90% confidence intervals (CI), estimates of adults upstream of RBDD (Adult Estimate), estimated female to male sex ratios, estimated females, estimates of female fecundity, calculated juveniles per estimated female (recruits per female) and egg-to-fry survival estimates (ETF) by brood year (BY) for Chinook sampled at RBDD rotary traps between July 2002 and June 2013.

BY	FRY EQ Passage	Lower 90% CI	Upper 90% CI	Adult Estimate	Sex Ratio (F: M) ¹		Estimated Females	Fecundity ²	Recruits per Female	ETF
2002	7,635,469	2,811,132	13,144,325	7337	0.77	0.23	5,670	4,923	1,347	27.4%
2003	5,781,519	3,525,098	8,073,129	8133	0.64	0.36	5,179	4,854	1,116	23.0%
2004	3,677,989	2,129,297	5,232,037	8635	0.37	0.63	3,185	5,515	1,155	20.9%
2005	8,943,194	4,791,726	13,277,637	15730	0.56	0.44	8,807	5,500	1,015	18.5%
2006	7,298,838	4,150,323	10,453,765	17205	0.50	0.50	8,626	5,484	846	15.4%
2007	1,637,804	1,062,780	2,218,745	2488	0.61	0.39	1,517	5,112	1,080	21.1%
2008	1,371,739	858,933	1,885,141	2850	0.51	0.49	1,443	5,424	951	17.5%
2009	4,972,954	2,790,092	7,160,098	4537	0.60	0.40	2,702	5,519	1,840	33.3%
2010	1,572,628	969,016	2,181,572	1533	0.53	0.47	813	5,161	1,934	37.5%
2011	996,621	671,779	1,321,708	824	0.51	0.49	424	4,832	2,351	48.6%
2012	1,789,259	1,157,240	2,421,277	2581	0.58	0.42	1,491	4,518	1,200	26.6%
Mean	4,152,547	2,265,220	6,124,494	6,532	0.56	0.44	3,623	5,167	1,349	26.4%
CV	70.1%	64.0%	74.9%	85.7%	17.9%	22.9%	83.4%	6.7%	35.5%	37.9%

¹ Annual sex ratio values based on annual carcass survey estimates of female recoveries.

² Female fecundity estimates based on annual values from LSNFH winter Chinook spawning data collected between 2002 and 2012.

Table 6d. Spring Chinook fry-equivalent production estimates, lower and upper 90% confidence intervals (CI), estimates of adults upstream of RBDD (Adult Estimate), estimated female to male sex ratios, estimated females, estimates of female fecundity, calculated juveniles per estimated female (recruits per female) and egg-to-fry survival estimates (ETF) by brood year (BY) for Chinook sampled at RBDD rotary traps between October 16, 2002 and September 30, 2013.

BY	FRY EQ Passage	Lower 90% CI	Upper 90% CI	Adult Estimate	Sex Ratio (F: M) ¹	Estimated Females	Fecundity ²	Recruits per Female	ETF
2002	360,352	142,134	657,043	608	0.46 0.54	280	5,078	1,288	25.4%
2003	714,086	293,095	1,187,827	319	0.46 0.54	147	5,078	4,866	95.8%
2004	624,079	255,886	1,029,162	575	0.46 0.54	265	5,078	2,359	46.5%
2005	747,026	146,488	1,695,236	189	0.46 0.54	87	5,078	8,592	169.2%
2006	594,511	328,845	860,757	353	0.46 0.54	162	5,078	3,661	72.1%
2007	392,451	242,563	544,184	767	0.46 0.54	353	5,078	1,112	21.9%
2008	251,795	96,737	406,863	305	0.46 0.54	140	5,078	1,795	35.3%
2009	591,549	238,710	945,904	314	0.46 0.54	144	5,078	4,095	80.7%
2010	207,793	80,320	344,475	208	0.46 0.54	96	5,078	2,172	42.8%
2011	251,444	130,051	382,077	167	0.46 0.54	77	5,078	3,273	64.5%
2012	451,705	238,187	665,825	868	0.46 0.54	399	5,078	1,131	22.3%
Mean	471,527	199,365	792,668	425		195		3,122	61.5%
CV	40.9%	41.7%	51.5%	56.8%		56.8%		70.8%	70.8%

¹ Sex ratio value of (0.46:0.54) is equivalent to the average ratio for fall Chinook between 2003 and 2012 used in Table 6a.

² Female fecundity estimates based on average of winter, fall, and late-fall hatchery data provided by CNFH and LSNFH; Table 6a-6c above.

Table 7. Green Sturgeon annual capture, catch per unit volume (CPUV) and total length summaries for sturgeon captured by RBDD rotary traps between calendar year (CY) 2002 and 2012.

CY	Captures	CPUV fish/ac-ft	Min TL (mm)	Max TL (mm)	Mean (mm)	Median (mm)
2002	35	0.3	23	52	28.8	27.5
2003	360	1.9	22	188	27.8	27
2004	266	1.0	21	58	30.5	29
2005	271	1.1	24	65	28.9	27
2006	193	0.8	21	79	30.5	28
2007	19	0.1	25	49	29.6	27
2008	0	0.0	-	-	-	-
2009	32	0.2	24	47	28.0	26
2010	70	0.5	20	36	27.1	27
2011	3701	20.1	18	86	27.4	27
2012	288	1.4	21	41	27.2	27
Ave	475.9	2.5	21.9	70.1	28.6	27.3
SD	1077.4	5.9	2.1	44.4	1.3	0.8
CV	226.4%	236.3%	9.7%	63.3%	4.5%	2.9%

Table 8a. Unidentified Lamprey ammocoetes annual capture, catch per unit volume (CPUV) and total length summaries for ammocoetes captured by RBDD rotary traps between water year (WY) 2003 and 2013.

WY	Captures	CPUV Fish/ac-ft	Min TL (mm)	Max TL (mm)	Mean (mm)	Median (mm)
2003	908	7.30	14	144	98	100
2004	925	6.80	27	191	105	108
2005	1415	11.65	22	159	104	108
2006	657	4.45	52	186	112	115
2007	556	5.16	29	155	105	111
2008	385	3.64	41	146	101	108
2009	593	5.53	41	150	106	112
2010	935	11.45	45	166	111	114
2011	859	7.07	30	186	111	117
2012	455	5.11	27	155	100	104
2013	632	6.45	25	160	103	107
Mean	756.4	6.8	32.1	163.5	105.1	109.5
SD	291.3	2.6	11.3	16.8	4.7	5.0
CV	38.5%	38.5%	35.1%	10.3%	4.5%	4.6%

Table 8b. Pacific Lamprey macrothemia and adult annual capture, catch per unit volume (CPUV) and total length summaries for macrothemia captured by RBDD rotary traps between water year (WY) 2003 and 2013.

WY	Captures	CPUV Fish/ac-ft	Min TL (mm)	Max TL (mm)	Mean (mm)	Median (mm)
2003	204	2.16	100	693	261	131
2004	478	3.91	96	630	149	125
2005	4645	45.00	72	665	137	126
2006	417	5.62	98	700	136	125
2007	3107	34.08	96	660	150	128
2008	5252	40.29	78	580	139	128
2009	2938	81.24	91	834	132	124
2010	699	32.30	80	819	136	125
2011	2747	68.18	92	620	140	129
2012	3464	112.76	86	500	136	127
2013	1734	25.63	88	617	131	127
Mean	2335.0	41.0	88.8	665.3	149.7	126.8
SD	1759.4	34.7	9.0	97.1	37.3	2.1
CV	75.3%	84.5%	10.2%	14.6%	24.9%	1.6%

Table 9a. Summary of fall Chinook abiotic sample conditions at RBDD rotary traps during dates of capture by brood year (BY).

BY	Dates of Capture			H ₂ O Temperature (°F)			Discharge (CFS)			Turbidity (NTU)		
	Initial	Final	Days	Min	Max	Ave	Min	Max	Ave	Min	Max	Ave
2002	4-Dec	30-Aug	269	47	61	55	6,390	86,500	17,471	0.5	240.2	19.6
2003	9-Dec	15-Aug	250	46	62	55	7,380	92,800	18,707	2.0	413.5	21.8
2004	8-Dec	29-Aug	264	46	63	56	5,390	76,200	13,315	1.9	626.5	24.6
2005	3-Dec	29-Aug	269	47	61	53	6,450	118,000	27,279	1.6	731.7	22.5
2006	10-Dec	26-Aug	259	46	62	55	6,030	45,400	10,628	1.6	90.0	8.0
2007	7-Dec	2-Sep	270	44	62	55	5,210	44,600	10,127	1.5	233.3	11.1
2008	5-Dec	4-Sep	273	45	64	56	4,160	33,000	9,297	2.1	129.8	12.0
2009	10-Dec	21-Aug	254	45	61	54	5,260	95,100	17,531	1.3	162.6	10.3
2010	7-Dec	29-Aug	265	45	61	54	5,260	95,100	17,331	1.3	162.6	10.2
2011	10-Dec	2-Sep	267	45	65	55	4,800	35,200	10,281	1.4	180.6	8.8
2012	2-Dec	23-Aug	264	44	64	56	5,330	70,400	11,323	1.5	315.5	9.9
Mean	7-Dec	27-Aug	264	45	62	55	5,605	72,027	14,844	1.5	298.7	14.4
SD			7	1.1	1.4	0.8	890	28,600	5,442	0.4	209.6	6.3
CV			3%	2%	2%	1%	16%	40%	37%	28%	70%	44%

Table 9b. Summary of late-fall Chinook abiotic sample conditions at RBDD rotary traps during dates of capture by brood year (BY).

BY	Dates of Capture			H ₂ O Temperature (°F)			Discharge (CFS)			Turbidity (NTU)		
	Initial	Final	Days	Min	Max	Ave	Min	Max	Ave	Min	Max	Ave
2002	19-Apr	14-Jan	270	47	62	57	6,176	86,500	12,981	0.4	59.7	11.3
2003	3-Apr	6-Mar	338	46	61	55	6,310	92,800	16,650	0.9	413.5	20.9
2004	2-Apr	21-Jan	294	46	62	57	5,170	57,000	10,983	1.4	470.0	8.0
2005	2-Apr	22-Jan	295	48	63	57	6,050	118,000	17,431	1.6	731.7	24.4
2006	1-Apr	13-Jan	287	46	61	55	6,610	80,900	15,374	2.0	178.0	8.8
2007	4-Apr	9-Jan	280	46	62	57	5,490	38,600	10,035	1.3	198.0	5.7
2008	2-Apr	2-Mar	334	45	64	56	4,160	33,000	8,775	1.5	129.8	6.9
2009	3-Apr	1-Mar	332	46	64	57	3,920	60,400	9,855	1.9	250.6	14.2
2010	1-Apr	12-Jan	286	47	62	56	5,900	50,600	11,831	1.1	220.3	7.3
2011	1-Apr	27-Jan	301	45	61	55	5,570	57,400	11,888	2.0	68.5	5.5
2012	2-Apr	11-Jan	284	46	62	56	5,536	67,520	12,580	1.4	272.0	11.3
Mean	4-Apr	29-Jan	300	46	62	56	5,536	67,520	12,580	1.4	272.0	11.3
SD			24	0.9	1.0	0.7	849	25,109	2,829	0.5	198.7	6.2
CV			8%	2%	2%	1%	15%	37%	22%	34%	73%	55%

Table 9c. Summary of winter Chinook abiotic sample conditions at RBDD rotary traps during dates of capture by brood year (BY).

BY	Dates of Capture			H ₂ O Temperature (°F)			Discharge (CFS)			Turbidity (NTU)		
	Initial	Final	Days	Min	Max	Ave	Min	Max	Ave	Min	Max	Ave
2002	4-Jul	8-Apr	278	47	61	55	6,176	86,500	14,081	0.4	240.2	13.5
2003	16-Jul	17-Mar	245	46	61	54	6,310	92,800	16,809	0.9	413.5	22.8
2004	22-Jul	25-Mar	246	46	62	55	5,170	57,000	9,817	1.4	470.0	12.1
2005	25-Jul	17-Feb	207	48	61	55	6,450	118,000	19,174	1.6	731.7	19.7
2006	16-Jul	10-Mar	237	46	59	54	6,030	45,400	9,788	1.6	90.0	7.2
2007	18-Jul	4-Apr	261	44	62	54	5,210	44,600	9,318	1.3	233.3	11.3
2008	30-Jul	24-Apr	268	45	64	55	4,160	33,000	7,647	1.5	129.8	8.2
2009	26-Jul	30-Mar	247	46	64	55	3,920	60,400	9,303	1.9	250.6	15.0
2010	18-Jul	7-Apr	263	45	61	54	5,260	95,100	14,941	1.1	162.6	8.6
2011	12-Aug	31-Mar	232	45	60	53	4,800	35,200	8,646	1.7	180.6	7.0
2012	23-Jul	19-Apr	270	46	61	55	5,349	66,800	11,952	1.3	290.2	12.5
Mean	22-Jul	28-Mar	250	46	61	55	5,349	66,800	11,952	1.3	290.2	12.5
SD			20	1.1	1.5	0.8	843	27,776	3,767	0.4	185.4	5.1
CV			8%	2%	2%	1%	16%	42%	32%	31%	64%	41%

Table 9d. Summary of spring Chinook abiotic sample conditions at RBDD rotary traps during dates of capture by brood year (BY).

BY	Dates of Capture			H ₂ O Temperature (°F)			Discharge (CFS)			Turbidity (NTU)		
	Initial	Final	Days	Min	Max	Ave	Min	Max	Ave	Min	Max	Ave
2002	16-Oct	29-May	225	47	61	54	6,176	86,500	16,877	0.4	240.2	19.1
2003	16-Oct	11-Jun	239	46	62	54	6,310	92,800	17,267	0.9	413.5	23.0
2004	16-Oct	3-Jun	230	46	63	54	5,170	76,200	11,612	1.4	626.5	27.6
2005	16-Oct	3-Jun	230	47	61	52	6,450	118,000	28,158	1.6	731.7	25.3
2006	16-Oct	26-May	222	46	62	53	6,030	45,400	8,630	1.6	90.0	8.3
2007	16-Oct	12-Jun	240	44	61	53	5,210	44,600	8,823	1.3	233.3	11.4
2008	16-Oct	7-Jun	234	45	64	54	4,160	33,000	7,841	1.7	129.8	10.1
2009	16-Oct	25-May	221	46	62	54	3,920	60,400	9,495	1.9	250.6	17.1
2010	16-Oct	12-Jun	239	45	61	53	5,260	95,100	16,656	1.3	162.6	9.9
2011	16-Oct	27-May	224	45	65	53	4,800	35,200	8,344	1.7	180.6	8.8
2012	16-Oct	23-Jun	250	46	62	53	5,349	68,720	13,370	1.4	305.9	16.0
Mean	16-Oct	4-Jun	232	46	62	53	5,349	68,720	13,370	1.4	305.9	16.0
SD			9	1.0	1.4	0.6	843	27,696	6,116	0.4	205.5	7.0
CV			4%	2%	2%	1%	16%	40%	46%	30%	67%	43%

Table 9e. Summary of *O. mykiss* abiotic sample conditions at RBDD rotary traps during dates of capture by calendar year (CY).

CY	Dates of Capture			H ₂ O Temperature (°F)			Discharge (CFS)			Turbidity (NTU)		
	Initial	Final	Days	Min	Max	Ave	Min	Max	Ave	Min	Max	Ave
2002 ¹	-	-	-	-	-	-	-	-	-	-	-	-
2003	19-Jan	30-Dec	345	46	61	56	6,310	56,800	13,677	0.9	240.2	16.4
2004	6-Jan	17-Dec	346	46	62	56	5,170	92,800	14,613	1.4	413.5	9.3
2005	1-Jan	29-Dec	362	46	63	56	5,890	94,700	12,661	1.6	626.5	20.1
2006	3-Jan	30-Dec	361	47	61	54	6,610	82,900	20,803	2.0	190.5	11.4
2007	16-Jan	27-Dec	345	46	62	56	5,510	45,400	9,596	1.3	74.5	6.4
2008	6-Jan	28-Dec	357	44	64	56	4,610	44,600	9,478	1.5	233.3	9.0
2009	12-Jan	25-Dec	347	45	64	57	4,020	33,000	8,775	1.9	129.8	10.3
2010	15-Jan	12-Dec	331	47	62	56	5,150	60,400	11,194	1.1	250.6	12.4
2011	1-Jan	30-Dec	363	45	61	55	5,260	95,100	13,833	1.3	162.6	7.2
2012	17-Jan	14-Dec	332	45	65	56	4,800	70,400	10,557	1.2	315.5	11.0
Mean	10-Jan	23-Dec	349	46	63	56	5,333	67,610	12,519	1.4	263.7	11.4
SD			12	0.9	1.3	0.8	783	22,986	3,551	0.3	159.1	4.1
CV			3%	2%	2%	1%	15%	34%	28%	24%	60%	37%

¹ Sampling did not begin until mid-April of 2002 and this year not included in analyses.

Table 9f. Summary of Green Sturgeon abiotic sample conditions at RBDD rotary traps during dates of capture by calendar year (CY).

CY	Dates of Capture			H ₂ O Temperature (°F)			Discharge (CFS)			Turbidity (NTU)		
	Initial	Final	Days	Min	Max	Ave	Min	Max	Ave	Min	Max	Ave
2002	7-May	16-Jul	70	55	60	58	9,317	15,680	13,038	0.9	16.3	3.5
2003	13-Jun	11-Nov	151	52	61	58	6,950	16,000	10,802	0.9	48.6	6.5
2004	4-May	29-Jul	86	55	60	58	9,560	16,700	14,210	3.0	18.3	4.9
2005	7-May	13-Aug	98	54	61	58	10,200	76,200	18,614	2.3	626.5	26.4
2006	10-Jun	25-Aug	76	56	59	57	12,800	15,600	14,579	3.4	13.9	5.7
2007	11-May	24-Jul	74	55	61	58	9,790	17,000	12,905	1.7	50.4	4.5
2008	-	-	0	-	-	-	-	-	-	-	-	-
2009	11-May	16-Jul	66	58	64	61	9,460	13,700	11,226	4.1	34.4	13.5
2010	26-May	29-Aug	95	55	61	58	9,150	18,300	13,143	1.6	22.0	5.4
2011	16-May	27-Aug	103	52	61	58	10,400	24,800	14,059	3.6	23.5	6.8
2012	1-May	26-Jun	56	55	61	58	8,763	21,398	12,258	2.2	85.4	7.7
Mean	17-May	12-Aug	88	55	61	58	9,639	23,538	13,483	2.4	93.9	8.5
SD			27	1.7	1.2	0.9	1,464	18,782	2,181	1.1	188.4	6.9
CV			31%	3%	2%	2%	15%	80%	16%	47%	201%	81%

Table 9g. Summary of Lamprey *spp.* abiotic sample conditions at RBDD rotary traps during dates of capture by water year (WY).

WY	Dates of Capture			H ₂ O Temperature (°F)			Discharge (CFS)			Turbidity (NTU)		
	Initial	Final	Days	Min	Max	Ave	Min	Max	Ave	Min	Max	Ave
2003	1-Oct	27-Sep	361	47	61	56	6,176	86,500	15,033	0.4	240.2	15.1
2004	1-Oct	29-Sep	364	46	62	55	6,310	92,800	15,528	0.9	413.5	16.3
2005	2-Oct	29-Sep	362	46	63	56	5,170	76,200	11,800	1.4	626.5	18.6
2006	1-Oct	29-Sep	363	47	61	54	6,450	118,000	22,724	1.6	731.7	17.9
2007	1-Oct	29-Sep	363	46	62	55	6,030	45,400	9,832	1.6	90.0	7.3
2008	1-Oct	29-Sep	364	44	63	56	5,210	44,600	9,342	1.3	233.3	8.8
2009	1-Oct	29-Sep	363	45	64	57	4,160	33,000	8,791	1.6	129.8	10.5
2010	1-Oct	30-Sep	364	46	62	56	3,920	60,400	10,241	1.1	250.6	12.1
2011	3-Oct	30-Sep	362	45	61	55	5,260	95,100	15,022	1.3	162.6	8.4
2012	3-Oct	27-Sep	360	45	65	55	4,800	35,200	9,753	1.2	180.6	7.1
2013	5-Oct	28-Sep	358	44	64	56	5,330	70,400	10,479	1.1	315.5	8.5
Mean	2-Oct	29-Sep	362	46	63	56	5,347	68,873	12,595	1.2	306.8	11.9
SD			2	1.1	1.3	0.7	843	27,701	4,177	0.3	205.5	4.4
CV			1%	2%	2%	1%	16%	40%	33%	29%	67%	37%

Figures

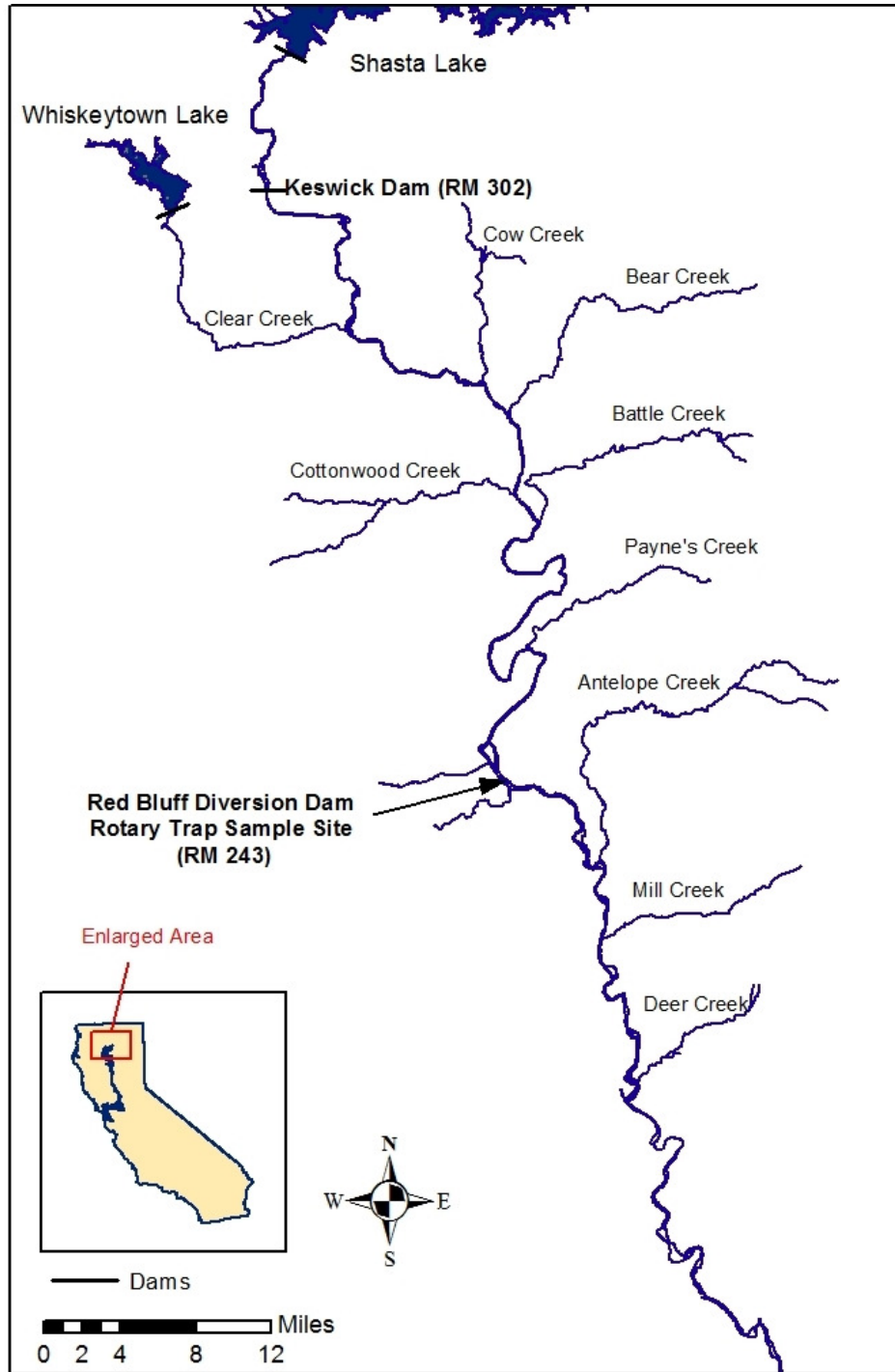


Figure 1. Location of Red Bluff Diversion Dam rotary trap sample site on the Sacramento River, California (RM 243).

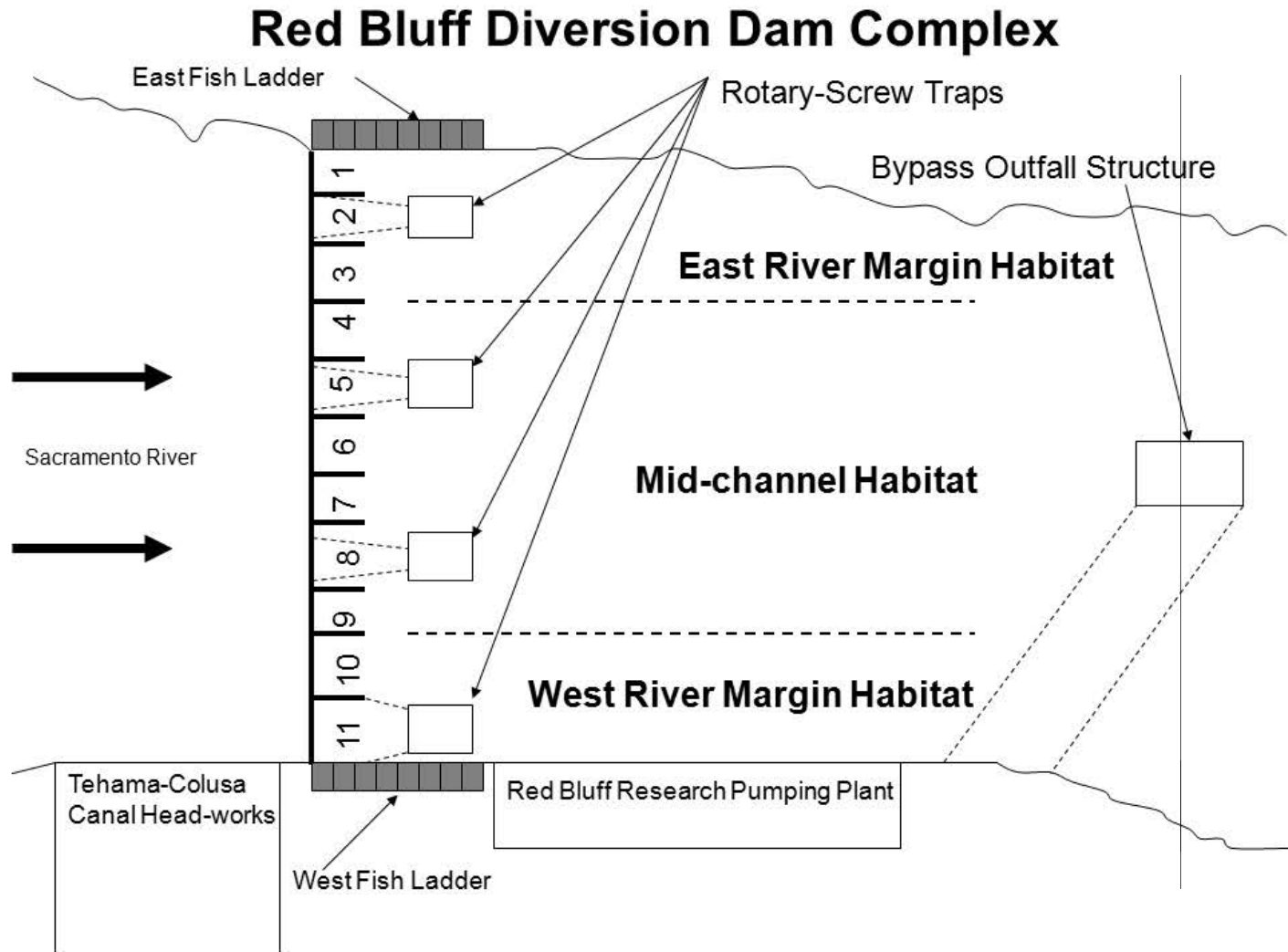


Figure 2. Rotary-screw trap sampling transect at Red Bluff Diversion Dam Site (RM 243) on the Sacramento River, California.

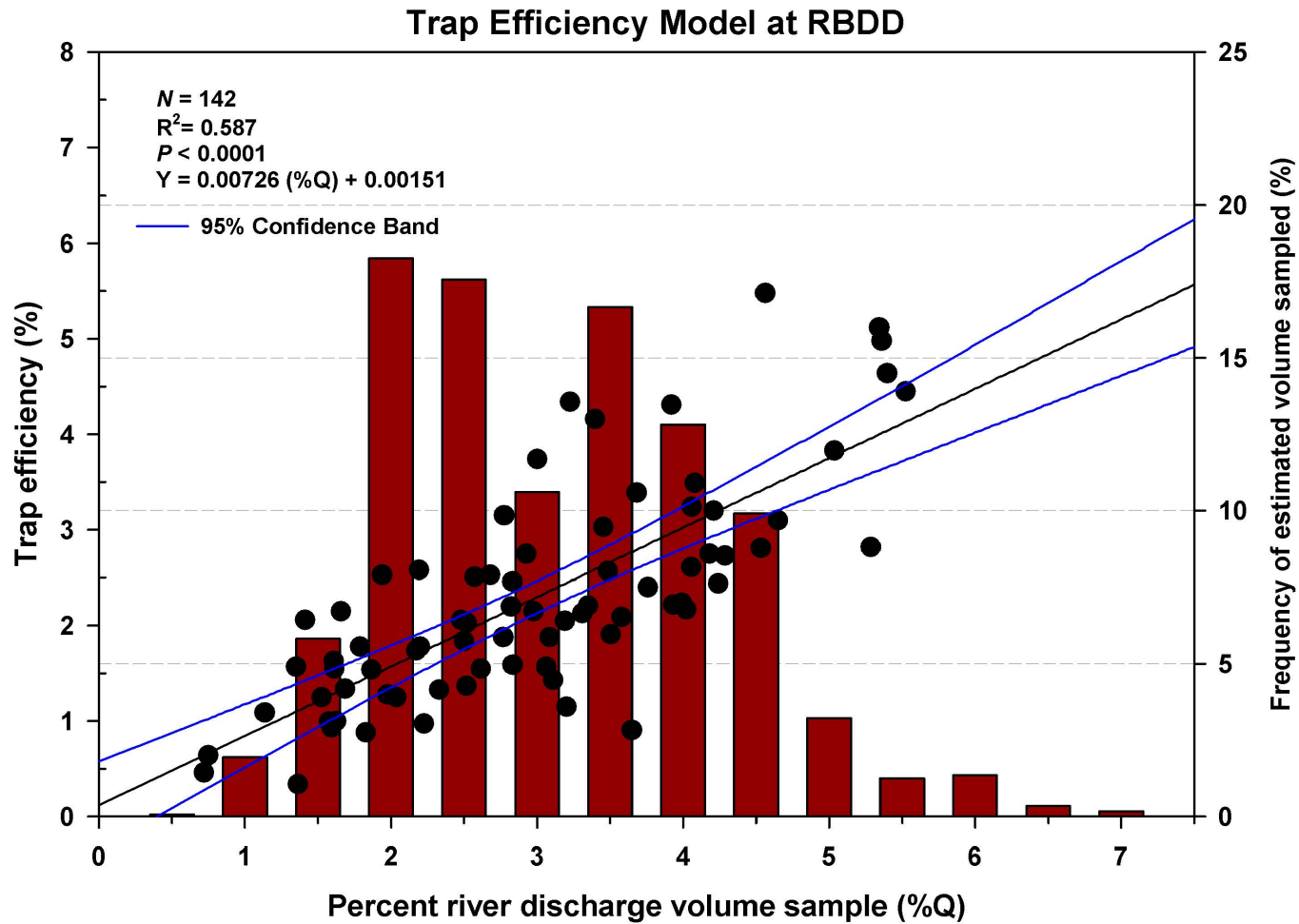


Figure 3. Trap efficiency model for combined 8-ft diameter rotary traps at Red Bluff Diversion Dam (RM 243), Sacramento River, CA. Mark-recapture trials ($N = 142$) were used to estimate trap efficiencies. Histogram indicates percentage of time traps sampled various levels (half percent bins) of river discharge between April 2002 and September 2013.

BY 2002-2012 Fall Chinook Capture Fork Length Summaries

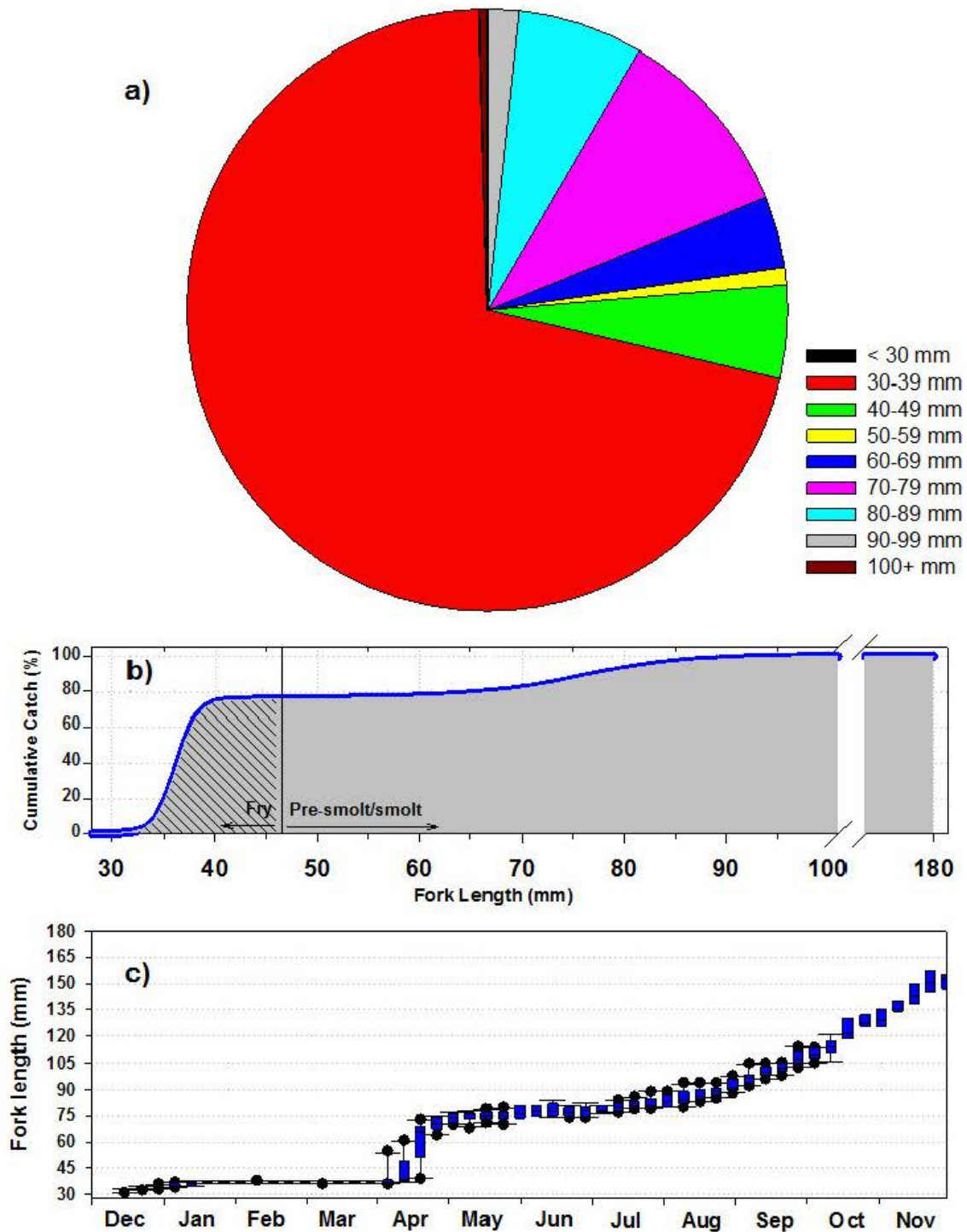


Figure 4. Fall Chinook fork length (a) capture proportions, (b) cumulative capture size curve, and (c) average weekly median boxplots for fall Chinook sampled by rotary traps at RBDD between December 2002 and September 2013.

BY 2002- 2012 Late-Fall Chinook Capture Fork Length Summaries

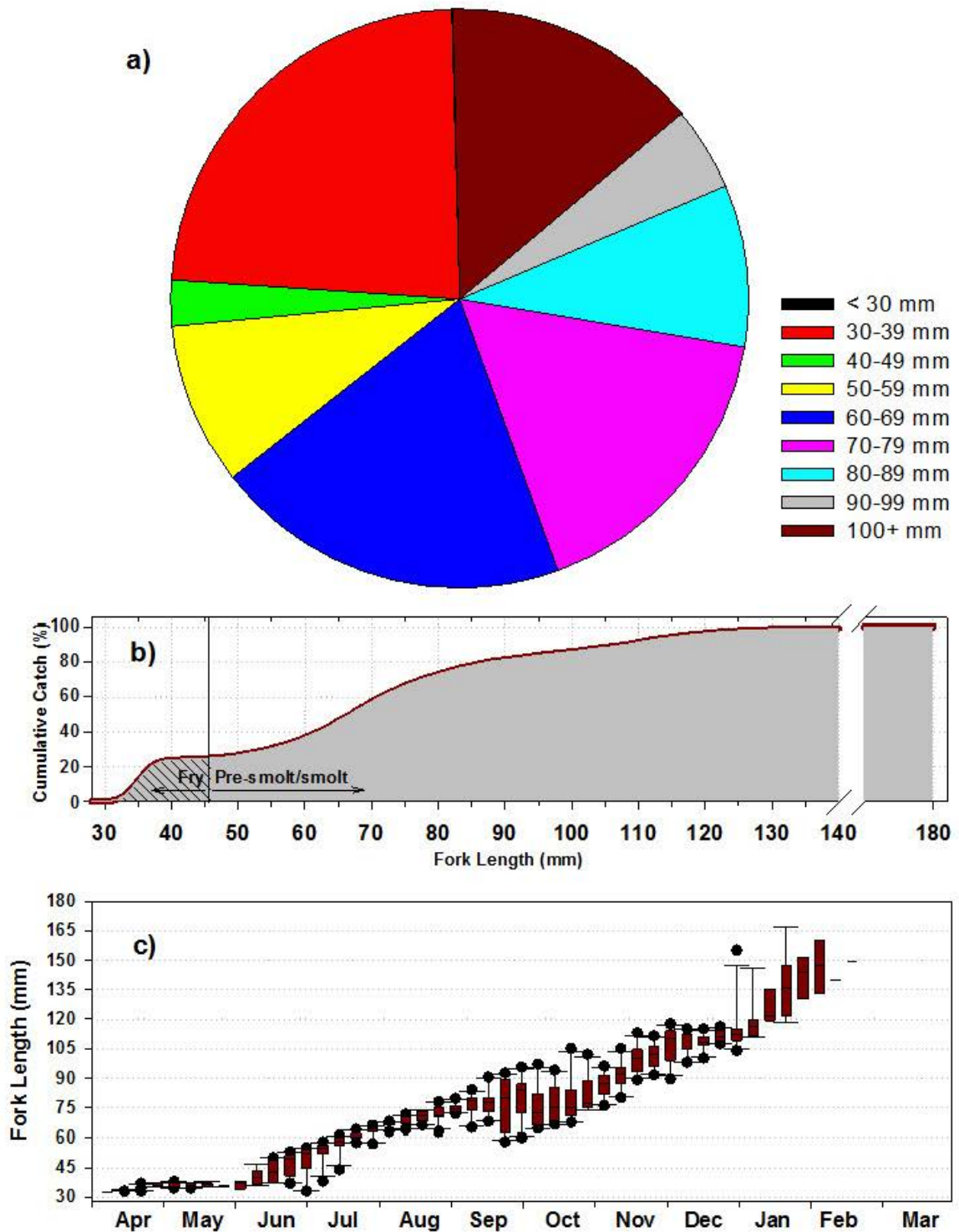


Figure 5. Late-fall Chinook fork length (a) capture proportions, (b) cumulative capture size curve, and (c) average weekly median boxplots for late-fall Chinook sampled by rotary traps at RBDD between April 2002 and March 2013.

BY 2002-2012 Winter Chinook Capture Fork Length Summaries

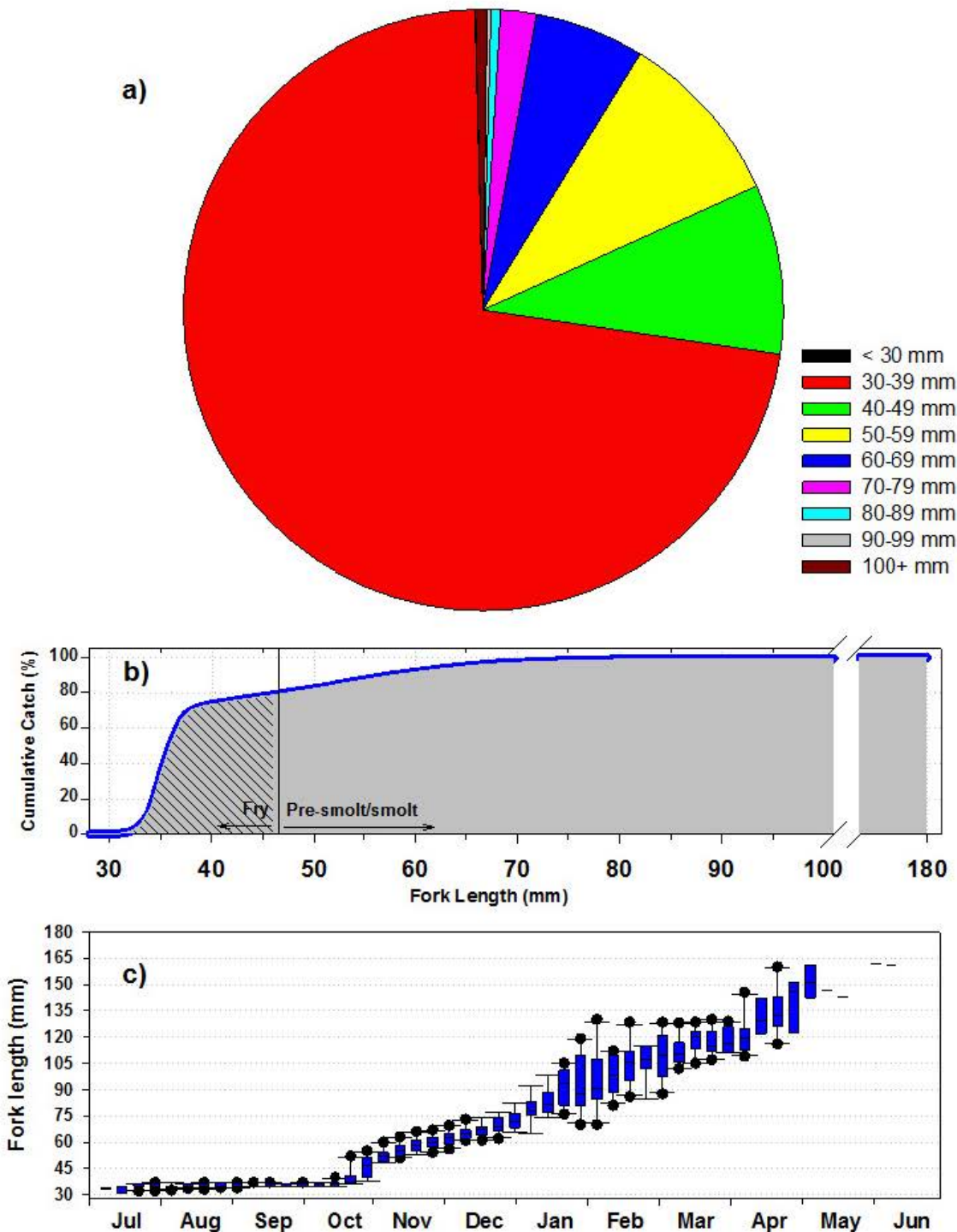


Figure 6. Winter Chinook fork length (a) capture proportions, (b) cumulative capture size curve, and (c) average weekly median boxplots for winter Chinook sampled by rotary traps at RBDD between July 2002 and June 2013.

BY 2002- 2012 Spring Chinook Capture Fork Length Summaries

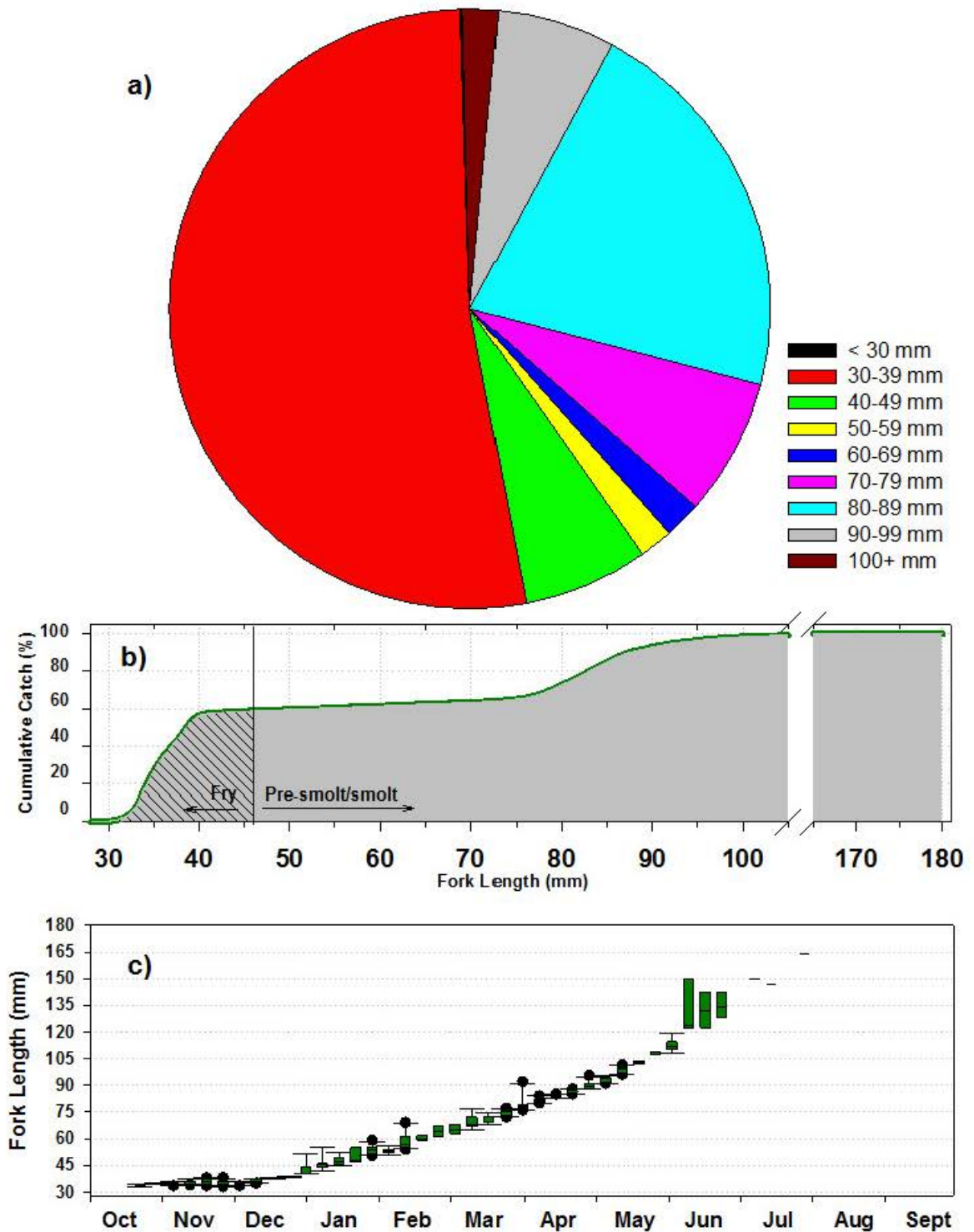


Figure 7. Spring Chinook fork length (a) capture proportions, (b) cumulative capture size curve, and (c) average weekly median boxplots for spring Chinook sampled by rotary traps at RBDD between October 2002 and September 2013.

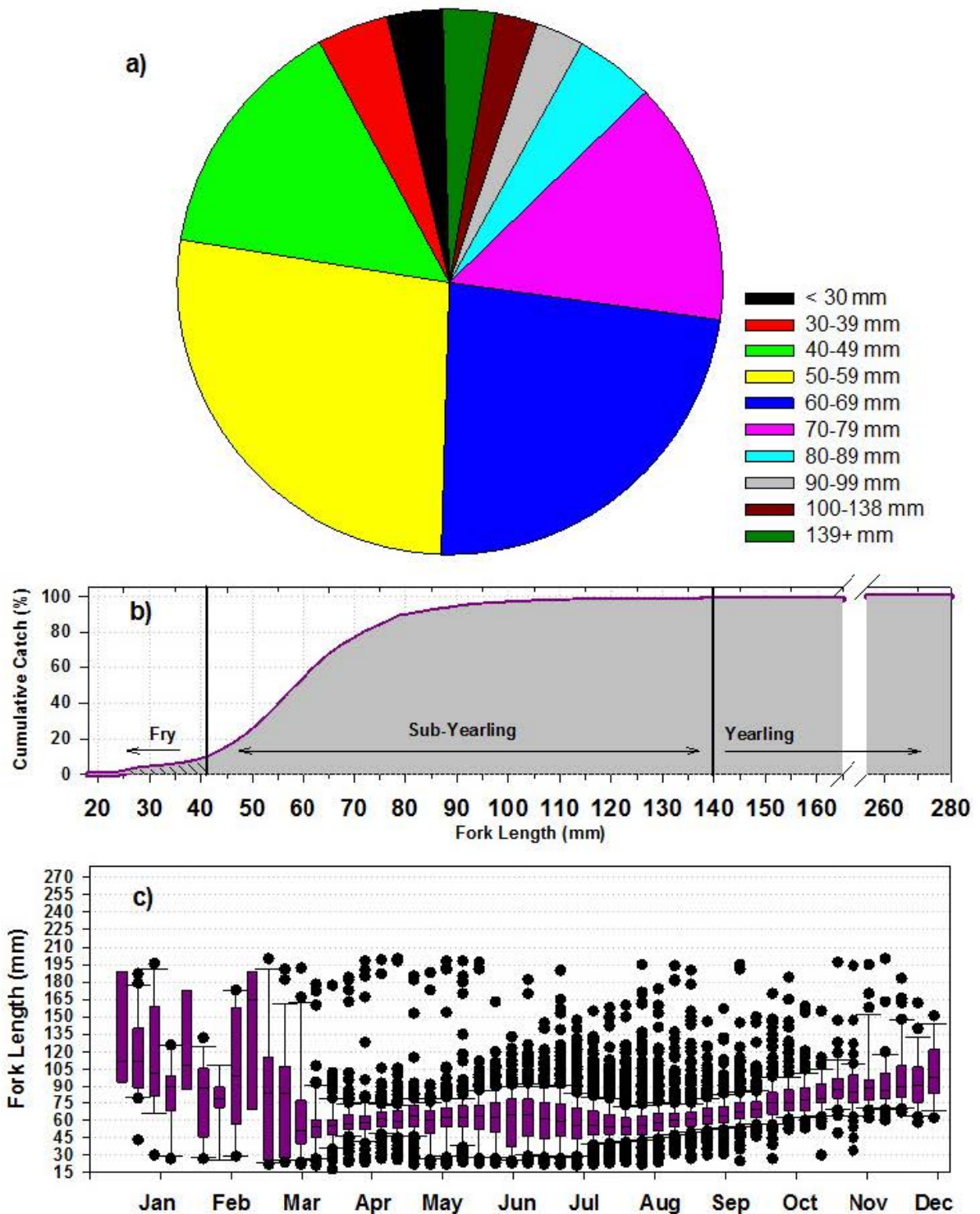
CY 2002-2012 *O. mykiss* Capture Fork Length Summaries

Figure 8. *O. mykiss* fork length (a) capture proportions, (b) cumulative capture size curve, and (c) average weekly median boxplots for *O. mykiss* sampled by rotary traps at RBDD between April 2002 and December 2012.

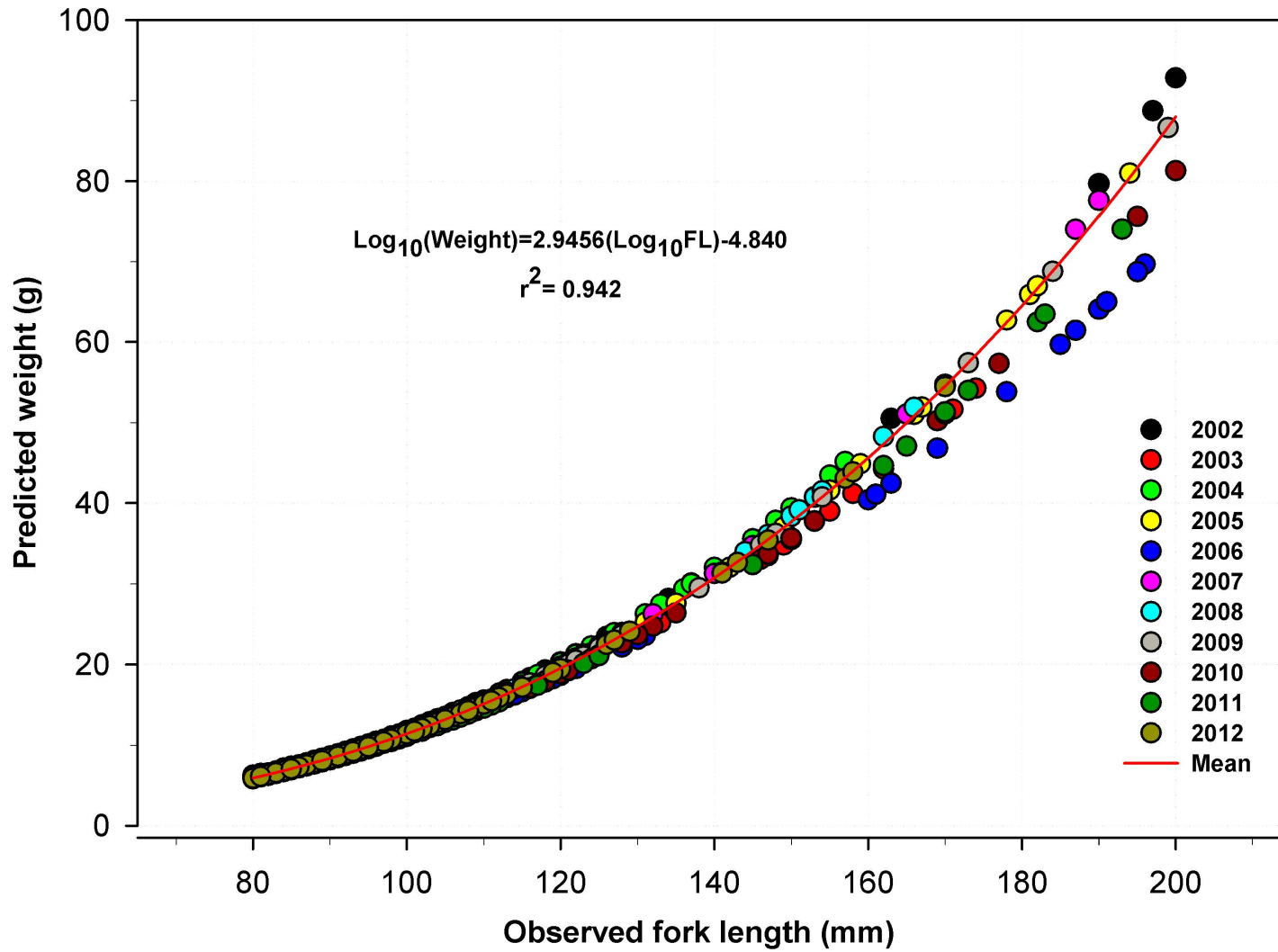


Figure 9. Predicted weight (g) for *O. mykiss* with measured fork lengths (FL) between 80 and 200 mm using annual weight-length regression equation.

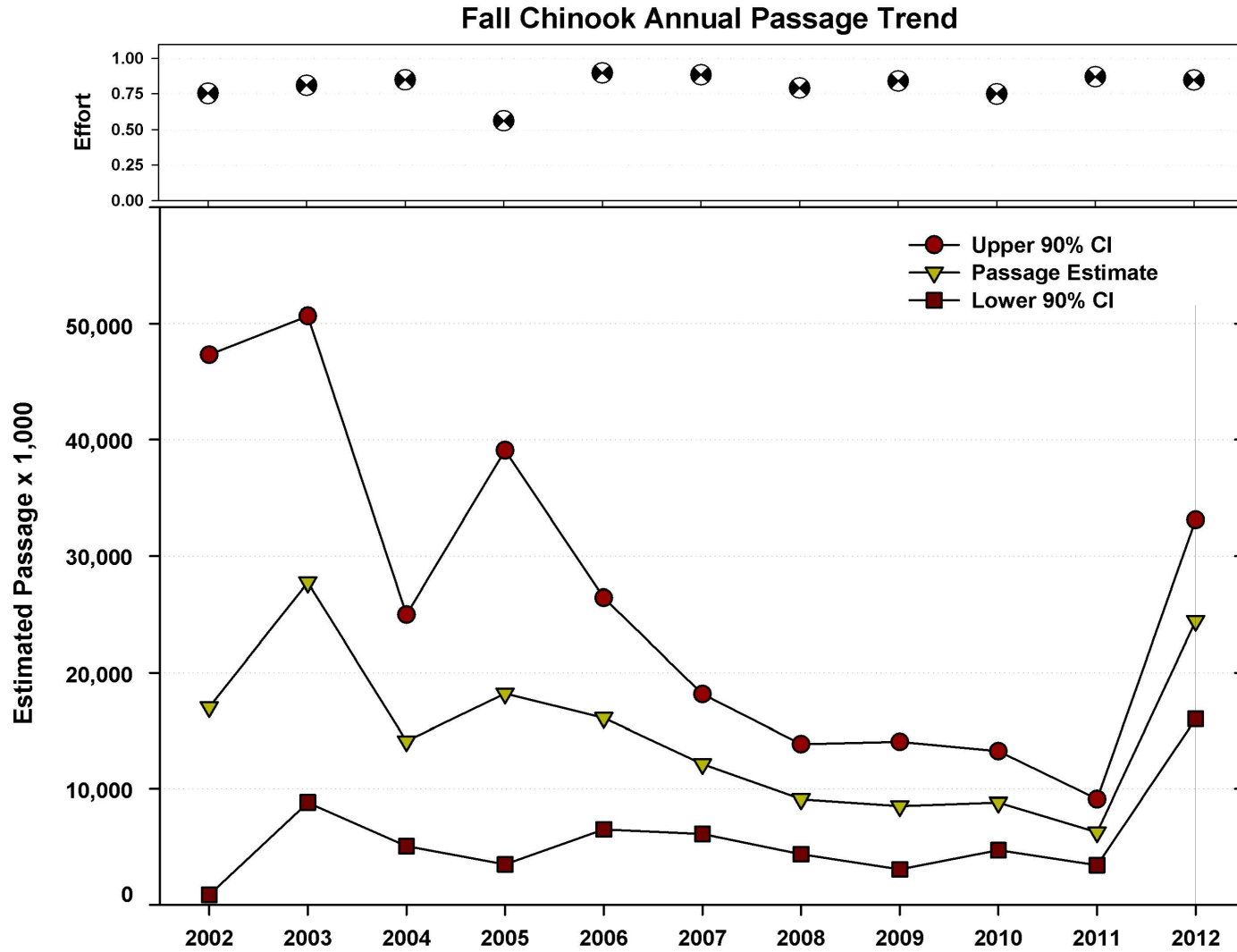


Figure 10. RBDD rotary trap fall Chinook annual sample effort and passage estimates with 90% confidence intervals (CI) for the period December 2002 through September 2013

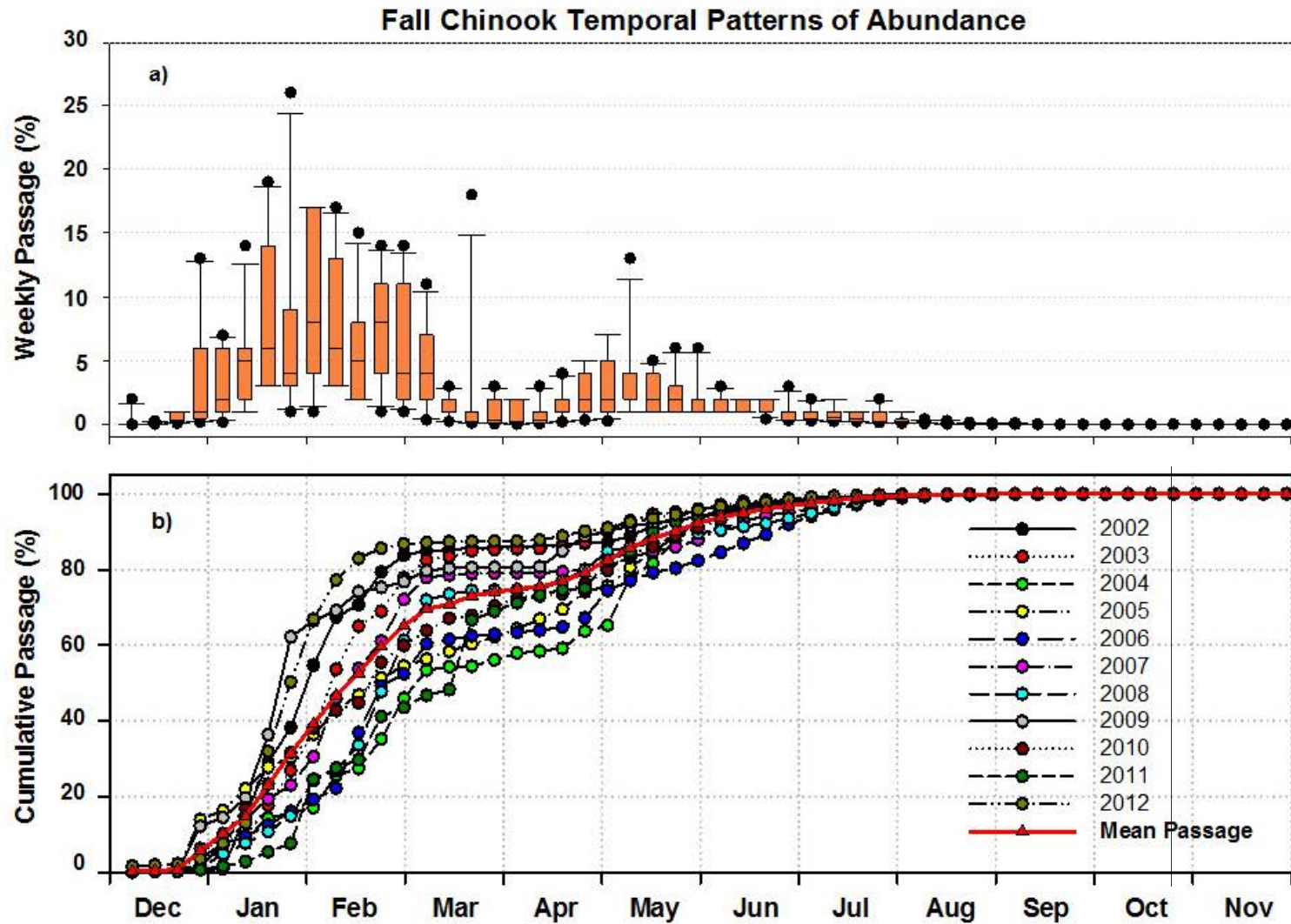


Figure 11. RBDD rotary trap fall Chinook (a) boxplots of weekly passage estimates relative to annual total passage estimates and (b) cumulative weekly passage with 11-year mean passage trend line for the period December 2002 through September 2013.

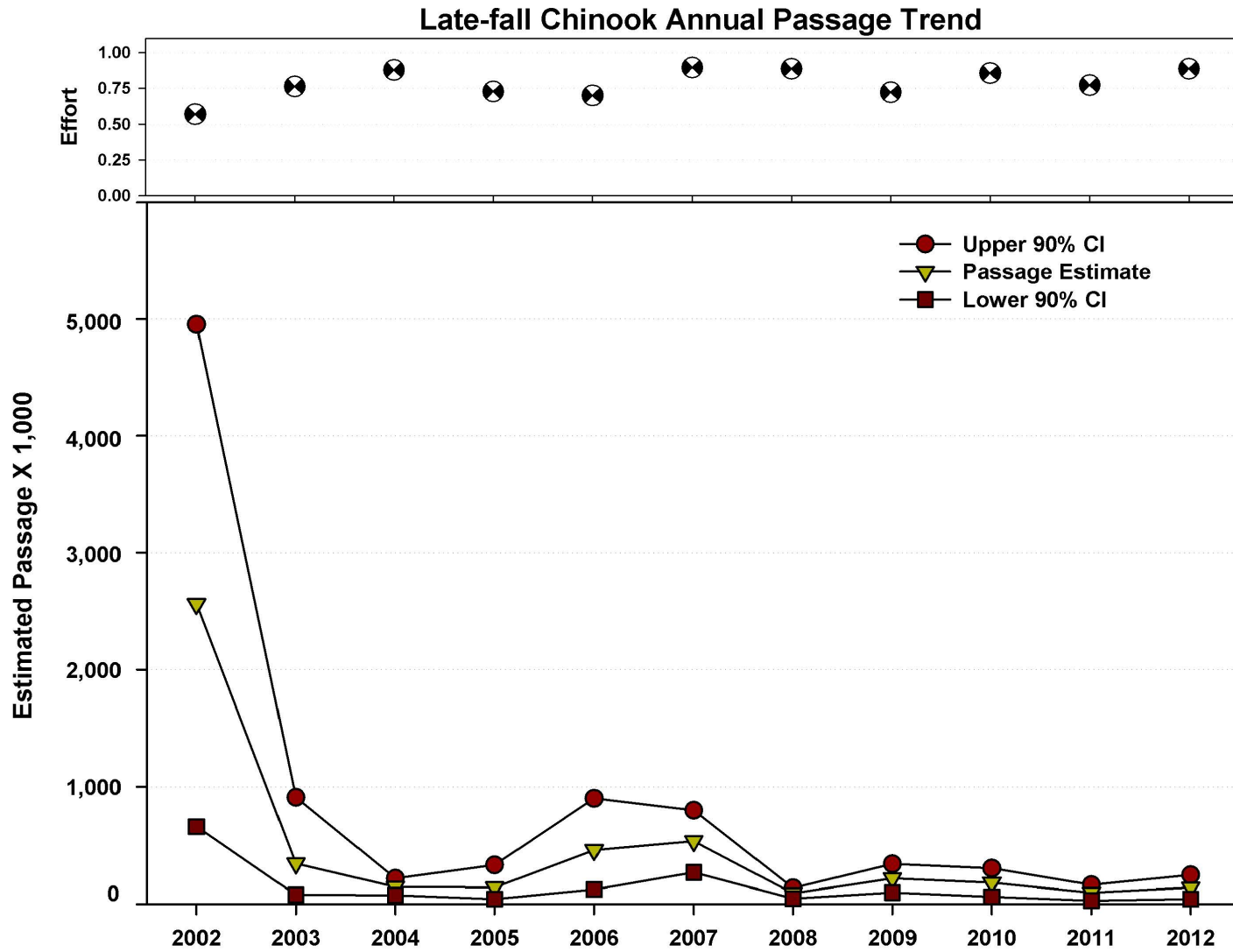


Figure 12. RBDD rotary trap late-fall Chinook annual sample effort and passage estimates with 90% confidence intervals (CI) for the period April 2002 through March 2013.

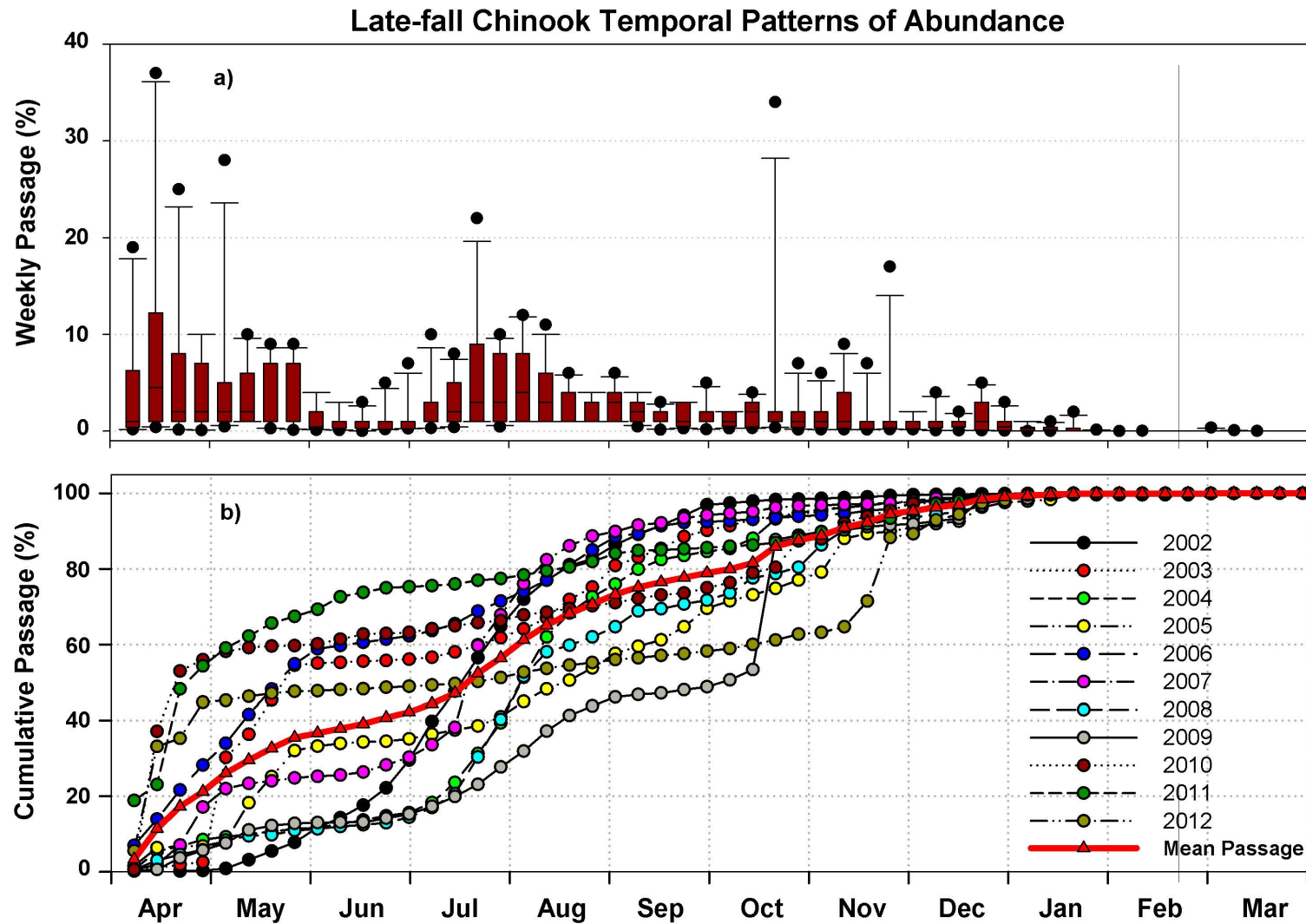


Figure 13. RBDD rotary trap late-fall Chinook (a) boxplots of weekly passage estimates relative to annual total passage estimates and (b) cumulative weekly passage with 11-year mean passage trend line for the period April 2002 through March 2013.

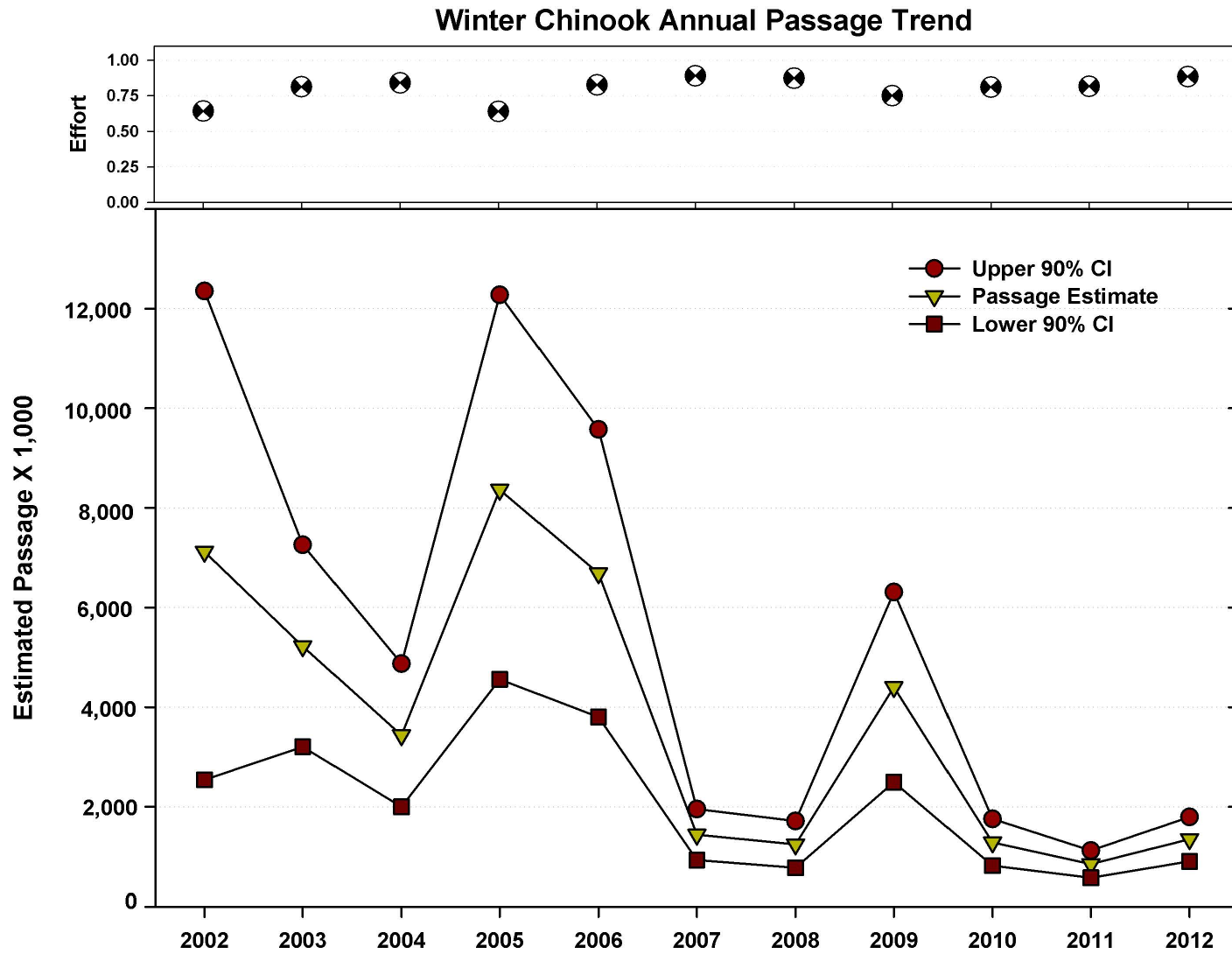


Figure 14. RBDD rotary trap winter Chinook annual sample effort and passage estimates with 90% confidence intervals (CI) for the period July 2002 through June 2013.

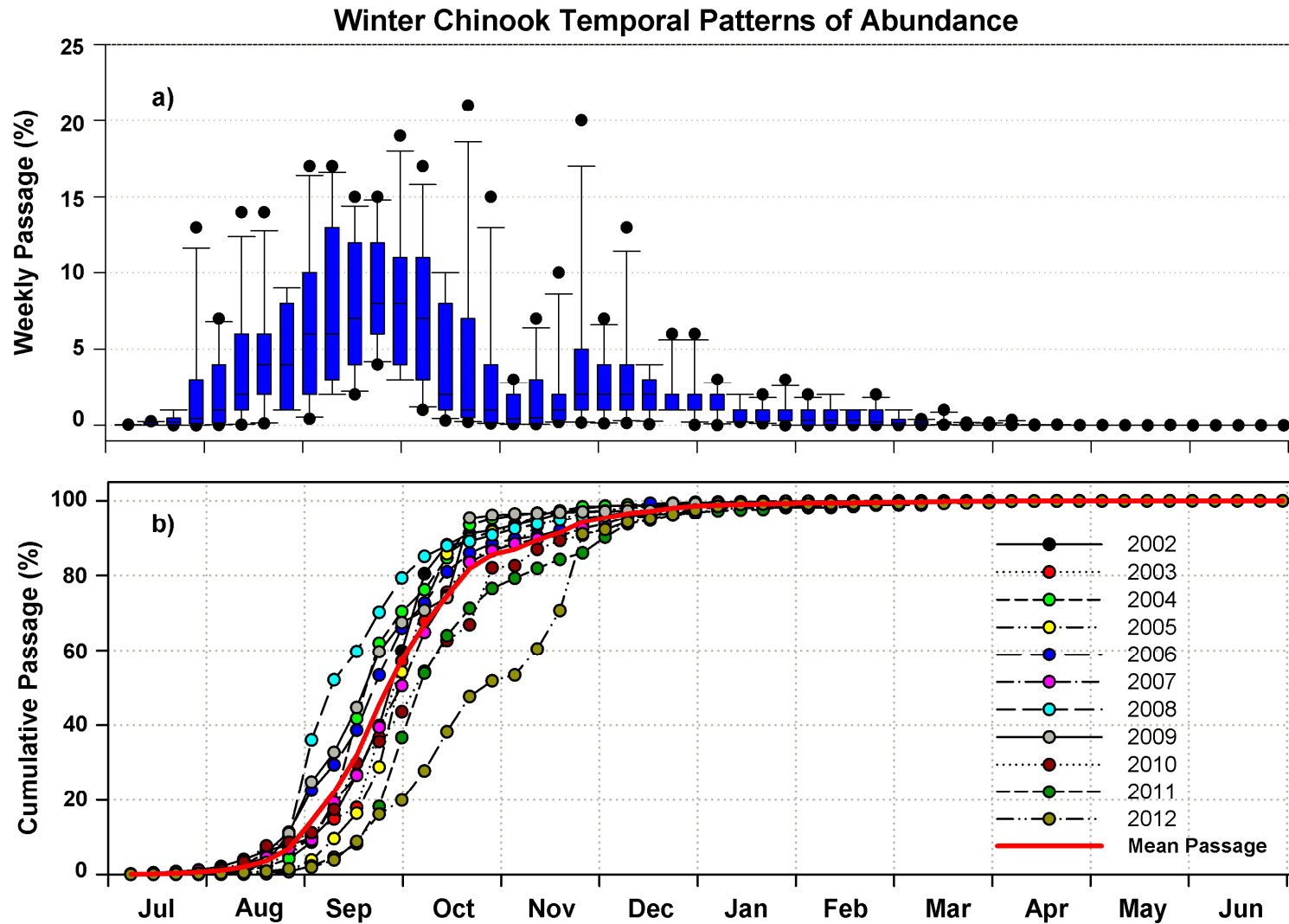


Figure 15. RBDD rotary trap winter Chinook (a) boxplots of weekly passage estimates relative to annual total passage estimates and (b) cumulative weekly passage with 11-year mean passage trend line for the period July 2002 through June 2013.

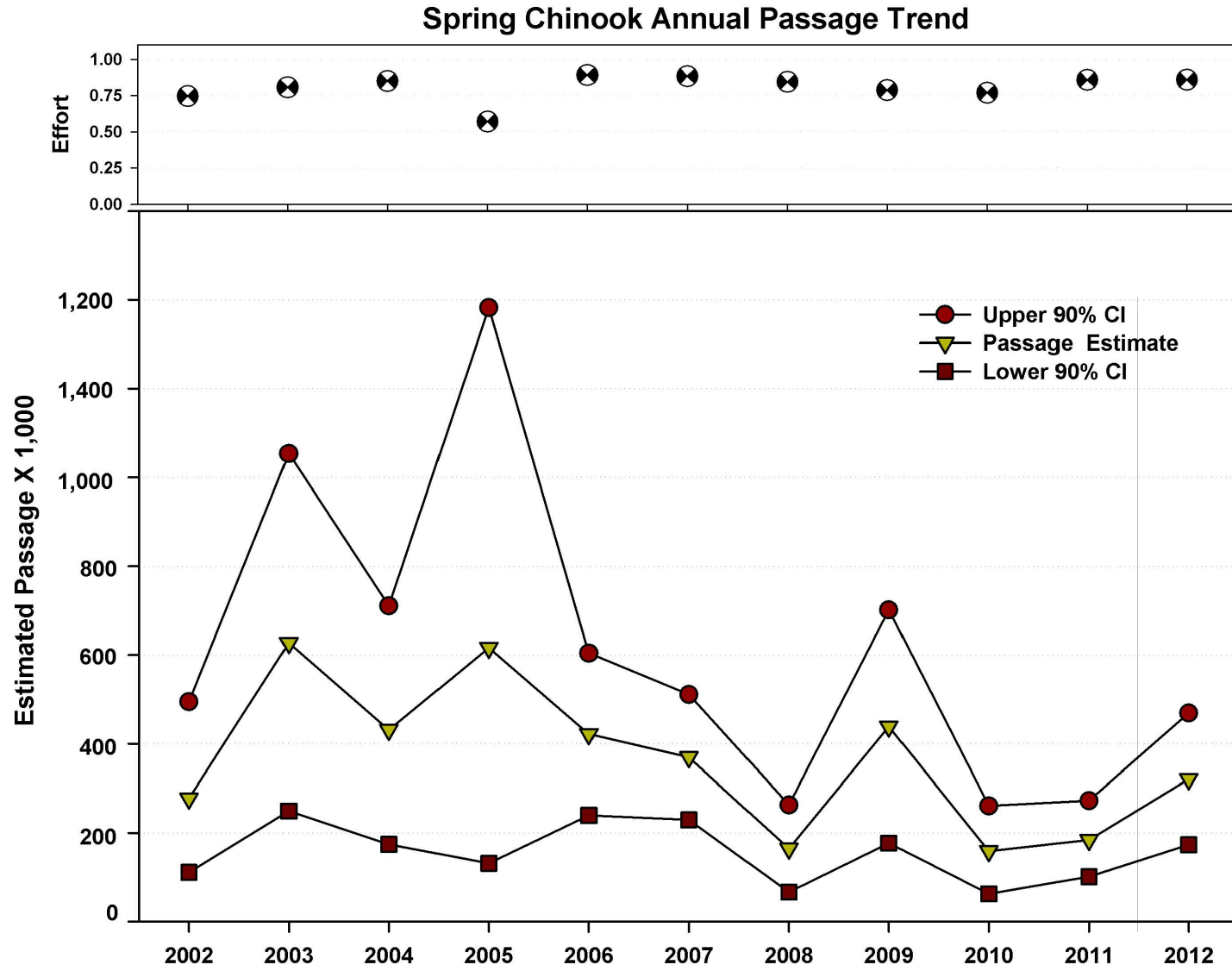


Figure 16. RBDD rotary trap spring Chinook annual sample effort and passage estimates with 90% confidence intervals (CI) for the period October 2002 through September 2013.

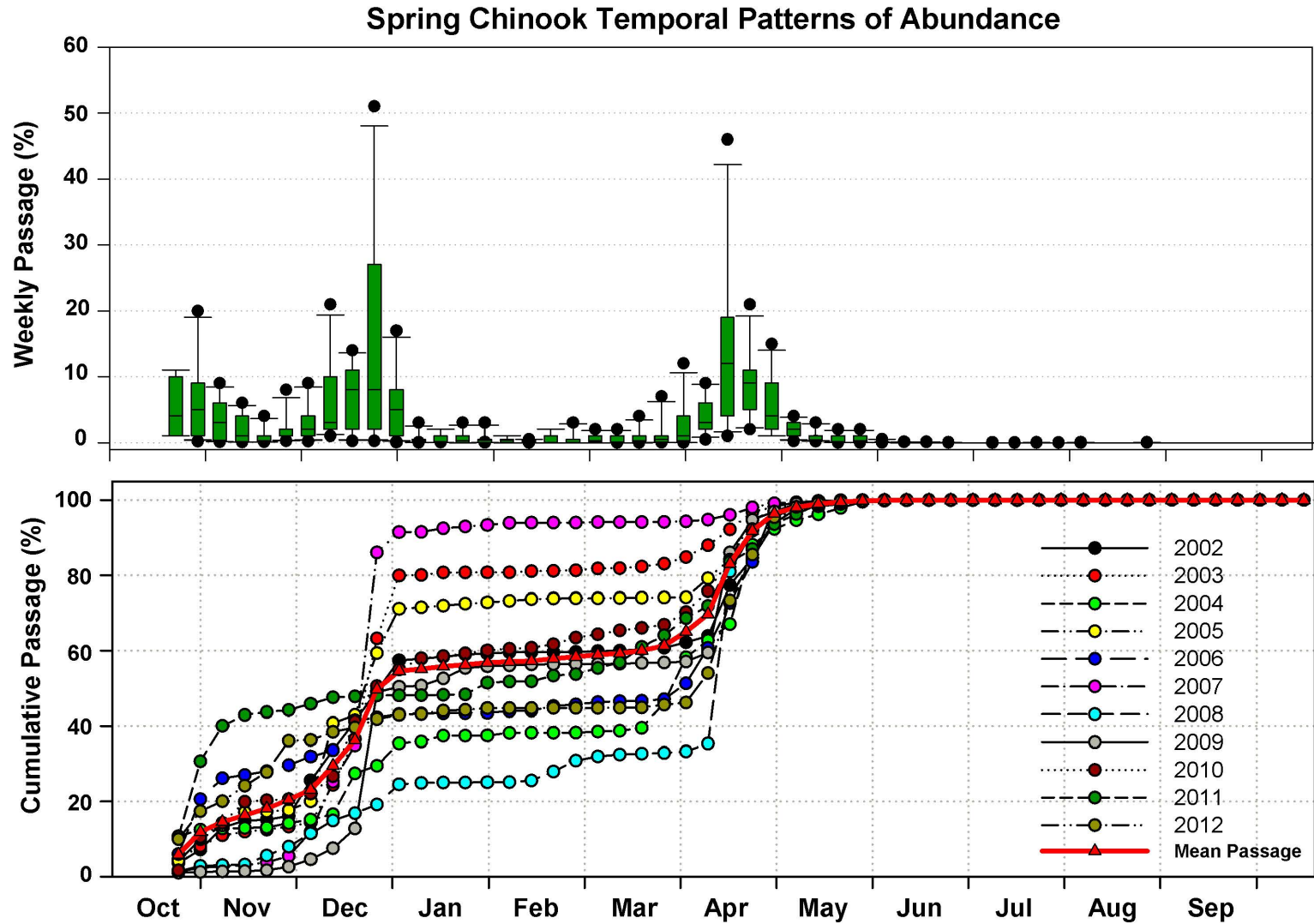


Figure 17. RBDD rotary trap spring Chinook (a) boxplots of weekly passage estimates relative to annual total passage estimates and (b) cumulative weekly passage with 11-year mean passage trend line for the period October 2002 through September 2013.

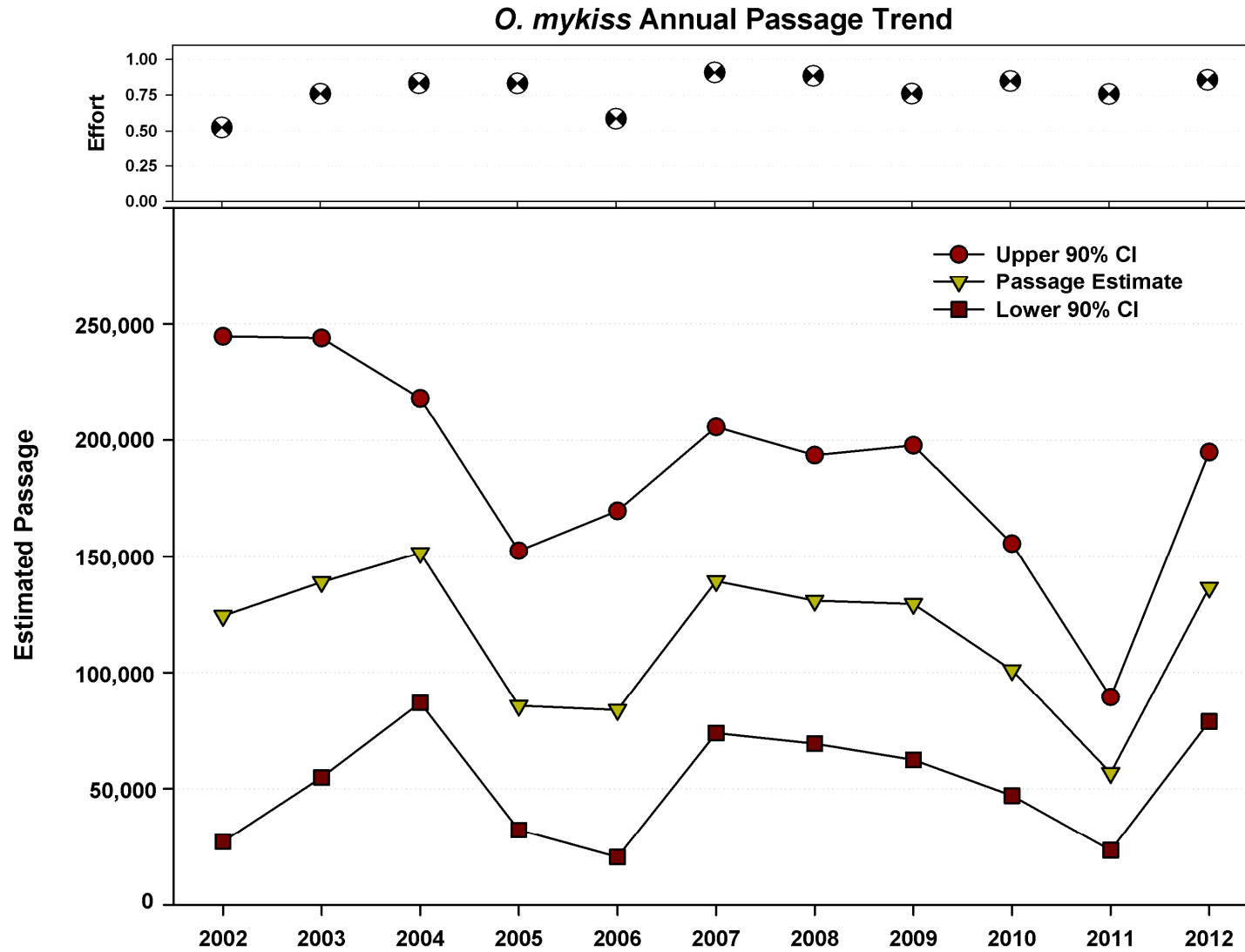


Figure 18. RBDD rotary trap *O. mykiss* annual sample effort and passage estimates with 90% confidence intervals (CI) for the period April 2002 through December 2012.

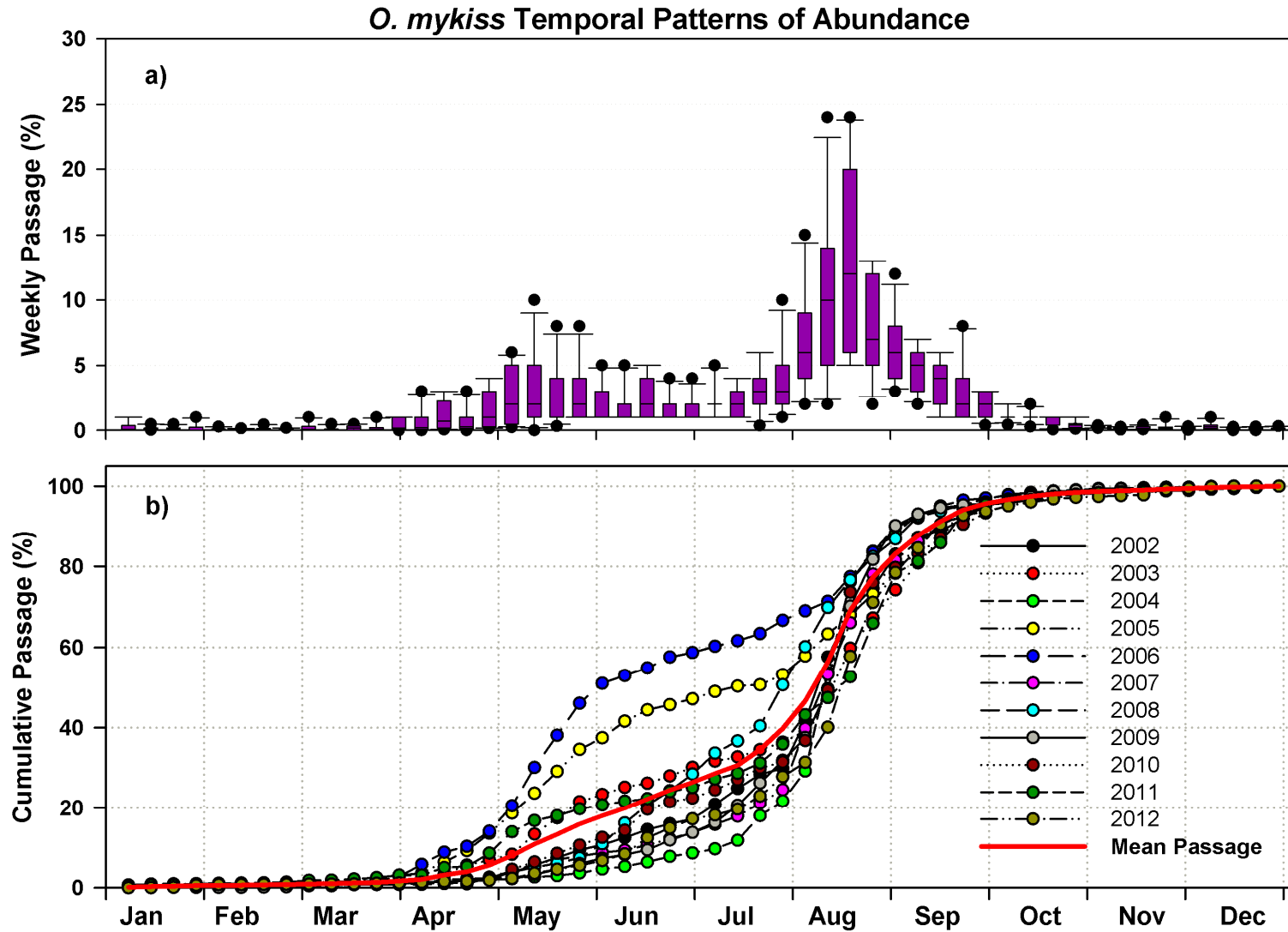


Figure 19. RBDD rotary trap *O. mykiss* (a) boxplots of weekly passage estimates relative to annual total passage estimates and (b) cumulative weekly passage with 11-year mean passage trend line for the period April 2002 through December 2012.

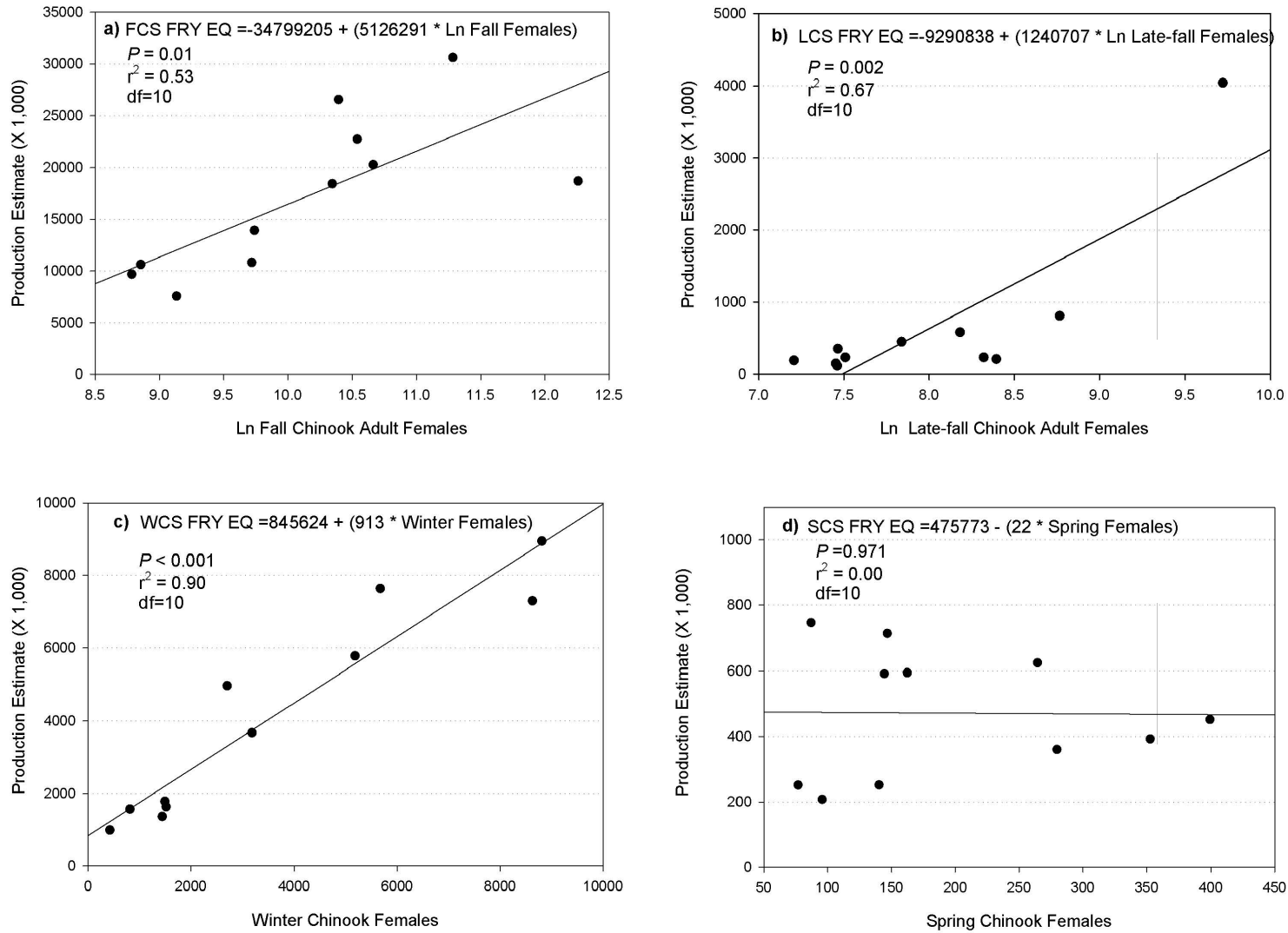


Figure 20. Relationships between a) fall, b) late-fall, c) winter, and d) spring Chinook fry-equivalent production estimates and estimated number of female adult Chinook salmon upstream of RBDD between 2002 and 2012. Note: fall and late-fall adult females were natural log transformed due to extraordinary escapement values estimated for the year 2002.

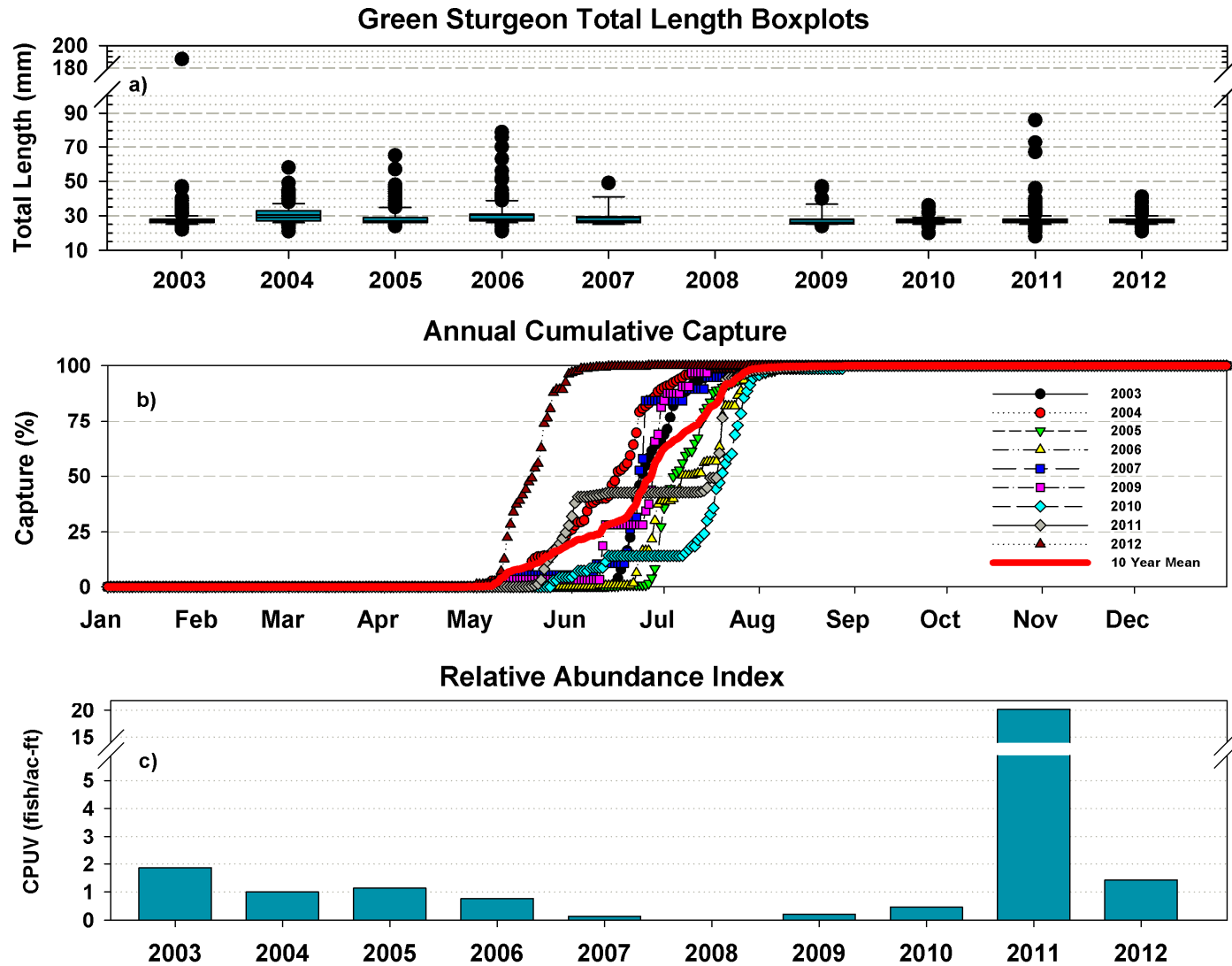


Figure 21. Green sturgeon a) annual total length capture boxplots, b) annual cumulative capture trends with 10-year mean trend line, and c) relative abundance indices. All fish captured by rotary trap at RBDD (RM 243) on the Upper Sacramento River, CA between 2003 and 2012. Data from 2002 excluded from analysis due to limited effort and USBR Crown Flow study resulting in incomparable sampling regimes and results.

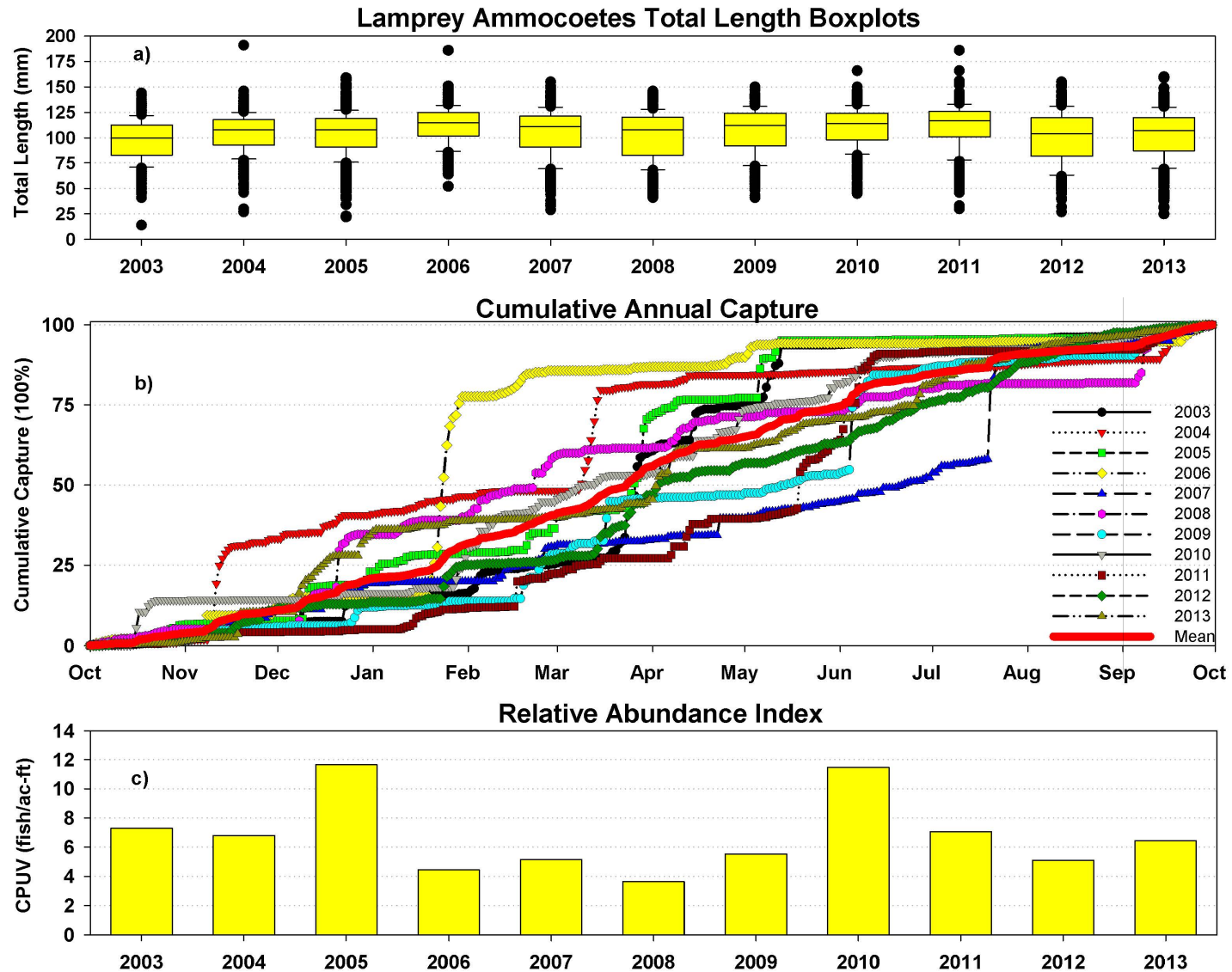


Figure 22. Unidentified lamprey ammocoetes a) total length distribution box plots, b) cumulative annual capture trends, and c) relative abundance indices from rotary trap samples collected between October 1, 2002 and September 30, 2013 by water year from the Sacramento River, CA at the RBDD (RM 243).

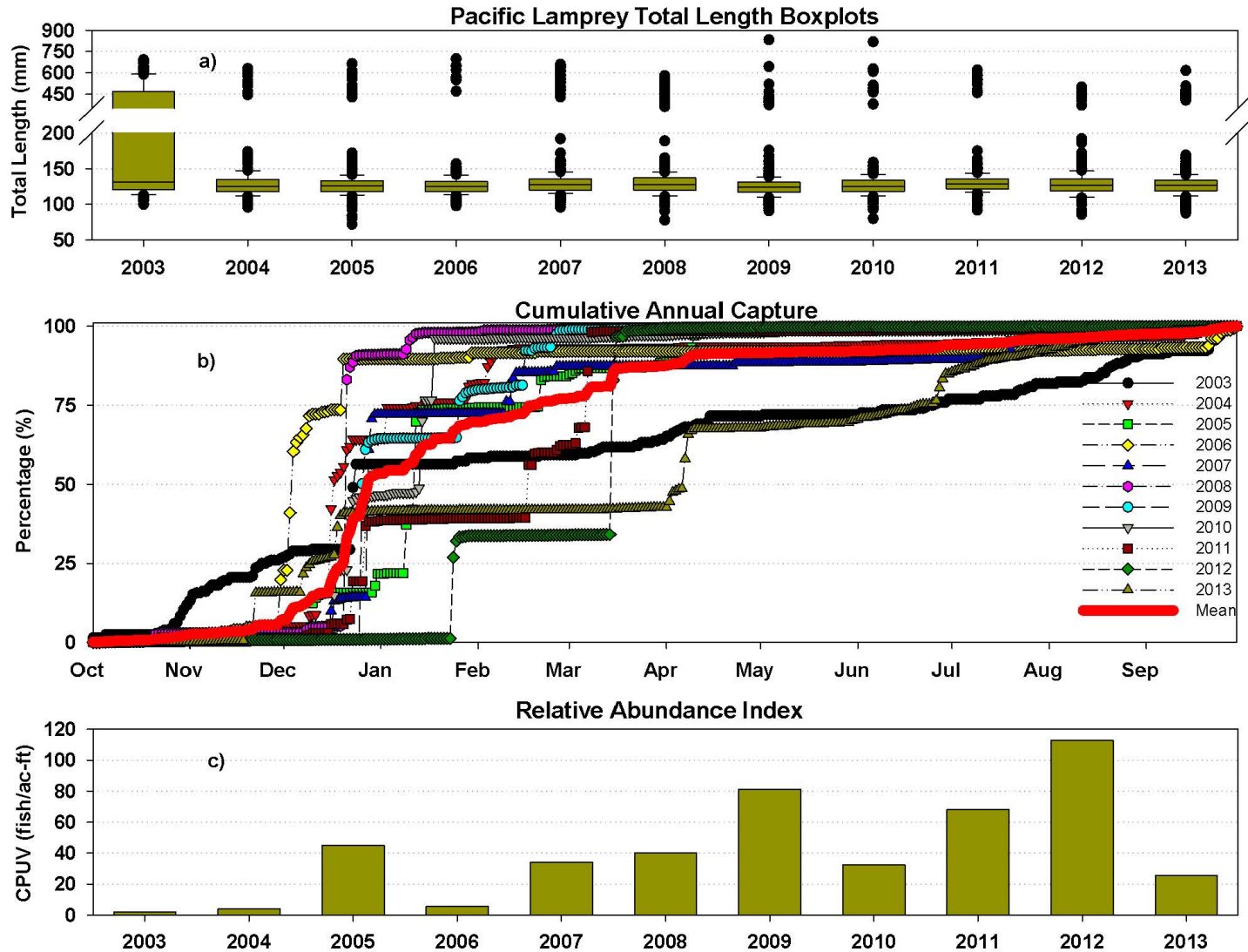


Figure 23. Pacific Lamprey (*macrophthalmia* and adults) a) total length distribution box plots, b) cumulative annual capture trends, and c) relative abundance indices from rotary trap samples collected between October 1, 2002 and September 30, 2013 by water year from the Sacramento River, CA at the RBDD (RM 243).

Green Sturgeon Relative Abundance Environmental Covariate Analyses

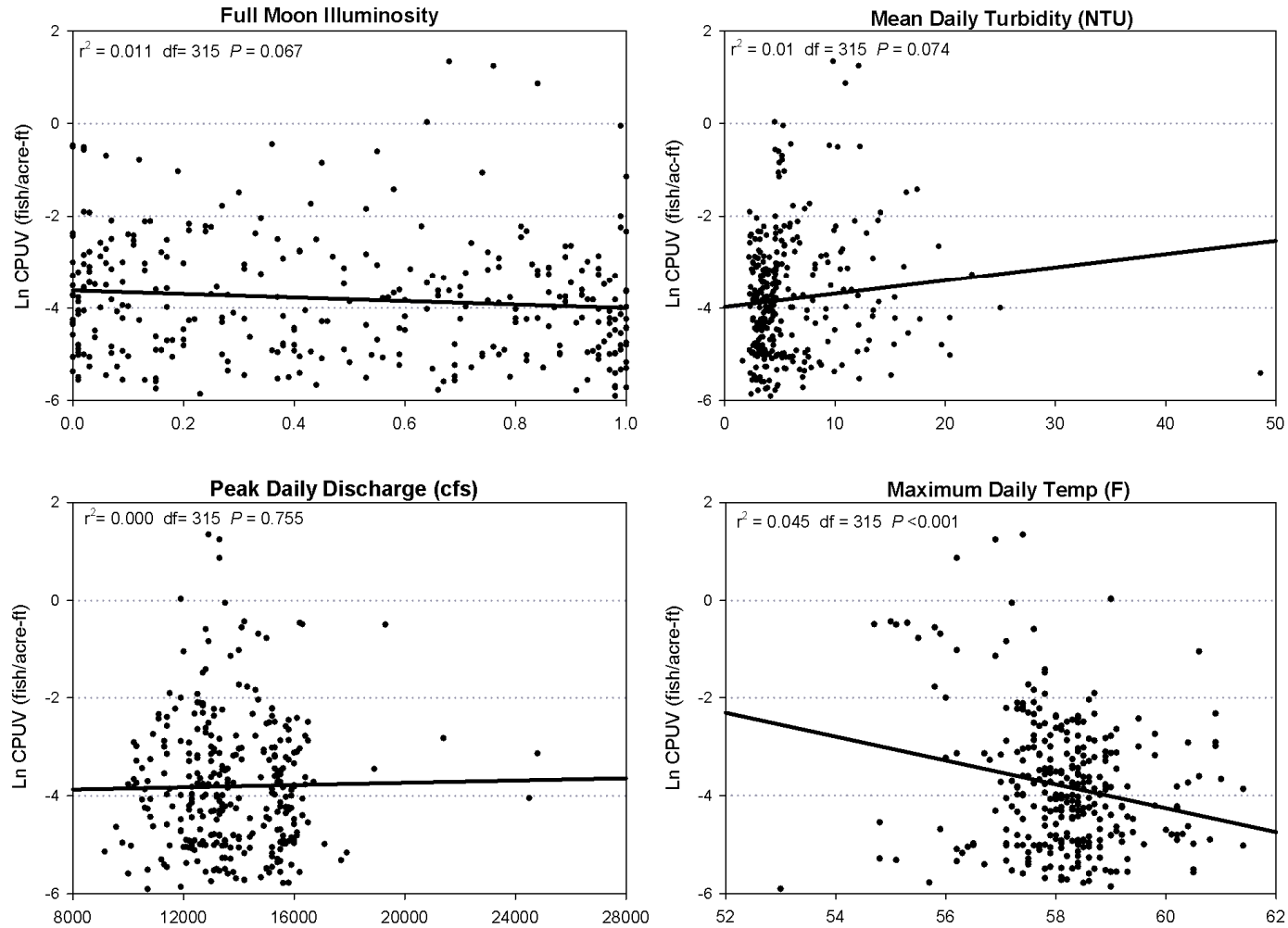


Figure 24. Regression analysis results of natural log (Ln) Green Sturgeon catch per unit volume (CPUV) and a) full moon illuminosity, b) mean daily turbidity, c) peak daily discharge and d) maximum daily temperatures at RBDD. All fish captured by rotary trap at RBDD (RM 243) on the Upper Sacramento River, CA between 2003 and 2012. Data from 2002 excluded from analysis due to limited effort and USBR Crown Flow study resulting in incomparable sampling regimes and results.

Lamprey Relative Abundance Environmental Covariate Analyses

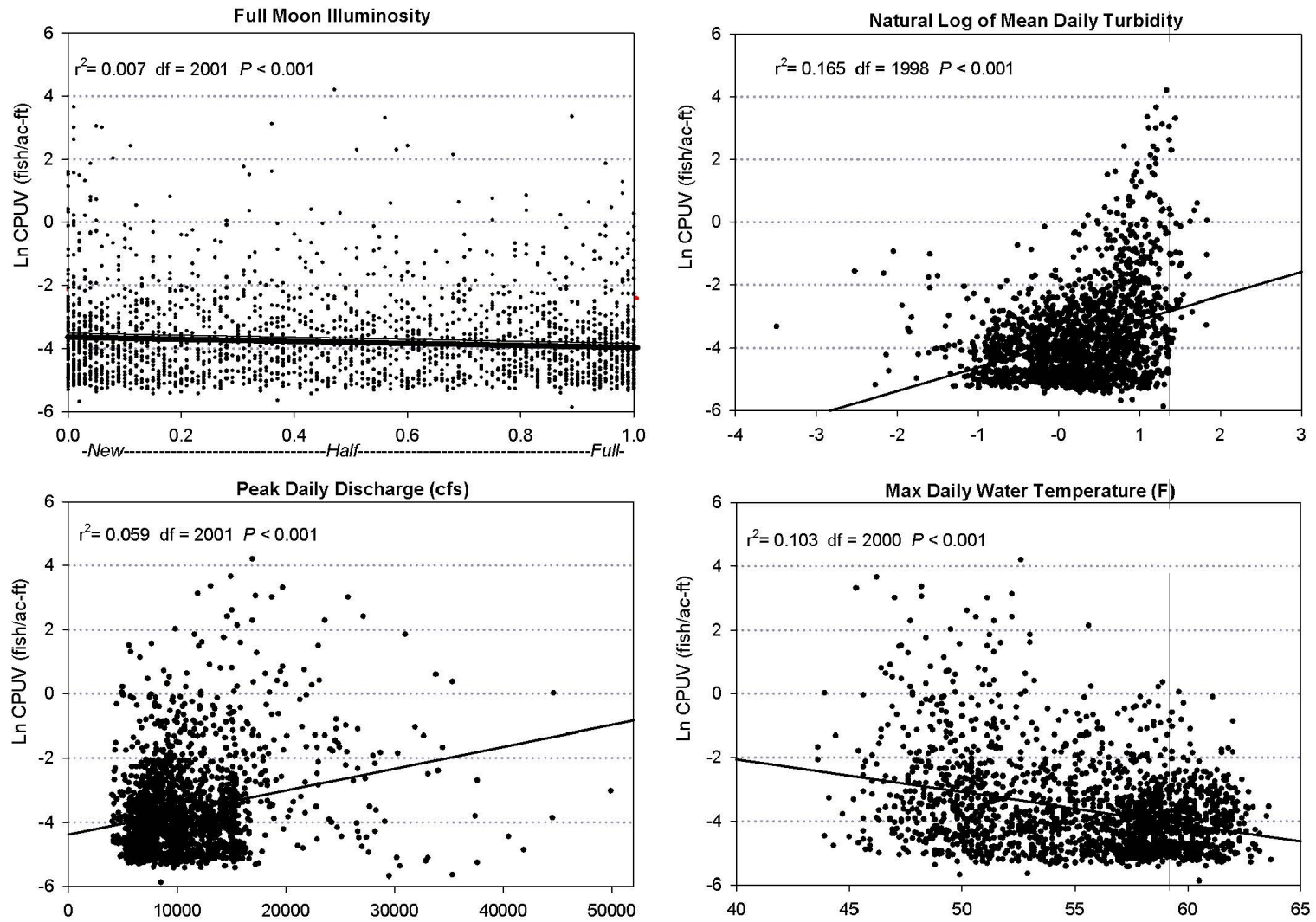


Figure 25. Regression analysis results of natural log (Ln) Lamprey *spp.* catch per unit volume (CPUV) and a) full moon illuminosity, b) Ln mean daily turbidity, c) peak daily discharge and d) maximum daily temperatures at RBDD. All fish captured by rotary trap at RBDD (RM 243) on the Upper Sacramento River, CA between water year 2003 and 2013.

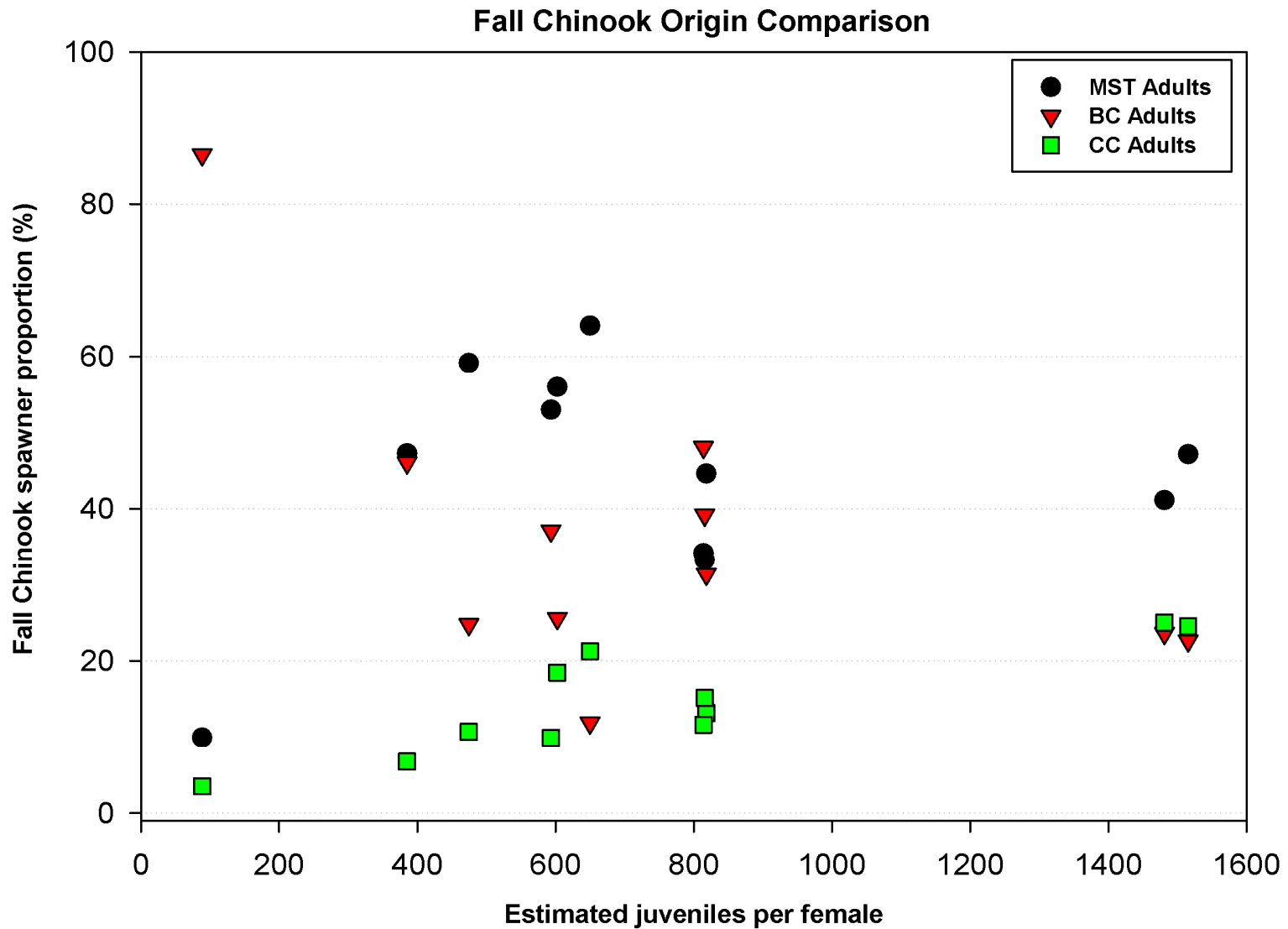


Figure 26. Comparison of estimated juveniles produced per estimated number of females in relation to distribution of fall Chinook spawners in the mainstem Sacramento River (MST), Battle Creek (BC), and Clear Creek (CC) between years 2002 and 2012.

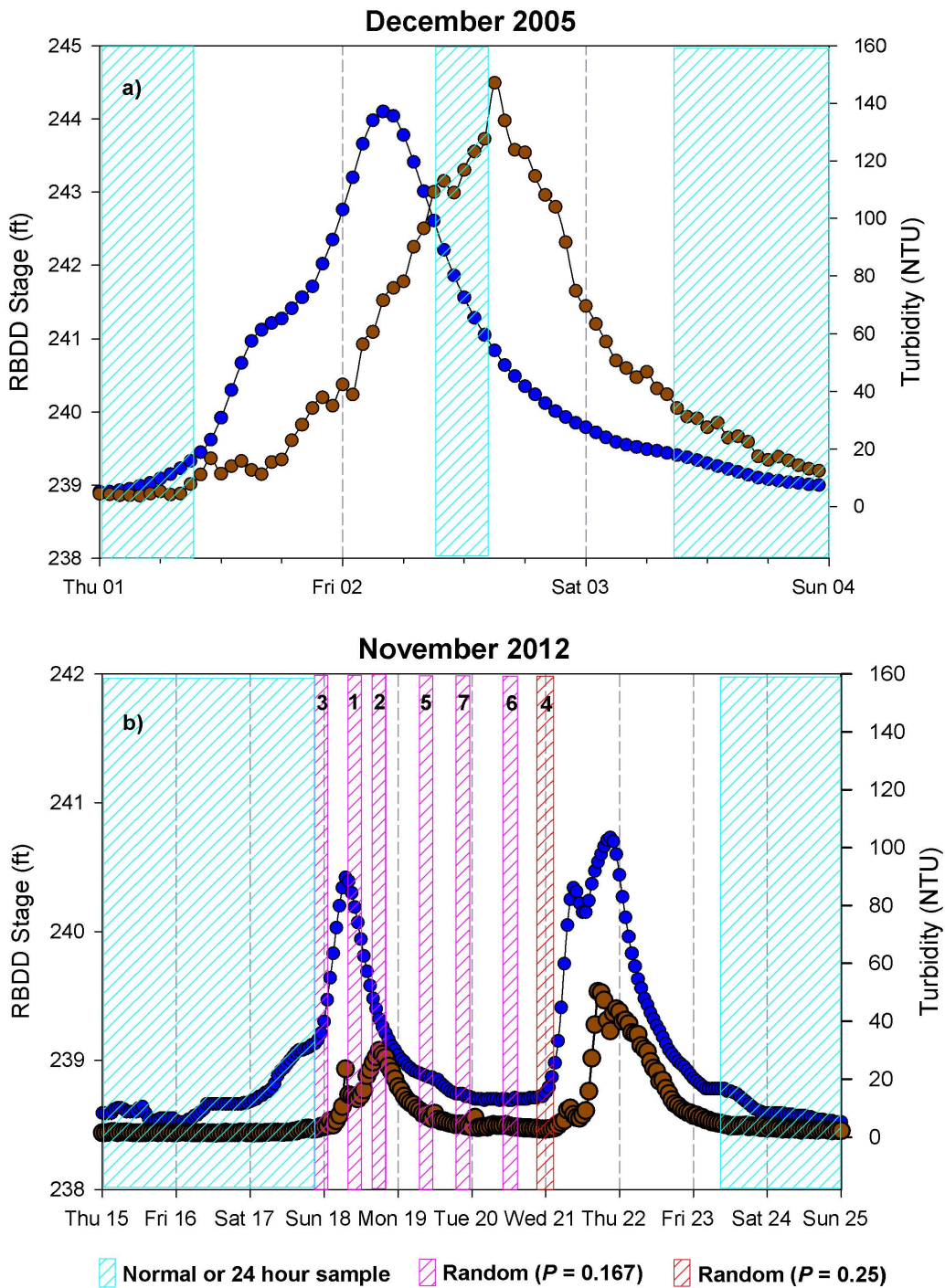


Figure 27. Timing comparison of RBDD stage (i.e., discharge level) and turbidity measurements along with sample collection times for storm events on a) December 1-4, 2005 and b) November 15-25, 2012. Numerals within sample period boxes in figure b indicate rank of standardized Chinook passage totals from greatest (1) to least (7).

APPENDIX 1

Appendix 1: List of Tables

Table	Page
A1. Summary of RBDD rotary trap annual effort, fall Chinook fry (<46 mm FL) passage estimates and lower and upper 90% confidence intervals (CI), by brood year for the period December 2002 through September 2013	108
A2. Summary of RBDD rotary trap annual effort, fall Chinook pre-smolt/smolt (>45 mm FL) passage estimates and lower and upper 90% confidence intervals (CI), by brood year for the period December 2002 through September 2013	108
A3. Summary of RBDD rotary trap annual effort, late-fall Chinook fry (<46 mm FL) passage estimates and lower and upper 90% confidence intervals (CI), by brood year for the period April 2002 through March 2013	109
A4. Summary of RBDD rotary trap annual effort, late-fall Chinook pre-smolt/smolt (>45 mm FL) passage estimates and lower and upper 90% confidence intervals (CI), by brood year for the period April 2002 through March 2013	109
A5. Summary of RBDD rotary trap annual effort, winter Chinook fry (<46 mm FL) passage estimates and lower and upper 90% confidence intervals (CI), by brood year for the period July 2002 through June 2013.....	110
A6. Summary of RBDD rotary trap annual effort, winter Chinook pre-smolt/smolt (>45 mm FL) passage estimates and lower and upper 90% confidence intervals (CI), by brood year for the period July 2002 through June 2013	110
A7. Summary of RBDD rotary trap annual effort, spring Chinook fry (<46 mm FL) passage estimates and lower and upper 90% confidence intervals (CI), by brood year for the period October 2002 through September 2013.....	111
A8. Summary of RBDD rotary trap annual effort, spring Chinook pre-smolt/smolt (>45 mm FL) passage estimates and lower and upper 90% confidence intervals (CI), by brood year for the period October 2002 through September 2013	111
A9. River Lamprey, <i>Lampetra ayresi</i> , annual capture, catch per unit volume (CPUV) and total length summaries for River Lamprey captured by RBDD rotary traps between water year (WY) 2003 and 2013	112
A10. Pacific Brook Lamprey, <i>Lampetra pacifica</i> , annual capture, catch per unit volume (CPUV) and total length summaries for Pacific Brook Lamprey captured by RBDD rotary traps between water year (WY) 2003 and 2013.....	112

Fall Chinook

Table A1. Summary of RBDD rotary trap annual effort, fall Chinook fry (<46 mm FL) passage estimates and lower and upper 90% confidence intervals (CI), by brood year for the period December 2002 through September 2013.

Brood Year	Effort	Estimated Fry		
		Passage	Low 90% CI	Up 90% CI
2002	0.76	14,687,984	348,386	42,027,818
2003	0.81	23,612,094	6,953,966	44,283,689
2004	0.85	7,946,496	3,449,094	12,447,378
2005	0.56	11,740,225	2,452,034	24,687,255
2006	0.90	10,152,406	3,458,524	17,567,355
2007	0.88	9,594,099	4,834,813	14,353,810
2008	0.79	6,684,332	3,335,617	10,033,164
2009	0.84	6,900,302	2,190,210	11,662,489
2010	0.75	6,302,961	3,432,017	9,502,694
2011	0.87	4,437,956	2,380,436	6,498,878
2012	0.85	21,375,192	14,332,396	28,700,826

Table A2. Summary of RBDD rotary trap annual effort, fall Chinook pre-smolt/smolt (>45 mm FL) passage estimates and lower and upper 90% confidence intervals (CI), by brood year for the period December 2002 through September 2013.

Brood Year	Effort	Estimated		
		Smolt Passage	Low 90% CI	Up 90% CI
2002	0.76	2,350,433	505,837	5,318,021
2003	0.81	4,124,773	1,879,521	6,393,281
2004	0.85	6,161,742	1,626,946	12,527,167
2005	0.56	6,470,030	1,041,939	14,426,210
2006	0.90	5,955,245	3,056,683	8,855,302
2007	0.88	2,537,504	1,291,848	3,821,912
2008	0.79	2,431,215	1,034,851	3,827,754
2009	0.84	1,632,074	868,002	2,396,298
2010	0.75	2,539,519	1,288,830	3,850,851
2011	0.87	1,833,305	1,029,403	2,637,509
2012	0.85	3,054,227	1,692,494	4,416,322

Late-Fall Chinook

Table A3. Summary of RBDD rotary trap annual effort, late-fall Chinook fry (<46 mm FL) passage estimates and lower and upper 90% confidence intervals (CI), by brood year for the period April 2002 through March 2013.

Brood Year	Effort	Estimated Fry		
		Passage	Low 90% CI	Up 90% CI
2002	0.57	442,393	84,832	901,368
2003	0.76	196,271	4,562	683,458
2004	0.88	24,382	8,802	40,591
2005	0.73	50,274	5,723	175,598
2006	0.70	284,999	41,006	634,496
2007	0.90	144,688	54,397	235,201
2008	0.89	10,489	4,347	17,813
2009	0.72	29,568	13,126	46,360
2010	0.86	113,667	26,705	200,935
2011	0.77	69,686	18,487	120,996
2012	0.89	67,479	9,925	136,431

Table A4. Summary of RBDD rotary trap annual effort, late-fall Chinook pre-smolt/smolt (>45 mm FL) passage estimates and lower and upper 90% confidence intervals (CI), by brood year for the period April 2002 through March 2013.

Brood Year	Effort	Estimated		
		Smolt Passage	Low 90% CI	Up 90% CI
2002	0.57	2,117,122	569,453	4,093,545
2003	0.76	149,976	72,089	230,841
2004	0.88	122,779	64,498	181,783
2005	0.73	93,407	35,067	160,738
2006	0.70	175,269	82,005	273,572
2007	0.90	390,932	213,642	568,595
2008	0.89	81,506	41,983	121,166
2009	0.72	190,256	83,201	297,652
2010	0.86	69,771	33,929	106,575
2011	0.77	27,354	9,535	45,914
2012	0.89	73,055	32,567	113,633

Winter Chinook

Table A5. Summary of RBDD rotary trap annual effort, winter Chinook fry (<46 mm FL) passage estimates and lower and upper 90% confidence intervals (CI), by brood year for the period July 2002 through June 2013.

Brood Year	Effort	Estimated Fry		
		Passage	Low 90% CI	Up 90% CI
2002	0.64	6,381,286	2,156,758	11,217,962
2003	0.81	4,420,296	2,743,637	6,096,955
2004	0.84	3,087,102	1,812,619	4,361,584
2005	0.64	7,533,380	4,225,130	10,841,630
2006	0.83	5,813,140	3,307,323	8,318,957
2007	0.89	1,158,791	744,804	1,572,817
2008	0.87	1,063,919	662,381	1,465,748
2009	0.75	3,587,134	2,076,422	5,098,125
2010	0.81	875,049	603,549	1,146,644
2011	0.82	638,056	441,983	834,289
2012	0.89	722,048	545,751	898,345

Table A6. Summary of RBDD rotary trap annual effort, winter Chinook pre-smolt/smolt (>45 mm FL) passage estimates and lower and upper 90% confidence intervals (CI), by brood year for the period July 2002 through June 2013.

Brood Year	Effort	Estimated		
		Smolt Passage	Low 90% CI	Up 90% CI
2002	0.64	737,755	373,538	1,149,079
2003	0.81	800,719	453,256	1,169,559
2004	0.84	347,581	179,502	519,265
2005	0.64	829,302	324,860	1,442,763
2006	0.83	873,940	487,244	1,264,701
2007	0.89	281,773	180,254	387,123
2008	0.87	181,071	110,592	252,089
2009	0.75	815,188	410,512	1,222,586
2010	0.81	410,341	210,252	613,810
2011	0.82	210,920	130,861	291,312
2012	0.89	627,771	354,764	900,897

Spring Chinook

Table A7. Summary of RBDD rotary trap annual effort, spring Chinook fry (<46 mm FL) passage estimates and lower and upper 90% confidence intervals (CI), by brood year for the period October 2002 through September 2013.

Brood Year	Effort	Estimated Fry		
		Passage	Low 90% CI	Up 90% CI
2002	0.75	159,084	67,900	255,023
2003	0.81	502,386	189,371	857,899
2004	0.85	155,053	59,655	250,451
2005	0.57	427,719	111,396	925,898
2006	0.89	174,186	114,642	233,907
2007	0.89	336,714	212,765	460,712
2008	0.85	40,213	26,016	54,448
2009	0.79	219,627	91,683	347,845
2010	0.77	89,213	39,829	138,597
2011	0.86	88,355	63,469	113,274
2012	0.86	134,028	82,843	185,271

Table A8. Summary of RBDD rotary trap annual effort, spring Chinook pre-smolt/smolt (>45 mm FL) passage estimates and lower and upper 90% confidence intervals (CI), by brood year for the period October 2002 through September 2013.

Brood Year	Effort	Estimated		
		Smolt Passage	Low 90% CI	Up 90% CI
2002	0.75	118,393	43,022	239,870
2003	0.81	124,529	59,434	197,777
2004	0.85	275,898	113,564	460,990
2005	0.57	187,828	19,676	460,441
2006	0.89	247,250	123,621	371,968
2007	0.89	32,787	15,894	51,271
2008	0.85	124,460	40,130	208,954
2009	0.79	218,778	83,930	354,607
2010	0.77	69,753	21,938	123,577
2011	0.86	95,935	37,782	159,702
2012	0.86	186,869	89,566	284,936

Table A9. River Lamprey, *Lampetra ayresi*, annual capture, catch per unit volume (CPUV) and total length summaries for River Lamprey captured by RBDD rotary traps between water year (WY) 2003 and 2013.

WY	Catch	CPUV Fish/ac-ft	Min TL (mm)	Max TL (mm)	Mean (mm)	Median (mm)
2003	0	0.00	-	-	-	-
2004	1	0.01	102	102	102	-
2005	0	0.00	-	-	-	-
2006	0	0.00	-	-	-	-
2007	0	0.00	-	-	-	-
2008	0	0.00	-	-	-	-
2009	0	0.00	-	-	-	-
2010	1	0.01	110	110	110	-
2011	26	0.23	99	151	121	121
2012	4	0.02	128	168	144	140
2013	0	0.00	-	-	-	-
Mean	2.9	0.02	109.8	132.8	119.3	130.5
SD	7.8	0.07	13.0	31.8	18.2	13.4
CV	266.5%	279.2%	11.9%	24.0%	15.3%	10.3%

Table A10. Pacific Brook Lamprey, *Lampetra pacifica*, annual capture, catch per unit volume (CPUV) and total length summaries for Pacific Brook Lamprey captured by RBDD rotary traps between water year (WY) 2003 and 2013.

WY	Catch	CPUV Fish/ac-ft	Min TL (mm)	Max TL (mm)	Mean (mm)	Median (mm)
2003	6	0.06	98	132	116	114.5
2004	1	0.01	159	159	159	-
2005	0	0.00	-	-	-	-
2006	0	0.00	-	-	-	-
2007	0	0.00	-	-	-	-
2008	0	0.00	-	-	-	-
2009	0	0.00	-	-	-	-
2010	1	0.02	120	120	120	120
2011	1	0.01	147	147	147	147
2012	6	0.04	112	156	138	142
2013	21	0.12	110	148	124	122
Mean	3.3	0.02	124.3	143.7	134.0	129.1
SD	6.3	0.04	23.6	14.9	16.9	14.4
CV	192.8%	159.7%	19.0%	10.4%	12.6%	11.2%

APPENDIX 2

Appendix 2: List of Figures

Figure	Page
A1. Brood year 2002 winter Chinook fry passage with moon illuminosity indicated by background shading (peak of light gray equals full moon), mean daily water temperatures (red), and peak daily flows (blue) at Red Bluff Diversion Dam.....	117
A2. Brood year 2003 winter Chinook fry passage with moon illuminosity indicated by background shading (peak of light gray equals full moon), mean daily water temperatures (red), and peak daily flows (blue) at Red Bluff Diversion Dam.....	118
A3. Brood year 2004 winter Chinook fry passage with moon illuminosity indicated by background shading (peak of light gray equals full moon), mean daily water temperatures (red), and peak daily flows (blue) at Red Bluff Diversion Dam.....	119
A4. Brood year 2005 winter Chinook fry passage with moon illuminosity indicated by background shading (peak of light gray equals full moon), mean daily water temperatures (red), and peak daily flows (blue) at Red Bluff Diversion Dam.....	120
A5. Brood year 2006 winter Chinook fry passage with moon illuminosity indicated by background shading (peak of light gray equals full moon), mean daily water temperatures (red), and peak daily flows (blue) at Red Bluff Diversion Dam.....	121
A6. Brood year 2007 winter Chinook fry passage with moon illuminosity indicated by background shading (peak of light gray equals full moon), mean daily water temperatures (red), and peak daily flows (blue) at Red Bluff Diversion Dam.....	122
A7. Brood year 2008 winter Chinook fry passage with moon illuminosity indicated by background shading (peak of light gray equals full moon), mean daily water temperatures (red), and peak daily flows (blue) at Red Bluff Diversion Dam.....	123
A8. Brood year 2009 winter Chinook fry passage with moon illuminosity indicated by background shading (peak of light gray equals full moon), mean daily water temperatures (red), and peak daily flows (blue) at Red Bluff Diversion Dam.....	124
A9. Brood year 2010 winter Chinook fry passage with moon illuminosity indicated by background shading (peak of light gray equals full moon), mean daily water temperatures (red), and peak daily flows (blue) at Red Bluff Diversion Dam.....	125
A10. Brood year 2011 winter Chinook fry passage with moon illuminosity indicated by background shading (peak of light gray equals full moon), mean daily water temperatures (red), and peak daily flows (blue) at Red Bluff Diversion Dam.....	126

Appendix 2: List of Figures continued

Figure	Page
A11. Brood year 2012 winter Chinook fry passage with moon illuminosity indicated by background shading (peak of light gray equals full moon), mean daily water temperatures (red), and peak daily flows (blue) at Red Bluff Diversion Dam.....	127
A12. Brood year 2002 winter Chinook pre-smolt/smolt passage with moon illuminosity indicated by background shading (peak of light gray equals full moon), mean daily water temperatures (red), and peak daily flows (blue) at Red Bluff Diversion Dam	128
A13. Brood year 2003 winter Chinook pre-smolt/smolt passage with moon illuminosity indicated by background shading (peak of light gray equals full moon), mean daily water temperatures (red), and peak daily flows (blue) at Red Bluff Diversion Dam	129
A14. Brood year 2004 winter Chinook pre-smolt/smolt passage with moon illuminosity indicated by background shading (peak of light gray equals full moon), mean daily water temperatures (red), and peak daily flows (blue) at Red Bluff Diversion Dam	130
A15. Brood year 2005 winter Chinook pre-smolt/smolt passage with moon illuminosity indicated by background shading (peak of light gray equals full moon), mean daily water temperatures (red), and peak daily flows (blue) at Red Bluff Diversion Dam	131
A16. Brood year 2006 winter Chinook pre-smolt/smolt passage with moon illuminosity indicated by background shading (peak of light gray equals full moon), mean daily water temperatures (red), and peak daily flows (blue) at Red Bluff Diversion Dam	132
A17. Brood year 2007 winter Chinook pre-smolt/smolt passage with moon illuminosity indicated by background shading (peak of light gray equals full moon), mean daily water temperatures (red), and peak daily flows (blue) at Red Bluff Diversion Dam	133
A18. Brood year 2008 winter Chinook pre-smolt/smolt passage with moon illuminosity indicated by background shading (peak of light gray equals full moon), mean daily water temperatures (red), and peak daily flows (blue) at Red Bluff Diversion Dam	134
A19. Brood year 2009 winter Chinook pre-smolt/smolt passage with moon illuminosity indicated by background shading (peak of light gray equals full moon), mean daily water temperatures (red), and peak daily flows (blue) at Red Bluff Diversion Dam	135
A20. Brood year 2010 winter Chinook pre-smolt/smolt passage with moon illuminosity indicated by background shading (peak of light gray equals full moon), mean daily water temperatures (red), and peak daily flows (blue) at Red Bluff Diversion Dam	136

Appendix 2: List of Figures continued

Figure	Page
A21. Brood year 2011 winter Chinook pre-smolt/smolt passage with moon illuminosity indicated by background shading (peak of light gray equals full moon), mean daily water temperatures (red), and peak daily flows (blue) at Red Bluff Diversion Dam 137	
A22. Brood year 2012 winter Chinook pre-smolt/smolt passage with moon illuminosity indicated by background shading (peak of light gray equals full moon), mean daily water temperatures (red), and peak daily flows (blue) at Red Bluff Diversion Dam 138	

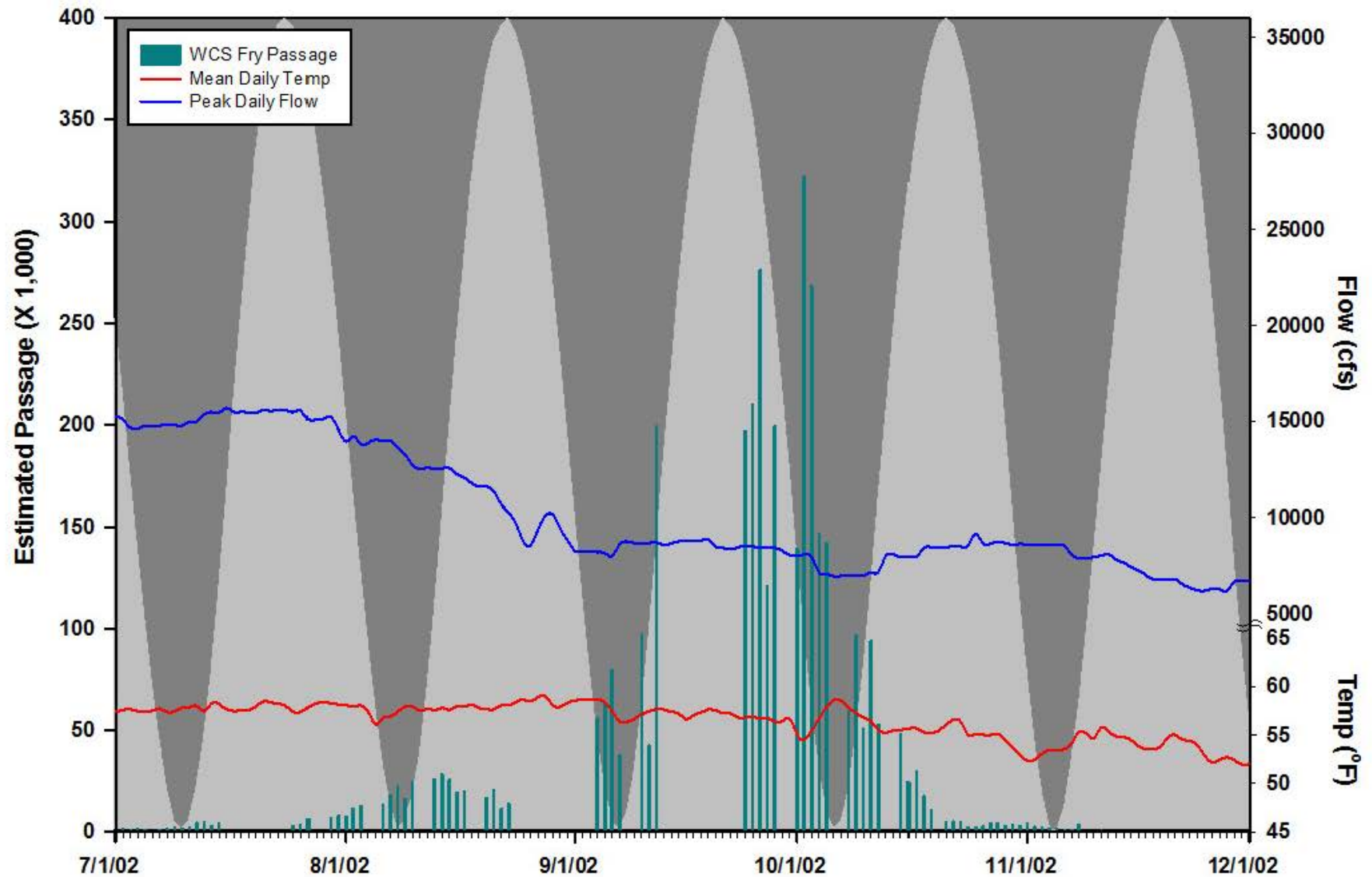


Figure A1. Brood Year 2002 winter Chinook fry passage with moon illuminosity indicated by background shading (peak of light gray equals full moon), mean daily water temperatures (red), and peak daily flows (blue) at Red Bluff Diversion Dam.

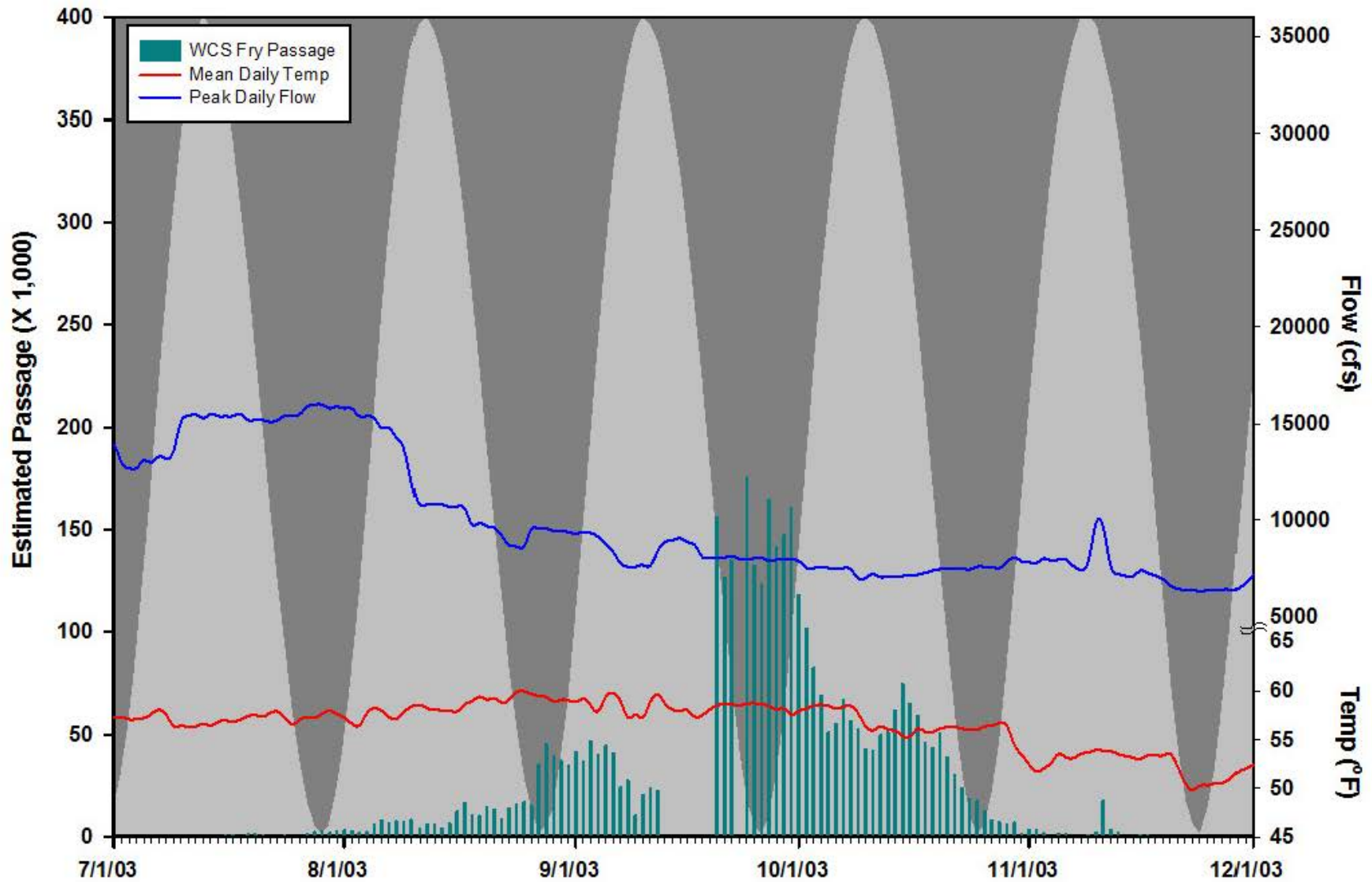


Figure A2. Brood Year 2003 winter Chinook fry passage with moon illuminosity indicated by back ground shading (peak of light gray equals full moon), mean daily water temperatures (red), and peak daily flows (blue) at Red Bluff Diversion Dam.

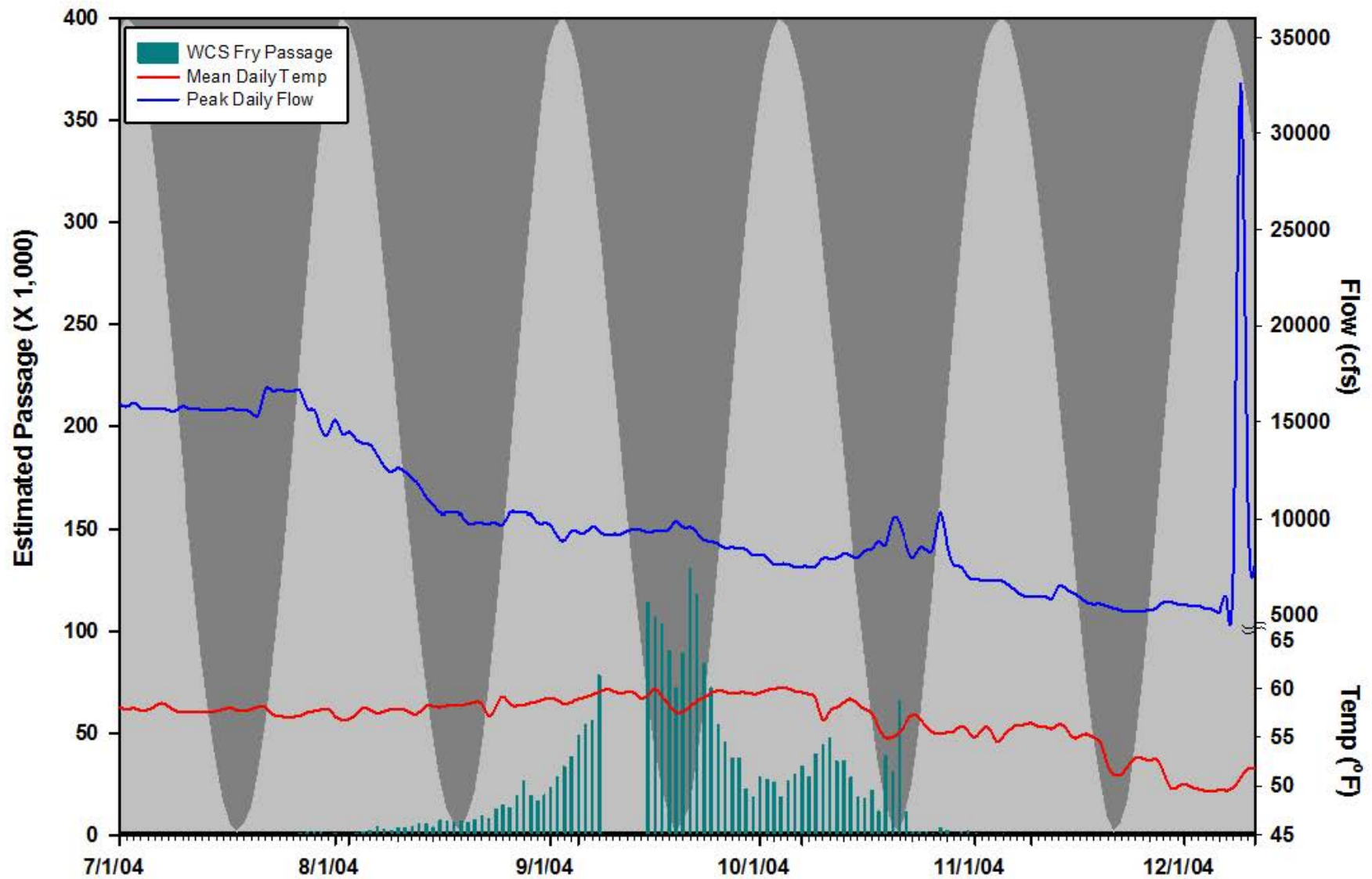


Figure A3. Brood Year 2004 winter Chinook fry passage with moon illuminosity indicated by back ground shading (peak of light gray equals full moon), mean daily water temperatures (red), and peak daily flows (blue) at Red Bluff Diversion Dam.

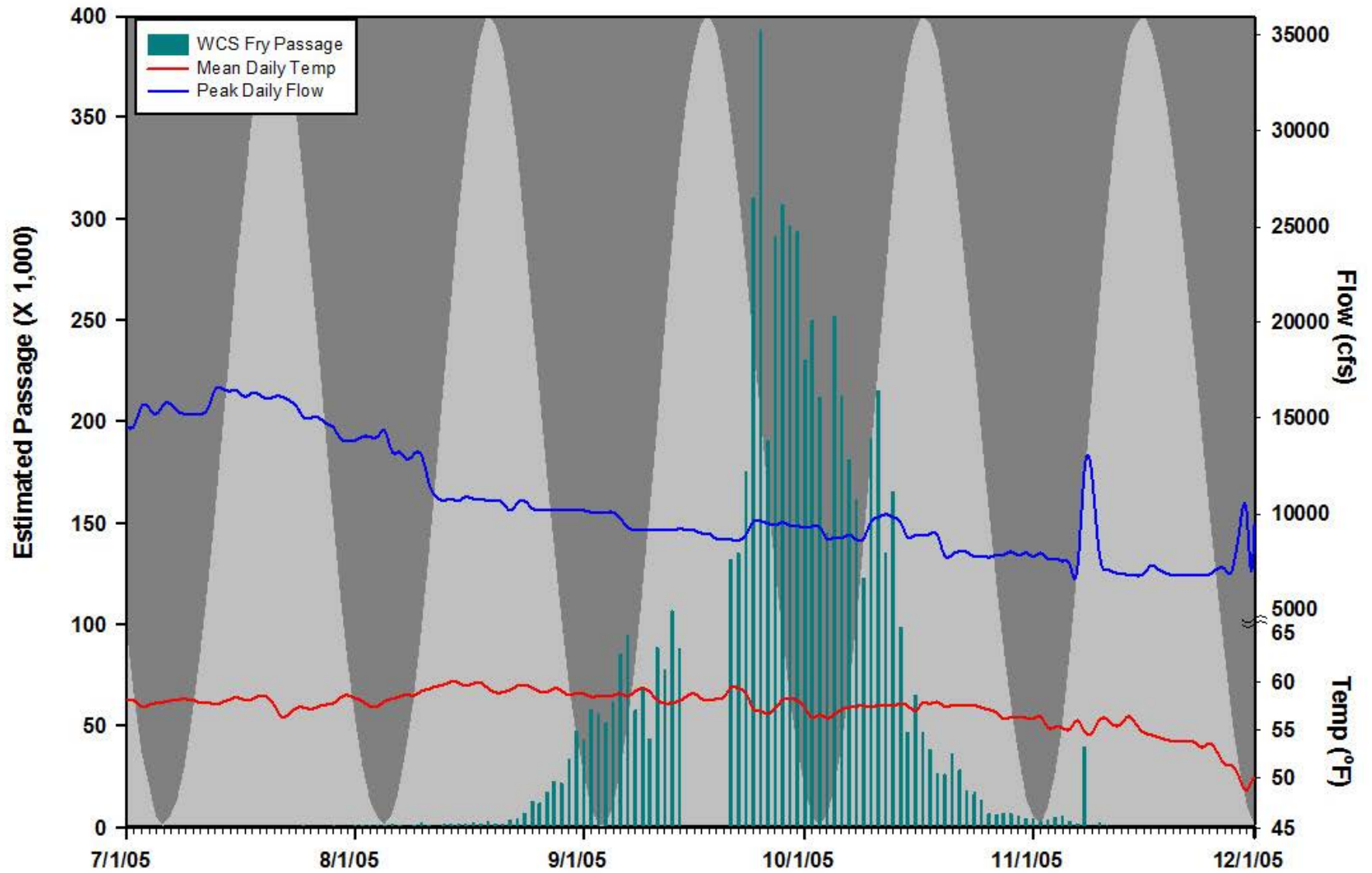


Figure A4. Brood Year 2005 winter Chinook fry passage with moon illuminosity indicated by back ground shading (peak of light gray equals full moon), mean daily water temperatures (red), and peak daily flows (blue) at Red Bluff Diversion Dam.

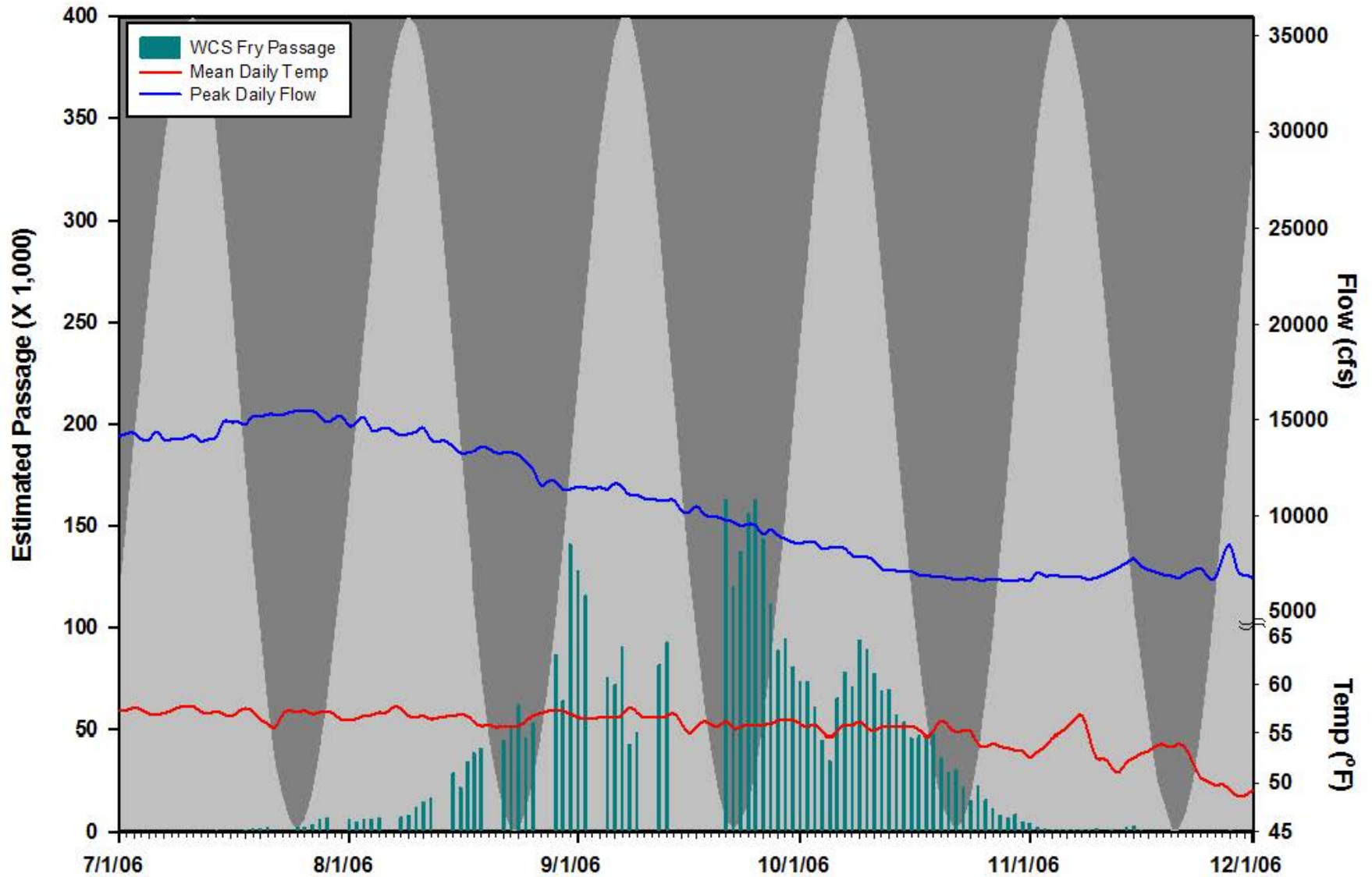


Figure A5. Brood Year 2006 winter Chinook fry passage with moon illuminosity indicated by back ground shading (peak of light gray equals full moon), mean daily water temperatures (red), and peak daily flows (blue) at Red Bluff Diversion Dam.

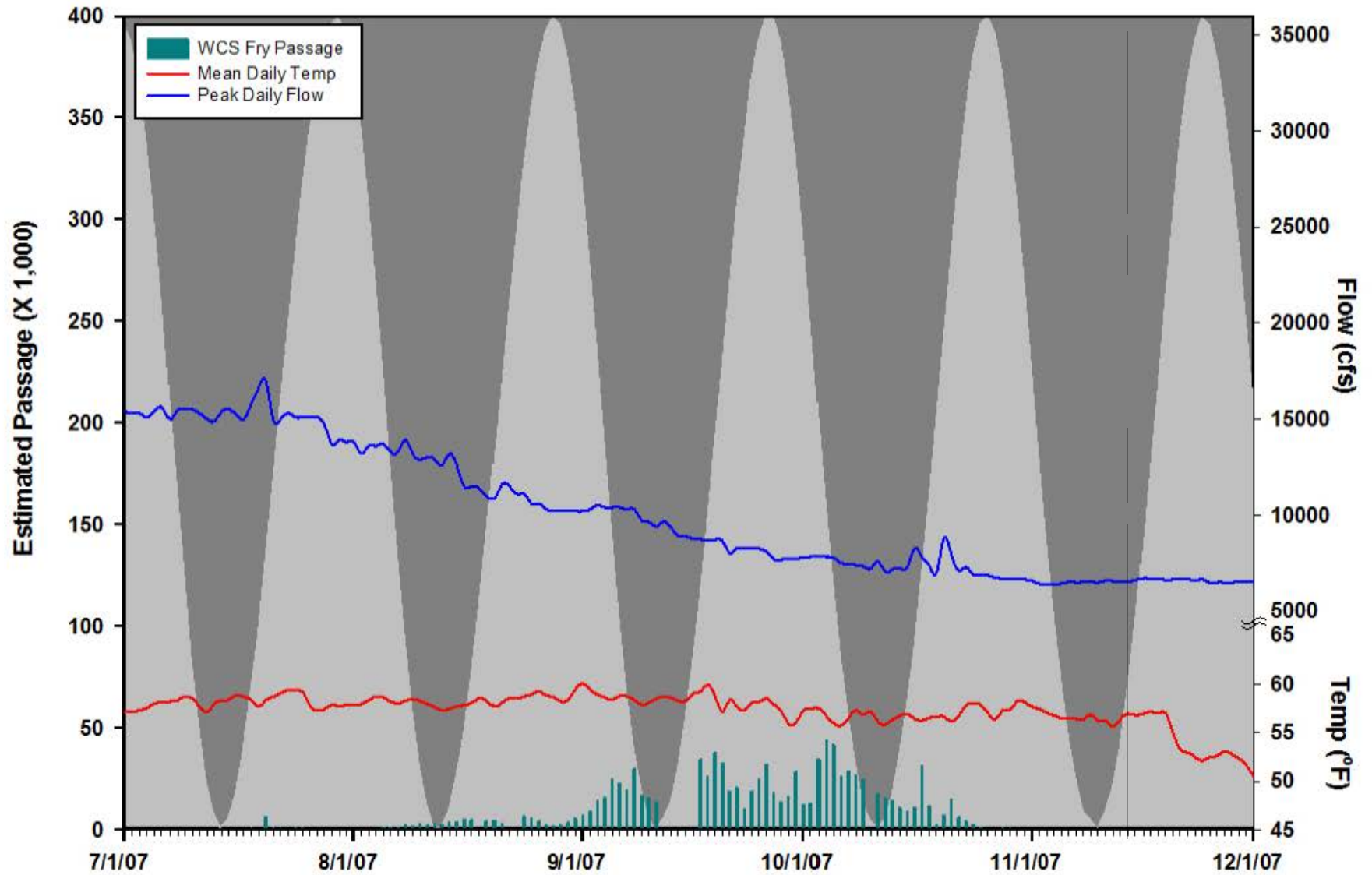


Figure A6. Brood Year 2007 winter Chinook fry passage with moon illuminosity indicated by back ground shading (peak of light gray equals full moon), mean daily water temperatures (red), and peak daily flows (blue) at Red Bluff Diversion Dam.

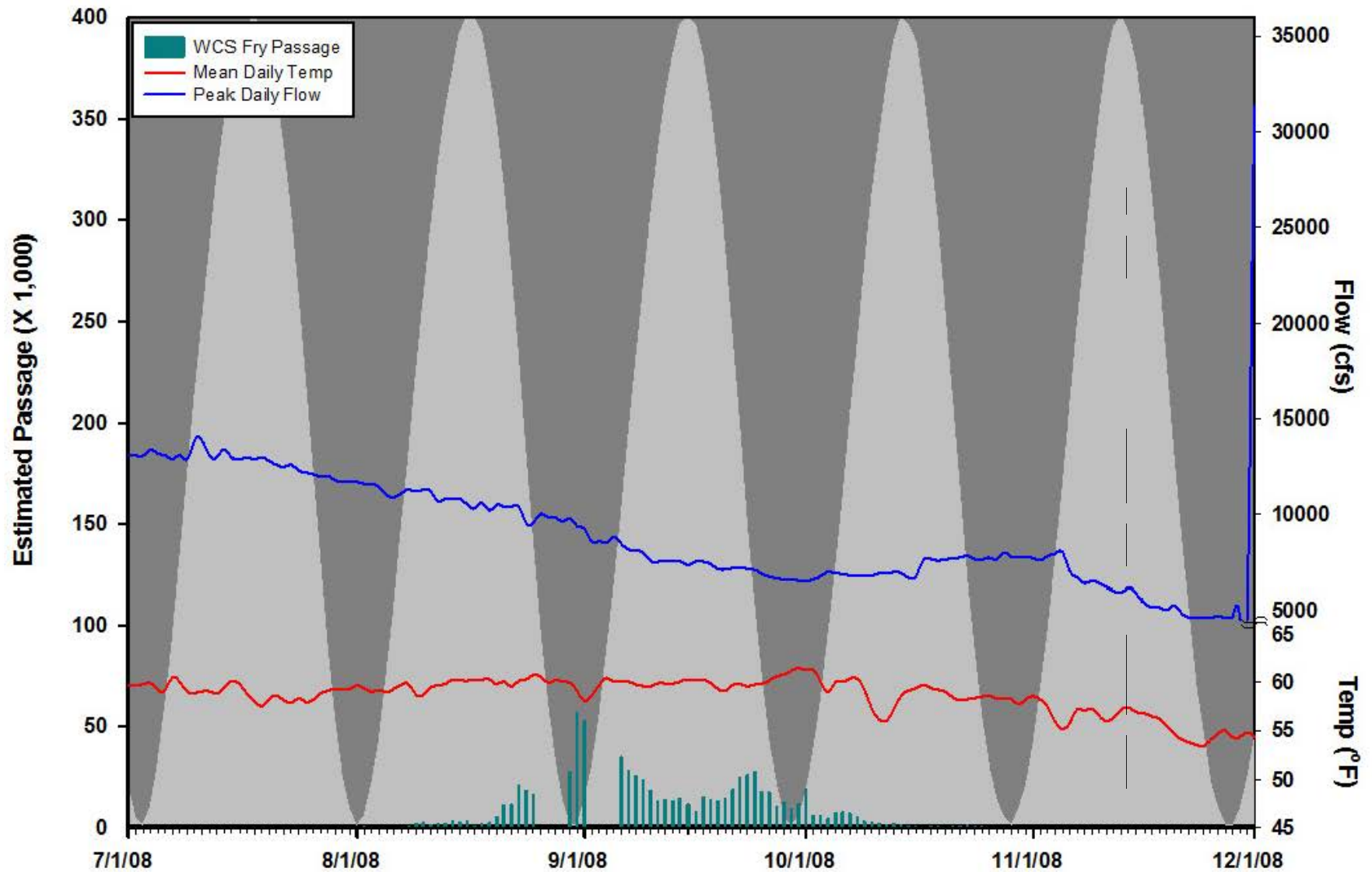


Figure A7. Brood Year 2008 winter Chinook fry passage with moon illuminosity indicated by back ground shading (peak of light gray equals full moon), mean daily water temperatures (red), and peak daily flows (blue) at Red Bluff Diversion Dam.

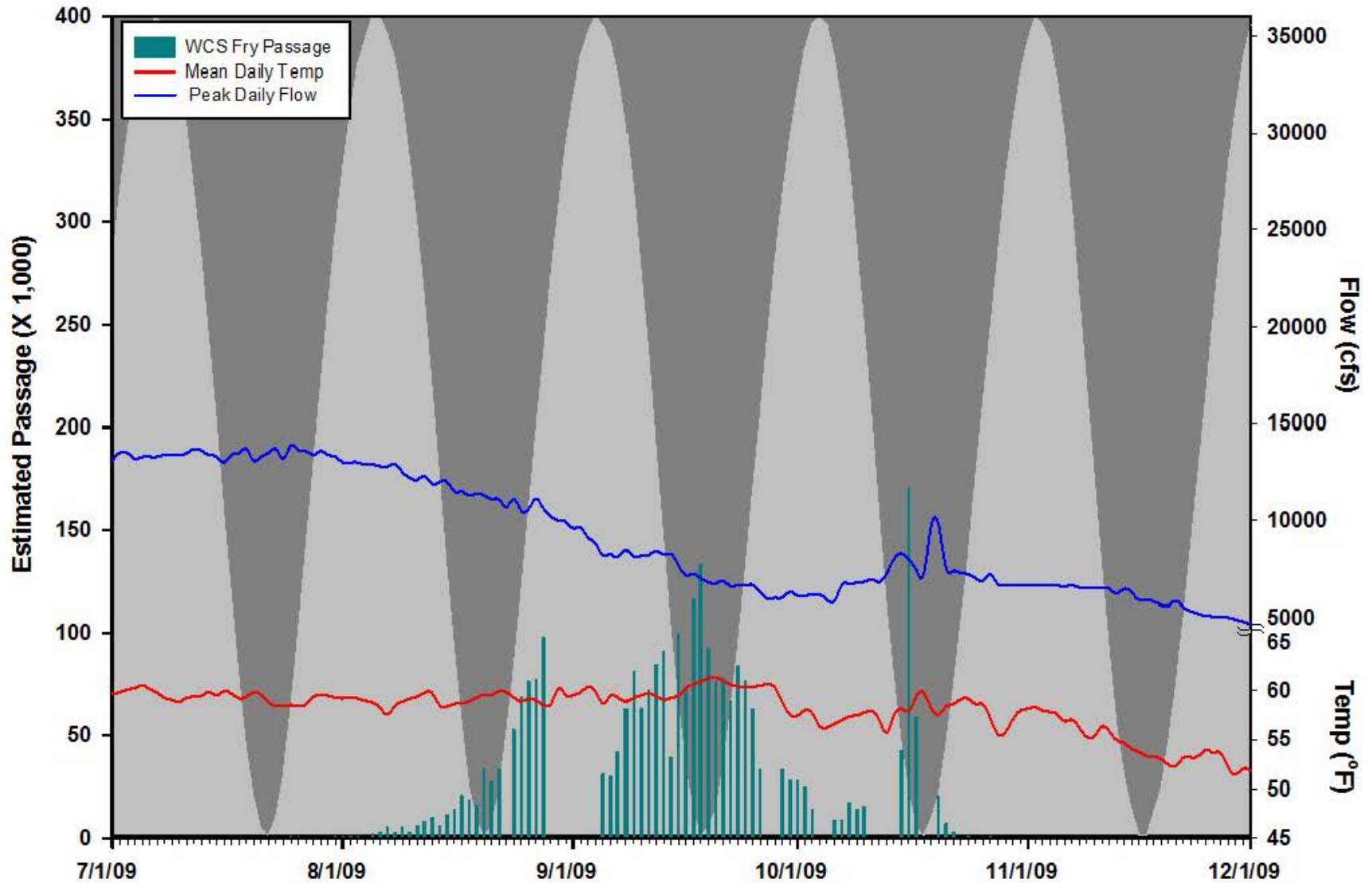


Figure A8. Brood Year 2009 winter Chinook fry passage with moon illuminosity indicated by back ground shading (peak of light gray equals full moon), mean daily water temperatures (red), and peak daily flows (blue) at Red Bluff Diversion Dam.

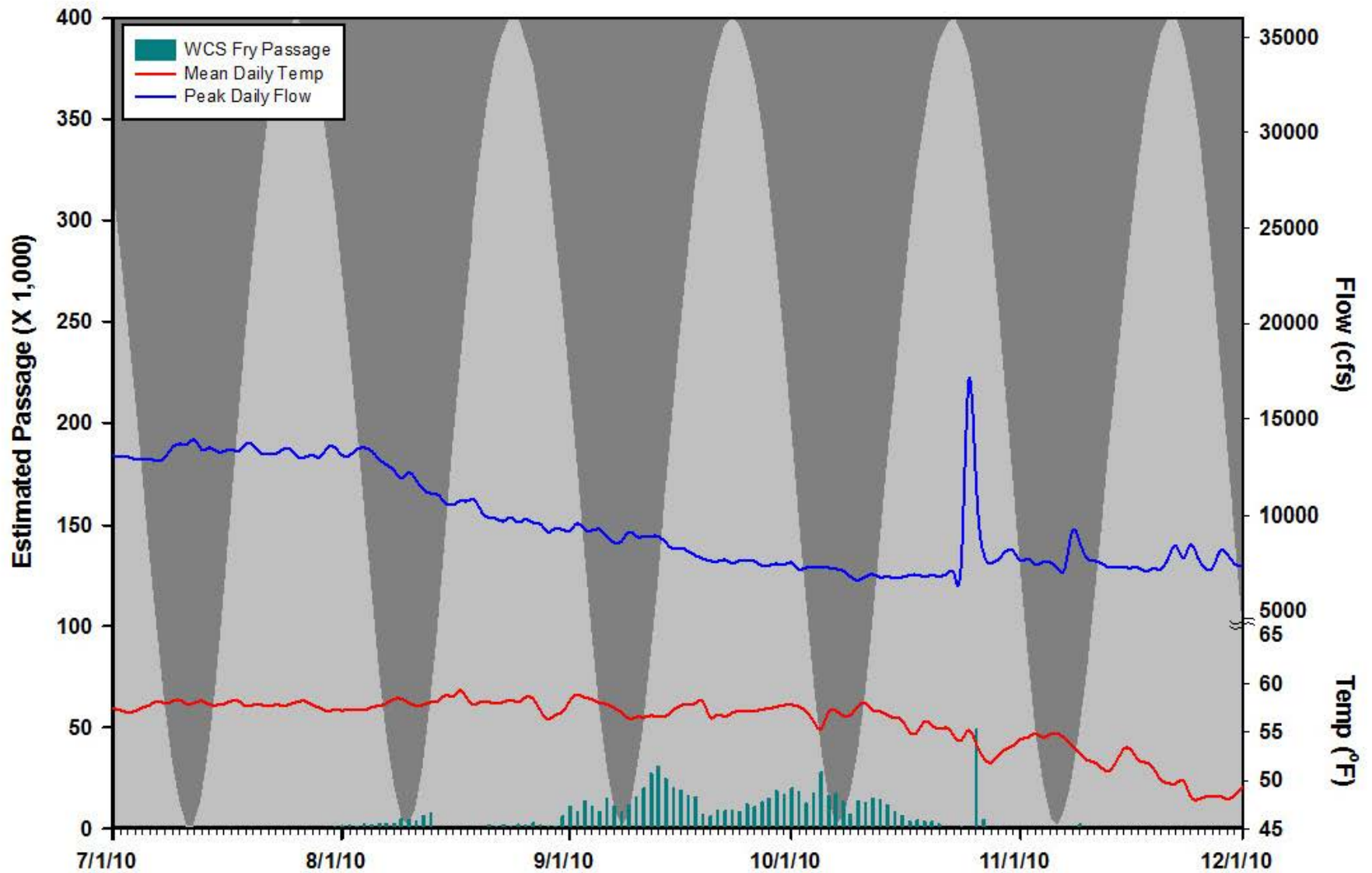


Figure A9. Brood Year 2010 winter Chinook fry passage with moon illuminosity indicated by back ground shading (peak of light gray equals full moon), mean daily water temperatures (red), and peak daily flows (blue) at Red Bluff Diversion Dam.

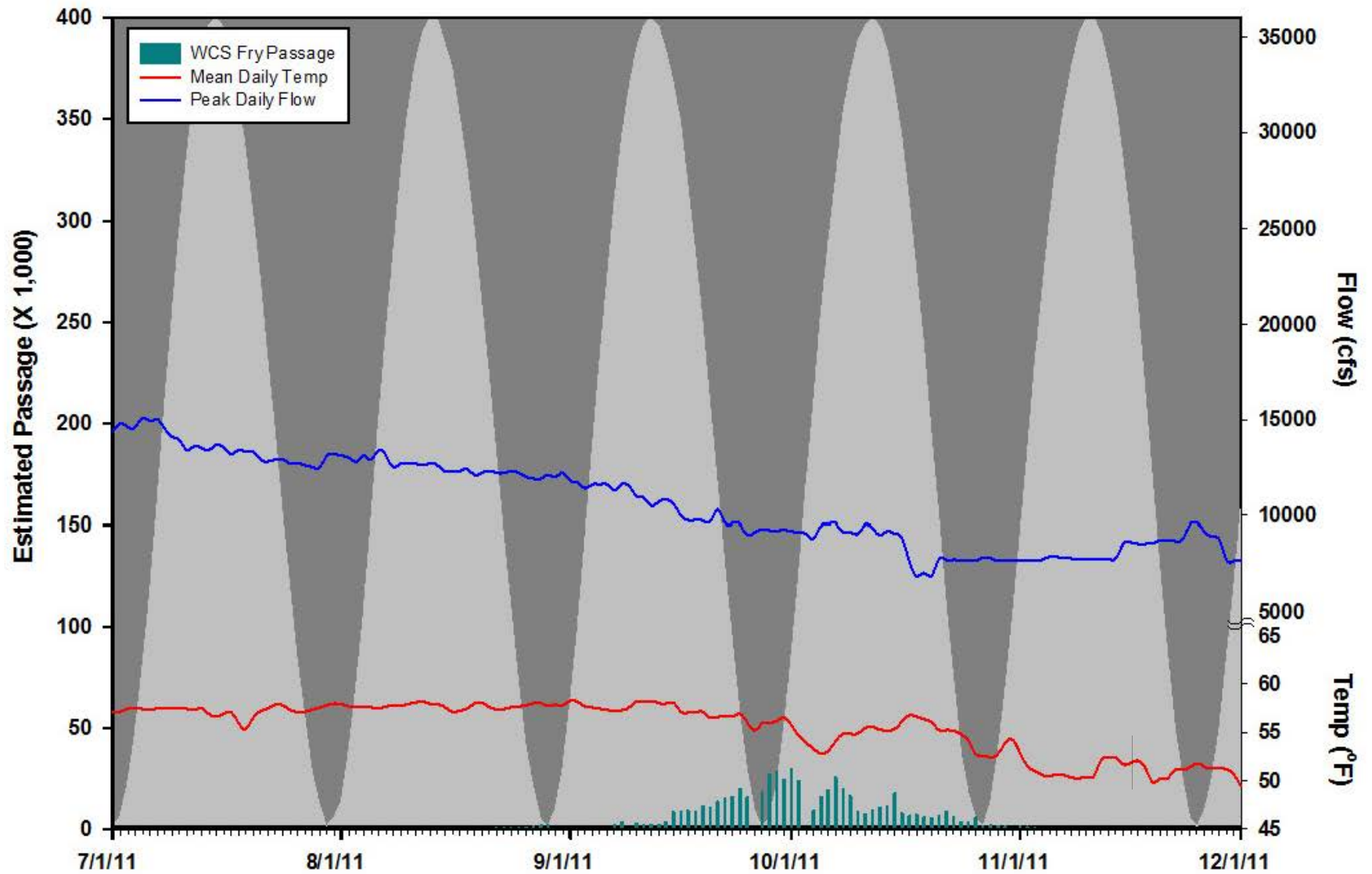


Figure A10. Brood Year 2011 winter Chinook fry passage with moon illuminosity indicated by back ground shading (peak of light gray equals full moon), mean daily water temperatures (red), and peak daily flows (blue) at Red Bluff Diversion Dam.

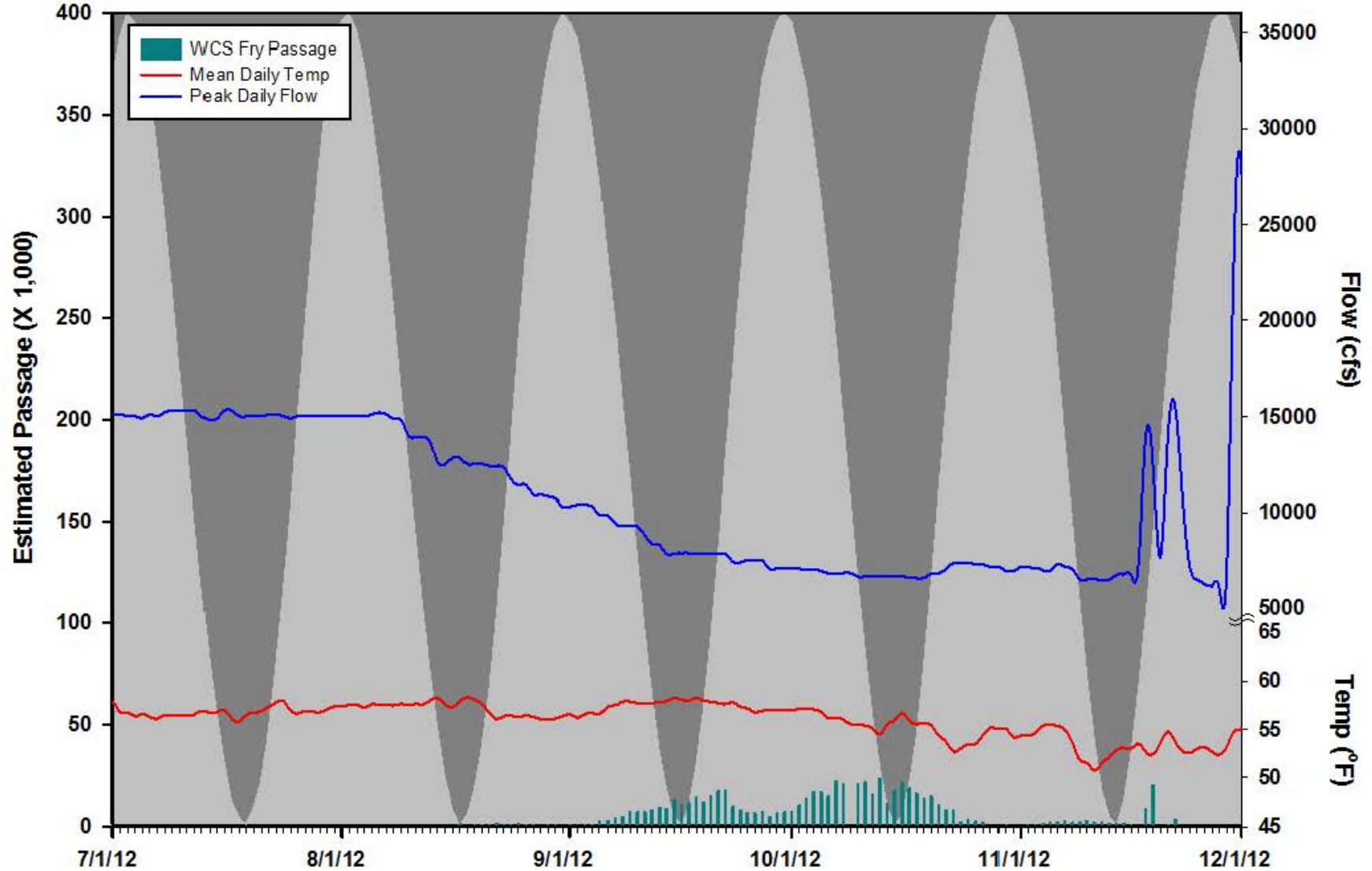


Figure A11. Brood Year 2012 winter Chinook fry passage with moon illuminosity indicated by back ground shading (peak of light gray equals full moon), mean daily water temperatures (red), and peak daily flows (blue) at Red Bluff Diversion Dam.

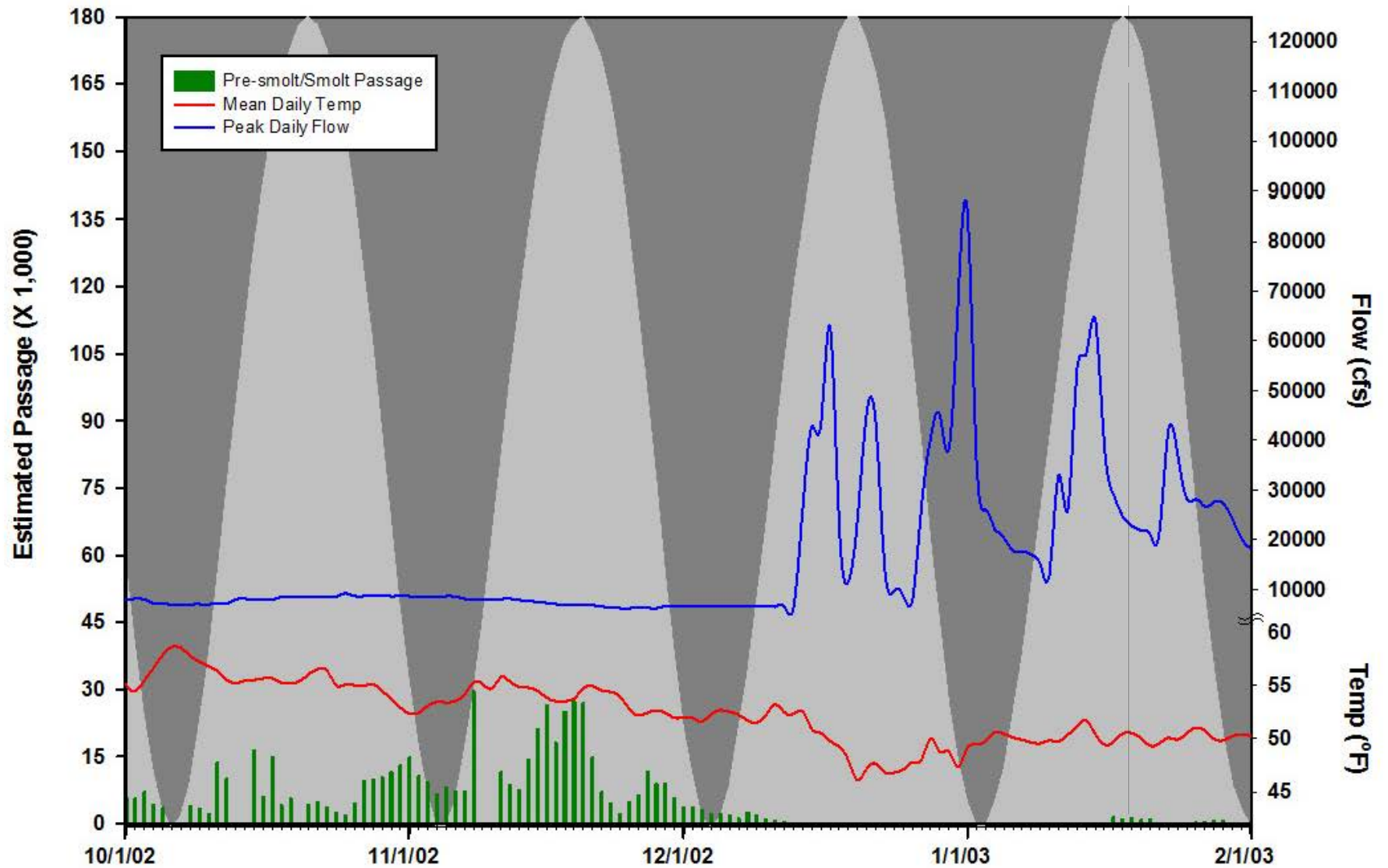


Figure A12. Brood Year 2002 winter Chinook pre-smolt/smolt passage with moon illuminosity indicated by back ground shading (peak of light gray equals full moon), mean daily water temperatures (red), and peak daily flows (blue) at Red Bluff Diversion Dam.

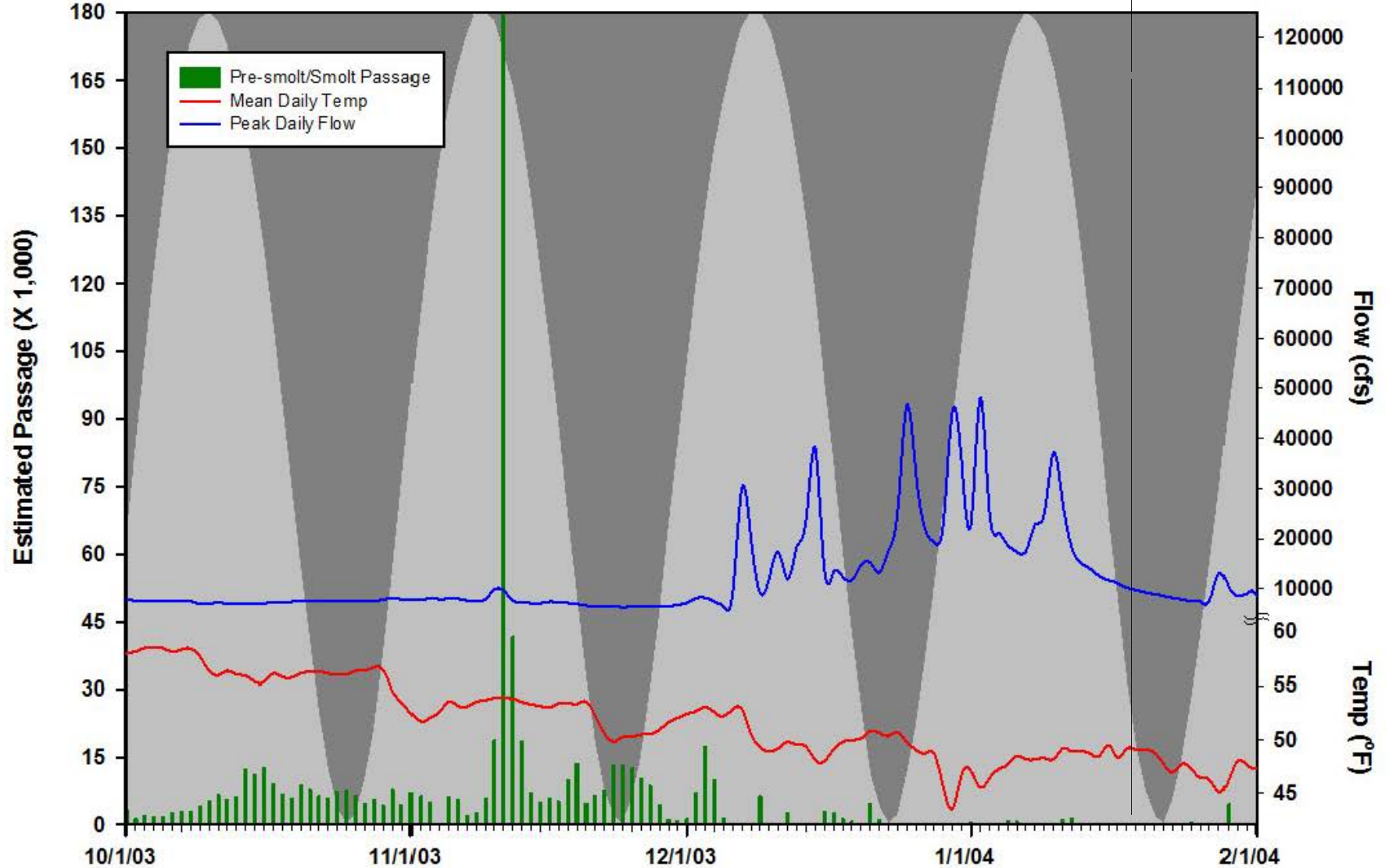


Figure A13. Brood Year 2003 winter Chinook pre-smolt/smolt passage with moon illuminosity indicated by back ground shading (peak of light gray equals full moon), mean daily water temperatures (red), and peak daily flows (blue) at Red Bluff Diversion Dam.

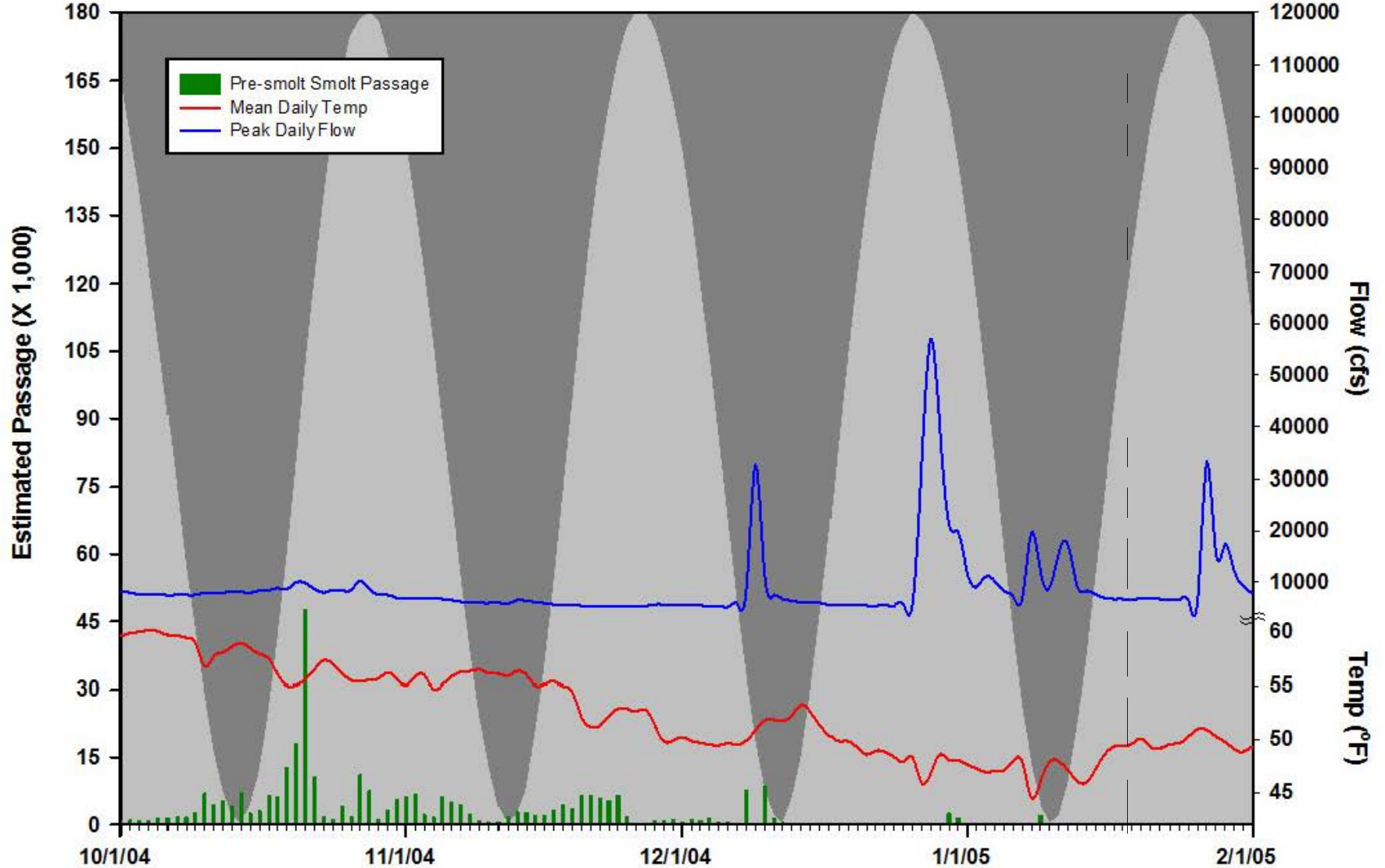


Figure A14. Brood Year 2004 winter Chinook pre-smolt/smolt passage with moon illuminosity indicated by back ground shading (peak of light gray equals full moon), mean daily water temperatures (red), and peak daily flows (blue) at Red Bluff Diversion Dam.

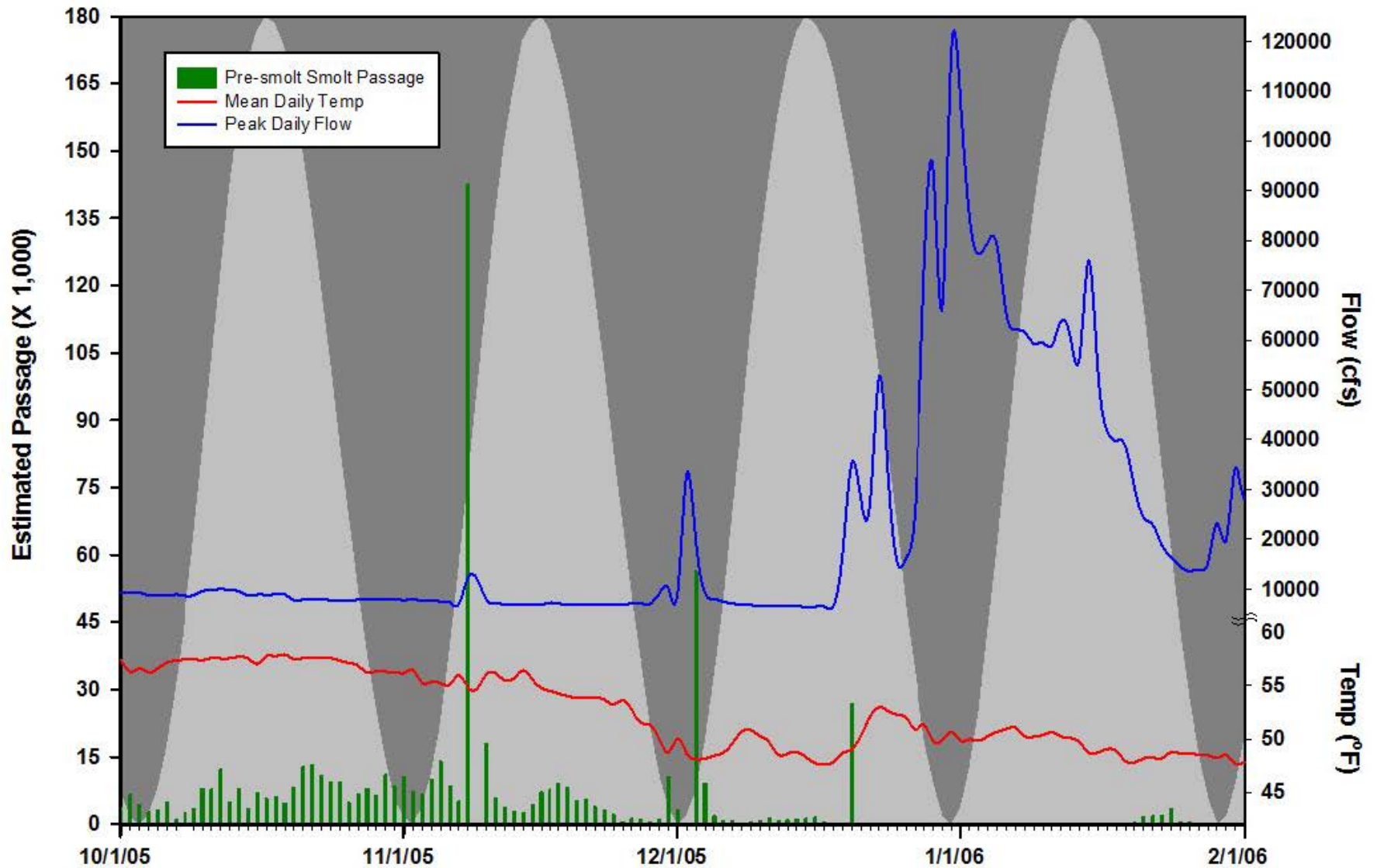


Figure A15. Brood Year 2005 winter Chinook pre-smolt/smolt passage with moon illuminosity indicated by back ground shading (peak of light gray equals full moon), mean daily water temperatures (red), and peak daily flows (blue) at Red Bluff Diversion Dam.

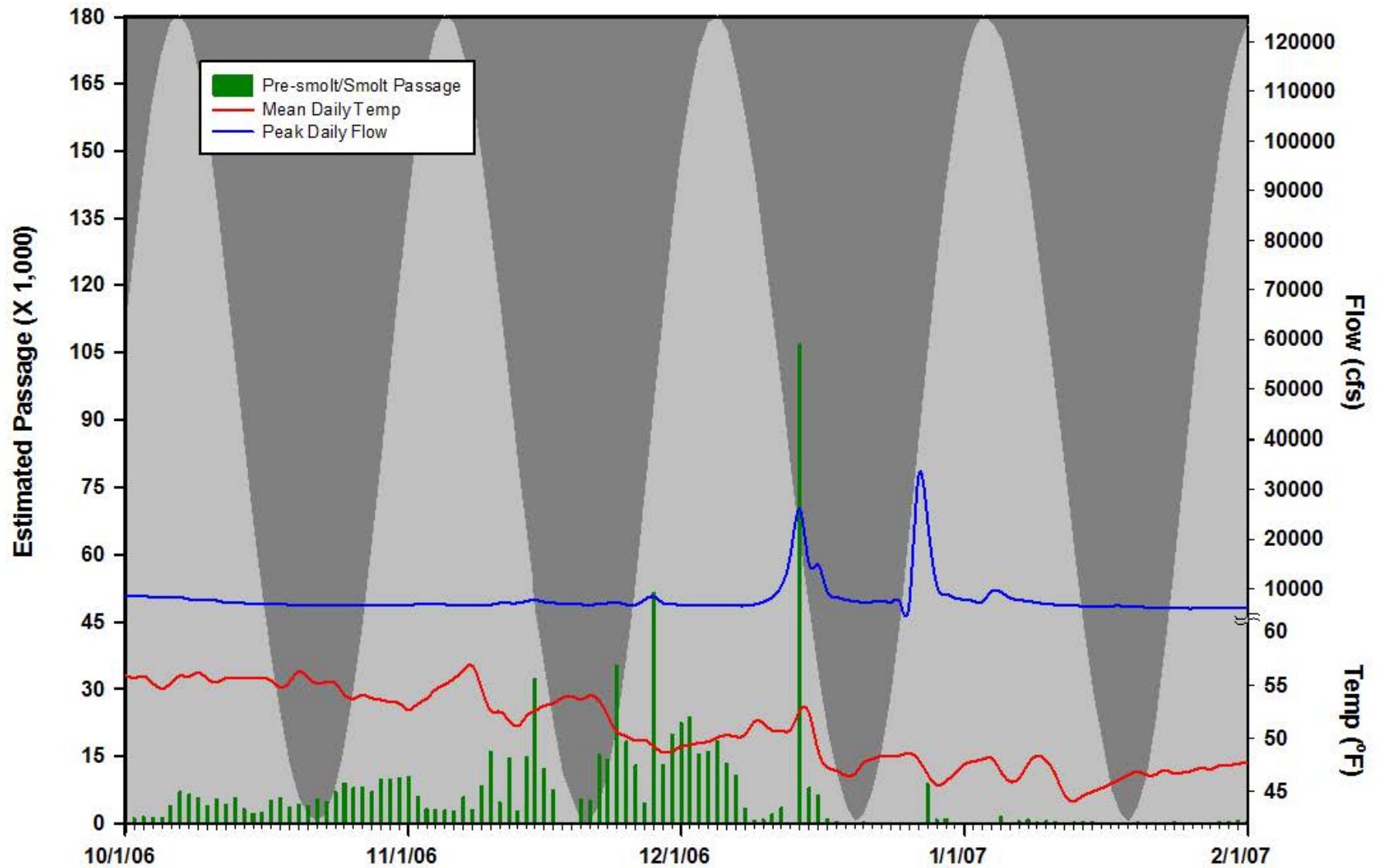


Figure A16. Brood Year 2006 winter Chinook pre-smolt/smolt passage with moon illuminosity indicated by back ground shading (peak of light gray equals full moon), mean daily water temperatures (red), and peak daily flows (blue) at Red Bluff Diversion Dam.

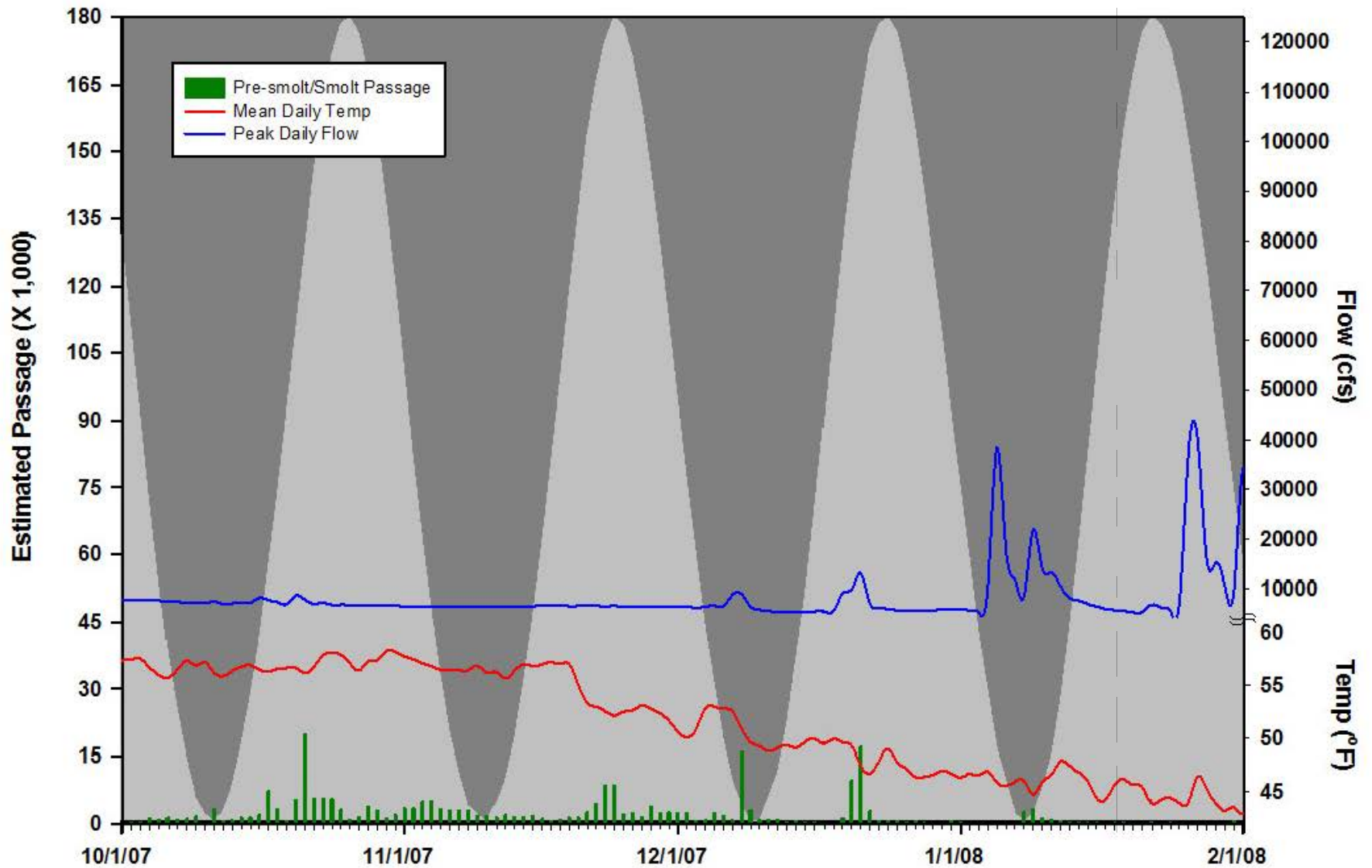


Figure A17. Brood Year 2007 winter Chinook pre-smolt/smolt passage with moon illuminosity indicated by back ground shading (peak of light gray equals full moon), mean daily water temperatures (red), and peak daily flows (blue) at Red Bluff Diversion Dam.

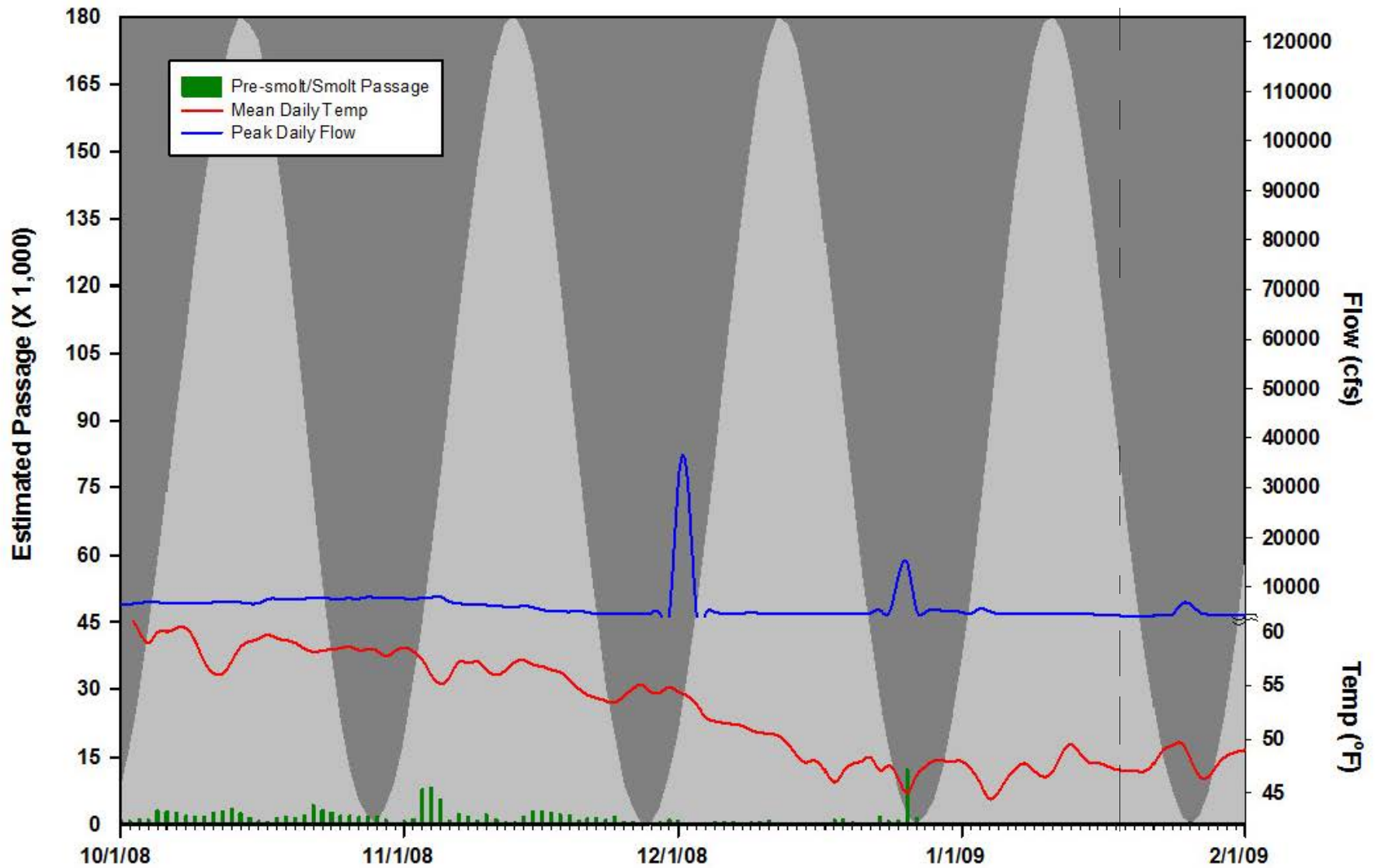


Figure A18. Brood Year 2008 winter Chinook pre-smolt/smolt passage with moon illuminosity indicated by back ground shading (peak of light gray equals full moon), mean daily water temperatures (red), and peak daily flows (blue) at Red Bluff Diversion Dam.

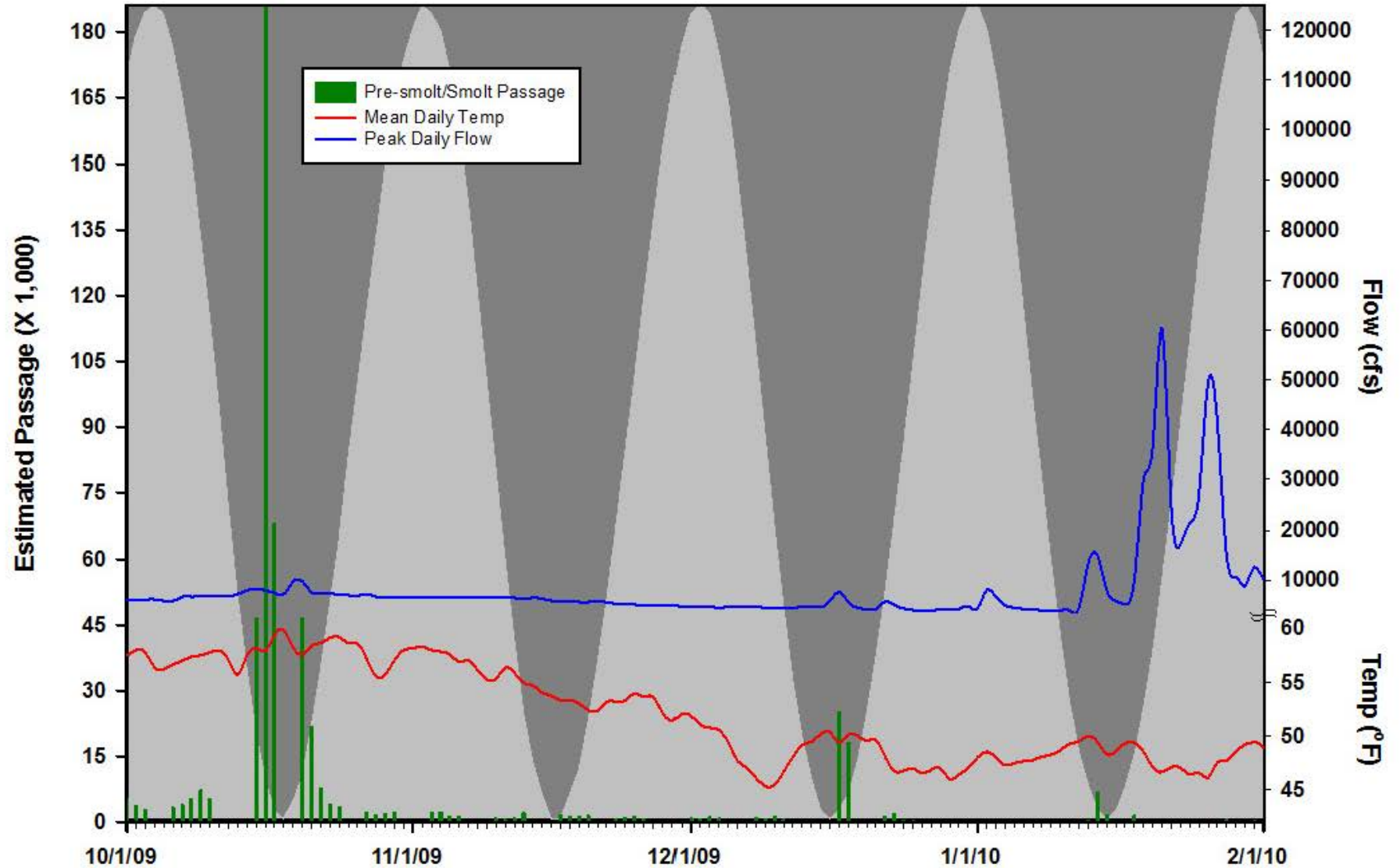


Figure A19. Brood Year 2009 winter Chinook pre-smolt/smolt passage with moon illuminosity indicated by back ground shading (peak of light gray equals full moon), mean daily water temperatures (red), and peak daily flows (blue) at Red Bluff Diversion Dam.

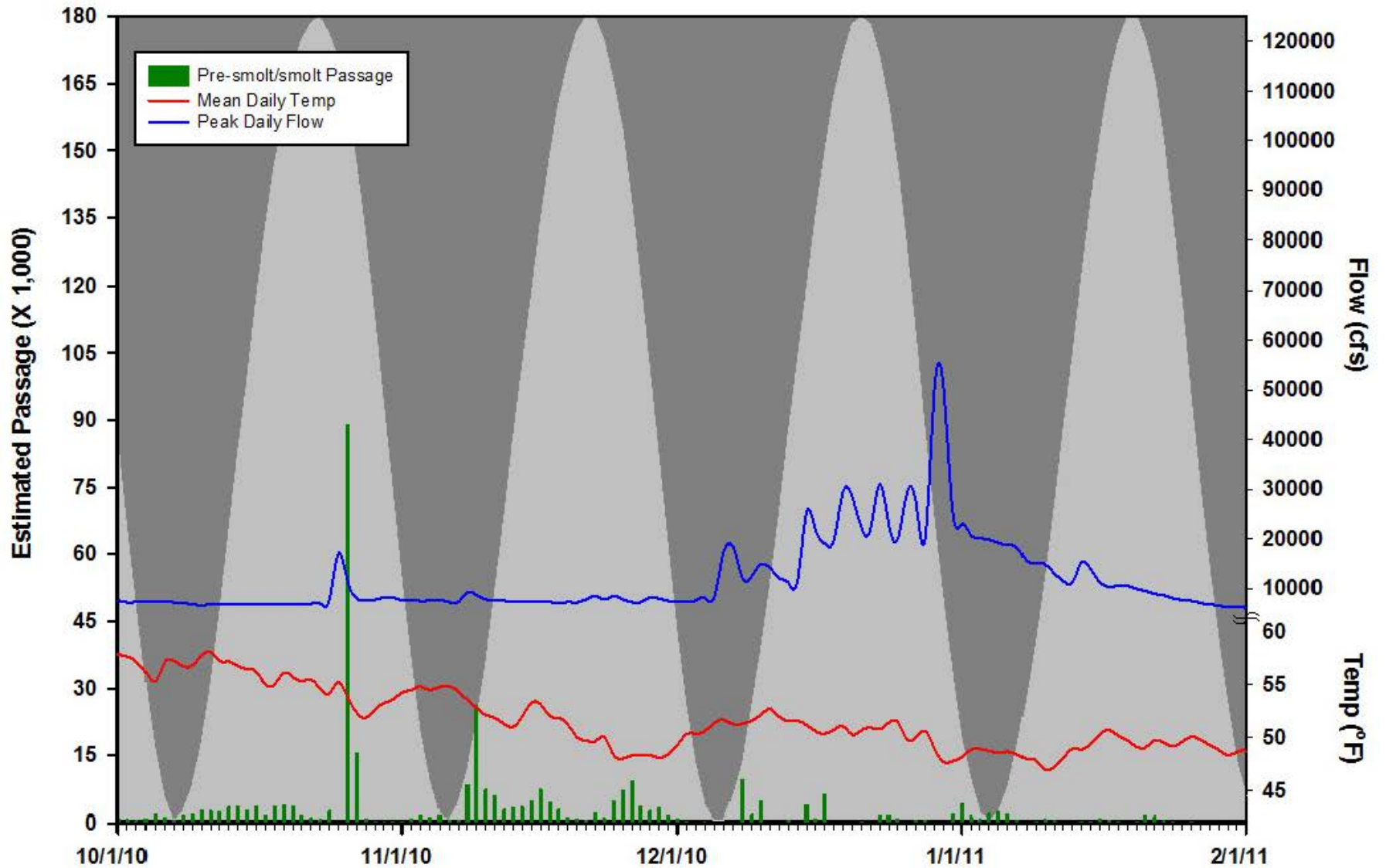


Figure A20. Brood Year 2010 winter Chinook pre-smolt/smolt passage with moon illuminosity indicated by back ground shading (peak of light gray equals full moon), mean daily water temperatures (red), and peak daily flows (blue) at Red Bluff Diversion Dam.

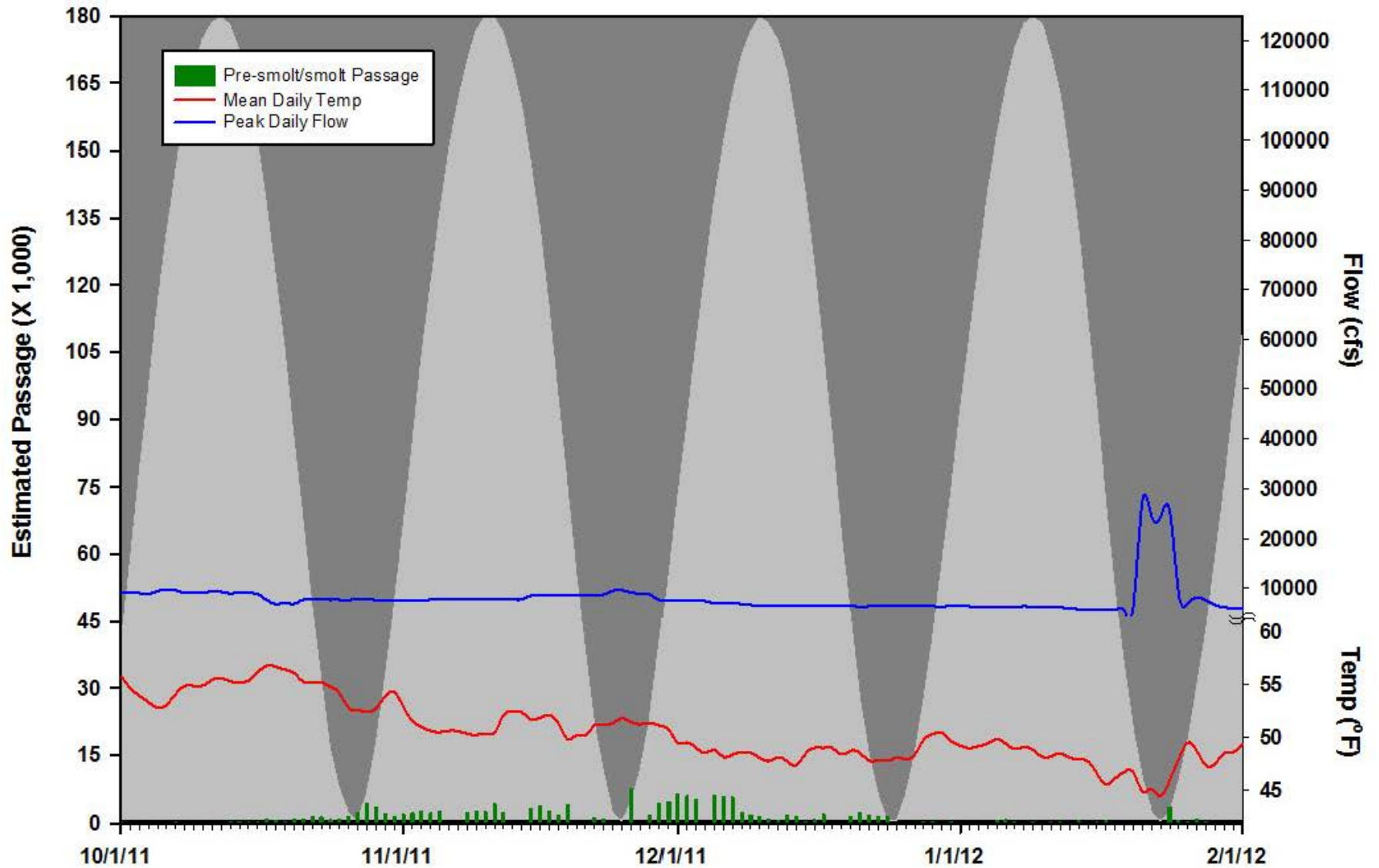


Figure A21. Brood Year 2011 winter Chinook pre-smolt/smolt passage with moon illuminosity indicated by back ground shading (peak of light gray equals full moon), mean daily water temperatures (red), and peak daily flows (blue) at Red Bluff Diversion Dam.

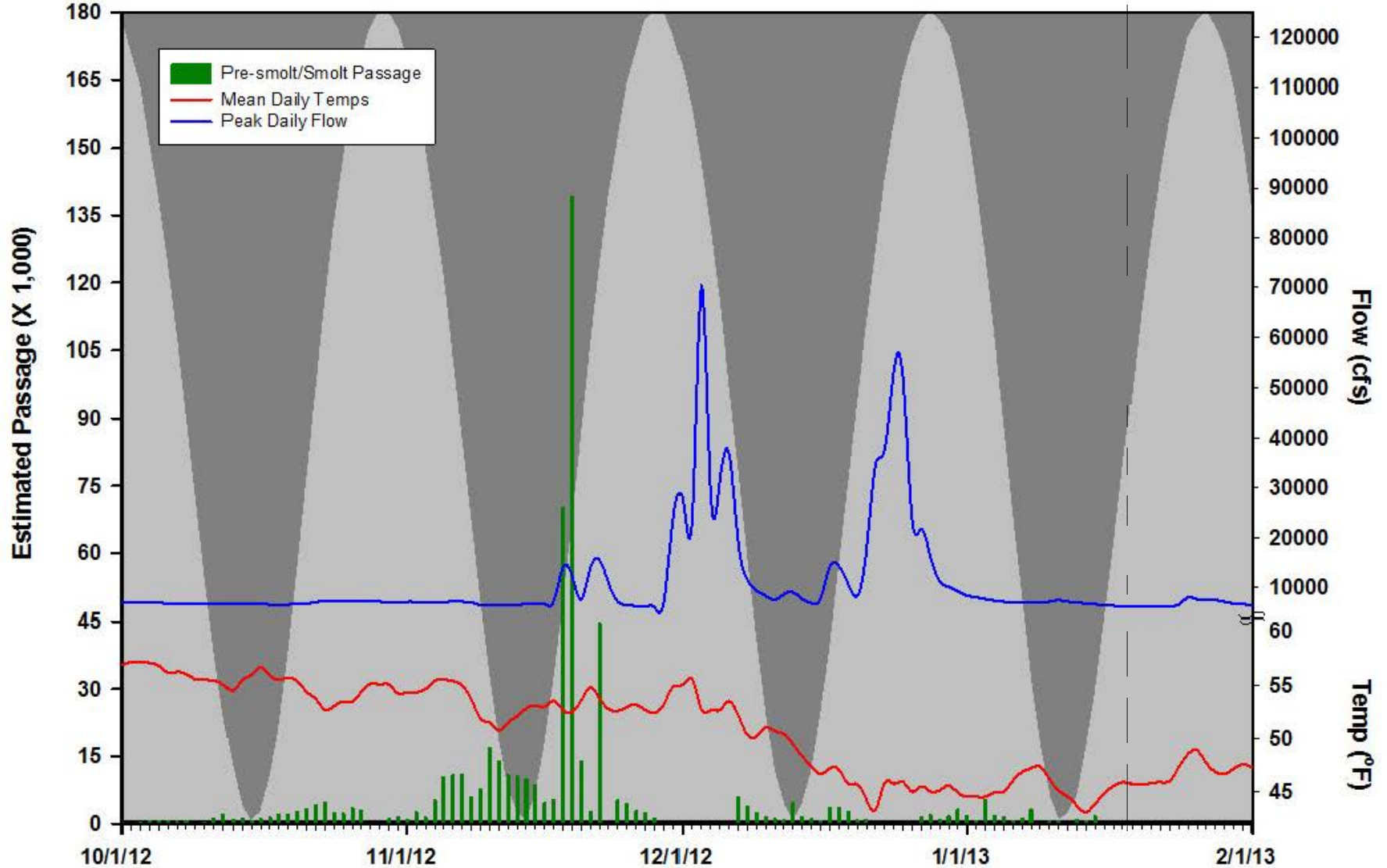
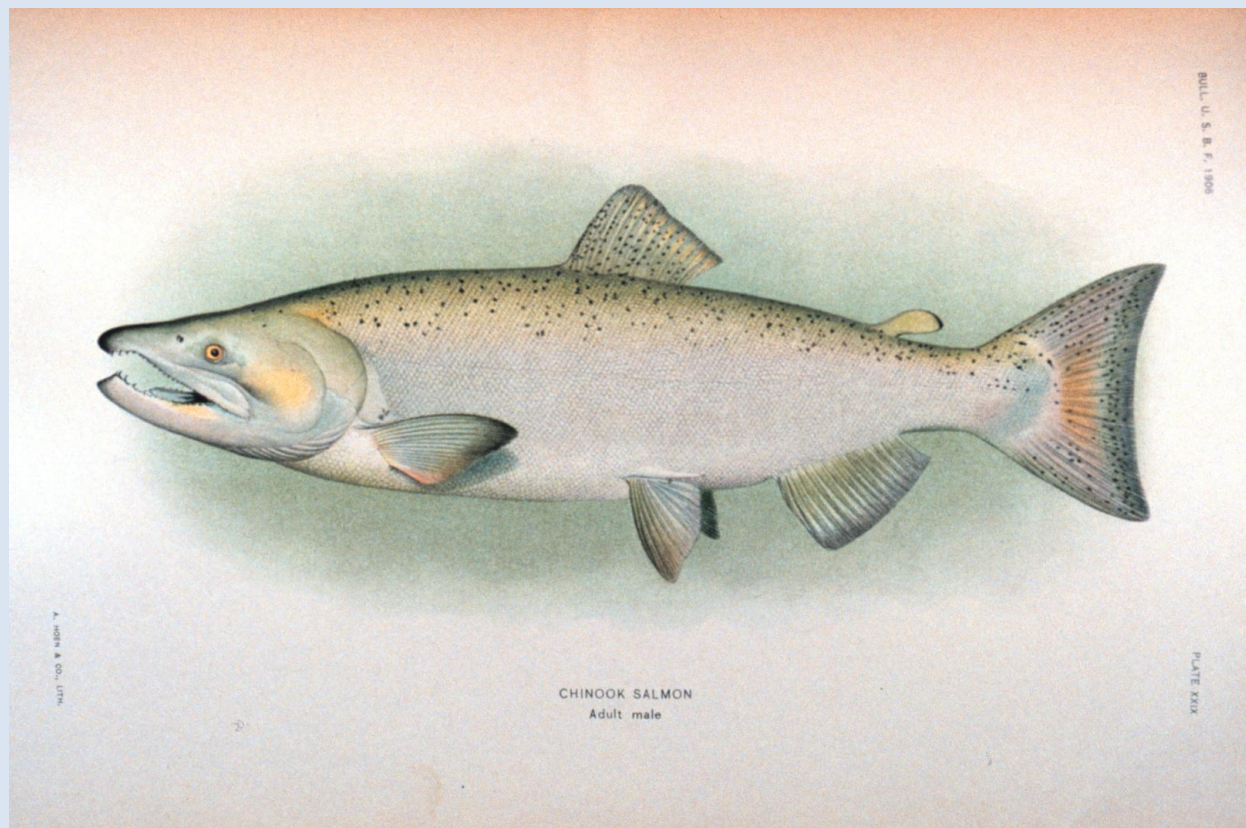


Figure A22. Brood Year 2012 winter Chinook pre-smolt/smolt passage with moon illuminosity indicated by back ground shading (peak of light gray equals full moon), mean daily water temperatures (red), and peak daily flows (blue) at Red Bluff Diversion Dam.



DRERIP Delta Conceptual Model

Life History Conceptual Model for Chinook Salmon & Steelhead

Oncorhynchus tshawytscha & *Oncorhynchus mykiss*

Prepared by: John G. Williams, Consultant. jgwill@dcn.org

September 2010

Life History Conceptual Model for Chinook Salmon & Steelhead DRERIP Delta Conceptual Model

Peer Review Chronology:

- Submitted November 2008
- Scientific Peer Review
- Author Revisions per Review
- Approved by Editor, Dr. Jim Anderson, Univ. of Washington September 2010

Suggested Citation: Williams, G. J. 2010. Life History Conceptual Model for Chinook salmon and Steelhead. DRERIP Delta Conceptual Model. Sacramento (CA): Delta Regional Ecosystem Restoration Implementation Plan. http://www.dfg.ca.gov/ERP/drerip_conceptual_models.asp

For further inquiries on the DRERIP Delta Conceptual Models, please contact Hildie Spautz at hspautz@dfg.ca.gov or Mike Hoover at Michael_Hoover@fws.gov.

Graphic of *Oncorhynchus tshawytscha* shown on the cover is provided by the National Oceanic and Atmospheric Administration. Department of Commerce. NOAA's Historic Fisheries Collection # fish3007. 1906.

PREFACE

This Conceptual Model is part of a suite of conceptual models which collectively articulate the current scientific understanding of important aspects of the Sacramento-San Joaquin River Delta ecosystem. The conceptual models are designed to aid in the identification and evaluation of ecosystem restoration actions in the Delta and to structure scientific information such that it can be used to inform public policy decisions.

The DRERIP Delta Conceptual Models include both ecosystem element models (including process, habitat, and stressor models) and species life history models. The models were prepared by teams of experts using common guidance documents developed to promote consistency in the format and terminology of the models at http://www.dfg.ca.gov/ERP/conceptual_models.asp.

The DRERIP Delta Conceptual Models are qualitative models which describe current understanding of how the system works. They are designed and intended to be used by experts to identify and evaluate potential restoration actions. They are not quantitative, numeric computer models that can be “run” to determine the effects of actions. Rather they are designed to facilitate informed discussions regarding expected outcomes resulting from restoration actions and the scientific basis for those expectations. The structure of many of the DRERIP Delta Conceptual Models can serve as the basis for future development of quantitative models.

Each of the DRERIP Delta Conceptual Models has been subject to a rigorous scientific peer review process, as described on the DFG-DRERIP website and as chronicled on the title page of the model. The scientific peer review was overseen by Dr. Jim Anderson, at University of Washington for all species models and by Dr. Denise Reed, University of New Orleans, for all ecosystem models.

The DRERIP Delta Conceptual models will be updated and refined over time as new information is developed, and/or as the models are used and the need for further refinements or clarifications are identified.

CONTENTS

I.	INTRODUCTION	1
A.	On nomenclature:	2
II.	BIOLOGY	4
A.	The life cycle of anadromous salmonids.....	4
B.	Adult size, fecundity, and survival by life stage of Chinook and steelhead	9
C.	Age distribution of Chinook and steelhead.	11
D.	Juvenile Growth	12
E.	Temperature tolerance.....	14
F.	Dissolved oxygen.....	15
III.	DISTRIBUTIONS.....	15
A.	Historical distributions.....	15
B.	Current geographical distributions	17
C.	Population Trends.....	21
IV.	ECOLOGY	24
A.	Adult life history patterns	24
B.	Navigation by adults	25
C.	Juvenile life history patterns.....	27
D.	Juvenile migration rate	36
E.	Navigation by juveniles	39
F.	Steelhead juvenile life history patterns	39
G.	The adaptive landscape	40
H.	Local adaptation.....	41
I.	Understanding salmonid life history diversity	42
J.	Use Of habitats:	43
K.	Habitat use by run.....	50
L.	Environmental constraints on life history patterns	53
M.	Predation.....	53
V.	ANTHROPOGENIC STRESSORS IN THE DELTA.....	54
A.	Climate Change	54
B.	Levees	54
C.	Diversions.....	55
D.	Hatchery influence.....	61
E.	Toxics	62
F.	Dissolved Oxygen	62
G.	Water temperature.....	62
H.	Predation.....	63
VI.	OUTCOMES.....	63
VII.	FUTURE RESEARCH	64
VIII.	REFERENCES.....	67

I. INTRODUCTION

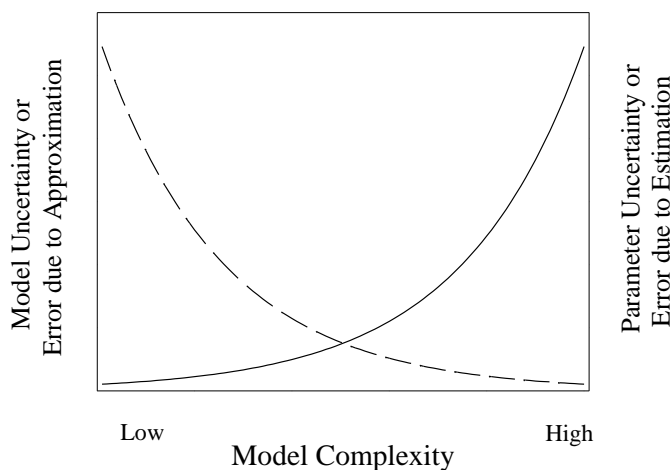
This report constitutes the conceptual model for Chinook and steelhead for the Delta Regional Ecosystem Restoration Implementation Plan (DRERIP). The report describes conceptual models, not numerical models, but several important considerations apply to both kinds, especially when they are used for management of living natural resources. First, the proper purpose of models is to help people think, not to think for them. Ignoring this can be disastrous, as exemplified by the current economic crisis. The world of credit default swaps was built on highly sophisticated models that persuaded many intelligent people that the associated risk was negligible, but they failed to recognize that a market based on houses that people could not pay for from their earnings is unsustainable.

In short, the most important “output” of a good conceptual or numerical model is clear thinking. To help people think, the model must be focused on selected features of the world that are thought to be important for the purpose at hand: in this case, management of the Delta. A model that tries to include everything will be too complex to be useful for this purpose.

Second, to be useful for management of natural living resources, numerical models must be unrealistic, because our knowledge of such resources is incomplete, and is based on data that includes measurement errors. According to Ludwig’s paradox, “Effective management models cannot be realistic” (Ludwig 1994:516), because two kinds of uncertainty must be balanced (Figure I-1; see Ch. 14 in Williams (2006) for elaboration of this point).

In our view, something similar applies to conceptual models of natural systems: to be useful, they must be simple. A schematic of the wiring in some electronic device is a conceptual model that may be useful as well as complex, but trying to develop a similar schematic of an ecosystem or part of an ecosystem is not useful, because our knowledge of such a system is much less complete than our knowledge of engineered devices, and we have only estimates of the relevant parameters.

Figure 1. Conceptual model of the trade-off between model uncertainty (dashed line) and parameter or estimation uncertainty (solid line). In a good predictive model these two types of uncertainty are balanced. Redrawn from Ludwig (1994). See Ch. 14 in Williams (2006) for more discussion of this matter.



Finally, reality is too complex to capture with a single model. Eric Lander, a noted geneticist who co-chairs President Obama’s Council of Advisors on Science and Technology,

recently remarked that “You can never capture something like an economy, a genome or an ecosystem with one model or one taxonomy – it all depends on the questions you want to ask” (NY Times, 11/11/08). Models are tools that we use to try to think, and multi-purpose tools generally do nothing well.

Therefore, although the complete life cycle of Chinook and steelhead is described here, the parts or aspects of the cycle that we think may be affected by management of the Delta are emphasized, and we try to keep it as simple as possible. More detail on most of the topics described here can be found in Quinn (2005), or in Williams (2006), from which this document draws very heavily.

A. On nomenclature:

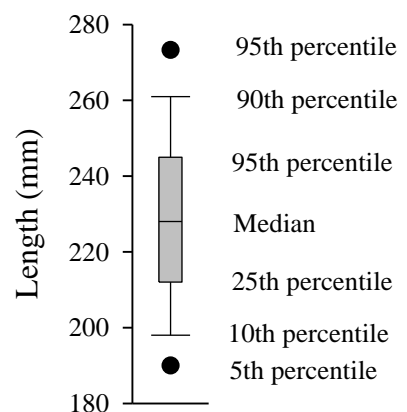
In the literature on Central Valley Chinook and steelhead, several terms are used with different meanings, which does not help an already difficult situation. For example, most people describe the area from the Golden Gate to the limit of tidal influence as the estuary, but MacFarlane and Norton (2002) apply that term only to the area influenced by the salinity of the ocean, essentially the area downstream from the Delta. This has caused many people to misunderstand their article. Similarly, the term ‘fry’ has been used to describe fish less than some length, such as 50 or 60 or 70 mm, with fish larger than that described as ‘smolts,’ although sometimes the distinction is between fry and ‘fingerlings,’ or fry and parr. Recently, CDFG has started describing fish in terms of physiological state rather than length; that is as fry, parr, silvery parr, or smolts, which is more appropriate for scientific purposes. Here, however, we often retreat to more traditional usage, and will refer to fry and fingerlings, with a division somewhere around 55 to 60 mm fork length. The term fingerling seems useful because it is a reminder that we are talking about small fish. By smolts we mean fish that are migrating rapidly and are well along in the physiological processes associated with smolting.

We use the term “salmon” to refer to both Chinook and steelhead, since both are members of the genus *Oncorhynchus*, the Pacific salmon, and steelhead were commonly called salmon in the 19th Century.

We distinguish ‘wild’ and ‘naturally produced’ fish by the extent of the hatchery influence in the population; the progeny of hatchery fish spawning in the wild are naturally produced.

All lengths given are fork lengths, unless otherwise noted.

Several of the figures in the report are “box plots,” which are conventional in science but may be unfamiliar to some readers. Box plots show distributions, as illustrated at right (with extra labeling) for the distribution of lengths of 346 unmarked juvenile steelhead captured at Chipps Island. If plots show more than two filled circles, they represent all outliers beyond the 10th and 90th percentiles.



Others of the figures show the factors influencing the probability of surviving the transition from one life stage to the next. These figures are numbered separately from the others, and follow the conventions for the DRERIP conceptual models.

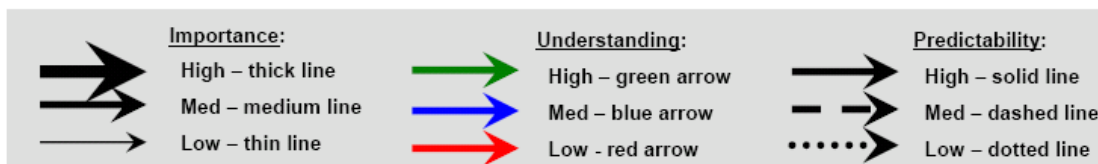
Linkages are depicted as arrows between cause (drivers) and effect (outcomes);

The **direction** of the effect is indicated by plus or minus signs;

The **importance** or magnitude of the effect is shown by line thickness;

Understanding about the relationship based on established literature knowledge is shown by line color;

The **predictability** of the effect is shown by line type.



These figures reflect the current understanding of Central Valley Chinook and steelhead, but they should be viewed with attention to the obvious limits to our understanding; for example, we did not anticipate the crash of the fall Chinook population in recent years, or do we understand why it increased before it crashed. Uncertainty does not justify inaction, but neither should it be ignored.

II. Biology

The Delta provides habitat for two species of Pacific salmon, Chinook (*Oncorhynchus tshawytscha*) and steelhead (*O. mykiss*). There are substantial differences between the species, but they are enough alike to treat them together for the conceptual models. Much less information is available on steelhead in the Central Valley than on Chinook, however. Lindley et al. (2007) commented that "... we are unable to assess the status of the Central Valley steelhead ESU with our framework because almost all of its roughly 80 populations are classified as data deficient." For the same reason, steelhead are given less attention here than they deserve.

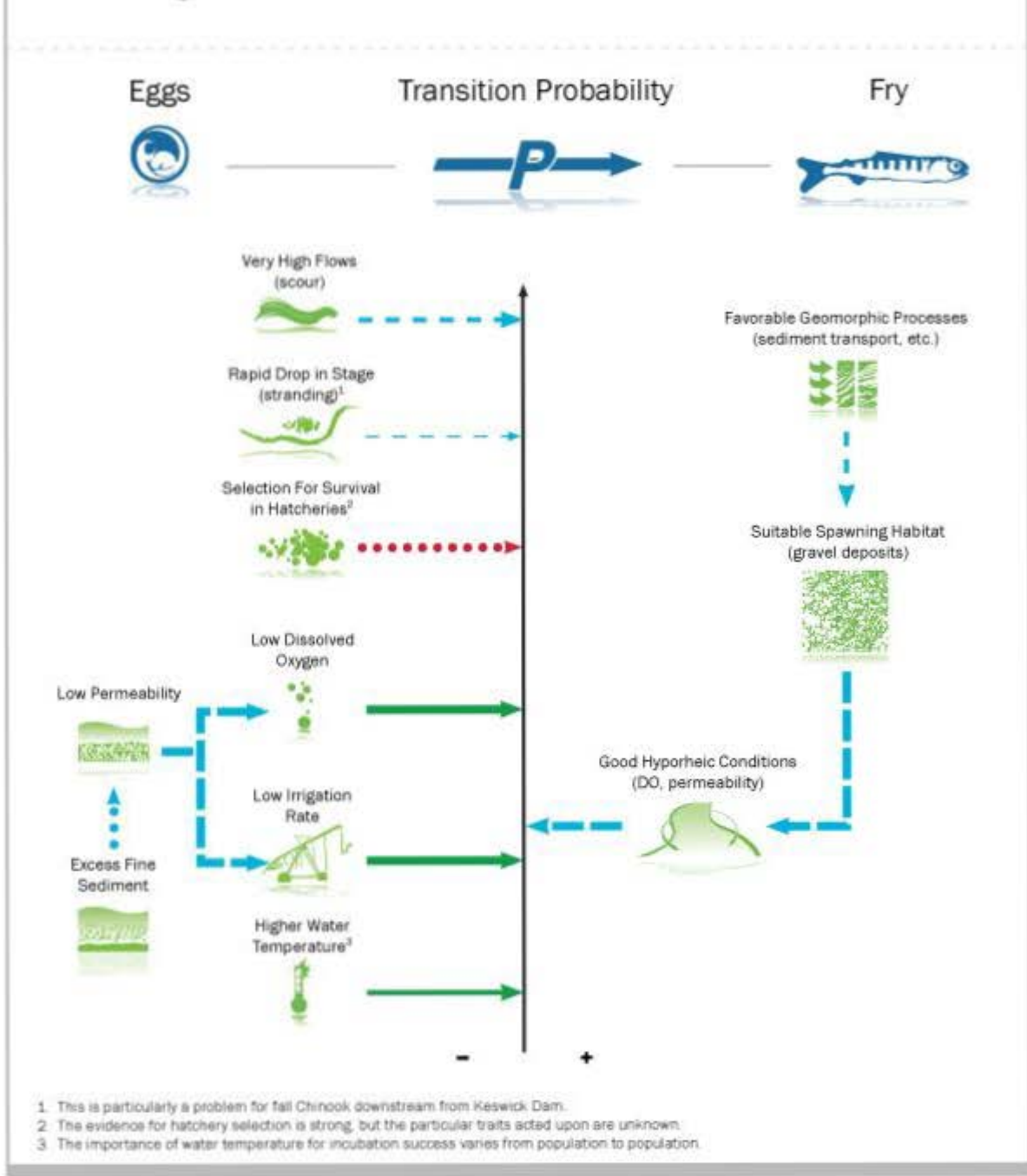
Pacific salmon typically are anadromous. That is, they reproduce in fresh water, but migrate to the ocean to gain most of their growth. There are many exceptions, however, such as rainbow trout (non-anadromous *O. mykiss*), and there is a great deal of variation in life history patterns among the anadromous fish. A conceptual model that helps explain this diversity in life histories is described in the ecology chapter, but the emphasis here is on fish that migrate through or at least to the Delta, and so are directly influenced by management of the Delta.

A. The life cycle of anadromous salmonids

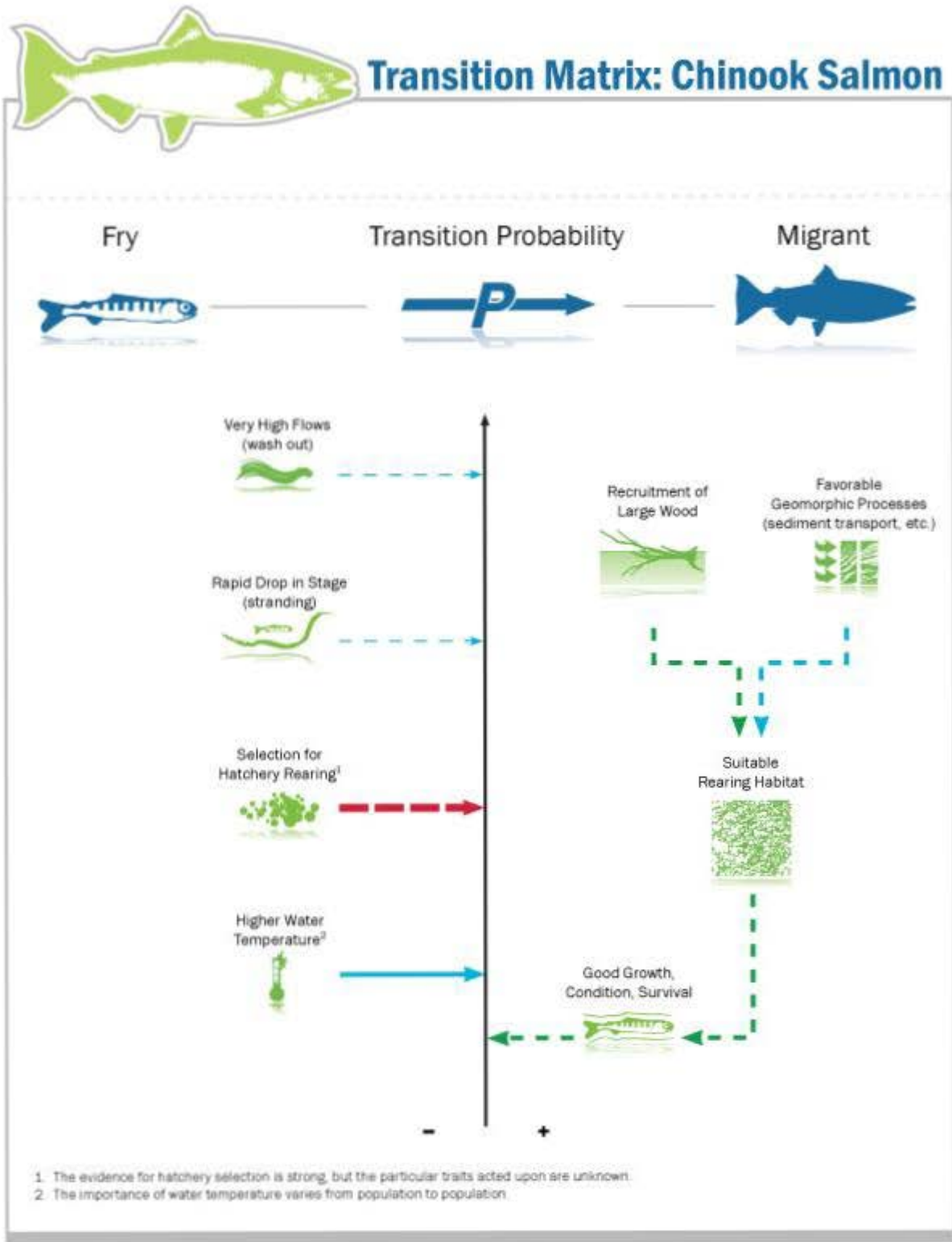
Figure 1 depicts the natural life history of anadromous salmonids. Adult females dig nests called redds in gravel-bedded streams, the eggs are fertilized by males as the female deposits them in the redd, and the female covers the eggs with gravel. Embryos develop and hatch in the gravel, and the larval fish, called alevins, remain there and grow, nourished by egg yolk attached to their bellies. Around the time the remaining yolk is enveloped by the growing fish, the fish emerge from the gravel into the overlying stream as fry, ~ 25 mm long for steelhead, and 35 mm for Chinook. Factors affecting the transition from egg to fry are depicted in Life Stage Transition Figure 1.

Although pink and chum salmon (*O. gorbuscha* and *O. keta*) migrate to sea directly after emerging, most salmon rear for months to years in fresh or brackish water before doing so. As the fish grow, they develop scales and dark vertical bands called parr marks on their sides that make the fish less visible in streams (Quinn 2005). Small parr are sometimes called fingerlings. Later, the fish go through various physiological changes that prepare them for living in salt water: externally, their shape changes, the parr marks fade, and the fish develop silvery sides and bellies that make them less visible from below. At this stage they are called smolts. Steelhead in Central Valley streams normally migrate at one or two years old. The age at which Chinook begin migrating is highly variable, however, as described in Chapter 4; the environmental factors affecting survival to the beginning of migration are depicted in Life Stage Transition Figure 2.

Transition Matrix: Chinook Salmon



Life Stage Transition 1.



Life Stage Transition 2

with a sharply different salt concentration is easier if it is done gradually, and temporary residence in an estuary allows this to occur.

For Chinook and steelhead in the Central Valley, the natural anadromous life history must be amended to include reproduction and juvenile rearing in hatcheries (Figure 2), which annually produce upwards of 30 million Chinook and 1.5 million steelhead (Williams 2006). In Central Valley rivers with hatcheries, hatchery and naturally spawning salmon are best regarded as single, integrated populations that reproduce in one of two very different habitats. Harvest is included in Figure 3, a conceptual model from Goodman (2005). Harvest is a desired outcome of management, and the rate of harvest is an important management “knob” that affects the extent of the influence of hatchery fish on the genetics of naturally reproducing fish (Goodman 2004, 2005). As this suggests, it is misleading to think of the salmonid life cycle as frozen in time. To the contrary, populations and their life histories can evolve rapidly enough that management should take evolution into account (Wilson 1997; Stearns and Hendry 2004). This is discussed below in terms of local adaptation.

Figure 2. Conceptual model combining the natural and hatchery life cycles, copied from USFWS, Warm Springs Hatchery. Note that natural reproduction seems somewhat truncated in the image.

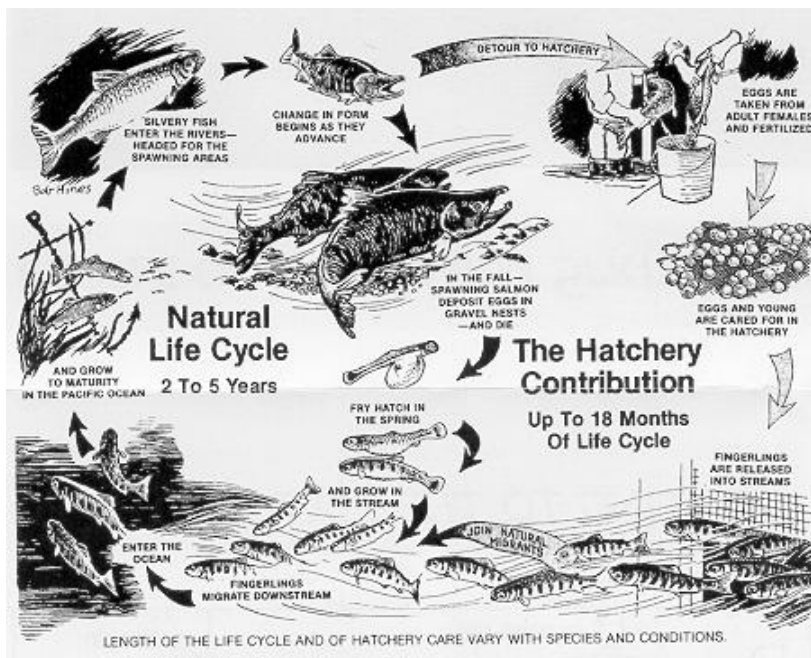
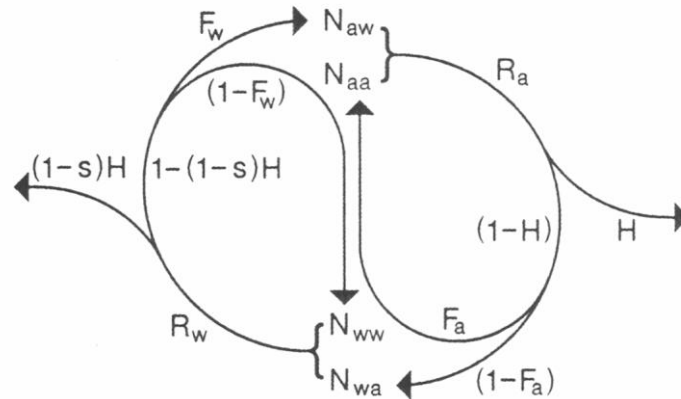


Figure 3, life cycle schematic, including hatchery production and harvest. N_{xy} is the number of spawner of origin y in habitat x , where w is natural and a is hatchery. R_y are the recruits, and F_y are the fractions of the natural and hatchery recruits taken into the hatchery. H is harvest, and s is the harvest selectivity for hatchery fish. Modified from Goodman (2004)



The juvenile life histories of Central Valley Chinook are highly variable, and the young fish enter the ocean at lengths ranging roughly from 75 to 250 mm (Williams 2006). The habitats where they gain most of this growth are also variable: at the extremes, some migrate rapidly through the Delta and grow mainly in the bays before entering the ocean, while others remain and rear in the gravel-bedded parts of the streams where they incubated and then migrate rapidly through the lower rivers, the Delta and the bays. This is discussed in more detail in the ecology chapter. Less is known about steelhead, but in the Central Valley they probably gain most of their growth in the gravel-bedded reaches. Most pass Chipps Island between ~ 215 and 245 mm in length (see the box plot in the Introduction).

B. Adult size, fecundity, and survival by life stage of Chinook and steelhead:

Chinook and steelhead have relatively few, large eggs, compared to most fishes of similar size, and average egg to fry survival is correspondingly high. However, although average egg to fry survival is high, it is also highly variable, and may be zero in many cases (Williams 2006).

Quinn (2005) compiled data from published studies on life-stage specific size and survival of wild or naturally reproducing Pacific salmon populations, and his results for Chinook and steelhead are presented in Table 1. Some studies reported survival from egg to fry or fry to smolt, and others estimated survival from egg to smolt. Quinn calculated separate estimates of adults per female using both sets of estimates, and the uncertainty in current knowledge is reflected in the different results from these two approaches. These data are from populations subject to fishing, which absorbs the surplus implied by adults per female being greater than two.

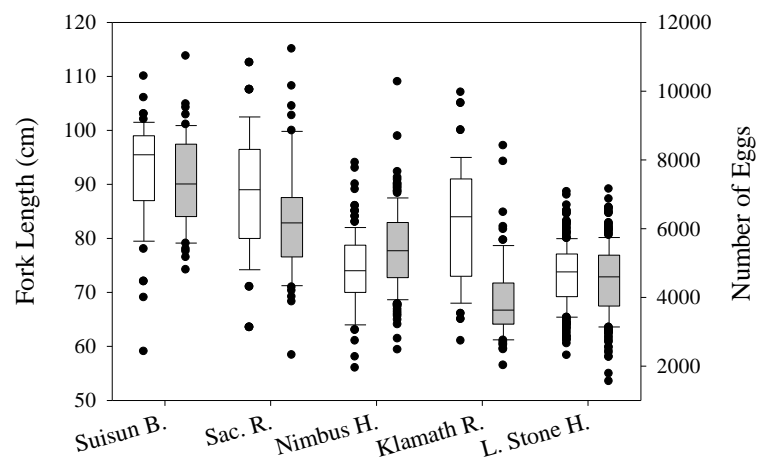
Table 1. Size, fecundity and survival estimates for Chinook and steelhead, copied from Quinn (2005).

Life History Stage	Chinook	Steelhead
Female Length (mm)	871	721
Fecundity	5401	4923
Egg size (mg)	300	150
Egg to fry survival	0.380	0.293
Fry size (mm)	35	28
Fry to smolt survival	0.101	0.135
Smolt size (mm)	60-120	200
Smolt to adult survival	0.031	0.130
Adults per female¹	6.4	25.5
Egg to smolt survival	0.104	0.014
Adults per female²	17.5	9.2

1. Calculated using egg to fry and fry to smolt survival estimates.
2. Calculated using egg to smolt survival estimates.

Historical data show that Central Valley Chinook used to be larger and more fecund than the averages given in Table 1 (Figure 4). On the other hand, Central Valley steelhead were smaller (Table 2). Current fecundity data for Central Valley Chinook are remarkably scarce, except for winter-run, but fall Chinook from a sample taken from the American River were small but fecund for their size (Figure 4). Note the lower fecundity of Klamath River Chinook for their size, which may reflect the steeper gradient and more arduous migration for fall Chinook in that river.

Figure 4. Distributions of size (open boxes) and fecundity (shaded boxes) for fall Chinook salmon collected in Suisun Bay ~ 1920, the Sacramento River ~ 1940, River Klamath River ~ 1920, and Nimbus Hatchery on the American River, 1997, and for winter Chinook from Livingston Stone Hatchery. Data from McGregor 1923b, Hanson et al. 1940, Kris Vyverberg, DFG, and John Rueth, USFWS. Copied from Williams (2006).



C. Age distribution of Chinook and steelhead.

One important aspect of life history variation among Chinook and steelhead can be summarized by tables showing the time spent in fresh and salt water. For most Chinook and steelhead, time can be specified in terms of winters in fresh water, as in Table 2, although some Chinook migrate past Chipps Island during the winter. Unfortunately, good information on the current age distributions of Chinook and steelhead in the Central Valley is only now becoming available. Table 2 gives qualitative “guesstimates” for Central Valley Chinook, based partly on data for one year in the Feather River given in Williams (2006). Table 3 gives quantitative data on four common life history patterns for Central Valley Steelhead in a somewhat different format, but the data are old and include only fish on their first spawning run, so older fish are not tabulated.

Table 2: Adult life history variation in Central Valley Chinook, based on various studies described in Williams (2006)

Winters in Fresh Water	Winters at Sea				
	1	2	3	4	5
0	Common	Common	Common	Scarce	~ nil
1	No data	Some	Some	Very scarce	~ nil

Table 3. Fork length in centimeters of Central Valley steelhead at various life stages, estimated from scale measurements of steelhead on their first spawning migration, for four life history patterns (age at return = years in freshwater/years in salt water). Data from Table 1 in Hallock et al. (1961).

Age at return	No. of fish	Length at salt water entry	Length at end of year 1	Length at end of year 2	Length at end of year 3	Length at capture
1/1	17	20.3	12.2			33.0
1/2	10	18.3	12.2	33.5		52.1
2/1	30	22.9	10.7	19.8		40.6
2/2	26	21.3	9.4	18.0	41.9	59.2

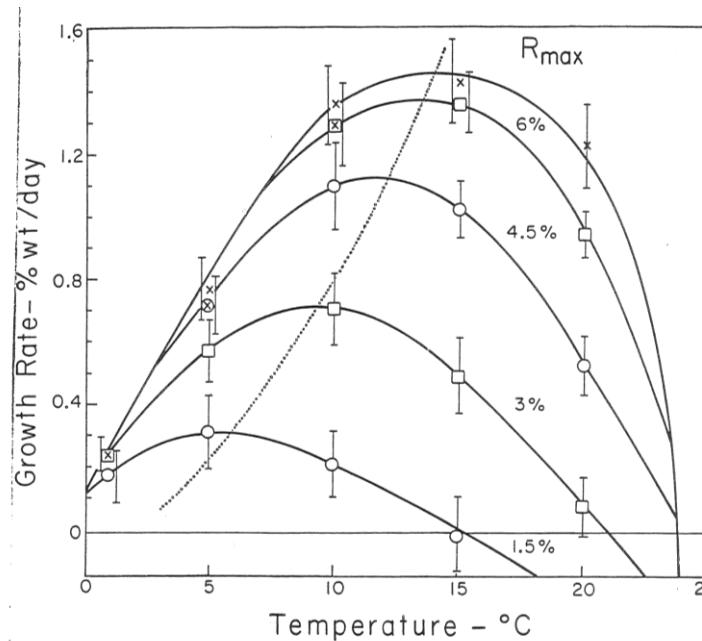
Variation in age at maturity buffers the population against environmental variation, since the consequences of reproductive failure or heavy mortality in early ocean life in any one year will be spread over several subsequent years, although the strength of this effect may be less than some suppose (Hill et al. 2003). Unfortunately, it appears that the age distribution of Central Valley Chinook has been reduced by about a year, probably by ocean harvest (Williams 2006).

Four sea-winter Chinook used to be common in the Central Valley, and there were a few five sea-winter fish, based on scale samples taken in 1919 and 1921 (Clark 1928). Only a few four sea-winter fish now occur. A rather different change has occurred with steelhead; it seems that many now forgo anadromy altogether, as discussed in the ecology chapter.

D. Juvenile Growth

The growth of juvenile salmon is strongly influenced by temperature and the amount of food available, known as “ration” in experimental studies. The best data are available for sockeye (*O. nerka*), shown in Figure 5, but the same general pattern applies to Chinook and steelhead, except that the temperature for maximum growth is higher. Based on studies of Central Valley fish, the growth of fish fed to satiety in good laboratory conditions peaks at around 19°C for Chinook and steelhead (Marine 2004, Myric and Cech 2000, 2001, 2002; 2004), although one study (Rich 1987) found maximum growth at a lower temperature; see Williams (2006) for more discussion of these studies.

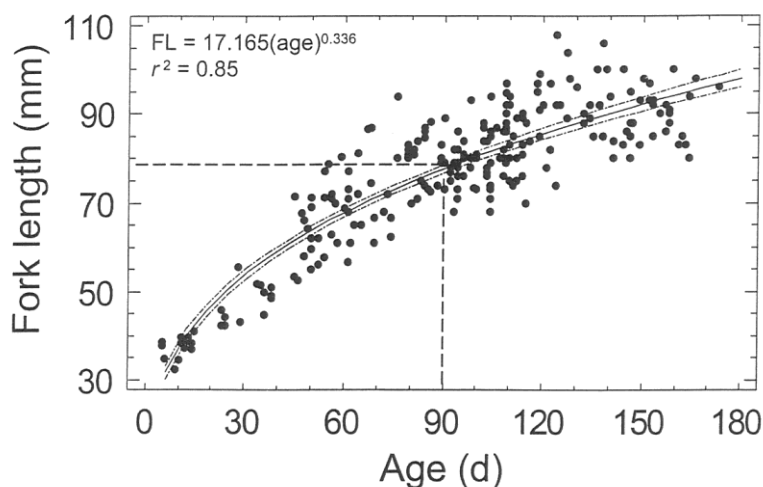
Figure 5. The relation between growth rate and temperature for different levels of ration for juvenile sockeye salmon. The dotted line connects temperature of maximum growth at each level of ration. Bars are two standard errors. Ration levels are given in percent body dry weight. Copied from Brett et al. 1969



Thus, temperature and ration are both “drivers” of juvenile growth, but other factors such as day length and the individual fish’s developmental program affect it as well, as discussed in the ecology chapter. Size and life-stage also affects growth, as growth in smaller fish is relatively more rapid, and growth (in weight) slows during smolting (Weatherby and Gill 1995). Growth also varies among individuals, even in laboratory conditions, as indicated by the error bars in Figure 9. Scofield (1920) noted regarding Klamath River Chinook that “Although from the same brood, hatchery practice and rearing pond, there was great variation in the size of the yearlings at the time of marking, the extremes in length being 1 3/16 to 5 inches ...” Data on the size at age of naturally produced Chinook in the American River and the bays show considerable variability (Titus et al. 2004; Figure 6), and a larger sample from the American River reported by

Castleberry et al. (1993) showed even more: the length of fish with ~125 otolith increments varied from about 40 to 80 mm. As another complication, fish of a given length vary in weight and in lipid content, which can be viewed as energy stored for future growth as well as future activity. In at least some populations of stream-type Chinook, day-length at emergence strongly influences juvenile growth (Clarke et al. 1992). In other words, growth is not a simple response to current environmental conditions, and fish in some sense “decide” how fast to grow. An obvious way that juvenile salmon can regulate their growth is behavioral. A fish may move up into the water column to feed, but risk being eaten itself, or it can burrow into the gravel and hide. Theory suggests that fish should adjust their behavior to minimize mortality per unit of growth, and observations support this idea (e.g., Bradford and Higgins 2001).

Figure 6. Size at age of juvenile Chinook salmon from the American River and from the San Francisco Estuary. Copied from Titus et al. (2004), courtesy of the American Fisheries Society.



Unpublished individual growth rates estimated from otolith microstructure, using the methods reported in Titus et al. (2004), vary from 0.27 mm d^{-1} to 1.05 mm d^{-1} . Interestingly, juvenile Chinook sampled in various Central Valley rivers grew faster on average than fish sampled in the Delta: 0.57 v. 0.54 mm d^{-1} (Rob Titus, DFG, pers. comm. 2008). Kjelson et al. (1982) reported that the growth of tagged fry released into the Delta mm averaged 0.86 mm d^{-1} in 1980 and 0.53 mm d^{-1} in 1981. This indicates that year to year variation in food availability in the Delta may be significant, and longer term variation may be important as well. Data on the size at date of fish collected at Chipps Island or the pumps should offer insight on this issue, as well as whether growth in the Delta is density-dependent.

Using hatchery fish in enclosures, Jeffres et al. (2008) found that juvenile Chinook grew more rapidly on the vegetated Cosumnes River floodplain when it was inundated than in the river, either within or upstream of the tidally influenced area. Food was very abundant, and the fish grew well even though the water temperature averaged 21°C for a week, with daily maxima up to 25°C . This underscores the relationship between the availability of food and temperature tolerance implied in Figure 5.

An 11 year study by NMFS found that on average juvenile fall Chinook grow slowly in length (0.33 mm d^{-1}) and hardly at all in weight during their migration through the bays, from Chipps Island to the Gulf of the Farallones, although they grow rapidly once they reach the gulf (MacFarlane and Norton 2002; MacFarlane et al. 2005, B. MacFarlane, pers. comm. 2008). Given that survival in the ocean is size-dependent, this raises the questions whether the human modification of the bays, especially loss of tidal wetlands (Nichols et al. 1986; Lotze et al. 2006), has adversely affected Chinook and steelhead, and whether naturally produced juveniles suffer from competition with hatchery fish in the bays. These questions deserve further study.

E. Temperature tolerance:

Salmon are ectotherms (cold-blooded), so their body temperatures are close to that of the water around them. Salmon do not tolerate warm water, and the Delta and lower rivers are unsuitable habitat for them in summer. However, salmon's response to temperature is affected by factors such as the availability of food, as discussed above, so, like growth, the temperature tolerance of salmon is affected by other factors in the environment.

Large embryos probably are the life stage least tolerant of warm water, because their metabolic rate increases with temperature, but they obtain oxygen and dispose of metabolic wastes only by diffusion through the egg wall. In laboratory studies with constant temperature through incubation (egg and alevin life-stages), mortality starts to increase at about 12 or 13°C, and increases sharply around 14 or 15°C (Williams 2006). In consequence, Central Valley streams are not suitable spawning habitat in summer except at high elevations, or where special circumstances such as inflows from large springs or releases from deep reservoirs keep the water cool. However, early-stage embryos seem somewhat more tolerant of warm water (Geist et al. 2006), so that Chinook spawning at 15 or 16°C in the fall may avoid harm if normal seasonal cooling occurs.

Juveniles tolerate temperatures of 20°C or even higher, provided food is abundant and the habitat is otherwise good, as in the Cosumnes River floodplain study described above. Juvenile steelhead probably are even more tolerant, as evidenced by the more southerly limit of their natural range. However, such warm temperatures do induce stress. At daily mean temperatures above 18-19°C, juvenile steelhead in the Navarro River develop elevated levels of a heat-shock protein, hsp 72 (Werner et al. 2005). At the least, this imposes a metabolic cost.

Adult Chinook can also tolerate about 20°C (Williams 2006). In Butte Creek in 2002 and 2003, adult spring Chinook suffered heavy mortality from columnaris, a bacterium, following more than a few days with mean temperatures > 21°C. There is also evidence of prespawning damage to gametes in 2002 (Williams 2006), so conditions in Butte Creek (Figure 7) probably represent the thermal limit for populations of spring Chinook, and global warming makes the prospect for the Butte Creek population dim.

Although juvenile steelhead and some juvenile Chinook stay in Butte Creek through the summer, they do not have to contend with predatory fishes there. This is not the case in the

Delta, or the larger rivers. Since the metabolic and digestive rates of predatory fishes also increase with temperature, so does the risk of predation for small salmon. Coded-wire tag studies have shown that survival in the Delta begins to decrease at temperatures that juveniles survive easily in the tributaries (Baker et al. 1995), probably because of increased predation. Whatever the cause, the lower rivers and Delta are too warm for juvenile Chinook and steelhead in the summer

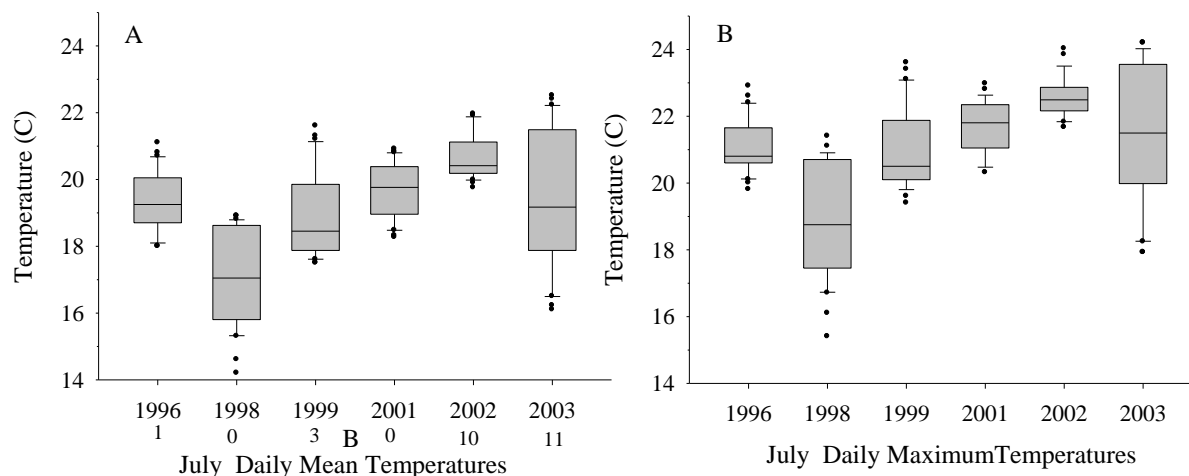


Figure 7. Daily mean (A) and daily maximum (B) water temperatures at the Pool 4 monitoring site in the reach of holding habitat on Butte Creek: The number of days with mean > 21°C in each year is shown below the date in A. July 2002 was consistently warm; July 2003 was cool early but warm later. Copied from Williams (2006); data from CDWR and CDFG.

F. Dissolved oxygen

The oxygen in water molecules is tightly bound to a carbon atom, but fish can take up dissolved oxygen through their gills. Generally, there is enough dissolved oxygen for Chinook and steelhead in flowing streams, but eggs and alevins are often under some level of oxygen stress (Williams 2006). This is particularly true for Central Valley fish, since the metabolic demands of the organism increase with temperature, the amount of dissolved oxygen that water can hold varies inversely with temperature, and fish in Central Valley streams generally incubate at relatively high temperatures. In the surface streams, dissolved oxygen is mainly an issue on the San Joaquin River near Stockton, where low flow and high biological demand in late summer and fall causes a “DO sag” (Lee and Jones-Lee 2003; Jassby and Van Nieuwenhuyse 2005). The low DO may delay migration up the San Joaquin River by adult fall Chinook, as discussed in the stressors chapter.

III. Distributions:

A. Historical distributions:

Chinook and steelhead were once widely distributed in Central Valley rivers, going just about anywhere they could swim. The past distribution of Chinook has been estimated from

historical accounts by Yoshiyama et al. (1996; 2001). Lindley et al. (2004, 2006) estimated that there were about 18 independent populations of spring Chinook, 4 independent populations of winter Chinook, and 81 independent populations of steelhead, based largely on the historical data compiled by Yoshiyama et al. (1996), and on factors such as stream gradient, basin size, and temperature. Winter Chinook inhabited streams in volcanic terrain in the upper Sacramento drainage where large springs provided substantial inflows of cool groundwater year-round: the McCloud, Little Sacramento, and Pit rivers, and Battle Creek. Spring-run probably were the most widely distributed Chinook; they ascended rivers to high enough elevations that summer temperatures remained tolerable, and because they migrated during spring snowmelt runoff, they could pass over barriers that were impassable during lower flows. Fall Chinook spawned at lower elevations than other runs, but also used accessible higher elevation habitat such as the McCloud River. However, they remained separate from other runs by spawning later in the fall than spring Chinook (Williams 2006), but earlier than late fall-run. There is little information on the natural range of late-fall Chinook (Williams 2006), but evidently they spawned at high enough elevation that the streams remained habitable for the juveniles through the summer, and spawned later than fall-run. Steelhead presumably went higher into watersheds and into smaller tributaries than Chinook, but good information on their natural range is also lacking (McEwan 2001).

Since salmon are anadromous, the distribution of any population includes habitats between the spawning grounds in gravel-bed streams and the oceans, including the Delta. Juveniles can and do swim upstream, so Chinook habitat in the Central Valley extends into small tributaries, such as Rock Creek near Chico, that are dry in the summer and do not support spawning (Maslin et al. 1999). These are relatively warm and biologically productive, and the young salmon grow rapidly there. As many as a million juveniles may still use these habitats.

Salmon habitat also extended widely across the valley floor. Historically, during the winter and spring, the rivers were not contained by their channels, and spread out over large areas, especially in the Sacramento Valley (Kelley 1989), to provide extensive floodplain habitat for juvenile salmon (Williams 2006). The overbank habitat along the lower rivers graded into the extensive tidal marsh habitat of the Delta and the bays. Although data are lacking, it seems likely that juvenile salmon historically used tidal and subtidal habitats all across the Delta. In a report on studies of Chinook in 1897 and 1898, Scofield (1899) described a few fish collected in the bays and the Delta, and observed that:

If this small number of salmon taken in salt water represents, as it unquestionably does, the first big movement of young salmon out of the river, it at first appears that more of them should have been found, but when we consider the vast expanse of territory the lower Sacramento covers with its many channels and bayous, to say nothing of San Pablo and Suisun bays, it is not so strange that so few were found—in fact, the strange part of it is that so many were found—and we can realize the vast number that must have distributed themselves in these waters.

B. Current geographical distributions:

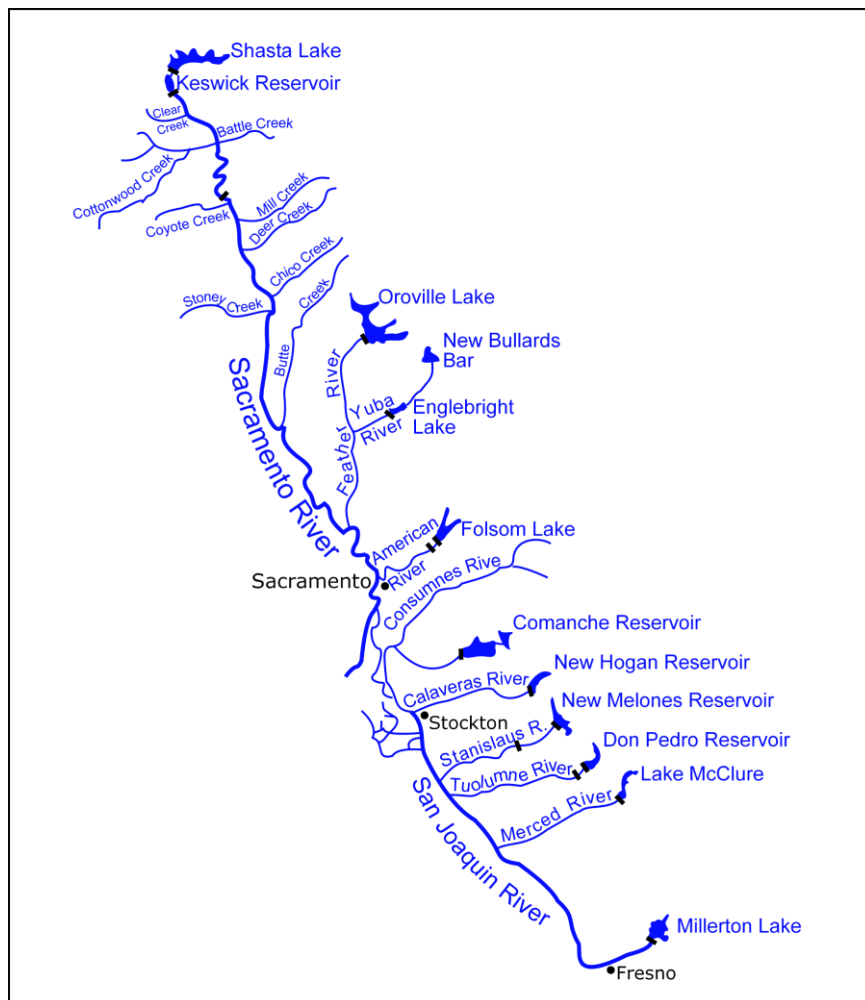
Current distributions of Chinook and steelhead are sharply constrained by impassible dams (Figure 8), or, on the San Joaquin River, by diversions. Fall Chinook, which still have access to the part of their natural range below the dams, are now most widely distributed, and are the only Chinook in the San Joaquin River and Delta tributaries. Winter Chinook persist only in the Sacramento River below Keswick Dam. Independent populations of spring Chinook remain in Mill, Deer, and Butte creeks, where migrations are not blocked by dams. Chinook enter the Feather and Yuba rivers in spring and hold over through the summer, but genetically the Feather River fish are very similar to fall-run, and the population is heavily influenced by hatchery fish; the same is probably true of the Yuba River population. Small populations of spring Chinook occur in several other Sacramento River tributaries such as Clear and Chico creeks, and a few nominal spring Chinook are reported in the mainstem. Late fall Chinook persist in the Sacramento River and apparently occur in various tributaries, but whether the tributary populations are viable is uncertain. *O. mykiss* remain widely distributed, but the number of naturally reproducing anadromous fish seems to be small, perhaps a few thousand, and there are few good data on them (Lindley et al. 2004, 2007; Williams 2006).

Along the streams and in the Delta, levees constrain the current distribution of juvenile salmon to the channels, except for the Butte Sink, the Sutter and Yolo bypasses (Figure 9), unleveed reaches of the Consumes River, and remnant tidal marshes in the Delta. Levees also block most of the tidal wetlands around the bay (Atwater et al. 1979). The loss of overbank and tidal habitat for juvenile rearing may rival the importance of the loss of upstream habitat for spawning. For example, habitat in the Butte Sinks and the Sutter Bypass probably accounts for the recent success of Butte Creek spring Chinook. The Yolo Bypass and the overbank habitat along the Consumes River provide good habitat when juvenile Chinook have access to them (Sommer et al. 2001, 2005; Jeffres et al. 2008).

Formerly an extensive tidal marsh, the Delta is now a web of constrained channels (Figure 10). The distribution of juvenile Chinook in the Delta in spring has been studied and described Erkkila et al. (1950) and by the Interagency Ecological Program (Kjelson et al. 1982; Brandes and McClain 2001). The IEP monitors the current distribution of juvenile Chinook in the Delta by seine surveys (Low 2005; Pipel 2005). Generally, density is highest along and near the Sacramento River, but juveniles occur throughout the Delta. The strong tidal flows in the Delta probably provide a sufficient explanation for the dispersal of juveniles, which preceded export pumping (Erkkila et al. 1950), but exports, active dispersal, and other factors probably affect it.

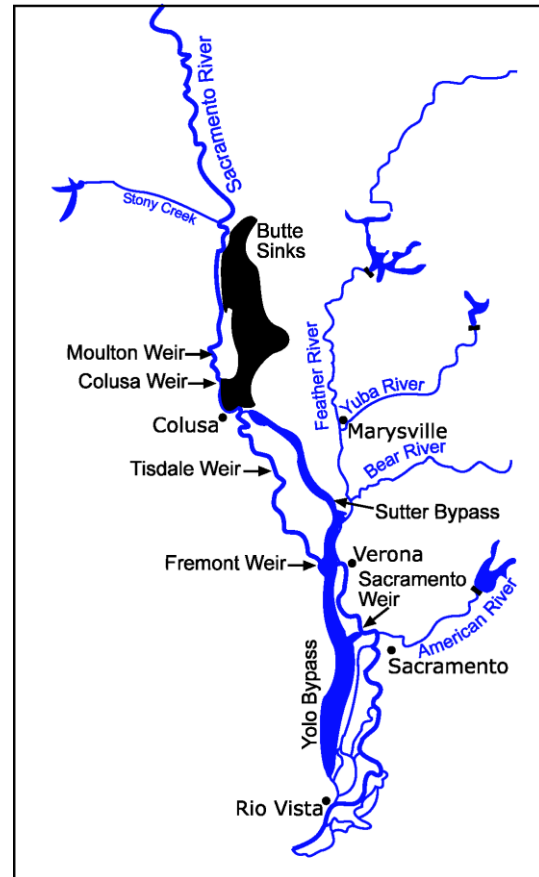
Like the juveniles, adult Chinook are widely distributed around the Delta, based on old tagging studies (Hallock et al. 1970) and the gill net fishery that existed until the 1950s. Presumably, steelhead are also distributed throughout the Delta, again with a concentration along and near the Sacramento River, but data are few.

Figure 8. Dams on Central Valley rivers. All major Central Valley rivers are blocked by large, impassable dams. Comanche Reservoir is on the Mokelumne River, and Friant Dam impounds Millerton Lake. The Red Bluff Diversion Dam is just upstream from Coyote Creek. Note that the rivers without dams are drawn ending at arbitrary points, not the upstream limit for anadromous fish. Copied from Williams (2006).



The distribution of juveniles in the bays is not well known. A few small juveniles are collected around the margins of the bays in the IEP seine surveys (SSJEFRO 2003) and in Suisun Marsh (e.g., Mattern et al. 2002). Fry use moderately saline (15-20 ppm) habitats in other estuaries (Healey 1991), so the salinity of much of the bays should not be an obstacle for them, even in dry years. NMFS has collected larger juveniles in the channels in April to June (MacFarlane and Norton 2002), but overall, data on distributions in the bay are sparse.

Figure 9. The flood bypass system along the Sacramento River. Water passes from the river through several weirs into the Butte Sinks, from which it flows into the Sutter Bypass, and then across the Sacramento River to the Yolo Bypass, which flows into the Delta. Copied from Williams (2006).



The distribution and production of hatchery salmon are summarized in Table 4. Hatchery Chinook returning as adults probably occur in all salmon streams, since hatchery fish stray more often than naturally produced fish. For example, five or six percent of the fall Chinook examined during carcass surveys on Mill and Deer creeks in 2003 and 2004 lacked adipose fins, and since only a small fraction of hatchery fall Chinook were marked at the time, a large proportion of the runs in those streams must have been straying hatchery fish (Williams 2006). The Joint Hatchery Review Committee (JHRC 2001) estimated that the straying rate of hatchery fish trucked around the Delta is over 70%, which helps explain the lack of detectable genetic variation among Central Valley populations of fall Chinook, described by Banks et al. (2000) and by Williamson and May (2005).

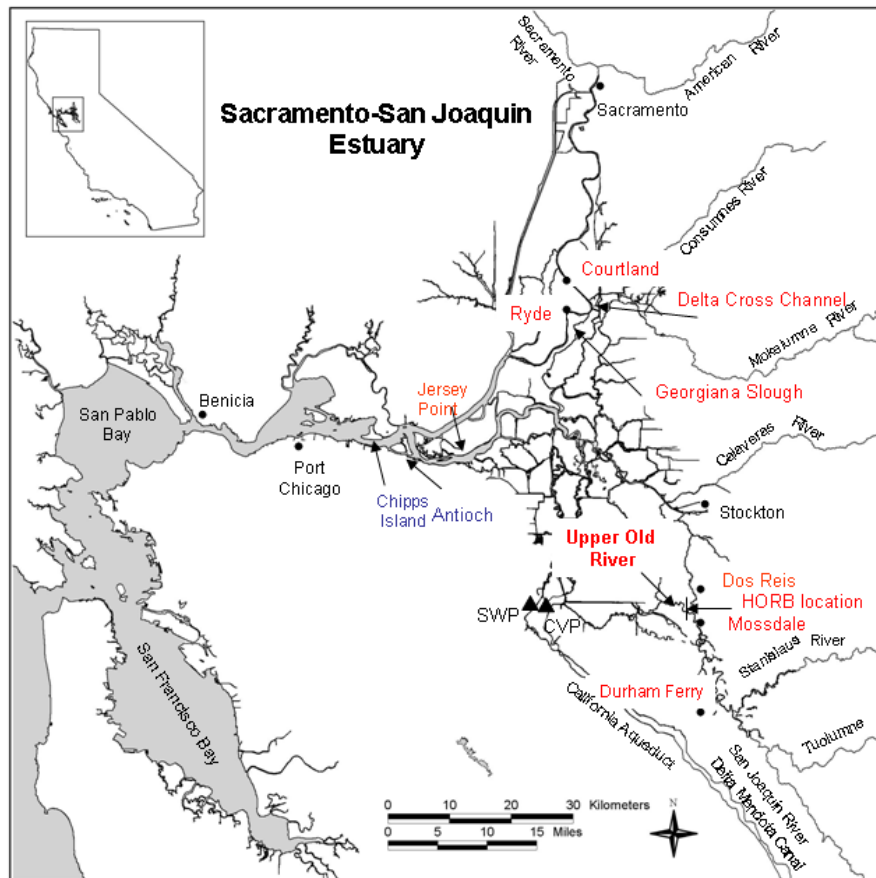


Figure 10. The Delta and bays. Locations marked in red figure importantly in IEP coded-wire tag studies. Sherwood Harbor, mentioned in the text, is not shown but is close to Sacramento. Copied from Newman (2008).

Table 4. Production and release data for salmon and steelhead in the Central Valley, data from JHRC (2001, Appendix V) and Brown et al. (2004). (JHRC) M = mitigation, E = enhancement. Coleman National Fish Hatchery is on Battle Creek, and Livingston Stone is on the Sacramento River near Keswick Dam. Fish with coded-wire tags (cwt) also are marked by removing the adipose fin.

Hatchery	Species or Run	Production Goal (millions)	Maximum Egg Take (millions)	Tag or Marks	Size and Time of Release	Release Location
Coleman	Fall	12, smolts		25% cwt BY 06 +	90/lb. Apr.	Battle Creek ¹
Coleman	Late-Fall	1, smolts		100% cwt	13-14/lb. Nov.-Jan	Battle Creek
Coleman	Steelhead	0.6, smolts		100% ad-clip, some cwt	~4/lb Jan.	75% Balls Ferry; 25% Battle Creek
Livingston Stone	Winter	0.2, smolts		100% cwt	~85 mm Jan.	Sac. R. at Redding
Feather River	Spring	5, smolts	7	100% cwt	May-June	50% F. R., 50% S. P. Bay
Feather River	Fall	M 6, smolts E 2, post-smolts	12	25% cwt BY 06 +	April-June	San Pablo Bay
Feather River	Steelhead	0.45, yearlings		Ad-clip		
Nimbus	Fall	4, smolts				San Pablo Bay
Nimbus	Steelhead	0.43, yearlings		100% ad-clip		
Mokelumne River	Fall	M 1, smolts M 0.5 post smolts E 2, post-smolts		25% cwt BY 06 +	May-July Sept.-Nov. May-June	various Lower M. R. San Pablo B.
Mokelumne River	Steelhead	0.1	0.25	100% ad-clip	Jan.	Lower M. R.
Merced River	Fall	0.96, smolts or yearling		100% cwt	Apr. – June Oct. – Dec	Merced R. + exper. releases elsewhere

C. Population Trends

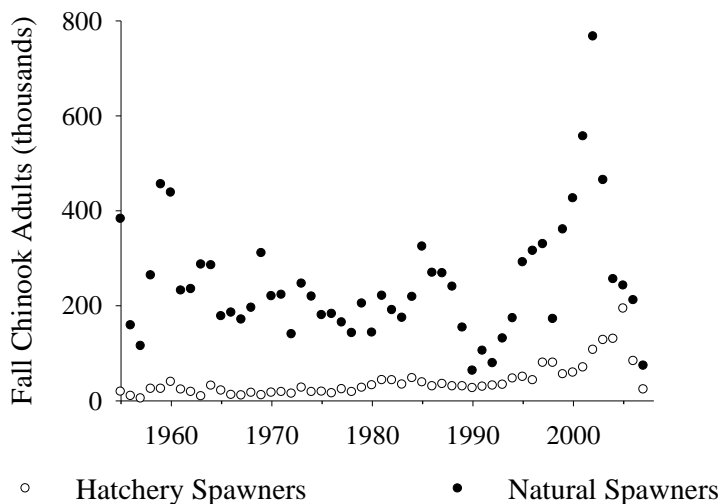
1. Fall Chinook

Returns of fall Chinook have fallen sharply from very high levels a few years ago (Figure 11). The decline is particularly striking because ocean harvest was well below normal levels for several years, and was shut down entirely in 2008. Poor ocean conditions have been identified as the proximate cause of the collapse by Lindley et al. (2009), in a report to the Pacific Fishery Management Council. However, the report also noted that “Degradation and simplification of freshwater and estuary habitats over a century and a half of development have changed the Central Valley Chinook salmon complex from a highly diverse collection of numerous wild

¹ A million fall Chinook from Coleman were trucked past the Delta in 2008.

populations to one dominated by fall Chinook from four large hatcheries.” Figure 10 understates hatchery influence, since many of the natural spawners are hatchery fish. A recent haphazard sample of about 100 from the party-boat fishery was 90% hatchery fish (Barnett-Johnson et al. 2007).

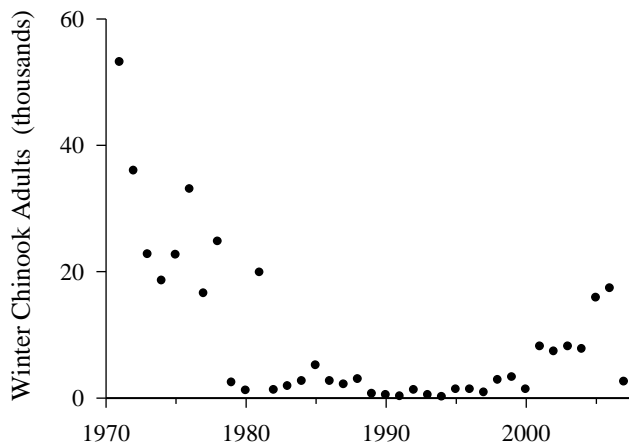
Figure 11. Returns of fall Chinook to Central Valley rivers (filled circles) and to Central Valley hatcheries (open circles). Data from CDFG. Recent years are preliminary.



2. Winter Chinook

After several years of increases, the number of winter Chinook returning to the Sacramento River declined sharply in 2007, although not as much as fall-run (Figure 12).

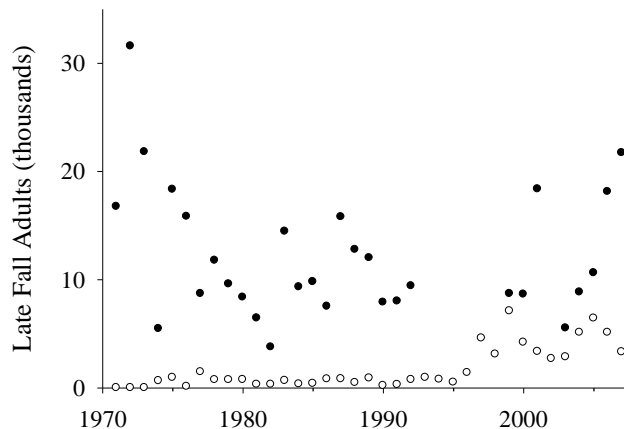
Figure 12. Returns of Winter Chinook to the Sacramento River. Data from CDFG. Recent years are preliminary.



3. Late fall Chinook

Returns of late fall Chinook have increased in recent years, in marked contrast to fall Chinook (Figure 13). As with fall Chinook, hatchery returns increased sharply after 1995. As discussed in the next chapter, late fall Chinook enter the ocean in winter, at a much larger size than fall Chinook, and this may explain why they responded differently to ocean conditions than fall Chinook.

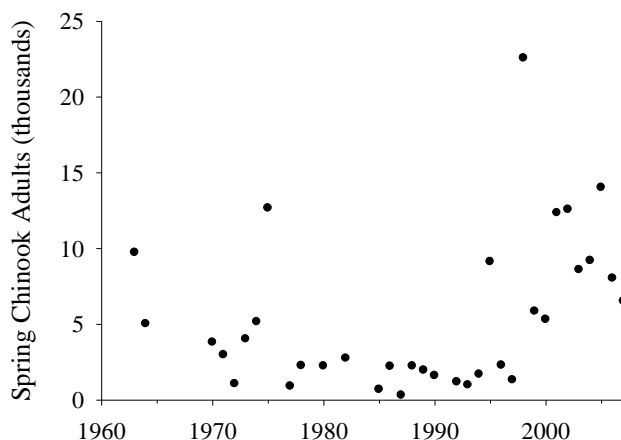
Figure 13. Returns of late fall Chinook to the upper Sacramento River (filled circles) and to Coleman Hatchery (open circles). Data from CDFG. Recent years are preliminary.



4. Spring Chinook

Spring Chinook have declined in recent years, especially in Mill and Deer creeks, but not as severely as fall Chinook (Figure 14). Spring-run from Butte Creek leave the Delta at about the same time and size as fingerling-migrant fall Chinook (see below), but for unknown reasons the spring Chinook suffered less from poor ocean conditions than did fall Chinook. There is essentially no hatchery influence on the Butte, Mill and Deer creek populations. Curiously, returns of hatchery-dominated Feather River spring Chinook were up in 2007, as were returns to the Sacramento River mainstem, which may be largely Feather River hatchery strays.

Figure 14. Returns of spring Chinook to the Mill, Deer, and Butte creeks. Data from CDFG. Recent years are preliminary.



5. Steelhead

There are few data on the abundance of wild or naturally produced adult steelhead in the Central Valley, now that they are no longer forced to pass a ladder at the Red Bluff Diversion Dam, and it is very hard to distinguish anadromous steelhead from large resident *O. mykiss* on the spawning grounds. Based on the number of unmarked juveniles captured at Chipps Island, however, the number of spawning females may average three or four thousand (Williams 2006).

IV. Ecology

A. Adult life history patterns

Chinook in the Central Valley usually are classified into four separate runs, named for the season in which adults enter fresh water: fall, late-fall, winter, and spring. Central Valley steelhead now enter fresh water mainly in fall, although a few adults of both species migrate up the Sacramento River even in the summer (Williams 2006). Winter Chinook are listed as endangered under the federal Endangered Species Act (ESA), and spring Chinook and steelhead are listed as threatened.

Fall Chinook generally enter fresh water as temperatures decline in the fall, in an advanced state of sexual maturation, and begin spawning when the water temperature declines to 15 or 16°C (Williams 2006). The timing of spawning varies somewhat from river to river and year to year (Table 5). Late-fall Chinook follow the fall-run into the rivers, but also spawn fairly soon after arriving on the spawning grounds. Winter and spring Chinook, however, typically hold in fresh water for several months to complete sexual maturation before they spawn. These different patterns are sometimes called “ocean maturing” and “stream maturing.”

Genetic evidence (Figure 15) indicates that the spring Chinook in Butte Creek are a separate lineage from those in Mill and Deer creeks, and spring Chinook in the Feather River are closely related to fall Chinook. Thus, the four named runs correspond generally but not completely with genetic lineages. Steelhead in the American and Mokelumne rivers are descended from a coastal stock brought to Nimbus Hatchery after the native run failed to thrive in hatchery culture (McEwan 2001).

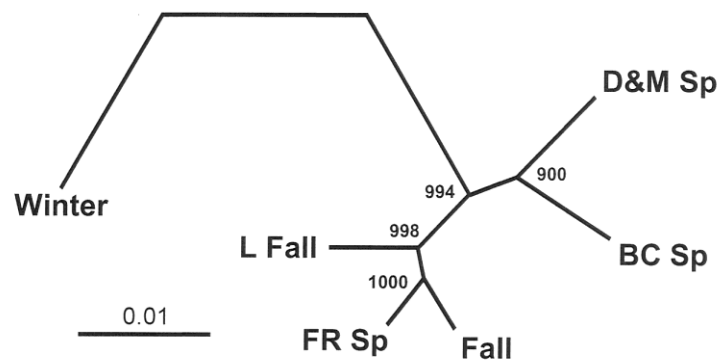


Figure 15. Genetic relationships among runs of Central Valley Chinook, based on distances (Cavalli-Sforza and Edwards) calculated from 12 microsatellite loci. The clustering analysis (UPGMA) distinguishes spring-run from Deer and Mill creeks (D&M Sp) and Butte Creek (BC Sp). Numbers next to nodes show the number of bootstrap trees, out of 1,000, showing this node. Nominal spring-run from the Feather River (FR Sp) group close to fall-run. Other genetic studies, reviewed by Hedgecock et al. (2001) have produced similar results. Copied from Hedgecock 2002.

Table 5. The estimated range in the time of spawning by Chinook salmon in various Central Valley rivers, summarized from tables 6-1 to 6-4 in Williams (2006).

Run:	5% by	Peak	95% by
Fall	mid-Sep. to late Oct.	Mid-Oct to late Nov.	early Nov. to late Dec.
Late-fall	early to late Dec.	late Dec. to late Jan.	late March to early April
Winter	early to mid-May	early June to early July	early to mid-August
Spring	late Aug. to early Sept.	Sept. to early Oct.	mid to late Oct.

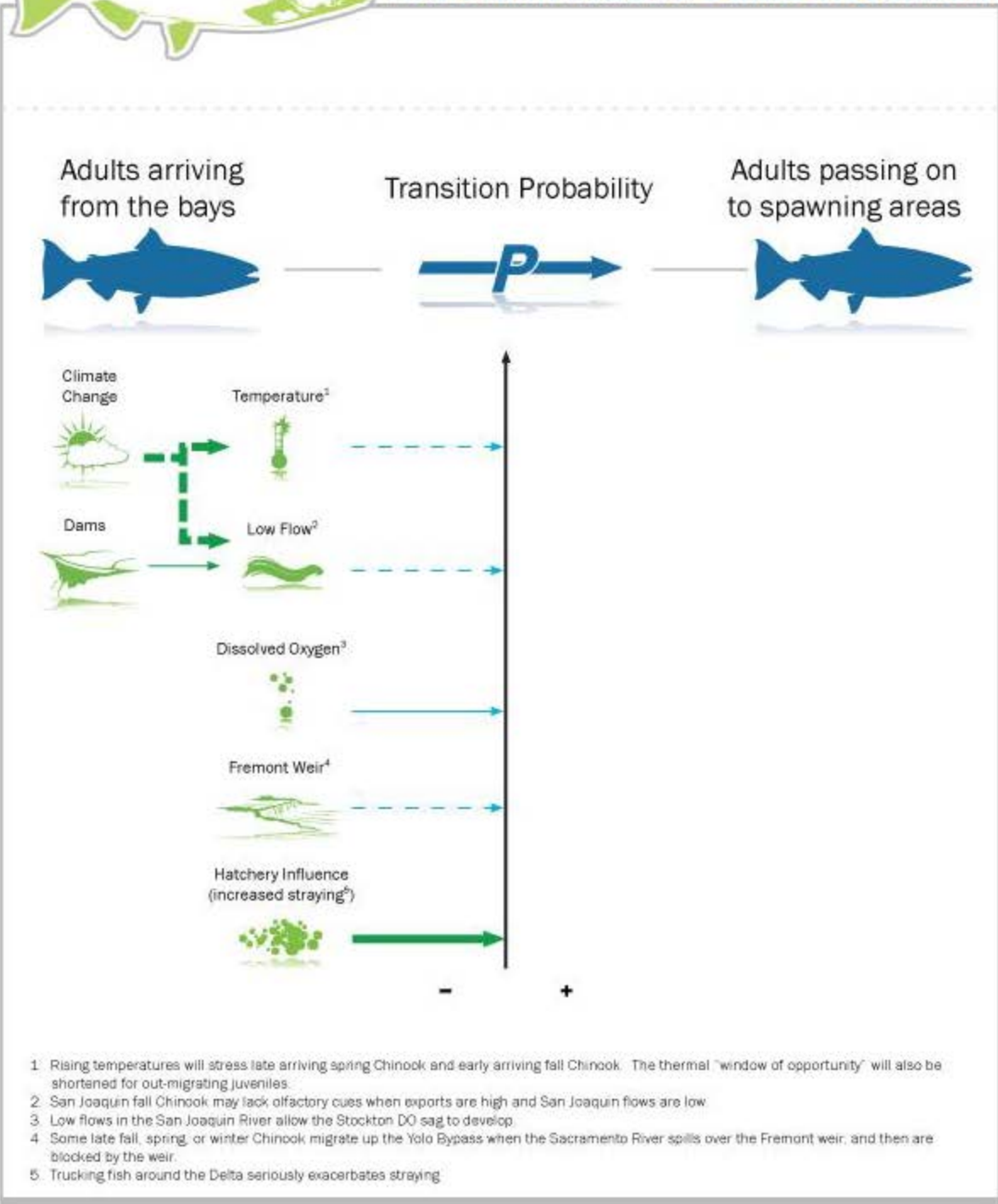
Like genetic lineages, management units of Chinook correspond generally but not exactly with the four named runs. In particular, for Endangered Species Act (ESA) purposes, fall and late fall Chinook are lumped together, as are all spring-run. Harvest is managed largely in terms of “Sacramento Fall Chinook”, which ignores fall Chinook in the San Joaquin system and in the Mokelumne and Cosumnes rivers, which flow directly to the Delta.

Steelhead migrate up the Sacramento River mainly from August through November, but some do so in all months (Hallock et al. 1961; McEwan 2001), and a summer-run may have existed historically (McEwan 2001). Although steelhead enter freshwater mainly in the fall, they are often called winter-run. The fall or winter-run steelhead spawn mainly from late December through April (Hallock et al. 1961; Hannon et al. 2003). Only few steelhead now migrate into San Joaquin River tributaries (Williams 2006).

B. Navigation by adults

Although the details remain uncertain, maturing salmon apparently find their way back to the vicinity of their natal stream using celestial and magnetic cues, and then shift mainly to their sense of smell to guide the rest of their migration (Quinn 2005). Maturing Chinook and steelhead migrating back to Central Valley rivers must pass through the Delta. Tagging studies showed that Chinook may spend weeks in the Delta (Hallock et al 1970), as they do in other estuaries (Olson and Quinn 1993), but some pass through quickly. Given the extent to which fish linger in the Delta, delays of a day or two at the Montezuma Slough gates or the Delta Cross Channel seem unlikely to be significant (Williams 2006). On the other hand, adult winter-run that try to migrate up the Yolo Bypass may find themselves trapped there. Factors reducing the survival of adults migrating through the Delta are summarized in Life Stage Transition Figure 3.

Transition Matrix: Chinook Salmon



Life Stage Transition 3

C. Juvenile life history patterns:

Early in the 20th Century, biologists recognized that some juvenile Chinook migrate to sea in the spring of their first year, while others remain in the stream through a winter and migrate the following spring. These were called “ocean-type” and “stream-type” (Gilbert 1913), but this dichotomy does not capture the actual range of juvenile life history patterns, since late fall and winter Chinook migrate downstream and into the bays during the fall and winter, and spring and fall Chinook may remain near the spawning areas for only a few days or for several months. Accordingly, juvenile Chinook of widely different sizes can be found in different Central Valley habitats (Figure 16). Although they are really points on a continuum, it seems possible to distinguish six different life history patterns for juvenile Chinook in the Central Valley, ranked below in terms of increasing amounts of time spent in fresh water. Similarly variable patterns have been described in other rivers (Burke 2004). Life history patterns can also be distinguished in terms of the habitats in which juveniles mainly rear (Figure 16).

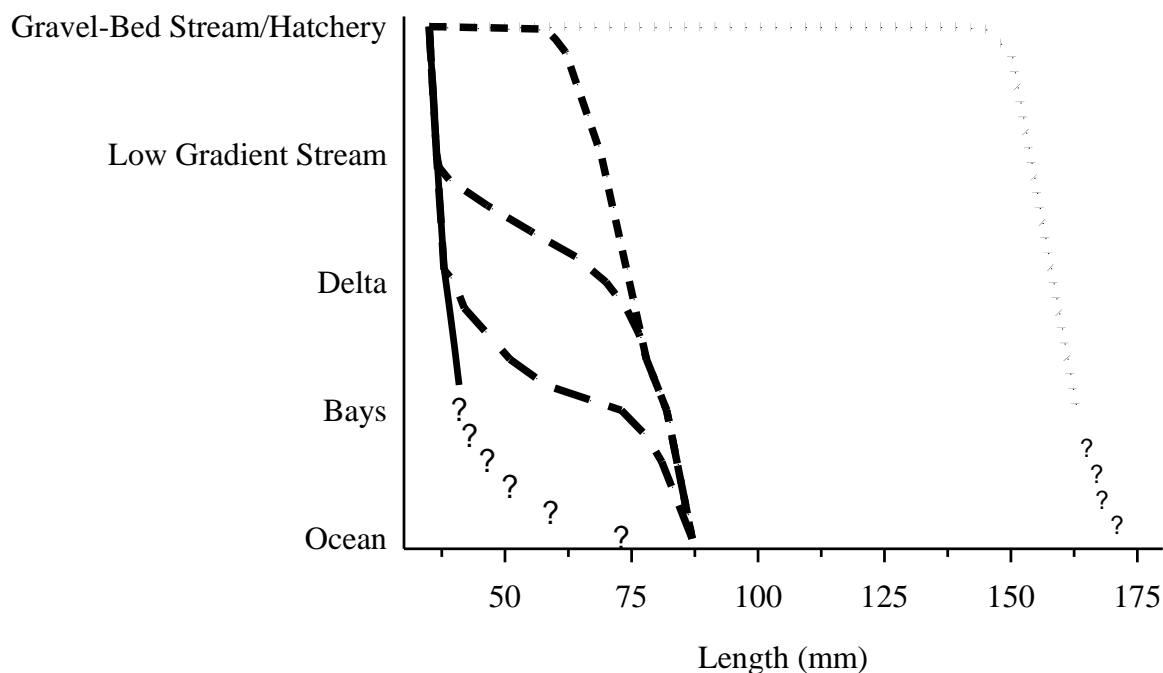


Figure 16. Conceptual “juvenile life-history space”. Lines show representative trajectories of growth and migration for juvenile Chinook. Fry emerge at ~35 mm, and may migrate directly to the bays; what they do when they get there is poorly understood. Many fish migrate directly to the Delta and rear there (long dashed line); if they survive, they migrate through the bays to ocean. Some fry migrate to the lower rivers and rear there before migrating through the Delta and bays (medium dashed line). Other fry emerge and remain in the gravel-bed reaches of the stream until they migrate, generally in spring, as fingerlings (short dashed line), while others remain in the gravel-bed stream through the summer and migrate as larger juveniles. How long they remain in the bays is unknown. Except for fry, lengths are actually highly variable, so properly the figure should show broad smears rather than discrete lines.

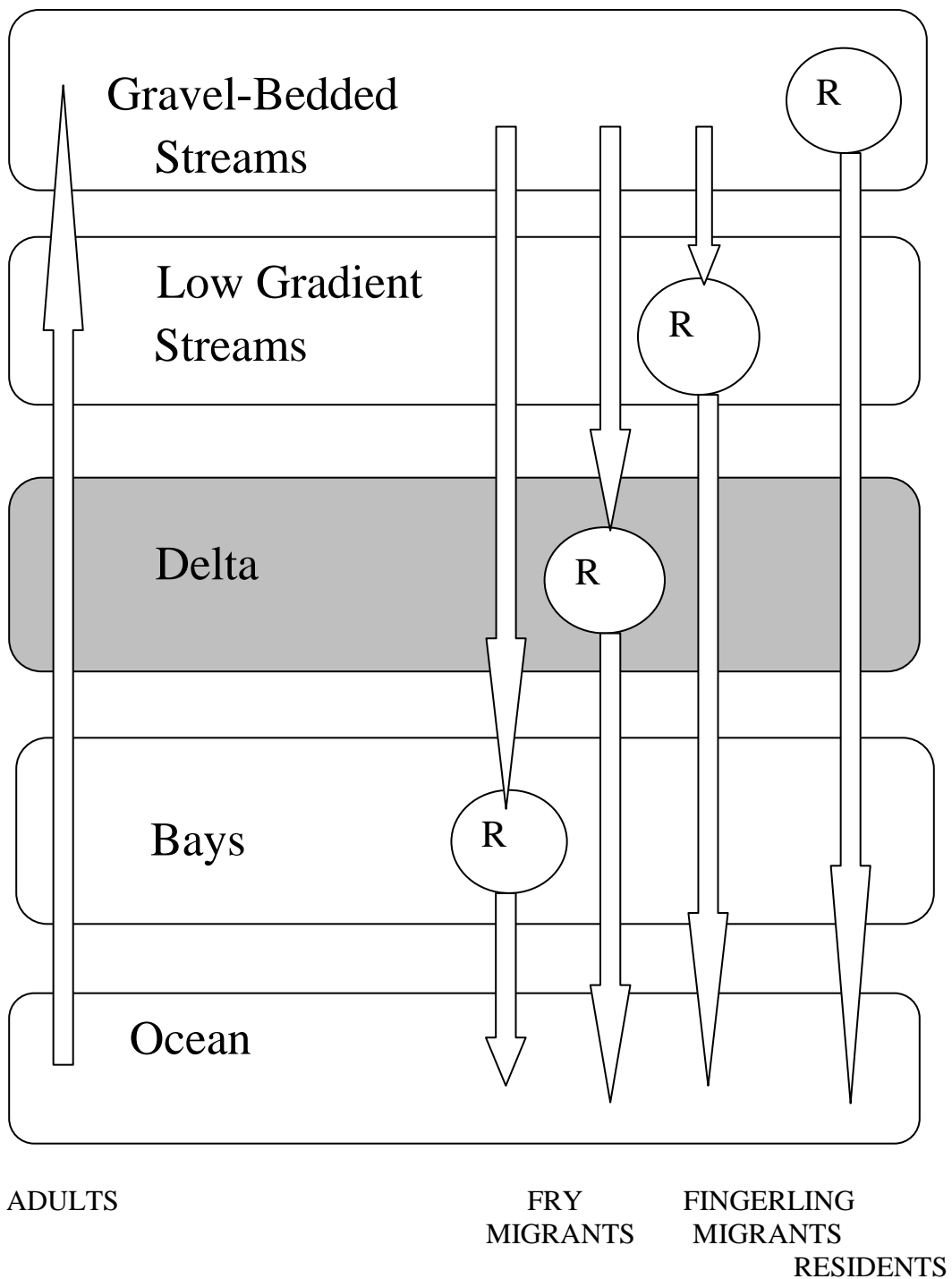


Figure 17. Schematic of the Chinook life-cycle, with arrows indicating migration and circles indicating the habitat in fish following different life-history patterns primarily rear.

Fry migrants to the bays migrate to brackish water soon after emerging from the gravel. Hatton and Clark (1942) captured significant numbers of ~40 mm juveniles at Martinez in mid-March, 1939, when flows in the rivers were low enough that these fish must have moved voluntarily through Suisun Bay. Similarly-sized fish are captured in the Chipps Island trawl, especially in wet years, although the capture efficiency of the trawl is probably low for fish of this size (Williams 2006). Modest numbers of fry were captured in seines in Suisun, San Pablo and San Francisco bays in 1980, although fewer were taken in 1981 (Kjelson et al. 1982). Only a few such fish are captured by the Interagency Ecological Program seine monitoring around the bays (SSJEFRO 2003), but this may reflect the large area over which such fish may be distributed. This life history may have been more common in the past, when more brackish tidal marsh habitat was available to them.

Fry migrants to the Delta also migrate downstream soon after emergence, but remain in the Delta and rear there before migrating into the bays. This is probably the most common life history pattern among juveniles, based on monitoring passage into the lower rivers (e.g. Figure 18), but the percentage that survive is unknown. Presumably, Chinook following this life history historically reared in the then-abundant tidal habitat in the Delta (Williams 2006).

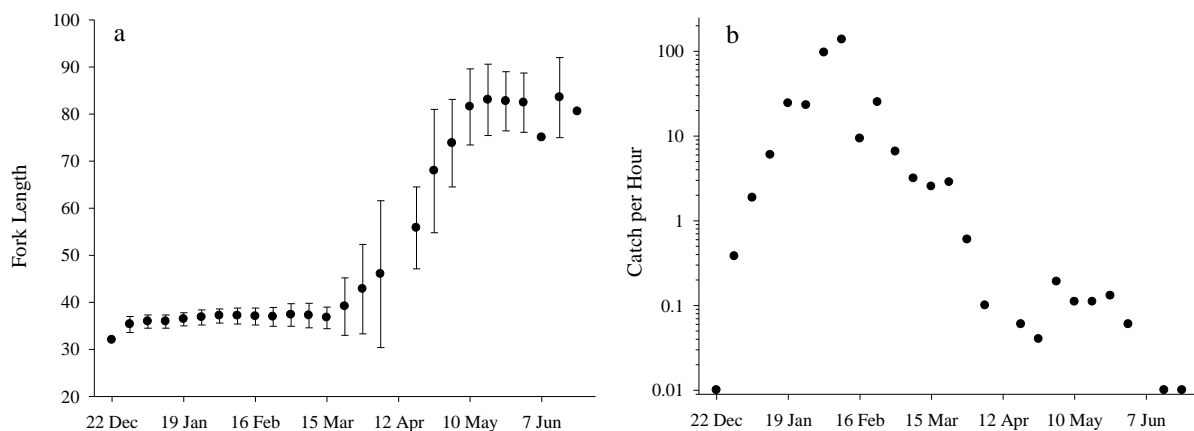
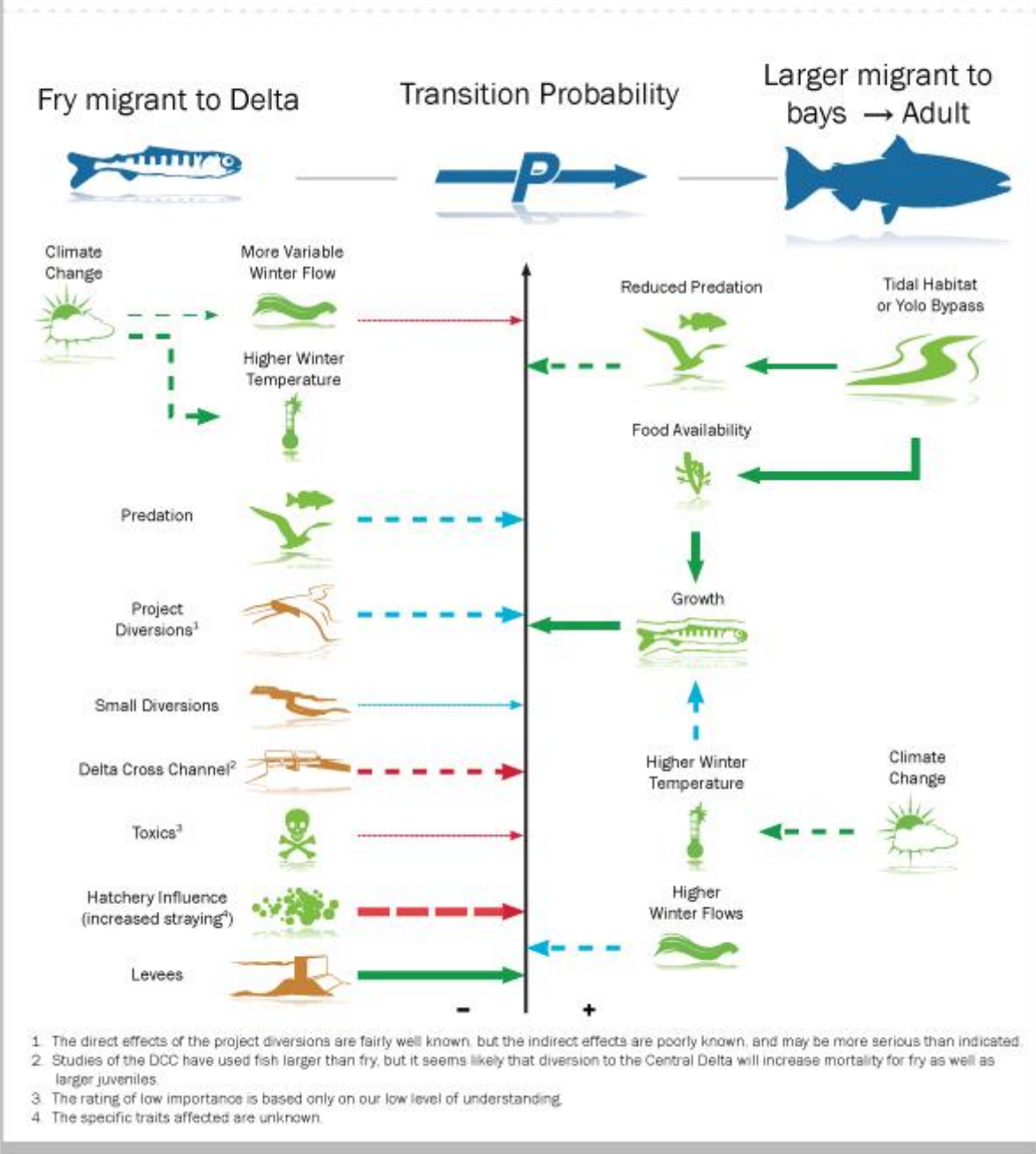


Figure 18. Mean length (a) and catch per hour (b) of juvenile fall Chinook salmon sampled in screw traps in 1999-2000 on the lower American River near the downstream limit of spawning habitat. Error bars show standard deviations. Note log scale in (b); the catch dropped sharply as size increased in March. Dates are approximately the middle of the sampling period. Data from Snider and Titus (2001); figure copied from Williams (2006).

Various factors influence the survival of fry migrants in the Delta, as summarized in the Life Stage Transition Figure 4. The negative factors (stressors) are discussed in Ch. 5; evidence for the positive effect of tidal or overbank habitat is discussed later in this chapter.

Transition Matrix: Chinook Salmon



Life Stage Transition 4

Fry migrants to low gradient streams move quickly downstream from the gravel-bed reaches where spawning occurs and rear in low gradient reaches in the valley floor before migrating rapidly through the Delta. Butte Creek spring-run exemplify this life history. Many Butte Creek spring-run fry are captured and tagged near Chico as they migrate into the Central Valley. The size of fish recaptured at Sherwood Harbor, near Sacramento, indicates that they mainly rear upstream of the Delta, presumably in the Butte Sinks or the Sutter Bypass, until they are > 70 mm; then they move rapidly through the Delta (Figure 19). The Yolo Bypass offers similar habitat to Sacramento River populations when water spills into it over the Freemont Weir, and several studies indicate that fish do well there (Sommer et al. 2001, 2005)

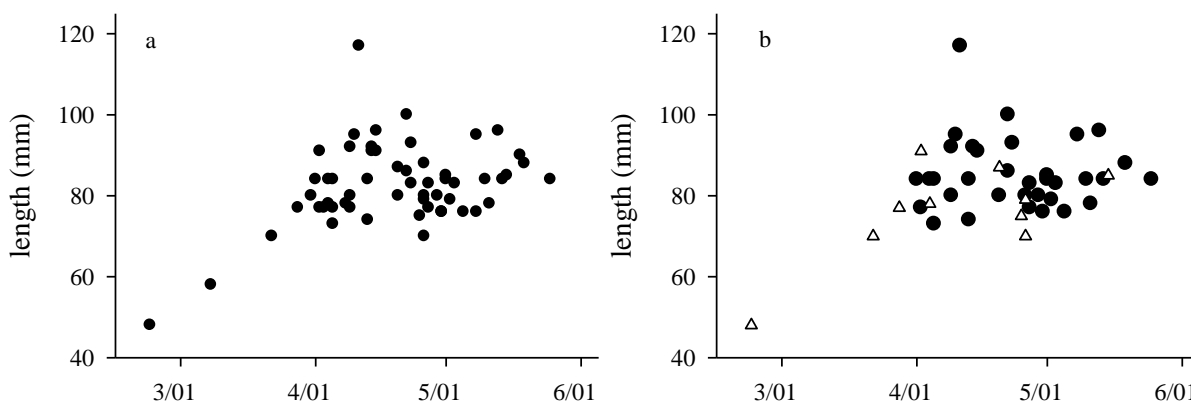
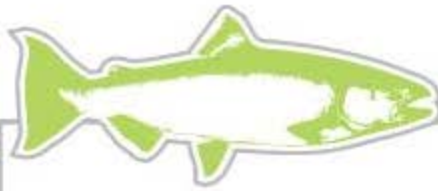
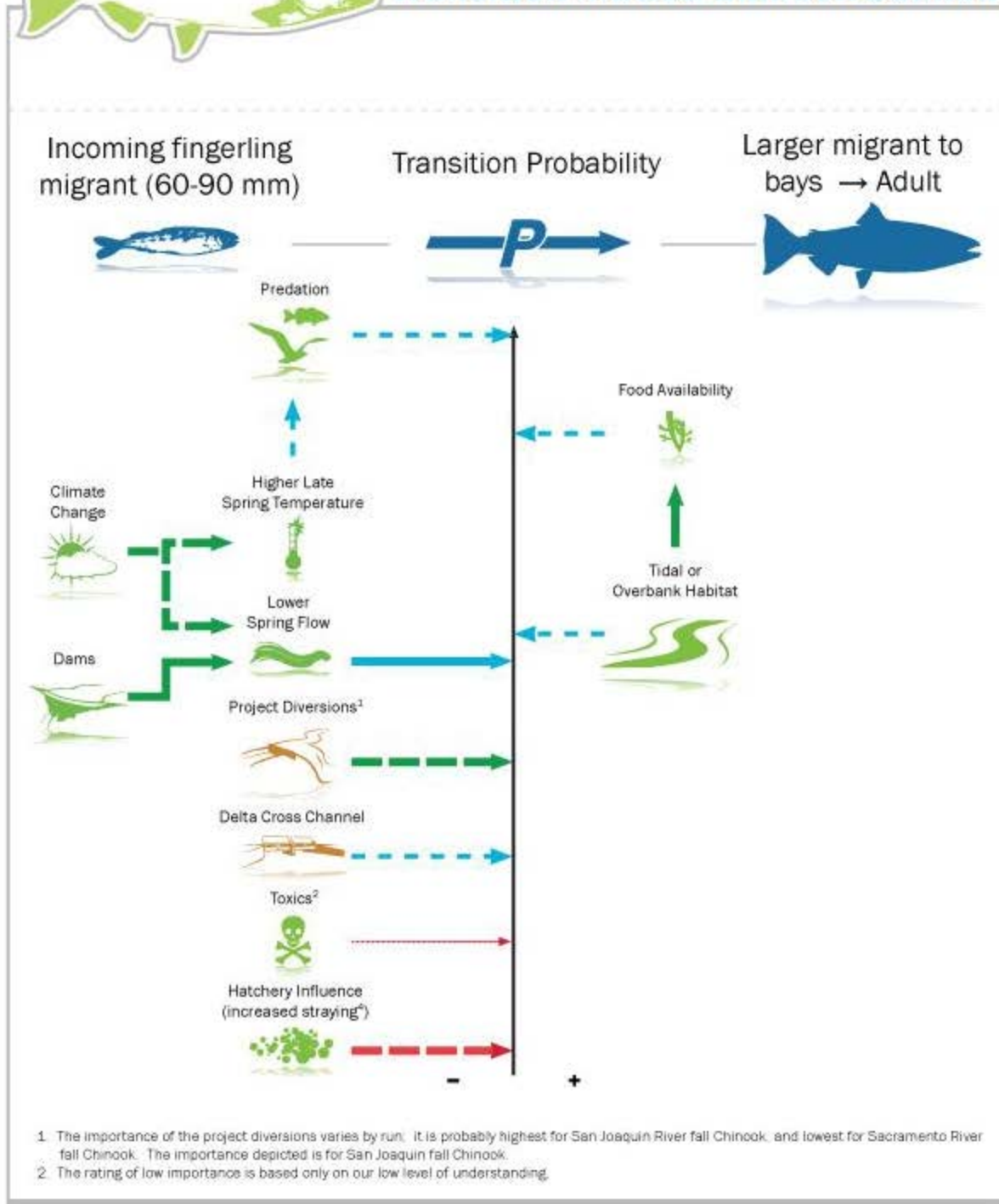


Figure 19: A. Size at date of capture of coded-wire tagged Butte Creek spring Chinook (n = 57), for all capture locations from Knights Landing to Chipps Island. B. As above, for Chipps Island (circles, n = 34) and Sherwood Island (triangles, n = 10). Data from USFWS, Stockton.

Fingerling migrants remain in gravel-bed reaches for a few months, and then migrate as larger (generally > 60 mm) parr or silvery parr, in late spring if they are fall-run. The second, smaller May mode in Figure 18b reflects this life history, which is followed by a larger proportion of the juveniles in the Mokelumne River and San Joaquin River tributaries than in the Sacramento River and tributaries, although there is considerable variation from year to year in the proportions (Williams 2006, Figure 20). The larger migrants are often called smolts, although few of them have reached this stage physiologically (e.g., Snider and Titus 2001). This life history pattern has received the most attention from managers. For example, most of the USFS coded-wire tag survival studies apply to this group. The life history of hatchery fall Chinook released into the river also approximates this pattern, since the hatchery fish are released at generally > 65 mm and most move rapidly downstream. Some move downstream very rapidly, in hatchery trucks, and are released into the bays, to avoid mortality in the Delta (Williams 2006). Factors influencing the survival of fingerling migrants to the Delta are shown in Life Stage Transition Figure 5.



Transition Matrix: Chinook Salmon



Life Stage Transition 5

Winter Chinook seem mainly to have a somewhat different juvenile life history, although the data are too sparse to support strong statements on the matter. Most of the naturally produced fish begin migrating as fry, but they seem to migrate slowly, reaching the lower Sacramento River in November (Figure 21), and generally not reaching the Delta pumps until February. More is known about the migration of hatchery winter-run, discussed below, since they are tagged, but their behavior seems to be different.

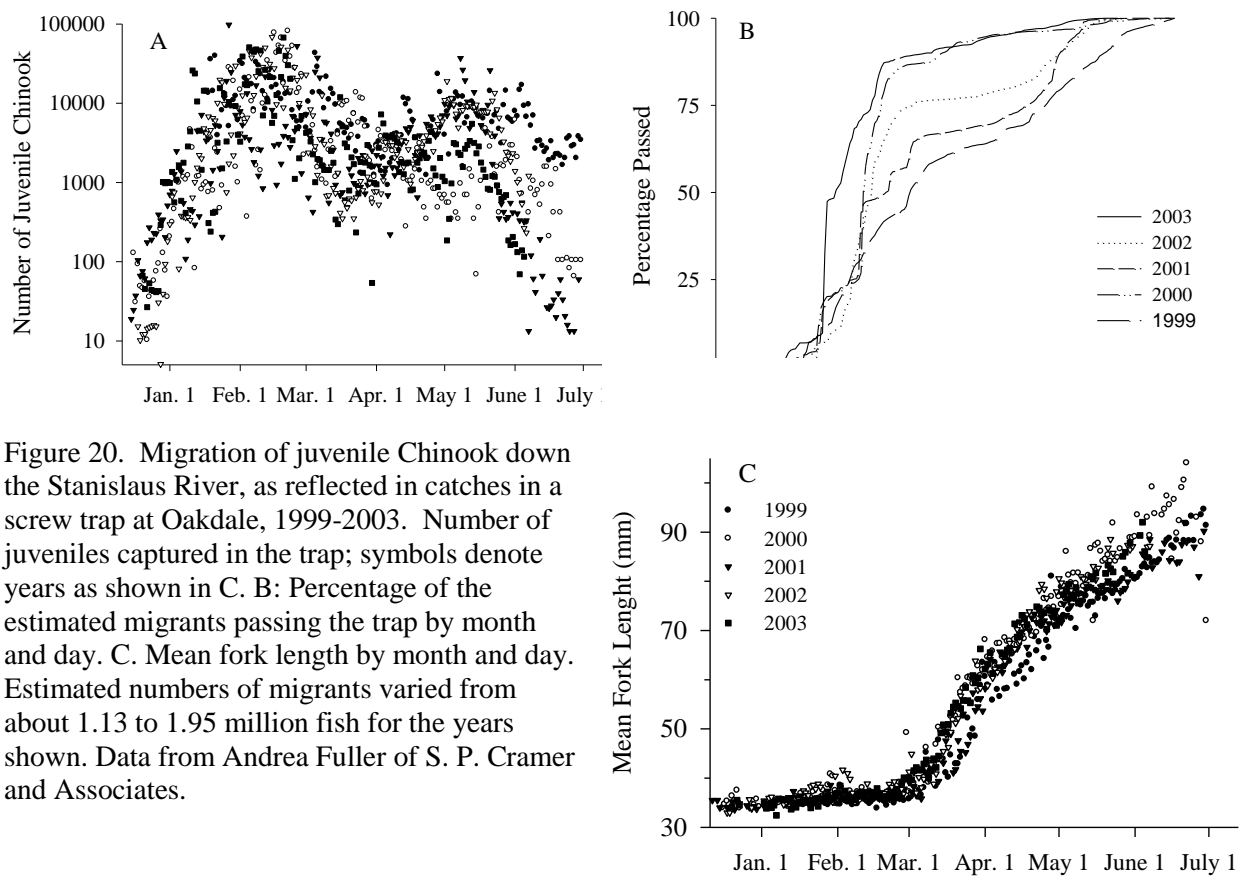
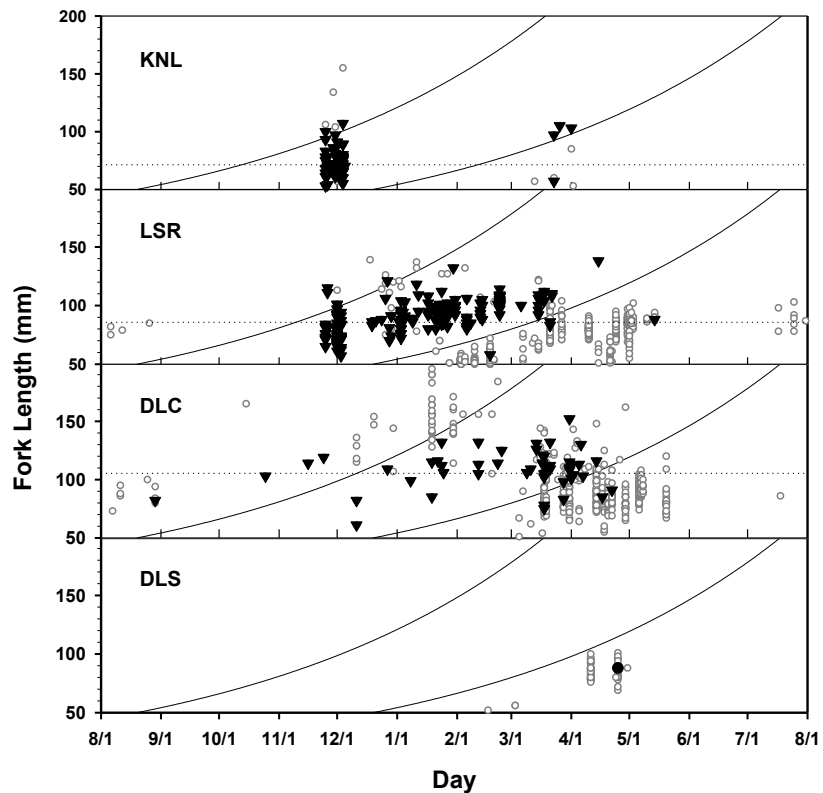


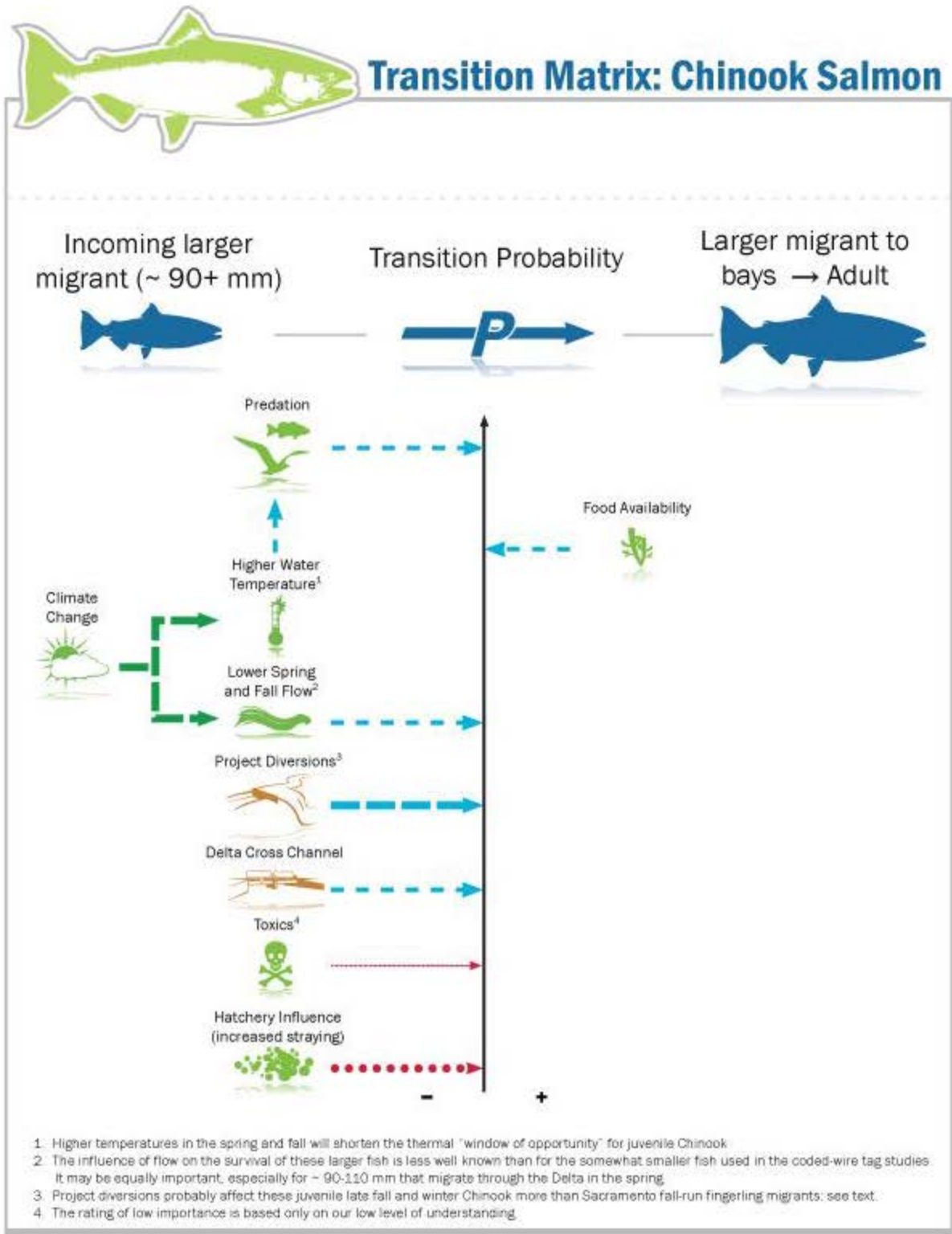
Figure 20. Migration of juvenile Chinook down the Stanislaus River, as reflected in catches in a screw trap at Oakdale, 1999-2003. Number of juveniles captured in the trap; symbols denote years as shown in C. B: Percentage of the estimated migrants passing the trap by month and day. C: Mean fork length by month and day. Estimated numbers of migrants varied from about 1.13 to 1.95 million fish for the years shown. Data from Andrea Fuller of S. P. Cramer and Associates.

Figure 21. Fork length and day of capture for juvenile Chinook assigned to runs by Hedgecock et al. (2002) for four areas from the IEP monitoring: Knights Landing (KNL), the lower Sacramento River (LSR), the central Delta (DLC), and southern Delta (DLS). Winter Chinook are shown by black triangles, other Chinook by open circles; dotted lines show mean lengths for winter-run at the site. The curved lines show length at date criteria for winter-run. Copied from Hedgecock (2002).



Fingerling residents remain in the gravel-bed reaches of the streams through the summer, and then migrate in fall or winter, generally at a length of 90 mm or more. This is probably the typical life history of late fall Chinook, and apparently it is being adopted by some fall Chinook below dams such as Keswick Dam on the Sacramento River that release cool water through the summer (Williams 2006). Many spring-run also follow this pattern; even in Mill and Deer creeks, most older juvenile spring-run migrate into the valley in November to January (Williams 2006).

Classic stream-type Chinook hatch in the spring, remain in the gravel-bed reaches of the stream through the winter, and migrate the following spring as smolts. This life history may have been more common before dams blocked most high elevation habitat, where low winter temperatures inhibit growth. Life Stage Transition Figures 6 shows the factors affecting the survival of the fingerling resident and stream-type juveniles in the Delta.



Life Stage Transition 6

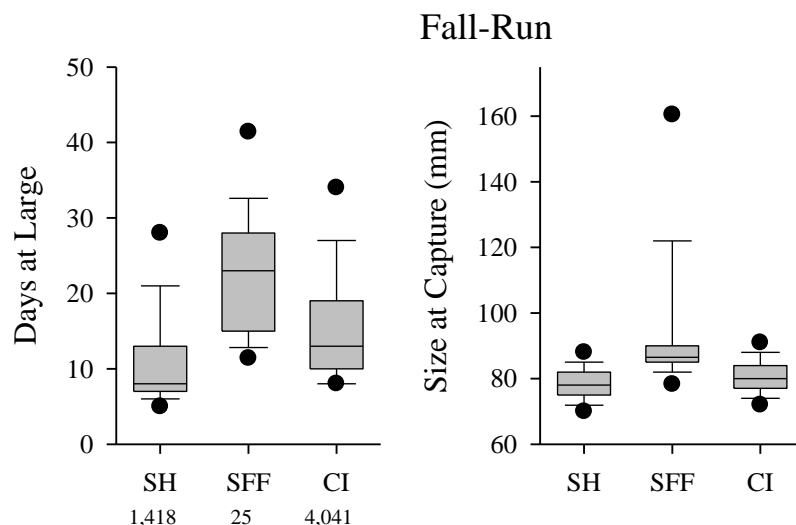
D. Juvenile migration rate

Juvenile migration is a complex matter, as suggested by the diversity of life history patterns described above, and despite many studies much about it remains unclear (Høgåsen 1998). If we take migration as a deliberate movement from one place to another, it is not even always clear whether juvenile salmon are migrating, or simply dispersing passively downstream. It is sometimes obvious that fry are being swept downstream (Williams 2006), but the downstream movement of large numbers of fry even during periods of low flows has seemed deliberate to most Central Valley biologists, starting with Rutter (1904).

The migration rates and schedules of wild and naturally produced Chinook are highly variable, as implied by the diversity of life history patterns described above. Only a few Central Valley data are available, (Williams 2006), not enough to provide good estimates, except for Butte Creek spring Chinook (Figure 19). The migration rate of tagged hatchery fish can be estimated from the number of days between the release and recapture of fish collected in monitoring programs, but hatchery fish may have different migratory behavior, so these data are most useful for comparisons among hatchery populations. All hatchery winter and late fall Chinook have been given coded-wire tags for some time, as have fall Chinook from the Merced River Hatchery, and about 8% of fall Chinook from Coleman Hatchery were tagged from 1995-2002; 25% of fall Chinook are now marked, so more data are accumulating rapidly.

Fall Chinook released from Coleman Hatchery migrate rapidly, with median travels time of 8 days to Sherwood Harbor, near Sacramento, and 13 day to Chipps Island (Figure 22). This suggests that the migration rate slows as the fish approach the Delta, since it is about 365 km from the hatchery to Sherwood Harbor, and only about 80 more to Chipps Island. The change from riverine flow to bi-directional tidal flow may account for the change in pace. Remarkably few of the fall Chinook released at Coleman have been recovered at the pumps (34 compared to 4,041 at Chipps Island), but those that do take longer to get there. Either they were larger to begin with, or they grew well ($\sim 0.8 \text{ mm d}^{-1}$) along the way.

Figure 22. Days at large, size at capture, and release date of tagged fall Chinook released at Coleman Hatchery, and recaptured at Sherwood Harbor (SH, n = 1,418) the state fish facilities (SFF, n = 25), and Chipps Island (CI, n = 4,041). Seven fish collected at the federal fish facilities and two released in January as yearlings are not shown. Sample sizes are given below X-axis labels on the left panel. Data from USFSW.



Coleman late fall Chinook do not migrate quite as rapidly to Sherwood Harbor as Coleman fall-run, despite their greater size (Figure 23). However, they appear to move more rapidly from Sacramento to Chipps Island. More Coleman late fall have been recovered at the pumps than at Chipps Island (3,898 v 3,008), very different from the fall-run. Much of this difference may be due to lower diversion rates and more intensive sampling at Chipps Island during the spring, but it seems that other factors such as migratory behavior must be involved as well.

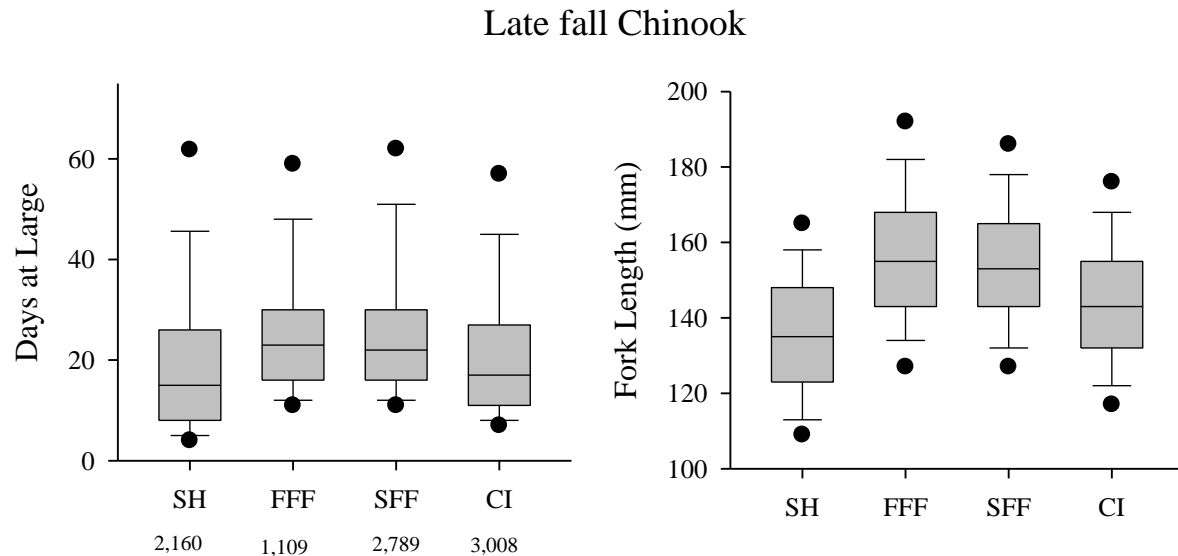


Figure 23. Days at large and size at capture of tagged late fall Chinook released at Coleman Hatchery, and recaptured at Sherwood Harbor (SH), the federal fish facilities (FFF), the state fish facilities (SFF), and Chipps Island (CI). Sample sizes are given below the labels on the X-axis, left panel. Data from USFWS.

Winter Chinook from Livingston Stone Hatchery at Keswick migrate more slowly, with median travel times of 24 days to Sherwood Harbor and 45 days to Chipps Island (Figure 24), again suggesting that migration slows approaching the Delta. Travel time to the pumps is not as long as to Chipps Island, different from the case with fall or late fall Chinook, although the hatchery winter-run collected at the pumps are larger on average than those at Chipps Island, as with fall and late fall. It seems likely that some biology that we do not understand is involved here.

L.S. Winter-Run

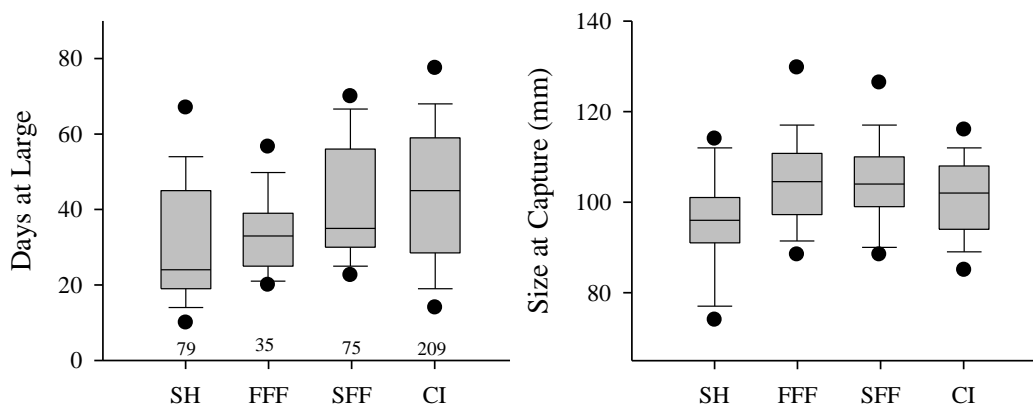


Figure 24. Days at large and size at capture of tagged winter Chinook released at Livingston Stone, and recaptured at Sherwood Harbor (SH), the federal fish facilities (FFF), the state fish facilities (SFF), and Chipps Island (CI). Sample sizes are given above the labels on the X-axis, left panel. Data from USFWS.

It is tempting to study the migratory behavior of hatchery fish because we have data with which to work, but we should remember that wild or naturally produced fish may behave differently. Hedgecock et al. (2002) analyzed tissue samples from juvenile Chinook at the pumps, and reported the length and capture date of 711 fish identified as winter-run using microsatellite DNA; they were intermediate in size between the hatchery late fall and winter Chinook, and arrived at the pumps slightly later in the year than hatchery winter-run (Figure 25), although they began migrating downstream sooner. Fortunately, it is now possible to obtain a good deal of information about the migratory history of wild and naturally produced Central Valley Chinook and steelhead by microchemical analyses of their otoliths (Barnett-Johnson et al. 2008; Phillis et al. 2008; Malamud-Roam et al. 2008). Such information is needed if we are to manage the Delta for the benefit of wild and naturally produced fish, rather than hatchery fish.

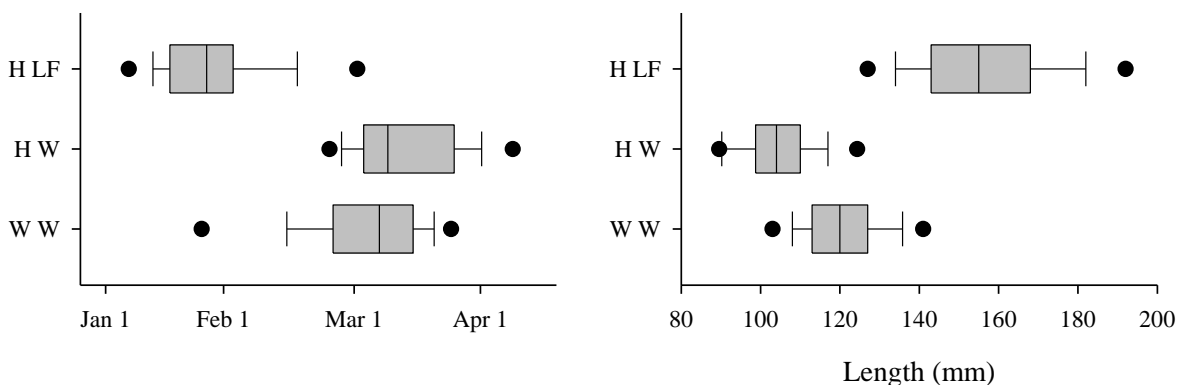


Figure 25. Distributions of dates of capture and length at capture for hatchery late fall-run (H LF), hatchery winter-run (H W), and wild winter-run (W W) at the state and federal fish facilities. Data from USFWS and Hedgecock (2002).

E. Navigation by juveniles

The sequential odor hypothesis (Harden Jones 1978) is the current working model for homing in anadromous salmon in fresh water. That is, juveniles learn a series of odors during their seaward migration, and then follow these in reverse order on their return. There is also evidence that other genetic factors may affect homing in fresh water (Quinn 2005), but these seem to be secondary. The sequential odor hypothesis implies that hatchery fish that are trucked to the bays should stray more often than fish that swim there, and this is observed (SRFCRT 1994). This raises the concern that staying hatchery fish may interbreed with locally adapted natural populations and reduce their fitness, as may have happened with fall Chinook in Mill and Deer creeks (Williams 2006).

The mechanisms by which juveniles find their way to the sea are less well known than the mechanisms by which they find their way back. In some situations, simply swimming (or drifting) downstream seems a sufficient mechanism, but in other cases, such as the complex migration of juvenile sockeye through chains of lakes (Quinn 2005), it would be hopelessly inadequate. Besides using current, juveniles can orient themselves by the position of the sun and the plane of polarization of sunlight, and by the Earth's magnetic field (Høgåsen 1998; Quinn 2005). In the Delta, tidal flows dwarf net seaward flows (Kimmerer 2004), and mechanisms besides sensing current seems necessary for navigation, especially for rapid migration through the Delta.

F. Steelhead juvenile life history patterns

The life histories of *O. mykiss* are even more variable than those of Chinook, but not much information is available on Central Valley populations; Lindley et al. (2007) described the status of populations on streams that do not have hatcheries as "data deficient." Figure 1 applies for anadromous *O. mykiss*, steelhead, but it seems that many *O. mykiss* in Central Valley streams either do not migrate, or else do not migrate beyond the large rivers or the Delta (Williams 2006). This is a recent development that may reflect evolutionary as well as environmental change. In rivers such as the Sacramento, Yuba, or Stanislaus, populations of large resident *O. mykiss* have developed where summer releases of cool water from dams provides good habitat for them.

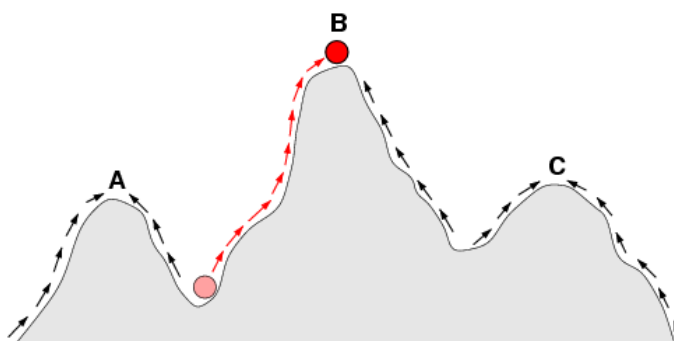
As far as is known, steelhead in the Central Valley follow a stream-type life history. Most naturally produced steelhead from the native lineage migrate to sea after two winters in fresh water, although fish from the American River grow rapidly, and migrate after one winter. Some American River fish, called "half-pounders" by anglers, may migrate only as far as the Delta or bays and then return. Hatchery steelhead also grow rapidly and migrate when released, after one winter in fresh water, but there is evidence from the sex ratios of steelhead captured at Knights Landing and Chipps Island that some hatchery males may not migrate beyond the Delta. (Rob Titus, DFG, pers. comm. 2008).

G. The adaptive landscape

Hatchery culture modifies the natural life cycle in several important ways: mates are selected by hatchery personnel rather than the fish, mortality during the egg and alevin stages are sharply reduced, and fish are canalized into a single juvenile life history pattern. There is good evidence that hatchery populations evolve to become more fit for a hatchery-based life cycle, and less fit for a natural life cycle. Older evidence is summarized in Williams (2006), but recent evidence from a study of steelhead in the Hood River, Oregon, is even stronger. By comparing the reproductive success of naturally spawning steelhead with one or two hatchery parents, Araki et al. (2007) demonstrated a rapid loss of fitness for natural reproduction.

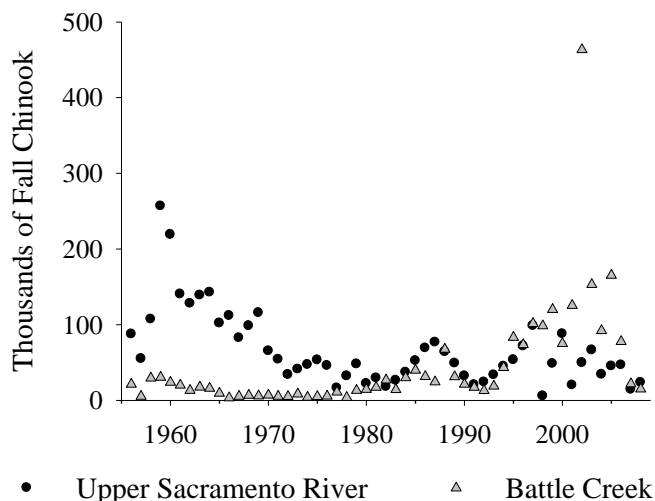
The ‘adaptive landscape’ is a conceptual model that helps explain this. For an organism in a given environment, there is a level of fitness associated with each combination of genes, or more specifically, of alleles (think of fitness as the propensity to have descendents). This can be visualized for one or two genetic dimensions, and for two dimensions looks like a topographic map, but with contours of equal fitness rather than elevation. The conceptual model can be applied to populations, except that each dimension shows the frequency of an allele in a population. Then, natural selection will tend to move the population “uphill,” toward higher fitness, although when genes interact or multiple alleles affect the trait, there may be multiple fitness peaks, some higher than others (Figure 26).

Figure 26. Cartoon of an adaptive landscape, in for one genetic dimension. The vertical distance shows fitness, and the horizontal axis shows combinations of gene frequencies. Arrows show the direction of selection, and the red ball shows a population evolving from lower to higher fitness. Copied from Wikipedia.



From this point of view, consider the situation of a population that lives in two different environments, each with its own adaptive landscape, such as a salmon population that reproduces both in a river and in a hatchery. There are two possible outcomes. Either the population will shift toward the fitness peak in one habitat or the other, or it will be caught somewhere in the middle, with intermediate fitness in both habitats. This can be modeled; Figure 3 is from a paper describing such a model, and it shows that a shift toward one peak or the other can happen suddenly. Data on fall Chinook in the upper Sacramento River suggests that such a shift may have occurred in that population, perhaps in the generations from the late 1970 to the early 1990s (Figure 27). Neither natural nor artificial selection can maximize the fitness of a population for both environments.

Figure 27. Number of adult fall Chinook returning to the upper Sacramento River (above Red Bluff) and to Battle Creek, including Coleman Hatchery. Assuming that these represent the naturally reproducing and hatchery components of the run, the run is now dominated by hatchery fish.



H. Local adaptation

Even streams in the same geographical area may provide different environmental challenges for salmon populations, and the strong tendency of salmon to return to their natal stream allows local adaptation to develop. Transplantation experiments in New Zealand, where Chinook were introduced about a century ago, show that such adaptation can develop fairly quickly. Although cases where local adaptation has been rigorously demonstrated are relatively few (Quinn 2005), there are many situations in which it seems highly likely, such as Atlantic salmon from an upper tributary of a river in Scotland that start their downstream migration sooner than salmon from a lower tributary (Stewart et al. 2006). As a local example, coded-wire tag studies suggest that juvenile Chinook from the Merced River survive better when released into the San Joaquin River than juveniles from the Feather River (Newman 2008). Traits related to juvenile migration seem a logical target for selection leading to local adaptation; for example, it seems likely that juvenile Chinook from the Sacramento River would benefit from an inherent tendency to bear to the right when they sense tidal flow reversals.

Estuaries are generally places of high biological productivity, and also provide habitat where juvenile salmon can rear and grow. For Chinook and steelhead, the importance of estuaries as juvenile rearing habitat varies inversely with the size at which the fish enter the estuaries, as indicated by the review of life history patterns above. This conceptual model is so simple that it seems unnecessary to render it in a graphic, but it is basic for assessing the importance of restoration activities in the Delta for the various runs. Spring Chinook, or at least the Butte Creek population, pass quickly through the Delta, so habitat restoration there seems unlikely to do much for them. The same is probably true for late fall Chinook, and for steelhead. Fall Chinook, however, probably would benefit strongly from tidal marsh restoration. The case for winter Chinook seems equivocal.

The life cycle of anadromous salmonids requires that the fish pass through estuaries at least twice in their lives. Navigating through a large estuary is not a simple matter, so it is important

that human activities not interfere with the navigational abilities by which salmon find their way. There is concern that various contaminants may do that, as discussed below.

I. Understanding salmonid life history diversity

There is great variability in the timing with which salmonids pass through the various stages shown in Figure 1, even within single species such as Chinook and steelhead, as discussed above. This variation is best understood for Atlantic salmon, for which a conceptual model has been developed by John Thorpe and colleagues (e.g., Thorpe et al. 1998).

The basic facts of Atlantic salmon life-history that the model seeks to explain are these. Atlantic salmon spawn in the fall, with fry emerging in the spring. The distribution of fry sizes is approximately normal at emergence, but then becomes bimodal, at least in some conditions (Thorpe 1977; Thorpe et al. 1998). In such conditions, all surviving fry feed actively early in their first summer, but the slower-growing ones restrict feeding in late summer and spend most of the winter hiding in the gravel in the streambed, while others continue actively feeding through the winter. Fish that continue feeding typically migrate in the spring, after one year in freshwater. Most of the slower-growing group then feeds actively through their second year, and then migrates to the sea, but a fraction again restricts feeding, and spends a third year in freshwater. After migrating, the fish spend a variable number of years in the ocean before returning to spawn.

The conceptual model posits a set of condition-dependent "switches" that affect or control such aspects of behavior as feeding, migration, and maturation. Individual variation in the thresholds for the switches and variation in environmental conditions can then produce the observed variation in life-history patterns. The model embodies two important generalizations about salmonid life histories: that there are photoperiodically-based "windows" of time in which life-history choices are made, and that these choices are based on the condition of the fish at some prior time, as well as on the condition of the fish shortly before the decision becomes manifest by, say, smolting or by sexual maturation (Shapovalov and Taft 1954; Thorpe 1989). Marc Mangel has developed this conceptual model into a numerical model (e.g., Mangel 1994), and with support from CALFED is currently extending and developing it for steelhead, in a form that also allows assessment of evolution in response to altered environmental conditions (Mangel and Satterthwaite 2008; Satterthwaite et al. 2009a, b). This helps explain the shift toward a resident life history in some populations of Central Valley *O. mykiss*.

The typical steelhead life-history is similar to that of Atlantic salmon, except that steelhead spawn in the late winter or spring, and some fish follow a resident life-history, especially in coastal California streams (Satterthwaite et al. 2009b). The reason this can be advantageous is sometimes obvious; for example, the Carmel River did not reach the ocean for three years during the drought of the late 1980s, and fish that probably would have been anadromous if they had had the chance were observed spawning in the upstream reaches where flow persisted. A resident life-history also seems to be developing in some Central Valley rivers where releases of cool water from reservoirs maintain good habitat for large trout through the summer (Williams

2006). However, the optimal life-history for a steelhead depends on the interactions among several environmental factors and the attributes of the particular fish (Satterthwaite et al. 2009a), so simple generalizations are hazardous.

Many Chinook salmon migrate downstream shortly after emergence, so it is clear that this model must be modified before it can be applied to them, but the fundamental insight remains that a fairly simple developmental program, together with environmental variation and genetic variation in thresholds for the switches and in the timing of the developmental windows, can account for the observed variation in life-history patterns within and among species of Pacific salmon. At least for some spring-run Chinook, a photoperiod-sensitive switch determines whether fish follow an ocean-type or stream-type juvenile life-history pattern (Clarke et al. 1992). Typically, these fish spawn at high enough altitude that winters are cold and embryos and alevins develop slowly (the incubation period is strongly temperature-dependent). Accordingly, fry emerge well after the winter solstice, and do not experience very short-day photoperiods until the following winter. This causes them to grow slowly, and as suggested by the model they do not migrate. If the fry are exposed experimentally to a short-day photoperiod, however, they will grow rapidly and adopt an ocean-type life history, migrating in their first year. This would explain why Spring Chinook in Butte Creek, which are restricted to < 350 m elevation, mostly migrate in their first spring.

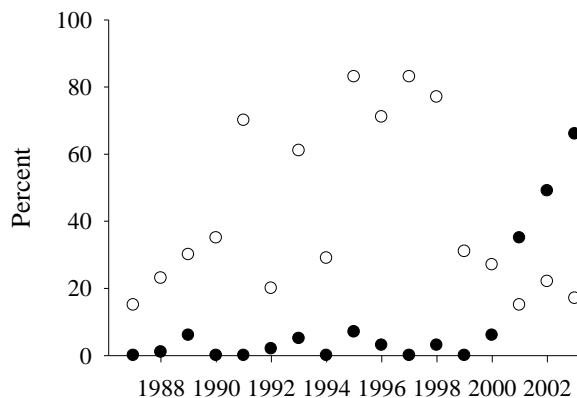
J. Use Of habitats:

1. Gravel-bed streams:

Apart from hatcheries, salmon reproduce and spend their early life in gravel-bed streams. Generally, the fish select redd sites where water flows through the gravel, such as at the tail of a pool where water downwells into the gravel, or where it upwells in the gravel bar below (Williams 2006). Water flowing through the gravel carries oxygen to the developing embryos or alevins, and carries away metabolic wastes. Some gradient in the stream is needed for suitable spawning habitat, but not much. For example, Rutter (1904) mapped fall Chinook spawning beds as far downstream as Tehama, near the Mill Creek confluence, although early commercial vessels could navigate beyond Tehama to Red Bluff.

Current distributions of spawning habitat for major Central Valley Chinook populations are well known from spawner surveys that are conducted to estimate adult returns (Low 2005; Pipel 2005), and uncertainly about most of the others is constrained by terminal dams or natural barriers. Although spawning extends well downstream, it tends to be concentrated near the barriers (Williams 2006). This is nicely illustrated by the upstream shift in the distribution of spawning by winter Chinook after passage was improved over the Anderson-Cottonwood Irrigation District (ACID) dam at Redding (Figure 28). Steelhead spawning is harder to observe, since the fish and their redds are smaller, they spawn in the winter when the water is often turbid, and it is very difficult to distinguish spawning by steelhead and similarly sized resident *O. mykiss*.

Figure 28. Percentage of winter-run redds observed above the ACID Dam (filled circles) between the dam and the Highway 44 bridge (open circles) in CDFG aerial surveys. Data from Doug Killam, CDFG, Red Bluff; copied from Williams (2006).



Redds occupy an area, and the area of suitable spawning habitat in a stream is limited. Females compete for spawning sites, and after spawning defend them for as long as they can. This limits the population that a given stream can support, and is one mechanism for the more general phenomenon of density-dependent mortality. That is, except at very low numbers, the survival or reproduction of members of a population tends to decrease as abundance increases. It is likely that density-dependent mortality among salmon occurs during other life-stages besides spawning, but not much is known about this for Central Valley populations (Williams 2006). One possibility is competition between hatchery and naturally produced Chinook in the Delta, bays, and Gulf of the Farallones. Kjelson et al. (1982:409) noted that “The problem of exceeding estuarine rearing capacity [through hatchery releases] is of some concern in the Sacramento-San Joaquin (hatchery releases total about 26 million smolts annually), but as yet has not been studied.” Many hatchery fish are now trucked around the Delta, but the point remains valid, especially for the bays.

Juvenile salmon can live at high densities if food is abundant, as demonstrated by hatcheries, but the rearing capacity of streams is more limited. Especially in smaller streams, fry tend to establish and defend territories, unless they migrate. The size of the territories increases with the size of the fish, imposing a limit on the number of fish that an area of stream can support that decreases as the fish grow. To what extent migratory fish in Central Valley are pushed out of some upstream habitat is unclear, since juveniles in larger rivers tend to form schools (Williams 2006), but density-dependent migration has been incorporated into models of salmon populations in rivers, for example Greene and Beechie (2004). It is clear, however, that a stream-type life history cannot support as large a population in a given stream as an ocean-type life history (Quinn 2005). This makes it unlikely that steelhead were ever as abundant as Chinook in the Central Valley.

2. Low gradient streams:

As juvenile Chinook or steelhead migrate downstream into the Central Valley proper, they encounter low gradient reaches with fine-grained beds. Historically, during the winter and spring, the rivers were not contained by their channels and spread out over large areas, especially in the Sacramento Valley (Kelley 1989). This graded almost imperceptibly into the Delta, so

there was not a clear distinction between the Delta and flooded overbank habitat farther upstream, especially in the Sacramento Valley (Williams 2006). The low gradient rivers now flow mostly in confined channels with steep banks, but remnants of this formerly extensive habitat remain in the Butte Sinks and the Sutter and Yolo bypasses, and along unleeved reaches of the Cosumnes River.

When the Cosumnes River spreads out over its floodplain, juvenile fall Chinook do so as well (Moyle et al. 2007). The fish grow rapidly there (Figure 29), and most move back into the river as the water level declines and floodplain drains. Similarly, juvenile salmon pass into the bypasses, and also grow well there (Sommer et al. 2001, 2005). Other fishes also use this habitat, and although many are stranded when water levels recede, these are mostly the introduced species; stranding losses of Chinook and other native species are usually modest (Sommer et al. 2005; Jeffres et al. 2008).

Figure 29. Comparison of juvenile Chinook from one enclosure on the Cosumnes River floodplain and from another in the river downstream, which is tidal in this reach and so part of the Delta. Copied from Jeffres et al. 2008.



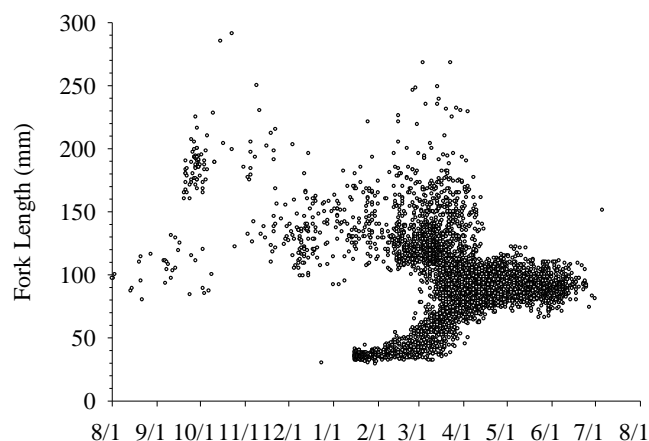
3. The Delta:

Geographical boundaries are usually more discrete on maps than on landscapes, as exemplified by the boundary of the Delta, defined here on the upstream side by the limit of tidal influence. Historically, the Delta was a vast tidal wetland (Atwater et al. 1979; TBI 1998), but most Delta channels are now confined by levees and have steep banks, like the low gradient river reaches upstream.

The diversity of juvenile Chinook in the Delta is reflected in the size at date of fish captured at the state and federal pumps (Figure 30). Larger juveniles, ~100+ mm, begin to appear at the pumps in August. The number of larger juveniles increases into March, then drops quickly in early April; it is unclear where a line should be drawn here between fingerling residents and classic stream-type. Fry migrants to the Delta, ~40 mm, begin to appear in January, and continue through most of March. Larger fry migrants, fry residents, and some fry migrants to low

gradient streams, begin to appear in March, followed by fingerling migrants and continue through June, when the Delta becomes too warm for juvenile salmon.

Figure 30. Juvenile Chinook at the Delta diversions; size at date of 6,752 juvenile Chinook sampled at the CVP and SWP diversion facilities in the Delta from August 1995 through July 2001. Data from Hedgecock (2002).



Based on studies of other estuaries, Chinook that migrate to the estuary as fry tend to rear there for some time, while Chinook that rear to fingerling size (~ 60 mm) or more somewhere upstream tend to pass through the estuary more rapidly (Healey 1991; Burke 2004). Small Chinook occupy mainly shallow water around the margins of the estuary, often moving up into tidal marsh channels on the flood tide, and retreating back to subtidal areas late on the ebb tide (e.g., Levy and Northcote 1982). The juveniles tend to move into deeper water and down the estuary as they grow (Healey 1980; 1991). Juvenile Chinook are opportunistic feeders, and reports on diet vary from study to study, but broad patterns are evident. Smaller juveniles occupying marsh channels often feed heavily on larval and pupal chironomids (e.g., Shreffler et al. 1992; Lott 2004). This has been observed in a remnant tidal marsh in the Delta (Simenstad et al. 2000), as well as in overbank habitats close to the Delta (Sommer et al. 2001, 2005; Jeffres et al. 2008). As the fish grow, larger prey become more important, and as they move farther offshore and into deeper water, their diet shifts toward prey that are available there.

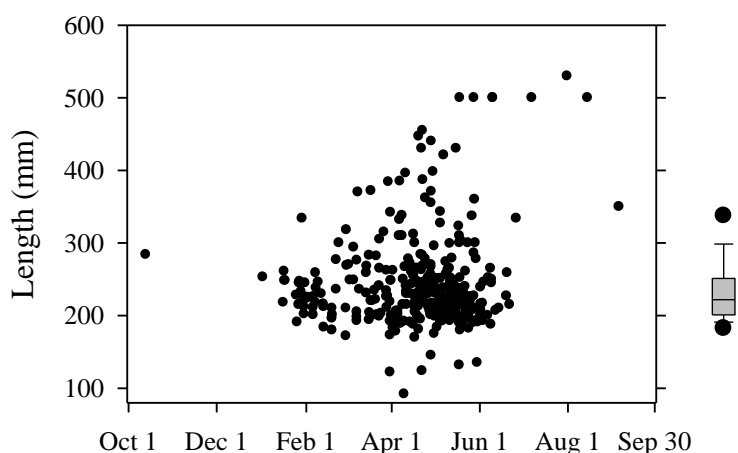
Most habitat in the Delta is now subtidal, because most channels are leveed with steep banks, and the prey available for fry reflect this. The best data are from Kjelson et al. (1982), who summarized their own and earlier studies as follows:

Crustacea and insects dominated fry stomach contents, with an increase in crustacea ingestion downstream. Cladocera and diptera were consumed frequently in the Delta, while in brackish San Pablo and San Francisco Bays, consumption of copepods, amphipods, and fish larvae increased. Similar food habits were described for older fry and smolts in Delta studies by Rutter (1904), Ganssle (1966), and Sasaki (1966).

Kjelson et al. (1982) called fish < 70 mm fry, but their samples included many fish < 50 mm. Larger juveniles sampled at Chipps Island more recently fed mainly on amphipods (*corophium*), but also postlarval crabs, flies, shrimp, and (non-fly) insects (MacFarlane and Norton 2002).

Naturally produced juvenile steelhead from the Sacramento system move past Knights Landing into the lower river in winter and spring, but mainly in April and May (Titus et al. 2004). Naturally produced juvenile steelhead are captured in the Chipps Island trawl are about the same size, mostly 200 to 250 mm long (Figure 31), suggesting a rapid migration. There are no data on the rate at which they move through the bays or how much they grow there. A few steelhead also migrate out of the Mokelumne River and San Joaquin River tributaries (Williams 2006).

Figure 31. Size and date of capture of 346 unmarked juvenile steelhead from the Chipps Island Trawl from 1999-2008. The box plot at right summarizes the size distribution. The larger fish may be kelts. Data from USFWS.



Studies on coastal streams (e.g., Bond 2006) show that lagoons can be very important habitat for juvenile steelhead. However, steelhead entering the Delta are older and much larger than the fish entering the lagoons in the coastal streams, so it is unlikely that these findings apply to the Delta.

4. The bays:

Habitat use in the bays probably is like that in the Delta, with larger juveniles mainly using deeper water farther from shore, and smaller juveniles mainly using shallower water and marsh channels around the margins. More small juveniles are captured in or entering the bays in wet years (Kjelson et al. 1982, Brandes and McLain 2001), but they have also been found there in dry years (Hatton and Clark 1942). A few are found in Suisun Marsh (e.g., Mattern et al. 2002).

Juvenile Chinook migrating through the bays from April through June were sampled in open water with trawls by NMFS, from 1995 to 2005. Most of these were fall Chinook, but some could have been ocean-type spring Chinook, which migrate at the same time (Fig. 19). On average, fish captured near the Golden Gate were 18 days older than fish captured near Chipps Island, and about 6 mm longer, but hardly any heavier (B. MacFarlane, NMFS, pers. comm.).

2008, Figure 32). The slow growth may reflect anthropogenic changes in the bays, as noted above, since early descriptions (e.g., Scofield 1913) suggest abundant food for Chinook. If so, such degradation of the bays is probably a significant problem for fall and spring Chinook, since survival in the ocean presumably increases with fish size and condition.

Figure 32 Size and condition of juvenile fall Chinook in the bays and ocean during 2005. Copied from Lindley et al. (2009). Note that “Estuary Entry” refers to Suisun Bay.

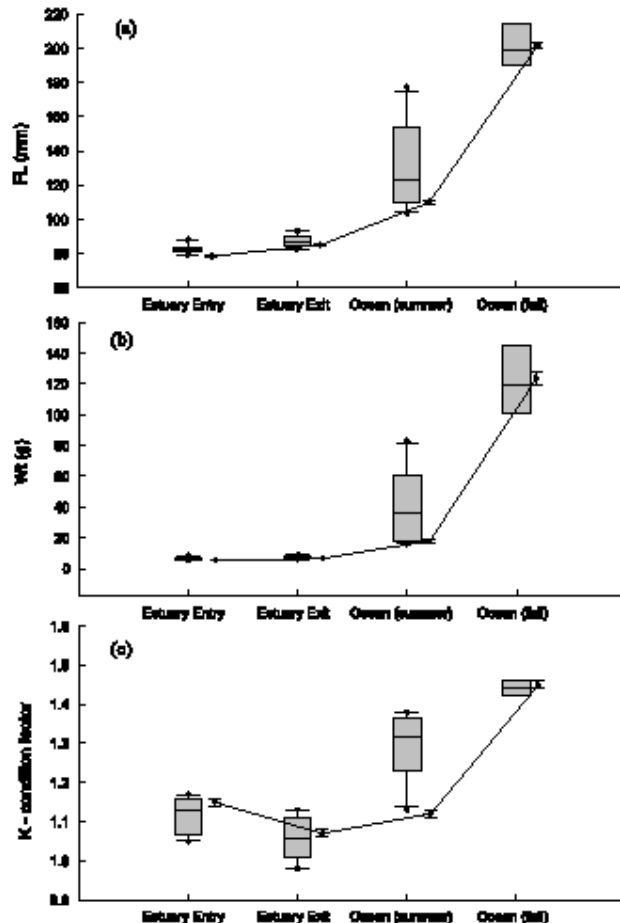
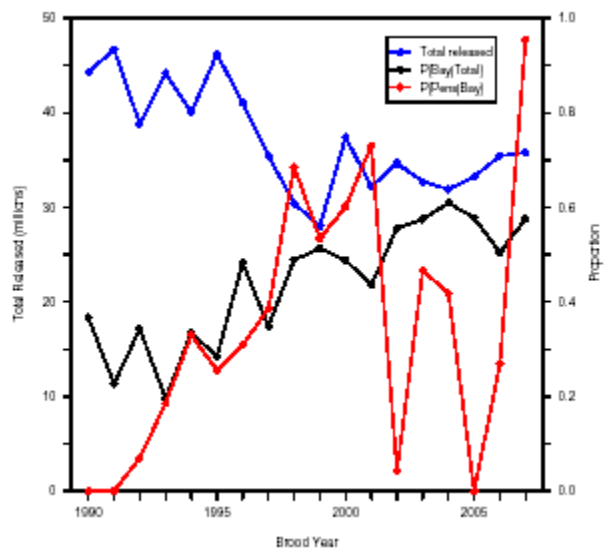


Figure 16: Changes in (a) fork length, (b) weight, and (c) condition (K) of juvenile Chinook salmon during estuarine and early ocean phases of their life cycle. Boxes and whiskers represent the mean, standard deviation and 90% central interval for fish collected in San Francisco Estuary (entry = Suisun Bay, exit = Golden Gate) during May and June and coastal ocean between 1998-2004; points connected by the solid line represent the means (± 1 SE) of fish collected in the same areas in 2005. Unpublished data of B. MacFarlane.

Poor growth in the bays also implies a strong potential for density-dependent mortality or reductions in growth, since many millions of hatchery smolts are released into the bays (Figure 33). This should be regarded as a serious problem unless new evidence suggests otherwise.

Figure 33: Total releases of hatchery fall Chinook, proportion of releases made to the bay, and the proportion of bay releases acclimatized in net pens. Unpublished data of CDFG and USFWS. Copied from Lindley et al. 2009.



5. The ocean:

Juvenile Chinook and steelhead leaving the bays enter the Gulf of the Farallones, a shallow and somewhat protected area, where they grow rapidly. From an eleven years study by NMFS, the mean and standard deviation of the length of fish entering the gulf were 87.1 and 10.4 mm; the same statistics for age (since hatching) were 153 and 22 days. Initially, the density of juveniles Chinook is highest in eddies on either side of the Golden Gate, but by September most have moved northward along the coast (B, MacFarlane, NMFS, pers. comm. 2008).

Data on the size and condition of juvenile fall Chinook in 2005 show that conditions in the ocean during the summer probably were responsible for the poor survival returns in 2007, since the size and condition of the fish were unusually small and poor (Figure 32). A statement to the contrary in Williams (2006) is mistaken. Unfortunately, such data have not been collected since 2005.

Most Central Valley Chinook, and probably steelhead as well, remain over the coastal shelf, rather than moving out into the open ocean as many salmon do at higher latitudes. Central Valley Chinook range mainly between Monterey Bay and the Columbia River, although a few go farther north or as far south as Point Conception (Williams 2006).

Juvenile steelhead from Scott Creek, on the San Mateo County coast, survive very poorly if they enter the ocean smaller than 140 mm (Bond 2006). Why smaller juvenile Chinook can successfully enter the ocean is uncertain, but higher biological productivity in summer and the protected conditions in the Gulf of the Farallones probably explain it. Conditions in the gulf can differ from conditions along the open coast farther north, which could weaken the correlation between the abundance of Chinook in the Central Valley and in coastal rivers.

K. Habitat use by run

Winter Chinook spawn in the summer, and because embryos are the most temperature sensitive life stage, winter Chinook require summer water temperatures $< \sim 14^{\circ}\text{C}$. Historically, this limited them to upper Sacramento River tributaries that drain basalt or porous lava terrain, and receive large amounts of cool water in the summer from springs (Lindley et al. 2004). Currently, winter-run spawn in the Sacramento River, downstream from Keswick Dam, where releases of water from Lake Shasta keep temperatures cool. Passage of juvenile winter-run past the Red Bluff Diversion Dam (RBDD) is well documented (Figure 34); most juveniles pass the dam as fry, in August and September. The size of the fish increases beginning in October, but the numbers drop off. The fish here are classified to runs by size and date, and so assignment involves some error, but the method is more reliable here than farther downstream, at least for smaller fish (Williams 2006).

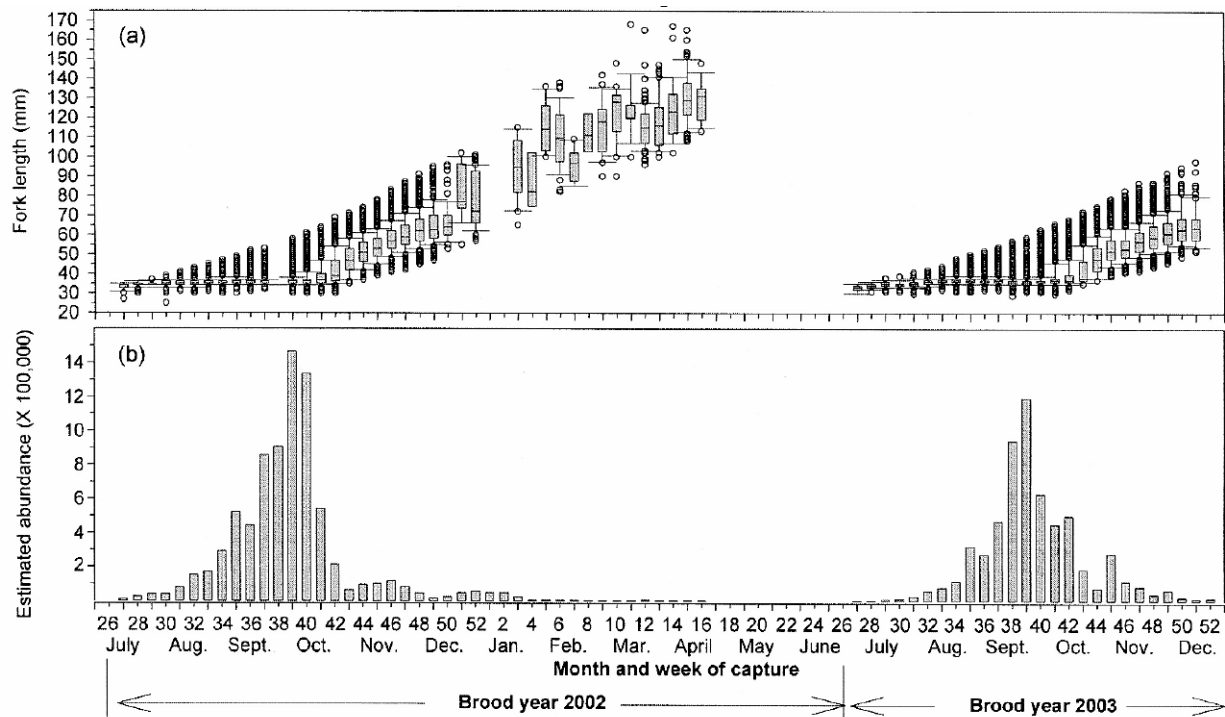


Figure 34. Size distributions (a) and numbers (b) of winter-run size juvenile Chinook salmon captured in screw traps at the RBDD in July 2002 through December 2003. Box plots in (a) show the 10th, 25th, 50th, 75, and 90th percentiles, plus outliers. Note that the outliers simply trace the size criteria when abundance is high. Classification accuracy is probably better for smaller fish. Copied from Gaines and Poytress (2004).

What juvenile winter-run do once they pass the RBDD is less well known, because the size-at-date criteria for assigning fish to runs do not work so well, and because monitoring farther downstream is less intensive. Based on a relatively small sample identified genetically, only a few winter-run reach the lower Sacramento and the Delta before late November (Figure 21). Winter-run appear at the pumps mostly in February and March, at an average length of 121 mm

(Figure 35). Generally, the data suggest a slow migration, but the relative survival of the smaller and larger migrants past the RBDD is unknown, so inferences about the migration rate and timing of the survivors are highly uncertain. Work in progress at UC Berkeley using microchemical analyses of adult otoliths (Ingram 2008) may clarify this. Tissue samples from fish captured at Chipps Island are now being analyzed to assign fish to runs, so more information should soon be available about the size and time at which winter Chinook move into the bays.

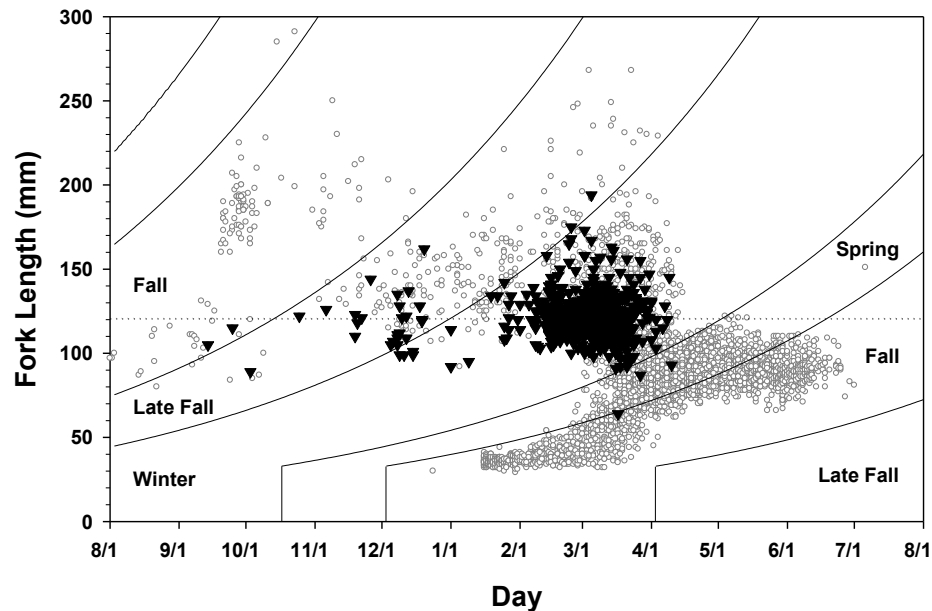


Figure 35. Distribution, by fork length and day of capture, of 6,752 juvenile Chinook salmon with assignable genotypes over a six-year period, from August 1995 through July 2001. The 711 juveniles assigned to winter-run are shown by dark inverted triangles; fish assigned to other runs are shown by open circles. Note that each symbol may represent more than one fish, and that many non-winter-run are obscured by the tight cluster of winter-run. Mean fork length of winter run juveniles (121 mm) is shown by the dotted line. The figure and most of the caption are copied from Figure 1 in Hedgecock (2002).

Adult spring Chinook hold over in streams during the summer, but do not spawn until the water temperature is declining in the fall (Table 4). They can tolerate summer water temperatures up to $\sim 20^{\circ}\text{C}$ daily average, as documented by careful monitoring in Butte Creek, although this presumably involves considerable stress. There is some evidence that gametes are less tolerant than the adults, so temperature stress may lead to reproductive failure even if spawning occurs (Williams 2006). Juveniles that remain in the stream over the summer must tolerate at least the same and perhaps higher temperatures.

Particularly in Butte Creek, most juveniles move down into the valley in spring, mainly as fry but also as larger (50 -100 mm) juveniles (Figure 36). Even larger juveniles migrate into the valley in fall, winter, and spring, but their numbers are very low by late winter. (Note that the X-

ax2s on this figure are logarithmic.) Tagging studies show that fry migrants from Butte Creek rear for some time in the Butte Sinks or Sutter Bypass before they migrate through the Delta (Figure 18). Similar information is not available for spring Chinook from Mill and Deer creeks, but it could be developed by studies of otolith microchemistry.

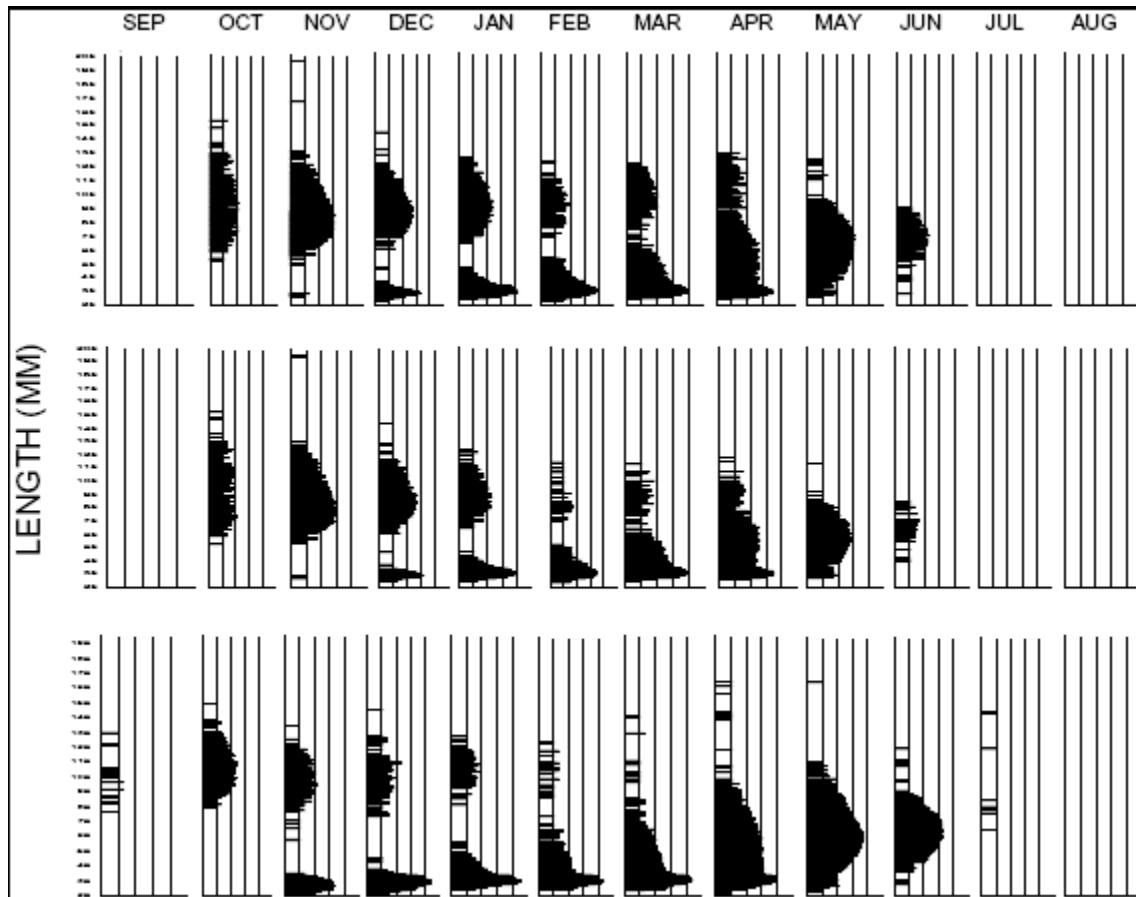


Figure 36. Length and time distribution of juvenile spring Chinook in Mill (top), Deer, and Butte (bottom) creeks. The scale of the x-axis is \log_{10} , from 1 to 10,000; the length scale is linear from 25 to 195. Copied from Lindley et al. 2004

Late-fall Chinook are present only as juveniles in the summer, and probably can tolerate about the same temperatures as the other runs. The historical distribution of their spawning habitat is not documented, but it may have been a lower elevation subset of the spring-run distribution. Naturally produced late-fall Chinook juveniles are thought to migrate to the Delta in the fall; the Chippis Island genetic sampling should clarify the timing of their migration into the bays.

Fall Chinook typically are not present during the summer, since adults normally enter fresh water as temperatures are declining, and the juveniles normally out-migrate in the spring. Some juveniles now hold over through the summer and pass through the Delta in the fall, for example

the group around 160 to 210 mm in September in Figure 30 (Williams 2006). It may be that some fall-run have always followed this life history, but summer releases of cool water from some dams make it more viable. Because fall Chinook are the most abundant run, and the only run in San Joaquin system and Delta tributaries, the traditional monitoring programs provide much more information about their behavior than about the other runs (e.g., Figure 34).

L. Environmental constraints on life history patterns:

There are at least three significant constraints on salmon life history patterns in the Central Valley. High summer water temperature is the most serious, since Chinook and steelhead one way or another must avoid thermally unsuitable habitat in the lower elevation rivers and the Delta. For example, juvenile Chinook in the Central Valley do not migrate to the Delta during the summer, although juvenile Chinook do migrate into estuaries in other rivers during that season. Similarly, as noted above, adult winter and spring Chinook are restricted to habitats that are thermally suited to spawning or holding during the summer. This constraint will become more serious as the climate warms. Butte Creek spring Chinook are most at risk; they are restricted to elevations below 350 m, and already suffer significant mortality in some years (Williams 2006).

Conditions in the ocean and probably in the bays are another constraint on juvenile life history patterns. The biological productivity of the coastal ocean and the Gulf of Farallones rises sharply in the spring when changes in the coastal winds make currents shift to predominantly southward flow, which induces upwelling of nutrient-rich water from the coastal shelf and slope (Ainley 1990; Williams 2006). The timing of this spring transition varies from year to year, and can strongly affect factors such as the nesting success of seabirds. Although direct evidence is lacking, it seems reasonable to expect that the survival rate of juvenile salmon increases with increasing biological productivity in the gulf, and Roth et al. (2007) have reported a relationship between seabird nesting success, which also depends on the productivity of the gulf, and the subsequent abundance of fall Chinook. Thus, juvenile Chinook that enter the ocean during times of lower productivity may be less likely to survive, especially if they are small. The importance of ocean conditions has been emphasized by the recent crash in the abundance of fall Chinook, for which poor ocean conditions seem the most likely proximate cause (Lindley et al. 2009).

M. Predation:

Many juvenile Chinook and steelhead are eaten in the Delta by other fishes, but high juvenile mortality is normal, so simply showing that significant predation occurs does demonstrate that something is “wrong.” Given that on average a female produces over a thousand fry (Table 1), we should expect that in natural conditions most will be eaten.

There is good evidence that predation in the Delta is significant. For example, studies of the survival of tagged hatchery fish show that fish released into Georgiana Slough survive ~45% as well as fish released into the Sacramento River nearby (Newman 2008), and acoustic tag studies indicate that increased predation there is probably the main reason for the difference, although fish released into the slough are also much more likely to be entrained at the pumps (K.

Newman, USFS, pers. comm. 2008). Similarly, Baker et al. (1995) found that the survival of tagged juvenile fall Chinook decreased as temperature rose above about 18°C. This is well within the physiological tolerance of the fish, so it seems likely that a decrease in survival results from the increased appetite of predators at temperatures that are not directly lethal for the salmon (Williams 2006). Similar increases in mortality at relatively low temperatures have been observed in the Columbia River (Anderson 2003).

The actual extent of predation remains uncertain, however, especially for smaller juveniles. The tagging studies were done with hatchery fish, and hatchery fish, especially those recently released, may be more susceptible to predation than naturally produced fish. In a modeling study, Lindley and Mohr (2003) found that the influence of striped bass predation on winter Chinook abundance probably was small, although more significant influence could not be ruled out. Nobriga et al. (2003) found relatively few Chinook in the stomachs of black and striped bass in shallow water, where small Chinook are more likely to occur, and Nobriga et al. (2006) did not find them in the stomachs of Sacramento pikeminnow.

V. ANTHROPOGENIC STRESSORS IN THE DELTA

Anthropogenic stressors in the Delta and current understanding of them are summarized in tables 7 and 8, and described below.

A. Climate Change

High water temperature is a major stressor for Chinook and steelhead in the Delta as well as in Central Valley rivers and streams. Temperature in late spring is an important predictor of the survival juvenile Chinook (Baker et al. 1995; Newman and Rice 2002; Newman 2003; Figure 32). The Delta is too warm in the summer for salmon, and Central Valley salmon have life history patterns that largely keep them out of the Delta during that season. This is a natural condition that was noted over a century ago (Rutter 1904). Water temperature in the Delta is determined primarily by atmospheric conditions, so anthropogenic climate change is already making the Delta warmer, and continued climate warming will increase the seasonal periods when the Delta is unfavorable or unsuitable for salmon.

Climate change in the Central Valley will affect different runs and life histories differently. Populations or life histories that remain in fresh water over the summer are most obviously at risk, but even ocean-type Chinook that rear upstream for some period before migrating will face a shorter period of favorable thermal conditions. Fry migrants may fare better by comparison, but may also face worsened ocean conditions. Climate change is the greatest long-term challenge facing Central Valley salmon (Williams 2006).

B. Levees

Levees impose a major stress on juvenile Chinook by blocking their access to tidal habitat (or to overbank habitat farther upstream), and confining them to habitat in the channels. This problem has been compounded in the Delta by subsidence of the Delta islands, so that in most

cases removing the levees would create subtidal ponds rather than restore the marsh habitat that used to exist there. The severity of this stress is greatest for fall Chinook, since it obstructs what was probably their predominant life history pattern. That is, the levees impose a greater stress on the fry migrant life histories that seem best able to tolerate climate change.

C. Diversions

1. Project diversions

Entrainment of juveniles in diversions at the state and federal pumps in the Delta is an obvious problem, but also a difficult one to assess. Samples of the fish that are collected for salvage are counted, providing an estimate of the total number collected, but an unknown number of fish are lost to predation near the pumps or bypass the collection facilities. Mark-recapture studies have been conducted to try to estimate mortality in the forebay at the state pumps, but these have used hatchery fish that may suffer higher mortality than naturally produced fish or hatchery fish that have been at large for some time (Williams 2006). The uncertainty in these estimates of “pre-salvage survival” compromises direct assessments of the harm done by the pumps. As a further complication, there is additional but poorly known “indirect” mortality farther from the pumps, but attributable to modification of Delta circulation patterns or other conditions associated with the pumps.

As an alternative to sampling at the pumps, the USFWS has conducted a long series of experimental releases of tagged hatchery fish that were recovered by trawling at Chipps Island or in the ocean fishery. Then, estimates were made of the effects of export pumping and other variables on the survival of the tagged fish. Two major analyses of these data have been published (Newman and Rice 2002, Newman 2003), and the results of these studies are compared in Figure 37. The magnitude of the coefficients shows the estimated strength of the influence of the associated variable, and the error bars show the associated statistical uncertainty. The effects of the exports/flow ratio is clearly strong using one analytical approach, and almost strong using the other. (See Williams 2006, Ch. 10 and Appendix B, for a more extensive comparison of these analyses).

Table 7. Summary of anthropogenic stressors in the Delta.

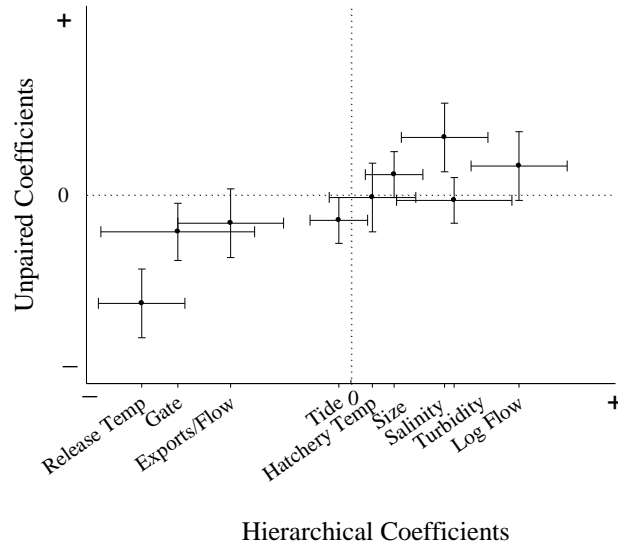
Life Stage	Stressors in the Delta						
	Levees	Water Temperature	Project Diversions	Smaller Diversions	Toxics	Hydrograph Modification	Gates and Barriers
Fry	Block access to tidal habitat	Increase predation	Entrainment, Indirect mortality	Entrainment (probably minor)	Inhibit imprinting. homing	Delay migration, change migration timing	Divert fish to Central Delta (SR fish) or South Delta (SJR fish)
Fingerlings	Block access to tidal habitat	Increase predation, physiological stress	Entrainment, Indirect mortality		Inhibit imprinting. homing	Increase late spring water temperature	Divert fish to Central Delta (SR fish) or South Delta (SJR fish)
Smolts (90+ mm)		Increase predation, physiological stress	Entrainment, Indirect mortality		Inhibit imprinting. homing	Increase late spring water temperature	Divert fish to Central Delta (SR fish) or South Delta (SJR fish)
Adults		Physiological stress	Delay migration to San Joaquin tribs		Inhibit homing?		Delay migration?

Life Stage	Stressors in the Delta		
	Hatchery Influence	Predation by introduced fishes	Dissolved Oxygen
Fry	Genetic effects from naturally spawning hatchery fish	Increases with water temperature	
Fingerlings	Genetic effects from naturally spawning hatchery fish, completion with hatchery fish	Increases with water temperature	
Smolts (90+ mm)	Genetic effects from naturally spawning hatchery fish, completion with hatchery fish	Increases with water temperature	
Adults	Genetic effects from naturally spawning hatchery fish, completion with hatchery fish, mortality from hatchery supported fishery		Low DO can delay migration of adults into the San Joaquin River.

Table 8. Summary of understanding of anthropogenic stressors in the Delta. U, I, and P are the estimated understanding, importance, and predictability of the stressors, with ranges from 1 (low) to 4 (high).

	Levees	Water Temperature	Project Diversions	Smaller Diversions	Toxics	Hydrograph Modification	Gates and Barriers	Hatchery Influence	Predation by introduced fishes	Dissolved Oxygen
Fry	U = 4 I = 4 P = 4	U = 3 I = 3 P = 3	U = 3 I = 3 P = 3	U = 3 I = 2 P = 2	U = 2 I = ? P = 1	U = 4 I = 4 P = 4	U = 2 I = 3 P = 2	U = 2 I = 4 P = 4	U = 3 I = 3 P = 3	U = 4 I = 1 P = 4
Fingerlings	U = 4 I = 3 P = 4	U = 4 I = 4 P = 4	U = 4 I = 4 P = 4	U = 3 I = 2 P = 2	U = 2 I = ? P = 1	U = 4 I = 4 P = 4	U = 3 I = 3 P = 3	U = 3 I = 4 P = 4	U = 3 I = 3 P = 3	U = 4 I = 1 P = 4
Smolts (90+ mm)	U = 3 I = 3 P = 4	U = I = P =	U = 3 I = 4 P = 3	U = I = P =	U = 2 I = ? P = 1	U = 3 I = 3 P = 4	U = 4 I = 3 P = 4	U = 3 I = 4 P = 4	U = 3 I = 3 P = 3	U = 4 I = 1 P = 4
Adults	U = 4 I = 1 P =	U = 3 I = 3 P = 3	U = I = P =	U = I = P =	U = 2 I = ? P = 1	U = I = P =	U = 4 I = 3 P = 3	U = 4 I = 4 P = 4	U = 4 I = 1 P = 4	U = 3 I = 2 P = 3

Figure 37.. Comparison of estimated coefficients plus/minus two standard errors for the unpaired analysis of Newman and Rice (2002) and the hierarchical analysis of Newman (2003) with release-specific capture probabilities. Copied from Williams 2006.



More recently, Newman (2008) has analyzed the results of several coded wire tag studies designed to address more specific questions, and summarized his results as follows:

For the most part, the substantive conclusions from the [Bayesian hierarchical model] analyses, summarized below, were consistent with previous USFWS analyses.

Delta Cross Channel: There was modest evidence, 64 to 70% probability, that survival of Courtland releases, relative to the survival of Ryde releases, increased when the gate was closed.

Interior: Survival for the interior Delta releases was estimated to be about 44% of the survival for the Sacramento River releases.

Delta Action 8: There was a negative association between export volume and relative survival, i.e., a 98% chance that as exports increased, relative survival decreased. Environmental variation in the relative survival was very large, however; e.g., for one paired release the actual relative survival at a low export level could with high probability be lower than relative survival at a high export level for another paired release.

VAMP: (a) The expected probability of surviving to Jersey Point was consistently larger for fish staying in the San Joaquin River (say passing Dos Reis) than fish entering Old River, but the magnitude of the difference varied between models somewhat; (b) thus if the HORB effectively keeps fish from entering Old River, survival of out-migrants should increase; (c) there was a positive association between flow at Dos Reis and subsequent survival from Dos Reis and Jersey Point, and if data from 2003 and later were eliminated from analysis the strength of the association increased and a positive association between flow in Old River and survival in Old River appeared; (d) associations between water export levels and survival probabilities were weak to negligible. Given complexity and number of potential models for the VAMP data, however, a more thorough model selection procedure using Reversible Jump MCMC is recommended

A shift in survival studies is underway. The studies described above used coded-wire tags, which identify batches of fish rather than individual fish, and require that fish be sacrificed for recovery of the tag. In the last few years, acoustic tags have largely replaced coded-wire tags for experimental studies, although coded-wire tags are still used to mark production releases of hatchery fish. Fish with the acoustic tags are individually marked and can be tracked remotely, which allows for addressing questions at much finer spatial and temporal scales, and for multiple detections of the same fish.

Results of acoustic tag studies in the Central Valley are beginning to appear in journals (e.g., Perry et al. In press), but have been reported mainly in talks. Unpublished work at the Delta Cross Channel indicates that the tidal and day/night cycles strongly influence the percentage of fish that pass into the central Delta through the Delta Cross Channel in the fall, which suggests that careful operation of the gate might reduce the effect of diversions through the gate on late fall and winter Chinook (Brau et al. 2007). The acoustic tag studies confirm that survival in the interior Delta is lower than in the Sacramento River. However, although visualization techniques make the data from these studies compelling, the acoustic tag studies are unlikely to be a panacea. Perry et al. (In press) and Perry and Skalski (2009) found that the survival of tagged late fall Chinook varies considerably among years and Delta channels, which suggests that considerable data will be needed before results can be relied upon, and the survival of fish with acoustic tags (e.g., those reported by Lindley et al. 2008) seems too low to be representative of a self-sustaining population. Most importantly, all studies to date have used hatchery fish, which may behave differently than naturally produced fish.

Yet another approach to analyzing the effects of the state and federal diversions uses data from the non-experimental releases of coded-wire tagged fish, usually at or near the hatchery. This approach has the advantage that fish may be exhibiting more natural migratory behavior than fish released in or near the Delta. By comparing recoveries of tagged fish at the pumps and at Chipps Island, Kimmerer (2008) estimated the percentage of fish from Coleman and Livingston Stone hatcheries leaving the Delta that are collected in the salvage facilities at the pumps, as a function of export flow (Figure 38). The analysis required some strong assumptions, so the detailed results should be regarded with due caution. One problem is that the Coleman Hatchery data include both fall and late fall Chinook, and it appears that late fall Chinook have a greater propensity to turn up at the pumps (Figure 39, Table 7). Nevertheless, the percentages of winter and especially late fall Chinook that are salvaged during periods of high exports is surely significant, especially if pre-screen mortality is high.

Figure 38. Relationship of estimated proportional salvage of tagged smolts at the fish facilities, PS, to export flow. Small symbols represent data based on six or fewer fish caught, which were not used in determining the line. Lines are from a generalized linear model with log link function and variance proportional to the mean ($p < 0.0001$, 57 df), with source of fish as a categorical variable. Thick lines are predictions for fish from each hatchery; thin lines are upper 90% confidence limits of the predicted mean values. Copied from Kimmerer 2008.

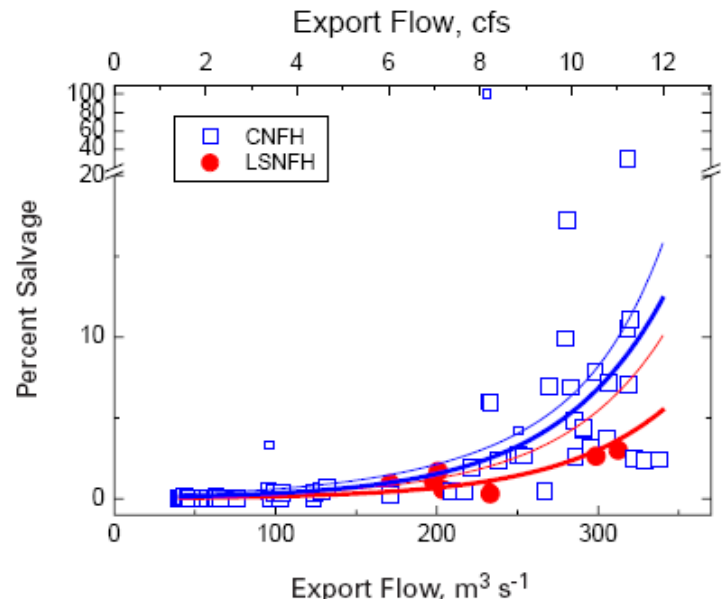
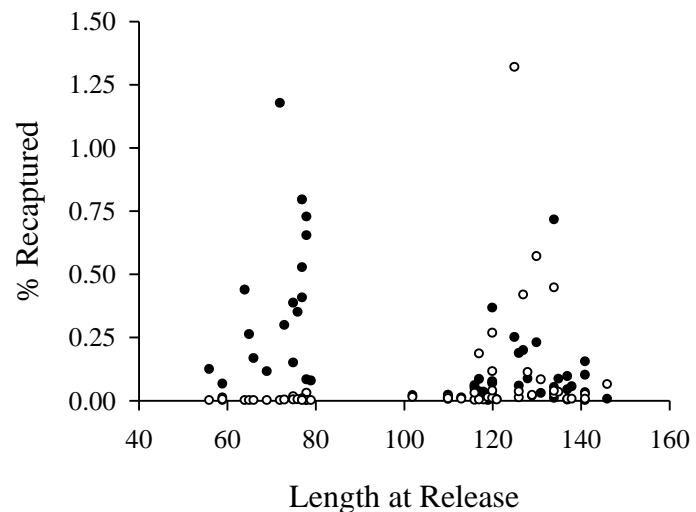


Figure 39. Recaptures of tagged juvenile fall and late fall Chinook at Chipps Island (filled circles) and the state and federal pumps (open circles). Fall Chinook (< 80 mm) are taken at the pumps much less frequently than late fall-run. Note that recaptures are not expanded to account for the limited duration of sampling, as was done for Figure 38). Data from Table 2 in Kimmerer (2008).



Based on a simple tabulation of recoveries of tagged juvenile Chinook released at the hatcheries, the state and federal pumps entrain a much higher proportion of winter-run and late fall-run migrants from the Sacramento River, and fall-run migrants from the San Joaquin River, compared with captures at Chipps Island; few Butte Creek spring-run show up at the pumps, and even fewer fall Chinook released from Coleman Hatchery do so (Table 9). Geography probably explains the much greater propensity of Merced River fall Chinook to appear at the pumps, low pumping rates during spring help explain the low number of Coleman fall-run and Butte Creek spring-run, and more frequent sampling at Chipps Island in the spring affect the numbers taken there, so the differences reflected in the table are more apparent than real. Nevertheless, the differences in the ratios of the numbers taken at the pumps and at Chipps Island are so large that it seems likely that behavioral differences among the runs are also involved. The data deserve more analysis.

Table 9: The number of marked or tagged fish recorded at the state and federal pumps and at Chipps Island: winter Chinook from Livingston Stone Hatchery, late fall Chinook from Coleman Hatchery, wild Butte Creek spring Chinook, fall Chinook from Merced River Hatchery, and steelhead from all hatcheries. Only fish released at or near the hatcheries are tallied. Data from USFWS.

	# at pumps	# at Chipps	Ratio
LS Winter	110	209	0.53
C Late Fall	3,898	3,008	1.30
BC Spring	3	34	0.09
C Fall	34	4,041	0.008
M Fall	2,570	250	10.28
Steelhead	507	177	2.86

Finally, based simply on the numbers of fish that are recovered at the pumps compared to the numbers that migrate into the Delta, the direct effects of the pumps seem not to be a major hazard for fry migrants to the Delta, at least when they are small.

2. Smaller diversions:

There are thousands of smaller diversions on Central Valley rivers and the Delta, most unscreened or poorly screened. These entrain some Chinook or steelhead, but the effects of these on salmon populations is uncertain (Moyle and Israel 2005). A recent study in the Delta by Nobriga et al. (2004) found that large numbers of larval and postlarval fishes were entrained in an unscreened diversion, but most of these were small non-native species. Generally, smaller fish are more vulnerable to entrainment than larger fish, and small Chinook are in the Delta mainly during the winter and early spring when diversion rates are low. Diversions on smaller streams may take a significant fraction of the flow, even if the absolute amount is small, and these may have a greater effect on the local populations. In light of the equivocal evidence for effects on populations, Moyle and Israel (2005) recommended that public money not be spent on screens “unless the projects have a strong evaluation component to them, including intensive before and after studies.”

D. Hatchery influence

Hatchery salmon can have negative effects on naturally reproducing salmon for various reasons, reviewed in Williams (2006). For example, hatchery Chinook presumably compete with naturally produced fish, in the Delta and especially in the bays, as noted above. Large numbers of hatchery fish may also attract predators that reduce the survival of naturally produced fish, as has occurred in streams (Nickelson 2003), and probably occurs with the ocean fishery. The presence of hatchery fish may also conceal or divert attention from the condition of wild or naturally reproducing fish. This is particularly the case when few hatchery fish are marked, as with fall Chinook until a few years ago. We will learn more about the extent of this problem this

year and next, when hatchery broods of fall Chinook with 25% marking return to spawn. In a related problem, conducting survival experiments with hatchery fish will tend to encourage management of the Delta to benefit fish that behave in the same way. If wild or naturally produced behave differently (figures 28, 29 and 36), this may be to their detriment. Similarly, attention to hatchery fish may need to neglect of fry migrants to the bays and Delta.

More serious and persistent are genetic changes, resulting from selection for a life cycle that involves reproduction in a hatchery, rather than a stream (Myers et al. 2004; Araki et al. 2007; 2008). In recognition of this, Lindley et al. (2007) included the degree of hatchery influence among criteria for viability of ESA-listed Central Valley salmon populations. Based on these criteria, Central Valley fall Chinook are at high risk of extinction.

Hatchery salmon tend to stray more than wild salmon (Williams 2006), and the practice of trucking juveniles around the Delta strongly increases straying (JHRC 2001). Straying presumably magnifies the harm from hatchery fish spawning in rivers by extending the effects of domestication selection into populations in streams that do not have hatcheries, such as fall Chinook in Mill and Deer creeks.

E. Toxics

Toxics in the Delta are a potential stressor for salmon, but the extent of the problem is unknown (I. Werner, UCD, pers. comm. 10/08). The main potential problems are ammonia, pyrethroid pesticides, and copper. Besides direct effects, ammonia reduces resistance to disease (Ackerman et al. 2006). The most likely effects from pyrethroid, organophosphate and copper pesticides are damage to the olfactory system (Schulz et al. 2000; Sandahl et al. 2004; Hecht et al. 2007) that can impair homing and predator avoidance. Past sources of acute toxicity, such as the Iron Mountain Mine, have been mostly abated.

F. Dissolved Oxygen

Dissolved oxygen concentrations on the San Joaquin River near Stockton can be low enough to block migration of adult salmon (Hallock et al. 1970; Alabaster 1989). This is a continuing problem, resulting from complex interactions among factors such as diversion of San Joaquin River water toward the Delta pumps, modifications of channel morphology to allow shipping, and wastewater discharge, that is the subject of considerable recent work (e.g., Lee and Jones-Lee 2003; Jassby and Van Nieuwenhuyse 2005) and a current test mitigation project by DWR (http://baydeltaoffice.water.ca.gov/sdb/af/index_af.cfm). Usually this problem eases in late October.

G. Water temperature

Hallock et al. (1970) reported that water warmer than 21°C blocks migration of Chinook into the San Joaquin River and water warmer than 19°C inhibits it. However, data from the new weir on the Stanislaus River indicate that in 2003 over 500 Chinook passed through water 21°C daily average, or warmer, in the lower San Joaquin River (SRFG 2004). The role of temperature in blocking migration should be clarified as data from this weir or others that may be installed on

other tributaries accumulate. Whether migration through such warm water harms gametes should also be considered.

H. Predation

Predation is natural, but human modification of the Delta can increase it, for example through increased predation associated with the pumps and the Delta Cross Channel. Striped bass and black bass, introduced species, are important predators on juvenile salmon in the Delta. Predation seems the most likely reason for the lower survival of migrating juvenile salmon in the interior Delta, discussed above. Tidal channels are thought to provide protection from predatory fishes (Lott 2004 and citations therein), so the loss of tidal habitat may increase predation. Predation by humans, harvest, is usually a serious stressor on Central Valley Chinook populations, but not in the Delta. See Chapter 13 in Williams (2006) for a discussion of ocean harvest of Central Valley Chinook.

VI. Outcomes

A logical desired outcome for Chinook and steelhead is recovery of the fish listed under the Endangered Species Act, or, more specifically, that winter and spring Chinook and steelhead should meet the viability criteria given in Lindley et al. (2007), and that the unlisted fall and late-fall Chinook should also meet these criteria. These criteria deal mainly with abundance and hatchery influence at the population level, and also with spatial diversity at the ESU or DPS level. However, for several reasons, these outcomes are only marginally useful for assessing management of the Delta. First, some of these criteria, such as the need for additional independent populations of winter Chinook, are unrelated to management of the Delta. Second, because so much of the life cycle of Chinook and steelhead occurs away from the Delta, and survival in these other habitats can be highly variable, even major improvements in Delta conditions would be unlikely to give a clear signal in abundance data until many years had passed (Bradford et al. 2005). The boom and bust of Central Valley fall Chinook over the last fifteen years illustrate the problem with using abundance alone as an indicator of success. Nevertheless, abundance and the viability criteria are surely important for assessing the overall effects of salmon and steelhead management and restoration efforts, of which Delta activities are an important part.

For assessing management of the Delta, monitoring the abundance of juveniles leaving the Delta and the bays seems more useful, but also seems very difficult to do well. Kimmerer (2008) used the Chipps Island trawl data to try to estimate the abundance of juvenile Chinook leaving the Delta, but the estimates depend on a number of strong assumptions and are of unknown accuracy and precision, and the trawl captures smaller fish less efficiently (Williams 2006). Trying to estimate the numbers coming into the Delta would face the same problems, at least downstream from the Red Bluff Diversion Dam, which presents an unusually favorable site for monitoring. Estimating the number of juveniles leaving the bays seems impossible.

Focusing on estimates of growth, growth rate and condition of juveniles rearing in and leaving the Delta should be more useful, particularly because data already exist from an 11-year NMFS program that sampled juveniles in the bays and the Gulf of the Farallones from 1995 to 2005 that provide a baseline, and allowed Lindley et al. (2009) to reach a much more robust conclusion about the collapse of the fall Chinook population than would have been possible otherwise (see Figure 32). Results from early years of the study have been published (MacFarlane and Norton 2002; MacFarlane et al. 2005), and a summary paper is in review (B. MacFarlane, pers. comm., April. 2009). There are also data on size at date from the USFWS trawling at Chipps Island. These data could be used to set quantitative targets for size at date and condition of juvenile Chinook leaving the Delta, and also to test whether there is a relationship between size at date and condition of juveniles leaving the Delta and subsequent adult returns.

Given that sublethal exposure to pesticides or other contaminants in the Delta can disrupt the olfactory system of juvenile salmon and interfere with normal imprinting, a natural rate of straying would be a desirable outcome of management of contaminants. However, straying is difficult to measure, and the natural rate of straying is not precisely known, so setting an outcome for management of toxics in terms of straying does not seem feasible. Setting targets in terms of concentrations of toxics that affect olfaction of fishes in the laboratory, or cause other harm, seems more realistic.

VII. Future Research

The suggestions below for future research try to go beyond the usual questions about the survival of tagged hatchery fish. They are based on the notion that we cannot do a good job of managing something unless we know how it works, and there are still major gaps in our understanding of how Chinook and steelhead populations work.

What are the life-history patterns followed by naturally produced juveniles from different Chinook lineages and populations? When and at what size do they enter and leave the Delta? What are the relative contributions of the different life history patterns to adult returns?

These questions can be addressed regarding lineages through genetic assignment of juveniles sampled in existing monitoring programs. This is currently underway for the sampling at Chipps Island, but it also seems important to clarify when and at what sizes the different lineages of Chinook come into the Delta, by genetic assignment of samples of fish collected in the Sherwood Harbor trawling. This seems especially important for winter Chinook, and would clarify to what extent hatchery late fall-Chinook can be used as surrogates for wild winter Chinook in survival and migration studies.

Genetic assignment should also be effective for spring Chinook, assuming that the Mill and Deer creek populations can be treated as one. It would not suffice for fall Chinook, which are too homogenous genetically to distinguish populations. However, the major populations of fall Chinook can be distinguished by microchemical analysis of otoliths (Barnett-Johnson et al. 2005; 2008), which takes advantage of geological variation along the Sierra Nevada and Cascade

Mountains. Analyses of the microstructure of otoliths collected from adults would provide information on the contributions of the different juvenile life history patterns to returns.

What determines the life-history patterns followed by Chinook and steelhead?

A modeling study to address this question for steelhead is already underway at UCSC, with funding by CALFED (Satterthwaite 2009a). However, even if the approach taken in this study is successful, much more information on the condition of juvenile steelhead and Chinook in the Central Valley will be needed to apply it fully. Fortunately, the data on growth and condition of juveniles suggested as appropriate for measuring the outcome of management of the Delta, from the point of view of salmon, will also be useful for developing the modeling approach.

How do juveniles navigate through the Delta?

Juvenile salmon may use celestial or magnetic cues to find their way through the Delta, as discussed above. Learning more about this may be useful, not from the point of view of installing giant magnets or search lights in the Delta to try to steer fish away from the pumps, but rather for understanding whether and how different groups of fish behave differently, and how hatchery practices, such as trucking fish around the Delta, might affect selection for such behavior. As a related question:

How do ATPase activity or other physiological variables correlate with or modify migratory behavior among Central Valley salmon?

There is a large and inconclusive literature on salmonids regarding this general topic, reviewed by Høgåsen (1998), but much of it is related to hatchery practices, rather than naturally produced fish, and it seems likely that the relations between physiological variables and migration will differ among different life-history types.

Ewing et al. (2001) describe migratory behavior of spring Chinook in the Rogue River, Oregon, that may be a model for the behavior of winter Chinook, although with a seasonal offset. Ewing et al. (2001) found that the migrating juveniles can be roughly divided into one group that migrates slowing down the margins of the channel and another group that migrates more rapidly down the center of the channel, with individuals shifting from the more slowly to the more rapidly migrating group over time. They also found that the status of individuals in this dichotomy can be assessed in terms of changing levels of gill Na^+/K^+ ATPase activity. If this story or some modification of it holds true for winter or late fall Chinook, this knowledge might improve monitoring and management of facilities in the Delta. It could also help answer a very applied question: can hatchery late fall Chinook be used as surrogates for wild winter Chinook?

Is migration a self-reinforcing behavior?

If migratory behavior is self-reinforcing, if the act of migration strengthens the physiological signals that promote migration, then studies of hatchery fish released into the Delta may not be representative of fish released at the hatchery, or of naturally produced fish.

What traits are involved in selection for fitness in a hatchery-based life-cycle?

It now seems settled that hatchery culture involves selection for fitness in a hatchery-based life-cycle, and against fitness in a natural life-cycle (Araki et al. 2007, 2008; Myers et al. 2004).

However, the particular traits selected for or against are not known, although it seems likely that multiple traits are involved (Araki et al. 2008). Traits affecting survival during the egg-alevin part of the cycle are good candidates, since the associated environments are radically different in hatcheries and in streams. In this regard, it is important to realize that hatchery culture does not simply relax selection for or against traits that affect survival in the wild. One reason is that hatcheries canalize fish into particular life histories, and so subject them to different conditions than they might have experienced otherwise (Goodman 2005). For example, steelhead from Coleman Hatchery smolt a year younger than most naturally produced Sacramento River steelhead. This means that Coleman steelhead will experience life in the Delta, bays and the ocean differently than naturally produced fish. Similarly, fall Chinook from Coleman are canalized into a fingerling migrant life-history, and will be subjected to different selective regimes than naturally produced fry migrants.

Does the spring transition in the Gulf of the Farallones define the beginning of a “smolt window” for Central Valley salmon?

Studies of salmon populations elsewhere have suggested that the timing of ocean entry strongly affects smolt survival, and that the timing of ocean entry has evolved in response (e.g., Tallman and Healey 1994). For Central Valley salmon, the spring transition in the Gulf of the Farallones to a regime dominated by upwelling (Ainley 1990; Williams 2006) seems a logical candidate for the beginning of such a period of higher survival. It is easy to see how the migration timing of fall Chinook or fry-migrant spring Chinook would fit such a conceptual model, but the larger juveniles that migrate down the Sacramento River during late fall and winter would seem not to fit. However, if the timing with which wild juvenile winter Chinook appear at the pumps (Figure 18) reflects the timing with which they leave the Delta, and if their migration through the bays is slow, then winter-run might indeed fit this model. This might be tested by comparing the timing of an increase in growth rate from the otolith microstructure of returning adults with the timing of ocean entry estimated from otolith microchemistry. As an alternative hypothesis, it could be that survival of winter-migrant juvenile Chinook depends on reaching a large enough size, as appears to be the case with coastal steelhead (Hayes et al. 2008).

Does food availability in the estuary limit the growth and subsequent survival of juvenile salmon? Does competition with hatchery fish adversely affect naturally produced fish in the estuary?

Recent estimates of the growth rates of juvenile Chinook in the Delta and especially in the bays seem low (Figure 32). Data on size at date from the Chipps Island trawling records and from recoveries at the state and federal pumps could be compiled to check for year to year variation and longer term trends in size at date, and data from monitoring in the rivers could be used to try to separate the effects on size of conditions in the Delta and in the rivers. Similarly, an index of food availability for juvenile salmon might be constructed from the long IEP monitoring records in the Delta. The indices of growth or of food availability might be used as covariates in statistical analyses of survival. Data on growth and condition of fish from the 1995-2005 NMFS monitoring could be used for detailed assessments for those years. The NMFS samples could also be classified as hatchery or naturally produced based on otolith microstructure, so that these groups of fish could be analyzed separately.

VIII. References

- Ackerman, PA, Wicks, BJ, Iwama, GK, Randall, DJ. 2006. Low levels of environmental ammonia increases susceptibility to disease in Chinook salmon smolts. *Physiological and Biochemical Zoology* 79:695-707.
- Ainley, DG. 1990. Seasonal and annual patterns in the marine environment near the Farallones. In: Ainley, DG, Bockelheide, RJ, editors. *Seabirds of the Farallon Islands*. Stanford University Press.
- Alabaster, JS. 1989. The dissolved oxygen and temperature requirements of king salmon, *Oncorhynchus tshawytscha*, in the San Joaquin Delta, California. *Journal of Fish Biology* 34:331-332.
- Anderson, JJ. 2003. Toward a resolution of the flow/survival debate and the impacts of flow augmentation and water withdrawal in the Columbia/Snake River system. Seattle: Columbia Basin Research, School of Aquatic and Fishery Science, University of Washington.
- Araki, H, Berejikian, BA, Ford, MJ, Blouin, MS. 2008. Fitness of hatchery-reared salmonids in the wild. *Evolutionary Applications* 1:342-355.
- Araki, H, Cooper, B, Blouin, MS. 2007. Genetic effects of captive breeding cause a rapid, cumulative fitness decline in the wild. *Science* 318:100-103.
- Atwater, BF, Conrad, SF, Dowden, JN, Hedel, CW, MacDonald, RL, Savage, W. 1979. History, landforms, and vegetation of the estuary's tidal marshes. In: Conomos, TJ, Editor. *San Francisco Bay, the urbanized estuary*. AAAS. p. 347385.
- Baker, PF, Speed, TP, Ligon, FK. 1995. Estimating the influence of temperature on the survival of Chinook salmon smolts (*Oncorhynchus tshawytscha*) migrating through the Sacramento - San Joaquin River Delta of California. *Canadian Journal of Fisheries and Aquatic Sciences* 52:855-863.
- Banks, MA, Rashbrook, VK, Calvaetta, MJ, Dean, CA, Hedgecock, D. 2000. Analysis of microsatellite DNA resolves genetic structure and diversity of Chinook salmon (*Oncorhynchus tshawytscha*) in California's Central Valley. *Canadian Journal of Fisheries and Aquatic Sciences* 57:915-927.
- Barnett-Johnson, R, Garza, JC, Grimes, CB, MacFarlane, RB. 2008. Linking freshwater sources of Chinook salmon to their ocean distributions using genes and otolith signatures of origin. Abstracts, 5th Biennial CALFED Science Conference; Sacramento, CA. p. p. 74.
- Barnett-Johnson, R, Grimes, CB, Royer, CF, Donohoe, CJ. 2007. Identifying the contribution of wild and hatchery Chinook salmon (*Oncorhynchus tshawytscha*) to the ocean fishery using otolith microstructure as natural tags. *Canadian Journal of Fisheries and Aquatic Sciences* 64:1683-1692. doi:10.1139/Fo7-129
- Barnett-Johnson, R, Ramos, FC, Grimes, CB, MacFarlane, RB. 2005. Validation of Sr isotopes in otoliths by laser ablation multicollector inductively coupled plasma mass spectrometry (LA-MC-ICPMS): opening avenues in fisheries science applications. *Canadian Journal of Fisheries and Aquatic Sciences* 62:2425-2430.
- Bond, MH. 2006. Importance of estuarine rearing to central California steelhead (*Oncorhynchus mykiss*) growth and marine survival. University of California Santa Cruz.
- Bottom, DL, Jones, KK, Cornwell, TJ, Gray, A, Simenstad, CA. 2005. Patterns of Chinook salmon migration and residency in the Salmon River estuary (Oregon). *Estuarine, Coastal and Shelf Science* 64:79-93.
- Bradford, MJ, Higgins, PS. 2001. Habitat-, season-, and size specific variation in diel activity patterns of juvenile Chinook salmon (*Oncorhynchus tshawytscha*) and steelhead trout (*Oncorhynchus mykiss*). *Canadian Journal of Fisheries and Aquatic Sciences* 58:365-374.
- Bradford, MJ, Korman, J, Higgins, PS. 2005. Using confidence intervals to estimate the response of salmon populations (*Oncorhynchus* spp.) to experimental habitat alterations. *Canadian Journal of Fisheries and Aquatic Sciences* 62:2716-2726.
- Brandes, PL, McLain, JS. 2001. Juvenile Chinook salmon abundance, distribution, and survival in the Sacramento-San Joaquin estuary. In: Brown, RL, editor. *Contributions to the biology of Central Valley salmonids*, Vol 2. Fish Bulletin No. 179. Sacramento: California Department of Fish and Game. p. 39-138.
- Brau, J., A. Blake, and R. Perry. 2007. Sacramento/San Joaquin River Delta regional salmon outmigration study plan: Developing understanding for management and restoration. Available: http://baydeltaoffice.water.ca.gov/ndelta/salmon/documents/RegionalSalmonStudyPlan_2008.01.07.pdf. (May 2009).
- Brett, JR, Shelbourn, JE, Shoop, CT. 1969. Growth rate and body composition of fingerling sockeye salmon, *Oncorhynchus nerka*, in relation to temperature and ration size. *Journal of the Fisheries Research Board of Canada* 26:2363-2394.
- Brown, R, Cavallo, B, Jones, K. 2004. The effects of the Feather River Hatchery on naturally spawning salmonids.

- California Department of Water Resources.
- Burke, Jennifer L. Life histories of juvenile Chinook salmon in the Columbia River estuary, 1916 to the present: MS thesis, Oregon State University; 2004.
- Castleberry, DT, Cech, JJr, Saiki, MK, Martin, BA. 1993. Growth, condition and physiological performance of juvenile salmonids from the American River, February through July, 1992. Dixon, California: U. S. Fish and Wildlife Service.
- Clark, GH. 1928. Sacramento- San Joaquin salmon (*Oncorhynchus tshawytscha*) fishery of California. Fish Bulletin 17:1-73.
- Clarke, WC, Whithler, RE, Shelbourn, JE. 1992. Genetic control of juvenile life history pattern in Chinook salmon (*Oncorhynchus tshawytscha*). Canadian Journal of Fisheries and Aquatic Sciences 49:2300-2306.
- Clarke, WC, Hirano, T. 1995. Osmoregulation. In: Groot, C, Margolis, L, Clarke, WC, editors. Physiological ecology of Pacific salmon. Vancouver, British Columbia: UBC Press. p. 317-438.
- Erkkila, LF, Moffett, JW, Cope, OB, Smith, BR, Nielson, RS. 1950. Sacramento - San Joaquin Delta Fishery Resources: Effects of Tracy Pumping Plant and Delta Cross Channel. Sacramento, California: U.S. Fish and Wildlife Service. Special Scientific Report: Fisheries No. 56.
- Ewing, RD, Ewing, GS, Satterthwaite, TD. 2001. Changes in gill Na⁺, K⁺-ATPase specific activity during seaward migration of wild juvenile Chinook salmon. Journal of Fish Biology 58:1414-1426.
- Geist, DR, Abernathy, CS, Hand, KD, Cullinan, VI, Chandler, JA, Groves, PA. 2006. Survival, development, and growth of fall Chinook salmon embryos, alevins, and fry exposed to variable thermal and dissolved oxygen regimes. Transactions of the American Fisheries Society 135:1462-1477. doi:10.1577/T05-294.1
- Gilbert, CH. 1913. Age at maturity of the Pacific coast salmon of the genus *Oncorhynchus*. Bulletin of the Bureau of Fisheries.
- Goodman, D. 2004. Salmon supplementation: demography, evolution, and risk assessment. In: Nickum, MJ, Mazik, PM, Nickum, JG, MacKinley, DD, editors. Propagated fish in resource management. American Fisheries Society, Symposium 44. Bethesda, Maryland: American Fisheries Society. p. 217-232.
- Goodman, D. 2005. Selection equilibrium for hatchery and wild spawning fitness in integrated breeding programs. Canadian Journal of Fisheries and Aquatic Sciences 62:374-389.
- Greene, CM, Beechie, TJ. 2004. Consequences of potential density-dependent mechanisms on recovery of ocean-type Chinook salmon (*Oncorhynchus tshawytscha*). Canadian Journal of Fisheries and Aquatic Sciences 61:590-602.
- Hallock, RJ, Elwell, RF, Fry, DHJr. 1970. Migrations of adult king salmon (*Oncorhynchus tshawytscha*) in the San Joaquin Delta as demonstrated by the use of sonic tags. Fish Bulletin 151. California Department of Fish and Game.
- Hallock, RJ, Van Woert, WF, Shapovalov, L. 1961. An evaluation of stocking hatchery-reared steelhead rainbow trout (*Salmo gairdnerii gairdnerii*) in the Sacramento River System. Fish Bulletin No. 114. California Department of Fish and Game.
- Hannon, J, Healey, M, Deason, B. 2003. American River steelhead (*Oncorhynchus mykiss*) spawning, 2001-2003. Sacramento, California: U. S. Bureau of Reclamation and California Department of Fish and Game.
- Hanson, HA, Smith, OR, Needham, PR. 1940. An investigation of fish salvage problems in relation to Shasta Dam. Special Scientific Report # 10. Washington, D. C.: U. S. Bureau of Fisheries.
- Harden Jones, FR. 1978. Fish Migration. London: Arnold.
- Hatton, SR, Clark, GH. 1942. A second progress report on the Central Valley fisheries investigation. California Fish and Game 28:116-123.
- Hayes, Sean A.; Hanson, Chad V.; Macfarlane, R. B., and Bond, Morgan H. 2008. Marine survival of steelhead (*Oncorhynchus mykiss*) enhanced by a seasonally closed estuary. Canadian Journal of Fisheries and Aquatic Sciences.; 65: 2242-2252.
- Healey, MC. 1991. Life history of Chinook salmon (*Oncorhynchus tshawytscha*). In: Groot, C, Margolis, L, editors. Pacific salmon life histories. p. 311-394.
- Healey, MC. 1980. Utilization of the Nanaimo River estuary by juvenile Chinook salmon, *Oncorhynchus tshawytscha*. Fishery Bulletin 77:653-668.
- Hecht, SA, Baldwin, DH, Mebane, CA, Hawkes, T, Gross, SJ, Scholz, NL. 2007. An overview of sensory effects on juvenile salmonids exposed to dissolved copper. D. S. Dept. Commerce, NOAA Tech. Memo. NMFS-NWFSC-83.
- Hedgecock, D, Banks, MA, Rasbrook, VK, Dean, CA, Blankenship, SM. 2001. Applications of population genetics to conservation of Chinook salmon diversity in the Central Valley. In: Brown, RL, editor. Contributions to the biology of Central Valley salmonids. Fish Bulletin .1. p. 45-70.

- Hedgecock, D. 2002. Microsatellite DNA for the management and protection of California's Central Valley Chinook salmon (*Oncorhynchus tshawytscha*). University of California, Davis, Bodega Marine Laboratory.
- Hill, MF, Botsford, LW, Hastings, A. 2003. The effects of spawning age distribution on salmon persistence in fluctuating environments. *Journal of Animal Ecology* 72:736-744.
- Høggåsen, HR. 1998. Physiological changes associated with the diadromous migration of salmonids. *Canadian Special Publication of Fisheries and Aquatic Sciences* 127.
- Ingram, L. 2008. The role of the San Francisco Bay-Delta in juvenile rearing for winter and spring run Chinook salmon, to be determined by otolith microchemistry. Supplemental proposal to CALFED, 2007 Supplemental PSP.
- Jassby, A, Van Nieuwenhuysse, EE. 2005. Low dissolved oxygen in an estuarine channel (San Joaquin River, California): mechanisms and models based on long-term time series. *San Francisco Estuary and Watershed Science* (online serial) 3:Article 2. <http://repositories.cdlib.org/jmie/sfews/vol2/iss2/art2>.
- Jeffres, CA, Opperma, JJ, Moyle, PB. 2008. Ephemeral floodplain habitats provide best growth conditions for juvenile Chinook salmon in a California River. *Environmental Biology of Fishes* In press: DOI: 10.1007/s10641-008-9367-1
- Joint Hatchery Review Committee (JHRC). 2001. Final Report on Anadromous Salmonid Fish Hatcheries in California, Review Draft. California Department of Fish and Game and National Marine Fisheries Service Southwest Region.
- Kelley, R. 1989. *Battling the inland sea*. Berkeley: University of California Press.
- Kimmerer, WJ. 2004. Open water processes of the San Francisco Estuary: from physical forcing to biological response. *San Francisco Estuary and Watershed Science* (online serial) 2:Article 1. <http://repositories.cdlib.org/jmie/sfews/vol2/iss1/art1>.
- Kimmerer, WJ. 2008. Losses of Sacramento River Chinook salmon and Delta smelt to entrainment in water diversions in the Sacramento-San Joaquin Delta. *San Francisco Estuary and Watershed Science* 6:Article 2. <http://repositories.cdlib.org/jmie/sfews/vol6/iss2/art2/>
- Kjelson, MA, Raquel, PF, Fisher, FW. 1982. Life history of fall-run juvenile Chinook salmon, *Oncorhynchus tshawytscha*, in the Sacramento-San Joaquin Estuary, California. In: Kennedy, VS, editor. *Estuarine comparisons*. New York: Academic Press. p. 393-411.
- Kostow, KE. 2004. Differences in juvenile phenotypes and survival between hatchery stocks and a natural population provide evidence for modified selection due to captive breeding. *Canadian Journal of Fisheries and Aquatic Sciences* 61:577-589.
- Lee, GF, Jones-Lee, A. 2003. Synthesis and discussion of findings on the causes and factors influencing low DO in the San Joaquin River deep water ship channel near Stockton, CA: including 2002 data. El Macero, CA: G. Fred Lee & Associates.
- Levy, DA, Northcote, TG. 1982. Juvenile salmon residency in a marsh area of the Fraser River estuary. *Canadian Journal of Fisheries and Aquatic Sciences* 39:270-276.
- Lindely, ST, Schick Robert S., Agrawal, A, Goslin, M, Pearson, TE, Mora, E, Anderson, JJ, May, BP, Greene, S, Hanson, C, Low, A, McEwan, DR, MacFarlane, RB, Swanson, C, Williams, JG. 2006. Historical population structure of Central Valley steelhead and its alteration by dams. *San Francisco Estuary and Watershed Science* Volume 4:Article 3. <http://repositories.cdlib.org/jmie/sfews/vol4/iss1/art3>
- Lindely, ST, Schick Robert S., Mora, E, Adams, PB, Anderson, JJ, Greene, S, Hanson, CMBP, McEwan, DR, MacFarlane, RB, Swanson, C, Williams, JG. 2007. Framework for assessing viability of threatened and endangered Chinook salmon and steelhead in the Sacramento-San Joaquin Basin. *San Francisco Estuary and Watershed Science* Volume 5 :Article 4. <http://repositories.cdlib.org/jmie/sfews/vol5/iss1/art4>
- Lindley, ST, Michel, C, Sandstrom, PT. 2008. Estimating reach-specific smolt survival rates and the factors affecting them from acoustic tagging data. 5th Biennial CALFED Science Conference; Sacramento, CA.
- Lindley, ST, Mohr, MS. 2003. Modeling the effects of striped bass (*Morone saxatilis*) on the population viability of Sacramento River winter-run Chinook salmon (*Oncorhynchus tshawytscha*). *Fishery Bulletin* 101:321-331.
- Lindley, ST, Schick, R, May, BP, Anderson, JJ, Greene, S, Hanson, C, Low, A, McEwan, D, MacFarlane, RB, Swanson, C, Williams, JG. 2004. Population structure of threatened and endangered Chinook salmon ESUs in California's Central Valley Basin. NOAA-TN-NMFS-SWFSC-370.
- Lindley, S. T.; Grimes, C. B.; Mohr, M. S.; Peterson, W.; Stein, J.; Anderson, J. R.; Botsford, L. W.; Botton, D. L.; Busack, C. A.; Collier, T. K.; Ferguson, J.; Garza, J. C.; Grover, A. M.; Hankin, D. G.; Kope, R. G.; Lawson, P. W.; Low, A.; MacFarlane, R. B.; Moore, K.; Plamer-Zwahlen, M.; Schwing, F. B.; Smith, J.; Tracy, C.; Webb, R.; Wells, B. K., and Williams, T. H. 2009. What caused the Sacramento River fall Chinook stock collapse? National Marine Fisheries Service, Southwest Fisheries Science Center. NOAA_TM_SWFSC-447.

- Lott, MA. 2004. Habitat-specific feeding ecology of ocean-type juvenile Chinook salmon in the lower Columbia River estuary. MS Thesis, University of Washington, School of Aquatic and Fishery Science.
- Lotze, JK, Lenihan, HS, Bourque, BJ, Bradbury, RH, Cooke, RG, Kay, MC, Kidwell, SM, Kirby, MX, Peterson, CH, Jackson, JB. 2006. Depletion, degradation, and recovery potential of estuaries and coastal seas. *Science* 312:1806-1809.
- Low, A. 2005. Existing program summary: Central Valley salmon and steelhead monitoring programs . Sacramento, California: California Department of Fish and Game.
- Ludwig, D. 1994. Uncertainty and fisheries management. In: Levin, SA, editor. *Frontiers in Mathematical Biology*. Springer-Verlag. p. 516-528.
- MacFarlane, BR, Ralston, S, Royer, C, Norton, EC. 2005. Juvenile Chinook salmon (*Oncorhynchus tshawytscha*) growth on the Central California coast during the 1980 El Niño and the 1999 La Niña. *Fisheries Oceanography* 14:321-332.
- MacFarlane, RB, Norton, EC. 2002. Physiological ecology of juvenile Chinook salmon (*Oncorhynchus tshawytscha*) at the southern end of their distribution, the San Francisco Estuary and the Gulf of the Farallones, California. *Fishery Bulletin* 100:244-257.
- Malamud-Roam, FP, Phillis, C, Ingram, L, Weber, PK. 2008. San Francisco Bay Estuary habitat use determined by otolith stable isotopes. Abstracts, 5th Biennial CALFED Science Conference; Sacramento, CA. p. p. 157.
- Mangel, M. 1994. Climate change and salmonid life history changes. *Deep-Sea Research II* 41:75-106.
- Mangel, M, Satterthwaite, WH. 2008. Combining proximate and ultimate approaches to understand life history variation in salmonids with application to fisheries, conservation, and aquaculture. *Butte tin of Marine Science* 83:107-130.
- Marine, KR, Cech, JJJr. 2004. Effects of high temperature on growth, smoltification, and predator avoidance in juvenile Sacramento River Chinook salmon. *North American Journal of Fisheries Management* 24:198-210.
- Maslin, P, Kindopp, J, Storm, C. 1999. Intermittent streams as rearing habitat for Sacramento River Chinook salmon (*Oncorhynchus tshawytscha*): 1999 update. California State University Chico, Dept. of Biological Sciences.
- Mattern, SA, Moyle, PB, Pierce, LC. 2002. Native and alien fishes in a California estuarine marsh: twenty-one years of changing assemblages. *Transactions of the American Fisheries Society* 131:797-816.
- McEwan, D, Nelson, J. 1991. Steelhead restoration plan for the American River. Sacramento, California: California Department of Fish and Game.
- McEwan, D. 2001. Central Valley Steelhead. In: Brown, RL, Editor. *Contributions to the biology of Central Valley salmonids*, Fish Bulletin 179. Fish Bulletin 179.1. California Department of Fish and Game. p. 1-44.
- McGregor, EA. 1923. Notes on the egg yield of Sacramento River king salmon. *California Fish and Game* 9:134-138.
- Moyle, PB. 2002. *Inland Fishes of California*. University of California Press.
- Moyle, PB, Crain, PK, Whitener, K. 2007. Patterns in the use of a restored California floodplain by native and alien fishes. *San Francisco Estuary and Watershed Science* vol. 5, issue 3, article 1:1-27. <http://repositories.edlib.org/jmi/sfews/vol5/iss3/art1>
- Moyle, PB, Israel, JA. 2005. Untested assumptions: effectiveness of screening diversions for conservation of fish populations. *Fisheries* 30:20-28.
- Myers, RA, Levin, SA, Lande, R, James, FC, Murdock, WW, Paine, RT. 2004. Hatcheries and endangered salmon. *Science* 303:1980.
- Myrick, CA, Cech, JJJr. 2002. Growth of American River fall-run Chinook salmon in California's Central Valley: temperature and ration effects. *California Fish and Game* 88:35-44.
- Myrick, CA, Cech, JJJr. 2001. Temperature effects on Chinook salmon and steelhead: a review focusing on California's Central Valley populations. <http://www.cwemf.org>: Bay-Delta Modeling Forum.
- Myrick, CA, Cech, JJJr. 2004. Temperature effects on juvenile anadromous salmonids in California's central valley: what don't we know. *Reviews in Fish Biology and Fisheries* 14:113-123.
- Myrick, CA, Cech, JJJr. 2000. Temperature influences on California rainbow trout physiological performance. *Fish Physiology and Biochemistry* 22:245-254.
- Newman, KB. 2008. An evaluation of four Sacramento-San Joaquin River Delta juvenile salmon survival studies. Stockton, Ca: USFWS.
- Newman, KB. 2003. Modeling paired release-recovery data in the presence of survival and capture heterogeneity with application to marked juvenile salmon. *Statistical Modeling* 3:157-177.
- Newman, KB, Rice, J. 2002. Modeling the survival of Chinook salmon smolts outmigrating through the lower Sacramento River system. *Journal of the American Statistical Association* 97:983-993.

- Nichols, FH, Cloern, JE, Luoma, S, Peterson, DH. 1986. The modification of an estuary. *Science* 231:567-573.
- Nickleston, T. 2003. The influence of hatchery coho salmon (*Oncorhynchus kisutch*) on the productivity of wild coho salmon populations in Oregon coastal basins. *Canadian Journal of Fisheries and Aquatic Sciences* 60:1050-1056.
- Nobriga, M, Matica, Z, Hymnson, Z. 2004. Evaluating entrainment vulnerability to agricultural irrigation diversions: a comparison among open-water fishes. *American Fisheries Society Symposium* 39. p. 281-295.
- Nobriga, ML, Feyrer, F, Baxter, RD. 2006. Aspects of Sacramento pikeminnow biology in nearshore habitats of the Sacramento-San Joaquin Delta, California. *Western North American Naturalist* 66:106-114.
- Nobriga, ML, Baxter, R. 2003. Baby steps toward a conceptual model of predation in the Delta: preliminary results from the shallow water habitat predator-prey dynamics study. *IEP Newsletter* 16:19-27.
- Olson, AF, Quinn, TP. 1993. Vertical and horizontal movements of adult Chinook salmon *Oncorhynchus tshawytscha* in the Columbia River estuary. *Fishery Bulletin* 91:171-181.
- Perry, RW, Brandes PL, Sandstrom, PT, Ammann, A, MacFarlane, B., Klimley, AP, and Skalski, JR. Estimating survival and migration route probabilities of juvenile Chinook salmon in the Sacramento-San Joaquin River Delta. In press. *North American Journal of Fisheries Management*.
- Perry, RW and Skalski, JR. 2009. Survival and migration route probabilities of juvenile Chinook salmon in the Sacramento-San Joaquin River Delta during the winter of 2008-2009. Report to the USFWS, Stockton, Ca.
- Phillis, C, Ingram, L, Weber, PK. 2008. River and estuary rearing of successfully spawned adult Chinook salmon, determined by otolith Sr isotopes. Abstracts, 5th Biennial CALFED Science Conference; Sacramento, CA. p. p. 75.
- Pipel, KA. 2005. Summary of monitoring activities for ESA-listed salmonids in California's Central Valley. NOAA-TM-NMFS-SWFSC-373.
- Quinn, TP. 2005. The behavior and ecology of Pacific salmon and trout. Bethesda, Maryland: American Fisheries Society.
- Rich, AA. 1987. Report on studies conducted by Sacramento County to determine the temperatures which optimize growth and survival in juvenile Chinook salmon (*Oncorhynchus tshawytscha*). Sacramento, California: McDonough, Holland & Allen.
- Roth, JE, Mill, KL, Sydeman, WJ. 2007. Chinook salmon (*Oncorhynchus tshawytscha*) seabird covariation of central California and possible forecasting applications. *Canadian Journal of Fisheries and Aquatic Sciences* 64:1080-1090.
- Rutter, C. 1904. Natural history of the Quinnot Salmon. *Bulletin of the United States Fish Commission* 22:65-142.
- Sacramento River Fall Chinook Review Team (SRFCRT). 1994. Sacramento River Fall Chinook Review Team Report. Portland, Oregon: Pacific Fishery Management Council.
- Sacramento-San Joaquin Estuary Fishery Resource Office (SSJEFRO). 2003. Abundance and survival of juvenile Chinook salmon in the Sacramento-San Joaquin Estuary. Stockton, California: U.S. Fish and Wildlife Service.
- Sandahl, JF, Baldwin, DH, Jenkins, JJ, Scholz, NL. 2004. Odor-evoked field potentials as indicators of sublethal neurotoxicity in juvenile coho salmon (*Oncorhynchus kisutch*) exposed to copper, chlorpyrifos, or esfenvalerate. *Canadian Journal of Fisheries and Aquatic Sciences* 61:404-413.
- Satterthwaite, W. H., M. P. Beakes, E. M. Collins, D. R. Swank, J. E. Merz, R. G. Titus, S. M. Sogard, and M. Mangel. 2009a. State-dependent life history models in a changing (and regulated) environment: steelhead in the California Central Valley. *Evolutionary Applications*. doi: 10.1111/j.1752-4571.2009.00103.x
- Satterthwaite, W. H., M. P. Beakes, E. M. Collins, D. R. Swank, J. E. Merz, R. G. Titus, S. M. Sogard, and M. Mangel. 2009b. Insights from a state dependent model of steelhead life history. *Transactions of the American Fisheries Society*. 2009b; 138:532-548.
- Scholz, NL, Truelove, NK, French, BL, Berejikian, BA, Quinn, TP, Casillas, E, Collier, TC. 2000. Diazinon disrupts antipredator and homing behaviors in Chinook salmon (*Oncorhynchus tshawytscha*). *Canadian Journal of Fisheries and Aquatic Sciences* 57:1911-1918.
- Scofield, NB. 1899. Notes on an investigation of the movement and rate of growth of the Quinnot salmon fry in the Sacramento River. Appendix to the Journals of Senate and Assembly of the thirty-third session of the legislature of the State of California.
- Scofield, N. B. A general report on a quinnat salmon investigation, carried on during the spring and summer of 1911. 1913. *Fish Bulletin* 1:35-41.
- Scofield, WL. 1920. King salmon marking experiment at Klamath River, 1919. *California Fish and Game* 6:101-103.
- Shapovalov, L, Taft, AC. 1954. The life histories of the steelhead rainbow trout (*Salmo gairdneri gairdneri*) and Silver Salmon (*Oncorhynchus kisutch*). Sacramento: California Department of Fish and Game. *Fish Bulletin*

No. 98.

- Shreffler, DK, Simenstad, CA, Thom, RM. 1992. Foraging by juvenile salmon in a restored estuarine wetland. *Estuaries* 15:204-213.
- Simenstad, CTJ, Higgins, H, Cordell, J, Orr, M, Williams, P, Grimaldo, L, Hymanson, Z, Reed, D. 2000. Sacramento/San Joaquin Delta breached levee wetland study (BREACH). Preliminary Report. Seattle, Washington: University of Washington, School of Fisheries.
- Skinner, JE. 1962. Fish and wildlife resources of the San Francisco Bay Area. Sacramento, California: California Department of Fish and Game.
- Snider, B, Titus, RG. 2001. Lower American River emigration survey, October 1997-September 1998. Sacramento, CA: California Department of Fish and Game, Stream Evaluation Unit. Technical Report No. 01-6.
- Sommer, TR, Nobroga, ML, Harrell, WC, Batham, W, Kimmerer, WJ. 2001. Floodplain rearing of juvenile Chinook salmon: evidence of enhanced growth and survival. *Canadian Journal of Fisheries and Aquatic Sciences* 58:325-333.
- Sommer, TR, Harrell, WC, Nobriga, M. 2005. Habitat use and stranding risk of juvenile Chinook salmon on a seasonal floodplain. *North American Journal of Fisheries Management* 25:1493-1504.
- Stearns, SC, Hendry, AP. 2004. The salmonid contribution to key issues in evolution. *Evolution illuminated: salmon and their relatives*. New York: Oxford University Press.
- Stewart, DC, Middlemas, SJ, Youngson, AF. 2006. Population structuring in Atlantic salmon (*Salmo salar*): evidence of genetic influence on the timing of smolt migration in sub-catchment stocks. *Ecology of Freshwater Fish* 15:552-558.
- Tallman, RF, Healey, MC. 1994. Phenotypic differentiation in seasonal ecotypes of chum salmon, *Oncorhynchus keta*. *Canadian Journal of Fisheries and Aquatic Sciences* 48:661-671.
- The Bay Institute (TBI). 1998. From the Sierra to the sea: the ecological history of the San Francisco Bay-Delta watershed. Novato, California: The Bay Institute. http://www.bay.org/sierra_to_the_sea.htm (2005)
- Thorpe, JE. 1977. bimodal distribution of lengths of juvenile Atlantic salmon (*Salmo salar* L.) under artificial rearing conditions. *Journal of Fish Biology* 11:175-184.
- Thorpe, JE. 1989. Developmental variation within salmon populations. *Journal of Fish Biology* 35(Supplement A):295-303.
- Thorpe, JE, Mangel, M, Metcalfe, NB, Huntingford, FA. 1998. Modeling the proximate basis of salmonid life-history variation, with application to Atlantic salmon, *Salmo salar* L. *Evolutionary Ecology* 12:581-599.
- Titus, RG, Volkoff, MC, Snider, WM. 2004. Use of otolith microstructure to estimate growth rates of juvenile Chinook salmon from a Central Valley, California stock. In: Feyrer, FL, Brown, RL, Orsi, JJ, editors. *Early life history of fishes in the San Francisco Estuary and watershed*. American Fisheries Society Symposium 39. Bethesda, Maryland: American Fisheries Society. p. 181-202.
- Weatherley, AH, Gill, HS. 1995. Growth. In: Groot, C, Margolis, L, Clarke, WCC, editors. *Physiological ecology of Pacific salmon*. Vancouver, British Columbia: University of British Columbia Press.
- Werner, I, Smith, TB, Feliciano, J, Johnson, ML. 2005. Heat shock proteins in juvenile steelhead reflect thermal conditions in the Navarro River Watershed, California. *Transactions of the American Fisheries Society* 134:399-410.
- Williams, JG. 2006. Central Valley salmon: a perspective on Chinook and steelhead in the Central Valley of California. *San Francisco Estuary and Watershed Science* 4: <http://repositories.cdlib.org/jmie/sfews/vol4/iss3/art2>
- Williamson, KS, May, B. 2005. Homogenization of fall-run Chinook salmon gene pools in the Central Valley of California, USA. *North American Journal of Fisheries Management* 25:993-1009.
- Wilson, MF. 1997. Variation in salmonid life histories: patterns and perspectives. Portland, Oregon: USDA, Forests Service, Pacific Northwest Research Station. Research Paper.
- Yoshiyama, RM, Gerstung, ER, Fisher, FW, Moyle, PB. 2001. Historical and present distribution of Chinook salmon in the Central Valley drainage of California. In: Brown, RL, editor. *Fish Bulletin 179: Contributions to the biology of Central Valley salmonids*. 1. Sacramento: p. 71-176.
- Yoshiyama, RM, Gerstung, ER, Fisher, FW, Moyle, PB. 1996. Historical and present distributions of Chinook salmon in the Central Valley drainage of California. In: *Sierra Nevada Ecosystem Project, Status of the Sierra Nevada, Volume III. Final Report*. p. 309-362.



Response of juvenile Chinook salmon to managed flow: lessons learned from a population at the southern extent of their range in North America

S. C. ZEUG, K. SELLHEIM & C. WATRY,

Cramer Fish Sciences, Auburn, CA, USA

J. D. WIKERT

U.S. Fish and Wildlife Service, Lodi, CA, USA

J. MERZ

Cramer Fish Sciences, Auburn, CA, USA

Abstract Fourteen years (1996–2009) of juvenile Chinook salmon, *Oncorhynchus tshawytscha* (Walbaum), migration data on the regulated Stanislaus River, California, USA were used to evaluate how survival, migration strategy and fish size respond to flow regime, temperature and spawner density. An information theoretic approach was used to select the best approximating models for each of four demographic metrics. Greater cumulative discharge and variance in discharge during the migration period resulted in higher survival indices and a larger proportion of juveniles migrating as pre-smolts. The size of pre-smolt migrants was positively associated with spawner density, whereas smolt migrant size was negatively associated with temperature and positively associated with discharge. Monte Carlo techniques indicated high certainty in relationships between flow and survival, but relationships with juvenile size were less certain and additional research is needed to elucidate causal relationships. Flow is an integral part of the habitat template many aquatic species are adapted to, and mismatches between flow and life history traits can reduce the success of migration and the diversity of migratory life history strategies. The analyses presented here can be used to assist in the development of flow schedules to support the persistence of salmon in the Stanislaus River and provide implications for populations in other regulated rivers with limited and variable water supply.

KEY WORDS: California, life history, Monte Carlo, river regulation, screw trap, survival.

Introduction

Pacific salmon, *Oncorhynchus* spp., stock abundances exhibit large temporal fluctuations that, in part, are determined by co-varying environmental parameters that characterise regional climatic conditions. This is not surprising given the profound effect freshwater flow has upon the physical, chemical and biological processes in streams, estuaries and associated coastal waters (Albright 1983; Junk *et al.* 1989; Wilcock *et al.* 1996). The freshwater hydrograph influences water temperature and quality, creation and maintenance of channel

complexity, seasonal activation of floodplain habitats, regulation of primary productivity and stimulation of migration in aquatic species (Dingle 1996; Poff *et al.* 1997; Ahearn *et al.* 2006). Particulate organic and inorganic matter, as well as juvenile salmon, are carried seaward by freshwater flow and incorporated into coastal marine food chains. In turn, conditions within coastal waters influence the health, survival and reproductive success of adult salmon returning to natal streams, causing a biological feedback on long-term health and success of salmon stocks (Mantua *et al.* 1997; Greene *et al.* 2005).

Correspondence: Steven Zeug, Cramer Fish Sciences, 13300 New Airport Road Suite 102, Auburn, CA 95602, USA (e-mail: stevez@fishsciences.net)

Salmon streams throughout the northern hemisphere have undergone dramatic and long-term anthropogenic changes including damming, mining, levee construction, hydropower generation and floodplain disconnection. Such effects have altered hydrologic, sediment and temperature regimes and impacted the native flora and fauna of these systems (Merritt & Cooper 2000; Trush *et al.* 2000; Vinson 2001). The associated decline of salmon populations that support valuable commercial and recreational fisheries has triggered efforts to design flow regimes for regulated rivers that provide conditions suitable to support self-sustaining populations. Yet, there remains a lack of information regarding the responses of different salmon life stages to specific environmental variables that can be used to inform flow strategies. Given the demands for large-scale water regulation and diversion within lotic ecosystems, effective resource management requires an understanding of how environmental conditions affect salmon (i.e. quantity, quality and migration strategy) during the freshwater portion of a given population's life cycle (Hoekstra *et al.* 2007; Nislow & Armstrong 2012).

It was hypothesised that juvenile salmon would demonstrate demographic responses to inter-annual variation in flow magnitude, flow variance and temperature. This hypothesis was tested by modeling how independent variables affected the proportion of juveniles transitioning from rearing to migration using an index of survival, the life stage when migration out of the natal stream was initiated and fish size. For this effort, 14 years of juvenile Chinook salmon migration data were collected at two locations on the Stanislaus River, California, USA, a highly regulated stream with an extant population of naturally reproducing Chinook salmon, *Oncorhynchus tshawytscha* (Walbaum). The monitoring sites included the downstream extent of identified Chinook salmon spawning habitat that was used to estimate fry abundance and the downstream extent of rearing used to estimate the abundance of Chinook salmon emigrating out of the natal stream. These analyses provide resource managers with essential information that can be used to better inform flow management for Chinook salmon in the Stanislaus River and provide implications for relationships between environmental drivers and Chinook salmon ecology in other regulated rivers.

Methods

Study site

The Stanislaus River drains approximately 2400 km² from the western slope of the central Sierra Nevada Mountains to its confluence with the San Joaquin River.

The watershed has a Mediterranean climate with dry summers, and approximately 90% of the annual precipitation occurs between November and April. Historically, relatively low-magnitude flow pulses occurred from late autumn until early spring in response to rainfall in the lower watershed followed by a snow melt-driven pulse from spring through early summer. In the 20th century, more than 40 dams were constructed on the Stanislaus River for flood protection, power generation, irrigation and municipal water supply. Collectively, these dams have the capacity to store 240% of the average annual runoff in the catchment and have reduced the amount of habitat available to Chinook salmon by 53% (Yoshiyama *et al.* 2001). Goodwin Dam (GDW), located at river kilometre (rkm) 94, is currently the upstream migration barrier to adult Chinook salmon and demarks the upstream end of the lower Stanislaus River (Fig. 1). Most fall-run Chinook salmon spawning in the lower Stanislaus River (LSR) occurs in the 29-km reach below GDW (from GDW to ~rkm 66); however, spawning has been observed as far downstream as rkm 53.1.

New Melones Dam, completed in 1979, impounds a reservoir that accounts for approximately 85% of the total storage capacity in the system and is the primary instrument of flow regulation in conjunction with GDW that serves as a re-regulating facility for the larger reservoir. In the years since New Melones Dam operation began, the LSR (below GWD) has changed from a dynamic river system, characterised by depositional and scour features, to a relatively static and entrenched system (Kondolf & Batalla 2005). Annual mean daily discharge has been reduced from 48 to 23 m³ s⁻¹ with mean 30-day maximum discharge reduced from 137 to 38 m³ s⁻¹ (Brown & Bauer 2009). Vegetation encroachment into the active channel, as well as urban and agricultural development, has altered the natural river channel-floodplain connection and has led to the coarsening of bed material, particularly within spawning habitat between Goodwin Dam and Honolulu Bar (Fig. 1).

Fall-run Chinook salmon freshwater life stages and timing

Similar to many anadromous salmonids, California Central Valley fall-run Chinook salmon exhibit distinct life stages that occur during specific time periods (Merz *et al.* 2013). In general, adults migrate from the Pacific Ocean to natal streams between August and December and spawning is initiated shortly after (peak from early October to late November). Chinook salmon require relatively cool, clear, flowing streams with appropriate substrate for successful spawning (Zeug *et al.* 2013), incubation and emergence (Tappel & Bjornn 1983).

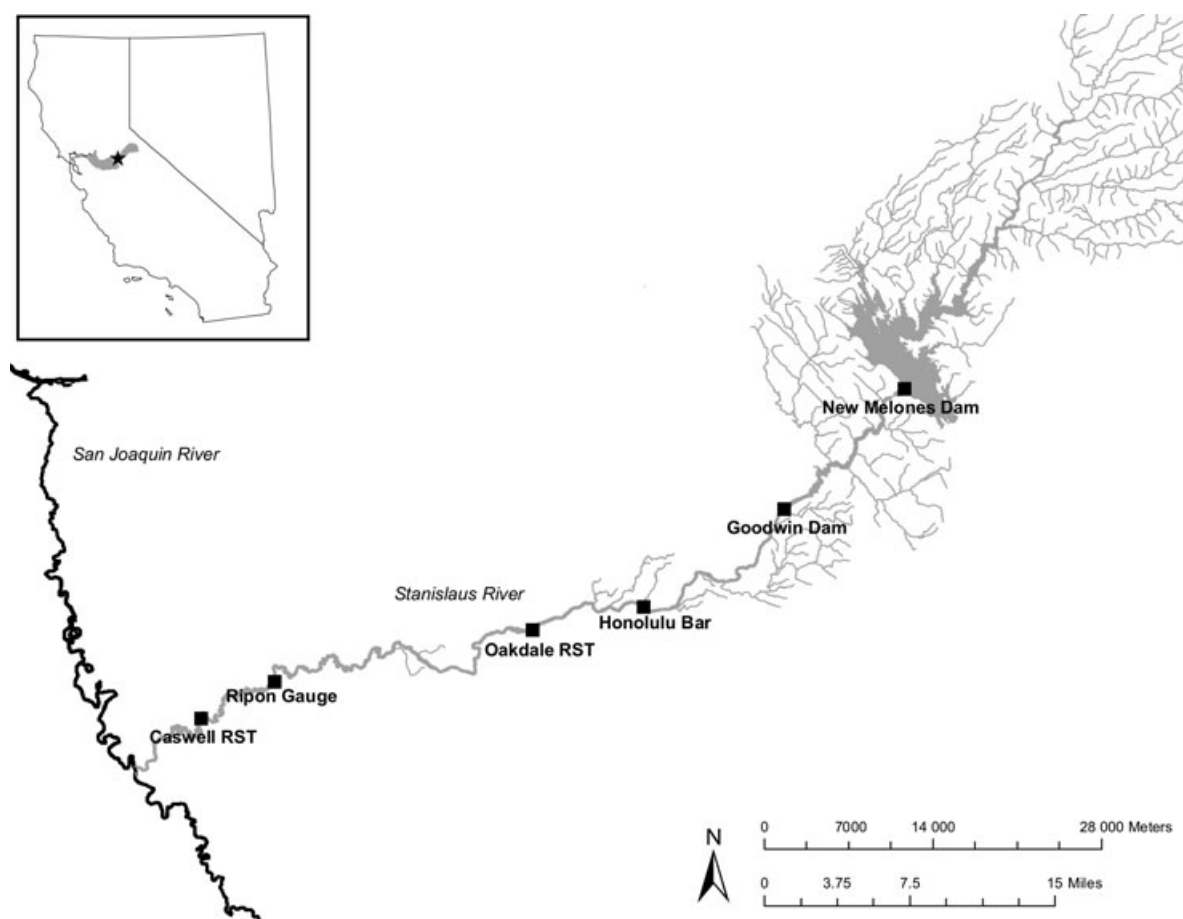


Figure 1. Location of the lower Stanislaus River, California and the location of rotary screw traps (RST) and other relevant features within the study area.

Incubation typically occurs from October through March, and emigration occurs from late December to early July.

Environmental variables

A suite of variables was measured to characterise LSR hydrologic and temperature regimes during the study period (Table 1). To facilitate comparisons of environmental conditions across years, a uniform range of days for each year was created to represent the juvenile rearing and emigration period. The beginning of the period was calculated as the day that 2.5% of cumulative juvenile Chinook salmon catch was observed for each year and averaged across years (mean = day of the year 17). The end date was calculated as the day that 97.5% of cumulative catch was observed for each year and averaged across years (mean = day of the year 147). These start and endpoints were assumed to represent conditions

the majority of juveniles experienced as they reared and migrated downstream through the LSR.

Hydrologic variables included in the analysis were cumulative discharge during the rearing period and variance in discharge during the rearing period. Mean daily flow was obtained from the United States Geological Survey stream gauge on the Stanislaus River located near Ripon, CA (Fig. 1) and converted to total daily flow ($\text{m}^3 \text{day}^{-1}$). To calculate cumulative flow, total daily flow was summed for the rearing period (130 days) each year (Table 1). Variance in flow was calculated as the sample variance of the total daily flow ($\text{m}^3 \text{day}^{-1}$) during the 130-day rearing period. Flow variation provides a mechanism for habitat creation and activation (e.g. bar formation, floodplain inundation) and has been identified as a trigger for fish migration and overall changes in metabolism (Raymond 1968; Hvidsten *et al.* 1995; Baker & Morhardt 2001).

Table 1. Environmental variables and estimates of Chinook salmon spawner abundance in the Stanislaus River during 1996–2009

Year	Cumulative discharge $\times 10^8$ (m ³)	Discharge variance $\times 10^9$ (m ³)	Degree days	Spawner abundance
1996	6.12	6.02	1602	168
1997	10.66	6.39	1838	5588
1998	8.07	5.33	1489	3087
1999	7.02	4.61	1533	4349
2000	4.78	3.75	1710	8498
2001	2.22	1.01	1767	7033
2002	2.23	0.52	1696	7787
2003	2.02	0.29	1773	5902
2004	1.68	0.41	1847	4015
2005	1.89	1.05	1849	1427
2006	11.02	8.90	1449	1923
2007	3.27	0.56	1659	443
2008	2.34	0.83	1639	865
2009	1.62	0.47	1737	595

Degree-days were used to represent the overall water temperatures that juvenile Chinook salmon were exposed to during the rearing period each year. Temperature data were obtained from the United States Geological Survey gauge on the Stanislaus River located near Ripon, CA (11303000). Degree-days were calculated by summing the mean temperature for each day during the juvenile rearing period. The use of degree-days for calculating the temperature-dependent development of poikilotherms is widely accepted as a basis for building phenology and population dynamics models (Taylor & McPhail 1985; Roltsch *et al.* 1999), and accumulated thermal units (analogous to degree-days) have been shown to initiate physiological changes linked to outmigration behavior of juvenile Chinook salmon (Sykes & Shrimpton 2010).

In addition to the three physical parameters described above, the number of adult spawners was acquired for each study year. These data were used to account for potential density-dependent effects on the demographic metrics. Spawner numbers were estimated by annual carcass surveys performed by the California Department of Fish and Wildlife and obtained from their 'Grand Tab' data base file available at <https://nrm.dfg.ca.gov/FileHandler.ashx?documentversionid=33911XXX>.

Fish sampling

Rotary screw traps (2.4-m diameter cone; manufactured by E.G. Solutions, Corvallis, OR, USA), were operated at two locations from 1996 to 2009 to index survival between the traps and estimate the size and life stage of juvenile Chinook salmon emigrating from the system. Rotary screw traps (RSTs) are commonly used in the

Pacific Northwest to monitor impacts of river management (e.g. habitat restoration, flow manipulation, dam management) on wild stocks (Volkhardt *et al.* 2007; Merz *et al.* 2013). Rotary screw traps are potentially powerful tools for validating assumptions regarding the effects of watershed restoration programs and land-use policies on fish populations (Solazzi *et al.* 2000; Johnson *et al.* 2005). These traps can also be used to assess survival between life stages, such as egg-to-smolt survival or parr-to-smolt overwinter survival (Solazzi *et al.* 2000; Johnson *et al.* 2005) and the effects of environmental parameters on migration timing and development (Sykes *et al.* 2009; Sykes & Shrimpton 2010).

The upstream RST was located at Oakdale (rkm 64.3; Fig. 1), which is immediately downstream from the majority of spawning habitat (hereafter referred to as the upstream trap). The upstream trap was assumed to provide a measure of juvenile Chinook salmon production from the spawning reach (Merz *et al.* 2013). The Caswell trap located at the lower extent of LSR rearing habitat (rkm 12.9) approximately 9 km from the San Joaquin River confluence (hereafter referred to as the downstream trap) was used to provide an estimate of out-migrating juveniles. Therefore, the lower trap provides a measure of size and survival of juvenile Chinook salmon exposed to the rearing reach just before exiting the LSR. Trap operations and configurations did not change among years at the upstream site where a single trap was operated. At the downstream site, two traps were operated in tandem for years 1996–2008; however, due to low flow and changes to site channel conditions, the trapping operation was relocated approximately 50 m downstream in 2009 to a site that would only accommodate a single trap.

Operation of LSR RSTs generally followed guidelines outlined in standard protocols [CAMP (Comprehensive Assessment & Monitoring Program) 1997; Volkhardt *et al.* 2007]. Traps were deployed each year between mid-December and mid-January, and sampling was terminated when at least seven consecutive days of trapping resulted in zero catch. This typically occurred in June or July near the end of the Central Valley fall-run Chinook salmon emigration (Williams 2006). Traps were checked daily or multiple times per day depending on debris load. Trap cones were raised on days when sampling did not occur due to excess debris or dangerous conditions.

All Chinook salmon <200 mm fork length (FL) and not demonstrating secondary sexual characteristics (e.g. releasing milt, spawning coloration) were designated as juveniles. Chinook salmon in the LSR are considered 'ocean type' because they primarily emigrate from the system prior to their first winter and typically before July

(Clarke *et al.* 1994). However, there are at least two distinct migration strategies. Juveniles may emigrate from the LSR in winter or early spring prior to smoltification (fry and parr) and rear in the estuary or possibly other non-natal waters prior to ocean entry, or they may rear in the LSR and leave as smolts later in the spring (Limm & Marchetti 2009; Merz *et al.* 2013). To examine factors influencing interannual variation in out-migration strategy, juvenile Chinook salmon were sub-classified as pre-smolt and smolt life stages. Although specific life-stage designations (i.e. fry, parr or smolt) based on morphological characteristics were made in the field, there was considerable variability in the characteristics used to differentiate the life stages, depending on the year and personnel conducting the sampling. Therefore, a piecewise linear regression model for each year of data was used to provide a more objective temporal split between pre-smolt- and smolt-dominated migration periods. These models are commonly used to identify thresholds, or 'breakpoints', where the slope of a regression line changes (Betts *et al.* 2007; Muggeo 2008). First, fish lengths were plotted by date for each year and trap location to provide a visual representation of the pattern of change in fish size. Next, the segmented statistical package in R, which uses initial estimates of breakpoint(s) to iteratively fit a standard linear model to the data, was used to generate an estimated annual breakpoint value (Muggeo 2008). This value corresponded to a day for each year and was considered the 'smolt date' whereby all fish captured up to and including the smolt date were categorized as pre-smolts and all fish captured after the smolt date were categorised as smolts, regardless of previous life stage designation.

To derive accurate abundance estimates at each trap, it was first necessary to estimate RST efficiency for each site. Mark-recapture trials with juvenile Chinook salmon were performed to estimate trap efficiency at both sites. Experimental mark-recapture groups of both hatchery and natural-origin juveniles were used to estimate trap efficiencies at the upstream ($n = 185$) and downstream ($n = 247$) traps. Release group sizes ranged from 17 to 6737 depending on the availability of fish for the trial and were performed during periods of flow change and throughout the migration period to capture the range of efficiency variability. Fish were dye-marked using a photonic marking gun (MadaJet A1000, Carlstadt, NJ, USA) with dye on the caudal or anal fin. Releases occurred approximately 430 m upstream of the traps from the north bank at a narrow, deep area of the river. Fish releases occurred approximately 1 h after dark in small groups (5–10 individuals) to encourage mixing with natural (unmarked) Chinook salmon in the river, reduce schooling and mimic pulses in natural catch during

nighttime migration. Marked fish were transported in a non-motorised boat and released across the channel at various points away from the bank. Traps were processed starting 1 h after completing release activities. Additional recaptures were recorded with the subsequent catch. To avoid pseudoreplication in efficiency analyses, data were pooled when multiple releases occurred on the same date. The maximum number of days post release that marked fish were collected ranged from 5 to 17 at the downstream trap and from 9 to 39 at the upstream trap.

Data analysis

Logistic regression was used to develop a predictive model of daily trap efficiencies. The dependent variable in these models was the binomial probability of capture. Independent variables included flow (log transformed), temperature, turbidity, fork length at release and year. A model was fit with an intercept (β_0), and then each explanatory variable was entered one at a time. The variable with the greatest explanatory power was then included in the model, and the remaining variables were again entered one at a time. The procedure was terminated when none of the remaining variables had a statistically significant effect on capture at $\alpha = 0.05$. The final model for the upstream trap included flow (negative relationship) and a year effect. The final model for the downstream trap included significant negative relationships with flow and fish fork length and a year effect.

Daily catch of migrating juvenile Chinook salmon for each trap was estimated as:

$$\hat{n} = \frac{c}{\hat{q}}$$

where c is the number of Chinook salmon captured each day and q is the estimated trap efficiency for that day from the logistic model. Error estimates for daily catch were calculated using the methods described in Appendix 1. During some years, there were periods when traps were not fished. A weighted average of all observed counts for the 5 days before and 5 days after the missing value were used to estimate a missing value of daily count (c) within a sampling period. The weights were equal to 1 through 5, where daily values that were 1 day before and after the missing day were weighted as 5, values that were two days before and after the missing day were weighted as 4, and so on. Annual catch estimates were generated by summing daily catch and error estimates (Fig. 2).

Three variables were estimated to describe the demographics of the juvenile Chinook salmon cohort in each

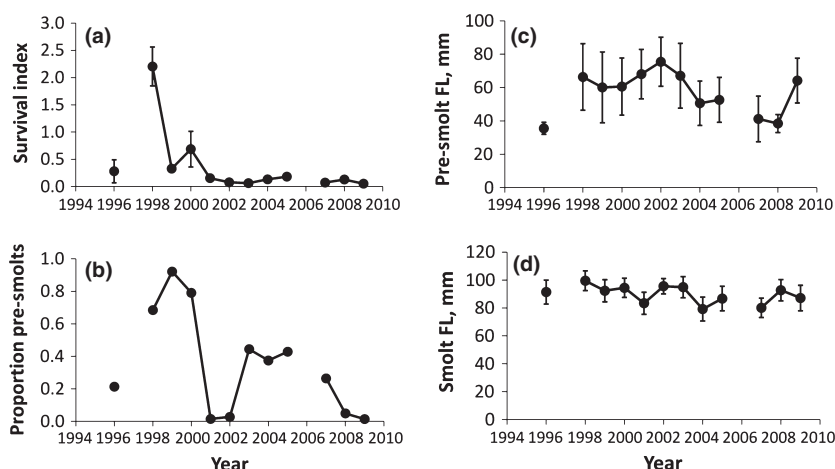


Figure 2. Demographic metrics (mean \pm SD) of the Stanislaus River juvenile Chinook salmon population during 1996–2009. (a) Survival index. (b) Proportion of migrants classified as pre-smolts. (c) Mean fork length (FL) of pre-smolt migrants. (d) Mean FL of smolt migrants.

year. First, annual catch estimates at each trap were used to index survival between the two traps:

$$S_i = \frac{\widehat{P}_D}{\widehat{P}_U}$$

where S_i is the index of survival, \widehat{P}_D is the estimated catch at the downstream trap and \widehat{P}_U is the estimated catch at the upstream trap (Fig. 2). Second, migration strategy was estimated as the proportion of all juveniles that migrated out of the system as pre-smolts in each year. Third, the fork length of juvenile emigrants was estimated in each study year. Fish length was separated by pre-smolts and smolts because portions of the population migrate at each stage. Migration strategy and fish length were modeled using only data from the downstream trap because this location captured fish that were actively migrating out of the system.

Prior to modeling the demographic metrics, a correlation analysis was performed on predictor variables to identify potential sources of multicollinearity. Correlations between all predictors were high (>0.70); thus, the full suite of predictor variables could not be included in the same statistical model without unacceptable variance inflation. Instead, four models were constructed (one for each demographic metric), and the strength of each predictor was evaluated using an information-theoretic approach.

For each of the four demographic metrics, the assumption of normality was tested with a Shapiro–Wilk test and auto correlation was tested with cross-correlation coefficients. When a parameter was identified as non-normal, an appropriate transformation was applied and the assumption of normality was retested. Four linear models were constructed for each demographic metric (16 total models) where the independent variables were: (1) cumu-

lative discharge; (2) discharge variance; (3) degree days and (4) spawner abundance. Akaike's information criterion corrected for small sample size (AIC_c) was used to evaluate the weight of evidence for each predictor. The difference in AIC_c values between each candidate model and the best model was calculated (ΔAIC_c), and models with a value <2 were considered to have similar support in the data (Burnham & Anderson 2002). Model weights ($AIC_c W$) also were calculated. These values are interpreted as the probability of each model being the 'best' of the four evaluated. The R^2 values of models with ΔAIC_c values <2 were used to evaluate overall model fit.

Finally, because estimates rather than observations were used as response variables in the linear models, Monte Carlo methods were used to reduce uncertainty in model estimates. One hundred re-samples of each response variable were performed for each year using a distribution informed by the sample mean and associated error. Abundance at each trap (used to calculate the survival index) was described by a negative binomial distribution, whereas a normal distribution was used for pre-smolt and smolt size. A predictor was considered to have good support in the data if the 95% confidence interval of its coefficient did not include zero.

Results

Survival

Indices for survival between the two traps ranged from 5% in 2009 to $>200\%$ in 1998 (Fig. 2). Fewer trap efficiency trials may have led to the survival index over 200% in 1998. As one of the survival estimates was $>100\%$, the data were scaled so that the value for 1998 was 100% and the values for all other years were

adjusted accordingly prior to use in statistical models. Following \log_{10} transformation, the data were found to be normal ($W = 0.909$, $P = 0.209$) and no autocorrelation was detected ($r = 0.36$, $P = 0.338$). Model selection based on ΔAIC_c values revealed that cumulative discharge and discharge variance had similar support for predicting survival, whereas degree days and the number of spawners were relatively poor predictors (Table 2). Both models had good overall fit to the data with R^2 values of 0.68 and 0.67 for cumulative discharge and discharge variance, respectively (Fig. 3). The coefficient in both models was positive indicating that survival increased as cumulative discharge and discharge variance increased (Table 3). The Monte Carlo exercise revealed that 94% of models that included cumulative discharge and 89% of models that included discharge variance had coefficients with confidence intervals that did not include zero suggesting low uncertainty for these relationships.

Migration strategy

The proportion of juvenile Chinook salmon that migrated as pre-smolts ranged from >0.92 in 1999 to 0.01 in 2001 and 2009 with a mean of 0.35 (SD = 0.32). Autocorrelation was not detected in the data ($r = 0.54$, $P = 0.136$), and the assumption of normality was met ($W = 0.905$, $P = 0.183$). Cumulative discharge was the best predictor of migration strategy, and discharge variance also had support in the data. However, the ΔAIC_c value of 2.11 for discharge variance was >2.00 that was the cutoff for assuming a similar level of support as the best fit model. (Table 2). Overall fit was good for models of cumulative discharge and dis-

charge variance with R^2 values of 0.43 and 0.33 respectively (Fig. 4). Similar to the survival models, the coefficients for both independent variables was positive indicating that more Chinook salmon juveniles migrated as pre-smolts when cumulative discharge and discharge variance were higher (Table 3). Monte Carlo estimates could not be generated for the migration strategy data because life stage-specific information was not consistently available from the efficiency tests to generate error estimates that could inform a distribution. All statistical analyses were performed with the program R (R Development Core Team 2012)

Pre-smolt migrant size

Juvenile Chinook salmon that emigrated as pre-smolts averaged 63.5 mm FL across all years with the smallest and largest pre-smolt emigrants observed in 1996 and 2002 (35.5 and 75.4 mm respectively). The data were normal following \log_{10} transformation ($W = 0.901$, $P = 0.163$), and autocorrelation was not significant ($r = 0.49$, $P = 0.182$). Spawner abundance was the only variable that accounted for size variation in pre-smolt migrants among years (Table 2). The R^2 value for this model was 0.51 indicating the model was a good fit to the data (Fig. 5). The size of pre-smolt migrants was greater in years with higher spawner abundance (Table 3). Models from the Monte Carlo exercise revealed only moderate certainty for the relationship with spawner density. Forty six percent of models yielded a coefficient with a confidence interval that did not include zero.

Smolt migrant size

Fork lengths of juveniles that emigrated as smolts averaged 86.8 mm across all years. The smallest smolt emigrants were observed in 2007 (80.1 mm) and the largest in 1998 (99.5 mm). Autocorrelation was not significant ($r = -0.170$, $P = 0.653$), and the logarithm-transformed data met the assumption of normality ($W = 0.933$, $P = 0.416$). Model selection indicated that three models were similarly supported predictors of smolt size (Table 2). The best model included degree days as the independent variable and competing models included cumulative discharge and discharge variance. All three competing models had moderately good fit with R^2 values of 0.31, 0.27 and 0.25 for degree days, cumulative discharge and discharge variance, respectively (Fig. 6). The coefficient for degree days was negative, whereas the coefficients for cumulative discharge and discharge variance were positive. The Monte Carlo exercise suggested high uncertainty in these relationships with $\leq 13\%$ of models for any of the three predictors having

Table 2. Results of the model selection exercise for juvenile Chinook salmon demographic metrics (response variable). Models for each response variable are listed in order from the most to least likely

Response variable	Predictor	AIC _c	ΔAIC_c	AIC _c W
Survival index	Cumulative discharge	8.75	0.00	0.58
	Discharge variance	9.42	0.67	0.41
	Degree days	17.83	9.08	<0.01
	Spawner abundance	22.32	13.57	<0.01
Proportion of pre-smolt migrants	Cumulative discharge	5.73	0.00	0.68
	Discharge variance	7.84	2.11	0.24
	Degree days	11.09	5.36	0.05
	Spawner abundance	11.94	6.21	0.03
Pre-smolt size	Spawner abundance	-21.81	0.00	0.96
	Discharge variance	-13.53	8.28	0.02
	Degree days	-13.38	8.43	0.01
	Cumulative discharge	-13.25	8.56	0.01
Smolt size	Degree days	-47.03	0.00	0.42
	Cumulative discharge	-46.17	0.86	0.27
	Discharge variance	-45.89	1.14	0.24
	Spawner abundance	-43.47	3.56	0.07

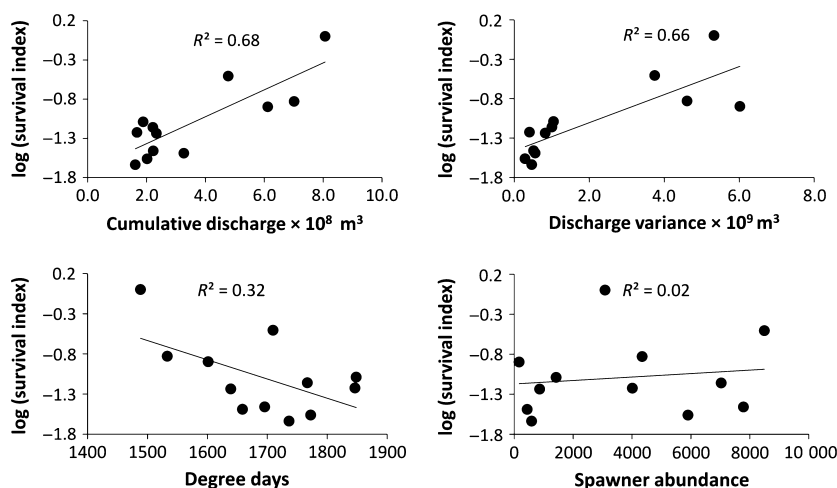


Figure 3. Relationships between the juvenile Chinook salmon survival index and four predictor variables.

Table 3. Coefficients and standard errors (in parentheses) for each predictor variable in linear models describing the four demographic metrics of juvenile Chinook salmon

Response variable	Cumulative discharge	Discharge variance	Degree days	Spawner abundance
Survival index	7.05×10^{-5} (1.52×10^{-5})	7.33×10^{-6} (1.64×10^{-6})	-0.002 (0.001)	2.16×10^{-5} (4.89×10^{-5})
Proportion of pre-smolt migrants	3.74×10^{-5} (1.34×10^{-5})	3.42×10^{-6} (1.54×10^{-6})	-0.001 (0.001)	2.48×10^{-5} (3.17×10^{-5})
Pre-smolt size	-1.28×10^{-6} (6.07×10^{-6})	-3.34×10^{-7} (6.32×10^{-7})	0.0001 (0.0002)	2.52×10^{-5} (7.78×10^{-6})
Smolt size	2.91×10^{-6} (1.54×10^{-6})	2.96×10^{-7} (1.64×10^{-7})	-1.57×10^{-4} (7.32×10^{-5})	2.87×10^{-6} (3.15×10^{-6})

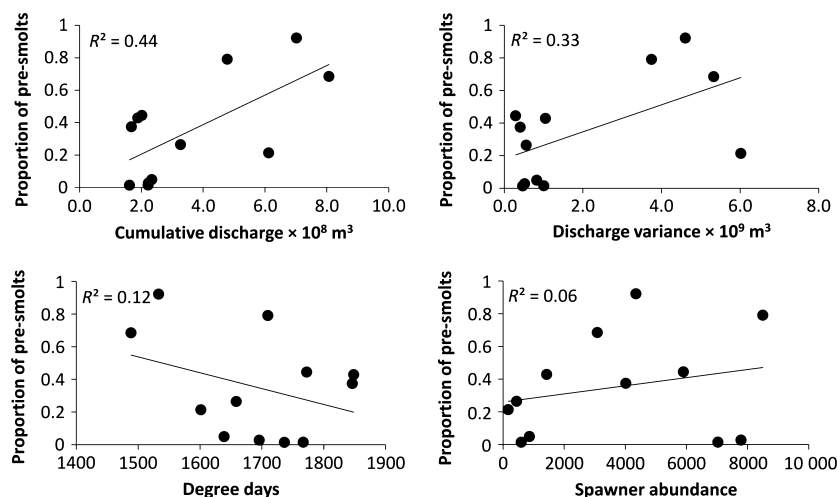


Figure 4. Relationships between the proportion of pre-smolt Chinook salmon migrants and four predictor variables.

coefficients with confidence intervals that did not include zero.

Discussion

The influence of flow regimes on the health of aquatic ecosystems has been widely recognised (Poff *et al.*

1997; Bunn & Arthington 2002). However, few studies have evaluated the demographic response of fish populations to flow regimes over multiple generations (Souchon *et al.* 2008). Analysis of 14 years of RST data on the LSR indicated that hydrology was a significant driver of several demographic characteristics of a Chinook salmon population. A strong positive response in survival, the

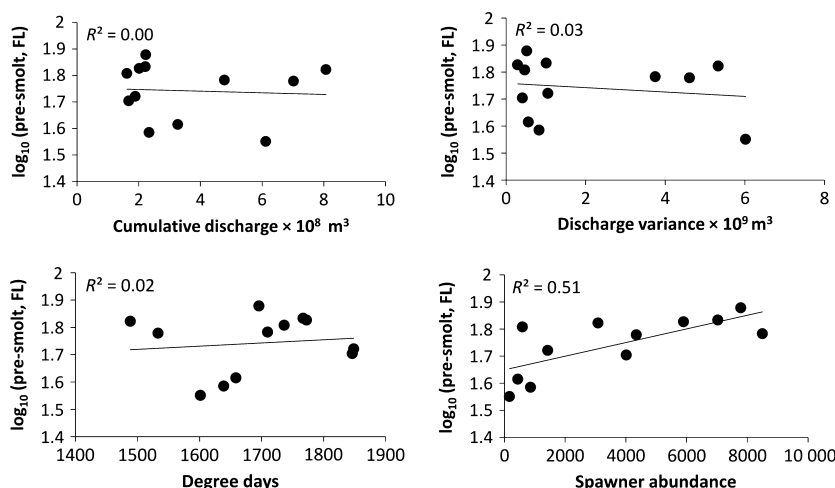


Figure 5. Relationships between the fork length (FL) of pre-smolt Chinook salmon migrants and four predictor variables.

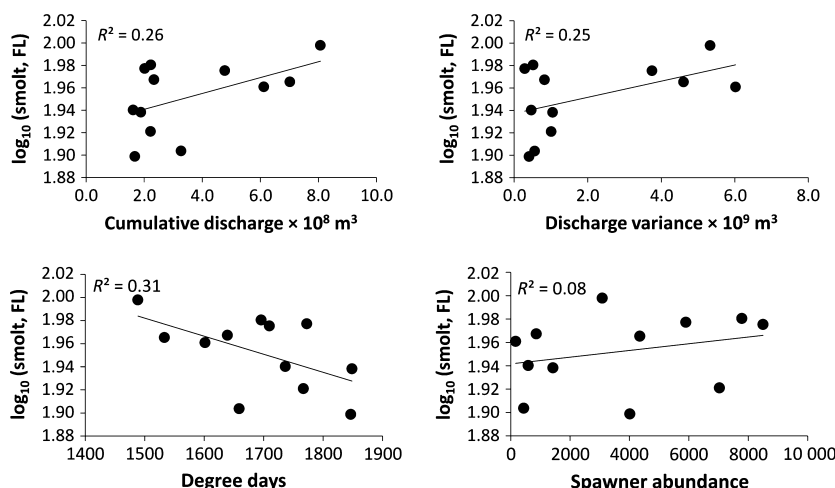


Figure 6. Relationships between the fork length (FL) of smolt Chinook salmon migrants and four predictor variables.

proportion of pre-smolt migrants and the size of smolts were observed when cumulative flow and flow variance were greater. Together, these data suggest that periods of high discharge in combination with high discharge variance are important for successful emigration as well as migrant size and the maintenance of diverse migration strategies.

Survival of migrating juveniles was higher when both cumulative discharge and discharge variance were greater. In a review of flow effects on salmonids, Nislow and Armstrong (2012) reported that reduced flow during the early emigration period was associated with lower growth and survival. Flow pulses provide fish access to seasonal habitats such as floodplains and side channels where food resources are often more abundant and predator densities lower (Junk *et al.* 1989; Bellmore *et al.* 2013). Chinook salmon rearing on California floodplains have been found to grow significantly

faster than fish in the main channel (Sommer *et al.* 2001; Jeffres *et al.* 2008). Since the construction of New Melones Dam, the LSR has become increasingly incised resulting in greater disconnection from its floodplain because greater flows are now required for floodplain inundation (Kondolf *et al.* 2001). A lack of access to off-channel habitats in years with low discharge and discharge variance may partially explain why low survival indices were observed. Higher velocities within the main channel may also reduce exposure time of migrating juveniles to predation within a specific stream reach (Cavallo *et al.* 2013). While turbidity data were not available, increased turbidity during high flow events might also influence behavior and success of emigrating juveniles (Gregory & Levings 1998), and this should be investigated further.

The proportion of Chinook salmon juveniles migrating as pre-smolts also responded positively to higher

cumulative discharge and discharge variance, supporting diversity in migration strategies (greater proportion of smolt migrants during lower discharge conditions, greater proportion of pre-smolt migrants during higher discharge conditions). It is unknown if LSR pre-smolt or smolt migrants survive better to later life stages; however, pre-smolt migrants from the Central Valley do survive and return as adults to spawn (Miller *et al.* 2010). The maintenance of multiple migration strategies can improve the persistence of salmon populations by spreading risk over space and time (Schindler *et al.* 2010). Reduction or elimination of the pre-smolt migration strategy by reducing cumulative discharge and discharge variance could have serious consequences for the LSR Chinook salmon population as risks associated with migration are increasingly concentrated into a relatively short time period (Carlson & Satterthwaite 2011).

The number of adult spawners was the only well supported predictor of pre-smolt size. Previous studies have found that marine-derived nutrients from spawner carcasses are incorporated into stream food webs that support juvenile salmon (Cederholm *et al.* 1999; Reimchen *et al.* 2002). Thus, increased spawner density may have increased productivity of invertebrate prey exploited by juvenile salmon or direct nutrient uptake from decomposing carcasses (Bilby *et al.* 1996). Alternatively, favorable ocean conditions that result in greater spawner returns may allow females to produce higher quality eggs that result in larger juveniles (Brooks *et al.* 1997; Heinimaa & Heinimaa 2004). However, caution should be used when interpreting this relationship. Negative density dependence may occur when spawner density exceeds the range observed during the years of this study. Thus, the relationship may not be linear across the range of potential spawner returns. Monte Carlo resamples of the data suggested there was only moderate certainty in this relationship. Additionally, both survival and the proportion of pre-smolt migrants could have stronger relationships with spawner density at levels above those observed during this study. The effects of quantity and quality of adult spawners on LSR juvenile offspring should also be evaluated further.

Juvenile size and water temperature at the time of Chinook salmon emigration can have a significant effect on ocean survival (Zeug & Cavallo 2013). Our results indicated that smolt size at emigration from the LSR had the strongest relationship with degree days. The Stanislaus River is located near the southern range limit of Chinook salmon spawning where temperatures can frequently exceed the optimum for the species (Myrick & Cech 2004; Williams 2006). Fish are strongly influenced by water temperature, which affects body temperature, growth rate, food consumption, food con-

version and other physiological functions (Houlihan *et al.* 1993; Azevedo *et al.* 1998). The negative relationship between smolt size and temperature suggests that temperatures may get high enough to impede growth in certain years. Monte Carlo resamples indicated high uncertainty in all relationships with smolt size. However, the negative effects of altered flow regimes can be exacerbated by temperatures outside of the optimum for juvenile salmonids (Nislow & Armstrong 2012), and further investigation of this issue in the LSR is warranted.

Despite strong relationships between hydrology and early Chinook salmon ontogeny and survival within the LSR, several considerations should be recognised when interpreting these results. Although RSTs are a tool frequently used to monitor migratory fishes (primarily salmon), they only provide indirect evidence of survival in relation to environmental conditions. More direct evidence can be obtained with techniques such as biotelemetry; however, long term data sets obtained with these technologies are not yet available for analysis, nor does such technology presently lend itself to earlier stages of salmon (i.e. fry-sized fish). Additionally, RSTs may be limited during periods of high flows when debris loads compromise trap operations and field personnel safety. This could mean that RSTs underestimate the number of juvenile salmon emigrating during these periods. It is likely that this aspect of RSTs contributed to the 1998 results when a greater number of Chinook salmon was estimated at the downstream trap. Finally, information theoretic methods can only select the best models from a candidate set. There may be predictors not examined here that better explain the data (e.g. predation rate) but were not available for analysis. If data on other potential predictors are available in the future, their fit can be evaluated against the predictors examined here. Regardless of these issues, RSTs provide robust, long-term monitoring data sets that are required to evaluate population-level responses to changes in flow regime (Souchon *et al.* 2008; Poff & Zimmerman 2010), and model selection identified several strong relationships between juvenile Chinook salmon and flow regime.

Pacific salmon life history diversity differs significantly across streams with different hydrologic regimes (Beechie *et al.* 2006). Conservation of such diversity is a critical element of recovery efforts, and preserving and restoring life history diversity depends in part on environmental factors affecting their expression (Schindler *et al.* 2010). This study found significant responses from juvenile Chinook salmon demography to variation in the LSR hydrologic regime. Although many methods have been used to establish sufficient flows for fish (Jowett 1997), strategies that mimic aspects of the natural flow regime are more likely to be successful (Richter *et al.*

1997). Flow regimes are an integral part of the habitat template to which aquatic species are adapted (Townsend & Hildrew 1994; Lytle & Poff 2004), and mismatches between flow and species life history traits (e.g. migration strategy) can create bottlenecks for population persistence (Schiemer *et al.* 2003). Reduced flow variance and cumulative flow were associated with reduced survival and the proportion of pre-smolt migrants. Although the volume of water released in regulated streams is paramount to fisheries management, stream flows during biologically important times of the year appear equally important (Kiernan *et al.* 2012). Together, these data suggest that cumulative discharge, discharge variance and water temperature are important environmental drivers, and they all should be included in the development of regulated flows to support the persistence of Chinook salmon populations and diverse life history strategies. While this study focused on a single Pacific salmon race in a highly regulated system, the analyses demonstrated here can be employed wherever migratory species and environmental parameters are adequately monitored.

Acknowledgments

The authors thank P. Bergman, B. Cavallo, R. Johnson, B. Pyper, W. Satterthwaite, A. Sturrock, D. Threlloff and M. Workman for helpful discussions on initial concepts for this manuscript. A. Gray and K. Jones provided significant input on an earlier draft. We greatly appreciate data collected by Cramer Fish Sciences, FishBio, the U.S. Bureau of Reclamation, and various entities that provided data utilized in this article. Funding for this project was provided by the U.S. Fish and Wildlife Service under contract 81332-6-G008. The findings and conclusions in this article are those of the authors and do not necessarily represent the views of the U.S. Fish and Wildlife Service. Mention of trade names does not constitute endorsement by the U.S. Government.

References

- Ahearn D.S., Viers J.H., Mount J.F. & Dahlgren R.A. (2006) Priming the productivity pump: flood pulse driven trends in suspended algal biomass distribution across a restored floodplain. *Freshwater Biology* **51**, 1417–1433.
- Albright L.J. (1983) Influence of river-ocean plumes upon bacterioplankton production of the Strait of Georgia, British Columbia. *Marine Ecology Progress Series* **12**, 107–113.
- Azevedo P.A., Cho C.Y., Leeson S. & Bureau D.P. (1998) Effects of feeding level and water temperature on growth, nutrient and energy utilization and waste outputs of rainbow trout (*Oncorhynchus mykiss*). *Aquatic Living Resources* **11**, 227–238.
- Baker P.F. & Morhardt J.E. (2001) Survival of Chinook salmon smolts in the Sacramento – San Joaquin Delta and Pacific Ocean. In: R.L. Brown (ed.) *Contributions to the Biology of Central Valley Salmonids*, Vol. 2. Sacramento, CA: California Department of Fish and Game, pp. 163–182.
- Beechie T., Buhle E., Ruckelshaus M., Fullerton A. & Holsinger L. (2006) Hydrologic regime and the conservation of salmon life history diversity. *Biological Conservation* **130**, 560–572.
- Bellmore J.R., Baxter C.V., Martens K. & Connolly P.J. (2013) The floodplain food web mosaic: a study of its importance to salmon and steelhead with implications for their recovery. *Ecological Applications* **23**, 189–207.
- Betts M., Forbes G. & Diamond A. (2007) Thresholds in songbird occurrence in relation to landscape structure. *Conservation Biology* **21**, 1046–1058.
- Bilby R.E., Fransen B.R. & Bisson P.A. (1996) Incorporation of nitrogen and carbon from spawning coho salmon into the trophic system of small streams: evidence from stable isotopes. *Canadian Journal of Fisheries and Aquatic Sciences* **53**, 164–173.
- Brooks S., Tyler C.R. & Sumpter J.P. (1997) Egg quality in fish: what makes a good egg? *Reviews in Fish Biology and Fisheries* **7**, 387–416.
- Brown L.R. & Bauer M.L. (2009) Effects of hydrologic infrastructure on flow regimes of California's Central Valley rivers: implications for fish populations. *River Research and Applications* **26**, 751–765.
- Bunn S.E. & Arthington A.H. (2002) Basic principles and ecological consequences of altered flow regimes for aquatic biodiversity. *Environmental Management* **30**, 492–507.
- Burnham K.P. & Anderson D.R. (2002) *Model Selection and Multimodel Inference: A Practical Information-Theoretic Approach*, 2nd edn. New York, NY: Springer, p. 488.
- CAMP (Comprehensive Assessment and Monitoring Program) (1997) *Standard Protocol for Rotary Screw Trap Sampling of Out-migrating Juvenile Salmonids*. Sacramento, CA: U. S. Fish and Wildlife Service, p. 10.
- Carlson S.M. & Satterthwaite W.H. (2011) Weakened portfolio effect in a collapsed salmon population complex. *Canadian Journal of Fisheries Aquatic Sciences* **68**, 1579–1589.
- Cavallo B., Merz J. & Setka J. (2013) Effects of predator and flow manipulation on Chinook salmon (*Oncorhynchus tshawytscha*) survival in an imperiled estuary. *Environmental Biology of Fishes* **96**, 393–403.
- Cederholm C.J., Kunze M.D., Murota T. & Sibatani A. (1999) Pacific salmon carcasses: essential contributions of nutrients and energy for aquatic and terrestrial ecosystems. *Fisheries* **24**, 6–15.
- Clarke W.C., Withler R.E. & Shelbourn J.E. (1994) Inheritance of smolting phenotypes in backcrosses of hybrid stream-type × ocean-type Chinook salmon (*Oncorhynchus tshawytscha*). *Estuaries* **17**, 13–25.
- Dingle H. (1996) *Migration: the Biology of Life on the Move*. Oxford, UK: Oxford University Press on Demand, p. 480.
- Gelman A., Carlin J.B., Stern H.S. & Rubin D.B. (1995) *Bayesian Data Analysis*. London: Chapman and Hall, p. 649.

- Greene C.M., Jensen D.W., Pess G.R. & Steel E.A. (2005) Effects of environmental conditions during stream, estuary, and ocean residency on Chinook salmon return rates in the Skagit River, Washington. *Transactions of the American Fisheries Society* **134**, 1562–1581.
- Gregory R.S. & Levings C.D. (1998) Turbidity reduces predation in migrating juvenile Pacific salmon. *Transactions of the American Fisheries Society* **127**, 275–285.
- Heinimaa S. & Heinimaa P. (2004) Effect of the female size on egg quality and fecundity of the wild Atlantic salmon in the sub-arctic River Teno. *Boreal Environment Research* **9**, 55–62.
- Hoekstra J.M., Bartz K.K., Ruckelshaus M.H., Moslemi J.M. & Harms T.K. (2007) Quantitative threat analysis for management of an imperiled species: Chinook salmon (*Oncorhynchus tshawytscha*). *Ecological Applications* **17**, 2061–2073.
- Houlihan D.F., Mathers E.M. & Foster A. (1993) Biochemical correlates of growth rate in fish. In: J.C. Rankin & F.B. Jensen (eds) *Fish Ecophysiology*. London: Chapman and Hall, pp. 45–71.
- Hvidsten N.A., Jensen A.J., Vivas H., Bakke O. & Heggeberget T.G. (1995) Downstream migration of Atlantic salmon smolts in relation to water flow, water temperature, moon phase and social interaction. *Nordic Journal of Freshwater Research* **70**, 38–48.
- Jeffres C.A., Opperman J.J. & Moyle P.B. (2008) Ephemeral floodplain habitats provide best growth conditions for juvenile Chinook salmon in a California river. *Environmental Biology of Fishes* **83**, 449–458.
- Johnson S.L., Rodgers J.D., Solazzi M.F. & Nickelson T.E. (2005) Effects of an increase in large wood on abundance and survival of juvenile salmonids (*Oncorhynchus* spp.) in an Oregon coastal stream. *Canadian Journal of Fisheries and Aquatic Sciences* **62**, 412–424.
- Jowett I.G. (1997) Instream flow methods: a comparison of approaches. *Regulated Rivers: Research and Management* **13**, 115–127.
- Junk W.J., Bayley P.B. & Sparks R.E. (1989) The flood pulse concept in river-floodplain systems. In: D.P. Dodge (ed.) *Proceedings of the International Large River Symposium*. Canadian Special Publication of Fisheries and Aquatic Sciences 106, pp. 110–127.
- Kiernan J.D., Moyle P.B. & Crain P.K. (2012) Restoring native fish assemblages to a regulated California stream using the natural flow regime concept. *Ecological Application* **22**, 1472–1482.
- Kondolf G.M. & Batalla R.J. (2005) Hydrological effects of dams and water diversions on rivers of Mediterranean-climate regions: examples from California. *Developments in Earth Surface Processes* **7**, 197–211.
- Kondolf G.M., Falzone A. & Schneider K.S. (2001) *Reconnaissance-level Assessment of Channel Change and Spawning Habitat on the Stanislaus River below Goodwin Dam*. Sacramento, CA: U.S. Fish and Wildlife Service, p. 60.
- Limm M.P. & Marchetti M.P. (2009) Juvenile Chinook salmon (*Oncorhynchus tshawytscha*) growth in off-channel and main-channel habitats on the Sacramento River, CA using otolith increment widths. *Environmental Biology of Fishes* **85**, 141–151.
- Lytle D.A. & Poff N.L. (2004) Adaptation to natural flow regimes. *Trends in Ecology and Evolution* **19**, 94–100.
- Mantua N.J., Hare S.R., Zhang Y., Wallace J.M. & Francis R.C. (1997) A Pacific interdecadal climate oscillation with impacts on salmon production. *Bulletin of the American Meteorological Society* **78**, 1069–1079.
- Merritt D.M. & Cooper D.J. (2000) Riparian vegetation and channel change in response to river regulation: a comparative study of regulated and unregulated streams in the Green River Basin, USA. *Regulated Rivers: Research and Management* **16**, 543–564.
- Merz J.E., Workman M.L., Wikert J.D. & Cavallo B. (2013) Salmon lifecycle considerations to guide stream management: examples from California's Central Valley. *San Francisco Estuary and Watershed Science* **11**. jmie_sfews_13365. Available at: <http://www.escholarship.org/uc/item/30d7b0g7> (accessed 13 June 2013)
- Miller J.A., Gray A. & Merz J. (2010) Quantifying the contribution of juvenile migratory phenotypes in a population of Chinook salmon *Oncorhynchus tshawytscha*. *Marine Ecology Progress Series* **408**, 227–240.
- Mood A.M., Graybill F.A. & Boes D.C. (1974) *Introduction to the Theory of Statistics*, 3rd edn. New York, NY: McGraw-Hill, p. 480.
- Muggeo V.M. (2008) Segmented: an R package to fit regression models with broken-line relationships. *R News* **8**, 20–25.
- Myrick C.A. & Cech J.J. (2004) Temperature effects on juvenile anadromous salmonids in California's Central Valley: what don't we know? *Reviews in Fish Biology and Fisheries* **14**, 113–123.
- Neter J., Wasserman W. & Kutner M.H. (1990) *Applied Linear Statistical Models*, 3rd edn. Boston, MA: Irwin, p. 1408.
- Nislow K.H. & Armstrong J.D. (2012) Towards a life-history-based management framework for the effects of flow on juvenile salmonids in streams and rivers. *Fisheries Management and Ecology* **19**, 451–463.
- Poff N.L. & Zimmerman J.K.H. (2010) Ecological responses to altered flow regimes: a literature review to inform environmental flows science and management. *Freshwater Biology* **55**, 194–205.
- Poff N.L., Allan J.D., Bain M.B., Karr J.R., Prestegard K.L., Richter B.D. et al. (1997) The natural flow regime. *BioScience* **47**, 769–783.
- R Development Core Team (2012) *R: A Language and Environment for Statistical Computing*. R Foundation for Statistical Computing, ISBN 3-900051-07-0, Available at: <http://www.R-project.org/> (accessed 23 May 2012)
- Raymond H.L. (1968) Migration rates of yearling Chinook salmon in relation to flows and impoundments in the Columbia and Snake rivers. *Transactions of the American Fisheries Society* **97**, 356–359.
- Reimchen T.E., Mathewson D., Hocking M.D. & Moran J. (2002) Isotopic evidence for enrichment of salmon-derived nutrients in

- vegetation, soil and insects in riparian zones in coastal British Columbia. In: J.G. Stockner (ed.) *Nutrients in Salmonid Ecosystems: Sustaining Production and Biodiversity*. Bethesda, MD: American Fisheries Society Symposium 34, pp. 59–69.
- Richter B.D., Baumgartner J.V., Wigington R. & Braun D.P. (1997) How much water does a river really need? *Freshwater Biology* **37**, 231–249.
- Roltsch W.J., Zalom F.G., Strawn A.J., Strand J.F. & Pitcairn M.J. (1999) Evaluation of several degree-day estimation methods in California climates. *International Journal of Biometeorology* **42**, 169–176.
- Schiemer F., Keckeis H. & Kamler E. (2003) The early life history stages of riverine fish: ecophysiological and environmental bottlenecks. *Comparative Biochemistry and Physiology Part A* **133**, 439–449.
- Schindler D.E., Hilborn R., Chasco B., Boatright C.P., Quinn T.P., Rogers L.A. *et al.* (2010) Population diversity and the portfolio effect in an exploited species. *Nature* **465**, 609–613.
- Solazzi M.F., Nickelson T.E., Johnson S.L. & Rodgers J.D. (2000) Effects of increasing winter rearing habitat on abundance of salmonids in two coastal Oregon streams. *Canadian Journal of Fisheries and Aquatic Sciences* **57**, 906–914.
- Sommer T., Nobriga M.L., Harrell W.C., Batham W. & Kimmerer W.J. (2001) Floodplain rearing of juvenile Chinook salmon: evidence of enhanced growth and survival. *Canadian Journal of Fishery and Aquatic Sciences* **58**, 325–333.
- Souchon Y., Sabaton C., Deibel R., Reiser D., Kershner J., Gard M. *et al.* (2008) Detecting biological responses to flow management: missed opportunities; future directions. *River Research and Applications* **24**, 506–518.
- Sykes G.E. & Shrimpton J.M. (2010) Effect of temperature and current manipulation on smolting in Chinook salmon (*Oncorhynchus tshawytscha*): the relationship between migratory behavior and physiological development. *Canadian Journal of Fisheries and Aquatic Sciences* **67**, 191–201.
- Sykes G.E., Johnson C.J. & Shrimpton J.M. (2009) Temperature and flow effect on migration timing of Chinook salmon smolts. *Transactions of the American Fisheries Society* **138**, 1252–1265.
- Tappel P.D. & Bjornn T.C. (1983) A new method of relating size of spawning gravel to salmonid embryo survival. *North American Journal of Fisheries Management* **3**, 123–135.
- Taylor E.B. & McPhail J.D. (1985) Ontogeny of the startle response in young coho salmon, *Oncorhynchus kisutch*. *Transactions of the American Fisheries Society* **114**, 552–557.
- Townsend C.R. & Hildrew A.G. (1994) Species traits in relation to a habitat templet for river systems. *Freshwater Biology* **31**, 265–275.
- Trush W.J., McBain S.M. & Leopold L.B. (2000) Attributes of an alluvial river and their relation to water policy and management. *Proceedings of the National Academy of Sciences* **97**, 11858–11863.
- Vinson M.R. (2001) Long-term dynamics of an invertebrate assemblage downstream from a large dam. *Ecological Applications* **11**, 711–730.
- Volkhardt G.C., Johnson S.L., Miller B.A., Nickelson T.E. & Seiler D.E. (2007) Rotary screw traps and inclined plane screen traps. In: D.H. Johnson, B.M. Shrier, J.S. O'Neal, J.A. Knutzen, X. Augerot, T.A. O'Neil & T.N. Pearsons (eds) *Salmonid Field Protocols Handbook: Techniques for Assessing Status and Trends in Salmon and Trout Populations*. Bethesda, MD: American Fisheries Society, pp. 235–266.
- Wilcock P.R., Barta A.F., Shea C.C., Kondolf G.M., Matthews W.V.G. & Pitlick J.C. (1996) Observations of flow and sediment entrainment on a large gravel-bed river. *Water Resources Research* **32**, 2897–2909.
- Williams J.G. (2006) Central Valley salmon: a perspective on Chinook and steelhead in the Central Valley of California. *San Francisco Estuary and Watershed Science* **4**, Article 2. Available: <http://repositories.cdlib.org/jmie/sfews/vol4/iss3/art2/> (accessed 07 July 2007)
- Yoshiyama R.M., Gerstung E.R., Fisher F.W. & Moyle P.B. (2001) Historical and present distribution of Chinook salmon in the Central Valley of California. *California Department of Fish and Game Fish Bulletin* **179**, 71–176.
- Zeug S.C. & Cavallo B.J. (2013) Influence of estuary conditions on the recovery rate of coded wire tagged Chinook salmon (*Oncorhynchus tshawytscha*) in an ocean fishery. *Ecology of Freshwater Fish* **22**, 157–168.
- Zeug S.C., Sellheim K., Watry C., Rook B., Hannon J., Zimmerman J. *et al.* (2013) Gravel augmentation increases spawning utilization by anadromous salmonids: a case study from California, USA. *River Research and Applications* doi: 10.1002/rra.2680.

Appendix (1) The following describes the methods used to estimate the variance and confidence intervals for total annual juvenile Chinook salmon catch. It begins with a description of the variance of a given daily catch estimate (\hat{n}), and then extends the formulas to the total annual catch. As noted in the methods, daily catch was estimated by:

$$\hat{n} = \frac{c}{\hat{q}}, \quad (1)$$

where c was the observed daily count of trapped juveniles and \hat{q} was the estimated trap efficiency for that day. To simplify notation, \hat{q} is expressed in terms of the daily 'expansion factor' denoted e , where:

$$\hat{e} = \frac{1}{\hat{q}}. \quad (2)$$

Thus, the daily catch estimate (\hat{n}) can be expressed as the following product: $\hat{n} = \hat{e}c$. (3)

There are two sources of variability in \hat{n} . First, there is error associated with the estimation of trap efficiency via logistic regression, which will be expressed as error in \hat{e} . Second, there is sampling error associated with the

daily count (c), which is assumed to be a binomial variable. An estimate of the variance of \hat{n} is given by Goodman (1960):

$$\hat{\sigma}^2\{\hat{n}\} = \hat{e}^2 \cdot \hat{\sigma}^2\{c\} + c^2 \cdot \hat{\sigma}^2\{\hat{e}\} - \hat{\sigma}^2\{\hat{e}\} \cdot \hat{\sigma}^2\{c\} \quad (4)$$

To obtain a variance estimate for \hat{e} , it is first expressed in terms of the back-transformation of the logit function (see equation (4)). Substituting equation 2 into equation 4 and rearranging yields:

$$\hat{e} = 1 + \exp[-(\hat{\beta}_0 + \hat{\beta}_1 x)] = 1 + \exp(-\hat{y}), \quad (5)$$

where \hat{y} is the logit transform of the estimated trap efficiency \hat{q} (see equation (3)). Given that the distribution of \hat{y} is approximately normal, \hat{e} is assumed to be log-normally distributed with an estimator of variance given by Gelman *et al.* (1995, p. 478):

$$\hat{\sigma}^2\{\hat{e}\} = \exp(-2\hat{y}) * \exp(\hat{\sigma}^2\{\hat{y}\}) * [\exp(\hat{\sigma}^2\{\hat{y}\}) - 1] \quad (6)$$

The variance of \hat{y} , which is a prediction from a linear regression, can be expressed in matrix notation as (Neter *et al.* 1990, p. 215):

$$\hat{\sigma}^2\{\hat{y}\} = \mathbf{X}'\mathbf{s}^2\{\mathbf{b}\}\mathbf{X}, \quad (7)$$

where \mathbf{X} is a vector containing the daily values of the explanatory variables, \mathbf{X}' denotes the transpose of \mathbf{X} , and $\mathbf{s}^2\{\mathbf{b}\}$ denotes the scaled estimate of the variance-covariance matrix for the logistic regression coefficients ($\hat{\beta}$). Specifically,

$$\mathbf{X} = \begin{bmatrix} 1 \\ x \end{bmatrix}, \mathbf{X}' = [1 \quad x], \mathbf{s}^2\{\mathbf{b}\} = \hat{\phi} \begin{bmatrix} \hat{\sigma}^2\{\hat{\beta}_0\} & \hat{\sigma}\{\hat{\beta}_0, \hat{\beta}_1\} \\ \hat{\sigma}\{\hat{\beta}_0, \hat{\beta}_1\} & \hat{\sigma}^2\{\hat{\beta}_1\} \end{bmatrix}. \quad (8)$$

Here, x is the daily value of $\log(\text{flow})$. Note that the variance-covariance matrix for the logistic regression coefficients is multiplied (i.e. scaled) by the estimated dispersion parameter ($\hat{\phi}$) to account for extra-binomial variation. Equation 6 through equation 8 define the variance estimate for \hat{e} required in equation 4. Also required in equation 4 is the variance of c , the observed daily count of trapped juveniles. Assuming that c follows a binomial distribution conditional on daily catch (n) and trap efficiency (q) (i.e. $c \sim \text{Bin}(n, q)$), the theoretical variance for c would equal $nq(1-q)$. However, a more reasonable and conservative approach is to assume that c is subject to the same extra-binomial variation estimated for the trap-efficiency tests. Extra-binomial variation

would be expected due to unaccounted for factors affecting trap efficiency or characteristics of fish behavior, such as schooling. Thus, the variance of c is estimated as:

$$\hat{\sigma}^2 c = \hat{\phi} \hat{n} \hat{q} (1 - \hat{q}) \quad (9)$$

Equations A4 through A9 define the variance estimate for a given daily catch estimate (\hat{n}) given the estimated trap efficiency (\hat{q}) and trap count (c) for that day. The estimated total catch (N) of juveniles across days ($i = 1, 2, 3, \dots, k$) of the sampling season is the sum:

$$\hat{N} = \sum_{i=1}^k \hat{n}_i, \quad (10)$$

with associated variance (Mood *et al.* 1974, p. 179)

$$\hat{\sigma}^2\{\hat{N}\} = \sum_{i=1}^k \hat{\sigma}^2\{\hat{n}_i\} + 2 \sum_{i=1}^{k-1} \sum_{j>i}^k \hat{\sigma}\{\hat{n}_i, \hat{n}_j\}. \quad (11)$$

The left side of equation 11 is sum of the variances of the daily catch estimates as defined by equation 4. The right side denotes the sum of the covariances among all pairs of daily catch estimates. These covariances arise from the fact that all daily catch estimates are based on predictions of q derived from the same logistic regression. Following from equations 3 and 5, the covariance of any two catch estimates can be approximated as follows:

$$\hat{\sigma}\{\hat{n}_i, \hat{n}_j\} = (c_i \hat{e}_i) * (c_j \hat{e}_j) * (\mathbf{X}'\mathbf{s}^2\{\mathbf{b}\}\mathbf{X}), \quad (12)$$

where

$$\mathbf{X} = \begin{bmatrix} 1 & x_i \\ 1 & x_j \end{bmatrix}, \mathbf{X}' = \begin{bmatrix} 1 & 1 \\ x_i & x_j \end{bmatrix}. \quad (13)$$

Again, $\mathbf{s}^2\{\mathbf{b}\}$ denotes the scaled variance-covariance matrix for the logistic coefficients as in equation 8.

Approximate 95% confidence intervals for \hat{N} assuming log normally distributed error is given by:

$$95\%LCI\{\hat{N}\} = \frac{\hat{N}}{c}, \text{ and } 95\%UCI\{\hat{N}\} = \hat{N} * c, \quad (14)$$

where

$$c = \exp(Z_{\alpha/2}) * \sqrt{\log_e(1 + (\hat{\sigma}\{\hat{N}\}/\hat{N})^2)} \quad (15)$$